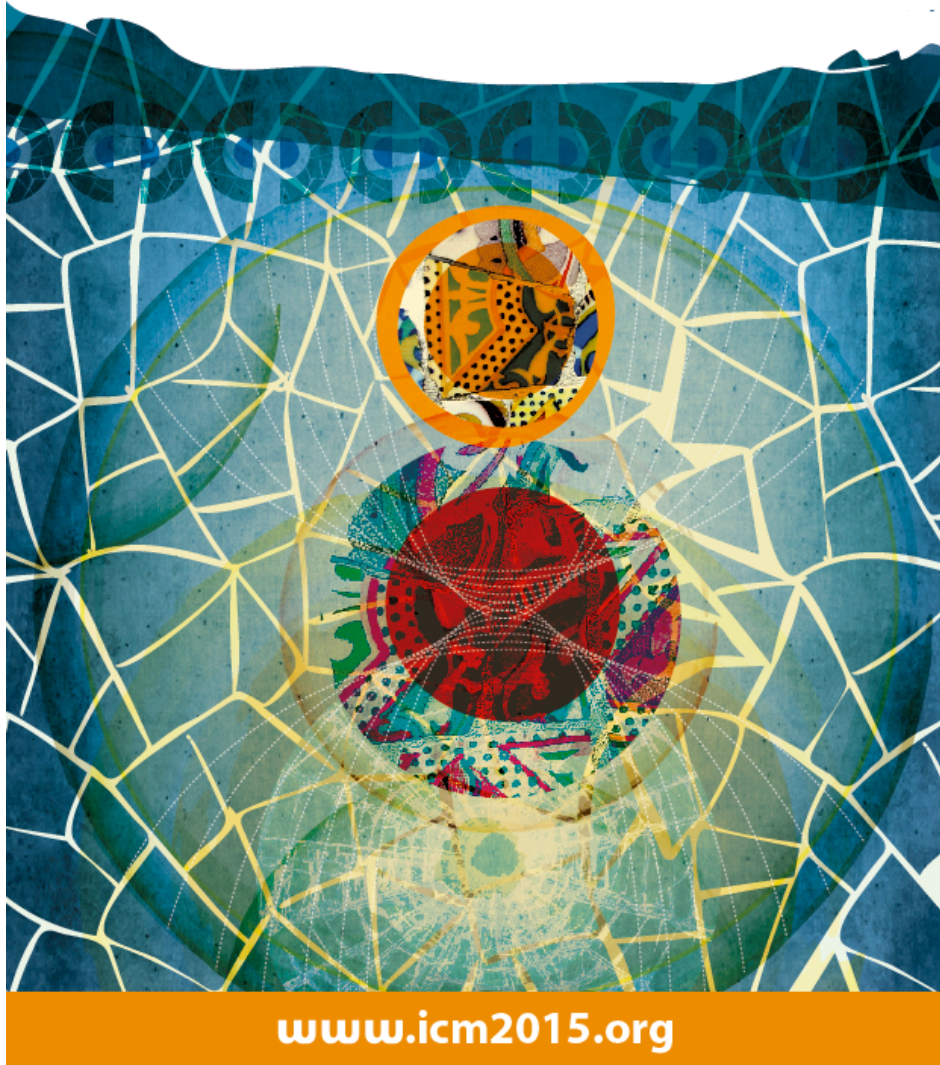
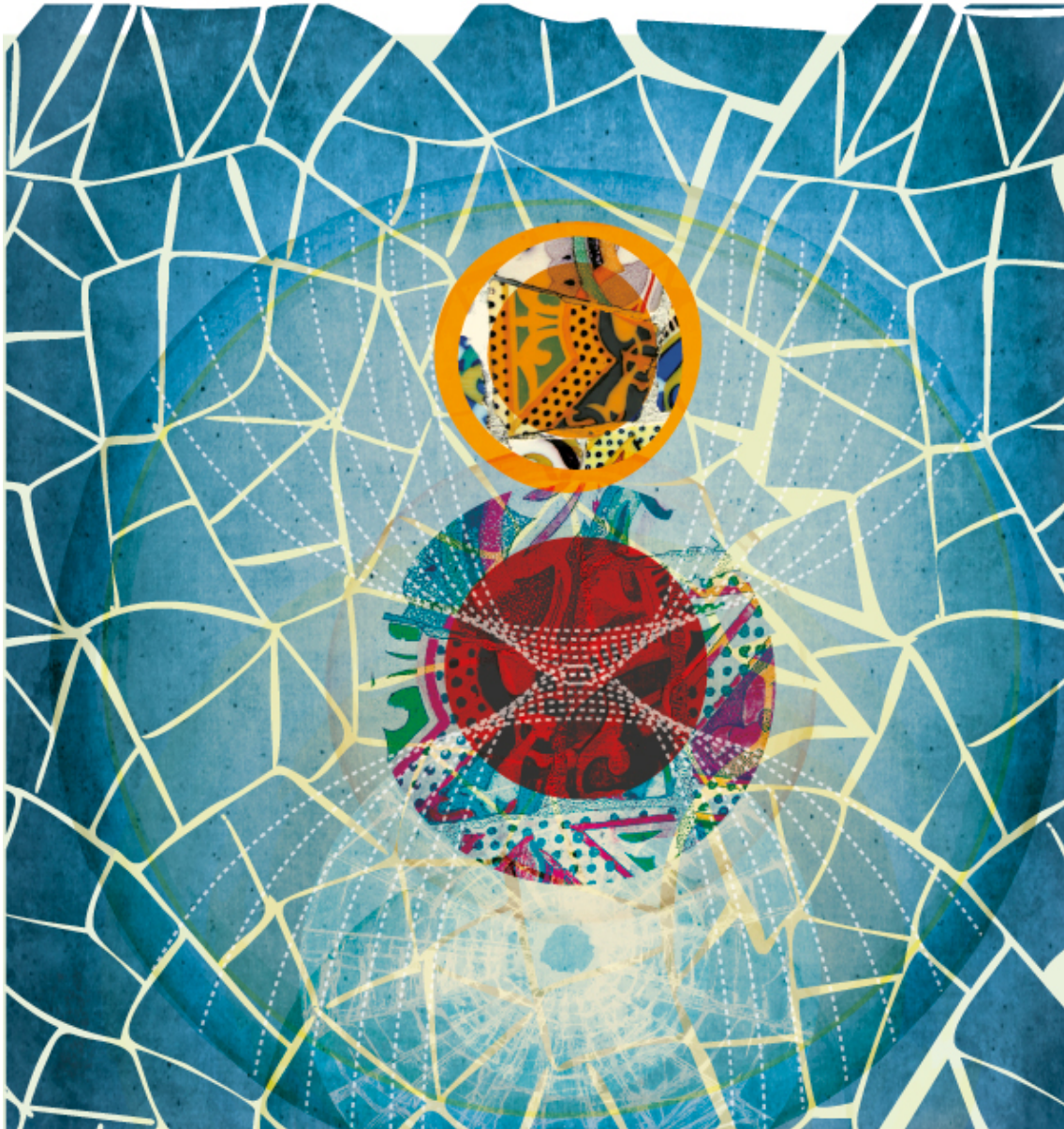


**20th International
Conference on
MAGNETISM**  JULY 5-10
2015
**BARCELONA
SPAIN**



Book of Abstracts

Plenary Lectures



PLENARY 1 - Continuous time quantum monte carlo methods: from quantum impurity models to real materials

A.J. Millis¹

1. Department of Physics, Columbia University, New York, United States

Continuous-time quantum Monte Carlo methods have revolutionized many-body physics by providing direct and accurate access to the real and imaginary time Green functions of a wide variety of quantum impurity models over wide temperature and parameter ranges. The ability to obtain results over wide spectral ranges makes the methods particularly useful as “solvers” for dynamical mean field theory. After a brief review of the history of the methods and the connection to dynamical mean field theory, this talk will explain what the methods really do, why they work well and in what situations they fail and where other methods are preferable. The methods will be illustrated with examples including magnetization dynamics and the splitting of the Kondo resonance in the nonequilibrium Anderson impurity model, properties of spin crossover molecules, and the dynamical mean field theory of correlated materials such as the rare earth nickelates and the copper - oxide high temperature superconductors.

My work in this area has been performed in collaboration with many scientists, including Philipp Werner, Emanuel Gull, Chris Marianetti and Hyowon Park and has been supported by the US National Science Foundation Division of Materials Research under grants 1006282 and 1308236 and the Basic Energy Sciences Division of the US Department of Energy under grant 046169.

PLENARY 2 - Golden era of modern magnetism

C.L. Chien¹

1. Johns Hopkins University, Baltimore, United States

Few could envision in the mid-1980s that magnetism, by then a well-established and mature field, would enter a golden era in which so many new phenomena could be realized in rapid succession, and some expeditiously exploited in new technologies. Beginning with the discovery of interlayer coupling and GMR, we had spin-valves, magnetic tunnel junctions, half-metals, spin transfer torque, spin Hall effect, domain wall motion, and countless other new subjects. In this talk, some recent examples in pure spin current phenomena and materials with Dzyaloshinskii-Moriya (DM) interaction will be given. We are truly blessed that after three decades the golden era continues unabated.

PLENARY 3 - Spin current generators

E. Saitoh^{1,2,3,4}

- 1. ERATO-SQR, JST, Saitama, Japan*
- 2. WPI-AIMR, Tohoku University, Miyagi, Japan*
- 3. Institute for Materials Research, Tohoku University, Miyagi, Japan*
- 4. ASRC, JAEA, Ibaraki, Japan*

Generation and utilization of a flow of spin angular momentum of electrons in condensed matter, called spin current, are the key challenge of today's nano-scale magnetism and spintronics. The discovery of the inverse spin Hall effect (ISHE) [1-3], the conversion of spin current into electric voltage via spin-orbit interaction, has allowed researchers to detect and utilize spin current directly, and, since then, many spin-current driven effects have been discovered by exploiting the ISHE. Here, such newly discovered spin-current effects will be

outlined, including light-spin conversion [1,4], plasmon-spin conversion, sound-spin conversion, and heat-spin conversion [5-6], and their common mechanism and future possible application will be discussed. Among them, a typical conversion effect is the spin Seebeck effect (SSE) [5], spin current generation from a temperature gradient. SSE has attracted a great deal of interest since it may realize new type thermo-electric convertors which make full use of the characteristic feature of spins: the non-reciprocal dynamics. This non-reciprocity allows a spin to rectify thermal fluctuation into unidirectional spin current via the spin pumping mechanism, which can be converted into electric power via the ISHE. Spins, working as a natural rectifier in magnets, may thus provide a versatile mechanism of energy conversion in condensed matter. I will show also that the rectification mechanism underlies various spin related phenomena which were found recently. At the end of my talk, spin current generation from mechanical motion of condensed matter will be discussed.

- [1] E. Saitoh et al., Applied Physics Letters 88 (2006) 182509
- [2] J. Wunderlich et al., Physical Review Letters 94 (2005) 047204
- [3] T. Kimura et al., Physical Review Letters 98 (2007) 156601
- [4] K. Uchida et al., Nature communications 6 (2015) 5910
- [5] K. Uchida et al., Nature materials 9 (2010) 894
- [6] T. An et al., Nature materials 12 (2013) 549

PLENARY 4 - Molecular spintronics

E. Coronado¹

1. ICMol. University of Valencia, Valencia, Spain

So far spintronics has been based on conventional materials like inorganic metals and semiconductors. A current trend in this area is that of incorporating molecules in the game. The resulting emergent field - namely molecular spintronics - is propelled by the possibility of preparing a second generation of spintronic devices based on molecular materials (organic spintronics) and by the possibility to manipulate the molecular spin individually (single-molecule nanospintronics). In this talk these trends will be illustrated with several examples taken from my own research: I) the fabrication of multifunctional molecular devices in which the light emission can be tuned through a magnetic field; II) The electrical addressing of the spin in molecular nanoobjects; III) the use of single-molecule nanomagnets as spin qubits.

PLENARY 5 - Magnetic materials for green technologies

O. Gutfleisch^{1,2}

1. TU Darmstadt, Material Science, Darmstadt, Germany

2. Fraunhofer Project Group Materials Recycling and Resource Strategy IWKS, Hanau, Germany

Due to their ubiquity, magnetic materials play an important role in improving the efficiency and performance of devices in electric power generation, conversion and transportation [1]. Permanent magnets are essential components in motors and generators of hybrid and electric cars, wind turbines, etc. Magnetocaloric materials could be the basis for a new solid state energy efficient cooling technique alternative to compressor based refrigeration [2]. Any improvements in magnetic materials will have a significant impact in these areas, on par with many "hot" energy materials (e.g. hydrogen storage, batteries, thermoelectrics, etc.). The talk focuses on rare earth and rare earth free permanent magnet and magnetocaloric materials with an emphasis on their optimization for energy and resource efficiency in terms of the usage of critical elements. The concept of criticality of strategic metals will be explained by

looking at demand, sustainability and the reality of alternatives of rare earths. Synthesis, characterization, and property evaluation of the materials will be examined considering their micromagnetic length scales and phase transition characteristics.

[1] Magnetic Materials and Devices for the 21st Century: Stronger, Lighter, and More Energy Efficient, *Adv. Mat.* 23 (2011) 821

[2] Giant magnetocaloric effect driven by structural transition, *Nature Mat.* 11 (2012) 620

Semi-plenary Lectures



MO.SP-1 - Adding magnetic functionalities to epitaxial grapheneR. Miranda^{1,2}1. *IMDEA Nanociencia, Madrid, Spain*2. *Dep. Física de la Materia Condensada, Universidad Autónoma de Madrid, Madrid, Spain*

The development of all-graphene spintronic devices requires that in addition to its capability to passively transmit spins over long distances, new magnetic functionalities are added to graphene. By growing epitaxially graphene on single crystal metal surfaces under UHV conditions [1] and either adsorbing molecules on it or intercalating heavy atoms below it, we show how to incorporate long range magnetic order or giant spin-orbit coupling, respectively, to graphene. I) Achieving long range magnetic order by a monolayer of electron acceptor molecules adsorbed on graphene /Ru(0001). Epitaxial graphene is spontaneously nanostructured forming an hexagonal array of 100 pm high nanodomains with a periodicity of 3 nm [2]. Cryogenic STM and Spectroscopy and DFT simulations show that TCNQ molecules deposited on gr/Ru(0001) acquire charge from the (doped) gr substrate and develop a sizeable magnetic moment revealed by a prominent Kondo resonance. The self-assembled molecular monolayer develops spatially-extended spin-split electronic bands. The predicted spin alignment in the ground state is visualized by spin-polarized STM at 4.6 K [3]. The system shows promising perspectives to become an effective spin filter device. II) Introducing a giant spin-orbit interaction on graphene/Ir(111) by intercalation of Pb. The intercalation of an ordered array of Pb atoms below graphene results in the appearance a series of sharp pseudo-Landau levels in the differential conductance revealed by STS at 4.6 K. The vicinity of Pb enhances by orders of magnitude the, usually negligible, spin-orbit interaction of graphene. The spatial variation of the spin-orbit coupling creates a pseudo-magnetic field that originates the observed pseudo-Landau levels [4].

[1] A.L. Vázquez de Parga et al, Phys. Rev. Lett. 100, 056807 (2008)

[2] B. Borca et al, Phys. Rev. Lett. 105, 036804 (2010)

[3] M. Garnica et al, Nature Physics 9, 368 (2013)

[4] F. Calleja et al, Nature Physics 11, 43 (2015)

MO.SP-2 - Magnetization dynamics of nanodots and fundamental limits of minimum energy dissipation during switchingG. Carlotti¹1. *University Of Perugia - Dipartimento di Fisica E Geologia, Perugia, Italy*

In this talk I will review recent results achieved by means of both micromagnetic simulations and Brillouin light scattering experiments at GHOST Laboratory, Perugia University, about the dynamical properties of either isolated or coupled magnetic nanodots [1,2,3]. The character of their spin-wave eigenmodes (frequency and spatial profile) exhibits peculiar properties when the lateral size D of the dots decreases below a critical value of about 150 nm. For in-plane magnetization, the inhomogeneity of the internal field and exchange-energy effects cause qualitative and quantitative differences in the spin wave spectrum, if compared to larger dots. For instance, the fundamental mode lies at the bottom of the spectrum and exhibits a maximum amplitude at the edges. This mode softens at an applied switching field with magnitude comparable to the coercive field, determining the initial steps of magnetization reversal. Therefore, a detailed knowledge of the eigenmodes spectrum of nanodots is also crucial to understand the switching process. To this respect, careful analysis of the fundamental limits of minimum energy consumption, during either conventional (irreversible)

[4] or adiabatic (reversible) switching [5], shows that dissipationless reversal is achievable, provided that both dynamic (arbitrarily slow application of external fields) and entropic reversibility (no free entropy increase) are insured [6]. These results can be relevant for the exploitation of deep-submicrometric magnetic dots as elemental switches in magnetic memory or storage devices, as well as in nano-magnetic logic applications and spin-torque oscillators.

[1] G. Carlotti et al., J. Phys. D: Appl. Phys., 47, 265001 (2014)

[2] G. Carlotti et al., J. Appl. Phys. 117, 17A316 (2015)

[3] G. Carlotti et al., J. Appl. Phys. 115, 17D119 (2014)

[4] G. Carlotti et al., Physica B 435, 4 (2014)

[5] M. Madami et al., Phys. Rev. B 90, 104405 (2014)

[6] M. Madami et al., submitted

MO.SP-3 - Ferromagnetism in Semiconductors and the Role of Localization

T. Dietl¹

1. Institute of Physics, Polish Academy of Sciences, Warsaw, Poland

The recent years have witnessed a rapid progress in the understanding of puzzling and controversial origin of ferromagnetism in various families of dilute magnetic semiconductors and insulators [1]. In the talk, an overview will be given on the relative importance of the dominant spin-spin exchange mechanisms in magnetically doped semiconductors, oxides, arsenides, and topological insulators, taking into account intra-band Ruderman-Kittel-Kasuya-Yosida interaction and the inter-band Bloembergen-Rowland mechanism as well as the short-range antiferromagnetic and ferromagnetic superexchange. The role of powerful element-specific and spin-sensitive nanocharacterization tools will be emphasized underlying that they have allowed to correlate magnetic properties with the distribution and location of magnetic ions in the host lattice. At the same time, photoemission results will be presented noting that they have provided direct information on the density of states of itinerant carriers. The importance of interplay between carrier-mediated ferromagnetism and carrier localization will be discussed in the context of studies on gated structures. These investigations have demonstrated the presence of electronic and magnetic phase separations on approaching the Anderson-Mott transition, the key element accounting for colossal magnetoresistance effects, a trade mark of magnetic semiconductors.

[1] see, T. Dietl. Nature Mater. 9 (2010) 965; T. Dietl and H. Ohno, Rev. Mod. Phys. 86 (2014) 187; T. Dietl, K. Sato, T. Fukushima, A. Bonanni, M. Jamet, A. Barski, S. Kuroda, M. Tanaka, Pham Nam Hai, and H. Katayama-Yoshida, arXiv:1412.8062

TU.SP-1 - Overview of Ce-115 based superconductors

J. Thompson¹

1. Los Alamos National Laboratory, New Mexico, United States

The Ce-115 heavy-fermion superconductors CeCoIn₅, CeIrIn₅ and CeRhIn₅ under applied pressure have revealed a remarkable variety of electronic states, none of which is understood well but some of which may be similar to those in other classes of electronically correlated materials. Magnetism in general and magnetic quantum criticality in particular are fundamentally the origin of these states, including superconductivity itself. Among other recently discovered states are one of coexisting magnetism and unconventional superconductivity whose coupling may lead to an exotic order [1], a pseudogap phase with seemingly dx₂-y₂ symmetry [2,3], and an unconventional type of quantum-critical state that favors the development of d-wave superconductivity [4,5,6]. This overview summarizes experimental evidence for these and related states and suggests areas where future work might be beneficial.

- [1] S. Gerber et al., Nature Phys. 10, 126 (2014)
- [2] B. Zhou et al., Nature Phys. 9, 474 (2013)
- [3] S. Wirth et al., J. Phys. Soc. Jpn. 83, 061009 (2014)
- [4] T. Park et al., Nature 456, 366 (2008)
- [5] L. Jiao et al., Proc. Natl. Acad. Sci. (USA) 112, 673 (2015)
- [6] S. Seo et al., Nature Commun (in press)

* In collaboration with many at Los Alamos and elsewhere whose insightful contributions have been essential. Work was performed under the auspices of the U.S. Department of Energy and supported by the Office of Basic Energy Sciences, Division of Materials Sciences and Engineering

TU.SP-2 - Phonons, Magnons and Spin Current

S. Maekawa¹

1. Advanced Science Research Center, Japan Atomic Energy Agency, Ibaraki, Japan

Phonons and magnons are the elementary excitations in a magnet. The interaction between them gives rise to a variety of magneto-acoustic and magneto-elastic effects. Since magnons carry spin angular momenta, the interaction provides an opportunity for phonons to contribute to spin-related phenomena. Spin current is a flow of spin angular momentum, and is converted to the charge current by the (inverse) spin Hall effect. Spin current carries energy and information as well. Here, we extend the magneto-acoustic and magneto-elastic effects by introducing spin current. In particular, the effects based on spin current in a hybrid system consisting of a non-magnetic metal such as Pt and a magnet including ferromagnet, antiferromagnet and ferrimagnet are examined. The spin Seebeck effect refers to the generation of a spin voltage caused by a temperature gradient in a magnet, which enables the thermal injection of spin current from the magnet into an attached non-magnetic metal. The inverse spin Hall effect converts the injected spin current into a transverse charge voltage, thereby producing electromotive force as in the conventional charge Seebeck device. Recent theoretical and experimental efforts have shown that magnons and phonons play crucial roles in the spin Seebeck effect. We present the theoretical basis of the spin Seebeck effect and other thermal spin effects.

TU.SP-3 - Quantum tunneling of the magnetic moment: From molecules to collective effects

J. Tejada¹

1. University Barcelona, Barcelona, Spain

Experimental work on quantum tunnelling of the magnetic moment performed at the University of Barcelona will be reviewed, starting with the discovery of quantum magnetic relaxation in nanoparticles and resonant spin tunnelling in molecular magnets. Collective quantum phenomena related to spin tunnelling will be discussed, such as quantum magnetic deflagration and superradiance. It will be argued that tunnel splitting in two-state systems introduces forces of quantum origin that can be measured in molecular magnets. Our most recent experiments with nanospheres of molecular magnets exhibiting extremely narrow quantum resonances will be reviewed.

References:

- 1.-E. M. Chudnovsky and J. Tejada, 'Lectures on Magnetism' Rinton Press (2006)
- 2.-E. M. Chudnovsky and J. Tejada, 'Macroscopic Quantum Tunneling of the Magnetic Moment'. Edited by Cambridge University Press (1998)
- 3.-J. R. Friedman, M. P. Sarachik, J. Tejada and R. Ziolo, Phys. Rev. Lett. 76, 3830 (1996)
- 4.-A.Hernández-Minguez, J.M. Hernandez, F. Macia, A. García Santiago, J. Tejada and P.V. Santos, Phys. Rev. Lett. 95, 217205 (2005)
- 5.- P.Subedi, S. Velez, F. Macia, M.P.Sarachik,, J.Tejada, S. Mukherjee, G. Christou and A. Kent, Phys. Rev. Lett, 110, 207203 (2013). Viwpoint :Firein a Quantum Forest, <http://physics.aps.org/articles/v6/53>
- 6.- W. Decelle, J. Vanacken, V.V. Moschalkov, J. Tejada, J.M Hernandez and F. Macia., Phys. Rev. Lett. 102, 027203 (2009)
- 7.- J. Tejada, E.M. Chudnovsky, J.M.Hernandez, and R. Amigo, Appl. Phys. Lett. 84, 2373 (2004)
- 8.- F.Macia, A. Hermamdez-Minguez, G.Abril, J.M. Hernandez, A. Garcia Santiago, J. Tejada; F. Parisi and P.V. Santos, Phys. Rev. 876, 174421 (2007)
- 9.- E. M. Chudnovsky, J. Tejada and R. Zarzuela, Quantum forces in solids with two-state systems, Phys. Rev. B88, 220409« (2013)
- 10, E. Molins, M. Gich, J.Tejada, J.M. Greneche and F. Macia, Europhys. Letters 108 , 47004 (2014). 11.- S. Lendinesíz et al.. Phys. Rev. B91, 024404 (2015)

TH.SP-1 - Novel topological phases in strongly correlated electron systems

L. Balents¹

1. Kavli Institute For Theoretical Physics, Santa Bárbara, United States

The role of topology in electronic systems is an active subject of research. Within a non-interacting quasi-particle picture, describing both weakly correlated insulators and superconductors, a rather complete classification of possible topological phases has been achieved, and of course topological insulators have been found and studied intensively experimentally.

The problem of correlated electrons is much richer, and requires updating the quasi-particle classification.

New topological phases and phenomena can occur only when electronic interactions are present. I will discuss some of the possible novel states that might be achieved in this way. I

will describe how gapped states may exhibit two distinct classes of topology: symmetry protected topological order, and intrinsic topological order.

I will also touch upon gapless states with topologically protected bulk gapless excitations.

Finally, I will spend some time describing applications of these ideas to the iridates.

TH.SP-2 - Electric manipulation of spin textures

A. Hoffmann¹

1. Materials Science Division, Argonne National Laboratory, Argonne, United States

Temporal and spatial magnetic spin textures have received increased interest, due to their potential for power-efficient information encoding and processing [1]. Examples of temporal spin textures are spin waves, and of spatial spin textures are magnetic skyrmions, which are stabilized by their distinct topology. Two types of electrical manipulation of these spin textures are discussed. First, local Oersted magnetic fields from charge currents can manipulate the propagation of spin waves. This can be used to guide spin waves through curved waveguides, where otherwise the propagation is suppressed by their inherently anisotropic dispersion in thin films [2]. This same concept is generalized for the switching of spin waves between multiple waveguides [3]. Second, magnetostatically-stabilized skyrmion bubbles can form in ferromagnet/heavy-element bilayers, where the interface gives rise to perpendicular magnetic anisotropy and a chiral Dzyaloshinskii-Moriya interaction [4]. These magnetic skyrmions are electrically manipulated utilizing spin Hall effects [5]. Furthermore, it is demonstrated that skyrmion generation via the spin Hall effect coupled to inhomogeneities in electrical charge currents occurs in a process that is similar to the droplet formation in surface-tension driven fluid flows. This provides a practical approach for skyrmion formation on demand. This work was supported by the U.S. Department of Energy, Office of Science, Materials Sciences and Engineering Division.

References:

1. A. Hoffmann and H. Schultheiß, *Curr. Opin. Solid State Mater. Sci.* (2014); doi:10.1016/j.cossms.2014.11.004
2. K. Vogt, H. Schultheiss, S. Jain, J. E. Pearson, A. Hoffmann, S. D. Bader, and B. Hillebrands, *Appl. Phys. Lett.* 101, 042410 (2012)
3. K. Vogt, F. Y. Fradin, J. E. Pearson, S. D. Bader, T. Sebastian, B. Hillebrands, A. Hoffmann, and H. Schultheiss, *Nature Commun.* 5, 3727 (2014)
4. W. Jiang, P. Upadhyaya, W. Zhang, G. Yu, M. B. Jungfleisch, F. Y. Fradin, J. E. Pearson, Y. Tserkovnyak, K. L. Wang, O. Heinonen, S. G. E. te Velthuis, and A. Hoffmann, (unpublished)
5. A. Hoffmann, *IEEE Trans. Magn.* 49, 5172 (2013)

TH.SP-3 - High temperature nanostructured superconductors: a tool towards a new era of high field magnetism*

X. Obradors¹

1. Institut de Ciència de Materials de Barcelona, ICMAB-CSIC, Campus de la UAB, Bellaterra, Spain

Achieving high current superconducting wires has been one of the most challenging objectives during all the High Temperature Superconductivity (HTS) era.

Extraordinary new ideas and materials developments have been demonstrated and second generation YBa₂Cu₃O₇ conductors (coated conductors, CCs) have emerged as an outstanding practical opportunity to generate high and ultrahigh magnetic fields.

The quasi-epitaxial multilayered film structure on flexible metallic substrates of CCs can be now achieved in very long lengths without the detrimental influence of grain boundaries. Additionally, a new boost in performance at high magnetic fields is being achieved when unique nanostructures are being introduced in these epitaxial films which allow reaching very high vortex pinning strengths. All these features make nanostructured CCs an enabling technology to develop practical high field large scale power applications and so opens a new era of high field magnetism.

In this talk I will present the major recent developments of the different CC architectures and the existing bottlenecks towards understanding the complex relationship between nanostructure and vortex pinning in HTS materials. Emphasis will be made in describing the diverse nanoscale structures allowing to enhance vortex pinning based on cost-effective chemical deposition approaches. Research progress in CC development in Europe, particularly in the scope of the European research program EUROTAPES (www.eurotapes.eu), will be reported.

* Research funded from EU-FP7 NMP-LA-2012-280432 EUROTAPES project

FR.SP-1 - Magnetocaloric effect: Challenges and opportunities

V. Pecharsky^{1,2}, Y. Mudryk¹, D. Paudyal¹, K. Gschneidner, jr.^{1,2}

1. Ames Laboratory, Iowa State University, Ames, United States

2. Department of Materials Science and Engineering, Iowa State University, Ames, United States

The discovery of the giant magnetocaloric effect in Gd₅Si₂Ge₂ and other R₅T₄ compounds (R = rare earth metal and T is a Group 14 element) generated a broad interest in the magnetocaloric effect and magnetic refrigeration near room temperature in particular, and in magnetostructural transitions in general. Reports on the giant magnetocaloric effect in other systems soon followed. These include MnFeP_xAs_{1-x} and related compounds, La(Fe_{1-x}Si_x)₁₃ and their hydrides, Mn(As_xSb_{1-x}), CoMnSi_xGe_{1-x} and related compounds, Ni₂MnGa and some closely related Heusler phases, and a few non-metallic systems, including manganites best known for their colossal magnetoresistance. A common feature observed in all materials that exhibit the giant magnetocaloric effect is the coupling of magnetic and elastic effects. In addition to the interplay between magnetic and lattice entropies, both of which are intrinsic materials' parameters that in principle can be modeled theoretically from first principles, extrinsic parameters such as microstructure and nanostructure, have been found to play a role in controlling both the magnetostructural transition(s) and magnetocaloric effect. Both the intrinsic and extrinsic parameters are, therefore, important in order to maximize magnetocaloric effect. The role of different control parameters and the potential pathways towards materials exhibiting advanced magnetocaloric effect will be discussed. This work is supported by the Materials Science and Engineering Division, Office of Basic Energy Sciences of the U.S. Department of Energy under contract No. DE-AC02-07CH11358 with Iowa State University.

FR.SP-3 - Ferromagnetic shape memory thin films: Structure and magnetic anisotropy

J.M. Barandiaran¹, V. Chernenko^{1,2}, I.R. Aseguinolaza¹

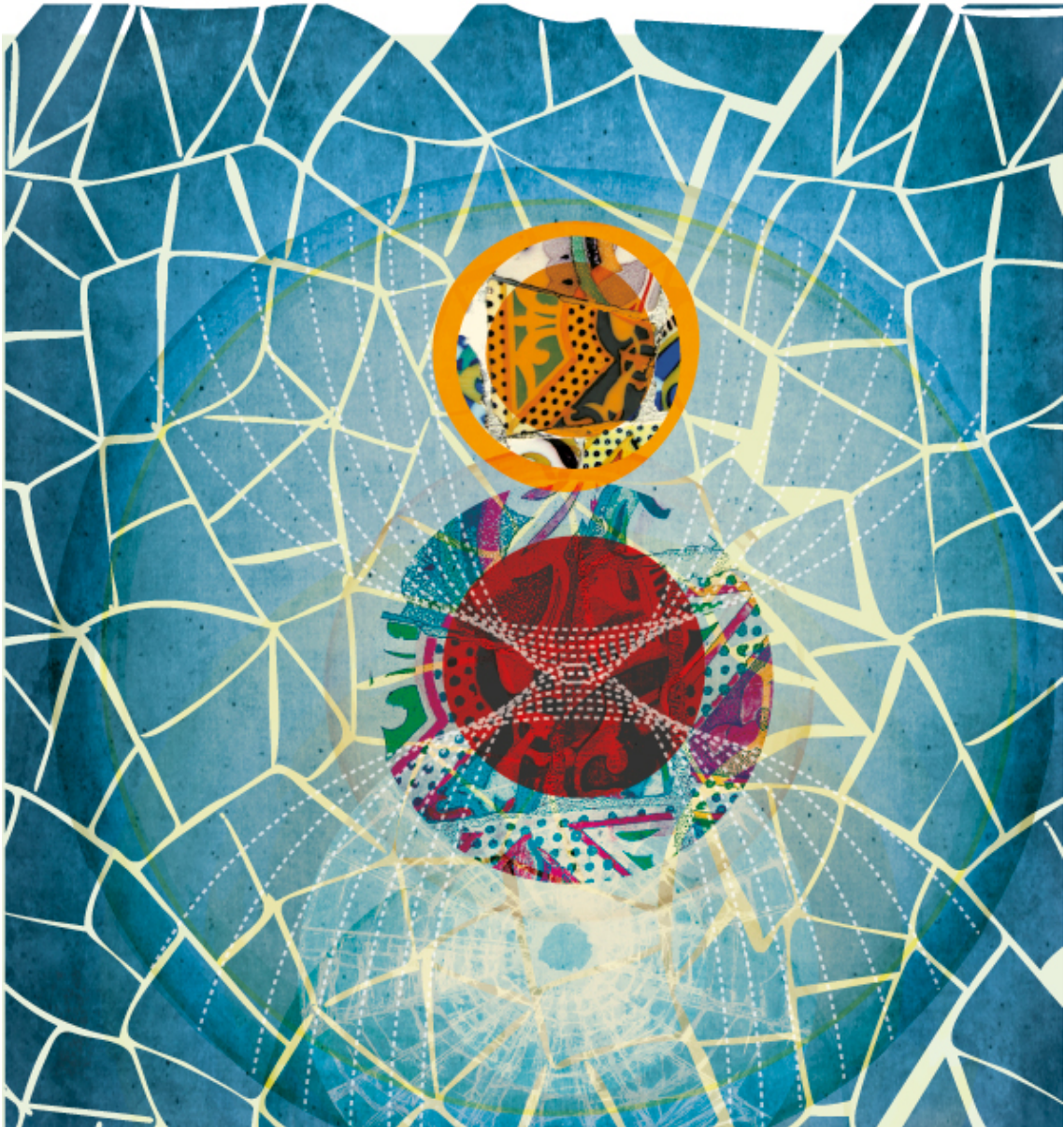
1. BCMaterials & Univ. of the Basque Country, Leioa, Spain

2. Ikerbasque, the Basque Foundation for Science, Bilbao, Spain

Ferromagnetic shape memory alloys (FSMA) such as off-stoichiometric Ni-Mn-Ga Heusler compounds, show the “magnetic-field-induced strain” (MFIS) effect, which is due to the mobile martensitic microstructure and the strong coupling between elastic and magnetic properties. Due to their high power density, these materials have a great potential to be used in magnetic MEMS.

In the present work we overview recent advances in submicron FSMA thin films. Particular emphasis is given to the structure of the films and to their magnetic anisotropy. Polycrystalline films deposited onto cold substrates have (220) out-of-plane fiber texture. Films grown onto hot substrates have epitaxial structures. The symmetry and strength of the magnetic anisotropy (MA) of the films have been studied by ferromagnetic resonance (FMR). They are controlled by the film crystallography, the martensitic nanostructure, the type of substrate and film thickness. The effect of the substrate in the anisotropy is demonstrated by comparing the in plane MA for a Ni-Mn-Ga film grown onto NaCl (001) and the out of plane oblique anisotropy in an identical film with the same texture deposited onto Si (001). Another important factor determining the MA is the film-substrate stress that determines the transformation volume strain. A reduction of the MA by one order of magnitude is found by FMR in single crystalline Ni-Mn-Ga films onto MgO (100). These results are explained in the framework of a magnetoelastic model of the martensite involving second- and forth-order magnetic anisotropy constants, which, thereof, can be evaluated from the experimental data. In these films the estimated value of the magnetic domain wall width is comparable with the width of the twins, indicating that the magnetic moment in neighbor twins are strongly coupled by the exchange interaction. Applications of single and double beam Si cantilevers, with deposited submicron Ni-Mn-Ga films are briefly discussed.

Special Lectures



A quick review of magnetism in Spain

A. Hernando

1. Instituto de Magnetismo Aplicado (UCM-ADIF-CSIC). Las Rozas, Madrid, Spain and Dept. Física de Materiales, Universidad Complutense de Madrid, Madrid, Spain

Magnetism has been in Spain the first scientific topic that acted as nucleus around which the spanish scientific community was born. Despite the previous existence of a few scientist, as the Nobel Price Santiago Ramón y Cajal, the experimental science was not here an usual and respected activity until the second decade of the XX century. Blas Cabrera, after visiting Pierre Weiss at Strasbourg, started a systematic experimental study of the magnetic susceptibility of rare earth compunds. The influence of Cabrera and his school on the firm establishment of some aspects of Atomic Physics and Quantum Mechanics, was emphasised by Van Vleck. In fact, the convergence of excelent quality multidimensional cultural aspects at the Residencia de Estudiantes in Madrid, close to the Instituto de Investigaciones Físicas, allowed us to refer to the first decades of the XX century as the Silver Age of the spanish culture. Guests of the Residencia were Salvador Dalí, Federico García Lorca and Luis Buñuel and was visited by Marie Curie, Erdwing Schrodinger and Albert Einstein among other scientists.

After revisiting Cabrera's contribution, the terrible effect of the Civil War on the spanish scientific productivity should be also analyzed. After the war a few researchers as S. Velayos continued the spanish tradition in Magnetism. It is true that Magnetism, as other research branches, undergoes an increasing growth since 1970 that reached a maximum expansion at the end of the eighties. In Spain a lot of competitive groups develop a remarkable activity nowadays, mainly at the University and Research Institutions depending of the state. A few companies also perform technological activities related to the field of Magnetism.

I have choosen a non exhaustive but representative set of spanish labs to illustrate and summarise the more competitive activity in magnetism research carried out in our country. Most of the active groups gather together as members of the Spanish Magnetic Club.

Highlights from 30 years of Magnetism

D. Givord

1. CNRS/Université Grenoble-Alpes, Institut Néel, Grenoble, France

Some of today's most active areas of magnetism derive from a series of discoveries that occurred in the 1980's. High Tc superconductivity gave an immense impulse to the study of strongly correlated electron systems. The development of high energy product NdFeB magnets revolutionized the design of motors and generators. The most important discovery of the period, namely giant magnetoresistance, has given birth to the new scientific domain of spintronics. During the same period, X-ray magnetic dichroism and Scanning Tunneling Microcopy, followed by other near-field microscopies, were discovered. These, together with enormous progress in magneto-optical studies and numerical simulations, have profoundly transformed the nature of studies dealing with magnetism and magnetic materials.

We have learned that complex magnetic orders may be stabilized and that magnetic ordering may even disappear under the influence of frustration, that domain walls are not simple planar objects, that magnetism and superconductivity are not always antagonistic, that an external magnetic field is not always needed to reverse magnetization and that magnetization is not needed to get a magnetic signal, that spin currents may exist independent of charge currents, that spin-orbit interactions may dramatically affect the magnetic properties of matter.

A number of new magnetic materials, from magnetic semiconductors to magnetocaloric materials and half-metallic alloys have been discovered. The study of the fundamental link generally existing between magnetic properties and microstructure, benefits from tremendous developments in characterization techniques, in particular aberration corrected TEM. The search for new materials is now guided by electronic structure calculations, and the material itself may be a complex magnetic object, designed in the so-called materials engineering approach. Finally, new domains of applications have emerged for magnetism, the two most significant being in the fields of green energy and bio-medical engineering.

Highly Efficient Current Induced Domain Wall Motion in Synthetic Antiferromagnetic Racetracks

S. Parkin^{1,2}

1. IBM Almaden Research Center, San Jose, California, United States

2. Max Planck Institute for Microstructure Physics, Halle, Germany

Memory-storage devices based on the current controlled motion of domain walls in magnetic racetracks promise performance and reliability beyond that of conventional magnetic disk drives and solid state storage devices (1). The materials and structures underlying racetrack memory have evolved over 4 major stages over the past decade (see Figure). Racetracks that are formed from atomically thin, perpendicularly magnetized nano-wires, interfaced with adjacent metal layers with high spin-orbit coupling, give rise to domain walls (DWs) possessing a chiral Néel structure. Domain walls that have a chiral structure, stabilized via a Dzyaloshinskii-Moriya Interaction, can be moved very efficiently with current via a chiral spin torque mechanism that relies on spin currents generated by the spin Hall effect (2). We show that DWs can be driven even more efficiently in synthetic antiferromagnetic (SAF) racetracks due to an even larger chiral exchange-coupling torque with DW velocities that can exceed 1,000 m/sec (3). The magnitude of the spin currents will also be discussed (4).

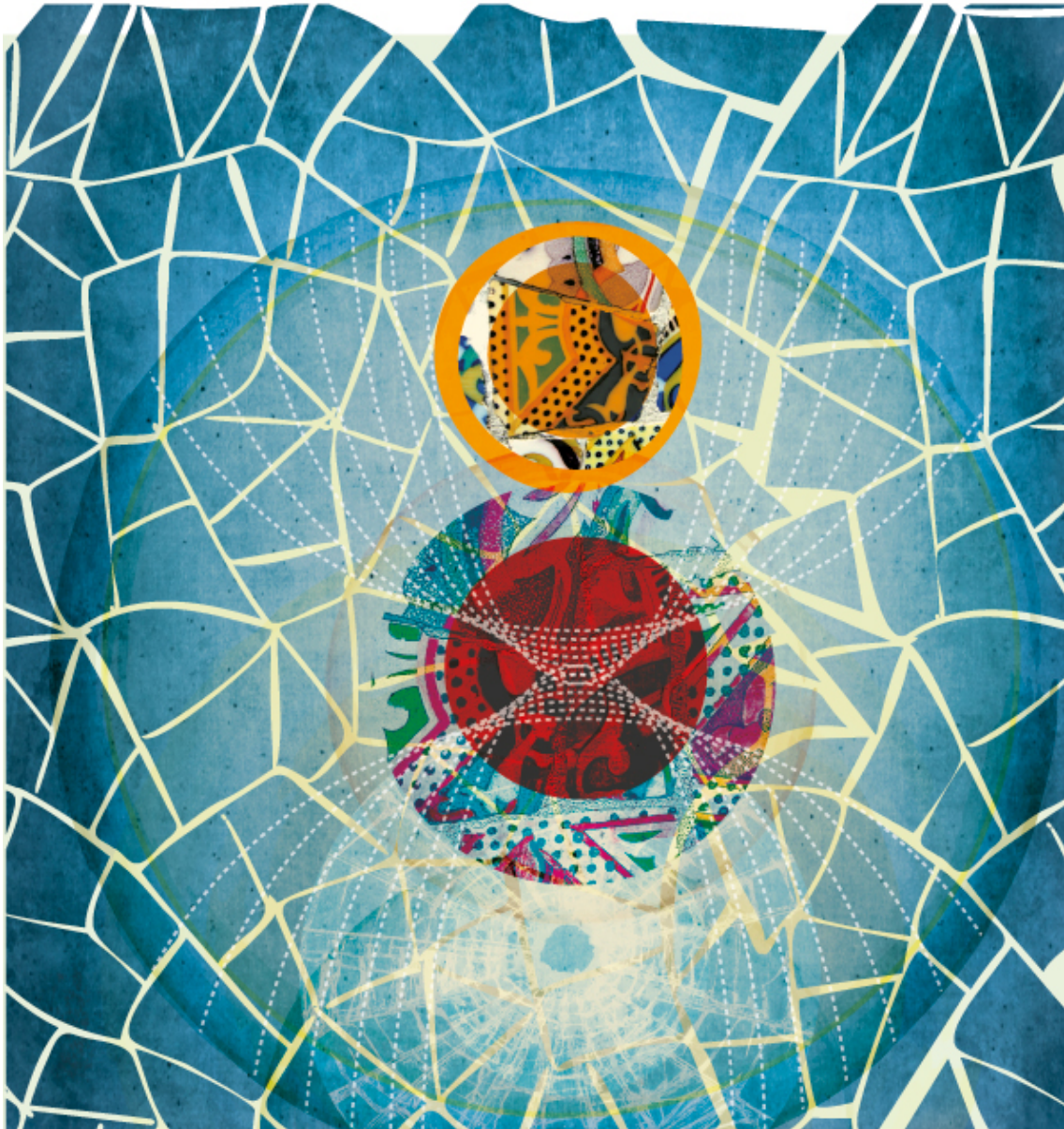
1. S. S. P. Parkin, S.-H. Yang, *Memory on the Racetrack. Nature Nanotech.* **10**, 195 (2015).

2. K.-S. Ryu, L. Thomas, S.-H. Yang, S. S. P. Parkin, *Nat. Nanotech.* **8**, 527 (2013).

3. S.-H. Yang, K.-S. Ryu, S. S. P. Parkin, *Nat. Nanotech.* **10**, 221 (2015).

4. W. Zhang, W. Han, X. Jiang, S.-H. Yang, S. S. P. Parkin, *Nat. Phys.* **27 April 2015**.

Symposium Lectures



MO.SYM 1 - Topological magnetismR. Moessner¹*1. MPI-PKS, Dresden, Germany*

Topological states of matter differ from conventional ones in that they look disordered but are in fact not at all featureless. Instead, they exhibit many remarkable phenomena related to their highly unusual low-energy degrees of freedom -- emergent gauge fields and fractionalised quasiparticles. This talk aims to provide a brief introduction to these phenomena, and will discuss recent developments in theory and experiment on quantum spin liquids and ices, in particular with view to dynamical response properties. It will also touch on the remarkably rich interplay of topology and disorder.

MO.SYM 2 - Low carrier concentration crystals of the topological insulator $\text{Bi}_{2-x}\text{Sb}_x\text{Te}_{3-y}\text{Se}_y$: a magnetotransport studyA. De Visser¹, Y. Pan¹, J. Angevaere¹, Y. Kai Huang¹, M. Golden¹, M. Snelder², A. Brinkman², S. Wiedmann³, U. Zeitler³*1. University of Amsterdam, Amsterdam, The Netherlands**2. University Twente, Enschede, The Netherlands**3. Radboud University, Nijmegen, The Netherlands*

Recently, it was demonstrated that the material system $(\text{Bi,Sb})_2(\text{Te,Se})_3$ (in short BSTS) can be prepared as genuine topological insulator (TI) with surface dominated transport (Ren et al., PRB 84, 165311, 2011). In our work to further optimize the TI properties we found that a record high resistivity and bulk-insulating behaviour, combined with a low carrier density, can be achieved for the composition $\text{Bi}_{1.46}\text{Sb}_{0.54}\text{Te}_{1.7}\text{Se}_{1.3}$ (Pan et al., New J. Phys. 16, 123035, 2014). The analysis within a parallel resistor model of the resistance measured for crystals with different thicknesses shows that the surface contribution to the electrical transport amounts to 97 % when the sample thickness is reduced to 1 micrometer. The magnetoconductance of exfoliated BSTS nanoflakes shows 2D weak anti-localization with the fit parameter α close to - 1 as expected for topological surface states. Magnetotransport experiments in high magnetic fields reveal 2D Shubnikov-de Haas (SdH) oscillations. By using the Lifshitz-Kosevich formalism, important transport parameters of the surface states, such as the carrier density, cyclotron mass and quantum mobility, were obtained. We also elaborate on the finite Berry phase, the hall mark for topological surface states, extracted from the SdH signal.

MO.SYM 3 - Transport and induced superconductivity in the topological surface and edge states of HgTeC. Brüne¹*1. Experimentelle Physik 3 Universität Würzburg, Würzburg, Germany*

HgTe is a semimetal with an inverted bandstructure in which the Γ_8 band is above the Γ_6 band. Due to the semimetallic nature of the bulk material topological insulator behavior can only be observed when a band gap is opened. This can be achieved by either applying tensile strain to a bulk HgTe layer or in HgTe quantum well structures above a critical thickness. The former, strained bulk HgTe, is a 3-dimensional topological insulator while the latter is a 2 dimensional TI.

This talk will focus on the transport properties of the topological surface and edge states in HgTe. Furthermore the properties of induced superconductivity in this edge/surface states is investigated

MO.SYM 4 - Topology in Heusler compounds - from a materials perspective

C. Felser¹, B. Yan¹, C. Shekhar¹, Y. Chen²

1. *Max Planck Institute Chemical Physics For Solids, Dresden, Germany*

2. *Oxford University, Oxford, United Kingdom*

Topological insulators and Weyl metals are a hot topic in condensed matter physics and materials science. Heusler compounds are a remarkable class of materials with more than 1,000 members and a wide range of extraordinary multifunctionalities including half-metallic high-temperature ferri- and ferromagnets and tunable topological insulators with a high potential for spintronics and energy technologies. The tunability of this class of materials is exceptional and nearly every functionality can be designed. Therefore it is not surprising that we were able to design Heusler compounds with a band inversion and a non-trivial topology for multifunctional topological insulators (TI). The topological state in these zero-gap semiconductors can be created by applying strain or by designing an appropriate quantum well structure, similar to the case of HgTe. Many of these ternary zero-gap semiconductors (LnAuPb, LnPdBi, LnPtSb and LnPtBi) contain the rare-earth element Ln, which can realize additional properties ranging from superconductivity (for example LaPtBi) to magnetism (for example GdPtBi) and heavy fermion behavior (for example YbPtBi). These properties can open new research directions in realizing the quantized anomalous Hall effect and topological superconductors. C1b Heusler compounds have been grown as single crystals and as thin films. The control of the defects, the charge carriers and mobilities can be optimized. The band inversion is proven by ARPES. Heusler compounds are similar to a stuffed diamond, correspondingly, it should be possible to find the “high Z” equivalent of graphene in a graphite-like structure or in other related structure types with 18 valence electrons and with inverted bands. Dirac cones and Weyl points can occur at the critical points. Weyl points, a new class of topological phases was predicted in NbP, NbAs and TaP. We found ultrahigh magneto resistance, mobilities and Fermi arcs in this class, proving their topological electronic state.

MO.SYM 5 - A spin-anisotropic harmonic honeycomb iridate

R. McDonald¹, K. Modic¹, T. Smidt¹, I. Kimchi¹, N. Breznay¹, A. Biffin¹, S. Choi¹, R. Johnson¹, R. Coldea¹, P. Watkins-Curry¹

1. *Los Alamos National Laboratory, New Mexico, United States*

Oxygen octahedra are prolific building blocks of correlated electron systems, for example, the numerous corner-sharing structures of the Ruddlesden-Popper series, that host phenomena ranging from high temperature superconductivity to exotic magnetism. In contrast, three dimensional structures with edge-sharing octahedra are relatively rare. The interest in exploring such structures originates from the the threefold coordination of edge-sharing octahedra that frustrates the nearest neighbor interactions.

Iridium-based oxides (iridates) open a further dimension to this problem by introducing strong spin-orbit interactions, such that the Mott physics has a strong orbital character. In the layered honeycomb iridates this is thought to generate highly spin-anisotropic interactions, coupling the spin orientation to a given spatial direction of exchange and leading to further frustration of magnetism. As a result quantum dynamics are expected to dominate the properties of these

materials. The potential for new physics emerging from such interactions has driven much scientific excitement; most recently in the search for a new quantum spin liquid, first discussed by Kitaev. In this talk I present a three dimensional iridate structure that has the same local connectivity as the layered honeycomb. The temperature dependence of the magnetic susceptibility exhibits a striking reordering of the magnetic anisotropy, giving evidence for highly spin-anisotropic exchange interactions.

Furthermore, the basic structural units of this material suggest the possibility of a new family of structures, the 'harmonic honeycomb' iridates. This compound thus provides a unique and exciting glimpse into the physics of a new class of frustrated and strongly spin-orbit coupled Mott insulators.

TU.SYM 1 - Two dimensional spin-orbitronics (skyrmions in multilayers, 2D conversion between charge and spin currents)

F. Albert¹

1. Unité Mixte de Physique CNRS/Thales And Université Paris Sud, Palaiseau, France

The exploitation of the Spin-Orbit Coupling (SOC) has recently opened new directions for the development of spintronics. My talk is on SOC-induced effects in 2D systems with a special focus on two topics:

- 1) Interface-induced magnetic skyrmions;
- 2) Conversion between charge and spin currents at surfaces and interfaces.

1) Interface-induced skyrmions at room temperature in multilayers: I will present i) the main features predicted by DFT calculations for the Dzyaloshinskii-Moriya Interactions (DMI) at the interfaces of magnetic layers with heavy metals, ii) what can be expected from micromagnetic simulations for the properties (nucleation, current-induced motion) of interface-induced individual skyrmions in thin films and multilayers, iii) experimental results at room temperature on skyrmions in (Pt/Co/Ir)_{xn} multilayers. I will also assess the potential of skyrmions for technological applications.

2) Conversion between charge and spin current by SOC at surfaces and interfaces: report of the results of spin pumping experiments on the spin to charge conversion by Rashba, topological insulator or oxide interfaces; discussion of the application of SOC torques to the motion of magnetic domain walls and the switching of nanomagnets.

I acknowledge the collaborations of K. Bouzehouane, A. Barthelemy, M. Bibes, V. Cros, C. Deranlot, K. Garcia, J-M. George, J. Grollier, E. Jacquet, H. Jaffres, E. Lesne, C. Moreau-Luchaire, N. Reyren, J-C. Rojas-Sanchez, J. Sampaio, N. Van Horne at UMP CNRS-Thales, S. Rohart, J. Sampaio, A. Thiaville at LPS Orsay, J-P. Attane, M. Chshiev, G. Desfond, Yu Fu, S. Gambarelli, M. Jamet, A Marty, S. Oyarzun, J-C. Rojas-Sanchez, C Vergnaux, L. Vila, H. Yang at CEA Grenoble, C. Moutafis, J. Raabe, C.A. Vaz, P. Warnicke, P. Wohlhüter at PSI Villigen, M. Weigand at MPIIS Stuttgart, Y. Ohtsubo at Osaka University, P. Lefevre, F. Bertran, A. Taleb-Ibrahimi at Synchrotron SOLEIL, J-M. De Teresa at ICM Univ-Zaragoza

TU.SYM 2 - Spin-orbitronics with skyrmions in chiral magnets

C. Pfleiderer¹

1. Technische Universität München, Munich, Germany

The emergence, stability and decay of skyrmions in chiral magnets and the associated emergent electrodynamics are reviewed. The non-zero topological winding, which corresponds to precisely one quantum of emergent magnetic flux, mediates an extremely efficient coupling between the conduction electrons and the magnetic properties. This emergent flux leads to a topological Hall signal, spin transfer torques at ultra-low current densities and emergent electric fields. Additionally skyrmions are characterised by an exceptional stability, which cannot be simply suppressed under large hydrostatic pressures or doping.

TU.SYM 3 - Spin hall effect and chiral magnetism in metallic heterostructures

M. Hayashi¹

1. National Institute For Materials Science, Tsukuba, Japan

Strong spin orbit effects in thin film heterostructures consisting of a perpendicularly magnetized ultrathin magnetic layer sandwiched between a heavy metal (HM) layer and an oxide layer have opened new paradigms to control magnetic moments electrically. We have studied spin transport and magnetic properties of CoFeB/MgO based heterostructures with heavy metal (e.g. Hf, Ta, W, Re) underlayers. We find that the HM layer generates large enough spin current via the spin Hall effect that can significantly influence the transport properties of the system and enables manipulation of the CoFeB layer magnetic moments. The amount of spin current generated via the spin Hall effect is probed by the spin Hall magnetoresistance (SMR): a large SMR is observed in the W underlayer films. We also find that a strong chiral magnetic order emerges at the W/CoFeB interface owing to the Dzyaloshinskii-Moriya interaction (DMI). The influence of the interface on the SMR and DMI will be discussed.

Acknowledgment:

MEXT Grant-in-Aid, MEXT R & D Next-Generation Information Technology

TU.SYM 4 - Magnonic charge pumping via spin-orbit coupling

Chiara Ciccarelli¹, Kjetil Hals², Andrew Irvine¹, Vit Novak³, Yaroslav Tserkovnyak⁴, Hidekazu Kurebayashi^{5,6}, Arne Brataas², Andrew Ferguson¹

1. University of Cambridge, Cambridge, United Kingdom

2. Norwegian University of Science and Technology, Trondheim, Norway

3. Institute of Physics ASCR, Prague, Czech Republic

4. University of California, Berkeley, United States

5. University College London, London, United Kingdom

6. PRESTO, Japan Science and Technology Agency

Spin pumping represents a convenient way to electrically detect magnetization dynamics. In this case, however, a secondary spin-charge conversion element, such as heavy metals with large spin Hall angle, is required to convert the spin current into a charge signal. Here, we report the experimental observation of charge pumping in which a precessing ferromagnet pumps a charge current, demonstrating direct conversion of magnons into high-frequency currents via the relativistic spin-orbit interaction. The generated electric current, unlike spin currents generated by spin-pumping, can be directly detected without the need of any additional spin-charge conversion mechanism. The charge-pumping phenomenon is generic

and gives a deeper understanding of its reciprocal effect, the spin orbit torque, which is currently attracting interest for its potential in manipulating magnetic information.

TU.SYM 5 - Chiral magnetic skyrmions in ultrathin films and heterostructures: inside from materials-specific theory

S. Blügel¹

1. Peter Grünberg Institut and Institute for Advanced Simulation, Forschungszentrum, Jülich, Germany

Ultrathin magnetic films and heterostructures provide a fantastic playground for the stabilization, manipulation and usage of magnetic skyrmions - topological magnetization solitons - magnetic entities with particle like properties that may open a new vista for spintronics. A crucial quantity for the skyrmion formation is the Dzyaloshinskii-Moriya interaction (DMI), whose presence in thin films could be established in a concerted effort of first-principles theory and spin-polarized scanning tunnelling microscopy [1]. It could be shown that the spin-orbit interaction and the structure inversion-asymmetry in these systems result in a DMI that is strong enough to give rise to one-dimensional and two-dimensional lattices [2] of chiral spin-textures as well as chiral domain walls. Even single skyrmions [3] could be induced. In retrospect, it is surprising how little is known about the DMI in these metallic systems. In this talk I give some insight into the DMI, the relation to the transport properties of electrons such as the THE and AHE in connection to the spin texture of a skyrmion, and discuss possibilities to tailor the magnetic interactions to enlarge the materials base to stabilize single skyrmions in films and heterostructures.

[1] M. Bode et al., Nature 447, 190 (2007)

[2] S. Heinze et al., Nature Physics 7, 713 (2011)

[3] Romming et al., Science 341, 636 (2013)

WE.SYM 1 - Membrane damage caused by magnetic hyperthermia on microglial cells

M.P. Calatayud^{1,2}, E. Soler¹, T. Torres^{1,2,3}, E. Campos⁴, C. Junquera⁵, M.R. Ibarra^{1,2,3}, G. Goya^{1,2}

1. Nanoscience Institute of Aragón, University of Zaragoza, Zaragoza, Spain

2. Department of Condensed Matter Physics, University of Zaragoza, Zaragoza, Spain

3. Laboratory of Advanced Microscopies (LMA), Zaragoza, Spain

4. Departamento de Física, CINVESTAV-IPN Col. San Pedro Zacatenco, México City, México

5. Dept. Anatomía e Histología, Facultad de Medicina, Universidad de Zaragoza, Zaragoza, Spain

We present experimental evidence demonstrating the suitability of Fe₃O₄-based magnetic nanoparticles (MNPs) to target microglial BV2 cells and to provoke cell death by magnetic hyperthermia. The MNPs, of 30-40 nm, were in situ functionalized with two different polymers, poly-acrylic-acid (PAA) and Lauric-Acid (LA) to control the final particle size for maximum heating efficiency. The measured specific power absorption (SPA) in water under alternating magnetic fields ($f = 560$ kHz, $H = 23.9$ kA/m) was within the 400 - 600 W/g range, and dropped to ≈ 250 W/g and < 150 W/g in culture medium for PAA-MNPs and LA-MNPs, respectively. The analysis of the MNPs distribution at the intracellular level showed vesicle-trapped MNPs agglomerates spread along the cytoplasm, as well as large (~ 0.5 - 0.9 μ m) clusters attached to the cell membrane. In vitro magnetic and water-bath hyperthermia experiments performed in pellets of microglial MNPs-loaded BV2 cells, designed to reach a

constant temperature of 46°C for 30 minutes, yielded a decrease of cell viability down to 25 % for both heating methods. Structural analysis of the cell structures after magnetic and water-bath hyperthermia under these conditions simulating a glial micro-tumor environment showed large amount of damage at the cellular level. It is demonstrated that those regions where the cell membrane is damaged are correlated to the MNPs clusters location. The drastic rupture of the cell and internal membranes suggest that a necrotic process triggered by the MNPs could be the main cause of cell death during hyperthermia.

WE.SYM 2 - Engineered nanoparticles for magnetic particle imaging: tailoring physics and chemistry to clinical applications

K. Krishnan ¹

1. University of Washington, Seattle, United States

The performance - sensitivity and spatial resolution - of Magnetic Particle Imaging (MPI), a new medical imaging technology for whole-body imaging of magnetic tracers, depends largely on the structural, chemical and magnetic characteristics of the tracers, in addition to instrumentation parameters. As the first biomedical imaging technique that truly depends on magnetic relaxation dynamics of nanoscale materials, MPI requires highly optimized and biocompatible magnetite nanoparticle tracers to generate good-quality images. Here, we describe the development of the most optimal tracers for MPI with magnetic properties that were designed using a sound theoretical framework, an organic synthetic route leading to highly phase-pure and monodisperse magnetite nanocrystals, subsequent phase-transfer and functionalization to ensure biocompatibility and adequate in vivo circulation. In phantom MPI imaging, with image reconstruction in either real or Fourier space, these optimized tracers showed more than 4x times signal-to-noise ratio and improved spatial resolution (50% better) than existing, commercial tracers; the latter approaching sub-mm resolution at 6T/m field gradients critical for translational applications in angiography and molecular imaging of cancer. Finally, we have established a flexible platform for functionalization of the magnetic cores with PEG (to increase water solubility, enhance circulation time up to ~160 minutes, and improve shelf life), dyes (to turn them into multimodal - MRI, MPI and NIRF - contrast agents and used to further enhance studies of their biodistribution with significant anatomical detail in rodent models) and ligands (such as Lactoferrin with specific affinity for glioma cells) tailored for targeted molecular imaging. These critical results, that pave the way for improved clinically relevant MPI performance, will be discussed with emphasis on the tracer response to both the alternating magnetic field and the biological environment.

This work was supported by NIH grants 1R01EB013689-01/NIBIB & 1R41EB013520-01.

WE.SYM 3 - Can the synthesis technology and properties of magnetite nanoparticles cater the needs of biomedical applications?

J. Balachandran ¹, H Mamiya ²

1. The University of Shiga Prefecture, Hikone, Japan

2. National Institute of Materials Science, Tsukuba, Japan

Magnetite nanoparticles of different sizes are considered as the potential magnetic seeds for various biomedical applications such as magnetic hyperthermia, magnetic imaging and drug delivery from the standpoint of their magnetic property and biocompatibility. As a consequence, several techniques have been proposed to synthesize mostly spherical magnetite particles with various diameters and narrow size distribution and their application in

biomedicine is being actively pursued. This presentation will focus on the application of magnetite particles for magnetic hyperthermia from the perspective of numerical simulation, experimental verification and the practical limits posed on the magnetic properties using the synthesis techniques available at present. First, the results of the numerical simulation study undertaken to compare the magnetic loss in rotatable magnetite nanoparticles in an aqueous phase with that of non-rotatable nanoparticles anchored to localized structures in the context of magnetic heat dissipation will be discussed. Secondly, the technology available for the synthesis of magnetite nanoparticles and their magnetic properties as well as the experimental findings on the heat dissipation properties of magnetite particles with varying magnetic properties under different alternating magnetic field strengths and frequencies will be discussed. Finally, the validity of the interpretation of the experimental observation of magnetite nanoparticles using the existing theories will be discussed. It should be noted that the experimental results obtained in heat dissipation experiments are generally being explained based on models that does not consider the magnetic interaction effects into account though the magnetic interaction is inevitably present. The preparation of magnetic interaction-free magnetite particles with diameters considered suitable for magnetic hyperthermia applications and estimation of their magnetic properties will also be presented. Results obtained reveals that the potential of magnetite particles as a magnetic thermal seeds will be limited unless additional steps are taken to nurture their properties to suit the operating conditions.

WE.SYM 4 - Albumin-SPIONs: protein surface binding, nanoparticles uptake and fate in cells and *C. elegans*

A. Roig¹

1. Institut de Ciència de Materials de Barcelona (ICMAB-CSIC), Bellaterra, Spain

Superparamagnetic iron oxide nanoparticles (SPIONs) are demonstrating huge potential in nanomedicine. SPIONs are investigated as MRI contrast agents, in hyperthermia treatment, for drug delivery, targeting therapies, biosensing and magnetic separation. However, the stability of SPIONs in complex biological environments remains a challenge and simple biocompatible surface coatings to stabilize nanoparticles, avoid agglomeration, enhance their therapeutic effect and prevent their dissolution, are currently being investigated. Albumin is the most abundant protein in serum with many important physiological functions in the circulatory system. Moreover, one of the first FDA-approved nanomedical products (Abraxane[®]) is a formulation of paclitaxel-albumin nanoparticles where the presence of albumin facilitates the transport of paclitaxel through the endothelial cells enhancing its accumulation in the tumor. I will show that bovine serum albumin (BSA) stabilizes SPIONs by controlling their aggregation and improving their colloidal stability in biological media. Moreover, BSA forms a protein corona around the nanoparticles modifying their initial surface chemistry and providing a new but distinct bio-identity to the nanoparticles when exposed to biological media, cells and organisms. Binding affinity, conformation changes of BSA upon binding to the SPIONs and the effects on cytotoxicity, cellular uptake, distribution and fate of nanoparticles in presence of albumin will be reported. Finally, nanoparticles assessment in a simple animal model, *C. elegans*, will also be presented. In particular, based on its transparency, short life cycle, differentiated anatomy and ease of cultivation, *C. elegans* is a suited model organism for in vivo NP evaluation within the synthetic laboratory (Figure 1). Interestingly, results confirm in vitro observations regarding enhanced stability of BSA-coated SPIONs in biological environment, and reduced interaction with cells. Furthermore, all findings indicate the protective effects of the protein both to the nanoparticles and to the worms especially at high concentrations.

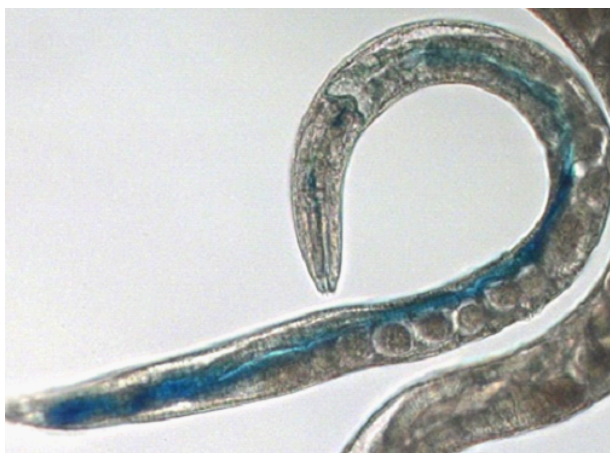


Figure1. Prussian Blue stained *C. elegans*: where SPIONs appear blue

WE.SYM 5 - Dual drug carrier for thermo-chemotherapy of cancer

D. Bahadur^{1,2}, L. Pradhan¹, A.K. DSwain²

1. Center For Research In Nanotechnology and Science, Indian Institute of Technology-Bombay, Mumbai, India

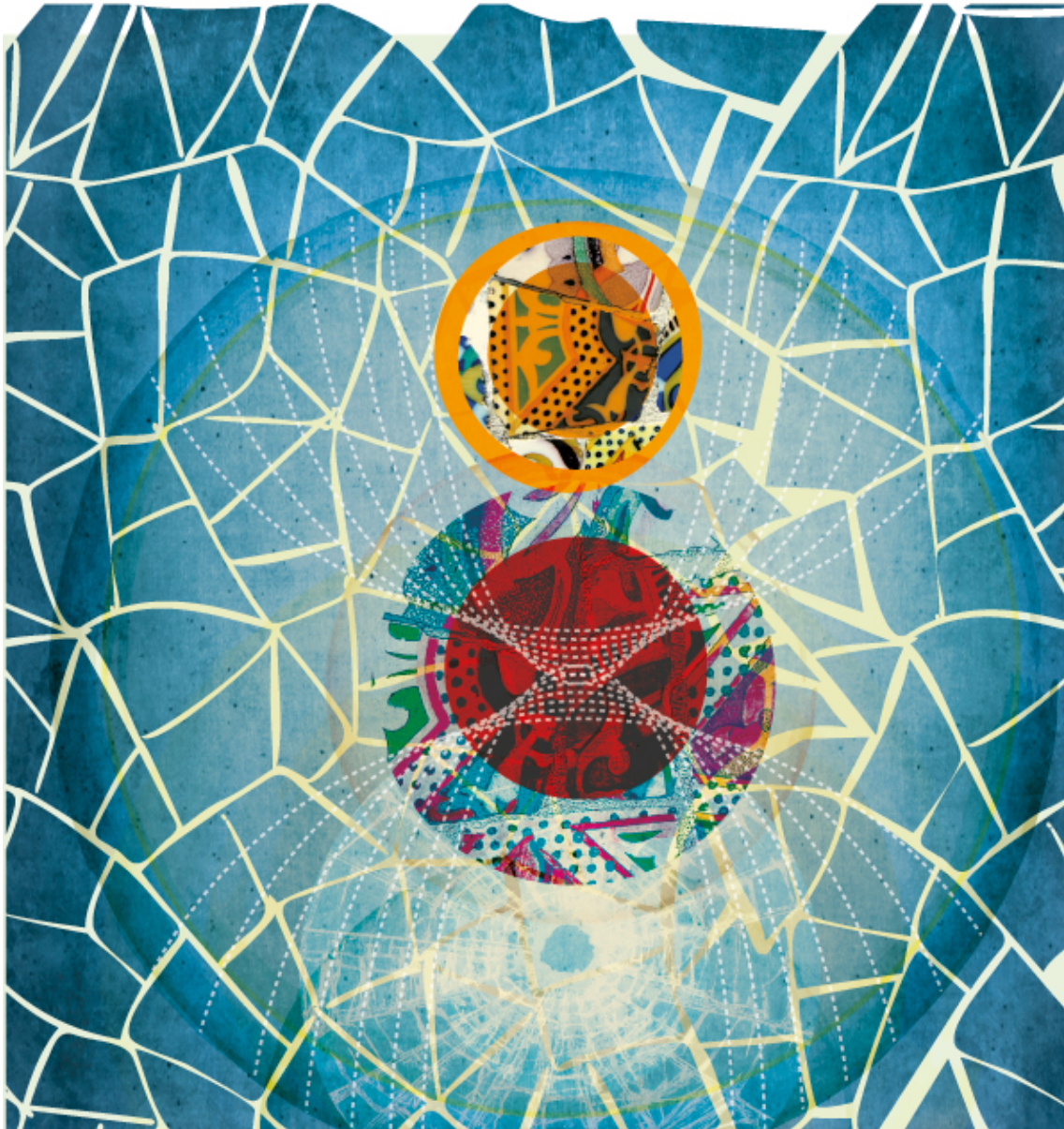
2. Department of Metallurgical Engineering and Materials Science, Indian Institute of Technology, Mumbai, India

We discuss here two different amphiphilic drug carrier systems for simultaneous thermo chemotherapy. A pH and thermo sensitive dual drug delivery system (DDDS) consisting of thin lipid layer encapsulated mesoporous magnetite nanoassemblies (MMNA) has been developed which can deliver two anticancer drugs simultaneously. Hydrophilic (Doxorubicin) and hydrophobic (Paclitaxel) drugs are used to examine the loading/releasing efficiency. This hybrid system was investigated for its ability to provide heat under AC magnetic field (ACMF). A high loading efficiency and sustained release are realized. An enhanced release of ~72 and ~68% is recorded for DOX and TXL respectively during the first hour with application of ACMF (~43 °C). Higher in vitro cytotoxic effect is observed with two drugs compared to individual ones in HeLa, MCF-7 and HepG2 cancer cells. With an application of ACMF for ten minutes, the cell killing efficiency is improved substantially due to simultaneous thermo-chemotherapy. Confocal microscopy confirms the internalization of drug by cells and their morphological changes during thermo-chemotherapy. We will also discuss some animal experiments. We also report here a novel nanocomposite of Fe₃O₄-graphene, stabilized with bio polymers that proves to be an effective dual drug carrier and also responsive to hyperthermia for effective cancer treatment. The nanocomposite is stabilized due to covalent functionalization of the two polymers (PVP and PVA) with Fe₃O₄-graphene (PIG). DOX and PTXL conjugated PIG exhibit a sustained release profile at acidic pH-4.3 compared to physiological pH-7.4 and controlled drug release under AC magnetic field is observed. The cellular toxicity assay suggests that the PIG has good cytocompatibility up to 2.5 mg/ml on L929 and HeLa cell lines. But higher cytotoxicity effect is observed with DOX-PIG and PTXL-PIG at 2.5 mg/ml on HeLa cell line.

References:

1. Lina Pradhan, R. Srivasta, D. Bahadur, "pH and thermo-sensitive thin lipid layer coated mesoporous magnetic nanoassemblies as a dual drug delivery system towards thermo-chemotherapy of cancer", *Acta Biomaterialia*, 10, 2976-2987 (2014)
2. S. Chandra, S. Nigam, D. Bahadur, "Combining unique properties of dendrimers and magnetic nanoparticles towards cancer theranostics", *Journal of Biomedical Nanotechnology*, 10, 32-49 (2014)

Invited & Contributed



MO.A.1_I1 - Superconductivity of Sr₂RuO₄: Current challengesY. Maeno¹*1. Department of Physics, Kyoto University, Kyoto, Japan*

In this talk, we will summarize the key experimental facts known so far concerning the superconducting symmetry of Sr₂RuO₄, a leading candidate of the spin-triplet, “p+ip” chiral superconductor with T_c = 1.50 K [1]. After introducing recent NMR results strengthening the evidence for spin-triplet pairing [2], we discuss how other key results [3-7], especially those evidencing the first-order superconducting transition under the accurately-aligned in-plane fields [3, 4], might resolve the outstanding issue of its superconducting symmetry. We also introduce other important approaches trying to demonstrate the phenomena specific to spin-triplet pairing. One such approach is the presence of half-quantum fluxoid (HQF) states observed in the magnetization of micro-rings of single-crystalline Sr₂RuO₄ [8]. Such states are expected to emerge in an Equal-Spin-Pairing (ESP) triplet superconductor. We describe our recent results attempting to confirm the HQF states by Little-Parks oscillations in micro-rings. Another approach is to establish long-range proximity effects of spin-triplet pairs into a ferromagnet. We have recently developed a hybrid system consisting of epitaxial thin film of ferromagnetic SrRuO₃ deposited on Sr₂RuO₄ [9]. It is expected that the range and the magnetic-domain-dependence of the proximity effect provide vital information about the nature of superconducting symmetry in Sr₂RuO₄.

[1] Y. Maeno, S. Kittaka, T. Nomura, S. Yonezawa, and K. Ishida, J. Phys. Soc. Jpn. 81, 011009 (2012)

[2] K. Miyake, J. Phys. Soc. Jpn. 83, 053701 (2014); K. Ishida et al., preprint (2014)

[3] S. Yonezawa, T. Kajikawa, and Y. Maeno, Phys. Rev. Lett. 110, 077003 (2013)

[4] S. Kittaka, A. Kasahara, T. Sakakibara, D. Shibata, S. Yonezawa, Y. Maeno, K. Tenya, and K. Machida, Phys. Rev. B 90, 220502(R) (2014)

[5] C. N. Veenstra, Z.-H. Zhu, M. Raichle, B. M. Ludbrook, A. Nicolaou, B. Slomski, G. Landolt, S. Kittaka, Y. Maeno, J. H. Dil, I. S. Elfimov, M.W. Haverkort, A. Damascelli, Phys. Rev. Lett. 112, 127002 (2014)

[6] S. Kashiwaya, H. Kashiwaya, K. Saitoh, Y. Mawatari, Y. Tanaka, Physica E 55, 25-29 (2014)

[7] C. W. Hicks, D. O. Brodsky, E. A. Yelland, A. S. Gibbs, J. A. N. Bruin, M. E. Barber, S. D. Edkins, K. Nishimura, S. Yonezawa, Y. Maeno, A. P. Mackenzie, Science 344, 283 (2014)

[8] J. Jang, D. G. Ferguson, V. Vakaryuk, R. Budakian, S. B. Chung, P. M. Goldbart, and Y. Maeno, Science 331, 186 (2011)

[9] M. S. Anwar, Y. J. Shin, S. R. Lee, S. J. Kang, Y. Sugimoto, S. Yonezawa, T. W. Noh, and Y. Maeno, Appl. Phys. Express 8, 015502 (2015)

MO.A.1_O2 - Controlling superconductivity by tunable AFM QCPs in the heavy fermion compound CeRhIn₅

T. Park¹, S. Seo¹, E. Park¹, E.D. Bauer², F. Ronning², J.N. Kim³, J.H. Shim³, J.D. Thompson²

1. Sungkyunkwan University, Seoul, South Korea

2. Los Alamos National Laboratory, New Mexico, United States

3. POSTECH, Gyeongsangbuk-do, South Korea

Magnetic impurities have been known to be detrimental to superconductivity because they break the Cooper pairs. In various classes of unconventional superconductors, the superconducting phase is located adjacent to a magnetic phase, suggesting that superconductivity may thrive in spite of magnetism. This viewpoint, however, has faced a challenge since the presence of a hidden quantum critical point was explicitly revealed inside the dome of superconductivity in the heavy fermion compound CeRhIn₅. In spite of this, the question has remained whether the superconductivity arises in spite of the QCP or because of the QCP. Even though the discovery of a hidden quantum critical point indicates that the spectrum of singular quantum fluctuations are responsible not only for the strange metallic state, but also for the Cooper pairing, a lack of further examples of a hidden QCP has raised a doubt on the role of quantum critical fluctuations in producing superconductivity. In this presentation, we show that the superconducting phase rigidly shifts commensurately with the QCP as a function of pressure and doping CeRhIn₅. The precise pinning of the SC phase by the tunable QCPs indicates that the singular quantum fluctuations are responsible for the unconventional superconductivity in CeRhIn₅. These discoveries, though specific to CeRhIn₅, could be broadly applicable to the SC mechanism of diverse classes of unconventional superconductors. We acknowledge support by a NRF grant funded by the Ministry of Science, ICT and Future Planning (No. 2012R1A3A2048816).

References:

S. Seo et al. Nature Communications (To be published)

MO.A.1_O3 - Antiferromagnetic order and spatial modulation in high field superconducting phase of CeCoIn₅

R. Ikeda¹, Y. Hatakeyama¹

1. Department of Physics, Kyoto University, Kyoto, Japan

For more than ten years, the issue on the high field superconducting phase (HFSP) of the heavy-fermion material CeCoIn₅ remains unresolved. Originally, this phase has been identified with a FFLO vortex phase [1]. After that, HFSP has been called as a Q-phase since the discovery of a long-ranged antiferromagnetic or spin-density-wave (SDW) order in the phase. The recent observation of a discontinuous change of the SDW q-vector via in-plane rotation of the magnetic field [2] in HFSP is crucial and corroborates the presence of a spatial modulation of the superconducting order in the phase. However, it is not easy to theoretically justify the presence of the pi-triplet superconducting order proposed as the origin of such a spatial modulation in Ref.[2]. We show in the present report that the original FFLO picture [1] of HFSP, modified in the way of taking account of the SDW order induced by the strong paramagnetic pair-breaking peculiar to this material [3], can nicely explain the discontinuous change of the SDW q-vector upon the field rotation [4]. The origin of the sudden change of the q-vector in this theory is a pinning of the q-vector to the FFLO nodal plane. By combining this result and agreements with other experimental data [5] altogether, we argue that the HFSP of CeCoIn₅ can be understood based only on the strong paramagnetic pair-breaking in this material.

[1] A. Bianchi et al., Phys. Rev. Lett. 91, 187004(2003) ; H.Adachi and R.Ikeda, Phys. Rev. B 68, 184510 (2003)

[2] S. Gerber et al., Nature Physics 10, 126 (2014)

[3] R. Ikeda et al., Phys. Rev. B 82, 060510(R) (2010)

[4] Y. Hatakeyama and R. Ikeda, Phys.Rev. B (to appear in March, 2015) ; arXiv:1412.2898

[5] For instance, K. Kumagai et al., Phys. Rev. Lett. 106, 137004 (2011)

MO.A.1_O4 - Heat capacity measurements on UBe₁₃ in rotated magnetic fields: anisotropic response in the normal state and the absence of nodal quasiparticles

Y. Shimizu¹, S. Kittaka¹, T. Sakakibara¹, Y. Haga², E. Yamamoto², H. Amitsuka³, Y. Tsutsumi⁴, K. Machida⁵

1. *The Institute for Solid State Physics, The University of Tokyo, Tokyo, Japan*

2. *Advanced Science Research Center, Japan Atomic Energy Agency, Ibaraki, Japan*

3. *Graduate School of Science, Hokkaido University, Hokkaido, Japan*

4. *Condensed Matter Theory Laboratory, RIKEN, Saitama, Japan*

5. *Department of Physics, Okayama University, Okayama, Japan*

Since the discovery of the heavy-fermion superconductivity in cerium and uranium based f-electron materials three decades ago, intensive experimental and theoretical works have been done in order to elucidate the unconventional pairing mechanisms that are widely believed to differ from conventional Debye-phonon mediated attraction. One of the most important issues is to clarify the gap structures of unconventional superconductors, which intimately reflect the pairing interactions. The oldest uranium heavy-fermion superconductor UBe₁₃, which crystallizes in a cubic structure, exhibits unconventional superconductivity at T_c~0.85 K [1]. In spite of numerous works, true nature of the superconductivity of UBe₁₃ as well as the origin of its non-Fermi-liquid normal state has remained elusive. In order to obtain information about the superconducting gap structure, we studied the low-energy quasiparticle excitations in the superconducting state of UBe₁₃ by means of heat capacity (C) measurements in a rotating field [2]. Quite unexpectedly, the magnetic-field dependence of C(H) is linear in H with no angular dependence at low magnetic fields in the SC state, implying that the gap is fully open over the Fermi surfaces [2]. Our observation contrasts starkly with previous expectations over more than 30 years [3] that the strongly correlated heavy f electrons favor a nodal superconducting gap to avoid the strong Coulomb repulsive force. We also observed a characteristic cubic anisotropy at high fields above 2 T with a maximum (minimum) for H || [001] ([111]), both in the normal as well as in the SC states. This oscillation possibly originates from the anisotropic response of the heavy quasiparticle bands, and might be a key to understand the anomalous properties of UBe₁₃.

[1] H. R. Ott et al., Phys. Rev. Lett. 50, 1595 (1983)

[2] Y. Shimizu et al., arXiv :1411.1504. [3] H. R. Ott et al., Phys. Rev. Lett. 52, 1915 (1984)

MO.A.1_O5 - Pr₂Pt₃Ge₅ - A novel magnetic superconductor?

J. Gavilano¹, D. Mazzone¹, R. Sibille², M. Bartkowiak², O. Zaharko¹, M. Mansson¹, J. Schefer¹, M. Frontzek¹, M. Kenzelmann²

1. *Laboratory for Neutron Scattering and Imaging, Paul Scherrer Institut, Villigen, Switzerland*
2. *Laboratory for Developments and Methods, Paul Scherrer Institute, Villigen, Switzerland*

Strong magnetic spin fluctuations are present in many unconventional superconductors. Although the two mechanisms, magnetic order and superconductivity, are often of competing nature, in many cases the two phenomena not only coexist, but also they depend on each other for their existence. For instance, for many unconventional superconductors spin fluctuations, which mediate the magnetic order, are necessary for the formation of Cooper pairs in [1, 2]. It is, therefore, crucial to understand in detail the properties of known materials which display both magnetism and superconductivity. For this reason Pr₂Pt₃Ge₅ has recently gained interest in the research community. This material displays a relatively high superconducting transition temperature $T_c = 7.8$ K and two antiferromagnetic (AF) transitions at $T_{N1} = 3.4$ and $T_{N2} = 4.1$ K, deep in the superconducting phase. It was suggested that Pr₂Pt₃Ge₅ is a multiple-gap superconductor with possibly a substantial amount of anisotropy in the superconducting properties [3]. We have studied the two AF phases of this compound by means of neutron scattering and found some very unexpected results. We have identified the propagation vectors and the magnetic structures of the two AF phases existing in the superconducting phase. The HT-phase boundary separating the normal state and the two magnetically ordered phases provides insights on the question of a possible coupling of superconductivity and magnetism in Pr₂Pt₃Ge₅.

References:

- [1] J. Flouquet et al., Nature. 7, 22 (2006)
- [2] P. Monthoux et al., Nature. 450, 1177 (2007)
- [3] N. H. Sung et al., Phys. Rev. B. 86, 224507 (2012)

MO.A.2_I1 - Phase competition and Fermi surface reconstruction by charge density-wave order in cuprate superconductors

N. Doiron-Leyraud¹, G. Grissonnanche¹, S. Badoux², O. Cyr-Choinière¹, R. Liang^{3,4}, D. Bonn^{3,4}, W. Hardy^{3,4}, B. Vignolle², C. Proust^{2,4}, L. Taillefer^{1,3}

1. *Université de Sherbrooke, Sherbrooke, Canada*

2. *Laboratoire National des Champs Magnétiques Intenses, Toulouse, France*

3. *University of British Columbia, Vancouver, Canada*

4. *Canadian Institute for Advanced Research, Toronto, Canada*

Recent developments have convincingly shown that charge density-wave (CDW) modulations are a universal property of cuprate superconductors and this has opened up a new era of research in the field. Understanding the origin of the CDW and its relation to the key features of cuprates, namely the superconducting state, the pseudogap phase, and the Fermi surface, are currently at the center of attention. To examine the interplay between the CDW and superconductivity, we have performed the first direct measurement of the upper critical field H_{c2} in the cuprate $YBa_2Cu_3O_y$ [1], which provides a thermodynamic measure of the strength of superconductivity across the temperature-doping phase diagram. Our measurements reveal a strong suppression of H_{c2} and of the condensation energy precisely where the CDW is strongest, and peaks in H_{c2} where the CDW vanishes, showing clearly a phase competition between the two phenomena. In the field-induced normal state above H_{c2} , our quantum oscillations measurements on $YBa_2Cu_3O_y$ reveal the presence of both electron and hole pockets, whose size and mass agree with the Fermi surface expected from a reconstruction by the measured CDW [2]. In this regime, our measurements of the thermal Hall conductivity at low temperatures demonstrate that the Wiedemann-Franz law is valid above H_{c2} , implying that the fundamental excitations are Landau quasiparticles carrying charge and entropy, suggestive of a Fermi-liquid state [3].

References:

[1] G. Grissonnanche, N. Doiron-Leyraud, and L. Taillefer, *Nature Communications* 5, 3280 (2014)

[2] N. Doiron-Leyraud, L. Taillefer, and C. Proust, *Nature Communications* (in press); arXiv:1409.2788

[3] G. Grissonnanche, N. Doiron-Leyraud, and L. Taillefer, preprint (2015)

MO.A.2_O2 - The evolution of microwave conductivity in $\text{YBa}_2\text{Cu}_3\text{O}_{6+x}$ across the superconducting dome

J. Baglo¹, J. Day², P. Dosanjh², R. Liang², W. Hardy², D. Bonn²

1. *Cavendish Laboratory, University of Cambridge, Cambridge, United Kingdom*

2. *Department of Physics and Astronomy, University of British Columbia, Vancouver, Canada*

The rich phenomenology displayed in the phase diagram of the high- T_c cuprates continues to be an active arena of investigation. Recent experimental and theoretical work appears to be converging on a picture of separate spin and charge order phase transitions, well-below and near optimal doping, respectively - along with associated Fermi surface reconstruction. As sensitive probes of the low-energy electrodynamics, microwave spectroscopy techniques are well-suited for characterizing the effects of such changes in electronic structure deep within the superconducting state. I will present the results of our survey of the complex microwave conductivity of YBCO over a wide range of oxygen contents, from 6.49 to 6.998, and discuss their implications for the evolution of electronic structure with doping. In particular, I will highlight the apparent absence of a peak in penetration depth near the proposed $p \sim 0.18$ quantum critical point (QCP), contrasting with its presence near the antiferromagnetic QCP of the pnictide superconductors. I will also discuss the surprising relationship we observed between quasiparticle scattering lifetimes and oxygen ordering, which carries important implications for quantum oscillation measurements.

MO.A.2_O3 - Magnetoresistance in the pseudogap phase of the high-T_c cuprate HgBa₂CuO_{4+δ}

M. Chan¹, K. Modic¹, B. Ramshaw¹, R. McDonald¹, N. Harrison¹, Y. Li², Y. Tang², M. Greven², S. Badoux³, W. Tabis², B. Vignolle³, J. Béard³, X. Zhao⁴, N. Barisic⁵,

1. *National High Magnetic Field Laboratory, Los Alamos, United States*

2. *University of Minnesota, Minneapolis, United States*

3. *Laboratoire National des Champs Magnétiques Intenses, Toulouse, France*

4. *State Key Lab of Inorganic Synthesis and Preparative Chemistry, Jilin University, China*

5. *Institute of Solid State Physics, Vienna University of Technology, Austria*

Besides high- T_c superconductivity, the identification of the pseudogap state in underdoped cuprates, which is characterized by the partial gapping of the Fermi surface below a characteristic temperature T*, remains a contentious issue within the field. Early electrical transport studies in the cuprates indicated highly anomalous behavior inconsistent with conventional Fermi-liquid descriptions in this regime. We report planar resistivity (ρ) and transverse magnetoresistance (MR) measurements for underdoped HgBa₂CuO_{4+δ} (Hg1201). Contrary to the long-standing view that Kohler's rule is strongly violated in underdoped cuprates, we find that it is in fact satisfied in the pseudogap phase of Hg1201 for temperatures above T_c [Phys. Rev. Lett. 113, 177005 (2014)]. The transverse MR shows a quadratic field dependence, $\delta\rho/\rho_0=aH^2$, with $a(T)\propto T^{-4}$. In combination with the observed $\rho\propto T^2$ dependence, this is consistent with a single Fermi-liquid quasiparticle scattering rate. A consequence of these results is that the pseudogap regime should feature a largely temperature independent Fermi surface. Furthermore, measurements of Hg1201 at low temperatures in a magnetic field sufficient to suppress superconductivity reveal Shubnikov-de Haas oscillations² [Nat. Phys. 9, 761 (2013)] which confirms the generality of small Fermi surfaces in underdoped cuprates first observed in YBa₂Cu₃O_{6+x}. Recent measurements in magnetic fields up to 90 T reveal only a single oscillatory frequency in contrast to the multiple frequencies observed in YBCO. Finally, the effective electron mass diverges upon underdoping, indicating a possible quantum critical point on the underdoped side of the superconducting dome.

MO.A.2_O4 - Observation of charge order in electron-doped cuprates

R. Greene¹, E. da Silva Neto², R. Comin², Y. Jiang¹, J. Higgins¹, A. Damascelli²

1. *University of Maryland, College Park, United States*

2. *University of British Columbia, Vancouver, Canada*

The origin of high-T_c superconductivity in the strongly correlated cuprates is still a mystery, 29 years after its discovery. In the hole-doped cuprates a “pseudogap phase” is found in the underdoped part of the phase diagram and this is believed to be related to the cause of the high-T_c superconductivity. A few years ago, charge order was found in the hole-doped cuprates and this was thought to be the cause of the quantum oscillations found in the “pseudogap” region and perhaps related to the origin of the high-T_c superconductivity. Here we report the first observation of charge order (CO) in the electron-doped cuprates from resonant x-ray scattering experiments. This is an unexpected result since the electron-doped cuprates do not have a “pseudogap phase” and their physics is believed to be dominated by antiferromagnetism and its associated spin fluctuations. Moreover, the temperature onset of the CO is unusual and is not related to the onset of the spin fluctuations or to the quantum oscillations. The CO is incommensurate, short ranged (as found in hole-doped cuprates), and has an unusual doping dependence. Since the origin of the high-T_c superconductivity is the same in all the cuprates (both p- and n-types), the CO found in the n-doped cuprates suggests that neither the “pseudogap” nor the CO are related to the origin of the high-T_c superconductivity in the cuprates. Our preliminary results on the CO in n-type cuprates is published in *Science* 347, 282 (2015).

MO.A.2_O5 - Hybridization and formation of coherent heavy fermions: Non-Fermi liquid detection with point contact spectroscopy

L.H. Greene¹, S. Narasimwodeyar¹, M. Dwyer¹, W.K. Park¹, P.C. Canfield², E.D. Bauer³, P.H. Tobash³, R.E. Baumbach³, F. Ronning³, J.L. Sarrao³, J.D. Thompson³

1. *University of Illinois at Urbana-Champaign, Champaign, United States*

2. *Ames Laboratory and Iowa State University, Ames, United States*

3. *Los Alamos National Laboratory, New Mexico, United States*

Point contact spectroscopy (PCS) is a well-developed bulk spectroscopic probe used to detect bosonic excitations through classical quasiparticle scattering; and superconducting gap structure and symmetry through Andreev scattering. We have found this technique to be surprisingly sensitive to a density of states arising from non-Fermi liquid behavior in systems with strong electron correlations where we used this technique to identify electron nematic phases in the Fe pnictides and chalcogenides [1]; and developed a quantum mechanical theory to account for this.[2] We have applied this to elucidate microscopic understanding of the hybridization process in heavy electron systems. Using PCS, we have shown the hybridization gap in a heavy-fermion URu₂Si₂ opens well above the hidden order transition. [3] Recently we have shown that for the non-superconducting, non-magnetic intermediate valence compound YbAl₃ exhibits a “slow crossover” to a coherent state [3,4]. We show how PCS is used to provide a more rigorous identification of the onset of the hybridization process.

[1] H. Z. Arham, et al., Phys. Rev. B 85, 214515; 1-4 (2012); Wei-Cheng Lee et al., Rev. B 86 245113; 1-5 (2012). Wei-Cheng Lee et al., Int’l J. Mod. Phys. B 27 1330014-39 (2013)

[2] Wei-Cheng Lee, et al., (PNAS) 112, 651-656 (2015)

[3] W. K. Park et al., Phys. Rev. Lett. 108, 246403 (2012); W. K. Park et al., Philos. Mag. 94, 3737 (2014)

[4] W. K. Park et al., arXiv:1411.7073, submitted to Phys. Rev. Lett.

[4] S. Burdin and V. Zlatić, Phys. Rev. B 79, 115139 (2009). Work at UIUC is supported by NSF DMR-1206766 and for Fe-based the Center for Emergent Superconductivity, by an EFRC under DE-AC0298CH1088, Ames Lab is supported by DE-AC02-07CH11358, and LANL under the auspices of the U.S. DOE, Office of Science

MO.A.3_O1 - Electronic, magnetic and structural properties in Fe-based superconductorsL. Simonelli¹, T. Mizokawa², N.L. Saini³1. *Alba Cells Synchrotron, Barcelona, Spain*2. *Department of Physics and Department of Complexity Science and Engineering, University of Tokyo, Chiba, Japan*3. *Dip. di Fisica, Università di Roma "La Sapienza", Roma, Italy*

The discovery of superconductivity in FeSe (11)-type chalcogenides has been an important finding to progress in the understanding of Fe-based superconductors (pnictides and chalcogenides) since it has emphasized the central role played by the ubiquitous Fe-Fe planes and interacting anion (pnictogen or chalcogen) atoms. FeSe (11)-type chalcogenides have been widely regarded as a model systems to explore the physics of Fe-based superconductors [1] since lacking the spacer layers present in the most common (1111)- and (122)-type pnictides it presents the easiest crystal structure. Moreover FeSe shows a huge enhancement of the superconducting transition temperature (T_c) under high pressure [2]. This high sensitivity to pressure underlines the delicate balance between electronic and structural properties in defining its physical properties. FeSe layers have been successfully intercalated by alkaline atoms (K, Rb, Cs), with intercalated chalcogenides showing superconductivity at 32 K [3-7], unlike the (11)-type of chalcogenides (maximum T_c : 15 K). (122)-type chalcogenides are non stoichiometric systems displaying a complex phase diagram [8], coexisting phases [9-11], a remarkably large iron magnetic moment and a magnetic order that at low temperatures coexists with bulk superconductivity [12-13]. High-energy spectroscopies are unique tools to investigate at the same time the evolution of the electronic and magnetic properties as a function of hydrostatic and chemical pressure. Here we report on the electronic and magnetic properties of Fe-based superconductors by x-ray emission (XES) and high resolution absorption spectroscopy (XAS). Comparing the effects of temperature, and hydrostatic and chemical pressure we identify clear correlations between structural, electronic, and magnetic properties, and superconductivity [1,9,14-16].

References:

- [1] L. Simonelli et al., *J. Phys.: Condens. Matter* 24, 415501 (2012)
- [2] S. Medvedev, et al., *Nature Materials* 8, 630-633 (2009)
- [3] J. Guo, et al., *Phys. Rev. B* 82, 180520 (2010)
- [4] Y. Mizuguchi, et al., *Appl. Phys. Lett.* 98, 042511 (2011)
- [5] J. J. Ying et al., *Phys. Rev. B* 83, 212502 (2011)
- [6] A. Krzton-Maziopa, et al., *J. Phys.: Condens. Matter* 23, 052203 (2011)
- [7] Ming-Hu Fang et al., *EPL* 94, 27009 (2011)
- [8] Y. J. Yan et al., *Sci. Rep.* 2, 212 (2012)
- [9] L. Simonelli et al., *Phys. Rev. B* 85, 224510 (2012)
- [10] Ricci et al. *Supercond. Sci. Technol.* 24 No 8, 082002 (2011)
- [11] Y. Liu et al., *Phys. Rev. B* 86, 144507 (2012)
- [12] W. Bao et al., *Chin. Phys. Lett.* 28, 086104 (2011)
- [13] V. Pomjakushin et al., *Phys. Rev. B* 83, 144410 (2011); V. Pomjakushin et al., *J. Phys.: Condens. Matter* 23, 156003 (2011)
- [14] L. Simonelli et al., *Phys. Rev. B* 90, 214516 (2014)
- [15] A. Iadecola et al., 2012 *J. Phys.: Condens. Matter* 24 115701; B. Joseph et al., *Phys. Rev. B* 82, 020502 (R) 2010
- [16] L. Simonelli et al., in progress

MO.A.3_O2 - Unconventional superconductivity in double quantum dots

M. Governale¹, B. Sothmann², S. Weiss³, J. König³

1. Victoria University of Wellington, Wellington, New Zealand

2. Université de Genève, Geneva, Switzerland

3. Universität Duisburg-Essen, Essen, Germany

The formation of electron pairs is a prerequisite for superconductivity. The fermionic nature of electrons leads to four different classes of superconducting correlations with definite symmetries in spin, space, and time (frequency) under exchange of two electrons forming a Cooper pair. Even-frequency singlet (odd in spin and even in space) is the most common type of pairing and occurs in standard s-wave and high-temperature d-wave superconductors. Even-frequency triplet pairing (even in spin and odd in space) is less common, an example being strontium ruthenate [1]. The concept of odd-frequency triplet correlations emerges in the context of superconductor-ferromagnet heterostructures [2]. Finally, odd-frequency singlet superconductivity has not been experimentally observed so far.

We show that double-quantum dots (DQDs) in proximity to a conventional s-wave superconductor are ideal systems to generate and study all four types of superconducting correlations in a single device [3]. In particular, we consider two single-level quantum dots, tunnel-coupled to a common superconducting lead in the presence of non-collinear magnetic fields.

This type of system shows an interesting interplay between superconducting correlations and Coulomb interaction [4]. We define even- and odd-frequency order parameters for the DQD and determine how they depend on gate voltages and external magnetic fields. Interestingly, we find that the odd-frequency order parameters can be expressed in terms of the even-frequency counterparts together with local and non-local expectation values of charge and spin on the DQD. Finally, we propose two detection schemes for unconventional superconductivity, based on either Josephson or Andreev spectroscopy.

[1] A.P. Mackenzie and Y. Maeno, Rev. Mod. Phys. 75, 657 (2003)

[2] F.S. Bergeret, A.F. Volkov, and K.B. Efetov, Rev. Mod. Phys. 77, 1321 (2005)

[3] B. Sothmann, S. Weiss, M. Governale, and J. König, Phys. Rev. B 90, 220501(R) (2014)

[4] A. Martín-Rodero and A. Levy Yeyati, Advances in Physics 60, 899 (2011)

MO.A.3_O3 - Electronic structure, spin excitations, and orbital ordering in a three-orbital model for iron pnictides

S. Ghosh¹, A. Singh¹

1. Indian Institute of Technology, Kanpur, India

A three-orbital itinerant-electron model involving d_{xz} , d_{yz} , and d_{xy} Fe 3d orbital is proposed for iron pnictides towards understanding the $(\pi, 0)$ ordered magnetism and magnetic excitations in these materials. It is shown that this model simultaneously reproduces several experimentally observed features such as circular hole and elliptical electron pockets in the electronic Fermi surface structure, quantitatively correct spin wave dispersion, as well as the ferro-orbital order between the d_{xz} and d_{yz} orbital.

MO.A.3_O4 - Superconductivity in SrPt₃P: An NMR study and comparison with non-centrosymmetric LaPt₃Si and CePt₃SiT. Shiroka^{1,2}, H.R. Ott^{1,2}, M. Pikulski¹, N.D. Zhigadlo¹, B. Batlogg¹, J. Mesot^{1,2}

1. *Laboratorium für Festkörperphysik, ETH Zurich, Zurich, Switzerland*
2. *Paul Scherrer Institut, Villigen PSI, Switzerland*

The unusual properties of non-centrosymmetric superconductors, characterized by sizable antisymmetric spin-orbit couplings due to the lack of crystalline inversion symmetry, have attracted considerable interest [1]. However, the exact origin of their unconventional behaviour remains an open question. To identify the special features of this class of superconductors, we studied the properties of the centrosymmetric compound SrPt₃P [2] and compare them with available results for the LaPt₃Si (T_c = 0.6 K) [3] and CePt₃Si (T_c = 0.75 K) [4], which adopt crystal structures that only differ in the arrangement of the Pt octahedra from that of SrPt₃P.

Normal and superconducting properties of SrPt₃P (T_c = 8.5 K) were investigated via ³¹P NMR and magnetometry, indicating a weakly correlated normal state and an s-wave type superconductivity [5], respectively. A sharp drop of the (metallic) Knight shift below T_c, associated with a concomitant steep increase of the linewidth and a Hebel-Slichter type variation of the 1/(T₁T) ratio, are all consistent with an s-wave pairing in SrPt₃P.

While SrPt₃P and LaPt₃Si follow a perfect Korringa law down to T_c, the 1/(T₁T) ratio of CePt₃Si is enhanced upon cooling due to the development of 4f-derived magnetic fluctuations. Electronically, both SrPt₃Si and LaPt₃Si are simple metals. The former exhibits conventional type-II superconductivity, while the nature of the superconducting state of the latter is not well established [6]. The superconductivity of CePt₃Si emerges from a heavy-electron state coexisting with antiferromagnetic order. The key differences between the considered centro- and non-centrosymmetric superconductors seem to be due to both the symmetry of the crystal lattice and to the cations entering the chemical composition of the compounds.

1. E. Bauer and M. Sigrist, *Non-Centrosymmetric Superconductors*, LNP 847 (Springer, Berlin, 2012)
2. T. Takayama et al., *Phys. Rev. Lett.* 108, 237001 (2012)
3. M. Yogi et al., *Phys. Rev. Lett.* 93, 027003 (2004)
4. M. Yogi et al., *J. Phys. Chem. Solids* 67, 522 (2006)
5. T. Shiroka et al., submitted to *Phys. Rev. B*
6. I. Kawasaki et al., *J. Phys. Soc. Jpn.* 82, 084713 (2013)

MO.B.1_I1 - Antiferromagnetic coupling in ferrimagnetic hard-soft core/shell nanoparticles

M. Estrader¹, A. López-Ortega², A. Juhin³, S. Estradé^{4,5}, I. Golosovsky⁶, M. Sikora⁷, C. Carvallo³, G. Salazar-Alvarez⁸, M. Vasilakaki⁹, K.N. Trohidou⁹, M. Varela¹⁰, D. C. Stanley¹¹, M.J. Pechan¹¹, P. Sainctavit³, P. Glatzel¹², D.J. Keavney¹³, F. Peiró⁴, S. Suriñach¹⁴, M.D. Baró¹⁴, J. Nogués¹⁵

1. Dept. de Química Inorgánica, Univ. de Barcelona, Barcelona, Spain
2. INSTM and Dept. Di Chimica "U. Schi", Univ. Degli Studi di Firenze, Firenze, Italy
3. IMPMC, UMR CNRS 7590, Univ. Pierre Et Marie Curie, Paris, France
4. LENS, MIND-IN2UB, Dept. d'electrónica, Univ. de Barcelona, Barcelona, Spain
5. TEM-MAT, CCiT, Univ. de Barcelona, Barcelona, Spain
6. St. Petersburg Nuclear Physics Institute, Gatchina, St. Petersburg, Russia
7. AGH-Univ. of Science and Technology, PACS & ACMiN, Kraków, Poland
8. Dept. of Materials and Environmental Chemistry, Stockholm Univ., Stockholm, Sweden
9. INN, NCSR "Demokritos", Attiki, Greece
10. Materials Science & Technology Division, Oak Ridge National Laboratory, Oak Ridge, United States
11. Department of Physics, Miami Univ., Oxford, United States
12. ESRF, BP220, Grenoble, France
13. Advanced Photon Source, Argonne National Laboratory, Argonne, United States
14. Dept. de Física, Univ. Autònoma de Barcelona, Bellaterra, Spain
15. ICREA and ICN2 - Institut Catala de Nanociencia i Nanotecnologia, Campus UAB, Bellaterra, Spain

The coupling between different magnetic layers in thin film systems is usually ferromagnetic (FM) (layers parallel to each other). However, other types of couplings such as antiferromagnetic (AFM) (i.e., antiparallel layers) have also been reported. In contrast, the magnetic properties of bi-magnetic core/shell nanoparticles remain relatively unexplored. While Monte Carlo simulations have probed the effects of different types of interface couplings from the theoretical viewpoint (e.g., FM vs. AFM coupling), experimental work so far has only reported ferromagnetic coupling between the counterparts. Here we present the existence of an interfacial AFM coupling in ferrimagnetic (FiM) hard-soft core/shell nanoparticles based on iron and manganese oxides [1]. Narrow size distributed $\text{Fe}_3\text{O}_4/\text{Mn}_3\text{O}_4$ and $\text{Mn}_3\text{O}_4/\text{Fe}_3\text{O}_4$ core/shell, soft/hard and hard/soft, were synthesized by seeded growth. In contrast to conventional systems, the temperature dependence of the magnetization, M , and the ferromagnetic resonance field, H_r , show a downturn at the magnetic ordering temperature of the hard Mn_3O_4 phase ($T_C(\text{Mn}_3\text{O}_4)=40$ K). This decrease in M and H_r can be linked to an antiferromagnetic coupling between both phases, although the degree of AFM coupling is related to the quality of the interface (as determined by RIXS-MCD [2]). Moreover, element-selective X-ray magnetic circular dichroism (XMCD) spectra and hysteresis loops confirm that the magnetization of the Mn-containing phase lies opposite to the Fe-containing phase. Magnetometry hysteresis loops show that for small cooling fields the loop shifts towards negative fields similar to exchange bias in conventional FM/AFM systems. However, for large cooling fields the loops shift to the opposite direction, i.e., positive exchange bias. Finally, Monte-Carlo simulations clearly confirm that an AFM interface coupling leads to a magnetization decrease at low temperatures and a positive exchange bias for large cooling fields.

[1] M. Estrader et al. Nat. Commun. 4, 2960 (2013)

[2] A. Juhin et al. Nanoscale 6, 11911 (2014)

MO.B.1_O2 - Core/shell bimagnetic nanoparticles: magnetic interactions and magnetization reversal

G. Lavorato¹, E. Lima Jr¹, D. Peddis², D. Tobia¹, H. Troiani¹, E. Agostinelli², D. Fiorani², R. Zysler¹, E. Winkler¹

1. Centro Atómico Bariloche CNEA-CONICET, Bariloche, Argentina

2. Istituto di Struttura della Materia, CNR, Roma, Italia

Novel bimagnetic nanoparticles (NPs) have been recently proposed for the development of new magnetic materials and comprehensive studies are required in order to understand their complex properties. In this work we compared two core/shell magnetic systems: one formed by non-magnetic ZnO NPs surrounded by ferrimagnetic (FiM) CoFe₂O₄ shell and the other formed by CoO antiferromagnetic (AFM) NPs surrounded by FiM CoFe₂O₄ shell. As both systems present analogous size and morphology (spherical NPs formed by a ~4 nm core and a ~2 nm thick shell), some general issues about core/shell systems can be discussed. The results showed that CoO/ CoFe₂O₄ NPs present a mean blocking temperature (TB) of ~270 K, higher than the ~110 K observed for the ZnO/ CoFe₂O₄ system. The field dependence of TB and the temperature variation of HC were explained through the Stoner-Wohlfarth model for ZnO/ CoFe₂O₄, but deviations were found for CoO/ CoFe₂O₄ NPs due to intra-particle interactions. A higher thermal stability of MS up to room temperature and an HC enhancement up to ~27.8 kOe at 5 K were observed for the bimagnetic sample. Magnetic remanence studies revealed that, although weak dipolar inter-particle interactions are observed, they play a minor role in determining the magnetic behavior of the materials. Relaxation experiments clarified that the magnetization reversal process of CoFe₂O₄ is strongly dependent on the magnetic order of the core. At 10 K, activation volumes of 46 and 96 nm³, representing ~20 and 40% of the total shell volume, were found for CoO/ CoFe₂O₄ and ZnO/ CoFe₂O₄ NPs respectively. While the main characteristic of ZnO/ CoFe₂O₄ NPs is the high surface-to-volume ratio, the exchange coupling at the CoO/ CoFe₂O₄ interface rules the magnetization reversal and the NPs' thermal stability by inducing a larger energy barrier and promoting a smaller switching volume.

MO.B.1_O3 - Surface anisotropy and tunable exchange bias in core/shell and hollow magnetic nanoparticles

H. Srikanth¹, K. Stojak Repa¹, Z. Nemati¹, H. Khurshid¹, J. Alonso^{1,2}, M. Phan¹

1. *University of South Florida, Tampa, United States*

2. *BC Materials, Derio, Spain*

Core/shell Fe/ γ -Fe₂O₃ and hollow γ -Fe₂O₃ nanoparticles are very promising for applications in magnetic storage due to their enhanced properties (strong exchange bias (EB) and effective anisotropy) [1-3]. Surface and interface magnetism in these nanostructures are of current interest and we have explored this in several systems. High quality Fe/ γ -Fe₂O₃ core/shell, core/void/shell, and hollow nanoparticles were synthesized with two different mean sizes of 8 nm and 12 nm, and their magnetic properties including the exchange bias (EB) effect were systematically studied. We find that as the morphology changes from core/shell to core/void/shell, the magnetization of the system decays and inter-particle interactions become weaker, while the effective anisotropy and the EB effect increase. In the case of the hollow nanoparticles, the coupling between the inner and outer spin layers in the shell gives rise to an enhanced EB effect, which increases with increasing shell thickness. This indicates that the morphology of the shell plays a crucial role in these kinds of exchange-biased systems.

In addition, we have filled multiwalled carbon nanotubes (MWCNTs) with these magnetic nanoparticles using a novel magnetically-assisted capillary action method [4]. These nanostructures show tunable electromagnetic properties useful for advanced biomedical and microwave applications.

1. S. Chandra, H. Khurshid, W. F. Li, G. C. Hadjipanayis, M. H. Phan and H. Srikanth, *Physical Review B* 86, 014426 (2012)

2. H. Khurshid, M. H. Phan, P. Mukherjee and H. Srikanth, *Applied Physics Letters* 104, 072407 (2014)

3. S. Chandra, N. A. Frey Huls, M. H. Phan, S. Srinath, M. A. García, Youngmin Lee, Chao Wang, Shouheng Sun, O. Iglesias and H. Srikanth, *Nanotechnology* 25, 055712 (2014)

4. K. Stojak, S. Pal, H. Srikanth, C. Morales, J. Dewdney, T. Weller and J. Wang, *Nanotechnology* 22, 135602 (2011)

MO.B.1_O4 - Synthesis and magnetic properties of CoPt(core)-Fe/FeCo(shell) nanoparticles

J. Cuya¹, H. Miyamura¹, S. Ishio², J. Balachandran¹

1. *The University of Shiga Prefecture, Shiga Prefecture, Japan*

2. *Akita University, Akita, Japan*

The development and use of exchange coupled magnets in areas such as permanent magnets, magnetic recording, etc. is being strongly considered. In the nanometric range, the use of hard magnetic FePt/CoPt cores with soft magnetic shells such as Fe, FeCo have been commonly prepared; however, the control over their particle size and composition, which are important to obtain high energy densities, $(BH)_{max}$ are considered difficult. Here, the CoPt core with different composition and size were synthesized at high temperatures by heating cobalt acetate, dihydrogen hexachloroplatinate in alcoholic solution containing oleylamine as surfactant. Then, these particles were introduced into a mixture of oleylamine and oleic acid, containing cobalt and iron acetylacetonates. This suspension was heated to temperatures above 250 oC to obtain the $Fe_3O_4/CoFe_2O_4$ -coated CoPt particles. The formation of core-shell structured particles was confirmed by TEM-EDS mapping. Finally, these particles were heat treated at different temperatures under reducing atmosphere (3% H₂/Ar) to obtain soft-hard magnetic composites. As the annealing temperature was elevated, the particles underwent transition from oxide to alloy progressively, and this was clearly visible from structural and morphological analysis using XRD and TEM measurements. Though the formation of magnetically hard core and soft shell was anticipated, our results suggested the gradual transformation of oxide to alloy exhibiting a maximum coercivity of 1.1 kOe and a saturation magnetization of ~70 emu/g of sample heat treated at 500 oC. Although, we found that the magnetic properties, M_s and H_c , were affected by the annealing temperature and composition, pure Fe or FeCo phases were not observed; consequently the magnetic properties were lower due to the remaining oxides phases or the formation of FeCoPt alloy compounds.

MO.B.1_05 - Optimizing the magnetic properties of inverse antiferromagnetic-core / ferrimagnetic-shell nanoparticles

M. Vasilakaki¹, K. Trohidou¹, J. Nogués²

1. *Institute of Nanoscience and Nanotechnology, NCSR "Demokritos", Aghia Paraskevi, Attiki, Greece*

2. *ICREA and ICN2 - Institut Catala de Nanociencia i Nanotecnologia, Campus UAB, Bellaterra, Spain*

Bi-magnetic core/shell nanoparticles are gaining increasing interest due to their foreseen applications. Inverse antiferromagnetic(AFM)/ferrimagnetic(FiM) nanoparticles with soft AFM core and hard FiM shell are particularly appealing since they may overcome some of the limitations of conventional FiM/AFM systems. We study the magnetic behavior of these inverse AFM/FiM with the Metropolis Monte Carlo simulations technique. We present their magnetic properties as a function of the core and shell size. Our results show that the coercivity, HC, and the loop shift, Hex, present a non-monotonic dependence on the core diameter and the shell thickness, in very good agreement with the available experimental data [1]. Namely, for very small core sizes both coercivity and exchange bias Hex sharply increase as the core size becomes larger. At a certain size HC and Hex give a maximum and then they start to decrease. Also we observe an increase of the HC and Hex that is proportional to the FiM shell thickness for large AFM cores. Our microscopic study shows that the observed behavior arises from the competition between the AFM core spins and the hard FiM shell that expands over a wide range of core diameters leading to non-vanishing Hex even for very large cores. Based on the results, several possible ways to enhance the experimental performance of inverse core/shell nanoparticles are proposed here for diverse applications.

[1] G. Salazar-Alvarez, J. Sort, S. Suriñach, M.D. Baró, J. Nogués, J. Am.Chem. Soc. 2007, 129, 9102

MO.B.3_O1 - Transport properties of 1D magnetic nanochainJ.S. Lee ¹, Y.K. Kim ¹*1. Korea University, Seongbuk-gu, South Korea*

An understanding of transport characteristics of 1D chain-like nanostructures assembled from nanoparticles are of scientific interest. Compared with tremendous amount of literatures reported on magnetic 3D, 2D, and homogeneous 1D nanostructures, 1D nanochain related literatures are barely found. Therefore, the preparation and measurement of this type of superstructure would allow us to investigate the electronic conduction and magnetoresistance in arrays of magnetic nanoparticles and line out the effect of disorder and dimensionality of the same. At first, magnetite (Fe_3O_4) nanoparticles with diameters of about 100 nm were synthesized by a hydrothermal polyol method. They show ferrimagnetic properties such as M_s of 75 emu/g and H_c of 40 Oe. A pair of Ti/Au electrode was deposited by e-beam evaporation utilizing a shadow mask on a Si substrate covered with SiO_2 . Next, nanoparticles were aligned on the substrate by dropping under magnetic field. We have measured the electrical properties of the nanochain at various temperatures and magnetic fields by a physical property measurement system (PPMS). The current-voltage characteristic (I - V) of the nanochain was linear at RT with a resistance of 560 k Ω . The resistance increased monotonically with decreasing temperature, reaching ~ 20 G Ω at 40 K. For T below 160 K, the I - V characteristics became increasingly nonlinear, and, below 40 K, it became insulating. The nanochain device showed negative magnetoresistance reaching a value as high as 16 % at $T = 80$ K where $H = 50$ kOe and $V_{\text{bias}} = 0$. Applied field aligns the electronic spins of adjacent nanoparticles, thereby increasing the tunneling probability and conductance for electrons moving through the nanochain, leading to negative magnetoresistance.

MO.B.3_O2 - Hollow Fe₃O₄ nanospheres and their microwave applications

Z. Yang¹, Z. Li¹, Y. Wu¹, M. Chua¹, Y. Yang²

1. Temasek Laboratories, National University of Singapore, Singapore

2. School of Chemical and Biomedical Engineering, Nanyang Technological University, Singapore

Hollow Fe₃O₄ nanospheres with the diameter of 450 nm and the wall thickness of 80 nm were prepared using a simple Solvothermal process without using any templates. The density of prepared samples is 3.78 g/cm³ which is much lower than their solid counterparts. The composites filled with 60 wt% of these hollow spheres show the good high-frequency and attenuation properties. μ' is 2.8 and μ'' is 1.2 at 3 GHz. The broad bandwidth WP of 55 % for return loss RL<-10 dB is achieved at thickness between 0.3 and 0.4 cm. The density of the composite is only 2.71 g/cm³, which is lighter 24 and 47 %, as compared to commonly used ferrite and carbonyl iron composites with the same weight concentration. Therefore, the composites filled with hollow nanospheres are potential candidates for EM attenuation applications.

MO.B.3_O3 - Chemical order in cobalt-iron nano-objects probed by ferromagnetic nuclear resonance

Y. Shin^{1,2}, C. Garnero³, K. Soulantica³, L. Marie Lacroix³, B. Chaudret³, J.W. Wu², C. Meny^{1,2}

1. *Institut de Physique et Chimie des Matériaux de Strasbourg (IPCMS), Strasbourg, France*

2. *Department of Physics, CNRS-Ewha International Research Center, Ewha Womans University, Seoul, South Korea*

3. *Laboratoire de Physique et Chimie des Nano-objets (LPCNO), Toulouse, France*

Nano-objects are involved in many research fields from spintronics to medicine. The physico-chemical properties of these objects will depend on the size, shape, crystallographic structure and chemical composition of the nano-objects. In this work we investigate assemblies of nano-objects prepared by chemical routes. The assemblies of nano-objects show very narrow size distributions and well defined object shapes: spheres or cubes. The objects have been prepared with an equal ratio of Iron and Co. CoFe alloys can produce a rich variety of chemical orders [1] that are difficult to study by regular investigation techniques. Because of its sensitivity to the chemical environment of Cobalt, we have used Ferromagnetic Nuclear Resonance (FNR, i.e. Nuclear Magnetic Resonance for ferromagnets) to investigate the chemical order within these nano-objects. Indeed FNR has been extensively used for studying the chemical order in thin films and alloys [2] and more recently for studying the crystallographic structure of Co nanoparticles [3]. Our results show that although both kinds of nano-objects are prepared with similar methods, their chemical order is very different. While the spheres show a predominance of a B2 ordered CoFe alloy, the cubes FNR spectra suggest that the chemical composition in the objects is not homogeneous but present a composition gradient going from pure Fe to almost pure Co.

1. M. WOJCIK, J.P. JAY, P. PANISSOD, et al., Z. Phys. B 103, 5-12 (1997)

2. P. PANISSOD, C. MENY, Appl. Magn. Reson. 19, 447-460 (2000)

3. Y.F. LIU, I. FLOREA, O. ERSEN, C. PHAM-HUU, C. MENY, ChemCommun, 51, 145-148 (2015)

MO.B.3_O4 - A novel approach for the chemical synthesis of magnetically hard Co and Fe/Co composite nanoparticles

F.M. Abel¹, V. Tzitzios², D.J. Sellmyer³, G.C. Hadjipanayis¹

1. *Department of Physics and Astronomy, University of Delaware, Newark, United States*

2. *Institute of Materials Science, NCSR Demokritos, Attiki, Greece*

3. *Department of Physics and Astronomy, University of Nebraska, Lincoln, United States*

Non-rare earth based hard magnetic materials, with both high saturation magnetization and coercivity, are of great interest for the development of future magnets to replace the current rare earth magnets because of the limited supply of rare earths. In this study, we explore the possibility of producing hexagonal cobalt nanoparticles, and hexagonal cobalt coated with iron nanoparticles to produce materials with both high saturation magnetization and moderate coercivity. The nanoparticles were synthesized using anhydrous cobalt (II) chloride and iron (II) chloride by sodium borohydride reduction in tetraglyme with and without oleylamine under a nitrogen/hydrogen flow. The reactions were done at high temperatures allowing for the formation of as-made hexagonal cobalt, which was then coated with iron nanoparticles. The size of the particles was controlled by changing the concentration of oleylamine producing a large range of different sized particles. Magnetic properties were optimized by changing the temperature of the reaction. We obtained hexagonal Co nanoparticles with saturation magnetization of (129 emu/g) and coercivity of (350 Oe). We were also able to improve the saturation magnetization of the Co particles by coating with Fe nanoparticles achieving the value of 133emu/g.

Work supported by DOE-BES-DMSE, DE-FG02-04ER4612 and Samsung.

MO.C.1_I1 - Emergent interfacial phenomena in magnetic complex oxide heterostructures

S.G.E. Te Velthuis¹

1. Materials Science Division, Argonne National Laboratory, Lemont, United States

In recent years the interest in complex oxide heterostructures has significantly increased as a myriad of intriguing phenomena have been discovered, including emergent magnetic behavior and exotic superconducting and ferroelectric phases, related to modified bonding at the interfaces. We have investigated manganite/cuprate/manganite structures that form either superconducting spin switches or magnetic tunneling junctions, depending on the type of cuprate. In both cases we have successfully correlated the influence of an induced interfacial magnetic moment in the cuprate, experimentally detected with soft x-ray magnetic dichroism, to modified electric transport behavior. In magnetic tunneling junctions, an anomalous temperature dependence of the tunneling magnetoresistance is found to be attributed to the competition between the positive spin polarization of the manganite contacts and the negative spin-filter effect from the interface-induced magnetization [1]. In the same system a reversible, voltage-driven magnetization switching without assistance from a magnetic field was demonstrated and linked a magnetoelectric coupling arising from the orbital reconstruction at the interface [2]. These contributions are important as emergent interfacial magnetization appears ubiquitous and understanding its influence on macroscopic properties can provide many opportunities to engineer oxide spintronics with tailored properties. Work at ANL supported by US-DOE, Office of Science, BES, MSE.

[1] Yaohua Liu, F.A. Cuellar, Z. Sefrioui, J.W. Freeland, M.R. Fitzsimmons, C. Leon, J. Santamaria and S.G.E. te Velthuis, *Phys. Rev. Lett.* 111 (2013) 247203

[2] F.A. Cuellar, Y.H. Liu, J. Salafranca, N. Nemes, E. Iborra, G. Sánchez-Santolino, M. Varela, M. García Hernández, J.W. Freeland, M. Zhernenkov, M.R. Fitzsimmons, S. Okamoto, S.J. Pennycook, M. Bibes, A. BarthÚlÚmy, S.G.E. te Velthuis, Z. Sefrioui, C. Leon, J. Santamaria, *Nature Communications* 5 (2014) 4215

MO.C.1_O2 - Roughness influence in the barrier quality of ferroelectric/ferromagnetic tunnel junctions, model and experiments

M. Sirena¹, J. Gonzales Sutter¹, L. Avilés Félix¹, L. Beatriz Steren², R. Bernard³, J. Villegas³, J. Briatico³, N. Bergeal⁴, A. Zimmers⁴, J. Lesueur⁴

1. *Laboratorio de Resonancias Magnéticas & Instituto Balseiro (CNEA & UNCuyo), Bariloche, Argentina*

2. *Centro Atómico Constituyentes, Buenos Aires - Argentina*

3. *Unité Mixte de Physique CNRS/THALES, Université Paris Sud, Palaiseau Cedex, France*

4. *Laboratoire de Physique et d'étude des Matériaux, Paris, France*

Manganites have attracted a lot of attention due to the possibility of studying many physical problems related to the strong correlation between their structural, transport and magnetic properties and their potential use in many technological applications. A renewed interest in these compounds has appeared for the developing of manganite/ferroelectric composite systems with multiferroic nature. The origin of this interest is the possibility to develop new technological devices, such as ferromagnetic/ferroelectric tunnel junctions (TJ), with new flexibility and improved performance. In order to obtain systems with increasing reading rate and low head noise, very thin tunnel barriers are required and a good knowledge of the barrier characteristics becomes critical. Recently, conductive atomic force microscopy (CAFM) has become an important tool to characterize the tunnel barrier for TJ like devices (such as spin filters, superconducting Josephson Junctions, etc.). In this work a phenomenological approach has been developed to analyze the electrical transport through an insulating barrier in ferromagnetic/ferroelectric bilayers, using CAFM. We have found that $I(V) = A_0 \cdot V^\alpha$, where A_0 and α depend linearly with the barrier thickness. The model allows to obtain critical information for the development of magnetic TJ. Moreover, assuming a Gaussian distribution of the barrier thickness, it is possible to fit the measured current distribution and to study the thickness homogeneity of the barrier. The influence of the substrate in the electrical properties of the FE/FM bilayers was studied in the frame of this model. CAFM images of both series of samples present an important distribution of the current, which is generally ascribed to a distribution in the barrier thickness. However, MGO substrates with higher roughness were found to increase the barrier height distribution and increase the attenuation length in the material, reducing the barrier quality for the developing of multiferroic tunnel junctions.

MO.C.1_O3 - Magneto-electric coupling in $\text{Ca}_3\text{CoMnO}_6$ thin filmsJ. Saha¹, G. Sharma¹, S. Patnaik¹*1. Jawaharlal Nehru University, New Delhi, India*

We report on the growth and magneto-electric (ME) coupling of $\text{Ca}_3\text{CoMnO}_6$ thin films deposited by pulsed laser deposition technique. $\text{Ca}_3\text{CoMnO}_6$ is interesting because of its tunable inter-chain magnetic interactions that affects its ME coupling. Thin films of thickness 200nm have been grown on single crystal sapphire substrates (0001- Al_2O_3). Substrate temperature was kept at 750°C. The X-Ray diffraction pattern indicates sharp peaks corresponding to (110), (300), (330) planes. AFM measurements show a homogeneous growth of the film. An optical band gap of 1.73eV was estimated by UV visible spectroscopy. The anti-ferromagnetic transition is surprisingly increased to 39 K, much above its bulk value (15K). The increase in magnetic transition temperature is possibly due to stronger inter-chain interaction and strain caused by lattice mismatch. Due to canting, the thin films show ferrimagnetic like behavior at low temperature. For magneto-electric measurements separate films were grown. First a conducting layer of Gallium doped ZnO (100nm) was deposited on the sapphire. On top of the conducting layer 300nm film of $\text{Ca}_3\text{CoMnO}_6$ was deposited. Magneto-electric coupling is measured as a function of temperature. A large magneto-electric coupling was observed. The dielectric measurements show anomaly at 10 K and 40 K which are clearly visible at the first derivative of dielectric data. From direct polarization measurements we associate the 10 K transition to a magnetic structure driven ferroelectric phase. The magneto-capacitance data at 5 K and 30 K show substantial change in dielectric constant with magnetic field. The large magneto-electric coupling is also verified by polarization measurement, where 25% change in polarization is observed on the application of 5T external magnetic field.

MO.C.1_O4 - Magnetic and dielectric properties of BaTiO₃-Co Nano-composite films

Y. Zhang¹, N. Kobayashi², S. Ohnuma^{1,2}, M. Nose³, H. Masumoto¹

1. Tohoku University, Miyagi Prefecture, Japan

2. Research Institute for Electromagnetic Materials, Tokai-Mura, Japan

3. University of Toyama, Toyama Prefecture, Japan

[Introduction] Developments of electromagnetic devices require multi-functional materials, such as magnetic-dielectric films. Our early work has found that the MgF-FeCo nano-composite films show giant dielectric properties [1] and TiN-Co nano-composite films show good high-frequency magnetic properties [2]. The resistivity is important for obtain magnetic-dielectric properties. In this research, by employing high-resistivity complex oxides BaTiO₃ (BTO) as matrix material, the BTO-Co nano-composite films have been deposited to realize high resistivity, magnetization (Ms) and dielectric constant.

[Experiment] The BTO-Co nano-composite films were deposited onto Si, Pt/Si and quartz substrates by differential pressure sputtering (DPS) method [3], with two separated sputtering chambers for oxide (BTO) and metal (Co). Film structures were investigated by XRD, TEM. The chemical composition of the films was analyzed by XRF. The magnetic properties were measured with VSM. The dielectric properties were tested by LCR meter.

[Result] The BTO-Co nano-composite films consist of amorphous BTO matrix and Co nano-particles. Magnetic and dielectric properties of the BTO-Co films are affected by Co content. With the Co content increasing from 13 at.% to 39 at.%, the Ms increases from 0.01 to 0.20 T. The dielectric constant was tested at 1 kHz for BTO-Co films, and increases from about 10 to 70, as the Co content increasing up to 28 at.%. BTO-Co nano-composite film shows promising prospect for multi-functional materials.

1. N. Kobayashi, H. Masumoto, S. Takahashi, S. Maekawa, Nat. Commun., 5, 4417 (2014)

2. Y. W. Zhang, S. Ohnuma, and H. Masumoto, IEEE Transactions on Magnetics, vol. 47, pp. 3795-3798 (2011)

3. M. Nose, T. Kurimoto, A. Saiki, K. Matsuda, K. Terayama, J. Vac. Sci. Technol. A, 30 (2012)

MO.C.1_O5 - Temperature dependent transport measurements of epitaxially grown copper manganese arsenide

V.A. Hills¹, P. Wadley¹, R. Campion¹, V. Novak², K. Edmonds¹, B. Gallagher¹, T. Foxon¹, T. Jungwirth^{1,2}

1. School of Physics and Astronomy, University of Nottingham, Nottingham, United Kingdom

2. Institute of Physics ASCR, v.v.i., Prague, Czech Republic

Antiferromagnetic thin films are widely used in current magnetic sensing technologies, as they enable the pinning of magnetic domains at antiferromagnet/ferromagnet interfaces. One promising candidate is epitaxially grown CuMnAs [1]. CuMnAs grown in this way forms a simple collinear antiferromagnet that can be grown on conventional III-V semiconductors (GaAs and GaP) by MBE at (1:1:1) stoichiometry. It has been shown through neutron diffraction to have a Néel temperature of 485 ± 5 K. Using a sample held under vacuum it is possible to measure the longitudinal resistivity and see a cusp in the derivative corresponding to the Néel temperature. This method allows for a thickness study of the material to observe the dependence of Néel temperature on the layer thickness. We can also use this method to see the effect of alloying with phosphorous on CuMnAs and how this shifts the Néel temperature significantly.

[1] P. Wadley, et Al. Nat .Commun. 4:2322 (2013)

MO.C.2_I1 - Magnetic shape memory nano-disks: effects of lateral confinement on magnetism, martensitic behaviour and microstructure

F. Albertini¹, M. Campanini¹, L. Nasi¹, F. Casoli¹, P. Ranzieri¹, S. Fabbri^{1,2}, V. Chiesi¹, C. Magen³, V. Grillo⁴, F. Celgato⁵, G. Barrera⁵, P. Tiberto^{5,1}

1. IMEM-CNR, Parma, Italy

2. MIST E-R Laboratory, Bologna, Italy

3. LMA-INA, ARAID, University of Zaragoza, Spain

4. NANO-CNR, Modena, Italy

5. INRIM, Torino, Italy

Magnetic shape memory materials show a remarkable multifunctional phenomenology (e.g. “giant” magnetomechanical, magnetocaloric, elastocaloric properties) arising from the presence of a martensitic transformation and magnetically ordered states. [1]. Low-dimensional materials, mainly thin films, have recently attracted much interest for their great potential in applications (e.g. microactuators, valves, solid-state microrefrigerators) [2]. With respect to the bulk, they offer the further possibility of tuning properties by thickness and by suitable substrates and underlayers [3]. Patterned films and 2D nanostructures are nowadays a vast and unexplored field. The present paper is addressed to the study of the effect of lateral confinement in on-substrate and free-standing nanodisks. Epitaxial thin films of NiMnGa of thickness ranging from 10 to 200 nm were grown by sputtering r.f. on MgO substrates with and without a Cr underlayer. Patterned thin films were obtained by polystyrene-nanosphere lithography, a large-scale and inexpensive nanostructuring method. Freestanding nano-disks (d=160, 650nm) were subsequently obtained by removing Cr underlayer by selective chemical etching. A multiscale structural and magnetic study was performed by means of electron transmission microscopy (HREM, STEM-HAADF, electron diffraction, Lorentz microscopy), X-ray diffraction and reflectivity, AFM/MFM, AGFM and SQUID magnetometry and susceptometry. It was found that nano-disks of both sizes preserve the salient martensitic and magnetic properties of continuous films and are then exploitable in multifunctional applications. On the other hand the twin microstructure and its temperature dependence can be influenced by lateral confinement and release from substrate. This fact, mainly exploitable in shape memory and magnetic shape memory applications, paves the way to the realization of shape-controlled nano-actuators.

MO.C.2_O2 - Tuning magnetic anisotropy by structural strain in La₂CoMnO₆ thin films

R. Galceran¹, L. Balcells¹, J. Cisneros-Fernández¹, J. Roqueta², L. López-Mir¹, B. Bozzo¹, C. Frontera¹, B. Martínez¹

1. Instituto de Ciencia de Materiales de Barcelona, ICMAB – CSIC, Barcelona, Spain

2. Institut Català de Nanociència i Nanotecnologia, ICN2 (CSIC, CERCA), Barcelona, Spain

We report on the magnetic and structural properties of ferromagnetic-insulating La₂CoMnO₆ thin films grown by means of RF sputtering technique. Insulating ferromagnets are of interest because of the exchange splitting of the bands allowing obtaining tunnel barriers with different height for spin-up and spin-down carriers and spin filters. In addition, the possibility of controlling its magnetic anisotropy will also open the door to the implementation of devices based on the tunneling anisotropic magnetoresistance phenomenon. Our results indicate a close correlation between the film composition and their magnetic properties. Both Curie temperature and the features of the hysteresis loops turn out to be dependent on the oxygen stoichiometry. On the other hand, we also show that structural strain, due to film/substrate mismatch, allows controlling the magnetic anisotropy. We probe this by growing La₂CoMnO₆ film on top of different substrates and with different thermal treatments. While compressive strain induces in-plane magnetic anisotropy tensile strain promotes out-of-plane anisotropy.

MO.C.2_O3 - Stabilization of helical magnetic structures in thin multilayers

L. Dzemiantsova^{1,2}, G. Meier^{1,3}, R. Röhlsberger^{1,2}

1. The Hamburg Centre of Ultrafast Imaging, Hamburg, Germany

2. Deutsches Elektronen Synchrotron, Hamburg, Germany

3. Max-Planck Institute for the Structure and Dynamics of Matter, Hamburg, Germany

Robust and energetically efficient magnetic structures that employ the spin degree of freedom to store and process information are at the heart of modern spin-based technology. It has recently been shown that the transmission and processing of information without electric currents or external fields can be subjected to internal interactions such as exchange, Ruderman-Kittel-Kasuya-Yosida (RKKY) or dipolar interaction [1]. It has been pointed out theoretically that these interactions can stabilize magnetic helices which can be used for magnetic energy storage if they are produced experimentally at the nanoscale.

Based on micromagnetic simulations [2], we report on a novel helical magnetic structure in a soft magnetic thin film that is sandwiched between and exchange-coupled to two hard magnetic layers. We show that such a structure initially twisted in an external magnetic field, stays stable even without the presence of the field. The magnetic stability is determined by the energy minimization and results in an internal effective field created by the exchange interaction in the soft magnetic layer. Changing the angle between hard magnetic layers, the helix can be stable with any twist up to 270 degrees. We show that the helix stores magnetic energy of about 8 kilojoule per cubic meter, as well as that ferromagnetic resonances (FMR) dramatically increase with the helical twist due to the presence of the internal field. In particular, the lowest resonance frequency is approximately two higher compared to that when the trilayer shows a ferromagnetic order. Thin films with a stable helical order provide, therefore, a new route to store magnetic energy and to generate high frequency signals without any presence of external fields or currents on the smallest scale.

References:

[1]. E. Y. Vedmedenko et al., Phys. Rev. Lett., 112, 017206 (2014)

[2]. <http://micromagnum.informatik.uni-hamburg.de>

MO.C.2_I4 - Shape-critical properties of patterned permalloy thin films

R. Shull¹, Y.P. Kabanov², V. Gornakov², A. Chen¹, V. Nikitenko²

1. *National Institute of Standards and Technology, United States*

2. *Russian Academy of Science, Saint Petersburg, Russia*

Steady improvement of thin film growth and patterning techniques pushes the sample physical size towards ever-smaller dimensions. In this case, the magnetization reversal in thin films with restricted lateral sizes is mostly governed by the magnetostatic fields localized in their edges [1]. A domain structure in practically isotropic Permalloy (Py) thin-film meshes demonstrates a competition between the exchange, Zeeman, and magnetostatic energies [2] and has to determine new kinetic effects in such structures. We present both experimental and simulation results of the magnetization distribution and transformation during the reversal of microstructured Py thin films. The effect of shape and edges in the magnetic elements with reduced dimensions on the magnetization reversal of cross-shaped Ni₈₁Fe₁₉ (30nm) films were studied. The stripes of the patterned structures had 3 - 30 μm widths and ~100 Åm lengths. Remagnetization details in these structures were visualized by the magneto-optical indicator film (MOIF) technique. The hysteresis loops were measured in a VSM. The MOIF images revealed three different types of the domain structure formation and evolution in the samples during their magnetization reversal: I) spin rotation with growth and annihilation of a cross-tie structure in the stripes perpendicular to the applied field, II) nucleation and fast motion of specific magnetization fronts, which consist of a number of coupled vortices located along both edges, in the parallel to applied field stripes, and III) new macrodomain nucleation and domain wall motion in the larger size films. It was established that, in the first two cases that magnetostatic fields, which are formed on the edges of the stripes and their intersections, play a crucial role in the formation of spin inhomogeneities and switching of the samples.

[1] A. Hubert and R. Schafer, *Magnetic Domains*, 3th ed. Berlin, Springer, Germany, 2008

[2] R. D. Shull, et al., *IEEE Trans.Magn.*, 50, 2304004, 2014

MO.C.3_O1 - Mobile magnetic phase boundary in compositionally graded films

C. Miller¹, B. Kirby², H. Belliveau³, P. Keinzle², A. Grutter², P. Riego⁴, A. Berger⁴

1. Rochester Institute of Technology, Rochester, United States

2. NCNR, NIST, Gaithersburg, United States

3. University of South Florida, Tampa, United States

4. CIC nanoGUNE Consolider, Donostia San Sebastian, Spain

Polarized neutron reflectometry was used to study the temperature and magnetic field dependent magnetization depth profile of a Ni

$x(z)\text{Cu}_{1-x(z)}$ film in which the local composition, and thus magnetic ordering, depends on depth into the film. It is interesting to consider the magnetic profile when the $\text{Ni}_{x(z)}\text{Cu}_{1-x(z)}$ film at intermediate temperatures, i.e., when the graded structure forms a ferromagnet/paramagnet bilayer. The effective phase boundary moves progressively deeper into the sample with decreasing T , and increasing the applied field from 5 mT to 500 mT alters the shape of the profile. Thus, this system exhibits a magnetic phase boundary that can be moved continuously along the growth axis with temperature, and modified by field. Modeling the data with a mean-field exchange strength gradient theory, we find that with increasing temperature, the magnetized thickness of the film continuously decreases, indicating a continuous distribution of local ordering temperatures. The validity of this modeling is corroborated by comparing the integrated magnetization of the profiles to the net magnetic moment from VSM; there is excellent agreement between the PNR profiles and the magnetometry results. Thus, we observe evidence of a continuous vertical distribution of the effective T_C in a compositionally graded film. The data are consistent with profiles determined from a mean-field simulation, and indicate a phase boundary between paramagnetic and ferromagnetic regions that moves continuously along the growth axis with temperature.

MO.C.3_O2 - Deposition of soft anisotropic FeCoN films on mica substrates

Y. Wu¹, Y. Yang¹, Z. Yang¹, F. Ma¹, B. Zong¹, J. Ding¹

1. National University of Singapore, Singapore

In recent decades, ferromagnetic thin films have attracted intensive interest due to high microwave permeability. Traditionally, Si wafers or glasses are used as the substrates since the films are not able to self-support. However, for some practical applications, the rigid supporting substrates are unfavorable due to increased total volume of the material. It is imperative to find a suitable substrate which can be thinned down or removed from the deposited film. Mica exists as a promising candidate since it can be conveniently split into thin uniform layers with atomically flat surface. In this work, a series of sputtered FeCoN thin films were deposited on freshly cleaved mica sheets with different sputtering power, which was changed from 100 W to 1000 W. The effect on the static magnetic properties and microwave performance was investigated. Dramatic change in the static magnetic properties has been observed. Only the films deposited with moderate sputtering power (250 W - 350 W) exhibited pronounced in-plane anisotropy and a relative low coercivity of a few Oersted. When the deposition power was lower than 250 W or higher than 350 W, an in-plane isotropy was observed with significantly increased coercivity. Correspondingly, high microwave permeability was obtained for the films with soft in-plane anisotropy, which can be understood using Acher's Law. When the deposition power is 350 W, the imaginary permeability reaches the maximum value of 1774 and the corresponding f_r is 2.5 GHz. These soft FeCoN films on reducible mica substrates are promising for high-frequency applications in gigahertz.

MO.C.3_O3 - Study of the antiferromagnetic order in strained SrMnO₃ multiferroic thin films

L. Maurel¹, N. Marcano^{2,3}, T. Prokscha⁴, E. Langenberg^{1,5}, J. Blasco^{2,6}, R. Guzman¹, C. Magen^{1,6,7}, L. Morellon^{1,6}, M.R. Ibarra^{1,6}, J.A. Pardo^{1,8}, P.A. Algarabel^{2,6}

1. Instituto de Nanociencia de Aragón, Universidad de Zaragoza, Zaragoza, Spain
2. Instituto de Ciencia de Materiales de Aragón, Universidad de Zaragoza - Consejo Superior de Investigaciones Científicas, Zaragoza, Spain
3. Centro Universitario de la Defensa, Academia General Militar, Zaragoza, Spain
4. Laboratory for Muon Spin Spectroscopy, Paul Scherrer Institute, Villigen PSI, Switzerland
5. Centro de Investigación en Química Biológica y Materiales Moleculares, Universidad de Santiago de Compostela, Santiago de Compostela, Spain
6. Departamento de Física de la Materia Condensada, Universidad de Zaragoza, Zaragoza, Spain
7. Fundacion ARAID, Zaragoza, Spain
8. Departamento de Ciencia y Tecnología de Materiales y Fluidos, Universidad de Zaragoza, Zaragoza, Spain

The interest on the SrMnO₃ compound has increased owing to the theoretical prediction of a multiferroic state induced by epitaxial strain¹. In a recent paper², the presence of a polar state in strained SrMnO₃ thin films has been proven by second harmonic generation experiments. In this work we present the study of the magnetic properties of antiferromagnetic (AF) SrMnO₃ epitaxial thin films (10 nm in thickness) grown on different single-crystal substrates: LaAlO₃ (LAO), (LaAlO₃)_{0.3}(Sr₂AlTaO₆)_{0.7} (LSAT) and SrTiO₃ (STO), which provide epitaxial strain levels of -0.4, 1.7 and 2.5 % respectively. Néel temperature (T_N) of the films has been determined by performing muon spin relaxation (μSR) experiments by means of polarized low-energy muon beam at the Paul Scherrer Institute. Using these results and the theoretical calculations,¹ a temperature-strain magnetic phase diagram is proposed.

To get a deeper insight into the magnetic properties of the AF SrMnO₃ thin films, SrMnO₃/La_{0.7}Sr_{0.3}MnO₃ bilayers were grown on LAO, LSAT and STO substrates with a thickness of around 8 nm each, and their exchange bias (EB) effect was studied. In all samples the EB field shows an exponential dependence on temperature and vanishes well below T_N. Moreover, the EB field increases with increasing the epitaxial strain value in the SrMnO₃ film. The EB field thermal dependence has been explained assuming the existence of a spin-glass (SG) state as a result of competing magnetic orders and spin frustration at the SrMnO₃/La_{0.7}Sr_{0.3}MnO₃ interface³. The dependence on strain is originated by the changes induced in the SG interfacial state by the variation of the magnetic interactions on the epitaxial strain.

- 1.- Lee, J. H. & Rabe, M. K. , Phys. Rev. Lett. 104, 207204 (2010)
- 2.- Becher C. *et al.*, to be published (2015)
- 3.- Ding J. F. *et al.*, Phys. Rev. B 87, 054428 (2013)

MO.C.3_O4 - Exploiting magneto-optics as a gateway to the magnetism of Ce-YIG films grown on strongly paramagnetic garnet substrates

B. Casals¹, M. Espinola¹, G. Herranz¹, J. Fontcuberta¹

1. Icmab-Csic, Bellaterra, Spain

The insulating ferrimagnet yttrium iron garnet (YIG) has come under limelight over the years because of its remarkable properties that make it appealing for a wide range of applications. Traditionally, because of their outstanding high magneto-optic activity, YIGs have been considered the staple materials for nonreciprocal devices in optical communications. Additionally, the remarkably small damping parameters for spin waves have gathered a high interest for magnonics, spintronics and spin caloritronics. For these applications, the deposition of YIG thin films on gadolinium gallium garnet (GGG) crystals is usually a desirable requirement. Yet, in spite of the outstanding structural compatibility between YIG and GGG, the strong paramagnetic susceptibility of the latter is a serious shortcoming when it comes to the magnetic characterization, as strong magnetic signals from GGG substrates obscure severely the much weaker response of YIG thin films. Here we show that magneto-optics is a way around to circumvent this difficulty. The magneto-optic activity results from the interaction of polarized light with magnetic materials and the spectral response is extremely sensitive to the electronic structure. With this in mind, we have measured the Kerr rotation and ellipticity of both Ce-doped YIG thin films grown on GGG and bare GGG substrates. We used cerium as a dopant as it is known to enhance further the magneto-optic activity of YIG. Our extensive spectroscopic study in the visible helped to identify the particular wavelengths for which the rotation and ellipticity of GGG vanished, while the magneto-optic activity of Ce-YIG remained large. That allowed us to access the individual magnetic properties of the Ce-YIG films that were otherwise unreachable using conventional magnetometry. This methodology was instrumental to achieve thin films with optimized magnetic properties.

MO.D.1_I1 - Magnetic shape memory alloys for energy applications

L. Mañosa¹, A. Planes¹

1. Universitat de Barcelona, Barcelona, Spain

Magnetic shape memory alloys feature interesting functional properties associated with the martensitic transition they undergo. Prominent among these properties are the giant caloric effects that arise when the transition is driven by an external field such as magnetic field, uniaxial stress and hydrostatic pressure. The large isothermal entropy and adiabatic temperature changes associated with these caloric effects make these alloys excellent candidates for environmental friendly solid-state refrigerating devices with low energy consumption. In my talk I will survey recent results on the several caloric effects in magnetic shape memory alloys.

MO.D.1_O2 - Tuning magnetic properties of isotropic ferrite powders as a feasible alternative for permanent magnet applications

F.J. Pedrosa ^{1,2}, K. Golasinski ¹, J. Rial ¹, A. Quesada ³, F. Rubio-Marcos ³, M.N. Guzik ⁴, S. Deledda ⁴, J.F. Fernández ³, J. Camarero ^{1,5}, A. Bollero ¹

1. *IMDEA Nanoscience, Madrid, Spain*

2. *Ingeniería Magnética Aplicada, IMA S.L., Barcelona, Spain*

3. *Electroceramic Department, Instituto de Cerámica y Vidrio, CSIC, Madrid, Spain*

4. *Institute for Energy Technology, Kjeller, Norway*

5. *Dep. Física de la Materia Condensada, Instituto Nicolás Cabrera, UAM, Madrid, Spain*

Rare earth-based permanent magnets (RE-PMs) are used in a large number of nowadays technological applications. The rapidly increasing market of green technologies demands increased amounts of this type of magnets. This demand in combination with the strategically geographical distribution of REs (especially critical for heavy REs) make necessary the search of alternatives to these PMs in as many applications as possible. NANOPYME is a European project that addresses the design and development of high quality PMs based on ferrites [1]. In this work authors will show:

(a) Achievement of high-coercive cobalt ferrite (CoFe_2O_4) powders by using milling times as short as 1.5-6 minutes and in contrast with previous studies [2];

(b) Tuning of microstructure and magnetic properties by proper choice of heat treatment parameters for as-milled material, resulting in isotropic powders with enhanced $(\text{BH})_{\text{max}}$. CoFe_2O_4 powders were prepared by sol-gel and co-precipitation followed by heating in air. X-ray diffraction showed the presence of exclusively spinel CoFe_2O_4 phase.

Milling of the starting powders for only 90 seconds has led to powders with a high coercivity $H_c=4.1$ kOe (four times larger than that obtained for the starting powders) [3]. This coercivity in combination with values $M_s=63.5$ emu/g and $M_r=40$ emu/g result in a $(\text{BH})_{\text{max}}=12.6$ kJ/m³. The large coercivity is due to a combination of a fine microstructure and the stress anisotropy induced on the particles during milling. Heat treatment of the as-milled material results in isotropic powders with $(\text{BH})_{\text{max}}>18$ kJ/m³. The excellent combination of magnetic properties achieved by using extremely short milling times makes of these powders good candidates for PM applications.

Acknowledgements: Research supported by EU-FP7-NANOPYME Project (No. 310516)

References:

[1] NANOPYME: www.nanopyme-project.eu

[2] B.H. Liu and J. Ding, *Appl. Phys. Lett.* 88, 042506-1_3 (2006)

[3] F.J. Pedrosa et al. "High coercive CoFe_2O_4 powders obtained by ultrafast milling". Submitted

MO.D.1_O3 - phase formation and magnetic properties of the L10 phase in Mn-Ga alloys

T. Mix^{1,2}, K. Müller¹, T.G. Woodcock¹, L. Schultz^{1,2}

1. IFW Dresden, Institute for Metallic Materials, Dresden, Germany

2. Department of Physics, TU Dresden, Dresden, Germany

The Mn-Ga binary system contains an L10 phase (cP4; P4/mmm) with high magnetocrystalline anisotropy, which may be a suitable candidate for rare earth free permanent magnets. The aim of this work is to understand the formation and stability of the L10 phase and to optimise both the intrinsic and extrinsic magnetic properties of the alloys. Mn-Ga binary alloys with compositions in the range 50-70 at.% Mn were produced by arc melting and annealing. Phase formation was studied using thermal analysis, x-ray diffraction and magnetometry. Measurements of the magnetocrystalline anisotropy constant and anisotropy field were performed in applied magnetic fields of 14 T. The single-phase L10 structure was obtained in the range 55-65 at.% Mn by annealing the high temperature phases, which were retained at room temperature after casting. A saturation magnetisation of $\mu_0 M_s = 0.807$ T together with an anisotropy field of $\mu_0 H_a = 4.4$ T could be reached for the Mn₅₅Ga₄₅ alloy. With increasing Mn content the saturation magnetisation decreases, whereas the anisotropy field increased. Mechanically milled Mn₅₅Ga₄₅ powder had coercivity of $\mu_0 H_c = 0.393$ T, which was a twentyfold increase compared to the bulk material but the magnetisation was reduced (cf. powder: $\mu_0 M_{5T} = 0.576$ T, bulk: $\mu_0 M_{5T} = 0.780$ T). Annealing the powder at 400 °C led to recovery of the magnetisation but reduced the coercivity, which was still ten times as high as the bulk value. A degree of texture of 0.45 was achieved by magnetic alignment of the powder particles, leading to a remanence of 0.526 T. Furthermore, isotropic hot compacts of powders were produced with packing density from 83 to 99%, in which the improved coercivity of the powders was partially retained.

MO.D.1_O4 - Atomic-scale characterisation of phase boundaries in hot deformed Nd-Fe-Co-B-Ga magnets infiltrated with a Nd-Cu eutectic

T.G. Woodcock¹, Q.M. Ramasse², T. Shoji³, M. Yano³, A. Kato³, O. Gutfleisch⁴

1. IFW Dresden, Dresden, Germany

2. SuperSTEM Laboratory, Warrington, United Kingdom

3. Toyota Motor Corporation, Prefecture Aichi, Japan

4. TU Darmstadt, Darmstadt, Germany

In order to develop Nd-Fe-B magnets with high coercivity (H_c) at elevated temperature without using Dy-substitution, precise engineering of the microstructure is needed. Hot deformed Nd-Fe-Co-B-Ga magnets have therefore been infiltrated with a Nd-Cu eutectic liquid, resulting in a 71% increase in coercivity to $\mu_0 H_c = 2.4$ T without the use of Dy. Aberration-corrected scanning transmission electron microscopy and electron energy loss spectroscopy (EELS) have been used to reveal the structure and chemical composition of phase boundaries in the magnets on the atomic scale [1]. EELS elemental profiles resolved the composition of individual lattice planes and were correlated with corresponding High Angle Annular Dark Field (HAADF) images, which revealed the crystal structure at atomic resolution. The results showed that the Nd-Cu eutectic liquid penetrated the ≈ 1 nm thick intergranular regions. The H_c increase following infiltration was therefore attributed to improved volume fraction and distribution of the intergranular phases. Co enrichment in the outermost 1-2 unit cells at several surfaces of the $\text{Nd}_2(\text{Fe,Co})_{14}\text{B}$ crystals was shown for the infiltrated sample. The as-deformed sample did not appear to show this Co enrichment. Interfacial segregation of Cu between the $\text{Nd}_2(\text{Fe,Co})_{14}\text{B}$ and the Nd-rich intergranular phase was observed in the infiltrated sample. All the secondary phases measured here contained significantly less Fe and more Nd than $\text{Nd}_2(\text{Fe,Co})_{14}\text{B}$.

[1] T.G. Woodcock *et al.*, *Acta Materialia* 77, 2014, 111-124

MO.D.1_O5 - Bi doped Mn₂Sb: a novel rare-earth free permanent magnet materialK. Aanand¹, N. Singh¹, N. Chirstopher¹, A. Gupta¹, A. Dhar¹*1. National Physical Laboratory, Middlesex, United Kingdom*

The demand for high-performance permanent magnets is rapidly growing worldwide due to their extensive usage in a wide range of energy generation and conservation applications. However, due to the recent global shortage and rising costs of rare-earth (RE) elements, it becomes imperative to develop permanent-magnets, which are free of RE elements. In the present work, we report the synthesis of Bi doped Mn₂Sb, as a potential RE-free permanent magnetic material. Mn₂Sb, crystallizes in a Cu₂Sb-type tetragonal structure, having two non-equivalent atomic sites for Mn, which is anti-parallel to each other, resulting in ferrimagnetic state of this compound. However, suitable doping of Mn₂Sb, transforms it into a ferromagnet and hence it could be a potential material for a RE-free permanent magnet. In the present work, we investigate the effect of Bi alloying in Mn₂Sb, on the magnetic properties of the resulting compound. A series of Mn₂Sb:Bi_x (x= 0.8 to 1.2) alloys was prepared by repeated arc-melting of the constituent elements under a high-purity argon gas atmosphere. This arc-melted master alloy was subsequently melt-spun, at optimized process parameters, to obtain continuous nanocrystalline ribbons. Phase purity and lattice parameters were determined employing X-ray diffraction and its Rietveld refinement. FESEM and HRTEM studies were conducted on the synthesized nanocrystalline ribbons and these results were correlated with their resulting magnetic properties. The magnetic properties of melt-spun Mn₂SbBi ribbon sample exhibited a considerable improvement over their arc-melted counterparts. The coercivity of the melt-spun Bi doped Mn₂Sb, nanocrystalline ribbons, after optimized annealing treatment, was found to be ~ 6 kOe with a (BH)_{max} ~ 4 MGOe. Further efforts are being made to optimize the material processing and annealing parameters to further enhance the magnetic properties.

MO.D.2_I1 - Advances in magnetocaloric characterization

M. Solzi¹, G. Porcari¹, F. Cugini¹

1. Dipartimento di Fisica e Scienze della Terra - Università di Parma, Parma, Italy

Magnetocaloric devices are a new generation of refrigerators aiming at a more efficient production of cooling power. The recent discovery of materials [1] showing high and reversible changes of temperature and entropy in magnetic field ranges ($\Delta B = 1$ T) that are reasonable for real machines is now pushing the envelope [2].

Together with materials preparation, magnetocaloric characterization techniques are evolving: 1) to give reliable estimations of materials' reversible and irreversible thermomagnetic properties and 2) to explore the materials' response on wider frequency ranges [3]. In-field calorimetry and conventional direct temperature change probes belong to the first group [4,5]. Non-contact temperature change setups are on the other hand useful solutions to overcome, or reduce at least, the thermal capacity of the temperature sensor. These techniques belong to the second group identified above since their characteristic time constant can be even 3 orders of magnitude lower than the fastest thermocouples (20 ms) available. Non-contact temperature change techniques may give useful insight into materials dynamic magnetocaloric response and direct temperature change of low dimensionality systems [6].

[1] F. Guillou, G. Porcari, H. Yibole, N. van Dijk and E. Brück, *Adv. Mater.* 26, 2671 (2014)

[2] <https://www.youtube.com/watch?v=Py9laztpKzs>

[3] K. G. Sandeman, Magnetic measurement standardization, In *Magnetics Technology International*, 72-78 (2014)

[4] G. Porcari, F. Cugini, S. Fabbri, C. Pernechele, F. Albertini, M. Buzzi, M. Mangia, and M. Solzi, *Phys. Rev. B* 86, 104432 (2012)

[5] G. Porcari, M. Buzzi, F. Cugini, R. Pellicelli, C. Pernechele, L. Caron, E. Brück and M. Solzi, *Rev. Sci. Instrum.* 84, 073907 (2013)

[6] F. Cugini, G. Porcari and M. Solzi, *Rev. Sci. Instrum.* 85, 074902 (2014)

MO.D.2_O2 - Quasi-zero volume change 1st order phase transition on (Mn,Fe)₂(P,A) A = Ge, Si magnetocaloric compounds

L. Caron^{1,2}, G. Porcari^{2,3}, X.F. Miao², N.T. Trung², N.H. Dung⁴, M. Solzi³, E. Brück²

1. *Max Planck Institute for Chemical Physics of Solids, Dresden, Germany*

2. *Delft University of Technology, Delft, The Netherlands*

3. *Parma University, Parma, Italy*

4. *Institute Neel, Grenoble, France*

(Mn,Fe)₂(P,A) A = Ge, Si compounds are, to date, the most promising materials for use as active regenerators in magnetic refrigeration based on the magnetocaloric effect. These compounds show extremely sharp first order isosymmetric phase transitions between ferro and paramagnetic states. As a result very large entropy and adiabatic temperature changes are observed which can be tuned varying the Mn:Fe and P:A ratios. Through the phase transition, the hexagonal unit cell lattice parameters show large discontinuous changes in opposite directions. In materials showing low thermal hysteresis it has been observed that the changes in lattice parameters, although large, compensate each other, giving rise to near zero volume changes. From this scenario two questions arise. The first fundamental question is: if there is no volume change, why is there hysteresis? The second, practical question concerns applications: does the near zero volume change mean better structural stability over a refrigeration cycle? In this work we show how Mixed Magnetism, as the underlying mechanism for the large magnetocaloric effect in these materials, conciliates near zero volume change and hysteresis. Near zero volume changes were observed directly and indirectly using temperature dependent XRD and high pressure magnetometry. Finally, thermo-magnetic cycling was used to test physical stability and showed that these compounds remained stable through ~1000 thermo-magnetic cycles simulating operating conditions.

MO.D.2_O3 - Gd-Zn biphasic magnetic composites synthesized in a single preparation step: increasing refrigerant capacity without decreasing magnetic entropy change

J.Y. Law¹, L.M. Moreno-Ramírez¹, J.S. Blázquez¹, V. Franco¹, A. Conde¹

1. Sevilla University, Seville, Spain

Magnetocaloric composites have been shown to exhibit enhanced refrigerant capacity in comparison to pure phases. Nevertheless, to be realistically applicable in devices, it is essential that each of the existing phases in the composite present a large magnetocaloric response. To date, the typical approach to combine different phases involves the preparation of multilayers, mixing powders etc. However, these methods entail drawbacks, such as poor thermal conductivity between surfaces, additional preparation steps during the synthesis etc. Hence, in this work, we aim to use an alternative approach to develop, in a single fabrication step, a material with mixed constituent phases within the composite (Gd and GdZn) with large magnetocaloric response. Gd-Zn alloy series, with a global composition of Gd(50+x)Zn(50-x) (with x=0, 5, 15 and 25 at.%), were successfully obtained by induction melting. X-ray microdiffraction results reveal the homogeneity of all the prepared samples and indicate a combination of GdZn and Gd phases with different proportions. The minor content of oxides detected in all cases, indicates it as superficial oxidation. A ~50 % enhancement of the refrigerant capacity for an applied field of 1.5 T is obtained when x increases from x=0 to x=25 while maintaining the same values of peak magnetic entropy change in the vicinity of room temperature. Field dependent heat capacity curves also exhibit a broadened multipeak behavior which remains upon the application of magnetic field. This work was supported by Spanish MINECO and EU-FEDER (project MAT2013-45165-P) and the PAI of the Regional Government of Andalucía.

MO.D.2_O4 - Thermal Conductivity study of (Mn-Fe)P_{1-x}Si_x magnetocaloric materials with first and second order phase transitionsA. Davarpanah¹, X.F. Miao², L. Caron², E. Bruck², J.S. Amaral¹, V.S. Amaral¹

1. Department of Physics / CICECO - Aveiro Institute of Materials, University of Aveiro, Aveiro, Portugal

2. Department of Radiation Science & Technology, Delft University of Technology, Delft, The Netherlands

Magnetic refrigeration attracts much attention as an environmentally friendly and efficient cooling procedure. One of the most promising materials for applications are the MnFeP_{1-x}Si_x compounds. These rare-earth free alloys are composed of abundant raw materials, showing large magnetocaloric entropy and adiabatic temperature changes, small thermal hysteresis and enhanced mechanical stability. These compounds crystallize in the Fe₂P-type hexagonal structure and undergo a transition between the paramagnetic and ferromagnetic states at the Curie temperature T_c which can be tuned changing P/Si and Fe/Mn ratios.

Besides the magnetocaloric properties, thermal conductivity plays a critical role for practical applications. However, studies on thermal conductivity of magnetocaloric materials are seldom reported.

In this study, the Hot Disk Transient method was used to measure the temperature dependence of the thermal conductivity in Mn_{1.3}Fe_{0.65}P_{0.4}Si_{0.6} (T_c=297K, 2nd-order) and Mn_{1.25}Fe_{0.7}P_{0.45}Si_{0.55} (T_c= 303K, 1st-order). At 273K (in the ferromagnetic phase), we obtain thermal conductivity values of 2.06 and 1.62 W/mK for Mn_{1.3}Fe_{0.65}P_{0.4}Si_{0.6} and Mn_{1.25}Fe_{0.7}P_{0.45}Si_{0.55}, respectively. Notice that, the thermal conductivity of the 2nd order sample is consistently higher over the whole temperature range. The thermal conductivity of both samples rises with temperature (almost 100% going from 253K to 393K) with an abrupt change near T_c, which is stronger for the 1st-order sample. Both samples display the same behavior: above T_c the slope is steep, while below T_c the thermal conductivity is much less temperature dependent.

These features point to the role of the magnetic ordering influence on the electronic and structural properties on thermal transport. The role of the electronic contribution is expected to be of major importance, since the electrical resistivity of similar samples presents sharp anomalies and large changes near T_c, with correlation of electrical and thermal conductivities expected from Wiedemann-Franz Law.

References:

1. X. F. MIAO *et al.* PHYSICAL REVIEW B 89, 174429 (2014)
2. O. Tegus *et al.* Nature 415, 150-152 (2002)
3. M. Gustavsson *et al.* Int. J. Thermophysics, Vol. 27, No. 1, 195 (2006)

MO.D.2_O5 - Conventional and rotating magnetocaloric effects in RAI_2 (R=Ho and Nd)

N. Antunes De Oliveira¹, J. Caro Patiño¹, P. von Ranke¹

1. *Universidade do Estado do Rio de Janeiro, Rio de Janeiro, Brazil*

In this work we theoretically discuss the conventional and the rotating magnetocaloric effects in RAI_2 , which crystallize in cubic symmetry and exhibit large magnetocrystalline anisotropy due to the crystal electric field. For this purpose, we use a model of interacting magnetic moments including a term to account for the anisotropy [1]. First, we apply the model to calculate the entropy changes and the magnetocaloric quantities in $HoAl_2$. Our calculations show that the entropy changes exhibit the usual behavior when the magnetic field is applied along the easy magnetization direction $\langle 110 \rangle$. However, when the magnetic field variation is applied along the hard direction $\langle 100 \rangle$ anomalies appear on the magnetocaloric quantities ΔS_{iso} and ΔT_{ad} . These findings are in reasonable agreement with the available experimental data [2].

We also calculate the caloric quantities in $HoAl_2$ by fixing the magnitude of the magnetic field and rotating its direction. Our calculations show that the magnetocaloric quantities exhibit sizeable values when the magnetic field rotates from $\langle 111 \rangle$ to $\langle 110 \rangle$ direction. On the other hand, our calculations predict changes of sign in the caloric quantities when the constant magnetic field rotates from $\langle 100 \rangle$ to $\langle 110 \rangle$ direction. This very interesting fact, which is basically due to the magnetocrystalline anisotropy, needs experimental data to be confirmed. Our calculations show that both the conventional and rotating magnetocaloric quantities in $NdAl_2$ exhibit similar behavior.

[1] N. A. de Oliveira and P. J. von Ranke, Phys. Rep. 489, 89 (2010)

[2] M. Patra et al, Jour. Phys:Cond. Matt. 26, 046004 (2014)

MO.D.2_O6 - Magnetic entropy change in materials with first- order magnetic transitions under cyclingB. Kaeswurm¹, V. Franco², K.P. Skokov¹, M. Fries¹, T. Gottschall¹, O. Gutfleisch¹*1. Institut für Geo- und Materialwissenschaften, Technische Universität Darmstadt, Darmstadt, Germany**2. Departamento Física de la Materia Condensada, Universidad de Sevilla, Sevilla, Spain*

Materials exhibiting a first-order magnetic phase transition are of interest for application in magnetic refrigeration due to the large magnetocaloric effect (MCE) associated with the transition. This effect may be expressed in terms of an entropy change ΔS or in terms of an adiabatic temperature change ΔT_{ad} . ΔS is related to the heat that can be transferred by magnetic means, while ΔT_{ad} characterises the efficiency of heat transfer in an active magnetic regenerator cycle. In a non-regenerative cycle such as Carnot or Bryton, measurement of ΔT_{ad} provides information on the maximum achievable thermal span. Magnetic refrigeration occurs in cycles, which is usually not replicated in laboratory tests. Measurements of both magnetocaloric quantities can be obtained by direct or indirect means. Direct measurements of the MCE require dedicated devices which are not broadly available. ΔS is indirectly obtained from measurements of either magnetisation isotherms $M(H)_T$ or thermomagnetisation curves $M(T)_H$ and subsequent application of the Maxwell relation. For materials undergoing a first order phase transition, the measurement protocol should include the preparation of the sample by erasing its thermal and magnetic history and the material starts from a homogeneous state before any transition takes place. Consequently, the measurement of any subsequent cycle would produce unphysical results. Here we present a procedure on how the cyclic behaviour of the magnetocaloric effect can be determined from indirect measurements of entropy change. We select three model materials with a first order phase transition: (La,Pr)(Fe,Si)₁₃, Fe₂P-type (Mn_{1.25}Fe_{0.7}P_{0.5}Si_{0.5}) and a compound with Heusler structure (Ni₄₅Mn₃₈In₁₂Co₅). Our method provides a basis for the comparison of the suitability of different hysteretic magnetocaloric materials for their application in a refrigerator device, taking into account the material's response to periodic variations of field and temperature. The method allows extracting the cyclic magnetic entropy change from quasi-static measurements, without the need for dedicated devices.

MO.D.3_O1 - Neutron scattering study of J1-J2 zig-zag chains in SrDy₂O₄ frustrated magnet

N. Gauthier¹, A. Fennell², A. Désilets-Benoît³, B. Prévost³, A.D. Bianchi³, C. Niedermayer², M. Frontzek², C. Baines⁴, J. Ollivier⁵, L.P. Regnault⁵, G. Nilsen⁵, M. Kenzelmann¹

1. *Laboratory for Developments and Methods, Paul Scherrer Institut, Villigen, Switzerland*
2. *Laboratory for Neutron Scattering and Imaging, Paul Scherrer Institut, Villigen, Switzerland*
3. *Département de physique, Université de Montréal, Montréal, Canada*
4. *Laboratory for Muon Spin Spectroscopy, Paul Scherrer Institut, Villigen, Switzerland*
5. *Institut Laue-Langevin, Grenoble, France*

Competing interactions in geometrically frustrated magnets can lead to ground states with large degeneracies and open the way to novel states of matter. Compounds of SrR₂O₄ family (R=Gd, Tb, Dy, Ho, Er, Tm and Yb) have first been pointed out to be candidates for frustrated magnetism in 2005. Since then, various interesting properties have been observed in these systems: spin-liquid-like ground-states, coexistence of two different magnetic orderings, low-dimensional correlations, magnetization plateaus and magnetic field induced order. Zig-zag chains in the structure are thought to be an important source of frustration in these compounds. The physics in the zig-zag chains is equivalent to a 1D chain with nearest neighbour J₁ and next-nearest neighbour J₂ interactions, usually called Ising J₁-J₂ chain model. The presence of two inequivalent rare earth sites in the structure probably leads to the coexistence of two different orders in compounds such as SrHo₂O₄ and SrEr₂O₄. The SrDy₂O₄ compound is especially interesting because it does not feature long range order down to 50 mK, thus showing a high degree of frustration. Different neutron scattering techniques have been used to characterize the low temperature properties of SrDy₂O₄ and to understand the absence of long range order. Diffuse scattering indicates short range correlations mainly along the c-axis originating from only one of the two inequivalent sites. Inelastic neutron scattering reveals the presence of a dispersive crystal field level and a gap opening at 60 mK, whose origin is not understood at present. Under applied field, a 1/3 magnetization plateau has previously been observed. This field-induced phase features a propagation vector consistent with the up-up-down state expected from theory.

MO.D.3_O2 - Micromagnetic characterisation of gyroid nanostructures

D. Love¹, J. Llandro¹, A. Kovacs², A. Kakay², M. Scherer¹, C. Ciorra¹, U. Steiner¹, R. Dunin-Borkowski², C. Barnes¹

1. University of Cambridge, Department of Physics, Cambridge, United Kingdom
2. Forschungszentrum Juelich, Ernst Ruska-Centre, Juelich, Germany

Gyroids are 3D self-assembled artificial materials that consist of a periodic network of struts, similar to the tetrahedral arrangement of pyrochlores [1]. Through a precise excursion in temperature, block copolymers can be self-assembled into a gyroid network. Selective dissolution of the minority phase then leaves an organic template that can be filled electrochemically to form metallic gyroid nanostructures [2]. Gyroid films have found applications in photovoltaics [3], photonics [4], catalysis [5], electrochromics [6] and supercapacitors [7] due to their porosity and high surface area to volume ratio.

While basic bulk magnetometry of gyroid films has previously been presented [8], the random nucleation process of orientational domains during self-assembly prevents true micromagnetic understanding of the system. However, the gyroid geometry forms a fundamentally interesting network and a potentially frustrated artificial magnetic material in 3D whose micromagnetic states have so far been left uncharacterised.

Here we present the fabrication of suitable gyroid crystallites with single orientational domains, 42nm unit cells and features sizes down to 10nm, suspended on TEM grids for nanometre-resolution electron holography and tomography characterisation. The holography results reveal magnetic flux patterns that indicate magnetically frustrated behaviour as well as onion states within the gyroid network. We use bespoke micromagnetic modelling to further aid in the characterisation of this unique self-assembled 3D artificial magnetic material.

- [1] S. Bramwell, *et al.*, Science 294, 1495-1501 (2001)
- [2] M. Scherer, *et al.*, Advanced Materials 26, 2403-2407 (2014)
- [3] E. Crossland, *et al.*, Nano Letters 9, 2807-2812 (2009)
- [4] S. Vignolini, *et al.*, Advanced Materials 24, OP23-OP27 (2011)
- [5] G. Armatas, *et al.*, Nature 441, 1122-1125 (2006)
- [6] M. Scherer, *et al.*, Advanced Materials 24, 1217-1221 (2012)
- [7] D. Wei, *et al.*, Nano Letters 12, 1857-1862 (2012)
- [8] H.-Y. Hsueh, *et al.*, Advanced Materials 23, 3041-3046 (2011)

MO.D.3_O3 - Spin-excitation spectrum of the insulating skyrmion compound Cu_2OSeO_3

D. Inosov¹, P. Portnichenko¹, A. Cameron¹, M. Schmidt², J. Park³, D. Abernathy⁴, A. Schneidewind³

1. *Technische Universität Dresden, Dresden, Germany*

2. *Max Planck Institute for the Chemical Physics of Solids, Dresden, Germany*

3. *Forschungsneutronenquelle Heinz Maier-Leibnitz, Garching, Germany*

4. *Oak Ridge National Laboratory, Oak Ridge, United States*

In the multiferroic Cu_2OSeO_3 system, the interplay of interatomic exchange and the Dzyaloshinskii-Moriya (DM) interactions leads to the twisting and canting of magnetic moments and, consequently, to the formation of a spinespiral ground state. An exotic skyrmion-lattice arrangement can be further stabilized by the application of magnetic field. Here we employed a combination of time-of-flight and triple-axis neutron spectroscopy to investigate the complete spectrum of spin excitations in Cu_2OSeO_3 over energies ranging from sub-meV to 50-60 meV. Several magnon bands are observed, in qualitative agreement with theoretical predictions, although a significant quantitative adjustment of exchange interaction parameters is required to match the neutron-scattering data. The experimentally measured dynamical structure factor of the magnons will be also discussed in relationship to the real-space crystal structure of the material.

MO.D3_O4 - Scaling Laws in speckle dynamics on artificial spin ices

Y. Li¹, S. Morley², D. Laroze^{1,3}, C. Marrows², R. Stamps¹

1. *University of Glasgow, Glasgow, United Kingdom*

2. *University of Leeds, Leeds, United Kingdom*

3. *Universidad de Tarapaca, Arica, Chile*

Speckle is an interference pattern produced by scattering from an illuminated surface, and is able to provide unique information about correlations in the scatterers [1]. We discuss how speckle can provide information about relaxation processes occurring over widely different times scales for magnetisation dynamics in patterned magnetic structures known as artificial spin ice [2]. These arrays are strongly correlated two-dimensional arrays of sub-micron sized magnets designed to produce competition between interactions that can result in degeneracies and frustration. We show that for two-dimensional lattices one can define a characteristic length scale for the domain growth, which in the coarsening approximation can be described by a multiple time scales model. The amplitude scattering has a direct relation to characteristic lengths of the system [3]. The theoretical model describes well the experimental data on a square array.

References:

1. G. Beutier et al. , Rev. Sci. Instrum. 78, 093901 (2007)
2. R. F. Wang et al., Nature (London) 439, 303 (2006)
3. A. Sadiq and K. Binder, J. Stat. Phys. 35, 517 (1984)

MO.D3_O5 - Spin excitations in a highly frustrated antiferromagnet Ni₃B₂O₆ explored by far-infrared and Raman spectroscopy

R.V. Pisarev¹, M.A. Prosnikov¹, K.N. Boldyrev², A.D. Molchanova², M.N. Popova², V.Y. Davydov¹, A.N. Smirnov¹, R. Yu. Babkin³, Y.G. Pashkevich³

1. *Ioffe Physical Technical Institute, Russian Academy of Sciences, St. Petersburg, Russia*
2. *Institute of Spectroscopy, Russian Academy of Sciences, Troitsk, Moscow, Russia*
3. *A.A. Galkin Donetsk Physical Technical Institute, National Academy of Sciences, Ukraine*

Frustrated magnets are a hot topic of the up-to-date magnetism in which many fundamental problems remain unresolved. In this talk we present results of experimental and theoretical studies of one- and two-magnon excitations in an orthorhombic borate Ni₃B₂O₆ (Pnmg group #58, Z=2) in which magnetic Ni²⁺ ions (S=1) in the unit cell occupy 2*a* and 4*f* distinct positions. Interactions between magnetic ions leads to an antiferromagnetic ordering below $T_N=46$ K with the magnetic structure formed by two inter-penetrating ribbons ...*a-2f-a-2f*... running along the *x* axis with the spins along the *y* axis. Far-infrared and Raman spectroscopic studies revealed new bright features arising below T_N in the range below the lowest phonon frequencies. First of all, infrared studies showed two absorption bands at 17.2 and 26.5 cm⁻¹ in $H(\omega) || z$ polarization whereas only one band at 17.5 cm⁻¹ was observed in $H(\omega) || x$ polarization. All these infrared features showed sharp decrease of their frequency and intensity and completely disappeared at T_N . Such behavior together with the polarization properties of the bands allowed us to assign them to one-magnon intra-ribbon spin excitations formed by different single ion anisotropies of Ni²⁺ ions at 2*a* positions (26.5 cm⁻¹) and 4*f* positions (17.2 and 17.5 cm⁻¹). Raman studies allowed observation of new spectrally complicated bands in a broad range of 50-200 cm⁻¹ with a pronounced sharp peak at 92-94 cm⁻¹ with behavior typical for two-magnon excitations. They showed appreciable temperature dependence when approaching T_N from below but they survived even above T_N as broad tails distinguishable up to 180 K. We relate such behavior of one-magnon and two-magnon excitations with the quasi-one-dimensional magnetic structure of Ni₃B₂O₆ caused by highly frustrated interactions between the magnetic ribbons composed of Ni²⁺ ions at 2*a* and 4*f* positions.

This work is supported by the Russian projects 14.B25.31.0025, 15-02-04222a, 15-02-07451, and MK-3521-2015.2.

MO.E.1_I1 - Soft X-ray photoemission spectro-microscopy at the ALBA Synchrotron: applications in magnetism

L. Aballe¹, M. Foerster¹, E. Pellegrin¹, J. Nicolas¹, S. Ferrer¹

1. ALBA Synchrotron Light Facility, Cerdanyola, Spain

The PhotoEmission Electron Microscopy (PEEM) experimental station of the CIRCE soft X-ray beamline at the ALBA synchrotron is presented, together with representative results from magnetism. The station is based on an Elmitec LEEM III low energy electron microscope with energy analyser. Using electrons emitted from the sample upon excitation by the variable polarization X-ray photons, surface imaging with high chemical, structural, and magnetic sensitivity is performed down to a lateral resolution better than 20 nm [1]. PEEM with X-Ray Magnetic Circular Dichroism (XMCD) contrast is a versatile, non/invasive, and powerful tool for the study of magnetic materials and micro/nanomagnetic systems. It provides element specific magnetic contrast with high spatial resolution and sensitivity (low moment). Thanks to the azimuthal sample rotation and the near grazing X-ray incidence, full 3D magnetization information can be obtained. Using X-Ray Magnetic Linear Dichroism contrast, even antiferromagnetic domains can be imaged (XMLD-PEEM). In the energy domain, X-ray absorption (XAS) and Photoemission (XPS) spectra can be measured down to the spatial resolution of the microscope (spectro-microscopy) with sufficient quality to determine surface magnetic moments through sum rule analysis [2]. The experimental station comprises standard in-situ surface preparation techniques, complementary characterization techniques such as microspot electron diffraction, and allows the application of electric and (weak) magnetic fields in the variable temperature sample stage during measurements.

[1] The ALBA spectroscopic LEEM-PEEM experimental station: Layout and performance. L. Aballe, M. Foerster, E. Pellegrin, J. Nicolas, S. Ferrer. *J. Synch. Rad.*, in press (2015)

[2] Spin and orbital magnetic moment of reconstructed sqrt2xsqrt2R45 magnetite (001). L. Martín-García, R. Gargallo-Caballero, M. Monti, M. Foerster, J. F. Marco, L. Aballe, J. de la Figuera. *Phys. Rev. B* 91, 020408(R) (2015)

MO.E.1_O2 - Ferromagnetic nuclear resonance for studying materials for spintronics, optics, and catalysis

C. Meny¹, K. Leguen², J.M. Andre², P. Jonnard², D. Halley¹, J.F. Dayen¹, Y. Liu³, C. PhamHuu³

1. Institut de Physique et Chimie des Matériaux de Strasbourg (IPCMS), University of Strasbourg, Strasbourg, France

2. Sorbonne Université, UPMC Univ. Paris 06, Laboratoire de Chimie Physique-Matière et Rayonnement, Paris, France

3. Institut de Chimie et Procédés pour l'Énergie, l'Environnement et la Santé (ICPEES), University of Strasbourg, ECPM, Strasbourg, France

Nuclear Magnetic Resonance (NMR) is a technique that is very popular in medicine, chemistry or biology, but it is much less used for studying ferromagnetic materials. However when used for ferromagnetic materials, NMR (also called in this case Ferromagnetic Nuclear Resonance, FNR) has the ability to provide, simultaneously and at the same scale, information about the local structure (crystallographic structure, chemical environment) as well as about the local magnetic properties of the probed atoms. For this purpose we have developed 3D NMR spectra in ferromagnets that allow visualising simultaneously the structural and magnetic inhomogeneities into the studied samples [1]. The magnetic information is recorded in the form of a local magnetic stiffness (inverse of the transverse susceptibility). To further improve the field of application of FNR we have recently developed a new investigation methodology based on temperature depend measurements that is specifically devoted to the study of assemblies of nano-objects.

After presenting the particularities of NMR in ferromagnets, the use of FNR is exemplified through the study of systems for applications in spintronics, optics and catalysis. We will successively investigate the hybridization of cobalt atoms at the interface with graphene, the interface morphology of Co-based multilayers [2] and the crystallographic structure and chemical composition within the size distribution of Co-based nanoparticles [3].

1. P. PANISSOD, C. MENY, *Appl. Magn. Reson.* 19, 447-460 (2000)

2. K. LE GUEN, M.H. HU, J.M. ANDRE, P. JONNARD, P.S.K. ZHOU, H. LI, J.T. ZHU, Z.S. WANG, C. MENY, *J. Phys. Chem. C*, 114, 6484-6490 (2010)

3. Y.F. LIU, I. FLOREA, O. ERSEN, C. PHAM-HUU, C. MENY, *ChemCommun*, 51, 145-148 (2015)

MO.E.1_O3 - AGFM for magnetic characterization of samples in A.C. magnetic field

M. Pérez¹, R. Ranchal², I. De Mendizabal¹, P. Cobos¹, J.L. Mesa³, M. Díaz³, C. Aroca¹

1. *Universidad Politecnica de Madrid (ISOM), Madrid, Spain*

2. *Universidad Complutense de Madrid, Madrid, Spain*

3. *Instituto Nacional de Técnicas Aeroespacial (INTA), Madrid, Spain*

Vibrating Sample Magnetometers (VSM) [1] and Alternating Gradient Force Magnetometers (AGFM) [2] are commonly used techniques to characterize magnetic materials. They have a similar sensitivity, 10⁻⁵-10⁻⁶ emu for the VSM and 10⁻⁶-10⁻⁷ emu for the AGFM and both systems allow the application of relatively large magnetic fields. Nevertheless, they cannot be used to characterize samples in AC because in these two systems, the samples are magnetized under continuous magnetic fields. Inductive methods are required when a sample has to be characterized as a function of frequency [3]. The main limitations of these inductive methods are the maximum field that can be applied to magnetize the sample (around 0.015 T) and the temperature increase in the primary coil. We have designed and fabricated a magnetometer that can work both as an AGFM and as a susceptometer without any modification in the experimental set-up because of the electronics we have developed. Another innovation of our prototype is the possibility of being used to characterize samples in a wide range of frequencies, from 0 to 30 kHz. We have demonstrated the capability of measuring different odd harmonics in a wide range of frequencies for small quantities of ferro-, para- and diamagnetic materials. Our system has also proved to be more adequate than a commercial VSM to characterize small quantities of dia- and paramagnets. Spurious effects such as hysteresis are not observed when measuring few micrograms of this type samples in our system.

[1] S. Foner, Rev. Sci. Instrum. 30, 548 (1959)

[2] H. Zijlstra, Rev. Sci. Instrum., 41, 1241 (1970)

[3] P. Cobos, M. Maicas, M. Sanz, and C. Aroca, IEEE Trans. Magn. 47 (2011) 2360-2363

MO.E.1_O4 - Towards quantitative magnetic measurements with atomic spatial resolution

J. Ruzs¹, J.C. Idrobo², J. Spiegelberg¹, A. Edström¹

1. Department of Physics And Astronomy, Uppsala University, Uppsala, Sweden

2. Center for Nanophase Materials Sciences, Oak Ridge National Laboratory, Oak Ridge, United States

We present recent advances in electron magnetic circular dichroism (EMCD) - a measurement technique performed using transmission electron microscope (TEM). EMCD is an electron-microscopy analogue of the well-established x-ray magnetic circular dichroism (XMCD). State-of-the-art aberration corrected scanning TEM (STEM) routinely allow to reach atomic spatial resolution, which brings a promise of measuring MCD of individual atomic columns. Electron vortex beams and other electron probes, with phase profiles tuned to the symmetry of local neighborhood of the studied atomic column, were predicted to enable detection of EMCD signal at atomic resolution. Early experimental tests together with advanced statistical processing of large datasets provide indications of EMCD signal on Mn-edge of an antiferromagnetic compound LaMnAsO, extending the reach MCD studies also to the domain of antiferromagnetic compounds.

MO.E.1_O5 - Bidirectional and co-resonant quantitative magnetic force microscopy sensors

T. Muehl¹, C.F. Reiche¹, J. Koerner¹, S. Vock¹, V. Neu¹, L. Schultz^{1,2}, B. Buechner^{1,3}

1. IFW Dresden, Dresden, Germany

2. Institut Für Werkstoffwissenschaft, Dresden, Germany

3. Leibniz Institute For Solid State and Materials Research, Dresden, Germany

Dynamic operation modes of scanning force microscopy are very successful methods to study force-related properties of surfaces with high spatial resolution. Here, we report on a concept of bidirectional force gradient microscopy sensors that enables a direct, fast, and quantitative real space mapping of force component derivatives in both the perpendicular and a lateral direction. This novel technique relies solely on multiple-mode flexural cantilever oscillations related to vertical probe excitation and vertical deflection sensing [1]. In particular, our approach includes the capability of in-situ switching between the two measurement directions. Exploring this concept we present a bidirectional magnetic force microscopy (MFM) sensor setup, corresponding quantitative measurements, and data analysis with emphasis on the calculation of mode-dependent spring constants that are the basis of quantitative force gradient studies.

Furthermore, we introduce a co-resonant MFM sensor design which combines a conventional cantilever oscillator and a low-stiffness magnetic nanowire oscillator. According to a coupled harmonic oscillator model, this nanowire oscillator strongly influences the cantilever oscillation if nanowire and cantilever have similar resonance frequencies even though the spring constants and the effective masses of the two partial systems differ by orders of magnitude. Thus, the magnetic interaction of the oscillating magnetic nanowire with the sample stray field leads to a large frequency shift of the coupled MFM sensor system which can be measured at the cantilever using conventional methods.

Finally, we apply this high sensitivity co-resonant oscillator approach to the lateral mode of our bidirectional MFM sensors.

[1] C. F. Reiche, S. Vock, V. Neu, L. Schultz, B. Büchner, and T. Mühl, New J. Phys. 17, 013014 (2015)

MO.E.2_O1 - Sensitive nanoSQUIDs for magnetization reversal measurements on single magnetic nanoparticles, nanotubes and nanowires

M.J. Martínez-Pérez ¹, R. Wölbing ¹, A. Buchter ², M. Wyss ², C. Reiche ³, T. Mühl ³, B. Müller ¹, T. Schwarz ¹, A. Zorin ⁴, B. Büchner ³, J. Sesé ⁸, A. Fontcuberta i Morral ⁵, D. Grundler ^{6,7}, R. Kleiner ¹, M. Poggio ², D. Koelle ¹

1. *Physikalisches Institut, Universität Tübingen, Tübingen, Germany*

2. *Dept. of Physics, Univ. Basel, Basel, Switzerland*

3. *IFW Dresden, Dresden, Germany*

4. *PTB Braunschweig, Braunschweig, Germany*

5. *EPFL Lausanne, Lausanne, Switzerland*

6. *TU München, Munich, Germany*

7. *STI, EPFL Lausanne, Lausanne, Switzerland*

8. *Dpto. de Física de la Materia Condensada, Zaragoza, Spain*

We report on recent advances in the realization of high-performance nano-scale superconducting quantum interference devices (nanoSQUIDs), which can be used for continuous measurements of magnetization loops of single magnetic nanoparticles in strong magnetic fields (applied in the plane of the SQUID loop) up to the Tesla range at cryogenic temperatures. We fabricated YBa₂Cu₃O₇ SQUIDs based on submicron grain boundary junctions patterned by focused ion beam milling [1] and Nb SQUIDs based on Nb/HfTi/Nb junctions patterned by e-beam lithography [2]. The nanoSQUIDs show very low flux noise down to ~ 100 nPhi₀/sqrt(Hz) (Phi₀ is the magnetic flux quantum) in the thermal white noise limit at temperature T=4 K, yielding spin sensitivities of down to a few μ_B /sqrt(Hz) (μ_B is the Bohr magneton). This opens new possibilities in the study of non-equilibrium dynamics of small spin systems at low T. We will discuss issues related to further improvement of the spin sensitivity, challenges related to operation in strong magnetic fields and approaches to position magnetic nanoparticles in close vicinity to the nanoSQUIDs. As some proofs-of-principle, we demonstrate measurements on a Co nanoparticle, a Fe nanowire (embedded in a carbon nanotube) and a Ni nanotube. In the latter case, a novel multifunctional system has been used, combining flux detection by a nanoSQUID and torque magnetometry with a ferromagnetic nanotube, mounted on a soft cantilever, as a scanning tip [3]. This system can be used for the detection of magnetic states of a single nanotube [4].

[1] T. Schwarz et al., ACS Nano 7, 844 (2013)

[2] R. Wölbing et al., Appl. Phys. Lett. 102, 192601 (2013)

[3] J. Nagel et al., Phys. Rev. B 88, 064425 (2013)

[4] A. Buchter et al., Phys. Rev. Lett. 111, 067202 (2013)

MO.E.2_O2 - Three-axis low energy neutron spectroscopy at the institut laue-langevin

M. Boehm¹, S. Roux¹, J. Kulda¹, V. Sechovsky², P. Svoboda², J. Saroun³, P. Steffens¹

1. Institut Laue-Langevin, Grenoble, France

2. Faculty of Mathematics and Physics, Charles University, Prague, Czech Republic

3. Nuclear Physics Institute AS CR, Rez, Czech Republic

Neutron inelastic scattering studies using three-axis spectrometers (TAS) are indispensable for measuring elementary excitations of magnetic correlated systems. Although other experimental techniques (NMR, muon spin rotation) can provide valuable information on the same systems, neutron inelastic scattering remains the method yielding the most complete information on the role of space and time correlations and their interplay in the behavior of condensed matter systems. Moreover, neutrons couple with comparable strength to both the structural and magnetic degrees of freedom and the two scattering components can be quite cleanly separated using polarized neutron techniques.

The new cold neutron spectrometer *ThALES* at the Institut Laue-Langevin has been optimized for exploring correlated magnetic systems beyond the experimental possibilities of its predecessor IN14 spectrometer [1-3] in terms of data collection rate, kinematical range and neutron polarization analysis. *ThALES* will cover momentum transfers up to 2 \AA^{-1} and energy transfers up to 18 meV with enhanced energy resolution ($\sim 0.05 \text{ meV}$ at incident wavenumber $k_i = 1.5 \text{ \AA}^{-1}$). The modified spectrometer shielding can host high field measurements up to 15 T in the complete dynamical range, while the new Heusler monochromator will provide a polarized neutron flux comparable to the old IN14 in its unpolarized mode. The challenge of measuring magnetic excitations in mm^3 -sized samples has been addressed by combining the virtual source concept with a focusing guide and a Si 111 focusing monochromator.

The commissioning phase of *ThALES* will finish in spring 2015 and the instrument will be available to the user community from summer 2015. Results of the commissioning phase will be presented.

The *ThALES* project is a collaboration between ILL and Charles University, financed by the Czech Ministry of Science and Education (Project no. LM2010001).

[1] Boehm M., Roux S., Hiess A., Kulda J., JMMM 310 (2007), e965-e967

[2] Boehm M., Roux S., Hiess A., Kulda J., I. Saroun, Meas. Sci. Technol 19 (2008), p.034024

[3] Boehm M., Cermak P., Kulda J., Hiess A., Steffens P., Šaroun J., J. Phys. Soc. Jap. 82, Supplement, SA026 (2013)

MO.E.2_O3 - Nanoscale magnetic imaging using single nitrogen vacancy centers in diamond

M. Ganzhorn¹, P. Appel¹, L. Thiel¹, B. Shields¹, E. Neu², P. Maletinsky¹

1. *University of Basel, Basel, Switzerland*

2. *University of Saarland, Saarbrücken, Germany*

Recent developments in magnetic imaging have led to important advances in material science, mesoscopic physics or life science [1]. In particular, scanning probe based approaches such as magnetic resonance force microscopy [2] or SQUID based detection schemes [3] have proven to play a pioneering role as they enable nanoscale spatial resolution, combined with a high sensitivity for small magnetic fields. However, the performance of these magnetometers is still limited by factors such as detector size and operation at cryogenic temperature only [1]. In this context, magnetic imaging with the isolated electronic spin of a nitrogen vacancy (NV) center in diamond offers a promising alternative. The NV center's atomic size and exceptionally long spin coherence time, even at room temperature, enables magnetic imaging with spatial resolution of tens of nanometers and a magnetic field sensitivity in the nanotesla range over a broad range of temperatures [4]. Here we report on our approach to such a high performance NV center based magnetometer. We will give an overview of the quantitatively imaging of magnetic stray fields in various nanoscale magnetic systems, for instance in ferromagnetic nanorods. Quantitative probing the stray fields of nanomagnetic structures will in the future allow us to study and image the dynamics of domain walls [5], spin waves [6] or high frequency magnetic fields.

References:

1. L. Rondin et al., Rep. Prog. Phys. 77, 056503 (2014)
2. Y. Martín et al., Appl. Phys. Lett. 50, 1455 (1987)
3. D. Vasyukov et al., Nature Nano 8, 639 (2013)
4. Maletinsky et al., Nature Nano 7, 320 (2012)
5. J.-P. Tetienne, Science 344, 1366 (2014)
6. van der Sar et al., Arxiv 1410.6123 (2014)

MO.E.2_O4 - Ultra high-resolution magnetic imaging of perpendicular magnetic recording media by near-surface alternating magnetic force microscopy

S.R. Kapa¹, S. Okayasu¹, H. Qi², F. Zheng², G. Egawa¹, Y. Kinoshita², S. Yoshimura¹, H. Saito¹

1. Graduate School of Engineering and Resource Science, Akita University, Akita, Japan

2. Venture Business Laboratory, Akita University, Akita, Japan

Magnetic force microscopy (MFM) is a powerful tool to observe fine magnetic domain structure with high spatial resolution down to about 10nm. To improve the resolution, magnetic imaging at near surface is quite effective, while conventional MFM has a difficulty to detect magnetic force near sample surface where short range forces are dominant. Therefore we developed alternating magnetic force microscopy (A-MFM) which enables near-surface imaging of DC & AC magnetic fields with high spatial resolution [1-2]. A-MFM utilizes the frequency modulation (FM) of a cantilever oscillation generated by an off-resonance alternating magnetic force between a magnetic sample and a magnetic tip. For DC magnetic field imaging, A-MFM uses a soft magnetic tip of which magnetic moment is driven by an AC magnetic field to generate the alternating magnetic force. A-MFM can distinguish the zero level and the polarity of magnetic force. By using these merits, we can detect the amplitude and direction of perpendicular DC magnetic fields from the sample simultaneously. The spatial resolution of less than 10nm was obtained by soft magnetic crystalline FeCo tips. Here the resolution was determined by the half of the minimum wave length where MFM magnetic signal reaches white noise level for the A-MFM image. To obtain higher spatial resolution, development of a sharpened soft magnetic tip with high sensitivity is important. In the present study, we have developed high-magnetization amorphous FeCoB soft magnetic tips and optimized the measuring conditions of A-MFM by using the evaluation result of AC magnetic field response of the tips. Ultra high-spatial resolution less than 5nm was obtained for the images of CoCrPt-SiO₂ perpendicular magnetic recording media.

References:

- 1) W. Lu et al., Appl. Phys. Lett., 96, 143104. (2010)
- 2) H. Saito et al., J. Appl. Phys., 109, 07E330, (2011)

MO.E.2_O6 - Quantitative magnetic force microscopy: A method to determine physical properties of superconducting materials

U. Wolff¹, F. Rhein¹, S. Vock¹, H. Stopfel², N. Joshi³, S. Ízer³, H.J. Hug³, V. Neu¹, L. Schultz¹

1. IFW Dresden, Dresden, Germany

2. Department of Physics and Astronomy, Uppsala University, Uppsala, Sweden

3. Department of Physics, University of Basel, Basel, Switzerland

Since the discovery of superconducting materials research is focused on the applicability of these materials which has already succeeded in some areas of medicine and instrumentation. Nevertheless, the potential for energy storage and supply still can be exploited and therefore the understanding of the unconventional superconductivity needs to be improved.

The visualization and analysis of the flux line arrangement and the determination of the temperature dependent magnetic penetration depth $\lambda(T)$ of a $\text{BaFe}_2(\text{As}_{0.24}\text{P}_{0.76})_2$ single crystal is performed using low temperature magnetic force microscopy. The results of the statistical evaluation methods of the flux line distribution are indications of a disordered hexagonal flux line arrangement. By three different evaluation methods the temperature dependent magnetic penetration depth $\lambda(T)$ was determined. The first approach analyses the force gradient by means of a monopole-monopole-model (MMM) with unknown tip properties whereas in the second method the tip properties are well known. The last possibility is a deconvolution by means of the previous determined tip transfer function (TTF). The calculated magnetic penetration depth λ_{output} can be compared to the known λ_{input} . The three different approaches show clearly that the deconvolution method of the MFM data provides the best results and is ubiquitous applicable.

From the measured magnetic force microscopy images the material specific magnetic penetration depth $\lambda(0)$ can be determined by extrapolation of its temperature dependency. The quantitative analysis of the magnetic penetration depth $\lambda(T)$ results in a specific magnetic penetration depth $\lambda(0) = (239 \pm 40)$ nm for the investigated $\text{BaFe}_2(\text{As}_{0.24}\text{P}_{0.76})_2$ single crystal.

Quantitative magnetic force microscopy has been proven to be a powerful tool for the determination of physical properties of superconducting materials. Moreover, the deconvolution approach established in this work allows to investigate all kind of samples and is not dependent on the scan height and therefore ubiquitous applicable.

MO.E.3_I1 - Manipulation of hybrid magnetic nanostructures through exchange bias and interfacial strain

A. Fraile Rodríguez¹, M. García del Muro¹, M. Kovylyna¹, A.C. Basaran², I. Valmianski², Rafael Morales^{3,4}, J.G. Ramírez², F. Kronast⁵, M. A. Marcus⁶, A. Scholl⁶, I.K. Schuller², X. Batlle¹, A. Labarta¹

1. *Institut de Nanociència i Nanotecnologia, Universitat de Barcelona, Barcelona, Spain*
2. *Department of Physics and Center for Advanced Nanoscience, University of California San Diego, La Jolla, United States*
3. *Department of Chemical-Physics, BCMaterials, University of the Basque Country UPV/EHU, Leioa, Spain*
4. *IKERBASQUE, Basque Foundation for Science, Bilbao, Spain*
5. *Helmholtz-Zentrum Berlin für Materialien und Energie GmbH, Berlin, Germany*
6. *Advanced Light Source, Lawrence Berkeley National Laboratory, Berkeley, United States*

Nanoscale manipulation of thin film magnetic properties can be achieved through proximity effects in hybrid heterostructures. For example, the unidirectional anisotropy induced in FM films by the proximity with an antiferromagnetic (AF) layer upon cooling through the AF Néel temperature (TN) (exchange bias effect) is crucial in numerous applications. Recently, ferromagnetic/antiferromagnetic (FM/AF) nanostructures exhibiting both negative and positive exchange bias have been proposed as model systems for multistate switching memory units. Furthermore, the proximity of a FM film with a vanadium oxide results in a large and reversible modification of the magnetic properties due to the magnetoelastic anisotropy caused by the interfacial stress. In particular, large changes in coercivity in Ni/V₂O₃ bilayers across the structural phase transition (SPT) of V₂O₃ have been recently reported. In this work, we use synchrotron X-ray photoemission electron microscopy to analyze the spin configurations of model exchange biased Ni/FeF₂ nanostructures and Ni/V₂O₃ nanostructures. For the Ni/FeF₂ case, we show that a progressive spatial confinement of the bilayers, either through FM thickness variation or via antidot patterning the whole FM/AF heterostructure, actively controls the domain configuration of uncompensated spins in the AF. The final spin structure is determined by the balance between the competing FM and AF magnetic energies. The underlying mechanism of the AF domain formation in Ni/FeF₂ may be generic to other magnetic systems with complex non-collinear FM/AF spin structures. For the Ni/V₂O₃ bilayers, we find that the SPT in V₂O₃ induces nucleation of reversed Ni domains, and their fraction grows monotonically with the predominance of one of the coexisting structural phases. The changes in domain structure are fully reversible over the narrow temperature window of the SPT. A local distribution of transition temperatures is found across the sample. The lateral domain correlation length allows us to discern the SPT character.

MO.E.3_O2 - Nonlinear magneto-plasmonics in hybrid metal-ferromagnet multilayer structures

I. Razdolski¹, A. Kirilyuk¹, T. Rasing¹, D. Makarov², O. Schmidt², V. Temnov³

1. *Institute of Molecules and Materials, Radboud University Nijmegen, Nijmegen, The Netherlands*

2. *Institute for Integrative Nanosciences, IFW Dresden, Dresden, Germany*

3. *Institut des Molécules et Matériaux du Mans, UMR CNRS 6283, Université du Maine, Le Mans, France*

Linear magneto-plasmonics represents a new way to probe the electromagnetic field in metal-ferromagnet nano-structures and better understand nano-optical interactions [1,2]. Nonlinear magneto-plasmonics [3] aims to utilize plasmonic excitations to control the mechanisms and tailor the efficiencies of nonlinear light frequency conversion at the nanoscale. We investigate the mechanisms of magnetic second harmonic generation in a hybrid gold-cobalt-silver multilayer structure supporting propagating surface plasmon polaritons at both fundamental and second harmonic frequencies. Using Kretschmann experimental configuration we observe a huge magneto-optical intensity modulation (magnetic contrast of up to 33%) which is dominated by the excitation of surface plasmon polaritons at the second harmonic frequency, as shown by tuning the optical wavelength over the spectral region of strong plasmonic dispersion. Our proof-of-principle experiment, as well as a simple phenomenological theoretical description open up the pathway to novel magneto-plasmonic devices and contribute to the general understanding of nonlinear optics with electromagnetic surface waves.

References:

[1] V.V. Temnov, Nature Phot. 6, 728 (2012)

[2] G. Armelles et al., Adv. Opt. Mat. 1, 10 (2013)

[3] W. Zheng et al., Sci. Reports 4, 6191 (2014)

MO.E.3_O3 - Stability of single skyrmionic bits

J. Hagemeister¹, N. Romming¹, K. von Bergmann¹, E. Vedmedenko¹, R. Wiesendanger¹

1. University of Hamburg, Hamburg, Germany

The switching between topologically distinct skyrmionic and ferromagnetic states has been proposed as a bit-operation for information storage. Generally, long lifetimes of the bits in combination with short switching times are required for data storage devices. The lifetimes of skyrmions however, have not been addressed so far. To study the feasibility of the realization of skyrmionic bits, we have investigated their energy landscape in a broad range of magnetic fields and temperatures theoretically by means of classical Monte-Carlo (MC) simulations. A critical field B_c at which the mean lifetimes of the skyrmionic (Sk) and ferromagnetic (FM) states are identical has been identified. Notably, the field dependent mean lifetimes of the two states show a high asymmetry with respect to B_c in contrast to conventional uniaxial magnetic bits. The main reason for the asymmetry has been found to be a different field dependence of the skyrmionic and ferromagnetic activation energies. We were also able to correlate the stability of skyrmions in systems on discrete lattices with their attempt frequency rather than with their activation energy. We use this knowledge to propose a procedure permitting the determination of effective material parameters and the quantification of the MC time scale from the comparison of theoretical and experimental data.

MO.F.1_I1 - Antiferromagnetic spintronics

T. Jungwirth¹

1. Institute of Physics ASCR and University of Nottingham, Nottingham, United Kingdom

Louis Néel pointed out in his Nobel lecture that while abundant and interesting from theoretical viewpoint, antiferromagnets did not seem to have any applications. Indeed, the alternating directions of magnetic moments on individual atoms and the resulting zero net magnetization make antiferromagnets hard to control by tools common in ferromagnets. Strong coupling would be achieved if the externally generated field had a sign alternating on the scale of a lattice constant at which moments alternate in AFMs. However, generating such a field has been regarded unfeasible, hindering the research and applications of these abundant magnetic materials.

We have recently predicted [1] that relativistic quantum mechanics may offer staggered current induced fields with the sign alternating within the magnetic unit cell which can facilitate a reversible switching of a biaxial antiferromagnet by applying in-plane electrical currents along two orthogonal directions. The effect occurs in antiferromagnets with specific crystal and magnetic structures for which the spin sublattices form space-inversion partners. Among these materials is a high Néel temperature antiferromagnet, tetragonal-phase CuMnAs, which we have recently synthesized in the form of single-crystal epilayers structurally compatible with common semiconductors, such as Si or GaP [2]. Relativistic current-induced fields strongly coupled to the Néel order, combined with antiferromagnetic CuMnAs epilayers and micro-device anisotropic magnetoresistance, are the key elements that led to our demonstration of the electrical writing and read-out in an antiferromagnetic memory device [3].

References:

- [1] J. Zelezny, et al., Phys. Rev. Lett. 113, 157201 (2014)
- [2] P. Wadley, et al., Nat. Commun. 4, 2322 (2013)
- [3] P. Wadley et al. <http://arxiv.org/abs/1503.03765>

MO.F.1_O2 - High temperature spin dynamics studied by solid state nuclear resonance and electron paramagnetic resonance in $^{29}\text{Si}:\text{B}$ crystals

R. Morgunov¹, O. Koplak¹, A. Talantcev¹

1. Institute of Problems of Chemical Physics RAS, Moscow, Russia

The Si:B micro crystals enriched with ^{29}Si isotope were studied by high resolution nuclear magnetic resonance (NMR-MAS) and electron paramagnetic resonance (EPR) in the 300 - 800 K high temperatures range. Recovery of nuclear magnetization saturated by radiofrequency impulses obeys pure power-law kinetics at 300 K, while admixing exponential contribution takes place at 500 K. The power-law relaxation corresponds to direct electron-nuclear relaxation due to inhomogeneous distribution of paramagnetic centers, while exponential kinetics corresponds to nuclear spin diffusion mechanism. Effect of plastic deformation on boron centers EPR lines was found and its interrelation with NMR data is discussed. Inhomogeneous distribution of deformation defects is a most probable reason of the power-law kinetics of nuclear spin relaxation.

MO.F.1_O3 - Amplification of spin polarization using electro-nuclear spin-spin transistor

K. Olejník¹, R. Campion², Z. Soban¹, V. Novák¹, T. Jungwirth^{1,2}

1. *Institute of Physics, ASCR, v.v.i., Prague, Czech Republic*

2. *School of Physics and Astronomy, University of Nottingham, Nottingham, United Kingdom*

We experimentally demonstrate operation of an all electrical hybrid ferromagnetic metal/semiconductor (Fe/n-GaAs) device which utilizes dynamically polarized nuclear spins to control electrically injected electron spins in a GaAs channel. The operation principle of the device consists of two steps. In the first step a weak out-of-plane electron spin polarization is generated by the Spin Hall effect on sides of a cross-channel structure which is used for the dynamic polarization of GaAs nuclei (time necessary for nuclear spin polarization is on the order of minutes). In the second step the non-local spin Hanle experiment is performed: electrons are injected from an Fe injector with in-plane spin polarization and the non-local spin signal is detected on an adjacent Fe detector as function of external out-of-plane field. The precession of in-plane spins is manipulated by the nuclear spin polarization via hyperfine interaction. Under defined conditions the change of the width of the Hanle curve is a measure of the degree of the nuclear spin polarization and hence provides effective direct tool for determination of nuclear polarization. In our device, the subtle out-of-plane nuclear spin polarization (0.01-0.1%) controls precession of the strong in-plane spin polarization (1-10%) of injected electrons. From this perspective the device performs amplification of the original spin signal generated by SHE used for the polarization of nuclei. The amplification allows for convenient electrical detection of very weak spin polarization.

MO.F.1_O4 - Novel bulk form diluted magnetic semiconductors with decoupled charge and spin doping: Synthesis and NMR investigation

F. Ning¹

1. Zhejiang University, Zhejiang, China

The research of DMS has been mostly confined to the MBE-grown thin films. Recently, many bulk form DMSs that are derivatives of Fe-based superconductors have been reported, i.e., “111” DMS system I-II-V Li(Zn,Mn)As with TC ~ 50 K [1], “122” DMS system (Ba,K)(Zn,Mn)2As2 with TC ~ 230 K [2,3], “1111” DMS system (La_{1-x}Bax) (Zn_{1-x}Mnx)AsO with TC ~ 40 K [4]. These ferromagnets are all p-type, and have the advantage of decoupled spin and charge doping. In this talk, I will give an introduction of these novel DMSs, and talk about the NMR results of Li(1+y)Zn(1-x)MnxP [5], which has an identical cubic structure to that of III-V (Ga,Mn)As and II-VI (Zn,Mn)Se. We will show that the new 7Li NMR peak induced by Mn doping enabled us to probe local static and dynamic properties of Mn spins with NMR for the first time [6]. We present unequivocal experimental evidences that the ferromagnetic ordering is indeed caused by randomly substituted Mn in Zn sites, instead of Mn cluster or other magnetic impurities. This result is also confirmed by muon spin relaxation (muSR) measurement [7], which shows a nearly full ferromagnetic ordered volume. Our experimental results establish that Mn-Mn ferromagnetic interaction are not limited to the near-neighbor sites, but extend over many unit cells.

- [1] Z. Deng, F.L. Ning and C.Q.Jin* et al, N.C. 2, 422, (2011)
- [2] K. Zhao, F.L. Ning and C.Q.Jin* et al, N.C. 4, 1442, (2013)
- [3] K. Zhao and C.Q. Jin* et al, Chin. Sci. Bull. 59, 2524, (2014)
- [4] C. Ding and F.L. Ning* et al, PRB, 88, 041102(R), (2013)
- [5] Z. Deng, F.L. Ning and C.Q.Jin* et al, PRB, 88, 081203(R), (2013)
- [6] C. Ding and F.L. Ning* et al, PRB, 88, 041108(R), (2013)
- [7] F.L. Ning* and H.Y. Man et al, PRB 90,085123 (2014)

MO.F.1_05 - Spin-to-Charge conversion in 2d electron gas at LaAlO₃/SrTiO₃ Interfaces

Y. Fu¹, E. Lesne², J.C. Rojas-Sánchez², S. Oyarzun¹, N. Reyren², E. Jacquet², V. Cros², G. Desfonds¹, S. Gambarelli¹, J.P. Attané¹, M. Jamet¹, J.M. George², A. Fert², A. Barthélémy², L. Vila¹, H. Hares^{2,3}, M. Bibes²

1. *Institut Nanosciences et Cryogénie, CEA Grenoble, France*

2. *Unité Mixte de Physique CNRS/Thales, and Université Paris-Sud 11, Palaiseau, France*

3. *Peter Grünberg Institute, and Institute for Advanced Simulation, Jülich, Germany*

The Rashba effect is a manifestation of spin-orbit interaction (SOI) in solids, where the spin degeneracy associated with the spatial inversion symmetry is raised due to a symmetry-breaking electric field perpendicular to the heterointerface [1] and giving rise to field modulation effect at oxide LAO/STO interfaces like demonstrated very recently [2]. On the other hand, Edelstein was the first to realize that in a Rashba two-dimensional electron system, the flow of a charge current is accompanied by a non-zero spin accumulation coming from uncompensated spin-textured Fermi surfaces [3]. Recently, the converse effect, corresponding to a spin-to-charge conversion through SOI (inverse Edelstein effect or IEE), was demonstrated at Ag/Bi(111) interfaces [3]. We performed spin injection by ferromagnetic-resonance-(FMR)-spin-pumping on NiFe/LaAlO₃/SrTiO₃ heterostructures. Our results suggest an efficient spin-to-charge current conversion at the STO/LAO interface taking advantage of the IEE on the 2 dimension electron gas at low temperatures (around 10 K). Moreover, by applying a gate voltage at the SrTiO₃ substrate and perpendicular to the LAO/STO interface we are able to tune the spin-to-charge current conversion, with the charge current production depending on both the amplitude and the direction of the gate voltage. We interpret these results in terms of the large SOI in LaAlO₃/SrTiO₃ and will discuss the corresponding electrostatic modulation of the IEE by the back-gate voltage.

[1] Y. A. Bychkov & E. I. Rashba, *J. Phys. C* 17, 6039 (1984)

[2] G. Herranz et al., *Nat. Commun.* 6, 6028 (2015)

[3] V. M. Edelstein, *Solid State Commun.* 73, 233 (1990)

[4] J. C. Rojas-Sánchez et al., *Nat. Commun.* 4, 2944 (2013)

MO.F.2_I1 - Templated self assembly of magnetic nanostructures

C.A. Ross¹, S. Ohja¹, N. Aimon¹, W. Bai¹, K. Tu¹

1. Massachusetts Institute of Technology, Cambridge, United States

Self assembly techniques provide a route to the rapid synthesis of nanostructures whose long range order and registration can be controlled by pre-patterning the substrate lithographically. An example is the codeposition of immiscible spinel and perovskite oxide phases producing epitaxial thin film nanocomposites in which ferrimagnetic cobalt ferrite (CFO) pillars are embedded in a ferroelectric bismuth orthoferrite (BFO) matrix. The pillars form a regular array when templated by pits of pitch 60 nm and above made in the substrate, and have a strong magnetoelastic anisotropy due to lattice strain from the BFO matrix. The arrays show magnetoelectric switching, in which an electric field leads to strain in the BFO which is transferred to the CFO, lowering its total anisotropy and enabling switching to occur driven by the stray field of the neighboring pillars. In (Co,Ni)Fe₂O₄/BFO arrays with 100 nm period the interactions were sufficiently strong to produce a checkerboard pattern of up/down magnetic moments after ac demagnetization. The behavior is verified by a model of coupled dipoles with an anisotropy distribution. The second process is the use of templated block copolymer films for patterning of metallic magnetic films and multilayers into arrays of lines or dots with feature sizes of 10 nm and above. Liftoff, damascene and ion beam etching processes were used to produce Co dot arrays and MTJs with 50 nm diameter and their properties were compared, with ion beam etching producing a narrower switching field distribution. Co nanowires and junctions with 30 nm width were fabricated and magnetic force microscopy showed the presence of transverse domain walls, allowing their structure and interactions to be probed.

MO.F.2_O2 - Ni₈₀Fe₂₀ nanodisks by nanosphere lithography for biomedical applications

P. Tiberto¹, G. Barrera^{1,2}, F. Celegato¹, M. Coisson¹, G. Conta^{1,2}, F. Vinai¹, K. Martina³, M. Caporaso³, L. Serpe³, R. Canaparo³

1. *Inrim, Torino, Italy*

2. *Dipartimento di Chimica, Università di Torino, Torino, Italy*

3. *Dipartimento di Scienza e Tecnologia del Farmaco, Università di Torino, Torino, Italy*

Magnetic nanoparticles have been intensively studied for applications as contrast enhancement agents in magnetic resonance imaging, drug delivery and hyperthermia. The magnetic moment is exploited for target-directed delivery, detection, separation, and manipulation. Recent publications describe the preparation of composite materials suitable for biorecognition, targeting, multimodal imaging, and therapy. However, it is intrinsically difficult to control nanoparticles size and magnetic properties. Bottom-up nanolithography allows the production of nanodisks with controlled diameters and magnetic properties. In this work, the fabrication and magnetic behavior of Ni₈₀Fe₂₀ nanodisks suspended in ethanol are presented. Arrays of nanodisks were obtained by sputtering continuous Ni₈₀Fe₂₀ films on an optical resist, then by self-assembling commercially available polystyrene nanospheres (starting diameter 800 nm). After depositing a monolayer of nanospheres on the film surface, spheres diameter is reduced by plasma in Ar. Subsequently, magnetic material among the nanospheres is removed by sputter-etching. The removal of the remaining spheres is performed by sonication. Finally, the resist layer is dissolved in acetone resulting in freely nanodisks that are dispersed in ethanol. Room-temperature magnetic hysteresis curves have been recorded at several stages of the process indicating that the continuous film displays a typical soft magnetic behaviour. Patterning leads to a hysteresis loop having the typical shape of magnetisation vortex nucleation with a higher coercive field, as confirmed by AFM/MFM images. The free-standing nanodisks are characterised by a similar behavior, maintaining a vortex magnetisation process. SQUID magnetometry in the 5-300 K range has been exploited to study possible magnetostatic interactions among the disks. To assess the suitability of the nanodisks in targeted drug delivery, chemical bioderivatization has been taken into account. Bioderivatization was aimed to the production of a nanoscaled functional material that combine multiple functionalities for enhanced therapeutic efficacy. The in vitro toxicity assessment of the nanodisks will be discussed.

MO.F.2_O3 - Investigation of different magnetocrystalline anisotropies with FORC analysis in electrodeposited Co-Pt nanowires

M. Shahid Arshad^{1,2}, M.P. Proenca^{3,4}, S. Trafela¹, V. Neu⁵, M. Vazquez³, S. Kobe^{1,2,6}, K. Žužek Rožman¹

1. *Jožef Stefan Institute, Department for nanostructured materials K7, Ljubljana, Slovenia*
2. *Jožef Stefan International Postgraduate School, Ljubljana, Slovenia*
3. *Instituto de Ciencia de Materiales de Madrid, CSIC, Madrid, Spain*
4. *IFIMUP and IN—Institute of Nanoscience and Nanotechnology and Departamento Física e Astronomia, Universidade Porto, Porto, Portugal*
5. *IFW-Dresden, Institute for Metallic Materials, Dresden Germany*
6. *Center of Excellence on Nanoscience and Nanotechnology (CENN Nanocenter), Ljubljana, Slovenia*

Ferromagnetic nanowires (NWs) have potential application in magnetic sensors, biomedical applications and racetrack memory devices. In the present work, we have fabricated Co-Pt NWs via potentiostatic electrodeposition into two different membranes, polycarbonate (PC) and alumina (AAO) membrane with the same pore diameter. The deposition conditions were kept the same in both cases. XRD results showed that NWs fabricated in both membranes have *hcp* crystal structure. However, analysis on XRD showed that only NWs in AAO membranes have strong texturing perpendicular to the NWs long axis. The global hysteresis loop showed that NWs fabricated in both membranes have strong perpendicular anisotropy due to *hcp* phase. In order to obtain information about magnetostatic interactions in the NWs we performed Henkel plots which showed strong interaction between the NWs in both cases. The quantitative information about this interaction were possible with first order reversal curves (FORC) measurements. FORC measurement showed that local interactions (within the NWs) is stronger than mean field interaction effect between the NWs in both membranes. Interestingly, in AAO membrane in perpendicular field direction two distinct interaction peaks were obtained which is related to two different switching field distributions. It can be possible if two different kind of NWs are present in our system. For that reason Magnetic force microscope (MFM) imaging was applied to observe magnetic domain patterns on the basis of the magnetization profile in NWs lying horizontally on specially prepared Si substrates, used to locate the NWs under the MFM. We performed statistical analysis and found two different type of domain structures present in NWs in AAO membrane, probably the reason for two FORC peaks. Moreover, micromagnetic simulations (NMAG) on NWs confirmed that such two different domain structures (due to different anisotropies) can present different switching field distribution.

MO.F.2_O4 - Magnetic domain walls in interconnected nanowire structures

D. Burn¹, M. Chadha¹, L. Cohen¹, W. Branford¹

1. Imperial College London, London, United Kingdom

Magnetic meta-materials exhibit interesting and complex magnetisation behaviour which originates from nanoscale patterning in addition to the intrinsic properties of the magnetic material. Artificial spin ice is one such example where interconnected magnetic nanowires are arranged in a kagome network. Here, the collective behaviour originates from multiple magnetic domain walls (DWs) which propagate along nanowires and interact at vertices.[1,2] In this work, spatially resolved magnetisation reversal behaviour in a kagome artificial spin ice structure is investigated through focussed MOKE magnetometry. With the application of a magnetic field, magnetisation reversal due to the nucleation and propagation of magnetic DWs is observed. Varying the applied field direction relative to symmetry axes in the patterning allows us to bias particular sub-lattice directions giving physical insight into the DW propagation and vertex interactions taking place.

Localised pulsed-field injection techniques[3] allow the DW propagation behaviour to be probed at fields below the intrinsic nucleation field of the system. This means that the relative influence of the DW nucleation and propagation processes upon the magnetisation reversal can be differentiated. Furthermore, the localisation of the DW injection shows behaviour associated with the bulk of the sample in comparison to that resulting from boundary effects at the edges of the structure.

This research builds on our understanding of complex interconnected magnetic systems and opens pathways to further explore the manipulation of magnetic charges[4] and potential technological applications.

[1] D. Burn et.al. Phys. Rev. B 90, 144414 (2014)

[2] K. Zeissler et.al. Sci. Rep. 3, 1252 (2013)

[3] D. Burn et.al. Phys. Rev. B 88, 104422 (2013)

[4] E. Mengotti et.al. Nat. Phys. 7, 68 (2010)

We acknowledge Leverhulme Trust grant RPG_2012-692 and UK EPSRC grant EP/G004765/1 for funding.

MO.F.2_O5 - Segmented nanowires for multi-level high-density magnetic data storage: Modeling and experimental proof-of-concept

N. Del-Valle¹, S. Agramunt-Puig¹, E. Pellicer¹, J. Zhang¹, J. Nogués^{2,3}, C. Navau¹, A. Sanchez¹, J. Sort^{1,2}

1. *Universitat Autònoma De Barcelona, Barcelona, Spain*

2. *Institució Catalana de Recerca i Estudis Avançats (ICREA), Barcelona, Spain*

3. *ICN2 - Institut Català de Nanociència i Nanotecnologia, Bellaterra, Spain*

The use of arrays of high-aspect ratio magnetic nanowires (NWs) has been proposed in recent years as a promising strategy to increase the areal density of information in magnetic memories with out-to-plane magnetic anisotropy, while avoiding superparamagnetic effects. The recording density of such systems can be further enhanced by taking advantage of a multi-level magnetic storage approach. In such systems, each NW consists of N segments of different ferromagnetic materials (i.e., with dissimilar anisotropies and coercivities) separated by non-magnetic spacers, thus rendering N bits per wire. The success of such designs strongly depends on achieving a delicate balance between two opposing technological demands: the need for an ultra-high density of NWs per unit area (high density of NWs in close proximity) and the minimization of inter-wire and inter-segment dipolar interactions. Here we introduce a powerful model to evaluate the magnetic response of large arrays of NWs composed of two magnetic segments. The model, which is first validated by comparison with micromagnetic calculations, captures the essential aspects of the underlying physics in these systems while it is, at the same time, computationally tractable even for relatively large arrays of NWs. The minimum lateral and vertical distances rendering densely packed weakly-interacting NWs and segments are calculated in order to optimize the performance of this type of recording media. As a proof-of-concept of such designs, multisegmented NWs consisting of hard ferromagnetic (CoPt)/ non-magnetic (Cu) / soft ferromagnetic (Ni) segments have been prepared by electrodeposition. Clear step-like hysteresis loops with four possible remanent magnetization states are obtained. The magnetic orientation of the two ferromagnetic segments at remanence can be tailored to be either parallel or antiparallel, depending on the applied external magnetic field.

MO.F.3_O1 - Demonstration of spin-MOSFET using n-type Si at room temperature

M. Kameno^{1,2}, T. Sasaki³, Y. Ando², T. Shinjo², H. Koike³, T. Oikawa³, T. Suzuki⁴, M. Shiraishi²

1. *Osaka University, Osaka Prefecture, Japan*

2. *Kyoto University, Kyoto Prefecture, Japan*

3. *TDK Corporation, Tokyo, Japan*

4. *AIT, Akita, Japan*

Spin-metal-oxide-semiconductor-field-effect-transistors (spin-MOSFETs) hold the possibility of reconfigurable computing units on information-processing devices [1]. Spin-MOSFETs have been anticipated as the one of the powerful candidates for Beyond-CMOS devices based on spintronics. For developing spin-MOSFETs, silicon (Si) channel is well known as one of the promising materials since it is prevalent in electronics devices and has small spin orbit interaction, resulting in good spin coherence in Si. Spin transport in n-type Si channel up to RT has been achieved in our study [2], and spin transport properties, i.e., spin diffusion and spin drift have been revealed quantitatively in a degenerate state [3,4]. This time, we report the experimental demonstration of spin transport in a nondegenerate Si with a spin-MOSFET structure.

We fabricated spin valve devices on a Si-on-Insulator substrate, which consisted of a phosphorus-doped ($\sim 2 \times 10^{18} \text{ cm}^{-3}$) n-type channel. Beneath ferromagnetic electrodes (FMs), MgO tunneling barrier layers and highly-doped layer are prepared in order to decrease the thickness of Shottkey barrier. When the device was measured with the gap length of FMs as 21 μm , we successfully observed the Hanle-type spin precession signals by applying perpendicular magnetic field at RT [5]. We found that the effect of spin drift made the reasonable contribution to quite long-range spin transport in the nondegenerate Si channel. In addition, the successful gate-voltage-induced modulation of the spin signals was obtained with the Elliott-Yafet-type spin relaxation mechanism.

1. S. Datta and B. Das *Appl. Phys. Lett.* 56, 665 (1990)
2. T. Suzuki, M. Shiraishi, et al., *Appl. Phys. Exp.* 4, 023003 (2011)
3. M. Kameno et al., *Appl. Phys. Lett.* 101, 122413 (2012)
4. M. Kameno et al., *Appl. Phys. Lett.* 104, 092409 (2014)
5. T. Sasaki and M. Kameno et al., *Phys. Rev. Applied* 2, 034005 (2014)

MO.F.3_O2 - Spin pumping and spin-orbit effects in Ge

S. Oyarzun¹, F. Rortais¹, J.C. Rojas-Sánchez², P. Laczkowski², N. Reyren², C. Vergnaud¹, L. Vila¹, J.P. Attané¹, C. Beigné¹, C. Ducruet³, S. Gambarelli¹, J. Widiez⁴, A.K. Nandy⁵, S. Blügel⁵, H. Jaffrès², J.M. George², M. Jamet¹

1. *INAC/SP2M, CEA-Grenoble and Université Grenoble Alpes, Grenoble, France*

2. *Unité Mixte CNRS/Thales, Palaiseau, France*

3. *CROCUS Technology, Grenoble, France*

4. *LETI, CEA-Grenoble, Grenoble, France*

5. *Forschungszentrum Jülich, Jülich, Germany*

The field of spintronics is based on the manipulation of the spin degree of freedom. It uses the carrier spin angular momentum as a basic functional unit in addition to the charge. By combining charge and spin, a single electronic device could then integrate both logic and memory functions limiting power consumption and speeding up data processing. The first requirement of a semiconductor-based spintronic technology is the efficient generation of spin-polarized carriers into the device heterostructure made of Si or Ge (the materials of mainstream microelectronics) at room temperature. In this presentation, we focus on the generation of a sizeable spin population into Ge by spin pumping. Spin pumping corresponds to the generation of a pure spin current in the Ge film by exciting the ferromagnetic resonance of an adjacent ferromagnetic electrode with microwaves. The pure spin current is then detected using spin-orbit based effects. Our aim is to understand the basic mechanisms of spin pumping into Ge as well as the spin-to-charge conversion by inverse spin Hall effect (ISHE, bulk effect) and Rashba effect (interface effect). In particular, the influence of the doping type (n and p) and interface resistance on spin pumping-ISHE measurements in Ge will be shown. The influence of interface states is clearly demonstrated. Moreover, using the spin-split Rashba sub-surface states of the Ge(111) surface, we succeeded in demonstrating the giant conversion of a spin current generated by spin pumping into a charge current by the Rashba Edelstein effect. Our experimental findings are supported by ab-initio calculations.

MO.F.3_O3 - Impurity-assisted tunneling magnetoresistance: the physics behind electrical three-terminal Hanle experiments

O. Txoperena¹, Y. Song², L. Qing³, M. Gobbi^{1,4}, L.E. Hueso^{1,5}, H. Dery^{2,3}, F. Casanova^{1,5}

1. CIC nanoGUNE, Donostia - San Sebastian, Spain

2. Department of Electrical and Computer Engineering, University of Rochester, Rochester, United States

3. Department of Physics and Astronomy, University of Rochester, Rochester, United States

4. Université de Strasbourg, Institut de Science et d'Ingénierie Supramoléculaires (I.S.I.S.), Strasbourg, France

5. IKERBASQUE, Basque Foundation of Science, Bilbao, Spain

Injection of spins into semiconductors is essential for the integration of the spin functionality into conventional electronics. Insulating layers are often inserted between ferromagnetic metals and semiconductors for avoiding the conductivity mismatch and obtaining an efficient spin injection. This is the case when employing the so-called three-terminal (3T) setup, in which spin accumulation is induced and probed by a single magnetic tunnel contact, through the Hanle effect [1]. Since this geometry does not require submicron-sized fabrication processes, 3T-measurements have become very popular. However, it has been increasingly realized that the magnetoresistance (MR) reported depends much on the tunneling process and too little on the semiconductor [2,3].

In this work, we perform measurements with a 3T geometry on devices with aluminum-oxide sandwiched between different metallic electrodes [2,3]. First, we use two strategies for the tunnel barrier fabrication: single plasma-exposure oxidation, or multistep deposition and subsequent natural oxidation of aluminum thin films. The MR effect is observed in impurity-rich multistep tunnel barriers and suppressed in plasma-oxidized barriers where direct tunneling is dominant, meaning that the effect is entirely impurity-driven [3]. Second, we detect similar MR effects in ferromagnetic-insulator-nonmagnetic (FIN) and nonmagnetic-insulator-nonmagnetic (NIN) devices, demonstrating that spin accumulation is not being measured in our setup [3]. Last, we explain the observed MR effect with a theory that considers the magnetic-field-induced on/off switching of the tunneling current through impurities embedded in the tunnel barrier [3,4]. The reported effect is universal for any impurity-assisted tunneling process and provides an alternative interpretation to a widely used technique that employs the same ferromagnetic electrode to inject and detect spin accumulation.

[1] S.P.Dash et al., Nature 462, 491 (2009)

[2] O.Txoperena et al., Appl.Phys.Lett. 102, 192406 (2013)

[3] O.Txoperena et al., Phys.Rev.Lett. 113, 146601 (2014)

[4] Y.Song et al., Phys.Rev.Lett. 113, 047205 (2014)

MO.F.3_O4 - Spin noise spectroscopy of the spin hall effect

Y.V. Pershin¹, V.A. Slipko^{1,2}, N.A. Sinitsyn³

1. Department of Physics and Astronomy, University of South Carolina, Columbia, United States

2. Department of Physics and Technology, V. N. Karazin Kharkov National University, Kharkiv, Ukraine

3. Theoretical Division, Los Alamos National Laboratory, New Mexico, United States

While the method of semiconductor spin noise spectroscopy has attracted significant attention, it is not directly suitable to detect the spin Hall Effect in typical semiconductors. Recently, we have suggested a method of hybrid spin noise spectroscopy, which is based on a simultaneous analysis of spin and transverse voltage fluctuations [1]. One can show that in the spin Hall Effect regime, the spin fluctuations are dressed by charge dipoles that lead to the transverse voltage fluctuations. Therefore, the transverse voltage fluctuations (that could be measured electronically) correlate with the spin fluctuations (that could be measured optically). Moreover, the strength of the transverse voltage fluctuations is proportional to the spin Hall coefficient. These observations form the basis for the hybrid spin noise spectroscopy [1] that will be discussed in this talk from the theoretical point of view. We anticipate the potential of the spin noise spectroscopy to study the spin-charge coupling in semiconductors and other materials.

[1] V. A. Slipko, N. A. Sinitsyn, and Y. V. Pershin, Phys. Rev. B 88, 201102(R) (2013)

MO.G.1_I1 - A study of antiferromagnetic/ferromagnetic systems using X-ray magnetic dichroism

Z.Q. Qiu¹

1. University of California at Berkeley, Berkeley, United States

Epitaxial CoO/Fe/Ag(001) and NiO/Fe/Ag(001) systems allow an element-specific measurement of the ferromagnetic (FM) and antiferromagnetic (AFM) elements using X-ray Magnetic Circular Dichroism (XMCD) and X-ray Magnetic Linear Dichroism (XMLD), respectively. The response of the AFM spins to the FM spin rotation shows that the CoO spins consist of rotatable and frozen spins and that only the Fe uniaxial magnetic anisotropy follows the CoO frozen spins. For the softer NiO AFM materials, we show that the NiO spins can form a Mauri domain wall in Fe/NiO/Fe as the two Fe layer magnetizations twists. However, the Mauri domain wall forms only up to ~90 degree twisting angle, at which the NiO domain switches its chirality and unwinds as the twisting angle increases from 90 to 180 degrees. This result explains why the AFM order could induce a strong uniaxial anisotropy but a weak exchange bias in the FM layer.

MO.G.1_O2 - Topologically protected magnetic helix for energy storage

E. Vedmedenko¹

1. University of Hamburg, Hamburg, Germany

The novel generation of computers is supposed to be based on logical elements made of chains of magnetic atoms or nanomagnets. Any logical elements require energy supply, but use the energy not all the time. A key issue for technology's competitiveness is to figure out how to store energy when it isn't used. Here, we discover that it can be stored in magnetic helices with integer number of revolutions corresponding to the stationary states of a chain of magnetic elements coupled via the antiferromagnetic exchange, the dipolar or the RKKY interaction [1]. Based on simulations and a benchmarked prototype, this finding permitted to propose a magnetic energy storing element. To store energy one has to rotate one of the end-nanomagnets in a chain until the helix will click into one of the stationary states. At the later time the end-element may be released to deliver the energy on demand. The longer is a chain, the larger number of rotations can be stored. The stable magnetic helices can be also used to transfer information. To do so, one has to read out when a knot, created at one end of the chain will arrive at the other chain's end. The main advantage of the proposed concept is its scalability from the macro- to the atomic scale and applicability to the great diversity of systems with different interactions like e.g. magnetic multilayers, magnetic or molecular nanoarrays and colloids.

[1] E. Y. Vedmedenko, D. Altwein, Phys. Rev. Lett. 112, 083012 (2014)
<http://journals.aps.org/prl/abstract/10.1103/PhysRevLett.112.017206>

MO.G.1_O3 - Atomistic spin dynamics and effective models of AFM/FM multilayer systems

I. Stockem¹, C. Schröder¹, G. Reiss²

1. *Department of Engineering Sciences and Mathematics, University of Applied Sciences Bielefeld, Bielefeld, Germany*

2. *Department of Physics, Center for Spinelectronic Materials and Devices, Bielefeld University, Bielefeld, Germany*

Antiferromagnets (AFM) are of growing interest for spintronic applications. Traditionally they are used as passive elements to statically fix the magnetization of the ferromagnetic (FM) layer in spin valves and magnetic tunnel junctions by exchange bias [1]. We have investigated two stacks, where the AFM plays a key role as an active element. The first system is a Co/Cr₂O₃ stack with a perpendicular anisotropy (PEB) and a switchable exchange bias [2]. Here the AFM is used to pin the magnetization of the FM and a strong field pulse can reverse the exchange bias direction.

The second system is a NiFe/IrMn/MgO/Pt stack showing spin-valve-like magnetoresistance [3]. The huge magnetoresistance is based on the tunneling anisotropic magnetoresistance effect of the IrMn/MgO interface (AFM-TAMR) in combination with the rotation of the antiferromagnetic moments that are pinned to the magnetic moments of the FM layer. Depending on the geometry and the interactions within and between layers, the AFM pins the FM magnetization or the FM rotates the AFM magnetization. We have studied the magnetization dynamics of these FM-AFM stacks subject to an external field for the two systems described above. We will discuss first a simplified effective model that can identify the basic mechanisms of the magnetization dynamics. Next, we will compare these results with atomistic spin dynamics simulations of the full scale systems [4]. To include finite temperature effects, we couple the system to a heat bath. The results show, that the orientation of the magnetic moments can be quite complex depending on the next neighbor interactions.

[1] S. S. P. Parkin, in *Spin Dependent Transport in Magnetic Nanostructures*, Taylor and Francis, London (2002)

[2] Y. Shiratsuchi et al., *Appl. Phys. Lett.* 100, 262413 (2012)

[3] B. G. Park et al., *Nature Materials*, Vol. 10, 2983 (2011)

[4] I. Stockem, S. Muschak, C. Schröder, DPG Spring Meeting 2015, Mar. 15-20, Berlin

MO.G.1_O4 - Enhancement of Blocking Temperature of Cr₂O₃/Co Perpendicular Exchange Coupling System with Thin Cr₂O₃ Layer

T. Nozaki¹, N. Shimomura², S.P. Pati³, M. Sahashi⁴

1. Tohoku University, Miyagi Prefecture, Japan

Magnetization reversal using Magneto-electric (ME) effect and perpendicular exchange bias (PEB) in antiferromagnetic (AF) Cr₂O₃ thin film has been established [1]. For the applications, thin Cr₂O₃ is required. But with decreasing thickness, blocking temperature (TB) of PEB in thin Cr₂O₃/Co exchange coupling system decreases due to the product of AF anisotropy and thickness (KAF*tAF) become smaller than exchange coupling energy JK [2]. To obtain sufficient TB using thin Cr₂O₃ layer, increase of AF anisotropy KAF is essential. In this study, we tried to enhance the TB in thin Cr₂O₃ layer by inducing lattice strain.

Sample design is c-Al₂O₃ sub. /Pt 25 or Fe₂O₃ 20/ Cr₂O₃ 20/metal spacer/Co 1/Pt 5 (nm). Samples are fabricated by using a RF-DC magnetron sputtering. Magnetic properties were measured by SQUID magnetometer. Structural characterizations were performed by XRD and TEM measurement. Metal spacer is inserted at Cr₂O₃/Co interface to control the exchange coupling energy JK. A higher TB was obtained in Fe₂O₃-buffered Cr₂O₃ sample compared with Pt- buffered sample, while the exchange coupling energies of both samples are almost identical. . In case of Pt-buffer, TB was limited to 150 K. On the other hand, much higher TB (~260 K) was obtained for Fe₂O₃-buffered sample. ~260 K was almost identical to the Neel temperature TN of this sample. Since the change in TB correlate with change in the lattice parameters, we believe this is due to the enhancement of KAF by lattice strain. That is, we succeed to obtain TB ~ TN using only 20nm thick Cr₂O₃ layer. This work was partly funded by ALCA Program of JST and ImPACT Program of Council for Science, Technology and Innovation (Cabinet Office, Japan Government).

[1] T. Ashida et al., Appl. Phys. Lett., 104, 152409 (2014)

[2] Y. Shiratsuchi et al., Appl. Phys. Express, 3, 113001 (2010)

MO.G.1_O5 - A quantitative description of the bias-field and coercive field in exchange-bias systems. Application to Mn₂Au

D. Givord^{1,2}, V.M.T.S. Barthem², A.Y. Ramos¹, H.C.N. Tolentino³, L.E. Fernández-Outon⁴, F. Herrera-Aragón⁵, W.A.A. Macedo⁵, A. Bernard-Mantel¹, L. Ranno¹

1. CNRS/Univ. Grenoble-Alpes, Institut Neel, Grenoble, France

2. Instituto de Física, Universidade Federal do Rio de Janeiro, Rio de Janeiro, Brazil

3. Laboratório Nacional de Luz Síncrotron, LNLS/CNPq, Campinas, Brazil

4. Departamento de Física, Universidade Federal de Minas Gerais, Belo Horizonte, Brazil

5. Laboratório de Física Aplicada, Centro de Desenvolvimento da Tecnologia Nuclear, Belo Horizonte, Brazil

Exchange-bias describes the peculiar magnetic properties characterizing exchange-coupled antiferromagnetic-ferromagnetic (AFM-FM) systems: shifted hysteresis cycle and additional ferromagnetic coercivity. It is attributed to the existence of some un-compensated magnetic moments in the antiferromagnetic material at the interface with the ferromagnetic one. The establishment of exchange-bias requires that a uniaxial direction be defined e.g. cooling under an applied magnetic field. Beyond this qualitative understanding, exchange-bias resists a quantitative description.

In the present study, we demonstrate that reversal of the ferromagnetic layer moment is fundamentally different whether it occurs from the “positive” initial orientation (defined by the field applied during cooling) or from the “negative” reversed orientation. This is due to moment reconfiguration under the effect of the interfacial AFM-FM coupling, which occurs for the negative orientation of the ferromagnetic layer, and transforms the reversed state, usually assumed to be a state of maximum coupling energy, into a metastable magnetic state. A simple expression is derived relating the bias-field, H_{eb} , and the coercive field, H_c .

At finite temperature, another phenomenon is involved in the magnetization processes of exchange-bias systems, namely thermal activation, which is acting on essentially exchange-decoupled AFM grains, as discussed in particular by O’Grady et al. [1]. Taking both above phenomena into account, a quasi-quantitative description of the temperature dependence of both H_{eb} and H_c is demonstrated for two different exchange-bias samples, involving antiferromagnetic Mn₂Au. The generality of the model will be further discussed.

[1] K. O’Grady, L.E.Fernández-Outon, G.Vallejo-Fernández J. Magn. Mater. 322, 883 (2010)

MO.G.2_I1 - Accelerated discovery of high-performance magnets

S. Sanvito¹

1. School of Physics, AMBER and CRANN Institute, Trinity College, Dublin, United Kingdom

Magnetic materials underpin a vast and diverse range of modern technologies, going from data storage to energy production and use. However, the choice of magnets for mainstream applications is limited to a few dozens and the development of a new high-performance magnetic compound is a long and often unpredictable process. Here we describe a systematic pathway to the discovery of novel magnetic materials for multiple applications, which demonstrates an unprecedented throughput and speed up in the discovery process. We have constructed a massive electronic structures library for Heusler alloys containing 236,856 materials. We have then extracted those magnetic compounds with specific electronic properties, such as half-metallicity and large magnetization density, and finally established whether these can be fabricated at thermodynamical equilibrium. A full analysis for stability has been carried out on a sub-set of 36,000 intermetallic Heuslers. This has identified 249 stable, including 21 new magnets. Our work paves the way for large scale design of novel magnetic materials at unprecedented speed.

MO.G.2_O2 - Cluster monte carlo algorithms for fept hamiltonianA. Lyberatos¹, G. Parker²1. *University of Crete, Crete, Greece*2. *HGST, a Western Digital Company, San José, United States*

The temperature dependence of the magnetization, susceptibility and specific heat of FePt in the critical region close to T_c is required for calculation of critical exponents and for multiscale modeling. The accuracy of single flip (Metropolis) Monte Carlo algorithms is limited by a) the critical fluctuations of the magnetization and energy and b) the divergence of the correlation time $\tau \sim \xi^z$, where ξ is the bulk spin correlation length and z is the dynamic exponent (critical slowing down). Critical fluctuations are an innate physical feature of any model, however, cluster flipping algorithms were proposed to solve the problem of critical slowing down for Ising and Heisenberg Hamiltonians with nearest neighbor interactions [1] and Ising models with long range interactions [2].

The case of a Heisenberg Hamiltonian with long range interactions has not been treated to our knowledge before. The classical spin Hamiltonian of FePt [3] also includes magnetic anisotropy and antiferromagnetic exchange coupling for some Fe-Fe pairs. We developed hybrid Metropolis/Swendsen-Wang and Metropolis/Wolff algorithms for FePt. Cluster moves must preserve the anisotropy energy and Metropolis steps are included to satisfy the requirement of ergodicity. The temperature dependence of the magnetization (Fig.1) and susceptibility are found to be in good agreement with the Metropolis algorithm, so the algorithms also satisfy the detailed balance condition. The Wolff algorithm has the advantage of reduced memory requirements. An estimate of the dynamic exponent $z = 2.13 \pm 0.05$ was obtained by plotting the correlation time as a function of grain size (Fig.2) at the Curie temperature for bulk FePt estimated as $T_c=677$ K [4]. It is shown that in the critical region the results are affected by the presence of a percolation cluster involving most of the spins in the grain, and we discuss efforts to control the cluster size using Niedermayer's algorithm.

References:

[1] U.Wolff, PRL 62, 361 (1989)

[2] K. Fukui and S. Todo, J. Comp. Phys. 228, 262 (2009)

[3] O. N. Mryasov, U. Nowak, K. Y. Guslienko and R.W. Chantrell, Europhys. Lett. 69, 805 (2005)

[4] O. Hovorka et al., APL 101, 052406 (2012)

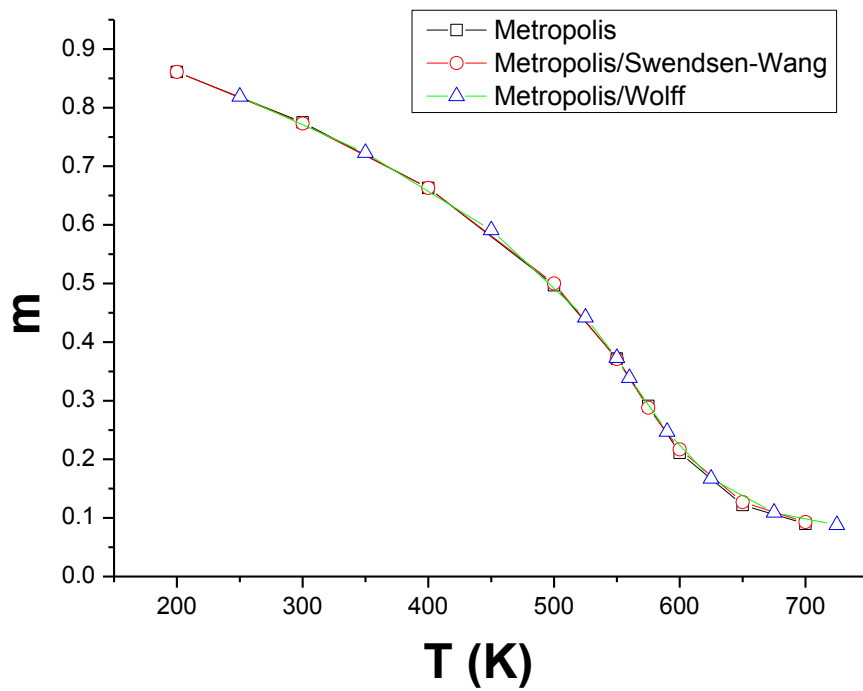


Fig.1 Temperature dependence of the reduced magnetization $m=M(T)/M(0)$ and a FePt grain.

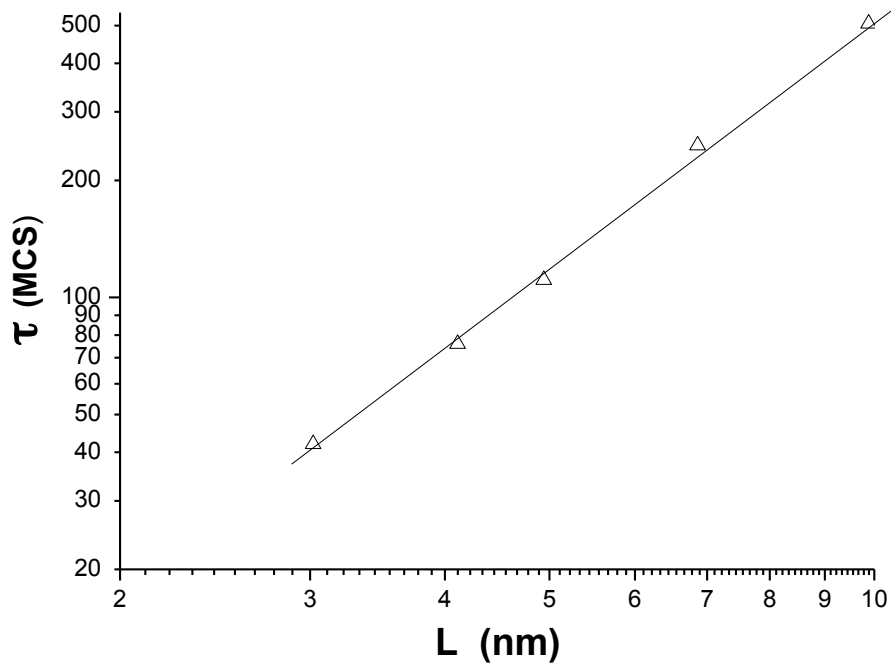


Fig.2 Correlation time (τ) of the fluctuations of the magnitude of the magnetization of a cubic FePt grain as a function of the grain size (L), plotted on a logarithmic scale. The Monte Carlo simulation was performed using the Metropolis/Wolff algorithm at the critical temperature $T_c=677$ K.

MO.G.2_O3 - Bimodal distribution of blocking temperature for exchange-bias ferromagnetic/antiferromagnetic bilayers: a granular Monte Carlo study with less stable magnetic regions spread over the interface

D. Ledue¹, G. Lhoutellier¹, R. Patte¹, F. Barbe¹, B. Dieny², V. Baltz²

1. GPM UMR 6634 CNRS-Université & INSA De Rouen, Saint-Étienne-du-Rouvray, France

2. SPINTEC, Univ. Grenoble-Alpes/CNRS/INAC-CEA, Saint-Martin-d'Hères, France

In exchange bias based devices, ferromagnetic/antiferromagnetic (F/AF) disordered interfacial spins which exhibit low freezing temperatures contribute to the alteration of the exchange bias properties. In particular, the blocking temperature distributions (DTB) earlier observed experimentally show two contributions: the common high-temperature peak due to the antiferromagnetic grain volume distribution and a less usual low-temperature contribution presumably attributed to disordered interfacial spins [1,2]. Here, our goal is to propose a granular level model which can reproduce bimodal DTB. To that purpose, the model includes small magnetic grains with weaker anisotropy and smaller interfacial coupling at the F/AF interface to account for the disordered interfacial spins. Then, the experimental 'Soeya et al' protocol [3] with a sufficiently low reference-temperature $T_m = 4K$ [1] is reproduced by Monte Carlo simulations to calculate the DTB. As a result, the bimodal character of blocking temperature distributions is reproduced and varying the amount of these smaller magnetic grains tunes the low-temperature contribution of the distribution. These simulations therefore validate the assumption that less stable magnetic regions spread over the F/AF interface may originate the bimodal character of DTB, as earlier brought forward by experimentalists to explain their results. In addition, because of the heterogeneities of the interface in presence of less stable small grains, our simulations show that such bilayers cannot be described using a simple model of uniform rotation of the ferromagnetic layer interacting with an average interfacial coupling [4].

[1] V. Baltz, B. Rodmacq, A. Zarefy, L. Lechevallier, and B. Dieny, Phys. Rev. B 81, 052404 (2010)

[2] K. Akmalidinov, S. Auffret, I. Joumard, B. Dieny, and V. Baltz, Appl. Phys. Lett. 103, 042415 (2013)

[3] S. Soeya, T. Imagawa, K. Mitsuoka, and S. Narishige, J. Appl. Phys. 76, 5356 (1994)

[4] G. Lhoutellier, D. Ledue, R. Patte, F. Barbe, B. Dieny, and V. Baltz, J. Phys. D: Appl. Phys. 48, 115001 (2015)

MO.G.2_I4 - Vortex nonlinear dynamics

C. Serpico¹, M. d'Aquino², S. Perna¹, A. Quercia¹

1. DIETI, University of Naples Federico II, Naples, Italy

2. Department of Engineering, University of Naples Parthenope, Naples, Italy

This work is devoted to the analysis of spin-torque nano-oscillators (STNOs) based on spin-valve structure with the free layer in a vortex state. This type of STNO promises to have an important role in forthcoming microwave communication technologies [1],[2]. In vortex-based STNOs, the magnetization oscillation typically occurs through a gyrotropic motion of the vortex and can be reasonably well described by a reduced set of variables such as the position of the vortex core. In order to design STNOs with sufficient emitted power, it is crucial to gain an understanding of the dynamics of such oscillators in regimes where the vortex is driven far from equilibrium, in nonlinear regimes. In this paper, we present a theoretical treatment of injection locking and nonlinear resonance of vortex oscillations, driven by AC injected currents and applied fields, based on a Thiele-like model of vortex core dynamics. By exploiting separation of time scales and using appropriate averaging technique[3], we derive equations which are applicable to the study of phase-locking for arbitrary large vortex core motion. The bifurcation diagram of nonlinear vortex core dynamics is obtained which enables one to have a comprehensive understanding of phase-locking and nonlinear resonance phenomena.

References:

[1] D. C. Ralph and M. D. Stiles, J. Magn. Mater. 320, 1190 (2008)

[2] P. Villard et al. IEEE J. Solid-State Circuits 45, 214

[3] N. N. Bogoliubov and Yu. A. Mitropolskii, Asymptotic Methods in the Theory of Nonlinear Oscillations. New York: Gordon and Breach, 1961

MO.G.3_O1 - Magnetic field dependence of phonons in the terbium gallium garnet

M. Mori¹, A. Spencer-Smith², O. Sushkov², S. Maekawa¹

1. *Japan Atomic Energy Agency, Ibaraki, Japan*

2. *University of New South Wales, Sydney, Australia*

When a magnetic field is applied perpendicular to a heat current in a terbium gallium garnet (TGG), $Tb_3Ga_5O_{12}$, a transverse temperature gradient is induced in the third perpendicular direction [1,2]. This is the ügphonon Hall effect (PHE)üh. Since the effect takes place at low temperature (~ 5 K) in the insulator, there are no mobile charges such as electrons nor holes to assist the thermal transport. Phonons are not charged and hence cannot be induced by the Lorentz force such as the Hall effect. Spin-orbit interaction for phonons is not obvious unlike the spin Hall effect for electrons. Furthermore, the TGG is a paramagnet around 5 K, at which the PHE is observed. Hence, one cannot expect a considerable contribution from magnons unlike the magnon Hall effect [3]. Therefore, an origin of the PHE is non-trivial and a fundamental question in condensed matter physics.

In this talk, we show that the PHE originates from the resonant skew scattering of phonons by quasi-doublet states at superstoichiometric Tb^{3+} ions [3]. Phonons interact with the crystal field due to the electrostatic interaction of lattice with electric multipole moments of the ion. Thus, the scattering of phonons can be attributed to the coupling of lattice strain and the quadrupole moments of Tb^{3+} ions. The phonon Hall angle (S), given by the ratio of off-diagonal and diagonal thermal conductivities divided by the magnitude of the magnetic field, is calculated using Boltzmann transport theory. Obtained magnitude of the effect is in agreement with experiments. It is also shown that S significantly grows with temperature, and a magnetic field can modulate the dispersion relation of phonons due to the coupling of lattice strain and the quadrupole moments of Tb^{3+} ions.

References:

[1] C. Strohm et al., Phys. Rev. Lett. 95, 155901 (2005)

[2] A. V. Inyushkin and A. N. Taldenkov, JETP Lett. 86, 379 (2007)

[3] Y. Onose et al., Science 329, 297 (2010). [4] M. Mori et al., Phys. Rev. Lett. 113, 265901 (2014)

MO.G.3_O2 - Magnetic susceptibility anisotropy in noncentrosymmetric CePt₃Si due to rashba-type spin-orbit coupling

B. Fak^{1,2}, V. Mineev²

1. *Institut Laue-Langevin, Grenoble, France*

2. *CEA and University, Grenoble Alpes, France*

Noncentrosymmetric metals with tetragonal structure are characterized by an antisymmetric Rashba-type spin-orbit interaction, which has been predicted to give rise to an anomalous spin susceptibility. We have studied the normal phase of the heavy-fermion unconventional superconductor CePt₃Si using polarized inelastic neutron scattering. Our measurements show a clear anisotropy in the spin susceptibility, in qualitative agreement with theoretical calculations based on the Hubbard model. The observed effect is larger than predicted, which may be due to the strong spin-orbit coupling of rare-earth heavy fermions.

MO.G.3_O3 - Distribution of relaxation times in the skyrmion compound Cu_2OSeO_3

I. Zivkovic^{1,2}, I. Levatic¹, V. Surija¹, H. Berger²

1. *Institute of Physics, Zagreb, Croatia*

2. *Institute of Condensed Matter Physics, Lausanne, Switzerland*

The investigation of skyrmions presents many challenging aspects to science. Some of the fundamental questions about the formation and the stability of the skyrmion lattice are still open, while at the same time there are several possible routes for the application of skyrmions, especially in spintronics. Skyrmions are whirls of spins, resembling the magnetic vortex in type-II superconductors. Skyrmions can form a long range ordered state called the skyrmion lattice, which can be found in several chiral magnets. The best known examples are conductive MnSi and insulating Cu_2OSeO_3 .

We present here the results of our investigation [1] of Cu_2OSeO_3 and the phase transitions that surround the skyrmion pocket. Although it has been suggested that the skyrmion lattice disintegrates through the first-order phase transition both into the paramagnetic (disordered) state as well as into the conical state, we have found a significant difference between the two. The conical-skyrmion lattice phase boundary is characterized by a wide dissipation region, as revealed by our high-sensitivity ac susceptibility measurements. Within the skyrmion phase one can follow a dissipation profile which demonstrates the presence of a distribution of relaxation times, usually found in spin-glass and superparamagnetic systems. Here, we present evidence that the distribution is intrinsic to the skyrmion lattice and not due to impurities.

References:

[1] I. Levatic, PRB 90, 224412 (2014)

MO.G.3_O4 - Guiding of a zigzag spin spiral by local uniaxial strain relief

P. Hsu¹, A. Finco¹, L. Schmidt¹, A. Kubetzka¹, K. von Bergmann¹, R. Wiesendanger¹

1. Department of Physics, University of Hamburg, Hamburg, Germany

Spin spirals typically result from competing magnetic interactions. In the presence of a sizable Dzyaloshinskii-Moriya interaction (DMI), the spin spirals exhibit a unique rotational sense and their periodicity is governed by the ratio of the exchange and DM-interaction strength. Here, we study the double-layer (DL) Fe grown on Ir(111) by means of spin-polarized scanning tunneling microscopy (SP-STM). We observe periodic reconstruction lines with a spacing of about 3.3-3.7 nm as a consequence of uniaxial strain relief induced by lattice mismatch. Using vectorial field-dependent spin mapping, a cycloidal spin spiral of a typical period of about 1.1 nm with unique rotational sense has been resolved. Interestingly, the spiral wavefronts are guided by the reconstruction lines, leading to three rotational domains. This is in contrast to the spin spirals found in the pseudomorphic area, which are propagating isotropically. Not only the wavevector of spin spirals is linked to the reconstruction lines, but also the wavefront is tied to the local symmetry of the atom arrangement which results in a zigzag shape. Furthermore, an atomic scale canting of spins with respect to reconstructions lines has been observed, which is proposed to originate either from DMI or alternatively from magneto-crystalline anisotropy. The zigzag spin spiral state is stable without magnetic phase transition under external out-of-plane field up to 9 Tesla.

MO.H.1_I1 - Spin-torque nanodevices for bio-inspired computing

J. Grollier¹

1. CNRS Thales, Palaiseau, France

Biological systems have impressive computing abilities. We, humans, are able to recognize people we barely know in just a fraction of second, even in a crowd. And we do this incredibly complex task with 10^4 times less power than any supercomputer! It therefore makes sense to take inspiration from biology to build data processing systems to perform low power 'cognitive' tasks on-chip and complement our traditional microprocessors. As biological systems, bio-inspired hardware should be composed of a huge number of computing nodes and connections in order to be efficient (there are 10^{11} neurons and 10^{15} synapses in the brain). While CMOS technology might appear as the most mature technique to build such systems, it suffers from the high number of transistors required to imitate synapses and neurons, and the related power dissipation issues. Fabricating devices that can emulate synapses and neurons at the nanoscale therefore appears as the key for the development of dense, efficient bio-inspired chips. In this talk, I will highlight that spin torque nanodevices, as multi-functional and tunable nonlinear dynamical nano-components, are interesting building blocks for the hardware implementation of bio-inspired models. In particular, they appear to be well suited for adapting on the nanoscale computing models inspired from the brain non-linear dynamics. I will describe the first steps that we achieved towards this long-term goal, including the realization of spin torques synapses, and noise-enhanced synchronization of stochastic oscillators.

MO.H.1_O2 - Current-induced spin orbit torques and magnetization switching in antiferromagnet/ferromagnet/oxide structures

B. Park¹

1. Kaist, Daejeon, republic of Korea

The utilization of antiferromagnetic (AFM) materials in spintronics as an active element has recently been reported in magnetic tunnel junctions and AFM memories. Moreover, an observation of a large inverse spin Hall effect (ISHE) demonstrates its sizable spin-orbit coupling (SOC). Those results imply that the AFM can replace heavy-metal (HM) as underlayer in the HM/ferromagnet(FM)/oxide based devices, which are intensively investigated because of the potentials in a low-power magnetization switching and a high speed domain wall motion. The spin Hall effect in HM layer and/or interfacial Rashba effect can generate so-called spin-orbit torque (SOT), of which magnitude and sign mostly relies on the SOC of the HM or HM/FM interface. Therefore, the non-negligible magnitude of the SOT from the AFM can be expected due to its large SOC.

In this work, we investigated the SOTs in a perpendicularly magnetized AFM IrMn/CoFeB/MgO heterostructures using harmonic lock-in measurements. It was observed that the sign of the SOT of the AFM IrMn underlayer is opposite to that of the Ta measured in Ta/CFB/MgO structure, implying a positive spin Hall angle of IrMn, while the magnitude of the SOT is comparable to that of Ta. We also performed switching experiments where an in-plane pulsed-current of 50us was applied while sweeping the longitudinal magnetic field. The magnetization of the samples can be switched by applying an in-plane current pulse and an in-plane magnetic field. The preferred magnetization direction for a certain current polarity and in-plane field direction is reversed as the IrMn layer is replaced with the Ta layer. Furthermore, we controlled the magnetization direction of the AFM layer and explored the effect on the SOTs and current-induced switching properties.

MO.H.1_O3 - Spin-orbit torque switching in a ferromagnet/antiferromagnet bilayer systemS. Fukami^{1,2}, C. Zhang³, S. DuttaGupta³, H. Ohno^{1,2,3,4}

1. CSIS, Tohoku University, Miyagi Prefecture, Japan
2. CIES, Tohoku University, Miyagi Prefecture, Japan
3. LNS, RIEC, Tohoku University, Miyagi Prefecture, Japan
4. WPI-AIMR, Tohoku University, Miyagi Prefecture, Japan

Spin-orbit torque (SOT)-induced magnetization switching[1-3] has attracted great attention due to its potential to be used in three-terminal spintronics devices that can achieve high-speed and high-reliability operation[4]. Up to now, the study on SOT switching has been focused on ferromagnet/non-magnet (FM/NM) bilayer structure. Here we show that ferromagnet/antiferromagnet (FM/AFM) bilayer system also exhibit the SOT large enough to induce magnetization switching. Furthermore, we elucidate the following two characteristics unique to the FM/AFM system: (I) ability to switch the perpendicular magnetization with no external field; (II) memristor-like behavior where the portion of reversed magnetization can be controlled in an analog manner.

We here study current-induced magnetization switching in Hall devices made of antiferromagnetic PtMn and ferromagnetic Co/Ni multilayer at room temperature. Magnetization curves of blanket films show that the Co/Ni multilayer has perpendicular easy axis with an in-plane unidirectional anisotropy originating from the exchange bias of PtMn layer. The magnetization switching at zero field is observed with the current density of about 6×10^{10} A/m², which is comparable to the one obtained in a Ta/CoFeB/MgO system with the same device geometry[3]. The direction of switching reverses when the direction of exchange bias is reversed or a large external field opposite to the bias is applied, indicating that Slonczewski-like SOT is the origin of the switching whose direction is determined by the exchange bias. Sign of the SOT is opposite to the Ta/CoFeB/MgO, which is consistent with a previous report on inverse spin Hall effect in PtMn[5]. We also find that the Hall resistance varies continuously with the magnitude of the applied current, indicating that the device works as a memristor, which is useful for bio-inspired computing.

This work was supported by R&D project for ICT Key Technology of MEXT, R&D Subsidiary Program of METI and ImPACT Program of CSTI.

References:

- [1] I. Miron et al. Nature 476, 189 (2011)
- [2] L. Liu et al. Science 336, 555 (2012)
- [3] C. Zhang et al. J. Appl. Phys. 115, 17C714 (2014)
- [4] S. Fukami et al. IEEE Trans. Magn.50, 3401006 (2014)
- [5] W. Zhang et al. Phys. Rev. Lett. 113, 196602 (2014)

MO.H.1_O4 - Magnetization manipulation by spin orbitronic effects in permalloy/heavy metal doped copper bilayers

M. Gabor¹, C. Tiusan¹, M. Belmeguenai², F. Zighem², S. Colis³, D. Lacour⁴, M. Hehn⁴

1. *Center for Superconductivity, Spintronics and Surface Science, Technical University of Cluj-Napoca, Cluj-Napoca, Romania*

2. *Laboratoire des Sciences des Procédés et des Matériaux, CNRS-Université Paris XIII, Villetaneuse, France*

3. *Institut de Physique et Chimie des Matériaux de Strasbourg (IPCMS), UMR 7504 UDS-CNRS and Université de Strasbourg (UDS-ECPM), Strasbourg, France*

4. *Institut Jean Lamour, CNRS, Université de Lorraine, Vandoeuvre, France*

Spin-orbit interaction (SOI) in heavy nonmagnetic metal/ferromagnetic metal bilayers attracted considerable interest due to the possibility to generate transverse pure spin currents via the spin Hall effect using in-plane charge currents. The spin current generated in the nonmagnetic layer diffuses in the ferromagnetic layer and exerts a torque on its magnetization. This provides important perspectives for novel spintronic devices with a spin torque control of magnetization switching.

Our study was performed in bilayers based on permalloy (Py) and a nonmagnetic adjacent layer constituted by a Cu conductive matrix doped with heavy metals impurities (Ir, Bi). As expected [1], this provides a large and tunable spin Hall angle via the extrinsic skew scattering contribution to the spin Hall effect. Prior to magneto-electric characterization, the samples have been lithographically patterned in stripes with Hall transverse contacts. Then, on these microstructures, a quasi-static technique has been used to evaluate the spin orbital field generated in Cu(Ir,Bi)/permalloy bilayers with different heavy metal impurity concentrations. This technique involves the generation of the spin orbital field by applying a direct current and the compensation of the spin orbital field using an external applied magnetic field [2]. Then, the statically measured spin-torque induced field in the Cu(Ir,Bi)/permalloy bilayer samples has been compared with the one measured in conventional [Pt (or Ta in the high resistive phase)]/permalloy bilayers [3,4]. We demonstrate similar orbital fields in less conventional Cu(Ir)/Py (60 A/m) as compared to the more conventional Pt/Py bilayers (80 A/m), at a charge current density of around 1010 A/m².

Eventually, the quasi-static magneto-electric characterization results in patterned stripes have been confronted with dynamic ferromagnetic resonance experiments. This correlated analysis demonstrates the direct correspondence between the spin pumping by spin-orbitronic effects and the Gilbert damping enhancement in permalloy layer adjacent to nonmagnetic metallic layers with enhanced SOI.

References:

[1] Y. Niimi et al., Phys. Rev. Lett. 106, 126601 (2011); Y. Niimi et al., Phys. Rev. Lett. 109, 156602 (2012)

[2] Xin Fan et al., Nat. Communications 4, 1799, (2013)

[2] I. M. Miron, et al., Nature 476, 189 (2011)

[3] L. Liu, Y. Niimi et al., Science 336, 555 (2012)

MO.H.1_05 - Spin-orbit torque induced magnetization switching in Ta/CoFeB/MgO heterostructure with a diameter down to 30 nmC. Zhang¹, S. Fukami^{2,3}, H. Sato^{2,3}, F. Matsukura^{1,2,4}, H. Ohno^{1,2,3,4}

1. Laboratory for Nanoelectronics and Spintronics, Research Institute of Electrical Communication, Tohoku University, Miyagi Prefecture, Japan

2. Center for Spintronics Integrated Systems, Tohoku University, Miyagi Prefecture, Japan

3. Center for Innovative Integrated Electronic Systems, Tohoku University, Miyagi Prefecture, Japan

4. WPI Advanced Institute for Materials Research, Tohoku University, Miyagi Prefecture, Japan

Recently, magnetization switching via spin-orbit torque (SOT) attracts increasing attention as a new switching method for magnetic tunnel junction devices¹⁻³, and much effort has been made on Ta/CoFeB/MgO system. Among them, a large discrepancy in the magnitude of switching current density J_{th} has been found¹⁻⁴, which may be related to the different device sizes and/or different measurement conditions. To address the origin of this discrepancy, we here systematically investigate SOT switching in Ta/CoFeB/MgO structures with various sizes (down to 30 nm) in various conditions.

We fabricate Hall devices from a film with a stack structure of substrate/Ta(5)/CoFeB(1.2)/MgO(1.5)/Ta(1) (nm), in which a CoFeB dot with various diameters D is prepared on a Ta channel. Switching probability P_{sw} is measured using pulsed currents with various durations τ under various in-plane magnetic fields H_x along the current direction. In the range $D = 30\sim 80$ nm, $J_{th} \sim 3 \times 10^{12}$ A/m² is almost independent of D at $\tau = 10$ ns and $\mu_0 H_x = 20$ mT. The obtained J_{th} is more than one order of magnitude larger than that of micrometer-sized devices where the switching is more likely to be initiated with nucleation reversal followed by domain wall motion. We analyze the τ dependence of P_{sw} for the device with a 40 nm dot by using a theoretical model⁵ with the effective spin Hall angle θ_{SH} , effective anisotropy field $\mu_0 H_K^{eff}$, and thermal stability factor $E/k_B T$ as adjustable parameters. As τ decreases from 100 μ s to 5 ns, θ_{SH} and $\mu_0 H_K^{eff}$ are almost constant (0.2 and 0.5 T), whereas $E/k_B T$ increases from 64 ± 11 to 98 ± 11 , reflecting the decrease of the Joule heating due to the high current density.

This work was supported by R&D project for ICT Key Technology of MEXT, R&D Subsidiary Program of METI, and ImpACT Program of CSTI.

References:

[1] I. M. Miron *et al.*, Nature 476, 189 (2011)

[2] L. Q. Liu *et al.*, Science 336, 555 (2012)

[3] M. Cubukcu *et al.*, Appl. Phys. Lett. 104, 042406 (2014)

MO.H.2_I1 - Spin pumping through a topological insulator probed by x-ray detected ferromagnetic resonance

A.I. Figueroa¹, A.A. Baker^{1,2}, L.J. Collins-McIntyre², G. van der Laan¹, T. Hesjedal¹

1. *Magnetic Spectroscopy Group, Diamond Light Source, Didcot, United Kingdom*

2. *Department of Physics, Clarendon Laboratory, University of Oxford, Oxford, United Kingdom*

In the field of spintronics, the generation of a pure spin current (without macroscopic charge flow) through spin pumping of a ferromagnetic (FM) layer is crucial for the new generation of dissipation-less devices. Microwave driven ferromagnetic resonance (FMR) can generate a pure spin current that enters adjacent layers, allowing for both magnetization reversal (through the spin transfer torque) and to probe of the spin coherence properties of non-magnetic (NM) materials. However, standard FMR is unable to study multilayer dynamics directly, since the measurement averages over the contributions of the whole system. The synchrotron radiation-based technique of x-ray detected FMR (XFMR), offers an elegant solution to this drawback, giving access to element-, site-, and layer-specific dynamical measurements in heterostructures [M. Marcham et al., Phys. Rev. B 87, 180403 (2013); G.B.S. Stenning et al., New J. Phys. 17, 013019 (2015)]. In this work, we present selected examples of how XFMR has provided unique information to understand spin pumping and spin transfer torque effects on magnetic heterostructures. We describe our most recent results of spin pumping through a topological insulator (TI) layer in a pseudo-spin valve heterostructure, where we demonstrate that TIs function as efficient spin sinks, while also allowing a limited dynamic coupling between ferromagnetic layers [A. A. Baker et al., Sci. Rep. 5, 7907 (2015)]. These results shed new light on the spin dynamics of this novel materials class, and suggest future directions for the development of room temperature TI-based spintronics.

MO.H.2_O2 - Control of the spin-wave relaxation in a magnetic insulator of macroscopic dimensions via spin-transfer torque

V. Lauer¹, D.A. Bozhko⁰, T. Brächer¹, P. Pirro¹, V.I. Vasyuchka¹, A.A. Serga¹, M.B. Jungfleisch³, M. Agrawal¹, Y.V. Kobljanskyj⁴, G.A. Melkov⁴, C. Dubs⁵, B. Hillebrands¹, A.V. Chumak¹

1. *Fachbereich Physik and Forschungszentrum OPTIMAS, Technische Universität Kaiserslautern, Kaiserslautern, Germany*

2. *Graduate School Materials Science in Mainz, Gottlieb-Daimler-Strasse 47, Kaiserslautern, Germany*

3. *Materials Science Division, Argonne National Laboratory, Argonne, Illinois, United States*

4. *Faculty of Radio Physics, Taras Shevchenko National University of Kyiv, Kyiv, Ukraine*

5. *INNOVENT e.V. Technologieentwicklung, Jena, Germany*

It was shown recently, that in the magnetic insulator yttrium iron garnet (YIG) the spin-wave damping can be controlled by means of spin-orbit torque (STT) [1]. For this purpose, a dc current was applied to an adjacent Pt layer generating a spin current via the spin Hall effect (SHE), that consequently transferred angular momentum into the YIG layer. In those studies, a micro-structured YIG/Pt disk of 5 μm diameter was used to demonstrate the damping control. However, one of the main advantages of the SHE-STT-based damping compensation is its predicted applicability to a system of macroscopic dimensions. Here, we present experimental studies of the SHE-STT-based spin-wave relaxation control in a YIG(100 nm)/Pt(10 nm) sample with dimensions 4 x 2 mm^2 . The change of the relaxation frequency with the applied dc current was determined from the investigations of the threshold of the parallel parametric instability [2]. The parametrically excited spin waves were detected by Brillouin light scattering (BLS) spectroscopy that allowed for the determination of the threshold values of the pumping magnetic field. The dc current, as well as the pumping magnetic field were pulsed (pulse duration to repetition time as 1:100), in order to avoid effects associated with parasitic heating. In contrast to [1], with the parallel pumping geometry we investigated the SHE-STT-based relaxation variation for spin waves with large wavenumbers of $k = 1\text{E}4$ rad/cm. We found that the relaxation frequency changes linearly with the dc current and can be tuned by $\pm 7.5\%$ for a current density of $5\text{E}10$ A/m², which was the largest current density used in the experiment. The tuning direction depends on the current direction with respect to the magnetizing field polarity.

References:

[1] A. Hamadeh et al., Phys. Rev. Lett. 113, 197203 (2014)

[2] C. W. Sandweg et al., Phys. Rev. Lett. 106, 216601 (2011)

MO.H.2_O4 - Low linewidth high frequency spin hall nano-oscillators

A. Awad¹, P. Dürrenfeld¹, A. Houshang¹, E. Lacocca¹, M. Ranjbar¹, R. Dumas¹, J. Akerman^{1,2}

1. *Department of Physics, University of Gothenburg, Göteborg, Sweden*

2. *Materials Physics, School of ICT, KTH-Royal Institute of Technology, Kista, Sweden*

The recent demonstration of so called Spin hall Nano-Oscillators (SHNOs)^{1,2} driven by pure spin currents has greatly increased the versatility of spin transfer torque (STT) driven devices. In comparison with the much more studied Spin Torque Nano-Oscillators (STNOs) where a spin-polarized current is injected in a current perpendicular to plane (CPP) geometry, the auto-oscillations in SHNOs are driven by a laterally injected spin currents in between two low-resistance needles, which allow for direct optical access to the magnetically active region. As a consequence, SHNOs allow for simultaneous measurement and characterization of their magnetization dynamics via wide range of different techniques ranging from electrical measurement to optical techniques such as micro-focused scanning Brillouin Light Scattering (u-BLS). What is not yet clear is the impact of the tilted field on the dynamics of such devices, and the nature and interplay mechanism of the multimode operation at room temperature. In order to study in depth the effect of field tilting and room temperature operation a sample SHNO device is prepared of thin bilayer with Py(5nm)/Pt(6nm). The spin injection is concentrated to a nanometric region via focusing the charge current flow in small region of the Pt. Here we, for the first time, demonstrate SHNO operation in tilted magnetic fields. We demonstrate improved spectral characteristics of the electrical signals with linewidths below 2 MHz at room temperature. The electrically detected modes are spatially resolved via u-BLS that permits the observation and the understanding of the excited modes. We show the existence of two different oscillation modes, a self-localised solitonic bullet mode and a field-localized linear mode. Micromagnetic simulations, using Mumax33, shed additional light on both modes and their mutual interplay, including significant mode-hopping between the two.

References:

1. Demidov, V. E. et al. *Nat. Mater.* 11, 1028 (2012)
2. Liu, R. H., Lim, W. L. & Urazhdin, S. *Phys. Rev. Lett.* 110, 147601 (2013)
3. Vansteenkiste, A. et al. *AIP Adv.* 4, 107133 (2014)

MO.H.2_O5 - Effect of spin-transfer-torque induced dynamics of a synthetic antiferromagnetic reference layer on a spin-torque diode spectrum

R. Matsumoto¹, H. Kubota¹, T. Yamaji¹, H. Arai¹, S. Yuasa¹, H. Imamura¹

1. National Institute of Advanced Industrial Science and Technology (AIST), Tokyo, Japan

Quantitative understanding of the spin-transfer-torque (STT) acting on a synthetic antiferromagnetic reference layer is important for the development of future spin-valve (SV) devices such as STT-MRAMs. The size of the SV devices tend to become smaller and smaller, and a large current pulse needs to be applied for a very fast magnetization switching. In such tough situations the STT induced magnetization dynamics in the reference layer cannot be neglected. Until now, the STT acting only on the free layer has been quantitatively understood by the spin torque diode (STD) effect [1]. Here, an RF current is rectified by the SV device which synchronizes the RF current and magnetoresistance oscillation caused by the STT [2]. In this study, the STD effect of the SV with the reference layer is theoretically analyzed [3]. Based on the macrospin model the analytical expression of the STD spectrum is derived. The obtained result enables us to analyze the STT acting on the reference layer. The peak of the STD spectrum at the resonance frequencies of the reference layer changes its sign depending on the magnitude of the STT which is generated by the RF current injected from the pinned layer.

This work was supported by JSPS KAKENHI Grant Number 25790045.

References:

- [1] H. Kubota et al., Nature Phys. 4, 37 (2007) and J. Sankey et al., Nature Phys. 4, 67 (2007)
- [2] A. A. Tulapurkar et al., Nature 438, 339 (2005)
- [3] R. Matsumoto et al. , Jpn. J. Appl. Phys. 53, 123001 (2014)

MO.H.3_O1 - Control of chaos in magnetic vortex structure formation

K. Lee¹, H. Han¹, S. Lee¹, M. Im², J. Hong³, P. Fischer²

1. School of Materials Science and Engineering, KIST-UNIST Ulsan Center For Convergent Materials, Ulsan National Institute of Science And Technology (UNIST), Ulsan, Republic of Korea

2. Lawrence Berkeley National Laboratory, United States

3. Daegu Gyeongbuk Institute of Science and Technology, Daegu, Republic of Korea

Novel spin textures such as magnetic vortex structures have recently been attracted much interests due to their interesting and unique non-trivial topological properties, but also for potential applications in information technologies due to increased storage densities with lower power consumption and robust high frequency oscillations with easy tuning methods. An important milestone to utilize such systems in applications is a fully reliable control of vortex structures, which requires a complete understanding and controlling of the dynamic behavior in their formation process. It has been known that a chirality of vortex can be controlled by forming vortex structures in asymmetric circular nanodisks; the chirality is determined by the saturation direction before a forming of vortex structures from the saturation states under in-plane magnetic field, whereas the polarity occurs randomly during the formation of vortex structure. From our micromagnetic simulations, it is found that the typical behavior of chaos, known as the butterfly effect, in vortex polarity formations on asymmetric disks. Very small fluctuation of initial spin configuration can affect the whole dynamic process of vortex formation and thus, the polarity occurs randomly. However, we found that the resultant polarity direction can be manipulated by applying very small external in-plane magnetic fields with a few Oe along the perpendicular direction to the saturation direction; the direction of the external in-plane magnetic field determines the polarity of the vortex structure. Interestingly, such small external fields do not vary the formation dynamics but choose the way of formation dynamics to one polarity. They turn the polarity formation process in asymmetric nanodisks into deterministic one. Our results offer fundamental understandings on chaos in spin structure formations as well as novel methods to manipulate by means of controlling the chaos.

MO.H.3_O2 - Skyrmions at room temperature: From magnetic thin films to magnetic multilayers

C. Moreau-Luchaire¹, C. Moutafis², N. Reyren¹, J. Sampaio¹, N. Van Horne¹, C. Vaz², K. Bouzehouane¹, K. García¹, C. Deranlot¹, P. Warnicke¹, P. Wöhlhüter², J.M. George¹, M. Weigand³, J. Raabe², V. Cros¹, A. Fert¹

1. Unité Mixte CNRS/Thales and Université Paris Sud, Palaiseau, France

2. Swiss Light Source, Paul Scherrer Institute, Villigen, Switzerland

3. Max Planck Institute for Intelligent Systems, Stuttgart, Germany

Facing the ever-growing demand for data storage will most probably require a new paradigm. Magnetic skyrmions are anticipated to solve this issue as they are arguably the smallest spin textures in magnetic thin films in nature. Numerical simulations have shown that the interfacial Dzyaloshinskii-Moriya interaction (DMI) can stabilize such skyrmions in nanoscale disks or tracks for a large range of DMI amplitudes. We designed cobalt-based multilayered thin films where the cobalt layer is sandwiched between two heavy metals providing additive interfacial DMI. We acquired maps of the magnetization by using scanning transmission X-ray microscopy combined with the XMCD effect at different perpendicular magnetic fields, evidencing magnetic bubble-like domains in these multilayers. From two different analysis of the magnetic domain configurations, we evaluate a DMI amplitude as large as 2 mJ/m² in Pt|Co|Ir. The good agreement of the size dependence and the stability of the bubble domains are strong evidences that these domains are skyrmions. The value of D is further confirmed by studying the typical width of the worm domains observed at zero magnetic field, indicating consistency in the analysis. This discovery of stable skyrmions at room temperature in a technologically relevant material opens the way for device applications in a near future.

MO.H.3_O3 - Broadband microwave spectroscopy on the skyrmion lattice phase of different chiral magnets

D. Grundler¹, I. Stasinopoulos², J. Waizner³, M. Garst³, A. Bauer⁴, S. Weichselbaumer², H. Berger⁵, T. Schwarze², C. Pfleiderer⁴

1. *Institut des Matériaux, École Polytechnique Fédérale de Lausanne, Lausanne, Switzerland*

2. *Lehrstuhl für Physik funktionaler Schichtsysteme, Technische Universität München, Munich, Germany*

3. *Institute of Theoretical Physics, University of Cologne, Köln, Germany*

4. *Lehrstuhl für Topologie korrelierter Systeme, Technische Universität München, Munich, Germany*

5. *Institut de Physique de la Matière Complexe, École Polytechnique Fédérale de Lausanne, Lausanne, Switzerland*

Recently topological spin solitons, so-called skyrmions, have been discovered in chiral magnets. Strikingly, the skyrmions have been evidenced in all three materials classes needed for modern information technology, i.e., metallic, semiconducting and insulating materials. It has already been argued that such nanoscale spin structures might allow for advanced storage or high-frequency device concepts that exploit the exceptional emergent electrodynamics of these compounds. For this, an accurate and unified quantitative account of the dynamics and resonant responses induced by microwave fields is key.

We report broadband spectroscopy of the collective spin excitations in the metallic, semiconducting and insulating chiral magnets MnSi, Fe_{1-x}CoxSi and Cu₂OSeO₃, respectively. Using differently designed coplanar waveguides (CPWs) and a cryogenic magnetocryostat we explore the resonant eigenmodes across the entire magnetic phase diagrams depending on temperature and magnetic field strength. We observe that the spectral weights of different modes expected for the skyrmion lattice phase depend decisively on the design of the CPW and the orientation of the bulk chiral magnets. Our observations are in agreement with a theoretical approach taking into account dipolar interactions [1]. Using two material-specific parameters that quantify the chiral and the critical field energy we achieve a precise quantitative modelling. The detailed understanding of both eigenfrequencies and the spectral weight of modes is relevant for purpose-designed applications based on the resonant response of the different chiral magnets with tailored electric conductivity.

Financial support through DFG TRR80, SFB608, German Excellence Cluster Nanosystems Initiative Munich, TUM Graduate School, and ERC-AdG (291079 TOPFIT) is gratefully acknowledged.

References:

[1] T. Schwarze et al., *Nature Mater.* (2015), doi:10.1038/nmat4223

MO.H.3_O4 - Observation of local magnetization dynamics in helimagnetic FeGe

P. Schönherr¹, A. Dussaux¹, K. Chang¹, N. Kanazawa², Y. Tokura⁰, C. Degen¹, M. Fiebig¹, D. Meier¹

1. *ETH Zürich, Zürich, Switzerland*
2. *University of Tokyo, Tokyo, Japan*
3. *Riken, Wako, Japan*

Magnetic whirls, so-called skyrmions, emerge in various chiral magnets and attract tremendous attention due to their exotic properties. For example, skyrmions can be moved at ultra-low current densities and give rise to the topological Hall Effect. Despite the intense research on skyrmion materials little is known about their actual magnetic ground state. This includes fundamental aspects such as the thermal stability, local magnetization dynamics, spin-defect interactions and related consequences for their technological utilization. The fragmented knowledge is partially due to the challenging experimental access and the general difficulty to image antiferromagnetic order at the nanoscale.

Here, we present spatially resolved investigations of the helimagnetic ground state in the skyrmion system FeGe using magnetic force microscopy (MFM) and diamond nitrogen-vacancy (NV) center magnetometry. Our MFM measurements reveal local temperature-driven changes in the magnetic domain structure as well as jump-like collective movements of the helical spin texture. By using single NV centers as non-invasive nano-probe, we demonstrate that these magnetization dynamics are intrinsic to the spin system. We attribute the detected variations in the magnetic microstructure to thermally activated Barkhausen jumps that occur due to spin-defect interactions. Such Barkhausen jumps are usually neglected regarding the performance of magnetic bulk materials, but may play a vital role for the use of skyrmions and helimagnetism in future nanotechnologies.

MO.I.1_I1 - Room-temperature edge magnetism in graphene nanoribbons

L. Tapasztó¹, G. Magda¹, I. Hagymasi², P. Vancso¹, C. Hwang³, L. P. Biro²

1. *Hungarian Academy of Sciences - 2D Nanoelectronics Research Group, Budapest, Hungary*

2. *Wigner Research Centre for Physics - Institute of Solid State Physics and Optics, Budapest, Hungary*

3. *Korea Research Institute of Standards and Science - Center for Nanometrology, Daejeon, South Korea*

Atomic vacancies of the graphene lattice are known to host unpaired spins. However, it is not clear under which conditions such magnetic moments can couple together to form long-range magnetic order. Here we propose that in contrast to random defect distributions, atomic scale engineering of graphene edges with precisely zigzag crystallographic orientation - comprising edge atoms only from one sub-lattice of the bipartite graphene lattice - can give rise to a robust magnetic order along the edges. We employ a nanofabrication technique [1] based on Scanning Tunneling Microscopy to define graphene nanoribbons with such edge orientation. Tunneling spectroscopy investigations revealed a sharp semiconductor-metal transition for zigzag graphene nanoribbons as a function of their width. This has been identified as a signature of magnetic order emerging along the ribbon edges. The transition was attributed to the switching of the magnetic coupling between opposite ribbon edges from antiferromagnetic to ferromagnetic configuration [2].

References:

[1] L. Tapasztó et al. *Nature Nanotechnol.* 3, 397 (2008)

[2] G.Z Magda and L. Tapasztó, *Nature* 514, 608 (2014)

MO.I.1_O2 - Emergent one-dimensional magnetism in a metal and a semiconductor

I. Zaliznyak¹, A. Savici², O. Garlea², S. Chang³, R. Hu¹, C. Petrovic¹

1. *CMPMSD, Brookhaven National Laboratory, New York City, United States*

2. *NSD, Oak Ridge National Laboratory, Oak Ridge, United States*

3. *NIST Center for Neutron Research, Gaithersburg, United States*

The nature of magnetism which emerges in strongly correlated metals and semiconductors presents one of the most challenging and fundamental problems in physics of these systems. It is also widely believed to be of profound practical importance, rendering much of their fascinating behaviors, such as the unconventional high-temperature superconductivity, and others. Here we report a neutron scattering studies of the $\text{Fe}(1-x)\text{Cr}(x)\text{Sb}_2$ materials, where an unusual one-dimensional magnetic dynamics emerges as material evolves from a parent material, a partially metallic narrow-gap semiconductor FeSb_2 , to a wide-gap semiconductor CrSb_2 , which is a quasi-one-dimensional (1D) $S=1$ spin-chain system. The magnetic response emerges at $x \sim 0.5$, where the material has an effectively half-filled band, and one could naively expect $S=1/2$ spin system. We, however, observe an unusual dynamical magnetic response of quasi-1D nature, where magnetic susceptibility likely originates from local spins, whose interactions nevertheless are determined by the Fermi surface nesting properties. Our observations are perhaps the first case where the emergent magnetic dynamics in a doped metal/semiconductor can be uniquely identified with an interplay of strong correlation and Fermi surface nesting, eventually rendering an unusual quasi-1D spin system.

MO.I.1_O3 - Longitudinal and transverse zeeman ladders in the ising-like chain antiferromagnet $\text{BaCo}_2\text{V}_2\text{O}_8$

S. Petit¹, B. Grenier², V. Simonet³, L.P. Regnault², S. Raymond², B. Canals³, E. Canevet⁴, C. Berthier⁵, P. Lejay³

1. LLB, CEA-CNRS, Gif Sur Yvette, France

2. CEA, INAC-SPSMS, Grenoble, France

3. CNRS, Institut Néel, Grenoble, France

4. Institut Laue-Langevin, CS 20156, Grenoble, France

5. CNRS, Laboratoire National des Champs Magnétiques Intenses, Grenoble, France

The nature of the excitations in spin half antiferromagnets is a topic of considerable current interest in the field of quantum magnetism. The one-dimensional case is especially interesting as quantum fluctuations melt the classical long-range Néel order. The ground state remains disordered, with a spin excitation spectrum consisting of a continuum composed of pairs of spinons. Physical realizations of 1D systems, however, eventually order at very low temperature, owing to a small coupling between chains. The metamorphosis of the continuum of spinons that accompany this dimensional crossover towards a 3D state is an appealing issue. In this context, we explore the spin dynamics emerging from the Néel phase of the chain compound antiferromagnet $\text{BaCo}_2\text{V}_2\text{O}_8$ [1,2]. Our inelastic neutron scattering study reveals unconventional discrete spin excitations, so called Zeeman ladders, understood in terms of spinon confinement, due to the interchain attractive linear potential. These excitations consist of two interlaced series of modes, respectively, with transverse and longitudinal polarization. The latter, which correspond to a longitudinal fluctuation of the ordered moment, have no classical counterpart and are related to the zero-point fluctuations that weaken the ordered moment in weakly coupled quantum chains. Our analysis reveals that $\text{BaCo}_2\text{V}_2\text{O}_8$, with moderate Ising anisotropy and sizable interchain interactions, remarkably fulfills the conditions necessary for the observation of discrete long-lived longitudinal excitations [2].

References:

[1] E. Canevet, B. Grenier, M. Klanjšek, M. Horvatić, C. Berthier, V. Simonet, and P. Lejay, Phys. Rev. B 87, 054408 (2013)

[2] B. Grenier, S. Petit, V. Simonet, E. Canevet, L. P. Regnault, S. Raymond, B. Canals, C. Berthier, and P. Lejay, Phys. Rev. Lett. 114, 017201 (2015)

MO.I.1_O4 - Pressure-induced quantum phase transitions in low-dimensional organic quantum magnets

J. Möller¹, G. Perren¹, A. Mannig¹, A. Zheludev¹

1. ETH Zürich, Zürich, Switzerland

We discuss several spectacular examples of pressure-induced quantum phase transitions in low-dimensional organic quantum magnets. Organic systems offer 'soft' molecular frameworks and more accessible energy scales compared to inorganic oxides and thus enable a strong coupling between lattice and magnetism, providing a fruitful playground for exploring quantum critical physics. We will focus on the pressure-induced quantum phase transition in the frustrated quantum spin liquid piperazinium hexachlorodocuprate (PHCC). Recent MuSR experiments on PHCC have shown the existence of a quantum critical point (QCP) around 4.3 kbar separating the low-pressure quantum spin liquid from high-pressure magnetically ordered phases [1]. This work was in apparent contradiction with previous inelastic neutron scattering (INS) experiments [2] which observed no closing of the gap in this pressure range. In very recent INS experiments, we have observed Goldstone modes in the dynamic structure factor at 10 kbar [3]. This demonstrates long-range (magnetic) order at this pressure, in good agreement with the MuSR findings and the presence of a pressure-induced quantum critical point at moderate pressure [1]. We suggest an explanation for the apparent contradiction with the previous INS study [2]. Our discussion on PHCC will be complemented with other recent examples from our group concerning the study of QPTs in a number of organic quantum magnets using a range of techniques.

References:

- [1] M. Thede et al., Phys. Rev. Lett. 112, 087204 (2014)
- [2] T. Hong et al., Phys. Rev. B 82, 184424 (2010)
- [3] G. Perren et al. (in preparation)

MO.I.1_05 - Phonon-modulated magnetic interactions and spin Tomonaga-Luttinger liquid in the p-orbital antiferromagnet CsO₂

M. Klanjsek^{1,2}, D. Arcon^{1,3}

1. Jozef Stefan Institute, Ljubljana, Slovenia

2. EN-FIST Centre of Excellence, Ljubljana, Slovenia

3. Faculty of Mathematics and Physics, University of Ljubljana, Ljubljana, Slovenia

Quantum magnetism is a term encompassing phenomena like Tomonaga-Luttinger liquid, Bose-Einstein condensation of magnons or spin-liquid behavior, which occur in d-orbital electron systems where spins are decoupled from orbital and lattice degrees of freedom. In p-orbital electron systems, such a decoupling is not possible due to a stronger interplay of various degrees of freedom, a prototypical example being molecular solids based on magnetic O₂⁻ magnetic anions: alkali superoxides, AO₂ [1], and alkali sesquioxides, A₄O₆ [2] where A is the alkali metal. A recent important X-ray and Raman scattering study of CsO₂ demonstrated the ordering of O₂⁻ p orbitals below the structural phase transition at 70 K, which leads to the formation of one-dimensional antiferromagnetic spin-1/2 chains in an otherwise two-dimensional magnetic lattice [1]. Using nuclear magnetic resonance, we show that the low-temperature phase of CsO₂ exhibits a Tomonaga-Luttinger-liquid behavior, while the librations of O₂⁻ 'dumbbells' in the high-temperature phase lead to a strongly temperature-dependent magnetic exchange interactions [3]. These are, respectively, the first example of quantum magnetism in a p-orbital system and the first demonstration of the phononic modulation of magnetic interactions, a phenomenon proposed in the 1970s that may be relevant for a range of other molecular solids.

References:

[1] S. Riyadi et al., Phys. Rev. Lett. 108, 217206 (2012)

[2] D. Arcon, K. Anderle, M. Klanjsek et al., Phys. Rev. B 88, 224409 (2013)

[3] M. Klanjsek et al., arXiv:1409.4818 (2014)

MO.I.2_I1 - Strong magneto-chiral dichroism detected by hard X-rays in a molecular helixR. Sessoli¹, A. Rogalev², F. Wilhelm², M.E. Boulon¹, M. Mannini¹, L. Poggini¹, A. Caneschi¹ N1. *University of Florence, Florence, Italy*2. *ESRF, Grenoble, France*

Chiral magnetic structures have been recently the focus of intense research because they offer the possibility to store information in topological protected structures like skyrmions. Chirality and magnetism are also directly connected in the interaction between matter and electromagnetic radiation through the magneto-chiral dichroism and birefringence[1]. Magneto-chiral dichroism, a non-reciprocal effect with different absorption of unpolarized light by systems with opposite chirality in the presence of a magnetic field, is a fascinating phenomenon that has been suggested to be at the origin of homochirality of life on the earth and observed only recently.[2] It is in general very weak, being assumed in first approximation to be related to the product of natural and magnetic circular dichroism, and only few examples are available in literature with limited information on the factors that originate the phenomenon. We report here a detailed synchrotron investigation [3] of the magneto-chiral effect detected at the 3d-metal K edge in two isostructural molecular helices comprising either isotropic Manganese(II) or anisotropic Cobalt(II) bridged by stable organic radicals. The experiments have revealed a strong magneto-chiral dichroism associated with the non-collinear spin structure of the Cobalt(II) derivative, which is also the archetype of Single-Chain Magnets, i.e. one-dimensional structures showing magnetic bistability due to short-range magnetic correlation. The magneto-chiral dichroism has an unusual symmetry, it is odd with respect to both parity and time-reversal symmetry but is invariant with respect to their product. It is closely related to the anapole moment, which in this particular case is originated from the toroidal orbital currents of the cobalt atoms. Orbital toroidal currents are of relevance for many phenomena, ranging from multiferroicity to superconductivity.

References:

[1] G.L.J.A. Rikken and E. Raupach, *Nature* 390, 493 (1997)[2] L. D.Barron, in *Physical Origin of Homochirality in Life*, ed. by D.B. Cline AIP, Woodbury, NY, 1996[3] R. Sessoli et al. , *Nature Phys.* 11, 69 (2015)

MO.I.2_O2 - B-T phase diagram of solid oxygen in the megagauss region

T. Nomura¹, Y.H. Matsuda¹, S. Takeyama¹, A. Matsuo¹, K. Kindo¹, T. C. Kobayashi²

1. *ISSP Univ. of Tokyo, Tokyo, Japan*

2. *Okayama University, Okayama, Japan*

Solid oxygen is known as the only antiferromagnetic insulator consisting of single chemical species. In addition to the van der Waals force, the exchange interaction between O₂ molecules contributes to the condensation energy of the solid oxygen, leading to a strong interplay between the magnetic and structural systems. Nowadays, a novel phase of solid oxygen is discovered by applying the magnetic field as high as 130 T [1]. This is the 8th phase of solid oxygen, and we call theta phase. Up to now, it is suggested that the theta phase is characterized by the large magnetic susceptibility and isotropic crystal structure [1]. In this study, we conducted two kinds of measurements, magnetization and magneto-transmission, to determine the B-T phase diagram. The field induced phase transition to the theta phase is observed at below 42 K, and the results in the two measurements are in good agreement. The transition field (H_c) from the lower field phases to the theta phase is almost temperature-independent, and the phase boundary is as steep as dH_c/dT~-10 K/T. By the analysis using the magnetic Clausius-Clapeyron equation, it is suggested that the entropy change in this phase transition is rather small. This result means that the theta phase is explicitly distinguished from the gamma phase, which is the plastic phase characterized by molecular rotation and large entropy. Therefore, it is concluded that the molecular axis is ordered in the theta phase as same with the alpha and beta phases.

References:

[1] T. Nomura et al., Phys. Rev. Lett. 112, 247201 (2014)

MO.I.2_O3 - Light-Induced spin-state switching of an Fe(II) complex adsorbed on HOPG

M. Bernien¹, H. Naggert², L.M. Arruda¹, L. Kipgen¹, F. Nickel¹, J. Miguel¹, C.F. Hermanns¹, A. Krüger¹, D. Krüger¹, E. Schierle³, E. Weschke³, F. Tuczek², W. Kuch¹

1. Institut für Experimentalphysik, Freie Universität Berlin, Berlin, Germany

2. Institut für Anorganische Chemie, Christian-Albrechts-Universität zu Kiel, Kiel, Germany

3. Helmholtz-Zentrum Berlin für Materialien und Energie, Berlin, Germany

Using magnetic molecules as building blocks for spintronic devices is a promising approach for miniaturization of functional units since it provides structural control and reproducibility on the atomic level by the chemical design of the molecules. We have studied submonolayers of the Fe(II) spin-crossover complex [Fe(bpz)2(phen)] (bpz=dihydrobis(pyrazolyl)borate, phen=1,10-phenanthroline) by x-ray absorption spectroscopy and x-ray magnetic circular dichroism. Such molecules are appealing because they possess a metastable spin state that can be switched by external stimuli, such as temperature or light. They can thus function as tiny molecular magnetic switches that can be controlled optically. However, if these complexes are immobilized on a solid surface, the spin transition is often quenched due to the interaction with the substrate. Using highly oriented pyrolytic graphite (HOPG) as a weakly interacting substrate we show that even molecules that are in direct contact with a solid surface can undergo a spin-crossover transition as a function of temperature. The transition temperature of $T_{1/2} = 161$ K is the same as for the bulk material, but the transition is much more gradual due to the isolated character of the complexes in the molecular layer. X-ray magnetic circular dichroism shows that the spin of [Fe(bpz)2(phen)] can be switched from $S=0$ (low spin) to $S=2$ (high spin) using green light of 520 nm wavelength at $T = 4.8$ K. The light-induced switching process is highly efficient with a time constant of 18.9 s, leading to a complete spin conversion from low spin to high spin. Increasing the temperature to 65 K resets the molecules back to their low-spin state. We can thus switch the magnetic moment of [Fe(bpz)2(phen)] in direct contact with an HOPG surface reversibly, where it is switched on by illumination with green light and off by increasing the temperature.

Financial support by the DFG (Sfb 658 and 677) is gratefully acknowledged.

MO.I.2_O4 - Intracluster interactions in 2butterfly" {Fe₃LnO₂} molecules with non-Kramers Ln = Tb and Ho

L. Badía-Romano¹, J. Rubín², F. Bartolomé¹, J. Luzón³, D. Prodius⁴, C. Turta⁴, V. Mereacre⁴, A. Rogalev⁵, F. Wilhelm⁵, J. Bartolomé¹

1. Instituto de Ciencia de Materiales de Aragón, Departamento de Física de la Materia Condensada, CSIC Universidad de Zaragoza, Zaragoza, Spain

2. Instituto de Ciencia de Materiales de Aragón, Departamento de Ciencia de Materiales e Ingeniería Metalúrgica, CSIC Universidad de Zaragoza, Zaragoza, Spain

3. Instituto de Ciencia de Materiales de Aragón, CSIC Universidad de Zaragoza, and Centro Universitario de la Defensa, Zaragoza, Spain

4. Institute of Chemistry, Academy of Sciences of Moldova, Chisinau, Republic of Moldova

5. European Synchrotron Radiation Facility, Grenoble, France

The intramolecular exchange interactions within the single-molecule magnet (SMM) "butterfly" molecule [Fe₃Ln(μ₃-O)₂(CCl₃COO)₈(H₂O)(THF)₃], where Ln(III) represents a lanthanide cation, have been determined by a combination of x-ray magnetic circular dichroism (XMCD) and vibrating sample magnetometry (VSM) along with an interaction model [1]. The three Fe atoms can be considered as a self-unit with total spin $S_{Fe_3}=5/2$ [2]. We have studied compounds with Ln=Tb and Ho, both with non-Kramers lanthanides and high uniaxial anisotropy, and with Ln=Lu, and Y(III) as pseudolanthanide that supply a nonmagnetic Ln reference case. Using the element selective of the XMCD magnetometry, measured at the Ln L_{2,3} edges, together with the VSM measurements, the local magnetization of the Ln ion and the Fe₃ subcluster, as a function of the field and low temperature (T≈2.5 K), has been determined separately. These results are described quantitatively in the framework of a theoretical model based on the effective spin Hamiltonian, which considers the competing effects of intracluster interactions and the external applied magnetic field [1]. The Ln-Fe₃ exchange interaction within the {Fe₃LnO₂} cluster has been determined to be antiferromagnetic, in both Tb and Ho compounds, with $J_{Tb-Fe_3} = -0.13$ K and $J_{Ho-Fe_3} = -0.18$ K, respectively. In both cases, a field-induced reorientation of the Fe₃ and Ln spins from antiparallel to parallel orientation takes place at a threshold field $\mu_0H = 1.1$ and 2 T, for the {Fe₃TbO₂} and {Fe₃HoO₂} compounds, respectively. By comparison with other compounds of the series, it is concluded that the Fe₃ subcluster magnetization polarizability decreases in the trend {Fe₃YO₂}→{Fe₃TbO₂}→{Fe₃HoO₂}→ {Fe₃DyO₂}, because of the increasing opposition of the exchange antiferromagnetic field caused by the Ln ion. It is the Ln ion which dominates the anisotropy of the molecule.

References:

[1] L. Badía-Romano *et al.*, PRB 87, 184403 (2013)

[2] J. Bartolomé *et al.*, PRB 80, 014430 (2009)

MO.I.2_05 - Landing functional molecular spin clusters on surfaces

M. Affronte¹

1. Università Di Modena E Reggio Emilia, Modena, Italy

Molecular nanomagnets have shown fascinating behaviour when observed as collection in 3D assemblies. Yet, one may wonder to what extent properties and functionalities of such systems survive when individual molecular units are extracted from crystalline environment and deposited on surfaces. First challenge is to learn to deposit and characterize molecular units in clean and safe way. Second challenge is the organization of molecules on surface by exploiting both self assembling or functional grafting. Then, we wish to control and understand interactions with different surfaces. Final goal is to exploit this control to fabricate hybrid devices where functionalities of individual molecular spin are combined with other active nanosystems, such as carbon-based circuits. I propose here to glimpse some of these aspects through the keyhole of our recent results and to discuss issues and achievements by presenting examples from our experiences.

MO.I.3_O1 - Probing hidden orders with resonant inelastic X-ray scattering

L. Savary¹, T. Senthil¹

1. Massachusetts Institute of Technology, Cambridge, United States

We propose a general scheme for the derivation of the signals resonant inelastic x-ray scattering (RIXS) gives access to. In particular, we find that RIXS allows to directly detect many hidden orders, such as spin nematic, bond nematic, vector and scalar spin chiralities. In the derivation, we choose to take the point of view of effective operators, leaving microscopic details unspecified, but still keeping explicit experimentally controllable parameters, like the incoming and outgoing polarizations. (In other words, here we ask not what microscopic processes can lead to a specific outcome, but, rather, what couplings are in principle possible.) This approach allows to systematically enumerate all possible origins of contributions to a general RIXS signal, a highly desirable feature, especially in light of some recent controversies. We emphasize that, although symmetry-based approaches have been put forth in scattering techniques in the past, the generality of the derivation and that of the results as well as the conclusions drawn from the latter are new. Although we mainly focus on magnetic insulators, for which we give a number of examples, our analysis carries over to systems with charge degrees of freedom, which we briefly address. We hope this work will help guide theorists and experimentalists alike in the design and interpretation of RIXS experiments.

MO.I.3_O2 - Femtosecond dynamics of magnetic excitations from resonant inelastic x-ray scattering

S. Kourtis¹

1. TCM Group, Cavendish Laboratory, University of Cambridge, Cambridge, United Kingdom

Taking spinon excitations in the quantum antiferromagnet CaCu_2O_3 as an example, we demonstrate that femtosecond dynamics of magnetic electronic excitations can be probed by direct resonant inelastic x-ray scattering (RIXS). To this end, we isolate the contributions of single and double spin-flip excitations in experimental RIXS spectra, identify the physical mechanisms that cause them, and determine their respective time scales. By comparing theory and experiment, we find that double spin flips need a finite amount of time to be generated, rendering them sensitive to the core-hole lifetime, whereas single spin flips are, to a very good approximation, independent of it. This shows that RIXS can grant access to time-domain dynamics of excitations and illustrates how RIXS experiments can distinguish between excitations in correlated electron systems based on their different time dependence.

MO.I.3_O3 - Spin and charge interplay of interacting and frustrated electrons on the 1/3-filled Kagome lattice

A. Ralko¹, K. Ferhat

1. Neel Institute, Grenoble, France

Geometrical frustration is at the center of intense theoretical and experimental research activity of nowadays condensed matter, thanks to the extremely rich and exotic quantum magnetic phases unravelled these last years. Together with the correlations, the frustration also affects the charge degrees of freedom, and by competing with the spins, makes room for unconventional physics. This is particularly true on the Kagome lattice, the most frustrated two-dimensional lattice.

At 1/3 filling and under correlations, electrons on such a geometry obey local 'ice-rule' constraints that make the classical ground state to be massively degenerate. We show that the interplay between the charges and the spins, together with the frustration allow for unconventional physics. In particular, we establish the presence of two peculiar states of matter driven by the strong quantum fluctuations. The first one consists of polarized droplets of metal standing on the hexagons of the lattice, and an enlarged kagome pinned charge order, inversely polarized, on the remaining sites. The second, obeying a local ice-rule type constraint on the triangles of the kagome site, is driven by an antiferromagnetically coupling of spins and is constituted of disconnected 6-spin rings. Those phases perfectly illustrate the importance of the frustration on charge ordered systems, as well as the strong resulting interplay with the spins.

K.Ferhat and A. Ralko, Phys. Rev. B 89, 155141 (2014)

MO.I.3_O4 - Magnetic field dependence of 6 K anomaly in spin liquid state of k-(BEDT-TTF)₂Cu₂(CN)₃ investigated by ¹³C NMRK. Miyagawa¹, K. Umeda¹, K. Kanoda¹*1. University of Tokyo, Tokyo, Japan*

The family of quasi-two dimensional organic conductors, k-(BEDT-TTF)₂X, is a prototype for investigating the Mott physics. The salt with X=Cu[N(CN)₂]Cl is a Mott insulator with an anisotropic triangular lattice, which shows an antiferromagnetic ordering with a moment of 0.45μB. On the other hand, another Mott insulator with X=Cu₂(CN)₃ shows no magnetic ordering due to the quasi-triangular lattice, while J is estimated at 250 K from spin susceptibility. We previously reported NMR experiments that show anomalous behavior around 6 K; an enhancement of ¹³C NMR line broadening and a marked decrease in the Knight shift and the nuclear spin-lattice relaxation rate, 1/T₁, below 6 K. Yet, the measurements of heat capacity, thermal conductivity and lattice constant found peculiarities that occur at approximately the same temperature. Thus, it is believed that the 6 K anomaly is a key phenomenon for clarifying the nature of the spin liquid of this material. To look further into the 6-K anomaly in of k-(BEDT-TTF)₂Cu₂(CN)₃, we have investigated the external-field strength and direction dependences of ¹³C NMR spectra and 1/T₁ up to 15 T. The external field is applied to parallel and perpendicular to conducting plane, and rotated between the two geometries. We have found the line broadening and shift decrease persistent up to 15 T, regardless of the field geometry. The accelerated fall-off of 1/T₁ below 10K and levelling-off below 6 K remains essentially unchanged in both field directions up to 15 T. This indicates that the orbital degrees of freedom is not responsible for 6 K anomaly and that a simple spin singlet transition does not explain that, either.

We also mention the NMR studies of k-(BEDT-TTF)₄Hg_{3-d}X₈ (X=Br,d=2.89 and Cl,d=2.78) that have an isotropic triangular lattice and a band filling 11% and 22% away from a half, namely a candidate of a doped spin liquid.

MO.J.2_I1 - Spin transport in molecular films: beyond conventional spin valves

L.E. Hueso^{1,2}, X. Sun¹, A. Bedoya-Pinto¹, M. Gobbi¹, H. Prima-García³, S. Gómez-Miralles³, E. Coronado³, F. Casanova^{1,2}

1. CIC NanoGUNE, San Sebastian, Spain

2. IKERBASQUE, Basque Foundation for Science, Bilbao, Spain

3. ICMOL, Universidad de Valencia, Valencia, Spain

Spin injection and transport into molecular semiconductors has attracted great interest recently, especially due to the small sources of spin decoherence in these materials [1]. However, there are still many open questions in this nascent field which range from the actual spin transport mechanisms across the molecular layers to the integration of molecular functionalities into spintronic devices. In this talk I will review several recent experimental highlights from our group. As a common link, they all share the use of novel molecules for spin transport with the development of meticulous fabrication techniques for vertical molecular-based spin valves.

By using bathocuproine (BCP) and fluorinated copper phthalocyanine (FCuPc) we have unambiguously proved that spin transport occurs via molecular levels, finally disregarding any eventual role of metallic filaments or defects in the electronic transport [2,3]. Our experiments point out to the critical role of the interfacial barriers for carrier injection into the molecular levels. Moreover, in the FCuPc case we have shown concomitant spin transport and photoresponse. Thanks to the emergence of two molecular-based properties, four distinguishable resistance states adjustable by light and/or magnetic field can be configured in a simple 2-bit memory cell [3]. On a more fundamental side, I will present spin valves based on rare-earth quinolines. In spite of the very different magnetic behaviour of the molecules (either paramagnetic or diamagnetic) involved, the magnetoresistance of the devices is largely unaffected thus pointing out to the major role of molecular orbitals in the spin transport [4].

References:

[1] V. Dediu, L.E. Hueso et al., *Nature Mater.* 8, 707 (2009)

[2] X. Sun et al., *Nature Commun.* 4, 2794 (2013)

[3] X. Sun et al., submitted [4] A. Bedoya-Pinto et al., submitted

MO.J.2_O2 - Voltage-controlled inversion of tunnel magnetoresistance in epitaxial spin valve based on graphene

F. Godel¹, V. Kamalakar², B. Doudin¹, Y. Henry¹, D. Halley¹, J.F. Dayen¹

1. *Ipcms-Cnrs, Strasbourg, France*

2. *Chalmers University of Technology, Göteborg, Sweden*

The large spin filtering effect predicted at the graphene/Nickel(111) interface [1] has recently driven major effort to build and characterize current perpendicular to plane (CPP) spin valve based on graphene [2,3]. Here, we report the fabrication and characterization of CPP epitaxial Magnetic Tunnel Junctions (MTJs) made by Molecular Beam Epitaxy: a 3 nm thick MgO barrier followed by a 50 nm Cobalt top electrode are deposited on CVD graphene directly grown on top of a Nickel thin film. We perform X-Ray Diffraction measurements to confirm the good quality and the (111) orientation of the MgO and ferromagnetic layers. The X-ray Photoelectron Spectroscopy also reveals the absence of oxidation of the bottom Nickel electrode, confirming its passivation by the graphene layers and leading to the use of the unique properties of Graphene Protected Ferromagnetic Electrode (GPFE) for spintronics applications [3,4]. In our junctions, we observe tunneling magnetoresistance (TMR) signals for different active area, from 1 μm^2 to 1000 μm^2 , with a resistance-area product in the range of 10-100 $\text{M}\Omega\cdot\mu\text{m}^2$, indicating the good quality of the tunnel barrier. Varying the applied bias voltage across the junction, a reproducible and scalable bias dependence of TMR is observed: it can be explained using a model of phonon-assisted transport mechanisms that relies on the peculiarity of the band structure and spin density of states at the hybrid graphene/Ni interface [1,4].

References:

- [1] Karpan et al. PRL 99 (2007)
- [2] Cobas et al. Nano Lett. 12 (2012)
- [3] Dlubak et al. ACS Nano 6 (2012)
- [4] Godel et al. APL 105 (2014)

MO.J.2_O3 - Spin dependent electron scattering in graphene nanostructures on Ni(111)

A. García-Lekue^{1,2}, T. Balashov³, M. Olle³, G. Ceballos³, A. Arnau⁰, P. Gambardella⁰, D. Sánchez-Portal^{1,4}, A. Mugarza³

1. Donostia International Physics Center (DIPC), San Sebastian, Spain
2. IKERBASQUE, Basque Foundation for Science, Bilbao, Spain
3. Catalan Institute of Nanoscience and Nanotechnology (ICN2), Bellaterra, Spain
4. Centro de Física de Materiales CFM - MPC, Centro Mixto CSIC-UPV, San Sebastián, Spain
5. Dpto. de Física de Materiales UPV/EHU, Facultad de Química, San Sebastián, Spain
6. Institució Catalana de Recerca i Estudis Avancats (ICREA), Barcelona, Spain
7. Department of Materials, ETH Zurich, Zurich, Switzerland

The electronic structure at the interface between graphene and metal contacts determines the charge and spin injection efficiency into graphene and is therefore a fundamental issue for the performance of nanodevices. The graphene-Ni interface represents an interesting case where the strong interaction with the ferromagnetic substrate opens hybridization gaps and induces magnetic moments [1,2]. Consequently, graphene is predicted to behave as a perfect spin filter in contact with a magnetic Ni electrode.

Previous studies focused on electron injection perpendicular to this interface. We investigate electron scattering in the most common current-in-plane geometry. For that purpose we grow graphene nanoislands on Ni(111) with varying geometry and atomically controlled edges. The shape can be selected by controlling the reaction temperature during the CVD growth [3], whereas the stacking with the substrate stabilizes different edge configurations depending on their relative orientation [4]. The electronic and scattering properties of the nanoislands are studied by combining local tunnelling spectroscopy and ab initio calculations [5]. We find that the hybridization between graphene and Ni states results in strongly reflecting graphene edges. Quantum interference patterns formed around the islands reveal a spin-dependent scattering of the Shockley bands of Ni, which we attribute to their distinct coupling to bulk states. Moreover, we find a strong dependence of the scattering amplitude on the atomic structure of the edges, depending on the orbital character and energy of the surface states.

References:

- [1] V.M. Karpan et al., Phys. Rev. Lett. 99, 176602 (2007)
- [2] M. Weser et al., Appl. Phys. Lett. 96, 012504 (2010)
- [3] M. Olle et al., Nano Lett. 12, 4431 (2012)
- [4] M. Olle et al., J. Chem. Phys. C 119, 4072 (2015)
- [5] A. García-Lekue et al., Phys. Rev. Lett. 112, 066802 (2014)

MO.J.2_O4 - Electrical detection of switching and photoconductivity in spin-crossover nanorods assembled by dielectrophoresis between interdigitated electrodes

C. Lefter², J. Dugay¹, R. Tan¹, A. Rotaru³, I.A. Gural'skiy⁴, S. Tricard², L. Salmon², J. Carrey¹, G. Molnar², A. Bousseksou²

1. *Laboratoire de Physique et Chimie des Nano-Objets, CNRS UMR 5215 et Université de Toulouse, France*

2. *Laboratoire de Chimie de Coordination, CNRS UPR-8241 and Université de Toulouse, France*

3. *Faculty of Electrical Engineering and Computer Science, Stefan cel Mare University, Suceava, Romania*

4. *Department of Chemistry, National Taras Shevchenko University, Kiev, Ukraine*

Switching the electronic or magnetic states of molecules or assemblies of molecules is one of the foremost paradigms in molecular electronics. Up to now numerous switchable molecular compounds have been synthesized, involving different physical phenomena, but the common challenge remains the construction of active devices. In particular, devices based on charge transport properties attract a great deal of attention, due to the substantial technological developments accomplished to probe charge transport down to the single molecule level. Here we focus on the charge transport properties of the $[\text{Fe}(\text{Htrz})_2(\text{trz})](\text{BF}_4)$ (Htrz = 1H-1,2,4-triazole) coordination network, which displays molecular spin-state switching. We used electric-field assisted directed assembly to organize high aspect-ratio spin crossover nanorods between interdigitated electrodes with a high degree of alignment. The temperature-dependent current-voltage characteristics of each device revealed a bistability of the current intensity associated with the spin-state switching. We also studied the effect of light irradiation on the electrical conductance of the samples. By illuminating the sample with different wavelengths (between 295 and 655 nm) either in air or under a nitrogen atmosphere we observed both a reversible and an irreversible change of the current flowing in the device. The reversible process consists of an abrupt decrease of the current intensity (ca. 10-50%) upon light irradiation, while the irreversible process is characterized by a slow, but continuous increase in time of the current, which persists also in the dark. These photo-induced processes were only detected in the high conductance low-spin state of the complex. On switching the rods to the high spin state the conductance decreases by two orders of magnitude and - as a consequence - the photo-effect vanishes. These results appeal perspectives for nano-scale switching and memory devices.

A. Rotaru et al., *Adv. Materials* 25, 1745 (2013) C. Lefter et al., *Phys. Chem. Chem. Phys.*, 2015, 10.1039/C4CP05250A

MO.J.2_O5 - XMCD investigation of the magnetic anisotropy of Co and Fe adatoms and clusters adsorbed on Gr/Pt(111)

P. Gargiani¹, H. Babu Vasili¹, J. Herrero¹, E. Pellegrin¹, A. Barla², M. Valvidares¹

1. ALBA Synchrotron Light Source, Cerdanyola del Vallés, Spain

2. Istituto di Struttura della Materia, ISM CNR, Area Science Park Basovizza, Trieste, Italy

Graphene, due to its peculiar electronic and transport properties is considered one of the most promising candidates for the development of novel electronic devices.[1] Being formed by a light element such as carbon, graphene is appealing as a material for spintronic application showing large spin diffusion lengths in spin-transport devices. Manipulating its magnetic properties via chemical modification [2], exchange coupling [3] or with magnetic adatom impurities [4-6] may facilitate the possibility to actually use it for such applications. Transition metal adatoms and cluster supported on graphene can be used as a model system to investigate the role of the interaction between the adatom 3d orbitals and the graphene substrate, leading to different magnetic properties of the impurities and clusters. In this study, we have investigated the magnetic configuration and in particular the magnetic anisotropy of Co and Fe adatoms and small clusters deposited on a graphene layer (grown via the CVD method on a Pt(111) substrate) by means of X-ray Absorption Spectroscopy (XAS) and X-ray Magnetic Circular Dichroism (XMCD) experiments. The results show that both Co and Fe adatoms on graphene are characterized by a planar magnetic anisotropy in contrast to Fe and Co adsorbed on Pt(111). The magnetic anisotropy energy (MAE) has been determined by angle- and field-dependent XMCD measurements showing that Co atoms are characterized by a higher anisotropy than Fe. The differences may be interpreted as being related to the orbital character of the two atomic species.

References:

- [1] K. S. Novoselov, et al. Nature 490, 192 (2012).; K. S. Novoselov, A. K. Geim, S.V. Morozov, D. Jiang, Y. Zhang, S. V. Dubonos. I. V. Grigorieva, A. A. Firsov, Science 306, 666 (2004)
- [2] J. Balakrishnan, et al. Nat. Phys. 9, 284 (2013). L. Xie, et al., Appl. Phys. Lett. 98, 193113 (2011)
- [3] M. Weser, et al. Phys. Chem. Chem. Phys. 13, 7534 (2011)
- [4] Eelbo, et al. Phys. Rev. Lett. 2013, 110, 136804
- [5] Donati, et al. Phys. Rev. Lett. 2013, 111, 236801; Donati et al. Phys. Rev. Lett. 113, 177201 (2014)
- [6] V. Sessi et al. New Journal of Physics 16, 062001 (2014)

MO.J.3_O1 - Sub-20 femtosecond opto-magnetic excitation and the ultimately fast spin dynamics in a Heisenberg antiferromagnet

D. Bossini¹, S. Dal Conte², Y. Hashimoto¹, A. Secchi¹, R. Pisarev³, G. Cerullo², T. Rasing¹, A. Kimel¹

1. *Institute for Molecules and Materials, Radboud University Nijmegen, Nijmegen, The Netherlands*

2. *IFN-CNR, Dipartimento di Fisica, Politecnico di Milan, Milan, Italy*

3. *A. F. Ioffe Physical-Technical Institute, Russian Academy of Sciences, St. Petersburg, Russian Federation*

The ability to generate, control and detect spin excitations is one of the main challenges in the recently emerged areas of magnonics [1] and spintronics [2], which might revolutionize the information processing technology [3]. Opto-magnetism provides an effective tool to control spins with light [4]. Recently, it has been demonstrated that the generation and control of spin waves in the centre of the Brillouin zone [4] and in the vicinity of it [5] can be effectively achieved on the femtosecond time scale. It is also known that light can access high wave vector spin waves [6]. However, the femtosecond magnetic dynamics following the ultrafast laser excitation of spin waves at the edges of the Brillouin zone has not been disclosed yet. Here we show that such coherent magnons are excited in the Heisenberg antiferromagnet KNiF₃, by sub-20 femtosecond laser pulses. The fastest possible dynamics of the order parameter, which follows the generation of the high wave vector magnons, appears to be significantly different from what can be anticipated on the basis of previous experiments in the frequency domain [7]. In particular, we demonstrate that the off-resonant optical excitation of the 22 THz magnetic mode allows the femtosecond coherent control of the antiferromagnetic order parameter. Our experiment discloses the pathways of the energy transfer between light and spins, resulting in an unprecedented ultrafast magnetic dynamics in an antiferromagnet.

References:

- [1] S. Demokritov et al., *Magnonics - From Fundamentals to Applications* (2013)
- [2] M. Wu et al., *Recent Advances in Magnetic Insulators* (2013)
- [3] T. Satoh et al., *Nat. Phot.* 9, 25 (2014)
- [4] A. Kirilyuk et al., *Rev. Mod. Phys.* 82, 2731 (2010)
- [5] T. Satoh et al., *Nat. Phot.* 6, 662 (2012)
- [6] M. Cottam et al., *Light Scattering in Magnetic Solids* (1986)
- [7] S. Chinn et al., *Phys. Rev. B* 3, 1709 (1971)

MO.J.3_O2 - Parametric Amplification of Spin Waves Using Bulk Acoustic Waves

P. Chowdhury¹, P. Dhagat¹, A. Jander¹

1. Oregon State University, Corvallis, United States

Spin waves are a promising prospect for the development of spin-based information processing devices, where they can be used as information carriers in logic devices and for transmitting information along spin wave buses between devices. However, the large intrinsic spin wave damping in most known magnetic materials limits the utilization of spin waves for interconnects. Viable amplification mechanisms for spin waves are therefore crucial to make further progress in the field. In this work, we investigate a novel technique of parametric amplification of spin waves using bulk acoustic waves. The device used for our experiment consists of a thin film acoustic transducer fabricated on one side of a gadolinium gallium garnet (GGG) substrate with an epitaxial Yttrium Iron Garnet (YIG) film on the opposite side. Longitudinal bulk acoustic waves generated by the transducer resonate in the GGG, a low acoustic loss substrate and couple into the YIG film. This induces strain in the YIG film which by inverse magnetostrictive effect, modulates the anisotropy of the YIG film at the same frequency as the acoustic waves. Parametric amplification may be achieved by driving this anisotropy variation at twice the frequency of the spin wave. The acoustic resonator was impedance matched to be driven at an acoustic resonance at 2.4632 GHz, exactly twice the frequency of the backward volume spin wave excited at 1.2316 GHz with a bias field of 10.1 mT in the YIG film. The intensity of the transmitted spin wave is seen to increase as a function of the acoustic power indicating modulation of the spin wave by acoustic energy. A threshold acoustic power of 160 mW is observed for parametric pumping. No such spin wave amplification was observed by driving the acoustic transducer off-resonance, thus confirming that the modulation is indeed related to the presence of acoustic waves.

MO.J.3_O3 - Spin-Orbit torques driven ferromagnetic resonance in ultrathin YIG disks

M. Collet¹, O. d'Allivy Kelly¹, R. Bernard¹, E. Jacquet¹, P. Bortolotti¹, V. Cros¹, A. Anane¹, X. De Milly², G. De Loubens², V.V. Naletov^{2,3}, O. Klein^{2,4}, J.L. Prieto⁵, M. Muñoz⁶

1. *Unité Mixte de Physique CNRS/Thales And Université Paris Sud, Palaiseau, France*
2. *Service de Physique de l'État Condensé, CEA Saclay, Gif-sur-Yvette, France*
3. *Institute of Physics, Kazan Federal University, Kazan, Russia*
4. *SPINTEC, UMR CEA/CNRS/UJF-Grenoble 1/Grenoble-INP, Grenoble, France*
5. *Instituto de Sistemas Optoelectronicos y Microtecnologia (UPM), Madrid, Spain*
6. *Instituto de Microelectronica de Madrid (CNM, CSIC), Madrid, Spain*

Spin Transfer induced high frequency dynamics has been up to now mainly studied in magnetic materials that are metallic as the spin current acting on the magnetization flows together with a charge current. Recently, this constrain has been released in using the Spin Orbit Interaction as a source of spin current through Spin Hall Effect (SHE) or Rashba effect. In this case, the spin current flows perpendicular to the charge current and thus opens the field of spin torque induced auto-oscillators to the wide family of insulating magnetic materials.

We have fabricated magnetic micro-disks (1 to 4 Åm) based on $Y_3Fe_5O_{12}$ (YIG) (20nm/Pt(7nm) bilayer. In a previous study, we demonstrate that our ultrathin YIG films grown by Pulsed Laser Ablation have excellent dynamical properties with a Gilbert damping that can be as low as $2.3 \cdot 10^{-4}$. DC electrical contacts as well as radio-frequency inductively coupled antennas have been lithographically defined on the top of each disk.

In this study, we demonstrate that spin wave modes can be excited by simply injecting a dc current in the top Pt layer of the YIG/Pt disks. The threshold density current necessary to overcome the damping is \sim a few 10^{11} A.m⁻², in excellent agreement with theoretical predictions. This result proves that the Spin Orbit torque due to SHE is efficient enough to drive the YIG magnetization dynamics at a frequency that we can actually relate to the ferromagnetic resonance mode. These auto-oscillations can be detected either by Inverse SHE on the Pt electrode or inductively using a spectrum analyzer connected to the antennas. Note that these YIG auto-oscillations are limited to a narrow range of current and field and that their amplitudes remain small. We believe that the demonstration of the electrical control of YIG dynamics in artificial microstructures paves the path to active magnonic devices.

Mo.J.3_O4 - Theory of Current-induced Spin Torque Resonance of Magnetic Insulators

T. Chiba¹, M. Schreier², G.E.W. Bauer⁰, S. Takahashi¹

1. *Institute for Materials Research, Tohoku University, Japan*

2. *Walther-Meissner Institut, Garching, Germany*

3. *WPI-AIMR, Tohoku University, Japan*

4. *Kavli Institute of NanoScience, Delft University of Technology, The Netherlands*

The magnetic insulator yttrium iron garnet (YIG) has attracted much attention as a new spintronic material for magnetic information technology because of its very low magnetization damping. Near-dissipationless propagation of spin waves makes YIG application to low power data transmission and logic devices. A crucial breakthrough is the discovery that the magnetization in YIG can be excited electrically by Pt contacts, thereby creating an interface between electronic-spintronic and magnonic circuits. However, the current-induced spin wave excitation is a strongly non-linear process and the critical threshold currents found by the experiment have not yet been explained. Here we suggest a simpler method to get to grips with the current-magnetization interaction in the YIG/Pt system without a problematic threshold, viz. by employing the recently discovered spin Hall magnetoresistance (SMR) to detect current-induced spin torque ferromagnetic resonance (ST-FMR). We study the alternating current-induced magnetization dynamics of a magnetic insulator, such as YIG, through the spin transfer effect by heavy normal metal, such as Pt, contacts. Based on the drift-diffusion spin model with quantum mechanical boundary conditions and the Landau-Lifshitz-Gilbert equation with a current-induced oscillating spin transfer torque, we find that a dc voltage is generated in the normal metal as an SMR-induced rectification effect. We also model the ST-FMR for all magnetization directions and in the presence of field-like spin-orbit torques. The dc voltage as a function of an external magnetic field or current frequency has recently been measured the current-induced magnetization dynamics of magnetic insulators, which also shows that ac spin pumping is reversible to the ST-FMR. Our results may expose crucial information on the spin-orbit coupling between currents and magnetization.

References:

[1] Y. Kajiwara et al., *Nature* 464, 262 (2010).

[2] H. Nakayama et al., *Phys. Rev. Lett.*, 110, 206601 (2013).

[3] L. Liu et al., *Phys. Rev. Lett.*, 106, 036601 (2011).

[4] T. Chiba et al., *Phys. Rev. Applied* 2, 034003 (2014); T. Chiba et al., arXiv:1409.8406.

[5] M. Schreier, T. Chiba et al., arXiv:1412.7460.

TU.A.1_I1 - Magnetic properties evolution vs. microstructure in Fe-Mn-Si-B-P-Cu submicron wires

N. Lupu^{1,2}, A. Makino^{2,3}, S. Corodeanu¹, P. Sharma³, A. Takeuchi³, H. Chiriac¹

1. National Institute of Research and Development for Technical Physics, Iasi, Rumania
2. Cooperative Research and Development Center for Advanced Materials, Institute for Materials Research, Tohoku University, Sendai, Japan
3. Research and Development Center for Ultra High Efficiency Nano-crystalline Soft Magnetic Materials, Institute for Materials Research, Tohoku University, Sendai, Japan

The soft magnetic nanocrystalline materials are playing an increasing role in specific applications, namely energy efficient magnetic devices, power electronics, electrically powered vehicles and nuclear reactors [1]. Here we report on the preparation of $\text{Fe}_{85-x}\text{Mn}_x\text{Si}_2\text{B}_8\text{P}_4\text{Cu}_1$ ($x = 0; 1; 3$ at.%) glass-coated submicron wires with metallic nucleus diameters (Φ_m) between 600 nm and 1.2 μm and the glass coating thickness (tg) of 4÷5 μm , with the aim to study the dependence of their magnetic properties on the diameter of the metallic core and structural changes induced by one-step and/or two-step annealing at different temperatures (T_a) ranging between 250 and 5500C. All samples are magnetically bistable, irrespective of dimensions and structure. The larger the Mn content the smaller the coercive and switching fields are. The bistability is preserved even for the annealed samples, this being a characteristic of the uniaxially magnetized materials indicating the formation of a central magnetic domain in the amorphous state. However, the submicron wires annealed below 4250C are much softer (the coercive field decreases), whilst after annealing above 4250C the coercivity increases significantly as the results of the increase of the grains size over the critical limit. Additionally, for the same total diameter, the smaller the diameter of the metallic core the larger the coercive field is. The measurement of the domain wall velocity (velocities of over 1500 m/s are obtained for optimum nanocrystalline structures) offers a more accurate image over the microstructure developed in glass-coated submicron wires than the conventional magnetic measurements (permeability and switching field). Despite the fact that the nanograins have similar sizes after annealing, the increase in their number after annealing at higher temperatures results in a slightly different mechanism for the magnetization processes, with the nucleation of the larger number of small irregular domains competing with the displacement of the domain walls.

This work was jointly supported by the Cooperative Research and Development Center for Advanced Materials, IMR, Tohoku University and the Romanian NUCLEU Programme (Project PN 09-43 01 02).

References:

- [1] R. Hasegawa, J. Magn. Mater. 324 (2012) 3555

TU.A.1_O2 - Circular magnetization process in a Co-rich microwire with negative magnetostriction

N. Usov¹, S. Gudoshnikov²

1. Pushkov Institute of Terrestrial Magnetism, Ionosphere and Radio Wave Propagation RAS, Moscow, Russian Federation

2. National University of Science and Technology MIS&S, Moscow, Russian Federation

The small angle magnetization rotation method is widely used [1] to determine magnetostriction constants of amorphous ferromagnetic microwires. Here, the wire is nearly uniformly magnetized in magnetic field $H > H_a$, where H_a is the anisotropy field, and its longitudinal magnetization component undergoes small oscillations at the frequency $2f$ under the influence of a circular magnetic field of alternating current, $I(t) = I_0 \sin(2\pi f t)$. These oscillations give rise to electro-motive force (EMF) arising in the receiving pick-up coil wound around the microwire. In this report it is experimentally shown that for amorphous Co-rich microwire with negative magnetostriction in the range of low magnetic fields, $|H| < H_a$, there are two different oscillation modes of the longitudinal magnetization component depending on the alternating current amplitude. When I_0 is less than the critical value, $I_0 < I_{0c}(H)$, the first harmonic gives the main contribution to the EMF signal. However, at $I_0 > I_{0c}(H)$ a significant contribution of the second EMF harmonic appears. As numerical simulation of the circular magnetization process shows, in the latter case the reversal of the circular magnetization component occurs twice during the period. When compared with the numerical simulation data, the measurement of the relation $I_{0c}(H)$ at different applied tensile stresses allows to determine the microwire saturation magnetization and the magnetostriction constant.

S.A. Gudoshnikov wishes to acknowledge support of the program of Russian Ministry of Education and Science (Grant No 2014/113).

References:

[1] A. Zhukov, V. Zhukova, J.M. Blanco, A.F. Cobeño, M. Vazquez, J. Gonzalez. J. Magn. Magn. Mater. 258-259 (2003) 151

TU.A.1_O3 - Heating influence on magnetic structure in Co and Fe rich amorphous microwires

A. Chizhik¹, A. Stupakiewicz², A. ², A. Zhukov^{1,3}, J. González¹

1. *Universidad del Pais Vasco, Leioa, Spain*

2. *University of Bialystok, Białystok, Poland*

3. *IKERBASQUE, Bilbao, Spain*

The influence of changing temperature on stable operation of magnetic sensors that use microwires as active elements, is the subject of the present work. The investigations have been performed using magneto-optical Kerr effect (MOKE) technique in Co- and Fe- rich magnetic glass covered microwires within 300-550 K temperature range. The images of surface magnetic domains have been obtained by means of MOKE microscope with a thermo-controlled system. It was found different types of domain structure depending on the temperature and the microwire composition. These types are characterised by the different domain period and the angle of the inclination of domain walls. The MOKE hysteresis loops reflect the transformation of surface domain structure. It was established the direct correlation between the domain structures and hysteresis loops. In particular, the coexistence of domain walls with different value of mobility has been found. Also it was observed original mechanism of the domain structure transformation: sharp change in the domain structure without movement of the domain walls. During increasing of the external magnetic field only the switching of the magnetization occurs in surface magnetic domains. The existence of the complex domain structures is considered in the frame of the complex stresses distribution. The value and the sign of internal stresses experience considerable change near the interface between the metallic nucleus and glass-coating.

TU.A.1_O4 - Visualizing decoupling in nanocrystalline alloys: FORC-temperature analysis

M. Rivas¹, J.C. Martínez-García¹, P. Gorriá¹

1. Departamento de Física & IUTA, Universidad de Oviedo, Gijón, Spain

Nanocrystalline microstructures obtained by partial devitrification of ferromagnetic glassy metals present a variety of magnetic behaviors ranging from ultra-soft to semi-hard or hard depending on the strength of the ferromagnetic coupling among nanograins. This is in turn conditioned, not only by the morphology and volume fraction of the crystalline phase, but very importantly by the magnetic characteristics of the amorphous spacer. In this work, the temperature-dependent coupling/decoupling of a Fe-based two-phase nanocrystalline system is analyzed. The main novelty of the study resides on the chosen technique: First-Order Reversal Curves (FORC) analysis proves its competency to discriminate different magnetic phases and explore their internal and mutual magnetic interactions. The 2D-representation of the FORC diagram provides a portrait of the different phases, visualized as separate colored spots whose position is directly related to the corresponding critical fields; the spatial distribution of the colors is associated to the magnetic interactions between the two phases or among the constituents within a particular phase. The FORC diagrams of samples obtained after different thermal treatments, from annealing temperatures in the onset of the first crystallization point to well above it, reveal two strongly coupled phases (amorphous and nanocrystalline) at room temperature. Except for the samples annealed at higher temperatures, the patterns show a gradual weakening of the coupling when heating up. Well above the amorphous phase Curie temperature a complex pattern is revealed corresponding exclusively to the crystalline phase.

TU.A.1_O5 - Enhanced magneto-optical properties of Ce:YIG thin films grown on GGG substrates

L. Beran¹, M.C. Onbasli², M. Zahradnik¹, J. Dusek¹, M. Kucera¹, J. Mistrik³, M. Veis¹, C.A. Ross²

1. Charles University in Prague, Faculty of Mathematics and Physics, Prague, Czech Republic
2. Department of Materials Science and Engineering, Massachusetts Institute of Technology, Cambridge, United States
3. University of Pardubice, Faculty of Chemical Technology, Pardubice, Czech Republic

Recent development in intergrated photonics calls for the on-chip integration of non-reciprocal optical elements based on magneto-optical effects. However, this relies on the preparation of high quality magneto-optical materials in form of thin films with well defined optical and magneto-optical properties. Cerium-doped Yttrium Iron Garnet (Ce:YIG) is one of the materials used for magento-optical applications. Although strong Faraday rotation (3300 deg/cm at 1.55 μm) [1] and high transparency in visible and infrared region were observed on bulk samples, thin films of this matrial still lack these properties and exhibit lower than bulk magneto-optical figure of merit (defined as Faraday rotation over optical loss). Here we present a systematic optical and magneto-optical study of 80 nm and 14 nm thick single crystal Ce:YIG films grown on (100), (110) and (111) GGG substrates by pulse laser deposition. X-ray and VSM measurements confirmed bulk-like structural and magnetic properties. Spectroscopic ellipsometry together with magneto-optical spectroscopy in Kerr and Faraday configurations were employed to derive the complete dielectric permittivity tensor of this material in the photon energy range from 1.2 to 5.6 eV. Obtained experimental data clearly demonstrated the influence of the substrate orientation on optical and magneto-optical properties as well as on magnetic coercivity and squareness (magnetic remanence over saturation moment) of investigated samples. A strong enhancement of magneto-optical properties was observed in films on (111) GGG substrates. The Faraday rotation reached 30000 deg/cm at a wavelength of 780 nm and 6000 deg/cm at 1550 nm, exceeding the bulk values.

References:

- [1] T. Shintaku, A. Tate, S. Mino, Appl. Phys. Lett. 71 (12), 1640 (1997)

TU.A.2_I1 - Coercivity enhancement in hybrid systems

J. de La Venta¹, J.G. Ramírez², T. Saerbeck³, S. Wang⁴, I. Valmianski², I. K. Schuller²

1. *Department of Physics, Colorado State University, Fort Collins, United States*

2. *Department of Physics and Center for Advanced Nanoscience, University of California San Diego, La Jolla, United States*

3. *Institut Laue-Langevin, Grenoble, France*

4. *Materials Science Division, Lawrence Berkeley National Laboratory, Berkeley, United States*

The coupling of electronic, magnetic, and structural properties from one material into another when in close physical proximity can induce novel functionalities in hybrid materials. Hybrid materials allow the engineering of new material properties by creative uses of proximity effects, for example when different length or time scales are competing in each material. Interesting possibilities arise when ferromagnets are in proximity to oxides that undergo a structural phase transition (SPT). In a series of recent studies we have shown the possibility of inducing large changes of magnetization and coercivity of ferromagnetic films brought in contact with two members of the vanadium oxide family, VO₂ and V₂O₃ (1, 2). Some of these hybrid structures show a 500 % coercivity enhancement across the phase transition. Our results show that the strain produced by the thermally induced SPT and the nanoscale phase coexistence across the first-order phase transition of the oxides are responsible for the observations in these hybrid materials. The results suggest the existence of similar effects in other hybrid materials with first-order structural phase transitions and give rise to interesting and perhaps useful properties.

Work supported by US-AFOSR and US-DOE.

References:

[1]. J. de la Venta, S. Wang, T. Saerbeck, J. G. Ramírez, I. Valmianski and Ivan K. Schuller. Coercivity Enhancement in V₂O₃/Ni Bilayers Driven by Nanoscale Phase Coexistence. *Appl. Phys. Lett.* 104, 062410, (2014)

[2]. T. Saerbeck, J. de la Venta, S. Wang, J. G. Ramírez, M. Erekhinsky, I. Valmianski and Ivan K. Schuller. Coupling of magnetism and structural phase transitions by interfacial strain. *J. Mater. Res.* 29, 2353, (2014)

TU.A.2_O2 - Exchange correlation length in nanocrystalline soft magnetic materials

K. Suzuki¹, N. Ito¹, J. Garitaonandia², A. Michels³, G. Herzer⁴, M. Lokamani⁵, R. Schaefer⁵

1. Monash University, Malvern East, Australia

2. University of the Basque Country, Leioa, Spain

3. University of Luxembourg, Walferdange, Luxembourg

4. Vacuumschmelze GmbH, Hanau, Germany

5. Leibniz Institute for Solid State and Materials Research, Dresden, Germany

The excellent magnetic softness of Fe based melt-spun nanocrystalline alloys is primarily due to averaging of the local magnetocrystalline anisotropy energy of grains over the exchange correlation length (L_{ex}). Hence, this characteristic length has been discussed extensively in many literatures. However, experimental observation of L_{ex} has been rather limited and the current understanding of the excellent magnetic softness relies on theoretical arguments based on the random anisotropy model (RAM). Our aim is to investigate L_{ex} of nanocrystalline soft magnetic materials experimentally by means of the Kerr microscopy and thereby verifying RAM. Two nanocrystalline $Fe_{84}Nb_6B_{10}$ samples were prepared by annealing a melt-spun amorphous precursor alloy under a static field (TFA) or under a rotating field (RFA) at 898 K for 1.8 ks. The applied field ($\mu_0 H$) was 0.8 T. Due to the static field, an induced uniaxial magnetic anisotropy (K_u) of 100 J/m^3 was confirmed for TFA. The remanence ratio of RFA was above 0.5, indicating that K_u is negligible and the random magnetocrystalline anisotropy ($\langle K_1 \rangle$) governs the magnetization process in RFA. Well-defined regular 180° domain walls were seen on the Kerr images obtained from TFA and the average surface wall width is $0.33 \pm 0.05 \text{ } \mu\text{m}$. 180° domain walls were also seen on RFA. However, the wall width tends to fluctuate considerably and the average width is $1.64 \pm 0.5 \text{ } \mu\text{m}$. These wall widths suggest that the exchange length in RFA is approximately 5 times larger than that in TFA. Since L_{ex} is inversely proportional to the square root of anisotropy energy, the observed wall width indicates that $\langle K_1 \rangle$ in RFA is as small as 4 J/m^3 . This value agrees exceptionally well with $\langle K_1 \rangle$ estimated from RAM (5 J/m^3) for the nanocrystalline $Fe_{84}Nb_6B_{10}$ sample (grain size of 10 nm and crystalline fraction of 0.7).

TU.A.2_O3 - Drastic reduction of Ni-Zn ferrites during consolidation by spark plasma sintering (SPS)

Y. Flores-Arias ¹, T. Gaudisson ², S. Ammar ², R. Valenzuela ¹

1. *Instituto de Investigaciones en Materiales, Universidad Nacional Autónoma de México, México D.F., México*

2. *ITODYS, Université Paris-Diderot, PRES Sorbonne Paris Cité, Paris, France*

The consolidation of ferrite nanoparticles (NPs) can provide nanostructured materials with novel and interesting magnetic properties, especially for electronics applications. Spark plasma sintering (SPS) has shown many advantages to perform this sintering; it is an extremely fast method [1] which can be operated at very low temperatures as compared with the classic solid state sintering. To achieve high densities it is typically needed a sintering process at 1200°C for 8 hours. By using the SPS method, 500°C for 10 minutes is enough to reach such densities [2]. However, for some cases, particularly for NiZn ferrites with high Zn content, significant differences between the expected and the obtained magnetic properties have been observed. In this work, we report on the consolidation of $Zn_{0.7}Ni_{0.3}Fe_2O_4$ ferrite nanoparticles by SPS, their structural characterization, and their magnetic properties. The initial ferrite NPs were synthesized by the polyol method, leading to NPs about 8 nm, with a blocking temperature ~ 70 K. These NPs were consolidated by SPS at 600 °C for 10 min, resulting in a polycrystalline solid with grains ~ 160 nm. Magnetization saturation and Curie temperature, however, exhibited values significantly higher than those reported for the bulk ferrite of this composition. X-ray diffraction patterns revealed a small content of metallic Ni for the SPS samples. The experimental results are interpreted in terms of a partial reduction of Ni to a metallic second phase, and the occupation of the spinel sites left by Ni_{2+} by Fe_{2+} reduced from Fe_{3+} . A good agreement with the magnetic properties of $Zn_{0.7}Ni_{0.3-y}Fe_{2+y}Fe_{3+2}O_4$ [3], where y is the reduced cation concentration (Ni and Fe), is obtained.

References:

[1] Z.A. Muniret al. J. Mater Sci. 41[3] 763-777 (2006)

[2] R. Valenzuela et al. J. Supercond. Nov Magn. 25, 2389-2393 (2012)

[3] R. Valenzuela. Magnetic Ceramics. Cambridge University Press (2005), p. 131

TU.A.2_O4 - Development of a very low loss MnZn ferrite for power applications

V. Tsakaloudi¹, V. Zaspalis^{1,2}

1. Centre for Research and Technology Hellas-CERTH, Thessaloniki, Greece

2. Aristotle University of Thessaloniki-AUTH, Thessaloniki, Greece

Current market trends of the switching power supplies industry indicate the demand of even lower energy losses in power conversion systems that maintain satisfactory initial permeability levels. Thus, the need for medium frequency power conversion ferrite materials in the magnetic components that exhibit optimal performance at operation conditions of 100 kHz, 200 mT is continuous. In this work the development of a polycrystalline MnZn ferrite material that satisfies this demand, exhibiting initial permeability above 2500 units and very low power losses at medium frequencies is presented. The MnZn ferrite samples were prepared following the ceramic process of solid state reaction and sintering was performed under controlled atmosphere conditions. The combinatorial role of TiO₂ and CoO together with Zn content, as well as the effects of the process parameters on the magnetic performance of the MnZn ferrite were evaluated. It is shown that the development of the adequate polycrystalline microstructure that is characterized by a) high sintered density, b) homogenous grain size that is free of morphological or chemical pinning effects and c) high resistivity grain boundary structure can be achieved by means of appropriate compositional and dopant adjustment, anisotropy control and specific resistivity optimization. The newly developed MnZn ferrite is characterized by high sintered density of 4.91 g/cm³, initial magnetic permeability of 2512 (at 10 kHz, 0.1 mT, 25° C), high saturation magnetic flux density of 560 mT (at 10 kHz, 1200 A/m, 25 °C) and very low power losses of 224 mW/cm³ (at 100 kHz, 200 mT, 100° C) combined with very low power losses of 470 mW/cm³ even at room temperature, establishing it as ideal for power applications.

TU.A.2_05 - Study of the induced anisotropy in field annealed Hitperm alloys by Mössbauer spectroscopy and Kerr microscopy

J. S. Blázquez¹, J. Marcin², F. Andrejka², V. Franco¹, A. Conde¹, I. Skorvanek²

1. *Departamento de Física de la Materia Condensada, ICM-SE CSIC, Universidad de Sevilla, Sevilla, Spain*

2. *Institute of Experimental Physics, Slovak Academy of Sciences, Kosice, Slovakia*

Samples of $\text{Fe}_{39}\text{Co}_{39}\text{Nb}_6\text{B}_{15}\text{Cu}_1$ alloy were nanocrystallized under zero field annealing (ZF) and transverse field annealing (TF) (640 kA/m, parallel to the ribbon plane and transverse to its axis). For TF sample, induced anisotropy $K=860 \text{ J/m}^3$ and anisotropy field $H_K=1390 \text{ A/m}$ were obtained. A reduction in coercivity with respect to ZF sample (16 and 45 A/m, respectively) is also observed as wiping out the domain structure during TF prevents the unwanted effect of domain walls stabilization that occurs for ZF sample. Kerr microscopy show a well defined parallel domain structure, transversally oriented to the ribbon axis for TF unlike for ZF sample, for which a disordered pattern is observed with large and small domains at the surface of the ribbon. Although Mössbauer spectra are clearly different for the two studied samples, they confirm that there is no significant difference between the hyperfine field (HF) distributions of TF and ZF samples. The site contributions (inner core of nanocrystals) are also very similar for both samples, without differences in the average values of HF and the isomer shift. In fact, the only significant difference is the angle between the gamma radiation and the magnetic moments, Θ . Whereas for TF samples $\Theta=\pi/2$ rad, in agreement with the well defined domain structure observed by Kerr microscopy, ZF samples show $\Theta=0.91$ rad, close to a random orientation and much smaller than that of as-cast amorphous samples, indicating that moments change their orientation to out of the ribbon plane during ZF unlike during TF annealing.

Work supported by Spanish MICINN and EU FEDER (Project MAT2013-45165-P), PAI (Project P10-FQM-6462) and Slovak projects NANOKOP Nr. ITMS 26110230061 NanoCEXmat Nr. ITMS 26220120019, APVV-0492-11, VEGA2/0192/13 and MNT ERA NET II STREAM.

TU.A.3_O1 - Magnetization of underdoped YBCO above the irreversibility line

J.F. Yu¹, I. Kokanovic^{2,3}, J. Day⁴, R. Liang⁴, W. Hardy⁴, D. Bonn⁴, A. McCollam⁵, S. Julian^{1,6}, J. Cooper³

1. Department of Physics, University of Toronto, Toronto, Canada

2. Department of Physics, University of Zagreb, Zagreb, Croatia

3. Cavendish Laboratory, University of Cambridge, Cambridge, United Kingdom

4. Department of Physics and Astronomy, University of British Columbia, Vancouver, Canada

5. High Field Magnet Laboratory, Nijmegen, The Netherlands

6. Canadian Institute for Advanced Research, Toronto, Canada

Theory [1] and early results from Nernst and torque experiments [2] suggest that in underdoped cuprates a large vortex liquid phase persists even at zero temperature. The issue of the existence of such a phase at high magnetic field is especially pressing as quantum oscillations (QO) have been observed just above the vortex melting field in underdoped YBCO [3] and there is still intense debate about whether Cooper pairs persist in the region of the H-T plane where quantum oscillations are seen. Two recent experiments on underdoped YBCO ($p=0.11$) have given conflicting answers to this question: Grissonnanche et al. showed through thermal conductivity measurements that there is a sharp feature at 22T which corresponds to the extrapolation of the irreversibility field at $T = 0K$ and they interpret this signature as H_{c2} [4]; Fan Yu et al. found through high field torque magnetometry that the diamagnetism persists above 22T and conclude that the vortex-liquid phase exists well above 22T [5]. We performed our own torque measurements on underdoped YBCO ($p=0.12$) at fields up to 33T and temperature down to 4.5K. Our results are qualitatively similar to Fan Yu et al. [5], however there are important quantitative differences both below T_c and in the normal state. Detailed analysis suggests that the most likely scenario involves weak superconductivity above 22T that is heavily suppressed by competition with the charge density wave instability seen by X-ray scattering [7].

References:

[1] Senthil, T. & Lee, P. A. Phys. Rev. B 79, 245116 (2009)

[2] Li Lu, et al. Phys. Rev. B 81, 054510 (2010)

[3] Doiron-Leyraud et al. Nature 447, 565 (2007)

[4] Grissonnanche, G. et al. Nature Communications 5, 3280 (2014)

[5] Yu Fan et al. arXiv:1402.7371

[6] Kokanovic, I. et al. Euro. Phys. Lett. 98, 57011 (2012)

[7] Chang, J. et al. Nature Physics, 8, 871 (2012)

TU.A.3_O2 - Ferro-type order of magneto-electric quadrupoles in the pseudo-gap phase of $\text{YBa}_2\text{Cu}_3\text{O}_6 + x$

S.W. Lovesey^{1,2}, D.D. Khalyavin², U. Staub³

1. ISIS Facility, STFC Oxfordshire, United Kingdom

2. Diamond Light Source Ltd, Oxfordshire, United Kingdom

3. Swiss Light Source, Paul Scherrer Institut, Villigen, Switzerland

Magnetolectric effects are important for materials, in which magnetism couples to electronic degrees of freedom due to the absence of inversion symmetry. These effects can be related to basic multipole moments beyond those of the charge, the magnetic dipole and the electric quadrupole (orbitals). These atomic multipoles are magnetic and break inversion symmetry (magnetolectric) and they have been previously found in multiferroics such as GaFeO_3 [1, 2] and CuO [3]. However, their importance as order parameter for the electronic phase remains unclear. Here we apply these concepts to $\text{YBa}_2\text{Cu}_3\text{O}_6 + x$ in its pseudo gap phase. Our theory [4] allows us to fully describe previously observed neutron Bragg intensities indicative of magnetic order in the pseudo-gap phase of $\text{YBa}_2\text{Cu}_3\text{O}_6 + x$. Magnetic diffraction intensities, collected using polarization analysis, are explained by magnetolectric quadrupoles at in-plane Cu sites arranged in a simple ferro-type motif. An absence of conventional spin and orbital angular momentum dipoles in our theory is compatible with the occurrence of superconductivity at low temperature. This strongly suggests that these multipoles are the primary order-parameter in the pseudo-gap phase.

References:

- [1] T. Arima, J. H. Jung, M. Matsubara, M. Kubota, J. P. He, Y. Kaneko, and Y. Tokura, *J. Phys. Soc. Jpn.* 74, 1419 (2005)
- [2] U. Staub, Y. Bodenthin, C. Piamonteze, M. García-Fernández, V. Scagnoli, M. Garganourakis, S. Koohpayeh, D. Fort, and S. W. Lovesey, *Phys. Rev. B* 80, 140410 (2009)
- [3] V. Scagnoli, U. Staub, Y. Bodenthin, R. A. de Souza, M. García-Fernández, M. Garganourakis, A. T. Boothroyd, D. Prabhakaran, and S. W. Lovesey, *Science* 332, 696 (2011)
- [4] S. W. Lovesey, D. D. Khalyavin, and U. Staub, arXiv:1501.02427 (2015)

TU.A.3_O3 - The SU(2) symmetry in cuprate superconductors

C. Pépin¹

1. *IPhT, CEA – Saclay, France*

In this talk we review the recent theoretical approach to the theory of high temperature superconductors, which considers the SU(2) rotation between d-wave pairing and the charge sector as a main player in the physics of these compounds [1-4]. We first discuss the role of this symmetry in the physics of the pG phase, its relation with AFM fluctuations and the recently observed charge orders in the under doped regime. We show recent numerical findings suggesting that the splitting of the SU(2) symmetry is minimal for a wide range of parameters, and gets smaller and smaller as the coupling is increased [4]. We argue that the collective mode associated with this symmetry corresponds to the A_{1g} resonance observed in Raman scattering at 41 meV around optimal doping.

References:

- [1] K.B.Efetov, H.Meier & C.Pépin, Nat. Phys. 9, 442 (2013)
- [2] H.Meier, M.Einenkel, C.Pépin & K.B.Efetov, PRB 88, 020506; PRB 89,195115 (2014)
- [3] C.Pépin, V. S.de Carvalho, T.Kloss & X.Montiel, PRB 90, 195207 (2014)
- [4] T.Kloss, X.Montiel & C.Pépin, arXiv:1501.05324

TU.A.3_O4 - The spin glass phase in cuprates and iron-based high temperature superconductors

J. Mydosh¹

1. Kamerlingh Onnes Laboratory, Leiden, The Netherlands

For over 40 years the spin glass (SG) problem has intrigued the magnetic community and generated an enormous spin-off into many diverse non-magnetic areas. Lately there has been fresh stimulation of SG behavior from the newly discovered randomly doped materials, e.g., the high T_c superconductors. Here the phase diagram of temperature versus the various doping included an antiferromagnetic phase which becomes weakened and disappears into the superconducting dome. Generally there is a small coexisting wedge between the antiferromagnetism and the superconductor that displays SG behavior. The extent of the SDW is defined by the doping that creates magnetic disorder. Many years ago a proposed SG model was the incommensurate SDW but not of the long-range phase transition type. Instead a short-range (SR), randomly propagating, finite correlation length SDW was detected by neutron scattering in some canonical SG. Now we wish to use this SR-SDW model to describe the SG-like behavior claimed in the cuprates and pnictides. We present experimental evidence for the this overlapping SG-superconducting state [1].

References:

[1] J. A. Mydosh, Rep.Prog.Phys. 78(2015) in press

TU.A.3_O5 - High-pressure phase diagram and electronic structure of FeSe

T. Terashima¹

1. National Institute For Materials Science, Tsukuba, Japan

FeSe is an intriguing member of the iron-based superconductors. It undergoes a structural transition at $T_s \sim 90$ K but no antiferromagnetic transition at ambient pressure. Although the superconducting transition temperature T_c at ambient pressure is low, ~ 8 K, it can be enhanced remarkably by pressure or in single-layer films.

We have performed resistance and ac magnetic susceptibility measurements on FeSe single crystals under high pressure up to 27 kbar. Our resistance data clearly show anomalies most likely associated with the pressure-induced antiferromagnetic transition, which was previously suggested by μ SR measurements [M. Bendele et al., PRL 104, 087003 (2010)]. The superconducting and antiferromagnetic transitions exhibit an intriguing interplay: Both transition temperatures increase with pressure as if the two orders cooperate, but the superconducting transition broadens when the antiferromagnetism coexists as if the two orders compete. The structural transition temperature is quickly suppressed by pressure and the transition line almost meets the antiferromagnetic one at ~ 18 kbar, the highest pressure where the transition was observed. The antiferromagnetic transition line however shows no clear kink indicating the point where the two transition lines meet. This might indicate that the two orders are nearly independent.

We have also performed Shubnikov-de Haas measurements [T. Terashima et al., PRB 90, 144517 (2014)]. We have found that the Fermi surface at ambient pressure is surprisingly different from that predicted by band structure calculations. It most likely consists of one hole and one electron cylinder at the zone center and corner, respectively. The carrier number is one order-of-magnitude smaller than predicted. Simple band-energy shifts and renormalization cannot explain these observations. Clearly, elaborated theories incorporating correlations and orbital ordering together are necessary. We will further report how the Fermi surface evolves with pressure.

TU.B.2_I1 - Exchange bias effect in CoO@Fe₃O₄ core-shell octahedron-shaped nanoparticles

V. Salgueiriño¹, N. Fontaíña-Troitiño¹, B. Rodríguez-González¹, B. Rivas-Murias²

1. *Universidade de Vigo, Vigo, Spain*

2. *CIQUS-Universidade de Santiago de Compostela, Santiago de Compostela, Spain*

Increased coercive and tunable exchange bias field values were registered in hybrid CoO@Fe₃O₄ core-shell octahedron-shaped nanoparticles of different average edge length. The metal cation chemical potential at the interface between the antiferromagnetic and ferrimagnetic oxides, captured as the dynamic variable, causes the effective magnetic anisotropy to increase and the type of interface to change after growing the magnetite shell epitaxially onto the cobalt oxide {111} surface facets, and consequently, to tune the exchange bias effect.

TU.B.2_O2 - Determination of the local oxidation state of transition metals in 3D: application to magnetic nanoparticles

S. Estrade¹, P. Torruella¹, R. Arenal², L. Yedra¹, A. Eljarrat¹, L. López-conesa¹, M. Estrader³, A. López-Ortega⁴, G. Salazar-Alvarez⁵, J. Nogués⁶, F. Peiro¹

1. LENS, MIND-IN2UB, Universitat de Barcelona, Barcelona, Spain

2. Laboratorio de Microscopías Avanzadas (LMA), Instituto de Nanociencia de Aragón (INA), Universidad de Zaragoza, Zaragoza, Spain

3. Departament de Química Inorgànica, Universitat de Barcelona, Barcelona, Spain

4. INSTM and Dipartimento di Chimica "U. Schiff", Università degli Studi di Firenze, Firenze, Italy

5. Department of Materials and Environmental Chemistry, Arrhenius Laboratory, Stockholm University, Stockholm, Sweden

6. Departament de Física, Universitat Autònoma de Barcelona & ICN2 - Institut Català de Nanociència i Nanotecnologia, Campus UAB & Institució Catalana de Recerca i Estudis Avançats (ICREA), Barcelona, Spain

Although electron energy loss (EEL) spectrum volume tomography enables access to 3D chemical information at the nanoscale, it has never been used to elucidate the 3D-distribution of oxidation states. Here we present the first EELS-tomography 3D-reconstruction of oxidation states in a nanoheterostructured system with high spatial resolution. The success of the data analysis relies on the optimized use of multivariate analysis (which is very effective in handling large number of spectra) and the novel use of compressed sensing (which allows reliable 3D-reconstructions even with a limited number of datasets) in tomography algorithms. The feasibility to perform complex spectra treatment in spectrum volume tomography opens the door to a wide range of applications in solving complex nanostructures. In the presented case (45-nm wide FeO/Fe₃O₄ core/shell cubic nanoparticles), due to the similarities in the composition and effective atomic number of the compounds, high angle annular dark field (HAADF) imaging could not be used to resolve the structure, justifying the need of a more sophisticated approach. As an alternative, EELS fine structure is used to obtain information on the iron oxidation state, thus making it possible to distinguish between Fe²⁺ and Fe³⁺. However, there is the limitation that EELS projects the information of the 3D nanoparticle into a 2D map. To overcome this issue, EELS spectrum image data-sets are considered for 3D tomographic reconstruction after data processing. The reconstruction not only contains information on the chemical composition of the sample but also on the oxidation state of iron at each voxel.

TU.B.2_O3 - Effect of the oxygen content in the reaction environment on size and shape of CoFe₂O₄ nanoparticles: morphological analysis by aspect maps.

G. Muscas^{3,4,5}, G. Singh¹, W.R. Glomm², R. Mathieu⁵, P. Anil Kumar⁵, G. Concas⁴, E. Agostinelli³, D. Peddis³

1. Department of Materials Science and Engineering, Norwegian University of Science and Technology (NTNU), Trondheim, Norway

2. SINTEF Materials and Chemistry, Biotechnology and Nanomedicine Sector, Trondheim, Norway

3. Istituto di Struttura della Materia – CNR, Rome, Italy

4. Dipartimento di Fisica, Università di Cagliari, Cagliari, Italy

5. Department of Engineering Sciences, Uppsala University, Uppsala, Sweden

Advanced synthesis approaches are necessary to achieve a strict control of the structural, morphological and chemical properties of nanomaterials, being at the basis of the reproducible manipulation of their physical behavior. In fact, any advanced application of nanoparticles (NPs) system will also rely on the achievement of such control, especially for magnetic nanoparticles that are complex physical objects, whose properties greatly differ from their parent massive material, being particularly sensitive to the particle size [1].

Within this context, the synthesis of spinel ferrite nanoparticles (MeFe₂O₄, Me = Fe²⁺, Co²⁺, Ni²⁺, Zn²⁺, ...) with controlled morpho-structural features represents an important issue due to the strong interest from both a fundamental and a technological point of view (e.g., MRI, hyperthermia, drug delivery, catalysis).

Crystalline cobalt ferrite nanoparticles were prepared by a modified high temperature thermal decomposition (HTD) synthesis of acetylacetonate precursors [1,2]. This approach was improved introducing a strict control on the residual oxygen in the reaction environment. A detailed analysis of the effect of the oxygen content on the growth mechanism was carried out analyzing TEM images through a statistical approach and using aspect maps [3].

The aspect maps allowed to follow the growth process of nanoparticles and to select the optimal value of residual pressure to produce particles size of ~ 19 nm and a narrow size distribution (polydispersity 0.4 nm⁻¹). The magnetic measurements showed an improvement of the switching field distribution (SFD) which is a key parameter for technological applications. Furthermore, our results suggest that particles with larger sizes can be also stabilized.

References:

[1] D. Peddis et al., Chem. Mater. 25 (2013) 2–10

[2] S. Sun, et al., J. Am. Chem. Soc. 126 (2004) 126–132

[3] G. Muscas et al., Chem. Mater. *in publication*

TU.B.2_O4 - Magneto-optical investigation on the multiphase and stability of Fe oxide nanoparticles

G. Campo¹, C. de Julian Fernández^{2,1}, M. Albino¹, C. Innocenti¹, F. Pineider^{3,1}, V. Bonanni^{3,1}, A. Caneschi¹, C. Sangregorio^{4,1}

1. *INSTM and University of Florence, Florence, Italy*

2. *IMEM – CNR, Parma, Italy*

3. *ISTM – CNR, Milan, Italy*

4. *ICCOM – CNR, Sesto Fiorentino, Italy*

Spinel ferrites magnetic nanoparticles have promising potential in different fields of application as magnetic recording, spintronics, sensoristics and biomedicine. Unlike their bulk counterparts, where the composition can be considered mainly as homogeneous, in nanosized magnetic ferrites the increased surface/volume ratio can give rise to a faster oxidation process, leading to a not pure chemical structure. Traditional magnetic measurements do not allow for discriminating between the different magnetic phases, in particular between the magnetite and the maghemite. Their magnetic properties have been analyzed by several studies but the possible oxidation of Fe²⁺ ions of the metastable magnetite phase to Fe³⁺ of maghemite can be relevant for the physical properties of the nanosystem.

Magnetic circular dichroism (MCD) spectroscopy, being sensitive to specific electronic transitions[1], represents a simple and valid alternative to other expensive investigation techniques for the detection of different cationic species. In this study spherical iron oxide nanoparticles with increasing size between 5 to 10 nm are investigated by MCD in the nUV-vis-nIR range [2].

Moreover the time evolution of different nanoparticles is monitored to investigate the progressive oxidation. The measurements show the presence of two definite spectral structures, whose intensity evolved in time, likely originated by different magnetic contributions. The analysis of the MO hysteresis loops allows the deconvolution of the two phases. The results support the hypothesis of two distinct magnetic phases, related to the presence magnetite and maghemite, which transformation is size dependent.

This work has been financed by the EC through FP7-214107-2 NANOMAGMA, and by Fondazione Cariplo through Project No. 2010-0612.

References:

[1] W.F.J. Fontijn, J. Appl. Phys. 85 (1999) 5100

[2] G. Campo et al. Chem. Mater. 27 (2015) 466-473

TU.B.2_O5 - Synthesis, structural and magnetic properties of CdFe₂O₄ ferrite

J.Z. Msomi¹

1. School of Physics, University of KwaZulu-Natal, Durban, South Africa

Nanoparticles of CdFe₂O₄ with particle size of about 10 nm have been synthesized by high energy ball milling and co-precipitation processes. The synthesis route appears to have some effects on the properties. The compounds have been characterized by X-ray diffraction, Fourier Transform Infrared (FTIR), transmission electron microscopy (TEM), Mössbauer and magnetization measurements. The XRD pattern of CdFe₂O₄ provides information about single-phase formation of spinel structure with cubic symmetry. The FTIR measurements between 400 and 4000 cm⁻¹ indicate intrinsic cation vibration of the spinel structure. The Mössbauer spectra were recorded at 4 K and 300 K. The hyperfine fields appear to be highly sensitive on particle size. The evolution of the properties as a function of particle size is also presented.

TU.B.3_O1 - Anisotropic Interaction of Ferromagnetic Nanoparticles Intercalated Inside Carbon Nanotubes

S. Prischepa¹, A. Danilyuk¹, I. Komissarov¹, V. Labunov¹, F. Le Normand², A. Derory³, J. Manel Hernández⁴, J. Tejada⁴

1. *Belarusian State University of Informatics and Radioelectronics, Minsk, Bielorrussia*

2. *Laboratory of Engineering, Informatics and Imagery (ICube), University of Strasbourg and CNRS, Strasbourg, France*

3. *IPCMS, University of Strasbourg and CNRS, Strasbourg, France*

4. *University of Barcelona, Barcelona, Spain*

We investigate magnetic properties of iron based nanoparticles (NPs) intercalated into carbon nanotube (CNT) aligned arrays for magnetic fields oriented both along and perpendicular to the CNT axes. Samples have been synthesized by floating catalyst chemical vapor deposition. We show that for the parallel field the interplay between the exchange coupling and magnetic anisotropy depends both on the NP content N_c and temperature T . For low N_c and T the magnetic anisotropy dominates [1]. Temperature increase leads to strengthening of the exchange interaction. Moreover, analyzing the law of the approach to saturation we have obtained evidence of long range coherent magnetic anisotropy at low T which takes place between NPs belonging to a single nanotube [2]. This magnetic order is strengthened by the CNT alignment and is due to the peculiar influence of the inner magnetic properties of CNTs. Increase in concentration of NPs destroys the coherent anisotropy. For the perpendicular field the exchange interaction dominates in the whole studied temperature range (2-300K) independently on the N_c value. This is because NPs belonging to different CNTs have to be considered in this case. Consequently, coherent anisotropy is destroyed due to loss of orientation of CNTs, and the exchange interaction is maintained by the indirect exchange via the conduction electrons of different CNTs, arbitrarily contacting each other.

References:

[1] A.L. Danilyuk et al. Carbon 68, 337 (2014)

[2] A.L. Danilyuk et al. New J. Phys. 2015, accepted

TU.B.3_O2 - Static and dynamic magnetization behavior of magnetic multi-core nanoparticles

C. Johansson¹, F. Ahrentorp¹, A. Sarwe¹, J. Blomgren¹, C. Jonasson¹, R. Stjernberg Bejhed², E. Wetterskog², P. Svedlindh², F. Ludwig³, F. Westphal⁴, C. Grüttner⁴, R. Costo⁵, M.P. Morales⁵, L. Zeng⁶, S. Gustafsson⁶, E. Olsson⁶, E. Schaller⁷

1. Acreo Swedish ICT AB, Göteborg, Sweden

2. Department of Engineering Sciences, Division of Solid State Physics, Uppsala University, Uppsala, Sweden

3. Institute of Electrical Measurement and Fundamental Electrical Engineering, Braunschweig, Germany.

4. Micromod Partikeltechnologie GmbH, Rostock, Germany

5. Instituto de Ciencia de Materiales de Madrid, ICMM-CSIC, Madrid, Spain

6. Department of Applied Physics, Chalmers University of Technology, Göteborg, Sweden

7. Chalmers Industriteknik, Chalmers Science Park, SE-412 88 Göteborg, Sweden

Magnetic multi-core nanoparticles consist of several magnetic single-domain nanocrystals positioned in different types of geometrical configurations (particle morphology). Depending on the nanocrystal size, particle morphology and the multi-core particle size, different types of magnetic behavior can be obtained. The result depends strongly on the interrelation between the nanocrystal size distribution, multi-core particle morphology and size. Thus, the magnetization process of the multi-core particle ensemble depends on both the individual magnetic moments of the nanocrystals as well as on the total effective magnetic moment of the particle (that depends on both the magnetic moment values and moment orientations of the individual nanocrystals). In this work, we use different analysis techniques, such as static magnetization, AC susceptometry (ACS), TEM, DLS, field rotation, and magnetorelaxometry (MRX), as well as modeling using Monte-Carlo techniques and Langevin dynamics in order to study the properties of different multi-core particles and also how the properties are different compared to single-core particles. Iron oxide based multi-core nanoparticle systems with mean particle diameters from 60 nm to 150 nm and nanocrystal mean sizes in the range of 15 nm - 30 nm are studied. From the ACS, MRX and field rotation analysis we can see that Brownian relaxation is the dominant process with some minor fast relaxation due to the Néel process. The size analysis result from the ACS and MRX method is in good agreement with the TEM and DLS data. The intrinsic saturation magnetization at 300 K obtained from DC magnetization is in the range of 340 kA/m and 390 kA/m, typical for iron oxide nanocrystals. DC magnetization and ACS results show that the low field magnetization process is different for the studied multi-core systems and is explained by differences in nanocrystal size and particle morphology. Work is supported by EC FP7 NMP NanoMag project (grant no. 604448).

TU.B.3_03 - Quantifying dipolar interaction effects in Fe oxide nanoparticles coated with oleic acid or silica by comparison with simulations

C. Moya¹, O. Iglesias¹, X. Batlle¹, A. Labarta¹

1. Dpt. Física Fonamental and IN2UB, Universitat de Barcelona, Barcelona, Spain

Distinguishing surface from interaction effects on the magnetic properties of nanoparticle assemblies is a complicated task due to their concomitance. In order to separate both effects, uniform variation of the interparticle distance in an assembly, avoiding also aggregation, is desirable but this cannot be simply achieved by changing the concentration. In this work, we present a detailed magnetic study of 5 nm non-aggregated Fe oxide nanoparticles, with narrow size distribution, synthesized by the organic decomposition method. By using oleic acid (S1) or silica (S2) to coat particles from the same batch, we could study the magnetic properties of a unique assembly with (S1) or without (S2) interactions among the particles, guaranteeing that the only difference between them is the mean interparticle distance. This was clearly corroborated by the excellent H/T scaling of isothermal magnetization curves for S2 which was not observed for S1, and the correspondent features in ZFC/FC processes. The effects of interactions on the dynamics were characterized by measuring the time dependence of the thermoremanence after application of different fields during the FC process. The effective energy barrier distributions extracted from a scaling analysis of relaxation curves have maxima at higher values and extend to higher energies for S1 than for S2. Moreover, the maximum and shape of the distribution for the interacting sample S1, progressively reduces as the field applied during the FC prior to relaxation increases. The results of dipolar field and energy barrier histograms obtained by Monte Carlo simulations of macrospin assemblies with different concentrations allow to demonstrate that the observed phenomenology is due to interactions. Comparison of numerical with experimental results allows quantification of the dipolar interaction effects on the energy barriers.

This work is supported by Spanish MINECO (MAT2012-33037), Catalan DURSI (2014SGR220) and EU FEDER funds (Una manera de hacer Europa)

TU.B.3_O4 - MnBi magnetic nanoparticles: New synthesis to realize rare-earth replacement nanomaterials

M. Rowe¹, E. Skoropata², Y. Wroczynskyj², J. van Lierop²

1. *Toyota Research Institute of North America, United States*
2. *University of Manitoba, Winnipeg, Canada*

There are few candidate magnetic materials that show promise of competing in energy product with rare-earth permanent magnets. MnBi, when formed correctly in an exchange coupled magnetic nanocomposite with a soft magnetic phase, is one of these few candidates. For over 50 years now, the production of MnBi has been challenging. The peritectic nature of molten Mn and Bi restricts formation of the intermetallic. The obvious solutions of melt spinning suffers from the drawbacks of MnBi forming in either a matrix of Mn or Bi, ill suiting it for formation of a nanocomposite with soft magnetic material. Ferromagnetic MnBi nanoparticles have been synthesized from a new reagent material known as Mn Ligated Anionic Element Reagent Complex (Mn LAERC), which is a construction of Mn and lithium borohydride, ligated by undecyl cyanide, as shown by FT IR analysis peaks versus literature values and authentic samples of the component materials. The Mn LAERC is used to produce MnBi nanoparticles simply and in large scale (gram quantities) through a solution based reduction of bismuth carboxylates. SEM EDX analysis of the as-synthesized MnBi nanoparticles agree with the powder XRD that nanoparticles are indeed being formed. $M(H)$ hysteresis loop data of these crude, magnetically aligned, nanoparticles show a magnetic coercivity (H_c) value of 660 Oe, with a magnetization saturation (M_s) of 0.28 emu/g at 300 K. Because the MnBi nanoparticle synthesis is kinetically fast (almost instantaneous), a large amount of crystalline disorder is expected to occur in the material. This notion is supported by the improvement that can be realized in the crude nanoparticles. A simple 2 hour long annealing process is effected to increase these magnetic performance values to $H_c = 1800$ Oe and $M_s = 25$ emu/g at 300 K, which increase to $H_c = 7960$ Oe and $M_s = 19$ emu/g at 400 K with an energy product of 2.8 MGOe.

TU.C.1_I1 - 3D Curved Magnetic Surfaces

D. Makarov¹, R. Streubel¹, M. Melzer¹, D. Karnaushenko¹, G. Lin¹, P. Fischer², F. Kronast³, U. K. Röbber⁴, O. G. Schmidt¹

1. *Institute for Integrative Nanosciences, IFW Dresden, Dresden, Germany*
2. *Center for X-ray Optics, Lawrence Berkeley National Laboratory, Berkeley, United States*
3. *Helmholtz-Zentrum Berlin für Materialien und Energie GmbH, Berlin, Germany*
4. *Institute for Theoretical Solid State Physics, IFW Dresden, Dresden, Germany*

Conventionally magnetic films and structures are fabricated on flat surfaces. The topology of curved surfaces has only recently started to be explored and leads to new fundamental physics and applied device ideas. Advancing in this field calls for the understanding of the magnetic responses of thin films on curved surfaces. Here, two basic geometries, i.e. hemi-spherical [1,2] and tubular [3,4], will be addressed. To enable the microscopic characterization of 3D architectures, we put forth the concept of magnetic soft x-ray tomography. This concept will be introduced and the angle- and layer-resolved imaging of rolled-up tubes [4,5] will be presented. Based on this knowledge, we fabricated flexible [6,7], printable [8] and stretchable [9] magnetic sensorics. The unique mechanical properties open up new application potential of magnetic field sensors for printable electronics and smart skins, allowing to sense and manipulate objects of the surrounding us physical as well as digital world [10]. This work is supported in part via ERC project SMaRT number 306277 and FET programme under FET-Open grant number 618083.

References:

- [1] T. Ulbrich et al., Phys. Rev. Lett. 96, 077202 (2006)
- [2] D. Makarov et al., Appl. Phys. Lett. 93, 153112 (2008)
- [3] E. Smith et al., Phys. Rev. Lett. 107, 097204 (2011)
- [4] R. Streubel et al., Nano Lett. 14, 3981 (2014)
- [5] R. Streubel et al., Adv. Mater. 26, 316 (2014)
- [6] G. Lin et al., Lab Chip 14, 4050 (2014)
- [7] M. Melzer et al., Adv. Mater. DOI: 10.1002/adma.201405027
- [8] D. Karnaushenko et al., Adv. Mater. 24, 4518 (2012) & Adv. Mater. 27, 880 (2015)
- [9] M. Melzer et al., Nano Lett. 11, 2522 (2011) & Adv. Mater. DOI: 10.1002/adma.201403998
- [10] M. Melzer et al., Nature Commun. 6, 6080 (2015)

TU.C.1_O2 - A New Path to Spin Engineering in Ultrathin Magnetic Layer Systems

K. Schlage¹, D. Erb¹, H. Wille¹, L. Bocklage^{1,2}, D. Schumacher¹, J. Comfort¹, R. Röhlberger^{1,2}

1. *Deutsches Elektronen-Synchrotron DESY, Hamburg, Germany*

2. *The Hamburg Centre for Ultrafast Imaging, Hamburg, Germany*

Spintronics with its multifaceted applications requires control over the magnetic properties of thin films. However, in conventional ferromagnetic thin film preparation, the magnetic anisotropy and coercivity cannot be chosen unrestrictedly, limiting the flexibility of spintronic multilayer device design. We demonstrate that the field-dependent magnetization behavior can be adjusted completely freely and set separately for the individual magnetic layers in a multilayer system by using oblique incidence deposition (OID). While the polar angle of deposition can be used to adjust the coercive field of practically every sputter deposited magnetic thin film in a range of 1 mT to 50 mT, the azimuthal orientation of deposition can be used to precisely define the orientation of its in-plane easy axis.

We demonstrate the capabilities of the new method by preparation of model systems with tailor-made magnetic properties: First, by stacking thin films with non-parallel in-plane easy axes of magnetization, multilayer hybrids are fabricated which are switchable between different ground states (ferromagnetic, ferrimagnetic, antiferromagnetic). Second, multilayers composed of thin films with different switching fields demonstrate the possible adaptability of magnetic field sensors to particular applications. In order to pinpoint the microscopic mechanism that leads to these features we have employed high-resolution magnetic x-ray scattering, magneto-optical Kerr effect measurements and cross-sectional TEM studies. Applicable to a wide range of material combination the proposed approach can provide access to diverse new routes in fundamental research and multilayer device design [1].

References:

[1] Kai Schlage, Denise Erb, Ralf Röhlberger, H.-C. Wille, Lars Bocklage, Daniel Schumacher. Method of producing a multilayer magnetoelectronic device and magnetoelectronic device. European Patent: P91642 (2014)

TU.C.1_O3 - Helimagnetic thin films: surface reconstruction, surface spin-waves and magnetization

H.T. Diep¹, S. El Hog¹

1. LPTM, University of Cergy-Pontoise, CNRS, Cergy-Pontoise, France

We study surface spin configuration, surface spin-waves and temperature-dependent surface magnetization in quantum Heisenberg helimagnetic thin films using the Green's function technique. We show that the helical angle is strongly modified at the surface and a few beneath layers. The ground-state spin configuration across the film is shown as a function of the interaction J_2 between next-nearest neighbors along the c-axis perpendicular to the film surface. The spin-wave spectrum is calculated for the non-collinear spin configuration. The surface localized spin-wave modes are identified. Using the spectrum, we calculate the layer magnetizations across the film as functions of temperature T , J_2 and surface anisotropy. Effects of quantum fluctuations at low T are shown and discussed. In particular, we show effects of surface exchange interaction on the zero-point spin contraction and the existence of a crossover between layer magnetizations at very low T . We also show and discuss the case of a helimagnetic nanotube.

TU.C.1_O4 - Direct imaging of the magnetic dead layer in strained manganite thin films

L.A. Rodríguez González^{1,2,3,4}, L. Marin^{2,3,5,6}, C. Magén^{2,3,4,7}, E. Snoeck^{1,4}, R. Arras^{1,4}, I. Lucas^{2,3,7}, L. Morellón^{2,3}, P.A. Algarabel^{3,5}, J.M. De Teresa^{2,3,4,5}, M.R. Ibarra^{2,3,4,5}

1. CEMES-CNRS, Toulouse, France
2. Laboratorio de Microscopias Avanzadas (LMA), Instituto de Nanociencia de Aragón (INA), Universidad de Zaragoza, Zaragoza, Spain
3. Departamento de Física de la Materia Condensada, Universidad de Zaragoza, Zaragoza, Spain
4. Transpyrenean Associated Laboratory for Electron Microscopy (TALEM), CEMES-INA, CNRS-Universidad de Zaragoza, Toulouse, France
5. Instituto de Ciencia de Materiales de Aragón (ICMA), Universidad de Zaragoza, Zaragoza, Spain
6. LAAS-CNRS, Toulouse, France
7. Fundación ARAID, Zaragoza, Spain

The substrate-induced strain effect in epitaxial manganite thin films is one of the main factors that produces dramatic changes in their magnetic and transport properties. In the past, different indirect methods have been employed to elucidate the reasons of these phenomena detecting, for instance, the appearance of a non-ferromagnetic/insulating layer, also called dead layer [1-3]. In this work, we show the first experimental image obtained by electron holography at low temperature of the formation of this dead layer. In the case of epitaxial strained $\text{La}_{2/3}\text{Ca}_{1/3}\text{MnO}_3$ thin films, we directly visualized that such dead layer is produced in the topmost surface of the film. Macroscopic magnetization measurements, as well as theoretical calculation have demonstrated that this layer has an antiferromagnetic (AF) behavior, and is produced by the epitaxial strain induced by the substrate [4]. In addition, we showed that by a suitable tuning of the out-of-plane lattice parameter of the film (i.e. reducing the c/a ratio of the film), such a dead layer can be avoided. In summary, we can control the appearance of an AF layer at the surface of the manganite being of interest for possible exchange bias applications.

References:

- [1] J. W. Freeland, et. al., J. Phys.: Condens. Matter 19 (2007) 315210
- [2] D. Pesquera, et. al., Nat. Commun. 3 (2012) 1189
- [3] S. Valencia, et. al., J. Phys.: Condens. Matter 26 (2014) 166001
- [4] L. Marin, et. al., Nano Lett., 15 (2015) 492-497

TU.C.1_O5 - Magnetic hardening through exchange bias in Fe/NiO bilayers grown onto nanoporous Al₂O₃ membranes

E. Navarro ¹, M. Alonso ¹, F. Cebollada ², F.J. Palomares ¹, J.M. Gonzalez ¹, L. Soriano ³, A. Gutierrez ³

1. Instituto de Ciencia de Materiales de Madrid – CSIC, Madrid, Spain

2. Escuela Técnica Superior de Ingenieros de Telecomunicaciones-UPM, Madrid, Spain

3. Depto. de Física Aplicada and Instituto de Ciencia de Materiales Nicolás Cabrera-UAM, Madrid, Spain

The occurrence of ferro-antiferromagnetic (F-AF) interfaces in Fe/NiO bilayers brings about the possibility of significantly varying the Fe layer hysteretic properties through the uniaxial anisotropy induced by the presence of unbalanced antiferromagnetic phase moments at that interface. In this work, we report on the Fe-thickness (5 - 20 nm) and temperature dependencies of the hysteretic parameters measured in Fe/NiO (200 nm)/ Al₂O₃ (nanoporous membranes). The Fe layers were deposited using pulsed laser ablation whereas the NiO ones were fabricated by means of magnetron sputtering on top of the Al₂O₃ membranes. Sample morphology was examined by both scanning electron and atomic force microscopies, which evidenced that the Fe/NiO bilayer maintained the Al₂O₃ membrane nanopores and grew in a six-fold columnar way around each original nanopore. The in-plane hysteresis loops measured (vibrating sample magnetometer) by field cooling the samples down to different temperatures below RT evidenced the occurrence of coercive forces larger than that associated to the Fe anisotropy field and also significant loop displacements, both of them clearly associable to the occurrence of exchange bias at the Fe/NiO interface. Also, and interestingly from the standpoint of the hysteresis control, the Fe thickness dependence of the coercivity evidence that the interphase coupling fundamentally influences the nucleation at the interface of a reversed domain whose propagation rules the Fe columns switching.

TU.C.2_I1 - Random Fields in Magnets and Superconductors: The Role of Topology

E. Chudnovsky¹, T. Proctor¹, D. Garanin¹

1. Lehman College and Graduate School of the City University of New York, Bronx, United States

Random fields in magnets and superconductors have been discussed for decades but their effect on the long-range order was not fully understood. Recently it has been argued that the answer depends on the topology of the order parameter. The n -component fixed-length continuous-symmetry order parameter in d dimensions, interacting with the random field, exhibits glassy behavior at $n < d + 1$ due to the pinning of singularities. Presence of nonsingular topological objects at $n = d + 1$ leads to a weak metastability. At $n > d + 1$ topological defects are absent and the behavior of the system is fully reversible, characterized by the exponential decay of correlations. Theoretical arguments have been confirmed numerically on lattices of up to one billion sites. Along the same lines the effects of magnetic impurities on the ferromagnetic order and random anisotropy effects in amorphous and sintered magnets have been studied. Our findings shed new light on properties of pinned charge density waves and properties of pinned flux lattices in superconductors.

This work is supported by the grant No. DE-FG02-93ER45487 funded by the U.S. Department of Energy, Office of Science.

TU.C.2_O2 - Relation between crystallographic chirality and spin chirality in chiral helimagnets studied by polarized small angle neutron scattering and muon spin rotation

K. Ohishi¹, Y. Kousaka², N. Ikeda³, T. Ogura³, T. Yoshii³, E. Proskurina³, J. Akimitsu³, J. Suzuki¹, H. Hiraka⁴, A. Koda⁴, M. Miyagawa², S. Nishihara², K. Inoue², J.I. Kishine⁵

1. CROSS

2. Hiroshima University, Hiroshima-Shi, Japan

3. Aoyama-Gakuin University, Tokyo, Japan

4. KEK-IMSS, Ibaraki, Japan

5. The Open University of Japan, Chiba, Japan

Recently, numerous experimental and theoretical studies have focused on chiral helimagnets in which antisymmetric Dzyaloshinskii-Moriya interactions induce long-range modulation of the magnetic order. Because they provide an opportunity to observe stable magnetic topological structure such as whirls of magnetization called skyrmions and, a spiral helimagnetic order that can be deformed by an external field such as the chiral soliton lattice (CSL) that is observed when a magnetic field is applied perpendicular to the helical axis in $\text{Cr}_{1/3}\text{NbS}_2$. Most of inorganic chiral magnetic materials form racemic-twinned crystals, having the left and right-handed crystalline domains in a specimen so that it is difficult to study the relation between crystallographic and magnetic structures. However, MnSi is known as one of unique examples to form only left-handed crystal structure, and the helimagnetic chirality follows the crystalline chirality. Moreover, our group succeeded in controlling the crystallographic chirality and obtained mm-sized single crystals of chiral helimagnet CsCuCl_3 . X-ray diffraction measurements show that each crystal adopts either a right or left-handed crystallographic chirality only. In order to elucidate the existence of CSL in MnSi and to clarify the relation between crystallographic and magnetic structures in CsCuCl_3 , we performed polarized small angle neutron scattering (SANS) and muon spin rotation measurements. The polarized SANS experiments detected the higher harmonics indexed as $(2\delta, 2\delta, -2\delta)$ under the applied field non-parallel to the helical axis. By evaluating the difference in intensities between the up and down-spin incident neutrons, it had the left-handed incommensurate magnetic structures. These results are well interpreted by formation of the left-handed CSL. Muon spin precession signals were observed in both the crystals under a zero field below T_N . Temperature dependence of the precession frequencies behaves the same way, suggesting that the right and left-handed samples are a pair of complete isomers in terms of both crystallographic and magnetic structures.

TU.C.2_O3 - Two step pressure induced collapse of magnetic order and fluctuating chiral phase in MnGe Chiral magnet

I. Mirebeau¹, M. Deutsch¹, N. Martín¹, P. Bonville², T. Hansen³, M.T. Fernández-Díaz³, F. Bert⁴, D. Andreica⁵, A. Amato⁶, L. Fomicheva⁷, A. Tsvyashchenko⁷, U. Roessler⁸

1. CEA-Saclay, DSM/IRAMIS/ Laboratoire Léon Brillouin, Gif-sur-Yvette, France

2. CEA- Saclay, DSM/IRAMIS/ SPEC, Gif-Sur-Yvette, France

3. Institut Laue Langevin, Grenoble, France

4. LPS, Université Paris-Sud, Orsay, France

5. Faculty of Physics, Babes-Bolyai University, Cluj-Napoca, Romania

6. Laboratory for Muon Spin Spectroscopy, Villigen, Switzerland

7. Vereshchagin Institute for High Pressure Physics, Troitsk, Moscow, Russia

8. Leibniz Institute for Solid State and Material Research IFW, Dresden, Germany

Cubic helimagnets such as MnSi or FeGe are model cases of pressure-induced collapse of band ferromagnetism in metals, accompanied with exotic partial order and chiral spin textures [1]. Their long wavelength helical structures arise from the spin orbit coupling, the Dzyaloshinskii-Moryia anisotropy perturbing the ferromagnetic exchange.

MnGe stands out owing to its much shorter helix pitch and high magnetic moment [2], yielding a giant Topological Hall Effect [3]. Using high pressure neutron diffraction, we show that helical order in MnGe transforms around 6 GPa from a high spin to a low spin state, recalling the weak ferromagnetism of MnSi at ambient pressure. Above 6 GPa an intermediate magnetoelastic state with strong spin fluctuations likely accommodates the volume mismatch between high spin and low spin regions. Helical order collapses only above 10 GPa, suggesting a second transition from a low spin to a non-magnetic state, in agreement with ab initio calculations [4].

At ambient pressure, we studied the spin fluctuations versus temperature by combining neutrons with Mössbauer spectroscopy on a 57Fe-doped sample [5], and recently with Muon Spin Resonance (MuSr). A inhomogeneous chiral phase is stabilized in a very large temperature range (TN±70K) around the Néel temperature (TN=170K), where fluctuating moments with short range ferromagnetic correlations coexist with frozen moments involved in the helical order. This coexistence is clearly detected on the MuSR spectra, and the temperature dependence of the fluctuating fraction well agrees with that deduced from Mössbauer spectroscopy. This unusual broad transition to paramagnetism, also studied by small angle neutron scattering [6] suggests a dynamical phase separation triggered by temperature. Our results show that in MnGe, as in MnSi and FeGe [7], spin fluctuations play an important role in the pressure induced spin transitions.

References:

- [1] C. Pfleiderer et al Nature 427,(227), (2004)
- [2] O. L. Makarova et al PRB 85, 205205, (2012)
- [3] N. Kanazawa et al PRL 106, 156603, (2011)
- [4] M. Deutsch et al PRB RC, 89, 180407R (2014)
- [5] M. Deutsch et al PRB 90, 144201, (2014)
- [6] E. Altynbaev et al PRB 90, 174420, (2014)
- [7] A. Barla et al PRL144, 016803 (2015)

TU.C.2_O4 - Long Periodic Helimagnetic Ordering in CrM_3S_6 ($M = \text{Nb, Ta}$)

Y. Kousaka^{1,2}, T. Ogura³, J. Zhang^{4,5}, P. Miao⁴, S. Torii⁴, T. Kamiyama^{4,6}, J. Campo⁷, K. Inoue^{1,8}, J. Akimitsu³

1. Graduate School of Science, Hiroshima University, Japan
2. Center for Chiral Science, Hiroshima University, Japan
3. Department of Physics and Mathematics, Aoyama-Gakuin University, Japan
4. Institute of Materials Structure Science, KEK, Japan
5. Institute of High Energy Physics, Chinese Academy of Science, China
6. Graduate University for Advanced Studies (Sokendai), Japan
7. CSIC-Universidad de Zaragoza, Spain
8. Institute for Advanced Materials Research, Hiroshima University, Japan

Recently, large attention has been paid to the chiral helimagnetic compounds, allowing an asymmetric Dzyaloshinskii-Moriya (DM) interaction. Under an applied magnetic field, it forms unique magnetic structures such as Skyrmion and chiral magnetic soliton lattice.

However, there have been few experimental results due to the difficulty to synthesize the suitable materials to realize such research. In chiral helical magnetic structures, the pitch angle, mainly determined by the ratio of exchange interaction and DM interaction, is usually very small. As a result, the helimagnetic period can be hundreds of angstroms. Therefore sometimes the angle resolution of thermal neutron diffraction experiments is not high enough to separate fundamental Bragg peaks and magnetic satellite peaks. As consequence, some compounds with chiral helimagnetic ordering may be easily misinterpreted as ferromagnetic ordering.

In order to observe the long periodic helimagnetic structure, we performed neutron diffraction experiments at BL08 (SuperHRPD) in the Materials and Life Science Experimental Facility (MLF) of J-PARC in Japan. By means of super high-resolution powder neutron diffraction in SuperHRPD, we observed very long periodical magnetic satellite peaks in CrM_3S_6 ($M = \text{Nb}$ and Ta) compounds. Magnetic structure analysis indicates these compounds forms helimagnetic structure.

TU.C.2_O5 - Microscopic theory of dzyaloshinskii-moriya coupling and related exchange-relativistic effects

A. Moskvina¹

1. Ural Federal University, Sverdlovsk Oblast, Russia

I present an overview of the microscopic theory of Dzyaloshinskii-Moriya coupling and other related exchange-relativistic effects such as exchange anisotropy, antisymmetric magnetoelectric coupling, antisymmetric magnetogyrotropic effects, and electron-nuclear antisymmetric supertransferred hyperfine interactions in strongly correlated 3d-based compounds. Theoretical results are applied to different classes of 3d compounds from conventional weak ferromagnets (FeF₃, Fe₂O₃, RFeO₃, RCrO₃,...) to unconventional systems such as weak ferrimagnets (e.g., RFe_(1-x)Cr_xO₃), helimagnets (e.g., CsCuCl₃, MnSi), cuprates (La₂CuO₄,...), and different multiferroics. Particular emphasis will be placed on the role of crystal field effects, the sense and direction of the Dzyaloshinskii vector, its dependence on the superexchange bonding geometry, and other subtle features of exchange-relativistic effects. A critical analysis will be given of different approaches to exchange-relativistic coupling based on the cluster and band calculations.

The work was supported by the Government of the Russian Federation Program 02.A03.21.0006 and by the Ministry of Education and Science of the Russian Federation, projects Nos. 1437 and 2725.

TU.C.3_O1 - New results for triangular-lattice quantum antiferromagnets in a magnetic field

G. Marmorini¹, D. Yamamoto², I. Danshita¹

1. *YITP Kyoto, Kyoto, Japan*

2. *Waseda Institute for Advanced Studies, Tokyo, Japan*

Frustrated antiferromagnets are a very rich class of physical systems, in which various new phases of matter are expected to be realized. From a theoretical point of view, however, they present challenging difficulties and typically defy a full quantum treatment. Restricting to a specific region of the parameter space, namely the one of high applied magnetic field, the problem can be solved within the dilute Bose gas of magnons. This also provides benchmarks for a numerical approach based on cluster mean-field theory, with which we determine the ground-state phase diagram of the prototypical spin-1/2 XXZ model on the triangular lattice and explain the magnetization process of $\text{Ba}_3\text{CoSb}_2\text{O}_9$. In a more complicated model with competing exchange interactions we find a new phase characterized by striped chiral order. We will also touch upon the relation between three-magnon scattering and a first-order phase transition between coplanar states, which is currently an open problem.

TU.C.3_O2 - Study of magnetic phase transitions and magnetostriction by means of reversible villari effect

S. Kustov¹, A. el Hichou¹, M.L. Corró¹

1. Departament de Física, Universitat de Les Illes Balears, Palma de Mallorca, Spain

A new technique referred to as mechanomagnetic spectroscopy (MMS) has been used to study the peculiarities of magnetic phase transitions and of magnetoelastic coupling in different magnetically ordered phases of several materials: single and polycrystalline Ni-Fe-Ga-(Co) shape memory alloys, rare earth polycrystalline Dy and such classical ferromagnetic transition elements as Fe and Ni. The method is based on registration of the reversible Villari effect (RVE) as the main experimental parameter [1].

Experimental results obtained for the shape memory alloys belonging to the Ni-Fe-Ga family [2,3], both in the martensitic and cubic phase, point to the existence of a certain domain in the H-T plane, which corresponds to the variation of the sign of magnetoelastic coupling (Villari critical points). The upper temperature limit of this domain is usually very close to the Curie temperature. In single crystalline cubic Ni-Fe-Ga samples such anomaly is found only for the λ_{100} mode of lattice strain.

The highly sensitive method used allows us to study the RVE in ferro-, antiferro- and paramagnetic phases of polycrystalline Dy. We found strong differences in the magnetic hysteresis between cooling to and heating from the ferromagnetic phase as well as time dependence of magnetoelastic coupling in the antiferromagnetic phase. The last effect has been attributed to the relaxation of internal stresses induced during thermal cycling and antiferro-ferromagnetic transition of the first order. A magnetic transition on heating from ferromagnetic phase was observed and related with the helix-fan transition, which was previously considered to occur only on cooling.

References:

- [1] S. Kustov, M.L. Corró, this Conference
- [2] Kustov S, Corró M L, Cesari E, Pérez-Landazabal J I and Recarte V, 2010 J. Phys. D: Appl. Phys. 43 175002
- [3] Corró M L, Chumlyakov Y I, Torrens-Serra J and Kustov S, 2013 J. Phys. D: Appl. Phys. 46 375002

TU.C.3_O3 - Magnetic ordering in magnetic shape memory alloy Ni-Mn-In-Co

K. Ollefs¹, C. Schöppner², I. Titov^{2,3}, R. Meckenstock², F. Wilhelm¹, A. Rogalev¹, J. Liu³, O. Gutfleisch³, M. Farle², H. Wende², M. Acet²

1. *European Synchrotron Radiation Facility (ESRF), Grenoble, France*

2. *Fakultät für Physik and Center for Nanointegration Duisburg-Essen (CeNIDE), Universität Duisburg-Essen, Duisburg, Germany*

3. *Faculty of Physics, M.V.Lomonosov Moscow State University, Moscow, Russia*

4. *Materials Science, Technische Universität Darmstadt, Darmstadt, Germany*

Structural and magnetic properties across the martensite-austenite phase transitions in the shape memory alloy $\text{Ni}_{45}\text{Mn}_{37}\text{In}_{13}\text{Co}_5$ are studied using complementary experimental techniques: ferromagnetic resonance, macroscopic magnetization measurements and x-ray magnetic circular dichroism in the temperature range from 5 K to 450 K [1].

Magnetization measurements exhibit a zero-field-cooled-curve and the field-cooled-curve (and field-warmed) splitting for $T < 30$ K, which indicates the presence of a field and history dependent magnetic state of the sample. This reveals spin glass like behaviour. While in the martensite state the sample shows a low but finite magnetization, in the austenite state the magnetization is increased and the sample is ferromagnetic.

In the ferromagnetic resonance experiments different resonance lines are observed which show coexisting antiferromagnetic and ferromagnetic correlations for the martensite phase and ferromagnetic and paramagnetic correlations in the austenite phase.

Ni and Co K-edge x-ray magnetic circular dichroism measurements confirm an assignment of ferromagnetic resonance lines purely to Ni and Co for a wide temperature range from 125 K to 225 K. Hence, combined ferromagnetic resonance and x-ray magnetic circular dichroism analysis allows to interpret the ferromagnetic resonance measurements in an element selective manner in the alloy.

Financial support by DFG, SPP 1599 is acknowledged.

References:

[1] K. Ollefs, Ch. Schöppner, I. Titov, R. Meckenstock, F. Wilhelm, A. Rogalev, J. Liu, O. Gutfleisch, M. Farle, H. Wende, and M. Acet, submitted to Phys.Rev.B 2015

TU.C.3_O4 - The influence of the magnetic structure on phase transformations in Ni-Mn-Sn heusler alloys - a phase diagram

K. Zaleski¹, M. Ekholm², B. Alling², I.A. Abrikosov², J. Dubowik³

1. NanoBioMedical Centre, Adam Mickiewicz University, Poznan, Poland

2. Department of Physics, Chemistry and Biology, Linköping University, Linköping, Sweden

3. Institute of Molecular Physics, Polish Academy of Sciences, Poznan, Poland

Ni-Mn-Z (Z = Ga, In, Sn, Sb) Heusler alloys belong to a class of magnetic shape memory alloys, in which a martensitic transformation takes place in a ferromagnetic state. This magnetostructural transformation leads to field-induced strains, magnetocaloric effect, modification of exchange coupling, large magnetoresistance, etc. The aforementioned effects depend strongly on the magnetic structure of the alloy, which often changes with the composition. We present the phase diagram of $\text{Ni}_{50}\text{Mn}_{50-x}\text{Sn}_x$ ($0 \leq x \leq 25$) obtained by means of ab initio calculations and Mean Field Approximation. The phase diagram includes temperatures of martensitic transformation (TM) estimated from a difference of calculated total energies of austenite and martensite phase. It also includes the estimated values of Curie temperature of austenite phase (TCA) and Curie and Néel temperatures of martensite phase (TCM, TNM). The calculated values are in good agreement with the experimental ones.

TU.C.3_O5 - Spin-stripe phase in a frustrated spin chain

M. Pregelj¹, A. Zorko¹, O. Zaharko², H. Nojiri³, H. Berger⁴, L. Chapon⁵, D. Ar on^{1,6}

1. Jozef Stefan Institute, Ljubljana, Slovenia

2. Laboratory for Neutron Scattering, PSI, Villigen, Switzerland

3. Institute for Materials Research, Tohoku University, Sendai, Japan

4. Ecole polytechnique f ed erale de Lausanne, CH-1015 Lausanne, Switzerland

5. Institut Laue-Langevin, Grenoble, France

6. Faculty of Mathematics and Physics, University of Ljubljana, Ljubljana, Slovenia

Periodic modulations of various shapes and sizes are encountered in a variety of natural systems, where at least two rival states are present [1]. In strongly correlated electron field such behavior has typically been associated with competition between short- and long-range interactions, e.g., between exchange and dipole-dipole interactions in the case of ferromagnetic thin films. Here we show that spin-stripe textures may develop also in antiferromagnets, where long-range dipole-dipole magnetic interactions are absent. Employing magnetic susceptibility, high-field magnetization, specific heat, and neutron diffraction measurements, we find beta-TeVO₄ [2] to be a nearly perfect realization of a frustrated ferromagnetic spin-1/2 chain [3], namely, a zigzag chain with competing ferromagnetic nearest-neighbor (NN) interaction J_1 and the antiferromagnetic next-nearest neighbor (NNN) interaction J_2 . The ground state of this system has vector-chiral (VC) correlations, while at higher magnetic fields collinear spin-density-wave (SDW) states evolve. Surprisingly though, in a narrow field/temperature range between these two parent states, we discover a remarkable spin strip phase with temperature-dependent nanometer-scale modulation. We associate its existence with weak frustrated short-range interchain exchange interactions, which hereby release the degeneracy of the VC and SDW states present in that particular field range. Effect of interchain interactions may be further assisted by the symmetry allowed electric polarization. The proposed concept provides an alternative route for the stripe formation in strongly correlated electron systems and may help understanding other widespread, yet still elusive, stripe-related phenomena.

References:

[1] M. Seul and D. Andelman, Science 267, 476 (1995)

[2] Y. Savina et al., Phys. Rev. B 84, 104447 (2011)

[3] M. Pregelj et al., in review (2015)

TU.D.1_I1 - Thermalization and exotic frustration in artificial spin ice

P. Schiffer¹, I. Gilbert¹, S. Zhang², C. Nisoli³, G. Chern³

1. *University of Illinois at Urbana-Champaign, Champaign, United States*

2. *Argonne National Laboratory, Lemont, United States*

3. *Los Alamos National Laboratory, New Mexico, United States*

Artificial spin ice consists of arrays of lithographically fabricated single-domain ferromagnetic elements, arranged in different geometries such that the magnetostatic interactions between the moments are frustrated. We have probed a number of different lattice geometries and find both local ordering and disordered states that match classic models for frustrated spin systems.

Our recent work has focused on thermalization of these arrays as well as investigation of lattice geometries that are unavailable in natural systems and are specifically designed to exhibit unusual behavior associated with frustration, e.g., the shakti lattice. Thermalization reveals ordering both of the moments and of the effective magnetic charges that characterize correlated many-body dynamics in these systems.

TU.D.1_O2 - Spin correlations in the randomness-induced quantum spin-liquid state of the spin-1/2 kagome Heisenberg antiferromagnet -- application to herbertsmithite --

T. Shimokawa¹, K. Watanabe¹, H. Kawamura¹

1. Osaka University, Osaka Prefecture, Japan

Herbertsmithite, the spin-1/2 Heisenberg antiferromagnet on the kagome lattice, has attracted considerable interest of researchers as a promising candidate of the possible quantum spin-liquid state [1]. Recent theoretical study has suggested that the effect of the quenched randomness might be important in understanding the nature of the quantum spin-liquid of this material [2]. Namely, the spin-1/2 antiferromagnetic Heisenberg model on the kagome lattice with the bond-random exchange interaction was observed to exhibit a gapless spin-liquid-like ground state, i.e., the random singlet (or the valence-bond glass) state [2,3]. In this study, we investigate the spin correlations of the random-bond spin-1/2 antiferromagnetic Heisenberg model on the kagome lattice by means of an exact diagonalization method to get further insight into the spin-liquid-like ground state of the model. We pay special attention to the dynamical structure factor of the model, with systematically varying the extent of the quenched randomness. The result is compared with the recent inelastic neutron-scattering data on a single-crystal herbertsmithite [4]. Good qualitative agreement is then obtained including a broad peak-like behavior without any gap signature at lower energies and a flat plateau-like behavior at higher energies, supporting the view that the experimentally observed quantum spin liquid state of herbertsmithite might indeed be the random singlet state.

References:

- [1] D. E. Freedman, et al : J. Am. Chem. Soc. 132 (2010) 16185
- [2] K. Watanabe, et al : J. Phys. Soc. Jpn. 83 (2014) 034714
- [3] H. Kawamura, et al : J. Phys. Soc. Jpn. 83 (2014) 103704
- [4] T. -H. Han, et al : Nature 492 (2012) 406

TU.D.1_O3 - Magnetic excitations and phase diagram of the hyperkagome garnets Gd₃Ga₅O₁₂ and Gd₃Al₅O₁₂

O. Florea¹, E. Lhotel¹, P. Deen², H. Jacobsen³, A. Wildes⁴, C. Knee⁵, P. Henry²

1. Institut Neel, Grenoble, France
2. European Spallation Source, Lund, Sweden
3. Niels Bohr Institute, Copenhagen, Denmark
4. Institut Laue-Langevin, Grenoble, France
5. Chalmers University of Technology, Göteborg, Sweden

Antiferromagnets on the hyperkagome lattice generate a great interest in frustrated magnetism. Indeed, on this highly frustrated 3D lattice, the ground state is highly degenerate, resulting in unconventional spin liquid behavior and emergent excitations. Gd₃Ga₅O₁₂ (GGG) is one of the few realizations of this model system, the magnetic Gd ions being on two interpenetrating corner sharing triangular sublattices. Many studies have been devoted to this compound, without giving a clear understanding of its (H,T) phase diagram. No long range order was found down to 25mK, despite a Curie-Weiss temperature of -2K, but a spin freezing was reported below 140mK [1].

We present a new approach to understand the puzzling physics of GGG by combining neutrons scattering and magnetization measurements, and comparing these measurements with the homologous compound Gd₃Al₅O₁₂ (GAG). We recently showed that the rich phase diagram of GGG can be understood in terms of competing interactions with loops of spins, trimers and decagons in addition to antiferromagnetic, ferromagnetic and incommensurate order. The phase diagram centers around a multiphase convergence to a single point at 0.9T and 350mK [2]. In GAG, the lattice parameter is slightly smaller than in GGG and a transition was reported in specific heat around T_c=170mK [3]. Our magnetization measurements evidence a spin freezing below 270mK, and an anomaly around T_c. However neutron scattering only observed short range correlations down to the lowest temperature (60mK), revealing a complex ground state in the manner of GGG. The phase diagram for GAG is also reminiscent of that for GGG. We expect that these results will clarify the mechanisms that stabilize fragile ground states and unusual excitations in these 3D frustrated systems.

References:

- [1] P. Schiffer et al, PRL 73, 2500 (1994)
- [2] P.P. Deen et al, PRB 91, 014419 (2015)
- [3] J.A. Quilliam et al, PRB 87, 174421 (2013)

TU.D.1_O4 - Spin liquid ground state in a vanadium based $S=1/2$ trimerized kagome compoundJ.C. Orain¹, F. Bert¹, P. Mendels¹, L. Clark², F.H. Aidoudi², P. Lightfoot², R.E. Morris²*1. Laboratoire de Physique des Solides, Université Paris-Sud, Orsay, France**2. School of Chemistry and EaSTChem, University of St. Andrews, St. Andrews, United Kingdom*

The search for quantum spin liquid states such as the resonant valence bond state (RVB) formed by the macroscopic resonance between the various spin singlet coverings of the lattice, is a major challenge in both experimental and theoretical condensed matter research [1]. The prime candidate to host this state of matter is the $S=1/2$ Kagome antiferromagnet (KAFM) in two dimensions. Among the rare experimental realizations of the KAFM model the recently synthesized compound, $[\text{NH}_4]_2[\text{C}_7\text{H}_{14}\text{N}][\text{V}_7\text{O}_6\text{F}_{18}]$ (DQVOF) [2], is the first one to host magnetically active V^{4+} (d^1) ions rather than more usual Cu^{2+} (d^9) thus allowing to investigate the effects of different perturbations to the ideal Heisenberg Hamiltonian. Further, this compound seems to be the first experimental realization of the trimerized Kagome model, formed by two different equilateral triangles, initially theoretically studied by M. Mambrini and F. Mila [3]. Our low temperature magnetization and specific heat results suggest that DQVOF is a good candidate for the $S=1/2$ KAFM physics despite a complex structure [4]. Besides, the low temperature specific heat and μSR studies evidence a gapless spin liquid behaviour down to 40mK. Recent NMR studies unveil the intrinsic susceptibility of the Kagome layers which is hidden in the macroscopic measurements by the Curie like interlayer V^{3+} contribution. Under strong magnetic fields, those studies revealed a spin gap of about 15 K ($J/4$). As a consequence, this material exhibits an exotic excitation spectrum, with a continuum of non magnetic excitations, quite reminiscent of the short range RVB physics which could be remarkably favoured by the trimerization of the Kagome model.

References:

[1] L. Balents, Nature 464, 199 (2010)

[2] F. H. Aidoudi and al, Nat. Chem. 3, 801 (2011)

[3] M. Mambrini and F. Mila, Eur. Phys. J. B. 17, 651-659 (2000)

[4] L. Clark and al, Phys. Rev. Lett. 110, 207208 (2013)

TU.D.1_05 - Thermal, transport, and spectral properties of generic quantum spin ice beyond the mean-field theory

S. Onoda¹

1. Riken, Wako, Japan

Quantum spin fluctuations in spin-ice related materials have attracted current great interest in a quest of bosonic U(1) quantum spin liquids hosting unconventional excitations, including deconfined spin-ice monopoles and emergent artificial photons. Reliably describing the nature of these novel excitations beyond naive mean-field approaches is indispensable for properly understanding experiments in relevant materials, such as $\text{Pr}_2\text{Zr}_2\text{O}_7$, $\text{Yb}_2\text{Ti}_2\text{O}_7$, and $\text{Tb}_2\text{Ti}_2\text{O}_7$. Here, taking into account fluctuations of both gauge fields and spinons (spin-ice monopoles) beyond the mean field theory, we revisit the zero- and finite-temperature phase diagram of the generic nearest-neighbor quantum spin ice model and uncover the spectral properties. Weakly first-order transitions due to the spinon condensation via the Higgs mechanism have been reproduced as in the mean-field theory. Furthermore, a finite-temperature confinement-deconfinement crossover has been obtained as a classical to quantum spin ice crossover obtained by quantum Monte-Carlo simulations. This sharply contrasts to a mean-field theory predicting a finite-temperature confinement-deconfinement phase transition. A simple confined phase showing any simple 2-in, 2-out magnetic structure is not stable because it does not gain the kinetic energy of spinons. Effects of the applied magnetic field are also examined. In particular, the $\langle 111 \rangle$ magnetic field can induce a quantum criticality of spinons as 2-in, 2-out states become locally degenerate with 3-in, 1-out states. Then, transport properties of spinons are discussed.

TU.D.2_I1 - Fluctuations and all-in / all-out state in the Ising antiferromagnet Nd₂Zr₂O₇

E. Lhotel¹, S. Petit², M.C. Hatnean³, S. Guitteny², C. Colin¹, J. Robert¹, I. Mirebeau², M.R. Lees³, G. Balakrishnan³

1. Institut Néel CNRS, Grenoble, France
2. Laboratoire Léon Brillouin CEA Saclay, Saclay, France
3. University of Warwick, Coventry, United Kingdom

Pyrochlore compounds (R₂M₂O₇, R=rare-earth, M=metal) are a rich playground for exploring magnetic frustration in a corner-sharing tetrahedron lattice. Depending on the rare-earth element, different spin anisotropy (Ising, easy-plane, Heisenberg) and interactions (antiferromagnetic, ferromagnetic, long-range, anisotropic) come into play, so that exotic phases such as spin-ices or spin liquids can be stabilized [1].

We have investigated single crystals of Nd₂Zr₂O₇, in which the Nd₃₊ magnetic moments exhibit a strong local <111> Ising anisotropy with an effective value of about 2.4μB [2]. Magnetization measurements performed along the [100], [110] and [111] axes of a crystal down to 70 mK, together with powder neutron diffraction experiments, reveal that Nd₂Zr₂O₇ undergoes an antiferromagnetic transition at 285 mK towards an all-in / all-out state. In addition, measurements as a function of field allow us to establish the full (H,T) phase diagram in the three directions of the applied field. This compound exhibits a metamagnetic transition towards an ordered spin ice state around 1000 Oe, associated with strong time dependent effects. Nd₂Zr₂O₇ thus appears as a model system of antiferromagnetic Ising spins on the pyrochlore lattice.

These findings are important since conventional ideas usually associate the all-in / all-out structure with the simple canonical un-frustrated case. However, surprisingly, our experiments demonstrate that the magnetic moment is only partially ordered (0.6μB), while the full moment of 2.4μB is recovered in the field induced phases. These findings point to the predominance of quantum fluctuations, and show that this case is a lot more complicated than it first appears.

References:

- [1] J.S. Gardner et al., Rev. Mod. Phys. 82, 53 (2010)
- [2] M. Ciomaga Hatnean et al., submitted to Phys. Rev. B

TU.D.2_O2 - What is the nature of the ground state in the stoichiometric pyrochlore $\text{Yb}_2\text{Ti}_2\text{O}_7$?

E. Kermarrec^{1,2}, K. Ross³, J. Gaudet¹, N. Butch⁴, H. Dabkowska^{1,5}, B. Gaulin^{1,5,6}

1. *Department of Physics and Astronomy, McMaster University, Hamilton, Canada*

2. *Laboratoire National des Champs Magnétiques Intenses, Grenoble, France*

3. *Colorado State University, Fort Collins, United States*

4. *NIST Center for Neutron Research, Gaithersburg, United States*

5. *Brockhouse Institute for Materials Research, Hamilton, Canada*

6. *Canadian Institute for Advanced Research, Toronto, Canada*

Rare-earth pyrochlores magnets are known to be prime examples of the rich physics generated by magnetic frustration. Among them, $\text{Yb}_2\text{Ti}_2\text{O}_7$ has attracted a lot of attention recently due to the exciting possibility that it could host a Quantum Spin Liquid (QSL) state below a first-order transition observed in specific heat at $T_c = 265\text{mK}$. However, the nature of the ground-state in $\text{Yb}_2\text{Ti}_2\text{O}_7$ is greatly debated, and several studies find some evidences for long range ferromagnetic order below T_c . Moreover, these experimental observations seem to vary from sample to sample, perhaps due to a slightly off-stoichiometry affecting real materials. We will present low temperature neutron scattering measurements carried out on a well characterized polycrystalline sample of stoichiometric $\text{Yb}_2\text{Ti}_2\text{O}_7$.

Our measurements reveal that there is change of intensity at nuclear Bragg positions upon warming which does not occur sharply at T_c , and which is consistent with an ordered moment size of $\sim 1.1 \mu\text{B}$ (58% of the saturation moment). The inelastic excitations at low temperature suggest the presence of dispersive modes coexisting with incoherent low energy fluctuations. The data is very reminiscent to what was recently found on the related pyrochlore compound $\text{Yb}_2\text{Ti}_2\text{O}_7$.

Our results suggest that the ground state in nominally pure $\text{Yb}_2\text{Ti}_2\text{O}_7$ is not a conventional ordered ferromagnet, but instead involves only partial polarization of the magnetic moments coexisting with a disordered component, a situation reminiscent of the partially polarized QSL called the Coulomb Ferromagnetic phase.

TU.D.2_O3 - Anisotropy tuned magnetic order in pyrochlore iridates

E. Lefrançois^{1,2}, V. Simonet², R. Ballou², E. Lhotel², P. Lejay², P. Manuel³, D. Khalyavin³, L.C. Chapon¹

1. Institut Laue-Langevin, Grenoble, France

2. Institut Néel, CNRS & Université, Grenoble, France

3. ISIS Facility, STFC, Rutherford Appleton Laboratory, Swindon, United Kingdom

Attention of the condensed matter community was recently attracted by the pyrochlore iridates $R_2\text{Ir}_2\text{O}_7$ (R = rare-earth ion) where magnetic frustration, strong spin-orbit coupling associated to the Ir^{4+} ions and magnetocrystalline anisotropy associated to the rare earth ions coexist and may lead to exotic magnetic phases and unprecedented electronic transport properties. These compounds exhibit a metal-insulator transition at the temperature corresponding to the onset of the Ir^{4+} magnetic ordering. The transition temperature and the high-temperature electronic state both depend on the rare-earth ion [Matsuhira et al., JPSJ 80 (2011) 094701]. We studied $\text{Er}_2\text{Ir}_2\text{O}_7$ and $\text{Tb}_2\text{Ir}_2\text{O}_7$ by means of magnetization measurement and neutron diffraction on polycrystalline samples. A bifurcation between the zero-field-cooled and field-cooled magnetic susceptibility was observed at respectively 140 K and 130 K, which is attributed to the Ir^{4+} magnetic moment ordering. The neutron diffraction patterns revealed magnetic Bragg peaks below 40 K in $\text{Tb}_2\text{Ir}_2\text{O}_7$. We show that these result from a freezing of the Tb^{3+} magnetic moments, induced by the Ir-Tb exchange, along their local 3-fold axis to form the so-called all-in/all-out magnetic configuration. On the other hand, no evidence of magnetic ordering was found in $\text{Er}_2\text{Ir}_2\text{O}_7$ down to 2K by neutron diffraction, though measurements on a magnetometer equipped with a dilution refrigerator show an extra thermomagnetic hysteresis suggesting a possible freezing below 0.6 K. The contrasting behaviors between $\text{Er}_2\text{Ir}_2\text{O}_7$ and $\text{Tb}_2\text{Ir}_2\text{O}_7$ are explained as being inherent to the change of magnetocrystalline anisotropy between Er (easy-plane) and Tb (easy-axis), which respectively competes against or is consistent with the molecular field associated with the Iridium magnetism [arXiv: 1502.00787]. This in turn strongly supports an all-in/all-out magnetic order on the Ir pyrochlore sublattice, which was awaited as a signature of the topological nature of the low temperature insulating state [Wan et al., PRB 83 (2011) 205101].

TU.D.2_I4 - Quantum order-by-disorder and excitations of anisotropic Kagome antiferromagnets

S. Chernyshev¹, M. Zhitomirsky²

1. *University of California, Irvine, United States*

2. *CEA, Grenoble, France*

In our work we advance theoretical understanding of the quantum effects in kagome-lattice antiferromagnets and provide deep insight into the quantum order-by-disorder mechanism, important for the broad class of realistic frustrated spin systems. We challenge general expectation that quantum fluctuations simply follow thermal ones in selecting the ground state and present a rare example of the situation when quantum order-by-disorder effect defies this trend and yields the ground state that is different from one favored by thermal fluctuations. We also demonstrate that the order selection is generated by topologically non-trivial tunneling processes, making loops around elementary hexagons. We proposed phase diagram of the model and suggest further theoretical studies [1]. Further progress is made in understanding the spectral properties of realistic kagome-lattice antiferromagnets such as Fe-jarosite, for which we demonstrate a remarkable wipe-out effect for a significant portion of their spectrum. This phenomenon is related to the existence of the so-called 'flat mode',---a ubiquitous feature of the kagome-lattice and other highly-frustrated antiferromagnets,---and is due to decay process involving two of such modes.

References:

[1] A. L. Chernyshev and M. E. Zhitomirsky, *Phys. Rev. Lett.* 113, 237202 (2014)

TU.D.3_O1 - In-situ neutron investigation of hydrogen absorption kinetics in La(FexSi_{1-x})¹³ magnetocaloric alloys for room-temperature refrigeration application

X. Hai ^{1,2}, C. Mayer ², C.V. Colin ¹, S. Miraglia ¹

1. Univ. Grenoble Alpes, Institut Néel, Grenoble, France

2. Erasteel SAS, Tour Maine Montparnasse, Paris, France

The La(FexSi_{1-x})¹³ system has attracted wide interest due to its large magnetocaloric effect and tunable transition temperature and nature. Hydrogen interstitials can adjust the temperature range near room-temperature. However, fully hydrogenated alloys are unstable upon heating. In order to get a precise knowledge of the hydrogen location and sequential filling of the interstitial sites, an in-situ high-flux neutron diffraction experiment is performed at Institut Laue Langevin. Moreover, carbon is added as a secondary interstitial element to investigate the site accommodation.

Two interstitial sites (48f and 24d) are considered for hydrogen or carbon accommodation. Refinements confirm that carbon and hydrogen are accommodated in the 24d octahedral site. Knowing that the volume of the interstitial site plays a major role in the stability, we have analyzed the variation of selected Fe-Fe distances of the Fe/Si icosahedral cluster in the course of interstitial insertion. This variation is related to that of the lattice parameter and reveals the one-to-one correspondence between lattice parameter and the Fe-Fe bond.

This time-resolved experiment makes it possible to analyze the absorption and desorption kinetics in the framework of the Avrami model. Results show slower hydrogen kinetics in carbon-containing compounds. It is proposed that there are distinctive diffusion paths for the interstitial atoms in the lattice. The pre-occupied interstitial carbon atoms distort the interstitial hole and this may lead to the blocking of the diffusion paths, depressing rate of the hydrogen absorption/release.

Within the desorption schemes, an asymptotic residual hydrogen concentration is observed for both cases regardless of the presence of carbon. Additional thermal activation is therefore necessary to achieve complete hydrogen desorption. Further investigation with substituted samples (by Ce and/or Mn) is planned to illustrate a substituting effect in the interstitial site space.

TU.D.3_O2 - Prototype energy harvesting device using high permeability amorphous ribbon

J. Samaniego ¹, A. Mitra ², C. Gómez-Polo ¹

1. *Universidad Pública de Navarra, Pamplona, Spain*

2. *CSIR - National Metallurgical Laboratory, Jamshedpur, India*

Energy harvesting on a miniature scale based on the utilisation of various properties of materials like piezoelectric, electromagnetic, electrostatic, thermoelectric etc. have generated considerable research interest over the years. In such devices the spent energies have been reused to develop miniature sized power generating system to replace the extensive use of the storage batteries.

Among the available energy harvesting systems, vibration based miniaturized generators have recently attracted a great deal of interest within both the academic community and industry, as a potential inexhaustible source for low-power devices [1,2] due to their better mechanical reliability and higher output signal. The present work is related to the development of a prototype vibration based energy harvesting device using high permeability Co-based amorphous ribbon and NdFeB permanent magnet. Two sets of coils having 1000 turns each were placed in mutually perpendicular direction for measuring the pick-up voltages generated due to the relative vibration of the permanent magnet. The dimension and resistance of each coil were 20mm x 7mm x 5mm and 70 Ohm respectively. Two sets of multiple poles NdFeB magnets separated by a distance were placed on a spring. The maximum flux density of the NdFeB magnet was 0.4T. Rapidly solidified high permeability $\text{Co}_{66}\text{Si}_{16}\text{B}_{12}\text{Fe}_4\text{Mo}_2$ ribbon was used to couple the flux from the permanent magnet to the coil. Four layers of the ribbon (30mmx5 mmx25 μm) were used to couple the flux of the permanent magnet to the pick-up coils. The entire system was made to vibrate using linear vibrator. Maximum pick-up voltages were obtained at a vibrating frequency of 14.5 Hz with a full width at half maximum as 9 Hz.

Acknowledgement: The financial support to one of the authors (AM) from Ministry of Education, Govt. of Spain under Campus of International Excellence Programme is gratefully acknowledged.

TU.D.3_O3 - An in-situ computed tomography study of the magnetovolume transition in $\text{LaFe}_{11.8}\text{Si}_{1.2}$

A. Waske¹, A. Funk^{1,2}, A. Rack³, J. Eckert^{1,2}

1. *Institute for Complex Materials, Dresden, Germany*
2. *Institute for Materials Science, Dresden, Germany*
3. *ID - 19, ESRF, Grenoble, France*

First-order transitions in magnetocaloric materials are the source of strong changes in their magnetization and entropy, giving rise to large magnetocaloric effects. These kind of transitions show interesting phenomena, like phase coexistence and thermal arrest. The way each phase nucleates from the other phase is largely unknown at a microscopic level, besides this being important not only from a fundamental point of view, but also for technical aspects like choosing the geometry of the sample or identifying an upper limit for the cycling frequency.

In $\text{La}(\text{Fe},\text{Si})^{13}$, an isostructural first-order transition occurs at the critical temperature T_C , which retains the structural symmetry of the crystal but leads to an abrupt increase in the lattice parameter. We apply low-temperature in-situ computed tomography on magnetocaloric $\text{La}(\text{Fe},\text{Si})^{13}$ to study the magnetovolume transition as a function of temperature. The in-situ experiments have been carried out at the beamline ID 19 at the ESRF in Grenoble (France). A stream of cold nitrogen gas was used to drive the magnetocaloric material through the phase transition upon cooling. Using this method, we show how the transition proceeds through a small sample of $\text{LaFe}_{11.8}\text{Si}_{1.2}$ upon cooling by tracking the subvolumes that turn at each temperature step around the critical temperature T_C . We observe that the regions which perform the magnetovolume transition first are determined by the surface morphology, and that there are big differences in the evolution of the phase transition for flat and rough sample regions. These findings connect microstructural aspects of the first-order transition to important properties like hysteresis and kinetics of the phase transition and can therefore help to tailor magnetocaloric materials towards application.

TU.D.3_O4 - Element resolved thermodynamics of magnetocaloric LaFe_{13-x}Si_x

H. Wende¹, M. Gruner^{1,2}, W. Keune^{1,3}, B. Roldán Cuenya⁴, C. Weis¹, J. Landers¹, S. Makarov^{1,3}, D. Klar¹, M.Y. Hu⁵, E.E. Alp⁵, M. Krautz², O. Gutfleisch⁶

1. University of Duisburg-Essen, Faculty of Physics and Center for Nanointegration Duisburg-Essen (CENIDE), Germany
2. IFW Dresden, Germany
3. Max Planck Institute of Microstructure Physics, Halle, Germany
4. Department of Physics, Ruhr-University Bochum, Germany
5. Advanced Photon Source, Argonne National Laboratory, United States
6. Materials Science, TU Darmstadt, Germany

Ferroc materials allow for a significant adiabatic temperature change induced by realistic electrical and magnetic fields, under pressure and external stress [1]. This approves their use in solid state refrigeration concepts, which offer an energy efficient alternative to the classical gas-compressor scheme. A good cooling material is characterized by a large isothermal entropy change $|\Delta S_{\text{iso}}|$, which determines the latent heat to be taken up during a first-order transformation in conjunction with a high adiabatic temperature change $|\Delta T_{\text{ad}}|$, which controls the operating range. Apart from the prototype Gd-based systems, a large number of suitable materials have evolved, which undergo a magnetic first-order transition and perform well with respect to both quantities, and LaFe_{13-x}Si_x-based compounds are found among the best [2, 3]. They consist of largely abundant components and are significantly less expensive than Gd- or Rh-based alloys. By combination of two independent approaches, nuclear resonant inelastic x-ray scattering (NRIXS) and first principles calculations in the framework of density functional theory, we demonstrate significant changes in the element-resolved vibrational density of states across the first-order transition from the ferromagnetic low temperature to the paramagnetic high temperature phase of LaFe_{13-x}Si_x [4]. These changes originate from the itinerant electron metamagnetism associated with Fe and lead to a pronounced magneto-elastic softening despite the large volume decrease at the transition. The increase in lattice entropy associated with the Fe subsystem is significant and contributes cooperatively with the magnetic and electronic entropy changes to the excellent magneto- and barocaloric properties.

References:

- [1] K. A. Gschneidner Jr., V. K. Pecharsky, and A. O. Tsokol, Rep. Prog. Phys. 68, 1479 (2005)
- [2] S. Fujieda, A. Fujita, and K. Fukamichi, Appl. Phys. Lett. 81, 1276 (2002)
- [3] J. Lyubina, R. Schäfer, N. Martín, L. Schultz, and O. Gutfleisch, Adv. Mater. 22, 3735 (2010)
- [4] M. E. Gruner, W. Keune, B. Roldan Cuenya, C. Weis, J. Landers, S. I. Makarov, D. Klar, M. Y. Hu, E. E. Alp, J. Zhao, M. Krautz, O. Gutfleisch, and H. Wende, Phys. Rev. Lett. 114, 057202 (2015)

TU.E.1_O1 - Magnetic phase diagram and ordered ground state in GdMn₂O₅ multiferroic studied by x-ray and neutron scattering.

A. Bombardi¹, C. Vecchini^{1,2}, L. Chapon³, P. Radaelli⁴, S. Cheong⁵

1. *Diamond Light Source Ltd., Harwell Science and Innovation Campus, Didcot, Oxfordshire, United Kingdom*

2. *National National Physical Laboratory Hampton Road, Teddington, Middlesex, United Kingdom*

3. *Institut Laue-Langevin, Grenoble, France*

4. *Department of Physics, University of Oxford, Parks Road, Oxford, United Kingdom*

5. *Rutgers Center for Emergent Materials and Department of Physics and Astronomy, Rutgers University, Piscataway, United States*

We recently reported giant tunability of ferroelectric polarization ($\Delta P=5000 \mu\text{C}/\text{m}^2$) in the multiferroic GdMn₂O₅ with external magnetic fields[1]. The zero field magnetic model determined from x-ray magnetic scattering indicates that the Gd-Mn symmetric exchange striction plays a major role in the tunable ferroelectricity of GdMn₂O₅, differently from other members of the same family. The Gd spins plays a key role in the giant magnetoelectric coupling in GdMn₂O₅. Magnetic field polarization measurements evidenced a very strong polarization dependence showing a sign reversal upon switching or increasing ($H>6\text{T}$) magnetic field. Here we present the magnetic phase diagram as determined from recently performed neutron diffraction experiments on an isotopically pure sample. This investigation is crucial to our understanding of the giant polarization reversal observed in this sample [2].

References:

[1] N. Lee et al, Phys. Rev. Lett. 110, 137203 (2013)

[2] C. Vecchini et al in preparation

TU.E.1_O2 - Magnetic structure of LuFe₂O₄ studied by soft x-ray magnetic circular dichroismS. Lafuerza¹, J. García², G. Subías², J. Blasco², J. Herrero-Martín³

1. European Synchrotron Radiation Facility (ESRF), Grenoble, France
2. Instituto de Ciencia de Materiales de Aragón (ICMA), Zaragoza, Spain
3. ALBA Synchrotron, Barcelona, Spain

The mixed-valence oxide LuFe₂O₄ is among the most studied multiferroic candidates since a new type of ferroelectricity based on charge ordering (CO) of Fe⁺² and Fe⁺³ was postulated below T_{CO} ≈ 320 K [1]. LuFe₂O₄ shows ferrimagnetic ordering with T_N ≈ 240 K and therefore both the electric and magnetic orderings would interestingly occur at high transition temperatures. Regrettably, the ferroelectric character of LuFe₂O₄ has been discarded in the light of new electric properties measurements [2]. This finding has been further supported by results of x-ray absorption spectroscopy [3], resonant x-ray scattering and high resolution powder diffraction [4] that agree with the presence of multimodal Fe valence distributions Fe^{+2.5±δ} below T_{CO} and T_N in which the maximum charge disproportionation is such that δ ≈ 0.25 electrons, far from the pure ionic CO model.

In the view of these results, the generally accepted ferrimagnetic ordering for LuFe₂O₄ in terms of Fe⁺²/Fe⁺³ ionic species needs to be revisited. We have performed x-ray magnetic circular dichroism (XMCD) measurements at the Fe L_{2,3}-edges in polycrystalline and single crystal samples of LuFe₂O₄. These measurements were carried out at BL29-BOREAS beamline of ALBA synchrotron (Spain) by using both total electron yield and fluorescence yield for the x-ray absorption spectra detection. The XMCD signal magnitude reproduces the strong anisotropy found in the macroscopic magnetization between the *c*-axis and the *ab*-plane of the hexagonal structure. Regarding the spectral features, two contributions with opposite sign are obtained in agreement with an antiferromagnetic coupling between two sublattices. Our experimental results along with multiplet theory calculations lead us to propose an alternative ferrimagnetic model for LuFe₂O₄. In our spin-ordering model the moments of Fe^{+2.2} and Fe^{+2.5} are aligned parallel (↑) to the applied magnetic field while the Fe^{+2.8} moments are antiparallel (↓) as opposed to the initially established model Fe²⁺ (↑) + 1/3Fe³⁺ (↑) + 2/3Fe³⁺ (↓).

References:

- [1] N. Ikeda *et al.*, Nature, 436, 1136 (2005).
- [2] S. Lafuerza *et al.*, Phys. Rev. B, 88, 085130 (2013).
- [3] S. Lafuerza *et al.*, Phys. Rev. B, 89, 045129 (2014).
- [4] S. Lafuerza *et al.*, Europhys. Lett. 107, 47002 (2014).

TU.E.1_O3 - Multiferroic perovskite RMnO_3 crystalline films studied by resonant soft and hard X-ray diffraction

W. Windsor¹, L. Rettig¹, A. Alberca¹, M. Ramakrishnan¹, K. Shimamoto², S. Huang¹, Y. Hu², V. Scagnoli¹, T. Lippert², C. Schneider², U. Staub¹

1. *Swiss Light Source, Paul Scherrer Institut, Villigen, Switzerland*

2. *General Energy Research Department, Paul Scherrer Institut, Villigen, Switzerland*

RMnO_3 perovskites with heavier R ions (R = Ho, Tm, Yb, Lu) are type-II multiferroics known to acquire significantly large electric polarizations when magnetic order sets in (~10 times larger than in TbMnO_3 [1]). These prototypical multiferroics are of great theoretical interest due to the ambiguity surrounding the mechanisms driving the multiferroic behavior [2,3]. Unfortunately the absence of high quality crystals of the heavy-R species has limited experimental work. Here we present a synchrotron X-ray diffraction study of high-quality single-crystalline o- RMnO_3 films with R=Ho, Tm, Yb and Lu. We will show that the magnetic order and the ferroelectric structural distortion appear concomitantly, and are directly controlled by epitaxial strain [4].

For this we directly probed the Mn magnetic structure with resonant magnetic diffraction at the Mn L-edges, and we probed the ferroelectric behavior through the appearance of symmetry-forbidden charge reflections. These are directly sensitive to the lowering of crystal symmetry at the multiferroic transition due to the ferroelectric structural distortion, and allow estimating how much the atoms actually move within the unit cell. We will also show that epitaxial films differ from bulk, as their magnetic structure is incommensurate, and not a "pure" E-type. A model for the magnetic order induced by the Mn on the R ion will also be discussed.

References:

- [1] Ishiwata et al., Phys. Rev B 81, 100411(R) (2010)
- [2] Federova et al., arXiv:1412.3702 [cond-mat.mtrl-sci] (2014)
- [3] Mochizuki et al., Phys. Rev. B 84, 144409 (2011)
- [4] Windsor et al., Phys. Rev. Lett. 113, 167202 (2014)

TU.E.1_O4 - Neutron scattering investigations of bulk and thin film multiferroic LuFeO₃

W. Ratcliff¹, S. Disseler¹, X. Luo², Y.S. Oh³, R. Hu³, J. Lynn¹, J. Borchers¹, C. Brooks⁴, J. Mundy⁴, J. Moyer⁵, D.A. Tenne⁶, P. Schiffer⁵, D. Muller⁴, J. Lau¹, D. Schlom⁴

1. NIST, Maryland, United States

2. Pohang University of Science and Technology, Pohang, Republic of Korea

3. Rutgers University, New Jersey, United States

4. Cornell University, New York, United States

5. University of Illinois, Illinois, United States

6. Boise State University, Idaho, United States

In this talk, we discuss our recent measurements on the hexagonal LuFeO₃ multiferroic in thin film and bulk forms.

While the ferroelectric order sets in at ~1000 K, magnetic order occurs at a far lower temperature.

We present results for MBE grown films on YSZ and Al₂O₃ substrates of thicknesses ranging from 22-250 nm in thickness.

In all cases the antiferromagnetic transition temperature is < 160 K. We also present our data on doping stabilized bulk LuFeO₃ in which we determine how the crystallographic structure influences the magnetic structure.

We also present the results of inelastic measurements in which we determine the basic exchange parameters for this compound.

TU.E.1_O5 - A high-pressure misfit-related polymorph of LuFe₂O₄ with room temperature antiferromagnetic order

F. Damay¹, M. Poiénar², M. Hervieu³, A. Guesdon³, J. Bourgeois^{1,3}, T. Hansen⁴, E. Elkaim⁵, J. Haines², P. Hermet², L. Konczewicz², T. Hammouda⁶, J. Rouquette², C. Martín³

1. Laboratoire Leon Brillouin, Gif sur Yvette, France

2. Institut Charles Gerhardt, Montpellier, France

3. Laboratoire CRISMAT, Caen, France

4. Institut Laue-Langevin, Grenoble, France

5. Synchrotron Soleil, Saint-Aubin, France

6. Laboratoire Magmas & Volcans, Clermont-Ferrand, France

Branded for its potential electronic ferroelectricity [1], [2], charge-ordered LuFe₂O₄ [3] has a layered Fe triangular framework, whose topology is source of degeneracy, both at the charge and spin levels. A high-pressure form of this material, LuFe₂O₄-*hp*, metastable at ambient pressure and temperature, was recently identified [4], but a comprehensive structural investigation of this compound was impaired by complex twinning mechanisms and modulation phenomena, the latter possibly related to charge ordering.

In this work, new samples of the high-pressure form of LuFe₂O₄ have been synthesised and thoroughly characterized by synchrotron X-ray, electron and neutron diffraction, combined with density functional theory (DFT) calculations and transport measurements. Although the pseudo-triangular lattice of the Lu layer is preserved in LuFe₂O₄-*hp*, the structure of the more deformable Fe bilayer changes to rectangular. LuFe₂O₄-*hp* is thus characterized by an original *misfit*-like monoclinic structure, accommodating a buckled triangular [Lu]_∞ layer and two shifted adjacent rectangular [Fe]_∞ planes belonging to a distorted rock salt-type layer. The release of the geometric frustration of the Fe magnetic lattice in the *hp* form leads to collinear antiferromagnetic ordering at T_N = 380 K, the room-temperature magnetic ground state of LuFe₂O₄-*hp* bearing close resemblance to that of NaCl-type monoxide FeO [5]. A stable stripe-like CO configuration is derived from DFT calculations of LuFe₂O₄-*hp*, though transport measurements are not conclusive as to whether, and in which temperature range, LuFe₂O₄-*hp* could be charge-ordered. The room-temperature coexistence of charge and magnetic orders in this material remains therefore an open issue.

References:

- [1] N. Ikeda, et al., Y. Murakami, K. Yoshii, S. Mori, Y. Horibe, and H. Kito, Nature 436, 1136 (2005)
- [2] S. W. Cheong and M. Mostovoy, Nature Materials 6, 13 (2007)
- [3] Y. Yamada, et al., Physical Review B 62, 12167 (2000)
- [4] J. Rouquette, et al., Physical Review Letters 105, 237203 (2010)
- [5] W. L. Roth, Phys. Rev. 110, 1333 (1958)

TU.E.1_O6 - Ultrafast spin dynamics of optically and THz excited TbMnO₃

T. Kubacka¹, J. Johnson², M. Hoffmann³, C. Vicario², S. de Jong³, P. Beaud², S. Grübel², S-W. Huang², L. Huber¹, L. Patthey², Y.D. Chuang⁴, J.J. Turner³, G.L. Dakovski³, S.L. Johnson¹, U. Staub²

1. *ETH Zurich, Zurich, Switzerland*

2. *Paul Scherrer Institut, Villigen, Switzerland*

3. *SLAC National Accelerator Laboratory, Menlo Park, United States*

4. *Lawrence Berkely National Laboratory, Berkeley, United States*

We present a study on the ultrafast spin dynamics in multiferroic TbMnO₃, the model spin-cycloid multiferroic where the ferroelectric polarization arises directly from the frustrated magnetic order. We discuss the magnetic and structural response of multiferroic TbMnO₃ to short cycle THz pulses and to excitations with 800 nm electromagnetic radiation. In the first case, we show that this excitation resonantly drives an electromagnon, which is studied by ultrafast resonant x-ray diffraction. [1] We can quantitatively determine its spin motion in real time and estimate the E-field strength required for switching the polarization. In the second case we excite mainly d-d intersite transitions of Mn, which leads to a suppression of magnetic order within 5-20 ps after excitation. This is unexpectedly slow compared to other multiferroics such as CuO. [2] This slow decay is attributed to a non-thermal melting of magnetic order, indicating that the excited electronic system transfers energy slowly to heat the spin system. Whether this energy is mediated by the lattice due to the creation of a small polaron or simple lattice heating could be addressed in the future by probing other diffraction peaks sensitive to lattice and charge order. The lack of any significant change in the scattering wavevector indicates that despite ultrafast pump, the extremely low magnon group velocity prohibits fast changes in the spin-spiral length.

References:

[1] T. Kubacka et al., *Science* 343, 1333 (2014)

[2] S. L. Johnson et al., *Phys. Rev. Lett.* 108, 037203 (2012)

TU.E.2_O1 - Giant Magnetoelectric effect in FeCo and FeCo/Ag films on (011) oriented PIN-PMN-PT

M. Staruch¹, P. Finkel¹

1. Naval Research Laboratory, Washington, United States

To engineer large magnetoelectric coupling in composites, it is necessary to optimize the properties of both the magnetic and ferroelectric components. There has recently been much interest in single crystals of relaxor ferroelectric $\text{Pb}(\text{In}_{1/2}\text{Nb}_{1/2})\text{O}_3\text{-Pb}(\text{Mg}_{1/3}\text{Nb}_{2/3})\text{O}_3\text{-PbTiO}_3$ (PIN-PMN-PT) due to high piezoelectric coefficient with larger linear range and temperature stability than binary relaxors, which could provide for large tunability of the magnetization. In this work, thin films of FeCo and FeCo/Ag multilayers were deposited on (011) PIN-PMN-PT crystals. The coercive field was significantly decreased in the multilayer film, which also showed a larger piezomagnetic coefficient at a lower magnetic field as compared to FeCo. Angular dependence measurements of the magnetization show an in-plane easy axis that is rotated with an electric field applied to the PIN-PMN-PT crystal. Giant converse magnetoelectric coupling up to $2 \times 10^{-6} \text{ s m}^{-1}$ were observed in heterostructural composites with both FeCo and FeCo/Ag.

This work was funded by the Office of Naval Research (ONR) through the Naval Research Laboratory Basic Research Program.

TU.E.2_O2 - $Mn_{1-x}Co_xWO_4$: $x = 0.135$ and $x = 0.15$: a study of the multiferroic state under high pressure

M. Gooch¹, N. Poudel¹, B. Lorenz¹, K.C. Liang¹, Y.Q. Wang¹, Y.Y. Sun¹, J. Wang², J. Fernández-Baca², F. Ye², C.W. Chu^{1,3}

1. Texas Center for Superconductivity at The University of Houston, Houston, United States

2. Oak Ridge National Lab, Oak Ridge, United States

3. Lawrence Berkeley National Lab, Berkeley, United States

It is well understood that multiferroic materials are sensitive to small perturbations induced through chemical substitution, magnetic and electric fields, or external pressure. One such system is $Mn_{1-x}Co_xWO_4$, which has an interesting and complex phase diagrams where two multiferroic phase coexist at $x = 0.15$. At this boundary on the phase diagram the conical spin extends to lower temperature, in addition to the a-c spiral spin structure forming below 7 K. On either side of the boundary we have a spiral spin structure for $x < 0.15$ and a conical spin for $x > 0.15$. To gain further insight into this system, high pressure measurements were conducted up to 18 kbars. Beginning with $x = 0.135$, only an a-axis polarization is observed at ambient pressure, which is consistent with the a-c spiral by symmetry. However, with increasing pressure a b-axis component of the polarization is observed and the a-axis component is decreasing. At the highest pressure measured, no a-axis polarization is observed and the polarization of the b-axis is comparable to the ambient data for $x = 0.17$. High pressure polarization measurements for the $x = 0.15$ are consistent with the previously mentioned measurements, where with pressure an increase in the polarization is observed. The effect of external pressure on the $Mn_{1-x}Co_xWO_4$ system can be described as similar to Co doping. Suggesting we have a polarization flop, where the a-c spiral is stabilized into the conical spin leading to the increased polarization that is observed.

TU.E.2_O3 - Magon-phonon interactions in hexagonal multiferroic YMnO₃

A. Kreisel¹, S. Mukherjee¹, B.M. Andersen¹, T. Schäffer¹, S. Holm¹, K. Lefmann¹, N.C.R. Momsen¹, J. Larsen², A. Fennell³, U. Stuhr³, Z. Yamani⁴

1. Niels Bohr Institute, University of Copenhagen, Copenhagen, Denmark

2. Institute of Physics, Technical University of Denmark, Lyngby, Denmark

3. Laboratory of Neutron Scattering, Paul Scherrer Institute, Villigen, Switzerland

4. Chalk River National Laboratory, Ontario, Canada

The multiferroic material YMnO₃ is known to show a large spin lattice coupling such that the spin and lattice degrees of freedom influence various properties, as for example the thermal conductivity that is found to have an anomalous contribution. The magnetoelastic modes have been measured recently in neutron diffraction experiments and linked to certain spectral features in Raman signals. Starting from a Heisenberg model on a triangular lattice with single ion anisotropies, we investigate the spin-phonon coupling via the magnetostriction mechanism and derive a coupled magnon-phonon model valid in the entire Brillouin zone. Within a spin-wave approach, where the coupling yields a hybrid magnon-phonon mode, we calculate the dynamic structure factor and compare to recent experimental neutron results.

TU.E.2_04 - Field-induced phase transitions and magnetoferroelectricity in the perfect triangular lattice antiferromagnet RbFe(MoO₄)₂ in a vertical magnetic field

H. Mitamura¹, R. Watanuki², N. Onozaki², Y. Amou², Y. Kono¹, S. Kittaka¹, Y. Shimura¹, I. Yamamoto², K. Suzuki², T. Sakakibara¹

1. *Institute for Solid State Physics, The University of Tokyo, Tokyo, Japan*

2. *Faculty of Engineering, Yokohama National University, Yokohama, United States*

The perfect triangular-lattice antiferromagnet RbFe(MoO₄)₂ (RFMO), in which Fe³⁺ carries spin 5/2, orders at TN=3.9 K in a planar spin structure characterized by the ordering vector $q=(1/3,1/3,0.458)$, an in-plane 120-degree rotation with helicity along the c axis [1]. Interestingly, RFMO exhibits ferroelectricity below TN [1], and its origin has recently been identified to be due solely to the in-plane triangular-spin chirality [2]. Indeed, the obtained phase diagram for the electric polarization (P // c) with B // c plane [2] agrees well with the one theoretically predicted for the spin chirality of a Heisenberg spin triangular lattice antiferromagnet [3]. However, not much has been known for the field evolution of chirality with B // c axis [4].

We performed P(B), dielectric constant and magnetization (M) measurements on RFMO in high magnetic fields applied along the c axis. Whereas M(B) at T=1.5 K monotonically increases with B up to the saturation at B=21 T, P(B) disappears about 14 T, far below the saturation point. In a field range $13 \leq B \leq 14$ T, the temperature variation of the dielectric constant shows double peaks below 2.8 K, indicating two successive transitions. These results strongly suggest the presence of a new high-field phase; the magnetic structure changes from a low-field conical state having chirality to a high-field coplanar non-collinear structure without chirality. The obtained phase diagram is in agreement with a theoretical prediction on hexagonal XY-like Heisenberg antiferromagnets [5].

References:

- [1] M. Kenzelmann et al., Phys. Rev. Lett. 98, 267205 (2007).
- [2] H. Mitamura et al., Phys. Rev. Lett. 113, 147202 (2014).
- [3] H. Kawamura and S. Miyashita, J. Phys. Soc. Jpn. 54, 4530 (1985).
- [4] L.E. Svistov et al., Phys. Rev. B 74, 024412 (2006).
- [5] S. Watarai et al., J. Phys. Soc. Jpn. 70, 532 (2001).

TU.E.2_05 - Study of spin-lattice competition through hydrostatic pressure in CdCr₂S₄G. Oliveira^{1,2}, A. Dos Santos³, Z. Gai⁴, J. Pedro Araújo², A.M. Lima Lopes², A.M. Pereira²*1. CFNUL - Centro de Física Nuclear, Universidade de Lisboa, Lisboa, Portugal**2. IFIMUP and IN-Institute of Nanoscience and Nanotechnology, Departamento de Física e Astronomia da Faculdade de Ciências da Universidade do Porto, Porto, Portugal**3. Quantum Condensed Matter Division, Oak Ridge National Laboratory, Oak Ridge, United States**4. Center for Nanophase Materials Sciences, Oak Ridge National Laboratory, Oak Ridge, United States*

Modern society has a critical demand for materials with multifunctional physical properties. They have become an integrating part of many applications, especially those that display a strong coupling between magnetic and polar degrees of freedom, the so-called magnetoelectrics. These materials, promise a paradigm-shift on technologies for magnetic data storage, high-frequency magnetic devices, spintronics, and micro-electromechanical systems. The clear determination of the complex interplay between electronic, magnetic, and lattice degrees of freedom usually is the solution to explain the mechanisms behind the exhibited physical properties. Among the numerous materials with an intimate coupling between all the degrees of freedom are the group of ACr₂X₄ spinels (A=Zn,Cd,Hg;X=O,S,Se). The tight alliance between structural, vibrational, magnetic, and charge degrees of freedom, makes the variation of lattice by external pressure an appealing route for studying the physical properties of these materials. Measuring the pressure dependence of the magnetic transition temperature may assist in getting new insights about the ordering mechanism and its relationship to the electronic structure (e.g. disordered local moments coupled with frustration mechanisms). In fact, external pressures are known to control bond lengths and bond angles as well as the degree of overlap between electron orbitals in solids. A shift and/or split of the energy levels and changes in exchange interactions strength in response to pressure variations can also occur. External press. when compared to the chemical press., is a cleaner tool to avoid substitutional induced disorder and spurious effects due to different chemical compositions. Several studies reported structural and electronic transitions under pressure for various Cr-based spinels. Nevertheless, studies on the relaxor-like temperature zone are not yet reported. Our results of dc magnetisation measurements under hydrostatic pressure for the CdCr₂S₄ spinel compound will be presented. The measurements have been performed on a polycrystalline sample under different applied hydrostatic pressures (up to 14 kbar) in the 30-220K temperature range (with 30e applied magnetic field). The anomalous behaviour of the magnetic susceptibility indicates that the local-cluster- phase that exists at low applied magnetic fields persists with applied pressures up to 14kbar and has a dependency on the applied pressure.

TU.E.2_06 - Dual ferroic properties of hexagonal ferrite ceramics BaFe₁₂O₁₉ and SrFe₁₂O₁₉

L. Panina¹, V. Kostishyn¹, L. Kozhitov¹, A. Timofeev¹, A. Zyuzin²

1. National University of Science And Technology MISIS, Moscow, Russia

2. Science and Technology Institute of Interbranch Information, Moscow, Russia

Coexistence of ferromagnetism and large ferroelectricity has been observed in hexaferrites BaFe₁₂O₁₉ and SrFe₁₂O₁₉ prepared by a standard ceramic technique from high-purity raw materials. The addition of boron oxide at the stage of wet milling makes it possible not only to restrict the grain size (with the average value of 300-400 nm) but also to increase the bulk resistivity. The latter is of primary importance to realise ferroelectric properties. The prepared polycrystalline samples had a single hexagonal phase, which was confirmed by X-ray diffraction patterns. The magnetic hysteresis is consistent with hard magnetic behaviour having the remanence induction of 3700 G and coercivity of 2 kOe. Large spontaneous polarisation in the range of 25-30 fC/cm² and coercivity of 100-200 kV/m were observed by measuring the electric hysteresis loops. A strong coupling between magnetic and electric ordering was confirmed by measuring the magnetoelectric parameter, magnetodielectric ratio and magnetic hysteresis in the presence of electric field. The obtained results are compared with the available data on multiferroic properties of widely studied BiFeO₃ films [1]. The magnetic properties of hexaferrites are much greater and the magnetoelectric coupling is stronger. On the other hand, the observed multiferroic properties are similar to those reported for corresponding hexaferrites sintered by polymer precursor technique [2]. This suggest great application potential of M-type hexaferrites in devices utilising magnetoelectric coupling.

References:

- [1]A.A. Amirov, A.B. Batdalov, S.N. Kallaev et al. Physics of the Solid State, V.51, p.1123 (2009)
[2]Guolong Tan, Xiuna Chen. J. of Magn. Magn. Mat., V. 327, p. 87 (2013)

TU.E.3_I1 - Transport with bose-einstein magnon condensates

B. Hillebrands¹, P. Clausen¹, D.A. Bozhko^{1,2}, V.I. Vasyuchka¹, G.A. Melkov³, A.A. Serga¹

1. *Fachbereich Physik and Landesforschungszentrum OPTIMAS, Technische Universität Kaiserslautern, Germany*

2. *Graduate School Materials Science In Mainz, Kaiserslautern, Germany*

3. *Faculty of Radiophysics, Electronics and Computer Systems, Taras Shevchenko National University of Kyiv, Ukraine*

The field of magnonics addresses the transfer and processing of information by spin waves and their quanta, magnons. Magnons are bosons and, thus, they can condense into a macroscopic quantum state. Condensates of magnons relate to Bose-Einstein condensates (BEC), and they spontaneously form a spatially extended, coherent ground state, which can be established independently of the magnon excitation mechanism even at room temperature. It is expected that magnon condensates can move in a form of a supercurrent, which represents a novel type of macroscopic quantum transport phenomenon analogous to the low-temperature effects of superconductivity and superfluidity. Magnon supercurrents constitute the transport of angular momentum, which is driven by a phase gradient in the magnon-condensate wave function. In this presentation, first experimental evidence of a magnonic supercurrent will be presented and its further implications will be discussed. The magnon supercurrent is created in a magnon BEC subject to a thermal gradient which imposes the phase gradient.

TU.E.3_O2 - Controlling the magnetic properties of spinel ferrite nanoparticles by chemical tuning

*C. Sangregorio*¹, M. Albino², V. Bonanni², G. Campo², P. Ghigna³, J.M. Greneche⁴, D. Peddis⁵, F. Pineider², N. Yaacob⁴, C. de Julián Fernández⁶

1. CNR-ICCOM & INSTM, Sesto Fiorentino, Italy
2. INSTM-LaMM, Dip. di Chimica "U. Schiff", Univ. di Firenze, Sesto Fiorentino, Italy
3. Dip. Di Fisica, Univ. di Pavia, Pavia, Italy
4. Universit  du Maine, Laboratoire de Physique de l'Etat Condense, Le Mans, France
5. CNR-ISM, Monterotondo Scalo, Italy
6. CNR-IMEM & INSTM, Parma, Italy

Magnetic nanoparticles, MNP, are expected to have a tremendous impact on several technological fields, ranging from electronics, to spintronics and clinical applications, one of the most prominent reasons being the possibility of fine tuning their physical properties to match the required optimal values. The feasibility of such a control requires the exact knowledge of the effect of size, morphology, structure and chemical composition on the magnetic properties of the final product. However, much information is still missing, mostly because of the difficulty in controlling independently each of the above parameters. However, the recent development of improved wet-chemistry syntheses, allowing for a tighter control on the MNP's features, has boosted a renewed interest in the field. In this contribution we present an in-depth investigation of the magnetic properties of a family of doped ferrite MNPs of formula $\text{Co}_x\text{Ni}_{1-x}\text{Fe}_2\text{O}_4$ whose magnetic anisotropy was systematically varied by controlling the relative amount of divalent ions ($0 \leq x \leq 1$). TEM and XRD analysis showed that all samples comprise highly crystalline, monodisperse, spherical particles with average size of 6 nm. Temperature- and field-dependent magnetic measurements displayed a strong dependence of the magnetic properties on the chemical composition; indeed, upon rising, x a high increase of both magnetic anisotropy and magnetization saturation is observed. Magneto-optical spectra, XMCD at Fe, Co and Ni L-edges and high-field temperature variable Mossbauer spectra allowed to explain the observed behavior, not only in terms of the intrinsic magneto-crystalline anisotropy of the cationic species involved, but also concerning their distribution between Td and Oh cavities in the spinel structure. In addition, a spin canted structure which becomes less prominent with increasing the Ni content was evidenced. Altogether these results underline the large tunability of the physical properties of this appealing class of nanomaterials. Research funded by project MAGNANO (INSTM-Regione Lombardia).

TU.E.3_O3 - Ledge-type Co/L1₀-FePt exchange-coupled composites

T. Speliotis¹, G. Giannopoulos¹, D. Niarchos¹, W. Li², G. Hadjipanayis², G. Barucca³, E. Agostinelli⁴, D. Fiorani⁴, S. Laureti⁴, D. Peddis⁴, A.M. Testa⁴, G. Varvaro⁴

1. *Institute of Materials Science, NCSR Demokritos, Athens, Greece*

2. *Department of Physics, University of Delaware, Newark, United States*

3. *SIMAU, Università Politecnica delle Marche, Ancona, Italy*

4. *Istituto Di Struttura Della Materia - CNR, Monterotondo Scalo, Roma, Italy*

FePt-based exchange-coupled composite (ECC) systems, consisting of a magnetically hard L1₀-FePt phase exchange coupled to a softer ferromagnetic material (such as Fe, Co, FeCo, [Co/Pd(Pt)]_n) are one of the most promising candidates for future ultra-high density (> 1 Tbit/in²) perpendicular magnetic recording media. Tuning both intrinsic and extrinsic properties of the two components allows simultaneously achieving high thermal stability and low switching fields [1,2]. The phase boundary between the two materials can be sharp or graded, and the cross-sectional shape of the magnetic phases is identical in conventional ECC, while in the ledge-type ECCs the soft section is more extended covering adjacent and discrete hard elements [3]. In this communication, the effect of the thickness of a soft Co layer, $3 < t_{\text{h}}(\text{Co}) < 20$ nm, on the magnetic behavior of ledge-type Co-fcc(100)/L1₀-FePt(001) nanocomposites deposited on an MgO (100) substrate is systematically studied by combining morpho-structural analyses (XRD, SAED, HRTEM) and angular magnetic measurements (vector VSM). Starting from a FePt film consisting of isolated L1₀-FePt(001) islands, the ledge-type structure was obtained by depositing a Co layer that either covered the FePt islands or filled up the inter-island region, gradually forming a continuous layer with the increase of $t_{\text{h}}(\text{Co})$. Magnetic measurements revealed a significant reduction of the switching field, which is well below the writing field of currently available write heads for $t_{\text{h}}(\text{Co}) > 5$ nm, the system still maintaining a perpendicular anisotropy up to $t_{\text{h}}(\text{Co}) < 9.5$ nm. Recoil loops measurements confirmed the exchange-coupled behavior, corroborating the potential interest for future magnetic recording media.

References:

[1] G. Varvaro et al., JMMM 368 (2014) 415

[2] D. Goll et al., Phys. Status Solidi A 210 (2013) 1261

[3] D. Goll et al., APL 93 (2008) 152512

TU.F.1_I1 - STS studies on correlated f-electron systems: Kondo lattice, quantum criticality and topological Kondo insulator

S. Wirth¹, S. Seiro¹, S. Rößler¹, L. Jiao¹, S. Hartmann¹, C. Krellner², C. Geibel¹, D. Kim³, Z. Fisk³, S. Kirchner⁴, Q. Si⁵, F. Steglich¹, L.H. Tjeng¹

1. *Max-Planck Institute for Chemical Physics of Solids Dresden, Dresden, Germany*

2. *Physics Institute, Goethe University, Frankfurt, Germany*

3. *University of California, Irvine, United States*

4. *Center for Correlated Matter, Zhejiang University, Hangzhou, China*

5. *Dept. of Physics and Astronomy, Rice University, Houston, United States*

Electronic correlations give rise to a plethora of interesting phenomena and phases. For example, hybridization between 4f and conduction electrons in heavy fermion metals may result in the generation of low-energy scales that can induce quantum criticality and unconventional superconductivity. One of the most important techniques that helped shaping our understanding of nonlocal correlations, both magnetic and superconducting, has been scanning tunneling spectroscopy (STS) with its unique ability to give local, microscopic information that directly relates to the one-particle Green's function. We combine STS with bulk measurements (specifically magnetotransport, thermopower and x-ray diffraction) to obtain complementary information on different length scales. We studied the temperature evolution of hybridization effects and Kondo lattice coherence as observed by STS, focusing on the model heavy fermion metal YbRh₂Si₂ and the intermediate-valence insulator SmB₆. Our STM and STS studies on high-quality single crystals of Yb(Rh_{1-x}Mx)2Si₂ (M = Co, Ir) focus on the evolution of the signatures of the development of Kondo lattice coherence upon lowering the temperature. We also show how Kondo coherence connects with quantum criticality. These results by STS are compared to magnetotransport and thermodynamic measurements, as well as to findings on other heavy fermion materials. Low-temperature in-situ cleaving of SmB₆ single crystals mostly resulted in reconstructed surfaces, while non-reconstructed patches were found less frequently. The different surface terminations give rise to marked differences in the STS results. Moreover, small non-reconstructed areas exhibit a diminished conductance at zero bias whereas larger ones can be described by a Fano resonance, confirming the hybridization picture typically considered for this material. All types of surfaces, reconstructed and non-reconstructed, displayed a finite zero-bias conductance of considerable magnitude confirming the robustness of the metallic surface states. Results obtained by STS on other strongly correlated materials are also discussed.

TU.F.1_O2 - Fermi surface instabilities in CeRh₂Si₂ at high magnetic field and pressure

A. Pourret^{1,2}, A. Palacio-Morales^{1,2}, G. Knebel^{1,2}, D. Braithwaite^{1,2}, G. Seyfarth³, M. Suzuki⁴, D. Aoki^{1,2,5}, J. Flouquet^{1,2}

1. Univ. Grenoble Alpes, INAC-SPSMS, Grenoble, France

2. CEA, INAC-SPSMS, Grenoble, France

3. Laboratoire National des Champs Magnétiques Intenses, - INSA, Grenoble and Toulouse, France

4. RIKEN Center for Emergent Matter Science, Wako, Saitama, Japan

5. Institute for Materials Research, Tohoku University, Oarai, Ibaraki, Japan

The interplay between spin fluctuations, valence fluctuations and charge ordering with Fermi surface (FS) instabilities is a key point in the understanding of quantum criticality in itinerant electronic systems. Heavy fermion materials are important examples as their low renormalized characteristic temperature give the opportunity to switch for example from long range antiferromagnetic (AF) to paramagnetic (PM) ground states under moderated pressure of few GPa and to recover, by applying magnetic field, a polarized paramagnetic state (PPM) above the AF-PM transition at H_c . We present thermoelectric power (TEP) studies under pressure and high magnetic fields in the antiferromagnetic heavy fermion compound CeRh₂Si₂ at low temperature. Under magnetic field, the observation of large quantum oscillations in the TEP, $S(H)$, in the AF phase and the sudden disappearance of these oscillations when entering in the polarized paramagnetic state at H_c state points out an important reconstruction of the FS. Under pressure, the strong increase of S/T at low temperature near the critical pressure P_c , corresponding to the collapse of the AF order, implies the interplay of FS change and low energy excitations driven by spin and valence fluctuations. The difference between TEP signal in the PPM state above H_c and in the paramagnetic state above P_c can be explained by different FS. New band structure calculations at $P = 0$ stress that in the AF phase the 4f contribution at the Fermi level (EF) is weak while it is the main component in the PM domain. By analogy to previous work on CeRu₂Si₂, in the PPM phase of CeRh₂Si₂ the 4f contribution at EF will drop.

TU.F.1_O3 - ARPES study of CeRh₂Si₂: Paradigmatic 4f spectral response in an enigmatic Kondo lattice

D. Vyalikh¹, C. Geibel²

1. *Institute of Solid State Physics, Dresden University of Technology, Dresden, Germany*

2. *Max Planck Institute for Chemical Physics of Solids, Saarbrücken, Germany*

CeRh₂Si₂ is an intensively studied antiferromagnetic Kondo lattice system, which presents a striking duality in the properties of the 4f electrons: The large 4f entropy of Rln2 just above TN = 35 K and the large value of the ordered moment mAF = 1.4 μB points to a fully localized 4f electron, while other properties, e.g. the width of the quasielastic line in inelastic neutron scattering, indicate a Kondo scale of about 33 K implying a strong 4f hybridization. The way how to reconcile these conflicting observations is yet not clear. Here we present an angle resolved photoemission study of this compound. Thanks to the nice cleavability of our single crystals and our knowledge on the surface state in homologues RERh₂Si₂ compounds (RE = Yb, Eu, Gd), we were able to discriminate between different surface terminations and to obtain distinct and highly resolved ARPES spectra for both the Si-terminated and the Ce-terminated surfaces. The former ones are representative for strongly correlated 4f states as present in bulk CeRh₂Si₂, the latter ones are representative for weakly hybridized Ce as expected at the surface. The differences in these spectra reflect the differing in the f- hybridization strengths: The pronounced 4f0 peak in the 4f spectral function of the Ce terminated surface gets suppressed in the signal of the Si-terminated surface due to stronger f-d hybridization. In contrast, for the latter we observe a fine structure near the Fermi edge which reflects the crystal electric field splitting of the "magnetic" 4f1 configuration, a signature which is absent for the weakly hybridized surface Ce. Analyzing this 'bulk' 4f1 signal along with recent specific heat data provides direct evidence why the simple picture for Kondo lattices cannot account for the exceptional dual nature of the 4f electrons in CeRh₂Si₂.

TU.F.1_O4 - Large fermi-surface antiferromagnetism in the Kondo lattice model

R. Peters¹, N. Kawakami²

1. *Riken, Wako, Japan*

2. *Kyoto University, Kyoto, Japan*

Using large-scale inhomogeneous dynamical mean field theory, we theoretically study the antiferromagnetic phase of the Kondo lattice model on a square lattice away from half filling. In previous works, authors have focused on the Neel state, which is the energetically stable state exactly at half filling. However, doping the system, the perfect Neel state is not commensurate with the Fermi momentum. In this situation, the system can gain energy by forming a long-range spin density wave (SDW), where the amplitude of the local polarization spatially oscillates. In this talk, we will analyze the properties of these SDWs. We will study static as well as dynamical correlations. We find that the transition between the SDW phase and the paramagnetic phase changes its character depending on the coupling strength. While for strong coupling, we observe the expected continuous transition between the SDW state and the paramagnetic state, the transition seems to be of first order for weak coupling strengths. Analyzing dynamical correlation functions, we observe a Lifshitz transition within the antiferromagnetic phase. However, looking at the Fermi surface and spin-spin-correlation functions, we conclude that the volume of the Fermi surface behaves smoothly within the SDW phase as well as across the phase boundary between the SDW phase and the paramagnetic phase. The SDW phase in the Kondo lattice model away from half filling is metallic with the local moments participating in the Fermi surface.

TU.F.1_O5 - Experimental Investigation on Magnetism and Pressure induced Superconductivity in CeCu₂Si₂, CeCu₂Ge₂, and CeAu₂Si₂G. Werner Scheerer¹, G. Girit¹, Z. Ren¹, G. Lapertot², D. Jaccard¹

1. DPMC - University of Geneva, Geneva, Switzerland

2. SPSMS, CEA-INAC/UJF, Grenoble, France

We present studies on Ce-based heavy-fermion single crystals, via resistivity, ac-susceptibility, ac-specific heat, and thermopower techniques in pressurized environment (up to 20 GPa) and under magnetic field (up to 8.5 T, 15 T at zero pressure).

In CeCu₂Si₂, the superconducting-transition temperature T_{SC} rises strongly, between the low-pressure region (~ 2 GPa) where T_{SC} is almost constant and the pressure $p_V \sim 4.5$ GPa where T_{SC} is maximum [1]. In this intermediate pressure range, the width of the SC-transition is found to be strongly sample-dependent, which is presumably due to surface quality (cleaved/polished). Here, a high T_{SC}^{onset} is due to partial or surface superconductivity, as shown by resistivity measured with nonlinear contacts.

Recently, we discovered pressure-induced SC deep inside the AF-phase of CeAu₂Si₂ ($p_c \sim 22.5$ GPa), where SC sets in at 11.8 GPa, which corresponds to $p_c - 11$ GPa [2]. Likewise, it is known that in CeCu₂Ge₂ superconductivity sets in at $p_c \sim 10$ GPa [3]. One can imagine that under specific conditions SC will be established at zero pressure in CeCu₂Ge₂. Therefore, we did zero-pressure measurements on CeCu₂Ge₂ in magnetic fields. T_N is found to be field-resistant at least up to 15 T. In the range 8 - 12 T, several crossover-like anomalies were observed, indicating successive field-induced modifications of the AF-structure.

High-pressure measurements on CeAu₂Si₂ were carried out to refine its phase diagram. We observe an interplay between a pressure-induced, progressive change of the magnetic structure and the establishment of partial superconductivity deep inside the AF-phase. Furthermore, an unusual behavior of the magnetism is revealed: while T_N decreases with increasing pressure, the magnetic phase becomes much more stable in magnetic field. For $p = 0$, AF is suppressed by $\mu_0 H = 5$ T, but for pressures above 7 GPa, AF survives beyond 8 T.

References:

- [1] G. Seyfarth, A.-S. Rüetschi, K. Sengupta, A. Georges, D. Jaccard, S. Watanabe, and K. Miyake: Phys. Rev. B 85, 205105 (2012)
- [2] Z. Ren, L. V. Pourovskii, G. Girit, G. Lapertot, A. Georges, and D. Jaccard, Phys. Rev. X, 4, 031055 (2014)
- [3] E. Vargoz, D. Jaccard, J. Magn. Magn. Mater. 177 - 181, 294 - 295 (1998)

TU.F.3_O1 - Chirality density wave of the “hidden order” phase in URu₂Si₂

G. Blumberg¹, K. Haule¹, H. Kung¹, John Mydosh², R. Baumbach³, E. Bauer³

1. *Rutgers University, Piscataway, United States*

2. *Kamerlingh Onnes Laboratory, Leiden University, Leiden, The Netherlands*

3. *Los Alamos National Laboratory, Los Alamos, New Mexico, United States*

A second-order phase transition in a physical system is associated with the emergence of an order parameter and a spontaneous symmetry breaking. The heavy fermion superconductor URu₂Si₂ has a “hidden order” (HO) phase below the temperature of 17.5 K; the symmetry of the associated order parameter has remained ambiguous. Here we use polarization resolved Raman spectroscopy to specify the symmetry of the low energy excitations above and below the HO transition. We determine that the HO parameter breaks local vertical and diagonal reflection symmetries at the uranium sites, resulting in crystal field states with distinct chiral properties, which order to a commensurate chirality density wave ground state. ScienceExpress 10.1126/science.1259729

TU.F.3_O2 - Cubic hastatic order

R. Flint¹

1. Iowa State University, Ames, United States

Typical Kondo systems are built from ions with an odd number of f-electrons, which allow the hybridization between the local moments and conduction electrons to be treated as a scalar and leads to the development of a non-symmetry breaking heavy Fermi liquid ground state via a crossover. However, if the local moment ground state is instead a non-Kramers doublet (requiring an even number of f-electrons), the hybridization mixing the Kramers conduction electrons and non-Kramers local moment must be spinorial in nature, and the resulting heavy Fermi liquid must also break some symmetry and therefore develop at a phase transition. This kind of hastatic order was proposed to describe the hidden order state in the tetragonal URu₂Si₂ [1], however the non-Kramers nature of the U ground state is controversial. Motivated by Pr based cubic compounds with clear non-Kramers doublet ground states like PrInAg₂ [2] and PrMg₃ [3], we study the emergence of time-reversal symmetry breaking hastatic order in a two-channel Anderson model based on the quadrupolar Gamma₃ doublet [4] using a slave boson approach.

References:

- [1] Premala Chandra, Piers Coleman and Rebecca Flint, Nature 493, 621 (2013)
- [2] A. Yatskar, W. P. Beyermann, R. Movshovich and P. C. Canfield, Phys. Rev. Lett. 77, 3637 (1996)
- [3] A. Andreeff et al, Phys. Status Solidi B 98, 283 (1981)
- [4] D.L. Cox, J. Magn. Magn. Mat. 76, 53 (1988)

TU.F.3_O3 - Heavy fermion superconductivity and double multipolar transition in PrV₂Al₂₀Y. Matsumoto¹, M. Tsujimoto¹, A. Sakai¹, T. Tomita¹, S. Nakatsuji¹

1. ISSP, Univ. of Tokyo, Tokyo, Japan

Novel quantum phases may arise from f electrons' orbital degrees of freedom through hybridization with conduction electrons. In particular, quadrupole Kondo effect, originally suggested as a single ion effect in the nonmagnetic cubic G_3 crystal electric field doublet [1], has attracted a lot of attention because of its non-Fermi liquid ground state. It is an interesting open question what happens in the lattice systems. To study this, the material should be clean enough and the hybridization should be large. However, there has been no prototypical system that satisfies both requirements.

On the other hand, recent studies have revealed that PrT₂Al₂₀ ($T = \text{Ti, V}$) are ideal systems to study the quadrupole Kondo effect and quantum criticality arising from orbital degrees of freedom [2-4]. The both systems have the nonmagnetic cubic Γ_3 crystal electric field doublet. In addition, the hybridization is strong as is evident in many physical properties.

We found that both exhibit heavy fermion superconductivity inside the multipole ordering phases [3-5]. Especially, in the case of PrV₂Al₂₀, the effective mass is highly enhanced ($m^*/m_0 \sim 140$) even at ambient pressure, revealing even stronger hybridization in PrV₂Al₂₀ [5]. This observation indicates the first realization of the novel superconductivity arising from the orbital fluctuation of the f electrons at ambient pressure.

While PrTi₂Al₂₀ exhibits a ferro-quadrupole ordering at 2.0 K, our recent success in growing the pure crystals has allowed us to reveal that PrV₂Al₂₀ exhibits double multipolar orderings at $T = 0.65$ and 0.75 K [5]. The specific heat exhibits the T^4 power law behavior below 0.5 K indicating the formation of the gapless mode due to strong orbital fluctuation. Although the origin of the double transition is not clear so far, the response to the magnetic field is anisotropic reflecting the anisotropic nature of the order parameter.

References:

- [1] D. L. Cox, PRL 59, 1240 (1987)
- [2] A. Sakai, and S. Nakatsuji, JPSJ 80, 063701 (2011). *References therein*
- [3] A. Sakai *et al.*, JPSJ 81, 083702 (2012)
- [4] K. Matsubayashi *et al.*, PRL 109, 187004 (2012).
- [5] M. Tsujimoto *et al.*, PRL 113, 267001 (2014). *References therein*

TU.F.3_O4 - Observation of a magnetic-resonance excitation mode in the Kondo insulator CeFe₂Al₁₀J.M. Mignot¹*1. Laboratoire Leon Brillouin, CEA-CNRS, Gif sur Yvette, France*

Kondo insulators (KI) form an important class of strongly correlated electron systems. Their ground state is typically a nonmagnetic singlet, with a spin-gap in their magnetic excitation spectrum. The possible competition between the KI state and a long-range antiferromagnetic order is an interesting, yet unsettled, problem.

The family of orthorhombic compounds CeT₂Al₁₀ (T: Fe, Ru, Os) offers a unique opportunity to study this phenomenon, since changing the transition metal element T drives the system from a KI behavior (CeFe₂Al₁₀) to a more complex situation (CeRu₂Al₁₀, CeOs₂Al₁₀), in which the development of the KI state is disrupted by the onset of AFM order. In the latter two compounds, previous elastic and inelastic neutron scattering (INS) studies have characterized the ordered magnetic structure and revealed the existence of a spin gap and magnonlike excitations in the magnetic response, whose dispersion implies unusually large anisotropy in the exchange interactions. It has been suggested that these systems are located close to a localized-itinerant transition.

Here we report [1] new single-crystal INS experiments on CeFe₂Al₁₀. The data indicate that a spin gap develops in the magnetic dynamic response below about 50 K, with a magnetic excitation branch dispersing from $E = 10.2 \pm 0.5$ meV at $\mathbf{q} = (0,1,0)$ (Y zone-boundary point) to approximately 12 meV at the top of the branch. The excitation shows a pronounced polarization of the magnetic fluctuations along a, the easy anisotropy axis. This spectral component, observed in the absence of long-range magnetic order, is contrasted with that previously found in CeRu₂Al₁₀, where the modes had transverse character and existed only in the antiferromagnetic state. It is ascribed to a “magnetic exciton” mechanism similar to that reported previously for other KI compounds such as SmB₆ or YbB₁₂.

References:

[1] J.-M. Mignot *et al.* Phys. Rev. B **89** (2014) 161103(R)

TU.G.1_I1 - Origin of ferromagnetism and critical behaviour in insulating (Ga,Mn)NM. Sawicki¹*1. Institute of Physics, Warsaw, Poland*

After a decade of contradicting reports, the last years have witnessed a breakthrough progress in the understanding of magnetism of (Ga,Mn)N. Due to the strong p-d hybridization the Mn^{2+/3+} acceptor level occupies the mid band gap position in GaN precluding the existence of carrier-mediated spin-spin coupling. Nevertheless, in uncompensated films, where Mn³⁺ ions prevail, the superexchange interaction becomes ferromagnetic for all Mn-Mn distances resulting in a ferromagnetic order persisting up to the Curie temperature $T_C=13$ K for $x=0.10$, yet retaining their insulating character. The experimentally established $T_C(x) \sim x^{2.2}$ supports the superexchange scenario as the same exponent describes the dependence of spin-glass freezing temperatures on x in Mn- and Co-doped DMSs, in which the antiferromagnetic superexchange is the established spin coupling mechanism. Moreover, the experimental T_C values are in a remarkable agreement with those obtained from the tight-binding and Monte Carlo simulations of ferromagnetic superexchange between Mn³⁺ ions in zinc-blende GaN. This finding indicates that (Ga,Mn)N emerges as a model system making it possible to explore properties specific to dilute ferromagnetic insulators. Having in hand a system with short-range ferromagnetic interactions between randomly distributed localized spins, we address experimentally the fundamental and long-standing question on how disorder influences the critical behaviour of continuous phase transitions. Our results confirm experimentally that in contrast to the magnetically clean case ($x=1$) the Curie transition in the dilute alloys studied here is characterised by an effective γ which exhibits a strong maximum above T_C , a behaviour anticipated by a renormalization-group theory. Surprisingly, however, our results point to a certain smearing of the transition which is likely to result from macroscopic inhomogeneities in Mn distribution inherent to virtually all real magnetic alloys.

This work was supported in part by the (Polish) National Science Centre through projects: PRELUDIUM (UMO-2012/07/N/ST3/03146) and OPUS (UMO-2013/09/B/ST3/04175).

Tu.G.1_O2 - Electronic structure of (Ga,Mn)As revisited: an alternative view on the -Battle of the bands-

K. Karlsson¹, J. Kanski², L. Ilver², I. Ulfat³, M. Leandersson⁴, J. Sadowski⁴, I. Di Marco⁵

1. *Department of Engineering Sciences, University of Skövde, Skövde, Sweden*

2. *Department of Applied Physics, Chalmers University of Technology, Göteborg, Sweden*

3. *Department of Physics, University of Karachi, Karachi, Pakistan*

4. *MAX IV Laboratory, Lund University, Lund, Sweden*

5. *Department of Physics and Astronomy, Uppsala University, Uppsala, Sweden*

The detailed nature of electronic states mediating ferromagnetic coupling in dilute magnetic semiconductors, specifically (Ga,Mn)As, has been an issue of long debate. Two confronting models have been discussed emphasizing host band vs. impurity band carriers. Using angle resolved photoemission we are for the first time able to identify a highly dispersive Mn-induced energy band. Our results show that the electronic structure of the (Ga,Mn)As system is significantly modified from that of GaAs. Most importantly, the bands in the region of valence band maximum are distorted and extend into the band gap region of GaAs. For Mn concentrations above 1% Mn the band reaches the Fermi level, and can thus host the delocalized holes needed for ferromagnetic coupling.

TU.G.1_O3 - Laser-induced ultrafast modification of electron-spin dynamics in GaAs with adjacent ferromagnetic epilayer

D. Butkovičová¹, P. Nývlec¹, K. Olejník², V. Novák², T. Janda¹, F.k Trojának¹, T. Jungwirth²

1. Charles University, Prague, Czech Republic

2. The Academy of Sciences of the Czech Republic, Prague, Czech Republic

Absorption of circularly-polarized light leads in semiconductors to photo-injection of carriers that have spin polarized along the light propagation direction. If an external magnetic field is applied perpendicularly to this direction the photo-injected electron-spins precess around this field. The time-evolution of the electron spin orientation can be determined by measuring the time-resolved magneto-optical signal due to polar Kerr effect. We investigated electron-spin dynamics in GaAs covered by a thin (~ 20 nm) epitaxial layer of ferromagnetic semiconductor (Ga,Mn)As with various Mn doping [1] at temperature of 15 K and using the light tuned above the GaAs band gap. Since the light penetration depth (~ 1 μm) is much larger than the thickness of (Ga,Mn)As, optical spin-injection takes place in both the ferromagnetic film and the GaAs substrate. We observed that the direction of electron-spins photo-injected in GaAs is ultrafast reoriented due to the presence of (Ga,Mn)As which is reflected in a substantial (up to 180 degrees) initial phase shift of the measured oscillations with respect to the signal measured in bare GaAs. This phase shift is developed within very short time (< 50 ps) after the laser pulse impact on the surface of the sample. The value of the phase shift depends on the Mn concentration in (Ga,Mn)As and on temperature. If an insulating barrier is embedded between the ferromagnet and GaAs the phase shift disappears which suggests that the electron-spin reorientation is related to an electron transfer between ferromagnet and the adjacent paramagnetic GaAs.

References:

[1] Nývlec et al, Nature Communications 4, 1422 (2013)

TU.G.1_O4 - Substitutional and metallic cobalt in ZnO films with aluminium

W. Dizayee¹, X. Li², H. Blythe¹, S. Heald³, M. Fox¹, G. Gehring¹

1. *The University of Sheffield, Sheffield, United Kingdom*

2. *Shanxi Normal University, Xi'an, China*

3. *Argonne National Laboratory, Lemont, United States*

The study of Zn_{1-x}Co_xO has excited much interest due to its possible use in spintronic devices. There are some samples where the Co is present only as Co²⁺ on Zn sites that are magnetic at room temperature with small coercive fields, typically less than 100 Oe at room temperature and less than 200 Oe at helium temperatures. There are other samples where the magnetisation is obviously due to metallic nanoparticles. We use x-ray near edge absorption, magnetometry and MCD to investigate if these two types of magnetism can coexist and if so if they are coupled together. We compared samples with, and without, small concentrations of Al. The fraction of Co ions present as metallic cobalt was determined by x-ray near edge absorption and EXAFS. The fraction of the saturation magnetism at low temperatures that might be assigned to the fraction of the sample that was present as metallic clusters was found to be ~0.2 assuming that the magnetic moment of Co atom in a metallic cluster was 1.78 Bohr magnetons, thus indicating that both components were present in our samples. Optical MCD is a very powerful technique to determine the relative importance of both types of magnetism because the MCD signals from metallic Co and from the matrix of ZnCoO containing Co²⁺ have different energy spectra. The MCD spectrum, taken at remanence to avoid any paramagnetic contamination, allows for an estimate of the strength of the signal from both components and MCD loops determines the coercive field for each component. It was found that samples of Zn_{1-x}Co_xO could be described in terms of two independent contributions to the magnetisation whereas the coercive field for the sample that contained Al was the same for both components at all temperatures and hence magnetism of both components are coupled.

TU.G.1_05 - Atomic-scale magnetic properties of truly 3d-diluted ZnO investigated with emission Mössbauer spectroscopy

R. Mantovan¹, H.P. Gunnlaugsson^{2,3}, K. Johnston⁴, H. Masenda⁵, T. Esmann Mølholt⁶, D. Naidoo⁵, M. Ncube⁵, S. Shayestehaminzadeh⁶, K. Bharuth-Ram^{7,8}, M. Fanciulli^{1,9}, H.P. Gislason⁶, G. Langouche², S. Ólafsson⁵, L.M.C. Pereira², U. Wahl¹⁰, P. Torelli¹¹, G. Weyer³

1. Laboratorio MDM IMM-CNR, Agrate Brianza, Italy
2. KU Leuven, Instituut voor Kern-en Stralings Fysika, Leuven, Belgium
3. Department of Physics and Astronomy, Aarhus University, Aarhus, Denmark
4. Physics Department, ISOLDE/CERN, Geneva, Switzerland
5. School of Physics, University of the Witwatersrand, Johannesburg, South Africa
6. Science Institute, University of Iceland, Reykjavik, Iceland
7. School of Physics, Durban University of Technology, Durban, South Africa
8. iThemba LABS, Somerset West, South Africa
9. Dipartimento di Scienza dei Materiali, Università di Milano Bicocca, Milan, Italy
10. Centro de Ciências e Tecnologias Nucleares, Instituto Superior Técnico, Universidade de Lisboa, Sacavém, Portugal
11. Laboratorio TASC, IOM-CNR, Trieste, Italy

In the search for dilute magnetic semiconductors and oxides, typical (and critical) issues concern the potential presence of extrinsic contamination and/or unwanted precipitates of 3d-atoms being the source of ferromagnetism, when investigated by volume-integrating techniques. In the recent years, contradictory results have been reported in very similar systems, under apparently comparable preparation conditions. In this contribution, the magnetic properties at the atomic level of Fe atoms incorporated in ZnO, in a concentration range of more than five orders of magnitude from 1×10^{-5} to 2.2 at.% are probed using emission ^{57}Fe Mössbauer spectroscopy on implanted ^{57}Mn and ^{57}Co produced at ISOLDE/CERN. In the ultra-dilute regime (10^{-5} at. %), the system shows isolated paramagnetic Fe^{3+} ions with a spin-lattice type of relaxation. At higher concentrations (between 0.02 and 0.2 at. %) a transition to spin-spin type of relaxation between neighboring Fe^{3+} is observed, without any signature of magnetic ordering up to 2.2 at.% [1]. Our results suggest that the absence of room temperature magnetic ordering in wide band gap and truly diluted semiconductors could be a general conclusion, attributable to the absence of efficient mechanisms to mediate long-range interactions.

References:

- [1] Mantovan et al., *Advanced Electronic Materials*, accepted (2015), doi: 10.1002/aelm.201400039

Tu.G.2_I1 - Exchange bias of spring-like domain walls

R. Morales¹, A.C. Basaran², J.E. Villegas³, D. Navas⁴, N. Soriano⁵, B. Mora⁵, C. Redondo⁵, X. Batlle⁶, I.K. Schuller²

1. *Department of Chemical-Physics & BCMaterials, University of the Basque Country UPV/EHU, and IKERBASQUE, Basque Foundation for Science, Bilbao, Spain*

2. *Department of Physics and Center for Advanced Nanoscience, University of California San Diego, United States*

3. *Unité Mixte de Physique CNRS/Thales, Palaiseau, and Université Paris Sud, France*

4. *IFIMUP-IN and Departamento Física e Astronomia, Universidade do Porto, Portugal*

5. *Department of Chemical-Physics, University of the Basque Country UPV/EHU, Leioa, Spain*

6. *Departament de Física Fonamental and Institut de Nanociència i Nanotecnologia, Universitat de Barcelona, Barcelona, Spain*

The exchange coupling between antiferromagnetic (AFM) and ferromagnetic (FM) materials yields a shift of the hysteresis loop along the magnetic field axis. The magnitude of this shift is known as exchange bias field, H_{eb} . It was experimentally and theoretically demonstrated that H_{eb} decreases with the FM thickness, following an inverse proportionality law, which is assumed to be valid for any FM thickness thinner than the ferromagnetic correlation length [1]. We demonstrate that AFM/FM bilayers with spring-like domain walls can break the inverse proportionality law even for FM thicknesses smaller than the ferromagnetic correlation length. $FeF_2/NiFe$ bilayers with NiFe thicknesses between 10 and 140 nm were deposited by electron beam evaporation. This magnetic system shows spring-like domain walls, parallel to the AFM/FM interface, at low temperature. The thickness dependence of H_{eb} significantly deviates from the inverse proportionality law as the NiFe thickness increases. The exchange bias magnitude of spring-like domain walls is always lower than the predicted by the inverse proportionality law. A model of magnetization planes parallel to the interface accounts for the experimental results. Both the shape of the hysteresis loops and the magnitude of H_{eb} were reproduced in excellent agreement with the experiment [2]. Moreover, the thermal evolution of the FM spin structure leads to an anomalous temperature dependence of H_{eb} . These findings reveal the importance of the FM domain structure on exchange bias.

Work supported by Spanish MINECO FIS2013-45469 and MAT2012-33037, EU FP7- IRSES-2012-318901, Catalan DUSI 2014SGR220, EU FEDER (Una manera de hacer Europa), University of Barcelona, and the U.S. Office of Basic Energy Science, U.S. Department of Energy, BES-DMS funded by the Department of Energy's Office of Basic Energy Science, DMR under Grant No. DE FG02 87ER-45332.

References:

[1] J. Nogués and I. K. Schuller, *J. Magn. Magn. Mater.* 192, 203 (1999)

[2] R. Morales et al. *Phys. Rev. Lett.* in-press

TU.G.2_O2 - The Importance of bulk antiferromagnetic spins in exchange bias

T. Saerbeck¹, A.C. Basaran², J. de la Venta³, H. Huckfeldt⁴, A. Ehresmann⁴, I.K. Schuller²,

1. *Institut Laue-Langevin, Grenoble, France*

2. *Department of Physics and Center for Advanced Nanoscience, University of California San Diego, La Jolla, United States*

3. *Department of Physics, Colorado State University, Fort Collins, United States*

4. *Institute of Physics and Center for Interdisciplinary Nanostructure Science and Technology, University of Kassel, Kassel, Germany*

The role of interfacial and bulk antiferromagnetic spins in the exchange bias (EB) phenomenon is a topic of ongoing discussion. While it is generally established that the antiferromagnetic bulk must affect the EB, the interface, near interface and regions far away from the interface are most often not clearly distinguished.

We used an EB geometry in which the antiferromagnetic FeF₂ layer is grown atop of the ferromagnetic Ni layer, and employed light ion irradiation to selectively create defects at and far away from the ferromagnetic/antiferromagnetic interface. Several sets of Ni/FeF₂ thin films capped with an inert Au layer were irradiated with He-ions of constant energy and dose. The penetration depth of the He-ions was controlled by the thickness of the nonmagnetic Au capping layers. This leads to a varying depth profile of vacancies induced in the thin film structure, which was confirmed by numerical simulations. A quantitative comparison of structural and magnetic characterizations before and after the bombardment of each sample revealed changes in the EB. The experiment allows to simultaneously detect and separate contributions from all layers and depths involved in the EB phenomenon. A substantial reduction in EB magnitude is observed even for vacancy profiles leaving the interface unaltered. These studies show that defect creation in the antiferromagnetic bulk far away from the interface has an effect and therefore the AF bulk must play a crucial role in the determination of EB.

This work was supported by the Office of Basic Energy Science, U.S. Department of Energy, under Grant No. DE FG02-87ER-45332.

References:

[1] A.C. Basaran, T. Saerbeck, J. de la Venta, H. Huckfeldt, A. Ehresmann and I.K. Schuller, *Applied Physics Letters* 105, 072403 (2014)

TU.G.2_O3 - Isothermal switching of in-plane exchange bias in orthogonal coupled DyCo/NiFe bilayer

D. Lott¹, K. Chen²

1. Helmholtz Zentrum Geesthacht, Geesthacht, Germany

2. Synchrotron SOLEIL, Gif-sur-Yvette, France

Alloys of rare-earth elements and 3d transition metals became recently again in the focus of attention due their rich variety of magnetic effects owed to the different anisotropies of both material classes [1,2,3]. In this paper, dual in-plane exchange bias effects were found in the orthogonal coupled Dy₂₀Co₈₀/NiFe bilayer at room temperature. Particularly interesting, the direction of the exchange bias effect can be switched by changing solely the direction of the perpendicular magnetic fields in relative moderate fields of about 200mT. The in-plane exchange bias keeps stable even at external in-plane magnetic fields of more than 6T. The underlying mechanism behind the extraordinary effect was investigated with magnetic optical Kerr effect (MOKE), X-ray magnetic circular dichroism (XMCD) and polarized neutron reflectometry measurements (PNR). The exchange bias in NiFe is caused by the interface exchange coupling to the DyCo layer, while the exchange bias in DyCo layer is due to the formation of chirality in its spin structure formed during the deposition on NiFe. Latter indicates a Dzyaloshinskii-Moriya like term in the interacting energy originating from the broken inversion symmetry at the interface between both magnetic layers.

References:

- [1] S. Mangin, et. al, Phys. Rev. B, 74, 0244414 (2006), S. Mangin et.al, Phys. Rev. B 80, 224424 (2009), S. Mangin et.al, Phys. Rev. Lett. 82, 4336 (1999)
- [2] F. Radu, R. Abrudan, I. Radu, D. schmitz H. Zabel, Nat. Communications, 3, 715(2012)
- [3] V. V. Polyakov and G. I. Frolov, Magnetic Materials for Radio Engineering and Electronics (Krasnoyarsk,1988), pp. 219223 [in Russian], V. A. Seredkin, S. V. Stolyar, G. I. Frolov and V. Yu. Yakovchuk, Technical Physics Letters, 30, 820-822 (2004)

TU.G.2_O4 - Extraordinary 'EB-like' phenomenon in orthogonally coupled ferromagnets: SmCo₅ (perpendicular) /CoFeB and /NiFe (in-plane) bilayers

A. Bollero¹, F.J. Pedrosa¹, J.L. Fdez Cuñado¹, J. Camarero^{1,2}, M. Seifert³, V. Neu³, V. Baltz⁴, D. Serantes⁵, O. Chubykalo-Fesenko⁵, R. Pérez del Real⁵, M. Vázquez⁵, L. Schultz³, B. Dieny⁴, R. Miranda^{1,2}

1. IMDEA Nanoscience, Madrid, Spain

2. Dep. de Física Materia Condensada, Inst. Nicolás Cabrera, UAM, Madrid, Spain

3. IFW Dresden, Institute for Metallic Materials, Dresden, Germany

4. SPINTEC, UMR-8191 CNRS/CEA-INAC/UJF, Grenoble, France

5. ICMM, Instituto de Ciencias de Materiales de Madrid, CSIC, Madrid, Spain

The present work focuses in a completely new exchange bias (EB)-like phenomenon observed in orthogonally coupled ferromagnetic (F) bilayers by comparison with previous studies done on [Pt/Co]-NiFe [1-3]. As an important conclusion of those studies, the strength of the out-of-plane anisotropy of the underlayer F has been shown to be decisive to guarantee appearance of EB effects, through creation of a metastable magnetic state in the bilayer. SmCo₅ possesses the largest known uniaxial magnetocrystalline anisotropy of $K_u=14$ MJ/m³ at room temperature as a bulk phase.

Following these observations we have designed a new system consisting of a hard magnet epitaxial SmCo₅ film with perpendicular anisotropy [4] in interaction with a soft magnetic layer (CoFeB and NiFe) with in-plane anisotropy through a Cr/Pt spacer of varying thickness. By contrast with conventional EB films, this system shows -independently of the nature of the soft layer (CoFeB or NiFe)- extraordinary features induced without changing the magnetic history of the system and measured by vectorial-MOKE (v-MOKE):

- In-plane loop shift with no need of any post-depositional treatment by comparison with conventional F-AF bilayers.
- Unprecedented effect consisting of pinning of exclusively the ascending hysteresis loop branch in a 90° rotation. This allows for tuning, not only the magnitude, but also the sign of the bias field.

The influence of varying the thickness of the spacer existing between both F layers on the EB-like effects has been studied in detail, proving that the observed phenomena are a result of competing anisotropies of the orthogonally coupled ferromagnets.

References:

- [1] J. Sort et al., Phys. Rev. B 70, 174431 (2004).
- [2] A. Bollero et al., Phys. Rev. B 73, 144407 (2006)
- [3] A. Bollero et al., Phys. Rev. B 84, 094423 (2011)
- [4] M. Seifert et al., Appl. Phys. Lett. 94, 022501 (2009)

TU.G.2_O5 - Crystal structure and magnetic exchange bias effect in UO₂/Fe₃O₄ deposited on different substrates

E. Tereshina¹, Z. Bao², L. Havela³, S. Danis³, A. Mackova⁴, T. Gouder⁵, R. Caciuffo⁵

1. *Institute of Physics ASCR, Prague, Czech Republic*

2. *PANalytical B.V., Almelo, The Netherlands*

3. *Department of Condensed Matter Physics, Faculty of Mathematics and Physics, Charles University, Prague, Czech Republic*

4. *Tandetron Laboratory, Nuclear Physics Institute of Academy of Sciences of the Czech Republic, Rez, Prague, Czech Republic*

5. *European Commission, Joint Research Centre (JRC), Institute for Transuranium Elements (ITU), Karlsruhe, Germany*

Exchange-biased [1] antiferromagnetic/ferromagnetic bilayers are of a great technological value for advanced electronics production [2]. In this work, we studied crystal structure and exchange bias (EB) effect in UO₂ (bulk Néel temperature TN 30.8 K) combined with Fe₃O₄. The use of particular substrates for the UO₂ films production can play a crucial role in the properties of deposited material [3]. We used reactive sputter deposition from metallic targets to prepare sets of samples with different thicknesses of magnetic layers using commercially available LaAlO₃ (100), CaF₂ (100) and (111) substrates. The stoichiometry of each deposited layer was controlled by X-ray Photoelectron Spectroscopy. Epitaxial growth of the UO₂ films was revealed by X-ray diffraction for all substrates while the layer of magnetite was found to be twinned [4]. LaAlO₃-based films were further characterized by means of Transmission Electron Microscopy. Rutherford Backscattering Spectroscopy (RBS) used for the CaF₂-based films showed no intermixing at the interface. The magnetic study of the UO₂/Fe₃O₄ bilayers showed EB exceeding 2000 Oe at 5 K. Interestingly, exchange bias did not vanish at TN of UO₂. Non-zero values of EB were observed up to 125 K, where a Verwey transition in magnetite takes place.

The work has been supported by the Czech Science Foundation, grant No. 13-25866P. The samples were prepared in the framework of the EARL project of the European Commission Joint Research Centre, ITU Karlsruhe. RBS measurements were carried out at the CANAM infrastructure of the NPI ASCR Rez supported through MŠMT project No. LM2011019.

References:

- 1) W. H. Meiklejohn and C. P. Bean, Phys. Rev. B, 102 1413, (1956)
- 2) B. Dieny et al., Phys. Rev. B, 43 1297 (1991)
- 3) Z. Bao et al., Phys. Rev. B 88, 134426 (2013)
- 4) E. A. Tereshina et al., Appl. Phys. Lett., 105 122405 (2014)

TU.G.3_O1 - Thermal and spatial confinement effects in exchange coupled IrMn/NiFe dot arrays

F. Spizzo¹, E. Bonfiglioli¹, M. Tamisari^{1,2}, A. Gerardino³, G. Barucca⁴, A. Notargiacomo³, F. Chinni¹, L. Del Bianco⁵

1. Dipartimento di Fisica e Scienze della Terra, Università di Ferrara, Ferrara, Italy

2. Dipartimento di Fisica e Geologia, CNISM Università di Perugia, Perugia, Italy

3. Istituto di Fotonica e Nanotecnologie, Roma, Italy

4. Dipartimento SIMAU, Università Politecnica delle Marche, Ancona, Italy

5. Dipartimento di Fisica e Astronomia, Università di Bologna, Bologna, Italy

We present a comprehensive study of the exchange bias phenomenon (EB) in an antiferromagnetic (AF)/ferromagnetic (FM) continuous film and in arrays of square dots with different size (D), aimed at elucidating thermal and spatial confinement effects on the AF/FM exchange coupling and their correlation with the AF structural and magnetic properties. For this purpose, an AF/FM Ir₂₅Mn₇₅[10 nm]/Ni₈₀Fe₂₀[5 nm] continuous film and arrays of square dots (D = 1000 nm, 500 nm and 300 nm) were prepared by electron beam lithography and lift-off using dc-sputtering. Structural investigations by electron microscopy techniques indicated that the AF layer consists of nanograins (mean size ~ 10 nm), but also clearly revealed the existence of a structurally disordered IrMn region (2-3 nm thick) at the interface with the NiFe phase. The magnetic properties, in particular the temperature dependence of the exchange field Hex and coercivity HC, were studied by SQUID and MOKE measurements. At room temperature, Hex decreases with reducing the size of the dots and it is absent in the smallest ones, whereas the opposite trend is visible at T = 10 K (Hex ~ 1140 Oe for D = 300 nm). The EB mechanism and its thermal evolution have been explained through a phenomenological model [1] that combines spatial confinement effects with other crucial items concerning the AF phase: the magnetothermal stability of the IrMn nanograins, the glassy magnetic nature of the structurally disordered IrMn region, the stabilization of a low-temperature (T < 100 K) frozen collective regime of the IrMn interfacial spins, implying the appearance of a length of magnetic correlation among them. The model predictions have been supported by micromagnetic calculations, satisfactorily reproducing the experimental findings.

This research work has been sponsored by MIUR under project FIRB2010-NANOREST.

References:

[1] F. Spizzo et al., Phys. Rev. B 91 (2015) 064410

TU.G.3_O2 - Bridging amount of disordered magnetic phases located over ferromagnetic/antiferromagnetic thin films and cell to cell variability of exchange bias in corresponding TA-MRAM chips

K. Akmalidinov ^{1,2,3,4}, L. Frangou ^{1,2,3}, C. Ducruet ⁴, C. Portemont ⁴, J. Pereira ⁴, I. Joumard ^{1,2,3}, B. Dieny ^{1,2,3}, J. Alvarez-Hérault ⁴, V. Baltz ^{1,2,3}

1. Univ. Grenoble Alpes, SPINTEC, Grenoble, France

2. CNRS, SPINTEC, Grenoble, France

3. CEA, INAC-SPINTEC, Grenoble, France

4. CROCUS Technology, Grenoble, France

Spintronics devices and in particular thermally assisted magnetic random access memories (TA-MRAM) use ferromagnetic/antiferromagnetic (F/AF) exchange biased bilayers: one for reference and one for storage. A TA-MRAM consists in a matrix of memory-cells where each cells carries a bit of information. For improved performances, lowering the cell to cell variability of the storage layer exchange bias is necessary. In this study, we prove that disordered magnetic phases, which exhibit low freezing temperatures and are located over the F/AF thin film, are the main cause of such variability once the layers are nanofabricated into a device. In particular, we show that the less the amount of disordered magnetic phases, the lower the cell to cell variability of exchange bias. More precisely, the amount of disordered magnetic phases was varied by sputtering different TA-MRAM stacks with various AFs in the storage layer: IrMn, FeMn and their alloys [1]. Blocking temperature distributions were measured to quantify the amount of disordered magnetic phases at the wafer level [2]. The wafers were then patterned to obtain two series of TA-MRAM chips on CMOS with circular magnetic cells of diameter 140 and 200 nm. The cells were then tested electrically. Finally, the resulting loop shift cumulative distribution functions accounting for the cell to cell variability of exchange bias were correlated to the initial amount of disordered magnetic phases. In addition to bridging the gap between fundamental disordered magnetic phases and a technological application, we also demonstrate here that blocking temperature distributions are a versatile method to qualify TA-MRAM production batches before processing [3].

References:

[1] K. Akmalidinov et al, J. Appl. Phys. 115, 17B718 (2014)

[2] V. Baltz et al, Phys. Rev. B 81, 052404 (2010)

[3] K. Akmalidinov et al, unpublished

TU.G.3_O3 - Phase diagram in exchange biased CoTb/[Co/Pt] multilayer based magnetic tunnel junctions

M. Bersweiler¹, D. Lacour¹, K. Dumesnil¹, F. Montaigne¹, M. Hehn¹

1. Institut Jean Lamour, Nancy, France

The magnetic properties of [Pt/Co]₄/MgO/[Co/Pt]₃/Co/CoTb full stack have been studied. Since the strength of the coupling between the Co layers through the Pt decreases rapidly when the Pt thickness increases, two reversal modes of the hard electrode have been highlighted at room temperature. For thin Pt thicknesses, the simultaneous reversal of the [Co/Pt]₃/Co multilayer and of the CoTb layers is observed whereas for large Pt thicknesses, the reversal occurs in two steps (first reversal of the [Co/Pt]₃ multilayer followed by the Co/CoTb reversal for larger applied fields). At low temperatures, the drastic increase of the anisotropy and the decrease of the magnetization in CoTb prevents its reversal, leading either to a spring magnet behavior for thin Pt thicknesses or to an exchange bias behavior for large Pt thicknesses. Finally, it is possible to stabilize a remanent intermediate magnetization state with the persistence of domains in the hard electrode. The different magnetic behaviors observed by magnetometry have been reproduced by micromagnetic calculations and summarized in original phase diagrams.

The magneto-transport properties of patterned MTJs have been explored to investigate how the various magnetic behaviors affect the transport properties. Beyond the usual cases where the applied field can reverse both electrodes, the resistance versus magnetic field characteristics have highlighted two interesting behaviors for magnetic fields in the range of the hard electrode magnetization reversal: (i) if the magnetic field is large enough to reverse the [Co/Pt] multilayer without CoTb reversal, the R(H) loops exhibit some common characteristics with M(H) : an exchange biased loop or a reversible spring magnet behavior. This last property is very attractive and could be used in the development of magneto-resistive sensor at room temperature and high fields; (ii) if the magnetic field is large enough to reverse the [Co/Pt] multilayer in the hard electrode and a part of the CoTb layer, the development of magnetic domains in the hard electrode gives rise to a domains duplication phenomenon from the hard to the soft electrode. This is nicely observed via the occurrence of a low resistance intermediate state.

TU.G.3_O4 - Search for exchange bias effect in antiferromagnetic Heusler alloy - ferromagnet bilayers

E. Simon¹, S. Khmelevskiy¹, R. Yanes-Diaz², L. Szunyogh¹, U. Nowak²

1. *Department of Theoretical Physics, Budapest University of Technology and Economics, Budapest, Hungary*

2. *Department of Physics, University of Konstanz, Konstanz, Germany*

The growing technological demand for spintronics applications raised increased interest for searching novel antiferromagnets (AFM). Promising candidates are the full Heusler compounds like Ni₂MnAl in the B2 phase or Ru₂MnZ (Z= Si, Ge) having Néel temperature above the room temperature. In this contribution we present a theoretical attempt to explore the possibility for exchange bias (EB) effect in bilayers formed by these AFM Heusler alloys and ferromagnetic (FM) metals like Fe and Co. Our approach is based on a combination of ab initio calculations and spin-dynamics simulations. We use the relativistic Screened Korringa-Kohn-Rostoker method to determine the electronic structure of the bilayer self-consistently and the relativistic torque method to derive exchange interactions in the system. In particular, by using the latter method we go beyond the usual Heisenberg model as it allows for calculating tensorial interactions that, beyond the isotropic interactions, account for two-site anisotropies and Dzyaloshinsky-Moriya interactions (DMI). In case of Ni₂MnAl/Fe bilayer we find AFM interface Fe-Mn coupling and sizable DMI in the interface Fe layer. In the interface Fe and Mn layers we calculated in-plane magnetic anisotropy. In case of Ni₂MnAl/Co bilayer the interface Mn-Co coupling is FM, the DMI's in the interface Mn and Co layers have similar magnitudes, and the interface Co layer exhibits a large out-of-plane magnetic anisotropy. By using the tensorial exchange interactions we performed simulations to determine the hysteresis loops of ordered Ni₂MnAl/Fe bilayers for different thicknesses of the AFM and FM layers. Our preliminary findings, however, indicate that for perfect Ni₂MnAl/Fe bilayers there is no (in-plane) EB effect. A possible way to generate EB is to consider defects in the AFM layer.

This work was supported by the European Commission via the Collaborative Project HAFIR (Project No. 604398).

TU.G.3_05 - IrMn/MgO-based tunneling junctions for room temperature antiferromagnet spintronics: effect of MgO and IrMn thickness

M. Cantoni¹, C. Rinaldi¹, L. Baldrati¹, S. Bertoli¹, M. Asa¹, D. Petti¹, E. Albisetti¹, R. Bertacco¹

1. Politecnico Di Milan, Milano, Italy

Memory elements based on pure antiferromagnetic templates (AF) have recently deserved large interest, because of their high packaging density (absence of stray fields) and robustness versus external perturbations. In a previous work [1], we demonstrated that in Ta/MgO/IrMn(2.5 nm) tunnelling junctions distinct metastable resistance states can be set by field cooling (FC) the heterostructures from above the Néel temperature (~ 170 K), with the external magnetic field along different orientations. Tunneling Anisotropic Magnetoresistance (TAMR) [2] up to 10% upon field cooling along the in-plane or out-of-plane direction provided the first demonstration of an electrically readable magnetic memory device, in which the information is stored within the AF active layer.

As a first step in order to extend the operation of the device to room temperature (RT), we studied the temperature dependence of the exchange bias versus the IrMn thickness in Si/SiO₂//CoFeB/IrMn(t)/Ru and Si/SiO₂//CoFeB/IrMn(t)/MgO/Ru structures. We demonstrated that, in structures without MgO, $t=3.5$ nm already presents a Blocking temperature larger than RT. Anyway, for $t < 6$ nm the presence of MgO suppresses the exchange bias (present if the MgO layer is removed), whereas $t = 6$ nm guarantees operating temperature above 180 °C.

Being IrMn/MgO an essential building block of AF spintronics, we investigated by photoemission spectroscopy this enabling/disabling influence of MgO on IrMn. We found that MgO plays a fundamental role in preserving the IrMn interface stoichiometry (Ir_{0.22}Mn_{0.78}), while in its absence a strong Mn depletion takes place (Ir_{0.47}Mn_{0.53}). The correlation between this chemical effect and the magnetic properties is currently under investigation.

IrMn/MgO/Ru tunneling junctions have finally been realized, with t ranging from 2.5 nm to 8 nm, in order to test the feasibility of TAMR at room temperature.

References:

[1] D. Petti et al., Appl. Phys. Lett. 102, 192404 (2013)

[2] A. B. Shick, Phys. Rev. B 81, 212409 (2010)

TU.H.1_I1 - Zero-field precession and suppression of the output power due to the biasdependence of the TMR in MgO-based spin-torque oscillators

E. Kowalska^{1,2}, V. Sluka¹, C. Fowley¹, A. Kakay¹, Y. Aleksandrov^{1,2}, J. Lindner¹, J. Fassbender^{1,2}, A.M. Deac¹

1. Helmholtz-Zentrum Dresden - Rossendorf, Institute of Ion Beam Physics and Materials Research, Bautzner Landstrasse 400, 01328 Dresden, Germany

2. Institute of Solid State Physics, TU Dresden, Zellescher Weg 16, 01069 Dresden, Germany

Spin-torque nano-oscillators (STNOs) are novel devices which may be exploited for wireless communication applications [1-3]. In particular, it has recently been demonstrated that STNOs utilizing an in-plane magnetized polarizer (also acting as read-out layer) and out-of-plane magnetized free layer allow for the full parallel-to-antiparallel resistance variation to be exploited in the limit of 90° precession angle, thereby maximizing the output power [1]. However, for this specific geometry, steady-state precession can only be sustained if the spin-transfer torque exhibits an asymmetric dependence on the angle between the free and the polarizing layer, such as in the case of fully metallic devices [1]. Nevertheless, it has recently been reported that dynamics have been experimentally observed in similarly designed MgO-based magnetic tunnel junctions (MTJs) under constant applied electrical current, in spite of the fact that such devices do not exhibit any asymmetry in the spin-torque angular dependence [4,5]. These results have so far been interpreted based on the formalism for metallic devices.

Here, we explore potential mechanisms for sustaining steady-state precession in MgO-based STNOs with this specific geometry. To this end, we analytically and numerically solve the Landau-Lifshitz-Gilbert-Slonczewski equation under a constant perpendicular applied current and field. We take into account both the angular and the bias dependence of the resistance of the nanopillar in order to convert the current into voltage, which is the relevant parameter in an MgO-MTJ. The field-like torque is neglected. We demonstrate that the angular dependence of the resistance introduces sufficient asymmetry of the in-plane spin-torque term to sustain precession in this system, but the bias dependence of the resistance gradually quenches this asymmetry as the current is increased and consequently suppresses precession above a given threshold. We furthermore prove that in an STNO with circular cross-section an external field is required to observe steady-state dynamics, but this constraint is lifted when introducing an in-plane easy axis, which opens new avenues to be explored for designing devices for mobile communication.

References:

- [1] W. H. Rippard, A. M. Deac, M. R. Puffall, et al., Physical Review B 81, 014426 (2010).
- [2] A. M. Deac, A. Fukushima, H. Kubota, et al., Nature Physics 4, 308 (2008).
- [3] S. I. Kiselev, J. C. Sankey, I. N. Krivorotov, et al., Nature 425, 380 (2003).
- [4] H. Kubota, K. Yakushiji, A. Fukushima, et al., Applied Physics Express 6, 103003 (2013).
- [5] T. Taniguchi, H. Arai, S. Tsunegi, et al., Applied Physics Express 6, 123003 (2013).

TU.H.1_O2 - Tunability versus deviation sensitivity in a nonlinear vortex oscillator

S. Y. Martin^{1,2}, C. Thirion³, C. Hoarau³, C. Baraduc², B. Diény²

1. Hitachi Cambridge Laboratory, Cambridge, United Kingdom

2. SPINTEC, UMR-8191, CEA-INAC/CNRS/UJF-Grenoble 1/Grenoble-INP, Grenoble, France

3. Institut Néel, CNRS et Université Joseph Fourier, Grenoble, France

We studied vortex oscillators based on ultra-low resistance magnetic tunnel junctions in which vortex is driven into a periodic motion by spin transfer torque (STT). The vortex oscillations are observed when the junction is subjected to a large dc bias current. The dc current produces both a large Oersted field which contributes to the vortex nucleation and a STT that starts the vortex oscillation [1].

Frequency modulation experiments were performed on this vortex oscillator for a wide range of modulation frequency, up to 10% of the oscillator frequency (about 500 MHz). A thorough analysis of the intermodulation products shows that the key parameter that describes these experiments is frequency-current dependence.

So we have developed an analysis based on modulation theory to treat the whole set of data at once. It appears that the description previously used to describe modulation experiments where the modulation frequency was much less than the natural frequency, does not apply when the modulation frequency is a significant fraction of the natural frequency. More precisely, the vortex response time appears to play a significant role, so that the concept of deviation sensitivity has to be introduced to explain the observations. Until now, deviation sensitivity was overlooked in the case of spintronic oscillators: it corresponds to the dynamical dependence of the oscillator frequency with an applied current that varies with time. We show that this frequency dependence differs strongly from that of a quasi-static experiment. Finally, we emphasize that the concept of deviation sensitivity differs significantly from the tunability discussed so far in the context of macrospin oscillators [2].

References:

[1] S.Y. Martin et al, PRB84, 144434 (2011), arXiv:1107.0867

[2] S.Y. Martin et al, PRB88, 024421 (2013), arXiv:1306.5552

TU.H.1_O3 - Self-injection on vortex spin torque oscillator using a delayed feedback circuit

S. Tsunegi^{1,2}, E. Grimaldi¹, R. Lebrun¹, A. Jenkins¹, J. Grollier¹, H. Kubota², K. Yakushiji², A. Fukushima², S. Yuasa², V. Cros¹

1. *Unité Mixte de Physique CNRS/Thales and Université Paris Sud, France*

2. *National Institute of Advanced Industrial Science and Technology (AIST), Spintronics Research Center, Tsukuba, Japan*

Towards the self-synchronization in arrays of Spin Torque Oscillators (STO), an important question is to understand the role of the phase difference $\Delta\varphi$ between a STO on the main features of the output rf signal. This issue is not only important to improve the rf properties of STOs but also for the potential implementation of neuro-inspired magnetic memories [1].

Here, we investigate the mechanism of self-injection using a delay line of STOs and notably the influence of $\Delta\varphi$ [2]. In order to re-inject the rf-signal generated from STO into the STO itself, we used the reflection at the close end. A tunable delay line is inserted in the circuit to control the $\Delta\varphi$; $\Delta\varphi=2\pi f_{ini} \Delta t +\pi$, where f_{ini} is the STO frequency without re-injection and Δt is the total delay time of lines. The rf signal generated by the STO after a re-injection is measured through a directional coupler.

The main results are that we clearly observed a 2π dependence with the phase difference $\Delta\varphi$ of the STO frequency, the linewidth, and the emission power as expected from theory [3]. Moreover, we find that when $\Delta\varphi$ is appropriately tuned, the spectral linewidth is strongly decreased and the emitted power increased compared with their respective values without re-injection. This first demonstration of an optimization of rf properties through an optimized delayed self-injection represent a key advance toward the mutual synchronization of two oscillators as the physical mechanisms are equivalent for both synchronizations.

The authors acknowledge the financial support from EU grant (MOSAIC No. ICT-FP7- n.317950) and from ANR agency (SPINNOVA) and. E.G. acknowledges DGA-CNES for support.

References:

[1] N. Locatelli, V. Cros, and J. Grollier, *Nat Mater* 13, 11 (2014)

[2] Y. Zhou, et. al., *J. Appl. Phys.* 101 09A510 (2007)

[3] K. Guru, et. al., *APL* (to be submitted)

TU.H.1_O4 - From perfect fractional injection locking to electrical synchronization of two vortex based spin-transfer nano-oscillator

R. Lebrun¹, S. Tsunegi^{1,2}, A. Jenkins¹, A. Dussaux¹, N. Locatelli¹, E. Grimaldi¹, H. Kubota², P. Bortolotti³, K. Yakushiji², A. Fukushima², J. Grollier¹, V. Cros^{1,3}

1. UMR CNRS/Thales & Université Paris Sud, France

2. National Institute of Advanced Industrial Science and Technology (AIST), Spintronics Research Center, Tsukuba, Japan

3. Thales TRT, France

In the last decade, large expectations have been anticipated on how the rich physics of spin transfer nano-oscillators could give birth to a new generation of multi-functional microwave spintronic devices [1]. Indeed, it has been often emphasized that their nonlinear behavior gives a unique opportunity to tune their radiofrequency properties but at the cost of large phase noise, not compatible with targeted applications.

To tackle this issue, a solution would be to rely on their synchronization to a reference external signal [2] or achieve mutual synchronization of multiple oscillators. However the largely reported presence of phase slips in the locked regime has non-controllable impact on these oscillators, and so an associated spectral linewidth that remains in the kHz range. Here we investigate the mechanism leading to a perfectly phase locked double vortex based STNO [3] to an external rf current F_s at multiple integer as well as half integer oscillator frequencies, with an associated phase noise down to -90dBc/Hz at 1 kHz frequency offset.

Furthermore we highlight that the physical mechanisms at play for the oscillator to be locked are very sensitive to the source and the symmetry of the spin transfer forces, allowing fractional synchronization without the presence of any phase slip events. The improved understanding of the locking behaviour gives us the opportunity to present an efficient electrical synchronization of two oscillators in series with a locking bandwidth of a few MHz. These results open the way to an efficient synchronization of multiple spin transfer oscillators which would be a real breakthrough towards applications in advanced rf devices or novel family of neuro-inspired memories.

References:

[1] N. Locatelli, V. Cros, and J. Grollier, Nat Mater 13, 11 (2014)

[2] R. Lebrun, arXiv:1502.03485 (2015)

[3] R. Lebrun, N. Locatelli, S. Tsunegi, J. Grollier, V. Cros, F. Abreu Araujo, H. Kubota, K. Yakushiji, A. Fukushima, and S. Yuasa, Physical Review Applied 2, (2014)

TU.H.1_O5 - Very Large Amplitude Power Spin Transfer Torque Nano-Oscillators with intermediate MgO barrier thickness

J. D. Costa^{1,2}, S. Serrano-Guisan¹, E. Paz¹, J. Borme¹, M. Tarequzzman¹, J. Ventura², R. Ferreira¹, P.P. Freitas¹

1. *International Iberian Nanotechnology Laboratory (INL), Braga (Portugal)*

2. *IN-IFIMUP, Porto (Portugal)*

Spin Transfer Torque Nano-Oscillators (STNOs) are one of the best examples of Spintronic devices exploring the spin transfer mechanism with a strong position to reach real world commercial applications. However, some requirements such as a large output power ($P_{out} \sim 1 \mu W$) and narrow linewidths ($\Gamma < 1$ MHz) were not reached yet. Among the many different implementations of STNOs, those based in Magnetic Tunnel Junctions (MTJs) look the most likely to provide large output oscillations thanks to the large tunneling magnetoresistance effect obtained in CoFeB/MgO/CoFeB stacks.

Here, a MTJ stack incorporating a MgO wedge (RA ranging from $\sim 50 \Omega \mu m^2$ to below $1 \Omega \mu m^2$ over an 8 inch wafer) was deposited with the purpose of clarifying the tradeoffs between endurance to large currents and reliability in ultra-thin and thin MgO barriers. Circular devices with diameters of 200 nm were then fabricated. Upon nanofabrication the static electrical properties of the nanopillars were measured and TMR ratios up to 100% achieved. The dynamic properties of some devices were then studied by measuring the RF emission and extracting key figures of merit (output power, line width, frequency, etc.) as a function of biasing conditions (field and voltage/current) for MTJs in different positions along the MgO wedge covering different ranges of RxA values. Besides oscillations in the RxA region approaching $RxA \sim 1 \Omega \mu m^2$, which is usually the target in MTJ based STNO applications, clear and good quality oscillations were also obtained in devices with intermediate MgO. A Very high output power of the order of $1 \mu W$ for $20 \Omega \mu m^2$ could be achieved.

To the best of our knowledge, this is the largest reported integrated power output obtained from a homogenous nano-oscillator. Besides the large integrated power output, the device also exhibits a reasonable linewidth and tunability in the frequency range.

TU.H.2_I1 - Quantum Critical Behavior in Quasicrystals and Approximant Crystals

N.Sato¹, S. Matsukawa¹, K. Nobe¹, K. Imura¹, K. Deguchi¹, T. Ishimasa²

1. *Department of Physics, Nagoya University, Japan*

2. *Department of Applied Physics, Hokkaido University, Japan*

Quasicrystals (QCs) are intermetallic alloys that possess aperiodic structures with diffraction symmetries forbidden to the conventional crystals. It is believed that their electronic states are critical, neither extended nor localized. Experimentally distinguishing such the critical state remains a formidable challenge. In the Au-Al-Yb QC, we observed quantum critical phenomena that are characterized by similar critical indices to those of Yb-based heavy fermions [1]. In contrast, no divergence was observed in the Au-Al-Yb approximant crystal (AC), a phase whose unit cell has atomic decorations (i.e., icosahedral clusters of atoms) that look like the QC and forms the body-centered cubic lattice in the present case. These results lead us to suggest that the observed quantum criticality in the QC is related to the critical state unique to the QCs. To gain further information on the physical properties, we studied the substitution effect of constituent elements on the magnetism and found that the Au-Al-Yb QC and AC are located near the border of the divalent and trivalent states of the Yb ion [2]. Recently, we found that there are two ACs with the Tsai-type cluster that show superconductivity at low temperatures [3]. In the presentation, we review the magnetic properties of these novel QCs and ACs. The effect of hydrostatic pressure and magnetic field on the unconventional quantum criticality of the Yb-based QCs and ACs as well as Ce-based ACs will be also presented.

References:

[1] K. Deguchi et al., *Nature Mat.* 11, 1013 (2012)

[2] S. Matsukawa et al., *J. Phys. Soc. Jpn.* 83, 034705 (2014)

[3] K. Deguchi et al., *J. Phys. Soc. Jpn.* 84, 023705 (2015)

TU.H.2_O2 - Multiple quantum phase transitions in CeRhIn₅

H. Yuan¹, L. Jiao¹, Z. Weng¹, Y. Chen¹, F. Steglich^{1,2}, D. Graf³, J. Singleton⁴, M. Jaime⁴, E. Bauer⁴, J. Thompson⁴

1. Center for Correlated Matter and Department of Physics, Zhejiang University, China

2. Max Planck Institute for Chemical Physics of Solids, Germany

3. National High Magnetic Field Laboratory, Florida State University, United States

4. Los Alamos National Laboratory, Los Alamos, United States

CeRhIn₅ provides a prototype compound for studying quantum criticality and its interplay with superconductivity. Application of pressure suppresses the antiferromagnetic (AF) order and gives rise to superconductivity [1]. A sharp change of Fermi surface was observed just at the pressure-tuning AF quantum critical point (QCP) [2], which was argued to support the scenario of local quantum criticality [3]. By means of measuring the dHvA oscillations and specific heat in a pulsed magnetic field, we have recently demonstrated the existence of a field-induced AF QCP around $B_{c0}=50\text{T}$ in this compound [4]. A sharp reconstruction of Fermi surface was observed well inside the AF state, i.e., around $B_0^*=31\text{T}$, which might correspond to a localized-itinerant transition of Ce 4f-electrons attributed to the Kondo effect. These results suggest that multiple quantum phase transitions may exist in CeRhIn₅ which can be classified by the measurements of Fermi surface topology[4]. We further explored the multiple QCPs of CeRhIn₅ by mapping its pressure-magnetic field phase diagram with measurements of the Hall resistivity and magnetoresistivity under combined extreme conditions of high pressure and high magnetic field.

References:

[1] T. Park, et. al., Nature 440, 65 (2006)

[2] H. Shishido, R. Settai, H. Harima, Y. ōnuki, J Phys Soc Jpn 74,1103 (2005)

[3] Q. Si, F. Steglich, Science 329,1161 (2010)

[4] L. Jiao et al., PNAS 112, 673 (2015)

TU.H.2_O3 - Frustration at the Quantum Phase Transition in CePdAl

V. Fritsch^{1,2}, A. Sakai¹, S. Lucas³, Z. Hüsge³, K. Grube², W. Kittler², C. Taubenheim², E. Green⁴, O. Stockert³, H. v. Löhneysen²

1. *Universität Augsburg, Institut für Physik, Experimentalphysik 6, Germany*

2. *Karlsruher Institut für Technologie (KIT), Germany*

3. *Max-Planck-Institut für chemische Physik fester Stoffe, Dresden, Germany*

4. *Helmholtz-Zentrum Dresden-Rossendorf, Germany*

CePdAl crystallizes in the hexagonal ZrNiAl structure, where the magnetic ions form a distorted kagomú lattice. At $T_{\text{N}} = 2.7$ K the onset of antiferromagnetic (AF) order is observed. Neutron scattering experiments [1] revealed a partial frustration in the distorted kagomú planes of this structure: two-thirds of the Ce moments form ferromagnetic chains, which are antiferromagnetically coupled, the remaining third do not participate in any long-range order. Along the c-axis the magnetic moments exhibit an amplitude modulation. Accordingly, the kagomú planes are stacked on top of each other, resulting in corrugated AF planes parallel to the c-axis formed by the ordered magnetic moments, which are separated by the frustrated moments [2]. The substitution of Pd with Ni in CePdAl tunes the system to a quantum critical point exhibiting an unconventional critical behavior [2].

I will present measurements of the thermodynamic properties, especially of the specific heat and the electrical resistivity, of single crystalline CePd_(1-x)Ni_(x)Al down to very low temperatures as well as neutron scattering experiments, in order to explore the effect of magnetic frustration on the quantum critical behavior and discuss the possible emergence of a partial spin liquid state in CePdAl.

References:

[1] A. Dönni et al., J. Phys.: Condens. Matter 8, 11213 (1996)

[2] V. Fritsch et al., Phys. Rev. B 89, 054416 (2014)

TU.H.2_O4 - Non-Fermi-liquid behavior in the THz response of CeCoIn₅

M. Scheffler¹, U. S. Pracht¹, M. Dressel¹, M. Shimozawa², R. Endo², T. Terashima³, T. Shibauchi^{2,4}, Y. Matsuda²

1. *Physikalisches Institut, Universität Stuttgart, Germany*

2. *Department of Physics, Kyoto University, Japan*

3. *Research Center for Low Temperature and Materials Science, Kyoto University, Japan*

4. *Department of Advanced Materials Science, University of Tokyo, Japan*

Heavy fermions are a prime material class to study the physics of quantum phase transitions. In particular, non-Fermi-liquid behavior related to quantum criticality has been observed in several heavy-fermion compounds. While the charge transport as a function of temperature has been studied in great detail for several quantum-critical heavy-fermion metals, including CeCoIn₅, the frequency dependence, directly revealing the charge dynamics, has been studied much less. This is mostly due to the severe experimental difficulties involved, namely optical spectroscopy on highly reflective metals at very low frequencies and temperatures. We overcome these difficulties by THz transmission measurements (detecting amplitude and phase of the THz signal) on high-quality thin films of CeCoIn₅. We are particularly interested in the extended temperature range (above the superconducting transition) where the dc resistivity of CeCoIn₅ exhibits a linear temperature dependence, which is a signature of non-Fermi-liquid behavior.

We have measured the optical response of CeCoIn₅ at temperatures down to 3 K and at frequencies between 0.2 and 1.1 THz, i.e. at matching energy scales of the non-Fermi-liquid regime. We find characteristic metallic behavior in the THz response, and in particular we can follow the transport relaxation rate move through our spectral range upon cooling. Using the extended Drude formalism, we deduce the frequency dependence of relaxation rate and effective mass of the charge carriers. Here we find a strong increase of the relaxation rate with increasing frequency that demonstrates optical non-Fermi-liquid behavior and which even surpasses the temperature dependence at zero frequency. The effective mass also exhibits a strong temperature dependence, which allows us to observe the evolution of the heavy-fermion state upon cooling.

TU.H.2_O5 - Microscopic investigation of electronic inhomogeneity induced by substitutions in a quantum critical metal CeCoIn5

E. Bauer¹, H. Sakai², F. Ronning¹, J.-X. Zhu¹, N. Wakeham¹, H. Yasuoka¹, Y. Tokunaga², S. Kambe², J. D. Thompson¹

1. Los Alamos National Laboratory, New Mexico, United States

2. Advanced Science Research Center, Japan Atomic Energy Agency, Japan

Chemical substitutions are used commonly to tune a magnetic transition to zero temperature, but the resulting non-Fermi liquid (NFL) behavior is non-universal. CeCoIn5 is an unconventional superconductor that belongs to the CeTIn5 (T=Co, Rh, Ir) family, and is known to lie in close proximity to an AFM QCP at ambient pressure [1, 2]. Due to the high purity of the parent materials we can study how controlled amounts of disorder influence these phenomena. A very small amount of Cd (5s2) substitution for In (5s25p) in CeCoIn5 induces long-range AFM order [3]. Applying pressure to CeCo(In,Cd)5 suppresses the AFM; however, the fluctuations and the signatures at this P-induced AFM QCP are absent [4]. In the case of Sn (5s25p2) substitution in CeCoIn5, magnetic order is not induced, and instead the AFM fluctuations are suppressed as the system is driven away from the AFM QCP [5,6]. In a rigid band picture, changing the electron count by of order $\pm 1\%$ per unit cell should have a negligible effect on the global band structure, and it, therefore, seems puzzling that two non-magnetic dopants on the In sites could produce vastly different responses at the QCP. Though Sn substitutions introduce a rather homogeneous electronic state suppressing the AFM fluctuations, Cd substitutions intrinsically produce an electronic heterogeneous state. We show here that Cd dopants in CeCoIn5 enhance antiferromagnetic behavior by inducing localized moments in their immediate vicinity. These substituents induce very different local electronic environments as observed by site dependent spin lattice relaxation rates $1/T_1$ that influence the NFL behavior. The effects found here illustrate the need for care in interpreting NFL properties determined by macroscopic measurements.

References:

- [1] C. Petrovic et al, J. Phys.: Condens. Matter 13, L337 (2001)
- [2] H. Sakai et al. Phys. Rev. Lett. 107, 137001 (2011)
- [3] L. D. Pham et al. Phys. Rev. Lett. 97, 056404 (2006)
- [4] S. Seo et al. Nature Physics 10, 120 (2014)
- [5] E. D. Bauer et al. Phys. Rev. B 73, 245109 (2006)
- [6] K. Gofryk et al. Phys. Rev. Lett. 109, 186402 (2012)

TU.H.3_I1 - Dynamics of chiral spin systems: soliton lattices, defects and spinwaves

R. Stamps¹

1. *University of Glasgow, Glasgow, United Kingdom*

In this talk, I will discuss unusual features associated with chiral interactions and geometries that lead to chiral ordering. A central theme of the talk will be chirality in spin systems and its manifestation as skyrmionic and helicoidal textures, the possibility of its emergence in artificially designed structures, and potentials for its application. [1,2] Interface induced Dzyaloshinskii interactions can have significant effects on domain wall structure and mobility in thin ferromagnetic films. Moreover, spin wave propagation can be strongly affected, especially in regards to scattering from magnetic domain walls. [3] Lastly, I comment on new ways of probing chirality in crystals using a type of electronic vortex state. Electrons in these states carry spin and angular momentum, and have great potential for use in electron microscopy as new types of probes. [4]

References:

1. Silva, R. L., Secchin, L. D. , Moura-Melo, W. A. , Pereira, A. R., and Stamps, R. L. (2014) Emergence of skyrmion lattices and bimerons in chiral magnetic thin films with nonmagnetic impurities. *Physical Review B*, 89 (5). 054434
2. Togawa, Y., McVitie, S., Stamps, R.L., et al. (2015) Discrete accumulation of chiral spin solitons.
3. Borys, Garcia-Sanchez, F., Kim, J.-V., and Stamps, R. L. (2015) Spin wave eigenmodes of Dzyaloshinskii domain walls.
4. Greenshields C., Stamps R. L., Frank-Arnold, S., *New Journal of Physics*, 14, 103040 (2012); Greenshields, C., Stamps, R. L., Frank-Arnold, S., Barnett, S. Is Angular Momentum Conserved in Electron Vortex Beams? *Physical Review Letters*, 113 (10). p. 240404

TU.H.3_O2 - Asymmetric Wave Propagation in Skyrmion String in Chiral Magnets

J. Iwasaki¹, C. Schütte², N. Nagaosa³

1. *University of Tokyo, Tokyo, Japan*

2. *Universität zu Köln, Köln, Germany*

3. *RIKEN, Saitama, Japan*

Skyrmion, a topological field configuration first introduced in nuclear physics as a model of hadrons, has now been observed in magnets, known as magnetic skyrmion. In particular, magnetic skyrmion appears ubiquitously in chiral magnets or multi-layered magnets, where the Dzyaloshinskii-Moriya interaction (DMI) due to broken inversion symmetry stabilizes its swirling structure. In the bulk of chiral magnets, two-dimensional skyrmions in xy -plane are stacked up along z -axis, forming a pillar-like object, which we call skyrmion string.

Although there are numerous works on the dynamical properties of magnetic skyrmion such as the dynamics induced by electric current and that by magnons, the most of them focus only on its two-dimensional motion. Here, we move to higher dimension and investigate the dynamics of skyrmion string in three dimensions. We first study, by the micromagnetic simulation based on the Landau-Lifshitz-Gilbert equation, how a wave propagates in skyrmion string, and find that the waves propagating $+z$ - and $-z$ -directions are not equivalent. Next, we look into the origin of this asymmetric feature. The simple analysis under the assumption that the skyrmion texture in xy -plane is rigid fails to produce the asymmetry. It is described by the coupling between the skyrmion string and surrounding magnons, which has k_z -linear term in its dispersion relation in the presence of the DMI. Finally, we confirm in the numerical simulation that the wave propagation is symmetric when we artificially switch off the DMI in z -direction.

TU.H.3_O3 - Neutron spin-echo spectroscopy of spin fluctuations in the skyrmion lattice phase of MnSi

F. Haslbeck¹, J. Kindervater¹, A. Bauer¹, W. Häußler^{1,2}, P. Böni¹, C. Pfleiderer¹

1. Physics Department, TU Munich, Germany

2. Heinz Maier-Leibnitz Zentrum, TU Munich, Germany

Recent theoretical studies suggest that the skyrmion lattice phase in chiral magnets such as MnSi is stabilised by thermal spin fluctuations [1,2]. We report an experimental study of the quasielastic spectrum of spin fluctuations in the skyrmion lattice phase of MnSi. Using the so called MIEZE spin-echo technique at the spectrometer RESEDA at FRM II we achieved an unprecedented resolution below 1 μeV going well beyond a first preliminary study [3]. Applying a magnetic field parallel and perpendicular to the neutron beam allowed us to study the fluctuations in and out of plane of the skyrmion lattice.

TU.I.1_I1 - Spin-wave logic devices

A. Chumak¹

1. Fachbereich Physik and Landesforschungszentrum OPTIMAS, Technische Universität Kaiserslautern, Kaiserslautern, Germany

With the fast growth in the volume of information being processed, researchers are charged with the primary task of finding new ways for fast and efficient processing and transfer of data. Spin excitations - spin waves and their quanta magnons - open up a very promising branch of high-speed and low-power information processing. Down-to-nm wavelengths, GHz-to-THz frequency range, Joule-heat-less transfer of spin information, and access to novel wave-based computing concepts allow for the development of a novel technology without drawbacks inherent in modern semiconductor electronics. In my talk, I will discuss exclusively magnon-based processing of digital data. After a brief overview of previous realizations of spin-wave logic gates, recent progress in the field will be discussed on the basis of two novel devices. The first one is a functioning magnon transistor [1], which is required for single-chip data processing solely within a magnonic system (see Fig. 1a). We have demonstrated that a magnon current can be efficiently controlled by another. The second device, which is of large potential for computing, is the magnon majority gate. The first micro-scale design of the majority gate was demonstrated recently using micromagnetic simulations (see Fig. 1b) [2]. A novel design of the majority gate operating with isotropic spin waves in normally-magnetized structure will be presented. A full adder, which consists of 28 transistors in CMOS technology, can be constructed using 3 majority gates only. The potential of magnon-based logic devices will be discussed with respect to miniaturization aspects [3] and the reduced power consumption.

References:

- [1] A. V. Chumak, A. A. Serga, and B. Hillebrands, *Nat. Commun.* 5, 4700 (2014)
- [2] S. Klingler, et al., *Appl. Phys. Lett.* 105, 152410 (2014)
- [3] P. Pirro, et al., *Appl. Phys. Lett.* 104, 012402 (2014)

TU.I.1_O2 - Novel paths for rf applications based on spintronics

P. Bortolotti¹, A. Anane¹, M. Collet¹, D. Crete¹, V. Cros¹, O. d'Allivy Kelly¹, E. Grimaldi¹, J. Grollier¹, A. Jenkins¹, J. Kermorvant¹, B. Marcilhac¹, R. Lebrun¹

1. Unité Mixte de Physique CNRS/Thale, France

Spintronics consists of manipulating electronic spins rather than, or in addition to, charges through electrical currents and/or magnetic fields. This technology has revolutionized the market of read-head applications and other types of magnetic sensors. Recently, a lot of promising studies have been done for active elements such as memories [1], spin transistors and more generally logic spin gates [2]; however, those functionalities are far from being implemented into real devices. Nevertheless, we believe that concerning radio-frequency (rf) applications, spintronics is now mature enough to propose interesting and industrially attractive active functionalities [3] and to foster the development of a new generation of rf devices such as filters, frequency detectors, synthesizers, etcà Here we will present some of our recent works on the subject. 1) A synthesizer based on vortex spin-transfer nano oscillator (STNO): a magnetic tunnel junction (MTJ) where the free layer is in the magnetic vortex configuration. 2) A new type of STNO frequency detector based on vortex core expulsion. 3) Novel STNO-based associative memories; by mimicking the behavior of our brain, we will consider an array of STNOs and take advantage of their mutual synchronization to perform associative memory functionalities. 4) Magnonic devices, i.e., the use of spin wave excitations (magnons) for information treatment. Information can be encoded in the phase of the magnetostatic spin waves and easily manipulated; miniaturized and low energy consumption devices, for both logic and rf functionalities, can indeed be conceived.

I acknowledge financial support from ANR agency (SPINNOVA ANR-11-NANO-0016; MEMOS ANR-14-CE26-0021-03; NANOSWITI ANR-11-BS10-003-05) and EU FP7 grant (MOSAIC No. ICT-FP7-n317950).

References:

1. D. Apalkov et al., J. Emerg. Technol. Comput. Syst. 9, 1550 (2013)
2. A. Chumak et al., Nat. Commun. 5, 4700 (2014) and ref. therein
3. N. Locatelli et al., Nature Mater. 13, 11 (2014)

TU.I.1_O3 - Ultra-compact device based on spin valve sensors coupled to flux concentrators with sub-micrometer gaps

D. Leitao^{1,2}, P. Coelho¹, J. Valadeiro^{1,2}, A. Silva^{1,2}, J. Borme³, L. Melo^{1,2}, S. Cardoso^{1,2}, P. Freitas^{1,3}

1. INESC-M, Lisbon, Portugal

2. University of Lisbon, Lisbon, Portugal

3. International Iberian Nanotechnology Laboratory, Braga, Portugal

Recent developments in magnetic field imaging techniques have demonstrated the advantages of using magnetoresistive (MR) sensors as active element. MR sensors give a direct quantification of the magnetic fields and their dimensions set the measurement's spatial resolution. Still, miniaturizing MR sensors leads to a significant increase in the demagnetizing effects thus decreasing field sensitivity (S). In turn, smaller sensor sizes also lead to large intrinsic noise levels.

We demonstrate a hybrid device with improved sensitivity by placing nanoscale spin-valve (SV) sensors within sub-2 μ m gap magnetic flux concentrators (MFCs), towards downsized magnetic field mapping. The SV stack (deposited by ion beam deposition) consisting of Ta 2/NiFe 3/MnIr 8/CoFe 3.3/Ru 8/CoFe 3.3/Cu 2.5/CoFe 2/NiFe 2/Ru 0.8/NiFe 2.5/Ta 10 (nm) was engineered to deliver improved sensitivity when nanopatterned and was defined by e-beam lithography and ion milling etching (1.3 μ m \times 500nm), displaying an overall MR \sim 5%. The sensors were then placed in the gap of two 600nm thick CoZrNb MFCs. The MFCs (pole=2 μ m; 100 \times 50 μ m²) were patterned by e-beam lithography and lift-off using PMMA (1.2 μ m). Our process guarantees that a challenging pole-sensor (P-S) distance down to 400nm is achieved with thick MFCs, thus ensuring maximum field gains. We successfully achieved MFCs with a very clean gap profile and pole geometrical features yielding closure magnetic domain structures, crucial for these dimensions.

NanoSVs-MFCs showed S=0.28%/Oe for P-S=1100nm, increasing to S \sim 0.37%/Oe for P-S=650nm, showing then a maximum value S=0.46%/Oe for P-S=570nm, corresponding to field gains of 15x, 21x and 23x, respectively (compared to isolated sensors). For the smallest P-S=400nm a decrease to S=0.37%/Oe was observed. This suggests the onset of considerable magnetostatic coupling between MFC-poles, which overrides the partial SV guiding effect. In summary, the optimized sensors combine high spatial resolution (500nm) and high field sensitivity (0.46%/Oe) in a small footprint device (100 \times 100 μ m²).

TU.I.1_O4 - Nanopatterning reconfigurable magnetic landscapes via thermally assisted scanning probe lithography

E. Albisetti^{1,2}, D. Petti¹, M. Pancaldi³, J. Curtis², W. King⁴, A. Papp⁵, G. Csaba⁵, W. Porod⁵, P. Vavassori³, E. Riedo², Bertacco^{1,7}

1. *Department of Physics, Politecnico di Milano, Milano, Italy*

2. *School of Physics, Georgia Institute of Technology, Atlanta, United States*

3. *CIC nanoGUNE Consolider, San Sebastian, Spain*

4. *Department of Mechanical Science and Engineering, University of Illinois Urbana-Champaign, Urbana, United States*

5. *Center for Nano Science and Technology, University of Notre Dame, Notre Dame, United States*

6. *IKERBASQUE, Basque Foundation for Science, Bilbao, Spain*

7. *IFN-CNR, c/o Politecnico di Milano, Milano, Italy*

The search for novel tools for controlling magnetism at the nanoscale is crucial for the development of new paradigms in optics, electronics and spintronics. So far, the patterning of magnetic nanostructures has been mainly achieved through irreversible structural or chemical modifications [1-3]. Here, we propose a new concept, that we call 'thermally assisted magnetic scanning probe lithography' (tam-SPL), for creating reconfigurable magnetic nanopatterns by crafting at the nanoscale the magnetic anisotropy landscape of a ferromagnetic layer exchange-coupled to an antiferromagnetic one. By performing a highly localized field cooling with the hot tip of a scanning probe microscope, magnetic structures, with arbitrarily oriented magnetization and tunable unidirectional anisotropy, are patterned without modifying the film chemistry and topography. The proposed technique is straightforward and combines the full reversibility and stability of exchange bias, as the same pattern can be written and reset many times, with the resolution and versatility of scanning probe lithography. In particular, we demonstrate the patterning of arbitrarily shaped domains with dimension down to 250 nm in a continuous CoFeB/IrMn/Ru exchange-bias trilayer grown by magnetron sputtering. By combining magnetic force microscopy, magneto-optical Kerr effect microscopy and micromagnetic simulations we show that, via tam-SPL, it is possible to locally control the micromagnetic configuration and unidirectional anisotropy of the magnetic layer with nanoscale precision. This opens unforeseen possibilities for the development of novel metamaterials with finely tuned magnetic properties as well as reconfigurable computing device architectures. In particular, we discuss the application of our technique to the fabrication of magnonic devices, namely phase shifters and magnonic crystals with controllable and reconfigurable band gaps.

References:

[1] C. Chappert et al., *Science* 280, 1919-1922 (1998)

[2] G.M. McClelland et al., *Appl. Phys. Lett.* 81, 1483 (2002)

[3] S. Kim et al., *Nat. Nanotechnol.* 7, 567-71 (2012)

TU.I.1_O5 - Precision Spintronics in Novel Ultrathin Magneto-Electronic Devices

K. Schlage¹, L. Bocklage^{1,2}, D. Erb¹, H. Wille¹, R. Roehlsberger^{1,2}

1. *Deutsches Elektronen-Synchrotron DESY, Hamburg, Germany*

2. *The Hamburg Centre for Ultrafast Imaging, Hamburg, Germany*

Next information and sensor technology is based on progress in spintronic multilayer design. The interlayer coupling approach used to engineer the magnetization profiles in these systems imposes fundamental limitations on the adjustability of their magneto-electronic response. We demonstrate that oblique incidence deposition (OID) can be used in a facile way to freely adjust the magneto-electronic properties in ultra-thin multilayer devices made from any magnetic material, with any non-magnetic spacer layer. The functionality of these devices is not based on interlayer coupling but solely depends on the magnetic anisotropy of the individual layers. In this new class of layered materials crossed multilayer easy axes with adjustable opening angle and custom-made switching fields (1 - 100 mT) of the individual layers can be precisely realized for the first time. Low and high-field magneto-electronic multilayers and spin-valve systems with tailor-made magneto-resistive functionality can be fabricated in a simple fashion from the same type of multilayer systems (identical layer structure and chemical composition) by adjusting the magnetic properties via oblique incidence deposition.

Irrespective of the interface roughness that goes along with the deposition via OID a very clean and strong magneto-resistive signal is obtained in ferromagnetic/nonmagnetic/ferromagnetic building trilayers that multiplies by simple stacking of such building blocks. Thus new routes are opened up for magnetic multilayer design, and the functionality of spintronic devices can be adjusted to particular applications with unprecedented accuracy [1].

References:

[1] Kai Schlage, Denise Erb, Ralf Röhlsberger, H.-C. Wille, Lars Bocklage, Daniel Schumacher. Method of producing a multilayer magnetoelectronic device and magnetoelectronic device. European Patent: P91642 (2014)

TU.I.2_O2 - Novel ways of shaping magnetic fields with superconducting-ferromagnetic metamaterials

A. Sanchez¹, J. Prat-Camps¹, C. Navau¹

1. *Universitat Autònoma Barcelona, Barcelona, Spain*

With the discovery of the transformation optics technique, many new possibilities of generating, transmitting and controlling electromagnetic waves have become possible, including electromagnetic cloaks and perfect lenses. This technique has also been recently successfully applied to the case of static magnetic fields. Here in this work we report on how transformation optics applied to static magnetic fields results in a variety of new possibilities for transmission and guidance of magnetic fields and energy. We discuss in particular how magnetic fields can be cloaked [1], can be concentrated in a given space with unprecedented values [2,3], and can even be transmitted to arbitrary long distances through magnetic hoses [4], similar to light transmitted in optical fibers. We also discuss why static magnetic fields make an ideal case for application of these ideas: many interesting designs require extreme values of the material properties (magnetic permeability in this case) and, for the case of magnetic fields, available superconductors and soft ferromagnets exist to provide both extreme permeability values (zero and infinite, respectively), as well as intermediate values. All these novel possibilities for magnetic fields achieved with metamaterials will be also experimentally demonstrated using superconducting and ferromagnetic hybrid systems.

References:

- [1] F. Gömory, M. Soloviyov, J. èouc, C. Navau, J. Prat-Camps, and A. Sanchez, *Science* 335, 1466 (2012)
- [2] C. Navau, J. Prat-Camps, and A. Sanchez, *Phys. Rev. Lett.* 109, 263903 (2012)
- [3] J. Prat-Camps, C. Navau, and A. Sanchez, *App. Phys. Lett.* 105, 234101 (2014)
- [4] C. Navau, J. Prat-Camps, O. Romero-Isart, J.I. Cirac, and A. Sanchez, *Phys. Rev. Lett.* 112, 253901 (2014)

TU.I.2_O3 - Thin-film magneto-impedance structures with very large sensitivityE. Fernández², A. García-Arribas^{1,2}, A. V. Svalov¹, N. G. V. Kurlyandskaya¹, J. M. Barandiaran^{1,2}*1. Departamento de Electricidad y Electrónica, Universidad Del País Vasco, UPV/EHU, Bilbao, Spain**2. BCMaterials, Universidad Del País Vasco, UPV/EHU, Bilbao, Spain*

Thin film-based Magneto-Impedance (MI) structures are well suited for developing highly sensitive magnetic microsensors, which can be directly integrated into microelectronic circuits. Permalloy (Py) based structures benefit from well-established preparation procedures and enhanced structural stability over amorphous based sensors. In previous studies we have concluded that sputtered Py (Ni₈₁Fe₁₉) films lose their soft magnetic properties for thickness above a critical value (about 200 nm). Py films below that limit display excellent properties with only slight differences between 50 nm and 100 nm thick films. Thicker (up to 1 micron) multilayer structures keeping soft properties can be obtained by inserting thin spacers between Py layers. Additionally, the MI performance is greatly enhanced in sandwiched structures composed by a non-magnetic conductive layer between two magnetic structures. The best results are expected when the thickness of the non-magnetic layer equals the magnetic ones. In this work we determine the combination of magnetic and non-magnetic layers that maximizes the MI performance, maintaining an open flux configuration (Py not enclosing the central non-magnetic conductor), which permits the fabrication of the complete stack of layers in a single process.

Samples with a sandwiched multilayer structure defined as [Py(100 nm)/Ti(6 nm)]₄/Cu(400 nm)/[Ti(6 nm)/Py(100 nm)]₄ have been prepared by magnetron sputtering and photolithography, having different dimensions. They were magnetically characterized by magneto-optical Kerr effect, displaying a well-defined transversal anisotropy. The MI was measured in a network analyzer using a microstrip test-fixture. The MI ratio $(Z-Z_{min})/Z_{min} \hat{=}$ 100 reaches values of 350 %, the largest ratios reported for thin film Py-based structures. The sensitivity, calculated as the field derivative of the MI ratio, reaches 300 %/Oe. The MI ratio is somewhat lower than the one reported previously for amorphous CoSiB/Ag/CoSiB with closed-flux structure, but the sensitivity is six times larger. These figures compare favorably with wire-based MI devices.

TU.I.2_O4 - Bioinspired Nanocomposite Tactile Sensor

A. Alfadhel¹, J. Kosel¹

1. Computer, Electrical and Mathematical Sciences and Engineering Division (CEMSE), King Abdullah University of Science And Technology (KAUST), Thuwal, Saudi Arabia

The current progress in fields like robotics or biomedical engineering requires the development of wearable and flexible sensing technologies that combine miniaturization with a high sensitivity and low power consumption. In this context, tactile sensors are required that have a high sensitivity and low power consumption.

We report the fabrication and characterization of a novel tactile sensor that consists of an array of 1 mm long and 200 μm in diameter bioinspired cilia integrated on a giant magneto-impedance (GMI) magnetic field sensing element for a wide range of tactile sensing applications including soft robotics, smart prosthesis, surgical tools, or flow sensing. The cilia are fabricated from a permanent magnetic and highly elastic nanocomposite that is made of iron nanowires (NWs) incorporated into polydimethylsiloxane (PDMS). The permanent magnetism stems from the high magnetization of iron NWs at remanence, which is due to the strong shape anisotropy.

The operating principle of the sensor is based on detecting the change of the stray magnetic field, created by the permanent magnetic cilia when deflected by an external force (e.g. hand touch). A GMI sensor, which offers a good compromise between sensitivity and fabrication complexity, and has potential for wireless operation, is utilized to measure the change in the magnetic field upon the deflection of the cilia.

The tactile sensing element has a high sensitivity of about 11.5 $\text{m}\Omega/\text{mN}$ (46 $\text{m}\Omega/\text{kPa}$) and a resolution of 1.4 mN (0.35 kPa). Its operating range is between 0-100 mN (0-25 kPa) with an extremely low power consumption of 80 nW . The developed tactile sensor is fabricated on rigid and flexible substrates and it can measure more than one property such as flow, vibration, orientation, or the texture of a contacted object, with easily modifiable performance and operating range.

TU.I.2_O5 - Low Frequency Plasmonic State in FeNi/Cu Hybrid Granular Composite Materials

T.Tsutaoka¹, H. Massango¹, T. Kasagi², S. Yamamoto³, K. Hatakeyama³

1. *Hiroshima University, Hiroshima, Japan*

2. *National Institute of Technology, Tokuyama College, Japan*

3. *University of Hyogo, Japan*

Left handed (LH) substances with simultaneously negative values of permittivity (ENG) and permeability (MNG) have been the most popular of the metamaterials due to their property of negative refractive index. The double negative (DNG) electromagnetic properties have been observed in granular composite materials in several GHz range [1, 2]. In this study, the FeNi/Cu hybrid granular composite materials has been prepared to investigate the electromagnetic properties by measuring the relative complex permeability and the relative complex permittivity spectra over the microwave frequency range with the goal to achieve the double negative permeability and permittivity spectra without the external magnetic field. The composite materials $(\text{Cu}_x\text{FeNi}_{1-x})_y\text{PPS}_{1-y}$, where x and y are the volume fraction of particles and PPS denotes the poly-phenylene sulfide resin, were prepared by mixing Cu and FeNi powder with PPS resin powder, heated the mixture at 300°C and pressing at a pressure of 31.8 MPa in the cooling process down to the room temperature. The samples were shaped in the toroidal form (inner diameter of 3 mm and outer diameter of 7 mm) with the thickness of about 1 mm. The permittivity and permeability spectra were measured by transmission/reflection method using the standard 7/3 mm coaxial airline techniques in the frequency range from 10 MHz to 20 GHz.

The permittivity spectra of $(\text{Cu}_{0.24}\text{FeNi}_{0.76})_{0.85}\text{PPS}_{0.15}$ indicated the Drude type ENG characteristic bellow 4.5 GHz. In this composite, the negative permeability was also obtained by the magnetic resonance of FeNi particles. Hence, combining these two ENG and MNG properties, a DNG characteristic can be obtained in the frequency range from 300 MHz to 1.8 GHz without the external magnetic field.

References:

[1] T. Tsutaoka et al., Appl. Phys. Lett., 103, (2013) 261906

[2] Z.-C. Shi et al., J. Mater. Chem. C, 1 (2013) 1633-1637

TU.I.2_O6 - Microwave shape resonance in magnetic microwires tuned by giant magnetoimpedance effect: sensing applications

V. Lopez Dominguez¹, E. Riccardi², K. Osiak³, P. Marín¹, A. Hernando¹

1. *Instituto De Magnetismo Aplicado, Universidad Complutense De Madrid-CSIC-ADIF, Madrid, Spain*

2. *Department of Structures for Engineering and Architecture University of Naples Federico II, Naples, Italy*

3. *Faculty of Materials Science and Engineering, Warsaw University of Technology, Warsaw, Poland*

Glass-covered amorphous magnetic microwires present a diameter in the range of microns and a magnetoelastic anisotropy influenced by mechanical stress and amorphous microstructure [1-2]. These characteristics besides the strong interactions that present magnetic microwires with electromagnetic microwaves make them ideal candidates for technological and medical applications [3-4]. In our present work we propose a new theoretical framework about the interaction of electromagnetic microwaves and Co-based magnetic microwires exhibiting giant magnetoimpedance effect. Such interaction induces an electrical current along the microwire [5] that depends on its impedance, as well as on the relation between its length and the wavelength of the microwave. Furthermore, our numerical results reveal a direct dependence of the total impedance of the microwire on its magnetic permeability, which can be tuned by an external magnetic field or stress. These theoretical results were compared with the experimental microwave spectrum of Co-based magnetic microwires (radius 33 μm) in the microwave range between 500 MHz and 20 GHz. Particularly, it was measured the relative variations of the scattering coefficient S_{21} induced by the application of an ac-bias magnetic field. As our theory predicts, depending on the length of the magnetic microwire there are a set of frequencies in which the variations of the scattering coefficient are maxima (shape resonance frequencies). In addition, at the shape resonance frequencies the maximum variation of the scattering coefficient occurs at the coercive field of the microwire (maxima variations of the magnetic permeability). Consequently, a suitable combination of magnetoimpedance effect and shape resonances opens the perspective to use this system as a wireless field and stress micro sensor element.

References:

- [1] L. Kraus, G. Infante, Z. Frait, and M. Vazquez, *Phys. Rev. B* 83, 174438 (2011)
- [2] A. Zhukov, J. Gonzalez, J. M. Blanco, M. Vázquez, and V. Larin, *Journal of Materials Research* 15, 2107 (2000)
- [3] P. Marín, M. Vázquez, J. Arcas, and A. Hernando, *J. Magn. Magn. Mater.* 254-255, 624 (2003)
- [4] C. Herrero-Gómez, A. M. Aragón, M. Hernando-Rydings, P. Marín, and A. Hernando, *Applied Physics Letters* 105, 092405 (2014)
- [5] G. Hanson, *Antennas and Propagation, IEEE Transactions on* 53, 3426 (2005)

TU.I.3_O1 - Evidence of a spin-polarized resonant surface state in (111) $\text{Sm}_{1-x}\text{Gd}_x\text{Al}_2$, a zero-magnetization ferromagnetK. Dumesnil¹, M. Bersweiler¹, D. Lacour¹, M. Hehn¹, P. Lefevre²*1. Institut Jean Lamour, Université de Lorraine and CNRS, Nancy, France**2. Synchrotron SOLEIL, Gif sur Yvette, France*

An important challenge in the field of spin-dependent tunnelling consists in developing materials to design electrodes with specific properties. A material with both high spin-polarization and very small or zero magnetization would thus constitute a perfectly stable electrode. In this context, the $\text{Sm}_{1-x}\text{Gd}_x\text{Al}_2$ (SGA) compound is of paramount interest: it can be considered as a zero-magnetization ferromagnet and a finite TMR value has been namely measured at its compensation point in SGA-based MTJ.

In order to unravel electronic transport properties in such MTJs and to get a deeper understanding of surface electronic properties of this original material, synchrotron-based Angle Resolved- and Spin Resolved-PhotoEmission Spectroscopy experiments have been performed for MBE-grown (111) $\text{Sm}_{1-x}\text{Gd}_x\text{Al}_2$ epitaxial films. Electronic band structure calculations (LSDA+U+SO, Wien2k code) complete this study.

ARPES experiments have evidenced an intense electron pocket, strongly localized around $\bar{\Gamma}$ and close to the Fermi level, with in-plane quasi free electron like isotropic dispersion and much reduced dispersion in the perpendicular direction. This electronic state exhibits a₁ symmetry and its spectral weight is strongly enhanced for an incident photon energy around 34eV. These various characteristics, combined with the observed sensitivity to surface conditions and with electronic calculations (for bulk and surface), strongly suggest the presence of a resonant surface state of 5d character, likely built on the bulk electron pocket developing around L points. First SRPES have evidenced the low temperature positive spin polarization at the Fermi level of this resonant surface state. It also appears to interestingly survive in a MgO (2ML thick)-covered $\text{Sm}_{1-x}\text{Gd}_x\text{Al}_2$ epitaxial film.

Such an electronic state should influence the transport properties of SGA-based MTJ, as it has been reported in other crystalline systems. A specific anomaly, indeed observed in the conductance characteristic, likely originates from the SGA resonant surface state highlighted by photoemission spectroscopy.

TU.I.3_O2 - Ab-initio calculations of Gilbert damping parameters in doped Permalloy systems.

L. Bergqvist¹, F. Pan¹, A. Bergman², A. Delin¹

1. *KTH Royal Institute of Technology, Stockholm, Sweden*

2. *Uppsala University, Uppsala, Sweden*

The Gilbert damping is perhaps the most important material parameter for magnetization dynamics. It is a measure of the strength of the dissipative processes in a magnetic dynamical system, for instance spin-flip scattering due to spin-orbit, scattering against phonons and magnons etc. In applications, a low damping is normally wanted to minimize losses. Experimentally it is normally measured using ferromagnetic resonance (FMR) but until recently, ab-initio calculations were scarce due to the complexity of such calculations. However, recent advances and developments in the computational tools, Gilbert damping is nowadays more accessible in calculations for a variety of materials. Here, we present a systematic investigation of Gilbert damping from ab-initio calculations using linear response formalism as implemented within the Korringa Kohn Rostoker (KKR) framework, including analysis of the temperature effects from phonons and magnons as well from the underlying band structure. In particular, we focus on the technologically important material Permalloy (Py), known for its low damping, doped with heavy elements like Au, Ag and Pt and compare the results with recent experimental measurements. The trends with respect to concentration of doping elements and temperature dependence are found to agree well with each other. By changing element and doping concentration, the Gilbert damping can be varied within a large interval and together with exchange interactions and anisotropy, all material specific parameters in atomistic spin dynamics simulations (ASD) are calculated within the same computational framework. We also present results on Heusler alloys, which is an important class of materials for spintronics applications, due to its intrinsic spin polarization and low damping.

TU.I.3_O3 - Experimental evidences of first-time reported (100) in-plane easy axis in magnetite films grown onto different single-crystal substrates

J. Fdez Cuñado¹, Y. F. Pedrosa^{1,2}, M. Sanz³, M. Oujja³, E. Rebollar³, J. Marco³, J. de la Figuera³, M. Monti³, M. Castillejo³, M. García-Hernández⁴, F. Mompeán⁴, N.M. Nemes⁵, N. Balint⁶, J. Camarero^{1,7}, A. Bollero¹

1. IMDEA Nanoscience, Madrid, Spain

2. Ingeniería Magnética Aplicada, IMA S.L., Barcelona, Spain

3. Instituto Química Física Rocasolano, CSIC, Madrid, Spain

4. Instituto Ciencias de Materiales de Madrid, CSIC, Madrid, Spain

5. Dep. Física Aplicada III, UCM, Madrid, Spain

6. Institute of Condensed Matter Physics, EPFL-SB-ICMP-LPMC, Lausanne, Switzerland

7. Dep. Física de la Materia Condensada, Instituto Nicolás Cabrera, UAM, Madrid, Spain

Magnetite (Fe₃O₄) is attracting much interest due to its robust ferrimagnetism down to nanometer thickness, good electrical conductivity and presumed half-metal character. Fe₃O₄ films are studied as ideal cases for designing improved bulk magnets [1] and have been tentatively used in spin-valves. Fe₃O₄ presents a low-temperature metal-insulator transition, proposed for spintronic applications. However, an open question is to what extent preparation can affect the detailed magnetic properties, such as the magnetic anisotropy axis.

Most of studies dealing with bulk and Fe₃O₄ films show room temperature (RT) in-plane <110> magnetic easy axis. By contrast, we show in this work the preparation of pure stoichiometric Fe₃O₄ thin films by IR-PLD [2], on different single-crystal substrates, with RT easy axes along the in-plane <100> directions [3], i.e. rotated by 45° respect to previous studies. Substrates of SrTiO₃, MgAl₂O₄ and MgO have been selected.

RT in-plane hysteresis loops were measured by vectorial-MOKE as a function of the direction of the applied field in 0°-360° range. The highest coercivity and remanence are found at 0°, 90°, 180° and 270° (i.e. <100>), thus orthogonal to each other, while the lowest coercivity values are found between them. This results in a well-defined four-fold symmetry indicative of biaxial magnetic anisotropy. In order to verify this result, ferromagnetic resonance (FMR) experiments have been carried out at 9.4 GHz frequency [4]. The angular dependence of the in-plane resonance field at RT proves that the easy axes are indeed the <100> directions. This result is supported by SPLEEM experiments and demonstrates the possibility of tuning the easy axis orientation in Fe₃O₄ films.

Acknowledgements: Research supported by EU-FP7-NANOPYME Project (No. 310516)

References:

[1] www.nanopyme-project.eu

[2] M. Sanz et al., Applied Surface Science 282, 642 (2013)

[3] M. Monti et al., J. Appl. Phys. 114, 223902 (2013)

[4] J.L.F. Cuñado et al. Submitted

TU.I.3_O4 - Orbital magnetism of coupled bands models

J. Fuchs^{1,2}, Arnaud Raoux^{2,3}, F. Piéchon², G. Montambaux²

1. *Laboratoire de Physique Théorique de la matière Condensée, CNRS and Université Pierre Et Marie Curie, Paris, France*

2. *Laboratoire de Physique des Solides, CNRS and Université Paris-Sud, France*

3. *Département de Physique, Ecole Normale Supérieure, Paris, France*

We develop a gauge-independent perturbation theory for the grand potential of itinerant electrons in two-dimensional tight-binding models in the presence of a perpendicular magnetic field. At first order in the field, we recover the result of the so-called* *{it modern theory of orbital magnetization}** and, at second order, deduce a new general formula for the orbital susceptibility. In the special case of two coupled bands, we relate the susceptibility to geometrical quantities such as the Berry curvature. Our results are applied to several two-band -- either gapless or gapped -- systems such as graphene, boron nitride, graphene bilayer, etc. We point out some surprising features in the orbital susceptibility -- such as in-gap diamagnetism or parabolic band edge paramagnetism -- coming from interband coupling. From that we draw general conclusions on the orbital magnetism of itinerant electrons in multi-band tight-binding models.

References:

Raoux et al., Phys. Rev. Lett. 112, 026402 (2014)

Raoux et al., Phys. Rev. B 91, 085120 (2015)

TU.J.1_I1 - Perpendicular magnetic tunnel junctions with single and double MgO barriers for STT-MRAM cells

L. Cuchet^{1,2,3}, A. Timopheev^{1,2,3}, P. Clement^{1,2,3}, B. Rodmacq^{1,2,3}, S. Auffret^{1,2,3}, C. Baraduc^{1,2,3}, R. Sousa^{1,2,3}, I. Prejbeanu^{1,2,3}, M. Chshiev^{1,2,3}, B. Dieny^{1,2,3}

1. Univ.Grenoble Alpes, INAC-SPINTEC, Grenoble,France

2. CEA, INAC-SPINTEC, F-38000 Grenoble, France

3. CNRS, SPINTEC, F-38000 Grenoble, France

STT-MRAM are about to become a main stream generic technology of non-volatile memories. Indeed, according to the ITRS, STT-MRAM are foreseen as the best contender to replace DRAM and SRAM as working memory in microelectronic circuits. Most of the research and development efforts on STT-MRAM are nowadays focused on out-of-plane magnetized magnetic tunnel junctions (MTJs) which offer better retention, lower write current for a given retention than their in-plane magnetized counterparts. The perpendicular anisotropy in these MTJs arises from the magnetic metal/oxide interface [1] partially balanced by the demagnetizing energy. In this work, the origin of this anisotropy has been clarified by ab-initio calculations and ways to increase it by doping of the bulk of the magnetic storage layer were proposed [2,3]. Single and double barrier MTJs were then prepared and characterized. Double barrier MTJs have the advantages of larger anisotropy and therefore longer retention, better resistance to high temperature anneals thanks to reduced Ta interdiffusion and improved resistance to electrical breakdown. Furthermore, by using two polarizing layers, they allow increasing the STT efficiency for writing and even to modulate the amplitude of the STT by using one of the polarizer as a read/write mode select layer. Finally, the influence of the field-like STT term (perpendicular torque) in the STT switching was also investigated. It is shown that this field-like term does not influence the critical current for magnetization switching which is dominated by the in-plane STT term. However, it influences the switching dynamics by modifying the precessional frequency.

References:

[1] S.Monso et al, Appl.Phys.Lett. 80, 4157-9 (2002)

[2] Yang H.Xet al, Phys.Rev.B 84, 054401 (2011)

[3] Hallal, A.et al, Phys.Rev.B 90, 064422 (2014)

TU.J.1_O2 - X-ray induced anisotropy change in Pt/Co/MgO trilayers

J. Vogel^{1,2}, S. Pizzini^{1,2}, T. Onur Montes³, A. Sala³, A. Locatelli³, L. Buda-Prejbeanu^{1,4,5}, G. Gaudin^{1,4,5}, O. Boulle^{1,4,5}

1. *Université Grenoble Alpes, Grenoble, France*
2. *CNRS, Institut Néel, 38042 Grenoble, France*
3. *Elettra - Sincrotrone Trieste S.C.p.A., Basovizza, Trieste, Italy*
4. *CEA, INAC, SPINTEC, Grenoble, France*
5. *CNRS, SPINTEC, Grenoble, France*

Magnetic microscopy using Photoemission Electron Microscopy (PEEM) on perpendicularly magnetized Pt/Co(0.85nm)/MgO trilayers revealed a significant increase in magnetic domain size upon irradiation with soft x-rays. Subsequent hysteresis loops taken by focused Kerr magnetometry show a large irreversible increase in coercivity and in remanence for the part of the sample that had been irradiated. The increase of the domain size, together with a decrease in domain wall width deduced from high-resolution PEEM images, are in agreement with an increase of the perpendicular magnetic anisotropy induced by the x-ray irradiation, probably caused by changes at the Co/MgO interface. Charging effects induced by the x-ray absorption can lead to the presence of an electric field at this interface, which is known to modify the anisotropy in this kind of Pt/Co/oxide systems due to electron transfer at the Co/oxide interface. In principle, this effect is reversible and disappears when the electric field is switched off, but it was shown more recently that in some types of Pt/Co/Ox stacks prolonged application of a positive electric field can lead to migration of Oxygen ions to the interface and thus to an increase of the magnetic anisotropy. Taking into account such modifications of the PMA is important when investigating this type of materials for skyrmions or domain wall dynamics using x-ray microscopy or x-ray holography techniques.

TU.J.1_O3 - Exchange bias-like effect in 2D patterned thin films with perpendicular magnetic anisotropy

A. Hierro-Rodriguez^{1,2}, J. Teixeira¹, M. Vélez³, L. Alvarez-Prado^{3,4}, N. J. Martín^{3,4}, J. Alameda^{3,4}

1. *IN-IFIMUP, Departamento de Física e Astronomia, Faculdade de Ciências, Universidade do Porto, Porto, Portugal.*

2. *INESC-TEC (Coordinated by INESC-Porto), Departamento de Física e Astronomia, Faculdade de Ciências, Universidade do Porto, Porto, Portugal.*

3. *Universidad de Oviedo, Dpto. de Física, Oviedo, Spain*

4. *Centro de Investigación en Nanomateriales y Nanotecnología - CINN (CSIC - Universidad de Oviedo - Principado de Asturias), El Entrego, Spain*

Patterned magnetic materials with Perpendicular Magnetic Anisotropy (PMA) are interesting systems both, from a fundamental research point of view [1] and also for application purposes [2, 3]. Usually, these systems consist in arrays of structures where the magnetic behavior is studied as a function of shape and/or structures density without changing the intrinsic magnetic properties. The use of extended films with a laterally nano/micro-structured magnetic property, introduce a new degree of freedom to get new building blocks that should be useful in the development of new magnetic devices. In this framework, the presented work shows how to fabricate 2D magnetically hard/soft composites by e-beam lithography plus dry etching techniques, based on sputter-deposited NdCo5 thin films with PMA. The laterally modulated parameter is the thin film's thickness, which leads to the modulation of the in-plane/out-of-plane magnetic anisotropies ratio. Due to this modulation, we are allowed to tune the magnetization reversal processes, leading to reproducible coercive field asymmetries (exchange bias-like effect) depending on magnetic history [4].

References:

[1] A. Hierro-Rodriguez et al, Phys. Rev. Lett. 109, 117202 (2012)

[2] J.I. Martín et al, J. Magn. Magn. Mater. 256, 449 (2003)

[3] A. Berger et al, Phys. Rev. B 82, 104423 (2010)

[4] A. Hierro-Rodriguez et al, Appl. Phys. Lett. 105, 102412 (2014)

TU.J.1_O4 - Perpendicular magnetic anisotropy in granular multilayers of CoPd alloyed nanoparticles

L. Gonzalez Vivas¹, A. I. Figueroa¹, F. Bartolomé¹, J. Rubén¹, L. García¹, C. Deranlot², F. Petroff², L. Ruiz³, J. M. Gonzalez-Calbet³, S. Pascarelli⁴, N.B. Brookes⁴, F. Wilhem⁴, M. Chorro⁴, A. Rogalev⁴, J. Bartolomé¹

1. Instituto De Ciencia De Materiales De Aragón (ICMA), CSIC- Universidad De Zaragoza. Departamento De Física De La Materia Condensada, Zaragoza, Spain

2. Unité Mixte de Physique CNRS/Thales, Palaiseau, France, and Université Paris-Sud, Orsay, France

3. Departamento de Química Inorgánica, Universidad Complutense de Madrid, Madrid, Spain

4. European Synchrotron Radiation Facility (ESRF) CS40220, Grenoble, France

Research on transition metal nanoparticles (NPs) embedded in or alloyed with high spin-orbit $4d$ and $5d$ elements aims to the tuning and control of the magnetic anisotropy energy for both the understanding of the physical phenomena and for technological purposes. In previous works we reported the enhancement of the magnetic anisotropy of assembled NPs systems by the type of the surrounding matrix. Capping Co NPs with noble metals like Cu, Ag, and Au (which does not diffuse on Co) results in the increase of the surface anisotropy. Alloyed bimetallic NPs of Co with W or Pt allow the modification of the intrinsic source of anisotropy (Phys. Rev. B 90, 174421, 2014). In the present work, we show that CoPd NPs present strong perpendicular magnetic anisotropy (PMA).

CoPd clusters of ~ 3 nm diameter were produced by sequential sputtering of Co on amorphous alumina and subsequent capping with Pd. This process is repeated N times in order to get a granular multilayer system. The particulate morphology was confirmed by HRTEM images, while XANES at the Co K edge proved the Co-Pd hybridization. The bimetallic $\text{Co}_{50}\text{Pd}_{50}$ alloy composition (identified also by XRD) as well as short-range order $L1_0$ -like phase have been revealed by EXAFS study at both Co K and Pd K edges. The collective magnetic behavior is temperature dependent and three magnetic phases are identified: hard ferromagnetic, soft-ferromagnetic and superparamagnetic. Magnetic total moments of about $2.7 m_B$ and of $0.4 m_B$ were found by XMCD at the $L_{2,3}$ edges for Co and Pd, respectively. PMA can be improved by increasing the amount of Pd in the sample preparation, since this directly affects the quality of the alloy and the structural properties. The PMA, on the order of 10^7 erg/cm³ at 5 K, is related to the short-range chemical order found in the CoPd NPs.

TU.J.1_O5 - Correlation between magnetic properties and chemical order in L10 FePtCu thin films studied by EXAFS

S. Laureti ¹, C. Brombacher ², D. Makarov ³, M. Albrecht ⁴, D. Peddis ¹, G. Varvaro ¹, F. D'Acapito ⁵

1. ISM-CNR, Area della Ricerca RM1, Monterotondo Scalo, Roma, Italy

2. Institute of Physics, Chemnitz University of Technology, Chemnitz, Germany

3. Institute for Integrative Nanosciences, Leibniz Institute for Solid State and Materials Research (IFW Dresden), Dresden, Germany

4. Institute of Physics, Augsburg University, Augsburg, Germany

5. CNR-IOM-OGG c/o ESRF, GILDA CRG, Grenoble, France

Nowadays, magnetic recording is a central technology in information storage, and a large part of the interest in nanoscaled magnetic films has been stimulated by their application to data storage [1]. In this contest, the chemically ordered FePt L10 phase is a material with a very high uniaxial magnetic anisotropy which provides the thermal stability for high density magnetic recording [2]. Furthermore, the addition of third elements allows tailoring the magnetic properties but also the onset annealing temperature for chemical ordering from the as deposited disordered FePt phase is strongly affected [3-5]. In this work we present an Extended X-ray Absorption Fine Structure (EXAFS) characterization of ternary FePtCu alloys at the Cu-K and Pt-LIII edges in order to describe the local environment around these elements and to compare the structural evolution as a function of the Cu content. The study allowed to distinguish experimentally the effects on the chemical order and lattice distortion induced by the Cu. We correlated the determined positions of the Cu atoms in the chemically ordered L10 lattice with the magnetic properties of FePtCu ternary alloys. In particular, the main effect is a linear reduction of the c/a ratio, while the non-monotonic behaviour of the chemical order is consistent with the variation of the magnetocrystalline anisotropy [6].

This work was supported by the EU FP7 project TERAMAGSTOR, by MIUR under project FIRB2010 - NANOREST and by the German Science Foundation (DFG)

References:

- [1] C. A. Ross, Annu. Rev. Mater. Res. 31 (2001) 203
- [2] D. Weller et al, Annu. Rev. Mater. Sci. 30 (2000) 611
- [3] J.-I. Ikemoto et al. IEEE Trans. Magn. 44 (2008) 3543
- [4] S. D. Willoughby, J. Appl. Phys. 95 (2004) 6583
- [5] C. Feng et al. Appl. Phys. Lett. 93 (2008) 152513
- [6] S. Laureti et al. J. Appl. Cryst. 47, (2014) 1722

TU.J.2_I1 - Spin torque oscillators based on perpendicular and tilted magnetic anisotropy materials

J. Akerman¹

1. University of Gothenburg, Gothenburg, Sweden

Nanocontact spin-torque oscillators (NC-STOs) provide an excellent environment for studying spin transfer torque (STT) driven nano-magnetic phenomena such as localized and propagating auto-oscillatory spin waves (SWs). While traditionally based on easy-plane anisotropy materials, the inclusion of perpendicular magnetic anisotropy materials have greatly expanded on both the physics and performance of these devices. For example, NC-STOs with perpendicular magnetic anisotropy (PMA) free layers were recently demonstrated, showing high-frequency operation in very low fields [1,2]. At higher fields, the same devices can nucleate and sustain so-called magnetic droplet solitons [3,4], stabilized by a combination of PMA and STT. In pillar STOs based on PMA materials in both the free and the fixed layer, the current dependence in in-plane magnetic fields can also be made very high [5]. To further expand the possibilities of NC-STOs based on easy-plane and PMA materials we recently also fabricated NC-STOs based on tilted anisotropy exchange springs [6].

In my talk I will report on these recent demonstrations, and the important role played by PMA and tilted anisotropies in NC-STOs.

References:

- [1] W. H. Rippard et. al. Phys. Rev. B, 81, 014426 (2010)
- [2] S. M. Mohseni et al, Phys. Status Solidi RRL 5, 432 (2011)
- [3] S. M. Mohseni et al, Science 339, 1295 (2013)
- [4] F. Macia et al, Nature Nanotechn. 9, 992 (2014)
- [5] T. Le et al, unpublished (2015)
- [6] T. Le et al, unpublished (2015)

TU.J.2_O2 - Electric-Field-Induced Magnetization Switching in Strained Au/FeCo/MgO Heterostructures

N. Kioussis¹, P. Vu¹

1. California State University Northridge, Northridge, United States

Voltage-controlled magnetic anisotropy (VCMA) plays a central role in the operation of the next-generation of magneto-electric random access memory (MeRAM). The major challenge in the development of the next-generation MeRAM is the low (< 100 fJ/(Vm)) magnetoelectric (ME) coefficient which in turn leads to high switching bit energy and high write voltage. Employing *ab initio* electronic structure calculations we demonstrate for the first time that epitaxial strain, which is ubiquitous in many heavy metal/ferromagnet/insulator trilayers, has a dramatic effect on VCMA of the Au/FeCo/MgO heterostructure. Strain can give rise to a wide range of novel VCMA behavior where the magnetic anisotropy can change from V- to a Λ -shape electric field dependence with *giant* ME coefficients which are asymmetric under voltage reversal. By tuning the epitaxial strain the ME coefficient can reach values as large as ~ 1800 fJ/(V.m) which in turn lead to magnetic switching in the low-electric-field regime. We will also present results for the nonlinear magnetoelastic coupling and the strain-induced spin-reorientation of the system. The underlying mechanism is the interplay between the modification of the MgO dielectric constant by strain and the changes of the spin-orbit coupled d-states at the interfaces due to the synergetic effect of strain and electric field. These findings open interesting prospects for exploiting strain engineering to harvest higher efficiency VCMA for the next generation MeRAM devices.

This research was supported by NSF Grant No. ERC-TANMS-1160504.

TU.J.2_O3 - Development of dual magnetic tunnel junctions with perpendicular anisotropy and double polarizing layers

L. Cuchet^{1,2,3}, B. Rodmacq^{1,2,3}, R. C. Sousa^{1,2,3}, S. Auffret^{1,2,3}, B. Dieny^{1,2,3}

1. Univ. Grenoble Alpes, INAC-SPINTEC, Grenoble, France
2. CEA, INAC-SPINTEC, Grenoble, France
3. CNRS, SPINTEC, Grenoble, France

Magnetic Tunnel Junctions (MTJs) with perpendicular anisotropy have been proved for many years to be attractive devices for STT-RAM applications. Among their numerous advantages, out-of-plane magnetized MTJs allow achieving significantly lower critical current density for spin-transfer-torque (STT) writing than their in-plane counterparts for a given specified retention. In the meantime, planar dual MTJs comprising two tunnel barriers were developed and shown to produce enhanced STT efficiency. Thus, in this study, we aimed at combining the advantages of both systems by developing double barrier MTJs with perpendicular anisotropy and two Synthetic AntiFerromagnetic (SAF) polarizing layers.

The first part of this work consisted in investigating the beneficial effect on the perpendicular anisotropy of the storage layer of sandwiching the latter between two MgO layers. A complete series of junctions with bottom SAF reference and increasing storage layer thickness enabled us to conclude that the effective (corrected from dead layers) critical thickness (out-of-plane to in-plane reorientation of the magnetization) increases from 1.1 to 2.4 nm if the standard Ta capping is replaced by MgO.

After developing junctions with a top SAF reference which transition fields were compatible with the bottom one, we combined them to create a full dual MTJ stack with perpendicular anisotropy. The functionality of such a structure was proved as the transitions of all individual magnetic layers could be clearly identified in the VSM measurements. Parallel and antiparallel configurations of the two polarizing layers can be stabilized which allows tuning the STT efficiency on the storage layer magnetization. Indeed, having antiparallel polarizing layers is equivalent to adding the two STT coming from them, whereas in the parallel configuration they subtract. We also developed composite SAF storage layers, with either Ru or Ta spacers, which are interesting to further reduce the magnetostatic interactions between the various parts of the stack.

TU.J.2_O4 - Evidence for In-Plane Tetragonal c-axis in Mn₃Ga Thin Films using Transmission Electron Microscopy

F. Casoli¹, J. Karel², P. Lupo³, L. Nasi¹, S. Fabbri^{1,4}, L. Righi^{1,5}, F. Albertini¹, C. Felser²

1. IMEM - CNR, Parma, Italy

2. Max-Planck-Institut für Chemische Physik fester Stoffe, Dresden, Germany

3. Information Storage Materials Laboratory, Department of Electrical and Computer Engineering, National University of Singapore, Singapore

4. MIST E-R Laboratory, Bologna, Italy

5. Dipartimento di Chimica, Università di Parma, Parma, Italy

Tetragonal Mn₃Ga films show exceptional magnetic and electronic properties, i.e., a unique combination of low magnetization, high uniaxial anisotropy, high Curie temperature, high spin polarization and low Gilbert damping, which make them very promising as ferromagnetic electrodes in Spin-Transfer-Torque Magnetic RAMs [1]. A few recent works have demonstrated epitaxial growth of this phase on MgO, SrTiO₃ or with Cr or Pt underlayers [2,3].

We have grown Mn_xGa_{1-x} (x=0.75,0.70) films with thickness 10 – 40 nm by RF sputtering on SrTiO₃(100) and fully characterized the films by structural and magnetometric techniques (X-Ray Diffraction – XRD; High Resolution Transmission Electron Microscopy – HRTEM; Atomic Force Microscopy - AFM; SQUID Magnetometry).

For both compositions and in all the considered thickness range the thin films exhibit perpendicular magnetic anisotropy with coercive fields between 1 – 2 T. HRTEM and XRD reveal that 40 nm samples grown at 300-350 °C show predominately the tetragonal phase epitaxial with perpendicular c-axis, but a fraction of in plane c-axes is also present; this structure results in a secondary magnetic component in the perpendicular magnetization. Growth at 300 °C with a reduced thickness or Mn concentration significantly decreases the presence of c-axis in the film plane, thus improving the magnetic properties. TEM is of critical importance in characterizing these materials, since conventional XRD cannot always identify the presence of additional crystallographic orientations although they can still affect the magnetic properties. Our study points to ways that the microstructure of these thin films can be controlled, which is critical for utilization of this material in spintronic devices.

References:

[1] B. Balke et al., Appl. Phys. Lett. 90 (2007) 152504

[2] H. Kurt et al., Phys. Status Solidi B 248 (2011) 2338

[3] M. Li et al., Appl. Phys. Lett. 103, 032410 (2013)

TU.J.2_05 - Logic gates from out-of-plane magnetized nanowires

R. Mansell¹, A. Beguivin¹, D. Petit¹, A. Fernández-Pacheco¹, J. Lee¹, R. Cowburn¹

1. Cavendish Laboratory, University of Cambridge, United Kingdom

Electronic devices rely on complex combinations of transistors in order to produce the logic functions which process data. It has been shown for in-plane magnetized systems that domain walls in nanowires can be used to reproduce all the necessary functionality required for logic operations. For perpendicularly magnetized layers implementation of logic gates is more difficult since the relatively large anisotropies cause the magnetization to become Ising-like, reducing the degrees of freedom of the system. However, the large data retention times and fast domain wall speeds of perpendicular materials make them attractive for logic applications. Here, we demonstrate the control of domain wall nucleation in nanowires made from Pt/CoFeB and Pt/Co multilayers simply by changing the width of the wire. By adding end pads we show that the nucleation occurs at the ends of the wires narrower than around 200 nm. This allows us to create asymmetric shaped nanowires where nucleation happens at one end. By placing such elements next to each other, the stray field from one element causes a bias field on the point of nucleation on the other that allows a NOT gate functionality. We demonstrate that a synchronous shift register can be made by chaining individual NOT gates together. For more complex devices we show through micromagnetic simulations how a Y-shaped junction between two nanowires can be used to create either an AND or an OR gate, where the functionality depends on the junction shape. This combination of gates forms the building blocks for complex logic devices in perpendicularly magnetized materials.

TU.J.3_O1 - The key role of thermal motion on the structure and magnetic properties of dithiazolyl-based bistable molecular materials

S. Vela^{1,2}, M. Deumal², M. Shiga³, J. Novoa², Jordi Ribas-Arino²

1. *Laboratoire de Chimie Quantique, Université de Strasbourg, Strasbourg, France.*

2. *Departament de Química Física and IQTCUB, Universitat de Barcelona, Barcelona, Spain*

3. *Center for Computational Science and E-Systems, Japan Atomic Energy Agency, 5-1-5, Kashiwanoha, Kashiwa, , Japan*

Recent years have witnessed a growing interest in the use of organic radicals as building blocks for bistable materials.[1] The family of 1,3,2-dithiazolyl (DTA) radicals has furnished spectacular examples of materials that undergo spin transitions between a low temperature (LT) diamagnetic phase and a high temperature (HT) paramagnetic phase.[2] The neutral radical 1,3,5-trithia-2,4,6-triazapentalenyl (TTTA) is the most prominent DTA-based compound, not least because its spin transition occurs with a wide thermal hysteresis loop that encompasses room temperature.[3] The LT phase of TTTA presents distorted π -stacks that comprise slipped pairs of nearly eclipsed radicals. The HT phase, in turn, presents regular π -stacks where each radical exhibits a slipped overlap with its two nearest neighbors along the stacking direction. I will explain the results of a recent piece of work, in which, by means of ab initio molecular dynamics simulations, we have demonstrated that the regular π -stacking motif of the HT polymorph of TTTA is not the minimum in the potential energy surface of the material. Instead, it is the result of a fast intra-stack pair exchange dynamics, whereby each radical continually exchange the adjacent TTTA neighbor (upper or lower) with which they form an eclipsed dimer. Such unique dynamics is the origin of a significant vibrational entropic gain and thereby it plays a key role in driving the LT  HT phase transition.[4] The importance of the vibrational motion in this material is not only essential to understand the structure, but also the magnetic properties of its HT-phase. I will demonstrate the need of a dynamic perspective of magnetism, and remark how this improved perspective challenges the usual static approach employed to rationalize the magnetic properties of molecular materials.[5] Finally, I will comment about the strategies that those findings open in the design of new bistable molecular materials.

References:

[1] R. Hicks. Nature Chem. 2011, 3, 189

[2] J.M. Rawson et al. J.Mater.Chem. 2006, 16, 2560

[3] W. Fujita, K. Awaga. Science, 1999, 286, 261

[4] Vela, S. et al. Nature Commun. 2014, 5

[5] Vela, S. et al. Chem.Sci. 2015. In press

TU.J.3_O2 - XMCD at the Fe K-edge in Fe Phthalocyanine on Au: an insight into the ground state

J. Bartolomé¹, C. R. Natoli², F. Bartolomé¹, O. Bunau¹, A. Figueroa³, L. García¹, M. Piantek⁴, J.I. Pascual⁵, I. K. Schuller⁶, T. Gredig⁷, F. Wilhelm⁸, A. Rogalev⁸, P. Kruger⁹

1. ICMA - Dept. Física de la Materia Condensada, CSIC - Universidad de Zaragoza

2. INFN - Laboratori Nazionali di Frascati, Frascati, Italy

3. Magnetic Spectroscopy Group, Diamond Light Source, Didcot, , United Kingdom

4. INA, Universidad de Zaragoza, Zaragoza, Spain

5. CIC nanoGUNE and Ikerbasque, Basque Foundation for Science, San Sebastian, Spain

6. Department of Physics and Center for Advanced Nanotechnology, University of California San Diego, La Jolla, California, United States

7. Department of Physics and Astronomy, California State University Long Beach, Long Beach, United States

8. ESRF-The European Synchrotron, Grenoble, France

9. Graduate School of Advanced Integration Science, Chiba University, 1-33 Yayoi-cho, Inage, Chiba, Japan

Metal Phthalocyanines (MPc) are robust planar organic molecules with interesting electronic, magnetic, and transport properties. Therefore, MPcs deposited on a substrate are one of the most studied organometallic materials suggested as building blocks on applications in nanodevices and spintronics. In iron phthalocyanine (FePc), the actual electronic structure of the ground state is still being questioned. This uncertainty affects any model one can construct out of these building blocks for a molecule onto a surface or in an epitaxial film

We have performed an experimental and theoretical study of a thick film of FePc on an Au(111) surface including magnetization measurements, STM and x-ray spectroscopic experiments (XMCD, XLPA) at the N K, Fe L_{2,3} and Fe K absorption edges

The observation of an anomalous quadrupolar signal in x-ray magnetic circular dichroism (XMCD) at the Fe K-edge of iron phthalocyanine films with an unexpected angular dependence is crucial to the determination of the FePc electronic ground state. Indeed, all ground states previously suggested for FePc are incompatible with the experimental data. Based on ab initio molecular orbital multiplet calculations of the isolated FePc molecule, we propose a new model for the magnetic ground state of the FePc film, which explains the XMCD data and reproduces the observed values of the orbital moments in the perpendicular and planar direction. The computed ground state corresponds to a spin triplet including 3A_{2g}, 3E_g, and 3E_g states.

TU.J.3_O3 - Exchange bias of TbPc2 molecular magnets on antiferromagnetic FeMn and ferromagnetic Fe films

C. Nistor ¹, C. Krull ², A. Mugarza ³, S. Stepanow ⁴, C. Stamm ⁵, M. Soares ⁶, S. Klyatskaya ⁷, M. Ruben ⁸, P. Gambardella ⁹

1. *ETH, Dept Mat, CH-8093 Zurich, Switzerland*
2. *Catalan Institute of Nanotechnology, E-08193 Barcelona, Spain*
3. *Catalan Institute of Nanotechnology, E-08193 Barcelona, Spain*
4. *ETH, Dept Mat, CH-8093 Zurich, Switzerland*
5. *ETH, Dept Mat, CH-8093 Zurich, Switzerland*
6. *ESRF, F-38043 Grenoble, France*
7. *KIT, Inst Nanotechnol, D-76344 Eggenstein Leopoldshafen, Germany*
8. *KIT, Inst Nanotechnol, D-76344 Eggenstein Leopoldshafen, Germany*
9. *ETH, Dept Mat, CH-8093 Zurich, Switzerland*

Improving the magnetic stability of single molecule magnets is a key issue facing molecular spintronics. In this study we use element-resolved x-ray magnetic circular dichroism to study the possibility of magnetically coupling TbPc2 to ultrathin FeMn and Fe films. TbPc2 deposited on Fe(4.6ML)/Cu(100) exhibits magnetic hysteresis as a consequence of antiferromagnetic exchange coupling to the interfacial Fe spins. TbPc2 deposited on FeMn(8 ML)/Cu(100) displays magnetic hysteresis and a vertical shift of the Tb magnetization curve, consistent with exchange bias generated by the interfacial uncompensated Fe spins. We demonstrate that the exchange coupling of TbPc2 to Fe and FeMn films can be controlled by doping the interface with electron-donor Li atoms.

TU.J.3_O4 - Spin spectroscopy of single magnetic molecules with a radio frequency scanning tunneling microscope

S. Müllegger¹, S. Tebi¹, R. Koch¹

1. Institute of Semiconductor and Solid State Physics, Johannes Kepler University Linz, Austria

The aim of this work is to combine the analytic power of magnetic resonance methods with the unrivalled spatial resolution and manipulation capability of the scanning tunneling microscope (STM). For this purpose, we have modified a commercial low temperature STM with a dedicated radio-frequency (rf) generation and detection system. Our STM is capable of adding a variable ac modulation between 10 MHz and 4 GHz to the dc tunneling current [1]. The frequency of the ac component is tuned into resonance with low energy (micro-electronvolt) transitions of the sample under investigation, in particular, spin transitions under a static external magnetic field of the order of 10 mT. The response signal is the dc tunneling conductance between the STM and the rf-excited sample obtained at different excitation frequencies. With our novel technique, we have studied single molecules of the archetypal Tb double-decker single molecule magnet adsorbed on Au(111) at 5 K. We demonstrate the successful resonant spectroscopy of the complete manifold of nuclear and electronic magnetic transitions of single quantum spins in single magnetic molecules within the experimental bandwidth [2]. In particular, we achieve sub-nanometer spatial resolution combined with single-spin sensitivity. The method of resonant radio-frequency scanning tunneling spectroscopy (rf-STTS) offers, atom-by-atom, unprecedented analytic power and spin control, which may impact diverse fields of nanoscience and nanotechnology.

References:

- [1] S. Müllegger et al., Nanotechnology 25, 135705 (2014)
- [2] S. Müllegger et al., Phys. Rev. Lett. 113, 133001 (2014)

WE.A1_O1 - Spin fluctuations in superconducting iron selenide (FeSe) and derivatives

M. Rahn¹, R. Ewings², S. Sedlmaier³, S. Clarke³, A. Boothroyd¹

1. *Department of Physics, Oxford University, United Kingdom*

2. *ISIS Facility, STFC Rutherford Appleton Laboratory, United Kingdom*

3. *Department of Chemistry, Oxford University, United Kingdom*

Experiments on iron-based superconductors have shown that spin fluctuations persist into the superconducting state and are linked to superconductivity. Mechanisms involving spin fluctuations are therefore highly attractive and in addition offer a possible route to higher superconducting transition temperatures. Superconductors based on FeSe layers exhibit some very distinct properties, including the ability to raise T_c dramatically by application of pressure, by intercalation with alkali metals and molecular species, and by preparation as a monolayer on SrTiO₃.

In this presentation I will describe recent neutron scattering experiments that probe the spectrum of magnetic fluctuations in FeSe [1], and in superconductors built from FeSe intercalated with Cs [2] and with Li(NH₂)_x(NH₃)_y [3]. The spin fluctuations in these systems all have different characteristic wave vectors. In the case of FeSe, we observe highly dispersive paramagnon fluctuations emerging from the square-lattice wave vector $(\pi, 0)$, whereas in the other two superconductors the characteristic wave vector is of the form (π, γ) with $\gamma \approx \pi/2$. I will discuss these results in connection with the calculated electronic structure and pairing symmetry.

References:

[1] M. C. Rahn, R. A. Ewings, S. J. Sedlmaier, S. J. Clarke and A. T. Boothroyd, ArXiv:1502.03838

[2] A. E. Taylor, R. A. Ewings, T. G. Perring, J. S. White, P. Babkevich, A. Krzton-Maziopa, E. Pomjakushina, K. Conder, and A. T. Boothroyd, Phys. Rev. B 86, 094528 (2012)

[3] A. E. Taylor, S. J. Sedlmaier, S. J. Cassidy, E. A. Goremychkin, R. A. Ewings, T. G. Perring, S. J. Clarke, and A. T. Boothroyd, Phys. Rev. B 87, 220508(R) (2013)

WE.A1_O2 - Competing Magnetic Phases, and Emergent Defect States as a Source of Resistivity Anisotropy in the Nematic Phase of Iron Pnictides

B. M. Andersen¹

1. University of Copenhagen, Copenhagen, Denmark

The pronounced electronic anisotropy observed in several experiments probing the iron-based superconductors is currently a topic of great interest and controversy.[1] I will discuss novel disorder effects in the nematic phase above the transition temperature to the (π , 0) stripe ordered magnetic state but below the orthorhombic structural transition. The anisotropic spin fluctuations in this region can be frozen by disorder, to create elongated magnetic droplets whose anisotropy grows as the magnetic transition is approached. Such states act as strong anisotropic defect potentials that scatter with much higher probability perpendicular to their length than parallel, although the actual crystal symmetry breaking is tiny. From the calculated scattering potentials, relaxation rates, and conductivity in this region we conclude that such emergent defect states are essential for the transport anisotropy observed in experiments.[2] Thus, a full understanding of the transport anisotropy in iron pnictides requires both intrinsic nematic susceptibility and concomitant emergent impurity response. Below the spin density wave transition the nematogens freeze into dimer states that show many characteristics in agreement with STM measurements.[3] Finally, a study of competing non-colinear and non-homogeneous magnetic phases (in addition to the usual magnetic stripe order of the pnictides) will be provided. We map out the general phase diagram and investigate the effects of superconductivity, finding good qualitative agreement with recent experiments on these materials.

References:

- [1] R. M. Fernandes, A. V. Chubukov, and J. Schmalian, Nat. Phys. 10, 97 (2014)
- [2] M. N. Gastiasoro, I. Paul, Y. Wang, P. J. Hirschfeld, and B. M. Andersen, Phys. Rev. Lett. 113, 127001 (2014)
- [3] M. N. Gastiasoro, P. J. Hirschfeld, and B. M. Andersen, Phys. Rev. B 89, 100502(R) (2014)

WE.A.1_O3 - Synthesis and characterization of new heavy fermion compound CePdIn5

K. Uhlířová¹, J. Prokleska¹, B. Vondrackova¹, M. Kratochvílová¹, M. Dusek², J. Custers¹, V. Sechovsky¹

1. Charles University In Prague, Faculty of Mathematics And Physics, Department of Condensed Matter Physics, Praha, Czech Republic

2. Institute of Physics ASCR, Department of Structure Analysis, Praha, Czech Republic

The family of Ce_nTmIn_{3n+2m} ($n = 1, 2$; $m = 1$; $T =$ transition metal) heavy fermion compounds have been intensively studied group of materials due to presence of magnetic order and superconductivity in a broad range of the temperature-pressure phase diagram. Besides the well know $CeTIn_5$ and Ce_2TIn_{11} ($T = Co, Rh, Ir$) compounds, new materials $CePtIn_7$, Ce_2PtIn_8 , Ce_3PtIn_{11} , Ce_2PdIn_8 , $Ce_5Pd_2In_{19}$ and Ce_3PdIn_{11} have been discovered recently[1-4].

We report on synthesis and characterization of Ce_nPdIn_{3n+2m} , compounds with focus on an up to now "missing" compound $CePdIn_5$. Similar to other compounds, single crystals of $CePdIn_5$ we prepared by indium flux growth method. The compounds were characterized by microprobe analysis and single crystal x-ray diffraction. Samples for electrical resistivity measurement were fabricated by focused ion beam method combined with electron beam lithography. $CePdIn_5$ crystallizes in the $HoCoGa_{5-type}$ tetragonal structure with room temperature lattice parameters $a = 0.4693$ nm and $c = 0.7538$ nm. The compound remains paramagnetic down to 0.4 K where it becomes superconducting. Interestingly, following the dimensionality, the series goes from pure superconducting state in $CePdIn_5$ ($T_c = 0.4$ K) and Ce_2PdIn_8 ($T_c = 0.7$ K) via coexistence of superconductivity and antiferromagnetism in Ce_3PdIn_{11} ($T_c = 0.4$ K, $T_N = 1.7$ K) to pure antiferromagnetic $CeIn_3$ ($T_N = 10$ K) resembling the proposed generic phase diagram [4]. The scenario of coupling evolution of magnetism and superconductivity with dimensionality in the Ce_nTmIn_{3n+2m} compounds will be discussed.

References:

- [1] Z. M. Kurenbaeva et al. *Intermetallics* 16 (2008) 979
- [2] A. Tursina et al., *J. Sol. State Chem.* 200 (2013) 7
- [3] M. Kratochvílová et. al. *J. Cryst. Growth* 397 (2014) 47
- [4] Q. Si et. al. *Physica B* 378 (2006) 23

WE.A.1_O4 - Comparative orbital fluctuation study in iron pnictides by spectroscopic methods

Y. Koh^{1,49}, Y. Kim², N. J. Seo¹, M. Eom³, J. Kim³, B. Park⁴, J. Kim⁴, C. Kim¹

1. *Yonsei University, Seoul, Republic of Korea*

2. *Advanced Light Source, Berkeley, United States*

3. *Pohang University of Science and Technology, Pohang, Republic of Korea*

4. *Pohang Light Source, Pohang, Republic of Korea*

The most important and still remaining issue in iron based superconductor is on the superconducting pairing mechanism. As well as spin fluctuation, orbital fluctuation has been proposed as a candidate for the pairing in iron pnictides. The mechanism we consider is a pairing mechanism in which spin and orbital order fluctuations coexist and contribute to the pairing. Therefore, investigation of orbital fluctuation will give a valuable hint for understanding the superconductivity in iron pnictides.

In this presentation, we present comparative studies on orbital order fluctuations in doped BaFe₂As₂ system. To investigate orbital order fluctuation, X-ray linear dichroism and angle resolved photoemission were performed on doped BaFe₂As₂ single crystals. We observed different d_{yz} and d_{xz} orbital in occupations by X-ray linear dichroism and band splitting by angle resolved photoemission. Based on these results, we confirmed the existence of orbital order in doped BaFe₂As₂ system. Temperature dependence data were compared to previously reported X-ray linear dichroism and angle resolved photoemission data from electron doped BaFe₂As₂. Therefore, we found a weak orbital order fluctuation in isovalent doped BaFe₂As₂. This comparative study on orbital order fluctuation can help us understand novel states in which spin and orbital order fluctuations coexist.

WE.A.1_O5 - Nematic-driven anisotropic electronic properties of underdoped detwinned Ba(Fe_{1-x}Co_x)₂As₂ revealed by optical spectroscopy

L. Degiorgi¹

1. ETH Zurich, Department of Physics, Zurich, Switzerland

We collect optical reflectivity data as a function of temperature across the structural tetragonal-to-orthorhombic phase transition at T_S on Ba(Fe_{1-x}Co_x)₂As₂ for $x = 0, 2.5\%$ and 4.5% , with uniaxial and in-situ tunable applied pressure in order to detwin the sample and to exert on it an external symmetry breaking field. At $T < T_S$, we discover a remarkable optical anisotropy as a function of the applied pressure at energies far away from the Fermi level and very much reminiscent of a hysteretic-like behavior. Such an anisotropy turns into a reversible linear pressure dependence at $T \geq T_S$, suggesting a substantial nematic susceptibility. Moreover, the optical anisotropy gets progressively depleted with increasing Co-content in the underdoped regime, consistent with the doping dependence of the orthorhombicity but contrary to the non-monotonic behavior observed for the dc anisotropy. Our findings bear testimony for an important anisotropy of the electronic structure and thus underscore an electronic polarization upon (pressure) inducing and entering the nematic phase.

WE.A.1_O6 - Orbital-driven nematicity in FeSe

S. Baek¹, D. Efremov¹, J. Mok Ok², J. Sung Kim², J. van den Brink¹, B. Buechner¹

1. *IFW Dresden, Dresden, Germany*

2. *Pohang University of Science and Technology, Republic of Korea*

An important feature in Fe-based superconductors is that superconductivity occurs in the vicinity of nematic ordering - a lowering of the rotational symmetry preserving time-reversal invariance - as well as of magnetic order. The origin of the nematic symmetry breaking has been heavily debated, because lattice, orbital, and spin degrees of freedom are all directly linked one another from a symmetry point of view, and thus it is challenging to establish which ordering is primary. In this talk, I will present nuclear magnetic resonance (NMR) studies of the high-quality FeSe single crystals, demonstrating that orbital degrees of freedom drives the nematic order [1].

References:

[1] S.-H. Baek et al., Nature Materials 14, 210 (2015)

WE.A.2_O1 - Proximity effects in YBa₂Cu₃O₇/[Co/Pt]_n heterostructures

C. Visani¹, F. Cuellar¹, A. Verso², C. Nail¹, C. Deranlot¹, F.S. Bergeret², J.E. Villegas¹

1. *Unité Mixte De Physique CNRS/Thales, Palaiseau, and Université Paris Sud, Orsay, France*

2. *Centro De Física De Materiales, CSIC/UPV, San Sebastián, Spain*

We have investigated proximity effects in heterostructures that combine the high-temperature superconductor YBa₂Cu₃O₇ with either Co/Pt multilayers or single Pt thin films. The study is based on measurements across vertical junctions between those materials. The measurements provide information of the electronic density-of-states changes due to superconducting proximity effects. A large number of junctions have been measured. The presence of certain spectral features in the conductance spectra, such as energy gaps or zero-energy peaks, depends on the interface resistance and thickness of the different materials in the stack. The observed behaviors are explained considering short/long range proximity effects.

Work supported by the EU IRSES grant "COEFMAGNANO"

WE.A.2_O2 - Magnetic nanoparticles in MgB₂: vortex pinning, pair breaking and connectivity

E. Babic¹, N. Novosel¹, D. Pajic¹, Stipe Galic¹, K. Zadro¹, N. D.J. Drobac²

1. *University of Zagreb, Faculty of Science, Department of Physics, Zagreb, Croatia*

2. *Institute of Physics, Zagreb, Croatia*

Present status of ongoing study of the influence of single-domain magnetic nanoparticles (MNP) with size comparable to the coherence length of MgB₂ and superparamagnetic (SP) at/below room temperature on electromagnetic properties (resistivity, magnetization, connectivity, T_c, J_c etc.) of high quality MgB₂ wires is reported. In spite of conceptual importance (coexistence of magnetism and superconductivity, magnetic flux pinning) and technological potential (improvement of superconducting parameters) present results for the influence of MNPs on MgB₂ are inconclusive [1]. In order to shed more light on this problem we measured over sixty MgB₂ wires doped with different amounts of four types of MNPs: elemental magnets, magnetic borides, ferrites and rare earth oxides/borides. Both, coated (carbon, silica or dextrin shell) and uncoated MNPs were used in order to assess the effects of co-doping and interparticle interaction. The influence of the annealing temperature and of shape of MNPs (sphere or rod) were studied, too. The magnetic state of MNPs, both in as-obtained form and inside MgB₂ was determined via magnetization and ac susceptibility measurements. Transport and magnetic measurements were used in order to determine reliably characteristic fields and J_c of doped and virgin wires [1]. The competition between detrimental influence of magnetic inclusions (reduced connectivity, pair breaking) and enhanced flux pinning in doped wires leads to deterioration of electromagnetic properties at high MNP contents, whereas at light doping (<3 wt%) an enhancement of these properties was observed for several MNPs. For Ni and dextrin coated NiFe₂O₄ MNPs the enhancement of in-field J_c is comparable to that obtained by the best nonmagnetic dopants. In the case of the enhancement of the properties a detailed analysis indicates the contribution of magnetic flux pinning, including the first observation of the matching effects in vortex pinning on MNPs.

References:

[1] N. Novosel and E. Babic, *Physica C* 493 (2013) 119

WE.A.2_O3 - Spin orbital interplay and topology in the nematic phase of iron pnictides

B. Valenzuela¹, L. Fanfarillo¹, A. Cortijo¹, L. Benfatto²

1. *Instituto De Ciencia De Materiales De Madrid CSIC, Madrid, Spain*

2. *University of Rome, Rome, Italy*

Iron superconductors, discovered in 2008, are together with cuprates the two families of high temperature superconductors. As in cuprates, superconductivity emerges upon doping a magnetic state. There are also profound differences between the two families since iron superconductors are multiorbital systems. The Fermi surface has a vortex in the Gamma pocket from the yz and zx orbitals making it topologically non trivial. On the other hand, in the normal state iron superconductors present a nematic state. Nematic signatures have been also found in cuprates. The nematic phase is characterized by an x/y anisotropy and it has been observed by many experimental techniques. There is a strong debate about whether the orbital or the spin is behind the origin of nematicity. Understanding the nematic phase is believed to be key to understand high temperature superconductivity. Nematicity has been mostly described with a Landau model with magnetic origin [1]. However to date there is not an understanding of the role played by the vortex of the Gamma pocket. In this work we derive an effective model from a Hamiltonian and we calculate the spin susceptibility in the nematic phase[2]. We find that orbital fluctuations arise from spin fluctuation making both fluctuations potential candidates for the mechanism of superconductivity. We also find that the vortex at the Gamma pocket is behind the anisotropy observed in the spin susceptibility. The anisotropic spin fluctuation give an anisotropic response in resistivity experiments related to the resistivity anisotropy in the magnetic phase.[3]

References:

1. R.M. Fernandes, et al. Phys. Rev. B 85, 024534 (2012); R. M. Fernandes, et al. Nat. Phys. 10, 97 (2014)
2. L. Fanfarillo, A. Cortijo, and B. Valenzuela, arXiv:1410.8488. L. Fanfarillo, A. Cortijo, L. Benfatto and B. Valenzuela, in preparation
3. B. Valenzuela, E.Bascones and MJ.Calderón, Phys. Rev. Lett. 105 207202 (2010)

WE.A.2_O4 - Colossal superconducting spin valve effect and ultra-small exchange-splitting in epitaxial rare-earth-niobium trilayers

Y. Gu¹

1. University of Cambridge, Cambridge, United Kingdom

Epitaxial Ho/Nb/Ho and Dy/Nb/Dy superconducting spin valves (SSVs) show a reversible change in the zero-field critical temperature of ~400 mK and an infinite magnetoresistance on changing the relative magnetization of the Ho or Dy layers. Unlike transition metal SSVs which show much smaller change in the critical temperature values, our results can be quantitatively modelled. However, the fits require an extraordinarily low induced exchange splitting which is dramatically lower than known values for rare-earth Fermi-level electrons implying that new models for the magnetic proximity effect may be required.

WE.B.2_I1 - Design of interfaces for tuning magnetism in nanostructures

BOOK OF ABSTRACTS

M. Farle¹, S. Liébana Viñas¹, R. Salikhov¹, C. Bran², E. Palmero², B. Arvan², P. Toson¹, J. Fidler³, M. Spasova¹, U. Wiedwald¹, R. Pentcheva¹, V. Salguerino⁴, Z.A. Li¹

1. *Fakultät für Physik and Center for Nanointegration (CENIDE), Universität Duisburg-Essen, Duisburg, Germany*

2. *Institute of Materials Science of Madrid, CSIC, Madrid, Spain*

3. *Institute of Solid State Physics, Vienna University of Technology, Vienna, Austria*

4. *Departamento de Física Aplicada, Universidade de Vigo 36310, Vigo, Spain*

3d transition metal based magnetic nanowires (NWs) and particles might be suitable candidates for alternative rare-earth free alloys as novel permanent magnets. I will discuss the magnetic hardening of Fe₃₀Co₇₀ nanowires by means of magnetic pinning at the tips of the NWs. We observe that 3 nm FeCo oxide layers in contact with the FeCo NW increases the coercive field by 20%, indicating that domain wall nucleation starts at the tip of a magnetic NW. Micromagnetic simulations support our experimental findings showing that the increase of the coercive field can be achieved by controlling domain wall nucleation using antiferromagnetic capping layer at the nanowire tips. In a second example the design of a ferromagnetic interface within a special type of antiferromagnetic CoO / Co₃O₄ core/shell nanoparticle [1] is presented.

Financial support by DFG and European Union 'REFreePermMag' is acknowledged.

References:

[1] Zi-An Li et al., Scientific Reports 5 (2015) 7997

WE.B.2_O2 - Building Blocks of Artificial Square Spin Ice: Stray-Field Studies of Thermal Dynamics and Tuned Interactions.

M. Pohlit¹, F. Porrati¹, M. Huth¹, Y. Ohno², H. Ohno², J. Müller¹

1. Institute of Physics, Goethe-University Frankfurt, Frankfurt am Main, Germany

2. Laboratory for Nanoelectronics and Spintronics, Research Institute of Electrical Communication, Tohoku University, Sendai, Japan

Over the last decade, spin ice systems with their intricate interplay between disorder, frustration and degeneracy giving rise to fundamentally new phenomena like the occurrence of monopole excitations, came to the fore of intensive research interest. Due to the ability to tune the geometric shape and the possibility to access spatially-resolved magnetic properties, artificial spin ice systems, i.e. nanostructured arrays of macroscopic spins, were successfully employed as 2D model systems for their 3D equivalent. Here we present magnetic measurements performed on individual building blocks of artificial square spin ice. For this purpose a cobalt-based spin ice structure was grown by focused electron beam induced deposition (FEBID) onto the surface of a lithographically defined μm -sized Hall-sensor based on a two-dimensional electron gas of an AlGaAs/GaAs heterostructure. This setup provides continuous access to the array's stray field during magnetization reversal. Using relatively simple temperature and magnetic field protocols, individual microstates were prepared and thermally-activated switching was observed. Encouraged by these findings the inter-macrospin interaction was enhanced by growing -in a second deposition step- low energy irradiated nano-granular Pt-C at the lattice nodes. In this material, recently a small magnetic moment was observed at low temperatures[1]. Below $T=20\text{ K}$ we find a strongly enhanced coercivity of the nanocluster's hysteresis as a result of the altered coupling. The presented results will be accompanied by recent investigations of the magnetization reversal of an isolated non-interacting single macrospin element i.e. the fundamental building block of the investigated nanocluster itself. First order reversal curves (FORC) supported by micro-magnetic simulations were employed to study the inter- and intra-macrospin interactions in a model system with increasingly complex interactions.

References:

[1] F. Porrati et al 2014 J. Phys.: Condens. Matter 26 085302

WE.B.2_O3 - Tuning the melting temperature of artificial spin ice structures

S. Pappas¹, E. Östman¹, H. Stopfel¹, B. Hjörvarsson¹, V. Kapaklis¹

1. Uppsala University, Department of Physics and Astronomy, Uppsala, Sweden

Water ice is the archetype of geometric frustration, exhibiting disorder in the arrangement of oxygen -proton bonds [1]. Frustration is observed in many physical systems. Spin frustration in rare - earth pyrochlores is found to mimic the geometric frustration in water ice through the formation of spin ice structures. By mimicking the crystalline spin ice materials, we can create two dimensional arrangements of frustrated interacting nanomagnets, referred as artificial spin ice systems, with characteristic length scales and energies distinguishing them from spin systems frustrated at the atomic level due to competing interactions between the individual spins.

In this work, our goal is to realize and investigate thermally induced transitions in extended artificial square spin ice arrays. At thermal energies above the reversal energy barrier, the particles act as super-paramagnetic entities. The investigation of the thermally induced dynamics in an extended spin ice structure requires the magnetic excitations to be observable under experimental conditions [2,3]. To accomplish this, the magnetic properties of the islands and their interactions need to be adjusted to match the accessible temperature range. This is achieved through the choice of the intrinsic ordering temperature of the island material and the distance between the islands. The islands were made of δ -doped Pd(Fe) thin films and different periodicities for the square spin ice lattice were chosen. Photoemission electron microscopy with X-ray magnetic circular dichroism (PEEM-XMCD) in combination with magneto-optical Kerr effect (MOKE) measurements, confirm a dynamical premelting of the artificial spin ice structure at a temperature well below the intrinsic ordering temperature of the island material. The premelting temperature was found to be dependent on the lattice geometry.

References:

- [1] L. Pauling, J. Am. Chem. Soc. 57, 2680 (1935)
- [2] V. Kapaklis et al., Nature Nanotechnology 9, 514 (2014)
- [3] V. Kapaklis et al., New J. Phys. 14, 035009 (2012)

WE.B.2_O4 - Magnetic imaging of honeycomb artificial spin ice at low temperatures

K. Zeissler¹, M. Chadha¹, D. Burn¹, L. Cohen¹, W. Branford¹

1. Imperial College London, London, United Kingdom

Advances in nanotechnology have enabled the creation of complex single domain ferromagnetic constructs, allowing the study of ferromagnetic interactions influenced by geometry. Artificial spin ice is such a playground which marries geometrical order with magnetic frustration. Recently published measurements have shown unusual features in the magnetotransport signature of cobalt and permalloy honeycomb artificial spin ice below 50 K and 20 K respectively [1,2]. Here we explore the changes in the magnetic reversal of a connected artificial spin ice array fabricated from permalloy below and above this transition temperature using magnetic force microscopy. The imaging shows a change in the magnetic reversal process at low temperatures, which results in a striking number of ice rule violations. These ice rule violations are rare occurrences at room temperature in permalloy arrays where switching occurs via propagation of transverse domain walls [3-5]. We present a link between the domain wall chirality with our low temperature observations.

References:

- [1] Branford WR, et al. Emerging Chirality in Artificial Spin Ice. *Science*. 2012;335(6076):1597-600
- [2] Lee LB, et al. Effects of exchange bias on magnetotransport in permalloy kagome artificial spin ice. *New J. Phys.* 2015;17(023047)
- [3] Ladak S, et al. Monopole defects and magnetic Coulomb blockade. *New J Phys.* 2011;13(023023)
- [4] Zeissler K, et al. The non-random walk of chiral magnetic charge carriers in artificial spin ice. *Sci Rep.* 2013;3(1252)
- [5] Walton SK, et al. *New J. Phys.* 2015;17(013054)

WE.B.2_O5 - XMCD-PEEM Characterisation of Self-Assembled Artificial Magnetic Material based on Concavity Nanostructures

J. Llandro¹, D. Love¹, D. Mahendru¹, C. Ciorra¹, F. Maccherozzi², S. Dhesi², J. Herrero Albillos³, C. Barnes¹

1. *University of Cambridge, United Kingdom*

2. *Diamond Light Source, United Kingdom*

3. *Centro Universitario de la Defensa, Spain*

Patterning of magnetic films into interacting arrays of nanostructures has found employment in both applications such as bit-patterned media [1] and fundamental investigations into fields such as frustrated magnetism via the creation of artificial spin ices [2]. An elegant method to synthesise structured 2D and 3D magnetic arrays is nanosphere lithography, in which well-ordered, close-packed arrays of polystyrene beads are formed into a template which can be backfilled by metal electrodeposition to form an inverse-opal, or nanostructured array of part-spherical concavities [1].

Here, substrates coated with a monolayer of 1000nm diameter polystyrene beads were back-filled by electrodeposition of Cu. After a second electrodeposition step of 20nm Ni and NiFe layers and dissolution of the spheres, we thus obtained 2D hexagonal arrays of suspended triangular magnetic elements; these differ from the more typical kagomé artificial spin ices in that the elements sit at the vertices of the lattice [2]. Furthermore, the spacing between the elements was sensitive to the thickness of the Cu underlayer; by altering this thickness from just less to just greater than the spheres' radius, we prepared a sequence of samples of constant magnetic layer thickness in which the magnetostatic interaction between elements varied from weak to strong. We present the results of X-ray magnetic circular dichroism photoelectron emission microscopy (XMCD-PEEM) measurements taken at the I06 beamline of the Diamond Light Source (RAL, UK). These measurements were made challenging by the high topographic changes in our concavity samples, as well as shadowing and multiple scattering effects; samples prepared for XMCD-PEEM are typically therefore confined to a 2D plane. These results highlight XMCD-PEEM as a complementary high-resolution probe for magnetic films on substrates with high 3D texturing.

References:

[1] A. Zhukov et al., *App. Phys. Lett.* 88, 062511 (2006)

[2] E. Mengotti et al., *Nat. Physics* 7, 68 (2011).

WE.B.2_I6 - Vortices and antivortices on the move: a powerful tool to probe magnetic states in nanomagnets.

J. Vicent^{1,2}, J. del Valle¹, A. Gomez¹, E. Gonzalez^{1,2}

1. *Universidad Complutense, Madrid, Spain*

2. *IMDEA-Nanociencia, Madrid, Spain*

Superconductivity and magnetism are two cooperative effects which compete with each other. Recently, this antagonist behavior has been turned around, since magnetic nanostructures could enhance superconducting properties, among many examples we can notice the so-called domain wall superconductivity. In the present work we have followed the opposite approach; we show that superconductivity is an appropriate tool to probe the magnetic behavior of tiny nanomagnets. We have fabricated on Si substrates hybrid superconducting/magnetic nanostructures using a combination of different techniques as sputtering, electron beam lithography, and reactive ion etching. The hybrid samples are arrays of nanomagnets (Py, Pd/Co multilayers, Co, Fe and Ni) with different shapes embedded in Nb films. These samples are patterned to a cross-shaped bridge which allows magnetotransport measurements with the magnetic field applied perpendicular to the films. We show that moving superconducting vortices and antivortices discriminate among different magnetic states including magnetic vortex states; even they show very small stray magnetic fields. We show that we can explore in details the magnetization states using the dissipation output signals induced by the motion of superconducting vortices, and even more in some of the nanomagnets the remanent states can be measured and fine-tuned using the so-called ratchet effect.

WE.C.1_I.1 - SPIN DEGREES OF FREEDOM IN RELATIVISTIC FERROELECTRICS

S. Picozzi

1. Consiglio Nazionale Delle Ricerche CNR-SPIN, L'Aquila, Italy

By exploiting the interplay between spin and dipolar degrees of freedom via spin-orbit coupling in ferroelectric semiconductors, I will focus on the tight link between k-dependent spin-splitting in the electronic structure, spin-texture and electric polarization. Based on density functional simulations, I will show our theoretical predictions of a giant Rashba spin-splitting in “bulk” GeTe[1], prototype of novel multifunctional materials - labeled as Ferro-Electric Rashba Semi-Conductors (FERSC)[2] - where the chirality of the spin texture is one-to-one linked to polarization. As the latter can be induced/controlled/switched via an electric field in a non-volatile way, the integration of semiconductor spintronics with ferroelectricity is envisaged. In the last part of the talk, the connection between ferroelectricity and spin-degrees of freedom will be discussed by providing examples from different materials classes (oxides heterostructures, halides perovskites,[3] chalcogenides,[4] etc), all of them showing strong relativistic effects.

References:

- [1] D. Di Sante, P. Barone, R. Bertacco and S. Picozzi, *Adv. Mater.* 25, 509 (2013)
- [2] S. Picozzi, *Front. Physics* 2, 10 (2014)
- [3] A. Stroppa, D. Di Sante, P. Barone, M. Bokdam, G. Kresse, C. Franchini, M.-H. Whangbo, S. Picozzi, *Nature Communications*, 5, 5900 (2014)
- [4] E. Plekhanov, D. Di Sante, P. Barone and S. Picozzi, *Phys. Rev. B Rapid* 90, 161108(R) (2014)

WE.C.1_O2 - Tiny cause with huge impact: polar instability through strong magneto-electric-elastic coupling in bulk EuTiO3

A. Bussmann-Holder¹, P. Reuvekamp¹, K. Caslin¹, R. Kremer¹, J. Köhler¹

1. Max-Planck-Institute For Solid State Research, Germany

Multiferroic materials with combined polar, magnetic, and elastic orderings are at the forefront of scientific research in view of their multiple interactive couplings: magnetic order can be tuned by strain and an electric field, polar order can be triggered by a magnetic field and strain, and elastic properties are controlled by a magnetic and/or an electric field. Such materials are desirable for multiple applications. Even though the phenomenon of multiferroicity has been predicted long ago [1], its realization remains rare for rather simple reasons: typically polar order is achieved when a transition metal d^0 configuration is combined with highly polarizable anions, whereas magnetic order relies on a finite d_n configuration. Obviously these two requirements yield a certain incompatibility of the coexistence of the two phenomena which have been tried to overcome by combining magnetic layers with polar ones, by growing composites, and via strain engineering [2, 3]. Even though a rather large number of materials have been shown to exhibit the desired properties, the coupling between magnetic and polar order is either very weak, or the spontaneous polarization/magnetization appears at low temperature only and remains too small to be of technological interest. Here we propose a new strategy to achieve strong magnetic-polar coupling by deriving the soft mode frequency of EuTiO₃ as a function of its lattice parameters which exhibits unusual, yet very small temperature dependencies at high and low temperatures [4, 5]. Specifically we develop a route of how to induce ferroelectric order in bulk EuTiO₃ (ETO) by combining experimental results with theoretical concepts. We show that marginal changes in the lattice parameter of the order of 0.01% have a more than 1000% effect on the transverse optic soft mode of ETO and thus easily induce a ferroelectric instability.

WE.C.1_I4 - Coupled electricity and magnetism in solids: currents, dipoles and monopoles in frustrated systems and in magnetoelectrics

D. Khomskii¹

1. II. Physikalisches Institut, Universitaet Zu Koeln, Köln, Germany

The standard point of view is that at low energies Mott insulators exhibit only magnetic properties, while charge degrees of freedom are frozen out. I demonstrate that in general this is not true [1, 2]: for certain spin textures in frustrated magnets there may exist spontaneous circular currents in the ground state of insulators, proportional to the scalar chirality. For other spin structures there may exist spontaneous charge redistribution, which can lead to the appearance of dipole moments and possibly of the net spontaneous polarization. This is a novel, purely electronic mechanism of multiferroic behaviour. In particular I show [3] that such electric dipoles should exist in spin ice materials at every tetrahedra with three-in/one-out or one-in /three-out spin configurations, which are equivalent to magnetic monopoles [4]. Thus there should be an electric dipole attached to each magnetic monopole in spin ice. This leads to electric activity of magnetic monopoles, and opens the possibility to control magnetic monopoles by electric field. I will also discuss unconventional dynamics of magnetoelectric materials, in which there should be a magnetic monopole attached to each electric charge [5], which will then become what is known as a dyon. Several experimental manifestations of this effect will be discussed.

References:

- [1] L.N.Bulaevskii, C.D.Batista, M.V.Mostovoy and D.I.Khomskii, Phys.Rev.B 78, 028402 (2008)
- [2] D.I.Khomskii, JPCM 22, 164209 (2010)
- [3] D.I.Khomskii, Nature Communications 3, 904 (2012)
- [4] C.Castelnovo, R.Moessner and S.L.Sondhi, Nature 451, 42 (2008)
- [5] D.I.Khomskii, Nature Communications 5, 4793 (2014)

WE.C.2_I1 - Electronic and Magnetic Structure of Actinide Metals

G. Van Der Laan

1. Magnetic Spectroscopy Group, Diamond Light Source, Didcot, United Kingdom

In comparison to 3d or 4f metals, magnetism in actinides remains poorly understood due to experimental complications and the exotic behaviour of the 5f states [1]. In particular, plutonium metal is most especially vexing. Over the last five decades, theories proposed the presence of either ordered or disordered local moments at low temperatures. However, experiments such as magnetic susceptibility, electrical resistivity, nuclear magnetic resonance, specific heat, and elastic and inelastic neutron scattering show no evidence for ordered or disordered magnetic moments in any of the six phases of plutonium. Beyond plutonium, the magnetic structure of other actinides is an active area of research, given that temperature, pressure, and chemistry can quickly alter the magnetic structure of the 5f states. For instance, curium metal has an exceedingly large spin polarization that results in a total moment of $\sim 8 \mu_B/\text{atom}$, which influences the phase stability of the metal. Insight in the actinide ground state can be obtained from core-level X-ray absorption spectroscopy (XAS) and electron energy-loss spectroscopy (EELS) [2]. A sum rule relates the branching ratio of the core-level spectra measured by XAS or EELS to the expectation value of the angular part of the spin-orbit interaction [3].

References:

[1] K.T. Moore and G. van der Laan, *Rev. Mod. Phys.* 81, 235 (2009)

[2] K.T. Moore, G. van der Laan, R.G. Haire, M.A. Wall, A.J. Schwartz, P. Söderlind, *Phys. Rev. Lett.* 98, 236402 (2007)

[3] G. van der Laan, K.T. Moore, J.G. Tobin, B.W. Chung, M.A. Wall, A.J. Schwartz, *Phys. Rev. Lett.* 93, 097401 (2004)

WE.C.2_O2 - UH3 based ferromagnets - new look at old material

L. Havela¹, I. Tkach¹, M. Paukov¹, D. Drozdenko¹, M. Cieslar¹, B. Vondrackova¹, Z. Matej¹, A. V. Andreev², N.-T.H. Kim-Ngan³, I. Turek¹

1. Charles University, Faculty of Mathematics and Physics, Prague, Czech Republic

2. Institute of Physics, Academy of Sciences of the Czech Republic, Prague, Czech Republic

3. Institute of Physics, Pedagogical University Cracow, Poland

UH3 is the first discovered material with ferromagnetism purely based on 5f electronic states, known for more than half century. Although the U metal is Pauli paramagnet, reduced 5f-5f overlap in compounds allows for moment formation and ordering, typically if the U-U spacing exceed the Hill limit, i.e. about 340 pm. The stable form of UH3, known as beta-UH3, with its high $T_C = 165$ K is rather unusual, considering $d_{U-U} = 330$ pm. Properties of metastable alpha-UH3 with $d_{U-U} = 360$ pm could never be well established. Using the fact that alpha-UH3 is in fact bcc U with interstitials filled by H, we attempted to synthesize alpha-UH3 starting from the gamma-U alloys, with the bcc structure retained to room temperature by doping combined with ultrafast cooling. While up to 15% Zr mixed a contamination by beta-UH3 was obtained, 20% Zr yielded single phase alpha-UH3. The T_C value remains high and very similar to beta-UH3. One can see an increase up to 187 K for 15% , followed by a weak decrease. Magnetic moments remain close to 1 μ_B /U atom. An insight is provided by ab-initio calculations, revealing a charge transfer towards H, depopulating U-6d and 7s states, leaving almost pure 5f character around the Fermi level. The 5f magnetism exhibits a high coercivity ($\mu_0 H_c$ up to 5.5 T) and large spontaneous volume magnetostriction $3.2 \cdot 10^{-3}$. Even higher increase of T_C , reaching up to 203 K, can be achieved in analogous Mo stabilized hydrides, which yield an amorphous structure. The compounds represent, together with known hydrides of U6Fe and U6Co, a new group of robust 5f ferromagnet with small d_{U-U} but high T_C . Although common hydrides are fine powders, some of the new hydrides described as $(UH3)_{(1-x)}T_x$ remain monolithic, which allows to study transport and thermodynamic properties.

WE.C.2_O3 - Physical properties of an $\text{UFe}_{1-x}\text{Sb}_2$ single crystal

A.P. Gonçalves¹, M.S. Henriques^{1,2}, J.C. Waerenborgh¹, I. Èurlik³, S. Ilkovic³, M. Reiffers³, J. Ruzs⁴

1. C2TN, Campus Tecnológico e Nuclear, Instituto Superior Técnico, Universidade de Lisboa, Bobadela LRS, Portugal
2. Institute of Physics, ASCR, Prague, Czech Republic
3. Faculty of Humanities and Natural Sciences, University of Presov, Presov, Slovakia
4. Department of Physics and Astronomy, Uppsala University, Uppsala, Sweden

In the present work the crystal structure and electronic properties of the $\text{UFe}_{1-x}\text{Sb}_2$ compound were studied in a single crystal. XRD confirms that $\text{UFe}_{1-x}\text{Sb}_2$ crystallizes in the $\text{HfCuSb}_{2\text{-type}}$ structure. Magnetization, AC susceptibility, specific heat, and electrical transport indicate two consecutive magnetic transitions. According to the AC susceptibility results, the anomalies are connected with an antiferromagnetic state at $T_N = 25.5$ K that changes to a ferromagnetic ground state at $T_C = 21$ K. The specific heat in zero field exhibits a small kink at T_N that vanishes with increasing applied magnetic field, which is consistent with the onset of the magnetic transition. All the electronic properties exhibit large anisotropy. First principles calculations of electronic structure show an unusually steep local minimum in the density of states right at the Fermi level, providing a starting point for explaining the strong anisotropy of the material.

WE.C.2_O4 - Phasons, amplitude modes, and spin wave excitations in the amplitude-modulated magnetic structure of PrNi₂Si₂J. Blanco¹, B. Fak², J. Jensen³, M. Rotter⁴, A. Hiess⁵, D. Schmitt⁶, P.I Lejay⁷*1. University of Oviedo, oviedo, Spain**2. 2SPSMS, UMR-E CEA/UJF-Grenoble-I, INAC, Grenoble, France**3. Niels Bohr Institute, Copenhagen, Denmark**4. Max-Planck Institute for Chemical of Solids, Dresden, Germany**5. European Spallation Source ESS AB, Lund, Sweden**6. ISTERre, CENR, Université de Grenoble I, Grenoble, France**7. Institut Néel, Grenoble, France*

In incommensurate magnetic structures, the only low-energy mode that is expected to be is the pseudo-Goldstone mode of broken translations, known as a phason. This excitation is a purely longitudinal mode associated with the phase of the complex order parameter and represent a modulation of the magnetic moment only. This phason mode is quite unusual, where typically the low energy collective modes are transverse spin waves, which correspond to small rotations of the magnetic moments away from their ordered axes. In the spin-wave theory, longitudinal modes are often expected to be highly damped, and then hard to be observed. For a recent notable exception to this rule is the case of amplitude-modulated magnetic structure of PrNi₂Si₂. It presents a peculiar magnetic character: it is one of the few examples in nature where the magnetic ions, Pr³⁺, have a longitudinal amplitude-modulated magnetic structure below TN = 20 K, which is stable down to 0 K. In this way, the material is characterized by an Ising-type magnetic structure, where the magnetocrystalline anisotropy confines the magnetic moments along the c-axis. In most "equal-moment" systems the moments saturate at low temperatures, in which case the longitudinal excitations are quenched, allowing only the presence of transversely polarized spin waves. The magnetic excitations in the low-temperature amplitude-modulated magnetic structure of PrNi₂Si₂ have been investigated by inelastic neutron scattering [1]. The dispersions and intensities of both longitudinal and transverse excitations were measured along the high-symmetry directions. The modulated magnitude of the ordered moments implies that the longitudinally polarized magnetic excitations are more intense and dispersive than the usual transverse spin waves. Several well-defined longitudinal amplitude modes are observed to coexist with the longitudinal phason mode. The experimental results are in good overall agreement with predictions from the random-phase approximation, using exchange and crystal field parameters already established from the macroscopic properties and the paramagnetic excitations. At low energies in the neighborhood of the magnetic zone center, the magnetic phason appears to hybridize with an unidentified dispersionless mode.

References:

[1] J. A. Blanco et al., Phys. Rev. B 87 (2013) 104411

WE.C.2_O5 - Copexistence of trivalent and intermediate-valence Ce in CeRuSn studied by polarized neutrons

K. Prokes¹, S. Hartwig¹, A. Gukasov², J. Mydosh³, Y. Huang⁴, O. Niehaus⁵, R. Poettgen⁵

1. *Helmholtz-Zentrum Berlin, Berlin, Germany*

2. *LLB Saclay, Yvette, France*

3. *Kamerlingh Onnes Laboratory, Leiden University, Leiden, The Netherlands*

4. *University of Amsterdam, Amsterdam, The Netherlands*

5. *Westfälische-Wilhelms University Muenster, Muenster, Germany*

Spin densities in CeRuSn were determined at elevated and at low temperatures using polarized neutron diffraction. At 285 K, where the CeRuSn crystal structure, commensurate with the CeCoAl type, contains two different crystallographic Ce sites, we observe that one Ce site is clearly more susceptible to the applied magnetic field whereas the other is hardly polarizable. This finding clearly documents that distinctly different local environment of the two Ce sites causes the Ce ions to split into magnetic Ce³⁺ and non-magnetic Ce(4- δ)⁺ valence states. With lowering the temperature, the crystal structure transforms to a structure incommensurately modulated along the c axis. This leads to new inequivalent crystallographic Ce sites resulting in a re-distribution of spin densities. Our analysis using the simplest structural approximant shows that in this metallic system Ce ions co-exist in different valence states. Localized 4f states that fulfill the third Hund's rule are found to be close to the ideal Ce³⁺ state (at sites with the largest Ce-Ru interatomic distances) whereas Ce(4- δ)⁺ valence states are found to be itinerant and situated at Ce sites with much shorter Ce-Ru distances. This transition resembles to the famous alpha-gamma transition in elemental cerium.

WE.C.2_I6 - Coupling lanthanide-based molecular qubits to quantum circuits

F. Luis¹

1. Instituto de Ciencia de Materiales de Aragón, CSIC-University of Zaragoza, Zaragoza, Spain

The manipulation of quantum superpositions of bit states gives resources to crack tough computational problems, relevant to the design of new chemicals and materials, the safe data protection and communication and the efficient search in large data bases, which are beyond those affordable by any classical device. An outstanding challenge is to scale up quantum computation architectures to a level where they are of practical use. In recent years, magnetic molecular clusters have been proposed as suitable materials for the realization of the quantum hardware. We describe experiments performed at very low temperatures on simple molecules that contain either one or two weakly coupled lanthanide ions. The experiments show that these molecules can perform as, respectively, single qubits and two-qubit CNOT gates, i.e., that they can realize the basic ingredients of a universal quantum computer. Spin decoherence times T_2 have been measured on magnetically diluted crystals and frozen solutions, reaching values of the order of 500 ns at liquid Helium temperatures and allowing the observation of Rabi oscillations between different qubit states. We next discuss the coupling of such magnetic molecules to quantum superconducting circuits (SQUIDs and superconducting resonators) and how these hybrid devices can contribute to develop a magnetic quantum processor.

WE.D.1_I1 - Origin of hysteresis in multicaloric materials

S. Fähler¹, M. E. Gruner², H. Seiner³, R. Niemann¹, L. Schultz¹

1. IFW Dresden, Dresden, Germany

2. University of Duisburg-Essen, Essen, Germany

3. Institute of Thermomechanics, Academy of Sciences of Czech Republic, Prague, Czech Republic

Ferroc phase transitions driven by external magnetic, electric or stress fields promise more energy efficient solid state refrigeration. A key step towards this environmentally friendly technology was the use of first instead of second order phase transitions, which substantially increased the associated entropy change. However, a drawback of first order materials is the transformation hysteresis, which heats up the material and thus reduces or even eliminates the efficiency of a solid state cooling device. Despite this, hysteresis is often ignored when characterizing materials, e. g. by using the Maxwell relation or using only the first direct delta-T measurement instead of a complete cycle.

In this talk the structural and microstructural origin of hysteresis exemplarily for Heusler alloys will be analyzed. Starting point is the transient coexistence of both phases, which requires the formation of interfaces between both phases. As these interfaces disappear when the complete sample has transformed, the associated interface energy contributes to the hysteresis loss. In case that the transformation is associated with a reduction of crystal symmetry, the formation of a nanotwinned microstructure minimizes the interface energy. Accordingly the often observed coarsening process of twins contributes substantially to hysteresis. In addition the formation of a periodic structure requires ordering of nanotwins and thus part of the interaction energy, which drives the ordering process, is dissipated. Last, but not least the elastic energy from the volume change at the transformation is dissipated twice during a cooling cycle. This talk will outline the underlying mechanism, scaling laws, and key experiments, without going into the details of the theories used. These concepts may help to develop new materials and microstructures with reduced hysteresis.

This work is supported by DFG through SPP 1599 www.FerroicCooling.de

WE.D.1_O2 - Increasing the achievable state of order in Ni-Mn-based Heusler alloys

P. Neibecker¹, M. Leitner¹, G. Benka², W. Petry¹

1. *Heinz Maier-Leibnitz Zentrum (MLZ), Technische Universität München, Garching Germany*

2. *Physics Department, Technische Universität München, Garching, Germany*

Ni-Mn based Heusler alloys are a class of functional materials closely connected with recent breakthroughs in the areas of ferromagnetic shape memory alloys, magnetocaloric materials and potential halfmetallic materials for spintronics applications. Yet, the functionality of these materials sensitively depends on the alloy's composition and especially the state of atomic order. Ni-Mn based Heusler alloys usually crystallize in the high temperature A2 or B2 phase and undergo at lower temperatures a transition to the ferromagnetic L2₁ phase. However, in some promising alloy systems such as Ni₂MnAl, an inherently low degree of L2₁ order suppresses ferromagnetism and thereby impedes the fulfillment of their theoretical potential e.g. as ferromagnetic shape memory alloys. In our work, we discuss the ordering kinetics in the Ni₂MnAl system and demonstrate a pathway for tremendously increasing the achievable state of atomic order in these materials [1]. In general, the state of atomic order is a complex value consisting of many parameters necessary to do justice to both the long and short range atomic order. We demonstrate in our work the interplay of calorimetric and magnetic measurements in order to obtain a quite local probe for the atomic order adjusted in the alloy. Based on the described measurement routine, the increase of achievable order in the alloy via accelerated ordering kinetics by the usage of quenched-in excess vacancies is discussed. With our method, equilibrium order at temperatures as low as 623 K can be adjusted in Ni₂MnAl, while under equilibrium vacancy concentration order adjustment at these temperatures would take impractically long.

References:

[1] Neibecker, P., Leitner, M., Benka, G., Petry, W., Appl. Phys. Lett. 105, 261904 (2014)

WE.D.1_O3 - Characteristics of Intermartensitic Transitions in Ni-Mn Based Heusler Alloys

A. Çakir¹, L. Righi², F. Albertini³, M. Acet⁴, M. Farle⁴

1. *Metallurgical and Materials Engineering Department, Mugla University, Mugla, Turkey*
2. *Chemistry Department, Parma University, Parma, Italy*
3. *IMEM, National Research Council, Parma, Italy*
4. *Physics Department, Duisburg-Essen University, Duisburg, Germany*

Currently, Ni-Mn-based Heusler alloys are intensively investigated for their multifunctional properties such as magnetic shape-memory, magneto-caloric, and giant magneto-resistance effects, which make them promising materials for technological applications. Especially, the characterization and detailed knowledge of the properties of magneto-structural transition properties of these materials is vital for the correct choice of the temperature ranges of their usage. Our recent studies revealed that the martensitic structure for some compositions of Ni-Mn-Ga and Ni-Mn-Sn alloys cannot be stable on varying temperature conditions. Intermartensitic transitions occur at low temperatures, and the reverse intermartensitic transition does not occur before reaching nearly room temperature, exhibiting a broad thermal hysteresis. On decreasing temperature, the 5M and 7M modulated martensite phases, which are the most important structures for the presence of magnetic shape memory property, tend to transform to the non-modulated L10 martensite phase, as this phase is estimated in calculations to be the energetically more stable ground state. This broad hysteresis effect has to be taken into account in variable temperature environments so that the material can be used with desired capacity.

WE.D.1_O4 - Atomic and magnetic structure and magnetocaloric properties of AlFe₂B₂

J. Cedervall¹, M. Andersson², T. Sarkar², E. Delczeg³, L. Höggström³, T. Ericsson³, P. Nordblad², M. Sahlberg¹

1. Chemistry – Angstrom, Uppsala University, Uppsala, Sweden

2. Engineering Sciences, Uppsala University, Uppsala, Sweden

3. Physics and Astronomy, Uppsala University, Uppsala, Sweden

The use of magnetic cooling in refrigerators as a replacement for conventional gas cooling devices could lead to lower power consumption and less hazardous materials in the life cycle of the refrigerator. Recently, a new class of materials based on layered AlM₂B₂ (M = Fe, Mn, Cr) was proposed as a candidate compound for magnetocaloric applications.

Here we report a detailed study on the synthesis and magnetic properties of AlFe₂B₂. Single phase samples were prepared using high-temperature synthesis methods gaining high quality samples. Magnetic and crystallographic properties were studied with powder diffraction, Mössbauer spectroscopy and magnetic measurements. The study shows that AlFe₂B₂ is a ferromagnetic compound with a magnetic transition at T_c=285K. The saturation magnetization at 10K is 60 Am²kg⁻¹ and ΔS_m(5T)=-4.5JK⁻¹kg⁻¹ around room temperature.

Mössbauer spectroscopy confirms a ferromagnetic substance and shows good agreement with the magnetic measurements. Theoretical calculations were carried out using the spin polarized relativistic Korringa-Kohn-Rostoker (SPR-KKR) method. Applying the scalar relativistic full potential (fully relativistic) approach a magnetic moment of 2.67 (2.36) μ_B/f.u. was found. The Curie temperature was estimated to 250 K using a Monte Carlo method implemented in the UppASD code.

WE.D.1_O5 - Study of magneto-elastic properties in shape-memory Heusler alloys by resonant ultrasound spectroscopy

C. Salazar Mejía¹, N. O. Born¹, A. K. Nayak¹, C. Felser¹, M. Nicklas¹, J. Schiemer², M. A. Carpenter²

1. Max Planck Institute For Chemical Physics of Solids, Dresden, Germany

2. Department of Earth Sciences, University of Cambridge, Cambridge, United Kingdom

Resonant ultrasound spectroscopy (RUS) is a technique that has been widely used in the area of geosciences to measure the elastic properties of minerals, with direct relevance to the velocities of seismic waves through the earth. Over the last 20 years, it has become a versatile laboratory technique in materials science for measuring elastic constants and ultrasonic attenuation [1]. We have applied RUS to study the magneto-elastic properties in Heusler alloys. Heusler alloys that undergo a martensitic transformation have been shown to exhibit diverse functional properties such as the shape-memory effect [2], magnetic-driven superelasticity [3] and the giant magnetocaloric effect [4], which derive from magnetoelastic couplings. The study of the magneto-elastic properties in these materials is important both from fundamental and application points of view. We have studied polycrystalline Heusler alloys from the Ni-Mn-Ga and Ni-Mn-In families by RUS, in a temperature range that includes the ferromagnetic and the martensitic phase transitions. We have observed fundamental differences in the behavior of the crystal lattice at the martensitic transition, i.e., stiffening versus softening, determined by the presence or absence of a pre-martensitic transition and the relation between the Curie temperature and the martensitic-transformation temperature. We will discuss these results in connection with our previous magnetization [5] and calorimetric data [6].

References:

- [1] R.B. Schwarz and J.F. Vuorinen, J. Alloys Compd. 310, 243-250 (2000)
- [2] R. Kainuma, et al. Nature 439, 957-960 (2006)
- [3] T. Krenke, et al. Phys. Rev. B 75, 104414 (2007)
- [4] J. Liu, et al., Nature Materials, 11, 620-626 (2012)
- [5] A. K. Nayak, et al., Phys. Rev. B 90, 220408 (2014)
- [6] M. Ghorbani Zavareh, et al., arXiv: 1501.04430 (2015)

WE.D.2_I1 - Controlling L10 ordering and microstructures of FePt films

C. Lai¹, S. Huang¹, W. Wen¹, J. Liao¹, B. Yang¹, K. Chang²

1. National Tsing Hua University, Taiwan

2. Seagate Technology

The addition of C segregant into L10 FePt films reveals a well-isolated granular structure. However, columnar grains with a high aspect ratio are difficult to obtain due to the accumulation of C at top grain surface. Here, we present two approaches to promote the aspect ratio. We prepared samples with the layer structure of substrate/MgO (10 nm)/FePt-C (0-28 vol%). The FePt-C was deposited at 350 OC. TEM images show the increased C contents promote grain isolation with the inevitable accumulation of C at top grain surface, whose amount is also proportional to the FePt film thickness. To suppress the C accumulation, we decrease the FePt-C layer thickness using the FePt-C (28 vol%) (0 iv 3 nm)/ FePt-B (20 vol%) (7 nm) bilayers. In the absence of FePt-C underlayer, FePt-B reveals no ordering peaks due to the presence of Fe-B bonding. With the 3 nm FePt-C layer, the bilayer structure shows enhanced ordering with perpendicular coercivity of 13.6 kOe. The TEM images of the bilayer show the well-isolated grains with the average grain size of 8.88 nm; the continuous (001) lattice through bilayers was observed in each grain, leading to the aspect ratio of 1.21. The EDX results suggest the diffusion of C into the FePt-B layer. The XPS spectra indicate the FePt-C underlayer reduces the Fe-B bonding and promotes the B-C compounds. The results indicate that this bilayer structure can improve the aspect ratio of grains with the promotion of L10 ordering in the top FePt-B layer. In addition to the bilayer approach, we directly perform the Ar plasma treatment on the FePt-C (28 vol%) (7 nm) film, followed by the deposition of an additional FePt-C (4 nm) layer. The TEM image reveals columnar grains, indicating the post plasma treatment can promote the aspect ratio by removing the C accumulation.

WE.D.2_O2 - Reduction in switching field of perpendicularly magnetized L10-FePt nanodots exchange-coupled with soft magnetic Ni81Fe19 under RF field application

W. Zhou¹, T. Seki¹, H. Imamura², H. Arai², K. Takanashi¹

1. *Institute For Materials Research, Tohoku University, Japan*

2. *National Institute of Advanced Industrial Science and Technology, Japan*

In order to continue the everlasting increase of magnetic storage density, magnetic materials with high uniaxial magnetic anisotropy (K_u), e.g. L10-FePt, are indispensable to maintain the thermal stability of magnetization in nanoscale. On the other hand, to solve the writability problem due to high K_u , Seki et al. proposed an effective switching method called spin wave-assisted switching [1]. The exchange-coupled bilayer film consisting of a Permalloy (Ni81Fe19; Py) and an in-plane magnetized L10-FePt showed a spatially twisted magnetic structure, and the magnetization of hard magnetic L10-FePt was switched at a low magnetic field by exciting the spin wave in the soft magnetic Py. For practical applications, however, it is important to demonstrate the spin wave-assisted switching in a perpendicularly magnetized configuration, which is the purpose of this study. In this study, perpendicularly magnetized L10-FePt was exchange-coupled with Py. The exchange-coupled film was microfabricated into dots with a diameter around 260 nm, in order to reduce the out-of-plane demagnetizing field and form spatially twisted magnetic structures [2]. A coplanar waveguide and a signal generator were utilized to apply an RF field to the microfabricated dots. The switching fields of the FePt (H_{sw}) were evaluated from the anisotropic magnetoresistance curves. In case of no RF field, the resistance change was observed due to the twisted magnetic structure, and H_{sw} was obtained to be more than 8 kOe. When an RF field of 176 Oe was applied, no significant reduction of H_{sw} was observed with the RF frequency (f) from 6 to 10 GHz. However, H_{sw} was reduced to about 3 kOe at $f = 11$ GHz, which is attributable to the excitation of spin wave in Py.

References:

[1] T. Seki, et al., Nat. Commun., 4, 1726 (2013)

[2] W. Zhou, et al., J. Appl. Phys., 117, 013905 (2015)

WE.D.2_O3 - Free layer effective anisotropy thickness in high TMR top and bottom pinned perpendicular magnetic tunnel junctions

J. Swerts¹, S. Mertens¹, T. Lin¹, S. Couet¹, Y. Tomczak¹, E. Liu¹, W. Kim¹, G. Sankar Kar¹, S. Van Elshocht¹, A. Furnemont¹

1. Imec, Leuven, Belgium

Thermal stability of the free layer to ensure data retention is one of the key challenges for sub-20 nm spin-transfer-torque MRAM with perpendicular magnetic tunnel junctions (pMTJ). We have studied the impact of the position of the [Co/Pt]-based synthetic antiferromagnetic (SAF) on the effective anisotropy thickness ($k_{\text{eff}} \cdot t$) of the free layer and the tunnel magnetoresistance (TMR) in a CoFeB/MgO/CoFeB-based pMTJ. The stacks were deposited by PVD in a 300 mm Canon-Anelva EC7800 on smoothed Ta-based bottom electrodes (BE) (rms roughness ~ 0.05 nm) and they received a 300°C crystallization anneal. The TMR was measured by current in-plane tunneling and the $k_{\text{eff}} \cdot t$ of the free layer in the thickness range of 0.9 nm-1.5 nm by vibrating sample magnetometry. In the case of the top pinned (TP) stack, i.e. [Co/Pt]-SAF on top of the MTJ, $k_{\text{eff}} \cdot t$ values as high as 0.45 erg/cm² were obtained whereas in the case of the bottom pinned (BP) stacks, the maximum in $k_{\text{eff}} \cdot t$ was 0.25 erg/cm². The TMR of the TP stack reaches values up to 150 % at area resistance of 5 Ohm \cdot Åm² whereas the BP stack reaches TMR values up to 130 %. The roughness induced by the BP SAF at the MgO level reduces the TMR [1]. When reducing the roughness in the BP stack, the TMR increases up to 150 %, but the $k_{\text{eff}} \cdot t$ does not increase significantly. Besides, TP pMTJ's deposited on non-smoothed BE (rms roughness 0.6 nm) do not reveal a decrease in free layer $k_{\text{eff}} \cdot t$. That indicates that the deposition sequence, i.e. MgO on top of CoFeB in the TP case and CoFeB on top of MgO in the BP case, strongly influences the MgO-CoFeB interfacial properties, and thus leads to different free layer $k_{\text{eff}} \cdot t$ values.

References:

[1] G. Kar et al., IEDM 2014

WE.D.2_O4 - Layer-selective switching of a double-layer perpendicular magnetic nanodot using microwave-assisted switching technique

H. Suto¹, T. Nagasawa¹, K. Kudo¹, T. Kanao¹, K. Mizushima¹, R. Sato¹

1. Corporate Research & Development Center, Toshiba Corporation, Kawasaki, Japan

Increasing the recording density of hard disk drives by the conventional scheme of shrinking magnetic data bits is expected to reach the superparamagnetic limit. Given these circumstances, three-dimensional (3D) magnetic recording with multiple recording layers has been proposed. The implementation of 3D recording requires a writing method that can selectively switch the magnetization in a specific recording layer. In this study, we report the first experimental demonstration of layer-selective switching by means of microwave-assisted magnetization switching (MAS). We fabricated magnetic tunnel junction (MTJ) nanodot (200×200 nm) comprising two Co/Pt-multilayer-based perpendicular magnetic layers, a MgO barrier, and two in-plane magnetic layers. The lower perpendicular layer (LL) has higher perpendicular anisotropy than the upper perpendicular layer (UL), and they are antiferromagnetically coupled. The dipolar interaction and antiferromagnetic coupling between the LL and UL is weak enough to allow them to take down or up states individually. The in-plane magnetic layers serve to detect the switching of the LL and UL through the magnetoresistive effect. They are antiferromagnetically coupled to cancel the stray fields and pinned by an antiferromagnetic layer. By applying a perpendicular magnetic field to this sample with both the LL and UL magnetizations being down, the UL reverses first because of its smaller anisotropy. By simultaneously applying an in-plane microwave field, the following complex switching behavior appears. When the microwave frequency is low, the UL still reverses first. As the frequency increases, the UL switching field gradually decreases and then suddenly increases. By further increasing the frequency, the LL starts to reverse stochastically, and in a certain frequency range, selective switching of the LL is realized without fail, showing that MAS can realize layer-selective switching by tuning a microwave frequency. This work was supported by Strategic Promotion of Innovative Research and Development from Japan Science and Technology Agency, JST.

WE.D.2_O5 - Multi-bits memory cell using degenerated magnetic states in a synthetic antiferromagnetic reference layer

A. Fukushima¹, K. Yakushiji¹, M. Konoto¹, H. Kubota¹, H. Imamura¹, S. Yuasa¹

1. *National Institute of Advanced Industrial Science and Technology (AIST), Tsukuba, Japan*

A new concept of multi-bits magnetic memory cell is represented. The multi-bits is realized by combining a freedom of the magnetic free layer and that in the antiferromagnetically coupled reference layer in the perpendicularly magnetized magnetic tunnel junction (p-MTJ) [1]. The structure of the reference layer is (FeB/Ta/[Co/Pt]₃)/Ru/([Co/Pt]₆); the top and the bottom layer are coupled by Ru layer where the reference layer has two degrees of freedom of a head-to-head and a bottom-to-bottom magnetic configuration. A four-state memory cell is realized by combination of both freedom.

However, the states in the reference layer hardly detected by the whole magnetoresistance of the p-MTJ because the magnetoresistance change in the reference layer is negligible small. That means the resistance values are degenerated and two different minor loops exist depending on the different magnetic states in the reference layer. On the other hand, the two minor loops have different switching fields due to the different stray field at the free layer depending on the magnetic configuration of the reference layer.

These magnetic states in the reference layer can be differentiated by the two-step read-out, before and after applying a proper pulse-magnetic field which can identify the initial state in the reference layer. This method is similar to distinguishing different magnetic states in an in-plane magnetized spin-valve element [2]. We demonstrated that four different states in the p-MTJ can be distinguished by the two-step read-out. Unlike conventional multi-level MTJ cells [3], this method is a destructive read-out which means the half of initial states will be changed during the read-out. However, this method can assure practically large operation margins which is the same of that of a single MTJ at a little cost of operation speed.

References:

- [1] K. Yakushiji *et al.*, Applied Physics Express 6 (2013), 113006
- [2] Z. Wang and Y. Nakamura, Journal of Applied Physics 79 (1996), 6639
- [3] K. Tsunoda *et al.*, IEDM Tech. Dig. (2013), 3.3

WE.D.2_I6 - Heat-Assisted Magnetic Recording - Turning Plasmonics and FePt Media into a Product

B. Stipe¹, T. Matsumoto¹, S. Burgos¹, G. Parker¹, M. Grobis¹, B. Terris¹

1. HGST, A Western Digital Company, San Jose, United States

Heat Assisted Magnetic Recording (HAMR) has the potential to revolutionize the way data is written in HDDs by using a plasmonic antenna to focus near-field radiation from a laser onto a recording disk. The resulting heating of an ultra-high anisotropy and small-grain recording media (such as FePt ordered alloy) defines the location of the written bits and, in principle, allows for dramatically higher storage densities compared to conventional recording. In a typical HAMR head design, a waveguide delivers light from a laser diode to a plasmonic aperture or antenna located at the air-bearing surface. The plasmonic device creates an intense optical pattern in the near-field, heating the disk at the nanometer scale. We have previously shown a head design with a plasmonic transducer, called the “E-antenna” fabricated at the end of a waveguide and then used it for recording on granular media with spinstand and on patterned media with a static tester at up to 1 Tb/in² [1]. An alternative design, called the “nanobeak” has also been described by us [2]. In this talk, we will explain some of the main challenges remaining before commercialization of HAMR can occur, especially in the areas of antenna reliability and areal density improvement.

WE.E.1_I1 - Spin to charge current conversion in metal/oxide interfacesY. Otani^{1,2}, Y. Niimi^{1,2}, K. Kondou², S. Karube^{1,2}

1. ISSP University of Tokyo, Tokyo, Japan

2. RIEN-CEMS, Wako, Japan

Spin Hall effects are commonly utilized as a means to interconvert between charge- and spin-currents. As an alternative mechanism for this interconversion, Rashba-type spin splitting at the Bi (111)/Ag interface was recently used to perform the spin to charge conversion called inverse Rashba-Edelstein (IRE) effect [1].

We here demonstrate that the similar spin to charge conversion can be achieved by using nonmagnetic metal/oxide interfaces. The device typically consists of e-beam deposited Ni₈₀Fe₂₀(Py)(5nm)/Cu(15nm)/Bi₂O₃(10nm) trilayer structure with a dimension of 5 μm wide by 3 mm long. The ferromagnetic resonance (FMR) of Py layer was excited by a 9 GHz microwave using the coplanar wave guide with applying external magnetic fields, so that FMR of the Py layer induces the spin pumping to the adjacent Cu layer through which spin currents flow towards Cu/Oxide interface accross a Cu layer, and are converted into charge currents. This is clearly observed as characteristic absorption peaks at the resonance field in the dc voltage spectrum. In contrast the Py/Cu bilayers prepared as a reference exhibit no peaks at the resonance field in the dc voltage spectrum, indicating this conversion is due to the presence of the Bi₂O₃ layer. We have studied both Cu and Bi₂O₃ thickness dependences and found the conversion efficiency λ_{IRE} exhibited the Cu thickness dependence via the quality of a Cu layer which varies as a function of the thickness. Rashba parameter α_R was estimated to be -0.3 eVÅngstrom, about 30% of the reported value for Bi/Cu(111) interface [2]. Spin absorption experiments [3] also support the presence of spin to charge conversion in the Cu/Bi₂O₃ bilayer.

References:

- [1] J.C. Rojas Sánchez *et al*, Nature Commun. 4, 2944 (2013).
- [2] I. Gierz *et al*, Phys. Rev. B, 81, 245430 (2010).
- [3] Y. Niimi *et al*, Phys. Rev. Lett. 106, 126601 (2011).

WE.E.1_O2 - Magnetic characteristics of CoPd and FePd antidot arrays on nanoporated Al₂O₃ and TiO₂ Templates

A.Maximenko^{1,2}, M. Marszalek¹, J. Fedotova², A. Zarzycki¹, Y. Zabala¹, B. Jany³, F. Krok³

1. *The Henryk Niewodniczanski Institute of Nuclear Physics Polish Academy of Sciences, Krakow, Poland*
2. *Research Institute for Nuclear Problems of Belarusian State University, Minsk, Belarus*
3. *Institute of Physics, Jagiellonian University, Krakow, Poland*
4. *The Henryk Niewodniczanski Institute of Nuclear Physics Polish Academy of Sciences, Krakow, Poland*

Hard magnetic antidot arrays (AA) show promising results in the context of implementation in percolated perpendicular media designing. In this work the technology of hard magnetic FePd and CoPd AA fabrication is presented and correlation between surface morphology, structure and magnetic properties is discussed.

For the first time CoPd AA were fabricated by deposition of Co/Pd MLs on nanoporous TiO₂ grown on Ti foil and Si wafers. SEM images indicated that morphology of antidots on the TiO₂/Si is flattened as compared to antidots on the TiO₂/Ti. Therefore improved magnetic characteristics of antidots are discussed with respect to the morphology of initial TiO₂ template. XRR and XRD revealed at Co/Pd MLs interface a presence of Co_xPd_{1-x} quasi-alloy with stoichiometry and grain sizes dependent on the template type. Systematic analysis of magnetization curves evidenced perpendicular magnetic anisotropy. Coercive field enhancement and change of magnetization reversal mechanism from domain wall motion for continuous films to incoherent rotation for AA is associated with pinning of magnetic moments on antidots.

The FePd AA were formed on porous anodic aluminium oxide templates with bowl-shape cell structure with inclined intercellular regions. FePd ordered L10 structure was confirmed by XRD analysis after successive vacuum annealing of MLs at temperatures 530oC and 600oC. Angular dependencies of magnetization curves showed that continuous FePd film had in-plane magnetic anisotropy, while FePd AA revealed isotropic magnetic properties due to increased contribution of out-of-plane oriented magnetic moments. MFM images of antidots showed more complicated contrast, with dark nanodots and bright nanospheres. Thus, MFM measurements confirmed that in FePd AA the enhancement of out-of-plane magnetization component can be associated with complex distribution of magnetic moments due to developed surface topography.

WE.E.1_O3 - Nuclear Resonant GISAXS: Spatially resolved magnetic ordering and magnetization reorientation in a Fe film with periodically varying thickness.

D. Erb³, K. Schlage¹, L. Bocklage¹, R. Ruffer², H. C. Wille¹, R. Röhlsberger¹

1. *Deutsches Elektronen-Synchrotron DESY, Hamburg, Germany*

2. *European Synchrotron Radiation Facility ESRF, Grenoble, France*

3. *University of Hamburg, Hamburg, Germany*

We propose to merge Grazing Incidence Small Angle X-ray Scattering (GISAXS) [1] and Nuclear Resonant Scattering (NRS) [2] into a new method providing the magnetic information obtained from NRS with the in-plane spatial resolution of GISAXS. The nuclear resonant signal (carrying the magnetic information) undergoes the same scattering in q-space as the electronic signal (carrying the structural information): photons scattered non-resonantly or resonantly from different structural units of the film are separated due to the sample morphology and can be detected at different positions in the scattering pattern. To demonstrate this principle, we fabricated a sample, in which structural and magnetic heterogeneity are correlated: A substrate with parallel surface facets was prepared by heat treatment of M-plane sapphire. Sputter deposition of ⁵⁷Fe onto this substrate under non-normal incidence resulted in a continuous hardmagnetic ⁵⁷Fe film consisting of stripe-like regions with periodically varying thickness: Thicker film regions on the facet surfaces facing the sputtering source alternate with thinner film regions on the facet surfaces avert from the source. We investigated this sample in-situ during ⁵⁷Fe film growth and studied its response to external magnetic fields ex-situ. During film growth we observed the onset of ferromagnetic first in the thicker regions, then in the thinner regions. Upon applying an external magnetic field the magnetic moments in thick and thin regions are displaced from the easy axis of magnetization to different extents. [3] Thus we have demonstrated that nuclear resonant GISAXS can be a feasible method for obtaining information about the magnetic state of individual parts of a magnetically heterogeneous sample.

References:

[1] G. Renaud, R. Lazzari, and F. Leroy, *Surface Science Reports* 64 (2009) 255

[2] R. Röhlsberger, *Springer Tracts in Modern Physics* 208 (2004)

[3] D. Erb, Ph.D. thesis, University of Hamburg (2014)

WE.E.1_O4 - Towards magnetic tomography of 3D structures at the nanoscale

C. Donnelly^{1,2}, M. Guizar-Sicairos², V. Scagnoli^{1,2}, M. Holler², T. Huthwelker², A. Menzel², I. Vartiainen², E. Mueller², E. Kirk^{1,2}, S. Gliga^{1,2}, J. Raabe², L.J. Heyderman^{1,2}

1. *Laboratory for Mesoscopic Systems, Department of Materials, Zurich, Switzerland*

2. *Paul Scherrer Institute, Villigen, Switzerland*

Significant developments in a variety of fields including biology, photonics and magnetism have been achieved thanks to recent advances in fabrication techniques to create mesoscopic 3D structures [1, 2]. Further progress in these areas benefits from their full quantitative and structural characterization. We use resonant ptychographic tomography, combining quantitative hard X-ray phase imaging and resonant elastic scattering to achieve ab initio element-specific 3D characterization of a cobalt-coated artificial buckyball polymer scaffold at the nanoscale. By performing ptychographic X-ray tomography at and far from the Co K edge, we are able to locate and quantify the Co layer in our sample to a 3D spatial resolution of 25 nm [3]. With a quantitative determination of the electron density we can determine that the Co layer is oxidized, which is confirmed with microfluorescence experiments. Resonant ptychographic tomography enables element-specific characterization, which can be extended to many elements within a sample by taking additional measurements at their corresponding absorption edges. This combination of tomography with resonant scattering opens the door to the full determination of 3D electronic and magnetic functionality of materials, spatially resolved at the nanoscale.

References:

- [1] G. von Freymann et al., *Advanced Functional Materials* 20, 1038 (2010)
- [2] B. J. Nelson, I. K. Kaliakatsos and J. J. Abbott, *Annual Review of Biomedical Engineering* 12, 55 (2010)
- [3] C. Donnelly et al. *Phys. Rev. Lett.* 114, 115501 (2015)

WE.E.1_05 - Anisotropic magnetic-field-induced phase transition in MnAs nanoribbons

L.B. Steren^{1,2,3}, F. Fernández Baldis^{2,3,4}, M. Sirena^{2,4}, V.H. Etgens⁵, M. Eddrief⁵, C. Ulysse⁶, G. Faini⁶

1. *Centro Atómico Constituyentes, San Martín, Argentina*
2. *Consejo Nacional de Investigaciones Científicas y Técnicas, Buenos Aires, Argentina*
3. *Laboratorio Internacional Franco-Argentino en Nanociencias (LIFAN), Buenos Aires, Argentina*
4. *Centro Atómico Bariloche, Instituto Balseiro - CNEA & Univ. Nac. de Cuyo, Bariloche, Rio Negro, Argentina*
5. *Institut des NanoSciences de Paris, UPMC, Paris, France*
6. *LPN-CNRS, Route de Nozay, Marcoussis, France*

MnAs thin films are known to present a phase coexistence of regularly arranged ferromagnetic α and paramagnetic β stripes below the Curie temperature, when grown onto GaAs(100) substrates. The observation of the effect in nanostructures whose sizes matched the characteristic length of the α / β arrays allowed us to tune the phase coexistence regime by changing different parameters. In our work, we report the observation of a magneto-structural phase transition induced by magnetic field on MnAs nano-ribbons. The transformation of high-resistance paramagnetic regions into low-resistance ferromagnetic ones explains the sharp resistivity drops that are observed when critical magnetic fields are applied to the samples. The critical field required to induce the phase transition in MnAs, depends of the magnetic history and the temperature. As the temperature of the system increases, higher fields are needed to stabilize the ferromagnetic phase. The phenomenon is hysteretic, highly anisotropic and size dependent.

We show that confinement effects in MnAs ribbons produce extraordinary features in the field dependence of the MR. Our results highlights and provides with unique evidences of the magnetic-field phase-induced transition and its characteristics.

WE.E2_I1 - Towards computational design of correlated materials

R. Valenti¹

1. Goethe University Frankfurt, Frankfurt, Germany

The combination of ab initio density functional theory with dynamical mean field theory (DFT+DMFT) has been proven to be a powerful approach for describing correlation effects in solid state systems at the microscopic level.

In this talk we will focus on recent progress on this method and its application to known unconventional superconductors such as Fe-pnictides, or organic charge-transfer salts as well as use its predictive power for possible new correlated Dirac metals [1,2,3,4].

References:

- [1] I. I. Mazin et al. Nature Communications 5, 4261 (2014)
- [2] S. Backes et al. New J. Phys. 16, 083025 (2014)
- [3] D. Guterding et al. Phys. Rev. B 91, 041112(R) (2015)
- [4] J. Ferber et al. Phys. Rev. B 89, 205106 (2014)

WE.E2_O2 - Impact of electronic correlations on the equation of state and transport in the epsilon phase of iron

L. Poyurovskiy¹, J. Mravlje², M. Ferrero¹, O. Parcollet³, I. Abrikosov⁴

1. CPHT-Ecole Polytechnique, Palaiseau, France
2. Josef Stefan Institute, Ljubljana, Slovenija
3. IPhT, CEA, Gif-sur-Yvette, France
4. IFM, University of Linköping, Linköping, Sweden

We have studied theoretically the ferromagnetic cubic alpha and paramagnetic hexagonal epsilon phases of iron using a fully self-consistent ab initio dynamical mean-field theory (DMFT) approach. The equilibrium volumes, bulk moduli, equations of states of both phases, as well as the volume change across the alpha-epsilon transition and transition pressure are obtained in close agreement with experiment. A remarkable improvement is obtained for the epsilon phase, which bulk modulus is strongly overestimated within the standard density-functional-theory framework. A significant magnitude of DMFT corrections in epsilon-Fe is due to rather strong local dynamical correlations in this phase as evidenced by a drastic reduction of the calculated quasiparticle lifetime and enhancement of the effective mass across the alpha-epsilon transition. The calculated electron-electron-scattering contribution to resistivity consequently undergoes a step-wise increase across this transition, as observed in experiment. The calculated magnitude of the jump is, however, significantly underestimated pointing out to probable importance of non-local correlations. The implications of our results for the superconductivity and non-Fermi-liquid behavior of epsilon-Fe are discussed.

WE.E2_O3 - A new tool for analysing systems immersed in a magnetic field: the metric space approach to quantum mechanics

P. Sharp¹, I. D'Amico¹

1. University of York, Heslington, United Kingdom

Systems subject to external magnetic fields are not simply characterized by their particle densities or their wavefunction, as even their ground states may display a finite current. Current Density Functional Theory (CDFT) is the extension of Density Functional Theory (DFT) for systems subject to external magnetic fields. The core theorem of CDFT, prescribes that ground state wavefunctions are characterized uniquely only by knowledge of both the particle density and the paramagnetic current density (and vice versa).

The metric space approach to quantum mechanics is a new method analysing quantities of physical interest [1]. It is based on deriving from conservation laws 'natural' metrics for quantum mechanical quantities of physical interest, in our case wavefunctions and particle and paramagnetic current densities [2]. We demonstrate the power of this approach by considering many-body systems immersed in a magnetic field, with a finite ground state current. We characterize ground states through the mapping at the core of CDFT between wavefunctions and particle and paramagnetic current densities. This is shown to be a mapping between metric spaces associated to these quantities. We find there are regions of allowed and forbidden distances, a 'band structure' in metric space which directly arises from the conservation of the z-component of the angular momentum. We analyse this band structure both for systems with varying magnetic fields and for systems with a fixed magnetic field but varying confinement potential. In addition, in metric spaces and for the systems considered, the relevant mappings at the core of CDFT display distinctive signatures, including (piecewise) linearity at short and medium distances.

We argue that the uncovered features of the mappings could be used to build or test (single-particle) approximate solutions to many-body problems, e.g., within CDFT schemes.

References:

[1] I. D'Amico, et al. PRL 106, 050401 (2011)

[2] P. M. Sharp and I. D'Amico, PRB 89, 115137 (2014)

WE.E2_O4 - Nonequilibrium transport at a dissipative quantum phase transition

C. H. Chung^{1,2}, K. Le Hur^{3,4}, G. Finkelstein⁵, M. Vojta⁶, P. Woelfle^{7,8}

1. *Department of Electrophysics, National Chiao-Tung University, HsinChu, Taiwan*

2. *Physics Division, National Center for Theoretical Sciences, HsinChu, Taiwan,*

3. *Center for Theoretical Physics Ecole Polytechnique and CNRS, Palaiseau, France*

4. *Department of Physics and Applied Physics, Yale University, New Haven, Connecticut, United States*

5. *Department of Physics, Duke University, Durham, North Carolina, United States*

6. *Institut fuer Theoretische Physik, Technische Universitaet Dresden, Dresden, Germany*

7. *Institut fuer Theorie der Kondensierten Materie, KIT, Karlsruhe, Germany*

8. *Institut fuer Nanotechnologie, KIT, Karlsruhe, Germany*

The new theoretical development on quantum criticality out of equilibrium is studied in a paradigmatic dissipative resonant-level quantum dot subject to a voltage bias. A detailed derivation of a rigorous mapping of our system onto an effective Kondo model is presented. A controlled energy-dependent renormalization-group approach is applied to compute the nonequilibrium current in the presence of a finite bias voltage V . In the linear-response regime V close to 0, the system exhibits as a function of the dissipative strength a localized-delocalized quantum transition of the Kosterlitz-Thouless (KT) type. Fundamental issues are addressed: Does the bias voltage play the same role as temperature to smear out the transition? What is the scaling of the nonequilibrium conductance near the transition? At finite temperatures, we show that the conductance follows the equilibrium scaling for $V < T$, while it obeys a distinct nonequilibrium profile for $V > T$. Our results have direct relevance to experiments on a quantum dot coupled to a resistive environment, such as H. Mebrahtu et al., [Nature (London) 488, 61 (2012)].

References:

[1] Chung-Hou Chung, Karyn Le Hur, Gleb Finkelstein, Matthias Vojta, and Peter Woelfle, Phys. Rev. B 87, 245310 (2013)

[2] Chung-Hou Chung, Karyn Le Hur, Matthias Vojta, and Peter Woelfle, PRL, 102, 216803 (2009)

WE.E2_O5 - Unconventional superconductivity in the Hubbard and t-J models: Gutzwiller wave function solution

J. Kaczmarczyk^{1,2}, T. Schickling³, J. Bünemann³, J. Spałek²

1. *Institute of Science And Technology Austria, Klosterneuburg, Austria*

2. *Marian Smoluchowski Institute of Physics, Jagiellonian University, Krakow, Poland*

3. *Fachbereich Physik, Philipps Universität Marburg, Marburg, Germany*

The superconducting phase of the Hubbard and t-J models [1, 2] is analyzed within a novel diagrammatic expansion (DE-GWF) method [3]. The method allows one to treat Gutzwiller wave functions (GWF) with unprecedented accuracy. The lowest order of the method reproduces analytically [2] the Gutzwiller Approximation results. With the increasing order of the expansion the results of a truncated DE-GWF method converge to those of the variational Monte Carlo approach. Our method does not suffer from finite-size limitations, which allows us to study the Fermi surface deformations, i.e. nematic ('Pomeranchuk') phases, as well as their coexistence with superconductivity.

The low computational cost of our method allows constructing a detailed phase diagram for the superconducting phase in the Hubbard and t-J models [1, 2]. We obtain agreement with the experimental results: (i) the superconducting gap at the Fermi surface resembles d-wave only around the optimal doping and the corrections to this state are shown to arise from the longer range of the pairing; (ii) the nodal Fermi velocity is almost constant as a function of doping and agrees semi-quantitatively with the experimental results; (iii) the superconducting transition is driven by the kinetic-energy lowering for strong interactions.

It is possible to apply the method to more complicated model systems, e.g., periodic Anderson models, multi-layer Hubbard models, or multi-band Hubbard models. Work in all these directions is in progress. Also the study of non-local interactions and/or correlations should be feasible in the future.

References:

[1] J. Kaczmarczyk, J. Spałek, T. Schickling, J. Bünemann, Phys. Rev. B 88, 115127 (2013)

[2] J. Kaczmarczyk, J. Bünemann, J. Spałek, New J. Phys. 16 073018 (2014)

[3] J. Bünemann, T. Schickling, F. Gebhard, Europhys. Lett. 98, 27006 (2012)

WE.E2_O6 - Correlation-induced d-wave superconductivity within the Anderson-Kondo lattice model: A fully microscopic approach

J. Spałek^{1,2}, O. Howczak¹

1. Marian Smoluchowski Institute of Physics, Jagiellonian University, Krakow, Poland

2. Academic Centre for Materials and Nanotechnology, AGH University of Science and Technology, Krakow, Poland

We discuss the appearance of the d-wave superconductivity and its coexistence with magnetism within a fully microscopic Anderson-Kondo lattice model derived earlier [1]. The pairing originates from a competition between the Kondo interaction and the f-f superexchange.

We use the so-called statistically consistent Gutzwiller approximation [2]. The coexistence regimes of antiferromagnetism with superconductivity are determined and appear in the vicinity of the Kondo-insulating quantum critical point. We compare our results with those obtained in the Kondo-lattice limit, where the startling f-electrons are localized [3], as well as discuss the valence change [4] accompanying the onset of superconductivity.

References:

[1] O. Howczak, and J. Spałek, Anderson lattice with explicit Kondo coupling revisited: metamagnetism and the field-induced suppression of the heavy fermion state, *J. Phys.: Condens. Matter* 24, 205602 (2012) pp. 1-14; O. Howczak, J. Kaczmarczyk and J. Spałek, Pairing by Kondo interaction and magnetic phases in the Anderson-Kondo lattice model: Statistically consistent renormalized mean-field theory, in Special Issue: Quantum Criticality and Novel Phases, *Phys. Stat. Sol. B* 250, 609-614 (2013)

[2] M. M. Wysokinski, M. Abram, and J. Spałek, Ferromagnetism in UGe₂: A microscopic model, *Phys. Rev. B* 90, 081114(R) (2014); Criticalities in the itinerant ferromagnet UGe₂, *ibid.* 91, 081108(R) (2015)

[3] O. Bodensiek, R. Zitko, M. Vojta, M. Jarrell, and T. Pruschke, Unconventional Superconductivity from Local Spin Fluctuations in the Kondo Lattice, *Phys. Rev. Lett.* 110, 146406 (2013)

[4] S. Watanabe, A. Tsuruta, K. Miyake, and J. Flouquet, Magnetic-Field Control of Quantum Critical Points of Valence Transition, *Phys. Rev. Lett.* 100, 236401 (2008)

The work was partly supported by Grant TEAM from the Foundation for Polish Science (FNP) and by Grant MAESTRO, No.DEC-2012/04/A/ST3/00342 from the National Science Centre (NCN).

WE.E2_07 - Local-moment magnetism and heavy-fermion superconductivity

Q. Si¹

1. Rice University, Houston, United States

It is widely believed that quantum criticality underlies unconventional superconductivity in many antiferromagnetic heavy fermions. As such, these systems provide a prototypical setting to study (A) the nature of quantum criticality and (B) how it drives superconductivity. Major efforts in the community over the past decade have been devoted to addressing the first point (A). The central issue has been whether heavy fermion quantum criticality operates within the Landau framework, commonly referred to as being of the spin-density-wave type, or goes “beyond Landau”, in particular taking the form of Kondo destruction [1,2]. This talk will in part summarize the recent theoretical efforts along this direction. The developments above are just beginning to be taken into account in the studies about the second point (B). In particular, the Kondo destruction turns the quasiparticles on the entire Fermi surface to be critical, and it is important to study superconductivity beyond the BCS-Eliashberg approach. I will describe our recent development of the theoretical methods [3,4], which allowed the conclusion for lattice models [5] that the Kondo-destruction local quantum criticality promotes unconventional superconductivity. Implications for systems such as CeRhIn5 and CeCu₂Si₂ will be discussed.

[1] Q. Si et al, Nature 413, 804 (2001)

[2] P. Coleman et al., J. Phys.: Condens. Matt. 13, R723 (2001)

[3] J. H. Pixley, A. Cai, and Q. Si, Phys. Rev. B91, 125127 (2015)

[4] J. H. Pixley, L. Deng, K. Ingersent, and Q. Si, Phys. Rev. B (Rapid Commun.), in press (2015)

[5] J. H. Pixley et al., to be published (2015)

WE.F.1_I1 - A unified phase diagram of domain walls in 1d systems, ranging from strips to cylindrical wires

S. Jamet^{1,2}, N. Rougemaille^{1,2}, C. Thirion^{1,2}, J.C. Toussaint^{1,2}, O. Fruchart^{1,2}

1. Univ. Grenoble Alpes, Institut NEEL, Grenoble, France

2. CNRS, Institut NEEL, Grenoble, France

Domain wall (DW) motion under magnetic field or spin current is an important research topic. The knowledge of their micromagnetic inner structure is a prerequisite to understand their motion. The phase diagram of domain walls in flat strips is firmly established, with transverse and vortex walls. In wires (cylindrical or square) micromagnetism predicted either transverse or a new type of wall, called Bloch-point wall; experimental confirmations are only emerging. We provide analytical arguments together with numerical simulations (home-made FeeLLGood software) to sketch a unified phase diagram for a geometry ranging from flat strips to nanowires of (i) square and (ii) circular section. A major aim is to provide a simple view of the important features of DWs. To achieve this we order DWs in terms of their topology, and phase-transitions.

Transverse and vortex walls share the same topology, motivating the name transverse-vortex, with a flux of induction going across the structure (obtained through rotation by $\pi/2$ for a wire). The Bloch-point wall is of different topology, with magnetization essentially parallel to the surface at any location. Transition between these is of first order. We define indicators to quantify the few degrees of freedom such as an asymmetry and a curling, two features resulting from the driving force to decrease magnetostatic energy. For example, vorticity of magnetization around a given direction, either longitudinal or transverse, appears like a second-order transition when one or the two transverse dimensions are larger than circa seven times the dipolar exchange length. An asymmetry of the through-induction in transverse-vortex walls may appear when curling is not possible, eg for the already known transverse walls in flat and wide strips. Finally, analytical scaling laws were derived, eg for the length of walls in wires, scaling like radius squared.

References:

S. Jamet et al., in press (<http://fr.arxiv.org/abs/1412.0679>)

WE.F.1_O2 - Magnetic structure of core-shell iron-iron oxide nanowires

I. Ivanov¹, A. Alfadhel¹, M. Alnassar¹, M. Vazquez², J. Kosel¹

1. King Abdullah University of Science And Technology (KAUST), Thuwal, Saudi Arabia

2. Institute of Materials Science of Madrid, CSIC, Madrid, Spain

Over the past few years core-shell nanostructures have attracted considerable attention due to potential applications as multi-function materials in fields like nanomedicine, smart sensors or spintronics. In particular magnetite (Fe_3O_4) nanowires (NWs) are attractive for biomedical application due to their low-toxicity and biocompatibility. By creating Fe and Fe_3O_4 core-shell NWs, a tunable magnetic moment and controllable magnetic properties can be achieved, while at the same time a passivation layer is present. Polycrystalline and single crystal Fe NWs with 50 nm in diameter have been prepared by electrodeposition into alumina oxide membranes using two different aqueous solutions. NWs have been released from the membrane by dissolving the alumina. Core-shell iron-iron oxide structures have been fabricated by oxidizing the NWs in an oven at 150 °C for a time between 10 minutes and 72 hours in ambient atmosphere. To observe the evolution of the core-shell structure with annealing time, energy filtered TEM (EFTEM) together with electron diffraction analysis has been utilized. For the polycrystalline iron NWs, increasing the oxidation time results in a gradual decrease of the Fe core and an increase of the iron oxide shell thickness. After 24 hours, the oxidation is practically completed. In contrast, for the single crystal Fe NWs, the formation of the iron oxide shell is much slower. A maximum shell thickness of 12 nm was obtained after 72 hours of annealing time. In contrast to the Fe NWs, the magnetic reversal mechanism of core-shell NWs includes two separate regions, which correspond to the switching of the magnetite shell and the Fe core. Note that the oxidation process creates several pinning sites for domain walls along the polycrystalline core-shell NW. Therefore, the magnetic reversal process includes the formation of a multi-domain state, which remains after removing the field. The magnetic moment measured by electron holography is 2.0 T for the Fe core and 0.25 T for magnetite.

WE.F.1_O3 - Electron holography of magnetic states in cylindrical Co/Cu multilayered nanowires

N. Biziere¹, D. Reyes¹, B. Warot-Fonrose¹, T. Wade², C. Gatel¹

1. CEMES, UPR 8011 CNRS, Toulouse, France

2. LSI, UMR 7642 CEA/CNRS/Ecole Polytechnique, Ecole Polytechnique, Palaiseau, France

We present a complete structural and magnetic characterization of cylindrical Co/Cu multilayers performed combining Energy Filtered Transmission Electron Microscopy (EFTEM), electron holography and 3D micromagnetic simulations.

Nano-layers are grown by template synthesis from a single electrochemical bath. EFTEM allows for a precise geometrical and chemical characterization of the layers. We demonstrate a 10 % amount of Cu impurities in the Co. The layers are shown to grow tilted 10 to 20° about the perpendicular of the nanowire axis. The mean thickness of Co and Cu is 24 nm and 14 nm respectively with a mean diameter of 54 nm. Remanent magnetic states in Co layers are observed by electron holography with a 2 nm spatial resolution. 3D magnetic configurations are deduced from comparison of the experimental and calculated electron phase shift induced by the magnetization. Calculations are performed with OOMMF including structural parameters measured by EFTEM.

We demonstrate that the remanent magnetic states can exhibit two different configurations. The first one corresponds to an antiparallel coupling between the Co layer magnetizations. The second one corresponds to coupled magnetic vortices. We will show that the emergence of each remanent state depends upon the structural characteristic of the layers, with the possibility in some particular cases to switch from one configuration to the other by application of a saturation field in the appropriate direction. A quantitative analysis of the experimental electron phase shift allows determining that the magnetization and exchange values of the cobalt layers are around 15 % smaller than the bulk values, while the anisotropy is only 30 % of the bulk. This study proves the potential of electrodeposition for spintronic applications such as vortex based nano-oscillators.

WE.F.1_O4 - Magnetization reversal of a single modulated magnetic nanowire

C. Bran¹, E. Berganza¹, E. M. Palmero¹, R. P. del Real¹, A. Fraile Rodríguez², A. Asenjo¹, M. Vazquez¹

1. Instituto de Ciencia de Materiales de Madrid (ICMM)-CSIC, Madrid, Spain

2. Departament de Física Fonamental and Institut de Nanociència i Nanotecnologia (IN2UB), Universitat de Barcelona, Barcelona, Spain

The study of spin configuration of a modulated magnetic nanowire and the control over its magnetization reversal process becomes essential for the progress in advanced information storage, logic systems and sensing devices [1-2]. The modulated in diameter Co-based nanowires, electrodeposited into the pores of alumina membranes, have been released from the membranes and studied individually by HRTEM, MFM and XMCD-PEEM. The cylindrical modulated wires are formed by segments with diameters of around 150 nm, separated at every 400 nm by much shorter segments (modulations) with 170nm in diameter. The effect of competing anisotropies on the magnetic domain configuration is analyzed. CoFeCu nanowires present a bcc (110) crystalline structure, with a low magnetocrystalline anisotropy overcome by shape anisotropy, which redirects the magnetization along the nanowire axis. MFM and PEEM images show a strong magnetic contrast at the ends of the wire and a weaker contrast along the wires that seems to match the position of each modulation. Although the easy axis of the magnetization is along the axial direction and the remanent configuration is a single domain state, the magnetization of the nanowires is not homogeneous. The nanowires display contrast along the length due to increase of the stray field at the modulation regions. On the other hand, Co nanowires present hcp (110) crystalline structure with the easy axis of the magnetization perpendicular to the nanowire axis. The MFM and PEEM images show a more complex behavior indicating that, although a competition between anisotropies is expected, the magnetocrystalline anisotropy plays a dominant role in the magnetic domain configuration. Magnetic domains are formed all along the nanowire axis, in good agreement with micromagnetic simulations.

References:

- [1] D. A. Allwood, G. Xiong, C. C. Faulkner, D. Atkinson, D. Petit and R. P. Cowburn, Science, 309, 1688-1692 (2005)
- [2] S. Da Col, S. Jamet, N. Rougemaille, A. Locatelli, T. O. Montes, B. Santos Burgos, R. Afid, M. Darques, L. Cagnon, J. C. Toussaint, and O. Fruchart, Phys. Rev. B 89, 180405(R) (2014)

WE.F.1_O5 - Asymmetric spin wave propagation in thin films with Dzyaloshinskii-Moriya coupling

D. Cortés-Ortuño^{1,2}, N. M. Opazo-Damiani¹, R. Troncoso¹, R. Gallardo¹, [P. Landeros](#)¹

1. Departamento De Física, Universidad Técnica Federico Santa María, Valparaíso, Chile

2. Institute for Complex Systems Simulation, University of Southampton, Southampton, United Kingdom

We have developed a general theory that describes the spin wave spectra of ferromagnetic films with Dzyaloshinskii-Moriya interactions, either of bulk or interfacial nature. In agreement with recent experiments [1], we demonstrate that, in the case that a bias field saturates the film magnetization, the spin wave dispersion relation is asymmetric with wave vector inversion, for a variety of ferromagnetic films with Dzyaloshinskii-Moriya interaction (DMI) and different crystallographic classes [2]. It is also predicted that, for non-zero wave vectors, the resonance frequency and resonance field can increase or decrease depending on the spin wave vector orientation. We provide explicit formulae for the spin wave dispersion relation, for the spin-wave frequency asymmetry, as well as for the dynamic susceptibility tensor for a film under microwave excitation, which can be used to understand Ferromagnetic Resonance (FMR) as well as Brillouin Light Scattering (BLS) experiments in these classes of magnetic thin films. It is proposed that the measurement of the frequency asymmetry can be useful to obtain the strength (D) of the Dzyaloshinskii-Moriya interaction [2]. We also predicted that depending on relative angle between the magnetization and the wave-vector, the asymmetry could be observed or not depending on the type of DMI, which may be used to characterize such magnetic coupling. It is also expected that in the case that the magnetization is perpendicular to the plane of the film, the frequency asymmetry vanishes for every kind of DMI. For the case of interfacial DMI the frequency asymmetry is proportional to the sine of the angle between the magnetization and the wave-vector.

WE.F.2_I1 - Superconductivity in the layered iron-germanide YFe₂Ge₂

M. Grosche¹, K. Semeniuk¹, P. Reiss¹, J. Chen¹, Z. Feng², P. Logg¹, Y. Zou¹, G. Lampronti³

1. *Cavendish Laboratory, University of Cambridge, Cambridge, United Kingdom*

2. *London Centre of Nanotechnology, University College London, London, United Kingdom*

3. *Department of Earth Sciences, University of Cambridge, Cambridge, United Kingdom*

In the d-electron system YFe₂Ge₂, an unusually high Sommerfeld ratio of the specific heat capacity of order 100 mJ/(molK²) and a non Fermi-liquid power law temperature dependence of the electrical resistivity signal strong electronic correlations in an anomalous metallic state. Full resistive transitions, diamagnetic screening and heat capacity anomalies observed at the transition suggest that pure samples of YFe₂Ge₂ superconduct below 1.8 K [1]. DFT studies have put forward alternative proposals regarding the pairing mechanism in YFe₂Ge₂ [2].

The electronic structure and superconducting properties of YFe₂Ge₂ are discussed in the context of the closely related alkaline metal iron-arsenide superconductors (K/Rb/Cs)Fe₂As₂, which have similarly enhanced heat capacities as YFe₂Ge₂, and which have recently been shown to superconduct in the pressure-induced collapsed tetragonal structure [3].

References:

[1] Y. Zou et al, *Physica Status Solidi (RRL)* 8, 928 (2014)

[2] A. Subedi, *PRB* 89, 024504 (2014); D. J. Singh, *PRB* 024505, 89 (2014)

[3] J. J. Ying et al, *arXiv:1501.00330* (2015); Y. Nakajima et al., *PRB* 91, 060508(R) (2015)

WE.F2_O2 - Magnetic-field-induced Lifshitz transitions in heavy fermion materials

G. Zwicknagl¹

1. Institut F. Mathematische Physik, TU Braunschweig, Braunschweig, Germany

Recent results on the evolution with magnetic field of the Fermi surfaces in various Ce- and Yb-based heavy fermion compounds are reported. The heavy quasiparticles are calculated by means of the Renormalized Band method which explicitly accounts for the field-dependence of the g-factor enhancement and of the quasiparticle mass in a Kondo system [1]. The Zeeman splitting of the Kondo resonance induces a series of Lifshitz transitions. In YbRh₂Si₂, the theoretically predicted critical magnetic fields were shown to agree quantitatively with the positions of anomalies in transport properties [2,3]. Of particular interest is the influence of magnetic-field-induced Fermi surface transitions on Spin Density Wave instabilities as reflected in recent neutron scattering results.

References:

- [1] G. Zwicknagl, J. Phys.: Condens. Matter 23, 094215 (2011)
- [2] H. Pfau et al, Phys. Rev. Lett. 110, 256403 (2013); H. R. Naren et al, New J. Phys. 15, 093032 (2013)
- [3] A. Pourret et al., J. Phys. Soc. Jpn. 82 , 053704 (2013)

WE.F2_O3 - Fermi surface and upper critical field study of the ferromagnetic superconductor UCoGe under hydrostatic pressure

G. Bastien^{1,2}, G. Knebel^{1,2}, D. Aoki^{1,2,3}, S. Araki⁴, I. Sheikin⁵, J. Flouquet^{1,2}

1. Univ. Grenoble Alpes, INAC-SPSMS, Grenoble, France

2. INAC/SPSMS, CEA-Grenoble, Grenoble, France

3. IMR-Tohoku University, Oarai, Japan

4. Okayama University, department of physics, Okayama, Japan

5. Laboratoire Nationale des Champs Magnétiques Intenses, Grenoble, France

UCoGe is a ferromagnetic superconductor with a Curie temperature $T_C=2.7\text{K}$ and a superconducting transition temperature $T_{sc}=0.6\text{K}$. The Curie temperature decreases with pressure and vanishes at a critical pressure: $p_c=1\text{GPa}$ [1]. Superconductivity was observed both below p_c and above p_c with a maximum of T_{sc} just below the critical pressure. At ambient pressure in the ferromagnetic phase the upper critical field as a function of temperature shows an unusual upward curvature [2]. We report magnetoresistance and Hall effect measurements on UCoGe for field along the easy magnetization axis c as function of pressure in the ferromagnetic and paramagnetic states. At ambient pressure we observed several anomalies in the magnetoresistance and in the Hall effect for field up to 34T. These anomalies point to several Fermi surface instabilities as function of field. A clear signature of a Fermi surface reconstruction appears at $H=17\text{T}$ where a small quantum oscillation frequency is suppressed and a large frequency appears. Measurements of Shubnikov-de Haas oscillations under pressure up to 2.5 GPa indicate only a small evolution of Fermi surface properties with pressure. No Fermi surface reconstruction has been observed around the critical pressure p_c . Finally, the upper critical field of UCoGe for field along the c axis increases with pressure through the critical pressure p_c . The unusual upward curvature of the upper critical field is also enhanced above the critical pressure, while the ferromagnetic fluctuations are expected to be reduced.

References:

[1] E. Hassinger, D. Aoki, G. Knebel, J. Flouquet, J. Phys. Soc. Jpn. 77, 7, 073703 (2008)

[2] N. T. Huy, D. E. de Nijs, Y. K. Huang, and A. de Visser, Phys. Rev. Lett. 100, 077002 (2008)

WE.F2_O4 - NMR measurements on CeCoIn₅ /YbCoIn₅ superlattices: The interface state between heavy-fermion compound and normal metal

T. Yamanaka¹, M. Shimosawa², R. Endo¹, Y. Mizukami³, H. Shishido⁴, T. Terashima⁵, T. Shibauchi^{1,3}, Y. Matsuda¹, K. Ishida¹

1. Department of Physics, Kyoto University, Kyoto, Japan

2. Institute for Solid State Physics, the University of Tokyo, Tokyo, Japan

3. Department of Advanced Materials Science, the University of Tokyo, Tokyo, Japan

4. Department of Physics and Electronics, Osaka Prefecture University, Osaka Prefecture, Japan

5. Research Center for Low Temperature and Materials Science, Kyoto University, Kyoto, Japan

Recently, the technique of fabricating epitaxial superlattices consisting of heavy-fermion compounds and conventional metals has been developed and provides a new research field on f-electron systems[1,2]. For example, superlattice-superconductors CeCoIn₅/YbCoIn₅ show the strong enhancement of H_{c2}/T_c[2] where H_{c2} is superconducting upper critical field at T = 0 K and T_c is critical temperature. In these superlattices, the heterostructure would play a key role, but its magnetic and electronic properties are have not been explored at the microscopic level. To investigate the magnetic and electronic properties in each block-layer(BL) of the superlattices, we performed nuclear magnetic resonance(NMR) measurement, which is one of the most suitable microscopic probes, on the CeCoIn₅/YbCoIn₅ superlattices as well as the thin films of CeCoIn₅ and YbCoIn₅. By comparing the spectra of these samples, we succeeded in identifying the 115In NMR signals arising from the CeCoIn₅ and YbCoIn₅ layers in the superlattices, separately. We measured nuclear spin relaxation rate(1/T₁) in each BL, and found that 1/T₁ of Ce-BL is suppressed with decreasing thickness of Ce-BL, although 1/T₁ of Yb-BL is essentially unchanged with 1/T₁ of the YbCoIn₅ thin film. This suggests that each BL is isolated and the proximity of f-electron with magnetic moment to nonmagnetic Yb-BL is unlikely. In addition, we compared the NMR spectra obtained in superlattices with different thickness of Ce-BL, and identified 115In-NMR signals arising from interfaces of heterostructures. From the measurement of 1/T₁, we found that antiferromagnetic fluctuations are spatially varied along the c-axis even in the one Ce-BL.

References:

[1] H. Shishido, et al., Science 327, 980-983 (2010)

[2] Y. Mizukami, et al., Nature Phys. 7, 849 (2011)

WE.F2_O5 - RIXS investigations of charge excitations in Kondo-switching YbInCu₄

I. Jarrige¹, H. Yamaoka², N. Tsujii³, K. Ishii⁴, M. Upton⁵, D. Casa⁵, J. Kim⁵, T. Gog⁵, A. Kotani⁶, J. Hancock⁷

1. *Photon Sciences Directorate, Brookhaven National Laboratory, Upton, United States*
2. *RIKEN SPring-8 Center, Sayo, Hyogo, Japan*
3. *Quantum Beam Center, National Institute for Materials Science, Sengen, Tsukuba, Japan*
4. *Japan Atomic Energy Agency, Sayo, Hyogo, Japan*
5. *Advanced Photon Source, Argonne National Laboratory, Argonne, United States*
6. *Photon Factory, Institute of Materials Structure Science, High Energy Accelerator Research Organization, Tsukuba, Ibaraki, Japan*
7. *Department of Physics and Institute for Materials Science, University of Connecticut, Storrs, United States*

We present resonant inelastic X-ray scattering (RIXS) experiments investigating electronic structural changes in response to the unusual valence transition in YbInCu₄. This system features free local moment behavior above the transition ($T_v=42\text{K}$), and strongly screened moments below, implying an order-of magnitude change in the Kondo scale in response to changes in temperature. Our hard X-ray RIXS measurements at the L₃ edge of Yb are particularly sensitive to the itinerant states related to Yb 5d orbitals, and directly reveal the existence of a quasi-gap in the itinerant electronic band structure, as well as systematic shifts in spectral features implying movement of the Fermi level as the Yb valence changes. These observations highlight the central role of the itinerant gap influencing transition. Separate soft X-ray experiments at the M₅ edge are particularly sensitive to the localized Yb 4f orbital excitations, and give the first indication that the hybridization scale is apparent in these spectrum. These results, and pending order-of-magnitude improvements in the energy resolution of the RIXS technique portends a new day in the science of heavy fermions and valence fluctuating compounds.

References:

I. Jarrige, et al Physical Review Letters (accepted, February 2015)

WE.F2_06 - Classical and quantum criticalities in the itinerant ferromagnet UGe₂: A microscopic interpretation

M. Wysokinski¹, M. Abram¹, J. Spałek^{1,2}

1. Marian Smoluchowski Institute of Physics, Jagiellonian University, Krakow, Poland

2. Academic Centre For Materials and Nanotechnology, AGH University of Science and Technology, Krakow, Poland

We present [1,2] a microscopic interpretation of the complete magnetic phase diagram of the ferromagnetic superconductor UGe₂ as a function of applied magnetic field, pressure, and temperature, including its classical and quantum critical points. Our predictions are based on the Anderson Lattice Model tackled by the modified Gutzwiller approximation (SGA [3]). Appearance of two distinct ferromagnetic phases in our approach is associated with change of Fermi surface topology. Our predictions at temperature T=0 of magnetic and electronic properties compare favourably with the experimental findings of UGe₂ as seen in the neutron scattering, the magnetization data, and in the de Haas - van Alphen oscillations. For T>0, we provide a quantitative description of the all critical points observed in this compound [4], namely the critical ending point, the tricritical point, and the quantum critical ending point. Moreover, we propose that a new quantum critical point appears in close vicinity to the spin-triplet superconducting dome. We characterize it as a Lifshitz quantum critical point and suggest that it can be related to the appearance of quantum critical fluctuations near the Fermi-surface-topology instability, and hence is related to the onset of the spin-triplet superconductivity.

References:

- [1] M. M. Wysokinski, M. Abram, and J. Spałek, Ferromagnetism in UGe₂: A microscopic model, Phys. Rev. B 90, 081114(R) (2014)
- [2] M. M. Wysokinski, M. Abram, and J. Spałek, Criticalities in the itinerant ferromagnet UGe₂, Phys. Rev. B 91, 081108(R) (2014)
- [3] M. M. Wysokinski and J. Spałek, Properties of an almost localized Fermi liquid in an applied magnetic field revisited: a statistically consistent Gutzwiller approach, J. Phys.: Condens. Matter 26, 055601 (2014)
- [4] V. Taufour, D. Aoki, G. Knebel, and J. Flouquet, Pressure Dependence of the Magnetization in the Ferromagnetic Superconductor UGe₂, Phys. Rev. Lett. 89, 147005 (2010)

Support of the National Science Centre (NCN), Grant MAESTRO, No. DEC-2012/04/A/ST3/00342 and of the foundation for Polish Science (FNP), grant TEAM is acknowledged.

WE.F2_O7 - Symmetry of the excitations in the hidden order state of URu₂Si₂

M.A. Measson¹, J. Buhot¹, Y Gallais¹, A. Sacuto¹, M. Cazayous¹, D. Aoki², G. Lapertot²

1. *University Paris Diderot – CNRS, Paris, France*

2. *Univ. Grenoble Alpes / Tohoku University, Grenoble, France*

For three decades, the identity of the ordered phase, the so-called hidden order (HO), found in URu₂Si₂ at temperature below T₀=17.5 K has eluded researchers despite intensive experimental and theoretical investigations. We address here the question of the symmetry of the novel excitations emerging from the HO state, a key information to solve the long-standing question of its nature.

We have performed polarized electronic Raman scattering on URu₂Si₂ single crystals at low temperature down to 8 K in the hidden order state and under magnetic field up to 10 T. The hidden order state is characterized by a sharp excitation at 1.7 meV and a gap in the electronic continuum below 6.8 meV. Both Raman signatures are of pure Γ symmetry. By comparing the behavior of the Raman sharp excitation and the neutron resonance at Q₀=(0,0,1), we provide new evidence, constrained by selection rules of the two probes, that the hidden order state breaks the translational symmetry along the c axis such that Γ and Z points fold on top of each other. The observation of these distinct Raman features with a peculiar Γ symmetry as a signature of the hidden order phase places strong constraints on current theories of the hidden order in URu₂Si₂.

Symmetry of the Excitations in the Hidden Order State of URu₂Si₂

References:

Phys. Rev. Lett. 113 (2014) 266405. J. Buhot, M.-A. Measson, Y. Gallais, M. Cazayous, A. Sacuto, G. Lapertot, and D. Aoki

WE.G.1_I1 - Berry curvature, hall effect and topological edge modes of magnons

S. Murakami¹

1. Tokyo Institute of Technology, Meguro, Japan

In electronic systems, various interesting phenomena such as spin Hall effect, quantum Hall effect, and topological insulators originate from nonzero Berry curvature of Bloch wavefunctions. This Berry curvature is calculated from the Bloch wavefunction and characterizes a geometric aspect of the Bloch wavefunction in k-space. We theoretically pursue analogous phenomena for magnons (spin waves). Such phenomena for magnons require some sorts of spin-orbit coupling. While it was known previously that the Dzyaloshinskii-Moriya interaction plays this role, we proposed that the dipolar interaction also gives rise to nonzero Berry curvature. If we consider only the dipolar interaction in a thin-film ferromagnet in a long-wavelength regime, we can calculate an analytic form of the Berry curvature for each magnonic band, and only the magnetostatic forward volume-wave modes (i.e. magnetic field being out-of-plane) have a nonzero Berry curvature. When the exchange coupling is included, the magnonic bands are modified, and there occur a number of band anticrossing points. Around such an anticrossing point, the Berry curvature is enhanced. This Berry curvature gives rise to thermal Hall effect of magnons, and it also gives rise to a shift of wavepackets in reflection or refraction. We explain some experimental attempts to measure this shift. In analogy to the quantum Hall effect and topological insulators for electrons, we can design the magnon band structure to make it topological. By introducing some artificial spatial periodicity into the magnet, for example by fabricating nanostructures with two different magnets in a periodic structure or by making a periodic array of nanomagnets, we theoretically propose emergence of topological edge modes, analogous to the edge modes in electronic quantum Hall effect. The edge modes are chiral, and propagate along the edge of the magnet in one way. We call this a topological magnonic crystal.

WE.G.1_O2 - The inverse thickness proportionality of the interfacial Dzyaloshinskii-Moriya interaction on the Pt/Co(CoFeB)/Al₂O₃ inverse symmetry broken structure

J. Cho¹, N.H. Kim¹, S. Lee¹, J.S. Kim², R. Lavrijsen², A. Solignac², Y. Yin², D.S. Han², N. Hoof², H. Swagten², B. Koopmans², C.Y. You¹

1. Department of Physics, Inha University, Incheon, Republic of Korea

2. Department of Applied Physics, Center for NanoMaterials, Eindhoven University of Technology, Eindhoven, The Netherlands

In magnetic multilayer systems, a strong spin-orbit coupling at the interface between heavy metal and ferromagnetic layers can lead intriguing phenomena such as the perpendicular magnetic anisotropy (PMA), the spin Hall effect, the Rashba effect, and especially the interfacial Dzyaloshinskii-Moriya (IDM) interaction. The understanding of IDM interaction is important not only for the fundamental understanding of magnetic structure but also to spintronic applications based on the spin-orbit torque. Here, we demonstrate a novel experimental technique to observe the IDM interaction, so-called Brillouin light scattering (BLS). The non-reciprocal spin wave dispersions, systematically measured by BLS, allow determining the IDM energy densities. We fabricated Co and CoFeB thin film 1.0 to 3.0 nm, sandwiched Pt and Al₂O₃ layers using DC magnetron sputter. In order to precisely and systematically investigate this interface effect by means of BLS, two different methods (magnetic field dependence and incident angle dependence) as a function of the thickness of the Co and CoFeB are used. The quantitative magnetic layer thickness dependent measurements and careful analysis show the inverse proportionality of the frequency differences and confirm that the IDM interaction is indeed purely interfacial with maximum energy density of 1.2 (0.8) mJ/m² for 1.2-nm-thick Co (1.6-nm-thick CoFeB) with the Pt underlayer. Furthermore, two independent measurement methods, the magnetic field dependence and spin wave dispersion relations, allow us to confirm our results are free from artifacts such as different interface anisotropies of top and bottom interfaces.

WE.G.1_O3 - Deterministic magnetization switching driven by spin hall effect in ultrathin magnetic CoFeB/MgO heterostructures with tilted anisotropy

J. Torrejon^{1,2}, F. Garcia-Sanchez³, T. Taniguchi⁴, J. Sinha², S. Mitani², J.V. Kim³, M. Hayashi²

1. *Unité Mixte de Physique CNRS/Thales, Palaiseau, France*

2. *National Institute for Materials Science, Tsukuba, Japan*

3. *Institut d'Electronique Fondamentale, UMR CNRS 8622, Université Paris-Sud, Orsay, France*

4. *National Institute of Advanced Industrial Science and Technology (AIST), Spintronics Research Center, Tsukuba, Ibaraki, Japan*

In addition to conventional spin transfer torque (STT) [1,2], current-induced torques due to Rashba [3] and Spin Hall effects [4] (SHE) may open new paradigms for highly efficient magnetization reversal. In particular, the perpendicular magnetization switching by in-plane current in ultrathin ferromagnetic layer is attracting great interest owing to its potential for technological applications. However, the underlying mechanism of the switching process is yet to be identified. We report magnetization switching in wires (30 μm length and 5 μm width, respectively) patterned from CoFeB/MgO heterostructures with heavy metal (HM) underlayers: we focus in TaN underlayer however others HMs have been also explored (Hf, Ta and W). Using a Kerr microscopy, we study the threshold current needed to reverse magnetization as a function of pulse amplitude, pulse length and in-plane magnetic field. We observe distinct differences in the in-plane field dependence of the threshold switching current depending on the underlayer thickness. The STT is likely responsible for the switching for the thinner underlayer films whereas the SHE is the dominant mechanism for the thicker underlayer films. In the latter case, the switching process is asymmetric with respect to the initial magnetization state and the current direction. Such asymmetry cannot be explained by the action of the longitudinal (damping-like) and transverse (field-like) components of spin Hall torque. We find that the broken symmetry is ascribed to a slight tilt in the uniaxial anisotropy axis. The tilt develops during the film deposition process and strongly influences the magnetization switching with current[5]. Most importantly, the presence of such symmetry breaking anisotropy enables deterministic magnetization switching at zero external fields [5,6].

Acknowledgment: MEXT Grant-in-Aid, MEXT R & D Next-Generation Information Technology

References:

- [1] J. C. Slonczewski, JMMM 996. 159(1-2): p. L1-L7
- [2] J. A. Katine et al, PRL 2000. 84(14): p. 3149-3152
- [3] I. M. Miron et al, Nature 476, 189 (2011)
- [4] L. Liu et al, Science 336, 555 (2012)
- [5] J. Torrejon et al, arXiv:1410.7473 (2014)
- [6] L. You et al, arXiv: 1409.0620 (2014)

WE.G.1_O4 - Signatures of a two-dimensional ferromagnetic electron gas at the La_{0.7}Sr_{0.3}MnO₃ /SrTiO₃ interface arising from orbital reconstruction

M.J. Calderon^{1,2}, N.M. Nemes^{2,3}, J.I. Beltran^{1,3}, F.Y. Bruno^{2,3}, J. Garcia-Barriocanal^{2,3}, Z. Sefrioui^{2,3}, C. Leon^{2,3}, M. Garcia-Hernandez^{1,2}, M. C. Muñoz¹, L. Brey^{1,2}, J. Santamaria^{2,3}

1. Instituto de Ciencia de Materiales de Madrid, ICMM-CSIC, Madrid, Spain
2. Laboratorio de Heteroestructuras con aplicación en Spintronica, Unidad Asociada Consejo Superior de Investigaciones Científicas/Universidad Complutense Madrid, Madrid, Spain
3. Departamento de Física Aplicada III, Universidad Complutense de Madrid, Madrid, Spain

Electronic reconstruction at interfaces between different oxides is giving rise to a plethora of new functionalities and novel phenomena. Complex oxides are characterised by a strong interplay of the different degrees of freedom (orbital, spin and lattice) which can be engineered and modified at interfaces and surfaces. For instance, the interface between two insulating non-magnetic oxides (for instance, LaAlO₃ and SrTiO₃) can be metallic and ferromagnetic. Another example is that of heterostructures involving manganites, in which interfacial orbital and magnetic reconstructions can affect transport properties. This work constitutes a joint theoretical-experimental effort to understand the properties of a multilayer formed by a metallic ferromagnetic manganite oxide (La_{0.7}Sr_{0.3}MnO₃) and the insulating SrTiO₃. Magnetoresistance has been measured under a magnetic field which rotates with respect to the interface plane. In such a geometry, a peak in the magnetoresistance for a perpendicular magnetic field is expected and has been measured in other systems. However, our heterostructures also show an unexpected peak when the magnetic field is in plane. We have performed calculations of the resistivity in a model system which includes spin-orbit coupling. The results reveal that the unexpected in-plane maximum is due to transport through a two-dimensional ferromagnetic electron gas formed by orbital reconstruction at the manganite interface. These orbital and magnetic reconstructions are supported by X-ray linear dichroism and ab-initio calculations.

This work has been published in *Advanced Materials* 26, 7516 (2014).

WE.G.1_O5 - Spin-orbitronics: Investigation of the spin-to-charge current conversion by a topological insulator

J.C. Rojas-Sánchez^{1,2}, S. Oyarzun³, A. Marty³, C. Vergnaud³, G. Desfond³, S. Gambarelli³, M. Jamet³, Y. Ohtsubo⁴, P. Le Fèvre⁵, F. Bertran⁵, A. Taleb-Ibrahimi⁵, N. Reyren^{1,2}, J.M. George^{1,2}, A. Fert^{1,2}

1. *Unité Mixte De Physique CNRS/Thales, Palaiseau, France*

2. *Université Paris Sud, Orsay, France*

3. *CEA-Grenoble and Université Joseph Fourier, INAC, Grenoble, France*

4. *Graduate School of Frontier Biosciences, Osaka University, Osaka, Japan*

5. *Synchrotron SOLEIL, Gif sur Yvette, France*

We have used experiments of spin pumping by ferromagnetic resonance (FMR) to investigate the efficiency of the spin-to-charge current conversion (SCCC) by spin-orbit effects in different systems [1-4]. In 3D systems the SCCC can be obtained by the spin Hall Effect (SHE) and is then characterized by the dimensionless spin Hall angle, θ_{SHE} [1-3]. SCCC can also be obtained by the spin-orbit coupling of 2D surface or interface states, as in our recent experimental discovery of the Rashba-Edelstein Effect (REE) [4] at a Rashba interface. With 2D systems, the key parameter that accounts for the efficiency of the SCCC is a length, which is called λ_{REE} for the REE of Rashba states [4,5].

The largest effects with 2D systems can be anticipated from the exploitation of the surface states of topological insulators. However one fundamental question, which is not yet experimentally answered, concerns the protection of the topological character of surfaces states when other layers such as ferromagnetic or normal metal layers are placed in contact with the topological insulator. I will mainly focus on the case of the topological insulator α -Sn [6], and present our recent ARPES experiment at the Cassiopee beamline at Synchrotron Soleil where we attempted to address this question. I will then present results of spin pumping FMR experiments on the same set of samples demonstrating a highly efficient SCCC.

References:

- [1] J.-C. Rojas-Sánchez et al. PRL 112, 106602 (2014)
- [2] J.-C. Rojas-Sánchez et al. SPIE 9167, Spintronics VII, 916729 (2014)
- [3] P. Laczowski et al. APL 104, 142403 (2014)
- [4] J C Rojas Sánchez et al. Nat. Commun. 4:2944 (2013)
- [5] K. Shen et al. PRL 112, 096601 (2014)
- [6] Y. Ohtsubo et al., PRL 111, 216401 (2013)

WE.G2_I1 - Bulk magnon spin-current theory for the longitudinal spin-Seebeck effect

S. Rezende¹, R. Suárez², A. Azevedo¹

1. *Universidade Federal de Pernambuco, Recife, Brazil*

2. *Pontificia Universidad Católica de Chile, Santiago, Chile*

The longitudinal spin-Seebeck effect (LSSE) consists in the generation of a spin current parallel to a temperature gradient applied across the thickness of a bilayers made of a ferromagnetic insulator (FMI), such as yttrium iron garnet (YIG), and a normal metal (NM) such as platinum [1]. The LSSE can be detected by two effects: (1) A DC voltage generated along the NM layer due to the conversion of the spin current into a charge current perpendicular to the static magnetic field by means of the inverse spin Hall effect: (2) A change in the magnetic relaxation of the FMI measured by the linewidth of the ferromagnetic resonance absorption or by the attenuation of spin-wave packets propagating along the FMI film. Depending on the sign of the gradient the relaxation rate can be increased or decreased, leading in the latter case to an apparent amplification. We will present a model for the LSSE that relies on the bulk magnon spin current created by the temperature gradient across the thickness of the FMI [2]. We show that the spin current pumped into the NM layer by the magnon accumulation in the FMI provides continuity of the spin current at the FMI/NM interface and is essential for the existence of the LSSE. The results of the theory are in good agreement with experimental data for the variation of the DC voltage with the sample temperature and with the FMI layer thickness in YIG/Pt bilayers. The model also explains the observed control of the magnetic relaxation rate in YIG/Pt under a thermal gradient applied across the thickness of the bilayer.

References:

- [1] G. E. W. Bauer, E. Saitoh, and B. J. van Wees, *Nature Mat.* 11, 391 (2012)
- [2] S. M. Rezende et al., *Phys. Rev. B* 99, 014416 (2014)

WE.G2_O2 - Electric-field-induced magnetic anisotropy in a nanomagnet investigated on the atomic scale

J. P. Hermenau¹, A. Sonntag¹, A. Schlenhoff¹, J. Friedlein¹, S. Krause¹, R. Wiesendanger

1. University of Hamburg, Hamburg, Germany

One of the challenges in data storage applications is the control of magnetic anisotropy: To stabilize a magnetic bit against thermal magnetization reversal a large anisotropy is needed, while a low anisotropy is desired when writing information. A possible control mechanism could be the selective application of an electric field that has been shown to modify the surface anisotropy of magnetic thin films [1,2]. However, the influence on a single nano-scaled magnet is so far largely unexplored.

In our experiments we investigate the impact of the electric field by observing the thermally driven switching of an individual atomic-scale magnet with uniaxial magnetic anisotropy. The biased probe tip of a spin-polarized scanning tunneling microscope (SP-STM) allows to apply electric fields up to 6 GV/m to in-plane-magnetized Fe nanomagnets on W(110) consisting of about 100 atoms [3]. The telegraphic signal which reflects the magnetization reversals of the nanomagnet in the tunneling current of an SP-STM is recorded for different bias voltages. The analysis of the telegraphic signals shows that the electric field E can be used to increase or decrease the switching rate, depending on the sign of E . This is attributed to an electric-field induced anisotropy that favors in-plane magnetization for $E < 0$ and out-of-plane magnetization for $E > 0$. The interpretation is verified by changing from the in-plane Fe/W(110) to the out-of-plane Fe/Mo(110) system. [4] The results of our experiments reveal a method to control magnetic properties of individual nanomagnets without exploiting spin or charge currents.

References:

- [1] M. Weisheit et al., Science 315, 349 (2007)
- [2] T. Maruyama et al., Nat. Nanotechn. 4, 158 (2009)
- [3] S. Krause et al., Phys. Rev. Lett. 103, 127202 (2009)
- [4] A. Sonntag et al., Phys. Rev. Lett. 112, 017204 (2014)

WE.G2_O3 - Enhancement of rectified voltage using electric-field-induced ferromagnetic resonance under dc bias voltage

Y. Shiota^{1,2,3}, S. Miwa^{2,3}, S. Tamaru¹, T. Nozaki^{1,3}, H. Kubota^{1,3}, A. Fukushima^{1,3}, Y. Suzuki^{1,2,3}, S. Yuasa^{1,3}

1. AIST, Spintronics Research Center, Tsukuba, Ibaraki, Japan

2. Osaka Univ., Suita, Osaka, Japan

3. JST-CREST, Chiyoda-ku, Tokyo, Japan

Rectification of microwave using magnetic tunnel junction (MTJ) is the promising candidate for high sensitive microwave detector, as demonstrated in spin-torque diode. [1] However the high detection sensitivity has been observed under only a lower dc bias current than the destabilizing current of the free layer magnetization. In this study, we demonstrate enhancement of the rectified voltage using electric-field-induced ferromagnetic resonance (FMR) under a dc bias voltage, and achieved the high-output microwave voltage even in a large input rf power and a dc bias voltage. [2] An MTJ film was prepared by sputter deposition on thermally oxidized Si wafer: buffer layer/IrMn (10 nm)/Co₇₀Fe₃₀ (2.0 nm)/Ru (0.7 nm)/Co₁₆Fe₆₄B₂₀ (3.0 nm)/MgO (2.0 nm)/Co₁₆Fe₆₄B₂₀ (2.0 nm)/capping layer. The film was annealed at 300°C for 2.0 h in a 600-mT in-plane magnetic field, which defined the direction of exchange-bias on the pinned layer parallel to the long axis of MTJ pillars. We measured the homodyne detection voltage for the input RF frequency of 2.0 GHz as a function of external magnetic field with tilted angle from the film normal direction. Under zero bias voltage, the spectrum with anti-Lorentzian structure was observed in FMR excited by voltage-torque. Under bias voltage application of -1.0 V, the shape of spectrum changes from an anti-Lorentzian structure to a Lorentzian structure, and clear enhancement of the rectified voltage was observed. This can be understood by the non-linear effect due to the asymmetric magnetization-potential in the free layer. This work was partially supported by the Strategic AIST integrated R&D Program, gIMPULSE: Initiative for Most Power-Efficient Ultra-Large-Scale Data Exploration, and ImPACT Program of Council for Science, Technology and Innovation (Babinet Office, Government of Japan).

References:

- [1] S. Miwa et al., Nature Materials 13, 50 (2014)
- [2] Y. Shiota et al., Appl. Phys. Lett. 105, 192408 (2014)

WE.G2_O4 - Charge and strain control of interface magnetism

K. Dumesnil¹, M.R. Fittsimmons², N. Jaouen³, T. Maroutian⁴, J.M. Tonnerre⁵, B. Kirby⁶, B. Holladay⁷, E. Fohtung^{2,8}, E. Fullerton⁷, O. Shpyrko⁷, S. Sinha⁷, Q. Wang², A. Chen², Q. Jia²

1. Institut Jean Lamour, Université de Lorraine and CNRS, Nancy, France
2. Los Alamos National Laboratory, Los Alamos, United States
3. Synchrotron SOLEIL, Gif-sur-Yvette, France
4. Institut d'Electronique Fondamentale, Université Paris-Sud and CNRS, Orsay, France
5. Institut Néel, Université Grenoble Alpes and CNRS, Grenoble, France
6. NIST, Gaithersburg, United States
7. University of California at San Diego, La Jolla, United States
8. New Mexico State University, Las Cruces, United States

The development of materials that combine magnetic and electric order parameters (multiferroic materials) drives intense research activities since the coupling of both order parameters opens the way to the electric control of magnetization. Composite multiferroics (combining ferroelectric and magnetic materials) are currently developed to optimize order parameter coupling that is often weak in intrinsic multiferroics: the magnetoelectric coupling in heterostructures is achieved either by strain or by modulation of charge carrier density. In the field of charge-driven magnetoelectric coupling, complex magnetic oxides are particularly interesting candidates because of the high sensitivity of strongly correlated magnetic systems to competing electronic ground states.

In this study, the influence of an electric field applied to a $\text{La}_{0.67}\text{Sr}_{0.33}\text{MnO}_3$ (LSMO)/ $\text{Pb}(\text{Zr}_{0.2}\text{Ti}_{0.8})\text{O}_3$ (PZT)/Nb-doped SrTiO_3 (STO) heterostructure on the magnetization depth profile of the LSMO single crystal film has been explored by Resonant X-ray Magnetic Reflectivity (RXMR). First results show that the saturation magnetization ($H=1\text{kOe}$) of ferromagnetically ordered LSMO is not affected by the direction of the electric polarization of PZT. However, in the remanent state ($H=0$), the ferromagnetic thickness and remanent magnetization of the LSMO film appear to be reduced for the case of hole-charge accumulation at the LSMO/PZT interface.

In order to decouple electric-field induced and possible strain-induced effects from PZT, complementary neutron scattering experiments have been performed: LSMO films directly grown on Nb-doped STO have been submitted to either a bending strain or an electric field. Bending strain was applied to the sample using a four-point mechanical jig, while, in a separate experiment, charge was applied using an electric field produced by a parallel plate capacitor. This investigation shows that the bending strain affects the saturation magnetization, while the electric field affects the remanent magnetization of the LSMO film, thus confirming the electric origin of the effects observed in the LSMO remanent state by RXMR.

WE.G2_05 - Reversible electric control of magnetic anisotropy in CoFeB/BaTiO₃ heterostructures with perpendicular magnetic anisotropy

L. Baldrati¹, C. Rinaldi^{1,2}, M. Asa¹, M. Cantoni¹, S. Bertoli¹, R. Bertacco^{1,2}

1. *Department of Physics, Politecnico Di Milano, Milan, Italy*

2. *IFN-CNR Institute for Photonics and Nanotechnologies, Milan, Italy*

The electric control of magnetization represents a viable path to overcome the consumption and miniaturization limits of memory/logic spintronic devices. Magneto-electric coupling (MEC) in heterostructures made of ferroelectric and ferromagnetic materials is a promising route towards room-temperature electric-field-controlled magnetic devices. We have already demonstrated the on-off switching of the ferromagnetism in the interfacial Fe layers of the Fe/BaTiO₃ (BTO) system, via an electric field applied across the BTO. [1,2] Here we present recent results obtained on the CoFeB/BaTiO₃ interface. Ta(2.0 nm)/ CoFeB(~1 nm)/ BTO(150 nm)/ La_{0.7}Sr_{0.3}MnO₃(50 nm) stacks were grown on SrTiO₃ (001) substrates. Microcapacitors (100x70 microns) were patterned by means of optical lithography and ion beam etching. LSMO serves as a conducting and lattice matching layer while Ta is used for capping and stabilization of the out-of-plane anisotropy of the CoFeB layer. We found a magnetic coercive field variation up to 80% versus voltage applied to BTO. Noteworthy, the magnetization can be switched from upwards to downwards by reversing the voltage polarity across the BTO in a bias field of -5 mT. Reversing this uniform low bias field and addressing each pad via voltage pulses, allows to reversibly switch the magnetization of individual spintronic devices in a chip.

References:

[1] G. Radaelli et al, Nat. Comm. 5, 3404 (2014). [2] G. Radaelli et al, J. App. Phys. 115, 172604 (2014)

WE.G2_I6 - Electric field effects on metallic ferromagnetic thin layers and its applications

Y Suzuki¹, S. Miwa¹, K. Tanaka¹, K. Matsuda¹, N. F. Bonell¹, Ti Nozaki², Y. Shiota², W. Skowronski², K. Yakushiji², A. Fukushima², L.D. Duong², H. Kubota², S. Yuasa², M. Suzuki³, T. Nakamura³

1. *Osaka University, Graduate School of Engineering Science, Suita, Osaka Prefecture, Japan*

2. *Spintronics research center, AIST, Tsukuba, Japan*

3. *Spring-8, Sayo District, Hyogo Prefecture, Japan*

Magnetization control using an electric field at room temperature [1, 2] will be useful because of its expected ultra-low power consumption and coherent behavior. Magnetic anisotropy control using electric field at room temperature in all solid-state devices was first done using an Fe ultrathin film grown on Au(001) surface and covered by an MgO layer [2]. The effect was soon applied to switch magnetization coherently [3], to excite FMR [4], and to modulate spin waves [5]. However, theoretical understanding of the effect has not been satisfactory. The size of the effect are in rough agreement with theories, however, even the sign of the effect can be opposite. The main reason of this difficulty is because of insufficient control of interfaces in our samples, although the effect is very sensitive to it. In my talk, I will also address to those difficulties and mention to a recent progresses in understanding the mechanism through XAS and XMCD measurements.

References:

- [1] Weisheit, M. et al., *Science* 315, 349-351 (2007)
- [2] Maruyama, T. et al., *Nature Nanotech.* 4, 158-161 (2009)
- [3] Shiota, Y. et al., *Nature Materials*, 11, 39-43 (2012)
- [4] Nozaki, T. et al., *Nature Phys.* 8, 491 (2012)
- [5] Nawaoka, K. et al., *J. Appl. Phys.* 117, 17A905 (2015)
- [6] Bonell, F. et al., *Surface Science* 616, 125-130 (2013)
- [7] Bonell, F. et al., *Appl. Phys. Lett.* 102, 152401 (2013)

WE.H.1_I1 - Manipulation of magnetic skyrmions with spin-polarized STM

K. von Bergmann¹

1. University of Hamburg, Hamburg, Germany

The spin textures of ultra-thin magnetic layers exhibit surprising variety. The loss of inversion symmetry at the interface of magnetic layer and substrate gives rise to the so-called Dzyaloshinsky-Moriya interaction which favors non-collinear spin arrangements with unique rotational sense [1,2]. An ideal tool to investigate such systems down to the atomic scale is spin-polarized scanning tunneling microscopy, which has enabled the discovery of spin spirals with unique rotational sense at surfaces [2]. Recently, different interface-driven skyrmion lattices have been found [3,4], which can be viewed as a two-dimensional analogon to spin spirals. Depending on the involved magnetic interactions single particle-like skyrmions can be realized and their writing as well as the deletion based on local spin-polarized current injection has been demonstrated [4]. An external magnetic field is used to tune the energy landscape, and the temperature is adjusted to prevent thermally activated switching between topologically distinct states. Switching rate and direction can then be controlled by the parameters used for current injection. In addition to measurements with spin-polarized currents we demonstrate that skyrmions can be detected with non-spin-polarized currents due to spin-mixing effects in the non-collinear spin texture. The strength of this new magnetoresistive effect correlates with the angle between nearest neighbors. As this is expected to be a general phenomenon we propose to use it as an easy and reliable scheme to detect skyrmions in future spintronics devices.

References:

- [1] K. von Bergmann et al., J. Phys.: Cond. Mat. 26, 394002 (2014)
- [2] M. Bode et al., Nature 447, 190 (2007)
- [3] S. Heinze et al., Nature Phys. 7, 713 (2011)
- [4] N. Romming et al., Science 341, 636 (2013)

WE.H.1_O2 - Chaotic dynamics triggering stochastic vortex formation in asymmetric magnetic disks

M.Y. Im^{1,2}, K.S. Lee³, A. Vogel⁴, J.I. Hong², G. Meier^{4,5}, P. Fischer^{1,6}

1. Lawrence Berkeley National Lab, Berkeley, United States

2. Daegu Gyeongbuk Institute of Science and Technology, Daegu, Republic of Korea

3. Ulsan National Institute of Science and Technology, Ulsan, Republic of Korea

4. Universität Hamburg, Hamburg, Germany

5. The Hamburg Centre for Ultrafast Imaging, Hamburg, Germany

6. University of California, Santa Cruz, United States

Magnetic vortices are attracting enormous interests since they have fascinating topological spin structures for fundamental studies of nanoscale spin behavior and offer a great potential as building blocks in advanced magnetic technologies [1]. To realize the practical application of magnetic vortices, a completely reliable control over the vortex spin structure is mandatory but it has been assumed to be hampered by stochastic nature. Therefore, Controlling and understanding stochastic behavior in magnetic vortex systems is premium. So far, most studies have assumed that thermal fluctuations are the main source for stochastic behavior in magnetic processes [2]. In this work, we provide evidence that the ultrafast dynamics in the initial stage of vortex formation process can be a critical factor for the stochastic behavior observed at steady state in asymmetric magnetic disks [3]. It was found that the dynamics triggering the stochastic nature in the vortex formation has a characteristic of chaos, the butterfly effect, where minute changes significantly determine the final outcome of a process. We also demonstrate that the proper design of the geometry in asymmetric disks can lead to fully deterministic behavior. This work would have a significant impact to acquire a deeper and fundamental understanding of nanospin behavior paving a way for potential applications. This work was supported by the Director, Office of Science, Office of Basic Energy Sciences, Materials Sciences and Engineering Division, of the U.S. Department of Energy under Contract No. DE-AC02-05-CH11231. This research was also supported by Leading Foreign Research Institute Recruitment Program through the National Research Foundation (NRF) of Korea funded by the Ministry of Education, Science and Technology (MEST) (2012K1A4A3053565).

References:

[1] T. Shinjo et al. Science 289, 930 (2000)

[2] M.-Y. Im et al. Adv. Mater. 20, 1750 (2008)

[3] M.-Y. Im et al. Nat. Commun. 5, 5620 (2014)

WE.H.1_O3 - Spin dynamics at the helimagnetic phase transition of MnSi

A. Bauer¹, J. Kindervater¹, I. Stasinopoulos², F. Rucker¹, M. Garst³, M. Janoschek⁴, N. Martin^{1,5}, S. Mühlbauer⁵, W. Häußler^{1,5}, D. Grundler², P. Böni¹, C. Pfleiderer¹

1. Physik Department E21/E51, Technische Universität München, Garching, Germany

2. Physik Department E10, Technische Universität München, Garching, Germany

3. Institut für theoretische Physik, Universität zu Köln, Garching, Germany

4. Los Alamos National Laboratory, Los Alamos, United States

5. Heinz Maier-Leibnitz Zentrum (MLZ), Technische Universität München, Garching, Germany

In MnSi the transition from paramagnetism to helimagnetism in zero field is driven fluctuation-induced first-order by strongly interacting chiral fluctuations as described in the Brazovskii scenario [1]. Magnetic fields quench these fluctuations leading to a field-induced tricritical point (TCP) where the transition becomes mean-field second-order [2]. In addition, MnSi gives rise to a regular arrangement of spin whirls, the so-called skyrmion lattice, in finite fields just below the helimagnetic ordering temperature [3]. While it was established that the unwinding of these topologically non-trivial objects into a helimagnetic state is accomplished via emergent magnetic monopoles [4], it is still unknown how they crystallize from a paramagnetic state.

In order to address this question, we report a comprehensive study combining small-angle neutron scattering and neutron spin echo spectroscopy using the MIEZE technique, which allows to measure under applied magnetic field without loss of energy resolution. The quasi-elastic linewidth recorded by means of MIEZE shows a change of the characteristic spin fluctuations at the TCP, providing microscopic evidence for its existence. In the field range of the skyrmion lattice, our data suggest the presence of fluctuations with a skyrmionic character already above the onset of static order. These findings are supported by high-resolution specific heat data, measurements of the longitudinal and the transversal ac susceptibility, as well as by all-electrical broadband spectroscopy showing excitations in the GHz range that may be attributed the gyration of skyrmion-like objects [5].

References:

[1] M. Janoschek et al., PRB 87, 134407 (2013)

[2] A. Bauer et al., PRL 110, 177207 (2013)

[3] S. Mühlbauer et al., Science 323, 915 (2009)

[4] P. Milde et al., Science 340, 1076 (2013)

[5] T. Schwarze et al., Nature Mater., in press (2015)

WE.H.1_O4 - Influence of thermal fluctuations on magnetic vortex depinning

M. Kuepferling¹, E. Ferraro¹, A. Sola¹, C. Serpico², H. W. Schumacher³, N. Liebing³, P. Krzysteczko³, A. Fernandez Scarioni³, X. Hu³, S. Sievers³, K. Rott⁴, G. Reiss⁴

1. *Inrim, Torino, Italy*

2. *University Federico II, Napoli, Italy*

3. *PTB, Braunschweig, Germany*

4. *University of Bielefeld, Bielefeld, Germany*

The characterization of defects in ferromagnetic nanostructures is of special importance for magnetic data storage based on vortices or domain walls moving through nano-devices, since their presence may modify critically the vortex or domain wall dynamics [1,2]. In this paper we study experimentally the temperature dependence of frequency, line-width and power of the vortex oscillations in $\text{Co}_{40}\text{Fe}_{40}\text{B}_{20}(3\text{nm})/\text{MgO}(1.1\text{nm})/\text{Co}_{40}\text{Fe}_{40}\text{B}_{20}(2\text{nm})/\text{Ni}_{81}\text{Fe}_{19}(30\text{nm})$ magnetic tunnel junctions (MTJ) circular pillars ($d=460\text{nm}, 590\text{nm}, 780\text{nm}$) in presence of defects. Small power oscillations in MTJs caused by thermal fluctuations [3] are especially sensitive to defects that pin the vortex and change the oscillation frequency [4,5]. When applying an in-plane magnetic field the oscillation frequency exhibits maxima and steep minima at certain field values. While the frequency maxima correspond to the oscillations of the pinned vortex [2], the minima correspond to the field induced depinning of the vortex where the energy landscape becomes flat and large amplitude, high power oscillations occur. The depinning is influenced by thermal fluctuations which help to overcome the energy barrier. We analyze the temperature dependent power spectra by using a Thiele based model including a white noise term and numerically solve the stochastic differential equation. The vortex pinning by defects is taken into account by a Gaussian pinning potential. We find experimentally that at certain field values a Barkhausen-like [6] depinning at low temperatures ($<70\text{K}$) occurs, showing temperature and rate dependent field hysteresis. We attribute these frequency jumps to strong defects (e.g. inclusions). The frequency maxima, which correspond to pinning by small defects (e.g. surface roughness), show a frequency increase up to 1200MHz at 4K (with respect to 450MHz of the unpinned vortex), which corresponds according to our model to pinning potentials of -0.7eV to -0.9eV . The approach shows that the description of magnetization dynamics in terms of vortex core position is consistent with the experimental results also in presence of thermal fluctuations.

References:

- [1] Min, H., et al., Phys Rev Lett 104, 217201 (2010)
- [2] Zaspel, C.E., et al., Phys Rev B 87, 134425 (2013)
- [3] Wysin, G.M., et al., PRB 86, 104421 (2012)
- [4] Min, H., et al., Phys Rev B 83, 064411 (2011)
- [5] Dussaux, A., et al., Nat Comms 1, 8 (2010)
- [6] Burgess, J.A.J., et al., Science 339, 1051 (2013)

WE.H.1_05 - Observation of magnetic skyrmions at room temperature in ultrathin Pt/Co/MgO perpendicularly magnetized multilayers by XMCD-PEEM

O. Boulle ¹, S. Pizzini ², J. Vogel ², L. Buda-Prejbeanu ¹, O. Mentès ³, A. Locatelli ³, A. Sala ³, G. Gaudin ¹

1. *Spintec, Grenoble, France*

2. *Institut Néel, France*

3. *Elettra Sinchrotrone, Nanospectroscopy beamline, Trieste, Italy*

Magnetic skyrmions are currently attracting lots of attention due to their stability, their poor sensitivity to material defects and the fact that they can be moved by currents with very small densities, which opens a path for novel spintronics data storage devices. So far, magnetic skyrmions in thin films have only been observed on free surfaces under ultra-high vacuum and low temperature, which prevents any use for applications. Here we show that the large Dzyaloshinskii-Moriya interaction in ultrathin magnetic multilayers allows stabilizing skyrmions at room temperature in patterned structures. We carried out XMCD-PEEM magnetic imaging on the Nanospectroscopy beamline in Elettra, Italy in ultrathin Pt/Co/MgO/Ta perpendicularly magnetized multilayers. The high spatial resolution of the technique combined with the larger magnetic contrast for in-plane compared to out-of-plane magnetization allows the observation of the magnetization within the magnetic domain walls (DW). The observation of the multidomain structure in the unpatterned thin film reveals that the magnetization in the DW is oriented perpendicularly to the DW surface, with opposite orientations for up/down and down/up magnetic DW. DW are thus chiral Néel DW which is a signature of the Dzyaloshinskii-Moriya interaction. In patterned sub-micronic squares, we observed 200 nm wide magnetic bubbles delimited by chiral Néel DWs, which are identified as chiral Néel magnetic skyrmions.

WE.H.2_I1 - Metamagnetism in heavy fermion systems

G. Knebel^{1,2}, A. Pourret^{1,2}, D. Aoki^{1,2,3}, T. Combier^{1,2}, A. Palacio Morales^{1,2}, G. Lapertot^{1,2}, T. D. Matsuda⁴, J. Flouquet^{1,2}

1. Univ. Grenoble Alpes, INAC-SPSMS, Grenoble, France

2. CEA, INAC-SPSMS, Grenoble, France

3. Institute for Materials Research, Tohoku University, Oarai, Ibaraki, Japan

4. Tokyo Metropolitan University, Hachioji, Japan

In this presentation we will discuss examples of metamagnetism in different heavy fermion compounds. In the first part we will review recent transport experiments on the itinerant 5 f system UCoAl. This is a paramagnet at ambient pressure, i.e. the quantum critical point is located at slightly negative pressure, and presents a canonical compound to study metamagnetic phenomena and the wing structure of the generic T-p-H phase diagram of an ferromagnet. Under field the system undergoes a first order metamagnetic transition to a field-induced ferromagnetic state at the critical magnetic field $H_m = 0.7$ T. Hall effect, resistivity, and thermoelectric power measurements were performed up to 2 GPa and 13 T on a single crystal of UCoAl. Hall effect measurements indicate a critical pressure near 1.6 GPa and a critical field near 7 T, while the other transport experiment point to a higher critical pressure. The pressure – temperature - magnetic field phase diagram will be discussed in detail. In the second part of the talk we will discuss antiferromagnetic systems where the a Lifshitz-type transition of the Fermi surface occurs when the magnetization reaches a critical value. This will be discussed for the heavy fermion compounds CeRu₂Si₂ and YbRh₂Si₂. We will discuss different transport properties and compare them to Fermi surface studies with quantum oscillation experiments.

WE.H.2_O2 - Controlling the coupling among many-body Kondo states in atomically designed Co atomic structures

M. Moro-Lagares^{1,2}, M. Piantek^{1,2}, M.R. Ibarra^{1,2}, J. I. Pascual³, D. Serrate^{1,2}

1. INA-LMA, University of Zaragoza, Zaragoza, Spain

2. Condensed Matter Physics Dpt., University of Zaragoza, Zaragoza, Spain

3. CIC-Nanogune and IKERBASQUE, San Sebastian, Spain

We investigate the hybridization of Kondo many-body states as interactions through conduction electrons among them are controllably strengthened. As a model system, we use Kondo screened Co adatoms (TK=55 K) over the Ag(111) surface studied by scanning tunneling spectroscopy and atomic manipulation at a base temperature of 1.1 K. We obtain spatially resolved images of the Kondo many-body resonance as a function of proximity to and number of atomic neighbors, which exhibit non-local Kondo screening [1,2] away from the atoms centers for interatomic distances below 8.7 Å. This is interpreted as the formation of hybrid 1-D many-body states, and show distinct features compared to the case of hybridized one-particle wave functions in atomic wires. Increasing the number of neighbors at 5.8 Å, the energy scales of the hybridization and Kondo screening become comparable and, as a consequence, magnetic Ruderman-Kittel-Kasuya-Yosida (RKKY) interactions develop. RKKY correlations lift the spin degeneracy of the isolated Co states, and lead to the energy broadening of the Kondo spectral features[3,4]. The dependence of the broadening on the Co cluster structure is compared with the expected spin splitting from a Heisenberg spin-1/2 ferromagnetic model Hamiltonian, and reveals an RKKY spin coupling constant of about 1.5 meV (about TK/2). With the aid of structural design of atomic scale ensembles, our results show how indirect interactions mediate the transition from Kondo screened isolated impurities to a Kondo lattice, and finally to a RKKY correlated magnetic structure.

References:

- [1] N. Tsukahara et al., Phys. Rev. Lett. 106, 187201 (2011)
- [2] Y. Jiang et al., Science 333, 324 (2011)
- [3] J. Bork et al., Nature Phys. 7, 901 (2011)
- [4] H. Prüser et al., Nature Comm. 5, 5417 (2014)

WE.H.2_O3 - Ferromagnetic Kondo lattice behaviour of CeZn(Zn_{0.29}Si_{0.71})₂

H. Michor¹, F. Failamani², A. Grytsiv², G. Giester³, E. Bauer¹, P. Rogl²

1. *Institute of Solid State Physics, Vienna University of Technology, Vienna, Austria*

2. *Institute of Physical Chemistry, University of Vienna, Vienna, Austria*

3. *Institute of Mineralogy and Crystallography, University of Vienna, Vienna, Austria*

We report on the ferromagnetic Kondo lattice behavior of novel CeZn(Zn_{0.29}Si_{0.71})₂, which was studied by means of ac and dc magnetic susceptibility, specific heat and resistivity measurements on flux-grown single crystals as well as on sintered bulk samples. The orthorhombic CeNiSi₂-type phase CeZn(Zn_{0.29}Si_{0.71})₂ [space group Cmc₂m, a=0.42079(1), b=1.765218(3), c=0.41619(1) nm] was identified in the course of an investigation of the phase equilibria in the Ce-Zn-Si system (<33.3 at.% Ce) in Ref. [1]. Field dependent isothermal well as temperature dependent magnetisation measurements reveal ferromagnetic ordering of CeZn(Zn_{0.29}Si_{0.71})₂ below about T_C=4.4 K with a magnetically ordered moment near 1 μB/Ce at 1.9 K and 6 T. The corresponding specific heat anomaly at 4.4 K displays a significantly reduced magnitude as compared to the value expected from a basic local moment mean-field approach and is analysed in terms of a simple model for a ferromagnetic Kondo lattice system based on the resonant level model by Schotte and Schotte [2], thus, yielding parameters for the ferromagnetic exchange coupling J = 14.6 K and the Kondo temperature T_K = 5 K. The effective paramagnetic moment of Ce, μ_{eff} = 2.5 μB, obtained from a Curie-Weiss fit suggest that the ground state of Ce-ions in this compound is close to 3+.

References:

1. F. Failamani, A. Grytsiv, R. Podloucky, H. Michor, E. Bauer, P. Broz, G. Giester, P. Rogl, submitted to Physical Chemistry Chemical Physics
2. K. D. Schotte and U. Schotte, Phys. Lett. A 55 (1975) 38; C. D. Bredl, F. Steglich and K. D. Schotte, Z. f. Phys. B Condens. Matter 29 (1978) 327

WE.H.2_O4 - Multiple magnetic-field-induced transitions in the Kondo lattice YbNi₄P₂

A. Steppke¹, H. Pfau¹, R. Daou², D. Sun¹, K. Kliemt³, C. Krellner³, C. Geibel¹, F. Steglich¹, M. Brando¹, S. Friedemann⁴

1. *Max-Planck Institute for Chemical Physics of Solids, Dresden, Germany*
2. *Laboratoire CRISMAT, UMR 6508 du CNRS, ENSICAEN et Université de Caen, Caen, France*
3. *Institute of Physics, Goethe University Frankfurt, Frankfurt am Main, Germany*
4. *HH Wills Physics Laboratory, University of Bristol, Tyndall Avenue, United Kingdom*

YbNi₄P₂ is a ferromagnetic Kondo lattice system with a Kondo temperature of 8K and a small Curie temperature of 0.15K. It is close to a ferromagnetic quantum critical point, which can be induced by substitution of phosphorus by arsenic [1]. A magnetic field of 60mT applied along the crystallographic c-axis is also able to suppress the ferromagnetic order, above which YbNi₄P₂ is a field-polarized Fermi liquid. We performed thermopower, resistivity, and specific heat measurements to study the evolution of YbNi₄P₂ in magnetic fields up to 12T. While we observe signatures of strong fluctuations at small fields, our measurements detect multiple transitions at higher fields between 0.5T and 12T. To analyse the high field behaviour, we explore the validity of the Mott formula, relating the thermopower to electrical conductivity, which gives important information about scattering mechanisms especially around the observed transitions. Using the combination of the transport results with thermodynamic properties, we obtain further insights into the origin of the transitions in YbNi₄P₂. Some of them present characteristics similar to those identified as Lifshitz-type in previous studies on the two Kondo lattices YbRh₂Si₂ [2] and CeRu₂Si₂ [3]. Lifshitz-type transitions mark changes of the Fermi surface topology, but break no symmetries. Kondo lattice systems are ideal materials to study Lifshitz transitions, since the Zeeman energy and the electronic bandwidth are comparable.

References:

- [1] A. Steppke et al., *Science* 339 933 (2013)
- [2] H. Pfau et al., *Phys. Rev. Lett.* 110 256403 (2013)
- [3] H. Pfau et al., *Phys. Rev. B* 85 035127 (2012)

WE.H.2_O5 - Investigations of the stability of spin gap formation and the moment direction by electron doping on the Al site in CeRu₂Al₁₀

D.T. Adroja^{1,2}, A. Bhattacharyya^{1,2}, C. Ritter³, B. Fak³, A.D. Hillier¹, K. Hayashi⁴, Y. Muro⁴, A.M. Strydom², M.M. Koza³, T. Takabatake⁵

1. ISIS Facility, Rutherford Appleton Laboratory, Chilton, Didcot Oxon, United Kingdom
2. Highly Correlated Matter Research Group, Physics Department, University of Johannesburg, Auckland Park, South Africa
3. Institute Laue- Langevin, Grenoble, France
4. Faculty of Engineering, Toyama Prefectural University, Toyama, Japan
5. Department of Quantum matter, ADSM, and IAMR, Hiroshima University, Higashi-Hiroshima, Japan

The Kondo semiconductor CeRu₂Al₁₀ orders antiferromagnetically at TN=27 K in spite of the small ordered moment $\mu_{ord}=0.34\mu_B$. We have investigated the effect of electron doping (i.e. 3% Si) on the Al site in CeRu₂Al₁₀ on the direction and magnitude of the ordered state Ce moment as well as on the spin gap formation using muon spin rotation (μ SR), neutron diffraction (ND) and inelastic neutron scattering (INS). Our μ SR study shows a strong increase of the electronic relaxation rates and 2/3 drop in the initial symmetry below 19 K, indicating the long range magnetic ordering (at TN=18.5 K) with large internal fields (>800G) at the muon sites. The ND study confirmed a long range magnetic ordering of the Ce-moment with a propagation vector $k=[1\ 0\ 0]$. This is similar to the ordering observed in the parent compound CeRu₂Al₁₀, however, the direction of the ordered state moment along the a-axis and its size ($\mu_{ord}=1.3\mu_B$) are in sharp contrast to the small moment ($\mu_{ord}=0.34\mu_B$, TN=27 K) observed along the c-axis in CeRu₂Al₁₀. The INS study does not reveal any clear sign of spin gap excitations at 5 K, indicating that the spin gap has nearly closed with electron doping on the Al-site. These observations are very similar to those found for electron doping (i.e. Ir/Rh) on the Os/Ru site in CeOs₂Al₁₀/ CeRu₂Al₁₀ and shows that the effect of electron doping either on the transition metal site (T=Ru, Fe and Os) or on the Al site gives very similar changes in the magnetic and electronic properties of the Kondo semiconductors CeT₂Al₁₀. These results suggest that part of the spin gap excitations should be originating from the electron and hole pockets of the Fermi surface and provide a basis to develop and test realistic theoretical models to understand the physics of these compounds.

WE.H.2_I6 - The importance of orbital occupation in heavy fermion compounds investigated by means of x-ray spectroscopyA. Severing¹, F. Strigari¹, M. Sundermann¹, W. Thomas¹, H. Maurits W.², L. Hao Tjeng²1. *University of Cologne, Cologne, Germany*2. *Max-Planck Institute for Chemical Physics of Solids, Dresden, Germany*

The importance of k-dependent hybridization in heavy fermion compounds has been suggested by several authors (e.g. Ref.s[1-3]) and should be visible in the anisotropy of the 4f ground state wave function. However, standard experimental methods were lacking accuracy so that only recently it was shown with a new experimental approach that the orbital anisotropy correlates with a heavy fermion phase diagram, from magnetically ordered to superconducting [4]. Other theories even suggest orbital transitions as function of hybridization [5,6] but are still waiting to be challenged by experiment.

We investigate the orbital occupation of cerium heavy fermion compounds by means of soft x-ray absorption spectroscopy and hard x-ray non-resonant inelastic scattering. In the former the dipole selection rules of linearly polarized light give access to the ground state symmetry with unprecedented accuracy (see e.g. [4,7,8]). In the latter the multipole selection rules of the double differential scattering cross-section contains information about the orbital symmetry plus they yield information about the rotation of an orbital with fourfold symmetry, thus completing the crystal-field picture [9].

These methods have been successfully applied to several metallic as well as insulating-like heavy fermion compounds. Several examples shall be given and the importance of orbital occupation shall be stressed.

References:

- [1] K. Hanzawa, K. Yamada, K. Yosida, J. Phys. Soc. Jpn. 56, 678 (1987)
- [2] P.G. Pagliuso, et al., Physica B 320, 370 (2002)
- [3] J.H. Shim, K. Haule, G. Kotliar, Science 318, 1615 (2007)
- [4] T. Willers, F. Strigaria, Z. Hu, V. Sessi, N.B. Brookes, E.D. Bauer, J.L. Sarrao, J. D. Thompson, Arata Tanaka, S. Wirthb, L.H. Tjeng, Andrea Severinga, PNAS 112 (8), 2387 (2015)
- [5] K. Hattori, J. Phys. Soc. Jpn. 79, 114717 (2011)
- [6] L. V. Pourovskii, P. Hansmann, M. Ferrero, A. Georges, Phys. Rev. Lett. 112, 106407 (2014).
- [7] P. Hansmann, A. Severing, Z. Hu, M.W. Haverkort, C. F. Chang, S. Klein, A. Tanaka, H.H. Hsieh, H.-J. Lin, C. T. Chen, B. Fak, P. Lejay, and L. H. Tjeng, PRL 100, 066405 (2008)
- [8] F. Strigari, T. Willers, Y. Muro, K. Yutani, T. Takabatake, Z. Hu, Y.-Y. Chin, S. Agrestini, H.-J. Lin, C. T. Chen, A. Tanaka, M. W. Haverkort, L. H. Tjeng, and A. Severing, PRB 86, 081105(R) (2012)
- [9] T. Willers, F. Strigari, N. Hiraoka, Y. Q. Cai, M.W. Haverkort, K.-D. Tsuei, Y. F. Liao, S. Seiro, C. Geibel, F. Steglich, L. H. Tjeng, and A. Severing PRL 109, 046401 (2012)

WE.I.1_I1 - Interface-driven chiral spin textures in ultrathin magnetic films

G. Beach¹

1. Department of Materials Science and Engineering, Massachusetts Institute of Technology, Cambridge, United States

Spin orbit coupling at interfaces in ultrathin magnetic films can give rise to chiral magnetic textures such as homochiral domain walls and skyrmions, as well as current-induced torques that can effectively manipulate them [1-3]. This talk will describe the statics and dynamics of chiral spin textures in thin-film nanowires stabilized by the Dzyaloshinskii-Moriya interactions (DMI) at a heavy metal/ferromagnet interface. We show that the DMI depends strongly on the heavy metal, differing by a factor of ~ 20 between Pt and Ta [2], and describe the influence of strong DMI on domain wall dynamics [1,2] and spin Hall effect switching [3]. We present high-resolution magnetic imaging of static magnetic textures that directly reveal the role of DMI and allow its strength to be quantified [4]. Finally, we will describe how a gate voltage can be used to control interfacial magnetism and magnetic domain walls in nanowires by manipulating interfacial oxygen coordination and magnetic anisotropy at a ferromagnet/oxide interface [5].

References:

- [1] S. Emori, et al., *Nature Mater.* 12, 611 (2013)
- [2] S. Emori, et al., *Phys. Rev. B* 90, 184427 (2014)
- [3] N. Perez, et al., *Appl. Phys. Lett.* 104, 092403 (2014)
- [4] S. Woo, et al., arXiv:1502.07376 (2015)
- [5] U. Bauer, et al., *Nature Mater.* 14, 174 (2015)

WE.I.1_O2 - Chiral effects in domain wall velocity and nucleation in Pt/Co/MOx films: The influence of the Dzyaloshinskii-Moriya interaction

S. Pizzini¹, J. Vogel¹, S. Rohart², L. Buda-Prejbeanu³, M. Miron³, G. Gaudin³, O. Boulle³, E. Jué³, A. Thiaville²

1. CNRS, Institut Néel, Grenoble, France

2. Laboratoire de Physique des Solides, Univ. Paris-Sud, CNRS, Orsay, France

3. SPINTEC, CEA/CNRS/UJF/Grenoble-INP, INAC, Grenoble, France

Chiral effects in current or field-driven domain wall (DW) motion in Pt/Co/MOx stacks with perpendicular magnetic anisotropy can be explained by the presence of chiral Néel walls stabilised by the Dzyaloshinskii-Moriya interaction (DMI). We show that the nucleation of reversed domains in a microstructure is also chiral and affected by the presence of DMI. The nucleation of domains in Pt/Co(0.6nm)/MOx (M=Al,Gd) stacks, induced by a z-field in the presence of an x-field, has been studied by Kerr microscopy. Nucleation occurs preferentially at one edge of the sample, normal to the x-field, where the DW magnetisation is parallel to the x-field (S. Pizzini et al. PRL 2014). The edge where nucleation takes place, which depends in a chiral way on the initial domain magnetization and applied field directions, points to Néel walls with left-handed chirality, stabilised by negative DMI. The nucleation field at the edges strongly decreases as the x-field increases, unlike the nucleation within the film. This decrease of the nucleation field is due to the decrease of the DW energy with the x-field in the presence of DMI. The DW energy becomes negative for x-fields around 200 mT, and domains nucleate without a z-field. Field- and current-driven domain wall motion in Pt/Co/Gd/Ox samples has also been studied. We show that the field driven low speed regime (creep regime) is strongly influenced by the details of the Gd/Co interface and cannot always be explained by the models proposed so far.

WE.I.1_O3 - Electrical switching of the perpendicular magnetization in Pt/[Co/Ni]3/Al multilayers

J.C. Rojas-Sánchez^{1,2}, J. Sampaio³, P. Laczkowski^{1,2}, N. Reyren^{1,2}, C. Deranlot^{1,2}, S. Collin^{1,2}, K. Bouzehouane^{1,2}, V. Cros^{1,2}, N. H. Jaffrès^{1,2}, A. Mougin³, A. Fert^{1,2}, J.M. George^{1,2}

1. *Unité Mixte De Physique CNRS/Thales, Palaiseau, France*

2. *Université Paris Sud, Orsay, France*

3. *Laboratoire de Physique des Solides, Université Paris Sud, Orsay, France*

Electrical control of the magnetic and resistive states in spintronic nanostructures is highly desirable. The spin to charge current conversions (SCCC) due to spin-orbit (SO) coupling opens the way to manipulate the magnetization by electrical means. In particular, using spin pumping by ferromagnetic resonance (FMR) experiment, we investigated the SCCC induced by spin Hall effect (SHE) in metals such as Pt [1,2] or AuW [3]. We found spin Hall angles that are large enough to drive the magnetization by SHE-induced spin torques.

In the context of an active debate [4-7] about the magnetization reversal mechanism(s) by SO torques, we will present results demonstrating the control of the magnetization in Pt/(Co/Ni)3/Al multilayers with perpendicular magnetization driven by electrical current. Using both the anomalous Hall Effect and Kerr experiments in patterned Hall bars, we are able to establish a scenario for the reversal mechanism involving domain wall motions and SO torques induced by SHE in Pt. In our scenario, the Dzyaloshinskii-Moriya interaction (DMI) at the Pt/Co interface [8] plays only a minor role in the reversal mechanism.

References:

- [1] J.-C. Rojas-Sánchez et al. PRL 112, 106602 (2014)
- [2] J.-C. Rojas-Sánchez et al. SPIE 9167, Spintronics VII, 916729 (2014)
- [3] P. Laczkowski et al. APL 104, 142403 (2014)
- [4] A. V. Khvalkovskiy et al. PRB 87, 020402 (2013)
- [5] I. M. Miron et al. Nature 476, 189 (2011)
- [6] L. Liu et al. PRL 109, 096602 (2012)
- [7] N. Perez et al. APL 104, 092403 (2014)
- [8] K.-S. Ryu et al. Nature Nanotech. 8, 527 (2013)

WE.I.1_O4 - Influence of Joule heating on current-driven domain wall depinning

S. Moretti¹, V. Raposo¹, E. Martinez¹

1. *University of Salamanca, Salamanca, Spain*

The analysis of the current-induced domain wall depinning (CIDWD) in ferromagnetic strips is not only crucial for the development of logic [1] and storage applications [2], but it is also interesting from a fundamental point of view. Although these depinning processes have been widely studied experimentally [3], the underlying theory of the interaction between a spin polarized current and the local magnetization is not completely understood. Experiments are usually interpreted in terms of a model where the current only generates both adiabatic and non-adiabatic spin-transfer torques (STT) [4]. However, due to the conductive nature of the strips, the current also generates space- and time-dependent Joule heating (JH) which could influence significantly the depinning process, and consequently, result in a different estimation of the STT parameters. In this work we explore numerically the role of the JH on the CIDWD by coupling the magnetization dynamics with the heat transport for a Permalloy strip [5] on top of a Si/SiO₂ substrate, as in typical experiments [3]. We study the critical depinning current densities as a function of the applied field. Our results clearly indicate that JH has a strong influence on the depinning process, and in particular, it significantly reduces the value of the critical depinning current and leads to symmetric phase diagrams with respect to the direction of the flowing current, as usually obtained in experiments. This study suggests that thermal effects must be taken into account to extract realistic information about the STT phenomena.

References:

- [1] D. A. Allwood et al., *Science* 309, 1688 (2005)
- [2] S. S. P. Parkin, U.S. Patent No. US 683-400-5 (2004)
- [3] M. Hayashi et al. *Phys Rev. Lett.* 97, 207205 (2006)
- [4] A. Thiaville et al., *Europhys. Lett.* 69, 990 (2005)
- [5] E. Martinez et al., *Phys. Rev. Lett.* 98, 267202 (2007)

WE.I.1_05 - Perpendicularly magnetized spintronic memristor

S. Lequeux¹, J. Sampaio¹, R. Matsumoto², A. Fukushima², K. Yakushiji², S. Yuasa², V. Cros¹, J. Grollier¹

1. *Unité Mixte De Physique CNRS/Thales, Palaiseau, France*
2. *AIST, Tsukuba, Japon*

Memristive devices are tunable nano-resistors which can store and process information [1]. Among their most interesting applications are multi-level memories and plastic synapses in neuromorphic architectures, which both require these devices to present a large number of resistance states. Spintronics offers the possibility to engineer memristors based on purely electronic writing by displacing a domain wall (DW) in the free layer of a magnetic tunnel junction thanks to spin torque [2]. In this case, the number of resistance states is equal to the number of positions where the DW can stabilize [2-4]. Here, we will show how perpendicularly magnetized (PMA) junctions can be engineered to fabricate very efficient, multi-state spintronic memristors. Our systems are FeB/MgO/FeB magnetic tunnel junctions [5] shaped as stripes ($\sim 0.1 \times 1 \mu\text{m}^2$). As expected for a PMA system, the number of resistance states is largely increased compared to our first generation of memristor [2-4] and is sufficient for bio-inspired applications. We have optimized the width of the stripes in order to accommodate a DW with a magnetic configuration between the Bloch and Néel DW configurations. This offers the possibility to harness the Slonczewski torque (ST) in addition to the field-like-torque (which is generally smaller than the ST) to move the DW [6]. We will present the numerical 1D model that we have developed to highlight the contribution of each torque in the DW depinning process. In our junctions, we measure that the DW motion occurs for very low current densities (about $1\text{-}2 \cdot 10^6 \text{ A/cm}^2$) under perpendicularly injected current. This observation, together with the general trends for the depinning as a function of field, indicate that indeed, both torques are involved in the DW dynamics. In addition, we observe that the displacement and depinning of the DW is remarkably stochastic. Supported by our model, we interpret this behavior by the fact that in the hybrid Bloch/Neel DW that we have chosen to enhance the ST contribution, the intrinsic dynamics for the DW is the Walker regime.

This research was partly funded by the French Ministry of Defense (DGA) and the European Research Council (Stg 259068).

WE.I.2_I1 - Spin-caloritronics in magnetic tunnel junction nanodevices

S. Serrano-Guisan¹, N. Liebing², T. Böhnert¹, K. Rott³, E. Paz¹, R. Ferreira¹, G. Reiss³, H.W. Schumacher²

1. International Iberian Nanotechnology Laboratory, Braga, Portugal

2. Physikalisch-Technischen Bundesanstalt, Braunschweig, Germany

3. Universität Bielefeld, Bielefeld, Germany

Spin-caloritronics [1] is a new emerging field of spintronics where thermal gradients developed in nanostructured devices can play an active role to control and manipulate spin-based effects like thermally driven spin currents [2, 3] and heat driven magnetization reversal [4]. Such effects are very promising to improve energy efficiency in future devices as well as to develop novel applications for industry and metrology such as magnetic heat valves. However, to date, many concepts have only theoretical basis and need to be studied experimentally. Moreover, the large current densities involved in spin transfer torque effects in magnetic tunnel junction (MTJ) nanodevices imposes a better knowledge of the interplay of heat, charge and spin currents at such conditions. Here we will present a compilation of the observed spin-caloric properties in MTJ nanodevices like the large Tunneling Magneto-Seebeck (TMS) ratios [5, 6] and its angular dependence [5, 7], the Tunneling Magneto-Thermocurrent [8] and the possibility to explore thermal spin transfer torque effects on magnetization dynamics. We will also discuss the uncertainty of input parameters and its large influence on the calculated temperature profile through the nanostructure (and hence on the derived Seebeck coefficients) [9], and we will show some different approaches to minimize it. Moreover, in order to establish a reliable method to derive Seebeck coefficients different experimental techniques for magneto-thermoelectric measurements in MTJ nanodevices (optical heating [6], electrical heating [5] and ohmic nonlinear correction [10]) will be considered.

WE.I.2_I2 - Spin pumping and magnon-drag effect

M. Costache¹, G. Bridoux¹, I. Neumann¹, S. Valenzuela¹

1. Catalan Institute of Nanoscience And Nanotechnology (ICN2), Bellaterra, Spain

Spin related effects have been intensively studied using electrical transport methods, by measuring the spin diffusing length in metals and semiconductors. In addition to electrical transport, the thermoelectric properties of magnetic materials are increasingly gathering more attention. There, thermal magnons are expected to play a major role. However, despite intensive studies on the spin transport, the coupling between electrons and magnons in ferromagnetic metals remains poorly known. We demonstrate a conceptually new device that enables us to gather information on magnon-electron scattering and magnon-drag effects[1]. The device resembles a thermopile formed by a large number of pairs of ferromagnetic wires placed between a hot and a cold source and connected thermally in parallel and electrically in series. By controlling the relative orientation of the magnetization in pairs of wires, the magnon drag can be studied independently of the electron and phonon drag thermoelectric effects. Measurements as a function of temperature reveal the effect on magnon drag following a variation of magnon and phonon populations. These results demonstrate the feasibility of directly converting magnon dynamics of nanomagnets into an electrical signal and could pave the way to novel thermoelectric devices for energy harvesting. This research was funded by the Spanish Ministry of Science (MICINN/MAT2010-18065) and by the European Union (FP7/NANOFUNCTION-257375).

References:

[1] Magnon-drag thermopile, M.V. Costache, G.A. Bridoux, I. Neumann and S.O. Valenzuela, Nature Materials 11, 199-202 (2012)

WE.I.2_O3 - Observation of magnon hall effect and planar righi-leduc effect in py and yig ferromagnets

J.E. Wegrowe¹, B. Madon¹, D. Chung Pham¹, D. Lacour², M. Hehn², A. Anane³, V. Cros³, R. Bernard³

1. Ecole Polytechnique, LSI, CNRS and CEA/DSM/IRAMIS, Palaiseau, France

2. Institut Jean Lamour UMR 7198 CNRS, University de Lorraine, Nancy, France

3. Unité Mixte de Physique CNRS/Thales and Université Paris Sud, Palaiseau, France

Since 2008, some publications have reported a surprising magneto-voltaic signal measured on an electrode in response to a thermal excitation [1]. We show here that the corresponding magneto-voltaic voltage can be interpreted in terms of Magnon Hall and planar Righi-Leduc effects [2], due to the anisotropic temperature difference generated by the heat current. The transverse electrode plays the role of a thermocouple that measures locally the temperature difference. The predicted magneto-voltaic signal DV measured on the transverse electrode in response to a thermal heat current Q, along the (Ox) direction is given by the equation [2] :

$\Delta V = Q \Delta S [(\Delta r \sin(2\theta)\sin 2\varphi)/2 + r_H \cos\theta]$ (1) where θ and φ are the angle describing the assumed uniform magnetisation of the ferromagnetic layer, ΔS is the amplitude of the thermocouple, Δr is the Planar Righi-Leduc coefficient and r_H is the “magnon Hall” or equivalently “anomalous Righi-Leduc” coefficient. We experimentally checked that our signal follows Equation (1)

On the one hand, the Magnon Hall effect is analogous to the well-known anomalous Hall effect and to the anomalous Nernst effect. On the other hand, a second transverse force is observed, which is generated by the anisotropy of the ferromagnetic excitations. The two forces are due to the same ferromagnetic axial vector, which is responsible for both the anisotropy of the heat resistance and the breaking of the time invariance symmetry. *We conclude that both planar Righi-Leduc and magnon Hall effects should be a priori present in any ferromagnetic materials in the same manner as anomalous and planar Hall effects can be expected a priori in any ferromagnetic conductors.*

References:

[1] K. Uchida et al, “Observation of the spin Seebeck effect” Nature 455, 778-781 (2008).

[2] J.-E. Wegrowe et al “Anisotropic magnetothermal transport and spin Seebeck effect” Phys. Rev. B 89, 094409(2014)

WE.I.2_O4 - Giant spin pumping into a fluctuating ferromagnet near T_c

H. Adachi¹, Y. Ohnuma², E. Saitoh³, S. Maekawa¹

1. *Advanced Science Research Center, Japan Atomic Energy Agency, Ibaraki Prefecture, Japan*

2. *Institute for Materials Research, Tohoku University, Miyagi Prefecture, Japan*

3. *WPI, Advanced Institute for Materials Research, Tohoku University, Miyagi Prefecture, Japan*

There has been a growing demand for efficient means for generating spin currents as it is a key quantity in driving the functionality of spintronic devices. An emerging technique called 'spin pumping' [1], i.e., a spin injection from a precessing ferromagnet into an adjacent spin sink, is now established as a versatile method for the spin current generation. The spin pumping has an advantage that it is not accompanied by any charge transfer across the spin injector/spin sink interface and thus free from the impedance mismatch problem which often hinders a spin injection into semiconductors [2]. Here we theoretically demonstrate that, when an itinerant weak ferromagnet near its Curie temperature (T_c) is used as the spin sink, the resultant spin pumping is significantly amplified owing to the fluctuation enhancement of the spin conductance across the precessing ferromagnet/spin sink interface [3]. We also discuss the mechanism of the plasmonic spin pumping recently demonstrated for a Pt/YIG bilayer with Au nanoparticles being embedded [4].

References:

[1] Y. Tserkovnyak et al., Phys. Rev. Lett. 88, 117601 (2002)

[2] K. Ando et al., Nat. Mater. 10, 655 (2011)

[3] Y. Ohnuma, H. Adachi et al., Phys. Rev. B 89, 174417 (2014)

[4] K. Uchida, H. Adachi et al., Nat. Commun. 6, 5910 (2014)

WE.I.2_O5 - Tunnel magneto-Seebeck effect in Heusler compound tunnel junctions

A. Boehnke¹, U. Martens², M. von der Ehe², C. Franz³, M. Czerner³, K. Rott¹, A. Thomas¹, C. Heiliger³, G. Reiss¹, M. Münzenberg²

1. *Center for Spinelectronic Materials and Devices, Physics Department, Bielefeld University, Bielefeld, Germany*

2. *Institut Für Physik, Ernst-Moritz-Arndt-Universität Greifswald, Greifswald, Germany*

3. *I. Physikalisches Institut, Justus-Liebig-Universität Gießen, Gießen, Germany*

In recent spin caloritronic research, several groups have observed the tunnel magneto-Seebeck effect (TMS) in magnetic tunnel junctions (MTJs) incorporating CoFe electrodes and MgO tunnel barriers [1, 2]. Semiconducting materials are known to have large Seebeck coefficients. This is mainly attributed to the gap in their band structure and the asymmetric position of the Fermi-level. Accordingly, half-metals with a band-gap for only one spin-channel may have very different Seebeck coefficients for the majority and minority charge carriers. The tunnel magneto-Seebeck effect (TMS) is a powerful tool to investigate such spin-dependent Seebeck coefficients because separate spin-channels can be defined in magnetic tunnel junctions (MTJs). Here, we investigate the spin-dependent Seebeck coefficients of half-metallic Heusler compounds in Heusler/MgO/CoFe MTJs. In comparison to CoFeB/MgO/CoFeB MTJs with TMR ratios of 80 to 230 % and TMS ratios of 5 to 50 % we find for Co₂FeSi as electrode material TMS ratios of up to 100 % with TMR ratios in the same range. Furthermore, we observe an increase in the measured voltage signal from 10 to 30 μ V in CoFeB to 3 mV in Co₂FeSi based MTJs when heating with a laser power of 150 mW. In addition, thermocurrent measurements were carried out as a function of applied laser power.

Funding by DFG SPP 1538 is acknowledged.

References:

[1] Walter, M., et al. Nature Mater. 10, 742 (2011)

[2] Liebing, N., et al. Phys. Rev. Lett. 107, 177201 (2011)

WE.I.2_O6 - Heat production by diffusion of pure spin current

T. Taniguchi¹, W. Saslow²

1. *National Institute of Advanced Industrial Science And Technology, Kashiwa, Japan*

2. *Department of Physics, Texas A&M University, College Station, United States*

The generation of a pure spin current by spin pumping, the spin Seebeck effect, or the spin Hall effect, has attracted much attention both as fundamental physics and for spintronics device applications. One motivation to utilize a pure spin current, instead of a spin current associated with an electric current, is that it is expected to reduce power consumption in practical applications because of the absence of the Joule heating due to the electric current. In particular, spin pumping has been widely used to generate pure spin current in a ferromagnetic (F)/nonmagnetic (N) multilayer system [1]. However, both spin-flip and spin-diffusion processes within the bulk and across the F/N interface result in an increase of entropy and in heat production. Therefore the heat production is finite even for a system with pure spin current, even in the absence of an electric current. A quantitative evaluation of the heat production, i.e., the dissipation, due to pure spin current therefore is of great significance. This study presents a theory of dissipation due to pure spin current, based on spin-dependent transport theory and thermodynamics [2]. We derive a generalized Joule heating formula that includes both electric current and spin current. The theory is applied to investigate entropy production for spin pumping across an F/N multilayer. Entropy is produced at the interface because spin pumping irreversibly transfers both spin angular momentum and energy from the ferromagnet to the conduction electrons near the interface. We find that the rate of heating production is proportional to the enhancement of the Gilbert damping constant by spin pumping.

References:

[1] S. Mizukami et al., Phys. Rev. B 66, 104413 (2002). K. Ando et al., Phys. Rev. Lett. 101, 036601 (2008)

[2] T. Taniguchi and W. M. Saslow, Phys. Rev. B. 90, 214407 (2014)

WE.J.1_I1 - Novel applications of perpendicular magnetic anisotropy: 3-dimensional MRAM and cancer therapy

Russell Cowburn¹

1. University of Cambridge, Cambridge, United Kingdom

Most thin magnetic films have their magnetization lying in the plane of the film because of shape anisotropy. In recent years there has been a resurgence of interest in thin magnetic films which exhibit a magnetization easy axis along the surface normal due to so-called Perpendicular Magnetic Anisotropy (PMA). PMA has its origins in the symmetry breaking which occurs at surfaces and interfaces and can be strong enough to dominate the magnetic properties of some material systems. In this talk I describe two novel applications based on the PMA system Pt/CoFeB/Pt. Both take advantage of the strong Brown's paradox present in such materials, i.e. high anisotropy combined with low coercivity. In the first application, we use the PMA material system to design a serial shift register acting between RKKY-coupled magnetic layers which is able to synchronously shift data from the bottom of a heterostructure to the top [1]. Such a shift register could form the basis of a 3-dimensional MRAM cell. In the second application, we lithographically structure a high-moment synthetic antiferromagnet layer system into microelements which we then lift off into solution to form a ferrofluid with carefully designed magnetic properties. This ferrofluid is then used for mechanical-disruption cancer therapy both in-vitro and in-vivo against glioblastoma cancer cells.

References:

[1] Lavrijsen, Cowburn et al. Nature 493, 647 (2013)

WE.J.1_O2 - In operando magnetic writing head quantitatively mapped using electron holography

A. Masseboeuf¹, J. Einsle², R. Bowman², M. Bashir³, M. Gubbins³, C. Gatel¹, R. Cours¹, E. Snoeck¹

1. CNRS-CEMES & Université Paul Sabatier, Toulouse, France

2. Queens University, Belfast, United Kingdom

3. Seagate Technology, Londonderry, United Kingdom

Electron holography (EH) is an interferometric method using an electron beam particularly efficient for the quantitative studies of local magnetic fields with a resolution of the order of few nanometers over large field of view as large as few microns. We developed a new set-up allowing for the first time to quantitatively map in-situ in a TEM the induction field generated by the write pole in operating of a hard disk drive (HDD) developed by Seagate Technology for perpendicular magnetic recording.

The use of EH allows for a complete mapping of the magnetic fields generated by the writer as a function of the applied electrical current. The resulting quantified field maps demonstrate the key features desired for a writing magnetic pole : low spread of a high magnetic flux over a reduce area. Further, since the writers control electronics are designed to operate at GHz frequencies, we demonstrated the possibility of performing time resolved magnetic dynamic studies to obtain quantitative information about the damping of the magnetic induction as a function of the applied current frequency. The magnetic induction maps obtained by EH for various applied currents have been successfully simulated using micromagnetic simulation using the geometrical parameters of the writer.

WE.J.1_O3 - A development of advanced barium ferrite tape media

O. Shimizu¹, M. Oyanagi¹, Y. Kurihashi¹, A. Morooka¹, T. Harasawa¹

1. FUJIFILM Corporation, Tokyo, Japan

The total global volume of digital data is increasing at an explosive rate and is projected to reach 44 zettabytes (ZB) by 2020—10 times the volume of data estimated for 2013 [1]. Particulate media-based tape storage systems are widely used for data backup and archiving applications because of their low cost, stability of the recording media for long term data retention, and the reliability of information retrieval and reproduction. Therefore, the continuous increase in the storage capacity of magnetic tapes is important. In order to achieve a higher areal recording density, smaller magnetic particles are essential. We have developed a magnetic tape media using barium ferrite particles as small as 1350 nm³, which is approximately 30% smaller than those used in LTO6 barium ferrite tape (LTO6B) and less than 50% of those used in LTO6 metal particulate tape (LTO6M). The signal-to-noise ratio (SNR) of our tape was 3.5 dB and 10.5 dB higher than that of LTO6B and LTO6M, respectively, at 300 kfc. Such a high SNR was achieved not only because of the use of smaller magnetic particles, but also by using perpendicular orientation of magnetization and providing a smoother surface to reduce spaces between those particles. Surface roughness (Ra) of this tape was 2.0 nm compared with 2.4 nm in the case of LTO6B. Contribution of particle size, orientation, and surface roughness to SNR is estimated to be 1.5 dB, approximately 1 dB, and approximately 1 dB, respectively. The large increase in SNR from LTO6M is explained by the difference of transition parameter between barium ferrite media and metal particulate media.

References:

[1] IDC, "The Digital Universe of Opportunities: Rich Data and the Increasing Value of the Internet of Things," <http://www.emc.com/collateral/analyst-reports/idc-digital-universe-2014.pdf>

WE.J.1_O4 - Circuit architecture for NAND logic operation via STT-MTJ

D. Loy¹, S. Goolaup², W. Siang Lew³

1. Nanyang Technological University, Singapore

Spin-transfer torque (STT) magnetic random access memory is one of the most promising candidates for next-generation non-volatile memory and logic devices owing to its high endurance, fast read/write speed and low power consumption. The main component of magnetic random access memory is the magnetic tunnel junction (MTJ), which is a magnetic element comprising of two magnetic layers (free and fixed) sandwiching a thin insulating layer. In this work, we present a simplified circuit configuration based on a STT-MTJ structure that is capable of performing NAND logic operations. Our proposed STT-MTJ structure comprises of five terminals, with decoupled reading and writing operations. In this structure, two terminals are used for writing, two are used for reading and the remaining terminal is used for potential tapping. In the two terminals used for writing, magnetization switching of the free layer is carried out by current-induced domain wall motion between two oppositely-charged writing terminals. The three remaining terminals are used to provide complimentary output (reading) and for acting as a potential tap. Two 5-terminal STT-MTJ structures are connected in a circuit and corresponding branches have complementary high and low resistances. PSPICE was used to simulate the circuit architecture with the STT-MTJ terminals represented by their respective high and low resistance using variable resistors. Our simulation shows that in a circuit structure comprising of just two STT-MTJ devices, a NAND logic operation can be performed. The scalability of this logic circuit makes it superior over similar logic devices. In addition, modifications to the circuit logic operations could allow us to achieve different logic operations such as OR, NOT etc.

WE.J.1_O5 - Ferromagnetic tetragonal Heusler thin films for spintronic applications

J Jeong¹, Y. Ferrante^{1,2,3}, S. Faleev¹, M. Samant¹, C. Felser⁴, S. Parkin⁵

1. IBM Almaden Research, San Jose, United States
2. The Graduate School of Excellence 'Materials science in Mainz', Mainz, Germany
3. University of Kaiserslautern, Physics dept., Kaiserslautern, Germany
4. Max Planck Institute for Chemical Physics of Solids, Dresden, Germany
5. Max Planck Institute of Microstructure Physics, Halle (Saale), Germany

Heusler alloys are class of materials with X_2YZ or XYZ and structure L_{21} or C_{1b} where X and Y are from transition metals or Lanthanides and Z is from the main group element. Heusler alloys are of great interest both scientifically and technologically due to their nature of multifunctionality and tunability: topological insulators[1], the possible existence of skyrmions[2], and half-metallicity[3] or high spin polarization etc. A subset of Heusler alloys which show high perpendicular magnetic anisotropy originating from the tetragonal distortion of the unit cell are of great importance in spintronic applications. As an example, Mn-based alloys such as Mn_3Ge and $Mn_{2-x}Ga$ have been extensively studied in both bulk and thin films where Mn spin moments between two adjacent planes were coupled antiferromagnetically. In this work, ternary/quaternary Heusler thin films were deposited by cosputtering of various constituting elements on both amorphous (Si/SiO₂) or single crystal MgO(100) substrate with proper choices of buffer layers. These materials were chosen as candidates to have tetragonal distortion with ferromagnetic coupling between magnetic layers predicted by DFT calculation. Magnetization, magnetic anisotropy and the structural property of deposited Heusler alloy films were measured and compared with the property of Mn-based tetragonal ferrimagnetic Heuslers.

References:

- [1] Stanislav Chadov et. al, Nature Mat. 9, 541-545 2010
- [2] O. Meshcheriakova et. al, Phys. Rev. Lett. 113, 087203 2014
- [3] M. Jourdan et. al, Nature Com. 5, 3974. 2014

WE.J.2_I1 - Composition and morphology of Fe-Si interfaces and (Fe/Si)₃ multilayer nanostructures

J. Bartolomé¹, L. Badía-Romano¹, J. Rubín¹, F. Bartolomé¹, C. Magén², D.E. Bürgler³, J. Rubio-Zuazo⁴, G.R. Castro⁴, S.N. Varnakov⁵, I.A. Yakovlev⁵, I.A. Tarasov⁵, M.S. Platunov⁵, S.G. Ovchinnikov⁵

1. *Instituto De Ciencia De Materiales De Aragón, Zaragoza, Spain*

2. *Laboratorio de Microscopias Avanzadas (LMA) Instituto de Nanociencia de Aragón, Universidad de Zaragoza, Zaragoza, Spain*

3. *Peter Grünberg Institut (PGI-6), Forschungszentrum Jülich GmbH, Jülich, Germany*

4. *ApLine Spanish CRG at ESRF, Grenoble, France*

5. *L.V. Kirensky Institut of Physics, SB RAS, Ktasnoyarsk, Russia*

During the past two decades, the growth and characterization of ferromagnetic metal/semiconductor have received much attention. In particular, the Fe/Si multilayer magnetic structures are quite interesting since they are compatible with Si microchip technology. Their performance depends on the iron silicides formed at the interfaces since they can affect their physical properties and possible applications. In this work we focus on Fe/Si nanometric multilayer samples, which were prepared by thermal evaporation under ultrahigh vacuum onto a Si(100) substrate¹, and on on GaAs(100)/Fe(1 nm)/Ag(150 nm) buffer². The morphology of the Si-on Fe interface was studied by a combination of scanning transmission electron microscopy, X-ray reflectivity, angle resolved X-ray photoelectron spectroscopy, hard X-ray photoelectron spectroscopy and XMCD^{1,2,3}. The nterface thickness and roughness were determined. Moreover, the stable and metastable Fe silicide phases formed at both Fe-on-Si and Si-on-Fe interfaces were determined using conversion electron Mössbauer spectroscopy on multilayers with well separated Si-on-Fe and Fe-on-Si interfaces and when the Fe layer thickness is several nanometers thick. The reported examples of Fe/Si interfaces are reviewed and compared.

References:

1. L. Badía-Romano, J. Rubín, F. Bartolomé, C. Magén, J. Bartolomé, S.N. Varnakov, S.G. Ovchinnikov, J. Rubio-Zuazo, G.R. Castro, *J. of Alloys and Comp.* 627, 136-145 (2015)
2. L. Badía-Romano, J. Rubín, C. Magén, D. E. Bürgler, and J. Bartolomé, *J. of Appl. Phys.* 116, 023907 (2014)
3. M.S. Platunov, S.N. Varnakov, S.M. Zharkov, G.V. Bondarenko, E. Weschke, E. Schierle, and S. G. Ovchinnikov, *JETP Letters* 99(12), 706-711 (2014)

WE.J.2_O2 - Influence of the type of magnetic domain walls on magnetization reversal of bilayer permalloy-niobium nanostructures

L.S. Uspenskaya¹, S.V. Egorov¹

1. Institute of Solid State Physics RAS, Chernogolovka, Russia

For many years it was studied the problem how would be changed the magnetic domain structure of soft magnetic material under the influence of the vicinity of superconductor [1-5]. Here we report our recent results on the experimental study of low temperature behavior of magnetic domain structure of permalloy in bilayer hybrid films permalloy-niobium. Kinetics of magnetization reversal is studied in bilayer permalloy-niobium hybrid nanofilms by means of a magneto-optic visualization technique [6]. The Nb-sublayer is found to affect the width of magnetic domain walls, the type of the walls, the orientation of the walls, and the kinetics of magnetization reversal in permalloy. Moreover, the low temperature magnetization reversal dependence upon the high temperature prehistory is revealed for a permalloy layer with domain walls of Bloch type. The niobium retains the information about a magnetic pattern freezed in permalloy and causes its reproduction during magnetization reversal. The “memory” is intact under magnetic field cycling as well as under a current flow. The effect demonstrates the efficiency of magnetic pinning and opens a new method for reversible variation of electromagnetic properties of hybrid devices.

References:

- [1] A.I.Buzdin, Rev.Mod.Phys.77 (2005) 935
- [2] I.F.Lyuksyutov, V.L.Pokrovsky, Adv.Phys. 54 (2005) 67
- [3] E.B. Sonin, Phys.Rev.B 66 (2002) 100504
- [4] L.N. Bulaevskii, E.M.Chudnovsky, Phys.Rev.B 63 (2000) 012502
- [5] V. Vlasko-Vlasov, A.Buzdin, A.Melnikov et al., Phys.Rev.B 85 (2012) 064505
- [6] L.S. Uspenskaya, S.V. Egorov. Physica B 435 (2014) 160

WE.J.2_O3 - Comparative study of pair correlations in superconducting-magnetic hybrid systems

A. Bill¹, T. E. Baker², A. Richie-Halford³

1. *California State University Long Beach, Long Beach, United States*

2. *University of California, Irvine, United States*

3. *University of Washington, Seattle, United States*

The proximity of a superconductor to an inhomogeneous magnetic material induces singlet and triplet pair correlations. The amount of each component and their presence deep in the magnetic material strongly depends on the hybrid structure and in particular on the type of magnetic inhomogeneity. We present a comparative study of pair correlations in a diffusive magnetic Josephson junction involving a multilayer with misaligned magnetization, a cosine-type helical structure and the domain wall of an exchange spring. We demonstrate that the three systems induce qualitatively different mixtures of correlations.

Misaligned homogeneous films and continuously rotating magnetizations do not display the same physical state. The relative weight of different pairing correlations is discussed by analyzing the Gor'kov functions and the cascading proximity effect [1,2]. We find that so-called short range singlet correlations can be found deep in the magnetic material and compete with triplet correlations giving rise to the singlet-triplet 0- π transition introduced in [2].

References:

[1] T.E.Baker, A.Richie-Halford, O.E.Icreverzi, and A.Bill, *Europhys. Lett.* 107, 17001 (2014).

[2] T.E.Baker, A.Richie-Halford, and A.Bill, *New J.Phys.* 16, 093048 (2014). See also the video abstract!

We gratefully acknowledge support from the National Science Foundation (DMR-1309341). TEB graciously thanks the support of the Orange County Achievement Rewards for College Scientists Fellowship (ARCS).

WE.J.2_O4 - Flexible magnetic actuator-cum-electrically conducting sheet based on FeNi₃-bacterial cellulose nanocomposite

T. Vijayabaskaran¹, S. Vitta¹

1. Indian Institute of Technology Bombay, Bombay, India

Bacterial cellulose (BC), a highly porous reticulate hydrogel polymer which is biodegradable has been functionalized into a magnetic actuator which is also electrically conducting by the incorporation of FeNi₃ nanoparticles. These nanoparticles have been incorporated through an aqueous phase reduction technique and the resulting FeNi₃-BC hydrogel is made into flexible sheets by pressing at 65°C under different applied pressures. X-ray diffraction combined with SEM and TEM shows the presence of spherical FeNi₃ nanoparticles of size varying between 20 nm and 250 nm distributed in the reticulate BC matrix. The room temperature field dependent magnetization clearly shows a ferromagnetic behavior with saturation magnetization of 18.9 emu/g and a coercivity of 31 Oe, a soft magnetic characteristic of FeNi₃. Temperature dependent dc magnetization indicates the presence of superparamagnetic particles with a blocking temperature, T_B between 13 and 15 K. Temperature dependent ac susceptibility exhibits a frequency dependent maximum between ~15 and 16 K. The rate at which the susceptibility maximum shifts with applied frequency indicates the presence of interparticle interactions. To determine the extent and nature of these interactions, electrical conductivity was investigated. It is seen that the sheets are conducting with a conductivity of 6.8 S/cm and 41.2 S/cm at 300 K for the two applied pressures 9 and 26 MPa respectively and it increases with decrease in temperature. The conductivity exhibits a temperature dependence which is typical of metals with a positive temperature coefficient of resistivity. These electrical and magnetic studies of FeNi₃-BC composite clearly show (i) coexistence of larger ferromagnetic and smaller superparamagnetic FeNi₃ particles, (ii) existence of spinglass like behavior at low temperatures and (iii) increase in percolating conducting path with increase in applied pressure which also affects the magnetic behavior.

WE.J.2_O5 - The ultimate hard magnetic MFM tip - a new approach to advanced magnetic force microscopy imaging

V. Neu¹, T. Sturm¹, S. Vock¹, L. Schultz¹

1. IFW Dresden, Dresden, Germany

A novel magnetic force microscopy (MFM) tip has been developed which has unprecedented high coercivities of up to 2 T. Its largely improved stability against demagnetizing fields allows superior contrast detection when applied in external fields and for the investigation of modern permanent magnet materials with large stray fields.

The MFM tip is based on a 50 nm thin epitaxially grown SmCo₅ film with a single orientation of the magnetic easy axis along an in-plane substrate edge. A triangularly shaped piece of film/substrate with base length of 2 μm and height of 15 μm is separated from the as-grown sample by focused ion beam (FIB) and is attached to a Si cantilever.

The imaging performance is tested on (i) a Co/Pt multilayer sample with a fine-scaled band domain pattern (ca. 170 nm), and (ii) a coarse grained Sm₂Co₁₇ alloy, which develops a large scaled domain structure (1 – 5 μm) with large stray fields. Tip calibration routines known from quantitative MFM are applied to extract the tip transfer function of the novel MFM tip. It fully compares in imaging quality with commercially available tips concerning sensitivity and resolution. The superiority of these tips shows itself in the ability to observe clear domain contrast on top of the Sm₂Co₁₇ magnet. To fully probe the tip's stability against external fields, it has been successively demagnetized and the magnetization state of the tip has been evaluated from zero-field MFM measurements on the two reference samples. The tip reversal is constructed as a function of applied field and was found to occur at above 0.8 T, but also to depend on the reference sample. This seeming discrepancy can be resolved when considering a domain nucleation at the tip apex and a hindered (pinned) domain expansion into the tip interior.

WE.J.2_I6 - Josephson superconductor/ferromagnet/superconductor structures and their possible applications in superconducting digital and quantum logics

V. Ryazanov¹

1. Institute of Solid State Physics, Russian Academy of Sciences, Chernogolovka, Russia

Josephson hybrids based on superconductors (S), normal metals (N) and ferromagnets (F) attract increasing attention in the last decade. Among the achievements made on SFS sandwiches it should be noted implementation of the pi-junction (superconducting phase inverter) [1] and realization of SFS switches for ultra-low-power, high-density cryogenic memories [2]. Our recent observations are carried out on planar multiterminal S/F/N structures and related with quasiparticle and spin injection to Josephson junctions. (See [3,4], for example).

References:

- [1] V.V. Ryazanov, V. A. Oboznov, A.Yu. Rusanov, A.V. Veretennikov, A.A. Golubov, and J. Aarts, Phys. Rev. Lett. 86, 2427 (2001)
- [2] T. I. Larkin, V. V. Bol'ginov, V. S. Stolyarov, V. V. Ryazanov, I. V. Vernik, S. K. Tolpygo, O. A. Mukhanov, Appl. Phys. Lett. 100, 222601 (2012)
- [3] T. E. Golikova, F. Hübner, D. Beckmann, I. E. Batov, T. Yu. Karminskaya, M. Yu. Kupriyanov, A. A. Golubov, and V. V. Ryazanov. Phys. Rev. B 86, 064416 (2012). [4 T. E. Golikova, M. J. Wolf, D. Beckmann, I. E. Batov, I. V. Bobkova, A. M. Bobkov, and V. V. Ryazanov, Phys. Rev. B 89, 104507 (2014)

Th.A.1_O1 - Spin-lattice coupling and magnetocrystalline transition in $\text{Pr}_{0.50}\text{Sr}_{0.50}\text{CoO}_3$ investigated by x-ray absorption and neutron diffractionJ. Padilla-Pantoja¹, J. Herrero-Martín², B. Bozzo¹, C. Ritter³, J. Blasco⁴, J.L. García-Muñoz¹*1. Institut de Ciència de Materials de Barcelona, Bellaterra, Spain**2. ALBA Synchrotron Light Source, Cerdanyola del Vallès, Barcelona, Spain**3. Institute Laue Langevin, Grenoble, France**4. Instituto de Ciencia de Materiales de Aragón, Dep. Física de la Materia Condensada, CSIC-Universidad de Zaragoza, Zaragoza, Spain*

Cobalt-based perovskites are attracting much interest as strongly correlated electron systems due to the relevance of the cobalt spin state for their functional properties. The spin state of trivalent cobalt is a key feature in half-doped $\text{Pr}_{0.50}\text{Sr}_{0.50}\text{CoO}_3$ (A: Ca or Sr) perovskites. Here the spin-lattice coupling gives rise to non-conventional magnetic and electronic transitions whose interpretation has been controversial.

The macroscopic properties of $\text{Pr}_{0.50}\text{Sr}_{0.50}\text{CoO}_3$ (PSCO) noticeably differ from those in $\text{Pr}_{0.50}\text{Sr}_{0.50}\text{CoO}_3$ (PCCO), where a spin-state change has been proved to induce a partial Pr^{3+} to Pr^{4+} valence shift and a exotic metal-insulator transition around 80 K [1]. Recent works have confirmed the importance of the spin-lattice coupling in PSCO reporting magnetostructural changes at 120K. We have investigated the properties of PSCO (always metallic, and ferromagnetic below $T_C \sim 230$ K) across the unexpected magnetostructural transition at $T_S \sim 120$ K [2]. X-ray absorption experiments (XAS) at the Pr M_{4,5} and L₃ edges rule out any trace of Pr^{4+} below T_S , and a large density of empty Co t_{2g} states precludes pure nonmagnetic Co^{3+} ions at low temperature unlike the PCCO compound. In addition, the sudden changes in the magnetization at T_S have been investigated by XAS, X-ray magnetic circular dichroism (XMCD) at Co L_{2,3} edges, and by neutron diffraction down to 5 K, revealing that they are driven by a $I_{\text{mma}} \rightarrow I_{\text{4/mcm}}$ symmetry change and spin reorientation of Co moments. They present a significant orbital contribution, and an anomalous m_I/m_S evolution concomitant to the stretching of CoO_6 octahedra at 120 K. Sudden spin state changes are discarded in this system, whose properties differ from related $\text{Ln}_{0.50}\text{A}_{0.50}\text{CoO}_3$ (Ln: lanthanide) compounds.

References:

[1] J.L. García-Muñoz et al, Phys. Rev. B 84, 045104 (2011)

[2] J. Padilla-Pantoja et al, Inorg. Chem. 53, 8854 (2014), also Inorg. Chem. 53, 12297 (2014)

Th.A.1_O2 - Magnetic properties of the 3d-5d double perovskite Sr₂FeOsO₆: Microscopic insights from ab-initio density-functional theory study

S. Kanungo¹, B. Yan^{1,2}, M. Jansen^{1,3}, C. Felser¹

1. Max Planck Institute For Chemical Physics of Solids, Dresden, Germany

2. Max-Planck-Institut für Physik komplexer Systeme, Dresden, Germany

3. Max-Planck-Institut für Festkörperforschung, Stuttgart, Germany

Using density-functional theory calculations, we investigated the electronic and magnetic properties of the ordered 3d-5d double perovskite Sr₂FeOsO₆, which has recently drawn attention for interesting antiferromagnetic (AFM) phase transitions in experiment. The calculated effective magnetic exchange interactions for reveal the importance of long-range super-super-exchange interactions in this compound.

The competition between the weak ferromagnetic Os-O-Fe short-range interaction and strong antiferromagnetic Os-O-Fe-O-Os long-range interaction induces strong magnetic frustration along the crystallographic c axis. This frustration is proposed to drive the magnetic phase transition between two AFM phases and related lattice distortion, which were observed in experiment. To understand, whether this is a general trend or not we studied another 3d-5d double perovskite Sr₂CoOsO₆ [2], and this also shows similar type of trend in the magnetic exchange interactions, although in the low temperature Co and Os sub-lattices follow very different spin dynamics. Ab-initio calculations indicate that the weak effective exchange coupling between Co and Os sub-lattices, drives this difference in the ground states and spin dynamics of Co and Os, making Sr₂CoOsO₆ distinct from previously reported double-perovskite compounds.

References:

1. Sudipta Kanungo et.al; Phys. Rev. B 89,214414 (2014)
2. Binghai Yan et. al Phys, Rev. Lett. 112, 147202 (2014)]

Th.A.1_O3 - Field-induced spin-structural transition in ising chain CoV₂O₆

M. Nandi¹, N. Khan¹, D. Bhoi¹, A. Midya¹, P. Mandal¹

1. Saha Institute of Nuclear Physics, Kolkata, India

Recently, the quasi-one-dimensional (1D) spin-chain CoV₂O₆ has received attention to the scientific community due to several interesting features like 1/3 magnetization plateau, large single ion anisotropy etc. Both monoclinic α -CoV₂O₆ and triclinic γ -CoV₂O₆ undergo long-range antiferromagnetic transition below 15 and 7 K respectively and exhibit field-induced metamagnetic transitions at two critical fields H_{c1} and H_{c2} .

We have investigated the temperature (T) and magnetic field (H) dependence of magnetization, specific heat (C_p), and relative sample length change ($\Delta L/L_0$) for understanding the field-induced spin-structural change in CoV₂O₆. Specific heat and the coefficient of linear thermal expansion (α) of monoclinic CoV₂O₆ exhibit a sharp λ -like peak close to transition temperature (T_N) and a huge positive magnetostriction [$\Delta L(H)/L_0$] is also observed below T_N . The large value of magnetostriction below T_N suggests presence of strong spin-lattice coupling in α -CoV₂O₆. With the application of external magnetic field, a sharp and symmetric peak emerges below T_N in both $C_p(T)$ and $\alpha(T)$ due to field-induced ferrimagnetic/ferromagnetic-paramagnetic transitions and the sharp nature of the peak indicates that the transition is first-order.

References:

[1] M. Nandi, N. Khan, D. Bhoi, A. Midya, and P. Mandal. *J. Phys. Chem. C*, 118, (2014), pp.1668-1673

Th.A.1_O4 - Magnetic phase transitions and magnetic interactions in quasi-two-dimensional complex oxides based on brucite-like octahedral layersA. Kurbakov¹, A. Kunevich¹, A. Malyshev¹, V. Nalbandyan², E. Zvereva³

1. Petersburg Nuclear Physics Institute, Gatchina, Russia

2. Southern Federal University, Rostov-on-Don, Russia

3. Moscow State University, Moscow, Russia

The results of neutron powder diffraction study of the crystal structures and spin configurations in new complex oxides with the layered crystal structure are presented. New layered solid electrolyte $\text{Na}_2\text{Ni}_2\text{TeO}_6$ ($P6_3/mcm$) and quasi-two dimensional honeycomb oxides $\text{Na}_3\text{Co}_2\text{SbO}_6$, $\text{Li}_3\text{Ni}_2\text{SbO}_6$ and $\text{Na}_3\text{Ni}_2\text{SbO}_6$ ($C2/m$) were investigated. The studied substances established structural motives on the basis of edge-related oxygen octahedral layers between which there are alkali metal cations or low charging relatively large cations of d-elements. Magnetic cations in the oxygen-octahedral layers form honeycomb grids that on condition of antiferromagnetic type interaction between nearest neighbors can lead to frustration in the magnetic subsystem and the emergence of unusual types of magnetic moments ordering including non-collinear spiral structure.

The appearance of additional reflections related to antiferromagnetic ordering organization of the samples at T_N below 7K ($\text{Na}_3\text{Co}_2\text{SbO}_6$), 15K ($\text{Li}_3\text{Ni}_2\text{SbO}_6$), 17K ($\text{Na}_3\text{Ni}_2\text{SbO}_6$) and 26K ($\text{Na}_2\text{Ni}_2\text{TeO}_6$) is clearly visible on the low-temperature neutron diffraction measurements. At $T > T_N$ the magnetic susceptibility nicely follows the Curie-Weiss law with positive and negative temperatures: $\Theta \approx -25\text{K}$ ($\text{Na}_2\text{Ni}_2\text{TeO}_6$), -10K ($\text{Na}_3\text{Co}_2\text{SbO}_6$) indicating predominance of AFM interaction and $+8\text{K}$ ($\text{Li}_3\text{Ni}_2\text{SbO}_6$), $+12\text{K}$ ($\text{Na}_3\text{Ni}_2\text{SbO}_6$) with predominance of FM. However at low temperatures long-range AFM order is established at all oxides. Hence there is a delicate balance of competing AFM and FM interactions due to difference in character and sign of exchanges between Co^{2+} (Ni^{2+}) ions within the magnetic layer and between the layers.

Especially as it was possible to expect that primary superexchange interaction via half-occupied Co/Ni e_g (d_z^2 , $d_{x^2-y^2}$) orbitals to be FM since within mixed-cation layers of Co/Ni and Sb/Te the Co(Ni)-O-Co(Ni) cation-anion angles are close to 90° .

It is demonstrated that there is a clear correlation between fine specific features and temperature evolution of crystal structures, the corresponding types of low-temperature spin ordering, and physical properties all researched systems.

Th.A.1_O5 - Local magnetic behavior across the first order phase transition of the $\text{La}(\text{Fe}_{0.9}\text{Co}_{0.015}\text{Si}_{0.085})_{13}$ magneto caloric compound

C. Bennati^{1,2}, F. Laviano¹, M. Kuepferling², E. Olivetti², V. Basso², G. Ghigo¹

1. *Department of Applied Science and Technology, Politecnico di Torino, Turin, Italy*

2. *Istituto Nazionale di Ricerca Metrologica (INRIM), Turin, Italy*

$\text{La}(\text{Fe,Si})_{13}$ based compounds [1] are known to show a giant magneto-caloric effect (MCE) due to the first order nature of their magneto structural transitions which can be easily tuned by substitution by Co or Mn. Such substitutions might lead to phase inhomogeneities which can influence drastically the kinetics of the phase transition, an important feature in order to judge the materials performance in refrigeration cycles.

We studied the compound $\text{La}(\text{Fe}_{0.9}\text{Co}_{0.015}\text{Si}_{0.085})_{13}$ by a magneto optical imaging technique with indicator film (MOIF) in order to investigate the local magnetic behavior during the temperature driven phase transition. Isothermal hysteresis loops (up to 70 mT) were recorded to spatially resolve the magnetic response of the compound at constant temperatures around the Curie temperature, $T_c = 200$ K. The magnetic permeabilities in different areas of dimension $10\text{-}1000 \mu\text{m}^2$ were analyzed statistically and differences between the matrix and isolated grains of secondary phases were found. We observed soft ferromagnetic (FM) grains, which have a constant permeability across the entire temperature range (185-215 K) and, for $T < T_c$, paramagnetic isolated grains (PM) which show a wide distribution of permeabilities.

The evidence of minor phases at the surface is also confirmed by SEM analysis, where isolated islands of Fe-rich phase (FM grains) and La-rich phase (PM grains) were observed. The correlation and the interaction between the parent phase and the secondary magnetic phases is thus discussed at a local spatial scale. In fact, when sweeping the temperature across the phase transition, we find that (i) the new magnetic phase nucleates in different areas at slightly different temperatures, thus we recognize Co/Si graded grains in the matrix (i.e. T_c -graded grains), (ii) there exists a secondary phase that remains paramagnetic in the whole temperature range. These secondary phases and the T_c -graded grains influence the nucleation of the new magnetic phase (the transition always starts close to one of them) and act as pinning centres for the transition thus influencing the propagation of the transition front [2].

References:

[1] A. Fujita et al., J. Appl.Phys. 85, 4756 (1999)

[2] M. Kuepferling et al., J. Appl. Phys. 115, 17A925 (2014)

Th.A.1_O6 - Magnetism of sigma-phase Fe-Mo alloys: revealing spin-glass as the ground state

S. Dubiel¹, J. Przewoznik¹

1. AGH University of Science And Technology, Krakow, Poland

Sigma-phase (space group D144h - P42/mnm) is a member of Frank-Kasper family of phases. Among over 40 known binary alloys in which sigma-phase occurs, only sigma-phase in Fe-Cr and Fe-V alloys was known, until recently, to possess magnetic properties. Freshly, magnetism of sigma-phase was discovered in Fe-Re [1] and Fe-Mo [2] alloy systems. To further characterize the magnetism in the latter, an AC magnetic susceptibility study was carried out on a series of sigma-Fe(100-x)Mo(x) (x =47-53) samples. This contribution reports the first ever AC susceptibility results obtained on this kind of alloys. Clear evidence was found that a spin glass (SG) constitutes the ground magnetic state of the alloys and the SG temperature ranges between 34K for x=47 and 16K for x=53. The SG state was found to be magnetically heterogeneous as far as an irreversibility is concerned, and it can be divided into a weak- and a strong-irreversibility domains. Figures of merit are typical of metallic (canonical) spin glasses hinting that the RKKY interaction is responsible for the magnetism. In particular, a relative shift of the SG temperature per decade of frequency ranges between 0.012 and 0.013 and the dynamic exponent, $z\nu$, varies between 8 and 10.

References:

- [1] J. Cieslak, S. M. Dubiel, M. Reissner, J. Tobola, J. Appl. Phys., 116 (2014) 183902
- [2] J. Cieslak, S. M. Dubiel, M. Reissner, J. Tobola, arXiv:1411.2446 (2014)

Th.A.2_O1 - Magneto-elastic coupling across the first order transition in the distorted kagome lattice antiferromagnet Dy₃Ru₄Al₁₂

M.S. Henriques^{1,2}, D.I. Gorbunov^{1,3}, A.V. Andreev¹, A. Gukasov⁴, V. Petříček¹, Y. Skourski³, M. Vališka⁵, J. Prokleška⁵, D. Kriegner⁵, Z. Matěj⁵, A.P. Gonçalves²

1. Institute of Physics ASCR, Prague, Czech Republic

2. CCTN, IST/CFMCUL, University of Lisbon, Nuclear and Technological Campus, Bobadela, Portugal

3. Dresden High Magnetic Field Laboratory (HLD), Helmholtz-Zentrum Dresden-Rossendorf, Dresden, Germany

4. Laboratoire Léon Brillouin, CE de Saclay, Gif-sur-Yvette, France

5. Charles University in Prague, Faculty of Mathematics and Physics, Department of Condensed Matter Physics, Prague, Czech Republic

Dy₃Ru₄Al₁₂ crystallizes in the hexagonal Gd₃Ru₄Al₁₂ archetype structure, in which Dy atoms form corner sharing distorted kagome nets. A single crystal was grown and its physical properties were first studied by means of magnetization, neutron diffraction, specific heat and resistivity measurements. It was found that Dy₃Ru₄Al₁₂ orders antiferromagnetically at $T_N = 7$ K in a non-collinear monoclinic magnetic structure with $\mathbf{k} = (1/2 \ 0 \ 1/2)$. The transition is of first-order as indicated by the anomalies in the specific heat, resistivity and the intensity of magnetic reflections. Additionally, the magnetic ordering of the Dy atoms presents some fingerprints of geometrical frustration, which is manifested also by metamagnetic transitions in all lattice directions accompanied by large positive magnetoresistance up to 140%. This altogether indicates a complex balance among the RKKY exchange interactions, the crystal-field induced magnetic anisotropy and Zeeman energy.

Thermal expansion and low temperature X-ray diffraction were performed across the magnetic transition, confirming its first-order character. The linear thermal expansion is step-like with a change of $\Delta l/l \approx 3 \times 10^{-5}$ at the transition, highly anisotropic and hysteretic upon cooling and heating. Structural refinements suggest that there is no symmetry lowering down to 2.5 K, but coupling between the lattice and the spin was disclosed by anomalies in the variation of the lattice parameters with temperature in the vicinity of T_N . Moreover, further data analysis has shown that the distance between the near nearest Dy atoms reaches an absolute minimum close to the critical temperature.

Th.A.2_O2 - Chiral magnetism in rare-earth intermetallic compounds YbNi_3Al_9 and $\text{Yb}(\text{Ni}_{0.94}\text{Cu}_{0.06})_3\text{Al}_9$ S. Ohara¹, H. Ninomiya¹, Y. Matsumoto¹, Y. Kousaka², K. Ohishi³, J. Akimitsu⁴*1. Nagoya Institute of Technology, Nagoya, Japan**2. Graduate School of Science, Hiroshima University, Hiroshima, Japan**3. Research Center for Neutron Science and Technology, Comprehensive Research Organization for Science and Society (CROSS), Naka, Japan**4. Department of Physics and Mathematics, Aoyama-Gakuen University, Shibuya, Japan*

In chiral magnetic materials, the combined effect of symmetric ferro- (or antiferro-) magnetic and antisymmetric Dzyaloshinskii-Moriya (DM) interaction will give rise to a helical or a canted magnetic structure. In recent years, chiral magnets have attracted much attention because they exhibit new spin-configurations, such as a skyrmion in MnSi and a chiral soliton lattice in $\text{Cr}_{1/3}\text{NbS}_2$. However, only a few materials have been known for chiral magnets. Moreover, most of the work has been done on 3d transition-metal compounds but very few reports on 4f rare-earth intermetallic. Recently, we have succeeded in synthesizing a new chiral crystal of rare-earth intermetallic compounds RNi_3X_9 (R: rare-earth elements, X: Al and Ga). In this work, we report chiral crystal structure and chiral magnetism of YbNi_3Al_9 and $\text{Yb}(\text{Ni}_{0.94}\text{Cu}_{0.06})_3\text{Al}_9$. To study the chiral properties in 4f-magnetism, X-ray diffraction, polarized neutron scattering and magnetization measurements have been taken on the single crystalline samples. The crystal structures are identified as the trigonal ErNi_3Al_9 -type with chiral space group R32. YbNi_3Al_9 is a helimagnet below an ordering temperature of $T_m=3.4\text{K}$ with a magnetic wave vector $q=(0, 0, 0.8)$. We confirmed that the magnetic satellite intensities depend on incident neutron polarization for YbNi_3Al_9 . In magnetization process, a metamagnetic transition is observed at a magnetic field of $H_m=1\text{kOe}$ with the magnetic field applied perpendicular to c-axis at 2K. We can enhance both T_m and H_m by copper substitution. For $\text{Yb}(\text{Ni}_{0.94}\text{Cu}_{0.06})_3\text{Al}_9$, T_m and H_m are 6.5 K and 10 kOe, respectively. The magnetization process in $\text{Yb}(\text{Ni}_{0.94}\text{Cu}_{0.06})_3\text{Al}_9$ was very similar to that in uniaxial chiral magnet $\text{Cr}_{1/3}\text{NbS}_2$ and in good agreement with the theoretical result based on the chiral soliton lattice. We conclude that the magnetic ordering in $\text{Yb}(\text{Ni}_{1-x}\text{Cu}_x)_3\text{Al}_9$ ($x=0$ and 0.06) can be chiral helical due to combined effect of Ruderman-Kittel-Kasuya-Yosida (RKKY) and DM interactions in the chiral crystal.

Th.A.2_O3 - Observation of large anomalous Kerr rotations in the Skyrmionic Mott insulator Cu_2OSeO_3

R.B. Versteeg¹, S. Schöfer¹, A. Aqeel², T.T.M. Palstra², P.H.M. Van Loosdrecht¹

1. *University of Cologne - II. Physics Institute, Cologne, Germany*

2. *Zernike Institute for Advanced Materials, University of Groningen, Groningen, The Netherlands*

The Mott insulator Cu_2OSeO_3 has recently gained considerable scientific interest owing to the presence of a Skyrmion lattice phase. The Skyrmion phase is a magnetic topologically protected state, which manifests itself as a hexagonal lattice of spin vortices, and originates from a combination of different magnetic interactions. Together with their topologically protected nature, the nanometer size scale of Skyrmions may potentially allow them to be harnessed as bits in racetrack memory devices. The ability to achieve all-optical control of Skyrmions would add yet another degree of flexibility to Skyrmion-based devices. This, however, requires intimate knowledge of the magneto-optical properties of these materials, but to date, research in this realm has been limited.

Here, we present the first magneto-optical Kerr Effect (MOKE) spectroscopy study of the Skyrmion material Cu_2OSeO_3 , in order to lay the foundation for better understanding of the magneto-optical properties of this class of materials. of particular interest is our observation of a surprisingly large anomalous Kerr rotation as large as 10 degrees with a nontrivial magnetic field dependence. The light polarization rotation observed at the intersite- $d-d$ and charge transfer transitions allows for the mapping of the magnetic phase diagram of bulk Cu_2OSeO_3 . In addition to gaining insight into the nature of the magnetic phases of these materials, our observations open an exciting new avenue on the quest for optical manipulation of Skyrmionic matter.

Th.A.2_O4 - Observation of various magnetic field-induced states in MnGe with cubic B₂₀ type structure

R. Viennois¹, C. Reibel¹, D. Ravot¹, R. Debord², S. Pailhes²

1. Institut Charles Gerhardt, Université Montpellier, Montpellier, France

2. Institut Lumière Matière, Université Claude Bernard - Lyon 1, Villeurbanne, France

Transition metal compounds with the cubic B₂₀ crystal are interesting because of their very various and exotic magnetic properties induced notably by the lacks of inversion center and fourfold axis in their cubic symmetry structure. The most important discovery in this class of compound was phases containing skyrmions. Recently, the study of MnGe has shown the presence of helimagnetic ground state below about 170 K with short length helix and large topological Hall effect and Nernst effect below 100 K [1]. However the origin of these two effects is still controversial as recent neutron work has shown [2]. Until now, MnGe seemed to behave differently than other compounds with B20 structure as there is no report of A phases containing skyrmions and located at temperature just below the ordering temperature as e. g. in MnSi [3]. But, to date, no systematic study of the magnetic phase diagram of MnGe has been performed. In the present communication, we report our study of the magnetic phase diagram of MnGe by using ac susceptibility experiments. For the first time, we found the presence of several different magnetic field induced phases. First we found not only the presence of an A phase presumably due to the presence of skyrmions as in isostructural compound MnSi but with much broader existence range in the (H,T) domain. We also found second phase we call B at much lower temperatures whose magnetic signature is very similar to that of A phase. Clearly, further studies on these different new magnetic phases are necessary in order to understand the large topological Hall and Nernst effects in MnGe.

References:

[1] Y. Shiomi et al, Phys. Rev. B 88, 064409 (2013)

[2] M. Deutsch et al, Phys. Rev. B 90, 144401 (2014)

[3] S. Mühlbauer et al, Science 323, 5916 (2009)

Th.A.2_O5 - The stable magnetic phase of the Gd doped topological insulator, $\text{Bi}_{2-x}\text{Gd}_x\text{Te}_3$ E.H. Shin¹, M.H. Chung², M. Kim¹, H. Kim¹

1. Sookmyung Women's University, Seoul, Republic of Korea

2. Sogang University, Seoul, Republic of Korea

The discovery of three dimensional strong topological insulators (TI) such as Bi_2Se_3 , Bi_2Te_3 and Bi_2Sb_3 has intrigued many researchers. The surface metallicity in contrast to the insulating bulk state is known to be topologically protected and robust for impurities and disorders as long as the time reversal symmetry is preserved.

One of TI, Bi_2Te_3 was studied to examine whether topological surface state is robust when the transition metals such as Fe, Mn, and Co are doped. In this presentation, we report first-principles calculations on the crystal of $\text{Bi}_{2-x}\text{Gd}_x\text{Te}_3$ ($x = 0.021, 0.042, 0.063, 0.074, 0.083, 0.125$) to understand the effect of substitution of magnetic rare-earth element, Gd (Gd_{Bi}) on the surface metallicity and the magnetic property.

A single Gd_{Bi} 's in Bi_2Te_3 crystal ($x=0.021$) is calculated to carry a spin magnetic moment of $7 \mu_B$. Two Gd_{Bi} 's in Bi_2Te_3 crystal ($x=0.042$) prefer to be located in the first nearest neighbor sites in the Bi sublattice on a single Bi atomic layer of the same quintuple layer. The magnetic moments of two Gd_{Bi} 's remain unchanged ($7 \mu_B$) and the antiferromagnetic (AFM) configuration is more stable [$\Delta E (=E_{\text{AFM}}-E_{\text{FM}})$ is -2.36 meV] due to super-exchange interaction via the intervening Te atoms.

With the increased concentration of Gd, we found that Gd_{Bi} 's favor to be clustered than to be uniformly dispersed. For instance, Gd_{Bi} 's form a linear chain ($x=0.083$) or a hexagonal ring ($x=0.125$) in the single Bi atomic layer. In most of the clustered structures, the AFM ordering is calculated to be more stable than the FM ordering. Among the considered configurations, the hexagonal ring is most effective in stabilizing the AFM phase ($\Delta E=-14.7 \text{ meV}$).

Th.A.2_O6 - Magnetic order and excitations in the Magnetic Dirac Materials (Ca,Sr)MnBi₂

A. Princep¹, A. Boothroyd¹, Y. Guo¹, X. Zhang², P. Manuel³, D. Khalyavin³, I. Mazin⁴, Y. Shi², A Piovano⁵

1. *Department of Physics, University of Oxford, Clarendon Laboratory, Parks Road, Oxford, United Kingdom*
2. *Beijing National Laboratory for Condensed Matter Physics, Institute of Physics, Chinese Academy of Sciences, Beijing, China*
3. *ISIS Facility, Rutherford Appleton Laboratory, Chilton, Didcot, United Kingdom*
4. *Naval Research Laboratory, Washington DC 20375, United States*
5. *Institut Laue-Langevin (ILL), Grenoble, France*

The electronic spectrum of so-called Dirac materials such as graphene and topological insulators is linear. These linearly dispersing “Dirac cones” and associated pseudospins determine the peculiar properties of Dirac materials such as high electron mobility, an anomalous quantum Hall effect, and a large spin-hall effect. Typical Dirac cones are in general isotropic, but several hamiltonians have been investigated which show (for example) k-linear dispersion in one direction but k² dispersion in a perpendicular direction. SrMnBi₂ and CaMnBi₂ have been determined to host highly anisotropic 2D Dirac fermions in a square conducting layer of Bi, with pseudospin dynamics analogous to those of graphene. These two materials are not quite isostructural, but they show giant magnetoresistance and a large magnetothermopower, related to their unusual low temperature transport properties. This result is particularly exciting because the Bi (or other pnictogen) square net is a building block of many layered materials, and the possibility of coupling Dirac fermions to superconducting or magnetic order parameters (as, for instance, in CeNi₂Bi₂ or the hypothetical BaFePn₂) offers a rich playground for the generation and exploration of new physics. Through neutron diffraction and inelastic scattering measurements on single crystal and powder samples, we have shown that both materials exhibit a Neel-type in-plane AFM order with ordered moment of ~3.7 μB (substantially reduced from the free-ion value), broadly consistent with DFT calculations, and that the MnBi₄ layers are coupled ferromagnetically in CaMnBi₂ and antiferromagnetically in SrMnBi₂. The spectrum of excitations shows significant nearest and next-nearest neighbour exchanges, a much weaker inter-plane coupling, and a surprisingly large anisotropy gap. We will discuss the implications of these results, particularly with regard to possible novel ordered phases that could be produced with doping.

Th.A.2_07 - Magnetism of disordered Heusler alloys

M. Leitner¹, P. Neibecker¹, W. Petry¹

1. Technische Universität München, Munich, Germany

Heusler alloys constitute a class of systems with great potential for applications. Most of their appeal rests on the diverse aspects of magnetism in these materials, including the ferromagnetic shape-memory effect, the magnetocaloric effects, and half-metallicity. Due to their intermetallic nature, off-stoichiometry and site disorder constitute degrees of freedom additional to temperature. In previous work we have shown that in Ni₂MnAl well-defined states of order can be prepared, which are accessible via correspondingly varying magnetic transition temperatures [1]. Here we report on a detailed characterization of the peculiar magnetic behaviour, e.g. temperature- and field-dependent magnetization for specific states of order, with nearly constant ferromagnetic susceptibilities up to the highest fields. We present a microscopic model of how Mn/Al site disorder and site-specific ferro- and antiferromagnetic interactions of the Mn moments give rise to observed features as a function of field, temperature, and order.

References:

[1] P. Neibecker, M. Leitner, G. Benka, W. Petry, Appl. Phys. Lett. 105, 261904 (2014)

Th.A.3_O1 - High coercivity in rare earth-lean hot-deformed magnets by grain boundary infiltrationG. Hadjipanayis¹, R. Madugundo¹, D. Salazar Jaramillo², J.M. Barandiaran²*1. Department of Physics and Astronomy, University of Delaware, Newark, United States**2. BCMaterials, Technology Park of Biscay, Derio, Spain*

The recent rare-earth crisis led to worldwide efforts to develop rare-earth lean/free permanent magnets. In this report, we present our recent results on the enhancement of coercivity (Hc) in rare-earth lean Pr(Nd)-Fe-B melt-spun ribbons and hot-deformed magnets by grain boundary modification through infiltration using the low melting temperature eutectic alloys Pr-Cu, Pr-(Cu,Co). Alloys with compositions $\text{Nd}_{10}\text{Fe}_{84}\text{B}_6$, $\text{Pr}_{11.5}\text{Fe}_{81.5}\text{Ga}_1\text{B}_6$ and $\text{Pr}_{12.5}\text{Fe}_{80.5}\text{Ga}_1\text{B}_6$ prepared by arc-melting were melt-spun to produce thin ribbons. The ribbons were crushed to small flakes $<200\ \mu$ and hot-compacted at temperatures between 650-750 C. The compacts were hot-deformed to 75% of their original height at 750 – 850 °C. In $\text{Nd}_{10}\text{Fe}_{84}\text{B}_6$ ribbons, the infiltration was carried out by mixing the ribbon pieces with Pr-(Cu,Co) crushed powder and the mixture was heat-treated at 650°C for 1- 4 hours. In the case of hot-deformed magnets, a thin slice of Pr-Cu alloy, or Pr-(Co,Cu) alloy powder was placed on top of hot-deformed pieces and heat-treated at 650°C for 1 to 4 hours. The ratio of Pr-Cu or Pr-(Co-Cu) alloy to melt-spun ribbon or hot-deformed magnet was 1:5. In $\text{Nd}_{10}\text{Fe}_{84}\text{B}_6$ ribbons, the Hc increases from 5.3 to 23.8 kOe on infiltration with Pr-(Cu,Co) powder for 4 hours. The $\text{Pr}_{11.5}\text{Fe}_{81.5}\text{Ga}_1\text{B}_6$ and $\text{Pr}_{12.5}\text{Fe}_{80.5}\text{Ga}_1\text{B}_6$ hot-deformed magnets show an increase in Hc from 5.4 to 19.5 kOe and 8.4 to 26.4 kOe, respectively on infiltration with Pr-Cu alloy for 4 hours. The microstructure of the melt-spun ribbons and hot-deformed magnets before and after infiltration are currently being studied and the results will be presented and discussed. Work supported by Siemens and Bizkaia Talent AYD-000-195.

Th.A.3_O2 - Grain boundary modifications of hot-deformed Nd-Fe-B permanent magnets with low melting eutectics

S. Sawatzki¹, C. Kübel², S. Ener¹, O. Gutfleisch^{1,3}

1. TU Darmstadt, Materialwissenschaft, Darmstadt, Germany

2. KIT, Institute of Nanotechnology (INT) & Karlsruhe Nano Micro Facility (KNMF), Eggenstein-Leopoldshafen, Germany

3. Fraunhofer IWKS, Projektgruppe für Wertstoffkreisläufe und Ressourcenstrategie, 63457 Hanau, Germany

The grain boundary diffusion process (GBDP) increases coercivity in sintered Nd-Fe-B magnets without losing much in remanent magnetization by only using a very small amount of Dy [1]. Here low melting eutectics DyCu, DyNdCu and TbNdCu have been incorporated by two different methods: first, by mixing the powders together with Nd-Fe-B melt-spun ribbons before hot-compaction and hot-deformation and second, by coating the solid state hot-deformed magnet (conventional GBDP). For the first method the distribution of these eutectics within the nano grained sample has been optimized by grinding as well as by ball milling. For the ternary eutectic alloys, an uniform distribution was observed by scanning electron microscopy (SEM). This uniform distribution was attributed to the lower melting point of DyNdCu and TbNdCu compared to DyCu. Additional annealing of the hot-compacted magnets at 600°C leads to a diffusion of Dy or Tb into the Nd-Fe-B flakes, which was observed by transmission electron microscopy (TEM). This diffusion modifies the grain boundary phase and thus enhances coercivity without decreasing remanence. For die-upset magnets coercivity was suppressed due to grain growth nearby the rare earth rich flake boundaries during the deformation process and could not be increased by additional low temperature annealing. In contrast to this, the second method enhances coercivity during low temperature annealing but also reduces remanence.

References:

[1] Park et al. Proc. 16th Int. Workshop on RE Magnets and their Applications (Sendai, Japan) (2000) p.257

Th.A.3_O3 - High-coercivity Nd-Fe-B permanent magnets based on the electrophoretic deposition of TbF₃

M. Soderžnik¹, K. Üestüener², M. Katter², S. Kobe¹

1. *Jozef Stefan Institute, Ljubljana, Slovenia*

2. *Vacuumschmelze, Hanau, Germany*

In this study, our aim was to substantially improve the coercivity of Nd-Fe-B magnets, based on the electrophoretic deposition (EPD) of TbF₃ powder and subsequent annealing called the grain-boundary diffusion process. In order to retain the remanence as high as possible Nd-Fe-B magnets with a rather low amount of heavy rare earths (HRE) were used as starting material. The overall amount of HRE was 1.6 wt. % (0.1 wt. % of Dy and 1.5 wt. % of Tb). The magnets with the dimensions 12.5 mm × 8 mm × 3.5 mm were evenly coated with TbF₃ powder using the electrophoretic deposition. After the magnets were coated with TbF₃ powder, they were heat treated in vacuum at 875°C for 10 h followed by aging at 500°C for 1 h. The magnetic properties were measured with a Steingroever permeameter. Since the magnets could not be demagnetized at room temperature, the remanence and the coercivity were determined to be $B_r = 1.25$ T and $H_{cJ} = 1580$ kA/m at 70°C, respectively. Applying the temperature coefficients $TK(B_r) = -0.11$ %/K and $TK(H_{cJ}) = -0.63$ %/K, the remanence and coercivity are calculated to be 1,32 T and 2080 kA/m at room temperature, respectively. Using the grain-boundary diffusion process, based on the electrophoretic deposition of TbF₃, we have successfully enhanced the coercivity at room temperature to more than 2000 kA/m, while the remanence exceeded the ambitious value of 1.3 T.

Th.A.3_O4 - Sintering analysis of NdFeB material

B. Hugonnet¹, C. Rado¹, J.M. Missiaen^{2,3}, O. Tosoni¹, F. Servent¹

1. *Univ. Grenoble Alpes, CEA, Grenoble, France*

2. *Univ. Grenoble Alpes, SIMAP, Grenoble, France*

3. *CNRS, SIMAP, Grenoble, France*

NdFeB permanent magnets are used in a broad range of devices including high temperature applications such as electric motors for hybrid cars or wind turbines. Indeed, their high remanence lead to an important weight and size reduction compared to induction magnets. They should contain heavy rare earth (HRE) to conserve enough coercivity at their working temperature. Actually, the use of HRE is a problem because it is a high critical resource and it decreases the magnet remanence. Another possibility to increase the coercivity without using HRE is to work on the microstructure. Indeed, several improvements in magnetic properties of NdFeB magnets have been done since their discovery by decreasing the grain size and by controlling the thickness and the continuity of the grain boundary phase. However, up to date, this solution did not give coercivity required for high temperature application. This could come from the fact that the link between microstructure and coercivity is still empirical. Microstructure could be controlled by a full mastering of the manufacturing process. The steps of sintering and annealing of the NdFeB-aligned powders need to be well understood. The Nd-Rich phase contained in the NdFeB powders plays a role during the sintering and its repartition controls the final magnetic properties. Sintering mechanisms which are responsible for a different shrinkage perpendicular and parallel to the magnetization axis require further investigation. In this work several aspects of NdFeB sintering are discussed based on dilatometric experiments and microstructure observation of sintered magnets. Possible causes of the strong sintering anisotropy have been identified. Calculation of the sintering activation energy has been used to characterize if a liquid phase is present or not at the grain boundary between the magnetic grains. Finally the link between magnetic properties and grain morphology in sintered magnets has been explored.

Th.B.1_I1 - Magnetocaloric effect in type-I $\text{Eu}_8\text{Ga}_{16}\text{Ge}_{30}$ clathrate nanocrystals

H. Srikanth¹, A. Biswas^{1,2}, S. Chandra^{1,3}, S. Stefanoski^{1,4}, J. Blasquez⁵, J. Ipus⁵, A. Conde⁵, M.H. Phan¹, V. Franco⁵, G. Nolas¹

1. Department of Physics, University of South Florida, Tampa FL, United States

2. Ames Laboratory, Ames, IA, United States

3. EMT-INRS, Quebec, Canada

4. Carnegie Institute, Washington DC, United States

5. Physics Department, University of Sevilla, Sevilla, SPAIN

$\text{Eu}_8\text{Ga}_{16}\text{Ge}_{30}$ type-I clathrates have attracted growing attention owing to their intriguing thermoelectric, magnetic and magnetocaloric properties [1-3]. The presence of Eu makes them interesting from the magnetism perspective and also affords the possibility of combining magnetocaloric and thermoelectric functionalities in the same material. The effect of reduction of particle size on magnetism and magnetocaloric response in these materials is reported. Nanocrystalline samples of three different average particle sizes (~42 , 34 , and 15 nm) were prepared by high energy ball milling [3]. While ferromagnetic materials show a general trend of magnetic entropy change ($-\Delta S_M$) decreasing with reduction in particle size, in this system there exists a unique cross-over temperature ($T_{\text{cross}} \sim 25$ K) below which the reduction of particle size enhances $-\Delta S_M$ significantly. The largest value of $-\Delta S_M$ (~ 10 J/kg K for a field change of 5 T at 5 K) is obtained for the sample with particle size of 15 nm, making it a promising candidate for cryogenic magnetic cooling. The observed increase in $-\Delta S_M$ for nanocrystalline samples is attributed to the enhancement of the interactions between Eu ions residing in two different positions in the lattice and responsible for the low temperature transition. Interestingly, the 42-nm particle size sample exhibits a table-like MCE, desirable for ideal Ericsson-cycle magnetic refrigeration.

References:

[1] Nolas et al. in *Semiconductors and Semimetals*, V-69, ed. T. M. Tritt (Academic Press, 2001), p. 255

[2] M. H. Phan, V. Franco, A. Chaturvedi, S. Stefanoski, G. Nolas and H. Srikanth, *Phys. Rev. B*, 84, 054436 (2011)

[3] A. Biswas, S. Chandra, S. Stefanoski, J. S. Blasquez, J. J. Ipus, A. Conde, M. H. Phan, V. Franco, G. S. Nolas and H. Srikanth, *J. Appl. Phys.*, 117, 033903 (2015)

Th.B.1_O2 - Thermoelectricity and thermodiffusion in ferrofluids: Alternative path toward future thermoelectric energy materials

S. Nakamae¹, B.T. Huang¹, T. Salez¹, M. Bonetti¹, M. Roger¹, E. Dubois², C. Filomeno^{2,3}, R. Caneira Gomes^{2,3}, G. Demouchy², M. Kouyaté², V. Peyre², G. Mériquet², R. Perzynski²

1. *Service de Physique de l'Etat Condensé, Gif-sur-Yvette, France*

2. *Laboratoire Physicochimie de Electrolytes et Nanosystèmes Interfaciaux, UPMC, CNRS, Paris, France*

3. *Grupo de Fluidos Complexos, Instituto de Física & Instituto de Química, Universidade de Brasília, Brasília, Brazil*

The unique properties of magnetic nanoparticles and their interactions with their environment continue to give rise to innovative and surprising experimental possibilities outside the field of conventional magnetism. One such example is found in the field of magneto-thermal energy science (e.g., magneto-convection and magneto-caloric effects). In this presentation, we will introduce a hitherto underexplored energy application possibility for magnetic nanoparticles; namely, the thermoelectric energy conversion in ferrofluids. More specifically, we have determined experimentally both the thermoelectric (Seebeck) and thermodiffusion (Soret) coefficients of ionically stabilized ferrofluids made of maghemite nanoparticles dispersed in various non-magnetic liquid media (e.g., dimethyl sulfoxide, water and ionic liquids) under a temperature gradient. Both the thermoelectric voltage and the concentration gradient are measured as a function of nanoparticle concentration and analysed using existing theoretical models. The connection between the thermoelectric and thermodiffusion effects is revealed through a common parameter, the Eastman entropy of transfer of nanoparticles. This parameter characterizes the particle-solvent interactions and is generally proportional to the particle size. It is known to give rise to large Soret coefficients in colloidal suspensions including ferrofluids, and it is predicted to influence the Seebeck coefficients of carrier fluids. The values of the Eastman entropy of transfer obtained from both experiments are a few orders of magnitude larger than typical electrolyte ions and are in a quantitative agreement, lending support to the existing theoretical models. Simultaneously, our findings open a new research and technological path for magnetic nanoparticles in thermoelectric device applications.

Th.B.1_O3 - Reproducibility of barocaloric and magnetocaloric effects in Fe₄₉Rh₅₁

E. Stern-Taulats¹, A. Gràcia-Condal¹, A. Planes¹, L. Mañosa¹, P. Lloveras², M. Barrio², J.L. Tamarit², S. Pramanick³, S Majumdar³, C. Frontera⁴

1. *Departament d'Estructura i Constituents de la Matèria, Facultat de Física, Universitat de Barcelona, Barcelona, Spain*
2. *Departament de Física i Enginyeria Nuclear, ETSEIB, Universitat Politècnica de Catalunya, Barcelona, Spain*
3. *Department of Solid State Physics, Indian Association for the Cultivation of Science, Jadavpur, Kolkata, India*
4. *Institut de Ciència de Materials de Barcelona, Bellaterra, Spain*

Fe₄₉Rh₅₁ exhibits an antiferromagnetic-ferromagnetic first-order phase transition at 320K displaying subtle changes in magnetization, volume and entropy [1]. Recently, large barocaloric effect has been found [2] to arise in the vicinity of the transition which adds to the previously reported magnetocaloric [3] and elastocaloric effects [4]. Its first-order transition temperature presents unusually high sensitivity to pressure, magnetic field and stress resulting in large isothermal entropy (~12.5 J K⁻¹ kg⁻¹, in absolute terms) and adiabatic temperature (~8 K) changes in a wide temperature span (~20 K) when external fields are applied (2T or 2.5 kbar). Direct and indirect measurements of barocaloric and magnetocaloric effects in Fe₄₉Rh₅₁ are provided in order to characterize these caloric effects arising from material's interplay with external fields and their corresponding reversibility which becomes crucial either for applicational purposes such as solid state refrigeration and the understanding of the physical mechanisms involved in the AFM-FM first-order transition. A proper combination of applied fields can result in an optimization of Fe₄₉Rh₅₁ thermal response and a practical reduction of hysteresis effects associated to the first-order transition which can be responsible of a substantial loss of material's thermal response when subjected to field cycling.

References:

- [1] Shirane et al., Phys. Rev. 134, A1547 (1964)
- [2] Stern-Taulats et al., Phys. Rev. B 89, 214105 (2014)
- [3] Nikitin et al., Phys. Lett. 148, 363 (1990)
- [4] Nikitin et al., Phys. Lett. 171, 234 (1992)

Th.B.1_O4 - Magnetostructural phase transition in AlFe_2B_2 with magnetocaloric potential

L. Lewis¹, R. Barua¹, B. Lejeune¹, E. Stern-Taulats², L. Mañosa², A. Planes²

1. Department of Chemical Engineering, Northeastern University, Boston, United States
2. Departament D'Estructura I Constituents De Matèria, Facultat de Física, Universitat De Barcelona, Barcelona, Spain

Understanding correlations between composition and crystal structure is key to tailoring the response of functional magnetic materials. In particular, the ferromagnetic AlFe_2B_2 compound with the layered $\text{AlMn}_2\text{B}_{2\text{-type}}$ structure is reported to exhibit a magnetic transition of relevance for magnetocaloric cooling, with a reported entropy change AlFe_2B_2 at an applied magnetic field of 2 T. Results derived from magnetic, structural and calorimetric probes confirm a thermodynamically first-order magnetic phase change in AlFe_2B_2 in the vicinity of the Curie temperature of ~ 300 K.

Th.B.1_O5 - Giant magnetocaloric effect in alternating magnetic fields

A. Aliev¹, A. Batdalov¹, L. Khanov¹, A. Êamantsev², E. Dilmieva², A. Mashirov², V. Koledov², V. Shavrov², M. Topic²

1. *Amirkhanov Institute of Physics of Daghestan Scientific Center, RAS, Makhachkala, Russia*
2. *Kotelnikov Institute of Radio-engineering and Electronics of RAS, Moscow, Russia*

The solid state magnetic working body in the magnetic refrigerators is subjected to a strong alternating magnetic field. That is why the alternating magnetic field behavior is crucial for the properties of the prospective magnetocaloric materials. First of all the giant magnetocaloric effect (GMCE) should express itself in alternating magnetic field. GMCE is mainly observed in the substances where both magnetic and structural phase transitions (PTs) are present and merged in one magnetostructural PT. In these materials the total change of entropy at external magnetic field change may consists of two impacts: magnetic and lattice ones. They can be expected to depend strongly on the frequency of the magnetic field applied. The present work is devoted to the study of the GMCE and magnetostriction in the alloys $\text{Fe}_{48}\text{Rh}_{52}$, Ni-Mn-In and manganite $\text{Sm}_{1-x}\text{Sr}_x\text{MnO}_3$ in alternating magnetic field by the technique described elsewhere [1]. The magnetic-field-induced magnetostructural PTs in these materials (antiferro-ferromagnetic in the cases of $\text{Fe}_{48}\text{Rh}_{52}$ and Heusler alloy Ni-Mn-In, and para-ferromagnetic in case of $\text{Sm}_{1-x}\text{Sr}_x\text{MnO}_3$) are accompanied by the strong lattice volume changes which also gives an impact to entropy.

We report that the correlation is observed of magnetostriction and GMCE in these materials. Both MCE and magnetostriction are negligible in small alternating magnetic fields. Starting from some threshold magnetic field both MCE and magnetostriction express themselves. We come to the following conclusions: GMCE is strongly expressed in the alloys where antiferro-ferromagnetic PT is accompanied by lattice contraction (FeRh , and Ni-Mn-In) only in the fields stronger than that of needed for the shift the temperature of PT $T_{N+}(H)$ below the temperature of reverse transition in zero field $T_{N-}(0)$ (at $T_{N+}(H) < T < T_{N-}(0)$). In substances, like manganite $\text{Sm}_{1-x}\text{Sr}_x\text{MnO}_3$, in which ferro-paramagnetic PT is accompanied by the lattice expansion, the GMCE expresses at temperatures higher than T_{C+} in the regime of zero-field heating and below $T_{C+}(H)$ at $T_{C+} < T < T_{C+}(H)$.

References:

- [1] Aliev, A. M., Batdalov, A. B., Kamilov, I. K., et al. *Appl. Phys. Lett.* V. 97, 212505 (2010)

Th.B.2_I1 - Bismuth: Playground for quantum and spintronic experiments

S. Sangiao¹, M. del C. Martínez-Velarte¹, I. Lucas¹, César Magén^{1,2}, N. Marcano^{3,4}, J.M. Michalik^{1,4}, M. Viret⁵, L. Morellón¹, M.R. Ibarra¹, J.M. De Teresa^{1,4}

1. *Laboratorio de Microscopias Avanzadas (LMA), Instituto de Nanociencia de Aragón (INA), Universidad de Zaragoza, Zaragoza, Spain*

2. *Fundación ARAID, Zaragoza, Spain*

3. *Centro Universitario de la Defensa, Zaragoza, Spain*

4. *Instituto de Ciencia de Materiales de Aragón (ICMA), CSIC-Universidad de Zaragoza, Zaragoza, Spain*

5. *CEA Saclay, Gif-sur-Yvette, France*

Bismuth (Bi) films, nanowires and nanoconstrictions result into an exciting playground to investigate uncommon quantum and spintronic effects. This stems from the combination of the extraordinary physical properties of Bi and the low dimensionality of the system. In particular, claims of topologically-protected quantum transport in Bi nanostructures have been reported [1,2], as well as remarkable Spintronic effects due to the Rashba interaction at the Bi/Ag interface [3]. In the present contribution we will report some of the experiments carried out by our group in Bi nanostructures along last years. In particular, we will first stress the existing competition of bulk and surface states and its impact in the magnetotransport properties of Bi-films and nanowires [4-6]. Later, we will describe our results in Bi nanocontacts created by electromigration and by focused ion beam etching, which show sub-quantum-of-conductance transport due to a metal-insulator transition at the constriction long before rupture [7]. Finally, the consequences of the Rashba interaction at the Bi/Ag interface for the spin-to-charge conversion due to Inverse Rashba Edelstein Effect and its competition with the Inverse Spin Hall Effect will be shown [8].

References:

- [1] C. Sabater, et. al., Phys. Rev. Lett. 6 (2014) 20254
- [2] I. K. Drozdov, et. al., Nature Physics 10 (2014) 663
- [3] J. C. Rojas-Sánchez, et. al., Nature Communications 4 (2013) 3944
- [4] N. Marcano, et. al., Phys. Rev. B 82 (2010) 125326
- [5] N. Marcano, et. al., Appl. Phys. Lett. 96 (2010) 082110
- [6] S. Sangiao, et. al., EPL 95 (2011) 37002
- [7] S. Sangiao, et. al., Physical Chemistry Chemical Physics 15 (2013) 5132
- [8] S. Sangiao, et. al., Appl. Phys. Lett., in press

Th.B.2_O2 - Intrinsic conduction through topological surface states of insulating Bi₂Te₃ epitaxial thin films

K. Höfer¹, C. Becker¹, D. Rata¹, J. Swanson^{1,2}, P. Thalmeier¹, L.H. Tjeng¹

1. Max Planck Institute For Chemical Physics of Solids, Dresden, Germany
2. University of British Columbia, Vancouver, Canada

Topological insulators represent a new state of matter that open up new opportunities to create unique quantum particles. Many exciting experiments have been proposed by theory; yet, the main challenges for their successful realization are material quality and cleanliness of the experimental conditions. The presences of tiny amounts of defects in the bulk or contaminants at the surface can easily mask these phenomena. We present the preparation, structural and spectroscopic characterization of MBE-grown Bi₂Te₃ thin films which exhibit insulating bulk properties. Moreover, temperature dependent four-point-probe resistivity measurements of the Dirac states on surfaces that are intrinsically clean were conducted. The total amount of surface charge carriers is in the order of 10^{12}cm^{-2} and mobilities up to $4600\text{cm}^2/\text{Vs}$ are observed. Importantly, these results are achieved by carrying out the preparation and characterization all in-situ under ultra-high-vacuum conditions [1]. In order to preserve the surface integrity of the Bi₂Te₃ thin films during ex-situ experiments, e.g. high field measurements, appropriate capping layers need to be identified. We will show ARPES and transport results of a promising candidate, which provides protection against ambient conditions without influencing the electronic structure at the surface. This also opens a feasible route for future device fabrication.

References:

- [1] K. Hofer, C. Becker, D. Rata, J. Swanson, P. Thalmeier, and L.H. Tjeng PNAS, 2014, 111(42), 14979-14984

Th.B.2_O3 - Effect of Co adatoms on topological insulator Bi₂Se₂Te

M. C. Martinez-Velarte^{1,2}, M. Moro-Lagares^{1,2}, T. M. Riedemann³, T. A. Lograsso^{3,4}, L. Morellon^{1,2}, M. R. Ibarra^{1,2}, D. Serrate^{1,2}

1. *Institute of Nanoscience of Aragon (INA) and Laboratory for Advanced Microscopy (LMA), University of Zaragoza, Zaragoza, Spain*
2. *Dpto. de Física de la Materia Condensada, Universidad de Zaragoza, Zaragoza, Spain*
3. *Ames Laboratory, Ames, United States*
4. *Department of Materials Sciences and Engineering, Iowa State University, Ames, United States*

Topological Insulators (TIs) are a new electronic state of matter which has been amply investigated during the last years due to its unique properties which have great potential for spintronic applications. TIs are materials with a bulk energy gap and metallic surface states, both stemming from non-trivial topology of the electronic structure [1]. Due to time-reversal symmetry and spin-orbit coupling, the surface states behave as Dirac Fermions and exhibit a fully spin-polarised k-dependent spin-texture. As a result, electron backscattering becomes quantum-mechanically prohibited, and topological 2-D surface states are expected to be robust against non-magnetic defects.

A large number of Bi-based ternary compounds have been theoretically predicted and experimentally proved to be topological insulators. Band structure calculations of Bi₂Se₂Te have predicted a TI state, with an isolated Dirac Point [2]. ARPES measurements of the occupied density of states (DOS) near the Fermi level support these calculations [3]. Here we show low temperature (1.1 K) Scanning Tunnelling Microscopy (STM) and Spectroscopy (STS) measurements on a Bi₂Se₂Te single crystal, gaining large spatial resolution of both the occupied and unoccupied local DOS. Atomically resolved STM images of the crystal surface shows a binary chemical contrast which is likely due to Te and Se segregation in regions of a few nm in size.

Moreover, individual Co atoms were deposited on the crystal surface held at T<6K to prevent atom diffusion. Co adatoms show an atomic resonance peak on the STS spectra at around -550 mV, in accordance with recent works on Bi₂Se₃[4]. Importantly, valence and conduction bulk bands undergo a shift towards lower energies upon Co doping.

Furthermore, an external magnetic field allows us to set a preferential spin direction of the Co magnetic moment. Our energy resolved STS measurements unveil the role of electronic hybridization in the interaction between localised magnetic scattering centres and topological Dirac fermions on the surface.

Th.B.2_O4 - Semimetal-insulator transition in Dirac semimetals induced by long-range Coulomb interactions

A. Sekine¹, K. Nomura¹

1. Institute for Materials Research, Tohoku University, Sendai, Japan

Dirac semimetals in three dimensions have attracted much attention as a novel phase. They have gapless linear dispersions in the bulk, and the low-energy excitations are described by three-dimensional (3D) massless Dirac fermions. Hence they can be regarded as a 3D analog of graphene. Dirac semimetals such as Na₃Bi and Cd₃As₂ were experimentally observed recently [1,2]. It is notable that there exists large out-of-plane Fermi velocity anisotropy in the Dirac cones. One of the important meanings of the realization of Dirac semimetals is on the point that they can lead to various topological phases, since they lie next to various topological phases in the phase diagrams. In this work, we study theoretically the effects of strong $1/r$ Coulomb interactions in Dirac semimetals with N nodes. Due to the vanishing density of states near the Fermi level, the screening effect is expected to be weak in Dirac fermion systems. We particularly consider the cases of $N = 4$ and $N = 16$. Based on the $U(1)$ lattice gauge theory, we analyze the system from the strong coupling limit. In this study, the dynamically generated mass of Dirac fermions, known as the chiral condensate, serves as the order parameter for the semimetal-insulator transition. It is shown that the Dirac semimetal phases survive in the strong coupling limit when the out-of-plane Fermi velocity anisotropy is weak, whereas the mass gap is generated in the strong coupling limit when the anisotropy is strong [3]. This result can be understood as a kind of dimensional crossover.

References:

- [1] Z. K. Liu et al., *Science* 343, 864 (2014)
- [2] M. Neupane et al., *Nat. Commun.* 5, 3786 (2014)
- [3] A. Sekine and K. Nomura, *Phys. Rev. B* 90, 075137 (2014)

TH.B.2_O5 - Spin and charge current driven by magnetization dynamics on disordered surface of doped topological insulators

K. Taguchi¹, K. Shintani¹, Y. Tanaka¹

1. Department of Materials, Physics And Energy Engineering, Graduate School of Engineering, Nagoya University, Nagoya, Spain

Topological insulator (TI) is a new class of material, which has a gapless surface state, in which the spin and momentum are perfectly locked by the spin-orbit interactions. On the surface of the TI attached ferromagnetic material (FM), the magnetization of the FM plays the role of an effective vector potential for conduction electrons, which is like a vector potential of electromagnetic fields. Owing to the effective vector potential, the time-derivative of the magnetization can be regarded as an effective electric field, and the magnetization dynamics generates charge current on the surface even in the absence of applied electric fields[1-3]. This is called as the spin-charge conversion. The property on the surface of the TI can be applicable for spintronics devices. Existing works of the spin-charge conversion has been done on a clean surface of the TI, namely the ballistic transport regime. However, the actual charge transport on the surface of the TI is in the diffusive regime due to the nonmagnetic impurity scattering. We theoretically study spin and charge generation and transport on a disordered surface of a doped three-dimensional TI/magnetic insulator junction by using Green's function techniques. We show that the charge and spin current are induced not only by local but also by nonlocal magnetization dynamics through the nonmagnetic impurity scattering on the disordered surface of the TI. We also clarify that the nonlocal magnetization dynamics induces spin current, as well as charge density on the surface. Using these results, we discuss the magnetization dynamics due to the ferromagnetic resonance before and after the spin and charge generation on the disordered surface of the TI.

References:

1. P. Deorani, J. Son, K. Banerjee, N. Koirala, M. Brahlek, S. Oh, and H. Yang, Phys. Rev. B 90, 094403 (2014)
2. Y. Shiomi, K. Nomura, Y. Kajiwara, K. Eto, M. Novak, Kouji Segawa, Yoichi Ando, and E. Saitoh, Phys. Rev. Lett. 113 196601 (2014)
3. M. Jamali, J.-S. Lee, Y. Lv, Z. Zhao, N. Samarth, and J.-P. Wang, arXiv-1407.7940

Th.B.3_O1 - Measurement of the Sommerfeld Coefficient in hydrogenated and Mn doped La(Fe,Si)13

L.F. Cohen¹, L. Ghivelder², A. Nicotina², E. Lovell¹, Z. Gercsi¹, V. Basso³, A. Barzca⁴, M. Katter⁴

1. *Blackett Laboratory, Imperial College London, London, United Kingdom*
2. *Instituto de Física, Universidade Federal do Rio de Janeiro, Rio de Janeiro, Brazil*
3. *Istituto Nazionale di Ricerca Metrologica, Torino, Italy*
4. *Vacuumschmelze GmbH & Co. KG, Hanau, Germany*

La(Fe,Si)13 are itinerant ferromagnets with giant magnetoelastic coupling, exhibiting large magnetocaloric effect (MCE) associated with a first-order metamagnetic phase transition. Substitution of Si produces lattice contraction and hybridisation between the electronic orbitals of Si and Fe atoms resulting in elevation of T_c. Substitution of Mn is thought to isovalently enhance antiferromagnetic exchange, lowering T_c. T_c can also be shifted to near room temperature by hydrogen absorption. Theoretical progress has been made to describe the electronic properties and the influence of substitution and interstitial occupancy [1, 2], but detailed comparison with experiment is lacking. Here we measure the Sommerfeld coefficient (γ) extracted from the low temperature heat capacity in polycrystalline LaFeXMnYSiZ. Changes in magnitude of γ by 20-30% are observed with Mn substitution and introduction of hydrogen showing that there are significant changes taking place in the density of states at the Fermi level. Interestingly γ is of the order of 150- 200 mJ/mol K² significantly greater by about a factor of eight than that determined by recent band structure calculation [3], but similar to experimental reports of related itinerant compounds [4,5]. Mass enhancement in transition metals on the cusp of ferromagnetism is understood to be due to electron correlation effects brought about by spin fluctuations [6] but detailed understanding in La(Fe,Si)13 is lacking.

References:

- [1] A. Fujita and H. Yako Scripta Materialia 67, 578 (2012)
- [2] Z. Gercsi, K.G. Sandeman and A. Fujita arXiv:1407.7975 v1 [cond-mat..mtrl-sci]
- [3] M.E. Gruner et al., arXiv:1408.4009 v1 [cond-mat..mtrl-sci]
- [4] F. Wang et al., Chinese Physics B 17, 3087 (2008)
- [5] H. Michor et al., Phys Rev B 69, 081404 (2004)
- [6] M.J. Rice Phys Rev Lett 20, 1439 (1968)

This work is funded by the EC FP7 Grant agreement 310748 "DRREAM", EPSRC EP/G060940/1 and Science Without Borders CAPES grant CSF-PVE's -88887.063730/2014-00.

Th.B.3_O2 - Spin seebeck and anomalous nernst effect in magnetite epitaxial thin films grown on different substrates

M.H. Aguirre^{1,2,3}, A. Anadón Barcelona^{1,2}, R. Ramos¹, I. Lucas^{1,4}, P. Algarabel^{2,5}, L. Morellón^{1,2}, R. Ibarra^{1,2,3}

1. *Instituto de Nanociencia De Aragón. Universidad de Zaragoza. Zaragoza, Spain*
2. *Departamento de Física de la Materia Condensada, Universidad de Zaragoza, Zaragoza, Spain*
3. *Laboratorio de Microscopías Avanzadas, Universidad de Zaragoza, Zaragoza, Spain*
4. *Fundación ARAID, Zaragoza, Spain*
5. *Instituto de Ciencia de Materiales de Aragón, Universidad de Zaragoza and Consejo Superior de Investigaciones Científicas, Zaragoza, Spain*

The generation of spin currents without movement of charge is of crucial importance in spintronics that could allow computer speed and power consumption to move past limitations of current technologies. The spintronic can also be applied to some traditional technologies as thermoelectric converters. Regardless of the big amount of research in thermoelectrics, the efficiency of such devices has remained low due to the interdependence between the Seebeck effect, the resistivity and the thermal conductivity. Meanwhile, the Joule heating of electronic devices with finite size effect is another obstacle. One promising approach to overcome this set of problems and give versatility to thermoelectric devices is exploiting the spin of the electron, in addition to its charge and transport properties. The discovery of the spin Seebeck effect (SSE) [1] and more particularly its observation in magnetic insulators [2, 3] offers a new approach for thermoelectric energy conversion and sensors. The SSE provides a feasible way to drive a nonequilibrium spin current, as a result of a temperature gradient in magnetic materials. The spin dependent thermal transport of magnetite films on different substrates was studied, taking special care about the heat manipulation of the different substrate material (Al_2O_3 , MgAl_2O_4 , SrTiO_3 , MgO). In particular, the magneto-thermoelectric characteristics of magnetite film have been investigated by fine manipulation of heat flow. The Anomalous Nernst Effect (ANE) was measured to normalize and distinguish from the SSE signal. The interplay between the magnetization, temperature gradient, structure and nanostructural defects induced by the substrate have shown to have an important influence on the ANE and SSE voltage signals. ANE and SSE signal were maxima in $\text{Fe}_3\text{O}_4/\text{Al}_2\text{O}_3$ and $\text{Fe}_3\text{O}_4/\text{MgAl}_2\text{O}_4$, respectively. Nanostructural defects like antiphase boundaries in magnetite films were studied by aberration correction TEM and showed to have different patterning depending on the substrate of growth.

Th.B.3_O3 - Modeling specific heat and entropy change in La(Fe,Mn,Si)13-H compoundsM. Piazzì¹, C. Bennati¹, C. Curcio¹, M. Kuepferling¹, V. Basso¹*1. Istituto Nazionale Di Ricerca Metrologica (INRIM), Turin, Italy*

Two classes of magnetic materials are currently the most promising candidates for room-temperature magnetic cooling: the La(Fe,Si)₁₃ based [1] and the MnFe(P,X) (X=As, Ge, Si) based [2]. Both systems display first-order ferro- to paramagnetic phase transitions with an enhanced magnetocaloric effect (MCE). In hydrogenated La(Fe,Mn,Si)₁₃-H the MCE can be finely tuned by varying Mn content [1]. Modeling the behaviour of these systems is of primary importance for further optimising the materials. In this work we compare La(Fe,Mn,Si)₁₃-H data with a thermodynamic model that, taking into account magnetovolume effects, is able to display both first- and second-order transitions by smoothly varying the strength of the magnetoelastic coupling [4]. The magnetism is treated within the framework of localized electrons mean field theory (MFT) and lattice entropy is explicitly considered. We find that the model successfully describes the experimental entropy change at the phase transition, capturing also the variation from first- to second-order transitions. However the sharp peaks of the specific heat close to the transition temperature are insufficiently reproduced. This is a known problem related to the difficulty of MFT to shape the specific heat behaviour close to the Curie point, where spin correlations play a relevant role. Thus, to go beyond MFT, different strategies taking into account these correlations should be considered. Here we derive the magnetic entropy from the density of states, as obtained by the Wang-Landau sampling algorithm applied to Ising ferromagnet [5]. The resulting model allows to better capture the peculiar shapes of the specific heat peak at La(Fe,Mn,Si)₁₃-H phase transitions.

The research leading to these results has received funding from the European Community's 7th Framework Programme under grant agreement no. 310748 (project "DRREAM").

References:

- [1] A. Barcza et al., IEEE Trans. Magn. 47, 3391 (2011)
- [2] H. Yibole et al., J. Phys. D: Appl. Phys. 47, 075002 (2014)
- [3] V. Basso et al., Proc. of the 6th IIF-IIR Int. Conf. on Magnetic Refrigeration (2014)
- [4] V. Basso, J. Phys.:Condens. Matter 23, 226004 (2011)
- [5] R. Tamura et al., Appl. Phys. Lett. 104, 052415 (2014)

Th.B.3_O4 - Effect of irreversibility on the magnetocaloric effect of compounds with first-order transitions

R. Burriel¹, E. Palacios¹

1. Instituto de Ciencia de Materiales de Aragón (ICMA), Zaragoza, Spain

The use of magnetocaloric materials for cooling applications at room temperature requires high values of the magnetocaloric parameters. These high values are found in compounds with first-order transitions. Associated with the first-order character, there is a detrimental effect due to the inherent irreversibility of these transitions.

At the first-order magnetic transitions there is an entropy production due to the irreversibility. The elemental evaluation of the isothermal entropy change upon a field change, ΔS_T , from magnetization, heat capacity, or direct measurements, has an error and its value depends on the physical property used. Estimations of the entropy from heat measurements lack the entropy creation through the first-order transitions. Consequently, the transition entropies derived from heat capacity or direct measurements are not correct and the errors are shown to be proportional to the thermal hysteresis of the compound. In the case of magnetization measurements, the Clausius-Clapeyron equation is used to calculate the entropy of the transition from the magnetization jump and the temperature dependence of the transition field. This calculation lacks an irreversible term that is demonstrated to be equal to the temperature derivative of the free energy jump at the transition. Generally, this correction to the values derived from magnetization is higher than in the case of values derived from heat capacity data.

Apart from these corrections of the transition entropy, accounting for the irreversible entropy creation, there is a much higher spurious effect in ΔS_T values derived from the application of the Maxwell equation to isothermal magnetization data. They result in an unphysical ΔS_T spike that has been referred to as a colossal magnetocaloric effect. The values of the spike are shown to be proportional to the anomalous heat capacity at zero magnetic field. This effect is not related to irreversibility but happens only in compounds presenting thermal hysteresis.

TH.C.1_I1 - Magnetic nanostructures for magnonic and logic applications

A. Adeyeye¹

1. National University of Singapore, Singapore, Singapore

Magnetic nanostructures have attracted a lot of interest from researchers around the world in the last decade, both from a fundamental viewpoint and because of their potential in a wide range of emerging applications such as ultra high density storage, magnetic random access memory, spin logic and magnonics. The ability to synthesize high quality arrays of magnetic nanostructure with precise dimensionality control is crucial for reproducible magnetic switching processes. Key issues to be considered in the development of any nanofabrication techniques are critical dimension control, resolution, size and shape homogeneity, patterned area and alignment accuracy. With advances in lithographic and other controlled nanofabrication techniques, made possible by developments in nanotechnology, it is now possible to synthesize a wide range of high-quality magnetic nanostructures. The talk will focus on strategies developed in my group over the year for synthesizing high-quality complex magnetic nanostructures using photon based and charge based lithographic processes [1]. In addition, recent results on the static and dynamic properties of magnetic nanostructures obtained using a combination of magneto-optical Kerr effect measurements, magnetic force microscopy, broadband ferromagnetic resonance spectroscopy and Brillouin light scattering (BLS) spectroscopy will be presented. The dynamic behavior of various types of structures made from lithographically defined magnetic nanostructures will be discussed [2]. Results on the direct detection of neighboring dipolar interactions on a single nanomagnet using micro-focused BLS spectroscopy will be presented [3]. It will be shown that magnetic nanostructures can be designed to realize ferromagnetic and antiferromagnetic ground states for logic and magnonic applications [4].

References:

- [1] J. Ding and A.O. Adeyeye, *Advanced Functional Materials*, 23, 1684 (2013)
- [2] X.M. Liu et al., *Appl. Phys. Lett.*, 105, 052413 (2014)
- [3] G. Shimon and A.O. Adeyeye, *Advanced Electronic Materials* (in press, 2015)
- [4] A. Haldar and A. O. Adeyeye, *Appl. Phys. Lett.*, 106, 032404 (2015)

TH.C.1_O2 - Mechanical control of magnetic easy axis in a TbFeCo thin film deposited on a flexible substrate

S. Ota¹, D. Bang², H. Awano², T. Kozeki³, H. Akamine³, T. Fujii³, T. Namazu³, T. Takenobu⁴, T. Koyama¹, D. Chiba¹

1. Department of Applied Physics, Faculty of Engineering, The University of Tokyo, Tokyo, Japan

2. Information Storage Materials Laboratory, Toyota Technological Institute, Nagoya, Japan

3. Division of Mechanical Systems, Department of Mechanical and Systems Engineering, University of Hyogo, Himeji, Japan

4. Department of Applied Physics, Waseda University, Tokyo, Japan

Use of the inverse magnetostriction effect is known as one of the effective way to manipulate magnetization direction for magnetic storage devices [1]. The strain-induced change in the magnetic anisotropy in ferromagnetic thin films has been reported by directly bending the substrate [2], or in the configuration where the sample was mounted on a piezo device [3]. In this work, we have achieved to apply larger uniaxial strain over 2% on the thin film made of TbFeCo, one of the famous magnetostriction alloys, by simply stretching a flexible substrate on which the film was deposited. As a result, a clear switching in the easy axis has been observed. Pt(4 nm)/TbFeCo(6 nm)/Pt(4 nm) layers were deposited on the flexible substrate by magnetron sputtering. The sample was fabricated into Hall bar structure to measure the magnetization curve under the application of strain using the anomalous Hall effect. When the external strain was off, a square hysteresis loop was seen in the curve, indicating that the sample had the perpendicular magnetic anisotropy. We applied a tensile strain ε to the sample by stretching the substrate in the direction parallel to the current direction. As ε increased, both the coercivity and the squareness ratio of hysteresis loop decreased, and the hysteresis disappeared when ε was larger than 2%, indicating that the easy axis switched from the perpendicular to the in-plane direction. After that, by reducing ε to 0%, the coercivity and the squareness ratio returned almost to their initial values. The result evidences that the change in the magnetic anisotropy shown here was reversible.

TH.C.1_O3 - High-sensitivity dc field magnetometer using nonlinear resonance magnetoelectric effect

Y. Fetisov⁴, D. Burdin¹, D. Chashin², N. Ekonomov³

1. *Moscow State Technical University of Radio Engineering, Electronics and Automation, Moscow, Japan*

New type magnetometer using nonlinear resonance magnetoelectric (ME) effect in ferromagnetic-piezoelectric (FM-PE) structures is proposed. The magnetometer exploits nonlinear dependence of FM sample magnetostriction δ vs. magnetic field and piezoelectric effect to register the signal. This differs from the fluxgate magnetometers which use nonlinear dependence of FM sample magnetization vs. field and electromagnetic induction.

The magnetometer operates as follows. The FM-PE structure is placed in a low-frequency pumping field h with frequency f and measured dc magnetic field H . In order to avoid influence of the FM layer hysteresis, h should be bigger than saturation field. The signal with frequency $3f$ generated by the PE layer due to nonlinear ME effect is measured. Magnitude of the signal is proportional to the field H . Acoustic resonance of the structure is used to increase sensitivity of the magnetometer.

A prototype of the magnetometer was fabricated on the structure with dimensions 40×5 mm² containing 30 μ m thick Metglas layer and 400 μ m thick langatite layer. The pumping field of $h = 20$ Oe and $f = 1.5$ kHz was created by a coil. The frequency $3f$ coincided with the frequency of bending oscillations of the structure 4.5 kHz. In this case the output signal and, respectively, the sensitivity of the magnetometer was increased by acoustic quality factor $Q \sim 10^2$. Under resonance operation regime the magnetometer allowed registration of fields $H = 1$ mOe - 5 Oe and had sensitivity $u/H \sim 1$ V/Oe.

Thus, new type dc field magnetometer using nonlinear resonance magnetoelectric effect in FM-PE structures was suggested and fabricated. The ME magnetometer has ~ 2 order of magnitude higher sensitivity than well known fluxgate magnetometers.

The research was supported by the Ministry of Education and Science of Russia

TH.C.1_O4 - New susceptibility measurement devices and their calibration

J.L. Mesa Uña¹, M. Pérez¹, A. B. Fernandez², M. Maicas¹, C. Aroca¹, M. Díaz Michelena¹

1. *Universidad Politécnica De Madrid, Madrid, Spain*

2. *Instituto Nacional de Técnica Aeroespacial (INTA), Madrid, Spain*

Susceptibility measurements are very important for materials characterization because it is related to intrinsic properties of the matter like the capability to magnetize (real part) and the conductivity or spin relaxation (imaginary part). In order to cover this widely extended technique, we have developed several devices:

1. Laboratory High Resolution Susceptometer. This device can measure with high resolution the magnetic signal produced by a magnetic sample. It is based on a linear actuator and a set of coils: primary and secondary. The principle is similar to a VSM, but the main difference consist in the possibility to determine the ac magnetic permeability in a large frequency range (dc - 100 kHz).

2. Portable Susceptometer for planetary applications. Device based on an electrical resonant ferrite actuator. The measurement technique is based on impedance changes in an inductive core due to the presence of a magnetic material. This device is currently being developed for a Mars lander. Despite the importance of having absolute measurements of the susceptibility, the calibration of the devices is complicated and requires the manufacturing of reference probes. In this work we report on the calibration and latter measurements with the two susceptometers. The calibration of the system has been carried out using a set of reference probes controlling the composition and the concentration of ferro and ferri magnetic materials in a scarcely diamagnetic epoxy. The susceptibility measurements of natural samples (basalt, peridotite, terrace and clays) performed with the portable susceptometer show a good correlation with the results obtained with other well-known techniques (SQUID, VSM), with the advantage that we can perform measurements of the ac magnetic susceptibility at different frequencies. The measurements performed with the laboratory susceptometer demonstrates a high resolution (minimum signal around 10 - 20 Oe) and a good correlation in dc with results obtained with VSM.

TH.C.1_O5 - Magnetostrictive stress reconfigurable thin film resonators in vacuum for magnetic field sensing

P.Finkel¹, [M. Staruch¹](#)

1. US Naval Research Laboratory, Washington DC, United States

The magnetic response of microdevices is significantly enhanced at structural resonance allowing for improved sensitivity and signal-to-noise ratio. The magnetic field resolution of these devices can be further improved when operating in vacuum due to an increase in mechanical quality factor. In this work, free-standing thin film CoFe bridge resonators have been fabricated and investigated. A strong magnetic field dependence of the fundamental resonance frequency is a function of magnetic field orientation due to a large unidirectional anisotropy. Under vacuum, a quality factor of up to 25 times greater than at atmosphere was revealed as well as an increased magnetic field sensitivity. Such stress reconfigurable sensors offer the possibility of broadband sensing with high resolution, and may therefore represent a new approach to fully integrated resonant magnetic field sensing technology.

Th.C.2_I1 - Field-dependent Size and Shape of Single Magnetic Skyrmions

N. Romming¹, André Kubetzka¹, C. Hanneken¹, K. von Bergmann¹, R. Wiesendanger¹

1. Department of Physics, University of Hamburg, Hamburg, Germany

Magnetism in thin films can significantly deviate from commonly known magnetic configurations in bulk systems due to low dimensionality, hybridization effects, a change of the lattice constant, stacking and broken inversion symmetry at interfaces. This can lead to non-collinear spin states such as spin spirals or skyrmions. Especially skyrmions offer great potential as information carriers in future robust, high-density, and energy-efficient spintronic devices: in addition to their protected topology and nano-scale size, they can easily be moved by lateral spin currents and written as well as deleted by vertical spin-current injection [1]. While numerous theoretical and simulation studies have concentrated on individual skyrmions and their physical properties, no high-resolution experimental characterization of the internal spin structure of skyrmions has been reported up to now, even though the knowledge about their actual size and shape provides the foundation for predictions about the interactions of skyrmions with spin currents or their manipulation by external fields as envisaged in potential skyrmion-based device concepts. Here we investigate the atomic-scale spin structure of individual isolated skyrmions in an ultrathin film in real space by spin-polarized scanning tunneling microscopy. Their axial symmetry as well as their unique rotational sense is revealed by using both out-of-plane and in-plane sensitive tips. The size and shape of skyrmions change as a function of magnetic field. An analytical expression for the description of skyrmions is proposed and applied to connect the experimental data to the original theoretical model describing chiral skyrmions [2]. Thereby, the relevant material parameters responsible for skyrmion formation can be obtained.

References:

- [1] Romming, N., Hanneken, Ch., Menzel, M., Bickel, J. E., Wolter, B., von Bergmann, K., Kubetzka, A. & Wiesendanger, R. Writing and Deleting Single Magnetic Skyrmions. *Science* 341, 636 (2013)
- [2] Bogdanov, A. & Hubert, A. The Properties of Isolated Magnetic Vortices. *Phys. Status Solidi B* 186, 527 (1994)

Th.C.2_O2 - In-situ TEM study of temperature-dependent dichroism: Application to epitaxial MnAs/GaAs(001)

X.Fu¹, D. Demaille², V. Etgens², S. Joulié¹, G. Seine¹, R. Arras¹, V. Serin¹, B. Warot¹

1. CEMES-CNRS, Toulouse, France

2. UPMC (Université Pierre et Marie Curie), Paris, France

Epitaxial MnAs thin films grown on GaAs substrate, have attracted much attention over the last decades due to their magnetic properties and potential spintronic applications. In this work, we focus on investigating the temperature-dependent local magnetic behavior of MnAs/GaAs(001) by TEM (Transmission Electron Microscopy) techniques. Before that, the surface topography and magnetic domain structure are observed using AFM (atomic force microscopy) and MFM (magnetic force microscopy). It demonstrates the coexistence of the α ferromagnetic phase and the β paramagnetic phase, in a temperature range of around 30°C. HRTEM (High resolution transmission electron microscopy) image and EELS (electron energy loss spectroscopy) spectrum have been acquired at room temperature, and the α -MnAs ferromagnetic phase has been identified. The magnetic moment information has been then extracted from the manganese L-2,3 edge with an element-specific technique, EMCD (Electron energy-loss Magnetic Circular Dichroism). The spatial resolution reaches a few tens of nm. Local quantitative magnetic moment information is extracted from the dichroism signal with Sum Rule, and it is compared to DFT calculations. In a second step, the temperature of the sample is increased above 70°C in situ inside the microscope. In this condition, all the hexagonal α -MnAs phases are transformed into the orthorhombic β -MnAs ones. We follow the change of atomic structure and magnetic moment during and after the phase transition.

Th.C.2_O3 - Experimental evidence of ultra-small particles in magnetic metal-insulating nanogranular films

M. Garcia Del Muro¹, Z. Konstantinovic², A. Labarta¹, X. Batlle¹

1. *Dpt. Física Fonamental and IN2UB, Universitat de Barcelona, Barcelona, Spain*

2. *ICMAB-CSIC, Bellaterra, Spain*

Since the first work by Morup in 1983 describing a nanoparticles (NP) system where the superspins of all NP were correlated in a ferromagnetic-like way, many efforts have been devoted to completely understand what has been called superferromagnetism (SFM). So far, there is no clear understanding of the interaction leading to the SF order in an ensemble of nanoparticles embedded in a dielectric matrix, although it has been generally assumed that indirect exchange could be mediated by dispersed ions and ultrasmall paramagnetic nanoparticles between the superspin particles (SSP). Thus, it is believed that these so-called glue-particles would cause the magnetic percolation below the physical percolation, but without any direct experimental evidence. In this work, we prepared nanogranular Co-ZrO₂ films, and submitted to two subsequent annealings to bring on the nucleation of very small particles from the Co atoms dispersed in the matrix. High resolution TEM images unambiguously show the presence of ultra-small (below 1 nm) regions with crystalline structure, that were attributed to Co by EELS. Those very small particles appear filling the space between the nanoparticles observed by conventional TEM. Our previous work, have revealed that microstructural changes are critical for the ac electrical behaviour, and the usefulness of random R-C models in simulating real complex materials with microstructural disorder: R accounts for the tunneling conduction paths through ultra-small particles, and C for the capacitive conduction through the bigger SSP. In this work, numerical simulations reproduce the ac experimental results and provide physical parameters that are compatible with microstructural changes observed by TEM, strongly confirming the increasing presence of ultra-small particles in between the SSP by subsequent annealings.

Work supported by MINECO (MAT2012-33037), DURSI (2009SGR856), and EU FEDER funds (Una manera de hacer Europa).

Th.C.2_O4 - Low frequency dynamics of magnetic droplet solitons in spin transfer nanocontacts

F. Macia¹, J.M. Hernández¹, S. Lendínez¹, D. Backes², A.D. Kent²

1. *University of Barcelona, Barcelona, Spain*

2. *New York University, New York, United States*

Localized excitations that correspond to reversed dynamically precessing magnetic moments, known as magnetic droplet solitons, were predicted to occur in uniaxial magnets in the absence of damping. However, damping is present in all magnetic materials and suppresses these excitations. It is possible now to compensate damping in ferromagnetic thin films by spin transfer torques through electrical current flow in nanometer scale contacts. Recent experiments [1,2] have shown the existence of these magnetic objects and proved their stability [2]. We explored conditions that allow formation, stabilization, and annihilation of the droplet excitations. We report spectral measurements, on the GHz range, as a function of current and applied field that challenge existing theories. Additionally, we will report low frequency (~300 MHz) excitations associated to the magnetic droplet dynamics. We will show that the droplet hysteretic behavior in current and field, which is related to its stability, is also present in the high and low frequencies spectra. Finally, we will present our recent simulations and compare them with the results and the existing theory. FM is Supported by Catalan Government through COFUND FP7. FM, JMH and SL acknowledge the Spanish Government (grant no. MAT2011-23698). DB and ADK were supported by NSF-DMR-1309202 and in part by ARO-MURI, Grant No. W911NF-08-1-0317

References:

[1] S. M. Mohseni, et al., *Science* 339, 1295 (2013)

[2] F. Macia et al. *Nature Nanotechnology* 9, 992-996 (2014)

Th.C.2_O5 - Light irradiation-driven modifications of Pt/Co/Pt trilayers

A. Maziewski¹, I. Sveklo¹, J. Kisielewski¹, Z. Kurant¹, A. Bartnik², M. Jakubowski³, R. Sobierajski³, J. Peřka³, A. Wawro³

1. Faculty of Physics, University of Białystok, Warsaw, Poland

2. Institute of Optoelectronics, Military University of Technology, Warsaw, Poland

3. Institute of Physics, Polish Academy of Sciences, Warsaw, Poland

A series of Pt(111)/Co(001)/Pt(111) trilayer structures was epitaxially grown on Al₂O₃(001) by MBE technique. As-grown films with in-plane magnetization state were selected. Samples were irradiated using various single pulse irradiation sources: (i) femtosecond laser of 800 nm in wavelength, similarly as in Ref. [1]; (ii) 3 ns laser-plasma source of extreme ultraviolet (EUV) with the most intense emission in a relatively narrow spectral region, centered at wavelength 11 nm described in Ref. [2]. Irradiations were performed at a broad range of light energy densities. The highest applied densities modified locally the morphology of studied trilayers due to: (i) sputtering of ultrathin layers using femtosecond pulses and (ii) local melting by EUV. Atomic force microscopy was used to control the surface modifications. Both magneto-optical Kerr microscopy and magnetic force microscopy were used for magnetic properties studies. Using image processing of magneto-optical images, the maximal Kerr rotation, remanence and coercivity were determined as functions of irradiation fluence. Both light sources enabled creation of the irreversible magnetic out-of-plane magnetic state - the irradiation can locally induce the spin reorientation transition. Strong decrease of magnetic domain size was observed while approaching the spin-reorientation transition region. Maximum Kerr rotation increased with the applied light fluence. Investigated light irradiation driven modifications of Pt/Co/Pt trilayers are similar to those induced by Ga⁺ ions irradiation described in Ref. [3]. The research is supported by: Polish National Science Centre under the project no. DEC-2012/06/M/ST3/00475 and SYMPHONY project operated within the Foundation for Polish Science Team Programme co-financed by the EU European Regional Development Fund, OPIE 2007-2013.

References:

[1] J. Kisielewski, et al., Journal of Applied Physics, 115, 053906 (2014)

[2] A. Bartnik, et al., Nuclear Instruments and Methods in Physics Research A 647, 125 (2011).

[3] A. Maziewski, et al., Physical Review B 85, 054427 (2012)

Th.C.3_O1 - Evidence for nodal superconductivity in quasi-one-dimensional $K_2Cr_3As_3$

G. Pang¹, M. Smidman¹, W. Jiang¹, J. Bao¹, Z. Weng¹, Y. Wang¹, L. Jiao¹, J. Zhang¹, G. Cao¹, H. Yuan¹

1. Department of Physics And Center For Correlated Matter, Zhejiang University, Hangzhou, China

The newly discovered quasi-one-dimensional superconductor $K_2Cr_3As_3$ has attracted considerable interest [1]. Its crystal structure consists of double-walled tubes of $[Cr_3As_3]^{2-}$ that run along the c axis. Electronic structure calculations for $K_2Cr_3As_3$ reveal that three bands cross the Fermi level, two of which are one-dimensional and one is three-dimensional [2]. For a transition temperature of $T_c \approx 6.1K$, this compound shows a remarkably high upper critical field ($B_{c2}(0) \approx 31.2T$), far exceeding the Pauli limiting value [1]. In this presentation, we report measurements of the London penetration depth $\Delta\lambda(T)$ and superfluid density $\rho_s(T)$ of $K_2Cr_3As_3$ to probe its superconducting gap structure [3]. Linear behavior of $\Delta\lambda(T)$ is observed for $T \ll T_c$, instead of the exponential behavior of conventional superconductors, indicating that there are line nodes in the superconducting gap. Possible pairing states will be discussed by comparing different fits of $\rho_s(T)$. Our results provide strong evidence for unconventional behavior and may provide key information for identifying the pairing state of this novel superconductor.

References:

- [1]J. K. Bao et al., Superconductivity in quasi-one-dimensional $K_2Cr_3As_3$ with significant electron correlations. Phys.Rev.X.5, 011013
- [2]H. Jiang, G. H. Cao, and C. Cao, Electronic structure of quasi-one-dimensional superconductor $K_2Cr_3As_3$ from first-principles calculations. arXiv:1412.1309
- [3]G. M. Pang et al., Evidence for nodal superconductivity in quasi-one-dimensional $K_2Cr_3As_3$. arXiv:1501.01880

Th.C.3_O2 - Unveiling the magnetic state of iron in the superconducting pressure region

B. Lebert^{1,2}, J. Ablett¹, F. Baudalet¹, M. Casula², A. Juhin², G. Le Marchand², P. Munsch², A. Polian², J.P. Rueff¹, Z. Zhang^{1,2}, M. d'Astuto²

1. Synchrotron SOLEIL, L'Orme des Merisiers, Gif sur Yvette, France

2. Institut de Minéralogie et de Physique des Milieux Condensés (IMPMC), UMR CNRS 7590, Université Pierre et Marie, Paris, France

Iron undergoes a martensitic transition at 13 GPa and room temperature from ferromagnetic α -iron to apparently non-magnetic ϵ -iron. This phase is superconducting between 15 GPa and 30 GPa [1], which cannot be explained solely by conventional phonon pairing mechanisms. There is theoretical evidence that a magnetically mediated mechanism is involved, however the magnetism of ϵ -iron is disputed to this day. Mössbauer spectroscopy (MS) finds an upper limit of $0.05 \mu_B$ for the local moment [2], while other techniques suggest a larger local moment. For example, a study using $K\beta$ x-ray emission spectroscopy (XES) which found evidence of “remnant” magnetism above 15 GPa in the ϵ -iron [3].

We have also performed $K\beta$ XES, however using higher statistics and argon as a pressure medium, to explore the phase diagram of iron from 3 to 50 GPa and 4 to 583 K. Our results show the satellite's shape and position are stable in α -iron and then exhibit a sharp decrease in intensity, increase in width, and shift in energy at 15 GPa, coinciding with the onset of superconductivity. Increasing the pressure further, the satellite's intensity continues to decrease and disappears between 30 GPa and 50 GPa. As well, we found that the satellite shows no temperature trend between 4 K and 583 K. These results suggest that the local moments are from an intrinsic magnetism in the ϵ -iron phase, rather than a “remnant” magnetism from the ferromagnetic α -iron phase. Furthermore, the overlapping pressure existence regions strengthens the case for a magnetically mediated component. Contrasting our results to MS: we are either observing magnetic fluctuations faster than the timescale of MS, or we are observing a proposed anti-ferromagnetic ground state (afmII) known to have very weak hyperfine field [4].

References:

[1] K. Shimizu et al, *Nature* 412, 316 (2001)

[2] S. Nasu et al, *J. Phys. Condens. Matter* 14, 11167 (2002)

[3] A. Monza et al, *Phys. Rev. Lett.* 106, 247201 (2011)

[4] G. Steinle-Neumann, *Proc. Natl. Acad. Sci. U. S. A.* 101, 33 (2004)

Th.C.3_O3 - Fermi-surface topology and pairing symmetry in bis2-based layered superconductorsT. Hotta¹, T. Agatsuma¹*1. Department of Physics, Tokyo Metropolitan University, Hachioji, Japan*

Recently, new BiS₂-based layered superconductors have been discovered by Mizuguchi et al. This material group has the characteristic structure similar to high-T_c cuprate superconductors. Namely, BiS₂ superconducting layer is sandwiched by insulating blocking layers. Here we pick up LaO_{1-x}F_xBiS₂. The mother compound LaOBiS₂ is insulating, but by substituting F for O, we can dope electrons into the BiS₂ layer and the system becomes metallic. Then, superconductivity occurs and in particular, at x=0.5, the superconducting transition temperature T_c becomes maximum. Under high pressures, we obtain T_c over than 10 K. The minimum model to describe electronic structure of BiS₂ layer is the two-band Hamiltonian composed of Bi 6p_x and 6p_y orbitals on the two-dimensional square lattice, proposed by Usui et al. In this research, we analyze the two-dimensional two-band model including intra- and inter-orbital Coulomb interactions within a random phase approximation to derive the effective pairing interaction among quasi-particles. Then, we solve the gap equation to obtain T_c and the gap symmetry by focusing on the Fermi-surface topology. We find that T_c becomes maximum at x=0.6 and the corresponding gap symmetry is the extended s-wave. In this case, we find a couple of big Fermi-surface curves at the centers of Gamma and M points and the extended s-wave is considered to be preferable. An interesting point is the conversion of the gap symmetry from extended s-wave to d-wave, when we decrease x. At x=0.4, we obtain the d-wave gap, but the disconnected Fermi-surface curves around at X and Y points do not cross the line nodes of the d-wave gap. We emphasize that the variation of the Fermi-surface topology induces the conversion of the gap symmetry in this system.

Th.C.3_O4 - First-order superconducting transition of Sr_2RuO_4 investigated by magnetization and magnetic torque

S. Kittaka¹, A. Kasahara¹, T. Sakakibara¹, D. Shibata², S. Yonezawa², Y. Maeno², K. Tenya³, K. Machida⁴

1. *University of Tokyo, Tokyo, Japan*

2. *Kyoto University, Kyoto, Japan*

3. *Shinshu University, Matsumoto, Japan*

4. *Okayama University, Okayama, Japan*

The first-order superconducting transition, recently discovered in a long-standing candidate for a spin-triplet chiral-p-wave superconductor Sr_2RuO_4 , is mysterious because it is not expected within the present scenario of spin-triplet superconductivity [1]. To uncover its mechanism, we have measured the magnetization and the magnetic torque using an ultra-clean single crystal of Sr_2RuO_4 down to 0.1 K [2]. In this study, the magnetic field has been applied parallel to the ab plane with a high precision using a device we recently developed. Although the spin susceptibility has been considered to be invariant for the anticipated spin-triplet state, we observed a sharp magnetization jump of as large as 0.74 G, which is comparable to the prediction on the basis of microscopic calculation for a strongly Pauli-limited spin-singlet superconductor. The present work provides the keystone issues whose resolution is crucial in uncovering a "hidden" pair-breaking mechanism within the triplet-pairing scenario, or might urge the reconsideration of the order parameter in Sr_2RuO_4 .

References:

[1] S. Yonezawa, T. Kajikawa, and Y. Maeno, Phys. Rev. Lett. 110, 077003 (2013)

[2] S. Kittaka et al., Phys. Rev. B 90, 220502(R) (2014)

Th.D.1_I1 - Long distance spin-spin entanglement and coexistence of multiple bipartite entanglements

J.E. Lorenzo¹, S. Sahling², G. Remenyi¹, C. Paulsen¹, P. Monceau¹, C. Marin³, A. Revcolevschi⁴, L.P. Regnault³, S. Marin³

1. *Université Grenoble Alpes, Institut Néel, CNRS & UJF Grenoble, Grenoble, France*

2. *TU Dresden, Institut für Festkörperphysik, Dresden, Germany*

3. *SPSMS, CEA-INAC/UJF, IMAPEC, Grenoble, France*

4. *SP2M, Université Paris-Sud, Orsay, France*

Entanglement is a concept that has defied common sense since the discovery of quantum mechanics. Two particles are said to be entangled when the quantum state of each particle cannot be described independently, no matter how far apart in space and time these two particles are. We demonstrate experimentally that unpaired spins separated by several hundred Å entangle through a collection of spin singlets made up of antiferromagnetic spin-1/2 chains in a bulk material. Low-temperature magnetization and specific heat studies as a function of magnetic field reveal the occurrence of very dilute spin dimers and at least two quantum phase transitions related to the breaking of excited local triplets. The mechanism at the origin of the unpaired spins inside the quantum chains is the inter-modulation potential between two sublattices, and may be replicated using well-designed synthetic multilayers. Finally I will show that many different kind of entangled species (more than 6 here !!!) can coexist in the same compound without interfering.

References:

S. Sahling, et al. Nature Physics 2015 DOI: 10.1038/NPHYS3186

Th.D.1_O2 - Magnetic interactions in the two-dimensional strongly coupled dimer system malachite

M. Enderle¹, E. Canevet^{1,2,4}, B. Fak¹, R. Kremer³, J.H. Chun³

1. Institut Laue-Langevin, Grenoble, France

2. Laboratoire de Physique des Solides, Université Paris Sud, Orsay, France

3. Max-Planck Institute for Solid State Research, Stuttgart, Germany

4. Paul Scherrer Institut, Laboratory for Neutron Scattering and Imaging, Villigen PSI, Switzerland

The mineral malachite, $\text{Cu}_2(\text{OH})_2\text{CO}_3$, is known since the antiquity as a green pigment and gemstone, but its magnetic properties have only recently attracted attention. No phase transition has been observed between room temperature and 0.4 K, and initially it was assumed that the Cu^{2+} spins $1/2$ form alternating chains. We have studied the magnetic excitations of malachite using inelastic neutron scattering on a fully deuterated powder sample. The neutron scattering measurements show that malachite has a quantum spin-liquid ground state and that the excitation spectrum consists of dispersive gapped singlet-triplet excitations, characteristic of spin- $1/2$ dimer-forming Heisenberg antiferromagnets. The observed excitation spectrum is well described by a model based on the harmonic triplon approximation. We identify the main interactions which are all antiferromagnetic, and lead to a new two-dimensional dimerized coupling scheme with strong interdimer coupling. This coupling scheme places malachite between strongly coupled alternating chains, square lattice antiferromagnets, and infinite-legged ladders. The geometry of the interaction scheme resembles the staggered dimer lattice, with potential for unconventional quantum criticality.

Th.D.1_O3 - Possible quadrupolar quantum criticality in PrIr₂Zn₂₀

A. Sakai¹, K. Matsumoto², T. Onimaru², T. Takabatake², P. Gegenwart¹

1. *Universitat Augsburg, Institut Fur Physik, Experimentalphysik VI, Augsburg, Germany*

2. *Department of Quantum matter, Hiroshima University, Hiroshima, Japan*

Quantum critical points (QCPs), which emerge when magnetic order is suppressed by tuning control parameters like pressure or magnetic field, have attracted much attention. It is quite interesting to search for new types of QCPs such as quantum criticality arising from orbital (quadrupole) ordering.

The cage compound PrIr₂Zn₂₀ has the cubic nonmagnetic G₃ CEF ground state and shows antiferroquadrupolar (AFQ) ordering at $T_Q = 0.11$ K^[1]. In addition, it becomes superconducting at $T_c = 0.05$ K within the AFQ ordered state. The AFQ state is suppressed by application of a magnetic field of 5 T along [100] associated with the anomalous enhancement of Seebeck coefficient [2].

In this presentation, we will present the results of adiabatic magnetocaloric effect measurements down to 50 mK for $B // [100]$. A peak in the magnetic Grüneisen ratio at $B \sim 5$ T is observed, suggesting possible quadrupolar quantum criticality.

References:

[1] T. Onimaru, K. T. Matsumoto, Y. F. Inoue, K. Umeo, T. Sakakibara, Y. Karaki, M. Kubota, and T. Takabatake, *Phys. Rev. Lett.* 106, 177001 (2011)

[2] Tohru Ikeura, Takeshi Matsubara, Yo Machida, Koichi Izawa, Naohiro Nagasawa, Keisuke T. Matsumoto, Takahiro Onimaru, and Toshiro Takabatake, *JPS Conf. Proc.* 3, 011091 (2014)

Th.D.1_I4 - Fluctuation driven spiral magnetic order near criticality in PrPtAl

G. Abdul-Jabbar¹, D. Sokolov¹, C. O'Neill¹, C. Stock¹, D. Wermeille², F. Demmel³, F. Kruger^{3,4}, A. Green⁴, F. Levy-Bertrand⁵, B. Grenier⁶, A. Huxley¹

1. *University of Edinburgh, Edinburgh, United Kingdom*

2. *XMAS, ESRF, Grenoble, France*

3. *ISIS, STFC, Rutherford Appleton Laboratory, Harwell Oxford, United Kingdom*

4. *London Centre for Nanotechnology, University College London, London, United Kingdom*

5. *CNRS, Institut Neel, Grenoble, France*

6. *Universite Grenoble Alpes & CEA, INAC-SPSMS, Grenoble, France*

Fluctuations around quantum critical points are known to be responsible for many unexpected phenomena, e.g. the discontinuous phase transitions seen in itinerant ferromagnets at low temperatures. Such fluctuation-induced first-order behaviour is a consequence of the interplay between magnetic order parameter and soft electronic particle-hole fluctuations.

Using a fermionic version of the quantum order-by-disorder mechanism, we demonstrate that the ferromagnetic quantum critical point is unstable towards the formation of incommensurate spiral order. The key idea is that certain deformations of the Fermi surface associated with the onset of competing order enlarge the phase space available for low-energy particle-hole fluctuations and self-consistently lower the free energy.

We apply this theory to PrPtAl where spiral order on the border of ferromagnetism is observed in neutron and x-ray scattering experiments. In this system, the coupling of the itinerant electrons to the local Pr(3+) moments leads to magnetic anisotropies which have characteristic experimental consequences.

References:

'Modulated magnetism in PrPtAl', G. Abdul-Jabbar, D. A. Sokolov, C. D. O'Neill, C. Stock, D. Wermeille, F. Demmel, F. Kruger, A. G. Green, F. Levy-Bertrand, B. Grenier, and A. D. Huxley, *Nature Physics* (2015) doi:10.1038/nphys3238

Th.D.2_I1 - Quantum fluctuations in spin-ice-like Pr₂Zr₂O₇

C. Broholm¹

1. Johns Hopkins University, Baltimore, United States

Spin ice is a magnetic analogue of H₂O ice that harbors dense static disorder. Dipolar interactions between classical spins yield a frozen frustrated state with residual Pauling entropy and emergent magnetic monopolar quasi-particles. Introducing quantum fluctuations is of great interest as this could melt spin ice and allow coherent propagation of monopoles. Here we report experimental evidence for quantum dynamics of magnetic monopolar quasi-particles in a new class of spin ice based on exchange interactions, Pr₂Zr₂O₇ [1]. Narrow pinch-point features in otherwise diffuse elastic neutron scattering reflects adherence to a divergence free constraint for disordered spins on long time scales. Magnetic susceptibility and specific heat data correspondingly show activated dynamics and residual entropy below 0.1 K. In sharp contrast to conventional ice, however, more than 90% of the neutron scattering is inelastic and devoid of pinch points furnishing evidence for magnetic monopolar quantum fluctuations. The spectrum of inelastic scattering persists to significantly higher energies than expected based on estimates of the exchange constant from thermomagnetic measurements. The absence of wave vector dependence in this scattering indicates it is associated with local physics of the non-Kramers doublet.

Work at IQM was supported by DoE, Office of Basic Energy Sciences, Division of Materials Sciences and Engineering under Award DE-FG02-08ER46544.

References:

[1] "Quantum fluctuations in spin-ice-like Pr₂Zr₂O₇," K. Kimura, S. Nakatsuji, J.-J. Wen, C. Broholm, M. B. Stone, E. Nishibori, H. Sawa, Nature Communications 4, 1934 (2013)

Th.D.2_O2 - Spin liquid versus long range magnetic order in the frustrated body-centered tetragonal lattice

S. Burdin¹, C. Thomas², C. Pépin³, A. Ferraz⁴, C. Lacroix⁵

1. LOMA, CNRS & Bordeaux University, Bordeaux, France

2. Instituto de Física, UFRGS, Porto Alegre, Brazil

3. Institut de Physique Théorique, CEA-Saclay, France

4. International Institute of Physics, UFRGN, Natal, Brazil

5. Institut Néel, Université Grenoble Alpes, Grenoble, France

An $SU(n)$ generalization of the quantum Heisenberg model is studied in the geometrically frustrated body-centered tetragonal lattice (BCT-lattice) with antiferromagnetic interlayer coupling J_1 and intralayer first and second neighbor coupling J_2 and J_3 . Using a fermionic representation of the $SU(n)$ spin operators, we study the phase diagram characterizing the ground state of the system. For small n , we find that the most stable solutions correspond to the three different possible long range magnetic orders that are respectively governed by J_1 , J_2 , and J_3 . For large n , spin-liquid (SL) solutions are stabilized. The SL solution governed by J_1 breaks the lattice translation symmetry. This Modulated SL is associated to a commensurate ordering wave vector $(1,1,1)$. For intermediate values of n , we show how competition between J_1 , J_2 , and J_3 can tune the ground state from a magnetically ordered to a SL state. We then discuss the relevance of this scenario for correlated systems with BCT crystal structure.

Th.D.2_O3 - Emergence of a Connected Family of Chiral Spin Liquids on the Kagome Lattice

K. Essafi¹, L.D.C. Jaubert¹, O.J. Benton¹

1. Okinawa Institute of Science & Technology, Onna-Son, Japan

Competing interactions in frustrated magnets prevent ordering down to very low temperatures and stabilize exotic highly degenerate phases where strong correlations coexist with fluctuations. We study a general classical anisotropic Heisenberg model on the kagome lattice with all the nearest neighbour interactions allowed by the symmetry of the lattice. We obtain the complete $T=0$ phase diagram. In particular, we find a connected family of chiral spin liquids (SL) which can be described by a Coulomb gauge theory. Within this family, on one hand, some of the phases appear for relatively simple and realistic couplings which will be compared with experiments. And on the other hand, some of those SL can be mapped onto the well known Heisenberg antiferromagnet, but should not be mingled with it. This allows for a connected picture of spin liquids in kagome. The underlying chiral spin texture is especially promising when coupled with itinerant electrons.

Th.D.2_O4 - The role of interchain coupling and exchange anisotropy for the existence of quantum multipolar phases in strongly frustrated edge-shared CuO₂ chain compounds at high magnetic fields near saturation

S.L. Drechsler¹, S. Nishimoto¹, H. Rosner², J. van den Brink¹, R. Kuzian³, J. Richter⁴

1. *IFW-Dresden, Dresden, Germany*

2. *Max-Planck-Institute Chemische Physik fester Stoffe, Dresden, Germany*

3. *Institute of Materials Sciences, Kiyv, Ukraine*

4. *Institut f. Theoretische Physik, Universitaet Magdeburg, Germany*

Based on electronic structure calculations, fitting thermodynamic properties and high-energy spectra, the ferromagnetic nearest-neighbor and antiferromagnetic next-nearest neighbor intrachain as well as interchain (IC) exchange are determined for typical CuO₂-chain compounds: linarite, LiSbCuO₄, LiVCuO₄, Li₂CuO₂, Ca₂Y₂Cu₅O₁₀ etc.. The resulting spin-Hamiltonians including also exchange anisotropies are studied numerically for chain bundles within the DMRG-technique and semi-analytically for infinite number of nematic hains within the hardcore-boson method. The resulting phase diagrams for the IC and exchange anisotropy vs. frustration ratio for various multipolar phases and different realistic IC coupling geometries are established firstly. Except for the first three compounds mentioned above, realistic IC within isotropic models is found to be detrimental for the existence of exotic nematic and higher multipolar quantum phases whereas moderate easy-axis and XYZ-exchange anisotropies can stabilize them. The remaining three candidates are discussed in detail. In particular, from neutron diffraction data for linarite we found evidence for the existence of collinear longitudinal SDW states with short-range correlations of large multimagnon complexes., Epitaxial thin film under tension are proposed to weaken the detrimental IC for the other compounds.

Th.D.2_O5 - Projective symmetry of partons in the Kitaev honeycomb model

P. Mellado¹, O. Petrova², O. Tchernyshyov³

1. Department of Engineering and Sciences, Adolfo Ibañez University, Santiago, Chile

2. Max Planck Institute for the Physics of Complex Systems, Dresden, Germany

3. Department of Physics and Astronomy, Johns Hopkins University, Baltimore, United States

Low-energy states of quantum spin liquids are thought to involve partons living in a gauge-field background. We study the spectrum of Majorana fermions of Kitaev's honeycomb model on spherical clusters. The gauge field endows the partons with half-integer orbital angular momenta. As a consequence, the multiplicities reflect not the point-group symmetries of the cluster, but rather its projective symmetries, operations combining physical and gauge transformations. The projective symmetry group of the ground state is the double cover of the point group.

Th.D.3_O1 - A new spin-liquid antiferromagnet based on opposite-sign bi-triangles

C. Balz^{1,2}, B. Lake^{1,2}, N. Islam¹, Y. Singh¹, S. Toth³, J. Reuther^{1,4}, O. Prokhnenko¹, M. Reehuis¹, H. Ryll¹, R. Schoenemann⁵, H. Luetkens³, G. Simeoni⁶, E. Wheeler⁷, J. Rodriguez⁸, T. Guidi⁹

1. Helmholtz-Zentrum Berlin, Berlin, Germany
2. Technische Universität Berlin, Berlin, Germany
3. Paul Scherrer Institut, Villigen PSI, Switzerland
4. Freie Universität Berlin, Berlin, Germany
5. Helmholtz-Zentrum Dresden-Rossendorf, Dresden, Germany
6. Technische Universität München, Munich, Germany
7. Institut Laue Langevin, Grenoble, France
8. NIST Center for Neutron Research, Gaithersburg, United States
9. ISIS, Surrey, United Kingdom

Frustration due to competing magnetic exchange interactions can give rise to exotic ground states and excitations. In extreme cases long-range magnetic order is completely suppressed and fluctuations persist down to the lowest temperatures. Here, we present a new candidate compound for such a spin-liquid ground state built on spin-1/2 Cr⁵⁺ ions. In Ca₁₀Cr₇O₂₈, long-range magnetic order is absent down to a temperature of 19mK while the excitations are diffuse and gapless as shown by inelastic neutron scattering. Muon spin relaxation and AC susceptibility confirm the absence of static magnetism and reveal that the ground state is fully dynamical. Ca₁₀Cr₇O₂₈ can be driven towards long range ferromagnetic order by applying an external magnetic field of 12T. In contrast to the zero-field excitations, the excitations in the saturated state resemble sharp magnon modes, and by fitting their dispersions to linear spin wave theory the exchange constants were extracted. A mixture of FM and AFM interactions were found where the FM interactions are greater than the AFM interactions. The coupling scheme consists of bi-triangles where ferromagnetic triangles lie directly over antiferromagnetic triangles and the intertriangle coupling is ferromagnetic. The frustration arises from the opposite sign of the coupling within the two triangles and neither triangle can realize its intrinsic spin arrangement due to the intertriangle coupling. This motif forms a 2D bilayer structure where in each layer the AFM triangles are coupled to FM triangles via their corners in a kagome like arrangement. FRG calculations confirm the absence of long-range order and the spin-liquid ground state in this new type of frustrated system.

Th.D.3_O2 - Interplay of disorder and frustration in the diamond spin lattice antiferromagnet CoAl_2O_4

V. Kataev¹, M. Iakovleva^{1,2}, E. Vavilova^{1,2}, H.J. Grafe¹, S. Zimmermann^{1,3}, A. Alfonsov¹, H. Luetkens⁴, H.H. Klauss³, A. Maljuk¹, S. Wurmehl¹, B. Büchner^{1,3}

1. *Leibniz Institute For Solid State And Materials Research IFW Dresden, Dresden, Germany*
2. *Kazan E.K. Zavoisky Physical-Technical Institute of the Russian Academy of Sciences, Kazan, Russia*
3. *Institute for Solid State Physics, Technical University Dresden, Dresden, Germany*
4. *Laboratory for Muon-Spin Spectroscopy Paul Scherrer Institut, Villigen PSI, Switzerland*

We present a detailed experimental study with three local spin probe techniques, NMR, μSR and ESR, of magnetic properties of the CoAl_2O_4 single crystal where the Co spins form a frustrated spin lattice with the diamond structure. We find that in the studied single crystal the degree of structural disorder due to the Al-Co site inversion is optimally tuned to obtain insights onto its influence on the ground state and on the low energy magnetic dynamics of the frustrated diamond spin lattice. Inhomogeneous broadening of ESR and NMR lines at temperatures below 30 - 50 K indicates the growth of short-range spin correlations. The analysis of the NMR and μSR relaxation rates evidences a critical slowing down of spin fluctuations at a characteristic temperature $T^* = 8$ K which suggests the onset of a quasi-static order at this temperature. Most probably the spin order is short-range and unconventional which is manifested by the overdamped oscillations of the muon spin polarization and a continuous line broadening of ESR and NMR lines below T^* . Since in the phase diagram of the diamond spin lattice CoAl_2O_4 is located close to the special critical point which separates collinear and noncollinear spin phases, it appears in our results that Al atoms at the Co sites acting as quenched impurities smear the phase boundary between the two phases. This can yield a competition between the two ground states with the low-lying spin spiral excitations responsible for an inhomogeneous magnetic dynamics.

We argue that our experimental findings may have important implications for recent theories of an 'order by disorder' mechanism in the frustrated diamond spin lattice.

Th.D.3_O3 - Neutron diffraction study of uniaxial pressure control of spin frustration in isosceles triangular lattice Ising antiferromagnet CoNb_2O_6

S. Kobayashi¹, S. Hosaka², H. Tamatsukuri², T. Nakajima², S. Mitsuda², K. Prokes³, K. Kiefer³

1. *Iwate University, Faculty of Engineering, Iwate, Japan*

2. *Tokyo University of Science, Tokyo, Japan*

3. *Helmholtz-Zentrum Berlin, Berlin, Germany*

We have studied the effect of uniaxial pressure on magnetic ordering in an quasi-one-dimensional Ising antiferromagnet CoNb_2O_6 by single-crystal neutron diffraction in zero field in order to see a possible pressure control of frustrated exchange interactions of the isosceles triangular lattice. In CoNb_2O_6 , magnetic Co^{2+} ions form a quasi-1D ferromagnetic chains along the c-axis and form the frustrated lattice in the a-b plane. In zero field, the system exhibits successive magnetic phase transitions from the paramagnetic (PM) phase to the incommensurate (IC) sinusoidal magnetic phase characterized by the temperature-dependent propagation wave vector $Q_{\text{propa}} = (0 \ q \ 0)$ at $T_1 = 3.0$ K, and then to the noncollinear antiferromagnetic (AF) phase with $Q_{\text{propa}} = (0 \ 0.5 \ 0)$ at $T_2 = 1.9$ K. We found that under uniaxial pressure of 400 MPa along the a-axis, the temperature dependence of q in the IC phase is significantly modified. With decreasing temperature, IC peaks show up at $T \sim 2.98$ K at an incommensurate position of $q = 0.411$ which is larger than 0.377 of no applied pressure, then shift to the AF position of $q = 0.5$, and the magnetic phase transition from the IC to AF phases occurs at $T = 2.2$ K, which is higher than 1.9 K at no applied pressure. The energy consideration for an Ising model with exchange interactions up to 2nd neighbors suggests that a ratio of nearest neighbor to next-nearest neighbor interactions on the lattice significantly increases from 1.33 to 1.81 by an uniaxial pressure of 400 MPa. This clearly demonstrates that uniaxial pressure can control spin frustration of the isosceles triangular lattice through the anisotropic deformation of the lattice[1].

References:

[1] S. Kobayashi et al., Phys. Rev. B 90 (2014) 060412(R)

Th.D.3_O4 - New investigation of the magnetization plateau phases in the frustrated antiferromagnet TbB₄ by neutron diffraction in pulsed magnetic fields up to 40 T

F. Duc¹, W. Knafo¹, J. Billette¹, X. Tonon², F. Bourdarot³, E. Lelièvre-berna², E. Lorenzo⁴, P. Frings¹, L.P. Regnault³, F. Iga⁵, S. Michimura^{6,7}

1. *Lab. National Des Champs Magnetiques Intenses, Toulouse, France*

2. *Institut Laue Langevin, Grenoble, France*

3. *Univ. Grenoble Alpes and CEA, INAC-SPSMS-MDN, Grenoble, France*

4. *Institut N el, CNRS, Grenoble, France*

5. *College of Science, Ibaraki University, Mito, Japan*

6. *Research and Development Bureau*

7. *Graduate School of Science & Engineering, Saitama University, Saitama, Japan*

TbB₄ has a tetragonal structure in which the Tb ($J = 9/2$) ions network in the c-plane is equivalent to the geometrically frustrated Shastry-Sutherland lattice [1]. In zero-field, two successive antiferromagnetic transitions occur at $TN_1 \sim 44$ K and $TN_2 \sim 24$ K [2]. Remarkably, for $T \ll TN_2$, TbB₄ exhibits a multistep magnetization process above 16 T when the magnetic field is applied perpendicular to the magnetic easy plane [3]. In order to understand this devil-staircase-like magnetization process, the first ever-made neutron diffraction experiment in pulsed magnetic fields up to 30 T was carried out on the CRG spectrometer IN22 at the ILL in 2008 [4] allowing to propose a magnetic model for the $1/2MS$ state. Here, we present the re-investigation of the magnetic structures of the plateau phases in TbB₄ using the newly completed pulsed field neutron diffraction set-up developed in collaboration between the LNCMI-Toulouse, the CEA-Grenoble, the ILL and the Institut N el, Grenoble. This installation consists of a 40 T long pulse rapid cooling magnet mounted inside a specially designed cryostat allowing to cool the sample up to 2 K. The new limits offered by this set-up installed on the spectrometer IN22 provide new opportunities for the study of magnetic materials. In the study of TbB₄, several steps, clearly related to the structures of the different plateaus, were now detected at low temperature in the field dependence of the antiferromagnetic (100) reflection thanks to better counting statistics and temperature control. A single crystal of TbB₄ enriched with ¹¹⁵B was kindly provided by Nojiri et al.

References:

[1] Shastry and Sutherland, *Physica B+C* 108, 1069 (1981)

[2] Matsumura et al., *J. Phys. Soc. Jpn* 76, 015001 (2007)

[3] Yoshii et al., *Phys. Rev. Lett.* 101, 087202 (2008)

[4] Yoshii et al., *Phys. Rev. Lett.* 103, 077203 (2009)

Th.E.1_11 - Tuning spin order and spin excitations in multiferroic BiFeO₃ thin films

D. Sando¹, A. Agbelele², C. Toulouse³, J.P. Tetienne⁴, I. Gros⁴, V. Garcia¹, K. Garcia¹, S. Fusil¹, R. Ruffer⁵, B. Dkhil⁶, A. Barthélémy¹, V. Jacques⁴, M. Cazayous³, J. Juraszek², M. Bibes¹

1. *Unité Mixte de Physique CNRS/Thales, Palaiseau, France*

2. *Groupe de Physique des Matériaux, UMR 6634 CNRS-Université de Rouen, Rouen, France*

3. *Laboratoire Matériaux et Phénomènes Quantiques, CNRS-Université Paris-Diderot, Paris France*

4. *Laboratoire Aimé Cotton, CNRS, Université Paris-Sud, Orsay, France*

5. *European Synchrotron Radiation Facility, Grenoble, France*

6. *Laboratoire SPMS, UMR 8580 CNRS-Ecole Centrale Paris, Châtenay-Malabry, France*

Multiferroics are compounds that show ferroelectricity and magnetism. BiFeO₃, by far the most studied, has outstanding ferroelectric properties, a cycloidal magnetic order in the bulk, and many unexpected virtues such as conductive domain walls or a low bandgap of interest for photovoltaics [1]. While this flurry of properties make BiFeO₃ a paradigmatic multifunctional material, most are related to its ferroelectric character, and its other ferroic property - antiferromagnetism - has not been investigated extensively, especially in thin films. In this talk, we will bring insight into the rich spin physics of BiFeO₃ through various advanced techniques such as conversion-electron Mössbauer spectroscopy, Raman scattering and nuclear resonant scattering. We will show how the spin orders and the spin excitations can be tuned by epitaxial strain and magnetic fields, and discuss routes to map spin textures in real space and control them by electric fields.

References:

[1] D. Sando, A. Barthélémy and M. Bibes, J. Phys.: Condens. Matter. 26, 473201 (2014)

Th.E.1_O2 - Artificially synthesized chemical and magnetic structure at the domain walls of the epitaxial oxide TbMnO₃

C. Magén¹, S. Farokhipoor^{2,3}, C.J.M. Daumont^{3,4}, S. Venkatesan^{3,5}, E. Snoeck⁶, J. Iñiguez⁷, D. Rubí^{3,8}, M. Mostovoy³, B. Noheda³

1. *Laboratorio de Microscopias Avanzadas (LMA), Instituto de Nanociencia de Aragón (INA) - ARAID, Universidad de Zaragoza, Spain*

2. *Department of Materials Science, University of Cambridge, United Kingdom*

3. *Zernike Institute for Advanced Materials, University of Groningen, The Netherlands*

4. *GREMAN UMR7347, Tours, France*

5. *Ludwig-Maximilians University Muenchen, Germany*

6. *CEMES-CNRS, Toulouse, France*

7. *ICMAB, Campus UAB, Bellaterra, Spain*

8. *GIA & INN, CAC-CNEA, San Martin, Argentina*

Strain engineering can improve or induce new functional properties in thin films by epitaxial growth, particularly in multiferroic materials such as the terbium manganite. Bulk TbMnO₃ exhibits an antiferromagnetic ordering below 42 K and a spin spiral below 27 K, the latter inducing the inversion symmetry breaking that causes ferroelectricity [1]. However, in this work we show that epitaxially-strained TbMnO₃ on SrTiO₃ (001) grown by Pulsed Laser Deposition induces the formation of a novel chemical and magnetic structure, which orders ferromagnetically at 15 K with magnetic moments up to 0.15 μB/f.u. [2]. This new phase is synthesized at the domain walls (DWs) formed to accommodate the epitaxial strain caused by the large lattice mismatch with SrTiO₃. Ferromagnetism is strongly correlated with this strain-induced microstructure. The reduction of thickness induces an increase of the DW density, which scales with the increase of the magnetization [2].

Aberration-corrected Scanning Transmission Electron Microscopy (STEM) imaging combined with Electron-Energy Loss Spectroscopy (EELS) has been carried out in an FEI Titan at 300 kV to characterize locally the structural and chemical properties of this novel phase. STEM imaging evidences the abundance of [001]-oriented DWs and the local strain relaxation at the DWs. Atomic-resolution STEM-EELS chemical mapping demonstrates that the new structure synthesized at the DWs is characterized by the presence of spatially ordered Tb-deficient positions along [001], which are entirely replaced by Mn atoms. The substitution of alternate Tb positions by Mn gives rise to exotic atomic coordinations for these “wall” Mn atoms at the Tb position and first principles calculations demonstrate that the different magnetic parameters of “wall” Mn atoms perturb the local magnetic coupling around the DW to induce long-range ferromagnetism.

References:

[1] Y. Kimura et al., Nature 426, 55 (2003)

[2] S. Farokhipoor, C. Magén, et al., Nature 515, 379 (2014)

Th.E.1_O3 - Magnetoelastic coupling in BiFeO₃ (111) thin-films observed by non-resonant x-ray magnetic diffraction

N.W. Price^{1,2}, R. Johnson¹, W. Saenrang³, A. Bombardi², C. Eom³, P. Radaelli¹

1. *University of Oxford, United Kingdom*
2. *Diamond Light Source, United Kingdom*
3. *University of Wisconsin – Madison, United States*

The coupling between ferroelectric and long range magnetic order in multiferroic materials is not only interesting in terms of fundamental physics, but also holds great promise for application in future memory devices. With its room temperature multiferroicity and giant ferroelectric polarisation, BiFeO₃ is the most intensely investigated multiferroic and arguably the most promising multiferroic material for application in devices. BiFeO₃ thin films, upon which these devices are likely to be based, display a wide range of tuneable functionalities, which are highly sensitive to environmental and growth conditions. Understanding the subtle effects of these conditions is therefore of great importance if BiFeO₃ thin film devices are to be realised. We study the domain configuration of cycloidal multiferroic domains in 111(cubic)-oriented BiFeO₃ films with non-resonant magnetic x-ray diffraction. Comparing reciprocal space maps and post scatter polarisation analysis with simulations, we find that, contrary to previous reports, the crystal structure undergoes a small monoclinic distortion, unresolvable by any conventional crystallographic diffraction techniques, which splits the film into a coherent set of monoclinic twins related by the three-fold axis of the parent (R3c) rhombohedral phase. The distortion is coupled to the magnetic structure such that each of the three monoclinic twins chooses a corresponding magnetic propagation vector, giving rise to the observed characteristic magnetic diffraction signal. We also propose a twin law based on symmetry arguments and a microscopic model of the coupling between the distortion direction and magnetic propagation vector. Our results put an upper bound on the multiferroic domain size of order microns, which has significant implications for devices that would exploit the magnetic order in this material.

Th.E.1_I4 - Induced magnetism at correlated oxide interfacesJ. Santamaria¹*1. Universidad Complutense de Madrid, Madrid, Spain*

At oxide interfaces electron correlations underlie the nucleation of emerging ground states with exciting responses not appearing in the bulk counterparts of the constituents. This has driven an important effort towards the design of heterostructures with specific functionalities. In this talk I will examine several interface problems in oxide heterostructures with special focus on the possibility of creating novel interfacial magnetic states. They originate at the modification of the orbital occupancy resulting from the modified bonding at the interface. I will discuss the effect of these low dimensional magnetic states in determining the magnetic response of practical magnetic tunnel junctions. I will demonstrate the possibility of designing specific functionalities such as spin filtering or electric field control of interface magnetization. In particular I will show that at $\text{La}_{0.7}\text{Ca}_{0.3}\text{MnO}_3$ (LCMO) - $\text{PrBa}_2\text{Cu}_3\text{O}_7$ (PBCO) interfaces a Cu magnetic state is induced which can be controlled by an electric field [1]. At interfaces combining antiferromagnetic LaFeO_3 (LFO) and ferromagnetic $\text{La}_{0.7}\text{Sr}_{0.3}\text{MnO}_3$ (LSMO), we find that a net magnetic moment is induced at the LFO interface [2]. Using X-ray photoemission electron microscopy, we show that the ferromagnetic domain structure of the manganite electrodes is imprinted into the antiferromagnetic tunnel barrier, endowing it with spin selectivity. I will conclude with an outline of interesting future directions.

References:

- [1] F. A. Cuellar et al. Nature Commun. 5, 4215 (2014) doi:10.1038/ncomms5215
[2] F. Y. Bruno et al. Nature Commun. 6, 6306 (2015) doi:10.1038/ncomms7306

Work done in collaboration with F. A. Cuellar¹, J. Tornos¹, J. Garcia-Barriocanal¹, D. Arias¹, A. Rivera-Calzada¹, Z. Sefrioui¹, M. Varela¹, C. Leon¹, M. N. Grisolia², F. Y. Bruno², M. Bibes², and A. Barthélémy², M. Garcia Hernandez³, Y. H. Liu⁴, S. G. E. te Velthuis⁴, M. R. Fitzsimmons⁵, S. J. Pennycook⁶, S. Valencia⁷, R. Abrudan⁷, A.A. Ünal⁷

Th.E.2_I1 - Spin dynamics in multiferroic BiFeO₃: interplay of DM interaction and anisotropy

J. Jeong^{1,2}, M. Duc Le¹, E. Goremychkin³, T. Guidi³, K. Nakajima⁴, P. Bourges⁵, S. Petit⁵, S. Furukawa⁶, Y.B. Kim⁷, G.S. Jeon⁸, S. Kim⁹, S. Lee⁹, V. Kiryukhin¹⁰, S. Cheong¹⁰, J. Park^{1,2}

1. *Center for Correlated Electron Systems, Institute for Basic Science (IBS), Republic of Korea*
2. *Department of Physics and Astronomy, Seoul National University, Republic of Korea*
3. *ISIS Facility, STFC Rutherford Appleton Laboratory, United Kingdom*
4. *Neutron Science Section, MLF Division, J-PARC Center, Japan*
5. *Laboratoire Leon Brillouin, CEA-CNRS, France*
6. *Department of Physics, University of Tokyo, Japan*
7. *Department of Physics, University of Toronto, Canada*
8. *Department of Physics, Ewha Womans University, Republic of Korea*
9. *Neutron Science Division, Korea Atomic Energy Research Institute, Republic of Korea*
10. *Rutgers Center for Emergent Materials and Department of Physics and Astronomy, Rutgers University, United States*

Multiferroic materials have attracted huge interest for coexistence of ferroelectricity and magnetism, and coupling between them. BiFeO₃ is the only example that shows multiferroicity above room temperature. It also has a complex magnetic structure including the cycloid spin structure with an extremely long period. In order to understand the microscopic magnetic interactions, inelastic neutron scattering (INS) experiments were carried out using co-aligned single crystals. The magnon dispersion over the full Brillouin zone was measured for the first time, and the exchange interaction parameters between the nearest and the next nearest neighbors were determined [1]. For the further study on the detailed magnetic excitations at low energy, additional INS experiments were performed using the triple-axis spectrometer 4F₂ at LLB. The magnon dispersion was also calculated using the Hamiltonian that includes the Dzyaloshinskii-Moriya (DM) interaction and single-ion anisotropy (SIA), which are associated with the distortion of the FeO₆ octahedra. The unusual low-energy excitations in BiFeO₃ is understood by examining the interplay of DM interaction and easy-axis SIA, and thermal evolution of the parameters was determined, which agrees with structural changes qualitatively [2].

References:

- [1] Jaehong Jeong et al., Phys. Rev. Lett. 108, 077202 (2012)
[2] Jaehong Jeong et al., Phys. Rev. Lett. 113, 107202 (2014)

Th.E.2_O2 - Multiferroic Iron Oxide Thin Films at Room-Temperature

M. Gich¹, I. Fina^{2,3}, F. Sanchez¹, A. Morelli², J. Gázquez¹, M. Alexe³, J. Fontcuberta¹, A. Roig¹

1. *Institut de Ciència de Materials de Barcelona-CSIC, Bellaterra, Spain*

2. *Max Planck Institute of Microstructure Physics, Halle, Germany*

3. *Department of Physics, University of Warwick, Coventry, United Kingdom*

The quest for magnetoelectric multiferroics is driven by the promise of a novel generation of devices combining the best characteristics of ferromagnetic and ferroelectric materials. These cherished applications require materials displaying a substantial magnetization and electric polarization which are coupled and coexist well above room temperature. These properties are not commonly found in a single phase materials and candidates propelling the development of these technologies are still required. In this contribution, we will report on epitaxial epsilon-Fe₂O₃ thin films grown by Pulsed Laser Deposition on (111) SrTiO₃ and present recent data on its structural, magnetic and dielectric characterization. The films are ferromagnetic and ferroelectric at room temperature and display magnetization and polarization values at remanence of about 50 emu/cm³ and 1u C/cm² with a long retention. A magnetocapacitive response has also been detected indicating that the films present coupling between both ferroic orders. The chemical simplicity of epsilon-Fe₂O₃ represents a major advantage to overcome the challenges of stoichiometry and phase purity control that might be cumbersome in all other known room-temperature multiferroics.

References:

[1] M. Gich, I. Fina, et al., *Advanced Materials* 26, 4645(2014).

Th.E.2_O3 - Theory of antisymmetric spin-pair dependent electric polarization in multiferroic BiFeO₃

S. Miyahara¹, N. Furukawa²

1. *Fukuoka University, Fukuoka, Japan*

2. *Aoyama Gakuin University, Tokyo, Japan*

In magnetoelectric (ME) multiferroics, there is a strong coupling between magnetization M and electric polarization P and ME effects and electromagnon, electroactive magnon, processes arise. As typical ME couplings, spin dependent electric polarizations due to the exchange striction [1,2], the spin current mechanism [3-5], and the metal-ligand hybridization [6] mechanisms are well known and explain the ME coupling in various multiferroics. However, novel component of the spin induced electric polarization observed in BiFeO₃, where an electric polarization arises perpendicular to the cycloidal spin structures, cannot be explained by the known mechanisms [7]. We clarify the microscopic origin of a new mechanism, a generic coupling between the electric polarization and antisymmetric spin pair [1,8] and show that such a coupling explains the novel feature in BiFeO₃ [7]. Moreover, we discuss dynamical ME effects, i.e., electromagnon and toroidal magnon [9] processes, in BiFeO₃ and clarify the selection rule of an absorption due to magnon excitation. The results indicate that various non-collinear magnetic structures show multiferroic behaviors owing to the new mechanism.

References:

- [1] T. Moriya, J. Appl. Phys. 39, 1042 (1968)
- [2] T. Arima et al., Phys. Rev. Lett. 96, 097202 (2006)
- [3] H. Katsura, N. Nagaosa, and A. V. Balatsky, Phys. Rev. Lett. 95, 057205 (2005)
- [4] M. Mostovoy, Phys. Rev. Lett. 96, 067601 (2006)
- [5] I. A. Sergienko and E. Dagotto, Phys. Rev. B 73, 094434 (2006)
- [6] T. Arima, J. Phys. Soc. Japan 80, 052001 (2011)
- [7] M. Tokunaga et al., Nature Comm. 6, 5878 (2015)
- [8] T.A. Kaplan and S.D. Mahanti, Phys. Rev. B 83, 174432 (2011)
- [9] S. Miyahara and N. Furukawa, J. Phys. Soc. Japan 81, 023712 (2012)

Th.E.2_O4 - Non-volatile magnetoelectric memory effects in multiferroic BiFeO₃

M. Tokunaga¹, S. Kawachi¹, A. Miyake¹, T. Ito², H. Kuwahara³

1. The Institute For Solid State Physics, The University of Tokyo, Tokyo, Japan

2. National Institute of Advanced Industrial Science and Technology (AIST), Japan

3. Sophia University, Chiyoda, Japan

BiFeO₃ is one of the most extensively studied multiferroic materials owing to its multiferroicity at room temperature. To clarify its fundamentals, we studied magnetic and magnetoelectric properties of mono-domain crystals of BiFeO₃ synthesized with using the laser-diode heating floating-zone furnace in pulsed high magnetic fields up to 55 T. In magnetic fields applied normal to the ac-plane of the trigonal lattice, electric polarization along the c-axis steeply changes at the transition field from the cycloidal to the canted-antiferromagnetic phase, which can be simply explained as the spin-driven polarization in the cycloidal state through the spin current mechanism or the inverse effect of the Dzyaloshinskii-Moriya interaction. On the other hand, we found even larger change in the polarization normal to the c-axis in addition to it. This transverse, i.e. normal to the c-axis, polarization appears to change its magnitude once the crystal experiences the field cycle up to about 10 T. Such a non-volatile memory effect was observed even at room temperature, and will be used for the low-power consumption magnetoelectric memory devices in future. Main part of this study was published in M. Tokunaga et al., Nature Commun. 6, 5878 (2015).

Th.E.2_O5 - Suppression of mixed-phase areas in highly elongated BiFeO₃ thin films on NdAlO₃ substrates

C. Woo¹, J. Lee¹, K. Chu¹, B. Jang¹, Y. Kim², T. Koo³, P. Yang⁴, Y. Qi⁵, Z. Chen⁵, L. Chen⁵, C.C. Choi⁶, J.H. Shim⁶, C.H. Yang^{1,7}

1. Department of Physics, KAIST, Daejeon, Republic of Korea
2. Gumi Electronics & Information Technology Research Institute, Gumi, Gyungbuk, Korea
3. Pohang Accelerator Laboratory, Pohang, Gyungbuk, Korea
4. Singapore Synchrotron Light Source, National University of Singapore, Singapore, Singapore
5. School of Materials Science and Engineering, Nanyang Technological University, Singapore, Singapore
6. Department of Chemistry, POSTECH, Pohang, Gyungbuk, Korea
7. Institute for the NanoCentury, KAIST, Daejeon, Republic of Korea

Multiferroic bismuth ferrite (BiFeO₃; BFO) has received a great deal of attention because it has both ferroelectric and anti-ferromagnetic properties at room temperature. It also has been discovered that a highly-elongated phase of BFO (T-BFO) can be stabilized by the heteroepitaxial misfit strain between substrate and film.[1] It is expected that the T-BFO has totally different physical properties from bulk BFO (R-BFO) because of the large elongation along the c-axis direction ($c/a \sim 1.26$).[2] It is needed to grow very thick pure T-BFO films for investigating the physical properties of the new BFO phase in more reliable way with sufficient sample volume. However, if the film thickness is thicker than ~ 40 nm, mixed phase areas start to appear parasitically and the areas become larger with increasing the thickness as a consequence of strain relaxation. We grew a series of T-BFO films varying film thickness on both lanthanum aluminate (LaAlO₃, LAO) and neodymium aluminate (NdAlO₃, NAO) substrates and characterized their crystal structures through the x-ray diffraction, the reciprocal space maps and the high-resolution transmission microscopy. The surfaces morphology and ferroelectric domain structures were studied by using piezoresponse force microscopy. We found that the NAO substrates prevent the formation of mixed-phase areas, but the LAO substrates do not. Finally we discussed the fundamental mechanism of phase completion of BFO phase using first principles density functional calculation for the misfit strain dependent total energy.

Th.E.3_O1 - A comparative measurement technique for magnetic hyperthermia in nanoparticle suspensions

K. O'Grady^{1,2}, J. Zehner¹, F. Halpin¹, G. Vallejo-Fernández¹, J. Flatt¹, J. Timmis², V. Patel²

1. Department of Physics, University of York, Heslington, York, United Kingdom

2. Liquids Research Ltd, Unit 9 Mentec, Gwynedd, United Kingdom

We describe a new method for the determination of the heating power of magnetic nanoparticle colloids which have potential for application in the remedial treatment of malignant and non-malignant tumours. The method is based upon a comparison between the heating power observed when the colloid is exposed to an RF frequency magnetic field and that which is observed using a resistive electrical heater. A new measurement cell has been designed and constructed which eliminates the effects of convection and ensures that the magnetic field is uniform. The heat losses in the system are the same both under a magnetic field and Joule heating ensuring that the measurement of the heating power is determined accurately. The correlation between the initial heating rate dT/dt and the equivalent power that gives rise to that heating rate is excellent. The relationship shows a high degree of linearity ($r^2 > 0.99$) so that measurements of dT/dt generated by the action of the magnetic field can be directly converted to an equivalent heating power.

Th.E.3_O2 - Synthesis and unusual magnetic damping effect in silver-cobalt ferrite nanosystem

S. Sharma¹, M. Knobel¹, K. Pirota¹, F. Beron¹, G. Zoppellaro², J. M. Vargas³, D. Altbir⁴

1. *Instituto de Física Gleb Wataghin (IFGW), Universidade Estadual de Campinas (Unicamp), Campinas, SP, Brazil*

2. *Regional Centre of Advanced Technologies and Materials, Faculty of Science, Olomouc, Czech Republic*

3. *Institute of Nanoscience and nanotechnology, Centro Atomico Bariloche, Bariloche, Argentina*

4. *Universidad de Santiago de Chile (USACH), Santiago, Chile*

The synthesis and unusual magnetic anomaly in silver-cobalt ferrite nanosystem prepared by two-steps chemical route is reported. The static and dynamic magnetic response of silver-cobalt ferrite nanosystem is compared to pure CoFe_2O_4 nanoparticles. Our silver-cobalt ferrite nanosystem showed significant changes in their magnetic behavior, phenomenon that can be understood with the damping effect of magnetic relaxation due to hybridization of Ag and CoFe_2O_4 electronic structures. The observed magnetic properties are explained in terms of superparamagnetic Stoner-Wohlfarth and Neel-Arrhenius/Vogel-Fulcher models through micromagnetics simulations. It was observed that enhancing the phase homogeneity in the hetero nano-system was the leading morphological factor responsible for producing a strong enhancement in the effective energy barrier and reduction of the magnetic hardness.

Th.E.3_O3 - Adjustable magnetic properties of Fe₃O₄/silicon nanocomposites with respect to biomedical applications

P. Granitzer¹, K. Rumpf¹, P. Poelt², M. Reissner³

1. *Karl-Franzens-University Graz, Institute of Physics, Graz, Austria*

2. *University of Technology Graz, Institute for Electron Microscopy, Graz, Austria*

3. *Vienna University of Technology, Institute of Solid State Physics, Wien, Austria*

In the frame of this work we present a magnetic nanocomposite system which is appropriate to be used for magnetically guided drug delivery. As matrix for the incorporation of iron oxide nanoparticles nanostructured silicon is employed. The used magnetite nanoparticles are superparamagnetic due to their size and they are coated with an organic shell. Both materials are known to be biocompatible which has already been shown previously. Further preconditions of the nanocomposite are a magnetic moment as high as possible and a non-existent remanence when the external magnetic field is switched off. Concerning the adjustability of the magnetic properties of the system the loading of the porous silicon with iron oxide nanoparticles has been elucidated in detail and the growth of iron oxide structures within the pores has been investigated. The magnetic properties, especially the transition temperature between superparamagnetic behavior and blocked state (TB) of the nanocomposite can be controlled by the filling procedure. TB shifts to higher temperatures with increasing magnetic coupling between the particles. Dependent on the packing density as well as on the size of the particles within the pores the magnetic interactions can be modified and thus TB can be tuned. These investigations have been carried out for particle sizes between 4 and 12 nm. An optimization of the magnetization (high filling density as possible) and its correlation with the blocking temperature has been carried out. An assessment of the iron oxide deposition dependent on the template and the chemical parameters as well as of the magnetic properties in dependence on the particle size, inter-particle distance and template morphology of the nanocomposite will be presented.

TH.E3_O4 - Dipolar ferromagnetism of island-like agglomerates of Fe₃O₄ nanoparticles embedded in an epoxy matrixP. Allia¹, P. Tiberto², G. Barrera³, F. Bondioli⁴, C. Sciancalepore⁵, M. Messori⁵

1. *Politecnico Di Torino, Torino, Italy*
2. *INRIM, Torino, Italy*
3. *Università di Torino, Torino, Italy*
4. *Università di Parma, Parma, Italy*
5. *Università di Modena e Reggio Emilia, Modena, Italy*

Stable suspensions of magnetite nanoparticles were prepared through solvo-thermal treatment of Fe(AcAc)₃ dissolved in different amounts into 2-ethyl-exane-1,3-diol (Ex-diol). Epoxy nanocomposites were obtained by in-situ polymerization of bisphenol A diglycidyl ether (DGEBA) monomers directly within the Fe₃O₄ nanoparticles suspensions. The formulations were prepared by adding the nanoparticle suspensions to DGEBA in the range between 1 and 6 phr of Fe₃O₄ using a magnetic stirrer and an ultrasonic bath. The formulations were cast into silicone moulds with a cationic thermal initiator and cured at 130°C for 3 h. Dried nanopowders were characterized by XRD, Raman spectroscopy, TEM. The powders are composed of almost pure Fe₃O₄; XRD spectroscopy indicates that nanoparticles have a crystalline core surrounded by an amorphous shell. TEM images shows that the particles have spheroidal shape with diameters in the range 10-18 nm depending on the [Fe(AcAc)₃]/[Ex-diol] ratio. Epoxy nanocomposites were characterized by TEM, FT-IR and DSC. TEM images show that in all cases the nanoparticles are not evenly dispersed in the matrix and form an island-like structure of well-separated nanoparticle agglomerates; within each agglomerate the individual particles are mostly not in contact. Magnetic measurements were performed using a 70 kOe SQUID magnetometer in the temperature range 10 - 300 K. Flat, almost structureless FC-ZFC curves indicate a highly correlated magnetic response. Magnetization loops exhibit non-negligible hysteresis with a coercivity increasing with decreasing temperature; the low-field susceptibility exhibits a non-monotonic trend with temperature. Detailed comparison of the evidence from different magnetic measurements points to a ferromagnetic-like behavior of the embedded nanoparticles. However, the absence of contact interaction among adjacent nanoparticles in island-like agglomerates rules out the hypothesis of the presence of a standard ferromagnetic phase; the temperature dependence of both coercivity and low-field susceptibility indicate that the agglomerates can be considered as dipolar ferromagnets in the whole temperature range.

Th.F.1_I1 - Multiscale dynamics as the key to all-optical magnetization reversal

A. Kirilyuk¹

1. Radboud University, Institute For Molecules and Materials, Nijmegen, The Netherlands

In spite of recent extensive work on all-optical switching of magnetization, confusion persists as to its mechanism. Here we demonstrate, using various time-resolved imaging techniques, that this confusion is largely due to the fact that this phenomenon involves behavior on multiple scales, both in space and time. At 100's fs, independent demagnetization of sublattices is observed accompanied by spin diffusive processes at <10 nm distances, as shown by time-resolved X-ray scattering [1]. This is followed by the exchange spring driven behavior [2] with reversal and formation of skyrmion-like domains [3] at a few ps times. Later, very large scale coherent oscillations can be observed that accompany the growth of large domains [4]. Moreover, an extra dimension is added to the problem by the multilayered character [4] and the overall shape of the sample [5]. Therefore, only a combination of high-resolution spatial and time resolved techniques is able to follow these processes both in space and time.

References:

1. C.E. Graves et al, Nature Materials 12, 293 (2013)
2. A. Kirilyuk et al, Rep. Prog. Phys. 76 , 026501 (2013)
3. M. Finazzi et al, Phys. Rev. Lett. 110, 177205 (2013)
4. M. Savoini et al, submitted
5. L. Le Guyader et al, Nature Comm. 6, 5839 (2015)

Th.F.1_O2 - Controlling the magnetization dynamics with sequences of picosecond acoustic pulses

J. Kim¹, M. Vomir¹, J. Bigot¹

1. IPCMS, CNRS, Strasbourg, France

We show that using picosecond acoustic pulses is a versatile and efficient way of controlling the magnetization precession in ferromagnets [1]. Two or three longitudinal acoustic pulses, generated by femtosecond laser pulses, allow suppressing or enhancing the magnetic precession at any arbitrary time by controlling the delays T_{12} , T_{23} and the amplitude ratios E_{12} , E_{23} between optical pulses. We found that when using two acoustic pulses, the control is somehow restrictive because the occurrence of suppression or amplification is related to integers of half ($T_{12} = (m+1/2)T_{\text{prec}}$; $m=\text{integer}$) or full precession periods ($T_{12} = mT_{\text{prec}}$). However, in the case of three acoustic pulses as shown in Fig. 1(a), it is shown that the suppression of the magnetization precession can be always achieved with the proper T_{23} , producing general relations of $T_{12} = (m+1/2)T_{\text{prec}}+dT$ and $T_{12} = mT_{\text{prec}}+dT$ for the suppression and amplification, respectively. Figure 1(b) presents, furthermore, that even in case of acoustic pulses with different shapes, above relations are maintained meaning that only the delay dT is the core parameter to determine the coherent control of magnetization precession. These results will be useful for the precise control of magnetization dynamics at will without a restriction about the arrival time of the second pulse and its shape.

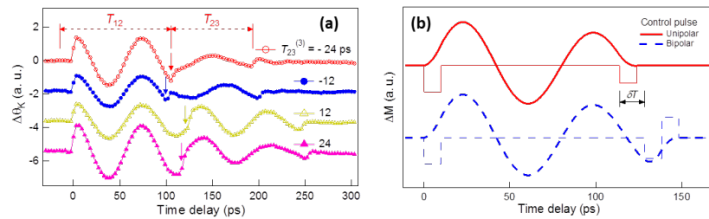


Figure 1. (a) Magnetization dynamics for various delays T_{12} and T_{23} (for $E_{23}=1$). (b) Simulation results of the magnetization precession with sequences of: two unipolar pulses (top) and unipolar + bipolar pulses (bottom).

References:

- [1] J.-W. Kim, M. Vomir, and J.-Y. Bigot, *Sci. Rep.* **5**, 8511 (2015).

Th.F.1_O3 - Femtosecond control of magnetism via resonant optical pumping of Dy ions in multisublattice magnet DyFeO₃

R. Mikhaylovskiy¹, T. Huisman¹, A. Popov², A. Zvezdin³, T. Rasing¹, R. Pisarev⁴, A. Kimel¹

1. *Radboud University Nijmegen, The Netherlands*

2. *National Research University of Electronic Technology, Russia*

3. *Prokhorov General Physics Institute, Russia*

4. *Ioffe Physical-Technical Institute, Russia*

Dielectric magnetic materials such as transition metal oxides appeared to be an excellent playground for the study of the mechanisms for light-spin interactions [1]. Unlike metals the electronic structure of dielectrics is well defined and allows one to trace how and how fast selective pumping of a specific electronic excitation results in magnetic changes. Although many of studied compounds contained rare-earth 4f -ions, their multi-sublattice nature have been often ignored and the experimental findings have been described in terms of off-resonant femtosecond excitation of the transition-metal 3d-ions (Mn,Fe,Co,Ni).

Here using terahertz emission spectroscopy we report that resonant optical pumping of f-f transitions of Dy³⁺-ions in the antiferromagnet DyFeO₃ with circularly-polarized femtosecond laser pulses has a dramatic effect on the laser-induced magnetization dynamics. Analysing the spectrum of the emitted THz radiation, its dependence on the pump polarization and photon energy, we infer that the resonant circularly-polarized optical pumping of Dy³⁺ magnetizes the ions on a femtosecond timescale. The resonantly induced ultrafast change of the magnetization reaches almost 1 %. We also observe a minimum in the efficiency of the Fe³⁺-spin-wave excitation for laser photon energies close to the resonance of Dy³⁺. This fact reveals that the resonant photo-induced magnetization and off-resonant excitation of the Fe³⁺-spin-waves via the inverse Faraday effect are competing processes.

References:

[1]. A. Kirilyuk, A. V. Kimel, and Th. Rasing. Ultrafast optical manipulation of magnetic order. *Rev. Mod. Phys.* 82, 2731 (2010)

Th.F.1_O4 - Low Gilbert damping and high magnetic anisotropy in L1₀-FePd epitaxial thin films grown on MgO and SrTiO₃ single crystal substratesS. Iihama¹, H. Naganuma¹, M. Oogane¹, S. Mizukami², Y. Ando¹

1. Department of Applied Physics, Tohoku University, Sendai, Japan

2. WPI-AIMR, Tohoku University, Sendai, Japan

Magnetic materials with a large perpendicular magnetic anisotropy (PMA) are very important for realizing high-density magnetic memory. L₁₀-ordered alloys, such as L₁₀-FePt, CoPt, and FePd, have a large PMA to achieve high thermal stability factor. On the other hand, reversal current of current-induced magnetization switching is proportional to Gilbert damping constant α and effective PMA constant K_u^{eff} . Therefore low α materials with large K_u^{eff} are necessary. Reported α of L₁₀-FePt film and Co/Pt multilayer showed very large, which may be caused by large spin-orbit coupling in Pt atom [1], while α of L₁₀-FePd has not been investigated intensively compared with that of L₁₀-FePt film. Here we demonstrate low α and high K_u^{eff} in L₁₀-FePd epitaxial thin films grown on MgO and SrTiO₃ single crystalline substrates [2, 3]. Samples were prepared by magnetron sputtering method. The films were deposited and annealed at various temperature to obtain the films having smooth surface and high chemical ordering. L₁₀-ordered phase for film with adequate substrate and annealing temperature was confirmed by X-ray diffraction. Magnetization curves for L₁₀-FePd film showed PMA and maximum K_u^{eff} is ~ 7 Merg/cm³. External field and field angle dependence of magnetization dynamics by Time-Resolved Magneto-Optical Kerr Effect were measured. Effective damping constant α_{eff} varied with external field and field angle. Very low α_{eff} of 0.007 was observed in particular sample. This α_{eff} is smallest among that of Fe- and Co- based materials with large PMA.

This work was supported by KAKENHI (24226001), Tanaka Co. Ltd grant, New Energy and Industrial Technology Development Organization (NEDO) for young scientists (11B07018d), FIRST program, and Grant-in-Aid for JSPS Fellows (26-4778)

References:

- [1] P. He *et al.* Phys. Rev. Lett. 110, 077203 (2013)
- [2] S. Iihama *et al.* Appl. Phys. Lett. 105, 142403 (2014).
- [3] S. Iihama *et al.* J. Magn. Soc. Jpn. (2015)

Th.F.1_O5 - Laser control of magnetizations, spin currents and orders in quantum magnets

M. Sato¹

1. Japan Atomic Energy Agency, Ibaraki, Japan

Recently, laser science has been rapidly developed and we can prepare various lasers in a wide frequency range. This development enables us to observe many sorts of driven quantum states by applying lasers to solid materials. For example, it is predicted that a topological state with a gapless chiral edge mode can appear when we apply a circularly polarized laser to two-dimensional Dirac electron systems [1], and after this prediction, a few experimental evidences for this laser-driven topological insulator have been reported [2]. Including these results, so far many studies for laser-driven systems have been focused mainly on electron systems. By contrast, recently, we have tried to theoretically find new laser-induced phenomena in insulating systems such as spin systems and multiferroics [3,4,5]. In the conference, I would like to show some of our recent theoretical results in this field. In particular, I will focus on the explanation that (i) for general quantum magnetic insulators, their uniform magnetization can be controlled by applying a circularly polarized laser WITHOUT any static magnetic field [3], and (ii) spin currents or spiral ordered states can also be induced by applying a circularly (more generally, elliptically) polarized laser to quantum multiferroic systems with a spin-chirality type magnetoelectric coupling [4].

References:

- [1] T. Oka and H. Aoki, Phys. Rev. B 79, 081406(R) (2009); T. Kitagawa, T. Oka, A. Brataas, L. Fu, and E. Demler, Phys. Rev. B 84, 235108 (2011)
- [2] Y. H. Wang, H. Steinberg, P. Jarillo-Herrero, and N. Gedik, Science 342, 453 (2013)
- [3] S. Takayoshi, M. Sato, and T. Oka, Phys. Rev. B 90, 214413 (2014)
- [4] M. Sato, S. Takayoshi, and T. Oka, in preparation
- [5] M. Sato, and Y. Sasaki, and T. Oka, arXiv:1404.2010

Th.F.2_I1 - Ultrafast demagnetization induced by hot electrons

N. Bergéard¹, G. Malinowski¹, M. Hehn¹, S. Mangin¹

1. Institut Jean Lamour, Université de Lorraine – CNRS, France

Ultrafast quenching of magnetization upon femtosecond laser excitation has been extensively studied during the last 20 years. However, possible mechanisms underlying the dissipation of angular momentum are still debated. Initially, direct excitation resulting in the absorption of the laser energy by the electronic system was considered as the only source, resulting in a subsequent loss of magnetization due to different particles quasi-particle interactions. Nevertheless, the role of hot electron transport in magnetic multilayers has been recently highlighted as a possible source for ultrafast demagnetization even though the results were strongly contested. In this work, we study ultrafast demagnetization dynamics in Glass/Ta/Pt/FM/Cu(x)/Pt(2) samples for x varying from 0 to 200 nm and with FM being either a Co/Pt or a Co/Ni multilayers. Both systems have a perpendicular magnetic anisotropy. The experiments were carried out pumping our samples with an 800 nm laser pulse from the front side and probing the induced change in magnetization from the back side (glass) with a 400 nm laser pulse. In order to control the excitation in our systems, we carefully determined the Cu layer absorption as a function of x and we extracted an attenuation length of 22 nm. In the case of the Co/Pt multilayer, a clear modification of the magnetization dynamics between direct optical excitation and excitation by hot electrons is observed when increasing the Cu thickness. However, no modification is measured in the case of the Co/Ni multilayers. These results show that demagnetization induced by hot electrons strongly depends on the nature of the ferromagnet. We infer that the slowing down of the dynamics is mainly due to the presence of the Pt which might increase the scattering of hot electrons.

Th.F.2_O2 - Enhancement of laser-induced ultrafast Demagnetization using localized surface plasmonsH. Xu¹, G. Hajisalem², G. Steeves¹, R. Gordon², B. Choi¹*1. Department of Physics And Astronomy, University of Victoria, Canada**2. Department of Electrical and Computer Engineering, University of Victoria, Canada*

Ferromagnetic thin films excited by laser pulses undergo ultrafast loss of magnetic order within several hundred femtoseconds, due to rapid energy transfer from thermalized electrons to the spin system. This is followed by a slower recovery over the picosecond timescale as electrons equilibrate with the phonons, and eventually to complete cooling via nanosecond lattice diffusion. The timescale of laser-induced ultrafast demagnetization is orders of magnitude below the limit imposed by conventional switching of magnetic order via magnetic field pulse, and has been the focus of considerable research. In this study we demonstrate that the demagnetization can be significantly increased without increasing the laser fluence by coating ferromagnetic thin films with gold nanorods (AuNRs) dimensionally-tuned to support localized surface plasmons (LSPs) near the peak laser frequency. The effect of plasmon resonance on the transient magnetization was investigated by drop-coating the ferromagnetic films with gold nanorods (AuNR), which support longitudinal surface plasmon resonance near the central wavelength of the pump laser. To independently verify the plasmon resonance effect of the AuNR coating, dark-field scattering spectra of the thin film samples were obtained with a white light source. Laser induced ultrafast magnetization were recorded for a range of pump fluences, $F \approx 0.08 - 0.26 \text{ mJ/cm}^2$, using a femtosecond Ti:sapphire laser in a pump-probe magneto-optic Kerr effect setup. For all experimental pump fluence used we observed an increased quenching of magnetic order in the AuNR-coated 20 nm thick $\text{Ni}_{80}\text{Fe}_{20}$ films. At the highest pump fluence ($F \sim 0.26 \text{ mJ/cm}^2$), the demagnetization signal ($\Delta M_z/M_s$) in the AuNR-coated sample is increased by $\sim 60\%$ compared to the uncoated sample. By extrapolating the linear fit of the data set, it was found that the uncoated sample would require a pump fluence $F \sim 0.42 \text{ mJ/cm}^2$ in order to achieve the same $\Delta M_z/M_s$ as the AuNR-coated sample at $F \sim 0.26 \text{ mJ/cm}^2$. The experimental results were qualitatively reproduced with simple model calculations based on mean-field theory.

Th.F.2_O3 - Ultrafast energy diffusivity dependency of all-optical magnetization switching in multi-layer structured GdFeCo thin filmsH. Yoshikawa¹, A. Tsukamoto²

1. Graduate School of Science And Technology, Nihon University, Chiyoda, Japan
2. College of Science and Technology, Nihon University, Chiyoda, Japan

Femtosecond laser pulse excite an all-optical magnetization switching (AOS) on multi-sub-lattice rare-earth transition-metal ferrimagnet thin films. This AOS phenomena originated from sub-lattice nature is fundamentally different from conventional magnetic field driven switching mechanism[1], [2]. In this study, we show the magnetic domain nucleation on multi-layered structures which have different properties of laser fluence absorption and diffusion, respectively [3]. A single femtosecond laser pulse was irradiated on the magnetic multi-layered thin films, SiN (60 nm)/ Gd₂₂Fe_{68.2}Co_{9.8} (l nm)/ SiN (m nm)/AlTi (n nm)/ glass sub. ({n,m,l} = {20,5,0}, {20,0,10}, {20,5,10}, {30,5,10}). To excite the materials we used regenerative amplified laser pulses at a wavelength of 800 nm. Each pulse had a Gaussian intensity profile, with a full width of a half maximum of 90 fs. The laser excitation create magnetic domains by AOS and/or multi-domains by thermo-magnetic nucleation (TMN) inside the area exceed each laser energy intensity threshold[2]. The time constant and degree of thermalization of electron, spin and lattice systems were changed with layer structure[3]. And, amount of ultrafast demagnetization (UD) is decided by the thickness of continuous metallic layer tmetal[3]. In this result, the domain sizes by TMN are lager in films which has thicker tmetal. UD of both {20,5,10} and {20,5,0} (tmetal=20 nm) are larger than it of {20,0,10} (tmetal=30 nm). However, the domain size of {20, 5, 10} by AOS is similar to it of {20,0,10}, and smaller than {20, 5, 0} ones. Furthermore, UD of {30,5,10} is similar to {20,0,10} ones. But, the magnetic domains werenüft created by AOS on {30,5,10}. These results mean that the created domain size by TMN simply depends on the laser fluence and tmetal. On the other hand, the created domain size by AOS depends on the energy diffusion process with electron, spin and lattice, too.

References:

- [1] T. A. Ostler, J. Barker, R. F. L. Evans, R. W. Chantrell, U. Atxitia, O. Chubykalo-Feseko, S. El. Moussaoui, L. Le Guyader, E. Mengotti, L. J. Heyderman, F. Nolting, A. Tsukamoto, A. Itoh, D. Afanasiev, B.A. Ivanov, A.M.Kalashnikova, K. Vahaplar, A. Kirilyuk, Th. Rasing and A. V. Kimel: Nature Comm. 3, 666 (2012)
- [2] H. Yoshikawa, S. Kogure, S. Toriumi, T. Sato, A. Tsukamoto, and A. Itoh: J. Magn. Soc. Jpn. 38, 139 (2014)
- [3] T. Sato, S. Toriumi, R. Shimizu, A. Tsukamoto, and A. Itoh: J. Magn. Soc. Jpn. 36, 82 (2012)

Th.F.2_O4 - Ultrafast control of the exchange interaction with electric fields

J. Mentink^{1,2}, K. Balzer², M. Eckstein²

1. *Radboud University Nijmegen, The Netherlands*

2. *University of Hamburg, Germany*

The strongest interaction between microscopic spins in magnetic materials is the exchange interaction J_{ex} . Therefore, ultrafast control of J_{ex} keeps the promise to control spins on ultimately fast timescales, potentially bypassing fundamental speed limits for the control of magnetism with magnetic fields. In this contribution we provide theoretical evidence that the exchange interaction can be manipulated on ultrashort timescales by strong electric field pulses [1,2]. Focusing on the prototype Mott-Hubbard insulator, we find very different effects for resonant and off-resonant photo-excitation. In the former case, the electron distribution is changed and the subsequent relaxation of photo-excited carriers causes an ultrafast reduction of J_{ex} . Conversely, off-resonant driving allows for an ultrafast and reversible control of J_{ex} , i.e., it is active while the field is on, but leaves the electronic state unexcited after the pulse is switched off. In the regime of weak-driving strength the modification of J_{ex} is proportional to the intensity of the electric field and we find that J_{ex} can be enhanced and reduced for frequencies below and above gap, respectively. Furthermore, for strong driving even the sign of the exchange interaction can be reversed and we show that this causes time reversal of the associated quantum spin dynamics.

References:

[1] J.H. Mentink and M. Eckstein, *Phys. Rev. Lett.* 113, 057201 (2014)

[2] J.H. Mentink, K. Balzer and M. Eckstein, arXiv:1407.4761, accepted for *Nature Communications* (2015)

Th.F.2_O5 - Terahertz-driven ultrafast magnetization dynamics in canted antiferromagnetic YFeO₃

J. Lee¹, T. Kim¹, S. Kovalev², Y. Tokunaga³, Y. Tokura³, M. Gensch²

1. *Gwangju Institute of Science and Technology (GIST), Gwangju, Korea*

2. *Helmholtz-Zentrum Dresden-Rossendorf, Dresden, Germany*

3. *RIKEN Center for Emergent Matter Science (CEMS), Wako, Saitama, Japan*

We investigate the coherent precessional motion of the magnetic moment in the canted antiferromagnetic YFeO₃ single crystal after excitation by the transient magnetic field of an ultra-short THz pulse. Time-resolved measurements of the magneto-optical response in the presence of external magnetic fields confirm the exclusive magnetic origin of the interaction between THz pulse and the spin system.. By tuning the spectral component of the input THz pulse around the quasi-ferromagnetic mode located near 0.3 THz, we have experimentally verified that the THz control of the spin state requires resonant excitation. We could confirm these results from the simulation based on the Landau-Lifshitz-Gilbert equation with two sub-lattice model for the canted antiferromagnet. Furthermore, we demonstrate that the spin state can be switched all-optically on a picosecond timescale using THz pulses of square and oscillating shapes. Whereas the oscillating THz pulse with a spectral component resonant with the magnetic excitations is necessary for an efficient magnetization switching, we study the possibility for a further reduction of the necessary THz field strength by examining influences of variations in the anisotropy energy and Dzyaloshinskii-Moriya interaction upon the switching behaviors.

Th.F.3_I1 - Advances in magnetic force microscopy

A. Asenjo¹, O. Iglesias-Freire¹, M. Jaafar¹, E. Berganza¹

1. Icomm-Csic, Madrid, Spain

During the past twenty years magnetic force microscopy (MFM) has become one of the most powerful general purpose methods for magnetic imaging. Apart from applications in quality control in the batch fabrication of magnetic devices, MFM has proven its relevance in fundamental research to gain information about the magnetic properties of the materials at the nanoscale. MFM can be applied under various environmental conditions and requires only little sample preparation. The quantitative data analysis, the tip-sample influence and the lateral resolution have been the most important challenges of this technique. New developments can be implemented in order to improve its potential. In the present work, MFM-based techniques developed in our group are described. MFM performed in external magnetic has led to a novel method of magnetometry at nanoscale [1,2] that can be used to study reversal magnetization processes in Py nanostripes [3] or CoFeCu nanowires. Regarding the spatial resolution, we show the advantage of using one side coated MFM probes [4] and how high lateral resolution magnetic images can be obtained by studying magnetic dissipation processes in MFM [5].

References:

- [1] M. Jaafar, R. Yanes, D. Perez de Lara, O. Chubykalo-Fesenko, A. Asenjo, J. V. Gonzalez Anguita, M. Vazquez and J. L. Vicent, Phys. Rev. B 81 054439. (2010)
- [2] M. Jaafar, L. Serrano-Ramón, O. Iglesias-Freire, A. Fernández-Pacheco, M. R. Ibarra, J.M. de Teresa, A. Asenjo, Nanosc. Res. Lett. 6 407 (2011)
- [3] O. Iglesias-Freire, M. Jaafar, L. Pérez, O. de Abril, M. Vázquez, A. Asenjo, J. Magn. Magn. Mater.,355 (2014) 152 - 157
- [4] O. Iglesias-Freire, M. Jaafar, E. Berganza and A. Asenjo, in press
- [5] O. Iglesias-Freire, J.R. Bates, Y. Miyahara, A. Asenjo, P.H. Grütter, Appl. Phys.Lett. 102 (2013) 022417

Th.F.3_I2 - Spin Dynamics of Magnetic Skyrmions and Domain Walls due to spin - orbit effects

M. Kläui¹

1. Institute of Physics, Johannes Gutenberg University Mainz, Mainz, Germany

Topological spin structures that emerge due to the Dzyaloshinskii-Moriya interaction (DMI), such as chiral domain walls and skyrmions possess a high stability and are of key importance for magnetic memories and logic devices [1,2]. We have investigated in detail the dynamics of domain walls [2] and we find that in addition to conventional spin transfer torque, also spin orbit torques play a key role [3]. By comparing the wall motion with current-induced magnetization switching in our systems, we can deduce the spin-orbit torques independently of the DMI [3] and we find that the motion observed Ta(5nm)/Co₂₀Fe₆₀B₂₀(1nm)/MgO(2nm) can be attributed to a DMI that is opposite to such stacks with a magnetic CoFe layer pointing to the B at the interface that governs the sign of the DMI [3]. For skyrmions we demonstrate for the first time that we can move a train of skyrmions in a “racetrack”-type device [1] due to spin-orbit torques reliably [4] and we find skyrmion lattices at room temperature in confined geometries [4]. Finally we study the field - induced dynamics of a magnetic bubble skyrmion [5]. The trajectory of the skyrmion’s position is accurately described by our quasi particle equation of motion. From a fit we are able to deduce the inertial mass of the magnetic bubble and find it to be much larger than inertia found in any other magnetic system, which can be attributed to the non-trivial topology [5].

References:

1. S. S. P. Parkin et al., Science 320, 190 (2008)
2. O. Boulle et al., Mater.Sci Eng R 72, 159 (2011)
3. R. Lo Conte et al.; Appl.Phys.Lett. 105, 122404 (2014); R. Lo Conte et al.; Phys.Rev B 91, 014433 (2015)
4. S. Woo et al., arxiv:1502.07376 (2015)
5. F. Büttner et al., Nature Phys. 11, 225 (2015)

Th.F.3_O3 - Development of 22 T VSM system using novel improvements in HTS conductor

J. Good¹, D. Bracanovic¹, T. Ritman-Meer¹

1. Cryogenic Ltd, London, United Kingdom

Current research has identified a need for greater magnetising fields during vibrating sample magnetometer (VSM) measurements and other measurement options. We present here the methodology involved in our development of a VSM system with 22 T superconducting magnet, a unique system and the highest field combined with a VSM anywhere in the world. Recent developments in HTS conductors have allowed greater reliability than previous coils made from YBCO and BISCO and thus facilitate the consistent achievement of higher magnetising fields at the sample with operation at 4.2 K rather than 2.2 K. Cryogenic Ltd wind HTS coils in both solenoid and pancake forms with an emphasis on solenoids, since they have been found to give a more reliable performance with less thermal transfer to the surrounding liquid helium. The 22T VSM system has been developed using 2G YBCO coated and BSSCO tape which exhibit critical currents up to 5 times greater than those seen in YBCO and BISCO at 4.2 K.

Th.G.1_I1 - Magnetic degrees of freedom in nanophotonics

R. Carminati¹

1. *ESPCI ParisTech, Paris, France*

Controlling the optical response of nanoscale devices using an external parameter is a key issue in active nanophotonics. The use of a magneto-optical (MO) effect, with the external static magnetic field as a control parameter, is receiving increasing attention. We will show that MO effects offer in principle many degrees of freedom to act upon light-matter interaction. They can be used to actively control resonant structures or to modulate field enhancements. Conversely, field enhancements can be used to boost the otherwise weak MO response of usual materials (including ferromagnetics). The discussion will be based on specific examples covering the coupling of an incident beam to surface plasmons [1], the use of geometric resonances on periodic gratings to enhance the MO response [2], and fluorescence energy transfer between dipole emitters [3]. We will also report on an experimental technique to quantify the relative importance of electric and magnetic dipole luminescence from a single nanosource. The technique allows one to measure the relative weights of the electric and magnetic contributions to the local density of states, a basic quantity in nanophotonics [4]. This result paves the way towards the full electric and magnetic characterization of nanostructures for the control of single emitter luminescence. I am indebted to H. Marinchio, R. Vincent, A. García-Martín, J.J. Sáenz and L. Aigouy for their key contributions to this work.

References:

- [1] R. Vincent, H. Marinchio, J.J. Sáenz and R. Carminati, *Phys. Rev. B* 90, 241412(R) (2014)
- [2] H. Marinchio, R. Carminati, A. García-Martín and J.J. Sáenz, *New J. Phys.* 16, 015007 (2014)
- [3] R. Vincent and R. Carminati, *Phys. Rev. B* 83, 165426 (2011)
- [4] L. Aigouy, A. Cazé, P. Gredin, M. Mortier and R. Carminati, *Phys. Rev. Lett.* 113, 076101 (2014)

TH.G.1_O2 - Magneto-optical mediated coupling of surface plasmon polaritons in 2D magnetoplasmonic crystals

P. Vavassori ^{1,2}, N. Maccaferri ¹, X. Inchausti ¹, A. García-Martín ³, J.C. Cuevas ⁴, D. Tripathy ⁵, A.O. Adeyeye ⁵

1. *CIC NanoGUNE, San Sebastian, Spain*

2. *IKERBASQUE, Basque Foundation for Science, Bilbao, Spain*

3. *IMM-Instituto de Microelectronica De Madrid (CNM-CSISC), Madrid, Spain*

4. *Departamento de Fisica Teorica de la Materia Condensada and Condensed Matter Physics Center (IFIMAC), Universidad Autonoma de Madrid, Madrid, Spain*

5. *Information Storage Materials Laboratory, Department of Electrical and Computer Engineering, National University of Singapore, Singapore*

A surface plasmon polariton (SPP) is a transverse magnetic mode electromagnetic wave propagating at a metal/dielectric interface, which is evanescently confined in the perpendicular direction to the interface. Similar to electrons in a crystal potential, the dispersion of SPP waves on a flat metal surface folds at the Brillouin zone boundaries to form a band structure when a periodic modulation of the metal surface is introduced, realizing what is called a two-dimensional plasmonic crystal. While in a film SPPs can couple only to p-polarized light in the free space, efficient coupling of free-space light, both p- and s-polarized to SPP waves can be achieved through diffraction in metal surfaces with periodic arrangements of sub-wavelength scale structures. We investigate here a two-dimensional plasmonic crystal with a periodic array of cylindrical holes in a ferromagnetic layer, namely a two-dimensional magneto-plasmonic crystal (2D-MPC). Nanostructured magnetic materials allow for intrinsic cross-coupling of plasmonic modes due to their inherent magneto-optical (MO) activity as demonstrated for localized surface plasmons [1]. The underlying idea explored in this work is that this phenomenon should occur also in 2D-MPCs under proper experimental conditions, namely having the MO coupling acting in the crystal plane. We show that this is indeed the case and demonstrate that magneto-optical activity mediated coupling between SPP waves, in combination with the 2D photonic band structure can be used to design metamaterials with tailored and enhanced MO response, moreover controllable via an external field. Thereby, our results disclose a novel way to exploit the SPPs mediated MO polarization conversion via plasmonic band engineering leading to enhancement of MO signals at desired wavelengths in view of potential applications of such 2D-MPCs as nanoscaled non-reciprocal polarization-dependent optical isolators.

References:

[1] N. Maccaferri et al., Phys. Rev. Lett. 111, 167401, (2013)

Th.G.1_O3 - Plasmon-mediated large enhancement of magneto-optical activity in colloidal magnetic metals

O. Herranz¹, G. Herranz¹

1. Icmab-Csic, Madrid, Spain

Magnetic properties may undergo dramatic changes at the nanoscale that, eventually, can be exploited as a basis for enhanced functionality. This is the case that we present here, in which we analyzed the rotation and ellipticity that magnetic nanoparticles exerted on the polarization of light. More specifically, we observed an outstanding increase of the magneto-optical activity at the frequencies of the plasmon resonances of the metallic magnetic nanoparticles, yielding a dramatic increase of the Verdet constant [1]. Furthermore, we have established an innovative theoretical framework in excellent quantitative agreement with the experimental data, endowing our model with a powerful predictive character for the interaction of polarized light with magnetic nanoclusters embedded in dielectric hosts. The relevance of our results goes well beyond the particular case of colloidal metals, as other systems such as metal inclusions in polymers or glasses containing small magnetic clusters can be as well considered. In addition, the observed large Verdet constants allow envisioning the exploitation of light polarization, instead as the commonly used reflectance, as a probe for plasmon-sensing devices. Our results provide new routes for plasmon-based biological and chemical detection.

References:

[1] O. Vlasin et al., Phys. Rev. Applied 2, 054003 (2014)

TH.G.1_O4 - Magnetic-field-induced photocurrent in metal-dielectric-semiconductor heterostructures based on cobalt nanoparticles SiO₂(Co)/GaAs

V. Pavlov¹, L. Lutsev¹, P. Usachev¹, A. Astretsov¹, A. Stognij², N. Novitskii², R. Pisarev¹

1. *Ioffe Physical-Technical Institute, Russian Academy of Sciences, St. Petersburg, Russia*

2. *Scientific and Practical Materials Research Centre, National Academy of Sciences of Belarus, Minsk, Belarus*

Magnetotransport phenomena in low dimensional systems have attracted much research attention due to their fundamental and applied importance. The purpose of the present study is to find novel combinational effects in heterostructures of silicon dioxide films containing cobalt nanoparticles SiO₂(Co) grown on n-GaAs substrate. The SiO₂(Co) films with a Co atomic concentration of 45-71 at. % were prepared on GaAs at temperature of 200 C from a composite cobalt-quartz target using the ion-beam deposition technique. We studied magnetic-field-induced photocurrent in these heterostructures in the avalanche regime. A strong photocurrent enhancement is observed for photon energies E above the GaAs bandgap E_g. The photocurrent is increased by a factor of about ten for the photon energy E = 1.5 eV in the magnetic field H = 1.65 kOe for the SiO₂(Co)/GaAs heterostructure with a Co atomic concentration of 60%. This phenomenon is explained by a model describing electronic transitions in magnetic fields with the spin-dependent recombination process at deep impurity centers in the GaAs interface region. We developed a model taking into account the exchange interaction between electrons on the oxygen levels with 3d-electrons of Co nanoparticles via electrons in the accumulation layer and assuming that the exchange interaction is isotropic. In a magnetic field electron-hole recombination is suppressed. This leads to additional free electrons in the conduction band and holes in the valence band. As a result, photo-induced holes are accumulated in the barrier, the photocurrent grows and the avalanche feedback can be manipulated by the light. The photocurrent enhancement caused by applied magnetic field can be used in field-controlled avalanche diodes.

TH.G.1_O5 - Polariton-mediated ultrafast magneto-optical modulation

R. Subkhangulov¹, R. Mikaylovskiy¹, V. Kruglyak², T. Rasing¹, A. Kimel¹

1. *Institute for Molecules and Materials, Radboud University Nijmegen, Nijmegen, The Netherlands*

2. *School of Physics, University of Exeter, Exeter, United Kingdom*

Controlling the response of media at the (sub)picosecond time-scale or Terahertz (THz) frequencies is one of the most debated topics in contemporary condensed matter physics and photonics. Aside from a purely fundamental interest in ultrafast processes in condensed matter at the characteristic time-scales pertinent to electronic, spin and atomic motion, the attention to this topic has been continuously fueled by the demands for ever faster information processing. THz magneto-optical modulation at tunable frequencies can be achieved by employing spin resonances. Here we propose a novel approach for an ultrafast tunable magneto-optical modulation by means of a polaritonic excitation launched at the surface of a magneto-optical medium. This excitation together with the surface of the sample act on visible light as partially transparent mirrors, which form an interferometer expanding with a relativistic speed and consequently modulating the total magneto-optical response at THz frequencies. Using Terbium gallium garnet as test sample we succeeded to show the feasibility of such a magneto-optical modulation with frequencies up to 1.1 THz, continuously tunable with the help of an external magnetic field. Besides the novel concept of the ultrafast magneto-optical polarization modulation, our findings reveal the important role which polaritonic excitations can play for the interpretation of pump-probe magneto-optical experiments. We argue that further enhancement of the efficiency of the ultrafast polaritonic magneto-optical modulation is quite possible.

TH.G.2_I1 - Domain wall propagation along cylindrical nanoelements

D. Altbir¹, R. Neumann², M. Bahiana³, S. Allende¹, D. Görlitz⁴, K. Nielsch⁴

1. *Universidad de Santiago de Chile, Santiago, Chile*

2. *IBM Research, Río de Janeiro, Brazil*

3. *Instituto de Física, Universidade Federal do Rio de Janeiro, Rio de Janeiro, Brazil*

4. *Institute of Nanostructure and Solid State Physics, University of Hamburg, Hamburg, Germany*

The magnetization reversal of two and three-segment cylindrical nanoelements comprising of alternating nanowire and nanotube sections is investigated by means of Monte Carlo simulations. By choosing different parameters and materials for the tube and wire segments, the nucleation of vortex and transverse domain walls could be tailored, creating a manifold of different scenarios for the magnetization reversal. Such nanoelements may feature a three-state behaviour with an intermediate plateau in the hysteresis curve due to a metastable pinning of the domain walls at the wire-tube interfaces. In general, when there is only one material the arrival of the domain wall at the interface leads to a local minimum in the differential susceptibility, since the difference in nucleation field across the interface is not large enough to create a plateau. However, when different materials are used to harden (soften) the wire (tube) section, an intermediate plateau is formed due to the large difference of nucleation fields on each side of the interface. In these cases the width of the wall decreases notably as it reaches the interface, regardless of the reversal mode. It is important to highlight the absence of a preferential nucleation site for domain walls in the WTW elements because in these elements the tube ends are fixed to the hard wires, preventing the nucleation of domain walls at the interfaces. Moreover, because the tube is uniform, the wall can nucleate almost simultaneously in different places, opening the possibility of injecting walls simultaneously on both wires by varying the size of the tube. In summary, a novel feature in cylindrical nanostructures was found, which consists of the outward movement of the domain walls from the element body to the element tips. This might give rise to applications in which such nanoelements are used as domain wall delivering structures at its tips.

TH.G.2_O2 - Structural and magnetotransport properties of FeCo(1-x) nanowires prepared by focused electron beam induced deposition with a heteronuclear metal carbonyl precursor

F. Porrati¹, S. Barth², F. Biegger², C. Gspan³, H. Plank³, M. Huth¹

1. *Goethe University Frankfurt a. M., Institute of Physics, Frankfurt, Germany*

2. *Vienna University of Technology, Institute of Materials Chemistry, Getreidemarkt, Wien, Austria*

3. *Graz University of Technology, Institute for Electron Microscopy and Nanoanalysis, Graz, Austria*

Focused electron beam induced deposition (FEBID) is an emerging one-step lithographic technique used to prepare nanostructures down to the nanometer scale. In FEBID the molecules of a precursor gas injected in an scanning electron microscope decompose by interaction with the electron beam, forming a sample during the rastering process. Carbonyl precursors like $\text{Fe}(\text{CO})_5$ or $\text{Co}_2(\text{CO})_8$ are used for the preparation of magnetic nanostructures with potential employment in magnetic nanologic and sensor applications. Recently, it was shown that magnetic alloys could be prepared by FEBID by mixing two homonuclear precursor gases. As a novel, alternative route we show that Fe-Co alloy deposits can be directly obtained by using a heteronuclear precursor. Such a route, known for the preparation of magnetic thin films alloys in chemical vapor deposition, allows to obtain metallic nanostructures with the stoichiometry of the heteronuclear metal carbonyl compound. In the present work, FEBID deposits have been fabricated by means of the $\text{HFeCo}_3(\text{CO})_{12}$ precursor gas. The deposits contain up to 80 at% metal, i.e., ca. 60 at% Co, 20 at% Fe, 10 at% C and 10 at% O, as measured by EDX spectroscopy. Nanowires of various size down to a width of 50 nm and a thickness of 10 nm have been prepared and characterized by four-probe magnetotransport measurements. All the nanowires show metallic behavior in temperature dependent resistivity measurements with a resistivity at room temperature of about 44 μWcm for the smallest nanowire investigated. From the analysis of the Hall effect negative and positive values for the ordinary and the anomalous Hall coefficients were derived, respectively. The saturation magnetization is about 1.4 T, similar to Fe and Co based FEBID deposits known from the literature. Finally, the microstructure of the nanowires has been investigated by means of transmission electron microscopy.

TH.G.2_O3 - Investigating the dipolar interactions in assemblies of ferromagnetic nano-objects by Ferromagnetic Nuclear Resonance

I. Camara¹, Y. Shin^{1,2}, N. Liakakos³, C. Achkar³, M. Respaud³, K. Soulantica³, T. Blon³, M. Bailleul¹, C. Meny^{1,2}

1. *Institut de Physique et Chimie des Matériaux de Strasbourg (IPCMS), CNRS- University of Strasbourg, Strasbourg, France*

2. *Department of Physics, CNRS-Ewha International Research Center, Ewha Womans University, Seoul, South Korea*

3. *Laboratoire de Physique et Chimie des Nano-objets (LPCNO), INSA, Toulouse, France*

Nano-objects are studied in many research fields, spintronics, chemistry, biology, medicine... The properties of these objects will depend on their size, shape, crystallographic structure and chemical composition. When we consider ferromagnetic nano-objects that are organized in assemblies where they are closely packed, dipolar interactions will also strongly influence the magnetic properties of the system. The system under investigation has been prepared by chemical route and consists of single-crystalline cobalt nano-wires epitaxially grown on a flat substrate to form a hexagonal array of 1×10^{12} nanowires/cm² [1]. In this work we show that while Ferromagnetic Nuclear Resonance (FNR, i.e. Nuclear Magnetic Resonance for ferromagnets) has been extensively used for studying the structure and chemical order in thin films [2] and nanoparticles [3] it can also provide direct insight into the dipolar interaction between the nanowires. Indeed by measuring the Co FNR spectra of the sample in its remnant state and in its demagnetized state we observe a shift of the Co FNR lines. This line shift is a direct measurement of the dipolar field resulting from the film shape of the assembly of nanowires. The measured dipolar field is reduced compared to the one expected for a continuous film and is discussed in term of packing factor of the nanowire film.

References:

1. N. LIAKAKOS et al., Nano Lett. 14, 3481–3486 (2014)
2. P. PANISSOD, C. MENY, Appl. Magn. Reson. 19, 447-460 (2000)
3. Y.F. LIU, I. FLOREA, O. ERSEN, C. PHAM-HUU, C. MENY, ChemCommun, 51, 145-148 (2015)

TH.G.2_O4 - Magnetic anisotropy of (ZnTe)/Co core/shell nanowires grown by MBE

P. Misiuna¹, T. Wojciechowski¹, P. Dłużewski¹, B. Kurowska¹, M. Wiater¹, S. Lewińska¹, A. Ślowska-Waniewska¹, A. Wawro¹, E. Milińska¹, T. Wojtowicz¹, L.T. Baczewski¹

1. Institute of Physics Polish Academy of Sciences, Warsaw, Poland

A model object for magnetic anisotropy study such as (ZnTe)/Co core/shell nanowires forming a magnetic nanotubes with nonmagnetic core were grown by MBE technique [1]. Arrays of crystalline zinc telluride nanowires obtained by vapor-liquid-solid mechanism were covered with cobalt of different thicknesses. Structural characterization was performed using SEM, TEM and EDX techniques. In-depth structural analysis revealed that deposited cobalt shell is polycrystalline with crystal grains of both HCP and FCC structure. Increment of deposited Co thickness as well as the initial roughness of ZnTe core leads to a quasi-dendritic shape of Co shell. Cross-section study performed by FIB showed a hexagonal shape of the nanowires with an uniform Co shell structure. Vibrating sample magnetometry and magnetic force microscopy experiments revealed that magnetization hard-axis is parallel to the long axis of the nanowires, which is in agreement with other experimental results [2] and theoretical predictions for hollow Co nanotubes. Our experimental results show that exchange bias effect caused by a possible Co oxides formation and suggested by some authors [3] as a possible origin of such anisotropy direction is not responsible for the observed effect. Protection of Co shell against oxidation by Au cover layer does not influence the anisotropy direction of the nanostructures, but causes its slight magnetic softening.

References:

- [1] P.A. Misiuna *et al.*, Journal of Crystal Growth 412 (2015) 80–86
- [2] K. Tivakornsasithorn *et al.*, J. Vac. Sci. Technol. B, vol. 30, p. 02B115, 2012
- [3] K. M. Lebecki *et al.* *Physica B: Condensed Matter* (2008), 403(2-3), 360–363

TH.G.2_O5 - Manipulation of transverse domain wall profile for logic devices

R. Maddu¹, S. Goolaup¹, C. Murapaka¹, W. Lew¹

1. School of Physical And Mathematical Sciences, Nanyang Technological University, Singapore

The dynamics of domain walls (DWs) in magnetic nanowires (NWs) have been studied to be able to use for high-density non-volatile memories and spin logic devices. The success of these technologies will rely inevitably on the precise control and understanding of magnetic DWs in NWs. This has been a challenging task and much research has been devoted to accomplish these. Changes in the DW structure are significant in device applications where DW motion is controlled via interaction with artificial defects, as the detailed spin distribution in the wall affects the nature and strength of the pinning potential. In thin film narrow magnetic nanowires, the transverse DW (TDW) is the stable configuration. TDW has two degrees of freedom; magnetic charge and chirality. Another approach to describing TDW is to view it as a composite object of elementary topological defects. The edge defects have half-integer winding numbers, either $+ \frac{1}{2}$ or $- \frac{1}{2}$, representing the spin configuration of the DW at the edges of the nanowire. As such, the topological defects of DW are important parameter for future DW based devices. Although much progress has been made, DW-based devices with high reliability, for industrial applications are still elusive. In this work, we demonstrated a method to perform logic applications via the topological edge defects. We experimentally demonstrate the DW rectification and logical NOT (inverter) operation based on DW topological defects. The rectifier provides a pre-determined topological output independent of the type of the input TDW. On the other hand, the inverter always provides an output which is has opposite edge defects as compared to the input. Experimental verification of our technique was carried out using magnetic force microscopy.

TH.G.2_O6 - Manipulating vortex domain walls with mechanical strain

A. Rushforth¹, R. Beardsley¹, D. Parkes¹, S. Bowe¹, K. Edmonds¹, B. Gallagher¹, T. Hayward², J. Wheelwright², D. Allwood², A. Irvine³, C. Reardon⁴, S. Cavill⁴

1. *University of Nottingham, Nottingham, United Kingdom*

2. *University of Sheffield, Sheffield, United Kingdom*

3. *Cambridge University, Cambridge, United Kingdom*

4. *University of York, York, United Kingdom*

Controlling the motion of magnetic domain walls is an important objective for studying their fundamental properties and for potential applications in devices such as Racetrack memory, 3-terminal MRAM and logical processing architectures[1]. In the case of vortex domain walls in planar magnetic nanowires, it has been proposed that the chirality of the wall can serve as the method to encode information[2]. Practical implementations of domain walls in such technologies will require low power methods to control domain walls on the local scale. A promising route to low energy control of magnetisation is to use electric fields. In particular, the application of voltage-induced mechanical strain in hybrid piezoelectric/ferromagnetic devices has received much attention recently[3,4]. Using this approach, we have investigated the effect of a voltage-tunable strain-induced uniaxial anisotropy on the pinning fields and chirality of vortex domain walls in nanowires. Using x-ray magnetic circular dichroism photo-emission electron microscopy (XMCD-PEEM), magneto-optical Kerr effect (MOKE) microscopy and micromagnetic calculations we demonstrate that the chirality of the domain wall can be modified by the voltage induced-strain. Furthermore, we find that vortex domain walls with opposite chirality exhibit different depinning fields and an opposite dependence of the depinning field on the induced anisotropy when interacting with a notch in the nanowire. The behaviour is explained by the deformation of the domain wall at the notch which leads to different depinning mechanisms for the two chiralities. Our results point the way towards a low power design of chirality dependent domain wall gates in schemes for information storage and processing.

References:

[1] D.A. Allwood et al., Science 309, 1688 (2005)

[2] Omari, et al., Phys. Rev. Appl. 2, 044001 (2014)

[3] Hu et al., Nature Communications 2, 553 (2011)

[4] Lei et al., Nature Communications 4, 1378 (2013)

TH.G.3_O1 - Spin-orbit-induced orbital excitations in Sr₂RuO₄ and Ca₂RuO₄: a resonant inelastic X-ray scattering study

C.G. Fatuzzo¹, M. Dantz², S. Fatale¹, P. Olalde-Velasco², N. Shaik Bastien Dalla Piazza¹, S. Toth³, J. Pellicciari², R. Fittipaldi Antonio Vecchione^{4,5}, N.Kikugawa^{6,7}, J. S. Brooks⁷, H.M. Rønnow^{1,8}, M. Grioni¹, C. Rüegg^{3,9}, T. Schmitt², J. Chang^{1,10}

1. *Institute for Condensed Matter Physics, EPFL, Switzerland*
2. *Swiss Light Source, Paul Scherrer Institut, Switzerland*
3. *Laboratory for Neutron Scattering and Imaging, Paul Scherrer Institut, Switzerland*
4. *CNR-SPIN, I-84084 Fisciano, Salerno, Italy*
5. *Dipartimento di Fisica "E.R. Caianiello", Università di Salerno, Italy*
6. *National Institute for Materials Science, 1-2-1 Sengen, Tsukuba, Japan*
7. *National High Magnetic Field Laboratory, Tallahassee, United States*
8. *Institute for Solid State Physics (ISSP), University of Tokyo, Japan*
9. *Department of Quantum Matter Physics, University of Geneva, Switzerland*
10. *Physics Institute, University of Zurich (UZH), Switzerland*

Ruthenate-oxide materials attract much attention due to the interesting ground states they exhibit, such as unconventional superconductivity in Sr₂RuO₄ or Mott physics in Ca₂RuO₄. The role of electron correlations, Hund's coupling and spin-orbit interactions is still being debated and explored [1,2]. In this talk [3] we present a study on the Ru 4d-orbital occupation and excitations in (Ca/Sr)₂RuO₄, performed through a combination of X-ray Absorption Spectroscopy (XAS) and high resolution oxygen K-edge Resonant Inelastic X-ray Spectroscopy (RIXS). The ruthenium 4d orbital occupation and excitations were probed through their hybridization with the oxygen p-orbitals. A minimal model, taking into account crystal field splitting and spin-orbit coupling, is presented to account for the observations. Implications on electronic structure, Mott physics and superconductivity are discussed.

References:

1. T. Mizokawa et al., Phys. Rev. Lett. 87, 077202 (2001)
2. M. W. Haverkort et al., Phys. Rev. Lett. 101,026406 (2008)
3. C.G. Fatuzzo et al., submitted to Phys. Rev. Lett

TH.G.3_O2 - Evidence for XY anisotropy in Sr₂IrO₄ as revealed by magnetic critical scattering

J. Vale^{1,2}, S. Boseggia^{1,3}, H. Walker^{4,5}, R. Springell⁶, Z. Feng¹, E. Hunter⁷, R. Perry¹, D. Prabhakaran⁸, A. Boothroyd⁸, S. Collins³, H.M. Rønnow^{2,9}, D.F. McMorrow¹

1. *University College London, London, United Kingdom*
2. *Ecole Polytechnique Federale de Lausanne, Lausanne, Switzerland*
3. *Diamond Light Source, Oxfordshire, United Kingdom*
4. *Deutsches Elektronen Synchrotron DESY, Hamburg, Germany*
5. *ISIS Neutron and Muon Source, Oxfordshire, United Kingdom*
6. *University of Bristol, Bristol, United Kingdom*
7. *University of Edinburgh, Edinburgh, United Kingdom*
8. *University of Oxford, Oxford, United Kingdom*
9. *Institute of Solid State Physics, University of Tokyo, Tokyo, Japan*

The magnetic critical scattering in Sr₂IrO₄ has been characterized using X-ray resonant magnetic scattering (XRMS) both below and above the 3D antiferromagnetic ordering temperature, T_N. The order parameter critical exponent below T_N is found to be $\beta=0.195(4)$, in the range of the 2D XYh₄ universality class. Over an extended temperature range above T_N the amplitude and correlation length of the intrinsic critical fluctuations are well described by the 2D Heisenberg model with XY anisotropy. This contrasts with an earlier study of the critical scattering over a more limited range of temperature which found agreement with the theory of the isotropic 2D Heisenberg quantum antiferromagnet, developed to describe the critical fluctuations of the conventional Mott insulator La₂CuO₄ and related systems. Our study therefore establishes the importance of XY anisotropy in the low-energy effective Hamiltonian of Sr₂IrO₄, the prototypical spin-orbit Mott insulator.

TH.G.3_O3 - Orbital magnetism and spin-orbit effects in iridium oxides

M. A. Laguna-Marco¹, P. Kayser², J. A. Alonso², Y. Choi³, D. Haskel³

1. ICMA and Dpto de Física de la Materia Condensada, CSIC-Universidad de Zaragoza, Zaragoza, Spain

2. Instituto de Ciencia de Materiales de Madrid, CSIC, Madrid, Spain

3. Advanced Photon Source, Argonne National Laboratory, Argonne, United States

Element- and orbital-specific L_{2,3} edge x-ray absorption and magnetic circular dichroism measurements are used to probe the electronic ground state and magnetism of Ir(5d) states in iridium oxides like A₂MIrO₆ (A=Sr, La; M = Mg, Ca, Sc, Ti, Ni, Fe, Zn, In) and (Ba,Sr)IrO₃. All the studied compounds present a significant influence of spin-orbit interactions in the electronic ground state. Besides, comparison between different A₂MIrO₆ compounds indicates that the Ir 5d local magnetic moment shows different character depending on the oxidation state. Ir carries an orbital contribution comparable (or even bigger) to the spin contribution for Ir⁴⁺ and Ir⁵⁺ oxides while the orbital contribution is quenched for Ir⁶⁺ samples. The results for the A₂MIrO₆ system also indicate that Ir carries a sizable local magnetic moment with the value of the much smaller net magnetization strongly dependent upon the structural details in each double perovskite. In a similar way, the 3d-5d magnetic interaction is strongly dependent on the structural details such as bond lengths and angles. Thus, we found that the net moment of Ir orders parallel to the net magnetic moment of Fe and Ni in Sr₂FeIrO₆ and Sr₂NiIrO₆, respectively, whereas it aligns antiparallel in La₂NiIrO₆. The delicate interplay between lattice degrees of freedom, electronic bandwidth and exchange interactions in iridates is further illustrated by the disparate response of the magnetic properties of BaIrO₃ to chemical (doping) and physical pressure.

TH.G.3_O4 - Orbital and magnetic orderings in half-doped manganites thin films: the crucial role of strain and bandwidth

D. Pesquera¹, D. Gutiérrez¹, G. Radaelli², A. Barla³, F. Bondino⁴, E. Magnano⁴, F. Sánchez¹, R. Bertacco², J. Fontcuberta¹

1. Institut de Ciència de Materials de Barcelona (ICMAB-CSIC), Campus UAB, Bellaterra, Spain

2. LNESS - Dipartimento di Fisica - Politecnico di Milano, Como 22100, Italy

3. Istituto di Struttura della Materia, ISM CNR, S.S. 14 km 163.5, Area Science Park Basovizza (Ts), I-34149, Italy

4. IOM-CNR, S.S. 14 km 163.5, Area Science Park Basovizza (Ts), Italy.

Half-doped manganites $\text{La}_{0.5}\text{A}_{0.5}\text{MnO}_3$ (A=Sr,Ca) have received renewed attention because their ground state (ferromagnetic (FM) / metallic or antiferromagnetic (AF) / insulator) can be radically modified by engineering the bandwidth or the carrier density. This property makes half-doped manganites ideal materials to be integrated in reconfigurable tunneling junctions with potentially large electroresistance [1,2]. Progress in this direction and discrimination between strain and field-effects in ferroelectric/half-doped manganite heterostructures, and the much wanted field-induced metal-insulator transition at the interface [4], require detailed understanding of the epitaxial strain effects on the properties of ultrathin films which may modify or suppress orbital ordering. Here, exploring the temperature and magnetic field dependence of X-ray absorption linear and circular dichroism, we discern the orbital and magnetic orderings of $\text{La}_{0.5}\text{A}_{0.5}\text{MnO}_3$ (A = Ca and Sr) films and its complex evolution with strain and electronic bandwidth. Our results -combined with the structural, magnetic and electrical characterization of these films [3]- provide a guide for material's selection for optimal hybrid half-doped manganite/ferroelectric tunnel junctions.

References:

[1] J. D. Burton and E. Y. Tsybal, Phys. Rev. Lett. 106, 157203 (2011)

[2] Y. W. Yin, J. D. Burton, Y.-M. Kim, a Y. Borisevich, S. J. Pennycook, S. M. Yang, T. W. Noh, a Gruverman, X. G. Li, E. Y. Tsybal, and Q. Li, Nat. Mater. 12, 397 (2013)

[3] D. Gutiérrez, G. Radaelli, F. Sánchez, R. Bertacco, and J. Fontcuberta, Phys. Rev. B 89, 075107 (2014)

[4] G. Radaelli, D. Gutiérrez, F. Sánchez, M. Stenger, R. Bertacco and J. Fontcuberta, Adv. Mater. In press (2015)

TH.H.1_I1 - Efficient and safe magnetic iron oxide nanoparticles for biomedicine

M. Del Puerto Morales ¹

1. Instituto De Ciencia De Materiales De Madrid, Consejo Superior De Investigaciones Cientificas, Madrid, Spain

Magnetic nanoparticles based on iron oxides are utilized in vivo investigations, in diagnosis and therapy treatments for their no-toxicity, biodegradability and magnetic properties. Compared to the conventional, non-targeted methods of drug delivery, magnetic nanoparticles with proper surface modification and conjugated targeting ligands/molecules are promising drug carriers due to the better specificity to the target site that can be assisted with a magnet and the reduced adverse effects [1]. Recent efforts are focused in designing new multifunctional magnetic nanoparticles to address the problems found in biomedical applications [2]. For example, to improve the sensitivity and accuracy of MRI, other materials (organic and inorganic) responsible for different imaging modalities are combined with the nanoparticles [3, 4]. Therapeutic efficacy can be also improved by synthesizing MNPs and controlling the nanoparticle assembling [5]. However, biodistribution and metabolism of these new nanoparticles need to be better understood before serving as nanoplatforms for highly efficient diagnostic and therapeutic applications.

References:

- [1] Mejías R. et al., Biomaterials 32, 2938e2952, 2011
- [2] Gutiérrez L., Dalton Transactions 44, 2943-29-52, 2015
- [3] Ruiz A., Nanoscale 5, 11400-11408, 2013
- [4] Veintemillas S., Nanotechnology 2015, in press
- [5] Serantes D., J. Phys. Chem C, 118, 5927-5934, 2014

TH.H.1_O2 - Magnetic hyperthermia properties of nanoparticles inside lysosomes using kinetic Monte-Carlo simulations: influence of key parameters, of dipolar interactions and spatial variations of heating power

J. Carrey¹, R. Tan¹, M. Respaud¹

1. Laboratoire De Physique Et Chimie Des Nano-Objets, INSA Toulouse, CNRS, Université de Toulouse, Toulouse, France

Understanding the influence of dipolar interactions in magnetic hyperthermia experiments is of crucial importance for fine optimization of nanoparticle heating power. In this study, we use a kinetic Monte-Carlo algorithm to calculate hysteresis loops that correctly account for both time and temperature. This algorithm is shown to correctly reproduce the high-frequency hysteresis loop of both superparamagnetic and ferromagnetic NPs without any ad-hoc parameters. The algorithm is easily parallelizable which considerably decreases calculation time and enables the study of assemblies of several thousands of NPs. The heating power of magnetic nanoparticles dispersed inside spherical lysosomes is studied as a function of volume concentration, applied magnetic field, lysosome size, NP diameter and anisotropy. Magnetic interactions are shown to increase the coercive field, saturation field and hysteresis area of major loops. However, for minor loops, the heating power as a function of concentration can increase, decrease or display a bell shape, depending on the relationship between the applied magnetic field and the coercive/saturation fields of the nanoparticles. The heating power of a given nanoparticle is strongly influenced by a local concentration involving approximately 20 neighbors. Because this local concentration strongly decreases upon approaching the surface, the heating power increases or decreases in the vicinity of the lysosome membrane. The amplitude of variation reaches more than one order of magnitude in certain conditions. The amplitude and sign of this variation is comprehensively explained. Finally, implications of these various findings are discussed in the framework of magnetic hyperthermia optimization. It is concluded that feedback on two specific points from biology experiments is required for further advancement of nanoparticle optimization for magnetic hyperthermia. The present simulations will be an advantageous tool to optimize magnetic NPs heating power and interpret experimental results.

References:

R. P. Tan, J. Carrey and M. Respaud, Phys. Rev. B. 90, 214412 (2014)

TH.H.1_O3 - On-chip attomol level detection of proteins using forced magnetic bead transport

R. S. Bejhed¹, B. Tian¹, K. Eriksson¹, R. Brucas¹, S. Oscarsson², M. Strömberg¹, P. Svedlindh¹, K. Gunnarsson¹

1. *Uppsala University, Dep. of Engineering Sciences, Uppsala, Sweden*

2. *Stockholm University, Dep. of Organic Chemistry, Stockholm, Sweden*

Based on their unique properties, magnetic beads are well suited to be used as target labels in biosensor systems. Here, we present a chip-based biosensor system for protein detection comprising lines of micron-sized magnetic thin film elements. Under the influence of a rotating external magnetic field, the elements enable a forced transport of magnetic beads. Both the beads and a section of the chip (the detection area) were functionalized with capture molecules complementary to the target protein. Two approaches were tested, in which the target protein was labeled with the beads either on-chip or off-chip. In the on-chip labeling approach, the sample was incubated on the chip prior to the transport of the beads. In the off-chip labeling approach, the sample was incubated with the beads which were then transported across the chip. In both cases, the target protein will act as a cross-linker between the capture molecules on the beads and the detection area, resulting in the immobilization of beads on the detection area. The immobilized beads were detected using a standard optical microscope. When tested using avidin as capture molecule and biotinylated anti-avidin as target protein, both approaches resulted in a limit of detection (LOD) in the attomol range. The on-chip labeling approach proved to be the more sensitive approach, with a LOD of 1.7 attomol in a 5 μ l sample (target protein in PBS) and a dynamic range of five orders of magnitude for a total assay time of 1.5 hours. When testing the on-chip labeling approach on a sample of target protein in PBS with 10% serum, the LOD shifted to 34 attomol in a 5 μ l sample. The overall performance of our biosensor system compares well to similar systems and our next challenge will be to extend the system for multiplex detection.

TH.H.1_O4 - Towards an on-chip platform for the investigation of cellular functions via magnetic nanoparticles

D. Petti¹, M. Monticelli¹, E. Albisetti¹, D. Conca¹, A. Cattoni², M. Lupi³, D. Parazzoli⁴, R. Bertacco¹

1. *PoliFab - Politecnico Di Milan, Milan, Italy*

2. *Laboratoire de Photonique et de Nanostructures (LPN) – CNRS, France*

3. *Instituto di Ricerche Farmacologiche Mario Negri, Instituto di Ricerche Farmacologiche Mario Negri*

4. *IFOM-FIRC, Institute of Molecular Oncology, Milan, Italy*

In-vitro tests and analysis are of fundamental importance for investigating biological mechanisms in cells and bio-molecules. The application of controlled forces to activate specific and not well-known bio-pathways, mimicking the role of the cellular environment, is becoming a prominent approach in this field. Methods based on the remote manipulation of magnetic beads, via external magnetic fields, are receiving great attention because magnetic fields are not screened by biological or culture media. Moreover, magnetic nanoparticles manipulation does not involve relevant energy dissipation, which could eventually damage the cell structure. In this work, we present a non-invasive magnetic on-chip platform, exploiting magnetic Domain Wall Tweezers (DWTs) [1], based on the controlled nucleation and displacement of Domain Walls (DWs) in ferromagnetic conduits, for trapping and finely manipulating single superparamagnetic particle properly functionalized. To this scope, nanometric Ni₈₀Fe₂₀ rings are patterned on a chip where cells are afterwards cultured and a pair of DWs, which attract and drag magnetic nanoparticles, are nucleated and displaced through the application of a rotating in plane magnetic field. In this way, we demonstrate the possibility to handle with high resolution (down to 100 nm) magnetic beads to a target cell in order to assess controlled forces in the range of pN-nN [2] to mechanically and chemically activate relevant cellular pathways (e.g. genes activation) actually under investigation. Furthermore, cellular response to localized stimuli is monitored in real time by means of optical methods like confocal microscopy.

References:

[1] M. Donolato et al., *Adv. Mat.* 22, 2706-2710 (2010)

[2] M. Monticelli et al., accepted for publication in *J. Appl. Phys*

TH.H.1_O5 – “In-planta” penetration and translocation of Fe@C magnetic nanoparticles

C. Marquina^{1,2}, Z. Cifuentes³, M.J. Coronado⁴, E. Corredor⁵, L. Custardoy^{6,7}, J.M. de la Fuente¹, L. De Matteis⁶, R. Fernández-Pacheco^{6,7}, P. González-Melendi⁸, M.R. Ibarra^{2,6,7}, A. Pérez de Luque³, M.C. Risueño⁵, D. Rubiales⁹, M.P.S. Testillano⁵

1. Instituto De Ciencia De Materiales De Aragón (ICMA); CSIC-UZ, Zaragoza (Spain)
2. Departamento de Física de la Materia Condensada; Universidad de Zaragoza, Zaragoza (Spain)
3. IFAPA, Centro Alameda del Obispo, área de Mejora y Biotecnología; Junta de Andalucía, Córdoba (Spain)
4. Hospital Universitario Puerta de Hierro; Majadahonda, Madrid (Spain)
5. Centro de Investigaciones Biológicas (CIB); CSIC, Madrid, Spain
6. Instituto de Nanociencia de Aragón (INA); Universidad de Zaragoza, Zaragoza, Spain
7. Laboratorio de Microscopías Avanzadas (LMA); Universidad de Zaragoza, Zaragoza, Spain
8. ETSI Agrónomos; Universidad Politécnica de Madrid, Madrid, Spain
9. Instituto de Agricultura Sostenible (IAS); CSIC, Córdoba, Spain

Magnetic nanoparticles have been implemented in biotechnological and biomedical applications related to animal (in particular human) cells and pathologies. However, their use in plant research biology is far less studied, although it could lead to the development of interesting plant biotechnology applications. For this purpose the first stage is to work out the penetration and transport of the magnetic nanoparticles into living plants and plant cells and how they interact with plant cells and tissues [1]. We have synthesized biocompatible suspensions of iron-oxide carbon-coated nanoparticles, obtained by a gas-phase condensation method. They have been injected into pumpkin (*Cucurbita pepo*) living plants. The graphitic shell of our nanoparticles made possible their visualization into plant cells and tissues, using different microscopy techniques (fluorescence, confocal, light and electron microscopy). Moreover, their magnetic character allowed the nanoparticles to be positioned in the desired plant tissue by applying magnetic field gradients. In the absence of magnetic fields, the nanoparticles can as well travel along the vascular system, reaching different cell and tissues. Nanoparticles have been found both in the cytoplasm and in the extracellular space between cells. A size-based selection mechanism seems to be operating, probably involving cell walls and waxes acting as a barrier. Accumulation of nanoparticles was detected in leaf trichomes, suggesting a way for nanoparticles excretion/detoxification. With respect to cytotoxicity, it has been observed that cells containing nanoparticle agglomerates exhibited a cytoplasm denser than that of cells containing few nanoparticles. Damage at the plant level was not macroscopically evident. Although more studies are necessary to unveil the nanoparticles penetration and translocation mechanisms as well as their cyto- and phyto-toxicity, our results open a wide range of possibilities for using magnetic nanoparticles in general plant research and agronomy.

References:

- [1] P. González-Melendi, et al., *Annals of Botany* 101 (2008) 187-195

TH.H.2_I1 - Tumor ablation by exploiting magnetic nanoparticles and magnetic nanoparticle functionalization to achieve heat-mediated drug delivery and antibody tumor targeting

T. Pellegrino¹

1. *Istituto Italiano di Tecnologia, Geneve, Italy*

At the tumor, a macroscopically temperature increase above 46°C, can provoke tumor ablation and kill cancer cells in the so called hyperthermia treatment. Lately, we have investigated iron oxide nanocubes prepared by thermal decomposition methods, as heat mediators in magnetic hyperthermia. These magnetic nanoprobles when exposed to an alternating magnetic field can generate heat and retarder the tumor growth (J. Kolosnjaj-Tabi et al. ACS Nano, 2014, 8, 4268). Here, our latest progress on the synthesis and their stabilization in physiological environments of suitable materials for magnetic-based hyperthermia will be presented (P. Guardia et al. J. Mater. Chem. B, 2014,2, 4426).

I will also present an example of surface functionalization of iron oxide nanocubes with a thermo-responsive polymer shell able to release the drug content upon an increase of temperature above the body temperature and under field and frequency conditions that are non-armful for patients. Given the high heat specific absorption rates (SARs) of the nanocubes, their activation under AMF exposure and the consequent heat production, can be exploited to trigger doxorubicin drug release loaded within the polymer shell (H. Kakwere et al, ACS Appl. Mater. Interfaces, 2015, 7 (19), pp 10132–10145).

Finally, an *in vitro* and *in vivo* study of specific targeting of iron oxide nanoparticles towards ovarian cancer cells will be also presented. Upon surface functionalization of spherical magnetic nanoparticles of 20 nm in diameter with an human antibody fragment (MNP-20-AFRA), a better targeting is achieved by directly administration of MNP20-AFRA by loco-regional administration (Quarta A et al., Nanoscale, 2015, 7, 2336–2351). In this context, tumor-specific MNP not only accumulate to a greater extent in the neoplastic lesion, to a level that can be considered appropriate for a therapeutic intervention, but also MNP20-AFRA are retained in the targeted area longer and prevented from a rapid clearance of the nanoparticles out of the tumor tissues than the non-specific control (PEG coated nanoparticles which do not bear the antibody).

TH.H.2_O2 - Real-time analysis of magnetic hyperthermia experiments on living cells under a confocal microscope

V. Connord¹, P. Clerc², N. Hallali¹, D. El Hajj Diab², D. Fourmy², V. Gigoux², J. Carrey¹

1. *NanoMagnetism, LPCNO Toulouse, Toulouse, France*

2. *RCTC, INSERM Toulouse, Toulouse, France*

Applying a high-frequency alternating magnetic field (AMF) to tumor cells which have internalized magnetic nanoparticles (MNPs) can induce their apoptotic death [1]. However, the mechanisms responsible for this death are currently far from being understood. Their study was made difficult because it was previously impossible to observe cells during the AMF application. Using a new experimental setup we managed to remove this technological bottleneck. To achieve this, a high-frequency miniaturized electromagnet was manufactured [2]. Its small diameter permits its insertion into a cell culture box. It can generate a magnetic field on tumor cells while allowing their observation under a confocal microscope, a standard instrument in cell biology. Using this setup and fluorescence tags, several biological processes were revealed when AMF was applied on a gel containing tumoral cells with or without internalized MNPs. First, cell damages were observed exclusively on cells containing targeted MNPs. Real-time capture of two events suspected to play a key role in cell death induced by the magnetic field treatment were performed: lysosomal membrane permeabilization and ROS generation. These two phenomena were detected after 30 mn of AMF treatment only and thus occur at an early stage in the cascade of events leading eventually to cell death. We have also observed that, in some cells, lysosomes having accumulated MNPs could self-organize into needles under the influence of the AMF. This novel experimental approach is simple to develop and allows getting an insight into the cellular, molecular and physical mechanisms occurring during AMF application on living cells. We hope it will permit to understand the reason why cell death is observed in these magnetic hyperthermia conditions in spite that no increase of global temperature is perceptible.

References:

[1] C.Sanchez et al., ACS Nano 8, 1350 (2014)

[2] V. Connord et al., Small (2015)

TH.H.2_O3 - Exploiting the theranostic potential of dendronised-iron oxide nanoparticles

C. Blanco-Andujar¹, H. Dib¹, D. Mertz¹, E. Robinet², F. Meyer², D. Felder¹, S. Begin-Colin¹

1. *Institut de Physique et Chimie des Matériaux de Strasbourg (IPCMS), UMR-7504 CNRS-Université de Strasbourg, 23 rue du Loess, Strasbourg, France*

2. *INSERM 1121, Faculté de Chirurgie Dentaire, Université de Strasbourg, 11 rue Humann, Strasbourg, France*

Hepatocellular carcinoma is a public health burden, which constitutes the third cause of cancer mortality in the world.[1] Nonetheless, only unsatisfactory treatments with major side-effects and high cost are available. As a result, there is a need for new therapies that provide targeted cost-effective treatments that improve patient prognosis. Magnetic iron oxide nanoparticles (IONPs) are a suitable platform for the assembly of targeted entities with multiple functionalities. There is a wide range of methods for their synthesis; however, limited reproducibility, low stability, biocompatibility and limited targeting capabilities, have hampered the translation of these materials into practical tools for medical use. IONPs are commercially available as contrast agents for magnetic resonance imaging (MRI); but interest is now focused on their use as theranostic tools by incorporating a therapeutic capability to these agents. Magnetic hyperthermia (MH) has gained attention for the treatment of malignant tissue due to the possibility of limiting the treated area and enhancing drug efficiency. Herein, 10-30 nm IONPs with different magnetic anisotropies were synthesised and coated with multifunctional dendrons designed for drug loading.[2] These provided stable water suspensions suitable for in vivo use, which were tested for MRI and MH. In vitro tests compared the effect of MH induced drug release against direct drug exposure. Cell internalisation was studied as a function of drug and NPs concentration, as well as under MH treatment. To summarise, we have developed a synthesis and functionalisation method yielding stable drug-loaded dendronised-IONPs water suspensions. This nanoplatform has the potential to fulfil the need for a new theranostic tool for the treatment of hepatocellular carcinoma and other cancers due to its stability and therapeutic properties obtained by combining drug and hyperthermia effects.

References:

1. Ferlay J., et al. GLOBOCAN 2012 v1.0, Cancer Incidence and Mortality Worldwide: IARC CancerBase No. 11. 2013; Available from: <http://globocan.iarc.fr>
2. Walter, A., et al., Chemistry of Materials, 2014. 26(18): p. 5252-5264

TH.H.2_O4 - Lab-on-a-chip platform for detecting pathogenic DNA via magnetic tunnelling junction-based biosensors

D. Petti¹, E. Albisetti¹, P. Sharma¹, M. Massetti¹, F. Damin², G. Falduti³, M. Cretich², E. Marchisio³, M. Chiari², R. Bertacco¹

1. *Polifab - Politecnico Di Milan, Milan, Italy*

2. *Istituto di Chimica del Riconoscimento Molecolare- CNR, Milan, Italy*

3. *Dia.Pro Diagnostic BioProbes srl, Milan, Italy*

In recent years, the development of fabrication techniques to process materials in micro and nano-scale sized structures has deeply promoted the application of magnetoresistance in the fields of magnetic memories and biosensing. For the latter case, bioassays combining biosensors based on magnetic tunneling junctions (MTJ) with magnetic markers have been widely developed in order to detect concentration of specific molecules in the medium under inspection. The most widely used scheme relies on the detection of molecular recognition events between the probe molecules, bound onto the sensor surface, and the magnetically labeled target molecules, which bind specifically to the complementary probes [1]. The magnetic stray field of the superparamagnetic labels on the surface of the sensor causes a change in the electrical resistance of the sensor, which is related to the concentration of the immobilized target molecules.

In this work, we demonstrate the detection of natural DNA from different classes of pathogens, precisely Hepatitis E virus (HEV) and Pathogenic bacteria (Salmonella, Listeria monocytogenes) using a highly sensitive biosensing platform based on magnetic tunneling junction (MTJ) [2]. The sensing array consists of 11 MTJ-based rectangular sensors with lateral dimensions $3 \times 40 \mu\text{m}^2$, a TMR value of 75% and a sensitivity $S_0 = 17 \%/mT$ in the linear region. The results show that the platform successfully meets the requirements for the detection of hybridized natural DNA. Moreover, this work represents a fundamental step towards the integration of MTJ-based biosensing platforms in compact Lab-on-a-chip devices for the straightforward detection of pathogens in the agrifood industry and for further medical applications.

References:

[1] Albisetti, E., Petti, D. et al., Sensors and Actuators B 200 (2014) 39–46

[2] Albisetti, E., Petti, D. et al., Biosens. Bioelectron. 47, 213–7 (2013)

TH.H.2_O5 - Optomagnetic read-out system for detection of pathogens based on magnetic nanobead dynamics

R. S. Bejhed¹, T. Zardán Gómez de la Torre¹, M. Donolato², M. F. Hansen², M. Strömberg¹, P. Svedlindh¹

1. *Uppsala University, Dep. of Engineering Sciences, Uppsala, Sweden*

2. *Technical University of Denmark, Department of Micro- and Nanotechnology, Lyngby, Denmark*

The interest for research on new and improved strategies for the detection of pathogens is continuously growing. One strategy is to label the target entity by binding it to magnetic nanobeads equipped with detection probes. The dynamic behavior of nanobeads exposed to an AC magnetic field will be different for nanobeads with and without bound target. By probing the nanobead dynamics using a laser, this change in behavior can be measured as a modulation of the intensity of light transmitted through a cuvette holding the sample. Here, the complex second harmonic component, V_2 , of the transmitted light was measured as a function of the AC magnetic field frequency. A DNA target was recognized through padlock probe ligation followed by rolling circle amplification, resulting in micrometer sized DNA coils to which the nanobeads were bound. The read-out system was optimized and a turn-on response was found in the low frequency regime of the phase angle versus frequency spectrum calculated from V_2 . A limit of detection of 5 pM of *Vibrio cholerae* DNA coils was found for an assay time of less than two hours. [1] Additionally, a qualitative *Escherichia coli/Vibrio cholerae* bplex detection methodology was demonstrated.[2] This was accomplished by the binding of two different bead sizes to DNA coils from the two targets. This read-out system has a number of advantages in that it is easy to manage, sensitive, fast and built using inexpensive components therefore being an ample candidate for further research towards commercialization.

References:

[1] Bejhed et al., *Biosensors and Bioelectronics*, 2015, 66, 405-411

[2] Bejhed et al., *Biotechnology Journal*, 2015, doi: 10.1002/biot.201400615

TH.H.3_I1 - Spin-dependent thermoelectric phenomena in thin films of

La_{2/3}Sr_{1/3}MnO₃

C. Bui¹, F. Rivadulla¹

1. *Centro de Investigación en Química Biológica y Materiales Moleculares (CIQUS),
Universidad de Santiago de Compostela, 15782-Santiago de Compostela, Spain.*

The different density of states and Fermi velocities for the spin up/down population in ferromagnetic metals produce different conductivities for the opposite spin directions [1]. Therefore when the spin lifetime is larger than the momentum relaxation time, a *spin-dependent* Seebeck and Peltier coefficient are predicted, on the basis of the Onsager reciprocities [2]. On the other hand, the observation of a spin Seebeck effect (SSE) in magnetic insulators,[3,4,5] demonstrates that this must be different to the conventional Seebeck effect in magnetic conductors.

In this talk we will discuss the observation of an intrinsic planar Nernst effect (PNE) and anomalous Nernst effect (ANE) in thin films of La_{2/3}Sr_{1/3}MnO₃(LSMO). This material shows a fully spin polarized 3d band, and a $T_c \approx 360$ K, which motivated its extended use as a FM electrode in tunnel junctions. We show that through a very careful control of the thermal gradients in the thin films, the ANE can be completely suppressed and separated from the symmetric PNE response. We further demonstrate that there is a perfect correspondence between the magnetothermal effects and their electrical counterparts in LSMO. Our findings also establish an upper limit for the possible observation of SSE in this system.[6]

References:

- [1] L. Gravier, A. Fabian, A. Rudolf, A. Cachin, J.-E. Wegrone, J.-Ph. Ansernet, Spin-Dependent Thermopower in Co/Cu Multilayer Nanowires, *J. Mag. Mag. Mater.*271, 153 (2004).
- [2] J. M. Ziman, *Electrons and Phonons*, Oxford University Press, UK 1960.
- [3] K. Uchida, S. Takahashi, K. Harii, J. Ieda, W. Koshibae, K. Ando, S. Maekawa, E. Saitoh, Observation of the Spin Seebeck Effect, *Nature* 455, 778 (2008).
- [4] G. E. Bauer, E. Saitoh, B. J. v Wees, Spin Caloritronics, *Nat. Mat.*11, 391 (2012).
- [5] K. Uchida, T. Ota, H. Adachi, J. Xiao, T. Nonaka, Y. Kajiwara, G. E. W. Bauer, S. Maekawa, E. Saitoh, Thermal Spin Pumping and Manong-Phonon-Mediated Spin-Seebeck Effect, *J. Appl. Phys.* 111, 103903 (2012).
- [6] Cong Tinh Bui and F. Rivadulla, *Phys. Rev. B(R)* 90, 100403, (2014).

TH.H.3_O2 - Switchable field-tuned control of magnetic domain wall pinning along Co microwires by 3D e-beam lithographed structures

C. Blanco-Roldán^{1,2}, C. Quirós^{1,2}, G. Rodriguez-Rodriguez³, M. Vélez^{1,2}, J. I. Martín^{1,2}, J. M. Alameda^{1,2}

1. *Departamento de Física, Universidad de Oviedo, Oviedo, Spain*

2. *Centro de Investigación en Nanomateriales y Nanotecnología CINN (CSIC, Universidad de Oviedo), El Entrego, Spain*

3. *Madrid Institute for Advanced studies in Nanoscience (IMDEA nanoscience), Campus de Cantoblanco, Madrid, Spain*

Modern memory devices based on magnetic domain wall motion require precise control of the domain wall dynamics, making this a fundamental task to achieve in their development process. In this work we present how wall motion in a cobalt wire can be controlled by pinning or de-pinning it due to the effect of the magnetic stray field of a previously magnetized cobalt bridge structure that crosses over it. Co microwires and bridges are both patterned over a Si substrate by e-beam lithography, and grown by magnetron sputtering followed by a lift-off process. Typical sizes are 12 x 3µm length and 250nm thickness for the bridges, which rise 200nm on average over the 50 x 3µm length and 40nm thickness needle-like shaped wires. Magnetization process has been analyzed by Kerr Microscopy in longitudinal geometry. It can be seen that the Co bridge has a high remanence when magnetized with a 0.53T field in the direction perpendicular to its length, that can induce a pinning effect in the wire below it, even without being in contact. In this way, by changing the remanence state of the bridge coming from negative or positive saturation, pinning of the domain wall motion in the wire can be selected to occur in either the positive or the negative branch respectively of the wire's hysteresis loop when a low magnetic field between 15mT and -15mT is applied along the wire direction, lasting this effect around 2.6 ± 1.0 mT. This switchable pinning effect is also very reliable, taking place with a probability of more than 83%, making these 3D structures a good alternative to use as pinning sites because of its novel tunable capacity of selection between pinning and de-pinning effect as required, opening a wider range of options for the user to control domain wall dynamics.

TH.H.3_O3 - Domain wall nanosensors based on ultra-thin CoFeB films

J. Wells¹, J. H. Lee², R. Mansell², R. Cowburn², O. Kazakova¹

1. National Physical Laboratory, Teddington, Middlesex, United Kingdom

2. Thin Film Magnetism, Department of Physics, University of Cambridge, Cambridge, United Kingdom

Manipulation of magnetic domain walls (DWs) within nanostructures holds great promise for numerous applications, including high density memory, logic and sensor devices. Materials engineered to exhibit perpendicular magnetic anisotropy (PMA) exhibit advantageous properties, including narrow DWs, high thermal stability and low critical currents for DW propagation, which can be implemented in the construction of nanodevices. High sensitivity (down to single particle) detection and manipulation of magnetic nanoparticles (MNPs) is a rapidly developing area of research due to the potential for implementation in metrology and novel medical technologies. Through a variety of studies implementing ultrathin CoFeB(0.6nm)/Pt multilayers, we present a proof of concept for nanodevices based on the controlled nucleation and propagation of DW's through components formed from this PMA material. Reproducible low energy DW injection is demonstrated using precisely tailored device geometry. DW progress through the structures is observed using anomalous Hall effect measurements. These are conducted using both conventional Hall crosses, and also by probing the Hall voltage using overlying gold wires to minimise the disruption to smooth DW motion caused by pinning at Hall crosses in the first type of measurements. Field-driven DW motion modulated via geometrical pinning is demonstrated as a method of initialising the device for the capture of magnetic nanoparticles, and subsequently for probing the interaction between the DW and a MNP located in close proximity to it. The behaviour of clean, as-fabricated devices under varying field orientation is presented. Subsequent measurements of the devices after being decorated with commercially produced 1 micrometer MNPs are contrasted with the pristine devices. A possible method for applying ultra-thin film PMA sensors for single bead detection is evaluated. Further methods for improving the sensitivity of the devices are discussed.

TH.I.1_I1 - Spin-polarization in reciprocal space: analyzing the spin structure of electronic states by quasi-particle interference

M. Bode¹

1. Wuerzburg University, Würzburg, Germany

The detection of spin-dependent surface properties is an important prerequisite for the understanding of various electron-correlation effects. The experiments presented here evaluate to what extent the observation of interference patterns created by coherent electronic states, so-called quasi-particle interference (QPI), can be used to obtain information on the spin-polarization of electronic bands in k-space. First, ferromagnetic Ni(111) will be used as a test sample for the QPI technique. In the following we will present investigations of surface alloys of some heavy post transition metals with Ag(111), which provide giant Rashba-type spin-splittings, and of magnetically doped topological insulators. In both cases some very complex QPI patterns. The analysis of the energy dispersion of the observed features and the comparison with density functional theory calculations shows how the conservation of spin angular and orbital momentum influences the interference pattern.

Th.I.1_O2 - Eddy current interactions in a Ferromagnet-Normal metal bilayer structure, and its impact on ferromagnetic resonance lineshapes

V. Flovik¹, F. Macià², A. Kent³, E. Wahlstrøm¹

1. Norwegian University of Science And Technology, Trondheim, Norway

2. Universitat de Barcelona, Barcelona, Spain

3. New York University, New York, United States

In ferromagnetic resonance (FMR) experiments the shape of the absorption line carries valuable information. Recent experiments have used the difference in symmetry of the FMR lines to study spin pumping from a magnetic material to a normal metal. Hence, to interpret correctly experimental data involving FMR it is important to understand how eddy-currents can cause modifications to the measured lineshape. In this study, we investigate the contribution of eddy-currents to the FMR response in a ferromagnet-normal metal (FM/NM) bilayer structure. Eddy-current effects are usually considered negligible for a NM layer thickness below the microwave (MW) skin depth (approx. 800nm for Au at 10 GHz). However, we show that eddy-currents in thin NM layers (10-100 nm Au or Cu) induce a phase shift in the FMR excitation, resulting in an asymmetry of the measured absorption lines. Through systematic studies of how sample geometry and NM thickness affect the coupling between MW fields and eddy-current induced fields, we show that this coupling is tunable through changing the sample geometry and the NM layer thickness.

Th.I.1_O3 - Femtosecond control of spin-polarized photocurrents at the interfaces of metallic ferromagnetic heterostructures using circular polarized light

T. J. Huisman¹, R.V. Mikhaylovskiy¹, J.D. Costa^{2,3}, E. Paz², J. Ventura³, P.P. Freitas², Th. Rasing¹, A. V. Kimel¹

1. *Radboud University Nijmegen, Institute For Molecules And Materials, Nijmegen, The Netherlands*

2. *International Iberian Nanotechnology Laboratory, INL, Braga, Portugal*

3. *IN-IFIMUP, Porto, Portugal*

Controlling spin-polarized currents using circularly polarized light [1,2] could lead to the development of ultrafast spintronic devices driven by laser pulses operating at the femtosecond timescale. Here we demonstrate that such a helicity dependent photocurrent can be generated at interfaces of metallic heterostructures consisting of a single ferromagnetic layer and a non-magnetic one. In particular, using terahertz emission spectroscopy we show that the direction of the generated photocurrent is controlled by both the helicity of light and the magnetization of the sample. Similarly to the case of noncentrosymmetric semiconductors [1,2] we argue that the helicity and magnetization dependent interfacial photocurrent in metallic multilayers originates from a combination of the spin-orbit interaction and the lack of center of symmetry which is also known as the Rashba spin-orbit coupling.

References:

[1] S. D. Ganichev, E. L. Ivchenko, S. N. Danilov, E. Eroms, W. Wegscheider, D. Weiss, and W. Prettl, Conversion of Spin into Directed Electric Current in Quantum Wells, *Physical Review Letters*, 86, 4358 (2001)

[2] S. D. Ganichev, E. L. Ivchenko, V. V. Bel'kov, S. A. Tarasenko, M. Sollinger, D. Weiss, W. Wegscheider, and W. Prettl, Spin-galvanic effect, *Nature*, 417, 153 (2002)

TH.I.1_O4 - Spin Hall effect in spin glass systems

Y. Niimi¹, B. Gu^{2,3}, M. Kimata¹, Y. Omori¹, T. Ziman⁴, S. Maekawa^{2,3}, A. Fert⁵, Y. Otani^{1,6}

1. ISSP, University of Tokyo, Tokyo, Japan

2. Advanced Science Research Center, Japan Atomic Energy Agency, Japan

3. CREST, Japan Science and Technology Agency, Japan

4. CNRS and Institut Laue Langevin, Grenoble, France

5. CNRS/Thales, Palaiseau, France

6. RIKEN-CEMS, Saitama, Japan

Pure spin current, flow of spin angular momentum with no flow of charge, is a key physical quantity to realize low-power spintronics devices. The spin Hall effect (SHE) enables one to convert charge current into pure spin current via spin-orbit interaction. Unlike most work, that has focused primarily on the magnitude of the spin Hall angle, the conversion yield between charge and spin currents, we here demonstrate an example of employing the SHE as a probe of a fundamental response of the spin current to the random spin configurations in spin glass systems. For this purpose, we chose CuMnBi ternary alloys [1]. When there is no Bi impurity in CuMn, it shows no SHE in the spin transport but shows a typical cusp structure at the spin glass temperature T_g in the thermo-magnetic curves. Once a small concentration of Bi was added in CuMn, a large SHE was observed as shown in our previous work on Bi-doped Cu [2]. Most remarkable is that the SHE of CuMnBi starts to decrease at about $4T_g$ and becomes as little as seven times smaller at $0.5T_g$. A similar temperature dependence was also observed in anomalous Hall effects in the ternary alloys. These experimental results clearly show that a pure spin current induced by skew scattering at the Bi sites is strongly suppressed by fluctuating spins at the Mn sites even far above T_g , and can be qualitatively explained by the relative dynamics between the localized moment and the conduction electron spin.

References:

[1] A. Fert et al., J. Magn. Magn. Mater. 24, 231 (1981)

[2] Y. Niimi et al., Phys. Rev. Lett. 109, 156602 (2012)

Th.I.1_05 - Mn₂Au, a new material for antiferromagnetic spintronics

V.M.T.S. Barthem¹, C.V. Colin², R. Haettel², D. Givord^{1,2}

1. Instituto De Fisica, Universidade Federal do Rio de Janeiro, Rio de Janeiro, Brazil

2. CNRS/Université Grenoble-Alpes, Institut Néel, Grenoble, France

Mn₂Au crystallizes in the MoSi₂ tetragonal structure. In a recent study, it was demonstrated to be an antiferromagnet, with a Mn magnetic moment of around 4 mB and Néel temperature above 950 K, temperature at which the Mn₂Au phase decomposes [1]. The magnetic structure, as determined from powder neutron diffraction, is formed of a stack of ferromagnetic sheets, perpendicular to the uniaxial axis. The moment orientation alternates from one sheet to the next. The Mn moments are confined in the plane of the tetragonal structure. The high Néel temperature in a large moment Mn compound with an heavy element such as Au, where large spin-orbit coupling is expected, suggest that Mn₂Au might be a very promising material for antiferromagnetic spintronics. The fact that the Mn moments lie in the plane of the tetragonal structure is a priori beneficial for possible applications in devices, since the in-plane anisotropy is expected to be much less than the uniaxial one. The possibility to reorient the moments under field remains to be demonstrated. A powder neutron diffraction studies have been performed. Rather than a spin-flop transition, under field, it revealed that the grains rotated under the torque resulting from the anisotropy in the susceptibility. The easy direction, derived from the analysis of the variation in the intensity of the diffraction lines is [110]. To verify the conclusions of this analysis, an X-ray study has been performed, with a powder sample of which constituting grains were previously oriented under field.

References:

[1] V.M.T.S. Barthem, C.V. Colin, H. Mayaffre, M.-H. Julien and D. Givord, Nature Comm. DOI 10.1038/ncomms3892

Th.I.2_O1 - Current-Driven Magnetization Switching via Spin-Orbit Torque in Perpendicularly Magnetized Hf|CoFeB|(MgO or TaO_x) Films with Structural Asymmetry

M. Akyol^{1,2}, G. Yu¹, J. G. Alzate¹, P. Upadhyaya¹, X. Li¹, K. L. Wong¹, A. Ekicibil², P. K. Amiri¹, K. L. Wang¹

1. *University of California, Los Angeles (UCLA), United States*

2. *University of Cukurova, Adana, Turkey*

A charge current flowing inside the heavy metal layer can generate spin-currents flowing into the ferromagnetic layer, which results in SOTs on the magnetization of ferromagnetic layer¹⁻³. However, since the SOT cannot switch perpendicular magnetization deterministically due to the symmetric damping-like SOTs in each out-of-plane magnetization state, an external magnetic field along the current direction is needed to assist the SOTs for deterministic switching². Our previous results showed that current-driven perpendicular magnetization switching without external magnetic field is possible in such structures, when they exhibit structural asymmetry along the in-plane direction, in addition to the symmetry breaking along the z-direction of the structure^{3, 4}. In this work, we study the cap oxide layer effect on the new field-like (FL) torque resulting from this type of symmetry breaking. Specifically, we measure the effective FL-SOTs in the z-direction, H_z^{FL} which are perpendicular to current direction, when in-plane current flows in Hall-bar devices with Hf|CoFeB(wedge)|(TaO_x or MgO) material stacks. The results show that although this new H_z^{FL} is observed in MgO-capped samples, a very weak H_z^{FL} is seen in TaO_x-capped samples. The maximum effective FL-SOT, defined as H_z^{FL} per current density, i.e. $\beta_z = H_z^{FL}/J$, were found to be 18.2 Oe/10⁷ and 0.8 Oe/10⁷ Acm⁻² for MgO and TaO_x-capped samples, respectively. Depending on the magnitude of H_z^{FL} , we observed zero field magnetic switching with in-plane charge currents in the MgO-capped sample. However, an external magnetic field is necessary to switch the magnetization via in-plane electric current in the TaO_x-capped sample due to the small H_z^{FL} . These results indicate that the top interface between the ferromagnetic and oxide layers affects the generated H_z^{FL} torque significantly, and hence a simplified picture based solely on the choice of the bottom metal layer would not be sufficient to understand the switching behavior of these SOT devices. This is consistent with earlier reported results, which showed that the conventional damping-like and field-like SOTs are also stronger in MgO-capped samples compared to those in TaO_x-capped samples⁵. These new insights are important for the design of magnetic random access memory (MRAM) devices based on SOT switching.

Th.I.2_O2 - Chiral-based spin devices without a permanent magnet

O. Ben Dor¹, Y. Paltiel¹

1. The Hebrew University of Jerusalem, Jerusalem, Israel

As technology shrinks down in size nano-structures are likely to become primary components of future electronic devices. One such revolution would merge spintronics with standard Si-based technologies. Spintronics, or spin electronics, refers to the role played by electron spin in solid state physics, and to devices that specifically exploit spin properties instead of charge degrees of freedom. This yields a decrease in the device power consumption, an increase in the devices effective speed and allows higher densities. A new phenomenon, called the Chiral Induced Spin-Selectivity effect has become the basis of spin control and manipulation, where organic chiral self-assembled monolayer acts as an efficient spin filter. We are utilizing this phenomenon to achieve high density, low power, Si compatible logic devices. For example, a proof of concept for a new type of chiral-based memory device, without a permanent magnet was realized, whereas vertical spin torque is transferred into a thin ferromagnetic film thus decreasing the required current density in comparison with standard out of plane torque transfer [Nature communications doi:10.1038/ncomms3256]. We also show that local magnetization can be achieved optically. In this work, using chiral molecules and nano crystals, we achieve local spin-based magnetization generated optically at ambient temperatures [Nano Letters DOI: 10.1021/nl502391t]. Through the chiral layer, a spin torque can be transferred without permanent charge transfer from the nano crystals to a thin ferromagnetic layer, creating local perpendicular magnetization. We used Hall sensor configuration and Magnetic Atomic Force Microscopy to measure the induced local magnetization. At low temperatures, anomalous spin Hall effects were measured using a thin Ni layer. The results may lead to Si compatible electrically/optically controlled spintronics logic devices that will enable low power consumption, high density, and cheap fabrication.

Th.I.2_O3 - Spin current conversion in Bi thin films

M. Shiraishi^{1,2}, H. Emoto², Y. Ando¹, G. Eguchi¹, T. Shinjo¹, Y. Fuseya³, E. Shikoh²

1. *Kyoto University, Kyoto, Japan*

2. *Osaka University, Suita, Japan*

3. *The University of Electro-Communications, Cofu, Japan*

Spin conversion physics in Bi has been attracting strong attention, since Bi essentially possesses a strongly spin-orbit interaction and an efficiency of the conversion between a pure spin current to a charge current, such as the inverse spin Hall effect (ISHE) can be large [1]. Recently, detection of the inverse Rashba-Edelstein effect (IREE) in Ag/Bi was reported and this new spin current conversion mechanism in Bi is one of the hottest issues in physics of Bi [2,3]. From this motivation, we have investigated interplay between the ISHE and the IREE in Bi on YIG, the magnetic insulator, where a strong Rashba field can be expected at the interface. Spin current was dynamically injected from the YIG into the Bi, and an electromotive force was detected from the Bi. Since the electric current induced by the spin conversion in the Bi exhibited obvious thickness dependence of the Bi, only the ISHE took place in the Bi, i.e., the IREE was missing in the Bi/YIG [4]. Hall measurements of the Bi indicate that electrons are majority carriers, whereas both electrons and holes exist in the Bi, and the polarity of the ISHE is consistent with this result. The spin relaxation mechanism in the Bi was clarified to be the D'yakonove-Perel type from the weak anti-localization measurements and conductivity dependence of the spin-orbit length. The detail of the study is introduced in the presentation.

References:

- [1] H. Emoto, M. Shiraishi et al., J. Appl. Phys. 115, 17C507
- [2] J.-C. Rojas-Sanchez et al., Nature Comm. 4, 2944 (2013)
- [3] V.M. Edelstein, Solid State Comm. 73, 223 (1990)
- [4] H. Emoto, M. Shiraishi et al., submitted

Th.I.2_O4 – Spin-to-charge current conversion in Pt, Au and Bi

M. Isasa¹, M.C. Marínez-Velarte^{2,3}, E. Villamor¹, C. Magen^{2,3,4}, L. Morellón^{2,3}, J.M. De Teresa^{2,3,5}, M. R. Ibarra^{2,3}, M. Gradhand⁶, L. E. Hueso^{1,7}, F. Casanova^{1,7}

1. CIC Nanogune, Guipúzcoa, Spain
2. Laboratorio de Microscopías Avanzadas (LMA), Instituto de Nanociencia de Aragón (INA), Zaragoza, Spain
3. Departamento de Física de la Materia Condensada, Universidad de Zaragoza, Spain
4. Fundación ARAID, Zaragoza, Spain
5. Instituto de Ciencia de Materiales de Aragón (ICMA), Universidad de Zaragoza-CSIC, Zaragoza, Spain
6. H. H. Wills Physics Laboratory, University of Bristol, Bristol, United Kingdom
7. IKERBASQUE, Basque Foundation for Science, Bizkaia, Spain

Being able to create, manipulate and detect pure spin currents is one of the main challenges in the field of spintronics. One of the most promising approaches to generate and detect these currents is by using the spin Hall effect (SHE) and its inverse [1]. These phenomena allow a charge-to-spin current conversion (and its inverse) in a non-magnetic metal with a high spin-orbit coupling. The origin of the effect can be attributed to different intrinsic and extrinsic contributions, although the driving mechanism is still unclear for some materials. In this work, we have studied the spin-to-charge current conversion in platinum (Pt), gold (Au) and bismuth (Bi) using the spin absorption technique in a lateral spin valve geometry. With this technique, we can measure the spin Hall angle (the efficiency to convert spin into charge current) in Pt and Au. Moreover, its evolution with temperature allows us to identify the dominant scattering mechanisms behind the SHE. We have observed that, whereas the intrinsic mechanism dominates in Pt, extrinsic effects are more relevant in Au, including a previously ignored phonon contribution to skew scattering [2]. The spin-to-charge current conversion in Bi is more intriguing: in this case, we observe that spin currents are strongly absorbed at the metallic-Bi surface, creating a 2D charge current due to the inverse Rashba-Edelstein effect (IREE). By analyzing the IREE as a function of temperature, we are able to determine the origin of the effect, which arises from the spin-splitting of the bulk states due to the Rashba effect at the metallic-Bi surface [3].

References:

- [1] J.E. Hirsch, Phys. Rev. Lett. 83, 9 (1999)
- [2] M. Isasa et al., Phys. Rev. B 91, 024402 (2015)
- [3] M. Isasa et al., arXiv: 1409.8540 (2014)

Th.I.2_05 - Towards the control of the sign of spin Hall effect in the Cu alloys doped with 5d elements

Z. Xu¹, B. Gu¹, M. Mori¹, T. Ziman², S. Maekawa^{1,3}

1. *Advanced Science Research Center, Japan Atomic Energy Agency, Tokai, Japan*

2. *Institut Laue Langevin, Grenoble, France*

3. *ERATO, Japan Science and Technology Agency, Sendai, Japan*

The spin Hall effect (SHE), which converts the injected longitudinal charge current into the transverse spin current via the spin-orbit interaction, is crucial for the development of spintronic devices. The sign of the spin Hall angle (SHA) describes the direction of the induced transverse current. We perform a systematical analysis of the SHE in the dilute Cu alloys doped with a series of 5d elements, by the combined approach of density functional theory and Hartree-Fock approximation. We find out that not only the spin orbit interactions (SOI) in the 5d orbitals, but also the SOI in the 6p orbitals and the local correlations effects in the 5d orbitals of the impurities, are decisive to the sign of the SHA. Including all of these factors properly, we predict the sign of SHA for each alloy in the series, different from the previous theoretical calculations [1,2]. A positive SHA is obtained for CuIr alloys [3,4], which is consistent with experiment [5], while negative SHA are obtained for several alloys including CuOs and CuRe. Furthermore, we analyze the possibility to control the sign of SHA among the Cu alloys doped with 5d elements.

References:

[1] A. Fert, P. M. Levy, *Phys. Rev. Lett.* 106, 157208 (2011)

[2] A. Johansson, C. Herschbach, D. V. Fedorov, M. Gradhand, and I. Mertig, *J. Phys.: Condens. Matter* 26, 274207 (2014)

[3] Z. Xu, B. Gu, M. Mori, T. Ziman, and S. Maekawa, *Phys. Rev. Lett.* 114, 017202 (2015)

[4] Z. Xu, B. Gu, M. Mori, T. Ziman, and S. Maekawa, arXiv: 1411.7733

[5] Y. Niimi, M. Morota, D. H. Wei, C. Deranlot, M. Basletic, A. Hamzic, A. Fert, and Y. Otani, *Phys. Rev. Lett.* 106, 126601 (2011)

Th.I.2_O6 - Evidence of magnonic charge pumping in single layers of permalloy

A. Azevedo¹, R. Cunha¹, F. Estrada^{1,3}, O. Alves-Santos¹, J. Mendes¹, L. Vilela-Leão¹, R. Rodríguez-Suárez^{1,2}, S. Rezende²

1. Federal University of Pernambuco, Recife, Brazil

2. Pontificia Universidad Católica de Chile, Santiago de Chile, Chile

3. Universidad Michoacana de San Nicolás de Hidalgo, Morelia, Mexico

The generation of a DC voltage in single layers of Permalloy (Py=Ni₈₁Fe₁₉) when the magnetization is undergoing ferromagnetic resonance has been recently reported by few groups [1,2]. This phenomenon needs to be well understood because it affects the electrical measurements of the spin pumping voltage in ferromagnet/non-magnetic (FM/NM) metallic bilayers. In order to understand further the origin of the DC voltage generated in single layer of Py we investigated the angular dependence of the voltage for a series of films varying the thickness as described above. As well known in spin pumping experiments using bilayers of FM/NM, the voltage measured along the NM layer can be interpreted as a superposition of the spin pumping contribution (VSP) and the anisotropic magnetoresistance contribution (VAMR). In a previous paper we showed[3] that depending on the angular position, VAMR has symmetric and antisymmetric components in field scan, whereas VSP has only a symmetric component. Here we show that the in-plane dependence of both symmetric and antisymmetric signals cannot be explained as due to galvanomagnetic effects only. The results are well explained by a model that takes into account the addition to the anisotropic magnetoresistance signal the contribution of the recent discovered effect of magnonic charge pumping (MCP)[4] that converts magnetization dynamics into charge current by means of the spin orbit coupling. In our films we have shown that the perpendicular anisotropy field that arises as due to the symmetry breaking at the surface of the films can support the origin of the MCP effect. Research supported in Brazil by the agencies CNPq, CAPES, FINEP and FACEPE, in México by CONACYT and in Chile by the FONDECYT No. 1130705.

References:

- [1] A. Tsukahara, et al., Phys. Rev. B 89, 235317 (2014)
- [2] A. Azevedo, et al., Appl. Phys. Lett., 104, 152408 (2014)
- [3] A. Azevedo, et al., Phys. Rev. B 83, 144402 (2011)
- [4] C. Ciccarelli, et al. , Nature Nanotech. 10, 50-54 (2015)

Th.I.3_O1 - Self-assembled magnetic nanodot arrays growing on diblock copolymer templates: An in-situ study combining GISAXS and NRS.

D.Erb², K. Schlage¹, R. Röhlberger¹

1. *Deutsches Elektronen-Synchrotron DESY, Hamburg, Germany*

2. *University of Hamburg, Hamburg, Germany*

Large-area nanopatterning via self-assembly has gained considerable interest as an alternative to lithography-based techniques for nanostructure fabrication. We propose a routine for preparing highly ordered metallic nanostructure arrays using exclusively self-assembly processes. Further, we present in-situ structural and magnetic investigations of Fe nanodot arrays during formation by means of synchrotron-based resonant and non-resonant x-ray scattering techniques.

Periodically nanofaceted substrates are produced by high-temperature annealing of M-plane α -Al₂O₃ (sapphire). These substrates provide a preferential direction for the microphase separation of diblock copolymer thin films into surface-perpendicular chemical nanodomains. This results in templates with a periodic chemical surface patterning with a high degree of lateral long-range order [1]. Certain metals such as iron exhibit a pronounced selectivity for one of the copolymer blocks, and will only wet the corresponding template domains during sputter deposition [2]. Thus, the regular chemical surface pattern is translated into a highly ordered array of uniform three-dimensional metallic nanostructures [3].

This bottom-up preparation routine allows for in-situ investigation of structural and magnetic properties of the highly ordered metallic nanostructures during formation by Grazing Incidence Small Angle X-ray Scattering (GISAXS) and Nuclear Resonant Scattering (NRS): For Fe nanodots growing on diblock copolymer templates, in-situ GISAXS data provide the lateral arrangement of the nanodots and the development of their size and shape during Fe deposition. In-situ NRS yields quantitative information on the evolution of magnetic moment dynamics during nanostructure growth. We observe a phase transition from isotropic superparamagnetic fluctuations of the magnetic moments to anisotropic fluctuations with a frequency in the MHz regime. By combining GISAXS and NRS in an in-situ experiment it is thus possible to relate the stage of nanostructure growth to the magnetic state of the nanostructure array. [3]

References:

[1] S. Park et al., *Science* 323 (2009) 1030

[2] W. A. Lopes et al., *Nature* 414 (2001) 735

[3] D. Erb, Ph.D. thesis, University of Hamburg (2014)

Th.I.3_O2 - Magnetic antidot to dot transition in Co/Pd nanopatterned thin films with perpendicular magnetic anisotropy

M. Krupinski¹, A. Zarzycki¹, A. Szkudlarek², M. Giersig³, M. Marszalek¹

1. Institute of Nuclear Physics Polish Academy of Sciences, Kraków, Poland

2. Academic Centre for Materials and Nanotechnology, AGH University of Science and Technology, Kraków, Poland

3. Department of Physics, Freie Universitat Berlin, Berlin, Germany

The understanding how the patterning affects the magnetic phenomena is an important topic for magnetic recording media, sensors and actuators built as nanostructures on patterned substrates. This work presents magnetic behaviour of antidots and dots of Co/Pd thin films, which are suitable materials for high density magnetic recording. Periodic arrays of magnetic nanostructures have been fabricated by depositing Co/Pd multilayers on polystyrene masks prepared on Si wafers. This approach led to highly ordered magnetic arrays of antidots/dots with periods from 200 nm to 800 nm. Change of the preparation conditions allowed to obtain arrays of separated magnetic islands as well as arrays of antidotes with adjustable sizes. Flat, continuous films were simultaneously prepared on Si substrates as reference samples. The magnetic properties and magnetization switching exhibited strong dependence on the island and antidot size and separation distance. The easy axis of magnetization for all samples was normal to the sample plane. The perpendicular coercivity increased with the increase of antidot size, reaching maximum at 3000 Oe for the antidot size of around 80% of the period, and then diminished to the value of 800 Oe characteristic for flat films. The change was more pronounced at low temperatures and it is related to modification of magnetic domain sizes and shapes observed by MFM. For narrow range of nanostructure sizes, the samples have revealed interesting behaviour, in which a morphologically antidot array behaves magnetically as an array of isolated dots. Additionally, field cooling measurements demonstrated significant amount of paramagnetic phase, which can be associated with magnetic dead phase appearing on the edge of nanostructures. The influence of samples morphology on coercivity and magnetization switching characteristics was also confirmed by the micromagnetic modelling, showing similar trend of magnetic properties changes with size and separation of the nanostructures.

Th.I.3_O3 - Anisotropy and dipolar interactions in an ultra-dense array of single-crystalline cobalt nanowires

T. Blon¹, N. Liakakos¹, C. Achkar¹, I. Camara², M. Bailleul², V. Pierron-Bohnes², Y. Henry², B. Chaudret¹, M. Respaud¹, K. Soulantica¹

1. *Laboratoire de Physique et Chimie des Nano-objets, INSA, Toulouse, France*

2. *IPCMS, UMR7504 CNRS-Université de Strasbourg, Strasbourg, France*

Up to now, ferromagnetic nanowires (NWs) were mainly synthesized by electrodeposition of metals in nanoporous templates resulting in polycrystalline NWs of relatively large diameters and packed at moderate densities. Recently, we reported the epitaxial solution growth of single-crystalline hcp Co nanowires of 6 nm in diameter. Without any template, they grow vertically on a un-patterned Pt(111) film and are spontaneously arranged in hexagonal arrays of 1012 NWs/cm² [1]. These properties confer a high interest of this system in future ultrahigh magnetic recording. We present here a detailed magnetic study of such a Co NW array in terms of coercivity, dipolar interactions and magnetocrystalline anisotropy. Despite important dipolar interactions, a high perpendicular anisotropy is obtained due to the combination of the magnetocrystalline and shape anisotropies which both act along the wire axis: at 300 K, the anisotropy is $K_{\text{eff}} = 2.4 \times 10^5 \text{ J/m}^3$ with a coercive field $H_c = 0.35 \text{ T}$. This coercive field reaches 0.62 T at 4 K, without any Co/Co oxide exchange bias effect. This demonstrates that the NWs are intrinsically oxygen free Co nano-objects. Contrary to electrodeposited nanowires, the measured temperature dependence of H_c cannot be explained by the Stoner-Wohlfarth/Néel-Brown model. On the other hand, the angular dependence of H_c suggests a coherent rotation of the magnetization. The easy axis hysteresis loops are sheared due to dipolar interactions. We demonstrated that the $M(H)$ slope at H_c is related to the packing fraction $P=0.38$ of the NW array. Also, ferromagnetic nuclear resonance measurements indicate a shift in the Co spectra related to the dipolar field and packing fraction. In an alternative approach to understanding the anisotropy, we used ferromagnetic resonance and magnetic torque measurements. Both underline the important dipolar interactions and reveal a magnetocrystalline anisotropy larger than expected suggesting the presence of a surface anisotropy.

References:

[1]. N. Liakakos, Nano Lett. 14 3481 (2014)

Th.I.3_O4 - Reversal mechanism, switching field distribution and dipolar frustrations in Co/Pt bit pattern media based on AAO auto-assembled hexagonal array of nanobumps

T. Hauet¹, L. Piraux², S. K. Srivastava², V. A. Antohe², D. Lacour¹, M. Hehn¹, F. Montaigne¹, J. Schwenk³, M. A. Marioni³, H. J. Hug⁴, O. Hovorka⁵, A. Berger⁵, S. Mangin¹, F. Abreu Araujo²

1. *Institut Jean Lamour, Lorraine, France*

2. *Institute of Condensed Matter and Nanosciences, Belgium*

3. *Empa, Dübendorf, Switzerland*

4. *Institute of Physics, Universität Basel, Switzerland*

5. *CIC nanoGUNE, Gipúzcoa, Spain*

We present a new method for designing low-cost densely-packed magnetic particle assemblies on 2D curved substrates with perpendicular magnetic anisotropy (PMA) [1]. This process involves the growth of magnetic nanocaps on the back of nanoporous anodic alumina templates (AAO), which is a typical self-ordered nanopore-array material formed by the electrochemical oxidation of Al in acidic solutions. As a proof of concept, we have studied a hexagonally close-packed array of [Co(0.4nm)/Pt(0.7nm)]₄ nanocaps deposited on bumps having about 100 nm and 50nm lateral modulation period. During the talk, we will present a careful study of the magnetization reversal mechanisms in such assembly of Co/Pt nanobumps. Using Extraordinary Hall Effect (EHE) and SQUID-VSM measurements, we will provide macroscopic characterization of reversal mechanisms in terms of the switching fields and switching field distribution (SFD) as a function of field angle and temperature [2]. Then bump-by-bump magnetization reversal mechanism will be proved by high-resolution magnetic force microscopy under magnetic field [2]. The role of inter-bump exchange coupling and dipolar coupling are enlightened. We will show that the magnetic hysteresis loops from flat films and bumpy films are very different because of reduction of direct exchange coupling between bumps and because of the triangular lattice. Then we will focus on isolating the origins of switching field distribution (SFD) in this system, namely dipolar interactions, intrinsic anisotropy distribution and template packing faults [2]. Finally we will further discuss the influence of triangular dipolar frustrations on the energy stability of demagnetized and half-switched states based on an Ising model including local exchange coupling, as well as the impact of intrinsic SFD and lattice defects [2].

References:

[1] L. Piraux et al., Appl. Phys. Lett. 101, 013110 (2012)

[2] T. Hauet et al., Phys. Rev. B 89, 174421 (2014)

TH.I.3_O5 - Magnetotransport in La(2/3)Ca(1/3)MnO(3) thin films with on-surface deposited Py nanostructures

W. Yanez¹, V. Vlaminck¹, J. Hoffman², A. Hoffmann², D. Niebieskikwiat¹

1. *Universidad San Francisco de Quito, Quito, Ecuador*

2. *Argonne National Laboratory, Argonne, United States*

We study the magnetotransport properties of thin films of La(2/3)Ca(1/3)MnO(3) with Permalloy (Py) nanodots deposited on the film surface, as a function of temperature, magnetic field and the size of the nanodots (100 and 200nm). Results of electrical resistivity show that there is a local proximity effect of the Py nanodots on the manganite film, associated to an interface exchange interaction. To some extent, this effect can be regarded as an applied magnetic field, i.e. electrical resistivity is reduced and the insulator-to-metal transition is shifted to higher temperatures.

Th.J.1_I1 - Advances in Magnetic Structure Determination. Instruments and Methods

J. Rodriguez-Carvajal¹

1. Institut Laue-Langevin, Grenoble, France

Magnetic Crystallography concerns the description and determination of the magnetization density in solids. A magnetic structure is a particular spatial arrangement of magnetic moments setting up below the ordering temperature. The determination of magnetic structures is mainly done using neutron diffraction (powder and single crystals) and in special cases the use of polarized neutrons is necessary to solve ambiguities in the interpretation of neutron diffraction data. The importance of magnetic structures for understanding the electronic and magnetic properties of condensed matter is testified by the huge number and impact of scientific papers appearing from the beginning of the nineties concerned with spin ordering in superconductors, giant magnetoresistance compounds, frustrated magnets and multiferroics. The symmetry properties of magnetic structures are traditionally described using two different approaches: the magnetic Shubnikov groups [1] and the group representation analysis [2-3]. Contrary to the major part of periodic arrangement of atoms, many magnetic structures are non-commensurate: the periodicity of the magnetic moments is not commensurate with the underlying crystal structure; this is one of the reasons why the representation approach is presently dominant. In this talk we shall describe briefly how these approaches work and the advantages of the new trend towards the use of magnetic superspace groups [4]. A review of the most important methods in magnetic neutron scattering as well as in the symmetry concepts will be presented. The current analytical tools and methods for determining magnetic structures and their symmetry will briefly be described.

References:

- [1] W. Opechowski, Crystallographic and Metacrystallographic Groups, Elsevier Science Publishers B.V., Amsterdam 1986
- [2] E.F. Bertaut, Acta Cryst A24, 1968, 217
- [3] Y.A. Izyumov, V.E. Naish and R.P. Ozerov, Neutron diffraction of magnetic materials, Plenum Publishing Corporation, New York 1991
- [4] J.M. Pérez-Mato, J.L. Riberiro, V. Petricek and M.I. Aroyo, J. Phys.: Condens. Matter 24 (2012), 163201

Th.J.1_O2 - A case study in magnetic pair distribution function (mPDF) analysis: local magnetic structure of MnO

B. Frandsen¹, S. Billinge^{2,3}

1. Department of Physics, Columbia University, United States

2. Department of Applied Physics and Applied Mathematics, Columbia University, United States

3. Condensed Matter Physics and Materials Science, Brookhaven National Laboratory, United States

The magnetic pair distribution function (mPDF) has recently been introduced as a method for quantitatively investigating local magnetic structure through neutron total scattering measurements. In analogy with the more familiar atomic pair distribution function (PDF), this technique involves Fourier transforming Bragg and diffuse scattering to access both short- and long-range correlations directly in real space, providing a highly intuitive view into the local magnetic structure of a material. Here, we present neutron total scattering measurements of the canonical antiferromagnet MnO as the first experimental demonstration of this new technique. Our analysis successfully recovers the known antiferromagnetic structure of MnO, thus verifying the recently derived mPDF equations. Combined atomic and magnetic PDF refinements suggest a local monoclinic distortion at low temperature with a preferred spin axis along the pseudocubic [11-2] direction. We have also conducted temperature-dependent measurements to investigate quantitatively the temperature evolution of the magnetic correlations in this material, including the short-range correlations that persist well above the Neel temperature. The successful application of the mPDF technique to MnO is a promising development and suggests that this technique can be a valuable tool for studying local magnetic structure in a wide class of materials.

Th.J.1_O3 - Magnetic behavior of a $\text{Mn}_{0.85}\text{Co}_{0.15}\text{WO}_4$ multiferroic crystal investigated by Resonant magnetic x-ray scattering

J. Herrero-Martín^{1,2}, A.N. Dobrynin³, C. Mazzoli⁴, P. Steadman³, P. Bencok³, R. Fan³, A.A. Mukhin⁵, V. Skumryev^{6,7}, J. L. García-Muñoz²

1. ALBA Synchrotron Light Source, Barcelona, Spain
2. Institut de Ciència de Materials de Barcelona (ICMAB-CSIC), Barcelona, Spain
3. Diamond Light Source, Didcot, Oxfordshire, United Kingdom
4. Dipartimento di Fisica, Politecnico di Milan, Milan, Italy
5. Prokhorov General Physics Institute, Russian Academy of Science, Moscow, Russia
6. Institució Catalana de Recerca i Estudis Avançats (ICREA), Barcelona, Spain
7. Departament de Física, Universitat Autònoma de Barcelona, Barcelona, Spain

Magnetically frustrated MnWO_4 (Hübnerite) and the $(\text{Mn},\text{Co})\text{WO}_4$ extended family are considered reference models where to study the mutual interaction between spins and polar orders and to investigate the magnetic control of the electric polarization. In $\text{Mn}_{1-x}\text{Co}_x\text{WO}_4$ improper multiferroics (MFs) Co favors a strong competition between its magnetocrystalline anisotropy (McA) and the Mn-Mn exchange interactions, stabilizes the ferroelectric (FE) behavior of MnWO_4 and produces an extraordinarily rich T-x phase diagram with a large number of different FE phases and magnetic structures. This family of MFs is intrinsically inhomogeneous since the two different magnetic ions (Mn and Co) occupy the same crystallographic position. In this work we investigate the precise magnetic behavior of a MF crystal of the critical composition $\text{Mn}_{0.85}\text{Co}_{0.15}\text{WO}_4$ above its FE transition. Resonant x-ray magnetic scattering (RXMS) experiments have allowed us to study the collinear AF4 phase of $\text{Mn}_{0.85}\text{Co}_{0.15}\text{WO}_4$ beyond the average description provided by neutron diffraction. Thanks to RXMS chemical selectivity we have observed that Co moments arrange antiferromagnetically following their own strong uniaxial McA, although the collinear order of Mn spins point to a different direction. This implies intrinsic remarkable deviations of the spin arrangement at local scale from the description extracted from neutron data. These element-resolved magnetic results call for reexamining the phase diagram of this model family of MFs beyond the average descriptions previously used.

Th.J.1_O4 - Disentangling the spin and orbital moments in the heavy fermion system CeRu₂Al₁₀ using polarised x-rays

P. Dean¹, P. Hatton¹, A. Dobrynin², T. Takabatake³, Y. Muro³

1. *Department of Physics, Durham University, United Kingdom*

2. *Diamond Light Source, Harwell Science and Innovation Campus, Didcot, Oxfordshire, United Kingdom*

3. *Institute for Advanced Materials Research, Hiroshima University, Hiroshima, Japan*

Non-resonant magnetic x-ray scattering (NRMXS) is a technique that is sensitive to both the orbital and spin magnetic moments of a system, however NRMXS is very weak so very high quality crystals are required. NRXMS can be used to determine the ratio of spin and orbital moments[1][2]. Resonant x-ray scattering (RXS), taking advantage of the polarisation dependence of magnetic scattering and can be used to determine complex spin (spin-orbit coupled J moment) structures in systems as it is highly directionally sensitive and small spin cantings can be measured and quantified. RXS has the advantage of element selectivity as well as a many-fold increase in the observed signal[3][4][5]. By combining these two techniques a number of other parameters can be determined as well as the spin-orbit ratio we can now experimentally verify the sign of the spin-orbit coupling. We are also able to determine a spin and orbital magnetic structures. We have studied CeRu₂Al₁₀ that has a complex cage-like structure surrounding the cerium atoms with large bond distances. From the Ce-Ce separation the magnetic transition temperature (as predicted by the RKKY interaction) is expected to be around 2 K, in reality transitions are observed close to 30 K[6]. CeRu₂Al₁₀ is a Kondo semiconducting heavy fermion system, which displays similar properties in its phase transitions to those of the hidden order transition in the heavy fermion superconductor URu₂Si₂[7][8]. Many systems studied to date using NRMXS have been 3d transition metal oxide perovskite structures in which the orbital moment is quenched by the crystalline electric field. In CeRu₂Al₁₀ the cerium orbital moment is expected to be largely unquenched as the nearest neighbors are separated by >3Å so any crystal field quenching will be minimal this is compounded by the fact that the magnetism is contained within the highly localized f-orbitals which are screened by the outer electrons.

References:

- [1] J.P.Hill and D.F.McMorrow, *Acta.Cryst.*, A52:236,1996
- [2] V.Fernández, C.Vettier, et al. *Phys.Rev.B* 57:7870,1998
- [3] J.P.Hannon, G.T.Trammell, et al. *Phys.Rev.Lett.*, 61:1245,1988
- [4] C.Detlefs, M.Sanchez del Rio, and C.Mazzoli. *Eur.Phys.J Spec.Top.*, 208:359,2012
- [5] M.Blume and D.Gibbs. *Phys.Rev.B*, 37:1779,1988
- [6] T.Nishioka and Y.Kawamura et al. *J.Phys.Soc.Jpn.*, 78:123705,2009
- [7] E.D.Isaacs, D.B.McWhan et al. *Phys.Rev.Lett.*, 65:3185,1990
- [8] C.S.Lue, H.F.Lui et al. *Phys.Rev.B*, 85:245116,2012

Th.J.1_O5 - First-principles molecular spin dynamics study on the magnetic structure of mn-based alloys with Cu₃Au-type crystal structureT. Uchida¹, N. Kimura¹, Y. Kakehashi²1. *Hokkaido University of Science, Hokkaido, Japan*2. *University of the Ryukyus, Okinawa, Japan*

The Mn-based ordered alloys Mn₃X (X=Pt, Rh, Ir) with a Cu₃Au-type crystal structure are known as three-dimensional frustrated itinerant magnets in which anti-ferromagnetic Mn local magnetic moments form an octahedron. Neutron diffraction experiments suggest that below the Neel temperature Mn₃Rh and Mn₃Ir exhibit a single ordered phase: triangular magnetic structure, while Mn₃Pt exhibits two ordered phases: triangular magnetic structure for T < 400K and collinear antiferromagnetic structure for 400K < T < 475K, the latter phase accompanying tetragonal distortion with volume expansion. The physical origin of their magnetic structure has not been clarified yet. In order to understand the magnetic structure from the theoretical point of view, we have investigated the magnetic structure by means of the first-principles Molecular Spin Dynamics (MSD) method [1,2]. The theory is based on the first-principles TB-LMTO Hamiltonian combined with the functional integral method and the isothermal MSD technique, and allows us to determine automatically the magnetic structures of itinerant magnets at finite temperatures. In the present analysis, we have adopted 4*4*4 Cu₃Au unit cells for MSD calculations, and fixed the volume to their room-temperature values. Numerical results at 25 K for Mn₃X (X=Pt, Rh, Ir) show triangular magnetic structure, being consistent with experiment. With increasing temperature from 25 K, Mn₃Pt exhibits first-order transition to a low-moment phase around 350K accompanying the development of Mn-Eg DOS peak at Fermi energy, while Mn₃Rh and Mn₃Ir show no such transition below the Neel temperature. We present detailed results of analysis of the magnetic structure by means of the MSD using site-dependent effective medium.

References:

- [1] Y. Kakehashi, S. Akbar, and N. Kimura, PRB 57, 8354 (1998)
- [2] T. Uchida, N. Kimura, and Y. Kakehashi, JKPS 62, 1748 (2013)

Th.J.2_I1 - On the dual fermion approach to charge order, spin frustration, and transport

S. Kirchner¹

1. Center For Correlated Matter, Zhejiang University, Hangzhou, China

Self-consistent dynamical approximations for strongly correlated fermion systems are particularly successful in capturing the dynamical competition of local correlations. In these, the effect of spatially extended degrees of freedom is usually only taken into account in a mean field fashion or as a secondary effect. As a result, critical exponents associated with phase transitions of the model have mean field character. Here, we demonstrate that a particular diagrammatic multijscale method, the dual fermion method[1], anchored around local approximations are indeed capable of capturing the non meanfield nature of the critical point of the lattice model and to correctly describe the transition to mean field like behavior as the number of spatial dimensions increases [2]. In spin models with frustrated interactions, relevant to a wide range of materials, e.g. the charge-transfer salts, the layered cobaltates, the delafossites, this approach is able to capture the dynamic interplay between electronic correlation and geometric frustration [3]. The dual fermion method can be extended to tackle systems far from equilibrium and has recently been used to interpret nonlinear transport data in strongly correlated nanostructures[4,5]. Strongly correlated electron systems, dynamical mean field theory and its extensions, dual fermions.

References:

- [1] A. N. Rubtsov, M. I. Katsnelson, and A. I. Lichtenstein, PRB (2008) 77, 033101
- [2] A. Antipov, E. Gull, & S. Kirchner, PRL, (2014) 112, 226401
- [3] G. Li, A. E. Antipov, A. N. Rubtsov, S. Kirchner, & W. Hanke, PRB(R) (2014) 89, 161118
- [4] E. Munoz, C. Bolech, & S. Kirchner, PRL, (2013) 110, 016601
- [5] E. Munoz, C. Bolech, & S. Kirchner, PRL, (2013) 111, 089702

Th.J.2_O2 - Colossal thermopower deep inside the SDW state of (TMTSF)₂PF₆

Y. Machida¹, X. Lin³, K. Izawa¹, W. Kang², K. Behnia³

1. *Tokyo Institute of Technology, Tokyo, Japan*

2. *Ewha Womans University, Seoul, Republic of Korea*

3. *ESPCI, Paris, France*

We present a study of low-temperature Seebeck coefficient of (TMTSF)₂PF₆, the first pressure-induced organic superconductor. At ambient pressure, the system undergoes a Spin-Density-Wave transition at $T_{\text{SDW}} \sim 12$ K. In the ordered state, the opening of the gap leads to an activated electric conductivity and a large thermoelectric response. Below 1K, the resistivity saturates in the Variable Range Hopping (VRH) regime. By extending for the first time the Seebeck coefficient measurements below 1K, we uncovered an extraordinary large thermoelectric response in the VRH regime. The Seebeck coefficient was found to attain the colossal value of $S \sim -40$ mV/K. This is by far the largest Seebeck coefficient reported in any system in this temperature range and points to an unidentified source of entropy available to hopping electrons not seen in other semiconductors.

Th.J.2_O4 - Determination of the sign of the Dzyaloshinskii-Moriya interaction in crystals

Andrei Rogalev¹, V. E. Dmitrienko², F. de Bergevin¹, E. N. Ovchinnikova³, F. Wilhelm¹, J. Kokubun⁴

1. ESRF, Grenoble, France
2. Institute of Crystallography, Moscow, Russia
3. Moscow State University, Moscow, Russia
4. Tokyo University of Science, Tokyo, Japan

Dzyaloshinskii-Moriya (DM) interaction, which is characterized by the so-called DM vector, is the key element in the physics of multiferroics, that's why so many efforts are devoted to its theoretical and experimental studies. However, the value and the sign of DM vector are not determined by symmetry and depend on details of magnetic and electronic structures. There were very sophisticated ab-initio calculations of the DM vector [1] but they are still waiting for experimental proof. Recently it was shown [2] that the DM sign could be deduced from resonant X-ray scattering experiment but interpretation relies on results of very sophisticated calculations. Another method using X-ray diffraction was recently suggested [3] to measure the sign of the DM vector in crystals. It is based on the interference between non-resonant magnetic scattering and multiple wave diffraction (which acts as a reference wave) which makes this approach model independent. However to make the interference observable one has to use circularly polarized X-rays at photon energies chosen to be far from an absorption edge. We have applied this new technique to a hematite Fe_2O_3 single crystal in which absence of local inversion symmetry gives rise to DM interaction which in turn leads to a small canting of Fe spin magnetic moments. The obtained experimental results show astonishingly good agreement with those of multiple-wave calculations and allow us to unambiguously determine the sign of the Dzyaloshinskii-Moriya interaction in hematite. The developed technique can be used even for not very perfect crystals.

References:

- [1] V.V. Mazurenko and V.I. Anisimov, Phys. Rev. B 71, 184434 (2005)
- [2] V.E. Dmitrienko et al, Nature Physics 10, 202 (2014)
- [3] V. E. Dmitrienko et al, JETP Lett. 92, 383 (2010)

Th.J.2_05 - Spin excitons in heavy fermion semi-metals

P. Riseborough¹

1. Physics Department, Temple University, Philadelphia, United States

Recently, a spin exciton dispersion relation has been observed in the paramagnetic semi-metal $\text{CeFe}_2\text{Al}_{10}$ via inelastic neutron scattering. The dispersion relation exhibits a characteristic minimum at the same reciprocal lattice vector that characterizes the antiferromagnetic state of a related compound. This coincidence, suggests that the spin exciton is a signature of pre-critical fluctuations. We investigate a theoretical model which describes a Lifshitz transition between the heavy fermion semi-conducting and the heavy fermion semi-metallic states. We relate the DOS states to the DOS inferred from experiments and investigate the effect of doping on the magnetic states.

Th.J.3_I1 - Anatomy of Dzyaloshinskii-Moriya Interaction at Co/Pt Interfaces

H. Yang¹, A. Thiaville², S. Rohart², A. Fert³, M. Chshiev¹

1. Univ. Grenoble Alpes, INAC-SPINTEC, Grenoble, France; CNRS, SPINTEC, Grenoble, France; And CEA, INAC-SPINTEC, Grenoble, France

2. Laboratoire de Physique des Solides, Univ. Paris-Sud, Orsay, France

3. Unité Mixte de Physique CNRS/Thales, Palaiseau, France and Univ. Paris-Sud, Orsay, France

Dzyaloshinskii-Moriya Interaction (DMI) [1] is recognized recently to play a crucial role at ferromagnetic (FM) and heavy nonmagnetic metals (NM) interfaces to create magnetic skyrmions [2]. DMI also plays an essential role for fast domain wall dynamics driven by spin-orbit torques [3]. Here, we clarify the main features and microscopic mechanisms of DMI in Co/Pt bilayers by ab-initio calculations. We find that the large anticlockwise DMI of the bilayers has a predominant contribution from DMI pair couplings between the spins of interfacial Co layer. This DMI between the interface Co spins is directly related to the change of the SOC energy in the adjacent Pt layer when the Co spin chirality is reversed consistent with Fert-Levy picture [4]. We found next that DMI does not extend significantly into other Co layers and is very weak between the proximity-induced spins in Pt. It was suggested [5] that DMI at FM/NM interfaces is directly related to the proximity induced moment in NM. However, we find the opposite result, i.e. Pt moment reduction slightly increases the DMI [6]. We performed calculations for other bilayers and found DMI of clockwise chirality for Co/Au and Co/Ir interfaces. The finding of opposite chiralities for Pt and Ir when both are below or both above Co leads to the interesting prediction of additive effects and large DMI when Co is between Pt and Ir.

References:

- [1] I. E. Dzyaloshinskii, Sov. Phys. JETP 5, 1259 (1957); T. Moriya, Phys. Rev. 120, 91 (1960)
- [2] A. Fert et al. Nat. Nanotech. 8, 152 (2013)
- [3] A. Thiaville, et al, Europhys. Lett. 100, 57002 (2012)
- [4] A. Fert and P. Levy, Phys. Rev. Lett. 44, 1538-1541 (1980)
- [5] K. Ryu et al, Nat. Nanotech. 8, 527 (2013)
- [6] H. Yang et al, arXiv:1501.05511

TH.J.3_O2 - Thermodynamic Properties of Pr_{1-x}Dy_xCoO₃ PerovskiteN.K. Gaur¹, R. Thakur¹*1. Barkatullah University, Bhopal, Madhya Pradesh, India*

The interest in LaCoO₃ cobaltates is associated with an occurrence of thermally induced transitions from low-spin (LS) to high-spin (HS) or intermediate-spin (IS) state as well as with a possibility to vary the transport and magnetic properties by heterovalent substitution on the La and/or Co sites. The parent compound lanthanum cobaltate LaCoO₃ shows an insulating ground state based on the diamagnetic LS state of Co^{III} ions. At room temperature LaCoO₃ and lanthanum gallate LaGaO₃ possess rhombohedrally distorted crystal structure of perovskite. The main focus of the present paper is to investigate the effect of isovalent substitution in LaCoO₃ of diamagnetic gallium ions Ga³⁺ with a completely filled 3d shell (3d¹⁰) for paramagnetic ions Co³⁺ with a partially filled 3d shell (3d⁶) on the elastic and thermal properties formed LaCo_{1-x}Ga_xO₃ as promising materials for fabricating membranes and other articles for electronic technology.

The specific heat and thermal expansion coefficient of LaCo_{1-x}Ga_xO₃ (0.01≤x≤1) has been studied as a function of temperature (10K≤T≤1000K) by means of a Rigid Ion Model (RIM) after modifying its framework to incorporate the van der Waals interactions. In this paper the functional relation between charge and size mismatch and the thermal properties is determined and compared with the available reports. The Debye temperatures obtained from the lattice contributions are found to be in somewhat closer agreement with the available experimental data. The thermal expansion and specific heat values revealed by using MRIM are in closer agreement with the available experimental data for some concentrations (x) of LaCo_{1-x}Ga_xO₃. In addition, the results on the bulk modulus (B), cohesive energy (ϕ), molecular force constant (f), Reststrahlen frequency (u_o) and Gruneisen parameter (γ) are also discussed.

Th.J.3_O3 - Stoner Magnetism in an Inversion Layer

D. Golosov¹

1. Dept. of Physics and the Resnick Institute, Bar-Ilan University, Ramat Gan, Israel

Motivated by recent experimental work on magnetic properties of Si-MOSFETs, we perform a calculation of magnetisation and susceptibility of electrons in an inversion layer, while taking into account the co-ordinate dependence of electron wave function in the direction perpendicular to the plane. It is assumed that the inversion-layer carriers interact via a contact repulsive potential, which is treated at a mean-field level, resulting in a self-consistent change of profile of the wave functions. We find that the results differ significantly from those obtained in the pure 2DEG case (where no provision is made for a quantum motion in the transverse direction). Specifically, the critical value of interaction needed to attain the ferromagnetic (Stoner) instability is decreased, and the Stoner criterion is therefore relaxed. Results are discussed in the context of the available experimental data.

Fr.A.1_I1 - Magnetic Properties of FeCo₂B and the effect of doping by 5d elements

A. Edström¹, M. Werwinski¹, J. Ruzs¹, O. Eriksson¹, K.P. Skokov², I.A. Radulov², S. Ener², M. D. Kuz'min², J. Hong², M. Fries², D.Y. Karpenkov², O. Gutfleisch², P. Toson³, J. Fidler³

1. Uppsala University, Uppsala, Sweden

2. Technische Universität Darmstadt, Darmstadt, Germany

3. Vienna University of Technology, Wien, Austria

We present a thorough investigation, combining electronic structure theory and experiments, into the magnetic properties of the tetragonal (FeCo)₂B system. This system is interesting e.g. in the context of novel permanent magnet materials due to relatively large magnetocrystalline anisotropy energy (MAE) in a certain range of alloy concentrations. We briefly discuss challenges in obtaining a good description of the alloy from the theory perspective. After obtaining a good understanding of the ternary (FeCo)₂B system, we address the question of how to further improve the MAE of this material. We show, using density functional theory based calculations, that the MAE can be increased substantially by doping small amounts, 2.5-5 at.%, of certain 5d elements on the FeCo site which is then verified in experiments.

Fr.A.1_O2 - Magnetic field effects on reaction-sintering of MnBi

Y. Mitsui¹, K. Abemitsu¹, R.Y. Umetsu², K. Takahashi², K. Koyama¹

1. Graduate School of Science And Engineering, Kagoshima University, Kagoshima, Japan

2. Institute for Materials Research, Tohoku University, Miyagi, Japan

Ferromagnetic compound MnBi has known to have a large magnetic anisotropy above room temperature. It is reported that in-field heat treatment realized the change of phase equilibrium and anisotropic microstructure of Bi-Mn alloy [1,2]. In addition, recently, we found that the solid-state reaction sintering process from Mn + Bi to MnBi was also influenced by magnetic fields [3]. In general, liquid-state sintering is denser than solid-state sintering. Therefore, investigation of magnetic field effects on liquid-state sintering is also necessary for improving the magnetic properties of Bi-Mn alloy. In this study, magnetic field effects on solid-state and liquid-state reaction sintering of MnBi were investigated. Crystal orientation, fraction of the ferromagnetic MnBi phase, and magnetic properties were evaluated by X-ray diffraction and magnetization measurements. It is found that reacted fraction of MnBi were enhanced by the application of magnetic field of 15 T for solid-state sintering. In contract to this, the enhancement of reaction was not observed clearly for liquid-state sintering. The fraction of ferromagnetic MnBi phase synthesized by in-field heat treatment was 80wt.%. Both of in-field solid-state and liquid-state sintered samples realized the highly crystal orientation of MnBi phase along the magnetic field direction. The Lotgering factor of the MnBi phase reached to be ~1. Due to the crystal orientation, anisotropic magnetic properties exhibits for in-field sintered samples. The anisotropy field of the sample was evaluated to be 4 T.

References:

- [1] Y. Mitsui, et al., Mater. Trans. 54 (2013) 242-245
- [2] Y. Liu et al., Solid State Commun. 138 (2006) 104-109
- [3] Y. Mitsui, et al., J. Alloy. Compd. 615 (2014) 131-134

Fr.A.1_O3 - The importance of strong electronic correlations in rare-earth free hard magnets

F. Ronning¹, J. Zhu¹, M.Janoschek¹, R. Rosenberg², J. Criginski Cezar³, E. Bauer¹, C. Batista¹, J.Thompson¹

1. *Los Alamos National Laboratory, United States*

2. *Advanced Photon Source, Argonne National Laboratory, United States*

3. *Laboratório Nacional de Luz Síncrotron, Brazil*

Correlated electron effects, which are normally underestimated in band-structure calculations, play a crucial role in the development of the orbital component of the magnetic moments in many materials. Because magnetic anisotropy arises from this orbital component, the ability to include correlation effects has profound consequences on our predictive power of the magneto crystalline anisotropy energy (MAE) of strong magnets. We show that incorporating the local effects of electronic correlations with dynamical mean-field theory provides reliable estimates of the orbital moment (measured by XMCD), the mass enhancement (measured by heat capacity), and the MAE of YCo₅ [1]. In addition, due to the importance of electronic correlations on the MAE we argue that one can adopt a 'molecular' type approach to designing new hard magnet materials. One such material we investigate is Fe₃GeTe₂, which despite its low Curie temperature is useful to test design principles. XMCD and heat capacity measurements illustrate that electronic correlations are again effective in producing a large MAE in Fe₃GeTe₂, and suggest additional routes to develop new materials.

References:

[1] J.-X. Zhu, et al. Phys. Rev. X, 4, 021027 (2014)

Fr.A.1_O4 - BH enhancement in SrFe₁₂O₁₉ hybrid nanocomposites

A.M. Aragón¹, A. Quesada², A. Bollero³, S. Deledda⁴, J.F. Fernández², A. Hernando¹, P. Marín¹

1. Instituto De Magnetismo Aplicado (UCM-ADIF), Las Rozas, Madrid, Spain

2. Instituto de Cerámica y Vidrio, CSIC, Madrid, Spain

3. IMDEA Nanoscience, Madrid, Spain

4. Institute for Energy Technology, Kjeller, Norway

The increasing demand of permanent magnets has boosted research to reduce the use of rare earths in their production [1]. A number of studies have been carried out to obtain biphasic materials composed of a hard magnetic phase and a soft one, coupled by exchange magnetic interaction. [2, 3] In this work, we have fabricated hybrid isotropic nanocomposites made of Sr-ferrite and ferromagnetic metals. We have used SrFe₁₂O₁₉ (H_c=4550 Oe and M_s(2T)=70 emu/g) as hard phase and Fe and FeCo-rich milled nanocrystalline powder (H_c=3-70 Oe, M_s(2T)=150 and 200 emu/g) as soft phase. A high energy ball milling procedure has been developed to obtain a homogeneous dispersion. Structural properties of the individual phases are preserved during milling. No amorphization or decomposition in secondary phases was observed. The average particle size of the soft phase is well above the critical threshold for effective exchange-coupling, nevertheless, magnetic properties were surprisingly improved in the nanocomposite. An enhancement of 27% in maximum energy product was reached as a consequence of 14% increase in remanence value, 17% increase in magnetic saturation and 28% decrease in coercivity. Recoil and DC demagnetization curves were carried out in order to elucidate the nature of the magnetic interactions between hard and soft phases, observing some of the typical features of exchange-spring magnets. For instance, a higher slope was observed in nanocomposites recoil curves as compared with pure Sr-ferrite. Susceptibility values were 2.4·10⁻⁴ for SrFe₁₂O₁₉ and 4.8 · 10⁻⁴ for the hybrid nanocomposite. In addition, the remanence to intrinsic coercivity ratio was 1.25. Finally, single phase behaviour was confirmed by analysing the switching field from the derivative hysteresis loop at 5K. These results suggest the possibility of improving the magnetic properties in hard-soft composites without the need for average particle sizes of the soft phase below the critical threshold.

Acknowledgements:

This work was supported by Project FP7-NMP-2012-SMALL-6 NANOPYME “Nanocrystalline Permanent Magnets Based on Hybrid Metal-Ferrites” (nº 310516).

References:

[1] <http://nanopyme-project.eu/>

[2] Hadjipanayis, G. JMMM 200, (1999) 373-391

[3] M.J. Molaei et al. Materials Characterization 101 (2015) 78-82

Fr.A.1_O5 - Magnetism of ferromagnetic bulk MnBi phases made from MnBi nanoparticlesE. Skoropata^{1,2}, J. Freeland³, M. Rowe², J. van Lierop¹*1. University of Manitoba, Winnipeg, Canada**2. Toyota Research Institute of North America, Chicago, United States**3. Argonne National Laboratory, Lemont, United States*

Due to MnBi having the unique quality of an increasing magnetic anisotropy with rising temperature, for over fifty years MnBi-based systems have been investigated for fundamental interest, and recently pursued aggressively as a rare-earth replacement in permanent magnet composites. To date, the required low-temperature phase (LTP) has been produced mainly in small quantities using laborious methods such as melt spinning followed by numerous grinding and heating processes. We have developed a novel synthesis for large (gram-scale) quantities of MnBi nanoparticles using a wet chemical method, followed by a single hot press sintering to create bulk MnBi. Hysteresis (M(H)) loops of the as-made MnBi indicated a ferromagnetic phase with a small saturation magnetization and coercivity ($M_S = 0.084$ emu/g and $H_C = 170$ Oe; $BH_{max} = 1 \times 10^{-3}$ MGOe at 400 K), and $H_C(T)$ which decreased with increasing temperature; a non-LTP ferromagnetic phase. Hot pressing nanoparticles at 150°C to 160°C for 1 to 4 hours resulted in bulk samples with large H_C 's having the LTP's requisite positive $H_C(T)$; $H_C = 11.7 - 15.4$ kOe and $BH_{max} = 0.2 - 3.4$ MGOe at 400 K. Interestingly, M(H) shapes indicated multiple ferromagnetic phases whose preferential formation resulted from pressing conditions. X-ray absorption spectra over the Mn L_{3,2} edges showed octahedrally coordinated Mn with clear d₅ configuration multiplet features, indicating electron localization. This suggested that a change in stoichiometry or microstructure, rather than Mn coordination environment, was the source of the changes in the overall magnetism. X-ray magnetic circular dichroism (XMCD) spectra of the as-made MnBi show virtually no detectable signal, indicating a very weak Mn magnetization, while the pressed MnBi samples all exhibited XMCD spectra at 10 K in 25 kOe; results consistent with the substantial improvements to the overall magnetism between as-made and hot pressed systems. Our novel synthesis and processing approach produces high anisotropy LTP MnBi, providing a new and simple route to preparing this highly desirable magnetic material.

Fr.A.2_I1 - Micromagnetics of rare-earth efficient permanent magnets?

T. Schrefl^{1, 2, 3, 4, 5}

1. *Center For Integrated Sensor Systems, Danube University Krems, Austria*
2. *St. Poelten University of Applied Sciences, St. Poelten, Austria*
3. *Universität Duisburg-Essen, Duisburg, Germany*
4. *Technische Universität Darmstadt, Darmstadt, Germany*
5. *Toyota Motor Corp., Toyota City, Japan*

Through the advance in computer methods classical experiments in permanent magnets can be explained by micromagnetic simulations. We show that the angle dependence of coercivity in hot deformed $\text{Nd}_2\text{Fe}_{14}\text{B}$ based magnets may be attributed to surface defects with a thickness of 1 nm to 3 nm. The grain size dependence of the coercive field of permanent magnets was found to be a result of local demagnetizing field that cause the nucleation of reversed domains near the edges of the grain. Using micromagnetic simulations we investigate the potential of multiphase nano-structured permanent magnets that show excellent magnetic properties with a reduced rare earth content. Based on micromagnetic simulations we propose a magnet with a grain size of around 100 nm. Each grain has a core-shell structure. The shell with a thickness of around 3 nm to 4 nm is made of $\text{Nd}_2\text{Fe}_{14}\text{B}$. The core might be a single semi-hard phase made of $(\text{FeCo})_2\text{B}$ or a nano-structured mixture of $\text{Nd}_2\text{Fe}_{14}\text{B}$ and FeCo . In the later case an optimal structure consists of about 20 nm sized FeCo cubes embedded in a $\text{Nd}_2\text{Fe}_{14}\text{B}$ matrix whereby the thickness of the matrix phase is 4 nm to 5 nm. We apply non-zero temperature micromagnetic simulations which take into account thermal fluctuations, in order to compute the remanence, the coercivity, and the energy product of different structures. Hard shell ($\text{Nd}_2\text{Fe}_{14}\text{B}$) - single phase core ($(\text{FeCo})_2\text{B}$) magnets show an energy product of 225 kJ/m at 450 K. Replacing the core with a nano-structured hard / soft mixture the energy product was calculated to be 380 kJ/m. In this magnet the volume fraction of $\text{Nd}_2\text{Fe}_{14}\text{B}$ was reduced by 40 percent as compared to a single phase $\text{Nd}_2\text{Fe}_{14}\text{B}$ hot deformed magnet. Work supported by MagHEM.

Fr.A.2_O2 - Micromagnetic simulations on the role of grain-boundary phase in Nd₂Fe₁₄B magnets

M. Yi^{1,2}, O. Gutfleisch¹, B. Xu¹

1. Technische Universität Darmstadt, Hessen, Germany
2. Beihang University (BUAA), Beijing, China

In the fields such as hybrid electric vehicles and wind turbine generators whose maximum operating temperature is typically ~160 °C, the coercive field of Nd-Fe-B magnets is reduced to an unacceptably low value. One way to obtain high coercive field at elevated temperature is to add the heavy rare-earth elements Dy or Tb, however, conventionally at the cost of remanence. Dy and Tb are scarce natural resources. This has motivated extensive research on enhancing the coercivity and keeping the remanence while minimizing the Dy or Tb usage. 'Grain boundary diffusion process' (GBDP) has been developed, whereby Dy is considered to diffuse through the grain boundaries and a (Nd,Dy)₂Fe₁₄B shell forms around the Nd₂Fe₁₄B core. The (Nd,Dy)₂Fe₁₄B shell is generally thought as the origin for the enhancement in coercivity, as magnetization reversal is delayed to larger critical opposing field. In this contribution, three-dimensional micromagnetic simulations multigrain model based on experimental observation are performed to investigate the effect of microstructure on the coercivity of Dy-diffused Nd-Fe-B sintered magnets by micromagnetic simulation. In the model, the grain boundary, the triple junction, the (Nd,Dy)₂Fe₁₄B shell, the Nd₂Fe₁₄B core, and the defect region will be considered. The size and properties of these phases are tuned to optimize the effect. It is found that if both the grain boundary and triple junction are non-ferromagnetic, a very thin (Nd,Dy)₂Fe₁₄B shell is enough to remarkably increase the coercivity. The defect region, which is ferromagnetic but with much decreased magnetocrystalline anisotropy, can significantly reduce the coercivity through the nucleation or de-pinning of domain during the reversal process. Moreover, the effect of microstructure on the temperature dependent coercivity is also explored.

Fr.A.2_O3 - Optimization of permanent magnets performance by means of micromagnetic modelling

D. Berkov¹, S. Erokhin¹

1. General Numerics Research Lab E.V., Jena, Germany

Our new methodology for micromagnetic simulations of magnetic nanocomposites [1] has enabled the in-advance optimization of permanent magnets performance, whereby magnetic characteristics of a magnetic nanocomposite material consisting of two magnetic phases can be predicted before its actual manufacturing. Large magnetization of the “soft” phase material is supposed to be combined with a high coercivity due to the presence of magnetically 'hard' inclusions. Both phases should be exchange coupled in the optimal way to obtain a hysteresis loop with shape close to the rectangular one. Our method allows to study the dependence of macroscopic magnetic properties of such materials on structural and magnetic parameters of their constituting phases. We are able to model systems containing up to ~ 1000 hard grains, including the analysis of a non-trivial magnetization distribution in every grain. This approach leads to a very high statistical reliability of results. In our talk we present results concerning the dependence of hysteresis loops and energy products on magnetic and geometric parameters of nanocomposite materials, in particular, volume fractions of phases, grain shape and sizes, exchange weakening on intergrain boundaries. Our methodology also allows to study nanocomposites containing a considerable amount of pores, which are unavoidable by many production techniques. In particular, we show that both for the volume fraction of the 'soft' phase and the degree of the intergrain exchange weakening there exist optimal values, for which the maximal energy product is achieved. Another important question studied here is the single-domain critical size of magnetically soft grains. Only the 'soft' grains with sizes not exceeding this single-domain limit give significant contribution to the energy product of a magnet made of this material. We present corresponding results for several magnetic materials.

Financial support of the DFG project BE2464/10-3 and the EU-FP7 project 'NANOPYME' (310516) [www.nanopyme-project.eu] is greatly acknowledged

References:

[1] A. Michels, S. Erokhin, D. Berkov, and N. Gorn, *J. Magn. Mater. (Current Perspectives on Neutron Scattering)* 350 (2014) 55

Fr.A.2_O4 - First-principles study of the effect of Cu and NdOx in Nd₂Fe₁₄B magnets

Y. Tatetsu¹, T. Ozaki², S. Tsuneyuki^{1,2}, Y. Gohda^{1,3}

1. ESICMM, Department of Physics, The University of Tokyo, Tokyo, Japan

2. Institute for Solid State Physics, The University of Tokyo, Tokyo, Japan

3. Department of Materials Science and Engineering, Tokyo Institute of Technology, Tokyo, Japan

For the development of technologies, such as high performance computers, hybrid cars, etc., strong magnets are needed to enhance those performances. Among them, Nd₂Fe₁₄B is the strongest magnet so far. Recent experimental studies tells us that understanding of interactions between grain boundaries and main phases in Nd-Fe-B magnets might be important in order to know the mechanism of its coercivity and magnetic anisotropy energy (MAE). Until now, improvement of coercivity has been reported because of the existence of Nd oxides (NdOx) with fcc Nd sublattice[1]. Furthermore, the coercivity of Nd-Fe-B magnets are enhanced by the Nd-Cu grain boundary diffusion process[2]. From this study, Cu is supposed to be around the main phases. To clarify the mechanism of the enhancement of the coercivity of Nd-Fe-B magnets, Nd_{2-y}Cu_yFe₁₄B/NdOx system is a suitable system for the first step calculation by the density functional theory. We calculate this system using the computational code OpenMX[3]. Nd atoms are performed by open core potentials due to the well-localized 4f electrons and for computational costs. First, we calculated Nd_{1.75}Cu_{0.25}Fe₁₄B where one Nd site is substituted for Cu, and found that substituting Nd for Cu at the 4g site is more stable than at the 4f site from the comparison of total energies of these two phases. We determined the metastable structure of NdOx as Nd₄O (x = 0.25) with the zinc blend structure, which is in good agreement with the previous research[4]. We will also present how Cu existing at grain boundaries affects to the magnetic moments in bulk compared to Nd₂Fe₁₄B/Nd₄O.

References:

[1] T. Fukagawa and S. Hirosawa: Journal of Applied Physics 104, 013911 (2008)

[2] H. Sepehri-Amin et al.: Acta Materialia 61, 6622 (2013)

[3] <http://www.openmx-square.org>

[4] Y. Chen et al.: The Minerals, Metals and Materials Society, JOM 61, 1133 (2014)

Fr.A.2_O5 - Molecular field and CEF single ion calculation of the finite temperature intrinsic magnetic properties of $R_2M_{14}B$ intermetallic compounds (R=rare earth, M= Fe, Co)M. Ito ^{1,2}, M. Yano ², N. M. Dempsey ¹, D. Givord ^{1,3}*1. CNRS/Université Grenoble-Alpes, Institut Néel, Grenoble, France**2. Advanced Material Engineering Div., Toyota Motor Corporation**3. Instituto de Física, Universidade Federal do Rio de Janeiro, Rio de Janeiro, Brazil*

The hard magnetic properties of the “R-M-B” (R=rare earth, M=mainly Fe) magnets derive from the specific intrinsic magnetic properties encountered in the $R_2M_{14}B$ compounds. These are a large magnetization and high magnetocrystalline uniaxial anisotropy occurring at room temperature and above. The reference ternary phase used in these magnets is $Nd_2Fe_{14}B$. However, material optimization very often involves the partial substitution of another R element for Nd and that of Co for Fe. It is of special interest in such cases to be able to predict what will be the impact of a given atom substitution on the values of the magnetization and anisotropy and on their temperature dependence. The properties of all $R_2Fe_{14}B$ compounds across the rare-earth series (lanthanides + Y) have been previously studied as well as those of a number of $R_2Co_{14}B$ compounds. The temperature dependence of the transition metal magnetization may be approximated by a phenomenological expression and the rare-earth magnetism may be described within a model, in which the R-M interactions on the rare-earth sites are treated as a molecular field arising from the M atoms, and the magnetocrystalline anisotropy is attributed to the crystalline electric field acting on single ions. In the present study, this has been applied to the calculation of the magnetic properties of all ternary $R_2Fe_{14}B$ compounds. Good agreement with measurements demonstrates the applicability of the hypotheses made. The model has been extended to the calculation of the magnetic properties of pseudo ternary $(RR')_2(FeCo)_{14}B$ compounds. For compounds of which properties are experimentally known, very good agreement with calculation is obtained. Such calculations may constitute a powerful tool for optimizing the chemical composition of the hard magnetic phase used in real magnets, without the need of systematically studying the experimental magnetic properties of the compounds involved.

Fr.A.3_O1 - Permanent magnet demagnetization process considering the inclination of the demag field

S. Tiziane¹, N. Novello¹

1. LEE Srl., Milan, Italy

ABSTRACT: Computer simulations of the magnetizing process have been carried out by applying a numerical model to the theory of magnetization for magnetic materials. The numerical model is able to calculate the magnetization/demagnetization of the permanent magnet material according to its B-H curves[1]. This numerical model is combined with an existing finite element method model.

The aim of this work was to develop a tool able to simulate the behavior of an anisotropic sintered permanent magnet during the demagnetization process. The permanent magnet material that has been studied in this work is sintered Nd-Fe-B and it was modeled taking into account an average misalignment angle related to the magnet easy axis [2]. This model also takes into account different demagnetizing field directions, such as a demagnetizing field perpendicular to the orientation direction. A gaussian distribution of the average misalignment angle in the permanent magnet material is also taken into account as well as its variation. Demag curves have been calculated varying the misalignment angle and the intensity and direction of the external magnetic field. The simulations results are in perfect agreement with the $1/\cos\theta$ law [3]. The model can be applied in many magnetization and magnetic tuning applications.

Keywords: Alignment Angle, BH curve, Calibration, Demagnetization, FEA, Numerical Modeling, Nucleation, Pinning, Python

References:

- [1]. M. Enokizono and K. Matsumura, "Magnetic Field Analysis of Anisotropic Permanent Magnet Problems by Finite Element Method", *IEEE Trans. Magn.*, vol. 33, no. 2, 1997
- [2]. R.W. Gao, D.H. Zhang, Y.M. Zhang, W. Li, Y.S. Wang and X.J. Yu, "Effect of the intergrain interactions on the coercivity and its angular dependence for Nd(FeCo)B sintered magnets", *Journal of Magnetism and Magnetic Materials*, vol. 224, pp. 125-131, 2001
- [3] Y. Pastushenkov, K. Skokov, "Magnetic Domain Structure: Analysis of Magnetic Reversal in RE-3d Permanent Magnets", [*Journal of Iron and Steel Research, International, Vol. 13, Supplement 1*](#), pp. 79-86, 2006

Fr.A.3_O2 - Structure and magnetic properties of Sm-Co/Fe-Co multilayer films with in-plane magnetic anisotropies prepared on MgO(110) single-crystal substratesM. Ohtake¹, Y. Hotta¹, M. Yamada¹, A. Suzuki¹, M. Futamoto¹, F. Kirino², N. Inaba³

1. Chuo University, Hachioji, Japan

2. Tokyo University of the Arts, Tokyo, Japan

3. Yamagata University, Yamagata, Japan

Multilayer films consisting of exchange-coupled hard and soft magnetic layers have a potential to achieve high energy products and have been studied for permanent magnet applications. Sm₁₇Co₈₅ (at.%) ordered alloy with RT5 structure and Fe₆₅Co₃₅ alloy with bcc structure are typical high H_a and M_s materials, respectively. In order to investigate the basic structural and magnetic properties, it is useful to prepare epitaxial films on single-crystal substrates by employing a molecular beam epitaxy (MBE) system equipped with a reflection high-energy electron diffraction (RHEED) facility. In-situ RHEED can reveal the crystallographic properties of films during formation. In the present study, Sm₁₇Co₈₃/Fe₆₅Co₃₅ multilayer films are prepared on MgO(110) single-crystal substrates at 500 °C by MBE. The film layer structures are [Sm₁₇Co₈₃(x nm)/Fe₆₅Co₃₅(40- x nm)]₂/MgO (x = 10-30) and [Sm₁₇Co₈₃(40/ n nm)/Fe₆₅Co₃₅(40/ n nm)] _{n} /MgO (n = 2-4). The structure and the magnetic properties are investigated by RHEED, XRD, and VSM. 1st Sm-Co/Fe-Co bi-layer grows epitaxially on the substrate in the crystallographic orientation relationship of Sm-Co(1-100)[0001] || Fe-Co(211)[01-1],[0-11] || MgO(110)[001]. The Fe-Co layer consists of two bcc(211) variants whose orientations are rotated around the film normal by 180° each other, while the Sm-Co layer is a single-crystal of RT5 ordered structure with the c -axis lying in the film plane. 2nd Fe-Co layer of bcc(211) orientation also grows epitaxially on the 1st Sm-Co layer. However, 2nd Sm-Co layer formed on the 2nd Fe-Co layer involves amorphous and crystals with structures other than RT5. The crystallographic quality degrades with increasing the repetition number of n . As the Sm-Co layer thickness of x increases, the H_c value increases, whereas the M_s value decreases. On the other hand, the H_c value decreases as the repetition number of n increases. The magnetic properties are delicately influenced not only by the multilayer structure but also by the crystallographic properties of Sm-Co layers.

Fr.A.3_O3 - Magnetization reversal process of Nd-Fe-B sintered magnets observed by magnetic very small angle neutron scattering

K. Ono¹, M. Yano², T. Ueno³, K. Saito¹, T. Shoji², A. Manabe², A. Kato², Y. Kaneko⁴, Z. Fu⁵

1. High Energy Accelerator Research Organization (KEK), Ibaraki, Japan

2. TOYOTA Motor Co., Aichi, Japan

3. National Institute of Materials Science (NIMS), Ibaraki, Japan

4. Toyota Central R&D Labs. Inc., Japan

5. Forschungszentrum Jülich, Jülich, Germany

There have been strong interests in the mechanism of high coercivity in Nd-Fe-B sintered magnets due to increasing demands for automotive applications. Motors used in hybrid and electric vehicles are operating at high temperature and approximately more than 30% of Nd is substituted with Dy in the current Nd-Fe-B sintered magnets for automotive motor applications to increase the anisotropy field. Since Dy is comparatively rare natural resources with supply risks, a new technology that can increase the coercivity of Nd-Fe-B sintered magnets is strongly desired. Magnetic Small Angle Neutron Scattering (SANS) is very powerful to observe bulk magnetic microstructures of Nd-Fe-B nanocrystalline magnets [1-4]. The length scale of standard SANS instrument is not suitable for sintered magnets, i.e. magnet used for motors and industrial applications, since the grain size of sintered magnets is a few micrometer. The use of Very Small Angle Neutron Scattering (VSANS) is indispensable for sintered magnet. In this study, we performed VSANS experiments for Nd-Fe-B sintered magnet at KWS-3 in FRM-II, Munich, Germany. We observed clear changes in magnetic VSANS patterns for Nd-Fe-B sintered magnet in the q -range of $0.003 \sim 0.03 \text{ nm}^{-1}$ during magnetization reversal process. It is suggested that the change in magnetic microstructure inside the bulk sintered magnet is occurred with the size of $200 \sim 2,000 \text{ nm}$. We also found that there are two different origins for the change in magnetic VSANS intensity. In lower q region, magnetic scattering is mostly affected by macroscopic magnetization. On the other hand in higher q region, magnetic scattering is mostly caused by a formation of magnetic domains. This work was partly supported by the JST under Collaborative Research Based on Industrial Demand High Performance Magnets: Towards Innovative Development of Next Generation Magnets.

References:

[1] M. Yano et al, IEEE Trans. Magn. 48, 2804 (2012)

[2] M. Yano et al., J. Appl. Phys. 115, 17A730 (2014)

[3] T. Ueno et al., IEEE Trans. Magn. 50, 2103104 (2014)

[4] K. Saito et al., J. Appl. Phys. 117, 17B302 (2015)

Fr.B.1_I1 - Size-induced enhanced magnetoelectric effect in chromium oxide nanoclusters

D. Halley¹, N. Najjari¹, L. Joly¹, B. Doudin¹, Y. Henry¹

1. CNRS/Université de Strasbourg, Strasbourg, France

Magnetoelectric materials give the opportunity of controlling the magnetic dipole of a device by applying an electric field. This explains the renewed interest for magneto-electrics materials within the field of magnetic memories and spintronics. Nevertheless, the scarcity of the magneto-electric materials and the smallness of the magnetoelectric effects up to now prevent the expected application of these materials. Different ways to enhance the magnetoelectric coefficient are therefore investigated: for instance, theoretical predictions of a magneto-electric effect enhancement under strain have recently been put forward. We recently showed* a proof-of-principle experiment proving that large strains due to nanoscale size reduction are very efficient for increasing magnetoelectric coefficients by orders of magnitude. We studied the archetype magnetoelectric material, Cr₂O₃, which was deposited in the form of epitaxial clusters in a MgO matrix that induces a large epitaxial strain in the clusters. The MgO layer is thin enough to behave as a tunnel barrier: electrons can be injected from a Fe magnetic electrode into the Cr₂O₃ clusters by tunnel effect. This enables us to measure the tunnel magneto-resistance effect and by this way to probe the magnetisation of those nanometric clusters under voltage. This original technique showed that the highly strained clusters exhibit an unprecedented 600% change in magnetization magnitude under 1V applied to the MgO tunnel barrier: this effect is due to the enhancement of the magneto-electric coefficient of three orders of magnitude relative to bulk Cr₂O₃. Furthermore, a multiferroic phase, with both permanent magnetic and electric polarizations, is evidenced in those clusters, while bulk Cr₂O₃ is antiferromagnetic and paraelectric.

References:

*D. Halley, N. Najjari, H. Majjad, L. Joly, P. Ohresser, F. Scheurer, C. Ulhaq-Bouillet, S. Berciaud, B. Doudin and Y. Henry, Nature Communications, 5, 3167 (2014)

Fr.B.1_O2 - Relationship between the verwey temperature and the particle size in magnetite nanoparticles

L. Marcano¹, D. Muñoz Rodríguez², A. Muela^{2,3}, A. García Prieto^{3,4}, J. Alonso^{3,5}, L. Fernández Barquín⁶, M.L. Fdez-Gubieda^{1,3}

1. *Universidad Del País Vasco (UPV/EHU), Spain*
2. *Departamento de Inmunología, Microbiología y Parasitología, Universidad Del País Vasco (UPV/EHU), Spain*
3. *BCMaterials, Building NO.500, Technological Park of Biscay, Derio, Spain*
4. *Departamento de Física Aplicada I, Universidad Del País Vasco (UPV/EHU), Spain*
5. *Department of Physics, University of South Florida, Tampa, United States*
6. *Departamento CITIMAC, F. Ciencias, Universidad de Cantabria, Santander, Spain*

Bulk magnetite presents a characteristic sudden change in the structure and electrical conductivity around 120 K, the so-called Verwey transition [1]. In this work we have focused on the study of this transition in magnetite nanoparticles and its dependence with the particle size. However, magnetite nanoparticles are especially sensitive to oxidation and the resulting stoichiometry changes influence Verwey transition, making difficult to find any relation with the size. In the present work, we have used magnetite nanoparticles biosynthesized by magnetotactic bacteria *Magnetospirillum gryphiswaldense*. This kind of nanoparticles, also called magnetosomes, are surrounded by a 3-4 nm lipid bilayer and present a high structural and chemical quality with well-determined properties thanks to the highly precise biological control. Aiming to know the dependence between the Verwey temperature and particle size, we have followed and stopped the biomineralization process of these magnetosomes at different times after the bacterial incubation in a medium containing Fe(III)-citrate, performing a time-resolved study [2]. By XAS analysis, we have proved that the stoichiometry of the nanoparticles remains constant for the different stages of the biomineralization process, allowing us to study the relation between the particle size and the Verwey transition. TEM analysis shows a size evolution from 15 nm, in early stages of biomineralization, to 45 ± 3 nm with a narrow size distribution, around 8 nm, at the end of the process. Verwey temperature has been obtained performing zero field cooled - field cooled DC magnetization curve and AC-susceptibility. We have observed an increase in the Verwey temperature from approximately 80 K, for fifteen-nanometer particles, to 107 K at the end of the biomineralization process.

References:

- [1] F. Walz, *J. Phys. Condens. Matter* 14, R285 (2002)
- [2] M. L. Fdez-Gubieda, A. Muela, J. Alonso, A. García-Prieto, L. Olivi, R. Fernández-Pacheco, and J. M. Barandiarán, *ACS Nano* 7, 3297 (2013)

Fr.B.1_O3 - Core/shell magnetism in NiO nanoparticles

A. Ionescu¹, J.F.K. Cooper¹, R.M. Langford¹, K. R.A. Ziebeck¹, C. H.W. Barnes¹, R. Gruar², C. Tighe², J. A. Darr², N.T.K. Thanh³, B. Ouladdiaf⁴

1. *Cavendish Laboratory, University of Cambridge, Cambridge, United Kingdom*

2. *Chemistry Department, University College London, United Kingdom*

3. *Davy-Faraday Research Laboratory, Royal Institution of Great Britain, London, United Kingdom*

4. *Institut Laue-Langevin, Grenoble, France*

Recently, magnetic nanoparticles (MNPs) have become a subject of intense research in a myriad of different fields, from catalysis and pattern formation to MRI contrast agents and for diagnoses in magnetic biosensors [1,2]. A feature common to both superparamagnetic and ferromagnetic MNPs is the addition of correction factors, which must be included when calculating their magnetisation compared to the expected bulk value. These factors are predominantly explained as accounting for finite size effects; however, the nature of these effects is as yet, unresolved [3]. The anomalous appearance of a ferromagnetic moment in nominally antiferromagnetic nanoparticles has been known about since Néel, but never well understood. We present proof of the core/shell model of magnetism in antiferromagnetic NiO nanoparticles (NP) using neutron diffraction. Nickel oxide nanoparticles were produced in a large quantity by a novel continuous hydrothermal flow synthesis method. The antiferromagnetic nature of the nanoparticles allowed the structural and the magnetic diffraction peaks to be completely separated. Using both the microstructure option in 'Fullprof' microstructure fitting suite and convolution techniques, we determined the NP consisted of an ordered antiferromagnetic core 5.2(2) nm in diameter surrounded by a disordered shell 0.7(2) nm thick. Further magnetic measurements showed that this disordered shell possess a significant polarisable magnetisation, up to a fifth that of pure nickel. They also indicate that two magnetic transitions occur between 400 and 10 K; around 350 K, there is a broad transition from paramagnetic to a form of superparamagnetism, then near 30 K there is a transition to a higher anisotropy state. Differences in field cooled and zero field cooled hysteresis loops were found, though with no evidence of exchange bias effects.

References:

[1] J. Llandro, J.J. Palfreyman, A. Ionescu, and C.H.W. Barnes, *Med. Biol. Eng. Comput.* 48, 977 (2010)

[2] N.T.K. Thanh, "Magnetic Nanoparticles: From Fabrication to Clinical Applications", Taylor and Francis (2012)

[3] J.F.K. Cooper, A. Ionescu, R.M. Langford et al., *Journal of Applied Physics* 114, 083906 (2013)

Fr.B.1_O4 - Interplay between microstructure and magnetism in transition metal oxide nanoparticles: towards the breakdown of the antiferromagnetic order

N. Rinaldi-Montes¹, P. Gorria¹, D. Martínez-Blanco², A. B. Fuertes³, I. Puente-Orench⁴, J.A. Blanco¹

1. *Departamento de Física, Universidad de Oviedo, Oviedo, Spain*

2. *Servicios Científico-Técnicos, Universidad de Oviedo, Oviedo, Spain*

3. *Instituto Nacional del Carbón, CSIC, Oviedo, Spain*

4. *Instituto de Ciencia de Materiales de Aragón, CSIC-Universidad de Zaragoza and Institut Laue-Langevin, Grenoble, France*

The possibility of tuning the magnetic behaviour of nanostructured 3d transition metal oxides has opened up the path for extensive research activity in the nanoscale world. In this work we report on how the antiferromagnetism of a bulk material can be broken when reducing its size below a given threshold [1]. As antiferromagnetic (AFM) systems need a high degree of symmetry in order to maintain a balanced magnetic structure, the magnetic frustration arising from size reduction is especially pronounced. We have combined the use of neutron diffraction, x-ray absorption spectroscopy and magnetic measurements in order to study the influence of NP diameter reduction on the microstructure and magnetism of NPs composed of materials that are AFM in their bulk forms (NiO, Cr₂O₃, CuO, MnO). Our findings reveal that size effects such as average undercoordination, bond relaxation and static disorder, induce surface spin frustration, which competes with the expected antiferromagnetism, giving rise to a threshold diameter for the nucleation of the AFM phase. Hence, the magnetic microstructure of the NPs changes from a core(AFM)/shell(spin-glass) morphology to a completely disordered magnetic state below a critical NP diameter. Finally, we have explored the link between the NP morphology and the emergence of the exchange bias effect, which arises as a consequence of the exchange interaction at the interface between two magnetic phases with different anisotropy energies.

Funding Source: Spanish MINECO (Project MAT2011-27573-C04) and MECD (Grant FPU12/03381).

References:

[1] N. Rinaldi-Montes et al., *Nanoscale* 6, 457 (2014)

Fr.B.1_O5 - Sorption study water contaminants by magnetic nanoparticles: a theoretical approach based on DFT calculations

S. Baltazar¹, M. Salgado¹

1. Departamento de Física, CEDENNA, Universidad de Santiago de Chile, Santiago de Chile, Chile

The study and application of magnetic iron nanoparticles for cleaning contaminated water have attracted a lot of attention during the last years in several regions around the world. In particular, the mechanism of arsenic and lead sorption from water using iron nanoparticles [1] has become increasingly interesting due to its applications in natural environment. The characterization of the materials, before and after the sorption processes, is considered in order to identify the new structures as a function of pH. In this context, a theoretical approach can be used to identify the interactions between Arsenic compounds and iron oxide nanoparticles performing ab initio calculations based on density functional theory [2] with the VASP package. In this case we considered the DFT+U method suitable for the study of strongly correlated systems such as iron oxides surfaces. In this work we present a theoretical study of the interaction of arsenic complexes in contact with different iron oxide surfaces such as Fe₃O₄ and FeO, which can be associated to the oxidation states found on iron nanoparticles. A detailed analysis of the structural changes, due to the interaction between arsenic compounds and the surface of magnetite, is presented. In particular electronic and magnetic properties such as charge density and magnetic dipolar momentum are reported as a function of the arsenic sorption process. We acknowledge the support of FONDECYT under grants 11100439, Conicyt Grant 79090022, ICM P10-061-F by Fondo de Innovación para la Competitividad-Minecon.

References:

- [1] S. Baltazar, A. Garcia, A. H. Romero, M. A. Rubio, N. Arancibia and D. Altbir, *Environ. Tech.* 35, 2365-2372 (2014)
- [2] D. M. Sherman and S. R. Randall, *Geochimica et Cosmochimica Acta*, 67, 4223-4230 (2003)

Fr.B.2_O1 – Element specific magnetic depth profiles of YBa₂Cu₃O₇/La_{0.7}Ca_{0.3}MnO₃ superlattices using X-ray resonant magnetic reflectometry

A. Alberca^{1,2}, M. A. Uribe-Laverde², K. Sen², I. Marozau², E. Perret², W.Y. Windsor¹, M. Ramakrishnan¹, L. Rettig¹, J. Stahn³, U. Staub¹, C. Bernhard²

1. *Swiss Light Source, Paul Scherrer Institut, Villigen, Switzerland*

2. *University of Fribourg, Department of Physics and Fribourg Centre for Nanomaterials, Fribourg, Switzerland*

3. *Laboratory for Neutron Scattering, Paul Scherrer Institut, Villigen, Switzerland*

The interactions arising at the interface between multilayers from complex oxides with strongly correlated electrons are subject of intense research. A prominent example of these interactions is the coupling between the antagonistic superconducting and ferromagnetic orders. In particular, the phenomena observed in superlattices made of high- T_c cuprate superconductors and ferromagnetic manganites, which comprise electronic and magnetic proximity effects (MPE), are yet to be fully understood. These effects are thought to be closely related to the strong electronic correlations and the intimate coupling between the magnetic, orbital and lattice degrees of freedom. For this reason, the study of these interactions and orders in the angstrom scale, with element specificity and with sensitivity to magnetic, orbital and charge orders is vital.

Here, we study the element specific magnetic depth profiles of YBa₂Cu₃O₇/La_{0.7}Ca_{0.3}MnO₃ (YBCO/LCMO) superlattices using Soft X-ray Resonant Magnetic Reflectometry (XRMR). In YBCO/LCMO superlattices, the MPE is characterized by the occurrence of a depleted layer on the manganite side of the interface and a small induced magnetization in the Cu atoms (0.25 μ_B per interfacial Cu ion) [1-3]. Using the element specific depth profiling capability we confirm that the Cu moments reside on the YBCO side and originate from the CuO₂ layer that is located right at the interface. We also show that the suppression of the Mn moment on the LCMO side is only a partial effect with interfacial Mn moments of 0.9 μ_B /Mn as compared to 2.4 μ_B /Mn near the center of the LCMO layer. Finally, our study confirms a strong asymmetry of the MPE, between the YBCO/LCMO and LCMO/YBCO interfaces, that was previously reported from polarized neutron reflectometry measurements.

References:

[1] D. K. Satpathy, *et al.*, PRL, 108, 197201, (2012)

[2] M. A. Uribe-Laverde, *et al.*, PRB, 90, 205135, (2014)

[3] M. A. Uribe-Laverde, *et al.*, PRB, 87, 115105 (2013)

Fr.B.2_O2 - Study of strong electronic correlations and superconductivity for KFe_2As_2 under pressure and for intercalated FeSe

H. O. Jeschke¹, D. Guterding¹, S. Backes¹, R. Valentí¹

1. *Goethe-Universität Frankfurt, Frankfurt, Germany*

We use density functional theory combined with dynamical mean field theory (DFT+DMFT) to study the effect of electronic correlations in KFe_2As_2 . We show that at ambient pressure, the Fermi surface that is seen in ARPES experiments can only be obtained if correlations are treated correctly [1]. In the recently discovered collapsed tetragonal phase of KFe_2As_2 at very high pressure, however, electronic correlations play a negligible role [2]. Within a random phase approximation spin-fluctuation approach we calculate the superconducting order parameter in the collapsed tetragonal phase. We suggest that the change of Fermi surface between low and high pressure is consistent with a change of superconducting order parameter from d-wave to $s \pm$. In a study of ammonia intercalated FeSe, we try to separate the effects of dimensionality (3D versus 2D) from the effects of charge doping. Our theory can explain the trends of T_c in this material [3].

References:

- [1] S. Backes, D. Guterding, H. O. Jeschke, R. Valentí, *New J. Phys.* 16, 085025 (2014)
- [2] D. Guterding, S. Backes, H. O. Jeschke, R. Valentí, arXiv:1501.03068v2
- [3] D. Guterding, H. O. Jeschke, P. J. Hirschfeld, R. Valentí, *Phys. Rev. B* 91, 041112(R) (2015)

Fr.B.2_O3 - Persistence of high-energy spin fluctuations in electron doped NaFeAsJ. Pelliciani¹, Y. Huang^{1,2}, M. Dantz¹, V. Bisogni¹, P. Olalde Velasco¹, C. Q. Jin², T. Schmitt¹1. *Swiss Light Source, Paul Scherrer Institute, Villigen, Switzerland*2. *Institute of Physics Chinese Academy of Science, Beijing, China*

Superconductivity in iron pnictides was discovered in 2008 [1] and a lot of effort has been devoted in order to explain their unconventional nature. As in other high temperature superconductors (HTSC), magnetism and superconductivity (SC) exhibit proximity, competition and/or coexistence in the phase diagram [2]. This indicates a strong connection between such phases and paved the way for the use of theories explaining SC as arising from magnetic fluctuations [3]. In this context the experimental characterization of static and dynamic magnetism is of vital importance in constraining theoretical models. The NaFe_{1-x}CoxAs series represents a contrasting case with the most studied BaFe_{2-x}CoxAs₂ compounds because of their much lower magnetic moment (ca 0.1 μ_B for NaFeAs vs. ca 1.3 μ_B for BaFe₂As₂) [2,4]. However, the T_c of their Co-doped compounds is pretty similar (21 K at x = 0.025 vs. 22 K at x = 0.2 for NaFe_{1-x}CoxAs and BaFe_{2-x}CoxAs₂, respectively [2, 4]). This situation turns out to be extremely interesting in order to elucidate the relation between static magnetic moments and spin fluctuations and eventually with superconductivity. Resonant Inelastic X-ray Scattering (RIXS) has proven to be a powerful spectroscopy for probing high energy spin fluctuations in HTSCs [5, 6, 7]. We present a high resolution Fe L₃ RIXS study of parent and superconducting NaFe_{1-x}CoxAs. Spectral shape decomposition reveals the persistence of broad dispersive magnetic excitations for all doping levels. In contrast to previous RIXS experiments on hole-doped BaFe₂As₂ compounds [6] the energy of such modes is not strongly affected by doping and the magnetic weight per iron atom of such excitations remains constant. However, renormalized per formula unit the magnetic weight decreases with doping. We argue that cobalt-doping is mainly tuning the electronic correlations without affecting the dispersion range of the magnetic excitations, only reducing their spectral weight.

References:

- [1] Y. Kamihara et al, J.Am.Chem.Soc. 130, 3296 (2008)
- [2] G.R. Stewart, Rev.Mod.Phys., 83, 1589 (2011)
- [3] D.J. Scalapino, Rev.Mod.Phys., 84, 1383 (2012)
- [4] D.C. Johnston, Advances in Physics Vol. 59, No. 6, 803 (2010)
- [5] L.J.P. Ament et al, Rev.Mod.Phys. 83, 705 (2011)
- [6] K.J. Zhou et al, Nat.Comm., 4, 1470 (2013)

Fr.B.2_O4 - Static Magnetic Order in Overdoped NaFe_{1-x}Cu_xAs Indicating a Mott Transition

S. Cheung¹, B. Frandsen¹, L. Liu¹, D. Wang^{1,2}, Y. Uemura¹, A. Hallas³, A. Millington³, T. Munsie³, M. Wilson³, G. Luke³, B. Chen⁴, L. Xing⁴, C. Jin⁴, C. Ding⁵, F. Ning⁵, Y. Nonaka⁶

1. Department of Physics, Columbia University, New York, New York, United States
2. Department of Applied Physics and Applied Mathematics, Columbia University, New York, New York, United States
3. Department of Physics and Astronomy, McMaster University, Hamilton, Ontario, Canada
4. Beijing National Laboratory for Condensed Matter Physics and Institute of Physics, Chinese Academy of Sciences, Beijing, China
5. Department of Physics, Zhejiang University, Hangzhou, China
6. Department of Physics, University of Tokyo, Bunkyo-ku, Tokyo, Japan

Since 2009, NaFeAs has attracted much attention for its notable superconducting dome upon electron-doping with Co, Cu, and Ni. In 2013, a Mott-insulating state was detected in highly overdoped NaFe_{1-x}Cu_xAs, unlike the metallic state in overdoped NaFe_{1-x}Co_xAs and NaFe_{1-x}Ni_xAs. An STM investigation by Wang [1] on overdoped NaFe_{1-x}Cu_xAs found signatures similar to those of underdoped cuprates, which have antiferromagnetic parent compounds. Subsequent magnetic susceptibility measurements of NaFe_{1-x}Cu_xAs indicate possible static magnetic ordering (SMO) in systems with Cu concentrations exceeding 25%, and recently, Song et al., [2] reported antiferromagnetic order in the 44% system from neutron scattering. We performed muon spin relaxation (MuSR) measurements on single crystals of NaFe_{1-x}Cu_xAs with x = 6, 15, 25, and 44% at TRIUMF. The asymmetry spectra observed in zero field (ZF-MuSR) revealed SMO in the 15, 25 and 44% systems. The 25% and 44% specimens show sharp transitions at TF ~ 20K and 60K, respectively, below which SMO rapidly develops in the entire volume fraction. The 15% compound possesses a gradual transition starting below 20K, with phase-separated paramagnetic and magnetically ordered volumes. This compound achieves SMO in a volume majority by 2K, with the moment size an order of magnitude smaller than those of the 25 and 44% systems. The 6% compound is paramagnetic down to 2K. The absence of sustained precession signals from ZF-MuSR, together with magnetic susceptibility cusps and history dependences, suggest possible spin-glass-like freezing in the 15, 25, and 44% compounds. Evolution from the Mott insulator to the superconducting dome involving a spin glass intermediary phase is reminiscent of the behavior of high-TC cuprates. The present investigation in NaFe_{1-x}Cu_xAs demonstrates the first case of a Mott transition in iron-based superconductors.

References:

- [1] Yayu Wang, Presentation: Super-PIRE REIMEI Workshop on Frontiers of Condensed Matter Physics, Beijing, March 2014
[2] Yu Song et al., Preprint

Fr.B.2_O5 - Successive AF-SC-AF phase transition and the quantum criticality in LaFeAsO_{1-x}H_x studied by nuclear magnetic resonance

N. Fujiwara¹, N. Kawaguchi¹, Y. Yamakawa², H. Kontani², S. Iimura³, S. Matsuishi³, H. Hosono³

1. *Kyoto University, Kyoto, Japan*

2. *Nagoya University, Nagoya, Japan*

3. *Tokyo Institute of Technology, Tokyo, Japan*

The prototypical iron-based high-T_c superconductors LaFeAsO_{1-x}H_x can accept high electron doping, which leads to two novel phenomena in the electronic phase diagram: (i) H doping leads to superconducting (SC) phase with double domes following a stripe-type antiferromagnetic (AF) phase, and (ii) further H doping leads to a second AF ordering [1] following double SC domes. We performed ⁷⁵As nuclear magnetic resonance in the heavily H-doped regime to investigate the second AF ordering in a microscopic viewpoint and the quantum criticality around the AF phase boundary (x=0.49). We found from the 1H linewidth and relaxation rate, 1/T₁ of ⁷⁵As that the SC phase is segregated from the second AF phase in the electronic phase diagram [2]. In the second AF phase, the relaxation rate divided by temperature, 1/T₁T exhibits a SDW-like gap: the gap decreases with decreasing H doping level and becomes almost zero at the AF phase boundary. Furthermore, the doping dependence of 1/T₁T exhibits the maximum at the AF phase boundary. These results suggest that the AF phase boundary corresponds to the quantum critical point.

References:

[1] N. Fujiwara, et al., Phys. Rev. Lett. 111 (2013) 097002

[2] R. Sakurai, et al. Phys. Rev. B 91 (2015) 064509

Fr.B.2_O6 - Microscopic coexistence of magnetism and superconductivity in $\text{Ca}_{1-x}\text{Na}_x\text{Fe}_2\text{As}_2$

H. Klauss¹, P. Materne¹, S. Kamusella¹, R. Sarkar¹, T. Goltz¹, H. Luetkens², L. Harnagea³, S. Wurmehl³, B. Büchner³, C. Timm⁴

1. TU Dresden, Institute of Solid State Physics, Dresden, Germany

2. Laboratory for Muon Spin Spectroscopy, Paul-Scherrer-Institut, Villigen PSI, Switzerland

3. IFW Dresden, Dresden, Germany

4. TU Dresden, Institute of Theoretical Physics, Dresden, Germany

We present Mössbauer spectroscopy and muon spin relaxation experiments on $\text{Ca}_{1-x}\text{Na}_x\text{Fe}_2\text{As}_2$ ($x = 0.35, 0.50, \text{ and } 0.67$). The parent compound CaFe_2As_2 shows spin-density-wave order below $T_N = 165$ K [1]. The magnetic phase transition is accompanied by a structural transition from a tetragonal to an orthorhombic structure [2]. Increasing the Na amount in $\text{Ca}_{1-x}\text{Na}_x\text{Fe}_2\text{As}_2$, the magnetostructural phase transition is suppressed [1].

Our microscopic study proves this suppression of the magnetic transition temperature as well as the magnetic order parameter with increasing x . For $x = 0.50$ we find a microscopic coexistence of magnetic and superconducting phases accompanied by a reduction of the magnetic order parameter below the superconducting transition temperature T_c .

A systematic comparison with other 122 pnictides reveals a linear correlation between the magnetic-order-parameter reduction and the ratio of the transition temperatures, T_c/T_N , which can be understood in the framework of Landau theory.

In the optimally doped specimen with $T_c \approx 34$ K, the temperature dependences of the penetration depth and of the superfluid density were obtained, which prove the presence of two superconducting s-wave gaps.

References:

[1] K. Zhao, Q. Q. Liu, X. C. Wang, Z. Deng, Y. X. Lv, J. L. Zhu, F. Y. Li, and C. Q. Jin, Phys. Rev. B 84, 184534 (2011)

[2] G. Wu, H. Chen, T. Wu, Y. L. Xie, Y. J. Yan, R. H. Liu, X. F. Wang, J. J. Ying, and X. H. Chen, Journal of Physics: Condensed Matter 20, 422201 (2008)

Fr.B.3_O1 - A novel superconductor in actinoid platinum metal borides

E. Bauer¹, C. Blaas-Schenner¹, D. Reith², W. Wolf², P. Rogl³, R. Podloucky³, E. Royanian¹, O. Sologub¹, H. Michor¹, E. Scheidt⁴, J. Bursik⁵, A. Goncalves⁶

1. *Vienna University of Technology, Wien, Austria*
2. *Materials Design, S.A.R.L., Montrouge, France*
3. *University of Vienna, Wien, Austria*
4. *University of Augsburg, Augsburg, Germany*
5. *Academy of Sciences of the Czech Republic, Prague, Czech Republic*
6. *Universidade de Lisboa, Lisboa, Portugal*

From a cursory investigation of phase relations in the systems {Th,U}-Pt-B at 900°C we observed the formation of novel compounds AnPt₃B of which ThPt₃B (a=0.4383(2) nm; Pm-3m) is a representative of the perovskites and UPt₃B (a=0.38906(3), c=0.52241(5) nm; P4mm) is isotopic with the non-centrosymmetric structure of CePt₃B. Characterization of physical properties for ThPt₃B reveals a superconducting transition at 0.75 K and an upper critical field at T = 0 below 0.6 Tesla. For non-superconducting UPt₃B a metallic resistivity behaviour was found in the entire temperature range. At lowest temperatures, spin fluctuations become evident and non-Fermi liquid features are observed from resistivity data. DFT calculations carried out for both compounds provide information about the electronic and phonic structure of these novel compounds.

Fr.B.3_O2 - Colossal thermoelectric effect due to Berry phase fluctuation in chiral superconductors

S. Fujimoto¹, H. Sumiyoshi²

1. *Department of Materials Engineering Science, Osaka University, Suita, Japan*

2. *Department of Physics, Kyoto University, Kyoto, Japan*

In chiral superconductors such as Sr_2RuO_4 (class D topological superconductor), and URu_2Si_2 (Weyl superconductor), Cooper pairs possess nonzero total angular momentum, breaking time-reversal symmetry. The chiral pairings accompanying the nontrivial Berry curvature give rise to exotic transverse transport such as the anomalous thermal Hall effect below the transition temperature T_c . It is naturally expected that even in the superconducting fluctuation regime near but above T_c , anomalous transverse transport may be raised by chiral superconducting fluctuations, which induce the Berry phase fluctuation. Here, we discuss this possibility [1]. We found that in the fluctuation regime above T_c , the anomalous Nernst effects can be raised by dynamical skew-scattering due to chiral superconducting fluctuations. This mechanism is in analogy with the skew-scattering mechanism of the anomalous Hall effect without Lorentz force. However, an important difference is that the skew-scattering due to chiral fluctuations is the dynamical Andreev scattering. Furthermore, this anomalous Nernst effects can be gigantic for cleaner samples. Our scenario successfully explains the recent experimental discovery of the colossal Nernst signal for URu_2Si_2 above T_c , which can not be understood within conventional theories of superconducting fluctuations [2]. We also comment on the application to Sr_2RuO_4 , and other topological superconductors with broken time-reversal symmetry.

References:

[1] H. Sumiyoshi and S. Fujimoto, *Physical Review B* 90, 184518 (2014)

[2] T. Yamashita, Y. Shimoyama, Y. Haga, T. D. Matsuda, E. Yamamoto, Y. Onuki, H. Sumiyoshi, S. Fujimoto, A. Levchenko, T. Shibauchi, and Y. Matsuda, *Nature Physics* 11, 17 (2015)

Fr.B.3_O3 - Quasiparticle interference in chiral superconductors and hidden order phase

P. Thalmeier¹, A. Akbari²

1. *Max Planck Institute For Chemical Physics of Solids, Dresden, Germany*

2. *Asia Pacific Center for Theoretical Physics and Department of Physics, POSTECH, Pohang, Gyeongbuk, Republic of Korea*

The technique of Bogoliubov quasiparticle interference (QPI) has recently been successfully used to investigate the symmetry of unconventional superconductors, in particular of heavy fermion compounds. It was demonstrated that QPI can distinguish between the d-wave singlet candidates of superconducting CeCoIn₅. A similar important system is URu₂Si₂ where presumably a chiral d-wave singlet superconducting (SC) state exists inside a multipolar hidden order (HO) phase. We develop a theory of QPI in the HO and coexisting SC phases using the exact solution of a multiorbital model for the heavy 5f quasiparticle bands. We show that hidden order leaves an imprint on the symmetry of QPI pattern that may be used to determine the essential question whether HO in URu₂Si₂ breaks the in-plane rotational symmetry or not. We also demonstrate that the chiral d-wave SC gap leads to a crossover to a quasi-2D QPI spectrum below T_c which sharpens the HO features. We compare the QPI signature in the HO phase with existing STM experimental results. Furthermore we predict the QPI spectrum for the multiband chiral p-wave triplet superconductor Sr₂RuO₄ [2] which is fully gapped on the active band and has nearly nodal gaps on passive bands. We show that this multigap structure should lead to a characteristic change of the QPI pattern as function of the bias voltage which can be used to confirm the nodes and minima positions of the gap structure.

References:

[1] A. Akbari and P. Thalmeier, Phys. Rev. B 90, 224511 (2014)

[2] A. Akbari and P. Thalmeier, Phys. Rev. B 88, 134519 (2013)

Fr.B.3_O4 - Superconductivity of Icosahedral Yb Approximants with Tsai-type Clusters

K. Deguchi¹, M. Nakayama¹, S. Matsukawa¹, K. Imura¹, K. Tanaka², T. Ishimasa², N. Sato¹

1. Department of Physics, Graduate School of Science, Nagoya University, Nagoya, Japan

2. Division of Applied Physics, Graduate School of Engineering, Hokkaido University, Sapporo, Japan

Quasicrystals (QC) have been quoted as the 3rd solid because they possess long-range, quasi-periodic structures with diffraction symmetries forbidden to crystals. Instead of extensive studies on the electronic structure, no long-range magnetic ordering has been observed although there are a few reports on superconductivity. For a periodic approximant crystal (AC), a phase whose composition is close to that of the QC and whose unit cell has atomic decorations similar to those of the QC, there are some reports on ferromagnetic or antiferromagnetic orderings. However, superconductivity has not been discovered thus far to the best of our knowledge.

Recently, a new type of magnetic QC and AC was discovered: the Au-Al-Yb QC exhibits novel quantum critical behaviour as observed in Yb-based heavy fermion materials with intermediate Yb valence, while the Au-Al-Yb AC shows heavy Fermi liquid behaviour. Since the diverging behaviour of the magnetic susceptibility as $T \rightarrow 0$ was only observed in the QC, the quantum critical state might correspond to an electronic state unique to the QCs, a critical state that is neither extended nor localized.

In the course of our research, we investigated Au-Ge-Yb system belongs to the 1/1 AC of a Tsai-type icosahedral QC. We have found two types of the Au-Ge-Yb ACs, which show superconductivity with transition temperatures T_c of 0.68 K and 0.36 K. The Tsai-type cluster center is occupied by Au and Ge ions in the former approximant, and by an Yb ion in the latter. For magnetism, the latter system shows a larger magnetization than the former. We present our low-temperature experiments on the electrical resistivity, magnetization, ac magnetic susceptibility, and specific heat of the Au-Ge-Yb ACs. We also discuss the relationship between magnetism and superconductivity in these new systems.

Fr.C.1_O1 - Topological surface states and double berry monopoles in the heavy fermion superconductor UPt₃

A. Nevidomskyy¹, P. Goswami²

1. *Department of Physics and Astronomy, Rice University, United States*

2. *Condensed Matter Theory Center, University of Maryland, United States*

The concept of topological states of matter has captured the imagination of physicists in the last decade, with possible applications to quantum computing. Traditionally, such topological phases are predicted to occur in fully gapped insulating or superconducting materials and are characterized by topologically protected gapless excitations on the surface. Here, I will demonstrate a generalization of this concept to metallic materials with gapless bulk excitations, focusing in particular on the B-phase of the heavy fermion superconductor UPt₃. Recent phase sensitive measurements provide strong evidence for the triplet, chiral pairing symmetry, which endow the Cooper pairs with orbital angular momentum $L_z = \pm 2$ along the c-axis. Such pairing supports both line and point nodes of the superconducting gap, and both types of nodal quasiparticles possess nontrivial topology in the momentum space. In particular, the point nodes located at the intersections of the closed Fermi surfaces with the c-axis are the double monopoles and anti-monopoles of the Berry curvature (referred to as 'double-Weyl points'). Consequently, we predict that the B phase should support an anomalous thermal Hall effect, various magneto-electric effects such as the polar Kerr effect, in addition to two topologically protected Fermi arcs on the (1,0,0) and (0,1,0) surfaces. The line node at the Fermi surface equator acts as a vortex loop in the momentum space and gives rise to the zero energy, dispersionless Andreev bound states on the (0,0,1) surface. At the transition from the B-phase to the A-phase, the time reversal symmetry is restored, and only the nodal ring survives inside the A-phase.

Fr.C.1_O2 - Superconductivity and antiferromagnetism in the half-Heusler compound HoPdBiA. Nikitin¹, X. Mao^{1,2}, Y. Pan¹, Y. Huang¹, B. Yan³, A. de Visser¹1. *Van der Waals - Zeeman Institute, University of Amsterdam, Amsterdam, The Netherlands*2. *Jimei University, Xiamen, China*3. *Max-Planck-Institut für Chemische Physik fester Stoffe, Dresden, Germany*

Half-Heusler compounds crystallize in a cubic structure. They attract ample attention because of their flexible electronic structure. Furthermore, electronic band structure calculations show selected half-Heusler compounds have an inverted band order, which makes them candidate topological semimetals or insulators (for a review see Ref. 1). Yet another interesting feature is that selected topological half-Heusler compounds, such as LaPtBi, YPtBi, LuPtBi and LuPdBi [1], are superconductors with $T_c \sim 1$ K. The band inversion, as well as the non-centrosymmetric crystal structure, is expected to give rise to unconventional superconductivity and theory predicts a mixed-parity Cooper-pair state. Recently, we reported a new member of this family: ErPdBi with a T_c of 1.22 K [2]. Moreover, ErPdBi shows antiferromagnetic order with a Néel temperature $T_N = 1.06$ K [2]. Here we report superconductivity in the presence of antiferromagnetic order in the related compound HoPdBi. Single crystals were prepared out of Bi flux. Transport measurements show superconductivity occurs below $T_c = 1.8$ K. The upper critical field, B_{c2} , has an unusual quasilinear temperature variation and reaches a value of 1 T for $T \rightarrow 0$. The Ho moments order antiferromagnetically with $T_N = 2.0$ K [3] and the AF phase boundary is located at $B_M \sim 3.6$ T for $T \rightarrow 0$. Thermal expansion measurements show a pronounced peak at the antiferromagnetic phase transition. Ac-susceptibility measurements indicate a superconducting volume fraction of 30 %, which suggests superconductivity and local-moment magnetism compete. Electronic structure calculations show HoPdBi has a topologically nontrivial band inversion. In the course of this work we learned that the occurrence of antiferromagnetism and superconductivity is a general feature of the rare earth palladium bismuthides [4].

References:

- [1] B.H. Yan and A. de Visser, MRS Bulletin 39 (2014) 859
- [2] Y. Pan et al., Europhys. Lett. 104 (2013) 27001
- [3] K. Gofryk et al. Phys. Rev. B 72 (2005) 094409
- [4] N. Nakajima et al., e-print arXiv:1501.04096v2

Fr.C.1_O3 - Linear magnetoresistance, weak antilocalization and Shubnikov-de Haas oscillations in the putative topological superconductor LuPdBi

O. Pavlosiuk¹, D. Kaczorowski¹, P. Wisniewski¹

1. Institute of Low Temperature and Structure Research, Polish Academy of Sciences

We present electronic transport and magnetic properties of single crystals of the half-Heusler phase LuPdBi, having theoretically predicted band inversion requisite for non-trivial topological properties [1]. The compound becomes superconducting below a critical temperature of 1.8 K, with a zero-temperature upper critical field of 2.3 T. Although superconducting transition is clearly reflected in the electrical resistivity and magnetic susceptibility data, no corresponding anomaly can be seen in the specific heat [2,3], alike reported for a few related superconductors: LuPtBi, YPtBi [4-6] and HoPdBi [7]. Temperature dependence of the electrical resistivity suggests existence of two parallel conduction channels: metallic and semiconducting, with the latter making negligible contribution at low temperatures. The magnetoresistance shows a weak antilocalization effect in small magnetic fields. In fields above about 1.5 T, the magnetoresistance becomes linear and does not saturate in fields up to 9 T, where it exceeds 200%. The linear magnetoresistance is observed up to room temperature. Below 10 K, it is accompanied by Shubnikov-de Haas oscillations revealing charge carriers with effective mass of 0.06 m_e and Berry phase very close to $1/2$ expected for Dirac-fermion surface states, thus corroborating topological nature of the material [2].

References:

- [1] H. Lin et al. Nature Mat. 9:546 (2010)
- [2] O. Pavlosiuk, D. Kaczorowski and P. Wisniewski, Sci. Rep. in print (2015)
- [3] Y. Nakajima et al. arXiv:1501.04096 (2015)
- [4] E. Mun et al. Phys. Rev. B 87:075120 (2013)
- [5] P. Pagliuso et al. APS March Meeting, Baltimore, abstr.: BAPS.2013.MAR.B13.13 (2013)
- [6] O. Pavlosiuk, D. Kaczorowski and P. Wisniewski, SCES'14, Grenoble, abstr.: Mo-101 (2014)
- [7] O. Pavlosiuk, D. Kaczorowski and P. Wisniewski - this conference poster

Fr.C.1_O4 - Discovery of superconductivity in Bi₂Te: evidence of universal behavior in an infinitely adaptive series under compression

R. Stillwell¹, J. Jeffries¹, S. McCall¹, Z. Jenei¹, S. Weir¹, Y. Vohra²

1. Lawrence Livermore National Laboratory, Livermore, United States

2. University of Alabama at Birmingham, Alabama, United States

The end members of the infinitely adaptive (Bi₂)_n(Bi₂Te₃)_m series, Bi and Bi₂Te₃, can be experimentally tuned to display topological surface states or superconductivity under appropriate conditions. An intermediate member of the series, Bi₂Te has been found to superconduct under similar conditions, transitioning from a semiconductor at ambient conditions to a metallic superconductor with a maximum T_c = 9.1 K at 14.5 GPa. This represents a move towards universal behavior in the infinitely adaptive (Bi₂)_n(Bi₂Te₃)_m series in which all of the superstructures converge into a metallic, superconducting state at high pressure.

Fr.C.1_O5 - Quantum oscillations in high magnetic fields, Berry phase, quantum Hall effect and superconductivity in Cu-doped bismuth selenide single crystalsS. I. Vedenev¹, T. Romanova^{1,2}, D. Knyazev^{1,2}, A. Sadakov^{1,2}*1. Lebedev Physical Institute of Russian Academy of Science, Moscow, Russia**2. International Laboratory of High Magnetic Fields and Low Temperatures, Wroclaw, Poland*

The discovery of a new class of materials 3D topological insulators (TIs) and topological superconductors (TSs) have generated a lot of excitement in condensed matter physics. Bi_2Se_3 attracted particular attention, because the intercalating copper between fivefold layers induces superconductivity below ~ 4 K. The surface electron modes of a TI are arranged in a single Dirac cone - the linear dispersion that describes massless particles. The circulating structure of the spins contributes a Berry's phase of π to the electronic wave function. Berry phase can be experimentally assessed by analyzing the Landau-level fan diagram of the Shubnikov-de Haas (SdH) oscillations due to the fact that longitudinal resistivity oscillates as $\Delta\rho_{xx} \sim \cos[2\pi(F/B_N) + \beta]$, where $-\beta$ is Berry Phase. Careful study of the π -Berry phase gives one of the key pieces of evidence for the Dirac nature of quasiparticles in TIs. Question about the value of the Berry phase in TI is still open, as there is no unambiguous experimental data in literature. In our experiment we tried to fix the question of the Berry phase value in TIs by means of magnetotransport measurements of high-quality single crystals of $\text{Bi}_{2-x}\text{Cu}_x\text{Se}_3$ in high magnetic fields up to 20 T and at temperatures down to 0.3 K. The 2D nature of the SdH oscillations in our samples was confirmed by sample rotation in magnetic field. From our data we assume that 2D SdH oscillations originating from several parallel 2D conducting channels in a $\text{Bi}_{2-x}\text{Cu}_x\text{Se}_3$ crystal. Also we show that quantum Hall effect can be observed when effective thickness of the conducting layer is less than fivefold layer in crystal structure. We also present experimental study of superconductivity in $\text{Bi}_{2-x}\text{Cu}_x\text{Se}_3$ single crystals. We have shown that the superconductivity in this 3D TI is well described by the extended Tinkham model for conventional thin-film superconductor.

Fr.C.1_O6 - Surface damage of SmB₆ through ion-irradiation

N. Wakeham¹, Y. Wang¹, Z. Fisk², F. Ronning¹, J. Thompson¹

1. *Los Alamos National Laboratory, New Mexico, United States*

2. *University of California, Irvine, California, United States*

SmB₆ is a Kondo insulator, but there is strong evidence for an intrinsic conductive surface state at low temperatures. Theoretical work indicates that SmB₆ may be a topological Kondo insulator with a topologically protected surface state that is robust against time-reversal invariant perturbations. To investigate this robustness, we have used non-magnetic ion-irradiation to damage the (001) surfaces of SmB₆ single crystals to varying depths, and have measured the resistivity as a function of temperature for each depth of damage. We observe a reduction in the residual resistivity with increasing depth of damage. Our data are consistent with a model in which the surface state is not destroyed by the ion-irradiation, but instead the damaged layer is poorly conducting and the initial surface state is reconstructed below the damage. This behavior is consistent with a surface state that is topologically protected. Investigations of time-reversal symmetry breaking perturbations of the surface layer, with magnetic ion-irradiation, will also be discussed.

Fr.C.2_I1 - Kondo Insulators: magnetism meets topology

P. Coleman^{1,2}, O. Erten¹

1. Center For Materials Theory, Dept Physics And Astronomy, Rutgers University, United States

2. Department of Physics, Royal Holloway, University of London, Egham, Surrey, United Kingdom

The electrons in Heavy fermion materials are subject to spin-orbit coupling interactions that greatly exceed their Kinetic energy. It has long been known that the spin orbit coupling stabilizes new kinds of heavy fermion metals, superconductors and 'Kondo insulators' against the competing state of magnetism. I will discuss the latest realization that spin orbit coupling can changing the topology of Kondo insulators, sometimes giving rise to Topological Kondo insulators[2,3] with surface Dirac cones. We'll specifically discuss SmB₆, a KI discovered 45 years ago, predicted to be topological in 2010[2], and tentatively confirmed to be so in a series of experimental studies of the past year[3,4,5]. I'll discuss a simple model for a topological Kondo insulator and discuss how Kondo breakdown at the surface has the effect of tuning the topological edge states from 'heavy' to 'light'. We'll review the status of the most recent measurements, including tentative spin polarized ARPES[5], de Haas van Alphen[6] and high field measurements that appear to support the idea that this is a strongly interacting topological insulator.

References:

[1] Work supported by DOE grant DE-FG02-99ER45790

[2] M. Dzero et al. Phys. Rev. Lett. 104, 106408 (2010)

[3] S. Wolgast et al, Phys. Rev. B, Rapid Comm., vol. 88, no. 18, p. 180405, Nov. 2013

[4] G. Li et al, arXiv:1306.5221 (2013)

[5] Nan Xu, X. Shi et al, Nature Communications 5:4566 (2014)

[6] S. Sebastian et al (unpublished) (2015)

Fr.C.2_O2 - Fermi surface of pressure metallised Mott insulator NiS₂

S. Friedemann¹, H. Chang², M. Gamza^{3,4}, W. Coniglio⁵, S. Tozer⁵, M. Grosche²

1. *HH Wills Laboratory, University of Bristol, United Kingdom*

2. *Cavendish Laboratory, University of Cambridge, United Kingdom*

3. *Royal Holloway University of London, United Kingdom*

4. *Jeremiah Horrocks Institute for Mathematics, Physics and Astrophysics, University of Central Lancashire, Preston, United Kingdom*

5. *National High Magnetic Field Laboratory, Tallahassee, United States*

Metals can turn into insulators when correlations become sufficiently strong. This is captured in the Mott-Hubbard model, where onsite Coulomb repulsion leads to the opening of a gap at the Fermi energy for a half-filled band. This insulating state is realised for instance in the parent compounds of cuprate superconductors. Whereas cuprates are turned into metals by controlling the filling via doping, the metallic state may also be recovered by controlling the ratio of Coulomb repulsion and kinetic energy, for instance by applied hydrostatic pressure. In proximity to the metal-insulator-transition the metal is strongly correlated and is expected to have a large Fermi surface comprising the full electron count in accordance with Luttinger's theorem. With the charge carrier count unchanged, the insulating state is predicted to be realised by localisation of electrons via divergent effective mass [1]. Here, we report resistivity and quantum oscillation measurements on the pressure-induced insulator-to-metal transition in the Mott insulator NiS₂. We demonstrate the quality of our single crystals and discuss the phase diagram for our samples. Our x-ray analysis as well as our high-pressure transport studies reveal an exceptionally low level of vacancies and impurities, a common challenge in the synthesis of NiS₂. The high quality of our crystals enabled us to perform quantum oscillation measurements for the first time in the high-pressure metallic phase of a Mott insulator. Our results on NiS₂ are consistent with the large Fermi surface obtained in DFT calculations and suggest a strong mass enhancement. We discuss these results in relation to models of NiS₂ including band-width controlled, filling controlled, and charge-transfer metal-to-insulator transitions.

References:

[1] W F Brinkman, T M Rice; Phys Rev B; 10 4302 (1970)

Fr.C.2_O3 - Pressure effect on the ferromagnetic-metal to ferromagnetic-insulator transition in $K_2Cr_8O_{16}$

Y. Ueda¹, T. Yamauchi²

1. *Toyota Physical And Chemical Research Institute, Nagakute, Japan*
2. *Institute for Solid State Physics, University of Tokyo, Tokyo, Japan*

There exists the general relation between magnetism and electronic transport properties that insulating transition metal oxides are typically antiferromagnetic, and ferromagnetism, particularly double-exchange (DE) ferromagnetism, goes hand in hand with metallicity. The chromium hollandite, $K_2Cr_8O_{16}$ is a DE ferromagnetic metal (FM). We found that this DE-FM phase transforms to an insulator, retaining fully polarized ferromagnetism [1]. We also revealed from the precise structure analysis and electronic structure calculations that this transition is caused by a Peierls instability in the quasi-one-dimensional column structure made of four coupled Cr-O chains rather than the double chains, namely the transition is a very rare example of the Peierls transition of fully spin-polarized electron systems [2]. The effect of opening of the band gap on DE-FM has been theoretically studied, which predicts novel ground state phase diagram [3]. Motivated by the theoretical study we have investigated the pressure effect on the ferromagnetic metal-insulator transition in $K_2Cr_8O_{16}$. The DE-FM phase is sharply suppressed, while the Peierls ferromagnetic insulator (FI) phase is considerably robust. As a result, the transition temperatures meet at approximately 3.5 GPa and 80 K. Above 3.5 GPa, the ferromagnetism disappears and the ground state becomes antiferromagnetic (AFI) or paramagnetic (PI). The magnetization and magnetoresistance measurements under high pressure suggest an intermediate insulator phase with partial spin polarization between the FI and AFI (PI) phases, which seems to realize the theoretical prediction.

References:

- [1] K. Hasegawa et al., Phys. Rev. Lett. 103 (2009) 146403
- [2] T. Toriyama et al., Phys. Rev. Lett. 107 (2011) 266402
- [3] S. Nishimoto and Y. Ohta, Phys. Rev. Lett. 109 (2012) 076401

Fr.C.2_O4 - Muon Spin Relaxation studies of Mott Transition Systems: RNiO_3 , $(\text{Ca,Sr})_2\text{RuO}_4$ and $(\text{Sr,Lu})_2\text{IrO}_4$

B. Frandsen¹, L. Liu¹, S. Cheung¹, Y. Uemura¹, T. Munsie², M. Wilson², A. Hallas², G. Luke², B. Chen³, C. Jin³, C. Ding⁴, F. Ning⁴, J. Alonso⁵, J. Ravichandran⁶, P. Kim⁶, C. Serrao⁷, R. Ramesh⁷, F. Nakamura⁸, Y. Maeno⁹

1. Department of Physics, Columbia University, United States
2. Department of Physics, McMaster University, Hamilton, Canada
3. Institute of Physics, Chinese Academy of Sciences, Beijing, China
4. Department of Physics, Zhejiang University, Hangzhou, China
5. Instituto de Ciencia de Materiales de Madrid (ICMM), CSIC, Madrid, Spain
6. Department of Physics, Harvard University, Cambridge, United States
7. Department of Materials Science and Engineering, UC Berkeley, Berkeley, United States
8. Kurume Institute of Technology, Kurume, Japan
9. Department of Physics, Kyoto University, Kyoto, Japan

The hallmark of a Mott insulator is a metal-insulator transition (MIT) upon cooling, which is often accompanied by the appearance of antiferromagnetic (AF) order. Frequently, the MIT and AF order can be suppressed by doping or pressure, resulting in a zero-temperature quantum phase transition. Here, we present detailed muon spin relaxation (muSR) measurements of three families of Mott insulators chosen from 3d, 4d, and 5d transition-metal oxides— RNiO_3 ($\text{R}=\text{Sm}, \text{Nd}, \text{Pr}, \text{La}$), $(\text{Sr,Lu})_2\text{IrO}_4$, and $(\text{Ca,Sr})_2\text{RuO}_4$ —to elucidate generic and system-specific behavior in the vicinity of the quantum critical point. We exploit the unique capability of muSR to independently determine the magnetically ordered volume fraction and the ordered moment size to examine first- and second-order behavior of the AF order. In all systems studied, we find that the magnetic order is suppressed near the quantum critical point through reduction of the ordered volume fraction, displaying a “stretched” Mott transition with significant phase separation between magnetic and paramagnetic regions over a wide temperature interval. We also find that the ordered moment size near the critical point remains constant in the nickelates but is gradually diminished in the other systems, in parallel with the reduced volume fraction. Finally, systems for which the MIT and AF transition coincide in temperature show first-order behavior of the moment size upon cooling, whereas systems for which the MIT and AF transition are decoupled show second-order behavior.

These observations may aid in gaining a deeper understanding of Mott physics.

Fr.C.2_05 - A population inversion observed in surface Dirac cone of topological insulator Sb_2Te_3

K. Sumida¹, S. Zhu¹, M. Taniguchi^{1,2}, Y. Ishida³, M. Ye⁴, K. Kokh^{5,6}, O. Tereshchenko^{6,7}, S. Shin³, A. Kimura¹

1. Graduate School of Science, Hiroshima University, Horoshima-shi, Japan
2. Hiroshima Synchrotron Radiation Center, Higashi-Hiroshima, Japan
3. Institute for Solid State Physics, University of Tokyo, Tokyo, Japan
4. Shanghai Institute of Microsystem and Information Technology, Chinese Academy of Science, Shanghai, China
5. Institute of Geology and Mineralogy, Siberian Branch, Russian Academy of Sciences, Moscow, Russia
6. Novosibirsk State University, Novosibirsk, Japan
7. Institute of Semiconductor Physics, Siberian Branch, Russian Academy of Sciences, Moscow, Russia

Topological insulators (TIs) show various properties such as a suppression of backscattering and spin-polarized massless Dirac fermion at the surface or interface. These properties are caused by topological surface states protected by time-reversal symmetry and a strong spin-orbit coupling. Therefore TIs are expected next-generation spintronic devices utilizing dissipationless spin current transport. Among so-far predicted binary chalcogenides, Bi_2Se_3 and Bi_2Te_3 have been experimentally established to be TIs possessing surface Dirac cones by using angle-resolved photoemission spectroscopy (ARPES). However, the topological characteristics of Bi_2Te_3 has not been sufficiently understood because the surface Dirac cone is almost located in the unoccupied state region due to its p-type character, which cannot be accessed by ARPES. Since Bi_2Te_3 is predicted to have a relatively large energy gap and an ideal massless Dirac surface state in sharp contrast to Bi_2Se_3 and Bi_2Te_3 , it is crucial to understand its Dirac Fermion characteristics from the electronic structure standpoint. Here we focus on time- and angle-resolved photoemission spectroscopy (TrARPES) implementing the pump-probe method. It allows us to observe not only unoccupied electronic state but also hot carrier dynamics. The TrARPES experiments were performed with linearly polarized pump (1.48 eV) and probe (5.92 eV) pulses caused by Ti:sapphire laser system at Institute of Solid State Physics in University of Tokyo. We have studied the Sb-rich [$\text{Sb}_{2.01}\text{Te}_{2.99}$ (ST#1)] and the Te-rich [$\text{Sb}_{1.98}\text{Te}_{3.02}$ (ST#2)] crystals, the former has the smaller hole carrier concentration than the latter. We have clearly observed the surface Dirac cones with Dirac points located at 188 meV and 218 meV for ST#1 and ST#2, respectively. For both samples, we observe a population inversion below and above the Dirac point. Moreover, it becomes clear in ST#2 that the decay time is shorter than ST#1 reflecting the difference in the size of the Fermi surface.

Fr.C.3_O1 - Magnetism of disordered Heusler alloys

M. Leitner¹, P. Neibecker¹, W. Petry¹

1. Technische Universität München, Germany

Heusler alloys constitute a class of systems with great potential for applications. Most of their appeal rests on the diverse aspects of magnetism in these materials, including the ferromagnetic shape-memory effect, the magnetocaloric effects, and half-metallicity. Due to their intermetallic nature, off-stoichiometry and site disorder constitute degrees of freedom additional to temperature. In previous work we have shown that in Ni₂MnAl well-defined states of order can be prepared, which are accessible via correspondingly varying magnetic transition temperatures [1]. Here we report on a detailed characterization of the peculiar magnetic behaviour, e.g. temperature- and field-dependent magnetization for specific states of order, with nearly constant ferromagnetic susceptibilities up to the highest fields. We present a microscopic model of how Mn/Al site disorder and site-specific ferro- and antiferromagnetic interactions of the Mn moments give rise to observed features as a function of field, temperature, and order.

References:

[1] P. Neibecker, M. Leitner, G. Benka, W. Petry, Appl. Phys. Lett. 105, 261904 (2014)

Fr.C.3_O3 - Unusual nonlinear magnon-magnon and magnon-phonon interaction in 2d triangular lattice of RMnO₃

J.G. Park^{1,2}, J. Oh^{1,2}, M. Duc Le^{1,2}, J. Jeong^{1,2}, H. Sim^{1,2}, H.H. Nahm¹, T.G. Perring³, K. Nakajima⁴, S. Ohira-Kawamura⁴, O. Yoshida⁵, H. Eisaki⁵

1. *Center for Correlated Electron Systems, Institute For Basic Science (IBS), Seoul, Republic of Korea*
2. *Department of Physics And Astronomy, Seoul National University, Seoul, Korea*
3. *ISIS Facility, STFC Rutherford Appleton Laboratory, Oxfordshire, United Kingdom*
4. *Neutron Science Section, MLF Division, J-PARC Center, Tokai, Ibaraki, Japan*
5. *National Institute of Advanced Industrial Science and Technology (AIST), Tsukuba, Japan*

Magnon is a fundamental and long-lived quasiparticle in solid, and so it is rather rare to observe them to decay. It has so far only been seen in a very limited case like one dimensional magnets or quantum magnets. However, it has been recently suggested theoretically [1] that such a rare event of magnon decay can occur even for classical spin systems when it meets certain conditions, i.e. noncollinear antiferromagnetic structures. This nonlinear magnon interaction is also predicted to be strongest for a two-dimensional triangular lattice. In this work, we have studied the spin dynamics of several such triangular lattice systems in the form of hexagonal magnanites, RMnO₃. RMnO₃ is one of extensively studied multiferroic materials, and was found to have a strong spin-lattice couple at the antiferromagnetic transition around 80 ~ 100 K [2]. Below the transition, it forms one of the so-called 120-degree structures, making it an ideal system to study the nonlinear magnon interaction. By measuring the spin waves over the full Brillouin zone, we have examined the fine details of the spin dispersion curves to find out that our data reveal the three key signatures of the nonlinear magnon interactions theoretically predicted [3]. More recently, we have extended this work to study a possible magnon-phonon coupling in our spin waves [4]. We will use our experimental results to test these two unusual interactions. Moreover, we will give not only qualitative but also quantitative descriptions of the two interactions in our data.

References:

- [1] M. E. Zhitomirsky and A. L. Chernyshev, *Rev. Mod. Phys.* 85, 219 (2013)
- [2] Seongsu Lee, et al., *Nature* 451, 805 (2008)
- [3] Joosung Oh, et al., *Phys. Rev. Lett.* 111, 257202 (2013): Editors' Suggestion
- [4] Joosung Oh, et al., (in preparation)

Fr.D.1_11 - The AC Wien effect and non-linear non-equilibrium susceptibility in spin ice

P. Holdsworth¹, V. Kaiser^{1,3}, S. Bramwell², R. Moessner³

1. *Ecole Normale Supérieure De Lyon, Lyon, France*

2. *London Centre for Nanotechnology, UCL, London, Great Britain*

3. *Max Planck, Dresden, MPIPKS, Germany*

We show that the Coulomb fluid of magnetic monopoles in spin ice (a "magnetolyte") exhibits the second Wien effect in the presence of an AC magnetic field [1]. This involves an increase of the monopole density -- a universal and robust enhancement for Coulomb systems in an external field [2] which in turn speeds up the magnetization dynamics. We predict that the monopole density increase is directly related to the non-linear magnetic response providing a signal of the Wien effect that is specific to magnetic systems. The non-linear non-equilibrium susceptibility is treated analytically within a phenomenological model. Through this study, we gain new insights into the AC version of the classic Wien effect. One striking discovery is that of a frequency window where the Wien effect for magnetolyte and electrolyte are indistinguishable, with the former exhibiting perfect symmetry between the charges as well as a new low-frequency regime where the growing magnetization counteracts the Wien effect and hinders any permanent currents. We discuss conditions required to observe our predictions of the AC Wien effect in the non-linear susceptibility of $\text{Dy}_2\text{Ti}_2\text{O}_7$.

References:

[1] V. Kaiser, S. T. Bramwell, P. C. W. Holdsworth, R. Moessner, arXiv:1412.4981

[2] V. Kaiser, S. T. Bramwell, P. C. W. Holdsworth, R. Moessner, *Nature Materials*, **12**, 1033-1037 doi :10.1038/nmat3729, (2013).

Fr.D.1_O2 - Magnetoelectricity of the spin-ice compound $\text{Ho}_2\text{Ti}_2\text{O}_7$

T. Herrmannsdörfer¹, R. Schönemann^{1,2}, E. Green¹, L. Opherden^{1,2}, R. Skrotzki^{1,2}, Z. Wang¹, H. Kaneko³, H. Suzuki³, J. Wosnitza^{1,2}

1. *Dresden High Magnetic Field Laboratory (HLD-EMFL), Helmholtz-Zentrum Dresden-Rossendorf, Dresden, Germany*

2. *Institut für Festkörperphysik, TU Dresden, Dresden, Germany*

3. *Faculty of Mathematics and Physics, Kanazawa University, Kanazawa, Japan*

The frustrated balance of competing spin-spin interactions leads to a wide spectrum of fascinating physical properties in the two pyrochlore compounds, $\text{Ho}_2\text{Ti}_2\text{O}_7$ and $\text{Dy}_2\text{Ti}_2\text{O}_7$. Their rare-earth magnetic moments obey the “ice rules” by mapping spin configurations which resemble the proton configurations in water ice, organize as interweaving networks of aligned dipoles, i.e. Dirac strings, and constitute thermally-excited point defects which behave as magnetic monopole charges at far separated string ends. Here we present a detailed investigation of the $\text{Ho}_2\text{Ti}_2\text{O}_7$ spin-ice compound by means of dc-magnetization, magnetic ac-susceptibility, as well as dielectric polarization measurements. Data have been taken both in a wide magnetic-field (up to 14 T) and temperature range (down to 30 mK). The dynamic magnetic susceptibility of $\text{Ho}_2\text{Ti}_2\text{O}_7$ shows a distinct maximum at the spin freezing temperature, $T_f = 1.3$ K, accompanied by a huge increase of the spin viscosity deduced from the ratio of imaginary and real susceptibility components. At the same temperature, we observe a decrease of the dielectric constant. Its temperature dependence below 1 K suggests the assumption that the dielectric properties of the pyrochlore compound are directly related to the density of magnetic monopole excitations. The magneto-electric coupling in $\text{Ho}_2\text{Ti}_2\text{O}_7$ emerges clearly by applying a symmetry-breaking magnetic field which allows for a manipulation of the density and orientation of Dirac strings. Our experiments provide a detailed insight into the magnetic-monopole physics of spin ice compounds and illustrate a manifold duality of spin and charge degrees of freedom in these materials.

Fr.D.1_O3 - Magnetic charge crystal phase embedded in a disordered spin lattice in thermally-active artificial spin ice

I. Chioar^{1,2}, Benjamin Canals^{1,2}, D. Lacour³, M. Hehn³, B. Santos Burgos⁴, T.O. Mentès⁴, A. Locatelli⁴, F. Montaigne³, N. Rougemaille^{1,2}

1. CNRS, Institut NEEL, Grenoble, France

2. Université Grenoble Alpes, Institut NEEL, Grenoble, France

3. Institut Jean Lamour, Université de Lorraine and CNRS, Vandoeuvre lès Nancy, France

4. Elettra - Sincrotrone Trieste S.C.p.A., S.S: 14 km 163.5 in AREA Science Park, Basovizza, Trieste, Italy

Artificial spin ices (ASI) are systems designed to explore the intriguing physics observed in magnetically frustrated materials. Generally fabricated by using lithography techniques, they offer almost infinite possibilities to construct a wide variety of spin models which can be accessed experimentally in a controlled manner [1]. ASI systems have been the subject of intense research in the last few years and have allowed the investigation of a rich physics and fascinating phenomena, such as the exploration of the extensively degenerate ground-state manifolds of spin ice systems, the evidence of new magnetic phases in purely two-dimensional lattices, and the observation of pseudo-excitations involving classical analogues of magnetic monopoles. In this contribution, we investigate magnetic frustration effects in thermally active ASI. Starting from a paramagnetic state, the system is cooled down below the Curie temperature of the constituent material. The resulting magnetic configurations show that our arrays are locally brought into a novel magnetic phase characterized by a magnetic charge crystal embedded in a disordered spin lattice. By studying our arrays on a larger scale, we find the unambiguous signature of an out-of-equilibrium physics that reveals the spin kinetics which lead to this exotic spin texture [2].

References:

[1] R. F. Wang et al., Nature 439, 303 (2006)

[2] I. A. Chioar et al., Phys. Rev. B 90, 220407 (2014)

Fr.D.1_O4 - Magnetic crystallography and 'jellyfish' structure of monopoles in spin ice

L. Jaubert¹, M. Udagawa², C. Castelnovo³, R. Moessner⁴

1. *Okinawa Institute of Science And Technology, Japan*
2. *University of Tokyo, Japan*
3. *University of Cambridge, United Kingdom*
4. *MPI-PKS Dresden, Germany*

Pyrochlore materials have proven to be fertile soil for the emergence of exotic physics such as magnetic monopoles in $\text{Dy}_2\text{Ti}_2\text{O}_7$ or the spontaneous Hall effect observed in $\text{Pr}_2\text{Ir}_2\text{O}_7$. In this talk, we shall review some of the recent developments in the physics of magnetic monopoles in spin ice, especially when magnetic and electric degrees of freedom are coupled together. As shown by Khomskii (Nature Comm. 2012), the spin texture of magnetic monopoles allow them to carry an electric dipole moment. We will show how such magneto-electric coupling opens the path for a magnetic analogue of crystallography by stabilizing long-range ordered crystals of magnetic charges. Here, this crystal takes the form of a double-layer structure of monopoles, reinforced by a magnetic field. This structure has been observed in $\text{Tb}_2\text{Ti}_2\text{O}_7$ under large [110] field which allows us to extract the typical size of electric dipole moments in rare-earth oxides. Furthermore, when coupled to itinerant electrons, magnetic moments are expected to interact via RKKY interactions. We will explain how, for some specific range of parameters, the resulting effective interaction between monopoles gives rise to a new kind of branching structure made of same-sign monopoles, which we figuratively name 'monopole jellyfish'. This jellyfish structure supports an emergent chirality able to encode time-reversal symmetry breaking which could be related to spontaneous Hall effect.

Fr.D.1_O5 - Magnetic phases up to 120 T in a triangular-lattice antiferromagnet CuCrO₂

A. Miyata¹, K. Ohgushi¹, S. Takeyama¹

1. ISSP, Univ. of Tokyo, Tokyo, Japan

A delafossite oxide CuCrO₂ is one of the typical multiferroic compounds in triangular-lattice antiferromagnets [1] and has shown a rich magnetic phase diagram under high magnetic fields due to the geometrical spin frustration [2, 3]. However the full magnetic phase diagram of CuCrO₂ has not yet been obtained due to its strong magnetic interactions (Curie-Weiss temperature is about -210 K [1].) We investigated the magnetic phases of CuCrO₂, using magnetization and magneto-optical measurements under ultrahigh magnetic fields of up to 120 T. A 1/3 magnetization plateau was newly observed around 100 T. Magneto-optical spectroscopy revealed the other distinct anomalies below and above the 1/3 plateau phase showing rich magnetic phases due to the interplay of its geometrical spin frustration and magnetic field.

References:

[1] K. Kimura et al. , Phys. Rev. Lett. 103, 107201 (2009)

[2] E. Mun et al., Phys. Rev. B 89, 054411 (2014)

[3] S.-Z. Lin et al., Phys. Rev. B 89 , 220405(R) (2014)

Fr.D.2_11 - First principles design of complex magnetic oxides

A. Ernst¹

1. Max Planck Institute of Microstructure Physics, Weinberg, Germany

The ability to predict material properties is a fundamental requirement for scientific and technological advancement. One of our most important research fields is the computational material design of oxidic materials. First-principles design of oxides is one of most ambitious challenges in modern computational physics. The electronic and magnetic properties of these materials are substantially affected by strongly localized electrons, complex crystalline structures, and mixed valencies of magnetic ions. To describe these specific features of oxides we develop ab-initio concepts that are put in state-of-the-art computer codes. Using efficient numerical algorithms and modern supercomputers we can simulate experiments and study properties of realistic systems. More specifically, our research on oxides is currently focused on study of crystalline structures of complex oxidic materials and their electronic and magnetic properties. A detailed description of these systems often involves a large number of degrees of freedom, especially when periodic surfaces or interfaces with large unit cells result from surface instabilities or misfits at interfaces. In my talk, I present our first-principles approach to design magnetic oxides, which are highly attractive for spintronic applications. The approach is based on the multiple-scattering theory and provides explicitly the Green function, which can be used in many applications such as spectroscopy, transport and many-body physics. Combined with the coherent-potential approximation this method can be used as well for the description of alloys and pseudo-alloys. An important feature of our method is the treatment of electronic correlation effects, which can be substantial in many complex oxides. In particular, we combine several approaches, designed for strongly correlated materials, to compute measurable quantities, which can be compared with available experiments. A such direct comparison enables us to adjust several important parameters such as the degree of electronic correlations, the oxidation states and the chemical composition of the investigated system. The efficiency of our approach will be illustrated by studies of several complex oxides, which are attractive for spintronic applications.

Fr.D.2_O2 - Half metallicity with huge room temperature spin polarization in the ferromagnetic Heusler compound Co₂MnSi

A. Kronenberg¹, J. Minar², J. Braun², S. Chadov³, B. Balke⁴, A. Gloskovskii⁵, M. Kolbe¹, H. J. Elmers¹, G. Schönhense¹, H. Ebert², C. Felser³, M. Kläui¹, M. Jourdan¹

1. *Physics, Mainz University, Germany*

2. *Chemistry, LMU München, Germany*

3. *MPI-CPfS, Dresden, Germany*

4. *Chemistry, Mainz University, Germany*

5. *DESY, Hamburg, Germany*

The magnitude of the room temperature spin polarization of ferromagnetic materials is a key property for their application in spin transport-based electronics. Thus Heusler compounds, due to their predicted bulk half-metallic properties, i.e. 100% spin polarization at the Fermi energy, are in the focus of interest. However, for most applications it is not the bulk but the surface or interface of the material, which is relevant. Investigating optimized thin films of the compound Co₂MnSi by in-situ spin-resolved UPS, we were able to demonstrate for the first time half-metallicity in combination with directly measured 93% spin polarization at room temperature in the surface region of a Heusler thin film [1]. Our novel band structure and photoemission calculations including all surface-related effects [2] show that the observation of a high spin polarization in a wide energy range below the Fermi energy is related to a stable surface resonance in the majority band of Co₂MnSi extending deep into the bulk of the material. Spin-integrated ex-situ HAXPES with a photon energy of 6 keV on Co₂MnSi thin films and spin-integrated in-situ UPS was carried out. The UPS and the HAXPES results fundamentally agree although the information depth of both experiments varies from less than 1 nm to 20 nm. Nearly quantitative agreement of the calculations with the experiments for both, UV and hard X-ray photon energies was obtained.

References:

[1] M. Jourdan et al. Nat. Commun. 5, 3974 (2014)

[2] J. Braun et al. New J. Phys. 16, 015005 (2014)

Fr.D.2_O4 - Observation of quantum oscillations on La-doped Sr₃Ir₂O₇ single crystals

Z. Feng¹, J. Bruin², E. Hunter³, R. Perry¹, D. Mcmorrow^{1,4}

1. London Centre For Nanotechnology, University College London, United Kingdom

2. High Field Magnetic Laboratory, Nijmegen, The Netherlands

3. School of Physics & Astronomy, The University of Edinburgh, Edinburgh, United Kingdom

4. Department of Physics and Astronomy, University College London, United Kingdom

In this presentation, I will report our recent measurements of quantum oscillations in La-doped Sr₃Ir₂O₇. The layered perovskite iridates are correlated insulators have recently attracted great interest since they are sharing key structural and electronic properties with the high-Tc cuprates. Intriguingly, many iridates systems that are predicted to be metallic or even superconducting theoretically turn out to be insulators. Studies on the electronic states of these system are still rare due to lack of metallic candidates. With our successfully prepared the metallic (La_xSr_{1-x})₃Ir₂O₇ x=0.03-0.08 samples, we carried out torque measurement with the high magnetic field at High Field Lab Nijmegen Netherlands. Quantum oscillations from the torque signal have been observed, giving us a direct evidence of the existence of Fermi pockets in these gapless samples. The features of Fermi surface are highly dependent to the doping level, which also reflects in the energy gap and metal insulation transition. Our quantum oscillation results are in good agreement with our previous results on the Angle-resolved photoemission spectroscopy (ARPES) and LDA+U calculations [1].

References:

[1]. A. de la Torre et al., Phys. Rev. Lett. 113, 256402 (2014)

Fr.D.2_O5 - Discrete atomic-like crystal-field states in LaCoO₃ , K₂CoF₄ and CoO MOTT insulators

R. Radwanski^{1,2}, D. Nalecz¹, Z. Ropka²

1. *Institute of Physics, Pedagogical University, Krakow, Poland*

2. *Center of Solid State Physics, Krakow, Poland*

CoO, K₂CoF₄ and LaCoO₃ are considered as prototype oxides with very strong electron correlations, not well theoretically described so far. We provide a first-principles consistent description of these monoxides, which reconciles their insulating ground state and a strong magnetism related to 3d electrons in the incomplete 3d shell. We work in the strongly-correlated crystal-field approach with forbidden charge fluctuations (large U). From really first-principles calculations we have evaluated a full set of the crystal-field coefficients accounting for lattice and local distortions for all these compounds. They are real potentials, in the atomic scale, in contrary to pseudopotentials usually introduced in modern theories. We have calculated the electronic structure both in the paramagnetic and magnetic state and the temperature dependence of the specific heat in 0-800 K range, reproducing the lambda-type peak at TN. For the formation of the magnetically-ordered state the spin-orbit coupling is fundamentally important. We have reproduced values of the magnetic moment and its direction in the crystal structure. We have found that small lattice off-octahedral distortions (tetragonal in case of CoO and K₂CoF₄) determine the direction of the magnetic moment. For these compounds we have found a quite substantial orbital magnetic moment, of 0.5-1.0 μ_B . Nonmagnetic state of LaCoO₃ can be also regarded as originating from the orbital magnetism. The discrete atomic-like states have been found by EPR experiments to be very thin in a sharp contrast to band theories. The maximal energy of the spin waves (40 meV) observed in CoO is, according to our calculations, the splitting of the ground-state doublet by magnetic interactions. According to the developed Quantum Atomistic Solid-State Theory (QUASST) we claim that the conventional crystal-field interactions should be evaluated the first for any meaningful description of magnetic and electronic properties of any 3d/4f/5f compound.

Fr.D.3_O1 - Prediction of magnetic ordering in layered technetium perovskite Sr_2TcO_4

A. Horvat¹, L. Pourovskii², M. Aichhorn³, J. Mravlje¹

1. *Jozef Stefan Institute, Ljubljana, Slovenia*

2. *Ecole Polytechnique, Palaiseau, France*

3. *TU Graz, Graz, Austria*

Technetium perovskites are scarcely investigated due to the radioactivity of Tc. Few years ago strong antiferromagnetism with transition temperatures reaching 1000K has been observed in cubic Tc perovskite. Magnetic properties of layered compound Sr_2TcO_4 have not been measured so far. By combination of density functional theory with the dynamical mean field theory we extract the exchange interactions and predict the ordering to be of the checkerboard type. The frustration in the bct lattice would suppress magnetic ordering if it was not for the dipole-dipole interactions. Including the dipole-dipole interactions we predict the ordering temperature to be 500K. We discuss the role of the Hund's rule coupling for strong magnetism in Tc perovskites and speculate on the possible superconductivity in doped Tc perovskites.

Fr.D.3_O2 - Inherent orbital-selective tunneling in a STM measurement

Y. Takahashi¹, K. Ienaga¹, N. Kawamura^{1,2}, T. Miyamachi¹, A. Ernst³, F. Komori¹

1. ISSP, Univ. of Tokyo, Japan

2. STRL, NHK, Japan

3. MPI, Halle, Germany

Surface morphology of materials is widely discussed based on the topographic image obtained by the scanning tunneling microscopy (STM) measurement. What should be taken care is that its image does not necessarily correspond to an actual atomic coordination at the surface, because it just reflects the electron tunneling probability between the tip and the surface states. In most cases, bias voltage V is the only parameter which causes the image change. In some compounds, however, it has been reported that the topographic images become totally different depending on the tip-surface distance d . Although it is another important parameter for the tunneling process, systematic experimental study on a d -dependent change of the images has not been conducted in any systems so far. For revealing the influence of d on the topographic images, we took a series of d -dependent topographic images of monoatomic-layer iron-nitride islands fabricated on Cu(001). When the tip became closer to the sample surface, topographic images changed to show a dimerized structure rather than a dot one. This investigation links two incompatible topographic images previously observed for iron nitrides of the same surface symmetry [1,2]. Accompanied by this image change, dI/dV spectra also showed the d dependency. These results imply that the surface states detected by the tip shifted from s/p to d due to a different decay length of each state.

References:

- 1) J. M. Gallego et al., Phys. Rev. Lett. 95, 136102 (2005)
- 2) Y. Takagi et al., Phys. Rev. B 81, 035422 (2010)

Fr.D.3_O3 - The magnetism, energetic stability and magneto-optical properties of the Rh₂Mn-Bi-Al and Ir₂Mn-Bi-Al alloys

D. Legut¹, J. Kudrnovsky², J. Hamrle¹

1. VSB-Technical University of Ostrava, Czech Republic
2. Institute of Physics ASCR, Prague, Czech Republic

We have performed first-principle calculations to investigate structural, electronic, magnetic, and optical properties of Rh₂MnAl and Ir₂MnAl Heusler alloys using density functional theory [1]. In contrast to the Refs. [2,3,4] where only the ferromagnetic ordering were considered, here we anticipated also antiferromagnetic ordering along [001] and [111] crystal axis. In accord with the experimental data our calculation showed that the Rh₂MnAl possesses the most stable spin ordering to be antiferromagnetic along [111] crystal axis[5], whereas in the case of the Ir₂MnAl in contrast to the Ref. [5] we obtained as the most stable spin configuration the ferromagnetic ordering. We found that the ferromagnetic ordering could be induced by a strain of a few percent. The enhancement of the MO effects is done by a substitution of heavier element Bi instead Al, i.e. Rh₂MnBi and Ir₂MnBi. However, at the same time the system comes to the verge of the thermodynamic stability [2]. Therefore, we investigated a mixed phases, i.e. Rh₂Mn(Al/Bi) and Ir₂Mn(Al/Bi) as well as the disorder of the pure Rh₂MnAl(Ir₂MnAl) and Rh₂MnBi(Ir₂MnBi) phases. The influence of the substitution as well as the disorder vs. ordered compound on the MO effects were investigated. The origin of the enhancement of the MO effects by the Bi substituted Heusler alloys is predominately by the hybridization and increase of the spin-orbit interaction (SOI). The work was supported by the Grant Agency of the Czech Republic, project reg. No. 13-30397S.

Fr.D.3_O4 - Origin of non-monotonic concentration and temperature dependence of magnetocrystalline anisotropy in $(\text{Fe}_{1-x}\text{Co}_x)_2\text{B}$ alloys

K. Belashchenko¹, I. Zhuravlev¹, L. Ke², M. Daene³, L. Benedict³, V. Antropov²

1. *University of Nebraska-Lincoln, Lincoln, United States*

2. *Ames Laboratory, Ames, United States*

3. *Lawrence Livermore National Laboratory, Livermore, United States*

Magnetocrystalline anisotropy energy K in $(\text{Fe}_{1-x}\text{Co}_x)_2\text{B}$ alloys exhibits an unusual, non-monotonic variation with concentration and temperature [1]. The origin of this behavior is elucidated using a detailed first-principles electronic structure analysis. Both chemical and spin disorder are treated within the coherent potential approximation. We find that concentration [2] and temperature dependence of K is reproduced in all important details. These features include three spin reorientation transitions as a function of concentration, a temperature-driven spin reorientation transition at the Fe-rich end, and non-monotonic temperature dependence at the Co-rich end. To understand the origin of these features, we analyze the electronic spectral functions as well as the spin and wave vector-resolved contributions to K . We find that the unusual variation of K is due to the varying occupation of the minority-spin bands as a function of x and T , spin-orbital selection rules, and band broadening induced by substitutional and thermal spin disorder. The latter effect is particularly important near the Co-rich end where a large positive contribution to K is made by a pair of nearly degenerate bands. We also find that at the optimal Co concentration of 30%, K depends strongly on the tetragonality and doubles under a modest 3% increase of the c/a ratio. This suggests that the magnetocrystalline anisotropy can be further enhanced using epitaxial or chemical strain.

[1] A. Iga, Jpn. J. Appl. Phys. 9, 415 (1970)

[2] K. D. Belashchenko et al., Appl. Phys. Lett. 106, 062408 (2015)

Fr.E.1_I1 - Electron Holography and Lorentz microscopy for quantitative measurements of local magnetic properties and in-situ experiments

E. Snoeck^{1,2,4}, C. Gatel^{1,4}, Cesar Magen^{2,4}, Aurelien Maseboeuf^{1,4}, Luis Alfredo Rodriguez^{1,2,4}, Thomas Blon^{3,4}, Lise Marie Lacroix^{3,4}, Francisco Bonilla^{3,4}

1. CEMES-CNRS 29, Toulouse, France

2. Laboratorio de Microscopias Avanzadas (LMA), Instituto de Nanociencia de Aragón (INA), Universidad de Zaragoza, Zaragoza, Spain

3. LPCNO-INSA, Av de Rangueil, Toulouse, France

4. Transpyrenean Associated Laboratory for Electron Microscopy (TALEM), CEMES-INA, CNRS-Universidad de Zaragoza, Zaragoza, Spain

Electron holography (EH) and Lorentz microscopy (LTEM) are powerful TEM methods particularly efficient for the quantitative studies of local electrostatic and magnetic fields with respective spatial resolution of the order of few nanometers for EH and few tens of nm for LTEM and over fields of view as large as few microns. In addition, both allow performing in-situ measurements for the analysis of magnetic reversal processes as function of external applied field or electric current at various temperatures. The basics of EH and LTEM will be presented and illustrated by recent results obtained on the size dependence of Fe nanocubes magnetic configurations at remanence for sizes varying between 15 to 30 nm and on the complete mapping of the magnetic fields generated by a Hard Disk Drive writer as a function of an applied electrical current in situ in a TEM [1]. In a last part, latest in-situ LTEM results on the reversal magnetization mechanisms obtained on magnetic Co antidot arrays of 160 nm when applying the magnetic field along the easy and the hard axis [2] will be presented. These local EH and LTEM magnetic measurements are comforted by successful micromagnetic simulationsthat will be presented .

References:

[1] In situ electron holography of the dynamic magnetic field emanating from a hard-disk drive writer J.F. Einsle, C. Gatel, A. Maseboeuf, R. Cours, M.A. Bashir, M. Gubbins, R. M. Bowman and E. Snoeck Nano Research, 1-9, Nov. 2014

[2] High resolution imaging of remanent and dynamic magnetic superdomain structures in high-density cobalt antidot arrays L.A. Rodriguez Gonzalez, C. Magen, E. Snoeck, C. Gatel, et al. Nanotechnology. 25 (2014) 385703

Fr.E.1_O2 - Scanning gate microscopy of domain wall nanosensor

H. Corte-León^{1,2}, P. Krzysteczko³, F. Marchi⁴, J. Motte⁴, H. Werner Schumacher³, V. Antonov², N. Dempsey⁴, O. Kazakova¹

1. National Physical Laboratory, Teddington, United Kingdom

2. Royal Holloway University of London, Egham, United Kingdom

3. Physikalisch-Technische Bundesanstalt, Braunschweig, Germany

4. Univ. Grenoble Alpes, Inst. NEEL, Grenoble, France

By measuring the change in the depinning field of a domain wall (DW) trapped in magnetic nanodevices it is possible to detect small magnetic moments, *e.g.* from magnetic beads (MB), and use such devices as nanosensors in metrological and biomedical applications^{1,2}. Changes in the magnetic state of these structures and, hence, presence/absence of a DW can be detected by measuring the electrical resistance of the device due to the anisotropic magnetoresistance effect (AMR)^{1,2}.

To study sensitivity of DW nanosensors to small magnetic moments, we present scanning gate microscopy studies of the interaction between a micromagnet and a DW nanosensor. The electrical resistance of an L-shaped permalloy DW-device with the width of 75 nm is measured in correspondence to a 3D position of the scanning probe. The custom-made probe comprises an NdFeB microsphere (\varnothing 1 μ m) attached to a non-magnetic AFM tip³⁻⁶. The presence/absence of a DW in the corner of the nanostructure is controlled by an in-plane external magnetic field. We demonstrate the stray-field mediated interaction between the micromagnet and the DW, which appears as the change in the AMR signal measured in the close proximity of the probe to the DW position (\sim 100 nm lateral distance).

Using this method, we reconstruct a 3D sensitivity map of the device, which provides a route for characterization of the device performance to non-uniform magnetic fields.

Financed by the EU FP7 NMP project NanoMag.

References:

¹ H. Corte-León, et al., *Sci. Rep.* 4, 6045 (2014).

² M. Donolato, et al., *Nanotechnology* 20, 385501 (2009).

³ J.W. Alldredge and J. Moreland, *J. Appl. Phys.* 112, 023905 (2012).

⁴ T. Uhlig, et al., *Nanotechnology* 25, 255501 (2014).

⁵ H. Campanella, et al., *Nanotechnology* 22, 505301 (2011).

⁶ S. Ponomareva, et al., *Adv. Mater. Res.* 872, 167 (2013).

Fr.E.1_O3 - Domain wall pinning in cylindrical nanowires

I. Ivanov¹, A. Chuvilin², J. Kosel¹

1. King Abdullah University of Science And Technology (KAUST), Thuwal, Saudi Arabia

2. CIC nanoGUNE Consolider, San Sebastian, Spain

Magnetic nanowires (NWs) growing inside of an isolating template perpendicular to the substrate are promising candidates for biomedical applications, sensors or to realize new types of 3D magnetic memory devices. In context of the later, it is crucial to have a possibility for controlled manipulation of domain walls (DWs) by periodic energy potentials. In order to realize such potentials, a local variation of the magnetocrystalline anisotropy can be used; for instance, multilayered Co(hcp)/Ni(fcc) cylindrical NWs. Recently, the possibility to grow single crystal hcp Co NWs with strong easy axis in-plane of the NW diameter has been demonstrated. In contrast, the magnetic behavior of Ni NWs is determined by the shape anisotropy; hence, the easy axis is parallel to the length of the Ni NW. Multilayer NWs with 45 nm in diameter have been prepared by the electrodeposition of Co and Ni into anodic alumina membranes by using two different aqueous electrolytes. The electroplating conditions for the Co segments were chosen to yield the magnetocrystalline anisotropy to be in-plane of the NW diameter. The length of the segments was controlled by the deposition time. NWs with 2, 4 and 5 layers have been prepared. Electron diffraction confirmed a very good crystal quality of the NWs, which allows us to grow multilayer NWs with single crystal Co and Ni segments. A sharp interface without the presence of oxygen between Co and Ni segments has been confirmed by electron energy loss spectroscopy (EELS) mapping. Our electron holography studies together with the magnetic force microscopy (MFM) showed the presence of an asymmetric stray field at the Co/Ni interface which might effectively pin the domain wall after the reversing of the magnetization of one of the segment. So the possibility to control DW propagation in cylindrical NWs by local variation of the magnetic anisotropy was successfully demonstrated.

Fr.E.1_O4 - Mechanomagnetic spectroscopy: an ultrasonic method to study magnetostriction

S. Kustov^{1,2}, M. Ll. Corró Moyà¹

1. *Departament De Física, Universitat De Les Illes Balears, Palma, Spain*

2. *ITMO University, St. Petersburg, Russia*

A technique for mechanomagnetic spectroscopy (MMS) [1] based on the Piezoelectric Ultrasonic Composite Oscillator Technique (PUCOT) [2] has been developed to study the reversible inverse magnetostriction (reversible Villari effect, RVE) over a wide range of periodic stress, temperatures and polarizing magnetic field H. The technique allows us to study simultaneously also elastic and anelastic properties. Measurements of RVE can be performed as a function of cyclic applied field at constant temperature or as a function of temperature at fixed H. Ultrasonic resonant oscillations near 100 kHz are induced in a piezoelectric oscillator which includes the sample. Due to the magnetoelastic coupling, the oscillatory stress produces a variation of the induction in magnetically ordered samples, which is measured by a small pickup coil. The amplitude and the phase of the stress-induced induction with respect to elastic strain/stress are determined. Based on the Maxwell relation, an algorithm is developed to estimate the static magnetostriction versus H from the RVE. Experimental studies were performed in a variety of materials, including well-known ferromagnets (Fe, Ni) as test objects [3], ferromagnetic polycrystalline and single crystalline shape memory materials (Ni-Fe-Ga) [3,4] and pure element (Dy) in ferro- and antiferromagnetic states. In contrast to other macroscopic techniques, MMS is not based on the measurement of total static strain, which includes thermal expansion. This important advantage allows us to study very weak magnetoelastic coupling, like in the antiferromagnetic phase of Dy, or for extremely weak at magnetic fields as low as the Earth's one (spontaneous magnetostriction).

References:

- [1] S. Kustov et al, 2006 Appl. Phys. Lett. 89 061917
- [2] S. Kustov et al, 2006 Mater. Sci. Eng. A 442 532
- [3] S. Kustov et al, 2010 J. Phys. D: Appl. Phys. 43 175002
- [4] M. L. Corró et al, 2013 J. Phys. D: Appl. Phys. 46 375002

Fr.E.1_O5 - Imaging magnetic domain patterns in 3D curved surfaces

R. Streubel¹, F. Kronast², P. Fischer^{3,4}, O. G. Schmidt^{1,5}, D. Makarov¹

1. *Institute for Integrative Nanosciences, IFW Dresden, Germany*

2. *Helmholtz-Zentrum Berlin für Materialien und Energie GmbH, Germany*

3. *Center for X-ray Optics, Lawrence Berkeley National Laboratory, CA, United States*

4. *Physics Department, UC Santa Cruz, CA, United States*

5. *Material Systems for Nanoelectronics, Chemnitz University of Technology, Germany*

Expanding 2D systems into the third dimension allows for modifying conventional or launching novel functionalities by tailoring curvature or shape of the magnetic 3D surfaces. These systems possess striking novel properties originating from curvature-driven effects, such as magnetochiral effects and topologically induced magnetization patterns due to a Dzyaloshinskii-like exchange interaction. A nanometer spatial resolution is required to image details of the magnetic domain pattern even if the curvature radii of these 3D surfaces is in the micrometer range. In this respect, neither magnetic neutron nor electron tomography can be applied. On the other hand, magnetic x-ray tomography (MXT) relying on x-ray magnetic circular dichroism (XMCD) with full-field microscopy has the potential to become a powerful tool to study these novel classes of 3D magnetic objects. We demonstrate its capabilities by reconstructing the 3D magnetization textures in hollow tubular objects. These objects are fabricated by rolling up planar nanomembranes with well-defined magnetic properties, i.e. in-plane or out-of-plane magnetic easy axes. The magnetic domain patterns are retrieved from a set of 2D images by applying reconstruction algorithms taking into account the vector property of the magnetization. By these means, the impact of the number of windings and of surface angles with respect to the initially applied magnetic field on the domain morphology (size and shape) is studied.

Supported by DFG (MA 5144/2-1), ERC under EU FP7 program (FP7/2007-2013)/ERC n.306277 and the Future and Emerging Technologies (FET) programme under FET-Open grant number 618083. PF acknowledges support from BES, MSED of the U.S. Department of Energy (DE-AC02-05-CH11231) and by Leading Foreign Research Institute Recruitment Program (2012K1A4A3053565) through the NRF of Korea funded by Ministry of Education, Science and Technology.

Fr.E.2_I1 - Studies of magnetic structures and magnetization dynamic using scanning transmission x-ray microscope

T. Tyliczszak¹

1. Advanced Light Source, Lawrence Berkeley National Laboratory, Berkeley, United States

There are many microscopic techniques used to analyze magnetic structures and dynamics of magnetization. One of the most versatile for characterization of bulk magnetic properties is soft x-ray transmission microscopy. It combines good lateral resolution and sub 100 ps time resolution with high sensitivity to magnetization. Magnetization sensitivity is due to X-ray Magnetic Circular Dichroism (XMCD) effect on absorption of circularly or elliptically polarized x-ray by metals. There are two types of x-ray transmission microscopes: full field microscope (often noted as TXM) and scanning transmission x-ray microscope (STXM). Both are used in magnetization studies but they offer somewhat different characteristics. The talk is based on the results obtained using STXM. The Scanning X-ray microscopes with magnetization measurements capabilities are operating at many synchrotron centers. Presented results are from the beamline 11.0.2 of the Advanced Light Source. Beamline 11.0.2 delivers linearly or elliptically polarized light in energy range from 80 eV up to 2000 eV. The scanning x-ray microscope can focus this beam to the size of about 30 nm using Fresnel zone plate. Samples are imaged by recording transmitted intensity as a function of sample position. Images can be recorded as a function of x-ray energy and/or x-ray polarization allowing for spectral analysis at given point of the image. The x-ray beam at the ALS has periodic structure of 500 MHz with a time uncertainty of about 70 ps. By using a fast avalanche photodiode detector it is possible to use the time structured x-ray beam to study dynamics. At the ALS STXM two different modes are used: "pulse-and-probe" and spatially resolved ferromagnetic resonance. The "pulse" is either magnetic or current fast pulse; the x-ray probe time response of magnetic layers. In SR-FMR experiments, the magnetization of the sample is excited by a continuous RF sine wave. In that way spin precession modes (in the GHz frequency range), modes of magnetic vortex movements (in the sub-GHz frequency range) or motion of domain walls can be studied. The frequency of the excitation has to be phase synchronized with the x-ray flashes of the synchrotron. Thus only multiples of the synchrotron bunch frequency can be addressed. Flexible field of view of STXM imaging allows to efficient studies of magnetic structures in different shape and thickness of magnetic nanostructures or complexes like spin ice structures. Latest development in combining transmission imaged and recording scattering patterns (Diffraction Enhanced STXM - ptychography) is significantly improving spatial resolution of x-ray imaging. Presently, at the ALS we can image magnetic structures with a resolution better than 10 nm. Although, dynamic measurements in this mode are more difficult, first results will be presented. Technical aspects of both methods will be presented by discussing examples of latest studies: imaging of spin transfer switching, and magnetic vortex core reversal by excitation with bursts of an alternating field².

Fr.E.2_O2 - A nanopaleomagnetic study of the early solar system by means of X-ray PEEM

J. Herrero-Albillos¹, J.F.J. Bryson², C. I. O'Bryen Nichols², R.J. Harrison², F. Kronast³

1. *Centro Universitario de la Defensa, Zaragoza, Spain, Zaragoza, Spain*

2. *University of Cambridge, Cambridge, United Kingdom*

3. *Helmholtz-Zentrum Berlin, BESSY II, Berlin, Germany*

Time-resolved records of the Earth's planetary magnetic field have been essential in understanding the dynamic history of our planet. Although most rocky planets, moons and asteroids of the solar system do not generate magnetic fields nowadays, they are thought to have generated dynamo fields in the early solar system. The nature and temporal evolution of those fields has remained enigmatic but its understanding could provide a unique insight into planetary evolution. In the case of asteroids, our foremost source of information regarding magnetic fields comes from meteorites. Meteoritic metallic material contains micro and millimeter size magnetic phases. Unfortunately, those phases are magnetically soft, and therefore they are not thought to provide accurate records of magnetic fields. However, regions containing nano-scale islands of tetrataenite (chemically ordered FeNi), found within the metal, have been recently proposed as reliable remanence carriers. In order to extract the information potentially recorded in those nano-islands, X-ray Photoelectron Emission Microscopy (PEEM) has been performed in a series of meteorites. This technique allows obtaining both magnetic and chemical maps with a spatial resolution down to 40 nm, in a field of view of 5 micrometers. A comparison of the magnetic signals and compositional maps furthers the understanding of the magnetic properties of the nano-islands and their interaction with the surrounding matrix. On the other hand, the experimental magnetization maps are compared with nano-magnetic simulations, giving rise to a time-resolved reading of magnetic remanence of the parent asteroids. The results suggest that an unconventional mechanisms acted in the early solar system giving rise to a long-lasting and widespread epoch of dynamo activity among small bodies in the early solar system, and might help to explain the long-lived magnetic activity observed in larger bodies, such as the moon.

References:

(Bryson et al. 2015, Nature, DOI 10.1038/nature14114)

Fr.E.2_O3 - Direct observation of the magnetocrystalline anisotropy axes in Fe_{3-x}O₄ nanoparticles by MFM

C. Moya¹, Ó. Iglesias-Freire^{2,3}, N. Pérez¹, X. Batlle¹, A. Labarta¹, A. Asenjo²

1. *Departament de Física Fonamental, Institut de Nanociència i Nanotecnologia, Universitat de Barcelona, Barcelona, Spain*

2. *Instituto de Ciencia de Materiales de Madrid (ICMM-CSIC), Cantoblanco, Madrid, Spain*

3. *Department of Physics, McGill University, Montreal, Canada*

Magnetic nanoparticles have potential applications in fundamental magnetism, biomedical applications and ultra-high density magnetic recording. Thermal stability of the particle magnetization is a crucial issue in most of those applications, so that direct observation of the magnetization reversal becomes of great interest to check the validity of models and theoretical assumptions. Despite several attempts found in the literature [1], [2], unambiguous correlation of the magnetic domain orientation to the crystalline structure is yet to be achieved. In our work, we present direct experimental imaging by variable-field magnetic force microscopy of the magnetic domain configuration in individual, cubic Fe_{3-x}O₄ nanoparticles of about 27 nm in size and high crystal quality [3]. Single domain structures have been shown, whose orientation and polarity result from both the magnetocrystalline easy axes of the particles and previous magnetic history. As the main result, we report on the direct observation of the easy axes in individual ferrimagnetic nanoparticles. Furthermore, the changes in the domain orientation with an external magnetic field have given evidence of a particle magnetization reversal mediated by a coherent rotation of the particle spins that has also been supported by micromagnetic calculations. This work was supported by Spanish MINECO (MAT2012-33037, CSD2010-00024 and MAT2013-48054-C2) and Catalan DURSI (2009SGR856, 2014SGR220).

References:

[1] Sievers, S; Braun, K; Eberbeck, D; Gustafsson, S; Olsson, E; Schumacher, H.W.; Siegner, U. *Small*. 2012, 8, 2675

[2] Li, X; Li, Z; Pang, D; Yoshimura, S; Saito, H. *Applied Physics Letters*, 2014, 104, 213106

[3] Guardia, P.; Pérez, N.; Labarta, A.; Batlle, X. *Langmuir*, 2009, 26, 5843

Fr.E.2_O4 - Ghost imaging protocol for magneto-optical applications

A. Caprile¹, A. Meda², I. R. Berchera², I. P. Degiovanni², A. Avella², A. Magni¹, M. Genovese², M. Pasquale¹

1. INRiM - Electromagnetism Division, Torino, Italy

2. INRiM - Optics Division, Torino, Italy

In this work, we develop a new approach to perform magneto-optical imaging, applying for the first time a high resolution Ghost Imaging (GI) protocol to reconstruct the image of Weiss domains within a magnetic sample. Thermal light GI is a technique that exploits intensity correlations between light beams to reconstruct the image of an object. Considering two intensity-correlated multi-speckles light beams, the first one illuminating an object and observed with a “bucket” detector (i.e. without any spatial resolution), the second one, that has never interacted with the object, revealed by a spatial resolving detector (like a CCD camera), the image of the object can be retrieved by correlating the outputs of the two detectors. Glauber’s second order correlation function normalized to the fluctuations of the beams is used to reconstruct the image of the sample. An imaging setup, implemented in order to obtain a spatial resolution sufficient to perform an efficient imaging of magnetic domains within an yttrium iron garnet (YIG) sample, has been realized. The outstanding magneto-optical properties of YIG, which possesses one of the highest Faraday rotation angle, make it the perfect material for a feasibility investigation of this new technique. The sample used here is a film of YIG of chemical composition $(\text{YSmCa})_3(\text{FeGe})_5\text{O}_{12}$ grown on gadolinium gallium garnet substrate. Ghost image reconstructions of domains of average size of 60 μm with opposite magnetization have been successfully retrieved. The investigated approach opens to the development of interesting innovative setups for magneto-optical microscopy, allowing operations in small volumes such as e.g. in cryostats, since no actuators to scan the sample or CCD close to the sample are needed, where, in perspective, the image of the domains can be obtained just inserting a tiny bundle of optical fibers in the proximity of the sample.

Fr.E.2_O5 - Neutron scattering in magnetic fields up to 26 teslas

O. Prokhnenko¹, M. Bartkowiak¹, W. Stein¹, N. Stuesser¹, H. Bleif¹, K. Prokes¹, M. Bird², P. Smeibidl¹, B. Lake¹

1. *Helmholtz-Zentrum Berlin, Germany*

2. *National High Magnetic Field Laboratory, Tallahassee, United States*

This year the user instrument suite of the Helmholtz-Zentrum Berlin (HZB) has been strengthened by a unique high-field facility for neutron scattering. Its main components are the High Field Magnet (HFM), the most powerful DC magnet for neutron scattering in the world, and the Extreme Environment Diffractometer (EXED), the dedicated neutron instrument. Built in collaboration with NHMFL (Tallahassee), the HFM is a horizontal field hybrid magnet. With help of resistive insert coils mounted in the room temperature bore of a superconducting solenoid, fields as high as 26 T can be obtained. The magnet operation requires complex technical infrastructure which comprises the 4 MW power supply, the water-cooling system for the resistive coil and the Helium-refrigerator for cooling the superconducting coil. Because of this infrastructure and magnet dimensions, the HFM is permanently installed on EXED. A special feature of the HFM is a pair of 30 degree conical openings at the ends of the resistive insert envisaged for neutron scattering access. To cover a sufficient Q-range in such a restricted geometry, EXED uses the time-of-flight (TOF) technique. It compensates the limited angular access by the extended wavelength range. Combined with 15 degree magnet rotation, it enables gapless coverage of Q-range from about 0.01 up to 12 Å⁻¹ for diffraction and small angle experiments. In addition to elastic capabilities, the instrument is being upgraded to direct TOF spectrometer mode. It will enable inelastic neutron scattering experiments over a limited Q-range < 1.8 Å⁻¹ with an energy resolution of a few percent and E_i < 25 meV. In this contribution the present status and capabilities of the HFM-EXED user facility will be presented together with the established procedures for planning the experiments and applying for the beamtime.

Fr.E.3_O1 - Domain wall on a magnetic helix with easy-tangential anisotropy

O. Pylypovskiy¹, D. Sheka¹, V. Kravchuk², D. Makarov³, O. Schmidt³, Y. Gaididei²

1. *Taras Shevchenko National University of Kyiv, Kyiv, Ukraine*

2. *Institute for Theoretical Physics, Kyiv, Ukraine*

3. *Institute for Integrative Nanosciences, IFW Dresden, Dresden, Germany*

Here, we demonstrate the curvature- and torsion-induced effects on the magnetization and the magnetic domain wall structure in 1D magnetic helices [1]. Coiling of a magnetic wire with the easy-axis anisotropy along the wire axis into a helix leads to an easy-tangential anisotropy and results in the following effects: (i) Appearance of an effective easy-plane anisotropy in a tangent-binormal-plane and rotation of the axis of the easy-axis anisotropy; (ii) Appearance of the effective Dzyaloshinskii term in the expression for the magnetic energy, which is proportional to the torsion and curvature of the wire [2]. Such a geometrical deformation from a straight wire into the helix can result in values of the Dzyaloshinskii constants comparable with estimations of surface induced ones in multilayer structures [3]. Domain walls in this curved system are described in the Frenet-Serret frame of reference offering the advantage that the magnetic anisotropy assumes the simplest form. The nonzero torsion results in the tilt of magnetization in the domain wall. This effect is similar to the one reported for structures with the intrinsic Dzyaloshinskii interaction [4]. The nonzero curvature results in coupling of the domain wall type (head-to-head or tail-to-tail) and the rotation of magnetization in the domain wall. All these effects are described analytically and confirmed by customized spin-lattice simulator SlaSi [5].

References:

- [1] D. Sheka, V. Kravchuk, K. Yershov, Yu. Gaididei, arXiv: 1502.06482 (2015)
- [2] Yu. Gaididei, V. Kravchuk, D. Sheka, PRL, 112, 257203 (2014)
- [3] O. Boulle et al, PRL, 111, 217203 (2013)
- [4] V. Kravchuk, JMMM, 367, 9 (2014)
- [5] <http://slasi.rpd.univ.kiev.ua>

Fr.E.3_O2 - Multi-vortex magnetic nanoparticles: a twin-functionalized agent for magnetomechanical cancer-cell destruction and hyperthermia

D. W. Wong¹, N. Liu¹, Y. Yang², W. Liang Gan¹, C. Boon Tan¹, M. Ramu¹, Jun Ding², W. Siang Lew¹, G. Sarjoosing¹

1. *Nanyang Technological University, Singapore*

2. *National University of Singapore, Singapore*

Magnetic nanoparticles show great potential for magnetic biomedical applications, such as magnetomechanical cancer-cell destruction and magnetic hyperthermia. The key advantage over the conventional cancer therapy is the non-invasive and localization of treatment of the cancer tumor, which minimizes the harmful side effects experienced by the patient. In this study, we prepared NiFe magnetic nanoparticles, with various thicknesses of 50 - 500 nm, via template-assisted pulsed electrodeposition and differential chemical etching technique. Our micromagnetic simulations have revealed that NiFe magnetic nanoparticles, with thickness of > 300 nm, forms a frustrated triple vortex state which produces a higher net magnetization that is stronger than the single vortex state. Therefore, a greater magnetic torque can be actuated, beneficial for various magnetic torque-based biomedical applications, such as magnetomechanical cell destruction. The magnetic torque have been verified by the light transmissivity dynamics of a suspension of magnetic nanoparticles, which shows a much higher magnetic moment for nanoparticles with thickness of 500 nm. In addition, we show that applying a small amplitude and low frequency magnetic field for only a few minutes was sufficient to initiate HeLa cells destruction in vitro. The observation of the loss of HeLa cell membrane integrity can be attributed to the targeted membrane rupture or magnetomechanical induced cell destruction. Among the different thicknesses tested, magnetic nanoparticles with a thickness of 500 nm had significant Specific absorption rate (SAR) values in clinical conditions and reached SAR values up to 2256 W/g at 366 kHz and 48 kA/m. Within a small amount of time (approximately ~251 s) and low iron concentration of 0.024 mg/mL, the temperature can be raised to 42°C, reducing the viability of the cancer cells. Hence, we demonstrate the capability of our magnetic nanoparticles as a twin-functionalized agent for magnetomechanical cancer-cell destruction and magnetic hyperthermia.

Fr.E.3_O3 - Nonlinearity of dynamic magnetization in a superparamagnetic clustered-particle suspension with regard to particle rotatability under oscillatory field

S. B. Trisnanto¹, Y. Kitamoto¹

1. Tokyo Institute of Technology, Tokyo, Japan

Inhomogeneous particle size distribution which includes cluster formation or local particle aggregation in a polydisperse magnetic-suspension is associable with high nonlinearity of magnetization response, owing to the significance of dipolar magnetism and other inter-particle interactions between neighboring particles. However, the nonlinearity arising from how magnetic nanoparticles suspended in a liquid medium interact with alternating magnetic field, cannot be sufficiently explained from exclusively understanding field-strength dependence of equilibrium susceptibility or the corresponding change in effective magnetic-moments. Additionally, the possibility of individual particles and even the clustered-particles to rotate under oscillatory magnetic field should potentially contribute to shaping curve of magnetization versus magnetic field. To characterize particle rotatability, we, therefore, concerned about rotational relaxation losses in correlation with imaginary part of magnetization. A superparamagnetic clustered-particle suspension which contains ~7 nm iron oxide nanoparticles coated with carboxydextran and dispersed in water so that the measured hydrodynamic-size was ~65 nm, was placed in a magnetosusceptometer and subjected to 0-65 Oe-rms of magnetic field strength with applied frequencies of 0.3, 3, 30, and 300 kHz, to initially measure its complex magnetic susceptibility. From further numerical analyses, we found that a typical nonlinear-curve of dynamic magnetization in the function of field strength at 300 Hz tends to be linear at 300 kHz, and highly field-dependent equilibrium-susceptibility at 300 Hz appears to be relatively-independent at 300 kHz, as well as the effective magnetic-moments. These generally demonstrate that magnetically-induced particle dynamics of the suspension is frequency-dependent. Furthermore, since the rotating particles generate friction losses which is comparative to the dissipation of magnetic energy, their existence should be observable as imaginary part of magnetization M'' . Our important finding is that at lower frequency, M'' reaches its saturation at lower field strength. This indicates that Brownian relaxation losses are constant after the saturation, thus emphasizing a confinement of particle rotations.

Fr.E.3_O4 - Insight into magnetic configurations in Fe nanocubes by micromagnetic simulations and electron holography

F. Bonilla¹, C. Gatel², L. Lacroix¹, A. Meffre¹, B. Warot-Fonrose², E. Snoeck², T. Blon¹

1. *Laboratoire de Physique et Chimie des Nano-objets (LPCNO), Toulouse, France*

2. *CEMES-CNRS, Toulouse, France*

Magnetic configurations in nanoparticles result from the competition between different magnetic terms. Such terms can arise from intrinsic parameters like composition, crystallinity, lattice deformations, and extrinsic parameters like size, shape and external fields. Here we present a theoretical and experimental study of the magnetic configuration dependence on intrinsic/extrinsic parameters for single ferromagnetic nanocubes with cubic magneto-crystalline anisotropy. First, we performed micromagnetic simulations with the OOMMF-3D package using bulk magnetic parameters of known materials with cubic anisotropy. By varying the nanocube size between 20 and 30 nm, the single domain limit (SDL) has been investigated. Thereby we observed a transition from the single-domain (SD) to the vortex state, where we found intermediate states like the $\langle 111 \rangle$ vortex (vortex-core along the cube $\langle 111 \rangle$ direction) or $\langle 111 \rangle$ SD. In another approach, we considered the extrinsic parameters like shape and applied magnetic field: we demonstrated that a deviation from the cubic shape affects the single domain limit and, furthermore, that magnetic history of nanocubes has a strong impact on the magnetic configuration at remanence. A second part of the presented work deals with the experimental evidence of magnetic configurations in ferromagnetic nanocubes. The particles studied were Fe nanocubes with controlled shape, composition, size and crystallinity [1]. These nanoparticles appear as a model system in nanomagnetism, nonetheless, experimental evidence of their SDL is a real challenge considering the small size range. Using electron holography (EH) we mapped the phase shift of the electron beam in a TEM corresponding to the magnetic induction in and outside the nanoparticles [2]. Thus, by combining EH and micromagnetic simulations, we have demonstrated the SDL in isolated Fe nanocubes with sizes ranging from 20 to 30 nm: as the size decreases, the magnetic configuration evolves from the vortex state to the SD one through the intermediate $\langle 111 \rangle$ vortex.

References:

[1] Lacroix L.M. et al. J. Am. Chem. Soc. 131, 549-557 (2009)

[2] Snoeck E. et al. Nano Lett. 8, 4293-4298 (2008)

Fr.F.1_I1 - Designer Nanomagnets

J. Rossier¹

1. Inl, Braga, Portugal

Progress in scanning tunneling microscopy (STM) makes it possible to assemble and probe with atomic precision structures made of one or a few magnetic atoms on a surface. Inelastic tunneling permits to probe the spin excitations of these designer nanomagnets, and spin-polarized STM permits to probe the atomic magnetization. In this talk I will discuss the fascinating properties of spin chains made of a few Fe atoms on top of Cu₂N/Cu(100) surface, paying attention to the interplay between magnetic anisotropy and Kondo interactions and the conditions for this type of system to behave classically or quantum mechanically.

Fr.F.1_O2 - Strange correlations in symmetry protected topological phases

P. Sengupta¹, K. Wierschem²

1. *Nanyang Technological University, Singapore*

2. *National Taiwan University, Taiwan*

Recently, a “strange correlator” has been proposed as a direct probe for the topological character of interacting Symmetry Protected Topological (SPT) phases. Using projective quantum Monte Carlo, we are able to directly access the strange correlator in a variety of phases, as well as to examine its critical behavior at the quantum phase transition between trivial and non-trivial symmetry protected topological phases. After finding the expected long-range behavior in these two symmetry conserving phases, we go on to verify the topological nature of two-leg and three-leg spin-1 Heisenberg antiferromagnetic ladders. This demonstrates the power of the strange correlator in distinguishing between trivial and non-trivial symmetry protected topological phases.

References:

- [1] K. Wierschem and P. Sengupta, 'Quenching the Haldane Gap in Spin-1 Heisenberg Antiferromagnets', Phys. Rev. Lett. 112, 247203 (2014)
- [2] K. Wierschem and P. Sengupta, 'Strange correlations in spin-1 Heisenberg antiferromagnets', Phys. Rev. B 90, 115157 (2014)

Fr.F.1_O3 - Electronic properties of transition metal atoms on Cu₂ N/Cu(100): a comparative study

A. Ferrón¹, J.L. Lado¹, J. Fernández-Rossier¹

1. International Iberian Nanotechnology Laboratory, Braga, Portugal

We study the electronic and magnetic properties of individual transition metal atoms (Ti, V, Cr, Mn, Fe, Co and Ni) deposited on a Cu₂ N/Cu(100) surface by means of spin-polarized density functional theory (DFT) and CI calculations. We focus our work on a comparative study of the various quantities, such as magnetic moment, orbital occupation, structural properties, hybridization with the substrate and spin polarization of the substrate, paying attention to the trends as the transition metal is changed. In addition we construct a multi-orbital Anderson Hamiltonian for the N electron problem in the open shell of the magnetic atom allowing charge fluctuation with the surrounding atoms, including both effects of spin-orbit and Coulomb repulsion. In this work we try to go beyond existing theoretical works by providing a comprehensive and comparative study of the electronic, magnetic and structural properties of these seven atoms including also Ni, for which there are no published calculations to the best of our knowledge. In the case of Mn, Fe and Co, we connect our results with the existing scanning tunneling microscope experiments.

References:

- [1] A. Ferrón, F. Delgado and J. Fernández-Rossier, Derivation of the spin Hamiltonians for Fe in MgO, in press, New J. Phys
- [2] A. Spinelli, B. Bryant, F. Delgado, J. Fernández-Rossier and A. F. Otte, Nature materials 13 (8), 782-785
- [3] J. C. Oberg, M Reyes Calvo, F. Delgado, M. Moro-Lagares, D. Serrate, D. Jacob, J. Fernández-Rossier, C. F. Hirjibehedin, Nature nanotechnology 9 (1), 64-68

Fr.F.1_O4 - Magnetism in rare earth quasicrystals: RKKY interactions and ordering

S. Thiem¹, J. Chalker¹

1. University of Oxford, Oxford, United Kingdom

We study magnetism in simple models for rare earth quasicrystals, by considering Ising spins on a quasiperiodic tiling, coupled via RKKY interactions. Computing these interactions from a tight-binding model on the tiling, we find that they are frustrated and strongly dependent on the local environment. Although such features are often associated with spin glass behaviour, we show using Monte Carlo simulations that the spin system has a phase transition to a low-temperature state with long-range quasiperiodic magnetic order.

Fr.F.1_05 - Spin and orbital contributions to relativistic magnetic interactions in strongly correlated systems

A. Secchi¹, A.I. Lichtenstein², M.I. Katsnelson¹

1. *Radboud University Nijmegen, Institute For Molecules And Materials, Nijmegen, The Netherlands*

2. *Universitat hamburg, Institut für Theoretische Physik, Hamburg, Germany*

The theory of magnetism is based on the effective description of a magnetic material in terms of a system of spins, coupled to external fields and interacting between themselves via magnetic interactions. The interactions' strengths are related to underlying microscopic electronic processes that can be fully captured only by considering realistic electronic models, including both single-particle and interaction terms. The complexity of the electronic processes leads to non-Heisenberg effects in magnetic metals and semiconductors, i.e., the lengths of magnetic moments and values of exchange parameters depend on the spin configuration for which they are computed, requiring ab-initio expressions. We present our theory of magnetic interactions in strongly correlated systems [1], a method that allows to compute the complete relativistic exchange tensors (including Dzyaloshinskii-Moriya interactions and anisotropic contributions to exchange) for the generalized multi-orbital Hubbard model, in the presence of arbitrarily strong relativistic couplings (such as spin-orbit and magnetic anisotropy) and external electromagnetic fields. The multi-orbital Hubbard model allows to describe relevant magnetic systems such as d and f materials, and we do not assume quenching of the orbital moments. The expressions for all the terms of the exchange tensors are given in terms of equilibrium electronic single- and two-particle Green's functions, which have to be computed from the electronic model, e.g., with the methods of Dynamical Mean-Field Theory. We show that the intrinsic spin and orbital degrees of freedom of the electrons, as well as their interplay, give distinct contributions to the strengths of the magnetic interactions, which can be separately accessed within our formalism. This is expected to be a relevant development in the study of rare earth magnets, where spin-orbit coupling is strong beyond perturbative approaches.

References:

[1] A. Secchi, A. I. Lichtenstein, and M. I. Katsnelson, arXiv:1412.6441 (submitted)

Fr.F.2_I1 - Topological defects in quantum spin-nematics

Y. Akagi¹, H. Ueda¹, N. Shannon¹

1. Okinawa Institute of Science And Technology, Okinawa, Japan

Topological defects play an important role in the theory of nematic phases in liquid crystals. However, relatively little is known about their role in quantum spin nematic phases which have no long-range dipole order and break only spin-rotational symmetry [1,2,3]. Here, we consider the topological defects in these nontrivial states. The model is the spin-1 bilinear biquadratic model on the triangular lattice [4,5,6]. We classify the defects by homotopy theory and numerical optimization approach, simulated annealing. We also discuss new type defects at particular point, which has global SU(3) symmetry.

References:

- [1] B. A. Ivanov, R. S. Khymyn, and A. K. Kolezhuk, Phys. Rev. Lett. 100, 047203 (2008)
- [2] T. Grover and T. Senthil, Phys. Rev. Lett. 107, 077203 (2011)
- [3] C. Xu and A. W. W. Ludwig, Phys. Rev. Lett, 108, 047202 (2012)
- [4] A. Lauchil, F. Mila and K. Penc, Phys. Rev. Lett. 97, 087205 (2006)
- [5] H. Tsunetsugu and M. Arikawa, J. Phys. Soc. Jpn. 75, 083701 (2006)
- [6] A. Smerald and N. Shannon, Phys. Rev. B 88, 184430 (2013)

Fr.F.2_O2 - Quantum molecular magnetism

S. Brechet¹, F. Reuse¹, K. Maschke¹, J. Ansermet¹

1. EPFL, Lausanne, Switzerland

Our theoretical description of quantum molecular magnetism is based on the quantum master equations, where the system consists of the electronic spin degrees of freedom and the bath consists of the remaining degrees of freedom. The system is weakly coupled and weakly correlated to the bath, which is at equilibrium on an appropriate time scale. The electrons satisfy the exclusion principle, which requires the tensorial product of the spin and orbital parts of the state to be antisymmetric under permutation. However, the symmetries of the parts of the state taken separately are determined by the irreducible unitary representations of the permutation group. The structure of the quantum master equations is also determined by these representations. The coupling between different isotypic components of the permutation group appearing in the quantum master equations leads to a description of magnetic dissipation at the molecular level and defines molecular spin selection rules. Thus, this theoretical description is expected to bring new and fundamental insight for molecular magnetism. In particular, it is expected to predict the non-trivial deflection of molecular clusters in a field gradient.

Fr.F.2_O3 - Micromagnetic simulations of three dimensional magnonic crystals

L. Spinu¹, A. Maksymov¹

1. AMRI & Physics, University of New Orleans, United States

Magnonic crystals (MC) are artificial assembly of “man-made” building blocks with tailored properties via their geometrical shaping and compositional modulation. This fact makes possible the confinement of solid state excitations and formation of a discrete spectrum of the allowed modes. Magnonic crystals open huge possibilities for device application as the frequency and strength of resonances related to the propagation of the magnons can be controlled by the geometry and magnetization configuration of meta-atoms.

In this work we use micromagnetics simulations to find the spectra and spatial profiles of collective spin-wave excitations in various three-dimensional (3D) arrays of magnetic nanoelements. Complicated shapes of magnetic elements forming three-dimensional magnonic crystals determine a rather complex structure of a spin wave spectrum of these individual nanosized elements. Thus, full scale micromagnetic simulations that go beyond the macrospin approximation are needed to accurately evaluate the structure of spin wave modes in these elements. The magnetization dynamics in nanosized magnetic elements is described by the Landau Lifshitz-Gilbert (LLG) equation that is solved using a Finite Difference Time Domain method.

A static magnetic field selects different ground states of the system while a transverse picosecond exponential magnetic pulse determines the magnetization dynamics in the system. The frequency response of 3D MC was extracted from the spatially and temporarily resolved data produced by micromagnetic simulations. A special attention was paid to the influence of the magnetic system ground state on the properties of the collective resonance modes, i.e. the possibility to dynamically reconfigure a ground state of 3D MCs.

Fr.F.2_O4 - Remote qubit manipulation by magnetic solitons

A. Cuccoli^{1,2}, D. Nuzzi^{1,2}, R. Vaia^{2,3}, P. Verrucchi^{1,2,3}

1. *Università Di Florence - Dipartimento Di Fisica E Astronomia, Florence, Italy*

2. *INFN - Sezione di Florence, Florence, Italy*

3. *Istituto di Sistemi Complessi del CNR, Roma, Italy*

One of the major difficulties met when solid-state realizations of quantum computers are proposed, is that of addressing and manipulating the single qubits of a quantum register without affecting the neighbouring ones. We here describe and discuss the proposal of using magnetic solitons propagating along spin chains as a suitable mean for qubit manipulation. Solitons are constant-profile, non-linear excitations, well localized in space and time, and their robustness against external perturbations, like thermal noise, makes them natural candidates for the faithful transmission of signals between distant parties. Mathematically, classical spin chains, in the limit of continuous support, are well known physical models for soliton propagation; experimentally, the observed thermal properties of quasi one-dimensional magnetic materials clearly display distinctive features which can be unambiguously interpreted as the contribution of soliton-like excitations, possibly renormalized by quantum corrections. In view of the possible use of solitons for qubit manipulation, we firstly propose a practical scheme to generate soliton-like excitations in discrete classical Heisenberg chains by applying a time-dependent magnetic field at the chain edge. We present a numerical investigation of the resulting dynamics of the discrete chain, showing the effective injection and propagation of solitons, and their robustness against thermal disorder. Moreover, we propose a setup where the generated soliton, travelling along the chain, eventually reaches a distant qubit, physically realized as a localized magnetic moment of spin 1/2, coupled to the chain, effectively acting on it as a time-dependent magnetic field able to manipulate its quantum state. Numerical results confirm that by a proper choice of the soliton shape and speed, and of the chain-qubit interaction, solitons are indeed suitable for the required task, giving the possibility to effectively control the qubit state by a non-dissipative mechanism, an additional beneficial property of the proposed scheme with respect to more conventional ones.

FR.F.2_O5 - Energy efficient thermally induced magnetization switching by tailoring the electron and phonon dynamics

T. Ostler¹, U. Atxitia^{2,3}, O. Chubykalo-Fesenko⁴, R. Chantrell¹

1. *Department of Physics, The University of York, Heslington, United Kingdom*

2. *Fachbereich Physik, Universität Konstanz, Konstanz, Germany*

3. *Zukunftskolleg, Universität Konstanz, Konstanz, Germany*

4. *Instituto de Ciencia de Materiales de Madrid, CSIC, Cantoblanco, Madrid, Spain*

The recently discovered thermally induced magnetization switching (TIMS) in ferrimagnets has received a lot of attention as it proceeds on the time-scale of picoseconds and occurs without the need for other slower additional external sources, such as a magnetic field. Whilst the energy per bit required to reverse the magnetization is low, the system temperature after the application of a pulse remains rather high for a few hundreds of picoseconds. In some cases the final temperature after the pulse is near the Curie temperature of the magnetic material and the heat transfer out of the system is governed by slower phonon processes. Thus, lowering the fluence required to reverse the magnetic state of a material by the TIMS mechanism is a key challenge since it could allow one to (i) realize an ultra-low power magnetic bit-recording scheme and (ii) avoid long lasting elevated temperatures. In considering the optimal set of physical characteristics we must first note that whilst TIMS is a magnetic process, it relies strongly on the underlying physics of the electronic and phononic systems. The focus of this work is to address, at least partially, this issue by demonstrating the properties of a candidate material that would give rise to a significant reduction of the laser power required to excite TIMS. Using large-scale computer simulations based on the stochastic Landau-Lifshitz-Gilbert equation, we have performed extensive analysis of the optimal physical quantities both electronic/phononic and magnetic for example; electron-phonon coupling, amount of rare earth and thermal bath coupling required for low energy TIMS. Significantly, we have shown that by optimizing the combination of the composition and the electron phonon coupling the fluence can be reduced by an order of magnitude. Our results can be used as a recipe to find potential materials exhibiting low energy TIMS.

Fr.F.3_I1 - Inelastic electronic transport in single-layer graphene and at the surface of topological insulator Bi_2Se_3

J. F. Sierra ¹, M. V. Costache ¹, I. Neumann ¹, S.O. Valenzuela ^{1,2}

1. ICN2 - Institut Catala de Nanociencia i Nanotecnologia, Campus UAB, Bellaterra, Barcelona, Spain

2. ICREA - Institució Catalana de Recerca i Estudis Avançats, Barcelona, Spain

Understanding of the heating, energy flow and relaxation of two-dimensional Dirac carriers in graphene and topological insulators is essential for the design of electronic devices based on these materials. Elastic scattering by disorder imposes a limit to the conductivity at low temperatures; nevertheless, as disorder is reduced, the limit at finite temperatures will be ultimately set by the intrinsic electron-phonon (e-ph) coupling. In this talk, I will discuss our current understanding about the e-ph coupling in graphene and in the Bi_2Se_3 family of materials. In particular, I will describe recent results on electric-field and temperature-dependent transport measurements in exfoliated thin Bi_2Se_3 crystals and on the generation of thermoelectric voltages due to hot electrons in graphene. In contrast to conventional metals with large Fermi surfaces, 2D Dirac electrons are largely decoupled from acoustic phonons leading to relatively low electron-lattice cooling rates. Temperature and bias dependent measurements reveal the presence of specific optical phonon modes that dominate the electronic response, with similar phenomenology in graphene and Bi_2Se_3 . However, the large difference in the energy of the relevant modes (200 meV and 8 meV, respectively) results in dramatically different bias and temperature dependent transport characteristics. While in Bi_2Se_3 the resistivity changes strongly even at low temperatures (<100 K), reflecting inelastic scattering due to the thermal activation of optical phonons, the restriction of the acoustic phonons that can scatter off electrons in graphene leads to very long cooling times and unconventional high-order cooling pathways assisted by disorder in the same temperature range.

Fr.F.3_O2 - Study of the field-induced virgin effect in Mn-Fe-P-Si room temperature magnetocaloric compounds

A. Bartok¹, M. Kustov², L. F. Cohen², A. Pasko¹, K. Zehani³, L. Bessais³, F. Mazaleyrat¹, M. LoBue¹

1. SATIE ENS-Cachan, France

2. Imperial College London, London, United Kingdom

3. ICMPE-CMTR, CNRS, France

Hexagonal Mn-Fe-P-Si compounds are known to represent a promising rare-earth-free road to room temperature magnetic refrigeration [1]. The giant magnetocaloric effect (MCE) has been studied in this system with particular emphasis on the tuning of critical temperature and magnitude of the entropy change as a function of the composition [2]. Many materials where the first-order transition is associated with a strong magneto-elastic coupling show a peculiar phenomenon referred as “virgin effect” [3, 4] consisting in a lower transition temperature T_c upon first cooling and in a different slope of the magnetization versus temperature curve. To separate extrinsic aspects (i.e. synthesis route, micro-structure) from the intrinsic ones (i.e. the composition) we focus our attention on the influence of sintering technique on the virgin effect in Mn-Fe-P-Si compounds. Powders with composition $Mn_{1.3}Fe_{0.65}P_{0.5}Si_{0.5}$ have been prepared by ball milling and solid-state reaction methods and consolidated using conventional and SPS sintering. Magnetic and calorimetric measurements show important differences upon first cooling, and slight differences on second cooling between the samples prepared by different synthesis routes. Further measurements using Hall-probe imaging in high magnetic field have been carried out. Virgin samples have been cooled down just above the critical temperature, and the first phase transition has been induced by application of a magnetic field. Bulk samples show staircase isothermal magnetization curves whereas powders show a smoother transition curve. Partial phase transitions have been observed by Hall-probe technique.

This research has received funding from the European Community's Seventh Framework Programme FP7/2007-2013 under grant agreement n 310748 (DRREAM).

References:

[1] N. H. Dung et al. , App. Phys Lett. 99, 092511 (2011)

[2] E. Bruck et al., Scripta Materialia, 67, 590 (2012)

[3] X. F. Miao et al., to be published: arXiv: 1412.8402

[4] A. Waske et al., Phys. Stat. Sol. RRL, 1-5 (2015) /DOI10.1002/pssr.201409484

Fr.F.3_O3 - Giant Magnetocaloric effect and thermopower in multiferroic Eu_{1-x}Ba_xTiO₃

R. Mahendiran¹, K. Rubi¹

1. National University of Singapore, Singapore

The cubic perovskite EuTiO₃ is an antiferromagnetic quantum paraelectric. Partial replacement of the divalent Eu by the divalent Ba induces ferromagnetism and ferroelectricity. We have investigated magnetocaloric effect and thermopower in Eu_{1-x}Ba_xTiO₃ series (0 < x < 1). Specific heat and thermal conductivity were also measured on selected composition. It is found that the parent compound EuTiO₃ exhibits the largest magnetic entropy change of 45 J/kg.K for a field of 5T at its Neel temperature (5.5 K) and an adiabatic temperature change of 16 K. The magnitude of the magnetic entropy change decreases with increasing Ba content. However, even the most diluted compound x = 0.9 shows an appreciable magnetic entropy change of 9 J/Kg.K at the cryogenic temperature. Thermopower is negative and large (S = 200-400 microvolt/K) in all these compounds and it increases in magnitude with increasing temperature. The giant magnetocaloric effect is attributed to suppression of spinfluctuations of Eu:4f moments.

Fr.G.1_I1 - Spin-transfer torque for nano-magnonics

S. Demokritov¹, V. Demidov¹, S. Urazhdin²

1. University of Muenster, Germany

2. Emory University, Atlanta, GA, United States

We discuss recent experiments on utilization of spin-transfer torque for excitation and amplification of spin waves propagating in microscopic magnonic guiding structures. We demonstrate a novel approach enabling efficient integration of spin-torque nano-oscillators with magnonic waveguides enabling directional transmission of spin waves excited by the spin-polarized electric current. We also show that the spin-transfer torque exerted by pure spin currents generated due to the spin-Hall effect can be used to reduce propagation losses of spin waves in microscopic magnonic waveguides

Fr.G.1_O2 - Direct microscopic observation of spin wave modes in nanoscaled antidot lattices

J. Gräfe¹, A. Gangwar², M. Noske¹, H. Stoll¹, C. H. Back², G. Schütz¹, E. J. Goering¹

1. *Max Planck Institute For Intelligent Systems, Stuttgart, Germany*

2. *Department of Physics, University of Regensburg, Regensburg, Germany*

Magnonic crystals are nanostructured metamaterials with periodically alternating magnetic properties, similar to photonic crystals, which have gained significant scientific interest. These nanostructures have great potential for technological applications in data processing and storage, and spintronics. A periodic variation is achieved by creating holes in a magnetic host material to form a so-called antidot lattice (ADL). The introduction of the artificial ADL allows to alternate the spin wave dispersion in the material and to form a spin wave guide or filter. The spin wave dispersion can be tuned by variation of antidot size and distance, and the externally applied magnetic field. However, reaching technologically relevant higher frequencies and short-range filtering requires nanosized ADLs. As the spin wave propagation in nanoscaled ADL cannot be visualized by time resolved Kerr microscopy, typical investigations use all electrical spin wave spectroscopy or Brillouin light scattering and are unable to directly image the propagation of spin waves in nanometer sized magnonic crystals. Here, we present results from advanced time resolved x-ray microscopy (MAXYMUS@BESSY) of spin wave propagation and the mechanisms behind selective transmission or damping in these magnonic crystals. Therefore, magnon modes spanning from 250 MHz up to 8 GHz were resonantly excited and the influence of a variable applied field was investigated. These measurements allowed the direct observation of the individual modes, their interaction with the ADL, and their respective localisation within the lattice. Furthermore, we deduce and visualise the mechanisms behind the tailorable band structure of this class of magnonic crystals and the selective transmission or damping. Understanding this mechanism allowed tuning the magnon propagation length within the ADL ranging from 0.5 to 15 μm . Additionally, our spin wave movies indicate that these mechanisms in magnonic crystals can be exploited to focus magnons laterally.

Fr.G.1_O3 - Unidirectional spin-wave edge modes in perpendicularly magnetized permalloy structures

B. Leven¹, F. Ciubotaru¹, A. V. Chumak¹, V. I. Vasyuchka¹, A. A. Serga¹, B. Hillebrands¹

1. Fachbereich Physik And Forschungszentrum Optimas, TU Kaiserslautern, Germany

The continuous increase of data transfer capacity and processing speed in information technology requires a permanent evaluation of the underlying processes. However, the currently established techniques in CMOS technology and even spintronic applications seem to approach their limits. Here, using spin-wave information processing - so-called magnon spintronics - offers a high potential for future technology solutions. The advantage of this field is that information transport is conducted solely by the spin system without electron transport, thus preventing Ohmic losses and allowing for lower energy consumption than in conventional technology. New concepts using spin waves in micro- and nano-sized magnetic structures have shown promising results for application in magnon spintronic devices, as e.g. the magnon transistor or spin-wave interference logic gates. In this field, out-of-plane magnetized magnetic structures offer an essential benefit compared to the in-plane magnetized structures used so far: in perpendicularly magnetized films the spin-wave dispersion is isotropic, as the propagation direction is always perpendicular to the magnetization direction. Therefore, even in geometrically complex spin-wave conductors the propagation control of spin waves can be easily achieved. Employing micromagnetic simulations we demonstrated the controllability of a unidirectional propagating spin-wave mode excited in an isotropic perpendicularly magnetized Ni₈₁Fe₁₉ medium which allows for information transport even if the symmetry of the sample geometry is broken. Even the propagation around a corner of 90° is feasible. We showed that by controlling the excitation frequency the character of the spin-wave emission can be tuned between isotropic and anisotropic. Even for the volume waves an anisotropic spin-wave emission with respect to the excitation antenna can be achieved. These results show the high potential for the realization of magnonic circuits based on perpendicularly magnetized spin-wave conductors.

Financial support by the DFG grant SE-1771/1-2 is gratefully acknowledged.

Fr.G.1_O4 - Towards graded-index magnonics: Steering spin waves in magnonic networks

C. Davies¹, A. Francis¹, A. Sadovnikov², S. Chertopalov³, M. Bryan⁴, S. Grishin², D. Allwood⁴, S. Nikitov⁵, Y. Sharaevskii², V. Kruglyak¹

1. University of Exeter, Devon, United Kingdom
2. Saratov State University, Saratov, Russia
3. Donetsk National University, Donetsk, Ucraina
4. University of Sheffield, Sheffield, United Kingdom
5. Kotel'nikov Institute of Radioengineering and Electronics, Russia

The dispersion of spin waves in the magnetostatic in dipole exchange regimes is inherently anisotropic [1]. We have used the time-resolved scanning Kerr microscopy [2] and micromagnetic simulations to study the propagation of spin waves across a T-junction of 5 μm wide Permalloy waveguides. The T-junctions were biased by a magnetic field applied at an angle to its symmetry axis. We demonstrate that the non-uniformity of the internal magnetic field and magnetization inherent to patterned magnetic structures creates a medium of graded refractive index for propagating magnetostatic spin waves and can be used to steer their propagation in magnonic architectures. This results in the T-junction structure acting as a field-controlled magnonic multiplexor. The character of the magnetisation and effective field non-uniformities can be tuned and potentially programmed using the applied magnetic field. Thus, our findings suggest a possibility of using the principles of the graded-index magnonics within a novel reconfigurable magnonic computing technology.

References:

- [1] A. G. Gurevich and G. A. Melkov, "*Magnetization oscillations and waves*" (Chemical Rubber Corp., New York, 1996)
- [2] Y. Au, T. Davison, E. Ahmad, P. S. Keatley, R. J. Hicken, and V. V. Kruglyak, *Appl. Phys. Lett.* 98, 122506 (2011)

Fr.G.1_05 - Effective way of spin-wave excitation in YIG-Pt structures

A. Serga¹, M. Agrawal¹, V. Vasyuchka¹, B. Hillebrands¹

1. Department of Physics and State Research Center OPTIMAS, University of Kaiserslautern, Kaiserslautern, Germany

The field of magnonics deals with the transfer and processing of information through the utilization of spin waves and their quanta, magnons. One of the main challenges for this field is the limited lifetime of magnons even in such a low-damping material as single crystal yttrium-iron-garnet (YIG). One possible way to overcome this issue is the compensation of the spin-wave damping via injection of a spin transfer torque to a magnetic medium using a spin-polarized electron current in an adjacent non-magnetic metal layer. The decrease in the damping of travelling spin waves in YIG-Pt bilayer-based waveguides connected to a dc current source has already been demonstrated. However, the absolute value of spin-wave attenuation in a Pt-covered YIG film is still unacceptably high for practical applications. To understand the nature of this decay we performed a systematic study of the influence of a thin Pt film on the spin-wave propagation in a 6.7 μm thick YIG waveguide. Spin waves were excited and detected by 50 μm wide microstrip antennas at frequencies around 7 GHz. Using different excitation geometries, we have found that the observed Pt-related decrease in a spin-wave amplitude is caused not by magnon relaxation processes, but by a reduction in a spin-wave excitation efficiency due to the electromagnetic shielding of microwave Oersted fields induced by the antennas. The shielding effect is strong even if the thickness of the Pt layer (2-10 nm) is significantly smaller than the microwave skin depth. By using of a novel excitation geometry, where the Pt layer faces the ground plane of a microstrip line, we have eliminated the shielding effect and achieved, thus, a drastic (up to 100 times) increase in the excitation efficiency of the Damon-Eshbach surface spin wave.

Financial support from the Deutsche Forschungsgemeinschaft within the SFB/TR49 is gratefully acknowledged.

Fr.G.2_I1 - Novel diluted ferromagnetic semiconductors iso-structural to FeAs superconductors

Y. Uemura¹, L. Liu¹, B. Frandsen¹, S. Cheung¹, B. Chen², Z. Deng², K. Zhao², C. Jin², C. Ding³, F. Ning³, G. Luke⁴, B. Gu⁵, S. Maekawa⁵

1. *Physics Dept., Columbia Univ., New York, United States*

2. *Institute of Physics, Chinese Academy of Science, Beijing, China*

3. *Dept. of Physics, Zhejiang Univ., Hangzhou, China*

4. *Dept. of Physics and Astronomy, McMaster Univ., Hamilton, Ontario, Canada*

5. *Advances Science Research Center, JAEA, Tokai, Japan*

In a prototypical diluted magnetic semiconductor (DMS) (Ga,Mn)As, substitution of Mn^{2+} and Ga^{3+} leads to a very small chemical solubility, availability of specimens limited to metastable thin films, and high sensitivity to heat treatment. In 2007, we applied MuSR to study (Ga,Mn)As films grown by MBE method [1], and demonstrated development of homogeneous ferromagnetic order in the full volume with a rather sharp transition below T_c for specimens with proper heat treatment. Subsequently we succeeded in synthesizing new DMS systems Li(Zn,Mn)As ([2] ferromagnetic T_c up to 50 K), (Ba,K)(Zn,Mn)₂As₂ ([3] T_c up to 200 K), and (La,Ba)(Zn,Mn)AsO ([4] T_c up to ~ 50 K). These systems have similar/identical crystal structures with those of FeAs superconductors LiFeAs, (Ba,K)Fe₂As₂, and LaFeAsO with a very good matching of lattice parameters. Thanks to isovalent (Zn,Mn) substitutions, these new DMS systems can be obtained as bulk specimens, with spin doping and charge doping achieved independently with each other. We performed MuSR studies in bulk specimens of these new DMS systems [2-4] and confirmed development of ferromagnetism in the full volume fraction, and found a linear correlation between spatially averaged ordered moment size and ferromagnetic T_c followed both by (Ga,Mn)As and the new DMS systems with a common slope. The linear correlation suggests common origin and mechanisms of ferromagnetic exchange interaction in all these four DMS systems. The only exception to this behavior was found in (Sr,Na)(Zn,Mn)₂As₂ (T_c up to ~ 20 K) [5] which has a hexagonal crystal structure different from that of (Ba,K)Fe₂As₂.

References:

[1] S.R. Dunsiger et al., *Nature Materials*, 9, 299-303 (2010)

[2] Z. Deng et al. *Nature Communications*, 2, 422 (2011)

[3] K. Zhao et al., *Nature Communications*, 4, 1422 (2013)

[4] C. Ding et al., *Phys. Rev. B* 88, 041102(R) (2013) [5] B.J. Chen et al. *Phys. Rev. B* 90, 155202 (2014)

Fr.G.2_I2 - Magnetic order at the (111) polar surfaces of SrTiO₃: a non-magnetic insulator

J. I. Beltrán^{1,2}, M. C. Muñoz¹

1. Instituto De Ciencia De Materiales De Madrid (ICMM) Consejo Superior De Investigaciones Científicas (CSIC), Madrid, Spain

2. Departamento de Física Aplicada III, Universidad Complutense de Madrid, Madrid, Spain

We show that intrinsic confined magnetic phases are realized at the two possible terminations of the (111) SrTiO₃ surface. SrTiO₃ is a transparent non-magnetic wide-band gap insulator, which crystallizes in the cubic perovskite structure, along the (111) direction it consists of alternating stacks of Ti and SrO₃ layers. Via ab-initio density functional calculations, we prove that the ideal terminated SrO₃ and Ti surfaces become metallic and magnetic. A confined half-metallic two dimensional hole gas is formed at the SrO₃ surface, while the Ti termination sustains a two-dimensional electron gas (2DEG). The breaking of translational symmetry at the surface generates a polar discontinuity -of opposite sign at the two different terminations-, which induces the electronic reconstruction. At the SrO₃ surface, the creation of confined oxygen 2p-holes in the otherwise full valence band of the oxide, induces the development of a spontaneous spin-polarization and the stabilization of the ferromagnetic ground state. Contrary, the 2DEG at the bare Ti surface, is formed by conduction Ti t_{2g} d-electrons. Associated with the metallic state a large spin-splitting and long range magnetic order develop. The two Ti surface layers, which form a buckled honeycomb lattice, couple antiferromagnetically. Our results evidence the crucial role of the confinement crystal direction, which determines the orbital ordering and related electron localization in real space. Quantum confinement is determinant for stabilizing the two-dimensional magnetic phase, and thus shaping the unconventional intrinsic magnetism. The confined magnetic phases at the SrTiO₃ surfaces hold interesting analogies with the oxygen 2p hole-induced ferromagnetism recently reported in non-magnetic oxide heterostructures [1,2].

References:

- [1] . S. Elfimow et al. Phys. Rev. Lett, 89, 216403 (2002); S. Gallego et al. J. Phys. Condens. Matter 17 L, 451 (2005)
- [2] R. Oja, et al. Phys. Rev. Lett, 109, 127207 (2012); C. Guglieri et al. Adv. Funct. Mater. 24, 2094 (2014)

FR.G.2_O3 - Defect induced magnetism in SiCS. Zhou¹, Y. Wang¹, Y. Liu¹, S. Gemming¹, M. Helm¹*1. Helmholtz-Zentrum Dresden-Rossendorf, Dresden, Germany*

Defect-induced magnetism is attracting intensive research interest. It not only challenges the traditional opinions about magnetism, but also has some potential applications in spin-electronics. SiC is a new candidate for the investigation of defect-induced ferromagnetism after graphitic materials and oxides due to its high material purity and crystalline quality [1, 2]. In this contribution, we made a comprehensive investigation on the structural and magnetic properties of ion implanted and neutron irradiated SiC sample. In combination with X-ray absorption spectroscopy and first-principles calculations, we try to understand the mechanism in a microscopic picture.

For neon or xenon ion implanted SiC, we identify a multi-magnetic-phase nature [3]. The magnetization of SiC can be decomposed into paramagnetic, superparamagnetic and ferromagnetic contributions. The ferromagnetic contribution persists well above room temperature and exhibits a pronounced magnetic anisotropy. By combining X-ray magnetic circular dichroism and first-principles calculations, we clarify that p-electrons of the nearest-neighbor carbon atoms around divacancies are mainly responsible for the long-range ferromagnetic coupling [4]. Thus, we provide a correlation between the collective magnetic phenomena and the specific electrons/orbitals.

With the aim to verify if a sample containing defects through its bulk volume can persist ferromagnetic coupling, we applied neutron irradiation to introduce defects into SiC [5]. Besides a weak ferromagnetic contribution, we observe a strong paramagnetism, scaling up with the neutron fluence. The ferromagnetic contribution only occurs in a narrow fluence window or after annealing. We speculate that defect-induced ferromagnetism rather locally appears in particular regions, like surface/interface/grain boundaries.

References:

- [1] L. Li, ... S. Zhou, Appl. Phys. Lett. 98, 222508 (2011)
- [2] Y. Wang, ... S. Zhou, Phys. Rev. B 90, 214435 (2014)
- [3] Y. Wang, ... S. Zhou, Phys. Rev. B 89, 014417 (2014)
- [4] Y. Wang, ... S. Zhou, Sci. Reports, accepted (2015)
- [5] Y. Wang, ..., S. Zhou, Phys. Rev. B, submitted (2015)

Fr.G.3_O1 - Intrinsic non-adiabatic spin-transfer torque

K. Kim¹, K. Lee², H. Lee³, M. Stiles¹

1. *National Institute of Standards And Technology, Gaithersburg, United States*

2. *Korea University, Seoul, Republic of Korea*

3. *Pohang University of Science and Technology, Pohang, Republic of Korea*

Spintronics, which allows electrical manipulation of magnetization, is not only of scientific interest, but also of importance for realization of non-volatile memory devices based on ferromagnetic nanostructures. Spin-transfer torque is one of the most important concepts in spintronics. In the standard understanding of spin-transfer torque, an external electric field generates an electrical current which interacts with local magnetization and in turn induces dynamics of magnetization. Thus, spin-transfer torque is usually considered as a current-induced effect. In this work, we study a system with a continuously varying magnetic texture and demonstrate a novel type of spin-transfer torque which originates from an applied electric field but not a current. In this sense, the result of this work is electric-field-induced rather than current-induced. Although both of them are proportional to the applied electric field, the most important difference between the two is that a current-induced contribution is proportional to electrical conductivity while an electric-field-induced contribution is not. We illustrate that our result is closely related to a recently reported electric-field-induced spin-orbit torque from Rashba spin-orbit coupling [1], even though it is derived from a system without spin-orbit coupling. We also demonstrate that the electric-field-induced spin-transfer torque has the same form as current-induced non-adiabatic spin-transfer torque in most practical cases. It is known that the non-adiabaticity usually originates from extrinsic origins such as spin scattering, however, our result gives a non-adiabatic spin-transfer torque only from an intrinsic origin. Since the non-adiabaticity is an important parameter for spin torque efficiency, our theory opens another possibility for enhancing spin torque efficiency.

References:

[1] H. Kurebayashi et al., *Nat. Nanotechnol.* 9, 211 (2014)

Fr.G.3_O2 - Quantifying optical spin-transfer torque on a coherently expanding magnetic domain wall by tuneable geometrical pinning

T. Janda^{1,4}, P. Roy², R. Otxoa², A. Ramsay², A. Irvine³, H. Reichlova^{1,4}, R. Campion⁵, B. Gallagher⁵, K. Olejnik⁴, Z. Soban⁴, F. Trojanek¹, L. Nadvornik^{1,4}, T. Jungwirth^{4,5}, P. Nemeč¹, J. Wunderlich^{2,4}

1. Faculty of Mathematics and Physics, Charles University in Prague, Czech Republic

2. Hitachi Cambridge Laboratory, Hitachi Europe Limited, Cambridge, United Kingdom

3. The Cavendish Laboratory, University of Cambridge, Cambridge, United Kingdom

4. Institute of Physics ASCR, Czech Republic

5. School of Physics and Astronomy, University of Nottingham, Nottingham, United Kingdom

We analyse light-polarization dependent domain wall (DW) motion induced by fast optical spin-transfer torque (oSTT) pulses [1, 2]. In our experiments, a single coherent domain wall is geometrically pinned [3] on the entrance of a microscopic Hall cross patterned from an epitaxially grown (Ga,Mn)(AsP) film with perpendicular magnetic anisotropy. The strength of the oSTT is determined by the polarization dependent minimum laser fluency required to overcome the in-situ tuneable geometrical pinning barrier. Position and displacement of the DW are monitored by anomalous Hall and magneto-optical Kerr microscopy measurements. Our experimental method allows us to separate light-polarization independent thermal effects from oSTT and shows that the oSTT is the dominant mechanism at laser-light wavelengths where the spin polarization of the photo-carriers is high. We confirm by micro-magnetic calculations based on the Landau-Lifshitz-Bloch equation [4] that continuous DW motion is realised by very fast oSTT pulses. In our experiments, the pulse duration is limited dominantly by the ~ 10 ps life-time of the photo-carriers which is much shorter than the ~ 1 ns reactive precession time of the DW magnetisation. Moreover, the continuous DW motion evidences the inertia of the DW because the ~ 10 ps short oSTT pulses are applied only every ~ 10 ns.

References:

[1] P. Nemeč et al., Nature Physics 8, 411-415 (2012)

[2] A. J. Ramsay et al., Phys. Rev. Lett., 114, 067202 (2015)

[3] J. Wunderlich et al., IEEE Trans. Mag. 37, 4, 2104 (2001)

[4] O. Chubykalo-Fesenko et al., Phys. Rev. B 74, 094436 (2006)

Fr.G.3_O3 - Reversible electric field driven magnetic domain wall motion

K. Franke¹, B. van de Wiele², Y. Shirahata³, S. Hämäläinen¹, T. Taniyama³, S. van Dijken¹

1. *NanoSpin, Department of Applied Physics, Aalto University School of Science, Aalto, Finland*

2. *Department of Electrical Energy, Systems and Automation, Ghent University, Ghent, Belgium*

3. *Materials and Structures Laboratory, Tokyo Institute of Technology, Nagatsuta, Midori-ku, Yokohama, Japan*

Control of magnetic domain wall motion by electric fields has recently attracted scientific attention because of its potential for magnetic logic and memory devices. Here, we report on a new mechanism for reversible and deterministic motion of magnetic domain walls using an electric field only. Full electric-field control over the magnetic domain-wall velocity in the absence of a magnetic field or spin-polarized electric current is demonstrated using epitaxial Fe films on single-crystal BaTiO₃ substrates with alternating in-plane (a domains) and out-of-plane (c domains) ferroelectric polarization [1]. The magnetic domain walls of the Fe film are strongly pinned onto the a-c boundaries of the BaTiO₃ substrate by abrupt changes in the symmetry and strength of magnetic anisotropy as a result of strain transfer and inverse magnetostriction [2]. Repeatable back-and-forth motion of a ferroelectric a-c boundary and a pinned magnetic domain wall is realized by the application of positive and negative out-of-plane voltage pulses. The domain-wall velocity is varied over 5 orders of magnitude by adjusting the electric-field strength. Patterning of the magnetic film reveals that near-180° transverse magnetic domain walls can be stabilized in magnetic nanowires on top of BaTiO₃ due to competing shape anisotropy. Moreover, the driving mechanism is not affected by pinning centers such as grain boundaries or notches that usually affect the motion of magnetic-field or electric-current driven magnetic domain walls.

References:

1. K. J. A. Franke, B. Van de Wiele, Y. Shirahata et al., *Phys. Rev. X* 5, 011010 (2015)
2. T. H. E. Lahtinen, Y. Shirahata, L. Yao et al., *Appl. Phys. Lett.* 101, 262405 (2012)

Fr.H.1_I1 - Multiple quantum critical points in a cubic heavy fermion system

S. Paschen¹

1. Vienna University of Technology, Wien, Austria

Quantum criticality is a key organizing principles for strongly correlated electron systems. In heavy fermion compounds different kinds of quantum critical behavior have been observed experimentally. To classify them, a global phase diagram has been suggested [1]. Magnetotransport measurements on tetragonal YbRh₂Si₂ revealed a Kondo breakdown quantum critical point (QCP) between an antiferromagnetic and a paramagnetic phase [2], as predicted for systems with reduced dimensionality [3]. More recently, similar magnetotransport signatures were observed in the cubic heavy fermion compound Ce₃Pd₂₀S₁₆ as the lower of two consecutive phase transitions is suppressed to zero [4]. Here, however, the QCP separates two different ordered phases. Indeed, in the 3D case, a Kondo breakdown QCP is expected between ordered portions of the global phase diagram [3,4]. Our investigations now focus on a second putative QCP in this system [5]. We acknowledge financial support from the European Research Council (ERC Advanced Grant No 227378) and the Austrian Science Fund (project I623-N16).

References:

- [1] Q. Si, Physica B 378-380, 23 (2006). Q. Si, Phys. Status Solidi B 247, 476 (2010)
- [2] S. Paschen et al., Nature 432, 881 (2004). S. Friedemann et al., Proc. Natl. Acad. Sci. 107, 14547 (2010)
- [3] Q. Si et al. Nature 413, 804 (2001). P. Coleman et al., J. Phys. Condens. Matter 13, R723 (2001). T. Senthil et al., Phys. Rev. B 69, 035111 (2004)
- [4] J. Custers, K.-A. Lorenzer, M. Müller, A. Prokofiev, A. Sidorenko, H. Winkler, A. M. Strydom, Y. Shimura, T. Sakakibara, R. Yu, Q. Si, and S. Paschen, Nature Materials 11, 189 (2012)
- [5] V. Martelli, J. Larrea J., J. Hänel, K.-A. Lorenzer, A. Prokofiev, S. Paschen et al., unpublished

Fr.H.1_O2 - Frustrated magnetism in $\text{Yb}_2\text{Fe}_{12}\text{P}_7$

K. Grube¹, S. Zaum^{1,2}, P. Schweiss¹, J. J. Hamlin³, I. K. Lum³, D. A. Zocco^{1,3}, R. E. Bumbach³, M. B. Maple³, H. v. Löhneysen^{1,2}

1. *Karlsruher Institut für Technologie, Institut für Festkörperphysik, Karlsruhe, Germany*

2. *Karlsruher Institut für Technologie, Physikalisches Institut, Karlsruhe, Germany*

3. *Department of Physics, University of California, San Diego, La Jolla, California, United States*

Intermetallic compounds containing Ce or Yb atoms are archetypes for quantum critical behavior close to long-range magnetic order. $\text{Yb}_2\text{Fe}_{12}\text{P}_7$ is characterized by a low magnetic transition temperature of TN approx. 1 K and the breakdown of Fermi-liquid behavior [1]. These properties suggest the proximity to a quantum critical point (QCP) caused by the subtle competition between Kondo and RKKY interactions. The non-Fermi-liquid behavior, however, extends to magnetic fields far beyond the range of the magnetically ordered phase and does not conform to the standard QCP scenario described by the Hertz-Millis-Moriya theory. We measured thermal expansion, magnetostriction and magnetization to determine the phase diagram for fields perpendicular to the c axis. The pressure dependence was studied up to 15 GPa using resistivity measurements in hydrostatic piston cylinder and diamond anvil cells. A comparison with specific-heat measurements reveals that in $\text{Yb}_2\text{Fe}_{12}\text{P}_7$ only a small fraction of the Yb moments participate in the long-range magnetic order. The Grüneisen ratio does not diverge for T zero temperature indicating that the non-Fermi-liquid behavior is not related to a nearby pressure-induced quantum criticality. Likewise, the tiny pressure dependences of the Sommerfeld coefficient and TN argue against a magnetic order that is weakened by the Kondo effect. In view of the unusual noncentrometric crystal structure, our observations might point to geometric frustration of the magnetic moments.

References:

[1] R. E. Baumbach et al., Phys. Rev. Lett. 105, 106403 (2010)

Fr.H.1_O3 - Thermodynamic singularities in the anisotropic stress Grüneisen ratios of quantum critical CeCu_{5.9}Au_{0.1}

K. Grube¹, S. Zaum^{1,2}, O. Stockert³, Q. Si⁴, H. v. Löhneysen^{1,2}

1. *Karlsruher Institut Für Technologie, Institut Für Festkörperphysik, Karlsruhe, Germany*

2. *Physikalisches Institut, Karlsruher Institut für Technologie, Karlsruhe, Germany*

3. *Max-Planck-Institut für Chemische Physik fester Stoffe, Dresden, Germany*

4. *Department of Physics and Astronomy, Rice University, Houston, United States*

Quantum criticality represents an established means for generating non-Fermi-liquid properties of an electron fluid. Spectroscopic studies in the heavy-fermion compound CeCu_{6-x}Au_x have provided evidence that spatial anisotropy influences the nature of the quantum critical point. To establish this feature as a robust effect, directional probes of thermodynamic properties are called for. Here, we introduce the notion that the anisotropic stress Grüneisen ratios constitute a direct measure of the presence and strength of thermodynamic singularities. We demonstrate this new approach to quantum criticality in CeCu_{5.9}Au_{0.1}, uncover the scaling behavior of the associated singularities, and reveal the rich entropy landscape in the vicinity of the quantum critical point.

Fr.H.1_O4 - Non-fermi liquid behaviors and distinct metal insulator transitions in perovskite SrIrO₃ epitaxial films

Y. H Jeong¹, Y. A. Biswas¹

1. Dept of Physics, POSTECH, Pohang, Republic of Korea

Understanding of metal insulator transitions in a strongly correlated system, driven by Anderson localization (disorder) and/or Mott localization (correlation), is a long standing problem in condensed matter physics. The prevailing fundamental question would be how these two mechanisms contrive to accomplish emergent anomalous behaviors. Here we have successfully grown high quality perovskite SrIrO₃ thin films, containing a strong spin orbit coupled 5d element Ir, on various substrates such as GdScO₃ (110), DyScO₃ (110), SrTiO₃ (001) and NdGaO₃ (110) with increasing lattice mismatch, in order to carry out a systematic study on the transport properties. We found that metal insulator transitions can be induced in this system; by either reducing thickness (on best lattice matched substrate) or changing degree of lattice strain (by lattice mismatch between film and substrates) of films. Surprisingly these two pathways seek two distinct types of metal insulator transitions; the former falls into disorder driven *Anderson* type whereas the latter turns out to be of unconventional *Mott-Anderson* type with the interplay of disorder and correlation. More interestingly, in the metallic phases of SrIrO₃, unusual non-Fermi liquid characteristics emerge in resistivity as $\Delta\rho \propto T^\varepsilon$ with ε evolving from 4/5 to 1 to 3/2 with increasing lattice strain. We discuss theoretical implications of these novel phenomena to shed light on the metal insulator transitions.

Fr.H.1_05 - On the superconducting instabilities of metals near quantum critical points

S. Raghu¹

1. Stanford University, California, United States

We study the dynamics of a metal near a quantum critical point. We study both the intermediate regime where the Landau damping of the boson can be neglected and the strongly overdamped regime where the order parameter is strongly Landau damped. Using renormalization group and large N analyses, we consider controllable regimes in which superconducting instabilities are enhanced near continuous quantum phase transitions. We present renormalization group treatments of singular enhancement of superconductivity in the Cooper channel due to the exchange of a gapless (critical) order parameter field. The resulting log-squared and higher order divergences are treated in systematic fashion. We also discuss regimes in which superconductivity develops out of a normal state that consists of ill-defined quasiparticles.

Fr.H.2_I1 - Conductive atomic force microscopy of magnetic tunnel junction nanopillars

S. Majetich¹, S. Piotrowski¹, S. Oberdick¹, M. Bapna¹, A. Abdelgawad¹, M. Matty¹

1. Carnegie Mellon University, Pittsburgh, Pennsylvania, United States

Conductive atomic force microscopy (C-AFM) enables scanning magnetoresistance measurements of individual nanostructures. Here we describe the application of C-AFM to CoFeB/MgO/CoFeB magnetic tunnel junctions as a function of their diameter. The CoFeB films were < 1.2 nm so that they exhibited perpendicular anisotropy. Electron beam lithography and nanoparticle masking were used with reactive ion etching to pattern CoFeB/MgO/CoFeB tunnel junctions with diameters down to 10 nm. After scanning electron microscopy was used to determine the nanopillar diameters, the samples were imaged with the C-AFM. Topography and conductivity maps of the nanopillar patterns were collected simultaneously. Measurements of resistance as a function of magnetic field and voltage bias were made with the Pt-coated probe tip in stable contact with individual nanopillars. When resistance-area product was unchanged by the patterning process, field-dependent switching was reliably observed. Major and minor hysteresis loops were collected as a function of the applied magnetic field to determine the effective anisotropy of the free layer. At fields close to the coercivity the tunnel current showed random telegraph noise, and the effective anisotropy was also calculated from the switching statistics and comparison with Landau-Lifshitz-Gilbert modeling of the magnetization dynamics. Voltage induced switching of the free layer was observed in devices larger than 80 nm. The regimes of magnetization reversal by coherent rotation and domain wall nucleation are discussed.

Fr.H.2_O2 - Ferritin-based multifunctional nanoparticles for magnetic fluid hyperthermia

C. Innocenti¹, A. Guerrini¹, E. Fantechi¹, M. Zanardelli², L. di Cesare Mannelli², C. Ghelardini², M. Fornara³, E. Falvo³, P. Ceci³, C. Sangregorio⁴

1. *INSTM-LaMM and Dip. di Chimica "U. Schiff", Univ. di Florence, Florence, Italy*

2. *Dip. NEUROFARBA - Sez. Farmacologia e Tossicologia, Univ. di Florence, Florence, Italy*

3. *CNR-IBPM, Dip. di Scienze Biochimiche "A. Rossi Fanelli", Univ. di Roma "La Sapienza", Rome, Italy*

4. *CNR-ICCOM and INSTM, Florence, Italy*

Magnetic nanoparticles (MNP) are fundamental building-blocks for developing innovative nanodevices with multi-fold therapeutic and diagnostic activities, including magnetic fluid hyperthermia (MFH), Magnetic Resonance Imaging (MRI) and targeting of tumor cells. Iron oxide MNPs mineralized within human H chain ferritin protein, HFt, represent a viable platform to achieve this goal as they offer multiple advantages. However, a major limitation is that their size cannot exceed the protein shell inner diameter (ca. 8 nm), which is not large enough to produce a significant MFH effect. In order to overcome this drawback while still exploiting the advantages provided by HFt, we developed two different approaches: first, we increased the magnetic anisotropy of 6-7 nm NPs@HFt by doping with small amount of Co²⁺ ions (Co-NPs@HFt) [1]; the second approach was based on HFt-NPs constructs obtained by conjugation with apo-HFt of larger, chemically synthesized, magnetite NPs (15-18 nm). In vitro tests showed that both constructs were highly biocompatible. The hyperthermic properties of Co-NPs@HFt and HFt-NPs were investigated through calorimetric technique and related to the structural and magnetic properties. A doping of 5% was found to enhance the hyperthermic efficiency of Co-NPs@HFt and to induce a significant reduction of cell viability when exposed to an alternating field, with clear indications of an advanced stage of apoptotic process. On the other hand, the same treatment performed with HFt-NPs had no effect on cell viability, despite their much larger hyperthermic performances with respect to Co-NPs@HFt. Confocal microscopy measurements performed on rhodamine labeled samples, showed that the different hyperthermic efficiency should be related with a different level of cell internalization, pointing out the fundamental role of cell-nanoparticles interactions with respect to large hyperthermic efficiency.

[Research funded by projects RINAME (Italian MIUR) and BaTMAN (CARIPO n.2013-0752)].

References:

[1] E. Fantechi et al., ACS Nano 8 (2014) 4705

Fr.H.2_O3 - Efficient, safe and fast magnetic targeting of stem cells in spinal cord injury

V. Zablotskii¹, O. Lunov¹, D. Tukmachev², E. Sykova², S. Kubinova², A. Dejneka¹

1. *Institute of Physics ASCR, Prague, Czech Republic*

2. *Institute of Experimental Medicine ASCR, Prague, Czech Republic*

Cell transplantation represents a promising therapy for the treatment of different diseases, including spinal cord injury (SCI). To achieve a significant therapeutic effect, the number of cells in the lesion should be a large enough [1]. We propose a new magnetic system consisting of two cylindrical magnets placed on a ring-shaped folder with the poles facing each other. First, we studied general patterns of different superparamagnetic iron oxide nanoparticles (SPIONs) engulfment by living cells and verified endocytosis mechanisms involved in SPIONs uptake. Second, SPION-labelled mesenchymal stem cells were subdurally transplanted and targeted by a magnetic field to the lesion site in a rat model of SCI. The calculated magnetic forces exerted on the transplanted cells in the lesion site correlated with the cell distribution found by histological analysis. We succeeded in efficiently delivering stem cells to lesions within the animal anaesthesia time period, 2 hours. In our experiments, in contrast to the control non-magnetic groups, the SPION-labelled cells were able to migrate from the trapping area to the lesion site. It is worth noting that the efficacy of conventional stem cell transplantation to the lesion site is low and variable, with typical delivery time to SCI varying from 12 to 24 h [2]. The efficacy of the proposed magnetic targeting strategy and the possibilities of reaching therapeutic concentrations were assessed together with physiological and biological factors that decrease the number of captured live cells at the lesion site, e.g., because of cell death in the target area, macrophage activity and/or the possible further removal of cells due to cerebrospinal fluid flow. A minimally invasive magnetic targeting strategy enabling fast cell retention after intrathecal transplantation was designed and tested in vivo. Its main advantage is the ability to reach a significantly higher concentration of SPION-labelled stem cells into the vicinity of a lesion site. Supported by MEYS of the CR (LO1309).

References:

1. V. Vanecek, V. Zablotskii, S. Forostyak, J. Ruzicka, et al. *Int. J. Nanomedicine* (2012) 7, 3719
2. D. Tukmachev, O. Lunov, V. Zablotskii, A. Dejneka, et al. *Nanoscale* (2015), DOI: 10.1039/C4NR05791K

Fr.H.2_O4 - Regulation of mesenchymal stem cell adipogenesis by oscillating high-gradient magnetic fields

O. Lunov¹, V. Zablotskii¹, E. Syková², Š. Kubinová^{1,2}, A. Dejneka¹

1. ASCR, Institute of Physics, Prague, Czech Republic

2. ASCR, Institute of Experimental Medicine, Prague, Czech Republic

Biological effects of magnetic field on intracellular molecular mechanisms attract significant interest^{1,2}. Here, we show that oscillating HGMF and mechanical vibration affect adipogenic differentiation of mesenchymal stem cells (MSCs) by the transmission of mechanical stress to the cell cytoskeleton, resulting in F-actin remodelling and subsequent down-regulation of adipogenic genes. Our findings propose an insight into the regulation of cellular nanomechanics, and provide a basis for better controlled down-regulation of stem cell adipogenesis by HGMF, which may facilitate the development of challenging therapeutic strategies suitable for the remote control of biological systems.

The adipogenesis was significantly down-regulated after 2 days and completely blocked after 7 days of HGMF as well as mechanical vibrations³. Furthermore, our study of the effects of mechanical and magnetic vibrations on the differentiation pathway of MSCs may give a first hint as to a force value that could be responsible for changes in cell fate. Down-regulation of adipogenesis of MSCs by oscillating high-gradient magnetic fields and mechanical vibration was caused by small mechanical forces 0.1-1 pN transmitted through the cytoskeleton to the nucleus and DNA. These force values are just above the thermal fluctuation forces of f-actin.³ Nevertheless, two days' worth of exposure of the MSCs to mechanical vibrations and oscillating magnetic induced alterations of adipogenic gene expression. We suggest a mechanism involving the following consequence of events in the transformation of MSCs upon oscillating HGMF: external magneto-mechanical stress → enhancement of actin filament tension → enhanced tension of the cell nucleus and DNA → change of gene expression → change in the differentiation pathway. Furthermore, we suppose that, this mechanism can be reversible due to the ability of cells to deform elastically in the operating ranges of the mechanical loading^{4,5}.

Supported by MEYS of the CR (LO1309).

References:

1. Zablotskii, V., *et al. PLoS One* 8, e70416 (2013)
2. Zablotskii, V., *et al. Biomaterials* 35, 3164-3171 (2014)
3. Zablotskii, V., *et al. Appl. Phys. Lett.* 105, 103702 (2014)
4. Kasza, K.E., *et al. Curr. Opin. Cell Biol.* 19, 101-107 (2007)
5. Guo, J., *et al. Proc. Natl. Acad. Sci. U. S. A.* 111, E5252-5261 (2014)

Fr.H.2_O5 - Halbach arrays consisting of cubic elements optimized for high field gradients in drug delivery applications

L. Barnsley¹, J. Owen¹, D. Carugo¹, E. Stride¹

1. Institute of Biomedical Engineering, Department of Engineering Science, University of Oxford, Oxford, United Kingdom

Magnetic drug targeting (MDT) has received a significant amount of attention from researchers as a method for highly localized delivery of therapy in a range of diseases, including cancer and stroke [1]. While MDT has significant advantages because it is non-invasive and magnetic fields can permeate the human body without being attenuated by tissue, there are a number of challenges that must be overcome before the technique is clinically viable [2]. Of particular importance is the need to develop systems that can deliver sufficient magnetic forces at useful tissue depths to overcome the hydrodynamic forces of blood flow in the targeted region [3]. In this paper, we present a series of designs of Halbach arrays optimized to retain magnetically tagged agents at distances up to 50 mm. By considering assembly forces, and field and force profiles, a particular design was selected and constructed. In vitro experiments to test the assembled array's capacity to retain magnetic microbubbles against flow demonstrated a factor of two increase in the relative intensity of retained microbubbles at 15 mm from the magnet when compared with a conventional, linear Halbach array. We propose that these designs are viable as light-weight, inexpensive options for MDT, particularly for applications for which size and portability are limiting factors, e.g. thrombolysis and combination therapies.

References:

- [1] A.S. Lübke, et. al. *Cancer Res*, 56, 4686 (1996)
- [2] Q.A. Pankhurst, et. al., *J. Phys. D: Appl. Phys.*, 36, R167 (2003)
- [3] M.E. Hayden and U.O. Höfeli, *J. Phys.: Condens. Matter*, 18, S2877 (2006)

FR.H.3_O1 - Helimagnetic spin order in Fe nanoisland on Cu(111)

S.Phark^{1,2}, J. Fischer², S. Ouazi², M. Corbetta², D. Sander², K. Nakamura³, J. Kirschner²

1. CCES, Institute for Basic Science, Seoul National University, Seoul, Korea

2. Max-Planck-Institut für Mikrostrukturphysik, Halle, Germany

3. Department of Physics Engineering, Mie University, Tsu, Japan

We report a combined spin-polarized scanning tunneling microscopy (SP-STM/S) and *ab initio* calculations of the magnetic state of individual nm small biatomic-layer-high Fe islands on Cu(111). Our study reveals a one-dimensional helimagnetic spin order, with a period of 1.28 nm, in Fe nanoislands where the topmost Fe is located in bridge-site of the surface Fe layer [1]. Energy-resolved SP-STs mapping provides spatially-resolved and spin-dependent electronic structure of this spin order. The wave vector describing the spin order remains constant in the energy range -0.8 to +0.6 eV, whereas the spin contrast varies and changes its sign near the Fermi energy. We discuss this energy dependence in view of the electronic structure associated with the helical spin density wave. Our results point at a novel aspect of SP-STM/S to characterize complex spin order with respect to its spin-dependent electronic density of states.

References:

[1] S. Phark *et al.*, *Nat. Commun.* doi: 10.1038/ncomms6183 (2014)

Fr.H.3_O2 - Magnetization reversal and topological defects in weak perpendicular anisotropy bifurcations

M. Velez^{1,2}, C. Blanco-Roldán^{1,2}, C. Quirós^{1,2}, A. Sorrentino³, A. Hierro-Rodriguez^{4,5}, L. M. Álvarez-Prado^{1,2}, R. Valcarcel³, M. Duch⁶, N. Torras⁶, J. Esteve⁶, J.I. Martín^{1,2}, J.M. Alameda^{1,2}, E. Pereiro³, S. Ferrer³

1. Dpto. Física, Universidad de Oviedo, Oviedo, Spain

2. Centro de Investigación en Nanomateriales y Nanotecnología, CINN (CSIC - Universidad de Oviedo), El Entrego, Spain

3. ALBA Synchrotron, Cerdanyola del Vallés, Spain

4. IN-IFIMUP, Departamento de Física e Astronomia, Faculdade de Ciências, Universidade do Porto, Porto, Portugal

5. INESC-TEC (Coordinated by INESC-Porto), Departamento de Física e Astronomia, Faculdade de Ciências, Universidade do Porto, Porto, Portugal

6. Centro Nacional de Microelectrónica, IMB - CNM, CSIC, Campus Universidad Autónoma de Barcelona, Bellaterra, Spain

Domain wall propagation in magnetic nanostructures with in-plane magnetic anisotropy is strongly affected by the presence of edge topological defects [1] (half vortices and antivortices) that can be tuned by the system geometry (antidots, notches in nanowires, bifurcations, à). Nanostructured weak perpendicular anisotropy materials, with comparable in-plane and out-of-plane magnetization components, introduce an additional complexity in which in-plane half-vortices can become coupled to topological defects in the out-of-plane magnetization stripe pattern (dislocations and disclinations) [2]. In this work we have studied domain wall propagation in magnetic bifurcations of weak perpendicular anisotropy amorphous Nd-Co alloy. The samples have been fabricated by a combined e-beam lithography, cosputtering and lift-off process on Si₃N₄ membranes and Si substrates. Samples were patterned in an “Y” geometry, 50 nm thick, 1 micron wide and 10 micron long. Magnetization reversal has been studied by magnetic Transmission X-ray Microscopy, Kerr microscopy and Magnetic Force Microscopy. First, a large in-plane field is applied along the “Y” symmetry direction in order to define in-plane easy axis. Then, a series of transverse field pulses allows us to nucleate and propagate a vortex wall in the nanostructure. This process results in an asymmetric configuration of each “Y” branch and modifies stripe domain configuration at the bifurcation due to the coupling between in-plane and out-of-plane topological defects.

References:

[1] O. Tchernyshyov and G.-W. Chernet, Phys. Rev. Lett. 95, 197204 (2005)

[2] A. Hierro-Rodriguez, R. Cid, M. Vélez, G. Rodriguez-Rodriguez, J. I. Martín, L. M. Álvarez-Prado, and J. M. Alameda, Phys. Rev. Lett. 109, 117202 (2012)

Fr.H.3_O3 - Suppression of transition from antiferromagnetic to weak ferromagnetic state in (0001) oriented α -Fe₂O₃ film by Ir doping

S. Prakash Pati¹, N. Shimomura¹, H. Hoshino¹, T. Nozaki¹, K. Mibu², M. Sahashi¹

1. Department of Electronic Engineering, Graduate School of Electronic Engineering, Tohoku University, Sendai, Japan

2. Graduate School of Engineering, Nagoya Institute of Technology, Nagoya, Japan

Antiferromagnets with high ordering temperature have attracted the attentions due to their potential application in spintronics devices. In this context, corundum structured hematite α -Fe₂O₃ is a most promising antiferromagnet having high Neel temperature (TN, 950K). But, a well-known spin reorientation from the [0001] axis to the (0001) basal plane occurs at Morin temperature TM, 263K [1]. This spin re-orientation is explained by the competition between magnetic dipolar anisotropy (KMD, in-plane anisotropy) and single-ion anisotropy (KFS, perpendicular anisotropy) [2]. The origin of weak ferromagnetism above TM is the Dzyaloshinskii-Moriya (D-M) interaction, where asymmetric exchange interaction between two neighboring spins results in a weak net magnetic moment in the (0001) plane. In this study, the successful observation of weak in-plane magnetic moment above TM in (0001) oriented Fe₂O₃ thin films and its suppression by Ir-doping is reported. This suppression of weak ferromagnetism leads to a conclusion of enhancement of Morin transition temperature. Fe₂O₃ and Ir-doped α -Fe₂O₃ films are fabricated by reactive sputtering of metal target using RF magnetron sputtering. A clear increase of in-plane magnetization for Fe₂O₃ film has been observed indicating Morin transition, while that was not observed for Ir-doping case. These results indicate that by Ir-doping, TM of Fe₂O₃ is dramatically enhanced. To clarify this assumption, conversion electron Mossbauer spectroscopy (CEMS) study has been employed at room temperature. The results for the quadrupole shift and the intensity ratio confirm that the spin direction of Fe₂O₃ is in-plane and that TM is below room temperature, while the spin direction of Ir-Fe₂O₃ is perpendicular to the film and TM should be higher than room temperature. This work was partly funded by ALCA Program of JST and ImPACT Program of Council for Science, Technology and Innovation (Cabinet Office, Japan Government).

References:

[1] F. J. Morin, Phys. Rev. 78, 819 (1950)

[2] J. O. Artman, J. C. Murphy, and S. Foner, Phys. Rev. 138, A912 (1965)

Fr.H.3_O4 - Modifying magnetic properties of an individual Co nanomagnet by circumferential contact with Fe

J. Fischer^{1,2}, S. Phark^{1,3}, M. Corbetta¹, H. Oka¹, D. Sander¹, J. Kirschner¹

1. Max-Planck-Institut für Mikrostrukturphysik, Halle, Germany

2. Departamento de Física, Universidade Federal de Santa Catarina, Florianópolis, Brazil

3. Center for Correlated Electron Systems, Institute for Basic Science, Seoul National University, Republic of Korea

Nanomagnets, due to reduced dimensionality, are characterized by a spatial variation of spin polarization and magnetic anisotropy [1,2] within an individual magnet, which often leads to a reduced magnetization stability [2]. Surface (or perimetric) engineering [3] has been employed to modify magnetic properties of nanomagnets. However, microscopic access to the local magnetic state in an individual nanomagnet [1,2] is called for to address the underlying mechanism. Here we report a tuning of the homogeneity of the spin-polarization in 10 - 20 nm size individual Co nanomagnets [1,2] by perimetrical contact with Fe [4,5]. Spin-polarized scanning tunneling spectroscopy resolves the spin-polarization of an individual island, with subnanometer spatial resolution. The study reveals uniform electronic states throughout the Co core with an atomically sharp interface at the Co-Fe border. We discuss the role of perimetrical contact for structural relaxation and for the local strain state, and we elucidate the impact on spin polarization and the magnetic anisotropy of single nanoislands.

References:

- [1] H. Oka et al., Science 327, 843 (2010).
- [2] S. Ouazi et al., Phys. Rev. Lett. 108, 107206 (2012).
- [3] S. Rusponi S. et al., Nat. Mater. 2, 546 (2003).
- [4] D. Sander et al., J. Phys.: Condens. Matter 26 394008 (2014).
- [5] S. Phark et al., Nat. Commun. doi: 10.1038/ncomms6183 (2014).

Fr.I.1_I1 - Dynamics and inertia of skyrmionic spin structures

C. Moutafis^{1,2}, F. Büttner³, A. Bisig^{3,4}, B. Krueger³, C. A.F. Vaz², P. Warnicke², M. Foerster³, M. Mawass³, M. Scheneider⁵, C. Günter⁵, J. Geilhufe⁶, C. V. Korff Schmising⁵, J. Mohanty⁵, B. Pfau⁵, S. Schaffert⁵, T. Schulz¹, M. Weigand⁷

1. School of Computer Science, University of Manchester, United Kingdom

2. Paul Scherrer Institute, Villigen, Switzerland.

3. Institute of Physics, Johannes Gutenberg Universität Mainz, Mainz, Germany, Universität Konstanz, Konstanz, Germany

5. Institut Für Optik Und Atomare Physik, Technische Universität Berlin, Berlin, Germany

6. Helmholtz Zentrum Berlin Für Materialien Und Energie GmbH, Berlin, Germany

7. Max Planck Institute For Intelligent Systems, Stuttgart, Germany

8. Department of Applied Physics, Center For NanoMaterials, Eindhoven University of Technology, Eindhoven, The Netherlands

Magnetic skyrmions are topologically protected particle-like spin structures, with a topology characterised by their Skyrmion number [1]. Numerical predictions suggest that they exhibit rich dynamical behaviour governed by their topology, such as the basic gyrotropic and breathing eigenmodes [1-3]. While recent advances have brought the static manipulation of skyrmions under control, their dynamical behaviour is largely unexplored experimentally. We provide here the first observation of the basic eigenmode dynamics of skyrmion bubbles. In particular, we present picosecond nanoscale imaging data i) of the gyrotropic mode of a single skyrmion bubble in the gigahertz regime [4] and ii) the breathing-like behaviour of a pair of skyrmionic configurations. The observed dynamical behaviour is used to confirm the skyrmion topology and show the existence of an unexpectedly large inertia that is key for accurately describing skyrmion dynamics [4]. These results demonstrate new ways for experimentally observing skyrmion dynamics and provide a framework for describing their behaviour. Furthermore, the results reveal a link between the dynamical behaviour of skyrmions and their distinct topology, with possible ramifications for Skyrmions research including recently proposed technological applications [5].

References:

[1] N. Nagaosa, & Y. Tokura, Nat. Nanotech. 8, 899-911 (2013)

[2] C. Moutafis, S. Komineas, J. A. C. Bland, Phys. Rev. B 79, 224429 (2009)

[3] I. Makhfudz, I., B. Krüger, O. Tchernyshyov, Phys. Rev. Lett. 109, 217201 (2012)

[4] F. Büttner, C. Moutafis, et al., Nature Physics, doi:10.1038/nphys3234, (2015)

[5] A. Fert, V. Cros, J. Sampaio, Nat. Nanotech. 8, 152-156 (2013)

Fr.I.1_O2 - High-frequency dynamic modes of a magnetic antivortex

K. Buchanan¹, G. Riley¹, J. Liu¹, A. Haldar¹, M. Asmat-Uceda¹

1. Colorado State University, Colorado, United States

Magnetic vortices have been studied extensively in recent years because of their rich physics as well as their potential for applications. Magnetic antivortices, the topological counterpart of the vortex state, have similar potential; however, comparatively few experimental investigations have been conducted because they are more difficult to create. This presentation will discuss experimental measurements of the high-frequency spin dynamics of a magnetic antivortex made using micro-focus Brillouin light scattering (micro-BLS). Permalloy nanostructures with a pound-key-like shape that promotes the reliable formation of AV's [1] were patterned on top of gold waveguides that were used to excite the structure. The pumping frequency was swept from 1-7 GHz and the BLS intensity from a ~250-nm spot focused at various locations on the patterned structure were recorded. BLS spectra corresponding to the three possible magnetic states were obtained: AV, saturated along the dynamic field, and saturated perpendicular to the dynamic field. Spatial scans reveal that the modes in the 5-6 GHz range occur primarily in the legs of the structure and the modes in this range are similar for all of the magnetic states. A mode observed at 3.4 GHz is, however, unique to the AV state and is associated primarily with dynamics within the AV (intersection) region. The experimental results will be compared with detailed micromagnetic simulations of the expected modes. This work was supported by DOE-BES ER46854.

References:

[1] A. Haldar and K. S. Buchanan, Appl. Phys. Lett., 102, 112401 (2013)

Fr.I.1_O3 - μ SR studies of dynamic spin fluctuations and the static order parameter of skyrmion systems

L. Liu¹, S. Cheung¹, T. Goko^{1,2}, B. Frandsen¹, E. Morenzoni², S. Dunsiger³, P. Boeni³, G. Luke⁴, C. Jin⁵, A. Fujimori⁶, N. Kanazawa^{6,7}, N. Nagaosa^{6,7}, S. Seki^{6,7}, Y. Tokura^{6,7}, M. Lee⁸, D. Reznik⁸, Y. Uemura¹

1. Columbia University, New York, United States
2. Paul Scherrer Institute, Switzerland
3. Technische Universität München, München, Germany
4. McMaster University, Hamilton, Canada
5. Chinese Academy of Sciences, Beijing, China
6. University of Tokyo, Tokyo, Japan
7. RIKEN center for Emergent Matter Science, Saitama, Japan
8. University of Colorado, Boulder, United States

Antiferromagnets with high ordering temperature have attracted the attentions due to their potential application in spintronics devices. In this context, corundum structured hematite (α -Fe₂O₃) is a most promising antiferromagnet having high Neel temperature (T_N , 950K). But, a well-known spin reorientation from the [0001] axis to the (0001) basal plane occurs at Morin temperature T_M , 263K [1]. This spin re-orientation is explained by the competition between magnetic dipolar anisotropy (K_{MD} , in-plane anisotropy) and single-ion anisotropy (K_{FS} , perpendicular anisotropy) [2]. The origin of weak ferromagnetism above T_M is the Dzyaloshinskii–Moriya (D-M) interaction, where asymmetric exchange interaction between two neighboring spins results in a weak net magnetic moment in the (0001) plane. In this study, the successful observation of weak in-plane magnetic moment above T_M in (0001) oriented Fe₂O₃ thin films and its suppression by Ir-doping is reported. This suppression of weak ferromagnetism leads to a conclusion of enhancement of Morin transition temperature. Fe₂O₃ and Ir-doped Fe₂O₃ films are fabricated by reactive sputtering of metal target using RF magnetron sputtering. A clear increase of in-plane magnetization for Fe₂O₃ film has been observed indicating Morin transition, while that was not observed for Ir-doping case. These results indicate that by Ir-doping, T_M of Fe₂O₃ is dramatically enhanced. To clarify this assumption, conversion electron Mössbauer spectroscopy (CEMS) study has been employed at room temperature. The results for the quadrupole shift and the intensity ratio confirm that the spin direction of α -Fe₂O₃ is in-plane and that T_M is below room temperature, while the spin direction of Ir-Fe₂O₃ is perpendicular to the film and T_M should be higher than room temperature.

This work was partly funded by ALCA Program of JST and ImpACT Program of Council for Science, Technology and Innovation (Cabinet Office, Japan Government).

References:

- [1] F. J. Morin, Phys. Rev. 78, 819 (1950).
- [2] J. O. Artman, J. C. Murphy, and S. Foner, Phys. Rev. 138, A912 (1965)

Fr.I.1_I4 - Low-frequency magnetization dynamics of vortex dot clusters

K. Gusliyenko^{1,2}, O. Sukhostavets¹

1. *Depto. Física De Materiales, Universidad Del País Vasco, UPV/EHU, San Sebastián, Spain*

2. *IKERBASQUE, the Basque Foundation for Science, Bilbao, Spain*

The lateral arrays of magnetic dots with submicron in-plane sizes attract a considerable attention due to the presence of a vortex (half-skyrmion) magnetization configuration in their ground states. The vortex core excited by external magnetic field or electric current oscillates in 100 MHz - 1 GHz range providing a narrow frequency linewidth. The coupled vortex oscillators are promising candidates for spin-torque nano-oscillators emitting microwaves. One of unresolved problems is synchronization of several nano-oscillators that would allow increasing essentially the generated microwave power. The need of close packing of such magnetic dots to increase the interdot magnetostatic interactions leads to necessity to consider the collective vortex dynamics in dot clusters. In the present paper we develop an analytical approach to the dynamics of coupled vortex dot oscillators. The clusters consist of N=3 or N=4 laterally placed cylindrical dots on a substrate in the form of equilateral triangles or squares. The interdot magnetostatic interaction is accounted via multipole decomposition on the inverse the dot center-to-center distance. The gyrotropic eigenfrequencies/eigenmodes of collective vortex oscillations are calculated analytically [1] and compared with recent broadband ferromagnetic resonance and X-ray imaging experiments on interacting clusters of permalloy dots. The calculated fine structures of the excitation spectra of N=3 and 4 dot clusters are similar. The splitting of the degenerated gyrotropic frequency of isolated dots about of 10-30 MHz is determined by interdot coupling integrals, which are expressed explicitly in the form of multipole decomposition. The fine structure of the dot spectra can be tuned by changing the vortex core polarizations by an external magnetic field. The spread of the collective mode frequencies is approximately 3 times larger for the antiparallel vortex core polarizations than for the aligned case.

References:

[1] O.V. Sukhostavets et al., Appl. Phys. Express 8, 023002 (2015), published on-line Jan. 8, 2015

Fr.I.2_I1 - Nonlinear unidirectional spin Hall magnetoresistance

P. Gambardella¹

1. Department of Materials, ETH Zurich, Switzerland

Magnetoresistive effects constitute a prominent manifestation of spin-orbit coupling and spin dependent conductivity in ferromagnets, with manifold applications in sensor technology. Most such effects, including the anisotropic magnetoresistance (AMR), giant magnetoresistance (GMR), and spin Hall magnetoresistance (SMR), do not distinguish between opposite orientations of the magnetization. Indeed, all linear MR are even with respect to the inversion of either the current or magnetization owing to the time reversal symmetry embodied in the Onsager's reciprocity relations. In noncentrosymmetric conductors, however, nonlinear resistive terms can give rise to an MR that is linear in the magnetization. In this talk, we report on a new MR effect¹ occurring in ferromagnet/normal metal bilayers with strong current-induced spin accumulation.²⁻⁴ The effect combines features that are typical of the current-in-plane GMR and spin Hall effect (SHE), whereby the spin accumulation induced by the SHE in the normal metal replaces one of the ferromagnetic polarizers of a typical GMR device. Differently from GMR, however, this effect introduces a nonlinear dependence of the resistance on the current, which gives it unique unidirectional properties: we show that the longitudinal resistance of Ta|Co and Pt|Co bilayers changes when reversing the polarity of the current or the sign of the magnetization. This unidirectional MR scales linearly with current density and has opposite sign in Ta and Pt, which we associate to the modulation of the FM/NM interface resistance due to the current-induced spin accumulation. We expect such a resistance to be a general feature of noncentrosymmetric magnetic systems with strong spin-orbit coupling, including magnetic semiconductors and topological insulators.

References:

- 1 C. O. Avci et al., arXiv:1502.06898
- 2 I. M. Miron et al., Nature Mater. 9, 230 (2010)
- 3 I. M. Miron et al., Nature 476, 189 (2011)
- 4 K. Garello et al., Nature Nanotech. 8, 587 (2013)

Fr.I.2_O2 - Influence of non-magnetic spacers on spin wave spectra in two-dimensional binary magnonic crystals

P. Malago¹, P. Gruszecki², L. Giovannini¹, M. Krawczyk²

1. *Dipartimento di Fisica e Scienze della Terra, Università di Ferrara, Ferrara, Italy*

2. *Faculty of Physocs, Adam Mickiewicz University In Poznan, Poznan, Poland*

We study theoretically the influence of a non-magnetic spacer between ferromagnetic dots and ferromagnetic matrix on the spectra of spin wave excitations in two-dimensional bi-component magnonic crystals. With the use of the dynamical matrix method supported by micromagnetic simulations we investigate structures that are inhomogeneous across the thickness, i.e., composed of square array of grooves in permalloy matrix partially filled with ferromagnetic dots. We show that the introduction of the non-magnetic spacers significantly modify the total magnetic field in magnonic crystals, especially at the edges of the grooves and dots. This allows effective manipulation of the magnonic band structure, especially of the spin waves localized at edges of the dots or in matrix's material, at the edges of grooves. These two types of edge modes can be identified in the same magnonic crystal with properly designed non-magnetic spacers. Moreover, we demonstrate that the frequencies of the spin waves in these structures are significantly influenced by the dot material. We show that, with a single ferromagnetic material, it is possible to design a two-dimensional magnonic crystal preserving simultaneously some properties of bi-component magnonic crystals and magnonic antidot lattice. Finally, the influence of the non-magnetic spacers on technologically relevant parameters, like group velocity and magnonic band width, is evaluated and its usefulness for applications discussed. The research has received funding from Polish National Science Centre project DEC-2-12/07/E/ST3/00538, from the European Union's Horizon 2020 programme under the Marie Skłodowska-Curie GA No 644348 (MagIC), and from MIUR-PRIN 2010-11 Project2010ECA8P3 'DyNanoMag'.

FR.I.2_O3 - Spin and orbital magnetic moment of reconstructed $\sqrt{2} \times \sqrt{2}R45^\circ$ magnetite(001)

L. Aballe¹, L. Martín-García², R. Gargallo-Caballero², M. Monti², M. Foerster¹, J. F. Marco², J. de la Figuera²

1. ALBA Synchrotron Light Facility, Barcelona, Spain

2. Instituto de Física-Química Rocasolano (CSIC), Madrid, Spain

Magnetite is a functional material with applications in a variety of fields ranging from catalysis to information storage or soil decontamination. It is ferrimagnetic with a high Curie temperature, a half-metal conductor, multiferroic at low temperatures and with a metal-insulator transition known for the last century. Despite its interest, many of its properties are still under discussion, from the origin of the metal-insulator transition to its half-metal character or even its magnetic moments. The experimental data scatter in this latter point, from vanishing orbital moments to giant ones, has been shown to strongly depend on the surface quality and preparation, since most studies make use of the surface-sensitive soft X-ray Magnetic Circular Dichroism (XMCD) technique[1]. We here present the magnetic properties of a well-characterized magnetite (001) surface, prepared by sputtering/annealing cycles providing the $\sqrt{2} \times \sqrt{2}R45^\circ$ reconstruction. The distribution of magnetic domains on the surface, as well as the near-surface magnetic moments were measured by XMCD-Photoemission Electron Microscopy with different kinetic energies of the secondary electrons, in order to vary the depth sensitivity[2]. A reduced total moment of $3.3 m_B$ and a ratio of about 0.10 between orbital and spin moment was found, which we attribute to the Fe²⁺-poor surface reconstruction[3].

References:

- 1) E. Goering, Phys. Stat. Sol. B, 248, 2345 (2013)
- 2) L. Martín-García et al, Phys. Rev. B 91, 020408(R) (2015)
- 3) R. Bliem et al, Science 346, 1215 (2014)

Fr.I.2_O4 - Imprinting magnetic chiral spin textures

R. Streubel¹, F. Kronast², U. K. Rössler³, O. G. Schmidt^{1,4}, P. Fischer^{5,6}, D. Makarov¹

1. Institute for Integrative Nanosciences, IFW Dresden, Germany

2. Helmholtz-Zentrum Berlin für Materialien und Energie GmbH, Germany

3. Institute for Theoretical Solid State Physics, IFW Dresden, Germany

4. Material Systems for Nanoelectronics, Chemnitz University of Technology, Germany

5. Center for X-ray Optics, Lawrence Berkeley National Laboratory, CA, United States

6. Physics Department, UC Santa Cruz, CA, United States

The unique properties of non-trivial topological states, e.g. magnetic skyrmions, may path the way towards novel spintronic devices. However, these spin textures have only been observed in special class of materials possessing non-centrosymmetric crystal structure and at low temperatures, which limits their application potential. We offer an alternate route to design magnetic heterostructures that resemble swirls, vortices or skyrmions with distinct topological charge densities at room temperature [1]. We will present results on nanostructures consisting of soft-magnetic 40 nm thick Ni₈₀Fe₂₀ and 5 nm thick Co/Pd multilayers separated by a Pd spacer (1 to 30 nm) mediating an interlayer exchange coupling strength that ranges from 0.1 to 2 mJ/m². Depending on the interlayer coupling either planar vortices or donut states are imprinted into the Co/Pd layers. Driving full or minor hysteresis loops allows to stabilize topologically distinct donut states with topological charges of about 1 and 0. Evidence for the stabilization of the predicted non-collinear spin textures in the Co/Pd layers is provided by direct imaging of the magnetization patterns utilizing X-ray magnetic circular dichroism (XMCD) with magnetic soft X-ray transmission microscopy (MTXM) and X-ray photoemission electron microscopy (XPEEM). Modifications in both core size and out-of-plane magnetization components with respect to vortices in nanopatterned soft-magnetic materials induce distinct magnetization dynamics with time dependent gyrofrequencies. Supported by DFG (MA 5144/2-1), ERC under EU FP7 program (FP7/2007-2013)/ERC n.306277 and FET programme under FET-Open grant number 618083. PF acknowledges support from BES, MSED of the U.S. Department of Energy (DE-AC02-05-CH11231) and by Leading Foreign Research Institute Recruitment Program (2012K1A4A3053565) through the NRF of Korea funded by MEST.

References:

[1] R. Streubel et al., Sci. Rep., accepted

Fr.I.2_O5 - Macroscopic and static measurement of interfacial Dzyaloshinskii-Moriya interaction

D. Han¹, Y. Yin¹, N. Kim^{2,3}, J. Kim¹, J. Koo¹, J. Cho², R. Lo Conte³, G. Karnad³, T. Schulz³, M. Klau³, H. Swagten¹, B. Koopmans¹, C.Y. You²

1. *Department of Applied Physics, Center For NanoMaterials, Eindhoven University of Technology, Eindhoven, The Netherlands*

2. *Department of Physics, Inha University, Incheon, Republic of Korea*

3. *Institut für Physik and Exzellenz Graduiertenschule Materials Science in Mainz, Johannes Gutenberg Universität Mainz, Mainz, Germany*

Dzyaloshinskii-Moriya interaction (DMI) in heavy metal/ferromagnetic thin film structures has recently drawn great attention [1-7]. Such interfacial DMI is known to be responsible for high domain-wall velocities [1-3] in perpendicularly magnetized layers and for the formation of a magnetic skyrmion state [5], which is expected to be promising for ultrafast and high-density storage devices. So far, several experimental methods to verify the interfacial DMI has been proposed [2,6,7]. However, since all those methods have been reliant upon the magnetization dynamics which requires specific measurement techniques and instruments including Brillouin light scattering, ferromagnetic resonance, and domain wall imaging, it is not trivial to experimentally address DMI, and therefore, the development of an easily accessible technique is still a challenge. Here, we present an asymmetric hysteresis loop in asymmetric nanostructures under an application of an in-plane bias field, which can be used for a static and macroscopic measurement of the interfacial DMI. The measured asymmetry is directly proportional to the strength of the in-plane field and the asymmetry created in the structure. Moreover, we show the dependence of the asymmetry on the adjacent top layer (X) in Pt/Co/X, which is expected to lead to different strengths of the DMI. With the help of analytical and numerical studies, we have also quantified the DMI in these systems, and those are generally in very good agreement with the previously reported values.

References:

- [1]. S. Emori et al., Nat. Mat. 23, 611 (2013)
- [2] J. Torrejon et al., Nat. Comm. 5, 4655 (2014)
- [3]. K. Ryu et al. Nat. Nanotech. 8, 527 (2013)
- [4] S. Pizzini et al., Phys. Rev. Lett. 113, 0407203 (2011)
- [5] J. Sampaio et al, Nat. Nanotech. 8, 839 (2013)
- [6] S.-G. Je et al., Phys. Rev. B 88, 214401 (2013)
- [7] K. Di et al., Phys. Rev. Lett. 114, 047201 (2015)

Fr.I.3_O1 - A Magnetic nano-skyrmion lattice observed in a si-wafer based multilayer system

S. Krause¹, A. Schlenhoff¹, P. Lindner¹, J. Friedlein¹, R. Wiesendanger¹, M. Weinl², M. Schreck², M. Albrecht²

1. *University of Hamburg, Hamburg, Germany*

2. *University of Augsburg, Augsburg, Germany*

Recently, an atomic-scale two-dimensional magnetic skyrmion lattice at the Fe/Ir(111) interface has been discovered using spin-polarized scanning tunneling microscopy (SP-STM).[1] Skyrmions offer new exciting possibilities for spintronic applications, using them as digital information carriers. For these applications the mass production of devices using multilayer growth on large-scale substrates is indispensable. In 2009, the heteroepitaxial growth of single crystal Ir(111) films on Si(111) wafers with yttria-stabilized zirconia buffer layers has been demonstrated.[2] For our study we epitaxially grow one monolayer of Fe on top of this multilayer substrate. The SP-STM experiments reveal a magnetic skyrmion lattice, being fully equivalent to the magnetic ground state that has previously been observed on an Ir(111) bulk single crystal substrate. In addition, it is found to be robust against local atomic lattice distortions induced by multilayer preparation. Our work paves the way towards spintronic applications of nano-skyrmions in ultrathin films and multilayer systems.

References:

[1] S. Heinze et al., Nature Physics 7, 713 (2011)

[2] S. Gsell et al., J. Cryst. Growth 311, 3731 (2009)

Fr.I.3_O2 - Conduction-electron mediated Dzyaloshinsky-Moriya interaction in pairs of adatoms revealed by ISTS

M. Steinbrecher¹, A. Ako Khajetoorians^{1,2}, M. Bouhassoune³, M. dos Santos Dias³, S. Lounis³, M. Ternes⁴, J. Wiebe¹, R. Wiesendanger¹

1. *Department of Physics, Universität Hamburg, Hamburg, Germany*

2. *Institute for Molecules and Materials, Radboud University, AJ Nijmegen, The Netherlands*

3. *Peter Grünberg Institut and Institute for Advanced Simulation, Forschungszentrum Jülich and JARA, Jülich, Germany*

4. *Max-Planck Institut für Festkörperphysik, Stuttgart, Germany*

Localized magnetic moments in a metal are coupled by indirect exchange interactions, which are mediated by the conduction electrons of the nonmagnetic host. For hosts with weak spin-orbit coupling, this exchange can be described by an isotropic Ruderman-Kittel-Kasuya-Yoshida (RKKY)-interaction. The damped oscillation of this interaction as a function of distance between ferromagnetic and antiferromagnetic coupling has already been observed [1]. However, for materials with strong spin-orbit coupling, such as platinum, an additional anisotropic Dzyaloshinskii-Moriya (DM) type term has to be considered [2,3]. In our work, we report for the first time a study of the distance dependency of this DM term in pairs of an Fe-H₂ Kondo complex and an Fe atom adsorbed on Pt(111). To this end, we used a scanning tunneling microscope in an ultrahigh vacuum facility at a very low temperature of 0.3 K. We have built several pairs of various distances and performed inelastic scanning tunneling spectroscopy (ISTS) above each atom in such pairs. This reveals a splitting of the Kondo resonance and a shift of the Fe atom spin-excitation, dependent on the strength of the isotropic and DM components of the RKKY interaction for the specific distance. By using a model including the coupling to the substrate electrons in 3rd order perturbation theory [4], we were able to extract the strength of both components and find that in our system the DM term is of similar magnitude as the isotropic exchange. These results are confirmed by first-principles calculations using the KKR method

References:

[1] L. Zhou et al., Nat. Phys. 6, 187 (2010)

[2] A. Fert et al., PRL 44, 1538 (1980)

[3] S. Lounis et al., PRL 108, 207202 (2012)

[4] Y.-H. Zhang et al., Nat. Comm. 4, 127203 (2013)

Fr.I.3_O3 - Magnetism of single Ho atoms on metal surfaces

R. Baltic¹, F. Donati¹, A. Singha¹, S. Stepanow², C. Wöckerlin¹, J. Dreiser³, P. Gambardella², S. Rusponi¹, H. Brune¹

1. *Institute of Condensed Matter Physics (ICMP), École Polytechnique Fédérale de Lausanne (EPFL), Lausanne, Switzerland*

2. *Department of Materials, ETH Zürich, Zürich, Switzerland*

3. *Swiss Light Source (SLS), Paul Scherrer Institute (PSI), Villigen PSI, Switzerland*

Systems consisting of single magnetic atoms adsorbed on solid surfaces represent the smallest possible realization of a magnet and have received much attention due to their potential applications in quantum computation. Moreover, they represent model systems for investigating the origin of the magnetic anisotropy energy (MAE) and fundamental magnetic interactions. The majority of the research so far has focused on transition metal (TM) atoms, and has resulted in the highest observed value of MAE, 58 meV, for Co on MgO[1]. Yet TMs have limited potential as single atom magnets due to their strong hybridization with the substrate which lowers their spin relaxation times. To overcome this problem, we propose to use rare earth (RE) elements. Their 4f electrons have much larger values of spin-orbit coupling than 3d electrons in TMs, and are highly localized. This should lead to less hybridization and therefore much larger values of MAE and longer spin relaxation times. Here we present x-ray absorption spectroscopy and magnetic circular dichroism measurements used to determine the electronic ground state and magnetic anisotropy of single Ho atoms adsorbed on platinum, copper and silver surfaces. In particular, for Ho on Pt(111) we reveal an intermediate $J_z = \pm 5.4$ ground state with no hysteresis [2]. This is in disagreement with scanning tunneling microscopy study by T. Miyamachi et al. [3], where authors claim single ion magnetic behavior with the maximal $J_z = \pm 8$ ground state. For Ho on the other two surfaces we find $J_z = \pm 6.7$ ground states, with different 4f occupations: 4f10 on Cu(111) and 4f11 on Ag(111) surface.

References:

[1] I. G. Rau et al., *Science* 344, 988 (2014)

[2] F. Donati et al., *Phys. Rev. Lett.* 113, 237201 (2014)

[3] T. Miyamachi et al., *Nature* 503, 242 (2013)

Fr.I.3_O4 - Molecular-driven magnetism on a reactive Cu-surface

A. Bedoya-Pinto¹, Y. Prado², S. Shi³, S. Lach⁴, A. Chuvilin^{1,6}, A. Altenhof⁴, A. Droghetti⁵, R. Kruthovostovs¹, F. Casanova^{1,6}, R. Hillenbrand^{1,6}, S. Sanvito⁵, C. Ziegler⁴, M. Fahlman³, E. Coronado², L. Hueso^{1,6}

1. CIC nanoGUNE, Donostia-San Sebastian, Spain

2. Instituto de Ciencia Molecular (ICMOL) Universidad de Valencia, Valencia, Spain

3. Department of Physics, Chemistry and Biology, Linköping University, Linköping, Sweden

4. Department of Physics and Research Center OPTIMAS, University of Kaiserslautern, Erwin-Schrödinger, Kaiserslautern, Germany

5. School of Physics, AMBER and CRANN, Trinity College, Dublin, Ireland

6. IKERBASQUE, Basque Foundation for Science, Bilbao, Spain

The adsorption of molecules on metal surfaces presents a rich variety of physical phenomena. Depending on the interaction strength, these phenomena move from the creation of interface dipoles for physisorbed molecules to hybridization and charge-transfer through covalent metal-molecule bonds via strong chemisorption [1]. In some cases, a strong interaction can even lead to a surface rearrangement [2] triggered by kinetic and electrochemical processes, and eventually account for the formation of novel hybrid phases. In this work, we study the interaction of novel rare-earth quinoline molecules (Tb₃q₉) with non-magnetic metallic surfaces. The molecules preserve their structural, chemical and magnetic properties when deposited onto noble metal (Au) and passivated (SiO₂) surfaces. However, the adsorption on reactive metals such as Cu induces a magnetic phase at the interface involving molecular Tb-atoms, as determined via SQUID magnetometry and element-specific X-ray magnetic circular dichroism (XMCD) [3]. Remarkably, the magnetic ordering persists up to room-temperature for the Tb₃q₉/Cu system and is linked to a chemically-triggered change in structure and stoichiometry of the interfacial species, as confirmed by infrared (IR), ultraviolet and X-ray photoemission spectroscopy (UPS/XPS). Cross-sectional transmission electron microscopy (TEM) and spectroscopy (EDX/EELS) investigations confirm the formation of a new phase involving both the high-spin metal atom present in the molecule (Tb) and the metallic surface atoms (Cu). The fact that these purpose-made molecules are able to trigger the creation of a new inorganic phase with robust magnetic properties at a non-magnetic metal surface underlines the importance and role of interfacial chemistry to crucially modify surface properties and thus design building blocks for spintronic applications.

References:

[1] Braun, S., Salaneck, W.R. & Fahlman, M. *Advanced Materials* 21, 1450-1472 (2009)

[2] Tseng, T.-C. et al. *Nature Chemistry* 2, 374-379 (2010)

[3] A. Bedoya-Pinto, et al. (submitted)

Fr.J.1_I1 - Quantum criticality and emergence of the T /B scaling in strongly correlated metals

Shinji Watanabe¹, Kazumasa Miyake²

1. *Kyushu Institute of Technology, Fukuoka, Japan*

2. *Toyota Physical and Chemical Research Institute Nagakute, Japan*

Unconventional quantum critical phenomena observed in the heavy-electron metal beta-YbAlB₄ have attracted much attention [1]. The criticality is common to those observed in YbRh₂Si₂ [2] and even in the quasicrystal Yb₁₅Al₃₄Au₅₁ [3], which has been proposed to be explained theoretically by critical Yb-valence fluctuations [4,5]. By developing the theoretical framework of the quantum valence criticality under a magnetic field, we analyze the scaling behavior over four decades of the ratio of temperature T to magnetic field B observed in the magnetization in beta-YbAlB₄ [1]. We show that the T /B-scaling behavior can appear near the quantum critical point of the valence transition [6]. The emergence of the T /B scaling indicates the presence of the small characteristic energy scale of the critical Yb-valence fluctuations. The key origin is clarified to be due to the atomic origin of the Yb-valence fluctuations under the strong local electron correlation, giving rise to the spatially localized critical mode. In the presentation, we overview the quantum critical phenomena of valence fluctuations and discuss the mechanism of the emergence of the T /B scaling. The possibility of new universality class formed by critical valence fluctuations will be also discussed toward understanding the unconventional criticality commonly observed in the Yb-based periodic-crystal and quasicrystal systems.

References:

- [1] Y. Matsumoto et al., *Science* 331, 316 (2011)
- [2] P. Gegenwart et al., *Phys. Rev. Lett.* 94, 076402 (2005)
- [3] K. Deguchi et al., *Nature Mat.* 11, 1013 (2012)
- [4] S. Watanabe and K. Miyake, *Phys. Rev. Lett.* 105, 186403 (2010)
- [5] S. Watanabe and K. Miyake, *J. Phys. Soc. Jpn.* 82, 083704 (2013)
- [6] S. Watanabe and K. Miyake, *J. Phys. Soc. Jpn.* 83, 103708 (2014)

Fr.J.1_O2 - Electronic correlations in Hund metals

E. Bascones¹, L. Fanfarillo¹

1. Instituto de Ciencia de Materiales de Madrid (ICMM-CSIC), Madrid, Spain

A new concept has emerged in the last years in correlated electron systems: the Hund metal. This name was coined within the context of iron superconductors and refers to a strongly correlated metallic state found in multi-orbital systems with Hund's coupling playing a key role in setting the correlations [1]. Until very recently [2] the nature of correlations in Hund metals has been controversial and not well understood. When the atoms become spin polarized the overlap between the atomic and single particle states decreases suppressing the quasiparticle weight. Nevertheless the system seems to be far from a Mott transition as the transition is not found for moderate increase of interactions. On the other hand the strong increase of correlations as half-filling is approached has led to a description of Hund metals as doped Mott insulators. This has led to a discussion on the role of Mott physics in these systems. We have addressed the correlations in multi-orbital systems as a function of interactions, number of orbitals and electronic filling. We have clarified the nature of correlations in Hund metals and solved the controversy between Hund and Mott systems [2]. Our calculations clearly show that the suppression of coherence in Hund metals is directly connected to the Mott insulating state at half-filling. However correlations due to Hund's coupling are intrinsically different to those in Mott states. This is observed in the charge fluctuations, which are only weakly reduced or even enhanced in Hund metals as the quasiparticle weight is suppressed, contrary to what happens in Mott correlated systems. We have shown that the dependence of correlations, energy scales, charge and spin fluctuations can be understood by looking at the hopping processes which are suppressed or promoted by Hund's coupling.

References:

- [1] -Coherence-incoherence crossover in the normal state of iron-oxypnictides and importance of the Hund's rule coupling, K. Haule and G. Kotliar, *New J. Phys.* 11, 025021 (2009)
- Spin freezing transition and non-Fermi liquid self-energy in a 3-orbital model, P. Werner, E. Gull, M. Troyer, A.J. Millis, *Phys. Rev. Lett.* 101, 166405 (2008)
- Strong electronic correlations from Hund's coupling. A. Georges, L. de Medici and J. Mravlje. *Annual Reviews of Condensed Matter Physics* 4, 137-178 (2013)
- [2] Correlations in multi-orbital systems and iron superconductors, L. Fanfarillo and E. Bascones, arXiv: 1501.04607

Fr.J.1_O3 - Competition between Hund's coupling and Kondo effect in an extended one-dimensional periodic Anderson model

I. Hagymasi¹, J. Solyom¹, O. Legeza¹

1. Wigner Research Centre For Physics, Budapest, Hungary

We study the ground-state properties of an extended periodic Anderson model with inter- and intraband interactions to understand the role of Hund's coupling between localized and itinerant electrons using the density-matrix renormalization group algorithm. By calculating the von Neumann entropies we show that two phase transitions occur as the hybridization is increased in the symmetric half-filled case due to the competition between hybridization and Hund's coupling. In the intermediate phase, which is bounded by two critical points, we found a dimerized ground state, while in the other two phases the ground state is spatially homogeneous (Haldane-like and Kondo-singlet-like). We also determine the entanglement diagram of the system by calculating the mutual information, which clarifies the structure of each phase.

Fr.J.1_I4 - Non-local correlations beyond DMFT and (quantum) criticality

K. Held¹

1. Vienna University of Technology, Wien, Austria

Dynamical mean field theory (DMFT) has been a big step forward for our understanding of electronic correlations. A major part of the electronic correlations, the local ones, are included. The arguably most fascinating physical phenomena of solid state physics, however, such as (quantum) criticality and the physics of high-T superconductors are based on non-local correlations. To address these problems, recently diagrammatic extensions of DMFT have been developed: dynamical vertex approximation[1], dual fermion approach, 1PI and DMF2RG [2]. Among others, these approaches allow for describing spin-fluctuation-mediated pseudogaps and for calculating critical exponents of the 3D Hubbard model [3]. Most recently, it could be shown that long-range fluctuations are the fate of the Mott-Hubbard transition in 2D [3]. I will also present our current efforts to calculate the critical behavior at a 3D antiferromagnetic quantum critical point.

References:

- [1] For a pedagogical introduction see K. Held, Dynamical vertex approximation, Lecture notes published in 'Autumn School on Correlated Electrons. DMFT at 25: Infinite Dimensions', ISBN 978-3-89336-953-9 [arXiv:1411.5191]
- [2] C. Taranto et al., PRL 112, 196402 (2014)
- [3] G. Rohringer et al., PRL 107, 256402 (2011)
- [4] T. Schaefer et al., PRB 91, 121107 (2015)
- [5] T. Schaefer et al., unpublished

Fr.J.2_I1 - Controlled optical switching of ferromagnetic thin films and nanostructures

E. Fullerton¹

1. Center of Magnetic Recording Research, University of California, San Diego, United States

The possibilities of manipulating magnetization without applied magnetic fields have attracted growing attention over the last fifteen years. The low-power manipulation of magnetization, preferably at ultra-short time scales, has become a fundamental challenge with implications for future magnetic information memory and storage technologies. I will discuss recent experiments on the optical manipulation of the magnetization of engineered materials and devices using 100 fs optical pulses. We demonstrate that all optical switching can be observed in a broad range of materials and not limited to selected rare-earth transition-metal alloy films as had been previously observed. We observe all optical switching in a variety of materials, including ferrimagnetic alloys, multilayers, heterostructures and rare-earth-free Co-Ir-based synthetic ferrimagnets [1] and most recently observe optical control of ferromagnetic films and granular recording media [2]. The latter discovery can enable breakthroughs for numerous applications since it exploits materials that are currently used in magnetic data storage, memories and logic technologies. In addition, this materials study of all-optical switching offers valuable insight into the underlying mechanisms involved in optical control of ferromagnetic materials. This work is supported, in part, by the ONR MURI program and is in collaboration with C.-H. Lambert, M. Gottwald, R. Tolley, V. Uhler, and Y. Fainman at UCSD, S. Alebrand, D. Steil, M. Cinchetti and M. Aeschlimann at University of Kaiserslautern, and M. Hehn, D. Lacour and S. Mangin at Université de Lorraine.

References:

- [1]. Mangin et al., Nature Materials 13, 286-292, (2014)
- [2] Lambert et al., submitted (2014)

Fr.J.2_I2 - Ultrafast thermally induced magnetization switching in structured systems

T. Ostler¹, C. Zhu^{1,2}, R. Evans¹, R. Chantrell¹

1. Department of Physics, University of York, York, United Kingdom

2. College of Electric Engineering, South China Agricultural University, Guangzhou, Guangdong, PR China

The recently discovered phenomenon of ultrafast Thermally Induced Magnetization Switching (TIMS) in ferrimagnets is an intriguing physical phenomenon with significant potential for ultrafast magnetic and spintronic devices. Predicted theoretically and found experimentally [1] in amorphous GdFeCo, the phenomenon arises from the excitation of a 2-magnon bound state [2] by an ultrafast laser pulse. The essential requirements for TIMS are two antiferromagnetically coupled sublattices with different longitudinal relaxation times. Here we will firstly outline the underlying physics of TIMS and proceed to describe some recent predictions of TIMS in complex structures including Gd/Fe multilayers and Synthetic Ferrimagnets (SFIM). The behaviour of the Gd/Fe multilayers depends strongly on the layer structure in a way which is related to the effective exchange field at the interfaces. This also has a strong bearing on the lifetime of the transient ferromagnetic-like state which drives the magnetization reversal and the laser power required to initiate TIMS. SFIM consisting of Fe/FePt bilayers separated by a material such as Ir or Rh to enforce AF coupling between the layers are also shown theoretically to exhibit TIMS, suggesting that the phenomenon can be extended beyond its current observation in amorphous ferrimagnets, leading to the design of materials and structures with possible applications in data storage.

References:

[1] T. A. Ostler et. Al., Nat. Commun., 3:666 doi: 10.1038/ncomms1666 (2012)

[2] J Barker, U Atxitia, T Ostler, O Hovorka, O Chubykalo-Fesenko, and R Chantrell, Sci. Rep. 3, 3262 (2012)

Fr.J.2_O3 - Magnetic switching dynamics due to ultrafast exchange scattering in a toy model of a ferrimagnetic alloy

H.C. Schneider¹, A. Baral¹

1. University of Kaiserslautern, Kaiserslautern, Germany

We numerically analyze ultrafast magnetic switching dynamics in the framework a 'toy model' that captures several important characteristics of ferrimagnetic alloy. [1] While existing theories for magnetic switching treat these materials by Heisenberg models for classical localized spins on different sublattices, we use a band picture, and standard microscopic interaction Hamiltonians. Our model consists of two spin-dependent carrier species: localized electrons in a flat band and delocalized (itinerant) electrons in a parabolic band. These are designed to resemble localized 4f-electrons in gadolinium and itinerant 3d-electrons in iron, respectively. The two electronic species are antiferromagnetically coupled via a mean-field exchange interaction, and a Stoner contribution provides an additional ferromagnetic coupling among the itinerant carriers. A standard microscopic electron-phonon interaction allows for energy dissipation from the itinerant carrier system. We calculate the one-particle spin-density matrices of both electronic species, and describe the dynamical contributions of the exchange interaction and carrier-phonon interaction at the level of Boltzmann scattering integrals. We demonstrate [2] that the exchange scattering (described by microscopic Boltzmann scattering integrals) between localized and delocalized carriers leads to an ultrafast redistribution of angular momentum between the two carrier species after ultrafast excitation, which we model be an instantaneous heating of the itinerant carrier system. We show that a transient ferromagnetic-like state can always be achieved by a sufficiently strong excitation. We find that this transient ferromagnetic-like state only leads to a complete magnetization switching for model parameters that also yield a compensation point in the equilibrium $M(T)$ curve.

References:

- [1] A. Baral and H. C. Schneider, Phys. Rev. B 90, 014427 (2014)
- [2] A. Baral and H. C. Schneider, Phys. Rev. B(R), in press

Fr.J.2_O4 - The role of the non-collinear magnetic structure on ultrafast laser-induced spin dynamics in NdFeCo and PrFeCo

J. Becker^{1,2}, A. Tsukamoto³, A. Kirilyuk¹, T. Rasing¹, J. Kees Maan², P. Christianen², A. Kimel¹

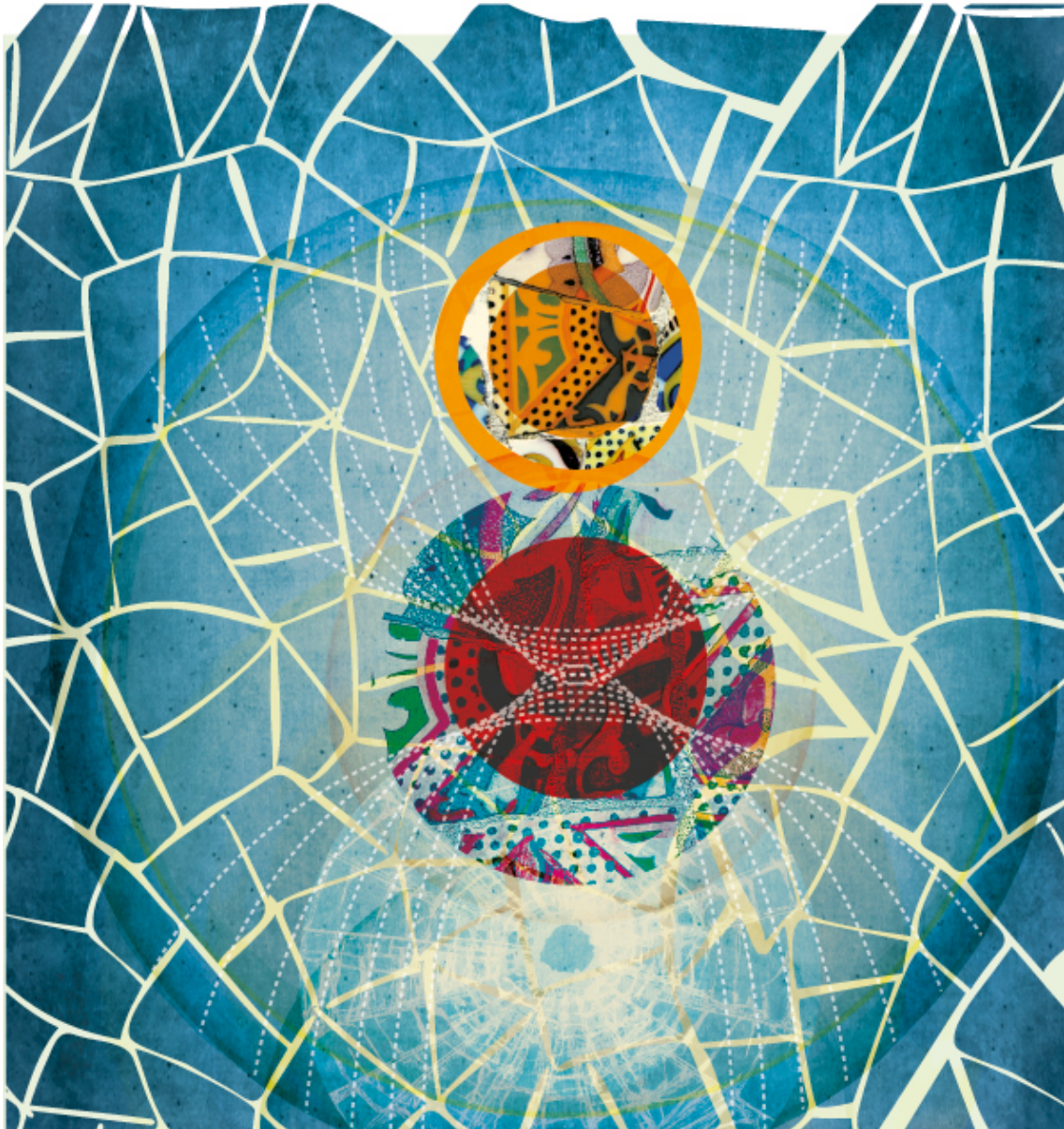
1. *Radboud University Nijmegen, Institute for Molecules and Materials, Nijmegen, The Netherlands*

2. *High Field Magnet Laboratory, Institute for Molecules and Materials, Radboud University Nijmegen, Nijmegen, The Netherlands*

3. *College of Science and Technology, Nihon University, Funabashi, Chiba, Japan*

Apart from conventional ferromagnetic and antiferromagnetic order, some materials display a more complex, non-collinear spin structure. These intriguing structures, ranging from completely disordered spin glass states to skyrmions, are formed due to competing magnetic interactions on a microscopic scale. Amorphous rare earth - transition metal (RE-TM) alloys are one class of materials which are known to have non-collinear magnetic structure. However, this special magnetic structure is rarely taken into account when investigating spin dynamics in these materials. We studied the amorphous light RE-TM alloys NdFeCo and PrFeCo using the time resolved magneto optical Kerr effect (TR-MOKE) and find that the spin-structure also undergoes dynamic changes that have severe consequences for the measured signal. From static MOKE measurements, we deduce that the TM sublattice of the NdFeCo and PrFeCo samples has a fan-like distribution of magnetic moments that closes upon increasing an external magnetic field. Investigating the magnetization dynamics, it is discovered that after excitation with a 100 fs laser pulse, two processes occur. The first process is well known and consists of an ultrafast demagnetization within 1 ps after the excitation and subsequent remagnetization of the longitudinal magnetization. The second process is the motion of the fan-structure itself. At first, the system reconstructs the magnetic order on a time-scale of 50-150 ps arriving at a state with a smaller opening angle of the fan. Subsequently, the original opening angle is restored on a time-scale of nanoseconds. Increasing the external magnetic field up to 0.6 T we can fully close the fan and thus suppress this second process.

Poster Presentations



MO.A-P02 - Distinct interplay between magnetism and superconductivity in $\text{Nd}_x\text{Ce}_{1-x}\text{CoIn}_5$

D. Mazzone¹, J. Gavilano¹, S. Raymond², L. Howald³, P. Dalmas de R\'eotier², A. Yaouanc², E. Ressouche², C. Baines⁴, M. Kenzelmann⁵

1. *Laboratory for Neutron Scattering and Imaging, Paul Scherrer Institut, Villigen, Switzerland*

2. *SPSMS, UMR-E 9001, CEA-INAC/UJF - Grenoble, France*

3. *Physik-Institut der Universit\'at Z\'urich, Zurich, Switzerland*

4. *Laboratory for Muon Spin Spectroscopy, Paul Scherrer Institut, Villigen, Switzerland*

5. *Laboratory for Developments and Methods, Paul Scherrer Institute, Villigen, Switzerland*

CeCoIn_5 is one of the most interesting and most intensively studied heavy-fermion (HF) systems. In CeCoIn_5 an antiferromagnetic (AF) phase develops at very low temperatures and high magnetic fields deep inside the superconducting phase. This incommensurated amplitude-modulated phase with $Q = (q, \pm q, 0.5)$, with $q = 0.45$, was named Q-phase [1] This intriguing phase has been matter of wide discussions and only recently it has been further clarified indicating a coupling of magnetism and the superconducting phase [2] Substituting Nd for Ce in CeCoIn_5 results in a rich phase diagram involving different phases: (i) HF ground state for CeCoIn_5 (ii) superconductivity and (iii) local magnetic moment magnetism for NdCoIn_5 [3]. A magnetically ordered phase develops deep inside the superconducting phase of $\text{Nd}_{0.05}\text{Ce}_{0.95}\text{CoIn}_5$ Results from thermal property measurements revealed a $T_c = 1.8$ K and $T_N = 0.9$ K at zero magnetic field [4]. Recently, Raymond et.al. found that the AF state $\text{Nd}_{0.05}\text{Ce}_{0.95}\text{CoIn}_5$ (at zero field) has the same propagation vector $Q' = (q, \pm q, 1/2)$, with $q = 0.45$, as the Q-phase in CeCoIn_5 [4] These unexpected results add interest to the discussion about the nature of the Q-phase.

Our latest muon and neutron measurements further confirmed a weak magnetic signal at Q' . Further investigations on $\text{Nd}_{0.05}\text{Ce}_{0.95}\text{CoIn}_5$ revealed the magnetic structure and phase diagram of the AF phase. However, while the propagation vector of the AF phase in $\text{Nd}_{0.05}\text{Ce}_{0.95}\text{CoIn}_5$ is similar to the Q-phase, we observe some drastic differences regarding the characteristic domain population (see Ref. [2]).

[1] M. Kenzelmann et al., Science. 321, 1652 (2008)

[2] S. Gerber et al., Nature Physics 10, 126 (2014)

[3] R. Hu et al., Phys. Rev. B 77, 165129 (2008)

[4] S. Raymond et al, J. Phys. Soc. Jpn., 83, 13707 (2014)

Mo.A-P04 - Pressure dependence of superconductivity on filled-skutterudite YOs4P12Y. Kawamura¹, H. Mikage¹, Yu Qi Chen¹, J. Hayashi¹, C. Sekine¹*1. Muroran Institute of Technology, Muroran, Japan*

Ternary metal pnictides with a general formula $\text{LnT}_4\text{X}_{12}$ (Ln=Lanthanide, T=Transition metal, X=Pnictogen) crystallize with a filled skutterudite structure (space group $\text{Im}\bar{3}$). $\text{YOs}_4\text{P}_{12}$ is one of filled skutterudite compounds, which shows superconductivity at $T_{\text{SC}} \sim 3 \text{ K}$ [1]. Among 19 filled-skutterudite compounds which have superconducting correlation, only two compounds show positive rate in pressure dependence of superconducting transition temperature (dT_{SC}/dP). One of them is $\text{LaFe}_4\text{P}_{12}$ and the other is $\text{YFe}_4\text{P}_{12}$ [2, 3]. When Fe is substituted by Ru or Os in $\text{LaFe}_4\text{P}_{12}$, dT_{SC}/dP becomes negative[1]. These difference can be explained from the density of states of electrons at Fermi level[4]. On the other hand, dT_{SC}/dP of $\text{YRu}_4\text{P}_{12}$ or $\text{YOs}_4\text{P}_{12}$ has not investigated and is intriguing. The purpose of this study is investigating the pressure dependence of T_{SC} on $\text{YOs}_4\text{P}_{12}$ and revealing the origin of its dT_{SC}/dP . We have succeeded in synthesizing $\text{YOs}_4\text{P}_{12}$ with high pressure and high temperature technique. Impurity is less than 2 %. We measured magnetization by incorporating opposed ceramic anvil pressure apparatus into MPMS. T_{SC} of $\text{YOs}_4\text{P}_{12}$ monotonically decreases with pressure in a rate of -0.11 K/GPa . In comparison with dT_{SC}/dP of $\text{YFe}_4\text{P}_{12}$ ($0.5 \sim 1.0 \text{ K/GPa}$ [3]), the sign of dT_{SC}/dP of $\text{YOs}_4\text{P}_{12}$ is reversed and the magnitude of it is very small. Because dT_{SC}/dP of $\text{LaFe}_4\text{P}_{12}$ is 0.72 K/GPa and that of $\text{LaOs}_4\text{P}_{12}$ is -0.095 K/GPa , the relation between $\text{YFe}_4\text{P}_{12}$ and $\text{YOs}_4\text{P}_{12}$ is the same as the relation between $\text{LaFe}_4\text{P}_{12}$ and $\text{LaOs}_4\text{P}_{12}$. Thus we propose the origin of dT_{SC}/dP of these compounds is the same.

[1] J. Hayashi et al., J. Phys.: Conf. Seri. 215 (2010) 012142

[2] L. E. DeLong and G. P. Meisner, Solid State Comm. 53 (1985) 119

[3] J. G. Cheng et al., Phys. Rev. B 88 (2013) 024514

[4] M. Nakazima et al., J. Phys. Soc. Jpn. 83 (2014) 065003

Mo.A-P05 - Raman response function assisted unveiling of the interplay of the coexistent CDW and PDW orders in hole doped cuprates

P. Goswami¹

1. D.B. College, University of Delhi, Delhi, India

The Raman response function (RRF), dependent on temperature T and the doping level p , is related to the real part of the longitudinal optical conductivity of a system like electron-doped or hole-doped cuprate and provides valuable information on the evolution of the carrier dynamics with T and p . We have calculated here RRF in the under-doped scenario where the partial density wave (PDW) and the charge density wave (CDW) instabilities, present at the hot spots of the spin-fermion (SF) model of hole doped cuprates, are linked by the (approximate) particle-hole symmetry of the SF model. The link is similar to that in the homogeneous d-wave superconductivity and the charge bond order. The combination of the CDW and PDW orders leads to a larger (SO(4)) symmetry. The corresponding ground state scenario could either be a 'stripe' order dominating or a 'checker-board' state. In the latter case, a chiral superconducting (SC) phase emerges upon lowering the temperature: coexistent SC solution could be accessed at the hot spots of the SF model where CDW/PDW order is also stabilized. We have also calculated RRF in this SC phase. We find that the RRF density or spectral weight density available for pairing in the PDW + CDW + SC phase does not change remarkably compared to that in the PDW/CDW phase. The chiral SC order may, thus, be considered as a by-product of the emergence of the CDW/PDW order.

Mo.A-P12 - Structural changes, transport and magnetic properties of Fe_{1.02}TeySe_{1-y-x}S_x compounds with ternary mixture of chalcogens

N. Baranov^{1,2}, A. Abouhaswa², A. Merentsov², N. Selezneva²

1. *Institute of Metal Physics, Ekaterinburg, Russia*

2. *Institute of Natural Sciences, Ural Federal University, Ekaterinburg, Russia*

This work aims to study the anion mixing effect on the crystal structure, superconducting and magnetic properties of FeSe-based compounds. Four series of polycrystalline samples with nominal compositions Fe_{1.02}TeySe_{1-y-x}S_x where ($y = 0.3, 0.4, 0.5, 0.6$) and ($x = 0, 0.1, 0.2, 0.3, 0.4, 0.5$) were prepared by a solid state reaction method. The synthesized samples have been studied by means of X-ray diffraction, electrical resistivity and magnetic susceptibility measurements. The substitution of S for Se keeping the constant tellurium concentrations in Fe_{1.02}TySe_{1-y-x}S_x is found to expand the crystal lattice in all samples despite the lower ionic radius of sulfur in comparison with selenium [1]. Together with the lattice expansion the substitution is observed to reduce the critical temperature of superconductivity in all series. The results of the magnetization measurements show that the materials exhibit bulk superconductivity, and the shielding volume fractions for all the samples decreases with increasing sulfur content. The results obtained in the present work show that the lattice, superconducting and magnetic properties of iron-chalcogen based superconductors can be tuned by the variation of S, Se and Te concentrations in the ternary chalcogen mixture. This work was supported by the Ministry of Education and Science of Russia (project No 1362) and by the program of the Ural Branch of RAS (project No 15-17-2-22).

[1] A.S. Abouhaswa et al., *Physica C*, 502 (2014) 10-13

Mo.A-P13 - Helical majorana fermions in $dx^2 - y^2 + i dxy$ -wave topological superconductivity of doped correlated quantum spin Hall insulators

Chung-Hou Chung^{1,2}, Shih-Jye Sun³, Yung-Yeh Chang¹, Wei-Feng Tsai⁴, A. Haim⁵, Y. Oreg⁵, F. Zhang^{6,7}

1. Department of Electrophysics, National Chiao-Tung University, HsinChu, Taiwan
2. Physics Division, National Center for Theoretical Sciences, HsinChu, Taiwan,
3. Department of Applied Physics National University of Kaohsiung, Kaohsiung, Taiwan
4. Department of Physics, National Sun Yat-Sen University, Kaohsiung, Taiwan
5. Department of Condensed Matter Physics, Weizmann Institute of Science, Rehovot, Israel
6. Department of Physics, Zhejiang University, Hangzhou, China
7. Collaborative Innovation Center of Advanced Microstructures, Nanjing, China

Large Hubbard U limit of the quantum spin Hall insulator in the form of the Kane-Mele model on a zigzag ribbon of honeycomb lattice near half filling is studied via a renormalized mean-field theory. The ground state exhibits time-reversal symmetry (TRS) breaking $dx^2 + i dxy$ -wave superconductivity, expected to support chiral edge states. To our surprise, however, at large spin-orbit coupling, the Z_2 phase with non-trivial spin Chern number in the pure Kane-Mele model is persistent into the TRS broken state (called “spin-Chern phase”), and has two pairs of counter-propagating helical Majorana fermion modes (MFs) at the edges. As the spin-orbit coupling is reduced, the system undergoes a novel topological quantum phase transition from the spin-Chern to chiral superconducting states. Our results demonstrate for the first time the 2D spin-singlet Z_2 topological superconductors which support helical MFs. Relevance of our results to adatom-doped graphene and irridate compounds is discussed.

Mo.A-P14 - Enhancement of superconductivity in multi-band systems by odd-parity mixing

M. Continentino¹, F. Deus¹, H. Caldas²

1. *Centro Brasileiro de Pesquisas Físicas, Rio de Janeiro, Brazil*

2. *Universidade Federal de São João Del Rei, São João del Rei, Brazil*

Hybridization is a key element in multi-band superconductors, such as, heavy fermions or high T_c cuprates. In these systems electrons coexisting at the common Fermi surface can arise from orbitals whose angular momenta differ by an odd number, like d-f or p-d orbitals. In this case the mixing between the electronic wave functions in different atomic sites is anti-symmetric in space which implies a k-dependent hybridization with the property $V(-k) = -V(k)$. This feature of hybridization has a profound effect in the properties of multi-band materials and in particular on their transport properties. We show that in two-band superconductors, anti-symmetric hybridization enhances superconductivity increasing its critical temperature. Since hybridization arises due to the overlap of atomic orbitals, it can be tuned by pressure acting as a control parameter in the exploration of the material's phase diagram. Our work also shows that tuning the mixing of anti-symmetric orbitals with pressure promotes a crossover from a weak type of superconductivity, associated with pairs of loosely coupled electrons, to one of tight pairs of strongly coupled quasi-particles forming a Bose-Einstein condensate. This occurs, even for a weak, fixed value of the interaction. As an additional feature of anti-symmetric mixing we discuss the possibility of generating Majorana fermions in a wire with superconductivity induced by the anti-symmetric mixing of its orbitals with those of a bulk superconductor.

Mo.A-P15 - Magnetically controlled long-range critical current suppression by ferromagnetic proximity effect

T. Wren^{1,2}, V. Petrashov², O. Kazakova¹

1. *National Physical Laboratory, Teddington, U.K.*

2. *Royal Holloway University of London, London, U.K.*

When a ferromagnet is in contact with a superconductor, the diffusion of spin polarised electrons from the ferromagnet into the superconductor suppresses the superconducting properties. Similarly, the superconducting electrons will diffuse into the ferromagnet, forming a base for the well-known proximity effect. Recently, it has been observed that non-collinear localised magnetic structures in proximity with superconductors can induce novel triplet superconducting currents^{1,2}, opening a possibility of manipulation of mesoscopic hybrid structures through control of the magnetic state.

In this work we investigate how switching between remnant magnetic states of submicron ferromagnetic element can be used to control superconducting properties in a simple bilayer mesoscopic structure consisting of an Al wire on top of a Ni disk. We observe that the critical current (I_c) of the hybrid device is suppressed and possesses a unique temperature dependence. In particular, the device exhibits SNS-like behaviour at temperatures $T \sim 0.5T_c - T_c$. The I_c suppression is long range in respect to the position of the Ni disk, causing a reduction of I_c in the aluminium wire up to 10 μm away from the ferromagnet. The same effect is observed when larger magnetic structures are used as heat sinks, eliminating local heating as the source of the I_c suppression. Finally, we show that the temperature dependence of I_c is dependent on the disks magnetic history both in the vicinity of the ferromagnet and far away from it. We interpret the long range suppression of critical current in terms of spin imbalance produced by the hybrid structure, indicating generation of a quasiparticle spin current and consequent suppression of superconducting properties.

1 I. Sosnin, H. Cho, V. Petrashov, and A. Volkov, Phys. Rev. Lett. 0 (2006)

2 J. Robinson, S. Piano, G. Burnell, C. Bell, and M. Blamire, Phys. Rev. B 76, 094522 (2007)

Mo.A-P16 - Asymmetric Andreev reflection

Z. Bak¹

1. Institute of Physics, Jan Dlugosz University, Częstochowa, Poland

We present theoretical study of the skew scattering at the Josephson junction. The resulting from skew scattering spin Hall effect /SHE/ observed in pure materials is rather small (below 0.5%), however, by now composite materials with 80% SHE were observed and this gave new impact to search for its applications. Most of SHE studies are devoted to bulk systems. Very recently an effect of asymmetric scattering at Josephson junction has been observed too. However, till now no microscopical mechanism behind it has been postulated. In our paper we present the model of asymmetric Andreev reflection at the Josephson junction that creates the SHE effect. The basic finding of our study is the prediction of a new resonance at Josephson junction which should effect in fluctuations of SHE.

As the Josephson current fluctuates with the eigenfrequency Ω^J the asymmetric Andreev reflection converts Josephson current into a transverse spin current (or Bose condensate). In this way there arises a forced condensate nano-oscillator which can have another characteristic eigenfrequency. When the nano-oscillator and Josephson eigenfrequencies are close to each other (or to their multiples) there arises a novel type of resonance.

Furthermore, we show that properly shaped Josephson junction interface can produce a skew scattering even if there is no significant spin-orbit interaction.

This offers new potential applications in spintronics based on the morphology of Josephson interfaces.

Mo.A-P17 - Dual-fermion approach to superconductivities in the two-dimensional kondo lattice

J. Otsuki¹

1. Tohoku Universit, Sendai , Japan

Heavy-fermion superconductivities in rare-earth and actinide materials appear near antiferromagnetic or ferromagnetic quantum critical point (QCP). Since this situation is similar to, e.g., cuprate superconductors, one might expect an unconventional superconductivity occurring in f-electron systems. However, since the origin of magnetism is different between d- and f-electron systems, superconductivities induced by those fluctuations can be different. We thus consider the following fundamental and explicit question: Provided that an f-electron system shows an antiferromagnetic ordering which has the same spin configuration as in cuprates, which types of superconductivities are favored around its QCP? We address this question using the two-dimensional Kondo lattice model, which exhibits a QCP between antiferromagnetism and heavy fermion states.

In order to address heavy-fermion superconductivities, we employ the dual-fermion approach and perform diagrammatic expansion around the dynamical mean-field theory (DMFT). With this formalism, we evaluate FLEX-type diagrams to incorporate low-energy spin excitations near antiferromagnetic QCP.

By numerical calculations using the continuous-time QMC, we found enhancement of superconducting fluctuations near antiferromagnetic QCP. However, unlike the Hubbard model, the d-wave pairing is not particularly favored, and other pairings such as p-wave and g-wave are almost degenerate. We discuss the origin of the competing superconductivities in view of the Fermi-surface structure, which varies according to formation of heavy quasiparticles.

Mo.A-P18 - Superconductivity in high entropy alloys

Z. Jaglicic¹, P. Koxelj², S. Vrtnik², A. Jelen², S. Jazbec², J. Luxnik², J. Dolinšek²

1. *University of Ljubljana, FGG And IMFM, Ljubljana, Slovenia*

2. *Jožef Stefan Institute, Ljubljana, Slovenia*

High entropy alloys (HEAs) are solid solution alloys that contain five or more principal elements in equal or near equal atomic percent [1]. High entropy of mixing can stabilize disordered solid solution phases with simple structures like a body-centred cubic or a face-centred cubic with small unit cells of the edge length about three angstroms only. Due to the problems in growing homogeneous samples of macroscopic size only few different HEAs have been studied so far. They show enhanced mechanical properties (e.g. hardness) while their physical properties remain mostly unexplored.

The HEA with the composition of $Ta_{34}Nb_{33}Hf_8Zr_{14}Ti_{11}$ (in at. %) has been synthesized and its physical properties determined. [2] The temperature dependent resistivity and susceptibility measurements show a transition to a superconducting state at a critical temperature of $T_c = 7.3$ K. A 100 % Meissner effect and temperature dependent specific heat measurements led us to the conclusion that the superconductivity is a bulk effect, where the entire specimen becomes superconducting below critical temperature. The magnetization curves between 2 K and 8 K show a typical type II superconductor behaviour with the first critical field of 32 mT at 2 K. The upper critical field extrapolated to $T = 0$ is approximately 8.3 T.

Very recently a superconductivity at even a little bit higher critical temperature of approx. 7.7 K has been detected in another HAE composed of transition metals Ta-Nb-Hf-Zn, showing superconductivity as a common feature of this type of HEAs.

[1] Y. Zhang et al, Progress in Materials Science 61 (2014) 1-93

[2] P. Koxelj et al, Phys. Rev. Lett. 113 (2014) 107001

Mo.A-P19 - Magnetic field dependence of the superconducting proximity effect in a two atomic layer thin metallic film

J. A. Fischer¹, M. Caminale¹, A. Alvaro Leon Vanegas¹, A Stepniak¹, H Oka¹, D Sander¹, Jürgen Kirschner¹

1. Max-Planck-Institut für Mikrostrukturphysik, Halle, Germany

The intriguing possibility to induce superconductivity in a metal, in direct contact with a superconductor, is under renewed interest for applications and for fundamental aspects [1]. The underlying phenomenon is commonly known as proximity effect. In this work we exploit the high spatial resolution of scanning tunneling spectroscopy at sub-K temperatures and in magnetic fields. We probe the differential conductance along a line from a superconducting 9 ML high Pb nanoisland into the surrounding two layer thin Pb/Ag wetting layer on a Si(111) substrate. A gap in the differential conductance indicates superconductivity of the Pb island. We observe an induced gap in the wetting layer, which decays with increasing distance from the Pb island. This proximity length is 21 nm at 0.38 K and 0 T. We find a non-trivial dependence of the proximity length on magnetic field. Surprisingly, we find that the magnetic field does not affect the induced superconductivity up to 0.3 T. However, larger fields of 0.6 T suppress superconductivity in the wetting layer, where the Pb island still remains superconducting. We discuss the unexpected robustness of induced superconductivity in view of the high electronic diffusivity in the metallic wetting layer.

[1] S. Guéron et al. Phys. Rev. Lett. 77, 3025 (1996); J. Xiang et al. Nat. Nano. 1, 208 (2006); J. Wang et al. Phys. Rev. Lett. 100, 197002 (2008)

Mo.A-P20 - A calorimetric investigation of RbFe₂As₂ single crystals

S. Khim¹, S. Aswartham¹, V. Grinenko¹, Christan G. F. Blum¹, F. Steckel¹, D.I Gruner¹, Anja U. B. Wolter¹, C. He¹, Stefan-Ludwig Drechsler¹, S. Wurmehl^{1,2}, B. Büchner^{1,2}

1. *Leibniz-Institute for Solid State and Materials Research, Dresden, Germany*

2. *Institut für Festkörperphysik, TU Dresden, Dresden, Germany*

We present physical properties of single crystals of the iron pnictide superconductor RbFe₂As₂. A bulk superconducting transition at $T_c \sim 2.7$ K was consistently observed in resistivity, magnetic susceptibility and specific heat measurements. While the normal state resistivity following a T^2 dependence at low T is that of a conventional metal, the magnetic susceptibility shows a deviation from a conventional Curie-Weiss behavior and an broad local maximum around 80 K. A large Sommerfeld coefficient, $\gamma_0 = 127$ mJ/mol K², was observed seemingly a common feature of heavily hole-doped '122' pnictides. We analyze the superconducting transition in the specific heat data by using the s -wave BCS two-gap model. The presence of a small gap is discussed as possible explanation to account for the large specific heat contribution far below T_c . The large H_{c2} anisotropy ratio, $\Gamma = H_{c2}^{ab}/H_{c2}^c \sim 7$ near T_c is also discussed within this multiband nature of the Fermi surface.

Mo.A-P21 - Collective spin fluctuations in stripe ordered $\text{La}_{1.875}\text{Ba}_{0.125}\text{CuO}_4$ detected by ^{139}La nuclear magnetic resonance

Seung-Ho Baek¹, M. Huecker², G. Gu², B. Buechner¹

1. IFW Dresden, Dresden, Germany

2. Brookhaven National Laboratory, Upton, NY, United States

We report ^{139}La nuclear magnetic resonance (NMR) studies performed on a $\text{La}_{1.875}\text{Ba}_{0.125}\text{CuO}_4$ single crystal. Right at the charge ordering temperature $T_{\text{CO}} = 54$ K, the ^{139}La spin-lattice relaxation rate $1/T_1$ sharply upturns, indicating that charge order triggers the slowing-down of spin fluctuations (SFs). In addition to the intradomain SFs, detailed temperature and field dependences of both $1/T_1$ and NMR signal intensity demonstrate that collective SFs develop below the spin ordering temperature $T_{\text{SO}} = 40$ K, implying the persistence of strong charge fluctuations (CFs) in the spin ordered state. We find that the collective SFs are rapidly suppressed with increasing magnetic field along the CuO_2 plane, which is well understood in terms of the enhanced spin order.

Mo.A-P23 - Magnetic properties of new filled skutterudite compound BaFe₄As₁₂

C. Sekine¹, T. Ishizaka¹, K. Nishine¹, Y. Kawamura¹, H. Gotou²

1. *Muroran Institute of Technology, Murora, Japan*

2. *Institute for Solid State Physics, University of Tokyo, Tokyo, Japan*

The filled skutterudite compounds, particularly P- and Sb-based compounds, have attracted much attention of their wide variety of strongly correlated electron behaviors, such as unconventional superconductivity, non-Fermi liquid behavior, anomalous metal-insulator transition, and multipole ordering. As-based filled skutterudite compounds also should be important for systematically investigating skutterudite systems. In fact, several compounds exhibit exotic properties, including superconductivity in LnRu₄As₁₂ (Ln = La, Pr) [1], canted ferromagnetic or ferrimagnetic phase transition in EuFe₄As₁₂ [2]. However, only preliminary studies have been conducted on the properties of As-based compounds because the compounds are quite difficult to prepare. High-pressure synthesis is a powerful technique for preparing As-based skutterudite compounds. New As-based filled skutterudite compound BaFe₄As₁₂ prepared under high pressure has been reported recently [3]. The temperature dependence of the electrical resistivity for BaFe₄As₁₂ reveals a metallic behavior and any anomalies were not observed down to low temperature. In this presentation, we report the magnetic properties for BaFe₄As₁₂. The magnetization, magnetic susceptibility and specific heat of BaFe₄As₁₂ were measured. The temperature dependence of the magnetic susceptibility shows a broad peak around 50K. This peak could be due to a spin fluctuation of Fe ions and suggests that this compound is an itinerant-electron metamagnet.

[1] I. Shirovani et al., Phys. Rev. B 56 (1997) 7866

[2] C. Sekine et al., J. Phys. Soc. Jpn. 78 (2009) 093707

[3] K. Takeda et al., J. Phys. Soc. Jpn. 80, SA029 (2011) SA029

Mo.A-P25 - X-ray photoelectron spectroscopy studies of the superconducting Mo₂B and Mo₂BC

R. Escamilla^{1,2}, E. Carvajal², L. Huerta¹, E. Verdín³, M. Cruz²

1. *Instituto de Investigaciones en Materiales-UNAM, Coyoacán, Mexico*

2. *ESIME-Culhuacán, Instituto Politécnico Nacional, Mexico, D. F., Mexico*

3. *Departamento de Física, Universidad de Sonora, Sonora, Mexico*

Mo₂BC polycrystalline sample was synthesized by the arc-melting method using Mo₂B as precursor. Studies of X-ray diffraction (XRD) showed that the phases are mainly single phase. Magnetization measurements showed a superconducting transition temperature (T_c) of about 7.0 and 5.2 K for Mo₂BC and Mo₂B, respectively. By X-ray photoelectron spectroscopy (XPS) the Mo 3d, C1s and B 1s core-levels were identified.

Mo.A-P27 - Interplay of charge density wave and superconductivity in BaPt₂As₂

C. Guo¹, W. Jiang¹, Y. Chen¹, Z. Weng¹, Y. Wang¹, L. Che¹, G. Pang¹, F. Gao¹, X. Lu¹, H. Yuan¹

1. Department of Physics And Center For Correlated Matter, Zhejiang University, Hangzhou, China

The newly discovered superconductor BaPt₂As₂ shows evidence for the coexistence of superconductivity (SC) and charge density wave (CDW) state [1]. In this presentation, we study the interplay of SC and CDW in this compound by measuring the electrical resistivity ρ (T) under pressure. Application of pressure suppresses the first-order CDW-like transition ($T_1=272$ K at $p=0$ kbar) and leads to a jump of T_c from $T_{c1}\approx 1.6$ K to $T_{c2}\approx 2$ K around $p_{c1}=6.7$ kbar. With further increasing pressure, a weak resistive anomaly remains around $T_2 \approx 200$ K and T_c slightly increases. Around $p_{c2}=17$ kbar, the resistive anomaly at T_2 develops into two pronounced first-order transitions; the one at higher temperature increases and the one at low temperature is suppressed with further increasing pressure. On the other hand, T_c undergoes another sharp increase at $p=p_{c2}$, with a nearly unchanged value at higher pressures. The nature of the pressure-induced resistivity anomalies at high temperatures remain unknown; they might be caused by a change of the CDW modulations or a structural transition. Our results suggest that BaPt₂As₂ provides a promising system to study the interplay of SC and CDW.

References:

[1] W. B. Jiang et al., Superconductivity and structural distortion in BaPt₂As₂. J. Phys.: Condens. Matter 27, 022202 (2015)

Mo.A-P28 - The in- and out-of-plane magnetisation of highly underdoped YBa₂Cu₃O_{6+x} single crystalsI. Kokanovic^{1,2}, J. Cooper²

1. Department of Physics, Faculty of Science, University of Zagreb, Zagreb, Croatia.
2. Cavendish Laboratory, University of Cambridge, Cambridge, United Kingdom

Measurements of static magnetic susceptibility $\chi_c(T)$ of YBa₂Cu₃O_{6+x} single crystals for magnetic field (H) applied along the c-axis, and $\chi_{ab}(T)$ for H in the ab-plane, can give useful information [1,2] about their thermodynamic properties which are still being hotly debated. We briefly review the main results of this work - the T-dependent anisotropy well above T_c arises from the pseudogap and the g-factor anisotropy, while at lower T there is evidence for Gaussian superconducting (s/c) fluctuations with a strong cut-off above 1.1 T_c. We then present new data for highly under-doped crystals with hole concentrations per CuO₂ plane, $p = 0.058$ to 0.073 , the region where neutron scattering studies [3] show competition between incommensurate magnetic short-range order and superconductivity. As found previously for polycrystalline samples [4], ordering the Cu-O chains increases T_c and substantially reduces the Curie term. At low T there is significant non-linear H dependence up to 5 T. In contrast to the spin susceptibility from the CuO₂ planes, the Curie terms are isotropic. Plots of $\chi_c(T)$ vs. $\chi_{ab}(T)$ show an unexpected result, the Curie terms disappear above a p-dependent onset temperature T_{Curie_onset} of order 200 K. We compare T_{Curie_onset}(p) with the pseudogap energy scale and the onset of charge density wave order ($x > 0.5$) and short-range magnetic order ($x < 0.5$).

For all six samples $\chi_D(T) = \chi_c(T) - \chi_{ab}(T)$ has a weakly T-dependent linear region at higher T where $\chi_D(0)$ is $1-2 \times 10^{-4}$ emu/mol. We analyse deviations from this linear behavior in terms of 2D or 3D Gaussian s/c fluctuations and the possibility of small superconducting regions with T_c ~ 60 K.

- [1] I. Kokanovic, et al., Europhys. Lett. 98, 57011 (2012)
- [2] I. Kokanovic, et al., Phys. Rev. B 88, 060505(R) (2013)
- [3] D. Haug, et al., Phys. Rev. Lett. 103, 017001 (2009)
- [4] J. Biscaras, et al., Phys. Rev. B 85, 134517 (2012)

Mo.A-P30 - Strong electronic correlations in the superconductors AFe₂As₂ (A = K, Rb, Cs)

K. Grube¹, F. Eilers¹, D. A. Zocco¹, P. Schweiss¹, R. Heid¹, H. Ikeda², T. Wolf¹, H. Löhneysen^{1,3}

1. *Institute of Solid State Physics, Karlsruhe Institute of Technology, Karlsruhe, Germany*

2. *Department of Physics, Ritsumeikan University, Kyoto, Japan*

3. *Physikalisches Institut, Karlsruhe Institute of Technology, Karlsruhe, Germany*

Superconductivity in iron pnictides and chalcogenides occurs in close proximity to antiferromagnetic order, giving rise to the assumption that superconductivity originates from electron-electron interactions. So far, experimental and theoretical studies underpin this assumption but have failed to unravel the pairing mechanism. A central question is the role of electronic correlations. We investigated the thermal expansion and magnetostriction of the stoichiometric compounds AFe₂As₂ with A = K, Rb, and Cs. The magnetostriction measurements exhibit quantum oscillations beyond the upper critical fields which allow determining the electronic structure and the effective quasiparticle masses m^* . With growing unit-cell volume along the AFe₂As₂ the strength of the electronic correlations exhibits a huge increase of m^* . This behavior is in line with the pressure dependence of the Sommerfeld coefficient determined from the thermal expansion above the superconducting transition temperature. Our measurements provide valuable input to explore the relation between crystal structure, electronic correlations and superconductivity on a more quantitative basis.

Mo.A-P31 - Spin-wave dispersion and magnetic exchange in antiferromagnetic Ca₂CuO₂Cl₂

M. d'Astuto¹, Mark M. P. Dean², A. Nicolaou³, J. Pelliciani⁴, B. Baptiste¹, R. Yu⁵, M. Azuma⁵, B. W. Lebert^{1,3}, A. Gauzzi¹, T. Schmitt⁴

1. IMPMC, UMR7590 UPMC-Sorbonne Universités - Paris, France

2. Department of Condensed Matter Physics and Materials Science, Brookhaven National Laboratory, Upton, NY, United States

3. Synchrotron SOLEIL, Gif-sur-Yvette, France

4. Swiss Light Source, Paul Scherrer Institut, Villigen, Switzerland

5. Materials and Structures Laboratory, Tokyo Institute of Technology, Yokohama, Japan

We measured the spin-wave dispersion in antiferromagnetic Ca₂CuO₂Cl₂ (CCOC) as a function of momentum transfer along the in-plane high symmetry directions in the Brillouin Zone using Cu L3-edge Resonant Inelastic X-Ray Scattering (RIXS) with the ADRESS spectrometer on the Swiss Light Source (SLS). Magnetic excitations in High Temperature Superconducting (HTS) cuprates have been widely studied in the last twenty years, as the possible boson exchanged in the Cooper pairing leading to superconductivity (see [1,2] and references therein). Using Inelastic Neutron Scattering (INS), many of the cuprates have been extensively investigated. However, several pieces of the puzzle are still open, largely because of the lack of a theoretical handling of correlated electronic systems beyond idealized, simplistic models. Recently RIXS [3], has emerged as an alternative probe of the same excitations. The new technique easily extends INS observation to higher energies [1], with the potential to also probe small volume crystals. However, the technique has mainly been used so far, in the case of HTS cuprates, to extend studies of compounds already measured by INS [2]. Here we study the parent compound of a HTS cuprate for which there are no available INS studies so far: Ca₂CuO₂Cl₂ [4,5]. The specific advantage of CCOC with respect to the already well-studied, and isostructural, **La_{2-x}Sr_xCuO₄** compound is that it is the only superconducting cuprate composed of low Z ions alone, which make it far more suitable for theoretical calculations compared to other HTS based on CuO₂ planes. In this study we refine the exchange parameters J of the spin Hamiltonian of CCOC based on the measured spin-wave dispersion. Future measurements will be done on the doped, superconducting compound, allowing a study of the paramagnon evolution under doping as done in more commonly studied '214' cuprates [2].

[1] M. Guarise et al., Phys. Rev. Lett. 105, 157006 (2010)

[2] M. P. M. Dean, et al, Nature Materials 12, 1019 (2013)

[3] M. P. M. Dean, Journal of Magnetism and Magnetic Materials 15, 3 (2015)

[4] Z. Hiroi, N. Kobayashi, M. Takano, Nature 371, 139 (1994)

[5] I. Yamada et al Phys.Rev. B 72 224503 (2002)

Mo.A-P32 - Charge-stripe Character of Magnetic Interactions of the Checkerboard Charge Ordered State

P. Freeman¹, S. Giblin², R. Mole³, K. Hradil⁴, P. Cermak⁵, D. Prabhakaran⁶

1. *University of Central Lancashire, Preston, England*

2. *Cardiff University*

3. *Bragg Institute, ANSTO*

4. *Technische Universität Wien*

5. *Jülich Centre for Neutron Science, Forschungszentrum Jülich*

6. *Oxford University, Oxford, U.K*

A breakthrough in understanding the magnetic interactions of the hole doped high temperature cuprate superconductors was made by discovery of a near identical hourglass shaped magnetic excitation spectrum in the non-superconducting charge ordered La_{5/3}Sr_{1/3}CoO₄ [1]. The underlying charge ordered structure of La_{2-x}Sr_xCoO₄ is however under debate, charge-stripes or checkerboard charge order?[2] The magnetism of an ideal checkerboard charge ordered state is spin frustrated, and we have previously shown how this spin frustration is lifted by magnetic stripe interactions in La_{3/2}Sr_{1/2}NiO₄[3]. In our present studies we wish to address how the magnetism of charge-stripe order develops in the charge-stripe ordered phase on doping towards the checkerboard charge order phase of La_{2-x}Sr_xNiO₄. We will present results on the magnetic ordering from ÁSR, and inelastic neutron scattering on charge ordered La_{2-x}Sr_xNiO₄, and discuss potential implication for understanding the magnetism of charge ordered La_{2-x}Sr_xCoO₄.

[1] A. T. Boothroyd, P. Babkevich, D. Prabhakaran and P. G. Freeman, *Nature* 471, 341 (2011)

[2] Y. Drees et al., *Nature Commun.* 4, 2449 (2013)

[3] P. G. Freeman et. al. *Phys. Rev. B* 71 (2005) 174412

Mo.A-P33 - Magnetic properties of GdT₂Zn₂₀ (T = Fe, Co) investigated by x-ray diffraction and spectroscopy

J. Mardegan¹, G. Fabbris^{2,3}, D. Haskel³, M. Avila⁴, C. Giles⁵

1. *Deutsches Elektronen-Synchrotron DESY, Hamburg, Germany*

2. *Department of Physics, Washington University, St. Louis, United States*

3. *Advanced Photon Source, Argonne National Laboratory, Lemont, United States*

4. *CCNH, Universidade Federal do ABC (UFABC), São Bernardo do Campo, Brazil*

5. *Instituto de Física 'Gleb Wataghin,' Universidade Estadual de Campinas, Campinas, São Paulo, Brazil*

In this work we report the magnetic and electronic properties investigated by synchrotron techniques on single crystals and powdered crystals of GdT₂Zn₂₀ (T = Fe, Co). These compounds belong to the complex cage-structure family RT₂Zn₂₀ (R - rare earth, T - transition metal) [1] in which several physical phenomena can be observed, such as superconductivity, magnetic ordering, nearly ferromagnetic Fermi-liquid and heavy fermion behavior [2-4], which are strongly affected by the replacement of Co by Fe ions into the polarizable medium of the cage structure. GdCo₂Zn₂₀ orders antiferromagnetically below T_N = 5.72(6) K, whereas the GdFe₂Zn₂₀ orders ferromagnetically at a remarkably high temperature of T_C = 86.5(3) K. High quality single crystals of GdCo₂Zn₂₀ were investigated by x-ray resonant magnetic scattering (XRMS) in which we observed a commensurate antiferromagnetic ordering with a magnetic propagation vector (c̄c̄c̄) below T_N. The distance between the Gd-Gd ions of around 6Å weakens the exchange interaction and helps explain this representative low temperature transition. The magnetic structure solved by XRMS revealed that only the Gd ions carry moment and that the Gd spins are aligned following the magnetic representation Γ_5 . In contrast, powdered crystals of GdFe₂Zn₂₀ investigated by x-ray absorption near-edge structure (XANES) and x-ray magnetic circular dichroism (XMCD) techniques performed below the Curie temperature displayed a strong magnetic signal around 12.5 % and 9.7 % for both Gd-L_{2,3} absorption edges, respectively. This magnetic signal arises from a splitting between the 5d states (up and down). The strong RKKY exchange interaction between the Gd-Gd ions, due to a high density of states at Fermi level, polarizes the medium and consequently an interesting and unusual magnetic signal of ~0.06 % is detected at the Zn K-edge. However, measurements at the Fe K-edge revealed an unexpected absence of magnetic contribution for the Fe ions.

Mo.A-P34 - Longitudinal spin excitations in iron-pnictide parent compoundsM. Fidrysiak¹*1. Wrocław University of Technology, Wrocław, Poland*

Recent observation [1] of sizable longitudinal spin excitations (LSEs) in the spin density wave (SDW) phase of Fe-pnictide parent compounds NaFeAs and BaFe₂As₂ has serious consequences. The suggested interpretation of the low energy LSEs as a bottom of particle-hole continuum implies a major role of itinerant electrons and calls into question relevance of local-moment approaches to these materials. I point out that the above mechanism is difficult to reconcile with optical spectroscopy and discuss the possibility that the LSEs originate from two-magnon (2M) processes which are free of this problem and do not sharply distinguish between localized and itinerant magnetism.

The 2M continuum obtained within the localized J₁-J₂ model, previously used to study spin waves in BaFe₂As₂, is shown to qualitatively reproduce observed LSEs, but predicted inelastic neutron scattering intensities are too low to explain the data. I discuss two mechanisms of 2M continuum enhancement, emphasizing either itinerant or localized electrons. The first relies on 2M continuum renormalization by virtual electronic excitations between magnetically split bands in the SDW phase of an itinerant antiferromagnet and is studied within a minimal two-band model with perfect nesting of hole- and electron-like Fermi surfaces (FSs). The second is based on proximity to a magnetic quantum phase transition, where the magnetic order is softened by quantum spin fluctuations, and is discussed within an effective non-linear sigma-model approach. The electronic mechanism enhances 2M contribution to LSEs in the regime of small FS taking part in the SDW instability, but is insufficient to account for reported intensities. The spin fluctuation mechanism, on the other hand, agrees qualitatively with observed LSEs and reproduces correct order of intensities for parameters relevant to BaFe₂As₂.

[1] C. Wang et al., Phys. Rev. X 3, 041036 (2013)

Mo.A-P36 - Magnetic investigation of silver sheathed Sr_{0.6}K_{0.4}Fe₂As₂ superconductor

M. Reissner¹, B. Brunner^{1,2}, P. Kovac², C. Yao³, Y. Zhang³, Y. Ma³

1. *Institute of Solid State Physics, TU Wien, Wien, Austria*

2. *Institute of Electrical Engineering, Slovak Academy of Sciences, Bratislava, Slovakia*

3. *Key Laboratory of Applied Superconductivity, Institute of Electrical Engineering, Chinese Academy of Sciences, Beijing, China*

In recent years 122-type iron-pnictides have become a perspective superconductor for high field applications. Although having low critical current densities J_c at low fields, they show extremely low field dependence at high magnetic fields (above 8 T). Due to improvements in preparation processes absolute values of 122-based tapes reach J_c values higher than 104 A/cm² at 10 T, which is necessary for applications. In this work we report on a magnetic investigation of silver sheathed Sr_{0.6}K_{0.4}Fe₂As₂ tape. The sample was prepared by ex-situ powder-in-tube technique (PIT). Sintered powder (900°C for 35 h) was ground and mixed with 5 wt% Sn, filled into Ag tubes and cold worked into tapes by drawing and flat rolling [1]. Transition temperature $T_c = 34.2$ K was achieved. Dc magnetic measurements were performed in fields up to 14 T between 4.2 K and T_c . From hysteresis loops irreversibility lines and magnetic critical current densities - obtained by Beans critical state model - were determined. From the relaxation measurements mean effective activation energies U according to Andersons flux creep theory were determined. The obtained U values are similar (< 40 meV at 4.2 K and 1 T) as for Bi2212 tapes, but an order of magnitude smaller in comparison with MgB₂ wires. U is practically field independent above 3 T in contrast to the other two superconductors, thus explaining the much higher J_c values at high fields. The obtained vortex matter phase diagram is compared to those obtained for ex-situ PIT prepared MgB₂ wires and silver sheathed Bi2212 tapes.

[1] X.Zhang et al, APL 104 (2014) 202601

Mo.A-P37 - Slowly-fluctuating magnetism and superconductivity in NdFeAsO_{1-x}F_x: new physics or déjà-vu?

T. Shiroka^{1,2}, G. Lamura³, P. Bonfó⁴, S. Sanna⁵, R. De Renzi⁴, M. Putti³, N. Zhigadlo¹, S. Katrych⁶, R. Khasanov², J. Karpinski^{1,6}

1. *Laboratorium Für Festkörperphysik, Zurich, Switzerland*

2. *Paul Scherrer Institut, Villigen, Switzerland*

3. *CNR-SPIN and Università di Genova, Genova, Italy*

4. *Dip.to di Fisica e Scienze della Terra, Università di Parma, Parma, Italy*

5. *Physics Department, University of Pavia and CNISM, Pavia, Italy*

6. *Laboratoire de Physique de la Matière Complexe, Lausanne, Switzerland*

Until recently, the Nd-based compounds belonging to the widely studied Ln-1111 family of superconducting iron-pnictides (with Ln a lanthanide), have not been explored in great detail due to considerable difficulties in their preparation. The recent availability of Nd-1111 samples, covering a wide range of fluorine doping, allowed us to address many open questions regarding the 1111 family, as e.g.: what is the role played by the different rare-earths, are the Ln-1111 compounds all alike at intermediate F-doping, can magnetic fluctuations appear in the intermediate-doping regime, etc.

With a focus on the magnetic-to-superconducting crossover region, our dc magnetometry and muon-spin spectroscopy (μ SR) investigations could show that Nd compounds confirm well-known aspects of 1111's, while exhibiting also new physics [1]. In particular:

– The FeAs long-range AF order at low fluorine doping ($x < 0.06$) is progressively replaced at intermediate doping ($x = 0.08$) by a short-range magnetic order, which coexists with superconductivity on a nanometric length scale. This result, together with the absence of magnetic order in high-fluorine ($x = 0.25$) superconducting samples, indicates a common behaviour within the Ln1111 pnictides (Ln being La, Sm, Ce, and Nd lanthanides [2,3,4]).

– Contrary to other Ln1111 cases, we detect sizable magnetic fluctuations (on the μ SR time scale) in the intermediate-doping range. Interestingly, this dynamic magnetic component persists down to low temperatures, until the short-range static magnetic order and the superconductivity develop over the whole sample volume. The nature of these fluctuations, as well as their possible relation with superconductivity, will be discussed.

[1] G. Lamura et al., Phys. Rev. B 91, 024513 (2015)

[2] G. Lamura et al., J. Phys.: Condens. Matter. 26, 295701 (2014)

[3] S. Sanna et al., Phys. Rev. B 80, 052503 (2009)

[4] T. Shiroka et al., Phys. Rev. B 84, 195123 (2011)

Mo.A-P38 - Tension failure of Nb-Cu superconductor alloy with fine grained structure in temperature range 4,2 - 300 K

J. Miskuf¹, K. Csach¹, A. Juríková¹, M. Huráková¹, E. Tabachnikova², I. Psaruk², M. Laktionova², A. Podolskiy²

1. *Institute of Experimentat Physics, Slovak Academy of Sciences, Košice, Slovakia*

2. *B. Verkin Institute for Low Temperature Physics and Engineering NASU, Charkov, Ukraine*

The problems of development of large scale and superconducting magnets generate hard requirements to structure materials of their windings. Properties of these materials should combine an extremely high robustness and good enough thermal and electrical conductivity. Mechanical and electromagnetic perturbation can destroy the superconductivity. In recent years the possibilities of enhancing the mechanical properties of metallic alloys, namely the yield strength, are studied. The focused thermomechanical treatment can help to decrease the grain size and increase the mechanical properties. The superconductor wire material with the composition of Nb₃Cu with the ultrafine grain structure was tested in uniaxial tension up to the failure in the temperature interval 4.2 - 300 K. It was observed that in the fine grained NbCu alloy the plastic nature of the deformation is saved up to the temperature of 4.2 K. The fractographic observations show that the failure is always ductile with developed shear zone. The void size respects the uniform structure with the low grain size. As the test temperature decreases, the yield strength increases more than the fracture stress. The small decrease in the plasticity at low temperatures is related to the total deformation changes from 6.1 to 3.5 %. This work was supported by the projects Nos. 26220120021 and 26110230097 provided in the frame of Structural funds of the European Union.

Mo.A-P39 - Effects of La doping on A-site ordered Cr perovskite oxides with Zhang-Rice state

M. Isobe¹, H. Sakurai², H. Takagi¹

1. *Max Planck Institute For Solid State Research, Stuttgart, Germany*

2. *National Institute for Materials Science, Tsukuba, Japan*

A-site ordered perovskite $\text{CaCu}_3\text{Cr}_4\text{O}_{12}$ is an attractive material that exhibits valence degeneracy [1] and also it can be a negative charge-transfer material. Besides, it has been observed an unusual Cu valence state (Zhang-Rice state) in the recent report [2]. It shows a metallic behavior without any phase transition above 2 K. We have therefore investigated the effects of La doping on this material. $\text{Ca}_{1-x}\text{La}_x\text{Cu}_3\text{Cr}_4\text{O}_{12}$ ($x=0.0, 0.2, 0.4, 0.6, 0.8, 1.0$) have been synthesized by solid state reaction under high pressure and high temperature conditions. In $\text{LaCu}_3\text{Cr}_4\text{O}_{12}$, we have observed a magnetic transition around 220K. Also the lattice constant shows a small discontinuity and the resistivity exhibits the some anomaly at the transition. Still the resistivity reveals the metallic behavior down to low temperature. The recent results of muon-spin rotation and relaxation measurements have suggested that the magnetic transition is an antiferromagnetic ordering [3]. The transition temperature decreases with decreasing the La content in $\text{Ca}_{1-x}\text{La}_x\text{Cu}_3\text{Cr}_4\text{O}_{12}$. Simultaneously it seems to be smeared out. We have not observed any superconductive behavior above 2 K in this system. We suppose that the charge and spin states of the Cu in this system are similar to those of the high T_c cuprates. However the CuO_4 planers are isolated in the crystal structure, then the CuO_2 planes cannot be constructed. Consequently it is considered that the superconductivity transition is suppressed to very low temperature.

[1] M. A. Subramanian et al., *J. Phys. Chem. Solid* 64, 1569 (2003)

[2] D. Meyers et al., *Sci. Rep* 3, 1834 (2013)

[3] J. Sugiyama et al., in preparation

Mo.A-P40 - Elastic softening in the orthorhombic compound YbPdGe

I. Ishii¹, Y. Noguchi¹, H. Goto¹, X. Xi¹, S. Kamikawa¹, K. Araki², K. Katoh², T. Suzuki¹

1. *Hiroshima University, Hiroshima-shi, Japan*

2. *National Defense Academy, Yokosuka, Japan*

The Yb-based compound YbPdGe with the orthorhombic YbAuSn-type structure shows a ferromagnetic phase transition at 11.4 K. At high temperatures, 4f-electrons of Yb³⁺ ions in YbPdGe have a localized character, and the crystal electric field (CEF) effect acts on its physical properties. On the other hand, the electronic specific heat coefficient estimated is 150 mJ/(mol K²) at low temperatures, indicating a heavy-fermion state. To investigate the phase transition at 11.4 K and the CEF effect, we carried out ultrasonic measurements on a single-crystalline YbPdGe sample. Characteristic elastic softening below 170 K is observed at high temperatures in the transverse elastic modulus C₆₆ in contrast to the longitudinal modulus C₂₂ without the softening. In the orthorhombic compound YbIrGe, the transverse moduli exhibit a similar elastic softening originating from the CEF effect, suggesting that the softening of C₆₆ in YbPdGe is also caused by the CEF effect. At the phase transition, C₂₂ and C₆₆ show abrupt elastic hardening and softening, respectively, due to the magnetostriction.

Mo.A-P41 - Excitonic condensation and superconductivity in Ta₂NiSe₅

Y. Ohta¹, T. Kaneko¹, K. Seki¹, T. Toriyama¹, T. Konishi¹

1. Chiba Universit, Chiba, Japan

The electron-hole pair (or exciton) condensation in thermal equilibrium into the excitonic insulator (EI) state has attracted renewed interest in recent years. A layered transition-metal chalcogenide Ta₂NiSe₅ is one such material, where the observed orthorhombic-to-monoclinic structural phase transition at 328 K has been discussed in terms of EI [1-4]. Recently, superconductivity was discovered in this material under high pressures [5]. We carried out the band structure calculation on Ta₂NiSe₅ and derived the three-chain Hubbard model with phonon degrees of freedom. We then applied the BCS mean-field theory to this model and showed that the excitonic condensation cooperatively induces the instability of the phonon mode at momentum $q = 0$, resulting in the structural phase transition [3]. We also applied the finite-temperature variational cluster approximation to the extended Falicov-Kimball model for Ta₂NiSe₅ and found that the calculated single-particle spectral function below and above the transition temperature reproduces the deformation of the band structure observed in experiment very well [4]. We also calculated the band structure under high pressures using the observed structural parameters and found that the quasi-one-dimensional band dispersions overlap to make the system semimetallic [5]. We discuss a possibility that the observed superconductivity may be due to the strong attractive interaction between electrons mediated by the excitonic fluctuations in a system of very low carrier densities.

[1] Y. Wakisaka et al., Phys. Rev. Lett. 103, 026402 (2009)

[2] Y. Wakisaka et al., J. Supercond. Nov. Magn. 25, 1231 (2012)

[3] T. Kaneko et al., Phys. Rev. B 87, 035121 (2013); 199902(E) (2013)

[4] K. Seki et al., Phys. Rev. B 90, 155116 (2014)

[5] K. Matsubayashi et al., in preparation

Mo.A-P42 - Novel electronic structures in ru-pnictides RuPn (Pn = P, As, Sb)H. Goto¹, T. Toriyama¹, T. Konishi¹, Y. Ohta¹*1. Chiba University, Chiba, Japan*

Recently, superconductivity has been discovered in Ru-pnictides, RuP and RuAs, under Rh doping [1]. These compounds crystallize in a MnP-type orthorhombic structure (space group Pnma), in which the RuPn₆ octahedra form a face-sharing chain along the a axis. The chains are connected by the edges and Ru ions form a distorted triangular lattice in the bc plane. The parent compounds RuP and RuAs show two sequential phase transitions: (i) a weak transition from a metal to a pseudogap phase at 330 K for RuP and at 280 K for RuAs, and (ii) a first-order transition to a nonmagnetic insulator at 270 K for RuP and at 200 K for RuAs. By Rh doping, these two phase transitions are suppressed and thus superconductivity occurs in the vicinity of the pseudogap phase.

In order to elucidate the microscopic origins of these phase transitions and consider the mechanism of superconductivity, we have carried out the first-principles electronic structure calculations using WIEN2k [2]. We found that there appear nearly degenerate flat bands just at the Fermi level in the metallic phase, which come mainly from the 4d_{xy} orbitals of Ru ions. The splitting of these bands accompanied by the spin-singlet formation may then be responsible for the observed metal-insulator transition and occurrence of the nonmagnetic insulator phase at low temperatures. These results are compared with the band structure calculated for RuSb that shows superconductivity without doping.

[1] D. Hirai, T. Takayama, D. Hashizume, and H. Takagi, Phys. Rev. B 85, 140509(R) (2012)

[2] P. Blaha, K. Schwarz, G. K. H. Madsen, D. Kvasnicka, and J. Luitz, WIEN2k (Technische Universitaet Wien, Austria, 2002)

Mo.A-P44 - Superconductivity under pressure in FeSe_{1-x}Te_x studied by dc magnetic measurements

K. Miyoshi¹, M. Kondo¹, K. Morishita¹, E. Mutou¹, G. Motoyama¹, K. Fujiwara¹, J. Takeuchi¹

1. Shimane University, Matsue, Japan.

FeSe_{1-x}Te_x is an iron-pnictide superconductor with the simplest crystal structure, which is composed by layers of edge sharing Fe(Se, Te)₄ tetrahedrons stacked along c-axis. In the end material FeSe (T_c=8 K), T_c has been found to be enhanced up to 34 K under hydrostatic pressure mainly due to the change of the crystal structure from orthorhombic to tetragonal one under pressure. On the other hand, superconductivity under pressure in FeSe_{1-x}Te_x is not sufficiently clarified. In the present work, we have studied the superconductivity under pressure in FeSe_{1-x}Te_x with x=0.7 (T_c=14 K) by the measurements of dc magnetization using high quality single crystal specimens, in which excess Fe included in the as-grown crystal was removed by annealing in Te vapor. It is found that T_c increases and makes a maximum of 15 K at 1 GPa but rapidly decreases above 1 GPa under hydrostatic pressure using liquid Ar as pressure transmitting media. In contrast, T_c is found to increase up to 18 K at 2.5 GPa then decrease gradually under nearly uniaxial pressure along c-axis using NaCl as pressure transmitting media. We have also found that T_c makes a maximum of 16 K at 1 GPa but is nearly pressure independent above 1 GPa under uniaxial pressure along a-axis using NaCl. These behaviors suggest that the superconductivity is suppressed by the isotropic stress but is enhanced (not changed) by the uniaxial stress along c-axis (a-axis).

Mo.A-P45 - Charge density wave and superconductivity in novel Pt-based superconductors : SrPt₂As₂ and LaPt₂Si₂

S. Kim¹, K. Kim¹, B.I. Min¹

1. Postech, Pohang, Korea

The intriguing coexistence of the charge density wave (CDW) and superconductivity in SrPt₂As₂ and LaPt₂Si₂ has been investigated based on the ab initio density functional theory band structure and phonon calculations. We have found that the CDW instability for the both cases arises from the Fermi surface nesting. The local split distortions Pt atoms in the [As-Pt-As] layers play an essential role in driving the five-fold supercell CDW instability as well as the phonon softening instability in SrPt₂As₂. By contrast, the CDW and phonon softening instabilities in LaPt₂Si₂ occur without split distortions of Pt atoms. The phonon calculations, however, suggest that the CDW and the superconductivity coexist in [X-Pt-X] layers (X = As or Si) for both cases.

Mo.A-P47 - Quantum criticality at the Lifshitz point in electron doped iron arsenides

S. Das¹, M. Laad², V. Tripathi³, J. Gillett⁴, S. Sebastian⁴

1. *University of Bristol, Bristol, United Kingdom*
2. *Institute of Mathematical Sciences, Chennai, India*
3. *Tata Institute of Fundamental Research, Mumbai, India*
4. *University of Cambridge, Cambridge, United Kingdom*

The twin issues regarding the nature of the normal state and the competing orders are crucial for the understanding of unconventional, high temperature superconductivity in the iron arsenide superconductors. Clear signatures of electronic anisotropy, in the temperature-doping phase diagram, has been observed from transport, STM, ARPES and neutron scattering measurements. Majority of the experimental evidence has been based on electron doped BaFe₂As₂ (Ba122) series. Over here we track the evolution of resistivity anisotropy in the sister SrFe₂As₂ (Sr122) series as a function of Co doping. Although there are differences in the phase diagrams of Ba122 and Sr122, in terms of splitting of the structural and magnetic transitions as well as the magnitude and position of the superconducting dome with respect to the magnetically ordered region, we find that the maximum magnitude of resistivity anisotropy in both the systems is very similar. The experimental finding is interpreted in terms of an underlying orbital selective Mott transition that gaps out the dxz states leading to a Lifshitz transition associated with the quantum critical point.

Mo.A-P48 - Cohabitating phases in metal doped BaFe₂As₂: a structural corroboration

M. E. Saleta^{1,2}, E. Granado¹, C. Adriano¹, D. Tobia¹, P. G. Pagliuso¹, R. R. Urbano¹

1. Instituto de Física "Gleb Wataghin", UNICAMP, Campinas (SP), Brazil

2. Brazilian Synchrotron Light Laboratory (LNLS), Campinas (SP), Brazil

The Fe-based superconductors involved great effort of the scientific community in the last few years. They present rich phase-diagrams and unusual superconducting pairing mechanism. In particular, the nature of the spin density wave (SDW) magnetic order, which is usually preceded by a tetragonal-to-orthorhombic structural transition, raised many debates. Our group has successfully grown good quality single crystals of BaFe₂As₂ (Ba122) pure and doped with Co and Cu ($x = 0.01$) in the Fe-site. The crystals were obtained by In-flux growth method.[1] Resistivity measurements showed that both doped samples present a phase transition at a critical temperature (T_0) close to 128K. In addition, a cohabitation of two phases (tetragonal/paramagnetic and orthorhombic/antiferromagnetic) around T_0 was suggested by our NMR measurements.[2] With the goal to corroborate with the existence of a region where the two phases cohabit, in this work we present a structural study on Co and Cu doped Ba122. We performed high-resolution X-ray diffraction experiment employing synchrotron radiation at Brazilian Synchrotron Light Laboratory (LNLS). We studied in detail the evolution on temperature of some characteristic diffraction peaks. In particular, we followed the reflections that split when the sample undergoes the transition from tetragonal (I4/mmm) to the orthorhombic (Fmmm) phase. Our experiment verifies that the phase transition occurs at a similar temperature that was reported from resistivity and susceptibility measurements. Moreover, we undoubtedly confirm that the tetragonal (PM) phase is cohabitating with the orthorhombic (SDW) one within a finite range of temperature around T_0 as previously reported by NMR.

[1] T.M.Garitezi, et al., Bras. J. Phys. 43 (2013), 223

[2] T.M.Garitezi, et al., J. Appl. Phys, 115 (2014) 17D711

Mo.A-P49 - Induced p-wave superfluidity in imbalanced fermi gases in a synthetic gauge field

H. Caldas^{1,2}, *M. Continentino*²

1. Departamento de Ciencias Naturais. Universidade Federal de São João del Rei, São João del-Rei, Brazil

2. Centro Brasileiro de Pesquisas Físicas, Rio de Janeiro, Brazil

We study pairing formation and the appearance of induced spin-triplet p-wave superfluidity in dilute three-dimensional imbalanced Fermi gases in the presence of a uniform non-Abelian gauge field. This gauge field generates a synthetic Rashba-type spin-orbit interaction which has remarkable consequences in the induced p-wave pairing gaps. Without the synthetic gauge field, the p-wave pairing occurs in one of the components due to the induced (second-order) interaction via an exchange of density fluctuations in the other component. We show that this p-wave superfluid gap induced by density fluctuations is greatly enhanced due to the Rashba-type spin-orbit coupling.

Mo.A-P50 - structural, electronic and magnetic properties of 42214 Fe-based superconductors

A. Continenza¹, F. Bucci^{1,2}, G. Profeta¹

1. *Università degli Studi dell'Aquila, Dept. of Physical and Chemical Sciences, L'Aquila, Italy*

2. *CNR, SPIN at Università degli Studi dell'Aquila, L'Aquila, Italy*

We present an ab-initio study of the newly discovered $L_4Fe_2As_2Te_{1-x}O_4$ superconductors, where L is a rare earth element (L= Pr, Sm, and Gd). This family represents a new entry on the Fe-based superconductor scenery, showing similar features to the other 1111 family and critical temperatures reaching the order of 40K. As the structure is layered with Fe-As planes intercalated by L-O and Te planes, there are new tools that could be adjusted to push the critical temperature towards higher values. To this end, we provide a detailed first principles study of the structural, electronic and magnetic properties of this 42214 family as a function of the L involved, Te-content and F-content. Our first-principles study is able to interpret the important role of the L element on the structure of these new compounds, especially acting on the As-atom height with respect to the Fe-planes, a parameter often considered to be strongly related to electronic correlation and to spin fluctuation strength. A careful comparison with experiments, shows that the ab-initio results give a reliable representation of these materials, even taking into account the non-perfect stoichiometry of the compounds. An antiferromagnetic-stripe low temperature phase is predicted, although not yet experimentally observed. Native Te-vacancies and fluorine substitution are shown to act as charge dopant, decreasing the nesting function and thus weakening the magnetic order. Finally, analysis of properties such as magnetic stability, As-height and electronic states at the Fermi level allows to draw a consistent picture of this compound family and to give predictions on how to improve the material properties and the critical temperature. We believe that our study will contribute to the understanding of this new compound family and of the all Fe-based superconducting material, where the interplay between structure, electronic and magnetic properties is very complex.

Mo.A-P52 - Isovalent substitution effect of P to As on magnetic characteristics of $\text{EuFe}_2\text{As}_2\text{-xPx}$ single crystals.

T. Kashiwagi¹, Y. Arakawa¹, T. Ishikawa¹, K. Kadowaki¹

1. University of Tsukuba, Tsukuba, Japan

$\text{EuFe}_2\text{As}_2\text{-xPx}$ system known as a member of the 122-system in Fe based superconductors has been studied in order to understand the characteristic features of the coexistence of magnetism and superconductivity. The mother compound of this system with $x = 0$ shows the spin-density wave order of Fe spins at $T_{SDW} = 190$ K and subsequently magnetic order of Eu^{2+} moment at $T_N = 19$ K. The isovalent substitution of P to As induces the superconductivity in this system and the T_c value increases up to 28 K around $x = 0.2$. It is also known that the superconducting region of x is narrower than that of other 122-systems. In order to understand the substitution effect of x in this system we have studied magnetic and transport properties of the under doped region of $\text{EuFe}_2\text{As}_2\text{-xPx}$ single crystals grown by the self-flux method. The magnetization curves and the transport characteristics in magnetic fields indicate the clear reduction of the exchange interaction and the uniaxial anisotropy of Eu ions with increasing x . In addition to that the in-plane anisotropy is also reduced with increasing the doping level of P according to the experimental results of the doping dependence of the in-plane fields transport measurements. The result of the increasing of the symmetry of the crystal fields is consistent with the X-ray experiments. We will discuss the substitution effect of P into As on the transport characteristic of this system comparing with the reported phase diagram of the 122-systems.

Mo.A-P53 - Elastic softening in HoFe₂Al₁₀

S. Kamikawa¹, I. Ishii¹, H. Goto¹, T. Fujita¹, F. Nakagawa¹, H. Tanida¹, M. Sera¹, T. Suzuki¹

1. Hiroshima University, Hiroshima-shi, Japan

The ternary compound HoFe₂Al₁₀ has the orthorhombic YbFe₂Al₁₀-type structure (space group Cmc₂m). The specific heat of HoFe₂Al₁₀ exhibits Schottky anomaly at around 1.5 K, suggesting energy gap of $\Delta \approx 3$ K under a crystalline electric field (CEF). To investigate the CEF effect in HoFe₂Al₁₀, we carried out specific heat and ultrasonic measurements on single crystalline samples. We found two Schottky anomalies at around 1.5 K and 20 K in magnetic specific heat. The transverse elastic modulus C₅₅ shows a characteristic elastic softening below 20 K, which is observed down to 2 K. We carried out the theoretical analysis. The two Schottky peaks and the softening of C₅₅ are reproduced by the 4f energy level scheme.

Mo.A-P54 - Superconductivity in LaPd₂Al(2-x)Ga_x compounds

P. Dolezal¹, M. Klicpera¹, J. Pasztorova², J. Prchal¹, P. Javorsky¹

1. Charles University In Prague, Faculty of Mathematics And Physics, (DCMP), Praha, Czech Republic

2. Pavol Jozef Safarik University in Kosice, Faculty of Science, (DCMP), Kosice - Stare Mesto, Slovak Republic

Tetragonal CeT₂X₂ compounds (T: d-element and X: p-element) reveal such physical properties as pressure-induced superconductivity, valence fluctuating phenomena or strong crystal field exciton-phonon coupling in CePd₂Al₂. The CeT₂X₂ compounds crystallize generally in centrosymmetric ThCr₂Si₂-type or CaBe₂Ge₂-type of crystal structure. Superconductivity in these compounds is almost exclusively connected to ThCr₂Si₂-type structure, where the inversion centre takes place at the atomic position of Ce. On the other hand, the compounds crystallizing in CaBe₂Ge₂-type structure (where the centre of inversion is out of any atomic position) reveal frequently the structure instability at low temperatures.

The non-magnetic LaPd₂Al(2-x)Ga_x compounds crystallize in centrosymmetric CaBe₂Ge₂-type structure and undergo a phase transition from tetragonal to lower symmetrical structure at low temperature. Our recent study [1] revealed the superconducting state in these compounds, which deviates substantially from the behaviour described by BCS theory: the positive curvature of field dependence of the superconducting transition temperature T_{sc}(H), non-exponential temperature dependence of the electronic specific heat in the superconducting state and significantly lower value of the weak-coupling BCS limit. The temperature of superconducting transition linearly increases with Ga content up to x = 1.6 and decreases again for LaPd₂Ga₂. Present study is focused on structural and superconducting transitions in LaPd₂Al(2-x)Ga₂ series investigated by means of electrical resistivity measurement under hydrostatic pressure and in external magnetic fields. The application of pressure leads to a decrease of T_{sc} and the dependence of the T_{sc}(H) is changed to a linear decreasing. The temperature of structural phase transition rises with increasing external pressure and moreover, another type of low-temperature crystal structure is induced by pressures > 0.7 GPa.

[1] M. Klicpera, J. Pásztorová, P. Javorský, Superconductor Science and Technology 085001, 27, (2014)

Mo.A-P55 - Pressure dependence of the magnetic order in CrAs

L. Keller¹, J. S. White¹, M. Frontzek¹, P. Babkevich², M. A. Susner³, Z. C. Sims³, A. S. Sefat³, H. M. Ronnow², C. Rüegg^{1,4}

1. *Laboratory for Neutron Scattering and Imaging, Paul Scherrer Institute, Villigen, Switzerland*
2. *Laboratory for Quantum Magnetism, Ecole Polytechnique de Lausanne, Lausanne Switzerland*
3. *Oak Ridge National Laboratory, Oak Ridge, United States*
4. *Department of Quantum Matter Physics, University of Geneva, Geneva, Switzerland*

The suppression of magnetic order with pressure concomitant with the appearance of pressure-induced superconductivity was recently discovered in CrAs. Here we present a neutron diffraction study of the pressure evolution of the helimagnetic ground state towards and in the vicinity of the superconducting phase. Neutron diffraction on polycrystalline CrAs was employed from zero pressure to 0.65 GPa and at various temperatures. The helimagnetic long-range order is sustained under pressure and the magnetic propagation vector does not show any considerable change. The average ordered magnetic moment is reduced from 1.73(2) μ_B at ambient pressure to 0.4(1) μ_B close to the critical pressure $P_c \approx 0.7$ GPa, at which magnetic order is completely suppressed. This indicates a reduction of the magnetic volume fraction and a large coexistence region of magnetic order and superconductivity. The width of the magnetic Bragg peaks strongly depends on temperature and pressure, showing a maximum in the region of the onset of superconductivity. We interpret this as associated with competing ground states in the vicinity of the superconducting phase.

Mo.A-P56 - Effective doping, pressure-induced metallization and magnetic phases in the BiS2 family of superconductors from first principles

C. Morice¹, E. Artacho^{1,2,3}, S. E. Dutton¹, D. Molnar¹, H.-Jin Kim¹, S. S. Saxena¹

1. *University of Cambridge, Cambridge, United Kingdom*

2. *Nanogune and DIPC, San Sebastian, Spain*

3. *Basque Foundation for Science, Ikerbasque, Bilbao, Spain*

The large variety of phenomena arising in the BiS2 family of materials is making these increasingly fascinating. A recent study of Bi4O4S3 has shown it to be a mixture of two phases. Using density functional theory, we explore the electronic structure of both the phases and demonstrate that the S2 layers dope the bismuth-sulphur bands, and this causes metallisation. We find that some compounds in the family have magnetic tendencies, in particular we find that Ce(O,F)BiS2 becomes ferromagnetic at low temperature, which has been confirmed experimentally since. We report the calculation of some magnetic coupling factors. In the Ln(O,F)BiS2 (Ln = La, Ce, Pr, Nd) subfamily of compounds, we show that the change of rare earth does not affect the Fermi surface, and predict that CeOBiS2 should display a pressure induced phase transition to a metallic, if not superconducting, phase under pressure. We also explore the influence of spin-orbit coupling on the electronic structure. [1] Effects of stoichiometric doping in superconducting Bi-O-S compounds (Accepted in J. Phys. Cond. Mat.) [2] Electronic and magnetic properties of superconducting LnOxF1-xBiS2 (Ln = La, Ce, Pr, and Nd) from first principles, arXiv:1312.2615

Mo.A-P57 - Magnetic ground states of superconducting $\text{Eu}(\text{Fe}_{1-x}\text{M}_x)_2\text{As}_2$ ($\text{M} = \text{Co}, \text{Ru}, \text{Ir}$) as revealed by single-crystal neutron diffractionW. Jin^{1,2}, S. Nandi^{1,2,3}, Y. Xiao¹, Y. Su², B. Thomas^{1,2}

1. Jülich Centre for Neutron Science JCNS and Peter Grünberg Institut PGI, JARA-FIT, Forschungszentrum Jülich GmbH, Jülich, Germany
2. Jülich Centre for Neutron Science JCNS, Forschungszentrum Jülich GmbH, Outstation at MLZ, Jülich, Germany
3. Indian Institute of Technology, New Delhi, India

Among various parent compounds of the Fe-based superconductors, EuFe_2As_2 is a unique member of the ternary “122” AFe_2As_2 ($\text{A} = \text{Ba}, \text{Sr}, \text{Ca}$, etc) family since it contains two magnetic sublattices and the A site is occupied by the S-state rare-earth Eu^{2+} ion possessing a $4f^7$ electronic configuration with an electron spin $S = 7/2$, corresponding to a theoretical effective magnetic moment of $7.94 \mu\text{B}$ [1]. Recently, we have investigated the magnetic ground states in superconducting $\text{Eu}(\text{Fe}_{1-x}\text{M}_x)_2\text{As}_2$ compounds with $3d$, $4d$ and $5d$ transition metal doping ($\text{M} = \text{Co}, \text{Ru}$ and Ir) by single-crystal neutron diffraction measurements, respectively. In all three systems, the Eu^{2+} moments were found to be ferromagnetically aligned along the crystallographic c direction in the ground state, coexisting with the superconductivity. In superconducting $\text{Eu}(\text{Fe}_{1-x}\text{Co}_x)_2\text{As}_2$ ($x = 0.18$) with superconducting transition temperature $T_{\text{SC}} = 8 \text{ K}$, the antiferromagnetism (AFM) of the Fe^{2+} moments still survives, although the spin-density-wave (SDW) order temperature is significantly suppressed to $T_{\text{N}} = 70 \text{ K}$ [2]. However, the Fe-SDW order is completely suppressed in optimally doped $\text{Eu}(\text{Fe}_{1-x}\text{Ru}_x)_2\text{As}_2$ ($x = 0.24$, $T_{\text{SC}} = 23 \text{ K}$) and $\text{Eu}(\text{Fe}_{1-x}\text{Ir}_x)_2\text{As}_2$ ($x = 0.12$, $T_{\text{SC}} = 22 \text{ K}$), attributed to stronger hybridization and more expanded bandwidth induced by $4d$ or $5d$ doping, as revealed by first-principles electronic structure calculations [3, 4]. Although the effect of transition-metal dopants in suppressing the Fe-SDW is different to some extent, they tend to modify the indirect Ruderman-Kittel-Kasuya-Yosida (RKKY) interaction among the Eu^{2+} spins in a similar way, tuning the magnetic order of the Eu sublattice from A-type AFM in the nonsuperconducting parent compound to FM in the superconducting doped compound. The coexistence of ferromagnetism and superconductivity in $\text{Eu}(\text{Fe}_{1-x}\text{M}_x)_2\text{As}_2$ is intriguing and a possible spontaneous vortex state might be responsible for the compromise between such two antagonistic phenomena.

References:

1. Y. Xiao, et al., Phys. Rev. B 80, 174424 (2009)
2. W. T. Jin, et al, Phys. Rev. B 88, 214516 (2013)
3. W. T. Jin, et al, in preparation
4. W. T. Jin, et al, Phys. Rev. B 91, 064506 (2015)

Mo.A-P58 - LaAlO₃/SrTiO₃ quantum wells: engineering 2D-superconductivity and rashba spin-orbit coupling by selective orbital occupancyG. Herranz¹, G. Singh², N. Bergeal², A. Jouan², J. Lesueur², J. Gázquez¹, M. Scigaj¹, N. Dix¹, F. Sánchez¹, J. Fontcuberta¹1. *Icmab-Csic, Bellaterra, Barcelona, Spain*2. *LPEM-UMR8213/CNRS-ESPCI ParisTech-UPMC, Paris, France*

The discovery of 2DEGs at the LaAlO₃/SrTiO₃ interface has been heralded as one of the most relevant topics in modern condensed matter. Unlike more conventional 2DEGs -based on III-V or II-VI semiconductors -, carriers at the LaAlO₃/SrTiO₃ interface populate narrow 3d-bands, where electronic correlations are strong. This gives way to complex electronic phases: 2D superconductivity, magnetism -and even the coexistence of both-. There is a growing consensus that the specific symmetry of the occupied t_{2g}-bands (d_{xy}, d_{xz}, d_{yz}) should play a vital role in the emergence of correlated states. Therefore, altering the orbital hierarchy of the electronic band structure of these 2DEGs is a way towards the understanding of the interrelationship between orbital symmetry and the 2DEG complex phases. With this in mind, our research has revealed the distinctive reconstructions of the electronic structure at the LaAlO₃/STiO₃ interface when the 2DEG quantum is confined either along [001] or [110]. We have seen that the degeneracy within the t_{2g} and the eg subbands of the t_{2g}-manifold is broken inversely depending on the crystal orientation, enabling selective orbital occupancy modulated by orientational tuning [1]. By carrying out electrostatic gating experiments in LaAlO₃/SrTiO₃ wells, we have shown that the 2DEG reconstruction driven by crystal orientation leads to remarkable changes in the 2DEG properties. In particular, the anisotropy of the 2D-superconductivity as well as the Rashba spin-orbit field strength can be largely modulated by controlling the 2DEG subband filling. Such an orientational tuning expands enormously the possibilities for electronic engineering of 2DEGs at LaAlO₃/SrTiO₃ interfaces and opens new research fields to extend our current understanding of the link between orbital symmetry and magnetism and superconductivity at LaAlO₃/SrTiO₃ quantum wells.

[1] D. Pesquera et al., Phys. Rev. Lett. 113, 156802 (2014); G. Herranz et al., Nat. Comms. 6, 6028 (2015)

Mo.A-P59 - New Insights in the phase diagram of URhGe

A. Gourgout^{1,2}, A Pourret^{1,2}, D. Aoki^{1,2,3}, J. Flouquet^{1,2}

1. CEA, INAC-SPSMS, Grenoble, France

2. Univ. Grenoble Alpes, INAC-SPSMS, Grenoble, France

3. Institute for Materials Research, Tohoku University, Oarai, Ibaraki, Japan

The exotic electronic properties near a ferromagnetic quantum critical point are not very well understood. In this study we focus on the superconducting ferromagnet URhGe. The remarkable feature in this compound presents the magnetic field induced superconducting phase associated to a spin re-orientation at HR 12T for H parallel to b-axis (hard magnetization axis). This spin re-orientation transition at HR is supposed to be associated with a topological change of the Fermi surface (FS) known as a Lifshitz type transition. In order to probe Fermi surface changes, we chose to measure thermoelectric power and Nernst effects on samples with different orientations of the thermal gradient (along and perpendicular to the easy magnetization axis, J along c, a and b-axis, respectively) with H parallel to b-axis. It is well known that thermoelectric power is particularly sensitive to any change of the FS. At low field, thermoelectric power as function of magnetic field shows small anomalies below HR possibly due to FS changes and a strong peak at HR. At very high magnetic fields, we observed quantum oscillations in the thermopower a frequency of 580 T. In addition, we detected anomalies in the different thermoelectric coefficients corresponding to two new energy scales that collapse at Hr. These low energy scales could possibly mark the appearance of a Fermi Liquid state at low temperature and confirm the presence of ferromagnetic fluctuations close to the QCP.

Mo.A-P60 - Enhancement of Tc due to pressure application in LaFeAsO_{1-x}H_x studied by NMR

N. Fujiwara¹, N. Kawaguchi¹, S. Iimura², S. Matsuishi², H. Hosono²

1. *Kyoto University, Kyoto, Japan*

2. *Tokyo Institute of Technology, Tokyo, Japan*

The prototypical iron-based high-T_c pnictide LaFeAsO_{1-x}H_x undergoes successive antiferromagnetic (AF)-superconducting (SC)-AF phase transition upon H doping. The superconducting phase has double-domes structure in the electronic phase diagram. Pressure application merges the double domes into a single dome, and the T_c minimum of 26 K at x=0.2 goes up to 45 K, the T_c maximum, by applying a pressure of 3.0 GPa. To investigate the high-T_c mechanism, we performed ⁷⁵As nuclear magnetic resonance at 3.0 GPa. The relaxation rate divided by temperature, 1/T₁T for x=0.2 exhibited monotonous increase with the increase in temperature above T_c, implying that spin fluctuations hardly have an effect on 1/T₁T at ambient pressure. By applying pressure, the T dependence above T_c was almost the same with that at ambient pressure, despite that the enhancement of T_c due to pressure application was confirmed from remarkable decrease in 1/T₁T below T_c. These features are also seen for 14% F-doped LaFeAsO_{1-x}F_x [1], suggesting that spin fluctuations are not essential to achieve high T_c in the La1111 series.

[1] T. Nakano, et al., Phys. Rev. B 81 (2010) 100510(R)

Mo.A-P61 - The nature of the metamagnetic transition in ferromagnetic superconductor UGe2

C. Lithgow¹, K. Kamenev¹, A. Huxley¹

1. The University of Edinburgh, Edinburgh, United Kingdom

The coexistence of ferromagnetism and superconductivity requires an unconventional electron-pairing mechanism, since the conventional theory of opposite-spin Cooper pairs is ruled out by the spin-alignment due to the ferromagnetic order. In ferromagnetic superconductor UGe2 the microscopic mechanism for superconductivity is as yet unknown, however the emergence of the superconducting state seems to be connected to the critical point where a metamagnetic transition between two different phases of ferromagnetism is suppressed, by high pressure, to zero Kelvin.

Hall effect and magnetoresistance measurements crossing this transition in temperature, pressure and magnetic field adds to our understanding of the nature of the different phases of ferromagnetism either side of the critical point and ultimately the nature of superconductivity in UGe2. Here we report the significant changes in the ordinary and anomalous Hall coefficients crossing the metamagnetic transition.

Mo.A-P63 - Doping effect on Pd site of quasi-one-dimensional Nb₂PdS₅

Z.-An Xu¹, C. Shen¹, B. Si¹, H. Bai¹, X. Yang¹, Q. Tao¹

1. Zhejiang University, Hangzhou, China

Polycrystalline Nb₂Pd_{1-x}RxS₅ (R=Ir, Ag, Ni, Pt) were synthesized by a solid-state method and superconductivity was investigated by measuring resistivity, Hall effect and magnetic susceptibility. While Ni and Pt are both isovalent dopants at Pd site, Ag (Ir) has one more (less) d electron compared to Pd, which is supposed to change the charge carrier density in the system. It is found that superconducting transition temperature (T_c) can be slightly enhanced by partial substitution of Ir on Pd, but the system is quickly suppressed to a metallic ground state with 30% Ag doping. Hall effect measurements show that Ir doping induces extra electron-type charge carriers to the system and Ag doping instead decreases the charge carrier density. A close correlation between T_c and charge carrier density can be established. Meanwhile T_c reaches a maximum around x=0.2 and finally vanishes with a semiconducting ground state for isovalent Pt doping. Ni doping shows a similar behavior. It is proposed that T_c may be tuned by chemical pressure induced by Pt or Ni doping.

We acknowledge the National Basic Research Program of China (Grant No. 2011CBA00103) and the National Science Foundation of China (Grant Nos. 11190023 and U1332209) for financial support.

Mo.A-P64 - Superconducting and quadrupolar properties of a dilute praseodymium system $Y_{1-x}Pr_xIr_2Zn_{20}$ for $x < 0.1$ Y. Yamane¹, K. Wakiya¹, K. Matsumoto¹, T. Onimaru¹, K. Umeo², T. Takabatake¹1. *Advanced Sciences of Matter, Hiroshima University, Hiroshima-shi, Japan*2. *Natural Science Center for Basic Research and Development, Hiroshima University, Hiroshima-shi, Japan*

Praseodymium-based compounds with $4f^2$ configuration exhibit interesting phenomena arising from hybridization between $4f$ and conduction electrons. The Pr^{3+} ion in a caged compound $PrIr_2Zn_{20}$ has the Γ_3 doublet CEF ground state with quadrupolar degrees of freedom. This system exhibits an antiferro-quadrupolar (AFQ) ordering at $T_Q = 0.11$ K and a superconducting transition at $T_C = 0.05$ K [1, 2]. The coexistence of the AFQ and superconducting state indicates that the quadrupole fluctuations possibly stabilize the superconducting state. In the present work, we have focused on a dilute Pr system $Y_{1-x}Pr_xIr_2Zn_{20}$ for $x < 0.1$ expecting that another type of the ground state would emerge from the Γ_3 doublet once the long-range AFQ order collapses by the Y substitution. We report on the measurements of the electrical resistivity, specific heat, and ac/dc magnetic susceptibility for polycrystals of $Y_{1-x}Pr_xIr_2Zn_{20}$ for $x < 0.1$.

We have found superconductivity in YIr_2Zn_{20} at $T_C = 0.13$ K from the Meissner diamagnetic signal in the AC magnetic susceptibility. The T_C does not change for x up to 0.026. The magnetic part of the specific heat C_m of $Y_{1-x}Pr_xIr_2Zn_{20}$ was estimated by subtracting the data for YIr_2Zn_{20} and $LaIr_2Zn_{20}$ mixed in an appropriate ratio.

For $x = 0.026$ and 0.085 , $C_m(T)$ shows a broad peak at around 9 K, which could be reproduced by a doublet-triplet two-level model. It indicates that the CEF ground state of dilute Pr^{3+} ion is the Γ_3 doublet as in $PrIr_2Zn_{20}$. Below 3 K, $C_m(T)/T$ follows $-\ln T$ dependence. These results will be discussed from the view point of the quadrupolar Kondo effect in the dilute system.

[1] T. Onimaru, *et al.*, J. Phys. Soc. Jpn. 79, 033704 (2010)[2] T. Onimaru *et al.*, Phys. Rev. Lett. 106, 177001 (2011)

Mo.A-P66 - Development of ferromagnet/spin-triplet superconductor hybrid to study proximity effects

M. S. Anwar¹, Y. Sugimoto¹, Y. J. Shin^{2,3}, S. J. Kang^{2,3}, Y. Tano⁴, S. R. Lee^{2,3}, R. Ishiguro^{4,5}, S. Yonezawa¹, H. Takayanagi⁴, T. W Noh^{2,3}

1. Department of Physics, Graduate School of Science, Kyoto University, Kyoto, Japan

2. Center for Correlated Electron Systems, Institute for Basic Science, Seoul, Korea

3. Department of Physics and Astronomy, Seoul National University, Seoul, Korea

4. Department of Applied Physics, Tokyo University of Science, Tokyo Japan

5. RIKEN Center for Emergent Matter Science, Saitama, Japan

Spin triplet superconductivity does not only exist in the bulk like Sr₂RuO₄ [1] but can also be generated at an interface between a spin-singlet superconductor (S) and a ferromagnet (F) via magnetic inhomogeneity [2]. However, there is another approach to realize the spin-triplet proximity effects with junctions between F and a spin-triplet superconductor (T). Theoretically, it has been predicted that spin-triplet proximity effect can be controlled by magnetization direction of F relative to the spin direction of the spin-triplet Cooper pairs [3].

We developed F/T hybrids by growing epitaxial ferromagnetic SrRuO₃ thin films on the *ab*-surface of Sr₂RuO₄ single crystals. The films are under compressive strain ($\approx 2\%$) and ferromagnetic order appears below 160 K [4]. Conductance vs voltage shows the superconducting transitions at a characteristic voltage of the order 5 μ V at 300 mK. Field dependent characteristic voltage reveals the presence of spin-triplet proximity effect at SrRuO₃/Sr₂RuO₄ interface. Our work will help opening a new field of research which may be called "Superspintronics".

[1] Y. Maeno, *et al.*, J. Phys. Soc. Jpn. 81, 011009 (2012)

[2] F. S. Bergret *et al.*, Phys. Rev. Lett. 86, 4096 (2001)

[3] P. M. R. Brydon, *et al.*, Phys. Rev. B 88, 054509 (2013)

[4] M. S. Anwar, *et al.*, Appl. Phys. Ex. 8, 015502 (2015)

Mo.A-P68 - Pressure effects on superconducting properties of $\text{FeSe}_{0.5}\text{Te}_{0.5}$ E. L. Martínez¹, Roberto Escudero¹*1. Iim, Unam, Coyoacán, México, D. F., Mexico*

During the last years, the compound $\text{FeSe}_{1-x}\text{Te}_x$ has been strongly studied in order to understand the changes in crystalline structure and critical temperature under hydrostatic pressure [1-3]. However, the superconducting parameters have been barely studied [4], and this paper proposed compares these parameters at different pressures. In this work we studied a high oriented sample of $\text{FeSe}_{0.5}\text{Te}_{0.5}$ using a high cell for MPMS (Quantum Design), Pb as in-situ manometer and Daphne 7373 oil as pressure media. We found that the superconducting properties of $\text{FeSe}_{0.5}\text{Te}_{0.5}$ were modified when an external pressure was applied during magnetic measurements. When the samples were subjected to pressures between 0.1 to 0.8 GPa, the critical temperature changed from 14.5 to 20 K with a rate of $dT_c/dP=7.37 \text{ K GPa}^{-1}$. The lower and upper critical magnetic fields ($H_{c1}(0)$ and $H_{c2}(0)$) were calculated from the experimental data and a linear fit near the T_c using a Werthamer-Helfand-Hohenberg (WHH) approximation [5]. $H_{c1}(0)$ increased from 0.1 to 0.5 T and H_{c2} changed from 2 to 18 T with external pressure, while the Ginzburg-Landau parameters were estimated between $K=3.37-10$, $\xi(0)= 11.74-4.4 \text{ nm}$ and $\lambda(0)=78-22 \text{ nm}$. In summary, the lower and upper critical fields increased, while the coherence length and penetration depth decreased. These facts indicated a gain in to the density of superconducting carriers.

References:

- [1] K. W. Yeh, et al, J. Phys. Soc. Jpn, 77, 152505 (2008)
- [2] D. Velasco-Soto, et al. J. Appl. Phys, 113, 7E138(2013)
- [3] A. Stemshorn, et al., High Press. Res., 29, 267 (2009)
- [4] Pietosa, J., et al. J. Phys. Condens, Matter 24 (2012)
- [5] L.F. Li, et al, Physica C, 470, 313 (2010)

Mo.A-P69 - A manifestation of latent superconductivity in ferromagnet via a proximity effect in FS structures

Y.i Proshin¹, M. Avdeev¹

1. Kazan Federal University, Kazan, Russia

It is well known that a proximity effect - an interplay between superconducting order parameter in S layers and magnetic order parameter in F layers in the artificial layered ferromagnet-superconductor (FS) structures - can lead to several striking phenomena. However, in standard approach to the proximity effect theories for these systems, a superconducting order parameter and an interelectronic interaction constant were neglected for a ferromagnet. Actually, an electron-electron interaction in a ferromagnet is in existence, but it is suppressed by strong exchange field. The interaction can be reveal itself only if an exchange field would be removed. In this virtual case, a ferromagnet is transformed to normal metal and this latent interaction can lead to superconducting correlations and, therefore, to a superconductivity onset with critical temperature T_{cf} , estimated by the BCS expression. We analyze such situation for dirty case basing on solutions of the Usadel equations. Changing different parameters of asymmetrical trilayers F1SF2 and F1F2S (thicknesses of layers, boundary transparencies, angle between magnetizations, external magnetic field, T_{cf} , and so on), we show that an existence of the electron-electron interaction in a ferromagnet can essentially change the phase diagrams of the FS systems. Thus, an appearance of latent superconductivity of F layers can be manifest itself in the proximity effect conditions. It will be especially expressed if magnetizations in both F layers have opposite signs. A peculiar kind of method of superconducting probing spectroscopy to detect unknown electronic parameters of F metals is proposed. Possible conditions for experimental observation of solitary superconductivity predicted us are also investigated.

The work is partially supported by Russian Government Program of Competitive Growth of Kazan Federal University. MA is also thankful to the RFBR (13-02-01202) for partial support.

Mo.A-P70 - Pressure dependence of superconducting and normal state properties in YFe₂Ge₂

K. Semeniuk¹, J. Chen¹, G. Lampronti², Y. Zou¹, M. Grosche¹

1. *Cavendish Laboratory, University of Cambridge, Cambridge, United Kingdom*

2. *Dept. of Earth Sciences, University of Cambridge, Cambridge, United Kingdom*

The paramagnetic d-electron system YFe₂Ge₂ displays an unusually high Sommerfeld ratio of the specific heat capacity $C/T \approx 100$ mJ/molK² at low temperature and can be tuned to the border of spin density wave order by partial substitution of Y with isoelectronic Lu [1], suggesting that YFe₂Ge₂ is located close to a spin density wave quantum critical point. Our ambient pressure, low temperature measurements reveal a $T^{3/2}$ power law temperature dependence of the electrical resistivity above a superconducting transition at about $T_c \approx 1.8$ K [2].

The similarity both in terms of crystal and electronic structure between YFe₂Ge₂ and the alkaline metal iron arsenide superconductors (K/Rb/Cs)Fe₂As₂ has motivated alternative proposals regarding the pairing mechanism [3]. We explore the role of the nearby spin density wave quantum critical point for superconductivity in YFe₂Ge₂ by high pressure measurements in high quality samples with residual resistivity ratios of up to 200.

References:

[1] S. Ran et al., *Phil. Mag.* 91, 4388 (2011)

[2] Y. Zou et al, *Physica Status Solidi (RRL)* 8, 928 (2014)

[3] A. Subedi, *PRB* 89 024504 (2014); D. J. Singh, *ibid.* 024505 (2014)

Mo.A-P71 - Competition of spin and charge orders in a model cuprate

Y. Panov¹, A. Moskvina¹, A. Chikov¹, I. Avvakumov¹

1. *Ural Federal University, Sverdlovsk Oblast, Russia*

The fascinating issue of an intertwining effect between bulk superconductivity and static magnetic order in cuprate superconductors has attracted a lot of attention for many years (see e.g.: [1]). Here we present a unified approach to the description of the variety of the local intra-unit-cell order parameters determining a low-energy physics in cuprates. We start with a minimal model with the on-site Hilbert space reduced to only three effective valence centers [CuO₄]^{7-,6-,5-} (nominally Cu^{1+;2+;3+}). Central point of the model implies the occurrence of unconventional on-site quantum superpositions of the three valence states characterized by different hole occupation: $n_h=0,1,2$ for Cu^{1+;2+;3+} centers, respectively, and different conventional spin: $s=1/2$ for Cu²⁺ center and $s=0$ for Cu^{1+;3+} centers. We develop an $S=1$ pseudospin model with a non-Heisenberg effective Hamiltonian that provides a physically clear description of 'the myriad of phases' from a bare parent antiferromagnetic insulating phase to a Fermi liquid in overdoped cuprates. Making use of a generalized mean-field approximation (MFA) and classical Monte-Carlo technique we demonstrate a competition of the spin and charge orders in terms of a simplified model Hamiltonian and the evolution of the phase diagram with the doping charge concentration n . The work was supported by the Government of the Russian Federation, Program 02.A03.21.0006 and by the Ministry of Education and Science of the Russian Federation, projects Nos. 1437 and 2725.

References:

[1] Z. Guguchia et.al., *New Journal of Physics*, 15, 093005 (2013)

Mo.A-P72 - Low-energy magnetic excitations in $\text{La}_{1.855}\text{Sr}_{0.145}\text{CuO}_4$ in the vicinity of a quantum-critical point

M. Pikulski¹, N. B. Christensen^{2,3}, L. Udby^{2,3}, C. Niedermayer⁴, K. Lefmann^{2,3}, H. M. Rønnow⁵, J. Ollivier⁶, H. Mutka⁶, T. Kurosawa⁷, N. Momono⁷, M. Oda⁷, J. Mesot^{1,4,8}, J. Chang⁹

1. *Laboratorium für Festkörperphysik, ETH Zürich, CH-8093 Zürich, Switzerland*

2. *Materials Research Department, Risø National Laboratory for Sustainable Energy, Roskilde, Denmark*

3. *Nano-Science Center, Niels Bohr Institute, University of Copenhagen, Copenhagen, Denmark*

4. *Paul Scherrer Institut, Villigen, Switzerland*

5. *Laboratory for Quantum Magnetism, École Polytechnique Fédérale de Lausanne (EPFL), CH-1015 Lausanne, Switzerland*

6. *Institut Laue-Langevin (ILL), Grenoble, France*

7. *Department of Physics, Hokkaido University, Sapporo, Japan*

8. *Laboratory for Neutron & Synchrotron Spectroscopy, École Polytechnique Fédérale de Lausanne (EPFL), Lausanne, Switzerland*

9. *Physik-Institut, Universität Zürich, Zürich, Switzerland*

We present a time-of-flight neutron-spectroscopy study of the high- T_C cuprate superconductor $\text{La}_{1.855}\text{Sr}_{0.145}\text{CuO}_4$ (LSCO). High instrumental energy-resolution allowed us to probe the low-energy incommensurate spin-excitations in the 0.2-2 meV range. In the normal state, we observe two resonance-like features in the excitation spectrum. Upon cooling into the superconducting phase, these resonances appear to be suppressed, while the spectral weight at the lowest accessible energy-transfers decreases only gradually. Our results are discussed in terms of competition between superconductivity and spin-density-wave order.

Mo.A-P73 - Electrostatic Doping under Pressure

D. McCann^{1,2}, K. Kamenev^{1,3}, A. Huxley^{1,2}

1. *Centre for Science at Extreme Conditions, University of Edinburgh, Edinburgh*

2. *School of Physics and Astronomy, University of Edinburgh, Edinburgh*

3. *School of Engineering, University of Edinburgh, Edinburgh*

Electrostatic doping allows continuous tuning through a materials phase diagram by application of high electric fields thus eliminating any potentially obscuring effects normally associated with chemical doping. Electric Double Layer devices make use of this effect to induce a 2D superconducting state at interfaces in a range of materials. One such device is the Electric Double Layer Capacitor which can detect the onset of superconductivity through AC susceptibility measurements. We make use of such a device in an attempt to electrostatically dope and tune the superconductivity in the cuprate compound $\text{La}_{1.93}\text{Sr}_{0.07}\text{CuO}_4$ as well as investigating whether application of pressure improves its efficiency.

Mo.A-P74 - Impurity defects in iron-doped Bi2212

S. Baar¹, N. Momono^{1, 2}, J. Suzuki², J. Soda², K. Kobayashi², H. Takano^{1,2}, Y. Amakai², T. Kurosawa³, M. Oda³, M. Ido³

1. *Division of Chemical and Material Engineering, Muroran Institute of Technology, Muroran, Japan*

2. *Division of Applied Sciences, Muroran Institute of Technology, Muroran, Japan*

3. *Department of Physics, Hokkaido University, Sapporo, Japan*

The origin of the pseudogap and its influence on the electronic state are believed to be the key factors in understanding the mechanism of the high temperature superconductivity in cuprates. The modulation structure of the Local Density of States (LDoS) distribution has been intensively studied as a possible origin of the pseudogap. Recently a charge order with a similar characteristic wave vector as the LDoS modulation in the pseudogap state has been reported by bulk-sensitive experiments. However the origin of the charge order and the LDoS modulation is not yet fully understood. In the present study, high-resolution and low-temperature Scanning Tunnelling Microscopy / Spectroscopy (STM/STS) measurements were used to obtain information about the Local Density of States (LDoS) distribution on the sample surface. The single crystal was grown using the Floating zone method. The transition temperature T_C of the sample was determined to be 82 K and 89 K. The STS measurements were made at 8.5 K. The processed samples were pure and iron-doped slabs of an overdoped $\text{Bi}_2\text{Sr}_2\text{CaCu}_2\text{O}_{8+\sigma}$ (Bi2212). The LDOS of the Fe-doped Bi2212 shows a suppressed superconducting gap with a shifted global minimum. The STM- and dI/dV - maps show impurity defects, which are suspected to be caused by the iron dopant. The fluctuations of the global minimum were mapped and compared to the locations of the impurities. Surprisingly, there were no correlations between the locations of the impurity defects and the global minimum variations. The Fe-doped sample was analysed while applying an external magnetic field, to further investigate the behaviour of the superconducting gap and the impurity sites.

Mo.A-P75 - Two superconducting phases separated by a Lifshitz transition in LaFeAs_{1-x}PxO

Z. -An Xu¹, Ch. Shen¹, B. Si¹, X. Yang¹, Y. Luo¹, C. Cao², Chunmu Feng¹, G. Cao¹

1. Zhejiang University, Hangzhou, China

2. Hangzhou Normal University, Hangzhou, China

Two distinct superconducting phases have recently been discovered in the P-doped 1111-type iron pnictide superconductors LaFeAs_{1-x}PxO (0 ≤ x ≤ 1). The first superconducting phase is centered around x = 0.3 and then superconductivity disappears as P content increases to x = 0.5. For x > 0.5, a second superconducting phase appears and T_c reaches a maximum at x = 0.7. We found that the upper critical field H_{c2} is significantly larger in the second superconducting phase although the maximum of T_c is close to each other. Hall effect and thermopower measurements reveal a distinct difference in the normal state transport properties between the two superconducting phases. Further study of Zn impurity effect implies that there could be a change in the superconducting pairing symmetry between the two superconducting states. First-principles band calculations suggest that there could be a Lifshitz transition around x = 0.5.

We acknowledge the National Basic Research Program of China (Grant Nos. 2011CBA00103 and 2014CB921203) and the National Science Foundation of China (Grant Nos. 11190023 and U1332209) for financial support.

Mo.A-P76 - Pseudogap and kinetic energy of unconventional superconductivity in the two-dimensional Hubbard model

E. Calegari¹, A. Lausmann¹, S. Magalhaes², C. M. Chaves³, A. Troper³

1. *Universidade Federal de Santa Maria, Santa Maria, Brazil*

2. *Universidade Federal Fluminense, Niterói, Brazil*

3. *Centro Brasileiro de Pesquisas Físicas, Rio de Janeiro, Brazil*

In conventional superconductors described by the Bardeen-Cooper-Schrieffer (BCS) theory, the transition from the normal to the superconducting state is accompanied by a reduction in the potential energy and an increase in the kinetic energy. On the other hand, in high-temperature superconductors the potential and the kinetic energies present an unconventional behavior that may be strongly related to the pseudogap phenomena. In this work, we analyzed the kinetic and potential energies in the superconducting state of the two-dimensional Hubbard model. The model includes hopping to first (t) and second (t_2) nearest neighbors and is investigated by the Green's function method within a n -pole approximation [1,2], which allows to consider superconductivity with d -wave pairing. In the present scenario, a pseudogap emerges near the anti-nodal points in the Fermi surface, when the strong coupling regime is reached. The obtained results show that in the low doping region, the system enters the strong coupling regime and the opening of a pseudogap is followed by a decreasing of the kinetic energy and an increasing of the potential energy. This result corroborate the scenario recently presented by Gull and Millis [3] that attributes the pseudogap to the strong correlations present in the underdoped regime. A phase diagram of Coulomb interaction U versus the occupation n is also presented. This phase diagram shows clearly that the pseudogap regime coincides with the strong coupling regime in which the kinetic and potential energies present an unconventional behavior. Finally, we show that the pseudogap and the unconventional behavior of the kinetic and potential energies are close related to strong antiferromagnetic correlations.

[1] L. M. Roth, Phys. Rev. 184, 451 (1969)

[2] J. Beenen and D. M. Edwards, Phys. Rev. B52, 13636 (1995)

[3] E. Gull and A. J. Millis, PRB 86, 241106 (2012)

Mo.A-P77 - Superconductivity in an antisymmetric diatomic s - p chain: application to BiS₂

G. Sousa¹, K.Foyevtsova^{2,3}, M Continentino¹, G. Martins⁴

1. *Centro Brasileiro de Pesquisas Físicas (CBPF), Rio de Janeiro, Brazil*

2. *Department of Physics & Astronomy, University of British Columbia, Vancouver, Canada*

3. *Quantum Matter Institute, University of British Columbia, Vancouver, Canada*

4. *Department of Physics, Oakland University, Rochester, United States*

We study the properties of a superconducting phase in a diatomic chain with two different atoms in the unit cell. One of the atoms contains an s- and a p-orbital while the other has just a p-orbital. The kinetic energy of the model has a hopping term between orbitals p (tpp) and an antisymmetric hybridization (V) between the orbitals s and p of the two different atoms. We add by hand a superconducting term that is treated at the mean-field level. By using the Green's function method, we calculate the superconducting order parameter and analyze the effect of tpp and V over it. This model was then applied to understand the superconducting phase of LaOBiS₂ [JPSJ 81, 114725 (2012)], whose electronic structure has been shown to be approximately one-dimensional [PRB 86, 220501 (2012)]. We model it as a chain of Bismuth (p-orbital) and Sulfur (s- and p-orbital) atoms. We were able to determine that, for tpp and V values consistent with those obtained from DFT calculations for LaOBiS₂, there exist a superconducting phase which is strongly dependent on variations in these hopping parameters. This is consistent with experimental findings in LaOBiS₂ showing a strong dependence of the superconducting phase with pressure [PRB 90, 220510 (2014)], which is well known to affect the value of hopping parameters and hybridization.

Mo.A-P78 - The transport measurement on $K_x\text{Fe}_{2-y}\text{Se}_2$ at high pressure

H. Fujita¹, T. Kagayama¹, K. Shimizu¹, Y. Yamamoto², J. Mizuki², M. Tanaka³, Y. Takano³, H. Yamaoka⁴

1. KYOKUGEN, Grad. Sch. Eng. Sci., Osaka Univ., Osaka, Japan

2. Fac. of Sci., Kwansei Gakuin University, Nishinomiya, Japan

3. NIMS, Tsukuba, Japan

4. RIKEN, Wakō, Japan

The superconductor FeSe has simpler crystal structure, and its T_c can be raised by doping alkali metal from 8 K to over 30 K. In addition, the K-doped FeSe has two separated superconducting phases with pressure and the T_c of the superconducting phase at higher pressure (SC-2) is 48 K at 12 GPa [1]. $K_x\text{Fe}_{2-y}\text{Se}_2$, has Fe-vacancies and two states, the metallic state and the insulator state. The phases co-exist and are decided by the order of iron vacancies [2]. In this study, the sample dependence of $K_x\text{Fe}_{2-y}\text{Se}_2$ is researched with transport measurement at high pressure. Four samples, which have different heat-treatment, were used. The SC-2 didn't appear in some samples, and every sample showed different temperature dependence of electric resistance. We will report the relation between differences of samples and their superconductivity in poster presentation.

[1] L. Sun et al., Nature 483 (2012) 67

[2] F. Chen et al., Phys. Rev. X 1 (2012) 021020

Mo.A-P79 - Magnetic measurements of superconducting $KxFe_2-ySe_2$ single crystals under high pressure

K. Miyoshi¹, M. Kondo¹, K. Morishita¹, G. Motoyama¹, K. Fujiwara¹, J. Takeuchi¹

1. Shimane University, Matsue, Japan

$KxFe_2-ySe_2$ is an FeSe based superconductor with $T_c=30$ K, having a crystal structure composed by intercalating K atoms between the layers of edge sharing FeSe₄ tetrahedrons, which is the unit layer in FeSe superconductor ($T_c=8$ K). In FeSe based superconductors, there is a general trend toward higher T_c as interlayer distance or length of c-axis increases, as expected from the fact that T_c of $(NH_3)_yAxFe_2Se_2$ (A=alkali metal) is ranging from 30 K to 44 K depending on the c-axis lattice parameter. The importance of interlayer distance for the superconductivity can be confirmed by the investigations on the superconductivity under physical pressure, which compresses the lattice volume. In the present work, we have performed the measurements of dc magnetization for $KxFe_2-ySe_2$ single crystal specimens both under hydrostatic and uniaxial pressure, using miniature diamond anvil cell. In the experiments, liquid Ar and NaCl were used as pressure transmitting media to generate hydrostatic and uniaxial pressure, respectively. It has been found that T_c is pressure independent below 2 GPa but decreases rapidly above 3 GPa, indicating that the superconductivity disappears at about 5 GPa, in case that liquid Ar is used as pressure transmitting media. On the other hand, T_c is found to decrease rapidly above 2 GPa and is extrapolated to 0 K at about 3 GPa, in case that the uniaxial pressure is applied along c-axis using NaCl as pressure transmitting media. These behaviors suggest that the c-axis lattice constant is one of the important factor to determine T_c , so that the lattice compression along c-axis destroys the superconductivity more effectively, showing consistency with the general trend mentioned above.

Mo.A-P80 - Improvement of high-pressure thermal expansion measurement using an active-dummy method with an application to the antiferromagnetic superconductor CeRhIn5K. Imura¹, M. Takahashi¹, K. Deguchi¹, N. Sato¹*1. Nagoya University, Nagoya, Japan*

Near a quantum critical point (QCP), where an ordering temperature goes down to zero temperature, there emerges a novel quantum state such as unconventional superconductivity. At a magnetic QCP, the Gruneisen constant diverges and hence thermal expansion measurements may be useful for studying physics of the QCP. In heavy fermions, the QCP can be achieved by the application of easily accessible magnitude of pressure. For high-pressure thermal expansion measurements, an active-dummy method using a strain-gauge is usually adopted. It is a powerful tool, but is not straightforwardly applied to the study on the QCP: the active-dummy method requires us to use two strain gauges, which are put on a sample and a dummy, and a small difference in their resistivity particularly below 4 K causes a spurious voltage that results in an error in the quantitative determination. In this paper, we present that such the spurious voltage can be reduced by selecting an appropriate pair of strain gauges. We also report the application of the method to thermal expansion measurements of CeRhIn5. At ambient pressure, CeRhIn5 exhibits an antiferromagnetic and superconducting transition below $T_N = 3.8$ K and $T_{sc} = 90$ mK, respectively [1]. Note that whether superconductivity at ambient pressure is of bulk origin remains to be under debate. With applying external pressure, T_N initially increases and shows a peak at 0.7 GPa, and then vanishes at a critical pressure $P_c \sim 2.1$ GPa. Besides a lot of experimental studies, a pressure-temperature phase diagram in the vicinity of P_c remains to be cleared. We measured the thermal expansion of CeRhIn5 using an appropriate pair of strain gauges, and obtained the pressure dependence of the thermal expansion at a constant temperature. From this result, we determine a phase transition line between the low-pressure antiferromagnetic state and high-pressure superconducting state.

[1] G. Chen et. al. Phys. Rev. Lett. 97, 017005 (2006)

Mo.A-P81 - Correlation between ferromagnetism and superconductivity in Y9Co7S. Kunikata¹, A. Takeda¹, K. Imura¹, K. Deguchi¹, N. K. Sato¹, S. Kittaka², T. Sakakibara²

1. Graduate School of Science, Nagoya University, Nagoya, Japan

2. Institute for Solid State Physics, University of Tokyo, Tokyo, Japan

Ferromagnetism (FM) and superconductivity (SC) have been considered to be antagonistic because FM spontaneous magnetization seems to be incompatible with SC diamagnetism. However, this simple consideration was overthrown by the discovery of UGe₂, URhGe, and UCoGe in which 5f electrons are responsible for both of itinerant FM and SC. This raises a question of that this unique feature may arise from some characteristic nature of 5f electrons. To clear this problem, we study Y9Co7, a candidate of ferromagnetic superconductor. Y9Co7 exhibits FM (TFM = 5 K) and SC (TSC = 2 K) at ambient pressure [1], although it is controversial if the FM is a long-range order. (According to our recent measurements, the 3rd harmonic magnetic susceptibility shows a negative broad peak as a function of temperature [2], indicative of cluster glass-like inhomogeneous state.) To further investigate the correlation of the long-range or short-range FM with SC, we measured the dc magnetization and the ac magnetic susceptibility at temperatures above and below TSC. We found that their magnetic field dependences are those in a conventional ferromagnet and a superconductor, in contrast to those of UCoGe in which the lower critical magnetic field (H_{c1}) is absent [3]. From these results, we suggest that Y9Co7 is a conventional type II superconductor and hence has no spontaneous vortex state. We also measured the ac magnetic susceptibility under pressure. As the pressure increases, TSC increases while the ac susceptibility just above TSC decreases, similarly observed in a previous report [4]. Then, we constructed a pressure vs. temperature phase diagram, in which TSC decreases while a paramagnetic Curie temperature decreases. From this result, we suggest that the ferromagnetism (ferromagnetic fluctuation) competes with SC.

[1] A. Kolodziejczyk et al., J. Phys. F: Metal Phys., 10 (1980) L333

[2] S. Kunikata et al, in preparation

[3] K. Deguchi et al., J. Phys. Soc. Jpn., 79 (2010) 083708

[4] C.Y. Huang et al. Solid State Commun., 45 (1983) 795

Mo.A-P83 - Cu-NMR Study of Single Crystal CeCu₂Si₂ under pressure

K. Fujiwara¹, C. Matsumura¹, Y. Suwada¹, T. Shirai¹, T. Kobayashi², S. Seiro³, C. Geibel³, F. Steglich³

1. Department of Materials Science, Shimane University, Matsue, Japan

2. Graduate School of Natural Science and Technology, Okayama University, Okayama, Japan

3. Max Planck Institute for Chemical Physics of Solids, Dresden, Germany

CeCu₂Si₂ shows significant increase in T_c around the critical pressure $P_c = 4.5$ GPa. It is proposed that superconducting mechanism around P_c results from the valence fluctuation of Ce ions. Our previous study revealed that the ⁶³Cu-NQR frequency (⁶³ ν_Q) suddenly deviated from the linear pressure dependence of ⁶³ ν_Q above 4 GPa, suggesting that Ce valence rapidly increases around P_c . Since valence transitions are not observed in powdered XRD measurement, valence crossover occurs in the narrow pressure range around P_c . Recently, theory of valence mediated superconductivity proposed that the valence transition appears with applying high magnetic field. Therefore we started to measure Cu-NMR of single crystal CeCu₂Si₂ in order to elucidate the field and pressure dependence of NQR frequency (ν_Q), and to search field-induced valence transitions. Since NMR spectrum of polycrystalline powder sample shows broad powder pattern, it is impossible to investigate the valence state. Under the magnetic field (= 8 T) parallel to a -axis and c -axis at ambient pressure, Knight shift is consistent with previous data obtained by the low field NMR and ν_Q is also consistent with that of NQR at zero field. We will report T -dependence of ν_Q under pressure and discuss valence and spin state, estimated by applying the field parallel to a -axis and c -axis.

Mo.A-P84 - Drastic enhancement of superconducting transition temperature in 112-type $\text{Ca}_{1-x}\text{RE}_x\text{FeAs}_2$ (RE = La, Ce, Pr, Nd) induced by negative chemical pressure

K. Kudo¹, Y. Kitahama¹, K. Fujimura¹, T. Mizukami¹, M. Nohara¹

1. Department of Physics, Okayama University, Okayama, Japan

The 112-type CaFeAs_2 is a recently discovered iron-based superconductor [1,2]. The compound crystallizes in a monoclinic structure and consists of alternately stacked FeAs and arsenic zigzag bond layers. It has been recognized that the rare earth (RE) substitution is necessary for stabilizing the 112 [1,2]. La-doped compounds show bulk superconductivity at 35 K [3], while Pr-, Nd-, Sm-, Eu-, and Gd-doped compounds show superconductivity at 10-15 K with a small shielding volume fraction of 5-20% [2,4]. Ce-doped compounds rarely exhibit superconductivity [4]. In this paper, we report that a negative chemical pressure induced by Sb doping increases the T_c of $\text{Ca}_{1-x}\text{La}_x\text{Fe}(\text{As}_{1-y}\text{Sb}_y)_2$ to 47 K [5], which is the second highest T_c after 1111-type iron-based superconductors. Moreover, we show that bulk superconductivity at 43, 43, and 43 K is induced by Sb doping of $\text{Ca}_{1-x}\text{RE}_x\text{FeAs}_2$ with RE = Ce, Pr, and Nd, respectively [5]. These results highly contrast with those of other iron-based superconductors, in which T_c is generally enhanced by a positive pressure. We found that an increase in the lattice parameter b , which modifies the As-Fe-As bond angle, is important for optimizing the superconductivity in the 112 phase [5]. The T_c might be increased above 50 K, if the b parameter can be increased to approximately equal a .

[1] N. Katayama et al., J. Phys. Soc. Jpn. 82, 123702 (2013)

[2] H. Yakita et al., J. Am. Chem. Soc. 136, 846 (2014)

[3] K. Kudo et al., J. Phys. Soc. Jpn. 83, 025001 (2014)

[4] A. Sala et al., Appl. Phys. Express 7, 073102 (2014)

[5] K. Kudo et al., J. Phys. Soc. Jpn. 83, 093705 (2014)

Mo.A-P85 - Superconductivity in the higher borides Zr_{1-x}Lu_xB₁₂ AND Y_{1-x}La_xB₆

N. Sluchanko¹, S. Gavrilkin², K. Mitsen², A. Azarevich¹, V. Glushkov¹, S. Demishev¹, A. Khoroshilov¹, N. Shitsevalova⁴, V. Filipov⁴, S. Gabani⁵, P. Szabo⁵, P. Szabo⁵, K. Szabo⁵, A. Kuznetsov³

1. Prokhorov General Physics Institute of RAS, Moscow, Russia

2. Lebedev Physical Institute of RAS, Moscow, Russia

3. National Research Nuclear University MEPhI, Moscow, Russia

4. Frantsevich Institute for Problems of Materials Science, NASU, Kiev, Ukraine

5. Institute of Experimental Physics SAS, Košice, Slovakia

In superconductors Zr_{1-x}Lu_xB₁₂ and Y_{1-x}La_xB₆ ($x < 0.1$) with a transition to cage-glass state at $T^* \approx 50-100$ K [1] heat capacity $C(T)$ and magnetization measurements have been carried out on high quality single crystals in magnetic fields up to 9 T in combination with point-contact spectroscopy studies of the superconducting energy gap. For these higher borides with critical temperatures in the range $T_c \approx 4.5-7.4$ K we have estimated the thermodynamic and upper critical fields, electron density of states' renormalization effect, electron-phonon interaction λ , superconducting gap $\Delta(T)$ [2] and pseudogap Δ^* . Our experiments reveal strong changes in aforementioned characteristics with variation of content x in these compounds with BCS-type superconductivity mediated by quasi-local vibrations of the ions of transition and rare earth metals (Y^{3+} , La^{3+} , Zr^{4+} and Lu^{3+}). We analyze step-by-step the transformation of II-order superconductivity with a wide range variation of the Ginzburg–Landau parameter $\kappa = 0.7-7$. We discuss also the development of the structural instability, the formation of two level systems, their role in the suppression of superconductivity and the nature of pseudogap in the RB₆ and RB₁₂ higher borides.

References:

[1] N. E. Sluchanko, A. N. Azarevich, A. V. Bogach, et al., JETP 113, 468 (2011)

[2] N. Sluchanko, S. Gavrilkin, K. Mitsen et al., J Supercond Nov Magn 26, 1663 (2013)

Mo.A-P86 - Precise phase control and superconductivity in $A_x(NH_3)_yFe_{2-d}Se_2$ system (A: Alkali and Alkali-earth metal)

T. Kambe¹, K. Ashida¹, J.-Hyun Lee¹, Y. Takahei¹, N. Nishimoto¹, T. Kimura¹, K. Kudo¹, M. Nohara¹

1. Okayama University, Okayama, Japan

The high- T_c superconducting phase is obtained by an intercalation of alkali or alkali-earth metals between the FeSe layers. For the solution method, the solvent molecules are intercalated simultaneously between the FeSe layers, and expand the interlayer spacing effectively. It is suggested that the T_c for this system increases with increasing the interlayer spacing [2]. Recently the T_c -dome as a function of the interlayer spacing was reported [3]. On the contrary, multi-phase character was also observed in the ammoniated FeSe system due to the difference in an amount of intercalants; solvent molecules and/or metal ions [4]. Thus, to extract the key parameter for the superconductivity in ammoniated FeSe system, it is important to control the superconducting phase precisely. Here, we present our synthesis method, and show the superconducting properties including the magnetization and resistivity experiments for $A_x(NH_3)_yFe_{2-d}Se_2$ samples. For example, in Ba doped FeSe sample, the magnetization and the resistivity experiments indicate that the onset- T_c is obtained to be 43 K, which is higher than the previous result (38 K). We will discuss the correlation between the structural parameters and superconducting transition of $A_x(NH_3)_yFe_{2-d}Se_2$ system in detail.

References:

- [1] M. Burrard-Lucas, et al., Nat. Materials, 12, 15 (2013)
- [2] Lu Zheng, et al., Phys Rev B. 88, 094521 (2013)
- [3] T. Hatakeda, et al., J. Phys. Soc. Jpn. 82 (2013) 123705
- [4] J. Guo, et al., Nat. Commun. 5:4756 (2014)

Mo.A-P88 - V substitution of Co in Nd(Co_{1-x}V_x)₂Si₂; A crossover from antiferro to ferromagnetismR. Roy Chowdhury¹, S. Dhara¹, B. Bandyopadhyay¹*1. Saha Institute of Nuclear Physics, Kolkata, India*

RT₂X₂ intermetallic compounds (R = rare earth, T = transition metal and X = Si) crystallize in the body centered tetragonal ThCr₂Si₂ type structure. Previous works suggest the R³⁺ ions are responsible for magnetism in the RCo₂Si₂ compounds, whereas Co does not carry any magnetic moment. In the work, non-magnetic Co has been substituted by V, having a larger atomic volume and a fewer number of d-electrons than Co. NdCo₂Si₂ shows antiferromagnetic transition at 34 K. Temperature dependence of magnetic susceptibility, in Nd(Co_{1-x}V_x)₂Si₂ (x = 0 to 0.35) follow ferrimagnetic behavior in between 50-300 K. Below ~ 30 K, the field dependence of magnetization curves tend to saturate at ~ 2 tesla and also coercivity is exhibited in hysteresis loops, indicating dominance of ferromagnetic interaction. Saturation magnetization moment M_s, increases with V content and for x = 0.35, M_s reaches to ~0.35-0.40 Bohr-magneton /f.u., much smaller than that of the rare earths. Susceptibility consists of a strong ferromagnetic part and paramagnetic part. The R³⁺ ions contribute to the paramagnetic part confirming the observed ferromagnetism to be originating from 3d moments. Also, in V doped samples exchange bias is observed which increase markedly below ~ 12 K where there is also a sharp decrease in the resistivity. Specific heat measurements of the parent compound show three transitions at ~ 13, 23 and 32 K respectively which are consistent with the magnetization data. Doped compounds show two sharp transitions at 26 K and 45 K respectively. For NdCo₂Si₂, magnetic entropy (S_{mag}) at transition 32K is about 52% of the total magnetic entropy value for Nd³⁺, and in the doped sample S_{mag} at transition temperature 45 K is about 69-70% of the total magnetic entropy. The measurements indicate that partial substitution of Co by V in NdCo₂Si₂ result in ferromagnetism coexisting with antiferromagnetism.

Mo.A-P89 - Anomalous ferromagnetic anomaly coexisting with superconductivity in layered superconductor CeO_{1-x}F_xBiS₂

T. Asano¹, T. Nakashima¹, R. Higashinaka, T. D. Matsuda, Y. Aoki

1. Tokyo Metropolitan University, Tokyo, Japan

BiS₂-based layered superconductors LnO_{1-x}F_xBiS₂ (Ln: rare earth) have been attracting much attention [1,2]. Among them, the coexistence of superconductivity and ferromagnetism has been revealed in CeO_{1-x}F_xBiS₂ by magnetic susceptibility measurements using polycrystalline samples [3]. To investigate this intriguing anomaly, we have studied the physical properties of CeO_{0.5}F_{0.5}BiS₂ using single crystals with the onset superconducting transition temperature of 3.2 K. The observed easy ab-plane anisotropy in the magnetization can be explained by a model that 4f –electrons of Ce ions are well localized with the crystalline-electric-field ground state of $J_z = \pm 1/2$ doublet as in undoped CeOBiS₂ [4]. It has been found that a ferromagnetic anomaly develops below 7 K along the c axis, even though this is the hard magnetization axis. The absence of specific heat anomaly around 7 K indicates that this is not a bulk thermodynamic phase transition. Instead, specific heat shows a profound -logT divergence below 3 K in a similar manner as observed in CeOBiS₂ [4]. This finding clearly demonstrates that the unprecedented type of quantum critical behavior found in CeOBiS₂ in the Ce-ion magnetic system remains almost unchanged even in the carrier doped CeO_{0.5}F_{0.5}BiS₂.

[1] Y. Mizuguchi et al, Phys. Rev. B, 86 , 220510(R) (2012)

[2] Y. Mizuguchi et al, J. Phys. Soc. Jpn. 81, 114725 (2012)

[3] S. Demura et al, J. Phys. Soc. Jpn. 84, 024709 (2015)

[4] R. Higashinaka et al, J. Phys. Soc. Jpn. 84, 023702 (2015)

Mo.A-P90 - NMR studies on the in-plane anisotropy of the iron pnictide LiFeAs

M. Toyoda¹, Y. Kobayashi¹, M. Itoh¹, M. Sato²

1. Nagoya University, Nagoya, Japan

2. Research Center for Neutron Science & Technology, CROSS, Naka, Japan

Possibility of the orbital fluctuation has been discussed as a mechanism of the superconducting (SC) pair in the iron pnictides with multi-orbitals, and various kinds of phenomena has been reported to demonstrate the presence of the orbital fluctuation. Among these phenomena, we have focused on physical properties with lower symmetry (the C_2 symmetry) within the Fe plane than the C_4 symmetry of the crystal structure. Until now, we have studied an in-plane anisotropy of the electric field gradient (EFG) at the As sites in the Co-doped $BaFe_2As_2$ using the ^{75}As NMR probe, and concluded that the static in-plane anisotropy of the electronic state is induced by Co impurities or defects in the Fe plane, which is consistent with the model of impurity-induced orbital order [1]. In this study, we present the results of ^{75}As NMR measurements on the iron pnictide LiFeAs which exhibits the SC transition at 18 K without atomic substitution. We found that the anisotropic parameter of EFG, h , at the As sites in the Fe plane is not zero even at 280 K and gradually increases with decreasing temperature, which may not be explained only by the yz/zx band splitting owing to spin-orbit coupling. The h value at 20 K is one order of magnitude less than the values in the superconducting Co-doped $BaFe_2As_2$. These results indicate that an amount of the defects within the Fe plane in LiFeAs is less than in $BaFe_2As_2$. The EFG anisotropy should be compared with the in-plane anisotropy of the other physical properties to discuss the anisotropic electronic state in this system.

[1] Y. Inoue *et al.*, Phys. Rev. B **85**, 224506 (2012).

Mo.A-P91 - Superconductivity in the doped ferromagnetic semiconductor samarium nitride

B. Ruck¹, E.-Maria Anton¹, F. Natali¹, S. Granville¹, S. Chong¹, U. Zuelicke¹, M. Governale¹, J. Trodahl¹, A. Engel², A. Moghaddam³

1. *Victoria University of Wellington, Wellington, New Zealand*

2. *Physics Institute of the University of Zürich, Zürich, Switzerland*

3. *Institute for Advanced Studies in Basic Sciences, Zanjan, Iran*

The rare-earth nitride series are especially attractive for fundamental studies in spintronics and magnetism. Many of the series are intrinsic ferromagnetic semiconductors, and they possess interesting magnetic states resulting from the interplay between the spin and orbital contributions to the magnetic moments. They thus exhibit such surprising properties as a magnetisation in direct opposition to the spin moments in light rare earth nitrides [1], magnetic moments with no net angular momentum in EuN [2], and ferromagnetically aligned spins with no net magnetisation in SmN [3]. The last is a result of near complete cancellation of the orbital and spin moments. Perhaps most remarkably we have very recently discovered superconductivity below 4 K in SmN. We have observed the superconductivity through both resistivity and magnetisation measurements in a series of SmN films. The superconductivity occurs deep within the ferromagnetic phase, suggesting spin-triplet electron pairing of superconducting electrons. We have developed a theoretical description of this novel superconducting phase based on pairing within a fully spin-polarised electron system.

[1] F. Natali, B.J. Ruck, N.O.V. Plank, H.J. Trodahl, S. Granville, C. Meyer, and W.R.L. Lambrecht, Rare-earth mononitrides, *Prog. Mats. Sci.* 58, 1316 (2013)

[2] Do Le Binh, B.J. Ruck, F. Natali, H. Warring, H.J. Trodahl, E.-M. Anton, C. Meyer, L. Ranno, F. Wilhelm, and A. Rogalev, Europium nitride: A novel diluted magnetic semiconductor, *Phys. Rev. Lett.* 111, 167206 (2013)

[3] C. Meyer, B.J. Ruck, J. Zhong, S. Granville, A.R.H. Preston, G.V.M. Williams, and H.J. Trodahl, Near-zero-moment ferromagnetism in the semiconductor SmN, *Phys. Rev. B* 78, 174406 (2008)

Mo.A-P92 - A half-quantum vortex in chiral or helical p-wave superconducting statesS. Kikuchi¹, Y. Kikuchi¹, T. Yoshioka¹, H. Tsuchiura¹, M. Sigrist²1. *Department of Applied Physics, Tohoku University, Sendai, Japan*2. *Theoretische Physik, Eidgenössisch Technische Hochschule (ETH), Zurich, Switzerland*

A half-quantum vortex (HQV) is expected to be found in the so-called A-phase of ³He and the chiral p-wave spin-triplet pairing superconducting state [1,2]. It is formed by a π -rotation of the superconducting phase and also a π -rotation of the d -vector around the vortex core. Thus the magnetic flux through a HQV is one-half of the flux quantum Φ_0 . HQVs are topologically possible objects, however, the energetic stability is a subtler question. Indeed, it has been pointed out that HQVs is unstable unless a weak spin-orbit coupling exists, based on phenomenological Ginzburg-Landau theory [3,4]. For experimental search of HQVs in real superconductors, it is useful to study the effects of material dependent factors on the stability of HQVs, such as the strength of the spin-orbit coupling, the anisotropy of the pairing interaction, the Fermi surface structure, and also the effects of magnetic field via a Zeemann coupling based on microscopic theory.

In this paper, as a first step, we study the quasiparticle states around a HQV or an impurity in a chiral or helical p-wave superconducting states in a square lattice tight-binding model based on the Bogoliubov-de Gennes theory. We confirmed that the zero-energy bound state, the so-called Majorana state, appears within the HQV [5], whereas it does not around the impurity. We also show the effects of spin-orbit interaction and Fermi surface structure.

[1] G. E. Volovik and V. P. Mineev, *Pis'ma Zh. Exp. Teor. Fiz.* 24 (1976) 605[2] D. A. Ivanov, *Phys. Rev. Lett.* 86 (2001) 268-271[3] S. B. Chung, H. Bluhm, and E. -A. Kim, *Phys. Rev. Lett.* 99 (2007) 197002[4] V. Vakaryuk and A. J. Leggett, *Phys. Rev. Lett.* 103 (2009) 057003[5] M. Kato, Y. Niwa, and K. Maki, *J. Phys.: Conf. Ser.* 150 (2009) 052103

Mo.A-P96 – La₃Co - superconductivity on the edge of ferromagnetismJ.Strychalska¹, M. Roman¹, B. Wiendlocha², A. Kozub¹, T. Klimczuk¹

1. Faculty of Applied Physics and Mathematics, Gdańsk University of Technology, Gdańsk, Poland

2. Faculty of Physics and Applied Computer Science, AGH Univeristy of Science and Technology, Kraków, Poland

A polycrystalline sample of La₃Co was synthesized by arc-melting of stoichiometric amount of lanthanum (purity 99.9%) and cobalt (purity 99.95%) and annealed at 500 degrees Celsius for three weeks. Physical properties were studied by measuring susceptibility, specific heat and resistivity. The temperature dependence of resistivity above transition temperature ($T_c=6$ K) discloses a metallic-like character ($d\rho/dT>0$). The residual resistivity ratio is $\rho_{(300K)}/\rho_{(8K)}=6$. Traces of unreacted lanthanum metal is detected by a sudden drop of resistivity below $T_c=6$ K. The second, sharp drop of $\rho(T)$ at 4.65 K is associated with the transition of La₃Co to the superconducting state. By plotting H_{c2} versus T and using the WHH expression we obtained upper critical field $\mu_0 H_{c2}=3.5$ T, that implies the superconducting coherence length $\xi_0=10$ nm. A clear heat capacity anomaly is observed below a transition temperature $T_c = 4.44$ K and confirms bulk superconductivity of La₃Co. The results of measuring the specific heat in magnetic field 3 T determined Sommerfeld coefficient $\gamma=31.1$ mJ mol⁻¹ K⁻² and Debye temperature $\theta_D=133$ K. The electron-phonon coupling constant estimated from the inverted McMillan formula (where $\mu^*=0.13$) was $\lambda_{ep}=0.82$. Using γ and the specific-heat-jump value $\Delta C/T_c$ at the superconducting transition temperature, we estimated $\Delta C/\gamma T_c$, suggesting intermediate-coupling superconductivity. Estimated value of zero-temperature lower critical field, complying the demagnetization factor $\mu_0 H_{c1}(0)=17.6$ mT. Using obtained values we calculated a Ginzburg-Landau superconducting penetration depth $\lambda_{GL}(0)=162$ nm. The Ginzburg-Landau parameter is $\kappa=16.7$, indicating that La₃Co is a II-type superconductor. We estimated the thermodynamic critical field $\mu_0 H_c=148$ mT.

Mo.A-P97 - K-doping effect in Ba_{1-x}K_xFe₂As₂ studied by x-ray emission and absorption spectroscopyS. Lafuerza Bielsa¹, L. de' Medici¹, F. Hardy², T. Wolf², C. Meingast², H. Wen³, P. Glatzel¹

1. ESRF (European Synchrotron Radiation Facility), Experiments Division, Beamline ID26

2. Karlsruhe Institut für Technologie, Institut für Festkörperphysik, Karlsruhe, Germany

3. Center for Superconducting Physics and Materials, National Laboratory of Solid State Microstructures & Department of Physics, Nanjing University, Nanjing, China

Since superconductivity was discovered in the layered iron arsenides Ba_{1-x}K_xFe₂As₂ by partial substitution of Ba²⁺ with K⁺ [1] i.e., by hole doping in the (FeAs)_z layers, these compounds have received a great deal of attention as they show a high transition temperature ($T_c \approx 38$ K for $x = 0.4$). Recently, a new scenario of selective Mott physics has been found to agree with and disentangle a wealth of experiments on mass enhancements in electron- and hole-doped BaFe₂As₂ [2]. Within this framework, Mott correlations increase with hole-doping and accordingly the fluctuating local moments in the paramagnetic phase are also expected to build up.

A direct method to probe the local magnetic moment is the core-to-core (CTC) K β x-ray emission spectroscopy (XES) technique, sensitive to the 3d spin due to the intra-atomic 3p-3d exchange interaction. We have then applied CTC Fe K β XES to obtain the evolution of the Fe local moment with K-doping in Ba_{1-x}K_xFe₂As₂. The experiment was carried out at beamline ID26 of the European Synchrotron Radiation Facility (ESRF) at room temperature on single crystals covering the range $0 \leq x \leq 1$. Besides, valence-to-core (VTC) Fe K β XES and high-energy resolution fluorescence-detected x-ray absorption near edge structure (HERFD-XANES) spectra at the Fe K-edge were also collected to characterize the Fe local electronic structure.

The CTC K β XES spectra indicate a monotonic increase of the Fe local spin moment upon K-doping which is, however, smaller than reported for other iron-based superconductors [3]. On the other hand, the VTC K β XES and HERFD-XANES spectra reflect an enhancement in the hybridization between As and Fe occupied and unoccupied states respectively with increasing K content. The observed small magnetic moment increase in hole-doped BaFe₂As₂ can thus be explained in terms of a spread of the Fe 3d orbitals due to the strong covalence.

[1] – M. Rotter *et al.*, Physical Review Letters 101, 107006 (2008)[2] – L. De Medici *et al.*, Physical Review Letters 112, 177001 (2014)[3] – H. Gretarsson *et al.*, Physical Review B 84, 100509(R) (2011)

Mo.A-P98 - Superconducting versus non-superconducting FeTe_{0.6}Se_{0.4} single crystals in high magnetic fields

K. Prokes¹, S. Hartwig¹, S. Wurmehl², E. Kampert³, J. Law³, T. Foerster³, C. Hess², M. Sculze², S. Landsgesell¹, B. Buechner²

1. Helmholtz-Zentrum, Berlin, Germany

2. IFW, Dresden, Germany

3. HZDR, Dresden, Germany

FeTe_{1-x}Se_x system, abbreviated in the literature as “11” represents structurally the simplest iron based system. These materials are rather unusual exhibiting huge upper critical fields that can be well above the Bardeen-Cooper-Schrieffer (BCS) paramagnetic limit, above which the pair-breaking Zeeman energy exceeds the binding energy of the Cooper pair. Recently, it has been noticed that samples prepared in different ways (starting from the same nominal composition) show physical properties that vary significantly. In this contribution we concentrate on the x=0.40 system. The two single crystal types have been prepared with a different cooling protocol. The fast-cooled sample shows superconductivity (SC) below 18 K but is on a microscopic scale inhomogeneous consisting from a matrix and large precipitates. The slowly cooled sample is of better crystalline quality, homogeneous but does not show SC down to 2 K. Excess of the interstitial iron within the matrix of the inhomogeneous crystal and within the homogeneous one is around 3 %. We have performed a series of high-field magnetoresistance and magnetization measurements on both types of crystals. The inhomogeneous sample exhibits H_{c2}(0)=45 (2) T for both field orientations. Anomalies connected with the destruction of the SC state by magnetic field are more pronounced for the a-axis direction than for the c-axis direction. The critical field decreases with the increasing temperature and for 16 K no anomaly could be observed. No significant anisotropy has been detected. Also for the homogeneous sample we have observed some traces of SC behavior. However, in overall, magnetoresistance curves for this sample show much smaller field variations pointing to only traces of SC phase in this sample. Thus, a very surprising result is observed: crystallographically homogeneous FeTe_{0.6}Se_{0.4} system appears to be non-superconducting in contrast to a multiphase system.

Mo.A-P100 - Superconducting properties and pseudogap from preformed Cooper pairs in the triclinic $(\text{CaFe}_{1-x}\text{Pt}_x\text{As})_{10}\text{Pt}_3\text{As}_8$

M. Surmach¹, Felix Brückner¹, S. Kamusella¹, R. Sarkar¹, P. Portnichenko¹, J. Park², G. Gambashidze³, H. Luetkens⁴, P. Biswas⁴, W. J. Choi⁵, Y.I. Seo⁵, Y.S. Kwon⁵, H. Klauss¹, D. Inosov¹

1. Technische Universität Dresden, Dresden, Germany

2. MLZ, Garching, Germany

3. MPI, Stuttgart, Germany

4. PSI, Villigen, Switzerland

5. DGIST, Daegu, Republic of Korea

Using μSR , INS and NMR, we investigated the novel Fe-based superconductor with a triclinic crystal structure $(\text{CaFe}_{1-x}\text{Pt}_x\text{As})_{10}\text{Pt}_3\text{As}_8$ ($T_c = 13$ K). The T -dependence of the superfluid density from the μSR measurements indicates the presence of two superconducting gaps. Our INS data revealed commensurate spin fluctuations at the $(\pi, 0)$ wave vector. Their intensity remains unchanged across T_c , indicating the absence of a spin resonance typical for many Fe-pnictides. Instead, we observed a peak around $\omega_0 = 7$ meV at the same wave vector, which persists above T_c and is characterized by the ratio $\omega_0/k_B T_c \approx 6.2$, i.e. significantly higher than typical values for the magnetic resonant modes in iron pnictides (~ 4.3). The T -dependence of magnetic intensity at 7 meV revealed an anomaly around $T^* = 45$ K related to the disappearance of this new mode. A suppression of the spin-lattice relaxation rate, $1/T_1 T$, observed by NMR immediately below T^* without any notable subsequent anomaly at T_c , indicates that T^* could mark the onset of a pseudogap in $(\text{CaFe}_{1-x}\text{Pt}_x\text{As})_{10}\text{Pt}_3\text{As}_8$, likely associated with the emergence of preformed Cooper pairs.

Mo.A-P101 - C-axis resistivity of superconducting FeSe single crystals: upper critical field and its angular behavior

T. Romanova¹, D. Knyazev¹, A. Sadakov¹, D. Chareev²

1. *Lebedev Physical Institute of Russian Academy of Science, Moscow, Russia*

2. *Institute of Experimental Mineralogy, Russian Academy of Sciences, Chernogolovka, Moscow, Russia*

FeSe is the simplest representative of iron-based superconducting family and can be considered as a model system to study mechanism of superconductivity in this class of materials. We report out-of-plane resistivity measurements for high quality superconducting FeSe single crystals in magnetic fields up to 9 Tesla. This superconductor proved to be slightly anisotropic in terms of upper critical field H_{c2} measured by in-plane resistivity [1]. Our goal was to study temperature and angular behavior of upper critical field in the $H \parallel ab$ geometry by out-of- plane resistivity measurements. For careful studying of C-axis resistivity we used direct R_c measurement technique that doesn't demand any additional mathematical models [2]. Temperature dependence of $H_{c2} \parallel c$ is in consistency with literature [1]. Derivative dH_{c2}/dT is -5.74 T/K and estimation of $H_{c2}(0)$ (WHH theory [3]) is 35.9 T. We studied superconducting transitions $R(B)$ in different in-plane field orientation (the measuring current is always perpendicular to magnetic field. H_{c2} obtained from magnetoresistance data exhibits anisotropic behavior.

[1]S.I. Vedenev et.al. PRB 75, 064512(2007)

[2]S. I. Vedenev, et.al. PRB 87, 134512 (2013)

[3] N. R. Werthamer, E. Helfand, and P. C. Hohenberg, Phys. Rev. 147,295 (1966)

Mo.A-P102 - Investigation of the magnetic character of oxy-pnictides via Spin Dilution

S. Sanna¹, P. Carretta¹, P. Bonfà², R. De Renzi², Y. Yiu³, M. McGuire⁴, A. Huq⁵, S. Nagler⁶, G. Lamura⁷, A. Martinelli⁷, M. Putti⁷

1. *Physics Department, University of Pavia, Pavia, Italy*

2. *Department of Physics and Earth Sciences, University of Parma, Parma, Italy*

3. *Department of Physics and Astronomy, University of Tennessee, Tennessee, United States*

4. *Materials Science and Technology Division, Oak Ridge National Laboratory, Tennessee, United States*

5. *Chemical and Engineering Materials Division, Oak Ridge National Laboratory, Tennessee, United States*

6. *CIRE, University of Tennessee, Tennessee, United States*

7. *CNR-SPIN and University of Genova, Genova, Italy*

Parent compounds of many iron-based high-temperature superconductors are metallic and magnetic, with a spin density wave character. At first sight, the metallic ground state suggests that magnetism originates from the Fermi surface nesting of itinerant electrons, consistently with band structure calculations. However there are several indications that electron correlations could be important and local moments might play a significant role together with itinerant electrons for magnetic, transport and superconducting properties [1].

Here we discuss the evolution of the magnetic and structural phase diagram of $\text{LnFe}_{1-x}\text{Ru}_x\text{AsO}$ for $\text{Ln} = \text{La}, \text{Pr}$ via diamagnetic Ru for Fe spin dilution. The substitution of Ru for Fe is isoelectronic [2,3], hence allowing for investigation of the underlying physics without the complication of extrinsic modifications of the Fermi surface.

Muon spin relaxation measurements show that the Ru/Fe spin dilution directly produces a gradual disruption of magnetism which eventually disappears at the dilution threshold $x=0.6$, significantly higher than plain square bond dilution, and coinciding with the threshold for the J1-J2 frustrated square-lattice, localized spin model [2]. Neutron diffraction measurements show that the structural tetragonal-to-orthorhombic transition is a close precursor of the magnetic transition up to $x\approx 0.4$, thus indicating a relevant magneto-elastic coupling within the FeAs layers [3,4]. These results can be described in the framework of the Ising-nematic scenario predicted for localized spins in the J1-J2 model, indicating that a model of localized degrees of freedom is a proper framework to describe the magnetic character of oxy-pnictides.

[1] e.g. see : P. Dai, J.Hu, E.Dagotto *Nature Physics* 8, 709 (2012)

[2] P. Bonfà et al., *Phys. Rev. B* 85, 054518 (2012); M. Mazzani et al., *Phys. Status Solidi B* 251, 974 (2014)

[3] A. Martinelli et al., *J. Phys.: Condens. Matter* 25, 395701 (2013)

[4] Y. Yiu, S. Sanna et al., *Phys. Rev. B* 90, 064515 (2014)

Mo.A-P104 - Phase diagrams for coexistence of localised magnetism and superconductivity from a microscopic model

N. Costa^{1,2}, J. Pimentel², M. ElMassalami¹, T. Paiva¹, R. Rocha dos Santos¹

1. Instituto de Física, Universidade Federal do Rio de Janeiro, Rio de Janeiro, Brazil

2. Departamento de Física, Universidade Federal do Piauí, Teresina, Brazil

Coexistence between superconductivity and magnetism is a topic of current interest as a unifying link between heavy fermions, borocarbides, iron pnictides, and possibly the cuprates. In view of this, working models which can reproduce several aspects of this coexistence can certainly contribute to a better understanding of the mechanisms at play. Here we consider a model consisting of localised spins interacting with conduction electrons through an exchange (Kondo) coupling, while the conduction electrons themselves are subject to an on-site pairing interaction; the presence of localised moments renders this model especially suitable to describe the borocarbides. We use a Hartree-Fock approximation in which the local spins are treated semi-classically, in the sense that their average values are modulated by a three-dimensional magnetic wavevector Q while the coupling with the conduction electrons is described in terms of fermion operators. This approach led us to obtain spiral magnetic phases with modulation wavevector depending on the coupling constants as well as on the conduction electron density, and on the temperature. We have found that for a range of parameters these spiral phases can coexist with an s-wave superconducting phase. Our main results are summarised as slices of the phase diagram, showing temperature vs. pairing interaction, temperature vs. Kondo coupling, and temperature vs. doping. For suitable combinations of the Hamiltonian parameters, these diagrams are in good agreement with experimental results for the borocarbides, obtained for different rare-earth elements, keeping the same transition metal, as well as for alloying the transition metal, for a given rare-earth element; in the latter case, the sequence of magnetic modes is adequately described by our model.

Mo.A-P107 - Superconductivity in YPt₂Si₂A. Pikul¹, G. Chajewski¹, P. Wiñniewski¹, M. Samsel-Czeka¹, D. Kaczorowski¹*1. Institute of Low Temperature And Structure Research, Polish Academy of Sciences, Warsaw, Poland*

The RT₂M₂ intermetallic phases (where R is a lanthanide or actinide, T – a transition or noble metal, and M – a *p*-electron element) are known to crystallize in two closely-related derivatives of the tetragonal BaAl₄-type structure: a non-centrosymmetric primitive one of the CaBe₂Ge₂-type (space group P4/nmm) and a body-centered one of the ThCr₂Si₂-type (space group I4/mmm). As shown by Shelton et al. [1], the primitive unit cell consistently favors superconductivity over the body-centered one (at least in experiments performed above 1.1 K). The main aim of our work was to examine this relationship between crystal structure and physical behavior in an extended series of Y-, La-, and Th-based RT₂M₂ phases. Here we present preliminary results obtained for YPt₂Si₂.

A polycrystalline button of YPt₂Si₂ was prepared by arc melting. Subsequently, half of it was annealed at 850°C for one week. X-ray powder diffraction revealed that both the as-cast fragment and the annealed one crystallize with the CaBe₂Ge₂-type structure (the lattice parameters for the latter are: $a = 4.1594(1)$ Å and $c = 9.8039(3)$ Å). Magnetic susceptibility, electrical resistivity and specific heat measurements, performed down to 0.35 K, showed that the as-cast sample becomes superconducting below about 1.7 K, while the annealed one at about 1.6 K, in agreement with the previous report [1]. Quantitative analysis of the magnetic susceptibility and specific heat data showed that the superconductivity in YPt₂Si₂ has a bulk character. Experiments performed in magnetic fields revealed that the transition can be suppressed by applying about 0.1 T for the as-cast specimen, and about 0.05 T for the annealed one.

[1] R. N. Shelton, H. F. Braun, W. Musick, Solid State Commun. 52 (1984) 797

Mo.A-P108 - Field-dependence of charge order in the cuprate high-temperature superconductor La_{2-x}Sr_xCuO₄

B. Lake^{1,2}, E. Schierle¹, E. Weschke¹, K. Siemensmeyer¹

1. Helmholtz Zentrum Berlin Für Materialien Und Energie, Berlin, Germany
2. Technical University Berlin, Berlin, Germany

In the cuprate high-T_c superconductors a number of competing and co-existing phases are present and their role in the mechanism of high-T_c superconductivity is still a matter of debate. The most important of these phases are spin and charge order whose origins have been related to stripe formation or Fermi surface nesting. While incommensurate spin fluctuations were observed in the optimally doped La_{2-x}Sr_xCuO₄, static spin order was observed in underdoped La_{2-x}Sr_xCuO₄. These features are altered by the onset of superconductivity e.g. the appearance of a spin gap in the fluctuations and the enhancement of static order. The effect of magnetic field on the magnetism has also been explored and found to enhance the fluctuations and spin order while partially suppressing the superconductivity. Charge order has also been found in a number of underdoped cuprates superconductors. The charge order is observed as incommensurate peaks around the nuclear Bragg positions with twice the incommensurate wavevector as for the magnetic peaks. They appears gradually at temperatures well above T_c and unlike the spin order, show a clear change at the superconducting transition temperature below which they become suppressed. We have investigated the charge order in underdoped La_{2-x}Sr_xCuO₄ (x=0.11, T_c=29K) using resonant soft X-ray diffraction. We find that charge peaks appear at ~60K and gradually increase with decreasing temperature down to T_c=29K below which they become partially suppressed. We have further investigated the effect of an applied magnetic field of 6T (parallel to the out-of-plane c direction) on the charge order. We show that the superconductivity-induced suppression is reversed by the field and that the charge peaks continue to increase below T_c for fields up to 6T. These results demonstrate the strong competition between charge order and superconductivity.

Mo.A-P109 - The high pressure - low temperature structural phase diagram of $K_xFe_{2-y}Se_2$

T. Giles¹, J. Poulten¹, M. Gamza¹, D. Daisenberger², H. Wilhelm², X. Chen³, P. Niklowitz¹

1. Royal Holloway, University of London, Egham, Surrey, United Kingdom

2. Diamond LightSource, Harwell Science and Innovation Campus, Didcot, United Kingdom

3. Hefei National Laboratory for Physical Sciences at Microscale and Department of Physics, University of Science and Technology of China, Hefei, People's Republic of China

There has been significant interest in Fe-based superconductors due to their high critical temperatures. Some iron-chalcogenide parent compounds display antiferromagnetic Mott insulating behaviour similar to the Cuprates. $K_xFe_{2-y}Se_2$ exhibits antiferromagnetism with $T_N \sim 550K$. The antiferromagnetic transition appears to be closely coupled to a structural transition which has been identified as the onset of an Fe-vacancy order. With careful tuning of the Fe-valence by varying x and y a superconducting phase can be reached [1]. High pressure measurements [2,3] show the Mott insulating state and superconductivity to be suppressed gradually before completely disappearing at a critical pressure of about 9 GPa. A second superconducting phase emerges on further increase of pressure, with a higher critical temperature.

In this work high pressure and low temperature x-ray powder diffraction was performed on insulating and superconducting samples of $K_xFe_{2-y}Se_2$ using a diamond anvil cell to investigate any correlation between the superconducting phase diagram and the structural properties. In particular we focused on the Fe-vacancy order transition, which was known to be located at about 9 GPa at room temperature [2]. Our measurements show that the Fe-vacancy order transition is pushed to slightly higher pressures at low temperatures and occurs near the onset of the second superconducting phase emphasizing the relevance of the Fe-vacancy order for the superconducting phase diagram of $K_xFe_{2-y}Se_2$.

[1] Y. J. Yan *et al.* Sci. Rep. 2 212 (2012)

[2] J. Guo *et al.* Phys. Rev. Lett, 108 197001 (2012)

[3] P. Gao *et al.* Phys Rev B, 89 094514 (2014)

Mo.A-P111 - Elastic softening and phase transition characteristics in YbPtGe

X. Xi¹, I. Ishii¹, Y. Noguchi¹, H. Goto¹, S. Kamikawa¹, K. Araki², K. Katoh², T. Suzuki¹

1. Hiroshima University, Hiroshima-Shi, Japan

2. National Defense Academy, Yokosuka, Japan

YbPtGe with the orthorhombic ϵ -TiNiSi-type structure is reported as a heavy-fermion ferromagnet with $T_c = 5.4$ K. Recent researches suggested its magnetic anisotropy can be ascribed to the crystal electric field (CEF) effect which acts on the eight-fold multiplet of the Yb^{3+} ion. In order to clarify the CEF effect and investigate the magnetic phase transition in this compound, ultrasonic measurements of YbPtGe and related theoretical calculation have been performed. The transverse elastic modulus C_{66} exhibits a softening characteristic with a peak of 180 K while the longitudinal modulus C_{33} mode shows a continuous hardening during all temperature range. According to the theoretical strain-susceptibility fitting of the transverse elastic modulus by the CEF parameter obtained from Katoh's research [1], we argue that the softening at higher temperature range ($>50\text{K}$) as the result of quadrupole interaction between the ground and excited Kramers doublets of CEF. With further decrease the temperature below T_c , C_{66} mode exhibits a step-like softening phenomenon which is quite different from that of C_{33} mode and the possible mechanism of this was discussed.

[1] K Katoh *et al.*, J. Phys. Soc. Jpn. 78 (2009) 104721

Mo.A-P112 - Fermi Surface measurement of TiNi_2Se_2 by quantum oscillations

X. Chen¹, H. Tan¹, S. K. Goh^{1,2}, P. Reiss¹, H. Wang³, Q. Mao^{3,4}, J. Yang⁴, M. Fang³, M. Sutherland¹

1. University of Cambridge, Cambridge, United Kingdom
2. The Chinese University of Hong Kong, Hong Kong, China
3. Zhejiang University, Hangzhou, China
4. Hangzhou Normal University, Hangzhou, China

TiNi_2Se_2 is a recently discovered nickel-chalcogenide superconductor ($T_c = 3.7\text{K}$). Measurements of the electronic heat capacity have revealed a Sommerfeld coefficient of $\gamma \sim 40\text{mJ/mol K}^2$, indicating an unusually large effective mass of $14 - 20 m_e$ [1]. Several important questions regarding this material, such as the pairing symmetry and its relations to the iron based superconductors and the cuprates are the subject of debate [1, 2]. Using the Shubnikov-de Haas technique, we report preliminary measurements of quantum oscillations in TiNi_2Se_2 . We compare our results to the expected Fermi surface obtained using band structure calculations in the LDA approximation. Measurements of the effective mass of the cyclotron orbits shed light on the possibility of heavy Fermion behavior in this material.

- [1] Wang, H. *et al.* Multiband Superconductivity of Heavy Electrons in a TiNi_2Se_2 Single Crystal. *Phys. Rev. Lett.* **111**, 207001 (2013)
- [2] Hong, X. C. *et al.* Multigap nodeless superconductivity in nickel chalcogenide TiNi_2Se_2 . *Phys. Rev. B* **90**, 060504 (2014)

Mo.B-P02 - Unusual magnetic ground states of novel $S = 1/2$ square-lattice antiferromagnets $\text{Sr}_2\text{NiO}_3\text{X}$ ($X = \text{F}, \text{Cl}$)

Y. Tsujimoto¹, K. Yamaura¹, T. Uchikoshi¹, T. Haku², T. Masuda²

1. National Institute For Materials Science, Tsukuba, Japan

2. Institute of Solid State Physics, The University of Tokyo, Tokyo, Japan

We present unusual magnetic properties of new quantum-spin square-lattice antiferromagnets, $\text{Sr}_2\text{NiO}_3\text{X}$ ($X = \text{F}, \text{Cl}$), synthesized by high-pressure technique. These compounds adopt K_2NiF_4 -type structure, but the preferential occupation of the halide ions at the apical positions causes the Ni center to take a square pyramidal coordination with five oxygen atoms. The nickel cation has the tri-valence state with low-spin state of $S = 1/2$. Interestingly, although these present compounds have a positive Weiss temperature, an antiferromagnetic ordering at 11 K takes place for $X = \text{Cl}$, and a spin freezing transition at 11 K for $X = \text{F}$. We discuss the magnetic ground states on the basis of a J_1 - J_2 model with AFM nearest neighbor (NN) interactions and FM 2nd NN interactions.

Mo.B-P03 - Valley-spin locked, tunable super-current transport in superconductor / normal silicene or germanene/ superconductor junction

P. Goswami¹

1. D.B. College, University of Delhi, Delhi, India

We start with the reduced silicene/germanene single-particle Hamiltonian in buckled 2D hexagonal lattice expressed in terms of Pauli matrices associated with the pseudo-spin. In these systems, where the Hamiltonian comprises of the Dirac kinetic energy, the spin-orbit coupling, and a mass term, the latter breaks the sub-lattice symmetry of the system's honeycomb structure and generates spin-split band gap with the help of the spin-orbit coupling. The buckled lattice generates a staggered sub-lattice potential between silicon atoms at A sites and B sites for an applied electric field E_z perpendicular to its plane. The physics of the system in the normal state is determined by two Dirac-like cones at K and K' points. By tuning E_z , one attains a critical value at which the system at the topological insulating phase goes to a semi-metal state where the 'spin down' upon the 'spin-up' band gap ratio (r) $\ll 1$ for the valley K, and $r \gg 1$ for the valley K'. This state is termed as the 'valley-spin-polarized-metal' (VSPM) due to the opposite spin-polarization of the K and K' valleys. The combination of a s-wave superconducting proximity effect with VSPM is the focal point of this communication due to the possibility of creating Majorana fermions in this manner. We briefly discuss the possibility of the majorana hosting in this scenario. We also focus on the signature of both local and crossed Andreev reflection process. We show that the super-current flowing in the superconductor /normal/ superconductor junction is in pure VSPM state and completely tunable by E_z . This finding, together with the fact that the Andreev reflection process is fully valley-spin polarized, show that silicene/germanene provide a remarkable platform for tunable super-current transport.

Mo.B-P04 - Nonlinear dielectric susceptibility in a multiferroic quantum magnet Sul-Cu₂Cl₄K. Povarov¹, A. Reichert¹, E. Wulf¹, A. Zheludev¹*1. Neutron Scattering And Magnetism, Laboratory For Solid State Physics, Zurich, Switzerland*

A $S=1/2$ spin tube Sul-Cu₂Cl₄ is a material, belonging simultaneously to the domains of quantum magnetism and multiferroicity. Being a highly frustrated gapped spin-liquid, it enters a helimagnetically ordered multiferroic phase as a result of magnetic field-induced quantum phase transition [1,2]. Previous measurements have already verified the presence of dielectric anomaly at the high-temperature phase transition boundary [3]. Our investigation shows that contrary to expectations dielectric susceptibility exhibits no criticality in the low-temperature limit. This implies the electric polarization itself is not an ordering parameter of the transition. The dielectric anomaly is studied in a wide range of temperatures and magnetic fields, down to 50 mK and up to 14 T. We track the phase boundary with a high precision and determine a crossover exponent of the phase transition to be $3/2$. This is consistent with the Bose-Einstein condensation universality class of the quantum phase transition, typical for the field-induced magnetic order in gapped quantum magnets. However, we observe an unexpected intrinsic nonlinearity in the dielectric susceptibility above the critical magnetic field. This nonlinearity manifests itself, for example, in generation of higher harmonics of the displacement current under applied radiofrequency voltage. Higher-order susceptibilities, appearing in the ordered phase, are determined from the displacement current harmonics. It is worth mentioning that in principle the anomaly in dielectric susceptibility of Sul-Cu₂Cl₄ is very small compared to most other multiferroic materials. This makes the highly pronounced nonlinear behavior even more surprising. Understanding this nonlinearity remains a challenge for the theory.

[1] V. Garlea et al., Phys. Rev. B 79 060404 (2009)

[2] A. Zheludev et al., Phys. Rev. B 80 214413 (2009) [3] F. Schrettle et al., Phys. Rev. B 87 121105 (2013)

Mo.B-P05 - Magnetic structure of quasi-one-dimensional frustrated antiferromagnet Cu₃Mo₂O₉

M. Hase¹, H. Kuroe², V. Pomjakushin³, L. Keller³, R. Tamura¹, N. Terada¹, Y. Matsushita¹, A. Doenni¹, T. Sekine²

1. National Institute For Materials Science (NIMS), Tsukuba, Japan

2. Sophia University, Tokyo, Japan

3. Paul Scherrer Institut (PSI), Villigen, Switzerland

Frustrated spin chains provide grounds for studies of exotic quantum phases caused by combination of frustration and quantum fluctuation. We have paid our attention to Cu₃Mo₂O₉. The spin system consists of antiferromagnetic (AF) uniform spin-1/2 chains and AF spin-1/2 dimers. Chains and dimers are connected and magnetic frustration appears. This cuprate exhibits both AF long-range order with tiny ferromagnetic components and electric polarization below the transition temperature $T_N = 7.9$ K. The ferromagnetic components appear only in finite magnetic fields parallel to the a or c axis. The ferromagnetic behavior disappears by slight substitution of Zn (0.2 %) for Cu sites. Several phase transitions and 2/3 magnetization plateau appear in magnetic fields. To understand these results, we determined the magnetic structure of Cu₃Mo₂O₉ in neutron powder diffraction experiments. Spins in chains are nearly disordered, whereas magnetic moments in dimers are ordered. Probably, magnetic frustration generates the partial disordered state. The space group at room temperature was considered to be orthorhombic Pnma (No. 62). From the previously reported electric polarization and the present observation of reflections forbidden in Pnma in X-ray powder diffraction experiments at room temperature, the exact space group must be monoclinic P2₁/m (No. 11) that is one of subgroups of Pnma. The ferromagnetic behavior in magnetic fields parallel to the a or c axis is possible in the magnetic structure..

Mo.B-P06 - Magnetic ground state of novel zigzag chain compounds, NaCr2O4 and Ca1-xNaxCr2O4, determined with muons and neutrons

J. Sugiyama¹, H. Nozaki¹, M. Harada¹, Y. Higuchi¹, H. Sakurai², E. Ansaldo³, J. Brewer^{4,5}, L. Keller⁶, V. Pomjakushin⁶, M. Mansson⁷

1. Toyota Central Research & Development Laboratories, Inc., Nagakute, Japan

2. National Institute for Materials Science (NIMS), Tsukuba, Japan

3. University of Saskatchewan, Saskatoon, Canada

4. University of British Columbia, Vancouver, Canada

5. TRIUMF, Vancouver, Canada

6. Paul Scherrer Institut, Villigen, Switzerland

7. KTH Royal Institute of Technology, Stockholm, Sweden

One-dimensional (1D) systems offer an intriguing example as relatively simple systems that display interesting magnetic phenomena and complex phases. This is in large part due to the competition between nearest-neighbor (intra-chain) and next-nearest-neighbor (inter-chain) interactions. Recently, the field of geometrically frustrated materials has been driven by the synthesis and discovery of new compounds in which the frustration can be tuned, particularly due to the progress of a high-pressure synthesis technique. Here, we report the results of muon-spin rotation and relaxation (μ SR) and neutron diffraction (ND) experiments on 1D zigzag-chain compounds, Ca_{1-x}Na_xCr₂O₄ [1], which is a solid solution system between CaCr₂O₄ and NaCr₂O₄. Both compounds possess a CaFe₂O₄-type Pnma structure. In the Ca_{1-x}Na_xCr₂O₄ lattice, the Cr₂O₄ double-chains, which are formed by a network of edge-sharing CrO₆ octahedra, align along the b-axis so as to make an irregular hexagonal one-dimensional (1D) channel. The end member compound, novel NaCr₂O₄ [1], is found to enter into an antiferromagnetic ordered state below T_N=124 K. The combined analyses both for the μ SR and ND data provides a unique spin structure including a canting angle of the Cr moments [2]. On the other hand, the other end member compound, CaCr₂O₄, μ SR measurements reveal the formation of a complex magnetic order below T_N=21 K, being consistent with an incommensurate AF proposed by neutron [3]. Moreover, we have studied the x=0.5, 0.75, and 0.85 samples to determine the variation of internal magnetic fields with x.

[1] H. Sakurai, Phys. Rev. B 89, 024416 (2014)

[2] H. Nozaki et al., Meeting Abstracts of Phys. Soc. Jpn. 68-1, 606 (2013)

[3] H. Sakurai et al., Angew. Chem. Int. Ed. 51, 6653 (2012)

[4] F. Damay et al., Phys. Rev. B 81, 214405 (2010)

Mo.B-P07 - Spin pseudogap in doped $S = 1/2$ Heisenberg antiferromagnetic spin chains

G. Simutis¹, S. Gvasaliya¹, A. Mohan², C. Hess², B. Büchner², A.L. Chernyshev³, I. Zaliznyak⁴, N. S. Beesetty⁵, A. Revcolevschi⁵, A. Zheludev¹

1. *ETH Zürich, Zürich, Switzerland*
2. *IFW Dresden, Dresden, Germany*
3. *University of California, Irvine, United States*
4. *Brookhaven National Laboratory, Upton, United States*
5. *ICMMO, Université Paris-Sud, Orsay cedex, France*

Due to the topology of one-dimensional objects, impurities always play an important role in their physical properties. An interesting case is the $S = 1/2$ Heisenberg antiferromagnetic spin chains with high exchange constant - SrCuO₂ and Sr₂CuO₃ - which were recently shown to exhibit an energy pseudogap in spin excitation spectrum upon introduction of impurities [1,2]. In an earlier study, we used neutron spectroscopy to obtain quantitative information about the effect of the Ni-doping in a spin chain material SrCuO₂ [2]. This material has a double-chain structure where the chains are arranged in pairs and coupled via weak and geometrically frustrated interactions. We suggested a model based on a theoretical study of broken chains [3] which explained the data very well and reproduced the universal scaling behavior.

In order to clarify the role of the double chain in the spin pseudogap physics, we performed a neutron scattering study on a Ni-doped single-chain material Sr₂CuO₃. The role of the double chain was found to be related to the number of effective chain breaks. The proposed model was found to explain the observations in both the single and double chain materials in a broad temperature range. An extended neutron scattering study of both materials will be presented.

[1] Hammerath et al., PRL 107, 017203 (2011) and PRB 89, 184410 (2014)

[2] Simutis et al, PRL 111 , 067204 (2013)

[3] Eggert et al, PRB 46 10866 (1992)

Mo.B-P08 - Influence of sample quality on the physical properties of the S=1 antiferromagnetic spin-ladder CaV(2)O(4)

S. Hiller¹, S. Guitarra¹, A. Caneiro², M. Salamon³, [D. Niebieskikwiat](#)¹

1. *Universidad San Francisco de Quito, Quito, Ecuador*

2. *Instituto Balseiro - Centro Atómico Bariloche, Bariloche, Argentina*

3. *University of Texas at Dallas, Richardson, United States*

In this work we study the magnetic and transport properties of different CaV(2)O(4) samples. This compound presents quasi one-dimensional (1D) V chains, with an antiferromagnetic (AFM) S=1 spin-ladder ground state. Due to this 1D characteristic, it is expected that the physical properties of CaV(2)O(4) are very sensitive to impurities, defects, and disorder in general. Indeed, different previous works show dissimilar results about the magnetic response of this vanadium-oxide. Here, we present results on samples prepared by different methods and conditions (solid-state and wet-chemical routes), showing the influence of the sample quality and preparation protocol on the physical properties of this material. Not only the magnetic and electric properties depend on the sample quality, also one of the important findings is that the nitrate decomposition route produces samples with a higher order temperature.

Mo.B-P09 - Low dimensional magnetism induced by chalcogen ordering.

M. Valldor¹, S. Huh^{1,2}, E. J. Hopkins^{1,2}, Y. Prots¹, P. Adler¹, U. Brukhardt¹, Y. Watier³, Z. Hu¹, C.-Yang Kuo¹, J. Chiang¹, T. Pi⁴, A. Tanaka⁵, L. Tjeng¹

1. Max Planck Institute For Chemical Physics of Solids, Dresden, Germany

2. University of British Columbia, Vancouver, Canada

3. ESRF, The European Synchrotron, Grenoble, France

4. Institute of Physics, National Chiao Tung University, Hsinchu, Taiwan

5. Department of Quantum Matter, ADSM, Hiroshima University, Higashi-Hiroshima, Japan

Today's solid state research focuses mostly on cations and treats anions as a homogenous matrix. Here, we follow a different approach. By designing the anionic lattice in materials, the ordering of two or more anions leads to the formation of anionic superstructures. The anionic order causes different environments, in which cations dwell. The position of a certain cation will now depend on its nature. A soft/hard cation will try to enter a site, neighboring as many soft/hard anions as possible, according to the HSAB rule. Moreover, if mixed valence is expected for the cation, a charge order might occur where a low/high oxidation states will choose soft/hard anions as next neighbors. Locally, the cations can be found with completely new coordination, often cancelling the local inversion symmetry and allowing for magneto-electric coupling. To exemplify this, spin-ladder compounds $A\text{Fe}_2\text{Ch}_2\text{O}$ ($A\text{E} = \text{Sr}, \text{Ba}$, $\text{Ch} = \text{S}, \text{Se}$) were synthesized having iron magnetically coupled along the ladders via Ch and over the rungs via O, which is different from the pure selenide or an oxide spin-ladder. Further, the heteroleptic coordination of iron causes an unusual electric field gradient to appear. The spin-spin coupling strengths and transition temperatures on these ladders are dependent on AE and Ch. A second example is $\text{Ba}_3\text{V}_2\text{S}_4\text{O}_3$, which possesses a quasi-one-dimensional atomic lattice due to ordering of S and O, where also a charge disproportionation coincides with the coordination of vanadium. Hence, V^{3+} ($S = 1$) is found in columns of face sharing VS_6 trigonal antiprisms, while O is found only next to V^{5+} . Although no long ranged spin order is observed, broad magnetic features are visible at high temperatures, probably related to spin excitations in the one-dimensional spin system. The structural polarity, as induced by the non-centrosymmetric crystal structure might play a role.

Mo.B-P11 - Quasi one dimensional magnetism in Mn_{1-x}Fe_xNb₂O₆ compounds

M. Hnedá^{1,2,3}, J. Cunha³, M. Gusmão³, O. Isnard^{1,2}

1. Institut Néel du CNRS, Grenoble, France

2. Université Grenoble Alpes - Joseph Fourier, Grenoble, France

3. Instituto de Física, Universidade Federal do Rio Grande do Sul, Porto Alegre, Brazil

Physical properties of ANb₂O₆ have attracted much interest due to their quasi-one dimensional magnetic behavior. The structure can be viewed as a stacking of slightly tilted oxygen octahedra surrounding the ions, forming zigzag chains along the c axis. In this work, we concentrate on the Mn_{1-x}Fe_xNb₂O₆ compounds (0 < x < 1) that present orthorhombic Pbcn crystal symmetry and exhibit the presence of weakly coupled chains. Several samples are investigated by both X-ray and neutron powder diffraction, specific heat and magnetic measurements. The cation chains are Heisenberg type (weak anisotropy) for Mn and Ising like chains (strong anisotropy) for Fe. In addition opposite behavior occurs in the extreme compounds since for A=Mn it is observed a negative Curie-Weiss temperature indicating dominant antiferromagnetic interactions. On the contrary, A=Fe shows a positive Curie-Weiss temperature which suggests dominating ferromagnetism coupling. Due competing interactions between the magnetic ions different magnetic structures can be obtained. MnNb₂O₆ presents a magnetic structure characterized by a propagation vector $k=(0,0,0)$ and FeNb₂O₆ by $k=(0,1/2,0)$ and $(1/2,\pm 1/2,0)$. We thus use the substitution of magnetic cations to change the interatomic distances and modify the exchange interactions between the magnetic ions both intra and inter magnetic chains. Specific heat measurements are presented down to 1.8K and discussed in the light of magnetic measurements and compared to results of neutron diffraction data.

Mo.B-P12 - Magnetic properties of quasi one-dimensional antiferromagnet BaCo₂Si₂O₇

M. Akaki¹, A. Okutani¹, D. Yoshizawa¹, H. Kuwahara², M. Hagiwara¹

1. *Center For Advanced High Magnetic Field Science, Graduate School of Science, Osaka University, Osaka, Japan*

2. *Department of Physics, Sophia University, Tokyo, Japan*

One-dimensional antiferromagnetic spin systems are known to exhibit various exotic magnetic properties caused by quantum fluctuations. The compounds with Co²⁺ under an octahedral crystal field are sometimes regarded as a fictitious spin (S) 1/2 one-dimensional Ising-like antiferromagnet. In contrast, the compounds with Co²⁺ ions under a tetrahedral crystal field usually show a Heisenberg-type magnetism with S = 3/2. In this study, we have investigated magnetic properties of quasi one-dimensional antiferromagnet BaCo₂Si₂O₇ single crystal in high magnetic fields. In BaCo₂Si₂O₇, CoO₄ tetrahedra are connected at their corners to form chains running along the c axis. BaCo₂Si₂O₇ shows a weak ferromagnetism below the Néel temperature T_N = 21 K [1, 2]. At 4.2 K, a large magnetic anisotropy was observed in the magnetization process measured in a pulsed high magnetic field. Below 13 T, the slope of the magnetization curve parallel to the c axis is smaller than that perpendicular to the c axis. This result suggests that the c axis is a magnetic easy axis. On applying magnetic fields further along the c axis, some magnetization jumps were observed around 14 T. These results suggest that BaCo₂Si₂O₇ shows an easy-axis magnetic anisotropy, and thus can be regarded as a one-dimensional Ising-like antiferromagnet. We will also present the experimental results of magnetostriction and electron spin resonance measurements of BaCo₂Si₂O₇ and discuss its magnetic properties.

[1] R. D. Adams et al., *Inorg. Chem.* 35, 3492 (1996)

[2] M. Akaki et al., *Physica B* 403, 1505 (2008)

Mo.B-P13 - Quantum coherence of strongly correlated defects in spins chainsS. Bertaina¹, C. Dutoit¹, J. Van Tol², M. Dressel³, B. Barbara⁴, A. Stepanov¹

1. Aix-Marseille Université, CNRS, IM2NP UMR7334, Marseille, France

2. NHMFL, FSU, Tallahassee, United States

3. Physikalisches Institut Universität Stuttgart, Stuttgart, Germany

4. Institut Neel, CNRS, Grenoble, France.

The coherence phenomenon of electron spin has attracted a great interest for the last decade due to its potential application for quantum information processing. Usually, electron spin qubits are made of paramagnetic impurities [1-4], which lose their coherence because of the environment interactions (spin bath, photon bath). Hereby we will present a completely new concept in the domain of quantum information. In Heisenberg spin chains, a non magnetic defect polarizes the surrounding spins and creates a quantum trapped soliton of total spin $S=1/2$. Since the correlated defect belongs to the chain, the isotropic Heisenberg exchange protects the correlated defect from the environment and highly reduces the loss of quantum memory. Using electron paramagnetic resonance (EPR), we observed the signal coming from quantum defects in the organic Heisenberg spin $S=1/2$ chain (TMTTF)₂X (X=PF₆,AsF₆ or SbF₆). The signal contains two lines: a main line (ML) from the uniform spin chain and a very sharp line (SL) attributed to the correlated defects. The linewidth of SL, about 0.1G, is one of the smallest ever observed in correlated impurities. The anisotropy of the g-factor of SL is exactly the same as that of ML and the intensity of SL doesn't follow the Curie behaviour of an isolated paramagnetic impurity. Using time domain EPR, we observed quantum coherence (Rabi oscillations) of strongly correlated defects in (TMTTF)₂PF₆ (preliminary results can be found here [5]). In this presentation, we will discuss the coherence properties of strongly correlated defects.

[1] Bertaina S. et al. Nature Nanotechnology 2, 39 - 42 (2007)

[2] Bertaina S. et al. Nature 453, 203 (2008)

[3] Morton, J. J. L et al Nature 455, 1085 (2008)

[4] Schlegel, C. et al. Phys. Rev. Lett 101, 147203 (2008)

[5] Bertaina et al. Phys. Rev. B R90, 060404 (2014)

Mo.B-P14 - Magnetic properties of layered one dimensional γ -CoV₂O₆ and NiV₂O₆ magnetic oxides: a comparative studyM. Lenertz^{1,2}, A. Dinia², S. Colis²*1. Laboratoire Léon Brillouin – CEA, Gif-sur-Yvette, France**2. Institut de Physique et Chimie des Matériaux de Strasbourg - Université de Strasbourg, Strasbourg, France*

Low-dimensional magnetic oxides show an increasing interest from the scientific community mainly due to their strong anisotropy, their magnetization variations showing plateaus corresponding to different magnetic configurations. In most cases, these properties result from magnetic frustrations. γ -CoV₂O₆ and NiV₂O₆ are such one dimensional magnetic oxides that exhibit an antiferromagnetic ground state and present a same triclinic crystal structure (P-1 space group). Recent studies have shown that the structural modulations in the γ -CoV₂O₆ chains' leads to more complex magnetic structures¹. While the synthesis and structural properties are generally well known, the magnetic properties of NiV₂O₆ have never been reported. The aim of this work is to study the magnetic properties of NiV₂O₆ with respect to the ones of the well known γ -CoV₂O₆. Our results show that the lattice parameters of NiV₂O₆ are slightly smaller than those of γ -CoV₂O₆ which can be understood on the basis of the smaller ionic radius of Ni²⁺ (0.055 nm) with respect to that of high-spin Co²⁺ (0.058 nm). The magnetic measurements indicate that both compounds are antiferromagnetic in the ground state, with Néel temperatures of 7K (for γ -CoV₂O₆) and 16K (for NiV₂O₆), in agreement with the smaller lattice parameters of NVO. The magnetization curves recorded at 1.8K show a stepped variation with sharp field-induced magnetic transitions. A magnetization plateau at one third of the saturation magnetization is observed for γ -CoV₂O₆ while only the onset of this plateau is visible for NiV₂O₆. The stronger coupling in NiV₂O₆ is also reflected in the MH loops by i) the larger field needed for the ferro- / ferri- magnetic transition, ii) the smaller slope corresponding to the antiferromagnetic state, iii) the absence of any hysteresis at 1.8K for NiV₂O₆, and iv) the much larger (estimated) saturation field of NiV₂O₆.

[1] Lenertz. et al. J. Phys. Chem. C 118, 13981 (2014)

Mo.B-P15 - Controlled bond disorder in the model spin ladder $(C_5H_{12}N)_2CuBr_4$

S. Ward^{1,2,3}, S. Furuya³, D. Biner⁴, K. W. Krämer⁴, M. Bohm⁵, T. Giamarchi³, D. F. McMorrow², C. Rüegg^{1,3}

1. *Laboratory for Neutron Scattering and Imaging, Paul Scherrer Institut, Villigen, Switzerland*
2. *London Centre for Nanotechnology and Department of Physics and Astronomy, University College London, London, United Kingdom*
3. *Department of Quantum Matter Physics, University of Geneva, Geneva, Switzerland*
4. *Department of Chemistry and Biochemistry, University of Bern, Bern, Switzerland*
5. *Institut Laue-Langevin, Grenoble*

Research in quantum magnetism depends strongly on the availability of prototypical model materials that serve as clean quantum simulators. One special low-dimensional spin geometry is the spin ladder, the study of which has recently become possible by the discovery of new model materials that are experimentally accessible in magnetic field, temperature and energy range. The possible realisation of controlled exchange randomness in such systems has become an exciting new direction. One such prototypical spin ladder material is the $S = 1/2$ Heisenberg antiferromagnetic 2-leg ladder $(C_5H_{12}N)_2CuX_4$ for $X=Br, Cl$ (BPCB, BPCC) which has chemical flexibility on the halogen site X.

We present work on the effects of random Chlorine substitution on BPCB, focusing on the average ladder superexchange parameters as a function of composition from magnetic susceptibility and providing a case study on the elementary excitation spectrum of a system with weak bond disorder as measured by inelastic neutron scattering (INS).

We find a strong compositional dependence of both ladder rung and leg exchange. The dispersion in the weakly bond disordered case shows a renormalized singlet-triplet mode, with a line shape that is reminiscent of magnon-magnon interaction, and components that are better described by localized modes. In a microscopic description, the statistical case of substitution is considered and applied to a model, which is solved by exact diagonalization. Numerical results and experimental data are compared, showing remarkable agreement. Hence we demonstrate the effects of bond disorder on the excitation spectrum of a one-dimensional system, realised in the spin ladder Hamiltonian.

[1] S. Ward, P. Bouillot, H. Ryll, K. Kiefer, K. Krämer, C. Rüegg, C. Kollath, and T. Giamarchi, *J. Phys.: Condens. Matter* 25, 4004 (2013)

[2] T. Tajiri, H. Deguchi, M. Mito, S. Takagi, H. Nojiri, T. Kawae, and K. Takeda, *Journal of Magnetism and Magnetic Materials* 272-276, 1070 (2004)

Mo.B-P16 - The spin structure on the ground state of the equilateral triangular spin tube CsCrF₄

K. Matsui¹, T. Goto¹, H. Manaka², Y. Miura³

1. Sophia University, Japan, Tokyo, Japan

2. Kagoshima University, Kagoshima, Japan

3. Suzuka National College of Technology, Suzuka, Japan

CsCrF₄ is $S = 3/2$ three-leg Heisenberg spin tube system, in which magnetic Cr³⁺ ions form equilateral triangles stacked along the leg direction without rotation. Due to low dimensionality and to the geometrical frustration within an equilateral triangle, the system is expected to have an exotic ground state, and has been believed to have the ground state of the spin liquid. However, quite recently, the existence of a magnetic phase transition has been suggested by μ SR and neutron scattering measurement. In order to investigate the magnetic structure at the low-temperatures, we have measured the temperature dependence of ¹⁹F/¹³³Cs-NMR spectra down to 0.31 K. First, from the temperature dependence of Knight shift in high temperature paramagnetic region above 20 K, the hyperfine coupling constant for each F-sites 6j, 3f(3g), 3g(3f) was determined to be -0.146, 0.345 and -0.636 T/ μ B, respectively. Next, in low temperatures, both ¹⁹F and ¹³³Cs-NMR spectra showed drastic broadening at 3 K, and at around 0.3 K, there appeared a wide plateau expanding at both the sides of the sharp central peak. The distance between the two edges at both sides tends to be 1.8 T. The observed abrupt broadening in spectra at 3 K indicates a long-range magnetic order of Cr³⁺ moments. Characteristic spectral profiles with sharp edges can be understood in terms of the contribution from each fluorine site as follows. 3g-sites are expected to contribute to the sharp central peak due to geometrical canceling between the two Cr sites above and below. For the hyperfine coupling constant of 6j is too small to carry the wide edge, its main contribution must be from 3f site, which indicate that the size of ordered moment of Cr³⁺ may be 2.6 or 1.42 μ B, depending on the determination of the hyperfine coupling constant of 3f site to be 0.345 or -0.636T/ μ B, respectively.

Mo.B-P17 - NMR study on the Ru-dimer system with valence fluctuationY. Hosoya¹, T. Goto¹, A. Endo¹, T. Hashimoto¹, M. Masuko¹, T. Hayashita¹, S. Iguchi², T. Sasaki²

1. Sophia University, Tokyo, Japan

2. IMR Tohoku University, Sendai, Japan

The ground state of $S=1/2$ spin dimer with the antiferromagnetic interaction is the singlet with a finite spin excitation gap. This nonmagnetic state shows the quantum phase transition to the magnetic state under high magnetic field, which is well known as the magnon-BEC reported in many spin dimer systems. The purpose of this study is to introduce a new method of valence fluctuation to cause a quantum phase transition in dimer systems.

The target compound is Ru-based binuclear complex $[\{\text{Ru}^{\text{III}}(\text{acac})_2\}_2(\text{m-OEt})]$, in which Ru takes the trivalent state with $S=1/2$. The valence state of ruthenium can be fine-tuned by changing the methyl group on the bidentate ligand, acetylacetonone to substituents with different electronegativity such as trifluoromethyl group.

We have investigated this substitution effect of CF_3 on their magnetic property by means of the magnetic susceptibility and the longitudinal nuclear spin relaxation rate T_1^{-1} of $^1\text{H}/^{19}\text{F}$ -NMR. The prepared samples were $[\{\text{Ru}^{\text{III}}(\text{acac})_2\}_2(\text{m-OEt})]$ and $[\{\text{Ru}^{\text{III}}(\text{fhma})_2\}_2(\text{m-OMe})]$. In the latter fhma system, half of methyl groups on bidentates are substituted with CF_3 . The two stereoisomers, in each compound, that is, D L type called meso form and D D: L L type called racemi, were separated by column chromatography.

Both the meso and racemi forms of acac system showed extremely small magnetic susceptibility with nearly flat temperature dependence between 4 and 200K, indicating they are in the spin singlet state with a gap comparable to the room temperature. In the fhma systems, while the meso form sample showed a behavior similar to acac systems, the racemi form sample exhibited large magnetic response: both the susceptibility and T_1^{-1} , these two scaled each other, increased prominently with increasing temperature, and the ratio to the other three reached 30 at 100K. This unique behavior in the fhma system of the racemi form may be caused by the slight change in the Ru valence due to CF_3 substitution.

Mo.B-P18 - Cu-NMR study of the quasi-one-dimensional antiferromagnet $\text{Cu}_3\text{Mo}_2\text{O}_9$

T. Kawase¹, H. Kuroe¹, K. Misoka¹, T. Hamasaki¹, T. Sekine¹, T. Goto¹, T. Sasaki², M. Hase³, K. Oka⁴, T. Ito⁴, H. Eisaki⁴

1. Department of Physics, Sophia University, Tokyo, Japan

2. Institute for Materials Research, Tohoku University, Sendai, Japan

3. National Institute for Materials Science (NIMS), Tsukuba, Japan

4. National Institute of Advanced Industrial Science and Technology (AIST), Japan

The target material of this research is a quasi-one-dimensional antiferromagnetic quantum spin system $\text{Cu}_3\text{Mo}_2\text{O}_9$, consisting of a spin-1/2 linear chain (Cu1) and spin-1/2 distorted dimer (Cu2 and Cu3) weakly interacting with each other. Existence of these three non-equivalent Cu sites and of the frustration effect routed in the tetrahedral structure formed by the nearest neighboring four Cu's suggested an unprecedented spin state. So far, the measurements of magnetization and specific heat by Hamasaki *et al.* have revealed that long range magnetic order occurs at $T_N = 7.9$ K. However the detailed magnetic structure in the ordered state is undissolved until now. In order to investigate the spin structure in the ordered state, we performed Cu-NMR measurements on a single crystal.

The single crystal with an approximate size of $2 \times 4 \times 10$ mm³ prepared by an infrared imaging furnace was set on the sample rotator in the cryo-cooled cryostat with a 12T superconducting magnet where $^{63/65}\text{Cu}$ -NMR spectra were obtained by a conventional spin-echo method. The field direction was rotated within an *ab*-plane. At 4.2K, we observed three sets of peak-groups, corresponding to the three inequivalent sites of Cu. Each peak group consists of many peaks corresponding to the eqq-splitting, the isotopes and the two chains in the unit cell connected with the glide symmetry.

From the detailed analysis of the temperature dependence and the field direction dependence of the resonance line shifts, the observed peaks have been successfully assigned to the three Cu sites. The internal magnetic fields of Cu1, Cu2 and Cu3 sites were determined to $0(\pm 0.2)\text{T}$, $4.7(\pm 0.4)\text{T}$ and $9.6\text{T}(\pm 0.9)$ in *H//c* respectively. One of the main conclusions of this study is that the Cu1 in the chain site has little magnetic moment and that Cu2 and Cu3 are magnetically asymmetric. These results are consistent with the recent neutron study by Hase *et al.*

Mo.B-P19 - Antiferromagnetic ground states and phase separation in doped AA-stacked bilayer graphene

A. Sboychakov^{1,2}, R. Akzyanov³, A. Rozhkov^{1,2,3}, A. Rakhmanov^{1,2,3}, F. Nori^{2,4}

1. *Institute for Theoretical and Applied Electrodynamics, Russian Academy of Sciences, Moscow, Russia*
2. *Advanced Science Institute, RIKEN, Wako-shi, Japan*
3. *Moscow Institute of Physics and Technology, Dolgoprudnyi, Russia*
4. *Department of Physics, University of Michigan, Ann Arbor, United States*

We study electronic properties of AA-stacked graphene bilayers. In the single-particle approximation such a system has one electron band and one hole band crossing the Fermi level. If the bilayer is undoped, the Fermi surfaces of these bands coincide. Such a band structure is unstable with respect to a set of spontaneous symmetry violations. Specifically, strong on-site Coulomb repulsion stabilizes antiferromagnetic order. At small doping and low temperatures, the homogeneous phase is unstable and experiences phase separation into an undoped antiferromagnetic insulator and a metal. The metallic phase can be either antiferromagnetic (commensurate or incommensurate) or paramagnetic depending on the system parameters. The incommensurate AFM phase is mathematically equivalent to the Fulde-Ferrel-Larkin-Ovchinnikov state in superconductors. We derive the phase diagram of the system on the doping-temperature plane and find that under certain conditions, the transition from the paramagnetic to the antiferromagnetic phase may demonstrate reentrance. When disorder is present, phase separation could manifest itself as a percolative insulator-metal transition driven by doping. The application of the transverse voltage induces the exciton order parameter on the antiferromagnetic background. The value of this second order parameter is proportional to the biased voltage and the value of the nearest-neighbor interplane Coulomb repulsion.

Mo.B-P20 - High field magnetization of single crystals of the $S=1/2$ quasi-1D Ising-like Antiferromagnet $\text{SrCo}_2\text{V}_2\text{O}_8$

A. Okutani¹, T. Kida¹, T. Usui², T. Kimura², M. Hagiwara¹

1. Center For Advanced High Magnetic Field of Science, Graduate School of Science, Osaka University, Osaka, Japan

2. Graduate School of Engineering Science, Osaka University, Osaka, Japan

Quantum spin systems in high magnetic fields have attracted much interest, since they sometimes show very fascinating phenomena. $\text{SrCo}_2\text{V}_2\text{O}_8$ is a quasi one-dimensional (1D) Co^{2+} spin system, which crystallizes in the tetragonal $I4_1cd$ space group [1]. The temperature evolution of magnetic susceptibility for the magnetic field $H \parallel c$ (chain direction) exhibits broad maxima around 40 K and a rapid drop below 5 K. From the specific heat measurements, the Néel temperature is determined to be 4.8 K at $H=0$. With increasing magnetic fields for $H \parallel c$, the transition temperature shifts lower, and the field-induced Néel order to disorder transition occurs at about 4 T when at 2 K [2]. Such magnetic behavior is similar to $\text{BaCo}_2\text{V}_2\text{O}_8$ (tetragonal $I4_1/acd$), which is known as $S=1/2$ quasi-1D Ising-like antiferromagnet [3]. We report the results of the high field magnetization measurements at 1.4 K on single crystal samples of $\text{SrCo}_2\text{V}_2\text{O}_8$, which were grown by the floating-zone method, to investigate the difference between $\text{SrCo}_2\text{V}_2\text{O}_8$ and $\text{BaCo}_2\text{V}_2\text{O}_8$. For $H \parallel c$ -axis, the magnetic transition from the ordered to disordered state and an anomaly on the magnetization curve were observed at 4.0 T and 25.1 T, respectively, and the saturation field is 29.5 T. On the other hand, the magnetization achieves saturation at 45.5 T for $H \parallel [110]$, but the magnetization gradually increases in magnetic fields of up to 50 T for $H \parallel a$ -axis. We will report the similarities and differences in magnetization curves between $\text{SrCo}_2\text{V}_2\text{O}_8$ and $\text{BaCo}_2\text{V}_2\text{O}_8$ [4].

[1] D. Osterloh *et al.*, Z. Naturforsch. B 49, 923 (1994)

[2] Z. He *et al.*, Phys. Rev. B 73, 212406 (2006)

[3] Z. He *et al.*, Appl. Phys. Lett. 88, 132504 (2006)

[4] S. Kimura *et al.*, J. Phys.: Conf. Ser. 51, 99 (2006)

Mo.B-P21 - 1H-NMR study of spin-1/2 triple-chain magnet Cu₃(OH)₄MoO₄Y. Fujii¹, H. Kikuchi², K. Nakagawa², S. Takada², M. Fujisawa³*1. Research Center For Development of Far-Infrared Region, University of Fukui, Fukui, Japan**2. Department of Applied Physics, Faculty of Engineering, University of Fukui, Fukui, Japan**3. Technical Department, Tokyo Institute of Technology, Meguro, Tokyo, Japan*

Geometrically frustrated magnets on low dimensional lattices with $S=1/2$ spins have been attracting much interest because quantum effects are expected to appear without long range ordering (LRO). In Cu₃(OH)₄MoO₄ (mineral name: szenicsite), there exist a triple-chain structure of Cu²⁺ ($S=1/2$) which forms a ribbon of isosceles triangles. As is reported in our previous work [1], the magnetic susceptibility of Cu₃(OH)₄MoO₄ shows a broad maximum around 80 K and the magnetization increases smoothly up to 48 T. Further, no LRO is observed down to 2 K in the specific heat measurements. These results are approximately explained with a naive model of three identical antiferromagnetic spin-1/2 chains without interchain interactions. However, due to a divergent behavior of the susceptibility below 20 K, which is attributed to the contribution from impurities, intrinsic susceptibility of the bulk sample is still unclear. In order to study the magnetic ground state of Cu₃(OH)₄MoO₄ from a microscopic viewpoint, we have performed 1H-NMR measurements of Cu₃(OH)₄MoO₄. The width of the spectrum increased with decreasing temperature, suggesting the inhomogeneous broadening due to impurities. The shift of the spectrum, in contrast, showed a maximum around 100 K and decreased down to the lowest temperature of 1.5 K. These results support the picture of the antiferromagnetic chain model for Cu₃(OH)₄MoO₄. We will discuss our results comparing with magnetic properties of Cu₃(OH)₄SO₄ (mineral name: antlerite) [3] whose crystal structure is very similar to that of Cu₃(OH)₄MoO₄.

[1] M. Fujisawa et al.: J. Phys.: Conf. Ser. 320 (2011) 012031

[2] P. C. Burns: Mineral. Mag. 62 (1998) 461

[3] S. Vilminot et al.: J. Solid State Chem. 170 (2003) 255; S. Hara et al.: J. Phys. Soc. Jpn. 80 (2011) 043701; Y. Fujii et al.: J. Kor. Phys. Soc. 62 (2013) 2054

Mo.B-P22 - From order to randomness: an experimental investigation of disorder in a one-dimensional spin system

T. Shiroka^{1,2}, F. Eggenschwiler¹, M. Pikulski¹, M. Thede^{1,2}, A. Zheludev¹, H. Ott^{1,2}, J. Mesot^{1,2}

1. *Laboratorium Für Festkörperphysik, ETH Zurich, Zurich, Switzerland*

2. *Paul Scherrer Institut, Villigen PSI, Villigen, Switzerland*

Quantum fluctuations dominate the low-temperature physical properties of low-dimensional systems, such as 1D or 2D arrays of spins. Ordinary long-range order is suppressed and unusual magnetic states emerge. By their nature, 1D systems are particularly sensitive to disorder, which can break the translational invariance, introduce random couplings between individual spins, and lead to a so-called random singlet (RS) phase [1,2], characterized by couplings of spins at arbitrary distances to form weakly-bound singlets. What exactly happens when a regular spin-chain is exposed to an increasing degree of disorder is not well known. To address this question we considered BaCu₂Si₂O₇, a model material featuring weakly interacting $S = 1/2$ spin chains, and studied a series of this compound where, by systematically replacing Si with Ge, we achieve randomness in the Cu²⁺ exchange interactions. Since Heisenberg spin-1/2 chain materials are well recognized as strongly-interacting quantum systems, our series is perfectly well suited for clarifying the role of disorder in the 1D case [3,4]. Results of magnetometry measurements combined with those of local-probe ²⁹Si NMR studies, including lineshape, relaxation-time, as well as stretching-exponent data, were used to monitor the evolution of the disorder-related properties from BaCu₂Si₂O₇ to the maximally disordered BaCu₂SiGeO₇, with intermediate disorder steps. A low-degree of disorder suppresses the 3D ordering temperature quite effectively and, with maximum disorder, the system adopts the theoretically predicted RS phase. Our results are expected to trigger a more rigorous understanding of the role and significance of disorder in low-dimensional spin systems.

References:

1. S. K. Ma, C. Dasgupta, and C. K. Hu, Phys. Rev. Lett. 43, 1434 (1979)
2. D. S. Fisher, Phys. Rev. B 50, 3799 (1994)
3. T. Shiroka et al., Phys. Rev. Lett. 106, 137202 (2011)
4. T. Shiroka et al., Phys. Rev. B 88, 054422 (2013)

Mo.B-P23 - Spin-Orbit torques originated from topological surface states of Bi₂Se₃

Y. Wang¹, P. Deorani¹, K. Banerjee¹, N. Koirala², M. Brahlek², S. Oh², H. Yang¹

1. *Department of Electrical and Computer Engineering, National University of Singapore, Singapore*

2. *Department of Physics & Astronomy, Rutgers Center for Emergent Materials, Institute for Advanced Materials, Devices and Nanotechnology, The State University of New Jersey, Newark, United States*

Recent progresses have demonstrated the manipulation of magnetization via spin-orbit coupling in heavy metal/ferromagnetic (FM) layer heterostructures. The search for new materials possessing a higher conversion efficiency between the charge currents and spin currents (i.e. higher spin-orbit torques) is crucial to realize next generation spintronic devices. The three dimensional topological insulators (TI) are a new class of quantum state of materials that have an insulating bulk and a topological surface state. They exhibit strong spin-orbit coupling and are expected to show a high charge to spin current conversion efficiency. In this work, we investigate the spin-orbit torques at different temperatures in Bi₂Se₃ (20 nm)/Co₄₀Fe₄₀B₂₀ (CFB, 5 nm) heterostructures by spin torque ferromagnetic resonance (ST-FMR) measurements. We find in our Bi₂Se₃/CFB, the charge-spin conversion efficiency shows an abrupt and nonlinear increase as temperature decreases. In the context of spin Hall mechanism, the spin Hall angle has been reported to be almost independent of temperature or in some cases a gradual increase as the temperature decreases. This indicates that the spin Hall effect from the Bi₂Se₃ bulk is not the dominant mechanism for our observation of temperature dependent spin-orbit torque in Bi₂Se₃/CFB. In addition, we have confirmed that the direction of in-plane spin polarization to the electron momentum in our Bi₂Se₃/CFB is consistent with that expected from the topological surface state of TIs (spin-momentum locking). The out-of-plane spin-orbit torque also shows an increasing trend as temperature decreases. We conclude that our observations especially in the low temperature range (less than ~ 50 K) could be correlated with the topological surface state in our Bi₂Se₃/Co₄₀Fe₄₀B₂₀ heterostructures.

Mo.B-P24 - off-diagonal spin-spin correlations in noncollinear antiferromagnets or in applied magnetic fields

A. Kruchkov¹, H. Ronnow¹, M. Zhitomirsky²

1. *Laboratory for Quantum Magnetism (LQM), École Polytechnique Fédérale de Lausanne (EPFL), Lausanne, Switzerland*

2. *Service de Physique Statistique, Magnétisme et Supraconductivité, UMR-E9001 CEA-INAC/UJF, Grenoble Cedex 9, France*

We study semi-analytically and numerically the contributions of the off-diagonal spin-spin correlators to the total dynamical structure factor of the system. The study mainly considers the square lattice Heisenberg antiferromagnet in the moderate magnetic field and also can be generalized for noncollinear structures.

Mo.B-P27 - Symmetry-protected topological phases/transition in spin-1/2 zigzag chains and the relevance to Rb₂Cu₂Mo₃O₁₂H. Ueda¹, S. Onoda^{1,2}*1. Condensed Matter Theory Laboratory, RIKEN, Wako-shi, Japan**2. RIKEN Center for Emergent Matter Science (CEMS), Wako-shi, Japan*

We study a ground-state phase diagram of frustrated spin-1/2 chains in the space of the nearest-neighbor ferromagnetic and second-neighbor antiferromagnetic exchange couplings J_1 and J_2 , the relative amplitude δ of the nearest-neighbor bond alternation, and the easy-plane XXZ exchange anisotropy, by means of a density-matrix renormalization group method for infinite systems [1]. We numerically identify projective representations for four distinct time-reversal invariant symmetry-protected topological (SPT) phases; two parity-symmetric dimer phases near the Heisenberg and XX limits and two parity-broken vector-chiral (VC) dimer phases in between. A small nearest-neighbor bond alternation induces a direct SPT transition between the two distinct VC dimer phases. We also find numerically that two Berezinskii-Kosterlitz-Thouless transitions, which occur from the gapless to the two distinct gapped VC phases in the case of $\delta = 0$, meet each other in the case of $\delta > 0$ at a Gaussian criticality of the same Tomonaga-Luttinger parameter value as in the SU(2)-symmetric case.

Besides, we obtain the model parameters for a relevant material Rb₂Cu₂Mo₃O₁₂, which explain overall experimental findings on the temperature dependence of the magnetic susceptibility, the spin excitation gap from the non-magnetic ground state, and the dynamical spin structure factor [2]. A spin-gapped vector-chiral order induced by a staggered scalar-chiral ring-exchange interaction under the magnetic field is proposed as a possible scenario for a field-induced ferroelectricity in the absence of long-range cycloidal magnetic order [3].

[1] H. Ueda, S. Onoda, Phys. Rev. B 90, 214425 (2014)

[2] H. Ueda, S. Onoda, Y. Yasui, et al., unpublished

[3] H. Ueda, S. Onoda, Phys. Rev. B 89, 024407 (2014)

Mo.B-P29 - Natural Mineral epidote in magnetic fields

K. Prokes¹, B. Klemke¹, J. Hoffmann¹

1. Helmholtz-Zentrum Berlin, Berlin, Germany

In this contribution we report on the magnetic properties of a natural mineral epidote. Epidote, which crystallizes in a monoclinic crystal structure with an approximate chemical formula $\text{Ca}_2(\text{Fe,Al})\text{Al}_2(\text{SiO}_4)(\text{Si}_2\text{O}_7)\text{O}(\text{OH})$, contains magnetically active Fe^{3+} ions that are in the high spin state. Iron atoms form weakly coupled linear chains extended along the b axis. We have measured the specific heat and magnetic bulk properties of a small natural single crystal of this material down to 0.04 K. Static magnetic field of up to 14 T applied along the three principal axes was used. We show that at low temperatures the magnetic response is weakly anisotropic. The magnetic susceptibility and the specific heat shows a broad maximum around 6 K that is affected by the applied magnetic field. Also the low-T specific heat upturn that is strongly magnetic dependent and exhibits a non-trivial dependence. We also report on the neutron diffraction results obtained at low temperatures and in magnetic fields of up to 7 T applied along the b axis. While no signature of a long-range magnetic order is found in zero field, increase of diffracted signal in magnetic fields indicate an induced magnetic order.

Mo.B-P30 - Effects of the underlying geometry on the physical properties of topological insulators

T. Melo¹, D. Viana¹, Y. Gomes², W. Moura-Melo¹, J. Fonseca¹, A. Pereira¹

1. *Departamento de Física, Universidade Federal de Viçosa, Viçosa, Brazil*

2. *Centro Brasileiro de Pesquisas Físicas, Rio de Janeiro, Brazil*

Three-dimensional topological insulators (3D TI's) come to be an exotic state of matter where non-trivial topology of the insulating bulk renders conducting electronic-type states at the borders. In addition, such metallic-like states propagate in a such a way that their spin and linear momentum are orthogonal each other over the surface, the so-called spin-momentum locking. A number of additional special properties make them potential candidates for several applications ranging from spintronics to quantum computation. Here, we would like to call the attention to some facts regarding how the underlying geometry of a 3D TI render it additional interesting effects. Indeed, in a conical TI an peculiar electric polarization comes about so that narrower (aperture angle < 30 degrees) cones tend to polarize towards the apex while in wider ones (aperture angle > 30 degrees) the polarization is reversed. On the other hand, on the surface of a genus-1 toroidal 3D TI there appear two Berry phases associated to the geometrical periodic boundary conditions. In turn, this yields infinitely degenerate zero-modes and two independent bound-states along the confined dimensions. In addition, whenever a laser beam is shed onto a micro-sized spherical 3D TI the response is so that a net controllable force tends to drift the sphere center (in usual dielectric spheres net force vanishes at the focus of the beam). Such a drift may be useful for optical tweezer applications in biology, for instance, while distending a DNA strip or a membrane. Financial support: Capes, CNPq and Fapemig (Brazilian agencies).

Mo.B-P31 - Genus one toroidal topological insulator

J. Fonseca¹, V. Carvalho-Santos², W. Moura-Melo¹, A. Pereira¹

1. *Universidade Federal de Viçosa, Viçosa, Brazil*

2. *Instituto Federal de Educação, Ciência e Tecnologia Baiano - Campus Senhor do Bonfim, Senhor do Bonfim, Brazil*

We consider the theoretical possibility of a toroidal topological insulator (TI). From a geometrical point of view the toroidal topological insulator is a good form to investigate the connection between geometry and topological properties of the TI because it has a variable Gaussian curvature, genus 1 and the sphere can be recovered as a limit case. An effective Hamiltonian that describes the surface states of a toroidal topological insulator is obtained and the bulk and surface spectrum are investigated. The toroidal TI supports zero-mode energy in your surface. The boundary conditions on surface wavefunction are discussed and the connection with two types of Berry phase. The authors are grateful to CNPq, FAPEMIG and CAPES (Brazilian agencies) for financial support.

Mo.C-P01 - Field and temperature dependence of spin fluctuations in ZrZn₂

P. Reiss¹, G. Lonzarich¹, F. Malte Grosche¹

1. Cavendish Laboratory, University of Cambridge, Cambridge, United Kingdom

ZrZn₂ is a low temperature band ferromagnet ($T_c \sim 28$ K), which displays non-Fermi liquid transport properties over a wide temperature range: above $T_{FL} \sim 1$ K and even beyond T_c , the electrical resistivity follows a power-law temperature dependence with an exponent $5/3$, whereas the electronic contribution to the thermal resistivity is linear in temperature. This has been explained in terms of a magnetic fluctuation model, which includes a self-consistent renormalisation for the magnetic susceptibility [1, 2]. Applied magnetic fields up to 9 T have been observed to increase the cross-over temperature T_{FL} to ~ 7 K. Previous calculations did not include effects of magnetic fields. We will present the results of an extended calculation which accounts for the role of applied field, allowing a comparison between high field resistivity measurements and the predictions of a magnetic fluctuation model. Furthermore we will show that the magnetic transition is expected to be continuous in this model. However this transition is characterised by a strongly temperature dependent coefficient $b(T)$ of the quartic term in a Landau-Ginzburg expansion. Moreover, $b(T)$ changes sign at T_c , with $b(T) < 0$ in the ordered phase.

[1] G. G. Lonzarich and L. Taillefer, J Phys C: Solid State Phys, 18, 4339-4371 (1985)

[2] R. Smith et al., Nature, 455, 1220-1223 (2008)

Mo.C-P02 - Effect of Ce Doping on Elastic and Thermal Properties of SrCoO₃R. Thakur¹, R. K. Thakur¹, N.K. Gaur¹

1. Barkatullah University, Bhopal, India

2. Barkatullah University, Bhopal, India

3. Barkatullah University, Bhopal, India

SrCoO₃ has a cubic perovskite crystallographic structure which adopts a long-range with Curie temperature of T_c=266K and is considered a candidate for realization of intermediate spin ground state. The elastic and thermodynamic properties for Sr_{1-x}Ce_xCoO₃ (0.05≤x≤0.45) with temperature have been investigated by using modified rigid ion model (MRIM). The computed results on the elastic constants (C₁₁, C₁₂ and C₄₄) are the first report on them. Using these elastic constants we have computed other elastic properties such as elastic constants (C₁₁, C₁₂, C₄₄), Cauchy pressure, Internal strain parameter, tetragonal shear modulus, Shear modulus and B/G ratio, Young's modulus, Poisson's ratio, Lamé's parameter, Anisotropy parameter, Transverse, Longitudinal and Average wave velocity.

The present values of Young moduli increases from Sr_{0.95}Ce_{0.05}CoO₃ to Sr_{0.55}Ce_{0.45}CoO₃ which indicates that Sr_{0.55}Ce_{0.45}CoO₃ is stiffer than Sr_{0.95}Ce_{0.05}CoO₃. The calculated anisotropy factors A for Sr_{1-x}Ce_xCoO₃ (0.05≤x≤0.45) are greater (or lesser) than 1 which indicates that these compounds have an elastically anisotropic character. Based on the calculated results, we conclude that these compounds belong to the class of metallic bonding material, i.e. they are ductile in behavior. Here, all C_{ij} constants for Sr_{1-x}Ce_xCoO₃ (0.05≤x≤0.45) compounds are positive and satisfy the generalized criteria for mechanically stable crystals: (C₁₁-C₁₂)>0, (C₁₁+2C₁₂)>0 and C₄₄>0. Therefore, we conclude that Ce doped SrCoO₃ should belong to metallic bonding materials by analyzing their elastic modulus. We have also reported the thermodynamic properties such as cohesive energy (φ), Molecular force constant (f), Reststrahlen frequency (u), Debye temperature (q_D) and Gruneisen parameter (g). On the basis of above discussion we have calculated the specific heat and thermal expansion coefficient for Sr_{1-x}Ce_xCoO₃ over the wide temperature range 1K ≤T≤ 300K.

Mo.C-P03 - First principles study of strain induced phase diagram and spin-orbit coupling in (SrIrO₃)_m/(SrTiO₃)₁ superlattice

W. Fan¹, T. Shirakawa^{1,2}, S. Yunoki^{1,2,3}

1. Computational Condensed Matter Physics Laboratory, RIKEN, Wako, Japan

2. Computational Materials Science Research Team-RIKEN Advanced Institute for Computational Science (AICS), Kobe, Japan

3. Computational Quantum Matter Research Team-RIKEN Center for Emergent Matter Science (CEMS), Wako, Japan

In order to understand the electronic and magnetic phase transitions under the condition of lattice distortion, strong spin-orbit coupling (SOC) and electron correlation in 5d iridates, especially to understand some recent experiments on thin films of iridates by strain engineering, we studied (SrIrO₃)_m/(SrTiO₃)₁ superlattice by using first principles methods. The band structures show sensitive dispersion behaviors. Under certain distortion (e.g. by means of IrO₆ octahedra rotation and Ir-O bond length), metal-insulator transition (MIT) takes place. The magnetic ground state is confirmed as the in-plane non-collinear antiferromagnetic insulating state with a large anisotropic magnetic exchange interaction, such as Dzyaloshinski-Moriya (DM) interaction. This is the signature of large SOC.

We further studied the phase diagram of (SrIrO₃)_m/(SrTiO₃)₁ under epitaxial strain and adjustable correlation (U), which may be manageable from experimental point of view. It turns out that four phases can appear, which are paramagnetic metal (PM), magnetic metal (MM), non-collinear antiferromagnetic insulator (NCAFI) and collinear antiferromagnetic insulator (CAFI). On the other hand, the strain also influences the SOC. To explain this SOC change, I considered the competition or cooperation of two factors involved: the effective electric field and d-p hybridization. It shows that SOC saturates under compressive while drops monotonically under tensile strain. Our work may be a theoretical guidance for experiments to realize various novel magnetic phases in 5d transition metal oxides.

Mo.C-P04 - Onsite magnetic moment and magnetocrystalline anisotropy studies of Lu-/Y- substituted NiFe₂O₄U. Kodam¹, R. Reddy V², Markandeyulu G¹

1. Indian Institute of Technology Madras, Chennai, Tamil Nadu, India

2. UGC-DAE Consortium for Scientific Research, University Campus, Khandwa Road, India

The NiFe_{2-x}R_xO₄ (x = 0, 0.05, 0.075, R = Lu and Y) compounds are seen to form in cubic inverse spinel phase with *Fd $\bar{3}m$* space group, from the XRD and Raman spectra results. The lattice constant value of NiFe₂O₄ is 8.3351(1) Å whereas, those of NiFe_{1.95}Lu/Y_{0.05}O₄ are 8.3459(3) Å and 8.3406(3) Å, respectively and those of NiFe_{1.925}Lu/Y_{0.075}O₄ are 8.3515(8) Å and 8.3411(1) Å respectively. The magnetic moments values of NiFe_{1.95}Lu/Y_{0.05}O₄ at 20 K are respectively 2.293 μ_B/fu and 2.347 μ_B/fu and those of NiFe_{1.925}Lu/Y_{0.075}O₄ are respectively 2.1 μ_B/fu and 2.173 μ_B/fu. These values are less than that of NiFe₂O₄ (2.364 μ_B/fu) the contraction is attributed to the substitution of Fe³⁺ by Lu³⁺/Y³⁺ in the B-site. The value of K₁, the first order magnetocrystalline anisotropy constant was obtained by the law of saturation method. The values of K₁ at 20 K of NiFe₂O₄ and NiFe_{1.95}Lu/Y_{0.05}O₄ are 42.19 kJ/m³, 36.29 kJ/m³ and 54.17 kJ/m³ respectively and those of NiFe_{1.925}Lu/Y_{0.075}O₄ are 74.6 kJ/m³ and 55.76 kJ/m³ respectively. The observed variation in the temperature dependent K₁ for all the compounds is explained on the basis of *single-ion* model. Mössbauer spectra recorded at 5 K, 300 K were fitted with two sextets corresponding to the Fe ions at the tetrahedral and octahedral sites. The effective magnetic moments of NiFe_{1.925}Lu/Y_{0.075}O₄ calculated from the Mössbauer spectra (at 5 K) are 2.49 μ_B/fu and 2.4 μ_B/fu respectively that are larger than the corresponding values from the magnetization measurements, probably due to the inversion parameter, which is less than 1.

Mo.C-P05 - Multiband spin-lattice relaxation in Gd³⁺-doped YCo₂Zn₂₀ probed by electron spin resonanceM. C. Baez¹, A. Naranjo-Uribe², J. M. Osorio-Guillén^{1,2}, C. Rettori^{1,3}, M. A. Avila¹

1. CCNH, Universidade Federal do ABC (UFABC), Santo André, Brazil

2. Instituto de Física, Universidad de Antioquia UdeA, Medellín, Colombia

3. Instituto de Física "Gleb Wataghin", Universidade Estadual de Campinas (UNICAMP), Campinas, Brazil

The understanding of the physical properties of complex materials with cage-like structures, such as the family RT₂Zn₂₀, have attracted the attention of many researchers focused in condensed matter physics. In this work, we perform temperature dependent Electron Spin Resonance (ESR) experiments on Gd³⁺ doped YCo₂Zn₂₀ intermetallic single crystals, (Y_{1-x}Gd_xCo₂Zn₂₀: 0.001 ≤ x ≤ 1.00) showing a Korringa-like relaxation rate $b = \frac{d(\Delta H)}{dT}$ of $b = 8.8(3)$ Oe/K and $b = 1.9(1)$ Oe/K for the lowest and highest concentration respectively. These results indicate that this system features an *exchange bottleneck* effect, also revealed by the *g*-shift ($\Delta g = g - 1.993$) that crosses from positive, $\Delta g = 0.026(10)$ for $x = 0.001$ (*unbottleneck* regime), to negative $\Delta g = -0.014(3)$ for $x = 1.00$ (*bottleneck* regime). Consequently, in this case we are able to identify the spin-lattice relaxation mechanism of the excited Gd³⁺ electron, which is processed via different types of conduction electrons. First-principles Density Functional Theory band structure calculations combined with heat capacity, DC magnetic susceptibility and ESR results allows to extract the exchange interaction parameters between the localized magnetic moments of Gd³⁺ and the different types of electrons present at the Fermi level (J_{fs} , J_{fp} and J_{fd}). The combination of experimental data and band structure calculations can provide a better understanding of the *RKKY* mechanism responsible for the antiferromagnetic order in the GdCo₂Zn₂₀ intermetallic compound in terms of microscopic parameters. We thank the financial support of FAPESP, CAPES and CNPq.

Mo.C-P06 - Anisotropy of magnetic interactions in complex Ir oxides from band structure calculations

A. Yaresko¹

1. Max Planck Institute For Solid State Research, Stuttgart, Germany

In complex Iridium oxides magnetic interactions become anisotropic due to strong spin-orbit interaction of Ir 5d electrons. In α -Li₂IrO₃ and α -Na₂IrO₃ Ir ions form a honeycomb lattice and their magnetic interaction are suggested to be strongly bond-dependent and to be described by a Kitaev model. Recently, another complex Ir oxide β -Li₂IrO₃ has been synthesized which is expected to be close to forming a Kitaev spin liquid. Ir ions in this compound form a "hyper-honeycomb" lattice, a three-dimensional analogue of the honeycomb lattice of α -Na₂IrO₃. We present results of LSDA+U band structure calculations for α -Na₂IrO₃ and β -Li₂IrO₃ with various magnetic configurations constrained by symmetry. It is shown that the change of the total energy cannot be described by an isotropic Heisenberg-like model and anisotropic interactions are at least as strong as the isotropic ones.

Mo.C-P07 - Asymmetric spinwave dispersion relations in the presence of interfacial Dzyaloshinskii-Moriya interaction using Brillouin light scattering

J. Cho¹, S. Ku Kang¹, C. You¹

1. Inha University, Incheon, South Korea

The Dzyaloshinskii-Moriya interaction which is known the antisymmetric component of the exchange interaction originates from the combination of strong spin-orbit coupling and low structural symmetry. However, it is also existed at the interface between a magnetic layer and a high spin-orbit coupling adjacent layer, so-called the interfacial Dzyaloshinskii-Moriya interaction (iDMI), which has been proposed by Fert [1, 2]. The Brillouin light scattering (BLS) is able to detect propagating spin wave excitations with $\pm k$ -wavevectors simultaneously. This non-contact inelastic light scattering method allows us to measure asymmetric spin wave dispersion relations due to the iDMI. In this study, we determine the iDMI energy on the heavy metal /ferromagnet/ Heavy metal structure by employing BLS. A series of 2-nm-thick CoFeB films with different heavy metal (Ta and Pt) are fabricated by dc magnetron sputtering. We find that symmetric dispersion relations (zero-iDM) on the symmetric Pt/CoFeB/Pt and Ta/CoFeB/Ta samples and clearly asymmetric dispersion relation (finite iDM) on the asymmetric Pt/CoFeB/Ta and Ta/CoFeB/Pt samples as the different chirality directions. In our result, different sign of asymmetry dispersion is arisen by different position of Pt/CoFeB interface. It means that Pt/CoFeB interface is leading the iDMI. Furthermore, it is revealed that the iDM energy density is $+0.64 \pm 0.05$ mJ/m² and -0.50 ± 0.1 mJ/m² for Pt/CoFeB/Ta and Ta/CoFeB/Pt samples, respectively.

[1] A Fert and M Levy, *Phys. Rev. Lett.* 44, 1538 (1980)

[2] A Fert, *Mater. Sci. Forum* 59-60, 439-480 (1990)

Mo.C-P08 - Rashba Spin-orbit torques in two-dimensional itinerant ferromagnets

A. Qaiumzadeh¹, R. Duine², M. Titov¹

1. *Radboud University, Nijmegen, Netherlands*

2. *Utrecht university, Utrecht, Netherlands*

Magnetization dynamics in single ferromagnets can be triggered by charge current in the presence of spin-orbit coupling. We investigate Rashba spin-orbit torques in metallic two-dimensional ferromagnets via functional Keldysh theory. A reactive, anti-damping-like spin-orbit torque, as well as a dissipative, eddy-like term are calculated microscopically, to the leading order in spin-orbit strength. By calculating the first vertex correction we show that the intrinsic anti-damping-like spin-orbit torque vanishes unless the scattering rate is spin-dependent.

Mo.C-P09 - High temperature magnetism of epsilon-Fe₂O₃ : the transition from hard to soft ferrimagnetism

M. Gich¹, J. Padilla¹, J. Nogués^{2,3}, J. Kreisel^{4,5}, A. Roig¹, J. L. Garcia-Muñoz¹

1. *Institut de Ciència de Materials de Barcelona, Barcelona, Spain*
2. *Institució Catalana de la Recerca i Estudis Avançats (ICREA), Barcelona, Spain*
3. *Institut Català de Nanociència i Nanotecnologia (ICN2), Bellaterra, Spain*
4. *Luxembourg Institute of Science and Technology, Sanem, Luxemburgo*
5. *University of Luxembourg, Walferdange, Luxemburg*

Despite being the less studied ferrimagnetic iron oxide, epsilon-Fe₂O₃ displays appealing room temperature properties such as a huge coercivity (20 kOe)[1] and multiferroicity[2]. This rich physics stems from a complex structure with four Fe³⁺ sublattices and it is related to the existence of a substantial spin-orbit coupling [3]. However, the structural details that give rise to these properties are still not understood. We have studied the magnetic properties of epsilon-Fe₂O₃ between room temperature and 925 K by magnetic, Raman and neutron diffraction measurements. Upon heating, the saturation magnetization undergoes a monotonical decrease but the coercivity and remanence sharply drop and vanish at 480 K. Above 500 K and up to 870K epsilon-Fe₂O₃ is ferrimagnetic and presents a soft magnetic behaviour. Interestingly, this transition from superhard to soft ferrimagnetism involves changes in the magnetic state and magnetostructural effects that are relevant for a better understanding of the origin of spin-lattice coupling in epsilon-Fe₂O₃.

[1] B. Jin et al. Adv.Mater. 16 (2004) 48

[2] M. Gich et al. Adv. Mater. 26 (2014) 4645

[3] Y. C. Tseng et al. Phys. Rev. B 79 (2009) 094404

Mo.C-P10 - Orbital and spin structures in transition metal compounds with face-sharing octahedra

K. Kugel¹, D. Khomskii², A. Sboychakov¹, S. Streltsov^{3,4}

1. *Institute for Theoretical and Applied Electrodynamics, Russian Academy of Sciences, Moscow, Russia*
2. *II. Physikalisches Institut, Universität zu Köln, Köln, Germany*
3. *Institute of Metal Physics, Ural Branch, Russian Academy of Sciences, Ekaterinburg, Russia*
4. *Ural Federal University, Ekaterinburg, Russia*

Specific features of orbital and spin structure of transition metal compounds in the case of the face-sharing MO_6 octahedra are analyzed. In this geometry, we consider the form of the spin-orbital Hamiltonian for transition metal ions with double (e_g^σ) or triple (t_{2g}) orbital degeneracy. Trigonal distortions typical of the structures with face-sharing octahedra lead to splitting of t_{2g} orbitals into an a_{1g} singlet and e_g^π doublet. For both doublets (e_g^σ and e_g^π), in the case of one electron or hole per site, we arrive at a symmetric model with the orbital and spin interaction of the Heisenberg type and the Hamiltonian of unexpectedly high symmetry: $\text{SU}(4)$. Thus, many real materials with this geometry can serve as a testing ground for checking the prediction of this interesting theoretical model. We also compare general trends in spin-orbital exchange interaction for three typical situations: those of MO_6 octahedra with common corner, common edge, and the present case of common face, which has not been considered yet.

Mo.C-P11 - XAS and XMCD study on Co doped Ga_{0.6}Fe_{1.4}O₃ films

D. Kim², J. Kim¹

1. Pohang Accelerator Laboratory, POSTECH, Pohang, Korea

2. Department of Physics, POSTECH, Pohang, Korea

GaFeO₃ is a well known piezoelectric ferrimagnet where electron and spin degree of freedoms are coupled. There are four different cationic sites, Ga₁(Td), Ga₂(Oh), Fe₁(Oh), and Fe₂(Oh) and Fe₁ and Fe₂ are antiferromagnetically coupled. But, in Ga_{2-x}Fe_xO₃ including GaFeO₃, there are site disorders depending on the x and the fabrication methods and resultantly they became ferrimagnets. In this work, we studied the electronic and magnetic structure of Co doped Ga_{0.6}Fe_{1.4}O₃ films by measuring X-ray absorption spectroscopy and X-ray magnetic circular dichroism on the L edges of Fe and Co. The XAS of Co L edges clearly show that doped Co ions takes the Fe sites and the ground state of them are d⁷ high spin state(Co²⁺) under Oh symmetry or its subgroup. It is also interesting that a few percent doping of Co makes a noticeable change in the XMCD spectra of host Fe. It indicates Co doping induces a big change in the site disorder of host ions too. Through these experimental results, we clearly explain why the total magnetization decreases by factors and the electronic leakage decreases by orders just by doping a few percent of Co ions to Ga_{0.6}Fe_{1.4}O₃ films.

Mo.C-P12 - Large anisotropic g-factor due to crystalline spin-orbit interaction in bismuth

Y. Fuseya¹, Z. Zhu², B. Fauque³, W. Kang⁴, B. Lenoir⁵, K. Behnia³

1. *University of Electro-Communications, Chofu, Japan*
2. *Wuhan National High Magnetic Field Center*
3. *Ecole Supérieure de Physique et de Chimie Industrielles, Paris, France*
4. *Ewha Womans University, Seoul, South Korea*
5. *Ecole Nationale Supérieure des Mines de Nancy, Nancy, France*

The g-factor mirrors the effect of the crystalline spin-orbit interaction, which is a central issue in contemporary solid state physics. It is a crucial task for various fields, such as spintronics, multiferroics, and topological insulators, to understand and manipulate the g-factor of solids. However, on the other hand, it has been a hard task. For example, the origin of large anisotropic g-factor of holes in bismuth has been a mystery for more than a half century; their Zeeman energy is more than twice larger than their cyclotron energy when the magnetic field is along the trigonal axis, but becomes vanishingly small for the perpendicular orientation. Here, we report a theoretical solution to this longstanding puzzle based on a relativistic k.p theory of multiple band. Furthermore, we also present new experimental results that show the crystalline spin-orbit interaction can be actually manipulated according to our new understandings. Our new approach opens a new direction for the study and manipulation of spin-orbit interaction with possible applications, such as for spintronics, multiferroics, and topological insulators.

Mo.C-P13 - Diluting magnetism in Honeycomb lattice Iridates and understanding magnetic exchange

S. Manni^{1,2}, Y. Tokiwa¹, P. Gegenwart¹

1. *I Physikalisches Institut, Georg-August-Universität Göttingen, Göttingen, Germany*

2. *Ames Laboratory and Department of Physics and Astronomy, Iowa State University, Ames, Iowa, United States*

Honeycomb lattice iridates $A_2\text{IrO}_3$ ($A = \text{Na, Li}$) has drawn immense interest in the correlated electron physics community due to its realization as a novel spin-orbit Mott insulator with very unusual magnetic structure and also due to controversial discussion in background of different models like localized Heisenberg-Kitaev (HK) model [1]. The cause of this controversy lying in deep of complicated interactions within honeycomb arrangement of Ir $S_{\text{eff}}=1/2$ moments. In our lab we have synthesized $A_2\text{IrO}_3$ in single and poly-crystalline form and characterized structurally, magnetically and thermodynamically. We have identified both the system has long range antiferromagnetic (AF) ordering below $T_N = 15$ K with strong AF interaction between Ir $S=1/2$ [2,3]. We have synthesized $A_2(\text{Ir}_{1-x}\text{Ti}_x)\text{O}_3$ single and poly-crystal for Na and Li system respectively to study systematic dilution of Ir magnetism by nonmagnetic Ti for better understanding of magnetic interactions. Upon dilution both Na and Li honeycomb system shows spin glass behavior but in Na system spin glass temperature (T_g) and AF Weiss temperature drops very sharply towards zero before percolation limit whereas for Li system these two parameters persist much above percolation limit. This signifies Na_2IrO_3 is fundamentally nearest neighbor interaction system and in Li_2IrO_3 further neighbor interactions are significantly important. We observe a smeared quantum phase transition for $x=0.5$ dilution in Li-system which is rare for a $S_{\text{eff}}=1/2$ antiferromagnetic system.[4] The result is published in Ref. [4]. Work Supported by ERASMUS MUNDUS and DFG.

[1] J. Chaloupka et. al. PRL 105, 027204 (2010)

[2] Y.Singh et. al. PRB 82, 064412 (2010)

[3] Y. Singh, S.Manni et.al. PRL 108, 127203 (2012)

[4] S. Manni et. al. in PRB B 89, 241102(R) (2014)

Mo.C-P14 - Neutron diffraction studies on the magnetic structure of a-RuCl₃C. Ritter¹, A. Jain², N. Sung², B. Kim²1. *Institut Laue Langevin*2. *Max Planck Institute for Solid State Research, Stuttgart, Germany*

The importance of the spin-orbit coupling (SOC) in determining the electronic ground state of transition metal oxides has recently been a focus of both theoretical and experimental efforts. On the theoretical side the Kitaev model, which describes the interactions of spins $J_{\text{eff}} = \zeta$ on a honeycomb lattice by including bond dependent exchange interactions resulting from the SOC, is a rare example of exactly solvable models with highly nontrivial properties such as a quantum spin-liquid state and fractional statistics. However, being highly artificial, the model is difficult to realize in a real-world material. A number of promising candidates have been proposed in strongly spin-orbit coupled 5d transition-metal oxides (such as Na₂IrO₃ and Li₂IrO₃), which have the requisite bond-directional interactions of the form in the Kitaev model. The search for the Kitaev spin-liquid has recently been extended to 4d transition-metal oxides with a-RuCl₃ as one of the possible candidates as it crystallizes in a layered structure where the Ru³⁺ ions sit on a honeycomb lattice and see a nearly perfect RuCl₆ octahedral environment. Although magnetic susceptibility data had indicated a finite-temperature long-range magnetic order, the determination of its magnetic structure is of crucial importance in assessing the proximity to the Kitaev quantum spin liquid state. Here we present the results from the first neutron powder diffraction measurements which strongly support the presence of a zigzag type magnetic order, quite similar to that of Na₂IrO₃. In the low temperature neutron diffraction patterns, we have observed two magnetic Bragg peaks which could be indexed with a propagation vector $\mathbf{k} = (\zeta, 0, \zeta)$. Using magnetic symmetry analysis, the refinement of these two peaks was possible with an allowed irreducible representation and confirmed the three-dimensional nature of the magnetic order despite the fact that neighboring Ru-Cl layers are weakly coupled by van der Waals forces.

Mo.C-P16 - Mechanism of the electron paramagnetic resonance line broadening in the hole doped manganites $\text{La}_{1-x}\text{Ca}_x\text{MnO}_3$

M. Auslender¹, E. Rozenberg², A. Shames

1. Ben Gurion University of the Negev, Department of Electrical and Computer Engineering, Beersheba, Israel

2. Ben Gurion University of the Negev, Department of Physics, Beersheba, Israel

Since the first experimental studies of electron paramagnetic resonance (EPR) in the hole doped manganites $\text{La}_{1-x}\text{Ca}_x\text{MnO}_3$ ($0 < x < 0.5$), it has been recognized that the EPR signal linewidth increases upon heating starting from some temperature above the Curie point, with no signs of saturation. In those and later publications on the base of measured temperature dependences of the EPR, different mechanisms of such a broadening, contradicting partially to each other even for the same manganites, were suggested such as: one-phonon spin-lattice relaxation of three- and four-valent Mn ions and small-polaron hopping. Most of those attributions, however, were made on the base of restricted data obtained on low-quality samples and/or in a narrow temperature range, and until nowadays, increasing the EPR linewidth has remained a puzzle. In this contribution, we address the mechanism of this phenomenon for both single- and polycrystalline samples in unprecedentedly wide range of Ca compositions and temperature. On the base of the temperature slope and absence of activation of the linewidth at $x > 0.2$, we substantiate ruling out both spin-phonon and polaron-hopping mechanisms, respectively. Moreover, the EPR g-factor data, allow us to argue that most of eg electrons of leave the formerly trivalent Mn sites to be more mobile bond-occupating ones, even at low x. This facilitates using the double exchange (DE) model for a theoretical description. Including the spin-orbital interaction of the charge carriers with the lattice and impurities, we calculate the contribution of the carriers to the EPR linewidth both for the case of weak and strong Hund exchange. The temperature dependences of the EPR linewidth obtained within our theory fit well the experimental data. A part of these results were communicated in JAP, 113, 17D705 (2013).

Mo.C-P17 - Magnetic order and Trigonal crystal field effects in Sr₃NiIrO₆

E. Lefrançois^{1,2}, L.C. Chapon¹, S. Virginie², P. Lejay², R. Ballou², D. Khalyavin³, S. Rayaprol⁴, E.V. Sampathkumaran⁵, D.T. Adroja^{3,6}, A.M. Pradipto⁷, S. Picozzi⁷, M. Moretti Sala⁸

1. Institut Laue-Langevin, Grenoble, France
2. Institut Néel, CNRS & Université Grenoble Alpes, Grenoble cedex 9, France
3. ISIS Facility, STFC, Rutherford Appleton Laboratory, Oxfordshire, United Kingdom
4. UGC-DAE CSR, Mumbai Center, Mumbai, India
5. Tata Institute of Fundamental Research, Mumbai, India
6. Physics Département, University of Johannesburg, Johannesburg, South Africa
7. CNR-SPIN, l'Aquila, Italy
8. European Synchrotron Radiation Facility, Grenoble, France

Oxides of the family A₃MM'O₆ (A = alkaline-earth metal, M, M' = transition metal) attracted a lot of attention because of their unconventional magnetic properties linked to the coexistence of low dimensionality, magnetic frustration and magnetocrystalline anisotropy. In these compounds, the M and M' ions form chains which are distributed on a triangular lattice. In consequence, the magnetism of the compounds with an easy-axis of anisotropy, which confines the magnetic moments along the chains direction, should be strongly frustrated. We studied the 5d-based compound Sr₃NiIrO₆, where the strong spin-orbit coupling on the Ir⁴⁺ ions might induce unexpected behaviors through spin-orbit entanglements. Single crystal magnetization, powder neutron diffraction and single crystal resonant inelastic scattering (RIXS) measurements were performed. The magnetization measurement revealed the existence of a large easy-axis anisotropy confining the Ni²⁺ and Ir⁴⁺ magnetic moments along the chains. Besides the zero-field cooled and field-cooled measurements show that there are two characteristic temperatures: T₁ = 70 K and T₂ = 17 K. The first temperature is associated with a deviation from a Curie-Weiss behavior and the appearance of magnetic order with propagation vector $k=(0,0,1)$. At T₂, the susceptibility reaches a maximum followed by a sudden drop. The magnetic structure can be determined from powder neutron diffraction only up to a global phase. However, symmetry arguments allowed determining the exact nature of the magnetic ground state below T₂, thus clarifying the universal magnetic properties of this family of compounds [PRB 90 (014408) 2014]. RIXS measurements allowed probing the electronic and magnetic excitations inside the t_{2g} triplet thus estimating the strength of the spin-orbit coupling as well as the amplitude of the trigonal distortion of the IrO₆ octahedra. Besides the low-temperature measurements also show the emergence of a non-dispersive magnon around 90 meV.

Mo.C-P19 - X-ray Magnetic circular dichroism in the spinel-type vanadium oxides AV_2O_4 (A=Mn,Fe)

K. Matsuura¹, H. Sagayama¹, Y. Nii¹, N. Duy Khanh², N. Abe¹, T. Arima¹

1. *The University of Tokyo, Tokyo, Japan*

2. *Tohoku University, Sendai, Japan*

Spinel-type vanadium oxides FeV_2O_4 and MnV_2O_4 are considered to exhibit different types of V^{3+} orbital order from each other. The orbital structure at V^{3+} in MnV_2O_4 has been reported as real-function type antiferroic orbital order and that in FeV_2O_4 as complex-function type ferro orbital order. In order to tackle this issue, temperature dependence of x-ray absorption spectrum (XAS) and x-ray magnetic circular dichroism (XMCD) spectrum are investigated in both the spinel compounds. XMCD spectroscopy is widely applied for estimating element-selective orbital and spin angular momenta in 3d transition metals and their compounds quantitatively by using simple formalisms of orbital and spin sum rules. The application of the sum rule to the obtained V edge XMCD spectra and the comparison with crystal field multiplet calculation suggest a real-function orbital ordered state with quenched orbital angular momenta in both FeV_2O_4 and MnV_2O_4 . A dissimilarity in XAS spectra implies a quantitative difference of the effect of trigonal distortion on the electronic structure between FeV_2O_4 and MnV_2O_4 .

Mo.C-P20 - Current induced switching in Transition-metal/Ferromagnetic multilayers

J. Kim¹, D. Kim¹, Y. Jang¹, B. Kim¹, K. Rhie¹

1. Department of Display and Semiconductor Physics, Korea University, Sejong, South Korea

The spin orbit torque (SOT) may lead to a better conceptual basis for developing 3-terminal magnetic memory cells [1]. After the Miron's work [2], many results shown that SOT is a good mechanism to change a magnetization direction of ferromagnetic layers which include a transition-metal (TM)/ferromagnetic (FM) multilayers structure. [3, 4] In this study, we use Pt/Co, FeZr(amorphous paramagnetic)/CoFeB, and Ta/CoFeB multilayers to understand an effect of SOT in each structure. In Pt (t1)/Co/Pt (t2) case, the thickness of both upper (t2) and lower (t1) Pt layers are varied separately. The sign of SOT is changed when t2 is thicker than t1, which means injected spin currents from upper and lower Pt layers have different spin directions. Since the amount of injected spin current is proportional to thickness of TM, one is able to observe the competitions of spins injected from upper and lower paramagnetic layers. The critical current to switch magnetization decreases with the increase of in plane magnetic field strength. And the sign of Hall voltage is changed when the direction of applied field is switched. We observed magnetic field dependence of switching current and thickness dependence of spin Hall sign

- [1] L. Liu, C. F. Pai, Y. Li, H. W. Tseng, D. C. Ralph, and R. A. Buhrman, Science 336, 555 (2012)
- [2] I. M. miron, k. Garello, G. Gaudin, P. J. Zermatten, M. V. Costache, S. Auffret, S. Bandiera, B. Rodmacq, A. Schuhl and P. Gambardella, Nature (Lond on) 476, 189 (2011)
- [3] K. Ando, S. Takahashi, k Harii, K. Sasage, J. Idea, S. Maekawa and E. Saitoh, Phys. Rev. Lett. 101, 036601 (2008)
- [4] L. Q. Liu, T. Moriyama, D. C. Ralph and R. A. Buhrman, Phys. Rev. Lett. 106, 036601 (2011)

Mo.C-P21 - 51V NMR study on the orbital degenerated system Sr₂VO₄ with the K₂NiF₄ type structure

Y. Kato¹, Y. Shimizu¹, Y. Kobayashi¹, M. Itoh¹, H. Sakurai², T. Kao^{2,3}, H. Yang³

1. *Department of Physics, Graduate School of Science, Nagoya University, Nagoya, Japan*

2. *National Institute for Materials Science, 1-1 Namiki, Tsukuba, Japan*

3. *Department of Physics, National Sun Yat-Sen University, Kaohsiung, Taiwan*

Sr₂VO₄ with the K₂NiF₄ type structure has attracted much attention as a 3d¹ system with the degenerated d_{xy}/d_{yz} orbital due to the tetragonal crystal field. Magnetic susceptibility shows a drop around 100 K where a structural transition takes place. Based on the first principle calculation combined with the path-integral renormalization group method, a stripe-type orbital and spin order, leading to the movement of the degeneracy, was proposed as a ground state. On the other hand, by taking account of the spin-orbit interaction for the degenerated orbital, the magnetic octupole transition was proposed to take place. However, the ground state and the mechanism of the phase transition have not been uncovered, although several experimental studies were performed. In this study we have made 51V NMR measurements on a powder sample to reveal local magnetic properties of Sr₂VO₄. We observed the 51V NMR spectrum with the negative Knight shift 51K having the hyperfine coupling constant due to the core polarization effect, $A = -110$ kOe/ μ_B , above 120 K, whereas a weak NMR spectrum was observed to become nonmagnetic in the temperature range 100-120 K where the paramagnetic spectrum coexists. Below 100 K, only a weak nonmagnetic spectrum was observed with 51K=0, indicating that there is partly a nonmagnetic V site. This might be ascribed to the orbital order, although it is inconsistent with the tetragonal structure reported below 100 K.

Mo.C-P22 - Tuning the spectroscopic g-factor in permalloy

C. Gonzalez^{1,2}, Y. Yin², R. Dumas², C. Garcia¹

1. *Departamento de Física, Universidad Tecnica Federico Santa Maria, Valparaiso, Chile*

2. *Department of Physics, University of Gothenburg, Gothenburg, Sweden*

It is predicted that the spin-orbit coupling (SOC) has a significant role in quenching the electronic orbital angular momentum in ferromagnets [1], that results in a small deviation of the spectroscopic g-factor (g) from 2. In this work we apply a recently published methodology [2] to measure the value of g with very high precision in thin films of permalloy doped with different concentrations of metals which have significant SOC: Ag, Pt and Au. The results shows a positive correlation between the value of g , the dopant concentration and the dopant's SOC.

[1] C. Kittel, Phys. Rev. 76, 743 (1949)

[2] Justin M. Shaw, Hans T. Nembach, T. J. Silva and Carl T. Boone, J. Appl. Phys. 114, 243906 (2013)

Mo.C-P23 - Spin-flip electron scattering in the Rashba surface alloy

S. Schirone¹, E. E. Krasovskii^{2,3,4}, G. Bihlmayer⁵, R. Piquerel¹, P. Gambardella^{1,6,7}, A. Mugarza¹

1. ICN2-Institut Catala de Nanociencia i Nanotecnologia, Campus UAB, Bellaterra, Barcelona Spain

2. Dpto. de Física de Materiales, Facultad de Ciencias Químicas, UPV/EHU, San Sebastián/Donostia, Spain

3. Donostia International Physics Center (DIPC), Paseo Manuel de Lardizabal 4, San Sebastián/Donostia, Spain

4. IKERBASQUE, Basque Foundation for Science, Bilbao, Spain

5. Peter Grünberg Institut and Institute for Advanced Simulation, Forschungszentrum Jülich and JARA, Jülich, Germany

6. ICREA - Institutio Catalana de Recerca i Estudis Avancats, Barcelona, Spain

7. Department of Materials, ETH Zurich, Zurich, Switzerland

Spin-orbit interaction (SOI) in metallic surfaces can lead to a splitting of the spin degeneracy and the emergence of particular spin textures that are related to the entanglement between spin and orbital momentum. This can lead to interesting electron scattering phenomena where backscattering is forbidden by time reversal symmetry, as observed for topological surface states [1]. Here we study effect of the spin texture on electron scattering at surfaces characterized by strong Rashba interaction. In the BiAg₂ surface alloy, which is characterized by the strongest to date Rashba effect [2,3], we find that an SOI-driven spin-flip mechanism opens new backscattering channels. The alloy is formed on the surface after the deposition of monolayer of Bismuth, which induces a reconstruction. The scattering has been studied using Scanning Tunnelling Microscopy and Spectroscopy (STM/STS). In this way we have studied electron confinement by measuring the interference patterns formed by surface electrons scattered from monoatomic steps. We find that scattering is determined by i) an unconventional orbital/spin texture of the surface bands, which give rise to transitions with combined orbital and spin flips, and ii) by its chemical composition, which defines a heterogeneous electron localization and potential landscape. The negligible leakage we observe across some step structures indicate a strong confinement effect, comparable to that observed in metals with marginal SOI such as Ag(111) [4]. The results describe a scenario that is far more complex than the conventional Rashba-type two dimensional free-electron gas.

References:

- [1] J. Seo, et al., Nature 466, 343 (2010)
- [2] C. Ast, et al., Phys. Rev. Lett. 98, 186807 (2007)
- [3] G. Bihlmayer, et al., Phys. Rev. B 75, 195414 (2007)
- [4] J. E. Ortega, et al., Phys. Rev. B 87, 115425 (2013)
- [5] S. Schirone et al., submitted

Mo.C-P25 - Current-induced spin polarization and spin-orbit torque in magnetized graphene with Rashba spin-orbit interaction

A. Dyrdal¹, J. Barnas

1. Faculty of Physics, Adam Mickiewicz University, Poznań, Poland

Electric current flowing in a system with spin-orbit interaction can induce spin polarization of conduction electrons. Such a nonequilibrium spin polarization in magnetic structures can generate a spin-orbit torque exerted on localized magnetic moments, and may lead to magnetization switching in the system.

Here, we consider theoretically current-induced spin polarization in graphene with Rashba spin-orbit interaction. To find the stationary nonequilibrium polarization in the linear response regime, we have used the Green's function formalism and derived analytical formulas for the induced spin polarization [A. Dyrdal, J. Barnas, and V. K. Dugaev, Phys. Rev. B 89, 075422 (2014)]. This polarization is oriented in the graphene plane and is normal to the current orientation. Furthermore, orientation of the spin polarization becomes reversed when the Fermi level (whose position can be controlled by an external gate voltage) crosses the Dirac points.

When graphene is deposited on a magnetic substrate, a nonzero equilibrium magnetization can be induced due to the proximity effect. In such a case, the other components of the current-induced spin polarization become nonzero, which in the lowest-order approximation depend linearly on the exchange field. We have derived analytical formulas for all components of the spin polarization. The spin-orbit torque exerted on the magnetization has also been determined.

Mo.D-P02 - Silicon-based current-controlled reconfigurable magnetoresistance logic device

X. Zhang¹, Z. Luo¹

1. School of Materials Science and Engineering, Tsinghua University, Beijing, China

Silicon-based complementary metal-oxide-semiconductor (CMOS) transistors have achieved great success. However, the traditional development pathway is approaching its fundamental limits. Magnetoelectronics logic, especially magnetic-field-based logic, shows promise for surpassing the development limits of CMOS logic and arouses profound attentions. Existing proposals of magnetic-field-based logic are based on exotic semiconductors and difficult for further technological implementation. Here, a kind of diode-assisted geometry-enhanced low-magnetic-field magnetoresistance (MR) mechanism is proposed [1]. It couples p-n junction's nonlinear transport characteristic and Lorentz force by geometry, and shows extremely large low-magnetic-field MR (>120% at 0.15 T). Further, it is applied to experimentally demonstrate current-controlled reconfigurable magnetoresistance logic on the silicon platform at room temperature. This logic device could perform all four basic Boolean logic including AND, OR, NAND and NOR in one device [2]. Combined with non-volatile magnetic memory, this logic architecture with unique magnetoelectric properties has the advantages of current-controlled reconfiguration, zero refresh consumption, instant-on performance and would bridge the processor-memory gap. Our findings would pave the way in silicon-based magnetoelectronics and offer a route to make a new kind of microprocessor with potential of high performance.

References:

- [1] C. H. Wan, X. Z. Zhang, X. L. Gao, J. M. Wang & X. Y. Tan, Geometrical enhancement of low-field magnetoresistance in silicon, *Nature* 477, 304-307 (2011)
- [2] Zhaochu Luo, Xiaozhong Zhang, Chengyue Xiong, Jiaojiao Chen, Silicon-Based Current-Controlled Reconfigurable Magnetoresistance Logic Combined with Non-Volatile Memory, *Advanced Functional materials*, online published on 10 NOV 2014. (DOI: 10.1002/adfm.201402955)

Mo.D-P03 - Magnetic tunnel junctions with semiconducting rare earth nitride electrodes

H. Warring¹, J. Trodahl¹, F. Natali¹, B. Ruck¹

1. The MacDiarmid Institute For Advanced Materials And Nanotechnology, Wellington, New Zealand

Magnetic tunnel junctions (MTJs) are predominantly based on conventional transition metal-based electrodes where the electrodes are only partially spin polarised, and hence the tunnel magnetoresistance (TMR) is limited. The TMR can be maximised by increasing the spin polarisation of the electrodes, as evidenced by studies of MTJs with half-metallic electrodes. Another class of materials which can harbour large spin polarisations are the ferromagnetic semiconductors. These materials are especially interesting for use in MTJs because in principle properties such as the carrier concentration and Fermi level can be tuned. The rare earth nitride series contains several examples of intrinsic ferromagnetic semiconductors, i.e., they are both ferromagnetic and semiconducting without the need for addition of dopant atoms. This combination gives them clear potential for creating and understanding spintronics devices. Although their physical properties have been widely studied, the rare earth nitrides have yet only been used in a small number of proof-of-concept devices. This talk will present developments in producing magnetic tunnel junctions using rare earth nitrides as the electrodes. An insulating GaN barrier separates two magnetic GdN electrodes in which the tunnelling current is modulated by the magnetisation of these layers. We find that the transport properties are heavily influenced by the electronic structure of the GdN electrodes. The Fermi level of the GdN is found to lie slightly above the middle of the GaN gap at low temperatures, consistent with recent predictions. Our results show that GdN tunnel junctions are promising candidates for further investigation into the role novel electrode materials can play in tuning the properties of magnetic tunnel junctions.

Mo.D-P04 - Experimental demonstration of Elliott-Yafet spin relaxation mechanism and room-temperature spin transport in highly-doped n-type Ge epilayers.

S. Dushenko¹, M. Koike¹, Y. Ando^{1,2}, T. Shinjo², M. Myronov³, M. Shiraishi^{1,2}

1. *Osaka University, Osaka, Japan*

2. *Kyoto University, Kyoto, Japan.*

3. *The University of Warwick, Coventry, United Kingdom*

Ge possesses much higher carrier mobility comparing to Si, thus it is possible for Ge-based spin transport devices to overcome scaling limits of the Si-based devices. However, in contrast to successful realization of spin transport in Si at room temperature (RT), spin transport in Ge is still limited to low temperatures. We report the first experimental realization of RT spin transport in n-Ge epilayers and temperature dependence of the spin relaxation time. Under ferromagnetic resonance conditions spins were injected from Py (Ni80Fe20) strip into 50 nm thick heavily n-type doped Ge epilayer with a phosphorous doping concentration of $1.0 \times 10^{19} \text{ cm}^{-3}$. After transport through the n-Ge channel spin current was absorbed into a metal strip with large spin-orbit interaction (Pt or Pd in our study) and converted into a charge current via inverse spin Hall effect (ISHE). Using theoretical model for our spin transport geometry we calculate generated ISHE voltage and extract spin diffusion length in the n-Ge channel, which is estimated to be $660 \pm 200 \text{ nm}$ at RT. Additionally using temperature dependence of the ISHE voltage and mobility in the n-Ge channel we determine spin relaxation mechanism in highly doped n-Ge. In the temperature range from 130 K to 297 K spin relaxation time decreased 2.2 times with increasing temperature [1]. Thus indicating dominance of the Elliott-Yafet spin relaxation mechanism in the highly doped n-Ge epilayers.

References:

1. S. Dushenko, M. Koike, Y. Ando, T. Shinjo, M. Myronov, and M. Shiraishi, submitted

Mo.D-P05 - Large magnetoresistance in silicon

X. Zhang¹, Z. Luo¹

1. Tsinghua University, Beijing, China

Large magnetoresistance in silicon Xiaozhong Zhang and Zhaochu Luo School of Materials Science and Engineering, Tsinghua University, Beijing 100084, China Magnetoresistance (MR) reported in some non-magnetic semiconductors particularly silicon has triggered considerable interest owing to the large magnitude of the effect. We showed that MR in lightly doped n-Si can be significantly enhanced by introducing diodes and proper design of the carrier path. We designed a four-terminal Si-based geometrical enhanced MR device whose room-temperature MR ratio reaching 30% at 0.065 T and 20000% at 1.2T, respectively, approaching the performance of commercial MR devices. The mechanism of this GEMR is: the diodes help to define a high resistive state (HRS) and a low resistive state (LRS) in device by their openness and closeness, respectively. The ratio of apparent resistance between HRS and LRS is determined by geometry of silicon wafer and electrodes. Magnetic field could induce a transition from LRS to HRS by reshaping potential and current distribution among silicon wafer, resulting in a giant enhancement of intrinsic MR [1,2]. We also propose a new nonlinear method to increase low-magnetic-field MR by forming a sharp resistance transition with high magnetic sensitivity in the S-shape negative differential conductance region [3]. This two-terminal Si-based micro-device with simple structure could work at low voltage (~4V) and a large low-magnetic-field MR could be achieved at room temperature (~1,000% at 0.05 T). These two performances approaching that of magnetic metal-based MR devices, would pave the way in silicon-based magnetoelectronics.

References:

- [1] C.H. Wan, X. Z. Zhang, X. L. Gao, J. M. Wang & X. Y. Tan, Nature 477, 304 (2011)
- [2] Zhaochu, Luo and Xiaozhong Zhang, J. Appl. Phys. 117, 17A302 (2015); doi: 10.1063/1.4906766
- [3] Hong-Guang Piao, et al, Large low-magnetic-field magnetoresistance in Silicon, (in submission)

Mo.D-P07 - Scattering matrix approach to the anomalous hall effect: 2D network model

P. Streda¹

1. Institute of Physics, ASCR, Prague, Czech Republic

The general theory of irreversible processes leads to the conclusion that the linear response to the dynamical force, represented by the electric field, has to be equivalent to that given by the statistical force, represented by the gradient of chemical potential. While the anomalous Hall current induced by the electric field has been intensively studied, nearly no attention has been devoted to the response of the chemical potential gradient, which is based on the scattering matrix approach. The nonzero magnetization of ferromagnetic materials is attributed to the existence of the spin-polarized bands. Within the tight-binding approach these bands originate in a network of overlapping atomic spin-polarized orbitals. The main attention is devoted to orbitals having nonzero orbital momentum. Considering the sample in the form of a hollow cylinder, the chemical potential difference between cylinder edges gives rise to a non-zero orbital momentum parallel with its axis. It is determined by the part of free currents forming loops around the cylinder axis, anomalous Hall current. Their general properties has been studied by using the simple two-dimensional network model. Point contact coupling between orbitals, characterized by the energy independent transition probability, has been considered. Longitudinal and Hall conductivity has been establish by the detail analysis of the scattering matrix structure for the cylindrical sample. It has been found that the network model on square lattice shows the topological phase transformation for transition probability just equal to one half. At this point the spin-orbit energy is changing its sign. Above this value the anomalous Hall conductivity approaches the quantized value within the energy gap regions. This quantization is connected with chiral edge states arising in samples having form of the strip as experimentally observed on magnetic topological insulators.

Mo.D-P08 - Hot electrons transport in devices combining tunnel and Schottky barriers

C. Vautrin¹, Y. Lu¹, S. L. Gall², G. Sala¹, S. Robert¹, O. Lenoble¹, F. Montaigne¹, M. Wu³, D. Lacour¹, M. Hehn¹

1. *Institut Jean Lamour*

2. *LPEP*

3. *Hefei National Laboratory for Physical Sciences at Microscale*

We have recently unveiled experimentally a new interfacial trapping phenomenon for hot electron injection in silicon[1]. The transport measurements indicate that an interfacial charge trapping and a backscattering-induced collector current limitation take place when the temperature is lower than 25K. This results in a rapid decrease of the magneto-current ratio. In this presentation we will demonstrate an electrical control of this trapping effect thanks to a magnetic tunnel transistor made on wafer bonded substrate [2]. A model taking into account the effects of both electric field and temperature will be presented. It closely reproduces the experimental results and allows extraction of the trapping binding energy (1.6 meV). Finally we will also discussed the difficulties encountered during realization of equivalent devices having out of plane magnetizations. Links between Schottky barriers preparation techniques and the existence of perpendicular magnetic anisotropy in a CoNi multilayer are established made. A solution to join in the same devices a Schottky barrier and perpendicular anisotropy will be revealed.

[1]Y. Lu, D. Lacour et al, Appl. Phys. Lett. 103, 022407 (2013)

[2]Y. Lu, D. Lacour et al, Appl. Phys. Lett. 104, 042408 (2014)

[3]C. Vautrin, D. Lacour et al, to be published (2015)

Mo.D-P09 - Spin dynamics in three coherently coupled quantum dots

B. Bułka¹, J. úuczak¹

1. Institute of Molecular Physics, Polish Academy of Sciences, Poznan, Poland

Di Vincenzo *et al.* [1] proposed a scheme for universal quantum computations which can be realized by a three spin system with exchange interactions in three quantum dots (TQD) where logical qubits are encoded in the doublet subspace. A main advantage of the TQD system is a purely electrical control of exchange interactions by gate potentials which act locally and provide much faster operations. Recently experimental efforts [2] were undertaken to get coherent spin manipulations in TQD according to Di Vincenzo's scheme.

Inspired by the experiments [2] we performed theoretical studies of spin dynamics activated by Landau-Zener passages between different charge states. The system is modeled by an extended Anderson Hamiltonian with time dependent positions of quantum dot levels. We show that due to spin Stark effect [3] one can activate the qubit states confining only to the doublet subspace (without the quadruplet state which was used in [2]). This new scheme operates within a decoherence-free subspace and is immune to decoherence processes. First spin dynamics is considered for a linear TQD system (corresponding to the experimental situation). However in this situation two doublet states are nonequivalent what restricts qubit operations. Therefore, we propose TQD in a triangular geometry as the qubit, where manipulations (preparation and single qubit operations) are performed by an electric field which breaks the symmetry of the system and changes spin entanglement.

This work was supported by the National Science Centre (Poland) under Contract DEC-2012/05/B/ST3/03208

[1] D.P. Di Vincenzo, *et al.*, Nature 408, 339 (2000)

[2] E.A. Laird, *et al.*, Phys. Rev. B 82, 075403 (2010); L. Gaudreau, *et al.*, Nat. Phys. 8, 54 (2012); S. Amaha, *et al.*, Phys. Rev. Lett. 110, 016803 (2013); Z. Shi, *et al.*, Phys. Rev. Lett. 108, 140503 (2012)

[3] B.R. Bułka, *et al.*, Phys. Rev. B 83, 035301 (2011)

Mo.D-P10 - Spin-glass behavior of Fe doped InAs prepared by ion implantation and pulsed laser annealing

Y. Yuan¹, H. Cai¹, M. Helm¹, S. Zhou¹

1. Helmholtz - Zentrum Dresden – Rossendorf, Dresden, Germany

Dilute magnetic semiconductors (DMSs) attracted great interests in the last several decades because of their potential for spintronic device [1]. III-V compounds especially GaAs based DMS has recently emerged as the most popular material for this new technology. However, that the low mobility of holes in p-type DMS limits the potential application in semiconductor spintronic devices. Therefore, the searching for n-type DMS is of interest.

The doping of Fe in InAs is attracting research attentions due to the possibility to fabricate n-type diluted magnetic semiconductors [2, 3]. However, the low solubility of Fe in InAs is the most difficulty to achieve InFeAs DMS. In this work, we obtain Fe doped InAs layers by ion implantation and pulsed laser annealing. This approach has shown success for preparing other III-V based DMSs [4, 5]. The formed InFeAs layers are proved to be epitaxial-like on InAs substrates. The prepared InFeAs layers reveal similar magnetic properties independent of their conductivity types. While the samples are lacking of characteristics of DMS, they appear to be spin-glass like, revealing such as time-dependent magnetization measurements reveal aging and memory effects.

1. T. Dietl et al., Science 287, 1019-1022 (2000)
2. M. Kobayashi et al., Appl. Phys. Lett., 105, 032403(2014)
3. P. Nam Hai et al., Appl. Phys. Lett., 101, 182403 (2012)
4. D. Bürger et al., Phys. Rev. B, 81, 115202 (2010)
5. M. Khalid et al., Phys. Rev. B, 89, 121301(R) (2014)

Mo.D-P11 - Spin filtering in double quantum dots Aharonov-Bohm ring under cubic Rashba spin orbit interaction

K. Kondo¹

1. Laboratory of Quantum Electronics, Research Institute For Electronic Science, Hokkaido University, Sapporo, Japan

A spin current generation without ferromagnetic metals is a key issue for spintronics devices. The spin orbit interaction (SOI) is expected to be a promising ingredient for the purpose. Especially, it is confirmed that the strength of Rashba SOI can be easily controlled by an external electric field. The theory of devices using SOI such as a spin-filter is very important in the field of spintronics. The spin-filtering devices can be used to generate and detect spin polarized currents. Many researchers have reported about the spin-filters using linear Rashba SOI. However, the spin-filters using cubic Rashba SOI are not yet reported. In this study, we investigate the spin filtering in double quantum dots Aharonov-Bohm (AB) ring under linear or cubic Rashba SOI. This AB ring consists of elongated quantum dots and quasi-one dimensional quantum nanowires under magnetic field. The spin transport is investigated from left nanowire to right nanowire in the above structure within tight binding approximation. In particular, we focus on the difference of spin filtering between linear and cubic Rashba SOI. The calculation is performed for the spin transmission with changing the penetrating magnetic flux for the AB ring subject to linear and cubic Rashba SOI, respectively. It is found that the perfect spin filtering is achieved for both linear and cubic Rashba SOI. This result indicates that this AB ring under Rashba SOI can be a promising device for spin current generation. Moreover, they behave in totally different ways in response to penetrating magnetic flux, which is attributed to linear and cubic behaviors in the in-plane momentum. This result enables us to make a distinction between linear and cubic Rashba SOI according to the peak position of the perfect spin filtering.

Mo.D-P12 - Electronic structure and transport properties of Bi₂Te₃ and Bi₂Se₃ with magnetic dopants

K. Carva¹, J. Kudrnovsk², M. ValiÜka¹, V. Hol^{2,1}

1. Charles University, Prague, Czech Republic
2. Institute of Physics, Prague, Czech Republic

The surface state in topological insulators is protected against perturbations that keep time-reversal symmetry. Magnetic impurities violate time-reversal symmetry and thus may affect largely transport properties of topological insulators connected with the forbidden backscattering. We concentrate on Bi₂Te₃ and Bi₂Se₃ doped with Mn and Cr. It is known that there are several locations for these dopants available in the host lattice. Ab initio calculations employing the tight-binding linear muffin tin orbital (TB-LMTO) method and the coherent potential approximation (CPA) have been performed for the case of Mn/Cr placed in an octahedral interstitial position or the substitution of one of Bi atoms by Mn/Cr. Big volume difference between Mn and Bi/Se atoms represents a challenge for this method. The dopant moment as well as its DOS is shown to vary significantly depending on its location in the lattice. The exchange interaction between magnetic dopants and its possible magnetic ordering has been studied. We also calculate the conductivity tensor by means of the linear response theory, a strong dependence on the type and location of defect is found here. Hence the defects can be used to control many of material properties. This information can also help in identification of the defect location in real samples.

Mo.D-P13 - Anomalous proportional dependence of spin RA product on tunnel RA product in CoFe/SiO₂/Si tunnel contacts

J. Lee¹, S. He^{1,2}, B. Kang¹, B. Cho¹

1. *School of Materials Science And Engineering, Gwangju Institute of Science And Technology (GIST), Gwangju, South Korea*

2. *Gruenberg Research Centre, Nanjing University of Posts and Telecommunications, Nanjing, China*

Efficient spin injection into a semiconductor is one of the most essential requirements in the field of semiconductor spintronics to realize novel spin-based devices, which utilize both the spin and charge functionality of electrons. In the past few years, electrical spin injection using 3-terminal Hanle technology has been widely reported in a variety of ferromagnet/tunnel oxide/semiconductor heterojunctions, in which an oxide tunnel barrier is employed to solve the conductivity mismatch between the metallic ferromagnet and the semiconductor. However, it has been found that the spin accumulation signal is highly sensitive to the thickness of the oxide barrier layer and its interfacial states [1-2]. Here, we systemically investigate the influence of tunnel resistance on the Hanle spin signal in CoFe/Silicon oxide/n+-Si structure. CoFe/SiO₂/Si samples with different levels of tunnel resistance were fabricated, in which silicon oxide tunnel barriers were formed by plasma oxidation of the heavily doped n-type Si and CoFe was deposited by magnetron sputtering without breaking vacuum. To our best knowledge, this is the first study of spin injection in ferromagnetic tunnel contact using silicon oxide tunnel barrier formed by plasma oxidation. Fig. 1(a) and (b) show the typical Hanle curves measured at different bias voltages at room temperature and Hanle and inverted Hanle curves measured at 90K, respectively. Anomalous proportional dependence of the spin RA product on tunnel RA product is observed, as shown in Fig. 1(c) and (d). This tendency is similar to that reported in NiFe/Al₂O₃/Si and Fe/MgO/Si junctions [2]. It is known that recently there has been intensive debate about both the origin of the Hanle signal and the role of the tunnel barrier in the tunneling process of spin polarized carriers [3]. Our work will provide more experimental evidence for the study of spin injection in ferromagnet/tunnel oxide/semiconductor heterojunctions.

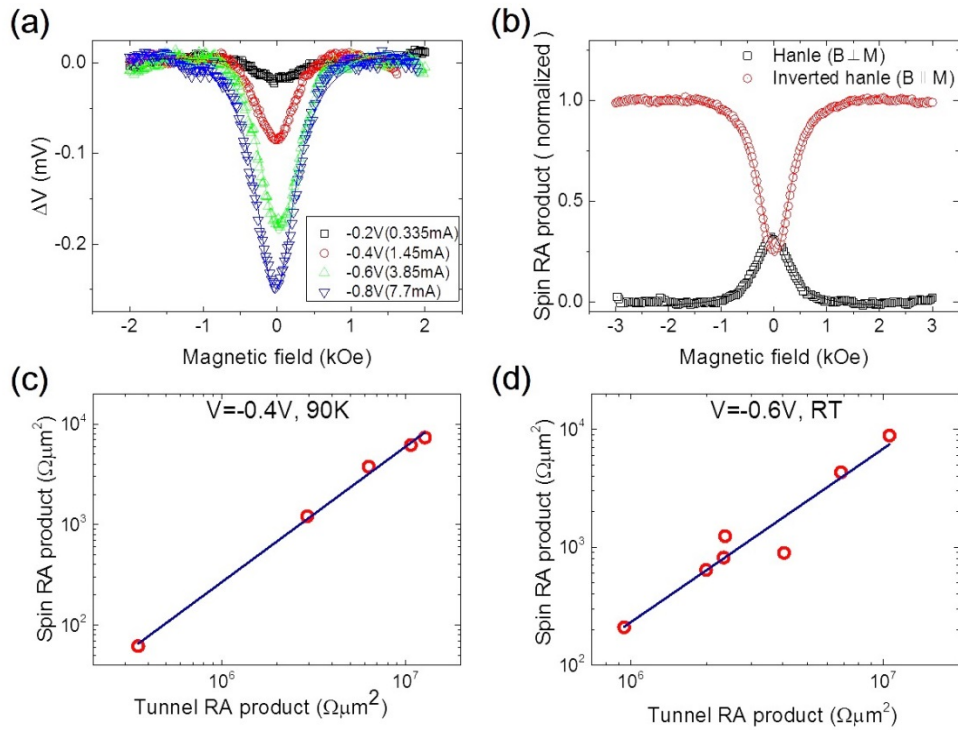


Fig. 1. Analysis of 3-terminal Hanle detection of CoFe/Silicon oxide/n-SOI junctions. (a) Hanle curves for spin injection measured at different bias voltages at room temperature. (b) Hanle and inverted Hanle curves measured at 90K. (c) and (d) Dependence of spin RA product on tunnel RA product.

References:

- [1] R. Jansen et al., *Semicond. Sci. and Technol.* 27, 083001 (2012)
- [2] S. Sharma et al., *Phys. Rev. B* 89, 075301 (2014)
- [3] O. Txoperena et al., *Appl. Phys. Lett.* 102, 192406 (2013)

Mo.D-P14 - Oxide diffusion barriers on GaAs(001)

A. Sarkar¹, S. Wang¹, R. Koch¹

1. Johannes Kepler University Linz, Linz, Austria

Thin oxide layers functioning as tunnel contacts and/or diffusion barriers between a ferromagnetic electrode and a semiconductor template are expected to improve the spin injection efficiency by reducing the loss of the electrons' spin polarization at the interface. We present our recent results on the growth and properties of thin films of two transition metal oxides, MgO and MoO₃, on GaAs(001)c(4×4) substrates, with emphasis on their structure, morphology, stress, strain relaxation, and electrical properties. Furthermore, as an exemplary diffusing element in GaAs(001) we investigated the interdiffusion across the oxide barrier by means of Fe/(MgO,MoO₃)/GaAs(001) heterostructures. The results on MoO₃/GaAs(001) will be compared with that of MgO(001)/GaAs(001).

Mo.D-P16 - Electrical spin injection and detection in Si nanowire with CoFeB/MgO contacts

J. Chang¹, T. Park¹, B. Min¹, Y. Park^{1,2}, M. Jo³, H. Choi²

1. *Korea Institute of Science And Technology, Seoul, South Korea*

2. *Yonsei University, Seoul, South Korea*

3. *Postech, Pohang, South Korea*

Semiconductor spintronics deals with the manipulation of spin degree of freedom for electronic applications in semiconductors, and holds a great promise for overcoming the limit of conventional charge-based electronics. Silicon is one of promising materials for semiconductor spintronics because of the compatibility with complementary metal-oxide semiconductor and its long spin life time. In addition, the one-dimensional nanowires with single crystallinity and clean surfaces can provide an outstanding platform to study the role of the dimensionality and size effects in semiconductor spintronics. Here we show the electrical spin injection and detection in Si nanowires with an enhanced spin injection efficiency using MgO tunnel barrier, and discuss the effect of nanowire geometry on spin signals. Si nanowires used in the experiments are prepared by chemical vapor deposition (CVD) using phosphorus as a dopant. It is found that the Si nanowires (diameter of 50-80 nm) are highly n-type semiconductor with low resistivity ($\sim 13 \text{ m}\Omega\cdot\text{cm}$ at room temperature). We employed the lateral spin-valve geometry with ferromagnetic CoFeB/MgO contacts for spin injection and detection. The non-local spin valve (NLSV) signal is as high as 380 mV with the current of 100 nA at 1.8 K. A clear memory effect is also observed as a function of the magnetic field at low temperature. A unique feature of the NLSV observed in the Si nanowire is non-flat background voltage which can be understood to Hanle curve superimposed on the NLSV signal owing to the shape distortion of CoFeB right on top of a Si nanowire. The local magnetization of CoFeB affected by shape distortion determines the orientation of injected spins and governs relative magnetization of both CoFeB electrodes. The shape of the nanowire contributes to the observed spin signal, which has never been observed in thin film devices.

Mo.D-P17 - Spin accumulation and transport signals in Heusler Co₂FeSi/MgO/n+-Si on insulator devices

Y. Saito¹, M. Ishikawa¹, T. Inokuchi¹, H. Sugiyama¹, K Hamaya², N. Tezuka³

1. Corporate R&D Center, Toshiba Corporation, Tokyo, Japan

2. Graduate School of Engineering Science, Osaka University, Osaka, Japan

3. Department of Materials Science, Tohoku University, Sendai, Japan

Efficient spin injection and detection are essential for spintronics. For this purpose, spin transport has been intensively studied in various kinds of materials. We have been observing spin accumulation signals in Si with relatively long spin relaxation time by measuring three-terminal and four-terminal Hanle signals for CoFe/MgO/n⁺-Si(100) devices [1], and observing local-MR and nonlocal (NL)-MR signals up to room temperature[2]. However, the estimated spin polarization was a small value of ~ 0.16 [2] and improving the spin polarization in Si is highly desired. On the other hand, spin devices with Co-based Heusler-compounds have been studied because of their enhancement in spin generation efficiency. In studies of spin polarization in semiconductors using Co₂FeSi, there have been some reports of efficient spin injection into Ge [3] and GaAs [4] channels. However, to our knowledge, there have been no reports for the case of Si channels.

In this study, we fabricated Heusler Co₂FeSi/MgO/Si on insulator (SOI) devices and examined spin accumulation and transport signals in n+-Si by NL four- and three-terminal Hanle measurements.

We prepared four-terminal devices with Co₂FeSi/MgO electrode on phosphorus-doped (~10¹⁹ cm⁻³) (100)-textured SOI substrates. After the native oxide layer on the surface of the SOI layer was removed with hydrofluoric acid, the MgO layer was deposited by electron beam evaporation method under 200 degree C. Co₂FeSi and Ru capping layers were then sputtered in the same ultra-high vacuum deposition system. We produced a single-crystalline MgO layer on the SOI.

As a result, from the observation of NL four-terminal Hanle signals, we found that the spin polarization in n+-Si estimated from the signals is enhanced by using a Co₂FeSi compared to the case of a CoFe electrode. We will also discuss the local-MR and NL-MR signals in Co₂FeSi/MgO/SOI devices.

This work was partly supported by IMPACT Program of Council for Science, Technology and Innovation (Cabinet Office, Government of Japan), and Grant-in-Aid for Scientific Research from JSPS.

[1] M. Ishikawa et al., Appl. Phys. Lett. 100, 252404 (2012)

[2] Y. Saito et al., J. Appl. Phys. 115, 17C514 (2014)

[3] K. Kasahara et al., Appl. Phys. Express 7, 033002 (2014). [4] T. Saito et al., Appl. Phys. Express 6, 103006 (2013)

Mo.D-P18 - Electrical spin injection in modulation doped GaAs using in-situ grown Fe/MgO

J. Chang¹, S. H. Shim^{1,2}, H. Kim¹, Y. Lee²

1. Korea Institute of Science and Technology, Seoul, South Korea

2. Korea University, Seoul, South Korea

The electrical spin injection from a ferromagnetic metal (FM) into a semiconductor (SC) and the conversion of the spin polarization in a SC into an electrical signal are the essential requirements for spin controlled devices in semiconductor. The careful control of the interface between FM and SC is a key to successful spin injection and introduction of tunnel barrier between FM and SC is a well-known way to overcome the conductivity mismatch problem. The Fe/MgO layer can be epitaxially grown on GaAs layer and forms a basic building block for the magnetic tunnel junction which allows coherent tunneling of Δ_1 Bloch state of Fe. The spin polarized charge transfer through Fe/MgO/GaAs heterostructures was studied using spin dependent photocurrent, but fully electrical spin injection through the heterostructure has not yet been reported.

We have studied spin accumulation in n-doped GaAs electrically injected from Fe electrode via MgO tunneling barrier using three terminal (3T) Hanle measurement. The control of Schottky barrier height and the depletion width by means of the doping-modulation at the interface dramatically improve spin injection efficiency. The whole Fe/MgO/GaAs heterostructures were prepared *in-situ* process using cluster MBE system without vacuum breaking by which both clean interface and high-quality tunnel barrier were obtained. Large Hanle signal of $\Delta V = 6.3$ mV at 10 K was detected and it is still sustained even at room temperature of 1.2 mV. The spin lifetime and spin diffusion length are measured to be 234 ps, and 0.97 μm respectively at 300 K. The bias dependence of the Hanle signal supports effective spin selectivity of injected electrons through epitaxial Fe/MgO/GaAs structure. Combination of in-situ grown MgO tunnel barrier and modulation doping technique appear to be very successful in spin injection to GaAs.

Mo.D-P19 - Spin transport through high-quality epitaxial Ge/Fe₃Si heterostructures in Cu-based lateral spin valves

M. Kawano¹, K. Santo¹, S. Oki¹, S. Yamada¹, T. Kanashima¹, K. Hamaya²

1. Osaka University, Osaka, Japan

2. Osaka University and JST-CREST, Osaka and Tokyo, Japan

We have so far demonstrated the epitaxial growth of high-quality Ge epilayers on a ferromagnetic Heusler compound, Fe₃Si, by low-temperature molecular beam epitaxy (LT-MBE).[1] If spin injection and detection across the Ge/Fe₃Si interfaces are demonstrated, the vertically stacked Ge/Fe₃Si structure can be used for vertical semiconductor spintronic devices. Here, we report the first observation of spin transport across the vertically stacked Ge/Fe₃Si interfaces by using non-local voltage measurements in Cu-based lateral spin valves (LSVs).

Ge(~50 nm)/Fe₃Si(~25 nm) structures were grown on a non-doped Si(111) substrate ($\rho = \sim 1000 \Omega\text{cm}$) by LT-MBE[1] and were processed into Ge/Fe₃Si electrodes with wire-shaped Cu channels in LSVs.[2] The junction size between Ge and Cu is about $150 \times 150 \text{ nm}^2$, and the center-to-center distance between the electrodes is about 300 nm. Since the sidewalls of the Ge/Fe₃Si electrodes in the LSVs were covered by insulator films, spin-polarized carriers were injected vertically from Fe₃Si to Ge and pure spin currents were transported laterally from Ge to Cu. Clear non-local spin signals were seen at various temperatures although the signal obtained at room temperature was about one order of magnitude smaller than that in LSVs without Ge epilayers.[2] This work indicates that the vertically stacked Ge/Fe₃Si structure which we developed can be used for vertical semiconductor spintronic devices.

This work was partly supported by Grant-in-Aid for Scientific Research on Innovative Areas 'Nano Spin Conversion Science' (No. 26103003) from JSPS, and Grant-in-Aid for Scientific Research(A) (No. 25246020) from JSPS. M.K. and S.O. acknowledge JSPS Research Fellowships for Young Scientists.

[1] M. Kawano *et al.*, Appl. Phys. Lett. 102, 121908 (2013)

[2] S. Oki *et al.*, Appl. Phys. Lett. 103, 212402 (2013)

Mo.D-P20 - MgO diffusion barriers for ferromagnetic electrodes on GaAs(001)A. Sarkar¹, S. Wang¹, R. Koch¹*1. Johannes Kepler University Linz, Linz, Austria*

Intermixing at the interface between high-spin-polarization ferromagnetic layers and semiconductor templates is expected to significantly reduce the spin injection efficiency of spin and magnetoelectronics devices and recommends the use of appropriate diffusion barriers. We report on the investigation of ultrathin MgO(001) films serving as diffusion barrier between ferromagnetic Fe electrodes and GaAs(001) semiconductor templates. Epitaxial MgO/GaAs(001) heterostructures were prepared at different growth temperatures in a multichamber III/V-semiconductor-MBE system [1]. Investigations with reflection high energy electron diffraction, x-ray diffraction and high resolution cross-sectional transmission electron microscopy (HRTEM) reveal the growth of single-crystal cubic MgO(001) film at 200 °C with MgO(001)[100] || GaAs(001)[100] and a 4 : 3 lattice registry. The surface of the MgO films, characterized by atomic force microscopy, exhibits a root mean square roughness of only 0.5 nm. In situ stress measurements reveal tensile stress as low as 1.7 GPa for a growth temperature of 200 °C in good agreement with the calculated residual misfit strain [1]. Finally, the effectivity of MgO as a diffusion barrier was investigated by growing epitaxial Fe/MgO/GaAs(001) heterostructures. Structural characterization of the heterostructures reveal a well-ordered crystalline growth and an epitaxial relation of Fe(001)[110] || MgO(001)[100] || GaAs(001)[100] in good agreement with the literature [2]. Auger electron spectroscopy depth-profiling and HRTEM evidence diffusion of Fe into MgO and for to thin MgO barriers further into GaAs(001). Our results recommend a MgO barrier thickness larger than 2.6 nm for its application as a reliable diffusion barrier on GaAs(001) in spintronics devices.[3]

References:

- [1] S. Wang, A. Sarkar, M. Gruber, and R. Koch, J. Appl. Phys. 114 (2013) 154511
- [2] C. Martínez Boubeta, E. Navarro, A. Cebollada, F. Briones, F. Peiró, and A. Cornet, J Cryst Growth 226 (2001) 223
- [3] A. Sarkar, S. Wang, W. Grafeneder, M. Arndt, and R. Koch, Nanotechnology (2014) submitted

Mo.D-P21 - Manipulation of the magnetism in (Ga,Mn)As films by organic molecules

X. Wang¹, H. Wang¹, D. Pan¹, T. Keiper², L. Li¹, X. Yu¹, J. Lu¹, E. Lochner², S. Molnár², P. Xiong², J. Zhao¹

1. *Institute of Semiconductors, CAS, Beijing, China*

2. *Department of Physics, Florida State University, Tallahassee, United States*

As widely accepted a kind of magnetic semiconductor with an intrinsic ferromagnetism, (Ga,Mn)As has attracted much attention in the recent years.[1,2] However, the highest Curie temperature (T_c) of 200 K obtained by combining heavy Mn doping, post-growth nano-patterning and annealing,[3] is still well below room temperature and limits its application in spintronic devices. In (Ga,Mn)As, since the holes from Mn doping are known to mediate the ferromagnetic interaction among the Mn ions, T_c may be controlled via variation of its carrier density by electrical gating.[4] Unfortunately, the tunable temperature range is limited, usually only several Kelvin. In this work, we demonstrate a novel way for effective manipulation of T_c in (Ga,Mn)As by organic molecules.[5] Organic charge-transfer molecules were deposited on the surface of (Ga,Mn)As films by either solution-based self-assembly or vacuum thermal evaporation, which led to large carrier density modulation. Electron donor (acceptor) molecules were found to decrease (increase) T_c. The maximum tunable value in T_c is up to 36 K. The experimental results are qualitatively consistent with the p-d Zener model proposed by Dietl et al.[6]. Moreover, through proper preparation of the (Ga,Mn)As surface, self-assembled monolayer patterns of organic molecules with sub-75 nanometer line width were successfully created via dip-pen nanolithography. These results may open a new pathway to controlled nanoscale manipulation of magnetism in magnetic semiconductor, with potential applications in reconfigurable, non-volatile and hybrid molecular nano-spintronics.

References:

[1] H. Ohno et al., Appl. Phys. Lett. 69(1996)363

[2] T. Dietl, and H. Ohno, Rev. Mod. Phys. 86 (2014)187

[3] L. Chen, X. Yang, F. H. Yang, J. H. Zhao, J. Misuraca, P. Xiong, and S. von Molnár, Nano Lett. 11(2011)2584

[4] H. Ohno, et al., Nature 408 (2000)944

[5] X. L. Wang, H. L. Wang, D. Pan, T. Keiper, L. X. Li, X. Z. Yu, J. Lu, E. Lochner, S. von Molnar, P. Xiong, and J. H. Zhao, A new pathway for manipulation of magnetism in magnetic semiconductor (Ga,Mn)As by organic molecules (to be submitted)

[6] T. Dietl, H. Ohno, F. Matsukura, J. Cibert, D. Ferrand, Science 287, (2000)1019

Mo.D-P22 - Effect of Mn impurities on the 3-terminal Hanle signals in ferromagnet/oxide tunnel contacts on a semiconductor

A. Spiesser¹, H. Saito¹, S. Yuasa¹, R. Jansen¹

1. National Institute of Advanced Industrial Science And Technology, Japan

In the last years, there have been lively discussions about the origin of the electrical spin signals observed in ferromagnet/insulator/semiconductor junctions. Many research groups have experimentally reported three-terminal Hanle signals that are orders of magnitude larger than what the standard theory predicts [1]. Nonetheless, the observed spin signals exhibit the typical features of precession of an induced non-equilibrium spin population, suggesting that intriguing physics is at play.

To explain the large spin voltage, two-step tunneling through localized states near the oxide/semiconductor interface or deep within the oxide was suggested [2,3]. However, this cannot explain the large spin accumulation signals that were recently observed in a direct Mn₅Ge₃ Schottky contact on Ge without an oxide tunnel barrier [4]. Nevertheless, one has to consider the possibility that some Mn atoms have diffused into the depletion region of the Ge and produced deep impurity levels in the Schottky tunnel barrier. Although previous studies have shown that the presence of impurities in magnetic tunnel junctions is detrimental for the spin transport [5], it is of interest to examine how impurities affect Hanle spin signals. Thus, we have intentionally inserted an amount of Mn impurities varying from 0.5 to 2 Å in the middle of a GeO₂ oxide tunnel barrier and investigated the effect on the three-terminal Hanle signal in Fe/GeO₂ junctions on p-type Ge(001) substrates. We have measured the Hanle and inverted Hanle effect and observed a strong decay of the spin signal with increasing amount of Mn. This shows that the presence of Mn impurities reduces the spin signal, rather than enhances it. The results, explained in terms of inelastic spin-exchange scattering of tunneling electrons by Mn ions, proves that enhanced Hanle spin signals are not due to tunneling via magnetic impurities.

References:

- [1] A. Fert et al., Phys. Rev. B 64, 184420 (2001)
- [2] M. Tran et al., Phys. Rev. Lett. 102, 036601 (2009)
- [3] O. Txoperena et al., Appl. Phys. Lett. 102, 192406 (2013)
- [4] A. Spiesser et al., Phys. Rev. B 90, 205213 (2014)
- [5] R. Jansen et al., Phys. Rev. B 61, 9047 (2000)

Mo.D-P23 - Spin transport in an n-type 4H-SiC channel

E. Shigematsu¹, Y. Ando¹, G. Eguchi¹, T. Shinjo¹, T. Kimoto¹, M. Shiraishi¹

1. Kyoto University, Kyoto, Japan

In a field of semiconductor spintronics, spin coherence is a crucial index for realization of spin transistors and quantum computation devices, and many attempts have been done to seek material with better spin coherence. Among Group-IV semiconductors, SiC, currently recognized as a potential wide-bandgap semiconductor for power device applications, is expected to have better spin coherence, because spin life time is proportional to the square of the bandgap in Elliott-Yafet mechanism [1]. In addition, 4H-SiC has spatial inversion symmetry, which exempts the Dresselhaus-type spin orbit interaction. Hence, an investigation of spin coherence in SiC can be an important research issue for further progress of group-IV spintronics. In this presentation, we show results on spin transport in n-type 4H-SiC by using dynamical spin pumping, which has been established in Si spintronics [2]. An n-type SiC epitaxial layer was grown on a semi-insulating SiC substrate. The patterns of NiFe (Permalloy, Py) and Pd were prepared by a lift-off method. In order to form an Ohmic contact, Ti was inserted beneath the Py and the Pd. Under the ferromagnetic resonance of the Py, an electromotive force (EMF) was observed from the Pd electrode. The sign of the EMF was inverted when the direction of the external magnetic field changes. Since the EMF of the self-induced inverse spin Hall effect (ISHE) in Py [3] and that of the ISHE in the Pd due to a spin current propagating through the SiC channel can be superimposed, we propose a procedure of separation of these two origins using an impedance matrix and discuss the spin-related properties of SiC.

[1] R. Elliot, Phys. Rev., 96, 266 (1954)

[2] E. Shikoh, M. Shiraishi et al., Phys. Rev. Lett., 110, 127201 (2013)

[3] A. Tsukahara, M. Shiraishi et al., Phys. Rev. B, 89, 235317 (2014)

Mo.D-P24 - All-electric spin transistor using perpendicular spins

H. Cheol Koo¹, J. Hoon Kim¹, J. Bae¹, B. Min¹, H. Kim¹, J. Chang¹, S. Hee Han¹

1. Korea Institute of Science And Technology, Seoul, South Korea

The spin-field-effect transistor (spin FET) is one of the most attractive devices in the field of spintronics because gate-controlled spin orientation modulates the channel conductance. The basic mechanism of the spin FET is that the injected spins precess around the Rashba field and gate field controls the spin precession angle. In a quantum well system with a structural asymmetry along the growth direction (z-axis), the electrons flowing along the x-direction produce the Rashba effective magnetic field along the y-axis. Thus, to induce spin precession of an injected spin, the injected spin orientation should be x or z direction. The neighboring ferromagnetic electrode causes the interference noise, so the perpendicular magnetization material (z-direction) is very attractive for high-density spin FET. In this research, we utilized Tb₂₀Fe₆₂Co₁₈/Co₄₀Fe₄₀B₂₀/MgO electrodes as drain and source in an InAs quantum well channel. The top Tb₂₀Fe₆₂Co₁₈ layer produces perpendicular magnetization and the Co₄₀Fe₄₀B₂₀ layer enhances the spin polarization of the injection electrons. In our system, the electrons injected with spin polarization along the z-axis precess under the influence of the Rashba field (B_{Ry}). The magnitude of electric field, E_z, can be modulated by a gate voltage, and the magnitude of the Rashba field is proportional to the electric field. Thus, the precession rate therefore changes as a function of gate voltage. The detector is also a Tb₂₀Fe₆₂Co₁₈/Co₄₀Fe₄₀B₂₀/MgO electrode with perpendicular magnetization. The channel conductance is high (low) when a detected spin has orientation parallel (anti-parallel) with that of the detector. The channel conductance oscillates periodically as a function of gate voltage. A gate voltage change of 2 V makes it possible to operate spin FET using perpendicular spins. We clearly observed that the gate field controls the spin orientation and the channel conductance without an external magnetic field.

Mo.D-P26 - Electrical spin injection and detection in homoepitaxial GaAs(110) layers

H. Kim¹, H. S. Kim^{1,2}, J. Shin¹, H. Chul Koo^{1,2}, J. Chang¹

1. *Center for Spintronics, Korea Institute of Science & Technology, Seoul, South Korea*
2. *KU-KIST Graduate School of Converging Science and Technology, Korea University, Seoul, South Korea*

GaAs quantum wells (QWs) on GaAs(110) substrates have attracted attentions for semiconductor spintronic device applications due to longer spin relaxation time compared to GaAs(001) channel. Furthermore, spin dephasing via the Dyakonov-Perel (DP) mechanism is strongly suppressed for growth-axis-oriented spins in the GaAs(110) QWs. As a result, much longer spin lifetime (of up to 10 ns) have been reported for GaAs(110) QWs compared to GaAs(001) QWs. For the realization of GaAs(110) channels of the longer spin relaxation time, the high quality epitaxial GaAs(110) growth is an essential ingredient. The homoepitaxial GaAs(110) growth, however, is more difficult than GaAs(001) growth because of the different arsenic incorporation due to the difference between nonpolar (110) and polar (001) surfaces. In this study, we carefully investigated the surface morphology evolutions and underlying pyramidal defects to implement the high quality GaAs(110) homoepitaxial growth by changing two key experimental parameters of layer thicknesses and growth temperatures. With the high quality of GaAs (110) channel excluding triangular-shaped surface defects and underlying stacking faults, we demonstrate spin transport from a ferromagnetic metal such as TbCoFe into the GaAs (110) channel to enhance the spin lifetime.

Mo.D-P27 - Spin injection in silicon and germanium: new elements for understanding

F. Rortais^{1,2}, S. Oyarzun^{1,2}, P. Laczkowski^{3,4}, J. Rojas-Sanchez^{3,4}, C. Vergnaud^{1,2}, C. Ducruet⁵, C. Beigné^{1,2}, N. Reyren^{3,4}, A. Marty^{1,2}, J. Attané^{1,2}, L. Villa^{1,2}, G. Desfonds^{6,7}, S. Gambarelli^{6,7}, J. Widiez⁸, H. Jaffrès^{3,4}, J. Georges^{3,4}, M. Jamet^{1,2}

1. CEA, INAC-SP2M, F-38000 Grenoble, France
2. Univ. Grenoble Alpes, INAC-SP2M, Grenoble, France
3. Unité Mixte de Physique CNRS/ThalPs, Campus Polytechnique, Palaiseau, France
4. Univ. Paris-Sud, Orsay, France
5. CROCUS-Technology, Grenoble, France
6. CEA, INAC-SCIB, Grenoble, France
7. Univ. Grenoble Alpes, INAC-SCIB, Grenoble, France
8. CEA, LETI, MINATEC Campus, Grenoble, France

Electrical spin injection from ferromagnetic metals to silicon (Si) and germanium (Ge) is the first and basic requirement for the development of spintronic devices and their integration with mainstream semiconductor (SC) technology. The main solution to avoid conductivity mismatch is to use a tunnel barrier between the ferromagnetic metal and the SC. However, electrical spin injection is still a challenge and raises other important issues in the interpretation of electrical spin signals. In particular, the possible presence of localized states within the insulating barrier or at the interface between it and the SC may lead to wrong conclusions. To study the exact origin of spin signals, we managed to measure 3 and 4 contacts devices of silicon-on-insulator (SOI) and germanium-on-insulator (GeOI). These materials allow us to apply back gate voltages to the SC channel to vary its resistivity and carrier mobility. We have grown Ta/CoFeB/MgO/SOI and GeOI samples with n and p type doping using variable MgO thicknesses. Following the possible defects coming from tunnel barrier, the signal will be controlled by the tunnel barrier thickness. Moreover we have used three different techniques to grow the MgO tunnel barrier: by sputtering of MgO or Mg followed by a plasma oxidation and e-beam evaporation of MgO. By changing the growth method we also expect different kinds of interface with possible defects. We focused on tunnel junction grown using Mg and plasma oxidation for silicon and germanium with different doping. We obtained very different temperature dependencies as expected. We are able to see a transition in temperature from the spin accumulation into interface states to the spin accumulation into the conduction band of n-Ge. For this purpose, both electrical and dynamical spin injection measurements were carried out as a function of temperature and bias voltage for different MgO tunnel barriers.

Mo.D-P29 - Spin selective transport through quantum ring with magnetic impurities

P. Dahan¹

1. School of Engineering At Ruppin Academic Center

A theory of magnetic impurities in quantum ring, QR, under magnetic field is formulated in terms of a resonance scattering model. We consider transition metal, substituting semiconductors QR and found that both short-range potential and resonance components of impurity scattering influence mainly the first QR energy level, near $k \approx 0$, $k = m + \Phi/\Phi_0$, m and Φ/Φ_0 are respectively the angular moment and flux.

Since the resonance scattering potential has a strong energy dependence characteristic, the spin up and spin down of the QR are modified with different energy values, δ_{\uparrow} and δ_{\downarrow} , respectively [1]. The zero-field spin splitting in the QR states involves various electronic effects. In particular, the polarized spin current can occur. The localized states in the QR serve as intermediate resonant states through which the tunneling takes place. Since the zero-field spin splitting of the first QR state is large, it can yield a very high spin polarization. This spin dependent transition property of the QR leads to enhanced transition probability for electrons populate a specific spin state, which results in polarization of the spin current. In principle, due to the above said effect such a system can be used as a spin filter and spin currents controller.

[1] P. Dahan et al., Phys. Rev. B 65 1653131 (2002)

Mo.D-P30 - Hybrid optical generation and electrical detection of spin in Germanium using magnetic tunnel junctions and inverse spin hall effect

A. Ferrari^{1,2}, F. Bottegoni³, C. Vergnaud⁴, M. Celebrano³, L. Ghirardini³, E. Sakat³, G. Isella³, M. Bollani⁵, P. Biagioni³, F. Rortais⁴, L. Vila⁴, J. Attané⁴, A. Marty⁴, C. Beigné⁴, C. Largeton⁶, F. Henry⁶, F. Ciccacci³, M. Finazzi³, M. Jamet³

1. Univ. Grenoble Alpes, Grenoble, France

2. CNRS, Institut Néel, 'Nanophysique et semiconducteurs' group, Grenoble, France

3. LNESS-Dipartimento di Fisica, Politecnico di Milano, Milano, Italy

4. INAC/SP2M, CEA-Université Joseph Fourier, Grenoble, France

5. CNR-IFN and LNESS, Como, Italy

6. LETI/DOPT/STM, CEA-Université Joseph Fourier, Grenoble, France

The integration of spintronics and photonics represents one of the most challenging tasks in modern optoelectronics. Among group-IV semiconductors, germanium plays a key role, owing to the large spin-orbit coupling, long electron spin lifetime and integrability with Si-based microelectronics. Although spin injection through optical orientation is a well-known technique, geometries that rely on optical excitation at normal light incidence provide a spin polarization vector perpendicular to the plane of the device, thus limiting their applicability in spintronic devices. However, it has recently been shown that two complementary in-plane spin populations can be optically generated in germanium by depositing a stripe-shaped platinum overlayer on top of the semiconductor. Spin generation can subsequently be electrically detected through the inverse spin-Hall effect (ISHE) measurements in the Pt layer or by using magnetic tunnel junctions (MTJs) in close proximity to the impinging light beam (at a distance less than the spin diffusion length L_{sf}). Here we will show our last results on optical generation and electrical detection of spin in Germanium using a confocal microscope setup and multi-terminal patterns comprising platinum stripes and CoFeB/MgO MTJs. In particular, MTJs are remarkably versatile probes since they can address different spin polarization components. This is possible either by fabricating MTJs with different well-defined remanence magnetization or by switching the magnetization with an external magnetic field. This combined electro-optical technique also allows to directly address the spin diffusion length and to quantify the spin current intensity injected into the ferromagnetic contact.

Mo.D-P31 - Suppression of spin decay in a laterally confined two-dimensional electron gas

P. Altmann¹, M. P. Walser¹, M. Kohda^{1,2}, C. Reichl³, W. Wegscheider³, G. Salis¹

1. *IBM Research, Zurich, Switzerland*

2. *Graduate School of Engineering, Tohoku University, Sendai, Japan*

3. *Solid State Physics Laboratory, ETH Zurich, Zurich, Switzerland*

The decay of spin polarization in a two-dimensional electron gas is often dominated by the intrinsic spin-orbit interaction through the Dyakonov Perel mechanism. If the electron gas is laterally confined to a wire structure with a width smaller than the spin-orbit length, the corresponding spin decay rate is predicted to be suppressed quadratically with the confinement width. We experimentally investigate this effect of lateral confinement on the dynamics of electron spins in etched GaAs wire structures of 1–80 μm width. Using time-resolved Kerr rotation measurements, we spatially map the diffusive expansion of locally excited spin polarization in individual wires. The decay of spin polarization is separated into a contribution from the dilution caused by spin diffusion, and an exponential decay of the excited spin eigenmode. We observe a strong suppression of spin dilution at the transition to one-dimensional diffusion [1]. The exponential spin lifetime increases with decreasing wire width. This effect is small in samples with almost balanced Rashba and Dresselhaus spin-orbit interactions. We find that for narrow wire widths, the spin lifetime approaches the value for a two-dimensional electron gas with perfectly balanced spin-orbit interaction, suggesting that these rates are both limited by the cubic Dresselhaus interaction.

[1] P. Altmann, M. P. Walser, C. Reichl, W. Wegscheider, and G. Salis, *Phys Rev. B* **90**, 201306(R) (2014).

Mo.E-P02 - Tuning of magnetoresistance in organic-based devices by interface engineering

H. Jang^{1,2}, O. Jurchescu², C. Richter¹

1. Semiconductor and Dimensional Metrology Division, National Institute of Standards and Technology, Gaithersburg, United States

2. Department of Physics, Wake Forest University, Winston-Salem, United States

Great efforts are underway to realize organic-based spintronics technologies including the exploration of the organic magnetoresistance (MR).[1] Organic MR is a unique magnetic field effect (MFE) on the electrical resistance of nonmagnetic organic semiconductor devices.[1] This unusual phenomenon has opened the door for developing novel applications such as organic spintronic devices and room temperature field sensors. While the underlying mechanisms for organic MR are still unsettled and debated,[1] it can be used as an experimental tool for improving the fundamental understanding of charge carrier transport mechanisms in organic semiconductor devices such as OLEDs.

In this presentation, we report a novel method of manipulating the organic MR in Alq₃ (tris-(8-hydroxyquinoline) aluminum) – based devices by simply adding a molecular self-assembled monolayer (SAM) at the interface between a metal electrode and an organic semiconductor.[2] SAMs have been known for their versatile use in various technological applications including their ability to alter the physical properties of an inorganic solid surface.[3] We show for the first time that the interfacial modification by simply inserting a fluorinated SAM (heptadecafluoro-1-decanethiol [CF₃(CF₂)₇(CH₂)₂SH] or F-SAM) in organic-based devices changes the sign of organic MR due to the change in relative strength of different MFE mechanisms coexisting in organic-based devices.[2] In addition, we utilize different MFE mechanisms coexisting in organic-based devices by adding a thin TPD (N,N'-Bis(3-methylphenyl)-N,N'-diphenylbenzidine) layer to create a system whose organic MR can be tuned by an external bias voltage.[2]

References

- [1] Wagemans, W. *et al.* The many faces of organic magnetoresistance. *SPIN* 1, 93-108 (2011)
- [2] Jang, H. –J. *et al.* Interface engineering to control magnetic field effects of organic-based devices by using a molecular self-assembled monolayer. *ACS Nano*, 8, 7192-7201 (2014)
- [3] Love, J. C. *et al.* Self-assembled monolayers of thiolates on metals as a form of nanotechnology. *Chem. Rev.* 105, 1103-1169 (2005)

Mo.E-P04 - Spin transistors based on single-molecule magnets

E. Burzuri¹, R. Gaudenzi¹, K. Park², A. Cornia³, Herre S. J. van der Zant¹

1. *Delft University of Technology, Delft, The Netherlands*

2. *Virginia Tech, Blacksburg, United States*

3. *University of Modena and Reggio Emilia, Modena, Italy*

Individual magnetic molecules embedded into electric circuits are envisaged as functional components in the emerging field of molecular spintronics. Single-molecule magnets (SMM), with high spin and high magnetic anisotropy are interesting candidates. We study three-terminal charge transport through individual Fe₄ SMM. In these transistors, an Fe₄ molecule is linked to two gold electrodes fabricated by self-breaking electromigration of a gold nanowire [1]. A third gate electrode is used to access different redox states of the molecule. The measurements reveal that the magnetic properties of the molecule are preserved and can be reversibly modified by adding a single electron into the molecule [2]. Interestingly, we observe that the current through the molecule can be significantly tuned by the presence of small transverse magnetic anisotropy perturbations [3] and individual vibrational modes of the molecule [4]. These two findings are of special relevance to use SMM as memory elements or qbits and opens the door to study quantum properties of the SMM such as quantum tunnelling and quantum interferences at the single molecule level. As a further step in the control of individual molecular spins, we work on ferromagnetic-functionalized graphene electrodes to inject spin-polarized currents into magnetic molecules.

[1] H. Park et al., *Appl. Phys. Lett.*, 1999, 75, 301; K. O'Neil et al., *Appl. Phys. Lett.* 2007, 90, 133109

[2] E. Burzuri et al, *Phys. Rev. Lett*, 2012, 109, 14203

[3] M. Misiorny, E. Burzuri et al, *Phys. Rev. B*. 2015, 91, 035442

[4] E. Burzuri et al, *Nano Lett*, 2014, 14, 3191

This work was supported by NWO (VENI) , OCW and by the EU FP7 Project 618082 ACMOL and the advanced ERC grant (Mols@Mols).

Mo.E-P05 - Cobalt states at a single Graphene/Co interface probed by ferromagnetic nuclear resonance

Y. shin^{1,2}, F. Godel¹, D. Halley¹, J. Francois Dayen¹, J. Weon Wu², C. Meny^{1,2}

1. *Institut de Physique et Chimie des Matériaux de Strasbourg (IPCMS), UMR 7504 CNRS-University of Strasbourg, Strasbourg, France*

2. *Department of Physics, CNRS-Ewha International Research Center, Ewha Womans University, South Korea*

Recent developments in spintronics involve the use of graphene layer because of its outstanding physico-chemical properties. In such hybrid devices their magnetic and transport properties will strongly depend on the contact with the ferromagnetic leads. [1] In order to understand the device properties it is therefore necessary to investigate the graphene/metal interfaces. Because of its sensitivity to the chemical environment of Cobalt, we have used Ferromagnetic Nuclear Resonance (FNR, i.e. Nuclear Magnetic Resonance for ferromagnets) to investigate the interface states of Cobalt atoms at a Graphene/Cobalt single interface. FNR is a unique tool to study the interfaces of Cobalt films and multilayers and has been widely used for investigating the interfaces with metallic or semiconducting layers [2,3]. In this work we have studied Cu/Graphene/Cobalt/Fe artificial structures deposited by MBE on copper foils. This architecture allows probing by FNR a single Graphene/Co interface since the Graphene/Co and Co/Fe interfaces result in contributions in different frequency ranges. Our investigations show that FNR is able to provide information about the local magnetic properties of the interfacial Co atoms. The influence of graphene on the electronic structure of Co extends over several atomic planes into the bulk of the cobalt films. The results will be discussed at the light of recently published computation results predicting very strong hybridization for Cobalt atoms at the interface with graphene.

1. F. GODEL (à) D. HALLEY, J.F. DAYEN, Appl. Phys. Lett., 105, 152407 (2014)

2. P. PANISSOD, C. MENY Appl. Magn. Reson. 19, 447-460 (2000)

3. N. YAACOUB, C. MENY, C. ULHAQ-BOUILLET, M. ACOSTA, P. PANISSOD Phys. Rev.B, 75, 174402,(2007)

Mo.E-P06 - Room Temperature Magnetoresistance in Single-Molecule Devices

E. Ruiz¹, D. Aravena¹, I. Díez-Perez¹, A. C. Aragonez¹, J. Antonio Real², J. Hihath³, J. I. Cerda⁴

1. *Universitat de Barcelona, Barcelona, Spain*

2. *Universitat de Valencia, Valencia, Spain*

3. *University of California, Davis, United States*

4. *Instituto de Ciencia de Materiales de Madrid, Madrid, Spain*

Controlling the spin of electrons in nanoscale electronic devices is one of the most promising topics toward devices with rapid and highly dense information storage. The interface magnetism or spinterface resulting from the interaction between a magnetic molecule and a metal surface, and vice versa, has become a key ingredient to engineering nanoscale molecular devices with novel functionalities. Here, we present a single-molecule wire displaying large (>10000%) magnetoresistance based on STM measurements. The molecular device is built by trapping individual spin crossover Fe(II) complexes between one Au and one ferromagnetic Ni electrode at room conditions. Large changes in the single-molecule conductance are measured when the electrons flow from the Au to either an alpha-up or a beta-down spin-polarized Ni electrode, the latter case being at least 100-fold more conductive than the former. The current flowing through such an interface appears to be strongly spin-polarized, thus resulting in the observed magnetoresistance effects depending upon the magnetic Ni polarization direction. The observation of strong magnetoresistance effects in a single-molecule device opens up a new door for the design and control of spin-polarized transport in nanoscale molecular devices at room temperature.

Mo.E-P07 - Magnetoresistance effect of magnetic tunnel junctions with an interface modified by [6]Cyclo-2,7-naphthylenes

K. Suzuki¹, T. Izumi^{2,3}, X. Zhang¹, A. Sugihara¹, S. Pham¹, H. Taka^{2,3}, S. Sato^{1,2,4}, H. Isobe^{1,2,4}, S. Mizukami¹

1. *Advanced Institute For Materials Research(AIMR), Tohoku University, Sendai, Japan*

2. *JST, ERATO, Isobe Degenerate π -Integration Project, Aoba-ku, Sendai, Japan*

3. *Corporate R&D Headquarters, Konica Minolta, Ishikawa-cho, Hachioji, Japan*

4. *Dept. of Chemistry, Graduate School of Science, Tohoku Univ., Aoba-ku, Sendai, Japan*

Organic-magnetic materials hybrid structures attracted much attention from the viewpoint of spin injection into the organic molecules [1,2] and new interface effects [3,4,5]. However, there were only few reports on these effects observed at room temperature (RT), thus it is interesting to explore the new materials/molecules hybrid structure exhibiting remarkable spin-dependent transport at RT. Here, we reports the fabrication of magnetic tunnel junctions with an insertion layer of the [6]cyclo-2,7-naphthylenes (CNAP) at interface between ferromagnetic electrode and insulating barrier and the characterization of spin-dependent transport properties. The CNAP is a new molecule synthesized recently, which has a conjugated pi-electron system, cyclic molecular structure, and excellent thermal stability up to about 600oC [6]. The junction devices were prepared by an organic-inorganic hybrid multi-chamber deposition system being equipped with an in-situ shadow-mask exchange system. The stacking structure was glass substrate/Co(50 nm)/AlOx(2 nm)/CNAP(d = 0-20 nm)/NiFe (30nm) and the junction area was 1.5 μ m²~1.8 mm². The MR ratio at RT for the junction without CNAP was 2.2%, whereas it increased with increasing d and then exhibited the maximum value, 5.6%, at d = 3 nm. Temperature dependence of the junction resistance showed a tunneling-like transport below d = 5 nm. This result indicated that the CNAP-modified NiFe interface could have a high spin polarization even at RT [7]. This work was supported by JST-ERATO and Murata Science Foundation. We thank H. Kiso for his assistance of device fabrications.

[1] V.A. Dediu, et.al., Nat. Mater. 8, 707 (2009)

[2] X. Zhang et. al., Nature Comm. 4, 1392 (2013)

[3] C. Barraud et. al., Nat. Phys. 6, 615 (2010)

[4] X. Zhang et. al., Appl. Phys. Lett. 99, 162509 (2011)

[5] K. V. Raman et. al., Nature 493, 509 (2013)

[6] W. Nakanishi et. al. Angewandte Chemie 123, 5435 (2011)

[7] K. Z. Suzuki et al., in-preparation

Mo.E-P09 - Ferromagnet - organic semiconductor interface for molecular spin electronic devicesS. Majumdar¹*1. Aalto University, Spoo, Finland*

Organic or hybrid inorganic-organic spintronics is the newly developing branch of spintronics where the advantages of both the large spin polarization of the ferromagnetic metals and half metals and long spin de-coherence lengths of the organic semiconductors are explored. For improved spintronic components, it is important to investigate material properties at the hetero-interfaces. In the present work, we have done structural, magnetic and transport characterization of interfaces comprised of a half-metallic ferromagnet La_{0.67}Sr_{0.33}MnO₃ (LSMO) and two different organic semiconductors namely Co-Pthalocyanine (CoPc) and rubrene. For the LSMO/CoPc interface, investigation of electronic, magnetic and magnetotransport properties indicate strong chemisorption of CoPc molecules on the LSMO surface improves the LSMO magnetic properties however at the same time the magnetoresistance (MR) of the CoPc coated LSMO increases which can be due to induce local trap states at the LSMO/CoPc interface where spin polarized charge carriers get trapped [1]. Similar increased MR of the LSMO-organic interface was observed for polymeric region-regular polyhexyl thiophene (RRP3HT) also [2]. For LSMO/rubrene interface, x-ray reflectivity measurements indicate a well-defined interface formation especially between vacuum-annealed LSMO and rubrene while x-ray photoemission measurements confirm a hybridization at the rubrene-LSMO interface. Magnetic measurements show due to this hybridization, ferromagnetic property of the LSMO improves whereas intentional disruption of this hybridization by insertion of AlO_x layer results in a decreased ferromagnetism at the hybrid interface [3]. These results demonstrate that by modifying the interface formation between organic semiconductors and half-metallic oxides, it is possible to engineer interface spin polarization properties which could lead to the desired control of the molecular spintronic components.

References:

- [1] S. Majumdar et al., *Spin* 4, 1440009 (2014)
- [2] M. Pesonen et al., *AIP Adv.* 3, 042102 (2013)
- [3] S. Majumdar et al. (communicated)

Mo.E-P10 - Effect of molecular ordering on spin transport in Fe/MgO/CuPc/Co hybrid junctions

Y. Jeong Bae¹, N. Jong Lee¹, J. Wade², J. Kim², A. Pratt³, T. Hee Kim¹

1. Ewha Womans University, Seoul, Suth Korea

2. Imperial College London, London, United Kingdom

In the last decade, there has been remarkable advancement in the filed of organic spintronics. However, the realization of highly effective organic spintronic devices working at room temperature still remains a challenge. Understanding and controlling organic-inorganic interfaces are crucial for manipulating spin-dependent transport in organic magnetic tunnel junctions. Molecular ordering of the organic film between two ferromagnetic (FM) layers could also play a key role in spin transport properties of the hybrid FM metal/organic systems. In this work, we prepared Fe(001)/MgO(001)/Cu-phthalocyanine (CuPc)/Co hybrid structures for magnetic tunnel junctions (MTJs). Fe(001) and Co FM metals are utilized as a spin injector and detector. The CuPc films of various thickness from 1.6 nm to 5 nm were deposited on a 1.6 nm-thick MgO(001) oxide layer grown on Fe(001). This MgO(001)/CuPc hybrid barrier offers a possible solution for improving the performance of organic MTJs. As a result, we observed magnetoresistance (MR) behavior of ~ 200% at 77K and ~ 10% at room-temperature (RT) for the MTJ with the hybrid 1.6 nm MgO(001)/1.6 nm CuPc barrier, whereas no significant MR effect was seen in the MTJs with a single barrier CuPc. A systematic study to analyze the interface (surface) properties was carried out by using metastable He de-excitation spectroscopy (MDS) and Raman spectroscopy. The CuPc films grown on the MgO(001) reveals a herringbone-type molecular arrangement as the sample temperature drops below 250 K. This phase transition of CuPc beyond MgO(001) could be related to the abrupt change of the junction resistance below 250 K. Obviously, our results indicate the molecular ordering is an important key for spin transport in organic films. The results of spin-polarized MDS study highlight the spin polarization induced in CuPc molecular orbitals by the enhanced intermolecular interactions.

Mo.E-P11 - Tailoring spin-textured interfaces with organic molecules

M. Cinchetti¹, B. Stadtmüller¹, J. Seidel¹, N. Haag¹, C. Tusche², J. Kirschner², M. Aeschlimann¹

1. *Department of Physics and Research Center OPTIMAS, University of Kaiserslautern, Kaiserslautern, Germany*

2. *Max-Planck-Institut für Mikrostrukturphysik, Halle, Germany*

The deposition of organic molecules on magnetic surfaces has revealed a very efficient and promising way to create interfaces with tailored spin properties [1]. The hybridization between the electronic bands at the surface of the magnet and the orbitals of the molecule can lead to a drastic change of the magnetic properties of the formed interface, like spin polarization, spin filtering [2] coercive field and exchange coupling strength. The versatility of organic molecules for spin applications is, however, not only limited to interfaces formed with magnetic materials, but extends to the much broader class of non-magnetic spin-textured materials, as recently demonstrated for magnetic skyrmions [3, 4]. Here, we have studied the electronic valence structure of the interface formed by PTCDA molecules adsorbed on a Pb/Ag(111) surface alloy by ARPES using a k-space microscope. The Pb/Ag(111) surface alloy shows a distinct spin-texture due to the Rashba-Bychkov effect [5]. We find that the band structure of the clean Pb/Ag(111) surface alloy is significantly modified by the adsorption of PTCDA, which we attribute to a change in the vertical relaxation of the positions of the Pb atoms in the surface alloy. This study indicates a new concept to tailor the spin texture of the Rashba system, namely by tuning the metal-organic interface “from the bottom”.

References:

- [1] J. S. Moodera, B. Koopmans, P.M. Oppeneer, MRS bulletin 39, 578 (2014)
- [2] S. Steil, N. Grohmann, M. Laux, A. Ruffing, D. Steil, M. Wiesenmayer, S. Mathias, O. L. A. Monti, M. Cinchetti, M. Aeschlimann, Nature Physics 9, 242 (2013)
- [3] J. Brede, J. et al. Nature Nanotech. 9, 1018 (2014)
- [4] M. Cinchetti, Nature Nanotech. 9, 965 (2014)
- [5] D. Pacilé et al., Phys. Rev. B 73, 245429 (2006)

Mo.E-P12 - Enhanced magnetic field effect in a top-emitting spin-OLED

N. Jong Lee¹, Y. J. Bae¹, H. Jung², C. Lee², E. Ito³, T. Hee Kim¹

1. Department of Physics, Ewha Womans University, Seoul, Republic of Korea

2. School of Electrical Engineering and Computer Science, Seoul National University, Seoul, Republic of Korea

3. Flucto-Order Functions Research Team, RIKEN Advanced Science Institute, Wako, Saitama, Japan

The magnetic field response of electroluminescence (EL) of organic light emitting devices (OLEDs) can be controlled by injecting spin-polarized carriers from ferromagnetic (FM) electrodes in principle. [1] However, in reality, the injection of fully spin-polarized carrier is difficult. [2] Also, the injected carriers can lose some of their spin information due to hyperfine interaction or spin-orbit interaction when moving through the organic materials before they emit light. In this work, we investigated a room-temperature (RT) spin-OLED with a magnetic anode such as bcc-Fe(001)\MgO(001) which is well known as a perfect spin filter. A semitransparent Al film was deposited on tris(8-hydroxyquinolato)aluminum (Alq₃) film as a cathode. For the Si(001)\MgO(001)\Fe(001)\MgO(001)\Cu-Phthalocyanine (CuPc)\N,N'-Bis(naphthalen-1-yl)-N,N'-bis(phenyl)-2,2'-dimethylbenzidine (α -NPD)\Alq₃\LiF\Al structure, magnetoelectroluminescence (MEL) of ~ 6% was observed at RT in a low magnetic field of 1 kG for an applied voltage in excess of ~ 5 volts while these measurements showed less than 3% for not fully spin polarized FM anodes (Py, Fe(001) and poly-Fe) without the thin MgO(001) overlayer.

In order to get information of the OLED operating process, such as charge distribution, carrier mobility, current density and etc., numerical analysis was performed by using the MOLED simulation model [3] provided for a typical OLED architecture consisting of an organic multilayered structure between two parallel planar electrodes. In addition, our experimental results were analyzed in the framework of the electron-hole pair (e-h pair) model. All these results strongly support that enhancement of MEL could be attributed to the spin-polarized hole injection from the epitaxial Fe(001)\MgO(001) bilayer.

[1] V. Alek Dediu et al., Nature Materials 8, 707 (2009)

[2] I. Bergenti et al., Org. Electron. 5, 309 (2004)

[3] H. Houili et al., Comp. Phys. Comm. 156, 108 (2003)

Mo.F-P01 - Massively parallel micromagnetic simulations of small-size nanoelements with applications to STT-MRAM devices

E. Semenova¹, D. Berkov¹

1. General Numerics Research Lab, Jena, Germany

In this contribution we present a new numerical method which allows massively parallel micromagnetic simulations of the magnetization reversal in small-size nanoelements by fully exploiting the high acceleration factor available on GPU architecture only for large systems. The major target of our new methodology is the simulation of magnetization dynamics in nanoelements with the size of several tens of nanometers. These elements are at present of the primary interest as attractive candidates for a new generation of conventional and spin-torque-based magnetic random access memory (MRAM) cells.

We apply our method to the analysis of the ST-induced magnetization switching in elliptical nanoelements. Being able to compute simultaneously magnetization reversal of up to 1000 MRAM cells, we could obtain the dependence of the switching time on the element size and the current with a very small statistical error.

Comparison with the macrospin approximation has shown that full-scale micromagnetic simulations are essential starting from the nanoelement size as small as $40 \times 50 \text{ nm}^2$. Switching times obtained by full-scale simulations are larger than those predicted by the macrospin approach; this difference rapidly grows with the nanoelement size. Detailed analysis of the switching statistics and the nature of the switching process (available only from full-scale simulations) allowed deep understanding of the magnetization reversal in such nanostructures. In particular, we have shown that for moderate element sizes (short ellipse axis $b = 40 \text{ nm}$, long axis $a = 60 - 90 \text{ nm}$) magnetization switches via the nucleation of small 'reversed' regions and their further growth. For $a > 90 \text{ nm}$ the reversal occurs via the propagation of the domain wall across the nanoellipse.

We also compare the switching statistics in dependence on the element size for the two cases, where either the total current through the MRAM cell or the current density is kept constant.

Mo.F-P02 - Magnetization dynamics of a single-domain magnet under a spin-polarized current with a tilted polarization

Z. Sun¹, T. Wang¹, Z. Wang¹

1. Soochow University, Suzhou, Jiangsu, China

Magnetization dynamics for a single-domain magnet under a spin-polarized current with any tilted polarization was investigated by solving the Landau-Lifshitz-Gilbert-Slonczewski equation. Taking into consideration the uniaxial magnetic anisotropy, the stationary-state solutions of the magnetization vectors can be analytically obtained by solving an algebraic cubic equation. It was found that one to three pairs of magnetization equilibrium states existed, depending on the current intensity and the direction of the spin polarization. The critical switching current threshold and reversal time for the magnetization reversal was also numerically found under different current polarization configurations with or without considering the spin polarized g-function. The work may be useful for designing in future spin transfer torque devices.

Mo.F-P03 - Temperature dependence of four terminal nonlocal spin signals with $\text{Co}_2\text{FeAl}_{0.5}\text{Si}_{0.5}/\text{n-GaAs}$ Schottky tunnel junctionsN. Tezuka¹, T. Saito¹, M. Matsuura¹, S. Sugimoto¹*1. Department of Materials Science, Graduate School of Engineering, Tohoku University, Sendai, Japan*

Semiconductor spintronics devices such as spin FETs and spin valve transistors have received much attention. In such applications, polarized spin electrons from ferromagnets must be injected into semiconductors at higher efficiency. Several groups have reported that spin injection/detection and spin transport in semiconductor, and have focused on using insulating barrier such as Al-oxide and MgO with a 3d transition ferromagnetic electrodes as spin injector/detector. We have reported spin signal for $\text{Co}_2\text{FeAl}_{0.5}\text{Si}_{0.5}/\text{n-GaAs}$ junctions with Schottky tunnel barrier.¹⁾ In this presentation, we will show temperature dependence of four terminal nonlocal spin signals with $\text{Co}_2\text{FeAl}_{0.5}\text{Si}_{0.5}/\text{n-GaAs}$ Schottky tunnel junctions. $\text{Co}_2\text{FeAl}_{0.5}\text{Si}_{0.5}$ (CFAS) Heusler alloy has high spin polarization which was estimated by tunnel magnetoresistance (TMR) effect.

Samples of n-GaAs 520 nm/n+GaAs 20nm/CFAS 10nm were deposited by molecular beam epitaxy on insulating GaAs substrates. CFAS were deposited with substrate temperature (T_{CFAS}) from room temperature to 400°C. Lateral spin transport devices for four terminal measurement were fabricated using conventional electron beam lithography and Ar ion milling. The planar dimension of spin injector and detector were $1 \times 20 \mu\text{m}^2$ and $2.5 \times 20 \mu\text{m}^2$, respectively, and the distance between them was 2.25 μm .

Magnetoresistance curves were obtained measured temperature from 10 K to 290K. It is clearly shown the voltage change ($\Delta V_{\text{nonlocal}}$) corresponding to magnetization switching of both CFAS electrodes. The spin signal of $\Delta V_{\text{nonlocal}}$ decreased with increasing measurement temperature. This temperature dependency might follow the spin diffusion length and conductance change in semiconductor channel. That means the spin injection/detection efficiency slightly changed, which is consistent with the result of temperature dependence of spin polarization of CFAS measured by a TMR effect. We will also show the temperature dependence of spin signal for the junctions with various distance between two CFAS electrodes, and will discuss the spin transport properties.

This work was partly supported by Grant-in-Aid for Scientific Research, and Strategic Japanese-German Joint Research Program "ASPIMATT" from JST.

References:

1) T. Saito, N. Tezuka, M. Matsuura, S. Sugimoto, Appl. Phys. Lett., 103, 122401 (2013) ; Appl. Phys. Express, 6, 103006 (2013)

Mo.F-P04 - Driven synchronization of multiple nano-contact spin torque oscillators

A. Houshang^{1,2}, E. Iacocca¹, P. Dürrenfeld¹, S. Radjai Sani³, J. Åkerman^{1,2,3}, R. K. Dumas^{1,2}

1. *Department of Physics, University of Gothenburg, Gothenburg, Sweden*

2. *NanOsc AB, Kista, Sweden*

3. *Materials Physics, School of ICT, Royal Institute of Technology (KTH), Kista, Sweden*

The synchronization of multiple nano-contact spin torque oscillators (NC-STOs) [1-3] is mediated by propagating spin waves (SWs) [4]. Additionally, it has been shown that the Oersted field generated in the vicinity of the NC can dramatically alter the emission pattern of SWs [5, 6], leading to highly anisotropic SW beams. In this work, we demonstrate that the Oersted field landscape of two nominally identical NCs, defined on top of an all metallic Co/Cu/NiFe pseudo-spin valve, can be dramatically different based on the geometry of the NCs. Synchronization is promoted (impeded) by the Oersted field landscape when the NCs are oriented vertically (horizontally) with respect to the in-plane magnetic field component. Additionally, the vertical positioning of the NCs gives rise to a unique Oersted field landscape that acts to localize, or trap, spin waves in a region just outside one of the NCs, as confirmed by micromagnetic simulations. Furthermore, it has been shown that in the vertical geometry, the frequency of the synchronized mode is driven by the frequency of the lower NC. This is made most evident in arrays where the NC diameters differ. Together, these phenomena establish a new kind of synchronization behavior. This work was supported by the European Commission FP7-ICT-2001-contract No 317950 "MOSAIC", VR, SSF, and the Knut and Alice Wallenberg Foundation.

[1] S. Kaka, et al., *Nature* 437, 389 (2005)

[2] F.B. Mancoff, et al., *Nature* 437, 393 (2005)

[3] S.R. Sani, et al., *Nat. Comm.* 4, 2731 (2013)

[4] M. Madami, et al., *Nat. Nanotechnol.* 6, 635 (2011)

[5] R.K. Dumas, et al., *Phys. Rev. Lett.* 110, 257202 (2013)

[6] M.A. Hoefer et al., *Phys. Rev B* 77, 144401 (2008)

Mo.F-P05 - Reducing the switching current with a Gilbert damping constant in a nanomagnet with perpendicular anisotropyKeisuke mada¹, K. Oomaru¹, S. Nakamura¹, T. Sato¹, Y. Nakatani¹

1. University of Electro-Communications, Chofu, Tokyo

Magnetoresistive random access memory using Spin torque switching (Spin-RAM) is one of the candidates as the next generation of non-volatile memory [1-5]. To realize high-density Spin-RAMs, it is required to be a low switching current (I_{sw}). In order to reduce I_{sw} , one possibility is to use the perpendicular magnetization with small damping constant (α) value and/or with small saturation magnetization (M_s), because it is expected that I_{sw} is proportional to $\alpha \cdot M_s \cdot H_k$ [1,4], where H_k is the perpendicular magnetic anisotropy. In this work, we simulated spin-current-induced magnetization switching in a perpendicularly magnetized nanomagnet using the macrospin model, which is the simplest model available that is comparable with the analytical model. We investigated the effect of α on I_{sw} with varying t_p , M_s and magnetocrystalline anisotropy K_u ($K_u \propto H_k$).

The material parameters used for the simulation were similar to those of CoFeB. The parameters used in the simulation are $M_s=600$ emu/cm³, $K_u=1.76 \times 10^6$ erg/cm³, spin polarization $P=1.0$, free layer volume $V=11.2^3$ nm³, initial magnetization angle $\vartheta_0=0.129$ rad and criteria angle $\vartheta'=p-0.129$ rad. The results show that reduction of α below a certain threshold (α_c) is ineffective in reducing I_{sw} for short t_p . When t_p is short, it is necessary to reduce both α and M_s simultaneously until α_c is reached to reduce I_{sw} . The results presented here offer a promising route for the design of ultrafast information storage and logic devices using current-induced magnetization switching [6].

This study was supported by New Energy and Industrial Technology Development Organization (NEDO) and Grant-in-Aid for JSPS Fellows.

- [1] *Phys. Rev. B.*, 62,570 (2000)
- [2] *Phys. Rev. Lett.* 84, 3149 (2000)
- [3] *J. Appl. Phys.*, 89, 6982 (2001)
- [4] *Nature Mater.* 5, 210 (2006)
- [5] *IEEE. Trans. Magn.*, 47, 6, 1599 (2011)
- [6] *Appl. Phys. Lett.* 106, 042402 (2015)

Mo.F-P06 - Point-Contact Spin Torque Oscillator with Highly Spin-Polarized Co₂(Fe, Mn)SiT. Yamamoto¹, T. Seki², T. Kubota¹, H. Yako¹, K. Takanashi¹

1. IMR, Tohoku Univ., Sendai, Japan

2. JST-PRESTO, Tokyo, Japan

Since the discovery of spin torque oscillation in a current-perpendicular-to-plane (CPP)-giant magnetoresistance (GMR) device, several types of spin torque oscillators (STOs) have been developed to achieve a large rf output power (P_{rf}) and a narrow spectral linewidth (Δf). Point-contact STOs have an advantage in narrow Δf , and rf oscillation has often been achieved at zero magnetic field. Generally, however, they show a smaller P_{rf} than those of CPP-GMR STOs. One promising material for high- P_{rf} STO is highly spin-polarized Co₂(Fe, Mn)Si (CFMS). Our group demonstrated a large P_{rf} in a CPP-GMR STO, and a micromagnetic simulation suggested the further enhancement of P_{rf} by improving the uniformity of the effective magnetic field in the CFMS layer. In this study, we fabricated point-contact STOs with CFMS, and investigated their oscillation characteristics.

CFMS (20) / Ag (5) / CFMS (5) (in nanometer) layered structures were prepared by an ultrahigh-vacuum magnetron sputtering system. The top CFMS layer was patterned into a mesa with an area of $20 \times 40 \mu\text{m}^2$, and a point-contact with a diameter of normally 140 nm was lithographically fabricated at the center of the CFMS mesa.

Fabricated STOs showed rf oscillations around 0.9 GHz with a narrow Δf of 3 MHz without external magnetic field. The low oscillation frequency is attributable to the gyration mode of magnetic vortex-like structure created in the CFMS layer, and the oscillation mode was changed by changing the applied current (I_{dc}). At $I_{dc} = 7.3$ mA, a large P_{rf} of 25.7 nW was obtained, which is the largest P_{rf} ever reported in all-metal STOs. The large P_{rf} and the narrow Δf are attributed to the high spin-polarization of CFMS and the advantage of point-contact geometry.

Mo.F-P07 - Magnetic phase transition and colossal magnetoresistive effect in Sm_{0.55}Sr_{0.45-x}Ag_xMnO₃ (0 ≤ x ≤ 0.10) system

M. Ahmad Bhat¹, D. Kumar², A. Shahee³, N.K. Gaur⁴

1. *Research Scholar*
2. *Scientist D*
3. *Research Scholar*
4. *Associate Professor*

In the present novel work, we have investigated the Structural, transport, magneto-transport and magnetization properties on single phase polycrystalline samples of silver doped disordered Sm_{0.55}Sr_{0.45}MnO₃ prepared via solid state reaction technology route. Rietveld refined x-ray diffraction results indicates an increase in lattice parameters and unit cell volume with Ag doping. The magnetization results show the presence of a first order paramagnetic to ferromagnetic transition; the transition temperature and amount of thermal hysteresis decreases on Ag doping. The transport, and magneto-transport results indicates decrease in metal to insulator transition, drastic increase in resistance and temperature coefficient of resistance (TCR %) with nearly unaffected colossal magnetoresistance effect. All these results indicate that at least a part of silver is incorporated in the lattice. SEM micrographs indicate that silver has also increased the grain growth sharpness and thus decrease the effect of grain boundary scattering. The significant value of TCR of ~43% of our samples indicates their applied nature for bolometric application. Keywords: Rietveld refinement, Metal - Insulator Transition Temperature, Temperature Coefficient of Resistance, First Order Magnetism.

Mo.F-P08 - Spin torque ferromagnetic resonance in a nano-contact geometry

M. Fazlali¹, P. Dürrenfeld¹, E. Iacocca^{1,2}, N. M. Dvornik¹, M. Haidar¹, M. Ranjbar¹, J. Åkerman^{1,2,3}, R. Dumas^{1,2}

1. *Physics Department, University of Gothenburg, Gothenburg, Sweden*

2. *NanOsc AB, Kista, Sweden*

3. *Material Physics, School of ICT, Royal Institute of Technology, Kista, Sweden*

Spin torque ferromagnetic resonance (ST-FMR) [1-4] is a widely used technique to probe the magnetodynamic response of individual sub-100 nm scale magnets. We present a quantitative experimental ST-FMR study of nanocontact spin torque oscillators (NC-STOs) over a wide range of frequencies, RF powers, and magnetic field angles. The material stack used is a fully metallic NiFe (free layer)/Cu (spacer)/Co (fixed layer) pseudo spin valve with a nominal NC diameter of 100 nm. The FMR resonances of both the Co and NiFe layers are observed and are well fit by the Kittel equation at all applied field angles. However, in contrast to conventional broadband FMR measurements on blanket films, our ST-FMR measurements reveal significantly more complex spectra consistent with not only the excitation of a uniform FMR mode, but additional higher order spin waves. Micromagnetic simulations highlight the importance role of not only ST, but also the RF current induced Oersted field in the vicinity of the NC, in generating the observed spectra.

This work was supported by the European Commission FP7-ICT-2011 contract No. 317950 "MOSAIC". Support from the Swedish Research Council (VR), the Swedish Foundation for Strategic Research (SSF), and the Knut and Alice Wallenberg Foundation is gratefully acknowledged.

[1] A. Tulapurkar, Y. Suzuki, A. Fukushima, H. Kubota, H. Maehara, K. Tsunekawa, D. D. Djayaprawira, N. Watanabe, and S. Yuasa, *Nature* 438, 339 (2005)

[2] C. Wang, H. Seinige, and M. Tsoi, *Low Temp. Phys.* 39, 247 (2013)

[3] J. C. Sankey, P. M. Braganca, A. G. F. Garcia, I. N. Krivorotov, R. A. Buhrman, and D. C. Ralph, *Phys. Rev. Lett.* 96, 227601 (2006)

[4] E. Evarts, M. Pufall, and W. Rippard, *J. Appl. Phys.* 113, 083903 (2013)

Mo.F-P09 - Theoretical investigation of spin transfer torque in antiferromagnetic and ferrimagnetic tunnel junctions

P. Merodio¹, A. Kalitsov^{1,2}, H. Béa¹, N. V. Baltz¹, M. Chshiev¹

1. SPINTEC, Univ. Grenoble Alpes, CNRS, CEA-INAC, Grenoble, France

2. MINT Center, University of Alabama, Tuscaloosa, AL, United States

We present a theoretical study of spin transfer torque (STT) [1,2] and tunnelling magnetoresistance (TMR) in antiferromagnets (AF) and ferrimagnet (FI) based tunnel junctions, where two magnetic metal electrodes, with at least one of them being FI or AF, are separated by a thin nonmagnetic insulating barrier. We found that electronic structure parameters such as the Fermi energy, band widths and the exchange splitting of the FI and AF electrodes strongly influence the STT and TMR properties including their bias dependence [3,4]. In particular, the STT spatial distribution within the leads shows nontrivial behavior, which can be explained in terms of interplay between exchange splittings of the two AF or FI sublattices. For example, for FI leads and due to their FI order, peculiar spin-modulated torque waves are observed. In addition, we identified the fundamental parameter for quantifying STT characteristic lengths in FI metals, which are also accessible to experiments for example by ferromagnetic resonance and spin pumping like in [5,6]. Such insights will be of importance for optimizing current induced magnetization reversal phenomena.

[1] A. S. Nñez et al., Phys. Rev. B 73, 214426 (2006)

[2] A. H. MacDonald and M. Tsoi, Phil. Trans. R. Soc. 396, 3098 (2011)

[3] P. Merodio et al, Phys. Rev. B. 90, 224422 (2014)

[4] P. Merodio et al, Appl. Phys. Lett. 105, 122403 (2014)

[5] A. Ghosh et al, Phys. Rev. Lett. 109, 127202 (2012)

[6] P. Merodio et al, Appl. Phys. Lett. 104, 032406 (2014)

Mo.F-P10 - Effectiveness of negative index of surface anisotropy

C. Mitsumata¹, M. Mizuguchi²

1. *National Institute For Materials Science, Tsukuba, Japan*

2. *Tohoku University, Sendai, Japan*

In recent years, the control of the magnetization reversal by the electric field has become the major stream of spintronics researches. The high frequency voltage control [1] showed hopeful potential for the low electric power consumption in there. The applied voltage also changed the surface anisotropy of metallic films [2], and it was possible to reduce the coercive force of magnetic films. [3] However, the magnitude change of a surface anisotropy restrictively reduced the coercive force. Contrastingly, the negative index of a surface anisotropy achieved the large reduction of a coercive force [4], even though mono atomic layer only became negative. On these techniques, the influence of the surface anisotropy in the spin torque oscillation (STO) system has been investigated in this paper. In the case of perpendicular magnetization system, it can be calculated that the magnetic torque due to the negative anisotropy enables to reduce the Gilbert damping torque in term of Landau-Lifshitz-Gilbert (LLG) equation. Namely, the gyro-magnetic precession term dominates the motion of spin in LLG equation. Also, in the high frequency voltage control, the increase of energy ratio of gyro-magnetic precession incrementally lowers the electric power consumption. Both reduction of coercive force and Gilbert damping assists to the low energy consumption in STO due to the spin transfer torque. Consequently, the negative index of a surface anisotropy is significantly effective for the continuous gyro magnetic precession in spintronics devices.

[1] T. Nozaki, et.al., Appl. Phys. Express, 7 073002 (2014)

[2] M. Weisheit, et.al., Science, 315 349 (2007)

[3] T. Seki, et.al., Appl. Phys. Lett., 98, 212505 (2011)

[4] C. Mitsumata, et.al., Appl. Phys. Express, 4 113002 (2011)

Mo.F-P12 - Spin-torque generated equilibria in spin Hall systems and their role in magnetic switching

S. Yan¹, Ya. B. Bazaliy¹

1. University of South Carolina, Columbia, United States

In a ferromagnet/heavy-metal bilayer device with strong spin Hall effect an in-plane current excites magnetic dynamics through spin torque. We analyze bilayers with perpendicular magnetization and calculate three-dimensional phase diagrams describing switching by external magnetic field at a fixed current. We then concentrate on the case of a field applied in the plane formed by the film normal and the current direction. Here we analytically study the evolution of both the conventional 'up'/'down' magnetic equilibria and the additional equilibria created by the spin torque. Expressions for the stability regions of all equilibria are derived, and the nature of switching at each critical boundary is discussed. The qualitative picture obtained this way predicts complex hysteresis patterns that should occur in bilayers. By analyzing the phase portraits of the system we show that when the spin torque induced equilibrium exists, switching between 'up' and 'down' states proceeds through it as an intermediate state. Using numeric simulations we analyze the switching time and compare it to that of a conventional spin torque device with collinear magnetizations of the polarizer and the free layer.

Mo.F-P13 - Narrow linewidth spin-torque oscillator driven by localized current in ferromagnetic nano-contacts

M. Al-Mahdawi¹, Y. Toda¹, Y. Shiokawa¹, M. Sahashi¹

1. Tohoku University, Sendai, Japan

Microwave nano-oscillators/detectors are sought after for applications like inter-/intra-chip communication, non-destructive testing, and lab-on-chip sensors. Spin-torque-driven oscillators of a ferromagnet by a spin-polarized current are a candidate for such a role [1]. However, due to the large frequency non-linearity, oscillation linewidth increases compared to linear auto-oscillators [2]. By device engineering, the non-linearity can be lowered and a smaller linewidth can be obtained [3]. Also, the expected presence of pin-holes and localized current in magnetic tunnel junctions was found to produce more coherent oscillations with different dynamics characteristics compared to more uniform junctions [4]. By combining both approaches, we were able to reach linewidths down to 2.3 MHz at 23-GHz oscillation frequency. The device stack was based on AlOx Nano-Oxide-Layer (NOL) with ferromagnetic Nano-Contacts (NCs) (thickness in nm): electrode layer/FeCo (5)/AlOx-NOL/FeCo (5)/Capping layer [5]. The film was fabricated into elliptical pillars with 2-to-1 aspect ratio. Measurement of a 160 nm x 80 nm pillar under conditions of 2.8-mA applied current, and 185-Oe field applied 80deg away from long axis, oscillations were observed having 23-GHz frequency and 2.27-MHz linewidth, resulting in a quality factor of more than 10000. Micromagnetic simulation showed the generation of propagating spin-waves (system's characteristic mode) from NCs. We will discuss the role of excitation from the NCs on the reduced non-linearity and linewidth, and the potential of NC-based spin-torque oscillators.

[1] Kiselev et al., Nature 425, 380 (2003)

[2] Slavin and V. Tiberkevich, Magn. IEEE Trans. On 45, 1875 (2009)

[3] Nagasawa et al., Appl. Phys. Lett. 105, 182406 (2014)

[4] Houssameddine et al., Appl. Phys. Lett. 93, 022505 (2008)

[5] Shiokawa et al., Magn. IEEE Trans. On 47, 3470 (2011)

Mo.F-P14 - Experimental evidence of Rashba spin orbit torque in Py/ β -Ta bilayer systemNi Behera¹, Sujeet Chaudhary², Di. K. Pandya³*1. Indian Institute of Technology Delhi, Delhi, India*

Rashba effect is an important phenomenon for generation of dissipation-less spin currents in ferromagnetic (FM) /paramagnetic (PM) hetero-structures. It is combination of both spin transfer torque (STT) and field like torque which originates from the interfacial spin Hall effect (SHE) phenomena. However at higher charge current the field like torque leads to Oersted field noise along with STT. In order to avoid such a problem we prefer to have dissipation less spin pumping mechanism with suitable choice of material system. So we explore the Py/ β -Ta bilayer system in which β -Ta plays an important role for obtaining such a condition. For getting maximum spin pumping effect it is necessary to optimize thickness of β -Ta layer. Thus we report the thickness (t_{Ta}) dependence of ferromagnetic resonance (FMR) linewidth (ΔH) of Py(18 nm) bilayer samples grown on Si(100)/SiO₂ substrates at room temperature by pulsed dc magnetron sputtering. The ΔH is found to vary linearly with frequency for all thicknesses of Ta, indicating the intrinsic origin of damping. The Gilbert's damping constant (α) obtained from linewidth fitting data. The α values of Py/ β -Ta bilayers are less than the bare Py layer and remain constant up to 6 nm Ta thickness. We ascribe this behavior to the effect of out of plane anti-damping spin orbit torque (SOT) also known as Rashba torque, which arises from Ta layer, acts on the in-plane magnetization of FM layer. Above the thickness 6 nm of Ta, there is slight increase in α values indicating that the decrease of anti-damping SOT beyond the $2\lambda_{SD}$, λ_{SD} being the spin diffusion length in Ta. We also determine the λ_{SD} and -ve value of interfacial spin mixing conductance ($g^{\uparrow\downarrow}$) from the fittings of the thickness dependent of change in α ($\Delta\alpha$). The determined values are about $\lambda_{SD} = 2.64$ nm (close to literature reported value 2.74 nm) and $g^{\uparrow\downarrow} = -1.5 \times 10^{18} \text{ m}^{-2}$ respectively.

Mo.F-P15 - Effects of Dzyaloshinskii-Moriya interaction on the spin transfer magnetization switching in magnetic tunnel junctions

J Sampaio¹, A. Khvalkovskiy², M. Kuteifan³, M. Cubukcu¹, D. Apalkov², V. Lomakin³, V. Cros¹, N. Reyren¹

1. Unité Mixte de Physique CNRS/Thales, Palaiseau, France

2. Samsung Electronics, Semiconductor R&D Center (Grandis), San Jose, United States

3. Department of Electrical and Computer Engineering, University of California at San Diego, La Jolla, United States

Magnetic tunnel junctions (MTJ) are at the center of the magnetic random access memories (MRAM) technology. Nowadays, the research and development efforts are focusing on perpendicularly magnetized layers in the MTJ, taking advantage of the anisotropy provided by spin-orbit coupling at the interfaces with heavy metals such as Pt or Ta [1]. Recently, interfaces between ferromagnetic and heavy metals are also studied in a more fundamental context, because an antisymmetric interaction might appear at interfaces, namely an interfacial Dzyaloshinskii-Moriya interaction (DMI) [2]. We will present a micromagnetic study of the reversal of the free layer magnetization direction by spin transfer torque under different amplitudes of the DMI. In particular, we will evaluate the energy barrier or equivalently the thermal stability and the minimal current density necessary for switching as a function of the DMI amplitude. Our numerical simulations show that the DMI, even with small amplitude, is detrimental for the operation of MRAM devices, and must hence be minimized in the corresponding MTJ structures. The amplitude of the DMI can probably be tuned in some extent by interface engineering using materials with opposite DMI amplitude [3].

This work was supported by the Samsung Global MRAM Innovation Program.

[1] A. V. Khvalkovskiy et al., J. Phys. D: Appl. Phys. 46, 074001 (2013)

[2] A. Thiaville et al., EPL 100, 57002 (2012)

[3] J. Sampaio et al., (to be published)

Mo.F-P16 - Spin torque oscillator under a quasiperiodic current

D. Laroze⁰, A. Cabanas², P. Caranivi², J. Gallas³

1. *University of Glasgow, Glasgow, Scotland*

2. *Universidad de Tarapaca, Arica, Chile*

3. *Universidade Federal da Paraíba, João Pessoa, Brazil*

We study the deterministic spin dynamics of a spin valve oscillator in the presence of a time dependent electric current using the Landau-Lifshitz-Gilbert-Slonzewski equation. In particular, we study the case when the current consists in a constant and a quasiperiodic time dependence term. We numerically characterize the dynamical behavior of the system by monitoring the Lyapunov exponents, and by calculating Poincaremsections and Fourier spectra. In addition, we calculate analytically the corresponding Melnikov function, which gives us the bifurcations of the homoclinic orbits. We find a rather complicated landscape of sometimes closely intermingled chaotic and non-chaotic areas in parameters space. Finally, we show that the system exhibits strange nonchaotic attractors.

Mo.F-P17 - High frequency oscillation above 10GHz in zero applied field with Rh/FeCo perpendicular free layer Spin-Torque-Oscillator

Y. Shiokawa¹, K. Sakamoto¹, M. K.O Al-Mahdawi¹, J. Jung¹, M. Sahashi¹

1. Department of Electronic Engineering, Tohoku University, Sendai, Japan

In order to realize the applications using Spin-Torque-Oscillator (STO), as the oscillator for wireless tip-to-tip communication, STO needs a high frequency above 10GHz in zero or low applied field. Some studies have reported the STOs with high frequency and high power realized by Out-of-Plane Precession (OPP) mode [1] [2], however, they must be applied a high perpendicular magnetic field. The Kittel's equation of OPP mode suggests that high frequency STO needs high applied field and/or uniaxial anisotropy field (H_a). In this study, we used the Rh/FeCo with high H_a [3] as free layer and we realized the high frequency oscillation with zero applied field.

We fabricated STO element with Sub./Rh 50/FeCo 2/AlOx NOL/FeCo 2.4/IrMn 7/Capping (nm). NOL (Nano-Oxide-Layer) as spacer layer was thin AlOx oxide layer with many Nano-Contacts (2 nm in diameter). The STO element size was 100 nm in diameter. The orientation of applied magnetic field was perpendicular to film plane.

We obtained the high effective internal field ($H_a - 4\pi M_{\text{eff}}$) of 4.7 ± 0.5 kOe from R-H curve. It was higher internal field than Pt/Co of 0.7 kOe we fabricated. And the high frequency of 10.2 GHz at zero applied field with 24 mA (3.1×10^8 A/cm²) was obtained. We analyzed the current dependence of frequency based on auto-oscillation model [4], and we obtained the threshold current I_{th} of 20 mA (2.6×10^8 A/cm²). According to theory [5], this high I_{th} might be caused by high H_a .

[1] W. H. Rippard, et al, Phys. Rev. B 70, 100406 (2004)

[2] H. Kubota, et al, Appl. Phys. Express 6, 103003 (2013)

[3] B. Lao, et al, IEEE Trans. Magn. 50, 2008704 (2014)

[4] A. Slavin, et al, IEEE Trans. Magn 45, 1875 (2009)

[5] T. Taniguchi, et al, IEEE Trans. Magn. 50, 1400404(2014)

Mo.F-P18 - Spin Hall magnetoresistance in cobalt ferrite thin films with different preferential axesT. Tainosho¹, S. Sharmin¹, T. Niizeki², H. Yanagihara¹, E. Kita¹1. *Inst. of Appl. Phys., Univ. of Tsukuba, Tsukuba, Japan*2. *WPI-AIMR, Tohoku Univ., Sendai, Japan*

The recently discovered spin Hall magnetoresistance (SMR) effect is an interesting phenomenon where the dependence of non-magnetic metal resistance on the magnetization of a ferromagnetic insulator may be attributed to the spin-mixing conductance at the interface. In this study, we report SMR at the interface between Pt/Co_{0.75}Fe_{2.25}O₄ (CFO) thin films with regards to magnetic anisotropy. Two CFO(001) films were epitaxially grown on MgO and MgAl₂O₄ (MAO) by the reactive magnetron sputtering technique. Pt Hall bars were then deposited on the CFO by the DC sputtering technique. Taking into consideration the lattice constants of the different substrates, the CFO(001) films were found to undergo either tensile (on MgO) or compressive (on MAO) stress and exhibit a magnetically preferential axis either out-of-plane (on MgO) or in-plane (on MAO). Moreover, the perpendicular saturation magnetization ($M_{s\perp}$) differs from that of in-plane ($M_{s\parallel}$) due to additional orbital angular momentum of Co²⁺ along [001] direction. From α -scans, i.e., angle dependent MR measurements (ADMR) with the rotation axis normal to the plane, the SMR ratios were found to be 0.074 and 0.073% for the bilayers on MgO and MAO, respectively, while the estimated spin mixing conductance (G_r) was 20.8 and 21.1 $\times 10^{14}$ ($\Omega^{-1}\cdot\text{m}^{-2}$), respectively. From β -scan, where the rotation axis along to the current, we obtained almost the same value of G_r for Pt/CFO/MgO as that from the α -scan despite $M_{s\perp}$ differing from $M_{s\parallel}$. Here, we assumed the value of spin Hall angle and spin diffusion length as 0.056 and 3.4 nm, respectively [1]. The G_r values are an order of magnitude larger than reported previously. We conclude that magnetic anisotropy or the existence of orbital moment does not have a significant effect on the SMR phenomenon. [1] Phys. Rev. Lett. 112, 106602 (2014)

Mo.F-P19 - Time-domain study of injection locked signal from a magnetic tunnel junction based spin torque oscillatorsR. Sharma¹, P. Dürrenfeld², J. Åkerman^{2,3}, P.K Muduli^{1,3}*1. Department of Physics, Indian Institute of Technology, Hauz Khas, New Delhi, India**2. Department of Physics, University of Gothenburg,, Gothenburg, Sweden**3. Materials Physics, School of ICT, KTH-Royal Institute of Technology, Kista, Sweden*

Spin torque nano-oscillators (STNOs) are nano-sized microwave devices where signals in the GHz range can be generated by steady magnetization precession of the free layer.¹⁻² STNOs are promising for wireless communication.³ However, practical applications of these devices are yet to be realized due to their large linewidth and low output power. A solution for these limitations is injection locking or parametric excitation.⁴⁻⁵ It produces a drastic reduction in linewidth and significant increase in power. Here, we report on a time domain study of injection locked STNO signals. The device under study shows a strong single mode at a frequency of 3.75 GHz at the field of 250 Oe near the threshold current of 6 mA and $\varphi = 196^\circ$, where φ is the angle between the free and the reference layer. An external signal of power 0 dBm is applied over the frequency range of $f_{ext} = 7-8$ GHz. A strong enhancement of the signal near twice of the frequency of the STNO (*i.e.*, $f_{ext} = 7.5 \pm 0.10$ GHz) is observed. The linewidth is found to significantly decrease from 115 to 13 MHz while the peak power shows an increase from 740 nV²/Hz to 3750 nV²/Hz. The frequency noise analysis of the locked signals shows a reduction of both white noise as well as $1/f$ noise observed in these devices.⁶ However, the instantaneous frequency calculated for 50 ns segments shows that the locking phenomenon is not perfect and the instantaneous frequency is within the locking range of $(f_{ext}/2 \pm 0.04)$ GHz for 60 % of time.

References:

- [1] L. Berger, Phys. Rev. B 54, 9353 (1996)
- [2] J. Slonczewski, J. Magn. Magn. Mater. 159, L1 (1996)
- [3] Hyun Seok Choi et al., Scientific Reports 4, 5486 (2014)
- [4] S. Urazhdin et al., Phys. Rev. Lett. 105, 237204 (2010)
- [5] P. Dürrenfeld et al., Appl. Phys. Lett. 104, 052410 (2014)
- [6] R. Sharma, et al., Appl. Phys. Lett. 105, 132404 (2014)

Mo.F-P20 - Spin wave eigenmodes excited by spin transfer torque in circular nanopillars: influence of lateral size and Oersted field studied by micromagnetic simulations

M. Pauselli^{1,2}, G. Carlotti¹

1. Dipartimento Di Fisica E Geologia Università Degli Studi Di Perugia, Perugia, Italy

2. Istituto officina dei Materiali del Consiglio Nazionale delle Ricerche (IOM-CNR), Sede di Perugia, c/o Dipartimento di Fisica, Perugia, Italy

It is well known that a spin-polarized current can excite persistent dynamics in nano-pillars once it overcomes a critical threshold, thanks to the energy balance between the Spin Transfer Torque (STT) and intrinsic damping. Under the application of a sufficiently strong external field, the precession occurs around the local energy minimum defined by the magnetic field direction. In this paper we present the results of a micromagnetic study of the low-amplitude, linear, eigenmodes excited by STT in circular Permalloy nanopillars, 5 nm thick, having a diameter of either 100 nm or 300 nm. Both in-plane and out-of-plane externally applied fields are considered, with emphasis given to the effect of the Oersted field (OeF) on the frequency and spatial symmetry of the excitations. In the case of an in-plane applied field, the main excited mode is localized at the dot edges, where it oscillates out-of-phase (in-phase) if the OeF is considered (neglected). The out-of-phase mode is at slightly larger frequency than the in-phase one, due to the exchange energy contribution. For the out-of-plane case, instead, the main mode excited taking into account the OeF is an orthoradial mode with zero amplitude in the center of the dot. This is completely different from the fundamental mode with maximum amplitude in the dot center that the current would excite, at lower frequency, neglecting the presence of the OeF. Therefore, it turns out that inclusion of the OeF has a major impact on the output of simulations, because it modifies the symmetry of the excitation and the specific subset of eigenmodes activated by the injected current. This findings make it clear that simplistic models where the OeF contribution is ignored are not suitable to reproduce the main features of the low-amplitude eigenmodes and this is relevant in view of a detailed understanding of experiments.

Mo.F-P21 - Shape anisotropy dependence for Large Power Coherent Microwave MgO/CoFeB based Spin Transfer Nano-oscillators close to the in-plane/out-of-plane anisotropy transition

M. Tarequzzaman¹, Santiago Serrano-Guisan¹, J. D. Costa¹, Borme¹, Elvira Paz¹, R. Ferreira¹, P. Freitas¹

1. INL - International Iberian Nanotechnology Laboratory, Braga, Portugal

Spin transfer nano-oscillators (STNOs) rely on the transfer of spin angular momentum from a spin-polarized current to a ferromagnet enabling to induce magnetic excitations like coherent magnetization precession. In order to implement such a technology several requirements like high emitted power ($P_{\text{out}} \sim 1\mu\text{W}$), narrow spectral linewidth ($L < 1$ MHz), high frequency operation (above GHz) and large tuneability are required. Very recently large power coherent microwave emission up to 300 nW and $L \sim 40$ MHz were observed in such MgO based magnetic tunnel junction (MTJ) nanopillar structures under out-of-plane magnetic fields [1, 2]. However, the operation frequency was still below the GHz regime.

Here we present spin transfer torque (STT) induced magnetization dynamic measurements in CoFeB/MgO/CoFeB based magnetic tunnel junction (MTJ) nanopillars with RA of $\sim 3 \Omega\text{-}\mu\text{m}^2$ and a free layer thickness of 1.4 nm. At such conditions, the free layer magnetization is still in plane, but very close to the transition at which the interfacial perpendicular magnetic anisotropy becomes dominant, driving the magnetization out-of-plane. This delicate equilibrium allows the free layer magnetization to move easily under the influence of a spin polarized current resulting in large emitted power. At the same time, the free layer still experiences an effective field which is strong enough to result in oscillations above 2GHz. Large emitted power up to 300 nW with narrow linewidths up to $L \sim 30$ MHz and operation frequency between 2.4 – 2.8 GHz is observed in such structures, showing a tuneability of 300 MHz/mA for current controlled coherent microwave emission larger than 30 nW. Shape anisotropy also plays a crucial role and different MTJ nanopillars shapes (circular, elliptical) and dimensions were characterized.

[1] Z. Zeng et al., ACS Nano 6, 6115 (2012)

[2] Z. Zeng et al., Sci. Rep. 3, 1426 (2013)

Mo.F-P22 - Experiment on spin current assisted magnetization reversal using spin pumping effect.

M. Takahashi¹, Y. Nozaki¹

1. Keio University, Tokyo, Japan

In ferromagnetic / nonmagnetic bilayers, a spin current can be produced by spin pumping effect which is owing to the transfer of spin angular momentum from the magnetization precession in the ferromagnetic layer. The spin current generated by spin pumping effect is generally measured using spin Hall effect. In this study, we tried to alternatively measure the spin current from the change in a coercive field of spin-valve (SV) films. If the spin current generated in one of the ferromagnetic layer is absorbed in another one, the coercive field will change due to the spin transfer torque (STT) from the spin current.

SV consisting of NiFe100 nm/Cu10 nm/NiFe10 nm was shaped into a rectangle with lateral size of $1 \times 100 \mu\text{m}^2$ using a conventional liftoff process. Underneath the SV, 4- μm -wide coplanar strip line was fabricated to apply microwave fields to the SV. From the giant-magnetoresistance measurement, the coercive fields of 10- and 100-nm-thick NiFe layers were found to be 62.4 and 91.4 Oe, respectively. By means of network analyzer ferromagnetic resonance (FMR) spectroscopy, we also measured FMR frequencies of the 10- and 100-nm-thick NiFe layers at remanent state (3.5 and 6 GHz, respectively). The dependence of coercive field in 10-nm-thick NiFe layer on the frequency of microwave field was measured. In the frequency range from 2 to 4 GHz, a decrease in coercive field caused by a microwave-assisted magnetization reversal was clearly observed. Further increase in the frequency up to 7 GHz causes an additional reduction in coercive field. This is attributed to the STT caused by the spin current from the harder NiFe layer in which FMR is excited by the microwave field. In the SV with parallel alignment of magnetization, spin current opposed to the magnetization that leads to the decrease in coercive field is considered to be generated.

Mo.F-P23 - Spin-Torque Oscillators: Energy Space Dynamics

Da. Pinn¹, D. Stei^{2,3}, A. Kent³

1. Unité Mixte de Physique CNRS/Thales, Palaiseau, France

2. Courant Institute of Mathematical Sciences, New York University, New York, United States

3. Department of Physics, New York University, New York, United States

The excitation of large-angle steady-state out-of-plane (OOP) magnetization precession in spin valves and magnetic tunnel junctions using a spin-polarized dc current has recently attracted much interest due to its technological implications for the development of robust wide-band tunable RF oscillators. In this presentation, the dynamics of a macrospin subject to both in-plane (IP) and out-of-plane spin-torques is explored analytically by constructing an effective energy-space evolution equation. We find that the magnetic free layer can be thought as being torqued by a spin-current polarized along an axis that is tilted with respect to the IP direction. Our theory predicts a surprisingly simple relationship among material parameters capable of discriminating between switching and IP/OOP oscillatory behavior. We conclude by emphasizing the importance of including an additional angular dependence to the torque on top of the usual phenomenological sinusoidal dependence. Our results agree with recent experiments involving in-plane magnetized spin-valve devices that incorporate both an OOP magnetized spin polarizing layer and an IP magnetized reference layer.

Mo.F-P24 - NON-LINEAR MODE INTERACTION BETWEEN SPIN TORQUE DRIVEN AND DAMPED MODES IN SPINTORQUE NANO-OSCILLATORS

Miguel Romera^{1,2,3}, E. Montebianco^{1,2,3}, F. Garcia Sanchez^{1,2,3}, B. Delaùt⁴, L. D. Buda-Prejbeanu^{1,2,3}, U. Ebels^{1,2,3}

1. Univ. Grenoble Alpes, Grenoble, France

2. CEA, INAC-SPINTEC, Grenoble, France

3. CNRS, SPINTEC, Grenoble, France

4. CEA-LETI, MINATEC, DRT/LETI/DIHS, Grenoble, France

Spin torque nano-oscillators (STNOs) have attracted much interest in recent years due to their potential use as a new type of nanoscale microwave generator or microwave detector. A standard STNO configuration contains an in-plane magnetized synthetic antiferromagnet (SyF) as a polarizer and an in-plane magnetized free layer. Most experimental observations on the excitations of such STNOs have been analyzed theoretically or numerically in the frame of a single layer model, where the free layer is considered independent with respect to the SyF whose magnetization is supposed to be fixed. However, experiments on spin valve nanopillars reveal non-continuous features such as kinks in the frequency-field dependence that cannot be explained within an independent free layer picture. Numerical macrospin simulations show that such kinks are due to a non-linear interaction between the spin torque driven mode and a damped mode. This interaction arises from the dipolar coupling between the free layer and the SyF and is mediated via the third harmonics of the STT driven mode. The kinks only occur at large applied currents and thus at large excitation amplitudes of the STT driven mode. Under these conditions, a new hybridized mode appears, characterized by a strong reduction of the linewidth. The reduced linewidth can be explained by a reduction of the non-linear contribution to the linewidth via an enhanced effective damping. Interestingly the effect depends also on the exchange interaction within the SyF. Upon reducing the exchange interaction strength by 30%, the current range of reduced linewidth is enhanced by a factor of two and the minimum linewidth is reduced by a factor of two. These results open strategies to optimize the design of STNOs in order to take advantage of the coupling mechanisms to improve microwave performances.

Mo.F-P25 - High frequency characterization of nanocontact spin torque oscillators with respect to altitude and azimuth angles of applied field

S. A. Hossein Banuazizi¹, S. R. Sani², S. Chung^{1,3}, M. Mohseni⁴, J. Jakerman^{1,3,5}

1. Department of Material and Nano Physics, School of Information and Communication Technology, KTH-Royal Institute of Technology, Kista, Sweden

2. Department of Physics, New York University, New York, United States

3. Department of Physics, University of Gothenburg, Gothenburg, Sweden

4. Department of Physics, Shahid Beheshti University, Tehran, Iran

5. NanOsc AB, Kista, Sweden

The Nano-Contact Spin Torque Oscillator (NC-STO) is a nano-scale electrical device with the capability of generating microwave signals over a wide range of GHz frequencies and with a wide, and rapid, current and field tunability [J. C. Slonczewski, J. Magn. Magn. Mater. 159, L1 (1996)]. NC-STOs are based on the phenomenon of spin momentum transfer and exhibit a very rich magnetodynamics dependent on device geometry, material properties, and experimental conditions. [F. J. Albert, et al., Phys. Rev. Lett. 89, 226802 (2002)]. In addition, to reach admirable spin transfer torque, it is consequential to investigate STO behavior in different conditions.

We have experimentally studied variation in spin-torque-driven oscillations of NiFe free-layer of NC-STOs as a function of field direction. We measured the oscillation behavior of identically fabricated circular NC-STOs with 2 degrees of freedom for applied field angles. The samples in this study are single NC-STOs with these layer structures: Pd8-Cu50-Co8-Cu7-NiFe4.5-Cu3-Pd3, and nominal NC diameter: 100 nm. Based on high capability and accuracy of our measurement set-up, we applied fixed magnetic field of 0.95 Tesla and dc current of 20 mA to our samples, then we characterized our NC-STOs with full altitude angle Θ scan from 0 to 360 degrees for 3 different azimuth angles of $\phi = -15, 0$ and 15 degrees.

Our results show totally inconsistent output with the geometrical symmetry of the device for different group of 12 symmetrically identical angles of the applied field (For example, 4 symmetric altitude angles $\Theta = 70, 110, 250$ and 290 degrees with 3 different azimuthal angles of $\phi = -15, 0$ and 15). The frequency of oscillation, microwave power and linewidth vary with field direction and polarity by hundreds of MHz, numbers of pW/GHz and hundreds of MHz, respectively. These results suggest some form of inhomogeneity in material and domain structures and also broken symmetry in geometry which cause a strong Θ and ϕ dependence of the oscillation behavior. From the point of view of potential reasons of the anisotropic frequency variations in these oscillators lead to obtain a deeper understanding and optimization of film growth and fabrication process.

Mo.F-P26 - Analytical model of a synthetic ferrimagnet spin torque oscillator: comparison of the self-polarized with the external polarizer caseB. Lacoste¹, M. Romera^{2,3,4}, U. Ebels^{2,3,4}, L. Prejbeanu-Buda⁰*1. International Iberian Nanotechnology Laboratory, Braga, Portugal**2. Univ. Grenoble Alpes, Grenoble, France**3. CEA, INAC-SPINTEC, Grenoble, France**4. CNRS, SPINTEC, Grenoble, France*

Spin-Torque Oscillators (STOs) are promising candidates for nanoscale radiofrequency devices. The most accepted theoretical model to describe the self-sustained oscillations of the magnetization in a STO, called here KTS model [1,2], describes well the dynamics of a single-layer (SL) free layer. We propose an extension of this model to two coupled layers. In real devices, coupling between the layers affects the magnetization dynamics, for example the coupling of the free layer with the reference layer via dipolar coupling [3]. Moreover, spin-transfer torque (STT) driven self-sustained oscillations can also be induced in a synthetic ferrimagnetic (SyF) that consists of two layers coupled via RKKY interaction and mutual STT. This can be achieved either by an external fixed polarizer [3,4] or in a self-polarized manner [5]. To describe such STT driven SyF excitations, the two coupled Landau-Lifschitz-Gilbert-Slonzcewski equations (one for each layer) are transformed to coupled complex equations. Assuming that the energy is almost constant along the STT-driven trajectories, the two equations are expressed in the coordinates of the linear (acoustic and optic) eigenmodes of the SyF. The final equations can be decomposed into conservative terms, describing the phase evolution, and dissipative terms, describing the amplitude evolution. The two equations are coupled to each other via the non-linear terms. The analytical results are validated by numerical simulations and only the important terms, mainly the diagonal terms, are kept. A major result is that the transition from the red-shift to blue-shift in the frequency-current dependence in a SyF with external polarizer can be explained by a vanishing of the non-linear coefficient. This is associated with a decrease in linewidth, interesting for applications. In the self-polarized SyF, the excited mode is optical-like, and the red-shift to blue-shift transition is found to be more complicated and to involve mode-mixing terms.

[1] A. Slavin and V. Tiberkevich, IEEE Trans. Magn. 44, 1916 (2008)

[2] J.V. Kim et al., PRL 100, 017207 (2008)

[3] S.C. Lee et al., Sci. Rep. 2, 531 (2012)

[4] D. Gusakova et al., Phys. Rev. B 79, 104406 (2009)

[5] T. Seki et al., Appl. Phys. Express 3, 033001 (2010)

Mo.F-P28 - Mechanical analogy for spin currents and torques in diffusive systems

Y. B. Bazaliy¹

1. University of South Carolina, Columbia, United States

We map the problem of spin-transfer torques in nanostructures with diffusive spin currents on a mechanical problem involving elastic strings connecting points of attachment that slide along the fixed straight rails. The obtained mechanical analogy provides a qualitative understanding of the effects of spin relaxation on spin torques and of the phenomenon of sign-changing angular dependence [1-3] of the spin torque efficiency factor $g(\theta)$.

[1] A. A. Kovalev, A. Brataas, and G. E. W. Bauer, Phys. Rev. B 66 224424 (2002)

[2] Jan Manschot, A. Brataas, and G. E. W. Bauer, Phys. Rev. B 69 092407 (2004)

[3] J. Barnas, A. Fert, M. Gmitra, I. Weymann, and V. K. Dugaev, Phys. Rev. B 72, 024426 (2005)

Mo.G-P03 - Investigation of Magnetostatic Spin Wave Resonance in Patterned Mu-metal Thinfilms

C. Deger¹, F. Yildiz², M. Ozdemir¹

1. *Marmara University, Physics Department, Goztepe, Istanbul, Turkey*

2. *Gebze Technical University, Physics Department, Istanbul Caddesi, Gebze, Turkey*

Nanosized magnetic films contain an outstanding rich physics, technological applications and more potential for novel scientific purposes. Thus researchers put lots of effort for understanding the nature of these films and constructing functional nano-scale materials. Spin wave phenomena is one of the attractive topic due to improve in magnetic recording and giving opportunity for investigating the dynamics of magnetic parameters. In this study behavior of spin waves was investigated in patterned μ -metal thin film both theoretically and experimentally. The μ -metal (111) thinfilms with 7 μm thickness were grown by thermal evaporation technique. Crystal structure and temperature dependence of static magnetic properties of the thinfilm were determined by XRD and VSM measurements. There was a small signal from (200) plane excepting (111) plane. Saturation magnetization and coercive field values of sample obtained from vibrating sample magnetometer are around 500 emu/cm³ and 10 Oe respectively. Dynamic and spin wave properties were investigated by FMR measurements for both continuous thinfilms and patterned structures. The patterns were square shaped, however size of squares were changed between 40-80 μm . Main mode and magnetostatic spin wave modes in patterned μ -metal thin films were observed. Theoretical model and computer program were developed for evaluation of the FMR spectra. Different dimensioned squares showed different spin wave modes and magnetic parameters.

Mo.G-P04 - Structural control of standing spin wave properties in exchange-coupled multilayer strips.X. Ya¹, k. Imamura¹, t. Tanaka¹, K. Matsuyama¹*1. ISEE Kyushu University Japan, Fukuoka, Japan*

Geometrically confined standing spin wave (SSW) has attracting intense research interests for practical application to power efficient SW based devices. The interlayer exchange coupling is promising to tune the magnetic properties for SW devices operated in a broad frequency range. In the present study, dynamics of the SSW in exchange-coupled multilayer strips with various layer structures has been systematically investigated by micromagnetic simulations. A multilayer strip (1 μm width) and overlaid conductors (100 nm width) along the long axis of the strip were supposed as a model structure for the SSW excitation and its inductive detection. The following material parameter set were assumed for the soft (s) and hard (h) layers; perpendicular anisotropy $H_k=13$ kOe (s), 14~23 kOe (h), damping constant $\alpha = 0.01$ (s,h), $M_s = 1000$ emu/cc (s,h). The SSWs of magnetostatic forward volume wave mode with the wave vector along the strip width direction were generated with conductor fields. Systematic simulations were carried out for strips with various total thicknesses t_t , the layer thickness ratio t_h/t_t (t_h , hard layer thickness), and the repetition number of unit structure N (ex. $N=2$, [s/h/s/h]).

Simulation results reveal that the SSW resonance frequency f_{res} can be continuously tuned from 4 GHz ($t_h/t_t = 0$, $t_t=30$ nm) to 23 GHz ($t_h/t_t = 1$). The f_{res} linearly increases with the increase of t_h/t_t for $N=3$, while the dependence becomes nonlinear for $N=1, 2$. The nonlinear dependence can be associated with non uniform magnetization precession along the film thickness direction in the relatively thick unit layer ($N=1, 2$). The coherent precession in the sublayers was found to be failed at the weak interlayer exchange coupling smaller than a threshold value, where the magnetization dynamics of each layer obey the individual shape and crystalline anisotropy.

Mo.G-P05 - Spin-wave frequency non-reciprocity in permalloy thin films

O. Gladii¹, M. Haidar^{1,2}, Henry¹, M. Kostylev³, M. Bailleul¹

1. *Institut de Physique et Chimie des Matériaux de Strasbourg, UMR7504 CNRS-Université de Strasbourg, Strasbourg, France*

2. *Department of Physics, University of Gothenburg, Göteborg, Sweden*

3. *School of Physics, The University of Western Australia, Crawley, Australia*

Propagating spin-waves can now be used as a powerful spectroscopic probe of magnetic interactions in ferromagnetic thin films. They have been used to measure the adiabatic and non-adiabatic spin-transfer torques, and very recently the Dzyaloshinskii-Moriya interaction. For such studies, it is essential to measure and interpret the frequency non-reciprocity, i.e. changes of frequency occurring when the spin-wave propagation direction is reversed. Since the early days of spin wave studies, frequency non-reciprocity is known to occur naturally in the so-called Magnetostatic Surface Wave configuration (when the magnetization direction and spin-wave wave-vector lie in the film plane and perpendicular to each other), as soon as the top-bottom symmetry of the magnetic film is broken. This had been observed in thick yttrium iron garnet films. In this work, we revisit this problem both experimentally and theoretically in the technologically more relevant case of thin ferromagnetic metal films. Propagating spin-wave spectroscopy measurements were performed for a set of permalloy films with different thicknesses ($t=6-40$ nm) and at different wave vectors ($k=1.55-7.8$ rad/Åm). The frequency non-reciprocity is seen to depend strongly on film thickness and wave-vector, with values ranging from 2 to 50 MHz. This behaviour was reproduced using both micromagnetic simulations and an approximate analytical model based on the Kalinikos-Slavin theory of dipole-exchange spin-wave. We found that the measured values could be correctly accounted for assuming the top and bottom film surfaces have different surface anisotropies with a difference of 0.19 mJ/m². This work shows that propagating spin wave measurements give access to ferromagnetic film asymmetries with high accuracy, which opens new perspectives for advanced magnetic characterization.

Mo.G-P06 - Spin waves in planar quasicrystals of Penrose tiling

J. W. Klos¹, D. Kumar², J. Rychly¹, M. Krawczyk¹, A. Adeyeye²

1. Faculty of Physics, Adam Mickiewicz University in Poznan, Poznan, Poland

2. Information Storage Materials Laboratory, Department of Electrical and Computer Engineering, National University of Singapore, Singapore

The investigated two-dimensional (2D) magnonic structures are the counterparts of the photonic quasicrystals [1] forming Penrose lattice. The considered magnonic systems possess however much richer physics due to magnetization pattern and inhomogeneous internal magnetic field influenced wave dynamics, additionally to the material structure which is common with photonic quasicrystals. Therefore, the studies of magnonic systems are challenging. We studied planar 2D quasicrystal in the form of thin slab composed of ferromagnetic inclusions (Co) embedded in ferromagnetic matrix (Py). The inclusions have a cylindrical shape and are located in the nodes of the Penrose lattice. We applied strong external magnetic field to saturate the system along specific in plane directions. The calculations were performed using plane wave method. We defined the supercell [2] which is a small fragment of the Penrose lattice. The periodic repetition of the supercell allows to cover the whole 2D plane without gaps and use the plane wave method. By extension of the size of the supercell we were able to approach the limit of quasiperiodic structure. We calculated the frequency spectra (density of states) of spin waves and the spatial profiles of dynamical components of the magnetization in dependence on direction of the magnetic field. We also traced the impact of the geometrical factors (filling fraction of inclusions, thickness of the structure) on the spectrum of spin waves.

We acknowledge the financial assistance from the Polish National Science Centre project No DEC-2-12/07/E/ST3/00538 and from European Union's Horizon 2020 research and innovation programme under the Marie Skłodowska-Curie GA No 644348 (MagIC).

[1] M. Notomi, H. Suzuki, T. Tamamura, K. Edagawa, Phys. Rev. Lett. 92 (2004) 123906

[2] K. Wang, S. David, A. Chelnokov, J. M. Lourtioz, J. Mod. Opt. 50, (2003) 2095

Mo.G-P07 - Spin wave propagation in Permalloy films under tangentially magnetic fields with an arbitrary direction

M. Nakayama¹, M. Tashima¹, S. Kasai², S. Mitani², T. Manago¹

1. *Fukuoka University, Fukuoka, Japan*

2. *National Institute for Materials Science, Tsukuba, Japan*

Spin wave propagation in ferromagnetic metals has attracted attention for novel spintronic devices such as signal transfer and signal processing.1-2) Spin wave propagation in ferromagnetic film has been investigated mainly on magnetostatic surface wave (MSSW), and there is a few papers for magnetostatic backward volume wave (MSBVW) and magnetostatic forward volume wave (MSFVW). These depend on the relationship between the magnetic field direction and propagation direction of spin waves. In order to design spin wave devices, the degree of freedom of a field direction is useful. In this paper, we investigated spin wave propagation in Permalloy (Py) films under tangentially fields with an arbitrary direction. The variations from MSSW to MSBVW are discussed. Py films with a thickness of 300 nm was prepared on a Si/SiO₂ substrate. After isolating with SiO₂ film, a pair of antennas for excitation and detection was formed. The distance between antennas were 5, 10, 20 μm. Spin wave transmission measurements were performed by a microprobe station with a electromagnet for applying in-plane magnetic field and a vector network analyzer. We defined the field angles to the antenna direction; $\theta = 0$ deg for the MSSW configuration, and $\theta = 90$ deg for the MSBVW configuration. As increasing field angles up to 45 deg, the spin wave resonant frequency decreased with almost same spectra shape. At more than 60 deg, the shapes have different characteristics. The signal intensity decreased with increasing the angle. The intensity becomes about half at 45 deg, and about 1/20~1/30 at 90 deg. We observed the MSBVW characteristics only in shortest antenna distance of 5 μm, which is reasonable because the attenuation length of MSBVW is very short. Thus, we successfully observed spin wave propagation from MSSW to MSBVW configurations.

Mo.G-P08 - High group velocity and large attenuation length of spin-waves in thick permalloy films

M. Ota¹, K. Yamanoi², S. Kasai³, S. Mitani³, T. Manago¹

1. *Fukuoka University, Fukuoka, Japan*

2. *Kyushu University, Fukuoka, Japan*

3. *National Institute for Materials Science, Tsukuba, Japan*

Spin waves have attracted much attention as a new transfer tool of the spin current. The advantage of the spin wave is its long-range propagation over a 10 μm -scale in a ferromagnetic metal such as Permalloy (Py), which is much larger than the spin diffusion length of the charge spin current. Spin wave devices using metal films, such as information transfer and logic operations using interference of spin-waves, expected to be suitable for integration with a Si process. In order to demonstrate these interference experiments, longer propagation length is favorable. In this paper, we investigated Py thickness dependence of the group velocity and attenuation length of spin waves. Py films with a thickness of 25 - 300 nm were prepared on a Si/SiO₂ substrate. After isolating with SiO₂ film, a pair of coplanar waveguides (CPWs) for excitation and detection antennas was formed, and the distance between two CPWs was varied from 10 - 300 μm . Spin-wave (magnetostatic surface spin-wave: MSSW) transmission measurements were performed using a sampling oscilloscope with a time domain reflection/transmission (TDR/TDT) unit. The group velocity of the MSSW increases in almost proportion to the Py thickness. It reaches to 67 $\mu\text{m}/\text{ns}$ for 300-nm-thick film. The MSSW spectra were clearly observed even in 200 μm of the antenna distance, although we previously reported that it was about 40~50 μm for Py thickness of 25 nm. However, for over 100 nm in Py thickness, the attenuation length hardly changes despite group velocity is faster. This suggests that damping for spin wave is enhanced in thick Py film. Further investigation is necessary to solve this issue. Thus, high group velocity and long range propagation of MSSW is realized by using thick Py films.

Mo.G-P09 - Graded-index magnonics with local electrical currents

C. Davies¹, V.Kruglyak¹

1. University of Exeter, Exeter, United Kingdom

It was recently reported [1] that a spin wave multiplexor could be realized using a network of Y-shaped Permalloy waveguides, mounted on a similar network of Y-shaped current-carrying wires. By switching the direction of the current, so that it flows under either arm of the structure, a local bias magnetic field can be introduced. This allows spin waves to be directed through either arm, with the direction toggled by the current. We demonstrate that the concept of graded-index magnonics can be used to explain the results of Vogt et al fully, by mapping the local spin wave group velocity distribution within the structure. First, we use finite element modelling to quantitatively solve Maxwell's equations to calculate the spatially-resolved non-uniform bias field across the network. Then, we use the Object-Orientated Micro-Magnetic Framework (OOMMF) to calculate the static magnetisation and effective field distribution in each simulation cell. We then use the dipole-exchange dispersion relation [2] to calculate the distribution of spin wave group velocity vectors across the Y-shaped structure. This enable us not only to explain the experimental results of Vogt et al but also to predict the optimal multiplexor geometry.

[1] K. Vogt et al, Nat. Commun. 5, 3727 (2014)

[2] B. A. Kalinikos and A. N. Slavin, J. Phys. C 19, 7013 (1986)

Mo.G-P10 - Spin wave excitations in artificial multiferroic yttrium iron garnet - zinc oxide layered structures

Y. Khivintsev^{1,2}, A. Kozhevnikov¹, S. Vysotsky^{1,2}, V. Sakharov¹, O. Kiryasova¹, A. Veselov¹, Y. Filimonov^{1,2}

1. *Saratov Branch of Kotelnikov Institute of Radio-engineering and Electronics of Russian Academy of Sciences, Saratov, Russia*

2. *Chernyshevsky Saratov State University, Saratov, Russia*

Combination of piezoelectric and ferromagnetic materials allows to tune magnetic properties through electrical control due to magnetostriction. In this work we experimentally studied spin wave (SW) excitations in such an artificial multiferroic in the form of yttrium iron garnet (YIG) - zinc oxide (ZnO) layered structure. Epitaxial YIG films on gadolinium gallium garnet (GGG) substrates were used in the experiment. ZnO films were grown on top of YIG by magnetron sputtering. Two types of samples were fabricated and tested. The first was coplanar waveguide (CPW) based on ZnO/YIG/GGG (structures #1) and in the second the microantennas for generation and detection of SW were fabricated on top of ZnO/YIG/GGG (structures #2). Also, in the second case YIG film was preliminary patterned in order to form 1D magnonic crystal and reduce YIG thickness between microantennas in order to realize wavelength conversation effect and examine shorter SW. Microwave measurements were done using a vector network analyzer along with a probe station with tangential magnetic bias field. For the structures #1 we observed absorption peak in the transmission characteristic corresponding to the ferromagnetic resonance (FMR). Position of the FMR peak was tunable not only by magnetic field but by voltage applied between the CPW signal line and ground planes as well (about 10 MHz at 1 kV). For the structures #2 we observed SW transmission band with stop bands corresponding to Bragg resonances. In this case voltage applied to electrodes fabricated on the sides of the SW beam for generation of tangential electric field in ZnO film caused oscillating changes in SW transmission characteristic. These changes were more pronounced (up to 7 dB/mm for electric field of 0.7 kV/mm) in the short wave part of the SW transmission band. This work was supported by RFBR (grants # 13-07-00941, 13-07-12421 and 14-07-00896).

Mo.G-P11 - Excitation of the spin wave beams with coplanar waveguide transducer

P. Gruszecki¹, A. E. Serebryannikov¹, W. Smigaj¹, M. Krawczyk¹

1. Faculty of Physics, Adam Mickiewicz University in Poznań, Poznań, Poland

In this paper, we propose a microwave transducer in non-uniform coplanar waveguide (CPW) geometry for excitation of spin wave (SW) beams in thin homogeneous ferromagnetic films. Traditional CPWs consist of three parallel wires made of a good conductor and generate a weak radio-frequency (RF) magnetic field when carrying microwave current. The magnetic field component that oscillates in the plane perpendicular to the CPW axis exerts a torque on the magnetization, which in turn induces coherent magnetization precession around the equilibrium direction. This disturbance can propagate in the form of a SW. The RF magnetic field distribution in the ferromagnetic film plane is inhomogeneous and determines the SW excitation efficiency, its wavelength and direction of propagation. Here, we exploit these properties to show how by varying the profile of the CPW along its axis we can mold the envelope of the generated SW. In particular, this enables excitation of SW beams with a customizable waist width, rather than SWs with a nearly planar front, as in standard CPWs.

We provide a qualitative description of our idea and validate it in numerical simulations. An electromagnetic solver is used to obtain the RF magnetic field generated by a microwave current flowing through the CPW; this field distribution is then input to micromagnetic simulations to find the profile of the excited SW beam. Finally, we propose an extension of the SW beam generator that allows excitation of two (or multiple) beams with a single CPW in the same ferromagnetic film. Other technologically relevant applications are discussed as well.

The research has received funding from Polish National Science Centre project DEC-2-12/07/E/ST3/00538 and from European Union's Horizon 2020 research and innovation programme under the Marie Skłodowska-Curie GA No 644348 (MagIC).

Mo.G-P12 - Microwave radiation from parametrically excited magnons

M. Mino¹, H. Kawahara¹

1. Okayama University, Okayama, Japan

Einstein condensation of nonequilibrium magnons at room temperature have been reported by many researchers. We study Microwave radiation from parametrically excited magnons in YIG. Measurements were performed with perpendicular and parallel pumping configurations. The radiation spectra are dependence on a pumping power, a shape of a sample and a pumping configuration. As the pumping power is increased, multi-frequency components of microwave radiation are observed simultaneously. For a spherical sample, microwave radiation from some magnetostatic modes, which are coupled on parametrically excited magnons, is observed. For a disk sample, radiation of a double frequency of a bottom mode and a frequency of a uniform mode are observed.

Mo.G-P13 - Stimulated thermalization of a parametrically driven magnon gas as a prerequisite for bose-einstein magnon condensation

D. A. Bozhko^{1,2}, P. Clausen¹, V. I. Vasyuchka¹, B. Hillebrands¹, G. A. Melkov³, A. A. Serga¹

1. *Fachbereich Physik and Landesforschungszentrum OPTIMAS, Technische Universität Kaiserslautern, Kaiserslautern, Germany*

2. *Graduate School Materials Science in Mainz, Kaiserslautern, Germany*

3. *Faculty of Radiophysics, Taras Shevchenko National University of Kyiv, Kyiv, Ukraine*

The realization of a Bose-Einstein condensation (BEC) of magnons is one of the great achievements in the area of quasi-particle gases, when the parametrically pumped magnon gas undergoes a phase transition leading to the spontaneous formation of a coherent state at the bottom of a spin-wave spectrum. Since the moment of this discovery, the physics of the parametrically driven magnon gases is under active theoretical and experimental investigation. Here, we report on the experimental insight into the evolution of a magnon gas determined by four-magnon scattering in the presence of the external pumping field. The experiment is performed using an in-plane magnetized single-crystal yttrium-iron-garnet film (YIG). In order to manipulate the magnon gas density, magnons were injected into YIG film using parallel parametric pumping. The temporal evolution of the magnon gas density was detected by the time- and wavevector-resolved Brillouin light scattering spectroscopy. We show that the magnons initially pumped to the transversal branch of the spin-wave spectrum do not scatter directly to the lowest energy states located at the longitudinal branch. Such a scattering is associated with the parametric excitation of the second group of short-wavelength magnons propagating at angles $< 90^\circ$ relative to the magnetization direction. Simultaneously, the initially excited transversal magnon group is suppressed by a mutual action of the second magnon group and the external pumping field. In conclusion, we suggest distinctly different phases of the thermalization process of a parametrically driven magnon gas: First, energy degenerated, parametric magnons are generated, which, secondly, scatter in a multistage magnon transfer process to the bottom of the magnon spectrum. The parametrically stimulated magnon thermalization is assumed as the essential precondition for the formation of the magnon Bose-Einstein condensate.

Financial support from the Deutsche Forschungsgemeinschaft within the SFB/TR49 is gratefully acknowledged.

Mo.G-P14 - Spin-wave modes in magnonic crystal waveguides and inverted waveguides.

M. Mansurova¹, J. Panke¹, M. Münzenberg²

1. *I. Physikalisches Institut, Georg-August-Universität Göttingen, Göttingen, Germany*

2. *Institut für Physik, Ernst-Moritz-Arndt-Universität Greifswald, Greifswald, Germany*

This work contributes to the understanding of spin waves behavior excited on periodically structured magnetic thin films (magnonic crystals). The examined sample consist of 50 nm CoFeB continuous film, where a square lattice of 1 μm antidots (3.5 μm lattice constant) has been produced using Focused Ion Beam (FIB). In addition to a uniform precession mode and perpendicular standing spin wave (PSSW) that are detected on continuous film, a Damon-Eshbach (DE) mode is supported by the magnonic crystal [1]. The excited DE mode wavevector is parallel to the lattice vector of the magnonic crystal, and its frequency is strongly dependent on magnonic crystal's lattice constant and its relative orientation to the applied magnetic field. In this work, we determine the spin-wave spectra of two kind of different structures on the magnonic crystal. First, a magnonic waveguide is realized by introducing 3-5 defect lines in the crystal structure. Second, a set of inverted waveguides consisting of n by 40 unit cells, where $n=2, 4, \dots, 20$ was produced. Spin-wave modes have been excited and observed optically by a double-modulated pump-probe technique using a pulsed (40 fs) 800nm laser. Magnetization oscillations are detected using time resolved magneto-optical Kerr effect (TRMOKE) and the fundamental frequencies are determined performing fast Fourier transform of the measured signal. We observe that a Damon-Eshbach mode is supported only on inverted waveguides of more than $n=6$ rows. On the other hand, this mode can also be detected on defect lines (waveguides) of as large as 5 rows of antidots. This sets a limit on the number of unit cell that are required to produce a collective behaviour of spin waves in a magnonic crystal. Support by DFG MU 1780/ 6-1 Photo-Magnonics project is acknowledged.

[1] B. Lenk, N. Abeling, J. Panke, M. Münzenberg, J. Appl. Phys. 112, 083921 (2012)

Mo.G-P15 - Twinned domain induced magnonic modes in La_{0.7}Sr_{0.3}MnO₃/SrTiO₃(001) thin films

E. Wahlström¹, F. Macià², J. E. Boscher¹, Å. Monsen¹, P. Nordblad³, R. Marhieu³, A. Kent⁴, T. Tybell¹

1. Norwegian University of Science And Technology, Trondheim, Norway

2. Universitat de Barcelona, Barcelona, Spain

3. Uppsala Universitet, Uppsala, Swedem

4. New York University, New York, United States

By defining a periodic magnetic structure it is possible to excite magnonic modes other than standard uniform magnetodynamic modes. However, a traditional top-down approach to define structures at length scales <100 nm is often challenging. Here we present a bottom up approach to such magnonic lattices. In order to achieve this we rely on epitaxial thin films of a prototypical perovskite, La_{0.7}Sr_{0.3}MnO₃, on top of SrTiO₃(001), with an intended structural twinned domain geometry, acting as a periodic perturbation for the magnonic lattice. Variable temperature ferromagnetic resonance spectroscopy provides evidence for additional magnonic modes. We will show that the origin of these modes can be related to a spatial modulation of the Curie temperature induced by the twin domain formation. This yields a temperature dependent magnetic variation in the saturation magnetization that forms the magnonic structure. We will discuss how film thickness and structural domain periodicity affects the excited modes. In particular the temperature dependence of the magnetic structure will be discussed and used in a model description of the system that accounts for the major features of FMR spectra.

Mo.G-P16 - Indirect vs direct magnonic band gap in two types of magnonic crystals: array of metallic stripes and array of grooves in YIG film

M. Mruczkiewicz¹, V. Bessonov^{2,3}, R. Gieniusz², U. Guzowska², A. Maziewski², A. Stognij⁴, M. Krawczyk¹

1. Faculty of Physics, Adam Mickiewicz University in Poznan, Poland

2. Faculty of Physics, University of Białystok, Białystok, Poland

3. Institute of Metal Physics, Ural Division of Russian Academy of Science, Yekaterinburg, Russia

4. Scientific-Practical Materials Research Center at National Academy of Sciences of Belarus, Minsk, Belarus

The magnonic band gaps in two types of the planar one-dimensional magnonic crystals comprised of the periodic array of the metallic stripes on yttrium iron garnet (YIG) film and YIG film with an array of grooves were analyzed experimentally and theoretically. In such periodic magnetic structures the propagating magnetostatic surface spin waves were excited and detected by microstripe transducers with vector network analyzer and by space resolved Brillouin light scattering spectroscopy. Properties of the magnonic band gaps were explained with the help of the finite element calculations in the frequency domain. The analysis of the imaginary component of the wavenumber of spin waves was found to be useful. The important influence of the nonreciprocal properties of spin wave dispersion induced by metallic stripes on the magnonic band gap width and the band gap width dependence on the external magnetic field has been shown. Indirect band gap and higher group velocity of spin waves in metallic magnonic crystal were identified as main cause of the wider band gap and steeper decrease of its width with increased external magnetic field as compared to the grooved magnonic crystal. The usefulness of both types of the magnonic crystals for potential applications and possibility for miniaturization are critically discussed.

The research has received funding from Polish National Science Centre project No. DEC-2-12/07/E/ST3/00538, the European Union's Horizon 2020 programme under the Marie Skłodowska-Curie GA No. 644348, SYMPHONY project operated within the Foundation for Polish Science Team Programme co-financed by the EU European Regional Development Fund, OPIE 2007-2013 and Megagrant of the RF No. 2013-220-04-350.

Mo.G-P17 - Detection of standing spin waves and investigation of the spin wave stabilities under high power excitations.

Y. Yokotani¹, K. Yamanoi¹, S. Yakata², T. Kimura⁰

1. Department of Physics, Kyushu University, Fukuoka, Japan

2. Department of Information Electronics, Fukuoka Institute of Technology, Fukuoka, Japan

3. Research Center for Quantum Nano-spin Science, Kyushu University, Fukuoka, Japan

The dynamical property of the spin wave and exploring their precise manipulation techniques have attracted much attention owing to its fast time scale in GHz range and high compatibility with a Si-based semiconductor integrated circuits. Especially, understanding the thermal stability and the non-linear response induced by the large amplitude RF magnetic field are indispensable for the practical application. Impedance transmission measurements based on the vector network analyzer is one of the representative method for investigating the spin wave. However, the detectable spin waves are limited by the electrode design because the interlinkage magnetic flux is canceled out. In this paper, we demonstrate a sensitive detection method for the spin wave excited by the patterned electrodes. The standing spin waves for various wavelengths are effectively detected through the anisotropic magnetoresistance. Our device consists of a ferromagnetic film and the ladder-type nonmagnetic Cu electrode, which are electrically separated each other by a SiO₂ film. An external magnetic field is applied along the Cu wire direction, and RF current flowing the ladder-type Cu wires generates the standing spin wave, which can be detected by the resistance of the Py film through AMR. We clearly observed the resonant features consisting of the multiple peaks in the induced voltage.

From the analysis, the resonant magnetic fields are well explained by the ferromagnetic resonance and the standing spin wave with the half wave length given by the fraction of the integer number of the electrode spacing. Nonlinear resonant feature was observed only in the ferromagnetic resonance when the large RF power for the ac current above 15 dBm is applied. The origin for the nonlinear behavior can be understood by the effective demagnetizing field due to the nonuniform precession with large cone angle.

Mo.G-P18 - Evaluation of the thermal spin injection driven by ferromagnetic resonance

K. Yamanoi¹, Y. Yokotani¹, S. Yakata², T. Kimura¹

1. *Department of Physics, Kyushu University, Fukuoka, Japan*

2. *FIT*

Thermal spin injection originating from the spin-dependent Seebeck effect is an attractive method for creating spin current without the use of the electricity. Recently, we have found that CoFeAl has a relatively large spin-dependent Seebeck coefficient because of its unique band structure.[1] In this method, producing the temperature gradient, which is the driving force for the thermal spin injection, is a key for the large spin-current generation and the seamless device integration. So far, the temperature gradient is produced by the Joule heating. On the other hand, since the ferromagnetic metal is known to be heated by ferromagnetic resonance (FMR), the thermal spin injection may be driven by the FMR. In addition, this can be another mechanism for the dynamical spin injection. In the present study, we focus on the thermal spin injection due to FMR heating.

First, we evaluate the temperature increase due to the FMR for several ferromagnetic thin film. The temperature change due to the FMR heating seems to increase with the damping constant of the ferromagnetic metal. Then, the efficiency of the thermal spin injection due to the FMR heating is evaluated by measuring the frequency dispersion of the FMR spectra in ferromagnetic metal/Cu bilayer system. A significant reduction of the frequency dispersion was clearly observed in CoFeAl/Cu system. This result strongly supports the large spin-dependent Seebeck coefficient for CoFeAl.

[1] S. Hu, H. Itoh, T. Kimura. *NPG Asia Mater.* 6, e 127 (2014)

Mo.G-P19 - Propagation of Volume Mode Spin Waves

L. Van Tilburg¹, F. Buijnsters¹, A. Fasolino¹, M. Katsnelson¹

1. Radboud University, Nijmegen, Netherlands

Spin waves are collective spin oscillations that play a role in many dynamical processes, and understanding their dynamics may lead to innovative ideas for new applications. In this poster we present preliminary results of a new numerical package for performing micromagnetic simulations of spin waves. Spin wave propagation and interactions are studied by solving the Landau-Lifshitz-Gilbert equation. As a benchmark simulation we reproduce the spin wave pattern found in recent experiments, with very good agreement. The properties of the spin wave dispersion for the Backwards Volume Magnetostatic Spin Waves (BVMSW) are investigated and we present results on modes with a group velocity of zero at nonzero k .

Mo.G-P20 - Division and multiplication of a ferromagnetic resonance frequency on the basis of the nonlinear microwave magnetoelastic transducer

V. Vlasov¹, L. Kotov², V. Shavrov³, V. Shcheglov³

1. *Institut Molécules Et Matériaux du Mans, UMR CNRS 6283, Université Du Maine, Le Mans, France*

2. *Syktyvkar State University, Syktyvkar, Russia*

3. *IRE Russian Academy of Sciences, Moscow, Russia*

The coupled oscillations of magnetization and elastic displacements in normally magnetized ferrite plate excited by the alternating magnetic field which frequency coincides with the frequency of a ferromagnetic resonance of a magnetic subsystem [1] are considered. When the resonant frequency of an elastic subsystem makes multiple part of resonant frequency of a magnetic subsystem, the excitation of elastic oscillations at the elastic resonance frequency represents process of division of initial frequency in the multiple relation is possible. When the resonant frequency of an elastic subsystem in multiple number of times exceeds frequency magnetic the multiplication of initial frequency in the multiple relation is possible. Processes of the division and multiplication of frequency are possible only in strongly nonlinear mode, and polarization of an exciting field has to be linear for the multiplication. Phase portraits of the excited elastic oscillations are constructed at division and multiplication cases. It is shown that the division and multiplication are observed only in that case when time of a relaxation of elastic oscillations not less than much exceeds time of a relaxation of the magnetic oscillations. The work was supported by RFBR (grant # 13-02-01401-a)

References:

1. V.S. Vlasov, L.N. Kotov, V.G. Shavrov, V.I. Shcheglov // Journal of Communications Technology and Electronics. 2009. V.54. No.7. P.821

Mo.G-P21 - Modeling of rf nonlinear dynamics of magnetoelastic oscillations in a ferrite layers

V. Vlasov¹, D. Pleshev², F. Asadullin², S. Poleshikov², L. Kotov³, V. Shavrov⁴, V. Shcheglov⁴

1. Institut Molécules Et Matériaux du Mans, UMR CNRS 6283, Université Du Maine, Le Mans, France

2. Saint-Petersburg state forest technical university named after S.M. Kirov, St-Petersburg, Russia

3. Syktyvkar State University, Syktyvkar, Russia

4. Institute of Radioengineering and Electronics of the Russian Academy of Sciences, Moscow, Russia

The system of ordinary differential equations described in the paper [1], is dealing with the electromagnetic excitation of nonlinear magnetoelastic oscillations in the normally magnetized ferrite plate when the parametric excitation of spin waves was blocked and is introduced in the given paper. The present paper deals with investigation of features of the magnetization vector nonlinear precession and the elastic displacement close to ferromagnetic resonance condition by two methods, the first one - by the eigenfunction expansion method and the second one - by the method of lines. The research was made for one-layer and two-layer ferrite plates. The case of the first elastic mode excitation is the only one that is considered in the research. The alternating circular polarized magnetic field was oriented in the plane of the plate. The systems of ordinary differential equations in nodes of the spatial grid were solved numerically by the Runge-Kutta 7-8 orders method with control of the integration at every step length. The time evolution of magnetic and elastic oscillations caused by the alternating field was analyzed. Dependences of magnetoelastic oscillation relaxation time on magnitudes of dc and alternating magnetic fields, saturation magnetization, the magnetoelasticity constant, magnetic and elastic relaxation parameters were determined. Magnetoelastic coupling efficiency in particular is determined by the ratio of the relaxation times of magnetic and elastic subsystems was revealed. Several regimes of precession changing each other by increase of the alternating field amplitude were identified. It was found that the magnetoelastic interaction changed the character of the observed precession regimes especially under the condition of the elastic resonance. In case of detuning the eigenfrequency of magnetic and elastic resonances, chaotic oscillation modes took place. The boundaries between regular and chaotic oscillations depending on the magnetic dissipation parameter, frequency and amplitude of the alternating field were determined.

The work is supported by RFBR (grant # 13-02-01401-a).

[1] V.S. Vlasov, L.N. Kotov, V.G. Shavrov, V.I. Shcheglov, J. Comm. Tech. El., 54 (2009) 821-832

Mo.G-P22 - Magnetisation dynamics of confined magnetic nanostructures controlled by voltage-induced mechanical strain

S. Bowe^{1,2}, R. Beardsley¹, D. Parkes¹, M. Wang¹, C. Reardon², K. Edmonds¹, B. Gallagher¹, A. Rushforth¹, S. Cavill^{2,3}

1. *School of Physics and Astronomy, University of Nottingham, Nottingham, United Kingdom*

2. *Diamond Light Source, Chilton, Didcot, Oxfordshire, United Kingdom*

3. *Department of Physics, University of York, Heslington, York, United Kingdom.*

Magnetic nanostructures containing flux closure and vortex domain configurations have potential applications ranging from information storage technologies to spin torque oscillators. The magnetisation dynamics of confined magnetic structures can be complex and consist of standing wave modes in regions with uniform magnetisation, oscillations of the domain wall structure[1] and gyration of the vortex core[2]. In our recent work we demonstrated how voltage induced strain can be used to significantly modify the configuration of magnetic flux closure domains in structures fabricated using Fe₈₁Ga₁₉[2]. Here we present investigations of the effects of a strain-induced uniaxial magnetic anisotropy on the magnetisation dynamics of Fe₈₁Ga₁₉ square structures in the flux closure configuration. Using time-resolved XMCD PEEM and micromagnetic simulations we find that an induced anisotropy energy of 10 to 40 KJ modifies the precession frequency of the uniform magnetic regions, the oscillations of the domain wall structure by up to 0.8GHz, and the gyration of the vortex cores by up to 150MHz in square objects between 500nm and 2000nm. This shift in frequency of oscillation is also accompanied by a reduction in the number of frequency modes present in the system from 3 to only one dominant mode. Our investigations show that inverse magnetostriction provides a promising route for tuning significantly the complex magnetisation dynamics of magnetic nanostructures.

[1] Bailleul et al., Phys. Rev. B 76, 224401 (2007)

[2] Parkes et al., Appl. Phys. Lett. 105, 062405 (2014)

Mo.G-P23 - Band structure of two-dimensional magnonic crystals with different antidot sizes: a micromagnetic study

R. Silvani¹, M. Madami¹, G. Gubbiotti², S. Tacchi², [G. Carlotti¹](#)

1. *University of Perugia - Dipartimento Di Fisica E Geologia, Perugia, Italy*

2. *CNR_IOM, UnitÓ di Perugia, Vía Pascoli, Perugia, Italy*

In the emerging field of magnon-spintronics, spin waves are exploited to carry and process information in materials with periodic modulation of their magnetic properties, named magnonic crystals (MCs). Here, one finds the appearance of allowed and forbidden frequency bands which can be exploited to tailor the spin wave dispersion as well as to design micro-devices operating in the GHz frequency range. In this paper, we present the results of advanced micromagnetic simulations performed using the open source GPU-accelerated code MuMax3. We consider two-dimensional MCs consisting of Permalloy (Ni80Fe20) square antidot lattices with a fixed periodicity $p=200$ nm and different hole sizes, namely 25 nm, 50 nm, and 100 nm. For each case, the band structure is analyzed in the Damon-Ehsbach (DE) configuration (wavevector perpendicular to the applied magnetic field) within the first three artificial Brillouin zones, with emphasis given to the dispersive character and spatial profile of the most prominent modes. It is shown that in the case of the smaller holes several modes have a finite group velocity, comparable to that of the DE mode of the unpatterned film. Instead, in the case of the larger holes, the eigenmodes are less dispersive and resemble stationary waves, localized within the minima of the highly-inhomogeneous internal field. To reduce the effect of such inhomogeneity of the internal field, arising at the hole edges, we studied bi-component MCs where the antidots are filled with a second magnetic material (e.g. Cobalt). In this case, one recovers the dispersive character of the modes even in presence of relatively large holes. Finally, we propose the realization of tunable magnonic filters based on the exploitation of the above antidot lattices.

This work was supported by the European Community (FP7/2007-2013) under Grant No. 318287 "LANDAUER" and by the MIUR under PRIN Project No. 2010ECA8P3 "DyNanoMag".

Mo.G-P24 - Spin wavevector dependent spin dynamics and damping processes on the magnetic nanowires

J. Cho¹, J. Yoon², F. Yuya³, K. Katsunori³, M. Jung⁴, Y. Suzuki³, C. You¹

1. Department of Physics, Inha University, Incheon, South Korea

2. Department of Electrical and Computer Engineering Faculty of Engineering, National University of Singapore, Singapore

3. Department of Materials Engineering Science, Osaka University, Osaka, Japan

4. Department of Physics, Sogang University, Seoul, South Korea

Ferromagnetic nanostructures have recently attracted much interest for the wide potential applications in high density magnetic recording media, logic devices and various spin orbit torque phenomena [1,2,3]. In many kinds of next generation nano spin devices, the damping process plays an important role in the devices performance. Therefore, more deep studies are needed to understand the damping processes in the nano devices structures including nanowires. In this study, we simulated the ferromagnetic resonance using micromagnetic with the different shape anisotropies in xy plane at zero temperature. In order to remove the finite size effect, we incorporated two-dimensional periodic boundary condition (PBC). The resonance frequencies are obtained by the fast Fourier transformation of time dependent M_x (transverse) and M_y (longitudinal). As the result, the demagnetization factor for longitudinal conditions, N_z (N_y) is increasing (decreasing) as decreasing the periodicity of PBC from 50 to 150 nm. In the transverse condition, N_z (N_y) is increasing (decreasing) as increasing the periodicity of PBC. In the macro-spin model, they must be identical, but micromagnetic simulation reveals the demagnetization factors different for two different magnetization states. The Gilbert damping constant for transverse case is increasing from 0.018 to 0.051 as the increasing periodicity of PBC, longitudinal case is almost constant as 0.021. Our finding can be explained by the wavevector dependent damping processes, which has been reported by K. Gilmore's theoretical work [4]. He claimed that the damping constant dramatically decrease from 0.2 to 0.05 as the wavevector decrease from zero to 1% of Brillouin zone edge at the low temperature.

[1] Stuart S. P. Parkin et. al., Science 320, 190 (2008)

[2] D. A. Allwood et. al., science 209, 1688 (2005)

[3] Ioan M. Miron et. al., Nature Materials 9, 230 (2010)

[4] Keith Gilmore et. al., Phys. Rev. B 79, 132407 (2009)

Mo.G-P25 - Spin-wave dynamics and the magnon Hall effect in the pyrochlore Lu₂V₂O₇

M. Mena^{1,2}, R. Perry¹³, T. Perring^{1,4}, D.O. Le⁵, S.O. Guerrero⁶, M. Storni⁶, D. Adroja⁴, U. Stuhr², M. Enderle⁷, C. Rüegg^{2,8}, D. McMorrow¹

1. London Centre For Nanotechnology, UCL, London, United Kingdom
2. Laboratory for Neutron Scattering and Imaging, Paul Scherrer Institute, Villigen, Switzerland
3. Centre for Science at Extreme Conditions, University of Edinburgh, Mayfield Road, Edinburgh, Scotland
4. ISIS Facility, STFC Rutherford Appleton Laboratory, Harwell Oxford, Didcot, United Kingdom
5. Helmholtz-Zentrum Berlin, Berlin, Germany
6. Condensed Matter Theory, Paul Scherrer Institute, Villigen, Switzerland
7. Institut Laue-Langevin ILL, Grenoble, France
8. DPMC-MaNEP, University of Geneva, Geneva, Switzerland

Members of the family Re₂V₂O₇ (Re = Yb, Tm, Lu) are quantum ferromagnetic insulators with pyrochlore structure that have been recently found to exhibit numerous exceptional properties including the magnon Hall effect, which is driven by the antisymmetric Dzyaloshinskii-Moryia interaction (DMI). Lu₂V₂O₇ has been identified as a potential dispersionless magnon medium and, as such, a prime candidate for magnonics and possibly the first magnon topological insulator [1,2,3]. We present the results of an inelastic neutron scattering study on the time-of-flight spectrometer MERLIN (ISIS, UK) to probe the spin dynamics of Lu₂V₂O₇. We observe well-defined spin waves and determine the spin Hamiltonian including its exchange parameters. The data is in agreement with a minimal model used to explain the magnon Hall effect, and allows to extract directly the ratio between the ferromagnetic exchange and the DMI, which is the driving parameter of the effect.

- [1] M. Mena, R. S. Perry, T. G. Perring, M. D. Le, S. Guerrero, M. Storni, D. T. Adroja, Ch. Rüegg and D. F. McMorrow, Phys. Rev. Lett. 113, 047202 (2014)
- [2] Y. Onose, T. Ideue, H. Katsura, Y. Shiomi, N. Nagaosa, and Y. Tokura, Science 329, 297 (2010)
- [3] L. Zhang, J. Ren, J.-S. Wang, and B. Li, Phys. Rev. B 87, 144101 (2013)

Mo.G-P26 - Spin wave dynamics in array of Py stripes with periodic and quasiperiodic order

J. Rychly¹, J. W. Klos¹, M. Mruczkiewicz¹, M. Krawczyk¹, P. Kuswik², M. Matczak², F. Lisiecki³, R. Gieniusz⁴, A. Maziewski⁴

1. Faculty of Physics, Adam Mickiewicz University in Poznan , Poznan, Poland

2. Institute of Molecular Physics, Polish Academy of Sciences, Poznan, Poland

3. Faculty of Technical Physics, Poznan University of Technology, Poznan, Poland

4. Faculty of Physics, University of Bialystok, Bialystok, Poland

We present investigation of the one-dimensional (1D) magnonic quasicrystals (MQs) made from infinitely long permalloy (Py) stripes separated by air. 30 nm thick, 700 nm (A) and 350 nm (B) wide Py stripes with 100 nm air gap are quasiperiodic ordered according to Fibonacci inflation rule. The number of stripes and total width of the structure are expressed by Fibonacci number F_n . The structure is saturated by external magnetic field applied along the stripes. In focus of our study are ferromagnetic resonance (FMR) and spin wave excitation spectra. Results obtained for MQs are compared with results for magnonic crystals (MCs) composed of periodic array of the same Py stripes and separations. We have proposed and realized quasiperiodic (and periodic) structures suitable for investigation of fractal properties of the spin wave spectra in nanoscale magnonics. We show, that dipole coupling existing in MQ is sufficient for formation of the collective spin wave excitations. Investigation of the MQ consisting of different number F_n of stripes provides the mechanism to explore the fractal nature of the spin wave spectra in MQs. We have found that for large MQs, multilevel structure of magnonic gaps exhibits property of self-similarity and FMR spectra with many absorption peaks. The magnonic gaps in MQs have been found also in frequency range below the first magnonic band gap in respective MC. Obtained results are promising for further experimental investigation and applications in magnonics, including its reprogrammable property. The research has received funding from Polish National Science Centre project DEC-2-12/07/E/ST3/00538, project SYMPHONY (program TEAM/2011-8/4) of the Foundation for Polish Science and from the EU's Horizon2020 research and innovation programme under the Marie Skłodowska-Curie GA No644348.

Mo.G-P27 - Spin-wave scattering by domain walls in ultrathin ferromagnetic films

F.Buijnsters¹, A. Fasolino¹, M. I. Katsnelson¹

1. Institute For Molecules And Materials, Radboud University Nijmegen, Nijmegen, Netherlands

There is an increasing focus on the essential role of the Dzyaloshinskii-Moriya (DM) interaction in the dynamics of magnetic structures in (ultra)thin films. For example, there are now strong indications that the DM interaction can greatly enhance the maximal propagation speed of a domain wall by stabilizing its internal structure [1]. At the same time, it has been claimed that the DM interaction does not influence the effect a domain wall has on spin waves that pass it [2]. Our calculations indicate that this conclusion is not general and that, in fact, the DM interaction can modify the interaction of spin waves with a domain wall in an essential way. We provide explicit analytical and numerical predictions on the magnitude of this effect. Our results show how the internal structure of the domain wall could be used as a novel switching element in the construction of magnonic devices beyond what was proposed in [3].

[1] K.-S. Ryu, L. Thomas, S.-H. Yang, S. Parkin, *Nature Nanotech.* 8, 527 (2013); S. Emori, U. Bauer, S.-M. Ahn, E. Martinez, G. S. D. Beach, *Nature Mater.* 12, 611 (2013)

[2] P. Yan, X. S. Wang, X. R. Wang, *Phys. Rev. Lett.* 107, 177207 (2011)

[3] R. Hertel, W. Wulfhekel, J. Kirschner, *Phys. Rev. Lett.* 93, 257202 (2004)

Mo.G-P29 - Broadband GHz magnetic susceptibility tensor of a synthetic antiferromagnet: experiment and semianalytical approach

D. E. Gonzalez-Chavez¹, E. Montebianco¹, R. Dutra¹, R. L. Sommer¹

1. Brazilian Center For Research In Physics, Rio de Janeiro, Brazil

A synthetic antiferromagnet (SAF) is one of the most basic magnetic coupled layered systems. It is composed by two ferromagnetic layers coupled antiferromagnetically through a thin metallic layer via the Ruderman-Kittel-Kasuya-Yosida interaction. Since the development of the spin valve structure, the SAF has been used as the replacement of the single, pinned or free, layers in read heads, magnetic random access memories and spin transfer torque oscillators (STOs). In particular, it is possible to enhance the output power of STOs by using appropriate SAF configurations. In this work we provide further insight on the effect of the SAF configuration by analyzing the ferromagnetic resonance response of a NiFe(20nm)/Ru(1nm)/NiFe(20nm)/IrMn(20nm) sample with SAF behavior by using vector network analyzer ferromagnetic resonance measurements with in-plane exciting RF field in, both, parallel and perpendicular directions relative to the applied static field direction. For both configurations we observe spectra with similar dispersion relations, with two resonant modes, but with absorption amplitudes on the resonant branches depending on the RF field direction. These amplitudes are related to the susceptibility tensor component probed by the RF field. We use the model explained in a previous work [1] to fully describe and reproduce the experimental results. From our model we calculate the susceptibility tensor and extract the magnetic moment oscillation amplitude and phases for each layer as a response to the RF field. A detailed analysis on the evolution of the oscillation amplitudes and phases with the applied field, on both resonant modes, is performed.

[1] D. E. Gonzalez-Chavez, R. Dutra, W. O. Rosa, T. L. Marcondes, A. Mello, and R. L. Sommer. Phys. Rev. B. 88, 104431 (2013)

Mo.G-P30 - Ferromagnetic resonance measurements of CoFeCrB alloys films for in-plane spin transfer torque devicesC. Lacroix¹, K Oguz², J. M. David Coey², D. Ménard¹

1. Polytechnique Montreal, Montreal, Canada
2. Trinity College Dublin, Dublin, Ireland

Decreasing the magnetization of the CoFeB free layer in MgO based magnetic tunnel junctions is desirable for reducing the critical current density J_c for spin transfer torque switching. While it has been reported that substituting Fe ions with Cr decreases the magnetization of the CoFeB layer and allows for reducing J_c by a factor of four*, the effect of Cr substitution on the damping mechanisms involved in the magnetization dynamics have yet to be clarified. Multilayers stacks of SiO₂(500 nm)/MgO(5 nm)/Co₄₀Fe_{40-x}Cr_xB₂₀(30 nm)/Ta(5 nm) were grown on a Si(001) substrate using a Shamrock sputtering system for $x = 0, 4, 8$ and 18 . The damping properties of the CoFeCrB films were investigated using angle-dependent and frequency dependent ferromagnetic resonance (FMR) in a resonant cavity (9.6 GHz) and in a shorted waveguide configuration (26 to 75 GHz). The magnetization M_s of the CoFeCrB films, determined from the fit of the resonance fields, show that M_s diminishes as the content of Cr increases, in agreement with SQUID magnetometry measurements. The g -factor, an indicator of spin-orbit coupling, equals 2.15 for $x = 0$, and diminishes as x increases, tending towards a value of 2 when M_s approaches zero. The linewidth of the FMR peaks increases with the content of Cr. The angular and frequency dependencies of the measured linewidth are fitted for all films ($x = 0, 4, 8$ and 18) assuming three different contributions: 1) an intrinsic damping modeled by a phenomenological Gilbert parameter, 2) an inhomogeneous broadening and 3) a two-magnon damping. Our results show that the Gilbert damping parameter decreases from 145 to 107 MHz as x increases. Furthermore, when $x = 0$ or 4 , the two-magnon damping is negligible in comparison to both the Gilbert damping and the inhomogeneous broadening. However, when $x = 8$ or 18 , a two-magnon damping is required to properly model the linewidth.

*Oguz et al. J. Appl. Phys. 111, 113904 (2012)

Mo.G-P31 - Spinwave dynamics in elliptical dots: experiment and simulations

R. Pinto¹, D. E. Gonzalez-Chavez¹, R. Sommer¹

1. Centro Brasileiro de Pesquisas Físicas, Rio de Janeiro, Brazil

The dynamical properties of patterned magnetic sub-micrometric elements have attracted an increasing interest in the last decade because of the observation of new effects induced by the lateral confinement on the spin excitation spectrum.

In this work we explore the magnetization dynamics of periodic arrays of Ni₈₀Fe₂₀ patterned elements using the vector network analyzer ferromagnetic resonance technique (VNA-FMR).

Two examples are presented: an array of disks with diameter of 1 μm and array of ellipses with dimensions of 2.4 μm x 1.4 μm, both with 50 nm thickness.

Our arrays were produced, onto a Si wafer, by combining e-beam lithography, magnetron sputtering and lift-off techniques. We were able to control the magnetostatic interaction in the arrays by varying the the spacing between the elements.

The samples were characterized by alternating gradient force magnetometry and magnetic force microscopy. The obtained M vs. H curves showed the typical behavior inherent to vortex states. From the broadband measurements we obtained the dispersion relations for fields up to ± 800 Oe, for two radio frequency field configurations ($h_{rf} \wedge H_{dc}$) and ($h_{rf} // H_{dc}$).

In the saturated states, where the magnetization of each element of the array is aligned to the external field, we observed the uniform Kittel and localized spin wave modes. On the other hand for the vortex states a rich structure of spin-wave modes was observed, such as modes with integral numbers, m and n, which represent the azimuthal and radial modes. Micromagnetic simulations were performed in order to have a further insight of the experimental results. With them we obtained the details of the excited spin eigenmodes in the frequency domain at a given bias field.

Mo.H-P01 - Influence of demagnetization field direction on domain structure and size of ultra-thin CoPt perpendicular anisotropy films

R. Hara¹, K. Hayakawa¹, H. Kawamura¹, R. Sugita¹

1. Department of Media And Telecommunications Engineering, Ibaraki University, Hitachi, Japan

CoPt based perpendicular anisotropy films have been studied for magnetic devices such as magnetic recording media, but there has been little discussion on the relationship between domain structure and the applied field direction for ultra-thin films. In this study, we clarify the influence of demagnetization field direction on domain structure and size of ultra-thin CoPt perpendicular anisotropy films. Samples whose structure was Pt(2 nm) / Co70Pt30(3-10 nm) / Ru(20 nm) / Pt(100 nm) / Glass substrate were prepared using an RF magnetron sputtering system, and were AC demagnetized with perpendicular or in-plane field. From MFM observations, it was found that the 3 nm thick CoPt film had irregular domain whose size was about 400 nm in the case of the perpendicular demagnetization, while it had mixed structure of irregular and maze domains whose size was about 200 nm in the case of the in-plane demagnetization. For the perpendicularly demagnetized 3 nm thick film, nuclei of reversed domain hardly emerge due to high perpendicular anisotropy, while for the in-plane demagnetized one, magnetization in in-plane direction easily rotates upward or downward because of being unstable. Therefore the domain size of the former is larger than that of the latter. The domain size monotonically decreased with increase of film thickness for both demagnetization directions, and the difference of the size between both demagnetization directions disappeared for the 10 nm thick film. For the 10 nm thick film, in both demagnetization directions the maze domain whose domain width was about 70 nm was observed. In conclusion, the domain size of perpendicularly demagnetized CoPt films was larger than that of in-plane demagnetized films for the thickness less than 10 nm, and for the 3 nm thick film the former was twice as large as the latter.

Mo.H-P02 - Stress-engineering of CoFe₂O₄ thin filmsI. Lucas^{1,2,3}, P. Jiménez-Cavero^{3,4}, B. Rivas-Murías⁵, C. Magén^{1,3,6}, F. Rivadulla⁵, L. Morellón^{2,3}1. *Fundación Araid, Zaragoza, Spain*2. *Instituto de Nanociencia de Aragón (INA), Universidad de Zaragoza, Zaragoza, Spain*3. *Departamento de Física de la Materia condensada, Universidad de Zaragoza, Zaragoza, Spain*4. *Instituto de Ciencia de Materiales de Aragón (ICMA), Universidad de Zaragoza, Zaragoza, Spain*5. *Centro de Investigación en Química Biológica y Materiales Moleculares (CIQUS), Universidad de Santiago de Compostela, Santiago de Compostela, Spain*6. *Laboratorio de Microscopias Avanzadas (LMA), Instituto de Nanociencia de Aragón (INA), Universidad de Zaragoza, Zaragoza, Spain*

The inverse spinel oxide CoFe₂O₄ (CFO) is an interesting and complicated material that has been object of intense research due to its interesting properties. The interest lies on the fact that this spinel is an attractive high magnetostrictive insulating material with large Curie temperature T_c and proved spin-filter efficiency [1-3]. The complication comes from the difficulty selecting the adequate substrate and deposition conditions to obtain the desired properties of CFO. Depending on the strain induced by the substrate and on the deposition conditions, the inversion degree of the spinel can be modified [4,5] affecting both magnetic and electric properties of CFO. In order to study the effect of ionic reorganization in the lattice under very different growth conditions, we have compared CFO thin films prepared by Pulsed Laser Deposition (PLD) and a chemical solution deposition method (Polymer Assisted Deposition, PAD). Samples of different thickness were deposited on MgAl₂O₄ (001) and MgO (001) substrates under different heat treatments, oxygen pressures and deposition rates to study the degree of ionic inversion and also to study the relaxation mechanisms of CFO on both substrates. All the samples have been structurally, magnetically and electrically characterized. The cation and defect distribution have been analyzed by Scanning Transmission Electron Microscopy (STEM), High Angle Annular Dark Field (HAADF) imaging and Electron Energy Loss Spectroscopy (EELS). Our study provides a guide to prepare thin films of these samples with the desired magnetic and electrical properties.

[1] R.M. Borzorth, et al. Phys. Rev. 99, 1788 (1955)

[2] Y. Chen, et al. IEEE Transactions on Magnetics 35, 3652 (1999)

[3] A.V. Ramos, et al. Appl. Phys. Lett. 91, 122107 (2007)

[4] Y.H. Hou, et al. J. Phys. 82, 1539 (2010)

[5] D. Fritsch et al. Appl. Phys. Lett. 99, 081916 (2011)

Mo.H-P03 - Spin-wave properties of IrMn/NiFe based spin-valves

G. Gubbiotti¹, Silvia Tacchi¹, M. Tamisari², L. Del Bianco³, E. Bonfiglioli², L. Giovannini², F. Spizzo², R. Zivieri²

1. *Consiglio Nazionale delle Ricerche- Istituto Officina dei Materiali (CNR-IOM)*

2. *Dipartimento di Fisica e Scienze della Terra, CNISM, Università di Ferrara, Ferrara, Italy*

3. *Dipartimento di Fisica ed Astronomia, Università di Bologna, Bologna, Italy*

Brillouin light scattering (BLS) was exploited to study the effect of the exchange coupling (EC) at the interface between antiferromagnetic (AF) and ferromagnetic layers on spin-wave properties in spin-valves (SVs). The stacking of the samples was Cu(5 nm)/IrMn(tu)/NiFe(5nm)/Cu(5nm)/NiFe(5nm)/IrMn(to); tu and to are the thicknesses of the AF IrMn (Ir₂₅Mn₇₅) underlayer and overlayer, respectively. Three different samples were studied: SVA (tu = 10 nm, to = 0 nm), SVB (tu = 10 nm, to = 6 nm), and a reference sample, SVR (tu = to = 0 nm). The samples were deposited by DC magnetron sputtering in a magnetic field of 400 Oe. The EC strongly affects the SV magnetization process by inducing a bias field (HB) on the pinned NiFe layer, that results in a shift of the NiFe loop along the measurement axis. BLS spectra were acquired by sweeping the applied field (H) over the upper branch of the hysteresis loop (from positive to negative saturation) and encompassing both the parallel (P) and antiparallel (AP) alignment of the NiFe layers. In the saturated state, in SVA and SVB the frequencies of the two measured modes increase with respect to the ones in SVR, and their frequency difference depends on H orientation with respect to HB direction. At the transition from the P to the AP alignment, the mode frequencies undergo an abrupt variation and the frequency dependence remarkably changes. The experimental frequencies are compared with those calculated by a theoretical model that includes in a phenomenological way the effects of the EC at the IrMn/NiFe interface[1]. For both the SVA and SVB samples, the accordance between experimental and theoretical frequencies is good in the P state, larger differences are present in the AP state.

[1] G. Gubbiotti et al., accepted for publication in J. Appl. Phys

Mo.H-P04 - Detail study of the physical properties in BiFeO₃/La₂/3Sr1/3MnO₃ bilayers.

C. Dominguez¹, J. Edward Ordoñez¹, M. Elena Gomez¹

1. *Thin Film Group, Department of Physics, Universidad del Valle, Cali, Colombia*

2. *Center of Excellence for Novel Materials - CENM, www.cenm.org, Cali, Colombia*

With multiferroic materials integrated into the spintronics, spins might be manipulated by an electric field, leading to the development of the next generation of low power consumption, magnetic memory storage, and high speed information technologies. Multiferroic BiFeO₃ (BFO) shows coexistence of ferroelectric (FE) and magnetic orders at room temperature with FE Curie temperature, TC-FE ~ 1100K and antiferromagnetic (AFM) Neel temperature, TN ~ 640K. In fact, the AFM order parameter in the multiferroic acts as a medium that indirectly couples the ferromagnetic (FM) ordering of a FM thin film and the FE ordering of the multiferroic. To study the AFM/FM coupling mechanics, we propose as strong FM candidate, half metallic manganite perovskite La₂/3Sr1/3MnO₃ (LSMO) has been widely used as a spin source in spintronics, with Curie temperature (TC ~350K). We have grown BFO/LSMO bilayers on (100) SrTiO₃ substrates by using DC and rf sputtering technique at pure oxygen pressures. Samples were structurally characterized by X-ray diffractometry; morphologically by statistical analysis of atomic force microscopy. Polarization curves in samples indicates the ferroelectric property of the BFO at room temperature. Magnetic characterization have been carried out by thermal demagnetization curves at zero field and at applied field cooling, as well as ZFC and FC isothermal magnetization curves.

Acknowledgments: This work was sponsored by Researchs Project No 110656933104, C.I.: 7917 COLCIENCIAS-UNIVALLE and C.I.: 7978 UNIVALLE

Mo.H-P06 - Co₈₀Pt₂₀ films with columnar grains and perpendicular magnetic properties produced by epitaxial deposition on Ru/Cu bilayers

S. Chen¹, C. Wen¹, C. Wang¹, T. Sun², C. Wang³, P. Kuo³

1. *Ming Chi University of Technology, New Taipei City, Taiwan*

2. *National Tsing Hua University, Hsinchu City, Taiwan*

3. *National Taiwan University, Taipei City, Taiwan*

Ordered Co₃Pt film is a promising material for high density recording media, due to its magnetocrystalline anisotropy constant being higher than that of current CoCrPt recording materials by a factor of around 10 times. Furthermore, the manufacturing temperature of Co₃Pt used for obtaining high perpendicular magnetic properties is similar to that used in current hard disk manufacture. However, single-layered Co₃Pt films incline towards in-plane magnetic anisotropy or random orientation, which cannot be utilized in perpendicular magnetic recording application. It has been reported that Co-rich Co-Pt films with high perpendicular magnetic properties can be achieved by introducing a Pt underlayer or Ru/Pt bilayer. However, the expensive Pt layer in the films would result in excessively high cost. In this study, the magnetic anisotropy of single-layered Co₈₀Pt₂₀ film with thickness of 50 nm deposited directly on glass substrates at ambient temperature inclines towards random orientation. It tends to an in-plane magnetic anisotropy by the introduction of a (10 1) texture of 30 nm Ru layer under the Co₈₀Pt₂₀ film. The perpendicular magnetic anisotropy would be increased slightly by inserting a 100 nm thick Cu layer between the Co₈₀Pt₂₀ and Ru layers. However, when the Cu layer is introduced under the Co₈₀Pt₂₀/Ru bilayer films, the magnetic anisotropy becomes perpendicular. This is because a fcc Cu (111) underlayer can promote hcp Ru (0002) seed layer to induce (0002) texture well in hcp Co₈₀Pt₂₀ magnetic layer, leading to a good perpendicular magnetic anisotropy of Co₈₀Pt₂₀ films. It is found that a columnar Co-rich Co-Pt nano-grains with perpendicular coercivity of 4580 Oe and perpendicular squareness of 0.77 can be achieved by depositing Co₈₀Pt₂₀(50 nm) film onto Ru(30 nm)/Cu(100 nm) bilayer films at ambient temperature. This Co₈₀Pt₂₀ film is a promising candidate for perpendicular magnetic recording media applications.

Mo.H-P07 - Tuning the magnetoimpedance response in NiFe/Cu/Co films through the magnetic interaction between ferromagnetic layers

E. Felix da Silva¹, M. Gamino², A. Marcos Helgueira de Andrade², R. Barreto da Silva³, M. Assolin Corrúa¹, F. Bohn¹

1. *Universidade Federal do Rio Grande do Norte, Natal, Brazil*

2. *Universidade Federal do Rio grande do Sul, Porto Alegre, Brazil*

3. *Universidade Federal de Santa Maria, Santa Maria, Brazil*

Magnetic materials exhibiting asymmetric magnetoimpedance effect are of large interest due to their potential for application in sensor devices. Asymmetric effects are obtained by inducing an asymmetric static magnetic configuration, usually done by magnetostatic interactions or exchange bias. In the present work, we investigate the quasi-static and dynamical magnetic behavior in ferromagnetic NiFe/Cu/Co films. We produce Ni₈₁Fe₁₉ (25 nm)/Cu(*t*_{Cu})/Co(50 nm) films, with *t*_{Cu}=0, 1.5, 3, 5, 7, and 10 nm, grown by magnetron sputtering. The quasi-static magnetic properties are investigated through magnetization and magnetoresistance measurements. Both are dependent on the thickness of the non-magnetic Cu spacer, and indicate a biphasic magnetic behavior for the films with Cu thicknesses above 3 nm. Magnetization dynamics is investigated through magnetoimpedance measurements obtained using a RF-impedance analyzer, in a frequency range between 0.1 and 3.0 GHz. The results present asymmetric magnetoimpedance in films with biphasic magnetic behavior. Besides, the magnetoimpedance response can be tailored by changing the thickness of the non-magnetic Cu spacer material and probe electrical current frequency. By considering this set of films, we verify the competition between two kinds of magnetic interactions between ferromagnetic layers: ferromagnetic exchange coupling and magnetostatic coupling. They are strongly dependent on the spacer thickness and affect in different ways the magnetic behavior. We show that the strength of the bias field increases with the thickness of the spacer and that the field value *H*=30 Oe corresponds to the magnitude of the effective coupling strength between the soft NiFe and hard Co layers, for films with *t*_{Cu}>3 nm. The results place films with biphasic magnetic behavior exhibiting magnetoresistance and asymmetric magnetoimpedance effect as very attractive candidates for application as probe element in the development of auto-biased linear magnetic field sensors.

Mo.H-P08 - Optical and magneto-optical interactions in permalloy thin and ultrathin films on Si substrates

Kristupas Kazimieras Tikuišis, Lukáš Beran, Petr Cejpek, Klára Uhlířová, Michal Urbánek, Marek Vaňatka, Martin Veis

1. *Faculty of Mathematics and Physics, Charles University in Prague, Prague, Czech Republic*
2. *Institute of Physical Engineering, Brno University of Technology, Brno, Czech Republic*
3. *CEITEC BUT, Brno University of Technology, Brno, Czech Republic*

Permalloy is a well-known magnetic alloy with high magnetic permeability, low coercivity and a very small magnetostriction which makes it promising material for various practical applications. Recently, novel spintronics concepts have been proposed, such as magnetic logic circuits, spin valves or MRAMs [1] employing permalloy layers. Although the functionality of these new spintronic devices is widely investigated by magneto-optical methods, only the spectral dependence of complex refractive index of permalloy is reported [2]. One could hardly find a precise spectral examination of its complete permittivity tensor, which describes both optical and magneto-optical interactions in this material. However, knowing it is necessary for theoretical predictions of the complex magneto-optical response of novel spintronic nanostructures. In this work, we present a systematic study of optical and magneto-optical properties of permalloy films in the photon energy range from 1.2 to 5.5 eV. The samples with nominal thicknesses of 10 nm and 150 nm were deposited onto Si substrates. They were examined by x-ray diffraction and atomic force microscopy to get information about their crystallinity, thickness and surface morphology. Spectroscopic ellipsometry and magneto-optical spectroscopy were performed at room temperature and the spectra of polar Kerr rotation and ellipticity were recorded in the magnetic field of 1.2 T, sufficient to magnetically saturate the samples. The spectral dependence of the diagonal and off-diagonal elements of permittivity tensor were deduced from ellipsometric and magneto-optical measurements using a Yeh's matrix formalism extended to absorbing media [3]. The spectra of both diagonal and off-diagonal elements of the permittivity tensor showed metallic behavior with notable differences, indicating a change of physical properties in ultrathin permalloy layers.

- [1] S. S. P. Parkin et al, *Science* 320, 190 (2008)
[2] R. Raueret et al, *Rev. Sci. Instrum.* 76, 023910 (2005)
[3] P. Yeh, *Surf. Sci.* 96, 41-53 (1980)

Mo.H-P09 - Thickness dependence of the dynamic magnetic behavior in Permalloy films

E. Felix Da Silva¹, R. Domingues Della Pace², M. Cara², A. Azevedo³, S. Rezende³, C. Chesman¹, M. Assolin Corrúa¹, F. Bohn¹

1. *Universidade Federal Do Rio Grande Do Norte, Natal, Brazil*
2. *Universidade Federal de Santa Maria, Santa Maria, Brazil*
3. *Universidade Federal de Pernambuco, Recife, Brazil*

The magnetization dynamics of systems with reduced dimensions have been extensively studied due to their technological relevance in a variety of devices. Spintronic devices use to operate with magnetization reversal times comparable to the natural ferromagnetic resonance (FMR) precession period, a behavior dependent on the intensity of the radio frequency field, shape of pulsed excitations, as well as on the structural properties and magnetic uniformity of the sample/device. Although FMR is useful to obtain the intrinsic magnetic properties of the material in saturated state, the properties of nonsaturated samples are rarely investigated due to the complexity of the magnetic configuration. In this work, we present an experimental investigation of the static and dynamic magnetic properties of ferromagnetic Ni₈₁Fe₁₉ films with thicknesses between 50 and 1000 nm. The quasi-static magnetic characterization is performed through magnetization curves. The dynamical magnetic behavior is studied through the traditional FMR experiment (at 9.4 GHz), FMR dispersion relations obtained with a vector network analyzer by measuring the reflection coefficient of a microstrip transmission line with the sample (from 50 MHz to 7 GHz), and magnetoimpedance measurements (from 100 MHz to 3 GHz). Considering the results, films thinner than 150 nm exhibit well-defined in-plane uniaxial magnetic anisotropy and one absorption peak in the FMR experiment, as well as just one ferromagnetic resonance mode in the FMR dispersion relations and magnetoimpedance curves. For films thicker than 200 nm, magnetization curves indicate isotropic in-plane magnetic properties with out-of-plane anisotropy contribution, a behavior related to the stress stored in the film, and to the columnar microstructure. FMR experiment presents more than one absorption peak, both suggesting the excitation of non-uniform modes. FMR dispersion relations and magnetoimpedance curves present complex magnetic behavior, depicted by several ferromagnetic resonance modes detected at relatively low fields. We discuss the results in terms of the mechanisms governing the dynamics at distinct frequency ranges, excitation modes, and quasi-static magnetic properties.

Mo.H-P12 - Experimental setup for investigation on magnetic thin layers by in-situ neutron reflectometry

J. Ye¹, W. Kreuzpaintner¹, B. Wiedemann¹, S. Mayr¹, A. Schmehl², T. Mairoser², A. Herrnberger², J. Moulin³, J. Stahn⁴, P. Korelis⁴, M. Haese-Seiller³, M. Pomm³, A. Paul¹, P. Böni¹, J. Mannhart⁵

1. Technische Universität München, München, Germany

2. Zentrum für elektronische Korrelation und Magnetismus, Universität Augsburg, Lehrstuhl für Experimentalphysik VI, Augsburg, Germany

3. Helmholtz Zentrum Geesthacht, Instrument REFSANS, Garching, Germany

4. Paul Scherrer Institut, Villigen, Switzerland

5. Max Planck Institut für Festkörperforschung, Stuttgart, Germany

Thin magnetic layers are used in many magneto-electronic devices. A thorough understanding of their texture and the coupling between them is, therefore, essential to improve functionality. In order to avoid the incorporation of impurities and surface contamination, these layers have to be grown under ultra-high-vacuum (UHV) conditions. An excellent method to analyze their structural and magnetic properties is polarized neutron reflectometry (PNR). Up to now, the sample growth and analysis have been performed in separate steps. The grown samples had to be removed from the vacuum after the growth process and put into the neutron beam line for analysis. This procedure is time consuming and leads to the sample being exposed to the environment which could alter their properties. In this contribution, a compact in-situ vacuum sputtering chamber with integrated DC and RF sputtering equipment for performing in-situ neutron reflectometry experiments will be presented. It can be easily transported and installed at neutron beam lines and combines both, deposition and measurement, into one single setup. This allows magnetic properties of thin films as a function of their thickness and composition to be investigated, both, quickly and on one single sample, at different evolutionary deposition steps. Despite the compactness of the device, no compromises regarding conditions for growth and measurement were made: A coil allows field dependent measurements and a cryostat with integrated heater can set the sample temperature in a range from 10K to 1000K. We constructed our device to be fully compatible to the REFSANS (FRM II) and the AMOR (PSI) ToF neutron reflectometers. At the later, we can perform PNR measurements using the state-of-the-art SELENE neutron optical setup which reduces measurement times from hours to several minutes.

The results of very promising measurements on Fe/Pd and Fe/Cr layers are shown in contributions by Sina Mayr and Wolfgang Kreuzpaintner.

Mo.H-P15 - Giant magnetoresistance and Magnetic properties of epilayers-perovskite LBMT0

M. Oumezzine¹, A. Catalin Galca², I. Pasuk², C. Florentina Chirila², A. Leca³, V. Kuncser³, A. Kuncser⁴, C. Ghica⁴, L.C. Tanase⁵, M. Oumezzine¹

1. *Laboratoire de Physico-Chimie des Matériaux, Faculté des Sciences de Monastir, Université de Monastir, Monastir, Tunisia*

2. *Laboratory of Multifunctional Materials and Structures, National Institute of Materials Physics, Magurele, Romania*

3. *Laboratory of Magnetism and Superconductivity, National Institute of Materials Physics, Magurele, Romania*

4. *Laboratory of Atomic Structures and Defects in Advanced Materials, National Institute of Materials Physics, Magurele, Romania*

5. *Laboratory of Nanoscale Condensed Matter Physics, National Institute of Materials Physics, Magurele, Romania*

An epitaxial thin film of $\text{La}_{0.67}\text{Ba}_{0.33}\text{Ti}_{0.02}\text{Mn}_{0.98}\text{O}_3$ (LBMT0) was synthesized using pulsed laser deposition technique (PLD) with a desirable thickness of 95 nm. The film grown on SrTiO_3 (0 0 1) substrates exhibited a paramagnetic-to-ferromagnetic second order phase transition at 291 K. The as-grown film displays a giant magnetoresistance (GMR) up to 150% at room temperature under 5T applied magnetic field.

Mo.H-P16 - Dependence of Curie temperature on the thickness of Pt layer in Co/Pt system

T. Koyama¹, A. Obinata¹, Y. Hibino¹, A. Hirohata^{2,3}, B. Kuerbanjiang³, V. Lazarov³, D. Chiba¹

1. *The University of Tokyo, Tokyo, Japan*

2. *PRESTO*

3. *University of York, Heslington, England, United Kingdom*

A Co ultra-thin film on Pt underlayer has attracted attention in the research field of spintronics because it brought new findings such as the realization of ferromagnetic phase transition by electric field in metal^{*1}. If the thickness of Co layer is below the characteristic length of the exchange interaction, the Curie temperature of the system becomes smaller than that of bulk Co. In this work, we show that not only the thickness of the Co layer^{*2} but also that of the adjacent Pt layer determines TC and the saturation magnetic moment of the system. We studied dependence of Curie temperature on thickness of ultra-thin Co and Pt layers in several series of perpendicularly magnetized (Pt/Co)/Pt samples. The Curie temperature and the saturation magnetic moment increased with the Co layer thickness and even with the thickness of the Pt layer, which is normally non-magnetic material. The Curie temperature was found to depend linearly on the total magnetic moment of the system and the coefficient of the linear fittings were the almost same, regardless of whether the thickness of the ferromagnetic Co layer or the Pt layer was varied. The Curie temperature increases also with the magnetic anisotropy, but no systematic dependence was observed on it. These results suggest that the magnetic moment induced in the Pt layer due the ferromagnetic proximity effect^{*3} plays a significant role in determining the Curie temperatures of such two-dimensional ferromagnetic systems. This work was partly supported by the PRESTO program of JST, Grants-in-aid for Scientific Research (S) from JSPS.

*1 D. Chiba et al., *Nature Mater.* 10, 853 (2011)

*2 C. M. Schneider et al., *Phys. Rev. Lett.* 64, 1059 (1990)

*3 M. Suzuki et al., *Phys. Rev. B* 72, 054430 (2005)

Mo.H-P17 - Sputtered thin films of Ti substituted barium hexaferrite for miniaturized components of electronic devices in the microwave range

N. Gutzeit¹, Bernd Halbedel², H. Romanus³, J. Müller^{1,3}

1. Technische Universität Ilmenau, Institute for Microelectronics and Nanoelectronics, Group of Electronics Technology, Ilmenau, Germany

2. Technische Universität Ilmenau, Institute of Materials Engineering, Group of Inorganic-Nonmetallic Materials, Ilmenau, Germany

3. Technische Universität Ilmenau, Center of Micro- and Nanotechnologies, Ilmenau, Germany

M-type barium hexaferrite thin films can be used for miniaturized components of electronic devices at microwave frequencies. Through the partial substitution of the iron ions by titanium ions the magnetic resonance frequency can be shifted to lower values. This paper will present the challenging manufacturing process by RF magnetron sputtering with the use of a self-made barium hexaferrite target at the Center of Micro and Nanotechnologies of the Technische Universität Ilmenau, Germany, as well as the characterization of the sputtered thin films. Barium ferrite thin films are sputtered on polycrystalline alumina substrates. The deposited, X-ray amorphous barium ferrite thin films are annealed after the sputtering process. The chemical composition is measured by EDX and ICP-OES. The influence of the titanium ion amount on the crystallization temperature is shown by X-ray diffraction and SEM images. The hexagonal barium hexaferrite phase is clearly proven by the measured diffractograms using the GID X-ray measurement method. The crystallites have a hexagonal, typical plate-like shape with dimensions at the nanometer scale. Results of static magnetic field measurements show the influences of the chemical composition and the peak temperature of the tempering process on the coercivity and the hysteresis loop.

Mo.H-P18 - Magnetic properties of irradiated Co₂MnSi Heusler alloys

I. ABDALLAH¹, N. BIZIERE¹, B. PECASSOU¹, G. BENASSAYAG¹, J. BOBO¹, E. SNOECK¹

1. CEMES, CNRS, Toulouse cedex 4, France

The Heusler alloys Co₂MnSi are ferromagnetic materials known for their high spin polarization and low magnetic damping parameter (α), making this material of particular interest for spintronic and radiofrequency devices. In this study, we demonstrate that the atomic disorder induced by He⁺ irradiation modifies the dynamic parameters of CMS in different ways as a function of the irradiation dose.

40 nm CMS films were prepared on MgO substrates using magnetron sputtering technique with a deposition temperature of 600° C and post annealed at 800°C. Irradiation with 150 KeV light He⁺ ions is then performed at doses between 10¹⁴ and 10¹⁷ ions/cm². Angular ferromagnetic resonance experiments were carried out in stripline geometry to extract the static (saturation magnetization $\mu_0 M_s$, the magneto-crystalline anisotropy field $\mu_0 H_k$) and dynamic (Gilbert coefficient α and extrinsic losses) magnetic parameters. Structural properties were investigated using X-Ray diffraction and Transmission Electron Microscopy (TEM).

We observed two different magnetic behaviors as a function of the irradiation dose. Below 10¹⁵ ions/cm², the extrinsic dynamic losses increase, while the static magnetic parameters and the gilbert constant remain constant. For higher doses, we observe a splitting of the FMR absorption peak appears, corresponding to a decrease of $\mu_0 M_s$ from 1.25 to 1.1 T while the anisotropy field increases by about 20%. Moreover, the damping coefficient can be multiplied by 2. These effects are shown to correspond to a crystallographic phase transition (L21/B2 or B2/A2) which goes along with an additional mechanical strain between the MgO and the CMS of the order of 0.2%. This is demonstrated by a shift in X-Ray diffraction peaks and by geometrical phase analysis from STEM-HAADF experiments.

Mo.H-P19 - Thickness dependent properties of Sr₂FeMoO₆ thin films grown on SrTiO₃ and (LaAlO₃)_{0.3}(Sr₂AlTaO₆)_{0.7} substrates

M. Saloaro¹, Il. Angervo¹, H. Huhtinen¹, P. Paturi¹

1. Wihuri Physical Laboratory, Department of Physics and Astronomy, University of Turku, Turku, Finland

The magnetoresistive Sr₂FeMoO₆ (SFMO) has high spin polarization and large intrinsic magnetoresistance at room temperature due to exceptionally high Curie temperature. Therefore, it has proven to be extremely promising material for novel spintronic applications. The applications require high quality thin films and therefore the the role of the substrate material and the film thickness is investigated. Two series of SFMO films with different pulse numbers from 250 to 10000 were made using pulsed laser deposition. The series were made on SrTiO₃ (STO-series) and (LaAlO₃)_{0.3}(Sr₂AlTaO₆)_{0.7} (LSAT-series) substrates, which have different lattice mismatch with SFMO (-1.05% and -1.88%, respectively). The characterization by X-ray diffraction shows that all the films were phase pure and fully textured. The in-plane strain in the LSAT-series was almost independent of the pulse number having an opposite sign to the lattice mismatch. In the STO-series the in-plane strain was compressive as expected from the mismatch and it decreased with increasing pulse number. The magnetic and resistivity behaviour had same tendency with both series. The Curie temperature and the saturation magnetization increased with pulse number up to 2000 pulses after which they were nearly constant. In the temperature dependence of the resistivity, a clear low temperature upturn indicating semiconductive spinchannel was observed in both series and it was notably larger in the films grown with lower pulse numbers. Considering the applications, the best properties are achieved when the pulse number is at least 2000. Major changes in magnetic properties were not observed between the series, but the structural properties suggest that the STO substrate with lower lattice mismatch should be used.

Mo.H-P20 - Defect induced enhanced low field magnetoresistance in Pr 0.6 Ca 0.4 MnO 3 thin films

T. Elovaara¹, S. Majumdar^{1,2}, H. Huhtinen¹, P. Paturi¹

1. Department of Physics and Astronomy, University of Turku, Turku, Finland

2. Department of Applied Physics, Aalto University School of Science, Espoo, Finland

We have investigated the effect of grain boundaries on the electronic transport properties of the colossal magnetoresistive low bandwidth manganite Pr 0.6 Ca 0.4 MnO 3 (PCMO) thin films. A series of PCMO films were prepared by pulsed laser deposition method on MgO substrate with varying deposition temperature. Characterizations of the structural, magnetic and magneto-transport properties show that the films prepared at lower ablation temperature contain higher amount of structural defects and an increasing amount of crystal orientations as the level of texturing decreases. According to the low field magnetoresistance (MR) measurements the poorly textured samples display an increased low field MR due to a grain boundary tunneling effect at low temperatures compared to the fully textured PCMO film on STO substrate. In the high field MR measurements, the samples also showed a colossal magnetoresistive insulator to metal (IMT) switching of almost eight orders of magnitude at low temperatures, and the IMT transition field could be reduced over 2 T by illuminating the sample.

Mo.H-P21 - Laterally confined magnonic waveguide with ferroelectric load

A. Sadovnikov¹, E. Beginin¹, S. Sheshukova¹, Y. Sharaevski¹, S. Nikitov^{1,2}

1. *Saratov State University, Nonlinear Processes Department, Saratov, Russia*

2. *Kotel'nikov Institute of Radio Engineering and Electronics of Russian Academy of Science, Moscow, Russia*

We report the experimental and numerical investigations of spin-electromagnetic waves propagating in laterally coupled finite-width multiferroic waveguide. We demonstrate the symmetric and asymmetric modes transformation when the coupled magnetic waveguide are loaded with the ferroelectric layer. Experimental study of eigenmodes of laterally confined multiferroic was performed by using microwave measurements techniques and space-resolved Brillouin light scattering spectroscopy. Numerical simulation was provided by the developed finite-element method (FEM) of electromagnetic eigenspectrum calculation. We show that the spatial distribution of magnetization of the width-modes in laterally confined multiferroic structure changes due to the electrodynamic coupling between the spin waves localized mainly in the finite-width ferrite layer and the electromagnetic waves propagating in the ferroelectric layer. Moreover the effectiveness of coupling depends on the mode number, propagating in the layered structure. This work was partially supported by scholarship of the President of the RF (SP-1551.2013.5), Grant from Russian Science Foundation (Project # 14-19-00760), by the Russian Foundation for Basic Research (Grant # 13-07-12409, 14-02-00976).

Mo.H-P22 - Magnetic waveguide arrays studied by Brillouin light scattering

A. Sadovnikov¹, Evgeny

1. Saratov State University, Nonlinear Processes Department, Saratov, Russia

We report the results of experimental investigation of the spin waves propagation in the laterally coupled planar YIG waveguide array by Brillouin light scattering (BLS) spectroscopy. Decomposition of eigenmodes reveals the width modes interference in the waveguide arrays. Due to the the symmetry breaking of the taper structure the spatial distribution of the magnetization corresponds to the superposition of the lowest odd modes ($m = 1,3$) in the input waveguide and the odd ($m = 1$) and even ($m = 2$) modes in central waveguide with a number $n=0$. Experimental studies of the frequency transmission coefficients, spatio-temporal dynamics of MSSW propagation and power transmission between waveguides in array were performed. The different levels of input RF power, different pulse-modulated and continuous microwave signals of different frequencies were considered. To explain the obtained experimental result we performed the numerical simulation with FDTD method (LLG equation). We demonstrate that in the coupled magnetic waveguides the phenomena of the spin wave coupling and discrete diffraction can be observed. Nonlinear propagation, interactions between waves and generation of discrete solitons are interesting field for further studies. This work was partially supported by scholarship of the President of the RF (SP-1551.2013.5), Grant from Russian Science Foundation (Project # 14-19-00760), by the Russian Foundation for Basic Research (Grant #15-07-05901, # 13-07-12409).

Mo.H-P23 - Ion Irradiation Induced Relaxation of Tensile Strain and Change in Directionality of Magnetic Domains in BaFeO_{3-δ} Thin Films

F. Aziz¹, M. Chandra¹, S. Das², M. Prajapat², K. Asokan³, K. R. Mavani¹

1. *Discipline of Physics, Indian Institute of Technology Indore, Madhya Pradesh, India*

2. *Department of Physics, Indian Institute of Science Education and Research Bhopal, Bhopal, India*

3. *Inter-University Accelerator Centre (IUAC), Aruna Asaf Ali Marg, New Delhi, India*

Perovskite BaFeO_{3-δ} (BFO) thin films (~ 250 nm), deposited on MgO (001) single-crystal wafers, were irradiated by ion beams of: (i) 200 MeV Ag⁺¹⁵ and (ii) 100 MeV O⁺⁷ (Series-1 and Series-2, respectively). These two series of films are investigated for structural and magnetic properties of BFO films at room temperature. There is a systematic variation in structure of the BFO films with increasing Ag⁺¹⁵ beam fluence, causing a relaxation of the tensile strain in the films. The Magnetic Force Microscopy (MFM) images show clear patterns of stripe-like magnetic domains of remanent magnetization, which were analyzed and studied by Fast Fourier Transformations. With increasing ion fluence, the formation of stripe-domains gradually changes the direction from 'one' crystallographic plane to 'two'. In contrast to Series-1, there are no systematic changes in the structure of Series-2 films. MFM patterns of Series-2 show gradually diffusing directionality of magnetic domains with increasing ion fluence. The simultaneous and systematic changes in strain and magnetic properties indicate correlated properties of BFO thin films at room temperature.

Mo.H-P25 - Strain induced magnetic anisotropy variation of CoFe₂O₄ films[§]

S. Park¹, Lee¹, C. Cho¹, J. Ba, J. Kim

1. Pusan National University, Busan, South Korea

2. Korea Basic Science Institute, Daejeon, South Korea

Co-based ferrite (CoFe₂O₄) is useful for high-density magnetic recording and magneto-optical media application due to its large magnetic anisotropy ($K_1 \sim 2.01 \times 10^6$ erg/cm³ in <100> orientation), magnetic elastic constant ($\lambda_s^p \sim -110 \times 10^{-6}$), high Curie temperature and excellent chemical stability. In order to fulfill the desired application, higher coercivity, smaller grain size, low surface roughness and low sample preparation temperature are required.

In this presentation, we showed magnetic anisotropy variation of CoFe₂O₄ films grown on MgO(001) and Al₂O₃(0001). Depending on the substrates and deposition temperature, the films exhibited different crystallinity and magnetic easy axis. These variations could be associated with the different strain state of films. With higher deposition temperature, films became isotropic. In the case of films grown on Al₂O₃(0001), strain state of the film changed from compressive to tensile with deposition temperature [1]. On the other hand, films grown on MgO(001) exhibited out-of-plane tensile state at lower deposition temperature and became less tensile state with increased deposition temperature. The room temperature in-plane and out-of-plane magnetic hysteresis loops showed a decreased out-of-plane anisotropy when the deposition temperature was increased. Simple uniaxial magnetic anisotropy energy calculation based on the experimental data showed a direct correlation between the uniaxial magnetic anisotropy direction and stress of the films. Furthermore, the deposition temperature-dependent cation distributions from X-ray photoelectron spectroscopy measurement revealed the possible microscopic origin of the magnetic anisotropy variation.

[§]This work is supported part by NRF Korea (2012R1A1A2005940, 2011-0031933).

[1] C.-W. Cho, D.Y. Lee, J.S. Bae and S. Park, J. Magn. Magn. Mater. 368, 149 (2014)

Mo.H-P26 - Interlayer thickness dependence of the magnetic coupling in FePt multilayered dots

Hirokazu¹, H. Iwama¹, M. Doi¹, T. Shima¹

1. Tohoku Gakuin University, Sendai, Japan

In order to apply to a next generation ultra high-density magnetic storage media, a lot of studies about the $L1_0$ ordered FePt thin film has been performed, because of its huge uniaxial magnetic anisotropy. It has been found that the coercivity of FePt thin film is increased by reducing the particle size. Besides, independent magnetization reversal of the top and bottom FePt layers have been observed in FePt multilayered film. In this study, $L1_0$ ordered FePt (001) circular dot arrays with FePt/MgO/FePt structure have been prepared and the relationship between the magnetic properties and the size of the dots and the interlayer thickness have also been investigated in order to obtain a design guideline for a high-density multi-level magnetic recording media. The FePt/MgO/FePt films were prepared by using a magnetron sputtering system. The thickness of the top and bottom FePt layers was fixed at 5 nm and 10 nm, respectively. While the thickness of MgO interlayer was 5 nm. The dots arrays were microfabricated from the continuous films through electron beam lithography method and Ar ion milling. The remarkable steps in the magnetization curves for the continuous multilayered films and the dots are clearly observed that indicate an independent magnetization reversal of the top and bottom FePt layers. These steps can be observed for the dots with $D = 0.8 \sim 3 \mu\text{m}^\phi$, however, they disappeared for the dots with $D = 0.3 \sim 0.7 \mu\text{m}^\phi$. The magnetic coupling behavior as a function of the size of the FePt/MgO/FePt dots and the thickness of the interlayer will be discussed in detail.

Mo.H-P28 - Unusual anisotropic magnetoresistance in single crystalline Fe films and Pt/Fe bilayers

J. Li¹, M. Jia¹, L. Sun¹, Z. Ding¹, H. Ding², Y. Wu¹

1. Fudan University, Shanghai, China

2. Nanjing university, Nanjing, China

Magnetoresistance (MR) is a fundamental transport property of magnetic thin films. Recently, a new MR effect named spin-Hall magnetoresistance (SMR) has been observed in Pt/YIG system [1] with the behavior of ρ_{xx} , which is distinctly different from the conventional anisotropic magnetoresistance (AMR) in polycrystalline magnetic films with ρ_{xx} [2]. It still remains an open question whether this MR behavior can be observed in single ferromagnetic film without the Pt layer. In this contribution, we report on a novel interfacial AMR effect in epitaxial Fe(001) films and an AMR enhancement in single crystal Pt/Fe(001) bilayers. For Fe/MgO(001) films, the resistivities show the behavior of ρ_{xx} up to 400nm, very similar to SMR in Pt/YIG system. The anisotropic resistivities ρ_{xx} , ρ_{yy} , and ρ_{zz} , show an apparent linear $1/t_{Fe}$ dependence. We also observed an enhancement of AMR [3] when capping a thin Pt layer on the Fe(001) thin films, and such enhancement of AMR can be attributed to the Pt magnetic moment in the conduction band induced by the spin dependent exchange scattering at Pt-Fe interface. Using a semi-classical model, we extracted the spin-diffusion length in Pt layer, which is 1.7-2.6 nm from 300K to 6K.

References:

- [1] H. Nakayama, et. al, Phys. Rev. Lett. 110, 206601 (2013)
- [2] T. R. McGuire, and R. I. Potter. IEEE Trans. Magn. 11, 1018 (1975)
- [3] J.X. Li, et. al, Phys. Rev. B 90, 214415 (2014)

Mo.H-P30 - Effects of the Layer Thickness on the Magnetic and Magneto-optical Properties of Sputtered and Annealed La_{0.66}Sr_{0.34}MnO₃ Thin Films on Silicon

M. Monecke¹, O. Ciubotariu¹, P. Richter¹, P. Thoma¹, G. Salvan¹, D. R.T. Zahn¹

1. Semiconductor Physics, Technische Universität Chemnitz, Chemnitz, Germany

La_{1-x}Sr_xMnO₃ is a conductive oxide which is crystallizing in a perovskite structure. The magnetic and electronic properties change with the concentration of strontium [1]. Moreover, the high spin polarization make this material an ideal electrode for spintronic applications. In particular, the composition La_{0.66}Sr_{0.34}MnO₃ (LSMO) was used in spintronic devices due to the nearly 100 % spin polarization at the Fermi level [2]. The electrodes are typically deposited by pulsed laser deposition on single crystalline substrates with similar lattice constants, e.g. SrTiO₃ [3], to obtain single crystalline layers. Here LSMO films with varying film thicknesses between 10 nm and 300 nm were deposited by magnetron sputtering at room temperature on silicon (111) substrates covered with a native oxide. The films were annealed in ambient atmosphere at 775 °C for 20 min, 1 h, 3 h, and 9 h. Afterwards the layers were investigated by Variable Angle Spectroscopic Ellipsometry (VASE), Magneto-Optical Kerr Effect (MOKE) spectroscopy, and Superconducting Quantum Interference Device (SQUID) Vibrating Sample Magnetometry (VSM). The main goal of this work is to understand how the magnetic properties, the dielectric function, and the magneto-optical response of post deposition annealed LSMO are influenced by the layer thickness and annealing time. The results show that the magnitude of the off-diagonal elements of the dielectric tensor decreases drastically when the layer thickness is smaller than 20 nm. Furthermore, the magnetic properties like remanence, coercive field, and Curie temperature increase with longer annealing times for films which are thicker than 20 nm.

[1] E. Dagotto et al. Physics Reports 344 (2001) doi: 10.1016/S0370-1573(00)00121-6

[2] J.-H. Park et al. Nature Vol 392 (1998) doi: 10.1038/ncomms5396

[3] W. Xu et al. Applied Physics Letters 90 (2007) doi: 10.1063/1.2435907

Mo.H-P31 - Spin wave eigenmodes of Dzyaloshinskii domain walls

P. Borys¹, Felipe G. Sanchez², J. Von Kim², R. Stamps¹

1. *University of Glasgow, Glasgow, Scotland*

2. *Institut d'Electronique Fondamentale, Univ. Paris-Sud, Orsay, France*

The Dzyaloshinskii-Moriya interaction (DMI) is an antisymmetric exchange interaction that arises in systems lacking inversion symmetry and possessing strong spin orbit coupling, such as ultrathin ferromagnetic films with heavy metal underlayers. It has been shown that the DMI stabilizes different kinds of chiral spin textures, such as Néel-type walls called Dzyaloshinskii domain walls that are favoured over Bloch-type walls. Here, we will present a theory for the spin wave eigenmodes of a Dzyaloshinskii domain wall. The mode frequencies for spin waves propagating parallel and perpendicular to the domain wall are computed using a continuum approximation. In contrast to Bloch-type walls, it is found that the spin wave potential associated with Dzyaloshinskii domain walls is not reflectionless, which leads to a finite scattering cross-section for interactions between spin waves and domain walls. Consequences for spin wave driven domain wall motion and band structures arising from periodic wall arrays are discussed.

Mo.H-P33 - Anomalous Hall Effect in antiferromagnetic Mn₅Si₃ films

C. Sürgers¹, G. Fischer¹, H. v. Löhneysen¹

1. Karlsruhe Institute of Technology, Karlsruhe, Germany

The anomalous Hall effect (AHE) in ferromagnets is usually assumed proportional to the magnetization. However, an AHE has been proposed to appear even in an antiferromagnet with a highly noncollinear and non-coplanar spin structure. Particularly interesting is a material which has collinear and non-collinear phases at different temperatures. This unusual situation arises in non-cubic antiferromagnetic Mn₅Si₃ with atoms Mn1 and Mn2 at two inequivalent lattice sites. In the long-range ordered antiferromagnetic AF2 phase between the Néel temperature TN₂ = 99K and TN₁ = 66 K, two third of the Mn2 atoms have moments oriented in a collinear fashion. In the AF1 phase below TN₁, the Mn1 atoms acquire a moment in addition to realigned Mn2 moments. The moments point into different directions forming a highly non-collinear magnetic structure attributed to topological frustration. The magnetic structure in the AF1 phase can be modified by a magnetic field thereby strengthening the AF2 arrangement. Here we show that a large AHE contribution develops in Mn₅Si₃ thin films well below the Néel temperature as soon as the spin arrangement changes from collinear (AF2) to non-collinear (AF1) with decreasing temperature [1]. The magnetic-field dependence of the AF1/AF2 phase boundary is in good agreement with earlier neutron scattering experiments. Furthermore, we demonstrate that the large AHE arising from collinearity is not observed when the material is turned ferromagnetic by carbon doping without changing its crystal structure. The results motivate future experimental work on the Hall effect in non-collinear antiferromagnets.

[1] C. Sürgers et al., Nat. Commun. 5:3400 (2014)

Mo.H-P34 - Proximity effects in Fe/Cr/Gd multilayers

V.V. Ustinov¹, M.V. Ryabukhina¹, E.A. Kravtsov¹, Y. Choi², D. Haskel², Y. Khaidukov³

1. *Institute of Metal Physics, Ekaterinburg, Russia*

2. *Advanced Photon Source, Argonne National Laboratory, Argonne, United States*

3. *Max Plank Institute for Solid State Research, Stuttgart, Germany*

Ferromagnetic 4f rare-earth/3d transition metal multilayers are popular model systems displaying a rich variety of magnetic phases in applied fields. Fe/Cr/Gd multilayers where Fe-Gd exchange coupling is mediated by antiferromagnetic Cr are promising systems where one may govern Fe-Gd interlayer exchange coupling by playing with Cr layer thickness and temperature. In our presentation we report on depth-resolved and element-specific magnetization density profiles in Fe(35 Å)/Cr(t Å)/Gd(50 Å), t = 0-8 Å multilayers determined by complementary application of SQUID-magnetometry, polarized neutron and resonant x-ray magnetic reflectometry. We show that the insertion of antiferromagnetic Cr spacer changes magnetic structure of multilayers as compared with Fe/Gd multilayers. First, it shifts the compensation point to lower temperatures. Second, it switches otherwise antiferromagnetic Fe-Gd interlayer magnetic ordering to noncollinear one - the thicker Cr spacer the more significant is the deviation from antiferromagnetic Fe-Gd interlayer ordering. Third, it leads to an enhancement of Gd magnetic moments in the interfacial regions near Fe. The effect is similar to that observed in Fe/Gd multilayers but the value of induced Gd magnetic moment is lower. Fourth, it causes to reduction of magnetic moments in the core of Gd layers even at very low temperatures.

Mo.H-P35 - Formation of ordered antiferromagnetic phase NiFeMn under thermo-magnetic treatment of manganese-permalloy bilayers

I.V. Blinov¹, T.P. Krinitsina¹, M.A. Milyaev¹, V.V. Popov¹, V.V. Proglyado¹, V.V. Ustinov¹

1. Institute of Metal Physics, Ekaterinburg, Russia

A method of formation of an ordered antiferromagnetic (AF) phase NiFeMn under thermo-magnetic treatment of manganese-permalloy bilayers has been suggested. A possibility of application of an AF alloy [NiFe](1-x)Mn(x) as a pinning layer in spin valves is studied. The results obtained can be used for fabrication of nanostructures with enhanced functional characteristics.

Samples including a disordered AF alloy [Ni₈₀Fe₂₀](1-x)Mn(x) were fabricated by magnetron sputtering on MPS-4000-C6 (Ulvac) device. For the formation of unidirectional anisotropy a permanent magnetic field of 110 Oe was applied under sputtering.

The as-prepared samples are characterized with a hysteresis loop shifted relative to the magnetic field axis. The surface density of energy of the exchange interaction at a FM/AF interface is found to be equal to 0.05 erg/cm², whereas the measured blocking temperature of the [Ni₈₀Fe₂₀](20nm)/[[Ni₈₀Fe₂₀](1-x)Mn(x)](50nm) system is about 150 Celsius degrees.

A higher blocking temperature 270 Celsius degrees has been obtained for the system Al₂O₃/[Ni₇₇Fe₂₃](5nm)/Mn(50nm)/[Ni₇₇Fe₂₃](30nm)/Ta(5nm) fabricated by electron-beam evaporation on Varian device and subjected to the thermo-magnetic treatment at 260 Celsius degrees for 4 hours. In this case the ordered AF phase NiFeMn is formed. The surface density of energy of the exchange interaction at a FM/AF interface in this case is 0.27 erg/cm². These values of blocking temperature and surface density of exchange energy are noticeably higher than those for the system [Ni₈₀Fe₂₀]/[Ni₈₀Fe₂₀](1-x)Mn(x), and are comparable with blocking temperature and surface density of exchange energy for the system with AF layer of IrMn.

The magnetoresistance of a spin valve including the AF alloy [NiFe](1-x)Mn(x) is 7.15 %.

Mo.H-P36 - CoFe₂O₄/Fe₃O₄ superlattices; MBE growth and magnetic properties

Q. Nguyen Van¹, Y. Shin², Rhim S. H.¹, A. Tuan Duong¹, M. Nguyen Thi¹, S. Cho¹, M. Christian²

1. Department of Physics, and Energy Harvest Storage Research Center, University of Ulsan, Ulsan, South Korea

2. Institute of Physics and Chemistry for Materials of Strasbourg, Strasbourg, France

Magnetite, Fe₃O₄, is a ferrimagnet with a cubic inverse spinel structure and exhibits a metal-insulator, Verwey, transition at about 120 K.[1] It is predicted to possess as half-metallic nature, 100% spin polarization, and high Curie temperature (850 K). Cobalt ferrite is one of the most important members of the ferrite family, which is characterized by its high coercivity, moderate magnetization and very high magnetocrystalline anisotropy. It has been reported that the CoFe₂O₄/Fe₃O₄ bilayers represent an unusual exchange-coupled system whose properties are due to the nature of the oxide-oxide super-exchange interactions at the interface[2]. In order to evaluate the effect of interface interactions on magnetic and transport properties of ferrite and cobalt ferrite, the CoFe₂O₄/Fe₃O₄ superlattices on MgO (100) substrate have been fabricated by molecular beam epitaxy (MBE) with the wave lengths of 50, and 200 Å, called 25(Å)/25(Å) and 100(Å)/100(Å), respectively. Streaky RHEED patterns in sample 25(Å)/25(Å) indicate a very smooth surface and interface between layers. High-magnification HAADF image and selected area electron diffraction (SAED) pattern in TEM cross section measurement indicated the successful growth of superlattices. Interestingly, magnetization curves showed a strong antiferromagnetic behavior, which was formed at the interfaces.

[1] D. Tripathy *et al.*, Appl. Phys. 101, 013904 (2007)

[2] AnaV.Ramos *et al.*, Phys.Rev.B 79, 014401 (2009)

Mo.H-P37 - Modification of Interfacial Magnetism in Weakly Strained Manganite films

N. Bingham^{1,2}, A. Suszka^{1,2}, C. Fernandes Vaz³, V. Franco⁴, L. Heyderman^{1,2}

1. *Laboratory for Micro- and Nanotechnology, Paul Scherrer Institute, Villigen, Switzerland*

2. *Laboratory for Mesoscopic Systems, Department of Materials, ETH Zurich, Zurich, Switzerland*

3. *Swiss Light Source, Paul Scherrer Institut, Villigen, Switzerland*

4. *Departamento de Física de la Materia Condensada, ICMSE-CSIC, Universidad de Sevilla, Sevilla, Spain*

Interfaces of thin film manganite heterostructures are of particular interest and are well-documented sites for fundamentally altered magnetism. Generally, much of the work in interfacial studies involves substrate-induced strain on the magnetic film. This results in changes of the film properties with the film adopting the in-plane symmetry of the substrate [1]. However, it is predicted that weakly strained films can induce the formation of nano/micro-scale phase separation in manganites leading to an enhancement of colossal magnetoresistance effects. We explored this modification of the magnetic structures in thin film manganites by investigating a strain-relaxed (50 nm) $\text{La}_{0.66}\text{Ca}_{0.33}\text{MnO}_3$ (LCMO) film capped with (5 nm) BaTiO_3 (BTO) and compared the results with those of an LCMO film without the addition of BTO. The films were deposited on MgO substrates via pulsed laser deposition. Temperature and field dependence of magnetization were measured in the temperature range of 5-300K and in magnetic fields up to 5 T. A paramagnetic to ferromagnetic transition of LCMO occurs at $T_c \sim 250$ K in both cases. However, for the LCMO/BTO sample there is a second transition at 150 K, which is attributed to the macroscopic modification in the magnetic behavior in the LCMO film at the rhombohedral to orthorhombic BTO structure transition. Magnetocaloric effect (MCE) measurements confirm this modification. X-ray absorption and x-ray magnetic circular dichroism data taken at the Mn L_{3,2} and Ti L_{3,2} edges at the SIM beamline, Swiss Light Source, show an electronic modification of the LCMO layer at the interface with the BTO film and identify primarily Mn²⁺ ions. These measurements also reveal sub-microscopic magnetic correlations above T_c on both the Mn and Ti edges, which could be attributed to local magnetization modification at the interface between LCMO and BTO layers above T_c .

[1] X. Moya, et al. Nature Mater. 12, 52-58 (2013)

Mo.H-P38 - Ferromagnetic and spin-wave resonances in multilayer nanogranular films [(Co₄₀Fe₄₀B₂₀)_x(SiO₂)_{100-x}/α -Si:H]_n and [(Co₄₀Fe₄₀B₂₀)_x(SiO₂)_{100-x}/SiO₂]_nE. Denisova¹, L. Chekanova¹, R. Iskhakov¹, Y. Kalinin², A. Sitnikov²

1. Kirensky Institute of Physics SB RA, Krasnoyarsk, Russia

2. Voronezh State Technical University, Voronezh, Russia

Multilayer films, consisting of granular (Co₄₀Fe₄₀B₂₀)_x(SiO₂)_{100-x} layers as thin as magnetic granule diameter alternating the a-Si:H or SiO₂ layers and the single layer films (Co₄₀Fe₄₀B₂₀)_x(SiO₂)_{100-x} (30 < X < 80) with the thickness much larger than the magnetic granule diameter have been investigated by means of ferromagnetic resonance (FMR) at 9.2 GHz.

The FMR spectrum for H applied parallel to the film plane consists of a single absorption line for all types of samples. It is found that the value of the resonance fields H_r is independent of metal layer thickness t (2.5 < t < 5 nm). The H_r magnitudes for multilayer [(Co₄₀Fe₄₀B₂₀)_x(SiO₂)_{100-x}/a-Si:H]_n films (for all thickness of the silicon layer) are larger than for single layer films with the same composition. From resonance fields we evaluated an effective shape anisotropy field of magnetic phase. The FMR linewidth of multilayer films is much less than for Co₄₀Fe₄₀B₂₀-SiO₂ films. When the external field is applied perpendicular to the film plane it is possible to observe multi-peaked spectra, due to resonance absorption by standing spin-wave resonance modes. There are up to 11 peaks in SWR spectrum of the Co₄₀Fe₄₀B₂₀-SiO₂ films. The separation of granular layers with a-Si:H or SiO₂ layer leads to a reduction in the number of SWR peaks. A surface resonance mode is observed for all samples. The surface anisotropy field is evaluated as a function of X (0.9 < K_s < 0.5 erg/sm²). It is found that the $H_r(n^2)$ (where n is the mode number) dependencies are non-linear. Such behavior is probably caused by the fluctuations of magnetic parameters (the magnetization and the ferromagnetic exchange coupling) in nanocomposite films. The magnetic properties of the films are discussed in relation with the microstructure of the multilayer systems.

Mo.H-P39 - Asymmetry in the Activity of Nucleation Centers in Ultrathin Pd/Co/Pd Trilayers

R. Shull¹, Y.L. Iunin², P.J. Chen¹, V.I. Nikitenko²

1. *National Institute of Standards and Technology, Gaithersburg, United States*

2. *Russian Academy of Science, Chernogolovka, Russia*

Normally, when a ferromagnet undergoes a magnetization reversal, the nucleation of domains with the opposite magnetization occurs at the same locations for opposite magnetic field directions. Recently, however, a new phenomenon of asymmetry in the activity of nucleation centers was revealed in Co/Pt films and multilayers [1]. In these cases, many nucleation sites for reversal domains were found to depend upon the direction of the reversal field. In order to determine if this new phenomenon is universal, we used Kerr microscopy to study in detail the domain nucleation and growth processes in Pd(10)/Co(0.2)/Pd(10 nm) trilayers sputtered on a MgO substrate at 300 K. As ultrathin Co/Pt and Co/Pd films and multilayers with perpendicular magnetic anisotropy have played an important role in magnetic data storage and advanced spintronic devices in recent years, this study is particularly timely. The experiments were performed as follows. First the sample was saturated by applying a magnetic field greater than the coercivity (HC) of the sample, followed by a gradual reduction and then reversal of the external field. During the field reduction and reversal, the nucleation and evolution of reversal domains was studied. Interestingly, just like in the Co/Pt system, asymmetrical magnetic domain nucleation centers were also observed in the Co/Pd trilayers of this study, where the reversal begins for one direction of magnetic field only. Thus, the asymmetry in the activity of nucleation centers is not specific to the Co/Pt system, but is a rather general phenomenon. It was also found here that applying a large enough perpendicular magnetic field (much greater than HC) suppresses the asymmetrical nucleation.

[1] Y. L. Iunin, Y. P. Kabanov, V. I. Nikitenko, X. M. Cheng, D. Clarke, O. A. Tretiakov, O. Tchernyshyov, A. J. Shapiro, R. D. Shull, and C. L. Chien, *Phys. Rev. Lett.* 98, 117204 (2007)

Mo.H-P40 - Tunnel transport through SrMnO₃ / La₂/3Sr1/3MnO₃ epitaxial bilayers investigated by CAFM.

P. Jiménez-Cavero^{1,2}, N. I. Lucas^{2,3,4}, L. Maurel^{2,4}, C. Magén^{2,3,4,5}, J. Angel Pardo^{4,6}, P. Antonio Algarabel^{1,2}, L. Morellón^{2,4}

1. Instituto de Ciencia de Materiales de Aragón, ICMA-CSIC, Universidad de Zaragoza, Zaragoza, Spain
2. Departamento de Física de la Materia condensada, Universidad de Zaragoza, Zaragoza, Spain
3. Fundación Araid, Zaragoza, Spain
4. Instituto de Nanociencia de Aragón (INA), Zaragoza, Spain
5. Laboratorio de Microscopias Avanzadas (LMA), Instituto de Nanociencia de Aragón (INA), Universidad de Zaragoza, Zaragoza, Spain
6. Departamento de Ciencia y Tecnología de Materiales y Fluidos, Universidad de Zaragoza, Zaragoza, Spain

Potential applications in spintronic devices such as non-volatile memories make tunnel junctions (MTJ) object of great interest. One of the main challenges in the field is finding materials showing high magnetoelectric effect, in which electric and/or magnetic field can control their magnetic and electric state. On this purpose, magnetic and electric properties of certain oxides may be engineered on demand by epitaxial growth on a substrate. In this work, epitaxial bilayers of La₂/3Sr1/3MnO₃ (≈23 nm) / SrMnO₃ (≈2.7 nm) were grown by pulsed laser deposition (PLD) on two different substrates: SrTiO₃ (STO) and (LaAlO₃)_{0.3}(SrAl_{0.5}Ta_{0.5}O₃)_{0.7} (LSAT), aiming at observing the impact of epitaxial strain on the tunnel transport properties. Recent theoretical calculations have proposed that SrMnO₃ becomes multiferroic under epitaxial strain [1]. Both samples were structurally characterized by reciprocal space maps as well as by scanning transmission electron microscopy, showing a lattice parameter deformation for SMO of in-plane +1.66% and out-of-plane -1.36% in the samples grown on LSAT, and in-plane +2.63% and out-of-plane -2.81% when substrate was STO. However, final volumes of the unit cell considering these deformations are very similar (~2% bigger than in bulk) for both samples within the experimental error. Tunnel transport properties were locally characterized by conductive atomic force microscopy (CAFM), using nanostencil lithography to deposit Au contacts on the sample. I(V) characteristic curves show that the thin SMO barriers retain the insulating behavior. I(V) curves were fitted to Simmons and Brinkman models [2,3], obtaining the characteristic parameters of the barriers. No difference was found between the average barrier heights, suggesting that the cell volume controls the characteristics of the barrier.

[1] J. H. Lee, M. K. Rabe, PRL 104, 207204 (2010)

[2] J. G. Simmons, JAP. 14, 1793 (1963)

[3] W. F. Brinkman et al, JAP 41, 1915 (1970)

Mo.H-P42 - Magnetization boundary conditions at a ferromagnetic interface of finite thickness

V. Kruglyak¹, O. Gorobets², Y. Gorobets³, A. Kuchko^{3,4}

1. *University of Exeter, Exeter, England, United Kingdom*
2. *National Technical University of Ukraine, Kiev, Ukraine*
3. *Institute of Magnetism of NAS of Ukraine, Kiev, Ukraine*
4. *Donetsk National University, Donetsk, Ukraine*

We have developed a systematic approach by which to derive boundary conditions at an interface between two ferromagnetic materials in the continuous medium approximation [1]. The approach treats the interface as a two-sublattice material, although the final equations connect magnetizations outside of the interface and therefore do not explicitly depend on its structure. Instead, the boundary conditions are defined in terms of some average properties of the interface, which may also have a finite thickness. In addition to the interface anisotropy and symmetric exchange coupling, this approach allows us to take into account coupling resulting from inversion symmetry breaking in the vicinity of the interface, such as the Dzyaloshinskii-Moriya antisymmetric exchange interaction. In the case of negligible interface anisotropy and Dzyaloshinskii-Moriya exchange parameters, the derived boundary conditions represent a generalization of those proposed earlier by Barnaś and Mills and are therefore named “generalized Barnaś-Mills boundary conditions”. We demonstrate how one could use the boundary conditions to extract parameters of the interface via fitting of appropriate experimental data. The developed theory could be applied to modeling of both linear and non-linear spin waves, including exchange, dipole-exchange, magnetostatic and retarded modes, as well as to calculations of non-uniform equilibrium micromagnetic configurations near the interface, with a direct impact on the research in magnonics and micromagnetism.

1. V. V. Kruglyak, O. Yu. Gorobets, Yu. I. Gorobets and A. N. Kuchko, *J. Phys.: Condens. Matter* 26 (2014) 406001

Mo.H-P43 - Thickness dependence of Gilbert damping of (Ru,MgO)/CoFeB/Ru trilayers

S. Bunyaev¹, A. García-García^{1,2}, A. Vieira Silva², J. M. Teixeira¹, J. Ventura¹, S. Cardoso², P. Freitas², G. Kakazei¹

1. IFIMUP-IN, Universidade do Porto, Porto, Portugal

2. INESC-MN/IN, Lisboa, Portugal

Gilbert damping α is a crucial parameter of magnetic materials that determines operating speed and energy effectiveness of spintronic and magnonic devices. CoFeB is suggested to be the most promising material for electrodes in magnetic tunnel junctions (MTJ) with MgO barriers, since it possess low damping values and can exhibit perpendicular magnetic anisotropy. However, available data of α dependence on CoFeB alloys thickness and buffer material remain incomplete and sometimes controversial. Two series of the samples (Ru,MgO)/(Co70Fe30)80B20/Ru were probed by broadband ferromagnetic resonance (FMR) in a frequency range from 1 to 20 GHz at room temperature. The thickness of CoFeB layer grown at room temperature via ion-beam sputtering was varied from 1.5 nm up to 40 nm. The method described in [1] was applied to obtain the FMR linewidth from complex magnetic permeability function. The approach proposed by Bilzer [2] was used then to extract α from the linewidth. As expected, increase of α with the CoFeB thickness decrease has been observed for both series. For the samples thinner than 20 nm the annealing at 330°C during one hour leads to α decrease for MgO buffer and to its increase for Ru one. The obtained results are important for the design of CoFeB based ultra-thin MTJs stacks that layers with different buffers. It is necessary to take into account the dependence of α on buffer material and annealing parameters.

References:

- [1] Kalarickal, S. S. et al. Ferromagnetic resonance linewidth in metallic thin films: Comparison of measurement methods. J. Appl. Phys. 99, 093909 (2006)
- [2] Bilzer, C. Microwave susceptibility of thin ferromagnetic films: Metrology and insight into magnetization dynamics. 181 (2007)

Mo.H-P44 - Annealing effects in Co/Ni multilayers

N. Soriano Gomez¹, H. Kilinc², H. Belliveau³, D. Navas⁴, C. Garcia⁵, C. W. Miller⁶, R. Morales^{7,8}

1. *Department of Chemical-Physics, University of the Basque Country UPV/EHU, Leioa, Spain*
2. *Physics Department, Bogazici University, Istanbul, Turkey*
3. *Physics Department, University of South Florida, Tampa FL, United States*
4. *4IFIMUP-IN and Departamento Física e Astronomia, Universidade do Porto, Porto, Portugal*
5. *Physics Department, Universidad Técnica Federico Santa María, Valparaiso, Chile*
6. *College of Science, Rochester Institute of Technology, Rochester NY, United States*
7. *Department of Chemical-Physics & BCMaterials, University of the Basque Country UPV/EHU, Leioa, Spain*
8. *IKERBASQUE, Basque Foundation for Science, Bilbao, Spain*

Co/Ni multilayers can exhibit an effective anisotropy with in-plane and/or out-of-plane components. The balance between these two orthogonal anisotropies depends on the growth conditions and the structural parameters of the multilayer, but it can be altered by subsequent thermal treatments. In this work we analyze the annealing effects on the magnetization reversal curves of “as grown” samples and post-annealed multilayers. In-plane and out-of-plane hysteresis loops were obtained at room temperature for three sets of measurements; (i) Co/Ni multilayers deposited at room temperature, (ii) Co/Ni multilayers deposited at high temperature, and (iii) post-annealing of Co/Ni multilayers deposited at room temperature. A significant change was observed in samples exposed to high temperatures, either during deposition or post-annealing. Remanent magnetization becomes null in both cases. X-ray diffractograms and surface roughness characterization by atomic force microscopy show that the microstructure is significantly affected by deposition or annealing temperatures. Surface roughness increases with temperature, which has a strong effect on the Co-Ni interface and consequently on the magnetic properties of the multilayers.

This work was supported by EU-FP7-IRSES-2012-318901, MICINN-FIS2008-06249, and NSF-ECCS.

Mo.H-P45 - Transverse Kerr effect transformation of by normal metal film atop ferromagnetic metal surface

V. Skidanov¹

1. Institute For Design Problems In Microelectronics RAS

Recent years observation of magneto-optical signal from additional ferromagnetic layer is considered as a promising way to enhance sensitivity of biochips based on plasmonic properties of noble metals.

The present report is devoted to experimental investigation of possibility to enhance magneto-optical signal by additional normal transition metal layer with nanoscale thickness. It is shown that the presence of normal transition metal layer with thickness up to 100 nm atop or/and under ferromagnetic metal significantly modifies magneto-optical reply of the film structure.

Inversion of the transverse Kerr effect is seen clearly when white light falls on the Cr layer side. Value and sign dependence of magneto-optical signal upon thickness of normal layer was found so that the inversed signal amplitude can exceed signal amplitude from pure Py film.

Up to three-fold enhancement of the magneto-optical signal was observed in configuration when light falls on the thin Py layer (≤ 10 nm) atop normal metal layer with thickness more than 20-30 nm. Thin normal metal underlayer (< 20 nm) leads to signal reduction.

Investigations were made with a wide number of normal transition metals with different filling of atomic shells 3d, 4d and 5d (Ti, Cr, Mo, Ta, Re, Pt, W). It was shown that the influence of normal metal layer rigorously depends upon filling of atomic d-shell of the metal. Inversed signal amplitude gradually reduced with d-shell filling. The most amplitude of inversed signal was observed for Ti and Ta coatings. No signal inversion was observed for Cu and Au coatings with filled 3d and 5d atomic shells. But two-fold enhancement of magneto-optical signal from Py film was found with Cu or Au layers underneath.

Mo.H-P46 - Domain wall propagation in Co/Pt-wedge/Co film with perpendicular anisotropy

M. Matczak^{1,2}, R. Schöfer^{3,4}, M. Urbaniak¹, B. Szymański¹, P. Kuwik¹, F. Stobiecki^{1,2}

1. Institute of Molecular Physics, Polish Academy of Sciences, Poznan, Poland

2. NanoBioMedical Centre, Adam Mickiewicz University, Poznan, Poland

3. Leibniz Institute for Solid State and Materials Research (IFW) Dresden, Institut für Metallische Materialien, Dresden, Germany

4. Dresden University of Technology, Institute for Materials Science, Dresden, Germany

Domain wall (DW) propagation in layers with perpendicular anisotropy, that is controlled by a uniform magnetic field, has the potential to be used for the transport of magnetic beads by the moving stray-field trap of a moving DW [1] or in sensors registering the maximum values of varying magnetic fields [2].

A magnetic multilayer of the structure substrate//Pt(15nm)/Co(0.8nm)/Pt-wedge(0-7nm)/Co(0.6nm)/Pt(2nm) was deposited by magnetron sputtering in a UHV system. The thickness of the Pt-spacer (tPt) changed from 0 to 7nm over a length of 18 mm. For tPt < 2.6 nm, the magnetization reversal of the Co-layers occurs cooperatively, and for larger tPt sequentially. The Co-layer with 0.6 nm thickness (CoS) has a lower switching field and is magnetically softer than the tCo = 0.8 nm layer (CoH). In the 2.6 < tPt < 3.0 nm range there are significant changes of the switching field due to a strong gradient of an interaction field H_{mls} (the field defines the position of the center of the minor hysteresis loop). For tPt > 3.0 nm, H_{mls} is about zero and the switching fields of the Co-layers are equal to their respective coercive fields. Interestingly, in a region of the sample with strong interaction gradient, the magnetization reversal in the CoS layer takes place reversibly by the propagation of a single straight DW. To explain this specific nature of magnetization reversal in the CoS layer, DW propagation velocity measurements were performed in an area characterized by a negligible interaction (H_{mls} ~ 0) and in a region with the gradient of the ferromagnetic interaction |dH_{mls}/dx| > 0. In the x-range with no interaction, the distance travelled by the DW, (dx), in a given magnetic field H, is proportional to the duration of the field pulse (dt), and the v(H) dependence is typical for creep propagation [3]. However, in the area with an interaction gradient H_{mls}, dx/dt is a decreasing function of the pulse duration. Thus, in the presence of the ferromagnetic interaction gradient, a strong suppression of the thermally activated DW propagation is observed.

[1] APL 100 (16), 162402, 2012

[2] J. Phys. Chem. B 111, 13479, 2007

[3] PRL 99, 217208, 2007

Mo.H-P47 - Magnetic anisotropy field in amorphous alloy and thin film with composition Co₆₇Fe₄Mo₁Si₁₇B₁₁: measurement by means of ferromagnetic resonance and low-field microwave absorption.

E. Lopez Molina^{1,2}, H. Montiel², G. Alvarez³, A. Conde Gallardo⁴, R. Zamorano⁴

1. Instituto de Investigaciones en Materiales, Universidad Nacional Autonoma de Mexico, Coyoacan, Mexico D.F., Mexico

2. Centro de Ciencias Aplicadas y Desarrollo Tecnológico, Universidad Nacional Autonoma de Mexico, Coyoacan, Mexico D. F. Mexico

3. Escuela Superior de Fisica y Matematicas IPN, San Pedro Zacatenco, Mexico D.F., Mexico

4. Departamento de Fisica CINVESTAV-IPN, San Pedro Zacatenco, Mexico D.F., Mexico

In this work, we analyze the magnetic anisotropy field of amorphous alloy as-cast and thin film with composition Co₆₇Fe₄Mo₁Si₁₇B₁₁ (Vitrovac6030). The amorphous alloy was obtained from VACUUMSCHMELZE GmbH & Co. KG, where this alloy was used as a target to grow thin films, being deposited by means of dc magnetron sputtering on a glass substrate; with a 3x10⁻² mbar Argon pressure and sputtering power of 0.834 Watts. X-ray Diffraction patterns show similar amorphous structures between Vitrovac6030 as-cast and Vitrovac6030 thin film. Magnetic measurements confirm that the amorphous alloy has ultra-soft ferromagnetic properties with a coercive field of 0.035 G; while the thin film has a coercive field of 17 G, indicating a partial loss of ultra-soft ferromagnetic properties, and it is due to magneto-elastic contributions promoted by deposition method and the interface between substrate and the thin film. Magnetic anisotropy was analyzed by means of ferromagnetic resonance (FMR) and low-field microwave absorption (LFMA) measurements. FMR measurements of Vitrovac6030 as-cast shows a typical spectrum of Cobalt-based alloys, with transversal magnetic anisotropy; while the thin film has a broad FMR line, associated with a wide distribution relaxation times due to magneto-elastic contributions, originating by deposit method. LFMA measurements show a similar behavior that FMR and this suggests an increment in magnetic anisotropy field by magneto-elastic effects.

Authors acknowledge to the PAPIIT-UNAM IG100314 project for the financial support.

Mo.H-P48 - The influence of deposit method on magnetic anisotropy field of CoFe₂O₄ thin films obtained by means of pulsed laser deposition.

E. Moreno^{1,2}, M. Montiel Sánchez², R. Castañeda Guzman², G. Alvarez Lucio³, A. Conde Gallardo⁴

1. Instituto de Investigaciones en Materiales, Universidad Nacional Autónoma de México
2. Centro de Ciencias Aplicadas y Desarrollo Tecnológico, Universidad Nacional Autónoma de México, Coyoacan, México D. F., Mexico
3. Escuela Superior de Física y Matemáticas IPN, San Pedro Zacatenco, México D.F., México
4. Departamento de Física CINVESTAV-IPN, México D.F., México

Cobalt ferrite (CoFe₂O₄) is a magnetic oxide with an inverse spinel type structure, and that it gives origin to their magnetic properties, also had been proposed as a component in magnetoelectric multilayer for technological applications development. In this work, thin films of cobalt ferrite were obtained by means of pulsed laser deposition (PLD); at vacuum pressure of ~10⁻⁶ Torr, with a constant oxygen pressure of 15 mTorr. The thin films were grown on a substrate of amorphous quartz and silicon <100>. The X-ray diffraction shows a preferential growth of crystallites in the direction <400> for both types of substrates. Atomic force microscopy shows a wide distribution of particle size. Magnetometry measurements show a high coercive field around of 2000 Oe in both substrates, and it is associated to an increment of magnetic anisotropy of particles due to preferential growth. Ferromagnetic resonance (FMR) spectra show two resonant absorptions associated with different magnetic phases, one phase corresponding to superparamagnetic particles and the other resonant absorption is associated with monodomain particles.

The authors acknowledge the financial support of DGAPA-UNAM, through the grants PAPIIT IG100314. Everardo Lopez M. is grateful to PAEP-UNAM and CONACYT-Mexico, through financial support and scholarship.

Mo.H-P49 - Electronic properties and magnetic moment distribution on perovskite type slabs

J. Pilo Gonzalez¹, J. Rosas Huerta¹, E. Carvajal Quiroz¹, M. Cruz-Irisson¹, O. Navarro Chávez²

1. Instituto Politécnico Nacional, ESIME-Cul, Coyoacan, México D. F., Mexico

2. Universidad Nacional Autónoma de México, IIM-Unidad Morelia

Perovskite type slabs were excised from the Sr₂FeMoO₆, SrFeO₃ and SrMoO₃ bulk double perovskites (SFMO, SFO and SMO, respectively), leaving (001) free surfaces. Supercells were built up for each slab, keeping a 10Å initial free space, to optimize the geometry. Once the minimum energy state was identified, the electronic and magnetic properties of the [001] oriented slabs have been calculated within the Density Functional Theory (DFT) scheme, with the Hubbard-corrected Local Density Approximation (LDA+U) and using the CA-PZ functional [1]. Magnetic moment for each atom in the systems was calculated; spin values for the Mo atoms are 0.25ħ, 0.27ħ and 0.26ħ for the SrMoO₃ slab system case and they are aligned ferromagnetically. Contrarily, Mo magnetic moments in the Sr₂FeMoO₃ slab system align antiferromagnetically to the corresponding Fe atoms. The Densities of States (DOS) and band structures were calculated also to study the electronic behaviors. The vacuum region change, decreasing as geometry stabilizes (10Å to 9.743Å for the SrMoO₃ case) and the *t*_{2g} and *e*_g states roles were discussed contrasting with what is found to bulk materials [2].

This work was partially supported by COFAA-IPN, the multidisciplinary projects 2014-1640 and 2014-1641 from SIP-Instituto Politécnico Nacional, PAPIIT-IN100313 from Universidad Nacional Autónoma de México. J. Pilo and J. L. Rosas want to acknowledge the graduate fellowship from Consejo Nacional de Ciencia y Tecnología.

[1] D. M. Ceperley, B. J. Alder, *Phys. Rev. Lett.*, 45(7), 566 (1980)

[2] E. Carvajal, R. Oviedo-Roa, M. Cruz-Irisson and O. Navarro, *Rev. Mex. Fís. S*, 58(2), 171 (2012)

Mo.H-P50 - Preparation and magnetic properties of NiFe₂O₄ / ZnFe₂O₄ bilayers

Mahender C¹, Prabhu R.², Sahu B.N², S. Prasad², Venkataramani¹

1. *Department of Metallurgical Engineering and Materials Science, Indian Institute of Technology Bombay, Bombay, India*

2. *Department of Physics, Indian Institute of Technology Bombay, Bombay, India*

NiZnferrite (NZF), a versatile material used in various applications, requires high temperature processing and stoichiometric target to get proper magnetic properties, when deposited in thin film form. In this paper, we have deposited NiFe₂O₄ (NiF) and ZnFe₂O₄ (ZnF) bilayer of different thicknesses from two binary ferrite targets (NiF and ZnF). By annealing the bilayer at different temperatures we could obtain a good control on the magnetic properties. We first deposited NiF film (170 nm) on fused quartz substrate. The ZnF films with different thicknesses (20 to 350 nm) were deposited on top of this film to form a set of bilayers. These samples were deposited at room temperature and annealed in air at various temperatures for 2 hrs. The $4\pi M_s$ values of the as deposited bilayers continuously decreased from 0.45 kG to 0.2 kG with increase in ZnF layer thickness. But the $4\pi M_s$ values of bilayers annealed at 650 °C initially increased from 3.1 kG with the ZnF film thickness and reached a maximum of 6.5 kG for total film thickness 330 nm. It then drops to 3kG when ZnF thickness exceeds the thickness of NiF layer. The maximum spontaneous magnetization value of bilayers is near to bulk value 6.6 kG of Ni_{0.7}Zn_{0.3}Fe₂O₄ at 10 K. The variation in $4\pi M_s$ of bilayers with increasing ZnF layer thickness nearly follows the trend of magnetization curve of bulk Ni_{1-x}Zn_xFe₂O₄ with Zn concentration (x). A cross sectional TEM image of NZF bilayers with thickness 370 nm shows that there is inter diffusion between the two layers. In these set of experiments we are in a position to control the Zn substitution in NiF through diffusion across the bilayers and see the effect of Zn composition of nano crystalline grain sizes in NZF thin films.

Mo.H-P51 - Ferromagnetic-antiferromagnetic transition in [001]-oriented L1₀ FeMnPt filmsT. Hasegawa¹, S. Kimura¹, K. Ito¹, S. Ishio¹, A. S. Kamzin², A. A. Valiullin², C. Barton³, T. Thomson³1. *Department of Materials Science and Engineering, Akita University, Akita, Japan*2. *Ioffe Physical Technical Institute, Russian Academy of Sciences, Moscow, Russia*3. *School of Computer Science, University of Manchester, Manchester, England, United Kingdom*

The [001]-oriented L1₀ (CuAu I type) FePt thin films have attracted much interest because the perpendicular magnetization is expected to have applications for storage media and spintronic devices due to a high magnetization ($M_s \sim 1100 \text{ emu/cm}^3$) and a high magnetocrystalline anisotropy ($K_u \sim 7.0 \times 10^7 \text{ erg/cm}^3$) caused by the atomic arrangement having alternating Fe and Pt layers along the *c* axis. By replacing Fe with Mn in the equiatomic FePt bulk alloy, significant antiferromagnetic (AF) ordering is stabilized [1]. However, there are very few reports on the magnetic phase diagram of films. In this work, [001]-oriented L1₀ (Fe_{1-x}Mn_x)₆₀Pt₄₀ films (6.12 nm thick) were prepared. The films were deposited on (100) MgO substrates by magnetron sputtering method, and those were subsequently annealed at 973 K for 10 minutes. The degree of order parameters was approximately 0.89 in all of the films. The lattice constant *c* decreased with *x*, and the gradients abruptly changed at around $x \sim 0.54$, while the gradient of the films with $x > 0.60$ increases in the bulk system [1]. The magnetic phase diagram is determined. At room temperature, the films with $0 \leq x \leq 0.52$ were in a ferromagnetic (FM) phase with a coercivity of several kilo-oersteds. The films with $0 \leq x \leq 0.54$ shows FM-paramagnetic (PM) transition at Curie temperature, and the films with $0.52 \leq x \leq 0.60$ show AF-FM-PM or AF-PM transition. At $x = 0.52$, which is close to the critical composition of the FM-AF phase change at room temperature, the K_u was about $1.3 \times 10^7 \text{ erg/cm}^3$ which is sufficient for the high-density magnetic storage media over 6 Tbit/in².

[1] A.Z. Menshikov et al., *J. Magn. Magn. Mater.* 65 (1987) 159

This work was supported by NEDO (11B07008d).

Mo.H-P52 - Epitaxially Textured PCMO Thin Films Under Considerably Low Substrate Temperature

M. Nyman¹, T. Elovaara¹, J. Tikkanen¹, S. Majumdar², H. Huhtinen¹, P. Paturi¹

1. *University of Turku, Turku, Finland*

2. *Aalto University, Espoo, Finland*

Among the perovskite manganites, a small-bandwidth compound of $\text{Pr}_{1-x}\text{Ca}_x\text{MnO}_3$ (PCMO), with fascinating electrical and magnetic properties like colossal magnetoresistance (CMR), coexistence of phase-separated regions, first order irreversible metamagnetic transition, large magnetocaloric effect and enormous resistive switching under optical or electrical excitation, has received a lot of technological and scientific interests and these phenomena have led to huge potential in the photovoltaic, magnetic data storage and memory applications. However, the applications are usually based on nearly atomically flat structures requiring high quality thin films of individual layer materials. Therefore, the optimization of the pulsed laser deposition (PLD) process, where the influence of the substrate temperature plays a significant role, is one of the main focus when developing novel multi-purpose thin films for wide-ranging future emerging-energy technologies. In this paper, we report the growth of well-crystallized and epitaxially textured PCMO thin films on SrTiO_3 substrates by pulsed laser deposition at a considerably low substrate temperature of as low as 450 C without high-temperature post-annealing treatments. Although a strong ferromagnetic interaction as well as large irreversible metamagnetic transition with a training effect have been observed for films grown at 450 C, the in-plane and out-of-plane lattice ordering is slightly improved with increasing substrate temperature. Therefore, the lowest magnetic field of 2 T for melting the insulating charge-ordering state at 70 K has been observed for films grown with substrate temperature between 550 and 600 C. The nucleation and growth of PCMO substrate at exceptionally low substrate temperature is qualitatively modelled by the combination of the kinetic energies and redox potential of the components of the ablation plasma, while the heat flow from the substrate is assumed to be less important. The results are of extreme importance for the future generation of energy-efficient oxide thin film fabrication routes for novel technology solutions.

Mo.H-P53 - Electrical, structural and morphological properties of epitaxially-grown Cr_{100-x}Cox alloy films

C. Sheppard¹, A. Prinsloo¹, M. Kadam¹, E. Fullerton², D. Dekadjevi³, P. Elies³, J. Richy³

1. *University of Johannesburg, Johannesburg, South Africa*
2. *University of California San Diego, La Jolla, United States*
3. *Université de Bretagne Occidentale, Brest, France*

Comparison between Cr in bulk and thin film forms revealed that dimensionality plays an important role in modifying the spin-density-wave (SDW) structure [1]. The present study extends these investigations to include epitaxially-grown Cr_{100-x}Cox thin films, with $0 < x < 8$ and thickness 200 nm. These samples were prepared on MgO(100) substrates using DC magnetron co-sputtering. Hall coefficients for these films, determined on cooling from 350K to 2K in a constant magnetic field, exhibit a change in majority charge carriers with variation in temperature and concentration. The Néel temperatures (TN) of the films were determined from anomalies observed at TN in electrical resistance measurements as a function of temperature. The TN-x phase diagram obtained for these samples indicates a decrease in TN values up to $x = 2.6$, where after the TN values increase and peak at about 5 at.% Co. This TN-x behavior is reminiscent of that seen for bulk Cr-Co, where a triple point (L) is observed for a concentration $x_L = 1.3$ at a temperature $T_L = 280$ K [2]. However, in the case of epitaxial Cr-Co thin films, L is shifted to $x_L = 2.6$ and T_L is decreased to 220 K. Interestingly, XRD analyses on the Cr_{100-x}Cox thin films indicate that for samples with x approximately equal to x_L the crystal coherence length in growth direction (100) is a maximum, while the mosaicity is a minimum. In addition, AFM studies indicate that the film roughness is also a minimum at x_L , where well defined cubical structures are observed. For films with $x < x_L$, small elongated angular structures are seen, while for films with $x > x_L$ large tilted cubic structures are formed. Thus, the behavior of the TN-x curve seems to reflect both the intrinsic magnetic properties and growth changes with increasing Co content.

[1] Zabel H 1999 J.Phys. Condens. Matter 11 9303

[2] Fawcett E et al. 1994 Rev. Mod. Phys. 66 25

Mo.H-P54 - Tunneling anisotropic magnetoresistance in oxide heterostructures

L. Balcells¹, R. Galceran¹, C. Frontera¹, B. Bozzo¹, A. Pomar¹, J. Cisneros¹, Z. Konstantinovic¹, B. Martinez¹

1. Instituto de Ciencia de Materiales de Barcelona – CSIC, Spain

Magnetic tunneling junctions (MTJ) are solid candidates for the development of a new generation of magnetic random access memories (MRAM). However, in spite of the intense work already done, some technical challenges, such as the uniformity of the magnetic properties of the electrodes, the insulating barrier uniformity or the thermal stability, are still not fully resolved. It has been recently shown that magnetoresistance in magnetic tunneling junctions may also depend on the orientation of the magnetization with respect to the crystallographic axes or to the direction of the current flow, in what is called tunneling anisotropic magnetoresistance (TAMR). The use of TAMR response would drastically simplify the technological implementation of MTJ since much of the above mentioned technical challenges will be suppressed. In this work we report on measurements of TAMR response as a function of temperature and magnetic field in different oxide heterostructures such as La₂/3Sr₁/3 MnO₃/AlLaO₃/Pt and La₂/3Sr₁/3 MnO₃/MgO/Pt in which TAMR responses of about 4% at low temperature have been measured.

Mo.H-P55 - Magnetotransport properties and morphology of epitaxial Fe/MgO granular multilayers

A. Vovk¹, A. García-García², Y. Pogorelov², J. A. Pardo^{3,4}, P. Štrichovanec³, C. Magén^{3,5}, J. M. De Teresa^{3,6}, L. Morellón^{3,6}, P. Algarabel⁶, M. Ricardo Ibarra^{3,6}, G. Kakazei²

1. BioISI/FCUL Universidade de Lisboa, Lisboa, Portugal

2. Departamento de Física, IFIMUP and INN, Universidade do Porto, Porto, Portugal

3. Instituto de Nanociencia de Aragón, Universidad de Zaragoza, Zaragoza, PSain

4. DCTMF, Universidad de Zaragoza, Spain

5. Fundación ARAID, Zaragoza, Spain

6. ICMA, Universidad de Zaragoza-CSIC, Spain

Discontinuous metal-insulator multilayers (DMIMs) are a particular kind of granular cermets containing a continuous insulating and a discontinuous (granular) metal layer. They exhibit moderate tunneling magnetoresistance (TMR) ratio but an enhanced low-field sensitivity [1], which makes them promising candidates for magnetic sensors.

Recently [2] our Fe(0.6 nm)/MgO (3.0 nm) DMIMs show increase in TMR ratio by a factor of ~ 4.5 with deposition temperature (T_s) for samples deposited on MgO single-crystal, remaining constant for samples deposited on glass. This was explained by enhanced degree of (001) texturing of MgO layers with T_s .

In this work we discuss the role of T_s on Fe island growth mode onto MgO layers taking into account previous researches by Boubeta *et al.* [3]. While low T_s yields flat surfaces, high temperature results in a 3D Fe growth. Magnetization measurements above blocking temperature exhibit sizeable deviation from common Langevin behavior. The experimental data were fitted using an extended model that accounts the island shape anisotropy and dipolar interactions between islands. It allows to determine and to elucidate the oblate spheroidal shape and size of Fe islands. Calculated values can be used to estimate correlations between magnetic moments of Fe neighboring islands. Results are compared with transport and magnetotransport measurements.

[1] G.N. Kakazei *et al.*, J. Appl. Phys. 90, 4044 (2001)

[2] A. García-García *et al.*, Appl. Phys. Lett. 98, 122502 (2011)

[3] C. Martínez Boubeta *et al.*, J. Phys.: Condens. Matter 15, R1123 (2003)

Mo.H-P56 - In-situ neutron reflectometry during thin film growth by sputter deposition

W. Kreuzpaintner¹, B. Wiedemann¹, J. Ye¹, S. Mayr¹, A. Paul¹, A. Schmehl², T. Mairoser², A. Herrnberger², J. Stahn⁴, J. Moulin³, M. Haese-Seiler³, P. Korelis⁴, M. Pomm³, P. Böni¹, J. Mannhart⁵

1. *Technische Universität München, Physik-Department E-21, Garching, Germany*
2. *Zentrum für elektronische Korrelation und Magnetismus, Universität Augsburg, Lehrstuhl für Experimentalphysik VI, Augsburg, Germany*
3. *Helmholtz Zentrum Geesthacht, Institut für Werkstoffforschung, Abteilung WPN, Instrument REFSANS, Lichtenbergstr. 1, 85747 Garching FRM II*
4. *Paul Scherrer Institut, Laboratory for Neutron Scattering, Villigen, Switzerland*
5. *Max Planck Institute for Solid State Research, Stuttgart,*

Thin magnetic layers and heterostructures thereof are the basic building blocks of a large number of magneto-electronic devices. Their performance strongly relies on the magnetic properties of the layers, which are functions of their morphology, and on the coupling between them. Since these parameters can change during the process of growth, it is important for the understanding and optimization of magnetoelectronic devices to not only accurately monitor the structural but also the magnetic properties during the process of growth. While the structural characterization of thin films during growth by various techniques is common practice (as e.g. commonly done by RHEED/LEED, STM or synchrotron radiation), the in-situ measurement of the magnetic properties of films using (polarised) neutron reflectometry is a challenging task. Within a collaboration of TU München, University Augsburg and MPI Stuttgart, we operate a mobile sputtering facility for the growth and in-situ monitoring of magnetic multilayers, which can be installed at suitable neutron beamlines. In this contribution, first proof of principle (unpolarised and polarised) in-situ neutron reflectivity measurements carried out at the ToF reflectometer REFSANS at the FRM II neutron source and at the AMOR beamline at PSI will be presented. At the latter, use of the SELENE neutron optical concept allows very fast polarised neutron reflectivity measurements to be performed.

Mo.H-P57 - Influence of strain on the magnetic properties of LaMnO₃ thin films

A. Pomar¹, J. Roqueta², J. Santiso², L. Balcells¹, C. Frontera¹, B. Bozzo¹, Z. Konstantinovic¹, N. BaguPs^{1,2}, F. Sandiumenge¹, B. Martínez¹

1. *Instituto de Ciencia de Materiales de Barcelona (ICMAB-CSIC), Spain*

2. *Institut Catala de Nanociencia i Nanotecnologia, ICN2 (CSIC-ICN), Spain*

We present a detailed investigation of the epitaxial growth of LaMnO₃ thin films on single crystalline SrTiO₃ substrates by Pulsed laser deposition. A progressive evolution of the magnetic and transport properties as a function of oxygen pressure during deposition has been found. A concomitant modification of the film structure has been studied by high-resolution x-ray diffraction. Our results show that films grown at low PO₂ are partially relaxed and they exhibit an antiferromagnetic/insulating behavior similar to their bulk counterpart. On the contrary, films grown under highly oxidizing atmospheres are fully strained and they present a strong ferromagnetic character while still electrically insulating. We interpret these findings in terms of different strain-induced orbital orderings. We will also discuss the possibility of tuning the functional properties of LaMnO₃ by modifying the residual stress imposed by the substrate.

Mo.H-P58 - Probing short range order mediated tunable spontaneous magnetization in Zn_{0.95}Co_{0.05}O epitaxial films by x-ray absorption

P. Satyarthi¹, S. Ghosh², P. Kumar³, D. Kanjilal⁴, H. Schmidt⁵, S. Zhou⁶, P. Srivastava⁷

1. Nanotech laboratory, Indian Institute of Technology Delhi, New Delhi, India

2. Nanotech laboratory, Indian Institute of Technology Delhi, New Delhi, India

3. Inter University Accelerator Centre, Aruna Asaf Ali Marg, New Delhi, India

4. Inter University Accelerator Centre, Aruna Asaf Ali Marg, New Delhi, India

5. Department of Materials for Nanoelectronics, Chemnitz University of Technology, Chemnitz, Germany

6. Helmholtz-Zentrum Dresden-Rossendorf, Institute of Ion Beam Physics and Materials Research, Dresden, Germany

7. Nanotech laboratory, Indian Institute of Technology Delhi, New Delhi, India

Over the past decades, a fairly large number of studies have explored spin dependent magnetization in Zn_{1-x}M_xO (M=transition metal) based diluted magnetic semiconductors by putting special emphasis on the variation of transition metal concentration and co-doping of additional element [1, 2]. However, origin of spontaneous magnetization is still debated to originate either from substitution and/or segregation of transition metal [1, 2] or solely from defects [3]. To address these aforementioned issues, we have investigated tunable spontaneous magnetization triggered in paramagnetic Zn_{0.95}Co_{0.05}O films (Co=5% only) using non magnetic 500 KeV xenon ion irradiation for their potential application in next generation spintronics. The origin of spontaneous magnetization is understood from different degree of bound magnetic polaron stabilization [4] underlined through alteration in short range ordering near the Zn and Co cations in extended x-ray absorption fine structure analysis at Zn and Co K edges. Temperature and magnetic field dependent x-ray circular dichroism measurements at Co L_{2,3} edge consistently provide purely paramagnetic contribution of Co sublattice in as deposited Zn_{0.95}Co_{0.05}O film. However, coexistence of paramagnetic and ferromagnetic contribution persists in post irradiated Zn_{0.95}Co_{0.05}O films.

[1] J. M. D. Coey, M. Venkatesan, and C. B. Fitzgerald, Nature Mater. 4, 173 (2005)

[2] P. Satyarthi, S. Ghosh, et al., J. Appl. Phys. 113, 183708 (2013)

[3] M. Gacic, G. Jakob, et al., Phys. Rev. B 75, 205206 (2007)

[4] T. Kaspar, J. Fiedler, et al., IEEE Elec. Dev. Lett. 34, 1271 (2013); APL Materials 2, 076101 (2014)

Mo.H-P61 - Study of dynamic and static magnetic properties of inverse opal-like structures based on Co and Ni

I. Shishkin¹, A. Mistonov^{1,2}, N. Grigoryeva¹, S. Grigoriev^{1,2}, D.Menzel³

1. Faculty of Physics, Saint Petersburg State University, Saint Petersburg, Russia

2. Petersburg Nuclear Physics Institute, Gatchina, Russia

3. Institut für Physik der Kondensierten Materie Technische Universität, Braunschweig, Germany

Inverse opal-like structures (IOLS) can be synthesized by filling the voids of opal templates with suitable structure-forming precursors and subsequent removal of the initial microspheres to leave three-dimensionally ordered porous materials. The inverse opals based on the ferromagnetic metals (Ni, Co, etc) represent a new class of the 3-dimensional nanoscale ferromagnetic structures, which are geometrically frustrated at room temperature. Method of ultra small-angle diffraction of synchrotron radiation has shown that the synthesized samples have presumably face-centered cubic ordering of the spherical voids with a period of 760 ± 10 nm. By small-angle neutron diffraction intensities of magnetic scattering as a function of external magnetic field for crystallographic planes of 202-family were obtained. It is assumed that the magnetic structure of inverse opals is a system of 4 magnetic subsystems, directed along four different 111 axes of the fcc structure. Different subsystems are magnetizing in different critical fields, so the magnetic scattering function has a stepped look. One can distinguish critical values of the magnetic field – coercivity; inflection field point; field point, where two branches come together; saturation field. By SQUID-magnetometry were obtained remagnetization curves for Co and Ni IOLS of the thickness in the range from 0.25 μm to 13 μm . This measurements were taken at temperatures of 5, 20, 45, 75, 180, 250, 300 K. For all the dependencies the critical fields were determined. They increase with IOLS thickness increasing that indicates presence of a magnetic connection between the layers. It was found also that magnetic hardness of material and developed porous surface affect on the temperature behavior of the film.

Mo.H-P62 - Comparison of FORC Results Obtained on L10 FeCuPt Measured by Three Different Methods

V. Provenzano¹, J. W. Lau¹, D. A. Gilbert^{1,2}, P. Silwal¹, K. B. Stritch¹, J. Liao³, C. Lai³, K. Liu²

1. *National Institute of Standards And Technology, Gaithersburg, United States*

2. *University of California -Davis, Physics Department, Davis, CA United States*

3. *National Tsing Hua University, Dept. of Materials Science and Engineering, Taiwan*

The first-order reversal curve (FORC) method is a simple, yet versatile “magnetic fingerprinting” technique for revealing extremely detailed information about a magnetic material, from which magnetic properties-structure correlations can be inferred. So far the technique has been often used for qualitative studies of magnetic phases and magnetization reversal mechanisms [1]. It also has the potential to become a fully quantitative technique for determining key magnetic characteristics such as magnetic interactions and distributions [2]. The default option for FORC measurements has been the vibrating sample magnetometry (VSM) or the alternating gradient magnetometry. An essential component needed to transform the FORC technique to a widely applicable and fully quantitative method, is the ability to yield reliable and reproducible FORC data and distributions acquired by different instruments, analogous to comparing crystal structures probed by X-ray diffraction vs. neutron scattering. To this end, FORC measurements were performed using the anomalous Hall effect (AHE) and magneto-optical Kerr effect (MOKE) methods, which are complementary to magnetometry techniques for acquiring FORC data. In this paper we present the FORC results obtained on a series of FeCuPt films that had undergone rapid thermal annealing between 300 °C to 400 °C (in this range, FePt transforms from a predominantly disordered A1 phase to a L10 phase). The FORC results measured by the three methods, show both basic similarities and key differences. The differences are mainly because the VSM-FORC is sensitive to the magnetization across the entire sample, so is the AHE transport-based FORC, but conduction-path dependent; while the MOKE-based FORC is magneto-optical dependent on the sample local structure. These results demonstrate the validity of AHE-FORC and MOKE-FORC in probing essential magnetic characteristics of the samples, while providing additional and complementary capabilities to magnetometry-based FORC that are very useful for developing the best practice protocol for FORC data acquisition.

References:

[1] J. E. Davies, O. Hellwig, E. E. Fullerton, G. Denbeaux, J. B. Kortright and Kai Liu, *Phys. Rev. B*, 70, 224434 (2004)

[2] D. A. Gilbert, G. T. Zimanyi, R. K. Dumas, M. Winklhofer, A. Gomez, N. Eibagi, J. L. Vicent, and Kai Liu, *Sci. Rep.* 4, 4204 (2014)

Mo.H-P63 - Up-scaling strained, increased coercivity [Fe-Co/Au-Cu]_n multilayers, towards Rare Earth free Permanent Magnets applications

G. Giannopoulos¹, R. Salikhov², L. Reichel³, A. Markou⁴, I. Panagiotopoulos⁵, M. Farle⁶, S. Fähler⁷, V. Psycharis⁸, D. Niarchos⁹

1. INN, NCSR Demokritos, Athens, Greece

2. Fakultät für Physik and Center for Nanointegration (CeNIDE), Universität Duisburg-Essen, Duisburg, Germany

3. IFW Dresden, PO Box 270116, Dresden, Germany, TU Dresden, Institute for Materials Science, Dresden, Germany

4. Department of Materials Science and Engineering, University of Ioannina, Ioannina, Greece

5. Department of Materials Science and Engineering, University of Ioannina, Ioannina, Greece

6. Fakultät für Physik and Center for Nanointegration (CeNIDE), Universität Duisburg-Essen, Duisburg, Germany

7. IFW Dresden, Dresden, Germany

8. INN, NCSR Demokritos, Athens, Greece

9. INN, NCSR Demokritos, Athens, Greece

Fe-Co is proposed as a possible candidate alloy for permanent magnet applications due to its high magnetic moment. Apart from this, high magnetocrystalline anisotropy and coercivity is required for permanent magnets. In this work we present sputtered thin Fe-Co/ Au-Cu multilayer films doped with Carbon, in order to stabilize metastable tetragonal phases, by straining the unit cell and thus inducing magnetocrystalline anisotropy in the system [1]. By adding Carbon we can stabilize the strain and increase the magnetocrystalline anisotropy of the system [2]. In order to maintain the strain in the magnetic Fe-Co thin films, preventing the partial strain relaxation which we have observed as film thickness increases [3], we followed a multilayer (up to 24 layers) Fe-Co / Au-Cu approach, where variable thickness Fe-Co (1-3nm) and Au-Cu(1-3nm) layers were deposited on MgO (100) substrate at 300°C. By employing this structure, strain is induced from both sides.

X-ray, SQUID and FMR measurements were performed. An intense Fe-Co (002) peak also indicates an epitaxial growth on Au-Cu buffer. There is also a peak shift of almost 0.5° compared to the theoretical value of $2\theta = 65.31^\circ$ which indicates a tetragonal distortion in the Fe-Co-C layers. In all multilayer samples, the easy axis of magnetization is in plane. A Magnetocrystalline Anisotropy Energy of about 0.4 MJ/m³ is found in [Fe₄₅Co₅₅(3 nm)/Au₃₀Cu₇₀(1 nm)]₁₂ system. Thus, our multilayer approach supports significantly the thickness scaling up of Fe-Co films preserving large perpendicular magnetocrystalline anisotropy. Furthermore a coercivity of about 900Oe was observed, which is a step forward towards permanent magnets applications.

Acknowledgements

We acknowledge funding of the EU through FP7-REFREEPERMAG

References

[1] T. Burkert et al, PRL 93, 027203 (2004)

[2] E. K. Delczeg-Czirjak et al, Phys Rev B 89, 144403 (2014)

[3] L. Reichel et al, J. Appl. Phys. 116, 213901 (2014)

Mo.H-P64 - Anomalous change and development of anisotropic residual stress at the initial stage of FeCo film growth

S. Nakagawa¹, H. Hayashibara¹, Y. Takamura¹

1. Tokyo Institute of Technology, Tokyo, Japan

An anisotropic residual stress induced by sputter-deposition process is one of the method to cause uniaxial in-plane magnetic anisotropy in FeCo(B) thin films[1]. We developed the in-situ stress observation system of the anisotropic internal stress at the initial stage of the film growth by detecting displacement of cantilever substrate during the film deposition process to clarify initiation and accumulation of the internal stress σ . Since the thickness of the cantilever substrates is as thin as 30 micron, the deviation of the cantilever caused by the film stress can be detected by the laser displacement sensor during the initial stage of the film growth.

It is well known that low and high Ar gas pressure cause compressive and tensile internal stress, respectively, to the films prepared by sputter-deposition. However, the σ of all the films prepared at various Ar gas pressure shows tensile stress at the initial stage of the film growth. The tensile stress at the early stage is caused by the formation of island structure and their agglomeration on the substrate. The critical thickness of the film t_p where the stress changes from tensile to compressive is around 1.5 to 8 nm depending on the surface energies of the film materials and that of the substrate. FeCo films prepared at low Ar gas pressure shows the anomalous change of the internal stress which indicates two critical thickness t_p around $t = 3.3$ and 7.8 nm. The critical thickness would be t_{p1} considering surface energy. The origins of t_{p2} may be related to magnetic interaction during the island growth or structural transition of alloys. Development of anisotropic residual stress can be also detected during the film formation after the continuous layer developed..

[1] A. Hashimoto, K. Hirata, T. Matsuu, S. Saito, and S. Nakagawa, IEEE Trans. Magn. 44, 3899 (2008).

Mo.H-P65 - Electrical control of magnetism in Heusler alloy $\text{Co}_2\text{FeAl}_{0.5}\text{Si}_{0.5}$ at room temperature

H. Wang¹, Y. Wu², H. Yu², Y. Jiang², J. Zhao¹

1. Institute of Semiconductors, Chinese Academy of Sciences, Beijing, China

2. School of Materials Science and Engineering, University of Science and Technology Beijing, Beijing, China

Magnetic materials with perpendicular magnetic anisotropy have received much attention due to its advantages in the application of spintronics devices, such as high integration density and low damping constant. For the aim of low-power operation, electrical manipulation of the magnetism is in urgent need, and much progress has been achieved such as the electrical switching of FeCo and CoFeB ultrathin magnetic films. Here, we show the electric field effects on the magnetism of Heusler alloy $\text{Co}_2\text{FeAl}_{0.5}\text{Si}_{0.5}$ ultrathin films with perpendicular magnetic anisotropy. The $\text{Co}_2\text{FeAl}_{0.5}\text{Si}_{0.5}$ samples were prepared by magnetron sputtering, in which the Pt buffer layer and the MgO cap layer make the $\text{Co}_2\text{FeAl}_{0.5}\text{Si}_{0.5}$ film perpendicularly magnetized. The samples were then fabricated into field-effect devices consisting of a top gate electrode, a dielectric insulator and a 10 to 30 μm wide channel. High-k dielectric HfO_2 with the thickness of 50 nm was deposited by atomic layer deposition (ALD), and the anomalous Hall effect was used to detect the local magnetization in the vicinity of the Hall probes. The Hall resistance R_{xy} , which is proportional to the perpendicular component of the magnetization, was recorded under different gate electric fields. An obvious dependence of the coercive field on gating voltage was observed from a 0.8 nm thick film, while a clear change of the magnetic anisotropy was obtained from a 1.1 nm thick one. $\text{Co}_2\text{FeAl}_{0.5}\text{Si}_{0.5}$ films thinner than 0.5 nm tend to show superparamagnetic behaviors at room temperature, and those films thicker than 2.0 nm show indistinguishable change under various gating voltages. It has been shown that the changing in the number of electrons plays a central role in enhancing or reducing the overall magnetic coupling in magnetic films, which is even strong enough and leads to the variation of Curie temperature. Here, the modulation of the coercive field and magnetic anisotropy with the gating voltage is certainly related to the carrier density variation near the interface between the magnetic film and the insulator. However, its dependence on the sample thickness is still an open question and needs to be further investigated.

Mo.H-P66 - Anisotropic magnetoresistance of Heusler-type half-metal ferromagnet and antiferromagnet bilayer thin films

T. Hajiri¹, M. Matsushita¹, M. Nishiwaki¹, H. Tanaka¹, K. Ueda¹, H. Asano¹

1. Department of Crystalline Materials Science, Nagoya University, Nagoya, Japan

Recently, a magnetization switching using a spin-polarized current is attracting interest because a spin-polarized current can alter the magnetic orientation of an antiferromagnetic layer [1,2]. The critical current for magnetization switching on antiferromagnet is 10^{-2} times smaller than that of ferromagnet [1]. A magnetization switching can be observed by an anisotropic magnetoresistance effect on antiferromagnet/ferromagnet exchange-coupled bilayer [3]. Besides, the sign of an anisotropic magnetoresistance effect includes the information about ferromagnetic half-metallicity [4]. We thus studied an anisotropic magnetoresistance effect on half-metallic ferromagnet (HMFM) Fe₂CrSi thin films and HMFM-Fe₂CrSi /antiferromagnet Ru₂MnGe bilayer thin films. Anisotropic magnetoresistance ratio - 0.17 % was observed on Fe₂CrSi, suggesting that Fe₂CrSi can be half-metallic. On the other hand, we succeeded in fabricating Ru₂MnGe with Neel temperature $T_N = 381$ K, which is higher than that of previous report ($T_N = 353$ K) [5]. Using these compounds, we fabricated Ru₂MnGe/Fe₂CrSi exchange-coupled bilayer. Large anisotropic magnetoresistance ratio more than -1.0 % was observed on Fe₂CrSi/Ru₂MnGe exchange-coupled bilayer. Besides, the shift of anisotropic magnetoresistance curve due to exchange bias was observed along field-cool direction. We would like to discuss the anisotropic magnetoresistance ratio for thickness dependent bilayers.

[1] A. S. Nunez et al., Phys. Rev. B 73, 214426 (2006)

[2] X. L. Tang et al., Appl. Phys. Lett. 91, 122504 (2007)

[3] H. Sakakibara et al., to be published in Annual Magnetism and Magnetic Materials Conference proceedings

[4] S. Kokado et al., J. Phys. Soc. Jpn. 81, 024705 (2012). [5] N. Fukatani et al., IEEE Trans. Mag. 48, 3211 (2012)

Mo.H-P67 - Thermally activated diffusion in Cu/Co/IrMn/Pt multilayers investigated by atom probe tomography

J. Le Breton¹, F. Letellier¹, R. Lardé¹, L. Lechevallier^{1,2}, V. Baltz³, K. Akmalidinov^{3,4}, S. Auffret³, B. Dieny³

1. *Groupe de Physique des Matériaux - UMR 6634 CNRS, Université et INSA de Rouen, France*

2. *Département GEII, Université de Cergy-Pontoise, France*

3. *SPINTEC - UMR 8191 CNRS, INAC-CEA, Université Joseph Fourier Grenoble 1, France*

4. *CROCUS Technology Grenoble, France*

Because thermal treatments are required to functionalize magnetic multilayers, chemical species diffusion can occur, which may lead to magnetic properties deterioration. This is the case for field cooling and post-deposition annealing treatments.

Atom Probe Tomography (APT) analysis being a very useful tool for the investigation of diffusion effects during thermal processes, we have investigated atomic diffusion in Cu/Co/IrMn/Pt exchange biased structures with various Pt cap, by APT. Three dimensional spatial distributions of atoms were obtained via analysis of Cu/Co/IrMn/Pt multilayers annealed at different temperatures (375, 475 and 525°C). The reconstructions obtained at different steps revealed gradual Mn diffusion in Co and Pt grains at Co/IrMn and IrMn/Pt interfaces respectively. Mn diffusion is revealed, first along Pt grain boundaries, and then laterally from the grain boundaries toward the inner parts of the Pt grains.

We estimated the diffusion lengths of Mn and Pt, through grain boundaries (d_{GB}) and within grains (d_L) for various annealing temperatures and for our typical experimental annealing time (1h). At both 375 and 475°C, the diffusion lengths are such that $d_{GB} \gg d_L$, meaning that grain boundaries indeed act as short diffusion circuits at such temperatures. An important increase of the lattice diffusion length d_L of Mn occurs between 375 and 475°C, implying that Mn diffusion through the grains interfaces is activated between 375 and 475°C, leading to the formation of Pt-Mn mixed regions at the IrMn/Pt interface for annealing temperatures higher than about 400°C, in agreement with previous investigations. These results are consistent with the larger affinity between Mn and Pt atoms than between Mn and Ir.

These structural data were correlated to the films exchange bias properties. The influence of the topmost Pt capping layer thickness, i.e. the effect of the Pt atoms reservoir pumping Mn out of the IrMn layer, turned out to be crucial.

Mo.H-P69 - The resistive switching and magnetic properties of CuO and Cu₂O films deposited by magnetron sputtering CuO target

Y. Hu¹, Z. Li¹

1. Department of Applied Physics, National University of Kaohsiung, Kaohsiung, Taiwan

It is known that oxygen flux is one of the key parameters to obtain Cu₂O films by magnetron sputtering metallic Cu target. More (less) oxygen flux would result in CuO (Cu₂O) phase preferentially and it is difficult to obtain pure Cu₂O or CuO phases by merely adjusting the oxygen flux. This work aims to prepare Cu₂O or CuO thin films by magnetron sputtering CuO (99.995%) target with different ambient gases. All of the samples were deposited on silicon substrates at 250°C. X-ray diffraction and Raman spectroscopy results show that the samples grown in Ar and O₂ ambient gases display the characteristic peaks of CuO, while those deposited in Ar and N₂ exhibit instead the characteristic peaks of Cu₂O. The results confirm that Cu₂O and CuO films were successfully prepared by sputtering a ceramic CuO target under proper ambient gases. Scanning electron microscopy and atomic force microscopy images reveal that both the grain size and surface roughness of Cu₂O film are larger than those of CuO film. Besides, both Cu₂O and CuO films displayed bipolar resistive switching properties, which are thought relevant to point defects. We measured the M-H curves of both Cu₂O and CuO films in low and high resistance states. Interestingly, the CuO film displays paramagnetic only, while the Cu₂O film displays paramagnetic and paramagnetic + ferromagnetic in low and high resistance states, respectively. For the Cu₂O film in high resistance state, we confirmed that the electric conduction is Schottky emission, and suggested that oxygen vacancies near the interface between electrode and Cu₂O film are responsible for the observed weak ferromagnetism.

Mo.H-P70 - Probing uncommensurated magnetic structures in thin films with GISANS

B. Wiedemann¹, S. Zhang², Y. Khaydukov^{3,4}, T. Hesjedal², O. Softwedel^{3,4}, T. Keller^{3,4}, S. Mühlbauer⁵, A. Chacon¹, C. Pfleiderer¹, P. Böni¹

1. Physik Department, Technischer Universität München, München, Germany

2. Clarendon Laboratory, Department of Physics, University of Oxford, United Kingdom

3. Max-Planck-Institut für Festkörperforschung, Stuttgart, Germany

4. Max-Planck-Society, Outstation at FRM II, München, Germany

5. Forschungsneutronenquelle Heinz Maier Leibnitz, Technische Universität München, München, Germany

The discovery of a regular arrangement of magnetic whirls in bulk samples of MnSi has drawn big interest in the scientific community and inspired new techniques for the study of uncommensurated magnetic structures. Due to their non-trivial topology these so called skyrmions may not be destroyed by smooth changes of the local magnetization and are great candidates for future magnetic storage technologies. Lately many experiments have been performed on thin samples of chiral crystals in the search of the skyrmion lattice, but the results have been inconclusive. New methods of probing thin samples for uncommensurated magnetic structures are needed. In this study we present the results of Grazing-incidence small-angle neutron scattering (GISANS) experiments on epitaxial thin films of MnSi and discuss the magnetic structure in our samples consisting of an out of plane helix in the context of the effects of uniaxial anisotropies and dimensionality.

Mo.H-P71 - Magnetic and dielectric properties of hexagonal ErFeO₃ thin film

H. Yokota¹, T. Nozue¹, M. Fukunaga², S. Nakamura^{3,4}, A. Fuwa⁵

1. Dept. of Phys., Chiba Univ., Chiba, Japan

2. Dept. of Phys., Okayama Univ., Okayama, Japan

3. Dept. of Science and Engineering, Teikyo Univ., Itabashi, Tokyo, Japan

4. Advance Research Center of Science and Engineering, Waseda Univ., Tokyo, Japan

5. Dept. of Science and Engineering, Waseda Univ., Tokyo, Japan

Hexagonal ErFeO₃ thin film was fabricated by using pulsed laser deposition method. X-ray diffraction measurement (XRD) confirmed that *c*-axis oriented ErFeO₃ thin film was obtained without impurity or secondary phases. Temperature dependences of lattice constant were measured by XRD and no structural phase transition was detected between 20K and 900K. Additionally, super lattice reflections were observed by XRD. This result indicated that the crystal structure is determined as non-centrosymmetric P6₃cm which suggests ErFeO₃ thin film is ferroelectric at room temperature. The double wave method also confirmed the ferroelectricity and the obtained spontaneous polarization is 90nC/cm² at room temperature. Static magnetic measurements were carried out by a magnetic property measurement system (MPMS). When the weak magnetic field was applied along the *c* axis of the thin film, temperature dependence of the magnetization showed thermal history blow 120K. Weak ferromagnetism was observed in this temperature range and the spontaneous magnetization was 0.14m_B/f.u. at 30K. Mossbauer spectroscopy was carried out with ⁵⁷Fe-enriched ErFeO₃ thin film deposited on Al₂O₃ (0001) substrate. The measurements were performed in transmission geometry using ⁵⁷Co-in Rh as the γ -ray source. The Doppler velocity was calibrated with an Fe metal foil measured at room temperature. The paramagnetic spectrum at room temperature consists of an asymmetric doublet. The isomer shift and the quadrupole splitting are 0.299 and 2.12mm/s, respectively, indicating that the Fe ions are in high spin Fe³⁺ state and located in the distorted pentahedral oxygen coordination. Below 120 K, the magnetically ordered spectra were observed. It suggests that the Fe³⁺ spin is inclined toward *c* axis from the *c* plane and it induces weak ferromagnetism.

Mo.H-P72 - Electronic and magnetic structures of vanadium phthalocyanine monolayer and multilayer films prepared on Ag(111)

K. Eguchi¹, T. Nakagawa², Y. Takagi², T. Yokoyama²

1. Nagoya University, Nagoya, Japan

2. Institute for Molecular Science, Okazaki, Japan

Up to the present, many kinds of metal phthalocyanines (MPcs) have been synthesized after the discovery of CuPc in 1927. In the 3d-transition-metal series, 3d-MPcs composed of a phthalocyanine ligand and a metal center have been synthesized for M = Ti, Cr-Zn, while the synthesis of ScPc and VPc have not been successful, because they are unstable under the atmospheric condition. To systematically understand the electronic states of the central metal, the synthesis of the whole series of the 3d-MPcs is strongly required. In this study, VPc was synthesized on a Ag substrate surface under an ultra-high vacuum (UHV) condition and the electronic and magnetic properties of VPc was investigated by x-ray photoelectron spectroscopy (XPS), x-ray absorption spectroscopy (XAS), and x-ray magnetic circular dichroism (XMCD). The VPc monolayer was fabricated by directly depositing the V atoms on an H2Pc monolayer under UHV conditions. The VPc multilayer was synthesized by repeated VPc monolayer deposition and subsequent sample annealing at approximately 450 K. The N 1s XPS of these samples showed a remarkable reduction in the peak assigned to H-bonded N atoms concomitant with the appearance of a new peak attributed to V-bonded N atoms close to the peak of iminic N. Additionally, the oxidation state of V estimated from the V 2p XPS peak position corresponded to 1.6 and 2.4 in the monolayer and multilayer samples, respectively. These results clearly imply that the VPc monolayer and multilayer were successfully obtained. The main ground state electronic configuration of the V center was found to be 2Eg by angle-dependent V L-edge XAS. The results of XMCD suggested that VPc shows a paramagnetic state on the Ag surface but an antiferromagnetic state in the multilayer.

Mo.H-P74 - Formation of $L1_0$ phase by rapid thermal annealing for sputtered FeNi thin films

M. Mizuguchi¹, T. Tashiro¹, K. Sato¹, T. Konno¹, K. Takanashi¹

1. Tohoku University, Sendai, Japan

Large uniaxial magnetic anisotropy materials are extremely promising for the application to high-density magnetic storage devices or permanent magnets. In particular, an $L1_0$ -ordered FePt alloy reveals extremely large magnetic anisotropy, therefore numerous studies on the fabrication of FePt films have been reported. However, it is an essential problem that Pt is a noble metal, thus development of a material revealing large magnetic anisotropy without any noble elements is strongly needed. In this paper, we successfully formed $L1_0$ -ordered FeNi phase, which is also known to show large magnetic anisotropy, by rapid thermal annealing (RTA) for sputtered films. Sputtering and RTA conditions were varied, and crystallographic and magnetic properties were precisely investigated. FeNi films with various thicknesses were prepared by co-deposition using magnetron sputtering on MgO(001) substrates at room temperature. After deposition, FeNi films were annealed in vacuum by using an RTA system with an infrared lamp. Crystallographic properties of films were investigated by x-ray diffraction (XRD) and transmission electron microscopy (TEM). Magnetic properties were characterized by a superconducting quantum interference device. Superlattice peaks indicating the $L1_0$ -ordered FeNi phase were observed in XRD patterns only for films with the RTA treatment. TEM observations in FeNi films with the RTA treatment also revealed the clear superlattice spots in transmission electron diffraction patterns. It was also found that $L1_0$ -formed areas were dispersed in FeNi layers. Magnetization curves also changed with the annealing temperature and the annealing time, which implied the successful formation of $L1_0$ -ordered FeNi. In addition, the enhancement of coercivity and remanent magnetization was observed associated with the appearance of $L1_0$ phase.

Mo.H-P75 - Strain-induced spin reorientation of bcc-like iron films grown on Cu(001)

E.C. Corredor^{1,2,3}, M. Ciria^{1,2}, J. I. Arnaudas^{2,3}, F. Lofink⁴, S. Rössler⁴, R. Frömter⁴, H. Oepen⁴

1. Instituto de Ciencia de Materiales de Aragón, Consejo Superior de Investigaciones Científicas

2. Departamento de Física de la Materia Condensada, Universidad de Zaragoza, Zaragoza, Spain

3. Instituto de Nanociencia de Aragón, Universidad de Zaragoza, Zaragoza, Spain

4. Institut für Angewandte Physik, Universität Hamburg, Hamburg, Germany

Magnetic properties are strongly influenced by the structure and the strain state of the material as is observed in Fe/Cu(001) epitaxial ultrathin films [1]. We address, using a microscopic approach, the question for the magnetization orientation within the transition regime from the onset of in-plane magnetization to the almost isotropic behavior with an effective magnetic easy axis parallel to the Cu <100> directions [2]. The in-plane orientation of the magnetization vector M in bcc-like Fe(110) films grown on Cu(001) by e-beam evaporation is determined, in situ, by means of scanning electron microscopy with polarization analysis (SEMPA)[3]. For thicknesses of 2 nm, slightly above the fcc/bcc phase transition, it is found that M is oriented along the <110> directions of the Cu(001) substrate. Following the Pitsch orientational relationship these correspond to magnetically hard <1-11> axes of bulk iron. This finding is in strong contrast to the behavior reported for thicker films (above 3 nm) of bcc Fe/Cu(001), where the <100> directions of the substrate are preferred. The magnetoelastic (ME) contribution to the magnetic anisotropy energy is discussed, inferring that the presence of a shear strain is mandatory to explain the spin reorientation. The shear strain in the Fe (110) plane is calculated utilizing results of previous He scattering experiments [4]. Using bulk ME constants, it is found that in each crystallite M deviates by 10 degrees from the bcc Fe <1-11> directions, which are collinear with the fcc Cu <110> axes. Hence, with four different structural variants, a fourfold effective magnetic anisotropy has to be expected.

[1] M. Wuttig, et al, Surf. Sci. 331-333 Part A, 659 (1995)

[2] R. Naik, et al., Phys. Rev. B 48, 1008 (1993)

[3] Edna C. Corredor et al., Phys Rev. B 90, 184410 (2014)

[4] T. Bernhard, et al Phys. Rev.Lett. 95, 087601 (2005)

Mo.H-P76 - Influence of elastically pinned domain walls on magnetization reversal in multiferroic heterostructures

A. Casiraghi¹, T. Rincón Domínguez¹, S. Rößler², K. Franke¹, S. Hämläinen¹, D. López González¹, R. Frömter², H. Peter Oepen², S. Van Dijken¹

1. *NanoSpin, Department of Applied Physics, Aalto University, Espoo, Finland*

2. *Universität Hamburg, Institut für Angewandte Physik, Hamburg, Germany*

Recent years have witnessed an increased interest in the study of magnetoelectric multiferroic systems [1], which represent a possible route towards electric-field control of magnetism. A promising approach exploits one-to-one domain correlations in elastically coupled ferroelectric and ferromagnetic systems [2]. In these multiferroic heterostructures, magnetic domain walls are firmly pinned on top of ferroelectric domain boundaries [2]. Here, we investigate the influence of pinned magnetic domain walls on the magnetization reversal process in a Co₄₀Fe₄₀B₂₀ wedge film (thickness up to 150 nm) that is elastically coupled to a ferroelectric BaTiO₃ substrate. We use magneto-optical Kerr microscopy to show that the magnetic field direction can be used for versatile switching between two distinctive magnetization reversal mechanisms, namely (1) double switching events involving every second stripe domain at a time or (2) synchronized switching of all domains. Furthermore, scaling of the switching fields with domain width and film thickness are also found to depend on field orientation. These results are explained by considering the dissimilar energies of the two types of pinned magnetic domain walls, magnetically charged or uncharged, that are formed in the system depending on whether the magnetic field is applied perpendicular or parallel to the stripe domains, respectively [3]. The local tunability of magnetic switching processes that can be attained in these fully correlated multiferroic heterostructures could be exploited as a platform to explore novel magnetic device concepts.

[1] M. Fiebig, *J. Phys. D: Appl. Phys.* 38 R123 (2005); W. Eerenstein, et al., *Nature* 442, 759 (2006); R. Ramesh and N.A. Spaldin, *Nat. Mater.* 6, 21 (2007)

[2] T.H.E. Lahtinen, et al., *Adv. Mater.* 23 3187 (2011)

[3] K.J.A. Franke, et al., *Phys. Rev. B* 85 094423 (2012)

Mo.H-P77 - Temperature dependence of magnon contribution to resistivity in permalloy thin films

V. Mohanan Parakkat¹, A. Roy¹, A. P.S. Kumar¹

1. IISc, Bengaluru, India

We investigate the contribution of thermally generated magnons towards the electrical resistivity of permalloy(Py) films by high field magnetoresistance(MR) measurements. In ferromagnets, the electrical resistivity contribution by the electron magnon scattering can be suppressed by application of high enough magnetic field. The temperature dependence of magnon contribution of resistivity in Py has not been previously reported in literature. Thin films of Py were grown by PLD (of thickness 17nm) and sputtering (of thickness 20nm) on thermally oxidized silicon. MR measurements on films were carried out by applying field in the direction of current i.e. in longitudinal geometry. The application of field in the plane of the films and along current direction minimizes the effect of anisotropic magnetoresistance; also it is easier to saturate these films in the plane than out of plane. A linear decrement of resistance at high field above the technical saturation (in plane saturation field of Py < 0.01T) of the ferromagnetic films, points towards the suppression of the resistivity arising from the spin flip scattering interaction mediated by thermal magnons. The high field (above 1Tesla) slope in the MR is measured as a function of temperature. This quantifies the contribution of magnonic part of resistivity in these films. Higher the temperature, larger is the contribution of magnons to resistivity, hence greater will be the slope. The high field MR measurement is a sensitive tool for probing the behavior of the ferromagnetic systems after its saturation when other direct magnetometric techniques fail to detect minute changes in magnetization. The value of the slope of MR at room temperature for both films are comparable to the value reported for Ni film grown by molecular beam epitaxy, which is possibly because Py is a Ni rich alloy (~81%).

Mo.H-P78 - Optical and Magneto-optical Spectroscopy of partially ordered Co₂MnSi

D. Kral¹, R. Silber², L. Beran¹, T. Kubota³, Y. Ando³, J. Pistora², M. Veis¹, J. Hamrle²

1. Charles University In Prague, Faculty of Mathematics And Physics, Prague Czech Republic

2. Department of Physics and Nanotechnology Centre, VSB - Technical University of Ostrava, Ostrava-Poruba, Czech Republic

3. Department of Applied Physics, Graduate School of Engineering, Tohoku University, Sendai, Japan.

In the last years Co₂-based Heusler compounds received considerable attention as they exhibit relatively high Currie temperature and spin polarization [1]. These properties make them promising candidates for applications in novel spintronic devices. However, their structural, magnetic, optical and electronic properties are strongly correlated making the structural disorder an important parameter to consider. Co₂MnSi Heusler compound can exhibit various types of ordering, such as B2 (ordered Co sublattices, and statistical occupation of the two other crystallographic sites by Mn and Si in Co₂MnSi) and L₂₁ ordering where the Mn and Si occupy distinct sublattices [2]. Therefore it is an ideal model structure to study as it exhibits transition from B2 to L₂₁ crystallographic ordering with increasing annealing temperature [3].

In this work, we present a systematic study of optical and magneto-optical properties of Co₂MnSi thin films with focus on different annealing temperatures. Spectroscopic ellipsometry as well as magneto-optical Kerr effect (MOKE) spectroscopy in linear and quadratic configurations were used as experimental techniques. Studied samples consisted of 30 nm thick Co₂MnSi layers epitaxially grown by inductively coupled plasma-assisted magnetron sputtering on a single MgO crystal substrate buffered with a 40 nm-thick Cr layer. The samples were capped with a 1.3 nm-thick Al layer. To achieve different degrees of crystallographic ordering, the samples were annealed at temperatures ranging from 300°C up to 500°C. Experimental data clearly showed differences in linear and quadratic MOKE spectra with different annealing temperatures suggesting an influence of L₂₁ ordering. For more detailed analysis, a spectral dependence of complete permittivity tensor was deduced from experimental data using advanced theoretical modeling.

[1] S. Wurmehl, et al., Appl. Phys. Lett. 88, 032503 (2006)

[2] S. Trudel, et al., J. Phys. D: Appl. Phys. 43, 193001 (2010)

[3] O. Gaier, et al., J. Appl. Phys. 103, 103910 (2008)

Mo.H-P79 - Crystal structure changes and interfacial mixing in Co/Si thin films investigated by Ferromagnetic Nuclear Resonance

Y. Shin^{1,2}, A. Tuan Duong³, S. Cho³, C. Meny^{1,2}

1. *Institut de Physique et Chimie des Materiaux de Strasbourg (IPCMS), UMR 7504 CNRS-University of Strasbourg, Strasbourg Cedex 02, France*

2. *Department of Physics, CNRS-Ewha International Research Center, Ewha Womans University, Seoul, South Korea*

3. *Department of Physics and Energy Harvest Storage Research Center, University of Ulsan, Ulsan, South Korea*

The deposition of Co layers on Si substrates and their reactions with Si are important issues in modern microelectronics technology. Indeed the interface between metal and semiconductor determines the device performance. In this work, Co films were grown on Si(001) and Si(111) substrates with a temperature range from room temperature to 500 °C. For investigating the Co structure inside the films and the formation of Co silicide at their interfaces, we performed ⁵⁹Co Ferromagnetic Nuclear Resonance (Nuclear Magnetic Resonance in ferromagnets, FNR) measurements. We have observed that the dominant phase of Co was changed from hcp to fcc as the growth temperatures increase from room temperature to 300 °C. Surprisingly the detail study of the FNR measurements versus the deposition temperature shows that the diffusion process does not follow a monotonous behavior. This seems to be related to the ratio of fcc and hcp Co. The formation of fcc Co seems to limit the amount of intermixing at the Co/Si interface for both growth direction. No FNR signals were obtained for the films prepared above 400 °C, since the elements of the substrates are diffusing into the Co layer up to the top of the surfaces. The structural properties of the samples will be compared to their transport properties.

Mo.H-P80 - Multifunctional Fe-Au heterogeneous thin-films

A. Conde-Rubio¹, M. Kovylna¹, A. Labarta¹, X. Batlle¹

1. Dept. Física Fonamental, Universitat de Barcelona and Institut de Nanociència i Nanotecnologia, Barcelona, Spain

Fe-Au heterogeneous thin-films have been deposited by radio frequency (RF) magnetron sputtering [1]. Nanostructural characterization, including transmission and electron microscopy, atomic and magnetic force microscopy and quantitative nanomechanical measurements, shows the granular nature of the thin films, while interferometric measurements reveal a well controlled surface roughness on the order of a few nanometers. Magnetic and optical properties are of special interest for the implementation of these compounds in the fabrication of multifunctional nanoparticles for biological applications such as hyperthermia treatments, magnetic resonance imaging enhancement, sensors, guided drug delivery to tumour cells etc [2]. By changing the Fe/Au composition, the RF power and the deposition time, a transition from superparamagnetism to ferromagnetic-like behavior can be observed in both magnetization and magnetoresistance measurements. In particular, superparamagnetism is present at room temperature in those alloys with lower Fe content, giving rise to giant magnetoresistance with non hysteretical behaviour. The absence of remanence should prevent particle agglomeration from magnetic interactions, which is one of the main drawbacks for bioapplications. Optical measurements revealed a maximum in the absorbance coming from the Au. This peak in the optical absorbance makes them suitable as a starting material for the fabrication of Fe-Au nanoparticles with an appropriate optical response for biological applications. By changing the size, shape and embedding medium the maximum absorbance region could be shifted to the near infrared, where biological tissue has high transmittivity. The financial support of the Spanish MINECO MAT2012-33037 and Catalan DURSI 2009SGR856 projects and the European Union FEDER funds (Una manera de hacer Europa) are acknowledged. A. Conde-Rubio acknowledges Spanish MINECO for a Ph.D. contract (BES-2013-065377).

[1] X. Batlle and A. Labarta, J. Phys. D: Appl. Phys. 35 (2002) R15-R42

[2] P. Tartaj et al., J. Phys. D: Appl. Phys. 36, (2003) R182-R197

Mo.H-P81 - Scanning SQUID-on-tip microscopy with single spin sensitivity for the study of magnetic materials

E. Lachman¹, Y. Anahory¹, N. Hoovinakatte¹, J. Cuppens², A. Young³, Y. Myasoedov¹, M. Huber⁴, E. Zeldov¹

1. *Department of Condensed Matter Physics, Weizmann Institute of Science, Rehovot, Israel*

2. *Physics and engineering of Nano-devices group, Institut Catala de Nanotecnologia, Cerdanyola, Barcelona, Spain*

3. *Department of Physics, UC Santa Barbara, Santa Barbara, United States*

4. *University of Colorado, Denver, United States*

We present a nano SQUID-On-Tip (SOT) based scanning microscope for the study of magnetic materials. The self-aligned method allows fabrication of SQUIDs residing on the edge of a sharp pipette with diameter down to 50 nm. As a result high spatial resolution of 50 nm, and spin sensitivity of 0.38 Bohr magneton is achieved, which is about two orders of magnitude more sensitive than any SQUID reported to date. The Scanning SOT Microscope (SSM) integrates the SOT into a scanning system operating at 3He temperatures (300mK) - a temperature which enables the use of different SOT materials such as Al, In and Pb. The low temperature and the SOT's unique geometry enable us to scan at high fields: 0.3T for Al and In, and as high as 2T for the Pb SOT's which is about three orders of magnitude above the typical Scanning SQUID. We will show that the use of scanning SQUID-On-Tip microscopy can unveil new physics in the field of magnetism and current distribution at the nano scale. As an example of such a study, results from imaging the surface magnetization of magnetically doped topological insulators will be presented. These measurements demonstrate the unique ability of the SOT to have sub-Gauss sensitivity at high fields.

References: D. Vasyukov, Y. Anahory et al. Nature Nanotech. 8 639 (2013) Finkler, A. et al. Rev. Sci. Instrum. 83, 073702 (2012)

Mo.H-P82 - Magnetic properties changes in ion beam irradiated Fe/Pt multilayers

A. Marynowska¹, A. Petrouchik¹, A. Wawro¹, S. Lewińska¹, A. Slawska-Waniewska¹, E. Dynowska¹, R. Böttger², J. Fassbender², L. Tomasz Baczewski¹

1. Institute of Physics Polish Academy of Sciences, Warsaw, Poland

2. Helmholtz Zentrum Dresden-Rossendorf, Dresden, Germany

L1₀ FePt alloys are promising candidates for future applications as high density recording media or as magnonic crystals due to its high magnetic anisotropy up to 7.0×10^7 ergs/cm². L1₀ FePt is often fabricated by post-annealing of Fe/Pt multilayers which allows switching of magnetization easy axis from in-plane (multilayers) to out-of-plane (L1₀ alloy) direction. As an alternative method of controlling magnetization easy axis direction and simultaneously allowing patterning we applied ion beam irradiation of Fe/Pt multilayers in order to create L1₀ phase in intermixed region.

Changes of magnetic properties of irradiated Fe/Pt multilayers were studied in order to verify a possibility of L1₀ structure formation in the intermixed regions. Six series of Fe/Pt multilayers of different bilayer thickness and total number of bilayers were grown using MBE and subsequently irradiated with Ne⁺ ions of different energies and doses (10^{14} - 10^{16} ions/cm²) evaluated *a priori* with TRIDYN simulations. RHEED, LEED and STM *in-situ* measurements and *ex-situ* XRD revealed epitaxial growth and good quality of interfaces. All as grown multilayers showed in-plane magnetization easy axis as revealed by VSM M(H) measurements.

Full switching of magnetization easy axis from in-plane to out-of-plane direction was not achieved after ion irradiation but certain amount of perpendicularly magnetized phase appeared in most of irradiated samples. XRD spectra measured after irradiation revealed structural changes in multilayers responsible for modification of magnetic properties. Simultaneously extremely interesting effect of quasi-oscillating changes of magnetic properties such as remanence and coercivity in the out-of-plane direction of the applied magnetic field with increasing ion dose was found in some series of samples.

Mo.H-P83 - Interplay between interparticle interactions and particles' anisotropy in magnetic granular multilayers

M. Vasilakaki¹, G. Margaris¹, K. Trohidou¹, J. Balogh², L. Kiss²

1. *Institute of Nanoscience Nanotechnology, NCSR "Demokritos", Athens, Greece*

2. *Institute for Solid State Physics and Optics, Wigner RCP HAS, Budapest, Hungary*

The role of the interplay between interparticle interactions and magnetic anisotropy on the magnetic behavior of Fe/Ag multilayers has been studied for two different morphologies of the Fe grains inside the layers, using the Monte Carlo simulations technique¹. The simulations have been performed for heterostructures with 2, 3, 5 and 10 granular Fe layers.

The Zero Field Cooled (ZFC) magnetization curves for different values of the in plane applied field have been calculated with dominant the in plane anisotropy axes orientation². Our simulations showed that the strong competition between the anisotropy and the interparticle interactions in the granular multilayers with non-uniform Fe particle distribution inside the layers because of the in plane frustration of the nanoparticles moments coupling, results in higher blocking temperatures than those of a uniform system. The observed decrease of the blocking temperature with the cooling field for all these heterostructures is attributed to the fact that as the cooling field increases it masks the competition between the in plane and the out of plane interactions³. This effect is stronger in the monolayers and bilayers and weaker in multilayers because of the in plane field orientation.

[1] G. Margaris, K. N. Trohidou, V. Iannotti, G. Ausanio, L. Lanotte, and D. Fiorani, PRB 86, 214425 (2012)

[2] J. Balogh, Cs. Fetzler, D. Kaptás, L. F. Kiss, I. S. Szucs, I. Dézsi and I. Vincze, phys. stat. sol (a) 205,1828-1830 (2008)

[3] M. Knobel , W.C. Nunes , H. Winnischofer , T.C.R. Rocha ,L.M. Socolovsky , C.L. Mayorga b, D. Zanchet Journal of Non-Crystalline Solids 353, 743–747 (2007)

Mo.H-P84 - Cationic distribution and anomalous magnetic properties of epitaxial CoFe_2O_4 thin films probed by x-ray magnetic circular dichroism

V. Hari Babu¹, P. Gargiani¹, M. Valvidares¹, E. Pellegrin¹, F. Sánchez², G. Herranz², J. Fontcuberta²

1. ALBA Synchrotron Light Source, Cerdanyola del Vallès, Barcelona, Spain

2. Institut de Ciència de Materials de Barcelona (ICMAB-CSIC), Campus UAB, Bellaterra, Barcelona, Spain

Investigation of the epitaxial thin films made of insulating ferromagnets (e.g., cobalt-ferrites) has received a renewed attention due to their central role in spintronic devices involving the spin Hall effect [1]. The spin magnetoresistance (SMR) is generally known to depend upon the film orientation and consequently the chemical nature of the exposed film surface. Among other recent works on cobalt ferrite films [2], we report on the cationic distribution due to the fact that the SMR is mainly controlled by the interface orbital magnetic moments.

We have fabricated epitaxial CoFe_2O_4 (CFO) films on $\text{SrTiO}_3(001)$ and $\text{SrTiO}_3(111)$ substrates with different thicknesses (2-48 nm) by pulsed laser deposition. We employed x-ray absorption spectroscopy to investigate the electronic charge distribution and element-specific x-ray magnetic circular dichroism (XMCD) to unravel the spin and orbital magnetic moments of Fe/Co ions and their site occupancy. With the decreasing film thickness, the CFO films exhibit non-saturation in the magnetization and reduced magnetic moments. For example, 14 nm thick CFO films exhibit a net moment of $1.34 \mu_B/\text{f.u.}$ which is smaller than the bulk moment ($3 \mu_B/\text{f.u.}$). Spectral fingerprinting in the XMCD data reveal the presence of $\text{Co}^{2+}(T_d)$ (20% of Co) and $\text{Fe}^{2+}(O_h)$ cations, resulting in the smaller macroscopic moment by the interplay of reduced Fe^{2+} moments and the modified ferrimagnetic alignment in the partially inverse spinel structure. The CFO films exhibit anomalous magnetic properties, including a two-step magnetization reversal and a reduced coercivity with the film thickness. The site-dependent Fe/Co XMCD hysteresis loops hint at the existence of antiphase boundaries by exhibiting a non-saturation at higher magnetic fields. Our results show that the small changes in the cation ordering lead to significant changes in the magnetic properties.

[1] Isasa, *et al.*, Appl. Phys. Lett. 105, 142402 (2014)

[2] Moyer, *et al.*, Phys. Rev. B 84, 054447 (2011)

Mo.H-P85 - Magnetic properties of surfactant assisted grown ultrathin Cr films on Fe(001)

A. Brambilla¹, A. Picone¹, A. Calloni¹, G. Berti¹, M. Riva¹, G. Bussetti¹, M. Finazzi¹, L. Du¹, F. Ciccacci¹

1. Dipartimento Di Fisica, Politecnico Di Milano, Milan, Italy

Interfaces between ferromagnetic and antiferromagnetic materials are widely investigated systems, characterized in particular by interesting magnetic phenomena such as exchange bias. The case of the Cr/Fe interface is of particular relevance, due to the well-known mediating role of thin Cr films in exchange coupled superlattices and in GMR multilayers [1]. The Cr/Fe(001) system was extensively studied in the past (see e.g. Refs. 1,2), particularly by focusing on the surface morphology and on the chemical interactions occurring at the interfaces. By scanning tunneling microscopy (STM) and low-energy electron diffraction (LEED) [3], we have shown that a sharp Cr/Fe interface can be obtained through growth on the pre-oxidized Fe(001)-p(1x1)O surface, with different resulting configurations at different growth temperatures. In particular, at 300 °C a single layer of chromium oxide has been stabilized on the Fe(001) surface. We discuss the magnetic properties of such ultrathin Cr structures on Fe(001) as investigated by means of X-ray Magnetic Circular Dichroism (XMCD) and by Spin-Polarized PhotoEmission Spectroscopy (SPES). The monolayer-range Cr oxide films show an antiparallel coupling with respect to the underlying Fe substrate [4]. When the thickness is increased, SPES provides evidence of the immediate onset of an antiferromagnetic stacking of the magnetization of Cr (001) atomic layers right from the Cr/Fe(001) interface, in contrast with previous experiments, in which the stacking was observed to begin after a few monolayers, the delay being ascribed to chemical alloying at the interface [2]. These results are particularly interesting in view of embedding such a controlled interface in low-dimensional magnetic devices.

[1] J. Bland, B. Heinrich, Ultrathin Magnetic Structures, Springer, 1994

[2] J. Unguris et al., Phys. Rev. Lett. 69 (1992) 1125

[3] A. Picone, et al., Phys. Rev. B 81, 115450 (2010)

[4] A. Brambilla et al., J. Appl. Phys. 114, 123905 (2013)

Mo.H-P86 - Geometrical effects on Barkhausen noise in a thin film

A. Roy¹, A. P. S. Kumar¹

1. Indian Institute of Science, Karnataka, India

All nucleation models of Barkhausen noise exhibit a crossover from non-universal to universal avalanche statistics as the magnitude of the quenched disorder crosses the critical disorder RC . The universal region is characterized by power law distributions of avalanche sizes, durations and power spectra, each characterized by a critical exponent, which is characteristic to the universality class to which the system belongs. Below RC , critical scaling properties break down and extrinsic features depending on the disorder magnitude, system size etc., dominate the size distributions. We have observed, for the first time, a crossover from universal to non-universal behaviour in the same sample by changing the measurement configuration. Our system consists of thin films of Fe grown by PLD on GaAs(001) substrates under UHV. Barkhausen noise was measured through planar Hall effect on 100 μ m wide Hall bars fabricated from these films. The external field was rotated out of plane of the sample and angular dependence was recorded. It was seen that the avalanche size distributions were non-universal when the applied field was in plane or close to it, with characteristic finite-size features. When the field was rotated significantly out-of plane, the size distribution changed to universal, with the power-law exponent approaching critical exponent values found in the literature. This phenomenon was remarkable as both the types of distributions were exhibited by the same samples without any change in the defect concentration. A nucleation model described as a Random Anisotropy Ising model has been employed to shed some light on this strange phenomenon. Simulations of the model have shown that it exhibits an identical sub-critical to critical transition as the angle between the external field and the anisotropy direction is increased. Our observations are explained in the light of this model assisted by micromagnetic simulations.

Mo.H-P87 - Suppression of Barkhausen noise mediated by collapse of the domain state due to strong inter-layer exchange bias

A. Roy¹, V. P. Mohanan¹, A. P. S. Kumar¹

1. Indian Institute of Science, Karnataka, India

We discuss the effects of interlayer exchange coupling on the magnetization reversal of a thin ferromagnetic films grown by pulsed laser ablation under UHV. In particular, we observe a change in the reversal mode of Fe upon exchange biasing with antiferromagnetic FeMn. Reversal mechanism was studied by measuring Planar Hall effect on Hall bars fabricated out of the thin films, as well as by MOKE magnetometry. In the first case, 15nm thick Fe films capped with 5nm of Au on GaAs was studied. The hysteresis showed magnetization reversal by domain wall motion characterized by discrete steps in the magnetic signal. Statistics of the jumps recorded by both the methods, showed a power law distribution, with an exponent ~ 2.5 . Apart from confirming the presence of Barkhausen noise, this measurement indicated a sample with very low disorder, due to the value of the exponent > 1.5 characteristic of a sub-critical disorder level. In the second case, a sample GaAs-Fe(15nm)-FeMn(15nm)-Au(5nm) was studied. Magnetization reversal was characterized by smooth continuous M-H curves reminiscent of rotation mode of reversal. Exchange bias was measured by 2 methods. Planar Hall effect gave an exchange bias of ~ 13 Oe. In this case Barkhausen noise was absent. The observation may be understood by considering a strong exchange coupling between the Fe-FeMn layers. Strong exchange coupling implies that when a domain wall is created in the ferromagnetic layer, a corresponding wall is created in the AF layer also. In order to create a domain wall in FeMn, an additional energy cost due to the exchange energy of FeMn is required for domain wall formation. In the first sample the cost of domain formation was lower than the magnetocrystalline energy barrier to rotation whereas in the second case, the additional energy requirement offset the energy balance in favor of the rotation mode.

Mo.H-P88 - Atomistic studies of domain wall dynamics in Co/Ni multilayers interfaced with heavy metal layers

J. Chico¹, K. Koumouras¹, O. Eriksson¹, L. Bergqvist², A. Bergman¹

1. Department of Physics And Astronomy, Uppsala University, Uppsala, Sweden

2. Department of Nano and Materials Physics, Royal Institute of Technology (KTH), Stockholm, Sweden

Materials with perpendicular magnetic anisotropy (PMA) are great candidates for spintronic applications where domain wall motion is a key ingredient. Experimental observations^{1,2} on Co/Ni multilayers interfaced with heavy metals such as Pt indicate that the contributions from Dzyaloshinskii-Moriya interactions (DMI) and the Spin Hall Effect (SHE) can here lead to domain wall speeds higher than the ones expected from the conventional spin transfer torque (STT). Given the narrow domain walls typically present in these PMA materials, electronic structure calculations and an atomistic description of their dynamics can give valuable insights in the underlying mechanisms that determine the domain wall velocities. In the present work the influence of the DMI and the SHE on the domain wall dynamics is studied by a combination of first principle methods and atomistic spin dynamics simulations. The chosen systems are Co/Ni multilayers on top of underlayers of Pt, Pd, Ir and Au, which are chosen for their high spin orbit coupling and to facilitate comparison with experiments. We have characterized magnetic properties such as interatomic exchange interactions, magnetocrystalline anisotropy, and damping by means of first-principles electronic structure calculations and based on these parameters we have then performed atomistic Landau-Lifshitz-Gilbert-Slonczewski based simulations on the dynamics of domain walls present in the materials. As experimentally observed, we find that the DMI stabilizes a Néel domain wall instead of a Bloch wall and that the choice of interfacing metal strongly determines the velocities of the domain walls.

Mo.H-P89 - Heusler ferrimagnetic multilayers with a perpendicular magnetic anisotropyQ. Ma¹, X. Zhang¹, T. Miyazaki¹, S. Mizukami¹

1. WPI-AIMR, Tohoku Univ., Sendai, Japan

One of the issues in spintronics is to explore magnetic materials exhibiting a large perpendicular magnetic anisotropy (PMA), small magnetization, and small Gilbert damping for applications, such as spin-transfer-torque magnetic random access memory [1,2]. There are many ordered alloys exhibiting large PMA, e.g., FePt, whereas those also have large saturation magnetizations [3]. Thus it is meaningful to investigate another class of magnetic materials. In this study we investigate a Heusler-based ferrimagnetic multilayers (MLs) with PMA. The MLs consist of a tetragonal ordered compound Mn-Ga and cubic Heusler alloy Co₂FeAl (CFA), which have a strong uniaxial and weak magnetic anisotropy, respectively, and the both materials exhibit low Gilbert damping constants [4, 5]. Because of antiferromagnetic coupling at the MnGa/CFA interface [6], the MLs may exhibit artificial ferrimagnetism. The epitaxial MLs were grown by a sputtering method. By changing each layer thickness, the MLs exhibited widely tunable magnetic properties with the respective magnetization and the effective PMA constant varying from ~ 0 to 400 emu/cm³ and from -2 (in-plane magnetization) to 8 Merg/cm³ (out-of-plane magnetization). The coercivity values for the out-of-plane magnetized MLs increased up to 15 kOe, corresponding to the compensation of magnetization for MLs. These properties are suitable for spin-transfer-torque applications [7].

This work is partially supported by KAKENHI (No. 24686001), Asahi Glass Foundation, and ASPIMATT (JST).

[1] H. Yoda et al., *Curr. Appl. Phys.*, 10, e87 (2010)

[2] K. Yamada et al., *Appl. Phys. Lett.*, 106, 042402 (2015)

[3] D. Weller et al., *IEEE Trans. Magn.* 36, 10 (2000)

[4] S. Mizukami et al., *Phys. Rev. Lett.*, 106, 117201 (2011)

[5] S. Mizukami et al., *J. Appl. Phys.*, 105, 07D306 (2009)

[6] Q. L. Ma et al., *J. Appl. Phys.*, 116, 233904 (2014)

[7] Q. L. Ma et al., *Sci. Rep.* 5, 7863 (2015)

Mo.H-P90 - Magneto-structural characterization and local probing of inhomogeneity effects on NI-MN-GA thin films

M. Pereira¹, L. Gomes¹, J. Amaral¹, N. Silva¹, A. Lourenço¹, V. Amaral¹

1. Department of Physics and CICECO, University of Aveiro, Aveiro, Portugal,

Ni₂MnGa is a ferromagnetic-shape-memory alloy with properties that show great potential for applications, especially in thin film form. Ni₂MnGa thin films were simultaneously deposited by UHV-magnetron-RF sputtering at 400 C on Si, Al₂O₃, MgO and SrTiO₃ substrates. Thicknesses between 10 and 160nm were obtained. Structural properties studied by XRD and microscopy techniques revealed low crystallinity and growing contribution of the martensitic phase as film thickness increase. Magnetic measurements by VSM and SQUID of magnetization vs magnetic field at 300K revealed ferromagnetic behavior with saturation magnetization ranging from 30 to 200 emu/cm³. Magnetization vs temperature measurements showed no sign of the martensitic transformation between 5K and 380K. Curie temperatures (TC) of the films increase with Ni content, as expected. There is no dependence of TC on the thickness of films deposited on MgO. For 20nm thick films, TC values vary according to the substrate. For 160nm thick films, TC remains the same for all substrates. The resistance versus temperature (R-T) curves obtained by the four-point method showed an abnormal initial thermal hysteresis and changes that suggest dependency on temporal effects as well as on structural effects. The R-T measurements under an external applied magnetic field showed an expected displacement of the structural transition. Scanning Probe Microscopy measurements at different temperatures show that different areas of the sample do not undergo the martensitic transformation simultaneously which is consistent with R-T results and may originate from compositional inhomogeneity. The use of Scanning Thermal Microscopy allows a local approach to the study of structural transition temperatures in these films. It consists in externally assisting the thermal nano-probe to induce local structural transitions while measuring the temperature at which changes on the morphology of the surface signal the structural transformation.

Mo.H-P91 - Tailoring of Gilbert damping constant and magnetic anisotropy of $\text{Co}_{20}\text{Fe}_{60}\text{B}_{20}$ thin films by excess Cobalt incorporationD. Jhahria¹, D. K. Pandya¹, S. Chaudhary¹*1. Thin Film Laboratory, Physics Department, Indian Institute of Technology Delhi, Delhi, India*

Spintronics based microwave devices and switching current density in spin transfer torque based applications are sensitive to damping constant α and magnetic anisotropy H_k . In this regard, we have co-sputtered the $\text{Co}_{20}\text{Fe}_{60}\text{B}_{20}$ and Co targets to bring systematic changes in the film-composition and film-stress which would lead to tuning of α and H_k as per the need of the device application. The amorphous CoFeB (30nm) thin films were co-sputter deposited with constant power of 120 W supplied to the $\text{Co}_{20}\text{Fe}_{60}\text{B}_{20}$ target and the Co target power was varied from 0-70 W to prepare Co-00, 30, 40, 50, 60 and 70 samples. The relative Fe/Co concentration ratio determined from EDAX decreased from 2.9 to 1.0. Owing to co-sputtering from CoFeB and Co targets, the Boron concentration is expected to decrease in the films. Magneto-optical Kerr effect (MOKE) measurement showed monotonous decrease in coercivity H_c from 23 Oe in Co-00 ($\text{Co}_{20}\text{Fe}_{60}\text{B}_{20}$) films to 11 Oe in Co-50 ($\text{Co}_{34}\text{Fe}_{50}\text{B}_{16}$) films followed by a small rise thereafter. The Co-00 film exhibited highest anisotropy field $H_{k\text{-static}}$ of 170 Oe which is generally attributed to high anisotropic stress. In Co-50 co-sputtered film it drops down to 70 Oe and slightly increases thereafter like H_c . The observed ferromagnetic resonance (FMR) spectra (5-12 GHz) of all the films were fitted based on Landau-Lifshitz-Gilbert (LLG) equation. Results showed that the dynamic anisotropy $H_{k\text{-dynamic}}$ mimics $H_{k\text{-static}}$. The α damping parameter also followed similar behavior as that of H_k , with minimum value of 0.0045 ± 0.00008 in Co-50 film compared to the highest value of $\alpha = 0.0084 \pm 0.00009$ in the Co-00 film. This interrelationship of α and H_k can be understood from grain boundary-two magnon scattering model. We thus establish a systematic correlation and tuning of H_c , H_k and α on excess Co addition in this technologically important $\text{Co}_{20}\text{Fe}_{60}\text{B}_{20}$ alloy system.

Mo.H-P92 - Influence of substituting Te for S on magnetization of EuS thin films

S. Senba¹, Y. Ueda², R. Kakimaru², S. Sakawaki², H. Asada², K. Kishimoto², T. Koyanagi²

1. Department of Electrical Engineering, National Institute of Technology, Ube College, Ube, Japan

2. Department of Electronic Devices Engineering, Graduate School of Science and Engineering, Yamaguchi University, Yamaguchi, Japan

Physical characteristics such as magnetic, optical, and electronic properties of europium chalcogenides have been studied extensively. Recently, EuS thin film has received much attention in fundamental studies of spin injection devices. In this study, we have investigated influence of partially substituting Te for S on epitaxial growth and magnetization of EuS thin films in order to manipulate the magnetic properties. We have successfully grown EuS_{1-x}Te_x (100) epitaxial films on InP (100) substrates using molecular beam epitaxy at substrate temperatures from 180 to 250°C. The result of roughness average (Ra) value measured by AFM indicates that smooth surface is obtained at around 200°C. The full width at half-maximum (FWHM) of the x-ray diffraction peak decreases with increasing of Te composition x and becomes smaller around x=0.2. Magnetization curves of all samples obtained by using a SQUID magnetometer shows clear hysteresis behaviors, implying the well-defined ferromagnetism. Substituting effect on a coercive force is relatively small, although Curie temperature of EuS_{1-x}Te_x films decreases with the increase of x. The ferromagnetic order would be weakened due to the antiferromagnetic exchange interaction induced by Te substitution.

Mo.H-P94 - Structural and magnetic properties of (ultra)thin LaSrMnO films

G. Varvaro¹, P. Graziosi², L. Del Bianco^{1,3}, A. Maria Testa¹, M. Calbucci², I. Bergenti², F. Liscio⁴, S. Milita⁴, V. Alek Dediu²

1. *Istituto Di Struttura Della Materia, CNR, Monterotondo Scalo (Roma), Italy*
2. *Istituto per lo Studio dei Materiali Nanostrutturati, CNR, Bologna, Italy*
3. *Dipartimento di Fisica e Astronomia, Università di Bologna, Bologna, Italy*
4. *Istituto per la Microelettronica e i Microsistemi, CNR, Bologna, Italy*

Ferromagnetic metallic manganites are employed as prototypical spin injectors in several systems in order to reveal insights in a variety of spin related effects [1,2]. In particular, the La_{0.7}Sr_{0.3}MnO₃ (LSMO) compound has stimulated an intense study since, in bulk form, it has one of the highest ferromagnetic transition temperature $T_c = 370$ K. Understanding and controlling the morpho-structural and magnetic properties of LSMO films as a function of thickness is crucial for realizing applications that commonly demand for ultrathin layers. For this purpose, LSMO films in the thickness range of 4 - 16 nm were deposited on single-crystal (001) SrTiO₃ substrates by means of channel spark ablation [3]. The temperature and angular dependence of the magnetic properties were studied by a vector Vibrating Sample Magnetometer, in conjunction to structural and morphological results. Even the thinnest sample shows ferromagnetism ($T_c = 250$ K) and T_c enhances with increasing t_h , reaching a value of about 315 K for $t_h = 16$ nm. This gradual approach towards the ferromagnetic properties of bulk LSMO follows a strain driven trend from fully strained films with weakened magnetism towards robust magnetism with a sudden change at about 6 nm. Moreover, with increasing the temperature from 100 K up to 300 K, a change of the magnetic anisotropy from a biaxial to a dominant uniaxial symmetry was clearly observed in all the films. Such a behaviour - probably related to a crossover from a low-temperature regime, where crystalline anisotropy dominates, to a high-temperature one, governed by magnetoelastic anisotropy - occurs progressively, with a substantial isotropic behaviour actually existing in a narrow temperature range.

[1] M. Bowen et al. *J. Phys.: Condens. Matter* 19 (2007) 315208

[2] I. Bergenti et al., *Philos. Trans. R. Soc. A* 369 (2011) 3054

[3] P. Graziosi et al., *Thin Solid Films* 534 (2013) 83

Mo.H-P95 - Onset of in-plane ferromagnetism and magnetic anisotropy of MBE-deposited Fe films on MOCVD GaN(0001)

J. Kim¹, A. Ionescu¹, R. Mansell¹, J. Cooper², N. Steinke², C. Kinane², S. Langridge², F. Oehler³, C. Barnes¹

1. *Thin Film Magnetism Group, Cavendish Laboratory, University of Cambridge, Cambridge, United Kingdom*

2. *ISIS, Rutherford Appleton Laboratory, Chilton, Didcot, Oxfordshire, United Kingdom*

3. *Department of Materials Science and Metallurgy, University of Cambridge, United Kingdom*

Fe/GaN heterostructures – a sister material system to the much-studied Fe/GaAs structures – provide excellent test grounds for future spintronic devices thanks to long spin lifetimes predicted in GaN [1] and the high thermal stability of the Fe/GaN interface [2]. Previous studies of Fe growth on GaN(0001) substrates demonstrated triple-domain Fe(110) growth [3] and six-fold magnetic anisotropy for Fe films with 5 – 70 nm thickness [4]. However, magnetic properties of ultra-thin (< 5nm) Fe films and the effect of the Fe/GaN interface remain a topic of active research.

In this work, thin Fe films with thickness between 1 and 10 nm were deposited by molecular beam epitaxy at room temperature (RT) on metal-organic chemical vapour deposited GaN(0001) substrates. *In-situ* reflecting high-energy electron diffraction patterns of GaN and Fe surfaces demonstrated a three-dimensional Fe growth up to 1 nm, and the doubling of Fe 1 x 1 streaks indicated Nishiyama-Wasserman (α -Fe (110) <001> // GaN (0001) <11-20>) and Kurdjumov-Sachs (α -Fe (110) <1-1-1> // GaN (0001) <11-20>) orientation relations as possible growth modes. Out-of-plane X-ray diffraction confirmed Fe(110) growth with estimated Fe domain sizes of around 20 nm. A linear relationship was observed between the saturation magnetisation per unit area and the Fe thickness, whose extrapolation suggested an onset of Fe in-plane ferromagnetism at around 0.6 nm (4 monolayers). Coercive fields measured along the *a*-axes (<11-20>) of GaN(0001) were found to increase from around 5 Oe at 1 nm to around 20 Oe at 10 nm at RT. Angular remanence measurements suggested dominant uniaxial magnetic anisotropy for Fe films thinner than 2.5 nm. For thicker films, signs of hexagonal anisotropies were observed with magnetic easy axes aligned with *m*-axes (<1-100>) of GaN(0001). This study of the magnetic properties of Fe thin films will be crucial in designing and processing future Fe/GaN diodes and transistors.

[1] S. Krishnamurthy *et al.*, Appl. Phys. Lett. 83, 1761 (2003)

[2] C. Gao *et al.*, Appl. Phys. Lett. 95, 111906 (2009)

[3] C. Gao *et al.*, Phys. Rev. B 82, 125415 (2010)

[4] R. Meijers *et al.*, Journal of Crystal Growth 283 500-507 (2005)

Mo.H-P96 - Structural and magnetic properties of epitaxial Fe/MgO/GaN(0001) heterostructures deposited by molecular beam epitaxy

N. Khalid^{1,2}, J. Kim¹, A. Ionescu¹, F. Oehler³, I. Farrer¹, R. Ahmad², T. Hussain⁴, C. Barnes¹

1. Cavendish Laboratory, University of Cambridge, Cambridge, United Kingdom

2. Department of Physics, Government College University, Lahore, Pakistan

3. Department of Materials Science and Metallurgy, University of Cambridge, United Kingdom

4. Centre for Advanced Studies in Physics, Government College University, Lahore, Pakistan

Ferromagnetic metal/semiconductor heterostructures with an oxide tunnelling-barrier in between have important technological implications in the context of spin-transport electronics [1,2]. Combining the spin-filtering properties of MgO [3] with the low spin-orbit interaction and subsequent long spin lifetime of GaN [4] makes such heterostructures promising candidates for spintronics research. In this paper, we studied the structural and magnetic properties of fully epitaxial Fe(110)/MgO(110)/GaN(0001) tunnel barrier structures grown by molecular beam epitaxy. The out-of-plane X-ray diffraction spectra showed an epitaxial Fe (110) film, while reflective high energy electron diffraction images confirmed the epitaxial growth of Fe(110) on top of epitaxial MgO(110) on GaN(0001). X-ray reflectivity measurements confirmed relatively smooth interfaces with roughness of approximately 0.3 nm and 0.7 nm for the MgO/GaN and Fe/MgO interfaces, respectively. In-situ magneto-optic Kerr effect measurements on Fe films indicated signs of ferromagnetism from as early as 1 nm at room temperature and demonstrated a rise in the coercive fields with increasing thickness. Angular remanence measurements on 5 nm Fe film displayed a strong uniaxial magnetic anisotropy with a weak cubic contribution, in contrast to the hexagonal anisotropy exhibited in the Fe(110)/GaN(0001) system [5]. This study of Fe/MgO/GaN system is expected to contribute in designing future GaN-based diodes and transistors.

[1] S. Datta and B. Das, Applied Physics Letters 56, 665 (1990)

[2] G. Schmidt et al., Physical Review B 62, R4790 (2000)

[3] J. Mathon and A. Umerski, Physical Review B 63, 220403 (2001)

[4] S. Krishnamurthy et al., Applied Physics Letters 83, 1761 (2003)

[5] J.-y. Kim et al., in preparation

Mo.H-P98 - Magnetic properties of DyCo5 and YCo5 amorphous alloys

C. Blanco-Roldán^{1,2}, A. Hierro-Rodríguez^{3,4}, J. Díaz^{1,2}, F. Valdés-Bango^{1,2}, P.Gargiani⁵, J. Miguel Teixeira³, C. Quirós^{1,2}, S. Manuel Valvidare⁵, J. M. Alameda^{1,2}

1. *Departamento de Física, Universidad de Oviedo, Oviedo, Spain*
2. *Centro de Investigación en Nanomateriales y Nanotecnología, CINN (CSIC - Universidad de Oviedo), El Entrego, Spain*
3. *IN-IFIMUP, Departamento de Física e Astronomia, Faculdade de Ciências, Universidade do Porto, Porto, Portugal*
4. *INESC-TEC (Coordinated by INESC-Porto), Departamento de Física e Astronomia, Faculdade de Ciências, Universidade do Porto, Porto, Portugal*
5. *ALBA Synchrotron Light Facility, Cerdanyola del Vallès, Catalonia, Spain*

Magnetic properties of 35 nm thick DyCo5 and YCo5 amorphous films have been studied from room temperature down to 5 K by Vibrating Sample Magnetometry (VSM, 9 T), Superconducting Quantum Interference Device (SQUID, 6 T), and X-ray Magnetic Circular Dichroism (XMCD, 6 T) at BOREAS beamline in Alba Synchrotron Light Facility. Two DyCo5 samples have been prepared with different magnetic properties. First sample, denoted DyCoC, is obtained by simultaneous co-sputtering of Dy and Co targets. Second sample is a multilayer, denoted DyCoM, obtained by alternating ultrathin pure Dy and Co layers, with thicknesses adjusted around a monolayer to give a similar average composition and total thickness than the first sample, but with a different local atomic environment. The same procedure has been applied to prepare two reference YCo5 samples. Magnetometry measurements with in-plane and out-of-plane applied magnetic fields indicate that DyCo films have perpendicular magnetic anisotropy (PMA) and show a ferrimagnetic behavior. However, there are differences between both samples in compensation temperature, which is 120 K for DyCoC and 90 K for DyCoM, and out-of-plane coercive fields, being magnetically softer the DyCoC film. On the contrary, reference YCo5 films have in-plane anisotropy. As YCo5 and DyCo5 are similar from the structural and chemical point of view, this indicates that there is no contribution of Co atoms to the PMA observed in the DyCo5 films. Finally, XMCD element selective hysteresis loops, acquired at photon energies corresponding to Co L3 and Dy M5 absorption edges, have been used to study the temperature evolution of the magnetic cones characteristic of sperimagnetic alloys.

Mo.H-P99 - Origin of Anisotropic Giant Magnetoresistance in magnetic nanostructures

P. Perna¹, D. Maccariello^{1,2}, F. Ajejas^{1,2}, J. Luis F. Cuñado^{1,2}, M. Muñoz³, J. Prieto⁴, A. Bollero¹, M. Angel Niño¹, J. Pedrosa¹, J. Camarero^{1,2}, R. Miranda^{1,2}

1. *IMDEA Nanociencia, Campus de Cantoblanco, Madrid, Spain*

2. *D.F.M.C., Universidad Autonoma de Madrid, Madrid, Spain*

3. *IMM (CNM-CSIC), Madrid, Spain*

4. *ISOM, UPM, Madrid, Spain*

The understanding of the magnetoresistance (MR) responses as related to the way how the magnetization reverses in any kind of magnetic material is of great interest, not only for fundamental study, but importantly also for the improvement of the current spintronics technology. In this work, we demonstrate that by having direct experimental access to the magnetization vector during the reversal (by using a vectorial-Kerr magnetometry) we can predict the magnetoresistive signals. We demonstrate so in spin-valve [1] and in its basic constituents, i.e. single FM layer [2] and bilayer FM / AFM. We performed RT angular and field resolved M-H loops and the corresponding simultaneous resistance changes, and demonstrate that the R(H) curves depend exclusively dependence on the reversal processes (ultimately dictated by magnetic anisotropy of the system). Very importantly, from the vectorial-resolved M-H we can experimentally determine the relative angle between the magnetization vectors of the two FM layers in spin-valve and the magnetic torque and the angle enclosed between the magnetization vector and the applied current direction in a single FM layer. This allows for the simulation and prediction of the giant magnetoresistance (GMR), anisotropic magnetoresistance (AMR) and Planar Hall Effect (PHE) in the whole angular range and for any magnetic field values.

[1] P. Perna et al. Phys. Rev. B 86, 024421 (2012)

[2] P. Perna et al. Appl. Phys. Lett. 104, 202407 (2014)

Mo.H-P100 - Fe Layer Induced Ferromagnetism in Pd: An *In-Situ* Polarised Neutron Reflectometry Study

S. Mayr¹, W Kreuzpaintner¹, J. Ye¹, A. Schmehl², T. Mairoser², A. Herrnberger², J. Stahn³, J. Moulin⁴, M. Haese-Seiller⁴, M. Pomm⁴, A. Paul¹, B. Hjörvarsson⁵, P. Böni¹, J. Mannhart⁶

1. Technische Universität München, München, Germany

2. Zentrum für elektronische Korrelation und Magnetismus, Universität Augsburg, Lehrstuhl für Experimentalphysik VI, Augsburg, Germany

3. Paul Scherrer Institut, Laboratory for Neutron Scattering, Villigen, Switzerland

4. Helmholtz Zentrum Geesthacht, Institut für Werkstoffforschung, Abteilung WPN, Instrument REFSANS, Geesthacht, Germany

5. Uppsala University, Department of Physics and Astronomy, Uppsala, Sweden

6. Max Planck Institute for Solid State Research, Stuttgart, Germany

Magnetic data storage systems are based on thin magnetic layers and heterostructures. For improving the functionality of existing devices and to develop new ones, a deep understanding of the properties of these layers and the coupling between them is essential. In this context not only the classic room temperature ferromagnets are of interest but also elements which can be polarised, like e.g. Pd, in which induced magnetism is observed when it is brought into contact with Fe. To monitor the structural and magnetic properties during the deposition process, *in-situ* polarised neutron reflectometry (PNR) is used as a novel analysis technique. These PNR experiments were carried out at the neutron reflectometer AMOR at PSI (Switzerland) using the Selene focusing optics to reduce measurement times.

In this contribution the evolution of the magnetism in polycrystalline Pd/Fe/Pd systems during its growth process will be presented. For only one monolayer of Fe deposited onto an initial Pd layer a high induced magnetic moment of approximately $1\mu_B$ was found in the Pd at the interface whereas the magnetic moment of the Fe is small compared to its bulk value. With more Pd deposited on top of the Fe layer, the magnetic moment of Fe increases while the induced magnetism in Pd decreases. An induced magnetisation of Pd was observed for a region of 7.5 Å on both sides of the Fe layer. The magnetic moment in Pd decreases with increasing distance from the Fe/Pd interface.

Mo.H-P101 - MAGNETIC PROPERTIES OF Fe-N THIN FILMS

C. Silva¹, A. Vovk¹, R. C. da Silva², P. Strichovanec³, P. A. Algarabel⁴, L. P. Ferreira, M. D. Carvalho⁶, M. Godinho¹, M. M. Cruz¹

1. *BioISI - Biosystems & Integrative Sciences Institute, Faculdade de Ciências, Universidade de Lisboa, Campo Grande, Lisboa, Portugal*

2. *IPFN, Instituto Superior Técnico, Universidade de Lisboa, Campus Tecnológico e Nuclear, E.N.10, Bobadela LRS, Lisboa, Portugal*

3. *INA, University of Zaragoza, Zaragoza, Spain*

4. *ICMA, University of Zaragoza-CSIC, Facultad de Ciencias, Zaragoza, Spain*

5. *Department of Physics, University of Coimbra, Coimbra, Portugal*

6. *Centro de Química e Bioquímica, Faculdade de Ciências, Universidade de Lisboa, Campo Grande, Lisboa, Portugal*

Iron nitride films are good candidates for spintronic applications due to their high magnetization, expected large spin polarization and chemical stability, combined with the ability to form sharp interfaces with semiconducting nitrides. In this work, Fe-N thin films were deposited by reactive sputtering in Ar+N₂ mixtures aiming at the production of cubic Fe₄N. In a first study both cubic Fe₄N and/or hexagonal Fe_{3+x}N ferromagnetic nitride films were obtained depending on the nitrogen concentration during growth. Since the production of the cubic nitride was intended, the nitrogen fraction in the mixture was fixed at 10% and 15% and two series of films were produced. Substrates with different crystalline structures (TiO₂, MgO and Al₂O₃) and specific orientations were selected to allow anisotropic induced strains. Ferromagnetic Fe₄N cubic films were obtained with good crystallinity, saturation magnetization values above 1.6 Bohr magneton per Fe ion and magnetic anisotropy correlated with the strain induced by the substrate.

This work was supported by Portuguese funds through FCT - Fundação para a Ciência e a Tecnologia project PTDC/FIS/102270/2008 and grant SFRH/BD/70150/2010.

Mo.H-P102 - Tantalum-mediated Epitaxial Crystallization of Fe₃O₄ Films

T. Hee Kim¹, J. Hyun Gook¹, N. Jong Lee¹, Y. Jeong Bae¹, A. Michel²

1. Ewha Womans University, Seoul, South Korea

2. CNRS - Universite de Poitiers – ENSMA, Poitiers, France

The mixed valence of magnetite (Fe₃O₄) possesses several interesting and useful properties including ferrimagnetism with a high Curie temperature of 850°C and redox surface chemistry, while band structure calculations predict room-temperature half-metallicity[1].

In this work, Ta-mediated crystallization in Fe₃O₄ thin films was investigated for its successful implementation into spintronic devices. Beyond unetched Si wafers, room temperature (RT) deposition of 5nm Ta/5nm MgO/30nm Fe₃O₄ trilayers was performed by rf-sputtering and followed by post-annealing for 1 hour under vacuum at various temperatures from 300°C to 500°C. After post-annealing at 450 °C, stabilization of the thin epitaxial magnetite (001) phase was observed by using X-ray diffractometry and reflectometry measurements and vibrating sample magnetometer. Moreover, the temperature dependence of resistivity showed a hallark feature of magnetite, the Verway transition at around 120 K. We focussd on the comparative study of the underlayer effects on structural and magnetic properties of sputtered Fe₃O₄ films. The effect of a Ta underlayer on the crystallization of magnetite film grown directly on SiO₂ is considerably stong. For the Fe₃O₄ films deposited on both MgO(001) and SiO₂ surface without the Ta underlayer, the structural and magnetic properties of polycrystalline Fe₃O₄ films were seen, revealing only the diffraction peak of the (311) family of Fe₃O₄ planes. Our results indicate that the 5 nm thick Ta inserted between the adjacent MgO and SiO₂ layers is effective in improving the texture and the roughness of Fe₃O₄ through the crystallization process of MgO and Ta after annealing. The surface properties also play an important role in the process of Ta metal-induced crystallization of Fe₃O₄. Ta metal acts as a nucleating agent for the crystallization of Fe₃O₄.

[1] A. Yanase and N. Hamada, J. Phys. Soc. Jpn. 68, 1607 (1999)

Mo.H-P103 - Seed layer improvements to multilayer Giant Magnetoresistance thin-films through the use of polarized neutron reflectometry

J. Davies¹, M. Torija¹, T. Turmanian², B. Kirby²

1. NVE Corporation, Eden Prairie, United States

2. Center for Neutron Research, National Institute of Standards and Technology, Gaithersburg, United States

Multilayer Giant Magnetoresistance (GMR) films are a core constituent of magnetoresistive sensor devices. In order to achieve optimal performance the film structure and properties the film must be carefully tailored and often unresolved performance issues remain. One of the more challenging issues to resolve through conventional transport and magnetometry measurements is the optimization of the RKKY coupling throughout the multilayer. We demonstrate the use of Polarized Neutron Reflectometry (PNR), while not an unfamiliar tool to understanding GMR and RKKY coupling in multilayers, to observe and understand the magnetic coupling in GMR multilayers and optimize the material properties. The film under study is a Ta/Py/[Cu/Py/Cu/CoFe]4/Cu/Ta multilayer grown by DC magnetron sputtering deposition. PNR results show significant rotation of the magnetization of the magnetic layers near the Ta/Py seed layer while the layers near have a good antiferromagnetic coupling consistent with strong 2nd order RKKY coupling. The rotation can be attributed to the Py portion of the seed layer being magnetically relaxed resulting in a tilting of the active layers' magnetization from a biquadratic-like coupling. Two approaches were then used in an attempt to improve the coupling. First, the copper layer separating the seed and active layers was thickened. This notably improved the GMR, but at the expense of a disproportionately reduced sheet resistance. Second, we substituted the Py seed for a compatible non-magnetic 5 nm Ruthenium also augments the GMR, indicating improved coupling and has the advantage of maintaining the proper resistivity. Thickening of the Ru layer to 10 nm reduces the multilayer performance and is likely due to the formation of (111) texturing.

Mo.H-P105 - The effect of Ta buffer layer on the microstructure, roughness and dead layer of CoFeB/MgO systems

J. Kanak¹, J. Wrona^{1,3}, M. Banasik¹, A. Zywczyk², W. Powroznik¹, M. Czapkiewicz¹, T. Stobiecki¹

1. *Department of Electronics, AGH University of Science and Technology, Krakow, Poland*

2. *Academic Center of Materials and Nanotechnology, AGH University of Science and Technology, Krakow, Poland*

3. *Singulus Technologies AG, Kahl am Main, Germany*

In this work we discuss structural and magnetic properties of samples with different thickness of Ta seed-buffer layer. Samples with structure: Ta (5, 10, 15) nm / wedge Co₄₀Fe₄₀B₂₀ 0.8-2.9 nm / MgO 5 nm/ Ta 3 nm were deposited on thermally oxidized Si(001) substrates and then annealed at 330°C for 20 min using Singulus Timaris PVD Cluster Tool system. The microstructure of the layers was characterized by x-ray diffraction (XRD) θ -2 θ , rocking curve and x-ray reflectivity measurements. Topography of the samples was investigated using an atomic force microscopy. The magnetic moment and effective anisotropy were determined from vibrating sample magnetometer (VSM) measurements.

XRD analysis shows that Ta in buffers has grown in amorphous phase or disoriented β structure and MgO has grown with highly (001)-oriented texture. Rocking curves measured at position MgO (200) exhibit changes depending on Ta buffer layer thickness. By comparing the full widths at half maximum (FWHM) obtained from rocking curve profiles fits, it was found that the strongest MgO texture was for buffer Ta 5 nm and it decreased successively with increasing of Ta thickness. The smallest buffer roughness was for Ta 5 nm thick and then increased with the thickness of Ta.

From the magnetic moment per unit area as a function of CoFeB layer the magnetic dead layer thickness was determined. It was found that the thickest dead layer was for the smoothest buffer Ta 5 nm while for the roughest buffer Ta 15 nm the dead layer was the thinnest.

Project was financed by the Polish National Science Center Grant DEC-2012/05/E/ST7/00240. T.S. acknowledges Swiss Contribution by NANOSPIN PSPB-045/2010 grant.

Mo.H-P106 - Growth and characterisation studies of the metamagnet Eu₃O₄ Thin Films Grown on Si and Graphene

R. Aboljadayel¹, G. Cheglakov¹, A. Ionescu¹, J. Rackham¹, C. Cimorra¹, P. Monteiro¹, D. Love¹, C. Barnes¹

1. TFM Group, Cavendish Laboratory, University of Cambridge, Cambridge, United Kingdom

Trieuropium tetroxide (Eu₃O₄) is a mixed-valence compound of Eu²⁺ and Eu³⁺ ions. Eu₃O₄ has an antiferromagnetic arrangement below 5 K and shows a metamagnetic behaviour in low magnetic fields, below the Néel temperature (T_N) [1]. The magnetic properties of this compound are determined mainly by the Eu³⁺, which has a high magnetic moment in comparison to Eu²⁺. This characteristic behaviour may be attributed to the interaction of 4f electrons with the conduction band which results in unique magnetic, structural and thermal properties [2]. Graphene is a promising material for spintronics applications due to its desirable properties such as its long spin-diffusion length and high electron mobility. So far no study on the Eu₃O₄/graphene system has been reported and this may well be due to the difficulty of growing Eu₃O₄, which is the unstable high temperature phase of Eu-oxides. Therefore, growing a single crystalline Eu₃O₄ and investigating the interface of this system would provide a fundamental understanding on the exchange coupling between a metamagnet and graphene. In this study, 25 nm Eu₃O₄ thick films were grown on Si/SiO₂ substrates and on graphene sheets by molecular beam epitaxy and capped with 5 nm of Au. Eu was deposited at high temperatures (300-600 °C) in an oxygen flux. The growth parameters such as the oxygen partial pressure, temperature and deposition rate were optimised to achieve a single crystalline Eu₃O₄ phase. The effect of the deposition conditions on the crystallinity of the films was studied by X-ray diffraction and reflection, where SQUID magnetometry was used to study their magnetic properties. The results show a successful growth of a crystalline, highly textured Eu₃O₄ (100) films with a Curie temperature of 5 K, which is in agreement with the value reported in [3]. This represents the first successful step towards integrating a metamagnetic “switch” in two widely used electronic substrates.

References:

- [1] K. Ahn et al., J. Appl. Phys. 106, 043918 (2009)
- [2] C. M. Varma Rev. Mod. Phys. 48, 219 (1976)
- [3] L. Holmes and M. Schieber, Phys. Rev. 167, 2 (1968)

Mo.H-P107 - Thermal cycling on the magnetostructural transition on thin film of $Gd_5Si_{1.3}Ge_{2.7}$

L. Pires^{1,2}, J. H. Belo¹, I. T. Gomes¹, R. L. Hadimani^{3,4}, D.L. Schlagel⁴, T.A. Lograsso^{4,5}, D.C. Jiles^{3,4}, A. M. Pereira¹, A. M. L. Lopes^{1,2}, J. P. Araújo¹

1. IFIMUP And IN - Institute of Nanoscience And Nanotechnology

2. CFNUL - Centro de Física Nuclear da Universidade de Lisboa, Lisboa, Portugal

3. Department of Electrical and Computer Engineering, Iowa State University, Ames, United States

4. Ames Laboratory, US Department of Energy, Iowa State University, Ames, United States

5. Division of Materials Science and Engineering, Ames Laboratory, Ames, United States

Nowadays, an interest in the study of MCE in materials with reduced dimensions has grown in order to produce miniaturized devices. For refrigeration systems based on magnetocaloric thin films it becomes necessary to study the influence of thermal cycles in order to simulate their behavior in a real device. In this work we investigated the influence of the thermal cycling of a $Gd_5Si_{1.3}Ge_{2.7}$ thin film on its microstructure, magnetic phase transition and magnetic entropy value. This thin film was deposited on a SiO_2 -covered Si substrate by a femtosecond pulsed laser. This study was performed by immersing the thin film in liquid nitrogen up to 450 cycles. In each cycle, the film was immersed in a bath for 30-60 seconds in order to ensure thermal equilibrium with the bath and then removed to rest in air, for 60 seconds. The magnetization curves show two magnetic transitions, one of first and other of second order. It is observed that the thermal cycling does not affect the high temperature (249 K) magnetic transition, whereas the lower temperature (197 K), which corresponds to a magnetostructural transition (MST), shows major differences. In fact, there is a clear decrease (16%) on the thermal hysteresis after the 450 cycles, showing a change on the phase transition dynamics. This decrease in the hysteresis occurs because of the reduction of the amount of phase undergoing the MST. Consequently this decrease of the MST affects the magnetocaloric effect. Hence, the thermal cycling causes a 19% decrease of the MCE peak value ($-DSm_{max}$ occurs at 193 K) because of the O(II) phase arresting. This phase is arrested due to the strong strain fields that are created after consecutive MST. Nonetheless, the MCE value shows a tendency to stabilize and reach an equilibrium state, which is crucial for future applications.

Mo.H-P108 - Magnetic percolation in Co/Ag multilayers grown by molecular beam epitaxy

E. Navarro¹, M. Alonso¹, A. Ruiz¹, F. Cebollada², F.J. Palomares¹, J.M. González¹, B. Martínez³, L. Balcells³

1. Instituto de Ciencia de Materiales de Madrid – CSIC, Madrid, Spain

2. Escuela Técnica Superior de Ingenieros de Telecomunicaciones-UPM, Madrid, Spain

3. Institut de Ciència de Materials de Barcelona-CSIC, Barcelona, Spain

We have fabricated, by molecular beam epitaxy, multi-layered (Co_x/Ag_y)_z/MgO samples (x and y give the number of nominal Co and Ag monolayers per period, respectively, and z gives the number of period repetitions). The total number of Comonolayers was kept constant at $x * z = 32$, whereas y varied from 4 up to 16 which resulted in a variation of the Co nominal volume concentration, given by $X_{Co} = x/(x + y)$, from 0.06 up to 0.72. The structure and periods pile up of the samples were examined by using x-rays (reflectometry, rocking curves and wide angle diffraction), whereas their morphology was investigated by means of transmission electron microscopy. From the x-rays data we concluded about the coherence of the structure along the direction perpendicular to the plane of the deposits. The results obtained from the transmission microscopy evidenced the presence of close-to-monodisperse Co clusters (having an average diameter of ca. 1.5 nm) in the samples having X_{Co} values below 0.14, progressively percolating into continuous Co layers with the increase of the nominal Co volume concentration. The hysteretic properties of the samples were measured in the temperature range from 5 up to 290 K by using a vibrating sample magnetometer under in-plane fields of up to 6 T. The corresponding data allowed us to evaluate the Co concentration dependence of the temperatures below which hysteresis was measurable in the different samples (e.g.: the samples with $X_{Co} > 0.3$ magnetically percolate at room temperature). Correlation of the low concentration hysteretic behaviour with the morphology data suggests that the global samples behaviour cannot be simply ascribed to a canonical superparamagnetic behaviour.

Mo.I-P01 - Influence of the seed layer on the exchange spring coupling of the NiFe/IrMn/Co trilayer

I. Castro Merino¹, V. Pedruzzi Nascimento², E. Passamani Caetano³, E. Baggio Saitovitch⁴

1. Centro Brasileiro de Pesquisas Físicas-CBPF, Rio de Janeiro, Brazil

2. Universidade Federal do Espírito Santo-UFES, Vitória, Espírito Santo, Brazil

3. Universidade Federal do Espírito Santo-UFES, Vitória, Espírito Santo, Brazil

4. Centro Brasileiro de Pesquisas Físicas-CBPF, Rio de Janeiro, Brazil

A systematic investigation, through structural and magnetic characterizations, is discussed regarding the influence of the crystallographic texture on the Exchange Spring observed in the NiFe/IrMn/Co trilayer grown on different seed layers (Cu or Ta) deposited at room temperature with Magnetron Sputtering technique. Using X-ray diffraction, it was shown that Ta and Cu seed layers provoke different degrees of (111) fcc-texture that directly affect the exchange bias and indirectly modify the exchange spring coupling behavior. Combining results from the combination of DC magnetization and ferromagnetic resonance techniques, performed at room temperature, it is provided a planar magnetic anisotropy and an understanding of the Exchange Bias and the Exchange Spring effects in NiFe/IrMn/Co heterostructures. DC magnetization data suggest that the Exchange Spring exists before the field cooling protocol. The Exchange Spring phenomenon was shown to be strongly dependent on the degree of [111] texture in the IrMn layer, which is, in turn, dependent on the seed layer deposited on Si(100) substrate. It has also been demonstrated, a posteriori, that a field cooling of 10 Oe is sufficient to set the Exchange Bias effect on both interfaces (NiFe/IrMn and IrMn/Co). In addition, it was observed that the highest Exchange Bias field occurs when an unstressed L12 IrMn structure is stabilized at 6-8 nm IrMn thickness intervals. Increasing the IrMn thickness, it was observed that the coupling angle between the Co and NiFe ferromagnetic layers increases for the Cu seed system, but it reduces for the Ta case. The results were explained considering: (i) different anisotropies of the Co and IrMn layers induced by the [111] texture and (ii) distinct Exchange Bias field in NiFe/IrMn and IrMn/Co interfaces in both systems. It was shown that the coupling angle is strongly correlated by both Exchange Bias and Exchange Spring effects.

Mo.I-P02 - Exchange bias induced at a Co₂FeAl_{0.5}Si_{0.5} /Cr interface

N. T. Chris Yu¹, A. Vick¹, N. Inami², K. Ono², A. Hirohata³

1. *Department of Physics, University of York, Heslington, England, United Kingdom*

2. *Institute of Materials Structure Science*

3. *Department of Electronics, University of York, Heslington, England, United Kingdom*

Four sets of epitaxial thin films were grown on MgO(110) substrates by an UHV molecular beam epitaxy (MBE) system. All samples have the structure of Cr (3nm)/Ag (30nm)/[CFAS (1nm-4nm)/Cr (0.9nm)]₃/MgO (3nm). An antiferromagnetic exchange coupling at the Cr/Co₂FeAl_{0.5}Si_{0.5} interface was achieved when the structure was even in the as deposited state. Owing to lattice mismatch, Cr lattices were stretched on the Heusler layer and induce an exchange coupling to the interfacial moments in the Heusler alloy layer [1]. Vibrating sample magnetometry was used for the magnetic measurement at room temperature. CFAS has been reported to be cubic to exhibit fourfold magnetic anisotropy [2]. However, it only shows uniaxial anisotropy in the thinner region which is not consistent with the theory but similar to ultrathin Fe film by lattice mismatch [3]. For 2 nm thick Heusler alloy sample, the magnetic anisotropy is found to be the maximum and it is tilted to 30° from the MgO[110] axis. This minor tilt agrees with the X-ray diffraction (XRD) result. The largest value of squareness (Mr/Ms) is 0.98 and the smallest Mr/Ms is 0.34 in 2 nm of Heusler alloy layers sample. By varying the thickness of both Cr and CFAS, Ms and Hc vary from 690 to 1060 emu/cm³ and 6 to 10 Oe, respectively. As the thickness of the Heusler alloy layer increases above 3 nm, Hc is found to decrease, which is the result of emerging bulk-like properties of the Heusler-alloy layers. These results indicate that the magnetic properties of the Heusler alloy films can be controlled by tuning the lattice matching.

1. C. A. Culbert et al, J. Appl. Phys. 103, 07D707 (2008)

2. C. Felser et al, Spintronics: From Materials to Devices, p. 326-327 (2013)

3. J.-B. LaloÛ et al., IEEE Trans Mag., VOL. 42, NO. 10, (2006)

Mo.I-P03 – Colossal exchange bias in a mixed oxide with intrinsic magneto-electronic phase separation

J. Lago¹, I. Zivkovic², I. Orue³, E. Legarra³, F. Plazaola³, I. Ruiz de Larramendi¹, R. Lopez-Antón⁴, T. Rojo^{1,5}

1. Dept. of Inorganic Chemistry, University of the Basque Country (UPVEHU), Bilbao, Spain

2. Laboratory for Quantum Magnetism, EPFL, Lausanne, Switzerland

3. Dept of Elect & Elect, University of the Basque Country (UPV-EHU), Bilbao, Spain

4. Univ. Castilla La Mancha, IRICA, Ciudad Real, Spain

5. CIC Energigune, Miñano, Spain

Exchange bias of a magnitude of up to 65 KOe has been observed in members of a family of doped orthoferrites $\text{La}_{1-x}\text{Sr}_x\text{Fe}_{1-y}\text{My}_{0.0-0.6}$ (where M = transition metal and $\delta \approx 0$) which is ascribed to the kinetic arrest of ferromagnetic clusters embedded in the antiferromagnetic matrix. The origin of these clusters is partly due to the disproportionation of the Fe(IV) sites in the lattice.

Mo.I-P04 - Independently tuning the interfacial and bulk contributions to exchange bias for ferromagnetic / (antiferromagnetic) thin films with (IrMn/Pt/FeMn) based composite antiferromagnets

L. Frangou^{1,2,3}, K. Akmalidinov^{1,2,3,4}, Cl. Ducruet⁴, I. Joumard^{1,2,3}, B. Dieny^{1,2,3}, V. Baltz^{1,2,3}

1. Univ. Grenoble Alpes, SPINTEC, Grenoble, France

2. CNRS, SPINTEC, Grenoble, France

3. CEA, INAC-SPINTEC, Grenoble, France

4. CROCUS Technology, Grenoble, France

Spintronics devices require a wide range of ferromagnetic/antiferromagnetic (F/AF) exchange bias properties and subsequently of AF materials. For example, the reference layer of thermally assisted magnetic random access memories (TA-MRAM) requires high blocking (TB) and Néel temperatures (TN). In contrast, for the storage layer, mostly moderate TB,N are needed [1]. Tunability of TB,N by adjusting the thermal stability of the AF bulk is thus desirable to minimize the write power consumption (related to TN) while insuring proper data retention (related to TB) on the device temperature operating range [2]. In addition to that, low-freezing spins behave like spin-glasses at the F/AF interface. Their random spread over the sheet film contributes to the bit-cell dispersion of exchange bias properties once the sheet film is processed into a functional MRAM chip. Mastering the quality of the F/AF interface is another issue to deal with in parallel. Here, the interfacial and bulk exchange bias properties were studied for (IrMn/Pt/FeMn) and (FeMn/Pt/IrMn) AFs, where the thicknesses of the IrMn and FeMn layers were varied. The F/AF magnetic interfacial qualities and the AF grains' thermal stability were probed via measurements of the low- and high-temperature contributions to the blocking-temperature distributions, respectively. For such F/AF bilayers with composite AFs, we observed that it was possible to tune independently the interfacial and bulk contributions to exchange bias.

[1] R. C. Sousa et al., CR Physique 6, 1013 (2005)

[2] V. Baltz et al., Phys. Rev. B 81, 052404 (2010); K. Akmalidinov et al., J. Appl. Phys. 115, 17B718 (2014)

Mo.I-P05 - Exchange bias in Co/CoO nanocaps and nanoislands

I. Panagiotopoulos¹, A. Ma. G. Akdogan², G. Hagjipanayis³

1. *Department of Materials Science and Engineering, University of Ioannina, Ioannina, Greece*

2. *Institut NEEL CNRS/UJF UPR2940, Grenoble cedex 9, France*

3. *Department of Physics and Astronomy, University of Delaware, Newark, United States*

Self-assembly of colloidal microspheres or nanospheres has been proven an effective strategy for bottom-up fabrication of ordered nanostructures. It is therefore suitable for the fabrication of model exchange biasing systems where precise control of microstructure is desirable [1-3]. In this work we present a study of exchange biasing phenomena in sputtered cobalt oxide/cobalt bilayers that have been nanostructured by using polystyrene spheres (970nm and 170nm) both as a template for the deposition of nanocaps and as a mask for the formation of triangular-like islands (330nm and 60nm respectively). Cobalt layers 30nm thick have been magnetron sputtered deposited and subsequently oxidized by prolonged heat treatment at 800°C in O₂ atmosphere to form a 15nm thick CoO layer. Upon field cooling under 30kOe, the nanocaps show coercivity $H_C = 1\text{kOe}$ and exchange biasing $H_{ex} = 0.4$ to 0.6 kOe that does not depend sensitively on the size compared to $H_C = 0.1\text{ kOe}$ and $H_{ex} = 0.27\text{ kOe}$ of a continuous film prepared under the same conditions. The nano-islands show $H_C = 1\text{kOe}$ and $H_{ex} = 0.37\text{ kOe}$ only for the smaller size. The H_C and H_{ex} values correlate well with blocking temperatures estimated by magnetization vs temperature measurements. Acknowledgement Research co-financed by the European Social Fund and Greek national funds through the Research Funding Program "ARCHIMEDES III".

[1] I.L. Guhr, S. van Dijken, G. Malinowski, P. Fischer, F. Springer, O. Hellwig and M. Albrecht, J. Phys. D: Appl. Phys. 40, 3005 (2007)

[2] Y. J. Zhang, Y. X. Wang, X. D. Meng, Y. Liu, X. Ding and J. H. Yang, J. Appl. Phys. 105, 083910 (2009)

[3] Sara Laureti, Sarah Y. Suck, Helge Haas, Eric Prestat, Olivier Bourgeois, and Dominique Givord, Phys. Rev. Lett. 108, 077205 (2012)

Mo.I-P06 - Exchange bias of epitaxially grown Ni₂MnAl/X bilayer (X: Fe, Co, Co₂MnSi)

T. Tsuchiya¹, T. Sugiyama¹, T. Kubota¹, K. Takanashi

1. Institute for Materials Research, Tohoku University, Sendai, Japan

Mn₃Ir is an antiferromagnetic material widely used in spin valve structure. Mn₃Ir has attractive properties of large exchange bias field and high blocking temperature. However, the high price and the scarcity of Ir are crucial problems. Antiferromagnetic Heusler alloys are promising materials for the replacement of Mn₃Ir. There have been only a few reports to date about the exchange bias properties of antiferromagnetic Heusler alloys^[1]. In this study, we have focused on Ni₂MnAl with a comparatively high Néel temperature, and structural, transport and magnetic properties of epitaxially grown Ni₂MnAl/X bilayers (X: Fe, Co, Co₂MnSi) have been investigated systematically.

Ni₂MnAl films with a thickness of 100 nm were prepared on MgO (100) single crystal substrates with different growth temperatures from RT to 600 °C by magnetron sputtering. A ferromagnetic X layer of 3 nm was deposited on the Ni₂MnAl film. The structural, transport and magnetic properties were measured by using a x-ray diffractometer, van der Pauw technique and a superconducting quantum interference device, respectively.

B2-ordered Ni₂MnAl (100) films were successfully grown on MgO (100) substrates. The temperature dependence of the electrical resistivity showed an anomaly at a temperature, which was varied from 220 to 300 K depending on the growth temperature of the film. The anomaly is considered to correspond to the Néel temperature. Loop shifts by exchange bias were observed in the magnetization curves at 10 K for Ni₂MnAl/X bilayers. Interfacial exchange coupling energy density for X = Co₂MnSi, Fe was deduced to be 0.03 erg/cm² that was higher than those for X = Co (0.015 erg/cm²), which implies better lattice matching causes higher J_k.

This work was supported by HARFIR (SICORP-EU) from the JST, and is a cooperative program (No. 14G0412) of the CRDAM-IMR, Tohoku University.

[1] X. Y. Dong, *et al.*, J. Cryst. Growth 254, 384 (2003)

Mo.I-P07 - Tuning structures and magnetism of NiFe/Cr-oxide bilayers via ion-beam bombardment and annealing

W.-R. Luo¹, K.-W. Lin¹, Y. Wroczynskyj², W.-T. Lo¹, [A. Ruotolo](#)³, J. V. Lierop²

1. National Chung Hsing University, Taichung, Taiwan

2. University of Manitoba, Winnipeg, Manitoba, Canada

3. City University of Hong Kong, Kowloon Tong, Hong Kong

The exchange bias effect has drawn significant research interest due to its potential in enabling current applications such as read/write heads, and future electric-field-control-based devices [1,2]. Previously, we have shown the in- and out-of-plane (applied magnetic field relative to substrate) exchange bias effects in NiFe/Cr-oxide bilayers [3]. To further study the implications of the upper limit of oxygen incorporation into Cr-oxide layers during deposition, as well as the effects that annealing the Cr-oxide layers can have on the magnetic properties, NiFe (~ 10 nm)/Cr-oxide (~ 15 nm) bilayers with oxygen content up to 41%O₂/Ar in the Cr-oxide layer were fabricated. While these films exhibited soft magnetic properties at room temperature, an enhanced coercive (H_c) and exchange bias field (H_{ex}) were observed at 10 K after a 10 kOe field-cooling (FC) process from 400 K. In addition, H_{ex} values were found to increase for films with increasing deposited oxygen content, from H_{ex} ~ -50 Oe for 30%O₂/Ar, to H_{ex} ~ -75 Oe for 41%O₂/Ar. In contrast, with annealing, a decreased H_{ex} (~ -25 Oe) for the NiFe/annealed Cr-oxide bilayers are attributed to a structural phase transition from AF Cr₂O₃ to Cr₃O₄, as determined by electron diffraction patterns and x-ray photoelectron spectroscopy. The temperature dependent low-field magnetization (M(T)) of the NiFe/Cr-oxide bilayers under FC and ZFC processes was characterized also. The different oxygen contents of the Cr-oxide layers played an important role in affecting the magnetization of ferromagnetic NiFe crystallites, as revealed by an alteration of the irreversibility temperatures (T_{irr}) and differences in M(T). Furthermore, the T_{irr} as well as alterations of H_{ex} in NiFe/Cr-oxide bilayer deposited on Al₂O₃(0001) substrates imply changes in spin structures by using single crystalline substrates.

Research was supported by MOST of Taiwan and NSERC and CFI of Canada.

[1] X. He et al., Nature Mater. 9, 579 (2010)

[2] K.-W. Lin et al., Appl. Phys. Lett. 100, 122409 (2012)

[3] K.-W. Lin and J.-Y. Guo, J. Appl. Phys. 104, 123913 (2008)

Mo.I-P08 - Dependence of the interfacial coupling in FeMn/NiFe/Cu/Co spin valves on the thickness of the Cu spacer

M. Sousa¹, P. Barreto¹, F. Pelegrini², E. Baggio-Saitovitch¹

1. *Centro Brasileiro de Pesquisas Físicas, Rio de Janeiro, Brazil*

2. *Instituto de Física, Universidade Federal de Goiás, Goiânia, Brazil*

The Ferromagnetic Resonance (FMR) technique was used to study the magnetic properties of Si(100)/Cu(20nm)/FeMn(40nm)/NiFe(5nm)/Cu(t)/Co(5nm)/Ta(10nm) spin valves with thickness of the Cu layer varying in the range 1-10 nm. The samples studied were produced using the magnetron sputtering technique, under constant Ar working pressure of 3×10^{-3} Torr and in the presence of an applied field of 400 Oe in order to set the unidirectional anisotropy. The FMR experiments were done at room temperature using a high sensitivity Bruker ESP-300 spectrometer operating at the X-band microwave frequency, with swept static magnetic field and the usual modulation and phase sensitive detection techniques. The in-plane angular variations of the absorption fields reveal the presence of uniaxial and unidirectional anisotropies in the samples. For the NiFe resonance mode, the effect of the interfacial coupling (exchange bias) at the FeMn/NiFe interface, is much higher than that due to the uniaxial anisotropy; for the Co resonance mode, only the effect of the uniaxial anisotropy is present. The anisotropy parameters were deduced from the experiments by assuming the formation of planar domains in the antiferromagnetic layer and a coherent rotation of the ferromagnetic magnetization. The exchange coupling field increases approximately linearly with the Cu thickness. Since the samples differ only by the thickness of the Cu spacer, this may be associated with the magnetic coupling between the NiFe and Co magnetizations mediated by the Cu layer, implying that the magnetostatic orange peel coupling is dominant in the system.

Mo.I-P09 - Photo-control of exchange bias in BiFeO₃/La₂/3Sr1/3MnO₃ thin films

J. Jung¹, K. Sung¹, T. Lee¹

1. Inha University, Incheon, South Korea

To date, electric fields have been widely used to control the magnetic properties of BiFeO₃-based antiferromagnet/ferromagnet heterostructures through application of an exchange bias. To extend the applicability of exchange bias, however, an alternative mechanism to electric fields is required. Here, we report the photo-control of exchange bias in BiFeO₃/La₂/3Sr1/3MnO₃ thin films on an SrTiO₃ substrate. Through an ex-situ pulsed laser deposition technique, we successfully synthesized epitaxial BiFeO₃/La₂/3Sr1/3MnO₃ thin films on SrTiO₃ substrates. By measuring magnetoresistance under light illumination, we investigated the effect of light illumination on resistance, exchange bias, and coercive field in BiFeO₃/La₂/3Sr1/3MnO₃ thin films. After illumination of red and blue lights, the exchange bias was sharply reduced compared to that measured in the dark. With increasing light intensity, the exchange bias under red and blue lights initially decreased to zero and then appeared again. It is possible to reasonably explain these behaviors by considering photo-injection from SrTiO₃ and the photo-conductivity of La₂/3Sr1/3MnO₃. This study may provide a fundamental understanding of the mechanism underlying photo-controlled exchange bias, which is significant for the development of new functional spintronic devices.

Mo.I-P10 - Angular dependent FORC studies on FeMn/Co exchange bias systems utilizing the magneto-optical Kerr effect

M. Schmidt¹, J. Gräfe¹, G. Schütz¹, E. Goering¹

1. Max Planck Institute For Intelligent Systems, Stuttgart, Germany

First order reversal curves (FORC) are a powerful method for magnetic sample characterization, separating all magnetic states of an investigated system according to their coercivity and internal interactions. A so called FORC distribution is calculated from a set of minor loops with appropriate reversal fields and displayed as a contour plot [1]. In our contribution, we will describe our approach for applying the MOKE technique to FORC measurements [2]. As an example of the application of MOKE-FORC complementary to conventional hysteresis measurements, we will present here angular dependent studies of two epitaxial FeMn/Co exchange bias (EB) systems with different crystalline orientations ((100) and (111)). With FORC, a clear difference in the magnetic characteristics of both sample types could be identified. The (100)-oriented sample exhibits an asymmetric switching mechanism regarding the ascending and descending hysteresis branches. Distinct influences of the crystalline anisotropy could be identified since also multiple reversal steps via the systems easy-axes were found, resulting in a splitting of the FORC distribution at the respective orientations. When switching the (111)-oriented samples, a strong smearing of the distribution could be observed away from the field-cooling direction as well as a higher symmetry of both hysteresis branches. The influence of the magnetocrystalline anisotropy on the magnetization reversal is weaker; the process is clearly dominated by the unidirectional anisotropy induced by field-cooling. Both results are supported by transverse MOKE measurements exhibiting angular characteristics coinciding with the shape of the FORC distributions. In conclusion, the angular dependent FORC diagrams clearly resolve the different reversal mechanisms in our samples and prove at the same time the feasibility of combining the FORC method with the quick and precise data acquisition process available in MOKE instruments.

[1] Pike, C. et al., JAP, (1999)

[2] Gräfe, J., Schmidt, M. et al., RSI, (2014)

Mo.I-P11 - Hard-soft magnetic composites prepared by wet-chemical method followed by Spark Plasma Sintering

P. Jenu¹, M. Topole¹, P. J. McGuinness¹, K. Zuzek Rozman¹, M. Stingaciu², M. Christensen², S. Kobe¹

1. Department for Nanostructured Materials, Jožef Stefan Institute, Ljubljana, Slovenia

2. Center for Materials Crystallography, Department of Chemistry and iNANO, Aarhus University, Aarhus, Denmark

Hard-soft exchange-coupled magnetic nanocomposites have gained a lot of attention in recent years due to enhanced magnetic properties compared to the pure phase material. In this study we have used a novel approach to synthesize exchange-coupled magnets based on Sr-ferrites (SFO). A negative charge on the surface of SFO particles was obtained with the adsorption of citric acid [1]. Hexadecyl-trimethyl-ammonium bromide adsorbed on the surfaces of CoFe or CoFe₂O₄ (CFO) nanoparticles provided a positive surface charge at operating pH (=10). Therefore, when mixing both suspensions, the oppositely charged surfaces were attracted and composites consisting of SFO platelets covered with CoFe or CFO nanospheres were formed. Dried composite powders were pressed and sintered with Spark Plasma Sintering (SPS) technique at various sintering temperatures and times. Transmission electron (TEM) and scanning electron (SEM) analysis confirmed the formation of composites consisting of hard SFO and soft CoFe or CFO magnetic phase. The knee in the hysteresis loops of dried powders indicated systems with two different magnetic phases. However, this knee disappeared in the sintered composites, which suggests the exchange interaction between hard and soft magnetic phase. Compared to the pure SFO the remanent magnetization of SFO-CFO composite increased (from 0.36 T to 0.41 T), while slight decrease in coercivity was observed (from 169.8 kA/m to 152.4 kA/m). The remarkable increase was observed also in BH_{max}, which was 21.9 kJ/m³ for SFO and 26.1 kJ/m³ for the SFO-CFO composite.

Acknowledgment: Research was supported by EU-FP7 NANOPYME Project (No. 310516) [<http://www.nanopyme-project.eu/>]. CEM for the use of TEM and SEM equipment. References: [1] Campelj S.; Makovec D.; Drofenik M. Preparation and properties of water-based magnetic fluids. J. Phys.: Condens. Matter 20, 204101 (2008)

Mo.I-P12 - Hybrid exchange-biased core@shell nanoparticles through the growth of polymer brushes : Synthesis, assembly and study of their magnetic properties

D. Toulemon¹, L. Ourry¹, T. Gaudisson¹, L. Mouton¹, S. Nowak¹, S. Ammar¹, F. Mammeri¹

1. ITODYS, Université Paris Diderot, CNRS UMR-7086, Paris, France

Tailoring the size of magnetic particles at the nanometer scale has led to the emergence of new magnetic properties, of great interest in various research topics including magnetic recording. One of the main challenges for the synthesis of such granular materials is the design of organized structures with enhanced tunable physical properties. Particularly, the thermal stability of the nanomaterials magnetization is critical for magnetic recording.

Several recent experimental studies have indicated that exchange coupled ferromagnetic (FM) and antiferromagnetic (AFM) nanostructures exhibit an improved thermal stability of the magnetization and all the features of exchange bias (EB).

Besides, in the case of core-shell FM-AFM exchange-biased nanoparticles (NPs), dipolar interactions may be of great importance and have to be considered. Despite an impressive number of works on exchange-biased systems, few of them deal with the interplay between EB and dipolar interactions. To study the relationships between EB and dipolar interaction, we propose to tune the NP-NP distance by growing polymer brushes on the surface of these nanoparticles.

We prepared, by the polyol process, highly crystallized nanoparticles (NPs) consisting in a Fe₃O₄ core perfectly epitaxied to a polycrystalline CoO shell. We choose to use the grafting from technique to grow poly(methyl methacrylate) (PMMA) chains directly on the surface of the nanoparticles. First, a brominated initiator was anchored to the particle surface. Then, radical polymerization (ATRP) was performed to grow PMMA brushes of controlled lengths.

At low temperature, it appears that increasing the average distance between the NPs increases the coercive field H_C and is decreasing the hysteresis loop shift, i.e. EB. These results emphasize the relationships between the dipolar interaction and the hysteresis loop shift in the magnetic NPs presenting EB properties.

Mo.I-P13 - Magnetic anisotropies of core-shell ferrite nanoparticles

F. Da Silva⁰, R. Aquino², F. A. Tourinho¹, J. Depeyrot¹, E. Dubois³, R. Perzynski³, V. I. Stepanov⁴, Y. L. Raikher⁴, G. Ballon⁵, A. Sulpice⁶

1. *Complex Fluids Group, Instituto de Física, UnB 70919-970, Brasília-DF, Brazil*

2. *Universidade de Brasília, Laboratório de Nanociência Ambiental e Aplicada, Complex Fluid Group, Faculdade UnB Planaltina, 70910-900, Brasília-DF, Brazil*

3. *Sorbonne Universités, UPMC Univ Paris 06, UMR 8234, PHENIX, Paris, France*

4. *Institute of Continuous Media Mechanics, Ural Branch of RAS, Perm, Russia*

5. *LNCMI-T, UPR 3228, CNRS-UJF-UPS-INSA, 31400, Toulouse, France*

6. *CRETA/CNRS-UJF BP166, 38042, Grenoble Cedex 9, France*

Magnetic core/shell nanoparticles (NP's) dispersed in a liquid carrier, present enhanced magneto-thermic effects, which may find their origin in exchange coupling properties of such NPs. We explore low temperature magnetic properties of individual NP's based on a MnFe_2O_4 core protected by a $\gamma\text{-Fe}_2\text{O}_3$ shell. Previous studies evidenced in such NPs a well-ordered ferrimagnetic core surrounded by a disordered surface layer frozen in a spin glass-like manner [1]. We investigate their magnetization, surface disorder and magnetic anisotropy properties. Thermal and field dependences of total magnetization are measured at 5T as a function of temperature and at 1.5K in a pulsed field experiment up to 52T. Total magnetization, analyzed as the sum of contributions from core and disordered surface, does not saturate even at very high fields because of misaligned surface spins. The core's magneto-dynamics is probed by FerroMagnetic Resonance (FMR). A theoretical analysis of these results points out the NP's uniaxial symmetry of the magnetic anisotropy energy of the core, which scales as the NPs surface. The deduced uniaxial anisotropy field H_{ani} parallel to the NP magnetic anisotropy axis is confirmed by first magnetization measurements and finds its origin in the exchange interaction at the core/shell interface. Besides, FMR measurements evidence another kind of exchange anisotropy field H_{iso} , which is rotatable, bidirectional and parallel to the applied field (264 kA/m). A third evidence of exchange interactions is found in the shift of hysteresis loops at various field cooling: exchange bias H_{ex} , which is scaling with H_{ani} [2,3].

We thank CAPES/COFECUB n°714/11, PICS/CNRS n°5939, FAP/DF, CNPq, CAPES and Perm Region - Russia.

[1] R. Aquino et al. Phys. Rev. B 72, 184435 (2005)

[2] F. G. Silva et al J. Phys. D: Appl. Phys. 46, 285003 (2013)

[3] R. Cabreira-Gomes et al. J. Magn. Magn. Mater. 368, 409 (2014)

Mo.I-P15 - Magnetization enhancement through exchange-coupling in CoFe₂O₄/CoFe₂ Nanocomposites

C. Granados-Miralles¹, A. Quesada², M. Stingaciu¹, F. Rubio-Marcos², F. J. Mompeán³, M. García-Hernández³, F. J. Pedrosa⁴, A. Bollero⁴, J. F. Fernández², M. Christensen¹

1. *Center for Materials Crystallography CMC, Department of Chemistry & iNANO, Aarhus University, Denmark*

2. *Instituto de Cerámica y Vidrio ICV-CSIC, Madrid, Spain*

3. *Instituto de Ciencia de Materiales de Madrid ICMM-CSIC, Madrid, Spain*

4. *IMDEA Nanoscience, Madrid, Spain*

Exchange-coupled magnets constitute a strategy for designing magnetic materials, not only intended for BH_{max} enhancement but also to fulfill the specific requirements of a broader spectrum of applications. Theory predicts a considerable improvement by coexistence of two magnetic phases of different nature (hard/soft). Numerous studies on the subject have been reported over the past few years. However, achieving effective exchange-coupling appears to be more challenging than expected. In this work, hydrothermally synthesized CoFe₂O₄ nanoparticles with an average size of approximately 10 nm were partially reduced through a mild thermal treatment in a reducing atmosphere. The aforementioned procedure gave rise to CoFe₂O₄ (hard)/CoFe₂ (soft) magnetic nanocomposites. Structural coherence of the two phases in case of partial reduction is presumably favored compared with bringing two different starting materials together. Rietveld refinement of high resolution powder x-ray diffraction data allowed quantitative analysis of compositional and microstructural features as function of reduction degree, revealing emergence of intermediate phases before the pure metal is finally formed. Magnetization measurements at room temperature showed a fivefold increase in BH_{max} with respect to the initial powders. A remanence value of 58 emu/g was preserved in this case, which is significantly higher than expected given the amount of soft phase present (approx. 40% metallic content). Magnetic hysteresis at low temperature and demagnetization curves indicate that an effective exchange-coupling is very likely to be the origin of the enhanced magnetic performance. The potential influence of these intermediate phases on the magnetic behavior is also examined. Research supported by EU-FP7 NANOPYME Project (No. 310516) [www.nanopyme-project.eu].

Mo.I-P16 - Negative rotatable anisotropy as a signature of antiparallel interface exchange coupling in exchange bias systems

D. Schafer¹, P. L. Grande¹, L. G. Pereira¹, G. de Medeiros Azevedo¹, A. Harres¹, M. A. de Sousa², F. Pelegrini², J. Geshev¹

1. *Instituto de Física, UFRGS, Porto Alegre, Brazil*

2. *Instituto de Física, UFG, Goiânia, Brazil*

The best-known manifestation of the exchange bias (EB) phenomenon, which occurs when a magnetically-hard material (usually an antiferromagnet) is coupled to a softer ferromagnet, is a hysteresis loop typically shifted at a direction opposite to that of the magnetic field applied during either sample growth or a post-deposition treatment. The intriguing positive EB (PEB), i.e., a shift in the applied field direction [1], is attributed to an antiparallel interface coupling. The present work addresses the origin of another fascinating EB feature, namely, the recently discovered negative rotatable anisotropy (RA) [2]. Rotatable uncompensated spins at ferromagnet/antiferromagnet interfaces are assumed to be responsible for the isotropic shift of the angular variation of the resonance field in ferromagnetic resonance (FMR) measurements through a RA field that rotates with the magnetization of the ferromagnet [3]. When the RA is positive, this shift is downward. Here we report on negative RA presented by as-made, annealed and ion-irradiated IrMn/NiFe bilayers. Opposite to the previous observations, an inverse correlation between RA and coercivity is observed. Also, the EB field, determined from hysteresis loop measurements, is higher than that obtained from FMR. All results are explained in terms of antiparallel coupling and magnetic-field-induced transitions, from antiparallel to parallel states, of uncompensated spins at the ferromagnet/antiferromagnet interface. This mechanism is also able to account for previously observed training-induced PEB and partial recovery of training after application of strong magnetic fields. We affirm that FMR-estimated negative RA is a signature of antiparallel interface coupling even in systems presenting conventional EB only.

1. W. H. Meikelejon and R. E. Carter, *J. Appl. Phys.* 30 (1959) 2020; J. Nogués et al., *Phys. Rev. Lett.* 76 (1996) 4624

2. S. Nicolodi et al., *Phys. Rev. B* 85 (2012) 224438

3. R. D. McMichael et al., *Phys. Rev. B* 58 (1998) 8605

Mo.I-P17 - Exchange bias effect in multilayers of NiFe/IrMn/Ta

P. Kern¹, J. Siqueira¹, O. Escobar¹, A. de Andrade², J. Rigue³, M. Carara¹

1. *Universidade Federal de Santa Maria, Santa Maria, Brazil*
2. *Universidade Federal do Rio Grande do Sul, Porto Alegre, Brazil*
3. *Instituto Federal Farroupilha, Camobi, Santa Maria, Brazil*

The exchange bias phenomenon occurs in thin films due to the coupling between a ferromagnetic layer adjacent to an antiferromagnetic one. The main observed manifestations of the exchange bias are the field shift in the magnetization curves and the increase in the coercive field when compared to the uncoupled ferromagnetic material. In this work, we have studied the presence of the exchange bias in Ni₈₁Fe₁₉(100 \uparrow)/Ir₂₀Mn₈₀(120 \downarrow)/Ta(30 \downarrow) multilayers, with different number of trilayers, grown by magnetron sputtering on Si(100) substrates at room temperature. The magnetic properties, such as bias and uniaxial anisotropy field as well as saturation magnetization, were determined through magnetization curves and ferromagnetic resonance (FMR). The magnetization measurements were obtained using an alternate gradient field magnetometer. The FMR dispersion relations were obtained by measuring, with a vector network analyzer (Rohde & Schwarz ZVB 14), the scattering parameter (S₁₁) of a microstrip transmission line loaded with the sample. The measuring frequency range was from 1 GHz to 8 GHz and the in plane magnetic field from -600 Oe to 600 Oe at different orientations relative to the anisotropy axis. The FMR dispersion relations were fitted to the Smit-Beljers equation. In order fit the data, the magnetization equilibrium angles were calculated by the minimization of the free magnetic energy which includes Zeeman, Uniaxial, Unidirectional and Magnetostatic energies. We show that this model fits very well the FMR experimental curves. We found that the anisotropy field values do not depend on the sample. We argue that the strong coupling between ferro and antiferro layers could explain this stationary value of anisotropy field.

Mo.I-P18 - Spring-magnet behaviour in annealed Fe₆₄Pd₃₆ thin films: exchange coupling between coexistent soft α -Fe and hard L1₀ FePd magnetic phases

S. Bahamida^{1,2}, A. Fnidiki², A. Laggoun¹, M. Coisson³, G. Barrera^{3,4}, F. Celegato³, P. Tiberto³, A. Guittoum⁵

1. *Research unit UR-MPE, University of Boumerdes, Boumerdes, Algeria*

2. *Material Physics Group UMR 6634 CNRS – University of Rouen, Saint-Etienne-du-Rouvray, France*

3. *INRIM, Nanoscience and Materials Division, Torino, Italy*

4. *Università degli Studi di Torino, Chemistry Department, Torino, Italy*

5. *Nuclear Research Centre of Algiers, Algiers, Algeria*

Fe₆₄Pd₃₆ thin films have been fabricated by thermal evaporation onto single-crystal Si (100) substrates. As-prepared thin films mainly display fcc phase. To promote the transformation to the L1₀ phase, samples have been annealed in vacuum at temperatures of 400 °C and 600 °C for one hour. Microstructural properties have been studied by X-ray diffraction. The magnetic properties were measured on a Quantum Design SQUID magnetometer and by ⁵⁷Fe Conversion Electron Mössbauer Spectroscopy (CEMS), as well as by alternating gradient magnetometry (FORC measurements) and AFM/MFM. X-ray diffraction results show that the as-prepared samples are composed of three magnetically soft phases: α -Fe and two disordered FePd and FePd₃ phases. After annealing at 400 °C, only α -Fe and disordered FePd phases are observed. Annealing at 600 °C shows the transformation of the disordered fcc FePd to the tetragonal ordered L1₀ FePd phase. The X-ray results are in agreement with Mössbauer measurements: the average hyperfine field decreases with annealing temperature, indicating the transformation from disordered fcc to ordered L1₀ phase. The room temperature hysteresis loops and their respective coercive fields, which increase from 56 to 106 and 310 Oe for samples as-prepared, annealed at 400 °C and at 600 °C respectively, confirm the structural transformations. Before and after annealing the saturation magnetization remains the same. After annealing at 600 °C, the hard L1₀ phase and the soft α -Fe phase coexist, but the hysteresis loops do not reveal magnetisation reversal occurring in two distinct steps. Conversely, first order reversal curves (FORC) measured on as-prepared and annealed samples show that in the film annealed at 600 °C a bias field might be attributed to exchange coupling between the two α -Fe and L10-FePd crystalline phases connected with each other within the interfaces phases.

Mo.I-P22 - Room temperature metastable behavior of exchange bias systems

R. Cichelero¹, A. Harres¹, J. E. Schmidt¹, L. G. Pereira¹, J. Geshev¹

1. Instituto de Física, UFRGS, Porto Alegre, Brazil

Although exchange bias (EB) [1] phenomenon has been studied extensively in the past few decades, some of its features still remain unexplained even almost sixty years after its discovery. Nevertheless, the effect is already widely used in spin-valve and magnetic-tunnel-junction devices. It is accepted that its origin lies in exchange coupling between a ferromagnet (FM) and uncompensated spins at the interface with an adjacent anti-ferromagnet (AF). Thus, understanding the role of magnetic interactions in AF/FM interfaces seems to be fundamental for achieving further development in the field. The present study reports on the time dependence of the EB field after the thin films have been subjected to post-deposition treatments such as ion bombardment (IB) and magnetic annealing upon application of a magnetic field. Evidences for such metastable behavior of thin films, observed after either IB [2,3] or annealing [4], have been recently reported. Once initialized the EB, our IrMn/CoFe and IrMn/Co bilayers were exposed to a saturating magnetic field during a certain time interval at room temperature. Subsequently, magnetization hysteresis loops were measured, also at room temperature, and the corresponding magnetic parameters (i.e., remnant magnetization, coercivity, etc.) were extracted. Depending on the EB-induction technique, the systems studied here showed rather distinct behaviors. E.g., after IB the films presented unstable magnetic states, enabling modifications of the EB field for a long time period after irradiation. For low IB fluences, the coercivity remained almost constant. The annealing, from the other hand, enabled energy configurations that eliminate or reduce treatment-induced thermal drift effects in our systems.

1. W. H. Meiklejohn and C. P. Bean, Phys. Rev. 102 (1956) 5
2. A. Ehresmann et al., J. Phys. D 38 (2005) 801
3. A. Paetzold and R. Röll, J. Appl. Phys. 91 (2002) 10
4. A. Ehresmann, Recent Res. Devel. Appl. Phys. 7 (2004) 1

Mo.I-P23 - Electric field effect in CoFeB/NiO exchange coupled system

K. Okabe¹, M. Kawakita¹, S. Yakata², T. Kawae^{3,4}, T. Kimura^{1,4}

1. *Department of Physics, Kyushu University, Fukuoka, Japan*

2. *Department of Information Electronics, Fukuoka Institute of Technology, Fukuoka, Japan*

3. *Department of Applied Quantum Physics and Nuclear Engineering, Kyushu University, Fukuoka, Japan*

4. *Research Center for Quantum Nano-Spin Sciences, Fukuoka, Japan*

Exchange bias caused by the interaction between the ferromagnetic thin film and anti-ferromagnetic film is utilized to fix the magnetization and is a key element in the operation of the magnetic field sensor and spin-based electric device. Depending on the purpose and situation, a metallic alloy or insulating magnetic oxide has been used as the anti-ferromagnet. On the other hand, the magnetic oxide film has also been used as a core channel for the resistive-switching memory. However, the magnetic properties of the magnetic oxide has not been considered intensively in the operation of the resistive memory. Since the resistance change corresponds to the modification of the electron state, it is natural to expect that the magnetic property is modified with the resistance change. This correlation between the electric and magnetic property may provide new insight in the nano-electronic device. For this purpose, we have investigated the electric field effect in a exchange-coupled CoFeB/NiO film. We have grown a CoFeB/NiO/W multi-layered film by using magnetron sputtering. We have evaluated the electron state of the NiO film from the vertical transport and also evaluated the magnetic property of the NiO from the exchange bias for the CoFeB film. In the vertical transport measurement, we have clearly observed the metal-insulator transition of the NiO film with bipolar signature. The switching voltage for the transition is smaller than other conventional resistive memory. This implies that the spin polarized electrode is effective for the transition. Moreover, the switching voltage is found to depend on the relative angle between the spin direction of the CoFeB and that of the NiO. In addition, the exchange bias was found to be modified by the resistance switching. Thus, these unique observed features strongly suggests that the spin plays an important role in the operation of the resistive memory.

Mo.I-P24 - Direct observation of controllable exchange bias configurations in Ni/FeF₂ nanostructures

A. F. Rodríguez¹, M. Kovylna¹, A. C. Basaran², R. Morales³, R. Morales⁴, J. Llobet⁵, X. Borrísé⁶, M. A. Marcus⁷, A. Scholl⁷, I. K. Schuller², X. Batlle¹, A. Labarta¹

1. *Dpt. Física Fonamental & Institut de Nanociència i Nanotecnologia, Universitat de Barcelona, Barcelona, Spain*

2. *Department of Physics and Center for Advanced Nanoscience, University of California San Diego, La Jolla, United States*

3. *Department of Chemical-Physics, BCMaterials, University of the Basque Country UPV/EHU, Leioa, Spain*

4. *IKERBASQUE, Basque Foundation for Science, Bilbao, Spain*

5. *Institut de Microelectrònica de Barcelona (IMB-CNM CSIC), Bellaterra, Spain*

6. *Institut Català de Nanociència i Nanotecnologia (ICN2), Bellaterra, Spain*

7. *Advanced Light Source, Lawrence Berkeley National Laboratory, Berkeley, United States*

Confining the dimensions and geometry of magnetic structures down to critical length scales such as the ferromagnetic exchange length or the domain wall width results in intriguing new phenomena not observed in the corresponding bulk material. Recently, ferromagnetic/antiferromagnetic (FM/AF) nanostructures exhibiting both negative and positive exchange bias (EB) have been proposed as model systems for multistate switching memory units [1, 2]. Patterning allows the control of writing fields and the design of the multistate cells [2]. In this work, we combine photoemission electron microscopy (PEEM) with X-ray magnetic circular dichroism (XMCD) to show that a progressive spatial confinement of a FM, either through thickness variation or laterally via patterning, drastically affects the AF domain structure in exchange-biased Ni/FeF₂ nanostructures. Imaging the magnetic domains at both sides of the FM/AF interface shows that the spin structure is determined by the balance between the competing FM and AF magnetic energies. For FM layer thicknesses below about 10 nm, competing interactions with the proximal AF system lead to tunable configurations of coexisting EB domains with opposite orientations. Antidot patterning of the Ni/FeF₂ heterostructures destabilizes the FM state, promoting the formation of additional inverted Ni domains below a critical antidot separation of the order of a few FeF₂ crystal domains. The underlying mechanism of the AF domain formation in Ni/FeF₂ may be generic to other magnetic systems with complex non-collinear FM/AF spin structures. This work was supported by Spanish MINECO (MAT2012-33037, FIS2013-45469), Catalan DURSI (2009SGR856), European Union FEDER funds (Una manera de hacer Europa), the EU FP7-PEOPLE-2012-IRSES, Project No. 318901, and the US-DOE grant number DE FG02-87ER-45332. A.F.R. acknowledges support from the MICIIN “Ramón y Cajal” Programme.

[1] Roshchin et al, International Patent Number: 05803831.6 1214 PCT/US2005025129 2005

[2] Morales et al, Appl. Phys. Lett. 2014, 104, 032401

Mo.I-P25 - Facile synthesis and exchange-bias in FeO/gamma-Fe₂O₃ core/shell nanoparticles

B. Leszczynski^{1,4}, V. Tzitzios², A. Aboud El-Gendy³, A. Skumiel¹, G. C. Hadjipanayis³, K. Zaleski⁴, S. Jurga^{1,4}

1. Department of Physics, Adam Mickiewicz University, Poznan, Poland

2. Institute of Materials Science, NCSR Demokritos, Greece

3. Department of Physics and Astronomy, University of Delaware, Newark, United States

4. NanoBioMedical Centre, Adam Mickiewicz University, Poznan, Poland

A facile chemical approach for the synthesis of Fe₂O₃/FeO core/shell nanoparticles is reported. The synthesis takes place by thermal decomposition of Fe(Oleat)₃ in tri-octyl-amine at 320°C. The core/shell morphology was confirmed by transmission electron microscopy (TEM and HR-TEM) analysis. The nanoparticles reveal a near spherical shape with an average diameter of 24 nm and core/shell morphology. The shell thickness was approximately 3.9 nm. A progressive oxidation for 40 days caused the shell thickness to increase to 4.8 nm. X-ray diffraction and VSM measurements showed the presence of wustite and maghemite/magnetite phases. Thermomagnetic measurements (M(T)) show an antiferromagnetic to paramagnetic transition at around 200 K which belongs to the wustite (FeO) phase while a minor inflection point in the ZFC M(T) was observed at 120 K which indicates the presence of magnetite (Verwey transition). Exchange bias behavior was also observed in the core/shell particles with a 250 Oe shift in the hysteresis loop at 50 K. A complete structural and magnetic characterization of the nanoparticles will be reported. Work Supported by IRSES NANOMAG.

Mo.I-P26 - Effects of short post-deposition heat treatment on structure and exchange bias in sputtered FeNi/FeMn system

P. Savin¹, J. Guzmán², V. Lepalovskij¹, A. Svalov¹, G. Kurlyandskaya³, A. Asenjo², V. Vas'kovskiy¹, M. Vazquez²

1. *Ural Federal University, Yekaterinburg, Russia*

2. *Instituto de Ciencia de Materiales, CSIC, Madrid, Spain*

3. *University of The Basque Country UPV-EHU, Bilbao, Spain*

Exchange anisotropy in layered structures can be created either by depositing an antiferromagnetic (AF) layer on a saturated ferromagnetic (FM) layer in a magnetic field or by cooling down the AF/FM system in a magnetic field after heating above the Néel temperature of the AF layer [1]. However, there is a still remaining challenge to determine the physical processes responsible for the formation of the exchange anisotropy in each one of the above mentioned methods.

In this work, we present a systematic study on the effect of post-deposition annealing in a magnetic field on the properties of Ta(5nm)/FeNi(40nm)/FeMn(20nm) (S1) and Ta(5nm)/FeNi(40nm)/FeMn(20nm)/FeNi(40nm) (S2) films.

It was found that the annealing at 200 °C during 5 min leads to a reduction of exchange field (H_{ex}) from 40 Oe to 27 Oe for S1 sample. A similar H_{ex} decrease was observed for the first FeNi layer in the S2 sample. The H_{ex} for the second FeNi layer is not changed substantially.

Careful analysis of X-ray diffraction patterns shows that such a heat treatment has no effect on the grain size and crystalline texture of the films.

Atomic force microscope studies shows that the samples in as-deposited state have a smoother surface than those after heat treatment which can be related with the increase of the interface roughness. Roughness variation for the S2 sample was more noticeable than for the S1 one. Change in the vacancies and/or dislocation density and formation of the new type of dislocation structures and stress relaxation at low temperature annealing can be responsible for the changes of the surface roughness.

Thus, H_{ex} changes after heat treatment are most likely caused by modification of interfacial roughness and unlikely by changes in the microstructure or/and composition of the antiferromagnetic FeMn layer.

[1] J. Nogués et al., Phys. Rep. 422 (2005) 65.

Mo.I-P27 - “Dependence of the exchange bias blocking temperature on the thickness of antiferromagnetic layer in the trilayered Si/Ta/NiFe/IrMn/NiFe/Ta thin-films”

C. Gritsenko¹, I. Dzhun, N. Chechenin, V. Rodionova

1. *Immanuel Kant Baltic Federal University, Kaliningrad, Russia*

2. *Lomonosov Moscow State University, Moscow, Russia*

Phenomenon of the shifting of the hysteresis loop along the field axis is called the exchange bias. It remains a topic of active investigation for last fifty years. The key issues are the understanding of the fundamental mechanisms controlling the magnitude of the exchange bias, the nature of exchange bias increasing in multilayered systems with few exchange interfaces and the development of the ways to enlarge the exchange bias blocking temperature. With this aim we have studied unidirectional anisotropy of the samples in the range of temperatures from 100 to 450K. We used thin films of Si/Ta/NiFe/IrMn/NiFe/Ta prepared by magnetron sputtering in magnetic field of 400 Oe. The thickness of the antiferromagnetic IrMn layer was changed from 2 to 50 nm. Magnetic moments of the samples were measured by vibrating sample magnetometer at 9 angles between the magnetization easy axis of samples and the direction of the magnetic field, from 0° to 360° with a step of 45°. Magnetic field was varied in the range of -500 - +500 Oe.

We have found how the exchange bias field depends on the thickness of the antiferromagnetic IrMn layer – it is a non-monotonic dependence with maximum (exchange bias field of 107 Oe) at the antiferromagnetic layer thickness of 10 nm. Also dependence of the exchange bias blocking temperature on the thickness of the antiferromagnetic layer was obtained. We have observed that the decreasing of the antiferromagnetic layer thickness leads to decreasing of the blocking temperature. The thickness of 5 nm is a critical one for appearance of the exchange bias in the studied trilayered structures at room temperature. These results were explained in the terms of sizes of antiferromagnetic grains which were estimated by atomic force microscope.

Mo.I-P28 - Exchange Bias down to the sub-nanometer regime

F. J. Ferraro^{1,2}, P. David^{1,2}, E. Mossang^{1,2}, A. Bernand-Mantel⁰, L. Ranno⁰

1. Univ. Grenoble Alpes, Inst. NEEL, F-38042 Grenoble, France

2. CNRS, Inst. NEEL, F-38042 Grenoble, France

Since its discovery in 1956, exchange bias (EB) has been commonly used in commercial sensors and memory cells to pin the direction of a ferromagnetic (FM) layer. Quantitative description of its mechanism is still incomplete and is a highly debated subject. In this work we developed a model sample to extend the study to the sub-nanometer regimes for both FM and antiferromagnetic (AFM) layers. This multilayer has the following structure: Si/Ta(5.5 nm)/Pt(2.5 nm)/Co(1.15 nm)/Al(wedge 0-3 nm). A plasma oxidation through the Al wedge allows to control the oxidation in a sub-nanometric scale and to create a Co (0.67 nm)/CoO (0.65 nm) stable magnetic bilayer. Using characterising tools such as VSM-SQUID magnetometry, extraordinary Hall effect and X-Ray reflectivity, we carefully analysed this structure. We evidence the EB effect, $HEB=0.65$ T at 5 K, which correspond to a surface energy of 0.55mJ/m^2 . The EB is preserved up to a 70 ± 5 K blocking temperature, which is only marginally reduced compared to nm-thick layers. We can quantitatively describe this results and by studying the remanence of the sample we could determine that CoO keeps a huge anisotropy (similar to the bulk value of 28 MJ/m^3) even in such a 0.65 nm-thick CoO layer. Modeling the complete magnetic response of the sample allows to rule out some EB mechanisms such as the ones assuming domain walls parallel to the interface.

Mo.I-P29 - The role of shape and interface roughness in the exchange bias effect in core-shell magnetic nanoparticles

D. Kechrakos¹, V. Dimitriadis¹, O. Chubykalo-Fesenko², V. Tsiantos³

1. *School of Pedagogical And Technological Education, Athens, Greece*

2. *Instituto de Ciencia de Materiales de Madrid, Madrid, Spain*

3. *Department of Electrical Engineering, East Macedonia and Thrace Institute of Technology, Kavala, Greece*

We study the isothermal magnetic hysteresis of cubical and spherical nanoparticles with FM core/AF shell morphology, in order to elucidate the sensitivity of the exchange bias effect to the shape of the particles and the structural imperfections at the core-shell interface. We use a classical Heisenberg Hamiltonian with local anisotropy for modelling the magnetic structure and the Metropolis Monte Carlo algorithm to study the field-cooled process and the isothermal hysteresis loop. The coercive and exchange bias fields for spherical and cubical nanoparticles with similar nominal sizes are compared. Our simulations at low temperature show that : (i) Cubical particles exhibit higher coercivity than spherical ones, however this situation can be reversed in strongly disordered interfaces. (ii) Cubical particles exhibit lower exchange bias field than spherical ones, owing to the lower number of uncompensated spins, a fact that stems from the geometrical shape of the FM-AF interface. (ii) The presence of interface disorder suppresses the exchange bias field in the case of uncompensated interfaces (spherical or cubical particles), while the opposite trend is observed for compensated interfaces (cubical particles, only). (iii) With increasing degree of interface disorder the differences between spherical and cubical particles are gradually smeared out, rendering the shape effects of minor importance. (iv) The atomic scale details of the interface disorder (alloying or roughness) are of secondary importance in the dependence of the exchange bias and coercive fields on the degree of disorder. Our results shed new light in the interpretation of recent experimental findings on the shape-dependent exchange-bias effect in core-shell nanoparticles.

Acknowledgment: Research co-financed by the European Social Fund and Greek national funds through the Research Funding Program ARCHIMEDES-III

Mo.I-P30 - Exchange bias effect in hybrid magnetic nanoparticles

A. Tzavellas¹, D. Kechrakos¹, V. Tzitzios², I. Panagiotopoulos³, H. Srikanth⁴, O. Chubykalo-Fesenko⁵, V. Dimitriadis¹, N. Moutis¹, E. Sideris¹, G. Hadjipanayis⁶

1. School of Pedagogical And Technological Education (ASPETE), Athens, Greece

2. Institute of Nanoscience and Nanotechnology, NCSR 'Demokritos', Athens, Greece

3. Department of Materials Science and Engineering, University of Ioannina Ioannina, Greece,

4. Department of Physics, University of South Florida, Tampa, United States

5. Instituto de Ciencia de Materiales de Madrid, Madrid, Spain

6. Department of Physics and Astronomy, University of Delaware, Newark, United States

Solution chemistry methods provide a versatile bottom-up approach for the growth of nanoparticles with tailor-made of sizes, shapes and material combinations. In the present work we use solution chemistry methods to grow Fe₂O₃/CoO hybrid nanoparticles with both the direct (FM grown on AF) and the inverted (AF grown on FM) morphology and various sizes. We use a combination of imaging techniques (TEM), magnetometry (SQUID) and computer simulations to understand the factors controlling the exchange bias effect in these hybrid nanoparticles. We observe an interesting behavior at low temperatures exhibiting strong time dependent phenomena (initial curves lying out of the hysteresis loop) and suppression of the exchange bias effect below a certain particle size. We model the morphology of the hybrid nanoparticles by two partially overlapping spherical particles of FM and AF material, described by a classical Heisenberg Hamiltonian with different local anisotropy terms for the core, the (free) surface and the interface region of each constituent spherical particle. We obtain the isothermal magnetic hysteresis after field-cooling using the Metropolis Monte Carlo algorithm and investigate the dependence of the exchange bias effect on the different geometrical lengths characterising the hybrid nanostructure (particle diameters, center-to-center distance) and the material parameters (exchange and anisotropy energy). Our simulations show that the exchange bias field: (i) shows a non-monotonous dependence on the degree of overlap between two spherical particles of fixed radii, following the change of the interface-to-volume ratio. (ii) shows a non-monotonous dependence on the ratio of the particles radii (RFM/RAF), (iii) vanishes below a critical value of the AF radius. Our simulation results support adequately the experimental measurements.

Acknowledgment: The authors from ASPETE, NCSR "Demokritos", University of Ioannina, ICMM and University of Delaware acknowledge financial support by the European Social Fund and Greek national funds through the Research Funding Program ARCHIMEDES-III

Mo.I-P31 - Probing the exchange bias training effect at the interface using XMCD

E. Jiménez¹, N. Mikuszeit², D. R. Cavicchia³, F. D'Orazio⁵, L. Rossi⁴

1. *The European Synchrotron, ESRF, Grenoble, France*

2. *Univ. Grenoble Alpes INAC-SPINTEC, CNRS INAC-SPINTEC,CEA INAC-SPINTEC, Grenoble, France*

3. *Institut für Angewandte Physik, Universität Hamburg, Hamburg, Germany*

4. *Dipartimento di Scienze Fisiche e Chimiche, Università degli studi del l'Aquila, L'Aquila, Italy*

5. *Dipartimento di Scienze Fisiche e Chimiche, Università degli studi del l'Aquila, L'Aquila, Italy*

Exchange bias is a well known effect used in applications such as spintronics, where it provides, e.g., the stability of a fixed magnetic layer. The effect is mainly an interface effect between a ferromagnet (FM) and, mostly, an antiferromagnet (AFM). It is commonly agreed on that at the interface of the FM/AFM system, pinned and unpinned uncompensated moments play the crucial role. Nevertheless, a full picture of all underlying microscopic mechanisms yet has to be developed. The amount and nature of the uncompensated moments depends among others on the interface quality. This influences coercivity enhancement, maximum exchange bias field, and the accordingly required field cooling procedure. We present results on in-plane magnetized Co based FMs on antiferromagnetic thin film containing Mn. The thin films are grown using rf-magnetron sputtering at room temperature. Magnetic characterization has been done using magnetometer measurements as well as X-ray circular dichroism (XMCD) measurements. After a field cooling procedure the magnetometer measurements show that the first hysteresis cycles do not represent the a stable system, but the well known training effect takes place. Over the first hysteresis loop the overall exchange bias changes until saturation is reached. We investigated systems during this training period. The element specific XMCD measurements allow to study the uncompensated moments of the antiferromagnet and their evolution in time when applying an external magnetic field. The amount of uncompensated moments decreases with time. The stronger the applied field and the longer the period it is applied, the more pronounced the decrease. The variation of uncompensated AFM moments is in good agreement with the typical decrease of EB during the training process. We can therefore correlate the EB field to the net amount of uncompensated moments. Different layer thicknesses show the same behavior, supporting the interfacial nature of the effect.

Mo.I-P32 - Comparison between a concentrated and a diluted superspin systems

D. Peddis¹, D. Fiorani¹, K. Trohidou³, M. Vasilakaki³, S. Baker², P. Nordblad⁴, R. Mathieu⁴, C. Binns²

1. ISM-CNR, Institute of Structure of Matter, Area della Ricerca di Roma, Roma, Italy
2. Department of Physics and Astronomy, University of Leicester, Leicester, United Kingdom
3. Institute of Nanoscience and Nanotechnology, NCSR 'Demokritos', Agghia Paraskevi, Attiki, Greece
4. Department of Engineering Sciences, Uppsala University, Uppsala, Sweden

Superspin glasses (SSG) exhibit slow dynamics which is qualitatively indistinguishable from that observed in atomic spin glasses, and typical glassy properties such as aging, memory and rejuvenation. The non-equilibrium dynamics of two different nanoparticle systems will be discussed:

- 1) a concentrated nanoparticle system: MnFe₂O₄ nanoparticles (<D> @ 2 nm),
- 2) a dilute nanoparticle system: Co particles (<D> @ 2 nm) embedded in an antiferromagnetic Mn matrix with a volume fraction of 4.7 % (Co@Mn 4.7%).

Zero Field Cooled (ZFC) and Field Cooled (FC) magnetization curves show the typical SSG behaviour for both systems, i.e. a sharp maximum at ~ 40 K and ~ 65 K for MnFe₂O₄ and Co@Mn (4.7%), respectively.

The MnFe₂O₄ system was found to exhibit a superspin glass phase transition, using ac-susceptibility and Mössbauer spectroscopy measurements. Non-equilibrium dynamics of the system has been studied by memory and rejuvenation measurements.

Co@Mn 4.7% represents a very interesting example of glassy behaviour in a dilute system. Generally, for such particle dilution in diamagnetic matrix (e.g. Co embedded in Ag matrix), dipolar interactions are weak and an ordinary blocking process of independent particle moments is observed. Nevertheless, a non-equilibrium dynamics typical of SSG is observed in this system. The reasons for the observation of SSG dynamics rely on the microstructural properties of this system, characterized by a significant Co-Mn alloying. By memory and rejuvenation experiments and Monte Carlo simulations we showed that the memory effects increase with the Co concentration and that both the interface exchange coupling and the dipolar interparticle interactions contribute to the observed dynamical behavior².

References:

[1] D. Peddis, M. Hudl, C. Binns, D. Fiorani, and P. Nordblad. *Aging Experiments in a Superspin Glass System of Co Particles in Mn Matrix*. *J. Phys. Conf. Ser.* 200, 72074 (2010)

[2] M. Vasilakaki, K.N. Trohidou, D. Peddis, D. Fiorani, R. Mathieu, M. Hudl, P. Nordblad, C. Binns, and S. Baker. *Memory Effects on the Magnetic Behavior of Assemblies of Nanoparticles with Ferromagnetic Core / Antiferromagnetic Shell Morphology*. *Phys. Rev. B* 140402, 1–5 (2013)

Mo.I-P33 - Modeling of the exchange bias behavior of Bi-Magnetic Nanoparticle assemblies

G. Margaris¹, K. Trohidou¹, J. Nogués²

1. *Institute of Nanoscience and Nanotechnology, NCSR "Demokritos", Aghia Paraskevi, Attiki, Greece*

2. *ICREA and ICN2 - Institut Catala de Nanociencia i Nanotecnologia, Campus UAB, Bellaterra, Spain*

Recently, bi-magnetic core/shell nanoparticles, where both core and shell are either ferromagnetic (FM), ferrimagnetic (FiM) or antiferromagnetic (AFM), are becoming increasingly appealing.[1] The synergetic combination of the properties of the two constituents and their interactions can enhance their performance. We present a novel mesoscopic method[2] based on a Monte-Carlo approach to simulate dense assemblies of bi-magnetic core/shell nanoparticles by reducing the number of spins to be simulated to the minimum necessary to satisfactorily represent their magnetic structure and introducing the adequate exchange parameters between them. We simulate the hysteresis loops and the temperature dependence of the magnetization, $M(T)$, of a 2D and a 3D random assembly of FM/AFM core/shell nanoparticles with high and low densities. The most prominent result of the simulation is the significant increase of both HC and HE for the large density of nanoparticles, where while $HE > HC$ for high densities, above the percolation threshold, it is opposite for low densities. Similarly, the results for $M(T)$ show that for higher densities the blocking temperature, TB, (i.e., the maximum of the zero field cooled $M(T)$) increases dramatically. Remarkably, all these features are consistent with the experimental results on Co/CoO nanoparticles assemblies[3].

[1] J. Nogués, V. Skumryev, J. Sort, S. Stoyanov and D. Givord, Phys. Rev. Lett. 97, 157203(2006)

[2] G. Margaris, KN Trohidou, J. Nogues, Adv. Mater. 24, Issue 31, pp4331-4336(2012)

[3] J. Nogués, J Sort, V. Langlais, V. Skumryev, S. Suriñach, J.S. Muñoz, M.D. Baró, Phys. Rep. 2005, 422, 65

Mo.I-P34 - Hysteresis properties of exchange coupled Fe-Ni/Tb-Co bilayers separated by ultrathin Ti spacer

N. Kulesh¹, K. Balymov¹, O. Adanakova¹, A. Svalov¹, V. Vas'kovskiy¹

1. Ural Federal University, Ekaterinburg, Russia

Thin films containing exchange coupled ferromagnetic (FM) and antiferromagnetic (AFM) layers are widely used in magnetic field sensors and spintronics devices. Typically Fe₂₀Ni₈₀ is used as a FM material and FeMn or IrMn as an AFM material. In this work we considered similar structures based on the amorphous Tb₂₇Co₇₃ ferrimagnetic layer instead of AFM and Fe₂₀Ni₈₀ or Fe₁₀Ni₉₀ as a material of the FM layer. Unlike antiferromagnetic materials Tb-Co has spontaneous magnetization, can induce large exchange bias field, and potentially has higher blocking temperature. Fe₁₀Ni₉₀ alloy was considered due to the large anisotropic magnetoresistance (AMR), relatively high coercivity and magnetostriction, which can potentially be utilized in deformation sensors.

Samples were prepared by ion beam sputtering of mosaic (Tb-Co) and alloyed (Fe-Ni) targets onto the glass substrates. Magnetic anisotropy of the Tb-Co layer was induced by application of the uniform in-plane magnetic field during the deposition process. Thicknesses of the main layers were 100 and 50 nm for Tb-Co and Fe-Ni respectively.

For all samples we observed expected reduction of the exchange bias field (H_{eb}) with thickness of the Ti spacer (L_{Ti}) increasing. Coercivity of both Fe₁₀Ni₉₀ and Fe₂₀Ni₈₀ layers remained about 0.2 Oe for L_{Ti} below 0.7 nm due to magnetization process taking place by magnetization rotation. As H_{eb} and magnetic susceptibility were modified by introduction of the nonmagnetic spacer and considering low coercivity, 20% higher AMR, and nearly the same magnetic susceptibility as observed for Fe₂₀Ni₈₀ layer, Fe₁₀Ni₉₀ can be successfully used instead of Fe₂₀Ni₈₀ in sensors applications. In order to verify the leading role of the uniaxial anisotropy in the formation of FM layers hysteresis properties, Co/Tb-Co films were obtained, which demonstrated coercivity below 1 Oe and relatively high magnetic susceptibility.

This work was supported by The Ministry of Education and Science of the Russian Federation, project No. 1362.

Mo.I-P35 - Interface exchange coupling in a CoPt/NiO bilayer

S. Laureti¹, L. Del Bianco², B. Detlefs³, E. Agostinelli¹, D. Peddis¹, A. Maria Testa¹, G. Varvaro¹, D. Fiorani¹

1. *ISM-CNR, Area della Ricerca RM1, Monterotondo Scalo, Roma, Italy*

2. *Dipartimento di Fisica e Astronomia, Università di Bologna, Bologna, Italy*

3. *European Synchrotron Radiation Facility, 6 Rue Jules Horowitz, Grenoble Cedex 9, France*

The effects originating from the proximity between the ferromagnetic and the antiferromagnetic phase in a CoPt/NiO bilayer, grown at 670 K by Pulsed Laser Deposition, have been investigated from the point of view of the chemical properties, by Hard X-ray Photoelectron Spectroscopy, HAXPES, and of the magnetic behavior (by measuring hysteresis loops in the temperature range 5-300 K both after cooling in zero external field and after cooling from T=380 K in a field of 1 T). At T=5 K, the coercivity, measured after zero-field-cooling, is ~168 mT, to be compared to that of a reference CoPt layer of ~87 mT. Such magnetic hardening of the ferromagnetic CoPt phase is ascribed to the magnetic exchange interaction at the interface with the antiferromagnetic NiO phase, which is also responsible for the horizontal shift of the loop, observed after field-cooling (exchange bias effect). Actually, the latter effect persists up to room temperature (exchange fields H_{ex} ~60 mT and ~8 mT were observed at T=5 and 300 K, respectively). Hence, it can be deduced that the CoPt and NiO phases are efficiently coupled by the exchange interaction, despite the chemical inhomogeneity observed at the interface region. In fact, the HAXPES analysis reveals that a chemical reduction of the NiO phase takes place in the interface region, resulting in the formation of metallic Ni. On the other hand, the interface chemical inhomogeneity is proposed to be at the origin of the peculiar shape of the field-cooled loop at T=5 K, featuring a double reversal of the magnetization[1].

This work has been supported by MIUR, under project FIRB2010 - NANOREST

[1] Laureti et al. *Thin Solid Films*, 543 (2013) 162

Mo.I-P36 - Exchange bias Study of Ni_{50.3}Mn_{36.9}Sb_{12.8}/BiFeO₃ heterostructures fabricated by magnetron sputtering

R. Barman¹, D. Kaur²

1. *Indian Institute of Technology Roorkee, Roorkee, India*

2. *Indian Institute of Technology Roorkee, Roorkee, India*

In the present study, we have reported the growth of Ni_{50.3}Mn_{36.9}Sb_{12.8}/BiFeO₃ heterostructure onto LaNiO₃ (LNO) coated Si (100) substrate by magnetron-sputtering at 5500C. The heterostructure exhibits preferred (220) and (001) orientations of Ni_{50.3}Mn_{36.9}Sb_{12.8} and BiFeO₃ respectively. Exchange bias field (EB) ~ 50 Oe was observed at 10 K in Ni_{50.3}Mn_{36.9}Sb_{12.8} thin film. This value of EB is enhanced to ~ 470 Oe at 10 K for Ni_{50.3}Mn_{36.9}Sb_{12.8}/BiFeO₃ heterostructure. The shifting of hysteresis loop was decreased with increasing of temperature, which is mainly due to the decoupling of FM-AFM spins at the interface. It is obtained from magnetic hysteresis loop characteristic that Saturation magnetization (Ms) is enhanced to 230 emu/cm³ in our heterostructure. This improvement of magnetization is due to the superexchange magnetic interaction between Fe³⁺ and Mn³⁺, occurring at the interface, combined with the compressive strain. On the other hand, a significant result for this heterostructure has been observed, EB~ 67 Oe at room temperature, which makes them a promising candidate for various multifunctional MEMS devices at room temperature.

Mo.I-P37 - Interfacial coupling induced symmetry-breaking of spin-orbit interaction in exchange biased systems

P. Perna¹, D. Maccariello^{1,2}, F. Ajejas^{1,2}, J. L. F. Cuñado^{1,2}, R. Guerrero¹, M. A. Niño¹, J. Pedrosa^{1,2}, A. Bollero¹, J. Camarero^{1,2}, R. Miranda^{1,2}

1. *IMDEA Nanociencia, Campus de Cantoblanco, Madrid, Spain*

2. *D.F.M.C., Universidad Autonoma de Madrid, Madrid, Spain*

In transition 3d metal systems the Spin-Orbit (SO) interaction arises from the coupling of the electron spin with its orbital motion. In order to minimize its energy, the system chooses preferential directions for the magnetization, modifying therefore its magnetic anisotropy. Since the SO coupling mixes the electron spin-up and spin-down states in the FM, it gives rise to a magnetization-direction dependent scattering rate, producing an anisotropic magnetoresistance (AMR) signal that depends on the angle enclosed by the magnetization vector and the injected electrical current [1]. In spintronics, the need of stabilizing and controlling the magnetoresistance (MR) output of device, is satisfied by resorting to ferromagnetic/antiferromagnetic (FM/AFM) structures in which the magnetization direction of the FM layer is pinned. In these systems an added anisotropy comes out from frustrated exchange interactions at FM/AFM interface, introducing a interfacial symmetry-breaking along the field axis determining a spin rearrangement in both layer surfaces [2]. Here, we investigate the symmetry-breaking effects of the SO interaction in exchange-biased FM/AFM polycrystalline Co/IrMn bilayer. This is done by performing angular- and field-dependent simultaneous measurements of the magnetoresistance and vectorial-resolved Kerr magnetization hysteresis loops [1,3]. We highlight the role of the exchange-bias induced magnetic anisotropy in determining asymmetric features of the field-driven angular anisotropic magnetoresistance curves, which are directly correlated to the magnetization reversal mechanisms. The experimental field dependent curves, including their asymmetries, gives direct visualization of SO chiral asymmetry which is intrinsic of an exchange-bias system.

[1] P. Perna et al. Appl. Phys. Lett. 104, 202407 (2014)

[2] J. Camarero, et al., Phys. Rev. Lett. 95, 057204 (2005); Phys. Rev. B 80, 014415 (2009); Appl. Phys. Lett. 95, 122508 (2009)

[3] P. Perna et al. Phys. Rev. B 86, 024421 (2012)

Mo.I-P38 - Modeling the exchange bias interaction in ferromagnetic/antiferromagnetic films and nanostructures

E. Bonfiglioli¹, P. Malagò¹, F. Chinni¹, F. Spizzo¹, M. Tamisari^{1,2}, L. Giovannini¹, L. Del Bianco^{1,3}

1. *Dipartimento di Fisica e Scienze della Terra, Università di Ferrara, Ferrara, Italy*

2. *Dipartimento di Fisica e Geologia, CNISM Università di Perugia, Perugia, Italy*

3. *Dipartimento di Fisica e Astronomia, Università di Bologna, Bologna, Italy*

A novel approach to model the exchange bias (EB) effect in ferromagnetic (FM)/antiferromagnetic (AFM) continuous films and nanodots is presented. The aim is to study both the EB magnetothermal stability and spatial confinement effects, key features for modern spintronic devices. The EB is due to the exchange coupling at the FM/AFM interface, and is featured by the exchange bias field (Hex), i.e. the horizontal shift of the hysteresis loop. To model the exchange coupling we used the three-dimensional Object Oriented MicroMagnetic Framework. The AFM phase was described as a collection of both fixed and rotatable spins (FSs and RSs, respectively) both interacting with the FM phase: the FSs have the role of pinning centers, i.e. they mirror the presence of regions with high anisotropy energy in the AFM phase, so they increase Hex; the RSs change their orientation following the FM magnetization, so they do not contribute to Hex. The calculations were performed for a continuous film and for squared dots with size (D) ranging from 1200 nm down to 300 nm. By changing the FSs to RSs relative fraction we accounted for confinement effects, confirming a reduction of the anisotropy energy for the AFM grains at the dot border. Moreover, by introducing spatial correlations among FSs we modeled the proven existence of a low temperature frozen collective regime of the interfacial AFM spins and its interplay with D. A good agreement was found between the results of the calculations and the experimental data [1]. Finally, we tested our model for the description of the dynamical properties of the FM/AFM system; we will present our results regarding the spin wave frequency dependence on the external magnetic field. This research was sponsored by MIUR-FIRB2010 project RBFR10E61T/NANOREST and PRIN2010-11 Project 2010ECA8P3/DyNanoMag.

[1] F. Spizzo et al., Phys. Rev. B 91 (2015) 064410

Mo.I-P39 - Spin flop transitions in exchange-biased structures

F. Pelegrini¹, D. Schafer², J. Geshev², V. Nascimento³, E. Baggio-Saitovitch⁴

1. *Universidade Federal de Goiás - Instituto de Física, Goiânia, Brazil*

2. *Universidade Federal do Rio Grande do Sul - Instituto de Física, Porto Alegre, Brazil*

3. *Universidade Federal do Espírito Santo - Departamento de Física, Vitória, Espírito Santo, Brazil*

Ferromagnetic Resonance (FMR) study of the exchange anisotropy of magnetron sputtered NiFe/IrMn bilayers and NiFe/FeMn/NiFe trilayers reveals that low field absorption modes also are excited by the microwave field. In particular, room temperature FMR experiments at frequency of 9.8 GHz, with swept static field and the usual modulation and phase sensitive detection techniques, reveal the excitation of three absorption modes at applied fields of 80, 86 and 95 Oe, for Ta(7nm)/NiFe(20nm)/IrMn(15nm)/Ta(5nm) bilayer, and at applied fields of 83, 98 and 123 Oe for WTi(7nm)/NiFe(30nm)/FeMn(13nm)/NiFe(10nm)/WTi(7nm) trilayer. The exchange-bias field, given by the angular variation of the in-plane absorption field of the uniform resonance mode, is equal to 85 Oe for the bilayer sample, and 83 Oe for the trilayer sample. For both structures, the spectra exhibit the three narrow and distinct low field absorption lines for the swept static magnetic field anti-parallel to the unidirectional anisotropy axis. They are attributed to spin flop transitions on the antiferromagnetic layer. As the field increases and the Zeeman energy grows, the spins on opposing sub-lattices cant towards the applied field and at a field H1 produce a net moment in this direction, at a field H2 neighboring spins become perpendicular to each other, at a field H3 the Zeeman energy overcomes the anti-ferromagnetic exchange and the antiferromagnetic layer is saturated. The bilayer sample was grown in the presence of a static magnetic field; the trilayer sample was grown in the absence of any applied field, but next subjected to a high field cooling process. The FMR results reveal that they have very similar magnetic parameters and confirm the equivalence of the distinct processes used to set the unidirectional anisotropy axis. The microwave absorption due to spin flop transitions reflects clearly the behavior of spins at the ferromagnetic-antiferromagnetic interface.

Mo.I-P40 - Magnetothermal behavior of the antiferromagnet in exchange-coupled NiFe/IrMn bilayers

E. Bonfiglioli¹, F. Chinni¹, F. Spizzo¹, M. Tamisari^{1,2}, L. Del Bianco^{1,3}

1. *Dipartimento di Fisica e Scienze della Terra, Università di Ferrara, Ferrara, Italy*

2. *Dipartimento di Fisica e Geologia, CNISM Università di Perugia, Perugia, Italy*

3. *Dipartimento di Fisica e Astronomia, Università di Bologna, Bologna, Italy*

The magnetothermal behavior of antiferromagnetic IrMn layers of different thickness ($t_{\text{AFM}} = 3, 6, 10$ nm) has been studied exploiting the exchange coupling with a ferromagnetic 5nm-thick NiFe layer. We have introduced an original protocol for the measurement of NiFe/IrMn sample magnetization as a function of temperature and time at different values of an external magnetic field H_{inv} , applied antiparallel with respect to the unidirectional exchange anisotropy [1]. This analysis probes the effective distribution of anisotropy energy barriers of the antiferromagnetic phase, as it is sensed by the coupled ferromagnetic layer. The NiFe/IrMn samples have been grown by DC magnetron sputtering at room temperature in a magnetic field of 400 Oe. At low temperature, $T < 100$ K, the barrier distribution features a peak, centered at $T \sim 20$ K, and this value is nearly independent on t_{AFM} and H_{inv} . For $T > 100$ K, a large peak is visible, and its position changes with t_{AFM} and H_{inv} . These results are consistent with the existence of a low-temperature magnetic regime in which the interfacial IrMn spins are frozen in a disordered glassy state and collectively involved in the exchange coupling mechanism. At $T \sim 100$ K, the collective state breaks up and only the interfacial IrMn spins which are tightly polarized by the IrMn nanograins, forming the bulk of the layer, are effectively involved in the exchange coupling. Therefore, for $T > 100$ K, the anisotropy energy barriers of bulk IrMn nanograins mainly give rise to the large peak in the distribution. The thermal evolution of the exchange field and of the coercivity in the three samples is discussed and coherently explained in the framework of this description. This research was sponsored by MIUR-FIRB2010 project RBFR10E61T/NANOREST.

[1] F. Spizzo et al., J. Phys.: Condens. Matter 25 (2013) 386001

Mo.I-P41 - Pressure effect on ferromagnetism and exchange bias in phase-separated (Bi,Ca)Mn_{1-x}Ru_xO₃ manganitesA. Wisniewski¹, I. Fita¹, V. Markovich², R. Puzniak¹*1. Institute of Physics, PAS, Warsaw, Poland**2. Department of Physics, Ben-Gurion University of The Negev, Beer-Sheva, Israel*

Pressure effect on magnetic state and exchange bias (EB) in phase-separated ferromagnetic/antiferromagnetic (FM/AFM) CaMn_{1-x}Ru_xO₃ ($0.06 \leq x \leq 0.15$) and Bi_{0.4}Ca_{0.6}Mn_{1-x}Ru_xO₃ ($x = 0.1, 0.2$) manganites was studied under a pressure up to 11 kbar. For both manganites, complex pressure and Ru-doping effects on EB and coercive fields may be explained with a model of size-variable (depending on Ru content and pressure) nanoscale FM droplets embedded in an AFM matrix. For CaMn_{1-x}Ru_xO₃, the observed enhancement of EB with increasing pressure is attributed to the reduction in the FM cluster size, evidenced by both pressure dependence of spontaneous FM moment and EB field dependence upon cooling field. The impact of FM droplet size on the EB was further evidenced by the magnetic field effect, which, in contrast to the pressure effect, leads to a growth of the FM droplets. The intricate coercive field dependencies on both pressure and Ru content are understandable in a view of the transition from the multidomain state to the single-domain one, induced by droplet size decrease with increasing pressure or with doping lowering. For Bi_{0.4}Ca_{0.6}Mn_{1-x}Ru_xO₃ charge-ordered manganite, it was found that the $x = 0.2$ composition is basically ferromagnetic while the low-doped ($x = 0.1$) one exhibits a FM cluster glass behavior and exchange bias effect at low temperatures. For this compound, both Ru-doping and external pressure act similarly, leading to a growth of the FM clusters and consequently to a suppression of the EB. The results show that for phase-separated FM/AFM manganites the EB effect may be smoothly controlled by pressure because of pressure-dependent size of FM clusters.

Mo.J-P01 - Full-potential KKR calculations for lattice distortion of point defects in Al, based on the generalized-gradient approximation

C. Liu¹, M. Asato², N. Fujima³, T. Hoshino³

1. Graduate School of Science and Technology, Shizuoka University, Shizuoka, Japan

2. National Institute of Technology, Niihama College, Niihama, Japan

3. Graduate School of Engineering, Shizuoka University, Shizuoka, Japan

In the previous papers [1, 2], we presented ab-initio data for the cohesive energies of Al and X (=Na-Si, Sc-Zn, Zr-Ag) and defect energies such as the solution energies of X impurities in Al, and the X-X and X-vacancy interaction energies in Al. In order to calculate the defect energies in Al, however, we neglected the distortion effect around the defects. It is easily expected that the distortion effect becomes important for the impurities with a large size-misfit, compared with the host atom [3]. We now study systematically the distortion effect. The calculations are based on the generalized-gradient approximation in the density functional formalism and the full-potential Korringa-Kohn-Rostoker Green's function method [4]. We already discussed the lattice distortion effect around single impurities (Sc-Ge) in Al [5].

In the present paper we show the calculated results for the lattice distortion of the two impurities X-X (X=Sc-Ge) in Al, being located at the 1st-nearest neighboring sites. The interatomic distance of the X-X bond lengthens for X=Sc, Mn, Fe, Co, Ni, Ga, and Ge while shortens for X=V, Cu, and Zn. We show that the calculated results for the lattice distortion of the two impurities X-X in Al are understood by considering the atomic sizes of X elements and the stronger Al-X (sp-d) bond compared with the X-X (d-d) bond, obtained by the present ab-initio calculations.

References:

- [1] T. Hoshino, M. Asato, and N. Fujima, *Intermetallics* 14 (2006), 908-912.
- [2] T. Hoshino, M. Asato, S. Tanaka, F. Nakamura, and N. Fujima, *Intermetallics* 14 (2006), 913-916.
- [3] M. Asato, C. Liu, K. Kawakami, N. Fujima, and T. Hoshino, *Mater. Trans.* 55 (2014), 1248-1256.
- [4] T. Hoshino, T. Mizuno, M. Asato, and H. Fukushima, *Mater. Trans.* 42 (2001), 2206-2215.
- [5] C. Liu, M. Asato, N. Fujima, and T. Hoshino, presented in The 15th-IUMRS conference, submitted to MRS-J.

Mo.J-P02 - Magnetism of 4d clusters compared to magnetism of 3d clusters: ab-initio study of free Rh and Fe clusters

O. Sipr¹, H. Ebert², J. Vackar¹, J. Minar^{2,3}

1. *Institute of Physics ASCR, Prague, Czech Republic*

2. *Ludwig-Maximilians-Universitat Munchen, Germany*

3. *University of West Bohemia, Pilsen, Czech Republic*

A fully relativistic ab-initio study of free Rh clusters of 13-135 atoms is performed to identify general trends concerning their magnetism. Special attention is paid to checking whether concepts which proved to be useful in interpreting magnetism of 3d metals are applicable to magnetism of 4d systems. By comparing theoretical results for free Rh clusters and for free Fe clusters, we demonstrate that some important intuitive concepts which proved to be useful when interpreting magnetism of 3d metals are not applicable for magnetism of 4d systems. In particular, there is no systematic relation between local magnetic moments and coordination numbers. On the other hand, the Stoner model appears to be well-suited as a criterion for the onset of magnetism of Rh clusters and, on the top of that, it can serve as a guide for the dependence of local magnetic moments on the local density of states at the Fermi level. Large orbital magnetic moments antiparallel to spin magnetic moments were found for some sites in Rh clusters, which might explain some earlier experimental results.

Mo.J-P03 - On the edge magnetism and energy gaps in graphenelike nanoribbons

S. Krompiewski¹

1. Institute of Molecular Physics, Polish Academy of Sciences, Poznan, Poland

This study aims to indicate the main factors responsible for formation of magnetic moments at edges of graphenelike nanoribbons. The attention is focused on the effect of: intrinsic spin-orbit coupling, zigzag nanoribbon's width, and perpendicular electric field. Of particular interest is the interplay of the edge magnetism and the energy band gap. It is shown that, with the increasing electric field, typically the following phases develop: magnetic insulator (with in-plane spins), nonmagnetic semimetal, and nonmagnetic insulator.

Acknowledgments_: Supported by the National Science Centre, through the decision No. DEC-2013/10/M/ST3/00488

Mo.J-P04 - Control of domain wall thickness by introducing spatial modulation of uniaxial anisotropy and exchange stiffness parameters

H. Arai^{1,2}, H. Imamura²

1. *Presto, Jst, Tokyo, Japan*
2. *AIST, Tsukuba, Japan*

A magnetic domain wall (DW) has been widely investigated for applications to spintronics devices such as Racetrack memory [1] and microwave oscillators [2]. In these applications, the DW must be pinned at a certain position to prevent undesired translational motion. Also the DW thickness must be controlled to improve device properties such as memory density and oscillation frequency. A common way to pin the DW and control its thickness is to build a geometrical constriction such as a notch. However, precise control of nano-sized notches is difficult without damaging the wire. In this study, we propose another approach to control the DW thickness and DW pinning by introducing spatial modulation of the exchange stiffness (A) and uniaxial-anisotropy (K) parameters to the system. We derived Euler-Lagrange equation and the Landau-Lifshitz-Gilbert equation taking into account of the spatial modulation of A and K . By analyzing the modulation as a perturbation, we showed that the modulation of A is more effective to modify the DW thickness than that of K . We numerically calculated the phase diagram of the DW properties on the wide range of modulation parameters, and showed that it can be classified into three regions: short DW is pinned, long DW is pinned, and DW is not pinned. This study is to appear in Jpn. J. Appl. Phys. (Rapid comm.)

References:

- [1] M. Hayashi, L. Thomas, R. Moriya, C. Rettner, and S. S. P. Parkin, *Science* 320, 209 (2008). S. S. P. Parkin, M. Hayashi, and L. Thomas, *Science* 320, 190 (2008)
- [2] L. Thomas, M. Hayashi, X. Jiang, R. Moriya, C. Rettner, and S. Parkin, *Science* 315, 1553 (2007). M. Franchin, T. Fischbacher, G. Bordignon, P. de Groot, and H. Fangohr, *Phys. Rev. B* 78, 054447 (2008). H. Arai, H. Tsukahara, and H. Imamura, *Appl. Phys. Lett.* 101, 092405 (2012)

Mo.J-P05 - Imprinting skyrmions in thin films by ferromagnetic and superconducting templates

C. Navau¹, N. Del-Valle¹, S. Agramunt¹, A. Sanchez¹

1. University Autonomous Barcelona, Bellaterra, Spain

Magnetic skyrmions are promising candidates as information carriers in a new generation of memories. How to nucleate and stabilize skyrmions is essential for their successful application to technology. By solving the dynamic Landau-Lifshitz-Gilbert equation, we theoretically demonstrate that arrays of skyrmions can be imprinted in ultrathin ferromagnetic films in large numbers by bringing a magnetic nanostructured template close to the film. Two kind of templates, allowed by present-day nanotechnologies, are studied: arrays of ferromagnetic nanorods (sources of dipolar magnetic fields) and superconducting vortices (sources of monopolar magnetic fields). Skyrmions are generated when exposing magnetic films to the template fields for short time of nanoseconds and remain stable after removing the template. This idea could open the possibility of to write large quantities of elements of few nanometers size in a fast way, which could be manipulate and read through the free surface of the film, for a future generation of magnetic memories.

Mo.J-P06 - Long-range order of classical dipoles on the kagome lattice

M. Maksymenko¹, V. Ravi Chandra², R. Moessner³

1. Department of Condensed Matter Physics, Weizmann Institute of Science, Rehovot, Israel

2. School of Physical Sciences, National Institute of Science Education and Research, Institute of Physics Campus, Bhubaneswar, India

3. Max-Planck-Institut für Physik komplexer Systeme, Dresden, Germany

We study the role of dipolar interactions in the system of classical spins on the highly frustrated two-dimensional kagome lattice. With a combination of the Luttinger-Tisza approach, numerical energy minimization, spin-wave analysis and parallel tempering Monte-Carlo we investigate the long-range orderings and finite-temperature phase transitions for a Hamiltonian containing both dipolar and nearest-neighbor interactions. We find two distinct low-temperature orderings. For weak and moderate dipolar interactions we observe a three-sublattice 120-degree order while for strong dipolar interactions we uncover a peculiar ferrimagnetic state with continuously varying net moment. For these orderings we study low-temperature excitations and corresponding finite-temperature phase transitions. The critical behavior for 120-degree state is consistent with Ising universality class, while for the ferrimagnetic state we obtain drifting exponents satisfying 'weak universality' hypothesis. Interestingly, the flat band of zero-energy spin-wave excitations in nearest-neighbor kagome antiferromagnet acquires a finite gap and minimal dispersion as dipolar interactions are added.

Mo.J-P07 - Spin glass state (SGS) and other seven fundamental magnetic structures with their symmetry groups in terms of the fibre bundle approach: Application to explain experiments on the temperature dependence of susceptibility in SGS

J. Warczewski¹, P. Gusin², D. Wojcieszuk³

1. *University of Silesia, Institute of Physics, ul. Uniwersytecka 4, Katowice, Poland*

2. *Wroclaw University of Technology, Faculty of Technology and Informatics, Jelenia Góra, Poland*

3. *University of Silesia, Institute of Physics, ul. Uniwersytecka 4, Katowice, Poland*

We present the description of all the eight fundamental magnetic structures and their symmetry groups including SGS in terms of the fibre bundle approach [1]. It turns out that the SGS structure consists in the appearance of the 3-dimensional Gaussian distribution of the orientations of all the separate atomic magnetic moments in the sample. Therefore, the magnetization vector M is also subject to the Gaussian-like distribution. Thus, the structure of the SGS is presented by M situated along the generatrix of a given cone whose axis coincides with the direction of an internal spontaneous magnetic field H indispensable for the SGS stability in a sample [2]. The axis of the 3-dimensional Gaussian distribution mentioned above coincides with the same direction. Any precession angle of M around H represents the symmetry operation of SGS once the angle between M and H remains constant. This means that the symmetry group of SGS is $SO(2)$. The temperature dependence of susceptibility of SGS in the alloys $Cu_{1-x}Mn_x$ ($x=1.08$ and 2.02) [3] can be explained on the basis of aforementioned relationship, namely: at ZFC it corresponds to the gradual degeneration of the Gaussian distribution of the magnetization vector with the increase of temperature, while at FC the effect is dominated by the external field F , which is usually much higher than H and it destroys instantaneously the primary Gaussian-like distribution of magnetic moments. We take in the account the interrelation of both fields and the frustration of orientations of the magnetic moments situated on the separate atoms with their given average kinetic energy depending on temperature.

[1] Warczewski, Gusin, Wojcieszuk, *Mol.Cryst.Liq.Cryst.*, 554(2012), 209-220

[2] Warczewski, Gusin, *J.Phys.:Condens.Matter*, 21(2009), 035402-035406

[3] Nagata, Keesom, Harrison, *Phys.Rev.*B19, 1633(1979)

Mo.J-P08 - Magnetization processes of CoPt antidot arrays

P. Gawronski¹, C. Bran², A. Asenjo², O. Chubykalo-Fesenko², I. Lucas³, R. Del Real², M. Vazquez²

1. AGH University of Science And Technology, Kraków, Poland

2. Instituto de Ciencia de Materiales de Madrid, CSIC, Madrid, Spain

3. Instituto de Nanociencia de Aragón (INA) Universidad de Zaragoza, Zaragoza, Spain

Magnetic properties of thin films can be controlled by the presence of holes or antidots, through their geometrical parameters such as the antidot diameter, separation between them and thickness of the film. The use of materials with perpendicular anisotropy such as CoPt provides an important route for potential application of these low dimensional nanostructures in magnetic recording, sensor or magnonic devices. In this work we study the magnetic behavior of antidot thin films with perpendicular anisotropy. The combined use of magnetometry, magnetic force microscopy (MFM) and the micromagnetic simulations give us an insight into the coercivity mechanisms of these materials. As a result of the competition between the perpendicular anisotropy and the thin film shape anisotropy, the hysteresis cycles becomes more inclined and the remanence decreases when the thin film thickness increases. To mimic the competition between the two anisotropies, micromagnetic simulations with fixed thin film thickness and varying the strength of the perpendicular anisotropy have been performed. To induce the broken hexagonal ordering symmetry, frequently observed the experimentally measured arrays, we rotated the lattice in half of the simulated array by 30 degrees, and filled the empty spaces by antidots. The numerically obtained values of coercivity grow with the diameter of the antidots for all investigated thicknesses of the arrays. The magnetic configurations at the remanence show the change of the domain structure from small domains localized at antidots to larger stripe domains. The simulated micromagnetic structures resemble those obtained by MFM in antidot thin films, prepared by electrodeposition in alumina membranes with the multilayer structure [Co(0.4nm)/Pt(0.7nm)]_x and varying the total thin film thickness.

Mo.J-P09 - First-principles calculations of the spin coupling between lanthanide adatoms and iron islandsC. de la Fuente¹, D. Coffey², J. L. Diez-Ferrer³, D. Serrate⁴, M. Ciria⁵, J. Arnaudus⁶

1. *Depto. Física de la Materia Condensada e ICMA, Univ. Zaragoza – CSIC, Zaragoza, Spain*
2. *Depto. Física de la Materia Condensada & LMA-INA, Universidad de Zaragoza, Zaragoza, Spain*
3. *Lab. Microscopías Avanzadas (LMA) & Inst. de Nanociencia de Aragón (INA), Univ. de Zaragoza, Zaragoza, Spain*
4. *Depto. Física de la Materia Condensada & LMA-INA, Universidad de Zaragoza, Zaragoza, Spain*
5. *Depto. Física de la Materia Condensada e ICMA, Univ. Zaragoza – CSIC, Zaragoza, Spain*
6. *Depto. Física de la Materia Condensada & LMA-INA, Universidad de Zaragoza, Zaragoza, Spain*

We performed a study of the electronic properties of Tm and Lu adatoms over an Fe monolayer on (110)W by using non-collinear spin polarized (SP) DFT-based first principles calculations, where LSDA+U is introduced for including the corresponding corrections when GGA fails, using $U = 0.8$ eV for Fe d-states and $U = 5.0$ eV for the adatom's 4f states. The spin-orbit coupling was also included to analyze the dependence of Kohn-Sham ground state energy on the direction of the magnetic moments. We performed a fully 3D structural optimization of an "adatom" + (3x3x1) supercell (217 atoms). Although the electronic structure of Tm adatoms is Tm³⁺, the 4f orbital and spin momenta are reduced by almost 50 % with respect to bulk Tm, what could be due to the existence of an important uniaxial magnetic anisotropy. The spontaneous 4f spin magnetic moment of Tm is almost fully aligned along [1 -1 0], which is the easy axis direction of the Fe monolayer, and shows a small tilting out of the (110) plane, of about 10°, towards [1 1 0] direction. On the other hand, we found that the Campbell mechanism proposed for Rare Earth-Transition Metal intermetallics, consisting in the antiferromagnetic (AF) coupling between the 5d Rare Earth spins and the 3d Fe spins, also holds at the single atom limit for both, Tm and Lu adatoms. Further, the analysis of conductance at different bias indicates that the major contribution is coming from dxz+dyz - states. The conductance calculations as well as the obtained AF coupling between 5d and 3d spin moments are in agreement with our spin polarized scanning tunneling microscopy experimental results.

Mo.J-P10 - A Methodology Study of the Hysteresis Loops by Monte Carlo Simulation

Z. Nehme¹, Y. Labaye¹, N. Yaacoub¹, R. Sayed Hassan^{1,2}, J. Greneche¹

1. IMMM, Université du Maine, CNRS UMR-6283, Le Mans, France

2. Faculté des Sciences, Université Libanaise, Elhadath, Beyrouth, Liban

During the last decades, the study of magnetic nanostructures has been the center of interest among the scientific community because of their increasing number of applications in various fields including catalysis, biotechnology [1], recording media (MRAM, à) [2]. Some magnetic properties are derived from the hysteresis loops the major characteristic of which is the coercive field. It comes into play in the study of various physical phenomena such magnetic anisotropy, exchange bias coupling that induces an additional anisotropy in materials [3], à. We are interested in the study of magnetic and structural exchange biased nanoparticles, as typically core@shell ones. For a detailed microscopic description of such spin system, the Monte Carlo MC method seems to be the most suitable one. But, simulating an hysteresis loop by means of MC can be affected by different numerical parameters such as the intrinsic algorithm dynamic, the field sweep speed, the field direction according to the anisotropy direction, the temperature, the magnetic anisotropy value, the reversal mechanism, à [4,5,6]. So, we need to understand the significance of the obtained numerical coercive field. We focused our study on the impact of varying the effective anisotropic constant on the coercive field for different temperatures by investigating the dynamics of different algorithms. A study of the angular acceptance move distribution has allowed us to check the validity of the implemented algorithm and to compare the dynamics generated by different algorithms in order to keep a good sampling of the phase space and to perform efficient simulations. The results show a linear dependence between the coercive field and the effective anisotropy constant for non-biased conditions. We conclude that the MC coercive field has a physical and numerical significance allowing us to describe correctly the magnetic properties for exchange biased nanoparticles.

[1] I. Safarik &al, Chem. Papers 63 (2009) 497

[2] B. D. Terris&al, J. Phys. D: Appl. Phys. 38 (2005) 199

[3] J. Nogués&al, Phys. Reports 422 (2005) 65

[4] M. Dimian&al, J. Appl. Phys. 91 (2002) 7625

[5] L. Berger&al, Phys. Rev. B 77 (2008) 104331

[6] K. J. Garcia-Otero&al, J. Magn. Magn. Mater. 203 (1999) 268

Mo.J-P12 - Micromagnetic study of inverse opal-like structures which exhibit spin ice behavior

I. Dubitskiy^{1,2}, A. Syromyatnikov^{1,2}, N. Grigoryeva¹, A. Mistonov^{1,2}, I. Shishkin^{1,2}, S. Grigoriev^{1,2}

1. Saint Petersburg State University, Saint Petersburg, Russia

2. Petersburg Nuclear Physics Institute, Gátchina, Russia

Artificial spin ice systems have attracted much attention in recent years [1]. They can be used as a model objects for the study of frustration phenomenon and magnetic excitations similar to those observed in pyrochlore spin ice materials. Most of artificial spin ice systems are two dimensional. Inverse opal-like structures (IOLS) are promising candidates to become first 3D artificial spin ice [2]. IOLS can be fabricated from opals by filling the voids between microspheres with another material (Co or Ni in our case). Later microspheres can be removed. Thus IOLS can be considered as a set of submicron metallic particles connected to each other via thin and long crosspieces (“legs”). The shapes of such particles resemble the shapes of the voids of face centered cubic (FCC) structure of opal and have quasi cubic and quasi tetrahedral forms. Such spatially ordered 3D structure of IOLS leads to a complex distribution of the magnetization in the sample [2,3]. One can think IOLS as 3D antidot array. We perform a micromagnetic calculation of magnetization distribution in IOLS unit cell using Nmag software [4]. External magnetic field was applied along IOLS principal axes and corresponding hysteresis curves were calculated. Results are in good quantitative agreement with experimental data (SQUID measurements) and suggest that IOLS exhibit spin ice behavior i.e. spin ice rule is fulfilled in quasicubes and quasitetrahedra in a wide range of magnetic field values.

[1] C. Nisoli et al. Reviews of Modern Physics, 85(4), 1473, (2013)

[2] A. A. Mistonov et al. Physical Review B, 87(22), 220408, (2013)

[3] S. V. Grigoriev et al. Phys. Rev. B 79, 045123 (2009)

[4] T. Fischbacher, M. Franchin, G. Bordignon, & H. Fangohr,. Magnetics, IEEE Transactions on, 43(6), 2896-2898, (2007)

Mo.J-P13 - Roles of grain boundaries in the coercivity of magnetic thin films investigated by a two-dimensional Ginzburg-Landau model

K. Iwano¹, C. Mitsumata², K. Ono¹

1. *High Energy Accelerator Research Organization (KEK), Tsukuba, Japan*
2. *National Institute for Materials Science (NIMS), Tsukuba, Japan*

Magnetic thin films, in which short-ranged exchange interaction and long-ranged dipole-dipole interaction most directly compete with each other, provide us a good stage to explore non-equilibrium physics from both experimental [1] and theoretical sides [2, 3]. Also, we expect that the analyses of hysteresis under various conditions will lead to a clue to increase the so-called coercivity drastically, which is a high demand from industrial fields.

Our model is a two-dimensional Ginzburg-Landau (GL) model, of which the conventional part corresponds to the exchange interaction and an anisotropy effect. Furthermore, it is augmented by terms corresponding to the dipole-dipole interaction and a grain-boundary phase. We apply a fast Fourier transform (FFT) to a discretized version of this continuum model, assuming a periodic boundary condition.

We prepare a regular arrangement of square grains separated by a non-magnetic grain boundary phase and investigate its behaviors under the reversal of the external magnetic field. We particularly find:

1. When the separation distance between the grains exceeds a certain distance, the hysteric curve is almost the same as that for a completely isolated grain.
2. With shorter separation distances, on the other hand, the coercive field decreases monotonically as a function of the distance. We interpret the above separation-distance dependence of the coercive field as due to the two-dimensional dipolar field, which takes the functional form of $1/r^2$ when it is integrated over a certain angle with keeping the same distance r .

[1] K. Ono et al, IEEE Magn. 47, 2672 (2011)

[2] K. Iwano, C. Mitsumata, and K. Ono, J. Appl. Phys. 115, 17D134 (2014)

[3] K. Iwano, C. Mitsumata, and K. Ono, J. Appl. Phys. 117, 17A704 (2015)

Mo.J-P14 - Laser heating and thermal stresses in the core-shell nanowiresI. Astefanoaei¹, I. Dumitru¹, A. Stancu¹

1. Alexandru Ioan Cuza University, Iasi, Romania

In the last years, the core-shell nanostructures as nanowires or nanoparticles are intensively used in the heat assisted magnetic recording (HAMR) [1, 2]. This technological procedure uses high anisotropy magnetic systems which can be switched with rather small fields. During the switching process the material is temporarily heated [3]. The induced thermal stress in the heating process becomes an important parameter to be known and controlled in the magnetization process of core-shell nanowires. This paper analyses the thermal stress produced by a laser heating source placed at one end of a core-shell type structure. The thermal field was computed using Fourier heat transport equation in Comsol Multiphysics. The internal stresses are essentially due to thermal gradients and different expansion characteristics of core and shell materials. The stress values computed by the thermo elastic formalism depend on the laser beam parameters (spot size, power etc.) and system characteristics (dimensions, thermal characteristics). The high order of the thermal stress magnitude (GPa) leads to a magnetoelastic energy of $8 \cdot 10^5$ (J/m³) which is comparable with the magnetocrystalline energy of FePt core. As a consequence, magnetic state of the system can be influenced significantly.

Different shell materials lead to different thermal stresses values in the magnetic core. A glass shell ensures a better thermal insulation and lower thermal gradients than alumina shell. The thermal stresses are lower in a system with glass shell, than alumina shell. As a consequence the magnetoelastic energy becomes smaller.

The thermal stress at the end of the laser heating process becomes an important parameter which needs to be carefully analyzed in the heating treatments of the magnetic materials. These results lead to a better understanding of the switching process in the magnetic materials.

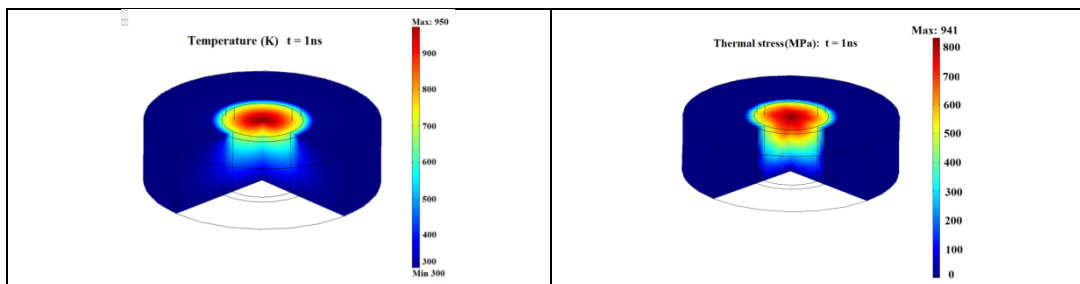


Fig. 1(a) The spatial temperature distribution in the core-shell system at $t = 1$ ns; (b) The radial stress distribution in the system at $t = 1$ ns;

Acknowledgement: Work was supported by Romanian CNCS-UEFISCDI Grant Nos. Grant Nos.PN-II-RU-TE-2012-3-0449.

References:

- [1] S. Sun, C. B. Murray, D. Weller, L. Folks, A. Moser, *Science*, 287 1989–1992 (2000)
- [2] B. X. Xu, Z. J. Liu, R. Ji, Y. T. Toh, J. F. Hu, J. M. Li, J. Zhang, K. D. Ye, C. W. Chia, *Journal of Applied Physics* 111 07B701 (2012)
- [3] S. N. Hsiao, S. H. Liu, *Applied Physics Letters* 101 182404 (2012)

Mo.J-P15 - Micromagnetic modelling of a magnetic nanoparticle including surface effects.

N. Ntallis¹, K. G. Efthimiadis¹, K. N. Trohidou²

1. Aristotle University, Thessaloniki, Greece

2. INN-Institute of Nanoscience and Nanotechnology, NCSR "Demokritos", Agia Paraskevi, Greece

The low temperature magnetic properties of magnetic nanoparticles as the size decreases are governed by surface effects [1]. Work has already been done by means of Monte Carlo (MC) [1] methods and micromagnetic approach, using core-shell type morphology [2], in order to investigate surface effects. In this work a micromagnetic model is presented for ferromagnetic nanoparticles where the surface is treated as a single layer. The model consists of two coupled magnetization vectors for the volume and boundary respectively. The evolution of each one is described by a partial differential equation (PDE) under the influence of an effective magnetic field as, arising from exchange interactions, magnetic anisotropy, Zeeman and dipole energy [3]. The two vectors interchange fluxes, based on the ratio a/l_x , where a is the effective width of the surface layer, and l_x is the exchange length. Simulations were made by means of the finite element method (FEM), on a spherical uniaxial particle by varying the strength and direction of the surface magnetic anisotropy and its diameter D . For a more comprehensive study FEM simulations for core-shell type and MC simulations also took place for the same magnetic parameters and assuming a simple cubic lattice by using a classical Heisenberg model [1]. The temperature was set to 0.01J and per external field value 2000MC steps are taken per spin. Results indicate that different anisotropy constant and direction influence H_s , the field where reversal takes place, in manner analogous to $1/(D)$. Our numerical results are in agreement with the micromagnetic core-shell type and the MC results for very small nano particle sizes and with experimental results. Moreover the computational cost of the effective layer model is lower than the core shell one, mainly due to discretization problems, thus can be easily extended to larger particles where dipole interactions count.

References:

- [1] K.N. Trohidou, "Monte Carlo studies on surface and interface effects of magnetic nanoparticles" . (2005) in Surface Effects in Magnetic Nanoparticles. Editor D. Fiorani. Springer
- [2] W. Scholz, D. Suess, T. Schrefl, J. Fidler, J. App. Phys. 95(2004) 6807
- [3] Ntallis .N, Eftimiadis K.G., JMMM, 363(2014) 152

Mo.J-P16 - Temperature-dependent exchange stiffness and domain wall width in hcp Co

R. Moreno Ortega¹, O. Chubycalo-Fesenko¹, M. del C. Munoz¹, L. Szunyogh², R. Evans³, R. Chantrell³

1. Instituto de Ciencias de Materiales de Madrid, CSIC, Madrid, Spain

2. Budapest University of Technology, Budapest, Hungary

3. Department of Physics, University of York, Heslington, York, , United Kingdom

Using a hierarchical multi-scale model we have evaluated the temperature dependence of the domain wall width and exchange stiffness in hexagonal close packed (hcp) Co. The exchange parameters were evaluated within the tight-binding approximation obtaining good agreement with previously published ab-initio calculations [1]. The Curie temperature was calculated using the atomistic simulations based on Langevin dynamics and the parameterized Heisenberg Hamiltonian, with good agreement with experimental values. The domain wall was created by imposing anti-periodic boundary conditions at either end of a nanowire of sufficient length to freely contain the domain walls. Our new approach allows the evaluation of the temperature dependence of the domain wall width at all temperatures up to and including the Curie temperature. In hcp Co we find a domain wall width of 30 nm, twice large as frequently assumed and exhibiting a monotonic increase with temperature. The domain wall width also shows some weak anisotropy, being slightly different in directions parallel and perpendicular to the c-axis of the crystal. In the range of low-to-intermediate temperatures the scaling relation of the exchange stiffness with magnetization is obtained both numerically with Langevin dynamics and analytically within a classical spectral density approach. The results constitute a basis for large-scale temperature-dependent micromagnetics, suitable, for example, for modeling heat-assisted magnetic recording or laser-induced magnetization dynamics.

[1] I. Turek, J. Kudrnovsky, V. Drchal, P. Bruno, and S. Blügel, Phys. Stat. Sol. (b) 236, 2, 318-324 (2003)

The authors acknowledge financial support from the EU project 'Femtospin'

Mo.J-P18 - Magnetic reversal modes in multisegmented nanowire arrays with long aspect ratio

S. Allende¹, E. Rando¹

1. Universidad de Santiago de Chile, Santiago, Chile

Multisegmented elements have been proposed for device storage, because they can store more than one bit depending on the number of elements and exhibit large magnetic stability of their states[1,2]. In this work a detailed numerical analysis of the magnetization reversal processes in multisegmented nanowire arrays was developed. The nanowires have a long aspect ratio and are formed by magnetic and non-magnetic sections alternately arranged in such a way that the array resembles magnetic layers separated by non-magnetic layers. Attention has been focused on the influence of magnetostatic interaction in the magnetic pattern formation of these magnetic nanostructures. Results from a magnetic correlation function among layers show that three different reversal modes can be detected depending on the number and distance between the magnetic segments. As a consequence of the different reversal modes, a non-monotonic behavior of the annihilation field in function of the distance between the layers is evidenced. Thus, these results are important for the production of magnetic devices with multisegmented nanowire arrays.

We acknowledge financial support from FONDECYT 11121214 and 1120356, Financiamiento Basal para Centros Científicos y Tecnológicos de Excelencia FB 0807, Concurso Inserción en la Academia-Folio 791220017.

[1] M. Albrecht, G. Hu, A. Moser, O. Hellwig, and B. D. Terris. *J. Appl. Phys.* 97, 103910 (2005)

[2] E. Cisternas and E. Vogel. *IEEE Trans. On. Mag.* 49, 4703 (2013)

Mo.J-P19 - Noise-induced effective potential for analysis of switching in spin-valves

S. Perna¹, C. Serpico¹, G. Bertotti², M. d'Aquino³, A. Quercia¹, I. D. Mayergoyz⁴

1. DIETI, University of Naples Federico II, Napoli, Italy

2. Istituto Nazionale di Ricerca Metrologica, Torino, Italy

3. Dipartimento di Ingegneria, Università di Napoli "Parthenope", Napoli, Italy

4. ECE Department and UMIACS, University of Maryland, College Park, United States

The magnetization dynamics in the nanosystems relevant to magnetic recording and spintronics technologies are stochastic in nature due to the presence of thermal fluctuations. This stochastic nature manifests itself in random transitions among coexisting steady states such as metastable magnetic equilibria or self-oscillatory regimes driven by spin-polarized currents. In this context there is a growing interest in studying the effects of fluctuations over a wide range of temperature across which the magnetic system undergoes superparamagnetic-like transitions[1]. In this paper, we carry out the analysis of a single-domain uniaxial nanomagnet subject to external field and spin-polarized currents while in contact with a thermal bath. Our starting point is the stochastic Landau-Lifshitz (LL) equation appropriately generalized to take into account the effect of spin-polarized currents [2]. We show that key information can be obtained by studying the properties of the noise-dependent effective potential that naturally arises from the averaging, with respect to rotations around the symmetry axis, of the Fokker-Planck equation [2] associated with the stochastic LL equation.

This potential contains a fluctuation-dependent part which is related to the presence of a noise-induced drift in the Fokker-Planck equation.

The study of bifurcation lines of the effective potential in the fields-temperature plane reveals an Astroid-like curve which enables to compute the values of injected current needed to switch the nanomagnet as function of temperature.

In this paper, the limit of applicability of the theory is studied by comparing the Astroid-like curve with the one determined numerically by estimating the switching values of the injected current computed at different temperatures on a certain time scale which depends by the temperature itself.

References:

[1] W. F. Brown, Phys. Rev. 130, 1677 (1963) [2] G. Bertotti et al, Nonlinear Magnetization Dynamics in Nanosystems, Elsevier, Oxford (2009)

Mo.J-P20 - Analysis of fast precessional switching in nanomagnets subject to hard-axis field pulses

M. d'Aquino¹, S. Perna², C. Serpico², A. Quercia², G. Bertotti³, I. D. Mayergoyz⁴

1. *Department of Engineering, University of Naples Parthenope, Naples, Italy*

2. *DIETI, University of Naples Federico II, Naples, Italy*

3. *Istituto Nazionale di Ricerca Metrologica, Turin, Italy*

4. *ECE Department and UMIACS, University of Maryland, College Park, United States*

The high-speed switching of magnetic particles is a central issue in magnetization dynamics for applications to magnetic recording nanotechnologies[1].

Several strategies have been analysed in recent years in order to circumvent the slow relaxation that occurs in switching an anisotropic nanomagnet through a large enough external field opposite to the initial magnetization. Possible more efficient alternatives include microwave-assisted switching[2] and precessional switching[3]. In the latter case, a field perpendicular to the initial magnetization, directed along the intermediate anisotropy axis, is applied to the particle. This method has been shown, both theoretically and experimentally, to yield much smaller switching times than conventional switching[3]. Nevertheless, in order to guarantee successful switching, an extremely precise timing of the field pulse has to be designed[4]. Recently, it has been also shown that ultra-fast and reliable precessional switching can be realized in anisotropic magnetic nanodots by using applied field pulses with two components: the larger one, directed along the particle hard-axis superimposed to a small bias field of appropriate amplitude[5].

In this work, we propose an analytical study of precessional switching of nanodots driven by hard-axis field pulses. In particular, we analytically derive closed-form expressions for critical fields, magnetization dynamics, pulse durations and timing tolerances for successful switching as function of material and geometrical parameters. Macrospin and micromagnetic simulations are performed to check the accuracy of the theoretical predictions. It is expected that this study will be instrumental to develop novel ultra-fast and reliable magnetization switching strategies.

References:

[1] J-P. Wang, *Nature Materials* 4, 191 - 192 (2005)

[2] C. Thirion et al., *Nature Mater.* 2, 524 (2003)

[3] S. Kaka et al., *Appl. Phys. Lett.* 80 (2002) 2958

[4] G. Bertotti et al., *IEEE Trans. Magn.* 39, 2501 (2003)

[5] M. d'Aquino et al., *IEEE Trans. Magn.* 50, 7100504 (2014)

Mo.J-P21 - Chaotic assisted switching of magnetic spin-valves

M. d'Aquino¹, A. Quercia², C. Serpico², G. Bertotti³, I. D. Mayergoyz⁴, S. Perna², P. Ansalone³

1. *Department of Engineering, University of Naples Parthenope, Naples, Italy*

2. *DIETI, University of Naples Federico II, Naples, Italy*

3. *Istituto Nazionale di Ricerca Metrologica, Turin, Italy*

4. *ECE Department and UMIACS, University of Maryland, College Park, United States*

Magnetization dynamics driven by microwave excitations has been extensively studied in connection with the phenomenon of ferromagnetic resonance[1] and, more recently, in connection with the possibility of using microwave field and microwave injected currents to achieve magnetization reversal under substantially reduced coercive fields[2,3]. In this paper, by using analytical techniques, we study the role of microwave excitations in assisting magnetization switching of a magnetic spin-valve-like nano-structure subject to both DC and microwave fields and injected currents. Magnetization dynamics is analyzed by means of the Landau-Lifshitz equation appropriately generalized to include the effect of spin-polarized currents. It is shown that a special role in the microwave excited dynamics is played by the presence, in the precessional dynamics, of saddle equilibria. The microwave perturbations of the dynamics around these saddle equilibria, at sufficiently large microwave excitations, give rise to homoclinic and heteroclinic phenomena. These phenomena produce chaotic type dynamics and, as a consequence of that, yield an effective reduction of the switching field. The analytical derivation of this reduction is the focus of this paper. The starting point is the characterization of homoclinic and heteroclinic trajectories of the unperturbed conservative dynamics by using elliptic functions. Then, the threshold values of microwave excitation amplitudes for producing heteroclinic and homoclinic entanglement are studied through an appropriate Melnikov function. Finally, by using the concept of lobe dynamics and basin erosion, we connect the reduction of coercive field to the presence of chaotic dynamics. The results of this treatment are instrumental to estimate the switching field by computing and measuring the extension of heteroclinic/homoclinic entanglement and basin erosion.

References:

[1] P. E. Wigen(Ed.), *Nonlinear Phenomena and Chaos In Magnetic Materials*, World Scientific Publishing, Singapore (1994)

[2] C. Thirion et al., *Nature Mater.* 2, 524 (2003)

[3] G. Bertotti et al., *J. Appl. Phys.* 105, 07B712, (2009)

Mo.J-P22 - Thermal stability and the size- and field-dependence of chiral profiles in ferromagnetic nanoparticles

N. Grisewood¹, H. Braun¹

1. School of Physics, University College Dublin, Dublin, Ireland

Understanding the behaviour of nonuniform profiles and the nature of size- and field-dependent transitions presents a fascinating challenge in magnetic systems and is of central importance for the design of magnetic recording media. Here we present an analytic model describing the magnetic free energy of a fine ferromagnetic nanoparticle deposited on an in-plane magnetized thin film substrate, and the resultant size-dependent chiral magnetic profiles which have been observed in recent photoemission experiments. As a bistable system, these chiral states may potentially be used for data storage or magnetic sensor purposes so we further consider thermally activated switching between the two chiral states. We analytically calculate the exact prefactor as a function of arbitrary size and field. Remarkably, we find a size-, and field-dependent transition where switching proceeds over a uniform barrier in small sample sizes and over a nonuniform barrier in larger sample sizes. We expect that the observation of such a phase transition should be readily realizable in experiments.

Mo.K-P03 - Magnetocaloric functional properties of $\text{Sm}_{0.6}\text{Sr}_{0.4}\text{MnO}_3$ manganite due to advanced nanostructured morphology

V. Andrade¹, S. Pedro², D. Rocco¹, M. Reis¹, A. Campos³, A. Coelho⁴, M. Escote⁵, A. Zenatti⁵

1. *Instituto de Física, Universidade Federal Fluminense, Niterói, Brasil*

2. *Departamento de Física, Universidade do Estado do Rio de Janeiro, Rio de Janeiro, Brasil*

3. *Divisão de Metrologia de Materiais, Instituto Nacional de Metrologia, Qualidade e Tecnologia, Duque de Caxias, Brasil*

4. *Instituto de Física 'Gleb Wataghin', Universidade Estadual de Campinas, Campinas, Brazil*

5. *Universidade Federal do ABC, Santo André, Brasil*

The magnetocaloric effect (MCE) is the key concept to produce new, advanced, freon-like free, low cost and environmental friendly magnetic refrigerators. Among several potential materials, $\text{Sm}_{0.6}\text{Sr}_{0.4}\text{MnO}_3$ manganite presents the highest MCE value in comparison to all other known manganites; however, it has a narrow useful temperature range. To overcome this problem we produced advanced nanostructures, namely nanoparticles and nanotubes of that highlighted manganite by using the pore wetting method. High resolution transmission electron microscopy revealed nanoparticle and nanotube diameters of 29 nm and 200 nm, respectively; and, in addition, this technique also showed that the wall of the nanotube is composed of nanoparticles with 15 nm of diameter. In fact, as desired, we could obtain a broader magnetic entropy change (ΔS_M) for the nanoparticles (in comparison to the bulk counterpart); but also an undesired M-shape profile for the nanotube sample was observed, due to the rising of a superparamagnetic behavior. These results also evidenced the existence of a nanoparticle size threshold below which the aim to make the transition wider is no longer valid. Finally, this effort is useful for the present knowledge on this issue and opens doors for deeper research on the evaluation of the magnetocaloric potential of nanostructures.

Mo.K-P04 - Vortex-state Permalloy nanodisks prepared by Colloidal Lithography for Biomedical Applications

M. Goiriena¹, A. García-Arribas^{1,2}, A. Svalov²

1. *BCMaterials, Universidad del Pais Vasco (UPV/EHU), Spain*

2. *Departamento de Electricidad y Electrónica, Universidad del Pais Vasco (UPV/EHU), Spain*

Magnetic nanoparticles are extensively studied for biomedical applications because their size are comparable to biological entities, while providing remote capabilities of actuation. Disk shaped ferromagnetic nanostructures display an attractive alternative to the chemically-synthesized oxide nanoparticles that are used normally. First, Permalloy (Py) nanodisks display much higher saturation magnetization and second, with the appropriate dimensions, they can present a spin vortex magnetic configuration, which leads to net zero magnetization at remanence, eliminating the problem of particle agglomeration. Therefore, Py nanodisks present a huge potential for biomedical applications, ranging from cancer cell destroy by hyperthermia or mechanical actuation to MRI contrast enhancement and drug delivery. In fact, micrometric disks has been shown to produce cell apoptosis by their mechanical oscillation under a low ac field. Disks in the nanometer scale might cross cell membrane expanding the biomedical possibilities.

The fabrication methods of nanostructures such as electron beam lithography or deep UV photolithography offer a high control on particle size and geometry, but they imply either a very low yield production or the use of state of the art and expensive equipment. As a satisfactory alternative, self-assembling routes provide high volume and low cost production of Py nanodisks. In this work we demonstrate the excellent capabilities of Hole-mask Colloidal Lithography (HCL) to produce high quality Py nanodisks with a yield adequate for biomedical applications (several micrograms per cm², approximately 1 miligram in a 2- $\frac{1}{2}$ wafer).

The parameters controlling the HCL process allow us to obtain Py nanodisks with different sizes that are characterized both morphological (SEM and AFM microscopies) and magnetically (SQUID and Kerr magnetometries). A well defined magnetic vortex state appears for dimensions that are compatible with previous phase diagrams. Effective procedures for releasing the fabricated nanodisks from the substrate are under development, which will permit in vitro biomedical experiments.

Mo.K-P05 - Skyrmion state stability in magnetic nanodots with perpendicular anisotropyK. Guslienko¹*1. Depto. Física de Materiales, Universidad del País Vasco, UPV/EHU*

Magnetic skyrmions recently attracted a lot of attention due to their small sizes (1-10 nm) assuming applications to ultra-high density magnetic recording and easy manipulation using spin-polarized currents. The skyrmions were observed in noncentrosymmetric weak ferromagnets MnSi, FeCoSi etc. It was established and widely accepted that the Dzyaloshinskii-Moriya (DM) exchange interaction plays decisive role in stabilization of such skyrmions. However, these materials have low Curie temperatures and need an external magnetic field to stabilize the skyrmions. Question: can the skyrmion state be stabilized in strong ferromagnets like Fe, Co without the DM interaction and bias magnetic field at room temperature? Stabilization of the skyrmion state in magnetic dots, stripes and other patterned nanostructures is of special interest. In this talk we demonstrate that the skyrmions can be stabilized in a nanodot by perpendicular anisotropy in absence of the external field and DM interaction. We consider a thin cylindrical dot with radius R and thickness L . We assume that L is about of the exchange length. We consider competition of the magnetic energies of three distinct magnetization states: perpendicular single domain (SD), vortex (V) and skyrmion (Sk). Then, we determine critical values of the anisotropy fields and dot sizes for transitions between the SD, V, and Sk states by comparing the energies of these stable (metastable) states and choosing a state with the minimal energy. We found that the skyrmion is the ground state of circular ferromagnetic nanodot without the DM exchange interaction and bias magnetic field for moderate perpendicular anisotropy fields $H_a = 2K/M_s$ (K is the uniaxial anisotropy constant, M_s is the saturation magnetization) within the range $H_{c1} < H_a < H_{c2}$. The critical anisotropy fields $H_{c1,2}(L,R)$ are functions of the dot sizes, L and R . The obtained Sk stability phase diagrams can serve as a benchmark for calculations of skyrmion dynamics in restricted geometry.

Mo.K-P06 - Instability thresholds for quantized spin waves in ferromagnetic nanowires under microwave pumping

Z. Haghshenasfard¹, M. Cottam¹

1. Department of Physics and Astronomy, University of Western Ontario, London, Canada

The spin-wave instability thresholds of parametric processes have been studied in ferromagnetic nanowires under conditions of pumping with a microwave field. The quantized spin waves are characterized by a one-dimensional wave vector along the nanowire length and spatial dependences of the amplitude in the transverse directions. The external applied magnetic field is taken to be either parallel to the longitudinal axis or in a perpendicular direction. In the latter situation the individual spins cant away from the axis and the static magnetization becomes spatially nonuniform. Both parallel (to the external field) pumping and perpendicular pumping geometries are considered and found to be quite distinct (e.g., the first-order Suhl effect in the latter case depends on three-magnon processes). Much of the previous work on nonlinear spin waves focused on effectively unbounded samples, or on macroscopic spheres or films, together with macroscopic theory. In nanowires with lateral dimensions less than about 200 nm the spatial quantization of the eigenmodes become predominant and our theory employs a microscopic (or Hamiltonian-based) dipole-exchange method analogous to that used recently for ultrathin films [1]. Numerical applications have been made to wires with different sizes and aspect ratios, as well as to magnetic materials with different relative strengths of the magnetic dipole-dipole and exchange interactions, including YIG and Permalloy (strong exchange) and EuO and EuS (weaker exchange). When our nanowire results are compared with those for macroscopic samples or for ultrathin films [1], it is found that the 'butterfly curves' (threshold field vs. applied field) are significantly modified and show more structural features. This is because the quantized spin waves are characterized by a one-dimensional (instead of two- or three-dimensional) wave vector and because of spatial nonuniformity of the magnetization.

[1] H. T. Nguyen and M. G. Cottam, Phys. Rev. B 89, 144424 (2014)

Mo.K-P07 - Quantification of nanowire uptake by living cells

M. Bogdan Margineanu¹, E. Jose Perez¹, K. Julfakyan¹, C. Sommer², M. Contreras¹, N. Khashab¹, J. Kosel¹, T. Ravasi¹

1. King Abdullah University of Science And Technology (KAUST), Thuwal, Saudi Arabia
2. Institute of Molecular Biotechnology of the Austrian Academy of Sciences (IMBA) Vienna, Austria,

Nanostructures have become increasingly important for different applications at cellular level. In order to understand how these nanostructures “behave” and for studying their internalization kinetics, several attempts have been made at tagging and investigating their interaction with living cells. In this study, magnetic iron nanowires with an iron oxide layer have been coated with (3-Aminopropyl)triethoxysilane (APTES), and subsequently labeled with a fluorogenic pH-dependent dye pHrodo Red, covalently bound to the aminosilane surface. Time-lapse live imaging of HCT 116 cells interacting with the labeled nanowires has been performed for 24 hours. As the pHrodo Red conjugated nanowires are non-fluorescent outside the cells but fluoresce brightly inside, internalized nanowires could be distinguished from non-internalized ones and their “behavior” inside the cells could be tracked for the respective time period. A computational framework dedicated to automatic analysis of live cell imaging data, Cecog Analyzer, has been adapted and used to classify the cells with internalized and non-internalized nanowires and subsequently determine the uptake percentage by cells at different time points. An uptake of 79 % by HCT 116 cells has been observed after 24 hours incubation at nanowire-to-cell ratios of 200. While the approach of using pHrodo Red for internalization studies is not novel in the literature, this is the first time it has been used for magnetic nanowires. To the best of our knowledge, this study also reports for the first time in the literature a time-resolved automatic analysis pipeline for quantification of nanowire uptake by cells. This pipeline has also been used for comparison studies with nickel nanowires and SPHERO Amino Magnetic particles, both coated with APTES and labeled with pHrodo Red. It has thus the potential to serve as a quantitative tool for studying the interaction of multiple nanostructures types with live cells in diverse experimental designs.

Mo.K-P08 - Magnetization reversal and domain wall motion in magnetic nanotubes

P. Landeros¹, J. Otálora¹

1. Departamento de Física, Universidad Técnica Federico Santa María, Valparaíso, Chile

We review our recent theoretical predictions on the magnetic properties of ferromagnetic nanotubes [1-6]. We start with a discussion of the actual equilibrium states and its relevance in the nucleation of vortex domain walls [2]. Then we show for long tubes, magnetization reversal is achieved by two mechanisms: propagation of a transverse or a vortex domain wall, which depends on the tube cross section [1]. We then present a theory based on collective coordinates for the field-induced dynamics of vortex domain walls [3,6]. We further propose that the injection either of magnetic field [4] or electric current pulses [5] can be used to control vortex domain walls in metallic ferromagnetic nanotubes. We show that the proper interplay between the tube geometry, and magnitude and duration of a current/field pulse, can be used to manipulate the position, velocity and chirality of vortex domain walls. Our calculations suggest that domain wall velocities greater than 1 km/s may be achieved for tube diameters of the order of 30 nm and increasing with it. We also find that the transition from steady to precessional domain wall motion occurs for very high electric current densities, of the order of 10^{13} A/m². Furthermore, the great stability displayed by such chiral magnetic configurations, and the reduced Ohmic losses provided by the current pulses, leading to highly reproducible and efficient domain wall reversal mechanisms.

[1] P. Landeros et al, Appl. Phys. Lett. 90, 102501 (2007)

[2] P. Landeros et al, Phys. Rev. B 79, 024404 (2009)

[3] P. Landeros et al, J. Appl. Phys. 108, 033917 (2010)

[4] J. A. Otálora et al, Appl. Phys. Lett. 100, 072407 (2012)

[5] J. A. Otálora et al, J. Phys.: Cond. Matt. 24, 436007 (2012)

[6] J. A. Otálora et al, J. Magn. Magn. Mater. 341, 86 (2013)

Mo.K-P09 - Aging effects on magnetic vanadium oxide nanotubes

M. E. Saleta^{1,2}, S. J.A. Figueroa², M. Granada³, H. E. Troiani³, R. D. Sánchez³, M. Malta⁴, R. M. Torresi⁵

1. Instituto de Física "Gleb Wataghin", Universidade de Campinas (UNICAMP), Campinas, Brazil
2. Brazilian Synchrotron Light Laboratory (LNLS), Campinas (SP), Brazil
3. Centro Atómico Bariloche (CNEA), S.C. de Barilohce, Argentina
4. Instituto de Química, Universidade Federal da Bahia (UFBA), Salvador, Brazil
5. Instituto de Química, Universidade de São Paulo (USP), São Paulo, Brazil

The vanadium oxide (VOx) nanotubes (NTs) are multiwall nano-structures constituted by alternating layers of VOx and a surfactant. The V-ions are in different oxidation states: the paramagnetic +4 (3d1) and the diamagnetic +5 (3d0). This coexistence of V oxidation states, with different magnetic behavior, gives rise to interesting and promising physical and chemical properties. Due to these characteristics the doped with other transition metal ions and undoped VOx-NTs, have demonstrated to be very versatile for possible technological-industrial applications such as cathode Li-ion and/or catalysis. In both applications the performance of the material is strongly associated with the ratio V4+/V5+ present in the nanostructure. Consequently, it is important to quantify the fraction of V ions and study different alternatives to vary these proportions. This allows to 'tune' the relationship V4+/V5+ suitable for each application. The possible use of these nanostructures as a technological component, such as batteries cathode, implies that the physico-chemical properties do not change across the time. The study of aging effects results primordial for possible applications and consequently the stability of the initial fraction V4+/V5+ in time. In this work we describe the results of a systematic study of the time evolution of the magnetic properties of VOx-NTs. For this completely characterization, we used electron spin resonance and dc-susceptibility techniques, which were supplemented with TEM microscopy and XANES. We observed that aging in normal environment conditions of pressure, temperature and humidity, that the +4 ions oxidize to +5. Although the multiwall tubular structure is maintained, this oxidation process produces a markedly change in its magnetic properties. Finally, this work allowed us to bring light to the question about the spread dispersion of data reported in VOx-NTs. In the scientific literature some authors reported in their quantifications around 50% of V4+, while others informed values close to 14%.

Mo.K-P10 - Magnetite Nanotubes and Nanorods: Microstructures and Magnetism

Feng Luo¹, Y. Chunjiang Jia², Lingdong Sun³, Kun Zheng⁴, Xiaodong Han⁴, Ze Zhang⁴, Naoaki Hayashi⁵, Mikio Takano⁵, Chunhua Yan³, N. N

1. IMDEA Nanoscience,

2. Shandong University, Madrid, Spain Jinan, China

3. Beijing National Laboratory for Molecular Sciences, State Key Laboratory of Rare Earth, Materials Chemistry and Applications, PKU-HKU Joint Laboratory in Rare Earth Materials and Bioinorganic Chemistry, Peking University, Beijing, China

4. Institute for Chemical Research, Kyoto University, Uji, Kyoto-fu, Japan

5. Microstructure & Properties of Advanced Materials, Beijing University of Technology, Beijing, China

We present a thermal transformation approach to prepare single crystalline Fe₃O₄ nanotubes and nanorods with α-Fe₂O₃ as precursors. Using various techniques, especially HRTEM, the microstructure of the magnetic Fe₃O₄ nanostructures and the crystallographic orientation-relationships between cubic Fe₃O₄ and trigonal α-Fe₂O₃ was extensively investigated. We got the electron microscopic evidence of all the four relations those are $\langle 111 \rangle_{\text{Fe}_3\text{O}_4} \parallel \langle 001 \rangle_{\alpha\text{-Fe}_2\text{O}_3}$, $\langle 112 \rangle_{\text{Fe}_3\text{O}_4} \parallel \langle 001 \rangle_{\alpha\text{-Fe}_2\text{O}_3}$, $\langle 113 \rangle_{\text{Fe}_3\text{O}_4} \parallel \langle 001 \rangle_{\alpha\text{-Fe}_2\text{O}_3}$, $\langle 115 \rangle_{\text{Fe}_3\text{O}_4} \parallel (001)_{\alpha\text{-Fe}_2\text{O}_3}$ deduced by Becker et al using X-ray texture goniometry technique in 1970s. (*J. Appl. Crystallogr.* 1977, 10, 77–78.). Furthermore, new orientation relations of α-Fe₂O₃ || Fe₃O₄, such as $\langle 001 \rangle_{\alpha\text{-Fe}_2\text{O}_3} \parallel \langle 100 \rangle_{\text{Fe}_3\text{O}_4}$, $\langle 001 \rangle_{\alpha\text{-Fe}_2\text{O}_3} \parallel \langle 110 \rangle_{\text{Fe}_3\text{O}_4}$, $\langle 001 \rangle_{\alpha\text{-Fe}_2\text{O}_3} \parallel \langle 120 \rangle_{\text{Fe}_3\text{O}_4}$, $\langle 001 \rangle_{\alpha\text{-Fe}_2\text{O}_3} \parallel \langle 122 \rangle_{\text{Fe}_3\text{O}_4}$, $\langle 001 \rangle_{\alpha\text{-Fe}_2\text{O}_3} \parallel \langle 123 \rangle_{\text{Fe}_3\text{O}_4}$, $\langle 001 \rangle_{\alpha\text{-Fe}_2\text{O}_3} \parallel \langle 233 \rangle_{\text{Fe}_3\text{O}_4}$, and $\langle 001 \rangle_{\alpha\text{-Fe}_2\text{O}_3} \parallel \langle 351 \rangle_{\text{Fe}_3\text{O}_4}$ were observed for the first time. In some tubes and rods, multiple fine-scale domains of the Fe₃O₄ were also detected, indicating the complexity of the microstructure of the Fe₃O₄ products. Compare with the Fe₃O₄ nanorods, the Fe₃O₄ nanotubes exhibit quite different magnetic properties due to the hollow geometry. There are two kinks near zero magnetization in the M-H loop of Fe₃O₄ nanotubes at 5K, which indicate the possibility of two vortex states with opposite directions. SQUID and MOKE both clearly indicate that the easy axis of Fe₃O₄ nanotubes is along the tube direction. While for the sample of Fe₃O₄ nanorods, although the magnetic easy axis is along the rod direction obtained from SQUID, both of the in-plane and out-of-plane direction are hard axis obtained from our measurements and due to the limitation of applied field in our MOKE system, we cannot saturate the sample in both directions. Since MOKE is very sensitive to the sample surface, the big difference between the data measured from SQUID and MOKE can be attributed to the imperfect surface microstructure of nanorods samples and also the possible dead layer or spin glass state may play an important role in the nanorods samples.

Mo.K-P11 - Influence of dipolar interactions on the magnetic states and hysteresis of ferromagnetic single-wall zigzag nanotubes

O. Iglesias¹, H. Salinas², J. Restrepo²

1. *Dpt. Física Fonamental and IN2UB, Universitat de Barcelona, Spain*

2. *Instituto de Física, Universidad de Antioquia, Medellín, Colombia*

We have studied the low temperature magnetic equilibrium configurations and hysteretic properties of magnetic nanotubes. The results have been obtained by Monte Carlo simulations of a lattice of Heisenberg magnetic moments residing on the cylindrical lattice of single-wall zigzag nanotubes which interact via competing short-range exchange (J) and long-range dipolar interactions (D). In order to ensure that the low temperature magnetic states correspond to the true ground states, a simulated annealing protocol was followed. Results reveal the occurrence of different low-temperature magnetic states depending of the degree of competition between the exchange and dipolar energies given by the parameter $\gamma=D/J$: collinear FM states at low γ , vortex states above a certain threshold γ^* , and interesting non-collinear helical states for intermediate values of γ . Concerning the order parameter, the magnitude of the rotational of the magnetization was computed and its dependence with the external field was analyzed in order to infer the switching fields. Results of the simulated hysteresis loops at low temperatures reveal the occurrence of different magnetization reversal mechanisms depending on orientation (perpendicular to or oriented along the length of the tube) of the external applied magnetic field. In each case, the shape of the hysteresis loops and the reversal mechanism is strongly dependent on γ . In particular, hysteresis loops become elongated and characterized by jumps or discrete steps along the cycle as γ increases and it becomes more competitive. Interpretation of that discrete character is given by direct visualization of the intermediate magnetic configurations in the vicinity of that jumps and analyzed by using convenient order parameters.

This work is supported by Spanish MINECO (MAT2012-33037), Catalan DURSI (2014SGR220) and European Union FEDER funds (Una manera de hacer Europa).

Mo.K-P12 - Controllable switching of transverse domain wall polarity in ferromagnetic planar nanowires: A prototype of 2 bits nonvolatile memory cell

S. Leonel¹, D. Toscano¹, P. Coura¹, F. Sato¹, B. Costa², M. Vazquez³

1. Universidade Federal de Juiz De Fora, Juiz de Fora, Brazil

2. Universidade Federal de Juiz de Fora, Juiz de Fora, Brazil

3. Institute of Materials Science of Madrid, Madrid, Spain

Micromagnetic simulations have been used to investigate the polarity reversal of the transverse domain wall in rectangular magnetic nanowires and the stabilization of the domain wall position after occurring the polarity reversal. One can control the wall position by modifying the local magnetic properties along the wire, which work as traps for pinning or blocking the wall. In order to stabilize the domain wall at predefined positions after a reversal of its polarity occurs, we have proposed the usage of a distribution of magnetic impurities consisting of two clusters. An example of application for this modified magnetic nanowire would be a nonvolatile memory cell, being able to store up to 2 bits of data per cell, which uses 4 states. The wall polarity switching was excited by application of a magnetic field pulse. For our typical pulse duration of 1 ns, we have found that the typical switching time is about 4 ns and the typical time interval from the pulse application to stabilization of the wall position is about 5 ns. Our result for switching time is of the same order of magnitude than the obtained in a previous work [1]. In contrast to previous studies on the polarity control, we showed that the polarity switching can be managed in a Permalloy nanowire with two traps, in our nanowire no local modification of system geometry is required [2] or no additional ferromagnetic layer [1]. Since the position and polarity of the wall can be controlled independently, the modified magnetic nanowire is attractive from a data storage perspective, because it would enable the realization of ultrafast and high-density nonvolatile memory devices.

[1] A. Vanhaverbeke, A. Bischof, and R. Allenspach, Phys. Rev. Lett. 101, 107202 (2008)

[2] O. A. Tretiakov, Y. Liu, and Ar. Abanov, Phys. Rev. Lett. 108, 247201 (2012)

Mo.K-P15 - Time-dependent factorial cumulants in quantum dots coupled to ferromagnetic leads

P. Stegmann¹, J. König¹, B. Sothmann²

1. *Theoretische Physik, Universität Duisburg-Essen and CENIDE, 47048 Duisburg, Germany*

2. *Département de Physique Théorique, Université de Genève, Geneva, Switzerland*

Recently, theoretical studies have shown that factorial cumulants provide a useful tool to probe interaction in electronic transport through nanostructures [1,2]. Sign changes of factorial cumulants as function of time indicate interaction, whereas in the absence of such sign changes the system can be described by an (effective) noninteracting Hamiltonian. In this sense, we demonstrate that a minimum number of transported electrons is necessary to recognize interaction. Below this critical number, the system appears effectively noninteracting. Furthermore, we derive a criterion for detecting interaction by analyzing the sign of the factorial cumulants in the long time limit. At last, we define a new kind of cumulants being more sensitive to interaction than the commonly used factorial cumulants. We demonstrate our results for a quantum dot and for a mesoscopic Stoner particle [3] weakly tunnel coupled to two ferromagnetic leads.

[1] D. Kambly, C. Flindt, and M. Büttiker, Phys. Rev. B 83, 075432 (2011)

[2] D. Kambly and C. Flindt, J. Comput. Electron. 12, 331 (2013)

[3] B. Sothmann, J. König, and Y. Gefen, Phys. Rev. Lett. 108, 166603 (2012)

Mo.K-P16 - Magnetization reversal of thin iron nanowires grown by focused-electron-beam-induced deposition

L. A. Rodríguez^{1,2}, L. Deen^{1,3}, R. Córdoba^{1,3}, C. Magén^{1,4}, E. Snoeck², B. Koopmans³, J. M. De Teresa^{1,5}

1. *Laboratorio de Microscopias Avanzadas (LMA), Instituto de Nanociencia de Aragón (INA), Universidad de Zaragoza, Zaragoza, Spain*

2. *CEMES-CNRS 29, Toulouse Cedex, France*

3. *Department of Applied Physics, Eindhoven University of Technology, MB Eindhoven, The Netherlands*

4. *Fundación ARAID, Zaragoza, Spain*

5. *Instituto de Ciencia de Materiales de Aragón (ICMA) and Departamento de Física de la Materia Condensada, CSIC-Universidad de Zaragoza, Zaragoza, Spain*

Iron nanostructures grown by Focused-Electron-Beam-Induced Deposition (FEBID) are promising for applications in magnetic sensing, storage and logic [1-3]. Such applications require precise design and determination of the coercive field (H_c), which depends on the nanostructure shape. In the present work, we have used the $\text{Fe}_2(\text{CO})_9$ precursor to grow iron nanowires by FEBID in the thickness range from 10 nm to 45 nm and width range from 50 nm to 500 nm. Such nanowires show Fe content between 80% and 85%, thus giving a high ferromagnetic signal. Magneto-optical Kerr characterization indicates that H_c decreases for increasing thickness and width, providing a route to control the magnetization reversal field via the modification of the nanowire dimensions. Transmission Electron Microscopy experiments indicate that these wires have a bell-type shape with a top-surface oxidation of about 5 nm. Such features are decisive in the actual value of H_c , as micromagnetic simulations demonstrate. These results are relevant to make appropriate designs of magnetic nanowires grown by FEBID.

References:

[1] J. M. De Teresa and A. Fernández-Pacheco, *Appl. Phys. A* 117 (2014) 1645

[2] R. Lavrijsen, et. al., *Nanotechnology* 22 (2011) 025302

[3] M. Gavagnin, et. al., *ACS Nano* 7 (2013) 777

Mo.K-P17 - Three-dimensional magnetic nanowires grown by focused-electron-beam-induced deposition

L. Serrano-Ramón^{1,2}, A. Fernández-Pacheco³, J. Pablo-Navarro⁴, L. A. Rodríguez^{1,2}, C. Magén^{1,5}, E. Snoeck², C. Gatel², M. R. Ibarra^{1,4}, J. M. De Teresa^{1,4}

1. *Laboratorio de Microscopias Avanzadas (LMA), Instituto de Nanociencia de Aragón (INA), Universidad de Zaragoza, Zaragoza, Spain*

2. *CEMES-CNRS 29, Toulouse Cedex, France*

3. *Cavendish Laboratory, University of Cambridge, Cambridge United Kingdom*

4. *Instituto de Ciencia de Materiales de Aragón (ICMA) and Departamento de Física de la Materia Condensada, CSIC-Universidad de Zaragoza, Zaragoza, Spain*

5. *Fundación ARAID, Zaragoza, Spain*

Three-dimensional (3D) magnetic nanowires have been grown by Focused-Electron-Beam-Induced Deposition (FEBID) using $\text{Co}_2(\text{CO})_8$ and $\text{Fe}_2(\text{CO})_9$ precursor gases and their magnetic properties characterized by Magneto-Optical Kerr Effect (MOKE) and Electron Holography (EH). Such 3D FEBID structures are being investigated for potential applications in magnetic sensing, storage and logic [1-3]. FEBID techniques are appropriate for the growth of these structures given the flexibility provided in terms of shape, resolution, used substrate, etc. In the present contribution, we will report the optimized growth conditions to simultaneously reach sub-100 nm resolution and high metal content. A pulsed FEBID strategy has been established as the most appropriate one. The role of heating during growth will be highlighted. The magnetic structure in the nanowires and the absolute value of the magnetization have been determined by EH. The magnetization reversal processes have been investigated by means of MOKE measurements in 3D standing nanowires as well as in nanowires felled on the substrate by means of a micro-manipulator.

References:

[1] M. Gavagnin, et. al., *ACS Applied Materials and Interfaces* 6 (2014) 20254

[2] A. Fernández-Pacheco, et. al., *Scientific Reports* 3 (2013) 1492

[3] J. H. Franken, et. al., *Advanced Functional Materials* 24 (2014) 3508

Mo.K-P20 - Magnetic properties of iron oxide nanotubes: Influence of the diameter of the nanotubes

A. Pereira^{1,2}, J. L. Palma^{1,2}, R. Zierold³, J. C. Denardin^{1,2}, M. Vázquez⁴, K. Nielsch³, J. Escrig^{1,2}

1. Departamento de Física, Universidad de Santiago de Chile, Santiago, Chile

2. Center for the Development of Nanoscience and Nanotechnology, Santiago, Chile

3. Institute of Applied Physics, University of Hamburg, Hamburg, Germany

4. Institute of Materials Science of Madrid, CSIC, Madrid, Spain

Among the different geometric types of objects, tubes offer an additional degree of freedom in their design as compared to wires, in that not only the length and diameter can be varied but also the thickness. This time we will show that changes in the diameter of the nanotubes strongly affect the mechanism of magnetization reversal and thereby the overall magnetic response. Our focus on iron oxides results from their unique position among the magnetic materials in terms of abundant availability and biocompatibility. Atomic layer deposition (ALD) of magnetic materials can be applied to ordered porous substrates to yield arrays of smooth tubes with a geometry that is tightly controlled and widely tunable. We have successfully used ALD to create Fe₂O₃ nanotubes in porous anodic alumina templates. Smooth tubes of 50, 60 and 75 nm outer diameters can be obtained. Subsequent reduction of the Fe₂O₃ material results in the formation of the strongly magnetic phase Fe₃O₄. The morphology and composition of the nanotubes were characterized by SEM and EDS analysis, respectively. In addition, hysteresis curves measured at different angles at which the external field is applied were measured using a magnetometer VSM. The dependence of the coercivity on the outer diameter is not monotonic: coercivity reaches its maximum at 60 nm outer diameter and then decreases for further increases in the diameter. We interpret this observation as arising from the coexistence of two distinct magnetization reversal modes in our system.

This work was supported by FONDECYT (Projects 1150952, 3130393, 3140073 and 1140195), Fondecup EQM120045 and Financiamiento Basal para Centros Científicos y Tecnológicos de Excelencia, under project FB0807.

Mo.K-P21 - Temperature dependent magnetic properties of ni nanotube arrays

A. Pereira^{1,2}, J. L. Palma^{1,2}, J. C. Denardin^{1,2}, J. Escrig^{1,2}

1. *Universidad de Santiago de Chile (USACH), Santiago, Chile*

2. *Center for the Development of Nanoscience and Nanotechnology (CEDENNA), Santiago, Chile*

Among the different geometric types of objects, tubes offer an additional degree of freedom in their design as compared to wires, in that not only the length and diameter can be varied but also the thickness. This time will show the effect of temperature on the magnetic properties of nickel nanotubes. Atomic layer deposition (ALD) of magnetic materials can be applied to ordered porous substrates to yield arrays of smooth tubes with a geometry that is tightly controlled and widely tunable. We have successfully used ALD to create NiO nanotubes in porous anodic alumina templates. Smooth tubes of 90 nm outer diameters can be obtained. Subsequent reduction of the NiO material results in the formation of Ni. The morphology of the nanotubes was characterized by scanning electron microscopy (SEM). In addition, hysteresis curves measured at different temperatures were measured using a magnetometer VSM. Finally, ZFC and FC curves were also measured.

This work was supported by FONDECYT (Projects 1150952, 3130393, 3140073 and 1140195), Fondecip EQM120045 and Financiamiento Basal para Centros Científicos y Tecnológicos de Excelencia, under project FB0807.

Mo.K-P22 - Skyrmion modes excitations and their hybridization induced by spin Hall effect spin torque

K. Lee¹, T. Shiino², B. Park²

1. School of Materials Science And Engineering, KIST-UNIST Ulsan Center For Convergent Materials, Ulsan National Institute of Science And Technology (UNIST), Ulsan, South Korea

2. Department of Materials Science and Engineering, KAIST, Daejeon, Republic of Korea

Skyrmions, a topological magnetic soliton found in a magnetic ultrathin film with large spin-orbit interaction through the interfacial Dzyaloshinskii-Moritya interaction (DMI), have been considered as a promising candidate of the information carriers in future spintronic devices. Recently, several micromagnetic simulation studies have predicted that a magnetic skyrmion can be nucleated and stabilized in a nano-sized ultrathin magnetic disk in the presence of the interfacial DMI. However, it has not been explored so far the current-induced skyrmion motion in a magnetic circular disk. In this study, we report on the micromagnetic simulation studies on excitation of skyrmion dynamic modes and their hybridizations induced by spin Hall effect spin torque (SHE-ST). From our simulations, it has been found that two distinct modes, gyrotropic motions as well as the breathing modes (variations of skyrmion size), can be excited resonantly by applying alternating current (AC) along in-plane direction only. In low frequency regime, 260 MHz for a monolayer nanodisk with 80-nm-diameter and the DMI constant $D = 3.0 \times 10^{-3} \text{ J/m}^2$, typical gyrotropic mode is excited. Interestingly, the breathing mode was excited by in-plane AC current in our simulations. We found that such breathing modes are excited indirectly; the in-plane AC current excites tiny vibrations of a skyrmion and resonant excitations of breathing modes are mediated by such vibrations of a skyrmion. This is because the distance of the skyrmion from the disk center determines the size of a skyrmion and thus, the vibrations of a skyrmion acts as a driving force of skyrmion breathing mode. Moreover, we found the hybridization of two distinct modes in high frequency regime. This may occur through the dynamical deformation of the skyrmion induced by the in-plane current-induced SHE-ST. Our findings and understandings open up novel methods to manipulate skyrmion dynamics for various applications of data storage and nano oscillator.

Mo.K-P23 - Domain Wall Dynamics in Parabolic WireK. Yershov^{1,2}, V. Kravchuk¹, D. Sheka³, Y. Gaididei¹, O. M. Volkov³1. *Bogolyubov Institute For Theoretical Physics, Kiev, Ukraine*2. *National University of "Kyiv-Mohyla Academy", Skovorody Str. 2, 04655 Kyiv, Ukraine*3. *Taras Shevchenko National University of Kyiv, Kiev, Ukraine*

The interaction of curvature and topologically nontrivial magnetization structures (e.g. domain walls) attract growing interest in fundamental studies and applications. Domain walls are topologically stable structures which can be used as key elements of nonvolatile magnetic memory devices [1]. In the racetrack domain wall magnetic memory [1] the sequence of bits of information in a nanowire is coded by sequence of magnetic domains separated by the domain walls of head-to-head and tail-to-tail types [2]. However, curvature parameters are an important characteristic of the wire in fabrication of memory devices. Vertical configuration of the racetrack magnetic memory consists of U-shaped nanowires [1] and therefore the domain wall properties on the curvilinear segment of the wire are very important.

Here we study both analytically and numerically the influence of curvature effects on the motion of a domain wall in parabolic curved wire. Using 1D approach developed in [3] we show that the domain wall is pinned by the effective potential induced by the curvature. In the case of infinitesimally small wall width $\Delta\kappa(s_0) \ll 1$ the pinning conditions can be written as $\kappa'(s_0) = 0$ and $\kappa(s_0)\kappa''(s_0) < 0$, where $\kappa(s_0)$ - the wire's curvature in the center of effective potential, Δ - wall width, prime denotes the derivative with respect to the arc length. We established that the domain wall motion frequency can be written as:

$$\omega = \omega_0 \pi \ell^2 \sqrt{|\kappa(s_0)\kappa''(s_0)|},$$

where $\omega_0 = 4\pi\gamma M_s$ with γ being the gyromagnetic ratio. The value of frequency of domain wall oscillations within the pinning potential increases with the increasing of curvature.

In order to verify our analytical predictions we performed numerical simulations of the Landau-Lifshitz equation using the NMAG code [4] and in house-developed simulator for a chain of discrete magnetic moments on the parabolic wire.

[1] Stuart S. P. Parkin, Masamitsu Hayashi, and Luc Thomas, *Science*, 320, 190 (2008).

[2] M. Kläui, *Journal of Physics: Condensed Matter*, 20, 313001 (2008).

[3] D. D. Sheka, V. P. Kravchuk, and Y. Gaididei, "Curvature effects in statics and dynamics of low dimensional magnets", *ArXiv e-prints* (2014), 1411.0646.

[4] T. Fischbacher, M. Franchin, G. Bordignon, and H. Fangohr, *IEEE Trans. Magn.* 43, 2896 (2007).

Mo.K-P24 - Magnetic properties of nanostructured CoNiFe-B alloy prepared by electroless platingD. Richardson^{1,2}, F.M.F. Rhen^{1,2}*1. Department of Physics and Energy, University of Limerick, Limerick, Ireland**2. Materials and Surface Science Institute, University of Limerick, Limerick, Ireland*

Electroless deposition requires the presence of a catalyst and it is a simple and cheap method for the preparation of metal and alloy. This method has been used for the preparation of non-magnetic nanotubes such as Cu [1] and Au [2]. We previously showed the preparation of electroless plated coaxial nanotubes [3]. Here, we carried out a systematic investigation of the magnetic properties and the nanostructure of electroless plated single wall CoNiFe-B into polycarbonate membrane with the formation of nanotubes. We show that the deposition of CoNiFe-B results in a nanostructure comprising nanotubes, nanoparticles and thin films. We prepared CoNiFe-B deposits by electroless plating into porous polycarbonate membranes and investigated the formation of the nanostructure using high-resolution scanning electron microscope images and magnetic measurements. The formation of the nanostructure occurs in five stages: nucleation, particle growth, percolation, film formation and films growth. High-resolution SEM images combined with magnetic measurements reveals that the nanostructure of the deposits consists of nanotubes, nanoparticles and thin film, which is directly linked to the stages of formation. Nanotubes with various lengths were obtained with typical values between 3 to 6 μ m and with wall thickness varying from 50 to 90 nm are obtained depending on deposition time. The magnetic measurements show that the nanostructured (Co₁₂Ni₆₀Fe₂₈)₈₈B₁₂ alloys have specific saturation magnetization of (88.6 \pm 7.7) JT⁻¹kg⁻¹ for samples plated from 2 to 60 min. Acknowledgements We also would like to thank Science Foundation Ireland (12/IP/1692) and IRCSET (RS/2011/270) for financial support.

[1] T. Chowdhury, D.P. Casey, J.F. Rohan, *Electrochem. Comm.* 11, 1203 (2009)[2] M. Wirtz, C.R. Martin, *Adv. Mater.* 15, 455 (2003)[3] J.F. Rohan, D.P. Casey, B.M. Ahern, F.M.F. Rhen, S. Roy, D. Fleming, S.E. Lawrence, *Electrochem. Comm.* 10, 1419 (2008)

Mo.K-P25 - Control of Domain Wall Nucleation in Cylindrical Nanowires

H. Mohammed¹, E. Vilanova Vidal¹, I. P. Ivanov¹, J. Kosel¹

1. King Abdullah University of Science And Technology, Thuwal, Saudi Arabia

Magnetic nanostripes have been a widely researched topic owing to their potential for data storage device applications. Attractive alternatives to nanostripes are cylindrical nanowires due to theoretical predictions showing the absence of Walker breakdown. For the realization of such a nanowire-based device, the controlled manipulation of magnetic domain walls (DWs) is fundamental both from a scientific and technological perspective.

Here we show that an overall reduction in the switching field of a nanowire allows the observation of pinning at internal defects and artificially introduced pinning sites. The reduction of the switching field is carried out by locally modifying the magnetic field at the end of a nanowire, where domain wall nucleation occurs. Pinning is observed via Magnetoresistance measurements (MR).

To demonstrate this, polycrystalline Nickel Nanowires were fabricated by electrodeposition into Anodic aluminium oxide templates. Au electrodes were then patterned onto an isolated nanowire to facilitate magnetoresistance measurements of the nanowire. For the purpose of manipulating the switching field, a permalloy (Py) pad was deposited onto one end of the nanowire.

The MR measurement in the case of the nanowire modified by the Permalloy pad demonstrates a 50% reduction in the switching field. This allows us to observe pinning at internal defects, which could not be detected otherwise. In addition to this, we introduced artificial pinning sites, which were reflected in the MR curve of the Permalloy modified nanowire. Furthermore, simulations confirm our experimental findings.

Mo.K-P26 - Identification and motion of magnetic domain walls in cylindrical nanowires

S. Da-Col^{1,2}, S. Jamet^{1,2}, N. Rougemaille^{1,2}, A. Locatelli³, T. Onur Montes³, R. Afid^{1,2}, L. Cagnon^{1,2}, J. Toussaint^{1,2}, O. Fruchart^{1,2}

1. Univ. Grenoble Alpes, Institut NEEL, Grenoble, France

2. CNRS, Institut NEEL, Grenoble, France

3. Elettra - Sincrotrone Trieste S.C.p.A., Trieste, Italy

The motion of magnetic domain walls along 1D systems has been an active field of research in the past 15 years. Beyond fundamental interest, an applied background is the search for low-power storage and computing schemes. Another prospect, yet even more challenging, is the concept of a three-dimensional data storage device proposed by IBM ten years ago, the race-track memory. Such a device would be based on dense arrays of cylindrical nanowires, where bits are coded in the form of magnetic domain walls along each wire. So far the focus has been set on flat strips fabricated by lithography, for ease of fabrication. To the contrary, domain walls in cylindrical nanowires was addressed mostly by theory and simulations. In these predictions, the expected physics is drastically different from the one encountered in the more traditional geometry of flat strips investigated so far. We report recent experiments that allowed the formal identification of the two predicted types of domain walls in cylindrical nanowires: of transverse and Bloch-point type, the latter being specific to wires [1]. This has been achieved applying XMCD-PEEM in an unusual shadow scheme to get information on the 3D magnetic structure of domain walls. The wires are made of permalloy, electroplated in anodized alumina templates. We also demonstrated that these domain walls may be moved rather easily along the wires, under the stimulus of an applied field. Propagation fields in the range 1-10mT have been evidenced, which is very similar to the strip counterparts. The propagation field at modulations of diameter made on purpose, either constrictions or protrusions, is shown to be several times larger.

[1] S. Da Col et al., Phys. Rev. B 89 (R), 180405 (2014)

Mo.K-P27 - Magnetic properties of hexagonally ordered nanowire and nanotube arrays

M. P. Proença¹, J. Ventura¹, C. T. Sousa¹, J. Escrig², M. Vázquez³, J. P. Araújo¹

1. IFIMUP And IN - Institute of Nanoscience And Nanotechnology And Dep. Física E Astronomia, Univ. Porto, Porto, Lisboa

2. Dep. Física, Univ. Santiago de Chile, and Center for the Development of Nanoscience and Nanotechnology, Santiago, Chile

3. Instituto de Ciencia de Materiales de Madrid - CSIC, Madrid, Spain

In this work, we present a study on the magnetic properties of highly ordered hexagonal arrays of Ni and Co nanowires (NWs) and nanotubes (NTs) electrodeposited in nanoporous alumina templates [1]. In particular, we describe a systematic comparative analysis on the magnetization reversal processes in ordered NW and NT arrays with different diameters ($d \sim 30 - 65$ nm). For this study we performed analytical calculations and experimental measurements of the angular dependence of the coercivity (H_c), allowing us to determine the reversal modes in NW and NT arrays [2]. The magnetization in Ni and Co NW arrays was found to reverse by means of the nucleation and propagation of a transverse domain wall. While for NT arrays a non-monotonic angular dependent H_c was observed for $d \geq 50$ nm, evidencing a transition between the vortex and the transverse reversal mode [3]. The magnetic interactions between NWs/NTs with different diameters were studied using first-order reversal curves (FORCs) [3,4]. From a quantitative analysis of the FORC measurements, we are able to obtain the profiles of the magnetic interactions and the coercive field distributions. In both NW and NT arrays, the magnetic interactions were found to increase with the diameter of the NWs/NTs, exhibiting higher values for NW arrays [3,5]. Finally, we also present experimental evidence of exchange-bias coupling in core-shell Co/CoO nanotubular structures [6].

[1] C.T. Sousa et al., Appl. Phys. Rev. 1, 031102 (2014)

[2] J. Escrig et al., Nanotechnology 18, 445706 (2007)

[3] M.P. Proenca et al., J. Appl. Phys. 113, 093907 (2013)

[4] C.-I. Dobrota and A. Stancu, J. Appl. Phys. 113, 043928 (2013)

[5] M.P. Proenca et al., J. Phys.: Condens. Matter 26, 116004 (2014)

[6] MP. Proenca et al., Phys. Rev. B 87, 134404 (2013)

Mo.K-P28 - Magnetic domain structure in epitaxial FeGa/MgO(001) wires

E. C. Corredor^{1,2,3}, M. Ciria^{1,2}, D. Coffey^{1,2}, J. I. Arnaudas^{2,3}

1. *Instituto de Ciencia de Materiales de Aragón, Consejo Superior de Investigaciones Científicas, Zaragoza, Spain*

2. *Departamento de Física de la Materia Condensada, Universidad de Zaragoza, Zaragoza, Spain*

3. *Instituto de Nanociencia de Aragón, Universidad de Zaragoza, Zaragoza, Spain*

Nanostructures with a defined geometry are important for the development of technological applications. The patterning processes changes the strain state of the nanostructures, and through the magnetoelastic (ME) contribution to the magnetic anisotropy, can be used to control the domain structure [1]. In this work magnetostrictive Galfenol (FeGa with about 20 % of Ga) strained epitaxial films grown on MgO(001) with thicknesses of 10 nm were patterned as lines using focused ion beam milling. The width w ranges are between 100 nm and 1000 nm, the long axis is along both the [100] and [110] in-plane directions of the film and the line length l is larger than the width ($w/l > 0.5$). Magnetic force microscopy (MFM) has been used to reveal the domain structure. The cubic magnetic anisotropy is small (K about -5 kJ/m³) a value that foresees a domain structure independent of the crystal direction of the wire axis. Nevertheless MFM images show that the domain structures are markedly different for [110] and [100]-wires. For [100]-wires a high remanence single domain structure is present for wires with w up to 1000 nm; similar structures are observed for [110]-wires if $w < 300$ nm, however above that width a multidomain structure appears. Micromagnetic simulations indicate that a uniaxial anisotropy, that enhances the shape anisotropy, precludes the formation of Landau or Diamond multidomain states in the galfenol wires. The ME contribution, which is proportional to the ME stress coefficient B_1 for [100]-wires and B_2 for [110]-wires, can address the observed behavior because B_1 is larger than B_2 and the latter changes its sign depending on slight variations in the range of composition of the film [2].

[1] M. Ciria, et al, Phys Rev. B 80, 094417 (2009)

[2] A. E. Clark et al, J. Appl. Phys. 93, 8621 (2003)

Mo.K-P29 - Domain Wall annihilation via Phase Correction in Cylindrical Nanowires

S. Goolaup¹, R. Maddu¹, W. Siang Lew¹

1. Nanyang Technological University, Singapore

Ferromagnetic cylindrical nanowire opens a new avenue for high speed domain wall (DW) memory due to its natural geometry for the 3D design of race track memory and the absence of the Walker breakdown. For memory applications, multiple DWs need to be created and propagated along the nanowire to separate the data. The motion of a transverse DW (TDW) in a cylindrical nanowire is linear and accompanied by the rotation of the transverse component of the DW around the long axis of the nanowire. In planar structures, depending on topological defects associated with the TDW, the interaction between adjacent DWs may lead to annihilation or the formation of a stable bound state. In this work, we show that the TDW interaction in cylindrical nanowires is highly dependent on the phase of the rotational component of the transverse domain wall. The interaction of two TDWs with the same phase of rotation leads to complete annihilation and emission of spin waves within the nanowire conduit. Any mismatch in the phase between the rotational components of two TDWs leads to the formation of a short-lived bound state DW configuration. Depending on the polarity of the phase mismatch, the bound state favours a particular longitudinal motion along the conduit, whereby it eventually annihilates. The maximum length scale over which the bound state is found to be stable occurs when the phase mismatch between the two TDWs is 180° . The annihilation of the bound state happens the TDWs correct the phase mistracking between their rotational components. Our results show that this is achieved via an increase in speed of the rotational component of one of the TDW within the bound configuration.

Mo.K-P30 - Mechanism of magnetic switching in rapidly solidified amorphous nanowires

T. Ovari¹, C. Rotarescu¹, A. Atitoaie¹, H. Chiriac¹

1. National Institute of R&D For Technical Physics, Iasi, Romania

Amorphous glass-coated nanowires with metallic core diameters from 90 to 900 nm have been recently prepared by glass-coated melt spinning. Here we investigate the magnetic switching in rapidly quenched amorphous nanowires prepared from alloys with the nominal compositions Fe_{77.5}Si_{7.5}B₁₅, with large and positive magnetostriction, and (Co_{0.94}Fe_{0.06})_{72.5}Si_{12.5}B₁₅, with small and negative magnetostriction. We measured their bulk and surface hysteresis loops, which show a fully bistable magnetic behavior in both cases, with the switching field being one order of magnitude smaller in the nearly zero magnetostrictive samples (hundreds of A/m as compared to kA/m for the highly magnetostrictive ones). The switching mechanism was analyzed in order to understand the key factors that influence the magnetization reversal and to employ them in tailoring the magnetic characteristics of the nanowires for the potential sensing applications. The magnetization reversal mechanism has been also studied by micromagnetic methods, which allowed us to simulate the hysteresis loops and to understand the main contributions to the magnetic anisotropy, i.e. shape and magnetoelastic terms, as well as to visualize the distribution of the magnetic moments at each value of the applied field, and in this way to monitor the possible nucleation of domains with reversed magnetization and the subsequent propagation of the newly formed domain walls along the nanowires. The results show that magnetization switching starts at both ends of the nanowires, irrespective of their magnetostriction. This is for the first time that a detailed analysis of the magnetization switching mechanism was performed for this novel type of magnetic nanowires, the results being essential for their future use in the development of micro and nanosensors, as well as for potential applications in magnetic logic devices. This work was supported by UEFISCDI through contract no. 46/2013 (project PN-II-ID-PCE-2012-4-0424).

Mo.K-P31 - Manipulation of the magnetization reversal in ferromagnetic nanostructures grown by Focused Electron Beam Induced Deposition

R. Córdoba¹, D. Han¹, B. Koopmans¹

1. Eindhoven University of Technology, Department of Applied Physics, MB Eindhoven, The Netherlands

The manipulation of magnetization is becoming crucial for future applications in spintronics. For instance, the magnetization reversal has been widely investigated for magnetic random access memories. In monodomain nanostructures, this reversal process basically consists of the nucleation of a domain wall and of its propagation, switching the magnetization. The nucleation and propagation processes are governed by magnetic properties of materials as well as structural parameters of the nanostructures. Exploring the magnetization reversal process at the nanoscale may profit from emerging methods for patterning structures at the nanoscale using focused electron or ion beams. As an example, the fabrication of ferromagnetic nanostructures by means of focused electron beam induced deposition (FEBID) has been demonstrated as an attractive alternative method [1,2]. In the present contribution, we report the magnetic reversal behaviors in a novel set of magnetic nanostructures fabricated by FEBID. We manipulate the magnetization reversal in Fe FEBID nanostructures varying the scanning strategy of this direct-write technique. In particular, we are able to control their coercive field as a function of the engineered thickness modulation in one direction. The magnetization reversal of these structures has been investigated by magneto-optical Kerr microscopy, where magnetic images are taken as a function of the applied magnetic field, and supported by micromagnetic simulations. This will make possible the investigation of the magnetization reversal processes in complex structures created using this novel strategy, which could have a great potential for the transfer of magnetic information.

References:

[1] R. Lavrijsen, et. al., Nanotechnology 22 (2011) 025302

[2] R. Córdoba, Functional Nanostructures fabricated by Focused Electron/Ion Beam Induced Deposition. Springer Thesis (2014)

Mo.K-P33 - Thermodynamic properties of anisotropic triangular lattices obtained from finite-temperature exact-diagonalization

B. Schmidt¹, P. Thalmeier¹

1. Max-Planck-Institut für chemische Physik fester Stoffe, Dresden, Germany

We present results of our systematic investigation of the thermodynamic properties of anisotropic triangular lattices with exchange anisotropy J_2/J_1 .

Here J_1 is the exchange coupling along two sides of the triangle, different from J_2 along the third side. In particular, we discuss the specific heat c_V and magnetic susceptibility χ . Our numerical tool is the finite-temperature Lanczos method, which is based on an iterative exact diagonalization (ED) of the model Hamiltonian describing the lattice.

For the ED procedure, we tile the lattice with clusters of size N up to 28 sites where the thermodynamic limit behavior of c_V and χ is already stable.

With this unbiased method we are able to investigate the full phase diagram of the model where both constants J_1 and J_2 can be ferro- and antiferromagnetic. Our description allows in particular for a smooth interpolation between the special cases square lattice ($J_2 = 0$), isotropic triangular lattice ($J_2 = J_1$), and one-dimensional chains ($J_1 = 0$). For the latter, our calculations reproduce the well-known infinite-chain results.

For a given anisotropy ratio J_2/J_1 , we determine the temperature dependence of c_V and χ with their characteristic broad peaks. We extract peak values and positions T_{\max} and show their systematic variation as a function of J_2/J_1 , which is very important for the analysis of experimental thermodynamic data, in particular of the susceptibility χ . To demonstrate the usefulness of the FTL method, we apply our findings to the prominent triangular compound Cs_2CuCl_4 . We perform an overall fit to the temperature dependence of its susceptibility and find values $J_1 = 0.11$ meV and $J_2 = 0.38$ meV which are in excellent agreement with those obtained from neutron scattering data above the saturation field.

Mo.L-P01 - Magneto-mechanical property of the Fe₅₅Co₁₇Ga₂₈ alloyS. U. Jen¹, Y. C. Lin¹*1. Institute of Physics, Academia Sinica, Taipei, Taiwan*

Fe₅₅Co₁₇Ga₂₈ alloy was made in an induction furnace, and then slowly cooled to room temperature (RT). The structural property of the as-cast alloy was examined by an x-ray diffractometer. From the diffraction pattern, we conclude that the major phase in the alloy is the A2 phase, and the minor phases may contain the D03, D019, and L12 phases. The magnetic hysteresis loop was measured by the vibration sample magnetometer: saturation magnetization $M_s = 113$ emu/g, and coercivity $H_c = 4$ Oe. Complex permeability ($\mu \equiv \mu' - i\mu''$) as a function of frequency (f) was obtained by using an LCZ meter. At 20 Hz (low- f), μ' equals to 280. The mechanical properties, such as Young's modulus (E), shear modulus (G), flexure damping rate (RF), and torsion damping rate (RT), were measured as a function of magnetic field (H), respectively, by the impulse excitation of vibration (IEV) method. The ΔE or ΔG effect is defined as $\Delta E/E \equiv [E_s - E_o]/E_s$, or $\Delta G/G \equiv [G_s - G_o]/G_s$, where subscript "s" means the near saturation state @ $H = 3.0$ KOe, and the subscript "o" means the zero-field state. Moreover, the flexural magneto-mechanical coupling coefficient (KE) and the torsional magneto-mechanical coupling coefficient (KG) can be calculated from the following definitions: $(KE)^2/[1 - (KE)^2] \equiv \Delta E/E_s$ and $(KG)^2/[1 - (KG)^2] \equiv \Delta G/G_s$ [1]. Thus, $KE = 11.8$ to 15.7% and $KG = 14.1$ to 15.2% for the Fe₅₅Co₁₇Ga₂₈ alloy.

[1] G. Engdahl, *Handbook of Giant Magnetostrictive Materials*, San Diego, Academic Press, 2000

Mo.L-P02 - Magnetocaloric effect studies on MnSb and MnSbR_{0.05} (R: Nd, Er)R. Pothala¹, Markandeyulu G¹*1. Indian Institute of Technology Madras, Chennai, India*

The search for materials exhibiting second order magnetic transition (SOMT) accompanied by large change in magnetic entropy (ΔS_M) close to transition temperature and at low applied fields has been important in high temperature magnetic refrigeration technology. Magnetocaloric effect studies (MCE) in SOMT materials are helpful to identify materials with high the efficiency of magnetic refrigeration, as they are free from the thermal hysteresis. The study of ΔS_M close to the Curie temperature (T_C) at applied fields ≤ 1.5 kOe in MnSb, MnSbR_{0.05} (R: Nd and Er), materials exhibiting SOMP, are presented in this paper.. Polycrystalline samples of MnSb, MnSbR_{0.05} (R: Nd and Er) were prepared by solid state reaction. XRD patterns reveal that all the samples were crystallized in the hexagonal NiAs-type of structure (space group D_{6h}^4 -P6₃/mmc). Magnetic transition was observed from the temperature variation magnetization at 500 Oe. The positive slope at all points of M^2 at and below T_C in the Arrott plot (M^2 vs. H/M) confirms the second-order magnetic transition behavior in all these materials. The temperature dependence of ΔS_M was determined close to T_C (591 K, of all the compounds studied) from isothermal magnetization plots in a magnetic field change from 0 – 15 kOe. The largest values of ΔS_M , $(\Delta S_M)_{max}$ observed in MnSbNd_{0.05}, MnSb and MnSbEr_{0.05} at H = 15 kOe are respectively, 0.57 J/kg K, 0.72 J/kg K and 0.99 J/kg K. The $(\Delta S_M)_{max}$ observed at H = 15 kOe, in MnSbEr_{0.05} is relatively large at high temperatures compared with those reported for high temperature MCE materials. On the other hand, a plateau type of behavior is seen at $(\Delta S_M)_{max}$ for MnSb, indicating that MnSb is useful for the practical applications in magnetic refrigeration, over a wide range of temperatures.

Mo.L-P03 - Peculiarities of giant magnetocaloric effect in Ni₅₀Mn₃₅In₁₅ alloys in the vicinity of martensitic transition

I. Rodionov¹, Y. Koshkid'ko^{2,3}, J. Cwik³, A. Quetz⁴, S. Pandey⁴, A. Aryal⁴, I. Dubenko⁴, S. Stadler⁵, N. Ali⁴, I. Titov¹, M. Blinov¹, V. Prudnikov¹, [E. Lähderanta](#)⁶, I. Zakharchuk⁶, A. Granovsky¹

1. *Lomonosov Moscow State University, Faculty of Physics, Moscow, Russia*

2. *VSB-Technical University of Ostrava, Ostrava-Poruba, Czech Republic*

3. *International Laboratory of High Magnetic Fields and Low Temperatures, Wroclaw, Poland*

4. *Department of Physics, Southern Illinois University, Carbondale, United States*

5. *Department of Physics & Astronomy, Louisiana State University, Baton Rouge, LA United States*

6. *Lappeenranta University of Technology, Lappeenranta, Finland*

We present results of direct measurements of magnetocaloric effect in moderate and strong magnetic fields in Ni₅₀Mn₃₅In₁₅ alloys. The polycrystalline samples were obtained by the conventional arc-melting technique, their composition was checked by EDX, the structural properties were studied by XRD, and magnetic properties were investigated with VCM (Lake Shore) and SQUID (Quantum Design). The adiabatic changes of temperature in magnetic fields up to 1.8 T was obtained with MagEq MMS 801set-up. For measurements in the field of 14 T of Bitter magnet we used the extraction method and specially designed home made set-up. We observed the abrupt martensitic transition (MT) from ferromagnetic austenitic state to martensite with low magnetization at 319 K and this temperature does not depend on magnetic field. Magnetic measurements confirm the presence of strong antiferromagnetic correlations in both martensitic and austenitic phases. In the vicinity of MT (H=1.6 T) changes at heating the sample from - 1.1 K to +0.9 K but (14 T) changes from -11 K to +6. The transition region of MT does not exceed 2.5 K. We connect such unusual behavior for this composition with strong antiferromagnetic correlations, which are suppressed by strong magnetic fields. Therefore large values of magnetocaloric effect in Ni-Mn-In alloys may be due to the magnetic field induced MT and by the suppression of intrinsic antiferromagnetic correlations.

The work was supported by European Social Foundation (No CZ.1.07/2.3.00/30.0016 and No LO1203), by the Office of Basic Energy Sciences, Material Science Division of the U.S. Department of Energy (DOE Grant No. DE-FG02-06ER46291 and DE-FG02-13ER46946) and by Russian Foundation for Basic Research (Grant No 15-02-02077 and 15-52-78080).

Mo.L-P05 - Theoretical investigation of the coupling between the electrocaloric and magnetocaloric effects in quantum paraelectric EuTiO_3

P. V. Ranke¹, P. Ribeiro¹, A. Carvalho², B. Alho¹, T. Alvarenga¹, E. Nobrega¹, A. Caldas¹, V. Sousa¹, P. Lopes¹, N. Oliveira¹

1. Instituto de Física Armando Dias Tavares, UERJ, Rio de Janeiro, Brazil

2. Laboratório Nacional de Luz Síncrotron, CNPEM, Campinas, Brazil

The magnetocaloric (MCE) and electrocaloric (ECE) effects correspond to a change in temperature of a material upon magnetic field and electric field variation, respectively. Quantitatively, these effects are characterized by the entropy change in an isothermal process ΔS_T and by the temperature change in an adiabatic process ΔT_{ad} upon the field variation [1]. EuTiO_3 exhibits a type-G antiferromagnetic structure with strong coupling between electric and magnetic properties around its Néel temperature $T_N = 5.5$ K. In this work the electrical polarization and the magnetization dependence on temperature, electric and magnetic fields were investigated through a microscopic model. The Hamiltonian of the EuTiO_3 system describes the ferroelectric subsystem, the magnetic subsystem and the coupling between the two subsystems. In molecular field approximation, the coupling interaction is embodied by the antiferromagnetic exchange parameter and by the pseudo-electric-spin interaction parameter [2]. The temperature dependence of ΔS_T in EuTiO_3 was calculated under simultaneous variations of electric and magnetic field. The peak in the ΔS_T -MCE can be tuned by the electrical field intensity and this process was scribed to the increasing of the antiferromagnetic interaction upon electric polatization. Besides, around T_N , an outstanding result was predicted in which the EuTiO_3 can absorbs or eliminate heat, in an isothermal process, upon magnetic field change from zero to 1 T, depending on the electric field intensity.

[1] N. A. de Oliveira, P. J. von Ranke, Phys. Rep. 89 (2010) 489

[2] H Wu, Q. Jiang, W. Z. Shen, Physics Letters A 330 (2004) 358

Mo.L-P07 - Giant reversible rotating magnetocaloric effect in $\text{KEr}(\text{MoO}_4)_2$ V. Tkáč^{1,2}, A. Orendáčová¹, M. Orendáč¹, A. G. Anders³, A. Feher¹1. *Institute of Physics, P. J. Šafárik University, Košice, Slovak Republic*2. *Department of Condensed Matter Physics, Faculty of Mathematics And Physics, Charles University, Prague, Czech Republic*3. *B. I. Verkin Institute for Low Temperature Physics and Engineering of NASU, Lenin, Kharkov, Ukraine*

Experimental and theoretical studies of $\text{KEr}(\text{MoO}_4)_2$ – a quasi-low-dimensional Ising magnet, were performed at temperatures above 2 K and magnetic fields up to 5 T. Previous studies in magnetic field [1] revealed a shift of a magnetic phase transition down to temperatures far below a zero-field value, $T_c = 0.9$ K. Thus, the investigation above 2 K excludes any possibility of the interplay between long-range magnetic correlations and crystal field effects (CEF). Correspondingly, magnetization data along the easy axis a can be described within a CEF model, while a description along the hard axis b , fails due to the occurrence of a field-induced Jahn-Teller effect [2]. In the field applied along the easy axis, large conventional magnetocaloric effect (MCE) was found from experimental data around 10 K ($-\Delta S_{\text{max}} = 14$ J/kg K) for 5 T and even higher values ($-\Delta S_{\text{max}} = 16$ J/kg K) can be expected around 12 K for 7 T, when applying the CEF model. A huge magnetic anisotropy in the ab plane leads to a large rotating MCE, $-\Delta S_{R, \text{max}} = 10$ and 13 J/kg K obtained by a simple rotating the single crystal within the ab plane in the constant magnetic field 2 and 5 T, respectively. The highest anisotropy of MCE was reported in HoMn_2O_5 [3] with $-\Delta S_{\text{max}} \approx 12.4$ J/kg K for 7 T, but only $-\Delta S_{\text{max}} \approx 3$ J/kg K for 2 T. Large ΔS_R values with no hysteresis losses and rather wide working temperature spans imply that $\text{KEr}(\text{MoO}_4)_2$ may serve as a promising candidate for the implementation of a compact rotary magnetic cryorefrigerator.

[1] A. Orendáčová et al., Phys. Rev. B 65, 014420 (2001)

[2] V. I. Kutko, Low Temp. Phys. 31, 1 (2005)

[3] M. Balli et al, Appl. Phys. Lett. 104, 232402 (2014)

Mo.L-P08 - KINETICS OF PHASE TRANSITIONS IN MAGNETOCALORIC MATERIALS

A. Kamantsev¹, V. Koledov¹, V. Shavrov¹, I. Tereshina², D. Kuzmin³, I. Bychkov³

1. *Kotelnikov IRE RAS, Moscow, Russia*

2. *Baikov Institute of Metallurgy and Material Science of RAS, Moscow, Russia*

3. *Chelyabinsk State University, Chelyabinsk, Russia*

The problem of rate of phase transitions (PTs) requires an indispensable solution, because the creation of new technologies based on “giant” effects in vicinity of PTs in magnetic materials is impossible without solving of this problem. The magnetocaloric effect reaches its peaks near the PTs in magnetics, therefore knowledge of PT's rate is necessary for creation of new technology of magnetic refrigeration at room temperature. The rate of PT limits the frequency of thermodynamic cycles. Accordingly, the power of refrigeration will depend on the frequency of cycles, and it is difficult to judge the profitability and competitiveness of the creation of this machine without determining the parameters of power. In this paper, we present a new technique for experimental study of the kinetics of the magnetic PTs under low alternating magnetic field, and the theoretical calculations of respective kinetic processes. The new dynamic thermo-magnetometer (DTM) is proposed for solving the problem of the experimental study the rate of the magnetic PT with response time of 10 ms. DTM is designed for measuring the time dependence of the magnetic susceptibility of thin plates of ferromagnets at an abrupt temperature change in water flow. The experimental measurements of the magnetic susceptibility of the samples were carried out with the help of a three-coil differential transformer. An AC signal with a frequency of 1-10 kHz was supplied to the outside coils. The measured signal was taken from the central coil. The temperatures of both samples and water were measured using thin differential thermocouples. As a result of experiments for Gd near $T_c = 20$ C relaxation time of magnetization is about 50 ms. Then the frequency of the cycles of a magnetic refrigerator with a working body made of Gd plates will be restricted to a value of $f = 10$ Hz.

Mo.L-P11 - Enhancement of Thermal Stability and Soft Magnetic Properties of High Induction (Fe(1-x)Co_x)₇₉Si_{8.5}B_{8.5}Nb₃Cu₁ (x= 0,0.05, 0.35) Nanocrystalline AlloysR. K. Roy¹, A. K. Panda¹, A. Mitra¹*1. MST Division, CSIR-National Metallurgical Laboratory, Jamshedpur, India*

The next generation soft magnetic alloys demand higher saturation induction than that of Fe based amorphous alloys (FINEMET) and a low core loss than that of Si steel. The increased thermal stability and high temperature magnetic properties are also prerequisites for their wide application in the harsh environment. In view of this requirement, the phenomena of nanocrystallization and associated high temperature magnetic properties have been investigated in two Co-substituted alloys (#FC05 and #FC35) with nominal compositions of (Fe_{1-x}Co_x)₇₉Si_{8.5}B_{8.5}Nb₃Cu₁ (x= 0.05, 0.35), respectively. Alloys were prepared by melt spinning technique and followed by annealing treatment in inert atmosphere to induce nanocrystallization. As-cast alloys are amorphous, and onsets of primary crystallization (Tx₁) and secondary crystallization (Tx₂) temperatures of #FC05 are 443 and 623°C and that of #FC35 are 437 and 582°C, respectively. With more Co incorporation, as examined in #FC35, the drop in Tx₂ is far drastic as compared to Tx₁. Thus, thermal stability ($\Delta T_x = T_{x_2} - T_{x_1}$) against secondary crystallization and activation energy (Q) for primary crystallization is higher for a minimal amount Co addition (#FC05), evaluated as $\Delta T_{x\#FC05} = 180^\circ\text{C}$, $\Delta T_{x\#FC35} = 145^\circ\text{C}$, $Q_{\#FC05} = 258\text{kJ/mol}$ and $Q_{\#FC35} = 235\text{kJ/mol}$. Additionally, alloy FC#05 although shows a relatively lower saturation induction (M_s) than #FC35, its coercivity (H_c) is considerably superior than the later [$M_{s\#FC05} = 1.46\text{T}$, $M_{s\#FC35} = 1.53\text{T}$, $H_{c\#FC05} = 4.4\text{A/m}$, $H_{c\#FC35} = 22.4\text{A/m}$]. Nanocrystallization process of annealed alloy is a consequence of α -FeCo crystallite formation and some non-magnetic phases. Annealing at 500°C confirms comparatively superior magnetic properties of #FC05 (M_s=1.62T, H_c=44.97A/m) than that of #FC35 (M_s 1.69T and H_c of 377.4A/m), which is attributed to more structural instability in annealed #FC35 and better grain refinement of annealed #FC05. Therefore, it is concluded that a small amount of Co addition is advantageous for improving thermal stability and high temperature magnetic properties.

Mo.L-P12 - Structural and magnetic characterization of CoNiAl and CoNiGa pseudo-Heusler superelastic alloys

J. Mino^{1,2}, V. Komanicky¹, M. Ipatov², A. Zhukov^{2,3}, V. Zhukova², R. Varga¹, Zuzana Vargova¹

1. *Institute of Physics, Faculty of Science, UPJS, Kosice, Slovakia*

2. *Dpto. Fisica de Materiales, Fac. Quimicas, UPV/EHU, San Sebastian, Spain*

3. *IKERBASQUE, Basque Foundation for Science, Bilbao, Spain*

Magnetic superelastic alloys are perspective materials, which can be used as sensors and actuators [1]. Properties of superelastic change are mostly influenced by martensitic transformation, which can be triggered by stress, temperature and, in the case of magnetic alloys, also by magnetic field change. The CoNiX (X=Al,Ga) superelastic pseudo-Heusler alloys are usually prepared by arc-melting with additional annealing [2]. However, with a melt-spinning method annealing can be avoided or significantly reduced, still with good quality of highly textured polycrystalline ribbons [3]. The structural and magnetic properties of melt-spoon CoNiGa and CoNiAl ribbons have been investigated. Structural examination by SEM revealed polycrystalline structure with grain size varied in the orders of micrograms. Magnetic measurements were carried by PPMS. Temperature dependence of magnetization shows martensitic transformation at the temperature around 123K for CoNiGa and 50K for CoNiAl. By measuring the hysteresis loop the relative volume fraction of both phases around the transformation temperature can be estimated.

Support: NanoCEXmat Nr. ITMS 26220120019, Slovak VEGA grant. No. 1/0060/13, APVV-0027-11.

[1] J. M. Jani, M. Leary, A. Subic, M. A. Gibson; *Materials & Design*, Vol 56, pp 1078-1113 (2014)

[2] K. Oikawa, T. Ota, F. Gejima, T. Ohmori, R. Kainuma, K. Ishida, *Materials transactions*, Vol 42, No. 11 pp 2472-2475 (2001)

[3] J.L. Sánchez Llamazares, T. Sanchez, J.D. Santos et al., *Applied Physics Letters*, Vol. 92 (2008)

Mo.L-P13 - A new method for determining the Curie temperature from magnetocaloric measurementsL. M. Moreno-Ramírez¹, V. Franco¹, A. Conde¹, M. Marsilius², G. Herzer²1. *Dpto. Física de la Materia Condensada, ICMSE-CSIC, Universidad de Sevilla, Sevilla, Spain*2. *Vacuumschmelze GmbH & Co KG, Grüner Weg 37, Hanau, Germany*

The usual methods for the determination of the Curie temperature (T_C) are either affected by the value of the applied field (e.g. the inflection point of magnetization curves), depend on the chosen values of the critical exponents (Arrott plots) or they are iterative procedures like Kouvel-Fisher method [1]. Although in the literature the position of the magnetic entropy change peak (T_{peak}) is usually identified as the Curie temperature of the sample, this is only true in terms of a mean field approximation. Actually, T_{peak} can be field dependent. The field dependence of the magnetic entropy change (ΔS_M) can be expressed as a power law of the field $\Delta S_M = aH^n$. It has been previously demonstrated [2] that $n(T_{peak}) = n(T_C)$. Making use of this property, in this work we propose an alternative method for the determination of T_C that provides values which are field independent and does not require an iterative procedure: it consists in 1) the determination of T_{peak} from the $\Delta S_M(T)$ curve, 2) evaluate $n(T_{peak})$ and 3) identify the temperature $T < T_{peak}$ for which the $\Delta S_M(T)$ curve reveals the same exponent n for the field dependence, which corresponds to the Curie temperature of the sample. The validity of the method is illustrated with numerically simulated data obtained from the Arrott-Noakes equation of state [3] and experimental results of a Cr containing Fe-based amorphous alloy. This work was supported by Spanish MINECO and EU-FEDER (project MAT2013-45165-P) and the PAI of the Regional Government of Andalucía. $\Delta \alpha$

References

- [1] J. S. Kouvel and M. E. Fisher, Phys. Rev. 136 (1964) A1626
- [2] V. Franco, A. Conde, M.D. Kuzmin, J.M. Romero-Enrique, J. Appl. Phys. 105 (2009) 07A917
- [3] A. Arrott, J.E. Noakes, Phys. Rev. Lett. 19 (1967) 786–789

Mo.L-P14 - Analysis of the field dependence of magnetocaloric effect at the transition temperatures for biphasic systems

J.J. Ipus¹, L.M. Moreno-Ramirez¹, J.S. Blázquez¹, V. Franco¹, A. Conde¹

1. Departamento de Física de la Materia Condensada, ICMSE-CSIC, Universidad de Sevilla, Sevilla, Spain

The future application of magnetic refrigeration close to room temperature has increased the interest of the optimization of magnetocaloric materials. Therefore, it is necessary to compare data from different laboratories and acquired at different experimental conditions (e.g. magnetic field, H). In this sense, the study of the field dependence of the magnetic entropy change, $\Delta S_M = aH^n$, and the master curve analysis[1] are useful tools for this comparison. For single phase materials with second order phase transition, n is field independent at the Curie temperature, T_C , and related to the critical exponents of the transition. However, several factors can yield an incorrect determination of n , like the effect of the demagnetizing field and the multiphase character of some alloys. In this work, partially amorphous $\text{Fe}_{75}\text{Nb}_{10}\text{B}_{15}$ alloy was prepared by mechanical alloying[2]. Isothermal magnetization curves were corrected considering a demagnetizing factor of 1/3 and used to calculate ΔS_M . From the analysis of the field dependence of ΔS_M , the individual parameters of each phase were extracted under the approximation of two non-interacting phases (amorphous and bcc-Fe phases). For a constant H , the product $n \cdot |\Delta S_M|$ at T_C of the amorphous phase linearly decreases with increasing crystalline fraction, X_C . From the field dependence of the parameters of the linear fit, the characteristics of each phase are obtained. These agree well with typical ones found for other amorphous materials[1]. The described method can be easily extended to analyze other systems for which pure phase materials are difficult to obtain.

This work was supported by MINECO and EU FEDER (project MAT2013-45165-P) and the PAI of the Regional Government of Andalucía.

[1] V. Franco, et.al Appl. Phys. Lett 89(2006)222512

[2] J.J. Ipus, et.al Appl. Phys. Lett. 105(2014)172405

Mo.L-P15 - Study of Magnetocaloric Effect in the Pseudo Binary Laves-Phase Compounds

J. Aewik¹, Y. Koshkid'ko^{1,2}, A. Mikhailova³, N. Kolchugina³, K. Nenkov^{1,4}, A. Hackamer⁵, M. Miller¹

1. *International Laboratory of High Magnetic Fields And Low Temperatures, Wrocław, Poland*
2. *VSB-Technical University of Ostrava, Ostrava, Czech Republic*
3. *Baikov Institute of Metallurgy and Materials Science, Moscow, Russia*
4. *IFW Dresden, Institute of Metallic Materials, Dresden, Germany*
5. *Institute of Low Temperature and Structure Research, Wrocław, Poland*

The magnetocaloric effect is extensively studied experimentally and theoretically due to its potential applications for magnetic refrigeration as well as for further understanding the fundamental properties of the new materials. One of the most promising materials for use as a working component of the magnetic refrigerators in wide temperature range are Laves phase intermetallic compounds. This work reports magnetic and magnetocaloric properties of the polycrystalline series of Er-Fe-Al solid solutions. These samples were synthesized using high purity elements. Powder X-ray diffraction study have been performed at room temperature and analyzed using Rietveld refinement. Magnetization measurements were carried out using a vibration sample magnetometer with a step motor in applied fields up to 14 T using a Bitter-type magnet. The heat capacity was measured using Quantum Design PPMS 14 Heat Capacity System in a temperature range of 2-295 K without the magnetic field and in a magnetic field of 1 and 2 T. Structural investigation showed the formation of the cubic C15 structure and the hexagonal C14 structure depends on the composition. The magnetic ordering temperature decreases from 273 K for ErFe_{1.64}Al_{0.36} to 28 K for ErFe_{0.5}Al_{1.5}. Magnetization measurements in strong magnetic fields showed the complex mechanism of magnetic saturation in the studied compounds. The magnetocaloric effect has been estimated both in terms of isothermal magnetic entropy change and adiabatic temperature change in magnetic fields up to maximum 2 T. The effect of increasing Al amount in ErFe_{2-x}Al_x samples on magnetic and magnetocaloric properties will be discussed.

Mo.L-P16 - Shedding light on first-order magnetostructural transitions

M. Boeije¹, F. Guillou¹, Yibole¹, X. Miao¹, P. Roy², N. van Dijk¹, R. de Groot², E. Brück¹

1. TU Delft, Delft, Netherlands

2. Radboud University Nijmegen, Nijmegen, Netherlands

Magnetic cooling is a highly efficient refrigeration technique which could replace the traditional vapour compression cycle in the future. The driving force for this effect is a change in entropy between high and low temperature phases and the material can be switched between these states by applying an external magnetic field. For most magnetic materials, only the magnetic entropy plays a role in this transition. In addition to a magnetic contribution, the more promising magnetocaloric materials also show a change in crystal structure. All these transitions are of first order, and range from a small volume changes to changes in crystal symmetry. Apart from the lattice entropy, electronic entropy also plays a role and when the signs of these changes are the same, they can amount to a huge entropy change. Our focus is on materials which exhibit small changes in volume, like found in Fe₂P and La(Fe,Si)₁₃ materials. These materials can have very low thermal hysteresis and tend to have better mechanical stability. Unfortunately, these materials are scarce and the mechanism which links the various entropy contributions is not fully understood. We present experimental evidence which show how the coupling between magnetism and crystal structure takes place, with an Fe₂P based material as example. Using X-ray absorption and diffraction experiments, it was found that a redistribution of electron density takes place across the transition. The redistribution is consistent with the classical picture of the forming of a covalent bond while losing the magnetization. This discovery provides direct evidence of a predicted form of magnetism, called mixed magnetism. We now understand how these materials work and where to look in finding new promising materials.

Mo.L-P17 - Giant irreversible inverse and large reversible magnetocaloric effect in (Dy_{0.6}Gd_{0.4})₅Pd₂ intermetallic compound

T. Paramanik¹, I. Das¹

1. CMP Division, Saha Institute of Nuclear Physics, Kolkata, India

Detailed structural, magnetic and magnetocaloric study has been performed on polycrystalline (Dy_{0.6}Gd_{0.4})₅Pd₂ compound. Magnetic measurement shows large irreversibility both in temperature and magnetic field cycling has been observed in low temperature region. A large reversible magnetic entropy change has been observed over a wide temperature range. The peak value of magnetocaloric entropy change ~ 7.2 J/kg-K for 7 T magnetic field change has been observed around 87.5 K. Giant positive irreversible magnetic entropy change (~ 14.8 J/kg-K at 3 K for 7 T magnetic field change) below 25 K from zero-field-cooled isothermal magnetization measurement, which is associated with the internal entropy production. The possibility of the origin of the giant irreversible positive entropy change has been discussed. Validity of Maxwell's relation to evaluate reversible magnetocaloric entropy change from magnetization measurement has been described. An estimation of internal entropy production and its thermal dependence has been presented from thermodynamical analysis.

Mo.L-P18 - Magnetic investigation on MnNiGe_{0.9}Al_{0.1} alloyP. Dutta¹, D. Das¹, S. Chatterjee¹*1. UGC-DAE Consortium For Scientific Research, Kolkata Centre, Kolkata, India*

We present a systematic magnetic investigation on an Al doped Mn-Ni-Ge magnetic equiatomic alloy (MEA) of nominal composition MnNiGe_{0.9}Al_{0.1}. The undoped MnNiGe alloy undergoes first order martensitic phase transition (MPT) from the high temperature hexagonal Ni₂In-type structure to the low temperature orthorhombic TiNiSi-type structure at 470K during cooling and orders antiferromagnetically (AFM) below 346K. Al doping in Ge site results decrease in structural transition temperature and causes changes in lattice parameters that induces ferromagnetism in this intrinsically AFM system. Magnetization vs. Temperature ($M - T$) data in presence of 100 Oe magnetic field reveals that, on cooling, the alloy undergoes paramagnetic (PM) to ferromagnetic (FM) transition around 190K and FM to AFM transition around 115K along with MPT. Observation of clear thermal hysteresis between field cooling and field cooled heating magnetization data around the MPT confirms the first order nature of the transition. Three distinct magnetic regions are clearly observed in the isothermal $M-H$ data. The negative slope of the Arrot plot near FM to AFM transition and the positive slope near the PM to FM transition indicate first and second order transitions respectively that prompted us to investigate the magnetocaloric effect (MCE) in the sample. Change in entropy (DS) on application of H is a measure of MCE. A large inverse MCE has been observed around the MPT ($DS = 15$ J/kg-K for 0-50 kOe at 115K), whereas DS is found to be negative around the FM to PM transition ($DS = -5$ J/kg-K for 0-50 kOe at 190K). Relative cooling powers are found to be -150.4 J/kg and 142.92 J/kg for 0-50 kOe at 115K and 190K respectively. This work reveals that the studied material is a good addition to the list of presently available intermetallic alloys having magneto-functional properties.

Mo.L-P19 - Influence of high pressure oxygenation on the structure and magnetic properties of la-ca-sr-mn-o perovskite ceramic material

K. Zmorayová¹, V. Antal¹, S. Piovarèi¹, V. Kavečanský¹, J. Kováč¹, L. Vojtková¹, P. Diko¹, M. Kaňuchová²

1. *Institute of Experimental Physics, Slovak Academy of Sciences In Košice, Košice, Slovakia*

2. *The Technical University of Košice, Košice, Slovakia*

In this contribution, the influence of high pressure oxygenation on the structure and magnetisation behaviour of $\text{La}_{0.67}\text{Ca}_{0.3}\text{Sr}_{0.03}\text{MnO}_3$ (LCSM) perovskite ceramics was investigated. The LCSM perovskite ceramic material was prepared by conventional solid state synthesis in air and subsequently sintered at 1520°C . The sample for study of oxygen influence was additionally treated by high pressure oxygenation (HPO) at following conditions: 800°C for 1 hour, cooling to room temperature at 95 bar pressure of pure oxygen atmosphere. The purity and grain size of studied sample was checked by a scanning electronic microscope (SEM) and analysis by energy dispersive spectrometer (EDS) which confirmed the uniform distribution of elements in the sample. The formation of the LCSM perovskite ceramic material and changes in the oxidation states of elements were studied by X-ray photoelectron spectroscopy (XPS) and by thermogravimetric measurement (TG). XPS measurements showed changes in the valence of Mn^{3+} to Mn^{4+} after high pressure oxidation caused by the mass changes of the oxygen content in the samples, which was confirmed by TG measurement. For determination of the Curie temperature the small sample pieces were measured by a Magnetic Property Measurement System (MPMS). The magnetization measurements showed that the high-pressure oxidation shifts the thermomagnetic curves toward lower temperatures.

Mo.L-P20 - Structural, optical and magneto-optical studies of martensitic transformation in magnetic shape memory alloy Ni₂MnGa

P. Cejpek¹, L. Beran¹, R. Antoš¹, V. Holý¹, M. Veis¹, O. Heczko²

1. Charles University In Prague, Prague, Czech Republic

2. Institute of Physics, Academy of Science of Czech Republic, Prague, Czech Republic

Magnetic shape memory alloys have the outstanding property, which allows their straining [1] in moderate magnetic fields (< 1T). Among these alloys Ni₂MnGa is a good model system in which the macroscopic deformation occurs due to magnetically induced structural reorientation of martensite. Therefore the martensitic transformation to low symmetry phase is a key for the existence of the shape memory effect and its deep understanding is necessary for future applications of these alloys. In this work, the structure of the Ni_{50.1}Mn_{28.4}Ga_{21.5} was systematically studied by X-ray diffraction, especially with the reciprocal space mapping. The structure is monoclinic, which slightly differs from the tetragonal martensite. Measured reciprocal maps contain more diffraction spots, which occur due to the mosaic blocks and the twinning. The satellite maxima have been measured too. There were four of them between each of the proper diffraction spots. That proves the 10M modulated structure. Temperature dependent reciprocal maps around 040 diffraction peak have been measured. The structure transition to cubic austenite phase was observed with notable hysteresis. The transition occurs at 68°C during the heating and at 56°C during the cooling. To get the information about the changes in electronic structure during the transformation, optical and magneto-optical methods were employed as well. Namely the spectroscopic ellipsometry and Kerr magneto-optical spectroscopy in the photon energy range from 1.2 to 5.6 eV. Magneto-optical spectra of polar and longitudinal Kerr rotation as well as spectra of ellipsometric parameters Ψ and Δ exhibited significant changes when crossing the transformation temperature. These changes correlated with XRD observations and were explained by change of optical properties of Ni₂MnGa due to differences in electron density of states at Fermi energy in martensite and austenite phases.

[1] Sozinov, et al., Mat. Sci. Eng. A 378 (2004), 399

Mo.L-P23 - Magnetic and magnetothermal properties of the melt-spun $(\text{Gd}_{1-x}\text{Tb}_x)_{75}\text{Co}_{25}$ and $(\text{Gd}_{1-x}\text{Y}_x)_{75}\text{Co}_{25}$ alloys

D. Shishkin^{1,2}, A. Volegov², A. Chirkova^{1,2,3}, K.i Nenkov³, N. Baranov^{1,2}

1. *Institute of Metal Physics, Russian Academy of Science, Ekaterinburg, Russia*

2. *Institute of Natural Sciences, Ural Federal University, Ekaterinburg, Russia*

3. *IFW Dresden, Dresden, Germany*

This work aims to study the magnetic and magnetothermal properties of melt-spun $(\text{Gd}_{1-x}\text{Tb}_x)_{75}\text{Co}_{25}$ and $(\text{Gd}_{1-x}\text{Y}_x)_{75}\text{Co}_{25}$ alloys. The samples were prepared by a melt-spinning technique. The isothermal magnetic entropy change, ΔS_M , was calculated from the temperature dependences of the magnetization measured in magnetic fields up to 50 kOe by using the thermodynamic Maxwell relation.

The Gd_3Co compound is an antiferromagnet with the Néel temperature $T_N \approx 131$ K and with zero magnetic moment on Co atoms. The amorphization of Gd_3Co modifies its magnetic state to the ferromagnetic-like behavior, leads to the appearance of a magnetic moment on Co atoms and improves the magnetocaloric properties in comparison with the crystalline counterpart [1]. Specific heat measurements performed in the present work have revealed that the liquid-quenched $\text{Gd}_{75}\text{Co}_{25}$ alloy exhibits a lower value of the electronic specific heat coefficient than the crystalline sample ($257 \text{ mJ kg}^{-1} \text{ K}^{-2}$ and $319 \text{ mJ kg}^{-1} \text{ K}^{-2}$, respectively). Unlike the metallic character of the resistivity behavior in the crystalline Gd_3Co the $\rho(T)$ dependence for the liquid-quenched sample shows a weak thermally activated behavior. For the melt-spun $(\text{Gd}_{1-x}\text{Y}_x)_{75}\text{Co}_{25}$ alloys, the substitution of Y for Gd reduces the magnetic ordering temperature and ΔS_M value. The amorphous $(\text{Gd}_{1-x}\text{Tb}_x)_{75}\text{Co}_{25}$ alloys are found to exhibit the ΔS_M value about of $8.7 \pm 0.5 \text{ J kg}^{-1} \text{ K}^{-1}$ in the wide temperature range between 75 K and 170 K. Moreover, amorphous samples show much higher refrigerant capacities in comparison with their crystalline counterparts.

This work was supported by the program of the Ural Branch of RAS (Project No 15-17-2-22) and RFBR (Grant No. 14-02-31865).

[1] D.A. Shishkin et.al., The Physics of Metals and Metallography. 113 (2012) 460

Mo.L-P24 - Magnetic behaviour of martensite in metamagnetic Ni-Co-Mn-Ga alloys

C. Seguí¹, E. Cesari¹, P. Lázpita²

1. *Departament de Física. Universitat Illes Balears, Palma de Marllorca, Spain*

2. *Departamento de Electricidad y Electrónica. Universidad del País Vasco, Leioa, Spain*

Ferromagnetic Ni-Co-Mn-Ga shape memory alloys show, for a certain range of Co content, metamagnetic behavior, as they undergo martensitic transformation (MT) between ferromagnetic austenite (Aferro) and paramagnetic -or weak magnetic- martensite (mpara). The temperatures of the structural and magnetic transitions depend on composition and atomic order. The austenite L21 order degree can be modified by selected thermal treatments; namely, quenched-in disorder after quench raises the MT temperatures, and lowers both austenite and martensite Curie temperatures, whereas order improvement during post-quench ageing promotes recovery of all transformation temperatures. Such opposite changes make that, for a given composition, the transformation sequence on cooling/heating depends on the atomic order; for example, poorly ordered high e/a alloys display Apara-mpara MT, evolving to Aferro-mpara as ordering improves, while for low e/a the MT changes from Aferro-mpara to Aferro-mferro. Consequently, combined composition and thermal treatment allows for MT between any magnetic state of austenite and martensite. In previous works we have made progress in understanding the mutual influence between atomic and magnetic order and its effect on the transformation entropy. However, there are still several issues that require detailed analysis to be well understood. These include the magnetic nature of martensite. At low magnetic fields, magnetization in martensite is small but seemingly not zero; this could be due to antiferromagnetic rather than paramagnetic behavior of martensite, as suggested for some metamagnetic alloys including Ni-Co-Mn-Ga, but this is still a matter of discussion. In the present work, the magnetic state of martensite has been studied in detail for the Ni₄₃Co₇Mn₃₀Ga₂₀ alloy. Its evolution as a function of atomic order shows that the magnetic order of the -as called- paramagnetic martensite increases as the austenite switches Apara to Aferro; in the ordered state, the martensite is ferromagnetic (or ferrimagnetic) rather than paramagnetic, as revealed by the magnetization vs field curves.

Mo.L-P25 - Rotational Electromagnetic Energy Harvesting System

D. Dinulovic¹, M. Haug¹, T. Petrovic²

1. *Wurth Elektronik EiSos, Germany*

2. *University of Nis, Niš, Serbia*

Abstract

This paper presents development of a rotational electromagnetic energy harvesting transducer. Transducer is driven mechanically by pushing the button; therefore, a mechanical energy will be converted in to an electrical energy. The energy harvesting (EH) transducer consists of multilayer planar coils embedded in to PCB, of multipolar NdFeB hart magnets, and of mechanical system for movement conversion. The EH transducer generate an energy of 3mJ at load of 10Ω. The maximal open circuit output voltage is higher as 2V and maximal short circuit output current is higher as 800mA.

Introduction

Main advantage of rotational electromagnetic transducers regarding to oscillatory electromagnetic transducers is independence to the oscillating frequency.

The harvester will be powered by pushing the button. The linear movement of the button will be transformed into a rotational movement by movement conversion mechanism. On this way, a rotor consisting of hart magnets will be rotated above the stator with coils. Therefore, an electrical voltage will be induced. These transducers are capable to achieve higher energy density as other electromagnetic transducers [1].

Design

The whole energy harvester system is modular and consists of 3 modules: (A) mechanism for motion conversion, (B) electromagnetic energy harvesting part, (C) power management system (PMS) with RF transmitter.

The electromagnetic transducer consists of movable part (rotor) and stationary part (stator). The rotor consists of 8 multi-pole hart magnet segments of NdFeB mounted on soft magnetic Co-alloy sheet metal with high saturation flux density. As a stator serves one coil system consisting of 8 coils divided in two phases. Coils are embedded into PCB.

Both parts, the stator and the rotor, are mounted on axis forming a defined air gap between.

An induced voltage will be “managed” using power management system. The AC voltage will be converted into DC voltage and set to a regulated output voltage i.e. 1.8V. This voltage will be used for power an RFID transmitter.

References:

[1]D.P. Arnold, „Review of Microscale Magnetic Power Generation”, IEEE Transaction on Magnetics, Vol. 43, No. 11, 2007, pp. 3940 – 3951.

Mo.L-P26 - Comparison of conventional sintering and spark plasma sintering routes for the fabrication of magnetocaloric Mn-Fe-P-Si compounds

A. Bartok¹, A. Pasko¹, K. Zehani², L. Bessais², F. Mazaleyrat¹, V. Russier², M. LoBue¹

1. SATIE, ENS Cachan, CNRS, Universite Paris-Saclay, , Cachan, France

2. ICMPE, CNRS, Universite Paris 12, Thiais, France

Hexagonal Mn-Fe-P-Si compounds are known to represent an extremely attractive rare-earth-free system for applications in room-temperature magnetic refrigeration [1]. The giant magnetocaloric effect (MCE) associated to a magneto-elastic first-order phase transition has been studied in this system with particular emphasis on the tuning of critical temperature, entropy change and thermal hysteresis as a function of the chemical composition [2]. MCE properties are also extremely sensitive to the preparation route [3, 4]. A systematic comparison between three bulk samples, with composition $\text{Mn}_{1.3}\text{Fe}_{0.65}\text{P}_{0.5}\text{Si}_{0.5}$, prepared respectively by conventional sintering and by spark plasma sintering (SPS) under different pressures, and a powder of the same composition prepared by high-energy ball milling is presented. Here we focus on the behavior of samples after the first cooling (i.e. the so-called virgin effect will be treated elsewhere). We show that the magnetic entropy change, derived from isothermal magnetization curves measured in a magnetic field up to 5 T, and Arrott plots are strongly affected by the preparation route. The observed differences are interpreted with emphasis on the role of microstructure and porosity. The way in which microstructure can affect the transition due to magneto-elastic coupling is discussed.

Mo.L-P27 - Pressure induced magnetic and magnetocaloric properties in Mn rich Mn-Ni-Sn Heusler alloysJ. Sharma¹, K. G. Suresh¹, A. A. Coelho²*1. Indian Institute of Technology Bombay, Mumbai, India**2. Instituto de Física "Gleb Wataghin", Universidade Estadual de Campinas-UNICAMP, Sao Paulo, Brazil*

In recent years Ni-Mn-Z (Z= Ga, Sn, Sb and In) Heusler alloys have attracted enormous attention owing to their multifunctional properties such as giant magnetocaloric effect (MCE) and large magnetoresistance, at their first order magnetostructural (martensitic) transition. Magnetic properties of these alloys are strongly influenced by Mn-Mn exchange interaction, which can be altered by either chemical substitution or applying pressure. Recently effect of pressure has been reported in many Ni rich Ni-Mn-Z alloys. However, no such reports are available for Mn rich Mn-Ni-Z alloys. In this paper, we have investigated the effect of pressure on the martensitic transition, magnetic and magnetocaloric properties of Mn rich $\text{Mn}_{50}\text{Ni}_{39+x}\text{Sn}_{11-x}$ ($x=0$ and 2) Heusler alloys. Polycrystalline samples were prepared by arc melting method. Magnetization measurements at different applied pressures have been performed using SQUID attached with a Cu-Be clamp type pressure cell. Both alloys undergo the martensitic transition and the transition temperature (T_M) has been found to increase with increase of pressure, whereas it decreases with increase in field. For $x = 2$, $T_M \sim 299$ K (RT) at ambient pressure ($P = 0$) and becomes ~ 339 K for $P = 10.4$ kbar, which is attributed to the stabilization of the martensite phase. A splitting between ZFC and FC curves has been observed at low temperatures, which is attributed to the coexistence of antiferromagnetic and ferromagnetic exchange interactions. Pressure effect on MCE has been studied by isothermal magnetic entropy change (ΔS_M). ΔS_M has been found to increase with increase of x , and a large value of $\Delta S_M \sim 6.45$ J/kg.K has been observed at $\sim \text{RT}$ (at $P = 0$) for $x = 2$. However it has been found to decrease with increase of pressure, but the peak temperature of ΔS_M vs. T peak increases. Therefore, hydrostatic pressure can be used to tune magnetic and magnetocaloric properties over a wide temperature span around RT in these alloys.

Mo.L-P28 - Enhancement of coercivity through Nd-Cu eutectic reaction for Nd-Fe-B thin films

R. Nakagawa¹, T. Shima¹

1. *Tohoku-Gakuin University, Sendai, Japan*

In this study, in order to enhance a hard magnetic properties and microstructure modification for the Nd-Fe-B thin films through Nd-Cu eutectic reaction, Nd-Fe-B/ Nd-Cu multilayer thin films have been prepared and their structure and magnetic properties have been investigated. The samples were prepared by using an UHV compatible magnetron sputtering system. The base pressure is below 5×10^{-8} Pa. First of all, a epitaxial Mo buffer layer of 20 nm was deposited onto MgO (100) single crystal substrates at room temperature (R.T.) Subsequently, the substrates were cooled to 500 °C and the Nd-Fe-B layer and the Nd-Cu cap layer were deposited. The nominal thickness of the Nd-Fe-B layer was fixed at 16 nm and Nd-Cu layer was fixed at 0.75 nm. Then, the samples were annealed from 500 °C to 600 °C for 60 min for the crystallization of Nd-Fe-B/ Nd-Cu layer. Finally, a protective Mo layer of 10 nm was deposited at R.T.. In order to see the effect of annealing temperature, T_a was varied. All the films were measured in the perpendicular direction to the film plane and in the in-plane direction. Nd-Fe-B layer began to crystallize at $T_a = 500$ °C and highest H_c of 29.2 kOe and good squareness were obtained at $T_a = 550$ °C. The alloy composition of Nd and Cu is close to eutectic point, and H_c is thought to increase by the diffusion of the Nd-Cu alloy layer to the grain boundary phase. However, remarkable reduction of H_c was observed at $T_a = 600$ °C.

Mo.L-P29 - Microstructural control of Nd-Fe-B materials sintered using electric Field Assisted Sintering Techniques (FAST)

E. Castle¹, S. Grasso¹, M. Reece¹, R. Sheridan², A. Walton²

1. *Queen Mary, University of London, London, United Kingdom*

2. *University of Birmingham, Birmingham, United Kingdom*

In order to address the growing need for high coercivity, Dy-free Nd-Fe-B permanent magnets for automotive applications, it has long been recognised that enhanced microstructural control over the grain size, alignment and grain boundary phase distribution and composition will be key [1,2]. In the present work, electric Field Assisted Sintering Techniques (FAST) have been employed in order to rapidly consolidate both commercially available melt-spun materials and recycled hydrogenation, disproportionation, desorption, recombination (HDDR) processed materials. The effect of starting material, pre-sintering preparation method and sintering conditions on the density, final microstructure and magnetic properties has been investigated. It is shown that a good degree of microstructural control can be achieved as well as consolidation to full density. Consequently, it is shown that a range of magnetic properties can be achieved, including both isotropic and anisotropic magnets; using fabrication techniques which require much less time and energy as compared to conventional processing methods.

Acknowledgements: Research supported by EU-FP7 MAG-DRIVE project (No. 605348) [<http://www.mag-drive-fp7.eu/>]

[1] K. H. Muller, D. Eckert, A. Handstein, P. Nothnagel, and J. Schneider, *J. Magn. Magn. Mater.*, 83, (1991) 195

[2] J. D. Livingston, *J. Appl. Phys.*, 57, (1985) 4137

Mo.L-P31 - The magnetic properties and magnetocaloric effect in Mn_{1-x}Ni_xCoGeQ. Ren¹, W. Hutchison¹, J. Wang², A. Studer³, S. Cadogan¹, S. Campbell¹

1. PEMS, University of New South Wales, Canberra, Australia

2. ISEM, University of Wollongong, Wollongong, Australia

3. Bragg Institute, Australian Nuclear Science and Technology Organisation, Lucas Heights, Australia

Refrigeration based on magnetic cooling *via* the magnetocaloric effect offers potential as an alternative to conventional gas-compression systems [1]. MnCoGe-based compounds show promise for magnetic refrigeration and have been extensively investigated over the last decade [e.g. 2]. These compounds have two crystallographic structures: nominally low temperature TiNiSi-type orthorhombic structure (*Pnma*) and the high temperature Ni₂In-type hexagonal structure (*P6₃/mmc*). When the structural transition temperature between the two structures is 'tuned' between the respective Curie temperatures of the phases (~345 K for the orthorhombic phase and ~275 K for the hexagonal phase in MnCoGe [2]), a direct change from a ferromagnetic orthorhombic phase to a paramagnetic hexagonal phase can result [2]. For a such a magneto-structural transition, the lattice and magnetic entropy changes occur simultaneously, thereby providing scope for observation of a large magnetocaloric effect [3].

The crystallographic structures and magnetic properties of annealed Mn_{1-x}Ni_xCoGe ($x = 0.03, 0.04, 0.05, 0.06$ and 0.07) have been investigated using x-ray diffraction ($T = 18-310$ K) together with neutron diffraction measurements carried out for Mn_{0.95}Ni_{0.05}CoGe in the range $T = 5-320$ K in addition to magnetisation measurements ($T = 5-340$ K). The outcomes from our experiments demonstrate the formation of magneto-structural transitions within the series. The magnetic entropy changes have been derived in the conventional way from a series of isothermal magnetisation experiments, e.g. $-\Delta S_m \sim -8.8$ J kg⁻¹ K⁻¹ for a magnetic field change of $\Delta B = 0-5$ T in Mn_{0.95}Ni_{0.05}CoGe.

[1] E. Brück, *J. Phys. D: Appl. Phys.* 38, R381 (2005)[2] N. T. Trung, L. Zhang, L. Caron, K. H. J. Buschow and E. Brück, *Appl. Phys. Lett.* 96, 172504 (2010)[3] J. Liu, T. Gottschall, K. P. Skokov, J. D. Moore and O. Gutfleisch, *Nat. Mater.* 11, 620 (2012)

Mo.L-P32 - Direct and inverse thermal magnetocaloric effect obtained from non-adiabatic measurements: $Gd_{0.5}Pr_{0.5}Al_2$ compound case

A. Carvalho¹, C. Salazar Mejía², A. Gomes²

1. *Laboratório Nacional de Luz Síncrotron, CNPEM, Campinas, Brazil*

2. *Instituto de Física, UFRJ, Rio de Janeiro, Brazil*

In the last two decades, there was an increasing interest on the research of the magnetocaloric effect (MCE), mainly due the possibility of applying it to heat up or cool down objects, using different thermomagnetic cycles, such as, Ericsson, Stirling or Brayton cycles. Direct measurement of the MCE is usually referred only to the adiabatic temperature change (ΔT_S), and in this case, the magnetic material is directly attached to a temperature sensor and its response is monitored while the applied magnetic field is altered. Although the direct measurement of ΔT_S seems to be a trivial task, it is not the case in terms of experimental procedures.

In this work, we apply to $Gd_{0.5}Pr_{0.5}Al_2$ compound a new methodology to obtain the ΔT_S curve from non-adiabatic temperature changes measurements. Around the magnetic transition temperature, we have obtained positive ΔT_S values (direct MCE). Below 60 K, we have obtained negative ΔT_S values (inverse MCE), in great agreement with results from calorimetric measurements [1]. Above 60 K, the divergences between MCE from calorimetry and MCE from direct measurements increase with temperature, which is an indication of any kind of problem with the calorimetric measurements in Ref. [1].

[1] A. Magnus G. Carvalho *et al.*, J. Magn. Magn. Mat. 321, 3014 (2009).

Mo.L-P33 - Giant Magnetic Entropy Change in $\text{La}_{0.6}\text{Ce}_{0.4}\text{Fe}_{11.5}\text{Si}_{1.5}$ Alloy Exhibiting First- and Second-Order Phase TransitionsT. D. Thanh¹, W. Z. Nan¹, B. Y. Jeon², T. S. You², T. L. Phan³, S. C. Yu¹

1. Department of Physics, Chungbuk National University, Cheongju, South Korea

2. Department of Chemistry, Chungbuk National University, Cheongju, Korea

3. Department of Physics, Hankuk University of Foreign Studies, Yongin, South Korea

In this work, a polycrystalline alloy ingot $\text{La}_{0.6}\text{Ce}_{0.4}\text{Fe}_{11.5}\text{Si}_{1.5}$ was prepared by an arc-melting method. Magnetic measurements versus temperature (50-300 K) and magnetic field (0-30 kOe) were performed on a vibrating sample magnetometer. The magnetic results reveal the sample exhibiting a ferromagnetic-paramagnetic phase transition at $T_c = 170$ K. Interestingly, the H/M versus M^2 curves at low-field ($H \leq 10$ kOe) show a positive slope, corresponding to the second-order phase transition (SOPT), whereas, a negative slope corresponding to the first-order phase transition (FOPT) was observed at high-field ($H > 10$ kOe). These suggest that a coexistence of FOPT and SOPT properties in $\text{La}_{0.6}\text{Ce}_{0.4}\text{Fe}_{11.5}\text{Si}_{1.5}$. Basing on $M(H)$ isotherms, $\Delta S_m(T)$ data for sample under the maximum magnetic field change $H = 5-30$ kOe (with step of 5 kOe) were calculated. As a result, $|\Delta S_m(T)|$ reaches the maximum ($|\Delta S_{\max}|$) around T_c and increases with an increasing H . With $H = 10, 20,$ and 30 kOe, $|\Delta S_{\max}|$ values are 13.2, 26.0, and 33.2 $\text{J}\cdot\text{kg}^{-1}\cdot\text{K}^{-1}$, respectively. On the other hand, the magnetic cooling efficiency of refrigerants can be, in simple cases, evaluated by $\text{RCP} = |\Delta S_{\max}| \times \delta T_{\text{FWHM}}$, where δT_{FWHM} is the full width at half maximum of $\Delta S_m(T)$ curve. Depending on H , the RCP value is found to be 59.4, 130.0, and 199.2 $\text{J}\cdot\text{kg}^{-1}$ for $H = 10, 20,$ and 30 kOe, respectively. Also, the results reveal that all $\Delta S_m(T)$ curves at low-field ($H \leq 10$ kOe) are collapsed into a universal curve, which is obtained by normalizing $\Delta S_m(T)/\Delta S_{\max}$ versus $\vartheta = (T - T_c)/(T_r - T_c)$; here, T_r is the reference temperature. In contrast, $\Delta S_m(T)/\Delta S_{\max}$ versus ϑ curves in the high-field case ($H > 10$ kOe) do not overlap into a universal curve, indicating an existence of the FOPT property. This nature of the observed phenomena is discussed thoroughly.

Mo.L-P35 - 3D nano-architected multiferroic CuO electrodes for high-performance supercapacitors

K. Lu¹, M. Deng¹, C. Song², C. Wang², Y. Tseng², J. Chen¹

1. National Synchrotron Radiation Research Center (NSRRC), Hsinchu, Taiwan

2. Department of Materials Science and Engineering, National Chiao Tung University, Hsinchu, Taiwan

We prepared nano-architected multiferroic CuO electrodes with a 3D hierarchically porous structure and an excellent supercapacitive performance. These nano-architected CuO electrodes were processed through co-deposition of a Ni–Cu layer on Ni foam, selective etching of Cu from the Ni–Cu film (leaving tentacle-like nanoporous Ni), and anodic deposition of CuO nanoribbons (NRs) on the tentacle-like nanoporous Ni/Ni foam substrate. Because of its unique nano-architecture, the prepared CuO nanoribbon-on-Ni-nanoporous/Ni foam (CNRNP) electrode shows exceptional performance of energy storage relative to a conventional version of the electrode. The CNRNP electrode has also a superior kinetic performance relative to CuO nanoflake-on-Ni foam (CNFNF) and flake-like CuO (FLC) electrodes. Besides its excellent cyclic stability, an exceptionally large specific capacitance of 880 and 800 F g⁻¹ (deducting the substrate capacitance from the total) for the CNRNP electrode is obtained at scan rates of 10 and 200 mV s⁻¹, respectively. The excellent pseudocapacitive characteristics of CNRNP electrodes associated with the variation of the Cu oxidation state during charge and discharge cycles were elucidated with *in situ* X-ray absorption near-edge structure (XANES) spectra.

Mo.L-P37 - Direct measurements of the crucial characteristics of MCE refrigeration in high magnetic fields in a Gd sample

E. Dilmieva¹, V. Koledov¹, A. Kamantsev¹, V. Shavrov¹, A. Mashirov¹, I. Tereshina², V. Nizhankovskii³

1. *Kotelnikov Institute of Radio Engineering And Electronics of RAS, Moscow, Russia*

2. *International Laboratory of High Magnetic Fields & Low Temperatures of PAN, Wroclaw, Poland*

3. *Baikov Institute of Metallurgy and Material Science of RAS, Moscow, Russia*

The coefficient of performance (COP) of cooling process is the relation of heat transferred from a cold body to a hot body of the refrigerator to the mechanical work spent for one thermodynamic cycle. For the purpose of experimental study of the process of magnetic cooling by Gd working body and direct estimation the COP the new technique was developed. It allows to determine at the same time the magnetocaloric effect (MCE) and the magnetization (M) of materials versus magnetic field (H) in quasiadiabatic mode. The full cycle of magnetic cooling was tested on Gd sample in the field of the Bitter magnet up to 12 T. The temperature growth is equal to $\Delta T_{\text{on}} = 13,5$ K at turning on magnetic field 12 T. The temperature drop is equal to $\Delta T_{\text{off}} = -19$ K at turning off the magnetic field. The resulting temperature change of the sample under cycle of magnetic field turning on/off is equal to $\Delta T_{\text{total}} = -5,5$ K. ΔT_{total} is a consequence of the process of magnetic cooling. The *in situ* measurement shows that M(H) dependence of the Gd sample during the process has hysteretic character. The calculation of integral of HdM on a closed loop allows one to determine the work of magnetic field during cooling cycle and to calculate the COP of magnetic cooling process. By calculating COP it is found that at initial sample temperature $T_0 = 298$ K and the magnetic field change 12 T, $\text{COP} = 15$. By reducing the magnetic field to $H = 2$ T, COP increases $\text{COP} = 92$. The fundamental restrictions on COP are imposed by Carnot's theorem. $\text{COP}_{\text{Carnot}}(T_0=298, H=2\text{T})= 600$, $\text{COP}_{\text{Carnot}}(T_0=298, H=12\text{T})= 60$. The reasons for which the COP found by experimental estimation is significantly lower than $\text{COP}_{\text{Carnot}}$ are discussed.

Mo.L-P39 - Magnetocaloric effect of La(Fe,Si,Co)₁₃ compounds as measured in pulsed magnetic fields

M. Ghorbani-Zavareh ^{1,2}, Y. Skourski ¹, K.P. Skokov ³, J. Wosnitza ^{1,2}, O. Gutfleisch ³

1. *Hochfeld-Magnetlabor Dresden (HLD-EMFL), Helmholtz-Zentrum Dresden-Rossendorf, Dresden, Germany*

2. *Institut für Festkörperphysik, TU Dresden, Dresden, Germany*

3. *Technische Universität Darmstadt, Institut für Materialwissenschaft, Darmstadt, Germany*

We report on direct measurements of the magnetocaloric effect (MCE) and magneto-volume effects of La(Fe,Si,Co)₁₃ compounds, which are promising candidates for magnetic refrigeration applications as they undergo a metamagnetic transition associated with considerable entropy change. The nature of the transition can be changed from first to second order as well as the temperature of the transition can be tuned by varying the Co concentration. The MCE of two compounds with different Co concentrations and transition temperatures of 199 K (first order) and 254 K (second order) have been measured in pulsed magnetic fields up to 50 T. The compound with first-order transition shows half of the net magnitude of the MCE already at low fields (2-10 T). Whereas the MCE of the compound with second-order transition grows gradually. The MCE in both compounds reaches similar values of about 18 K at maximum field of 50 T. Results obtained in pulsed magnetic fields of 2 T are in a good agreement with data from quasi-static-field measurements. These phenomena are driven by an itinerant-electron metamagnetic transition accompanied by a volume change of the sample. Magnetostriction measurements performed in both static and pulsed magnetic fields show an irreversible magnetovolume effect of about ~1%. The entropy change, ΔS , was evaluated from specific-heat measurements in static fields. Pulsed-field magnetization of both compounds was measured in fields up to 60 T in a nearly adiabatic regime and compared to steady-field isothermal measurements. The differences between the two are discussed and explained involving the measured MCE values.

Mo.L-P40 - Influence of structural disorder on normal and inverse magnetocaloric effect in $Y_{1-x}Gd_xCo_2$ ($0 \leq x \leq 1$) compoundsN. Pierunek¹, Z. Śniadecki¹, V. Franco², B. Idzikowski¹

1. Institute of Molecular Physics Polish Academy of Sciences, Poznań, Poland

2. Condensed Matter Physics Department, Sevilla University, Spain

YCo_2 compound is an exchange-enhanced Pauli paramagnet on the verge of being magnetic. Ferromagnetic long-range ordering can be induced by topological or chemical disorder [1]. The influence of Gd substitution and quenched-in free volumes and vacancies on the magnetic properties of as cast and annealed $Y_{1-x}Gd_xCo_2$ ($0 \leq x \leq 1$) compounds is studied by means of X-ray diffraction and vibrating sample magnetometry. Investigated systems crystallize in the $MgCu_2$ -type Laves phase ($Fd\bar{3}m$ space group) [2]. Magnetic entropy changes $\Delta S_M(T, \mu_0 H)$ and refrigerant cooling power RCP parameter were determined on the basis of $M(H)$ curves and results have been correlated to the presence of structural disorder [3]. Changes in values of ΔS_{Mpk} (maximum of ΔS_M peak), δT_{FWHM} (full width at half maximum) and RCP parameters with structural ordering (after isothermal annealing procedure) are clearly visible. For $Gd_{0.6}Y_{0.4}Co_2$ compound ($T_C = 282$ K) in as-quenched state the ΔS_{Mpk} , δT_{fwhm} and RCP are equal to 2.12 J/kgK, 75 K and 122 J/kg, respectively for magnetic field changes from 0 to 5 T. Through isothermal annealing ($T = 700^\circ C$, $\tau_a = 60$ min.) crystalline structure reaches lower free energy level, which directly affects the MCE properties. ΔS_{Mpk} is equal to 2.15 J/kgK, but δT_{fwhm} value drops with annealing by ca. 15% as well as RCP parameter. Structural disorder significantly broadens the magnetic transition and the temperature-dependent magnetic entropy changes in investigated compounds.

[1] Z. Śniadecki *et al.*, J. Appl. Phys. 115 (2014) 17E129[2] A. Wiśniewski *et al.*, J. All. Compd. 618 (2015) 258-262[3] A. Biswas *et al.*, J. Appl. Phys. 115 (2014) 17A318

Mo.L-P41 - Origin of martensitic phase transition in ferromagnetic shape memory alloy Ni-Fe(Co)-Ga thin film

K. Sumida¹, K. Shirai¹, S. Zhu¹, M. Taniguchi^{1,2}, M. Ye³, S. Ueda⁴, Y. Takeda⁵, Y. Saitoh⁵, I. Rodriguez⁶, J. Barandiaran⁶

1. Graduate School of Science, Hiroshima University, Hiroshima, Japan

2. Hiroshima Synchrotron Radiation Center, Hiroshima, Japan

3. Shanghai Institute of Microsystem and Information Technology, Chinese Academy of Science, Shanghai, China

4. Synchrotron X-ray Station at SPring-8, National Institute for Materials Science, Hyogo, Japan

5. Condensed Matter Science Division, Japan Atomic Energy Agency, Ibaraki, Japan

6. BCMaterials & University of Basque Country, Derio, Spain

7. Ikerbasque, Basque Foundation for Science, Bilbao, Spain

Heusler-type ferromagnetic shape memory alloys have attracted much attention over the last two decades due to their magnetoelastic, magnetocaloric and thermoelectric effects. Martensitic phase transition (MPT) is a key factor responsible for the unique properties. The Ni-Fe(Co)-Ga alloys are known to show a good ductility in sharp contrast to the most famous Ni-Mn-Ga alloys. Moreover, Curie temperature can be raised to by doping the ternary Ni-Fe-Ga alloys with Co. To unveil the underlying mechanism of MPT for Ni-Fe(Co)-Ga alloy film from the electronic structure viewpoint, we have done a bulk sensitive hard X-ray photoelectron spectroscopy (HAXPES), element-selective soft X-ray magnetic circular dichroism (XMCD) and first-principles calculations. The HAXPES and XMCD measurements were performed at BL15XU and BL23SU of SPring-8, respectively. First-principles calculations were done for the parent Ni₂FeGa alloy by using WIEN2k program package. The HAXPES results showed a drastic change of the electronic structure near Fermi energy (EF) and the observed hysteretic behavior was confirmed a close relation with the MPT. Moreover the spectral weight near EF was transferred to higher binding energy on cooling through the MPT. Namely, a pseudo-gap appeared in the low temperature phase. In addition, the Ni 3d, Fe 3d and Co 3d spin magnetic moments increased across the MPT. Especially, the Ni 3d moment increased to approximately 2 times larger value. The first-principles calculations also explained the formation of the pseudo-gap and the enhanced Ni 3d spin magnetic moment in the tetragonal phase. Thus we can conclude that the band Jahn-Teller distortion is the key mechanism of the MPT. The experiments at BL15XU and BL23SU were performed with the approval of NIMS and the approval of JAEA at SPring-8 (Proposal Nos.2013B3880, 2013B4910, 2014A3880, and 2014A4903).

Mo.L-P42 - The magnetic and magnetocaloric properties of $\text{CoMnGe}_{1-x}\text{Ga}_x\text{B}_{0.015}$ I. Dincer¹, G. Durak¹, E. Yüzüak², Y. Elerman¹

1. Department of Engineering Physics, Faculty of Engineering, Ankara University, Besevler, Ankara, Turkey

2. Department of Nanotechnology Engineering, Faculty of Engineering, Recep Tayyip Erdogan University, Rize, Turkey

The increasing attention has been attracted the magnetic cooling technologies due to its high efficiency and environmental friendliness. Recently, many experimental and theoretical studies are performed to investigate the magnetocaloric materials show first-order magnetostructural phase transition. CoMnGe alloy has particular interested because this alloy undergoes martensitic structural transition from hexagonal structure (space group: $P6_3/mmc$) to orthorhombic structure (space group: $Pnma$) at 420 K. The Curie temperature of this alloy is 355 K. The magnetic and structural phase transitions cannot overlap for CoMnGe alloy. There are so many methods to decrease the structural phase transition down to room temperature and overlap with Curie temperature because magnetic and magnetocaloric properties are very sensitive to interatomic distance in CoMnGe alloy. The $\text{CoMnGe}_{0.95}\text{Ga}_{0.05}$ alloy exhibits simultaneous structural and magnetic phase transitions around 310 K and the temperature dependent Synchrotron measurements reveal that ($\Delta V/V$) of alloy is 3.9% which is comparable to the $\text{CoMnGeB}_{0.02}$ system ($\Delta V/V=4.2\%$). Due to the presence of coinciding structural and magnetic phase transitions, huge magnetocaloric effect and also giant $\Delta V/V$, this alloy is considered to have a high potential for magnetic cooling applications. The magnetic and magnetocaloric properties of $\text{CoMnGe}_{1-x}\text{Ga}_x\text{B}_{0.015}$ ($x=0.05$ and 0.06) alloys have been investigated by using calorimetric, X-ray diffraction and magnetic measurements. Our results show that the structural and magnetic phase transitions in alloys are tailored by the substitution of Ga for Ge. The alloys exhibit a giant magnetocaloric effect due to coexistence of magnetic and Martensitic phase transitions at the same temperatures. The entropy change values range from -22.1 ($x=0.05$) to -27.1 J/kg.K ($x=0.06$) for $\Delta H = 7$ T and are proportional to the volume differences of the phases involved in the transition. These results on boron doped CoMn(Ge-Ga) alloys would set a good example for other types of magnetocaloric materials and could open up new possibilities for searching new magnetocaloric materials.

Mo.L-P43 - The Effect of the Substitution of Cu and Al for Mn on Magnetic and Magnetocaloric Properties of Ni₅₀Mn₃₄In₁₆Y. Elerman¹, M. Kaya¹, M. Mirac Cicek¹, I. Dincer¹*1. Department of Engineering Physics, Faculty of Engineering, Ankara University, 06100 Besevler, Ankara, Turkey*

Recent experimental and theoretical researches reveal that in Ni₅₀Mn₃₄In₁₆ Heusler alloy, extra Mn atoms partially occupy In sites and they exhibit antiferromagnetic coupling [1, 2]. According to *ab-initio* calculations and Monte Carlo methods, decreasing of magnetic exchange interactions in this alloy can lead to increase magnetic cooling properties around structural transition region, doping the alloy with nonmagnetic atoms. In accordance with these results, we investigated the influence of Cu and Al substitution for Mn on magnetic and magnetocaloric properties has been investigated by using calorimetric and magnetic measurements. We found that martensitic transition temperature ($T_m=(A_f+M_s)/2$) shifts to higher temperatures with Cu and Al substitutions as a result of decreasing of the magnetic exchange interactions with respect to the Ni₅₀Mn₃₄In₁₆. The isothermal magnetization curves around the martensitic transition temperatures show a typical metamagnetic behavior. Associated with that, large positive values of magnetic entropy changes around structural transition region are determined by using the Maxwell relation. The maximum magnetic entropy change values are found to be 25.2 and 13.0 J.kg⁻¹.K⁻¹ for Ni_{48.8}Mn_{34.3}Cu_{1.7}In_{15.2} (S1) [1] and Ni_{51.67}Mn_{31.84}Al_{1.32}In_{15.17} (S2) in a magnetic field change (ΔH) of 2 T, respectively. Furthermore, it is necessary to take into account that magnetocaloric materials are desired to have a large relative cooling power (RCP). The calculated RCP values are found 91.5 and 85.8 J.kg⁻¹ under $\Delta H=2$ T for S1 and S2, respectively. In summary, the results show the general tendency of increasing T_m from 200 K [3] to 266.5 and 278 K for S1 and S2 with the substitution of Cu and Al for Mn in Ni₅₀Mn₃₄In₁₆, respectively. It is observed that Cu and Al doping in Ni₅₀Mn₃₄In₁₆ alloy has not only shifted the T_m and improved magnetocaloric properties towards higher temperature, but has also increased the RCP values [1, 3].

References:

- [1] M. Kaya, S.Yildirim, E.Yüzüak, I.Dincer, R.Ellialtioglu, Y.Elerman. J. Magn. Magn. Mat. 368 (2014) 191
- [2] V.V. Sokolovskiy, V.D. Buchelnikov, V.V. Khovaylo, S.V. Taskaev, P. Entel, International Journal of refrigeration 37 (2014) 273
- [3] V.K. Sharma, M.K. Chattopadhyay, S.B. Roy, J. Phys. D 40 (2007) 1869

Mo.L-P44 - Visualization of crack evolution in field cycled $\text{LaFe}_{11.8}\text{Si}_{1.2}$

A. Funk¹, A. Waske¹, J. Eckert^{1,2}

1. Institute for Complex Materials, IFW Dresden, Helmholtzstraße, Dresden, Germany

2. Institute for Material Science, TU Dresden, Helmholtzstraße, Dresden, Germany

Based on solid state materials with a high magnetocaloric effect (MCE), magnetic refrigeration is a promising alternative to conventional gas-compression cooling techniques [1]. Such materials, e.g. $\text{La}(\text{Fe},\text{Si})_{13}$, Mn-Fe-P-X and Heusler alloys, commonly show a 1st order phase transition with simultaneous structural and magnetic changes that can be induced by an external magnetic field or temperature. The resulting volume change of $\text{La}(\text{Fe},\text{Si})_{13}$ can reach up to 1,5 vol.% in a moderate magnetic field ($\mu_0H = 2 \text{ T}$) [2]. Field or temperature cycling leads to cracks in bulk material, therefore its mechanical stability and refrigeration performance suffer drastically over time. However, Waske et al. observed an intermediate state before the material falls apart: Interlocked particles of thermally cycled $\text{La}(\text{Fe},\text{Si})_{13}$, conserve the 1st order MC behaviour of the bulk material after 40 cycles [3]. In this work, the transition of $\text{LaFe}_{11.8}\text{Si}_{1.2}$ close to its transition temperature is magnetically induced in a field up to $\mu_0H = 2 \text{ T}$ over several cycles. X-ray computed tomography (XCT) as a non-destructive imaging technique was applied to observe the crack evolution of a $\text{LaFe}_{11.8}\text{Si}_{1.2}$ bulk sample after certain cycling steps. Since field cycling was performed in a SQUID, magnetization behaviour is correlated to CT-microstructure comprehensively. Moreover, the degradation of the entropy change with decreasing particle cohesion was observed by magnetometry of a reference sample for different cycling numbers. The presented results help to understand the crack mechanism and the correlation to the giant MCE in $\text{La}(\text{Fe},\text{Si})_{13}$ and 1st order MC materials. This understanding is crucial in order to develop new material combinations, i.e. composites, in order to retain both, the large MCE and mechanical integrity for long term stability.

References:

- [1] Gutfleisch et al., Adv. Mater. 23, 2011
- [2] Jia et al., J. Phys. Cond. Matter 18, 2006
- [3] Waske et al., Phys. Status Solidi RRL, 2015

Mo.L-P45 - Magnetic properties of magnetostrictive galfenol nanowiresI. Ivanov¹, M. Alnassar¹, M. Vazquez², J. Kosel¹

1. King Abdullah University of Science And Technology (KAUST), Thuwal, Saudi Arabia

2. Institute of Materials Science of Madrid, CSIC, Madrid, Spain

Magnetostrictive nanowires (NWs) have attracted increasing attention due to their potential applications as functional elements in advanced nanoscale sensors, actuators or energy harvesters. Galfenol $\text{Fe}_{80}\text{Ga}_{20}$ is one of the most promising magnetostrictive materials. Single-crystal bulk Galfenol exhibits magnetostriction constants up to 400 ppm and attractive mechanical properties (high elastic modulus and tensile strength). Therefore, developing single-crystal Galfenol as NWs could lead to extremely efficient NW-based devices. Among various fabrication methods, electrodeposition into porous aluminum oxide templates (AOT) is a competitive, simple technique for the controlled preparation of high-quality NWs. 50 nm FeGa NWs were fabricated by DC electrodeposition. Electrodeposition was carried at a bias of between -1.1V and -1.5V to achieve the desired Ga content. For studies of individual NWs by transmission electron microscopy (TEM) and magnetic force microscopy (MFM), the AOT was dissolved. As observed by TEM the NWs are straight with a uniform diameter, smooth surface and single-crystal structure along the whole NWs' length (a few μm). The alloy composition is $\text{Fe}_{86}\text{Ga}_{14}$ (Energy dispersive X-ray analysis). Electron diffraction patterns confirmed the bcc structure with a lattice parameter of 2.95 Å and an angle of 20 deg between the NW's long axis and the strongest magnetostrictive axis $\langle 100 \rangle$.

Vibrating sample magnetometer measurements of the NWs array revealed the strong effect of shape anisotropy on magnetic properties. The magnetization curve perpendicular to the NWs axis exhibits two distinct regimes of low and high permeability which is typical for single-crystal bulk galfenol. A single domain magnetic structure at remanence has been observed by MFM. The coercivity of individual NWs measured by MFM and Lorenz microscopy is a bit higher than the one measured by VSM for the array, as expected. A variable magnetic field MFM study revealed two interesting remanence states depending on the strength of the external magnetic field.

Mo.L-P47 - Effects of pressure on the magnetic, structural, and Griffiths-like transitions in magnetocaloric R₅(SixGe_{1-x})₄ (R= Tb and Dy)

N. Marcano Aguado^{1,2}, P. Algarabel Lafuente^{2,3}, J. Rodríguez Fernández⁴, J. Herrero-Albillos^{1,2}, C. Magén Domínguez^{3,5,6}, J.P Araújo⁷, A. Pereira⁷, J. H. Belo⁷, Y. Mudryk⁸, V. K. Pecharsky⁸

1. Centro Universitario de la Defensa, Academia General Militar, Zaragoza, Spain
2. Instituto de Ciencia de Materiales de Aragón, Universidad de Zaragoza - Consejo Superior de Investigaciones Científicas, Zaragoza, Spain
3. Departamento de Física de la Materia Condensada, Universidad de Zaragoza, Zaragoza, Spain
4. Departamento CITIMAC, Universidad de Cantabria, 39005 Santander, Spain
5. Instituto de Nanociencia de Aragón, Universidad de Zaragoza, Zaragoza, Spain
6. Fundación ARAID, Zaragoza, Spain
7. IFIMUP and IN-Institute of Nanoscience and Nanotechnology, Departamento de Física da Faculdade de Ciências, Universidade do Porto, Porto, Portugal
8. Ames Laboratory, U.S. Department of Energy, Iowa State University, Ames, Iowa, USA
9. Department of Materials Science and Engineering, Iowa State University, Ames, Iowa, United States

The discovery of the giant magnetocaloric effect in Gd₅Si₂Ge₂ has attracted a strong interest in the study of other R₅(SiGe)₄-type (R= rare earth) compounds in order to understand the relationship between their structural and magnetic properties. The R₅(SiGe)₄ compounds are known for the appearance of a Griffiths-like phase (GP) at characteristic temperature T* above the long-range order temperature (TN,C). The GP has been reported in several R₅(SiGe)₄ compounds with either the monoclinic Gd₅Si₂Ge₂-type (M) or the orthorhombic Sm₅Ge₄-type (O(II)) of crystal structure [1]. Two interesting examples are Dy₅Si₃Ge and Tb_{4.925}La_{0.075}Si₂Ge₂. At room temperature both compounds crystallize in the M structure. As the temperature decreases they show a GP phase below T* > TN,C. The long-range ordered phase is antiferromagnetic (AF) for Dy₅Si₃Ge [2] and ferromagnetic (FM) for Tb_{4.925}La_{0.075}Si₂Ge₂ [3]. At TS they show a structural transition from the M-type to the orthorhombic O(I)-type structure. The hydrostatic pressure (P) strongly affects both TS and TN,C. In this work we report on a study of the pressure effect on the different phase transitions in Dy₅Si₃Ge and Tb_{4.925}La_{0.075}Si₂Ge₂ by measuring the magnetization under different applied magnetic field protocols up to 50 kOe and P up to 10 kbar in the temperature range 5 K < T < 300 K. At low applied magnetic field Ts strongly increases with increasing P, whereas TN and TC show a weak increasing dependence on P. Such difference in the pressure dependence enables the coupling of the magnetic and structural transitions above a critical pressure. The Griffiths-like phase temperature T* shows a weak temperature dependence increasing linearly with pressure.

- 1.- Pereira A. M. et al, Phys. Rev. B. 82, 172406 (2010)
- 2.- Marcano N. et al, Phys. Rev. B. 88, 214429 (2013)
- 3.- Belo J. H. et al, Phys. Rev. B. 86, 014403 (2012)

Mo.L-P48 - Experimental investigation and FEM simulation of epoxy-bonded magnetocaloric composites

B. Weise¹, M. Bierdel¹, B. Pulko², K. P. Skokov³, O. Gutfleisch³, A. Kitanovski⁴, A. Waske¹, J. Eckert^{1,2}

1. IFW Dresden, Institute for Complex Materials, Dresden, Germany

2. TU Dresden, Faculty of Mechanical Engineering, Dresden, Germany

3. TU Darmstadt, Department of Materials Science, Darmstadt, Germany

4. University of Ljubljana, Faculty of Mechanical Engineering, Ljubljana, Slovenia

Refrigeration based on the magnetocaloric effect (MCE) is considered to be environmentally friendly, due to reducing the energy consumption and therefore improving the energy efficiency of cooling devices. La-Fe-Si based materials are a promising candidate, because of its good magnetocaloric properties, a comparatively low material price and Curie temperatures that can be tuned by varying the alloying components. In Active Magnetic Regenerators (AMR) often plate-shaped magnetocaloric materials are used. This geometry can easily be realized by producing composites of magnetocaloric particles in an epoxy matrix.

Epoxy-bonded magnetocaloric composites with different particle sizes of magnetocaloric La-Fe-Co-Si were characterized by determining their magnetic properties, as well as the temperature- and field-dependent specific heat capacity ($c_p(T,H)$). For comparison, sintered La-Fe-Co-Si was measured. Entropy change ΔS and adiabatic temperature change ΔT_{ad} was calculated and compared with calculations from magnetic measurements (ΔS_{mag}) and direct measurements (ΔT_{direct}). Furthermore, by using X-ray Computed Tomography (XCT) exact volume fractions of the active magnetocaloric material, the epoxy and the porosity were studied. Moreover the particles of active magnetocaloric material were analyzed concerning their size and shape. We will discuss the magnitude of the magnetocaloric effect with respect to the fraction of active magnetic material in the composite as well as anisotropies originating from the manufacturing process. This is shown in the particle orientation within the composite and hence in the anisotropy of the properties. Additionally, the thermal conductivity, which is an often underestimated property in the development of MCE devices, was investigated in experiment and simulation. For this purpose, the structural data determined by XCT was used to feed FEM calculations with real geometry data. By simulation, anisotropic thermal conductivity of the plates was revealed.

Mo.L-P49 - Magnetocaloric properties of purified Gd: assessing structural and impurity aspects

I. Tereshina^{1,2}, G. Burkhanov², E. Tereshina³, G. Politova², V. Chzhan², O. Chistyakov², N. Kolchugina², H. Drulis⁴, M. Paukov⁵, L. Havela⁵

1. Department of Physics, M.V. Lomonosov Moscow State University, Moscow, Russia

2. Baikov Institute of Metallurgy and Material Science Russian Academy of Sciences, Moscow, Russia

3. Institute of Physics, Academy of Sciences of Czech Republic, Prague, Czech Republic

4. Institute of Low Temperature and Structure Research, Polish Academy of Sciences, Wroclaw, Poland

5. Charles University, Faculty of Mathematics and Physics, Department of Condensed Matter Physics, Prague, Czech Republic

The magnetocaloric, thermal and manufacturing properties of Gd make it currently the best material for room-temperature magnetic refrigeration [1]. Here we study high-purity Gd samples with the structure variation from coarse-grain to nanocrystalline obtained as a result of distillation procedure. Samples cut out of structurally inhomogeneous regions consisting of needle-shaped crystals of cross section 0.5-2.5 micrometers with near-c-axis orientation embedded in a matrix of nanosized (30 - 100 nm) grains [2] demonstrate strong anisotropy of electrical and magnetic properties. Further, several a-GdH_x solid solutions were obtained by hydriding the parent pure metal to different hydrogen concentrations. The maximum hydrogen content determined volumetrically reached 0.22 +/- 0.02 at.H/f.u. For the end sample GdH_{0.22}, the relative volume change upon hydrogenation DV/V is about 1%. As shown by Atomic Force Microscopy, the grains increased in size to 200-400 nm after hydrogenation. Magnetocaloric effect was studied using direct and indirect methods. Opposite trends in the MCE response to hydrogen charging with respect to the crystal's orientation within the samples was observed and the mechanisms interrelating the unique inhomogeneous structural morphology with the impurity behavior were proposed. As an overall assessment, the Curie temperatures of a-GdH_x solid solutions increase from 291 K up to 295 K when increasing hydrogen concentration x from zero to 0.22. Hydrogenation is found to broaden the ferromagnetic-to-paramagnetic phase transition and strongly increases the relative cooling power of Gd. The Curie temperature increase upon hydriding of pure Gd together with large MCE at elevated temperatures ensure avenue to application in future magnetic refrigeration, heat pump and power generation devices.

[1] Gschneidner K. A. Jr., Pecharsky V. K., Thirty years of near room temperature magnetic cooling: Where we are today and future prospect Int. J. Refrigeration 31, 945-961 (2008)

[2] G.S. Burkhanov, N.B. Kolchugina, E.A. Tereshina, I.S. Tereshina, G.A. Politova, V.B. Chzhan, D. Badurski, O.D. Chistyakov, M. Paukov, H. Drulis, L. Havela, Applied Physics Letters, 2014, v. 104, p. 242402(5)

Mo.L-P51 - Effect of Fe substitution on Ni₅₀Mn₃₅In₁₅ Heusler alloysM. Halder¹, Penkey Suresh¹, N. K. G. Suresh¹*1. Department of Physics, Indian Institute of Technology Bombay, Bombay, India*

The off-stoichiometric Ni-Mn-In Heusler alloys have drawn significant research interest in the recent years. The properties of these alloys are strongly affected by composition, magnetic field, etc., and some of the compounds exhibit multifunctional properties such as exchange bias, giant magnetocaloric effect, and magnetic shape memory effect, by virtue of the martensite phase transformation (MPT). The phase diagram of the Ni₅₀Mn_{50-y}In_y system has been studied in details in literature [1]. These alloys undergo a first order austenite to martensite phase transformation with lowering of temperature, particularly in the composition range $y = 15$ to 16 [1]. Ni₅₀Mn₃₅In₁₅ is reported to show MPT and large magnetocaloric effect [2].

We have investigated structural and magnetic properties of Ni₅₀Mn₃₅In₁₅ and effect of Fe substitution in Ni₅₀Mn₃₅In₁₅ *i.e.* Ni₄₈Fe₂Mn₃₅In₁₅. Room temperature x-ray diffraction shows that Ni₅₀Mn₃₅In₁₅ has two phases, cubic and other (which we were unable to index) phase *i.e.*, both austenitic and martensite phases coexist [2], while Ni₄₈Fe₂Mn₃₅In₁₅ shows pure cubic structure *i.e.* austenitic phase [3]. From magnetization measurements, in Ni₅₀Mn₃₅In₁₅, we observe MPT at about 311 K. The Curie temperatures of the austenite and the martensite phases are 313 and 189 K, respectively. In the case of Ni₄₈Fe₂Mn₃₅In₁₅, there is only one magnetic transition at 316 K with no MPT. This indicates that the martensite phase, which is present in Ni₅₀Mn₃₅In₁₅, gets suppressed when Ni is substituted by Fe, which stabilizes the austenite phase. The absence of MPT in the case of Ni₄₈Fe₂Mn₃₅In₁₅ has been explained on the bases of valence electron concentration e/a . The magnetic entropy change has been evaluated and the maximum value is found to be 7.6 and 2.7 J kg⁻¹ K⁻¹ for Ni₅₀Mn₃₅In₁₅ and Ni₄₈Fe₂Mn₃₅In₁₅, respectively, for a field variation of 20 kOe.

Mo.L-P52 - Structural and magnetic properties of FeRh_{1-x}Co_x

K. Takahashi¹, K. Ohtake¹, K. Koyama², K. Watanabe¹

1. *Institute For Materials Research, Tohoku University, Sendai, Japan*

2. *Graduate School of Science and Engineering, Kagoshima University, Kagoshima, Japan*

Ordered FeRh alloys around the equiatomic composition with an ordered B2 (CsCl-type) structure exhibit peculiar magnetic and structural properties. The compound shows a first-order transition from the antiferromagnetic (AFM) to the ferromagnetic (FM) phase accompanied by an isotropic volume expansion of about 1%. In this study, FeRh_{1-x}Co_x, substituting Co for part of Rh to control the AFM-FM transition temperature to around room temperature, was studied in order to investigate the relationship between magnetic and structural properties affected by the magnetic field. The magnetization was measured using a conventional SQUID magnetometer in magnetic fields up to 7 T and in the temperature range from 10 to 400 K. X-ray diffraction measurements with FeK α radiation were performed in magnetic fields up to 5 T and at temperatures ranging from 10 K to room temperature. The isostructural transformation due to the field-induced AFM-FM phase transition was directly observed by the X-ray measurements, and the lattice parameter was found to be expanded by 0.3% at the phase transition. The magnetocaloric property was also evaluated from the magnetization measurements, which shows excellent capability comparable to that of FeRh.

Mo.L-P53 - Magnetocaloric effect in Ni-Fe-Ga-Co-Al Heusler alloysF. Tolea¹, M. Sofronie¹, A. Daniela Crisan¹, M. Valeanu¹*1. National Institute of Materials Physics, Magurele, Romania*

The magnetocaloric effect (MCE) around room temperature is an environmentally friendly alternative to conventional refrigeration. In recent years, ferromagnetic shape memory alloys (FSMA) have received much attention as new magnetic materials with high magnetocaloric characteristics. The functionality of the FSMA is related to the martensite and magnetic order-disorder transformations; both, the martensitic (T_M) and Curie temperatures (T_C), may be tailor by doping the alloys with other elements (to change the electronic concentration, e/a) or by suitable thermal treatments (to change the atomic order) so that, alloys with concomitant or sequential structural and magnetic phase transition may be obtained. Recent studies have shown that the entropy change associated to the martensite transformation in FSMA increase as the temperature difference between T_C and T_M decreases.

The off-stoichiometric Ni-Fe-Ga based Heusler alloy have been found good candidate to replace the brittle Ni-Mn-Ga in various applications including magnetic refrigeration. The presence of the secondary phase responsible for its better ductility, may be prevent by suitable quenching preparation techniques, like melt spinning, ribbons preserving a relative good malleability. In addition, concerning the magnetocaloric applications, it is assumed that the thin melt-spun ribbons assure a more efficient heat transfer.

In the present work we investigate the entropy changes and the relative cooling power (RCP) in $Ni_{52}Fe_{20}Ga_{23}Co_3Al_2$ based Heusler alloy with concomitant or sequential structural and magnetic phase transition prepared as bulk ($T_C = 373$ K, $T_M = 253$ K) and as ribbons in as prepared state ($T_C = T_M = 378$ K) or subjected to a thermal treatment ($T_C = 388$ K, $T_M = 334$ K) for atomic ordering. For a magnetostructural transformation the as prepared ribbons show almost the same entropy variation with that obtained in bulk alloy (between -8 and -10 J/KgK) but the RCP is much enhanced.

Mo.L-P54 - Magnetic properties of soft magnetic thin ribbons prepared by an electroplating method

T. Yanai¹, Y. Watanabe¹, M. Otsubo¹, N. Shimoya², K. Fujisaki², M. Nakano¹, H. Fukunaga¹

1. Nagasaki University, Nagasaki, Japan

2. Toyota Technological Institute, Chicago, United States

As it is well-known that a reduction in thicknesses of soft magnetic materials is one of effective methods to reduce an eddy current loss, soft magnetic thin ribbons are widely used for high-frequency driven electric machines. Typical soft magnetic thin ribbons, such as amorphous ones and nano-crystalline ones, are produced by rapid quenching methods, and their thickness are approximately 0.02 mm. In present study, we fabricated Fe-Ni-based thin ribbons (< 0.02 mm) prepared by an electroplating method, and evaluated the magnetic properties of the toroidal core prepared from the thin ribbons. We electroplated Fe-Ni-based thin films on a Cu sheet (L350 ~ W5 ~ T0.3 mm), and then the films were peeled off physically from the Cu sheet. Consequently, we obtained the ribbon-shaped Fe-Ni thin films with Fe composition of approximately 22 at.%. The Fe-Ni thin ribbon (0.0092 mm-thick) were formed into toroidal core (D = 48 mm), and ac magnetic properties of the toroidal core were evaluated at $B_m = 0.9$ T in the frequency range from 50 Hz to 200 kHz. In order to compare high frequency properties, we also evaluated ac magnetic properties of a toroidal core prepared from a 0.025 mm-thick amorphous ribbon (2605HB1, Hitachi Metals, Ltd.). Although the amorphous core showed low iron loss in low frequency region, the loss of the amorphous core showed higher value compared with that of the Fe-Ni one in high frequency region (> 50 kHz). As an eddy current loss in a typical metric soft magnetic material becomes dominantly in the high frequency region, we found that the prepared Fe-Ni thin ribbon is an effective material for high frequency driving.

Mo.L-P55 - A new method for maximizing magnetic refrigeration efficiency in antiferromagnets

R. Tamura¹, S. Tanaka², T. Ohno³, H. Kitazawa⁴

1. *International Center for Young Scientists, National Institute for Materials Science, Ibaraki, Japan*

2. *Yukawa Institute for Theoretical Physics, Kyoto University, Kyoto, Japan*

3. *Computational Materials Science Unit, National Institute for Materials Science, Ibaraki, Japan*

4. *Quantum Beam Unit, National Institute for Materials Science, Ibaraki, Japan*

Magnetic refrigeration is a promising candidate as a next-generation cooling technology that can solve environmental and noise problems. The key to the magnetic refrigeration is the change of behavior of magnetic entropy in magnetic materials under different magnetic fields, which is known as the magnetocaloric effect (MCE). It has been recognized that ferromagnets are the most suitable materials for magnetic refrigeration because of their large magnetic field response near the phase transition temperature. Recently, the MCEs in nonferromagnets such as antiferromagnets and random spin systems have been studied experimentally. However, the fundamental theory relating MCE to the magnetic structure was not established. The purpose of this work is to formulate a fundamental theory for the relationship between MCE and magnetic structure, and to propose a method for maximizing the magnetic refrigeration efficiency. We consider the A-, C-, and G-type antiferromagnets that are typical ordered antiferromagnetic structures and compare the MCE in nonferromagnets with that in the ferromagnets by the Monte Carlo simulations and the mean-field treatments. In the isothermal process, the magnetic entropy monotonically increases as the magnetic field decreases in the ferromagnets. On the other hand, in the antiferromagnets, the magnetic entropy exhibits nonmonotonic behavior as a function of the magnetic field. Based on the fact, we propose a new protocol for applying magnetic field to obtain the maximum magnetic entropy change in the antiferromagnets. By using the same proposed protocol, the adiabatic temperature change and the cooling capacity such as the relative cooling power (RCP) are also maximized. We emphasize that the proposed protocol can be widely applied to any magnetic materials to achieve the maximum efficiency of magnetic refrigeration, not just antiferromagnets.

Mo.L-P56 - Mechanical and corrosion properties of La(Fe,Si)₁₃ for magnetic refrigeration technology

B. Kaeswurm¹, S. Sharma¹, A. Barcza², P. Geiger¹, M. Vögler¹, K.E. Johanns¹, N. Wilson³, M. Katter², O. Gutfleisch¹

1. *Institut für Geo- und Materialwissenschaften, Technische Universität Darmstadt, Darmstadt, Germany*

2. *Vacuumschmelze GmbH & Co. KG, Hanau, Germany*

3. *Camfridge Ltd, Cambridge, United Kingdom*

Magnetic refrigeration is an environmentally friendly and efficient technology which may replace conventional vapour cycle refrigeration in the near future. In order for a magnetocaloric material to be used as a heat exchanger, it needs not only to show the appropriate magnetocaloric properties and high thermal conductivity, but also mechanical and chemical stability as well as ease of machinability. We investigate the corrosion and mechanical properties of Co containing La(Fe,Si)₁₃. While water provides efficient heat transfer, it causes La(Fe,Si)₁₃ to corrode easily. In order to investigate the corrosion properties, heat exchanger plates were submerged in various testing fluids and removed for testing at regular intervals. For reference, samples were kept in air and argon atmosphere. A range of testing fluids with thermal conductivity $k = 0.1$ to 0.6 W/mK and specific heat capacity $c = 1$ to 4.2 J/kg K were chosen.

Samples of different Co content with different Curie Temperatures T_C near room temperature and well-defined geometry were used to investigate the mechanical properties of the material. The flexural strength σ was examined using four point bending under ASTM C1161. For increasing Co content, which corresponds to a higher T_C , a lower σ was observed. Resonance frequency damping analysis (ASTM E 1879-99) was applied in order to study the Youngs modulus as a function of temperature. The data correlates to the temperature dependence of the magnetic and crystallographic properties of the material.

The research leading to these results received funding from the EC FP 7/2007-2013 under grant agreement n°310748 (DRREAM).

Mo.L-P57 - EBSD analysis of {111}-Conjugated Interfaces in Mn-Al-C permanent magnetic materials

F. Bittner^{1,2}, L. Schultz^{1,2}, T. George Woodcock¹

1. IFW Dresden, Dresden, Germany

2. Department of Materials Science, TU Dresden, Dresden, Germany

Mn-Al based materials have the potential for application as rare earth free permanent magnets. Coercivity strongly depends on microstructure and the presence of defects in the Mn-Al materials is particularly important. In order to optimise the coercivity, it is therefore necessary to have detailed knowledge of the microstructural features which appear in these magnets, especially the types of defects, their formation mechanisms and the effect of processing on their fractions. MnAl and MnAl-C have the L10 crystal structure and planar defects, conjugated on {111} planes, similar to twins, are well known in these materials from the results of transmission electron microscopy (TEM). Electron backscattered diffraction (EBSD) offers an advantage over TEM for the analysis of interfaces as much larger areas can be studied, yielding more representative data. Mn-Al-C materials have therefore been studied in the heat treated and hot worked states using EBSD. Three crystallographically different {111}-conjugated twin-like defects, distinguished by different rotation angles about the normal to {111}, were found to be the dominant interfaces in the heat treated material. Previously only one of these interfaces has been reported in similar materials by TEM. In the hot worked sample, {111}-conjugated interfaces characterised by a rotation of 180° about the normal to {111} appeared frequently, probably as a result of the associated dynamic recrystallization, while the other two interfacial types were suppressed.

Mo.L-P58 - Influence of Nb content on high temperature magnetic properties of FeCo based high induction alloys

R.K. Roy¹, A. K. Panda¹, A. Mitra¹, M.E. McHenry²

1. *NDE & Magnetic Materials Gr., MST Division, CSIR-National Metallurgical Laboratory, Jamshedpur, India*

2. *Department of Materials Science and Engineering, Carnegie Mellon University, Pittsburgh, United States*

Research on the enhancement of soft magnetic properties in high induction alloys has been extensively studied in last two decades due to their potential use of transformers, motors and sensors for use in energy, transportation, defense and aerospace sectors. Prior research targeted reaching inductions of silicon steels and high temperature magnetic properties so that these materials can effectively perform in severe environments. In this work, Nb influence has been investigated in FeCo based alloys with nominal compositions of $(\text{Fe}_{0.65}\text{Co}_{0.35})_{85-y}\text{Si}_{2.8}\text{B}_{11.2}\text{Nb}_y\text{Cu}_1$ ($y= 0, 1, 2$ and 3) extending the composition range reported in [1]. Alloys were prepared in the form of ribbons by a single roller melt spinning technique, and subsequently annealed in inert atmosphere to induce nanocrystallization. The increasing Nb content increases not only amorphization of alloys but also the onsets of primary crystallization (T_{x1}) and secondary crystallization (T_{x2}) temperatures of alloys. Thus, thermal stability ($T_{x2} - T_{x1}$) and activation energy (Q) for primary crystallization are increased with more Nb addition. Higher Nb containing alloy ($y=3$) demonstrates saturation induction (M_s) of 1.62-1.68T and coercivity (H_c) of 66-82 A/m within temperature ranges of 400–550°C, whereas Nb free alloy exhibits very high M_s of 1.86-1.91T and H_c of 407-452A/m at the same temperature range. The hindrance of crystallite growth through higher Nb content and resulting fine (~20nm) crystallites are main reasons for enhanced soft magnetic properties in the former alloy. With increasing Nb, the residual amorphous phase is stabilized at high temperature and, therefore, amorphous Curie temperature (T_c) increases for those alloys. We conclude that an optimum amount Nb content is prerequisite for the enhancement of thermal stability and high temperature magnetic properties of FeCo based high induction alloys.

1. S.J. Kernion, V. Keylin, J. Huth, and M.E. McHenry. "Secondary Crystallization in $(\text{Fe}_{65}\text{Co}_{35})_{79.5+x}\text{B}_{13}\text{Nb}_{4-x}\text{Si}_2\text{Cu}_{1.5}$ and $(\text{Fe}_{65}\text{Co}_{35})_{83}\text{B}_{10}\text{Nb}_4\text{Si}_2\text{Cu}_1$ Nanocomposite Alloys". *J. Appl. Phys.* 111, 07A329-31,(2012)

Mo.L-P59 - Magnetocaloric effect and Magnetothermopower in $\text{Pr}_{0.5}\text{Sr}_{0.5}\text{MnO}_3$

R. Mahendiran¹, D.V. Maheswar Repaka¹

1. National University of Singapore, Singapore, Singapore

Materials that show more than one magnetic phase transition can be exploited for magnetic refrigeration over a wide temperature range. The manganite, $\text{Pr}_{0.5}\text{Sr}_{0.5}\text{MnO}_3$ upon cooling from room temperature undergoes a second order ferromagnetic transition ($T_C = 260$ K) followed by a first-order antiferromagnetic transition around 135 K. We have studied magnetocaloric effect and magnetothermopower in this compound. It is found that the magnetic entropy change at the ferromagnetic- antiferromagnetic transition ($\Delta S_m = 7$ J/Kg. K for $\Delta H = 5$ T) is three times larger than its value at the ferromagnetic transition. The results are compared with $\text{Pr}_{0.46}\text{Sr}_{0.54}\text{MnO}_3$ which undergoes a paramagnetic to antiferromagnetic transition without an intermediate ferromagnetic state.

The effect of magnetic field on thermopower is more dramatic. Magnetothermopower of nearly 100% is found at the ferromagnetic -antiferromagnetic phase boundary whereas the magnetothermopower changes by 40% around the paramagnetic-ferromagnetic phase boundary. We discuss possible connection between the magnetic entropy change and magnetothermopower. Coexistence of large magnetothermopower and magnetocaloric effect make this compound interesting for energy saving applications.

Mo.L-P60 - Enhanced electrical resistivity after rapid cool of the specimens in layered oxide Li_xCoO_2

K. Miyoshi¹, K. Manami¹, G. Motoyama¹, K. Fujiwara¹, J. Takeuchi¹, R. Sasai¹, S. Nishigori²

1. Department of Materials Science, Shimane University, Matsue, Japan.

2. Department of Materials Analysis, ICSR, Shimane University, Matsue, Japan

Li_xCoO_2 is practically used as a high energy cathode material in commercial Li ion batteries, having a structure consisting of CoO_2 layers and interlayers of Li atoms alternatively stacked along c-axis. In Li_xCoO_2 , charge ordering of $\text{Co}^{3+}/\text{Co}^{4+}$ occurs below $T_S=155$ K and is closely linked with ordering of Li ions via Coulomb interactions below $T_F=120$ K, above which Li ions begin to diffuse as in a liquid state. Recent observations by scanning tunneling electron microscope and density functional theory for $\text{Li}_{0.66}\text{CoO}_2$ have revealed that the surface CoO_2 layer shows a metallic electronic state with a characteristic ordering pattern of $\text{Co}^{3+}/\text{Co}^{4+}$ (=2:1) but also shows an insulating state with disordered structures, depending on the location of the surface.

The latter disordered state is produced by inhomogeneity in Li-ordering patterns, which is thought to be enhanced by cooling rapidly from a liquid state down to the temperature far below T_F , as in an amorphous metal. Thus, it is expected that the sample after rapid cool shows an enhanced resistivity. In the present work, we have performed the measurements of electrical resistivity as a function of temperature for Li_xCoO_2 using single crystal specimens in order to confirm whether or not electrical resistivity depends on the cooling rate of the sample as mentioned above. It has been found that electrical resistivity after rapid cool becomes 30-50% larger compared with that after slow cool below $T_S=155$ K especially for the specimens with $x=0.6-0.7$.

Mo.L-P61 - Effect of the induced internal stresses on the martensitic transition and magnetic properties of Ni-Mn-Ga glass-coated microwires

S. Shevyrталov¹, A. Zhukov^{2,3}, V. Zhukova², V. Rodionova¹

1. *Institute of Physics & Technology, Immanuel Kant Baltic Federal University, Kaliningrad, Russia*

2. *Dpto. Física de Materiales, Fac. Químicas, sUPV/EHU, San Sebastian, Spain*

3. *IKERBASQUE, Basque Foundation for Science, Bilbao, Spain*

Heusler alloys with Ni-Mn-X (Ga, In, Sb, Sn) composition have attracted significant attention due to their functional properties that are originating from the coupling between the magnetic and structural ordering. Thin glass-coated microwires might be of interest in this aspect because of the possibility to tune the strength of the internal stresses in the metallic nucleus by changing the diameters ratio (d/D – define the mechanical stresses inside the metallic nucleus) and by the thermal treatment. Both theoretically [1] and experimentally [2] there was demonstrated the possibility to change the temperatures of the structural transition by external pressure.

In this abstract we report on the results of investigation of the glass-coated microwires with different ratios of the diameters d/D 0.4÷0.8 prepared by the Taylor-Ulitovsky technique from $Ni_{49,5}Mn_{25,4}Ga_{25,1}$ Heusler alloy. Fabricated microwires were annealed at 773 K for 30 min to establish the structural ordering. Magnetic properties of the annealed microwires were investigated by vibrating sample magnetometer in the temperature range 77-450 K in the magnetic fields up to 12 kOe. Hysteresis loops were observed for two positions of the microwire (with the axis directed along and perpendicular to the magnetic field direction). Martensitic transitions were detected by differential scanning calorimetry method in the temperature range 150-450 K and by collecting magnetization vs temperature curves in the different magnetic fields (10 Oe, 1 kOe and 10 kOe).

All measurements were repeated for the same piece of the microwire after the glass-coating removal to determine the influence of the internal stresses induced by the glass coating.

It has been shown that the internal stresses affects considerably magnetic properties of the microwires that results in the decreasing of the magnetization and in the shifting down of the Curie temperature for about 10 K and of the temperature of the structural transition by 8 K.

1. A. Vasil'ev et. al., *Physics-Usppekhi*, 173, № 6, 577-605 (2002)
2. T. Kanomata et. al., *JMMM*. 65, 76 (1987)

Mo.L-P62 - Influence of Pr substitution for La on the structural, magnetic and magnetocaloric properties of $(\text{La}_{1-x}\text{Pr}_x)_{2/3}\text{Ba}_{1/3}\text{MnO}_3$ manganitesA. Bezerghéanu¹, C. Bazil Cizmas¹, I. Grigore Deac², R. Tetean²1. *Transilvania University of Brasov, Dept. Electrical Engineering & Applied Physics, Brasov, Romania*2. *Babes-Bolyai University, Faculty of Physics, Cluj-Napoca, Romania*

Structural, magnetic and magnetocaloric properties of $(\text{La}_{1-x}\text{Pr}_x)_{2/3}\text{Ba}_{1/3}\text{MnO}_3$, ($x=0; 0.2; 0.4; 0.6; 0.8$ and 1.0) manganites with perovskite type structure are reported. The samples were prepared by the conventional ceramic method, noting that the final sintering was carried out in air at 1300°C . The crystal structure was checked by X-ray diffraction (XRD). The XRD patterns showed the presence of a majority rhombohedral phase (GS: $R\bar{3}c$, $Z=6$), for all compounds. The lattice parameters decrease by increasing the Pr content and therefore the cell volume decrease linearly from 413.8 \AA^3 for $x=1$ to 408.9 \AA^3 for $x=0$. The magnetic measurements were performed in the temperature range $4.2\text{-}700 \text{ K}$ and external magnetic fields up to 7 T . The Curie temperatures (T_C), determined by thermomagnetic analysis, linearly decrease from $\sim 350 \text{ K}$ for $x=0$ to 197 K for $x=1$. The Arrots plots shows a second order magnetic phase transition at T_C , for all compounds. The saturation magnetic moments at 5 K also decreases from $3.7 \mu_B/\text{f.u.}$ for $x=0$ to $3.4 \mu_B/\text{f.u.}$ for $x=1$. The magnetic entropy changes, $|\Delta S_m(T, 0\text{-}B)|$, were determined from magnetization isotherms measured around T_C , using the Maxwell equation. Large $|\Delta S_m|$ value has been obtained for all samples. As example, for a magnetic field change from 0T to 5T , we have obtained $|\Delta S_m|=2.6 \text{ J/kgK}$ with relative cooling power $RCP=172 \text{ J/kg}$ for $x=0$ and respectively, $|\Delta S_m|=4.5 \text{ J/kgK}$ with $RCP=232 \text{ J/kg}$ for $x=1$. Considering the possibility to tune the transition temperatures with composition the potential use of these materials in magnetic refrigeration is also discussed.

Mo.L-P63 - Study of the magnetocaloric effect in (Pr,Dy)₂Fe₁₇ and Pr₂(Fe,Al)₁₇ intermetallic compounds

K. Zehani¹, R. Guetari^{1,2}, N. Mliki², L. Bessais¹

1. CMTR, ICMPE, UMR7182, CNRS-UPEC, Thiais, France

2. LMOP, Faculté des Sciences de Tunis, Université Tunis El Manar, Tunis, Tunisia

The Pr₂Fe₁₇ compound is a potential candidate for low cost magnetocaloric materials with a significant relative cooling power (RCP) around room temperature (280 K).

In this work, we present the results of the substitution of dysprosium for praseodymium and of the substitution of aluminum for iron in Pr₂Fe₁₇. The polycrystalline Pr_{2-x}Dy_xFe₁₇ (x = 0.125, 0.25, 0.375, and 0.5) and Pr₂Fe_{17-y}Al_y (y = 0, 0.25, 0.5, 0.75, 1) were prepared by arc melting under a high purity argon and homogenized at 1373K to minimize the amount of other possible impurity phases. The samples were characterized using powder X ray diffraction and were refined using Rietveld method with Fullprof program. All the samples crystallize in the R $\bar{3}$ m of the rhombohedral Th₂Zn₁₇ type structure. The lattice parameters increase with the Al and Dy content. The Curie temperature increases with Dy content (from 285 K at x = 0 to 314 K at x = 0.5) and Al content (from 285 K at y = 0 to 361 K at y = 1). This variation is due to an electronic effect.

The magnetic entropy change ΔS_m was estimated from isothermal magnetization curves for all samples. For Pr_{1.75}Dy_{0.25}Fe₁₇, the magnetic entropy increases up to a maximum $T_C = 305$ K of $\Delta S_m = 7.5$ J.kg⁻¹K⁻¹ ($T_C = 305$ K and $\Delta H = 5$ T). However, for Pr₂Fe_{17-y}Al_y, ΔS_m decreases with Al content from 5.5 J.kg⁻¹K⁻¹ (x = 0) to 4.2 J.kg⁻¹.K⁻¹ (x = 1) at $\mu_0H = 5$ T.

The analysis of the magnetic ordering transition using the Landau theory and the Arrott's plots have been carried out.

Keywords: Rare-earth intermetallics, Curie temperature, Magnetization, Magnetocaloric effects

Mo.L-P64 - Large magnetocaloric effect and magnetic properties in ErCoAlD. X. Li¹, Y. Homma¹, F. Honda¹, T. Yamamura², D. Aoki¹*1. Institute for Materials Research, Tohoku University, Oarai, Ibaraki, Japan**2. Institute for Materials Research, Tohoku University, Sendai, Japan*

Recent years, exploration of magnetic refrigerant material used in different temperature ranges has been attracted much attention. We are particularly interested in the magnetic materials that exhibit large magnetocaloric effect (MCE) and high relative cooling power (RCP), and can be used for liquefaction of hydrogen. Intermetallic compound ErCoAl is a worthwhile material, which crystallizes in the hexagonal MgZn₂-type structure and undergoes a ferromagnetic (FM) transition at the temperature near 20 K. As a potential magnetic refrigerant material for liquefaction of hydrogen, large MCE is expected for this alloy.

We have carried out a systematic study on magnetic properties and MCE of polycrystalline ErCoAl by measuring the temperature dependences of magnetic susceptibility, electrical resistivity and specific heat in various magnetic fields, and the field dependence magnetization in various temperatures. The experimental results indicate that ErCoAl undergoes a second-order FM transition at $T_c = 16$ K. The low field susceptibility curve shows a sharp rise around T_c while a rapid decrease in resistivity curve and a large peak in specific heat curve are clearly observed in zero field at the temperatures just below T_c . The important finding in this work is that both magnetic and calorimetric measurements reveal a large MCE for ErCoAl around 16 K. The maximum magnetic entropy change, adiabatic temperature change and relative cooling power are determined to be 15.5 J/kg/K, 6.0 K and 284 J/kg, respectively, for a field change of 5 T. It is worth emphasizing that the large MCE can be observed for ErCoAl even in a small field change (~ 2 T) that can be generated by a permanent magnet. These results indicate that ErCoAl has better refrigeration performance at the temperatures near 20 K, and thus can be considered as the potential magnetic refrigerant material for liquefaction of hydrogen.

Mo.L-P65 - New synthetic route for HoN particles as magnetic refrigerant in hydrogen re-liquefaction system

D. Kim¹, J. Ahn¹, C. Choi¹

1. Korea Institute of Materials Science, Changwon, Republik of Korea

For hydrogen energy system, liquefied hydrogen is suitable for storage and transportation, because it provides the highest hydrogen densities with respect to both mass and volume. In order to establish this refrigeration technology, it is necessary to obtain the efficient and reliable magnetic refrigerant that possesses a large magnetocaloric effect (MCE) near the boiling point of hydrogen. Rare-earth (RE) nitrides such as ErN, HoN, TbN etc have low transition temperatures and show high magnetic entropy change in cryogenic temperature. So, RE-nitrides have been studied for the application to magnetocaloric materials in low temperature considering re-liquefaction system in hydrogen storage. Among them, Holmium nitride (HoN) was selected from its excellent MCE around 20 K and successfully synthesized to nanoparticles by plasma arc discharge process and microwave-assisted sol-gel method respectively. X-ray diffraction patterns showed the six sharp peaks exactly corresponded to each plane of crystallographic structure of HoN in both cases. Also, the nanocrystallite depicts a clear lattice arrangement that belongs to the planes (111) with 0.28 nm interplaner spacing of HoN cubic crystal structure. Physical Property Measurement System (PPMS) was employed to measure the magnetic properties at various temperatures and applied fields. Magnetic entropy changes for as-synthesized particles calculated from the magnetization data set reached maximum value to 27.5 JK-1kg-1 by plasma arc discharge process and 36.6 JK-1kg-1 by microwave-assisted sol-gel method, which are comparable or superior to that of intermetallic compounds having a transition temperature around 20 K such as DyNi₂, HoAl₂ and (Gd_{0.1}Dy_{0.9})Ni₂. Accordingly, HoN particles prepared in this work can be a promising candidate for magnetic refrigerant in hydrogen re-liquefaction system.

Mo.L-P66 - Field-induced Martensitic Transformation in $\text{MnCo}_{0.92}\text{Fe}_{0.08}\text{Ge}$

K. Ozono¹, Y. Mitsui¹, R. Umetsu², K. Takahashi², M. Hiroi¹, K. Koyama¹

1. *Department of Physics and Space, Graduate School of Science and Engineering, Kagoshima University, Kagoshima, Japan*

2. *Institute for Materials Research, Tohoku University*

Ferromagnetic materials, which show martensitic transformation, have attracted considerable attention as magnetic field-controlled materials, because some of them exhibit magnetic-field-induced martensitic transformation, giant magneto-resistance effect, magneto-caloric effect, etc. [1, 2] MnCoGe is a ferromagnet with Curie temperature T_C of 335 K. It has been reported that MnCoGe causes the martensitic transformation from hexagonal Ni_2In type austenitic phase to orthorhombic TiNiSi type martensitic phase in the vicinity of 420 K. Recently, Li et al. and Lin et al. have been reported that the martensitic transformation temperature and T_C of $\text{MnCo}_{1-x}\text{Fe}_x\text{Ge}$ compounds are decreasing with increasing the substitution contents x . [3, 4] In our previous studies, it was found that $\text{MnCo}_{1-x}\text{Fe}_x\text{Ge}$ for $0.07 < x < 0.10$ shows the magnetic phase transition from paramagnetic to ferromagnetic and is accompanied by the martensitic transformation. This result suggests that $\text{MnCo}_{1-x}\text{Fe}_x\text{Ge}$ for $0.07 < x < 0.10$ shows the field-induced martensitic transformation in the vicinity of T_C . In this work, we have studied the magnetic and structural properties of $\text{MnCo}_{0.92}\text{Fe}_{0.08}\text{Ge}$ by using a high-field X-ray diffraction (XRD) system in magnetic fields up to 5 T. The obtained XRD patterns shows the diffraction peaks of the hexagonal phase with paramagnetic decrease and the peaks of the orthorhombic phase with ferromagnetic increase with increasing magnetic fields at 276 K. Consequently, we observed a field-induced martensitic transformation from hexagonal to orthorhombic by applying magnetic fields for $\text{MnCo}_{0.92}\text{Fe}_{0.08}\text{Ge}$.

[1] K. Koyama et al.: *Appl. Phys. Lett.* 88 (2006) 132505

[2] K. Koyama et al.: *Appl. Phys. Lett.* 89 (2006) 182510

[3] G.J. Li et al.: *J. Magn. Magn. Mater.* 322 (2013) 146-150

[4] S. Lin et al.: *IEEE Trans on Magn.* 42 (2006) 3776-3778

Mo.L-P67 - Effect of Mn-deficient on magnetocaloric effect in non-stoichiometric $\text{La}_{0.8}\text{Ca}_{0.2}\text{MnO}_{3+\delta}$ D. Nanto¹, B. Kurniawan², N. Chebotaev³, A. Telegin³, S.C. Yu⁴

1. Dept. of Physics Education, Syarif Hidayatullah State Islamic University, Banten, Indonesia

2. Dept. of Physics, University of Indonesia

3. Institute of Metal Physics, UB of RAS

4. Dept. of Physics, Chungbuk National University

In present work, influence of Mn-deficient on magnetocaloric effect (MCE) in Oxygen-excessive polycrystalline $\text{La}_{0.8}\text{Ca}_{0.2}\text{MnO}_{3+\delta}$ and $\text{La}_{0.8}\text{Ca}_{0.2}\text{Mn}_{0.975}\text{O}_{3+\delta}$ samples has been investigated. Both samples were prepared by conventional solid-state reaction method. Detail Oxygen treatment on the samples could be found elsewhere [1]. Magnetic properties for those samples were investigated by means of a vibrating sample magnetometer (VSM). Excessive Oxygen led to T_C decrease for $\text{La}_{0.8}\text{Ca}_{0.2}\text{MnO}_{3+\delta}$ compared to $\text{La}_{0.8}\text{Ca}_{0.2}\text{MnO}_3$ [2]. Figure 1 shows thermo-magnetization curves, $M(T)$, for Mn-deficient samples with $T_C \sim 144$ K for $\text{La}_{0.8}\text{Ca}_{0.2}\text{Mn}_{0.975}\text{O}_{3+\delta}$ and $T_C \sim 190$ K for $\text{La}_{0.8}\text{Ca}_{0.2}\text{MnO}_{3+\delta}$. Maximum magnetic entropy change of Mn-deficient $\text{La}_{0.8}\text{Ca}_{0.2}\text{Mn}_{0.975}\text{O}_{3+\delta}$ ($-\Delta S_{M \max} = 0.67 \text{ Jkg}^{-1}\text{K}^{-1}$) decreases significantly compared to the maximum entropy change of $\text{La}_{0.8}\text{Ca}_{0.2}\text{MnO}_{3+\delta}$ ($-\Delta S_{M \max} = 1.34 \text{ Jkg}^{-1}\text{K}^{-1}$) under external field of 10 kOe as shown in Fig. 2. Even the maximum magnetic entropy change of $\text{La}_{0.8}\text{Ca}_{0.2}\text{MnO}_{3+\delta}$ much higher than $\text{La}_{0.8}\text{Ca}_{0.2}\text{Mn}_{0.975}\text{O}_{3+\delta}$, however, refrigerant capacity of $\text{La}_{0.8}\text{Ca}_{0.2}\text{Mn}_{0.975}\text{O}_{3+\delta}$ (37.4 J/kg) higher than $\text{La}_{0.8}\text{Ca}_{0.2}\text{MnO}_{3+\delta}$ (26.8 J/kg). H/M versus M^2 curve shows that both cases exhibit second order magnetic phase transition due to positive slope. Interestingly enough, we find $M(T)$ curve has the magnetization of Mn-deficient $\text{La}_{0.8}\text{Ca}_{0.2}\text{Mn}_{0.975}\text{O}_{3+\delta}$ increases than the case of $\text{La}_{0.8}\text{Ca}_{0.2}\text{MnO}_{3+\delta}$ under low applied fields less than 100 Oe but decreases under high applied fields greater than 7 kOe, which is considered to be caused by excessive Oxygens. Moreover, the maximum entropy change of Mn-deficient $\text{La}_{0.8}\text{Ca}_{0.2}\text{Mn}_{0.975}\text{O}_{3+\delta}$ decreases than that of $\text{La}_{0.8}\text{Ca}_{0.2}\text{MnO}_{3+\delta}$ as well as the T_C without changing the second order behavior of the magnetic phase transition.

Mo.L-P68 - Critical exponents and EXAFS study of Non-stoichiometric $\text{Nd}_{0.5}\text{Sr}_{0.5}\text{MnO}_3$ Single Crystalline

D. Nanto¹, B. Kurniawan², S. Telegin³, A. Telegin³, S.C. Yu⁴

1. *Dep Syarif Hidayatullah State Islamic University, Jakarta, Indonesia*

2. *Dept. of Physics, University of Indonesia, Indonesia*

3. *Institute of Metal Physics, UB of RAS, Ekaterinburg, Russia*

4. *Dept. of Physics, Chungbuk National University, Cheongju, South Korea*

Non-stoichiometric $\text{Nd}_{0.5}\text{Sr}_{0.5}\text{MnO}_3$ (NSMO) single crystalline has been grown by the floating zone method. The slight non-stoichiometric NSMO single crystalline system raises the Curie temperature around 30 K towards room temperature without degradation of the refrigerant capacity (RC) and temperature span corresponding to the full width at half maximum of ΔS_{max} (ΔT_{FWHM}) compared to pure single crystalline NSMO system.[1] Here we study in detail critical behavior of non-stoichiometric NSMO. By using the modified Arrott plot method, the critical parameters were obtained to be T_C 267.05 K, $\beta=0.488 \pm 0.007$, and $\gamma= 1.005 \pm 0.048$ as shown in figure 1. The values of β obtained is close to expected the mean-field theory ($\beta = 0.5$ and $\gamma = 1$). Compared to pure single crystalline NSMO system the critical parameters obtained are relatively similar those are $\beta = 0.58$ and $\gamma = 1.02$ [2]. Such the results demonstrate an existence of ferromagnetic long-range order in both pure single crystalline and nonstoichiometric NSMO system. To find out other perspective, we perform local structure study around the central atom of Mn by using extended X-ray absorption fine structure (EXAFS) measured at Pohang Accelerator Laboratory (PAL), South Korea. Figure 2 shows absorption of photon energy NSMO non-stoichiometric compare to Mn-foil.

Mo.L-P69 - Investigation of Structural, Magnetic and Magnetocaloric Properties of $(\text{La}_{1-x}\text{Pr}_x)\text{Ag}_{0.85}\text{MnO}_3$ ($x = 0.0, 0.2$) PerovskitesA.O. Ayaş¹, M. Akyol², S. Kılıç Çetin², G. Akça², A. Ekicibil², Bekir Özçelik²

1. Department of Mechatronic Engineering, Faculty of Technology, Adiyaman University, Adiyaman, Turkey

2. Department of Physics, Faculty of Sciences and Letters, Çukurova University, Adana, Turkey

We study the Pr substitution into the La-site effect on magnetocaloric properties in $(\text{La}_{1-x}\text{Pr}_x)\text{Ag}_{0.85}\text{MnO}_3$ ($x=0.0$ and 0.2) polycrystalline compounds prepared by the sol-gel method. The structural and magnetic properties of both polycrystalline compounds are investigated by X-ray Diffraction (XRD), Scanning Electron Microscope (SEM) and Energy-Dispersive X-ray spectrum (EDX) methods. The crystal structures of both samples have been found hexagonal, closed packed structure determined from XRD analysis. SEM images showed that the particles are closely packed with each other in both samples. In addition, the average particle size dropped from 1.23 to 1.03 μm when the Pr added into the structure. We also performed EDX measurement for elemental analysis of each sample. The EDX spectrum showed that there is no any impurity elements coming from the producing and/or sintering process in both samples. Temperature dependence of magnetization, $M(T)$ measurements were performed to determine the Curie temperatures, T_C of both samples. External magnetic field dependence of magnetization, $M(H)$, measurements were performed to determine the magnetic entropy changing (ΔS_M) and saturation magnetizations, M_s of both samples. The critical transition temperatures from ferromagnetic to paramagnetic phase are found as 262 and 216 K in $\text{La}_{0.85}\text{Ag}_{0.15}\text{MnO}_3$ and $(\text{La}_{0.8}\text{Pr}_{0.2})\text{Ag}_{0.15}\text{MnO}_3$, respectively. In addition, the magnetic entropy changing, is calculated at around this transition temperature by using $M(H)$ data. It is found that the values are decreased from 7.90 to 4.96 J/kgK under 5T external magnetic field when Pr substituted into the structure. Furthermore, the relative cooling power (RCP) values are found as 213.32 and 263.02 J/kg in $\text{La}_{0.85}\text{Ag}_{0.15}\text{MnO}_3$ and $(\text{La}_{0.8}\text{Pr}_{0.2})\text{Ag}_{0.15}\text{MnO}_3$, respectively. These findings could potentially be used to engineer of magnetocaloric cooling systems with comparatively high magnetic entropy changing and cooling power in $(\text{La}_{1-x}\text{Pr}_x)\text{Ag}_{0.85}\text{MnO}_3$ ($x=0.0$ and 0.2) samples.

Keywords: Magnetic properties, Magnetocaloric effect, Magnetic entropy, Sol-gel method.

Mo.L-P70 - Relaxation dynamics across the first-order metamagnetic phase transition in magnetocaloric La(Fe,Mn,Si)₁₃

E. Lovell¹, M. Bratko¹, A.D. Caplin¹, L.F. Cohen¹, A. Barzca², M. Katter²

1. *Blackett Laboratory Imperial College London United Kingdom, London, United Kingdom*

2. *Vacuumschmelze GmbH & Co. KG, Hanau, Germany*

LaFe_{13-x}Si_x is of considerable interest due to their large magnetic entropy and adiabatic temperature changes and small magnetic hysteresis when field-driven through their first-order metamagnetic transition [1]. This transition is easily tuned by introduction of hydrogen interstitially [2] or by substitution of appropriate elements. Recently it has been shown that LaFe_{13-x}Si_x shows significant long-time magnetic relaxation across the phase transition related to the first order nature of the transition, with a strong dependence on internal demagnetising fields [3,4]. In addition we have observed in one composition $x = 1.4$, the magnetic relaxation rate slows down as the temperature is increased from T_c towards a tri-critical point (T_{crit}) known to exist in the H-T phase diagram, indicating that the dynamics are not Arrhenius or athermal [4]. We have speculated that these observations suggest that the dynamics are governed by the degree of superheating or supercooling. In order to investigate this further we have examined the magnetic relaxation rate in a series of LaFe_{1-x-y}Mn_ySi_x samples as a function of Mn concentration. We also use a sensitive ac calorimetry probe to separate the heat capacity from the latent heat, in order to characterise the strength of the first order character [5]. We report on the relaxation dynamics across this series of samples and report the correlation with the magnitude of the latent heat. This work is in part funded by the European Community's 7th Framework Programme under Grant agreement 310748 "DRREAM" and also the EPSRC EP/G060940/1.

References:

- [1] F. Hu et al, Appl. Phys. Lett. 78, 3675 (2001)
- [2] A. Fujita et al, Phys. Rev. B 67, 104416 (2003)
- [3] H. Yako et al, IEEE Trans. Mag. 47, 2482 (2011)
- [4] E. Lovell et al, Adv. Energy Mater. 1401639 (2014)
- [5] K. Morrison et al, Phil. Mag. 92, 292 (2012)

Mo.L-P71 - Temperature dependence of the electrical resistivity for the Heusler alloy system $\text{Ni}_2\text{Mn}_{1-x}\text{Cr}_x\text{Ga}$

Y. Adachi¹, M. Fujio², T. Kanomata³, R.Y. Umetsu⁴, X. Xu⁵, R. Kainuma⁵

1. Graduate School of Science and Engineering, Yamagata University, Yonezawa, Japan
2. Faculty of Engineering, Yamagata University, Yonezawa, Japan
3. Research Institute for Engineering and Technology, Tohoku Gakuin University, Sendai, Japan
4. Institute for Materials Research, Tohoku University, Sendai, Japan
5. Department of Materials Science, Graduate School of Engineering, Tohoku University, Sendai, Japan

Much attention has been paid to the ferromagnetic shape memory alloys (FSMAs) due to their application potential as actuators, sensors and magnetocaloric materials. Heusler alloy Ni_2MnGa is a well-known FSMA with the Curie temperature (T_C) of 376 K and the martensitic transition temperature (T_M) of 202 K [1]. T_C and T_M depend on the kind and quantity of the doping atoms as reported in $\text{Ni}_2\text{Mn}_{1-x}\text{M}_x\text{Ga}$ ($M=\text{Co}$, Ni , and Cu) alloy system [2-4]. Some researchers have reported that T_M is mapped to the average number of valence electrons per atom (e/a) [2]. Co , Ni and Cu atoms have the more valence electrons than Mn atom, but Cr atom has less. As far as we know, there is no data for T_C and T_M of the Cr -doped Ni_2MnGa . In this study, the temperature dependence of the electrical resistivity r of $\text{Ni}_2\text{Mn}_{1-x}\text{Cr}_x\text{MnGa}$ ($x=0 - 0.15$) has been measured. Two anomalies on the r - T curves for all samples are observed. These anomalies correspond to the magnetic and structural phase transition at T_C and T_M , respectively. On the basis of the experimental results, the T - x phase diagram of $\text{Ni}_2\text{Mn}_{1-x}\text{Cr}_x\text{Ga}$ is given.

- [1] P.J. Webster *et al.*, *Phil. Mag. B*, 49 (1984) 295
[2] M. Khan *et al.*, *J. Appl. Phys.* 97 (2005) 10M304
[3] V.V. Khovaylo *et al.*, *Phys. Rev. B*, 72 (2005) 224408
[4] M. Kataoka *et al.*, *Phys. Rev. B*, 82 (2010) 214423

Mo.L-P72 - Magnetic structure and magnetocaloric properties of $\text{Ho}(\text{Co}_{1-x}\text{Fe}_x)_2$ quasibinary intermetallic compounds

M. Anikin¹, E. Tarasov¹, A. Pirogov¹, N. Kudrevatykh¹, A. Zinin¹

1. Ural Federal University, Ekaterinburg, Russian Federation

We have studied crystal and magnetic structures, magnetic and magnetocaloric properties of $\text{Ho}(\text{Co}_{1-x}\text{Fe}_x)_2$ isostructural compounds ($x = 0.00, 0.04, 0.07, 0.12$) and made an assessment of a possibility of their application as material for a working body of magnetocaloric refrigerators.

Magnetic properties were measured with SQUID-magnetometer under the magnetic field up to $H = 70$ kOe over temperature range $5 \div 400$ K. Neutron diffraction (ND) experiments were carried out with the D-2 diffractometer, mounted on the reactor IVV-2M (Zarechny, Russia). The neutron wave length is 1.805 \AA .

It was found that temperature dependencies of the magnetic entropy change $\Delta S(T)$, calculated from magnetization isotherms, demonstrate a broadening of their maximums at temperatures below Curie point. The broadening rises both under magnetic field increasing and Fe-content. At $H = 50$ kOe the cooling capacity of the sample with $x = 0.12$ was found to be 583 J/kg , that is much higher than that 299 J/kg determined for $\text{Tb}(\text{Co}_{0.7}\text{Fe}_{0.3})_2$ in [1].

These unusual $\Delta S(T)$ dependences could be explained by a canted magnetic ordering in the Ho sublattice of doped compounds. This assumption is confirmed by results of ND-experiments at $T = 78 \text{ K}$ on the sample with $x = 0.12$, in which the average magnetic moment of Ho-atoms was found to be $7.8 \mu_B$ instead of $10.0 \mu_B$ for the Fe-free sample. Thus, it was possible to infer that Ho-magnetic moments near the Fe-atoms positions in MgCu_2 lattice are deflected from the global easy axis $[100]$ at the large angles. The average angle of this deflection for all Ho-magnetic moments was assessed as 38° .

This work has been supported by the UrFU State contracts № 1362 and № 2582.

Mo.L-P73 - Hydrogen-induced magnetic anisotropy and magnetocaloric effect in SmFeCoN. Mushnikov¹, A. Protasov¹, V. Gaviko¹, V. Lazukin¹*1. Institute of Metal Physics UB RAS, Ekaterinburg, Russian Federation*

Quasi-binary $\text{Sm}(\text{Fe}_{1-x}\text{Co}_x)_2$ intermetallics with the fcc MgCu_2 -type lattice are ferromagnets with the Curie temperatures 208-667 K depending on x value. The samarium sublattice provides a large anisotropic magnetostriction, and the crystal lattice undergoes rhombohedral magnetoelastic distortions which can be registered by x-ray diffraction. A characteristic feature of these intermetallics is their high activity to hydrogen. Powdered samples spontaneously absorb hydrogen from the atmosphere and form hydrides $\text{Sm}(\text{Fe}_{1-x}\text{Co}_x)_2\text{H}_{0.1-0.05}$. Hydrogen orders in the distorted lattice, which in turn enhances the rhombohedral distortions. The arrangement of the hydrogen ions can be modified by heating in magnetic field, which causes a uniaxial magnetic anisotropy.

We studied the magnetic and magnetothermal properties and structure of the SmFeCo compound containing spontaneously absorbed hydrogen. The compound has the Curie temperature 613 K and the room-temperature specific magnetization $45 \text{ Am}^2/\text{kg}$. After heating up to 350-450 K and subsequent cooling in magnetic field, the magnetization curves measured along the direction of thermomagnetic treatment and perpendicular to it were found to be substantially different because of an induced magnetic anisotropy. We determined optimum values of the temperatures and magnetic fields which provide the induced anisotropy energy up to $5.2 \times 10^5 \text{ J/m}^3$ at room temperature. It decreases down to zero with increasing temperature up to 350 K. Near this temperature, due to increasing of hydrogen mobility, we observed strong magnetic relaxation.

Using the results of temperature and field dependences of magnetization, we estimated the magnetocaloric effect caused by changing of mutual orientations of the easy axis and magnetic field direction. The MCE is positive, appeared in relatively weak magnetic fields and has a maximum at $\sim 320 \text{ K}$. The maximum value of the isothermal entropy change amounts to $1.8 \text{ J kg}^{-1}\text{K}^{-1}$. The adiabatic temperature changes for the hydrogen-containing SmFeCo are currently under study.

This work is partially supported by RFBR 13-02-96022 and UB RAS 15-17-2-22 grants.

Mo.L-P74 - Specific heat, magnetostriction and magnetocaloric effect in Fe₄₈Rh₅₂ alloy

A. Aliev¹, A. Batdalov¹, L. Khanov¹, A. Kamantsev², E. Dilmieva², A. Mashirov², V. Koledov², V. Shavrov², M. Topic²

1. *Amirkhanov Institute of Physics of Daghestan Scientific Center, RAS, Makhachkala, Russia*
2. *Kotelnikov Institute of Radio-engineering and Electronics of RAS, Moscow, Russia*

In the modern literature, there are no comprehensive data on the role of different mechanisms responsible for metamagnetic phase transition of the 1st order from antiferromagnetic (AFM) to ferromagnetic (FM) state observed in the alloys Fe-Rh. There is no theory satisfactorily describing the nature of this transition. The most popular idea is of an electronic nature of the transition, based on differences in the density of electronic states near the Fermi level in the FM and AFM- phases. The basis for this assumption is the experimentally observed difference in the coefficients of the electronic specific heat $\gamma=C_e/T$ in FM and AFM-states ($\gamma_{FM} > \gamma_{AFM}$) [1,2]. Since the direct measurement of γ_{FM} is not possible, the procedure was carried out by measuring the specific heat at low temperatures in magnetic fields exceeding the critical values. The experimentally measured value of the specific heat just before the AFM-FM transition and just after the transition must undergo a jump $\Delta C = (\gamma_{FM} - \gamma_{AFM})T_{cr}$. Using data on $\Delta\gamma \approx 0.048 \text{ J/kgK}^2$ [1,2] and $T_{cr} = 318 \text{ K}$, one can get $\Delta C_e = 15.26 \text{ J/kgK}$. Our experimental data $C_p(T)$ show that the expected discontinuity of ΔC cannot be observed.

Direct measurements of MCE were conducted using magnetic field modulation technique, with high ΔT accuracy measurements [3]. The temperature hysteresis, a significant difference in the magnitude of the effect at heating and cooling, as well as the splitting of the maximum of the effect in weak magnetic fields were detected. The observed phenomena are explained by the coexistence of FM and AFM-phase and low heterogeneity of the studied sample. Temperature hysteresis of MCE in strong magnetic fields demonstrate a qualitatively different form.

[1] P. Tu, A.J. Heeger et al. J. Appl. Phys. 40, 1368 (1969)

[2] N.V. Baranov, E.A. Barabanova. Journal of Alloys and Compounds 219, 139 (1995)

[3] A.M. Aliev. arXiv:1409.6898

Mo.L-P75 - Predictions of large magnetocaloric effects in Co- and Cr-substituted Heusler alloys using first-principles and Monte Carlo approaches

V. Sokolovskiy¹, V. Buchelnikov¹, M. Gruner², P. Entel²

1. Chelyabinsk State University, Chelyabinsk, Russia

2. Duisburg-Essen University, Essen, Germany

Ferromagnetic (FM) compounds with first-order magnetic phase transition and simultaneous structural changes have attracted interest due to emerging magnetocaloric effects (MCE) and their possible application in magnetic refrigeration technology [1]. Nowadays, Ni-Z-Mn-In (Z = Co, Fe, Cr, Si etc.) Heusler alloys have been widely investigated because of their potential applications as intelligent FM materials [1-3]. The additional element Z can bring a transformation sequence from martensite having low magnetization to FM austenite with high magnetization giving rise to better magnetocaloric properties. In this work we theoretically studied MCE in Ni-Co-Mn-Cr-In Heusler alloys by combining first principles with Monte Carlo approaches. We discuss the resulting complex spin configurations, temperature behavior of entropy as well as critical temperatures of phase transitions. Three types of composition with substitution of 5at.% Cr for Mn, In, and Ni have been discussed. The ab initio calculations have been carried out by using two kinds of 16-atom supercell Ni₇Co₁Mn₆In₂ with different both spin configurations and distributions of Mn and In at the In-sublattice. We have shown that different spin configurations lead to the small respective large magnetic moments of martensite and austenite. As a consequence, the substitution of 5% Co for Ni and 5% Cr for Mn results in a magnetostructural transition from FM austenite to antiferromagnetic martensite, which is accompanied by a spin-flip transition upon cooling. Large magnetization drop and giant inverse magnetocaloric effect can be achieved of $\Delta T_{ad} \sim -9$ K under magnetic field change of 2 T field across the structural transition.

This work is supported by RFBR Grant No. 14-02-01085, RSF Grant No. 14-12-00570\14, Ministry of Education and Science of RF No 3.2021.2014/K

[1] K.A. Gschneidner Jr., and V.K. Pecharsky, *Int. J. Refrig.* 31 (2008) 945

[2] X. Moya et al. *Nature Mater.* 13 (2014) 439

[3] V.V. Sokolovskiy et al. *Mater. Sci. Foundation* 81-82 (2015) 38

Mo.L-P76 - Direct measurements of the low-field magnetocaloric effect in low volume and thin film samples

J. Döntgen¹, J. Rudolph¹, T. Gottschall², O. Gutfleisch², S. Salomon³, A. Ludwig³, D. Hägele¹

1. *Arbeitsgruppe Spektroskopie der kondensierten Materie, Ruhr-Universität Bochum, Bochum, Germany*

2. *Institut für Materialwissenschaft, TU Darmstadt, Darmstadt, Germany*

3. *Institut für Werkstoffe, Ruhr-Universität Bochum, Bochum, Germany*

The search for materials that exhibit a large magnetocaloric effect (MCE) near room temperature endorses the systematic investigation of entire material classes with varying chemical composition. For this purpose material libraries can be prepared by thin film deposition on wafers. However, the direct measurement of the adiabatic temperature change ΔT in thin film samples is difficult due to the fast heat diffusion on small length scales.

We present direct measurements of ΔT in low volume and thin film samples [1]. Our newly developed experimental setup combines magnetomodulation with non-contact temperature measurements via detection of the sample's thermal radiation. The setup reaches sub-mK sensitivity and gives insights into the low-field behavior of the MCE, which is not accessible by standard calorimetry.

For the measurements of ΔT on a thin film, a 1.4 μm thick layer of Gd was deposited on a 1.1 μm thick membrane fabricated by micro-electro-mechanical systems technology. Temperature dependent measurements show a clear peak at 294K, as expected in the region of the ferromagnetic-paramagnetic phase transition.

Measurements on bulk metamagnetic $\text{LaFe}_{11.05}\text{Co}_{0.91}\text{Si}_{1.04}$ in magnetic field amplitudes of 4 mT to 45 mT show a strong broadening of the peak with increasing field amplitude. Different values for the temperature change are observed upon heating and cooling the sample, indicating a thermal hysteresis. Magnetic field dependent measurements on all samples show a quadratic dependence of ΔT at the peak temperature for weak external fields, contradicting earlier predictions. An analytic expression is derived from Landau-theory that correctly describes both the quadratic dependence of ΔT at low fields and the well known $H^{(2/3)}$ behavior at high fields.

[1] J. Döntgen et al., Appl. Phys. Lett. **106**, 032408 (2015)

Mo.L-P77 - Phase transformations and magnetocaloric effect in Ni-Mn-(Co)-In Heusler alloysV. Buchelnikov¹, R. Fayzullin¹, A. Mashirov², V. Koledov², V. Shavrov², S. Taskaev¹

1. Chelyabinsk State University, Chelyabisk, Russia

2. Kotelnikov Institute of Radioengineering and Electronics, Moscow, Russia

The magnetocaloric effect (MCE) is a phenomenon of adiabatic temperature change of the magnetic material induced by change of external magnetic field. Recent experimental studies have shown that Ni-Mn-(Co)-In Heusler alloys are also attractive for magnetic refrigeration [1, 2]. In this work, we study experimentally MCE in Ni_{1.81}Mn_{1.64}In_{0.55}, Ni_{1.73}Mn_{1.80}In_{0.47} and Ni_{1.72}Mn_{1.51}In_{0.49}Co_{0.28} Heusler alloys. Polycrystalline ingots with nominal compositions were prepared by an arc-melting method. The MCE measurements were performed by the setup produced by AMT&C [3]. The temperatures of phase transitions were determined from the thermomagnetic dependences in the temperature range of 50–400 K. The latent heat connected with the first-order transformation were determined by differential scanning calorimetry.

The magnetostructural transformation from the antiferromagnetic-like martensite to the ferromagnetic austenite phase in the all compositions was found. The giant inverse MCE (DT_{ad} = -3.72 K) is observed at the magnetostructural phase transition temperature (T_m=230 K) in Ni_{1.81}Mn_{1.64}In_{0.55} alloy. For Ni_{1.73}Mn_{1.80}In_{0.47} and Ni_{1.72}Mn_{1.51}In_{0.49}Co_{0.28} alloys maximum values of MCE are somewhat smaller: DT_{ad} are -2.1 K (at T_m=292 K) and -2.4 K (at T_m=311 K) for DH=2 T, respectively. Maximum positive value of MCE in Ni_{1.81}Mn_{1.64}In_{0.55} and Ni_{1.72}Mn_{1.51}In_{0.49}Co_{0.28} (DT_{ad} = 1.8 K at T_c=320 K and DT_{ad} = 1.4 K at T_c=327 K, respectively) observed at Curie temperature. This work was supported by RFBR (Grant No. 14-02-01085, preparation of samples), RSF (Grants No. 14-12-00570, MCE measurements, No. 14-22-00279, magnetic measurements) and Ministry of Education and Science RF (Grant No. 3.2021.2014/K, DSK measurements).

1. J. Liu, T. Gottschall, K.P. Skokov, et al., *Nature Mater.*, 11, 620 (2012)2. V. Sokolovskiy, M. Zagrebin, V. Buchelnikov, *Mater. Science Found.*, 81-82, 38 (2015)3. A. Tishin, Yu. Spichkin, D. Kopeliovich, et al., *proc. 3rd Intern. Conf. Magn. Refrigeration at Room Temperature*, Des Moines. Iowa. USA, 2009, P. 173

Mo.L-P78 - MAGNETIC and structural analysis of MN rich MN-NI-SN alloys

J.J. Suñol¹, R. Coll¹, L. Escoda¹, M. Ipatov²

1. *University of Girona, Girona, Spain*

2. *SGIKER, University of Basque Country, Leioa, Spain*

In this work we analyse the thermomagnetic response and the structure transformation of three Mn rich alloys of the Mn-Ni-Sn system: $Mn_{50}Ni_{40}Sn_{10}$, $Mn_{50}Ni_{42.5}Sn_{7.5}$ and $Mn_{50}Ni_{45}Sn_5$ (at. %). Previous studies concluded that these materials are prospective for the development of magnetically driven sensors, actuators and working substances for magnetic refrigeration. Characteristic temperatures of the martensitic transformation were determined from differential scanning calorimetry (DSC) measurements. Structure and microstructure was examined by X-Ray diffraction (XRD) and scanning electron microscopy (SEM) linked with an energy dispersive X-ray spectrometry (EDX) device. Temperature and field dependences on magnetization were measured with a vibrating sample magnetometer (VSM) and PPMS. The temperature dependence of the magnetization $M(T)$ was measured at our values of applied magnetic field from 50 Oe up to 50 kOe. Martensitic transformation temperatures decrease as the intensity of the applied magnetic field increases. Thus, magnetic field stabilizes the high temperature austenite phase. Magnetization values of 40 emu/g were obtained (austenite phase). The Curie temperature ranged from 250 to 350 K. Complementary AC magnetic susceptibility measurements were also performed. Transformation temperatures are lower than those obtained in Ni rich Ni-Mn-Sn alloys.

Acknowledgements: Financial support from project MAT2013-47231-C2-2-P

Mo.L-P79 - The effects of hydrogenation and Mn doping on the first order nature of the metamagnetic transition in $\text{La}(\text{Fe,Si})_{13}$

M. Bratko¹, Y. E. Lovell¹ N, J. Turcaud¹ N, D. Caplin¹ N, L.F. Cohen¹ N, V. Basso² N, M. Kupferling² N, C. Curcio² N, C. Bennati² N, A. Barzca³ N

1. Imperial College London, London, United Kingdom

2. Istituto Nazionale di Ricerca Metrologica, Torino, Italy

3. Vacuumschmelze GmbH & Co. KG, Hanau, Germany

Magnetocaloric effect (MCE) is the isothermal entropy change or adiabatic temperature change induced by external magnetic field and it forms the basis for solid state refrigeration near room temperature. For successful application, large MCE is required in relatively small fields below 2 T. $\text{La}(\text{Fe,Si})_{13}$ based compounds are promising candidates exhibiting large MCE associated with a first-order metamagnetic phase transition above the T_c . Importantly, the T_c can be shifted to near room temperature by hydrogen absorption while sustaining the large MCE [1].

The effect of hydrogenation on the metamagnetic phase transition is not fully understood. Here we investigate the impact of hydrogenation on the first order nature of the phase transition in $\text{LaFe}_{11.33}\text{Mn}_{0.37}\text{Si}_{1.30}$, where Mn doping has been used to tune the T_c of fully hydrogenated state to 283 K. We use our unique microcalorimeter which operates in two distinct setups allowing us to measure the latent heat and the reversible changes in heat capacity separately. Thus we can quantify the first order and the second order contribution to the entropy change. We do so in the dehydrogenated and fully hydrogenated state showing significant decrease in the first order contribution to the total MCE in the hydrogenated state. In the dehydrogenated state we perform this analysis across a series of $\text{La}(\text{Fe,Mn,Si})_{13}$ compounds with increasing Si and Mn content showing a transition from relatively strongly first order phase transition to a second order phase transition. Across the series we observe tricritical points where the metamagnetic phase transition becomes fully second order. The tricritical points appear closer to the T_c with the suppression of first order phase transition by composition.

[1] Fujita A. et al., Phys. Rev. B 67, 104416

This work is in part funded by the European Community's 7th Framework Programme under Grant agreement 310748 "DRREAM" and also the EPSRC EP/G060940/1

Mo.L-P80 - Magnetocaloric effect in Gd - Y alloys

M. Drobosyuk¹, S. Taskaev¹, M. Ulyanov¹, D. Bataev¹, R. Fayzullin¹, V. Buchelnikov¹

1. Chelyabinsk State University, Chelyabinsk, Russian Federation

The magnetocaloric effect (MCE) is the ability of magnetic materials to heat up or cool down then they are placed in or removed from an external magnetic field. The magnetic materials with large values of MCE can be applied as work substances in magnetic cooling devices. In this work, we study experimentally MCE of Gd - Y alloys.

Polycrystalline ingots with Gd - Y nominal compositions were prepared by a conventional arc-melting method. Samples were cut from the middle part of the ingots.

The magnetocaloric measurements were performed by the Magnetocaloric Measuring Setup produced by Advanced Magnetic Technologies and Consulting Ltd (AMT&C). The adiabatic temperature change ΔT_{ad} was measured by a direct method in this setup. . Magnetic field up to 2 T was created by Halbach permanent magnet magnetic field source. Signals from the thermocouple and Hall probe were recorded simultaneously what allowed us to measure ΔT_{ad} as a function of magnetic field H . Temperature was stabilized with accuracy of ~ 0.05 K. The measurements were performed in a temperature interval from 220 to 290 K.

Temperature dependencies of ΔT_{ad} for one of Gd_{100-x}Y_x alloys for the magnetic field change $\Delta H = 2$ T are shown in Figure 1. It is seen that all the alloys exhibit the positive MCE typical for 2nd order transition. The maximal MCE is observed at the Curie point and it's value of ΔT_{ad} is 2.68 K.

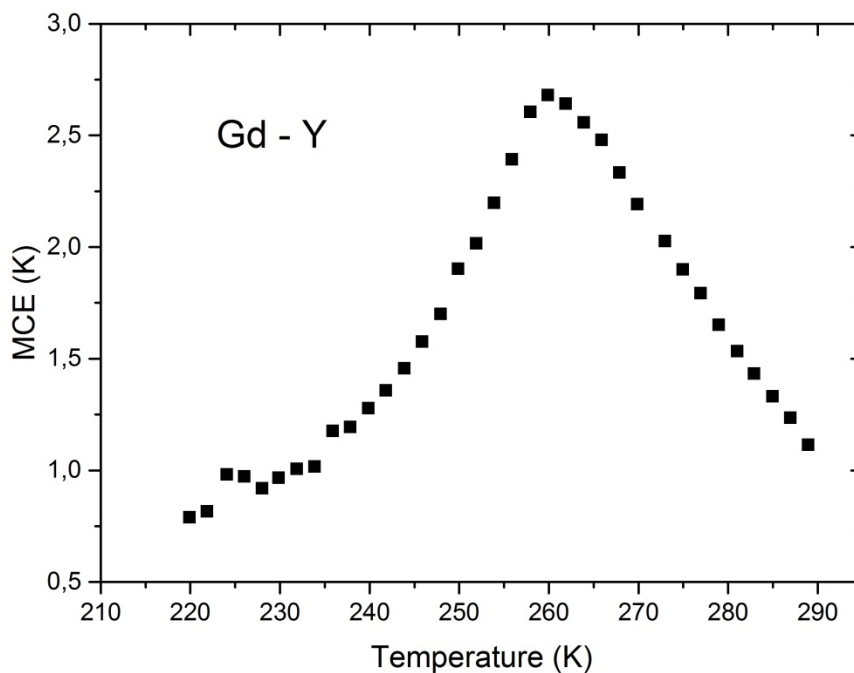


Fig. 1. Adiabatic temperature change in Gd-Y alloy

Mo.L-P81 - Thermal and rheological properties of water based ferrofluids and their applicability as quenching media

J. Župan¹, M. Majić Renjo¹

1. University of Zagreb, Faculty of Mechanical Engineering And Naval Architecture, Quenching Research Centre (QRC), Zagreb, Croatia

Water based ferrofluids present a new energy transfer fluid with tunable properties. Previous research has shown the increase in thermal conductivity of water based nanofluids with the addition of iron oxide. Such increased thermal properties show great potential for use in heat transfer. In this paper, several nanofluids were prepared with two step method. Iron (II,III) oxide nanoparticles with average particle size less than 50 nm were added to deionized water in following concentration: 0.01, 0.1, 0.5 and 1 g/L. Their thermal and rheological properties were measured at 20, 40 and 60 °C. Results showed increase in thermal conductivity and viscosity with increase in the addition of nanoparticles at all three temperature levels. The biggest increase was observed at 20°C. For this research, all of the prepared nanofluids were tested as immersion quenching liquid according to ISO 9950 standard. Besides still conditions, quenching experiments were conducted under the magnetic field at two levels, 500 and 1000 Gauss. The magnetic field effect was least present at 60°C with almost no influence on the cooling curve and cooling rates. At lower temperature levels quenching under the magnetic field shortened the full film boiling phase and increased the maximum cooling rate.

Mo.L-P82 - Two Dumbbell-shaped M_5Gd_4 Heterometallic Clusters exhibiting well magnetocaloric effectJ.P. Tong¹, X.J. Xu¹, D.J. Yang¹, K. Zhang¹, J. Tao²

1. Xiangyang Noncommissioned Officers School, Xiangyang, China

2. Xiamen University, Fujian, China

Heterometallic 3d-4f complexes have been intensively studied owing to the rapid development in molecular magnetic properties. Many Gd-containing complexes display fascinating magnetocaloric effect due to spin multiplicity of Gd(III) ions. So far, lots of Gd-containing complexes have been synthesized, in which tetranuclear cuboidal species are highly concerned because intracluster ferromagnetic exchanges and thus high-spin ground states are often obtainable so that they are potential candidates used in low-temperature refrigeration.

Herein, we obtained two dumbbell-shaped heterometallic clusters **Co₅Gd₄** and **Ni₅Gd₄**. The skeleton can be viewed as two {M₂Ln₂} cubanes connected via an M(II) ion. The magnetic entropy changes of **Co₅Gd₄** and **Ni₅Gd₄** are calculated from magnetization data according to the Maxwell equation. The largest $-\Delta S_m$ values at 3.5 K for 7 T are 31.0 J Kg⁻¹ K⁻¹ for **Co₅Gd₄** and 37.3 J Kg⁻¹ K⁻¹ for **Ni₅Gd₄**, respectively. Ni₅Gd₄ shows large MCE taking advantage of intramolecular ferromagnetic interactions and considerable metal-to-ligand mass ratio.

References:

- [1] Wernsdorfer, W.; Sessoli, R. *Science* 1999, 284, 133
- [2] Benelli, C.; Gatteschi, D. *Chem. Rev.* 2002, 102, 2369
- [3] Sessoli, R. *Angew. Chem. Int. Ed.* 2012, 51, 45

Mo.L-P83 - Direct measurements of giant adiabatic temperature change in FeRh alloys under cyclic conditions

A. Chirkova¹, K.P. Skokov², T. Gottschall², O. Gutfleisch², L. Schultz¹, N.V. Baranov^{3,4}, T.G. Woodcock¹

1. IFW Dresden, Germany, Dresden, Germany

2. TU Darmstadt, Darmstadt, Germany

3. Ural Federal University, Yekaterinburg, Russia

4. Institute of Metal Physics, Yekaterinburg, Russia

Materials exhibiting a large magnetocaloric effect (MCE) can be exploited for solid-state magnetic refrigeration. The presence of a first order metamagnetic transition in a material has the disadvantage of a hysteresis, which can reduce the MCE. It is very important to carefully estimate the MCE under cyclic conditions close to those in a potential magnetic refrigerator [1] in order to avoid the overestimation that happens when only the first application of the magnetic field is considered. FeRh exhibits one of the largest MCE displayed at a metamagnetic transition from an antiferromagnetic (AF) to ferromagnetic (FM) state near room temperature and this is characterised by a large adiabatic temperature change (ATC). FeRh has a large hysteresis (about 20 K in 0.5T) and is an ideal model system for magnetocaloric materials with a hysteretic transition. It has been estimated that the magnetic entropy change in FeRh does not decrease significantly even after repeated applications of a magnetic field [2], however so far direct measurements of the MCE under cyclic conditions have not been reported. In the current work, direct measurements of the ATC during cycling of binary Fe-Rh have been carried out. The results showed that in Fe₄₉Rh₅₁, the ATC was 9.2 K on the first application of the 2T field and it remained constant at 6.2 K during repeated cycling. Despite the presence of the hysteresis at the AF-FM transition, this directly measured value of the ATC is higher than in Gd and demonstrates the potential of materials with a first order metamagnetic transition for application in magnetic refrigeration technology.

[1] K. P. Skokov, V. V Khovaylo, K.-H. Muller, J. D. Moore, J. Liu, and O. Gutfleisch, J. Appl. Phys. 111, 07A910 (2012)

[2] M. Manekar and S. B. Roy, J. Phys. D: Appl. Phys. 41, 192004 (2008)

Mo.L-P84 - $(\text{Mn}_{55}\text{Al}_{45})_{100}\text{B}_2$ and $\text{Mn}_{55}\text{Al}_{45}\text{Ga}_5$ - promising permanent magnetic materials

Sofia Kontos¹, Klas Gunnarson¹, H.ailiang Fang², P. Svedlindh¹, Martin Sahlberg²

1. Uppsala University, Engineering Sciences, Uppsala, Sweden

2. Uppsala University, Chemistry, Uppsala, Sweden

Due to magnetic properties potentially superior to ferrites and lack of rare earth contents, Mn-Al alloys are promising candidates for permanent magnets. Besides, they show good mechanical properties, machinability and corrosion resistance. The ferromagnetic tetragonal τ -phase has a strong uniaxial anisotropy which is a prerequisite for achieving a high coercivity. τ -phase is usually formed from the nonmagnetic hexagonal ϵ -phase by annealing a quenched alloy with 50-60% of Mn. Since both phases are metastable at room temperature, different alloying elements are used to stabilize the phase.

Magnetic and crystallographic properties were obtained by X-ray diffraction and vibrating sample magnetometry measurements. By alloying $\text{Mn}_{55}\text{Al}_{45}$ with B or Ga to $(\text{Mn}_{55}\text{Al}_{45})_{100}\text{B}_2$ and $\text{Mn}_{55}\text{Al}_{45}\text{Ga}_5$, respectively, τ -phase was achieved from high temperature synthesis methods. Subsequently the samples were annealed at 1000°C and quenched in water. The magnetization was measured as a function of applied field up to 7.2 MA/m at room temperature before and after a relaxation process.

For $(\text{Mn}_{55}\text{Al}_{45})_{100}\text{B}_2$ and $\text{Mn}_{55}\text{Al}_{45}\text{Ga}_5$, the saturation magnetizations are 0.42 MA/m and 0.50 MA/m and the coercivities 0.26 MA/m and 0.22 MA/m, respectively. The quantities were measured directly after annealing and quenching. After relaxation, the saturation magnetizations are slightly increased to 0.50 MA/m and 0.51 MA/m, however, at the expense of coercivities which decreased to 0.15 MA/m and 0.11 MA/m. The squareness factor M_r/M_s of the samples were 0.3-0.4 for all samples.

Mo.L-P85 - Ab-initio based analytical evaluation of entropy in magnetocaloric materials with first order phase transitions

M. Piazza¹, V. Basso¹, J. Zemen², K. Sandeman^{2,3}

1. *Istituto Nazionale di Ricerca Metrologica, Torino, Italy*

2. *Blackett Laboratory, Imperial College London, London, United Kingdom*

3. *Brooklyn College, CUNY, New York, United States*

The possibility to predict first order magnetic phase transition from first principles would boost the theory-led discovery of novel compounds with enhanced magnetocaloric effect. However this task is a challenging one. Spin polarised density functional theory (SDFT) can foreshadow Curie points [1], but can say little about first order transitions where magnetoelastic effects and spin disorder at finite temperature play relevant effects. Possible solutions include the application of the disordered local moment (DLM) picture [2], that has been recently applied to antiferromagnets [3]. Here we investigate an approach complementary to Ref. [3], based on multilevel modeling: ab-initio SDFT and mean field thermodynamic theory (MFT) [4]. On the one hand SDFT provides the local moments, the ground state energy and the electronic density of states. On the other hand MFT allows for the analytical evaluation of the magnetic entropy and magnetoelastic contributions. In this way we evaluate by SDFT the magnetic configurations of a system and we derive by MFT the temperature dependence of the free energy. We test this approach with relevant magnetocaloric compounds: La(Fe,Si)₁₃ [5] and Mn-based antiperovskites (AXMn₃, with X=C, N and A metal element) [6]. For the antiperovskites we find that adding the localized spin contribution is necessary to achieve good agreement with the measured T_t, since the electronic entropy alone would overestimate the value. The research leading to these results has received funding from the EC FP7 under Grant agreement 310748 'DRREAM'.

[1] G. Bihlmayer, Density Functional Theory of Magnetism, in Handbook of Magnetism and Advanced Magnetic Materials (H. Kronmuller and S. Parkin, Eds.) J. Wiley & Sons, Ltd. (2007).

[2] B. L. Gyorffy et al. J. Phys. F 15, 1337 (1985)

[3] J. B. Staunton et al. Phys. Rev. B 89, 054427 (2014)

[4] V. Basso, J. Phys.: Condens. Matter 23, 226004 (2011)

[5] Z. Gercsi et al., arXiv:1407.7975 [cond-mat.mtrl-sci] (2014)

[6] T. Peng et al. Chinese Phys. B 22, 067501 (2013)

Mo.L-P88 - Ferrites in the low-power wireless power transfer systems

B. Stergiou¹, V. Zaspalis¹

1. Laboratory of Inorganic Materials, Centre for Research and Technology – Hellas, Thessaloniki, Greece

The emerging trend of wireless charging in electronic device market has revived the research interest in wireless power transfer systems and pushed magnetic materials design towards certain specifications. In typical inductive power transfer applications, the demand for efficient inductive coupling and elaborate manipulation of magnetic fields indicate the critical role of magnetic materials. Thus, the main objective of this investigation is to monitor the impact of magnetic material properties on the basic characteristics of a low-power wireless power transfer system.

For this examination, two different compositions of NiZn and NiCuZn spinel ferrites were fabricated with the conventional solid-state reactions route. Specifically, disc and toroidal specimens were pressed at the constant density of 3gr/cm^3 and sintered at different top temperatures from 1000°C to 1300°C . The varying composition and sintering temperature ensured the appearance of different material properties, which facilitated the derivation of their influence on the overall performance. To this end, the ring-shaped ferrite samples were initially characterized in terms of the saturation magnetization B_{sat} , complex permeability μ^* and power loss density P_v in various frequency ranges from 20kHz to 1GHz. The variations of these properties were clearly correlated with the recorded structural and microstructural aspects of the materials. Moreover, by employing the produced disc-shaped ferrite specimens, we have measured their shielding effectiveness in the near field and studied their effect as substrate material on the inductance L and quality factor Q of standard planar spiral coils with emphasis on the 100-200kHz frequency range, which is defined by the respective prevalent standards. Finally, the impact of high saturation and permeability planar ferrite on the coupling efficiency was verified and quantified by means of an evaluation low-power wireless power transfer module.

This work was supported by the IKY fellowships of excellence for postgraduate studies in Greece - Siemens program.

Mo.L-P89 - Magnetocaloric effect in some magnetic materials in alternating magnetic fields

A. Aliev¹, A. Batdalov¹, A. Gamzatov¹, L. Khanov¹, V. Koledov², V. Shavrov²

1. *Amirkhanov Institute of Physics of Daghestan Scientific Center, RAS, Makhachkala, Russia*

2. *Kotelnikov Institute of Radio-engineering and Electronics of RAS, Moscow, Russia*

The creation of magnetic refrigerators remains an actual and alluring idea. Today the compact sources of high magnetic fields exist; the alloys with large values of magnetocaloric effect (MCE) are obtained. But an important question is scarcely explored. The magnetocaloric materials in refrigerators will be affected by external alternating magnetic field. But it is not clear how will the magnetocaloric effect behave under alternating magnetic fields. Whether a magnetocaloric material will have time to exchange energy with surrounding heat exchanger under such conditions?

In this work we present the modulating method of the direct measurement of magnetocaloric effect, alternating magnetic field source, and experimental results of magnetocaloric effect in different materials, including gadolinium, some manganites, and Heusler and FeRh alloys under alternating magnetic fields up to 25 Hz. In some of the studied materials no significant dependence of the MCE on frequency of magnetic field change is observed. In some Heusler alloys and manganite compounds, MCE strongly depends on the frequency of magnetic field changes, and can even vanish at high frequencies.

Possible reasons for the frequency dependence of MCE could be the long time relaxation processes at magnetic phase transitions and irreversibility around the first order magnetostructural phase transitions. The results show that the frequency dependence of MCE should be considered for the choice of materials for magnetic refrigerators.

Mo.L-P90 - Anodic iron oxide nanotubes: Structural and magnetic characterization

A. Apolinário¹, C. T. Sousa¹, A. M. Pereira¹, M. P. Fernandez¹, G. Oliveira¹, J. Azevedo^{1,2}, J. Ventura¹, L. Andrade², A. M. Mendes², J.P. Araújo¹

1. IFIMUP-IN - Universidade Do Porto, Porto, Portugal

2. LEPAE - Universidade Do Porto, Porto, Portugal

Highly-ordered hematite (α -Fe₂O₃) nanotubes (NTs) have gained relevance for application in hydrogen production by water splitting (photoelectrochemical cells) [1] due to its narrow band gap about 2.0-2.2 eV, which collects up to 40% of the solar spectrum energy. However, the hematite materials have poor electron mobility that results into high electron-hole recombination rate and, short hole diffusion length. In order to overcome these drawbacks, nanostructuring techniques have been proven useful for increasing the performance of the hematite's photoresponse [2]. In this work, we synthesized iron oxide NTs starting from an iron foil in fluoride containing electrolytes via an electrochemical anodization method. The NTs' geometry depend on different anodizing parameters (electrolyte type, concentration, pH, time, temperature and applied potential) that determine the relevant tube features (length, pore diameter and wall thickness). Fast-growth of iron NTs arrays were obtained with an anodization potential of 50 V in an ethylene glycol solution containing NH₄F (0.5 wt%) and H₂O (2 wt%) at 45°C. Through scanning electron microscopy (SEM) it was determined the NTs morphology, unveiling NTs features, diameter and length. Afterwards, the as-prepared NT samples were annealed under different conditions, time and temperature, in an oxygen atmosphere in order to obtain crystalline iron oxide NTs. It was observed that after 1h the iron oxide NTs start to crystallize at temperatures above 400°C. The X-ray diffraction spectrum discloses that 2 iron oxide phases are always present: magnetite (Fe₃O₄) and α -Fe₂O₃. These achievements were further corroborated by the temperature dependence of magnetization measurements, namely by the presence of a breakdown of magnetization magnitude at $T_V \sim 120$ K, arising from the electronic transition of Fe₃O₄ (Verwey transition). Additionally, and one anomaly at $T_M \sim 190$ K is also presented due to the antiferromagnetic spin flop transition of the α -Fe₂O₃ (Morin transition). The isothermal hysteresis loop proves that all the oxide NTs are ferromagnetic at room temperature with coercive fields ~ 150 Oe and up to 400 Oe for low temperatures.

References:

[1] M.Gratzel, Photoelectrochemical cells, *Nature*, 414 (2001) 338–344

[2] R.V.D. Krol, Y. Liang, J. Schoonman, *Journal of Materials Chemistry*, 18 (2008) 2311-2320

Mo.L-P92 - Influence of quenching and heat-treatment parameters on the antiferromagnetic-ferromagnetic phase transitions in Fe₄₉Rh₅₁ alloys

V. Rodionov¹, V. Rodionova¹, S. Shevyrtalov¹, M. Annaorazov¹

1. Immanuel Kant Baltic Federal University, Kaliningrad, Russia

The nearly equiatomic Fe–Rh alloys when heated without an external influences to critical temperature suffer the first-order antiferromagnetic–ferromagnetic transition. The reverse transition takes place at lower temperature. The width of thermal hysteresis can be varied by the changing of alloy's chemical content, preparation technique of the samples, heat- and mechanical treatment in wide range of temperatures. To decrease the hysteresis - it is important for technical applications. Moreover, each subsequent measurement leads to changing of the antiferromagnetic–ferromagnetic transition temperature. This research work was aimed to find quenching and heat-treatment parameters of equiatomic Fe–Rh alloy for achieving of the extremely narrow thermal hysteresis and repeatable results. The quenching was performed in different temperature range: from 1370 K down to 990 K, from 1208 down to 790, from 1073 down to 278 K. At highest temperatures (temperature of exposition) the alloy was kept for 5-400 min. The heat-treatment was performed at 1273 K for 20-72 hours and 1100 K for 20-72 hours with cooling rate of 10 K/hour. Vibrating sample magnetometer by Lake Shore was used for measurements of magnetic moment versus temperature in range of 100-950 K. The optimal parameters of quenching and heat-treatment were determined to observe thermal hysteresis of 15 K. The increasing of the temperature of exposition time leads to decreasing of temperature of transition на 14 K.

Mo.L-P93 - Ni-Mn-Sn-Co metamagnetic shape memory thin filmsI.R. Aseguinolaza^{1,2}, A.V. Svalov¹, V.A. Chernenko^{1,2,3}, J.M. Barandiaran^{1,2}1. *University of The Basque Country (UPV/EHU), Bilbao, Spain*2. *BCMaterials, Technology Park of Biscay, Derio, Spain*3. *Ikerbasque, the Basque foundation for Science, Bilbao, Spain*

Magnetic shape memory alloys (MSMAs) represent a promising kind of smart materials because of their ability to undergo large strains (>10%) under a moderate external magnetic field. This effect arises from the magnetostructural coupling in the martensitic phase. Among these compounds, metamagnetic shape memory alloys (MMSMAs) [1] show additionally the magnetic field induced reverse martensitic transformation due to the big and sudden magnetization increase from the martensite to the austenite. Such phenomenon enables the large inverse magnetocaloric and large magnetoresistance effects, making these materials appropriate for applications like magnetic refrigeration. Beyond their bulk applicability, their micro- or nanoscale functionality is especially interesting in view of the enhanced properties of the MMSMAs when they are reduced to those dimensions, as in the case of thin films [2]. On the one hand, the high area/volume ratio of the films increases the heat transfer rate per unit mass allowing high-frequency temperature actuation. On the other hand, the magnetically controlled resistivity through phase transformation permits a potential implementation in microelectronic systems. In this work, Ni-Mn-Sn-Co MMSMA 1 μm -thick films have been sputter-deposited from two pre-alloyed Ni_{46.1}Mn_{38.9}Sn_{10.1}Co_{4.9} and Ni_{44.8}Mn_{37.7}Sn_{10.8}Co_{6.7} targets, using a 150 W power and a 500 °C substrate temperature for both Si/SiO₂ and single-crystalline MgO (001) substrates. The film compositions have been studied as a function of the Ar pressure exhibiting a systematic increase of Ni and decrease of Mn contents as the pressure increases. The martensitic transformation of the films has been characterized by means of magnetic and electric resistivity measurements as a function of temperature, taking place near the room temperature and revealing a narrower transformation interval as the Ni content increases. The observed magnetization drop upon direct transformation reaches up to 42% while the electric resistivity changes by 64%, making these films suitable for the mentioned applications.

[1] R. Kainuma, Y. Imano, W. Ito, Y. Sutou, H. Morito, S. Okamoto, O. Kitakami, K. Oikawa, A. Fujita, T. Kanomata and K. Ishida, *Nature* 439, 957 (2006)

[2] R. Niemann, L. Schultz and S. Föhler, *J. Appl. Phys.* 111, 093909 (2012)

TU.A-P01 - Magneto-electric coupling, magnetoresistance and magnetocaloric effect in Ba rich quantum paraelectrics : $\text{Eu}_{0.4}\text{Ba}_{0.6}\text{TiO}_3$

R. Mahendiran¹

1. National University of Singapore, Singapore, Singapore

While BaTiO_3 is a well known ferroelectric of displacive type, ferroelectric transition is impeded in EuTiO_3 , presumably by quantum fluctuations. We have synthesized $\text{Eu}_{1-x}\text{Ba}_x\text{TiO}_3$ for a wide x from x = 0 to 1 and studied magnetism, magnetoelectric coupling, dc and ac magnetoresistance, magnetothermopower and magnetocaloric effect. Giant magnetic entropy change ($> 20 \text{ J/kg.K}$) at below 20 K has been found. Resistivity and dielectric studies indicate that charge carriers are coupled to Eu^{2+} 4f local spins. Our results indicate a correlation between magnetocapacitance and magnetoresistance in the Ba-rich compound x = 0.6. I will give overview of the physical properties of the Ba rich compositions investigated.

TU.A-P03 - Photostriction in multiferroic BiFeO₃

B. Kundys¹

1. Institut De Physique Et De Chimie Des Matériaux De Strasbourg, Strasbourg, France

The multiferroic BiFeO₃ belongs to the group of photostrictive materials [1] where the photovoltaic effect [2] linked with elastic interactions induces the deformation by light [3]. In this work we study the wavelength dependence of photostriction in BiFeO₃ and its correlation with photocurrent. As light energy decreases, the photostriction effect in a single crystal of BiFeO₃ shows a monotonous dependence and follows the photocurrent with a some delay. The light-induced charge excitation mechanism and direct light coupling to ferroelectric polarization can be used to understand such a correlation. By increasing excitation energy at the given wavelength some remnant strain levels can be observable after light is off. Therefore it appears to be extremely important to distinguish between the photostriction in spontaneous and saturated ferroelectric states. Based on recent experiments [4,5], the analogy to remnant strain effects can also be seen in photostriction. Depositing ferromagnetic film on such a photostrictive material results in its interesting photo-magneto-resistive behaviour that can be used for the light-controlled logic and memory applications in both optics and magnetic straintronics with photostrictive elements.

References:

- [1] B. Kundys, Appl. Phys. Rev. 2, 011301 (2015)
- [2] T. Choi, S. Lee, Y. J. Choi, V. Kiryukhin, & S.W. Cheong, Science 324, 63-66 (2009)
- [3] B. Kundys, M. Viret, D. Colson, D. O. Kundys, Nature Materials, 9, 803 (2010)
- [4] B. Kundys, V. Iurchuk, C. Meny, H. Majjad, B. Doudin, Appl. Phys. Lett. 104, 232905 (2014)
- [5] V. Iurchuk, B. Doudin, B. Kundys, J. Phys.: Condens. Matter (Fast track) 26 292202 (2014)

TU.A-P07 - Physical properties of Single Crystals of A-site ordered manganites REBaMn₂O₆ (RE = rear earth)

S. Yamada¹, K. Higuchi¹, T. Sasaki¹, H. Aoki¹, H. Sagayama², T.H. Arima³

1. Department of Materials System Science, Yokohama City University, Kanagawa, Japan

2. Institute of Materials Structure, High Energy Accelerator Research Organization, Ibaraki, Japan

3. Department of Advanced Materials Science, The University of Tokyo, Chiba, Japan

We have succeeded in growth of single crystals of A-site ordered perovskite manganites, REBaMn₂O₆ (RE = Sm, Eu, Tb, Gd, Dy, and Y), and investigated the physical properties. We categorize the materials into three groups in terms of the difference in magnetic properties between the single crystals (SCs) and the Pulverized samples (PSs). The first group is the compound with RE = Sm and Eu which has small magnetic moments. In contrast to the temperature dependence of magnetization of the SCs, that of the PSs does not exhibit an anomaly at ~ 200 K which is the charge rearrangement temperature and has a broad peak between the charge ordering (~ 400 K) and the rearrangement (~200 K) temperature. The second group is the compounds with RE = Y which has no magnetic moment. The temperature dependence of magnetization of the SC is the same as that of the PS. The last group is the compound with RE = Tb, Gd and Dy which has large magnetic moments, the temperature dependences of magnetization of the SCs are also same as that of the PSs. However, these magnetizations are not mainly caused by the magnetic moments manganese ions but those of rear earth ions. These results indicate when the rare earth ions have small magnetic moments in comparison with that of the manganese ions, these temperature dependence of magnetization strongly depend on the size of the samples.

We can clearly observe anomalies in temperature dependence of magnetization and electrical resistivity of the single crystals, which enable us to determine the magnetic and electric phase transition temperatures. In particular, the obtained Neel temperatures are different from the ones proposed by previously studies using polycrystalline samples. We revise the magnetic and electric phase diagram of REBaMn₂O₆.

TU.A-P08 - Structural and physical properties of multiferroic $\text{Bi}_{1-x}\text{RE}_x\text{FeO}_3$ powders (RE = Nd^{3+} , Eu^{3+}) synthesized by the sol-gel method

T. Slimani Tlempani¹, T. El Bahraoui¹, M. Taibi², G. Schmerber³, A. Belayachi¹, M. Abd-Lefdil¹, A. Dinia³

1. University of Mohammed V, Materials Physics Laboratory, Rabat, Morocco

2. University of Mohammed V, Laboratoire de Physico-Chimie des Matériaux Inorganiques et Organiques, Ecole Normale Supérieure Rabat-Morocco, Rabat, Morocco

3. IPCMS, CNRS-Université de Strasbourg, Strasbourg, France

Interrelation of magnetic and electric properties allow to manipulate transport and create new devices for writing and saving of information. Among the substances with the strong correlation between the magnetic and electrical properties are the disordered systems. Electron doping of manganese monoselenide of $\text{Mn}_{1-x}\text{Gd}_x\text{Se}$ ($0 \leq x \leq 0.7$) solid solutions may cause the chemical phase separation and nonuniform magnetic states. The aim of this work is to study the mechanism of the electrical resistivity and interrelation between the electric and magnetic subsystems depend on compounds, temperature and magnetic field. Solid solutions, as well as limit compounds MnSe and GdSe, have an antiferromagnetic ordering with $T_N=136$ K and $T_N=34$ K. The magnetic susceptibility was measured in the 77-900 K temperature range. The Neel temperature is monotonically decreased with gadolinium concentration and achieve to $T_N=88$ K for $\text{Mn}_{0.3}\text{Gd}_{0.7}\text{Se}$. The magnetic permeability and relaxation time were studied in the range of frequencies 10 Hz-100 kHz at temperatures $80 \text{ K} < T < 400 \text{ K}$. Prehistory dependence of magnetic moment at cooling without magnetic field and in magnetic field is found. The electrical resistance of $\text{Gd}_x\text{Mn}_{1-x}\text{Se}$ solid solutions has been measured at magnetic field $H=0.8$ T and at zero magnetic field within the $100 \text{ K} < T < 500 \text{ K}$ temperature range. The resistance minimum is observed at two temperatures. On heating, the composition with $x = 0.05$ exhibits the change of magnetoresistance sign from negative to positive and the magnetoresistance peak near the transition to the magnetically ordered state and at $T=375$ K. The experimental data are interpreted in the framework of the model involving the orbital ordering of electrons and the arising electrical polarization leading to the changes in the spectral density of states for electrons in the vicinity of the chemical potential in the applied magnetic field.

TU.A-P09 - Magnetic properties of the CaBaCo₃FeO₇J. Blasco¹, V. Cuartero², J. García¹, G. Subías¹, J. A. Rodríguez-Velamazán^{1,3}

1. *Instituto De Ciencia De Materiales De Aragón, CSIC-Universidad De Zaragoza, Zaragoza, Spain*
2. *ESRF-The European Synchrotron, Grenoble, France*
3. *Institute Laue Langevin, Grenoble, France*

We here report the magnetic properties of CaBaCo₃FeO₇, an isostructural compound of the ferrimagnetic pyroelectric CaBaCo₄O₇. The structure is non-centrosymmetric with Co/Fe atoms in tetrahedral coordination in four non-equivalent sites. The Co(Fe)-O sublattice is composed by Co(Fe)O₄ tetrahedra sharing corners giving rise to a geometrically frustrated network (Kagomé layer) regarding magnetic interactions. Replacing a quarter of Co atoms by Fe leads to a drastic change in the magnetic properties of the system. CaBaCo₄O₇ undergoes a ferrimagnetic transition at TC~64 K coupled to the occurrence of spontaneous electric polarization along the c-axis. The partial substitution of Co with Fe leads to a strong magnetization decrease and the disappearing of spontaneous magnetization at low temperature. In addition, the magnetic susceptibility of CaBaCo₃FeO₇ between 5 and 300 K does not obey a Curie-Weiss law and shows a rounded anomaly close to 160 K. In order to disentangle these differences, neutron diffraction measurements were performed in both samples. CaBaCo₃FeO₇ shows a magnetic structure below ~64 K with a propagation vector $k=0$ and the Co moments lie in the ab-plane forming zigzag chains along b-axis with a ferromagnetic component in the whole Kagomé layer in agreement with previous studies. The neutron thermodiffractograms of CaBaCo₃FeO₇ reveals an antiferromagnetic contribution below 160 K. The new magnetic Bragg peaks follow the propagation vector $k= (1/3, 0, 0)$ and moments mainly lie in the ac-plane forming a conic arrangement, new for this family of compounds. Refinements of neutron patterns performed above the magnetic transition indicate that the replacement of Co by Fe is not random but the Fe atoms preferentially occupy two of the four crystallographic sites. This may agree with an isovalent substitution of Co³⁺ with Fe³⁺ and changes in the magnetic interactions in Co(Fe) sublattice leading to the stabilization of a different magnetic structure.

TU.A-P10 - Metamagnetic transitions in $R_2\text{CoMnO}_6$ (R=Yb, Lu) magnetoelectric double perovskites

J. Blasco¹, J. García¹, G. Subías¹, J. Stankiewicz¹, J.L. García-Muñoz², C. Ritter³, J.A. Rodríguez-Velamazán^{1,3}

1. Instituto De Ciencia De Materiales De Aragón, CSIC-Universidad De Zaragoza, Zaragoza, Spain

2. Institut de Ciència de Materials de Barcelona, CSIC, Campus univ. de Bellaterra, Bellaterra, Spain

3. Institute Laue Langevin, Grenoble, France

$R_2\text{CoMnO}_6$ compounds, with R = Yb or Lu, adopt the crystal structure of a double perovskite with an almost perfect ordering of Co and Mn atoms in the B-position. The crystal structure is strongly distorted and the competitive magnetic interactions between neighbor atoms and next-neighbor atoms lead to the development of an E-type antiferromagnetic ordering at low temperature. This feature differentiates these compounds from $\text{La}_2\text{CoMnO}_6$ where a collinear ferromagnetic order is observed. Magnetic transition in distorted $R_2\text{CoMnO}_6$ samples is coupled to a large anomaly in the real part of the electric permittivity suggesting that these materials are very close to improper multiferroics. We have found that the dielectric anomaly disappears under a magnetic field of 5 T revealing a negative magnetocapacitance for these compounds. In order to identify the causes of this behavior, neutron diffraction patterns were collected in different conditions of temperature and external magnetic field for three selected samples: $\text{Yb}_2\text{CoMnO}_6$, YbLuCoMnO_6 and $\text{Lu}_2\text{CoMnO}_6$.

Above a critical value the external magnetic field induces similar changes in the neutron patterns of the three samples: The E-type magnetic peaks vanish whilst the intensity of some nuclear peaks increases. This fact reveals that these samples undergo a metamagnetic transition from E-type antiferromagnet into collinear ferromagnet. The critical field to produce this transition depends on the composition (higher for Lu than for Yb) and on the temperature (decreases as temperature increases). Measurements of the isothermal magnetization as function of magnetic field also show turning points at the critical field where the phase transition is produced. These measurements show hysteresis loops revealing spontaneous magnetization and an increase of coercivity as the temperature decreases. The combination of both hysteresis loops and neutron diffraction patterns allowed us to outline the H-T phase diagram that reveals the magnetic states present in these samples.

TU.A-P11 - Optical activity in multiferroic ferroborate

A.M. Kuzmenko ², A. Shuvaev ¹, V. Dziom ¹, A. Pimenov ¹, M. Schiebl ¹, A.A. Mukhin ², V.Y. Ivanov ², L.N. Bezmaternykh ³, A. Pimenov ¹

1. *Vienna University of Technology, Vienna, Austria*

2. *Prokhorov General Physics Institute, Russian Academy of Sciences, Moscow, Russia*

3. *L.V. Kirensky Institute of Physics Siberian Branch of RAS, Krasnoyarsk, Russia*

In contrast to well-studied multiferroic manganites with a spiral structure, the electric polarization in multiferroic borates is induced within collinear antiferromagnetic structure and can easily be switched by small static fields. Because of specific symmetry conditions, static and dynamic properties in borates are directly connected, which leads to giant magnetoelectric and magnetodielectric effects. Here we prove experimentally and theoretically that the giant magnetodielectric effect in samarium ferroborate $\text{SmFe}_3(\text{BO}_3)_4$ is of intrinsic origin and is caused by an unusually large electromagnon situated in the microwave range. This electromagnon reveals strong optical activity, which leads to a nonreciprocal propagation of the terahertz light.

TU.A-P12 - Giant Magnetoelectric Effect in FeCo and FeCo/Ag films on (011) oriented PIN-PMN-PT

M. Staruch¹, P. Finkel¹

1. Naval Research Laboratory, Washington, United States

To engineer large magnetoelectric coupling in composites, it is necessary to optimize the properties of both the magnetic and ferroelectric components. There has recently been much interest in single crystals of relaxor ferroelectric $\text{Pb}(\text{In}_{1/2}\text{Nb}_{1/2})\text{O}_3\text{-Pb}(\text{Mg}_{1/3}\text{Nb}_{2/3})\text{O}_3\text{-PbTiO}_3$ (PIN-PMN-PT) due to high piezoelectric coefficient with larger linear range and temperature stability than binary relaxors, which could provide for large tunability of the magnetization. In this work, thin films of FeCo and FeCo/Ag multilayers were deposited on (011) PIN-PMN-PT crystals. The coercive field was significantly decreased in the multilayer film, which also showed a larger piezomagnetic coefficient at a lower magnetic field as compared to FeCo. Angular dependence measurements of the magnetization show an in-plane easy axis that is rotated with an electric field applied to the PIN-PMN-PT crystal. Giant converse magnetoelectric coupling up to $2 \times 10^{-6} \text{ s m}^{-1}$ were observed in heterostructural composites with both FeCo and FeCo/Ag.

This work was funded by the Office of Naval Research (ONR) through the Naval Research Laboratory Basic Research Program.

TU.A-P13 - Role of Tb single ion Ising-nature on the magnetic anisotropy on TbMnO₃ under applied magnetic fields

V. Cuartero¹, S. Lafuerza¹, G. Subias², J. Garcia², E. Schierle³, J. Blasco², J. Herrero-Albillos^{2,4}

1. *European Synchrotron Radiation Facility, Grenoble, France*
2. *Instituto de Ciencia de Materiales de Aragón, Departamento de Física de la Materia Condensada, CSIC-Universidad de Zaragoza, Zaragoza, Spain*
3. *Helmholtz Zentrum Berlin Mat & Energie, Berlin, Germany*
4. *Centro Universitario de la Defensa, Universidad de Zaragoza, Zaragoza, Spain*

TbMnO₃ is a prototypical spin driven multiferroic material: magnetic competing interactions lead to a noncollinear ordering of Mn₃₊ moments oriented in the bc plane below 27 K and to the appearance of a spontaneous electric polarization (Ps). The short range ordering of Tb moments occurs at TN(Tb)=7 K. The inversion symmetry breaking due to the anisotropic magnetic interactions of Mn moments is commonly ascribed to be responsible for ferroelectricity. However, in an applied magnetic field, the strong magnetic anisotropy from Tb-spins appears to be important for the flop of the Mn cycloid with magnetic field and therefore, the flop of Ps from c- to a-axis. In order to disentangle the magnetic contributions responsible for the macroscopic magnetic anisotropic behavior under applied magnetic fields on TbMnO₃, the differentiated role of Mn and Tb ions has been investigated by soft x-ray magnetic circular dichroism (XMCD) at Tb M_{4,5} and Mn L_{2,3} edges, as a function of temperature and the intensity and direction of the applied magnetic field. Integrated XMCD signals at the Tb M_{4,5}-edge as a function of the magnetic field highly reproduce the macroscopic magnetic anisotropy at low temperatures, with the Tb moments staying along their Ising axis within the ab plane. However, a weak XMCD signal is observed at the Mn L_{2,3}-edge. These results point out that Tb₃₊ single ion anisotropy is the only responsible for the magnetic anisotropy on this multiferroic compound at high magnetic fields. Moreover, we found a negligible magnetic coupling between Mn and Tb at low temperatures under an applied magnetic field. We conclude that Tb₃₊ single-ion anisotropy is responsible for the magnetic anisotropy on TbMnO₃ at high magnetic fields and also plays a highly relevant role on its magnetic field-induced electric polarization flop.

TU.A-P14 - Theoretical prediction of spin-valley coupling in 5d transition-metal oxides

K. Yamauchi¹, P. Barone², T. Shishidou³, T. Oguchi¹, S. Picozzi²

1. *ISIR-Sanken, Osaka University, Osaka, Japan*

2. *CNR-SPIN, Genova, Italy*

3. *AdSM, Hiroshima University, Hiroshima, Japan*

Spin-orbit coupling plays a considerably important role in spintronic phenomena, such as magnetoelectric effects, magnetic anisotropy, etc. Among them, the Rashba effect, which removes the spin degeneracy in non-magnetic materials, has appealing potential for spin-FET applications. Although the Rashba effect commonly occurs at interfaces or surfaces where inversion symmetry is broken, it was recently suggested that Rashba splitting might also occur in non-centrosymmetric (polar or ferroelectric) bulk materials, such as BiTeI or GeTe. When the Rashba splitting extends over two valleys in k space and results in two non-degenerate spin states, it is called spin-valley coupling. For example, a monolayer of MoS₂ shows a valley Hall effect due to a strong spin-valley coupling. Based on an *ab initio* materials-design approach, we study “bulk spin-valley coupling” in newly designed perovskite oxides. Aiming at a sizable spin splitting, low-spin 5d transition metal ions are embedded in host ferroelectric oxides with LiNbO₃-type structure. Our calculations clarified that the spin-orbit coupling splits t_{2g} orbital states of the transition metal ion into $j_z=+1/2$ and $j_z=-1/2$ states at the valence-band top around K and K' points in the hexagonal Brillouin zone. In this talk, the microscopic mechanism for the spin-valley coupling in our novel oxide system will be discussed and compared with the monolayer MoS₂ case.

This work is supported by a Grant-in-Aid for Young Scientists (B) from the Japan Society for the Promotion of Science (No 26800186).

TU.A-P15 - Crossover from paramagnetism to superparamagnetism in zinc ferrite nanoparticles: X-Ray Absorption Spectroscopy studyS. Gautam¹, J. Pal Singh², R.C. Srivastva³, K. Asokan⁴, D. Kanjilal⁴, K. Hwa Chae²

1. Dr. SSB, University Institute of Chemical Engg. & Tech., Panjab University Chandigarh, Chandigarh, India
2. Advanced Analysis Center, Korea Institute of Science & Technology, Seoul, South Korea
3. Deptt of Physics, Govind Ballabh Pant Univ. of Agri and Tech, Pantnagar, Uttarakhand, India
4. Materials Science Division, Inter University Accelerator Centre, New Delhi, India

Magnetism in zinc ferrite nanoparticles has been topic of great understanding due to presence of different magnetic ordering like ferromagnetic, ferromagnetic and antiferromagnetism [1]. In this work zinc ferrite nanoparticles were investigated, which exhibit superparamagnetic as well as paramagnetic behaviour. Zinc ferrite nanoparticles of different sizes (61 nm (ZF61), 32 nm (ZF32), 19 nm (ZF19), and 13 nm (ZF13))were synthesized by nitrate method. The samples ZF61 and ZF32 exhibit paramagnetic nature, while samples ZF19 and ZF13 are superparamagnetic [2]. Crossover from paramagnetism to superparamagnetism has been studied using NEXAFS spectra at Fe L-edge and O K-edge (figure not shown). Fe L-edge spectra exhibit spectral features at 709, 711, 722, 724 eV, which occurs due to Fe (2p) core level in effect of spin-orbit coupling give rise to degenerate state $2p_{3/2}$ (~708 eV) and $2p_{1/2}$ (~721 eV). Presence of octahedral crystal fields lifts the degeneracy of the $2p_{3/2}$ and $2p_{1/2}$ levels so that two levels with t_{2g} and e_g symmetry [2]. The spectral features present in the spectra favors the ferromagnetic high spin $3d^5$ configuration of Fe. In ferrites, Fe L-edge spectra occur due to Fe (2p) core level. Though the shape of spectral features of Fe L-edge spectra for all samples is almost same however spectra for samples ZF32 and ZF61 have more intense spectral features. These spectral features are more distinguished in difference spectra. O K-edge spectra exhibit spectral features ~ 527 eV (A2), 530 eV(B2), 534eV (C2), 538 eV (D2), 545 eV (E3). The variation of e_g and t_{2g} feature in O K-edge is varied with respect to the annealing (size) effect. The behavior is also supported by Fe L-edge spectra. Spectral features for ZF61 and ZF32 are enhanced than that of ZF19 and ZF13. It may be contemplated that the strengthening of the local electronic structure of zinc ferrite nanoparticle and successfully correlated the spin-orbit coupling with the magnetic properties and hence strengthening of density of states.

References:

1. S.H. Lee, C. Broholm, W. Ratcliffe, et al., Nature 418 (2002) 856
2. Jitendra Pal Singh, Gagan Dixit et al., Bull. Mat. Sci. 36 (2013) 751-754

TU.A-P16 - Charge ordering, Ferroelectric, and Magnetic Domains in LuFe₂O₄ Observed by Scanning Probe Microscopy

Y.H. Jeong¹, I. Yang¹

1. Dept of Physics, POSTECH, Kyungbuk, Republic of Korea

LuFe₂O₄ is a multiferroic system which exhibits charge order, ferroelectricity, and ferrimagnetism simultaneously below ~230 K. The ferroelectric/charge order domains of LuFe₂O₄ are imaged with both piezoresponse force microscopy (PFM) and electrostatic force microscopy (EFM), while the magnetic domains are characterized by magnetic force microscopy (MFM). Comparison of PFM and EFM results suggest that the proposed ferroelectricity in LuFe₂O₄ is not of usual displacive type but of electronic origin. Simultaneous characterization of ferroelectric/charge order and magnetic domains by EFM and MFM, respectively, on the same surface of LuFe₂O₄ reveals that both domains have irregular patterns of similar shape, but the length scales are quite different. The domain size is approximately 100 nm for the ferroelectric domains while the magnetic domain size is much larger and gets as large as 1 μ m. We also demonstrate that the origin of the formation of irregular domains in LuFe₂O₄ is not extrinsic but intrinsic.

TU.A-P17 - Polarization modulation induced by a magnetic field in polar oxide α -Cu₂V₂O₇Y.H. Jeong¹, Y. Lee¹, S. Lee²

1. Dept of Physics, POSTECH, Kyungbuk, Republic of Korea

2. Dept of Physics, Univ of Virginia, Charlottesville, United States

α -Cu₂V₂O₇ is a complex oxide material with an unusual polar structure and antiferromagnetic ground state. We have investigated the variation of induced electric polarization under a magnetic field in this canted antiferromagnet with flux grown single crystalline samples. We have also thoroughly examined the currently available theoretical models to account for the magnetically induced polarization variation in α -Cu₂V₂O₇.

The crystal structure of α -Cu₂V₂O₇ adopts a orthorhombic structure with space group *Fdd2* (no. 43), and the lattice parameters of $a = 20.66 \text{ \AA}$, $b = 8.39 \text{ \AA}$, and $c = 6.44 \text{ \AA}$. α -Cu₂V₂O₇ consists of cross-linking chains of CuO₅ polyhedra with one chain parallel to the [011] direction and another parallel to [0-11] direction. These chains are then separated by V₂O₇ anion groups. While all copper atomic positions are equivalent above Neel temperature T_N , but below T_N four Cu sites must be considered independently since the spin directions are different in each Cu ion. Of five oxygen ions surrounding the Cu ion, four oxygen ions show shorter bonds of $1.91 \sim 1.94 \text{ \AA}$ to Cu and one oxygen a longer bond of 2.56 \AA .

Currently there are several available microscopic models for magnetically induced ferroelectricity. The most prevailing model is the spin current mechanism, or equivalently the inverse Dzyaloshinskii-Moriya mechanism. In a crystal which contains multiple inequivalent magnetic sites, the collinear spin structure may also induce ferroelectricity due to magnetostriction. The third one, which is less known, is the magnetic-metal-ligand *p-d* hybridization mechanism. While the magnetically induced polarization modulation of α -Cu₂V₂O₇ cannot be accounted for by the spin current model nor by the exchange striction mechanism, it is adequately described by the spin-dependent *p-d* hybridization between the transition metal Cu and ligand O via the spin-orbit interaction. We discuss the implication of the present result from the viewpoint of multiferroics materials search.

TU.A-P18 - The magnetic properties of SrCo₂Ti₂Fe₈O₁₉ compound

M. Mihalik¹, M. Mihalik¹, M. Zentková¹, V. Eremenko², V. Sirenko², A. Mikhailovich Balbashov³

1. *Institute of Experimental Physics SaS, Košice, Slovak Republic*

2. *B. I. Verkin Institute for Low Temperature Physics and Engineering, Kharkov, Ukraine*

3. *Moscow power engineering institute, Moscow, Russian Federation*

An increasing degree of interest has been paid to hexaferrites since their discovery in 1950s due to their interesting magnetic, ferroelectric and multiferroic properties which determine application potential of hexaferrites in the field of permanent magnets, microwave or data storage devices. We present the magnetic measurements performed on M-type hexaferrite SrCo₂Ti₂Fe₈O₁₉ single crystal. We have found that the compound orders magnetically at a little bit higher temperature (TC = 768 K) than the parent, SrFe₁₂O₁₉ compound (TC = 732 K) [1]. SrCo₂Ti₂Fe₈O₁₉ undergoes another order-to-order magnetic phase transition at T₁ = 380 K and the magnetization data exhibit additional maximum at 329 K. The bifurcation point of zero-field-cooled (ZFC) and field-cooled (FC) curves was found to be T_b = 763 K, but at lower temperatures the ZFC curve crosses FC curve two times: at 384 K and 345 K. The hysteresis loops measured at T = 350 K with magnetic field applied in basal plane reach magnetization 36 Am²kg⁻¹ at applied magnetic field of 5 T and the hysteresis loop has coercivity of -800 Am⁻¹. At temperature T = 500 K (above T₁) the hysteresis loop has coercivity of 3.2 kAm⁻¹, but the highest-reachable magnetization at field of 5 T amounts 11.5 Am²kg⁻¹.

The imaginary part of AC susceptibility exhibit frequency-dependent maximum, which occurs at temperature below 40 K at frequency 1 Hz and increases to 75 K for frequency 884 Hz. This observation might signal the dynamics and the complexity of the magnetic structure.

Concluding, the magnetization data suggest that SrCo₂Ti₂Fe₈O₁₉ compound can have application potential at room temperature and elevated temperatures. This compound can be used also for basic studies of magnetic dynamics of M-type hexaferrites.

[1] R. C. Pullar, Prog. Mat. Sci. 57 (2012), 1191-1334

TU.A-P19 - Magnetic and magnetodielectric behavior of GdCrTiO₅ and its implications

T. Basu¹, K. Singh¹, K.K. Iyer¹, E.V. Sampathkumaran¹

1. Tata Institute of Fundamental Research, Mumbai, India

The compound NdCrTiO₅, consisting of two magnetic sub-lattices (Nd and Cr), shows magnetodielectric (MDE) coupling and magnetism induced ferroelectricity around magnetic ordering temperature (T_N = 21 K) [1]. It is believed that Cr sublattice orders at T_N, whereas Nd sub-lattice orders near 11 K.

Here, we report the results of our investigation of dc magnetization (M), heat-capacity (C), and dielectric behavior of the Gd analogue GdCrTiO₅ down to 2K. We do not find any evidence down to 2 K for the long-range magnetic ordering of the Gd sub lattice; however, M(T) and C(T) data reveal some features around 10 K, attributable to magnetic ordering from Cr. Thus, T_N for the sub-lattice in the Gd case is suppressed with respect to that in the Nd case. Another point of emphasis is that, at the same temperature, dielectric constant exhibits a weak anomaly, which gets stronger with the application of external magnetic fields, supporting the existence of MDE coupling. This relative weakness of MDE behavior in comparison with that in the Nd case is surprising considering larger magnetic moment on Gd. On the basis of these results, we speculate that 4f-anisotropy and/or 4f-hybridization (which is stronger in light rare-earths) play a dominant role over the magnitude of the rare-earth magnetic moment in deciding T_N as well as MDE coupling in this series.

[1]. J. Hwang et al, Phys. Rev. B 85, 024415 (2012)

TU.A-P20 - Magnetic ordering in multiferroics Ba(Fe,Nb)O₃ AND Pb(Fe,Nb)O₃ observed by mssbauer spectrometry

T. Kmjec¹, J. Kohout¹, K. Zaveta¹, D. Kubaniova¹, V.V. Laguta², I.P. Raevsky³

1. Faculty of Mathematics and Physics, Charles University in Prague, Prague, Czech Republic

2. Institute of Physics, Academy of Sciences of the Czech Republic, v. v. i., Prague, Czech Republic

3. Department of Physics and Research Institute of Physics, Southern Federal University, Rostov on Don, Russia

The multiferroic materials Ba(Fe,Nb)O₃(BFN) and Pb(Fe,Nb)O₃(PFN) studied in this work belong to the family of single-phase perovskites exhibiting high value of dielectric permittivity [1]. The aim of our study was to estimate the value of the transition temperature to magnetically ordered state from the temperature dependences of the hyperfine parameters. Tablets of ceramics of BFN and PFN were prepared by solid state reaction.

Our samples were characterized by XRD to check phase composition, crystal structure and lattice constant(s). Their chemical composition and homogeneity were confirmed by SEM and XRF. Sample BFN is single phase whose crystal structure at room temperature was found to be cubic (Pm-3m) with a=4.06(3) Å [2]. Two phases were identified in PFN sample: pure monoclinic (C1m1) PFN (~97.2%) with a=5,67(6) Å, b=5,67(3) Å, c=4,02(8) Å, beta=89.826(5)°, [3] and as impurity FCC (F4/m-32/m) alfa-LiFeO₂ (~2.8%) with a=4,16(1) Å. The Mssbauer spectra were acquired in the temperature range 4.2-300 K with in-field spectra taken in external fields up to 6 T at 4.2 K. In summary, magnetic ordering transition was found in a relatively wide range of temperatures around 30 K (BFN) and 40-80 K (PFN). The spectra of both BFN and PFN at 4.2 K are consistent with random distribution of Fe and Nd atoms. In-field spectra of BFN indicate antiferromagnetic ordering while in PFN two sublattices with magnetization oriented parallel and antiparallel to the applied field exist. Temperature dependences of Isomer Shift above the magnetic transition temperature correspond to the second order Doppler shift.

Acknowledgements: This work was supported by the research grants GACR No. 13-11473S and GAUK No.: 8313/2013

[1] I. P. Raevski, et al., J. Appl. Phys., 93 (2003) 4130-4136

[2] S. Eitsayeam et al., Current Applied Physics 9 (2009) 993-996 [3] V. Bonny et al., Solid State Commun. 102(1997) 347

TU.A-P21 - Anisotropic orbital occupation and Jahn-Teller distortion of orthorhombic YMnO₃ epitaxial films: a combined experimental and theoretical study on polarization-dependent x-ray absorption spectroscopy

J.M. Chen¹, S.C. Haw^{1,2}, J.M. Lee¹, S.A. Chen^{1,2}, K.T. Lu¹, P.A. Lin³, C.H. Lee², M.T. Lee¹, T.W. Pi¹, Z. Hu⁴

1. National Synchrotron Radiation Research Center, Hsinchu, Taiwan

2. Department of Engineering and System Science, National Tsing Hua University, Hsinchu, Taiwan

3. Department of Physics, National Tsing Hua University, Hsinchu, Taiwan

4. Max Planck Institute for Chemical Physics of Solids, Dresden, Germany

The b-axis oriented orthorhombic YMnO₃ (o-YMnO₃) epitaxial films on a YAlO₃ (010) substrate were fabricated with pulsed-laser deposition. The anisotropic orbital occupation and Jahn-Teller (JT) distortion of an o-YMnO₃ film were investigated with polarization-dependent x-ray absorption spectra and configuration-interaction multiplet-cluster calculations. A significant energy difference, ~3.8 eV, for the main white line along E//b and E//a in polarization-dependent Mn K-edge spectra of o-YMnO₃ indicates an extraordinary JT distortion and significant anisotropic Mn-O bonding within the ab plane in the o-YMnO₃ film. Most importantly, although the orbital occupation of 3d electrons in o-YMnO₃ films is almost the same as that in single crystalline o-DyMnO₃, the JT distortion of o-YMnO₃ films is larger than that of single crystalline o-DyMnO₃, deduced from the multiplet calculations. We speculate that this JT distortion predominantly contributes to the origin of the cycloidal spin deformation in bulk o-YMnO₃, because of a suppressed nearest-neighbor (NN) superexchange interaction and an enhanced next-nearest-neighbor (NNN) superexchange interaction. These complementary results provide insight into the origin of the E-type magnetic configuration of o-YMnO₃.

TU.A-P22 - Uniaxial-stress control of spin-driven ferroelectricity in multiferroic Ba₂CoGe₂O₇

T. Nakajima¹, Y. Tokunaga^{1,3}, V. Kocsis^{1,2}, Y. Taguchi¹, Y. Tokura^{1,4}, T.H. Arima^{1,3}

1. RIKEN Center For Emergent Matter Science, Saitama, Japan

2. Department of Physics, Budapest University of Technology and Economics, Budapest, Hungary

3. Department of Advanced Materials Science, University of Tokyo, Chiba, Japan

4. Department of Applied Physics and Quantum-Phase Electronics Center, University of Tokyo, Tokyo, Japan

We demonstrate that spin-driven ferroelectricity in a tetragonal multiferroic Ba₂CoGe₂O₇ is controlled by applying uniaxial stress. This system is known to exhibit a simple collinear antiferromagnetic order, in which the magnetic moments are aligned along the a or b axis, below TN = 6.7 K [1]. By applying a magnetic field of ~0.4 T along the [110] direction, the magnetic moments are rotated so as to be perpendicular to the magnetic field. This rotation breaks the fourfold rotoinversion symmetry of the crystal, and consequently spontaneous electric polarization appears along the c axis [2]. In the present study, we performed pyroelectric measurements under applied compressive uniaxial stress of up to 100 MPa along the [110] direction, in zero magnetic field. As a result, we found that the field-induced ferroelectric phase is also induced by the application of uniaxial stress, which can affect the magnetic anisotropy of the Co²⁺ ions through tiny deformation of the crystal. We have also demonstrated that magnetic-field variations of the spin-driven electric polarization can be tuned by the application of the uniaxial stress. These results suggest that an application of 'anisotropic' stress, which is the simplest way to control symmetry of matter, can induce a variety of cross-correlated phenomena in spin-driven multiferroics.

This work has been published as Phys. Rev. Lett. 114, 067201 (2015).

References:

[1] M. Soda et al., Phys. Rev. Lett. 112, 127205 (2014)

[2] H. Murakawa et al., Phys. Rev. Lett. 105, 137202 (2010)

TU.A-P23 - Evolution of magnetic and crystallographic transition in $\text{Cu}_{1-x}\text{Zn}_x\text{Fe}_2\text{O}_4$ studied by neutron powder diffractionF. Chang¹, M. Avdeev², J. Bertinshaw¹, G. Deng², X. Wang³, C Ulrich^{1,2}*1. School of Physics, University of New South Wales, Kensington, Australia**2. The Bragg Institute, Australia Nuclear Science and Technology Organization, Lucas Heights, Australia**3. The Institute for Superconducting & Electronic Materials, University of Wollongong, Wollongong, Australia*

CuFe_2O_4 is a highly interesting material as a ferrimagnet with an unusual high ordering temperature up to 780 K, while ZnFe_2O_4 is a frustrated spin system with antiferromagnetic order below 10 K. High and high intensity neutron powder diffraction were applied to study the crystallographic and magnetic phase transition in $\text{Cu}_{1-x}\text{Zn}_x\text{Fe}_2\text{O}_4$ from 4 K to 750 K, combined with magnetization measurement from 10 K to 950 K. Fully inverse CuFe_2O_4 was obtained with all the Cu^{2+} occupying the octahedral sites. Structural phase transition from cubic to tetragonal phase was observed, which is caused by Jahn-Teller Cu^{2+} ions with two-fold e_g orbital degeneracy, resulting in the stretching of CuO_6 octahedra along c axis. Ferrimagnetic order was observed with spin ordered along c axis in CuFe_2O_4 . Short-range antiferromagnetic scattering peak was observed below 10 K in cubic ZnFe_2O_4 and this ordering is strongly restrained by addition of slightly amount of Cu^{2+} ions. All the doped $\text{Cu}_{1-x}\text{Zn}_x\text{Fe}_2\text{O}_4$ ($x = 0.2 - 0.8$) samples crystallize cubic structure and form ferrimagnetic spin configuration. Upon doping, ferrimagnetic order temperature was gradually reduced from 789 K. Collinear spin setting was observed and no indication of frustration was found even up to doping rate of $x = 0.8$. Highly frustrated $\text{Cu}_{0.04}\text{Zn}_{0.96}\text{Fe}_2\text{O}_4$ and ZnFe_2O_4 behave short-range antiferromagnetic order, as well as high Curie-Weiss temperature ($T_{\text{CW}} = 112$ K and 43 K, respectively) induced by the competing between ferromagnetic interaction from first-nearest neighbour and antiferromagnetic interaction from the third-nearest neighbour in tetrahedron formed by Fe ions on B sites.

TU.A-P24 - Strain-induced multiferroicity in antiferromagnetic SrMnO₃ thin films

L. Maurel^{1,2}, C. Becher³, U. Aschauer³, M. Lilenblum³, R. Guzman^{1,4}, C. Magen^{1,4,5}, D. Meier³, E. Langenberg¹, M. Trassin³, J. Blasco^{2,6}

1. Instituto De Nanociencia De Aragón, Universidad de Zaragoza, Zaragoza, Spain
2. Departamento de Física de la Materia Condensada, Universidad de Zaragoza, Zaragoza, Spain
3. Department of Materials, ETH Zürich, Zurich, Switzerland
4. Laboratorio de Microscopías Avanzadas (LMA), Instituto de Nanociencia de Aragón, Universidad de Zaragoza, Zaragoza, Spain
5. Fundación ARAID, Zaragoza, Spain
6. Instituto de Ciencia de Materiales de Aragón, Universidad de Zaragoza-CSIC, Zaragoza, Spain
7. Forschungszentrum Jülich, Peter-Grünberg-Institut (PGI-6), Jülich, Germany, currently at: Institut für Optik und Atomare Physik, Berlin, Germany
8. Departamento de Ciencia y Tecnología de Materiales y Fluidos, Universidad de Zaragoza, Zaragoza, Spain

Multiferroic materials exhibiting two or more ferroic orders have gained a lot of interest owing to the development of new mechanisms that increase the coupling between their properties. This development is expected to give rise to new devices where the electric control of the magnetic properties would open new concepts in the field of the data storage. One very promising mechanism is by means of strain engineering, where the artificial expansion of the unit cell in the perovskite system AMnO₃ (where A is an alkaline-earth cation such as Ca, Sr or Ba) is predicted to bring the system into a multiferroic state[1]. Two different approaches have been chosen to induce multiferroicity in this system: first of all, theoretical calculations[2] predicted a ferroelectric state in epitaxially strained SrMnO₃ thin films; secondly, above 45% Ba doping in bulk SrMnO₃ was shown to induce a ferroelectric behavior[3]. In this work we have used pulsed laser deposition to grow strained epitaxial SrMnO₃ thin films, and X-ray diffraction and transmission electron microscopy to show their high crystal quality and strain state. Then, through second harmonic generation measurements we have shown the emergence of a polar state induced by epitaxial strain. Furthermore, in agreement with theoretical studies in similar materials[4], we have found that epitaxial strain induces the formation of oxygen vacancies, concomitantly increasing the unit cell volume more than expected by the elastic deformation alone. Our observations using scanning probe microscopy, together with first-principle calculations, show that these defects get ordered and give rise to oxygen-deficient insulating walls separating conducting polar nanodomains.

- [1] S. Bhattacharjee et al., PRL 102, 117602 (2009)
[2] J. H. Lee and K. M. Rabe., PRB 104, 207204 (2010)
[3] H. Sakai et al., PRL 107, 137601 (2011)
[4] U. Aschauer et al., PRB 88, 054111 (2013)

TU.A-P26 - Pseudocubic phase stabilization of epitaxial (Sr_{1-x}Ba_x)MnO₃ thin films

E. Langenberg^{1,2}, R. Guzmán^{1,3}, L. Maurel^{1,4}, L. Martínez de Baños¹, L. Morellón^{1,4}, R. Ibarra^{1,4}, J. Blasco^{4,5}, C. Magén^{1,3,6}, P.A. Algarabel^{4,5}, J.A. Pardo^{1,7}

1. Institute of Nanoscience of Aragon (University of Zaragoza), Zaragoza, Spain
2. Centro de Investigación en Química Biológica y Materiales Moleculares (CIQUS), University of Santiago de Compostela, Santiago de Compostela, Spain
3. Laboratorio de Microscopías Avanzadas, Institute of Nanoscience of Aragon (University of Zaragoza), Zaragoza, Spain
4. Departamento de Física de la Materia Condensada, University of Zaragoza, Zaragoza, Spain
5. Instituto de Ciencia de Materiales de Aragón, University of Zaragoza-CSIC, Zaragoza, Spain
6. Fundación ARAID, Zaragoza, Spain
7. Departamento de Ciencia y Tecnología de Materiales y Fluidos, University of Zaragoza, Zaragoza, Spain

The possibility of controlling the magnetization (polarization) by an electric (magnetic) field in materials displaying ferroelectric and magnetic order in the same phase, so-called multiferroic materials, has triggered great amount of research in the last few years. However, very few of them have been proved to show strong magnetoelectric coupling, mainly due to the different mechanisms of ferroelectricity and magnetism in these compounds. Exception could be found, though, in perovskite AMnO₃ system (A = Ca, Sr, Ba), in which Mn⁴⁺ is expected to be able to drive both the magnetic order and the required non-centrosymmetric distortion for ferroelectric order. Yet ferroelectricity is allowed in this system, solely, when the unit cell volume is large enough to promote Mn off-centring [1], which may be achieved by using increasingly larger A cation, as partially replacing Sr with Ba [2]. However, increasing the size of the A-cation also destabilizes the perovskite structure, becoming different hexagonal polymorphs the ground state phase [3].

Here, we report the pseudocubic phase stabilization of (Sr_{1-x}Ba_x)MnO₃, 0.1 ≤ x ≤ 0.5, (SBMO) epitaxial thin films grown by pulsed laser deposition from bulk polycrystalline hexagonal phase targets onto (001)-oriented perovskite substrates. X-ray diffraction measurements show that, under appropriate deposition conditions, the perovskite pseudocubic phase with cube-on-cube growth is stabilized over the non-ferroelectric hexagonal phase. Moreover, we have managed to grow epitaxial tensile strained SBMO films, ranging from 0% to 4% strain. Selected films were observed by aberration corrected scanning transmission electron microscopy, which proves the homogeneity and defect-free crystal quality of the films, and corroborate the epitaxial coherent growth and the pseudocubic structure of the films.

[1] S. Bhattacharjee *et al.*, *Phys. Rev. Lett.* 102, 117602 (2009)

[2] H. Sakai *et al.*, *Phys. Rev. Lett.* 107, 137601 (2011)

[3] J. M. Rondinelli *et al.*, *Phys. Rev. B* 79, 205119 (2009)

TU.A-P27 - Electric Control of the Local Magnetic Moment in Multiferroic Compound $\text{Ba}_2\text{CoGe}_2\text{O}_7$

M. Soda¹, S. Hayashida¹, B. Roessli², M. Mansson², J. White², M. Matsumoto³, R. Shiina⁴, T. Masuda¹

1. Neutron Science Laboratory, Institute for Solid State Physics, University of Tokyo, Chiba, Japan

2. Laboratory for Neutron Scattering and Imaging, Paul Scherrer Institut, Villigen, Switzerland

3. Department of Physics, Shizuoka University, Shizuoka-Ken, Japan

4. Department of Materials Science and Technology, Niigata University, Niigata, Japan

Electric control of a local-magnetic moment is studied in multiferroics $\text{Ba}_2\text{CoGe}_2\text{O}_7$ by using a polarized-neutron-diffraction technique. Below 6.7 K, $\text{Ba}_2\text{CoGe}_2\text{O}_7$ exhibits a collinear-antiferromagnetic structure with the easy axis along $\langle 100 \rangle$ directions and an antiferroelectric order with the polarization axis along [001] direction. The magnitude and direction of the electric polarization depend on the local relationship between the Co spin and the O ions in a local CoO_4 tetrahedron, which is explained by the spin-dependent d-p hybridization mechanism. The result of the neutron experiment shows that the magnetic intensities at the Q-points with $h > 0$ and $k > 0$ decrease with applying an electric field along the c-axis. In contrast the magnetic intensities at the Q-points with $h > 0$ and $k < 0$ increase with the field. On the assumption that the polarization direction does not deviate from the c-axis, the spin-dependent d-p hybridization mechanism leads to the constraint that the magnetic moment is confined in the c-plane. Then, the electric-field dependence of the intensities is consistent with the model that the direction of the magnetic moment rotates from $\langle 100 \rangle$ to [110] with the field. The present study revealed the novel magnetoelectric effect that the direction of the local-magnetic moment is controlled continuously by the electric field.

TU.A-P28 - Tunable metamagnetic transitions in a mixed-valent ferromagnet

N. Lee¹, H.Y. Choi¹, M.S. Seo², S.Y. Park², Y.J. Jo³, Y.J. Choi¹

1. *Yonsei University, Seoul, Republic of Korea*

2. *Korea Basic Science Institute, Seoul, Republic of Korea*

3. *Kyungpook University, Daegu, Republic of Korea*

Metamagnetic transition which undergoes an abrupt increase of magnetization in a magnetic field is a crucial subject in magnetism, motivated by a desire to enhance certain functionalities utilizing different means of tuning parameters. Here we present remarkable controllability of metamagnetic transitions in our first-synthesized double perovskite single crystals of $\text{Eu}_2\text{CoMnO}_6$ in which ferromagnetic order emerges below $T_c=122$ K along the crystallographic c axis. In an as-grown crystal, magnetic susceptibility exhibits a pronounced peak at ~ 117 K indicating a spin-glass behavior, and isothermal magnetization at 5 K reveals a metamagnetic transition. We demonstrate the control of relative portions of ferromagnetic and spin-glass states by annealing the crystals in different gas environments, resulting in the retardation (after Ar-annealing) and bifurcation (after O₂-annealing) of the metamagnetic transition. This remarkable variation offers an efficient approach of manipulating metamagnetic transitions.

TU.A-P29 - Strong ferromagnetic-dielectric coupling in multiferroic Lu₂CoMnO₆ single crystals

N. Lee¹, H.Y. Choi¹, Y.J. Jo², M.S. Seo³, S.Y. Park³, Y.J. Choi¹

1. *Yonsei University, Seoul, Republic of Korea*

2. *Kyungpook National University, Daegu, Republic of Korea*

3. *Korea Basic Science Institute, Seoul, Republic of Korea*

We have grown single crystals of multiferroic double-perovskite Lu₂CoMnO₆ and studied the directional dependence of their magnetic and dielectric properties. The ferromagnetic order emerges below $T_C=48$ K along the crystallographic c axis. Dielectric anomaly arises along the b axis at T_C , contrary to the polycrystalline work suggesting ferroelectricity along the c axis. Through the strongly coupled ferromagnetic and dielectric states, the highly non-linear variation of both dielectric constant and magnetization was achieved in application of magnetic fields. This concurrent tunability provides an efficient route to manipulation of multiple order parameters in multiferroics.

TU.A-P30 - Key features of the magnetic and magnetoelectric properties of rare-earth multiferroic $\text{HoFe}_3(\text{BO}_3)_4$

Y.F. Popov¹, A.I. Popov^{2,3}, G.P. Vorob'ev¹, V.Y. Ivanov⁴, A.A. Mukhin⁴, N. Kostyuchenko^{2,4}, A.K. Zvezdin^{2,4}

1. *Lomonosov Moscow State University, Moscow, Russia*

2. *Moscow Institute of Physics and Technology, Dolgoprudny, Moscow region, Russia*

3. *National Research University of Electronic Technology, Zelenograd, Moscow, Russia*

4. *A. M. Prokhorov General Physics Institute of Russian Academy of Sciences, Moscow, Russia*

Recently a new class of multiferroics, rare-earth $\text{RFe}_3(\text{BO}_3)_4$ ferroborates have been discovered [1]. Among them holmium iron borates $\text{HoFe}_3(\text{BO}_3)_4$ is of substantial interest due to its rich magnetic and magnetoelectric properties including low temperature spontaneous spin-reorientation as well as quite a large (in terms of potential applications) value of the magnetoelectric effect [1-3].

In the present work, we have studied experimentally and theoretically the magnetic and magnetoelectric properties of rare-earth iron borates using holmium iron borate as an example. We measured magnetization, magnetic susceptibility and polarization of $\text{HoFe}_3(\text{BO}_3)_4$ single crystals. The measurement of the field dependences up to 200 kOe of the magnetoelectric polarization along the a axis, Pa revealed that the longitudinal, Pa(Ha) and transverse, Pa(Hb) magnetoelectric effects have the opposite signs and magnetically induced polarization changes its sign in a field close to the field of exchange between Ho^{3+} and Fe^{3+} ions. These dependences agree well with theoretical predictions based on the symmetry of the compounds. Energy levels and wave functions Ho^{3+} ion were defined. A self-consistent description of the magnetization, magnetic susceptibility and electric polarization has been made. The quantum theory of the magnetoelectric effect developed in [4] has been applied to $\text{HoFe}_3(\text{BO}_3)_4$. We show that the leading role in the origins of the magnetoelectric effect belongs to the single-ion mechanisms: the electron mechanism linked to the magnetic field-induced electric dipole moment in the 4f -electron shell, and the ion mechanism connected to electric polarization arising from the relative spatial shift of the ions in magnetic field.

1. A. M. Kadomtseva, Yu. F. Popov, G. P. Vorobev, A. P. Pyatakov, et al, *Low Temp. Phys.* 36, 511 (2010)

2. K.-C. Liang, R. P. Chaudhury, B. Lorenz, Y. Y. Sun, L. N. Bezmaternykh, I. A. Gudim, V. L. Temerov and C. W. Chu, *Phys. Rev. B*, 80, 104424 (2009)

3. A. M. Kadomtseva, G. P. Vorob'ev, Yu. F. Popov, A. P. Pyatakov, A. A. Mukhin, V. Yu. Ivanov, A. K. Zvezdin, et al, *JETP*, Vol. 114, 810 (2012)

4. A. I. Popov, D. I. Plokhov, and A. K. Zvezdin, *Phys. Rev. B*, 87, 024413 (2013)

TU.A-P33 - Large low field room temperature magneto-dielectric response from $(\text{Sr}_{0.5}\text{Ba}_{0.5})\text{Nb}_2\text{O}_6$ / $\text{Co}(\text{Cr}_{0.4}\text{Fe}_{1.6})\text{O}_4$ bulk 3-0 composites

S. Vitta², S. Rathore¹

1. *Indian Institute of Technology Bombay, Mumbai, India*

Bulk magnetodielectric composites with a 3-0 configuration comprising of ferroelectric-magnetostrictive phases have been synthesized using $(\text{Sr}_{0.5}\text{Ba}_{0.5})\text{Nb}_2\text{O}_6$ / $\text{Co}(\text{Cr}_{0.4}\text{Fe}_{1.6})\text{O}_4$ as the two constituents respectively. The ferroelectric phase made by a dual stage sintering process has a uniform grain size of 15 μm while the magnetostrictive phase has a grain size of 2 - 3 μm . Composites synthesized by conventional solid state processing using these two constituents exhibits large magnetodielectric coupling at room temperature which increases with increasing magnetic field. The composite with 30 % magnetostrictive phase distributed uniformly in the ferroelectric phase has the most desirable microstructure and exhibits a large coupling with 3.2 % change in the dielectric constant at 1 kHz and 8 kOe magnetic field. This change in dielectric constant decreases when the fraction of magnetostrictive phase is varied, indicating that 30 % is the optimal value to realize large coupling between the two phases. The change in magnetodielectric constant upon application of an external magnetic field could be due to the inherent magnetoresistance of the magnetic component. These result however confirm that 3D percolation causes the coupling to decrease in composites.

TU.A-P34 - Effect of magnetic and non-magnetic substitution on properties of magnetoelectric $\text{Ba}_3\text{NbFe}_3\text{Si}_2\text{O}_{14}$

S.S. Rathore^{1,2}, S. Vitta¹

1. *Indian Institute of Technology Bombay, Mumbai, India*

2. *University of Petroleum and Energy Studies, Dehradun, India*

The effect of partial substitution of Fe with magnetic and non-magnetic Mn and Cu respectively has been studied in the magnetoelectric compound $\text{Ba}_3\text{NbFe}_3\text{Si}_2\text{O}_{14}$. The variation in crystal and magnetic structure with temperature studied using neutron diffraction in the temperature range 6 K to 300 K shows that substitution does not change the crystal structure. The magnetic structure is observed to be similar to the parent compound with triangular and spiral arrangement of Fe_3^+ moments along a-b plane and c-axis respectively. However, a small change in pitch of the magnetic spiral has been observed due to substitution which leads to a change in interaction strength. The susceptibility shows that up to 10 at. % Cu substitution no change in antiferromagnetic ordering temperature $T_N \sim 26$ K is observed whereas for 10 at. % Mn substitution it is reduced to ~ 21.5 K. The effect on magnetic properties is more evident in field dependent magnetization studies. The parent compound exhibits a ferromagnetic component along with paramagnetic and antiferromagnetic phases. A partial and nearly complete suppression of the ferromagnetic component was observed for Mn and Cu substituted $\text{Ba}_3\text{NbFe}_3\text{Si}_2\text{O}_{14}$ respectively. The change in magnetic properties is attributed to the variation in exchange path length which changes the interaction strength and hence the magnetic properties.

TU.A-P35 - Dielectric and Magnetic Properties of Two-Phase Composite System: Mn-Zn or Ni-Zn ferrites in Dielectric Matrices

M. Salem¹, L. Panina¹, A. Morchenko¹, V. Kostishyn¹, O. Hemedat², A. El-Raouf Tawfik

1. National University of Science And Technology, Islamabad, Pakistan

2. Faculty of Science, Physics Department, Tanta University, Tanta, Egypt

Novel two-phase powder composites of Zn-substituted spinel ferrites $\text{Cu}_{0.6}\text{Zn}_{0.4}\text{Fe}_2\text{O}_4$ (CZF) and ferroelectric barium titanate (BT) BaTiO_3 were prepared by high energy ball milling technique [1] starting from raw materials. Increasing the milling time, it was possible to obtain powders with micrograins having a nanocrystalline structure. The structural parameters of the composite system $(1-x)$ CZF + (x) BT (where x changes from 0 to 1) were deduced from the analysis of X-ray diffraction patterns which were consistent with the existence of two piezoelectric and piezomagnetic phases. The magnetoelectric (ME) effect is due to the mechanical coupling between the ferrite and ferroelectric phases. The maximum of the ME coefficient of about 0.25 mV/cm/Oe is observed at 400 Oe for 40% BT phase. Very similar values for ME are also seen for 80% BT phase. In the latter case, a clear electrical dipole hysteresis is detected as well, demonstrating the ferroelectric properties of the prepared composites. Further increase in the ferrite phase led to irregular hysteresis loops because of decrease in resistivity causing the leakage current problems. As expected, the magnetic permeability of the composites decreases when increasing BT content but less than twice when the ferrite phase is decreased from 100% to 20%. The permeability increases with frequency for all concentrations. When increasing BT content, the dielectric constant at room temperature increases, while the dielectric loss decreases. These properties suggest the potential for applications in tunable high frequency materials and devices such as electrically controlled microwave phase shifters, ferromagnetic resonance devices, and magnetically controlled electro-optic or piezoelectric devices [2].

References:

- [1] A.Rittidech, P. Khotsongkram, American Journal of Applied Sciences 3 (3): 1760-1762, 2006
- [2] O.M. Hemedat, A.Tawfik, M.A.Amer, B.M.Kamal and D.E.ElRefaay, JMM 324, 3229-3237(2012)

TU.A-P36 - Reversible spin ordering transition by an electric field near a multiferroic triple phase point

B.-K. Jang¹, J.H. Lee¹, K.E. Kim¹, H. Jang², K.T Ko³, M.H. Jung⁴, T.Y. Koo⁵, Y.H Jeong⁴, H. Ohldag², J.S. Lee²

1. Department of Physics, KAIST, Daejeon, Republic of Korea

2. Stanford Synchrotron Radiation Lightsource, SLAC National Accelerator Laboratory, Menlo Park, United States

3. Max Planck Institute for Chemical Physics of Solids, Dresden, Germany

4. Department of Physics, POSTECH, Kyungbuk, Republic of Korea

5. Pohang Accelerator Laboratory, POSTECH, Gyeongbuk, Republic of Korea

A phase boundary of competing phases has played a key role in exotic phenomena such as colossal magnetoresistance (1), morphotropic phase boundary (2), and metal-insulator transition (3). Bismuth ferrite (BiFeO₃, BFO) has been heavily studied due to its multiferroicity at room temperature. A highly-elongated tetragonal-like BFO shows a concurrent phase transition of multiple order parameters near room temperature (4). In this work, we applied the phase proximity concept into the highly-elongated tetragonal-like BFO. By introducing chemical substitution into the tetragonal-like BFO, the concurrent transition temperature decreases simultaneously, and then bifurcates, thereby producing a multiferroic triple phase point. Near the triple phase point, the as-grown spin disordered state can be switched into a spin ordered state by means of an electrical writing. Phenomenological theory was employed to understand how the phase proximity in multiferroic system can offer a non-volatile spin order transition by an electric field in a reversible way. Our findings offer a promising route toward enhancing inter-coupled phenomena in multiferroic systems.

1. S. Jin et al., Thousandfold change in resistivity in magnetoresistive La-Ca-Mn-O Films. Science 264, 413-415 (1994)

2. M. Ahart et al., Origin of morphotropic phase boundaries in ferroelectrics. Nature 451, 545-548 (2008)

3. J. H. Park et al., Measurement of a solid-state triple point at the metal-insulator transition in VO₂. Nature 500, 431-434 (2013)

4. K.-T. Ko et al., Concurrent transition of ferroelectric and magnetic ordering near room temperature. Nature Communications 2, 567 (2011)

TU.A-P37 - XANES: A probing tool for mixed valence, modified magnetismH. Singh¹, M.N. Singh¹, A.K. Sinha¹*1. Indus Synchrotrons Utilization Division, Raja Ramanna Centre for Advanced Technology Indore, India*

X-ray Absorption Near Edge Structure (XANES) is extremely sensitive to the oxidation state, hybridization effect of orbitals and electronic state of the probed element in the sample. Mixed valence manganites, cobaltites etc. have already drawn great attention to the fundamental as well as application based science. We, on the other hand, show the effect of mixed valency of transition metals (TM) in TM (Co/Mn) based oxides using XANES. For this, we have taken two samples Co_3TeO_6 (CTO) and $\text{Co}_{2.5}\text{Mn}_{0.5}\text{TeO}_6$ (CMTO) prepared by conventional solid state reaction route. In the former, observations of $\text{Co}^{2+}/3+$ using XANES agrees well with the high field dc magnetization as well as first principles total energy calculations (Singh et al., JAP 116 (2014)). Existence of Co^{3+} in ceramic CTO does not diminish multiferroic property observed earlier in single crystal (with Co^{2+}), but actually enhances some of the observables. For example; the magnetization on our ceramic sample under 1 T is comparable to that measured for single crystal in a magnetic field of 14 T. While, the observation of $\text{Co}^{2+}/3+$ and $\text{Mn}^{2+}/3+$ using XANES in CMTO not only enhances the Neel temperature from 26 K (CTO) to 45 K (CMTO) but also short range robust ferromagnetism is observed at around 185 K (Singh et al., JAP 116 (2014)). This spectroscopic technique can also be used as a tool to extract the concentration of the corresponding mixed valence states, where linear combination fit of the unknown sample as a combination of the corresponding standards provides the quantitative information. Not only the oxidation state but one can easily observe the coordination geometry (tetra/octahedra) of the probed element which plays a significant role in most of the ferroelectrics and/or multiferroics. Aforementioned XANES measurements (transmission as well as fluorescence mode) has been done at BL-12, Indus -2 Synchrotron Source India.

TU.A-P38 - A comparison in multiferroic coupling between triangular lattice polytypes of hexagonal and rhombohedral AgFeO₂N. Terada¹, D. Khalyavin², P. Manuel², Y Tsujimoto¹, A. Belik¹

1. National Institute For Materials Science, Tsukuba, Japan

2. ISIS facility, STFC Rutherford Appleton Laboratory, Harwell Oxford, United Kingdom

In order to study an influence of a parent symmetry on coupling between spin order and ferroelectricity in spin-order-driven multiferroics, we have investigated magnetic and ferroelectric orderings of a triangular lattice antiferromagnet 2H-AgFeO₂ by neutron diffraction, magnetic susceptibility, specific heat, pyroelectric current, dielectric constant measurements. This compound has the space group of hexagonal $P6_3/mmc$, and is known as a polytype of rhombohedral 3R-AgFeO₂ ($R-3m$) with multiferroic behaviors that has been reported in our previous work. (N. Terada et al, *Phys. Rev. Lett.* **109** 097203 (2012)) Although these compounds have similar triangular lattice structures, the magnetic orderings and ferroelectricity of 2H-AgFeO₂ are significantly different from those of 3R-AgFeO₂.

Ferroelectric polarization, $P \sim 5$ mC/m² appears below 11 K in 2H-AgFeO₂, concomitant with a polar nature of the magnetic ordering. For $11 \text{ K} \leq T \leq 18 \text{ K}$, an incommensurate spin density wave ordering (ICM1) (magnetic point group $mmm1'$) is realized. Below 14 K, a proper screw ordering (ICM2) appears as a minor phase, which is coexistent with other phases. No ferroelectric polarization associated with the ICM2 phase was observed due to the nonpolar point group $2221'$. The spiral order with cycloid and proper screw components (ICM3) emerges below 11 K. Based on the deduced magnetic point group $21'$ in the ICM3 phase, we conclude that the ferroelectric polarization in 2H-AgFeO₂ is parallel to the hexagonal c axis and is yielded by the inverse Dzyaloshinskii -Moriya effect with $\mathbf{p}_1 \propto \mathbf{r}_{ij} \times (\mathbf{S}_i \times \mathbf{S}_j)$. Unlike polytype rhombohedral 3R-AgFeO₂, the additional contribution, $\mathbf{p}_2 \propto \mathbf{S}_i \times \mathbf{S}_j$, does not exist due to the symmetry constraint in the hexagonal 2H-AgFeO₂.

TU.A-P39 - Negative magneto-dielectric coupling in ceramic multiferroic Co_3TeO_6

H. Singh¹, G. Sharma², H. Ghosh¹, S. Patnaik², A. K. Sinha¹

1. *Indus Synchrotrons Utilization Division, Raja Ramanna Center for Advanced Technology, Indore, India*

2. *School of Physical Sciences, Jawaharlal Nehru University, New Delhi, India*

The coupling phenomena among various ferroic order parameter e.g. mutual control of P by M, in multiferroics have attracted great attention due to their promising potential applications as spintronics and magnetic data storage devices, in future. We have made an attempt to find out the microscopic mechanisms (exchange-striction, spin-current model and the p-d hybridization) for magnetically driven ferroelectricity in type II multiferroic Co_3TeO_6 (CTO) which shows interesting physical as well as low temperatures magnetic properties (Singh et al., JAP 116 (2014)). To probe the same, magneto-dielectric measurements are performed. Our dielectric constant shows a sharp peak at around $T_2 = 17.4$ K (at zero magnetic field). This anomaly in dielectric constant shows suppression in magnitude with the application of magnetic fields. With fields, this T_2 (= T_{N2} , the Neel temperature, observed in magnetization) shifts towards lower temperature indicating strong coupling between magnetic and electrical order. There are several reports on magneto-dielectric coupling which deal with the nature of the magnetic ordering and the role of the magnetic phases can be employed to explain the magneto-dielectric behaviour of our ceramic CTO. Following similar observations, our CTO shows negative magneto-dielectric shift i.e. lowering of overall magnitude of dielectric constant in higher magnetic fields, a behaviour expected for AFM transition, and could be related to the spiral spin structure (in the frame of spin current model - spin current induced by two non collinear spins realizes a nonzero electric dipole moment). This also supports the observation by Wang et al., PRB 88 (2013) that the spontaneous polarization is not caused purely by the incommensurate magnetic order. However, till date there is no report which deals with ferroelectric nature of CTO in term of spiral magnetic order. This could also explain the change in the polarization and dielectric constant with magnetic fields in CTO.

TU.A-P40 - Magnetoelectric effect in diamagnetic sillenites

K. Filar¹, V.I. Nizhankovskii¹

1. International Laboratory of High Magnetic Fields And Low Temperatures, Wroclaw, Poland

The magnetoelectric effect - an electric polarization induced by a magnetic field - is observed in ferromagnetic or, at least, paramagnetic structures [1,2].

But if an elementary cell is non-centrosymmetrical then it's possible to see the magnetoelectric effect even in a diamagnetic crystal [3]. Such observations haven't been published till now.

Measurements were done for $\text{Bi}_{12}\text{TiO}_{20}$ (BTO), $\text{Bi}_{12}\text{SiO}_{20}$ (BSO) and $\text{Bi}_{12}\text{GeO}_{20}$ (BGO) single crystals, that have non-centrosymmetrical cubic structure and they belong to the I23 space group [4]. The BTO was doped with chromium at level of 0.0015 wt%, whereas BSO and BGO were pure crystals.

The magnetic moment measurements were made by using VSM magnetometer in 14 Tesla superconducting magnet (Oxford Instruments), while measurements of the magnetoelectric effect were done by means of field modulation technique and Keithley 642 electrometer.

Measurements of magnetization vs. magnetic field show that both materials are diamagnetic, but with some paramagnetic contribution for Cr-doped BTO. Results for dependence of polarization derivative vs. magnetic field demonstrate that magnetoelectric effect exists in both materials, but is much bigger for Cr-doped BTO. It is caused by chromium doping in BTO and only by some magnetic impurities in BSO. Actual polarization was received after integration dP/dH signal.

Moreover, for these two single crystals, the influence of light exposure on the magnetoelectric effect was investigated. It has been shown that, the longer the exposure time is, the effect become smaller, especially after annealing in vacuum. It is caused by traps generated by oxygen vacancies in crystal.

[1] M. Fiebig, V.V. Eremenko and I.E. Chupis, "Magnetoelectric Interaction Phenomena in Crystals", NATO Science Series, II. Mathematics, Physics and Chemistry - vol. 164, Kluwer Academic Publishers, (2004)

[2] W. Eerenstein, N. D. Mathur & J. F. Scott, "Multiferroic and magnetoelectric materials", Nature, Vol. 442, (2006)

[3] H. Schmid, "Some symmetry aspects of ferroics and single phase multi-ferroics", J. Phys.: Condens. Matter 20 (2008) 434201

[4] S. C. Abrahams, P. B. Jamieson, and J. L. Bernstein, "Crystal Structure of Piezoelectric Bismuth Germanium Oxide $\text{Bi}_{12}\text{GeO}_{20}$ ", J. Chem. Phys. v.47 4034 (1967)

TU.A-P41 - Cone→Planar→Uniaxial transitions in $\text{Sr}_{(3-x)}\text{Ba}_x\text{Co}_2\text{Fe}_{24}\text{O}_{41}$ multiferroicsY. Santos¹, B. Andrade², M. Macedo¹

1. Federal University of Sergipe - Physics Department, São Cristóvão, Brazil

2. Instituto Federal de Alagoas – Piranhas, Piranhas, Brazil

Multiferroics were produced by proteic sol-gel process. The effect of the replacement of the Sr^{2+} ions with Ba^{2+} ions in Cone→Planar→Uniaxial transitions was investigated by magnetometry and structural analysis obtained with the Rietveld refinement. The volume expansion and the distortion of the unit cell were observed as a function of the amount of Ba^{2+} ions, as the ionic radius of Ba^{2+} (1.35 Å) is higher than that of Sr^{2+} (1.12 Å). The MxT magnetization curves showed changes in the magnetocrystalline anisotropy of the samples as a function of the amount of Ba^{2+} . The cone→planar transition was observed in the temperature range of 375–400 K, and occurred at lower temperatures as the amount of Ba^{2+} increased. The planar→uniaxial transition of the easy magnetization axis was found in the temperature range of 500–563 K. The temperature at which this transition occurs is proportional to the amount of Ba^{2+} ions. The Cone→Planar→Uniaxial transitions are also related to the behavior of the effective magnetic moment of the Co ions. The MxH curves at room temperature showed an increase of the coercive field H_c and the remanent magnetization M_r in the range of 10.4–14 emu/g and 1.1–1.7 emu/g, respectively; the saturation magnetization M_s , approximately equal to 47 emu/g, remained identical for all the concentrations. A strong magnetic anisotropy was found when the applied field was parallel or perpendicular to the sample, with M_r ranging from 0.9 to 3.3 emu/g. The substitution induced a change in the bond angle Fe(4)–O(2)–Fe(5) stabilizing the spiral magnetic order, contributing to the changes observed in H_c , and also facilitating the superexchange interaction. Controlling the amount of Ba can be an efficient mechanism to produce multiferroics that are best suited for this type of application.

TU.A-P42 - Magnetodielectric frequency behavior in nanoparticulated BTO-CFO multiferroic composites

U. Acevedo Salas¹, R. Lopez Noda^{1,2}, S. Ammar³, F. Calderón Piñar⁴, R. Valenzuela¹

1. *Instituto De Investigaciones En Materiales, Universidad Nacional Autónoma De México, Mexico District Federal, Mexico*

2. *Departamento de Física Aplicada, Instituto de Cibernética, Matemática y Física, ICIMAF, CITMA, Havana, Cuba*

3. *ITODYS, Université Paris Diderot, PRES Sorbonne Paris Cité, Paris, France*

4. *Instituto de Ciencia y Tecnología de Materiales, Universidad de La Habana, Havana, Cuba*

Magnetodielectric (MD) effects in different materials have exhibited many contributions, from purely magnetoresistance and Maxwell-Wagner effects, to induced stress arising from direct magnetoelectric coupling [1-3]. In this work, we report an investigation of the MD response (or magnetocapacitance MC) in nanoparticulated BTO-CFO composites consolidated by Spark Plasma Sintering (SPS). The electrical conductivity was measured simultaneously as a function of magnetic field (- 1200 to + 1200 kA/m), temperature (40-210°C), and as a function of frequency in the 5 Hz-1 MHz range, as typically in impedance spectroscopy. By using the Jonscher's universal relaxation law, the activation energies for long-range conductivity and hopping conductivity could be resolved [4]. Both activation energies exhibited a critical behavior for values about the coercive field of CFO, and also about the Curie point for BTO, thus confirming the magnetoelectric coupling in the nanoparticulated BTO-CFO.

References:

[1] G. Catalan, Appl. Phys. Lett. 88, 102902, 2006

[2] S. A. Gridnev, A. V. Kalgin & V. A. Chernykh, Int. Ferroelectrics: An Intern. J., 109 (1), 70-75, 2009

[3] M. M. Sutar, S. R. Jigajeni, A. N. Tarale, et al, J. Mater. Sci.: Mater. Electron. 25, 3771-3778, 2014

[4] R. L. Noda, U. Acevedo, R. Valenzuela, et al, IEEE Trans. OnMagn., 50 (11), 8002304, 2014

TU.A-P43 - Magnetic and magnetoelectric dynamical Mn/rare-earth coupling in RMnO₃ multiferroics

V. Simonet¹, L. Chaix², S. deBrion¹, X. Fabrèges³, S. Petit³, R. Ballou¹, A. Cano⁴, L.P. Regnault⁵, E. Ressouche⁵, J. Ollivier²

1. Institut Néel, CNRS/Grenoble Alpes, Grenoble, France
2. Institut Laue Langevin, Grenoble, France
3. Laboratoire Léon Brillouin, CEA/CNRS, Gif-sur-Yvette, France
4. ICMCB, Université Bordeaux, Pessac, France
5. MDN/SPSMS/INAC, CEA, Grenoble, France
6. synchrotron SOLEIL, Gif-sur-Yvette, France

The interest for spintronic and spins/charges controls motivates material science research in the field of multiferroicity, magnetoelectric effect, and magnonics. Signatures of dynamical magnetoelectric coupling have already been observed in the form of magnons dressed with electric charges, hence excitable via an electric field [Pimenov et al. Nat. Phys, 2, 97 (2006)]. Coupling two complementary experimental techniques, THz/FIR spectroscopy on synchrotron source and inelastic neutron scattering, we have focused on two members of the multiferroics hexagonal manganites RMnO₃, with R=Er and Ho. These compounds order electrically below 800 K and magnetically around 80 K with a 120° frustrated arrangement of the Mn³⁺ ions. We have fully characterized the low energy spectra (magnon, phonon, crystal field transitions) of these compounds and their excitation rules as regards the electric and magnetic fields of the THz wave. In ErMnO₃, we have observed the complete loss of the magnetic character of a magnon transmuted into an electroactive excitation [Chaix, et al. Phys. Rev. Lett. 112, 137201 (2014)]. We attribute this magnetoelectric dynamical process to the hybridization between a crystal field level transition of the Er magnetic rare earth and a Mn magnon. In HoMnO₃, spectacular modifications of the Mn spin waves and Ho crystal field level transitions are observed at a temperature of 40 K when a spin reorientation of the Mn magnetic moments occurs, together with the ordering of some Ho ions [Fabrèges et al. Phys. Rev. Lett. 103, 067204 (2009)]. At lower temperature, the spin waves dispersion perpendicular to the Mn triangular planes vanishes, the Mn ordered structure being maintained in the molecular field of the rare earth ions. Both studies highlight the crucial role of the strong coupling between the Mn and rare earths in the dynamical properties of these hexagonal manganites.

TU.A-P44 - Effects of in-plane strain on charge/orbital ordering in $\text{La}_{0.5}\text{Ca}_{0.5}\text{MnO}_3$ thin films

J.Y. Juang¹, J.W. Mi¹, T. Tsai¹, Y.F. Hsiao¹, Y.W. Jiang¹, Y.M. Chang¹, C.W. Luo¹, K.H. Wu¹, J.Y. Lin², T.M. Uen¹

1. Department of Electrophysics, National Chiao Tung University, Hsinchu, Taiwan

2. Institute of Physics, National Chiao Tung University, Hsinchu, Taiwan

A series of 20-nm-thick perovskite (010)- $\text{La}_{0.5}\text{Ca}_{0.5}\text{MnO}_3$ (LCMO) thin films were grown on SrTiO_3 (110) and LaAlO_3 (110) substrates by pulsed laser deposition. Depending on the in-plane strain state of the films, the charge/orbital ordering (COO) behavior, manifested as resistivity hysteresis near the COO temperature, was found to appear only when measuring along certain crystalline orientation. Moreover, the orientation along which COO occurs can be changed when the in-plane strain state was changed from tensile to compressive. The results suggest that there exist two versions CE state, namely the “charge stacked” and “Wigner crystal”, in LCMO films grown on different substrates. These results suggest that the strain-induced variations in Mn 3d orbitals may have altered the competition between super-exchange and double-exchange interactions in the CE-type phases.

TU.A-P45 - Direct observation of polar state in multiferroic (Sr_{1-x}Ba_x)MnO₃

R. Guzman¹, E. Langenberg², L. Maurel^{2,3}, P.A. Algarabel^{3,4}, J.A. Pardo^{2,5}, C. Magen^{1,2,6}

1. *Laboratorio de Microscopías Avanzadas (LMA), Instituto de Nanociencia de Aragón (INA), Universidad de Zaragoza, Zaragoza, Spain*

2. *Instituto de Nanociencia de Aragón, Universidad de Zaragoza, Zaragoza, Spain*

3. *Departamento de Física de la Materia Condensada, Universidad de Zaragoza, Zaragoza, Spain*

4. *Instituto de Ciencia de Materiales de Aragón, Universidad de Zaragoza-CSIC, Zaragoza, Spain*

5. *Departamento de Ciencia y Tecnología de Materiales y Fluidos, Universidad de Zaragoza, Zaragoza, Spain*

6. *Fundación ARAID, Zaragoza, Spain*

Multiferroic materials showing simultaneous magnetic and ferroelectric ordering have become the subject of intensive research in the last decade. Recent theoretical predictions and experiments suggest that paraelectric SrMnO₃ with the cubic ABO₃ perovskite structure could become ferroelectric upon artificial expansion of the unit cell, either by epitaxial strain [1] or partial substitution of Sr for Ba [2]. This would give rise to a new class of multiferroic perovskites where ferroelectricity would be driven by off-centering of the magnetic cation Mn⁴⁺.

In this work we show pseudocubic (Sr_{1-x}Ba_x)MnO₃, 0.1 ≤ x ≤ 0.2, (SBMO) epitaxial thin films grown by pulsed laser deposition from bulk polycrystalline hexagonal phase targets onto (001)-oriented perovskite substrates. Strain analysis of High Angle Annular Dark Field (HAADF) images by aberration-corrected Scanning Transmission Electron Microscopy (STEM) confirms the epitaxial coherent growth and the pseudocubic structure of the films. By simultaneous HAADF and Annular Bright Field (ABF) imaging we have confirmed the polar state of the SBMO films. This technique reveals significant displacements of the Mn atomic positions in addition to a strong shift of the oxygen atoms, leading to distorted MnO₆ octaedra. Quantitative mapping of local atomic displacements with picometer resolution is carried out by the precise structural analysis of atomic resolution ABF images [110]. Displacement mapping of large areas reveal extended domain walls due to the progressive spatial variation of the O-Mn relative positions in Sr_{0.8}Ba_{0.2}MnO₃ samples.

References:

[1] J. H. Lee and K. M. Rabe, Phys. Rev. Lett. 104, 207204 (2010)

[2] H. Sakai et al., Phys. Rev. Lett. 107, 137601 (2011)

TU.A-P46 - Unravelling the basic mechanisms in magnetoelectric TbMn_{1-x}Fe_xO₃ system

M. Mihalik¹, M. Mihalik¹, M. Zentková¹, M. Vavra^{1,2}, D. Passos³, R. Vilarinho³, D. Mota³, A. Almeida³, A. Moreira³, P. Tavares⁴

1. Institute of Experimental Physics, Slovak Academy of Sciences, Košice, Slovak Republic

2. P. J. Šáfárik University, Faculty of Science, Kosice, Slovak Republic

3. IFIMUP-IN, Departamento de Física e Astronomia da Faculdade de Ciências, Universidade do Porto, Rua do Campo Alegre, Porto, Portugal

4. Centro de Química, Universidade de Trás-os-Montes e Alto Douro, Vila Real, Portugal

5. Institute of Nuclear Physics, Polish Academy of Sciences, Kraków, Poland

6. Institute of Mathematics, Physics and Mechanics & Faculty of Civil and Geodetic Engineering, University of Ljubljana, Slovenia

Multiferroics, where spontaneous long-range magnetic and dipolar order coexist, show a rich fundamental physics with potential for multifunctional applications. TbMnO₃ is a multiferroic compound, exhibiting magnetic ordering of Mn ions, with a sinusoidally modulated collinear magnetic structure along the a-axis (Pnma space group) below TN = 41 K. This magnetic structure changes to a cycloidal phase below Ts = 28 K, which is accompanied by the emergence of a spontaneous electric polarization along the b-axis, accordingly to Dzyaloshinskii-Moriya model. On further cooling, Tb₃₊ spins order independently from the Mn₃₊ sublattice at T1 = 7 K [1, 2]. In order to tune the balance between the competitive ferro- and antiferromagnetic interactions leading to frustrated magnetic structures, we have studied the effect of Fe₃₊ substitution for Mn₃₊ on selected physical properties of TbMn_{1-x}Fe_xO₃, with x=0 to 0.05. Fe₃₊ has the same radius as Mn₃₊ but while Mn₃₊ is Jahn-Teller active, Fe₃₊ is not. In our work we present a detailed characterization of the structural, thermal, magnetic, polar and magnetoelectric properties of the TbMn_{1-x}Fe_xO₃ system as well as a lattice dynamical study at low temperatures by Raman spectroscopy. We have found that already at x=0.05 ferroelectricity is lost and below this concentration there is a strong dependence of the magnetoelectric response on Fe concentration. The temperature dependence of the Raman modes of MnO₆ units has revealed a shift relative to the pure anharmonic temperature dependence of the phonon frequency. The relation between spin-spin correlation function and anomalous Raman mode frequency behaviour is evidenced enabling the determination of spin-phonon coupling. A phase diagram for this system is proposed.

[1] N. Aliouane et al. Journal of Physics: Condensed Matter, Vol. 20 (2008) 434215

[2] Kimura T et al., Journal of Physics: Condensed Matter, Vol. 20 (2008) 434204

TU.A-P47 - Single-crystal growth and magnetic properties of multiferroic triangular-lattice antiferromagnet 3R-AgFeO₂ and alpha-NaFeO₂

Y. Ikedo¹, H. Sato¹, N. Terada², K. Kindo³, A. Matsuo³, M. Tokunaga³, A. Miyake³

1. *Department of Physics, Chuo University, Bunkyo-Ku, Japan*

2. *National Institute for Materials Science, Ibaraki, Japan*

3. *Institute for Solid State Physics, University of Tokyo, Chiba, Japan*

3R-AgFeO₂ and alpha-NaFeO₂ are two-dimensional triangular-lattice antiferromagnets with rhombohedral symmetry. Recently, it has been reported that the both compounds have non-collinear magnetic phases accompanied by a dielectric polarization. In spite of several powder studies, there have been no investigations on single crystals. We succeeded in growing single crystals of 3R-AgFeO₂ and alpha-NaFeO₂ by a hydrothermal method. Using them, anisotropic measurements of the magnetic susceptibilities, the magnetizations and the dielectric properties were carried out under high magnetic field up to 60 T. The magnetic susceptibility of 3R-AgFeO₂ under a magnetic field along the c axis reveals two-step magnetic phase transitions at 15 and 7 K. The magnetization curve of 3R-AgFeO₂ at 1.3 K exhibits anomalies corresponding to the 1/5 and 1/3 magnetic plateaus at 12.5 T and 27 T, respectively when the field is applied along the c axis. On the other hand, the magnetization curve under magnetic fields along the a axis is almost linear except for a small bend at 40 T. alpha-NaFeO₂ undergoes two-step phase transitions at 9 and 5 K. The decrease in the magnetic susceptibility below 9 K is more pronounced under magnetic field along c axis. The magnetic susceptibility steeply drops at 5 K with a thermal hysteresis. These behaviors are consistent with the neutron results. The magnetization curve of alpha-NaFeO₂ exhibits multi-step phase transitions under the field along the both c and a axes. Field-induced transitions are detected at 5.2, 8.5 and 13.5 T under the c-axis fields, 3.3, 8.5 and 13.6 T under the a-axis fields. A dielectric polarization is observed under magnetic fields between 5.2 and 13.5 T along the c axis.

TU.A-P49 - Effect of partial substitution of Fe^{3+} with Al^{3+} on the magnetic and dielectric properties of Z-type hexaferrite, $\text{Sr}_3\text{Co}_2\text{Fe}_{24}\text{O}_{41}$ S. Tiwari¹, S. Vitta¹*1. Indian Institute of Technology, Bombay, India*

Hexaferrites have non-collinear magnetic structures which facilitate multiferroicity to be induced at elevated temperatures. A Z-type compound, $\text{Sr}_3\text{Co}_2\text{Fe}_{24}\text{O}_{41}$ has been chosen for investigation as it has cycloidal or conical magnetic structure at room temperature. Partial substitution of Fe^{3+} with Al^{3+} allows tuning of the magnetic structure and hence magnetoelectric coupling. In the present work $\text{Sr}_3\text{Co}_2(\text{Fe}_{1-x}\text{Al}_x)_{24}\text{O}_{41}$ with $x=0$ and 0.019 compounds have been synthesized using standard solid state techniques. Structural characterization shows that both the compounds are single phase with a hexagonal crystal structure, $\text{P6}_3/\text{mmc}$. Secondary and backscattered electron images show the presence of plate like grains with no secondary phases. The variation of magnetization M with temperature T at different external fields, 100, 500 and 1000 Oe has been measured under two different conditions, ZFC and FC, to determine magnetic structural changes. In the unsubstituted compound a single hump in the magnetization was observed at ~ 370 K while the substituted compound exhibits additional peak at lower temperature. The position of these peaks in the substituted compound has been found to shift with changing magnetic field. These peaks indicate that the magnetic structure undergoes modification on changing either the T or external field. The room temperature hysteresis shows that the $x=0$ compound has a simple ferromagnetic behavior while the substituted compound exhibits discontinuities – a step like M variation indicative of successive evolution of the magnetic structure at different fields. The dielectric permittivity and resistivity of the two compounds at room temperature has been investigated in the frequency range 1Hz to 1MHz. In both the compounds permittivity and resistivity decrease with increasing frequency. The permittivity of unsubstituted compound however is higher compare to the substituted compound at low frequency. The resistivity of $x=0$ compound decreases from $10^6 \Omega\text{m}$ to $6 \times 10^4 \Omega\text{m}$ while for $x=0.019$ it decreases from $10^7 \Omega\text{m}$ to $6 \times 10^4 \Omega\text{m}$.

TU.A-P50 - Magnetostriction of $\text{Cu}_3\text{Mo}_2\text{O}_9$ under the pulsed magnetic fields

S. Nishikawa¹, Y. Hirata¹, H. Kuroe¹, T. Sekine¹, S. Kawachi², A. Miyake², M. Tokunaga², M. Hase³, K. Oka⁴, T. Ito⁴

1. Sophia Univ., Tokyo, Japan

2. Institute for Solid State Physics, The University of Tokyo, Tokyo, Japan

3. National Institute for Materials Science (NIMS), Ibaraki, Japan

4. National Institute of Advanced Industrial Science and Technology (AIST), Ibaraki, Japan

We report some anomalies due to magnetically induced phase transitions, e.g., the plateau states, in the magnetostriction curve of $\text{Cu}_3\text{Mo}_2\text{O}_9$.

$\text{Cu}_3\text{Mo}_2\text{O}_9$ is a multiferroic material which exhibits the slightly canted antiferromagnetic and ferroelectric phase below $T_N = 8$ K [1, 2]. The cross correlation effects between the spin and the charge systems and the magnetically induced phase transitions, including the one to the magnetization plateau state above 50 T, are observed in $\text{Cu}_3\text{Mo}_2\text{O}_9$ [3]. Our main focus is the cross correlation effects between the spin and the lattice systems under pulsed magnetic fields up to 57 T. We measure the longitudinal magnetostriction at 1.6 K by using the capacitance technique [4].

When $H//a$, the lattice constant decreases with increasing magnetic fields up to 19 T and shows sudden increase with hysteresis at 19 T, where the magnetization also increases suddenly [3,5]. And it shows the magnetostriction plateau above 52 T, where the magnetization plateau is observed [3]. Also, when $H//c$, the lattice constant increases with increasing magnetic field up to 8 T and turns to decrease at the magnetic fields above 8 T. It shows a small anomaly at 18.6 T, where the magnetization jump is observed [3,5]. It also shows the magnetostriction plateau at the magnetic fields where the magnetization plateau is observed. The magnetic-field dependence of magnetostriction resembles that of the squared magnetization, suggesting the cross correlation effects between the lattice and the spin systems in $\text{Cu}_3\text{Mo}_2\text{O}_9$.

[1] T. Hamasaki et al., Phys. Rev. B 77 (2008) 134419

[2] H. Kuroe et al., Phys. Soc. Jpn. 80 (2011) 093705

[3] H. Kuroe et al., JPS Conf. Proc. 3 (2014) 014036

[4] G. Kido Physica B 155 (1989) 199

[5] T. Hamasaki et al., J. Phys: Conf. Ser. 150 (2009) 042047

TU.A-P52 - Multiferroic properties of $(\text{Cu,Zn})_3(\text{Mo,W})_2\text{O}_9$

Y. Hirata¹, S. Nishikawa¹, K. Aoki¹, R. Kino¹, H. Kuroe¹, T. Sekine¹, M. Hase², K. Oka³, T. Ito³, H. Eisaki³

1. Sophia Univ., Tokyo, Japan

2. National Institute for Materials Science (NIMS), Ibaraki, Japan

3. National Institute of Advanced Industrial Science and Technology (AIST), Ibaraki, Japan

The substitution effects on $\text{Cu}_3\text{Mo}_2\text{O}_9$ is presented. The parent material has a distorted tetrahedral quasi-one-dimensional spin structure made from the Cu^{2+} ions with the spin moments of $S = 1/2$. From this spin structure, geometrical frustration and quantum fluctuation are expected to appear simultaneously. We have found that $\text{Cu}_3\text{Mo}_2\text{O}_9$ is a multiferroic material, where the weak ferromagnetic component of the spin moments and the ferroelectricity coexist below $T_N = 8 \text{ K}$ [1,2].

In $(\text{Cu,Zn})_3\text{Mo}_2\text{O}_9$, the direct substitution of the nonmagnetic Zn^{2+} ions for the magnetic Cu^{2+} ones introduces the spin defects into the spin system [3,4]. In the case of $\text{Cu}_3(\text{Mo,W})_2\text{O}_9$, the nonmagnetic Mo^{6+} ions replace the nonmagnetic W^{6+} ones. The disorder is introduced indirectly into the spin chain through the lattice system. We have synthesized the single crystals of $(\text{Cu,Zn})_3(\text{Mo,W})_2\text{O}_9$ with the continuous solid state crystallization [5]. We have studied these direct and indirect substitution effects on $(\text{Cu,Zn})_3(\text{Mo,W})_2\text{O}_9$ and have published some results in the Zn-substituted systems [3,5,6]. In this report we present our recent results of the magnetization, the specific heat, and the dielectric constant in $(\text{Cu,Zn})_3(\text{Mo,W})_2\text{O}_9$. I explain the similarity and difference between W- and Zn-substitution effects.

I focus the temperature-impurity-concentration-ratio phase diagram. In both of the W- and the Zn- substituted systems, the phase transition temperature decreases linearly. The efficiency of the W substitution is much weaker than that of the Zn substitution.

[1] T. Hamasaki et al., Phys. Rev. B 77 (2008) 134419

[2] H. Kuroe et al., J. Phys. Soc. Jpn. 80 (2011) 083705

[3] M. Hase et al., J. Phys. Soc. Jpn. 77 (2008) 034706

[4] H. Kuroe et al., J. Kor. Phys. Soc. 63 (2013) 542

[5] K. Oka et al., J. Cryst. Growth 334 (2011) 108

[6] H. Kuroe et al., JPS Conf. Proc. 2 (2014) 010206

TU.A-P53 - Muon-spin rotation in multiferroic $\text{Cu}_3\text{Mo}_2\text{O}_9$ under electric fields

H. Kuroe¹, H. Kuwahara¹, T. Sekine¹, I. Watanabe², A.R. Raselli³, M. Elender³, P.K. Biswas³, M. Hase⁴, K. Oka⁵, T. Ito⁵

1. Sophia Univ., Tokyo, Japan

2. RIKEN Nishina Center, Saitama, Japan

3. Paul Scherrer Institute (PSI), Villigen, Switzerland

4. National Institute for Materials Science (NIMS), Ibaraki, Japan

5. National Institute of Advanced Industrial Science and Technology (AIST), Ibaraki, Japan

The muon spin relaxation/rotation/resonance (mSR) measurements under electric field give helpful information to study the electrically induced magnetism, *e.g.*, the cross correlation effects in multiferroic materials.

In this presentation, we report the electric-field application system up to 500 V newly developed for Dolly spectrometer at PSI. We also present, as a main subject of this research, the electric-field effects on the mSR spectrum in $\text{Cu}_3\text{Mo}_2\text{O}_9$.

This compound has a multiferroic phase below $T_N = 8$ K [1, 2]. Below T_N , a slightly canted antiferromagnetic long-range magnetic order appears. Two kinds of the internal magnetic fields at the muon stopping sites are clearly observed as the beating oscillation in the muon-spin rotation spectrum below T_N [3]. The mSR spectrum is related to the phase transition at T_N because the temperature dependence of the averaged internal-field amplitude reflects the order parameter of this phase transition. In this presentation, we clarify that the mSR spectrum depends on the electric fields along the *c* axis of the crystal. In this direction, the spontaneous electric polarization appears.

From the fitting of the mSR spectra in time and frequency domains, we conclude that the observation of the electric-field dependence on mSR spectra clearly demonstrates the change of the internal electric fields induced by the application of the external electric fields.

[1] T. Hamasaki *et al.*, Phys. Rev. B **77** (2008) 134419

[2] H. Kuroe *et al.*, J. Phys. Soc. Jpn. **80** (2011) 093705

[3] H. Kuroe *et al.*, JPS Conf. Proc. **2** (2014) 010206

TU.A-P54 - Interplay between electronic correlation and charge transport properties of self-doped multiferroic oxides $\text{CuCr}_{1-x}\text{O}_2$ ($0 < x < 0.1$)

D.C. Ling¹, S.B. Singh¹, L.T. Yang¹, Y.F. Wang¹, Y.C. Shao¹, C.W. Chiang¹, K.T. Lin¹, W.F. Pong¹

1. Dept. of Physics, Tamkang University, Taipei, Taiwan

We have performed x-ray absorption near-edge structure (XANES), extended x-ray absorption fine structure (EXAFS), valence-band photoemission spectroscopy (VB-PES) measurements on layered multiferroic oxides $\text{CuCr}_{1-x}\text{O}_2$ with $0 < x < 0.1$ to elucidate the interplay between electronic correlation and charge transport properties. The Cu L_{3,2}- and O K-edge XANES spectra reveal a gradual increase in the valence state of Cu from Cu^{1+} to Cu^{2+} and the presence of excess holes at the O sites due to the generation of Cu^{2+} , indicative of a strong hybridization between Cu 3d and O 2p states. VB-PES spectra show that the spectral weight of the occupied O 2p valence states shifts about 3 eV toward delocalized O 2p-Cu 3d hybridized states with increasing Cr deficiency, accompanied by a decrease of the density of states of the Cu 3d and O 2p valence states near the Fermi level. These findings provide direct evidence that the increase in the p-type conductivity over a wide range of temperature predominantly arises from Cr-deficiency-induced changes in the electronic structures.

TU.A-P55 - Oxygen vacancy mediation of magnetoelectric coupling in W-type strontium hexaferrites doped with Ce³⁺ ion

B. Andrade¹, M. Macedo²

1. Instituto Federal De Alagoas – Piranhas, Piranhas, Brazil

2. Federal University of Sergipe - Physics Department, São Cristóvão, Brazil

W-type strontium hexaferrite was prepared by proteic sol-gel process. The effects of the Ce substitution on the structural and magnetic properties were investigated by X-ray diffraction, X-ray fluorescence, scanning electron microscopy, magnetometry, differential scanning calorimetry, and impedance spectroscopy. The results revealed the increase of lattice parameters and unit cell volume in function of Ce³⁺ concentration in W-type hexaferrite. This finding indicated the complete substitution of Sr²⁺ by Ce³⁺. The value of the saturation magnetization of all the samples was approximately 66.3 ± 0.7 emu/g, whereas the Curie temperature was invariant with the doping ($T_c = 475$ °C). The remanence, coercivity, and activation energy increased with the Ce³⁺ doping. The insertion of a dopant ion led to the creation of oxygen vacancies and the reduction of Fe³⁺ to Fe²⁺ in the octahedral site. Thus, the concentration of cerium ions indicated a possible coupling between the electric and magnetic fields. The Mr/MS ratio suggested that W-type hexaferrites doped with Ce³⁺ have multiple domains and coercivity lower than 100 Oe. As a result, this material is a potential candidate for magnetoelectric and electromagnetic devices.

TU.A-P56 - Structural and magnetic properties of M-type $\text{Sr}_{1-x}\text{Mg}_x\text{Fe}_{12}\text{O}_{19}$ M. Macedo¹, B. Andrade², Y. Santos¹

1. Federal University of Sergipe - Physics Department, , São Cristóvão, Brazil

2. Instituto Federal de Alagoas – Piranhas, Piranhas, Brazil

$\text{Sr}_{1-x}\text{Mg}_x\text{Fe}_{12}\text{O}_{19}$ nanocrystals were obtained via proteic sol-gel process with the molar ratio $\text{Fe}/\text{Sr}_{1-x}\text{Mg}_x = 12$ ($x = 0.0-1.0$). The materials were characterized by scanning electron microscopy (SEM), X-ray diffraction (XRD), and magnetometry. XRD results showed: for $x \leq 0.2$ a hexagonal phase; for $0.2 < x < 0.8$ a mixture of $\text{Sr}_{1-x}\text{Mg}_x\text{Fe}_{12}\text{O}_{19}$ and few traces of $\alpha\text{-Fe}_2\text{O}_3$; and for $x > 0.8$, the phase $\alpha\text{-Fe}_2\text{O}_3$. The c/a ratio falls 3% for $x < 0.8$, due to the different ionic radii between Mg^{2+} and Sr^{2+} . SEM results showed a morphological structure with wide distribution in particle size. The FC-ZFC curves obtained from the magnetization versus temperature with a field of 100 Oe for $x > 0.8$ showed a marked elevation of 250 K. This transition was attributed to the reorientation of spins typically found in the hematite, which gradually disappeared as the hexagonal phase formed. The maximum values of M_s , M_r , H_c and M_r/M_s found at $x = 0.2$ were 66.0 emu/g, 30.0 emu/g, 538.0 Oe and 0.5, respectively. For $x > 0.2$ a sharp drop in these quantities was observed, reaching saturation at $x = 0.8$. The increase of the magnetic properties for $x = 0.2$ can be explained by hyperfine field of the 12k- and 2b-site as a result of superexchange interaction energy for Fe-O-Fe. Above this doping, the reduction of the magnetization can be explained by magnetic dilution. The reason M_r/M_s suggests that the presence of Mg^{2+} in the structure leads to the formation of single domain particles to multiple magnetic domains. This study showed that low magnesium doping leads to an increase of the magnetic properties of strontium hexaferrite.

TU.A-P57 - Magnetic and Magneto-optical properties of films of multiferroic GdMnO₃ grown on SrTiO₃ (100) and LSAT (100) and (111)H. Albargi¹, H. Blythe¹, A.M. Fox¹, G. Gehring¹, V. Chichkov², N. Andreev²1. *The University of Sheffield, Sheffield, United Kingdom*2. *National University of Science and Technology "MISIS"*

Bulk GdMnO₃ is a canted antiferromagnet below ~ 40K and ferroelectric below ~8K and is orthorhombic with axes $a = 5.310 \text{ \AA}$, $b = 5.840 \text{ \AA}$, $c = 7.430 \text{ \AA}$. The magnetization is expected to depend strongly on strain because of the coupling between the spin structure and the ferroelectricity. We investigate the effects strain on films that are grown epitaxially on LSAT(100) and (111) and compare the results with epitaxial films grown on SrTiO₃ (100) [1]. The magnetic properties have been studied using a SQUID magnetometer to obtain ZFC/FC and hysteresis loops data for magnetic fields both in and out of the plane. The strain due to the substrates causes substantial differences in the magnetic properties. The canting of the Mn moments is enhanced and a strong easy plane anisotropy is induced by the strain caused by the LSAT(100) that is larger than that induced by SrTiO₃ (100) due to the extra compressive strain in plane. The saturation magnetization of the film grown on LSAT(111) are reduced and almost isotropic. The Curie constant found by fitting the ZFC plot to a Curie law is also smaller for the films grown LSAT(111). The in-plane compression of the film grown on LSAT(100) causes a strong enhancement of the strength of the inter-site transition between Mn ions and a large enhancement of the magnetic circular dichroism (MCD) around 2eV relative to the films grown on SrTiO₃ (100). In contrast the MCD is suppressed for the film grown on LSAT(111). Thus large changes may be induced in GdMnO₃ by growing thin epitaxial films on suitably chosen substrates. In particular a marked enhancement of the saturation magnetization and the coercive field may be obtained by growing on LSAT (100).

[1] Al-Qahtani, et al Journal of Physics: Conference Series 391 012083 (2012)

TU.A-P58 - Anisotropy, Magnetostriction and Inverse Magnetoelectric effect in Dy substituted Ni FerriteA. Majumder¹, K. Ugendar¹, A. Baby K. B.¹, V. Chunchu¹, M. G¹*1. Indian Institute of Technology Madras, Chennai, India*

NiFe₂O₄ and NiFe_{1.9}Dy_{0.1}O₄ compounds prepared by solid state reaction were found to crystallize in the cubic inverse spinel phase as confirmed by XRD and Raman studies. The saturation values of magnetization (M_s) of NiFe₂O₄ and NiFe_{1.9}Dy_{0.1}O₄, at 300 K, are 50.1 emu/g and 44 emu/g respectively and at 20 K, the respective values are 56.4 emu/g and 53.2 emu/g. The M-H data were fit to the law of approach to saturation (LAS) and $K_1(T)$, the first order magnetocrystalline anisotropy constant, was obtained. The values of K_1 of NiFe₂O₄ and NiFe_{1.9}Dy_{0.1}O₄ at 20 K are 42.2 kJ/m³ and 121.2 kJ/m³ respectively and K_1 at 300 K are 33 kJ/m³ and 55.1 kJ/m³ respectively. The observed increase in K_1 is attributed to the large negative anisotropy value of Dy. From the $\ln K_1(T)$ vs $\ln M(T)$ plot, the anisotropy of NiFe_{1.9}Dy_{0.1}O₄ is seen to be more sensitive to temperature than NiFe₂O₄, explaining the lower value of M_s of the former, at 20 K. The saturation magnetostriction (λ_s) values at 300 K of NiFe₂O₄ and NiFe_{1.9}Dy_{0.1}O₄ are -32×10^{-6} and -35×10^{-6} , respectively, the increase being contributed by that of the Dy³⁺ ion. Ferroelectricity, magnetocapacitance and magnetoelectric effect have been reported on Dy substituted Ni ferrite. All the above made possible the observation of inverse magnetoelectric effect in NiFe_{1.9}Dy_{0.1}O₄. A circular pellet of the sample was electrically poled in a field of 0.3 kV/cm and the magnetic field was determined by measuring a change in impedance of a soft magnetic ribbon kept above the pellet. The impedance was measured at 5 MHz, the frequency at which, the magnetoimpedance of the ribbon was the largest (28%). The magnetic field developed due to poled NiFe_{1.9}Dy_{0.1}O₄ was determined as 1.2 Oe (~96 A/m or 0.1 mT).

TU.A-P59 - 'One-way transparency of light' in multiferroic CuB_2O_4

S. Toyoda¹, N. Abe¹, S. Kimura², Y. Matsuda³, T. Nomura³, A. Ikeda³, S. Takeyama³, T.H. Arima¹

1. *Department of Advanced Materials Science, University of Tokyo, Chiba, Japan*

2. *Institute for Materials Research, Tohoku University, Sendai, Japan*

3. *Institute for Solid State Physics, University of Tokyo, Chiba, Japan*

The response of matter to light is described in terms of electric response and magnetic response. In multiferroic materials, the responses can interfere with each other, resulting in a change in optical absorption with the reversal of the propagating direction of light. If the electric response is as large as the magnetic response, the material should be transparent for the light propagating in one direction, while it should absorb light propagating in the opposite direction. It has been reported that CuB_2O_4 shows giant directional dichroism at 1.40 eV which corresponds to the intratomic $d_{(x^2-y^2)}-d_{xy}$ transition of Cu^{2+} holes in the canted antiferromagnetic phase below 21 K [1]. The optical absorption coefficient changes by a factor of three with the reversal of the propagation direction of light. In this study, we investigate the directional dichroism in high magnetic fields up to 52 T. The directional dichroism is enhanced with magnetic field. The ratio of the optical absorption coefficient is as large as 1000 % at 52 T for the light $E // [110]$ and $B // c$ -axis. The enhancement of the directional dichroism is explained by a modification of the electric and magnetic transition dipole moments with the canting of the spin direction of Cu^{2+} . Furthermore we predicted that the electric dipole transition should be as large as the magnetic dipole transition at 52 T by rotating the sample around $[110]$ axis by 45 degrees, because the magnetic dipole transition decreases with reduction of the c -component of the magnetic field of light. In fact, the absorption peak disappears for the light propagating in one direction. In other words, we succeeded in realization of 'one-way transparency of light'.

[1]M.Saito, K.Taniguchi, T.Arima, J. Phys. Soc. Jpn 77, 013705(2008)

TU.A-P60 - 'One-way transparency of light' in multiferroic CuB₂O₄

S. Toyoda¹, N. Abe¹, S. Kimura², Y.H. Matsuda³, T. Nomura³, A. Ikeda³, S. Takeyama³, T.H. Arima¹

1. *Department of Advanced Materials Science, The University of Tokyo, Chiba, Japan*

2. *Institute for Materials Research, Tohoku University, Sendai, Japan*

3. *Institute for Solid State Physics, University of Tokyo, Chiba, Japan*

The response of matter to light is described in terms of electric response and magnetic response. In multiferroic materials, the responses can interfere with each other, resulting in a change in optical absorption with the reversal of the propagating direction of light. If the electric response is as large as the magnetic response, the material should be transparent for the light propagating in one direction, while it should absorb light propagating in the opposite direction.

It has been reported that CuB₂O₄ shows giant directional dichroism at 1.40 eV which corresponds to the intratomic $d_{x^2-y^2} - d_{xy}$ transition of Cu²⁺ holes in the canted antiferromagnetic phase below 21 K [1]. The optical absorption coefficient changes by a factor of three with the reversal of the propagation direction of light.

In this study, we investigate the directional dichroism in high magnetic fields up to 52 T. The directional dichroism is enhanced with magnetic field. The ratio of the optical absorption coefficient is as large as 1000 % at 52 T for the light E || [110] and B || c-axis. The enhancement of the directional dichroism is explained by a modification of the electric and magnetic transition dipole moments with the canting of the spin direction of Cu²⁺. Furthermore we predicted that the electric dipole transition should be as large as the magnetic dipole transition at 52 T by rotating the sample around [110] axis by 45 degrees, because the magnetic dipole transition decreases with reduction of the c-component of the magnetic field of light. In fact, the absorption peak disappears for the light propagating in one direction. In other words, we succeeded in realization of "one-way transparency of light".

[1]M.Saito, K.Taniguchi, T.Arima, J. Phys. Soc. Jpn 77, 013705(2008)

TU.A-P61 - Weak ferromagnetic transition induced by structure phase transition in chiral antiferromagnet $\text{Ba}_3\text{Fe}_2\text{O}_5\text{Cl}_2$

N. Abe¹, S. Shiozawa¹, N. Netsu¹, K. Nguyen¹, K. Matsuura¹, H. Sagayama², A. Nakao³, Y. Tokunaga¹, T.H. Arima¹

1. *Department of Advanced Materials Science, University of Tokyo, Chiba, Japan*

2. *Institute of Materials Structure Science, KEK, Ibaraki, Japan*

3. *Research Center for Neutron Science and Technology, CROSS, Ibaraki, Japan*

Coupling of the crystal chirality and the magnetism in material causes interesting phenomena such as chiral soliton lattice, skyrmion, and magnetochiral dichroism. $\text{Ba}_3\text{Fe}_2\text{O}_5\text{Cl}_2$ is a chiral magnetic insulator of space group I213. Each magnetic Fe^{3+} ion is located at the center of oxygen tetrahedron. Neighboring FeO_4 tetrahedra connected by sharing a corner, which leads to fairly strong antiferromagnetic superexchange interaction. Because of a previous study provided no information about magnetic and dielectric properties, we grow large single crystals and reveal the physical properties of $\text{Ba}_3\text{Fe}_2\text{O}_5\text{Cl}_2$.

We succeeded in growing large single crystals by using floating zone method. A magnetization measurement shows that weak ferromagnetic moment appears below 137K. Dielectric constant also shows an anomaly at the magnetic transition temperature. In order to clarify the mechanism of the phase transition, we performed a single crystal structure analysis by using synchrotron x-ray diffraction at BL-8A, Photon Factory, Japan, and single crystal magnetic structure analysis by using pulsed neutron diffraction at BL-18, MLF, J-PARC, Japan. The crystal structure clearly shows that the crystal structure changes from cubic to orthorhombic at the magnetic phase transition temperature. From the result of the crystal structure analysis, Fe sites are split into two univalent sites in the low temperature phase. We also performed a magnetic structure analysis for the high temperature phase. We found that Fe magnetic moments are arranged antiferromagnetically. Therefore we can conclude that antiferromagnetic to weak ferromagnetic transition is induced by the structure phase transition. This phase transition would be controlled by applying uniaxial pressure or magnetic field.

TU.A-P62 - Strain induced phase separation in thin films of half-doped $\text{La}_{0.5}\text{Sr}_{0.5}\text{MnO}_3$ manganites: 55Mn NMR studies

M. Wojcik¹, E. Jedryka¹, G. Radaelli^{2,3}, D. Gutiérrez², F. Sánchez², J. Fontcuberta²

1. *Institute of Physics, Polish Academy of Sciences, Warsaw, Poland*

2. *Institut de Ciència de Materials de Barcelona (ICMAB-CSIC), Bellaterra, Spain*

3. *Istituto Italiano di Tecnologia, Smart Materials, Nanophysics Department, Genova, Italy*

Half-doped manganites $\text{La}_{1-x}\text{A}_x\text{MnO}_3$ (where A is a divalent ion and $x=0.5$) recently attracted a renewed attention because their ground state (ferromagnetic or antiferromagnetic, metallic or insulator) can be easily modified by engineering the bandwidth or modifying the carrier density. The aim of this study is to explore how epitaxial strain affects the magnetic and electric ground state in films of $\text{La}_{0.5}\text{Sr}_{0.5}\text{MnO}_3$ (LSMO-05) by using 55Mn NMR resonance as probe to local magnetism and charge localization. Various oxide substrates with a different lattice mismatch to LSMO-05 were used in order to induce different strain effect (tensile or compressive strain). 55Mn NMR spin echo experiments have been carried out at 4.2 K on films with thickness of 20 and 35 nm. The NMR spectra consist of the Mn^{4+} line and the resonance line corresponding to Mn in a mixed valence state revealing the presence of hole localized and hole itinerant states, respectively. The analysis of NMR data leads to the following conclusions: (1) Strain induces a separation into antiferromagnetic and ferromagnetic phases rather than reducing an overall magnetization of a film, which could be suggested by the macroscopic magnetization measurements. (2) A degree of phase separation depends on the film thickness and on magnetic history of the film. (3) 55Mn NMR frequency (55Mn hyperfine field) observed at manganese ions participating in the double exchange interaction is surprisingly high compared to that expected for this composition ($x=0.5$) and similar to the frequency observed for the optimally doped composition ($x=0.3$). This observation strongly suggests that besides phase separation also the electronic charge redistribution takes place between the ferromagnetic and the antiferromagnetic phases.

TU.A-P63 - Overlayer-induced reconstruction of Mn orbitals in manganite thin films studied by ^{55}Mn NMRM. Wojcik¹, E. Jedryka¹, D. Pesquera², F. Sánchez², G. Herranz², J. Fontcuberta²*1. Institute of Physics, Polish Academy of Sciences, Warsaw, Poland**2. Institut De Ciència De Materials De Barcelona (ICMAB-CSIC), Bellaterra, Spain*

Optimally doped manganite $\text{La}_{2/3}\text{Sr}_{1/3}\text{MnO}_3$ (LSMO) is prospective for use in spintronic devices, which involve contact of a manganite layer with other materials (mainly other perovskite oxides - ABO_3), leading to deterioration of magnetic and conducting properties of manganite film. Here, we use ^{55}Mn NMR as a probe of charge distribution and of Mn spin state in LSMO ultra thin films to study the effect of strain and bonding at the interface between manganite and ABO_3 capping layer. A series of LSMO thin films were grown by PLD deposition on the (001) STO- TiO_2 terminated substrates. Three of these films were respectively capped with SrTiO_3 (STO), SrZrO_3 (SZO) or LaAlO_3 (LAO), while the fourth remained uncapped and served as a reference. Based on the characteristic features of ^{55}Mn NMR spectra, the contributions from the two interfaces (with substrate and with capping) have been disentangled. The NMR line around 375 MHz corresponds to the mixed valence state of Mn ions within the main ferromagnetic and metallic phase (FMM) governed by double exchange (DE) interaction. Intensity of this line varies with the capping material and reveals a dramatic role of an open surface in breaking degeneracy of Mn $e_g(3d)$ orbitals, diminishing the strength of DE and converting a few upper atomic layers of the manganite film into antiferromagnetic (AF) phase. Depending on the capping material, parameters such as lattice mismatch to manganite, symmetry (s, d) and space expansion (3d, 4d) of the wave function of the B atom (Al, Ti, Zr), the local symmetry of Mn atoms in the upper layers is altered. In case of capping with LAO and STO (to less extend), this brings back the degeneracy of Mn $e_g(3d)$ orbitals and recovers the DE phase, whereas in case of SZO, the asymmetry of the Mn $e_g(3d)$ orbitals is strengthened, leading to expansion of the AF phase.

TU.A-P65 - Peculiar Magnetoelectric Coupling in BaTiO₃:Fe₁₁₃ppm

C. De Oliveira Amorim¹, F. Figueiras^{1,2}, J. de Sequeira Amaral^{1,2}, P. Tavares³, M.d.R. Correia⁴, E. Alves⁵, J. Rocha⁵, V.d.S. Amaral¹

1. *Physics Department & CICECO, University of Aveiro, Aveiro, Portugal*

2. *IFIMUP-IN, Science Faculty, Porto University, Porto, Portugal*

3. *Chemistry Center, Trás-os-Montes & Alto-Douro University, Vila Real, Portugal*

4. *Physics Department & I3N, Aveiro University, Aveiro, Portugal*

5. *C2TN, Instituto Superior Técnico, Campus Tecnológico e Nuclear, Bobadela, Portugal*

Multiferroics is one prominent area of Physics due to the outstanding applications that arise from these materials which led to the study of composites of ferroic materials, namely composites of ferromagnetic and ferroelectric archetypes.

We show results regarding polycrystalline BaTiO₃ which contained an overall 113 ppm of Fe. Despite this tiny concentration, abrupt variations in the magnetization ($\approx 600\%$) are seen in temperature dependent magnetic curve around $T \approx 330\text{K}$ and $T \approx 373\text{K}$.

This result is correlated with the BaTiO₃ ferroelectric phase transitions. Such effect was never seen even in works where bulk BaTiO₃ was doped/mixed with higher concentrations of Fe (similar effects were only seen in thin films composites). Raman Spectroscopy analysis of the 520cm^{-1} and the 487cm^{-1} vibrational modes confirms this correlation, revealing a magnetoelectric coupling in the BaTiO₃:Fe_{113ppm} phase transitions.

EDS mapping reveals that Fe distribution through the BaTiO₃ is quite inhomogeneous, tending to aggregate in specific locations we believe being in the vicinity (around/between/inside) of the grain boundaries which should have a preponderant role in the reported magnetoelectric coupling.

BaTiO₃ thermal treatments show that the magnetoelectric coupling persists for temperatures as high as 1200°C . Although, for $T \geq 1300^\circ\text{C}$ treatments the abrupt variations of the magnetization vanish and the magnetic curve assumes the shape of a typical paramagnetic Curie curve, suggesting the dispersion of the Fe ions all over the BaTiO₃ matrix.

Fe ion implantation in BaTiO₃ single crystals was made to confirm the importance of grain boundaries and in fact even for local Fe concentrations as high as 1% do not show any signs of a magnetoelectric coupling in the magnetization curve, having instead a magnetization behavior similar to the one obtained for the $T \geq 1300^\circ\text{C}$ thermal treatments.

We also discuss DFT calculations as well as others' experimental data to suggest possible mechanisms for this peculiar magnetoelectric coupling.

TU.A-P66 - Huge Resistive Change in Tunnel Junctions Using the Multiferroic BiFeO₃ BarrierT. Ichinose¹, H. Naganuma¹, M. Oogane¹, Y. Ando¹*1. Tohoku University, Japan*

Tunnel electroresistance (TER) effect in ferroelectric tunnel junctions has attracted much attention because the high resistance change was achieved ~106% by switching ferroelectric polarization [1]. If we use multiferroic materials as a tunneling barrier having magneto-electric (ME) coupling, an extremely weak magnetic field can be detected through both of ME effect and TER effect; which is a noble concept of high-sensitive magnetic field sensors. In this study, (001)-La:SrTiO₃ sub./BiFeO₃(0.8-3.2)/CoFe(4)/Ru(5) (in nm) tunnel junctions were prepared by r.f. magnetron sputtering, and its structural, ferroelectric, and electric conductive properties were systematically investigated. TEM observation using pattern analysis of nano-beam diffraction revealed that the BiFeO₃ barrier has rhombohedral structure even though the film thickness was only 3.2 nm. It should be noted that the rhombohedral symmetry of BiFeO₃ has ME effect above room temperature. Switching spectroscopy PFM confirmed that the ferroelectric polarization of BiFeO₃ barrier was switched. The current-voltage (I-V) curves for the junctions with various BiFeO₃ barrier thicknesses were asymmetric, and the current was drastically decreased at negative bias; which indicated that the junction resistance strongly depended on the polarization direction. The resistance ratio between upward-polarization-state and downward-polarization-state was estimated to be 107%. 10 times larger resistance ratio than that of the previous report should be caused by extremely low resistance in downward-polarization-state. The barrier height lowering in downward-polarization-state should lead the conduction of the electrons with high energy than that of barrier height. The asymmetric I-V curves were observed even if the BiFeO₃ thickness was decreased from 3.2 to 0.8 nm. This study was partly supported by KAKENHI (No. 25600067, 24226001) and JST ASPI-MATT.

[1] H. Yamada et al., ACS Nano 7, 5385 (2013)

TU.A-P67 - Tests for electromagnetic effects on a toroidal magnetic ordered state of UNi₄BH. Saito¹, K. Uenishi¹, N. Miura¹, C. Tabata¹, H. Hidaka¹, T. Yanagisawa¹, H. Amitsuka¹*1. Graduate School of Science, Hokkaido University, Hokkaido, Japan*

Toroidal moment is one of the parameters that describe the strength of the magnetoelectric effect. In the last several years, the toroidal order, which is the ordered periodic array of toroidal moments, has attracted much interest in connection with multiferroic insulating materials. Last year, S. Hayami et al. showed theoretically that such an exotic order can occur in metallic systems, and electric currents can induce magnetization in such the toroidal ordered metal [1].

UNi₄B crystalizes in the orthorhombic structure with the symmetry *Cmcm* and U ions form a slightly distorted triangular lattice [2]. Below T_N (= 20.4 K), 2/3 of U ions gain ordered magnetic moments and make the vortices in each triangular planes [3]. This magnetic structure is the same as the structure assumed in the above theory, so that UNi₄B may show the exotic electromagnetic phenomena predicted by the theory. To test the reality of the theoretical predictions, we performed the magnetization measurements with the electric currents applied in the toroidal magnetic ordered state of UNi₄B.

Magnetization parallel to [01-10] was measured with applying the electric current parallel to [1000] and [0001]. In our measurements, a variation of magnetization ΔM due to applied electric current was found in the direction of [01-10] below T_N for each setup of $I \parallel [1000]$ and $[0001]$. ΔM increases by cooling or applying larger currents. Reversing the current direction, ΔM changes its sign. ΔM is mostly independent of magnetic field. Those experimental results indicate that the electric currents in both the directions induce spontaneous magnetization parallel to [01-10] below T_N , confirming basically the theoretical predictions.

[1] S. Hayami *et al.*, Phys. Rev. B 90, 024432 (2014)

[2] Y. Haga *et al.*, Physica B 403 900-902 (2008)

[3] S. A. M. Mentink *et al.*, Phys. Rev. Lett. 73, 1031 (1994)

TU.A-P72 - Strain effect and multiferroic properties of $\text{Sr}_2\text{CrReO}_6$ / $\text{Ba}_x\text{Sr}_{1-x}\text{TiO}_3$ heterostructuresJ. So¹, F. Xu¹, K. Ito¹, T. Hajiri¹, K. Ueda¹, H. Asano¹*1. Nagoya University, Dept. of Crystalline Materials Science, Graduate School of Engineering*

Multiferroic heterostructure composed of ferromagnetic (FM) half-metal and ferroelectrics (FE), in which the coexistence of tunneling electroresistance (TER) and tunneling magnetoresistance (TMR) effects can be confirmed, are promising for future high-density memory devices. Double-perovskite ferrimagnetic half-metal $\text{Sr}_2\text{CrReO}_6$ with a high Curie temperature ($T_C = 635$ K)[1] exhibits large magnetocrystalline anisotropy[2], making it favorable to generate perpendicular magnetization. Therefore it is expected for spintronics applications at room temperature. However, there has been no study that utilized $\text{Sr}_2\text{CrReO}_6$ in multiferroic heterostructures. In this study, in order to evaluate the potential of $\text{Sr}_2\text{CrReO}_6$ as an electrode of multiferroic tunnel junctions, we used $\text{Ba}_x\text{Sr}_{1-x}\text{TiO}$ ($x = 0.2-0.7$) as buffer layers to induce strain and perpendicular magnetization in $\text{Sr}_2\text{CrReO}_6$ films. Then we grew $\text{Ba}_{0.7}\text{Sr}_{0.3}\text{TiO}_3$ as a dielectric layer on $\text{Sr}_2\text{CrReO}_6$ epitaxially and also systematically investigated the influence of strain on dielectric properties of $\text{Ba}_{0.7}\text{Sr}_{0.3}\text{TiO}_3$ layers.

Thin films of $\text{Sr}_2\text{CrReO}_6$ and $\text{Ba}_x\text{Sr}_{1-x}\text{TiO}$ ($x = 0.2-0.7$) were grown on LSAT (001), LAO (001) substrate by magnetron sputtering. The buffer layer $\text{Ba}_x\text{Sr}_{1-x}\text{TiO}$ has larger lattice constant than $\text{Sr}_2\text{CrReO}_6$ and induces larger tensile strain as x becomes bigger. We have confirmed the c/a value of 80nm $\text{Sr}_2\text{CrReO}_6$ goes smaller ($c/a = 0.998, 0.994$ and 0.991) as x increases ($x = 0.2, 0.4$ and 0.7). It was found that $\text{Sr}_2\text{CrReO}_6$ showed different longitudinal and perpendicular magnetization properties depending on its c/a value. Then we investigated electric properties of $\text{Ba}_{0.7}\text{Sr}_{0.3}\text{TiO}_3$ thin film on the $\text{Sr}_2\text{CrReO}_6$. We obtained the $2P_r$ values of $\text{Ba}_{0.7}\text{Sr}_{0.3}\text{TiO}_3$ are 28, 40, and 62 $\mu\text{C}/\text{cm}^2$ for thickness of 100, 50, 40 nm, respectively. The dielectric measurement result of $\text{Ba}_{0.7}\text{Sr}_{0.3}\text{TiO}_3$ with different thickness shows that as $\text{Ba}_{0.7}\text{Sr}_{0.3}\text{TiO}_3$ layer becomes thinner, its property becomes better. The negative mismatch of -1.5% induced greater strain effect when $\text{Ba}_{0.7}\text{Sr}_{0.3}\text{TiO}_3$ becomes thinner. Therefore, $\text{Sr}_2\text{CrReO}_6/\text{Ba}_x\text{Sr}_{1-x}\text{TiO}_3$ heterostructure is a very potential substitute for multiferroic tunneling junctions aiming for the coexistence of TER and TMR effects at room temperature.

[1] H. Asano, et al., Appl. Phys. Lett. 85, 263 (2004)

[2] J. M. Lucy, et al., Phys. Rev. B 90, 180401 (2014)

TU.A-P73 - Magnetic- and electric-field control of magnetoelectric properties of CaBaCo₄O₇R. Oda¹, R. Kajihara¹, K. Nishida¹, M. Akaki², H. Kuroe¹, H. Kuwahara¹1. *Department of Physics, Sophia University*2. *Center for Advanced High Magnetic Field Science, Graduate School of Science, Osaka University*

The so-called "114" family compounds focused in this study have been intensively investigated as a novel magnetic system. One of these 114 compounds, CaBaCo₄O₇ with polar space group Pbn21, has recently attracted much interest owing to its giant change of electric polarization ΔP associated with the ferrimagnetic ordering below $T_c=64K$. One possible origin of ΔP is proposed to be magnetostriction, which is supported by the large change of lattice parameters at T_c . For further understanding of the large ΔP of magnetic origin, we have systematically investigated the magnetoelectric properties of pristine CaBaCo₄O₇ and its impurity-substituted derivative (Ca_{1-x}Y_x)BaCo₄O₇, (Ca_{1-x}Sr_x)BaCo₄O₇, Ca(Ba_{1-x}Sr_x)Co₄O₇, and CaBa(Co_{1-x}Fe_x)₄O₇ single crystals in magnetic and/or electric fields.

By applying magnetic fields, magnetic and dielectric transition temperature for CaBaCo₄O₇ increases, which is due to the stabilization of the ferrimagnetic phase. We have observed the large magnetocapacitance and magnetic-field-induced ΔP near above T_c . In addition, we have tried to detect the electric-field-induced magnetization by using a magnetometer with customized system. This is because the nonzero components, α_{23} and α_{32} , of linear magnetoelectric tensor are expected from a symmetry analysis for the magnetic point group of $m'm2'$. As a result, we have successfully observed the discernible change of magnetization within the ab plane as a function of applied electric field along the c axis up to $\pm 2.0MV/m$ below T_c , which is the first demonstration expressed as $M_b = \alpha_{32} E_c$. We have measured lattice striction for CaBaCo₄O₇ in magnetic fields by using a strain gauge attached along each principal axes. Then we have confirmed the large change of lattice striction: the magnetic easy ab plane expands, whereas the hard c axis shrinks at T_c with decreasing temperature. The observed large $\Delta L/L$ of about 10^{-4} also supports that the magnetostriction plays an important role in the appearance of large ΔP .

TU.A-P75 - Charge-Ordering induces magnetic axes rotation in organic materials (TMTTF)₂X (X=PF₆, AsF₆, SbF₆)C. Dutoit¹, S. Bertaina¹, M. Orio², M. Dressel³, A. Stepanov¹*1. Aix-Marseille Université, CNRS, IM2NP UMR7334, Marseille, France**2. Aix-Marseille Université, CNRS, iSm2 UMR7313, Marseille, France**3. Physikalisches Institut Universität Stuttgart, Stuttgart, Germany*

Charge-ordering (CO) phenomenon, also named charge disproportionation, has been intensively studied in the last decade in antiferromagnetic quantum spin chains (TMTTF)₂X with X = SbF₆, AsF₆, and PF₆. (TMTTF) molecules are arranged in a zig-zag configuration, forming stacks along the a direction. Above TCO, the charge is equally distributed between two TMTTF molecules. Below TCO, there is a charge disproportionation between two molecules TMTTF and the symmetry center is broken. All (TMTTF)₂X salts crystallize in the triclinic structure P-1. Experimentally, we studied the g tensor electron spin resonance (ESR) at 9.7GHz and the temperature dependence of the g tensor principal axes position was examined. We observed a rotation of up to 18° of the g-tensor principal axes around a direction in the temperature range from 300 to 15K for (TMTTF)₂SbF₆ salt. We discuss the possible origin of this rotation by comparing experimental results with the quantum-chemical calculation performed by DFT (using ORCA). g-tensor were obtained using the hybrid functional B3LYP and the EPR-II basis set. Considering only thermal contraction of TMTTF structure [2] as temperature decreases, the numerical calculation shows a rotation of only 2° between 300K and 4K. If one considers additionally a uniform anion displacement, experimentally reported in (TMTTF)₂PF₆ salt [1], one obtains a rotation of about 22° between 300K and 4K, which is in good agreement with the experimental value.

[1] Foury-Leylekian et al, Physica B 405 (2010) S95

[2] Furukawa, K. et al, J. Phys. Soc. Japan 78, 104713 (2009)

TU.A-P76 - Improper ferroelectricity in the $\sim 1 \mu\text{C cm}^{-2}$ range in the single-valent quadruple perovskite $\text{LaMn}_3\text{Mn}_4\text{O}_{12}$

A. Gauzzi¹, P. Bordet², C. Bellin¹, M. Verseils¹, A. Polian¹, Y. Klein¹, F. P. Milton³, A. Gualdi³, D. Dreifus³, P. S. Pizani³

1. Sorbonne Universités - UPMC - IMPMC, Paris, France

2. Institut Néel - CNRS, Grenoble, France

3. Universidade Federal de São Carlos, São Carlos, SP, Brazil

4. IMEM-CNR, Parma, Italy

Improper ferroelectrics, where the electric polarization is induced by a magnetic order, typically exhibit modest values of polarization, $P \sim 0.1 \mu\text{C cm}^{-2}$, which prevents their use as multiferroic materials. Here we report on values up to $\sim 1 \mu\text{C cm}^{-2}$ in the single-valent compound $\text{LaMn}_3\text{Mn}_4\text{O}_{12}$ [1], which belongs to the family of quadruple perovskites $AA'_3B_4O_{12}$ [2,3]. This value is ~ 4 times larger than the previous record value reported on the related mixed-valence compound $\text{CaMn}_3\text{Mn}_4\text{O}_{12}$ [4,5]. Our analysis of neutron diffraction, magnetization and pyroelectric current measurements shows that, in $\text{LaMn}_3\text{Mn}_4\text{O}_{12}$, the polarization is induced at $T_{N,B} = 78 \text{ K}$ by a C-type antiferromagnetic order of the Mn^{3+} ions at the octahedral B sites. The simplicity of the nuclear and magnetic structures and the observation of a sudden increase of the monoclinic b-angle at $T_{N,B}$ enable us to establish that the polarization is parallel to the ac-diagonal, which indicates that the magnetoelectric coupling is driven by exchange striction. An abrupt $\sim 2 \text{ cm}^{-1}$ softening of all Raman modes at $T_{N,B}$ and a 40% reduction of the specific heat by a 9 T field confirm the existence of a very large magnetoelastic coupling. Finally, the single-valent Mn^{3+} characteristics enable us to rule out the possible contribution of the charge ordering to the polarization.

1. A. Prodi *et al.*, Phys. Rev. B 79, 085105 (2009)

2. A. Deschanvres, B. Raveau, and F. Tollemer, Bull. Soc. Chem. Fr. 11, 4077 (1967)

3. A. Prodi *et al.*, Nature Mater. 3, 48 (2004)

4. G. Zhang *et al.*, Phys. Rev. B 84, 174413 (2011)

5. R. D. Johnson *et al.*, Phys. Rev. Lett. 108, 067201 (2012)

TU.A-P77 - Using pinned domain walls to implement magnetic logic gates in ferromagnetic-ferroelectric heterostructures

D. López González¹, A. Casiraghi¹, S. van Dijken¹

1. NanoSpin, Department of Applied Physics, Aalto University School of Science, Aalto, Finland

Local magnetic anisotropy modulations in continuous ferromagnetic films can be realized using pre-patterned substrates [1] or focused ion beam irradiation [2]. Alternatively, strain coupling between a ferroelectric substrate and a magnetic film can be used to induce regular magnetic stripe domains [3]. Because of strong pinning of magnetic domain walls onto ferroelectric boundaries, versatile control over the formation of magnetically charged and uncharged domain walls in an applied magnetic field can be achieved in such systems [4]. Here, we report on the effect of pinned magnetic domain walls on the magnetization reversal in a Co₄₀Fe₄₀B₂₀ wedge film on a ferroelectric BaTiO₃ substrate. We show that the distinctive energies of the two types of domain walls cause either a lateral modulation or a synchronization of magnetic switching, depending on field direction. Based on these findings, we propose a magnetic logic device consisting of three stripe domains, whereby the central domain reads out the magnetic state of the two adjacent domains. Depending on the applied bias field, AND, NOR, and NOT gates can be implemented. The concept is experimentally demonstrated and further supported by micromagnetic simulations.

[1] S.P. Li et al., Phys. Rev. Lett. 88, 087202 (2002)

[2] J. Fassbender and J. McCord, J. Magn. Mater. 320, 579 (2008)

[3] T.H.E. Lahtinen et al., Adv. Mater. 23, 3187 (2011)

[4] K.J.A. Franke et al. Phys. Rev. B 85, 094423 (2012)

TU.A-P78 - Exotic ferromagnetic ordering of polar magnetic PbVO₃ epitaxial thin films

S. Hee Oh¹, H. Jin¹, J. Cha², S. Hong², W. Jo¹

1. *Department of Physics, Ewha Woman University*

2. *Department of Physics and Graphene Research Institute, Sejong University*

Tetrahedron-based perovskite PbVO₃ (PVO) is an intriguing polar magnetic material because its strong tetragonal distortion allows VO₅ square-pyramidal structure rather than VO₆ octahedron. Bulk PVO is known to show the unique features of 2-dimensional antiferromagnetic ordering and large pyroelectric polarization. The c-axis lattice parameter of the PVO films epitaxially grown on LaAlO₃(001) and SrTiO₃(001) substrates is abnormally elongated by 5% and 6.5%, respectively [1]. Atomic ordering of Pb and V shows an interesting configuration onto La and Al or Sr and Ti. In a single-crystal bulk, the ground state of magnetic ordering of PVO is degenerated by C- and G-type configurations [2] and its transition temperature is reported as $T_N = 47\text{K}$ [3]. In our theoretical study using the first-principle calculations, a ferromagnetic ordering is found to be stable in the elongated PVO thin-films. Our magnetic measurement exhibits a clue for this exotic phase at low temperature, which is a direct evidence for change of the exchange interaction between two adjacent dxy electrons of the V⁺⁴ ions. The phenomenon is attributed to the elongation of the c-axis lattice parameter of the PVO thin-films.

[1] S. H. Oh et al., J. Phys. D: Appl. Phys. 47, 245302 (2014)

[2] D. Singh, Phys. Rev. B 73, 094102 (2006)

[3] K. Oka et al. Inorg. Chem. 47, 7355 (2008)

TU.A-P79 - Magnetic properties and Magnetoelectric coupling of vacancy doped hexagonal $\text{LuMn}_x\text{O}_{3+\delta}$ ceramics

A. Baghizadeh¹, J.M. Vieira¹, J.S. Amaral, M.P Gr̃a

1. CICECO, Dep. of Materials And Ceramics Engineering

Vacancy doping on A-site or B-site of the h- $\text{LuMn}_x\text{O}_{3+\delta}$ ($x=\text{Mn}/\text{Lu}$) ceramics were used to explore the dependency of the lattice parameters and magnetic properties to doping. Ceramics samples were sintered via solid state route in the range of $0.92 \leq x \leq 1.12$, and the study extended to investigate the effect of sintering time. The concomitant occurrences of planar defects, nano-scale domains inside the crystalline grains of the main phase and secondary phases as impurities are further investigated by electron microscopy for samples on either sides of the stability range of hexagonal $\text{LuMn}_x\text{O}_{3+\delta}$ phase. It is found that within the solid stability limit and different sintering conditions studied in this work, the lattice structure preserves the hexagonal P63cm crystalline structure. Shrinkage of the lattice parameters as x goes from 0.92 to 1.12 is found. The AFM transition with Neel ordering temperature around 90 K is observed for all samples under study. The trend of change in T_N is decreasing as the x value is increased, showing higher values for lower x values. The irreversibility observed in FC and ZFC magnetization measurements of all samples starts at T_N and is independent from sintering conditions. Magneto-electric coupling could be revealed for all samples in measurements of the complex dielectric constant. Measured dielectric and magnetic properties coupled to lattice change are connected to the vacancy doping of either A-site or B-site.

This work was developed within the project CICECO-Aveiro Institute of Materials (Ref. FCT UID/CTM/50011/2013)

TU.A-P81 - Excitonic Multipole Order in a d-p Model with Parity MixingY. Sugita¹, S. Hayami¹, Y. Motome¹*1. Department of Applied Physics, University of Tokyo, Tokyo, Japan*

Multipole orders have attracted much attention in condensed matter physics, as they lead to exotic electronic, transport, and optical properties. Recently, unconventional multipole orders associated with conventional electronic symmetry breaking have been of great interests. A typical example is found in several pyrochlore compounds, such as Os and Ir pyrochlores. In these compounds, a noncoplanar all-in/all-out type magnetic (dipole) order was discussed as a magnetic octupole order. Similar multipole orders (magnetic toroidal and quadrupole orders) were discussed on a zigzag chain and a honeycomb lattice, paying attention to the effects of the atomic spin-orbit coupling and the mixing of different parity orbitals. In these previous works, however, multipole orders always appear subsidiary to the lower-rank electronic orders. Thus it is important to explore the possibility of pure, primary multipole ordering for deeper understanding of the multipole physics. In order to search such primary multipole orders, we consider a simple d-p model on a zigzag chain, which incorporates the spin-orbit coupling and the parity mixing. The model is considered as an extension of the multi-orbital Hubbard model discussed for excitonic orders. Using the Hartree-Fock approximation, we obtain the ground-state phase diagram of this model at half filling in a wide range of intra and interorbital Coulomb interactions. The result shows that a pure multipole ordered phase appears as an intermediate phase between the band insulating phase with the d-p hybridization gap and the antiferromagnetic phase caused by the strong intraorbital Coulomb interaction. The intermediate phase has a magnetic quadrupole order with an excitonic nature from the orbital mixing, which is stabilized by the spin-orbit coupling and the parity mixing. We also find that the multipole ordered phase exhibits a peculiar band deformation with a shift of the band bottom in the momentum space in an applied magnetic field.

TU.A-P82 - Effect of Fe doping on magnetic properties of RMnO₃ single crystals (R = Gd and Dy)

J. Lazrovský¹, V. Viktor¹, M. Mihalik¹, M. Mihalik¹, M. Zentkovský¹, J. Briančin², K. Uhlířovský³, M. Kratochvílovský³, M. Fitta⁴

1. *Institute of Experimental Physics, Slovak Academy of Sciences, Watsonova 47, Košice, Slovak Republic*

2. *Institute of Geotechnics, Slovak Academy of Sciences, Košice, Slovak Republic*

3. *Department of Condensed Matter Physics, Faculty of Mathematics and Physics, Charles University in Prague, Prague, Czech Republic*

4. *Institute of Nuclear Physics, Polish Academy of Sciences, Kraków, Poland*

In our work we study effect of Fe doping on thermal and magnetic properties of GdMnO₃ and DyMnO₃ single crystals. In GdMnO₃ a ferroelectric phase appears in magnetic field $H = 1$ T and DyMnO₃ shows a ferroelectric order even at $H = 0$ [1]. GdMnO₃ orders magnetically below $T_N(\text{Mn}) = 43$ K and undergoes the second transition at $T_N(\text{Gd}) \sim 6.5$ K [1]. DyMnO₃ exhibits magnetic ordering below $T_N(\text{Mn}) = 41$ K, where Mn-spins order in a longitudinal spin density wave propagating along the b-direction; this structure changes to a cycloidal phase below $T_s(\text{Mn}) = 18$ K and another ordering appears at $T_N(\text{Dy}) \sim 6.5$ K [1, 2]. The cycloidal Mn-spin structure, with the inverse Dzyaloshinskii-Moriya interaction is the driving force for ferroelectric order and frustration is mechanism of multiferroicity [3]. Magnetic frustration can be tuned by modifications of exchange interactions e.g. by substitution. Single crystals of RMn_{1-x}Fe_xO₃, where R = Gd, Dy and $x = 0.00, 0.01, 0.02, 0.05, 0.1$, were grown by optical floating zone method in order to verify this assumption. All crystals adopt the orthorhombic crystal structure, space group Pbnm. The crystal lattice parameters change linearly and volume of the elementary cell decreases with Fe doping. Temperature of all characteristic transitions decreases with doping as it is indicated e.g. by the decrease of the maximum in heat capacity at $T_N(\text{Mn})$ from 38.5 K to 33 K and from 41.5 K to 31.5 K for Dy and Gd samples, respectively. No sign of transition to the cycloidal phase was observed for $x > 0.02$. Magnetization measurements confirmed that c-axis is the hard magnetic axis. [1] T. Kimura et al.: Phys. Rev. B 71 (2005) 224425. [2] T. Kimura et al.: J. Phys.: Condens. Matter 20 (2008) 434204. [3] S-W. Cheong et al: Nat. Mater. 6 (2007) 13.

TU.A-P83 - Determination of incommensurate magnetic structures using symmetry argumentsI. Urcelay-Olabarria¹, J.M. Pérez-Mato¹, E. Ressouche², J.L. García-Muñoz³*1. Departamento de Física de la Materia Condensada, Facultad de Ciencia y Tecnología, Universidad del País Vasco, UPV-EHU, Leioa, Spain**2. SPSMS, UMR-E CEA/UJF-Grenoble 1, INAC, Grenoble, France**3. Institut de Ciència de Materials de Barcelona, ICMA-B-CSIC, Campus universitari de Bellaterra, Bellaterra, Spain*

Determining a magnetic structure from neutron diffraction data can be a rather tough problem, and frequently the data analysis is manually constrained in order to achieve a satisfactory convergence. Nevertheless, in most of the cases those constraints are made using arbitrary criteria, and this is more evidenced in the field of incommensurate magnetic structures (ICMS). In this work we show how the use of the superspace symmetry formalism allows to rationalize not only the data treatment, but also the physical properties induced by a magnetic ordering.

The ICMSs in $Mn_{1-x}Co_xWO_4$ have been studied using symmetry arguments. $MnWO_4$ is a multiferroic material in which the magnetic order of one of its magnetic phases induces ferroelectricity. Like most multiferroic materials $MnWO_4$ is extremely sensitive to small perturbations. It turned out that doping with Co^{2+} is particularly interesting since it strongly stabilizes the multiferroic phase at low temperatures, and moreover, by increasing the cobalt amount in the crystals its properties change (electric polarization flops from the b axis to the ac plane). This change of orientation is linked to a symmetry change. The ICMS of the $x = 0$ and $x = 0.10$ compounds, have been studied thoroughly. We have found, not only the symmetry of the magnetic structures and their intrinsic restrictions, but also information about the tensor properties, such as ferroelectric and magnetostructural properties: in the paramagnetic state, there is a unique independent magnetic atom in the crystallographic unit cell in both cases, but when the system enters into the multiferroic phase, this is no-longer true. In the multiferroic phase of $MnWO_4$, the two Mn atoms in the unit cell become symmetry independent, whereas in the $x = 0.10$ substituted compound, they are still symmetry-related. This difference is related to the change of the electric polarization.

TU.A-P85 - Phase transitions and magnetoelectric coupling in $\text{Bi}_{1-x}\text{A}_x\text{FeO}_3$ (A=La, Nd) multiferroic ceramicsA. Amirov¹, I. Kamilov¹, D. Yousupov², L. Reznichenko², O. Razumovskaya², I. Verbenko²

1. Institute of Physics, Dagestan Scientific Center of Russian Academy of Sciences, Makhachkala, Russia

2. Institutes of Physics, South Federal University

Compounds on base of BiFeO_3 are very perspective multiferroic materials due to high temperature of magnetic and ferroelectric phase transitions, bad conductivity and simple chemical structure [1-2].

High quality ceramics were synthesized on the basic of $\text{Bi}_{1-x}\text{A}_x\text{FeO}_3$ (A=La, Nd; $x=0-0.2$) solid solutions. Their crystal and grain structure, Mossbauer spectra, dielectric, magnetic, thermal characteristics were studied. The ac-susceptibility vs. temperature curve of BiFeO_3 has a sharp peak at 646 K which corresponds to the antiferromagnetic phase transition T_N and it is confirmed by literature data [3]. The anomalies of dielectric permeability, spacing parameter, thermal conductivity and heat capacity near temperature of antiferromagnetic order T_N were observed in all samples and it is related with correlation between magnetic and ferroelectric subsystem which is typical for multiferroics. The magnetization of pure BiFeO_3 is small and grows linearly with magnetic field. The substitution Bi by La or Nd changes the temperature of the antiferromagnetic order and increases the magnetization of BiFeO_3 . The magnetic properties change occurs not only on account of magnetic moment and ionic radiuses, but also because of La and Nd ions magnetic moments anisotropy.

The samples were also studied for the presence of the magnetodielectric effect (magnetocapacitance), which is a change in the permittivity of the sample caused by the application of a magnetic field

$$\frac{\Delta\varepsilon(H)}{\varepsilon(0)} = \frac{\varepsilon(H) - \varepsilon(0)}{\varepsilon(0)},$$

where $\varepsilon(H)$ and $\varepsilon(0)$ are the permittivities in a magnetic field and in the absence of it, respectively. The measurement results showed an increase in magnetodielectric effect is associated with an increase in the degree of interaction between the dipole and magnetic subsystems. The slower increase of magnetocapacitance in the range $0.05 \leq x \leq 0.1$ associated with the change of predominant mechanism in the solid solutions, as in $0.15 \leq x \leq 0.2$ - with the existence of invar effect due to the appearance of a new monoclinic phase.

- [1]. J. Wang et al., *Science* 299, 1719 (2003)
- [2]. A.K. Zvezdin and A.P. Pyatakov, *Sov. Phys. Usp.* 47, 8 (2004)
- [3]. Sosnowska and A. K. Zvezdin, *J. Magn. Magn. Mater* 140-44, 167 (1995)

TU.A-P86 - Superficial strain effect on magnetic anisotropy of BaTiO₃/La₂/3Sr₁/3MnO₃ bilayers

J.E. Ordoñez¹, L. Marín², L. Alfredo Rodríguez³, M.E Gómez¹, P. Algarabel^{4,5}, J.A. Pardo⁶, L. Morellón^{4,6}, C. Magen^{4,7,8}, P. Prieto^{1,9}, M. Ricardo Ibarra^{4,7}

1. Universidad Del Valle, Cali, Colombia

2. LAAS-CNRS 7, Toulouse, France

3. CEMES-CNRS 29, Toulouse, France

4. Departamento de Física de la Materia Condensada, Universidad de Zaragoza, Zaragoza, Spain

5. ICMA-CSIC, Universidad de Zaragoza, Zaragoza, Spain

6. INA, Universidad de Zaragoza, Zaragoza, Spain

7. LMA-INA, Universidad de Zaragoza, Zaragoza, Spain

8. Fundación ARAID, Zaragoza, Spain

In multiferroic heterostructures magnetoelectric coupling between a ferroelectric material and a ferromagnetic film has been extensively studied during the last decade and various interaction mechanisms have been identified as promising routes towards exclusively electric-field controlled magnetism. In strain-coupled systems, direct correlations between the polarization direction within ferroelectric domains and the locally-induced magnetic anisotropy have been demonstrated [1-2]. We have fabricated bilayer thin films of the ferromagnetic (FM) La₂/3Sr₁/3MnO₃ (tLSMO=100 nm) and ferroelectric (FE) BaTiO₃ (tBTO=100 nm) on (001) oriented SrTiO₃ (STO), (LaAlO₃)_{0.3}(Sr₂TaAlO₆)_{0.7} (LSAT) and LaAlO₃ (LAO) substrates as a possible route to design heterostructures with artificial magnetoelectric coupling. Reciprocal space map analysis revealed that, while the LSMO grew epitaxially strained, the BTO film grew relaxing its single-crystal structure through dislocations formed in the LSMO-BTO interface. Magnetization-temperature curves prove the ferromagnetic order for all bilayers at room temperature, with magnetization between 280-320 emu/cm³, making possible a multiferroic behaviour at room temperature. Magnetic anisotropy analysis through magnetization hysteresis loops performed at 300 K, with the magnetic field applied along different in-plane crystallographic directions, showed that the bilayer grown on STO (001) substrate presented a change in the magnetic anisotropy from biaxial magnetic ordering (observed in the LSMO/STO (001) single-layer) to uniaxial magnetic ordering (BTO/LSMO/STO (001) bilayer) due to strain induced by the BTO layer on the top of LSMO layer. This effect has not been observed in the bilayers grown on LSAT and LAO substrates. This result revealed that the superficial strain effect only induced a uniaxial anisotropy when the LSMO film was grown with a tensile strain.

Acknowledgments: This work has been supported by "Research Projects CI 7917-CC 10510 contract 0002-2013 COLCIENCIAS and CI 7978 UNIVALLE.

[1] Y.-H. Chu et al., Nature Materials, 7, 478 (2008)

[2] R. Streube et al., Phys. Rev. B 87, 054410 (2013)

TU.A-P87 - Magnetic and structural features of multiferroic $\text{EuFe}_3(\text{BO}_3)_4$: Spectroscopic studies

K. Boldyrev¹, M. Popova¹, D. Erofeev^{1,2}, T. Stanislavchuk³, B. Malkin⁴, L. Bezmaternykh⁵, I. Gudim⁵

1. Institute of Spectroscopy, Russian Academy of Sciences, Troitsk, Moscow, Russia
2. Moscow institute of physics and technology, Dolgoprudnyj, Moscow region, Russia
3. Department of Physics, New Jersey Institute of Technology, Newark, NJ, United States
4. Kazan Federal University, Kazan, Russia
5. Kirensky Institute of Physics, Siberian Branch of the Russian Academy of Sciences, Krasnoyarsk, Russia

Rare-earth iron borates with general formula $\text{RFe}_3(\text{BO}_3)_4$ ($\text{R} = \text{Y}, \text{Pr-Er}$) have a structure of the natural mineral huntite (SG R32). Iron borates with an ionic radius of R smaller than that of Sm undergo a structural phase transition into the SG P3121 at the temperature T_S inversely proportional to the ionic radius of R^{3+} . $\text{EuFe}_3(\text{BO}_3)_4$ has the lowest T_S . $T_S=88\text{K}$ and $T_S=58\text{K}$ were reported for powder samples prepared by solid-phase synthesis [1] and for a single crystal [2], respectively. In the present work we study how and why the method of sample growth influences structural, magnetic, and spectroscopic properties of $\text{EuFe}_3(\text{BO}_3)_4$. We compare optical spectra of $\text{EuFe}_3(\text{BO}_3)_4$ crystals grown by flux-melting technique using (i) $\text{Bi}_2\text{Mo}_3\text{O}_{12}$ and (ii) Li_2WO_4 based fluxes. The spectra clearly evidence $T_S=58\text{K}$ for the sample (i) and $T_S=83\text{K}$ for the (ii) one, whereas $T_N=34\text{K}$ for both samples. Obviously, lower T_S for the sample (i) is connected with entering of a “big” Bi^{3+} ion from the flux into positions of Eu^{3+} . Our estimate gives $7\pm 2\%$ for Bi concentration in the sample (i). Bi impurity manifests itself also by a presence of extra lines in the spectra, due to Eu^{3+} located near Bi impurities. Using high-resolution polarized spectra of the “pure” (ii) crystal, we have determined energies and symmetries of the Eu^{3+} crystal-field (CF) levels for both R32 and P3121 phases. CF calculations were performed and CF parameters were determined. To describe the spectral data for a magnetically ordered state, the anisotropic orbitally-dependent exchange Hamiltonian was considered. These results form a basis for a correct description of magnetic and magnetoelectric properties of $\text{EuFe}_3(\text{BO}_3)_4$.

This work was supported by the Russian Science Foundation (Grant¹ 14-12-01033).

[1] Y. Hinatsu et.al., J. Solid State Chem. 172, 438 (2003)

[2] M. N. Popova, J. Magn. Magn. Mater. 321, 716 (2009)

TU.A-P88 - New dipolar ordering of $(\text{C}_2\text{H}_5\text{NH}_3)_2\text{CuCl}_4$ below 26 K

T. Sakami¹, T. Ohtani¹, X. Xi¹, T. Suzuki¹

1. Department of Quantum Matter, ADSM, Hiroshima University, Higashi-Hiroshima, Japan

Perovskite-type layered structure compounds with the chemical formula $(\text{C}_2\text{H}_5\text{NH}_3)_2\text{MeCl}_4$ (Me = Transition metal) have been intensively investigated due to the interests in the mechanism of successive transition. Many of these compounds show not only magnetic order but also ferroelasticity. We have studied dielectric properties of $(\text{C}_2\text{H}_5\text{NH}_3)_2\text{CuCl}_4$ (hereafter EACuC) known as antiferromagnet below 10 K and found out a clear anomaly at 26 K in the temperature dependence of the dielectric constant. To confirm this transition, we carried out the x-ray diffraction experiments of single-crystalline samples and found that the centrosymmetry was lifted below 26 K. These experimental results strongly suggests that EACuC has a new dipolar ordering at low temperatures.

TU.A-P89 - Jahn-Teller distortions study in Sm(Nd)MnO₃ Manganites

R. Teixeira^{1,2}, G. Nuno Pinho Oliveira^{1,2}, M. Barbosa², J. Nuno Gonçalves³, J. Schell⁴, T. Melo Mendonça^{2,5}, J. Guilherme Correia⁶, A.M. Lima Lopes², J. Pedro Araujo²

1. CFNUL - Centro de Física Nuclear, University of Lisbon, Lisbon, Portugal
2. IFIMUP and IN-Institute of Nanoscience and Nanotechnology, University of Porto, Porto, Portugal
3. CICECO and Department of Physics, University of Aveiro, Aveiro, Portugal
4. Helmholtz-Institut für Strahlen- und Kernphysik, University of Bonn, Bonn, Germany
5. CERN, Geneva, Switzerland
6. Centro de Ciências e Tecnologias Nucleares, Instituto Superior Técnico, University of Lisbon, Bobadela, Portugal

Manganites and their exquisite electronic properties have been extensively studied in the last decade due to both fundamental interest and possible applications of colossal magnetoresistance, magnetocaloric and multiferroic properties [1,2]. Additionally, low-cost AMnO₃ and doped manganites have shown promising results for catalysts solutions [3,4]. In these systems orbital occupancy of the metal ion, orbital order and the Jahn-Teller effect have a critical role on the macroscopic material's properties.

In this work it will be presented the evolution of the local Jahn-Teller distortion across the Jahn-Teller phase transition as function of temperature studied with the perturbed angular correlation technique. In the case of NdMnO₃ a single phase scenario is proposed. In addition, ab initio calculations were performed and the results will be discussed in light of the experimental electric field gradient (EFG) measurements.

1. Magnetic and magnetoelectric excitations in multiferroic manganites, A M Shuvaev, A A Mukhin and A Pimenov, *J. Phys.: Condens. Matter* 23 113201 (2011)
2. Electric Field Control of Terahertz Polarization in a Multiferroic Manganite with Electromagnons, A. Shuvaev, V. Dziom, Anna Pimenov et al., *Phys. Rev. Lett.* 111, 227201 (2013)
3. Design principles for oxygen-reduction activity on perovskite oxide catalysts for fuel cells and metal-air batteries, J. Suntivich, H. Gasteiger, N. Yabuuchi et al., *Nature Chemistry* 3, 546–550 (2011)
4. AMnO₃ (A=La, Nd, Sm) and Sm_{1-x}Sr_xMnO₃ perovskites as combustion catalysts: structural, redox and catalytic properties, P. Ciambelli, S. Cimino, S. Rossi et al., *Applied Catalysis B: Environmental* 24 243–253 (2000)

TU.A-P90 - Inelastic neutron scattering on multiferroics NdFe₃(BO₃)₄

S. Hayashida¹, M. Soda¹, S. Itoh², T. Yokoo², K. Ohgushi³, D. Kawana¹, T. Masuda¹

1. Neutron Science Laboratory, Institute for Solid State Physics, University of Tokyo, Chiba, Japan

2. Neutron Science Division, Institute of Material Structure Science, High Energy Accelerator Research Organization, Ibaraki, Japan

3. Department of Physics, Tohoku University, Sendai, Japan

The rare-earth ferrobates RFe₃(BO₃)₄ (R = rare-earth metal) are a new series of multiferroic compounds containing R³⁺ and Fe³⁺ (3d⁵ S = 5/2) as magnetic ions. Variety of the magnetic anisotropy of the R³⁺ moments (R = Y, Pr, Nd, Sm, Gd and Tb) and that of the interaction between the Fe³⁺ and R³⁺ moments, f-d coupling, induce diverse magnetoelectric effects with respect to the R³⁺ ions [1]. In these compounds the mechanism of the magnetoelectricity is explained by the spin-dependent metal-ligand hybridization model [2,3]. We performed inelastic neutron scattering experiment to explore the magnetic excitations in NdFe₃(BO₃)₄. The obtained spectra are analyzed by the spin-wave calculation to identify the magnetic Hamiltonian. It is revealed that Fe³⁺ chains along the c - axis are weakly coupled and that they strongly interact with Nd³⁺ moments. The anisotropy of Fe³⁺ moment is easy-axis type and that of Nd³⁺ moment is easy-plane type. The origin of the Fe³⁺ anisotropy is discussed in terms of single-ion anisotropy, magnetic-dipole interaction, and the polarization interaction in the framework of the crystal symmetry. None of the three explains the direction of the anisotropy, suggesting that undetectably small distortion is the origin of the anisotropy.

[1] A. M. Kadomtseva et. al., Low Temp. Phys. 36, 511 (2010)

[2] A. I. Popov et. al., Phys. Rev. B 87, 024413 (2013)

[3] T. Kurumaji et. al., Phys. Rev. B 89, 195126 (2014)

TU.A-P91 - Angular-dependent magnetic properties of exchange-coupled ferromagnetic and multiferroic BiFeO₃ thin films

J. Camarero¹, P. Perna², J.L.F. Cuñado^{1,2}, F. Ajejas¹, S.L. de las Heras², C. Rodrigo¹, R. Miranda^{1,2}, J. Albille³, C. Deranlot³, A. Barthélémy³

1. *Universidad Autonoma De Madrid, Madrid, Spain*

2. *IMDEA nanoscience, Madrid, Spain*

3. *Unite Mixte de Physique CNRS/Thales, Palaiseau, France*

The interfacial exchange coupling between a ferromagnetic (FM) and a multiferroic BiFeO₃ (BFO) layer is investigated. FM/BFO bilayers with different FM intrinsic anisotropy and BFO film with different structure have been used, in order to explore the influence of the intrinsic FM anisotropy and the magnetic configuration of the BFO film. BFO and 5%-Mn doped BFO (BFO-Mn) thin films were grown by pulsed laser deposition onto (001)-oriented SrRuO₃ (SRO) and SrTiO₃ (STO) surfaces [1]. Co, Fe, Ni, and CoFeB thin films were sputtered in a separate chamber at 300K in a magnetic field of 200 Oe, after a short plasma cleaning. The samples were capped by 10 nm of Au layer for ex-situ characterization. The BFO films are fully strained epitaxial heterostructures [2] and display an antiferromagnetic (AFM) behaviour at room temperature, as derived by the non-negligible exchange bias values found for any FM/BFO bilayer. High resolution vectorial magneto-optic Kerr effect (v-MOKE) measurements have been performed at room temperature by using a v-MOKE setup with simultaneous and quantitative determination of the two in-plane magnetization components [3]. The angular dependence of the hysteresis phenomena, remanence, coercivity, exchange bias, and magnetization reversal processes, as well as the accurate determination of the characteristic magnetization directions and magnetic anisotropies are discussed. The data show that the angular-dependent properties are strongly affected by the intrinsic anisotropy of the FM layer and the structure of the BFO layer. The largest exchange bias effects are found for CoFeB films exchange-coupled with BFO films grown onto oriented-(001) metallic SRO surfaces. Numerical simulations based on a modified Stoner-Wohlfarth model confirm that the competition between the unidirectional anisotropy, due to the interfacial coupling, and the anisotropy of the FM layer is the key parameter to understand the experimental observations.

[1] J. Allibe, et al. Appl. Phys. Lett. 95, 182503 (2009)

[2] H. Béa, et al. Philos. Mag. Lett. 87, 165 (2007)

[3] E. Jiménez, et al. Rev. Sci. Instrum. 85, 053904 (2014)

TU.A-P93 - Magnetic order, anisotropy and ferroelectricity in frustrated $Mn_{1-x}Co_xWO_4$ multiferroics at high doping

J.L. García-Muñoz¹, J. Herrero-Martín², I. Urcelay-Olabarria³, J. Padilla-Pantoja¹, B. Bozzo¹, V. Pomjakushin⁴, E. Ressouche⁵, A.A. Mukhin⁶, V. Yu Ivanov⁶, V. Skumryev⁷

1. *Institut de Ciència de Materials de Barcelona, ICMA-B-CSIC, Campus universitari de Bellaterra, Bellaterra, Spain*
2. *ALBA Synchrotron Light Source, 08290 Cerdanyola del Vallès, Barcelona, Spain*
3. *BCMaterials, Technological Park of Biscay, Derio, and Dep. de Física de la Materia Condensada, Universidad del País Vasco, UPV-EHU, Zaragoza, Spain*
4. *Lab. for Neutron Scattering, Paul Scherrer Institute, Villigen PSI, Switzerland*
5. *SPSMS, UMR-E CEA/UJF-Grenoble 1, INAC, Grenoble, France*
6. *Prokhorov General Physics Institute, Russian Academy of Science, Moscow,*
7. *Institut Català de Recerca i Estudis Avançats (ICREA), Barcelona, Spain; and Dep. de Física, Univ. Autònoma de Barcelona, Bellaterra, Spain*

We have investigated a variety of coupled magnetic and ferroelectric phase transitions in $Mn_{1-x}Co_xWO_4$ multiferroics by single crystal and powder neutron diffraction, symmetry analysis and polarization measurements. The competition between the magnetic anisotropy and the isotropic exchange interactions or the external field produces a rich variety of competing multiferroic magnetoelectric phases, in which the anisotropy of the ferroelectricity behaves according to the inverse Dzyaloshinskii-Moriya model.

Spin-orbit coupling effects associated to the presence of $Co^{+2}O_6$ octahedra strongly modify the magnetic anisotropy and produce changes in the magnetic structures. Up to five distinct collinear and non-collinear spin orders (commensurate and incommensurate) compete in $Mn_{1-x}Co_xWO_4$ multiferroics with Co concentrations in the range $x \approx 0.12-0.15$.

Here we report the investigation of the magnetic and ferroelectric properties of these frustrated oxides in the highly-doped regime ($0.15 \leq x \leq 0.50$, above the complex $x \approx 0.15$ composition). The evolution of the magnetic behavior has been investigated and described up to the composition with $x=0.50$. The results obtained allow to extend our understanding of the magnetic and ferroelectric phase diagram up to $x=1$. We have found that the magnetic and ferroelectric properties in the high doping range can be rationalized in terms of the influence of Co atoms on the competition between commensurate collinear (AF4) and incommensurate cycloidal (AF2) spin structures. Finally, powder and single-crystal neutron results are faced to previous resonant magnetic x-ray scattering studies using soft x-rays and full polarization analysis.

TU.A-P94 - Magnetoelectric effect in CoFe alloy/Piezoelectric/CoFe alloy three-layered structures

K. Chichay¹, L. Fetisov², V. Rodionova¹, M. Shamonin³, Y. Fetisov²

1. Immanuel Kant Baltic Federal University, Kaliningrad, Russia

2. Moscow State Technical University of Radio Engineering, Electronics and Automation, Moscow, Russia

3. Regensburg University of Applied Sciences, Faculty of Electrical Engineering and Information Technology, Regensburg, Germany

Multiferroic materials are interesting from both applied and fundamental points of view: there are many applications in microelectronic, magnetic memory devices, sensor technologies and energy harvesting area and at the same time there are few challenges related, for example, interactions between electric and magnetic properties in these materials. Recently much attention has been paid to studies of magnetoelectric effect in layered multiferroic structures, which consist of ferroelectric and ferromagnetic phases. In this work we investigated the magnetoelectric effect in planar composite structures consisting of 3 layers: piezoelectric layer located between two ferromagnetic layers. Piezoelectric material was the same for all structures - Vibrit 1100. Three different types of cobalt-iron alloys were used as ferromagnetic layers. Three-layered structures based on different magnetic materials had various thicknesses: Vacoflux 48 - 0,2 mm, Vacoflux 50 - 0,35 mm and Vacodur 50 - 0,3 mm. The magnetoelectric properties of the three-layered structures with cobalt-iron alloys were compared with three-layered structure with nickel. Magnetoelectric effect was measured using the technique of harmonic modulation of magnetic field. Constant magnetic field was varied in range from 0 to 3000 Oe, amplitude of applied alternating magnetic field was 0-10 Oe and frequency range was 0,1-223 kHz. Resonances were observed at a frequencies of 212,38 kHz, 206,36 kHz, 217,5 kHz and 217,12 kHz for the structures with Ni, Vacoflux 48, Vacoflux 50 and Vacodur 50 layers, respectively. The values of magnetoelectric effect were found to be larger for three-layered structures with cobalt-iron alloys. The magnetoelectric effect magnitude for structure with Ni-ferromagnetic layer was only 0,41 V/(cm*Oe) while the largest magnetoelectric effect value for cobalt-iron alloys structures was 10,25 V/(cm*Oe) - for multiferroic based on Vacoflux 48 material.

TU.A-P95 - Enhanced magnetism and electrical behavior of Co-doped KNbO₃

J.A. Astudillo Lagos¹, J.L. Izquierdo², A. Gómez³, M. Castro⁴, O. Morán⁵, G. Bolaños⁶

1. *Universidad del Cauca, Departamento de Física, Laboratorio de Bajas Temperaturas, Popayán, Colombia*
2. *Universidad Nacional de Colombia, Campus Medellín, Departamento de Física, Laboratorio de Materiales Cerámicos y Vítreos, Medellín, Colombia*
3. *Universidad Nacional de Colombia, Campus Medellín, Facultad de Minas, Laboratorio de Caracterización de Materiales, Medellín, Colombia*
4. *Universidad Nacional de Mar del Plata, Facultad de Ingeniería, INTEMA, Mar del Plata, Argentina*
5. *Universidad Nacional de Colombia, Campus Medellín, Facultad de Minas, Laboratorio de Caracterización de Materiales, Medellín, Colombia*
6. *Universidad del Cauca, Departamento de Física, Laboratorio de Bajas Temperaturas, Popayán, Colombia*

Polycrystalline KNb_{1-x}Co_xO₃ (x = 0, 0.05, 0.1) samples were synthesized by standard solid-state reaction and their electrical and magnetic properties carefully studied. Special attention is paid to the thermal treatments in order to obtain a single-phase compound. In this regard, the KNb_{1-x}Co_xO₃ pellets have been preheated at 850° C for 12 hours, and then sintered at 900° C for 12 hours in air atmosphere. The X-ray diffraction patterns of the Co-doped samples show a systematic shift of their peaks to the right side as compared to those of the pristine compound (x=0). Morphological analysis of the compounds evidences that the crystallite size increases by increasing Co content. The magnetic response of the pellets is detected by sensible measurements of the magnetization as a function of the temperature and external magnetic field. An increased ferromagnetism by Co-doping is observed at temperatures as high as room temperature. In turn, measurements of the resistivity as a function of the magnetic field show high values of the magnetoresistance. In addition, the dielectric and conducting properties of the samples were studied by means of complex impedance spectroscopy at temperatures above 300 K. Measurements of the electric polarization as a function of the electric field indicate the presence of ferroelectricity in the analyzed samples.

TU.A-P97 - Electric tuning of magnetization dynamics and negative magnetic permeability in nanoscale composite multiferroics

C. Jia¹

1. Lanzhou University, Lanzhou, China

Steering magnetism by electric fields upon interfacing ferromagnetic (FM) and ferroelectric (FE) materials to achieve an emergent multiferroic response bears a great potential for nanoscale devices with novel functionalities.

FM/FE heterostructures allow, for instance, the electrical manipulation of magnetic anisotropy via interfacial magnetoelectric (ME) couplings. A charge-mediated ME effect is believed to be generally weak and active in only a few angstroms. Here we present an experimental evidence uncovering a new magnon-driven, strong ME effect acting on the nanometer range. For $\text{Co}_{92}\text{Zr}_8$ (20 nm) film deposited on ferroelectric PMN-PT we show via ferromagnetic resonance (FMR) that this type of linear ME allows for electrical control of simultaneously the magnetization precession *and* its damping, both of which are key elements for magnetic switching and spintronics. The experiments unravel further an electric-field-induced negative magnetic permeability effect, pointing so to a new class of optical negative-index metamaterials based on multiferroics.

TU.A-P98 - Stabilization of the multiferroic spin cycloid in Ni₃V₂O by light Co-doping

N. Qureshi¹, E. Ressouche², A.A. Mukhin³, V.Y. Ivanov³, S.N. Barilo⁴, S.V. Shiryaev⁴, V. Skumryev⁵

1. Institut Laue-Langevin, Grenoble, France

2. SPSMS, UMR-E CEA/UJF-Grenoble I, INAC, Grenoble, France

3. Prokhorov General Physics Institute, Russian Academy of Sciences, Moscow, Russia

4. Institute of Solid State and Semiconductor Physics, National Academy of Sciences of Belarus, Minsk, Belarus

5. Institució Catalana De Recerca I Estudis Avançats (ICREA), and Departament De Física, Universitat Autònoma De Barcelona, Bellaterra, Spain

Multiferroic lightly Co-doped Ni₃V₂O₈ was investigated by macroscopic measurements and neutron diffraction on single-crystal samples. Doping Co into the parent compound suppresses the sequence of four magnetic phase transitions [1], and only two magnetically ordered phases - the paraelectric high-temperature incommensurate (HTI) phase and the ferroelectric low-temperature incommensurate (LTI) phase - can be observed. Interestingly, the LTI multiferroic phase with a cycloidal magnetic structure is stabilized down to at least 1.8 K. The resulting symmetry-adapted magnetic structures of both phases show subtle differences to those observed in the parent compound. The stabilization of the LTI phase together with a wider temperature stability range of the HTI phase in comparison to Ni₃V₂O can be explained by a simple model [2], which takes into account the interplay between the single-ion easy-axis anisotropy due to Co doping and the ratio between the competing next-nearest-neighbor and nearest-neighbor interactions.

[1] G. Lawes et al., Phys. Rev. Lett. 93, 247201 (2004)

[2] M. Kenzelmann et al., Phys. Rev. B 74, 014429 (2006)

TU.A-P99 - Preparation of ferromagnetic-insulating double perovskites of transition metal oxides for spintronic applications

E.V. Pannunzio Miner ^{1,2}, L. López Mir ¹, R. Galcerán ¹, J. Cisneros-Fernández ¹, Ll. Balcells ¹, C. Frontera ¹, B. Martínez ¹

1. *Institut De Ciència De Materials De Barcelona (ICMAB-CSIC), Barcelona, Spain*

2. *INFIQC-CONICET, Dpto De Fisicoquímica, Fac. Ciencias Químicas, UNC. Córdoba, Argentina*

We have explored the preparation of different transition metal oxides with double perovskite structure with the aim of obtaining insulating materials with ferromagnetic order with high Curie temperature. New ferromagnetic insulating (FM-I) materials are interesting as candidates for active insulating barriers in spin filters. We have started with two known systems: La₂CoMnO₆ and La₂NiMnO₆. The first one was prepared by solid state reaction and the second one by the sol-gel method in order to favor cationic ordering and reducing sintering temperature. In both cases, x-ray diffraction measurements disregard the presence of impurities. The degree of cationic ordering has been estimated from low temperature magnetic properties. The use of alternative 3d cations is currently under investigation with the aim to prepare new FM-I materials with Curie points above RT.

TU.A-P100 - Local electrical control of the Ferromagnetic/Antiferromagnetic transition in FeRh just above room temperature

S. Valencia¹, L.C. Phillips², A.A. Ünal¹, F. Kronast¹, R.O. Cherifi², V. Ivanovskaya², A. Zobelli³, I.C. Infante⁴, E. Jacquet², N. Guiblin⁴

1. Helmholtz-Zentrum Berlin Für Materialien Und Energie, Berlin, Germany

2. Unité Mixte De Physique CNRS/Thales, Palaiseau & Université Paris-Sud, Orsay, France

3. Laboratoire De Physique Des Solides, Université Paris-Sud, CNRS UMR 8502, Orsay, France

4. Laboratoire SPMS, UMR 8580, Ecole Centrale Paris-CNRS, Grande Voie Des Vignes, Châttenay-Malabry, France

Coupling between different ferroic orders in artificial multiferroic structures might allow electrical control of macroscopic magnetic properties such as for example magnetization and coercive field. Here we show by means of element specific X-Ray PEEM microscopy the possibility to locally switch (isothermally) by means of a voltage between the ferromagnetic and antiferromagnetic phase of epitaxial FeRh thin films grown on top of ferroelastic BaTiO₃ [Ref. 1]. The resultant magnetoelectric coupling is larger and more reversible than previously reported from macroscopic measurements [Ref. 2]. Our results emphasize the importance of nanoscale ferroic domain structure and the promise of first-order transition materials to achieve enhanced coupling in artificial multiferroics.

References:

[1] L. C. Phillips, A. A. Ünal, F. Kronast, R. O. Cherifi, V. Ivanovskaya, A. Zobelli, I. C. Infante, E. Jacquet, N. Guiblin, B. Dkhil, A. Barthélémy, M. Bibes and S. Valencia. Scientific Reports 2015, (in-press)

[2] R.O. Cherifi, V. Ivanovskaya, L.C. Phillips, A. Zobelli, I.C. Infante, E. Jaquet, V. Garcia, S. Fusil, P.R. Briddon, N. Guiblin, A. Mougin, A.A. Ünal, F. Kronast, S. Valencia, B. Dkhil, A. Barthélémy and M. Bibes. Nature Materials 13, 345 (2014)

TU.B-P01 - Study of d-electron correlations in skutterudite-related $Ce_3M_4Sn_{13}$ (M = Co, Rh, and Ru)

Andrzej Ślebarski¹, J. Goraus¹, P. Witas¹, L. Kalinowski¹, M. Fijałkowski¹

1. Institute of Physics, University of Silesia, Katowice, Poland

In the past few years, the number of intermetallic compounds based on rare earth and transition metals and having coexistence of f- and d-electron correlations increases [1]. We present the electric transport, thermodynamic properties and electronic structure of $Ce_3M_4Sn_{13}$ heavy fermions, where M is d-electron metal (Co, Rh, and Ru). A comparison of DFT electronic structure calculations and the XPS data gives evidence for strong Coulomb correlation among metal M d-electron states. We note the large impact of d-electron correlation, which is clearly observed in the change of Ce 5p states located about 18 eV in the valence bands. The influence of the d-electron correlations is also manifested by the positive magnetoresistivity of $Ce_3Rh_4Sn_{13}$, $Ce_3Ru_4Sn_{13}$ and the La-doped alloys, and strong enhancement of the low-temperature electronic specific heat coefficient in $C(T)/T$ data.

1] A. Ślebarski, J. Goraus, P. Witas, L. Kalinowski, and M. Fijałkowski, Phys. Rev. B, 2014

TU.B-P02 - Conduction Electron Spin Resonance in the heavy fermions α -YbAl_{1-x}Fe_xB₄ ($x < 0.55$) and their reference compound α -LuAlB₄

P. Pagliuso¹, L.M. Holanda², G.G. Lesseux¹, E.T. Magnavita³, R.A. Ribeiro³, S. Nakatsuji⁴, K. Kuga⁴, Z. Fisk⁵, S.B. Oseroff⁶, R.R. Urbano¹

1. GPOMS-IFGW-Unicamp, Campinas, Brazil

2. Universidade Federal Rural do Semi-Árido, Pau dos Ferros, Brazil

3. CCNH, Universidade Federal do ABC (UFABC), Santo Andre, Brazil

4. Institute for solid State Physics (ISSP), University of Tokyo, Kashiwa, Japan

5. University of California, Irvine, United States

6. San Diego State University, San Diego, United States

In this work, we report Electron Spin Resonance (ESR) studies on the α -YbAl_{1-x}Fe_xB₄ ($x < 0.55$) heavy fermions series and on their reference compound α -LuAlB₄.

For all studied compounds, the observed ESR signal strikes as a Conduction Electron Spin Resonance (CESR) response in the entire temperature range ($10 \text{ K} \leq T \leq 300 \text{ K}$). This observation is in clear contrast to the behavior found in the heavy fermion superconductor ($T_c \sim 0.8 \text{ K}$) β -YbAlB₄, for which a striking and unprecedented ESR signal was found. This unusual ESR response (named *Kondo quasiparticles spin resonance* (KQSR))[1] behaves as a CESR at high temperatures and acquires characteristics of the Yb³⁺ local moment ESR at low temperature. We discuss the difference between the ESR responses in β -YbAlB₄ and α -YbAl_{1-x}Fe_xB₄ ($x < 0.55$) considering the fact that proximity to a quantum critical point may be essential to the occurrence of a KQSR signal.

[1] L. M. Holanda, J. M. Vargas, W. Iwamoto, C. Rettori, S. Nakatsuji, K. Kuga, Z. Fisk, S. B. Oseroff, and P. G. Pagliuso, Phys. Rev. Letters 107, 026402 (2011)

TU.B-P03 - Static magnetic order in A-site ordered perovskite, $\text{LaCu}_3\text{Cr}_4\text{O}_{12}$, probed with muon-spin spectroscopy

J. Sugiyama¹, H. Nozaki¹, I. Umegaki¹, E. Ansaldo², J. Brewer^{3,4}, H. Sakurai⁵, M. Isobe⁶, H. Takagi⁶

1. Toyota Central Research & Development Laboratories, Inc., Nagakuyte, Japan

2. University of Saskatchewan, Saskatoon, Canada

3. University of British Columbia, Vancouver, Canada

4. TRIUMF, Vancouver, Canada

5. National Institute for Materials Science (NIMS), Tsukuda, Japan

6. Max Planck Institute for Solid State Research, Stuttgart, Germany

The microscopic magnetic nature of a novel A-site ordered chromium perovskite, $\text{LaCu}_3\text{Cr}_4\text{O}_{12}$, has been studied with muon-spin rotation and relaxation (μSR) measurements down to 1.8 K using a powder sample. Here, the sample was synthesized with a high-pressure technique above 6 GPa and 1200 C [1]. In the $\text{LaCu}_3\text{Cr}_4\text{O}_{12}$ lattice, the 3/4 of the A site are occupied by Cu^{2+} ion so as to make isolated CuO_4 planes [2]. Since the related compounds, $\text{CaCu}_3\text{Ru}_4\text{O}_{12}$ [3] and $\text{CaCu}_3\text{Ru}_4\text{O}_{12}$ [4], show a heavy-fermion like behavior without magnetic order down to the lowest temperature measured, the A-site ordered perovskites are thought to be a candidate for exhibiting a quantum phase transition.

Magnetization and resistivity measurements indicated the presence of a magnetic transition at $T_m=220$ K together with a metal-to-metal transition [1]. Moreover, since the magnetization versus temperature curve showed a step-like decrease at T_m with decreasing temperature, it was thought that a spin-singlet like state is formed below T_m . However, μSR measurements demonstrates the appearance of static antiferromagnetic (AF) order below T_m , i.e. $T_m=T_N$. Thus, both negative chemical pressure and electron-doping due to the substitution for Ca by La is found to induce AF order, implying the presence of a quantum phase transition in this system.

[1] M. Isobe, H. Sakurai, and H. Takagi, Meeting Abstracts of Phys. Soc. Jpn. 69, 386 (2014)

[2] P. M. Woodward, Acta Crystallogr., Sect. B 53, 32 (1997); *ibid* 53, 44 (1997)

[3] W. Kobayashi et al., J. Phys. Soc. Jpn. 73, 2373 (2004)

[4] M. A. Subramanian et al., J. Phys. Chem. Solid 64, 1569 (2003)

TU.B-P05 - Clarification of the crystal-field ground state in the Kondo semiconductor CeNiSn

F. Strigari¹, M. Sundermann¹, Z. Hu², K.A. McEwen⁶, D. Fort³, K. Kummer⁴, N.B. Brookes⁴, A. Tanaka⁵, M.W. Haverkort², L.H. Tjeng²

1. *Institute of Physics II, University of Cologne, Cologne, Germany*

2. *Max Planck Institute for Chemical Physics of Solids, Dresden, Germany*

3. *Department of Metallurgy and Materials, University of Birmingham, Birmingham, United Kingdom*

4. *European Synchrotron Radiation Facility (ESRF), Grenoble, France*

5. *Department of Quantum Matter, AdSM, Hiroshima University, Higashi-Hiroshima, Japan*

6. *Department of Physics and Astronomy, University College London, London, United Kingdom*

The local electronic structure of the f electrons in Kondo-insulating materials is known to be of major importance for transport and magnetic properties, and in particular for the generation of the hybridization gap. CeNiSn, one of the first narrow-gap Kondo semiconductors, has been intensively studied in the past [1] and many explanations for the low-temperature behavior have been suggested, all of which stress the significance of the 4f crystal-field ground state [2-4]. However, an unambiguous direct experimental detection of the ground state is still pending. By exploiting the potential of polarization-dependent x-ray absorption spectroscopy at the Ce M_{4,5} edge at low temperature [5], we have determined the crystal-field ground-state wave function of CeNiSn. Furthermore, the energies of the excited Kramers' doublets can be estimated from the temperature dependence of the linear dichroism. The obtained crystal-field scheme is in good agreement with a possible solution found for Cu-doped CeNiSn [6] and supports the theoretical framework of Moreno and Coleman [4] for the understanding of the narrow pseudo-gap and the low-temperature characteristics of the Kondo-insulating behavior.

[1] P. S. Riseborough, *Adv. Phys.* 49, 257 (2000)

[2] K. A. Kikoin et al., *Phys. Rev. B* 59, 15070 (1999); Y. Kagan et al., *Phys. Rev. B* 55, 12348 (1997)

[3] H. Ikeda and K. Miyake, *J. Phys. Soc. Jpn.* 65, 1769 (1996); M. Miyazawa and K. Yamada, *J. Phys. Soc. Jpn.* 72, 2033 (2003)

[4] J. Moreno and P. Coleman, *Phys. Rev. Lett.* 84, 342 (2000)

[5] see e.g. P. Hansmann et al., *Phys. Rev. Lett.* 100, 066405 (2008); Willers et al., *Phys. Rev. B* 81, 195114 (2010); or Strigari et al., *Phys. Rev. B* 86, 081105(R) (2012)

[6] J.-Y. So et al., *Phys. Rev. B* 71, 214441 (2005)

TU.B-P08 - Transport properties of Field-Insensitive Heavy-Fermion Compound $\text{SmTa}_2\text{Al}_{20}$

A. Yamada¹, R. Higashinaka¹, T.D. Matsuda¹, Y. Aoki¹, H. Sato¹

1. Department of Physics, Tokyo Metropolitan University, Tokyo, Japan

RTX₂₀ (R: rare earth, T :transition metal, X :Al and Zn) crystallizing in the cubic CeCr₂Al₂₀-type structure with the space group #227, have attracted much attention due to their novel physical properties. In SmT₂Al₂₀ family, Kondo-like behaviors unusually insensitive to magnetic field (such as -logT dependent resistivity and large mass enhancement) were found, suggesting a non-magnetic mechanism of the formation of the heavy-fermion state. In order to reveal the origin of the field-insensitive nature, we performed detailed studies of electrical transport properties in SmTa₂Al₂₀, putting emphasis on the field dependence, and those of La-substitution for Sm site. We found transverse magnetoresistance (MR) roughly follows H² dependence in low-field condition in SmTa₂Al₂₀, which indicates that the suppression of Kondo scattering by magnetic field is quite small compared with the positive ordinary MR due to the cyclotron motion of conduction electrons. We also found strong deviation from Kohler's rule (i.e. strong enhancement of MR with decreasing temperature down to the lowest temperature, 0.5 K). In the same temperature range between 2 and 50 K, Hall coefficient shows evident temperature dependence. These facts indicate that the scattering probability of conduction electrons has a huge wave-number dependence in the ground state. Furthermore, we have confirmed that such field-insensitive behaviors appear even in the Sm-diluted system.

TU.B-P09 - Powder x-ray diffraction study of caged magnetic compound DyFe₂Zn₂₀ at low temperature

N. Kishii¹, S. Tateno¹, M. Ohashi¹, Y. Isikawa²

1. Kanazawa University, Kanazawa, Japan

2. Toyama University, Toyama-Takaoka, Japan

High-angle X-ray powder diffraction measurements show that the crystal structure of the caged magnetic compound DyFe₂Zn₂₀ is tetragonal while almost all RT₂X₂₀ compounds are cubic. The lattice parameters were estimated at temperatures between 14 K and 300 K. No structural transition was observed and the ratio between the a- and c-axes was found to be almost constant, i.e. $c/a \sim 0.989 \pm 0.0034$ between 14 K and 300 K. The large magnetic anisotropy observed may be related to the low structural symmetry of DyFe₂Zn₂₀.

TU.B-P10 - Itinerant-Localized Transitions in Magnetic Phases of the Periodic Anderson Model

K. Kubo¹

1. Advanced Science Research Center, Japan Atomic Energy Agency, Ibaraki, Japan

In recent years, Fermi-surface reconstruction, which is called a Lifshitz transition, has been discussed as a possible origin of anomalies in magnetic phases of several f-electron materials. To clarify the characteristics of the Lifshitz transitions, we investigate magnetically ordered states of the periodic Anderson model by applying the variational Monte Carlo method. As variational wavefunctions, we use the Gutzwiller wavefunctions for the paramagnetic, antiferromagnetic, and ferromagnetic states. For each state, we evaluate energy and determine the variational parameters in the wavefunction which minimize energy. Then, we compare energy between different magnetic states.

Around half-filling, we find an antiferromagnetic phase, and far away from half-filling, we find a ferromagnetic phase as the ground state. Inside the both magnetic phases, Lifshitz transitions take place. At the Lifshitz transitions, the sizes of the ordered moments change. In order to understand the transitions further, we also analyze the f-electron contribution to the Fermi surface by evaluating the jumps in the momentum distribution function at the Fermi momenta. Then, we find that, in the large ordered-moment states, the f-electron contribution to the Fermi surface becomes small. This observation clearly shows that these Lifshitz transitions are itinerant-localized transitions of the f electrons.

TU.B-P11 - Double-k commensurate magnetic order in NdFe₂Al₁₀

J. Robert¹, F. Damay¹, K. Saito^{1,3}, A.M. Bataille¹, F. Porcher¹, G. André¹, A. Gukasov¹, J.M. Mignot¹, H. Tanida², M. Sera²

1. Laboratoire Léon Brillouin, CEA-CNRS, CEA/Saclay, Gif sur Yvette, France

2. Department of Quantum Matter, ADSM, Hiroshima University, Higashi-Hiroshima, Japan

3. Present address: Institute of Materials Structure Science, KEK, 1-1 Oho, Tsukuba, Ibaraki, Japan

The orthorhombic compound NdFe₂Al₁₀ has been studied by powder and single-crystal neutron diffraction [1]. Below $T_N = 3.9$ K, the Nd³⁺ magnetic moments order in a double-k [$k_1 = (0, 3/4, 0)$, $k_2 = (0, 1/4, 0)$] collinear magnetic structure, whose unit cell consists of four orthorhombic units in the b direction. The refinements show that this structure consists of (0 1 0) ferromagnetic planes stacked along b, in which the moments are oriented parallel to a (the easy anisotropy axis according to bulk magnetization measurements) and nearly equal in magnitude (approx. 1.7–1.9 Bohr magneton). The alternating eight-plane sequence providing the best agreement to the data turns out to be that which yields the lowest exchange energy if one assumes antiferromagnetic near-neighbor exchange interactions with $J_1 \gg J_2, J_3$. With increasing temperature, the single-crystal measurements indicate the suppression of the k_2 component at $T = 2.7$ K, supporting the idea that the anomalies previously observed around 2–2.5 K correspond to a squaring transition. In a magnetic field applied along the a axis, the magnetic Bragg satellites disappear at $H_c = 2.45$ T, in agreement with earlier measurements. Comparisons are made with related magnetic orders reported previously for CeT₂Al₁₀ (T = Ru, Os) [2] and TbFe₂Al₁₀ [3].

[1] J. Robert et al., Phys. Rev. B 90 (2014) 224425

[2] J. Robert et al., Phys. Rev. B 82 (2010) 100404(R), 2010; D. D. Khalyavin et al., Phys. Rev. B 82 (2010) 100405(R); H. Kato et al., J. Phys. Soc. Jpn. Suppl. 80 (2011) 073701

[3] M. Reehuis et al., J. Phys.: Condens. Matter 15 (2003) 1773

TU.B-P12 - CeRh₆Si₄ : An intermediate valent cerium compoundT. Gruner¹, C. Geibel¹*1. Max Planck Institute for Chemical Physics of Solids, Dresden, Germany*

The ternary Ce-Rh-Si system comprises a huge number of compounds crystallising in different structure types and with a broad spectrum of properties. Particularly interesting is the change of the Ce-valence from stable trivalent Ce with completely localized 4f electrons, as e.g. in CeRh₃Si₂ [1], to a strongly intermediate valence state with fully delocalised 4f electrons, as e.g. in CeRh₃. While the binary Ce-Si and Ce-Rh compounds show a continuous evolution of the valence as a function of Rh or Si content, presently available results for ternary compounds do not indicate a simple relation between composition and valence. Here we present a study of the compound CeRh₆Si₄. It crystallises in a rather simple hexagonal structure [2], in which the Ce sublattice presents some quasi-one-dimensional character which might lead to interesting properties. The presence of four different CeRh_xSi_y compounds in a very small composition region makes the preparation of pure CeRh₆Si₄ delicate. By starting from a slightly off-stoichiometric composition, we were able to prepare rather pure samples as evidenced by energy-dispersive X-ray spectroscopy, powder X-ray diffraction, and a comparatively high residual resistivity ratio of 31. Analysis of magnetic susceptibility and X-ray LIII absorption edge measurements indicate an intermediate valent state, with a Ce valence of approximately 3.2 and a characteristic energy of about 260K. Thus the f-hybridisation is much stronger in CeRh₆Si₄ than in the nearby CeRh₃Si₂. We analyse the expected relation between distance to ligands and 4f-hybridisation by comparing a number of Ce-Rh-Si compounds.

TU.B-P13 - Thermodynamic properties of CeRh₂Si₂: Evidence for a meta-orbital transition?

P. Kushwaha¹, N. Caroca-Canales¹, D.V. Vyalikh², C. Geibel¹

1. *Max Planck Institute for Chemical Physics of Solids, Dresden, Germany*

2. *Institute of Solid State Physics, Dresden University of Technology, Dresden, Germany*

CeRh₂Si₂ is an intensively studied antiferromagnetic Kondo lattice system, which presents a striking duality in the properties of the 4f electrons: The large 4f entropy of Rln2 just above TN = 35 K and the large value of the ordered moment mAF = 1.4 μB points to a fully localized 4f electron, while other properties, e.g. the width of the quasi elastic line in inelastic neutron scattering (INS), indicate a Kondo scale of about 33 K implying a significant 4f hybridization. We have determined the 4f specific heat of CeRh₂Si₂ up to 300 K and analyzed the data using a standard approach with three crystal electric field (CEF) doublets subject to different Kondo scales. This analysis confirms the contradiction between TK = 33 K as deduced from INS and the large entropy just above TN, and indicates that the excited CEF levels are very broad in energy. It implies a strong hybridization for at least one of the excited CEF level, as recently suggested by photoemission spectroscopy. Our analysis indicate that the simple standard picture for Kondo lattice is not applicable for CeRh₂Si₂. By combining our results with previous ones obtained under pressure, we show that the Kondo scales has to increases strongly within the small pressure range between P = 0 and the critical pressure Pc at which antiferromagnetism is suppressed, in contrast to other Kondo lattice systems. This indicates that the simple Doniach scenario is not applicable, and that a further mechanism is needed to account for the properties of CeRh₂Si₂ near Pc. The combination of large entropy at TN, strong hybridization of an excited CEF level, and large increase of TK in the small pressure range up to Pc suggest the occurrence of a meta-orbital transition.

TU.B-P14 - Heavy fermion behavior in itinerant ferromagnet CeCrGe₃ and possible existence of a quantum bi-critical point in CeCr_{1-x}Ti_xGe₃Z. Hossain¹, D. Das¹, T. Gruner², C. Geibel²*1. Department of Physics, Indian Institute of Technology, Kanpur, India**2. Max-Planck Institute for Chemical Physics of Solids, Dresden, Germany*

New and exotic phases including unconventional superconductivity are often discovered near quantum critical point (QCP). It is widely believed that magnetic fluctuations near the QCP play a key role in stabilizing the superconductivity in a wide class of materials like heavy fermions, pnictides, high T_c cuprates etc. Ce based intermetallic compounds are of particular interest for studying quantum phase transition as the magnetism of Ce-compounds can quite conveniently be tuned by doping or by applying pressure. Many Ce-based compounds have been investigated and tuned toward QCP. However, ferromagnetic (FM) QCPs in Ce-compounds are quite rare. In this context, our discovery of heavy fermion behaviour in the trivalent Ce compound CeCrGe₃ is quite remarkable. It exhibits enhanced value of Sommerfeld coefficient (~ 130 mJ/mol/K²) and FM ordered state due to the ordering of itinerant Cr moments (T_c=70K)[1]. Moreover, our attempt to suppress the FM ordering of Cr by Ti substitution strongly suggests a possible existence of a quantum bi-critical point in this system[2]. We have performed a systematic study on polycrystalline CeCr_{1-x}Ti_xGe₃ (0 < x < 1) using magnetic susceptibility, isothermal magnetization, specific heat and electrical resistivity measurements[1,2]. Our results also show that upon Ti substitution the Cr- ordering temperature is gradually suppressed down to T_C = 7K for x = 0.7K beyond which Ce moment ordering starts to dominate and a crossover between Cr and Ce moment ordering is observed[2].

[1] D. Das et al. J. Phys.: Condens. Matter, 26, 106001 (2014)

[2] D. Das et al. J. Phys.: Condens. Matter, 27, 016004 (2015)

TU.B-P15 - A combined full multiplet and configuration interaction analysis of hard x-ray photoelectron spectroscopy data of cerium compounds with strong plasmons

M. Sundermann¹, F. Strigari¹, T. Willers¹, E.D. Bauer², J.L. Sarrao², J.D. Thompson², P. Lejay³, A. Tanaka⁴, J. Weinen⁵, Y.F. Liao⁶

1. *Institute of Physics II, University of Cologne, Cologne, Germany*

2. *Los Alamos National Laboratory, Los Alamos, New Mexico, United States*

3. *Institut NEEL - CNRS, Grenoble, France*

4. *Department of Quantum Matter, AdSM, Hiroshima University, Higashi-Hiroshima 739-8530, Japan*

5. *Max Planck Institute for Chemical Physics of Solids, Dresden, Germany*

6. *National Synchrotron Radiation Research Center, Hsinchu, Taiwan*

Photoemission spectroscopy (PES) has been shown to be very powerful in determining valences and configuration interaction parameters of heavy fermion compounds. However, the surface sensitivity has always been a big drawback [1]. Using hard x-rays which are available at third generation synchrotrons increases the probing depth so that bulk representative results can be obtained [2]. We have performed such hard x-ray core level PES (HAXPES) experiments at the Taiwan beamline BL12XU at Spring-8 in Japan with incident photon energy of 6.47 keV. Several heavy fermion and intermediate valence compounds were probed and their 4f occupancy and configuration interaction parameters have been quantitatively determined by combining full multiplet calculations with an Anderson Impurity Model (AIM) within a single ligand state approximation [3]. This combination has the advantage that even strong plasmon excitations in the spectra can be corrected for. Results for intermediate valent CePd₃ [4], the ferromagnetic and strongly hybridized giant crystal-field system CeRh₃B₂ [5], the heavy fermion compounds CeRu₂Si₂ [6] and CeMIn₅ with M=Co, Rh, and Ir [7] will be shown. We find 4f contributions of 22% for CePd₃, 14% for CeRh₃B₂, 7% for CeRu₂Si₂ and of only 3-5% for the three CeMIn₅ compounds. In particular the Ce 3d HAXPES data of the latter family suffer from strong plasmons.

[1] C. Laubschat et al., Phys. Rev. Lett. 65, 1639 (1990)

[2] C. Dallera et al., Appl. Phys. Lett. 85, 4532 (2004)

[3] F. Strigari et al., J. Electron Spectrosc. Relat. Phenom. 199, 56-63 (2015)

[4] V.R. Fanelli et al. J. Phys. Cond. Matter 26, 225602 (2014) and Ref.s therein

[5] S. Raymond et al. Phys. Rev. B 82, 094416 (2010) and Ref.s therein.

[6] J. Flouquet in Prog. in Low Temp. Phys. VX, p. 139 (2005) and Ref.s therein

[7] J.L. Sarrao and J.D. Thompson, J. Phys. Soc. Jpn. 76, 051013 (2007) and Ref.s therein

TU.B-P17 - Crystal Field of Superstoichiometric Samarium Dihydride (SmH_{2+d})O. Nakamura¹, M. Sakai², K. Matsubayashi³, Y. Uwatoko³

1. Faculty of Engineering, Okayama University of Science, Okayama, Japan

2. Faculty of Engineering, Saitama University, Saitama, Japan

3. Institute for Solid State Physics, University of Tokyo, Tokyo, Japan

Stoichiometric samarium dihydride (SmH_{2+d}) has been known as an antiferromagnet with $T_N=9.7$ K from the magnetic susceptibility measurement[1]. T_N was determined to be 9.6 K from the temperature dependence measurement of the resistivity [2]. For superstoichiometric case ($d>0$), T_N decreases as d increases[2], and is 8 K at $d=0.16$. Temperature effect on the resistivity at T_N becomes broad. For stoichiometric case ($d=0$), T_N is determined to be 6.75 K from specific heat measurement [3]. An analysis of the specific heat data suggests that stoichiometric samarium dihydride may have the mixed valence with ground state G_7 [3]. However a non-negligible value of d is possibly present in their sample[4]. In the previous study, we reported the grand state of the G_7 and the mixed valence of superstoichiometric samarium dihydride($\text{SmH}_{2+d}:d=0.16$) [5]. However, it was insufficient consideration for Sm^{3+} of Van Vleck term. In the present study, We fully take into account the Van Vleck term and newly analyzed the grand state of the crystal field from the magnetic susceptibility measurement newly performed in the paramagnetic region ($T>T_N$). We have carried out the fitting procedure of the specific heat of paramagnetic region. It follows from the present analysis that in $\text{SmH}_{2.16}$, all Sm ion are Sm^{3+} having ground state G_8 and the Sommerfeld coefficient g is 150 $\text{mJ}/(\text{K}^2 \text{ mole})$.

[1] O. J. Zogal, Phys. Stat. Sol. (b) 117 (1983) 717

[2] P. Vajda, J. N. Daou and J. P. Burger, Phys. Rev. B 40 (1989)500

[3] J. Opyrchal and Z. Biega, Solid State Commun. 26 (1978)965

[4] P. Vajda :in (Eds) K. A. Gscheidner, L. Eyring, Handbook on the Physics and Chemistry of Rare Earths Elsevier Science B.V 1995, Chap. 20

[5] O.Nakamura, Y.Tanaka, K.Nakazawa, T.Nakano, M.Sakai, S.Orimo,Y.Uwatoko, J.Magn Magn Mat. 310(2007)e65

TU.B-P18 - Relation between Heavy Quasi Particles and Crystal Electric Field Multiplet in f2-Configuration Based Systems

T. Hinokihara¹, A. Tsuruta², K. Miyake³

1. *Department of Physics, University of Tokyo, Bunkyo-ku, Japan*

2. *Department of Materials Engineering Science, Osaka University, Osaka, Japan*

3. *Toyota Physical and Chemical Research Institute, Nagakute, Japan*

Heavy electron systems with f2-configuration basis such as U compounds are known for showing various phases which depend on the crystalline electric field (CEF) multiplet. In order to discuss such various phases, it is significant to analyze quasiparticle states and interaction between quasiparticles in f2-configuration based system. We analyzed quasiparticle energy levels and renormalization factors in three orbital ($j=5/2$) periodic Anderson model with CEF effect. We calculated the system by using slave boson mean field approximation which is introduced auxiliary boson operators up to triple occupied states at each local site. As a result, we clarified the several quasiparticle bands which related to CEF ground state are strongly renormalized. In addition, an enormous flat band which is inconsistent with renormalization factor appears at Fermi energy because of several quasiparticle energy levels tend to degenerate at Fermi energy. This result suggests the direct hopping between f-electrons becomes effectively significant to a shape of Fermi surface at heavy Fermi liquid state in the f2-configuration based system. It is possible to explain the Fermi surface structure and heavy effective mass in UPt3 .

TU.B-P19 - Break-Junction tunneling spectroscopy of Kondo semiconductors CeT₂Al₁₀ (T = Fe, Os)

J. Kawabata¹, Y. Yamada¹, T. Takabatake^{1,2}, Y. Sakai³, A. Sugimoto³, T. Ekino³, Y. Muro⁴

1. Graduate School of Advanced Sciences of Matter, Higashi-Hiroshima, Japan

2. Institute for Advanced Materials Research, Miyagi, Japan

3. Graduate School of Integrated Arts and Sciences, Hiroshima University, Higashi-Hiroshima, Japan

4. Liberal Arts and Sciences, Faculty of Engineering, Toyama Prefectural University, Izumi, Japan

The Kondo semiconductor CeOs₂Al₁₀ exhibits an antiferromagnetic (AFM) order at $T_N = 28.5$ K, whose temperature is unexpectedly high for the small ordered moment of $0.3 m_B/\text{Ce}$ [1,2]. On cooling below 60 K, opening of a hybridization gap of 30 meV was observed by polarized optical conductivity [3] and photoemission measurements [4]. At around 38 K ($T > T_N$), openings of a charge gap of 20 meV and a spin gap of 11 meV were observed, respectively, by polarized optical conductivity [3] and inelastic neutron scattering [2] experiments. For better understanding of the relationship between these gap openings and the unusual AFM order, we have performed a tunneling spectroscopic study of single crystals of CeFe₂Al₁₀ and CeOs₂Al₁₀ by the break-junction technique [5]. For CeFe₂Al₁₀ without AFM, we observed two distinct gaps with $V_1 = 600$ mV and $V_2 = 150$ mV, where V represents the peak-to-peak voltage difference in the tunneling conductance in the semiconductor - insulator - semiconductor design of the break junction. The former gap appears at $T < 60$ K and the later develops at $T < 30$ K. In CeOs₂Al₁₀, we observed three structures; $V_1 = 400$ mV appearing at $T < 60$ K is the c - f hybridization gap, $V_{AF} = 200$ mV at $T < T_N$ is attributable to AFM, and the development of $V_2 = 100$ mV at $T < 16$ K coincides with the semiconducting increase in the resistivity. The magnitude of V_1 and V_2 in CeFe₂Al₁₀ are 1.5 times larger than those in CeOs₂Al₁₀, respectively. This result is consistent with the higher T_K in CeFe₂Al₁₀ than in CeOs₂Al₁₀. For both compounds, no significant anisotropy was observed neither in the gap value nor the opening temperature.

[1] Y. Muro *et al.*, Phys. Rev. B 81, 214401 (2010). [2] D. T. Adroja *et al.*, Phys. Rev. B 82, 104405 (2010)

[3] S. Kimura *et al.*, Phys. Rev. B 81, 056404 (2011). [4] T. Ishiga *et al.*, J. Phys. Soc. Jpn 83, 084717, (2014)

[5] T. Ekino *et al.*, Phys. Rev. Lett. 75, 4262 (1995)

TU.B-P20 - Under-compensation effect in the Kondo insulator (Yb,Tm)B₁₂

K. Nemkovski¹, P. Alekseev^{2,3}, J.M. Mignot⁴, A. Ivanov⁵, S. Rols⁵, V. Filipov⁶, N. Shitsevalova⁶

1. Forschungszentrum Jülich GmbH, Jülich Centre For Neutron Science, Outstation At MLZ, Garching, Germany

2. National Research Centre "Kurchatov Institute", Moscow, Russia

3. National Research Nuclear University "MEPhI", Moscow, Russia

4. Laboratoire Léon Brillouin, CEA-CNRS, CEA/Saclay, Gif sur Yvette, France

5. Institut Laue-Langevin, Grenoble, France

6. I. N. Frantsevich Institute for Problems of Materials Science, Kiev, Ukraine

We present an inelastic neutron scattering study of the influence of isoelectronic Tm substitution on the low-energy structure and temperature dependence of the dynamical magnetic response in Yb_{1-x}Tm_xB₁₂ ($x = 0, 0.08, 0.15,$ and 0.75) and Lu_{0.92}Tm_{0.08}B₁₂ solid solutions [1].

Substantial changes have been observed in the spectral structure and temperature evolution of the Yb contribution to the inelastic response for a rather low content of magnetic Tm ions. The spin-exciton-like resonance mode near 15 meV is steeply suppressed at the lowest measured Tm concentration ($x = 0.08$). The spin gap is replaced by a pseudogap at concentrations lower than 0.15. These results point to a specific effect of impurities carrying a magnetic moment (Tm, as compared to Lu or Zr) in a Kondo insulator, which is thought to reflect the "under-compensation" of Yb magnetic moments, originally screened in pure YbB₁₂. A parallel is made with the strong effect of Tm substitution on the temperature dependence of the Seebeck coefficient in Yb_{1-x}Tm_xB₁₂, which was reported previously [2].

This work was partly supported by the RFBR grant 14-22-01002.

[1] P.A. Alekssev et al., Phys. Rev. B 89 (2014) 115121

[2] N. E. Sluchanko et al., JETP Lett. 89 (2009) 256

TU.B-P21 - Magnetic excitations through the hidden order transition in URu₂Si₂

N. Butch^{1,2,3}, M. Manley⁴, J. Jeffries³, M. Janoschek⁵, K. Huang⁶, B. Maple⁶, A. Said⁷, B. Leu⁷, J. Lynn¹

1. NIST Center For Neutron Research, Gaithersburg, Maryland
2. CNAM, Dept. of Physics, University of Maryland, College Park, United States
3. Lawrence Livermore National Laboratory, Livermore, United States
4. Oak Ridge National Laboratory, Oak Ridge, United States
5. Los Alamos National Laboratory, Los Alamos, United States
6. Dept. of Physics, University of California, San Diego, United States
7. Advanced Photon Source, Argonne National Laboratory, Argonne, United States

Using inelastic neutron and x-ray scattering, we looked for signs of incipient symmetry breaking in the lattice and magnetic excitations of URu₂Si₂. The phonons do not show any dramatic temperature dependence. New measurements of the magnetic excitations allow us to estimate the effective moment responsible for the dynamic susceptibility in the hidden order phase. The magnetic excitations resemble the effects of strong electron correlations, whose overall symmetry looks the same above and below the hidden order phase transition. N. P. Butch, et al., Phys. Rev. B 91, 035128 (2015)

TU.B-P22 - Magnetic order in USb₂ at high pressures

J. Jeffries¹, N. Butch², R. Stillwell¹, S. Weir¹

1. Lawrence Livermore National Laboratory, Livermore, United States

2. NCSR, National Institute of Standards and Technology, Gaithersburg, Maryland

USb₂ is a member of the uranium dipnictide family, and exhibits antiferromagnetism at the relatively high temperature of 203 K. Strong anisotropy in the physical properties has been measured and predicted, including two-dimensional electronic structure. These observations point to strong hybridization of the U 5f states, and suggest that high pressures could substantially perturb the magnetic state and electronic structure of the system. Though the uranium dipnictides have been studied extensively at ambient pressure, few studies have applied significant pressures to these materials. In this presentation, we will report high-pressure electrical transport and structural characterization of USb₂ using diamond anvil cell techniques.

This work was supported by LDRD (14-ERD-041). Lawrence Livermore National Laboratory is operated by Lawrence Livermore National Security, LLC, for the U.S. Department of Energy, National Nuclear Security Administration under Contract DE-AC52-07NA27344.

TU.B-P23 - Inelastic neutron scattering measurement and low-temperature properties of CePd₂(Al,Ga)₂ compoundsM. Klicpera ^{1,2}, M. Boehm ², M. Marek Koza ², S. Rols ², P. Dolezal ¹, P. Javorsky ¹

1. Charles University In Prague, Prague, Czech Republic

2. Institut Laue-Langevin, Grenoble, France

CeT₂X₂ compounds, where T = transition d-metal and X = p-metal, crystallizing in centrosymmetric CaBe₂Ge₂-type tetragonal structure form relatively large family of intermetallics with a variety of interesting electronic properties. The electronic ground state in these compounds strongly depends on the competition between the RKKY and Kondo interaction, but also on the influence of the crystal electric field on the single 4f electron of Ce. The strong interaction between crystal field (CF) excitons and lattice vibrations in CePd₂Al₂ leading to the additional peak in energy spectrum (vibron quasi-bound state is formed) [1] is another highly interesting property of CeT₂X₂ compounds. The presented study focuses on CePd₂Al_{2-x}Ga_x compounds, investigated by means of bulk measurements and mainly inelastic neutron scattering experiments. The change of the crystal structure from tetragonal to orthorhombic (for Al rich compounds [1]) or triclinic (for Ga rich compounds [2]) and its influence on the vibron state in these compounds is discussed. The non-magnetic La analogues, undergoing the same structural phase transitions as their cerium counterparts, were investigated as well. The temperature of this structural transition is much higher in the La-counterparts than in Ce-based compounds for x<0.8, whereas for x>1.0, the opposite trend is observed. The energy spectrum of tetragonal CePd₂Al₂ exhibits three CF-like peaks at energies 1.5, 7.4 and 16 meV. First peak is shifted by structural transition (to orthorhombic structure) to 3.7 meV, while the others remain at almost the same energy. Similar behavior is observed also for compound with x=0.8, whereas for the rest of the series only two CF peaks were found.

[1] L.C. Chapon, E.A. Goremychkin, R. Osborn, B.D. Rainford, S. Short, Physica B 378-380, 819 (2006)

[2] J. Kitagawa, M. Ishikawa, J. Phys. Soc. Japan 68, 2380-2383 (1999)

TU.B-P24 - Valence fluctuation mediated quantum criticality in heavy fermions

R.U.H. Wani¹, N. Rao Dasari², V. N.S.³

1. *Jawaharlal Nehru Center for Advanced Scientific Resaerch, Karnataka, India*

2. *TSU, JNCASR, Bangalore, India*

3. *TSU, JNCASR, Bangalore, India*

Spin fluctuations lead to quantum criticality in heavy fermion systems in which there are many competing interactions like Kondo interaction, RKKY interaction and the effect of lattice coherence. However it is charge/valence degree of freedom rather than spin which is associated with quantum criticality in certain heavy fermion systems. To capture the effect of valence fluctuations in these systems we have investigated extended Periodic Anderson(e-PAM) model within the framework of dynamical mean field theory(DMFT) using continous time quantum Monte Carlo(CT-QMC) as an impurity solver. In the e-PAM there is an additional repulsive interaction $U_f c$ between localized f electrons and conduction electrons. In our preliminary calculations we have found that f level occupancy decreases as we increase the orbital energy of f electrons and this decrease becomes very steep at higher values of $U_f c$.

TU.B-P25 - Quantum Criticality and Valence Fluctuation Study for Ce- and Yb-based Compounds Probed by 3d-2p Resonant X-ray Emission Spectroscopy

N. Kawamura¹, H. Tonai², M. Mizumaki¹, T. Uozumi², S. Watanabe³

1. Japan Synchrotron Radiation Research Institute (JASRI/SPring-8), Sayo-gun, Japan

2. Osaka Prefecture University, Sakai, Japan

3. Kyushu Institute of Technology, Kitakyushu, Japan

Recently, quantum criticality for Ce- and Yb-based compounds in the heavy fermion (HF) system has been discussed from a viewpoint of valence fluctuation [1]. In this vision, the valence state (f electrons; ν_f) and d-f intra-atomic interaction (Udf) are important parameters to explain several anomalous phenomena observed near the quantum critical point (QCP). To determine parameters ν_f and Udf for several Ce and Yb compounds, resonant X-ray emission spectroscopy (RXES) measurement at Ce and Yb L3-edge (2p-4f, 5d excitations) has been performed at BL39XU of SPring-8, and theoretical calculation based on the impurity Anderson model (IAM) combined with a first principle band structure calculation has been used to analyze the experimental results. To verify the applicability of IAM framework, RXES spectra for CeO₂ are analyzed and ν_f and Udf values are estimated. The RXES spectrum around pre-edge region of X-ray absorption spectroscopy (XAS), which is necessary to determine Udf value, is well reproduced by the calculation. The parameters $\nu_f = 0.59$ and Udf = 3.0 eV are estimated through the IAM analysis of the spectra. Moreover, the parameters obtained by the calculation well reproduce the experimental results for not only high-resolution XAS spectrum (partial fluorescence yield; PFY) but also X-ray photoemission spectrum and RXES for 3d core [2, 3]. The ν_f and Udf values for the Ce- and Yb-based HF compounds with ThCr₂Si₂-type structure are mainly estimated by analyzing RXES and PFY spectra to discuss the quantum criticality from a viewpoint of valence fluctuation mechanism.

[1] S. Watanabe, et al., Phys. Rev. Lett. 105 (2010) 186403

[2] E. Wuilloud et al., Phys. Rev. Lett. 53 (1984) 202

[3] S. M. Butorin et al., J. Alloys Compounds 225 (1995) 230

TU.B-P26 - Isotropic magnon dispersion in A-type CeCu₂Si₂Z. Huesges¹, K. Schmalzl², C. Geibel¹, F. Steglich¹, O. Stockert¹1. *MPI Chemical Physics of Solids, Dresden, Germany*2. *Institut Laue-Langevin, Grenoble, France*

Paramagnons are supposed to provide the pairing glue for unconventional superconductors, not only for the cuprates, but also for heavy-fermion superconductors. For CeCu₂Si₂ there is indeed good evidence from inelastic neutron scattering that spin fluctuations drive the superconductivity, which has been studied by comparing the spin susceptibility in the normal and the superconducting state [1,2]. An interesting question is the relation of the paramagnons to the magnons in the antiferromagnetic state. Recently Le Tacon et al. have measured the dispersion of several members of the YBa₂Cu₃O_{6+x} family and found a striking similarity of the magnons in the antiferromagnetic parent compound with paramagnons in samples of varying doping levels [3]. Here, we present the measurement of the magnon dispersion in A-type CeCu₂Si₂ by inelastic neutron scattering, and compare it to previous results of S-type crystals [1,2]. We find that the dispersion is almost identical in the antiferromagnetic state, in the paramagnetic state of A-type CeCu₂Si₂ (T just above TN) and in the paramagnetic state of S-type CeCu₂Si₂ (B above Bc2). The inelastic response only differs in the correlation length and lifetime, which are increased in the ordered state, and the magnitude of the susceptibility, which is enhanced for the A-type crystal due to a weakening of the Kondo effect. In contrast to the cuprates, the magnetism in CeCu₂Si₂ is 3-dimensional, evident from the nesting-driven ordering vector of (0.22 0.22 0.52). Thus we have measured the dispersion not only along [110], but also along [001]. We find that the dispersion and the correlation length are very similar for both directions, confirming the 3D-nature of magnetic interactions in CeCu₂Si₂.

[1] J. Arndt et al., PRL 106 (2011), 246401

[2] O. Stockert, et al, Nature Physics 7 (2011), 119

[3] M. Le Tacon, et al, Nature Physics 7 (2011), 725

TU.B-P27 - Magnetic properties of heavy fermion antiferromagnet YbRhGe

S. Nakamura¹, K. Araki², K. Katoh², T. Nojima¹, A. Ochiai³

1. IMR, Tohoku University, Sendai, Japan

2. Dept. Appl. Phys., National Defense Academy, Yokosuka, Japan

3. Dept. Phys., Tohoku University, Sendai, Japan

We investigate magnetic properties and magnetic phase transitions of heavy fermion antiferromagnet ($T_N=5.9$ K) YbRhGe down to 0.5 K and up to 8 T. YbRhGe is the ternary compound having an orthorhombic TiNiSi-type crystal structure which belongs to space group Pnma. The Rh and Ge ions comprise hexagons nearly parallel to the ab-plane and the Yb ions form zigzag chains along the c-axis. YbRhGe is interesting as a spin system with characteristic crystal structure where the Kondo effect and the antiferromagnetic RKKY interaction compete with each other. Recently, an additional phase transition was found by specific heat measurements at 1 K. However, details of magnetic properties of YbRhGe at low temperatures have been revealed yet. We have synthesized single crystals of YbRhGe and measured magnetic properties by using SQUID magnetometers and a Faraday magnetometer. The magnetic susceptibility for $H//a$ rapidly increases with decreasing temperature below 3 K and becomes to be temperature independent below 1 K. This indicates an antiferromagnetic order at 1 K. Both the spin structure of the local moments and the degrees of magnetic freedom carried by the heavy Fermi liquid may change at this additional phase transition temperature. The magnetization processes of YbRhGe at 0.5 K indicate multi-transitions in the spin structure. Spin flips have been observed not only in the fields directed along the hard axis (c-axis) but also in the fields along the easy axis (a-axis). The complex magnetization processes strongly suggest competitive RKKY interactions in the spin system.

TU.B-P28 - Magnetic properties of a novel $\text{CeCo}_{0.715}\text{Si}_{2.285}$ compound

J. Moudrik¹, J. Prokleška¹, I. Císarova², J. Pospíšil¹, V. Sechovský¹, M. Klicpera³, B. Ouladdiaf³

1. Charles University In Prague, Faculty of Mathematics and Physics, DCMP, Prague, Czech Republic

2. Charles University In Prague, Faculty of Science, DIC, Prague, Czech Republic

3. Institut Laue-Langevin, Grenoble, France

We report on the basic physical properties of a novel $\text{CeCo}_{0.715}\text{Si}_{2.285}$ compound, mainly its rich magnetic phase diagram. Using the Czochralski method (single) crystals have been grown for the first time. The compound crystallizes in the I-42m space group structure with extremely prolonged unit cell ($a=4.12\text{Å}$, $c=32.84\text{Å}$).

In a zero magnetic field it orders antiferromagnetically at $T_N=10.5\text{K}$ with another order-to-order transition at 9.5K . Under application of a magnetic field along the c-axis it manifests numerous magnetic phases in small fields ($B<500\text{mT}$), similar to the so-called 'devil's staircase' systems, however, having the high field state stable with respect to field removal. Above 1T the magnetization is almost unchanged up to 14T (maximum magnetic field applied within our study) and quite reduced ($0.3\mu\text{B}/\text{Ce}$) with respect to the free Ce^{3+} ion. The compound also exhibits strong hysteresis of magnetization in temperature and magnetic field. For fields applied along the a-axis a typical behavior for the antiferromagnetic hard axis is observed.

TU.B-P29 - Magnetic and Electronic properties of $R\text{Cr}_2\text{Al}_{20}$ T. Namiki¹, S. Tsuchimoto¹, Q. Lei¹, K. Nishimura¹*1. University of Toyama, Toyama, Japan*

Recently, cage-structured compounds such as filled skutterudites have attracted much attention due to the novel properties such as the heavy fermion behavior and the first observation of unconventional superconductivity in the Pr-based filled skutterudites, and multiple ordering. These novel properties are coming from the low-lying crystal electric field (CEF) due to the crystal structure. Among them, the compounds $RT_2\text{Al}_{20}$ (R : rare earth, T : transition metal) also have the caged and cubic structure. These compounds also show the novel properties. However, only a few compounds ($R = \text{Pr}, \text{Sm}$) are studied. To clarify these novel properties, systematic studies are important. Recently, we were succeeded in growing new $R\text{Cr}_2\text{Al}_{20}$ (R : Nd, Ho) crystals, and studied magnetic and electronic properties. $R\text{Cr}_2\text{Al}_{20}$ were made by the arc melting method. The obtained samples were measured by the Powder X-ray diffraction analysis. Most of the observed diffraction lines are indexable using $\text{CeCr}_2\text{Al}_{20}$ type structure and lattice parameters are determined. The obtained values are consistent with previous reports. The temperature dependences of the resistivity ρ for $R\text{Cr}_2\text{Al}_{20}$ show the metallic behaviors down to ~ 2 K, and no anomaly is observed. The residual resistivity ratio (RRR) becomes ~ 3 .

TU.B-P30 - Strong ferromagnetism at the surface of an antiferromagnet EuRh_2Si_2

A. Chikina^{1,2}, M. Höppner^{1,3}, S. Seiro⁴, K. Kummer⁵, S. Danzenböcher¹, A. Generalov¹, M. Güttler¹, E.V. Chulkov^{6,7}, Y.M. Koroteev^{7,8}, C. Geibel⁴

1. *University of Technology Dresden, Dresden, Germany*

2. *St. Petersburg State University, St. Petersburg, Russia*

3. *Max Planck Institute for Solid State Research, Stuttgart, Germany*

4. *Max Planck Institute for Chemical Physics of Solids, Dresden, Germany*

5. *European Synchrotron Radiation Facility, Grenoble, France*

6. *Donostia International Physics Center (DIPC), Departamento de Física de Materiales and CFM-MPC UPV/EHU, San Sebastian, Spain*

7. *Tomsk State University, Tomsk, Russia*

8. *Institute of Strength Physics and Materials Science of Siberian Branch Russian Academy of Sciences, Tomsk, Russia*

Layered compounds are possible candidates for quasi-two dimensional phenomena both in the bulk and particularly at the surface. Here we consider the tetragonal antiferromagnet EuRh_2Si_2 , which consists of Eu atom arranged on a square lattice, separated by Si-Rh-Si trilayers. The pure spin moments of the Eu-atoms are ferromagnetically ordered in-plane, while neighbouring Eu-planes are coupled antiferromagnetically to each other below an ordering temperature of $T_N = 24.5$ K. Here we show that large exchange coupling of a Si-derived Shockley surface state to the outermost Eu-layer that is located four atomic layers below the surface of the antiferromagnetic compound EuRh_2Si_2 . The resulting exchange splitting provides direct information on the temperature dependent magnetism in the discussed Eu layer and at reveals an ordering temperature of 4f moments close to the surface is notably higher than than the bulk T_N .

TU.B-P31 - Relationship between onset of RKKY interaction and Ce element in Ce-based (RE-Gd)Ni; (RE=Ce, Y, Lu) compoundsK. Yano¹, K. Nishimura², T. Namiki³, T. Ohta⁴*1. Nihon University, Chiyoda, Japan**2. University of Toyama, Toyama, Japan**3. University of Toyama, Toyama, Japan**4. Quantum Design of Japan, Tokyo, Japan*

The Ce-based (Ce-Gd)Ni compound system, which are composed of a heavy fermion compound CeNi and a ferri-magnet GdNi, shows a peculiar $\mu_0 H$ relationship in $M(T)$ at Gd-poor contents of 0.10...0.2 and this unusual behavior in $M(T)$ can be found to stem from a collapse-like decrease of RKKY interaction J_{Gd-Gd} by using molecular field analysis. Accordingly, the unusual linear behavior does reflect the collapse-like decrease of RKKY interaction between Gd and Gd in the compounds and whether this collapse of RKKY interaction is confined to some characteristics of Ce element or not becomes an interesting and important problem. In order to investigate this problem, the system of (RE-Gd)Ni, where Ce is replaced by non-magnetic RE (Rare Earth) element such as Y and Lu, are suitable. The system of (Y-Gd)Ni, where Ce is substituted by Y, has been preliminary studied and in this system, RKKY interaction seems to revive and does not collapse. Although Y is often classified as RE element, Y has no 4f, 5d and 6s electrons characteristic to RE. In this study, we deal mainly with (Lu-Gd)Ni system in Gd-poor content of 0.10 and 0.15, respectively. In (Lu-Gd)Ni system at Gd-poor content, the $M(T)$ behaves normally curved lines and does not take linear relationship. At present, the collapse-like decrease of RKKY interaction is highly possible to be attributed to some peculiar characteristics of Ce element.

TU.B-P32 - Low temperature anomalies of the magnetic heat capacity of $\text{Ho}_x\text{Lu}_{1-x}\text{B}_{12}$

A. Khoroshilov¹, N. Sluchanko², A. Bogach², V. Glushkov^{1,2}, S. Demishev^{1,2}, V. Filippov³, N. Shitsevalova³, S. Gabani⁴, K. Flachbart⁴

1. Moscow Institute of Physics And Technology, Dolgoprudny, Russia

2. A.M. Prokhorov General Physics Institute of RAS, Moscow, Russia

3. Institute for Problems of Materials Science, NAS of Ukraine, Kiev, Ukraine

4. Institute of Experimental Physics, SAS, Kosice, Slovakia

Heat capacity $C(T,H)$ measurements have been carried out on high quality single crystals of $\text{Ho}_x\text{Lu}_{1-x}\text{B}_{12}$ solid solutions ($x \leq 1$) in a wide range of temperatures (0.07 – 300 K) and in external magnetic field up to 90 kOe. For holmium concentrations $x \geq 0.2$ antiferromagnetic phase transition have been detected (Fig 1a) and it was found that Neel temperature $T_N(x)$ changes about linearly in the range of 1-7.4 K. Detailed investigations of the specific heat within the framework of approach developed in [1] allowed us to separate vibration, electron and magnetic contributions to heat capacity. The analysis allows concluding in favor of low temperature magnetic C_m and nuclear C_n components in heat capacity. The first one may be described as a three-level Schottky anomaly attributed to Γ_5 triplet ground state of Ho^{3+} ions [2] with Zeeman splitting in the external magnetic field. The second contribution appears due to hyperfine splitting of holmium nuclear levels, and it can be described very well in terms of a nuclear multi-level Schottky anomaly (see Figs 1b, 1c). The hyperfine field on holmium nuclear is estimated ($H_{\text{hf}} = 4000\text{-}8000$ kOe) in combination with effective g-factors of Zeeman splitting of the ground state multiplet of Ho^{3+} -ions ($g_1=4.7\pm 0.1$ and $g_2=10.4\pm 0.1$) for all $\text{Ho}_x\text{Lu}_{1-x}\text{B}_{12}$ crystals studied. A comparison between the specific heat data and the magnetoresistance results [3] was finally carried out providing with arguments in favor of additional spin-polaron component both in the charge transport and in thermal properties of $\text{Ho}_x\text{Lu}_{1-x}\text{B}_{12}$.

[1] N.E. Sluchanko, Azarevich A.N., Bogach A.V. et al., *JETP* **140** (2011) 536-552

[2] K. Siemensmeyer, K. Habicht, Th. Lonkai et al., *J. Low Temp. Phys.* **146** (2007) 581-605

[3] N.E. Sluchanko, Khoroshilov A.L., Anisimov M.A. et al., *arXiv:1412.0497 [cond-mat.str-el]*

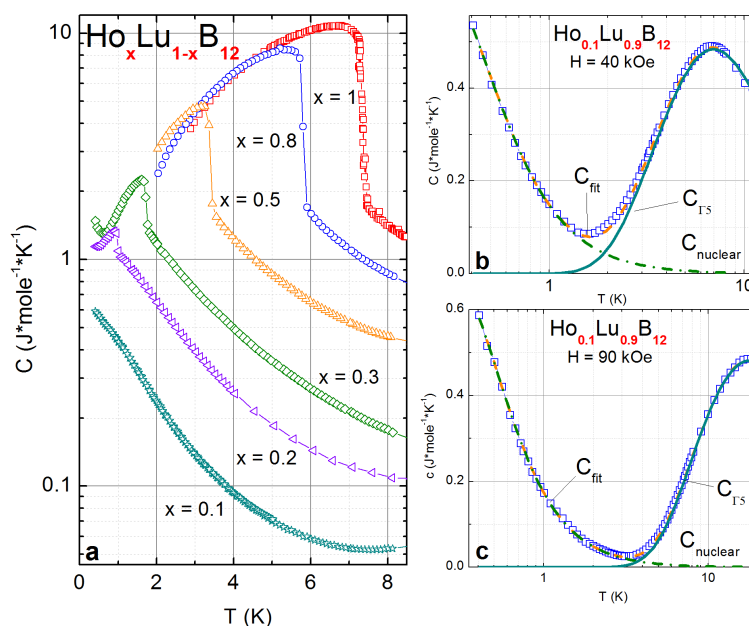


Fig 1. Low temperature heat capacity of $\text{Ho}_x\text{Lu}_{1-x}\text{B}_{12}$ (a), of $\text{Ho}_{0.1}\text{Lu}_{0.9}\text{B}_{12}$ in magnetic field of $H = 40$ kOe (b), and $H = 90$ kOe (c).

TU.B-P33 - Anomalous thermal expansion of intermediate valence YbAl₃ nanometric alloys

L. Fernandez Barquin¹, M. de la Fuente Rodríguez¹, C. Echevarria-Bonet^{1,7}, D.P. Rojas², J.C. Gómez Sal¹, J.I. Espeso¹, P. Gorria³, A. Garcia-Prieto⁴, M.L. Fdez-Gubieda⁴, E. Bauer⁵

1. Universidad de Cantabria, Santander, Spain
2. Universidad Politécnica de Madrid, Madrid, Spain
3. Universidad de Oviedo, Oviedo, Spain
4. Universidad del País Vasco, Bilbao, Spain
5. Technische Universität Wien, Wien, Austria
6. ALBA-CELLS, Barcelona, Spain
7. Institute for Energy Technology, Kjeller, Norway

The Strongly Correlated Electron System YbAl₃ alloy has attracted attention due to the fact that it exhibits a variety of cutting-edge physical phenomena [1]. Recently, we have undergone a thorough study of YbAl₃ nanoparticles. X-ray absorption measurements supported the decrease of the valence with the reduction of the size of the particles, related to the increase of the Yb²⁺ contribution [2]. The effect was related to the surface/volume ratio increase due to the downsizing of the particles. We have recently carried out an X-ray diffraction ($\lambda = 0.4126$ Å, YbAl₃ > 99 %) experiment at ALBA synchrotron facility. A careful crystallographic Rietveld analysis has revealed an intriguing behaviour of the thermal expansion (α) of these YbAl₃ nanoparticles at $80 \leq T \leq 300$ K. The lattice parameter variation of the $D = 10$ nm nanoparticles (milled during 70 h) shows an unexpected change of slope around 180 K. It should be noted that heat capacity did not exhibit any sign of transition at this temperature. It is of paramount significance that the $\alpha = 7.5 \cdot 10^{-6} \text{ K}^{-1}$ value inferred from the linear variation below 200 K is within the values reported for the bulk alloy, whereas the one ($\alpha = 1.5 \cdot 10^{-6} \text{ K}^{-1}$) extracted for $T > 200$ K is anomalously small. The latter α value is approaching those reported for Zero Thermal Expansion (ZTE) compounds [3]. In consequence, the use of the size as a parameter.

[1] A. L. Cornelius *et al.*, Phys. Rev. Lett. 88 (2002) 117201

[2] D. P. Rojas *et al.*, Phys. Rev B 78, 094412 (2008)

[3] J. R. Salvador *et al.*, Nature. 425 (2003) 702

TU.B-P34 - Magnetic, thermal and electronic properties of nanosized YbAl₂ alloys

D.P. Rojas¹, L. Fernandez Barquin², J.C. Gomez sal², J.I. Espeso², J. Rodriguez Fernandez², J. Chaboy³

1. *Universidad Politécnica De Madrid, Madrid, Spain*

2. *Universidad de Cantabria, Santander, Spain*

3. *CSIC- Universidad de Zaragoza, Zaragoza, Spain*

The bulk YbAl₂ alloy has been subject of comprehensive studies because it interesting properties associated to the intermediate valence behavior. It was observed that the value of its mean valence increases from 2.15 at low temperatures up to 2.4 at room temperature [1]. In the present work the effects of the mechanical milling on the structural, magnetic, thermal and electronic properties of this alloy are reported. The analysis of the X-ray diffraction data indicates that for 20 h of milling time the particle size reduces down to 47 nm and the lattice strain reaches the value of 0.2 %. Measurements of the magnetic and thermal properties present a similar tendency to that observed in the parent intermediate valence alloy YbAl₃ with a reduction of the value of the magnetization and the presence of additional contributions in the specific heat due to the phonon softening [2,3]. In addition, the XANES spectra shows an increase of the Yb²⁺ contribution associated to the size reduction, and specifically to the atoms sitting at the surface of the nanoparticles. Interestingly, with the further increase of the milling time up to 70 h and 120 h, a metallurgical transformation to the YbAl₃ phase takes place. The results are discussed as the influence of size effects on the above mentioned properties.

[1] T. Görlach, C. Pfeleiderer, K. Grube, and H. v. Löhneysen, Phys. Rev B, 71, 033101 (2005)

[2] D. P. Rojas et.al, Phys. Rev B 78, 094412 (2008)

[3] D. P. Rojas et.al, Nanotechnology 21, 445702 (2010)

TU.B-P36 - Magnetism in UBeGe

R. Gumeniuk^{1,2}, W. Schnelle², U. Burkhardt², H. Borrmann², A. Leithe-Jasper², Y. Grin²

1. *Institute For Experimental Physics, TU Bergakademie Freiberg, Germany*

2. *MPI CPFS, Dresden, Germany*

UBeGe and ThBeGe crystallize with ZrBeSi type of structure. UBeGe is a ferromagnet with $T_C = 157$ K and with a large coercive field of 0.55 T. The low field measurements indicate a rather low anisotropy of this ferromagnet. The experimentally determined saturation moment of 2.43 μ_B /U-atom at 7 T agrees well with the theoretically calculated one (LSDA+U) of 2.1 μ_B /U-atom. In the paramagnetic range Curie-Weiss behaviour with $\mu_{eff} = 3.2 \mu_B$ and $\vartheta_p = 160$ K is observed, in agreement with the strong ferromagnetic interactions. Electrical resistivity and specific heat capacity of UBeGe show strong second-order type anomalies at T_C . All these findings would indicate a well localized character of U 5f electrons in studied germanide, which was already expected from the crystal structure. ThBeGe is a simple metallic system with low density of states at the Fermi, which was confirmed by theoretical calculations and measurements of electrical resistivity and specific heat.

TU.B-P38 - Valence state of Tm in YbB₆ and YB₆

H. Sato¹, H Nagata², F. Iga³, K. Mimura⁴, S. Ueda⁵, K. Fukuda⁶, Y. Tobita⁷, K. Ishii⁷, K. Hayashi⁷, Y. Osanai⁷

1. Hiroshima Synchrotron Radiation Center, Hiroshima University
2. Graduate School of Science, Hiroshima University
3. College of Science, Ibaraki University, Ibaraki, Japan
4. Graduate School of Engineering, Osaka Prefecture University, Osaka, Japan
5. Synchrotron X-ray Station at SPring-8, National Institute for Materials Science
6. Graduate School of Advanced Sciences of Matter, Hiroshima University
7. Graduate School of Science and Engineering, Ibaraki University
8. Institute for Solid State Physics, University of Tokyo

The rare-earth hexaborides RB₆ with the CaB₆ cubic structure exhibit a wide variety of physical properties depending on the R ion such as an antiferroquadrupole order in CeB₆ and valence fluctuation in the narrow-band gap semiconductor SmB₆. However, there has been no report for the synthesis of TmB₆. The lattice parameters of the solid solutions La_{1-x}Tm_xB₆ and Yb_{1-x}Tm_xB₆ suggested that TmB₆ would be a valence fluctuation compound [1]. In this study, we have investigated electronic structure of Yb_{1-x}Tm_xB₆ and Y_{1-x}Tm_xB₆ by means of hard x-ray photoemission spectroscopy (HAXPES) at $h\nu = 5.95$ keV carried out at BL15XU of SPring-8. The valence states of Tm ions have been directly probed by the Tm 3d HAXPES. We found that the Tm valence state changes depending on the host materials YbB₆ and YB₆. Only Tm³⁺ components are detected in the Tm 3d HAXPES spectra of Yb_{1-x}Tm_xB₆ ($x=0.1, 0.2$), indicating that Tm ion is substituted for Yb as a trivalent state. The Yb valence remains in a divalent state as in YbB₆. The Yb_{2+ 4f_{7/2}} peak at about 1 eV below the Fermi level is shifted to the deeper binding energy side. This shift suggests that the Yb₂₊ state is stabilized due to the Tm substitution. On the other hand, the Tm 3d spectra of Y_{1-x}Tm_xB₆ ($x=0.35$) clearly indicate strong fluctuation of Tm valence in Y_{1-x}Tm_xB₆. On cooling, the Tm²⁺ (Tm³⁺) component increases (decreases) as often observed in the Yb-based valence fluctuation compounds [2]. In fact, the Tm valence deduced from the Tm 3d spectra decreases from $\nu=2.75$ at 300 K to $\nu=2.56$ at 20 K.

[1] M. Kasaya et al., J. Magn. Mater. 389, 31-34 (1983)

[2] For example, Y. Utsumi et al., Phys. Rev. B86, 115114 (2012)

TU.B-P39 - Single crystal growth and electronic state of UPd₂Cd₂₀H. Doto¹, Y. Hirose², F. Honda³, D. Li³, D. Aoki³, R. Settai²

1. Graduate School of Science And Technology, Niigata University, Niigata, Japan

2. Department of Physics, Niigata University, Niigata, Japan

3. Institute for Materials Research, Tohoku University, Sendai, Japan

UT₂X₂₀ (T = Transition Metal, X = Al, Zn) crystallizes in the cubic CeCr₂Al₂₀ type structure and shows characteristic behavior. For example, the heavy fermion compound UIr₂Zn₂₀ has a large electronic specific heat coefficient of about 400 mJ/mol·K² and UMn₂Al₂₀ shows a ferromagnetic transition[1,2]. Recently, Burnett et al. found new compounds RNi₂Cd₂₀ (R = Rare Earth)[3].

We succeeded in growing single crystals of a new compound UPd₂Cd₂₀ by the Cd self-flux method, which is found to be the CeCr₂Al₂₀ type structure. The electrical resistivity slightly increases with decreasing temperature, and shows a maximum at 25 K. Below 5 K, the resistivity rapidly decreases and follows the Fermi liquid relation $\rho = \rho_0 + AT^2$ with $\rho_0 = 5.4 \mu\Omega\cdot\text{cm}$ and $A = 2.4 \mu\Omega\cdot\text{cm}/\text{K}^2$, where ρ_0 is a residual resistivity, and A is a coefficient which relates to effective mass. The observed A value is about 2 times larger than that of heavy fermion compound UIr₂Zn₂₀, implying that UPd₂Cd₂₀ forms the heavy fermion state[4]. The temperature dependence of the magnetic susceptibility follows the Curie-Weiss law above 30 K with the effective magnetic moment $\mu_{\text{eff}} = 3.44 \mu_B/\text{U}$. The obtained value of μ_{eff} is close to the value for U³⁺ or for U⁴⁺ ionic state. The magnetic susceptibility indicates a broad maximum at 6 K and an abrupt decrease at 5 K, suggesting an antiferromagnetic ordering.

Experimental results strongly suggest that UPd₂Cd₂₀ is a new heavy fermion antiferromagnet.

[1] E. D. Bauer, et al. : J. Magn. Magn. Mater. 310 (2007) 449

[2] C. H. Wang, et al. : Phys. Rev. B 82 (2010) 094406

[3] V.W. Burnett, et al. : J. Solid State Chem. 215 (2014) 114

[4] Y. Hirose, et al. : J. Phys. : Conf. Ser. 391 (2012) 012021

TU.B-P40 - Fragile antiferromagnetism in a new Shastry-Sutherland lattice compound $\text{Yb}_2\text{Ru}_3\text{Ga}_{10}$ Y. Muro¹, T. Fukuhara¹, T. Kuwai²

1. Faculty of Engineering, Toyama Prefectural University, Toyama, Japan

2. Graduate School of Science and Engineering, University of Toyama, Toyama, Japan

Combination between Kondo effect and geometrical frustration attracts much interest on the heavy fermion physics[1]. For ytterbium systems, peculiar magnetic properties due to the above combination were observed in a Shastry-Sutherland lattice (SSL) system $\text{Yb}_2\text{Pt}_2\text{Pb}$ [2]. In this presentation, we report the single-crystal study of a new Yb-based SSL compound $\text{Yb}_2\text{Ru}_3\text{Ga}_{10}$ by measuring the magnetic susceptibility, electrical resistivity, and specific heat. Yb atoms in $\text{Yb}_2\text{Ru}_3\text{Ga}_{10}$, crystallizing in a new tetragonal structure type[3], occupy the 4g site of the space group $P4/mbm$ and form the SSL on (001) plane. Single-crystalline samples were grown by a Ga self-flux method. The magnetic susceptibility at $B // [100]$, $C_{[100]}$, shows a Curie-Weiss behavior between 50 K and 300 K while the $C_{[001]}$ shows a small temperature dependence. This anisotropic susceptibility indicates that the Yb 4f moments lie in (001) due to the crystal-field effect. The electrical resistivity below 30 K shows a $-\log T$ behavior, indicating that $\text{Yb}_2\text{Ru}_3\text{Ga}_{10}$ is a new Kondo-lattice compound. Below 1.4 K, we observed a sharp anomaly accompanying a small hump due to an antiferromagnetic transition with the transition temperature $T_N = 1.4$ K. This transition disappears at only 0.2 T for $B // [100]$, while T_N survives at 1.4 K for $B = 1$ T // [001]. The disappearance of antiferromagnetic order at weak magnetic field and anisotropic phase diagram in $\text{Yb}_2\text{Ru}_3\text{Ga}_{10}$ should result from the magnetic frustration arising from the SSL.

[1] P. Coleman and A. H. Nevidomskyy, J. Low Temp. Phys. **161** (2010) 161[2] M. S. Kim and M. C. Aronson, Phys. Rev. Lett. **110** (2013) 017201[3] M. Schlüter and W. Jeitschko, Inorg. Chem. **40**, 6362 (2001)

TU.B-P41 - Theoretical investigation of the linear and the nonlinear magnetic susceptibility of URu_2Si_2 compoundA. Lausmann¹, B. Pedrolo¹, E. Calegari¹, S. Magalhães², P Riseborough³1. *Universidade Federal de Santa Maria, Santa Maria, Brazil*2. *Universidade Federal Fluminense, Niterói, Brazil*3. *Temple University, Philadelphia, United States*

In the last three decades, the heavy fermion compound URu_2Si_2 has attracted much attention mainly due to its unusual behavior. In the absence of an external magnetic field, the specific heat exhibits an anomaly which indicates a phase transition to a unknown ordered state. This phase transition occurs at 17.5 K and the ordered state is known as a Hidden Order phase [1]. Results of magnetic torque experiments on tiny crystals of URu_2Si_2 show that, below the ordered temperature T_{HO} , the magnetic susceptibility becomes anisotropic [2]. Moreover, measurements in URu_2Si_2 compound show that the nonlinear susceptibility exhibits a strong anomaly at T_{HO} resembling the specific heat anomaly [3]. Recently, a theory based in the underscreened Anderson Lattice Model has been proposed for describe the order parameter of the hidden order phase [4] in URu_2Si_2 . In the present work, this theory is employed to investigate both the linear and the nonlinear magnetic susceptibilities of the model of reference [4]. The magnetic susceptibilities are calculated for two distinct cases: for a magnetic field H_z parallel to the axis of quantization and for a magnetic field H_x perpendicular to the axis of quantization. The results show that when H_z is present, the linear magnetic susceptibility is strongly temperature dependent, whereas for H_x the linear magnetic susceptibility is only slightly temperature dependent. For a magnetic field parallel to the axis of quantization the nonlinear magnetic susceptibility presents an anomaly at T_{HO} , which is similarly to the anomaly observed in the specific heat. The present results are in qualitatively agreement with experimental results [2,3] on URu_2Si_2 .

[1] J. A. Mydosh and P.M. Opeeneer, Philosophical Magazine 94, 3642 (2014)

[2] R. Okazaki et. al., Science 331, 439-442 (2011)

[3] A.P Ramirez et. al., PRL 68, 2680 (1992) [4] P.S. Riseborough, B. Coqblin, and S.G. Magalhães, PRB 85, 165116 (2012)

TU.B-P42 - Thermal Expansion and Magnetostriction Measurements on Heavy-Fermion Compound YbCu₄Au

T. Takeuchi¹, Y. Hirose², R. Tsunoda³, F. Honda⁴, R. Settai²

1. *Low Temperature Center, Osaka University, Toyonaka, Osaka, Japan*

2. *Department of Physics, Niigata University, Niigata, Japan*

3. *Graduate School of Science and Technology, Niigata University, Niigata, Japan*

4. *IMR, Tohoku University, Oarai, Ibaraki, Japan*

The ternary intermetallic compound YbCu₄Au crystallizes in the AuBe₅-type cubic structure and shows a large electronic specific heat coefficient larger than 2 J/K²mol [1]. The antiferromagnetic order appears below T_N ~ 0.8 K with the ordered magnetic moment of 0.85 μ_B/Yb, which is substantially reduced with respect to that expected for the Gamma₇ ground state doublet [2]. It is noted that the temperature-magnetic field (T-H) phase diagram of YbCu₄Au is found to be very similar to that of YbRh₂Si₂, which is situated close to the quantum critical point[3,4]. In this study, we measured the specific heat, thermal expansion coefficient, and magnetostriction of polycrystalline samples in the temperature range down to 1.4 K in order to investigate further the T-H phase diagram of YbCu₄Au. The temperature dependence of the specific heat under H = 2 T shows a broad peak at T ~ 3 K, and this peak shifts to higher temperatures with increasing magnetic field. This broad peak was interpreted as the Schottky anomaly due to the Zeeman splitting of the Gamma₇ doublet [1]. Correspondingly, the thermal expansion coefficient under 2 T shows a broad peak centered at approximately 3 K, and this peak shifts to higher temperatures with further increase in the magnetic field. The magnetostriction up to 9 T indicates anomalous behaviors at temperatures below 15 K. These anomalies in the specific heat, thermal expansion coefficient, and magnetostriction are discussed in relation to the characteristic T-H phase diagram of YbCu₄Au [3,4].

[1] E. Bauer et al., Phys. Rev. B 50, 9300 (1994)

[2] E. Bauer et al., Physica B 234-236, 676 (1997)

[3] A. Yamamoto, S. Wada, and J. L. Sarrao, J. Phys. Soc. Jpn. 76, 063709 (2007). [4] S. Wada and A. Yamamoto, Physica B 403, 1202 (2008)

TU.B-P43 - Pressure effect of EuCu_9Sn_4 and EuZn_{13}

S. Satoh¹, Y. Hirose², S. Tomaru¹, S. Kurahashi¹, T. Takeuchi³, F. Honda⁴, D. Li⁴, D. Aoki⁴, K. Matsubayashi⁵, Y. Uwatoko⁵

1. Graduate School of Science And Technology, Niigata University, Niigata, Japan
2. Department of Physics, Niigata University, Niigata, Japan
3. Low Temperature Center, Osaka University, Osaka, Japan
4. Institute for Materials Research, Tohoku University, Sendai, Japan
5. Institute for Solid State Physics, Tokyo University, Chiba, Japan
6. Advanced Science Research Center, Japan Atomic Energy Agency, Ibaraki, Japan

The Eu ions can be either divalent or trivalent in compounds. The trivalent Eu ion doesn't exhibit a magnetism due to the total angular momentum $J=0$ in the ground state. On the other hand, the divalent Eu ion shows a magnetism with a larger volume compared to that of trivalent ion state. Pressure is expected to change the valence of Eu ions. For example, an antiferromagnet $\text{Eu}(\text{Pd}_{0.8}\text{Au}_{0.2})_2\text{Si}_2$ is found to indicate the valence transition above 1.2GPa[1]. In this study, we focused on an antiferromagnet EuCu_9Sn_4 and a ferromagnet EuZn_{13} with a similar crystal structure, and measured the temperature dependence of the electrical resistivity under pressure, in order to investigate the pressure effect in different magnetic ordered states. EuZn_{13} crystallizes in the cubic NaZn_{13} type structure[2], which has two types of caged-like structure formed by 12 Zn and 38 Zn atom surrounding Zn atom and Eu atom, respectively. EuCu_9Sn_4 crystallizes in the tetragonal LaFe_9Si_4 type structure, which forms distorted caged-like structures of NaZn_{13} type[3]. We succeeded in growing single crystals of EuCu_9Sn_4 and EuZn_{13} by the Sn and Zn self-flux method, respectively. Recently, we found that EuCu_9Sn_4 is an antiferromagnet with the easy plane type anisotropy perpendicular to the [001] direction[4]. The temperature dependence of the electrical resistivity of EuCu_9Sn_4 monotonically decreases with decreasing temperature, and indicates a rapid decrease at $T_N=8.7\text{K}$. With increasing pressure, T_N shows a minimum value of 8.2K at 4GPa. Above 8GPa, the resistivity indicates a hysteresis in the temperature range between 5 and 10K, which could be a sign of the first order valence transition.

- [1] M.M.Abd-Elmeguid et al., Phys. Rev. Lett. 55, 2467(1985)
[2] A. Landelli et al., J. Less-Common Met. 12, 333(1976)
[3] D. Mazzone et al., J. Alloy. Compd. 453, 24(2008)
[4] Y. Hirose, S. Satoh et al., to be published in J. Phys : Conf. Ser

TU.B-P44 - Study of valence in heavy-fermion single crystals under pulsed magnetic fields up to 30 T

A. Poux¹, F. Duc¹, W. Knafo¹, S. Pascarelli², D. Braithwaite³, O. Mathon², P. van der Linden², C. Strohm², V. Balédent⁴, X. Fabre¹

1. *Laboratoire National Des Champs Magnétiques Intenses - CNRS*

2. *ESRF, 6 rue Jules Horowitz, Grenoble, France*

3. *Univ. Grenoble Alpes and CEA, INAC-SPSMS, Grenoble, France*

4. *Laboratoire de Physique des Solides, Orsay, France*

5. *Synchrotron Soleil, L'Orme des Merisiers, Saint-Aubin, Gif-sur-Yvette, France*

6. *Institut Néel, Grenoble, France*

Heavy-fermions metals are characterized by a Fermi liquid regime with effective masses reaching hundred to several thousands times that of the free electron mass [1]. Strong electronic interactions can be tuned by pressure, doping, or magnetic field, which leads to magnetic quantum phase transitions where the effective mass is enhanced and exotic phenomena, as non-Fermi liquid and unconventional superconductivity, emerge. Recently, it has been proposed that changes of valence and valence fluctuations might play a significant role in these systems [2]. Valence changes occurring from tuning with high pressure or temperature have been extensively studied on several systems. Heavy fermion systems are also very sensitive to high magnetic fields [3], but the effect of field on the valence state requires magnetic fields higher than those readily available in synchrotron facilities and is still largely unexplored. In this contribution, we present the investigation of valence in Yb-based heavy fermions under fields up to 30 T at temperatures from 4 K to 300 K by x-ray absorption spectroscopy combining the use of a long-duration pulsed magnet developed by the LNCMI-Toulouse and a specially designed helium flow cryostat developed by the ESRF-Grenoble on the Energy-Dispersive-XAS beamline ID24. At low temperature, a small but measurable variation of valence is observed when the field is applied along the easy magnetic axis, while no variation of valence is found when the field is applied along the hard magnetic axis. This anisotropic effect is a signature of the interplay between the magnetic properties and the variation of valence, which is usually understood as a consequence of the Kondo delocalization of the f-electrons.

[1] J. Flouquet, *Prog. Low Temp. Phys.* 15, 139 (2005)

[2] S. Watanabe et al., *Phys. Rev. Lett.* 100, 236401 (2008)

[3] D. Aoki et al., *C. R. Physique* 14, 53 (2013)

TU.B-P45 - Crystallographic and Magnetic Properties of UAu₂Si₂

C. Tabata¹, S. Shimmura¹, N. Miura¹, H. Saito¹, H. Hidaka¹, Y. Ihara¹, H. Amitsuka¹

1. Graduate School of Science, Hokkaido University, Japan

The tetragonal UT₂Si₂ family (T: transition metals) has been one of the subjects of intense research during last three decades, providing fruitful opportunities for systematic understanding of 5f-electronic properties. Among the numerous studies of UT₂Si₂ compounds, there are only 5 reports about polycrystalline UAu₂Si₂, where it is said to be a heavy-fermion compound with a ferromagnetic ordered state below 20 K. In order to get further insight into the 5f-electronic properties of this compound, we synthesized polycrystalline UAu₂Si₂ and its isostructural nonmagnetic counterpart ThAu₂Si₂, and investigated their magnetic, thermal and transport properties by means of magnetization, specific-heat and electrical-resistivity measurements. In addition to these macroscopic measurements, we also performed X-ray-diffraction and ²⁹Si-NMR experiments on powdered sample to obtain microscopic information about the ordered state of UAu₂Si₂. In our detailed bulk measurements, we have found several unusual behaviors that seem to be inconsistent with those expected in normal ferromagnetic compounds as follows: The magnetization shows a distinct cusp anomaly at the transition temperature T₀ = 20 K in high magnetic fields above 5 T. The specific-heat jump at T₀ becomes not broader but more pronounced as the field increases. Moreover, the resistivity shows a Cr-like anomaly below T₀, which suggests opening of an energy gap at the Fermi surface. These experimental facts strongly suggest that the phase transition at T₀ may not be simply ferromagnetic, as previously reported, but intrinsically antiferromagnetic.

This hypothesis is supported by our preliminary results of the ²⁹Si-NMR experiments.

TU.B-P47 - NMR observation of quadrupole order and multipole fluctuations in PrTi₂Al₂₀

T. Taniguchi¹, M. Yoshida¹, H. Takeda¹, M. Takigawa¹, M. Tsujimoto¹, A. Sakai¹, S. Nakatsuji¹

1. Institute For Solid State Physics, University of Tokyo, Chiba, Japan

The intermetallic compound PrTi₂Al₂₀ shows a phase transition at 2 K [1,3] associated with the quadrupole moments of Pr ions, for which the ground state of crystal field is non-magnetic doublet [3]. Recent discovery of enhanced superconductivity under high pressure suggests novel mechanism for Cooper pairing due to quadrupole fluctuations [4]. Here we report results of Al-NMR in a single crystal PrTi₂Al₂₀. When a magnetic field is applied along the 111 direction, certain lines of the NMR spectrum split upon entering into the ordered phase, indicating breaking of the three-fold rotation symmetry due to field-induced magnetic dipole moment perpendicular to the field. This provides microscopic evidence for a symmetry-breaking ferro-quadrupole order of O₂₀ (3z²-r²) type. We discuss detailed field- and temperature-dependence of the induced dipole, which is proportional to the quadrupole order parameter. In addition, the nuclear relaxation rate (1/T₁) shows strong enhancement below 30 K and a sharp peak near the transition temperature. The possible origin of the nuclear relaxation is the field-induced dipoles associated with quadrupolar fluctuations or octupole moments. We present quantitative analysis of the multipolar fluctuations based on the field and orientation dependence of the nuclear relaxation rates.

[1] A. Sakai, *et al*, J. Phys. Soc. Jpn. 80, 063701 (2011)

[2] M. Koseki, *et al*, J. Phys. Soc. Jpn. 80, SA049 (2011)

[3] K. Matsubayashi, *et al*, Phys. Rev. Lett, 109, 18 (2012)

[4] T. J. Sato, *et al*, Phys. Rev. B 86, 184419 (2012)

TU.B-P48 - G_3 lattice instability of URu_2Si_2 highlighted by pulsed magnetic field

T. Yanagisawa¹, T. Murazumi¹, S. Mombetsu¹, H. Hidaka¹, H. Amitsuka¹, M. Akatsu², S. Yasin³, P.T Cong³, S. Zherlitsyn³, J. Wosnitza³

1. Department of Physics, Hokkaido University, Sapporo, Japan
2. Department of Physics, Niigata University, Niigata, Japan
3. Hochfeld-Magnetlabor Dresden, Helmholtz-Zentrum Dresden-Rossendorf, Niigata, Japan
4. Department of Physics, University of California San Diego, Niigata, Japan
5. Los Alamos National Laboratory, Niigata, Japan
6. CEA-Grenoble, Grenoble, France
7. Institute for Materials Research, Tohoku University, Niigata, Japan

Heavy-fermion superconductor URu_2Si_2 has been known to show an enigmatic second-ordered phase transition at 17.5 K, so called 'Hidden Order (HO)', whose order parameter still has remained unsolved. In high magnetic fields for $H \parallel [001]$ at low temperatures, URu_2Si_2 undergoes three meta-magnetic transitions in the range 35 and 39 T with a collapse of the HO phase. While, this compound also exhibits a strong hybridization between conduction electron and $5f$ electrons below $T^* \sim 50$ K in low-magnetic fields, the c - f hybridization is also suppressed in higher magnetic field region above 39 T. Our recent investigation of elastic constant $(C_{11}-C_{12})/2$ of URu_2Si_2 under pulsed-magnetic fields strongly suggests that the hybridized electronic state possesses an orthorhombic lattice instability with Γ_3 symmetry (x^2-y^2 type). In order to clarify the elastic response of the other symmetry-breaking strains in URu_2Si_2 under high-magnetic fields, we have measured elastic constants of transverse C_{44} , C_{66} ultrasonic modes and also longitudinal C_{11} and C_{33} ultrasonic modes of URu_2Si_2 single crystals by means of high-frequency ultrasonic measurements under pulsed-magnetic fields up to ~ 62 T for $H \parallel [001]$ in wide temperature range from 1.5 K to ~ 120 K. Elastic constants C_{33} , C_{44} and C_{66} exhibit successive step-like decreasing through the cascade-like meta-magnetic transition region and keep decreasing above 39 T, while C_{11} and $(C_{11}-C_{12})/2$, both of which are related to Γ_3 -symmetry response, show increasing in higher-magnetic-field region. Such clear contrast in the elastic responses strongly support the idea that the G_3 -type orthorhombic lattice instability is related to a symmetry-breaking band instability that arises due to the c - f hybridization, and is probably linked to the HO parameter of this compound.

TU.B-P49 - Magnetic, transport, and structural properties of caged compounds $\text{ROs}_2\text{Zn}_{20}$ (R=La-Nd)K. Wakiya¹, K. T. Matsumoto¹, N. Nagasawa¹, T. Onimaru¹, K. Umeo², T. Takabatake⁰*1. Graduate School of Advanced Sciences of Matter, Hiroshima University, Higashi-Hiroshima, Japan**2. Natural Science Center for Basic Research and Development, Hiroshima University, Higashi-Hiroshima, Japan**3. Institute for Advanced Materials Research, Hiroshima University, Hiroshima, Japan*

Cubic compounds $\text{RT}_2\text{Zn}_{20}$ (R: rare earth, T: Transition metal) have attracted much attention, because they show various phenomena such as heavy-fermion state, superconductivity, and multipole ordering [1-3]. From the cage-like structure, it is expected that low-energy vibrations of guest ions in the atomic cages may play a role in the physical properties. In fact, the first principles calculation of $\text{LaT}_2\text{Zn}_{20}$ (T=Ru, Ir) pointed out that the Zn atom at the 16c site in the R_2Zn_{12} cage is vibrating at low frequencies, and the vibration is probably related to the structural transition [3, 4]. In order to perform a systematic study on the magnetic, transport, and structural properties of $\text{RT}_2\text{Zn}_{20}$, we have synthesized a series of T=Os compounds with R=La, Ce, Pr, and Nd. We report on the electrical resistivity, magnetization, and specific heat measurements.

All the compounds of $\text{ROs}_2\text{Zn}_{20}$ undergo structural transitions, whose temperature decreases with lanthanide contraction. This suggests that the high-temperature structure is stable for smaller lattice volume. The observed relationship between the lattice volume and the transition temperature suggests that the low-energy vibration of the Zn atom at the 16c site plays a role in the structural transitions. The measurements of physical properties of $\text{ROs}_2\text{Zn}_{20}$ indicate that $\text{LaOs}_2\text{Zn}_{20}$ without 4f electron is a diamagnet with the electronic specific heat coefficient γ of 10.4 mJ/K² mol. $\text{CeOs}_2\text{Zn}_{20}$ is a valence fluctuating compound whose γ value is ten times larger than that of $\text{LaOs}_2\text{Zn}_{20}$. At low temperatures, $\text{PrOs}_2\text{Zn}_{20}$ displays a van-Vleck paramagnetic behavior, suggesting a non-magnetic ground state. $\text{NdOs}_2\text{Zn}_{20}$ shows a ferromagnetic transition at 0.6 K. These physical properties of $\text{ROs}_2\text{Zn}_{20}$ are in parallel with those of the isostructural compounds $\text{RRu}_2\text{Zn}_{20}$ (R=La-Nd) [2, 3, 5].

[1] M. S. Torikachvili et al., Proc. Natl. Acad. Sci. U.S.A. 104 9960 (2007)

[2] T. Onimaru et al., Phys. Rev. Lett. 106, 177001 (2011)

[3] T. Onimaru et al., J. Phys. Soc. Jpn. 79, 033704 (2010)

[4] T. Hasegawa et al., J. Phys. : Conf. Ser. 391, 012016 (2012)

[5] Y. Ishikawa et al., J. Phys. Soc. Jpn. 82 083711 (2013), and *ibid.* 82 123708 (2013)

TU.B-P50 - High-Frequency Ultrasonic Measurements of $\text{SmOs}_4\text{Sb}_{12}$ under Hydrostatic Pressure

S. Mombetsu¹, H. Inagaki¹, T. Murazumi¹, T. Yanagisawa¹, H. Hidaka¹, H. Amitsuka¹, P.C. Ho², M.B. Maple³

1. Department of Physics, Hokkaido University, Sapporo, Japan

2. Department of Physics, California State University, Fresno, United States

3. Department of Physics, University of California, Berkeley, United States

We have carried out ultrasonic measurements on the filled-skutterudite compound $\text{SmOs}_4\text{Sb}_{12}$ under hydrostatic pressure as high as 1.2 GPa and with frequency up to 250 MHz. This experiment is made possible by installing two semi-rigid coaxial cables into a piston cylinder pressure cell. The elastic constant C_{11} of the present compound shows ultrasonic dispersions (UDs) at ~ 20 K and ~ 60 K at the frequency of ~ 100 MHz under ambient pressure. The UD is considered to be caused by thermally-activated ionic motions, "Rattling", of the Sm-ion. Thus, the present study provides new information of hydrostatic pressure dependences of the UD and their relation to the heavy-electron state of this compound. As pressure increases, the UD which appears at higher temperature shifts to lower temperatures, which indicates decreasing of activation energy and/or increasing of relaxation time of the rattling. On the other hand, the UD which appears at lower temperature gradually disappears as pressure increases. We have also found that the elastic response in a low-temperature ordered phase below T_o (~ 2 K at ambient pressure) is dramatically changed by hydrostatic pressure. At 1.2 GPa, C_{11} shows rapid decrease of $\sim 3\%$ in the ordered phase in comparison with the change of $\sim 0.2\%$ under ambient pressure. The relatively large elastic anomaly implies that a lattice distortion is induced in the ordered phase by hydrostatic pressure. Below 80 K down to T_o , C_{11} also shows Curie-type softening, which is also enhanced with increasing pressure. The present results strongly suggest that $4f$ -electrons of the Sm ion become localized with increasing hydrostatic pressure and the quadrupole degrees of freedom play an important role in the phase transition.

TU.B-P51 - Magnetic and transport properties of mixed-valent europium sulfide EuPd_3S_4 S. Michimura^{1,2}, M. Tanahashi², H. Hirabayashi², K. Shibata², S. Katano², M. Kosaka²

1. Saitama University, Research And Development Bureau, Saitama, Japan

2. Saitama University, Graduate School of Science & Engineering, Saitama-shi, Japan

We have investigated the magnetic and transport properties of a ternary intermetallic compound EuPd_3S_4 . The mixed-valent behavior was previously reported from magnetization measurements and ^{151}Eu Mössbauer spectroscopy using polycrystalline samples [1]. EuPd_3S_4 undergoes an antiferromagnetic transition at $T_N = 3.4$ K [2]. The experimental results can be explained by assuming the valence of $\text{Eu}^{2.5+}$. In particular, two absorption peaks in Mössbauer spectra, which indicate the divalent and trivalent state, were well defined even at room temperatures. This result may suggest the charge ordered state, the ratio of $\text{Eu}^{3+} : \text{Eu}^{2+} = 1 : 1$. On the other hand, the broad maximum around 150 K in the temperature dependence of the thermoelectric power is reminiscent of the behavior observed in the valence fluctuation compounds [3]. Accordingly, the details of the valence state in this compound are still controversial.

In this study, we have succeeded in growing single crystalline samples by using chemical transport method. The saturation magnetization is determined to be $3.3 \mu_B$ at 1.8 K. This is almost the half of the expected value of $gJ = 7 \mu_B$, suggesting that the ratio of Eu valence is estimated to be $\text{Eu}^{3+} : \text{Eu}^{2+} = 1 : 1$. The evaluated magnetic entropy also supports this suggestion. Moreover, we have performed measurements of electrical resistivity and powder X-ray diffraction in high temperature regions in order to obtain an anomaly corresponding to a transition to the valence fluctuate state, if the charge ordered state is realized at room temperatures, such as Eu_4As_3 [4]. The resistivity of EuPd_3S_4 is linearly proportional to temperature up to 600 K, and lattice constant also increases monotonically with increasing temperature up to 900 K, without any transition. In many valence fluctuation compounds, the deviation from linear temperature dependence is observed on resistivity. We speculate that the charge ordered state is stabilized up to 900 K.

TU.B-P52 - Role of c-f hybridization to the mid-IR peaks in Ce compounds

S.I. Kimura¹, Y.S. Kwon², Y. Matsumoto³, H. Aoki⁴, O. Sakai⁵

1. *FBS and Physics Department, Osaka University, Osaka, Japan*

2. *Department of Emerging Materials Science, DGIST, Daegu, Korea*

3. *Department of Engineering Physics, Nagoya Institute of Technology, Aichi, Japan*

4. *Department of Physics, Tohoku University, Sendai, Japan*

5. *National Institute for Materials Science, Ibaraki, Japan*

Cerium and ytterbium based heavy fermion materials have characteristic peaks in the optical conductivity spectra in the middle infrared region (mid-IR peaks). The mid-IR peaks originate from the hybridization between conduction and 4f electrons, namely c-f hybridization [1]. The peak energies originate from the renormalization of the 4f states due to the electron correlation [2,3], i.e., the mid-IR peaks shift to the lower energy side with approaching to the quantum critical point (QCP) from the heavy fermion region in the Doniach phase diagram. Here, we show the alternative behavior of the mid-IR peaks in the local region of weaker c-f hybridization intensity than QCP.

We measured the optical conductivity spectra of isostructural antiferromagnetic compounds CeM_2Ge_2 (M = Cu, Ru, Rh, Ag) and compared with those of heavy fermions CeNi_2Ge_2 and CeCu_2Si_2 [4]. As a result, the mid-IR peak energy becomes minimized at slightly local side from QCP and upturn again with decreasing the c-f hybridization intensity. The origin of the behavior can be explained by a weak screening effect of the conduction electron to the 4f states and seems to be strongly related to the quantum criticality.

[1] H. Okamura et al., JPSJ 76, 023703 (2007)

[2] S. Kimura et al., JPSJ 78, 013710 (2009)

[3] S. Kimura, PRB 80, 073103 (2009)

[4] J. Sichelschmidt et al., JPCM 25, 065602 (2013)

TU.B-P53 - Anomalous low-energy excitations on LaB₆ investigated by Raman scattering measurements

T. Hasegawa¹, N. Ogita¹, F. Iga², M. Udagawa^{1,3}

1. Graduate School of Integrated Arts and Sciences, Hiroshima University, Higashi-Hiroshima, Japan

2. College of Science, Ibaraki University, Ibaraki, Japan

3. Institute for Advanced Material Research, Hiroshima University, Hiroshima, Japan

In phonon Raman scattering with different wavelength excitation, its peak energy does not depend on wavenumber of the excitation light, but peak intensity will change due to resonance effect. This invariance of the energy is because of a quite small scattering vector q in a Raman scattering process compared with reciprocal lattice vectors of crystals. However, when we observe excitations with linear dependence on q , e.g. an acoustic phonon or intra-band excitations of electrons, then, peak energy changes due to the wavenumber of excitation light. Intra-band excitation spectrum is broad and the energy of the maximum intensity is expected to be qvF with the Fermi velocity vF . Here, we present the dispersion relations of such electronic excitations in LaB₆, investigated by Raman scattering measurements. We have measured Raman spectra of LaB₆ on (100) and (110) surfaces from 4 K to 300 K. The wavelength of the incident light was varied from 458.0 nm to 632.8 nm. Below 400 cm⁻¹, there is no Raman active phonon mode, while two-phonon excitation due to the flat La vibration bands is found around 200 cm⁻¹. In addition to the two-phonon peak, the anomalous peaks have been clearly observed below 150 K. The peak energies strongly depend on the excitation light energy. In the (x,x) spectra on (100) surface, the peak energy is found at 210 cm⁻¹ for the 514.5 nm line of Ar⁺ laser. However, with the 632.8 nm line of He-Ne laser, it becomes at 30 cm⁻¹. The dispersion curve of this peak shows that the group velocity is about 1 % of velocity of light. It is typical magnitude of the Fermi velocity. This result suggests that the anomalous excitation is intra-band electronic excitations.

TU.B-P54 - Al-NMR study of single crystal CeAl₂ under high pressure

K. Fujiwara¹, T. Umezawa¹, K. Takamiya¹, G. Motoyama¹, K. Miyoshi¹, S. Nishigori²

1. *Department of Materials Science, Shimane University, Matsue, Japan*

2. *Interdisciplinary Center for Science Research, Shimane University, Matsue, Japan*

CeAl₂ is a typical heavy fermion compound ($T_N = 3.8$ K), that RKKY and the Kondo interaction compete at the low temperature. The electrical resistivity has two peaks owing to the Kondo effect and the crystal-field splitting of $4f$ levels. Two peaks merge around $P_C = 2.7$ GPa and T_N disappears at P_C . Similar behavior in the resistivity has been also observed in heavy fermion superconductor CeCu₂Si₂ around $P_C = 4.5$ GPa and T_C is quite enhanced at P_C . We have been measured Al-NMR under pressure in order to clarify valence and spin state of Ce ions near P_C . Single crystalline sample (RRR=100, $T_N = 3.9$ K) was prepared in tetra-arc furnace. In this work, we use the indenter pressure cell and the pressure-transmitting medium was Daphne oil 7373. Since CeAl₂ shows a cubic Laves structure, Al site has axial symmetry along (111) direction. Consequently, both Zeeman and nuclear quadrupole interaction (the principal axis: (111) direction) contribute to Al-NMR spectrum. Applying the magnetic field parallel to the (111) direction, energy degeneracy of nuclear spins was resolved, and NMR spectrum shows two inequivalent Al sites. On the other hand, since the (100) direction is 54.7 degrees to a principal axis, and the effect of the nuclear quadrupole interaction becomes zero, only one peak is observed. In this study, we report and discuss temperature and pressure dependence of Knight shift and nuclear relaxation ratio ($1/T_1$) along to (100) and (111) directions.

TU.B-P55 - Electronic structure of ThRu₂Si₂ studied by ARPES

S.I. Fujimori¹, M. Kobata¹, Y. Takeda¹, T. Okane¹, Y. Saitoh¹, A. Fujimori^{1,2}, H. Yamagami^{1,3}, Y. Matsumoto^{4,5}, E. Yamamoto⁵, Y. Haga⁵

1. Condensed Matter Science Division, Japan Atomic Energy Agency, Ibaraki, Japan
2. Department of Physics, University of Tokyo, Bunkyo-Ku, Japan
3. Department of Physics, Faculty of Science, Kyoto Sangyo University, Kyoto, Japan
4. Graduate School of Engineering, Nagoya Institute of Technology, Aichi, Japan
5. Advanced Science Research Center, Japan Atomic Energy Agency, Ibaraki, Japan

ThRu₂Si₂ is an isostructural compound of the heavy fermion superconductor URu₂Si₂ which shows the hidden order transition. Since ThRu₂Si₂ does not have 5f electrons, it is a good reference material to understand the contribution of U 5f electrons in the electronic structure of URu₂Si₂. In the present study, we have revealed the band structure and Fermi surface of ThRu₂Si₂ by angle resolved photoelectron spectroscopy (ARPES) using soft X-rays (hν=600-800 eV). The experimentally obtained band structure and Fermi surface are compared with those of URu₂Si₂ as well as the result of the band structure calculation. We have found that the states in the vicinity of EF are very different in ThRu₂Si₂ and URu₂Si₂, suggesting that U 5f electrons form itinerant bands in URu₂Si₂. The details of the electronic structure of ThRu₂Si₂ and the contributions from U 5f electrons in the band structure and Fermi surface of URu₂Si₂ are discussed.

TU.B-P57 - Novel heavy-fermion antiferromagnet YbRhGe with the TiNiSi-type structure

K. Araki¹, H. Tanaka¹, T. Kohei¹, S. Nakamura^{2,4}, T. Nojima^{2,4}, A. Ochiai^{3,4}, K. Katoh¹

1. Dept. Appl. Phys., National Defense Academy, Yokosuka-Shi, Japan

2. Inst. For Materials Research, Tohoku Univ, Sendai, Japan

3. Graduate School of Science, Tohoku Univ., Sendai, Japan

4. Univ. Centr. For Low Temp. Sci., Tohoku Univ., Sendai, Japan

YbTGe (T = transition metal) compounds are of much interest because they display a variety of attractive phenomena, such as magnetic ordering, heavy-fermion state, frustration, etc. Recently we have succeeded in growing large single crystals of YbRhGe with the TiNiSi-type orthorhombic structure, which was reported to be antiferromagnet with $T_N = 7$ K^{*1}. In order to investigate low-temperature properties, we have performed specific heat C , electrical resistivity ρ measurements down to 0.5 K and up to 9 T. These results revealed that YbRhGe undergoes the heavy-fermion state with the electric specific heat coefficient $\gamma \approx 220$ mJ/mol K² and the successive transition at $T_m = 1.0$ K below magnetic ordering at 6.0 K. The temperature dependence of ρ shows a superzone gap opening along only the c-axis below T_N . In magnetic fields applied along the a- and c-axes, the system undergoes a spin-flop state in contrast to no such behavior in the field applied along the b-axis. This suggests that the magnetic moments in the AF phase are lying within the ac-plane.

*1K. Katoh et al., J.M.M.M., 268 (2004) 212.

TU.B-P58 - Possible existence of partially disordered Sm ions in magnetically ordered state of Ising magnet SmPt_2Si_2 K. Fushiya¹, Ryuji Higashinaka¹, Tatsuma¹, D Matsuda¹, Yuji Aoki¹*1. Tokyo Metropolitan University, Tokyo, Japan*

$RT_2\text{Si}_2$ (R : rare earth; T : transition metal) are known to exhibit a variety of strongly correlated electron phenomena. For $R=\text{Sm}$, however, only a few reports have been made of systematic physical property investigations using single crystals [1]. Recently, we have succeeded in growing single crystals of SmPt_2Si_2 and have studied their magnetic properties [2]. It has been found that there are two magnetically ordered phases; an antiferromagnetically (AFM) ordered phase (I) setting in at $T_N=5.1$ K and a field induced magnetization plateau phase (II). In phase I, unlike the usual AFM states, a pronounced Curie-Weiss contribution remains in magnetic susceptibility, indicating the existence of “partially disordered” Sm ions. The realization of such inhomogeneous magnetic structures is attributable to geometric frustrations inherent in the crystal structure of $RT_2\text{Si}_2$; note that the axial-next-nearest-neighbor Ising (ANNNI) model accounts for the similar magnetic properties observed in UPd_2Si_2 .

The disordered Sm ions can form a Kondo sublattice through hybridization with conduction electrons [3], resulting in a quasiparticle mass enhancement. This may account for the largely increased electronic specific heat coefficient of $350\text{mJ}/\text{K}^2$ mol observed in phase I. SmPt_2Si_2 should provide an appropriate system in which one can study the ground-state properties of a “partial Kondo sublattice” immersed in a magnetically ordered phase.

[1] K. Hiebl, et al., J. Magn. Magn. Mater. 50, 39 (1984)

[2] K. Fushiya, et al., J. Phys. Soc. Jpn. 83, 113708 (2014)

[3] For theoretical studies, see, e.g., Y. Motome, et al., Phys. Rev. Lett. 105, 036403 (2010)

TU.B-P59 - Nature of heavy fermion state in $R_{0.01}La_{0.99}B_6$ (R=Ce, Ho)

M. Anisimov¹, V. Glushkov¹, S. Demishev¹, V. Voronov¹, S. Gavrilkin², K. Mitsen², N. Shitsevalova³, A. Levchenko³, V. Filippov³, A. Bogach¹, S. Gabani¹

1. *A.M. Prokhorov General Physics Institute of RAS, Moscow, Russia*

2. *Lebedev Physical Institute of RAS, Moscow, Russia*

3. *Institute for Problems of Materials Science of NASU, Kiev, Ukraine*

4. *Institute of Experimental Physics of SAS, Košice, Slovak Republic*

We present the results of complex study of resistivity, magnetoresistance, specific heat and magnetization of solid solutions $R_xLa_{1-x}B_6$ (R=Ce, Ho) in the regime of isolated magnetic impurity ($x \sim 1\%$). In the study it was of special interest to analyze comparatively the charge transport properties, when Kramers (Ce^{3+}) and non-Kramers (Ho^{3+}) ions are introduced in LaB_6 nonmagnetic matrix. The data obtained allow detecting the increase of resistivity with the temperature lowering both in $Ce_{0.01}La_{0.99}B_6$ and $Ho_{0.005}La_{0.995}B_6$ rare earth hexaborides. It was found that instead of logarithmic behavior $\Delta\rho_m(T) \sim -\ln T$, predicted by Kondo model, the magnetic contribution to resistivity obeys the power law $\Delta\rho_m(T) \sim T^{-\alpha}$, which corresponds to the regime of weak localization of charge carriers with the critical exponent values $\alpha \sim 0.39$ (Ho) and 0.5 (Ce) [1]. Moreover, the analysis of the negative magnetoresistance observed at liquid helium temperatures allows concluding in favor of the formation of many-body states of a spin-polaron type near the magnetic rare-earth ions in the LaB_6 matrix [2, 3]. In accordance with the aforementioned results a new approach to describe the heavy fermion formation in $R_{0.01}La_{0.99}B_6$ (R=Ce, Ho) is proposed.

[1] W.L.McMillan, Phys. Rev. B 24, 2739 (1981)

[2] N.E.Sluchanko, M.A.Anisimov et al., JETP Lett. 101, 36 (2015)

[3] M. Anisimov et al., JETP 116, 760 (2013).

TU.B-P60 - Intersite electron correlations in quasi-periodic systems

N. Takemori¹, A. Koga¹, H. Hafermann²

1. *Tokyo Institute of Technology, Tokyo, Japan*

2. *CNRS, Grenoble, France*

Quasicrystal systems have attracted considerable interest since its discovery [1]. An important feature is that the system does not have translational symmetry but rotational symmetry (e.g. 10-fold and 8-fold) which should yield nontrivial electric properties in the metallic quasicrystals. Recently, quantum critical behavior in $\text{Au}_{51}\text{Al}_{34}\text{Yb}_{15}$ has experimentally been realized [2], which stimulates further theoretical and experimental investigations on electron correlations in quasi-periodic systems.

To clarify how electron correlations affect low temperature properties in strongly correlated quasi-periodic systems, we study the repulsive Hubbard model on two-dimensional Penrose lattice. The model Hamiltonian is given as $H = \sum_{i,j} t_{ij} c_{i\sigma}^\dagger c_{j\sigma} - \sum_i U n_{i\uparrow} n_{i\downarrow}$ where $c_{i\sigma}$ denotes nearest neighbor site, $c_{i\sigma}^\dagger$ is the creation (annihilation) operator of a fermion at the i th site with spin σ , t_{ij} is the hopping integral, and U is the Coulomb interaction. In our previous paper, we have discussed the Mott transition in the model by means of the real-space dynamical mean field theory (RDMFT) [6], which incorporates local electron correlations. However, intersite correlations cannot be taken into account with RDMFT. In the present work, we make use of the real-space dual fermion approach [5], where intersite correlations are taken into account. We then study how magnetic correlations develop at low temperatures.

[1] D. Shechtman, et al., *Phys. Rev. Lett.* 53 1951 (1984)

[2] T. Tokihiro et al., *Phys. Rev. B* 38 5981 (1988)

[3] K. Deguchi., et al., *Nat. Mater.* 11, 1013-1016 (2012)

[4] H. Tsunetsugu, et al., *Phys. Rev. B* 43 8879-8891 (1991)

[5] A. N. Rubtsov et al., *Phys. Rev. B* 77, 033101 (2008)

[6] N. Takemori, and A. Koga., *J. Phys. Soc. Jpn.* 84, 023701 1-5 (2015); N. Takemori, and A. Koga., accepted for publication in *Journal of Physics: Conference Series*

TU.B-P61 - Influence of the Crystal Field on the Magnetic Properties of RENi_3Ga_9 (RE = Gd, Tb, Dy and Ho) single crystals

J. Duque¹, S. Silva¹, G. Mecena¹, T. Meneses¹

1. Federal University of Sergipe, São Cristóvão, Brazil

In this work, we report on X-ray, heat capacity and magnetization measurements in single crystals of RENi_3Ga_9 (RE = Gd, Tb, Dy and Ho) grown from the melt flux-gallium. X-ray analyses confirm that all samples belong to the trigonal (R32) space group. The T-dependence of the magnetic susceptibility reveals that these compounds order antiferromagnetically at low temperature ($T_N < 20$ K) and the evolution of their magnetic properties depends on the crystal-field ground-state configuration. The high-field magnetization measured at 2 K presents field induced transitions which can be related to the spin-flop and/or metamagnetic transitions. In particular case of DyNi_3Ga_9 , we have observed four successive field induced transitions. Finally, heat capacity data are consistent with the magnetic phase transition observed at low temperature in magnetization measurements.

TU.B-P63 - Charge dynamics of heavy fermions in CeCu₆ and YbRh₂Si₂ probed by microwave spectroscopy

K. Parkkinen^{1,2}, D. Hafner¹, M. Thiemann¹, M. Dressel¹, O. Stockert³, K. Grube⁴, H.V. Löhneysen^{4,5}, C. Krellner^{3,6}, C. Geibel³, F. Steglich³, M. Scheffler¹

1. *Physikalisches Institut, Universität Stuttgart, Stuttgart, Germany*

2. *University of Helsinki, Helsinki, Finland*

3. *Max-Planck-Institut für Chemische Physik fester Stoffe, Dresden, Germany*

4. *Institut für Festkörperphysik, Karlsruhe Institute of Technology (KIT), Karlsruhe, Germany*

5. *Physikalisches Institut, Karlsruhe Institute of Technology (KIT), Karlsruhe, Germany*

6. *Physikalisches Institut, Goethe-Universität Frankfurt, Frankfurt, Germany*

CeCu₆ and YbRh₂Si₂ are two well-known heavy-fermion metals with peculiar behavior related to an antiferromagnetic quantum phase transition. While CeCu₆ in the absence of magnetic field is a paramagnet with clear Fermi-liquid behavior at temperatures well below 1 K, YbRh₂Si₂ undergoes an antiferromagnetic phase transition at 70 mK (and zero magnetic field) and exhibits pronounced non-Fermi-liquid behavior at higher temperatures. While both materials have been studied in great detail using thermodynamic, magnetic, and transport techniques, there are only few spectroscopic studies that address the physics related to the quantum phase transitions in CeCu₆ and YbRh₂Si₂. Main challenges here are the involved energy and temperature scales well below 1 K. In the present work, we employ microwave spectroscopy to study the charge dynamics in these two materials at temperatures between 50 mK and 5 K and at frequencies between 2 GHz and 16 GHz.

We have recently developed a new spectroscopic approach, namely superconducting stripline resonators, to study the microwave conductivity of exotic metals and superconductors. While we previously addressed heavy fermions at 4He temperatures, we now implemented the technique into a dilution refrigerator, and we have performed microwave measurements on CeCu₆ and YbRh₂Si₂ single crystals. For CeCu₆ (and in zero magnetic field) we observe a smooth evolution of the microwave surface resistance throughout our complete temperature range, including the Fermi-liquid regime, and we find a substantial anisotropy. For YbRh₂Si₂, on the other hand, the temperature dependence of the microwave surface resistance exhibits pronounced anomalies, which we relate to the transitions between antiferromagnetic, Fermi-liquid, and non-Fermi-liquid regimes of the phase diagram for magnetic fields below 80 mT.

TU.B-P64 - trivalent uranium crystal-field states in UGa₂ and UPd₂Al₃ intermetallicsR. Radwanski^{1,2}, D. Nalecz¹, Z. Ropka²1. *Institute of Physics, Pedagogical University, Krakow, Poland*2. *Center of Solid State Physics, Krakow, Poland*

UPd₂Al₃ exhibits superconductivity coexisting below T_{sc} of 2 K with the antiferromagnetic state (T_N = 14 K) with substantial U magnetic moment. Apart of the surprising superconductivity there was long debate on the role played by *f* electrons, itinerant or localized, and a number of localized *f* electrons. One of the present authors (RJR) has claimed at the very beginning on the existence of the three localized *f* electrons, i.e. of the U³⁺ ion in UPd₂Al₃, in contrary to strong opposition of the "itinerant" community or of "two-localized-f-electrons" community. Much the same debate goes over description of UGa₂. UGa₂ is unique uranium compound being ferromagnet with T_c = 125 K. Our U³⁺ description (JMMM 140-144 (95) 1373) was covered by a 5f² claim (Phys. Rev. B 53 (1996) 9658) and later by a dual f-electron model. Recent studies [1] on the single-crystal specimen of UGa₂ have revealed a surprised increase of T_c with pressure but confirmed the strong ferromagnetic properties with a moment of 3.07 μB, 10% larger than the previous value. Magnetization curves have revealed (Ref. 37 in very strong anisotropy with the moments lying along the hexagonal *a* axis. The ferromagnetic state allows for the evaluation of the macroscopic anisotropy parameters. We have derived a new modified set of crystal-field (CEF) parameters in order to account for the observed larger magnetic moment. We have calculated the splitting of the lowest CEF state in the ferromagnetic state to be 98 K what we claim was seen in the inelastic-neutron scattering experiments and interpreted as a magnon gap of 7-8 meV (Ref. 37 in [1]).

Within the Quantum Atomistic Solid State theory (QUASST), claiming the preservation of the atomic-like states in a solid, we consistently have explained the ground-state properties and thermodynamics, both in the paramagnetic and magnetic state, together with the reproduction of the λ-type peak at the phase transition. In QUASST we look for solutions with an integer number of *f* electrons in contrary to a 5f-ligand hybridization model.

[1]. A. K. Kolomiets et al., Phys. Rev. B 91 (2015) 064405

TU.B-P66 - Quantum criticality in CeCu₂Ge₂?

P. Geselbracht¹, E. Faulhaber¹, M. Rotter², K. Schmalzl³, D. Quintero Castro⁴, M. Deppe⁵, O. Stockert⁵, M. Loewenhaupt⁶, A. Schneidewind⁷

1. Technische Universität München, Heinz Maier-Leibnitz Zentrum, Garching, Germany
2. McPhase Project, Dresden, Germany
3. Jülich Centre for Neutron Science at ILL Forschungszentrum Jülich GmbH, Grenoble, France
4. Helmholtz-Zentrum Berlin, Berlin, Germany
5. Max-Planck-Institut für Chemische Physik fester Stoffe, Dresden, Germany
6. Technische Universität Dresden, Dresden, Germany
7. Jülich Centre for Neutron Science at MLZ, Forschungszentrum Jülich GmbH, Garching, Germany

The heavy-fermion compound CeCu₂Ge₂ with tetragonal ThCr₂Si₂ structure establishes incommensurate antiferromagnetic order below $T_N = 4.1$ K with a propagation vector $k = (0.285 \ 0.285 \ 0.550)$ and Kondo compensated moments of $1.0 \mu_B/\text{Ce}$. The magnetic order was determined to be an amplitude-modulated magnetic structure with moments along the [1-10] direction, i.e., perpendicular to the propagation vector. Similar to the superconducting counterpart CeCu₂Si₂, comparable energy scales of the RKKY interaction and the Kondo screening lead to a complex magnetic B-T phase diagram. Crystalline electric field excitations of the Ce³⁺ moments ($J = 5/2$) do not play a role here, since the ground-state doublet is well separated from the excited states. Recently Singh et al. (Sci. Rep. 1, 117 (2011)) reported on quantum-critical behavior in the spin dynamics in CeCu₂Ge₂ when applying a magnetic field $B = 8$ T ($B \parallel [1-10]$). This observation triggered us to study the magnetic order and the spin dynamics of CeCu₂Si₂ in more detail at low temperatures (deep in the ordered state and close to T_N) and in magnetic fields up to 13.5 T ($B \parallel [1-10]$). In contrast to Singh et al. the transition at $B \sim 7.5 \dots 8$ T is clearly identified as a first-order transition with no appearance of quantum-critical behavior. At higher fields $B \sim 13$ T the magnetic superstructure peaks vanish and spectral weight of the spin excitations shifts to lower energies. However, quantum-critical behavior there is also not obvious. Additionally, we performed mean-field calculations of the spin-wave spectrum and the magnetic order in CeCu₂Ge₂ using McPhase. Given the limitations of the technique the spin-wave dispersions and the magnetic structure are well described. To further improve the theoretical modeling the partially itinerant nature of the 4f Ce magnetism in CeCu₂Ge₂ would have to be taken into account.

TU.B-P67 - $\text{Yb}_2\text{Ni}_{12}\text{Pn}_7$ (Pn = P,As): A promising system for studying valence fluctuations and quantum criticality

W. Jiang¹, L. Yang¹, C. Guo¹, J. Chen², Z. Hu³, J. Lee², Y. Wang¹, Y. Chen¹, M. Smidman¹, Z. Chen¹

1. *Center for Correlated Matter and Department of Physics, Zhejiang University, Hangzhou, China*

2. *National Synchrotron Radiation Research Center, Hsinchu, Taiwan*

3. *Max Planck Institute for Chemical Physics of Solids, Dresden, Germany*

We report measurements of the physical properties and electronic structure of the hexagonal compounds $\text{Yb}_2\text{Ni}_{12}\text{Pn}_7$ (Pn = P, As) [1] by measuring the electrical resistivity, magnetization, specific heat, partial fluorescence yield X-ray absorption spectra (PFY-XAS), and resonant X-ray emission spectra (RXES). These demonstrate a crossover upon reducing the unit cell volume, from a mixed valence state in $\text{Yb}_2\text{Ni}_{12}\text{As}_7$ to a heavy-fermion paramagnetic state in $\text{Yb}_2\text{Ni}_{12}\text{P}_7$, where the Yb is nearly trivalent. Upon applying pressure to $\text{Yb}_2\text{Ni}_{12}\text{P}_7$, the temperature at which Fermi liquid behavior is observed (TFL) is suppressed, suggesting the presence of a quantum critical point (QCP) [2] at around 2.8 GPa and there is little change in the Yb valence up to 30 GPa. However, there is a strong increase of the Yb valence for $\text{Yb}_2\text{Ni}_{12}\text{As}_7$ under pressure, before a near constant value is reached. The pressure dependence of the valence and lattice parameters are compared, indicating a correlation between structural and electronic changes. These results indicate that any magnetic QCP in this system is well separated from strong valence fluctuations.

[1] B. K. Cho, F. J. DiSalvo, J. S. Kim, G. R. Stewart and S. L. Bud'ko, *Physica B*. 253, 40-46 (1998)

[2] T. Nakano, R. Satoh, K. Tsuchiya, N. Takeda, K. Matsubayashi, and Y. Uwatoko, *J. Phys.: Conf. Ser.* 391, 012052 (2012)

TU.B-P69 - Possible signature of magnetic order inside the superconducting state at low magnetic fields in CeCoIn₅

C.F. Miclea¹, M. Niclas², A.C. Mota³, J.D. Thomson⁴, R. Movshovich⁴

1. National Institute for Materials Physics, Bucharest-Magurele, Romania

2. Max-Planck-Institute for Chemical Physics of Solids, Dresden, Germany

3. Solid State Laboratory, ETH Zurich, Zurich, Switzerland

4. Los Alamos National Laboratory, Los Alamos, New Mexico, United States

The presence of strong magnetic fluctuations manifested in the heavy fermion compound CeCoIn₅ by non Fermi-liquid behavior suggested that this compound is placed in the proximity of a magnetic quantum critical point. However no long range magnetic order has been reported so far. In this study we report on vortex dynamics, dc magnetization and penetration depth measurements in CeCoIn₅ down to low temperatures, T=50 mK. While the pinning is rather conventional for a clean limit superconductor which does not break spontaneously any additional symmetries besides the U(1)-gauge, a strong increase in the remnant magnetization, M_{rem} is observed around T approximately 0.3 K in low magnetic fields just high enough to put the sample in the Bean critical state. Moreover, this anomaly is corroborated by the DC magnetization and the penetration depth measurements at very low fields. We extended the vortex dynamics investigation to Pb irradiated CeCoIn₅. While the defects created by irradiation have a clear effect on the relaxation rates, the enhancement of M_{rem} still takes place at the same temperature. Our findings are consistent with the existence of a magnetically ordered phase, deep inside the superconducting state.

TU.B-P70 - XMCD study of ferromagnetism in YbCu₂Si₂ under pressureF. Wilhelm¹, D. Braithwaite², S. M. Ramos², E.N. Hering², G. Lapertot², A. Rogalev¹1. *European Synchrotron Radiation Facility (ESRF), Grenoble, France*2. *SPSMS, UMR-E CEA / UJF-Grenoble 1, INAC, Grenoble, France*

In rare-earth intermediate-valence (IV) compounds, the interplay between the magnetic and valence instability represents one of the most studied subjects, with the possibility of tuning the system to a magnetic quantum critical point (QCP), where strong spin and/or valence fluctuations are present. The Ce and Yb Kondo lattices are often considered to be electron/hole equivalents, however Yb compounds also offer a favorable opportunity for studying the role of the valence fluctuations in the quantum criticality, since applying pressure is expected to induce larger changes of the valence. YbCu₂Si₂ is an ideal prototype Yb system, obeying Doniach's phase diagram. By applying pressure, the system evolves from a paramagnetic state to an ordered one [1], reached at the critical pressure $P_c=7-8$ GPa. Recent a.c. susceptibility measurements under high pressure strongly suggested that the induced magnetic order is ferromagnetic (FM) [2]. Determining the nature of an ordered phase that occurs only above 8 GPa although, is not trivial. A direct confirmation of ferromagnetism in this compound is highly desirable, especially because systems presenting a FM QCP are quite rare. In this work, we report x-ray magnetic circular dichroism (XMCD) measurements at the L3-edge of Yb in YbCu₂Si₂ single crystal at 2K and under pressure up to 15GPa. The amplitude of the XMCD signal is proportional magnetization of the absorbing atom. For pressures higher than 7.5GPa, the field dependence of the XMCD signal shows a typical FM behavior with a tendency to saturate above $H=0.5$ T. Moreover, it was found to be small and almost constant at low pressure, followed by a strong increase above P_c , confirming the FM nature of the ordered phase.

[1] K. Alami-Yadria, H. Wilhelm, and D. Jaccard, *Eur. Phys. J. B* 6, 5-11 (1998)[2] A. Fernandez-Pañella, D. Braithwaite, B. Salce, G. Lapertot and J. Flouquet, *Physical Review B* 84, 134416 (2011)

TU.B-P72 - Crystal field in R_2RhIn_8 series studied by bulk measurements

P. Čermák¹, M. Prachařová², J. Zubáč², K. Pajskr², P. Javorský²

1. Forschungszentrum Jülich, Outstation At MLZ, Jülich, Germany

2. Charles University in Prague, Prague, Czech Republic

The influence of the anisotropy on the magnetic and superconducting properties of heavy fermion compounds has been studied for a long time. Previous studies on R_2RhIn_8 (where R is rare earth) showed, that magnetic structures are driven mainly by crystalline electric field (CEF) [1, 2, 3]. We have grown compounds with $R = Nd, Tb, Ho, Dy, Er$ and Tm and determined their magnetic structures [2, 3].

In this presentation, we are going to show detailed analysis of specific heat from 1.5 – 300K. Precise Schottky magnetic contribution is determined by subtraction of the electron and phonon specific heat determined from non-magnetic analogues with $R = La, Lu, Y$ [4]. Schottky specific heat and susceptibility temperature dependencies are then fitted simultaneously to obtain CEF energy levels. Determined second order B_2^0 CEF parameter is always dominant and its sign determines crystal anisotropy and theoretically calculated exchange constants matches determined crystal structures. The results are discussed in context of CEF and magnetic structures in heavy fermion superconductor Ce_2RhIn_8 , where also other effects come into the role.

The new open source software package for simultaneous fitting of specific heat and susceptibility will be introduced.

[1] P. Čermák et al., *J. Phys. Condens. Matter* 24 (2012) 206005

[2] P. Čermák et al., *Phys. Rev. B*, 89 (2014) 184409

[3] P. Čermák et al., submitted for publication, preprint: arxiv: 1409.0433

[4] P. Čermák et al., *Solid State Communications*, 163 (2013) 55–59

TU.B-P73 - Neutron scattering and high pressure transport properties in a rare correlated ferromagnet Nd₂PdSi₃

S. Saha¹, R. Wang¹, J. Paglione¹, J. Lynn², J. Jeffries³

1. *Center for Nanophysics and Advanced Materials, Department of Physics, University of Maryland, College Park, Maryland, United States*

2. *NIST Center for Neutron Research, National Institute of Standards and Technology, Gaithersburg, Maryland, United States*

3. *Condensed Matter and Materials Division, Lawrence Livermore National Laboratory, Livermore, California, United States*

The compound Nd₂PdSi₃ belongs to an A1B₂-derived ternary family (hexagonal structure, space group P6/mmm) showing many exotic properties [1-3]. This compound attracted recent attention: It is reported to order ferromagnetically below T₀~16 K, unlike the other members of this series that order antiferromagnetically. The magnetic ordering temperature T₀ is significantly enhanced with respect to the de Gennes-scaled value [3]. Studying polycrystalline sample, the effects of Nd (4f) hybridization on the magnetism is discussed, which is rare in an Nd-based intermetallic compound [3]. We have grown single crystals of Nd₂PdSi₃ using Czochralski method in a tetra arc furnace. We would like to present neutron scattering, magnetic, and transport properties under high pressure on Nd₂PdSi₃ and discuss about Nd (4f) hybridization.

References:

[1] S. R. Saha et al. , Phys. Rev. B 60, 12162 (1999)

[2] S. R. Saha et al. , Phys. Rev. B 62, 425 (2000)

[3] K. Mukherjee et al., Phys. Rev. B, 84, 184415 (2011)

TU.B-P74 - Magnetic and related properties of $Ce_3T_2Sn_7$ (where T = Ti, V, Cr, Co, Ni).G. Chajewski¹, A. Pikul¹*1. Institute of Low Temperature And Structure Research, Polish Academy of Sciences, Wroclaw, Poland*

Ternary cerium-based intermetallics attract great attention due to variety of intriguing low-temperature physical properties. Although it is commonly believed that their ground state is governed mainly by hybridization of 4f electrons of cerium with conduction band (s, p and d) electrons, there is still little known about the influence of particular groups of electrons on the properties of the f-electron systems. In order to shed more light on that issue we have performed comprehensive investigations of a series of isostructural phases $Ce_3T_2M_7$ (where T is a transition or noble metal and M stands for p-electron element). Here we present preliminary results obtained for a few stanides with Ti, V, Cr, Co and Ni.

Polycrystalline samples of $Ce_3Ti_2Sn_7$, $Ce_3V_2Sn_7$, $Ce_3Cr_2Sn_7$, $Ce_3Co_2Sn_7$ and $Ce_3Ni_2Sn_7$ were prepared by conventional arc melting the stoichiometric amounts of the constituents and studied by means of X-ray powder diffraction, magnetization, electrical transport and specific heat measurements. Rietveld refinement of the experimental powder diffraction patterns confirmed that all the phases studied crystallize in the orthorhombic $La_3Co_2Sn_7$ -type structure (space group *Cmmm*, no. 65) with lattice parameters close to those reported for $Ce_3Ni_2Sn_7$ – the only hitherto known compound of this family [1]. Magnetization of the compounds exhibits at elevated temperatures Curie-Weiss-like behavior with the effective magnetic moment close to that expected for a free Ce^{3+} ion. Only in $Ce_3Ni_2Sn_7$ and $Ce_3Co_2Sn_7$ the moments order antiferromagnetically below $T_N = 3.8$ K and 4.4 K respectively. Specific heat and transport properties of all phases studied show some features characteristic of dense Kondo systems.

[1] B. Chevalier, J. Etourneau, J. Mater. Chem. 9 (1999) 1789

TU.B-P75 - Low-temperature properties of the non-centrosymmetric heavy-fermion compound CeTAl₃ (T = Cu, Ag, Au, Pd, Pt)

C. Franz¹, R. Schönmann¹, J. Spallek¹, A. Regnat¹, A. Senyshyn², P. Cermak³, P.J. Cabre¹, A. Schneidewind³, A. Bauer¹, C. Pfleiderer¹

1. Physik Department E51, Technische Universität München, Garching, Germany

2. Forschungs-Neutronenquelle Heinz Maier-Leibnitz, Garching, Germany

3. Jülich Centre for Neutron Science JCNS, Outstation at MLZ, Garching, Germany

We report a comprehensive study of the series of non-centrosymmetric heavy-fermion compounds CeTAl₃ (T = Cu, Ag, Au, Pd, and Pt). Large single crystals have been prepared by means of optical float-zoning. The single-crystal ingots were characterized using Laue x-ray scattering, powder x-ray diffraction, and energy dispersive x-ray spectroscopy. For T = Cu, Au, Pd, and Pt the system crystallizes in the non-centrosymmetric I4mm crystal structure, while we observe a slight orthorhombic distortion for T = Ag. Subsequently, the magnetization, specific heat, and electrical resistivity were investigated down to temperatures of 200 mK and in magnetic fields of up to 14 T revealing typical heavy-fermion behavior. At low temperatures, CeCuAl₃ and CeAuAl₃ order antiferromagnetically, whereas CeAgAl₃ is a ferromagnet. Inelastic neutron scattering studies indicate the presence of so-called vibron modes, i.e., coupled modes of phonons and crystal electric field excitations.

TU.B-P76 - Thermal expansion and magnetostriction of heavy fermion CeRu₂Si₂ at millikelvin temperatures

D. Inoue¹, D. Kaido¹, Y. Yoshikawa¹, M. Minegishi¹, K. Matsumoto¹, S. Abe¹, S. Murayama²

1. Kanazawa University, Kanazawa, Japan

2. Muroran Institute of Technology, Muroran, Japan

CeRu₂Si₂ is well known as a typical heavy fermion compound, which generally exhibits the Landau-Fermi liquid (LFL) state that thermal expansion coefficient and magnetostriction coefficient were proportional to the temperature and magnetic field, respectively, below the Kondo temperature T_K . This compound has a ThCr₂Si₂-type crystal structure that the easy axis (c-axis) and the hard axis (a-axis) of magnetization indicate the metamagnetic behavior for B//c-axis. Here, we have measured linear thermal expansion and magnetostriction of single crystal CeRu₂Si₂ along the a-axis (B//a-axis) at temperature down to 12 mK and in magnetic fields up to 9 T. Our dilatometer using the capacitance method composed of the sample and the reference capacitor provides the high precision of $dL/L \sim 10^{-10}$ in millikelvin temperatures. In high-temperature region and high magnetic fields, thermal expansion and magnetostriction exhibited the LFL behavior in contrast to the metamagnetic behavior for B//c-axis and indicated a strong magnetic anisotropy between the direction parallel and perpendicular to the a-axis. Furthermore, we observed non-Fermi liquid behavior that showed the negative contribution about $T < 100$ mK and $B < 1$ T. Thermal expansion and magnetostriction have a close relationship with the partial derivative of entropy and magnetization with respect to pressure. Thus, these properties are apposite to investigate the pressure driven quantum critical point.

TU.B-P77 - Fermi Surface properties in impurity kondo effect : Quantum oscillation study on $Ce_xLa_{1-x}Ru_2Si_2$ and $U_xTh_{1-x}Ru_2Si_2$

Y. Matsumoto¹, Y. Haga², N. Tateiwa², N. Kimura³, H. Aoki³, E. Yamamoto², S. Ohara¹, Z. Fisk^{2,4}, H. Yamagami^{2,5}

1. Nagoya Institute of Technology, Nagoya, Japan
2. Japan Atomic Energy Agency, Ibaraki, Japan
3. Tohoku University, Sendai, Japan
4. University of California, Sacramento, United States
5. Kyoto Sangyo University, Kyoto, Japan

In strongly correlated f electron system, many anomalous properties, for example heavy fermion, non-Fermi liquid and unconventional superconductivity, takes place. To understand these properties, it is important to measure the electronic structure. Especially, it is concerned that the relation between Kondo effect and electronic structure is the most important key to reveal the electronic structure because the Kondo effect is likely to be the origin of the delocalized f electron from the de Haas-van Alphen (dHvA) effect measurements study of impurity Kondo state in $Ce_xLa_{1-x}Ru_2Si_2$. We have performed the quantum oscillation study of $Ce_xLa_{1-x}Ru_2Si_2$ alloy and $U_{1-x}Th_xRu_2Si_2$ to reveal the Fermi surface properties of typical heavy fermion compound $CeRu_2Si_2$ and URu_2Si_2 . From $LaRu_2Si_2$ with no f electron to $CeRu_2Si_2$ through impurity Kondo state, the Fermi surface continuously changes with Ce concentration. On the other hand, from $ThRu_2Si_2$ with no f electron to $x=0.03$, Fermi surfaces does not changes. Moreover, we regard $ThRu_2Si_2$ as a reference Ce^{4+} compound and compared the Fermi surfaces of $ThRu_2Si_2$ and those of $CeRu_2Si_2$. The results indicate that the topology of Fermi surfaces is similar each other.

TU.B-P78 - Single Crystal Growth and physical properties of $R_2Pt_6Ga_{15}$ (R=rare earth)

Y. Matsumoto¹, T. Ueda¹, S. Ohara¹

1. Nagoya Institute of Technology, Aichi, Japan

We have synthesized the single crystal $R_2Pt_6Ga_{15}$ (R=rare earth) with hexagonal $Sc_{0.67}Fe_2Si_5$ type structure. The magnetic R-ions form a two-dimensional triangle-lattice. The nearest R-R distance is 0.43nm in c-plane. While, the distance between triangle-lattice layers is about 8.7Å along c-axis, which is more than twice as long as the in-plane R-R distance.

We have measured the magnetic properties and specific heat of $R_2Pt_6Ga_{15}$. It is found that the antiferromagnetic order takes place in $R_2Pt_6Ga_{15}$ except R=Ce and Yb.

TU.C-P01 - Quantum criticality of spin liquids in novel insulators and magnetsV. Stephanovich¹, V. Shaginyan², E. Kirichenko¹1. *Opole University, Opole, Poland*2. *Petersburg Nuclear Physics Institute, Gatchina, Russia*

Strongly correlated Fermi systems are among the most intriguing and fundamental systems in physics, whose realization in some compounds is still under consideration. Quantum spin liquids are promising new phases, where exotic quantum states of matter could be realized. Here we consider a quantum spin liquid (QSL) made of hypothetical particles like chargeless fermionic spinons with spin $\frac{1}{2}$. The QSL can be conveniently realized in geometrically frustrated magnetic insulators like herbertsmithite [1], where important experimental facts have been gathered. We present a theory of the QSL thermodynamic properties. The essence of our theoretical approach is the notion of so-called fermion condensation quantum phase transition [2]. This transition occurs at zero temperature and leads to a quite specific state called fermion condensation. The manifestation of such effect is one more channel of Landau Fermi liquid instability (complimentary to Pomeranchuk criteria), which consists in unlimited increase of the effective mass of Landau quasiparticles which creates flat bands [2]. The application of this formalism permits to reveal the scaling behavior, which strongly resembles that observed in heavy-fermion (HF) metals and two-dimensional ^3He . We also describe the dynamic magnetic susceptibility of QSL compounds, which allows us to show that at low temperatures quasiparticles excitations, or spinons, form a continuum, and populate an approximately flat band crossing the Fermi level. Our analysis reveals that the properties of QSL compounds are similar to those of HF metals. Transport properties of the QSL compounds shed light on the QSL nature in them. Analysis of the heat conductivity detects its scaling behavior resembling those of both the spin-lattice relaxation rate and the magnetoresistivity. It reveals a strong magnetic field dependence of the spinons effective mass.

References:

1. J.S.Helton, K.Matan,M.P.Shores,E.A.Nytko,B.M.Bartlett,Y.Qiu,D.G.Nocera,Y.S.Lee, Phys. Rev. Lett. 104, 147201 (2010)
2. M. Ya. Amusia, K. G. Popov, V. R. Shaginyan, and V. A. Stephanovich, Theory of Heavy-Fermion Compounds - Theory of Strongly Correlated Fermi-Systems, Springer Series in Solid-State Sciences 182, (2014)

TU.C-P02 - Variation of magnetic phases in $\text{Sr}_{1-x}\text{Ca}_x\text{Co}_2\text{P}_2$ clarified with muon-spin spectroscopy

J. Sugiyama¹, H. Nozaki¹, M. Harada¹, I. Umegaki¹, K. Miwa¹, M. Imai², C. Michioka², K. Yoshimura², E. Ansaldo³, J. Brewer^{4,5}

1. Toyota Central Research & Development Laboratories, Inc., Nagakuyte, Japan

2. Kyoto University, Kyoto, Japan

3. University of Saskatchewan, Saskatoon, Canada

4. University of British Columbia, Vancouver, Canada

5. TRIUMF, Vancouver, Canada

6. Babes-Bolyai University, Cluj-Napoca, Romania

7. Paul Scherrer Institut, Villigen, Switzerland

8. KTH Royal Institute of Technology, Stockholm, Sweden

In order to elucidate the dependence of the magnetic ground state on the Ca content (x) in $\text{Sr}_{1-x}\text{Ca}_x\text{Co}_2\text{P}_2$ ($0 \leq x \leq 1$, ThCr_2Si_2 -type structure), we have performed muon-spin rotation and relaxation (μSR) experiments on $\text{Sr}_{1-x}\text{Ca}_x\text{Co}_2\text{P}_2$ powder samples mainly in a zero applied field [1]. The end member compound, SrCo_2P_2 is found to be paramagnetic down to 19 mK, which is consistent with recent single crystal [2]. As x increases, such a paramagnetic ground state is observed until $x = 0.45$ down to 1.8 K. Then, as x increases further, a short-range antiferromagnetic (AF) ordered phase appears at low temperatures for $0.48 \leq x \leq 0.75$, and finally, a long-range AF ordered phase is stabilized for $x > 0.75$. The internal magnetic field of the other end member compound, CaCo_2P_2 , is well consistent with that of the A-type AF order state, which was proposed from neutron scattering experiments [3]. The phase diagram determined with μSR is different from that proposed by macroscopic measurements [4]. The evolution of the magnetic order is connected to the shrinking of the c-axis length as a function of x, which naturally enhances the AF interaction between the two adjacent Co planes.

[1] J. Sugiyama et al., submitted to PRB

[2] A. Teruya et al., J. Phys. Soc. Jpn. 83, 113702 (2014)

[3] M. Reehuis et al., J. Alloys Compounds 266, 54 (1998)

[4] S. Jia et al., Phys. Rev. B 80, 165107 (2009)

TU.C-P03 - Quantum criticality of a Kondo quantum dot coupled to helical edge states of 2D interacting topological insulators

C.H. Chung^{1,2}, S. Silotri¹

1. *Department of Electrophysics, National Chiao-Tung University, HsinChu, Taiwan*

2. *Physics Division, National Center for Theoretical Sciences, HsinChu, Taiwan*

For two decades, the exotic quantum phase transition (QPT) between the one-channel Kondo (1CK) and two-channel Kondo (2CK) ground states has been predicted in a Kondo impurity coupled to two electron-electron interacting 1D Luttinger liquid leads via varying the electron interactions in the lead, defined by the Luttinger parameter $0 < K < 1$. The 1CK-2CK quantum critical point is at $K_c = 1/2$. However, no rigorous theoretical approaches are available so far to access this new quantum critical point due to the divergence of the intra-lead Kondo coupling near 2CK fixed point. We successfully address this long-standing issue of 1CK-2CK QPT in a modern context: in a Kondo quantum dot coupled to two leads made of helical edge states of interacting 2D topological (Quantum Spin Hall) insulators, known as the helical Luttinger liquids. We examine the SU(2) symmetry breaking anisotropic 2-channel Kondo model of our setup via a controlled field-theoretical perturbative renormalization group (RG) approach combined with bosonization and re-fermionization techniques. In the limit of strong electron interactions ($K \ll 1$), we find the 2CK phase is favored. However, for sufficiently weak interactions (K close 1), the 2CK state is unstable towards the 1CK fixed point again and the system undergoes a quantum phase transition between 1CK and 2CK quantum ground states as K or Kondo couplings are varied. The quantum critical and crossover behaviors for various thermodynamic quantities near the transition are obtained. Our study serves as the first example of the 1CK-2CK QPT that is accessible by a controlled theoretical approach.

References: Chung-Hou Chung* and Salman Silotri 2015 New J. Phys. 17, 013005 (193 downloads as of Feb. 6, 2015, presented in PSROC annual meeting, Jan. 30, 2015, National Tsing-Hua University, HsinChu, Taiwan)

TU.C-P04 - Yb-based quantum critical materials: Single crystal growth and characterization of YbRh₂Si₂ and YbNi₄P₂K. Kliemt¹, C. Butzke¹, C. Krellner¹*1. Goethe-University Frankfurt, Frankfurt, Germany*

Heavy fermion systems are model systems to unravel the exciting physics around quantum-phase transitions. Studying these emergent phenomena necessitates the preparation of large and high-quality single crystals. Here, we report on the optimization of the single-crystal growth for two Yb-based quantum critical materials, YbRh₂Si₂ and YbNi₄P₂.

The prototype heavyfermion system YbRh₂Si₂ is situated extremely close to an unconventional antiferromagnetic (AF) quantum critical point (QCP). The AF ordering (T_N = 70 mK) can be further lowered by chemically induced negative pressure using Ir-substitution. The QCP is reached for an Ir substitution of $x \sim 0.1$ in Yb(Rh_{1-x}Ir_x)₂Si₂ [1]. Here, we report on the optimization of the crystal growth of the substitution series as well as of the unsubstituted compound from an indium-flux. The latest crystal generation of YbRh₂Si₂ grown with that method exhibits a resistivity ratio $RR_{1.8K} \sim 33$. Furthermore, we report on our experiments to determine the melting point of YbRh₂Si₂, which reveal a melting point above 1800°C. In the heavy fermion metal, YbNi₄P₂, a ferromagnetic (FM) transition at T_C = 0.17K was observed recently [2] and a FM QCP is reached at $x \sim 0.1$ in YbNi₄(P_{1-x}As_x)₂ [3]. We report on the successful crystal growth of YbNi₄P₂ by Czochralski method out of a Ni-P self-flux from a levitated melt. Applying this method yields mm³ sized crystals. The obtained crystals were characterized by Laue X-ray scattering, X-ray powder diffraction, EDX microprobe analysis and resistivity measurements.

[1] S. Friedemann et al., Nature Phys. 5, 465 (2009)

[2] C. Krellner et al., New J. Phys. 13, 103014 (2011)

[3] A. Steppke et al., Science 339, 933 (2013)

TU.C-P05 - Crossover from non-Fermi liquid to Fermi liquid behavior and the superconductivity dome in heavy electron systems

P. Schlottmann¹

1. Florida State University, Tallahassee, United States

nested Fermi surface together with the remaining interaction between the carriers after the heavy particles are formed may give rise to itinerant antiferromagnetism. We consider an electron and a hole pocket, separated by a wave vector Q , and Fermi momenta $kF1$ and $kF2$, respectively [1]. The order is gradually suppressed by increasing the mismatch of the two Fermi momenta and a QCP is obtained as $T_N \rightarrow 0$. For critical mismatch of the Fermi vectors (tuned QCP) the specific heat over T increases as $-\ln(T)$ as T is lowered [1,2] and the linewidth of the quasi-particles is linear in T and $|Q|$. With increasing nesting mismatch and decreasing temperature the specific heat and the linewidth display a crossover from non-Fermi liquid ($\sim T$) to Fermi liquid ($\sim T^2$) behavior.

If in addition the vector Q is commensurate with the lattice (Umklapp with $Q = G/2$), pairs of electrons can be transferred between the pockets. To avoid the QCP this process may lead to superconductivity and a superconducting dome above the quantum critical point. We investigate the conditions under which such a dome arises [2].

[1] P. Schlottmann, Phys. Rev. B 59, 12379 (1999)

[2] P. Schlottmann, Phys. Rev. B 89, 014511 (2014)

TU.C-P06 - Non-linear quantum critical conductance in a dissipative resonant level through a double-barrier

C.H. Chung^{1,2}, C.Y. Lin¹, H. Baranger³, G. Finkelstein³

1. Department of Electrophysics, National Chiao-Tung University, HsinChu, Taiwan

2. Physics Division, National Center for Theoretical Sciences, HsinChu, Taiwan,

3. Department of Physics, Duke University, Durham, United States

The recent experiment by H.T. Mebrahtu et.al. (Nature Physics 9, 732 (2013)) demonstrated an exotic state of electronic matter obtained by fine-tuning to a quantum critical point (QCP) in a resonant level quantum dot coupled to an Ohmic dissipative nano-wire through a symmetrical double-barrier potential. At low temperatures T and bias voltages V across the dot, the deviation of conductance from perfect transmission shows a universal crossover from a power-law in V/T for $V > T$ (with an exponent related to the dissipation strength) to a constant for $V < T$, a signature of a non-Fermi liquid quantum critical behavior. However, there is lack of theoretical understanding of it. We theoretically address this issue by investigating the non-linear transport of the system at finite T and V in the resonant tunneling regime. Utilizing combined bosonization and re-fermionization, we map our model onto a voltage-biased spinless resonant level coupled to an effective new Luttinger liquid lead and compute the non-linear conductance via controlled frequency-dependent renormalization group (RG). We address the interplay between decoherence and Luttinger physics. Our results are in excellent agreement with the above-mentioned experiment.

TU.C-P07 - Quantum criticality of an itinerant 5f-electron ferromagnet: Ru doped UCoAlP. Opletal¹, Jan Prokleška¹, V Sechovský¹*1. Charles University In Prague, Faculty of Mathematics And Physics, Department of Condensed Matter Physics, Prague, Czech Republic*

UCoAl is an itinerant 5f-electron paramagnet appearing on the verge of ferromagnetism. It crystallizes in the hexagonal ZrNiAl-type structure and exhibits strong magnetocrystalline anisotropy with easy axis along the c-axis. At low temperatures it undergoes first-order metamagnetic phase transition (FOMPT) to ferromagnetic state with the critical magnetic field $B_c \sim 0.7$ T applied along the c-axis and the critical temperature $T_0 = 11$ K where FOMPT changes to crossover behavior. $B_c(T_0)$ increases (decreases) with applying hydrostatic pressure. FOMPT disappears at quantum critical point at $p = 1.5$ GPa and $B = 7$ T. This is in agreement with the generic H,p,T phase diagram for itinerant quantum ferromagnets. From this phase diagram and pressure experiments on UCoAl, the true ferromagnetic phase would appear in negative pressures $p \leq -0.2$ GPa, which cannot be put into practice. The unusual physics of UCoAl has been attracting researchers for many years. Frequent studies dealt with substituting Co by other d-elements. Depending on d-metal dopant and its amount, ground ferromagnetic or paramagnetic state, where FOMPT completely disappears is realized. It has been shown that as little as 1% of Ru substituted for Co leads to ferromagnetism with $T_C = 17$ K. By lowering nominal Ru content we move closer to the UCoAl ground state. We have grown single crystals of $\text{UCo}_{1-x}\text{Ru}_x\text{Al}$ for $x = 0.0025, 0.005$ and 0.01 and investigated the corresponding H,p,T magnetic phase diagram by magnetic, electrical resistivity, Hall Effect and thermal expansion measurements. $\text{UCo}_{0.9975}\text{Ru}_{0.0025}\text{Al}$ exhibits paramagnetic ground state and FOMPT with critical magnetic field $B_c \sim 0.55$ T. In $\text{UCo}_{0.995}\text{Ru}_{0.005}\text{Al}$ ground ferromagnetic state and FOMPT is observed. $\text{UCo}_{0.99}\text{Ru}_{0.01}\text{Al}$ exhibits same ground ferromagnetic state as in previous research. Evolution of magnetism in UCoAl and our single crystals within the generic H,p,T phase diagram of itinerant quantum ferromagnets will be discussed.

TU.C-P09 - Tuning $ZrFe_4Si_2$ by Ge substitution: Confirming the proximity to a magnetic quantum critical point

K. Weber^{1,2}, N. Mufti¹, T. Goltz², T. Woike³, H.H. Klaus², C. Bergmann¹, H. Rosner¹, C. Geibel¹

1. Max Planck Institute For Chemical Physics of Solids, Dresden, Germany

2. Institute of Solid State Physics, Dresden University of Technology, Dresden, Germany

3. Institute for Structural Physics, Dresden University of Technology, Dresden, Germany

Magnetic systems with reduced dimensionality or frustration are attracting strong interest because these features lead to an increase of quantum fluctuations which often results in unusual, very interesting properties. Our previous studies evidence the AFe_4X_2 family ($A = Y, Lu, Zr$ and $X = Ge, Si$) to cover the whole regime from frustrated antiferromagnetic (AFM) order up to the quantum critical point separating the frustrated AFM ground state from the paramagnetic ground state. $ZrFe_4Si_2$ showed evidence for an unusual type of weak magnetic order and was therefore suspected to be near the quantum critical point. In order to get a deeper insight into its ground state, we performed a detailed study of Ge substituted $ZrFe_4Si_2$, where Ge is suspected to stabilize the magnetic state because of a negative chemical pressure effect. We synthesized polycrystalline samples of $ZrFe_4(Si_{1-x}Ge_x)_2$ with $x = 2\%$ to 50% and investigated their magnetic, thermodynamic, structural and transport properties. As expected, with increasing Ge content the magnetic state is stabilized towards a well defined AFM order at high Ge content. This confirms the near-by quantum critical point in $ZrFe_4Si_2$.

TU.C-P10 - Electron doping effect on AeCo_2As_2 (Ae = Ca, Sr and Ba)

H. Ohta¹, E. Akabane¹, H. Katori¹

1. Institute of Engineering, Division of Advanced Applied Physics, Tokyo University of Agriculture And Technology, Koganei, Jpana

We synthesized solid solutions of $\text{Ae}(\text{Co}_{1-x}\text{Ni}_x)_2\text{As}_2$ (Ae = Ca, Sr and Ba) for studying electron doping effects on AeCo_2As_2 . As results of magnetic measurements, we found that SrCo_2As_2 , which is exchange-enhanced Pauli paramagnet, shows antiferromagnetic ordering with 10% of Ni substitution, despite their uncollapsed tetragonal structure. For the case of BaCo_2As_2 , Ni substitution does not induce magnetic ordering. However, the Weiss temperature of $\text{Ba}(\text{Co}_{1-x}\text{Ni}_x)_2\text{As}_2$ shows maximum at about $x = 0.15$, where the sample is almost magnetically ordering. These results show that AeCo_2As_2 with uncollapsed tetragonal structure have potential to magnetically order. They can not order possibly because their Fermi energy is slightly lower than peak position of density of states.

TU.C-P11 - Perfect Metal Phases of One-Dimensional and Anisotropic Higher-Dimensional Systems

M. Mulligan¹, E. Plamadeala², C. Nayak^{2,3}

1. Stanford University, Stanford, United States

2. University of California, Santa Barbara, United States

3. Microsoft Research, Station Q, Santa Barbara, United States

We show that a 1D quantum wire with 23 channels of interacting fermions has a perfect metal phase in which all weak perturbations that could destabilize this phase are irrelevant. Consequently, weak disorder does not localize it, a weak periodic potential does not open a gap, and contact with a superconductor also fails to open a gap. Similar phases occur for $N > 23$ channels of fermions, except for $N=25$, and for $8k$ channels of interacting bosons, with $k > 2$. Arrays of perfect metallic wires form higher-dimensional fermionic or bosonic perfect metals, albeit highly-anisotropic ones. We will also discuss aspects of transport in such perfect metal wire arrays.

TU.C-P12 - Magneto - crystalline anisotropy and non - Fermi - liquid behaviour in $\text{CeNi}_{1-x}\text{Co}_x\text{Ge}_2$ Z. Molčanová¹, M. Mihalik¹, M. Mihalik¹, M. Zentková¹, Viktor Kavečanský¹, J. Briančin²1. *Institute of Experimental Physics SAS, Košice, Slovak Republic*2. *Institute of Geotechnics SAS, Košice, Slovak Republic*

In our contribution we present results of magnetization, AC susceptibility, specific heat and electrical resistivity measurements of $\text{CeNi}_{1-x}\text{Co}_x\text{Ge}_2$ heavy fermion system ($0 < x < 1$) which were prepared by arc melting and grown by optical floating zone method in four mirror furnace. The parent compound CeNiGe_2 is an antiferromagnetic Kondo system that orders magnetically at $T_N = 3.9$ K and undergoes a spin structure rearrangement at $T_1 = 3.2$ K [1] while CeCoGe_2 is a nonmagnetic heavy-fermion Kondo compound with $j=5/2$ ground state and large Kondo temperature $T_K > 200$ K [2]. Our magnetization and electric resistivity measurements confirmed large magneto - crystalline anisotropy of the system. The susceptibility is strongly anisotropic over the whole temperature range studied but can be fitted with the Curie – Weiss law for all samples. The effective magnetic moments μ_{eff} does not change significantly and has been identified approximately to $2.55\mu_B$ for samples with low concentration of Co, but the paramagnetic Curie temperature changes very much with crystallographic orientation and chemical composition ranging from about – 80 K to small positive values. Heat capacity measurements revealed that characteristic feature of CeNiGe_2 , the double peak with maxima at $T_N = 3.6$ K and $T_1 = 2.9$ K, moves to smaller temperature and only single peak appears for sample containing small amount of Co. AC susceptibility results showed that the phase transition from the antiferromagnetic to the paramagnetic state is suppressed to lower temperatures with an increasing concentration of dopant. The maximum detected around 3.8 K for CeNiGe_2 decreases to 2.6K for $x = 0.05$ and the magnetic ordering is suppressed below 0.5 K at about $x = 0.3$.

[1] A.P. Pikul et al. *Journal of Physics: Condensed Matter*, Vol. 16 (2004) 6119[2] E. D. Mun et al. *Physical Review B* 69 (2004) 085113

TU.C-P13 - Non-fermi liquid behaviors in PrIr₂Zn₂₀: Effect of Ga substitutionT. Onimaru¹, K. Uenisi¹, K.T. Matsumoto¹, K. Wakiya¹, K. Umeo², T. Takabatake^{1,3}

1. Dept. Quantum Matter, AdSM, Hiroshima University, Higashi-Hiroshima, Japan

2. N-BARD, Hiroshima University, Hiroshima, Japan

3. IAMR, Hiroshima University, Higashi-Hiroshima, Japan

Praseodymium-based cubic compounds attract much attention because they show various phenomena arising from nonmagnetic degenerated ground states of 4f² configuration. In particular, a family of PrT₂X₂₀ (X=Al and Zn) show quadrupole order, heavy-fermion superconductivity, and structural transitions.[1-3] The crystalline electric field ground state of most PrT₂X₂₀ compounds is a non-Kramers gamma₃ doublet that possesses no magnetic dipoles but electric quadrupoles. Among them, PrIr₂Zn₂₀ undergoes an antiferroquadrupole order at T_Q=0.11 K and a superconducting transition at T_c=0.05 K.[1,2] In the temperature range 0.2<T<0.8 K, above T_Q, the magnetic specific heat C_m and the electrical resistivity rho(T) exhibit non-Fermi liquid (NFL) behavior; C_m/T and rho are proportional to -lnT and rootT, respectively, being characteristic of quadrupole Kondo effect.[4] In the present work, the origin of the NFL behavior have been studied by the measurements of rho, C, and the magnetic susceptibility of PrIr₂Zn₂₀-xGa_x for x<=1.0.

The lattice parameter for x=1.0 decreases by only 0.1 % from that for x=0. The values of residual resistivity for x=0.5 and 1.0 increase by one-order of magnitude from that for x=0. It prevents us from detecting a change of the rootT dependence of rho(T) observed for x=0. The -lnT dependence of C_m/T vanishes for x=0.5 and 1.0, and instead, C_m/T approaches a constant value on cooling below 0.6 K, indicating collapse of the NFL state. As T goes down to 2 K, chi(T) continues to increase, although that for x=0 remains constant below 5 K. The results indicate the unstable NFL state in PrIr₂Zn₂₀. The driving mechanism is likely to be either enhancement of hybridization between the 4f and conduction electrons due to the increase of 4p electron density or small splitting of the gamma₃ doublet due to the symmetry breaking at the Pr site.

[1] T. Onimaru *et al.*, J. Phys. Soc. Jpn. 79, 033704 (2010)[2] T. Onimaru *et al.*, Phys. Rev. Lett. 106, 177001 (2011)[3] A. Sakai *et al.*, J. Phys. Soc. Jpn. 80, 063701 (2011)

[4] D. L. Cox, Phys. Rev. Lett. 59, 1240 (1987)

TU.C-P14 - Substitution driven magnetic instabilities of non-Fermi liquid $Ce_3Pd_4Si_4$

E. Bauer¹, N. Robisc¹, K. Sirhan¹, I. Messner¹, R. Kurinjimala¹, B. Raab¹, F. Kneidinger¹, H. Michor¹, J. Sereni², A. Griбанov³

1. *Vienna University of Technology, Vienna, Austria*
2. *CAB Bariloche, San Carlos de Bariloche, Argentina*
3. *Moscow State University, Moscow, Russia*
4. *University of Vienna, Vienna, Austria*

An experimental study of ternary $Ce_3Pd_4Si_4$ evidenced non-Fermi liquid properties due to the proximity of this non-magnetic compound to a quantum critical point. The ground state observed for this Ce system appears to be a result of mutual interactions of the crystalline electric field, of the Kondo effect and of RKKY interactions. A subtle change of the balance of these interactions e.g., by pressure or by substitutions is expected to trigger some instability, presumably of magnetic origin. The aim of the present investigation is to reveal the response of the system when certain atoms in $Ce_3Pd_4Si_4$ are exchanged by different other appropriate elements. Here we will show how long range magnetic order in the substituted materials develops on a substitution of Ce/La, of Pd/Ni and of Si/Ge from a study of temperature, pressure and magnetic field dependent transport properties, of magnetization and of specific heat.

Work supported by the Austrian FWF, P22295.

TU.C-P15 - Theory for anomalous magneto transport of CeCu₂Si₂ under the pressure of sharp valence crossover

K. Miyake¹, S. Watanabe²

1. *Toyota Physical And Chemical Research Institute, Nagakute, Japan*
2. *Kyushu Institute of Technology, Kitakyushu, Japan*

Anomalous and unconventional temperature (T) and pressure (P) dependences of the Hall coefficient of CeCu₂Si₂ observed under the pressure [1,2], around which the valence of Ce is known to exhibit sharp crossover from the Kondo to the valence fluctuation regime, are shown to be understood by the effect of critical valence fluctuations (CVF) which explain a series of unconventional behaviors observed in CeCu₂Si₂ around P=5GPa, such as enhancements of the superconducting transition temperature and the residual resistivity, and T-linear dependence in the resistivity, and so on [3]. By borrowing the formalism for the superconducting fluctuation effect on the Hall coefficient [4], we calculate the P and T dependence of Hall conductivity and the Hall angle, together with the Nernst coefficient, reproducing the unconventional behaviors observed by a series of experiments [1,2].

- [1] G. Seyfarth, et al.: Phys. Rev. B 85, 205105 (2012)
[2] S. Araki, et al: SCES2014, Grenoble, Tu-225
[3] K. Miyake and S. Watanabe: J. Phys. Soc. Jpn. 83, 061006 (2014)
[4] H. Fukuyama, et al: Prog. Theor. Phys. 46, 1028 (1971)

TU.C-P16 - Strange Metal Without Magnetic CriticalityT. Tomita¹, K. Kuga², Y. Uwatoko¹, S. Nakatsuji¹

1. Institute For Solid State Physics (ISSP), University of Tokyo, Kashiwa, Japan

2. Center for Advanced High Magnetic Field Science, Graduate School of Science, Osaka University

Recently discovered heavy fermion superconductor β -YbAlB₄ exhibits unconventional quantum criticality despite strong mixed valency. This material is also first Yb-system that exhibits quantum criticality at zero field at ambient pressure. [1-3] Normally, in Yb systems, it is expected that a magnetic order connected to the quantum critical point is driven through application of pressure.

Here, we report our comprehensive study on the pressure vs temperature phase diagram constructed by using the electrical resistivity, magnetization and specific heat measurements of single crystals β -YbAl_{1-x}Fe_xB₄ down to the low temperature of 40 mK under pressure. We observed that non-Fermi liquid observed at ambient pressure is robust with application of pressure up to 0.4 GPa, beyond which a transition from non-Fermi-liquid to Fermi-liquid was observed. In further high pressure regime more than 2.5 GPa, the magnetic order was observed and T_N goes up with pressure, reaching 30 K under 8 GPa, extremely large scale for Yb heavy fermion compound. The same type of behavior is also confirmed in the Fe-doping as a function of chemical pressure. We will discuss the observation of strange metal 'phase' emergent nearby ambient pressure, which is separated from magnetic instability by Fermi liquid phase.[4]

[1] S. Nakatsuji, *et al.*, Nature Phys. 4, 603 (2008)

[1] M. Okawa, M. Matsunami, K. Ishizaka, R. Eguchi, M. Taguchi, A. Chainani, Y. Takata, M. Yabashi, K. Tamasaku, Y. Nishino, T. Ishikawa, K. Kuga, N. Horie, S. Nakatsuji, and S. Shin, Phys. Rev. Lett. 104, 247201 (2010)

[2] Y. Matsumoto, S. Nakatsuji, K. Kuga, Y. Karaki, Y. Shimura, T. Sakakibara, A. H. Nevidomskyy, Piers Coleman, Science 331, 316 (2011)

[3] T. Tomita, K. Kuga, Y. Uwatoko, P. Coleman, S. Nakatsuji, Preprint

TU.C-P17 - Non-Fermi liquid behavior in disordered Kondo systems $\text{Ce}_2\text{Co}_{0.8}\text{Si}_{3.2}$ and $\text{Ce}_2\text{Rh}_{0.4}\text{Co}_{0.4}\text{Si}_{3.2}$ D. Gnida¹, M. Szlawska¹, D. Kaczorowski¹*1. Institute of Low Temperature And Structure Research, Polish Academy of Sciences, Wroclaw, Poland*

The role of nonmagnetic disorder in Kondo lattice systems was investigated in single crystalline samples of $\text{Ce}_2\text{Co}_{0.8}\text{Si}_{3.2}$ and $\text{Ce}_2\text{Rh}_{0.4}\text{Co}_{0.4}\text{Si}_{3.2}$ by means of magnetic susceptibility, specific heat and magnetotransport measurements. Both compounds were characterized as Kondo paramagnets. Their low temperature thermodynamic properties are dominated by distinct non-Fermi liquid features, which manifests themselves as a power law divergence of the magnetic susceptibility and the heat capacity over temperature ratio [1, 2]. The temperature dependencies of the electrical resistivity, $r(T)$, are characteristic of Kondo lattice systems. Below the coherence temperature, the resistivity is changing in linear or quasi-linear manner down to 0.4 K or 2 K for $\text{Ce}_2\text{Co}_{0.8}\text{Si}_{3.2}$ and $\text{Ce}_2\text{Rh}_{0.4}\text{Co}_{0.4}\text{Si}_{3.2}$, respectively, which is in line with the non-Fermi liquid behaviour observed in the thermodynamic properties. For $\text{Ce}_2\text{Rh}_{0.4}\text{Co}_{0.4}\text{Si}_{3.2}$, some shallow minima are observed below 2 K in both components of the resistivity tensor. In the case of $\text{Ce}_2\text{Co}_{0.8}\text{Si}_{3.2}$, similar minima appear in magnetic fields $B > 3$ T, and their position shift to higher temperatures with increasing field. As both compounds exhibit a high residual resistivity ($r_0 > 200$ μOhmcm) and a small residual resistivity ratio (close to 1) it seems likely that the low-temperature upturns in $r(T)$ occur due to diffusive motion enhanced interactions between conduction electrons. Thus, the anomalous thermodynamic and transport properties of $\text{Ce}_2\text{Co}_{0.8}\text{Si}_{3.2}$ and $\text{Ce}_2\text{Rh}_{0.4}\text{Co}_{0.4}\text{Si}_{3.2}$ are mostly governed by the interplay of Kondo effect and RKKY interactions in the presence of sizable atomic disorder, which induces spatial fluctuations in the local density of states and hence smearing off the Kondo and RKKY characteristic energy scales.

This work was supported by the National Science Center (Poland) under Grant No.2011/03/D/ST3/02351.

[1] M. Szlawska, D. Kaczorowski, J. Phys.: Condens. Matter 25 (2013) 256601

[2] M. Szlawska, D. Kaczorowski, J. Phys.: Condens. Matter 26 (2014) 016004

TU.C-P18 - High-pressure effect on low-temperature properties of the approximant crystal to magnetic Au-Al-Yb quasicrystal

S. Matsukawa¹, M. Nakayama¹, T. Yamashiya¹, K. Nobe¹, K. Kamiya¹, K. Deguchi¹, K. Imura¹, H. Takakura², T. Ishimasa², N. Sato¹

1. Nagoya University, Nagoya, Japan

2. Hokkaido University, Sapporo, Japan

Quasicrystals are metallic alloys that possess long-range, quasiperiodic structures with diffraction symmetries forbidden to conventional crystals. The quasiperiodic structure leads us to expect that the electronic state of quasicrystals is different from that of conventional crystals and amorphous materials. More than 100 quasicrystals have been found to date since the discovery of the quasicrystal, but such a novel state had not been reported besides the recent finding of an unconventional quantum criticality in the Au-Al-Yb quasicrystal [1]. In this new type of quasicrystal, the magnetic susceptibility and the electronic specific heat coefficient diverge as $T \rightarrow 0$. In contrast, the Au-Al-Yb approximant crystal shows a conventional heavy fermion feature at low temperatures. Therefore, the unconventional quantum criticality of the magnetic quasicrystal may arise from a characteristic state unique to the quasicrystals.

We present here the high-pressure effect on the low-temperature properties of the Au-Al-Yb approximant. At ambient pressure, the inverse magnetic susceptibility of the approximant follows the power law, $1/c \propto T^{0.51} + \text{const.}$ at low temperatures. The inverse magnetic susceptibility extrapolated to zero temperature, $1/c(0)$, decreases monotonically with increasing pressure. With further increasing pressure, $1/c(0)$ turns to increase, suggesting the presence of a quantum critical point, although it is not clear at present whether the high-pressure state is a long-range ordered state or a glass-like short-range ordered state. This pressure dependence of the low temperature properties is in contrast to that of the magnetic Au-Al-Yb quasicrystal: $1/c(0)$ exhibits the quantum criticality ($1/c \propto T^{0.51}$) at any pressure studied. The comparison between the approximant and the quasicrystal strongly suggests that the unconventional quantum criticality of the magnetic quasicrystal is related to a characteristic state unique to the quasicrystal.

1. K. Deguchi, S. Matsukawa, N. K. Sato, T. Hattori, K. Ishida, H. Takakura and T. Ishimasa, Nature Materials 11 (2012), 1013

TU.C-P19 - Unconventional quantum critical behavior in nonmetallic CeOBiS₂: A mother phase of BiS₂-based superconductor

R. Higashinaka¹, T. Asano¹, T. Nakashima¹, K. Fushiya¹, Y. Mizuguchi¹, O. Miura¹, T. D. Matsuda¹, Y. Aoki¹

1. Tokyo Metropolitan University, Tokyo, Japan

BiS₂-based layered superconductors LnO_{1-x}F_xBiS₂ (Ln: rare earth) have been attracting much attention [1]. We have studied the low-temperature properties of CeOBiS₂ single crystals by electrical resistivity, magnetization, and specific heat measurements. Ce 4f-electrons are found to be in a well-localized state split by crystalline-electric-field (CEF) effects. The CEF ground state is a pure J_z = ±1/2 doublet, and excited doublets are located above 300 K. At low temperatures in zero field, we observe pronounced - log T divergence in the specific heat, revealing the presence of quantum critical fluctuations of 4f magnetic moments near a quantum critical point (QCP) [2]. Considering that CeOBiS₂ is a nonmetal, this phenomenon cannot be attributed to the competition between Kondo and the Ruderman-Kittel-Kasuya-Yosida (RKKY) interactions as in numerous f-electron-based strongly correlated metals. This fact indicates an unconventional mechanism for the QCP in CeOBiS₂. Magnetic interactions in a CeO block layer are probably mediated by superexchange interactions. The interactions among Ce ions can be expressed with the spin-1/2 XXZ model. In a 2D quantum spin-1/2 XXZ system along with the J₁-J₂ frustration, theoretical calculations show that no long-range order (LRO) appears in a certain parameter range called the “quantum paramagnetic phase” [3]. We suggest that CeOBiS₂ is the first material found to be located at a QCP among geometrically frustrated nonmetallic magnets.

[1] Y. Mizuguchi et al, Phys. Rev. B, 86 , 220510(R) (2012)

[2] R. Higashinaka et al, J. Phys. Soc. Jpn. 84, 023702 (2015)

[3] R. F. Bishop, P. H. Y. Li, R. Darradi, J. Schulenburg, and J. Richter, Phys. Rev. B 78, 054412 (2008)

TU.C-P20 - Exploring the vicinity of a quantum critical point with coplanar microwave resonators

D. Geiger¹, A. Sidorenko¹, D.H. Nguyen¹, L. Prochaska^{1,2}, S. Putz^{2,3}, J. Majer^{2,3}, H. Hübl⁴, R. Gross⁴, S. Paschen¹

1. *Institute of Solid State Physics, Vienna University of Technology, Vienna, Austria*

2. *Center for Micro and Nanostructures ZMNS, Vienna, Austria*

3. *Institute of Atomic and Subatomic Particles, Vienna, Austria*

4. *Walther-Meißner-Institut, Bayerische Akademie der Wissenschaften, Garching, Germany*

Close to a quantum critical point, the physical properties of metals may deviate drastically from the predictions of Fermi liquid theory. Compared to static electronic properties, probed by thermodynamic or electronic transport measurements for many quantum critical systems, much less is known about dynamical properties. Investigating the frequency response close to a quantum critical point requires specialized experimental conditions: very low temperatures and techniques that allow investigating very low-energy excitations. The latter can be achieved by using electromagnetic radiation in the microwave range. We apply coplanar waveguide resonators, installed in a dilution refrigerator, to couple the electrons of quantum-critical materials to microwave radiation in the low GHz range. The quality factor and resonance frequency of the transmitted signal are directly related to dynamic properties of the sample: the surface resistance and the surface reactance. For non-resonant experiments in a broad frequency range, high-quality thin films are needed. First perspectives towards this goal, applying molecular beam epitaxy, will also be presented.

We gratefully acknowledge financial support from the European Research Council (ERC Advanced Researcher Grant 227378), the Austrian Science Fund (FWF doctoral program W1243), and the U.S. Army Research Office (grant W911NF-14-1-0496).

TU.C-P21 - Correlation effects in One-Dimensional Quasiperiodic Anderson-Lattice ModelF. Matsuda¹, M. Tezuka¹, N. Kawakami¹*1. Department of Physics, Kyoto University, Kyoto, Japan*

Recently, heavy fermion systems in quasicrystals have attracted much attention after quantum critical phenomena were found in the quasicrystals. In the quasicrystal $\text{Yb}_{15}\text{Al}_{34}\text{Au}_{51}$, quantum criticality of valence fluctuations emerges, which is shown to be quite robust against pressure, while this robustness is not seen in its approximant crystals [1]. The research reported that low-temperature properties of magnetic susceptibility χ , NMR/NQR relaxation rate $(T_1T)^{-1}$, specific-heat coefficient C/T , and resistivity ρ agree very well with the theory of quantum valence criticality. A theoretical research to explain this robustness of quantum criticality has been done by considering a single cluster of $\text{Yb}_{15}\text{Al}_{34}\text{Au}_{51}$ [2].

Can this robustness of quantum criticality be seen in random systems or is it specific to quasiperiodic systems? To answer these questions, we focus on the effects of quasiperiodicity on the quantum criticality of valence fluctuations. We consider the one-dimensional (1D) quasiperiodic Anderson-lattice model, which has quasiperiodically ordered impurities. The sites with an f-orbital are ordered as "Fibonacci word", which is known as a method to construct 1D quasiperiodic orderings. To treat the correlation effect precisely, we use the density matrix renormalization group (DMRG) method. We find that a valence transition occurs in different ε_f at each site. This is consistent with the previous research, which showed that the robustness of quantum criticality comes from overlap of the critical regimes at each site. Moreover, we discuss the properties which are specific to the 1D quasiperiodic Anderson-lattice model, comparing it against periodic and random-potential models.

References:

- [1] K. Deguchi et al., Nature Materials 11, 1013 (2012)
- [2] S. Watanabe and K. Miyake, J. Phys. Soc. Jpn. 82, 083704 (2013)

TU.C-P22 - Common Anomalies of Transport Properties in PrTr₂Zn₂₀ (Tr = Ir, Rh) with Non-Kramers Doublet Ground State

T. Yoshida¹, Y. Machida¹, K. Izawa¹, Y. Shimada², N. Nagasawa², T. Onimaru², T. Takabatake²

1. Department of Condensed Matter Physics, Tokyo Institute of Technology, Tokyo, Japan

2. Graduate School of Advanced Science of Matters, Hiroshima University, Higashi-Hiroshima, Japan

Although possible interplay between quadrupole moments and conduction electrons including the non-magnetic Kondo effect has been considered both experimentally[1] and theoretically[2], it remains elusive now. PrTr₂Zn₂₀ (Tr = Ir, Rh) have emerged as rare and suitable playgrounds to examine this possibility because 4f-electrons of the Pr ions have the non-Kramers doublet ground state with a quadrupole degree of freedom. In addition, the strong hybridization is expectable due to a high coordination number of the Zn ions surrounding the Pr ion. At low temperatures, both compounds undergo an antiferro-quadrupolar transition below the certain transition temperatures TQ[3, 4]. Here, we present a study of the electric and thermoelectric transport properties of PrTr₂Zn₂₀ (Tr = Ir, Rh). Our electric resistivity measurements reveal the non-Fermi liquid behavior with an upward convex curve above TQ, and this characteristic normal-state resistivity is found to satisfy a scaling relation over the wide temperature and field range throughout the compounds. Moreover, on the verge of the quadrupole ordered phase under the magnetic fields, we find a dramatic enhancement of the Seebeck coefficient at low temperatures in both compounds. These features imply a common underlying mechanism presumably dominated by the interplay between quadrupole moments and conduction electrons.

References:

- [1] C. L. Seaman, et. al., J. Alloys Compd., 181, 327-338 (1992)
- [2] D. L. Cox, Phys. Rev. Lett., 59, 1240 (1987)
- [3] T. Onimaru, et. al., Phys. Rev. Lett., 106, 177001 (2011)
- [4] I. Ishii, et. al., Phys. Rev. B, 87, 205106 (2013)

TU.C-P23 - muSR-investigations on $\text{Nb}_{1-y}\text{Fe}_{2+y}$

S. Süllow¹, D. Rauch¹, M. Kraken¹, J. Litterst¹, H. Luetkens², A. Neubauer³, C. Pfleiderer³, W. Duncan⁴, M. Grosche⁵

1. TU Braunschweig, Braunschweig, Germany
2. PSI Villigen, Switzerland
3. TU München, München, Germany
4. Royal Holloway, University of London, United Kingdom
5. University of Cambridge, United Kingdom

We have investigated single crystals and polycrystals from the series $\text{Nb}_{1-y}\text{Fe}_{2+y}$, $-0.019 \leq y \leq 0.018$ by muon spin relaxation. With our study utilizing a microscopic experimental tool, we are able to access the full phase diagram previously established by bulk experimental techniques. In addition to the previously studied spin-density-wave phase and the ferromagnetic phase for Fe-rich material, with our data we can now verify the suppression of magnetic order at the quantum critical point at $y \sim 0.015$ on a microscopic level. Further, we establish the reentrance of magnetic order for larger y values, and compare the mSR signature for this supposedly ferromagnetic phase with that from the Fe-rich side of the phase diagram.

TU.C-P24 - Single-ion Kondo physics in the cage compound CeRh₄Al_{15.37}A. Strydom¹, V. Avzuragova², A. Tursina², S. Nesterenko²*1. Highly Correlated Matter Research Group, Physics Department, University of Johannesburg, Auckland Park 2006, South Africa**2. Department of Chemistry, Lomonosov Moscow State University, Moscow, Russia*

Crystal structures of rare-earth based systems with high aluminium content, such as CeT₂Al₁₀ (T=Fe, Ru, Os) [1], produce intermetallic compounds with unusual physical properties that test our understanding of correlated electron phenomena [2]. Aside from the 3-dimensional cage-type structure [2] of CeT₂Al₁₀ compounds, a more conspicuous aspect of these crystal structure types is that they have a 2-dimensional layered atomic arrangement [3]. Here we explore the physical properties of the new compound CeRh₄Al_{15.37}. It forms in a tetragonal crystal structure [4]. All the atoms are highly coordinated, including Ce with CN=20. Four Al sites have partial occupancy. At a nearest distance of $d_{\text{Ce-Ce}} \approx 7 \text{ \AA}$, the Ce ions are well isolated from each other in the lattice. Above 100 K the full free-ion Ce³⁺ magnetic moment governs the susceptibility. The specific heat $C_p(T)/T$ increases strongly below 6 K, and produces a quasi-logarithmic divergence over more than a decade in temperature. This persists down to 50 mK where $C_p(T)/T$ reaches a very high value of 0.9 J/mol.K². Our physical properties data collectively define CeRh₄Al_{15.37} as a Kondo lattice, but with heavy-electron 4f spins remaining in the single-ion Kondo state as $T \rightarrow 0$.

1. VMT Thiede, T. Ebel, and W. Jeitschko, J. Mater. Chem. 8 (1998) 125

2. AM Strydom, Physica B 404 (2009) 2981

3. B. Fehrmann, and W. Jeitschko, Inorg. Chem. 38 (1999) 3344

4. B. Fehrmann, and W. Jeitschko, J. Alloys. Comp. 298 (2000) 153

TU.C-P25 - Spin-fluctuation effects near the quantum phase transition of the ising-type itinerant ferromagnet URhAl

Y. Shimizu¹, D. Braithwaite², B. Salce², T. Combier², D. Aoki^{2,3}, J. Flouquet²

1. *The Institute for Solid State Physics, The University of Tokyo, Chiba, Japan*

2. *CEA-Grenoble, Grenoble, France*

3. *IMR, Tohoku University, Ibaraki, Japan*

It was believed that an itinerant magnetic compound usually has a quantum critical point (QCP), however, in itinerant ferromagnets, ZrZn₂, UGe₂, and metamagnet UCoAl, the first-order ferromagnetic wing structures have recently been found at low temperature from hydrostatic pressure experiments. In particular, the tri-critical point in UCoAl is estimated to exist at negative pressure of -0.2 GPa, and we cannot capture the whole picture of its ferromagnetic wing.

In order to gain further understanding of the spin-fluctuation effects as well as the QPT of the itinerant ferromagnetism, we focus on another ferromagnet URhAl, which has the same ZrNiAl crystal structure as UCoAl. Since the atomic radius of Rh is larger than that of Co, URhAl would be a system in which a negative pressure is applied for UCoAl.

By means of resistivity measurements for URhAl under pressure up to 7.5 GPa [1], we found that the critical pressure exists around $P_c \sim 5.2$ GPa. The Curie temperature disappears as a first-order phase transition, and the critical behavior of the Fermi-liquid regime cannot be described by a ferromagnetic QCP. However, near P_c , we also observed a large enhancement of the A coefficient of the Fermi-liquid resistivity term, and the resistivity is described rather by a non-Fermi-liquid regime, in which the exponent of resistivity is $n \sim 1.6-1.7$, close to the expected value for a ferromagnetic QCP. From the magnetic field dependence of resistivity, we observed an anomaly, which is consistent with the presence of a ferromagnetic wing. The nature of the first-order phase transition is probably weak, and the system is dominated by strong spin-fluctuations. An intermediate phase through a Fermi-surface change around the QPT may be possible in URhAl due to the strong spin-fluctuation effect, which persists substantially up to 7.5 GPa.

[1] Y. Shimizu et al., arXiv:1501.06701; accepted in Phys. Rev. B

TU.C-P26 - Electron spin resonance studies in the antiferromagnetic phase of YbRh_2Si_2

W. Voesch¹, C. Claus¹, M. Javaheri¹, M. Dressel¹, K. Kliemt², C. Krellner², J. Sichelschmidt³, C. Geibel³, M. Scheffler¹

1. *Physikalisches Institut, Universität Stuttgart, Stuttgart, Germany*

2. *Goethe-Universität Frankfurt, Physikalisches Institut, Frankfurt/Main, Frankfurt, Germany*

3. *Max-Planck-Institut für Chemische Physik fester Stoffe, Dresden, German*

The heavy-fermion material YbRh_2Si_2 is a model system to investigate strong electron-electron correlations. Weak antiferromagnetic order is observed below 70 mK in the absence of a magnetic field. At zero temperature, this antiferromagnetic order vanishes with an applied magnetic field of 60 mT at a quantum critical point. Electron spin resonance (ESR) is an established spectroscopic tool to study magnetism in solids and to characterize magnetic order. However, conventional ESR studies use frequencies with a corresponding magnetic field of 0.3 T (X-band) and larger and therefore cannot be used to investigate these interesting phases in YbRh_2Si_2 .

With the recent development of coplanar resonators, a wide range of low GHz frequencies are accessible for ESR which lead to corresponding magnetic fields down to 30 mT. In the case of YbRh_2Si_2 the lower frequencies are of main interest as one can investigate the antiferromagnetic, the non-Fermi-liquid and the Fermi-liquid phase. This work focuses on the antiferromagnetic phase and the transition to the paramagnetic regime. We observe clear signs of the antiferromagnetic transition in the experimental raw data (quality factor of the resonator) as well as in the deduced ESR parameters, namely the g factor and the linewidth.

Thus, these results provide opportunities to gain deeper insights in the antiferromagnetic state of YbRh_2Si_2 and the spin dynamics of the magnetic moments.

TU.C-P27 - Peculiar transport and phase diagram in non-Kramers doublet compounds with quadrupole degree of freedomK. Izawa¹, T. Yoshida¹, Y. Machida¹, K. Matsumoto², T. Onimaru², T. Takabatake², H. Suzuki³*1. Department of Physics, Tokyo Institute of Technology, Tokyo, Japan**2. Graduate School of Advanced Science of Matters, Hiroshima University, Higashi-Hiroshima, Japan**3. Advanced Technologies Division National Institute for Material Science, Ibaraki, Japan*

We report unusual transport coefficients of praseodymium compounds PrPb_3 and $\text{PrT}_2\text{Zn}_{20}$ ($T=\text{Ir, Rh}$). These compounds provide unique opportunities to study the nature of novel electronic states inherent in a multipole degree of freedom because they all have a non Kramers doublet ground state with multipole degeneracies. In fact, PrPb_3 exhibits an antiferroquadrupolar (AFQ) ordering with incommensurate/modulated structures at transition temperature T_Q [1], implying the presence of the RKKY type interaction between quadrupole moments. On the other hand, $\text{PrIr}_2\text{Zn}_{20}$ and $\text{PrRh}_2\text{Zn}_{20}$ show an antiferroquadrupolar ordering at T_Q followed by superconductivity deep inside the ordered phase [2], implying a close connection between quadrupole and superconductivity. Although these phenomena imply a crucial role of the hybridization between quadrupole moments and conduction electrons, the physics behind them is still far from being clarified. In this study, we carried out measurements of electric and thermoelectric coefficients of these Pr-based compounds to elucidate the nature of the novel electronic states characteristic of multipoles hybridized with conduction electrons. We found a μ g unusual non Fermi liquid (NFL) behavior of the resistivity with a convex curve above T_Q in PrPb_3 as well as $\text{PrT}_2\text{Zn}_{20}$. Interestingly, such unusual resistivity can be well expressed by a scaling function based on a quadrupolar Kondo lattice model [3] in the wide temperature and field range throughout these materials. Moreover, we also found a strong enhancement of the Seebeck coefficient as well as the coefficient of T^2 term of resistivity above the critical field of AFQ ordering at very low temperatures, implying the formation of a non-trivial quantum state due to the quadrupole degree of freedom.

References:

- [1] T. Onimaru et al., Phys. Rev. Lett. 94, 197201 (2005)
- [2] T. Onimaru, et. al., Phys. Rev. Lett., 106, 177001 (2011)
- [3] A.Tsuruta and K. Miyake, unpublished

TU.C-P28 - The effect of hydrostatic pressure on the electronic liquid crystal phase of $\text{Sr}_3\text{Ru}_2\text{O}_7$

D. Sun¹, S.A. Grigera^{2,3}, R. Perry⁴, A.P. Mackenzie^{2,5,6}, S.R. Julian^{1,5}

1. *University of Toronto, Toronto, Canada*
2. *University of St. Andrews, Saint Andrews, United Kingdom*
3. *Instituto de Física de Líquidos y Sistemas Biológicos, La Plata, Argentina*
4. *University College London, London, United Kingdom*
5. *Canadian Institute for Advanced Research, Toronto, Canada*
6. *Max Planck Institute for Chemical Physics of Solids, Dresden, Germany*

Electronic liquid crystal (ELC) phases are novel phases that have a special symmetry that lies between the Fermi liquid and the Wigner solid, with the symmetry controlled by electron-electron interactions. Hydrostatic pressure is a direct and effective parameter that can change the interactions between electrons and thus is a powerful tool to study the ELC phases. There is an ELC phase induced by the magnetic field in the bi-layer ruthenate $\text{Sr}_3\text{Ru}_2\text{O}_7$, signaled by a pronounced anisotropic peak in the resistivity within a very narrow field range. In our experiment, we studied the anomalous phase by applying hydrostatic pressure to a single crystal of $\text{Sr}_3\text{Ru}_2\text{O}_7$. With the magnetic field near the c-axis, the anisotropy of the ELC phase disappears at very low pressure and the corresponding peak in the resistivity is suppressed below 7.7 kbar. The results suggest that the ELC phase is driven by quantum criticality, which is closely related to the magnetic structure. This is in sharp contrast to the behavior of a second ELC phase, seen with the field aligned in the ab-plane, which is relatively unaffected by hydrostatic pressure [1].

[1] D. Sun, W. Wu, S.A. Grigera, R.S. Perry, A.P. Mackenzie and S.R. Julian, Phys. Rev. B 88 (2013) 235129

TU.C-P29 - Magnetic field-induced quantum criticality in pressurized CeNiAsO and CeNiAs_{0.65}P_{0.35}O

G. Pristas^{1,2}, J. Larrea J.^{1,3}, D. Geiger¹, H.M. Rønnow⁴, Z. Xu⁵, Q. Chen⁵, S. Paschen¹

1. Institute of Solid State Physics, Vienna University of Technology, Vienna, Austria

2. Institute of Experimental Physics, Slovak Academy of Sciences, Košice, Slovak Republic

3. Brazilian Center for Research in Physics, Rio de Janeiro, Brazil

4. Laboratory for Quantum Magnetism, École Polytechnique Fédérale de Lausanne, Lausanne, Switzerland

5. Department of Physics and State Key Laboratory of Silicon Materials, Zhejiang University, Hangzhou, China

A pressure-induced quantum critical point (QCP) with Kondo destruction was recently suggested to occur in the nickel oxypnictide CeNiAsO at 6.5 kbar [1]. Also partial substitution of As by P in CeNiAs_{1-x}P_xO was shown to drive the system through a QCP, situated somewhere between $x = 0.35$ and 0.4 . Here we present electrical transport measurements on both CeNiAsO and CeNiAs_{0.65}P_{0.35}O in pressures up to 15 kbar and magnetic fields up to 14 T, at temperatures down to 40 mK, an order of magnitude lower than in the previous work [1]. We construct a three-dimensional pressure-magnetic field-temperature phase diagram for both samples and locate quantum critical lines in the $T = 0$ K plane. Focus is on magnetic field-tuning of samples with fixed pressure near the critical pressure. Both isothermal magnetic field scans and isofield temperature dependencies will be presented.

We acknowledge the European Research Council (ERC Advanced Grant 227378) for financial support. JLJ also acknowledges the CNPq/MCTI-Brazil (Fellowship 306467/2014-3).

[1] Y. Luo, L. Pourovskii, S. E. Rowley, Y. Li, C. Feng, A. Georges, J. Dai, G. Cao, Z. Xu, Q. Si, and N. P. Ong, Nature Materials 13 (2014) 777

TU.C-P30 - Search for a Quantum Brazovskii phase transition in $Mn_{1-x}Fe_xSi$

J. Kindervater¹, S. Ernst¹, F. Haslbeck¹, T. Adams¹, A. Bauer¹, C. Franz^{1,2}, N. Martin^{1,2,3}, W. Häußler^{1,2}, M. Garst⁴, P. Böni¹, C. Pfleiderer¹

1. Physik Department, Technische Universität München, Garching, Germany

2. Heinz Maier-Leibnitz Zentrum (MLZ), Garching, Germany

3. CEA Saclay, DSM/IRAMIS/Laboratoire Leon Brillouin, Gif sur Yvette, France

4. Institute for Theoretical Physics, Universität zu Köln, Köln, Germany

Extensive high-pressure studies in MnSi revealed an extended parameter range with an unexplained non-Fermi liquid resistivity [1] and partial magnetic order [2] on time scales faster than μ -SR [3]. Detailed measurements of the Hall effect in addition recently identified a topological Hall contribution [4] as a key feature of the non-Fermi liquid regime characteristic of spin fluctuations supporting non-trivial topology akin the skyrmion lattice phase at ambient pressure [5]. However, due to the pressure cell quasi-elastic neutron scattering studies of the slow spin dynamics in the high pressure state of MnSi have not been possible so far. We have therefore revisited the nature of the spin dynamics in MnSi when helimagnetic order is suppressed by substitutional Fe-doping [6]. We explore the nature of the helimagnetic phase transition in $Mn_{1-x}Fe_xSi$, when helimagnetic order is suppressed under substitutional doping. In our study we combine small-angle neutron scattering and neutron resonance spin echo spectroscopy with measurements of the Hall effect, the ac susceptibility and the specific heat. Tracking the melting transition of long-range helimagnetic order under Fe-doping as combined with recent Hall effect measurements in $Mn_{1-x}Fe_xSi$ [7] we observe microscopic evidence suggesting the formation of a skyrmion liquid.

[1] C. Pfleiderer et al., Nature 414, 427 (2001); N. Doiron-Leyraud et al. Nature 425, 595 (2003)

[2] C. Pfleiderer et al., Nature 427, 227 (2004)

[3] Y. Uemura et al., Nature Physics 3, 29 (2007)

[4] R. Ritz et al., Nature 497, 231 (2013); R. Ritz et al., Phys. Rev. B 87, 134424 (2013)

[5] S. Mühlbauer et al., Science 323, 915 (2009)

[6] A. Bauer et al., Phys. Rev. B 85, 214418 (2012)

[7] C. Franz, et al., Phys. Rev. Lett. 112, 186601 (2014)

TU.C-P31 - Tetragonal iron monotelluride under extreme conditions

R. Viennois^{1,2}, S. Arsenijevic^{3,4}, R. Gaal³, L. Forro³, W. Knafo⁵, G. Ballon⁵, X. Fabrèges⁵, F. Duc⁵, J. Léotin⁵, C. Deftels⁶

1. Institut Charles Gerhardt, Université De Montpellier, Montpellier, France
2. DQMP, Université de Genève, Genève, Switzerland
3. Institute of Condensed Matter Physics, Swiss Federal Institute of Technology, EPFL, Switzerland
4. High Magnetic Field Laboratory, Institute for Molecules and Materials, Radboud University Nijmegen, 6525 ED Nijmegen, The Netherlands
5. LNCMI, UPR 3228, CNRS-UJF-UPS-INSA, Toulouse, France
6. ESRF, Grenoble, France

Tetragonal iron chalcogenides Fe_{1+x}Ch have attracted the attention because of their simple crystal structure, the absence of charge transfer reservoir layer and of arsenic. However, the partial filling of a second interstitial site by iron atoms has crucial effect on the physics of the Fe_{1+x}Ch , both on superconducting and magnetic properties of this family of compounds [1]. Recently, several interesting phenomena have been discovered in the non-superconducting parent compound Fe_{1+x}Te as a pressure-induced ferromagnetic transition [2] and a magnetic field induced irreversible transition [3]. In the present work, we will describe some of our recent works on the physical properties of Fe_{1+x}Te under extreme conditions, i. e. under high magnetic fields or under high pressures.

We have recently discovered an irreversible magnetic field induced transition in Fe_{1+x}Te at 53 T for $T = 2$ K whose critical field decreases strongly with temperature [3]. This transition occurs only for H perpendicular to c and is due to reorientation of the magnetic domains because it is closely related to the magnetic ground state of Fe_{1+x}Te . Our X-ray diffraction study of Fe_{1+x}Te under high pressure does not confirm the presence of collapsed phase reported previously [4]. In our transport and thermoelectric experiments under pressure, we have observed anomalies corresponding to the pressure-induced ferromagnetic phase above 1.6 GPa and thermal hysteresis at 1.4 GPa, which coincides with the orthorhombic structural phase [1]. More importantly, for that value of pressure the thermopower coefficient S/T diverges with a $\ln(1/T)$ dependence, signaling the existence of critical spin fluctuations at the crossover between the two magnetically ordered phases.

- [1] L. Malavasi, S. Margadonna, Chem. Soc. Rev. 41, 3897 (2012)
[2] M. Bendele et al, Phys. Rev. B 87, 060409(R) (2013)
[3] W. Knafo et al, Phys. Rev. B 87, 020404(R) (2013)
[4] Zhang et al, Phys. Rev. B 80, 144519 (2009)

TU.C-P32 - Magnetic field - temperature phase diagrams including modulated magnetic order near the border of ferromagnetism in NbFe₂

J. Poulten^{1,2}, P. Niklowitz¹, M. Hirschberger³, W. Duncan¹, A. Neubauer⁴, K. Seemann⁵, C. Peleiderer⁴, F. Malte Grosche⁶

1. Royal Holloway University of London, Egham, UK
2. Diamond Light Source, Harwell Science and Innovation Campus
3. Department of Physics, Princeton University
4. Fakultät für Physik, Technische Universität München
5. Forschungsneutronenquelle Heinz Maier-Leibnitz (FRM II), Technische Universität München
6. Cavendish Laboratory, University of Cambridge, Cambridge, UK

Many experimental studies suggest that ferromagnetic quantum critical points (FM QCPs) are hard to approach in real materials, as they are often replaced by a first order quantum phase transition. Nb_{1+y}Fe_{2-y} is a C14 Laves phase system which, in Fe-rich compositions, displays easy-axis ferromagnetism at low temperatures. This ferromagnetic order may be fully suppressed through precise tuning of y [1]. Near the critical composition, bulk measurements have shown Marginal Fermi liquid behaviour, as expected of a FM quantum critical point (QCP) [1]. However, the FM QCP itself appears to be masked by a modulated magnetic order, or spin density wave (SDW) [2], which represents a different route by which a FM QCP can be avoided. In this study we have explored the magnetic field – temperature phase diagrams of Fe-rich Nb_{1+y}Fe_{2-y} through neutron scattering. We have studied high quality single crystal samples of Nb_{1-y}Fe_{2+y}, grown in an optical floating zone furnace by performing neutron diffraction at the triple-axis spectrometer MIRA at FRM II in diffraction mode. The phase diagrams including the SDW for both **B**||c and **B**⊥c were obtained. The critical fields of the SDW phase were obtained for both field directions. The critical fields in the B||c case are an order of magnitude smaller than the critical fields in the B⊥c case. Our results are consistent with phase diagrams from bulk measurements.

TU.C-P33 - Tuning of the modulated magnetic order at the border of ferromagnetism in NbFe₂

P.G. Niklowitz¹, M. Gamza¹, M. Hirschberger², J. Poulten¹, W. Duncan¹, A. Neubauer³, P. Cermak⁴, A. Schneidewind⁴, K. Seemann⁴, E. Faulhaber⁴

1. *Department of Physics, Royal Holloway, University of London, Egham, TW20 0EX, U.K.*

2. *Department of Physics, Princeton University, NJ 08544, U.S.A.*

3. *Fakultät für Physik, Technische Universität München, 85748 Garching, Germany*

4. *Forschungsneutronenquelle Heinz Maier-Leibnitz (FRM II), Technische Universität München, 85748 Garching, Germany*

5. *Cavendish Laboratory, University of Cambridge, CB3 0HE, U.K.*

The border of ferromagnetism in the C14 Laves phase NbFe₂ is characterised by unusual low-temperature properties: signatures of marginal Fermi liquid behaviour are observed, consistent with ferromagnetic quantum criticality [1], but the ferromagnetic quantum critical point appears to be masked by an ordered state of different origin [2]. Recently we have directly observed the ordering wavevector q_1 of this state by neutron diffraction, showing that the ferromagnetic quantum critical point is masked by modulated magnetic order. Here we report on comprehensive B, T and y tuning of the modulated magnetic order. We have observed the evolution of the modulated magnetic order using neutron scattering studies on several single-crystalline Nb_{1-y}Fe_{2+y} samples ranging from Fe-rich to nearly stoichiometric composition. Our data reveals a significant dependence of q_1 on the different tuning parameters, which indicates to which extent the modulated magnetic order can be understood as emerging from ferromagnetic quantum criticality. We also report on pressure tuning of the modulated magnetic order. Electrical transport measurements on single crystals reveal that the modulated magnetic order can be fully suppressed by pressure. The region around the critical pressure is characterized by non-Fermi liquid behaviour, which suggests that the modulated order itself is a source of quantum criticality.

[1] M. Brando et al., Phys. Rev. Lett. 101, 026401 (2008)

[2] D. Rauch et al., arXiv1312.2357

TU.D-P01 - Magnetization jumps in $[\text{Mn}((\text{R/S})\text{-pn})]_2[\text{Mn}((\text{R/S})\text{-pn})_2(\text{H}_2\text{O})][\text{Cr}(\text{CN})_6]_2$ molecular magnets

M. Kirman¹, A. Talantsev¹, R. Morgunov¹

1. Institute of Problems of Chemical Physics of Russian Academy of Sciences

Recently, the authors [1] presented a theoretical calculation discontinuity of magnetization caused by a commensurate-to-incommensurate magnetic phase transition. Our purposes are experimental observing and identification of magnetization jumps in $[\text{Mn}((\text{R/S})\text{-pn})]_2[\text{Mn}((\text{R/S})\text{-pn})_2(\text{H}_2\text{O})][\text{Cr}(\text{CN})_6]_2$ chiral magnets described in [2,3]. We used SQUID magnetometer to obtain magnetic hysteresis loops of the sample at $T = 2-50$ K. The static magnetic field was stepwise swiped with the step $dH = 2 - 0.2$ Oe in the 0 - 50 kOe range.

Series of the magnetization jumps was observed. These jumps appeared in magnetic field close to coercive field. The starting field of magnetic jumps decreases as sample was heated. Observed jumps caused by quantized energy of spin soliton lattices of different periods. Transitions between these states was observed as steps on the field dependence of the magnetization.

Magnetization jumps caused by spin soliton formations were experimental observed in $[\text{Mn}((\text{R/S})\text{-pn})]_2[\text{Mn}((\text{R/S})\text{-pn})_2(\text{H}_2\text{O})][\text{Cr}(\text{CN})_6]_2$ molecular magnets.

The work was supported by the RFBR grant 14-02-31022, [15-02-05149](#).

[1] J. Kishine, G. Bostrem, A. S. Ovchinnikov et al., Phys. Rev. B 89, 014419 (2014)

[2] J. Kishine, K. Inoue, Y. Yoshida, Prog. Theor. Phys. Suppl. **159**, 82 (2005)

[3] R.B. Morgunov, M.V. Kirman, K. Inoue et al., Phys. Rev. B 77, 184 419 (2008)

TU.D-P02 - Single-ion magnet behavior of Co(II) in cyclodextrine-based multinuclear sandwich-type complexes

N. Nedelko¹, P. Aleshkevych¹, A. Kornowicz², J. Lewinski², A. Krzyzewski¹, S. Lewinska¹, A. Slawska-Waniewska¹

1. *Institute of Physics, Polish Academy of Sciences*

2. *Warsaw University of Technology*

In recent years, a novel group of materials known as mononuclear Single-Molecule Magnets (or Single-Ion Magnets (SIMs)) expands rapidly. Many interesting properties are revealed but not all of them are well described and understood, including the origin of the field-induced slow magnetic relaxations in SIMs containing 3d Kramers ions with an easy-plane magnetic anisotropy. We report the magnetic studies of the two Cyclodextrine-templated sandwich-type complexes $[(\gamma\text{-CD})_2\text{Co}_4\text{Li}_8(\text{H}_2\text{O})_{12}]$ (1) and $[(\alpha\text{-CD})_2\text{Co}_3\text{Li}_6(\text{H}_2\text{O})_9]$ (2) which contain the heterometallic rings $\{\text{Co}, \text{Li}, \text{Li}\}_4$ and $\{\text{Co}, \text{Li}, \text{Li}\}_3$, respectively. Each Co(II) center adopts distorted trigonal bipyramidal geometry with the CoO_5 environment. Variable temperature *ac/dc* magnetic measurements and X-band EPR spectrometry studies have shown that both in 1 and 2 the individual Co(II) ions (in high spin state, $S = 3/2$) endowed with positive value of zero-field splitting parameter D exhibit field-induced slow magnetic relaxations consistent with the SIMs behavior. Interestingly, the slow magnetization dynamics in 1 shows the nearly single relaxation process, whereas in 2 - two relaxation processes are evident. A comparison of the spin-relaxation pathways of Co(II) ions in 1 and 2 and their dependences on the applied static magnetic fields has been performed.

The research was partially performed in the laboratories founded by POIG.02.02.00-00-025/09.

TU.D-P03 - Magnetism of Mn(dppm)₂(OAc): Field induced slow magnetic relaxation of single five-coordinated Mn(III) ion

N. Nedelko¹, P. Aleshkevych¹, A. Kornowicz², J. Lewinski², A. Krzyzewski¹, S. Lewinska¹, A. Slawska-Waniewska¹

1. *Institute of Physics, Polish Academy of Sciences*

2. *Warsaw University of Technology*

The novel crystalline Mn(dppm)₂(OAc) compound (where OAc = acetate and dppm = (S)-diphenylpyrrolidinmethanolate) has been studied with variable temperature static and dynamic magnetic susceptibility measurements as well as X-band EPR spectrometry. The experimental data were analyzed within the spin-Hamiltonian formalism. The results obtained show that Mn(dppm)₂(OAc) incorporates Mn(III) centres in a high-spin state ($S = 2$). The compound studied exhibits paramagnetic behaviour in the temperature range 2 - 300 K with the influence of a ground state zero-field splitting effect ($D \sim -2 \text{ cm}^{-1}$) at the lowest temperatures. ac magnetic susceptibility measurements in the presence of dc magnetic field reveal a slow magnetization dynamics of mononuclear five-coordinated Mn(III) ions that is unexpected considering the assigned very small single ion anisotropy of Mn. The detailed investigations of the spin-relaxation processes and their dependences on the applied dc field have been performed to establish the origin of slowing of the relaxation dynamics and the nature of this Single-Ion Magnet like behaviour. Additionally, detailed EPR studies performed on a single crystal allowed to reveal the presence of Mn(II) impurity ions (below 1 %) built-in a regular crystalline structure. The super-hyperfine structure related to interaction of these ions with nucleus of two ¹⁴N ligands was observed.

The research was partially performed in the laboratories founded by POIG.02.02.00-00-025/09.

TU.D-P04 - Magnetostructural correlations in anion-radical salts $M(\text{bipy})_3(\text{TCNQ})_4$, where $M=\text{Co, Ni, Zn}$

A. Feher¹, D. Šoltéssová¹, Erik Èižmár¹, G. Vasylets², V. Starodub³

1. *Institute of Physics, Faculty of Science, P. J. Šaffrik University In Košice, Park Angelinum 9, 041 54 Košice, Slovakia*

2. *Applied Chemistry Department, V.N. Karazin Kharkiv National University, Svobody Sq. 4, 61022 Kharkiv, Ukraine*

3. *Institute of Chemistry, Jan Kochanowski University of Humanities and Sciences, 25-406 Kielce, Poland*

Materials based on anion-radical salts of 7,7',8,8'-tetracyanoquinodimethane (TCNQ) and containing transition-metal complex cations are very interesting for the study of their physical properties because of the tendency to form low-dimensional magnets. Three novel anion-radical salts $\text{Zn}(\text{bipy})_3(\text{TCNQ})_4 \cdot \text{H}_2\text{O}$, $\text{Co}(\text{bipy})_3(\text{TCNQ})_4 \cdot \text{H}_2\text{O}$ and $\text{Ni}(\text{bipy})_3(\text{TCNQ})_4 \cdot (\text{CH}_3)_2\text{CO}$ were synthesized and structurally characterized [1]. The lattice contains $[\text{M}^{\text{II}}(\text{bipy})_3]^{2+}$ cations (where $M = \text{Zn, Co}$ and Ni , $\text{bipy} = 2,2'$ -bipyridine) and two types of crystallographically independent TCNQ^- stacks. We present experimental results of the magnetic susceptibility (1.8 K–300 K) and magnetization measurements up to 7 T. All compounds exhibit structural tetramerization of anion-radical stacks leading to the creation of antiferromagnetic dimers with singlet ground state. While behaviour of compound containing Co ion can be described at low-temperatures by the presence of single-ion anisotropy, an indication of ferromagnetic coupling in the system containing Ni ion was observed. The experimental results were analysed by own algorithm employing EasySpin simulation package [2].

This work was supported by the Slovak Research and Development Agency under contract No. APVV-0132-11 and VEGA 1/0145/13.

[1] G. Vasylets et al., *Synthetic Metals* 191 (2014) 89

[2] S. Stoll et al., *Journal of Magnetic Resonance*, 178 (2006) 42–55

TU.D-P05 - Magneto-structural correlations of paramagnetic ionic liquids with 3D ordering in the solid state

A. García-Saiz¹, I. de Pedro¹, P. Migowski², I. Hernández¹, L. Fernández Barquín¹, I. Abrahams³, M. Motevalli³, J. Rodríguez Fernández¹

1. CITIMAC, Facultad de Ciencias, Universidad de Cantabria, Santander 39005, Spain

2. CITIMAC, Facultad de Ciencias, Universidad de Cantabria, Santander 39005, Spain

3. Materials Research Institute, Department of Chemistry and Biochemistry, School of Biological and Chemical Sciences, Queen Mary University of London, London E1 4NS, United Kingdom.

Paramagnetic Ionic Liquids (MILs) are promising new smart materials that allow adding further features to the typical properties of ionic liquids such as magnetic, photophysical or electrochromic behaviour which are due to the incorporated metal ions [1].

Here we present the thermal, structural and magnetic studies of two novel MILs, comprised of 1-ethyl-2,3-dimethylimidazolium (Edimim) cation and tetrahaloferrate(III) (FeX₄) (X = Cl and Br) anion. Their crystal structure is formed by layers of cations (in non-planar configuration) and anions stacked upon one another in a 3D manner with several non-bonding interactions: hydrogen bond, anion- π , and halide-halide. The field-cooled molar susceptibility (c_m) measured under 1 kOe of both compounds increases and reaches a maximum at approximately 2.9 K and 9 K for Edimim[FeCl₄] and Edimim[FeBr₄] respectively, indicating the existence of a long-range magnetic ordering, also observed in other compounds with the 1-ethyl-3-methylimidazolium (Emim) and 1,3-dimethylimidazolium (Dimim) cations [2-4]. At low temperatures, the heat capacity data of these MILs shows a I-type anomaly characteristic of a three-dimensional magnetic ordering. This anomaly becomes rounder and smaller in height as the applied magnetic field increases, shifting to lower temperatures, as expected for an antiferromagnetic ordering. The magneto-structural correlations give the evidence that the 3D magnetic ordering takes place via Fe-X---X-Fe interactions, displaying a higher superexchange magnetic interaction between the planes.

[1] a) B. Mallick; B. Balke; C. Felser; Mudring, A.-V. *Angew. Chem. Int. Ed.* 2008, 47 (40), 7635-7638. b) Okuhata, M.; Funasako, Y.; Takahashi, K.; Mochida, T. *Chem. Commun.* 2013, 49 (69), 7662-7664

[2] I. de Pedro, D. P. Rojas, J. Albo, P. Luis, A. Irabien, J. A. Blanco and J. Rodríguez Fernández, *J. Physics-Condensed Matter* 2010 22

[3] A. García-Saiz; P. Migowski; O. Vallcorba; J. Junquera; J. A. Blanco; J. A. González; M. T. Fernández-Díaz; J. Rius; J. Dupont; J. Rodríguez Fernández; I. de Pedro, *Chem. Eur. J.* 2014, 20 (1), 72-76

[4] A. García-Saiz; I. de Pedro; P. Migowski; O. Vallcorba; J. Junquera; J. A. Blanco; O. Fabelo; D. Sheptyakov; J. C. Waerenborgh; M. T. Fernandez-Diaz; J. Rius; J. Dupont; J.A. Gonzalez; J. R. Fernandez, *Inorg. Chem.* 2014, 53 (16), 8384-96

TU.D-P07 - Comparison of spin dynamics and magnetic properties in antiferromagnetic closed and open molecular Cr-based rings

F. Adelnia^{1,2}, F. Borsa², L. Bordonali², M. Mariani³, S. Bordignon⁴, T. Orlando², R. Winpenny⁵
G. Timco⁵, A. Lascialfari^{1,2}

1. Dipartimento Di Fisica And INSTM, Università Degli Studi Di Milano, Italy

2. Dipartimento di Fisica and INSTM, Università degli Studi di Pavia, Italy

3. Dipartimento di Fisica e Astronomia, Università degli studi di Bologna, Italy

4. Dipartimento di Fisica e Scienze della Terra, Università degli studi di Parma, Italy

5. School of Chemistry, University of Manchester, United Kingdom

The comparison of the magnetic properties of the closed molecular antiferromagnetic ring Cr₈ with the open ring Cr₈Zn shows that, while the nearest-neighbor exchange constant J_{Cr-Cr} changes only from ~ 16.9 K [1] in the closed ring to ~ 15.3 K [2] in the open one, the different spin topology has dramatic effects on the level spacing between the S=0 ground state and the excited magnetic states [3]. The aim of the present work is to explore the effect of spin topology on the spin dynamics by means of proton nuclear magnetic resonance and relaxation. The proton NMR measurements were performed in Cr₈ and Cr₈Zn in the temperature range 1.65 < T < 300 K at different external magnetic fields. The temperature dependence of 1/T₁ was found to be similar in both open and closed rings with a magnetic field dependent peak centered at a temperature of the order of the corresponding exchange constant J_{Cr-Cr}. No detectable effects due to changes in the low temperature energy levels separation, which were instead revealed in the magnetization measurements and related to the spin topology, were observed. The peak of 1/T₁(T) could be fitted with a single correlation frequency as in most molecular magnets [4]. A new feature, not previously observed, consisting in a well resolved smaller peak below 4 K and possibly related to a second correlation frequency of the magnetization [5], was also singled out.

[1] G. A. Timco et al., Chem Commun, 3649 (2005) DOI: 10.1039/b504912a

[2] A. Bianchi et al. Phys. Rev. B 79, 144422 (2009)

[3] Y. Furukawa et al, Phys. Rev. B 78, 092402 (2008)

[4] F. Borsa, Y. Furukawa and A. Lascialfari, in "New Developments in Magnetic Resonance " Springer and Verlagö eds. (2006)

[5] P. Santini et al., Phys. Rev. B 70, 134434 (2004)

TU.D-P08 - Raman scattering study of a chiral two-dimensional molecule-based magnetN. Ogita¹, T. Hasegawa¹, M. Udagawa¹, L. Li², K. Inoue²*1. Graduate School of Integrated Arts and Sci., Hiroshima University**2. Department of Chemistry and Institute for Advanced Materials Research, Hiroshima University*

Green needle-shaped crystals, $[\{\text{Cr}(\text{CN})_6\}\{\text{Mn}(\text{R/S})\text{-pnH}(\text{H}_2\text{O})\}](\text{H}_2\text{O})$; ((R/S)-pn=(R/S)-1,2-diaminopropane), is known as the two-dimensional chiral ferrimagnet of Cr^{3+} and Mn^{2+} below $T_c=38\text{K}$ [1]. The crystal structure is an orthorhombic (P212121 space group). The two-dimensional chiral network is constructed of $[\text{Cr}(\text{CN})_6]$ and Mn ion to form a bimetallic square, which is arranged almost perpendicular to the c-axis. One chiral (R/S)-pn ligand and two water molecules separate the Mn-Cr sheets, and (R/S)-pn coordinates to a Mn^{2+} ion in the sheets. Although the magnetic moment of Mn and Cr ions does not locate at chiral positions, the chiral structure of a molecule might give an unusual spin structure [2]. Therefore, to elucidate the lattice dynamics and the spin-lattice coupling, polarization and temperature dependence of the Raman spectra have been measured.

Among a lots of peaks in observed spectra, some peaks show the intensity difference between cross polarization spectra of (x,y) and (y,x). (a,b) denotes the polarization directions of incident(a) and scattered(b) light, respectively. This asymmetry of the Raman tensor can be regarded these peaks as the vibration of the magnetic moment or chiral atoms. In the temperature dependence of the stretching vibrations of cyanide, the energy decrease has been found at around T_c . This result denotes that the atomic vibration is affected by the spin structure. On the other hand, drastic spectral change, such as peak split and appearance, is observed at around 250K with decreasing temperature. This anomaly suggests the drastic change of the lattice, such as the structural transition, might occur at around 250K.

[1] K. Inoue, et al., *Angew. Chem., Int. Ed.* 42(2003) 4810[2] A. Hoshikawa et al., *JPSJ* 73 (2004) 2597

TU.D-P09 - Correlation between dielectric and magnetic properties on fullerene-based magnets

T. Kambe¹, K. Oshima¹

1. Okayama University

The orbital degeneracy plays an essential role in fullerene superconductors. The cooperative ordering of the ligand ions or molecules removes the orbital degeneracy of the C₆₀ and, then, leads to the spatial arrangement of the C₆₀'s orbitals. This should produce a coherent magnetic interaction among localized spins on C₆₀.

The α -phase of Tetra-*kis*-(dimethylamino)-ethylene C₆₀ (abbreviated as α -TDAE-C₆₀) is known as the first fullerene magnet, of which the ferromagnetic transition temperature, T_c , is as high as 16 K. Other α -TDAE-C₆₀ polymorph has different arrangement of orbitals and undergoes an antiferromagnetic transition around 7 K. We recently discovered the existence of permanent dielectric moments around C₆₀ in these magnets, and implied that the two polymorphs exhibit clear differences in their dielectric responses at room temperature [1]. In this presentation, we summarize the different character of dielectric properties for these polymorphs and discuss possibility of magneto-electric couplings.

Reference:

[1] Takashi Kambe and Kokichi Oshima, *Scientific Reports*, 4, 6419 (2014)

TU.D-P10 - Magnetic properties of FePc on In/Si(111) surface studied with ab initio calculations

J.M. Hyun¹, H. Kim¹

1. Department of Physics, Sookmyung Women's University,

Metal-organic systems have attracted much attention for potential applications in future electronic devices. Among these systems, metal phthalocyanine (MPc) represents one of the most promising classes because of its thermal and chemical stability. In recent years, there has been a variety of work performed on MPc systems such as FePc, CoPc, NiPc, and CuPc on graphene/Ni(111) [1-2] as well as on metallic surface [3-5]. However, it is scarcely known about them on nanostructured metal-semiconductor hybrid substrates. Theoretical analysis is highly required to understand issues such as the MPc-substrate interaction, which may affect the molecular adsorption mechanism and the magnetic properties on the metal/semiconductor hybrid surfaces. In this presentation, we report density functional theory (DFT) calculations on the FePc on Si(111)In-4×1. We have examined various adsorption sites on In chain, Si Seiwatz chain, and boundary area. The magnetic moment of an isolated FePc molecule is calculated to be $2 \mu_B$. Upon adsorption, the magnetic moment of FePc is reduced to about $1 \mu_B$ and $0 \mu_B$ on Si and In chains, respectively. The stable adsorption sites and electronic structure will be discussed.

This work has been supported by the Future-based Technology Development Program(Nano Fields) (No. 20120006200) and the EDISON program (No. 2012M3C1A6035684) through the National Research Foundation of Korea(NRF) funded by the Korea government(MEST).

- [1] J. Uihlein *et al.*, J. Chem. Phys. 138, 081101 (2013).
- [2] L. Massimi *et al.*, Beilstein J. Nanotechnol. 5, 308 (2014).
- [3] X. Lu *et al.*, J. Am. Chem. Soc. 118, 7197 (1996).
- [4] K. W. Hiips *et al.*, J. Phys. Chem. 100, 11207 (1996).
- [5] X. Lu *et al.*, J. Phys. Chem. B 101, 5391 (1997).

TU.D-P11 - A ferrimagnetic dodecnuclear Fe(III) complex exhibiting single-molecule magnet behaviorJ.P. Tong¹, X.J. Xu¹, D.J. Yang¹, Jun Tao¹*1. Xiangyang Noncommissioned Officers School, Xiamen University, Fujian, China*

Single- molecule magnets (SMMs) have attracted considerable attention these decades. The discovery of SMMs has immensely prompted the investigation of polynuclear magnetic clusters with high blocking temperature and slow magnetization relaxation. Commonly, metal ions with anisotropy (Mn^{3+} , Co^{2+} , Tb^{3+} , Dy^{3+} , etc.) are mostly introduced. And a molecule containing all high spin Fe(III) ions with anisotropy is rare.

Herein, we report a novel dodecnuclear Fe(III) cluster with ferrimagnetic magnetic property. Magnetic studies have revealed the ferromagnetic interactions within the $[Fe_4(OH)_4]$ core and among the eight peripheral Fe(III) ions as well as antiferromagnetic interactions between the $[Fe_4(OH)_4]$ core and the peripheral Fe(III) ions, thus resulting a ferrimagnetic cluster with ground state $ST = 10$. Molecular anisotropy mainly caused by the symmetry of the structure. The molecule has a S_4 symmetry, which indicates the presence of uniaxial with c axis. The ac susceptibilities show slightly frequency-dependent behavior at temperature range of 1.8-7K. And the out-of-phase susceptibilities slightly moved to higher temperature range when dc field increased, indicating the potential of the molecule as a SMM and not a spin glass state.

References:

- [1] Tong, J.-P.; Shao, F.; Tao, J.; Huang, R.-B.; Zheng, L.-S. *Inorg. Chem.* 2011, 50, 2067
- [2] Freedman, D. E.; Harman, W. H.; Harris, T. D.; Long, G. J.; Chang, C. J.; Long, J. R. *J. Am. Chem. Soc.* 2010, 132, 1224
- [3] Sessoli, R.; Gatteschi, D. *Angew. Chem. Int. Ed.* 2003, 42, 268

TU.D-P12 - Unexpected antiferromagnetic interaction of CrTPP molecules with bare cobalt thin film

M. Baljovic¹, J. Girovsky¹, K. Tarafder^{2,3}, J. Nowakowski¹, C. Wäckerlin⁴, D. Siewert⁵, A. Wäckerlin⁵, A. Kleibert⁶, N. Ballav⁷, T.A. Jung¹

1. *Laboratory For Micro And Nanotechnology, Paul Scherrer Institute*

2. *Uppsala University, Uppsala, Sweden*

3. *BITS, Shameerpet, Andhra Pradesh, India*

4. *LNS, EPFL, Lausanne Switzerland*

5. *University of Basel, Basel, Switzerland*

6. *Swiss Light Source, Paul Scherrer Institute, Villigen, Switzerland*

7. *Indian Institute of Science Education and Research (IISER), Pune, India*

Exchange coupling of spin-bearing metallo-organic complexes to ferromagnetic (FM) substrates leads to an exchange induced magnetic moment in the molecules [1,2]. Recent studies on square-planar 3d metal-porphyrins and -phthalocyanines adsorbed on bare magnetic substrates and oxygen covered magnetic substrates show FM and AFM alignment of molecular spins, respectively. Such magnetic ordering is mostly attributed to direct or indirect exchange coupling in the case of FM alignment of the Chromium spins versus the spins contained in the substrate atoms [2,3] and to superexchange coupling in the case of their AFM alignment [4]. In this contribution, a combined experimental and theoretical study on CrTPP molecules adsorbed on ferromagnetic substrates reveals an unexpected antiferromagnetic (AFM) exchange coupling of these molecules to bare cobalt substrates [5]. The experimentally observed AFM interaction is first confirmed by DFT+U calculations and alternatively described within the framework of Goodenough-Kanamori-Anderson (GKA) rules. According to the GKA model, the electrons from the less than half-filled 3d shell of the Chromium ion interact with those from the out-of-plane orbitals of the cobalt atoms via an indirect 90 degree exchange coupling mechanism mediated by the porphyrin's nitrogen atoms.

[1] A. Scheybal et al., Chem. Phys. Lett. 411, 214 (2005)

[2] N. Ballav et al., J. Phys. Chem. Lett. 4, 2303 (2013)

[3] A. Lodi Rizzini et al., Surface Science 630, 361 (2014)

[4] D. Chyralecka et al., J. Phys. Chem. Lett. 1, 1408 (2010)

[5] J. Girovsky et al., Phys. Rev. B 90, 220404(R) (2014)

TU.D-P13 - Neutron scattering signatures of the entanglement transition in molecular magnets: An exact-diagonalisation study

H. Irons^{1,2,3}, J. Quintanilla^{1,2,3}, T. Perring², L. Amico⁴, G. Aeppli^{6,7,8}, M.A. Martin-Delgado⁵

1. University of Kent
2. ISIS Neutron Facility
3. SEPnet and Hubbard Theory Consortium
4. MATIS-CNR-INFN & Dipartimento di Metodologie Fisiche e Chimiche (DMFCI), viale A. Doria 6, 95125 Catania, Italy
5. Departamento de Física Teórica I, Universidad Complutense, E-28040 Madrid, Spain
6. UCL Department of Physics and Astronomy and London Centre for Nanotechnology, University College London
7. Department of Synchrotron Radiation and Nanotechnology at the Paul Scherrer Institute (PSI)
8. Swiss Federal Institute of Technology Lausanne

The factorised state in 1D Antiferromagnetic chains with a transverse field has been known for a long time[Kurmann]. Recently this state has been linked to the Entanglement Transition[Marty]. When quantifying entanglement it is common to use local measures such as Quantum Discord[Campbell] and concurrence[Amico2008]. In contrast, many experimental probes such as neutron scattering rely on global measurements. Here we demonstrate theoretically, through exact diagonalisation, that the Entanglement Transition can be realised experimentally in molecular magnets above zero temperature. We predict a remarkable change in the finite-temperature neutron scattering cross section as the applied field passes through the Entanglement Transition.

References: J. Kurmann, et al, Physica A 112,235 (1982)

References: O Marty 10.1103/PhysRevB.89.125117

References: S. Campbell, J. Richens, N. Gullo, T. Busch, Phys. Rev A 88 062305 (2013)

References: L. Amico, Rev. Mod. Phys. 80, 517 (2008)

TU.D-P14 - Slow magnetic relaxation of Co-NIT ferrimagnetic chainsM. Novak¹, R. Allão Cassaro², M. Vaz³, P. Lahti⁴

1. Instituto de Física, Universidade Federal do Rio de Janeiro, Brazil

2. Instituto de Química, Universidade Federal do Rio de Janeiro, Brazil

3. Instituto de Química, Universidade Federal Fluminense, Brazil

4. Department of Chemistry, University of Massachusetts, Amherst, United States

Isolated highly anisotropic ferrimagnetic chains, known in the molecular magnetism community as Single Chain Magnets (SCM) present magnetic bistability due to slow magnetic relaxation similar to single molecule magnets (SMM). SCMs appear to have some advantage in reaching higher blocking temperatures, whose main ingredients are strong intrachain magnetic interactions and uniaxial anisotropy plus as weak as possible interchain interactions.

We have developed recently a new family of one-dimensional ferrimagnetic chain compounds containing nitronitroxide radicals with large polycyclic aromatic ring pendants. We have found an extremely large antiferromagnetic exchange interactions for a ferrimagnetic manganese(II) chain[1] and record blocking temperature for the isostructural cobalt(II) chain[2]. In these cobalt(II) chains, the large local anisotropy and strong metal-radical antiferromagnetic interaction are responsible for slow magnetic relaxations at low temperatures, with record blocking temperatures ($T_b \approx 14$ K) and among the highest coercive fields for molecular magnets ($H_c \approx 50$ kOe at 8 K). These promising improvements in T_b are attributed to strong intrachain exchange interaction, nearly parallel local anisotropy axis and high isolation of individual chains. The large distance between chains insured a vanishing interchain interaction and no magnetic ordering, allowing the full observation of the chains' magnetic switching dynamics. The Glauber-like relaxation shows two distinct Arrhenius relaxation processes attributed to finite size long and short chains. The low temperature hysteresis loops are consistent with the presence of two sets of chains, which unblocks at different fields. These chains do not fall in the Ising limit, and so is well suited to motivate further theoretical models and simulation developments.

[1] Vaz, M. G. F. et al. *Inorg. Chem.* 2012, 51, 3138[2] Vaz, M. G. F. et al. *Chemistry- A European Journal* 2014, 20, 5460

TU.D-P15 - A stochastic model for magnetic dynamics in single-molecule magnets

R. López-Ruiz ¹, P. Toderó de Almeida ¹, M.G.F. Vaz ², M.A. Novak ³, F. Béron ¹, K. Roberto Pirota ¹

1. *Unicamp*

2. *Universidade Federal Fluminense*

3. *Universidade Federal do Rio de Janeiro*

The work simulates the magnetization dynamics in superparamagnets with tunneling reversal possibility using a simple stochastic model which takes into account: (i) the thermal activation described by the occupation of levels according to the Boltzmann distribution and (ii) the possibility of tunnel effect described by the Landau-Zenner model.

Both hysteresis and relaxation simulation curves were compared experimentally using the Mn12 single-molecule magnet as a model system. The simulations are experimentally scalable allowing to quantify the time of the simulation stage. Despite being a simple simulation model, the simulations are consistent with a thermally-activated tunneling magnetization reversal phenomenology in which blocking temperature displaces with the variation of the physical parameters involved in the simulation. The relaxation curves present an exponential decay and its field-dependent characteristic relaxation time values give a robust interpretation of hysteresis loops. In terms of inversion mechanism competition, we can separate the quantum and the classical contributions to the characteristic relaxation time.

TU.E-P01 - Full-potential KKR calculations for electronic and magnetic properties of transition metal monosilicide MSi (M=Cr-Co) and mixtures of FeSi and CoSi, based on the generalized-gradient approximation

M. Asato¹, C. Liu², N. Fujima³, T. Hoshino³

1. *National Institute of Technology, Niihama College*

2. *Graduate School of Science and Technology, Shizuoka University*

3. *Graduate School of Engineering, Shizuoka University*

The cubic B20 structure transition metal monosilicides MSi (M=Cr-Co, 8 atoms per unit cell) are an interesting because they exhibit a wide variety of magnetic and transport behavior which reflects the importance of the details of the band structure near the Fermi surface [1]. Recently the mixtures (Fe(1-c)Co(c)Si) of FeSi and CoSi are expected as a new magnetic material exhibiting giant magnetoresistance [2]. The purpose of the present work is to clarify systematically the electronic and magnetic properties of MSi (M=Cr-Co) and Fe(1-c)Co(c)Si, by ab-initio calculations based on the generalized-gradient approximation in density functional formalism and the full-potential Korringa-Kohn-Rostoker Greenüfs function method [3]. The calculated results are summarized as follows: (1) The experimental results for the lattice parameters of MSi are reproduced within the error of 1% of the measured values; (2) The fundamental features of the experimental results such as nonmagnetic (NM) semiconductor of FeSi, NM semimetal of CoSi, and ferromagnetic (FM) metal of MnSi are understood by using the calculated DOS of NM state. The experimental results for FM or NM states of MSi are understood by the simple Stoner condition [4]; (3) The fundamental features of electronic and magnetic properties of Fe(1-c)Co(c)Si are understood by the virtual binary alloy (MSi) model where the nuclear charge of M is the concentration average of nuclear charges of Fe and Co.

References:

- [1] J. H. Wernick, G. K. Wertheim, and R. C. Sherwood, *Mater. Res. Bull.* 7 (1972), 1431-1441.
- [2] N. Manyala, Y. Sidis, J. F. DiTusa, G. Aeppli, D. P. Young, and Z. Fisk, *Nature (London)* 404 (2000), 581-584
- [3] M. Asato, M. Ohkubo, T. Hoshino, F. Nakamura, N. Fujima, and H. Tatsuoka, *Mater. Trans.* 49 (2008), 1760-1767
- [4] J. F. Janak, *Phys. Rev. B* 16 (1977), 255-262

TU.E-P02 - AA-stacked bilayer graphene in an applied electric field: Tunable antiferromagnetism and coexisting exciton order parameter

R. Akzyanov^{1,2,3}, A. Rakhmanov^{1,2,3,4}, A. Rozhkov⁰, A. Sboychakov^{3,4}, F. Nori^{4,5}

1. *All-Russian Research Institute of Automatics*
2. *Moscow Institute of Physics and Technology*
3. *Institute for Theoretical and Applied Electrodynamics*
4. *CEMS RIKEN*
5. *University of Michigan*

We study theoretically the electronic properties of AA-stacked bilayer graphene in a transverse electric field. The AA-BLG consists of two graphene layers, up and down. Each carbon atom of the upper layer is located above the corresponding atom of the lower layer. The strong on-site Coulomb repulsion stabilizes the antiferromagnetic order in such a system. The antiferromagnetic order is suppressed by the transverse bias voltage, at least partially. The interplane Coulomb repulsion and nonzero voltage stabilize an exciton order parameter. The exciton order parameter coexists with the antiferromagnetism and can be as large as several tens of meV for realistic values of the bias voltage and interaction constants. The application of a transverse bias voltage can be used to control the transport properties of the bilayer.

TU.E-P03 - Magnetic properties of $Ce_{n+1}Co_{3n+5}B_{2n}$ ($n = 0, 1, 2, 3$) compounds investigated by ^{59}Co NMRK. Shimizu¹, K. Kakiuchi¹, T. Ito², H. Ido²*1. Department Of Physics, Faculty Of Science, University Of Toyama, Toyama, Japan**2. Department Of Electronic Engineering, Tohoku Gakuin University, Sendai, Japan*

The compounds $Ce_{n+1}Co_{3n+5}B_{2n}$ ($n = 0, 1, 2, 3$ and ∞) have been known to show various interesting magnetic properties which depend on n . The complex magnetic properties of the compounds, however, have not been fully clarified. We present the ^{59}Co spin-echo NMR results on the compounds ($n = 0, 1, 2, 3$). In addition to the zero-field spectra, the field-swept spectra from non-magnetic Co are also observed for $Ce_3Co_{11}B_4$ and $Ce_2Co_7B_3$. These spectra arise from 3g-Co in $Ce_3Co_{11}B_4$ and 6i₂-Co in $Ce_2Co_7B_3$. In order to estimate the spin and orbital moments, m_{spin} and m_{orb} , for respective Co-sites in $Ce_{n+1}Co_{3n+5}B_{2n}$ we use the equation $H_{hf} = am_{spin} + bm_{orb}$ with the hyperfine coupling constants a of -110 kG/ m_B and b of 600 kG/ μ_B , which are estimated by the above equation with the experimental values of H_{hf} and theoretical values of spin and orbital moments for 2c- and 3g-Co atoms in $CeCo_5$ [1,2]. The magnitude of m_{spin} for 2c-Co is estimated to be ~ 1.2 m_B for $Ce_{n+1}Co_{3n+5}B_{2n}$ ($n = 0, 1, 2, 3$), and for 6i₁-Co in $Ce_3Co_{11}B_4$ and $Ce_2Co_7B_3$ the m_{spin} to be about 0.4 m_B , while m_{orb} of 2c-Co varies from ~ 0.3 in $CeCo_5$ to ~ 0.1 m_B in $Ce_2Co_7B_3$, and m_{orb} for the other sites are of the order of 0.08 to 0.01 m_B . These results are discussed together with energy band calculations[1] and magnetization measurements on $Ce_{n+1}Co_{3n+5}B_{2n}$ [3-5].

References:

- [1] T. Ito, H. Ido, J. Appl. Phys. 105 (2009) 07E511
- [2] L. Nordström et al., Phys. Rev. B 41 (1990) 9111
- [3] N.M. Hong et al., J. Appl. Phys. 73 (1993) 5917
- [4] H. Ido, Y. Yamaguchi, J. Magn. Magn. Mater. 272-276 (2004) e487
- [5] Y. Saito et al., J. Appl. Phys. 97 (2005) 10M520

TU.E-P04 - Optical investigation on the electronic structure of FeGe thin film

Y. Lee¹, S. Cho²

1. *Soongsil University, Seoul, South Korea*

2. *Ulsan University, Ulsan, South Korea*

We investigated the electronic structures of the FeGe epitaxial films by using optical spectroscopy. The films were grown on an epi-ready semiconducting GaAs(100) substrate by molecular beam epitaxy. Electric and magnetic measurements revealed that our films show ferromagnetic-metallic behavior, and interestingly a complex M-H curve could be related to the skyrmion. In spectroscopic ellipsometry, we compared the optical conductivity spectra with the theoretical calculation. Infrared spectroscopy identified the formation of the low energy resonance mode. We discuss the low energy electrostatics of our films in relation to their unusual magnetic properties.

TU.E-P05 - Effect of annealing on magnetic and structural properties of half-metallic Co₂MnAl Heusler ribbons

T. Ryba¹, L. Galdun¹, Z. Vargova², M. Obaida³, K. Saksl⁴, M. Durisin⁴, V. Haskova¹, P. Szabo⁴, C. Garcia⁵, R. Varga¹

1. Institute Of Physics, Faculty Of Sciences, P. J. Safarik University, Kosice, Slovakia

2. Dept. Inorg. Chem., Fac. Sci., P. J. Safarik University, Kosice, Slovakia

3. Solid State Physics Department, National Research Centre, Giza, Egypt

4. IEF SAS, Watsonova 47, Kosice, Slovakia

5. Departamento de Fisica, Universidad Technica Federico Santa Maria, Valparaiso, Chile

The Heusler alloys are materials for many applications as spintronics, magnetocaloric cooling, sensors etc. [1]. Particularly, the applications in spintronics are significantly influenced by high value of magnetic moment, high spin polarization, high Curie temperature and small Gilbert damping. Half-metallic composition as Co₂MnAl is a typical example of full Heusler (L21 - structure) alloy with high calculated (100%) value of spin polarization [1-2]. This alloy is typically produced by arc-melting of pure elements and subsequent long-term annealing. On the other hand, rapid quenching (melt-spinnig) is a rapid method for preparation of large amount of homogeneous ribbons of Heusler alloy without necessity of further annealing. In the given contribution, we offer the comparison of structural and magnetic properties of annealed (48 hours at 990 K) and as-cast half-metallic rapidly quenched Co₂MnAl alloy. As-cast sample of Co₂MnAl exhibit B2 structure while annealed sample shows L21 structure. Hysteresis loops and temperature dependence of magnetization shows direction of easy magnetization in parallel direction and Curie temperature is above 700 K, chemical composition and orientation of grains were determined by SEM/EDX. Spin polarization of the sample was measured by point contact method, giving values of 76 % for as-cast sample and 72 % for annealed one. Value of spin polarization was not affected by annealing of sample. This results is in good agreement with the theory of Y-Z disorder [3].

This work was supported by NanoCEXmat ITMS 26220120035, VEGA 1/0060/13 and APVV-0027-11.

References:

- [1] T. Graf, C. Felser, S. S. P. Parkin, Progress in Solid State Chemistry, 39 (2011) 1
- [2] Y. Sakuraba, J. Nakata, M. Oogane, et al., Jap. J. of Appl. Phys., 44 (2005) 6535
- [3] Y. Miura, K. Nagao, M. Shirai, Phys. Rev. B, 69 (2004), 144413

TU.E-P06 - Dilute ferromagnetic InMnP

S. Zhou¹, M. Khalid¹, E. Weschke², W. Skorupa¹, M. Helm¹

1. *Helmholtz-Zentrum Dresden, Rossendorf, Germany*

2. *Helmholtz-Zentrum Berlin for Materials and Energy, Berlin, Germany*

We have synthesized a new magnetic semiconductor, InMnP, by Mn ion implantation and pulsed laser annealing [1, 2]. Clear ferromagnetic hysteresis loops and a perpendicular magnetic anisotropy are observed up to a Curie temperature of 42 K. Large values of negative magnetoresistance and magnetic circular dichroism as well as anomalous Hall effect are further evidences of a ferromagnetic order in InMnP. An effort is made to understand the transport mechanism in InMnP using the theoretical models. We find that the valence band of InP does not merge with the impurity band of the heavily doped InMnP (8 %). Our results suggest that impurity band conduction is a characteristic of Mn-doped InP and GaP which have deep Mn-acceptor levels.

[1] M. Khalid, et al., Phys. Rev. B 89, 121301(R) (2014)

[2] M. Khalid, et al., J. Appl. Phys. 117, 043906 (2015)

TU.E-P07 - First-principles study of spin-wave dispersion in FeCo alloy system with tetragonal distortion

Y. Kota¹, A. Sakuma²

1. *Fukushima National College of Technology, Fukushima, Japan*

2. *Tohoku University, Sendai, Japan*

Tetragonally distorted FeCo alloys are a strong candidate as novel hard-magnetic material without rare-earth elements. After the giant magnetocrystalline anisotropy of tetragonal FeCo alloys was predicted theoretically, many experimental trials have been performed to realize such a property. In previous studies, however, the Curie temperature of tetragonal FeCo alloys (especially in the disordered phase) was not investigated, though the Curie temperature is an essential property of ferromagnetic materials. Moreover, the stability of the ferromagnetic state in tetragonal FeCo alloys is unclear, whereas the ferromagnetic state in pure-Fe system tends to become unstable by tetragonal distortion. To verify these points, analyzing FeCo system deviated from the ferromagnetic ground state is an important topic. In this work, we study the spin-wave dispersion of tetragonal FeCo alloys to clarify the stability of the ferromagnetic state and the exchange stiffness constant. The electronic structure calculations of tetragonal FeCo alloys with the spin spiral structures are performed by using the tight-binding linear muffin-tin orbital method under the local spin-density approximation. Also the coherent potential approximation is adopted to deal with the substitutional disorder between Fe and Co atoms. The obtained results reveal that the ferromagnetic state is stable in tetragonal FeCo alloys, and that the exchange stiffness constant is about 70% compared with the stiffness constant of cubic FeCo. When the degree of the tetragonal distortion from the bcc structure is increased, the exchange stiffness constant decreases monotonically. Even so the Curie temperature estimated from the stiffness constant of tetragonal FeCo alloys is sufficiently higher than room temperature, and the tetragonal FeCo is utilizable as a hard-magnetic material.

TU.E-P08 - Investigating the metallic and insulating behaviors in NiCo₂O₄ thin films by X-ray absorption spectroscopy

Y.Y. Chin¹, Y. Bitla², J.C. Lin³, N. Chien², R.R. Liu⁴, Y.M. Zhu⁴, H.J. Liu², Q. Zhan⁴, H.J. Lin¹, C.T. Chen¹

1. National Synchrotron Radiation Research Center, Hsinchu, Taiwan

2. Department of Materials Science and Engineering, National Chiao Tung University, Hsinchu, Taiwan

3. Institute of Physics, Academia Sinica, Taipei, Taiwan

4. Department of Material Physics and Chemistry, University of Science and Technology Beijing, Beijing, China

5. Department of Physics, Durham University, Durham, United Kingdom

In the present work, we investigate distinct transport behaviors of NiCo₂O₄ thin films under different growth conditions by use of X-ray absorption spectroscopy and magnetic circular dichroism. Comparing the experimental spectra with the theoretical calculations, the valence and spin states of Co and Ni are determined. We found that the metallic and insulating behaviors in NiCo₂O₄ thin films could be understood by the percolation threshold. Besides, the increase of the resistivity at low temperature in the metallic phase may be linked to the change of the magnetization.

TU.E-P09 - Magnetic and resistivity properties in half-metallic glass-coated Co₂FeSi Heusler microwires

L. Galdun¹, T. Ryba¹, V. Prida², V. Zhukova³, A. Zhukov³, Z. Vargova¹, R. Varga¹

1. *Inst. Phys., Fac. Sci., UPJS, Kosice, Slovakia*

2. *Dpto. De Física, Universidad de Oviedo, Oviedo, Spain*

3. *Dpto. Física de Materiales, Fac. Químicas, UPV/EHU, San Sebastian, Spain*

Co₂-based Full Heusler alloys are one of the most promising materials predicted to exhibit 100% spin polarization at the Fermi energy level (E_F), which renders these alloys suitable candidates for spintronics applications. However the theoretical values of spin polarization for the half-metal Co₂FeSi with the highest Curie temperature (T_C 1100 K) and magnetic moment per unit cell ($m = 6m_B/f.u.$) are much higher as the values determined with point contact Andreev reflection (PCAR) spectroscopy. This phenomenon could be explained through the sensitivity of atomic order in L₂₁ phase, which is crucial for obtaining the spin-polarized material. [1].

One of the few disadvantages of Heusler alloy is their complex production process that usually consists of Arc melting of pure elements followed by long term annealing at high temperature. This process can be reduced by rapid quenching of master alloy that brings more homogeneous sample and no post treatment is necessary [2].

In the given contribution, we present the application of another type of rapid quenching production method using Taylor-Ulitovski technique to produce glass-coated microwire [3]. This method increases the quenching rate by one order (comparing to melt-spinning) and allows production of up to kilometres of the wire from 1g of master alloy. Basic structural and magnetic characterizations are provided. It is shown that due to a high quenching rate it is possible to achieve microwires, with polycrystalline L₂₁ structure and well defined magnetic anisotropy that are especially suitable for spintronics applications.

This work was supported by NanoCEXmat ITMS 26220120035, VEGA 1/0060/13 and APVV-0027-11.

[1] D. Bombor, Ch. Blum, O. Volkonskiy, et al., *Phys. Rev. Lett.* **110**, 066601, (2013)

[2] B. Hernando, J. L. S. Llamazares, J. D. Santos, et al., *Appl. Phys. Lett.* **92**, 042504, (2008)

[3] R. Varga, T. Ryba, Z. Vargova, et al., *Scripta Materialia* **65** (2011), 703

TU.E-P10 - Half-metallic ferromagnetism in Sn-doped perovskite ruthenates: A first-principles study

J. Yu¹, N. Kim¹, R. Kim¹

1. Seoul National University, Seoul, South Korea

The half-metallic ferromagnets are unusual materials which show metallic property in one spin channel and insulating property in the other spin channel. There have been many attempts in searching of new half-metallic materials after the pioneering work on the Mn-based Heusler alloys. Among them, perovskite oxides has attracted some attention as a promising class of materials for half metallic ferromagnets. Here we propose Sn-doped perovskite ruthenates as a new breed of perovskite oxides which can pose a range of properties from ferromagnetic metal to a large gap semiconductor, where a mixture of B-site ions, Ru and Sn, can generate possibly an emerging physical property like half-metallicity for some range of x , where x represents the ratio of Sn substituting Ru. To investigate the electronic and magnetic properties of Sn-doped perovskite ruthenium oxides, we carried out first-principles electronic structure calculations. From the calculation results, we demonstrate that the Sn-doped ruthenium oxides transforms from a ferromagnetic metal for $x < 0.5$ to a ferromagnetic half-metal for $0.5 < x < 0.7$ to an insulator for $x > 0.7$. The formation of half-metallic state in Sn-doped ruthenates evidently originates from the reduced hopping of Ru 4d electrons due to the presence of the substituted Sn elements between Ru atoms. The effect of tilting and rotation of RuO_6 octahedron is still present. But the angle of the octahedron is unchanged with increasing Sn doping and no further noticeable lattice distortion is observed in the fully relaxed lattice structures. We suggest that the realization of half-metallic ferromagnetic state in a perovskite oxide contribute to its possible memory and spintronic device applications.

TU.E-P11 - Effect of hydrogen on magnetic properties of ϵ -Fe₂O₃

D. Hirai^{1,2}, S. Tsuneyuki^{1,2,3}, Y. Gonda^{1,2,4}

1. Department of Physics, The University of Tokyo, Tokyo, Japan

2. Elements Strategy Initiative Center For Magnetic Materials, Tsukuba, Japan

3. Institute For Solid State Physics, The University of Tokyo, Tokyo, Japan

4. Department of Materials Science and Engineering, Tokyo Institute of Technology, Tokyo, Japan

ϵ -Fe₂O₃ has attracted attention for next-generation high-density magnetic recording media and high-frequency electromagnetic wave absorbers, due to its large coercivity [1]. However, this origin remains unelucidated.

In this study, we performed first-principles calculation to understand the magnetic properties. Our calculation is based on density functional theory. First, we show that the pristine ϵ -Fe₂O₃ exhibits zero magnetization in contrast to experiments showing a finite one [1]. To obtain a finite magnetization, we considered the influence of hydrogen on the magnetic properties. It is shown that hydrogen can be naturally included in ϵ -Fe₂O₃ from the discussion of formation energy. As a result of the introduction of hydrogen in the unit cell, we observed the finite spin magnetic moment of 1 μ_B . In addition, we found that the enhancement of magnetocrystalline anisotropy energy (MAE) compared to that of the pristine case. Based on the second-order perturbation scheme on the spin-orbit interaction [2,3], we clarified that this enhancement is originated from only a specific Fe site, which is nearest Fe site from the oxygen site bonding hydrogen. Further, we found that the spin-orbit coupling between occupied $dx^2-y^2\downarrow$ and unoccupied $dxy\downarrow$ of this Fe site is the most important for the MAE enhancement. Our study suggests that the existence of hydrogen plays a significant role on the magnetic properties.

References:

- [1] S. Ohkoshi *et al.*, Bull. Chem. Soc. Jpn. **86**, 897 (2013).
- [2] Z. Torbatian *et al.*, Appl. Phys. Lett. **104**, 242403 (2014).
- [3] D. Hirai *et al.*, to be submitted.

TU.E-P12 - X-ray and visible magnetic circular dichroism spectroscopy of $\text{Pr}_{1-x}\text{Sr}_x\text{MnO}_3$ thin films: Comparative studyA. Rogalev⁴, Y. Samoshkina¹, I. Edelman¹, A. Sokolov¹, K. Ollefs², N. Andreev³, V. Chichkov³

1. Kirensky Institute Of Physics, Krasnoyarsk, Russia
2. European Synchrotron Radiation Facility (ESRF), Grenoble, France
3. National University of Science and Technology 'MISIS', Moscow, Russia
4. European Synchrotron Radiation Facility (ESRF), Grenoble, France

$\text{Pr}_{1-x}\text{Sr}_x\text{MnO}_3$ polycrystalline films with $x = 0.2$ and 0.4 were prepared with the dc magnetron sputtering and investigated by x-ray magnetic circular dichroism (XMCD) at Mn K- and Pr L-edges and also by visible magnetic circular dichroism (MCD). The XANES (x-ray absorption near-edge structure) spectra were measured additionally. General shape of XMCD and XANES spectra at the Mn K-edge for the $\text{Pr}_{1-x}\text{Sr}_x\text{MnO}_3$ films is very similar to that for manganites of other composition presented in literature, in particular for the $\text{La}_{1-y}\text{Ca}_y\text{MnO}_3$. However, in the studied samples an evolution of XANES spectra is not observed when the doping element concentration increases, namely, there is no systematic energy shift and the enhancement of the pre-edge structure intensity at $E \sim 6557$ eV what were characteristic for the above-mentioned manganites. XMCD spectra at Mn K-edge also coincide for the both $\text{Pr}_{1-x}\text{Sr}_x\text{MnO}_3$ films but show the enhancement of dichroic signal with x increasing. Similar behavior is observed for XMCD and XANES spectra at the Pr L-edges. In the case of MCD in visible range, for the films with $x = 0.2$ and 0.4 we have traced the correlation of the MCD peculiarities in different spectral interval not only with the x value but with the conductivity type of samples. Thus, MCD spectroscopy seems to be sensitive method to study the electronic and magnetic structure of $\text{Pr}_{1-x}\text{Sr}_x\text{MnO}_3$. The observed MCD features were associated with the different ratios $\text{Mn}^{3+}/\text{Mn}^{4+}$ in the films and also with the presence of free charge carriers in the samples and explained in terms of electronic transitions. The behavior of XMCD and XANES spectra for $\text{Pr}_{1-x}\text{Sr}_x\text{MnO}_3$ films needs additional research.

The work was supported partly by RFBR, grant ¹14-02-01211, and Grant of President of Russian Federation No.NSh-2886.2014.2.

TU.E-P13 - Electronic structure and magnetic properties of $(\text{LaMnO}_3)_m/(\text{SrTiO}_3)_n$ Superlattices

A. Aezami¹, M. Reza Abolhassani², M. Elahi², M. Niayfar¹

1. *Department of physics, Science and Research Branch, Islamic Azad university, Ahwaz, Iran*

2. *Department of physics, Science and Research Branch, Islamic Azad University, Tehran, Iran*

We study the magnetic structure and Curie temperature of the $(\text{LaMnO}_3)_m/(\text{SrTiO}_3)_n$ superlattices (SL m - n) with $m=1, 2, 3$ and $n=1, 2, 3, 8$ based on density functional calculations using Quantum-Espresso open source code. We find that the electronic and magnetic structure changes with the thickness of the layer, which is in agreement with experimental results. The leakage of the Mn eg electrons from the LaMnO_3 side to the SrTiO_3 side show different magnetic structures. This in turn affects the interfacial magnetism via the superexchange interaction. Using Stoner model for all of these superlattices before and after adding U term on the Ti atoms, we have found that magnetic order of interfacial atoms of these superlattices changes to ferromagnetic by implying $U=5$ eV on the Ti atoms. The inclusion of electron-electron correlation with $U=5$ eV on the Ti atoms for all of the superlattices makes the 2DEG formed at the interface half-metallic. We found that the values of Curie temperature obtained (by mean field approximation) with $U=5$ eV on the Ti atoms are in good agreement with the experimental results.

TU.E-P14 - Quantum interference of surface-induced Friedel oscillations enhanced by Fermi-surface nesting in layered manganitesR. Yamamura¹, T. Hotta¹*1. Department Of Physics, Tokyo Metropolitan University, Hachioji, Japan*

In recent decades, some manganites have been focused as important materials for the cathodes in Li-ion batteries and catalysts in photosynthesis. Manganites work as cathodes and catalysts by the valence change mainly from Mn^{4+} to Mn^{3+} in the process of chemical reaction. Since such a reaction occurs on the surface of manganites, to achieve high efficiency as these materials, it is desirable to obtain the situation with Mn^{4+} ions on the surface and Mn^{3+} in the bulk. We can naively expect to realize this situation in metallic materials, but it is still unclear what microscopic mechanisms cause such valence imbalance of manganese ions between surface and bulk. To clarify this point, we have investigated imbalance of Mn^{3+} and Mn^{4+} ions between surface and bulk in layered manganites on the basis of an orbital degenerate double-exchange model with surfaces for several types of t_{2g} spin structures. First we confirm that the number of Mn^{4+} ions on the surface is larger than that in the bulk, explained by the surface-induced Friedel oscillation. The wavevector of Friedel oscillation is closely related with nesting vector along the direction of oscillation. Thus, when two Fermi-surface curves exist, we observe two Friedel oscillations with the wavevectors equal to the nesting vectors. In particular, when two nesting vectors possess similar values, quantum beat phenomena appear due to the interference between two Friedel oscillations and the number of Mn^{4+} ions is actually increased on the surface. Furthermore, we report the appearance of the arrangement of x^2-y^2 orbital on the surface in the three-dimensional ferromagnetic state.

A part of this presentation will be submitted as an original paper to Journal of the Physical Society of Japan and will be also presented at the meetings of the Physical Society of Japan.

TU.E-P15 - First-principles study for the chiral magnet $\text{Cr}(\text{NbS}_2)_3$ T. Shishidou¹*1. ADSM, Hiroshima University, Hiroshima-shi, Japan*

In the layered intercalated compound $\text{Cr}(\text{NbS}_2)_3$, Cr atoms order in the $\sqrt{3} \times \sqrt{3}$ superlattice and the arrangement of S atoms, octahedrally coordinating to Cr's, takes on chirality along c axis. In accord with the chiral crystal structure, Cr local moments ($S=3/2$) show long-period chiral magnetic structure ($L=48\text{nm}$). Furthermore, it is theoretically predicted that the chiral spin soliton lattice would emerge by applying a small magnetic field perpendicular to the c axis, and is actually proved experimentally. An anomaly in electrical conductivity is also observed, which shows clear dependency on the magnetic soliton density and makes this material attractive. It is widely believed that the neighboring spin interaction is ferromagnetic and competes with the Dzyaloshinsky-Moriya interaction, leading to the chiral magnetic order. However there has been no ab initio study, which discusses the electronic structure in detail and estimates the various magnetic interactions. In this study, aiming at discussing the crystal structure, the fundamental electronic structure, and the magneto crystalline anisotropy (MCA) of $\text{Cr}(\text{NbS}_2)_3$, we carry out density-functional theory calculations based on the all-electron FLAPW method. Since the magnetic chiral period is very long, we can approximately use a collinear ferromagnetic alignment for the present purpose. After the full structural relaxation, the S atoms exhibit the chiral arrangement accounting for the experiment. The Cr t_{2g} majority-spin states are believed to be well localized to form $S=3/2$. However, our study shows that the a_{1g} orbital of the t_{2g} manifold hybridizes strongly with Nb 4d states and bears an itinerant character. This orbital is considered to have some role on the Cr-Cr magnetic interaction and also to couple magnetically with conducting states. MCA is evaluated to be easy-plane type, being in agreement with experiment.

TU.E-P16 - Anomalous oxidation state of iron in two-leg ladder compound $Ba_6Fe_8S_{15}$

H. Aruga Katori¹, T. Adachi¹, H. Ohta¹, S. Nakamura^{2,3}, A. Fuwa⁴

1. Institute Of Engineering, Tokyo University Of Agriculture And Technology, Tokyo, Japan
2. Department of Science and Engineering, Teikyo University, Itabashi, Japan
3. Advanced Research Institute of Science and Engineering, Waseda University, Tokyo, Japan
4. Faculty of Science and Engineering, Waseda University, Tokyo, Japan

$Ba_6Fe_8S_{15}$ shows a tetragonal structure (space group $I4/m$), in which FeS_4 tetrahedra construct Fe_4S_{10} clusters. Infinite columns of the tetrahedrally coordinated irons in this cluster can be viewed as one-dimensional twisted two-leg ladders. There is only one crystallographic iron site in $Ba_6Fe_8S_{15}$, suggesting that the charge is delocalized and iron ion has an average valence of +2.25.

To clarify the oxidation state of iron and magnetism, we synthesized $Ba_6Fe_8S_{15}$ and performed the magnetization and Mössbauer spectroscopy measurements. Magnetization measurements were carried out using a vibrating sample magnetometer in the temperature range between 1.5 K and 300 K in fields up to 12 T. ^{57}Fe Mössbauer spectra were measured in conventional transmission geometry in the temperature range between 4.2 K and 300 K. The temperature dependence of magnetization observed in high temperature region shows a similar behavior to that of one-dimensional antiferromagnetic chain system. The Mössbauer spectra above 120 K indicate the existence of only a single quadrupole doublet, which is consistent with the evidence of one crystallographic Fe site. Below 110 K, however, we observed the spectra characterized by two kinds of magnetic hyperfine patterns, indicating an existence of complicated magnetic order. These spectra cannot be explained if the mixed valence state of Fe^{2+} and Fe^{3+} is realized. By analyzing Mössbauer spectra in detail, we discuss the oxidation state of iron including possibility of a structural phase transition and an electric charge ordering.

TU.E-P17 - Metal-Insulator Transition driven by all-in/all-out magnetic ordering in $\text{Cd}_2\text{Os}_2\text{O}_7$

C.H. Sohn¹, H.G. Jeong¹, H.S. Jin¹, J. Yamaura², S.Y. Kim¹, L.J. Sandilands¹, H.J. Park¹, K.W. Kim³, S.J. Moon⁴, D.Y. Cho⁵

1. *Center for Correlated Electron Systems, Institute for Basic Science, Seoul National University, Seoul, Korea*
2. *MCES, Tokyo Institute of Technology, Kanagawa, Japan*
3. *Department of Physics, Chungbuk University, Cheong-ju, Chungbuk, Korea*
4. *Department of Physics, Hanyang University, Seoul, Korea*
5. *Department of Physics, Chonbuk National University, Jeonju, Korea*
6. *ISSP, University of Tokyo, Kashiwa, Japan*

We investigate the metal-insulator transition driven by all-in/all-out (AIO antiferromagnetic ordering in 5d pyrochlores $\text{Cd}_2\text{Os}_2\text{O}_7$ using optical spectroscopy and first-principle calculations. The temperature dependence in band gap and free carrier density clearly reveals hidden sequential phase transitions, from paramagnetic metal to AIO metal to AIO insulator. The accompanied spectral weight transfer and first-principle calculations further show that the origin of such phase transitions is Lifshitz transition induced by AIO ordering. Our result clearly demonstrates how AIO ordering leads the metal-insulator transition in 5d pyrochlores and lays a groundwork for searching exotic phenomena including Weyl semimetal and quantum critical behaviors.

TU.E-P18 - Fabrication of epitaxial Mn₂CoAl films for spintronic applications using spin-gapless semiconductorsK. Ueda¹, S. Hirose¹, M. Nishiwaki¹, T. Hajiri¹, H. Asano¹*1. Nagoya University, Nagoya, Japan*

Spin-gapless semiconductors (SGS) are magnetic semiconductors with zero-gap and half-metallic characters simultaneously due to their special band structures, and they have high potential for fabricating novel spintronic devices. An inverse Heusler compound, Mn₂CoAl, is one of promising candidates for SGS because SGS-like transport properties (temperature-independent conductivity, linear MR, etc.) have already been reported for bulk Mn₂CoAl. Preparation of SGS in film form is necessary to fabricate devices. However, there are only several reports on the growth of Mn₂CoAl films, which have room for improvement. In this study, we have tried fabricating high-quality Mn₂CoAl films for spintronic applications using SGS.

Mn₂CoAl films were formed by ion-beam assisted sputtering (IBAS), which is effective to obtain Heusler films at lower growth temperature [1]. XRD measurements revealed epitaxial Mn₂CoAl films (Mn₂CoAl (001)[110]// MgAl₂O₄ (001)[100]) can be formed on MgAl₂O₄ substrates at the growth temperature (T_g) of 300~600°C. These films showed ferromagnetic hysteresis at room temperature. The c-axis lattice constant and saturation magnetization (M_s) increased as T_g decreased and they became 0.5792 nm and ~240 emu/cc with H_c of ~70 Oe for T_g= 300°C, which are comparable to those for bulk Mn₂CoAl (c= 0.5798 nm; M_s: ~350 emu/cc, H_c: ~100 Oe). One of possible reasons for smaller c-axis and M_s is interfacial reaction/diffusion between Mn₂CoAl and MgAl₂O₄ at higher T_g. The films showed semiconducting behaviors with very small activation energy of ~3 meV and relatively small resistivity of ~700 μΩcm for semiconductors, which agree well with zero band-gap features of SGS. The electron concentration and mobility deduced from Hall resistivity measurements (ρ_{xy}) is ~7*10²⁰ cm⁻³ and ~12 cm²/Vs at 4 K, which were comparable to reported values for Mn₂CoAl films. These results indicate high-quality Mn₂CoAl films can be obtained on MgAl₂O₄ by IBAS.

Reference:

[1] K. Ueda et al., Appl. Phys. Lett. 103 (2013) 052408

TU.E-P19 - Semiconducting behaviour of $\text{Ce}_3\text{Cu}_3\text{Sb}_4$ revisitedL. Kalinowski¹, P. Witas¹, M. Fijałkowski¹, J. Goraus¹, A. Ćelebarski¹*1. Institute of Physics, University Of Silesia, Katowice, Poland*

The recent complex investigations have shown $\text{Ce}_3\text{Cu}_3\text{Sb}_4$ as a ferromagnetic semiconductor [1,2] and a good material for thermoelectric applications [3,4]. The semiconducting properties of $\text{Ce}_3\text{Cu}_3\text{Sb}_4$ were, however, questioned [5] and activated behavior in resistivity was attributed to magnetic polaron effect. Our ab-initio calculations predict for this compound a broad energy gap located near the Fermi energy EF, which prefers the semimetallic character of $\text{Ce}_3\text{Cu}_3\text{Sb}_4$ and strong gradient of the density of states (DOS) at EF. The presence of the pseudogap near the Fermi level is fully supported by the resistivity vs. temperature experiment, which exhibits the activated behavior, while the gradient in DOS can enhance the thermoelectric properties of this material. Basing on the fully relativistic FPLO calculations we also investigated the band structure of the $\text{Ce}_3\text{Cu}_{3-x}\text{Ni}_x\text{Sb}_4$ alloys which did not show the significant change of the energy gap with alloying. However, thermopower of the $\text{Ce}_3\text{Cu}_{3-x}\text{Ni}_x\text{Sb}_4$ is strongly reduced. We interpret this effect as result of the change of DOS at the Fermi level. To evidence the effect, we also investigated the magnetic, electric transport, thermoelectric properties and Hall effect for $\text{Ce}_3\text{Cu}_{3-x}\text{Ni}_x\text{Sb}_4$.

References:

- 1] R. V. Skolozdra et al, Inorg. Mater. 29 (1993) 26
- 2] S. Patil et al., Solid State Commun. 99 (1996) 419
- 3] K. Fess et al. J. Appl. Phys. 83 (1998) 2568
- 4] C. D. Jones et al. Phys. Rev. B 60 (1999) 9518
- 5] P. Wachter et al. Phys. Rev. B 60 (1999) 9518

TU.E-P20 - De Haas-van Alphen effect and Fermi surface properties in ferromagnet LaCo₂P₂ and related compounds

A. Teruya¹, A. Nakamura¹, T. Takeuchi², F. Honda³, D. Aoki³, K. Matsubayashi⁴, Y. Uwatoko⁴, H. Harima⁵, K. Uchima⁶, M. Hedo⁷

1. Graduate School of Engineering and Science, University of the Ryukyus, Nishihara, Japan
Japan

2. Low Temperature Center, Osaka University, Osaka, Japan

3. Institute for Materials Research, Tohoku University, Sendai, Japan

4. Institute for Solid State Physics, University of Tokyo, Tokyo, Japan

5. Graduate School of Science, Kobe University, Kobe, Japan

6. General Education, Okinawa Christian Junior College, Nishihara, Japan

7. Faculty of Science, University of the Ryukyus, Nishihara, Japan, Japan

We grew high-quality single crystals of LaCo₂P₂ with the ThCr₂Si₂-type tetragonal structure by the Sn-flux method, and measured the electrical resistivity, specific heat, magnetic susceptibility, magnetization, and de Haas-van Alphen (dHvA) effect for a ferromagnet LaCo₂P₂, together with related compounds SrCo₂P₂ and EuCo₂P₂. An as-grown sample of LaCo₂P₂ is of a thin plate with the tetragonal (001) plane. The typical size is 2×2×0.5 mm³. The residual resistivity r_0 and residual resistivity ratio RRR are $r_0=1.17$ mWcm and RRR=69, respectively, indicating a high-quality sample. From the results of magnetic susceptibility and magnetization measurements, LaCo₂P₂ is a ferromagnet with a Curie temperature $T_C=130$ K and a saturated moment of 0.4 m_B/Co. Note that a magnetic easy-axis corresponds to the [100] direction. When the magnetic field is applied along a hard-axis of the tetragonal [001] direction, magnetization reaches the saturated moment in magnetic fields larger than 50 kOe. These experimental results are consistent with the previous report [1]. We thus carried out the dHvA experiment in magnetic fields ranging from 50 to 150 kOe. Main dHvA branches possess the dHvA frequencies $F=(2-7) \times 10^7$ Oe, where the dHvA frequency $F (=c\hbar S_F/2pe)$ is proportional to the maximum or minimum cross-sectional area of the Fermi surface S_F , which is shown as a unit of magnetic field. The corresponding cyclotron effective masses are (2-3) m_0 (m_0 : rest mass of an electron). The present relatively large cyclotron masses are due to the magnetic correlation of Co-3d electron, which are compared with much larger cyclotron masses of (3-7) m_0 for a nearly ferromagnet SrCo₂P₂ [2]. The strong correlation is realized in SrCo₂P₂.

[1] M. Reehuis et al., J. Magn. Magn. Mater. **138**, 85 (1994)

[2] A Teruya et al., J. Phys. Soc. Jpn. **83**, 113702 (2014)

TU.E-P21 - Spin stiffness constant of half-metallic ferrimagnet in Mn-based Heusler alloysR. Umetsu^{1,2}, T. Kanomata³

1. Tohoku University, Sendai, Japan

2. JST-PRESTO, Tokyo, Japan

3. Tohoku Gakuin University, Sendai, Japan

Mn-based Heusler alloys with half-metallic electronic structure have a potential candidate for the spintronics devices. Recently, many kinds of Mn-based Heusler alloys have been predicted as showing half-metallic electronic states from the first principle calculations [1,2]. In our experimental studies, some Mn-based Heusler alloys with high phase stability were suggested and their physical properties have been investigated. The spin stiffness constant, D , indicates thermal stability of the exchange interaction and such the excitation of the spin will relate to the performance of the devices. In the present study, we evaluated the value of D for Mn-based Heusler alloys and discuss the obtained values comparing with that for various Co-based Heusler alloys [3]. Polycrystalline specimens of Mn_2VAl and Mn_2CoGa were prepared by arc-melting or induction melting. After the identifications of the composition, microstructure and crystal structure, magnetic measurements were performed with a SQUID magnetometer up to 5 T and a vibrating sample magnetometer. The spontaneous magnetization was confirmed from the Arrott plot at each measured temperature. The Curie temperature, T_C , of Mn_2VAl , $Mn_{50}V_{20}Al_{30}$ and Mn_2CoGa were 768, 754 and 741 K, respectively. The value of D was evaluated from the temperature, T , dependence of the spontaneous magnetization in each specimen below 150 K, where linear dependence of $T^{3/2}$ was observed. The D values for these materials were obtained to be '5.2 - 5.4' meV-(nm)² and significantly larger than that for Co-based Heusler alloys (Co_2FeAl ; 4.7, Co_2MnSi ; 3.5, Co_2MnGa ; 2.4 meV-(nm)²) [3]. The strong exchange interaction would be the reason that the Mn-based Heusler alloys indicate high T_C even though they have not so large total magnetic moment.

References:

- [1] S. Ishida et al., J. Phys. Soc. Jpn. 53 (1984) 2718
- [2] R. Weht and W.E. Pickett, Phys. Rev. 60 (1999) 13006
- [3] R.Y. Umetsu, et al., IEEE Trans. Mag. 47 (2011) 2451

TU.E-P22 - Magnetic properties of the kondo insulator CeRu₄Sn₆

A. Sidorenko¹, H. Winkler¹, A. Prokofiev¹, S. Paschen¹

1. Institute of Solid State Physics, Vienna University of Technology, Austria

Kondo insulators (KIs) continue to attract attention as less explored relatives of the heavy fermion metals. CeRu₄Sn₆ is one of the rare examples of a KI with tetragonal crystal structure. Indications for a narrow gap formation somewhat below 100 K have been provided early on by electrical resistivity measurements on polycrystalline samples [1]. Electrical resistivity [2] and optical conductivity measurements [3] on a single crystals revealed a strong anisotropy, indicating the development of an anisotropic energy pseudogap. Here we present our magnetic property investigation of single crystalline CeRu₄Sn₆. The magnetic susceptibility as well as magnetic isotherms were studied in wide ranges of temperature (300 mK - 1000 K) and magnetic field applied along the principle crystallographic axes. It is discussed to which extent the results can be understood within the framework of a simple crystal electric field approach.

This work was supported by the European Research Council (ERC Advanced Researcher Grant 227378) and the U.S. Army Research office (grant W911NF-14-1-0496).

[1] I. Das and E. V. Sampathkumaran, Phys. Rev. B 46, 4250 (1992)

[2] H. Winkler, K.-A. Lorenzer, A. Prokofiev, and S. Paschen, J. Phys.: Conf. Series 391, (2012) 012077

[3] V. Guritanu, P. Wissgott, T. Weig, H. Winkler, J. Sichelschmidt, M. Scheffler, A. Prokofiev, S. Kimura, T. Iizuka, A. M. Strydom, M. Dressel, F. Steglich, K. Held, and S. Paschen, Phys. Rev. B 87, (2013) 115129

TU.E-P23 - Curie temperature within the electronic correlation formalism in double perovskites systems

O. Navarro¹, F. Estrada¹, M. Avignon²

1. *Instituto de Investigaciones en Materiales, UNAM, Mexico D.F., Mexico*

2. *Institut Néel, CNRS and Université Joseph Fourier, Grenoble, France*

The half-metallic ferromagnetic double perovskite Fe-Mo based compound is considered as an important material in view of its potential spintronic applications due to its high Curie temperature $T_C=420\text{K}$, complete spin polarization and substantial low-field magnetoresistance at room temperature [1]. So, It is fundamental to understand the role of electronic parameters controlling the half-metallic ground state and high Curie temperature in this system. In this work we present an electronic approach to study the Curie temperature behavior in double perovskites systems, this approach is based on a correlated electron picture with localized Fe-spins and conduction Mo-electrons interacting with the local spins via a double-exchange-type mechanism [2]. The Curie temperature behavior shows an enhancement with the on-site Hubbard electronic interaction.

Acknowledgements: This work has been partially supported by PAPIIT IN100313 from UNAM.

References:

[1] KI Kobayashi, T Kimura, H Sawada, K Terakura, Y Tokura, *Nature* 395 (1998) 677

[2] JR Suárez, F Estrada, O Navarro, M Avignon, *Eur. Phys. J. B* 84 (2011) 53-58

TU.E-P24 - Half-metallic properties of (001) surfaces of quaternary Heusler alloys CoFeCrZ (Z=Al and Ga): A first-principles studyJ.I. Lee¹, B. Bialek¹, D.C. KIm²1. *Inha University, Incheon, South Korea*2. *Halla University, Wonju-si, South Korea*

Half-metallic ferromagnets, which are characterized by complete spin polarization at the Fermi level, are perfect candidates for spintronic applications as sources of spin-polarized charge injection. Since the NiMnSb with half-Heusler structure was predicted to be a half-metal [1], various kinds of half metallic materials, such as ferrite, chromium oxide, manganese, transition metal pnictides, and chalcogenides were found. Heusler and half-Heusler structured half-metals have attracted much attention for the spintronics application, since their structures are compatible with the usual, zinc-blende structured, semiconductors. Recently, a first-principles study led to a prediction that quaternary Heusler compounds, CoFeCrZ (Z=Al, Ga) are excellent half-metallic ferromagnets [2]. In this study, we investigate the electronic and the magnetic properties at the (001) surfaces of CoFeCrAl and CoFeCrGa by means of the full-potential linearized augmented plane wave (FLAPW) method [3] within general gradient approximation [4]. We considered two types of surface termination: CoFe-terminated and CrZ-terminated surfaces, Z being either Al or Si. From the calculated total magnetic moments and the local density of states, we found that half-metallicity is preserved only the CrAl-terminated surface of the CoFeCrAl. The CrSi- and CoFe-terminated surfaces are almost half-metallic. The magnetic moment of the Cr atom at the CrAl(001) surface of CoFeCrAl is 2.98 bohr magneton, almost twice the bulk value. The magnetic moment of Co atom at the FeCo-terminated surface of CrFeCoAl is increased compared to the bulk value, while the magnetic moment of the Fe atom decreases to nearly zero from reported 1.63 bohr magneton bulk-like value [2].

References:

- [1] R. A. de Groot, F. M. Mueller, P. G. van Engen, K. H. J. Buschov, Phys. Rev. Lett. 50 (1983) 2024
- [2] G. Y. Gao, L. Hu, K. L. Yao, B. Luo, and N. Liu, J. Alloy. Compd 551 (2013) 539
- [3] E. Wimmer, H. Krakauer, M. Weinert, and A. J. Freeman, Phys. Rev. B 24 (1981) 864
- [4] J. P. Perdew, K. Burke and M. Ernzerhof, Phys. Rev. Lett. 77 (1996) 3865

TU.E-P25 - Magnetic exchange interaction between A'-site transition-metal ions in A-site-ordered perovskites

M. Toyoda^{1,2}, K. Yamauchi¹, T. Oguchi^{1,2}

1. *Institute Of Science And Industrial Research, Osaka University, Osaka, Japan*

2. *Japan Science and Technology Agency*

The magnetic exchange interaction has been studied in the A-site-ordered perovskite-structure oxides $AA'B_4O_{12}$ by using ab initio electronic structure calculations. These oxides are of special interest because they can contain magnetic transition-metal ions at a part of the A sites as well as at the B sites. In general, the A sites in perovskite-related structures are occupied by cations with larger ionic radii such as strontium and lanthanum. However, in this particular structure, octahedral rotation and tilting around B sites change the local oxygen coordination around 3/4 of the A sites (called A' sites) to an almost square-planar coordination. The spins at the A' sites interact with each other in a different manner than the B-site spins. In order to understand the magnetic exchange interaction between the A'-site spins, Heisenberg-type exchange coupling constants J are calculated for several compounds, such as $CaCu_3Ge_4O_{12}$, $CaCu_3Sn_4O_{12}$, $CaCu_3Ti_4O_{12}$, $YMn_3Al_4O_{12}$, and $LaMn_3V_4O_{12}$. It is found that the magnetic exchange interaction is comprehensively explained by super-exchange mechanism, the sign of which depends on the electronic configuration of the A'-site transition-metal ions.

TU.E-P26 - Spin gapless ferrimagnetism induced by triangular frustration in (111)-oriented FeX/GaX (X = N, P, and As) superlattices

M. Nakao¹

1. Department Of Precision Engineering, Tokai University, Toyko, Japan

We investigate the electronic and magnetic properties of iron pnictide monolayers in tetrahedrally coordinated FeX/GaX (X = N, P, and As) superlattices with (111) orientation to explore for spin gapless semiconductors, in which both electrons and holes can be fully spin polarized. Using density functional calculations, we find that the quasi-two-dimensional FeX monolayers embedded in compound semiconductors are always geometrically frustrated antiferromagnets regardless of their stacking sequence and separation. Here we treat the exchange-correlation functional within the spin-polarized generalized gradient approximation plus Hubbard U method to account for electron correlation; turning on an appropriate on-site Coulomb repulsion U leads the system to a spin gapless semiconducting state. There is a narrow gap between the conduction and valence bands for both the majority and minority spins, while there is no gap between the majority spin state in the valence band top and the minority spin state in the conduction band bottom. Among possible collinear spin arrangements, the magnetic ground state is a four-sublattice structure with an up-up-down-down (UUDD) configuration. Competing ferrimagnetic UUD three-sublattice and UUDD five-sublattice structures lie close in energy. Upon either electron doping or applying a magnetic field, the quasi-2D FX monolayers will exhibit spin gapless ferrimagnetism. We suggest that artificially synthesized frustrated systems are favorable candidates for a new class of spintronic materials.

TU.E-P27 - Electronic structure and magnetic properties of $(\text{LaMnO}_3)_m/(\text{SrTiO}_3)_n$ superlattices

A. Aezami¹, M. Reza Abolhassani², M. Elahi², M. Niyafar¹

1. *Science And Research Branch, Islamic Azad University, Ahwaz, Iran*

2. *Department of physics, Science and Research Branch, Islamic Azad University, Tehran, Iran*

We study the magnetic structure and Curie temperature of the $(\text{LaMnO}_3)_m/(\text{SrTiO}_3)_n$ superlattices (SL m - n) with $m=1, 2, 3$ and $n=1, 2, 3, 8$ based on density functional calculations using Quantum-Espresso open source code. We find that the electronic and magnetic structure changes with the thickness of the layer, which is in agreement with experimental results. The leakage of the Mn eg electrons from the LaMnO_3 side to the SrTiO_3 side show different magnetic structures. This in turn affects the interfacial magnetism via the superexchange interaction. Using Stoner model for all of these superlattices before and after adding U term on the Ti atoms, we have found that magnetic order of interfacial atoms of these superlattices changes to ferromagnetic by implying $U=5$ eV on the Ti atoms. The inclusion of electron-electron correlation with $U=5$ eV on the Ti atoms for all of the superlattices makes the 2DEG formed at the interface half-metallic. We found that the values of Curie temperature obtained (by mean field approximation) with $U=5$ eV on the Ti atoms are in good agreement with the experimental results.

TU.E-P28 - Chemical disorder and enhanced Curie temperature of $\text{Co}_{2-x}\text{Fe}_{1+x}\text{Si}$ Heusler alloys

J. Karel¹, J. Fischer¹, P. Adler¹, L. Wollmann¹, S. Fabbri², G. Fecher¹, F. Albertini², C. Felser¹

1. Max Planck Institute For Chemical Physics Of Solids, Dresden Germany

2. Institute of Materials for Electronics and Magnetism, Parma, Italy

Co_2 -based Heusler compounds are one of the most promising classes of materials for high performance spintronic devices, owing in part to their very high spin polarization; many of these compounds are theoretically predicted to be half-metallic ferromagnets, which exhibit 100% spin polarization at the Fermi energy. In this work, the magnetic and structural properties including the Curie temperature (TC) were investigated for a series of bulk $\text{Co}_{2-x}\text{Fe}_{1+x}\text{Si}$ ($0 < x < 1$) Heusler alloys. Co_2FeSi has the highest TC reported for a Heusler alloy, but we found an enhanced TC (14K greater than Co_2FeSi) for the middle composition ($x=0.4$) of the series. We will show that this increase seems to be connected to the local atomic Fe environments, which were probed using Mössbauer spectrometry. Namely, we find two different magnetic hyperfine fields corresponding to Fe in two different positions in the lattice. An occupancy change (Fe-Co disorder) on one of these positions leads to an enhanced hyperfine field for Fe in the other position, which scales with TC. Moreover, a very small change in lattice constants also follows the same trend in TC.

The valence electron concentration (N_v) is varied across this series; as N_v increases (x decreases), the local magnetic moment carried by Co also increases. These findings are supported by theoretical calculations of the local atomic moments and the exchange parameter.

TU.E-P29 - Magnetic structure of $\text{Hf}_{0.825}\text{Ta}_{0.175}\text{Fe}_2$ itinerant-electron system as probed by neutron diffraction under high pressureL.V.B. Diop^{1,2}, O. Isnard^{1,2}

1. Univ. Grenoble Alpes, Inst. Néel, Grenoble, France
2. CNRS, Inst. Néel, Grenoble, France

Laves phase compounds of $\text{Hf}_{1-x}\text{Ta}_x\text{Fe}_2$ are known as itinerant-electron magnets and have attracted a lot of attention due to their unusual magnetic and electronic properties and their potential applications in giant magnetoresistance and magnetic refrigeration. The pseudobinary system $\text{Hf}_{1-x}\text{Ta}_x\text{Fe}_2$ crystallizes in the hexagonal MgZn_2 -type structure (space group P63/mmc) in which the Fe atoms are located on two inequivalent crystal sites (2a and 6h) with the Hf/Ta atoms occupying the 4f site. Despite the enormous current interest in the $\text{Hf}_{1-x}\text{Ta}_x\text{Fe}_2$ compounds, there appear to have been no direct measurements of the magnetic structure in this series of compounds. The magnetic structures of these intriguing compounds remain unknown. We report here a detailed neutron powder diffraction study for a chosen composition $\text{Hf}_{0.825}\text{Ta}_{0.175}\text{Fe}_2$ as a function of both temperature and pressure. As main results, $\text{Hf}_{0.825}\text{Ta}_{0.175}\text{Fe}_2$ exhibits a temperature-induced first-order transition at 200 K from the ferromagnetic (FM) to the antiferromagnetic (AFM) state upon heating. In the FM state at 1.5 K the Fe-6h atoms have a magnetic moment of 1.48 μB and those Fe-2a a magnetic moment slightly lower 1.41 μB . On the other hand in the AFM state, the antiferromagnetic arrangement is only due to the Fe-6h atoms which carry a moment of 0.51 μB : they are ferromagnetically coupled within a given (001) layer and antiferromagnetically between successive layers along the c-axis, while the Fe-2a atoms do not carry any ordered magnetic moment. A remarkable spontaneous volume magnetostriction of $\Delta V/V = 0.88\%$ is observed at the FM-AFM transition. The application of hydrostatic pressure suppresses the low temperature FM ground state. It completely vanishes under pressures higher than 7.5 kbar, that corresponds to the decrease of volume of only 0.43%. The ferromagnetic order gets substituted by a new antiferromagnetic order under pressure.

TU.E-P30 - Spectral signatures of thermal spin disorder and excess Mn in half-metallic NiMnSb

K. Belashchenko¹, J. Weerasinghe¹, S. Mu¹, B. Pujari¹

1. University of Nebraska-Lincoln, Lincoln, Nebraska, United States

Effects of thermal spin disorder and excess Mn on the electronic spectrum of half-metallic NiMnSb are studied using first-principles calculations [1]. Temperature-dependent spin disorder, introduced within the vector disordered local moment model, causes the valence band at the Γ point to broaden and shift upwards, crossing the Fermi level and thereby closing the half-metallic gap above room temperature. The spectroscopic signatures of excess Mn on the Ni, Sb, and empty sites (Mn_{Ni} , Mn_{Sb} , and Mn_E) are analyzed. Mn_{Ni} is spectroscopically invisible. The relatively weak coupling of Mn_{Sb} and Mn_E spins to the host strongly deviates from the Heisenberg model, and the spin of Mn_E is canted in the ground state. While the half-metallic gap is preserved in the collinear ground state of Mn_{Sb} , thermal spin disorder of the weakly coupled Mn_{Sb} spins destroys it at low temperatures. This property of Mn_{Sb} may be the source of the observed low-temperature transport anomalies in NiMnSb.

Reference:

[1] K. D. Belashchenko, J. Weerasinghe, S. Mu, and B. S. Pujari, arXiv:1501.00969

TU.E-P31 - ESR study of heavily Na-doped low-silica X zeolite near the insulator-to-metal transitionT. Nakano¹, K. Mukai¹, S. Hayashi¹, Y. Nozue¹*1. Department of Physics, Osaka University, Osaka, Japan*

In low-silica X (LSX) zeolite, b-cages with an inner diameter of 0.7 nm and supercages (cavities) with that of 1.3 nm are arrayed in a double diamond structure. The chemical formula of Na-form LSX is given by $\text{Na}_{12}\text{Al}_{12}\text{Si}_{12}\text{O}_{48}$ per supercage (or b-cage). Cationic Na clusters can be generated in both cages by the loading of guest Na atoms. Non-magnetic insulating states have been observed up to high loading density of $n \sim 11$, where n indicates the number of guest Na atoms (or s-electrons) per supercage [1,2]. It has been proposed that the strong electron-phonon coupling of Na atoms stabilizes small multiple bipolarons, and the insulating state is realized in spite of such a heavy doping [2]. However, a sudden metallic transition occurs at $n > 12$, which is explained by a formation of mobile large polarons [2,3]. In the present work, we performed ESR experiments in order to examine the spin susceptibility c_{spin} near the insulator-to-metal transition. We precisely evaluated the absolute values of c_{spin} by analyzing the ESR intensity as well as the DC magnetization. In a metallic sample with the highest loading density, $n = 16.7$, a temperature-independent component is clearly observed. From the obtained value, $\sim 3 \times 10^{-7} \text{ emu/cm}^3$, the number of carriers can be estimated to be ~ 5 electrons per supercage if we assume the component originates from Pauli paramagnetism of free electrons. The sample at $n = 11.3$ shows an insulating behavior in the electrical resistivity. However, c_{spin} is found to contain the temperature-independent component with $\sim 1 \times 10^{-7} \text{ emu/cm}^3$, indicating a finite density of state at the Fermi level. These results indicate that it is necessary to take into account not only the polaron effect but also the weak localization in order to understand the mechanism of insulator-to-metal transition in this system.

References:

- [1] T. Nakano et al., J. Phys. Chem. Solids 71, 650 (2010)
- [2] Y. Nozue et al., J. Phys. Chem. Solids 73, 1538 (2012)
- [3] M. Igarashi et al., Phys. Rev. B 87, 075138 (2013)

TU.E-P33 - Pressure induced insulator to metal transition in neutral radical FBBO

D. Tian¹, S. Julian¹, S. Winter², A. Mailman², R. Oakley²

1. *Department of Physics, University Of Toronto, Toronto, Ontario, Canada*

2. *Department of Chemistry, University of Waterloo, Waterloo, Ontario, Canada*

Though first proposed by Haddon more than 40 years ago[1], a metallic half-filled neutral organic radical has yet to be realized, primarily due to the difficulties to overcome the large Coulomb barrier and narrow electronic bandwidth inherent in this kind of compound. The layered fluoro-substituted oxobenzene-bridged bisdithiazolyl, or FBBO, recently showed to exhibit a number of encouraging properties and has been identified as a promising candidate [2]. Though its conductivity remains activated under ambient conditions, FBBO was found to have a small Mott-Hubbard gap that can be closed at 3GPa [2], according to previous room temperature infrared absorption and transport experiments. In this report, we present further investigations of the conductive behaviors of FBBO under various pressures at low temperatures, by the means of four probe transport experiments in a diamond anvil cell. At 6.2GPa the sample exhibited a positive resistance/temperature profile and a room temperature resistance three orders of magnitude smaller than the first pressure at 2.6GPa, indicative of the transition to a metallic state. Hysteresis loops emerged below 1.4K in magneto-resistance measurements, suggesting a magnetic ground state in qualitative agreement with the weak canted AFM order found at ambient pressure [2,3].

References:

[1]Robert C. Haddon, Nature 1975, 256, 394

[2]Aaron Mailman et al., JACS, 2012, 134, 9886

[3]Stephen M. Winter et al., PRB, 2014, 89, 214403

TU.E-P34 - Spectral features of angle-resolved photoemission in a magnetic-polaron system

H.D. Kim¹

1. Center For Correlated Electron Systems, Seoul, Korea

EuB₆ is a well-known semimetal that has a ferromagnetic (FM) ground state with T_c = 15.5 K. It has attracted much attention because of a resistivity upturn just before the FM transition, which was ascribed to magnetic-polaron formation. Angle-resolved photoemission (ARPES) spectra in the FM phase show two clear exchange-split B 2p bands, which may originate from an antiferromagnetic Kondo coupling between B 2p and Eu 4f electrons. At high-enough temperature, where there is no resistivity anomaly, two bands completely merge together. But, at slightly higher temperature than T_c, there is a vestige of exchange-split band near the Fermi level (EF), while well below the EF, the two bands has already merged. In order to clarify this behavior, we simulated ARPES spectra with a Kondo lattice model. By treating a local moment as an Ising spin, the model was solved for a 40 x 40 lattice by the Monte Carlo method with the Metropolis algorithm. In order to probe enough k points for resolving a Fermi surface for a semimetallic system, we employed open boundary conditions. Calculated ARPES spectra show that two exchange-split bands in the FM phase merge at first well below the EF, while there are still split bands near the EF. At high-enough temperature, they become a single band. All these results explain quite well the observed ARPES spectra.

TU.E-P35 - Magnetic properties of Cr-based ternary compound CrAlGeS. Yoshinaga¹, Y. Mitsui¹, R. Umetsu², K. Koyama¹

1. Faculty of Science, Kagoshima University, Kagoshima, Japan

2. Institute for Materials Research, Tohoku University, Sendai, Japan

Mn-based compound MnAlGe with a tetragonal Cu₂Sb-type structure is ferromagnetic at the temperature below Curie temperature T_C of 518 K [1]. The compound has a large magnetic moment of 3.25 m_B and a magnetic anisotropy associated with the anisotropic crystal structure. Therefore, this compound has been considered to be one of the candidates for memory and spintronic devices. Cr substitution for Mn in the compound enhanced the saturation magnetization M_S and T_C [2]. According to the report of ternary phase diagram of Cr-Al-Ge, fully substituted compound CrAlGe exists as a stable phase. However, the structural and magnetic properties of CrAlGe are not characterized yet in details. In this study, we have performed X-ray diffraction (XRD) and magnetization measurements for CrAlGe in order to clarify the fundamental properties.

Polycrystalline CrAlGe was prepared by induction melting process of a mixture made of appropriate amounts of pure elements. The obtained ingots were annealed at 1073 K for 1 day and then quenched into water. XRD measurements were carried out at room temperature. Magnetization measurements were performed for $5 \leq T \leq 390$ K and magnetic fields B up to 5 T.

Our XRD analysis showed clearly that the crystal structure of CrAlGe is not the tetragonal Cu₂Sb-type but the orthorhombic TiSi₂-type with lattice parameters of $a = 0.4744$ nm, $b = 0.8229$ nm and $c = 0.8705$ nm. From detailed analysis, Cr atom occupied the 8a-site and both atoms of Al and Ge are at the 16f-site of the TiSi₂-type structure. CrAlGe is ferromagnetic and has $M_S = 0.2 m_B$ at 5 K and $T_C = 83$ K, suggesting that CrAlGe is a weak itinerant ferromagnet.

References:

[1] J.H. Wernick, et al., J. Appl. Phys., 32, 2495 (1961)

[2] R. Y. Umetsu *et al.*, IEEE Trans. Magn. , 11, 1001904 (2014)

TU.E-P36 - Electronic and magnetic properties of impurity hydrogen in semiconductors

K. Yoshizawa¹, Y. Iwazaki², Y. Gohda³, S. Tsuneyuki^{1,4}

1. Institute For Solid State Physics, The University Of Tokyo, Tokyo, Japan

2. Taiyo Yuden Co., Ltd., Tokyo, Japan

3. Dept. Mater. Sci. Eng., Tokyo Institute of Technology, Tokyo, Japan

4. Department of Physics, The University of Tokyo, Tokyo, Japan

Impurity hydrogen (H) affects the electronic and magnetic properties of semiconductors with three charge states (H^0 , H^+ , H^-).

We estimate H states in semiconductors (SiO_2 , TiO_2 , CdS, GaN, ZnO, and so on) by using first-principles calculation based on density functional theory (DFT). Total electron number in a supercell is changed to study the charge state of H (H^0 , H^+ , H^-) and the magnetic moment. The charge states are determined by Bader analysis after the optimization of semiconductors with a H atom. The calculation results show different H states for each semiconductor. SiO_2 takes three charge states (H^0 , H^+ , H^-), TiO_2 takes H^+ only, and the others take H^+ and H^- in the above semiconductors. In the example of SiO_2 , a neutral H atom is localized in interstice. When H is in H^+ state, the H atom is located near the O atom. The distance between H and O atoms is about 1.03Å, which is almost the same as the O-H bond length in H_2O of 0.96Å. Similarly, when H is in H^- , the H atom forms a Si-H bond of 1.33Å. The magnetic moment of H^0 is $1\mu_B$, and that of the H^+ and H^- is 0. We show the stable charge state by evaluating the defect-formation energy and discuss the cause of the H states by calculating the dielectric constant and the effective mass of the semiconductors in this poster.

We also understand H behavior by calculating the isotropic and anisotropic hyperfine coupling constants. Because muonium in crystals behaves similarly to H, muon spin rotation (μSR) has played an important role in identification of hydrogenlike states in semiconductors. We evaluate the accuracy of DFT calculation for H in semiconductors by the comparison with hyperfine parameters of μSR .

TU.E-P37 - Magnetism and insulator-to-metal transition of strongly correlated polarons in alkali-metal loaded zeolites

T. Nakano¹, G. Prasad Hettiarachchi¹, L.M. Kien¹, T. Goto¹, Y. Nozue¹

1. Department Of Physics, Graduate School Of Science, Osaka University, Osaka, Japan

Guest alkali-metals of Na, K and Rb can be loaded into regular nanospaces of host porous crystals of zeolites X, sodalite and P without changing their framework structures (cages and cavities). Magnetisms, such as ferromagnetism, antiferromagnetism and ferrimagnetism, have been observed depending on the framework structures of zeolites, kinds of alkali metals and the loading densities. An insulator-to-metal (IM) transition is observed with the increase in the loading density. These s-electrons have an interaction with the displacement of alkali-metal cations in nanospaces as well as the mutual interaction between them, which leads to the electron-phonon interaction (EP) and the electron correlation simultaneously. Hence, we will explain these electronic properties by the concept of strongly correlated polarons. Small polarons with magnetic moments, which are the self-trapped quantum states stabilized by the EP interaction, are formed as clusters in the regular nanospace. An insulating state is observed up to some amounts of loading density of alkali-metals. Large polarons, which are the extended states being mobile as free carriers, are generated with the increase in the loading density, and an IM transition occurs. The interactions between small polarons and between large and small polarons play an important role in magnetisms. When the EP interaction is large enough to combine two small polarons against a Coulomb repulsion, small bipolarons without magnetic moment are generated preferentially. These behaviors are generally understandable in the scheme of the electron transfer energy (t), the electron Coulomb repulsion energy (U), the EP interaction energy (S) and the s-electron density (n).

TU.E-P38 - ^{77}Se NMR study on the possible excitonic insulator Ta_2NiSe_5

S. Li¹, Y. Kobayashi¹, Masayuki Itoh¹

1. Department of Physics, Graduate School of Science, Nagoya University, Furo-cho, Chikusa-ku, Nagoya, Japan

The excitonic insulator is an exotic electronic state ascribed to the BCS or Bose-Einstein condensation of electron-hole pairs formed by the strong Coulomb interaction, if the binding energy is much higher than the energy gap between valence and conduction bands. Recently, Ta_2NiSe_5 was proposed as a candidate of the excitonic insulator on the basis of a Ta_{5d} conducting band and a flat $\text{Ni}_{3d}\text{-Se}_{4p}$ valance band observed by the ARPES experiment. Ta_2NiSe_5 is crystallized into the monoclinic structure. NiSe_4 tetrahedra form one chain along the a axis, whereas TaSe_6 octahedra form two chains beside the NiSe_4 chain. These chains form a layer along the c axis and the layers are weakly coupled via the Van der Waals interaction. Magnetic susceptibility shows a drop accompanied by the structural transition at $T_c=328$ K. Although intensive experimental and theoretical studies have been made after the ARPES study, it remains uncovered whether Ta_2NiSe_5 is an excitonic insulator or not below T_c . In this study, we have performed ^{77}Se NMR measurements on both powder and single crystal samples to study the local electronic and magnetic properties of Ta_2NiSe_5 . We observed powder NMR spectra coming from the three Se sites, Se_1 with neighboring one Ni and two Ta atoms, Se_2 with three Ta, and Se_3 with two Ni and two Ta. Each Se powder spectrum was found to have a so-called powder pattern governed by the isotropic and anisotropic Knight shifts. The observed Knight shifts, which decrease with lowering temperature below T_c , clearly show a nonmagnetic ground state. The nuclear spin-lattice relaxation rate was also found to show the activated temperature dependence below T_c .

TU.E-P39 - NMR/NQR studies on the phase transition in A-site-ordered perovskites $ACu_3Cr_4O_{12}$ (A= La and Bi)Y. Kobayashi¹, M. Iguchi¹, M. Itoh¹, M. Isobe², H. Takagi², H. Sakurai³, H. Takagi²*1. Department of Physics, Graduate School of Science, Nagoya University, Japan**2. Max Planck Institute For Solid State Research, Stuttgart, Germany**3. National Institute for Materials Science, Tsukuba, Japan*

Chromium oxides with a high-valence Cr ion exhibit anomalous physical properties owing to hybridization between Cr and O orbitals. One of such systems, the A-site-ordered perovskite $ACu_3Cr_4O_{12}$ with a mixed-valence Cr ion, is expected to have the inter-site charge transfer and the charge disproportionation as discussed in the iron oxides. In $ACu_3Cr_4O_{12}$ (A= La and Bi) which were recently synthesized, a phase transition was reported to take place with a structural change at $T_s \sim 220$ and 170 K for La and Bi, respectively. In this study, we have performed $63,65Cu$ -NMR/NQR and $53Cr$ -NMR measurements on powder samples to examine the valence states of the Cu and Cr ions at T_s in $ACu_3Cr_4O_{12}$ (A= La and Bi). In $LaCu_3Cr_4O_{12}$, the change observed at T_s in the $63,65Cu$ -NQR spectra show that the Cu valence change takes place, whereas the Cu Knight shift and the nuclear spin-lattice relaxation rate indicate that the Cu ion changes from a paramagnetic to non-magnetic state below T_c . This result means that the Cu valence may change from high-temperature Cu^{2+} ($3d^9$) to low-temperature Cu^{3+} ($3d^8$) or $Cu^{2+}L$ ($3d^9L$), where L denotes a hole in the $O2p$ orbital, owing to the inter-site charge transfer between the Cu and Cr ions. On the other hands, in $BiCu_3Cr_4O_{12}$, the $63,65Cu$ -NMR/NQR spectra show that the Cu ion is preserved to be in a divalent state through T_s .

TU.E-P40 - Electric field dependence of the induced magnetic moment of pd thin film

M. Kim¹, T. Quang¹, J.M. Hyun¹, H. Kim¹

1. Sookmyung Women's University, Seoul, South Korea

Electric field dependence of the magnetic properties in a Pd thin film on MgO (001) substrate is theoretically investigated within the density functional theory framework. The result reveals that the Pd, which is paramagnetic in bulk, prefers a ferromagnetic phase with the induced Pd spin magnetic moment of $0.31 \sim 0.34 \mu_B$ when it is grown epitaxially on the MgO (001) substrate due to the in-plane lattice expansion by 6.7%. Under the external electric field (EF) perpendicular to film surface, the induced Pd magnetic moments are modulated in different ways for each Pd layer. The modulation of the surface Pd moment emerges for the EF above a critical value, $E_c = 1.3 \text{ V/\AA}$, showing a non-linear variation with EF which can be explained by the linearized Stoner model, whereas the change of interface Pd moment exhibits a linear increase up to E_c and a non-linear variation above E_c . With the reversed EF, a similar EF-dependence was obtained for both the surface and the interface Pd moments, but with the different critical field of $E_c = -0.5 \text{ V/\AA}$. From the analysis of the site-projected and orbital-decomposed density of states, we found a strong correlation between the modulation of induced Pd moments and the Pd(d) states. This intriguing EF-induced variation of Pd magnetic moments was confirmed to be of purely electronic origin, and not related with ionic displacements.

TU.E-P41 - Tailoring of electronic and magnetic properties of bcc Fe- based high entropy alloys

K. Perzynska¹, K. Szymanski¹, A. Matwiejczyk¹, M. Biernacka¹, D. Oleszak², L. Hawelek³, J. Waliszewski¹, M. Gutowska⁴, T. Zajarniuk⁴, A. Szewczyk⁴

1. Faculty of Physics, University of Bialystok, Bialystok, Poland

2. Faculty of Materials Science and Engineering, Warsaw University of Technology, Warszawa, Poland

3. Institute of Non Ferrous Metals in Gliwice, Gliwice, Poland

4. Institute of Physics, Polish Academy of Sciences, Warszawa, Poland

Structural, electrical and magnetic properties of *bcc* Fe_{1-x}A_x alloys are presented, where the A corresponds to various compositions of the elements: A = (Co, Ga, Cr, V, Al, Ni, Ge, Si). The system is closely related to the known family of the High Entropy Alloys (HEA). The samples were synthesized by melt spinning technique and exhibit *bcc* type of structure. Systematic changes in the residual resistivity, magnetic moments, specific-heat and electronic structure with the A content are observed.

The change from metallic to the semiconductor-like behaviour of temperature dependence of the electrical resistivity $\rho(T)$ with an increase of dopants (x) has been observed. One possible explanation of this behaviour is a low density of electronic states at the Fermi level in samples. This behaviour was verified by measurement of the low-temperature specific-heat. Properties of the Fe_{1-x}A_x system with *bcc* structure for small x are generally similar to those of pure iron. So, at first step of data interpretation the constant magnetic contribution was subtracted from all samples. Despite the small magnetic contribution to specific-heat, this procedure apparently improves the linearity of C/T vs. T^2 at low temperature. The Debye temperatures and the electronic specific heat coefficients were determined from a linear plot of C/T vs. T^2 . The results show a linear decrease of the Debye temperature with concentration x . The electronic specific-heat parameter, γ , reaches a minimum at $x=0.4$. At this concentration change of sign of the temperature coefficient of resistivity was observed. The experimental results are compared to the results of electronic structure calculations.

TU.E-P42 - Thickness dependent dynamic study of ion-beam sputtered Co₂FeAl thin films

S. Akansel¹, A. Kumar¹, S. Husain², S. Chaudhary², P. Svedlindh¹

1. *Engineering sciences, Uppsala university, Uppsala, Sweden*

2. *Department of Physics, Indian Institute of Technology Delhi, Delhi, India*

The Co based Heusler alloy Co₂FeAl (CFA) is a promising material for spintronics due to its half-metallicity, high Curie temperature and low Gilbert damping constant (α), which are key requirements for spin devices. However, to obtain high quality CFA thin films is still a challenge and it has been found that the CFA thin film quality varies with the growth process and post deposition annealing treatment. Moreover, there are rarely any reports on the ion-beam sputter deposition of CFA thin films.

In the present work CFA thin films were deposited from a 99.5% pure Co₂FeAl target by reactive ion beam sputtering on HF-treated Si (100) substrates at the optimized deposition temperature of 300°C. A series of different thicknesses, 1.8, 3.3, 5.0, 6.6, 8.8, 12.4, 16.5 nm have been prepared and all samples were capped with a 5 nm Ta layer. The XRD measurements show that the films exhibit the disordered B2 crystallographic structure. The thickness dependent static and dynamic properties of the films were studied by SQUID magnetometry and out-of-plane VNA-FMR measurements in field-sweep mode. The saturation magnetization and coercivity of the samples varied with film thickness in the range of 459 to 766 emu/cc and 3 to 8 Oe, respectively. The thickness and frequency dependent variation of the line-width and resonance field were obtained and the results evidence an extrinsic contribution to the linewidth originating from the inhomogeneous and local variation of the effective demagnetization field contributions. The effective magnetization $4\mu M_{\text{eff}}$ and intrinsic α values were found to be in the range of 9 to 11.4 kG and 1.8×10^{-2} to 2×10^{-3} , respectively. The lowest value of $\alpha = 2 \times 10^{-3}$ is comparable to the smallest values observed for epitaxial CFA films.

TU.E-P43 - Moessbauer spectroscopy study of collapse-like decrease of Fe magnetic moment in amorphous (Fe-Cr)-B and Fe(Cr-Cu)-B alloys

K. Yano¹, H. Tange², S. Lee³, E. Kita³

1. *Nihon University, Japan, Chiyoda, Tokyo, Japan*

2. *Ehime University, Matsuyama, Japan*

3. *University of Tsukuba, Tsukuba, Japan*

4. *University of Tsukuba, Tsukuba, Japan*

There remains to be some unsolved problems and hard nuts to crack in magnetism for amorphous (a-) transition metal (TM)-metalloid alloys. One of them is a rapid decrease, that is, a collapse-like decrease of magnetic moment of TM such as Fe and Co substituted by Cr, V and so on in the so-called Slater-Pauling curve. This phenomenon has been found by Mizoguchi et al. in 1974 and thereafter there seems to have been no decisive improvements in this problem. In this study, the electronic states of Fe in a-(Fe-Cr)₈₀B₂₀ and a-{Fe(Cr-Cu)}₈₀B₂₀ alloys have been investigated by employing the Moessbauer spectroscopy. The hyper-fine field (the peak value of the distribution) decreases rapidly to 1.2 uB at Cr=0.15 (15 at %) in a-(Fe-Cr)₈₀B₂₀ alloys at 4.2 K and this result nearly correspond to the value obtained by magnetization measurement. However, the Moessbauer spectroscopy shows a characteristic profile at Cr=0.15 and it suggests that the substitution of Cr by non-magnetic TM element such as Cu can give some useful informations. Regarding this, the result is to be discussed at the Conference. Furthermore, at Cr=0.05 (5 at %), the Moessbauer spectroscopy reveals that the magnetization unexpectedly orients perpendicular to the film surface from 77 K to 4.2 K.

TU.E-P44 - Studies of ^{27}Al NMR in SrAl_4

H. Niki¹, N. Higa¹, H. Kuroshima¹, T. Toji¹, M. Morishima¹, M. Minei¹, M. Yogi¹, A. Nakamura¹, M. Hedo¹, T. Nakama¹

1. Department of Physics, Faculty of Science, University of The Ryukyus, Nishihara, Japan
2. Faculty of Science, Kobe University, Hyogo, Japan

A charge density wave (CDW) transition at $T_{\text{CDW}} = 243$ K and a structural phase (SP) transition at approximately 100 K occur in SrAl_4 with the BaAl_4 -type body center tetragonal structure, which is the non-4f-divalent-Sr reference compound of EuAl_4 [1]. To understand the behaviors of the CDW and SP transitions, the ^{27}Al NMR measurements in SrAl_4 have been carried out. Al atoms have two crystallographically inequivalent sites, denoted Al(I) and Al(II), respectively. High-quality single crystal of SrAl_4 was grown by the Al-self flux method. NMR measurements using the powder sample and single crystal of SrAl_4 have been done applying in the external magnetic field of approximately 6.5 T. The ^{27}Al NMR spectra corresponding to the sites I and II are obtained. The temperature dependence of Knight shifts of the ^{27}Al (I) and ^{27}Al (II) shows the different behaviors. The value of ^{27}Al (I) Knight shift is almost constant above TCDW, decreases monotonously below TCDW, has a step-like anomaly around at 100 K because of the structural transition, keeps constant until 50 K, and decreases below 50 K. However, the value of ^{27}Al (II) Knight shift keeps almost constant from room temperature to 4.2 K. The shift to the negative side of the Knight shift at the Al(I) site below TCDW is attributable to the core polarization of the d-electrons. The line width below TCDW is modulated by an electrical quadruple interaction between ^{27}Al nucleus and CDW charge modulation. The value of the $1/T_1T$ of ^{27}Al (I) takes an almost constant value above TCDW, decreases monotonously below TCDW, and keeps constant below 60 K. However, the value of the $1/T_1T$ of ^{27}Al (II) takes a constant value between 4.2 and 300 K. The density of state at the Fermi level below 60 K would be about 0.9 times less than that above TCDW.

TU.E-P45 - Influence of structural disorder on electronic structure and magnetic properties of YCo₂-based compounds

Z. Sniadecki¹, M. Werwinski²

1. Institute of Molecular Physics, Polish Academy of Sciences, Poznan, Poland

2. Department of Physics and Astronomy, Uppsala University, Uppsala, Sweden

The studied intermetallic compounds based on YCo₂ Pauli paramagnet [1] with Nb and Ti substitutions crystallize in C15 Laves phase structure. Samples obtained by melt-spinning process exhibit magnetic ordering induced by chemical and topological disorder. Experimentally observed ferrimagnetic ground states for YCo₂ systems with Y atoms substituted by Ti and Nb [2] find theoretical explanation on the basis of the electronic band structure calculations. FP-LAPW method (Full Potential--Linearized Augmented Plane Wave) implemented in the WIEN2k code was utilized to determine the site preference energies for the Nb and Ti substitutions in YCo₂, by systematic study of YCo₂ structures with point defects. The considered defects are vacancies and Nb and Ti substitutions on Y or Co sites. Calculations show that the Ti and Nb impurities strongly prefer to occupy the Y sites. Moreover, the considered point defects in place of Y stabilize the ferrimagnetic ground state stronger than the point defects on Co sites. The calculated magnetic moments on Co atoms are close to 1 μ_B and opposite to smaller (0.1 μ_B – 0.66 μ_B) moments localized on Y and dopants. Substitutions that enhance the lattice parameter induce magnetic ordering. The results of calculations are in good agreement with our measurements. The intermetallics with Nb and Ti content higher than 10 at.% tend to form multiphase systems.

References:

[1] K. H. J. Buschow, Phys. Scr. T1 (1982) 125-129

[2] Z. Sniadecki et al. J. Appl. Phys. 115 (2014) 17E129

TU.E-P46 - Relation between composition, crystal structure, and magnetic properties of $\text{Cu}_{1+x}\text{Mn}_{1-x}\text{As}$ compoundsB. Vondráèková¹, K. Uhlíøová¹, R. Tarasenko¹, F.J. Martínez-Casado², Z. Matij¹, V. Holý¹

1. Charles University In Prague, Faculty Of Mathematics And Physics, Praha, Czech Republic
2. Max IV Laboratory - Lund University, Lund, Sweden.

The central part of the Cu-Mn-As ternary system has become attractive after a recent rediscovery of CuMnAs, a material promising for applications in antiferromagnetic spintronics [1, 2]. CuMnAs crystallizes in an orthorhombic structure. It orders antiferromagnetically below the Néel temperature of 400 K and shows semi-metallic character. Experiments on thin films have shown that the orthorhombic CuMnAs compound can be epitaxially grown on GaAs substrate while tuned to tetragonal Cu_2Sb -type structure and enhanced Néel temperature $T_N=475$ K [1]. Single crystals of CuMnAs, $\text{Cu}_{1.1}\text{Mn}_{0.9}\text{As}$, CuMn_3As_2 , and a new compound $\text{Cu}_2\text{Mn}_4\text{As}_3$ were prepared from bismuth and lead flux. The samples were characterized by microprobe analysis and single crystal x-ray diffraction. It was confirmed that the stoichiometric CuMnAs crystallizes in orthorhombic structure with lattice parameters $a = 0.6577$ nm, $b = 0.3854$ nm, $c = 0.73096$ nm. While the Mn-rich samples CuMn_3As_2 and $\text{Cu}_2\text{Mn}_4\text{As}_3$ have orthorhombic structure with twice as large unit cell prolonged along the a -direction. The Cu-rich $\text{Cu}_{1.1}\text{Mn}_{0.9}\text{As}$ crystallizes in the Cu_2Sb -type tetragonal structure. Magnetization measurements have shown that the stoichiometric CuMnAs order antiferromagnetically with the Néel temperature between 340 K and 400 K, while the Néel temperature of the Cu-rich samples was well above 400 K, in agreement with study on thin films [1]. The new compound $\text{Cu}_2\text{Mn}_4\text{As}_3$ orders magnetically below 315 K. The type of the order is most likely antiferromagnetic, however, considering the type of crystals structure which has 3 independent Mn-sites, more complex magnetic structure can be expected. The magnetic anisotropy was found to be rather weak in all studied compounds.

References:

1. Wadley, P. et al., Nature Communications 4 (2013)
2. Maca, F. et al., J. Magn. Magn. Mater., 324(8), 1606 (2012)

TU.E-P47 - Magnetic phases in Single Crystals Mn₅Si₃

R.F. Luccas^{1,2,3}, A. Correa-Orellana^{1,2,3}, F.J. Mompean^{1,3}, M. García-Hernández^{1,3}, H. Suderow^{2,3}

1. Instituto de Ciencia de Materiales de Madrid, Consejo Superior de Investigaciones Científicas (ICMM-CSIC), Madrid, Spain

2. Laboratorio de Bajas Temperaturas, Departamento de Física de la Materia Condensada, Instituto de Ciencia de Materiales Nicolás Cabrera, Condensed Matter Physics Center (IFIMAC), Universidad Autónoma de Madrid, Madrid, Spain

3. Unidad Asociada de Bajas Temperaturas y Altos Campos Magnéticos, UAM, CSIC, Cantoblanco, Madrid, Spain

Transition metal magnets are characterized by having moments strongly linked to their local environment. This leads to a rich interplay between d-electron magnetism and nearest-neighbor interactions.[1] Topological non-trivial arrangement, like skyrmions in MnSi, have been trust important for developing new devices, however the Mn-Si family have been not extensively studied. In particular, previous neutron scattering in polycrystalline or powder samples of Mn₅Si₃ show several magnetic phases, with two magnetic transitions $T_N^1 = 60$ K and $T_N^2 = 90$ K. Below T_N^1 , spins are arranged in a non-collinear structure, showing local chirality. This phase is destroyed by a magnetic field of several Tesla, favoring the high temperature antiferromagnetic arrangement.[2]

In this work, a study of the phase diagram of the Mn₅Si₃ system is presented. Crystals of Mn₅Si₃ were grown out of Cu flux. Needles with typically 6 mm in length and a non-regular octagonal cross section of about 1 mm² were obtained. Magnetization measurements up to 7 T and down to 2 K were performed on individual needles along their main axis. Known magnetic transitions T_N^1 and T_N^2 were observed in combination with a new additional transition T_N^{1*} at 45 K. T_N^1 was observed magnetic field independent, whereas T_N^{1*} strongly decreases with the magnetic field. In addition, several transition were observed for the phase down T_N^{1*} when increasing field at a fixed temperature. Our measurements suggest that the low temperature magnetic non-collinear structure unwinds with the magnetic field through metamagnetic transitions. There is an additional intermediate magnetic phase between 45 K and 60 K, which is probably also non-collinear. The role of sample synthesis on the magnetic structure is briefly discussed.

[1] Naoto Nagaosa and Yoshinori Tokura, *Nature Nanotechnology* 8, 899 (2013).

[2] Christoph Sürgers, et al., *Nature Communications* 5, 3400 (2014).

TU.E-P48 - Polarized neutron reflectivity and atomic structure study of a $\text{Co}_2\text{FeSiAl}/\text{Si}(111)$ heterointerface

B. Kuerbanjiang¹, L. Lari¹, Z. Nedelkoski¹, S. Yamada², T. Saerbeck³, S. Glover⁴, P. Hasnip¹, T. Hase⁴, G. Bell⁴, A. Hirohata¹

1. *University Of York, Heslington, York, United Kingdom*

2. *Osaka University, Osaka, Japan*

3. *Institut Laue-Langevin, Grenoble, France*

4. *University of Warwick, Coventry, United Kingdom*

We study high-quality Heusler (Co_2FeSiAl) /Si heterointerfaces for silicon (Si)-based spintronic applications. Heusler alloys are predicted halfmetals (i.e 100% spin polarised materials at the Fermi level). Recent reports have shown that the integration of spin functionality into existing Si large-scale-integrated circuits technologies for next-generation semiconductor devices with ultra low power consumption [1]. To utilize Co_2FeSiAl as source and drain electrodes in Si-based spin transistors, the magnetic and structural properties at the interface should be explored since the Si atoms may diffuse at $\text{Co}_2\text{FeSiAl}/\text{Si}$ interfaces.

A 25 nm Co_2FeAlSi film was deposited on Si(111) substrate by molecular beam epitaxy at room temperature [2]. Using polarized neutron reflectivity on the sample, we observed a magnetic dead layer at the $\text{Co}_2\text{FeAlSi}/\text{Si}(111)$ heterointerface. Structural analysis with atomic resolution has been performed on this heterointerface to understand the origin of the magnetically dead layer. Based on the cross-sectional transmission electron microscopy images we construct atomistic models of this interface and explained possible causes of magnetic properties of the $\text{Co}_2\text{FeAlSi}/\text{Si}$ interface. Finally, we propose plausible atomic interface structures that would preserve halfmetallicity of the Co_2FeAlSi up to the very interface based on first principle electronic calculations.

References:

[1] H. Dery et al, Nature 447, 573 (2007)

[2] S. Yamada et al, Appl. Phys. Lett. 105, 071601 (2014)

TU.E-P49 - The effect of post annealing conditions on the iron oxides thin films grown on MgO(100)

B. Kuerbanjiang¹, D. Pingstone¹, C. Chirnside¹, L. Lari¹, S. Tear¹, V. Lazarov¹

1. *University Of York, Heslington, York, United Kingdom*

Growth defects, domain structures and off-stoichiometric compositional deviation are the cause of anomalous magnetic and transport properties of magnetite (Fe_3O_4) thin films. Post-annealing at high temperature of Fe_3O_4 films in a CO/CO_2 atmosphere results in a significant improvement of magnetic and magnetotransport properties [1,2] compared to bulk specimens. In this work, we present atomistic study on the oxidation of Fe thin films as well as FeO_x with aim to understand the correlation between the structure and functional properties of iron oxide films. Control of the oxidation, and structure was achieved by in-situ O-plasma annealing followed by ex-situ postannealing in CO/CO_2 gas mixture. By optimizing post-annealing conditions, we show the influence of annealing temperature and flux of CO/CO_2 gas mixture on the structure of the Fe oxide films by means of x-ray photo electron spectroscopy, magnetoresistance, alternating-gradient force magnetometer and transmission electron microscopy techniques.

References:

- [1] K. Matsuzaki et al., J. Phys. D: Appl. Phys. 46 022001 (2013)
- [2] D. Gilks et al., J. Appl. Phys. 115, 17C107 (2014)

TU.E-P51 - Transport properties of a metallic two-dimensional triangular antiferromagnet Ag_2CrO_2 T. Kida¹, A. Okutani¹, H. Yoshida², M. Hagiwara¹1. *Osaka University, Osaka, Japan*2. *Hokkaido University, Sapporo, Japan*

Geometrically frustrated conducting magnets exhibit unconventional anomalous Hall effects (AHE) that could be used to realize materials required for the emerging field of spintronics [1]. Ag_2CrO_2 is one of the suitable materials for investigating the relationship between geometrical frustration and the AHE. Ag_2CrO_2 consists of triangular lattice planes of CrO_2 , which are well separated by the metallic Ag_2 layers [2]. This compound is an $S=3/2$ (Cr^{3+} ion) frustrated triangular lattice antiferromagnet ($T_N = 24$ K) without orbital degrees of freedom. Recently, Matsuda et al. [3] have reported that a partially disordered state with 5 sublattices abruptly appears at T_N , accompanied by a structural distortion, and found anomalous magnetic excitations, which cannot be explained simply by linear spin-wave theory. In this study, we have investigated the transport properties of Ag_2CrO_2 and discussed the coupling with the magnetism in this compound. Polycrystalline samples of Ag_2CrO_2 were synthesized using a high-pressure technique [2]. The transport measurements were performed by using a conventional dc four-probe technique in a 16 T superconducting magnet. The resistivity of this compound displayed metallic behavior and an abrupt decrease at T_N . Below T_N , almost linear positive magnetoresistance was observed. On the other hand, just above T_N ($T = 25$ K), a large negative magnetoresistance of 38% at 8 T was observed. The absolute value of the negative magnetoresistance decreases with increasing temperature. The Hall resistance showed a non-linear behavior as a function of the magnetic field below T_N . These results suggest the transport properties of Ag_2CrO_2 are closely related to its unusual antiferromagnetic spin-structure.

References:

- [1] Y. Taguchi et al., *Science* 291, 2573 (2001)
- [2] M. Matsuda et al., *Phys. Rev. B* 85, 144407 (2012)
- [3] H. Yoshida et al., *J. Phys. Soc. Jpn.* 80, 123703 (2011)

TU.E-P53 - The ground-state phase diagram of the XXZ spin-s kagome antiferromagnetJ. Richter¹, O. Goetze¹*1. Institute for Theoretical Physics, University Magdeburg, Magdeburg, Germany*

We use the coupled cluster method at high orders of approximation in order to calculate the ground-state phase diagram of the XXZ spin-s kagome antiferromagnet with easy-plane anisotropy, i.e., the anisotropy parameter Δ varies between $\Delta=1$ (isotropic Heisenberg model) and $\Delta=0$ (XY model) [1,2]. Anisotropy as well as larger spin quantum numbers $s>1/2$ have relevance for the experimental research. Moreover, anisotropic spin models are of great interest with respect to engineering models of quantum magnetism on optical lattices. The interplay of frustration, quantum fluctuations and anisotropy leads to a rich ground-state phase diagram. We find that for the extreme quantum case, $s=1/2$, the ground state is magnetically disordered in the entire region $0 \leq \Delta \leq 1$. For $s=1$ the ground state is disordered for $0.818 < \Delta \leq 1$, it exhibits $\sqrt{3} \times \sqrt{3}$ magnetic long-range order for $0.281 < \Delta < 0.818$, and $q=0$ magnetic long-range order for $0 \leq \Delta < 0.281$. We confirm the recent unexpected result of Chernyshev and Zhitomirsky [3] that the selection of the ground state by quantum fluctuations is different for small Δ (XY limit) and for Δ close to one (Heisenberg limit), i.e., $q=0$ magnetic order is favored over $\sqrt{3} \times \sqrt{3}$ order for $0 \leq \Delta < \Delta_c$ and vice versa for $\Delta_c < \Delta \leq 1$.

We calculate the critical Δ_c as a function of the spin quantum number s .

References:

- [1] O. Götze, D.J.J. Farnell, R.F. Bishop, P.H.Y. Li, and J. Richter, Phys. Rev. B 84, 224428 (2011)
- [2] O. Götze and J. Richter, arXiv:1501.02146
- [3] A. L. Chernyshev and M. E. Zhitomirsky, Phys. Rev. Lett. 113, 237202 (2014)

TU.F-P03 - Preparation and characterization of poly-alpha-olefin-based ferrofluids

J.H. Kim¹, K. Park¹

1. Research Center For Advanced Magnetic Materials, Chungnam National University, Daejeon, South Korea

Magnetite of fine particles was synthesized by adding an excess ammonium hydroxide to a solution of iron (II) and (III) chlorides. Surfactants of oleic acid and span 80 were in turn applied to the magnetic particles as a combined stabilizer, and poly-alpha-olefin (PAO) 30 and 60 were used as liquid bases for low viscosity and for high viscosity, respectively. The ferrofluids were prepared with the concentrations of 200, 300, 400 and 500 mg/mL, which were characterized by density, dispersion, magnetization and viscosity. The fluid density varied from 0.98 g/mL to 1.27 g/mL in the PAO 30 base and from 1.01 g/mL to 1.30 g/mL in the PAO 60 base with increasing concentrations, depending on the density difference between two types of bases, and the dispersion percent of the stabilized fluids indicated about 80% at the lowest concentration for both bases. The saturation magnetization of the ferrofluids depended on the content of bare particles corresponding to the fluid concentration, exhibiting the values of 16 to 41 mT in proportion to the concentration from 200 mg/mL to 500 mg/mL. The viscosity variation with temperature was least at the 400 mg/mL PAO-30-based ferrofluid and the 300 mg/mL PAO-60-based ferrofluid. Considering the magnetic applications of ferrofluid, the highest possible concentration is more desirable.

TU.F-P04 - Magnetic and magnetoelectric properties of Fe₃O₄ nanocrystal self-assemblyS. Kohiki¹, Y. Nakamura¹, K. Akiyama-Hasegawa², M. Mitome², D. Tsuya²1. *Kyushu Institute of Technology, Kitakyushu, Japan*2. *National Institute for Materials Science, Tsukuba, Japan*

The red brick wall of traditional semiconductor electronics boosts development of a spin-polarized current switching device using negative magnetoresistance (MR) of Fe₃O₄ nanocrystal (NC) arrays. MR is defined as $MR = (R_H - R_0)/R_0$, where R_H and R_0 are the differential resistance in non-zero and zero magnetic fields, respectively. Enhancement of magnetic coupling between adjacent NCs leads larger MR. Here, we report ferromagnetism for Fe₃O₄ NC, the spin-glass state and MR larger than -50% for Fe₃O₄ NC arrays at 300 K. Fe₃O₄ is known to have fully spin-polarized ($P = 1$) carriers up to 840 K, while $P = 1$ at 300 K is still controversial. Fe₃O₄ NCs with the crystallite size of 38 nm were synthesized by refluxing a mixture of Iron(III) acetylacetonate, dibenzylether and oleic acid. A self-assembly of Fe₃O₄ NCs was fabricated via drop casting of colloidal particles on an insulator substrate. In three-dimensional systems of Fe₃O₄ NCs isolated by oleic acid thin layers, MR is connected to P and the relative magnetization of the system (m) by $MR \equiv P^2 m^2 / (1 + P^2 m^2)$. Here, m relates to the angle (ϑ) between the magnetic moment of adjacent NCs as $m^2 = \langle \cos \vartheta \rangle$. Both $P = 1$ and $m = 1$ conditions give rise to $MR = -50\%$. Fe₃O₄ NCs exhibited ferromagnetic hysteresis loop at 300 K with spontaneous magnetization of $1 \mu_B/\text{Fe}$. The NCs demonstrated cooling history-dependence indicating the superparamagnetic state for each NC below 300 K. Temperature-dependent AC susceptibility revealed the frustrated magnetic state above 300 K for the self-assembly of Fe₃O₄ NCs. Larger R_0 than R_H resulted in MR of -56%, which proves $P = 1$ for Fe₃O₄ NC even at 300 K. Thus, Fe₃O₄ NC is promising for a normally-OFF spin-dependent current switch device application.

TU.F-P05 - Effect of dextran coated superparamagnetic iron oxide nanoparticles during in vivo observation of the rats

A.M. Prodan^{1,2,3}, C. Steluta Ciobanu⁴, M. Beuran^{1,2}, C. Turculet^{1,2}, G. Teleanu¹, M. Motelica-Heino⁵, S. Sizaret⁵, D. Predoi⁴

1. Emergency Hospital Floreasca, Bucharest, Romania

2. Carol Davila University of Medicine and Pharmacy, Bucharest, Romania

3. University Politehnica of Bucharest, Faculty of Applied Chemistry and Materials Science, Department of Science and Engineering of Oxide Materials and Nanomaterials, Bucharest, Romania

4. National Institute of Materials Physics, Bucharest, Magurele, Romania

5. ISTO, UMR 7327 CNRS, Université d'Orléans, Orléans Cedex 2, France

The superparamagnetic iron oxide nanoparticles have attracted a lot of interest due to their widespread biomedical and diagnostic applications. In this study, we report the synthesis of dextran coated iron oxide magnetic nanoparticles (D-IONPs) with spherical shape uniform size distribution. The average grain size of the monodisperse D-IONPs deduced from the Transmission Electron Microscopy (TEM) is 7.5 (\pm 0.5) nm. The hydrodynamic diameter of D-IONPs determined by dynamic light scattering (DLS) was equal to 30 nm, approximately. The clear lattice fringe in the HR-TEM image demonstrates the well crystalline nature of resultant nanoparticles. The adsorption of dextran on surface of iron oxide was evidenced by Attenuated Total Reflectance Fourier transform Infrared (ATR-FTIR) spectroscopy. The magnetic hysteresis measurement of dextran coated maghemite nanoparticles showed a superparamagnetic compartment at room temperature. The tolerability of the D-IONPs was demonstrated by in vivo observation of rats during one month after intraperitoneal injection. The histological investigations were performed every 14 days. The hematology analysis data in rats after intraperitoneal injection of D-IONPs are presented. The results obtained after the 28 days from histological investigations and hematology analysis data in rats are comparable to those obtained for rats in the control group. Keywords: dextran, maghemite, superparamagnetic, in vivo, histological investigations

Acknowledgements: This work was financially supported by the PN-IIPT-PCCA-2013-4-0006 (131/01/07/2014) funded by the Ministry of Education- UEFISCDI and the Sectoral Operational Programme Human Resources Development 2007-2013 of the Ministry of European Funds through the Financial Agreement POSDRU/159/1.5/S/134398.

TU.F-P06 - Synthesis, self-organization and magnetism of iron oxide and Au-iron oxide core/shell nanocomposite particles

D. Muraca¹, S. Sharma¹, M. Knobel¹, P. Mendoza Zelis²

1. *Instituto de Física Gleb Wataghin (IFGW), Universidade Estadual De Campinas (Unicamp), Campinas, SP, Brazil*

2. *Instituto de Física La Plata CONICET, La Plata, Argentina*

This work reports a simple chemical synthesis of Au-iron oxide nanocomposites using Au nanoparticles seeds and their systematic oxidation in the presence of dry air atmosphere at various temperatures (125-250 C). It has been observed that the oxidation not only facilitate the self-organization of iron oxide nanoparticles, but also to switch these nanocomposites into core-shell Au-iron oxide structures. We have observed a systematic improvement in the core and shell shape through controlling the reaction time as well as the oxidation temperature. Spherical and spherical-triangle shaped core-shell structures have been synthesized at an optimum oxidation temperature of 125 C and 150 C for 30 minutes, whereas with the further increase in the temperature as well as oxidation time, there is a full amendment in the core-shell structures. The nanoparticle samples have been thoroughly characterized using X-ray diffraction (XRD), high-resolution transmission electron microscopy (HR-TEM), Mossbauer spectroscopy and superconducting quantum interference device (SQUID) magnetometer.

TU.F-P07 - Magnetic properties and crystal structure of DyMn₂O₅ nanoparticles embedded in mesoporous silicaT. Tajiri¹, Y. Ando², H. Deguchi², M. Mito², A. Kohno¹*1. Faculty of Science, Fukuoka University, Fukuoka, Japan**2. Faculty of Engineering, Kyushu Institute of Technology, Kitakyushu, Japan*

Magnetic properties and Crystal structure of nanoparticles differ from those of the bulk crystal owing to surface and finite size effects. In a rough approximation, the energy states of the magnetization vector of the particles can be modeled as a double well potential separated by barriers whose characteristics depend on the particle size and magnetic anisotropy. Recently, multiferroic materials have been widely studied because of the interesting physics such as magneto–electric effect. Multiferroic compound DyMn₂O₅ shows antiferromagnetic ordering of Mn moments at $T_N \approx 40$ K and commensurate–incommensurate magnetic transition at $T_N' \approx 27$ K. In addition, the Dy magnetic moments order below 8 K. DyMn₂O₅ undergoes a transition to a ferroelectric phase below T_N . We attempted to synthesize DyMn₂O₅ nanoparticles with few nanometers and investigated their magnetic properties and crystal structure. The DyMn₂O₅ nanoparticles were synthesized in pores of mesoporous silica. Powder X-ray diffraction (XRD) patterns for the DyMn₂O₅ nanoparticles exhibited some broad Bragg peaks, which were attributed to the crystal structure of bulk DyMn₂O₅. The XRD experimental results indicated that successful synthesis of the DyMn₂O₅ nanoparticles with average particle size of 7-20 nm. The lattice constant b of the nanoparticles increased monotonically with decreasing particle size, which suggested that the crystallographic structure distorted with decreasing particle size. We measured the temperature dependence dc magnetic susceptibility and magnetization curves for the nanoparticles. These results exhibited superparamagnetic behaviors. The evaluated Weiss temperature for the nanoparticles changed in sign and magnitude which decreased linearly with increasing particle size. These results suggested that the decrease in particle size induces the distortion of crystallographic structure and the changes in magnetic exchange interactions.

TU.F-P09 - Proton relaxometry and magnetic hyperthermia evaluation of gadolinium doped nickel ferrite nanoparticles

T. Yadavalli¹, S. Ramaswamy², G. Chandrasekharan¹, H. Annal Therese¹, R. Chennakesavulu³

1. *Nanotechnology Research Centre, SRM University, Kattankulathur, Tamilnadu, India*

2. *Accendere Knowledge Management, Annanagar, Chennai, Tamilnadu, India*

3. *Department of Pharmacy Practice, SRM University, Kattankulathur, Tamilnadu, India*

Based on our previous paper, a low temperature ferrous sulfate method was used for the synthesis of gadolinium doped nickel ferrites. However, post several unsuccessful attempts, doping experiments using hydrothermal synthesis method formed nanoscale nickel ferrites with a maximum doping concentration of 20%. The results were confirmed by X-ray diffraction studies with no phase separation at 20% dopant concentration. Samples with higher gadolinium concentration demonstrated the formation of multiple phases in addition to nickel. Low temperature and room temperature magnetic studies conducted on the samples, concluded that the samples NGFO-10 and NGFO-20 were potential candidates for relaxometry and magnetic hyperthermia studies due to their single phase property and high magnetic saturation values. Further, relaxometry studies established that nickel ferrite nanoparticles with 20% gadolinium dopant concentration had a high relaxation rate of 6.63 s⁻¹ at a concentration of 0.1 mg/mL. Further, four different concentrations of the same were subjected to magnetic hyperthermia based nanoparticle heating studies as a function of time. At a concentration of 1 mg/mL, samples attained a temperature of 68°C under 250 seconds concluding that gadolinium doped nickel ferrite nanoparticles are ideal candidates for magnetic theragnostic system

TU.F-P10 - Synthesis of Co doped AgFeO₂ delafossite nanoparticles

T. Yamazaki¹, K. Mori¹, M. Hachisu¹, S. Morimoto¹, K. Hyodo¹, Y. Ichiyanagi¹

1. Graduate School Of Yokohama National University, Yokohama, Japan

It is known that AgFeO₂ bulk crystal exhibits semiconductive material with two Néel temperatures of $T_{N1} = 15$ K and $T_{N2} = 9$ K, with ferroelectricity below 9 K. Cobalt doped delafossite nanoparticles AgFe_{1-x}Co_xO₂ ($0 \leq x \leq 0.3$) with an average diameter of approximately 10 nm were synthesized by co-precipitation method from silver nitrate and iron (III) nitrate, cobalt (II) nitrate and sodium hydroxide. Obtained samples were examined by X-ray powder diffraction (XRD), X-ray fluorescence (XRF), a TEM imaging and X-ray absorption fine structure (XAFS) measurement. The c axis of the lattice constants was shortened in accordance with increase Co-ion doping. XAFS analysis provided that Fe ions mainly exist in the valence of Fe³⁺ and Co ions also mainly exist in the valence of Co³⁺. The magnetic properties and the optical properties of the samples were measured by SQUID magnetometer and spectrophotometer. From the behavior of *M-T* curves of AgFe_{1-x}Co_xO₂ ($0 \leq x \leq 0.3$) nanoparticles, the magnetic transition temperature T_{N2} shifted higher than AgFeO₂ bulk crystal. While the T_{N2} shifted lower temperature as the Co-ion doping increased. Co doped AgFeO₂ nanoparticles were newly prepared, and magnetic and optical properties of these particles were clarified. (201 words)

TU.F-P11 - Evolution of complex magnetoresistance and perpendicular magnetic anisotropy in cobalt nanoparticles in silver matrix

D. Kumar¹, S. Chaudhary¹, D.K. Pandya¹

1. *Thin Film Laboratory, Physics Department, Indian Institute of Technology Delhi, New Delhi, India*

We report on the evolution of the perpendicular magnetic anisotropy and unusual complex magnetotransport behavior observed in cobalt nanoparticles embedded in a silver matrix. Thin silver films containing cobalt nanoparticles were deposited by co-sputtering technique with cobalt concentration varied from 11.8 to 45.1 at.%. These samples have been analyzed by temperature dependent magnetoresistance and magnetization, atomic force microscopy (AFM) and magnetic force microscopy (MFM) studies. Here we present our interesting finding of a transition from normal to complex magnetoresistance (MR) behavior, in conjunction with MFM evidence of the existence of a magnetic microstructure perpendicular to the film plane for 32.6% film that shows the complex behavior at 20 K. The dc-magnetization studies provide additional support to the presence of perpendicular magnetic anisotropy for this film. The perpendicular magnetic anisotropy gets reduced with the increase of cobalt concentration. The complex MR behavior also decreases with the increase of cobalt concentration. The room temperature MR, coercivity behavior and remanence to saturation magnetization ratio indicate the presence of direct ferromagnetic interactions due to the presence of ferromagnetic particles for $x \geq 32.6$ films. The observed complex MR behavior and perpendicular magnetic anisotropy are interpreted in terms of manifestation of the transition of interparticle magnetic interaction nature from dipolar to direct ferromagnetic ones.

TU.F-P12 - Excluded volume causes integer and fractional plateaus in magnetic colloidal ratchet currents

P. Tierno¹, T. Johansen², T. Fischer³

1. University Of Barcelona, Barcelona, Spain

2. University of Oslo, Oslo, Norway

3. University of Bayreuth, Bayreuth, Germany

We study the collective transport of paramagnetic colloids driven above a magnetic bubble lattice by an external rotating magnetic field. We measure a direct ratchet current which rises in integer and fractional steps with the field amplitude. The stepwise increase is caused by excluded volume interactions between the particles, which form composite clusters above the bubbles with mobile and immobile occupation sites. Transient energy minima located at the interstitials between the bubbles cause the colloids to hop from one composite cluster to the next with synchronous and period doubled modes of transport. The magnetic colloidal current may be polarized to make selective use of type up or type down interstitials.

TU.F-P13 - Depinning and collective dynamics of magnetically driven colloidal monolayers

P. Tierno¹

1. University Of Barcelona, Barcelona, Spain

We study the collective dynamics of interacting paramagnetic colloids transported via a magnetic ratchet effect above a modulated periodic potential. Upon increasing the modulation frequency, the particles undergo a series of dynamic transitions, from a continuous smectic flow to a disorder flow, and later enter into a two phase flow regime, ending in a complete pinned state. In the disordered phase, the system organizes into density waves due to traffic jams, as in granular systems, while the two phase flow regime shows strong similarities with plastic flow in vortex matter. Finally, it is shown that induced attractive interactions between the moving colloids lead to enhancement of the particle current due to formation of condensed chains traveling along the modulated landscape

TU.F-P14 - Enhanced room temperature ferromagnetism of Sol-Gel synthesized LaMnO₃ nanoparticles

C. Liu¹, B. Lee¹, P. Tola¹, D.H. Kim¹

1. Hankuk University Of Foreign Studies, Seoul, South Korea

Lanthanum-based perovskite-type oxides (LaMO₃) containing transition metals are well known as functional inorganic materials having wide applications such as electrodes for fuel cells, gas sensors, ion sensors, catalysts, and various biomedical materials. LaMO₃ has been reported to show interesting magnetic properties and broad electric properties induced by oxygen vacancies. In this work we investigated the effect of polyvinyl alcohol (PVA) on the magnetic properties of LaMO₃ nanoparticles synthesized by the sol-gel method. The precursor chemicals of La and Mn elements were first dissolved in a mixed solvent of acetic acid and methanol to get a clear precursor solution, then 6 wt% PVA of different volume (0, 5, 10, and 15 ml) was added. The final product was obtained by annealing the reaction precipitates at 700°C for 2 h. Although PVA did not seem to cause obvious effect on the crystallinity and composition of the LaMO₃ nanoparticles, the morphology and magnetic properties showed noticeable dependence on the amount of PVA added during the sol-gel process. The LaMO₃ nanoparticles became more porous when PVA solution was added, and the LaMO₃ nanoparticles prepared with 10 ml PVA showed much improved room temperature ferromagnetism despite the fact that bulk LaMO₃ shows antiferromagnetism with a Neel temperature of 140 K. X-ray photoelectron spectroscopy measurement revealed that the addition of PVA adjusted the amount of cation vacancies in the LaMO₃ nanoparticles. The amount of Mn⁴⁺ ions in LaMO₃ nanoparticles was increased with the addition of PVA solution, which directly affected the magnetic properties. Our results provide a simple approach to prepare LaMO₃ nanoparticles with enhanced room temperature ferromagnetism.

TU.F-P15 - Stability of patrons inscribed on arrays of magnetic nanowires

E. Vogel¹, J. Faundez¹, E. Cisternas¹

1. Universidad De La Frontera, Temuco, Chile

Magnetic nanowires trapped in the membranes used to produce them can be used to store information in the form of patterns representing shapes, symbols, or barcodes. In the present paper we calculate the repulsive interacting energy among the ferromagnetically oriented wires in the pattern contrasting with a random background. The starting point is the interaction between a pair of wires; an algorithm is designed to calculate all the interactions within the pattern without truncations due to distance between elements. Then two lines of thought are followed to test stability: A) The inscription of an opposite ferromagnetic band within the pattern of variable width w ; B) The detection of weak points within the pattern which are more lenient to reversion which could lead to loss of the stored information. Results are reported both by means of functional plots (i.e. dependence of the total repulsive energy per wire with respect to relevant parameters) and graphically (color coded maps showing particularly weak and strong points within the pattern with respect to possible magnetization reversals). Several letters in the Arial font are used as actual examples for previous analysis. Some of the main conclusions are: i) for w between 0.35 to 0.40 in units of the actual width of the pattern the best conditions for stability are reached; ii) wires in the periphery of the patterns are the most stable; iii) wires at the center of the pattern are the less stable under possible spontaneous reversal than can trigger a cascade of reversals leading to the fading away of the stored ferromagnetic domain. Several stabilization mechanisms are proposed. Acknowledgements: Fondecyt under contract 1150019 and Center for the Delopment of Nanoscience and Nanotechnology (CEDENNA) under contract FB0807.

TU.F-P16 - Magnetic anisotropy of maghemite nanoparticles probed by RF transverse susceptibility

A.I. Figueroa^{1,2}, J. Bartolomé¹, L.M. García¹, F. Bartolomé¹, A. Millán¹, F. Palacio¹

1. *Instituto de Ciencia de Materiales de Aragón, CSIC-Universidad de Zaragoza. Departamento de Física de la Materia Condensada, Zaragoza, Spain.*

2. *Magnetic Spectroscopy Group, Diamond Light Source, Didcot, United Kingdom*

The radio frequency (RF) magnetic transverse susceptibility (TS) technique has been used over the years with great success to study the magnetic anisotropy of different magnetic nanostructured systems [N.A. Frey. Surface and Interface Magnetism in Nanostructures and Thin Films. PhD thesis (University of South Florida, Tampa, 2008); A. I. Figueroa. Magnetic Nanoparticles. A Study by Synchrotron Radiation and RF Transverse Susceptibility. Springer International Publishing (2015)]. It is a powerful and sensitive technique to directly extract the magnetic anisotropy constant K_{eff} of nanoparticles systems and to study their interparticle interactions. Understanding these parameters in nanoparticle systems is of paramount importance to evaluate their potential applications in diverse fields like biomedicine. In this work, TS measurements on $\gamma\text{-Fe}_2\text{O}_3$ (maghemite) nanoparticles, with sizes between 5 and 13 nm in diameter, allow us to estimate their K_{eff} and examine its variation as a function of the particle size. The resulting K_{eff} values range from 4 to 8×10^4 erg/cm³, being on the order of the magnetocrystalline anisotropy in bulk maghemite. K_{eff} values increase as the particle diameter increases, which is consistent with an anisotropy enlargement with bigger core volume of the particles. Evidences of anisotropy field distribution given by the size distribution in the samples, and interparticle interactions that increase as the particle size increases are also observed in the TS measurements. Thus, the effects of interparticle interactions in this maghemite system overcome those of thermal fluctuations, in contrast with TS results obtained for other iron oxide particles such as SiO₂ – coated magnetite [A. I. Figueroa et. al., Nanotechnology 24, 155705 (2013)].

TU.F-P17 - Universal behaviour for magnetic entropy change in Ba-doped $\text{La}_{0.7}\text{Ca}_{0.3}\text{MnO}_3$ nanoparticlesT.D. Thanh^{1,2}, D.C. Linh², T.A. Ho¹, T.L. Phan³, S.K. Oh¹, S.C. Yu¹

1. Chungbuk National University, Cheongju, South Korea
2. Vietnam Academy of Science and Technology, Hanoi, Vietnam
3. Hankuk University of Foreign Studies, Yongin, South Korea

$\text{La}_{0.7}\text{Ca}_{0.3-x}\text{Ba}_x\text{MnO}_3$ ($x = 0, 0.025, \text{ and } 0.05$) nanoparticles with the crystallite size of $d_c = 39\text{-}45$ nm were synthesized by utilizing the solid-state reaction and mechanical ball milling methods. We have used the Banerjee's criteria, the mean-field, and the thermodynamic theories, and isothermal magnetization, $M(H)$, data around Curie temperature (T_C) to investigate the magnetic phase transformation and the temperature (T) and magnetic field (H) dependences of magnetic entropy change, $\Delta S_m(T, H)$, for nanoparticles. These exhibit the samples undergoing a second-order magnetic phase transition with an existence of the ferromagnetic short-range order in the samples. Under an applied magnetic field change $H = 30$ kOe, the maximum value of ΔS_m (denoted as $|\Delta S_{\text{max}}|$) are obtained about $4.4 \text{ J}\cdot\text{kg}^{-1}\cdot\text{K}^{-1}$ corresponding to a refrigerant capacity (RC) value about $140 \text{ J}\cdot\text{kg}^{-1}$. Field dependences of $|\Delta S_{\text{max}}|$ and RC can be expressed by the power laws, $|\Delta S_{\text{max}}| = a\cdot H^n$ and $\text{RC} = b\cdot H^N$, where a and b are coefficients, n and N are the field exponents, respectively. Interestingly, all the $\Delta S_m(T, H)$ curves measured at different applied fields are collapsed onto a universal curve, $\Delta S_m(T, H)/\Delta S_{\text{max}}$ versus $\vartheta = (T - T_C)/(T_r - T_C)$, where T_r is the reference temperature.

Keywords: Nanocrystallite manganites, Magnetocaloric effect, Magnetic phase transformation.

TU.F-P18 - Core-shell Ag@Fe₃O₄ brick-like nanoparticles for magnetic hyperthermia

M.E. Fortes Brollo¹, C. Sato², D. Muraca¹, R. López-Ruiz¹, K. Pirola¹, M. Knobel¹

1. Instituto de Física Gleb Wataghin, Unicamp, Campinas - Brazil

2. Brazilian Synchrotron Light Laboratory (LNLS) / Brazilian Center of Energy and Materials (CNPEM), Campinas - Brazil

Research on the heating efficiency of magnetic nanoparticles (NPs), under an alternating magnetic field for tumor treatment via hyperthermia has attracted a great interest in the last few years. Magnetite nanoparticles (Fe₃O₄) have shown excellent properties for this therapy, given their high values of energy dissipation. Coupled with an optical active noble metal such as Ag or Au, they could give rise to a wide variety of interesting phenomena, with potential application as markers for biological molecules, for example. Here we investigate the heating efficiency of multifunctional Ag (core)-magnetite (shell) nanoparticles. These NPs were synthesized by a rather simple synthetic route, resulting in compact, brick-like nanostructures (size) with interesting magnetic properties [1].

Magneto-hyperthermia was evaluated by means of the specific absorption rate (SAR) parameter, usually employed to evaluate the heat emission of a magnetic material when a resonant alternating magnetic field (frequency of 313 kHz) is applied. The results of our novel NPs were compared with pure magnetite and dimer (Ag-Fe₃O₄) NPs. The results indicate that these unique, compact core-shell NPs display SAR values similar to recent reported results of colloidal suspensions of plain magnetite with similar diameter, which are considered one of the best choices for in vivo applications.

Reference:

[1] M. E. F. Brollo, R. López-Ruiz, D. Muraca, S. J. A. Figueroa, K. Pirola, M. Knobel, "Compact Ag@Fe₃O₄ core-shell nanoparticles by means of single-step thermal decomposition reaction", Nature Scientific Reports (2014)

TU.F-P19 - Tailoring magnetic size-dependent properties of Co-ferrite nanoparticles for permanent magnet applicationsA. López-Ortega¹, E. Lottini¹, C.d.J. Fernandez², C. Sangregorio³*1. INSTM And Dipartimento Di Chimica, Firenze, Italy**2. INSTM and CNR-IMEM, Parma, Italy**3. INSTM and CNR-ICCOM, Sesto Fiorentino (Firenze), Italy*

Magnetic nanoparticles (NPs) have attracted a great interest in the last decades thanks to their novel fundamental properties emerging from their extremely reduced size. Special attention has been devoted to cobalt ferrite ($\text{Co}_x\text{Fe}_{3-x}\text{O}_4$) NPs due to their cheap manufacturing and high magnetic anisotropy. In particular, the application of cobalt ferrite in the realization of permanent magnet has attracted a renewed interest as an alternative to rare-earth base materials. Many works have been focused on the correlation between magnetic properties and stoichiometry, particle size and structural defects, demonstrating cobalt ferrite NPs are a promising candidate for permanent magnet application, although a global picture of the effect of each parameter on the final properties is still missing. Indeed, all these investigations have been limited to a short range of particle sizes and to confined temperatures. Therefore, a deeper understanding in structural, size-dependent and morphological effects on final physical properties appears necessary. Herein, we present the synthesis and investigation of a series of cobalt ferrite NPs with average size covering a broad range (from 4 to 60 nm), with narrow size distributions and controlled shape and stoichiometry. Structural, morphological and magnetic characterizations were carried out using several techniques, including transmission electron and helium ion microscopy, X-ray diffraction analysis and magnetometric measurements. The evolution of the magnetic properties was studied as a function of particle size and shape. In addition, we evaluated the (BH)max product, the figure of merit of permanent magnets, obtaining the maximum values ever reported in the literature for cobalt ferrite NPs (i.e., 2.1 MGOe (18 MJm⁻³) for 40 nm NPs) (see Fig. 1(i)). Finally, this study allowed us to settle the limits of cobalt ferrites for permanent magnet applications in base of the definition of the (BH)max product. (This research was supported by EU-FP7 NANOPYME Project (No. 310516)).

TU.F-P20 - Magnetic properties of mechanically alloyed bcc Fe-Pd influenced by hydrogen

Y. Jiraskova¹, J. Bursik¹, I. Turek¹, J. Cizek², O. Zivotsky³

1. Institute of Physics of Materials in Brno, Academy of Science of the Czech Republic, Brno Czech Republic

2. Charles University in Prague, Faculty of Mathematics and Physics, Department of Low Temperature Physics, Prague, Czech Republic

3. Department of Physics and RMTVC, VèB-Technical University of Ostrava, Ostrava, Czech Republic

Metastable Fe-Pd powder samples of nominal composition Fe₉₅Pd₅ were synthesized by mechanical alloying using a high-energy ball mill. Their fundamental properties, i.e., chemical and phase composition, lattice parameters, microstructure, morphology, grain size, macro- and micro-magnetic properties were monitored during milling procedure and discussed from the viewpoint of the milling atmosphere used. For these purposes the X-ray diffraction, Mössbauer spectrometry, high resolution scanning and transmission microscopy and magnetic measurements at room and elevated temperatures were applied. Two samples were prepared: the A sample was a mixture of Fe powder and of Pd powder pre-charged with hydrogen, the B sample was a mixture of Fe and Pd powders. The input Fe powder for both samples was annealed to remove oxides. Two objectives were followed: (i) the alloying of Fe and Pd(H) in A sample during milling under Ar atmosphere and (ii) the alloying of Fe and Pd in B sample during milling under hydrogen atmosphere. The A sample yields after 5 h of milling a slight decrease in saturation magnetization as compared to pure Fe, supported by a similar tendency of the hyperfine induction, but no highly defected interfacial phase has been observed. This phase appeared after further milling. On the contrary, the highly defected phase was detected after the same milling time (5 h under hydrogen) in sample B yielding a similar decreasing trend of magnetic behavior in the next steps and surprisingly a higher sensitivity to oxidation. The analyzed Henkel graphs point to negative magnetic interactions among the particles.

TU.F-P21 - On the interplay of dipolar interactions and surface spin disorder in colloidal maghemite nanocrystal clusters

A. Lappas¹, K. Brintakis^{1, 2}, A. Kostopoulou¹, M. Vasilakaki³, L. Manna⁴, A. Douvalis⁵, K. Trohidou³

1. *Institute of Electronic Structure and Laser (IESL), Foundation for Research and Technology - Hellas (FORTH), Heraklion, Greece*

2. *Department of Physics, Aristotle University of Thessaloniki, Thessaloniki, Greece*

3. *IAMPPNM, Department of Materials Science, NCSR Demokritos, Athens, Greece*

4. *Istituto Italiano di Tecnologia, Genova, Italy*

5. *Department of Physics, University of Ioannina, Ioannina, Greece*

Understanding the enhanced or collective magnetic properties of nanoscale systems made of multiple subunits is a key in their exploitation in various application fields extending from photocatalysis and magnetic storage to biomedicine. This study illustrates the controlled assembly of single-crystal, colloidal maghemite nanoparticles (NPs) via a high-temperature polyol-based pathway. The outcome is hydrophilic, size-tunable (50-90 nm) colloidal nanoclusters (CNCs), composed of crystallographically oriented maghemite NPs (10 nm). [1] Bulk ac/dc susceptibility of frozen aqueous dispersions and local-probe Mossbauer spectroscopy of such nanocolloids are complemented by Monte Carlo simulations. We discuss the impact on the microscopic interaction effects of the nanoparticle assembly process as this is dictated by the increasing volume fraction, ϕ , of the inorganic magnetic phase (i.e. from individual NPs to larger cluster-like nanoparticle assemblies). In addition to room-temperature ferrimagnetism, the study of the magnetic dynamics recognizes two different spin-dynamical regimes. Scaling-law analysis and Monte Carlo calculations suggest that a spin-glass state ($T_f < 70$ K) arises (i) in the individual NPs, from strong dipolar interactions and their impact on the surface spin disordering, whereas (ii) in the assembly of such NPs in clusters (with increased ϕ), from the interplay of dipolar interactions with an additional spin disorder due to the defected nanoparticle surface coordination environment. In this second case, the former interaction mechanism is responsible for the observed memory effects at the high-temperature superspin glass transition ($T_B < 200$ K). We suggest that the clarification of magneto-structural characteristics and coupling effects that influence the magnetization of a colloidal assembly of nanocrystals is essential in engineering functional nanoarchitectures for magnetically-driven technologies (e.g. MRI, magnetic hyperthermia etc).

Reference:

[1] A. Kostopoulou et al., *Nanoscale* **6**, 3764 (2014)

We acknowledge funding under the Action KRIPIS, project No MIS-448305 (PROENYL), of the GSRT/Ministry of Education, Greece and the European Regional Development Fund (NSRF 2007-2013)/EC.

TU.F-P22 - Influence of annealing process on the structure and magnetic behavior of $\text{Ba}_{0.5}\text{Co}_{0.5}\text{Fe}_2\text{O}_4$ nanoparticles

N. Osman¹, T. Moyo¹

1. University Of KwaZulu-Natal, Durban, South Africa

The structure and magnetic properties of $\text{Ba}_{0.5}\text{Co}_{0.5}\text{Fe}_2\text{O}_4$ nanoparticles were investigated for the as-synthesized and sample annealed at different temperatures of 300 °C, 400 °C, 500 °C and 600 °C. The phase structure was studied by means of X-ray powder diffraction (XRD). The XRD result revealed that the annealing process up to 500 °C decreases the sample microstrain and increases the crystallinity of the sample. The iron distribution and hyperfine interaction on the tetrahedral site and octahedral site for the as-prepared and sample annealed at different temperatures were studied using room temperature Mössbauer spectroscopy. The hyperfine field increases as the annealing temperature (TA) increases. The values of isomer shift show only the existence +3Fe. Investigation of the magnetic behavior for the as-prepared and the annealed samples was carried out using a mini-cryogen free VTI system in temperature range from 300 K to 4 K in the external magnetic fields of up to 5 T. The saturation magnetization decreases dramatically as the TA increases whereas the coercivity increases. The hysteresis loops as a function of measuring temperature show the effect of spin freezing. The values of the remanence (M_r) at 4 K decreases as the TA increases, whilst at 300 K, M_r increases with increasing TA. The measurement of reduced remanence shows cubic anisotropy for as-prepared and the samples annealed at different temperature.

TU.F-P23 - Dimensionality effects on the dynamics of dipolar interacting ferromagnetic fine particles: A monte carlo investigation

D. Brinis^{1,2}, D. Ledue², R. Patte², A. Laggoun¹

1. *Unité de Recherche MPE- Université de Boumerdes, Boumerdes, Algérie*

2. *Groupe de Physique des Matériaux, UMR 6634 CNRS - Université de Rouen, Saint-Etienne-du-Rouvray, France*

The magnetization dynamics of one- or two-dimensional self-organized assemblies of interacting nanoclusters [1] which are potential candidates for ultra-high density magnetic recording media was investigated using Monte Carlo simulations [2]. The study was focused on the temperature variation of the ac-susceptibility as well as the decay over time of the magnetization of cobalt nanoparticles having the same anisotropy axis. Evidence was found of significant dipolar interaction effects on the peak position of the imaginary part of the ac-susceptibility and on the relaxation time due to the common easy axis and the low-dimensionality of the assemblies even for low concentration (less than 10%). With increasing the strength of the dipolar interactions, the peak of the out-of-phase component shifts towards higher or lower temperatures depending on whether the magnetic moments are oriented in the plane assembly or perpendicular to it [3]. A peak shift towards higher (lower) temperatures is clearly linked to an increase (decrease) of the relaxation time. The relaxation time in the presence of dipolar interactions still follows an Arrhenius law [4] with an effective energy barrier which is either larger or smaller than the anisotropy energy barrier. It is also shown that random positions slightly strengthen the influence of dipolar interactions.

References:

[1] M. Pauly, B.P. Pichon, P. Panissod, S. Fleutot, P. Rodriguez, M. Drillon and S. Begin-Colin, *J. Mater. Chem.* 22, 6343 (2012)

[2] D.W. Heermann, *Computer Simulation Methods in Theoretical Physics*, 2nd Edition, Springer, Berlin, 1990. K. Binder, D.W. Heermann, *Monte Carlo Simulation in Statistical Physics*, 2nd Edition, Springer, Berlin, 1990

[3] D. Brinis, A. Laggoun, D. Ledue et R. Patte, *J. Appl. Phys.* 114, 173906, (2014)

[4] L. Néel, *Ann. Géophys.* 5, 99 (1949)

TU.F-P24 - Effect of Zn concentration on photonic crystals band structure of $\text{Co}_{1-x}\text{Zn}_x\text{Fe}_2\text{O}_4$ nanoparticules under an external perpendicular magnetic fieldG. Zambrano ¹, N. Porrás-Montenegro ², M.E. Gomez ¹, J. Alonso Lopez ^{1,3}, L.E. González ²*1. Thin Films Group, Universidad del Valle, , Cali, Colombia**2. Grupo de Física Teórica del Estado Sólido, Universidad del Valle, Cali, Colombia**3. CNYN-UNAM, Ensenada B.C., Mexico*

Ferrofluids based on $\text{Co}_{1-x}\text{Zn}_x\text{Fe}_2\text{O}_4$ magnetic nanoparticles are colloidal systems composed of a single domain of magnetic nanoparticles dispersed in a polar or a nonpolar carrier liquid. These kinds of systems are considered soft magnetic materials with interesting technological applications in nanotechnology, when the ferrofluids are placed in an external magnetic field. Morphological characterization of the $\text{Co}_{1-x}\text{Zn}_x\text{Fe}_2\text{O}_4$ magnetic nanoparticles was obtained through high-resolution transmission electron microscopy studies. In addition, we observed self-assemblies of $\text{Co}_{1-x}\text{Zn}_x\text{Fe}_2\text{O}_4$ magnetic nanoparticle aggregates forming columns in a hexagonal 2D photonic crystal, when the ferrofluid was encapsulated in a cell glass under the action of a tunable magnetic field applied perpendicular to the film. The dependence of the ferrofluid effective refractive index with the applied magnetic field strength was determined by laser interferometry measurements by using a Mach–Zehnder interferometer. To determine the optical response of 2D magneto-controllable photonic crystals based on ferrofluids under the action of a DC external magnetic field, the Maxwell-Garnett theory, the experimentally calculated effective refractive index, and the plane wave expansion method were used. The photonic band structure of 2-D photonic crystals for these ferrofluids were simulated, finding that the optical response of photonic crystal depends on the ferrofluid effective refractive index, the area ratio, the permittivity of magnetic columns, and on the composition of $\text{Co}_{1-x}\text{Zn}_x\text{Fe}_2\text{O}_4$ ferrofluids. The results showed that the photonic band structure of the ferrofluid with the least Zn concentration ($x = 0.25$) presented a complete band gap in the IR range ($\lambda \cong 10.6 \mu\text{m}$) at low perpendicular applied magnetic field. Finally, the procedure used in this work may be considered an alternative method to characterize the optical response of nanostructured ferrofluids in the presence of external magnetic fields. These results can be taken into account for technological applications of ferrofluids as magneto-controllable photonic crystals.

TU.F-P26 - Crystal Field Effects Of Er^{3+} In Cubic $\text{NaY}_{1-x}\text{Er}_x\text{F}_4$ Nanoparticles

A.F. Garcia-Flores¹, G. Lesseux², T. Caldonazo², D. Garcia³, R. Urbano², C. Rettori^{1,2}

1. Universidade Federal do ABC, CCNH, Santo André-SP, Brazil

2. Instituto de Física Gleb Wataghin, UNICAMP, Campinas-SP, Brazil

3. Centro Atómico Bariloche, S.C. de Bariloche, Río Negro, Argentina

In this work we report on the synthesis and the magnetic properties of $\text{NaY}_{1-x}\text{Er}_x\text{F}_4$ nanoparticles (NPs) doped with Er^{3+} ions (nominal concentration $x = 0.01$). The NPs were synthesized by thermal decomposition of trifluoroacetate precursors in a solution of octadecene and oleic acid at 300 °C. X-ray Diffraction (XRD) confirms their cubic crystallographic structure, $Fm-3m$. Transmission Electron Microscopy (TEM) images display that the synthesized NPs are nanopolyhedral and particle sizes vary from about 15 to 50 nm. The powder-like magnetic susceptibility data of the $\text{NaY}_{1-x}\text{Er}_x\text{F}_4$ NPs was fitted using a crystal field (CF) Hamiltonian appropriated for a $J = 15/2$ multiplet corresponding to Er^{3+} ions sited in cubic symmetry with $\mu_{\text{eff}} = 9.58\mu_{\text{B}}$ and $x = 0.008(1)$. The obtained 4th order CF parameter $B_{40} = 0.0096 \text{ K}$ ($B_{60} \ll B_{40}$) predicts an overall CF splitting of 318 K and a Γ_8 quadruplet ground state. By X-Band Electron Spin Resonance (ESR) experiments a Γ_7 doublet excited state with $g = 7.0(4)$ was detected, in agreement with the scheme of energy levels resulting from the magnetic susceptibility analysis.

TU.F-P29 - Structural changes in ferronematic liquid crystals studied by surface acoustic waves

Peter Bury¹, Štefan Hardoň¹, Jozef Kúdelčík¹, Peter Kopčanský², Milan Timko²

1. *Department Of Physics, Žilina University, Žilina, Slovakia*

2. *Institute of Experimental Physics, Slovak Academy of Science, Košice, Slovakia*

The response in attenuation of surface acoustic wave (SAW) of frequency 30 MHz propagating along ferronematic liquid crystals (6CHBT) to both electric and low magnetic field (up to 1.0 T) has been studied experimentally. Three low volume concentrations ($\Phi_1=1\times 10^{-5}$, $\Phi_2=5\times 10^{-5}$ and $\Phi_3=1\times 10^{-4}$) of spherical magnetic nanoparticles were added to liquid crystal during its isotropic phase. In contrast to undoped 6CHTB the distinctive SAW attenuation responses induced by both electric and magnetic fields in ferronematic liquid crystals below Fréedericksz transition have been observed suggesting structural changes. The geometrical re-ranking of magnetic nanoparticles was registered for some orientations of magnetic field, too. Observed results confirmed the significant influence of the presence of magnetic nanoparticles and their concentration on the structural properties of 6CHTB.

TU.F-P30 - Interactions in densely packed nanoparticle systems

M. Svante Andersson¹, R. Mathieu¹, P.S. Normile², S.S. Lee³, G. Singh⁴, P. Nordblad², J.A. De Toro¹

1. Department of Engineering Sciences, Uppsala University, Uppsala, Sweden

2. Instituto Regional de Investigación Científica Aplicada (IRICA) and Departamento de Física Aplicada, Universidad de Castilla-La Mancha, Ciudad Real, Spain

3. Institute of Bioengineering and Nanotechnology, Singapore, Singapore

4. Ugelstad Laboratory, Department of Materials Science and Engineering, Norwegian University of Science and Technology (NTNU), Trondheim, Norway

Spherical γ -Fe₂O₃ nanoparticles having a very narrow size distribution were packed using a hydraulic press which resulted in a filling fraction close to random close packing (64%). Three samples were made from 8, 9 and 11.5 nm particles. Reference samples were made by pressing the same particles coated with a thick silica shell. The references were used to determine the properties of the individual magnetic particles which are only very weakly interacting. From SQUID magnetometry it was found that all of the samples are superspin glasses exhibiting dynamic properties; aging, memory, rejuvenation and critical slowing down qualitatively similar to atomic spin glasses. The dependence of the freezing temperature as a function of particle size suggests that dipolar interactions dominate in these systems in spite of the direct contact between the particles.

TU.F-P31 - Autoresonant switching of the magnetization in single-domain nanoparticles

G. Klughertz¹, L. Friedland², G. Manfredi¹, P.A. Hervieux¹

1. *Institut de Physique et Chimie des Materiaux de Strasbourg, CNRS and Universite de Strasbourg, Strasbourg, France*

2. *Racah Institute of Physics, Hebrew Univesrity of Jerusalem, Jerusalem, Israel*

The ability to control the magnetization switching in nanoscale devices is a crucial step for the development of fast and reliable techniques to store and process information. Also, the quest for higher density in magnetic data storage implies future use of smaller nanoparticles with high magnetic anisotropy to overcome the superparamagnetic limit. But an increased anisotropy requires larger fields to reverse the magnetization of the nanoparticle, which is experimentally difficult experimentally. To elude this limitation, a microwave field can be combined with the static field [1], and it has been shown that the optimal microwave field should be modulated both in frequency and magnitude [2].

We investigate the magnetization reversal of single-domain Co nanoparticles with uniaxial anisotropy under the macrospin approximation. We show that the switching dynamics can be controlled efficiently by combining a static magnetic field with a microwave field with time-dependent frequency (autoresonance) [3]. According to the autoresonance theory, a nonlinear oscillator can be strongly excited by using a weak chirped frequency drive [4]. If the drive strength exceeds a threshold, the oscillator will stay phase-locked to the drive and excited to high amplitudes without any feedback.

We provide a full theoretical framework for the autoresonant switching technique, by exploiting the analogy between the magnetization state of a nanoparticle and a two-level quantum system [5], whereby the switching process can be interpreted as a population transfer. We derive the threshold amplitude of the microwave field and consider the effects of damping and thermal fluctuations. Finally, using a mean field approach, we show that dipolar interactions in a chain of nanoparticles tend to cancel out the effect of the temperature on the threshold.

References:

- [1] C. Thirion, W. Wernsdorfer and D. Mailly, *Nat. Mater.* 2, 524-527 (2003)
- [2] N. Barros, M. Rassam, H. Jirari and H. Kachkachi, *Phys. Rev. B* 83, 144418 (2011)
- [3] G. Klughertz, P.-A. Hervieux and G. Manfredi, *J. Phys. D: Appl. Phys.* 47, 345004 (2014)
- [4] J. Fajans and L. Friedland, *Am. J. Phys.* 69, 1096 (2001)
- [5] R. Feynman, F. L. Vernon, and R. W. Hellwarth, *J. Appl. Phys.* 28, 49 (1957)

TU.F-P32 - Magneto-optical study of ferritin with different iron content

M. Koralewski¹, L. Melnikova², M. Pochylski¹, Z. Mitroova², P. Kopcansky²

1. Faculty of Physics, Adam Mickiewicz University, Poznań, Poland

2. Institute Of Experimental Physics SAS, Košice, Slovakia

Ferritin is the iron-storage protein of living organisms. It consists of ferrihydrite-like mineral core surrounded by the apoferritin hollow sphere with diameter of about 12 nm, capable of accommodating up to 4500 iron atoms according to the specific requirements of the metabolism [1, 2]. Understanding the precise mechanisms of iron ions incorporation and release in ferritin in vivo is very important in relationship with many various diseases (cancer, neurodegenerative, cardiovascular) that could be caused by iron ions accumulation and overloading of ferritin biomacromolecules followed by the disruption of the normal storage function of this protein. In general, chemical composition of the ferritin core significantly differs between physiological and pathological occurrence [3]. Magneto-optical measurements of ferritins could be useful for qualitative and quantitative distinguishing of various mineral core structures [4].

Our work presents experimental investigation of magneto-optical properties of reconstructed and reduced horse spleen ferritin (HSF) core modified by the chemical process. Iron reduction of ferritin was done by partial core reduction of HSF followed by iron(II) chelation. Ferritin reconstruction was realized using the apoferritin shell, oxidant and iron(II) solution in anaerobic conditions. Magnetically induced optical birefringence (Δn) and Faraday rotation was measured at room temperature for aqueous suspensions of modified ferritins with different iron contents. It was shown that magnetic birefringence and Cotton-Mouton constant of studied aqueous suspensions provides evidence that the ferritin core behaves as a non-Euclidian solids and uptake and release process is not symmetrical. Both magneto-optical phenomena suggest that iron mineral with high magnetization do not appear in the synthetic core of ferritins.

References:

- [1] P. M. Harrison, P. Arosio, *Biochim. Biophys. Acta* 1275 (1996) 161
- [2] S.H. Banyard et al., *Nature* 271 (1978) 282
- [3] C. Quintana, *Mini-Rev. Med. Chem.* 7 (2007) 961; J. Dobson, *FEBS Lett.* 496 (2001) 1
- [4] M. Koralewski et al., *Nanotechnology* 23 (2012) 355704; *J. Magn. Magn. Mater.* 323 (2011) 2413.

The work was supported by the European Structural Funds (PROMATECH no. 26220220186) and PHYSNET no. 26110230097.

TU.F-P33 - High performance core-shell structured magnetic nanoparticles: Fabrication, characterization, and application

L. Wang¹, Y. Jin¹, J. Wang¹, A. Ferrie¹, Y. Chen¹

1. Corning Incorporated, Corning, United States of America

Heterostructured magnetic nanoparticles, such as core-shell structured magnetic nanoparticles (Mag@shell), are emerging as next generation materials due to their synergistically enhanced magnetism and multi-functionalities for various fields including high density magnetic storage, chemical catalysis, magnetic resonance imaging (MRI), and biomedical separation and diagnostics. In this presentation, we will review some of our recent work on the design and fabrication of core-shell structured magnetic nanoparticles with high performance capabilities. The core-shell structured magnetic nanoparticle examples in this presentation will include either inorganic shell or organic shell or both, e.g. Mag@gold, Mag@silver, and Mag@polymers. The core-shell structures were characterized and confirmed by a series of instruments and analysis methods including HRTEM, EDX hypermap element maps, XRD, XPS, and surface reactivity. The magnetic properties of Mag@shell were studied by a SQUID instrument, which showed differences between magnetic nanoparticles with shell and without shell in terms of blocking temperature, magnetization, and coercivities. These core-shelled magnetic nanoparticles have demonstrated feasibility and capability for different applications. The internal evaluation results showed some of our core-shell structures had comparable or better performance in biomedical separation and diagnostic applications than similar products currently in the market.

TU.F-P34 - Magnetostatic interactions in dense clusters of magnetic nanoparticles

N. Usov¹, O. Serebryakova¹

1. Pushkov Institute Of Terrestrial Magnetism, Ionosphere And Radio Wave Propagation RAS

A detailed numerical simulation of quasistatic hysteresis loops of dense quasispherical clusters of interacting magnetic nanoparticles is carried out. Both the clusters of magnetically soft and magnetically hard nanoparticles are considered. The clusters are characterized by an average particle diameter D , the cluster radius R_c , the particle saturation magnetization M_s , and the uniaxial anisotropy constant K . The number of particles in the cluster varies between $N = 30 - 120$. The particle centers are randomly distributed within the cluster, their easy anisotropy axes being randomly oriented. It is shown that a rare assembly of identical random clusters of nanoparticles can be characterized by two dimensionless parameters: 1) the intensity of mutual magnetostatic interaction, K/M_s^2 , and the average particle concentration within the cluster, $g = VN/V_c$. Here V is the nanoparticle volume, and V_c is the volume of the cluster, respectively. For magnetically soft nanoparticles, $K/M_s^2 \ll 1$, the universal hysteresis loops of the assembly are constructed. In the variables $(M/M_s, H/M_s)$ these hysteresis loops depend only on the particle filling factor g , which varies in the range $0 < g < 0.5$. The hysteresis loops of magnetically hard nanoparticles in the variables $(M/M_s, H/H_a)$, where $H_a = 2K/M_s$ is the anisotropy field, are close to the standard Stoner-Wohlfarth hysteresis loop.

TU.F-P35 - Preparation of ϵ -Fe₂O₃ nanoparticles by crystal structural transformation of iron oxide nanoparticles

R. Nishida¹, A. Muramatsu¹, M. Nakaya¹

1. Tohoku University, Sendai, Japan

Introduction : ϵ -Fe₂O₃ nanoparticles have received much attention from the industrial point of view due to their large coercivity at room temperature. However, it is very difficult to obtain single-phase ϵ -Fe₂O₃ nanoparticles, because ϵ -Fe₂O₃ phase is an intermediate phase on the transformation from γ -Fe₂O₃ phase to α -Fe₂O₃ phase. To prepare ϵ -Fe₂O₃ phase selectively, focusing on the formation energy of ϵ -Fe₂O₃ phase is important. In this study, the effects of treatment temperature and particle size on the formation of ϵ -Fe₂O₃ phase were investigated.

Experimental : FeO nanoparticles with the size of 24, 40 and 60 nm were synthesized by our previous method (*Chem. Lett.* 42, 863 (2013)). As-obtained nanoparticles were coated with SiO₂ shell to prevent their tremendous aggregation during heat treatment (*J. Chem. Chem. Eng.* 7, 1050 (2013)). The resulting SiO₂ coated FeO nanoparticles were treated at 1000 - 1200 °C in the air.

Results and Discussion : When 40 nm FeO nanoparticles with ca. 15 nm SiO₂ shell were treated, significant aggregation and increase in particle size were observed at every treatment temperatures. As-prepared nanoparticles were found the mixture of γ -Fe₂O₃, ϵ -Fe₂O₃ and α -Fe₂O₃ phases. When 40 nm FeO nanoparticles were treated to cover with ca. 40 nm SiO₂ shell, the particle aggregation was completely inhibited. The crystal structure was found to transform from γ -Fe₂O₃ phase to α -Fe₂O₃ phase via ϵ -Fe₂O₃ phase as the treatment temperature increased. The ϵ -Fe₂O₃ nanoparticles formed at 1100 °C showed large coercivity of 20.8 kOe at 300 K. As a result, the control in change in the crystal structure with temperature, under the complete inhibition against aggregation nor the growth in size, is the most important so that ϵ -Fe₂O₃ is selectively formed as a desired product. (Financial support by JSPS Grant-in-Aid for young Scientists (B) 24730121 M. Nakaya)

TU.F-P36 - Spin diffusion in nonlocal spin valves operated by spin pumping

L. Feiler¹, N. Kuhlmann¹, G. Meier^{1,2,3}

1. Institut für Nanostruktur- und Festkörperphysik, ehem. Institut für Angewandte Physik und Zentrum für Mikrostrukturforschung, Universität Hamburg, Hamburg, Germany

2. The Hamburg Centre for Ultrafast Imaging, Hamburg, Germany

3. Max-Planck Institute for the Structure and Dynamics of Matter, Hamburg, Germany

In the past years, high frequency properties of magnetic nanostructures became of great interest since they offer fundamental understanding of spin dynamics as well as new potential technological applications. We study lateral spin valves in nonlocal geometry [1], using the spin-pumping effect as injection mechanism [2]. A pure spin current that arises from a ferromagnetic nanostructure driven at ferromagnetic resonance (FMR) is injected into the adjacent normal metal. In addition a second ferromagnetic electrode enables to detect and quantify the pure spin current. We simultaneously measure the broadband FMR transmission and the nonlocal voltage, in order to be able to comprehensively interpret the data.

To calculate the spin diffusion length, in the experiments the power of high-frequency excitation is varied. The resulting power dependence of the non-local voltage is fitted to a model that includes the spin-current injection by spin pumping, its diffusive decay in the normal metal, and the heating of the device. The latter could cause a Seebeck contribution. For devices with a copper normal metal strip we estimate from the experimental data a spin-diffusion length of 174 nm at room temperature. The presented method allows to determine the spin-diffusion length within one sample and in a short measurement time in comparison to standard methods [3].

Financial support of the Deutsche Forschungsgemeinschaft via SFB 668, GK 1286 and the excellence cluster CUI is gratefully acknowledged.

References:

[1] N. Kuhlmann, C. Swoboda, A. Vogel, T. Matsuyama, and G. Meier, PRB 87, 104409 (2013)

[2] Y. Tserkovnyak, A. Brataas, and G.E.W. Bauer, PRL 88, 117601 (2002)

[3] F. Jedema, A. T. Filip, and B. J. van Wees, Nature 410, 345 (2001)

TU.F-P37 - Effects of milling conditions on nano-scale MnFe(P,Si) particles by surfactant-assisted high-energy ball milling

T. Nguyen¹, E.H. Bruck¹, N.H. van Dijk¹

1. FAME, RST, TU Delft

The effects of milling parameters on nano-scale MnFe(P,Si) particles obtained by surfactant-assisted high-energy ball milling have been investigated. The presence of surfactant oleic acid prevents the re-welding of crushed particles and enhances the dispersion of nanoparticles in the solvent during the ball milling. This is supported by the fact that without the surfactant, the heptane remained clear after milling while it changed color from transparent to brown when the surfactant was added to the milling process. The XRD peak intensity decreases and the peaks broaden with increasing milling time, indicating a decrease in grain size. With increasing the milling time, spontaneous magnetization becomes lower and thermal hysteresis becomes smaller. This may be due to a larger contribution of the surface states as a result of either a decrease in particle size or surface contamination. The surfactant concentration does not have a strong impact on the magnetic properties of the obtained nanoparticles which is consistent with the X-ray diffraction data showing the same patterns at different surfactant concentration.

TU.F-P38 - Effects of milling conditions on nano-scale MnFe(P,Si) particles by surfactant-assisted high-energy ball milling

T. Nguyen¹, E.H. Bruck¹, N.H. van Dijk¹

1. FAME, RST, TU Delft

The effects of milling conditions on nano-scale MnFe(P,Si) particles obtained by surfactant-assisted high-energy ball milling have been investigated. The presence of surfactant oleic acid prevents the re-welding of crushed particles and enhances the dispersion of nanoparticles in the solvent during the ball milling. This is supported by the fact that without the surfactant, the heptane remained clear after milling while it changed color from transparent to brown when the surfactant was added to the milling process. The XRD peak intensity decreases and the peaks broaden with increasing milling time, indicating a decrease in grain size. With increasing the milling time, spontaneous magnetization becomes lower and thermal hysteresis becomes smaller. This may be due to a larger contribution of the surface states as a result of either a decrease in particle size or surface contamination. The surfactant concentration does not have a strong impact on the magnetic properties of the obtained nanoparticles which is consistent with the X-ray diffraction data showing the same patterns at different surfactant concentration.

TU.F-P39 - Synthesis of iron-oxide nanoparticles. Size and shape effect on magnetic properties

J.M. Orozco¹, D. Muraca¹, S. Sharma¹, M. Knobel¹

1. Universidade Estadual De Campinas, Campinas, Brazil

Iron-Oxide nanoparticles with sizes between 5-18nm obtained by means of thermal decomposition and their static magnetic properties are reported. Sizes and shapes were tuned making small changes in the synthesis process (concentration of some of its reactivities were varied). Furthermore, in one case, the final step of the synthesis was modified allowing the reaction to have contact with room atmosphere obtaining an increment on the average size of the nanoparticles and different geometries. Structural characterization, X-ray diffraction and TEM images was performed in different samples and related with magnetic measurements. Zero Field Cooled and Field Cooled (ZFC/FC) magnetization at several applied fields as well as hysteresis loops at different temperatures were measured. From these data it was possible to infer blocking temperatures, coercive field, saturation magnetization and log-normal size distribution of the nanoparticles (based on conventional superparamagnetism modelling). Values of anisotropies from $\sim 2.8 \times 10^4 \text{ J/m}^3$ to $\sim 7.9 \times 10^4 \text{ J/m}^3$ and saturation magnetization at room temperature (from $\sim 37 \text{ A.m}^2/\text{kg}$ to $\sim 78 \text{ A.m}^2/\text{kg}$), were obtained, indicating a strong dependence on interactions, size and shape of the nanoparticles.

TU.F-P41 - Soft magnetic $Zn_xMn_{1-x}Fe_2O_4$ spinelsM. Schmidt¹, M. Christensen¹*1. Center for Materials Crystallography, Department of Chemistry and iNANO, Aarhus University, Aarhus, Denmark*

Soft magnetic nanoparticles with spinel structure has attracted significant attention due to potential applications in bio imaging and for permanent magnets.[1] By reducing the size below 10 nm it has been shown that superparamagnetic nanoparticles with very high magnetic saturation (175 emu/g) can be obtained.[2] The magnetic properties of the spinel structures are related to the position of the transition metals. The general formula of the spinel structure can be written as $[AII+]_{tet}[BIII+]_{oct}2O_4$, where A is the tetrahedral site normally preferred by the $^{2+}$ ion, while B is the octahedral site preferred by the $^{3+}$ ion. Ideally all the Zn^{2+} should be allocated on the tetrahedral site, however conventional powder X-ray diffraction cannot establish this and more advanced characterization techniques like EXAFS or neutron powder diffraction must be employed. We have prepared a series of spinel structures (Fd-3m, $a = 8.44 \text{ \AA}$) with formula $Zn_{1-x}Mn_xFe_2O_4$ ($x=0, 0.2, 0.4, 0.5, 0.6, 0.8, \text{ and } 1$) using hydrothermal synthesis from chloride precursors, which were precipitated using ammonia hydroxide. The magnetic properties of the compositions range were determined using vibrational sample magnetometry. In our studies we are not capable of reaching the high saturation magnetization values reported in the literature. In fact the pure Zn sample appears to be antiferromagnetic corroborate with Zn^{2+} occupying the A site. While for the Mixed Mn and Zn structures our findings suggests that Zn^{2+} , Mn^{2+} and Fe^{3+} is randomly distributed over the two A and B site in the spinel structure.

References:

- [1] Frey, N. A. et al. Magnetic nanoparticles: synthesis, functionalization, and applications in bioimaging and magnetic energy storage, *Chem. Soc. Rev.* 2009,38, 2532-2542
- [2] Jang J.-T. et al. Critical Enhancements of MRI Contrast and Hyperthermic Effects by Dopant-Controlled Magnetic Nanoparticles, *Angew. Chem. Int. Ed.* 2009, 48, 1234 -1238

TU.F-P42 - Structural and magnetic properties of cobalt ferrite nanoparticles obtained by laser ablation in liquid

G. Bulai¹, I. Dumitru¹, M. Pinteala², C. Focsa³, S. Gurlui¹

1. *Atmosphere Optics, Spectroscopy and Lasers Laboratory- LOASL, Faculty of Physics, Alexandru Ioan Cuza University, Iasi, Romania*

2. *Petru Poni Institute of Macromolecular Chemistry, 41A Gr. Ghica Voda Alley, Iasi, Romania*

3. *Laboratoire de Physique des Lasers, Atomes et Molécules (UMR 8523), Université Lille 1 Sciences et Technologies, Villeneuve d'Ascq, France*

Magnetic nanoparticles are extensively studied for applications which include flexible electronics, MRI imaging and drug delivery, multiple state memory elements, highly transparent magneto-optic materials, magnetic field sensors etc. The combination of cobalt ferrite polymer materials can account for significant advances in different technological areas. The study of polymer coated cobalt ferrite nanoparticles for cancer therapy applications is sustained by the interesting properties of both components (e.g. biocompatibility, magnetic response).

Our work was focused on studying both the influence of laser wavelength and fluence and solution type on the particle dimension, chemical and magnetic properties of the laser ablated nanoparticles. The cobalt ferrite target was obtained by conventional ceramic technique using commercially available pure oxides (Fe_2O_3 and Co_3O_4) as starting materials. The milled powders were pressed into disks at 250 MPa and sintered in air at 1250 °C for 5 hours with a 100 °C/h heating rate followed by a natural cooling to room temperature. The target was immersed in different solutions of distilled water, ethanol and PEG (Mw=4000 and 6000) in different concentrations. The nanoparticles were obtained using the first (1064 nm) and second harmonic (532 nm) of an Nd-YAG laser with a 10 ns pulse duration and 10Hz repetition rate. The laser radiation was focused on the single phase cobalt ferrite pellet by a 7 mm focal length lens and the fluence was varied from 4 to 12J/cm². The solutions were dried at 100 °C and the material was collected for further investigations. The structural and chemical properties of the obtained nanoparticles were studied by X-ray diffraction, scanning electron microscopy/energy dispersive X-Ray spectroscopy, transmission electron microscopy and dynamic light scattering. The magnetic response was investigated using a vibrating sample magnetometer. The obtained nanoparticles presented a spinel structure with particle dimensions and magnetization values depending on the laser fluence.

TU.F-P43 - Dopant effect on the magnetic and structural properties in $\text{Sn}_{1-x}\text{TM}_x\text{O}_y$ nanoparticles (TM = Co, Fe and Mn)

C. Meneses¹, T. Cunha², I. Costa², J. Duque¹, R. Lima³

1. *Universidade Federal De Sergipe, Departamento de Física, Campus de Itabaiana, Itabaiana, Brazil*

2. *Universidade Federal De Sergipe, Departamento de Física, Campus São Cristóvão, São Cristóvão, Brazil*

3. *Universidade Federal de Campina Grande - Unidade Acadêmica de Física, Campina Grande, Brazil*

In this work we have investigated the magnetic and structural properties in TM-doped SnO_y nanoparticles (TM = Fe, Co and Mn; y = 1 and 2) obtained using different chemical methods. The results of X-ray diffraction allied to the Rietveld refinement revealed that the samples present an average particle size from 4 to 60 nm. These results were confirmed by transmission and scanning electron microscopy. The optical band gap was estimated by UV-Vis and your values are close to 4 eV for both tin oxides. Fittings of magnetization curves as a function of temperature show only 1% and 20% of the ions are in a paramagnetic state for SnO₂ and SnO doped samples, respectively. The magnetization as a function of field curves show that all Fe-doped SnO_y samples present a ferromagnetic ordering at room temperature. We have observed also an increasing in the magnetization and a decreasing in your coercive field with increasing of the dopant concentration. Such ordering can be attributed to interaction between the diluted Fe ions, provided by possible defects in the crystal structure. The EPR results obtained at room temperature show two lines presenting g's close to 4,3 and 2, corresponding to the values of the ordered and paramagnetic components, respectively.

TU.F-P44 - Fe,Mn-dilution effect on the magnetic properties in $Zn_{1-x}(Fe,Mn)O$ nanoparticles

C. Meneses¹, I. Costa², T. Cunha², J. Almeida¹, J. Duque¹

1. *Universidade Federal De Sergipe, Departamento de Física, Campus de Itabaiana, Itabaiana, Brazil*

2. *Universidade Federal De Sergipe, Departamento de Física, Campus São Cristóvão, São Cristóvão, Brazil*

In this work we have studied the magnetic, optical and structural properties of ZnO nanoparticles pure and doped with different concentrations of Fe and Mn synthesized by three different synthesis methods; co-precipitation (CP), hydrothermal (SH) and thermal decomposition (DT). The samples were characterized by measurements of X-ray diffraction (XRD) and analyzed allied to Rietveld refinement method, absorption in the UV-Vis region, scanning and transmission electron microscopy (SEM and TEM), and magnetization measurements as a function of field and temperature (MvsT, MvsH). Through XRD analysis we have observed a dependence of the size with increasing temperature for both CP and SH methods well as a change in morphology with temperature for the samples system synthesized by SH. XRD analysis through the Williamson-Hall plot associated with the TEM images show that particles obtained by SH and CP methods present an anisotropic growth, different of the particles obtained by DT method, that they present a spherical-like shape. The XRD results for $Zn_{1-x}FexO$ systems obtained by the CP and SH present only one phase but from point of view magnetic properties we have observed that these samples present transition at low temperature ($T = 10K$) similar to an antiferromagnetic ordering. However, the $Zn_{1-x}FexO$ samples obtained by DT synthesis we have observed a paramagnetic behavior evidenced by MvsT curves. Therefore, at room temperature the MvsH curves indicated a ferromagnetic behavior. All $Zn_{1-x}MnxO$ ($x=0,01, 0,5$ e $0,10$) present a paramagnetic behavior. The UV-Vis results show for all systems a slow increase in gap band with increases of dopant concentration.

TU.F-P45 - Behavior of the magnetic hyperfine field in Fe₃O₄ nanoparticles doped with hafniumI. Matos¹, G. Cabrera-Pasca¹, R. Vianden², R. Saxena¹, A. Carbonari¹, J.A. Souza³1. *Ipen-Usp, São Paulo, Brazil*2. *HISKP, Bonn University, Bonn, Germany*3. *Universidade Federal Do ABC, Santo André, SP, Brazil*

Fe₃O₄ magnetic nanoparticles (MNPs) have been intensively investigated because their non-toxic and biocompatibility characteristics and due to its ability to become magnetized when exposed to a magnetic field, which is enhanced by the presence of superparamagnetism. These features make them good candidates for new biomedical applications, which include drug delivery, imaging, labeling and tracking cells. Fe₃O₄ has a cubic inverse spinel structure with two different A and B sites, with tetrahedral and octahedral coordination of oxygen, respectively. A-sites are occupied by Fe³⁺ ions whereas B-sites carry Fe²⁺ and Fe³⁺ ions in equal proportions. Doping Fe₃O₄ nanoparticles with other elements can tune its magnetic behavior and an investigation of the local effects of this doping within an atomic scale is necessary. In this work, we have investigated the local magnetic properties of Hf-doped Fe₃O₄ (5%) by perturbed γ - γ angular correlation (PAC) spectroscopy using ¹⁸¹Hf(¹⁸¹Ta) and ¹¹¹In(¹¹¹Cd) as probe nuclei. ¹⁸¹Hf(¹⁸¹Ta) probe nuclei were obtained by irradiating of Hf-doped Fe₃O₄ with thermal neutrons in the IEA-R1 research reactor of IPEN. Doped Fe₃O₄ samples were prepared by co-precipitation method. The structure of compounds were characterized by X-ray diffraction (XRD) and their morphology by transmission electron microscopy (TEM). XRD Results show that the samples crystallize in the expected structure with single phase. Magnetization measurements were also carried out and show an expected magnetic behavior with a blocking temperature around 100 K. PAC results for the measured temperatures with both compounds showed a pure time-dependent magnetic dipole interaction below 300 K, which is ascribed to the time dependence of the superparamagnetic behavior of the nanoparticles.

TU.F-P46 - Tuning the size of magnetic CoFe₂O₄ nanocrystallites - An in situ powder X-ray diffraction studyH. Lyder Andersen¹, M. Christensen¹*1. Center for Materials Crystallography, Department of Chemistry and iNANO, Aarhus University, Aarhus, Denmark*

Magnetic spinel ferrites, MFe₂O₄ (M = Co²⁺, Cu²⁺, Ni²⁺, etc.), are very important magnetic materials with many modern technological applications.[1] Notably, CoFe₂O₄ has a large magnetic anisotropy, high abundance and excellent chemical stability as well as a good saturation magnetization, mechanical hardness and relatively high Curie temperature (~793 K).[2] This makes CoFe₂O₄ an important magnetic material with a wide range of uses in e.g. magnetic recording media, ferrofluids and biomedicine.[3] In this study, the evolution of size and size distribution during hydrothermal synthesis of nanocrystalline CoFe₂O₄ has been investigated by in situ synchrotron powder X-ray diffraction (PXRD). Controlling the size and size distribution during CoFe₂O₄ nanocrystallite synthesis is a key issue as the electrical, optical and magnetic properties are highly dependent on the crystallite size.[4] Varying synthesis temperature or [OH⁻] concentration in the precursor proves to have no significant effect on the final volume-weighted nanocrystallite sizes (~12 nm) of CoFe₂O₄. However, analysis by whole powder pattern modeling of the [OH⁻] concentration series reveals a substantial difference in the number-weighted size distributions when varying the amount of base used. Furthermore, changing the metal ion concentration prior to NaOH addition in the precursor preparation gives a handle to control the nanoparticle sizes (~5-15 nm). The in situ experiments show almost instantaneous formation of the CoFe₂O₄ nanocrystallites, without significant growth or broadening of the size distribution after 60 s. Magnetic hysteresis curve measurements illustrate, how this facilitates the tailoring of materials with specific magnetic properties, as larger particles (~15 nm) exhibit hard magnetic properties while the smaller particles (~6-7 nm) are superparamagnetic. More information can be found in a recently published paper.[5]

References:

1. R. Valenzuela, Physics Research International, 2012, 2012
2. R. Skomski, J. Phys.: Condens. Matter, 2003, 15, R841-R896
3. D. S. Mathew and R. S. Juang, Chem. Eng. J., 2007, 129, 51-65
4. M. Artus, L. B. Tahar, F. Herbst, et al. Phys.: Condens. Matter, 2011, 23, 506001
5. H. L. Andersen and M. Christensen, Nanoscale, 2015

TU.F-P47 - Coexistence of superparamagnetic and spin glass behaviors in Co₃₀Cu₇₀ granular alloy and room temperature memory effect

S. Dhara¹, R. Roy Chowdhury¹, B. Bandyopadhyay¹

1. Saha Institute Of Nuclear Physics, Kolkata, India

Granular binary alloys display interesting magnetic and magneto-transport properties. We have studied the magnetic properties of Co₃₀Cu₇₀ alloy prepared by borohydride reduction of CoCl₂ and CuCl₂ solutions with CTAB as the capping agent. XRD studies shows diffraction peaks coming only from fcc Cu phase confirming alloy formation. From XRD line width and TEM micrographs average particle size is calculated as 15 nm. ICPOES studies confirms elemental compositions of the sample as Co-31.26% and Cu-68.74%. The temperature dependencies of magnetization in ZFC-FC protocols of Co₃₀Cu₇₀ shows branching which indicates superparamagnetism. Blocking temperature from ZFC-FC magnetization is 367K. The peak in the ZFC curve at 7K is coming for spin glass like short range magnetic interaction that is suppressed at high external magnetic field like 1 Tesla. We have study the memory effect Co₃₀Cu₇₀ sample. The difference between this ZFC magnetization with intermittent stop and the normal ZFC magnetization as a function of temperature shows a dip at the stopping temperature if there exist a spin glass like ordering. First we have chosen TS as 10 K but at this temperature MZFC-MZFC(ref) shows no dip. But when TS is 4 K, i.e., below the glassy temperature 7 K there is a dip in the difference. In the superparamagnetic region intermediate changes in condition, either by decreasing temperature or by switching field to zero, do not affect the relaxation mechanism. Rather, it repeats the previous history which is a signature of memory effect. At the room temperature the sample is in blocked state, it shows memory effect in room temperature. This room temperature memory is very important in technological application which causes by distribution of particle sizes of non-interacting superparamagnetic system. At the end, we conclude that the sample is superparamagnetic with a small glassy contribution in low temperatures and the sample shows room temperature memory effect.

TU.F-P48 - Characterization of biocompatible magnetic nanoparticles modified by PEG

M. Kubovcikova¹, I. Antal¹, M. Koneracka¹, V. Zavisova¹, J. Kovac¹, P. Kopcansky¹

1. Institute Of Experimental Physics, Slovak Academy Of Sciences Bratislava, Slovak

Magnetic fluids (MF) are stable colloidal suspensions of magnetic nanoparticles (around 10 nm in diameter) in a liquid carrier. To meet biomedical requirements they have to be superparamagnetic, and non-toxic. Due to their small size and superparamagnetic behaviour, MFs offer a variety of uses in the field of biomedicine. This paper deals with preparing magnetite nanoparticles sterically stabilized by sodium oleate and modified with polyethylene glycol (PEG, average molecular weight of 6 kDa) to produce biocompatible magnetic fluid (MFPEG). Characterization of prepared magnetic nanoparticles in terms of size distribution, thermal and colloidal stability and magnetic properties was carried out. Different methods such as dynamic light scattering (DLS), differential centrifugal sedimentation (DCS) and magnetic measurements were used to determine particle size distribution. The magnetic measurements confirmed superparamagnetic behaviour of samples at room temperature. Thermal stability of both MF and MFPEG was observed using DLS and via application of AC magnetic field, where changes in the temperature dependence of AC susceptibility were monitored. The out-of-phase component of the complex susceptibility as a function of applied field frequency was used for hydrodynamic diameter determination of modified magnetic nanoparticles. From the peak observed at 997 Hz we determined a Brownian relaxation time 1,6.10-4 s and consequently a hydrodynamic diameter of approx. 76 nm. This value correlates with the values obtained from DLS and DCS measurements with the output of 51.72 nm and 47.2 nm respectively for unmodified sample and 65.56 nm and 685 nm for MFPEG, respectively. Finally, the magnetic core diameter calculated from magnetic measurements was estimated to be 6.85 nm. The exact characterization of the prepared magnetic nanoparticles allows the further MF modification with specific biocompatible material (PEG), which offers good prospects of biomedical application.

Acknowledgement: This work was supported within project No. 26110230097 in frame of Structural Funds of European Union.

TU.F-P49 - Influence of magnetic nanoparticles on nematic to isotropic phase transition kinetics in liquid crystal mixture

K. Csach¹, A. Juríková¹, J. Miskuf¹, N. Tomasovicová¹, Z. Mitroová¹, V. Zavisová¹, M. Koneracká¹, P. Kopcanský¹, N. Éber², K. Fodor-Csorba², V. Vajda²

1. Institute Of Experimental Physics, Slovak Academy Of Sciences, Kosice, Slovakia

2. Institute for Solid State Physics and Optics, Wigner Research Centre for Physics, Hungarian Academy of Sciences, Budapest, Hungary

For practical purpose of liquid crystals, the mixtures of substances are used. The transition from crystalline to liquid phase is more complex and proceeds through several intermediate phases. The controlled nematic to isotropic phase transition is usually exploited in liquid crystal based displays.

The binary mixture of bent-core (10DCIPBBC) and rod-shaped (6008) liquid crystals (with the weight ratio of 1:1) was chosen as a model substance combining the properties of both types of the liquid crystals. The mixture was doped with the spherical and the rodlike magnetic nanoparticles with the concentrations of $7,5 \times 10^{-4}$ and $8,5 \times 10^{-4}$, respectively. DSC experiments were performed for the pure as well as the doped mixture at different heating rates ranging from 1 to 16 °C/min. The kinetics of nematic to isotropic phase transition was evaluated in the framework of the differential isoconversional method. The addition of the magnetic nanoparticles lowered the phase transition temperature. This effect is more intensive in the case of the rodlike magnetic nanoparticles. Measured enthalpy change decreased from the value of 2 J/g for the pure mixture to the value of about 1,5 J/g for the liquid crystal mixture modified by the magnetic nanoparticles. The calculated apparent activation energy showed non-monotonous behaviour and the sensitivity on the shape of added magnetic nanoparticles.

This work was supported by the projects Nos. 26220120021 and 26110230097 provided in the frame of Structural funds of the European Union.

TU.F-P50 - Influence of magnetic nanoparticles on phase transition temperatures in bent-core and rod-shaped liquid crystal mixture

A. Juríková¹, K. Csach¹, J. Miskuf¹, N. Tomasovicová¹, Z. Mitróová¹, V. Závisová¹, M. Koneracká¹, P. Kopcanský¹, N. Éber², K Fodor-Csorba²

1. *Institute Of Experimental Physics, Slovak Academy Of Sciences, Kosice, Slovakia*

2. *Institute for Solid State Physics and Optics, Wigner Research Centre for Physics, Hungarian Academy of Sciences, Budapest, Hungary*

Binary mixtures of bent-core and rod-shaped liquid crystals (LCs) are the subject of intensive research due to their potential applications. Whereas pure bent-core compounds have LC phases above room temperature, which limits their utility for many applications, mixtures of bent-core and rod-shaped molecules can extend the mesophase temperature range to near room temperature. We studied phase transitions of the binary mixture of bent-core and rod-shaped LCs with the weight ratio of 50:50 wt% using differential scanning calorimetry. Isotropic to nematic transition at the temperature above 90°C was followed by nematic to smectic transition below the temperature 40°C and by crystallization at sub-ambient temperature. The same transitions were observed for the mixture doped with two types of magnetic nanoparticles, spherical and rodlike. The influence of the nanoparticle shape on the transition temperatures in the bent-core and rod-shaped LC mixture was studied. The phase transition temperatures varied with cooling rates (2-10°C/min). The activation energies of the phase transitions in the LC mixtures were evaluated from linear fits of Kissinger plots. Doping the LC mixture with the magnetic nanoparticles caused the shift the transition temperatures at continuous cooling from the isotropic state. The isotropic to nematic phase transition temperature was shifted to lower temperatures by rodlike nanoparticles more than by spherical ones. Nematic to smectic and smectic to crystalline phase transition temperatures were lowered by doping the liquid crystal mixture with rodlike nanoparticles, whereas the spherical nanoparticles caused the shift towards the higher temperatures. The highest shift of the phase transition temperature (up to several °C) was observed for crystallization of the mixture doped by the rodlike nanoparticles. It was found that among the studied transitions the crystallization was the phase transition with the lowest apparent activation energy.

The work was supported by projects 26220120021 and 26110230097 provided in the frame of the European Union.

TU.F-P51 - Probing structural and chemical inhomogeneities in assemblies of nanoparticles with wide size distributions: A ferromagnetic nuclear resonance study of cobalt nanoparticles for producing synthetic fuel

Y. Liu¹, Y. Shin^{2,3}, C. PhamHuu¹, C. Meny^{2,3}

1. *Institut de Chimie et Procédés pour l'Énergie, l'Environnement et la Santé (ICPEES), UMR 7515 CNRS-University of Strasbourg, ECPM, 25, Strasbourg Cedex 02, France*

2. *Institut de Physique et Chimie des Matériaux de Strasbourg (IPCMS), UMR 7504 CNRS-University of Strasbourg, Strasbourg Cedex 02, France*

3. *Department of Physics, CNRS-Ewha International Research Center, Ewha Womans University, Seoul, South Korea*

Assemblies of nanoparticles are widely studied in many research fields such as spintronics, medicine or catalysis. Their properties will depend on the size, shape, crystallographic structure and chemical composition of the nano-particles. In addition, assemblies of nanoparticles often show wide size distributions making the interpretation of their properties even more complicated. Indeed the structure and the chemical order of the particles might change with the size of the particles within the particles size distributions. In this work we show that Ferromagnetic Nuclear Resonance (FNR, i.e. Nuclear Magnetic Resonance for ferromagnets) [1] allows mapping the structure and the chemical order of assemblies of nanoparticles within their size distributions. In this study we have investigated two types of assemblies of nanoparticles with wide size distributions. The first type of nanoparticles consists in Cobalt nanoparticles used in catalysis for producing synthetic fuel. We have shown that the smallest particles in the size distributions have mostly an hcp crystallographic structure while the largest ones have mostly an fcc structure [2]. This information provides a unique insight into the morphology of such distributions of nanoparticles. The results are correlated to the catalytic activity of the samples. In a second example we study the chemical composition inhomogeneities within the size distribution of CoFe nanoparticles.

References:

1. P. Panissod, C. Meny, *Appl. Magn. Reson.* 19, 447-460 (2000)
2. Y.F. Liu, I. Florea, O. Ersen, C. Pham-Huu, C. Meny, *ChemCommun*, 51, 145-148 (2015)

TU.F-P52 - Exchange-bias and collective magnetic behavior of random binary compacts of maghemite nanoparticles

J.A. De Toro ¹, M. Svante Andersson ², S.S. Lee ³, P.S. Normile ¹, P. Muñiz ¹, G. Singh ⁴, J.M. Colino ¹, R. Mathieu ², P. Nordblad ²

1. *Instituto Regional de Investigación Científica Aplicada (IRICA) and Departamento de Física Aplicada, Universidad de Castilla-La Mancha, Ciudad Real, Spain*

2. *Department of Engineering Sciences, Uppsala University*

3. *Institute of Bioengineering and Nanotechnology, Singapore*

4. *Department of Chemical Engineering, Norwegian University of Science and Technology*

The narrow size distribution achieved in the synthesis of maghemite nanoparticles [1] has allowed the accurate control of the bimodal size distribution resulting from the mixture of two types of almost monodispersed particles (9.0 and 11.5 nm in diameter). The mixing was performed in liquid solution to ensure a random distribution of the two populations. The solutions were then dried and the resulting powders compressed to form close-packed discs with different proportions of small (volume V) and big (volume 2V) nanoparticles. Superspin glass behavior with a single transition temperature (which increases linearly with the proportion of big particles) is observed across all the series, but the effective broadening of the size distribution smears out the transition peak observed in AC and DC magnetic susceptibility curves and affects the dynamical critical exponent. The temperature and frequency dependence of the magnetic susceptibility at and below the freezing temperature is discussed in detail. The end members of the series (pure small/big particles) exhibit different values of the exchange bias field, indicating the presence of a similarly thick magnetically disordered shell in the particles of each volume (a result confirmed from the difference between the 'Langevin magnetic size' and the TEM size). Furthermore, the strong dipolar interactions present in these random-close-packed systems [1] do not significantly affect the exchange bias of the individual particles, as concluded from the linear variation of this parameter across the concentration series. This result is discussed in the light of recent Montecarlo simulations on core/shell interacting particles [2].

References:

[1] J. A. De Toro, P. S. Normile, S. S. Lee et al., J. Phys. Chem. C 117, 10213 (2013)

[2] G. Margaris, K. N. Trohidou and J. Nogués, Adv. Mater. DOI 10.1002/adma.201200615 (2012)

TU.F-P53 - Interactions and surface effects in bimagnetic CoO_core/Co_{0.5}Ni_{0.5}Fe₂O₄_shell nanoparticles

G. Lavorato¹, E. Winkler¹, E. Lima Jr¹, D. Peddis², H. Troiani¹, E. Agostinelli², D. Fiorani², A. Ghirri³, D. Rinaldi³, R. Zysler¹

1. Centro Atómico Bariloche, S.C. de Bariloche, RN, Argentina

2. Istituto di Struttura della materia-CNR, Monterotondo (Rome), Italy

3. Università Politecnica delle Marche, Ancona, Italy

With the aim to investigate the surface effects on bimagnetic core/shell nanoparticles we have fabricated antiferromagnetic CoO nanoparticles encapsulated within a ferrimagnetic Co_{0.5}Ni_{0.5}Fe₂O₄ shell. The material was synthesized by seed-mediated growth high-temperature decomposition method, which leads to nanoparticles composed by ~ 2.4 nm CoO cores surrounded by a ~2 nm thick Co_{0.5}Ni_{0.5}Fe₂O₄ shell. We have analyzed the magnetic properties of two samples by ac and dc-magnetization measurements: the as-synthesized (A-sample) and the annealed in air at 573 K nanoparticles (B-sample). From the ac-susceptibility we have observed that the B-sample presents a single peak centered in the 150-200 K range, following a Vogel-Fulcher phenomenological law. On the contrary, the A-sample presents two peaks, one located in the 100-150 K range, which also follows the Vogel-Fulcher law and a low temperature maximum located at 2-5 K, which is weakly frequency sensitive. The Vogel-Fulcher dependence can be related to the progressive blocking of interacting magnetic supermoments and the fitting parameter indicates that the interactions are weaker in the as-synthesized sample. The ZFC-FC measurements confirm the superparamagnetic-blocked behavior, where the mean blocking temperatures are $\langle TB \rangle \sim 64$ K and $\langle TB \rangle \sim 104$ K for the A and B samples, respectively. Instead, the frequency dependence of the low temperature peak of the as-synthesized sample follows a Power Law compatible with spin-glass transition. Finally, it is important to mention that the annealed sample presents an enhanced coercivity (HC) with an exchange bias field (HEB), i.e. $HC \sim 13$ kOe and $HEB \sim 1.5$ kOe at 50 K, compared to the as-synthesized sample. These results indicate that the annealed bimagnetic nanoparticles behave as an exchange coupled system while the as-synthesized system presents weaker intraparticle interactions with a lower TB. In addition, the surface of the Co_{0.5}Ni_{0.5}Fe₂O₄ shell remains magnetically disordered and thermally fluctuates and freezes into a spin-glass-like state at a much lower temperature.

TU.F-P54 - Coffee ring effect analyzed by eddy current sensing in drying magnetite solution droplets

J.C. Martínez-García¹, A. Rascón¹, D. Lago-Cachón¹, M. Rivas¹, J.A. García¹

1. Departamento de Física & IUTA, Universidad de Oviedo. Edificio Departamental Este, Gijón, Spain

When a drop of particle dispersion is evaporated on a surface, the solid phase creates non-homogenous ring-shaped patterns, commonly known as coffee rings [1]. Different characteristics of the particles (size, covering, electrostatic charge and magnetic properties) or the liquid (pH and viscosity) influence the formation of these patterns [1]. Therefore, creating homogenous depositions of particles is not a simple task. In this work magnetic nanoparticles (MNP) have been dried onto glass slides and blotting paper strips and the resulting concentration pattern has been analyzed using an electromagnetic impedance-based sensor. The sensing principle has been recently identified by the authors [2] and is based on the eddy-current effects produced by the superparamagnetic character of the nanosized particles [2]. In this work the method is tested for 2D-scanning of the droplets. For room temperature-evaporated droplets more than 90% of the particles are located on the outer ring, occupying 30% of the surface. With the aim of achieving homogenous samples for sensing purposes, different temperature-controlled deposition protocols have been carried out and tested by means of the eddy-current sensor.

References:

- [1] R.B. Deegan et al., Nature 1997, 389, 827
- [2] D. Lago-Cachón et al., Nanotechnology 2013, 245501

TU.F-P55 - Bottom-up Structuring of Magnetic SrFe₁₂O₁₉ Nanoplatelets

M. Saura-Múzquiz¹, C. Granados-Miralles¹, M. Christensen¹

1. Center for Materials Crystallography, Department of Chemistry and iNANO, Aarhus University, Denmark

Hard magnetic materials are of key importance in a large variety of scientific and technological applications.[1, 2] The discovery of high performance rare-earth magnets directed the attention away from conventional magnets. However, recent geopolitical problems have sparked the need for new and cheaper rare-earth reduced/free magnetic materials consisting of more abundant elements.[3]

Nano-structuring of conventional magnetic ferrites has the potential to significantly improve their magnetic performance making them a viable alternative for certain applications.[4] An excellent candidate is the hexaferrite SrFe₁₂O₁₉ due to its pronounced magnetocrystalline anisotropy. Here, SrFe₁₂O₁₉ nanoparticles of various sizes have been synthesized using the Supercritical Hydrothermal Flow method. Control over the particle size has been achieved by varying synthesis parameters, such as pH, temperature and the metal concentration upon addition of the base. Results, obtained from Rietveld refinement of powder X-ray diffraction data, TEM and AFM, reveal a platelet-like shape of the nanoparticles, thin along the crystallographic *c*-axis (~3-8 nm), and large in the *ab*-plane (~20-60 nm). The aspect ratio of the nanoplatelets (*ab/c*) is variable, and highly dependent on particle size. Compaction of the tailored nanoplatelets into bulk magnets has been carried out through Spark Plasma Sintering, obtaining highly aligned nanocrystals. This leads to large enhancement of the magnetic properties, reaching a maximum of 25.11 kJ/m³.

This Research was partially supported by EU-FP7 NANOPYME Project (No. 310516) [www.nanopyme-project.eu]

References:

1. I. Matsui, *Jpn J Appl Phys* 1, 2006, **45**, 8302-8307
2. S. Tammaruckwattana and K. Ohyama, *Ieee Ind Elec*, 2013, 7157-7162
3. R. L. Moss, E. Tzimas, H. Kara, P. Willis and J. Kooroshy, *Critical Metals in Strategic Energy Technologies*, European Union, Luxembourg: Publications Office of the European Union, 2011
4. E. F. Kneller and R. Hawig, *Ieee T Magn*, 1991, **27**, 3588-3600

TU.F-P56 - X-ray magnetic circular dichroism of free, 3d transition metal molecules

V. Zamudio-Bayer¹, K. Hirsch², A. Langenberg², A. Lawicki², A. Terasaki^{3,4}, B. von Issendorff¹, T. Lau²

1. *University of Freiburg, Freiburg, Germany*

2. *Helmholtz-Zentrum Berlin, Berlin, Germany*

3. *Cluster Research Laboratory, Toyota Technological Institute*

4. *Kyushu University, Fukuoka, Japan*

Only recently was it possible for the first time to measure the x-ray magnetic circular dichroism (XMCD) of free, size selected clusters. This achievement opens up new possibilities to better understand how spin coupling and orbital magnetic moment in 3d transition metals develop from the isolated atom to the bulk material. With this in mind, we have now measured the XMCD of free 3d transition metal molecules consisting of two and three atoms, i.e. dimers and trimers. We have studied cationic homonuclear molecules of chromium, manganese, iron, and cobalt. The high complexity of the electronic structure of these smallest molecules is evidenced by the numerous attempts in the literature to theoretically describe their electronic ground states. For chromium and manganese, it turns out that the experimentally obtained x-ray absorption spectra and the XMCD show a very good agreement with simulated atomic spectra, indicating that the 3d orbitals remain atomically localized in the molecules and their ferromagnetic ground state arise from the dominating double-exchange contribution. In the case of iron and cobalt dimers, the application of the XMCD sum rules allows the resolution of spin and orbital contributions to the total magnetic moment in these molecules and to therefore determine their electronic ground state. The comparison with theoretical studies in the literature show that in the case of iron the calculations systematically underestimate the orbital magnetic moment.

TU.F-P57 - Spatially-resolved EELS analysis of antibody distribution on biofunctionalized magnetic nanoparticles

R. Arenal^{1,2,3}, L. De Matteis¹, L. Custardoy^{1,2}, A. Mayoral^{1,2}, M. Tence⁴, V. Grazú¹, J.M. de la Fuente⁵, C. Marquina^{5,6}, M.R. Ibarra^{1,2,6}

1. Instituto de Nanociencia de Aragón (INA); Universidad de Zaragoza, Zaragoza, Spain

2. Laboratorio de Microscopías Avanzadas (LMA); Universidad de Zaragoza, Zaragoza, Spain

3. Fundación ARAID; Gobierno de Aragón, Zaragoza, Spain

4. Laboratoire de Physique Solides; Université Paris-Sud, Orsay, France

5. Instituto De Ciencia De Materiales De Aragón (ICMA); CSIC-UZ, Zaragoza, Spain

6. Departamento de Física de la Materia Condensada; Universidad de Zaragoza, Zaragoza, Spain

We have made use of Spatially Resolved Electron Energy Loss Spectroscopy (SR-EELS) using Scanning Transmission Electron Microscopy (STEM) for the identification and determination of the spatial distribution of the components/elements of immuno-functionalized core-shell superparamagnetic nanoparticles at subnanometer scale [1].

Core-shell magnetic nanoparticles are commonly used in biomedical applications, as supports for macromolecules of biological interest. The shell, either organic or inorganic, allows in principle the use of different functionalization protocols to link a large variety of biological moieties, depending on the final purpose. The functionalization of nanoparticles with antibodies makes possible the use of the nanoparticles in applications based on immunorecognition processes, in which the particles act, for example, as carriers for targeted drug delivery, as labels for immuno-assays etc. An adequate immobilization strategy is critical to guarantee not only the stability of the antibody binding on the nanoparticle surface, but also its correct orientation. Therefore, detailed knowledge of the functionalized nanoparticle surface is crucial when working with nanoparticle-antibody conjugates. Some information can be obtained by means of biochemical techniques but there is still a need for characterization at microscopic level. The results obtained in our work have shown, for the first time to our knowledge, how SR-EELS measurements allow the study and direct identification of the biological moieties (protein G and anti-Horse Radish Peroxidase antibody, which were used in our model system) on the nanoparticle. Our findings provide information on their spatial localization/distribution on the nanoparticle surface. We conclude that the data obtained in this study, together with those gathered by conventional biochemistry techniques, provide insight into the efficiency and potential applications of these nanoparticles in biomedicine and related fields.

Reference:

[1] R. Arenal, L. de Matteis, L. Custardoy, A. Mayoral, M. Tence, V. Grazú, J. M. de la Fuente, C. Marquina, M. R. Ibarra, ACS Nano 7 (2013) 4006

TU.F-P58 - Structural and magnetic properties in co-deposited Fe-doped Yb films

C. Rojas-Ayala ^{1,2}, E. Passamani ³, M. Sousa ¹, F.J. Litterst ^{1,4}, E. Baggio-Saitovitch ¹

1. *Centro Brasileiro de Pesquisas Físicas, Rio de Janeiro, Brazil*

2. *Universidad Nacional Mayor de San Marcos, Facultad de Ciencias Físicas, Lima, Peru*

3. *Universidade Federal do Espírito Santo, Departamento de Física, Vitória, Brazil*

4. *Technische Universität Braunschweig, Institut für Physik der Kondensierten Materie, Braunschweig, Germany*

Structural and magnetic properties of co-deposited (x at.% Fe)Yb (x = 0.3 - 5.0) films have been investigated by X-ray absorption spectroscopy, Mössbauer spectroscopy and magnetization measurements. EXAFS analysis indicates a short-range order for Fe atoms, which is consistent with nano-sized Fe clusters. Room temperature Mössbauer spectra reveal three paramagnetic components that order magnetically at 4.2 K. Specifically, low temperature Mössbauer spectra show a broad magnetic hyperfine field distribution, which can be attributed to inhomogeneous inter-cluster interactions; compatible with susceptibility data that suggest spin-freezing behavior with weakly interacting clusters at temperatures below ca. 20 K. Our data indicate that the Fe clusters are in nanometer scale and for this reason, the gyromagnetic ratios, determined by ferromagnetic resonance experiments that is dependent on Fe concentration, display values smaller than that found for the metallic Fe-bulk.

TU.F-P59 - Pressure-dependence of the magnetic irreversibility in the disordered phase of Superantiferromagnetic TbCu₂ nanoparticles

M. De La Fuente Rodríguez¹, C. Echevarria-Bonet^{1,5}, D.P. Rojas², I. de Pedro^{1N}, J. Rodríguez Fernández¹, J.A. Blanco³, P. Gorria³, M.L Fdez-Gubieda⁴, L. Fernández Barquín¹

1. *Universidad de Cantabria, Santander, Spain*

2. *Universidad Politécnica de Madrid, Madrid, Spain*

3. *Universidad de Oviedo, Oviedo, Spain*

4. *Universidad del País Vasco/EHU, Leioa, Spain*

5. *Institut for Energy Technology*

Recent investigations on metallic nanoparticles of TbCu₂ produced by inert-gas high-energy milling have revealed the existence of a superantiferromagnetic state with a Néel temperature $T_N \approx 47$ K. On top of that ordered state, there is an evidence for a spin freezing $T_f \approx 9$ K due to the presence of surface of randomized moments [1]. The frozen moments interface provokes the existence of magnetic anisotropy giving rise to exchange bias [2]. The role of the magnetically disordered phase depends on the size of the nanoparticles and it is clearly affected by the magnetic field affecting the irreversibility [1]. However the dependence of the irreversible state with the pressure (P) is not so well analyzed. In this contribution we will show the effect in the Neel and freezing temperatures. The nanoparticle alloys have been obtained after different milling times ($0.5 \text{ h} \leq t \leq 15 \text{ h}$) with a reduction of the size ($D \leq 25 \text{ nm}$) and increase of microstrain ($\eta \leq 0.7 \%$), as revealed by X-ray diffraction. DC-magnetization ZFC-FC curves were obtained for $P \leq 11 \text{ kbar}$ at different cooling fields $H \leq 1 \text{ T}$. The results indicate that there is not a significant modification of the T_N values as expected. By contrast, The T_f values are reduced with increasing P indicating that magnetic moments become stiffer. As an indication, the variation of $T_f(P)$ with pressure is around 10% which is much smaller than $T_f(H) \approx 70 \%$ in the $t = 2 \text{ h}$ nanoalloy. The relative importance of the variation of T_f with pressure and field will be discussed. In this sense, in superparamagnetic core/shell nanoparticles the blocking temperature is also modified by pressure [3] and occurs in spin glasses of LaGdAu in which the T_f -decrease reaches $\Delta T_f/\Delta P = -14 \text{ mK kbar}^{-1}$ [4].

References:

- [1] C. Echevarria-Bonet et al., Phys. Rev. B 87, 180407(R) (2013)
- [2] C. Echevarria-Bonet et al., Submitted to Phys. Rev. B
- [3] Y. Komorida et al., J. Magn. Magn. Mat. 322, 2117 (2010)
- [4] F. Razavi and J. S. Schilling, J. Phys. F: Met. Phys. 13, L59 (1983)

TU.F-P60 - Co and Ni doping in iron oxide nanoparticles: A systematic study

T. Orlando¹, M. Albino², C. Innocenti², C. Sangregorio², M. Corti¹, A. Lascialfari³

1. *Department of Physics and INSTM, University Of Pavia, Pavia, Italy*

2. *Department of Chemistry 'U. Schiff' and INSTM, University of Florence, Florence, Italy*

3. *Department of Physics and INSTM, Università degli Studi di Milano, Milan, Italy*

The role of the magnetic material is crucial in determining the physical properties at the nanoscale. Several iron oxide nanostructures doped with cobalt, zinc or gadolinium have been already investigated, but a complete and systematic study on the effect of doping is still missing. In order to address this issue, five cobalt and nickel substituted ferrite ($\text{Co}_x\text{Ni}_y\text{Fe}_{3-x-y}\text{O}_4$) nanoparticles were ad hoc synthesized, having a fixed size (7 nm) and a step-by-step doping, going from “pure” Co-ferrite to “pure” Ni-ferrite. This allowed us to explore the influence of the doping avoiding any contribution coming from the size-effect or from the different synthesis procedure. A complete set of DC and AC susceptibility measurements were performed, allowing us to study both static and dynamic properties. The evolution of the magnetization, the blocking temperature and the parameters governing the magnetization reversal were explored as a function of doping. A deeper study about the magnetic anisotropy, directly connected with the lattice structure and the ions arrangements, was then performed. Using two distinct approaches, the effective anisotropy constant K_{eff} was estimated. The first relies on the direct estimation of the energy barrier from fit of the ZFC curve; the second allows the evaluation of K_{eff} from the value of the coercive field. Comparing the obtained data with the ones of undoped iron oxide nanoparticles having similar size, a clear trend connected to the amount and the kind of doping material was found. Specifically, the “pure” cobalt ferrite exhibits a very high anisotropy compared to all the other nanoparticles and, in general, the more is the cobalt doping, the higher is the anisotropy barrier. On the contrary, the anisotropy barrier of “pure” Ni-ferrite turns out to be even lower than the one of undoped maghemite particles, although the nickel ion is magnetic.

TU.F-P61 - Synthesis strategies of single-core magnetic nanoparticles

H. Gavilán¹, S. Veitemillas-Verdaguer¹, L. Gutiérrez¹, M. Puerto Morales¹

1. Institute Of Material Science (ICMM-CSIC) Cantoblanco, Madrid, Spain

Among other functional nanomaterials, magnetic iron oxide nanoparticles (MNPs) are especially promising as contrast enhancement agents for magnetic resonance imaging (MRI), drug carriers for disease treatment and heat mediators for cancer treatment by magnetic hyperthermia. Each of these biomedical applications requires MNPs with specific properties, and therefore it is of great importance to be able to control the shape, size and magnetic interaction of MNPs. Nowadays, just a few synthesis strategies and coating methods allow the production of single core nanoparticles, by preventing aggregation and minimizing the inter-particle interactions [1]. However not all the size ranges and varieties of shapes are covered by the synthesis of direct magnetic cores. We present a three-step aqueous approach to obtain Fe₃O₄ single-core particles based on the synthesis of antiferromagnetic nanoparticles, its coating and subsequent transformation to magnetite. This method has the advantage of the low inter-particle interactions of as-synthesized nanoparticles that allows the coating of the particles independently. In addition, it covers different size ranges and allows obtaining different morphologies that antiferromagnetic materials exhibit. This opens up new possibilities and interesting magnetic behaviours. Regarding hyperthermia for cancer treatment, different geometric shape leads to distinct shape anisotropy, resulting in significant difference in hysteresis loss and Specific Absorption Rates (SAR) values [2]. Recently, Serantes et al. found that the chain-like arrangement biomimicking magnetotactic bacteria could exhibit better heating performance than the randomly distributed system, implying the crucial role of shape anisotropy [3].

The careful control of the coating process of the antiferromagnetic particles allows the obtention of single-core antiferromagnetic nanoparticles that will remain as single core entities once their crystalline structures is transformed into magnetite. By fine-tuning the initial particles sizes and morphologies, we have produced a library of single core MNPs that may have very interesting properties for different biomedical applications.

TU.F-P62 - Mössbauer Study of Co-Ti ferrite nanoparticles for magnetic hyperthermia treatmentY. Ichiyanagi², A. Kamzin¹, K.E. Romachevsky¹, K. Mori²1. *Yokohama National University, Yokohama, Japan*2. *A. F. Ioffe Physico-Technical Institute of RAS, St Petersburg, Russia*

Study of magnetic hyperthermia treatment attracted attention recent years. Magnetic nanoparticles (MNPs) are sufficiently small to be introduced into cells, and some particles such as magnetite (Fe_3O_4) particles are known to be biocompatible with the human body.

In this study, functionalized MNPs, SiO_2 -shelled $\text{Co}_{1+x}\text{Ti}_x\text{Fe}_{2-2x}\text{O}_4$, ($0.2 \leq x \leq 0.5$) ferrite nanoparticles with average diameters ranging from 6 to 12 nm were produced by a wet chemical method. The use of these nanoparticles in hyperthermia treatments has been discussed on the basis of measurements of their AC magnetic susceptibilities.

Fig. 1 shows the X-ray diffraction patterns and Mössbauer spectra for the $\text{Co}_{1+x}\text{Ti}_x\text{Fe}_{2-2x}\text{O}_4$ ($x = 0.2, 0.3, 0.4, \text{ and } 0.5$) samples. Single-phase spinel structure was confirmed in all the different samples. The broad peak observed around 25° on X-ray diffraction patterns corresponds to amorphous SiO_2 .

The imaginary part of the AC magnetic susceptibility χ'' was measured for samples placed in a 1-Oe, 100-Hz AC magnetic field at room temperature. The optimum concentration of Ti ions was found to be that corresponding to $x = 0.3$ with diameter of 12 nm. This result was confirmed by the Mössbauer spectra, indicating that the Co-Ti ferrite at $x = 0.3$ was in a superparamagnetic state and this was determined from the AC magnetic susceptibility measurements. A temperature increase of about 10 K was observed in a 300-Oe, 10-kHz field. The determined values of T/dt ranged from 0.001 to 0.008 K/s, depending on the frequency and composition when a field with a fixed strength of 50 Oe was applied; when the frequency was fixed at 10 kHz, the determined values of $\Delta T/dt$ ranged from 0.05 to 0.9 K/s. These samples are expected to be used as thermal agents in magnetic hyperthermia treatment. In vitro experiment supported the drastic hyperthermia effect.

TU.F-P63 - Coherency of reversible magnetization changes in Ni nanorods

C. Schopphoven¹, A. Tschöpe¹, C. Dennis², R. Shull²

1. *Universität des Saarlandes, Campus D2.2, Saarbrücken, Germany*

2. *National Institute of Standards and Technology, Gaithersburg, United States of America*

Magnetic particles allow the contactless application of forces or torques through external magnetic fields, which enables the use of such particles as microrheological probes or as active components in soft magnetic actuators. Detailed characterization of the magnetic properties of the particles is of vital importance to correctly analyze microrheometric measurements or predict and optimize the system behavior of magnetically functionalized soft composites. The objective of this study was the characterization of reversible magnetization changes of cylindrical ferromagnetic nanoparticles in transverse homogeneous magnetic fields and the related magnetic torque acting on the particles.

We investigated uniaxial ferromagnetic nickel nanorods with a mean diameter of ~20 nm and a mean length of ~320 nm. The nanorods were synthesized by current-pulsed electrodeposition of Ni into porous alumina (AAO) templates. The particles were then released by dissolving the alumina layer and embedded in a mechanically stiff 10 wt % gelatin hydrogel matrix. Application of a homogeneous field during gelation resulted in a uniaxial texture of the sample. The field-dependent magnetization components parallel and perpendicular to the applied field in an angular range of 0°- 90° with respect to the sample texture axis were measured using a vector vibrating sample magnetometer (VSM). The resulting angles and values of the average magnetization vectors were then compared with the predictions of the Stoner-Wohlfarth model for coherent rotation.

At lower angles of the texture axis (0° - 70 °) the magnetization rotation was largely coherent over the entire field range of 0 - 1500 mT as indicated by a nearly constant total magnetization. At larger angles, the deviation from coherency was negligible for small field strength up to 100 mT. However, a significant drop of the total magnetization was observed in the case of high field strength and angles approaching 90 °, indicating incoherent rotation. These results provide the range of parameters in which the Stoner-Wohlfarth model with an experimentally determined effective anisotropy constant can be applied to describe the magnetic torque acting on the cylindrical ferromagnetic nanoparticles.

We acknowledge financial support by the German National Science Foundation (DFG Priority Program SPP 1681).

TU.F-P64 - Iron oxide-based magnetic nanostructures for enhanced theranostic applications

E. Fantechi^{1,2}, A. Roca¹, J. Nogués^{1,3}, C. Innocenti², M. Albino², C. Sangregorio⁴

1. Institut Català de Nanociència i Nanotecnologia (ICN2), Bellaterra, Spain

2. INSTM - Laboratorio di Magnetismo Molecolare (LA.M.M.), Dip. di Chimica, Università di Firenze, Firenze, Italy

3. Institució Catalana de Recerca i Estudis Avançats (ICREA), Barcelona, Spain

4. Consiglio Nazionale delle Ricerche - Istituto di Chimica dei Composti Organometallici (CNR-ICCOM), Firenze, Italy

Magnetic nanoparticles (MNPs) are excellent building-blocks for the development of innovative biomedical nanodevices with multi-fold therapeutic and diagnostic activities. Among the different applications of MNPs, one of the most promising is their use as heat mediators for Magnetic Fluid Hyperthermia (MFH), a thermal treatment of cancer that relies on the highest sensitivity of tumoral cells to temperature with respect to healthy ones. There is an increasing interest in improving the hyperthermia efficiency of MNPs for MFH, with the aim to reduce the dose required and improve the efficiency of the treatment. Up to now, the most investigated materials for MFH are the iron oxides magnetite and maghemite. In this contribution, we present two promising strategies for the enhancement of hyperthermic efficiency of these materials. In the first one, the magnetic and hyperthermic properties of the material are tuned through the partial or total substitution of Fe(II) with other bivalent cations, like Co(II) and Zn(II). Here we focus on highly monodisperse Co-doped [1,2] and Co/Zn-doped iron oxide-based MNPs, investigating the dependence of the hyperthermic efficacy on the magnetic and structural properties, and considering the role of magnetic anisotropy and saturation magnetization in increasing the heat release capability. A second promising strategy is the realization of magnetic-plasmonic nanosystems able to combine MFH with another hyperthermic therapy, i.e., Plasmonic Absorption Hyperthermia (PAH), in which plasmonic NPs generate heat when irradiated with laser light. In this contribution we focus on complex hetero-dimer magnetic-plasmonic nanostructures, based on iron oxide and gold. The results show that hetero-dimer nanoparticles exhibit plasmonic and magnetic properties similar to the ones of the different counterparts.

References:

[1] E. Fantechi, et al., J. Phys. Chem. C 2012 116 8261

[2] E. Fantechi, et al., J. Magn. Magn. Mat. 2015 380 365

TU.F-P65 - Spin-glass-like freezing of inner and outer surface layers in hollow maghemite nanoparticles.

H. Khurshid ¹, P. Lampen-Kelley ¹, O. Iglesias ², M.H. Phan ¹, M.L Saboungie ³, C. Sun ³, H. Srikanth ¹

1. Department of Physics, University of South Florida, Tampa, United States

2. Dpt. Física Fonamental and IN2UB, Universitat de Barcelona, Barcelona, Spain

3. Center for Nanoscale Materials, Argonne National Laboratory, Illinois, United States

Disorder among surface spins largely dominates the magnetic response of ultrafine magnetic particle systems. In this work, we examine time-dependent magnetization in high-quality, monodisperse hollow maghemite nanoparticles with a 15 nm outer diameter and enhanced surface-to-volume ratio. The nanoparticle ensemble exhibits spin-glass-like signatures in dc magnetic aging and memory protocols and ac magnetic susceptibility. The dynamics of the system slows near 50 K, and becomes frozen on experimental time scales below 20 K. Remanence curves indicate the development of magnetic irreversibility concurrent with the freezing of the spin dynamics. A strong exchange-bias effect and its training behavior point to highly frustrated surface spins that rearrange much more slowly than interior spins with bulk coordination. Monte Carlo simulations of a hollow particle reproducing the experimental morphology corroborated strongly disordered surface layers with complex energy landscapes that underlie both glass-like dynamics and magnetic irreversibility. Calculated hysteresis loops reveal that magnetic behavior is not identical at the inner and outer surfaces, with spins at the outer surface layer of the 15 nm hollow particles exhibiting a higher degree of frustration. Our study sheds light on the origin of spin-glass-like phenomena and the role of surface spins in magnetic hollow nanostructures.

This work is supported by Spanish MINECO (MAT2012-33037), Catalan DURSI (2014SGR220) and European Union FEDER funds (Una manera de hacer Europa).

TU.F-P66 - Dielectric and magnetic properties of α -Fe₂O₃ nanoparticles

J.W. Chen¹, Y.H. Huang¹, N. Rao G¹

1. Department Of Physics, National Taiwan University, Taipei, Taiwan

We have investigated the dielectric and magnetic properties of the α -Fe₂O₃ nanoparticles prepared by the co-precipitation method. Iron nitrite was used as a precursor material. X-ray diffraction reveals the obtained nanoparticles are of the rhombohedral structure with space group $R\bar{3}c$. The particles sizes were determined from the XRD peak width using the Sherrer relation. The size of the particles was found between 45 nm and 100 nm, depending on the annealing temperature T_A .

The magnetization of the samples were taken using a commercial SQUID in a field of 5 KOe between 2 K and 300 K. The results show a monotonic decrease of the Morin temperature T_M from 260 K to 254 K as the particle size reduces from 100 nm to 45 nm. Below T_M , features in the $M(T)$ curves were observed at ~ 110 K and ~ 20 K, respectively.

The real part dielectric constant $\epsilon'(T)$ curves of the samples exhibit distinct behaviors in different temperature regions. Below 110 K, ϵ' is almost independent of temperature and test frequency, and approaches to a constant value ϵ_s ($\epsilon_s < 20$, depending on the particle size). For $T > 110$ K, $\epsilon'(T)$ increases with increasing T and decreases as the test frequency increases. The loss tangent $\tan\delta$ exhibit a peak at the temperature near the inflection temperature observed in the $\epsilon'(T)$ curves.

Our results indicate that core-shell structure in the samples studied. The observed features in the $M(T)$ and $\epsilon'(T)$ curves at $T \sim 110$ K can be attributed to the Verwey transition due to existence of g -Fe₃O₄ in the shell of the nanoparticles.

TU.F-P67 - Beyond the effect of particle size: Influence of CoFe₂O₄ nanoparticle arrangements on magnetic properties

D. Peddis¹, C. Cannas², A. Musinu², A. Ardu², F. Orrù², D. Fiorani¹, S. Laureti¹, D. Rinaldi^{1,4,5}, G. Muscas^{1,3}, G. Concas³

1. Istituto di Struttura della Materia-CNR

2. Dipartimento di Scienze Chimiche e Geologiche, Università di Cagliari, Cagliari, Italy

3. Dipartimento di Fisica, Università di Cagliari, Cagliari, Italy

4. Dipartimento di Fisica e Ingegneria dei Materiali e del Territorio, Università Politecnica delle Marche, Ancona, Italy

5. Consorzio Nazionale Interuniversitario per le Scienze Fisiche della Materia (CNISM)

This paper focus on assemblies of CoFe₂O₄ nanoparticles, analyzing the influence of the synthesis method on nanoparticles arrangement and magnetic proprieties. Using synthesis procedures based on direct micelle (DM) and high thermal decomposition (HTD) of metalorganic precursors, are been prepared three samples of CoFe₂O₄ nanoparticles with the same average particles size of about 5 nm. HTD method allows to obtain high crystalline nanoparticle coated by oleic acid and self-assembled in hexagonal close packing (H-CoFe_{HTD}) [1]. The DM method results appropriate to prepare either individual irregular arrangement of CoFe₂O₄ nanoparticles (I-CoFe_{DM}) or secondary spherical iso-oriented nanoporous assemblies with a high surface area (S-CoFe_{DM}) [1]

Despite the same particle size, magnetization measurements of the HTD sample show tendency towards cubic anisotropy ($M_R/M_S \sim 0.7$), while in DM samples a uniaxial anisotropy ($M_R/M_S \sim 0.4$) is observed. The comparison between I-CoFe_{DM} and S-CoFe_{DM} samples indicates that the ordering of nanocrystals at the mesoscopic scale induces an increase of the coercive field ($\mu_0 H_c = \sim 1.17 \text{ T} \rightarrow \sim 1.45 \text{ T}$) and of the reduced remanent magnetization ($M_R/M_S: \sim 0.4 \rightarrow \sim 0.5$). The reason for these differences is discussed. In particular, a detailed study on interparticle interactions is carried out, highlighting the influence of the molecular coating and of the formation of spherical iso-oriented assemblies [2].

References:

[1] C. Cannas, et al., Chem. Mater. 20 (2008) 6364–6371

[2] D. Peddis et al. Chem. Mater. 25 (2013) 2–10

TU.F-P68 - Magnetic properties of small magnetite nanocrystals

G. Muscas^{1,3}, G. Concas³, C. Cannas², A. Musinu², A. Ardu², F. Orrù², D. Fiorani¹, S. Laureti¹, D. Rinaldi^{1,4,5}, G. Piccaluga²

1. Istituto di Struttura della Materia-CNR

2. Dipartimento di Scienze Chimiche e Geologiche, Università di Cagliari, Cagliari, Italy

3. Dipartimento di Fisica, Università di Cagliari, Cagliari, Italy

4. Dipartimento di Fisica e Ingegneria dei Materiali e del Territorio, Università Politecnica delle Marche, Ancona, Italy

5. Consorzio Nazionale Interuniversitario per le Scienze Fisiche della Materia (CNISM)

Among nanostructured magnetic materials, nanoparticles are unique complex physical objects. In fact, at the nanoscale magnetic single-domain particles are formed, leading to new supermagnetic behaviors, depending on nature and strength of interparticle interactions [1]. In addition, the physics of nanoparticles is influenced by the modification of the structural and electronic properties at the particle surface [2].

Nanoparticles of spinel ferrites are of great interest, not only for their technological applications but also from the point of view of fundamental science. In particular, magnetite (Fe_3O_4) has been one of the most widely studied and utilized magnetic materials in the life of humankind. It is characterized by high Curie temperature ($T_C = 850$ K in bulk magnetite) and nearly full spin polarization at room temperature, which make it a potential material for spintronics. [3].

This paper focuses on the study of the magnetic properties of 9 nm magnetite nanocrystals. XRD and TEM measurements indicate the presence of crystalline particles, with a fraction of them only partially crystallized or highly defective. The analysis of the temperature dependence of the zero-field-cooled/field-cooled magnetization and of the thermoremanent magnetization provides evidence of the existence of three magnetic regimes [4]: 1) a high temperature superparamagnetic (SPM) regime (300–100 K), centered at a broad maximum due to the blocking process of particles moments; 2) an intermediate regime (100–30 K), centered at a maximum at the Verwey transition; 3) a low temperature regime (below 30 K) centered at a peak identifying a collective super-spin-glass type transition of particles moments.

References:

[1] S. Bedanta and W. Kleemann J. Phys. D: Appl. Phys. 42 (2009) 1–28

[2] *Surface Effects in Magnetic Nanoparticles*; Fiorani, D., Ed.; Wiley: New York, 2005

[3] Bohra et al. J. Magn. Magn. Mater. 321 (2009) 3738– 374

[4] G. Muscas et al. J. Phys. Chem. C 117 (2013) 23378–23384

TU.F-P69 - Magnetic properties of transition metal co-doped TiO₂ nanoparticles and local structure analysis by XAFS measurements

M. Hachisu¹, K. Mori¹, K. Hyodo¹, S. Morimoto¹, T. Yamazaki¹, Y. Ichiyangi¹

1. Yokohama National University, Yokohama, Japan

Ti_{0.97-x}Co_{0.03}MxO₂ (M = Fe, Mn, Nb x = 0, 0.02, 0.04) nanoparticles encapsulated with amorphous SiO₂ were synthesized by our novel preparation method. An anatase TiO₂ single-phase structure was confirmed using X-ray diffraction. The particle size could be controlled to be about 5 nm. The composition of these nanoparticles was investigated by X-ray fluorescence analysis. The magnetization curves for the nanoparticles indicated ferromagnetic behavior at room temperature. The dependence of the electrical conductivity on the frequency was measured by an LCR meter, and the carrier concentration was determined. X-ray absorption fine structure spectra (XAFS) showed that the Ti⁴⁺, Fe³⁺, Mn²⁺:3+=1:2, and Co²⁺ states were dominant in our prepared samples. A reduction in the coordination number was also confirmed. Magnetization value was drastically improved where M = Fe, x = 0.02 sample. We concluded that the ferromagnetism interaction originated in oxygen vacancies around the transition metal ions and exchange ferromagnetic or antiferromagnetic interaction occurred between transition metal ions.

TU.F-P70 - AC magnetic susceptibility and hyperthermia effect in vitro experiment of cozn-ferrite nanoparticles

Y. Ichiyanagi¹, T. Yamazaki¹, S. Morimoto¹, K. Hyodo¹, K. Mori¹, M. Hachisu¹

1. *Yokohama National University, Yokohama, Japan*

CoZn-ferrite ($\text{Co}_{0.8}\text{Zn}_{0.2}\text{Fe}_2\text{O}_4$) nanoparticles (NPs) were prepared by the novel wet chemical method. Single phase spinel structure in amorphous SiO_2 was confirmed by X-ray diffraction patterns. Particle sizes were estimated between 5 and 17 nm. These magnetic particles were further functionalized for biomedical applications and cancer cell selective NPs were developed by conjugating with folic acid.

AC magnetic susceptibilities were measured by SQUID magnetometer. Temperature dependence of imaginary part of magnetic susceptibility χ'' for various particle sizes of Co-Zn ferrites suggested that the particle system followed Néel relaxation theory. The peaks corresponding to freezing temperature T_f shifted towards higher temperature side as the particle size increased. χ'' has a peak around 8 nm at 300 K, and this phenomenon indicated the most effective condition for heat dissipation upon an application of the external field. An AC field was found to cause an increase in temperature, with the 8 nm particles exhibiting the highest temperature increase as expected. In addition, *in vitro* experiments to study the hyperthermia effects of CoZn-ferrite particles on human cancer cells were carried out. Remarkable effect of magnetic hyperthermia was observed.

TU.F-P71 - Energy losses in bacterial magnetosomes

M. Timko¹, M. Molcan¹, J. Kovac¹, P. Kopcansky¹, A. Skumiel², H. Gojewski^{3,4}, S. Dutz⁵

1. *Institute of Experimental Physics SAS, Kosice, Slovakia*

2. *Institute of Acoustics, Adam Mickiewicz University, Poznan, Poland*

3. *Institute of Physics, Poznan University of Technology Poznan, Poland*

4. *Max Planck Institute of Colloids and Interfaces, Potsdam, Germany*

5. *Institute of Biomedical Engineering and Informatics, Technische Universität Ilmenau, Germany*

Magnetic losses in liquid suspension of magnetosomes can be investigated by analysis of minor hysteresis loops and specific absorption loss power determined calorimetrically. Hysteresis losses may be determined in a well-known manner by integrating the area of hysteresis loops, a measure of energy dissipated per cycle of magnetization reversal. It depends strongly on the field amplitude as well as the magnetic prehistory.

In our contribution we present the calculation of the energy contribution from hysteresis losses as a function of applied magnetic field. Losses were calculated from the minor hysteresis loops of magnetosomes extracted from *Magnetotacticum Spirillum-AMB1*. Samples of magnetosomes were divergent in length i.e. chains of magnetosomes have been modified due to mechanical effects during sonication. Specific absorption rate (SAR) values were 356 W/gmagnetite and 178 W/gmagnetite for samples IM (isolates magnetosomes) and SM (sonicated magnetosomes), respectively. These values were compared with results obtained from calorimetric measurements estimated at 10 kA/m and 508 kHz which were 963 W/gmagnetite and 463 W/gmagnetite for IM and SM samples, respectively. We can see that the obtained values for quasistatic experiments are lower comparing to the calorimetric measurement what largely reflecting higher relaxation during static measurements and thus a lower value of magnetic losses converted into heat.

This work was supported by project PhysNet 26110230097 .

TU.F-P72 - Arsenic adsorption in a magnetic stabilized bed made of magnetic aggregates based on hydrated iron oxides

A.M. Estevez¹, J.M Rodriguez¹, A. Alvaro¹, P. Augusto¹, C. Torrente¹, T. Castelo-Grande²

1. APLICAMA - Dep. Chem Engineering - Fac Chem Sciences - Univ Salamanca, Salamanca, Spain

2. LEPABE, Departamento de Engenharia Química, Faculdade de Engenharia da Universidade do Porto, Porto, Portugal

Arsenic contamination of waters represents a world-wide problem, and regions of Spain, North of Europe, Argentina, Bangladesh or India, are among the most problematic sites. Technologies have been investigated to handle this problem (e.g. precipitation, reverse osmosis). However all these technologies have been facing practical difficulties, which, together with the severity of the problem, implies the need to search for new methods for a more effective and economical elimination of arsenic in groundwater and surface water streams. Iron oxides have shown a high and effective capacity of water-contained arsenic adsorption. In the present work we have prepared magnetic aggregates based on hydrated iron oxide FeOOH - which high-adsorption capability was previously determined -, on magnetite and sodium alginate. These magnetic aggregates were then introduced in a magnetic stabilized bed (see Figure 1), through which arsenic contaminated water was driven.

Figure 1. Experimental Setup used: 1.- Deposit (Water and arsenic); 2.- Pumps; 3.- Valves; 4.- Flowmeter ; 5.- Thermometer; 6.- Manometers; 7.- Distributor; 8.- Solenoid; 9.- Adsorbent Bed of Particles. 10.- CC Power Source; 11.- Electrical Network; 12.-Sample Collection, 13.- Regenerator Deposit.

Results obtained show a good level of arsenic removal (26 mgAs/gFeOOH). Using higher magnetic field intensities leads to an improvement in the water flowrate that we are able to treat. A first-order adsorption kinetic has been proven to exist by the kinetic study done. Adsorption constants were also determined, as well as the influence of the main variables on their experimental values, and they increase at high arsenic concentrations, as well as when water flowrate increases. A hydrodynamic study was performed, as well as the determination of the pressure drops and the interstitial velocities, as well as the minimum fluidization and elutriation velocities.

TU.F-P73 - Nanomagnetic particles synthesis: Comparison of methods and applications

P. Augusto¹, C. Torrente¹, A.M Estevez¹, T. Castelo-Grande², D. Barbosa², M. Gonzalez¹, M. Diego¹, E. Martin¹, B. Rodriguez¹, A. Sanchez¹

1. *APLICAMA - Dep. Chem Engineering - Fac Chem Sciences - Univ Salamanca, Salamanca, Spain*

2. *LEPABE, Departamento de Engenharia Química, Faculdade de Engenharia da Universidade do Porto, Porto, Portugal*

Synthesis of nanomagnetic particles has experienced a boom in the last decade. However for practical reasons, and in the moment of choosing a manufacturing method, it is important to have a strong basis for a correct choice. Integrated Science, where in the same Research Project or Plan, the research is planned and followed from the initial production until the final applications, is amongst the most important driven goals set by the European Commission in the H2020 Programme. Therefore, in this work, we have investigated three of the mostly used magnetic particle synthesis methods - co-precipitation, microemulsion and pirolisis - and compared the final particles. We have produced magnetite particles in the micron size and found out that differences of pH of the magnitude of 1 do not influence the results. Then we have compared the different nanomagnetic particles produced by the three methods and concluded among others that: the co-precipitation method provides a cheap and simple way of manufacture, but there is an inherent heterogeneous distribution of sizes and, also, aggregates are hard to avoid; the microemulsion method provides a more homogenous distribution of sizes and avoids almost the formation of aggregates, but there are difficulties in getting the surfactant out of the particles, and it does not seem proper for larger-scale; in laser pirolisis the particles obtained show highly homogeneity and may even achieve high rates of magnetization, however it has problems when larger nanosized particles are in order. We then made a literature review of several applications: environmental applications (ex.: heavy metal removal), magnetic hyperthermia, enzyme immobilization and biotechnical applications, and by comparison with the characteristics of the particles obtained in the three different methods, arrived to the conclusion that each application has its own needs and that dependent on the final application a determined synthesis method is mostly appropriated.

TU.F-P76 - Novel structures and spin correlations in nanomagnets

D. Sellmyer¹, B. Balasubramanian¹, P. Manchanda¹, B. Das¹, T. George¹, P. Mukherjee¹, R. Skomski¹, G. Hadjipanayis²

1. Nebraska Center for Materials and Nanoscience and Department of Physics and Astronomy, University of Nebraska, Lincoln, United States

2. Department of Physics and Astronomy, University of Delaware, Newark, United States

Spin-polarized nanoparticles or clusters have attracted much interest due to novel magnetic properties and potential applications in nanoscale spintronics, ultra-high density magnetic recording, and permanent magnetism. Furthermore, the nonequilibrium fabrication process used for clusters and particles can also stabilize metastable structures and often leads to new crystal and spin structures. In this talk, we discuss our recent work on Co-Si and Mn-Si nanoclusters, which exhibit magnetic properties significantly different from the corresponding bulk alloys. This includes highly anisotropic Co₃Si and Mn₅Si₃, Co₂Si nanoclusters exhibiting very weak itinerant ferromagnetism, and MnSi and CoSi nanoclusters with B20-type crystal structures. The unique nanocluster properties will be explained using DFT first-principle calculations. This research is supported by US-DOE and NSF-DMREF.

TU.F-P78 - Energy losses in bacterial magnetosomes

M. Molcan¹, J. Kovac¹, P. Kopcansky¹, A. Skumiel², H. Gojzewski^{3,4}, S. Dutz^{5,6}, M Timko¹

1. *Institute of Experimental Physics, Slovak Academy of Sciences, Košice, Slovakia*

2. *Institute of Acoustics, Adam Mickiewicz University, Poznań, Poland*

3. *Institute of Physics, Poznań University of Technology, Poznań, Poland*

4. *Max Planck Institute of Colloids and Interfaces, Potsdam, Germany*

5. *Institute of Biomedical Engineering and Informatics, Technische Universität Ilmenau, Ilmenau, Germany*

6. *Department of Nano Biophotonics, Leibniz Institute of Photonic Technology, Jena, Germany*

Magnetic losses in liquid suspension of magnetosomes can be investigated by analysis of minor hysteresis loops and specific absorption loss power determined calorimetrically. Hysteresis losses may be determined in a well-known manner by integrating the area of hysteresis loops, a measure of energy dissipated per cycle of magnetization reversal. It depends strongly on the field amplitude as well as the magnetic prehistory.

In our contribution we present the calculation of the energy contribution from hysteresis losses as a function of applied magnetic field. Losses were calculated from the minor hysteresis loops of magnetosomes extracted from *Magnetotacticum Spirillum-AMB1*. Samples of magnetosomes were divergent in length i.e. chains of magnetosomes have been modified due to mechanical effects during sonication. Specific absorption rate (SAR) values were 356 W/gmagnetite and 178 W/gmagnetite for samples IM (isolates magnetosomes) and SM (sonicated magnetosomes), respectively.

These results are compatible with our calorimetric measurements of hyperthermia which were 963 W/gmagnetite and 463 W/gmagnetite for IM and SM samples, respectively.

All values were estimated at 10 kA/m and 508 kHz. We can see that the obtained values for quasistatic experiments are lower comparing to the calorimetric measurement what largely reflecting higher relaxation during static measurements and thus a lower value of magnetic losses converted into heat.

TU.F-P79 - Size-dependent electronic and magnetic properties of iron oxide and cobalt ferrite nanocrystals probed by synchrotron X-ray imaging and spectroscopyA. Fraile Rodríguez¹, C. Moya¹, N. Pérez¹, C. Piamonteze², X. Batlle¹, A. Labarta¹*1. Dpt. Física Fonamental and Institut de Nanociència i Nanotecnologia (IN2UB), Universitat de Barcelona, Barcelona, Spain**2. Swiss Light Source, Paul Scherrer Institut, Villigen-PSI, Switzerland*

Iron oxide-based nanoparticles (NP) have outstanding magnetic properties and promising applications for spin-filter devices, biomedicine, and catalysis. In addition to finite-size effects, a key issue for research is how the intrinsic magnetic properties of the individual particles are modified by their own electronic structure, chemistry, surface termination and crystallinity.

By combining synchrotron X-ray absorption spectra (XAS) with photoemission electron microscopy (PEEM), we analyze the electronic structure and chemical bonding of individual, $\text{Fe}_{3-x}\text{O}_4$ and $\text{Co}_x\text{Fe}_{3-x}\text{O}_4$ NP in the size range of 8 to 24 nm, synthesized by thermal decomposition of organometallic precursors [1], and deposited onto Si substrates. All the NP display high crystalline quality and macroscopic bulk-like magnetic properties [2,3]. However, the spectra from individual NP show that the variation of some synthesis parameters significantly alter the cationic distribution and the uniformity of magnetic phases [5]. In particular, 13-nm NP synthesized using oleic acid as a surfactant and iron oleate (III) as a metallic precursor are very homogeneous in stoichiometry, compatible with an Fe_3O_4 core surrounded by a thin $\gamma\text{-Fe}_2\text{O}_3$ shell. In contrast, 24-nm NP, synthesized with the same precursors but with a different solvent and no stabilizer, are inhomogeneous, composed of either a thick FeO or metallic Fe core surrounded by a thin Fe_3O_4 shell or an Fe_3O_4 core surrounded by a thin $\gamma\text{-Fe}_2\text{O}_3$ shell.

Furthermore, spatially-integrated X-ray magnetic circular dichroism (XMCD) spectra and element-specific hysteresis loops of mono-disperse assemblies of the $\text{Co}_x\text{Fe}_{3-x}\text{O}_4$ NP using both electron and fluorescence yields have enabled the deconvolution of the electronic and magnetic contributions of the NP surface from those of the inner core regions.

This work was supported by MINECO (MAT2012-33037), DURSI (2009SGR856 and 2014SGR220), and European Union FEDER funds (Una manera de hacer Europa). A.F.R. acknowledges support from the MICIIN “Ramón y Cajal” Programme.

References:

- [1] P. Guardia, A. Labarta, and X. Batlle, *J. Phys. Chem.* **115**, 390 (2010)
- [2] N. Pérez et al, *Appl. Phys. Lett.* **94**, 093108 (2009)
- [3] X. Batlle et al, *J. Appl. Phys.* **109**, 07B524 (2011)
- [4] X. Batlle, A. Labarta, and A. Fraile Rodríguez, *McGraw-Hill 2015 Yearbook of Science & Technology*, pp. 157 (2015)

TU.F-P80 - The role of the 1,2-hexadecanediol on the magnetic properties of Co-ferrite nanoparticles

C. Moya¹, M. del Puerto Morales², X. Batlle¹, A. Labarta¹

1. *Departament de Física Fonamental and Institut de Nanociència i Nanotecnologia (IN2UB), Universitat de Barcelona, Barcelona, Spain*

2. *Instituto de Ciencia de Materiales de Madrid, CSIC. Campus de Cantoblanco, Madrid, Spain*

Co-ferrite nanoparticles (NPs) are especially suitable for potential applications in biomedicine and in technology because of their high values of the magnetocrystalline anisotropy, saturation magnetization and the magneto-optical coefficients. However, Co-ferrite NPs in literature show magnetic properties with high variability depending on the preparation method, what limits the standardization of those procedures for large scale applications. Consequently, the choice of a suitable synthesis method, where one can get control of the size, shape, stoichiometry and the crystallinity of the particles, is of key importance to make progress in the fundamental understanding of the properties of nanoparticulate Co-ferrite systems as compared to those of bulk-counterparts. Within this framework, we report on the effect of the 1,2-hexadecanediol content on the structural and magnetic properties of CoFe_2O_4 nanoparticles synthesized by thermal decomposition of metal-organic precursors in 1-octadecene. Although pseudo-spherical particles having an average size of about 8 nm and similar stoichiometry have been observed in all studied samples, a high level of variability of the crystal quality and, in turn, of the magnetic properties has been found as a function of the amount of 1,2-hexadecanediol added to the reaction mixture. The magnetic study reveals that samples progress from glassy magnetic behavior to bulk-like, ferrimagnetic order as the crystal quality improves. The analysis of the reaction mixtures by Fourier transform infrared spectroscopy at various stages of the reaction shows the key role of the 1,2-hexadecanediol on favoring the decomposition of the metal-organic precursor, formation of an intermediate $\text{Co}^{2+}\text{Fe}^{3+}$ -oleate complex and, finally, the nucleation of nanoparticles at lower temperatures. This work was supported by Spanish MINECO (MAT2011-23641, MAT2012-33037, MAT2013-48054-C2), Catalan DURSI (2014SGR220) and European Union FEDER funds (Una manera de hacer Europa). C. Moya acknowledges Spanish MINECO for a Ph.D. contract (BES-2010-038075) and a three months stay at the ICMN-CSIC (Madrid).

TU.F-P81 - Designing new manganite/ferrite nanocomposites with tunable magnetic and electrical properties

G. Muscas^{1,2,3}, R. Mathieu³, A. Puri Kumar³, G. Concas², G. Varvaro¹, D. Peddis¹

1. *Istituto di Struttura della Materia - CNR, Monterotondo Scalo (RM), Italy*

2. *Dipartimento di Fisica, Università di Cagliari, Monserrato, Italy*

3. *Department of Engineering Sciences, Uppsala University, Uppsala, Sweden*

Entering the nanometer scale regime, the magnetic behavior changes dramatically with respect to the bulk state and new phenomena appear, such as Supermagnetism [1]. Nanostructured strongly electron correlated magnetic oxides represent a very interesting class of materials due to their electronic and magnetic properties and for their important technological applications (magnetic recording, biomedicine, ferrofluid technology, catalysis, etc.). In order to synthesize new or improved such transition metal oxide systems, we have developed new nanocomposites of Colossal Magneto-Resistance (CMR) manganites (i.e., $\text{La}_{1-x}\text{Ca}_x\text{MnO}_3$, LCMO) with a hard magnetic material as ferrites (i.e., CoFe_2O_4 , CFO). This class of composites has already attracted a great interest for the Tunnel Magneto-Resistance effect (TMR) [2], employed in actual hard drives. We propose a new approach to synthesize nanocomposites $\text{CoFe}_2\text{O}_4/\text{La}_{0.67}\text{Ca}_{0.33}\text{MnO}_3$, in order to maximize interphase interactions. A comparison between such nanocomposites (NC) and a mechanical mixing (N-MIX) of the same two phases in nanoparticle phase is carried out by a complete structural and morphological characterization, together with detailed magnetometry studies. All the results suggest that a strong coupling only occurs for the NC sample, whose magnetic behavior resembles that of an exchange-spring system [3] as clearly indicated by both the $M(H)$ curve (figure 1) and the associated switching field distribution.

[1] S. Bedanta and W. Kleemann, *J. Phys. D: Appl. Phys.* 42 (2009) 1-28

[2] P. Anil Kumar and D.D. Sarma, *Appl. Phys. Lett.* 100 (2012) 262407

[3] H. Fukunaga et al., *IEEE Trans. Magn.* 49 (2013) 3240-3243

TU.F-P82 - ESR study of YbNi₂ nanometric alloys

V. Ivanshin¹, E. Gataullin¹, D. Rojas², L. Fernández Barquín³

1. *Institute of Physics, Kazan Federal (Volga region) University, Kazan, Russia*

2. *Departamento de Física e Instalaciones-ETSAM, Universidad Politécnica de Madrid, Madrid, Spain*

3. *DCITIMAC, Facultad de Ciencias, Universidad de Cantabria, Santander, Spain*

We have investigated the structural and magnetic properties of the heavy-fermion YbNi₂ [1] crystalline alloy when submitted to high-energy ball milling. The sample was characterized by means of DC magnetic susceptibility and electron spin resonance (ESR) of the intrinsic Yb³⁺. The analysis of the x-ray diffraction data shows a reduction of the particle size down to 12 nm for 20 h of milling time. The ferromagnetic (FM) contribution practically disappears and a new magnetic phase arises at lower temperatures, below T_C, as observed in other rare earth FM alloys under mechanical milling [2]. In the vicinity of T_C = 10.5 K, the ESR parameters (linewidth and g-factor) show distinct anomalies, which can be associated with a presence of strong magnetic fluctuations at an onset of FM ordering. The Orbach-Aminov spin-lattice relaxation processes with the involvement of the first excited crystalline electric field level of Yb³⁺ at Δ ≈ 75 K dominate the electron spin dynamics of YbNi₂ in the paramagnetic phase [3]. The Yb³⁺ ions in bulk YbNi₂ are primarily located in almost perfect cubic crystal field. Data of ESR measurements demonstrate different types of distortions observed in the core and the surface regions of the nanocrystallites.

References:

[4] D.P. Rojas et al., *Solid State Commun.* 152 (2012) 1834.

[5] D.P. Rojas et al., *J. Phys: Cond. Matter* 19 (2007) 186214.

[6] E.M. Gataullin et al., *JPS Conf. Proc.* 3 (2014) 012028.

TU.F-P83 - Geometry-induced effects on domain walls on curved surfaces

O. Pylypovskyi¹, V. Kravchuk², D. Sheka¹, D. Makarov³, O. Schmidt³, Y. Gaididei²

1. *Taras Shevchenko National University of Kyiv, Kyiv, Ukraine*

2. *Institute for Theoretical Physics, Kyiv, Ukraine*

3. *Institute for Integrative Nanosciences, IFW Dresden, Dresden, Germany*

Curved surfaces of nanoobjects result in the effective anisotropy-like effects and Dzyaloshinskii-like terms in the exchange energy [1]. Geometry of the Moebius ring allows combining of curvature-induced [1] and topological effects [2]. They influence the magnetic ground state as well as the magnetization dynamics. We study numerically and analytically the impact of curvature on the magnetic domain walls in Moebius ring of different sizes and easy-normal anisotropy [3]. Moebius ring topology leads to appearance of either longitudinal or transversal domain walls in the ground state. While the former wall type is favorable for the system with strong anisotropy (large quality factor, the ratio between the anisotropy and magnetostatic energies), the latter one appears when the quality factor is close to one. A vortex state is observed when the quality factor is small.

Furthermore, we show that the geometry induced Dzyaloshinskii interaction influences on the structure of the domain walls and determines their location in the Moebius ring. Namely, we found the presence of the coupling between the geometrical chirality of the Moebius ring and the direction of the magnetization rotation (magnetic chirality) of the walls: (i) The transversal domain wall always has the magnetic chirality opposite to the chirality of the Moebius ring and has a favorable position on the ring. (ii) The longitudinal domain wall is placed along the central line of the Moebius ring and has the same magnetic chirality as the sample.

The developed analytical approach can be readily applied to investigate a variety of geometries with vector fields defined on them. As an example, peculiarities of the magnetic domain wall structures will be discussed for the uniformly twisted strips.

References:

[1] Yu.Gaididei, V.Kravchuk, D.Sheka, PRL, 112, 257203 (2014)

[2] M.Yoneya, K.Kuboki, M.Hayashi, PRB, 78, 064419 (2008)

[3] O.Pylypovskyi, V.Kravchuk, D.Sheka, D.Makarov, O.Schmidt, Yu.Gaididei, arXiv:1409.2049 (2014)

TU.F-P84 - Magnetic properties and relaxation processes in FePt nanoparticlesA. Zelenakova¹, V. Zelenak², J. Kovac³

1. *University of Pavol Jozef Safarik, Institute of Physics, Department of Condensed Matter Physics, Košice, Slovakia*

2. *University of Pavol Jozef Safarik, Institute of Chemistry, Department of Inorganic Chemistry, Košice, Slovakia*

3. *Institute of Experimental Physics, Slovak Academy of Sciences, Bratislava, Slovakia*

Magnetic nanoparticles exhibit unique properties in comparison with their corresponding bulk analogues, originating from the size and surface effects of the nanostructured materials. The chemically synthesized FePt nanoparticles are of special interest. It was shown recently that thermal treatment of chemically synthesized materials can induce the phase transformation from the disordered $A1$ phase, with low anisotropy, to the ordered $L1_0$ phase creating the nanomaterials with high magnetocrystalline anisotropy. In our work we have prepared and studied the FePt core-shell nanoparticles with Pt shell. The particles were synthesized by a reverse micelle method based on the process of the self-assembly of surfactants (CTAB). The method allowed us to control the spherical shape of the particles as well as their size by tuning the molar composition of the reactants. The structural characterization of the nanoparticles was made by powder X-ray diffraction, XANES (X-ray Near Edge Spectroscopy) measurements at absorption edges of Fe K (7112eV) and Pt L3 (11564eV), SAXS (Anomalous Small Angle X-ray Scattering) and HRTEM measurements. The measurements confirm the spherical, core-shell morphology of the prepared FePt particles, with the average diameter about 5 nm. The DC magnetic susceptibility, measured in ZFC and FC regimes using SQUID based magnetometer in temperature range of 2-300 K, shows on the unconventional behaviour of the sample with two blocking/freezing temperatures $T_{B1} \sim 5$ K and $T_{B2} \sim 25$ K, as determined from the two discrete maxima on the ZFC curve. The magnetization curves measured at different temperatures in the fields up to 5T confirm the existence of exchange bias. From the $M(H)$ at 300 K the magnetic moment $m_P \sim 250 \mu_B$ was calculated for as-prepared FePt nanoparticles. The magnetic relaxation study by AC susceptibilities (χ' and χ'') suggests the existence of strong dipolar interaction between nanoparticles. The characteristic relaxation time $\tau_0 \sim 2 \times 10^{-15}$ s, the measure of effective energy barrier $T_0 = 10$ K and effective anisotropy constant $K_{eff} = 2.6 \times 10^6$ J/m³ were estimated from the magnetic relaxation studies.

TU.F-P85 - Nanocomposite magnetic materials obtained by synthesis of Fe nanoparticles in presence of SrFe₁₂O₁₉ nanoparticles

V. Nachbaur¹, N. Maât¹, E. Folcke¹, M. Jean¹, J.M. Le Breton¹

1. Groupe de Physique des Matériaux - UMR 6634 CNRS, Université et INSA de Rouen, France

Rare earth magnetic materials are ubiquitous in our current way of life, and more particularly when they are used as permanent magnets. Due to supplying troubles, toxicity and high cost of these compounds, their replacement by more available and affordable materials is a very current topic. Designing nanocomposites with high magnetic coupling is currently the subject of numerous investigations, and appears as a very promising way to obtain new permanent magnet materials. With this aim, we have synthesized and investigated strontium hexaferrite - iron nanocomposites. Synthesis of strontium hexaferrite, with the stoichiometry SrFe₁₂O₁₉, has been achieved with a solvothermal process followed by ceramic treatment. By modifying experimental conditions, various shapes and sizes (micronic, sub-micronic and nanometric) are obtained. Iron nanocrystallites were obtained by reduction of FeCl₃ iron chloride with NaBH₄ sodium borohydride as reducing agent. Iron crystallites appear as filaments linked by one common crystallographic direction, with a dimension of few nanometers. To obtain SrFe₁₂O₁₉/Fe nanocomposites, iron nanocrystallites were synthesized in presence of hexaferrite nanoparticles. Nanocomposites have been characterized by X-ray diffraction, electron microscopy (SEM and TEM), and magnetic measurements (VSM and SQUID). The influence of nanostructure on magnetic properties is identified and interpreted. The properties of the nanocomposites are intermediate between those of SrFe₁₂O₁₉ and Fe phases. The occurrence of magnetic coupling between iron and strontium hexaferrite particles is discussed. Financial support of the French "Agence Nationale de la Recherche" (ANR), through the program "Investissement d'avenir" (ANR-10-LABX-00-01) LabExEMC3 is gratefully acknowledged.

TU.F-P86 - Chemical synthesis of SrFe₁₂O₁₉ nanoparticles: influence of processing parameters on structural and magnetic properties

N. Maât¹, J.M. Le Breton¹, E. Folcke¹, A. Rossigny¹, V. Nachbaur¹, M. Jean¹, R. Lardé¹

1. Groupe de Physique des Matériaux - UMR 6634 CNRS, Université et INSA de Rouen, France

Increasing the magnetic properties of SrFe₁₂O₁₉ hexaferrites by nanostructuration is one way to obtain rare-earth free new permanent magnet materials. We prepared SrFe₁₂O₁₉ nanostructured powders by hydrothermal processing of strontium and ferric nitrates in a Teflon lined bomb for temperature between 110 and 215°C and time between 5 and 90h. The influence of Fe/Sr ratio, synthesis temperature and synthesis time, on both structural and magnetic properties of the as-synthesized powders, was investigated. The powders were characterized by X-ray diffraction, transmission electron microscopy, scanning electron microscopy and VSM measurements. The first stages of formation of SrFe₁₂O₁₉ particles were investigated as well. The nanoparticles form in a crystalline state, grow first in the (a,b) plane of the hexagonal structure, and then in the c-direction. The results show that the best magnetic properties are obtained for a Fe/Sr ratio of 3, and synthesis at 170°C for 20h. These synthesis conditions correspond to the formation of single phase SrFe₁₂O₁₉ well-crystallized particles, about 200 nm large and about 30 nm thick. For a Fe/Sr ratio of 3, the powder is single phase, while for a higher ratio, Fe₂O₃ hematite is formed. For lower temperature and lower processing time, SrFe₁₂O₁₉ nanoparticles and secondary Sr₃Fe₂(OH)₁₂ phase coexist. For higher temperature and longer processing time, micrometric SrFe₁₂O₁₉ particles and Fe₂O₃ hematite phase coexist. Financial support of the French "Agence Nationale de la Recherche" (ANR), through the program "Investissement d'avenir" (ANR-10-LABX-00-01) LabExEMC3 is gratefully acknowledged.

TU.F-P87 - Size dependent magnetism in FeO/Fe₃O₄ Core/Shell nanoparticles

A.G. Roca¹, M. Estrader^{2,3}, A. Lopez-Ortega^{1,4}, S. Estrade^{5,6}, G. Salazar-Alvarez², D. Tobia⁷, E. Winkler⁷, I.V. Golosovsky⁸, W.A.A. Macedo⁹, M. Vasilakaki¹⁰

1. Institut Català de Nanociència i Nanotecnologia (ICN2), Campus UAB, Bellaterra, Spain
2. Dept. de Química Inorgànica, Univ. de Barcelona, Barcelona, Spain
3. Dept. of Materials and Environmental Chemistry, Stockholm Univ., Stockholm, Sweden
4. INSTM and Dipt. di Chimica α U. Schiff', Univ. degli Studi di Firenze, Firenze, Italy
5. TEM-MAT, SCT, Univ. de Barcelona, Barcelona, Spain
6. LENS-MIND-IN2UB, Dept. d'Electrònica, Univ. de Barcelona, Barcelona, Spain
7. Centro Atómico Bariloche, S.C. de Bariloche, Argentina
8. St. Petersburg Nuclear Physics Institute, Gatchina, St. Petersburg, Russia.
9. Centro de Desenvolvimento da Tecnologia Nuclear, Belo Horizonte, Brazil.
10. IAMPPMN, Dept. of Materials Science, NCSR α Demokritos', Attiki, Greece

The proposed use of exchange bias to overcome the superparamagnetic limit [1] triggered a renewed interest in bi-magnetic magnetic core/shell nanoparticles [2]. However, most of the studies are being carried out in ferromagnetic (FM) transition metal core and the corresponding antiferromagnetic (AFM) shell, (FM/AFM systems)[2]. In this work we present the study of the structural and magnetic properties of 'inverted' antiferromagnetic/ferrimagnetic (AFM/FiM) core/shell nanoparticles as opposed to the typical FM/AFM. The AFM/FiM nanoparticles were prepared by thermal decomposition of iron organic compounds leading to the AFM-core (FeO), which is passivated under air resulting in a FiM-shell (Fe₃O₄). Two extreme sizes of the AFM/FiM nanoparticles, small (9 nm) and large (45 nm), are investigated. The results show that while both systems exhibit some similar features, like exchange bias, there are also important differences [3]. The detailed characterization by neutron diffraction, Mössbauer, and electron spin resonance evidences that while the core in the large particles is antiferromagnetic and has a more bulk-like behavior, in the smaller ones the core is highly non-stoichiometric and strained, displaying no significant antiferromagnetism. Namely, while the large particles exhibit clear a transition at the Néel temperature, (TN) of the core (with an enhanced TN = 250 K) and a clear Verwey transition of the shell (despite its reduced thickness), the core in the small ones seems to be non-magnetic and the shell does not exhibit any Verwey transition. The results evidence that the spread of magnetic results in the literature for FeO/Fe₃O₄ nanoparticles stem from the strong size effects exhibited by this system and highlight the importance of ample characterization to fully understand the properties of nanostructured metal oxides.

References:

- [1] V. Skumryev, et al. Nature 2003, 423, 850
- [2] J. Nogués, et al. Phys. Rep. 2005, 422, 65
- [3] M. Estrader, et al Nanoscale 2015, 7, 3002

TU.F-P88 - Chemically synthesized $\text{Cu}_{1-x}\text{Fe}_x\text{Cr}_2\text{Se}_4$ nanoparticles. Morphology and magnetic properties

C.R. Lin ¹, C.C. Chen ¹, O. Li ^{1,2}, H.S. Hsu ¹, R. Ivantsov ², S. Zharkov ^{2,3}, I. Edelman ², D. Velikanov ², S. Ovchinnikov ^{2,3}

1. National Pingtung University, Pingtung City, Pingtung County, Taiwan

2. L. V. Kirensky Institute of Physics, Russian Academy of Sciences, Krasnoyarsk, Russia

3. Siberian Federal University, Krasnoyarsk, Russia

The work is devoted to the study of the morphology and magnetic properties of $\text{Cu}_{1-x}\text{Fe}_x\text{Cr}_2\text{Se}_4$ nanoparticles synthesized via thermal decomposition of metal nitrate or chloride salts and selenium powder with different ratios of the raw material components in the high-temperature organic solvent. Correlations between technological conditions and nanoparticles morphology, on one hand, and between the morphology and magnetic properties of nanoparticles, on the other hand, are obtained. According to the high-resolution transmission electron microscopy data (JEOL JEM-2100), nanoparticles of two types coexist for all raw material compositions: thin hexagon plates and thin belts (for nitrate salts) or rods (for chloride salts). Moreover, all the types of the nanoparticles are single crystalline ones with the CuCr_2Se_4 structure, besides the particles with $x=0.4$ demonstrate a more complicated structure. For some compositions, the belts gather into large conglomerates forming hierarchical particles. The magnetization temperature dependences of the nanoparticles demonstrate different shapes for FC and ZFC modes characteristic for heterogeneous systems such as super paramagnetic particles. However, contrary to usual situations, the magnetization maximum is observed not only in ZFC but also in the FC curve. The maxima positions and widths depend on the nanoparticle morphology. The Curie temperature for all the samples with $x=0$ is about 410 K; it decreases with the x value increase. Magnetic circular dichroism (MCD) in the region 1.2-3.5 eV demonstrates several extremes of different signs, which are close to the maxima positions, observed in the spectrum of the imaginary part of the off-diagonal component of the optical conductivity tensor for the CuCr_2Se_4 single crystal [1]. The similarity of the MCD spectra for all the samples evidences the same nanoparticle electronic structure independent of their morphology.

Reference:

[1] S. Bordacs, et al., New Journal of Physics 12 (2010) 053039

TU.F-P89 - Magnetic and EPR studies of electron-hole asymmetry in bulk and nanoparticles of $\text{Bi}_{1-x}\text{Ca}_x\text{MnO}_3$ ($x = 0.4, 0.6$): A comparison

G. Singh¹, S.V. Bhat²

1. Department of Physics, Indian Institute Of Science, Bangalore, India And National Physical Laboratory, New Delhi, India

2. Department of Physics, Indian Institute Of Science, Bangalore, India

Electron-hole asymmetry, which refers to the asymmetry in the phase diagram across $x = 0.5$ in doped rare earth manganites such as $\text{Re}_{1-x}\text{A}_x\text{MnO}_3$ (Re is a trivalent rare-earth ion such as La, Bi, Nd, Pr, Sm and A is a divalent alkaline earth ion such as Ca, Sr, Ba, Pb) is known to vanish on reducing the size of the particles to a few nanometers. Bismuth based manganites provide an interesting model system for comparison: e.g. though the doped rare earth manganites show disappearance of charge order (CO) on size reduction to nanoscale, CO in Bi manganites is found to be more robust. Here we study the effect of size reduction on magnetic properties and EPR parameters of electron ($x = 0.6$, BCE) and hole ($x = 0.4$, BCH) doped $\text{Bi}_{1-x}\text{Ca}_x\text{MnO}_3$ (BCMO). Nearly spherical nanoparticles ($D \sim 30$ nm) of BCMO were prepared by sol-gel synthesis and the bulk samples using the solid state reaction route. Magnetic and X-band EPR measurements were carried out on all the samples. Lineshape fitting was carried out using the double Lorentzian function accounting for clockwise and counterclockwise rotating components of the microwave field. It is found that the electron-hole asymmetry in the nanoparticles of electron doped ($x = 0.6$) and hole doped ($x = 0.4$) $\text{Bi}_{1-x}\text{Ca}_x\text{MnO}_3$ samples still persists. The values of the extracted EPR 'g' parameter for the bulk and the nano samples indicate that the electron-hole asymmetry has reduced but has not completely vanished in the BCMO samples.

TU.F-P90 - Preparation and magnetic properties of interaction-free magnetite nanoparticles

J. Balachandran¹, M. Fukunaga¹, I. Furukawa¹, J. Cuya¹, H. Mamiya², H. Miyamura¹

1. *The University Of Shiga Prefecture, Hikone, Japan*

2. *National Institute of Materials Science, Tsukuba, Japan*

Synthesis routes for magnetic oxide, metal and alloy nanoparticles (NPs) have witnessed unprecedented growth since the year 2000. Especially, the main focus has been on monodispersity, controllability of size, stability and composition of the NPs. However, despite the fact that considerable progress has been made in the size and size distribution control, the true magnetic characteristics of NPs is yet to be revealed due to interaction between particles. As a consequence, the application-oriented design of magnetic particles has become difficult. Thus in this study, we have attempted the preparation of interaction-free magnetite nanoparticle (MNPs) system, intending their application in the field of magnetic fluid hyperthermia, by coating the same with silica-shell of different thicknesses and measured their temperature dependence of magnetization and First Order Reversal Curve (FORC) analysis to evaluate the magnetic interaction qualitatively and quantitatively. First, magnetite particles with average diameter of 7.8 nm were synthesized by reducing goethite in 1-octadecene. Then, these magnetite particles were coated with silica shell thicknesses of 6.5, 13.7 and 20.8 nm. When zero-field cooled and field cooled temperature-dependent magnetization of these samples were measured, the peak of the normalized magnetization as a function of temperature shifted to lower temperature for increasing silica-shell thicknesses. And also, the low temperature increase in the field-cooled magnetization became pronounced as the silica-shell thickness became larger. These results indicated the decrease in magnetic interaction with the increase in inter particle distance caused by thicker silica-shell qualitatively. To measure the magnetic interaction between particles quantitatively, FORC analysis was performed on dry uncoated and silica-coated MNPs. The results suggested that the interaction field decreases with increasing silica-shell thickness of 6.5 and 14 nm, compared to uncoated magnetite particles. Furthermore, the preparation of an interaction-free sample was confirmed when the magnetite particles were coated with a silica shell thickness of 20.8 nm.

TU.F-P91 - Acoustic investigation of biocompatible magnetic fluid under magnetic field

P. Bury¹, J. Kúdelčík¹, S. Hardon¹, M. Kubovcikova², M. Timko², P. Kopčanský²

1. Department Of Physics, Žilina University

2. Institute of Experimental Physics, Slovak Academy of Science, Bratislava, Slovakia

The study of structural properties of biocompatible magnetic fluid (BCMF) is very important in view of their biomedical applications as magnetic drug targeting (MDT), magnetic resonance imaging (MRI), hyperthermia effect and so on. The behavior of BCMF in an external magnetic field was studied by acoustic spectroscopy. The linear increase, decrease and jump change of the external magnetic field up to 300 mT was applied and corresponding changes of acoustic attenuation were studied. The strong dependence of acoustic attenuation on magnetic field intensity, magnetic field sweep rate and time of exposure were observed. These effects are connected with the structural changes of magnetic nanoparticles in the water-based magnetic fluid when an external magnetic field is applied. The interaction between the magnetic field and the magnetic moments of the nanoparticles leads to the aggregation of magnetic nanoparticles and following clusters formation. Measurements were made also for several temperatures from the range of 15-30 °C to know the influence of thermal motion to cluster creation. The significant influence on the change of acoustic attenuation was observed, too. The obtained results are very important for MDT for example, for the using of optimal concentration of MNPs as it is impossible to use very concentrated BCMF due to the strong aggregation of MNP.

TU.F-P93 - Cobalt ferrite nanoparticles: A two phases behavior at low temperature

M. Saidani¹, W Belkacem¹, A. Bezergeanu², N. Mliki¹, C. Bazil Cizmas²

1. *Laboratoire Matériaux, Organisation et Propriétés, Faculté des Sciences de Tunis, Université de Tunis El Manar, Tunis, Tunisia*

2. *Transilvania University of Brasov, Dept. Electrical Engineering & Applied Physics, Brasov, Romania*

Studies of the $\text{Co}_x\text{Fe}_{3-x}\text{O}_4$ ($x = 0, 0.4, 0.8$ and 1) ferrite nanoparticles prepared by a solvothermal chemical route are herein presented. The microstructure has been studied by X-ray diffraction (XRD) and by transmission electron microscopy (TEM) and. The XRD patterns were mainly indexed with a cubic spinel structure. The TEM analysis shows a decrease of the mean size when x increases and HRTEM analysis for $x = 1.8$ exhibits a very irregular shape that can exert strains on the magnetic results. The magnetic dynamics behavior is investigated by measurements of magnetic hysteretic properties and zero field cooling (ZFC) susceptibility. These measurements were performed by VSM method in temperature range of 5K-700K and magnetic field up to 7T. The dependence of the irreversibility field, inversely proportional to the particle size, clearly indicates that the magnetic anisotropy of our particles finds its origin on the surface layer. The behavior of the magnetization at low temperature is interpreted in terms of surface interparticle interactions effects by means of the power Bloch law and the Kneller law. When increasing x from 1 to 1.4, no noticeable variations in the coercivity at 10 K has been detected whereas a decrease of the saturation magnetization has been found. This could be related to the effect of the value of the Co^{2+} magnetic moment which it is less than that of Fe^{3+} . The other samples exhibit a different behavior. Fitting the saturation magnetization dependence vs the temperature using the power $T^{3/2}$ Bloch law has confirmed the existence of the frustration of the surface moments. Also, for $x = 0$, we have identified the presence of the hematite with a ratio of 42 % while we didn't identify any additional phase (like maghemite or magnetite) for the other contents.

TU.F-P94 - Small angle neutron scattering and superspin glass behavior in compacts of as-received and 350 °C-annealed maghemite nanoparticles

P. Normile¹, D. Alba Venero², R. Fan³, S. King², G. Singh⁴, S.S. Lee⁵, D. Marques¹, P. Muñoz¹, J.A De Toro¹

1. *Instituto Regional de Investigación Científica Aplicada (IRICA) and Departamento de Física Aplicada, Universidad de Castilla-La Mancha, Ciudad Real, Spain*

2. *ISIS, STFC Rutherford Appleton Laboratory, Chilton, Didcot, United Kingdom*

3. *Diamond Light Source, Didcot, Oxon, England*

4. *Ugelstad Laboratory, Department of Materials Science and Engineering, Norwegian University of Science and Technology (NTNU), Trondheim, Norway*

5. *Institute of Bioengineering and Nanotechnology, 31 Biopolis Way, The Nanos, Singapore, Singapore*

A compact of highly monodisperse, essentially bare maghemite nanoparticles (NPs) was recently reported to exhibit model superspin glass (SSG) behavior [1]. Here, a similar compact together with a second compact of NPs from the same (washed) powder batch but annealed at 350 °C in air (prior to compaction) are studied by small angle neutron scattering (SANS). The purpose of the annealing is to boil off any small residue of the oleic acid surfactant (still coating the particles after washing) and thus provide “truly” bare maghemite particles. Transmission electron microscopy, however, suggests the annealing also yields an initial stage of particle coalescence. The second compact shows very similar scaling of the magnetic relaxation time in AC susceptibility to the first, but its SSG freezing transition (in DC magnetization) is 202 K compared to 165 K in the as-received NP compact. A structural correlation peak indicative of a random close packing (RCP) of spherical particles is clearly observed in the SANS from the first compact but is absent in that from the second, where a significantly wider particle size distribution (but just a 5 % larger mean diameter) is found. By recording the difference between SANS registered with and without a saturating magnetic field applied to the sample, a magnetic contribution to the scattering is identified in both compacts. Field is found to drive the majority of magnetic correlations to length scales beyond the capability of the experimental setup ($Q_{min} = 0.1 \text{ nm}^{-1}$) in both, however, differences in the temperature and field dependence of the magnetic scattering exist. For example, in the first compact, depending on its magnetic history, field also induces magnetic correlations at the position of the RCP correlation peak.

Reference:

[1] J. A. De Toro et al. (2013): Appl. Phys. Lett. 102, 183104 & J. Phys. Chem. C 117, 10213

TU.F-P95 - Exchange bias in $\text{Co}_x\text{Fe}_{1-x}\text{O}$ (AFM)| $\text{Co}_x\text{Fe}_{3-x}\text{O}_4$ (FiM) Core|Shell nanoparticlesE. Lottini^{1,2}, A. López-Ortega^{1,2}, G. Bertoni³, S. Turner⁴, C.d.J. Fernandez^{2,3}, C. Sangregorio^{2,5}1. *University Of Florence - Sesto Fiorentino, Firenze, Italy*2. *INSTM Sesto Fiorentino, Firenze, Italy*3. *CNR-IMEM, Parma, Italy*4. *EMAT, University of Antwerp, Antwerp, Belgium*5. *CNR-ICCOM, Sesto Fiorentino, Firenze, Italy*

The exchange bias effect, first reported by Meiklejohn and Bean in Co|Co ferromagnetic(FM)|antiferromagnetic(AFM) core-shell (CS) nanoparticles [1], manifests as a horizontal hysteresis loop shift and a coercivity increase due to interface coupling between AFM and FM or ferrimagnetic (FiM) phases. Interestingly, being an interface effect, exchange bias is only observed at the nanoscale. In the last decades main efforts were devoted to study exchange bias in thin films. However, with the increased capability of synthesizing CS nanoparticles with controlled features, the interest extended to these kinds of structures as well. Here, an investigation on inverted AFM|FiM CS nanoparticles of formula $\text{Co}_x\text{Fe}_{1-x}\text{O}$ | $\text{Co}_x\text{Fe}_{3-x}\text{O}_4$, is presented. Narrowly size distributed CS nanoparticles with mean diameter from 7 to 20 nm were synthesized by thermal decomposition of mixed iron and cobalt metal-oleate, leading to the formation of an AFM-core ($\text{Co}_x\text{Fe}_{1-x}\text{O}$) which is passivated under air yielding the corresponding FiM-shell ($\text{Co}_x\text{Fe}_{3-x}\text{O}_4$). The presence of a $\text{Co}_x\text{Fe}_{1-x}\text{O}$ | $\text{Co}_x\text{Fe}_{3-x}\text{O}_4$ CS structure was confirmed by X-ray Diffraction and Electron Energy Loss Spectroscopy analyses: all the samples are characterized by the presence of a constant FiM shell thickness ($t_{\text{Shell}}=2$ nm) and a variable AFM core diameter ($d_{\text{Core}}=7,11,16$ nm). Low temperature hysteresis loops revealed the presence of exchange bias and increased coercivity as indeed expected for a good exchange coupling between core and shell phases. Since the exchange bias effect is affected in an entangled way by the core and shell size [2], the synthesized NPs were used to systematically address the effect of the size of AFM counterpart which has been less studied than the FM size dependent properties. (Research supported by EU-FP7 NANOPYME Project (No. 310516) [www.nanopyme-project.eu] and EU-FP7 ESTEEM2 Project (No. 312483)).

References:

[1] Skumryev, V. et al. Nature 2003, 423, 850

[2] López-Ortega, A. et al. J. Am. Chem. Soc. 2010, 132, 9398

TU.F-P96 - Mössbauer and magnetic study of $\text{Co}(\text{Ti},\text{Sn})_x\text{Fe}_{2-x}\text{O}_4$ nanoferrites

J.Z. Msomi¹, N. Ngema¹, T. Moyo¹

1. School of Chemistry and Physics, University of KwaZulu-Natal, Durban, South Africa

Sn or Ti-substituted CoFe_2O_4 ferrite, $\text{Co}(\text{Ti},\text{Sn})_x\text{Fe}_{2-x}\text{O}_4$ ($0 \leq x \leq 1.0$, in steps of 0.1), fine powders with particle size of about 10 nm were synthesized by high energy ball milling. The compounds were also prepared by hydrothermal process to study the relationship between the preparation processes and the magnetic processes. TEM analysis shows formation of spherical nanoparticles with spherical nanoparticles. Our work indicates that the various synthesis routes can determine the properties of the magnetic nanoparticles. The properties of the nanosized specimen produced are compared to those of bulk samples reported in previously [1]. The Mössbauer spectra indicate ordered magnetic spin state in all the compounds. The evolution of the magnetic properties as a function of particle size is also presented.

Reference:

[1] V. Vaithyanathan, K. Ugendar, J. A. Chelvane, K. K. Bharati, S.S.R. Inbanathan, J. Magn. Mater. 382 (2015) 88.

TU.F-P98 - Structural and magnetic properties of CoFe_2O_4 nanoparticles diluted in SiO_2 amorphous matrix

J. Duque¹, H. C. Costa¹, J. S. Lima², A. Coelho³, T. Meneses¹

1. NPGFI, Federal University of Sergipe, São Cristóvão, Brazil

2. Unidade Acadêmica de Física, Universidade Federal de Campina Grande, Campina Grande, Brazil

3. Instituto de Física 'Gleb Wataghin' – UNICAMP, Campinas, Brazil

In this work, we carried out a systematic study of the structural and magnetic CoFe_2O_4 nanoparticles embedded inside a SiO_2 amorphous matrix. In order to control the mean distance between particles we have prepared via sol-gel method different samples changing the amount of Fe and Co salts and the tetraetilortossilicato (TEOS). X-ray, transmission electron microscopy and magnetization analysis allow us to estimate the particle mean size. Besides, all analyzed samples present single crystalline phase belonging to the spatial group $Fd\bar{3}m$. The T-dependence of the magnetization shows typical behaviors of a classical magnetic nanoparticle system, that is, a maximum in the ZFC curve and a thermal hysteresis in the low temperature region. It was observed a displacement of the maximum into high temperatures for increasing the CoFe_2O_4 nanoparticles in the SiO_2 matrix. The coercive data were fitted for using a generalized model which take account the particle size distribution of the system. Finally, we have attributed the change in maximum of ZFC curve and the decreasing in the effective anisotropy constant to the possible interparticle interactions.

TU.F-P100 - Ultrafast hyperthermia using Fe₃O₄ nanoparticles

V. Tzitzios¹, G. Basina², C. Hadjipanayis³, G. Hadjipanayis⁴

1. Institute of Materials Science, Demokritos, Athens, Greece

2. Department of Chemistry, University of Crete, Voutes, Heraklion, Greece

3. Department of Neurosurgery, Emory University School of Medicine, Winship Cancer Institute of Emory University, GA, United States

4. Department of Physics and Astronomy, University of Delaware, Newark, DE, United States

In the past few years, much work has been published on Fe₃O₄ nanoparticles especially on synthetic protocols to control their size, shape and surface functionality.¹ For optimal magnetic hyperthermia, the maximum Specific Loss Power (SLP) for isolated Fe₃O₄ nanoparticles was reported in the 10-15 nm size range.² More recently, it was reported that nano-assemblies of Fe₃O₄ nanoparticles can lead to significantly increased SLP values.^{1, 2, 3}

In this study, we report an alternative synthesis of Fe₃O₄ nano-assemblies based on a modified polyol method that uses Fe lactate as the iron source in the presence of poly-vinyl-pyrrolidone (PVP) as the morphogenetic and capping agent. The as-made PVP coated Fe₃O₄ nano-assemblies, were further functionalized by citrate ions in order to increase their water solubility. The nano-assemblies have a flower-like morphology with 30-40 nm mean diameter and consist of 6-8 nm mean diameter isolated Fe₃O₄ nanoparticles. The temperature profiles, obtained from hyperthermia measurements in water solution, showed an increase in temperature from 293 to 338 K ($\Delta T=45$ K) after only 79 sec of field exposure with a very high heating rate of 0.57 °C/sec in the case of citrate functionalized nanoparticles. Future in vitro hyperthermia studies on therapy-resistant human brain cancer (glioblastoma) cells will also be performed with the Fe₃O₄ nano-assemblies. In addition, distribution and in vivo hyperthermia studies will be performed by MRI in an intracranial rodent glioma model.

References:

1. Lartigue L., Alloyeau D., Kolosnjaj-Tabi J., Javed Y., Guardia P., Riedinger A., P  choux C., Pellegrino T., Wilhelm C., Gazeau F., *ACS Nano* 2013, 7 (5), pp 3939–3952
2. Fortin J-P, Wilhelm C., Servais J., M  nager C., Bacri J-C, Gazeau F., *J. Am. Chem. Soc.*, 2007, 129 (9), pp 2628–2635
3. Barickn K.C., Aslam M., Lin Y-P., Bahadur D., Prasad P.V., Dravid V. P., *J. Mater. Chem.*, 2009, 19, 7023-7029

TU.F-P101 - Surface oxidation effect on the verwey transition in cubic magnetite nanoparticles

M. Cöpkün¹, S. Çitođlu², T. Edvinsson³, E. Wetterskog⁴, P. Svedlindh⁴

1. Hacettepe University, Department of Physics Engineering, Beytepe, Ankara, Turkey

2. Hacettepe University, Department of Nanotechnology and Nanomedicine, Beytepe, Ankara, Turkey

3. Uppsala University, Department of Chemistry, Uppsala, Sweden

4. Uppsala University, Department of Engineering Sciences, Uppsala, Sweden

Cubic-shaped Fe₃O₄ nanoparticles (NPs) with a size of approximately 40 nm were synthesized by the reduction of Fe(acac)₃ as a precursor; benzyl ether and squalane as the solvent; and decanoic acid as the stabilizing ligand. We have investigated the influence of the oxidation on the magnetic properties of the NPs. The morphology, structure and magnetic properties of the NPs were investigated using analytical tools such as transmission electron microscopy, X-ray diffraction (XRD), thermogravimetric analyses, ferromagnetic resonance (FMR), micro-Raman spectroscopy and vibrating sample magnetometry. XRD analysis showed peaks characteristics of the Fe₃O₄ phase for the sample. The NPs exhibit ferrimagnetic properties with a relatively high saturation magnetization of 80 emu/mg at room temperature. In the zero-field-cooled and field-cooled magnetization curves a sharp Verwey transition at 120 K was observed for stoichiometric magnetite NPs. The Verwey transition was also observed in temperature dependent FMR measurements. The NPs oxidized in air at room temperature for a time period of a few months. In the oxidized NPs, the Verwey transition is broadened and shifted to lower temperatures due to a maghemite shell surrounding the NPs. Structural investigations by micro-Raman spectroscopy also revealed magnetite NPs with a partial surface oxidation to maghemite.

TU.F-P102 - SANS, Mössbauer and magnetic characterization of interacting iron oxide nanoparticles

P. Bender¹, D. Alba Venero¹, L. Fernández Barquín¹, R. Costo², J. Fock³, C. Frandsen³, M. Fougth Hansen³, S. Rogers⁴, E. Wetterskog⁵, P. Svedlindh⁵

1. CITIMAC, Universidad de Cantabria, Santander, Spain

2. Instituto de Ciencia de Materiales de Madrid, CSIC, Madrid, Spain

3. Department of Physics, Technical University of Denmark, Kgs. Lyngby, Denmark

4. ISIS-STFC, Rutherford Appleton Laboratory, United Kingdom

5. Faculty of Technology, Uppsala University, Uppsala, Sweden

6. Acreo Swedish ICT AB, Göteborg, Sweden

The magnetic properties of an ensemble of iron oxide nanoparticles (IO-NPs) primarily depend on the structural properties of the individual particles, but also on interparticle interactions, which has significant implications e.g. in biomedical applications such as hyperthermia. To standardize the magnetic parameters driving those applications is a need for the near future. In the present study two samples of IO-NPs with nearly identical average core diameters (10-11 nm), but with different interparticle distances, were characterized by Small Angle Neutron Scattering (SANS), Mössbauer and magnetization measurement. In the first sample, the particles were coated with an organic surfactant (DMSA) and aggregated to clusters consisting of several dozens individual particles. In contrast, the particles of the second sample were surrounded by a rigid silica shell with a thickness of about 30 nm, increasing the interparticle distance to at least 60 nm and as result significantly decreasing the amount of dipolar interactions. According to Mössbauer measurements the IO-NPs in both samples were predominantly composed of maghemite and exhibited low polydispersity < 6%, as verified by SANS. Hence, the two particle systems can be regarded as model systems to investigate the influence of dipolar interactions on the magnetization behavior of aggregated and nearly monodisperse IO-NPs. In this work the Zero-Field-Cooled and the Field-Cooled curves of both samples were adjusted by global fitting routines [1], which were modified e.g. to incorporate the influence of dipolar interactions. This work is part within a 18-institution consortium to standardize IO-NPs and is supported by EC FP7 NMP project NanoMag Project (grant no. 604448).

Reference:

[1] F. Tournus, E. Bonet, JMMM 323 1109-1117 (2011)

TU.F-P103 - The effect of pH on the structural and magnetic properties of MnFe₂O₄ nanoparticles synthesized via proteic sol-gel processN. Ferreira¹, S. Farias¹, M. Macêdo²

1. Departamento de Física, Universidade Federal do Amazonas, Manaus, Brazil

2. Departamento de Física, Universidade Federal de Sergipe, São Cristóvão, Brazil

During the past few decades, the design, preparation and characterization of spinel ferrite nanoparticles have been the subject of intense research not only for their fundamental scientific interest but also for their high potential for application in high-density magnetic recording, ferrofluids technology, magnetic resonance imaging, and biomedical drug delivery. In this work, we report the structural, microstructural, and magnetic properties of MnFe₂O₄ nanoparticles synthesized via proteic sol-gel method at different pondus hydrogenii (pH) value. Five solutions were prepared by adding 5g of Fe(NO₃)₃·9H₂O and 1g of C₄H₆MnO₄ to 25 mL of *in natura* coconut water. 1M NaOH solution slowly dropped in each one of the 5 solutions to change the pH values to 2, 4, 7, 10 and, 12. Then, the mixtures were polymerized to form the gels at 100°C for 24h and, after that, calcinated at 400°C for 1h to produce the nanoparticles. According to XRD and TEM studies, all MnFe₂O₄ samples were cubic spinel single phase with space group Fd-3m. The crystal lattice constant was decreased gradually from 0.8526 to 0.8464nm with pH increasing from 2 to 12. In addition, the average crystallite size, which is determined from Scherrer formula, was about 14-35nm. The magnetization results showed small hysteresis loops. The saturation magnetization increased from 51 emu/g to 65 emu/g with pH increasing from 2 to 12, which is among the best values reported so far. Meanwhile, the coercive force increased drastically from 6.7 to 73Oe. This behavior suggests that the variation of the cationic distribution between octahedral and tetrahedral sites contribute to the unique magnetic behavior of the samples at room temperature. Our results indicate that adjusting in pH *enhances* systematically the structural and magnetic properties of the MnFe₂O₄ nanoparticles synthesized via proteic sol-gel process.

TU.F-P104 - XRD, Mössbauer and magnetic study of $Mn_xMg_{0.5-x}Zn_{0.5}Fe_2O_4$ nanoparticles

W.B. Dlamini¹, J. Msomi¹, T. Moyo¹

1. University Of KwaZulu-Natal, Durban, South Africa

We report Mn substitution in Zn-Mg ferrite nanoparticles. Single phase nanoferrite powders bearing the chemical formula $Mn_xMg_{0.5-x}Zn_{0.5}Fe_2O_4$ ($0 \leq x \leq 0.5$ in steps of 0.1) were produced by co-precipitation technique. The compounds were characterized by X-ray diffraction, Mössbauer and VSM measurements. The particle size varies between 9 nm and 15 nm. Changes in the saturation magnetization and coercive fields with increasing Mn content have been observed. Mössbauer spectra reveal transformation from ordered to disordered magnetic spin state with increasing x . The variation of the magnetic parameters such as coercive fields and saturation magnetization as a function of temperature is also presented.

TU.F-P105 - Magnetic properties of $\text{Mg}_{0.5}\text{Co}_{0.5}\text{Fe}_2\text{O}_4$ and $\text{Mg}_{0.8}\text{Co}_{0.2}\text{Fe}_2\text{O}_4$: The effect of milling

W.B. Dlamini¹, J. Msomi¹, T. Moyo¹

1. University Of KwaZulu-Natal, Durban, South Africa

In the present work, $\text{Mg}_{0.5}\text{Co}_{0.5}\text{Fe}_2\text{O}_4$ and $\text{Mg}_{0.8}\text{Co}_{0.2}\text{Fe}_2\text{O}_4$ nanoparticles with particle diameters of about 15 nm were synthesized by glycol-thermal reaction. To further reduce the particle size and to study the effect of milling, the as prepared specimens were then milled for up to 40 hours. The properties of the as-prepared, milled and bulk compounds are compared. The phase purity and morphology of the compounds are investigated by X-ray diffraction, transmission electron microscopy and Fourier Transform infrared spectroscopy. The 57Fe Mössbauer effect spectra show ordered magnetic spin state in both $\text{Mg}_{0.5}\text{Co}_{0.5}\text{Fe}_2\text{O}_4$ and $\text{Mg}_{0.8}\text{Co}_{0.2}\text{Fe}_2\text{O}_4$ nanosized compounds. The M-H loops of the compounds have been traced using the Vibrating Sample Magnetometer (VSM). The magnetization data show an increase in coercive fields to a maximum value and then a reduction with further milling. This is explained on the basis of domain transformation from multi- to single-domain behaviour. The variation of magnetization as a function of temperature (FC and ZFC) is also presented.

TU.F-P106 - Modulation of interacting phenomena in iron oxide nanoparticle colloids

D. Cabrera¹, D. Ortega^{1,2,3}, G. Salas^{1,2}, F.J. Teran^{1,2}

1. *Imdea Nanociencia, Madrid, Spain*

2. *Unidad Asociada de Nanobiotecnología, CNB-CSIC ---IMDEA, Madrid, Spain*

3. *Institute of Biomedical Engineering, University College London, London, United Kingdom*

Iron oxide nanoparticles (IONP) have attracted much attention due to their capabilities acting as magnetic nanocarriers, hyperthermia mediators and/or contrast agents. Their applications in biomedicine mainly relies on their magnetic response, which can be significantly altered by magnetic dipolar interactions. Hence, controlling the latter is of great importance towards the clinical use of IONP as reliable actuators.

Here, we report on the influence of particle size, media viscosity as well as field amplitude (H) and frequency (f) conditions on interacting phenomena. We assess the specific absorption rate (SAR) and AC hysteresis loops of IONP colloids. Recently, a theoretical model was proposed[1] for describing magnetic dipolar interactions and their implications on tuning the dynamical magnetic response of IONP colloids when varying particle concentration. Our results indicate that SAR concentration dependence is tightly related to particle size. While large sizes (19 nm) show a non-monotonic behaviour with a relative SAR maximum within a given concentration range, small sizes (12 nm) show a progressive SAR decay until reaching a minimum which remains constant in the studied concentration range. The variation of H and f gives rise to a rich variety of behaviours resulting in a progressive SAR decay (at low-f) towards non-monotonic behaviour (at high-f). Relative SAR maxima occurring at given concentrations which tightly depend on H. Considering that $SAR = A \cdot f$, where A is the area of hysteresis loop, we have proven how magnetic parameters involved in the A determination (i.e. coercivity and remanence) differently change with IONP concentration. We also show the role of colloidal viscosity in shaping hysteresis loops with smaller squareness with respect to water dispersions, and consequently reducing the heating efficiency. Finally, we discuss the departure of our data from the currently available physical models (i.e. LRT or Stoner-Wohlfarth based models).

Reference:

[1]-Martinez-Boubeta et al.,*Adv.Funct.Mat.*2012,22,3737

TU.F-P107 - Effects of vanadium doping on the magnetism of FeCo and FeCo/SiO₂ Core/Shell nanoparticles

R. Desautels^{1,2}, J. Freeland³, M. Rowe², J. van Lierop¹

1. *University Of Manitoba, Winnipeg, Manitoba, Canada*

2. *Toyota Research Institute of North America, United States*

3. *Argonne National Laboratory, Lemont, United States*

The breadth of magnetically soft alloys accessible through traditional top-down metallurgical techniques is far narrower in nanoparticle form. Additionally, in magnetic nanoparticle systems, complex core/shell structures have been shown to exhibit unique and useful magnetism from interfacial effects. Core/shell nanoparticles are the ideal ingredient for today's high quality devices and other nanoscale technological applications, however, a detailed understanding of their magnetism is lacking. Furthermore, physical properties such as ductility are of significant importance for the fabrication of devices. Historically, vanadium has been added to increase the ductility of the ingredients used. Here, we report on the effects that vanadium doping of FeCo and FeCo/SiO₂ nanoparticles has had on their structure, composition and magnetism. X-ray powder diffraction experiments and transmission electron microscopy images have indicated that these nanoparticle (doped and not doped) were amorphous, and for the core/shell systems the silica coating encompassed the nanoparticles completely. X-ray absorption spectroscopy (XAS) and magnetic circular dichroism (XMCD) experiments indicated that these amorphous nanoparticles, free of oxygen contamination, formed complex strained systems. XAS spectra presented mixed metallic and non-metallic-like features, however, XMCD spectra were purely metallic-like. A marked increase of the nanoparticles coercivity as well as a decreased saturation magnetization occurred with V-doping in both FeCo nanoparticles and FeCo/SiO₂ core/shell nanoparticles, despite similar blocking temperatures. In addition, only V-doped FeCo/SiO₂ nanoparticles exhibited an exchange bias loop shift of 0.141(1) T at 5 K, likely from the formation of a V-oxide (identified by XAS spectra) interfacial region in-between the FeCo core and SiO₂ shell. Magnetic anisotropies were calculated from χ_{AC} susceptibility experiments and were an order-of-magnitude larger in comparison to the bulk counterparts of the nanoparticles, consistent with these high surface area systems.

TU.F-P108 - Iron/silicon/ silica nanoparticles synthesized via laser pyrolysis technique and thermal treatment

F. Dumitrache^{1,2}, C. Fleaca^{1,2}, I. Morjan¹, A. Badoi¹, A.M. Niculescu¹, O. Marinica³, L. Vekas⁴, E. Vasile²

1. *National Institute for Plasma, Laser and Radiation Physics (NILPRP), Bucharest, Romania*

2. *'Politehnica' University of Bucharest, Independentei 313, Bucharest, Romania*

3. *'Politehnica' University of Timisoara - Research Center for Engineering of Systems with Complex Fluids, Timisoara, Romania*

4. *Romanian Academy Timisoara branch, Timisoara, Romania*

A multitude of iron based nanoparticles, such as iron oxides, metallic iron embedded in polymer or amorphous carbon matrix, iron carbides or iron nitrides are found in many bio-medical, pharmaceutical, and industrial processes or products due to their magnetic properties. On the other hands, SiO₂ nanoparticles possess a low to an inert toxicity and no proved toxicological change in drug delivery applications. Therefore, composite nanoparticles with iron based core and silica shell should provide benefit properties: high magnetic susceptibility and low toxicity. Laser pyrolysis was used to synthesize almost spherical Fe@Si nanoparticles with superparamagnetic properties, high saturation magnetization (more than 50 emu/g), 8-12 nm mean size diameter and narrow size distribution. TEM, SAED, XRD, EDX and VSM (virgin curve and hysteresis loop) measurements were used for structural and magnetic characterization of as synthesized and thermal treated powders. In optimal conditions nanopowder with iron based core with silica shell were obtain. The both proposed nanomaterials, as synthesized and thermal treated, possess good water compatibility. Stable dispersions with 40 to 100 nm hydrodynamic diameter were realized using L-3,4-dihydroxyphenylalanine (L-Dopa) or sodium carboxymethylcellulose (CMC-Na) as stabilizers. Some suspensions with a high degree of nanoparticle concentrations (5, 10 or 20 g/l) have high saturation magnetization values, up to 5 Gs.

TU.F-P111 - Magnetic and structural characterization of the cobalt ferrite nanoparticles

T. Torres Molina^{1,2,3}, E. Lima Jr.⁴, A. Mayoral^{1,3}, A. Ibarra^{1,3}, C. Marquina^{2,5}, M.R. Ibarra^{1,2,3}, G.F. Goya^{1,2}

1. Instituto De Nanociencia De Aragón & Laboratorio De Microscopias Avanzadas, Universidad De Zaragoza, Zaragoza, Spain

2. Departamento de Física de la Materia Condensada, Facultad de Ciencias, Universidad de Zaragoza, Zaragoza, Spain

3. Laboratorio de Microscopias Avanzadas (LMA), Universidad de Zaragoza, Zaragoza, Spain

4. División Resonancias Magnéticas, Centro Atómico Bariloche/CONICET, S. C. Bariloche, Argentina

5. Instituto de Ciencia de Materiales de Aragón (ICMA), CSIC - Universidad de Zaragoza, Zaragoza, Spain

We present a systematic study on the structural and magnetic properties of $\text{Co}_x\text{Fe}_{3-x}\text{O}_4$ magnetic nanoparticles (MNPs) with sizes between 5 to 25 nm, prepared by thermal decomposition of $\text{Fe}(\text{acac})_3$ and $\text{Co}(\text{acac})_2$. The correlation between magnetic parameters and size, morphology and stoichiometry of the MNPs are analyzed. All samples were indexed within the Fd_3m space group as expected for cubic spinel crystal structure. A systematic deviation of the atomic Co:Fe ratio from the stoichiometric 1:2 value is present in all samples, and this composition is demonstrated to be present and homogeneous both at macroscopic and single-particle scale. Magnetization $M(T, H)$ data reflected the large crystalline magnetic anisotropy of the MNPs through high blocking temperatures (TB) and large coercive fields (HC ≈ 1.6 MA/m for $T = 5$ K). For the smallest particles ($\langle d \rangle = 5$ nm), surface spin disorder the $M(H)$ curves do not saturate up to $H = 11.2$ MA/m (14 T), suggesting the existence of a magnetically hard surface. The large magnetic anisotropy allowed seeing that the temperature dependence of HC (T) deviates from the usual $T^{1/2}$ law expected for thermally-driven magnetic (Neel) relaxation of single domain MNPs.

TU.F-P113 - Room temperature ferromagnetism in (Fe,Cr)-doped CeO_{2-δ} nanoparticles synthesized by proteic sol-gel processN. Ferreira¹*1. Departamento de Física, Universidade Federal do Amazonas, Manaus, Brazi*

Room-temperature ferromagnetic semiconductors have generated extraordinary research interest due to their potential applications in spintronic devices. More recently, theoretical studies have predicted room-temperature ferromagnetism mediated by doping with qualified transition metal in several inorganic oxides. Among these, cerium oxide (CeO₂) has been extensively studied because its electronic configuration and structural properties are similar to silicon. In the present study, Cr and Fe co-doped O_{2-δ} nanoparticles were synthesized successfully via proteic sol-gel process. The CeO₂, Ce_{0.95}Fe_{0.05}O_{2-δ} and Ce_{0.93}Fe_{0.05}Cr_{0.02}O_{2-δ} samples were prepared by dissolving Fe(NO₃)₃·9H₂O, Cr(NO₃)₂·9H₂O and Ce(NO₃)₃·6H₂O with suitable stoichiometries in coconut water (*Cocos Nucifera*). Then, the mixture was polymerized to form the gel at 100°C for 24h and, after that, calcinated at 400 °C for 1h to produce the nanoparticles. X-ray diffraction reveals that the CeO₂, Ce_{0.95}Fe_{0.05}O_{2-δ} as well as Ce_{0.93}Fe_{0.05}Cr_{0.02}O_{2-δ} nanoparticles were cubic in structure (fluorite phase) and no other secondary phase was found in all the samples indicating that Cr and Fe cations are substituted at the Ce sites. Transmission electron microscopy measurements show that the average size of these nanoparticles is in the range 10-20 nm. It was observed that all samples showed the Raman vibrational frequency around 468 cm⁻¹, which is the expected value for the vibrational mode of the Ce-O₈. CeO₂ nanoparticles exhibit diamagnetism while Ce_{0.95}Fe_{0.05}O_{2-δ} exhibit saturated hysteresis loop at room temperature indicating ferromagnetic behavior (M_s~0.13 emu/g). Moreover, the M-H curves at room temperature for the Ce_{0.93}Fe_{0.05}Cr_{0.02}O_{2-δ} nanoparticles indicated enhancement in ferromagnetism (M_s~0.34 emu/g). Our results demonstrate that proteic sol-gel process can be used to synthesize Fe and Cr doped CeO₂ nanoparticles with potential for spintronics applications.

TU.F-P114 - Synthesis, structural and magnetic properties of mixed Zinc-Cobalt ferrite nanoparticles

P. Copolla¹, G. Siqueira Gomide³, F. Gomes da Silva², F.L. de Oliveira Paula³, R. Aquino², J. Depeyrot³, F. Augusto Tourinho¹

1. Universidade de Brasília, Instituto de Química, Universidade de Brasília, Brasília, Brazil

2. Laboratório de Nanociência Ambiental e Aplicada, Grupo de Fluidos Complexos, Faculdade UnB Planaltina, Universidade de Brasília, Brasília, Brazil

3. Grupo de Fluidos Complexos, Instituto de Física, Universidade de Brasília, Brasília, Brazil

Magnetic ferrite nanoparticles (NPs) have attracted considerable attention because of their electrical, structural, optical and magnetic properties that lead to novel technological and biological applications. We currently elaborate ferrite based NPs in order to disperse them in water [1]. In this context, we have synthesized several samples of $\text{Co}_{(1-x)}\text{Zn}_x\text{Fe}_2\text{O}_4$ mixed ferrite NPs, each one with a different stoichiometric parameter x varying from 0.1 to 0.9. Our NPs, obtained by hydrothermal coprecipitation in alkaline medium, have their chemical composition checked by using atomic absorption spectroscopy and their structure by X-Ray Diffraction (XRD) experiments realized on powder samples. In addition, Transmission Electron Microscopy (TEM) pictures show their morphology and allow a mean size determination. It clearly indicates a mixture of nanospheres and nanocubes of similar sizes. This is described by an averaged size, which well matches the one deduced from XRD analysis, performed by Rietveld refinement. The diffractograms reveal for all samples a pure spinel structure, with zinc ions mostly located at tetrahedral sites and cobalt ions mainly distributed among octahedral sites. This is in agreement with a magnetization decrease with zinc content. Hysteresis loops measurements were performed at 300K and at 5K using a PPMS magnetometer. At 300K, we observed non-zero remanence and coercivity for higher cobalt content. At low temperature, coercivity and remanence also increase with increasing Co content. Furthermore, a sudden drop in the magnetization is observed close to remanence, being more pronounced for samples with higher cobalt content. This behavior is associated to both NPs with uniaxial and cubic anisotropies.

Acknowledgments This work was supported by the contracts CAPES/COFECUB nº 714/11 and the Brazilian agencies FAP/DF, CNPq, CAPES

Reference:

[1] J. A. Gomes, M. H. Sousa, F. A. Tourinho, R. Aquino, G. J. da Silva, J. Depeyrot, E. Dubois, R. Perzynski J. Phys. Chem. C 112. 6220 (2008)

TU.F-P115 - Towards ideal biotechnologically applicable magnetic particles with highly tunable perpendicularly magnetized synthetic anti-ferromagnets

T. Vemulkar¹, R. Mansell¹, D. Petit¹, R.P. Cowburn¹

1. Cavendish Laboratory, University of Cambridge, Cambridge, United Kingdom

The use of ferrofluids in biological applications has become an important area of technological innovation. We demonstrate the fabrication of zero remanence, low susceptibility and high moment ferrofluids for biotechnological applications via the lift off of lithographically patterned multilayer thin films. Perpendicularly magnetized CoFeB/Pt thin film bilayers that are antiferromagnetically coupled via RKKY interactions across a Pt/Ru/Pt spacer form the basic building block of this work. This bilayer system demonstrates sharp switching to saturation magnetization at a specific applied field. The RKKY coupling gives a zero remanence state with a low susceptibility, a necessity to prevent particle agglomeration in the ferrofluid. We then repeatedly stack this bilayer system 12 times to increase the moment of the magnetic stack independently of the other system parameters. This 12 times repeated bilayer system is sputtered on pre-patterned resist, and lifted off into solution to create a ferrofluid of particles that are 2 μm across. We demonstrate that the magnetic properties of the thin film are transferred to the particles in the solution. Polar magneto-optical Kerr effect hysteresis loops of individual particles recondensed on a substrate are compared to vibrating sample magnetometer hysteresis loops of both the thin film, and an aliquot of the ferrofluid. Interestingly, we see that the ferrofluid shows a slightly higher RKKY coupling strength as compared to the thin film, as well as zero remanence and very small low field susceptibility, less than half that of the thin film hard axis. We also demonstrate the ability to tune the magnetic anisotropy through the CoFeB thicknesses, the switching field via the RKKY coupling strength, and the total magnetic moment through the number of repeats of the bilayer building block. We use this work to outline a parameter space for the fabrication of these highly tunable synthetic ferrofluids for biotechnological applications.

Tu.F-P122 - Ferronematics in low magnetic fields

P. Kopcansky¹, N. Tomasovicova¹, V. Gdovinova¹, M. Timko¹, V. Zavisova¹, N. Eber², T. Toth-Katona², F. Royer³, D. Jamon³, C.K. Hu⁴

1. *Institute of Experimental Physics, Slovak Academy of Sciences, Kosice, Slovakia*

2. *Research Institute for Solid State Physics and Optics, Hungarian Academy of Sciences, Budapest, Hungary*

3. *Université de Saint Etienne, Saint Etienne, France*

4. *Institute of Physics, Academia Sinica, Taipei, Taiwan*

The orientational order of liquid crystals (LCs) can be controlled by magnetic or electric fields due to the anisotropy of dielectric permittivity or diamagnetic susceptibility. Very small anisotropy of the diamagnetic susceptibility of liquid crystals causes that liquid crystals are rather control by electric field in practise than by magnetic field. In order to increase the magnetic susceptibility of liquid crystals Brochard and de Gennes' introduce the great idea of doping them with fine magnetic particles so called ferronematics [1]. A linear magnetodielectric response has been detected in planarly oriented ferronematics samples far below the threshold of the magnetic Fredericksz transition in the presence of a weak orienting bias magnetic field (2mT) [2]. In our study, magneto-optical and dielectric properties of magnetic nanoparticle doped nematic LCs has been investigated by means of applying different orienting bias magnetic fields B_{bias} as well as electric fields E_{bias} . The liquid crystals 4-n-hexyl-4'-cyanobiphenyl (6CB) and 4-(trans-4'-n-hexylcyclohexyl)-isothiocyanatobenzene (6CHBT) were doped with spherical magnetite nanoparticles of 10nm in diameter. The obtained results ie linear magnetic field dependence of magnetoptical and magnetodielectric effects in low magnetic field region showed that bias fields allow controlling these effects of ferronematic samples. This can be used as liquid sensors for the mapping of magnetic field similar to mapping spacial distribution of temperature by liquid crystals for example.

This work was supported by Ministry of Education Agency for Structural Funds of EU in frame of project PhysNet 26110230097.

References:

[1] F. Brochard and P. G. De Gennes, "Theory of magnetic suspensions in liquid crystals," J. Phys., vol. 31, no. 7, pp. 691-708, 1970

[2] N. Tomašovičová, M. Timko, Z. Mitróová, M. Koneracká, M. Rajňák, N. Éber, T. Tóth-Katona, X. Chaud, J. Jadzyn and P. Kopčanský, Phys. Rev. E 87, 014501 (2013)

Tu.F-P123 - Magnetic moments in Pd nanoparticles: from sub- μm to sub-nm size

F. Bartolomé¹, U. Urdíroz-Urricelqui¹, L. Badía-Romano¹, M. Kovylna^{2,3}, A. Labarta², X. Batlle²

1. ICMA, Departamento de Física de la Materia Condensada, CSIC-Universidad de Zaragoza, Zaragoza, Spain
2. Departament de Física Fonamental and Institut de Nanociència i Nanotecnologia IN2UB, Universitat de Barcelona, Barcelona, Catalonia, Spain
3. University of Toronto, , Toronto, Canada

The understanding of magnetism at the ultimate length scale is one of the current frontiers in solid state physics. Some metals whose bulk material do not fulfill Stoner criterium to support ferromagnetic ordering, like Pd, may undergo a crossover to magnetic behavior by several ways: a neighboring magnetic material may polarize it, or more interestingly, a perturbation of the Pd coordination may cause the Pd to interact magnetically producing magnetic particles. We have prepared Pd₁₃ particles, supported in NaY and KL (iron-free) zeolites, in two chemical states: Pd₁₃ particles in the bare neutral cluster, and Pd₁₃ with absorbed H. The surface effects attributable to the loss of local symmetry are maximized in this clusters. These Pd₁₃ samples are model systems for this study on nano-magnetism as they are virtually monodisperse and the Pd loading of the zeolite is $\approx 6\%$ in weight, and therefore, the interaction between particles can be neglected. We have also prepared a series of high quality Pd nanoparticles by cosputtering, embedded in amorphous ZrO₂ within a wide size range (from 2 to 25 nm) and a very narrow size distribution. Particles are well isolated, with sharp particle-matrix interfaces due to immiscibility between the two phases. In-house characterization includes SEM and HR-TEM, EDX, EPS, and SQUID magnetometry. All the foregoing suggests that this is a clean system to study the spontaneous magnetic moment in Pd nanoparticles larger than 1.5 nm in diameter. The magnetization of the Pd₁₃ and larger Pd nanoparticles at $T = 1.8\text{K}$ shows a dominant diamagnetic signal, clearly accompanied by a paramagnetic curve. The data collection coalesces obeying a corresponding-states law which can be properly fitted to a $2 \mu\text{B}$ Langevin function. For the larger particles, a decreasing magnetic moment with increasing particle size is evidenced from experiments.

TU.G-P01 - [Co/Pt] multilayers structural, magnetic and electronic properties: role of the Pt thickness

K. Dumesnil¹, M. Bersweiler¹, D. Lacour¹, S. Robert¹, M. Hehn¹

1. Institut Jean Lamour, Université de Lorraine and CNRS, Nancy, France

[Co/Pt] multilayers constitute archetypes of perpendicularly magnetized systems and have been widely used for almost two decades in close connexion with the development of spintronic devices: magnetic tunnel junctions (MTJs), magnetic recording media, devices where the magnetization is manipulated by spin-transfer torque. Most attention has been focused on the origin and optimization of the strong perpendicular anisotropy, mainly exploring the role of Co thickness and interface morphology. This study aims in exploring more particularly the role of the Pt thickness and of oxide buffer layers as MgO and Al₂O₃, commonly used as insulating barriers in MTJs. Using [Co/Pt] multilayers as electrodes in MTJs may namely require their growth on such oxides, which could affect the interface morphology and consequently the magnetic and transport properties. Accurate structural, magnetic and transport investigations have been performed to correlate various properties of [Co(0.58nm)/Pt]₄ stackings (effective anisotropy, saturation magnetization, effective tunnel polarisation) to the interface morphology when varying the Pt thickness and the nature of the oxide buffer layer.

The results first highlight the prominent role played by the Pt thickness: increasing the Pt thickness tends to smooth the interfaces and then to improve the Perpendicular Magnetic Anisotropy (PMA). The roughness is however significantly increased when using an oxide buffer instead of Pt, especially for Al₂O₃, which leads to a reduced PMA. Simultaneously, rough interfaces (small Pt thickness and/or oxide buffers) obviously drive a large enhancement of the saturation magnetization via the polarization of Pt atoms in direct contact with Co.

Interestingly, the Pt thickness also appears to play an important role in the effective tunnel polarization, determined from Tunnel Magneto Resistance values in [Co/Pt]-based MTJs. A decrease of the low temperature effective spin polarization is observed versus Pt thickness, consistently with the exponential decay expected for the induced magnetic moment in the Pt layers.

TU.G-P02 - Perpendicular magnetic anisotropy and Gilbert damping study in amorphous FeTaC filmM. Nandi¹, B. Samantaray¹, A. Perumal², N. Khan¹, P. Mandal¹, R. Ranganathan¹

1. Saha Institute of Nuclear Physics, 1/AF Bidhannagar, Calcutta, India

2. Department of Physics, Indian Institute of Technology Guwahati, Guwahati, India

Spin transfer torque (STT) has greater credibility towards ultrafast spin dynamics in ferromagnets by switching the magnetization of spin valves and magnetic tunnel junctions. In STT devices, the low spin polarized current density which manipulates the magnetization reversal requires low the Gilbert damping constant (α) and high perpendicular magnetic anisotropy (PMA).¹ These material specification parameters ' α ' and PMA were explored in soft ferromagnetic thin film Fe₈₀Ta₂₀C₁₂ based alloy of thickness 200 nm by using micro-strip ferromagnetic resonance (MS-FMR) in broad band frequency range (4-18 GHz) at room temperature. The present film is magnetically isotropic in plane and the saturation magnetization ($4\pi M_s$) was found to be 7790 Oe from frequency dependence of resonance field (H_r) analysis. The out-of-plane angular dependence of H_r at different frequencies could be successfully modeled with experimental data by taking free energy density function (E) for thin film, where the total energy was contributed by Zeeman energy, effective demagnetization energy and perpendicular magnetic anisotropy energy. The parameters deduced from the analysis are listed as PMA constant, $K_{\perp} = 2 \times 10^5$ erg/cm³, effective magnetization, $4\pi M_{eff} = 7145$ Oe and Landé g factor, $g = 2.1$. The Gilbert damping constant (α) was analyzed from out-of-plane angular dependence of FMR line width (ΔH) by using Gilbert-type intrinsic damping and extrinsic damping due to anisotropy dispersion of magnitude and direction of effective magnetization.^{2,3} The ' α ' values increases monotonically with decrease in frequency and were found to vary from 6×10^{-3} to 1.2×10^{-2} in the frequency range of 10-4 GHz.

References:

1. Hyon-Seok Song, et al., Appl. Phys. Lett. 103, 022406 (2013)
2. X. Guo, et al., Appl. Phys. Lett. 105, 072411 (2014)
3. S. Mizukami, et al., Phys. Rev. B 66, 104413 (2002)
and have potential application in magneto-resistive random access memories (MRAM) and magnetic recording media

TU.G-P03 - Effects of process parameters on structures and perpendicular magnetic properties of Co-rich Co-Pt thin filmsS.C. Chen¹, J.Y. Chiou¹, C.K. Wen¹, S.T. Chen², P.C. Kuo²1. *Ming Chi University Of Technology, Taipei, Taiwan*2. *National Taiwan University, Taipei, Taiwan*

Materials having high magnetocrystalline anisotropy constant (K_u) are generally desirable for high density magnetic recording applications due to their thermal stability even with smaller grain size. The K_u of hcp Co_3Pt alloy films is as high as $2 \times 10^7 \text{ erg/cm}^3$, and the temperature required for obtaining high perpendicular magnetic properties is only 300°C . Therefore, Co_3Pt alloy film has significant potential to be utilized in ultra-high density (1Tb/in^2) magnetic recording media. It has been reported that Co-rich Co-Pt films with perpendicular magnetic properties can be achieved by introducing a Pt underlayer or Ru/Pt bilayers. The lattice parameter of Ag is close to Pt and both structures are fcc. Furthermore, compared to a Pt underlayer, the Ag does not change the composition ratio of Co to Pt in the Co_3Pt magnetic layer, and the cost of Ag is much lower than that of Pt. In this study, $\text{Co}_{80}\text{Pt}_{20}$ films were deposited onto Ru/Ag bilayer films. The perpendicular magnetic anisotropy was achieved by depositing $\text{Co}_{80}\text{Pt}_{20}$ film onto Ru/Ag bilayer films using an argon working pressure of 3 mTorr to sputter the Ru layer at ambient temperature. Its perpendicular coercivity and perpendicular squareness are 3980 Oe and 0.76, respectively. When the working pressure increases to above 10 mTorr, the perpendicular magnetic anisotropy of the films deteriorates greatly. However, both perpendicular coercivity and perpendicular squareness of the film can be increased to 4530 Oe and 0.82 respectively if the $\text{Co}_{80}\text{Pt}_{20}$ film is deposited on a higher texture Ru(0002)/Ag(111) bilayer that has been annealed at 300°C . When this $\text{Co}_{80}\text{Pt}_{20}/\text{Ru}/\text{Ag}$ multilayer film is subsequently post-annealed at 300°C , the perpendicular magnetic properties are improved further. The perpendicular coercivity and perpendicular squareness of the film are further increased to 5040 Oe and 0.87 respectively, which reveal its significant potential as perpendicular magnetic recording media for ultra-high density recording.

TU.G-P04 - perpendicular magnetic anisotropy of very thin L₁₀ FePt films

A. Kaidatzis¹, G. Giannopoulos¹, V. Psycharis¹, J.M. García-Martín², D. Niarchos¹

1. *Institute of Nanoscience and Nanotechnology, NCSR Demokritos, Athens, Greece*

2. *IMM-Instituto de Microelectrónica de Madrid (CNM-CSIC), Madrid, Spain*

Perpendicular Magnetic Anisotropy (PMA) materials, like L₁₀ FePt thin films [1, 2], are under intense study because of their high potential for applications in spintronics and magnetic storage. In this work, we investigated FePt films, with thickness between 1 nm and 5 nm, deposited on MgO (001) substrates at 500°C using magnetron sputtering. The films were characterized by means of X-ray diffraction, atomic/magnetic force microscopy (AFM/MFM), and anomalous Hall effect measurements. It is shown that the films have L₁₀ structure down to a thickness of 2.7 nm and clearly exhibit PMA, with remanent to saturation magnetisation ratio (M_r/M_s) equal to 1 and perpendicular coercivity H_{cp} equal to 14.8 kOe at 2.7 nm and 16 kOe at 5 nm FePt layer thickness. However, as the FePt film thickness is reduced, M_r/M_s and H_{cp} rapidly decrease, indicating the emergence of in-plane anisotropy and the presence of both L₁₀ and A1 phases. The surface morphology is typical of polycrystalline metallic films, with surface roughness between 0.5 and 0.8 nm and grain size between 15 nm and 25 nm. The only exception is the 1 nm thick film, which has 1.2 nm surface roughness, indicating that it is not continuous and revealing the island growth mechanism of FePt. Finally, MFM imaging of the 2.7 nm and 5 nm thick films reveals a magnetic domain size between 200 nm and 300 nm, much wider than the average grain size, indicating strong magnetic coupling between adjacent grains. It is concluded that as the FePt layer is getting thinner, higher energy is needed for the formation of the L₁₀ phase, thus leading to the need of depositing FePt at higher substrate temperature.

References:

[1] A. Perumal et al., Appl. Phys. Lett. 92, 132508 (2008)

[2] G. Giannopoulos et al., J. Magn. Magn. Mat. 325, 75 (2013)

TU.G-P06 - Magnetic properties of the interfaces of MgO/Fe and Pt/Fe studied by hard X-ray photoemission

S. Ueda¹, T. Tashiro², M. Mizuguchi², K. Takanashi²

1. Synchrotron X-ray Station at SPring-8, National Institute For Materials Science, Sayocho, Japan

2. Institute for Materials Research, Tohoku University, Sendai, Japan

It is known that a perpendicular magnetic anisotropy is induced by a hetero interface of non-magnetic and ferromagnetic materials [1]. To clarify the origin of the perpendicular magnetic anisotropy near the interface, a direct measurement of the electronic and magnetic properties of ferromagnetic materials near the interface is required. Recently, hard X-ray photoemission spectroscopy (HAXPES) [2] has been used to investigate electronic structures of buried layers [3] due to large inelastic mean-free-path (IMFP) of photoelectrons [4] in solids. We fabricated two samples of MgO(2 nm) and Pt(2 nm) capped Fe(20 nm) on MgO(001) substrates by sputtering in order to investigate the interface magnetic properties of MgO/Fe and Pt/Fe by means of HAXPES. The HAXPES measurements were performed at BL15XU of SPring-8 [2]. The Fe 2p_{3/2} HAXPES spectra for the both the samples showed a broad main peak with a clear shoulder structure in comparison with that for bulk polycrystalline Fe, although the spectra were measured in the normal emission geometry, in which the spectra were bulk sensitive. When we measured the spectra with near interface sensitive geometry (off-normal emission angle of 60 deg), the shoulder structure of Fe 2p_{3/2} spectra were evolved in comparison with that measured in the normal emission geometry. These results strongly suggest that near interface Fe has the larger orbital moment than bulk Fe. Thus we can conclude that this larger orbital moment of Fe is the origin of the perpendicular magnetic anisotropy near the interfaces of MgO/Fe and Pt/Fe.

References:

- [1] S. Ikeda et al., *Nature Mater.* 9, 721 (2010)
- [2] S. Ueda, *J. Electron Spectrosc. Rel. Phenom.* 190, 235 (2013)
- [3] S. Ueda et al., *Appl. Phys. Lett.* 104, 132402 (2014)
- [4] S. Tanuma, C. J. Powell, D. R. Penn, *Surf. Interf. Anal.* 21, 165 (1994)

TU.G-P07 - Structure and spin texture of FeCo ultrathin films on Cu₃Au(001)A. Cotta ¹, A. Ponce ¹, W. Macedo ¹*1. Centro de Desenvolvimento da Tecnologia Nuclear, Belo Horizonte, Brazil*

Tetragonally distorted Fe_{1-x}Co_x alloy films epitaxially grown on different face centered cubic substrates are a model system for perpendicular magnetic anisotropy (PMA). Depending on the level of tetragonal distortion in the system, the epitaxy can result in a strong PMA and films with perpendicular magnetization [1]. For equiatomic Fe-Co films on Rh(001), for example, the easy-magnetization axis can remain perpendicular up to 15 ML at room temperature (RT) [2]. Cu₃Au has an in-plane lattice constant of 3.75 Å, being very close to the predict value to result in FeCo films with a large PMA. A very recent work has shown that 11 ML FeCo on Cu₃Au(001) present in plane magnetization and, based on RHEED results, speculates that FeCo films thinner than 9 ML should present a tetragonal distortion suitable for perpendicular magnetic anisotropy [3]. In this work, we have determined the spin texture of FeCo films grown on Cu₃Au(001) at RT by molecular beam epitaxy (MBE) in ultra-high vacuum. The ⁵⁷FeCo films were prepared at room temperature by codeposition (disordered films) and by deposition of alternated Fe and Co monolayers (ordered films). The substrate and the films were characterized by using XPS, LEED and RHEED. Ex-situ conversion electron Mössbauer spectroscopy (CEMS), vibrating sample magnetometry and in-situ magneto-optical Kerr effect (MOKE) measurements were also conducted. The structure and magnetism of FeCo films up to 14 ML were investigated. Our results indicate that codeposited (disordered) FeCo/Cu₃Au(001) films show in plane magnetization. Films prepared by alternated ML of Fe and Co (ordered) present a strong PMA up to 7 ML. MOKE measurements on films with alternate Fe and Co atomic layers show an oscillatory behavior of the coercivity depending on the surface layer, suggesting stronger perpendicular anisotropy for Fe-terminated films when compared with Co-terminated films.

TU.G-P08 - Influence of high density plasma processes on magnetic properties and microstructures of FePt alloy films

S.C. Chen¹, T.H. Sun², S.U. Jen^{3,4}, C.K. Wen¹, J.Y. Chiou¹

1. *Ming Chi University Of Technology, New Taipei City, Taiwan*

2. *National Tsing Hua University, Hsinchu City, Taiwan*

3. *Academia Sinica, Taipei, Taiwan*

4. *National Taiwan Ocean University, Keelung, Taiwan*

L_{10} FePt film is considered a potential candidate for the future perpendicular magnetic recording media because its large magnetocrystalline anisotropy constant (K_u) of 7×10^7 erg/cm³. However, the structure of the L_{10} FePt phase is face-centered-tetragonal (fct) and normally has (111) preferred orientation, which makes the magnetic anisotropy of the film incline toward the film plane. In order to apply FePt film to perpendicular magnetic recording media, achievement of a high (001) texture of the L_{10} FePt films is necessary. Usually, the (001) textured FePt film could be achieved by depositing the film onto MgO, Cr and CrRu underlayers. However, these multilayer films would result in the higher cost and undesirable interdiffusions between the FePt magnetic layer and underlayers during post annealing process.

In this study, single-layered FePt films were deposited directly onto Corning 1737 glass substrates by both direct current magnetron sputtering (DCMS) and high power impulse magnetron sputtering (HIPIMS). These films were then post-annealed at 700 °C for 30 min in a vacuum of 1.0×10^{-6} Torr. It was found that single-layered FePt films with random orientation were achieved by using DCMS. However, FePt films with (001) texture showing high perpendicular magnetic properties were obtained by HIPIMS. Their perpendicular coercivity, saturation magnetization and perpendicular squareness are as high as 14.2 kOe, 624 emu/cm³ and 1, respectively, which reveal its great potential for use as next-generation perpendicular magnetic recording media for ultra-high density recording.

Keywords : Direct current magnetron sputtering, High power impulse magnetron sputtering (HIPIMS), Single-layered FePt films, Perpendicular magnetic anisotropy, Perpendicular magnetic properties

TU.G-P09 - Negative perpendicular anisotropy in NiFe₂O₄ (001) epitaxial film grown on MgAl₂O₄(001)

M. Matsumoto¹, H. Yanagihara¹, S. Sharmin¹, J.I. Inoue¹, E. Kita¹

1. Institute Of Applied Physics, University Of Tsukuba, Tsukuba, Japan

Magnetic materials with a large anisotropy constant are promising candidates for the exhibition of higher ferromagnetic resonance frequencies and therefore a possible extension of the operation frequencies of various magnetic devices. The magnetoelastic effect that arises due to a lattice misfit between a magnetic material and a substrate is one of the most effective approaches for enhancing the magnetic anisotropy of films. In this presentation, we report on the negative magnetic anisotropy of an epitaxial NiFe₂O₄ (001) film grown on MgAl₂O₄ (001) substrate. The film was grown by reactive rf-magnetron sputtering technique using an alloy target of NiFe with a composition of 1:2. Prior to the growth process, the substrate was heated to 400C to remove surface contamination. Growth temperature was kept at 300C and sputtering power was 100W. In situ RHEED experiments confirmed that the film was epitaxially grown. Magnetization measurements revealed that the easy axis lies in-plane and the hard axis is normal to the film. The saturation magnetization (Ms) was 227 emu/cm³ at room temperature. The anisotropic field for the out-of-plane MH-loop was close to 70 kOe which is more than 20 times greater than the demagnetization field of the film, indicating the existence of additional magnetic anisotropy with a negative constant. Effective anisotropy energy (K_{eff}) estimated from the difference between the two MH-loops was -7.94 emu/cm³. In addition, the torque experiment was also performed at room temperature to evaluate K_{eff}. The torque curves were analyzed by Miyajima's method and the extrapolated values of K_{eff} and Ms were -7.78 Memu/cm³ and 269 emu/cm³, thus showing good agreement with the MH-loop analysis. The observed large K_{eff} can be attributed to the magnetoelastic effect caused by the relatively large lattice misfit between NiFe₂O₄ and MgAl₂O₄.

TU.G-P10 - Rotatable magnetic anisotropy in anisotropy-graded FePt films induced by ion irradiation at low incidence angle

M.G. Pini¹, A. Rettori², S. Tacchi³, G. Gubbiotti³, M. Madami⁴, A. di Bona⁵, S. Valeri⁶, F. Albertini⁷, F. Casoli⁷, P. Ranzieri⁷

1. *Istituto Dei Sistemi Complessi Del CNR (CNR-ISC), Unità Di Firenze, Florence, Italy*
2. *Dipartimento di Fisica ed Astronomia, Università di Firenze, Sesto Fiorentino, Italy*
3. *Istituto Officina dei Materiali del CNR (CNR-IOM), Unità di Perugia, c/o Dipartimento di Fisica e Geologia, Università di Perugia, Perugia, Italy*
4. *Dipartimento di Fisica e Geologia, Università di Perugia, Perugia, Italy*
5. *Centro S3, c/o Istituto Nanoscienze del CNR (CNR-NANO), Modena, Italy*
6. *Dipartimento di Scienze Fisiche, Informatiche e Matematiche, Università di Modena e Reggio Emilia, Modena, Italy*
7. *Istituto dei Materiali per l'Elettronica e il Magnetismo del CNR (CNR-IMEM), Parma, Italy*
8. *Information Storage Materials Laboratory, Department of Electrical and Computer Engineering, National University of Singapore, Singapore*

Alternating gradient force magnetometry (AGFM), Brillouin light scattering (BLS) from thermally excited spin waves, and magnetic force microscopy (MFM) have been used to investigate the static and dynamic magnetic properties of a 15-nm-thick FePt film after Ar⁺ irradiation, performed at two different incidence angles, 85 and 45 degrees, with respect to the film normal. Ion irradiation turns the L10, chemically ordered, magnetically hard phase, into the A1, chemically disordered, magnetically soft phase [1], inducing an anisotropy gradient along the film normal. On changing the ion incidence angle, the ion penetration depth and the relative thicknesses of the soft and hard phases have been modified. We found that the sample irradiated at 45 degrees is characterized by a profound softening of the perpendicular magnetic anisotropy near the surface plane. Moreover, BLS measurements, performed at remanence as a function of the in-plane rotation angle, indicate the presence of a rotatable magnetic anisotropy [2]: namely, an anisotropy whose direction can only be rotated by changing the saturating field direction. The presence of this anisotropy can be ascribed to the competition between the moderate perpendicular magnetic anisotropy and the easy-plane shape energy. Finally, from the fit of the BLS frequency versus the intensity of the in-plane field H, the effective rotatable anisotropy field H_{rot} was estimated to be $H_{rot} \leq 510$ Oe for $H \leq 2$ kOe. The tunability of the zero-field frequency, obtained by Ar⁺ irradiation varying the incidence angle of the ion beam, may have large applications for microwave magnetic devices.

References:

- [1] A. di Bona et al., *Acta Materialia* 61 , 4840 (2013)
- [2] L. M. Alvarez-Prado et al., *Phys. Rev. B* 56 , 3306 (1997)

TU.G-P11 - Competing Nd and Co contributions to the perpendicular magnetic anisotropy of $\text{Nd}_x\text{Co}_{1-x}$ amorphous thin films first time observed by X-ray magnetic circular dichroismR. Cid Barreno ^{1,2}, J. Díaz ^{1,2}, H. Rubio ¹, J.M. Alameda ^{1,2}, S. Manuel Valvidares ³1. *Universidad De Oviedo, Oviedo, Spain*2. *Centro de Investigación en Nanomateriales y Nanotecnología, El Entrego, Asturias, Spain*3. *ALBA Synchrotron, Cerdanyola Del Vallès, Barcelona, Spain*

Many amorphous RE-TM alloys exhibit perpendicular magnetic anisotropy (PMA) [1] of discussed origin. The most accepted source of their PMA is single ion anisotropy at the RE sites [2]. Several $\text{Nd}_x\text{Co}_{1-x}$ amorphous thin films of different nominal compositions and Nd-Co multilayers with $\lambda < 1$ nm have been grown by DC-magnetron co-sputtering. EXAFS measurements only evidenced a large disorder at the Nd sites and segregation of Co atoms [3], while XMCD measurements demonstrate that the PMA is located at the RE 4f orbitals indeed [4]. The $\langle L_z \rangle / \langle S_z \rangle$ ratio in Nd is very close to the theoretical one at normal incidence, though it is not isotropic as expected for a 4f orbital, but always smaller in plane. Furthermore, the Co subnetwork presents an in-plane anisotropy crossed to it. The values of $\langle \mu_{\text{Nd}} \rangle$ support the existence of an asperomagnetic structure whose cone angle slightly changes with orientation. On the other hand, the effective exchange interaction Co-Nd ($J_{\text{Co-Nd}}$) determines the size of $\langle \mu_{\text{Nd}} \rangle$. We compare a multilayer (M) and a homogenous alloy (HA) with 21-22% Nd, but only M shows strong PMA. Despite their similar $\langle L_z \rangle / \langle S_z \rangle$ anisotropies for both specimens, their different values and thermal evolutions of $\langle \mu_{\text{Nd}} \rangle$ suggest that $J_{\text{Co-Nd}}(\text{M}) \geq 3 \cdot J_{\text{CoNd}}(\text{HA})$. Therefore, $J_{\text{Co-Nd}}$ is a key factor to make the PMA of the Nd sublattice overcome the shape anisotropy and the Co planar anisotropy.

[1] K.H.J. Buschow, Rep. Prog. Phys. 40:1179–1256 (1977)

[2] Y. Suzuki, S. Takayama, F. Kirino, and N. Ohta, IEEE Trans. Magn., 23:2275 (1987)

[3] J. Díaz, [R. Cid](#), [A. Hierro](#), [L.M. Álvarez-Prado](#), [C. Quirós](#) and [J.M. Alameda](#), J. Phys. Condens. Matter 25, 426002 (2013)

[4] R. Cid, J. Díaz, L.M. Álvarez-Prado, J.M. Alameda, S.M. Valvidares, J.C. Cezar and N.B. Brookes, J. Phys.: Conf. Ser. 200 072017 (2010)

TU.G-P12 - Synesthetic ferrimagnet of cubic Heusler/tetragonal Heusler Mn₃Ga bilayers with perpendicular magnetic anisotropyR. Ranjbar¹, K. Suzuki¹, A. Sugihara¹, Q. Ma¹, T. Miyazaki¹, S. Mizukami¹*1. WPI Advanced Institute For Materials Research, Tohoku University, Sendai, Japan*

Bilayer structure consisting of magnetic films with perpendicular magnetic anisotropy (PMA) and in-plane magnetic anisotropy show fully PMA when interfacial exchange coupling is strong enough. Such bilayers with negative interfacial exchange coupling, the so-called synesthetic PMA ferrimagnets are practically important to use in perpendicular magnetic tunnel junctions (p-MTJs) for high density spin-transfer-torque magnetoresistive random access memory (STT-MRAM) [1, 2]. Synesthetic PMA ferrimagnets consisting of L10 MnGa alloy with PMA and an ultra-thin ferromagnetic metal/alloy layer are one of the good candidate. We recently reported that the interfacial exchange coupling of the bilayer of L10 MnGa and Co-rich Fe-Co is antiferromagnetic and the strength is -3.0 erg/cm^2 and also tunnel magnetoresistance is 60% (120%) at room (low) temperature [3]. Here, we studied the bilayer of tetragonal Heusler D022 Mn₃Ga and cubic Heusler alloys (Co₂FeAl, Co₂FeSi, Co₂MnAl, and Co₂MnSi). Heusler (20 nm) / D022 Mn₃Ga (30 nm) bilayer films were fabricated with different post annealing temperature on (100) MgO substrate buffered and capped with Cr by using an ultrahigh vacuum magnetron sputtering system. The strongest antiferromagnetic coupling J_{ex} of -3.2 erg/cm^2 was observed in the Co₂MnSi / Mn₃Ga bilayer, in which the L21 ordered Co₂MnSi was epitaxially grown on Mn₃Ga layer and its saturation magnetization of 800 emu/cm^3 [4, 5]. To achieve ultra-thin synthetic ferrimagnet, the thickness of Co₂MnSi Heusler alloy and D022 Mn₃Ga were decreased. The bilayer with 1-nm-thick Co₂MnSi and 7.5-nm-thick D022-MnGa shows good PMA which makes this bilayer as good choice for making free electrode of p-MTJ based on MnGa alloy. This work was partially supported by the development of an infrastructure for normally-off computing technology project from NEDO and ASPIMATT (JST). R.R also thanks to Y. Kondo for his technical assistance and to the WPI program and JGC-S scholarship (Nikki).

References:

- [1] T. Hiratsuka, et al., J. Appl. Phys. 107, 09C714 (2010)
- [2] K. Yakushiji, et al., Appl. Phys. Express 6, 113006 (2013)
- [3] Q. L. Ma, et al., Phys. Rev. Lett. 112, 157202 (2014)
- [4] R. Ranjbar, et al., J. Appl. Phys. (in-press) [5] R. Ranjbar, et al., (submitted)

TU.G-P13 - Real-space calculations of uniaxial magnetic anisotropy at surfaces of bcc Fe films and of Y₂Fe₁₄B compoundsJ.I. Inoue¹, T. Yoshioka¹, H. Tsuchiura¹*1. Department of Applied Physics, Tohoku University, Sendai, Japan*

The fundamental origin of the magnetic anisotropy (MA) may be attributed to lowering of crystal symmetry and the spin-orbit interaction (SOI), and intensive search for high performance permanent magnets is currently conducted both experimentally and theoretically. Nevertheless, materials dependence of MA is unpredictably complicated. The complication could be partly due to structural inhomogeneity in magnets, such as grain boundaries and lattice disorder. Therefore, a theoretical approach to treat effects of grain boundaries and random lattice structures is desirable. To this end, we have developed real-space formalism to calculate MA energy for any lattice structures by expanding the thermodynamic potential in terms of SOI by using multi-orbital tight-binding model. By using the method, site-resolved MA is easily obtained with high numerical accuracy. The applicability has already been examined by comparing the numerical results with those obtained in the first-principles method [1]. Here we apply the method to calculate the uniaxial MA at bcc Fe (001) surfaces with several surface structures, and that at surfaces of Y₂Fe₁₄B compounds. Our findings are as follows:

- (1) The out-of-plane MA at bcc Fe (001) surface is strongly enhanced due to surface resonant states as compared with bulk MA. As a result, dependence of the out-of-plane MA at surface on charge density becomes stronger than that of bcc bulk Fe.
- (2) The uniaxial MA at surface sites of Y₂Fe₁₄B compounds is also enhanced. For example, in-plane MA at 4c-Fe sites on (001) surface becomes twice as large as the bulk value, and the uniaxial MA at 8j2-Fe sites on (010) surface is enhanced as compared with the bulk value. These results may implicate important roles of surface/interface Fe sites on the MA and magnetization process of ferromagnetic thin films and grains.

Reference:

[1] J. Inoue, T. Yoshioka, and H. Tsuchiura, J. Appl. Phys. to be published.

TU.G-P14 - Magnetic properties of amorphous Tb_xCo_{1-x} thin films grown in an in-plane external magnetic field by combinatorial magnetron sputteringGabriella Andersson¹, Y. Sebastian George¹, N. Andreas Frisk¹, N. Fridrik Magnus¹*1. Uppsala University, Department Of Physics And Astronomy, Uppsala, Sweden*

The magnetic properties of amorphous Tb_xCo_{1-x} thin films, with x ranging from 0.07 to 0.3, have been investigated using vibrating sample magnetometry (VSM), magneto-optical Kerr effect (MOKE), and magnetic force microscopy (MFM). The samples were deposited by DC magnetron sputtering on 10 mm by 60 mm rectangular strips of Si, with a native oxide layer. The combinatorial deposition from separate Tb and Co targets, placed at either end of the Si strip, yielded a continuous composition gradient along the strip, and an accompanying thickness gradient spanning 45-60 nm. Amorphous Al₇₀Zr₃₀ was used for buffer and cap layers. During deposition, a 100-mT external B-field was applied parallel to the substrate surface, perpendicular to the composition gradient, i.e. across the strip. Identical samples were also grown without this external field. As expected from previous studies [1], the amorphous TbCo films exhibit strong perpendicular magnetic anisotropy (PMA). However, we do observe changes in saturation field and coercivity with varying composition. Furthermore, there is a clear difference in domain structure, as observed by MFM, between samples grown with and without the in-plane B-field, indicating that this field has an impact on the magnetization, in spite of the strong PMA. MOKE magnetization loops confirm the presence of a small in-plane magnetization component. The effect of the growth field on the domain structure is most pronounced for the lower Tb concentrations (x = 0.07 - 0.09). VSM magnetization loops exhibit two-step switching, which is not observed in the corresponding MOKE data. This suggests that the lower and upper parts of the TbCo layers have different magnetic properties, which in turn may be a mechanism for creating the observed in-plane component.

Reference:

[1] X. Chen, Y. J. Wang, B. Q. Liang, Y. J. Tang, H. W. Zhao, J. Q. Xiao, J. Appl. Phys. 87, 6845 (2000), and references therein

TU.G-P15 - Anisotropy studies of Co and FeCo nanowires with Torque Magnetometry

N.M. Nemes¹, D. Gonzalez², C Bran², M. Garcia-Hernandez¹, M. Vazquez², T. Feher³

1. Laboratorio de Heteroestructuras con aplicación en Spintronica, Unidad Asociada Consejo Superior de Investigaciones Científicas/Universidad Complutense Madrid, Madrid, Spain

2. Instituto de Ciencia de Materiales de Madrid, Consejo Superior de Investigaciones Científicas, Madrid, Spain

3. Budapest University of Technology and Economics, Institute of Physics and Condensed Matter Research Group of the Hungarian Academy of Sciences, Budapest, Hungary

We report on torque magnetometry results to study the magnetic anisotropy of cobalt and iron-cobalt nanowires, grown by electrochemistry into nanoporous alumina templates. We look at the effects of shape and magnetocrystalline anisotropy. For comparison we also measured a 50 nm thick Permalloy film with in-plane anisotropy. We developed a technique of “torque rotations”, that is, we rotate the sample in a fixed magnetic induction, B , (between 100 G and 14 T) and fixed temperature (between 2 K and 300 K) and analyse the resulting torque vs. angle, θ , curves by comparing them to simulated torque rotations. We use various free energy models and for a given B minimize them to obtain the direction of equilibrium magnetization, M . We show that the high- B torque rotations are independent of B , can be described as $\sin(2*\theta)$, and reflect the leading anisotropy term ($K*V$, where V is the magnetic volume). On the contrary, the small- B rotations scale with B and have a distorted form. The transition from one behavior to another happens around the anisotropy field (K/M). In very small fields (below coercivity) the torque rotations change again and have $\sin(\theta)$ shape, as the magnetic moment is unmoved by B . This allows us to determine the total magnetic moment $m=M*V$, too.

TU.G-P16 - Fabrication of Mn₃Ga nanodisks using polystyrene nanosphere lithography

Julie Karel¹, F. Casoli², P. Lupo³, L. Nasi², P. Tiberto⁴, F. Celegato⁴, F. Albertini², C. Felser¹

1. Max Planck Institutue for Chemical Physics Of Solids, Dresden Germany

2. Institute of Materials for Electronics and Magnetism, Parma, Italy

3. Department of Electrical and Computer Engineering, National University of Singapore, , Singapore

4. INRIM, Torino, Italy

Mn₃Ga (y=2,3) in the metastable tetragonal D022 phase exhibits unique properties, which can be exploited for numerous spintronic devices such as spin-transfer-torque RAM [1]. This phase is also interesting for the development of permanent magnets with maximum energy products halfway between Nd₂Fe₁₄B and Ba(Sr)Fe₁₂O₁₉ [2]. Mn_xGa_{1-x} (x=0.75,0.70) films were grown by RF sputtering on heated SrTiO₃ (100) substrates. Through the control of growth parameters, thickness (10 - 40 nm) and composition, epitaxial films showing the tetragonal phase oriented primarily with the c-axis out of the film plane were obtained. The films exhibit perpendicular magnetic anisotropy with coercive fields in the range of 1 - 2 T and saturation magnetization between 100 - 250 kA/m. The saturation magnetization decreases with increasing x, consistent with previous reports; this trend arises from the antiferromagnetic alignment of Mn moments between the two Mn sublattices present in the D022 structure and preferential removal of Mn from only one sublattice with decreasing x.

Mn_xGa_{1-x} nanodisks were fabricated by assembling a monolayer of polystyrene nanospheres (PN) with a mean starting diameter of 800 nm on the thin film; subsequently, the PN size was reduced by reactive ion etching to obtain final dots of 500 - 600 nm in diameter. A sputter etching process in Ar⁺ plasma was used to remove the excess Mn_xGa_{1-x} film between the PNs. After the wet-lithography process, the nanodisks maintain the perpendicular magnetic anisotropy as shown by SQUID magnetometry and Magnetic Force Microscopy. The patterning process however results in partial structural disorder to the nanodisks, as evidenced by a kink around zero field in the perpendicular hysteresis curve.

References:

[1] J. Winterlik et al., Adv. Mater. 24, 6283 (2012)

[2] J.M.D. Coey, J. Phys.: Condens. Matter 26 064211 (2014)

TU.G-P17 - Perpendicular magnetic anisotropy of Co₂FeAl Heusler alloy thin films grown on flexible kapton substrates

M. Gabor¹, T. Petrisor jr.¹, C. Tiusan¹, M. Belmeguenai², F. Zighem², D. Faurie²

1. *Center for Superconductivity, Spintronics and Surface Science, Technical University of Cluj-Napoca, Cluj-Napoca, Romania*

2. *Laboratoire des Sciences des Procédés et des Matériaux, CNRS-Université Paris XIII, Villetaneuse, France*

The functional properties of devices on non-planar substrates are receiving increasing interest because of the new flexible electronics based-technologies. Magnetic thin films deposited on polymer substrate show tremendous potentialities in new flexible spintronics based-applications.

Within this context, the results of our study overcome several challenges. On flexible Kapton substrates we have successfully grown ferromagnetic polycrystalline thin films constituted by Co₂FeAl (CFA) Heusler alloy with large spin polarization and low Gilbert damping. By varying the thickness, the anisotropy of these films has been stabilized either in-plane or perpendicular-to-the plane. Then, correlating static (magnetometry) and dynamic magnetic studies (ferromagnetic resonance-FMR), we demonstrate the bending strain effect on the magnetic anisotropy properties of the CFA films. Ferromagnetic resonance analysis reveal significant bending effect on the magnetic anisotropy in 20nm thick CFA Heusler thin film grown on Kapton and glued on curved sample carriers with various radii. We attribute the measured effect to the interfacial strain transmission from the substrate to the film and to the relative large in-plane magnetostriction coefficient ($\lambda^{CFA}=13.8\times 10^{-6}$) [1]. These results have an important predictive character: if one targets the integration of the CFA in a flexible planar magnetoresistive device, the magnetostriction coefficient should be 10 times smaller in order to maintain the optimum magnetic anisotropy characteristics.

Furthermore, we demonstrate the realization of perpendicular magnetic anisotropy (PMA) in ultrathin polycrystalline CFA films grown on Kapton flexible substrates, attributed to the CFA/MgO interfacial anisotropy [2]. We show that the PMA is less influenced by the bending strain effect and remains stable up to relative large substrate curvatures. This point out the important potential of CFA to be integrated in PMA spintronic devices grown on flexible substrates.

References:

[1] M. Gueye, B. M. Wague, F. Zighem, M. Belmeguenai, M. S. Gabor, T. Petrisor Jr., C. Tiusan, S. Mercone, and D. Faurie, *Appl. Phys. Lett.* 105, 062409 (2014)

[2] M. S. Gabor, T. Petrisor, C. Tiusan, and T. Petrisor, *J. Appl. Phys.* 114, 063905 (2013)

TU.G-P18 - Magnetic anisotropy of $\text{Fe}_{1-y}\text{X}_y\text{Pt-L}_{10}$ [X = Cr, Mn, Co, Ni, Cu] bulk alloys.

R. Cuadrado¹, T.J. Klemmer², R.W. Chantrell¹

1. *Department of Physics, University of York, York, United Kingdom*

2. *Seagate Technology, Fremont, California, United States*

We demonstrate by means of fully relativistic first principles calculations that, by substitution of Fe by Cr, Mn, Co, Ni, or Cu in FePt-L_{10} bulk alloys, with fixed Pt content, it is possible to tune the magnetocrystalline anisotropy energy by adjusting the content of the non-magnetic species in the material. The changes in the geometry due to the inclusion of each element induces different values of the tetragonality and hence changes in the magnetic anisotropy and in the net magnetic moment. The site resolved magnetic moments of Fe increase with the X content while those of Pt and X are simultaneously reduced. The calculations are in good quantitative agreement with experimental data and demonstrate that models with fixed band structure but varying numbers of electrons per unit cell are insufficient to describe the experimental data for doped FePt-L_{10} alloys.

TU.G-P19 - Effect of Copper underlayer on perpendicular magnetic anisotropy in Co/Ni multilayers

M. Steblyy¹, A. Kolesnikov¹, A. Ognev¹, A. Samardak¹, A. Davydenko¹, L. Chebotkevich¹, A. Lara², F. Aliev²

1. *School of Natural Sciences, Far Eastern Federal University, Vladivostok, Russia*

2. *Fisica Materia Condensada, Universidad Autónoma de Madrid, Madrid, Spain*

The investigation of thin films and nanostructures with perpendicular magnetic anisotropy (PMA) is timely in terms of practical applications in spintronics and orbitronics. Co/Ni multilayers are promising materials due to low Gilbert damping ($\sim 0,02$), small switching currents and high thermal stability. Here we study magnetic properties and magnetization dynamics (by using VNA-FMR) of $[\text{Co}(0.3 \text{ nm})/\text{Ni}(t_{\text{Ni}})]_5$ multilayers with PMA produced by magnetron sputtering on Ta/Cu(t_{Cu}) buffer layers, where $t_{\text{Ni}} = 0.4$ to 0.55 nm, $t_{\text{Cu}} = 0$ to 10 nm. Our study reveals that magnetic anisotropy is strongly enhanced with introduction of copper underlayer ($t_{\text{Cu}} = 4.8$ nm) with respect to a control sample. Detailed analysis of the influence of Cu underlayer thickness and number of multilayers will be provided in order to determine relative importance of strain vs. purely electronic effects on magnetic anisotropy. Measurements of samples with different thicknesses of Cu show that a thicker copper layer also increases the switching field.

TU.G-P20 - Sputtering energy and perpendicular magnetic anisotropy of CoFeB

B. Kim¹, D. Kim¹, Y.J. Jang¹, J. Kim¹, K. Rhie¹

1. Department of Display and Semiconductor Physics, Korea University, Sejong, South Korea

Perpendicular-Magnetic tunnel junction (p-MTJs) structure is a good candidate for nonvolatile magnetoresistive random access memory (MRAM) devices [1, 2]. Both high quality of multi-layers and large anisotropic constant K are the essential requirements. The effect of sputtering energy for better perpendicular magnetic anisotropy (PMA) of CoFeB [3] is studied. SiO₂/X(2)/CoFeB(1.3)/MgO(2)/Ta(2) (in nm.) samples are grown by conventional magnetron sputtering techniques, where X is FeZr and Ta. The sputtering energy was controlled by changing sputtering pressure and distance between samples and sputtering gun. The sputtering particles may lose energy they arrive substrate, because they experience multiple scattering by Ar particles along the path to the substrate. Therefore, sputtering particle energy at substrate is small when both working pressure and distance is high. In a low sputtering energy case, sputtered particles cannot make a uniform surface and voids may be formed inside a film, which results lower film density. We observed that the film growth pattern changes from 2 dimensional to 3 dimensional growth by crossing a critical sputtering condition. The best pressure and distance to make the best film quality is less than 5mTorr and below 10.5 cm, respectively. Low resistivity and high anisotropic constant K could be achieved by controlling the sputtering energy.

References:

- [1] S. Ikeda, K. Miura, H. Yamamoto, K. Mizunuma, H. D. Gan, M. Endo, S. Kanai, J. Hayakawa, F. Matsukura, and H. Ohno, Nat. Mater. 9, 721 (2010)
- [2] W. X. Wang, Y. Yang, H. Naganuma, Y. Ando, R. C. Yu, and X. F. Han, Applied Physics Letters 99, 012502 (2011)
- [3] D. S. Kim, K. Y. Jung, S. J. Joo, Y. J. Jang, J. K. Hong, B. C. Lee, C. Y. You, J. H. Cho, M. Y. Kim, and K. Rhie, J. Magn. Mater. 374, 350 (2015)

TU.G-P21 - Large perpendicular magnetic anisotropy in magnetostrictive Fe_{1-x}Ga_x thin films

M. Barturen^{1,2,3,4}, J. Milano^{1,2,5}, M. Vázquez-Mansilla¹, C. Helman^{5,6}, M.A. Barral^{5,6}, A.M. Llois^{5,6}, M. Eddrief^{3,4,5}, M. Marangolo^{3,4,5}

1. CNEA-CONICET, Centro Atómico Bariloche, San Carlos de Bariloche, Argentina
2. Instituto Balseiro, Universidad Nacional de Cuyo, Centro Atómico Bariloche, San Carlos de Bariloche, Argentina
3. Sorbonne Universités, UPMC Univ Paris 06, UMR 7588, INSP, Paris, France
4. CNRS, UMR 7588, Institut des Nanosciences de Paris, Paris, France
5. LIFAN, Laboratorio Internacional Franco-Argentino en Nanociencias
6. CNEA, Centro Atómico Constituyentes, San Martín, Argentina

Nowadays, active research efforts are being carried out to stabilize out-of-plane magnetization in thin films and nanostructures. In this context, the change of the preferential direction of the magnetization from the commonly observed in-plane orientation to the direction perpendicular to the plane is usually referred to as perpendicular magnetic anisotropy (PMA). In this work we report the appearance of PMA in Fe_{1-x}Ga_x thin films grown onto ZnSe/GaAs(100). Fe_{1-x}Ga_x is well known for its magnetostrictive properties leading to industrial applications. Here, we show that magnetostrictive properties coexist with PMA in Fe_{1-x}Ga_x thin films. This arising anisotropy is related to the tetragonal metastable phase in as-grown samples recently reported [1]. By means of ferromagnetic resonance studies we measured PMA values up to 5x10⁵ J/m³. PMA is the origin of the magnetic stripe pattern observed by magnetic force microscopy (MFM). Interestingly, PMA vanishes when the cubic structure is recovered upon annealing at 300°C.

Despite the important values of the magnetoelastic constants measured via the cantilever method, the consequent magnetoelastic contribution to PMA is not enough to explain the observed anisotropy values in the distorted state. Ab initio calculations show that the chemical ordering plays a crucial role in the appearance of PMA. Through a phenomenological model we are able to explain that an excess of next nearest neighbour Ga pairs (B2-like ordering) along the perpendicular direction arises as the source of PMA in Fe_{1-x}Ga_x thin films.

References:

- [1] M. Eddrief et al., Phys. Rev. B 84, 161410 (2011)
- [2] M. Barturen et al. Appl. Phys. Lett. 101, 092404 (2012)
- [3] M. Barturen et al. Eur. Phys. J. B 86, 191 (2013)

TU.G-P24 - Estimation of Fe buffer layer for higher perpendicularly anisotropic magnetic property of L_{10} -FePt grains fabricated by Rapid Thermal AnnealingM. Imazato¹, A. Ogasawara¹, A. Tsukamoto²

1. Graduate School Of Science And Technology Nihon University, Chiyoda, Tokyo, Japan
2. College of Science and Technology, Nihon University, Japan, Chiyoda, Tokyo, Japan

We already reported that isolated several tens of nano-meters FePt grains were fabricated by Rapid Thermal Annealing (RTA) and Rapid cooling process (RCP) for Pt / Fe double layered ultra-thin film on SiO_x ¹. In this report, we aim to obtain perpendicularly higher anisotropic magnetic property originated from L_{10} ordered phase for FePt grains. We tuned composition of $\text{Fe}_x\text{Pt}_{100-x}$ ($x = 50 \sim 63.7$) deposited as Pt / Fe double layers on thermally oxidized Si substrate. The thickness of deposited double layer was 1.88 nm. After the fabrication of isolated FePt grains by RTA and RCP, relations between each compositions and corecivity (H_c) were $\{x, H_c\} = \{50, \approx 0\text{T}\}$, $\{55, < 0.2\text{T}\}$, $\{57, 2.6\text{T}\}$, $\{62, 4.2\text{T}\}$ and $\{63.7, 3.8\text{T}\}$, respectively. As the case of $x = 57, 62$ and 63.7 , large values of H_c were appeared. For $x = 62$, simple hard magnetic hysteresis loop was observed. However, in $x = 57$ and 63.7 , soft magnetic like properties also were observed below 1 Tesla and alsodisordered and non c-axis orientated peaks in XRD were mainly measured. Thus, we considered that the hard magnetic property was came from L_{10} -FePt phase in $x = 62$. Then, double layer was presumed to classify as $\text{Fe}_{50}\text{Pt}_{50}$ alloy layer of L_{10} ordered phase and 0.41 nm thick Fe buffer layer. Furthermore, we deposited different thick Pt / Fe double layered film (2.29 nm, $\text{Fe}_{60}\text{Pt}_{40}$). It consists from 0.41 nm of Fe buffer layer and 1.88 nm of Pt / Fe ($\text{Fe}_{50}\text{Pt}_{50}$) layer. We obtained FePt grains with high H_c about 4.7 Tesla and observed barely soft magnetic like contribution. These results indicate that Fe buffer layer (thickness = 0.41 nm) on thermally oxidized Si substrate was well effective for fabrication of perpendicularly higher anisotropic magnetic property originated from L_{10} ordered FePt phase.

Reference:

- 1) Y.Itoh, T.Aoyagi, A.Tsukamoto, K.Nakagawa, A.Itoh and T.Katayama: Jpn. J.Appl.Phys., 43, 12, 8040 (2004)

TU.G-P25 - Out of plane magnetic anisotropy and anisotropic magnetoresistance in epitaxial $\text{La}_{5/8-y}\text{Pr}_y\text{Ca}_{3/8}\text{MnO}_3$ ($y=0.4$) thin filmsLalit M. Kandpal¹, Y. P. K. Siwach¹, V. P. S. Awana¹, H. K. Singh¹*1. CSIR-National Physical Laboratory, New Delhi, India*

In the archetypical phase separated manganite $\text{La}_{5/8-y}\text{Pr}_y\text{Ca}_{3/8}\text{MnO}_3$ ($y=0.4$), the out of plane anisotropic magnetic and transport properties, which has not been paid much attention could provide a linkage between phase separation and anisotropy. In order to explore the linkage between phase separation and anisotropy, 42 nm thick epitaxial films were prepared by RF magnetron sputtering on (001) oriented SrTiO_3 substrates. The angular scaling of magnetization- magnetic field (M-H) data shows that the easy axis lies in the plane of the film while the hard axis is normal to it. The temperature dependent zero field cooled (ZFC), field cooled cooling (FCC) and field cooled warming (FCW) magnetization (M-T) measured at $H=100$ Oe applied parallel to film plane along the longest direction (M||) and normal to the film plane (ML) reveals large difference M|| and ML. This coupled with the M-H data confirms large out of plane magnetic anisotropy. Other prominent features that distinguish M|| and ML are, (i) considerably lower hysteresis in FCC-FCW ML-T, (ii) the peak in FCW M||-T at $T_P=42$ K is shifted to $T_P=18$ K in ML-T, (iii) the glass transition observed in M||-T at $T_g=31$ K disappears in ML-T. These results clearly show that the relative fraction of the coexisting phases, viz., ferromagnetic metallic (FMM) and antiferromagnetic/charge ordered insulator (AFM/COI) and hence degree of phase separation are sensitive to magnetic anisotropy. Colossal out of plane anisotropic observed also at $T>T_C$ but the AMR peaks disappear. The magnetic anisotropy is magnetoresistance (AMR) of -142 % and -115 % is observed in cooling and warming cycles. At $T<T_C$ the AMR-H data shows pronounced hysteresis and a peak which occurs at higher H in the field increasing cycle. The AMR-H hysteresis is due to coupled consequence of the magnetocrystalline and surface anisotropies and the FMM and AFM phases respond differently to it.

TU.G-P27 - Temperature dependence of perpendicular magnetic anisotropy in CoFeB thin films

Y. Fu¹, I. Barsukov², A. Goncalves^{2,3}, M. Spasova⁴, M. Farle⁴, C. Kuo⁵, J.P. Attané¹, L. Vila¹, I. Krivorotov²

1. Institut Nanosciences Et Cryogénie, CEA Grenoble, France

2. Physics and Astronomy, University of California, Irvine, United States

3. Centro Brasileiro de Pesquisas Fisicas, Rua Dr. Xavier Sigaud, 150, Rio de Janeiro, Brazil

4. Fakultät für Physik and Center for Nanointegration (CeNIDE), Universität Duisburg-Essen, Duisburg, Germany

5. Components Research, Intel, Hillsboro, United States

The uniaxial perpendicular magnetic anisotropy (PMA) of ferromagnetic layers is one of the most important factors that influence the performance of spintronic devices such as magnetic memory, magnetic sensors, and spin torque oscillators. Recently the Co-Fe-B alloys became popular in spintronics due to its strong PMA upon annealing [1] and the easy fabrication of CoFeB/MgO/CoFeB magnetic tunnel junctions (MTJs) with large tunneling magnetoresistance (TMR) [2]. The PMA in CoFeB possesses a second-order uniaxial term [3] that can be used to achieve ultrafast switching [4]. Understanding the factors controlling PMA in CoFeB thin films is of great importance for the development of MTJ-based spintronic devices. Here we report our studies on the temperature dependence (5 K - 295 K) of PMA in Ta/Co₂₀Fe₆₀B₂₀/MgO thin films with different Co₂₀Fe₆₀B₂₀ thicknesses by using ferromagnetic resonance (FMR) measurements. The temperature dependence of the first order PMA field B₁ shows a linear behavior, of which the slope of linear fit decreases monotonously with increasing thickness *d* and scales with *d*⁻³. B₁ at 0 K obtained by extrapolation increases with increasing thickness in the thickness range studied. For the CoFeB film with thickness of 1.3 nm that is close to the critical thickness 1.25 nm [5], an easy cone orientation of magnetization is realized at low temperatures, due to that the first and second order PMA fields are of the same order of magnitude. Based on the temperature dependences of the first and second order PMA fields, a thickness-temperature diagram of the Co₂₀Fe₆₀B₂₀ thin film was obtained, which illustrates different regions for easy-plane, easy-cone, and easy-normal orientations of magnetization, which would benefit further understanding of manipulation of PMA in CoFeB thin films for spintronic applications.

[1] S. Ikeda, K. Miura, et. al., Nat. Mater. 9, 721 (2010)

[2] S. Ikeda, J. Hayakawa, et. al., Appl. Phys. Lett. 93, 082508 (2008)

[3] J. Zhu, J. A. Katine, et. al., Phys. Rev. Lett. 108, 197203 (2012)

[4] D. Apalkov, A. Khvalkovskiy, et. al., Abstract GC-09, 58th Magnetism and Magnetic Materials Conference, 2013

[5] I. Barsukov, Yu Fu, et. al., Appl. Phys. Lett. 105, 152403 (2014)

TU.G-P28 - PNR studies of magnetization in Pt/Co/Pt trilayers irradiated by EUV light pulses

W. Szuszkiewicz¹, F. Ott², E. Dynowska¹, R. Minikayev¹, A. Bartnik³, I. Jacyna¹, D. Klinger¹, A. Wawro¹, R. Sobierajski¹, Z. Kurant⁴

1. *Institute of Physics Polish Academy of Sciences, Warsaw, Poland*

2. *Laboratoire Leon Brillouin, UMR-12 CEA-CNRS, CEA Saclay, Gif sur Yvette, France*

3. *Institute of Optoelectronics, Military University of Technology, Warsaw, Poland*

4. *Faculty of Physics, University of Białystok, ul. L. Ciołkowskiego, Białystok, Poland*

Magnetization reorientation driven by femtosecond, visible light pulses has been recently found in thin Pt/Co/Pt sandwiches and explained in terms of irradiation induced formation of Co-Pt alloy on the Co/Pt interface, exhibiting high perpendicular magnetic anisotropy [1]. In the present work we investigated the Pt/Co/Pt thin films whose in-plane magnetization state was modified by single, extreme ultraviolet (EUV) light pulses. The Co layers 3 nm or 10 nm thick placed in-between the Pt bottom and top layers with thickness close to 25 nm and 3 nm, respectively, were deposited by MBE method onto (0001)-oriented sapphire substrates. The samples were irradiated by 3 ns pulses from laser-plasma source with the most intense emission centered at wavelength 11 nm (see [2] for details). The structure of samples was characterized by X-ray diffraction and reflectivity methods. The polarized neutron reflectivity (PNR) is an effective tool to study depth profiles of in-plane magnetization in multilayers and, to some extent, depth profiles of constituent element distribution. The PNR measurements were performed at LLB with the use of PRISM spectrometer. Prior to the irradiation a presence of smooth and sharp interfaces was confirmed by all three methods above mentioned. The analogous results obtained for irradiated samples showed changes in their structures. Due to the formation of Pt-Co alloy the maximal value of magnetization in-plane slightly decreased. The thinner sample was more uniform than the second one. Results obtained for the thicker sample suggest a presence of a significant Co concentration gradient inside thick Pt buffer and more complex depth profile of in-plane magnetization.

This work was partially supported by the grant No. DEC-2012/06/M/ST3/00475 from National Science Centre (Poland).

References:

[1] J. Kisielewski et al., *Journal of Applied Physics* 115, 053906 (2014)

[2] A. Bartnik et al., *Nuclear Instruments and Methods in Physics Research A* 647, 125 (2011)

TU.H-P02 - Specific heat and thermal expansion of $\text{LaCo}_{1-x}\text{Ga}_x\text{O}_3$ cobaltatesN.K. Gaur¹, R. Thakur¹, R.K. Thakur¹

1. Barkatullah University, Bhopal, India

The interest in LaCoO_3 cobaltates is associated with an occurrence of thermally induced transitions from low-spin (LS) to high-spin (HS) or intermediate-spin (IS) state as well as with a possibility to vary the transport and magnetic properties by heterovalent substitution on the La and/or Co sites. The parent compound lanthanum cobaltate LaCoO_3 shows an insulating ground state based on the diamagnetic LS state of Co^{III} ions. At room temperature LaCoO_3 and lanthanum gallate LaGaO_3 possess rhombohedrally distorted crystal structure of perovskite. The main focus of the present paper is to investigate the effect of isovalent substitution in LaCoO_3 of diamagnetic gallium ions Ga^{3+} with a completely filled 3d shell ($3d^{10}$) for paramagnetic ions Co^{3+} with a partially filled 3d shell ($3d^6$) on the elastic and thermal properties formed $\text{LaCo}_{1-x}\text{Ga}_x\text{O}_3$ as promising materials for fabricating membranes and other articles for electronic technology.

The specific heat and thermal expansion coefficient of $\text{LaCo}_{1-x}\text{Ga}_x\text{O}_3$ ($0.01 \leq x \leq 1$) has been studied as a function of temperature ($10\text{K} \leq T \leq 1000\text{K}$) by means of a Rigid Ion Model (RIM) after modifying its framework to incorporate the van der Waals interactions. In this paper the functional relation between charge and size mismatch and the thermal properties is determined and compared with the available reports. The Debye temperatures obtained from the lattice contributions are found to be in somewhat closer agreement with the available experimental data. The thermal expansion and specific heat values revealed by using MRIM are in closer agreement with the available experimental data for some concentrations (x) of $\text{LaCo}_{1-x}\text{Ga}_x\text{O}_3$. In addition, the results on the bulk modulus (B), cohesive energy (ϕ), molecular force constant (f), Reststrahlen frequency (ν_0) and Gruneisen parameter (γ) are also discussed.

TU.H-P03 - Micromagnetic simulations of nanocomposites and their neutron scattering response

S. Erokhin¹, A. Michels², D. Berkov¹

1. *General Numerics Research Lab, Jena, Germany*

2. *Physics and Materials Science Research Unit, University of Luxembourg, Luxembourg*

Due to our recent achievements in micromagnetic simulations of nanocomposites [1], it is possible to study the magnetization state in a relatively large volume of a magnetic nanocomposite material. This talk includes physical examples of modelling of magnetic structure of soft nanocomposites and the corresponding small-angle neutron scattering (SANS) cross section, demonstrating the accuracy of our method. First, we present numerical studies of a nanocomposite of the Nanoperm type, consisting of iron-based crystallites embedded in an amorphous magnetically soft matrix. This alloy with high permeability demonstrates an unusual angular anisotropy of the experimental SANS cross-section. In order to find out the reason of this phenomenon, we have performed large-scale numerical simulations of the Nanoperm magnetization state in various fields. Our results have unambiguously demonstrated that this effect is due to the internal magneto-dipolar field arising around hard inclusions. The second example is a porous ferromagnet that possess the maximal magnetic inhomogeneity among nanocomposites due to the jump of the magnetization on the boundary between pore and material. This extreme case makes possible to show explicitly the anisotropic nature of magnetic correlations in this type of nanocomposites, employing numerical studies of spatial correlations functions of the magnetization distribution. Numerically calculated SANS cross-sections agree very well with experimental data obtained on real materials.

Our method allows to extract the individual contributions to the total magnetic SANS cross-section, which is a complicated combination of all magnetization components decorated by the interaction of neutrons with magnetodipolar stray field of magnetic moments. This analysis opens up new possibilities to obtain fundamental insights into the magnetic neutron scattering. This research was supported by the DFG Project BE 2464/10-3.

Reference:

[1] A. Michels, S. Erokhin, D. Berkov, and N. Gorn, (Current Perspectives on Neutron Scattering) *J. Magn. Magn. Mater.* 350, 55 (2014)

TU.H-P04 - Critical behaviors at low-field of Fe-Ni-Zr alloy ribbonsT.D. Thanh ^{1,2}, N.H. Dan ², T.L. Phan ³, S.C. Yu ¹

1. Chungbuk National University, Cheongju, South Korea

2. Vietnam Academy of Science and Technology, Hanoi, Vietnam

3. Hankuk University of Foreign Studies, Yongin, South Korea

In this work, we present a detailed study on the critical behavior at low-field (below 10 kOe) of the ferromagnetic-paramagnetic (FM-PM) phase transition in $\text{Fe}_{90-x}\text{Ni}_x\text{Zr}_{10}$ alloy ribbons with $x = 0-15$, which were prepared by a rapid-quenching method. The results reveal that the samples are almost amorphous with a very small volume fraction of the nano-crystalline. We point out that these alloy ribbons undergoing a second-order phase transition and the Curie temperature (T_C) depends strongly on Ni-concentration (x) increasing from 245 K (for $x = 0$) up to 403 K (for $x = 15$). Basing on isothermal magnetization data, $M(H)$, the values of the critical exponents β , γ , and δ around FM-PM phase transition were determined by using the modified Arrott plots and critical isotherm analyses. The $M(H)$ behavior in the critical region obeys the universal scaling law, $M(H, \varepsilon) = \varepsilon^\beta f_\pm(H/\varepsilon^{\beta+\gamma})$, which implies that plotting $M/|\varepsilon|^\beta$ versus $H/|\varepsilon|^{\beta+\gamma}$ makes all $M(H)$ data points falling into two universal branches corresponding to $T < T_C$ and $T > T_C$. The results obtained show that in the case of low Ni-concentrations, the β value ($\beta = 0.367$ and 0.396 for $x = 0$ and 5 , respectively) is close to that expected for the 3D-Heisenberg model revealing an existence of short-range FM interactions in $\text{Fe}_{90}\text{Zr}_{10}$ and $\text{Fe}_{85}\text{Ni}_5\text{Zr}_{10}$ alloy ribbons. In contrast, the falling of the β values in between the values of mean-field theory ($\beta = 0.5$) and the 3D-Heisenberg model ($\beta = 0.365$) for high Ni-concentration samples ($\beta = 0.436$ and 0.444 for $x = 10$ and 15 , respectively) indicates a coexistence of short- and long-range FM interactions. It means that the presence of Ni favors establishing FM long-range order. The nature of this phenomenon is carefully discussed.

Keywords: Critical behavior, Magnetic interactions, Amorphous magnetic materials.

TU.H-P06 - The Memory in Magnetic Systems

C. Appino¹

1. Inrim, Torino, Italy

Most of the features of ferromagnetic materials are embedded in their hysteresis loop [1]: a matter compelling one to focus the attention on the memory properties of magnetic systems. Starting from the landmark work of Preisach, where the memory effects of scalar hysteresis are suitably accounted for by means of the so called Preisach plane, a vector generalization to ensembles of Stoner-Wohlfarth particles has been recently proposed [2]. In this approach the stability properties of particles are described by adopting the conventional astroid representation, a strategy also exploited to discuss incoherent particle rotations [3]. On the other hand, in order to include the possibility of reversal by domain wall motion, a modification of the coherent rotation mechanism, graphically represented by a “truncated astroid”, has been proposed as well [4]. Within this framework, we present a general mathematical tool able to track the history of any magnetic system, with reversal of magnetization driven by reversible and irreversible rotations and domain wall displacements. Coupled to a vector hysteresis model, the procedure outlined allows one to decrease to a large extent the computational time needed to reproduce the hysteresis loop. Eventually, this instrument supplies a set of thermodynamic variables providing an estimate of the magnetic energy loss entailed by irreversible processes, and the consequent entropy production.

References:

- [1] “The Science of Hysteresis”, G Bertotti and I. Mayergoyz Editors, Academic Press (Elsevier), 2006
- [2] Carlo Appino, “Representation of Memory in Particle Assembly Hysteresis Models”, IEEE Trans. on Mag., VOL. 45, NO. 11, Nov. 2009
- [3] A. Stancu, C.Papusoi, L. Spinu, “Mixed -type model of hysteresis”, J. Magn. Magn. Mater. 150 (1995) 124-130
- [4] C. Appino, M. Valsania, V. Basso, “A vector hysteresis model including domain wall motion and coherent rotation”, Physica B 275 (2000) 103-106

TU.H-P07 - Forced volume magnetostriction of $Y_2Fe_{17-x}M_x$ (M=Al,Si,Ga)T. Kamimori¹, D. Haruna¹, H. Tange¹*1. Faculty Of Science, Ehime University, Matsuyama, Japan*

The substitutions of nonmagnetic elements for Fe in intermetallic compound R_2Fe_{17} increase the Curie temperature, T_C . This phenomenon is understood as Invar magnetism, $(dT_C/dV) > 0$. In reality, substitutions of Al and Ga for Fe increase both lattice volume and T_C . The values of (dT_C/dV) are $7.5(10^3 K/nm^3)$ for the Al substitution and 14 for Ga. On the contrary, the substitution of Si for Fe contracts lattice volume and increases T_C , $(dT_C/dV) = -63 < 0$. This is against the Invar magnetism. In this study, forced volume magnetostriction, $\partial\omega/\partial H$, was measured in $Y_2Fe_{17-x}M_x$ (M=Al,Si,Ga) compounds by means of 3-terminals capacitance method under magnetic field up to 1.5T. In all cases, the values of $\partial\omega/\partial H$ observed at R.T. were positive and decrease with increment of T_C by the substitutions. In all substitutions, the values of $dT_C/d(\partial\omega/\partial H)$ at R.T. are between $-1.7(10^2 K^{-1})$ and -3.7 . These phenomena indicate the substitution of Al,Si,Ga for Fe weakens magnetovolume effect of Y_2Fe_{17} with increment of T_C .

It is well-known, the origin of Invar effect is magnetovolume effect as expansion with appearance of magnetization. The results in this study indicate the increment of T_C by substitution of non magnetic elements for Fe in R_2Fe_{17} is not by the Invar effect itself but by the declining of the Invar magnetism.

TU.H-P09 - New medium frequency MnZn Ferrite with low losses over a broad temperature range

G. Kogias¹, V. Zaspalis¹

1. Center For Research And Technology-Hellas, Thessaloniki, Greece
2. Aristotle University of Thessaloniki, Thessaloniki, Greece

New and existing applications possess stronger demands on the performance of the magnetic cores, searching for both efficiency and miniaturization. The working conditions of the equipments require specific properties from the transformers and inductors in order to minimize magnetic power loss in the system. A relatively recent trend in the application market of magnetic components asks for the development of magnetic materials with low losses over broad temperature ranges. Some of these applications are automotive DC/DC converters in hybrid and electric vehicles, DC/DC converters in telecommunication and computing equipment, microinverters of photovoltaic systems or high power LED drivers for public lighting. In this article the development of a medium frequency MnZn ferrite polycrystalline material exhibiting low losses over broad temperature ranges is reported. The initial permeability is 1700 (10 kHz, 0.1 mT, 25°C) and the power losses at 500 kHz, 100 mT are 640 kW m⁻³ (25°C) and 650 kW m⁻³ (100°C). The improvements have been realized through optimizations in the design of the antiferrimagnetic unit cell lattice. The addition of Sn ions results to the increase of specific resistivity and as a result the losses at medium frequencies are decreased. The addition of Co ions possesses opposite anisotropy constant of the host lattice and with its introduction compensates the already existing lattice anisotropy. As a result it changes the temperature dependence of the anisotropy constant of the host lattice and leads to the increase of permeability and the decrease of losses. The previous results of the developed MnZn ferrite with low power loss values over a broad temperature range, establish it ideal for the above applications.

TU.H-P10 - Vector model for losses in non-oriented steel sheets

C. Appino¹

1. *Inrim, Torino, Italy*

The presence of two-dimensional (2D) magnetization processes in devices and electrical machines calls for the development of vector model for loss prediction. Starting from the Del Vecchio-Charap work [2], we developed a static model able to reproduce the 2D evolution of magnetization in soft non-oriented steel sheets: the most interesting case for applications. The material is assimilated to an ensemble of biaxial grains, each associated with a hysteron having two orthogonal easy axes. In each of them, the field driven irreversible switch of magnetization between the easy directions (Barkhausen jump: BJ) is governed by the value of local coercive field (about ten times smaller than the anisotropy fields); the ensemble of all these BJ accounts for the domain wall displacement. After the BJ, the local magnetization is brought to its energy minimum by the antagonism between anisotropy and Zeeman energy, so determining the reversible magnetization component. Domain wall reversible processes (bending) are not considered, whereas the role of macroscopic and internal demagnetizing fields is accounted for. The system average magnetization is obtained after integrating the outputs of single hysterons, each weighted by probability density functions suitably characterizing the material properties (i.e.: grain orientations, coercive and anisotropy fields). We have been able to reproduce the loss vs. polarization $W(J_p)$ evolution in several non-oriented materials, subjected to alternating and rotating fields. In particular, under circular induction, the W drop at high J_p was always found, without introducing “ad hoc” fitting functions. It is remarkable that the outlined approach can be extended to systems magnetized in dynamic conditions.

References:

- [1] C. Appino, C. Ragusa, and F. Fiorillo, “Can rotational magnetization be theoretically assessed?”, *IJAEM* 44 (2014), 355-370
- [2] R.M. Del Vecchio, S. H. Charap, “Two dimensional hysteresis model”, *IEEE Trans. Mag.* 20 (1984), 1437-1439

TU.H-P11 - magnetic and structural evolution of Nd₂Fe₁₄B nanoparticles doped with Co and Ni during surfactant-assisted ball-milling

J.S. Trujillo Hernandez¹, J. Anselmo Tabares¹, G.A. Pérez Alcázar¹

1. *Universidad Del Valle, Cali, Colombia*

In this work, powder produced by arc melting of the alloy Nd₁₆(Fe_{76-x}Co_x)B₈ with x = 0, 10, 20 and 25 (size distribution under 20 micrometers) was milled in a high-energy planetary ball-mill (Fritsch Pulverisette 5 with hardened steel balls) at a rotational speed of 300 rpm. The milling was performed in a protective argon atmosphere with the ball-to-powder weight ratio of 20/1 for milling times varying from 1 to 2 h. Hexane (55% of powder weight) was introduced in the mill as a solvent together with oleic acid (12% of powder weight) as surfactant. The powders obtained after milling was washed with ethanol. X-ray diffraction (XRD), Mossbauer spectroscopy (MS), and Vibrating Sample Magnetometry (VSM) measurements were performed in order to characterize the properties of the obtained samples. A PanAnalytical diffractometer with a Cu anode, a constant acceleration mode Mössbauer spectrometer with a 25 mCi 57Co (Rh) source, and a PPMS of Quantum Design were used, respectively, to obtain these measurements. The role of milling time and the presence of the surfactants proved to be critical for the final size, shape, structure and magnetism of the nanoparticles. In the beginning milling mostly improves exchange coupling between the Nd₂Fe₁₄B phase and soft magnetic phases. However, higher energy product value were achieved for nanostructures with sizes closer to the monodomain limit of Nd₂Fe₁₄B (50e100 nm).

Acknowledgment: This work was partially financed by “Centro de Excelencia de Nuevos Materiales CENM-Univalle.

TU.H-P12 - The effect of high energy ball - milling on the morphology and magnetic properties of $\text{Ho}(\text{Ni}_{0.5}\text{Co}_{0.5})_3$ compound

A. Bajorek^{1,2}, P. Skornia^{1,2}, K. Prusik^{2,3}, M. Wojtyniak^{2,3}, G. Chełkowska^{1,2}

1. A. Chelkowski Institute of Physics, University of Silesia, Katowice, Poland

2. Silesian Center for Education and Interdisciplinary Research, University of Silesia, Chorzów, Poland

3. Institute of Materials Science, University of Silesia, Chorzów, Poland

The aim of the presented study was to focus on the effect of mechanical grinding on the morphology and magnetic properties of $\text{Ho}(\text{Ni}_{0.5}\text{Co}_{0.5})_3$ intermetallic compound in order to improve its applicable magnetic parameters. First the polycrystalline $\text{Ho}(\text{Ni}_{0.5}\text{Co}_{0.5})_3$ bulk compound was crushed and pre-milled with a standard agate mortar. Then, such a mixture was grinded up to 80 h with frequency 30 Hz using Mixer Mill 400 (Retsch). The wet milling has been performed in dimethylformamide (DMF) using the Eppendorf vials and balls with a diameter of 2 mm made of ZrO_2 with balls to powder ratio about 10:1 by weight. After each stage of milling the morphology of the grinded material was investigated by using: dynamic light scattering DLS (Zetasizer Nano ZS Malvern Instruments), the scanning electron microscopy SEM (Jeol JSM 6480) and the X-ray diffraction XRD (Empyrean PANalytical). Additionally, after the last stage (80h) the transmission electron microscopy TEM (Jeol JEM 3010 UHR) and the atomic force microscopy AFM were applied. The magnetic properties has been determined based on wide-ranging SQUID magnetometer (Quantum Design MPMS, temperature from 1.9K to 400K and magnetic field up to 7T) series of different magnetic measurements.

The increase in the milling time leads to the reduction in the size of crystallites and the gradual amorphization of the starting material. Additionally, the presence of the nanoflakes with thickness even less than 100 nm was evidenced. Moreover, the increase in milling time results in the slight variation of the coercivity (H_c) and the *remanent-to-saturation* (M_r/M_s). The shape of the hysteresis loops varies across pulverization exhibiting a characteristic kink for higher milling time. Such a behaviour is due to the ultrafine grained structure and inhomogenities among magnetically ordered grains formed during HEBM.

TU.H-P13 - Partitioning of rare earth dopant and magnetic properties of RF3-doped Nd-Fe-B hot-pressed magnetJ.Y. Kim ¹, H.W. Kwon ¹, J.G. Lee ², J.H. Yu ²*1. Pukyong National University, Busan, South Korea**2. Korea Institute of Materials Science, South Korea*

With increasingly escalated need for high coercivity in many permanent magnet applications, rare earth fluoride (RF3) salts have been widely used for enhancing coercivity in the hot-pressed and die-upset Nd-Fe-B-type magnet. Melt-spun Nd-Fe-B flakes are mixed with RF3 and then hot-pressed and hot-deformed. Rare earth dopant from the doped RF3 substitutes some of Nd in either Nd₂Fe₁₄B matrix grain or Nd-rich grain boundary phase or both phases in the flake, thus enhancing coercivity. In this article, partitioning of the rare earth dopant in the Nd-Fe-B-type hot-pressed magnets doped with various RF3 and its effect on the magnetic properties were investigated. Commercial melt-spun flakes (MQU-F : Nd_{13.6}Fe_{73.6}Co_{6.6}Ga_{0.6}B_{5.6}) were mixed with 1.6 wt% RF3 (R = La, Ce, Pr, Nd, Dy) and then hot-pressed. Partitioning of the rare earth dopant was examined by SEM equipped with EDX and X-ray diffraction. RF3 (R = Pr, Nd, Dy)-doping led to an overall coercivity enhancement with respect to the un-doped magnet. The most profound coercivity enhancement (5.0 kOe) was achieved in the DyF₃-doped magnet pressed at 735 C, and this was attributed mostly to the substitution of Nd in Nd₂Fe₁₄B matrix grains in the flake by the dopant Dy from the DyF₃. NdF₃- and PrF₃-doping was most beneficial for enhancing coercivity (3.0, 3.5 kOe) in the magnet pressed at 700 C and below 670 C, respectively, and the improvement was attributed largely to the modification of Nd-rich grain boundary in the flakes by the dopant Nd, Pr. RF3 (R = La, Ce)-doping caused radical coercivity reduction in the magnet hot-pressed at higher temperature above 735 C, and this was attributed to the substitution of Nd in Nd₂Fe₁₄B matrix grain in the flake by the dopant La, Ce. Variation of magnetic properties caused by the RF3-doping was correlated with partitioning of the rare earth dopant.

TU.H-P14 - Direct imaging of Fe nanoclusters in a melt-spun FeSiBPCu alloy by aberration corrected high-resolution transmission electron microscopyK. Sato¹, K. Takenaka¹, A. Makino¹, Y. Hirotsu¹*1. Institute For Materials Research, Tohoku University, Sendai, Japan*

The newly developed FeSiBPCu nanocrystalline soft magnetic alloy contains more than 80at%Fe; which is the upper limit of the Fe content for single amorphous phase formation [1]. A proper heat treatment of an as-quenched ribbon is the key to obtain the excellent soft magnetic properties in this alloy ($H_c = 7-10$ A/m, $B_s = 1.88-1.94$ T). It has been suggested that small Fe clusters formed at an as-quenched state could act as the nucleation site for the α -Fe grains during the crystallization. However, detailed structure of an as-quenched FeSiBPCu alloy still remains an open question. In this study we hence intend to characterize atomic structures of a melt-spun $Fe_{85.2}Si_2B_8P_4Cu_{0.8}$ alloy by using spherical aberration (Cs) corrected high-resolution transmission electron microscopy (HRTEM). The Cs was adjusted to approximately $-1 \mu m$ and thus the theoretical optimal defocus becomes as small as 1.6 nm, which can effectively minimize possible imaging artifact. As a result, existence of a few nanometer-sized clusters was found in an amorphous matrix. The number density of such clusters reached as high as $9 \times 10^{12} cm^{-2}$. Some of the clusters show four-fold or six-fold atomic arrangements, implying existence of crystalline Fe clusters with the bcc structure [2]. Possible structural change due to electron irradiation can be excluded in the HRTEM observation using a CCD camera with a short acquisition time of 1s. Electron diffraction pattern obtained from a wide area shows only halo rings arising from amorphous structure. Thus modern Cs-corrected HRTEM unambiguously revealed the formation of a "heteroamorphous" structure in the as-quenched FeSiBPCu alloy. These extremely small nanoclusters with high number density must be responsible for a formation of high-density α -Fe nanocrystals produced by post-annealing.

References:

- [1] A. Makino et al., J. Appl. Phys. 105 (2009) 07A308
- [2] Y. Hirotsu and R. Akada, Jpn. J. Appl. Phys. 23 (1984) L479

TU.H-P15 - The effect of film thickness on the forming process and switching parameters of sol-gel prepared cobalt ferrite thin films

C. Liu¹, M. Mustaqima¹, D.H. Kim¹, B.W. Lee¹

1. Hankuk University Of Foreign Studies, Seoul, South Korea

The resistive switching (RS) phenomenon refers to the reproducible switching between a high resistance state (HRS) and a low resistance state (LRS) observed in a metal/oxide/metal (MOM) configuration. In the past 10 years, the RS effects in binary oxide materials such as NiO, TiO₂, and TaOx has been studied intensively for their potential applications in nonvolatile resistive random access memory (RRAM). More recently, ferrite materials have been discovered as potential RRAM materials showing excellent RS behaviors. Due to their ferromagnetic property and electrically insulating characteristics, ferrite materials have been considered as a good candidate for combining the magnetic and electrical switching behaviors in one device.

In this work we report the preparation of textured cobalt ferrite (CoFe₂O₄, CFO) thin films by sol-gel and spin-coating and the study on the RS properties of Pt/ CoFe₂O₄/Pt structures. The (111)-oriented polycrystalline CoFe₂O₄ thin films were prepared on Pt/TiO₂/SiO₂/Si substrate by spin-coating. Scanning electron spectroscopy revealed that the average layer thickness of one coating is about 60 nm. The thickness of the CFO thin film was adjusted by the number of coating varied from 1 to 4. All Pt/1-layered CFO/Pt structures showed a quite low resistance of a few ohms and no switching was observed. Most of the MOM structures based on 2-layered CFO thin films showed increased resistance around 10 Ω in the initial states, and unipolar resistive switching (URS) without forming process was observed. When the layer number increased to more than 3, the initial states of the Pt/CFO/Pt structures were of high resistance higher than 50 kΩ, and stable and repeatable URS with a HRS/LRS ratio about 1000 can be induced with a forming process. Based on the thickness dependence of the URS behavior observed, we analyzed the RS behaviors of the textured CFO thin films in detail with respect to the forming voltage and the conducting mechanism. Our results revealed that Pt/CFO/Pt structures with 2 or 3 layers of CFO thin films show the most stable RS behavior with a much narrow distribution in the set voltage.

TU.H-P16 - A novel experimental determination of the magnetometric self- demagnetization factor

N. Hillier¹, M. Hall¹, S. Turner¹, S. Harmon¹

1. National Physical Laboratory, Teddington, United Kingdom

Machine designers and advanced material manufacturers are in need of a robust, practical and accurate measurement technique, capable of determining permanent magnet properties for operating conditions. Recent techniques based on pulsed field magnetometry offer this capability, with the measurement of the full BH loop taking less than 100 ms. However, for these techniques to reach the required accuracy and robustness, detailed investigation into the associated correction factors is required. One such correction, which is associated with the geometry and susceptibility of the test sample, is the magnetometric self-demagnetization factor, ND. This correction and the associated phenomenon of self-demagnetization are explained in detail in the work of Chen et al. [1] and have thus far been theoretically calculated using an inductance model. This work will introduce a novel experimental determination of ND based upon a measurement of the working point polarisation, J_m , and the second quadrant demagnetization curve. In this study, a series of cylindrical NdFeB samples were investigated, with aspect ratios ranging from 1 up to 3, where 1 represents a cylinder 10 mm in length and 10 mm in diameter. The experimental and theoretical values of ND are presented and found to have discrepancies of up to 40%. This significant difference is attributed to over simplifications of the susceptibility used in the theoretical models. Data from the Pulsed Field Magnetometer (PFM) at the National Physical Laboratory is then processed using these values, with the experimentally determined ND resulting in behaviour closer to that of the known material behaviour. This paper will present for the first time these measurements of ND and discusses the complex self-demagnetization correction required to obtain material properties using a PFM.

Reference:

[1] D-X. Chen, J.A. Brug and R.B. Goldfarb, "Demagnetizing Factors for Cylinders", IEEE Transactions on Magnetics, vol. 27, pp. 3601-3619, July 1991

TU.H-P17 - Power density increasing design for railway vehicle traction motor using Halbach magnet array structure

H.W. Lee¹, H.W. Jun², K.D. Lee²

1. Korea National University Of Transportation, Chungju, South Korea

2. Hanyang University, Seoul, South Korea

Generally, traction motors for railway vehicles are inferior to that of electric vehicle in terms of power density. Traction motors for railway vehicles are relatively free of spatial constraints than motors electric vehicles, but in terms of whole system efficiency, increasing power density of traction motor is helpful. In this paper, neodymium magnet was used in permanent magnet synchronous motor design. The neodymium magnet is widely used in industry because its high energy density compared to other permanent magnet material. In this paper, using Halbach magnet array structure, power density of traction motor for 40kW class tram was elevated. This paper introduce detailed design process of the Halbach magnet array structure applied model, and check the effects on output characteristics by parameters like rotor shape, airgap diameter and pole ratio. Also, electrical output characteristics were compared between typical SPMSM model and Halbach magnet array model, which has same output. With electromagnetic analysis, the amount of power density elevation was confirmed, compared to Halbach model and typical SPMSM model. In addition, although there is a risk of occurring high torque ripple, achieve the same output characteristic as the prior SPMSM type motor by applying proper pole ratio.

TU.H-P18 - Application of the Jiles-Atherton model for the temperature dependence of magnetic hysteresis loops of amorphous alloys with perpendicular anisotropy

R. Szewczyk¹

1. Industrial Research Institute For Automation And Measurements PIAP, Warsaw, Poland

Cores made of amorphous alloys with perpendicular anisotropy are widely used as cores for precision current transformers. Such cores exhibit linear $B(H)$ characteristics with nearly constant permeability, and negligible coercive field of magnetic hysteresis loop.

However, both permeability and saturation flux density of such cores are temperature dependent. It should be highlighted, that this dependence has significant impact on characteristics of measuring devices, such as current transformers. On the other hand, the accurate model of temperature dependence of characteristic of anisotropic cores was still not presented. However, correction of Jiles-Atherton model of anhysteretic magnetization [1, 2] creates new possibility of such modelling. Magnetic hysteresis loop $B(H)$ of Nanoperm M-680 core produced by Magnetec was measured in the temperature range from -30 up to $+150$ °C. During the increase of temperature, the increase of amplitude permeability and significant decrease of saturation flux density B was observed.

On the base of experimental results, the modelling of $B(H)$ characteristics was carried out. Parameters of the Jiles-Atherton model of anisotropic anhysteretic magnetization were determined during the optimisation process, utilizing the simplex search method. As a result, very good agreement between experimental results of measurements of $B(H)$ characteristics and the results of modelling was achieved.

Results of modelling indicated the nearly linear decrease of average anisotropy energy density, when the temperature increases. Moreover, parameter a describing average domain wall density exhibits minima for the temperature about 40 °C.

Presented results confirm that the corrected Jiles-Atherton model enables modelling of temperature dependence of magnetic $B(H)$ hysteresis loops of amorphous alloys with perpendicular anisotropy. This model may be very useful for Spice-based modelling of measuring devices, such as precise current transformers.

[1] A. Ramesh, D. C. Jiles, J. Roderik, IEEE Trans. Magn. 32 (1996) 4234

[2] R. Szewczyk, Materials, 7 (2014) 5109

TU.H-P19 - Influence of grain boundaries on magnetization-reversal within Nd-Fe-B magnets

I. Kitagawa¹, J. Ushio¹, A. Sugawara¹, T. Nishiuchi²

1. *Central Research Laboratory, Hitachi Ltd., Kokubunji, Tokyo, Japan*

2. *Magnetic Materials Research Laboratory, Magnetic Materials Company, Hitachi Metals Ltd., Tokyo, Japan*

Creating a Nd-Fe-B magnet with high coercivity is a tremendous challenge. Understanding the correct picture of the magnetization-reversal process occurring in the magnet is one key to increasing the coercivity. To grasp the correct picture of the magnetization-reversal process, magnetization reversal in a multi-crystal-grain Nd-Fe-B magnet was studied by micromagnetics simulation.

In order to elucidate the mechanism of magnetization reversal, two computational models were used. One is for a numerical estimation of dependence of the intergrain interaction on the grain boundary (GB) width, magnetization of the GB phase and angle between easy axes of adjacent grains. We used a planar two-grain magnet model consisting of two plate-like grains connected by a GB phase. The other model examines intergrain interaction through the magnetization-reversal process occurring inside a realistic microstructure investigating the reversal mode changed by the property of GB. Moreover, a large-scale micromagnetics simulation package based on a voxel-mesh model, in which the demagnetization-field calculation is accelerated by massive graphics-processing units (GPUs) was also developed. The simulation results show that interaction energy through the grain-boundary phase increases with decreasing grain-boundary width. Grains with a nonmagnetic GB are isolated when the grain-boundary width is larger than 20 nm. Grains with a ferromagnetic GB are more strongly coupled than those with a nonmagnetic GB. The decrease in the interaction energy causes the reversal process to change from domain-wall-motion type to isolated-single-grain type. The simulation, moreover, reveals that the interaction energy decreases with increasing angle between the easy axes of adjacent grains. The magnetization-reversal process in a Nd-Fe-B sintered magnet is dominated by domain-wall motion, which is promoted by the ferromagnetic GB. Reducing magnetization in the GB phase is thus an effective way to enhance coercivity.

TU.H-P20 - Effect of pre-sintering on the magnetic properties of NdFeB sintered magnets diffusion -treated with Cu/Al mixed DyH₂ powder

M.W. Lee¹, H.S. Lee¹, T. Jang¹, T.H. Kim², S.R. Lee², H.J. Kim³

1. Sunmoon University, Asan, Chungcheongnam-do, South Korea

2. Korea University, Seoul, South Korea

3. R&D center of Jahwa electronics, Cheongwon-gun, South Korea

Grain-boundary diffusion treatment has been purposed as a heavy rare-earth (HRE) element saving method, where HRE atoms are allowed to diffuse from the surface of a NdFeB sintered magnet to its interior through grain boundaries upon heating. Since the magnet used for this treatment is almost fully dense, HRE atoms cannot easily diffuse into the magnet resulting in relatively shallow diffusion of HRE atoms. A pre-sintering process (PSP), for which a magnet is sintered as a primary step below 900 °C prior to a fully dense sintering at a higher temperature could improve the diffusion depth of HRE atoms like Dy by decreasing the density of NdFeB sintered body to 70 ~ 80 %. Furthermore, it is known that the elements of low melting point such as Cu and Al also improve the diffusivity of HRE atoms by improving wettability of Nd-rich grain boundary phase. The solubility of Cu to Nd₂Fe₁₄B phase is almost negligible whereas Al has some solubility to this main phase. In this work, we investigated the effect of pre-sintering process on the diffusion behavior of Dy in a NdFeB sintered magnet which was diffusion treated with Cu/Al mixed Dy source. The pre-sintering of a magnet was performed at 900 °C in vacuum and then the pre-sintered body was dipped in the solutions of DyH₂, DyH₂+Cu, and DyH₂+Al, respectively. The dipped pre-sintered body were then fully sintered at 1060 °C for 2 hrs followed by a subsequent annealing. The pre-sintering apparently improved the diffusivity of Dy atoms. The penetration of Dy into the magnet extended to 1500 μm from the surface when the DyH₂+Al solution was used as a Dy source resulting in the increase of coercivity more than 3 kOe. The experimental results will be discussed in detail in this presentation.

Acknowledgement:

This work is supported by the strategic Core Material Technology Development Program (No. 10043780) funded by the ministry of Trade, Industry and Energy (Korea).

TU.H-P21 - Synthesis and Magnetic Properties of $\text{SrZn}_x\text{Fe}_{(2-x)}\text{Fe}_{16}\text{O}_{27}$ ($0.0 \leq x \leq 2.0$)J.H. You¹, S.J. Choi¹, S. Lee¹, S.I. Yoo¹*1. Seoul National University, Seoul, South Korea*

Since strontium W-type hexaferrite (SrW) is stable at the high temperature region of 1350–1440°C in air, it is hard to obtain a pure phase of SrW at room temperature. Thus, there are some reports on the stabilization of SrW phase by substitution of Fe^{2+} ions with other divalent metal ions such as Mn, Zn, Co, and Ni. However these reports are on the full substitution for Fe^{2+} ions. Therefore, the effect of partial substitution on the properties has never been reported. Since we could obtain SrW pure phase at room temperature by annealing and subsequent furnace-cooling in a reduced oxygen atmosphere, we tried to prepare the Zn-substituted SrW bulk samples with the compositions of $\text{SrZn}_x\text{Fe}_{(2-x)}\text{Fe}_{16}\text{O}_{27}$ ($0.0 \leq x \leq 2.0$) in a reduced oxygen atmosphere, and identify the effects of Zn^{2+} substitutions on their magnetic properties. Furthermore, we tried to investigate the phase stability region change of $\text{SrZn}_x\text{Fe}_{(2-x)}\text{Fe}_{16}\text{O}_{27}$ with varying x. For this purpose, samples were annealed at the temperature region of 1100–1350°C for 2 h in $P_{\text{O}_2} = 10^{-3}$ atm. As a result, the saturation magnetization of the samples increased with increasing x from 0 to $x = 1.5$, and the phase stability region decreased with increasing x.

TU.H-P23 - Effect of milling energy and soft phase pre-milling on the microstructure and interphase exchange coupling of Nd₂Fe₁₄B/ α -Fe nanocomposites

S. Mican¹, R. Hirian¹, O. Isnard², I. Chicinaş³, V. Pop¹

1. Babes-Bolyai University, Faculty Of Physics, Cluj-Napoca, Romania

2. Institut Néel, CNRS, Université Grenoble Alpes, Grenoble, Cédex 9, France

3. Materials Sciences and Engineering Dept., Technical University of Cluj-Napoca, Cluj-Napoca, Romania

The effects of milling energy and soft phase pre-milling on the microstructure and interphase exchange coupling of Nd₂Fe₁₄B+10wt% α -Fe nanocomposites were investigated. The α -Fe crystallite size is critical for obtaining an efficient interphase exchange coupling. We thus try a pre-milling of the soft phase in order to obtain smaller α -Fe crystallite sizes. Also, the problem of damaging the Nd₂Fe₁₄B crystal structure during milling was addressed by using different milling energies. Nd₂Fe₁₄B+10wt% α -Fe powder samples were prepared through mechanical milling for 6h with \varnothing 10mm and \varnothing 15mm balls respectively. The starting soft phases consisted of commercial and 4h mechanically milled (MM) Fe powder annealed at 400°C for 4h. The milled nanocomposite samples were annealed under Ar at 700, 750 and 800°C for short times (0.5 to 3 minutes). X-ray diffraction (XRD) measurements showed the destruction Nd₂Fe₁₄B crystal structure, however, this effect was less pronounced after milling with \varnothing 15mm balls. The restoration of the Nd₂Fe₁₄B crystal structure after annealing was confirmed by XRD. The α -Fe crystallite sizes increase with annealing temperature/time, being roughly the same for both milling energies. Smaller α -Fe crystallite sizes were found for samples containing pre-milled Fe. The magnetic behavior was investigated from hysteresis curves and dM/dH vs. H plots. The samples milled at higher energies show a better interphase exchange coupling, however, milling at lower energies determined higher coercivities due to the reduced damaging of the Nd₂Fe₁₄B crystal structure. The best exchange coupling was obtained for samples annealed at 700°C for around 2 minutes, with a maximum coercive field of about 0.5T. By increasing annealing temperature/time, the interphase exchange coupling weakens due to increasingly larger α -Fe crystallites. Taking into account the milling energy and preparation conditions, the Nd₂Fe₁₄B/ α -Fe exchange coupling is analyzed.

TU.H-P24 - Structural and magnetic properties of mechanically milled $Mn_{50}Al_{46}M_4$ ($M = Mn, Ni$) alloysR. Hirian¹, S. Mican¹, O. Isnard², I. Chicinaş³, M. Coldea¹, V. Pop¹*1. Babes-Bolyai University, Faculty Of Physics, Cluj-Napoca, Romania**2. Institut Néel, CNRS, Université Grenoble Alpes, Grenoble, Cédex 9, France**3. Materials Sciences and Engineering Dept., Technical University of Cluj-Napoca, Cluj-Napoca, Romania*

The metastable τ -phase (tetragonal $L1_0$ structure) of the Mn-Al system was reported to have interesting magnetic properties for permanent magnet applications, the most stable composition being $Mn_{54}Al_{46}$. It was shown that the magnetic properties of the τ -phase can be improved through doping and mechanical milling. In this work, the structural and magnetic properties of milled $Mn_{50}Al_{46}M_4$ ($M=Mn, Ni$) alloys were investigated. The samples were prepared through induction melting, followed by mechanical ball milling up to 5h. The milled samples were annealed at 1050°C for 1h under Ar atmosphere followed by quenching in water. The as-cast samples were found to be phase mixtures. For $M=Mn$ the τ -phase was the main phase, while for $M=Ni$ the κ -phase (CsCl-type structure) was a majority phase. The as-milled samples showed a progressive broadening of the XRD peaks with milling time due to increased strain and defect density. Following annealing, the 5h MM samples were composed mainly of the τ -phase ($M=Mn$) and κ -phase ($M=Ni$) respectively.

The coercivity of the $Mn_{54}Al_{46}$ alloy increases with milling time, a value of 0.3T being obtained for a milling time of 0.5h. For milling times longer than 0.5h the coercivity decreases rapidly due to crystal structure damage which diminishes the anisotropy. The 5h MM annealed samples showed higher remanence and lower coercive field values than the as-milled samples, however both coercivity and remanence values were higher than those of the as-cast sample.

The as-milled $Mn_{50}Al_{46}Ni_4$ samples show the same magnetic behaviour vs. milling time as the one observed for $Mn_{54}Al_{46}$. However, the coercivity and remanence values are lower, due to the presence of the soft magnetic κ -phase. The 5h MM sample annealed at 1050°C for 1h showed both lower coercivity and remanence values than the as-milled samples, due to the κ -phase being the majority phase in this sample.

TU.H-P25 - Tic additive in neodymium iron boron magnets

Z. Mural¹, Y. Ilke Cakmakoglu¹, J. Link², L. Kollo¹, R. Veinthal¹

1. *Department of Materials Engineering, Tallinn University Of Technology, Tallinn, Estonia*

2. *National Institute of Chemical Physics and Biophysics, Tallinn, Estonia*

Since the discovery of the Nd₂Fe₁₄B compound in 1980s, continuous efforts are being made to enhance the magnetic properties of RE-based magnets by optimizing its microstructure and chemical composition. One of the strategies to increase coercivity of the magnets is by decreasing its grain size. The effect of small amounts (0.1 - 0.5 wt.%) of TiC nanoparticles on grain coarsening during sintering was studied in this work. Standard powder metallurgy route was used to prepare NdFeB magnets. The nanoparticles were added before or after jet milling. Adding the nanoparticles after the jet milling by simple mixing could not disperse the particles, resulting with agglomerates in the final microstructures. Introducing the nTiC prior to the jet milling was effective and nanoparticles were dispersed in the the final alloy, concentrating in the neodymium rich phase of the alloy. Although some grain refining effect was observed, no significant effect from nTiC additive on magnetic properties was found.

TU.H-P26 - Permalloy thin films on palladium activated self assembled monolayer for magnetics on silicon applications

R. Anthony^{1,2}, J. Rohan¹, C. Ó Mathúna^{1,2}

1. Tyndall National Institute, University College Cork, Dyke Parade, Cork, Ireland

2. Department of Electrical and Electronics Engineering, University College Cork, Cork, Ireland

Magnetic thin films of Permalloy (Py) have been extensively deposited as soft core materials for integrated magnetic components (micro-inductors and transformers) [1]. However, existing electroplating methods require an additional conductive seed layer resulting in undercutting of the core during patterning. We report an electroless deposition process for Py thin films on oxidised silicon substrates for magnetics on silicon applications. P-type Si (100) samples were immersed in an amino-propyltrimethoxy silane solution to form an adhesive self-assembled monolayer which was activated by palladium to realise a thin catalytic layer [2] (fig. 1). This was followed by electroless deposition of Py in a borane based bath. Well adhered smooth Py films up to 500 nm have been obtained at a deposition rate of 1.8 nm/second with 8.5 nm surface roughness.

The measured resistivity of $\sim 37 \mu\text{Ohm-cm}$ is higher than electroplated Permalloy thin films ($\sim 20 \mu\text{Ohm-cm}$). Energy dispersive X-ray analysis suggested $\sim 25\%$ Fe and $\sim 75\%$ Ni with negligible B content, typically less than 1% [3]. These isotropic deposits (fig. 2) possess easy and hard axes coercivities ~ 4.5 and ~ 6.95 Oe, respectively, as measured in BH loop tracer. High frequency characteristics were studied with a wide-band complex permeameter (up to 9 GHz). For a 110 nm thick deposit as expected from the skin depth equation, the initial permeability of the film measured at null field was ~ 2750 . Considerable increase in frequency roll off (fig. 3(a) and 3(b)) compared to previously reported Py films [4] is observed. This can be attributed to the presence of boron in the films which increases the resistivity, thereby reducing the high frequency eddy current losses.

The process for deposition of Py on non-conductive oxide films is ideal for MEMS structures with recessed regions, and applicable for deposition of other soft magnetic thin films on oxides.

Acknowledgement: The authors wish to acknowledge Central Fabrication Facilities (CFF) at Tyndall National Institute for their support; and European Union for funding the work through FP7 (Project: PowerSwipe) under Grant 318529.

Reference:

1. C. O. Mathuna, T. O' Donnell, N. Wang and K. Rinne, "Magnetic on silicon: an enabling technology for power supply on chip", IEEE Trans. Power Elec., vol. 20, no. 3, May 2005.

TU.H-P27 - Magnetic anisotropy and stress sensitivity of thin-gauge non-oriented electrical steels

S. Turner¹, N. Hillier¹, M. Hall¹, S. Harmon¹

1. National Physical Laboratory, Teddington, United Kingdom

The demand for high-performance electric motors, running at speeds in excess of 6000 rpm, has led to the production of thin gauge non-oriented electrical steels (0.2 mm and below) becoming more common place. Such materials restrict the generation of classical eddy current contributions, which increase with the square of frequency, and so offer a significant reduction in overall core loss. However, the processing required to reduce the gauge induces an unwanted magnetic anisotropy, which has a detrimental effect on permeability, power loss and performance under an applied stress. In this paper, the beneficial effects of thin gauge non-oriented electrical steels at higher frequencies are weighed against the corresponding detrimental influences of magnetic anisotropy and tensile stress. The results are compared to properties of thicker gauge laminations, demonstrating the advantages and disadvantages associated with each gauge. The DC magnetic properties of 0.2 mm non-oriented electrical steels were measured in both the rolling and transverse directions using a permeameter, where the latter shows a reduction in the maximum relative magnetic permeability of greater than 30%. These findings agree with ac measurements of specific total loss and apparent power for a peak polarization of 1.5 T measured at 50 Hz using both SST and Epstein frame methods. The DC magnetic properties under constant uniaxial tensile stress were also examined, by applying loads of up to 200 MPa in 50 MPa increments to strips cut in either the rolling or transverse direction. The magnetic properties were measured by applying a quasi-static DC magnetic field up to 3 kA/m, generating a full hysteresis loop at each increment. A 0.4% decrease in permeability per MPa was observed for both directions.

TU.H-P28 - Effect of Nd-Fe layer on the hard magnetic properties for Nd-Fe-B thin films

T. Furuuchi¹, M. Doi^{1,2}, T. Shima^{1,2}

1. Tohoku Gakuin University, Sendai, Japan

Since the discovery of Nd₂Fe₁₄B compound, Nd-Fe-B permanent magnets have been widely used for the applications such as sensors, actuators and motors, since they possess large magnetocrystalline anisotropy ($K_{u1} = 4.5 \times 10^6$ J/m³ at room temperature) and relatively high magnetization ($M_s = 1.6$ T) among all permanent magnets. The operating temperature of the traction motors for HEVs is approximately 200 °C, so heavy rare earth such as Dy and Tb is used for Nd-Fe-B sintered magnets for HEV motors. However, due to the scarce and localized natural resources of these elements, we are facing to the drastic reduction of the usage of these elements.

The present study demonstrates the effect of the thickness for particulate Nd-Fe-B thin films and also the effect of the composition of Nd-Fe cap layers, which constitute the grain boundary phase, for the Nd-Fe-B thin films on the structure and magnetic properties.

All the samples were prepared by co-sputtering of Nd (3N), Fe₈₀B₂₀ (at%) and Fe (4N) targets using an ultra high vacuum (UHV) compatible dc magnetron sputtering system. Structural analysis was performed by X-ray diffraction (XRD) with Cu-K α radiation. The magnetic properties were measured by a superconducting quantum interference device (SQUID) magnetometer.

From magnetization curves for Nd-Fe-B thin films at various film thicknesses, the squareness of the magnetization curve was improved for the film with $t_{\text{Nd-Fe-B}} = 10$ nm, and also relatively high coercivity H_c of 18.6 kOe was obtained. Subsequently, Nd-Fe alloy films was prepared for characterize magnetic properties in detail. No large H_c was observed for all the films. With increasing Nd content x in the Nd-Fe films, a saturation magnetization decreased and became zero at $x \geq 72.9$. Detailed structure and magnetic properties for Nd-Fe-B thin films with Nd-Fe alloy layer will be discussed at the conference.

TU.H-P29 - Microstructure and magnetic properties of highly condensed anisotropic MnBi system

Y.C. Chen¹, G. Gregori², S. Sawatzki³, B. Rheingans⁴, F. Qu⁴, S. Ener³, O. Gutfleisch³, H. Kronmüller¹, Gisela Schütz¹, Eberhard Goering¹

1. *Max-Planck-Institut für Intelligente Systeme, Stuttgart, Germany*

2. *Max-Planck-Institut für Festkörperforschung, Stuttgart, Germany*

3. *Institute of Materials Science, Technische Universität Darmstadt, Darmstadt, Germany*

4. *Institute of Materials Science, Universität Stuttgart, Stuttgart, Germany*

The low-temperature phase (LTP) of MnBi a promising rare-earth-free permanent magnet material due to high uniaxial magnetocrystalline anisotropy and an unusual positive temperature coefficient of coercivity (Hc).¹ However, it is still challenging to synthesize high performance powder and highly-compacted bulk samples so far. In this study, we will present that our MnBi powder shows remarkable magnetic properties, which are close to the reported maximum energy product (BH)_{max} values (~ 17.7 MGOe).² The high-LTP-content MnBi powder could be easily mass-produced with low-energy ball milling, leading to small particle size ranging from 0.1~5 μm.

To fabricate bulk magnets, the green samples were prepared through cold-pressing under an alignment field of 18 kOe. Subsequently, the high-performance anisotropic sintered samples were achieved by either hot-compaction or spark-plasma-sintering techniques. Different processing parameters such as sintering temperatures, pressing pressure and holding times were found to have great effect on the magnetic properties of the as-prepared magnets. A systematic work has been completed to investigate the physical properties of the as-prepared powders and corresponding compacted samples by using XRD, ICP-OES, SEM, DSC, MOKE and SQUID. It was found that the distinct microstructure of the hot- and SPS-compacted magnets give rise to different temperature-dependent magnetic properties and thermal stability. The coercivity behavior of these specimens was further studied by First Order Reversal Curves (FORC) measurements as a function of temperature. Combined with the results analyzed via hardening mechanism, we will provide a clear explanation for the influence of microstructure on the magnetic properties of hard magnetic behavior in the bulk MnBi systems.

TU.H-P30 - Effect of stress on hysteresis loops of crystalline and amorphous materials

O. Perevertov¹

1. Institute Of Physics, Academy Of Sciences, Na Slovance 2, Prague, Czech Republic

We compare influence of stress on magnetic hysteresis loops of iron-based steels and amorphous ribbons. Recently we have shown that for grain-oriented and non-oriented steels under all kinds of stresses changes in hysteresis loops measured at any direction could be described by the stressed-induced effective magnetic field, which was the product of two functions, a function of magnetization and a function of the stress [1]. In addition, the function of the stress was reduced to stress difference. So, we could get with very good accuracy the hysteresis curves for any stress from any two measured hysteresis curves simply by subtracting two curves and normalizing this function of magnetization by the stress difference to get the effective field per 1 MPa. Hysteresis loops on stressed amorphous ribbons have shown that this simple effective field approach developed for steels did not work for ribbons, the calculated curves were significantly different in shape from the measured ones. For steels the magnetocrystalline anisotropy is larger by orders of magnitude than any stress-induced anisotropy, so that the magnetization will be aligned along the crystal easy axes. The stress only causes an extra energy difference between the easy crystal axis. In contrast to steels, an amorphous ribbon usually consists of many regions with local uniaxial anisotropies given by local stresses. The applied stress changes this local anisotropies distribution. So, to describe accurately hysteresis loops of stressed amorphous ribbons it is necessary to use special models, different from that for polycrystalline materials. This work was supported by the Czech Science Foundation under Project 14-36566G.

Reference:

[1] O. Perevertov, R. Schäfer, Influence of applied compressive stress on the hysteresis curves and magnetic domain structure of grain-oriented transverse Fe-3%Si steel, *J. Phys. D: Appl. Phys.* 45(13) (2012) 135001

TU.H-P31 - Valence-specific magnetization of the ferrimagnetic oxyborate single crystals using soft and hard X-ray magnetic circular dichroism under high magnetic fields

S. Ovchinnikov^{1,2}, M. Platonov¹, N Kazak¹, Y. Knyazev², L. Bezmaternykh¹, A. Rogalev³, F. Wilhelm³, E. Weschke⁴, E. Schierle⁴, Y. Zubavichus⁵

1. *L.V. Kirensky Institute of Physics, SB RAS, Krasnoyarsk, Russia*

2. *Siberian Federal University, Krasnoyarsk, Russia*

3. *ESRF, CS40220, Grenoble, Cedex 9, France*

4. *HZB/BESSY II, Berlin, Germany*

5. *NRC Kurchatov Inst, Moscow, Russia*

The transition metal oxyborates with ludwigite crystal structure (space group $P6_3mm$) have been extensively studied due to a large variety of electrical and magnetic behaviours [1]. Unfortunately local electronic and magnetic properties of transition metals in these crystals remain practically unexplored. Here we report on the XAFS/XMCD studies of $Co_3O_2BO_3$ and $Co_2FeO_2BO_3$ oxyborate single crystals performed at the K- and L_{3,2}-edges of both cobalt and iron. These compounds are ferrimagnets with uniaxial anisotropy: $Co_3O_2BO_3$ (TC = 42 K), $Co_2FeO_2BO_3$ (TN₁ = 115 K, TN₂ = 70 K) shows an extraordinary increase in coercive field [1]. The XAFS/XMCD experiments have been performed at several beamlines (ID12 at the ESRF, UE46_PGM-1 at the BESSY II, K1.3b station at the NRC KI) under high magnetic fields and low temperatures. By comparing the XMCD results with the bulk magnetizations, the valence-specific magnetizations of Co^{2+} and Fe^{3+} ions are obtained [2]. Co^{2+} and Fe^{3+} ions show negative and positive valence-specific magnetizations, respectively. The signs of the valence-specific magnetizations of Co^{2+} and Fe^{3+} remain opposite, even if the system is in a paramagnetic phase. This is evidence of the robust antiferromagnetic interaction between Co^{2+} and Fe^{3+} ions. Surprisingly the field dependence of Co^{2+} and Fe^{3+} XMCD signals does not reproduce the high coercive field, as was observed macroscopically [1]. The observed data could be tentatively explained by a model considering the magnetic moments in Co and Fe sublattices being ordered antiparallel, while on top of that the cobalt sublattice being skewed. Possible correlation between the bulk magnetizations and the valence-specific magnetizations is discussed. This study was supported by the Russian Foundation for Basic Research (project nos. 13-02-00958-a, 13-02-00358-a, 14-02-31051-mol-a), and by the Council for Grants of the President of the Russian Federation (project nos. NSh-2886.2014.2, SP-938.2015.5). The work of one of coauthors (M.S.P.) was supported by the Krasnoyarsk Regional Fund of Science and Technical Activity Support, and by the program of Foundation for Promotion of Small Enterprises in Science and Technology ("UMNIK" program).

References:

[1] N.B. Ivanova, et al., JETP 113 (6), 1015 (2011)

[2] M.S. Platonov, et al., JETP Lett. 96, 650 (2013)

TU.H-P32 - Fabrication and characterization of iron phosphate-coated Fe metal powder

H.E. Kim¹, J.H. You¹, S. Choi¹, S.W. Lee¹, S.K. Kwon², S.I. Yoo¹

1. *Seoul National University, Seoul, South Korea*

2. *Samsung Electro-Mechanics, Suwon, South Korea*

Iron (Fe) metal powder with high saturation magnetization and low coercivity has been used as the core materials of inductors and transformers for high frequency applications. However, it is unavoidable to generate eddy current under AC field and critical at high frequencies. To minimize an eddy current loss, Fe metal powder has been coated with an insulating material.

For the same purpose, we tried to fabricate a core-shell structure composed of Fe core and iron phosphate shell. The iron phosphate coating was performed by the phosphating method with acetone solvent. The conditions of the iron phosphate coating, such as phosphate concentration and reaction time, were controlled in order to obtain a thin and uniform coating layer. Furthermore, to avoid the agglomeration of Fe metal powder, the solutions were stirred using a mechanical stirrer and/or an ultrasound treatment. The magnetic properties of Fe metal powder coated with iron phosphate were sensitive to these processing conditions. The 1mol% iron phosphate-coated Fe metal powder was observed the effectively reduced core loss values. However, the 1mol% iron phosphate-coated Fe metal powder with ultrasound treatment exhibited the decreased permeability and Q factor values while the coated powder with mechanical stirrer were observed no reduction of permeability and Q factor values. Details will be presented for a discussion.

TU.H-P33 - Study on hysteresis properties and domain behaviours in high purity Fe-(4-6)wt% Si alloys

Z. Lei¹, T. Horiuchi¹, I. Sasaki¹, C. Kaido², M. Takezawa¹, Y. Horibe¹, T. Ogawa³, H. Era¹

1. *Kyushu Institute Of Technology, Kitakyushu, Fukuoka, Japan*

2. *Kitakyushu National College of Technology, Kokuraminamiku, Kitakyushu, Fukuoka, Japan*

3. *Fukuoka Industrial Technology Center, Fukuoka, Japan*

High purity metallurgy has been desired for producing iron-silicon alloy in order to reduce hysteresis loss, which is drastically affected by inner impurities and crystallographic orientations. Currently, the impurities in iron silicon is minimized by a metallurgy method called Cold Crucible Levitation Melting (CCLM) which can separate melted alloy from crucible by magnetic induction. Combining the previous method as well as raw iron and silicon with a purity of 99.99wt% and 99.999wt%, high purity Fe-(4, 5 and 6)wt%Si specimens were achieved. Additionally, a new specimen called 3N Fe-4wt%Si was made by mixing Fe-4wt%Si with 0.1wt% carbon by CCLM. The permeability, coercivity and hysteresis loss of these four alloys were measured by automatic DC magnetization device. Furthermore, static domain structure and dynamic displacement-rotation behaviour under different applied fields, and effect of grain boundaries and precipitates on domain are studied by Lorentz TEM.

Permeability results shows that maximum permeability of 3N Fe-4wt%Si, Fe-(4, 5 and 6)wt%Si are 0.004, 0.010, 0.008 and 0.029 H/m, respectively. The average diameter of near-spheroidal grains in all specimens are similar with value of approximately 5 μm, which should not be considered as an influencing factor. Therefore, it can be seen that addition of carbon can decrease whereas increase of silicon can improve permeability. The relationships of flux density and hysteresis loss in Fe-(4, 5 and 6)wt%Si are all linear while in 3N Fe-4wt%Si it is nonlinear when flux density is below 1.2 T, which implies the pinning effect of impurities on domain displacement or rotation below certain applied field. The static domain structure results shows that domain patterns such as slab-like pattern with near-equivalent width and lancets pattern are observed, and complexity of domain patterns has close relationship with crystallographic orientations of grains and precipitates in the specimens.

TU.H-P34 - Comparison of the magnetic properties of submicron-sized strontium hexaferrite powders prepared with a top-down or a bottom-up approach

M. Topole¹, P. Jenuš¹, C. Granados², P. McGuinness¹, M. Christensen², K. Žužek Rožman¹, S. Kobe¹

1. Department for nanostructured materials, Jozef Stefan Institute, Ljubljana, Slovenia

2. Center for Materials Crystallography, Department of Chemistry and iNANO, Aarhus University, Denmark

In a search for the best strontium hexaferrite material with a particle size in the sub-micron range, suitable for use in a variety of magnetic applications, two possible methods of production were studied. 1) A top-down approach using high-energy planetary ball milling was introduced to reduce the particle size of a commercially available, strontium hexaferrite powder. 2) A hydrothermal synthesis was used for the bottom-up approach. For method 1) wet milling with ethanol as the milling medium was employed. The milling times were 4, 8 and 12 h. All of the powders were then dried in air at 60 °C for 12h and, in order to release the strain induced by the milling, annealed in air at 1100 °C for 1 hour. Scanning electron microscopy showed that submicron-sized particles were obtained. The best sample proved to be the one milled for 8 hours, where the BHmax was increased by 2%, compared to the original material. For the hydrothermal synthesis [1] 2), three different final temperatures were used (220, 230 and 240 °C) to obtain a pure phase of strontium hexaferrite with a submicron particle size. The materials synthesized with the hydrothermal method were also annealed at 1000 °C for 1 h for a fairer comparison with the milled powders. The hydrothermally synthesized sample with the purest hexaferrite phase composition was the one synthesized at 230 °C. When annealed at 1000 °C for 1 hour, its coercivity and remanence increased by more than a factor of two. The BHmax was increased from 1.90 to 9.23 kJ/m³.

Acknowledgement: CEM for the use of the equipment.

This research was supported by EU-FP7 NANOPYME Project (No. 310516). [2]

[1] Primc D., Drogenik M., Makovec D. Low-Temperature Hydrothermal Synthesis of Ultrafine Strontium Hexaferrite Nanoparticles. *European Journal of Inorganic Chemistry* 2011, 2011(25): 3802-3809

[2] NANOPYME Project: <http://www.nanopyme-project.eu/>

TU.H-P35 - Frozen orbital moment at rare earth M4,5 absorption edges in Nd based rare earth permanent magnets

S. Tripathi¹, Y. Chun Chen¹, T. Tietze¹, S. Schuppler², P. Nagel², M. Merz², G. Schütz¹, E. Goering¹

1. *Max Planck Institute For Intelligent Systems, Germany*

2. *Institute for Solid-State Physics, Karlsruhe Institute of technology, Eggenstei Leopoldshafen, Karlsruhe, Baden-Württemberg, Germany*

Rare earth permanent magnets (REPM) provide the highest energy product (50MGOe) at room temperature, however recently dramatic increase in prices for RE metals has occurred. We performed element specific XMCD investigation, in order to quantitatively determine the sub lattice magnetization of every single element, their interplay, influence on the magnetic properties and to check the applicability of the XMCD sum rules for M4,5 edge in the soft X-ray regime. We investigated highly textured Fe₁₅Nd₂B thin films (3400 Å) in comparison with reference soft magnetic multilayers of Fe (3.6 Å)/Nd (3.6 Å) (60 bilayer) at 6.5T. The most remarkable observation is the nearly vanishing orbital moment at the Nd site in the textured Fe₁₅Nd₂B thin film, while the multilayer system orbital moment ($m_l=2.71 \mu_B/\text{atom}$) is quite close to the expected Hund's rule value. As XMCD only probes rotatable magnetic moments, our results suggest strong pinning of RE orbital moments, even under magnetization reversal conditions. Thus sum rules allows to calculate accurately the spin magnetic moment values even for M4,5 edges. One can estimate the spin moment accurately using the correction given in [1]. This correction is mandatory for the proper estimation of the spin magnetic moment. Furthermore, from our experimental results it can be concluded that XMCD is a good tool to characterize the 4f spin magnetic moment values of rare earth compounds

References:

[1] Takeo Jo, J. Electron. Spectrosc. Relat. Phenom. 86 ,(1997),73-82

TU.H-P36 - From exchange-biased core@shell nanoparticles to hard magnetic nanostructured ceramics

T. Gaudisson^{1,2}, G. Franchesin¹, N. Flores-Martinez³, R. Valenzuela³, N. Yaacoub⁴, J. Grenèche⁴, F. Mazaleyrat², S. Ammar¹

1. ITODYS, Université Paris-Diderot, Sorbonne Paris Cité, Paris, France

2. SATIE, ENS CACHAN, Paris Saclay, Cachan, France

3. IIM, Universidad Nacional Autónoma de México, Mexico D.F., Mexico

4. IMMM, Université du Maine, LUNAM, Le Mans, France

Permanent magnets constitute an essential part of our modern societies, for motors and generators as well as for other electronic devices. The ever-growing technological demand has driven, since their discovery, the difficult task of improving the properties of these materials. Since 1960's, they are mainly based on rare earth (RE) alloys. Today, a focus is made on developing free RE magnets by improving the intrinsic anisotropy of RE free ferro- or ferrimagnetic high TC compounds by including other anisotropy sources such through shape anisotropy or intergrain exchange-coupling. Other original issues are explored consisting on the production of new ferromagnets such as cobalt carbide [1] and manganese alloys [2]. In this context, we propose to prepare exchange biased oxide-based core@shell nanoparticles and to consolidate them using Spark Plasma Sintering in order to design a new generation of magnets. The polyol process is a soft chemistry route. It is particularly efficient for seed mediated growth of nanocrystals in solutions [3]. It permitted us to prepare cobalt ferrite and cobalt monoxide composite nanostructured powders with the desired morphology and the required magnetic properties. These powders were sintered at 500°C under an uniaxial pressure of 100 MPa for 10 minutes. Interestingly, the resulting ceramics exhibit at low temperature enhanced coercivity and remanence, when they are cooled under a high magnetic field (>1T) below the CoO Néel temperature (298K). The deduced magnetic energy product (BH)_{max} from the hysteresis loops, recorded in these conditions, is found to be equivalent to that of bulk hexaferrites but one order smaller than that of state-of-art NdFeB alloys.

[1] V.G. Harris et al., J. Phys. D: Appl. Phys. 43 (2010) 165003

[2] A. Pasko et al., J. Phys.: Condens. Matter 26 (2014) 064203

[3] T. Gaudisson et al., J. Nanopart. Res. 16 (2014) 2359

TU.H-P37 - Evidence of dipolar magnetic interaction in melted Fe₅₀Al₅₀ samples

G. A. Perez Alcazar¹, H. Bustos², J. S. Trujillo¹, D. Oyola², Y. A. Rojas²

1. *Departamento De Fisica, Universidad Del Valle, Cali, Colombia*

2. *Departamento de Fisica, Universidad del Tolima, Cali Colombia*

Powders of the Fe₅₀Al₅₀ melted and heat treated samples were separated at different mean particle sizes as well as characterized based on their structural and magnetic properties. All the samples showed Fe-Al BCC and α -Fe phases as well as the same nanostructure. The powder with biggest particles, with particle size bigger than 105 μ m, presents the additional minority presence of FeO and Al₂O phases. The powders were found to be ferromagnetic at room temperature with a mean hyperfine magnetic field that increases with increasing particle size. The origin of this magnetic behaviour is attributed to the increment of magnetic dipolar interactions between the magnetic moment of each particle and the field produced by other magnetic moments of their surrounded particles. This field also increases as the particle size increases. Besides the dipolar magnetic interaction between particles, the Fe-Al and α -Fe grains present a ferromagnetic coupling between them.

TU.H-P38 - Fe-Pt / Fe-Co Nanocomposite films fabricated by electrochemical method

Y. Hayashi¹, S. Hashi¹, H. Kura², T. Yanai³, T. Ogawa², K. Ishiyama¹, M. Nakano³, H. Fukunaga³

1. *Research Institute of Electrical Communication, Tohoku University, Miyagi, Japan*

2. *Department of Electronic Engineering, Graduate School of Engineering, Tohoku University, Japan*

3. *Department of Electronic and Electrical Engineering, Graduate School of Engineering, Nagasaki University, Nagasaki, Japan*

Nanocomposite magnets have attracted considerable attention due to their high magnetic properties [1]. Control of their structure at nanoscale is important for achieving efficient exchange coupling among the hard and soft magnetic phases. There is one possibility to realize ordered nanostructure of the hard and soft magnetic phases by depositing other magnetic materials into vacant spaces between assembled magnetic nanoparticles (NPs). To achieve this aim, we have studied on electrochemical fabrication of nanocomposites containing magnetic NPs [2]. In this study, we fabricated nanocomposite films consisting of Fe-Co NPs in a L10 Fe-Pt matrix. The films were fabricated by a combination of electrophoretic deposition of Fe-Co NPs and electroplating of Fe-Pt. Then, the films were annealed to obtain L10 Fe-Pt. We investigated the magnetic properties and structure of the films. The M-H curves of the fabricated films showed magnetic single behavior. The coercivity of the films decreased from 10 to 6.5 kOe with an increase in the volume fraction of Fe-Co NPs (0 to 10 vol.%), while the magnetization increased from 660 to 760 emu/cc. In δM -H measurements, δM was initially positive due to the existence of exchange coupling, but it became negative after the reversal. This negative value indicates that magnetic interactions become dominant due to the presence of Fe-Co phase. This δM -H behavior is similar to behaviors in previous reports on nanocomposites applying magnetic nanoparticles [3]. Therefore, the nanocomposite films working exchange coupling between Fe-Co and L10 Fe-Pt phases were realized by this combination method.

Reference:

[1] E. F. Kneller, R. Hawig, IEEE Trans. Magn., 27, (1991) 3588

[2] Y. Hayashi, S. Hashi, K. Ishiyama, IEEE Trans. Magn., 48, (2012) 3170

[3] Y. Hou, S. Sun, C. Rong, J. P. Liu, Appl. Phys. Lett., 91 (2007) 153117

TU.H-P39 - Discontinuities of plastic deformation in amorphous alloys with different glass forming ability

M. Huráková¹, K. Csach¹, J. Miskuf¹, A. Juríková¹, S. Demcak², V. Ocelík³, J.Th.M. De Hosson³

1. *Institute Of Experimental Physics, Slovak Academy Of Sciences, Kosice, Slovakia*

2. *Department of Environmental Engineering, Faculty of Civil Engineering, Technical University of Kosice, Kosice, Slovakia*

3. *Department of Applied Physics, Faculty of Mathematics and Natural Sciences, University of Groningen, Groningen, The Netherlands*

Metallic glasses exhibit unique properties, including the high strength and the excellent soft magnetic properties (low coercive force and high permeability), which makes them attractive for practical applications. Recently, the Fe and Co rich composition with high glass forming ability was found out. Such metallic glasses exhibit the combination of the high strength and soft magnetic properties. For practical use knowledges about their mechanical properties are important. The strength is generally related to the microhardness. Due to the homogeneity of glassy structure, the micromechanism of the deformation in a small volume is similar as on the macroscopic level. To study the serrated plastic flow in different metallic glasses, nanoindentation experiments were performed for amorphous ribbons with different microhardness and glass forming ability. The metallic ribbons $\text{Fe}_{40}\text{Ni}_{40}\text{B}_{20}$, $\text{Cu}_{47}\text{Ti}_{35}\text{Zr}_{11}\text{Ni}_6\text{Si}_1$ and $\text{Zr}_{65}\text{Cu}_{17.5}\text{Ni}_{10}\text{Al}_{7.5}$ were studied at different loading rates from 0.05 to 100 mN.s⁻¹. We describe in details the differences in elemental discontinuities on the loading curves for the studied alloys. We found that the discontinuities began at the certain deformation independently on the ribbon properties. More developed discontinuities at higher deformations are created for the materials with lower microhardness and so lower strength.

This work was supported by the projects Nos. 26220120021 and 26110230097 provided in the frame of Structural funds of the European Union.

TU.H-P40 - Magnetic SANS study of a sintered Nd-Fe-B magnet: estimation of defect size

E. A. Périgo¹, E. Paul Gilbert², A. Michels¹

1. *University of Luxembourg, Luxembourg*

2. *Bragg Institute, ANSTO, Lucas Heights, Australia*

The magnetic microstructure of an isotropic sintered Nd-Fe-B permanent magnet has been studied at room temperature by means of unpolarized magnetic-field-dependent small-angle neutron scattering (SANS). Although the microstructure of the material consists of micron-sized Nd₂Fe₁₄B crystallites that are separated by a (low volume fraction) nanometer-sized Nd-rich phase, the SANS signal contains a significant contribution due to spin misalignment, which is evidenced by an enhanced scattering signal along the applied-field direction. The origin of this spin misalignment is presumably related to the perturbing effect of the Nd-rich interphases. Analysis of the SANS data in terms of the autocorrelation function of the spin misalignment provides an almost field-independent length scale $l_C \sim 40$ nm, which, for soft magnetic materials, is usually taken as a measure for the size of inhomogeneously magnetized regions around lattice imperfections. Comparison of our results with a phenomenological expression for l_C based on micromagnetic theory suggests that the large anisotropy field of the Nd₂Fe₁₄B phase (which is of the order of 8 T) reduces the size of gradients in the spin microstructure, so that, for hard magnetic materials, l_C represents the (field-independent) size of the characteristic defect in the microstructure.

TU.H-P41 - Steinmetz law in AC magnetic fields for iron-phenolformaldehyde resin soft magnetic composites

D. Olekšáková¹, V. Vojtek², P. Kollár², J. Füzér², R. Bureš³, M. Fáberová³

1. *Technical University In Košice, Košice, Slovakia*

2. *Institute of Physics, Faculty of Science, P.J. Šafárik University, Košice, Slovakia*

3. *Institute of Materials Research, Slovak Academy of Sciences, Košice, Slovakia*

The validity of Steinmetz law, describing the energy losses as a function of maximum flux density 0.1 T to 1.3 T has been verified in frequency range 100 Hz to 1.2 kHz for iron based soft magnetic composites (SMCs) with the effort to find a physical meaning of the coefficients in Steinmetz law. The Bertotti's statistical model was used for modification of Steinmetz law for DC magnetic field in which hysteresis energy loss $W_h = K_h \cdot (B_{max})^x$, (where B_{max} is the maximum flux density, K_h and x are constants) to the model for total energy losses, which appear when AC magnetic field is applied on soft magnetic composites. In this case for the total energy losses W_t is the dynamic energy loss W_d added to hysteresis loss $W_t = W_h + W_d$. For such a case we used for dynamic loss $W_d = K_v \cdot (B_{max})^y \cdot f$, where K_v and y are constants. The validity of this model was experimentally proven for investigated Fe-based SMCs at maximum flux density 0.3 T to 1.2 T. Finally, new "linear-elliptical model" based on "linear" model, for explanation of the hysteresis loss, described in [1], was created for explanation of total loss maximum flux density dependence in Fe-based SMCs and proved in frequency range 400 Hz to 1.2 kHz.

This work was supported by the Scientific Grant Agency of the Ministry of Education of Slovak Republic and the Slovak Academy of Science VEGA 1/0862/12 and KEGA 072TUKE-4/2014.

TU.H-P42 - Study of Dy diffusion in high-coercivity NdFeB magnets for electric-vehicle drive applications

K. Zagar¹, A. Kocjan¹, A. Kovács², M. Duchamp², R.E. Dunin-Borkowski², J. Mayer^{2,3}, P. McGuinness¹, S. Kobe¹

1. Jozef Stefan Institute, Ljubljana, Slovenia

2. Ernst Ruska-Centre for Microscopy and Spectroscopy with Electrons and Peter Grünberg Institute, Forschungszentrum Jülich, Jülich, Germany

3. RWTH Aachen, Aachen, Germany

In the present study, we report on the correlation between the magnetic properties and the distribution of the DyF₃ in the melt-spun Nd₂Fe₁₄B ribbons coated with the DyF₃ suspension, spark-plasma sintered (SPS) and annealed. The magnetic properties were measured at room temperature using a Steingroever permeameter. The addition of the DyF₃ up to 2.2 wt.% showed a positive and increasingly rapid effect on the coercivity (H_{ci}) of the heat-treated samples. The maximum H_{ci} of 1663 kA/m represents a 25% increase compared to the untreated sample. To observe the diffusion of DyF₃ as a function of heat-treatment process and correlate it with the magnetic properties, samples were investigated using aberration-corrected scanning transmission electron microscopy (FEI Titan 80-200). The analyses were carried out in the so-called wheel side regions of the SPS and the annealed samples. The energy dispersive X-ray spectroscopy (EDXS) maps of annealed samples revealed a Dy,Nd-Fe-B-rich shell structure around Nd-Fe-B core, while the SPS sample did not contain any Dy,Nd-rich shells around the Nd-Fe-B grains. Since the reliability of the EDXS analysis is compromised by overlapping of the Fe-K, Dy-L and Co-K lines, the electron energy loss (EEL) spectra of the same grains were recorded in order to separate the contribution of these elements and to provide reliable compositional maps. To unwrap the spectra the vertex component algorithm was applied and thus we determined Fe-L_{2,3}/Co L_{2,3}, Nd-M_{4,5}, Dy-M_{4,5}, F-K and O-K maps. In the case of annealed sample we observed the Dy,Nd-Fe-B phase formation in the shell around the pure Nd-Fe-B (core) grains. We can conclude that the 25% increase in H_{ci} is strongly linked to the heat-treatment process where Dy diffuses along grain boundaries into the outer parts of Nd-Fe-B grains and partially substitutes Nd to form a core-shell-like grains.

TU.H-P43 - Optimizing the magnetic properties of bulk Mn-Ga by severe plastic deformation and magnetic field annealing

S. Ener¹, K.P. Skokov¹, D. Yu. Karpenkov¹, M.D. Kuz'min¹, O. Gutfleisch^{1,2}

1. TU Darmstadt, Materialwissenschaft, Alarich-Weiß, Darmstadt, Germany

2.IWKS Hanau, Fraunhofer-Projektgruppe für Wertstoffkreisläufe und Ressourcenstrategie, Hanau, Germany

Mn₃-δGa thin films are regarded as a candidate for spin-torque transfer applications [1]. The distinguished perpendicular anisotropy of Mn₃Ga thin films results from the high positive effective anisotropy constant, $K_{eff} = 1.2 \text{ MJ/m}^3$ [2] and in this work we focused on how effectively one can convert the observed high anisotropy constant to coercivity for bulk samples. We demonstrate here an alternative production routine to the conventional sample preparation (arc melting and annealing) for the stabilization of Mn₇₀Ga₃₀ system in metastable D022 phase. We apply cold-rolling and annealing - with and without applied magnetic field - and study systematically the magnetic properties of Mn₇₀Ga₃₀. The best Mn₇₀Ga₃₀ material has been produced by arc melting followed by rolling and magnetic field-assisted annealing (24 h at 730 K in 1 T). The described procedure maximizes the content of the tetragonal D022 phase (known to be ferrimagnetic), raising the remanence to 0.239 T at room temperature. At the same time, the coercivity is as high as 1.24 T [3]. The MOKE and field dependent magnetic measurements indicates that the demagnetization mechanism most likely is the reversal of the magnetization by nucleation of reversed domains.

[1] B. Balke et al., Appl. Phys. Lett., 90 (2007), 152504

[2] F. Wu et al., Appl. Phys. Lett., 96 (2010), 042505

[3] S. Ener et al., Journal of Magnetism and Magnetic Materials, 382 (2015) 265-270

TU.H-P44 - Effect of WS₂/Al co-doping on the microstructural and magnetic properties of Nd-Fe-B sintered magnet

K.H. Bae¹, T.H. Kim¹, S.R. Lee¹, H.J. Kim², M.W. Lee³, T.S. Jang³

1. Dept. of Materials Science and Engineering, Korea University, Seoul, Republic of Korea

2. R&D Center of Jahwa Electronics Co. Ltd., Seoul, Republic of Korea

3. Dept. of Advanced Materials Engineering, Sunmoon University, Asan-s, Republic of Korea

One of possible ways to increase the coercivity of Nd-Fe-B magnets without addition of Dy is to refine the grain size as well as the improving the uniformity and crystallinity of Nd-rich grain boundary (GB) phase. The addition of refractory element (RFE) such as Mo, W, or Nb could suppress the grain growth during sintering or post-sintering annealing process. Especially, the RFE-sulfide powder addition is effective for Dy-saving because the formation of Dy segregated rare-earth rich (RE-rich, Nd-Dy-O) phase could be suppressed. The precipitates should be selectively formed only at the GB for efficient grain growth pinning. In this study, we investigated the effects of WS₂ (0~1.2 wt.%) addition together with Al (0.3 wt.%) on the microstructural and the magnetic properties of the magnet. Especially, the relationship between WS₂/Al co-doping condition and the magnetic properties are studied. The magnets (29.0Nd-3.0Dy-bal.Fe-1.0B-2.5M (wt.)) were sintered at 1070°C, and then the magnets were optimally annealed. The coercivity of the 0.6 wt.% WS₂/Al co-doped magnet increased the most (20.67 → 22.4 kOe) as compared to that of the solely WS₂-doped magnets. The average grain size of the 0.6 wt.% WS₂/Al co-doped magnet was the smallest (6.4 μm) as compared to those of the un-doped (7.6 μm) and 0.6 wt.% WS₂-doped (6.9 μm) magnet. The W-precipitates are selectively formed at the GB in the 0.6 wt.% WS₂/Al co-doped magnet because the fluidity of liquid Nd-rich phase increases by the Al addition. In addition, the formation of RE-rich phase was suppressed in the WS₂/Al co-doped magnet because of the reaction between the WS₂ and the RE-rich phase. However, the grain size was not decreased further with increasing the WS₂ content over 0.6 wt.%. The over-doped magnet deteriorated the magnetic properties because the precipitates are formed at the interior of the grains as well as at the GBs. Conclusively, coercivity enhancement of 8.3% could be obtained by addition of WS₂ (0.6 wt.%) together with Al (0.3 wt.%) resulting in the 0.8 wt.% Dy-saving.

TU.H-P45 - DC reversible and irreversible magnetization processes in Fe-based composite materials

P. Kollár¹, Z. Birèáková¹, J. Fúzer¹, M. Fáberová², R. Bureš²

1. Institute of Physics, Faculty of Science, Pavol Jozef Šafárik University, Košice, Slovakia

2. Institute of Materials Research, Slovak Academy of Sciences, Košice, Slovakia

Soft magnetic composites (SMCs) are a remarkable kind of soft magnetic materials consisting of small ferromagnetic particles insulated from each other. They exhibit very good electromagnetic properties as low classical losses and relatively low total energy losses (due to an insulating layer between iron powder particles) at medium and higher frequencies. On the other hand the increase of non-ferromagnetic content of the composite material increases the value of inner demagnetizing field leading to the decrease of the permeability.

The proportion of reversible and irreversible magnetization processes in iron-phenolphormaldehyde resin composite samples with different in magnetic particle size and resin content was studied. The investigation were focused on the magnetic permeability and DC and AC energy losses. The increase of the fraction of reversible magnetization processes (determined by means of the permeability measurements) at the expense of the irreversible magnetization processes, with the increasing resin content and with the reducing magnetic particle size, is explained by higher demagnetizing fields produced by magnetic particle surfaces resulting in lower number of movable domain walls. The magnetization process is then the more realized by magnetization vector rotation.

The similar fact was obtained also from the energy losses investigation - the excess losses were found to be higher for samples with higher resin content and lower particle size, explained by lower numbers of movable domain walls due to higher demagnetizing fields (meaning less irreversible processes) as well. The empirical relations between irreversible relative permeability and DC energy losses were found based on the Steinmetz law, the linear functions approximation and the Rayleigh law, enabling to predict the irreversible permeability in a wide range of magnetic induction values.

TU.H-P46 - Different metastable states of Hf₂Co₁₁B alloy as precursors for rare-earth free permanent magnetsA. Musiał^{1,2}, Z. Iniański¹, J. Marcin³, J. Kováčik³, I. Skorvanek³, B. Idzikowski¹

1. Institute of Molecular Physics, Polish Academy of Sciences, M. Smoluchowskiego, Poznan, Poland

2. NanoBioMedical Centre, Adam Mickiewicz University, Umultowska, Poznan, Poland

3. Institute of Experimental Physics, Slovak Academy of Sciences, Watsonova, Košice, Slovakia

New materials for the permanent magnets, especially the rare-earth free alloys, are of high importance for scientific community. Main focus is put on compounds, which exhibit a combination of high remanent magnetization, intrinsic coercive field and large energy product. High Curie temperature is also crucial factor which can be decisive in practical use.

The attention of this work has been focused on Hf₂Co₁₁B alloys. Amorphous and partially crystalline ribbons were produced using melt-spinning technique. Calorimetric measurements show three crystallization steps with the maxima temperatures at 594°C, 614°C and 654°C in amorphous sample. First two stages are connected with the crystallization of Hf₂Co₁₁ rhombohedral and orthorhombic phases. Thereafter HfCo₃B₂ phase appears. The X-ray diffraction patterns of partially crystalline sample in as-quenched state consist of peaks from Hf₂Co₁₁ phase in both mentioned forms with possible evidence of small amounts of HfCo₂ and fcc-Co. The occurrence of two Hf₂Co₁₁ phases is confirmed by temperature dependence of magnetization measurements. Two inflections corresponding to Curie temperatures of the orthorhombic and hard magnetic rhombohedral structures ($T_{Crhomb} = 488^\circ\text{C}$, $T_{Cortho} = 554^\circ\text{C}$) are visible on the M(T) curve.

The ribbon annealed from partially crystalline state is characterized by higher coercive field and magnetic anisotropy as compared to the sample annealed from initial amorphous state. We connect it with the existence of quenched-in nanocrystals of hard magnetic phase. Annealing at optimal conditions ($T_a = 570^\circ\text{C}$, $\tau_a = 60$ min) allowed to improve coercive field from 1.2 kOe to about 3 kOe and energy product from $|BH|_{max} = 5.3$ kJ/m³ to 21.2 kJ/m³ in partially crystalline alloy. These results are in good agreement with those reported in Ref. 1.

[1] B. Balamurugan et al., IEEE Trans. Magn. 49 (2013) 3330

Work was supported by the NCRD within the project no. POKL.04.03.00-00-015/12 and by Slovak APVV 0492-11

TU.H-P47 - A study on the anisotropic diffusion of Dy in the grain boundary diffusion processed Nd-Fe-B sintered magnet

T.H. Kim¹, K.H. Bae¹, S.R. Lee¹, S. Jin Yun¹, S. Ho Lim¹, H.J. Kim², M.W. Lee³, T.S. Jang³

1. Dept. of Materials Science and Engineering, Korea University, Seoul, Republic of Korea

2. R&D Center of Jahwa Electronics Co. Ltd., Cheongwon, Republic of Korea

3. Dept. of Advanced Materials Engineering, Sunmoon University, Asan, Republic of Korea

Developing a core-shell microstructure of Dy, which can be obtained by the grain boundary diffusion process (GBDP) using Dy-X (X = H or F) dip-coating or Dy vapor sorption method, is a promising way to enhance the H_c of the Nd-Fe-B sintered magnet without Br reduction. Dy-rich shells are preferentially formed depend on the crystal orientation of Nd₂Fe₁₄B phase at the Nd-rich grain boundary phase (GBP) interfaces. Anisotropic diffusion of Dy depends on the orientation of the magnet itself was also observed. We investigated the anisotropic diffusion mechanism of Dy in the DyH₂ dip-coated magnet in terms of crystallographic relationship between the GBP and the Nd₂Fe₁₄B phase. A method for further improving the H_c was suggested considering the anisotropic diffusion of Dy in the GBDP magnet. It was observed that the Dy-rich shells are formed only on particular side of the Nd₂Fe₁₄B phase at the Nd-rich GBP interface. Notably, we observed that the Dy-rich shell is formed when the c-axis of the Nd₂Fe₁₄B phase and the GBP are in parallel. In contrast, the Dy-rich shell is hard to form when the c-axis of the Nd₂Fe₁₄B phase is perpendicular to the GBP. According to the simulation results, the energy barrier for the migration of Dy along the c-axis of the Nd₂Fe₁₄B is 3.46 times larger than that along the a-axis of the Nd₂Fe₁₄B. In the point of the magnet orientation, the H_c of the GBDP magnet was enhanced (22.7 μ23.8 kOe) when the surface area perpendicular to the c-axis of the magnet (AC^a-) was increased (70 μ140 mm²). This result is contrary to the result of anisotropic diffusion of Dy in the Nd₂Fe₁₄B crystallographic orientation viewpoint. The detailed mechanism of anisotropic diffusion of Dy during the GBDP will be discussed in the point of the crystallographic orientation of the Nd₂Fe₁₄B phase and the change in the AC^a- before dip-coating process.

TU.H-P48 - Microwave properties of MnCuZn substituted BaFe₁₂O₁₉ in 0-26.5 GHz range

Z. Mehmedi^{1,2}, H. Sözeri¹, H. Kavas³, U. Topal¹, A. Baykal⁴, B. Aktas⁵

1. TUBITAK-UME, National Metrology Institute, Gebze-Kocaeli, Turkey

2. Fatih University, Bio-Nano Technology Engineering, Turkey

3. Istanbul Medeniyet University, Goztepe, Istanbul, Turkey

4. Department of Chemistry, Fatih University, B.Cekmece, Istanbul, Turkey

5. Gebze Technical University, Gebze-Kocaeli, Turkey

Barium hexaferrite particles were synthesized by replacing three cations having two valencies with two Fe³⁺ ions in the form of BaFe_{11.5-x}(Mn_{0.25}Cu_{0.25}Zn_{0.5})_xO₁₉, x=1, 2 and 3. Solid state reaction route was followed during the synthesis process. 1% boron was added to precursor before sintering as a catalyst to inhibit crystal growth and magnetic properties of the particles. Structural properties were investigated using X-ray diffractometer and scanning electron microscope. Magnetic properties were measured by vibrating sample magnetometer. A vector network analyzer was used in reflection/transmission mode to determine scattering parameters (S₁₁ and S₂₁) of samples placed in an airline in 0-18 GHz range and in between waveguides in 18-26.5 GHz. Magnetization and coercivity of samples decrease as MnCuZn content increases which can be explained by site preferences of substituted cations and their low magnetic moments compared to Fe³⁺ ions. The microwave energy was absorbed at two different frequencies in BaFe_{9.5}(Mn_{0.25}Cu_{0.25}Zn_{0.5})₂O₁₉ at 10.5 and 22.5 GHz with reflection losses of -23 dB and -15 dB, respectively. The mechanisms of the RLs are due to matching thickness at 10.5 GHz and magnetic/dielectric losses at 22.5 GHz.

TU.H-P49 - Investigation of microwave properties of Cu²⁺ substituted NiZn-ferrite with sample thickness in 0-26.5 GHz range

F.Genç^{1,2}, H. Sözeri¹, H. Kavas³, U. Topal¹, A. Baykal⁴, B. Aktaş⁵

1. TUBITAK-UME, National Metrology Institute, Gebze-Kocaeli, Turkey

2. Department of Physics, Gebze Technical University, Gebze-Kocaeli, Turkey

3. Department of Physics, Istanbul Medeniyet University, Goztepe, Istanbul, Turkey

4. Department of Chemistry, Fatih University, B.Cekmece, Istanbul, Turkey

Cu²⁺ substituted NiZn-ferrite powders were synthesized by solid state reaction route. 1 wt.% B₂O₃ was added to the precursor before sintering at 1100°C for 2 hours. Phase formation and morphology of the powders were investigated X-ray diffraction and scanning electron microscopy. Magnetic and microwave properties of samples were determined by vibrating sample magnetometer and vector network analyzer, respectively. Magnetization of the sample increases as nickel concentration increases up to x=0.45 in Ni_xZn_{0.8-x}Cu_{0.2}Fe₂O₄ with Ms value of 70 emu/g, and then, starts to decrease to 50 emu/g. Microwave measurements revealed that Ni_{0.3}Zn_{0.5}Cu_{0.2}Fe₂O₄ sample with 3mm thickness has better absorption properties. It has two reflection losses at frequencies of 12 and 18.5 GHz with -22.5 and -15 dB in magnitude. It was observed that as sample thickness increases absorption of microwaves occurs at low frequencies.

TU.H-P50 - Dielectric properties of $\text{AgY}_{1-x}\text{Gd}_x(\text{WO}_4)_2$ solid solutions

B. Sawicki¹, E. Tomaszewicz², M. Piątkowska², T. Groń¹, P. Urbanowicz¹, H. Duda¹, Z. Kukuła¹

1. Institute of Physics, University of Silesia, Katowice, Poland

2. Department of Inorganic and Analytical Chemistry, West Pomeranian University of Technology, Szczecin, Poland

Double molybdates and tungstates $\text{RE}(\text{MO}_4)_2$ (A = monovalent metal, e.g. an alkali metal or Ag, and Tl, RE – trivalent rare-earth metal, and M = Mo or W) are good laser hosts, and have potential applications in quantum electronics, visual display, and solid-state lighting. Low-temperature polymorphs of $\text{AgY}_{1-x}\text{Gd}_x(\text{WO}_4)_2$ solid solutions crystallize in monoclinic symmetry belonging to the $C2/m$ space group. The electrical resistivity and thermoelectric power measurements showed the insulating properties and n -type conduction [1]. The I - V characteristics showed a large emission of electrons for $(\text{Co,Mn})\text{Pr}_2\text{W}_2\text{O}_{10}$ and $\text{Cd}_{1-3x}\text{Gd}_{2x}\text{MoO}_4$ [2].

The main purpose of this study was to investigate the dielectric spectroscopy of $\text{AgY}_{1-x}\text{Gd}_x(\text{WO}_4)_2$ solid solutions for $x = 0.025$ and 1.0 . These studies showed low relative dielectric permittivity: $\epsilon_r \sim 4.4$ for $x = 1.0$ and $\epsilon_r \sim 6.1$ for $x = 0.025$, that substantially does not depend on temperature and frequency, due to the existence of deep trapping centers associated with high energy form of silver vacancies [3].

This work was supported by Ministry of Scientific Research and Information Technology (Poland) and funded from science resources: No. 1S-0300-500-1-05-06 and No. DS-518-10-020-3101.

- [1] B. Sawicki, E. Tomaszewicz, T. Groń, H. Duda, Z. Kukuła, J. Goraus, 43rd "Jaszowiec" International School & Conference on the Physics of Semiconductors, June 7– 12, 2014, Wisła Poland, TuP3, p.211
- [2] T. Groń, B. Sawicki, E. Tomaszewicz, H. Duda, EMN Meeting on Ceramics Energy, Materials, Nanotechnology, January 26-29, 2015 Orlando FL USA. Program & Abstract Book, Invited Speaker, p.76-78
- [3] R.O. Simmons, R.W. Balluffi, Phys. Rev. 119 (1960) 600

TU.H-P51 - Dynamics of magnetization processes in complex permeability spectra of Fe-based soft magnetic ribbons and powder cores

J. Fuzer¹, S. Dobak¹, P. Kollar¹

1. Institute of Physics, Faculty of Science, Pavol Jozef Šafárik University, Košice, Slovakia

Nowadays, amorphous and nanocrystalline soft magnetic alloys are a well-known group of magnetic materials, which are commercially produced on a large scale and exploited in a wide range of electronic applications, e.g. power transformers, inductive devices, magnetic sensors and actuators. In this study, the different character of magnetization mechanisms in as-quenched and annealed $\text{Fe}_{73}\text{Cu}_1\text{Nb}_3\text{Si}_{16}\text{B}_7$ ribbon and derived nanocrystalline powder cores was studied by using complex permeability spectroscopy. To apply an AC magnetic measuring field, a copper wire was wound around the core as a toroidal coil with several turns. To apply a DC magnetic field Helmholtz coil and electromagnet were used, respectively. An impedance analyzer (HP 4194A) equipped with a test fixture and controlled by a PC was used for measurements of these impedance parameters of the samples. The amplitude H_m of the AC magnetic field was calculated from the current flowing through the coil and geometrical dimensions of the core. The real and imaginary parts of the complex permeability were calculated on the basis of a series equivalent circuit.

We investigated the dynamics and relaxation of the reversible and irreversible domain wall movements, as the dominant magnetization processes in the samples, by means of the effects of the increasing AC and DC magnetic field amplitude on the complex permeability in a wide frequency range. In an amorphous ribbon, which was a precursor for preparation of powder cores, we observed two well-recognizable relaxation-dispersion regions corresponding to the domain wall displacements and bulging, respectively. The similar behavior was found for the annealed ribbon sample. However, in the bulk powder cores, only one dispersion region was present. From obtained spectra, the characteristic internal magnetic properties of the samples, such as relaxation frequencies of stepwise extinct magnetization processes and pinning fields, are extracted.

TU.H-P52 - Magnetic properties of mixed and vacuum/pressure impregnated Fe/SiO₂/shellac composites

J. Fuzerova¹, J.Fuzer², P. Kollar², E.Dudrova³, M.Kabatova³

1. Faculty of Mechanical Engineering, Technical University of Kosice, Slovakia

2. Institute of Physics, Faculty of Science, P.J. Safarik University, Kosice, Slovakia

3. Institute of Materials Research, Slovak Academy of Sciences, Kosice, Slovakia

Ring and cylindrical samples were made from Fe/(0.4-2wt.%)SiO₂/polymer composite materials based on irregularly and/or spherically shaped iron powder particles coated with sol-gel SiO₂ layer or with an addition of SiO₂ nano-powder. Soft magnetic composites (SMC) were prepared by two ways, by vacuum/pressure impregnation of low-temperature sintered Fe/SiO₂ compacts with shellac dissolved in ethanol as well as with thermoplast SL450 and for comparison also using a conventional procedure - by mixing the Fe/ SiO₂ powder with shellac dissolved in ethanol. In the present study, the effect of the iron particle shape way of adding SiO₂ and the effect of polymer type used to the nature of the insulating layer was investigated focusing on the complex permeability spectra, the DC and AC energy losses. The continuity and distribution of insulating layer in composites strongly depends on the shape of iron particles. The electric resistivity is a significant factor that influences eddy currents closely related to a damping of domain wall motion. A rather large resistivity extends a range of the sizeable real permeability to higher frequencies, where eddy current losses (classical and those due to domain wall motion) dominate the overall power losses. It is noteworthy that the magnetic properties strongly depend on the density, number of pores and non-magnetic phase. Creating a continuous insulating SiO₂/shellac layer with well insulating iron particles has led to acceptable values of electrical resistivity and coercivity, 776 μΩ.m and 178 A/m. This study demonstrates the possibility of producing the Fe based soft magnetic composites exhibiting good magnetic properties with tunable electric and magnetic properties.

TU.H-P53 - Specific heat of polycrystalline Ni₂InVO₆

T. Groń¹, E. Filipek², A. Paczeńska², H. Duda¹, A. Ślebarski¹, M. Fijałkowski¹

1. *Institute of Physics, University of Silesia, Katowice, Poland*

2. *Department of Inorganic and Analytical Chemistry, West Pomeranian University of Technology, Szczecin, Poland*

It is well known that oxide materials, which possess interesting physical and chemical properties, are necessary for various technical applications, *i.e.* as catalysts, pigments, elements of gas sensors and storage batteries. Ni₂InVO₆ is formed in the ternary NiO–V₂O₅–In₂O₃ system oxides [1]. Our previous magnetic studies showed the spin-glass-like behaviour below the freezing temperature $T_f = 5.0$ K [2]. Specific heat $C(T)$ was measured in the temperature range 1.8-240 K and in the external magnetic field up to $B = 6$ T using a Quantum Design PPMS platform.

The temperature specific heat capacity measurements showed a noticeable change in the slope of curve $C(T)$ and the broad peak in the curve $C(T)/T$ at T_f . This effect is clearly dependent on the applied magnetic field. Dependences of the differential $d[C(T)/T]/dT$ both in the zero magnetic field, and in the field of 6 T clearly showed the anomalous behaviour at T_f . So, the temperature dependence of heat capacity $C(T)$ and the anomalous shift of $d[C(T)/T]/dT$ towards low temperatures suggest the antiferromagnetic character of the magnetic glass state.

AŚ and MF thank the National Science Centre (NCN) for financial support, on the basis of Decision No. DEC-2012/07/B/ST3/03027.

[1] E. Filipek, A. Paczeńska, Patent No. P396804 (2014)

[2] T. Groń, E. Filipek, A. Paczeńska, M. Oboz, H. Duda, *SCTE 2014 - 19th International Conference on Solid Compounds of Transition Elements*, 21-26 June 2014, Genova, Italy, Book of Abstracts, p.143

TU.H-P54 - Spin wave propagation in yttrium iron garnet films grown on gadolinium gallium garnet and silicon substrates by ion beam evaporation

V. Sakharov¹, Y. Khivintsev^{1,2}, S. Vysotsky^{1,2}, Vl. Shadrov³, A. Stognij³, Y. Filimonov^{1,2}

1. *Saratov Branch of Kotelnikov Institute of Radio-engineering and Electronics of Russian Academy of Sciences, Saratov, Russia*

2. *Chernyshevsky Saratov State University, 410012, Saratov, Russia*

3. *Scientific and Practical Materials Research Centre of National Academy of Science of Belarus, Minsk, Belarus*

The effects of spin waves (SW) propagation in *ion-beam evaporated* yttrium iron garnet (YIG) films on gadolinium gallium garnet (GGG) and silicon (Si) substrates were examined for the first time. YIG films with thickness in the range of 0.2-0.6 micron were fabricated by deposition from yttrium oxide and iron oxide compound target using oxygen ion beam with following annealing. YIG/GGG has magnetization 1750 G and FMR linewidth 21 Oe while corresponding parameters of YIG/Si were 1450 G and 90 Oe. SW excitation and detection were performed with the coplanar micro-sized antennas fabricated directly on YIG films by lift-off technique. Measurements were done using a vector network analyzer along with a microwave probe station for tangential bias magnetic field geometry.

For both YIG/GGG and YIG/Si structures we observed excitation and propagation of the magnetostatic surface waves (MSSW). In the case of YIG/GGG the transmission signal corresponding to MSSW propagation was observed at distance between the antennas up to 200 micron and for wave numbers up to 5000 rad/cm whereas MSSW propagation in YIG/Si was only for 50 micron with maximum wave numbers around 2000 rad/cm. Gilbert damping derived from measured data for different distances between antennas in YIG/GGG structure was around 0.0025 and could reflect not only intrinsic losses but influence of two-magnon scattering due to film roughness.

This work was supported by Russian Foundation for Basic Research (projects # № 13-07-00941, 13-07-12421, 14-07-00896, and 14-07-90001) and Belarusian Republican Foundation for Fundamental Research (project # F14R-017).

Секция: Ferrites, Garnets and oxide materials

TU.H-P55 - Bulk CoNiFe-SiB amorphous and nanostructured alloys produced by plasma spray deposition and dynamic compaction: formation of soft magnetic properties

E. Denisova¹, L. Kuzovnikova², A. Kuzovnikov³, R. Iskhakov¹, A. Lepeshev⁴, I. Nemtsev⁵, V. Saunin⁶, S. Telegin⁶

1. L. V. Kirensky Institute of Physics SB RAS, Krasnoyarsk, Russian Federation

2. Krasnoyarsk Institute of Railways Transport, Krasnoyarsk, Russian Federation

3. JSC "Pulse technologies", Krasnoyarsk, Russian Federation

4. Siberian Federal University, Russian Federation

5. Krasnoyarsk Scientific Center SB RAS, Krasnoyarsk, Russian Federation

6. Siberian State Aerospace University, Russian Federation

This paper deals with progress in stabilization of amorphous or nanostructured state of bulk $\text{Co}_{58}\text{Fe}_5\text{Ni}_{10}\text{B}_{16}\text{Si}_{11}$ alloy prepared by different methods: plasma spray deposition and dynamic compaction. We focused on empirical rules for the achievement of local atomic configurations, structure with certain amorphous/nanocrystalline phase ratio, soft magnetic properties. The investigations of structure and magnetic properties of bulk samples were carried out by X-ray diffraction, electron microscopy and correlation magnetometry. The amorphous/crystalline phase ratio was estimated using the technique of magnetic phase analysis. The regimes of dynamic compaction and plasma spray deposition were selected so that the diffraction pattern, heat and temperature of crystallization, saturation magnetization (M_0 - 600 G), spin-wave stiffness (D - 117 meV Å²), and Curie temperature (T_c) of the bulk samples are identical to the same characteristics of amorphous $\text{Co}_{58}\text{Fe}_5\text{Ni}_{10}\text{B}_{16}\text{Si}_{11}$ ribbon produced by rapid quenching. It was found that the bulk amorphous coating and compact can be characterized as a heterophase system in which phase 1 with $T_c \sim 2600$ C comprises 90% of the volume and the phase 2 with $T_c \sim 5300$ C. The relaxation annealing of the $\text{Co}_{58}\text{Fe}_5\text{Ni}_{10}\text{B}_{16}\text{Si}_{11}$ bulk coating leads to a phase transition in this alloy in the precrystallization temperature range. At $T_{\text{ann}} \sim 3000$ C a ferromagnetic nanocrystalline phase 3 with $T_c \sim 3300$ C arises. The magnetic properties of the coating are correlated with changes in the microstructure. The appearance of nanocrystalline phase during relaxation heat treatment leads to a decrease of the coercivity and to an increase of the permeability. The coercivity and local magnetic anisotropy field of plasma spraying coating is less than that of the compact produced by dynamic compaction.

TU.H-P56 - Behaviors of magnetic properties and hardness in precipitation and recovery process on deformed Fe-Cu alloy

H. Kikuchi¹, T. Sasaki¹, F. Ito¹, T. Murakami¹

1. Iwate University, Morioka, Japan

Nondestructive evaluation using magnetic measurements is effective for investigating the integrity of nuclear reactor pressure vessel: good correlations exist generally between magnetic and mechanical properties, because both depend on the underlying microstructures. However, this good correlation has not observed on the deformed and aged Fe-Cu alloy experimentally, and the mechanism is unknown. An important issue to evaluate is how microstructural features contribute qualitatively and quantitatively to the magnetic and mechanical properties. Therefore, we prepared cold-rolled Fe-Cu alloys to induce dislocations, and annealed the alloys at 573 and 773K to alter the distribution of dislocations and to generate Cu precipitations. Then we evaluated the changes in coercivity and hardness, and discussed the relation between those properties and microstructural changes. The coercivity decreases with increasing aging in both treated temperature, and the slope of the reduction at 773K is larger than that at 573K. The hardness increases rapidly at the initial stage at 573K, while it increases gradually and peaks at 1000 hours at 773K. The increase in hardness is attributed to Cu precipitations, which is insensitive directly to domain wall movement, that is, magnetic properties. Previously, the idea has proposed: the precipitates occur preferentially around dislocations and compensate the internal stress around dislocations, which is attributed to decreases in coercivity. However, in this study, the hardness increases drastically due to Cu precipitation, whereas the coercivity decreases gently at 573K compared with at 773K. If Cu precipitation is dominant, the coercivity at 573K is expected to decrease more. This indicates Cu precipitation does not contribute to the decreases in coercivity. It is well known that recovery progresses in pure Fe matrix during aging and it contributes to the decreases in coercivity. This recover plays main role in the decrement of coercivity on the deformed and aged Fe-Cu alloy.

TU.H-P57 - Large-scale micromagnetics simulation for magnetization reversal process in Nd-Fe-B nanocrystalline magnets under periodic boundary condition

H. Tsukahara¹, K. Iwano¹, N. Inami¹, T. Ishikawa¹, C. Mitsumata^{1,2}, K. Ono¹

1. High Energy Accelerator Research Organization, Tsukuba, Japan
2. National Institute for Materials Science, Japan

The permanent magnet having high coercivity has been under intensive study because of their importance for high efficiency electric motors. Mechanism of the coercivity remains unclear and has been investigated during a long period. Especially, it has been expected that an origin of a discrepancy of the coercivity between experimental values and theoretical results that is calculated by magnetic anisotropy is magnetic defects [1]. Although magnetization reversal process is investigated solving Landau-Lifshitz-Gilbert using finite element method, the coercivity discrepancy cannot be explained quantitatively.

We performed large-scale micromagnetics simulation whose size is $1024 \times 1024 \times 1024 \text{ nm}^3$ with 2 nm mesh using Hitachi SR16000M1 supercomputer solving Landau-Lifshitz-Gilbert equation under periodic boundary condition to simulate bulk magnet and also to avoid macroscopic demagnetization. An effective field is constructed by an anisotropic, exchange, external and dipolar field. We choose different value for exchange stiffness constant between inter and intra grain interactions. Grains for Nd-Fe-B nanocrystalline magnet have about 160 nm in diameter and 50 nm in thickness. Fluctuation of crystal grain axis is realized using Box-Muller's method.

Simulation results show that the dipolar interaction plays an important role in magnetization reversal. As the external field approaches to a critical magnetic field, i.e. coercivity, the dipolar energy decreases in contrast to anisotropic energy. Thus the magnetic fluctuation is governed by the dipolar interaction. Additionally the coercivity of Nd-Fe-B nanocrystalline magnet is very sensitive to a fluctuation of the grains. When the easy axis of each grain has no fluctuation, the coercivity is 60 kOe. On the other hand, the coercivity becomes 38 kOe with a very small fluctuation. This work was partly supported by the JST under Collaborative Research Based on Industrial Demand "High Performance Magnets: Towards Innovative Development of Next Generation Magnets."

[1] H. Kronmuller et al., J. Magn. Magn. Mater. 74 291 (1988)

TU.H-P58 - Effect of current density for electroplated films prepared in a des-based bath

T. Yanai¹, K. Shiraishi¹, K. Azuma¹, Y. Watanabe¹, M. Nakano¹, H. Fukunaga¹

1. Nagasaki University, Japan

We have reported Fe and Fe-Ni films prepared from Deep-Eutectic-Solvent-based plating baths [1-2]. The DES-based baths showed high current efficiency (> 90 %), and we confirmed that the DES is a hopeful solvent for electroplating of Fe-based alloys. In this study, we evaluated the effect of the current density on the various properties of the as-plated Fe-Ni films.

The DES was prepared from the mixture of ethylene glycol (10 g) and choline chloride (10 g). FeCl₂·4H₂O (x g). NiCl₂·6H₂O (15 - x g) were added into the DES. The bath temperature was fixed at 373 K. The current density was varied from 13 to 667 mA/cm², keeping the total amount of the electric charge at 60 C.

We evaluated the effect of the current density on the Fe content of the as-plated films. The Fe content increased with increasing the current density from 13 to 70 mA/cm², and then showed almost constant values in the higher current density. This result indicates that high current density is suitable to plate the Fe-Ni films since the variation of the film composition against the current density is small. We also evaluated the effect of the current density on the current efficiency of the plating process. In this evaluation, the Fe content of the films were controlled at approximately 22 at.% by the change in the value of x since low coercivity was observed around this composition. We obtained high current efficiency (> 90 %) in a current density range from 30 to 133 mA/cm². From these results, we found that the moderate high current density (Approx. 100 mA/cm²) is suitable to obtain the Fe-Ni films efficiently.

[1] T. Yanai et al., J. Appl. Phys., 115, #17A344, (2014)

[2] T. Yanai et al., IEEE Trans. Magn., 50, #2008404, (2014)

TU.H-P59 - Magnetoelastic characteristics of the 13CrMo4-5 constructional steel and possibility of its modelling for non-destructive testing

D. Jackiewicz¹, R. Szewczyk¹, A. Bienkowski¹, M. Nowicki²

1. Institute of Metrology And Biomedical Engineering, Warszawa, Poland

2. Industrial Research Institute for Automation and Measurements, Warszawa, Poland

The magnetoelastic effect is very promising for non-destructive testing of construction elements, especially trusses. However, the main barrier for this application is lack of knowledge about magnetoelastic characteristics of constructional steels, as well as limited mathematical model-oriented description of magnetoelastic effect.

Rescaled truss structure was used for the investigation. It is made of the 13CrMo4-5 constructional steel, widely used in the energetic industry. The hysteresis loops measurements are done on the specially developed hysteresisgraph. The truss was supported on the bottom edge nodes. The mechanical force was vertically exerted on the upper central node of the truss by the oil hydraulic press.

Under the tensile stresses, value of the flux density B in the stretched sample first increase, and then, after reaching the Villari point, it starts to decrease. Moreover, under the compressive stresses, value of the flux density B in the compressed sample nonlinearly decreases. It should be highlighted, that these changes are relatively higher for lower values of the amplitude of magnetizing field H_m . This occurs due to the fact, that for lower values of magnetizing field H , participation of magnetoelastic energy in the total free energy in the sample's material is significantly higher.

Next, on the basis of measurements, magnetic hysteresis loops were modelled with Jiles-Atherton extended model. Results of the modelling utilising extended Jiles-Atherton model are consistent with results of experimental measurements, which is confirmed by high values of the determination coefficient, which exceeds 98% for each of the $B(H)$ magnetic hysteresis loop. Due to the high values of changes of magnetic characteristics under the stresses, and good agreement with the model, presented methodology is very promising for non-destructive methods of stress assessment in the steel constructional elements.

TU.H-P60 - Phase formation and magnetocaloric effect in (Pr,Nd)-Fe alloys prepared by rapidly quenched method

N. Dan¹, N. Ha², N. Yen¹, P. Thanh¹, T. Thanh^{1,3}, L. Phan³, S. Yu³

1. *Institute of Materials Science, Vietnam Academy of Science And Technology, 18 Hoang Quoc Viet, Hanoi, Vietnam*

2. *Hong Duc University, 565 Quang Trung, Dong Ve, Thanh Hoa, Vietnam*

3. *Chungbuk National University, Cheongju 361 - 763, Republic of Korea*

$\text{Pr}_{2-x}\text{Nd}_x\text{Fe}_{17}$ ($x = 0 - 2$) ribbons with thickness of about 15 μm were prepared by melt-spinning method. The alloy ribbons were then annealed at different temperatures (900 - 1100°C) for various time (0.25 - 2 h). The formation of the $(\text{Pr,Nd})_2\text{Fe}_{17}$ (2:17) crystalline phase in the alloys strongly depends on the Pr/Nd ratio and annealing conditions. Annealing time for the completed formation of the 2:17 phase in the rapidly quenched ribbons is greatly reduced in comparison with that of bulk alloys. Curie temperature, T_C , of the alloys can be controlled in room temperature region by changing Pr/Nd ratio. Maximum magnetic entropy change, $|\Delta S_m|_{\text{max}}$, of the alloys is quite high ($> 1.5 \text{ J.kg}^{-1}\text{K}^{-1}$ with $\Delta H = 12 \text{ kOe}$) in room temperature region. On the other hand, the full width at half the maximum peak of the magnetic entropy change is quite large (FWHM $> 50 \text{ K}$) making it possible for application in magnetic refrigerators at room temperature.

PACS number: 75.30.Sg, 07.20.Mc, 75.50.Kj

TU.H-P61 - Extraction and valorization of rare earth permanent magnets comprised in waste electrical and electronic equipment: the extrade project.

N. Maât¹, V. Nachbaur¹, J. Juraszek¹, R. Lardé¹, M. Jean¹, J. Le Breton¹, N. Menad²

1. CNRS-Groupe De Physique Des Matériaux UMR 6634, France

2. BRGM Bureau de Recherche Géologiques et Minières, Orléans, France

Rare earths are a group of chemical elements which are currently used in a very large number of technological applications and innovations. They have been classified, since July 2010, as strategic materials for the European Union, and their supply has become a capital issue for development and industry.

Exploitation of “urban mines”, in this case the electrical and electronic waste, has therefore emerged as a preferred choice, motivated by the substantial use of these elements by the industrialized countries.

In this context, the current research focuses on the improvement of the magnetic materials included in electrical and electronic waste, and their reintegration into the industrial circuit. The considered processes shall permit, from used Nd-Fe-B magnets, to synthesize new magnets with sufficient magnetic properties for applications.

Currents methods for recycling industrial scrap are based on hydrometallurgical, pyrometallurgical or solvent-extraction processes. Hydrogen decrepitation is also investigated in laboratories for recycling permanent magnets comprised in WEEE. Advantages and drawbacks of these processes are discussed here.

The Extrade project aims to develop new directions for retreatment of used magnets. As an alternative way we expose a process to remove the nickel metallic protective layers and recover the magnetic phase Nd₂Fe₁₄B. The process is based on a solvothermal treatment in hydrocarbons. Particular attention is paid to protocols that must be implemented to limit their oxidation during the various steps of the process.

This work is part of the project ANR-13-ECOT-0006-06 “EXTRADE”

TU.H-P62 - Milling and sintering of Nd-Fe-B magnets comprised in weee: a way for recycling rare earth permanent magnets.

N.Maât¹, V. Nachbaur¹, J. Juraszek¹, R. Lardé¹, M. Jean¹, J. Le Breton¹

1. Groupe de Physique des Matériaux, UMR 6634 CNRS, Université et INSA de Rouen, Saint Etienne du Rouvray, France

Rare earths are chemical elements used in a very large variety of devices and applications. Due to their high supplying costs, recycling is currently investigated both by industries and laboratories. Exploitation of urban mines has emerged as a solution for reducing rare earths consumption, with economical, environmental and geopolitical advantages. Currently, Nd-Fe-B permanent magnets are the most powerful magnetic materials commercialized. They are ubiquitous in common and high tech devices, and can be found in large quantities in waste stream. In our project we focus on Nd-Fe-B magnets comprised in WEEE (Waste Electrical and Electronic Equipment), and more particularly in hard disk drives. Due to the waste stream heterogeneity, classical production processes have to be adapted for processing new magnets from old ones. In this paper particular attention is paid to oxidation of the Nd₂Fe₁₄B magnetic phase during milling and sintering steps. Milling in hydrocarbons, aqueous or organic solvent is investigated. Powder purity and average grain size are analyzed. Samples are characterized by X-ray diffraction, SEM analysis, Mössbauer spectrometry and VSM measurements. The highest purity is obtained in ethyl acetate, wherein Nd₂Fe₁₄B phase is completely preserved with an average particle size of 10/ am. Sintering of recycled powders is performed with a Spark Plasma Sintering apparatus, which is slightly different from classical sintering processes. Influences of both powder purity and particle size on crystallographic, structural and magnetic properties of the sintered material are investigated. To avoid dissociation of the Nd₂Fe₁₄B phase upon sintering, high purity of the starting powder is required. The best results are obtained with powders having 10/ am diameter, sintered at 830°C for one hour under 40 MPa, and subsequently annealed at 950°C under vacuum for one hour.

This work is supported by the french “Agence Nationale de la Recherche”, in frame of the project ANR-13-ECOT-0006-06 'EXTRADE'.

TU.H-P63 - Coercivity enhancement in Ce-Fe-B magnets by Nd-Cu infiltration

M. Ito^{1,2,3}, M. Yano¹, N. Sakuma¹, H. Kishimoto¹, A. Manabe¹, T. Shoji¹, A. Kato¹, N. Dempsey^{2,3}, D. Givord^{2,3,4}

1. *Advanced Material Engineering Div., Toyota Motor Corporation, Susono, Japan*

2. *CNRS, Institut Néel, UPR 2940, Grenoble, France*

3. *Univ. Grenoble Alpes, Institut Néel, Grenoble, France*

4. *Instituto de Física, Universidade Federal do Rio de Janeiro, Rio de Janeiro, Brazil*

High performance permanent magnets are key components of electrical motors in electrical and hybrid cars, and the generators of wind turbines. These magnets almost exclusively consist of the $R_2Fe_{14}B$ ($R =$ rare-earth, Nd and Dy) phase. Nd and especially Dy are considered to be critical elements due to increasing demands. As a consequence, Ce-based intermetallic phases attract attention because of their potential applications in permanent magnets and the greater abundance of Ce compared to Nd and Dy. However the intrinsic magnetic properties, namely Curie temperature, saturation magnetization and anisotropy field, of $Ce_2Fe_{14}B$ are far inferior to those of $Nd_2Fe_{14}B$. To use Ce, the partial substitution of another R for Ce in rare-earth sites of $Ce_2Fe_{14}B$ and the optimization of microstructure are required to improve the extrinsic properties, in particular coercivity. In this study, Ce-based nano-structured core-shell-phase magnets were fabricated from rapidly quenched $Ce_2Fe_{14}B$ melt-spun ribbons. The melt-spun ribbons were sintered at 1020 K under a pressure of 100 MPa, then hot-deformed to a height reduction of about 80%. The hot-deformed magnets were infiltrated with liquid Nd-Cu eutectic alloy at 970 K for 165 minutes. These nano-structured magnets consist of core-shell grains separated by a grain boundary phase, the cores being semi-hard Ce-based 2-14-1 with the shells having a higher anisotropy owing to partial substitution of Nd for Ce. Microstructure observation by transmission electron microscopy, composition analysis by energy dispersive X-ray and magnetic property measurements have been performed.

From magnetization measurements made in the range 300 - 450 K, it was found that the coercivity of multi-phase magnets were improved compared to non-infiltrated and single-phase magnets (only core phase). These results indicate that the enhancement of coercivity was brought about by magnetic isolation of 2-14-1 phases by infiltration and the suppression of magnetization reversal by the high anisotropy shell.

TU.H-P64 - Magnetic and microstructural properties of MnBi thin films grown by an UHV sputtering system

H. Moon¹, S. Kim¹, M. Song¹, H. Lee¹, W. Lee¹

1. Department of Materials Science and Engineering, Yonsei University, Seodaemun-gu, Seoul, Republic of Korea

Low-temperature phase (LTP) of MnBi has attracted much attention because it has a larger coercivity than that of Nd-Fe-B at high temperature [1]. Moreover, it gives high potentiality as a hard magnetic core combined with soft magnetic shell, giving rise to further enhancement of $(BH)_{\max}$ in exchange-coupled core-shell magnet. It is estimated to overcome that of Nd-Fe-B. In this regards, there have been many efforts [2] to obtain the LTP-MnBi thin films for the exchange-coupled magnets. We synthesized LTP thin films on a glass substrate by UHV sputtering and vacuum annealing at 350°C. The deposition rate and annealing process were optimized to fabricate the single-phase of LTP. The magnetic and microstructural properties of the LTP-MnBi films were investigated as a function of Bi and Mn thicknesses. XRD results confirmed that all the films were well grown with the c-axis orientation. The highest value of $(BH)_{\max} \sim 6.6$ MGOe at room temperature was obtained in Bi(30nm)/Mn(20nm). We found that the ratio of Bi/Mn strongly has an effect on the magnetic properties of LTP-MnBi films. We will discuss exchange-coupled MnBi with various soft layers such as FeCo and Fe.

[1] T. Chen and W. E. Stutis, IEEE Trans. Magn, 10, 581-586 (1974)

[2] B. Li, W. Liu, X.G. Zhao, W.J. Gong, X.T. Zhao, H.L. Wang, D. Kim, C.J. Choi and Z.D. Zhang, J. Magn. Mater, 372, 12-15 (2014)

TU.H-P65 - A model for the dysprosium diffusion from a surface layer in NdFeB magnets

M. De Campos¹, J. de Castro¹

1. Federal Fluminense University, Brazil

It has been reported that Dysprosium addition by surface diffusion is an effective way to improving the coercivity of NdFeB magnets, saving the scarce Dysprosium. However, the Dysprosium diffusion is only effective for Nd₂Fe₁₄B samples with less than 5mm [1]. Nakamura et al [1] reported that after 20 hours (at 850oC) of heat treatment, coercivity of a depth below 5 mm was unaffected. Thus, kinetics is very important detail in this process. Additions of dysprosium as sulfides or oxides [2] near grain boundaries seem to be more effective for samples with larger volume, due to kinetic reasons. This article presents a model, based on 2nd law of Fick, for evaluating the surface diffusion of dysprosium from a Dy deposited layer or coating at the top of a NdFeB ternarium magnet. Variables as grain size and thickness of grain boundary phase are considered. The simulation confirms the results of Nakamura et al [1], and suggests that including Dy as Dy₂O₃ or Dy₂S₃ additives [2] may be more viable for improvement of coercivity with short time of heat treatment.

References:

- [1] H Nakamura, K Hirota, T Ohashi and T Minowa. J. Phys. D: Appl. Phys. 44 (2011) 064003
- [2] A. M. Gabay, M. Marinescu, W. F. Li, J. F. Liu, and G. C. Hadjipanayis. J. Appl. Phys., 109 (2011) 083916

TU.H-P66 - Suitable nanostructures for the application of the SW-CLC Model

M.De Campos¹, S. Romero²

1. *Federal Fluminense University, Brazil*

2. *Institute of Physics - University of Sao Paulo, Brazil*

The Stoner-Wohlfarth-Callen-Liu-Cullen (SW-CLC) model was originally proposed for amorphous magnetic alloys [1]. Application of SW-CLC for hard magnetic materials was pioneered by Hadjipanayis and Gaunt for PtFe [2] and by Hadjipanayis and Gong [3] for a Nd₂Fe₁₄B exchange coupled magnet. The SW-CLC model is only applicable for specific nanostructures. As discussed by Kneller and Hawig [4], the dimension of the soft phase has to be less than twice the domain wall thickness of the hard phase. Besides, the hard phase should be less than the single domain particle size, condition required by the Stoner-Wohlfarth model. The present study discusses the specific nanostructures where the SW-CLC model can be applied. A possibility is spherical grains of hard phase enveloped by a shell of the soft phase. Another possibility is very small grains of the nanophase inside the grains of the hard phase (inclusions). These inclusions of soft phase need to be separated by a distance of the order of twice the domain wall thickness [4]. Experimental conditions for application of the SW-CLC model are also discussed. Measurements obtained in Hysteresigraph are not adequate, because results obtained with this equipment show distortion the 1st quadrant of the hysteresis. The SW-CLC model should fit at least the 1st quadrant of the hysteresis. Thus, measurements obtained in VSM (Vibrating Sample Magnetometer) are more appropriate. For a better 1st quadrant experimental determination, samples with low demagnetizing field, (as for example parallelepipeds with dimensions 5 x1 x1 mm) are recommended.

References:

- [1] E. Callen, Y. J. Liu, E. R. Cullen. Phys. Rev. B 16 (1977) 263
- [2] G. Hadjipanayis, P. Gaunt. J. Appl. Phys. 52 (1981) 2093
- [3] G. C. Hadjipanayis, W. Gong. J. Appl. Phys. 64 (1988) 5559
- [4] E. F. Kneller, R. Hawig. IEEE Trans. Magn. 27 (1991)3588

TU.H-P67 - Fabrication and magnetic properties of $\text{Fe}_{81.4}\text{Si}_3\text{B}_{10}\text{P}_5\text{Cu}_{0.6}$ nano-crystalline powder coresY. Zhang¹, J. Luan¹, N. Yodoshi¹, P. Sharma¹, A. Makino¹*1. Institute for Materials Research, Tohoku University, Sendai, Japan*

Low core loss materials with high frequency characteristics and complex shapes can be obtained by powder metallurgy method. Usually Fe based materials with uniform nano-crystalline structure of α -Fe phase can exhibit high magnetic flux density and soft magnetic properties. Recently, amorphous powders were prepared by a newly method of spinning water atomization process (SWAP), which has a higher cooling rate than the conventional gas/water atomization methods. In present study, the $\text{Fe}_{81.4}\text{Si}_3\text{B}_{10}\text{P}_5\text{Cu}_{0.6}$ amorphous powders were compacted by cold-pressing and nano-crystallized by annealing. XRD and TEM were employed to identify the structure and the nano-crystalline grain size of the powder cores. The thermal stability and nano-crystallization behavior were analyzed by DSC. For the magnetic properties, hysteresis loop, magnetic permeability and core loss were measured by VSM, impedance analyzer and AC B-H analyzer, respectively. As a result, we focused on fabricating the powder cores of $\text{Fe}_{81.4}\text{Si}_3\text{B}_{10}\text{P}_5\text{Cu}_{0.6}$ with the particle size below 20 μm quenched by SWAP. After compacting and annealing at different temperature of $\sim 440 - 500$ $^{\circ}\text{C}$, nano-crystalline α -Fe grains can be obtained in the powder core annealed at 480 $^{\circ}\text{C}$. The average grain size related to the full-width at half-maximum of XRD peak is closed to 23 nm by estimated for core annealed at 480 $^{\circ}\text{C}$. Primary crystallization of α -Fe is completely finished as shown in the DSC curves. A constant initial permeability more than 50 was obtained upto the frequency range of tens of megahertz. At high frequency (> 100 kHz), powder cores exhibit low core loss due to relatively low eddy current loss resulting from the resin insulation.

TU.H-P68 - A soft/hard magnetic nanostructure based on multisegmented conical nanowires

A. Pereira^{1,2}, J. L. Palma^{1,2}, M. Vazquez³, J. Casagrande Denardin^{1,2}, J. Escrig^{1,2}

1. *Universidad De Santiago De Chile (USACH), Santiago, Chile*
2. *Center for the Development of Nanoscience and Nanotechnology (CEDENNA), Santiago, Chile*
3. *Institute of Materials Science of Madrid, CSIC, Madrid, Spain*

In this work we have introduced a new soft/hard nanostructure based on multisegmented CoNi nanowire arrays having diameters of around 110 nm and made of five segments with nominal compositions of Co, Co₆₆Ni₃₃, Co₅₀Ni₅₀, Co₃₃Ni₆₆ and Ni, each of which has a length of 800 nm, so that the total length of the multisegmented nanowire is 4 μm. These arrays have been synthesized by means of potentiostatic electrodeposition into the pores of hard-anodic alumina templates. The morphology, chemical composition and microstructure of the multisegmented CoNi nanowires were determined by high-resolution scanning electron microscopy, energy dispersive X-ray microanalysis, and powder X-ray diffraction method, respectively. The room temperature magnetic behavior of the multisegmented nanowire arrays is also studied and compared with CoNi nanowire arrays with homogeneous composition (non-segmented nanowires), synthesized in the same templates and having the same dimensions as the segmented ones. These nanostructures could be used to control the movement of magnetic domain walls. In this way, these nanostructures can be an alternative to store information or even perform logic functions.

We acknowledge financial support from Fondecyt under projects 3140073, 3130393, 1150952 and 1140195, the Financiamiento Basal para Centros Científicos y Tecnológicos de Excelencia, under Project FB0807, and the Spanish Ministry of Economía y Competitividad, MEC, under project i-LINK0783.

Pereira A., Palma J. L., Vázquez M., Denardin J. C., Escrig J. (2015). A soft/hard magnetic nanostructure based on multisegmented CoNi nanowires. *Phys. Chem. Chem. Phys.* 17, 5033.

TU.H-P69 - Enhancement of magnetic property of Nd-Fe-B powders prepared by reduction-diffusion processD. Kim¹, C. Chen², Y.k Seo¹, C.n Choi¹*1. Korea Institute of Materials Science, Republic of Korea**2. Korea University of Science and Technology, Republic of Korea*

Nd-Fe-B magnets have been fabricated by powder metallurgical routes, rapid quenching and reduction-diffusion (R-D) process. Compared with other methods, use of a relatively inexpensive Nd oxide as raw material and direct production of alloy powders suitable for further procedures can be pointed out as main advantages of R-D process. A novel route to prepare Nd-Fe-B magnetic powders by utilizing both spray drying and reduction-diffusion processes was designed and investigated in this study. Precursors were prepared by spray drying method using the aqueous solutions containing Nd salt, Fe salt and boric acid with stoichiometric ratios. Desalting of the precursors, milling and reduction in H₂ atmosphere were performed, followed by R-D process. It was revealed that the amount of Calcium (Ca) as reducing agent added in R-D step played an important role in the formation of Nd₂Fe₁₄B phase, because vigorous H₂ evolution and dissociated hydrogen might be diffused into the lattice of Nd₂Fe₁₄B interstitially to form Nd₂Fe₁₄BH_x (x=1-5) during washing of powders in water obtained after R-D with excessive amount of Ca. This is one of the critical reasons for low magnetic property of powders synthesized by R-D process. In order to make the powders smaller and homogeneous size, we carried out ball milling in ethanol before washing with water. Finally, Nd₂Fe₁₄B powders with high coercivity of more than 10 kOe were produced by adjusting the amount of Ca in reduction-diffusion (R-D) process. They showed spherical in shape with a mean size of 1 μm and maximum energy product (BH_{max}) was attained 17.8 MGOe.

TU.H-P70 - Coercivity enhancement in La coated Nd-Fe-B thin films

K. Koike¹, H. Ishikawa¹, D. Ogawa¹, H. Katao¹, T. Miyazaki², Y. Ando², M. Itakura³

1. Graduate school of Science and Engineering, Yamagata University, Japan

2. Graduate school of Engineering, Tohoku University, Japan

3. Interdisciplinary Graduate school of Engineering Science, Kyushu University, Japan

Achieving higher coercivity in sintered Nd-Fe-B magnets without using heavy rare-earth elements is one of the most crucial and urgent subjects, in view of the rapidly growing demand for high-performance motors such as those in electric or hybrid vehicles. At least two approaches have been known so far to increase coercivity in sintered Nd-Fe-B magnets. First one is the grain size refinement of the main Nd₂Fe₁₄B phase. The second approach is the interface control between the main and grain-boundary phases.

In order to investigate the relation between such interface state and the coercivity in sintered Nd-Fe-B magnets, we have been fabricating samples with the model interface between Nd₂Fe₁₄B and grain-boundary phases by using a thin-film technique [1-3]. We reported the coercivity enhancement phenomena in Nd-Fe-B films when the Nd overlayer was deposited and annealed at 500°C [1]. However, the origin of such a coercivity enhancement is still not clear. In this paper, we fabricated the similar Nd-Fe-B films but with the La overlayer and investigated their magnetic properties in order to approach the coercivity mechanism.

The Nd-Fe-B (20 nm)/La (20 nm) thin films were deposited on Al₂O₃(0001) substrate by using UHV sputtering technique. The coercivity of as-deposited Nd-Fe-B films without the La overlayer showed 9 kOe. We then deposited the La overlayer on this film. But the coercivity remained almost unchanged.

On the other hand, when annealed at 470°C, the coercivity of the Nd-Fe-B/La film increased significantly and reached 15 kOe. The SIMS, XRD, and high resolution TEM observation in this high coercivity film suggested the existence of hcp-La₂O₃ phases in the La layer.

[1] Koike, et al., J.Phys. Conf. Ser., 200 (2010) 082015

[2] Umezawa, et al., J. Korean Phys. Soc., 63 (2013) 616

[3] Koike, et al., J. Appl. Phys., 115 (2014) 17A735

TU.H-P71 - Magnetic property and magnetocaloric effect in Ni-Mn-(Sn,Sb,Al) heusler alloys

N.n Dan¹, N. Mai², V. Quang³, N.n Yen¹, P. Thanh¹, T. Thanh^{1,4}, L. Phan⁴, S.Yu⁴

1. *Institute of Materials Science, Vietnam Academy of Science and Technology, Vietnam*
2. *VNU University of Science, Nguyen Trai, Hanoi, Vietnam*
3. *Ha noi Pedagogical University, Xuan Hoa, Vinh Phuc, Vietnam*
4. *Chungbuk National University, Cheongju, Republic of Korea*

Ni-Mn-Z (Z = Sn, Sb, Al) Heusler alloys in forms of ingot and ribbon were prepared by using arc-melting and melt-spinning methods, respectively. Structure-property relationships in these systems of Heusler alloys were systematically investigated and compared. The results showed that structure, magnetic property and giant magnetocaloric effect (GMCE) of the alloys are strongly influenced by fabrication conditions such as quenching rate, annealing temperature, annealing time. The coexistence of ferromagnetic (FM) and antiferromagnetic (AFM) orders can be observed in these systems with appropriate compositions and fabrication conditions. The magnetic phase transitions can be controlled by changing composition and annealing conditions of the alloys. GMCEs with large magnitude and wide working temperature range have been obtained on these alloys showing their application potential for magnetic refrigeration technology.

TU.H-P72 - Effects of ordered phases on the structure and magnetic properties of Fe-9%Si-2%Cr powder

P. Jang¹, G. Choi²

1. Cheongju University, Cheongju, Republic of Korea

2. Changsung Corporation, Incheon, Republic of Korea

Miniaturized inductors with good electromagnetic properties have been required in recent mobile devices, for which operating frequency should be higher than 10 MHz and low electrical resistivity is also required for high dc current. The electrical resistivity of well-known Fe-6.5%Si alloys with excellent dc magnetic properties is too low for the high frequency application. Fe-Si powder cores with high silicon content have high electrical resistivity. However, ordered phases such as B2 and DO3 existing in disordered A2 phase appear in the alloys. The effects of size and distribution of the ordered phases on the electromagnetic properties of the Fe-Si alloys have not been well-studied. In this study, Fe-9%Si-2%Cr powder with a mean size of 14.4 μm was gas-atomized and then annealed at 25 - 650°C in nitrogen gas for 1 hr. In XRD analysis A2 and B2 phases existed in the as-atomized powder. The DO3 started to precipitate and volume fraction of B2 phase decreased after 550°C annealing which can be well-explained by the Fe-Si equilibrium phase diagram. However, B2 phase did not disappear even after 650°C annealing. The size of DO3 phase is 13 and 84 nm after 550 and 650°C annealing, respectively. The fine distribution of the DO3 phase can increase the electrical resistivity because of the high electron scattering in the interface between DO3 and A2 phases. DC magnetic properties were not so much influenced by the annealing so that the saturation magnetization and coercivity of the annealing powder were 150 A·m²/kg and 240-320 A/m, respectively.

TU.H-P74 - Structure and magnetic properties of sputtered $\text{Sm}_x\text{Co}_{100-x}$ ($20 < x < 32$) films prepared at low temperatures

F.M.F. Rhen^{1,2}, S. Belochapkin², F.P. Missell³

1. *Department of Physics and Energy, University of Limerick, Ireland*

2. *Materials and Surface Science Institute, University of Limerick, Ireland*

3. *Centro de Ciências Exatas e Tecnologia, Universidade de Caxias do Sul, Caxias do Sul, Brazil*

There is growing interest in using magnetic components in microelectromechanical systems (MEMS). If a MEMS device with two magnetic parts is scaled down by a factor k , the force between the two magnets scaled up by a factor k , making them favourable for integration over magnet-coil devices, in which interaction is scale invariant [1]. CMOS compatible technologies require processing temperatures typically below 400°C. The preparation of Sm-Co alloy with TbCu7 structure by sputtering has been demonstrated at low processing temperature of 350°C [2], showing the potential of this alloy for MEMS applications integrated with CMOS.

Here, we prepared $\text{Sm}_x\text{Co}_{100-x}$ ($20 < x < 32$) by sputtering onto heated silicon substrates at 350°C (623 K). The structure was investigated by X-rays diffraction (XRD) and transmission electron microscopy (TEM). Room temperature magnetic properties were measured with a vibrating sample magnetometer. We found that the (110) and (100) preferential orientations coexist in the films in different proportions depending on the Sm content. Coercivity and hysteresis loop shape are dependent on the Sm content and are correlated with the crystallographic orientation of SmCo_5 crystallites in the films.

Our investigation reveals that hexagonal SmCo_5 with preferential (110) orientation in the films is promoted by an excess of Sm during the sputtering process. Overall, these results show that hard magnetic properties of thick films with SmCo_5 phase can be obtained by sputtering at low temperatures with coercivity of up to $m_0H_C = 1.12$ T.

Acknowledgements: Dr. F.M.F Rhen and Professor F.P. Missell thank Science Foundation Ireland (12/IP/1692) and CNPq partial financial support, respectively.

References:

[1] O.Cugat, J.Delamare and G.Reyne, IEEE Trans. Magn. 39, 3607 (2003)

[2] A.Walther, D.Givord, N.M.Dempsey, K.Kholpkov, O.Gutfleish, J. Appl. Phys. 103, 043911 (2008)

TU.H-P75 - Effect of RF-Power on magnetic properties and FMR line width of RF-Sputtered Zn-Ferrite thin films

B. Sahu¹, N. Venkataramani², S. Prasad¹, R. Krishnan³

1. Department of Physics, IIT Bombay, Mumbai, India

2. Department of Metallurgical Engineering & Materials Science, IIT Bombay, Mumbai, India

3. Retired scientists, CNRS/Universite de Versailles-St-Quentin, Versailles, France

Zn-Ferrite (ZnFe_2O_4) shows a size dependent magnetic order with low FMR linewidth (ΔH), only when it is in nano sized. Nanocrystalline ZnFe_2O_4 films are known to show better FMR line shape and low ΔH when deposited by RF-sputtering, as against PLD. In this paper we report the effect of rf-power (P) and ex-situ annealing temperature (T_A) on magnetic and FMR properties of rf-magnetron sputtered films. The films were deposited in Ar atmosphere at ambient temperature on corning glass substrate with P varying between 30 to 150 watts. The as deposited films were annealed at T_A from 250-650 °C in air for 2hrs. The thickness of the films increased from 100 to 670 nm as P increased from 30 to 150 watt. The grain sizes also increased both with P and T_A . The spontaneous magnetizations ($4\pi M_s$) at 300 K increased from 480 G to 1930 G as P changed from 30 to 130 watt. For $P=150$ watt, the $4\pi M_s$ was 1760 G. $4\pi M_s$ values initially increased with the T_A up to 250 °C, then decreased, showing a paramagnetic like behavior for $T_A > 450$ °C. Parallel and perpendicular FMR measurement were carried out at 9.44 GHz. The peak to peak ΔH did not show monotonous behavior with the P and T_A . It was found that the films deposited at higher P , show larger ΔH . However, upon annealing ΔH decreases at higher rate for them than those deposited as low P . Minimum ΔH of 170 Oe for parallel and 115 Oe for perpendicular was obtained for the sample with $P=150$ watt and $T_A=450$ °C. These results can be explained on the basis of grain size dependence of magnetic order. The present results show that it is important to optimize both P and T_A for obtaining low linewidth in ZnFe_2O_4 thin films.

TU.H-P77 - Magnetic properties and X-ray photoemission of $\text{NaCo}_{2-x}\text{Ca}_x\text{O}_4$ ($x = 0.0, 0.1$ and 0.2)B. Kurniawan², D. Nanto¹, E. Ermawan², S. Poetardji², S.Yu³*1. Dept. of Physics Education, Syarif Hidayatullah State Islamic University, Indonesia**2. Dept. of Physics, University of Indonesia, Indonesia**3. Dept. of Physics, Chungbuk National University, Indonesia*

Spinel structure have drawn a lot of research interests for their exhibition of many unusual physical properties including high magnetic moment, magneto-resistance, half metallic behavior, potential applications in chemical sensors [1], catalytic activity [2], photo-conductive materials [3] and thermoelectric effect [4] which has great potential in the field of cooling, heating, generating power, and recovering waste heat. Co_3O_4 is an antiferromagnet ($T_N \sim 30$ K) [5]. Co rich compounds in spinel oxides could be of interesting in view of the diversity in magnetic properties (ferrimagnet, antiferromagnet and antiferromagnetic spin glass) and magneto-transport phenomena (colossal magnetoresistance). In present work, we have studied magnetic properties of polycrystalline $\text{NaCo}_{2-x}\text{Ca}_x\text{O}_4$ ($x = 0.0, 0.1$ and 0.2). The purpose of this paper is to study how the doped alkali metal Ca affects the magnetic property. Polycrystalline samples $\text{NaCo}_{2-x}\text{Ca}_x\text{O}_4$ were synthesized by conventional solid state reaction. The crystal structure was detected by x-ray diffraction (XRD) using $\text{Cu-K}\alpha$ radiation. Magnetic properties for those samples were investigated by means of a superconducting quantum interference device (SQUID) magnetometer. X-ray photoelectron spectroscopy (XPS) measurements were carried out to observe valance band energy on the sample. Figure 1 shows maximum magnetic hysteresis polycrystalline $\text{NaCo}_{2-x}\text{Ca}_x\text{O}_4$ ($x = 0.0, 0.1$ and 0.2) under external field of 20 kOe at 5 K. Figure 2 demonstrates binding energy on sample polycrystalline $\text{NaCo}_{2-x}\text{Ca}_x\text{O}_4$ ($x = 0.0, 0.1$ and 0.2). As Ca^{2+} increase chemical shift goes to lower binding energy indicting addition of electron. Considering charge neutrality into account, the sample will have chemical distribution may transform from $\text{Na}^{1+}\text{Co}^{3+}\text{Co}^{4+}\text{O}_4^{2-}$ to $\text{Na}^{1+}\text{Ca}^{2+}\text{Co}^{2+}\text{Co}^{3+}\text{O}_4$. Coupling magnetic interaction of $\text{Co}^{3+}/\text{Co}^{4+}$ to $\text{Co}^{2+}/\text{Co}^{3+}$ shows strong correlation to the enhancement of magnetization. Therefore, it is interesting to discuss in detail the mechanism of magnetic enhancement with X-ray photoemission result in full report work.

TU.H-P78 - Magnetic properties of hexaferrites obtained by spark plasma sintering of SrFe₁₂O₁₉ nanoparticles

JM. Le Breton¹, N. Maât¹, V. Nachbaur¹, E. Folcke¹, FX. Lefevre², Y. Bréard², A. Pautrat²

1. *Groupe de Physique des Matériaux - UMR 6634 CNRS, Université et INSA de Rouen, France*

2. *CRISMAT - UMR 6508 CNRS, Université de Caen et ENSICAEN, France*

The replacement of rare earth magnetic materials by more available and affordable materials is a very current topic. One way to obtain rare-earth free new permanent magnet materials is to increase the magnetic properties of SrFe₁₂O₁₉ hexaferrites by nanostructuration.

SrFe₁₂O₁₉ nanostructured powders were obtained by hydrothermal processing of strontium and ferric nitrates in a Teflon lined bomb at 170°C for 20h, with appropriate concentrations of starting materials. The as-prepared powders were sintered by spark plasma sintering (SPS) at 350°C under 700MPa. Both powders and sintered materials were characterized by X-ray diffraction, scanning electron microscopy and magnetic measurements.

The sintered materials appear to be homogeneous. They are composed of platelets elongated perpendicular to the pressing direction. Their size, about 200 nm large and about 50 nm thick, is similar to that of the starting powders, indicating that no grain growth occurred during SPS. The magnetic properties of the sintered materials were measured parallel and perpendicular to the pressing direction. A coercive field $\mu_0 H_C$ is about 1800 G is obtained (the coercive field of the starting powders is very low, being less than 50 G). A slight magnetic anisotropy is observed, related to the anisotropic shape of the grains. The saturation magnetization of the powders is preserved, being about 60emu/g.

Financial support of the French "Agence Nationale de la Recherche" (ANR), through the program "Investissement d'avenir" (ANR-10-LABX-00-01) LabExEMC3 is gratefully acknowledged.

TU.H-P79 - Crystallization process and magnetic properties of Fe-rich nanocrystals embedded on amorphous magnetic ribbons

J. Duque¹, B. Peixoto¹, G. Mecena¹, S. Silva¹, C. Mendonça¹, T. Meneses¹

1. NPGFI, Federal University of Sergipe, Sergipe, Brazil

In this work we use thermal analysis methods, X-ray diffraction and magnetization measurements to carry out a systematic study on amorphous magnetic materials. In this sense, as-quenched amorphous samples of $\text{Ni}_{40}\text{Fe}_{40}\text{P}_{14}\text{B}_6$ and $\text{Fe}_{76,5}\text{Cu}_1\text{Nb}_3\text{Si}_{13,5}\text{B}_6$ were used. We have interpreted the crystallization kinetics in terms of the Johnson/Mehl/Avrami (JMA) nucleation-growth model. X-ray diffraction data as function of temperature reveal that our samples consist of single phases of Fe-rich nanocrystals embedded in a residual amorphous phase. Magnetic measurements as function of temperature show a sharp decreases of the magnetization around 200 and 350C to $\text{Ni}_{40}\text{Fe}_{40}\text{P}_{14}\text{B}_6$ and $\text{Fe}_{76,5}\text{Cu}_1\text{Nb}_3\text{Si}_{13,5}\text{B}_6$, respectively, likely related to the Curie temperatures. TGA and magnetization curves show additional increases in the high temperature region which are attributed to the growth of the Fe-rich magnetic phases.

TU.H-P80 - Direct and converse magnetoelectric effect in BSPT-NFO co-fired laminate composite

D.Kumar S¹, Ramesh G¹, Subramanian V¹

1. Indian Institute of Technology Madras, India

The magnetoelectric (ME) properties of laminate composite consists of 0.373 BiScO₃- 0.627 PbTiO₃ (BSPT) as ferroelectric phase and NiFe₂O₄ (NFO) as ferrite phase is studied. The bi-layer laminate is prepared by stacking the individually calcined phases followed by co-fired technique at two different temperatures (i) 1100°C (B-N 1100) and (ii) 1200°C (B-N 1200). The effects of sintering temperature on ME coupling between the phases were investigated. The scanning electron microscopy (SEM) and energy dispersive X-ray (EDX) analysis across the interface indicates diffusion between the phases enhances with increase in sintering temperature. A well saturated ferroelectric loop is observed in both the samples and the saturation polarization decreases with increase in sintering temperature. The direct ME (DME) coefficient of B-N 1100 and B-N 1200 laminate shows a maximum value of 30 mV/(cm.Oe) and 20 mV/(cm.Oe) respectively where as the converse ME (CME) coefficient shows a maximum value of 0.04 (mG.cm)/V and 0.16 (mG.cm)/V respectively. Interestingly, the B-N 1100 sample shows a maximum DME effect whereas B-N 1200 sample shows a maximum CME effect which might be due to effect of sintering on the magnetic phase and the diffusion between the phases.

TU.H-P81 - Combinatorial development of Fe-Co-Nb thin film magnetic nanocomposites

V. Alexandrakis¹, W. Wallisch², S. Hamann¹, G. Varvaro³, J. Fidler², A. Ludwig¹

1. Ruhr-University Bochum, Faculty of Mechanical Engineering, Institute of Materials, Bochum, Germany

2. Institute of Solid State Physics, Vienna University of Technology, Vienna, Austria

3. Istituto di Struttura della Materia, CNR, Monterotondo Scalo, Roma, Italy

To date, rare earth (RE)-based magnetic materials are the best performing permanent magnets (PMs); they cover 65% of the market, while less expensive hexaferrites, characterized by a lower (BH)_{max} value but still high T_c, provide another 34% of the total [1]. Nowadays, RE supplies have become a bottleneck, thus stimulating an intense activity for the search of new materials with a reduced or even zero content of RE either to match/surpass the properties of the state-of-art RE-PMs or to bridge the gap between hexaferrites and RE-based PMs. Discovery of novel materials for PMs is challenging, as the performance of a PM mainly depends on coercivity and remanence, which are extrinsic properties strongly affected by both composition and microstructure, being then extremely difficult to be predicted by calculations. High-throughput experimentation and combinatorial fabrication of materials' libraries offer a quick assessment of materials properties, giving a guidance about which materials are promising for novel PMs. In this communication, combinatorial and high-throughput methods were applied for the fabrication and characterization of Fe-Co-Nb thin film composition spread type materials libraries. Nb was chosen as an alloying element for Fe-Co as it is in abundance with a low price and forms non-cubic binary structures with both Fe and Co. Structural analysis indicated the formation of a new ternary compound (Fe,Co)₃Nb with a hexagonal crystal structure embedded in a FeCo-based matrix. The magnetic measurements revealed that the film behave as a hard-soft magnetic composite, thus indicating that the new (Fe,Co)₃Nb phase is ferromagnetic. The reversal mechanism was also investigated and was found to be domain wall pinning type.

[1] O. Gutfleisch et al. Adv. Mat. 23 821 2011

[2] Goll et al. J. Phys.: Cond. Matter. 26 064208 2014

TU.H-P85 - Optical and magneto-optical properties of Bi substituted Nd iron garnets prepared by metal organic decomposition method

E. Jesenska^{1,2}, M.Sasaki¹, T. Hashinaka¹, G. Lou¹, M. Zahradnik², L. Ohnoutek², R. Antos², M. Veis², T. Ishibashi¹

1. Nagaoka University of Technology, Japan

2. Charles University In Prague, Prague, Czech Republic

Magnetic garnets have recently attracted a renewed attention as they manifest several magneto-electric, spintronic and magneto-optical (MO) phenomena, such as induction of polarization or magnetization by electromagnetic field, spin Seebeck effect, spin Hall magneto-resistance as well as high Faraday effect [1,2,3,4]. Because of their well-defined optical and magnetic properties, rare-earth magnetic garnets are interesting materials for applications in magnetic recording, non-reciprocal photonic devices (including optical isolators and circulators) and MO visualizers. Several techniques are used to grow their high quality thin films. Among them metal organic decomposition (MOD) method appears to be very promising, because it is inexpensive, simple, and guarantees highly uniform chemical composition and purity, combined with chemical stability [5]. Although yttrium iron garnets are mostly studied, neodymium iron garnets seems to have interesting properties, such as strong out-of-plane magnetic anisotropy.

In this work, we present systematic optical and MO studies of $\text{Nd}_2\text{BiFe}_{(5-x)}\text{Ga}_x\text{O}_{12}$ and $\text{Nd}_{0.5}\text{Bi}_{2.5}\text{Fe}_{(5-x)}\text{Ga}_x\text{O}_{12}$ ($x=0, 0.25, 0.5, 0.75, 1$) thin films prepared by MOD method on $\text{Gd}_3\text{Ga}_5\text{O}_{12}$ (111) substrates. Spectroscopic ellipsometry and MO spectroscopy were employed as characterization techniques. Faraday and Kerr MO spectra clearly demonstrated that the increasing Ga concentration decreases the spin-orbit coupling and influences the MO effect. A confrontation of ellipsometric and MO experimental data with advanced theoretical calculations provided a spectral dependence of complete permittivity tensors of studied materials in a wide spectral range.

[1] X. Ding, Adv.Mat.Res. 418-420, 1752 (2011)

[2] A. Kirahara, Nat.Mat. 11, 686 (2012)

[3] H. Nakayama, Phys.Rev.Lett. 110, 206601 (2013)

[4] T. Ishibashi, J.Cryst.Grow. 275 (2005) [5] T. Ishibashi, J.Appl.Phys.97, 013516 (2005)

TU.H-P87 - Co ferrite thin films on MgO (100) prepared by metal-organic decomposition method

T. Ishibashi¹, M. Sasaki¹, M. Ninomiya¹, T. Tsurui¹, K. Shinozaki¹, T. Komatsu¹, H. Yanagihara², E. Kita²

1. Nagaoka University of Technology, Japan

2. University of Tsukuba, Japan

Recently, stress-induced large magnetic anisotropy has been reported in the epitaxial Co ferrite thin films on MgO (100) substrates prepared by sputtering technique[1], showing the possibility of ferrite materials for strong permanent magnet or high-density magnetic recording media without using rare earth metals nor noble metals. In order to explore new ferrite materials, metal organic decomposition (MOD) method is promising because of good productivity with accurate chemical composition and uniformity. In this paper, we report on Co ferrite thin films prepared by MOD method. MOD solution with a composition of Co : Fe = 1 : 3 (Kojundo Chemical Lab Co.,Ltd.) was spin-coated on MgO (100) substrates with 3000 rpm for 30 s, followed by drying at 100°C for 10 - 30 min. In order to decompose organic materials and obtain precursor films, samples were pre-annealed at 450°C for 30 min. Finally, the samples were annealed at 700°C in air for 1 - 13 h for crystallization. The 400 diffraction peaks of Co ferrite were observed in the XRD measurement, indicating that Co ferrite films grown along <100> on the MgO (100) substrates. Magneto-optical spectra showed characteristic structures of Co ferrite having peaks at 1.8, 2.1, 2.2 eV. TEM combined with EDX measurement revealed that homogeneous thin films with a thickness of 42 nm were grown on the substrates and the chemical composition was Co : Fe = 1 : 4. Magnetic anisotropy field was found to be larger than 50 kOe. On the other hand, coercivity was as small as 4 kOe. We conclude that the MOD method is promising for preparation of ferrite films.

[1] T. Niizeki et al., J. App. Phys. Lett. 103, 162407 (2013)

TU.H-P88 - Refining of Mo permalloy powders (MPPs) by hydrogen and magnetic properties of core made of refined MPPs

Ji Young Byun¹, Kwang Deok Choi¹, G. Choi²

1. Material Architecturing Center, Korea Institute of Science and Technology, Republic of Korea

It has been well known that the hydrogen annealing of permalloy plates at high temperatures of 1,100-1,200°C enhances their magnetic properties drastically due to removal of non-metallic elements of carbon, oxygen, sulfur, etc. The same process, however, cannot be applied for refining the permalloy powders, because high-temperature annealing results in sintering of the powders. The approach in the present work was to add CaO powders to the Mo permalloy powders (MPP). Experimental results of hydrogen-annealing of the MPPs showed that CaO powders in the mixture of CaO and MPPs prevented MPPs from sintering, even though the mixture was treated at high temperatures of 900-1,000°C. Water-soluble CaO can be easily removed from the reaction mixture by magnetic separation in water medium. (S+O) contents in MPP were reduced from 900 ppm to less than 300 ppm when the mixtures were kept above 1 hr at 1000°C or 4 hrs at 950°C or 9hrs at 900°C. This indicates that each MPP is exposed to the hydrogen and (S+O) in the permalloy is removed by reactions with hydrogen to form H₂O and H₂S. Core losses of powder cores made of hydrogen-refined MPPs were observed to be lower than those of cores made of unrefined MPPs. Effects of the annealing temperature and time and the CaO amount in powder mixture on the contents of sulfur and oxygen, hardness, and grain size will be presented in detail in the poster.

TU.H-P89 - crystal field parameters for rare-earth permanent magnets: wannier function approach

T. Yoshioka¹, H. Tsuchiura¹, P. Novak²

1. *Department of Applied Physics, Tohoku University, Sendai, Japan*

2. *Institute of Physics of ASCR, Prague, Czech Republic*

Crystal electric fields (CEF) acting on the 4*f* electrons of rare-earth (RE) ions in RE permanent magnets play a dominant role in determining their magnetic anisotropy. The interaction between the anisotropic 4*f* electronic clouds of RE ions and the CEF of surrounding charges control the magnetic moments along a specific crystalline direction. The large magnetic anisotropy energy of RE magnets produced by the CEF is strongly believed to mainly dominate their coercivity. Thus, precise information of CEF is needed to study and to improve the magnetic anisotropy and coercivity of RE magnets.

Theoretically, there still remain problems to treat the 4*f* electrons of RE ions. The open-core method may give good results when 4*f* electrons are well-localized. Unfortunately, however, some RE magnets have been known to be not the case. Quite recently, a new method has been developed to carry out an accurate calculation of CFPs by using Wannier functions.[1] Now it is interesting to estimate the CFPs of RE magnets by using this method.

The CFPs for crystalline R₂Fe₁₄B have been obtained by the Wannier function approach, which enables us to visualize the 4*f* electron clouds. By diagonalizing CEF Hamiltonian based on the Wannier functions, we have confirmed that the low energy wave functions for R=Nd and Dy are expanded to the *a-b* plane, which result in the single-ion anisotropy along the *c*-axis. The 4*f* electron clouds in Nd ions are more expanded to radial direction than that in Dy ions reflected by the lanthanide contraction. On the other hand, we also calculate the CFPs of Nd ions around the surface of the crystalline Nd₂Fe₁₄B and have found that the Nd ions exposed on the (001) surface have 4*f* electron clouds extended to the *c*-axis accompanying the *c*-plane magnetic anisotropy. The results for CFPs are consistent with previous theoretical study. [2]

References:

[1] P. Novák, K. Knížek, and J. Kuneš, Phys. Rev. B Vol. 87 (2013) 205139

[2] H. Moriya, H. Tsuchiura, and A. Sakuma, J. Appl. Phys. 105 (2009) 07A740

TU.H-P90 - Effects of annealing on the structure and magnetic properties of Fe-Si-Cr flakes and composite sheets

P. Jang¹

1. Cheongju University, Cheongju, Republic of Korea

Gas atomized Fe-Si-Cr powder was used in the application of a bypass sheet in near field communication. The powder was ball-milled, annealed at different temperatures and then manufactured to the sheet. Changes in microstructure and magnetic properties were investigated by XRD, VSM and impedance analyzer. The as-milled Fe-Si-Cr flake consisted mainly of disordered A2 and ordered B2 phases while the atomized powder consisted of A2, B2 and DO₃ phases. Increases in the annealing temperature caused the formation of a DO₃ phase. At temperatures higher than 923 K, the final flake consisted of only A2 and DO₃ phases. Grain size increased abruptly from 823 K, while the size of the DO₃ phase increased rapidly from 623 K. Coercivity of the flake decreased after annealing, with the lowest coercivity obtained after 923 K annealing while saturation magnetization showed a minimum value of 928 kA/m after 523 K annealing. Sputtered Fe-12%Si films showed a highest electrical resistivity value of 191 $\mu\Omega\cdot\text{cm}$ after 623 K annealing while the resistivity of Fe-4%Si sputtered films decreased almost linearly with annealing temperature. Therefore it could be concluded that high permeability of the 623 K sheet at 13.56 MHz and low permeability of the 923 K sheet at 80 MHz were due to the high resistivity as well as nanostructure of the 623 K flake.

TU.H-P91 - Theoretical evaluation of temperature dependence of magnetic anisotropy constants of $R_2Fe_{14}B$ compounds

D. Miura¹, R. Sasaki¹, A. Sakuma¹

1. Applied Physics, Tohoku University, Japan

Sintered Nd-Fe-B permanent magnets have the largest maximum energy product of all permanent magnets, and are vital materials of high-performance magnetic devices. Unfortunately, the Nd-Fe-B magnet is unusable under the high temperature environment (above 500K) due to the lacking coercive force. In general, it is believed that the coercive force of rare-earth magnets including Nd-Fe-B magnets is dominated by magnetocrystalline anisotropy originated from both the crystalline electric field (CEF) and the exchange field acting on the 4f electronic system in rare-earth ions. However, there are few calculations for the temperature dependent magnetic anisotropy constants (MACs) based on the microscopic footing mentioned above. Our aims are to theoretically reproduce temperature dependence of various magnetic properties of $R_2Fe_{14}B$ (R stands for a rare-earth element) compounds and understand the coercive mechanism of rare-earth magnets from microscopic viewpoints. In this work, we calculate MACs (K_1 , K_2 , K_3) of $R_2Fe_{14}B$ compounds on the basis of a microscopic model. The Hamiltonian for the 4f electronic system in an R ion consists of the spin-orbit interaction, the CEF term and the exchange interaction with Fe spins. We define the MACs as the expansion coefficients, with respect to powers of trigonometric functions, of the Helmholtz free energy for the 4f electronic system. From analysis of temperature and angle dependence of the free energies, we can reproduce well the temperature dependences of the MACs agreeable with the experimental results in the quantitative level. Also we refer to the effects of first excited J multiplet on the MACs, and find it is important in a low-temperature region and becomes ignorable with increasing temperature.

TU.H-P92 - The influence of ac joule heating on the magnetic properties of thin finemet cold-drawn microwires

H. Chiriac¹, S. Corodeanu¹, A. Donac¹, V. Dobrea¹, G. Ababei¹, M. Lostun¹, T.A. Ovari¹, N. Lupu¹

1. National Institute of Research and Development for Technical Physics, Iasi, Romania

Amorphous and/or nanocrystalline microwires with enhanced soft magnetic properties are excellent as sensitive elements in sensors for the detection/measurement of ultra-low magnetic fields [1]. This type of sensing device could be also used for detecting small displacements, vibrations, and various mechanical deformations. In this paper, we studied the magnetic and magnetoelastic properties of FINEMET nanocrystalline wires with diameters ranging from 40 μm down to 10 μm , obtained by cold drawing FINEMET amorphous wires of 105 μm in diameter prepared by in-rotating-water spinning. Their unique magnetic properties are discussed considering the stresses induced during preparation and cold drawing, the stresses relief following annealing, the annealing-induced structural transformations (e.g., nanocrystallization) and the corresponding changes in the magnetic anisotropy. The different magnetic behavior observed after conventional annealing at 500⁰C and, respectively, 550⁰C, with the permeability reaching the maximum after annealing at 500⁰C and the giant magnetoimpedance (GMI) response being maximum after annealing at 550⁰C, can be ascribed to the different evolution of the nanocrystallization process in the center of the wire and on the surface, as confirmed by UHR-TEM studies. Furthermore, the cold drawn wires were annealed by Joule heating using a.c. currents of different frequencies (1÷10 MHz) to control the area of the cross section of the wire in which the nanocrystalline structure appears. The longitudinal magnetic permeability measurements corroborated with the GMI response and the surface measurements by magneto-optical Kerr magnetometry shown that, in the case of current annealing a well-defined circumferential or even oblique anisotropy are induced. The TEM studies emphasized also smaller nanograins on the surface compared with the inner core of the wires subjected to a.c. current annealing. Using different frequencies for the a.c. currents it was possible to control the magnitude of the longitudinal magnetic permeability and GMI response, accordingly with the requirements for different sensing applications.

This work was supported by the NUCLEU Programme (PN 09-43 01 01).

[1] H. Chiriac, S. Corodeanu, A. Donac, V. Dobrea, G. Ababei, G. Stoian, M. Lostun, T.-A. Ovari, and N. Lupu, J. Appl. Phys. 117 (2015) *in press*

TU.H-P93 - Magnetoelastic properties of amorphous $\text{Co}_{66}\text{Fe}_4\text{Ni}_1\text{B}_{14}\text{Si}_{15}$ alloys in compressive and tensile stress sensors applications

J.Salach¹

1. Institute of Metrology And Biomedical Engineering, Warsaw University of Technology, Warsaw, Poland

Amorphous magnetic materials are known very well in magnetic and electronic components. However, they are not widely known for their magnetoelastic properties for stress sensors applications. Reason of this state is character of these materials, which are typically in the form of ribbon or wire. Meanwhile, to obtain a high resolution of magnetoelastic sensors, uniform stresses distribution and closed magnetic circuit is necessary.

Paper presents the results of investigation of magnetoelastic properties of amorphous $\text{Co}_{66}\text{Fe}_4\text{Ni}_1\text{B}_{14}\text{Si}_{15}$ alloy. Ribbon was rolled up in a ring shaped samples and then annealed in temperature of selected values. The temperature was chosen in order to obtain the high permeability material without losing the high mechanical strength. Thus, a temperature of 350oC and 365oC was chosen. For comparison of of tested material magnetoelastic properties change, it was also investigated in as-quenched state. Investigation of magnetoelastic properties was performed for a range of tensile stress form 0 up to 3 MPa. This range was due to the mechanical strength of testing device. For compressive stresses, the attainable range was from 0 up to 10 MPa. These results indicate, that investigated materials have high magnetoelastic sensitivity, and after special preparation can be used for application in magnetoelastic sensors of compressive and tensile stresses. Significant changes of flux density in the samples suggest stable indication of proposed sensor, and resistance to external interference.

TU.H-P94 - Strain-controlled MO effect on highly Bi-substituted neodymium iron gallium garnet thin films

M. Sasaki¹, G. Lou¹, T. Hashinaka¹, A. Meguro¹, M. Ninomiya¹, T. Ishibashi¹, T. Taniyama²

1. *Nagaoka University of Technology, Nagaoka, Japan*

2. *Tokyo Institute of Technology, Tokyo, Japan*

Controlling magnetization of magneto-optic (MO) materials by voltage instead of electric current is expected to reduce power consumption and miniaturize functional elements in MO devices such as magneto-optic spatial light modulator (MO-SLM). One of the methods to control magnetization is to use reverse magnetostrictive effect using piezoelectric actuator [1] [2] [3]. In this study, highly Bi-substituted neodymium iron gallium garnet (NBIGG) thin films prepared on gadolinium gallium garnet (GGG) single crystal substrates were studied as a strain-mediated magnetoelectric coupling element. $\text{Nd}_{0.5}\text{Bi}_{2.5}\text{Fe}_{4.5}\text{Ga}_{0.5}\text{O}_{12}$ thin films were prepared by metal-organic decomposition method. The NBIGG films were cemented on the PZT polycrystals with two Au electrodes with a gap of 1mm. Tensile strain in the direction of the electrical field was applied to the NBIGG thin films, which was measured by a strain gauge on the PZT and was estimated to be approximately 3.5×10^{-4} at applied voltage 1.7kV. Strain-induced changes of coercivity H_c and saturation field in hysteresis loop were measured by the magneto-optical Kerr microscope. We found that H_c increased by maximum 10% and saturated Kerr rotation angle also changed by maximum 40% when the applied voltage was increased from 0V to 1.7kV. We also found that magnetic domain structures under the strain were not uniform because of spatial distribution of residual stress. We consider that it was caused by non-uniformity of adhesive or other artifact.

[1] A. Brandlmaier et al., Phys. Rev. B 77, 104445 (2008)

[2] S. Mito et al., J. Magn. Soc. Jpn., 32, 63 (2008)

[3] S. Geprags et al., Solid State Commun., 198, 7 (2014)

TU.H-P95 - Structural and magnetic properties of magnetically semi-hard $(\text{Fe}_x\text{Co}_{1-x})_3\text{B}$ compounds

S. Pal¹, S. Ener¹, M. Skokov¹, O. Gutfleisch^{1,2}

1. TU Darmstadt, Materialwissenschaft, Darmstadt, Germany

2. IWKS Hanau, Fraunhofer-Projektgruppe für Wertstoffkreisläufe und Ressourcenstrategie, Hanau, Germany

There has been some efforts in fabricating nano-composite exchange-spring magnets by combining large remanence (soft) phases, such as Fe and Fe-Co and strong-anisotropy (hard) phases, in order to improve the energy product $(BH)_{\text{max}}$ value. However, the soft phases affect coercivity negatively. It is expected that, apart from the magnetization improvement, the coercivity of nano-composite permanent magnets would be improved through the replacement of soft magnetic phase by a semi-hard magnetic phase. Here, we present a study on the $(\text{Fe}_x\text{Co}_{1-x})_3\text{B}$ ($x = 0.0, 0.1, 0.2$ and 0.3) compounds with the aim of synthesizing Fe_3B compound with tetragonal structure which is a metastable phase and exists in a narrow temperature range of 1150-1250 K. The $(\text{Fe}_x\text{Co}_{1-x})_3\text{B}$ compounds have been prepared by substitution of Fe atoms for Co atoms in Co_3B . A single phase orthorhombic structure was obtained by X-ray diffraction measurement for all compositions. Magnetic domain images obtained by Kerr microscopy show distinctive domains and reveal the presence of uniaxial magnetocrystalline anisotropy. The anisotropic nature was confirmed by the demagnetization curve measurements of the magnetically oriented single-crystalline particles which were obtained after crushing the ingots. The anisotropy constants and anisotropy field of the samples of magnetically oriented single-crystalline particles have been calculated. An anisotropy field of 2.2 T was obtained for Co_3B ($x = 0.0$), the anisotropy field was found to decrease with increasing Fe content reaching to a value of 1.5 T for $x = 0.3$. The Curie temperature for $(\text{Fe}_x\text{Co}_{1-x})_3\text{B}$ compound was found to increase from 750 K for $x = 0.0$ to 923 K for $x = 0.3$. These compounds with uniaxial magnetocrystalline anisotropy are promising materials to be used as semi-hard magnetic phase for the preparation of nanocomposite exchange-spring magnets.

TU.H-P96 - Effect of the Mn/Bi ratio on the microstructure and magnetic properties of melt-spun MnBi LTP alloys

M. Grigoras¹, M. Lostun¹, G. Ababaei¹, H. Chiriac¹, N. Lupu¹

1. National Institute of Research & Development For Technical Physics, Iasi, Romania

Recently, the free rare-earth permanent magnets become an attractive research topic. Among these, the low-temperature-phase (LTP) pure MnBi turned out to be a competitive candidate since it shows hexagonal NiAs-type crystal structure at RT and exhibit large magnetocrystalline anisotropy and positive temperature coefficient of coercivity [1]. The coercivity increases with temperature, reaching a maximum of 2.5 T at 540 K [2], making MnBi-based magnets an attractive alternative, especially for high temperatures applications. However, MnBi relatively saturation magnetization of about 75 Am²/kg at RT limits the (BH)_{max} to about 136 kJ/m³. To improve the magnetic properties, many efforts have been made to prepare MnBi compounds with pure LTP, but this proved to be a challenge up to now. In this respect, we report here the effect of the Mn/Bi ratio on the hard magnetic properties and microstructure of Mn_{100-x}Bi_x melt-spun ribbons prepared by rapid solidification (x=40,60 at.%). The alloy ingots were prepared by arc-melting from the constituent elements, followed by induction-melting in order to obtain better uniformity. MnBi-ribbons were obtained by melt-spinning using a copper wheel at different velocities. The ribbons were then annealed in vacuum, for different periods of time, at temperatures between 563 K and 673 K in order to obtain the pure LTP. We have managed to achieve a coercivity near 0.85 T at RT in Mn₅₀Bi₅₀ melt-spun ribbons, annealed at 573 K for 20 h, while the saturation magnetization was 61 Am²/kg. The microstructure of the annealed Mn₅₀Bi₅₀ melt-spun ribbon revealed a fine and uniform grains structure, with an average size of about 40 nm. By modifying the Mn/Bi ratio, the magnetic properties are enhanced and the grain structure refined.

This work was supported by the NUCLEU Programme (PN 09-43 02 01).

[1] X. Guo, et al, Phys.Rev.B 46,14578(1992)

[2] J. B. Yang, et al, Appl.Phys.Lett. 99,082505(2011)

TU.H-P97 - Grain boundary engineering of thin FeCo films: a route towards new hard magnetic materials

A. Backen^{1,2}, D. Le Roy^{1,2}, N. M. Dempsey^{1,2}, D. Givord^{1,2,3}

1. Institut Néel, CNRS, UPR 2940, Grenoble, France

2. Université Grenoble Alpes, Institut Néel, Grenoble, France

3. Instituto de Física, Universidade Federal do Rio de Janeiro, Rio de Janeiro, Brazil

Minimizing the content of rare earth (RE) elements in hard magnetic materials is one of the major challenges in magnet research today. High-coercivity RE-Fe-B magnets with heavy RE content below typically 1-2 % are being prepared by grain boundary diffusion processing. This permits an enhancement of the surface/interface hard magnetic properties, without affecting the magnetic properties within the grains themselves. We have applied this approach with the objective of preparing new types of hard magnetic materials, with properties intermediate between those of high performance RE-Fe-B and those of hard ferrites. FeCo-based alloys are very interesting in this context, because of their high spontaneous magnetization. FeCo sputtered films have been prepared with thickness in the range 20 - 200 nm. These films exhibit a columnar microstructure, which should be favorable for grain boundary diffusion from capping and buffer layers into the main layer. In films in which the FeCo layer is sandwiched between two Nd layers, annealing for 10 h at 675°C, leads to the development of a coercive field of up to 50 mT at 50 K. In these films, the FeCo peaks are no longer observed in XRD scans, and small peaks suggest the formation of the Nd₂Fe₁₇ phase. To avoid the consumption of FeCo, the FeCo layer may be separated from the Nd layer, by another transition metal layer, immiscible with Fe and Co, namely Ag. During annealing, the Nd diffuses into Ag, forming a low temperature eutectic. Nd is thus only available at the surface of the FeCo layer. For very thin layers FeCo layers (20nm), an increase in coercivity up to 65 mT is obtained after annealing. In the case of 200 nm-thick FeCo layers, the coercivity after annealing is about 13 mT. In both cases, the observed coercivity is almost temperature-independent which suggests the influence of shape anisotropy.

TU.H-P98 - Nanosized powder with preserved soft magnetic properties obtained by high energy and cryomilling techniques.

A. Aragón¹, M.Guzik², S. Deledda², A. Hernando¹, P. Marín¹

1. Instituto De Magnetismo Aplicado (UCM-ADIF), Las Rozas (Madrid), Spain
2. Institute for Energy Technology, Kjeller, Norway

Fe-based nanocrystalline alloys are well known because of their good soft magnetic properties, which make them suitable for specific applications. Several reports have shown that mechanical ball milling is an optimal processing technique to obtain amorphous or nanocrystalline powder to be used in compactation. [1-4] In this work, different milling techniques as High Energy Ball Milling (dry and wet) and cryomilling, have been used to obtain nanometer particle size powder of nanocrystalline Fe and FeCo based ribbons. We have studied the influence of selected milling technique in microstructure and magnetic soft properties of the final product have been studied. Induction of nanocrystallization before milling increased the brittleness of sample. Surfactant-assisted milling prevented particle agglomeration and milling at liquid nitrogen temperature decreased particle size in a shorter time. An average particle size between 300 nm and 900 nm was obtained. All samples showed low coercivity and high magnetic saturation values: 3-30 Oe and 125-150 emu/g for Fe-rich, and 10-70 Oe and 170-202 emu/g for FeCo-rich powder. Among all the samples, cryomilled ribbons presented the higher susceptibility values. This is explained by the increase of work hardness during milling performed at low temperatures, because of the augmented number of lattice defects. These structural properties in conjunction with the submicron grain size improve tensile strength and hardness of compacted samples.

Acknowledgements: This work was supported by Project FP7-NMP-2012-SMALL-6 NANOPYME "Nanocrystalline Permanent Magnets Based on Hybrid Metal-Ferrites" (nº 310516).

References:

- [1] J. Füzér, et al. IEEE Trans. Magn. 46, 2 (2010)
- [2] Y.Y. Suna, et al. J. Alloys Compd. 509, 6603-6608 (2011)
- [3] B.V. Neamt et al. J. Alloys Compd. 626, 49-55 (2015)
- [4] Hernando, A. et al. Phys. Rev. B. 69, 052501 (2004)

TU.H-P99 - Magnetic and structural analysis of mechanically alloyed Fe-Co based nanocrystalline alloys

J.J. Suñol¹, J. Bonastre¹, J. Saurina²

1. University of Girona, Girona, Spain

Mechanical alloying was used to prepare several FeCo based soft magnetic alloys as powder mixtures in a high-energy planetary ball mill under argon atmosphere. These materials have high saturation magnetization and also high Curie temperature. Structural, microstructural and magnetic behavior was followed by scanning electron microscopy (SEM), X-ray diffraction (XRD), differential scanning calorimetry (DSC) and vibrating sample magnetometry (VSM). Nanocrystalline structure was achieved at 40 hours of milling. It was found that the partial substitution of Fe by Co in nanocrystalline alloys is a way of extending their outstanding soft magnetic properties to higher temperatures. Furthermore, the nanocrystalline the nanostructured materials have a significant fraction of atoms in grain boundaries and crystallographic defects (voids, dislocations) which influences their magnetic properties. In these alloys, annealing improves soft magnetic behavior by reducing mechanically induced internal stress. Powdered samples were consolidated and sintered to obtain bulk materials in order to analyze their properties. However, high annealing temperatures should be avoided to prevent significant grain growth. Crystallization was also analyzed to determine the thermal stability from crystallization (activation energy, crystallization phase diagram) and to design experimental conditions to develop alloys with controlled nanocrystalline size.

Acknowledgements: Financial support from project MAT2013-47231-C2-2-P.

TU.H-P100 - Study of AC magnetic properties and core losses of Fe/Fe₃O₄ - epoxy resin soft magnetic composite

Laxminarayana T. A.¹, Subhendu Kumar Manna², Fernandes B. G.³, Venkataramani N.¹

1. *Department of Metallurgical Engineering and Materials Science, Indian Institute of Technology Bombay, Mumbai, India*

2. *Department of Physics, IIT Madras, Chennai, India*

3. *Department of Electrical Engineering, Indian Institute of Technology Bombay, Mumbai, India*

Soft magnetic composite (SMC) is an electrically insulated iron powder that can be used for high frequency electrical devices due to its low core losses and 3D magnetic flux. SMC for this study was prepared by coating of ultrafine Fe₃O₄ particles, synthesized by co-precipitation method, on atomized iron powder of particle size < 53 μm using epoxy resin as an intermediate binder between iron and Fe₃O₄. SEM images and XRD pattern confirmed the uniform coating of ultrafine Fe₃O₄ particles on the surface of iron powder. Further a toroid of OD = 35 mm, ID = 25 mm was prepared by cold compaction of coated iron powder under a compaction pressure of 1050 MPa and subsequently cured at 150°C for 1 hour in Argon atmosphere. For comparison of properties, a toroid with uncoated iron powder was also compacted at 1050 MPa and annealed at 600°C in Argon atmosphere. DC resistivity and AC B-H loops were recorded on these toroids. The coated iron has a resistivity greater than 20000 μΩcm, measured by four probe method. Magnetic Hysteresis loop and core loss of the toroids were measured by B-H Loop tracer in the frequency range 0 to 1500 Hz. Coated and uncoated iron cores exhibited a core loss of 91 W/kg and 693 W/kg respectively at 500 Hz and 1 Tesla. For uncoated iron powder a drastic change in losses observed as frequency is increased due to the dominant eddy current losses at high frequency. A new method to prepare coated iron powder that yielded properties comparable to commercial SMC sample like somaloy130i-1P from Hoganas, Sweden is reported. DC Induction value of coated iron powder and somaloy130i-1P at 10000 A/m are 1.35 Tesla and 1.4 Tesla respectively, with Core loss of 206 W/kg and 147 W/kg respectively at 1000 Hz and 1 Tesla.

TU.H-P101 - Tailoring the magneto-transport properties of ferromagnetic amorphous wires

T. Ovari¹, S. Corodeanu¹, H. Chiriac¹

1. National Institute of R&D For Technical Physics, Iasi, Romania

Co-based nearly zero magnetostrictive amorphous wires have been shown to exhibit a large magneto-impedance effect. Here we investigate the effect of tensile stresses on the magneto-impedance response of amorphous wires with various diameters, aimed for stress and vibration monitoring sensors, to understand the effect of wire dimensions and stress magnitude on their magneto-transport characteristics, and to optimize their properties for such applications. We measured the magneto-impedance effect in wire samples having 80, 100, and 120 microns in diameter, respectively. The experimental set-up allowed us to measure samples simultaneously subjected to dc magnetic field and mechanical stress, at various frequencies of the ac driving current between 1 and 50 MHz. The maximum tensile stress was 500 MPa. To describe the magneto-impedance effect, we employed the magneto-impedance ratio (MIR), defined as the relative variation of impedance at each value of the applied field. We observed that for the thinnest sample, the maximum MIR at 50 MHz increases over three times with applied stress. Frequency is also important: the maximum MIR increases from 160% to nearly 450% for the sample with 100 microns in diameter, when the frequency increases from 1 to 10 MHz. This trend is maintained as the frequency increases to 50 MHz, where the stronger skin effect pushes the MIR over 500%. In conclusion, wire size is a key factor in the magnitude of the magneto-impedance effect. Its non-linear influence on the magneto-transport behavior originates in the magnitude and orientation of the magnetoelastic anisotropy, its dependence on wire diameter, and its changes with applied stress. The results are essential for the practical choice of materials to be employed in vibration and stress monitoring applications, and for tailoring the magneto-transport properties of amorphous wires.

This work was supported by UEFISCDI through contract no. 37/2014 (project PN-II-PT-PCCA-2013-4-0471, SmartFlow).

TU.H-P102 - Cobalt doping effect on Ni-Zn-Cu ferrites produced by reactive sintering

A. Mercier¹, G. Chaplier¹, A. Pasko¹, V. Loyau¹, F. Mazaleyrat¹

1. SATIE, ENS Cachan, CNRS, France

The process Spark Plasma Sintering (SPS) can be used for reactive sintering, i.e. it is possible to synthesize and to sinter the material in a single step which greatly reduces production time. For example, it is possible to produce spinel ferrite parts by this technique. A mixture of simple oxides is placed in a graphite die between two pistons. The spinel phase is formed at the first heating stage (580°C), and then the ferrite is sintered during the second heating stage (800°C). Unlike the classical process, it is not necessary to go through the intermediate stage of calcination [1], and the total process duration is only 25 minutes.

It was demonstrated that Co-substitution in Ni-Zn-Cu ferrites can improve the magnetic properties in general and the losses at high frequency in particular [2]. However, there is a great dependency on the temperature, and for a given cobalt rate, there is a local maximum permeability matching the spin reorientation transition [3].

In addition, the properties depend on the sintering process. To our knowledge, there is still no study of the influence of cobalt in spinel ferrites manufactured by SPS. The chemical formula is $\text{Co}_x(\text{Ni}_{0.24}\text{Cu}_{0.20}\text{Zn}_{0.56})_{1-x}\text{Fe}_2\text{O}_4$ where the Co-substitution x varied from 0 to 7 centimoles. The magnetic measurements show that there is a maximum of the permeability for a doping of 3 centimoles. At room temperature, the static permeability $\mu_s=7$ and merit factor $\mu_{\text{sfr}}=1.5\text{Ghz}$. However, XRD shows that unreacted simple oxides remain that probably influence negatively the properties. The measurement of the permeability and the losses will be presented in a temperature range from 0 to 100 Celsius degrees.

[1] K. Zehani et al., J. App. Phys. 109, 07A504 (2011)

[2] T. Y. Byun et al., IEEE Trans. Magn. 35, 3445 (1999)

[3] A. Lucas et al., App Phys Lett. 97, 182502 (2010)

TU.H-P103 - Structural, morphological & magnetic studies on pristine and Gd-doped YBiO₃ particlesD. Bhatnagar¹, R. Chatterjee¹*1. Magnetics & Advanced Ceramics Laboratory, Physics Department, Indian Institute of Technology Delhi, New Delhi, India*

YBiO₃ has attracted attention of researchers due to its properties like high ionic conductivity, excellent photo-catalyst properties, as buffer layer for superconductor films and in recent times as possible topological insulator material. However the structural and magnetic behaviour of YBiO₃ is still not well explored. In this work, pristine and gadolinium (Gd) doped YBiO₃ particles were successfully synthesized through co-precipitation technique. Yttrium, Gadolinium and bismuth nitrate salts were chemically reacted at optimized conditions, forming nanometer-sized precipitates. After calcination and sintering treatment polycrystalline powders were obtained.

Microstructure of the samples was investigated using scanning electron microscopy (SEM). The X-ray diffraction measurement (XRD) confirmed that the particles crystallized with face centred cubic (FCC) fluorite structure in single phase. The refined XRD data shows that the lattice parameter increases from 5.42 Å (for x=0 sample) to 5.44 Å (for x=0.02 sample). With further increase in Gd doping (x=0.05 sample), the lattice parameter decreased to 5.42 Å. The observation of lattice scale imaging in high resolution transmission electron microscopy (HRTEM) data indicates good quality of the samples and the structural parameters obtained from selected area electron diffraction (SAED) pattern matched well with the XRD results.

Raman spectra of all samples ($0 \leq x \leq 0.05$) showed five Raman active phonon modes; consisting of one A_{1g}, one E_g, and three T_{2g} modes. Apart from this, magnetic properties of pristine and Gd-doped YBiO₃ samples were also explored using MPMS SQUID magnetometer. (YGd)BiO₃ samples showed soft (~10 Oe) saturating M-H loops indicating weak ferromagnetism; whereas, the parent YBiO₃ shows temperature dependent diamagnetic behaviour at higher field values.

References:

1. G. Pollefeyt et al., J. Mater. Chem. A, 1 (2013) 3613
2. H. Jin et al, Sci. Rep. 3 (2013) 1651

TU.H-P104 - Problems of measuring and modeling of compressive stresses influence on magnetic properties of Fe-based amorphous alloy in rayleigh region

M. Kachniarz¹, R. Szewczyk², A. Bienkowski², J. Salach²

1. Industrial Research Institute For Automation And Measurements PIAP, Warsaw, Poland

2. Warsaw University of Technology, Institute of Metrology and Biomedical Engineering, Warsaw, Poland

Fe-based amorphous alloys are used in many technical applications, like cores of the inductive components for electronics and sensors of mechanical stresses. For this applications it is important to study the influence of mechanical stress on the magnetic properties of Fe-based amorphous alloys (so called Villari effect).

Rayleigh region is referring to the first part of initial magnetization curve. It is the region of low magnetizing fields, where initial magnetization curve and hysteresis loop are described by second order equation with two coefficients: initial magnetic permeability and Rayleigh coefficient. Investigation of magnetic and magnetoelastic properties of amorphous alloys in Rayleigh region is important because most of inductive components is working under low magnetizing fields. For the investigation, Fe-based as quenched amorphous alloy 2605 S3A of chemical composition $\text{Fe}_{77}\text{Cr}_2\text{B}_{16}\text{Si}_5$ was chosen. The special measurement setup was developed using hydraulic press to apply compressive stress to the material.

Obtained results indicates that compressive stress has significant influence on the magnetic properties of investigated amorphous alloy. On the basis of obtained $B_m(H_m)$ characteristics, the dependence of initial magnetic permeability and Rayleigh coefficient on the compressive stress was designated. This dependence was modeled with polynomial equations. Developed model allow to calculate values of initial magnetic permeability and Rayleigh coefficient and simulate the shape of Rayleigh hysteresis loop depending on the compressive stresses acting on the material. Obtained modelling results show high compatibility with measurement data which indicates that developed model can be used to simulate influence of compressive stress on the magnetic properties of Fe-based amorphous alloys in Rayleigh region.

TU.H-P105 - Transformation of the magnetic nature of Li-Fe spinels due to substitution with Ba and Ti ionsP. Bhatia¹*1. Gurunanak College of Arts, Science And Commerce, Mumbai, India*

Spinel ferrites have been established as magnetic materials which occupy smaller volume, have low production cost and are easier to manufacture using ceramic technology. The ability of the spinel to distribute cations in the octahedral and tetrahedral sites in different manners, gives rise to varied physical and chemical properties. In the present work it is thought interesting to investigate the role of Li⁺, Ba²⁺, Fe³⁺, and Ti⁴⁺ in a spinel by reducing a pseudobrookite to a spinel using the formula (Li_xFe_{2-x})(Ba_{1-y}Ti_y)O₄ where x+y=1, with a view to combine different properties which these cations impart in different environment. Li_{0.9}Fe_{1.1}Ba_{0.1}Ti_{0.9}O₄ (SP1) and Li_{0.7}Fe_{1.3}Ba_{0.3}Ti_{0.7}O₄ (SP2) are formed and their structural and magnetic behaviour are reported here. X-Ray Diffraction patterns indicate the single phase spinel formation belonging to LiFe₅O₈ group. However, SP1 is cubic and SP2 exhibits tetragonal symmetry. Ba²⁺ prefers the tetrahedral sites. Interionic distances, radii of tetrahedral and octahedral interstices are determined. Their magnetic hysteresis loops are studied and the corresponding parameters related to magnetic nature of the two spinels are reported. The sharp, narrow hysteresis loops are typical of soft ferrites.

The larger saturation magnetization M_s, Coercive force H_c and magnetic moment of SP2 are in accordance with the cation distribution and larger quantity of Fe. The Fe content has increased substantially on the B site, strengthening the exchange interaction which perhaps is responsible for the absence of canting in SP2. On the other hand, Ti-rich spinel SP1 shows presence of canting as well as multi domains. Curie temperature is observed to be lowered with substitution and approaches the room temperature hinting at applications as a switch.

TU.H-P106 - Shape dependent spin switching and surface state in millimeter-sized single crystals of $R_2Fe_{14}B$ (R=Nd and Tb)

R. Sakaguchi¹, R. Saito¹, D. Ogawa¹, Y. Mizuno¹, K. Koike¹, Y. Ando², H. Kato¹

1. Graduate school of Science and Engineering, Yamagata University, Japan

2. Graduate school of Engineering, Tohoku University, Japan

In view of the rapidly-growing demand for high-performance motors, the most crucial and urgent problem in sintered Nd-Fe-B magnets is to achieve much higher coercivity without heavy rare-earth elements. What we should remember is that the magnetic anisotropy of $Nd_2Fe_{14}B$ is large enough to exhibit higher coercivity without adding Dy.

We have grown $Nd_2Fe_{14}B$ films with different values of lateral grain size d . The coercivity showed monotonous increase with decreasing d from 7 kOe ($d=300$ nm) to 16 kOe (70 nm). When we deposited the 60-nm-thick Nd overlayer on these films and annealed at 500 degree C, the coercivity was enhanced with the increment of about 10 kOe irrespective of the d value [1]. These results thus suggest the independence of the size and the interface effects in a spin-switching process in the $Nd_2Fe_{14}B$ system.

If this conjecture is correct, then even bulk-sized single crystals would exhibit finite coercivity by an appropriate interface control. In this work, we prepared millimeter-sized single crystals of $Nd_2Fe_{14}B$ and $Tb_2Fe_{14}B$, and investigated systematically the spin-switching properties by using SQUID and MOKE techniques.

We shaped the crystals into the two kinds of rectangular plates with the tetragonal (001) or (100) plane as a largest surface, without any protective coating. The SQUID measurements on the $Nd_2Fe_{14}B$ crystals showed that coercivity is negligibly small for both (001)- and (100)-cut plates. On the other hand, MOKE observation for the (100)-cut plate exhibited the finite "local coercivity" of about 1 kOe. In the case of $Tb_2Fe_{14}B$, even the SQUID measurement on the (100)-cut plate revealed the large coercivity of 5.2 kOe in striking contrast to the negligibly small coercivity of the (001)-cut plate. These results suggest a shape-dependent correlation between the crystallographic orientation of the 2-14-1 surface and the spin-switching process.

[1] Koike et al. in preparation

TU.H-P107 - Nanoanalytical TEM studies and micromagnetic modelling of (Nd,Pr)-Fe-B magnets

G. Zickler¹, P. Toson¹, A. Asali¹, J. Fidler¹

1. Institute of Solid State Physics, Vienna University of Technology, Vienna, Austria

The search for candidates of suitable magnetic materials and their expected behaviour as reduction of the dysprosium/terbium content is of great economic and scientific interest. On the basis of numerical finite element micromagnetics (FEM) we have analysed the influence of the microstructural features, such as intergranular grain boundary phases (GB) and misalignment of the hard magnetic grain, on the optimization of magnetization reversal processes in order to improve the coercive field of (Nd,Pr)-Fe-B magnets. The microstructural model of the grains and intergranular phases, which is used for theoretical simulations, has been derived from a detailed nanoanalytical TEM/STEM study of Dy/Tb free magnets with different rare earth (RE) content and coercive field. Different types of grain boundaries are distinguished, such as the ones which are responsible for the nucleation processes of reversed domains and the ones acting as hindrance for reversed domain expansion. Special attention is laid on the EDX and EELS analysis of GB with a thickness ranging from 2 - 5 nm. This analysis identified the GB to have about 40 at.% of Iron and 50 at.% of RE, which is in good agreement with recent three dimensional atom probe experiments [1]. FEM simulations have been carried out in order to study the influence of internal demagnetizing fields determined by the microstructure on the magnetization switching behaviour. Special emphasis was put on the influence of the GB and their magnetic properties, due to their substantial influence on the nucleation of reverse magnetic domains and the pinning of domain walls. GB with soft ferromagnetic properties have the most effective influence on the decrease of the coercive field.

[1] H. Sepehri-Amin, Acta Materialia 60 (2012) 819-830

The financial support from the EC-FP7 project ROMEO (no: 309729) is acknowledged. This TEM investigation was carried out using facilities at USTEM, TUW, Austria.

TU.H-P108 - Comparison of potential approximations in electronic structure calculations of magnetic anisotropy energy of PrCo₅ and Pr₂Fe₁₄BA. Asali¹, P. Toson¹, G. Zickler¹, J. Fidler¹*1. Institute for Solid State Physics, Vienna University of Technology, Austria*

We report on DFT calculations of the PrCo₅ and Pr₂Fe₁₄B compounds at 0K. The goal is to compare the dependence of results on the utilized potential approximation, GGA or LDA. The electronic structure is simulated using WIEN2k [1], a full-potential, linearized augmented plane wave code. Core electrons are treated relativistically and the self-consistence force calculation already includes the scalar relativistic effects. After the SR-SCF, the spin orbit coupling (SOC) is calculated. The magnetic anisotropy energy is calculated as the difference in energy values for easy and hard axis.

In general we note that GGA calculations are more stable (lower total energy) than LDA. All moments are in μ_B .

<u>PrCo5</u>	Pr_spin	Pr_orbital	Pr_total	Co(3g)
GGA:	-2.05	1.11	-0.94	1.73
LDA:	-2.00	1.44	-0.56	1.63
Literature:			3.2 [2]	1.7 [2]
<u>PrCo5</u>	Co(2c)	Co_all	PrCo5_tot	MAE [MJ/m ³]
GGA:	1.75	8.67	6.96	8.74
LDA:	1.69	8.26	7.12	-4.25
Literature:	1.7 [2]	8.5 [2]	11.7 [2]	7.6 [3] (Room Temp.)
<u>Pr2Fe14B</u>	Pr_spin	Pr_orbital	Pr_total	Fe_spin_mean
GGA:	-2.23	1.11	-1.12	2.39
LDA:	-2.03	1.55	-0.48	2.27
Literature:			0.8 [4]	2.2 [4]
<u>PrFe14B</u>	Fe_total_mean		Pr2Fe14B_total	MAE
GGA	2.43		29.74	0.46
LDA	2.31		30.27	5.94
Literature			32.3 [4]	4.0 [5]

We conclude that GGA calculations are more precise for the PrCo₅ system. For Pr₂Fe₁₄B systems our preliminary results show a better agreement for LDA with the experimental value.

The financial support of the EC-FP7 project ROMEO (309729) is acknowledged. The computational results have been achieved using the Vienna Scientific Cluster.

[1] K. Schwarz, P. Blaha, Comp. Mat. Sci. 28 (2003) 259-273

[2] Hummler et al, PRB: Condens. Matter 53 (1996) 3272–3289

[3] Patra et al. J. Phy. D: Appl. Phys. 47 (2014) 215001

[4] Sinnema et al: J. Magn. Magn. Mater. 44 (1984) 333–341

[5] Bolzoni et al.: J. Magn. Magn. Mater. 65 (1987) 123–127

TU.H-P109 - First principles study for the effect of spin fluctuation on the crystalline magnetic anisotropy in L10-type ordered alloysN. Kobayashi¹, K. Hyodo¹, A. Sakuma¹*1. Department of Applied Physics, Tohoku University, Japan*

For the application of high-density magnetic devices, thermal stability of magnetization in materials is one of the key factors. In almost hard-magnetic materials below Currie temperature, the thermal effect on magnetization is emerged as the fluctuation of its direction.

In this study, we investigated the influence of the spin fluctuation at finite temperature on the uniaxial magnetic anisotropy constant (K_u) on L1₀-type ordered alloys, such as FePt and CoPt. For the calculation, we employed the tight-binding linear muffin-tin orbital (TB-LMTO) method within the local spin density functional theory. The spin fluctuation was considered based on the disordered local moment picture (DLM), and the spin disorder was expressed through the random substitution ratio "x" in (Fe ↑)_{1-x}(Fe ↓)_x Pt, where the Fe ↑ and Fe ↓ respectively means the Fe atom having magnetic moment pointing to upward and downward. The disordered magnetization was taken into account by using coherent potential approximation (CPA).

The result showed that K_u decreased monotonically with the substitution ratio x as well as the total magnetic moment $\langle M \rangle$. From this data, we analyzed the relationship between K_u and $\langle M \rangle$, and found that K_u is proportional to n-th power of $\langle M \rangle$ ($n \doteq 2$) in both FePt and CoPt. This trend is similar to the experiment [1] and the previous first-principles calculation [2] using the functional integral method for the finite temperature magnetism. We conclude that the behavior of K_u of these alloys at finite temperature is well explained by a simple assumption of the Ising type fluctuation for the thermal excitation.

[1] S. Okamoto *et. al.*, Phys. Rev. B 66, 024413 (2002)

[2] J. B. Staunton *et. al.*, Phys. Rev. Lett., 93, 257204 (2004)

TU.H-P110 - Ab-initio study on the hard magnetic properties of MnBiP. Toson¹, A. Asali¹, G. r Zickler¹, J. Fidler¹*1. Institute of Solid State Physics, Vienna University of Technology, Vienna, Austria*

The low-temperature phase (LTP, space group 194) of MnBi has interesting properties suitable for permanent magnetic applications [1]. At low temperatures its spin configuration is in-plane but at $T = 80\text{K}$ a spin reorientation takes place and the magnetocrystalline anisotropy energy (MAE) increases with increasing temperature up to 2.1kJ/m^3 at $T = 500\text{K}$. At $T = 593\text{K}$ a first-order phase transition occurs reducing the c/a ratio [2]. These properties motivate a systematic study of the magnetic properties of MnBi in dependence on the change of lattice parameters with temperature.

Ab-initio calculations have been performed with the full-potential augmented plane wave code Wien2k [3] (V_{xc} : GGA, 10000 k-points). After a convergence of the scalar-relativistic calculation has been achieved (criterion: 10^{-9} Ry), the relativistic orbital contraction of the Bi s-states and the spin orbit coupling for two magnetisation directions have been introduced to determine the MAE. Orbital moments have been calculated afterwards with the density matrix.

The calculated magnetic moments $\mu_{\text{Mn}} = 3.88\mu_{\text{B}}$ ($\mu_{\text{Mn,spin}} = 3.79\mu_{\text{B}}$, $\mu_{\text{Mn,orb}} = 0.09\mu_{\text{B}}$) are higher than previously calculated moments ($3.39\text{--}3.69\mu_{\text{B}}$) but are in good agreement with experimental results ($3.82\text{--}4.25\mu_{\text{B}}$). Bi moments are aligned antiparallel to the Mn moments with $\mu_{\text{Bi}} = -0.12\mu_{\text{B}}$. The MAE at low temperature is overestimated (calculated: -3.1MJ/m^3 , experimental: -0.2MJ/m^3) but consistent with other DFT calculations [4]. The high temperature MAE of 2.14MJ/m^3 is in good agreement with experimental results (2.1MJ/m^3). Increasing the unit cell volume by 1.7% (with constant c/a ratio 1.43) causes an increase of MAE by 13.4% and a decrease of saturation polarisation by -0.8%. Increasing the c/a ratio by 4.4% causes a decrease in MAE by 21%.

Acknowledgements: The financial support of the EC-FP7 projects REFREPERMAG (280670) and ROMEO (309729) is acknowledged. The computational results presented have been achieved by using the Vienna Scientific Cluster (VSC).

References:

- [1] N.V.Rama Rao, A.M.Gabay, and G.C.Hadjipanayis, *J.Phys.Appl.Phys.* 46, 062001 (2013)
- [2] K.Adachi and S.Ogawa, in *Pnictides Chalcogenides I*, edited by H.P.J. Wijn (Springer-Verlag, Berlin/Heidelberg, 1988), pp. 180–181
- [3] K.Schwarz and P.Blaho, *Comput.Mater.Sci.* 28, 259 (2003)
- [4] K.V.Shanavas, D.Parker, and D.J.Singh, *Sci.Rep.* 4, 7222 (2014)

TU.H-P111 - Directly obtained τ phase MnAl for permanent magnetsH. Fang¹, S. Kontos², J. Cedervall¹, P. Svedlindh², K. Gunnarsson², M. Sahlberg¹*1. Uppsala University, Department of Chemistry – Ångström Laboratory, Uppsala, Sweden**2. Uppsala University, Engineering Sciences, Box 534, SE-75121 Uppsala, Sweden*

Tetragonal MnAl based materials (τ phase) are promising candidates to become a high performance permanent magnets. These materials might partly replace the conventional hard ferrites, Alnicos and bonded Nd-Fe-B magnets due to low cost and large availability of Mn and Al. A major challenge of the low temperature formed ferromagnetic τ -phase MnAl is its low stability. Carbon doping has proved to be an effective way to stabilize the ferromagnetic τ phase and significantly increase the magnetization of the material.

Mn₅₄Al₄₆ and (Mn_{0.55}Al_{0.45})₁₀₀C₂ alloys were synthesized through high temperature synthesis process. Both the Mn₅₄Al₄₆ and (Mn_{0.55}Al_{0.45})₁₀₀C₂ alloys directly formed the τ phase, thus bypassing the intermediate ϵ -phase. The XRD phase analysis shows that carbon doping dramatically promoted the formation and stability of τ phase in the (Mn_{0.55}Al_{0.45})₁₀₀C₂ alloy. The 9T VSM characterization is in agreement with the XRD phase analysis, with $M_{\text{sat}}=0.56\text{MA/m}$ (108emu/g), $H_c=0.045\text{MA/m}$, $K=1.3\text{MJ/m}^3$, $BH_{(\text{max})} = 50 \text{ kJ/m}^3$.

In order to increase the coercivity, samples were milled from 2 to 14 hours to decrease grain size. The milled samples were subsequently relaxed at 500°C for 1 hour. Phase analysis revealed that the milled samples were almost pure τ -phase, and that grain size decreased with increased milling time.

TU.H-P112 - Annealing effect on magnetic properties of hot-deformed Nd-Fe-B magnetsJ. Lee¹, H. Cha^{1,2}, L. Shu^{1,2}, J. Yu¹, H. Kwon³

1. Powder&Ceramics Division, Korea Institute of Materials Science, Changwon, Republic of Korea

2. School of Materials Science and Engineering, Pusan National University, Geumjeong-gu, Busan, Republic of Korea

3. Department of Materials Science and Engineering, Pukyong National University, Busan, Republic of Korea

Recently, there is emerging concern regarding the development of highly coercive Nd-Fe-B magnets without HRE elements due to their uneven distribution in the earth crust and low output, causing their prices to soar. To achieve high coercivity without HRE elements, it is now well known the control of microstructures such as grain size and grain boundary is of significant importance. Based upon these backgrounds, hot deformation has been employed to produce ultrafine-grained bulk Nd-Fe-B magnets. In this process, melt spun flakes are subjected to hot-pressing and subsequent die-upsetting process, which causes c-axis texture of Nd₂Fe₁₄B grain parallel to the pressing direction and the mechanism of texture formation has been extensively studied. Plenty of work is also reported regarding the role of intergranular phases on the coercivity with or without GBDP. On the other hand, the annealing effect of hot-deformed Nd-Fe-B magnet has not been well understood. In this study, we investigated the annealing effect on microstructure and magnetic properties of hot-deformed Nd-Fe-B magnets. The hot-deformed magnets were subjected to heat-treatment at various temperatures for 1h in vacuum (1st-PA) and then again annealed at constant temperature, 600°C (2nd-PA). The coercivity was largely enhanced about 2.4 kOe by annealing at 600°C. However, the coercivity was decreased at temperatures other than 600 and 700°C. After 2nd-PA, the coercivity of magnets which 1st-PA treated at above 700°C were also decreased despite the 2nd-PA temperature was low than melting point of Nd-rich phase. Low-temperature annealing could induce some defect or strain at interface between main phase and grain boundary phase due to difference of volume expansion at the below melting point of Nd-rich phase. In the case of high temperature, 800°C could cause grain growth and change in Nd-rich phase, resulting coercivity drop.

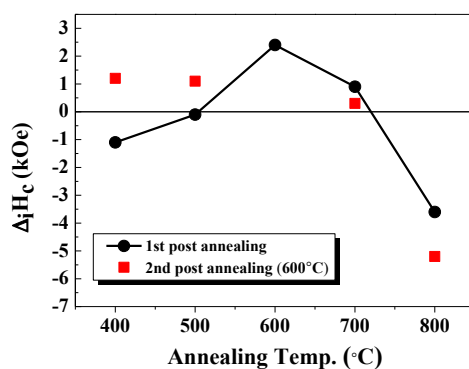


Fig. 1 Dependence of die-upset magnets' coercivities on various annealing temperatures

TU.H-P113 - High saturation magnetization of Fe-based amorphous / nanocrystalline ribbons

H. Yim¹

1. Sookmyung Women's University, Seoul, Republic of Korea

A novel Fe-based soft magnetic alloys with $\text{Fe}_{67-x}\text{Co}_{20}\text{Ti}_7\text{Zr}_6\text{B}_x$ ($x = 0, 2, 4, 6 \%$) were produced by melt-spinning technique and their thermal, mechanical and soft magnetic properties were investigated by differential scanning calorimetry, nano-indentation, and vibrating sample magnetometer, respectively. With boron addition into $\text{Fe}_{67-x}\text{Co}_{20}\text{Ti}_7\text{Zr}_6\text{B}_x$ system, thermal stability was increased. The ribbons exhibited fully amorphous phase except for the ribbon of $B = 0 \text{ at. } \%$ in $\text{Fe}_{67-x}\text{Co}_{20}\text{Ti}_7\text{Zr}_6\text{B}_x$ system. The ribbon of $\text{Fe}_{67}\text{Co}_{20}\text{Ti}_7\text{Zr}_6$ with $0 \text{ at. } \%$ of B has α -Fe particle embedded in amorphous phase. This means that only minor addition of B, $2 \text{ at. } \%$ can cause a drastic change in microstructure from nano-crystalline to a fully amorphous phase in this system. Among the ribbons, the nano-crystalline alloy of $\text{Fe}_{67}\text{Co}_{20}\text{Ti}_7\text{Zr}_6$ exhibited exceptionally good soft magnetic properties such as a low coercivity of 0.308 Oe and a high saturated magnetization of 190 emu/g (1.81 T) with the as-spun condition. Also, the ribbon has only α -Fe particles embedded in amorphous phase. These results of Fe-based ferromagnetic alloy system indicate that the Fe-Co-Ti-Zr-B alloy system has promising properties that are applicable to the soft-magnetic materials industry.

TU.H-P114 - Magnetic anisotropy of $\text{Nd}_{0.5}\text{Bi}_{2.5}\text{Fe}_{5-y}\text{Ga}_y\text{O}_{12}$ ($y = 0 \sim 1$) thin films on glass substrates prepared by metal organic decomposition (MOD) method

G. Lou¹, M. Sasaki¹, T. Kato², Sat Iwata², T. Ishibashi¹

1. Nagaoka University of Technology, Japan

2. Nagoya University, Japan

Recently, we have reported that $\text{Nd}_{0.5}\text{Bi}_{2.5}\text{Fe}_4\text{GaO}_{12}$ thin films on glass substrates were successfully prepared by metal-organic decomposition (MOD) method, exhibiting a large magneto-optical effect and perpendicular magnetic anisotropy [1]. In this paper, we report the magnetic anisotropy of the Nd iron garnets with various Ga substitutions.

$\text{Nd}_{0.5}\text{Bi}_{2.5}\text{Fe}_{5-y}\text{Ga}_y\text{O}_{12}$ ($y = 0, 0.25, 0.5, 0.75, 1$) thin films with a thickness of 200 nm were prepared on the 120 nm-thick $\text{Nd}_2\text{BiFe}_4\text{GaO}_{12}$ buffer layers on glass substrates (Eagle XG, Corning) by MOD method. MOD solutions were spin coated on glass substrates at 3000 rpm for 60 seconds, dried at 100 degrees Celsius for 10 minutes and pre-annealed at 450 degrees Celsius for 10 minutes. The thin films were then annealed for crystallization in a furnace at 700 degrees Celsius for 3 hours.

We have measured the Faraday hysteresis of $\text{Nd}_{0.5}\text{Bi}_{2.5}\text{Fe}_{5-y}\text{Ga}_y\text{O}_{12}$ thin films at the peak of the Faraday spectrum. When the Ga content is 0, the hysteresis was rectangular, indicating in-plane magnetic anisotropy, with Faraday rotation angle of 3.4 degrees and the coercive force of 0.13 kOe. By increasing Ga content, perpendicular magnetic anisotropy was obtained, where Faraday rotation angles decreased to 2.3 degrees and coercive force increased to 0.24 kOe for Ga content of 1. These results indicated that it is possible to control the magnetic anisotropy of $\text{Nd}_{0.5}\text{Bi}_{2.5}\text{Fe}_{5-y}\text{Ga}_y\text{O}_{12}$ thin films exhibiting the large Faraday effect. Anisotropy constant K_u of the films measured by torque measurements are also discussed.

[1] T. Yoshida, K. Oishi, T. Nishi, and T. Ishibashi, European Phys. J. Web of Conf., 75, 05009 (2014)

TU.H-P115 - SANS study of the initial magnetization process in nanocrystalline Nd-Fe-B magnets

K.Saito¹, T. Ueno², M. Yano³, T. Shoji³, N. Sakuma³, A. Manabe³, A. Kato³, E. Gilbert⁴, K. Ono¹

1. *High Energy Accelerator Research Organization, Japan*

2. *National Institute for Materials Science, Japan*

3. *Toyota Motor Corporation, Japan*

4. *Australian Nuclear Science and Technology Organization, Australia*

Physics inside permanent magnets is more complicated than most of the physicists think due to inhomogeneity and multiscale structures. The coercivity mechanism of hard magnets is a good example and it has been a center of attention recently in a pursuit of better hard magnets with high coercivity. On the other hand, the initial magnetization process has not been regarded as an important topic though it is also a physical phenomena where inhomogeneity and multiscale structures play crucial roles. In addition, experimental studies other than microscopic observations and magnetization measurements have been rarely reported so far. Small angle neutron scattering (SANS) is one of the most suitable method to observe the magnetization process and microstructures inside bulk magnets. We have conducted SANS experiments on the initial magnetization process in nanocrystalline Nd-Fe-B magnets with different microstructures to investigate the relation between microstructure and initial magnetization. Samples are nanocrystalline Nd-Fe-B magnets with no infiltration, NdCu-, and PrCu-infiltration. Cu alloy is expected to separate Nd₂Fe₁₄B grains and break the exchange interaction between the grains. SANS experiments were carried out at QUOKKA, ANSTO, Australia. Two-dimensional SANS images of the samples in the thermally-demagnetized state at 0 T show anisotropic features reflecting samples' microstructures. One-dimensional plots along directions parallel and perpendicular to the easy axis show different power law indices, indicating changes in smoothness of grain boundaries by the infiltrations. During the initial magnetization process, SANS intensities along the direction perpendicular to the easy axis increase drastically in low Q range. This reflects the development of magnetic domains. Plateau-like structure in magnetic field dependence of SANS intensities for lower Q range is observed in Cu alloy infiltrated samples, which corresponds to an effect of grain separation.

TU.H-P116 - Alnico V thin films with improved saturation magnetization and coercivity

F.Mohseni¹, M. Pereira¹, N.Fortunato¹, J. S. Amaral¹, A. C. Lourenço¹, J. M. Vieira²

1. *Department of Physics, University of Aveiro, 3810-193, Aveiro, Portugal*

2. *Department of Materials and Ceramic Engineering, University of Aveiro, Aveiro, Portugal*

The recent rare-earth element price crisis has motivated intensive research to develop new, high-performance rare-earth free permanent magnets [1]. Alnico V magnets, containing Al, Ni, Co and Fe, are nanostructured hard ferromagnets, a result of spinodal decomposition during heat treatments, and present coercivity values typically below 650 Oe [2]. Because of their high working temperatures and material sustainability, an increase of energy product would make Alnico a worthy substitute of Nd-based magnets. Recently, Alnico V thin-films on Silicon were shown to present coercivity values up to ~ 10 kOe. The unusually high coercivity value happens as the result of Si ions diffusion from substrate to the thin film which leads to the formation of a novel Body Centered Tetragonal Fe-Co-Si phase [3, 4]. Nonetheless, the diffusion mechanism, chemical composition and saturation magnetization of this novel phase require further studies.

The present investigation explores the effects of deposition temperature and post heat treatments on the magnetic properties and morphology of RF-sputtered Alnico V thin films on Si substrates. Samples with different thicknesses, with and without capping layers were prepared at different deposition temperatures. Post-deposition heat treatments in different Argon pressures, followed by quenching and slow-cooling, were also performed. We show that controlling deposition temperature can result in an increase of up to 40% of saturation magnetization compared to room-temperature deposited samples. Raising Argon pressure during heat treatments causes a considerable increase in coercivity, up to 4 times the coercivity of bulk Alnico V magnets. Unlike previous reports on high-coercivity Alnico V thin films, where quenching was required to obtain the novel BCT Fe-Co-Si phase, our results show no such correlation, pointing to different mechanisms at work. We discuss the origin behind these effects, and potential mechanisms to combine the observed increase in saturation magnetization and coercivity, leading to higher performance materials.

[1] N. Poudyal, J Ping Liu, J. Phys. D: Appl. Phys. 46 (2013) 043001

[2] K. H. J. Buschow, Rep. Prog. Phys. (1991) 54 1123

[3] O. Akdogan, G. C. Hadjipanayis, J. Phys: Conf. Series 200 (2010) 072001

[4] O. Akdogan, W. Li, G. Hadjipanayis, J Nanopart Res (2012) 14:891

TU.H-P117 - Mechanically induced superelastic effect in magnetic Fe-Ni-Co-Al-Ta-B rapidly quenched microwires

F. Borza¹, N. Lupu¹, I. Murgulescu¹, V. Dobrea¹, H. Chiriac¹

1. National Institute of Research & Development For Technical Physics, Iasi, Romania

Interest continues to grow in the development of high-performance materials with multifunctional properties which are very important for the miniaturization and simplification of devices, especially in the medical field such as microsurgery. One such example is the superelastic FeNiCoAlTaB shape memory alloy which exhibits tensile superelastic strains higher than 13% at room temperature in a <100> textured Fe_{40.95}Ni₂₈Co₁₇Al_{11.5}Ta_{2.5}B_{0.05} polycrystal which reaches strengths of >1 GPa [1]. In the attempt to reduce the steps involved in the thermo-mechanical processing of this materials we have used a cost effective technique, rapid quenching from the melt for the fabrication of these magnetic superelastic materials as wire-shaped materials.

Fe_{40.95}Ni₂₈Co₁₇Al_{11.5}Ta_{2.5}B_{0.05} wires with the diameter of 280 micrometers have been prepared by in rotating water spinning technique followed by successive cold-drawing down to 40 micrometers with the aim to achieve a higher than 97% reduction in the diameter of the wire when the superelastic effect occurs. From the magnetic point of view, cold-drawing Fe-Ni-Co-Al-Ta-B wires lead to the deterioration of soft magnetic properties at low fields (the magnetization and relative permeability decreases while the coercive field increases) but an important increase in the saturation magnetization from 0.6T to 1T has been observed in higher fields (maximum applied field of 30 kA/m). However, the most significant result is the induction of the superelastic effect of about 1% directly by cold-drawing, without intermediary thermomechanical treatments. The combination of relatively good magnetic and superelastic properties makes these materials potential candidates for applications in microsurgery as catheters. They can also replace the currently employed NiTi alloys in applications where radiotransparency is needed.

Acknowledgements: Work supported by the Romanian Ministry of Education and Research, NUCLEU Programme, project PN 09-43 02 03.

[1] Y. Tanaka, Y. Himuro, R. Kainuma, Y. Sutou, T. Omori, K. Ishida, Science 327 (2010) 1488-1490

TU.H-P118 - Spin reorientation temperature of ultrafine Nd₂Fe₁₄B particles: influence of exchange-coupling

S.K. Pal ^{1,2}, K.Müller ², L. Schultz ², O. Gutfleisch ¹

1. TU Darmstadt, Materialwissenschaft, Darmstadt, Germany

2. IFW Dresden, Institute for Metallic Materials, Dresden, Germany

High magnetocrystalline anisotropy materials such as SmCo₅ and Nd₂Fe₁₄B, are the most important materials for application in high-energy-density permanent magnets. The Nd₂Fe₁₄B compound is of significant importance for its high-energy-density value which originates from the unique combination of Nd, Fe and B atoms providing high anisotropy, magnetization and stability of crystal structure, respectively. It is of fundamental interest to study the influence of size of fine-grained particles on the intrinsic properties of Nd₂Fe₁₄B compound. Spin reorientation temperature (SRT), an intrinsic property, is a temperature-induced magnetic phase transition. Here, we report on the influence of exchange-coupling on the SRT value of ultrafine Nd₂Fe₁₄B particles. The ultrafine Nd₂Fe₁₄B particles of size ranging from 2 μm (consisting of hundreds of grains) to 300 nm (single-crystalline particles) were prepared by surfactant-assisted ball milling of hydrogenation disproportionation desorption and recombination (HDDR) processed Nd₂Fe₁₄B powder. The SRT values for ultrafine Nd₂Fe₁₄B particles of different sizes have been determined. The SRT value was found to increase from 129 K for HDDR powder (consisting of single-domain grains of average size 300 nm) to 134 K for ~2 μm particles consisting of hundreds of grains. The SRT value was increased further to 136 K for isolated single-crystalline particles (~300 nm size). A transformation of single-crystalline particles to polycrystalline flakes (with ~12 nm grain size) after intense ball milling results in decrease of SRT to a value of 128 K. The increase in the SRT value with decreasing particle size is thought to be due to the decrease in the extent of magnetic exchange-coupling. The decrease of the SRT value for polycrystalline nanoflakes can be attributed to the increased magnetic exchange-coupling between nanometer-sized grains in the flakes. These findings need to be considered when fabricating nanocrystalline or nanocomposite Nd₂Fe₁₄B magnets for low temperature application.

TU.H-P119 - Preparation of Co-based amorphous powders by wet mechanical alloying. The influence of Si and/or B substitution by Ti and/or Zr over their properties

B.V. Neamtu¹, H.F. Chicinas¹, T.F. Marinca¹, O. Isnard^{2,3}, I. Chicinas¹

1. *Technical University of Cluj-Napoca, Materials Science and Engineering Department, Cluj-Napoca, Romania*

2. *Universite de Grenoble Alpes, Institut Néel, Grenoble, France*

3. *Centre National de la Recherche Scientifique, Institut Néel, Grenoble, France*

Co-based amorphous powders were synthesized by wet mechanical alloying starting from elemental powder of Co, Fe, Ni, Si, B, Ti, Zr. The magnetic properties and thermal stability of the $\text{Co}_{70}\text{Fe}_4\text{Ni}_2\text{Si}_{15}\text{B}_9$ at% master alloy obtained by wet mechanical alloying were compared with the characteristics of the newly formed alloys in which the Si and/or B were substituted by Zr and/or Ti. The purpose of the above mentioned substitution experiments is mainly to increase the thermal stability of the amorphous phase, which will further allow higher sintering temperature. Early results reveal that regardless of the substitution type, the powders amorphisation occurs at the same milling duration (25 hours). The thermomagnetic measurements show that the Curie temperature of the amorphous phase increases with more than 50%. It was proved that substitution of 5 at.% of Si with Ti or Zr are leading to an increase of the saturation magnetization of the powder with about 49%. The values of the alloys saturation magnetization can be explained by a more dense random packed structure, leading thus to a stronger interaction of the magnetic atoms. Differential scanning calorimetry analysis evidenced that the substitution of Si with either Ti or Zr increases the crystallization temperature of the master alloy with over 100 °C. The as obtained powders can be further subjected to spark plasma sintering and due to their higher crystallization temperature, high density amorphous compacts can be obtained, for several applications, such as soft magnetic cores.

TU.H-P120 - Structural and magnetic characteristics of nanocrystalline iron-magnetite composite powder obtained by mechanosynthesis

T. Marinca¹, B. Neamtu¹, I. Chicinas¹, O. Isnard^{2,3}, H. Chicinas¹

1. *Materials Science and Engineering Department, Technical University of Cluj-Napoca, Cluj-Napoca, Romania*

2. *Universite de Grenoble Alpes, Institut Néel, Grenoble, France*

3. *Centre National de la Recherche Scientifique, Institut Néel, Grenoble, France*

The formation of iron-magnetite (Fe_3O_4) composite powder by mechanosynthesis and its structural and magnetic characteristics have been studied. The purpose for obtaining such type of composite is to enhance the magnetic characteristics of the magnetite. Iron-magnetite composite powder was synthesized using iron and hematite (Fe_2O_3) powder. The powder have been investigated by X-ray diffraction, differential scanning calorimetry, particle size analysis and magnetisation measurements. The Fe_3O_4 is progressively formed upon increasing milling time by the reaction of hematite with iron. After 600 minutes of milling the powder consists mainly in iron and magnetite phases. The magnetite and iron phases have the mean crystallite size after 600 minutes of milling of 8 and 19 nm respectively. The $\text{Fe}_3\text{O}_4/\text{Fe}$ composite powder is stable up to 540 °C independent on milling time, after this temperature a w^3 stite phase is formed. The powder magnetisation is diminished in the first period of mechanical milling during the formation of $\text{Fe}/\text{Fe}_2\text{O}_3$ composite particles. The next stage of milling leads to the formation of Fe_3O_4 phase and consequent the magnetisation of the powder significantly increases. Upon increasing the milling time from 120 up to 600 minutes a continuous increase of the powder magnetisation is noticed as a result of the progressive formation of Fe_3O_4 . The magnetisation of the milled composite $\text{Fe}_3\text{O}_4/\text{Fe}$ material is lower as compared to the theoretical one. This is due to the presence of some Fe_2O_3 residual phase and also to the surface defects. The annealing lead to the elimination of the residual phase and remove stresses induced by milling. An enhancement of the magnetic characteristics of the nanocrystalline composite powder was noticed after annealing.

TU.H-P121 - Temperature dependence of coercivity in $(\text{Mn}_{1-x}\text{Ti}_x)_{50}\text{Bi}_{50}$ alloysC. Curcio¹, E.S. Olivetti¹, L. Martino¹, M. Kuepferling¹, V. Basso¹

1. INRiM, Istituto Nazionale Di Ricerca Metrologica, Torino, Italy

nBi compound has a high uniaxial magnetocrystalline anisotropy which has the peculiar feature to increase with temperature up to 500 K where $K_u = 2.2 \text{ MJ/m}^3$. This makes the compound an interesting candidate as a rare-earth-free hard magnet, especially for high temperature applications. Several strategies were developed to optimize the coercivity by refining grain size without appreciable reduction of phase fraction and magnetization. Cryomilling and surfactant addition have been shown to be effective, but the production process becomes rather complex. Partial substitutions of Mn with different transition metals or rare-earth elements may increase the coercivity, at the expense of the saturation magnetization. Here we investigate the magnetic properties of $(\text{Mn}_{1-x}\text{Ti}_x)_{50}\text{Bi}_{50}$ polycrystalline alloys in which Mn is partially substituted by Ti. Samples were obtained by a preparation route that does not require melting of a master alloy: powders of Bi and $\text{Mn}_{1-x}\text{Ti}_x$ were mixed, compacted in pellets and annealed for 1 hour in an applied magnetic field of 1 T in order to promote the phase formation and the growth of aligned grains. We find that Ti is effective in increasing the coercivity without significant loss in magnetization, suggesting a role of Ti atoms in enhancing a fine microstructure. In order to understand the mechanism of the magnetization reversal of $(\text{Mn}_{1-x}\text{Ti}_x)_{50}\text{Bi}_{50}$ we study the temperature dependence of coercivity in the range 300-630 K. Through Kronmuller plot we estimate the αK and N_{eff} parameters, which take into account the effect of microstructure. The temperature dependence of coercivity for $x=0$ shows a regime for $T < 350 \text{ K}$ with $\alpha K=0.12$ and a regime for $T > 350 \text{ K}$ with $\alpha K=0.34$. For $x=0.02$ a single regime with $\alpha K=0.43$ is observed, which can be associated to a nucleation mechanism responsible for the increase of coercivity with respect to the $x=0$ case.

TU.H-P122 - Soft magnetic composite Fe₃O₄/Ni₃Fe obtained by mechanosynthesis and annealing, structural and magnetic characteristics

H. Chicinas¹, T. Marinca¹, B. Neamtu¹, I. Chicinas¹, O. Isnard^{2,3}

1. *Technical University of Cluj-Napoca, Materials Science and Engineering Department, Cluj-Napoca, Romania*

2. *Universite de Grenoble Alpes, Institut Néel, Grenoble, France*

3. *Centre National de la Recherche Scientifique, Institut Néel, Grenoble, France*

Soft magnetic Fe₃O₄/Ni₃Fe composite powder was obtained by mechanosynthesis and subsequent annealing, starting from Fe, Ni and Fe₂O₃ precursors. The aim is to produce a magnetic material that has soft magnetic characteristics as Ni-Fe alloy but with a higher electrical resistivity. The X-ray diffraction patterns of the milled samples, revealed the incipient formation of Fe₃O₄ for the sample milled for 3 hours. At 10 hours of milling, the formation of Ni₃Fe and Fe₃O₄ hasn't occurred completely, as a consequence a presence of a small amount of unreacted Fe₂O₃ can be found. After annealing the Fe₃O₄/Ni₃Fe composite is fully formed. DSC measurements revealed a decrease of the temperature required for the Fe₃O₄ formation upon increasing milling time, which reveals the fact that the amount of energy required for the formation of Fe₃O₄ can be attained by mechanical milling, heat treatment, or a combined method. The first magnetization curves reveal a two stage evolution for the milled samples. In the first stage, for milling times up to 4 hours, when the Fe₃O₄ particles are starting to form, the value of magnetization has a decrease tendency. For longer milling times, due to the progressive Fe₃O₄ and Ni₃Fe formation, the value of magnetization increases. The magnetization is diminished due to a presence of residual Fe₂O₃ phase, which has also been identified on the XRD pattern, yet for the sample milled 10 hours the magnetization has the highest value, due to complete formation of Ni₃Fe and its contribution.

TU.H-P124 - The influence of severe plastic deformation on magnetic properties of some 3-d based alloys perspective for rare-earth free permanent magnets

S.Taskaev¹, K. Skokov², V. Khovaylo^{3,4}, D.Gunderov⁵, D. Karpenkov², O. Gutfleisch²

1. Chelyabinsk State University, Chelyabinsk, Russian Federation

2. TU Darmstadt, Darmstadt, Germany

3. National University of Science and Technology, Moscow, Russian Federation

4. ITMO University, St. Petersburg, Russian Federation

5. Ufa State Aviation Technical University, Ufa, Russian Federation

After the development of Sm-Co and especially Nd-Fe-B magnets, these magnetic materials are essential components in many fields of technology, because of their ability to provide a strong magnetic flux. Nevertheless the crises of rare-earths during last few years open the discussion about rare-earths free permanent magnets [1].

The important properties of a permanent magnet include its coercivity, remanence and energy product [2]. There are essentially two means of achieving the large values of these properties necessary for today's applications. First, the microstructure of a material can be optimized (in our case with the help of high pressure torsion) to prevent the rotation of ferromagnetic domains. The second factor is the intrinsic spin-orbit coupling of electrons that forces spins to align with a particular crystallographic orientation, giving rise to the magnetocrystalline anisotropy energy of a material. Because the strength of spin-orbit coupling increases as the fourth power of an element's atomic number, maximizing the magnetocrystalline anisotropy energy is accomplished by utilizing heavier elements. Based on that, the aim of this work is to investigate the influence of high pressure torsion (HPT) on magnetic properties of some 3-d based intermetallic compounds, e.g. $\text{Ni}_{48}\text{Fe}_{48}\text{Zr}_4$, $\text{Fe}_{1.5}\text{Co}_{0.5}\text{BTa}_{0.3}$ and $\text{Co}_{80}\text{Zr}_{16}\text{B}_4$ alloys. HPT (Bridgemen's anvils) was performed under 5GPa pressure with 5 complete turns. Such high plastic deformation dramatically affect on microstructure of the samples reducing the grain size up to nanometer scale. It is shown that HPT and proper heat treatment affect to the magnetic properties of prepared compounds by a different ways. The found value of $H_c=2.25$ kOe on $\text{Co}_{80}\text{Zr}_{16}\text{B}_4$ HPT alloy is comparable with [3], where this compound was prepared by melt spun ribbon technique.

The authors gratefully acknowledge the financial support of the RF President MD-770.2014.2 grant.

References:

- [1] L.H. Lewis and F. Jimenez-Villacorata. Metallurgical and Materials Transactions A. S2 - V 44A, January 2013
- [2] Coey J. M. D. 2010 Magnetism and Magnetic Materials (New York: Cambridge University Press)
- [3] A. Mitra Ghemawata, M. Foldeakib, R.A. Dunlapb and R. C. O'Handlev. IEEE Transactions on Magnetism, V. 25, ¹5, September 1989

TU.H-P125 - Joint and separate effect of d/D and d on the magnetic properties of glass-coated amorphous ferromagnetic microwires

I. Machay¹, K. Chichay¹, A. Litvinova¹, I. Iglesias¹, N. Perov², V. Rodionova¹

1. *Immanuel Kant Baltic Federal University, Kaliningrad, Russian Federation*

2. *Faculty of physics, Lomonosov MSU, Moscow, Russian Federation*

Amorphous ferromagnetic glass-coated microwires are interesting materials because of their unusual micromagnetic structure and magnetic properties determined by the value and the distribution of the internal stresses and the magnetostriction coefficient of the metallic core simultaneously. The main stresses arise due to the difference between the thermal expansion coefficients of the metal and the glass. The value of these stresses depends on the ratio of the metal core diameter, d , and the total diameter of the glass-coated microwire, D . Also d has a strong influence on the magnetic properties of the microwires. Usually only the influence of d or d/D is considered. For the first time in this work we examined the magnetic properties depending on the microwire sizes not as a single-variable function of d or d/D but as a function of two variables - of d and d/D . Investigated microwires ($d \sim 2.5-20 \mu\text{m}$ and $d/D \sim 0.1-0.8$) were made from Fe-based alloy and have magnetic bistability. We investigated the magnetostatic properties of the microwires of different lengths using VSM. The length of microwires changed from 2 to 0.05 cm. The measurements of the magnetostriction coefficient were measured by small angle magnetization rotation method. We found that magnetostatic and magnetostrictive properties are changing under the influence of both d and d/D . We established that the influence of d/D on the magnetic properties is varied at different d and magnetic parameters (magnetostriction coefficient, coercivity) have non-monotonic dependence on d/D and d . The measured value of the magnetostriction coefficient was found to be $7 \cdot 10^{-6} - 1 \cdot 10^{-6}$ when d changes by a few μm . In addition, we demonstrated the strong joint influence of d/D and d on the critical length of the bistability. The smallest length was found to be 0.2 cm for the microwires with largest d/D and smallest d .

TU.H-P126 - High frequency properties of ferrite - Fe-Si-Al alloy soft magnetic composites

B. Stergiou¹, V.Zaspalis¹

1. Laboratory of Inorganic Materials, Centre for Research and Technology – Hellas, Greece

The need for shielding facilities and equipment against the increasingly high frequency electromagnetic waves has driven the extensive research on materials with the proper electromagnetic performance. In this direction, tailoring the properties of polymer composites with dielectric or magnetic fillers predominate in the respective studies and applications. The different approach of the present investigation lies in the synergy of ferrimagnetic ceramic and metallic materials, by the incorporation of Fe-based alloy particles in a ferrite matrix, in order to form rigid soft magnetic composites as efficient electromagnetic absorbers.

Specifically, Cu-substituted NiZn spinel ferrite powder was prepared with the conventional solid-state reactions technique and mixed with commercial Fe-Si-Al alloy powder (sendust) up to the content of 20% (v/v). For the mechanical reinforcement of the composites, they were doped with a glass compound, compacted in disc shape and finally annealed at the temperature from 600°C to 900°C.

The main objectives were to optimize the production process of the specific ceramic-alloy composites and study the effect of sendust addition on the composites' electromagnetic properties. Therefore, the employed starting powders were characterized as to their density, particle size and crystal structure. Moreover, the impact of the processing variables on the alloy structure and the microstructure of the composites was recorded by means of X-ray diffraction method, thermogravimetric analysis and scanning electron microscopy. Finally, the electromagnetic constitutive parameters of ring-shaped samples were measured in the frequency range 1MHz-6GHz and the respective return losses were calculated. The experimental findings indicate the cohesion between the ferrite and alloy compounds and the feasibility of preparing relatively dense composites at low temperature. Furthermore, despite the decrease of the magnetic properties with the addition of the alloy particles, the resultant shift of the permeability spectrum to higher frequencies highlights the potential use of such novel composites as electromagnetic wave absorbers.

TU.H-P128 - Electronic theory for the magnetic properties of Nd₂Fe₁₄B compounds

H. Tsuchiura^{1,2}, T. Yoshioka^{1,2}, P. Novák³

1. *Department of Applied Physics, Tohoku University, Japan*

2. *ESICMM, Tsukuba, Japan*

3. *Institute of Physics of ASCR, Prague, Czech Republic*

In view the energy-saving and renewable technology, theoretical understanding of the coercivity mechanisms of Nd-Fe-B is urgently needed. It has been widely accepted that the large magnetic anisotropic energy due to the Nd ions is the dominant factor of the coercivity of Nd-Fe-B magnets. For deeper understanding of the mechanism, it is necessary to study the magnetic anisotropy due to the Nd ions from the viewpoint of crystal field theory. Several recent experimental studies have revealed that local atomic structures around the grain boundaries of sintered Nd-Fe-B magnets significantly affect their coercivity [1]. Theoretically, we have found that the crystal field parameters (CFP) A_2^0 of Nd ions can be negative, implying the local in-plane anisotropy, if they are exposed on the (001) surface of the crystalline Nd₂Fe₁₄B [2]. We have also reported that such surface anisotropy anomaly may cause coercivity reduction of a single Nd₂Fe₁₄B particle by half of the anisotropy field H_K , based on a simple micromagnetic-type simulation [3].

In this talk, first we show the physical origin of the anomalous surface anisotropy by using newly developed CFP calculation technique, the so-called Wannierization method [4]. We find that the 4f clouds in Nd₂Fe₁₄B system are usually lie within the *c*-plane, but extend along the *c*-axis direction in the surface Nd ions. We also show the results of higher-order CFPs based on the Wannierization method, and discuss the spin-reorientation phenomena and coercivity of a single Nd₂Fe₁₄B particle.

[1] H. Sepehri-Amin, T. Ohkubo, T. Shima, and K. Hono, *Acta Mater.* 60, 819 (2012)

[2] H. Moriya, H. Tsuchiura, and A. Sakuma, *J. Appl. Phys.* 105, 07A740 (2009)

[3] C. Mitumata, H. Tsuchiura, and A. Sakuma, *Appl. Phys. Exp.* 4, 113002 (2011)

[4] P. Novák, K. Knížek, and J. Kuneš, *Phys. Rev. B* 87, 205139 (2013)

TU.H-P129 - Influence of the continuousness and thickness of the shell of the magnetically bi-phase microwires on the core/shell magnetostatic coupling

I. Iglesias¹, K.Chichay¹, J. Jimenez², R. Pérez del Real², M. Vazquez², V. Rodionova¹

1. *Immanuel Kant Baltic Federal University, Kaliningrad, Russian Federation*

2. *Materials Science Institute of Madrid, CSIC, Madrid, Spain*

Study of the multilayered magnetic systems is of great interest due to their high potential in the various applications ranging from magnetic recording media to multifunctional sensors. Magnetic behavior and peculiarities of the magnetization reversal of these systems have been studied by different methods. The magnetically bi-phase fully covered microwires have been studied since 2007. In 2014 a new type of the multilayered microwire was fabricated - partially covered bi-phase microwire. It consists of a ferromagnetic glass-coated microwire(core) and a ferromagnetic shell with magnetostriction constant of the opposite sign. The partially covered microwires are very promising for creation of the actuators. The first results of the investigation of the partially covered microwires demonstrated the dramatic difference between the magnetization reversal processes of the microwires with various continuousness. Particularly, the typical step-like behavior of the hysteresis loop for the fully covered microwires disappeared for the partially covered ones. The aim of this work was to analyze and compare magnetic behavior of partially and fully covered microwires and to establish the influence of the continuousness and thickness of the shell on the core/shell magnetostatic coupling. Partially and fully covered microwires were fabricated by combined quenching and drawing techniques and electroplating. The core and the shell were prepared from FeCo-, Fe-based and CoNi, FeNi materials, respectively. The cores have similar diameters. The shell has thicknesses ranging from hundreds of nanometers up to 5 micrometers. Magnetic measurements were carried out at room temperature by VSM. In both cases, the magnetostatic coupling of the magnetic phases results in appearance of the features on magnetization curves. The stray fields of the magnetic phases were estimated using the COMSOL for both types of microwires. The value and the distribution of these fields explain the mentioned difference. The increase in the shell thickness diminishes the difference between the magnetization processes.

TU.H-P130 - Structural and magnetic properties of substituted M-type barium hexagonal ferrite annealed at different temperaturesT. Ben Ghzaïel^{1,2}, W.Dhaoui¹, F. Mazaleyrat²*1. Université de Tunis El Manar Faculté des Sciences de Tunis, UR11ES18 Unité de Recherche de Chimie Minérale Appliquée, Tunis, Tunisie**2. SATIE, ENS Cachan, CNRS, Université Paris-Saclay, Cachan, France*

With increasing cost of earth-rare metals, researches have focused on earth-rare free permanent magnets. M-type barium hexaferrites (BaM) are good candidates due to their high stability[1], large magnetocrystalline anisotropy[2], high Curie temperature[3] and large magnetization[4]. In order to fulfil the properties required for this application, BaM ferrites with different substitutions were prepared to modify the structural and magnetic behaviour of M-type hexaferrite. The effect of ion substitution and annealing on the phase composition, Curie temperature and magnetic properties were investigated. In this work, BaMeFe₁₁O₁₉ where Me is trivalent transition metal ions (Al, Bi, Cr, Mn) were prepared by dynamic hydrothermal synthesis and then annealed at different temperatures from 900 to 1000°C for 2h. XRD results show partial formation of magnetoplumbite structure P63/mm, in the prepared samples for all substituted BaM ferrites.

The magnetic measurements of the powders with various substitutions revealed that the coercivity decreases while the magnetization increases with annealing temperature. High coercivity H_c= 4.8 KOe is observed for BaBiFe₁₁O₁₉. However, BaCrFe₁₁O₁₉ exhibited greater magnetization M_s=61.33 emu/g. Interestingly, BaBiFe₁₁O₁₉ curve shows two steps hysteresis loop at all annealing temperatures. This characteristic feature wasn't due to the presence of secondary phase which is attested XRD data. To understand the origin of this phenomenon, we have investigated the effect of applied temperature below 300 K on the magnetic properties. We observed that the magnetization increased with decreasing temperature from 300 to 100K but the two steps curves persisted. This phenomenon is attributed to a strong value of the fourth order anisotropy constant (k₂).

[1]P. Xu, X. Han, M. Wang, J. Phys. Chem. C, 111, (2007), 5866

[2]J. Smit, H. Wijn, Ferrites, Philips Technical Library, Eindhoven, Netherlands, (1959)

[3]H. Kojimi, E.P. Wohlfarth, Ferromagnetic Materials, North Holland, Amsterdam, (1982)

[4]P. Shi, S.D. Yoon, X. Zuo, J. Appl. Phys., 87, (2000), 4981

TU.H-P131 - A density functional theory study on the novel high coercivity BCT Fe-Co-Si phase

N. Fortunato¹, J. Gonçalves¹, J. S. Amaral^{1,2}

1. *Departamento de Física and CICECO, Universidade de Aveiro, Aveiro, Portugal*

2. *IFIMUP and IN-Institute of Nanoscience and Nanotechnology, Porto, Portugal*

High-performance hard magnetic materials are now commonplace, with a world market dominated by rare-earth (RE) magnets. RE elements, particularly heavy REs are critical materials, mainly due to limited global deposits, low sustainability and expensive extraction and processing. As such there is currently a considerable effort to develop new high-performance RE free hard magnetic materials[1].

Alnico is a permanent magnet material based on Fe, Ni, Co and Al, first discovered in the 1930's, where the coercivity arises from shape anisotropy. Alnico magnets typically show coercivities below 2kOe, and subsequently low energy products, around 10 MGOe, which compare poorly to the ~ 60 MGOe values of modern NdFeB-based alloys. Recently Hadjipanayis et al.[2] reported a high coercivity value of 6.5k Oe of Alnico thin films sputtered on silicon substrates. This was attributed to a high magnetocrystalline anisotropy of a new Fe_xCo_ySi_z body centered tetragonal (BCT) phase. While a Curie temperature value of ~305°C and structural data of this novel BCT phase were reported, there is currently no prediction for its stoichiometry, nor total magnetic moment. We here report on a Density Functional Theory (DFT) study to present a tentative composition range for this high Coercivity BCT phase, taking into account the experimental lattice parameters, correlated with T_c estimations via a mean-field model approximation together with magnetic exchange interaction parameters obtained via the Liechtenstein method [3], and the use of the Coherent Potential Approximation, as implemented in the SPR-KKR package [4]. We discuss the predicted magnetic saturation values, as crucial performance parameters for applications. The phase stability for the studied composition ranges is taken into account, which can be an important factor when considering the external effects (strain/epitaxy) that have led to the formation of this novel phase.

[1]- Jones N., Nature 472 22 (2011)

[2]-O. Akdogan and G. C. Hadjipanayis "Alnico thin films with high coercivities up to 6.9 kOe" J. Phys.: Conf. Ser. 200 072001 (2010)

[3]-A I Liechtenstein et al, J. Phys. F: Met. Phys. 14 L125 (1984)

[4]-The Munich SPR-KKR package, version 6.3, H. Ebert et al, <http://ebert.cup.uni-muenchen.de/SPRKKR>

TU.H-P132 - X-ray analysis of ordered Fe-Co thin films

N. Inami¹, T. Ueno², T. Hasegawa³, S. Ishio³, K. Ono¹

1. *High Energy Accelerator Research Organization (KEK), Japan*

2. *National Institute for Materials Science (NIMS), Japan*

3. *Akita University, Japan*

Magnetic materials, which do not contain rare metals, have been extensively studied. Fe-Co alloy is one of the candidates with both high magnetic anisotropy and high saturation magnetization. The magnetocrystalline anisotropy of body centered tetragonal type Fe-Co alloys has been reported by first-principles calculation. [1] In addition, the largest anisotropy has been realized at the lattice parameters ratio c/a of about 1.25. [2] Structural analysis of Fe-Co alloys is important for understanding the relationship between magnetic properties and the structure. To determine the long-range order parameters of ordered Fe-Co alloys precisely, X-ray diffraction measurements obtaining the diffraction from the ordered-lattice layer are indispensable. However, the measured diffraction from the ordered phase is rather weak using a standard X-ray tube, because the contrast of X-ray scattering in Fe and Co is very small. For a quantitative investigation, the X-ray analysis with the photon energy tuned around the absorption edge of Fe or Co using the anomalous scattering is rather important. In this study, the structure of FeCo thin films is investigated using synchrotron radiation X-ray diffraction. The FeCo (t nm)/Ta (2 nm) ($t = 5, 10, 20$) thin films were deposited on MgO substrates by sputtering. X-ray diffraction measurement was performed at BL-8A/B, Photon Factory in KEK with the photon energy of 7.1 keV corresponding to the K absorption edge of Fe. Long-range order parameter S were determined from the intensity ratio of 0 0 1 diffraction spots, which was reflected from superlattice, and 0 0 2 diffraction spots, which was reflected from fundamental lattice. The order parameter S of all the FeCo thin films was about 0.6 and the order parameters are considered to be originated from the relaxed lattice strain at the interface between FeCo films and MgO substrates. Magnetic properties were also measured by VSM and X-ray magnetic circular dichroism and the relationship between the order parameter and magnetic properties were investigated. This work was partly supported by Japan Science and Technology Agency (JST).

[1] T. Burkert, et al., Phys. Rev. Lett. 93, 027203 (2004)

[2] Y. Kota and A. Sakuma, Appl. Phys. Exp. 5, 113002 (2012)

TU.H-P133 - Effect of magnetic field annealing on magnetoimpedance in nanocrystalline Fe-Cu-Nb-Si-B bilayer ribbons

F. Andrejka¹, M. Varga¹, L. González-Legarreta¹, J. Marcin¹, J. Kováč¹, D. Janičkovič², P. Švec², I. Škorvánek¹

1. *Institute of Physics, Slovak Academy of Sciences, Bratislava, Slovakia*

2. *Institute of Experimental Physics, Slovak Academy of Sciences, Košice, Slovakia*

This work deals with the study of the influence of longitudinal or transverse magnetic field annealing on the magnetic properties of rapidly solidified Fe_{73.5}Cu₁Nb₃Si_{13.5}B₉ bilayer ribbons prepared by a special planar flow casting method from a single crucible with two nozzles close to each other and with a partition between them. In order to prepare nanocrystalline bilayers with improved soft magnetic properties, pieces of parent amorphous bilayer ribbon ~45 μm thick were isothermally annealed in external magnetic field with intensity of 640kA/m applied in the longitudinal (LF) or transverse (TF) direction to the ribbon length. Reference samples were annealed in a zero magnetic field (ZF). The effect of thermal processing in external magnetic field was examined by hysteresis loop measurements. A heat treatment under longitudinal field resulted in reduction of the coercivity as compared to the ZF-annealing. The lowest coercivity value ~ 0.6 A/m was found for the sample annealed at temperature 823 K for 1 hour. Sheared hysteresis loops with good field linearity and low coercivity (H_c ~ 1.4 A/m) were achieved after TF-annealing. The magnetoimpedance (MI) measurements were performed over a frequency range 0.1 – 10 MHz. The dependence of the MI ratio on the applied dc-magnetic field for the LF-annealed sample exhibited single peak structure. On the other hand, GMI response for TF - annealed sample showed two distinct maxima at ±H_k ~ 230A/m. The maximum values of impedance ratio (ΔZ/Z)_{max} and the field sensitivity η_{max} were 140% and 24%/Oe, respectively. The MI changes in field annealed bilayers were found to be markedly higher as compared to their single-layer counterparts, which makes them promising candidates for magnetoimpedance sensors.

Acknowledgement: This work has been supported by the projects APVV-0492-11, NanoCEXmat Nr. ITMS 26220120019 and VEGA2/0192/13.

TU.H-P136 - Structure and the magnetic properties of $RFe_{4.5}Si_{1.5}$ (R=Y, Dy, Gd)M. Gjoka¹, D.Niarchos¹, V.Psycharis¹*1. Institute of Nanoscience and Nanotechnology, NCSR Demokritos, Athens 15310, Greece*

The research on iron-based intermetallic compounds as possible candidates for permanent magnets still remains attractive. In this work we report our research on the possible new intermetallics $RFe_{4.5}Si_{1.5}$. Ingots were prepared by arc-melting elemental constituents of high purity (99.9%), with the starting composition $RFe_{4.5}Si_{1.5}$ and (R =Y, Dy, Gd), subsequently followed by annealing (wrapped in tantalum foil) in vacuum at 573-1173 K for three days and then fast quenching in water. X-ray diffraction (XRD) data of powder samples were obtained using Cu-K α radiation. The thermal phase transitions and the thermomagnetic analysis of the samples were examined using differential thermal analysis (DTA/TGM) measurements by Diamond Perkin-Elmer instrument at a heating rate of 10 °C/min under Ar flow. Magnetization isothermal measurements at various temperatures were recorded by VSM and SQUID magnetometry. The morphology and composition of the ribbon samples were determined using scanning electron microscopy (SEM) and dispersive X-ray microanalysis (EDX).

The samples present almost one magnetic transition in the interval 298-1173K. The Curie temperatures are 458, 475 and 545 K respectively for (YDy) $Fe_{4.5}Si_{1.5}$ (sample A) , $DyFe_{4.5}Si_{1.5}$ (sample B) and $GdFe_{4.5}Si_{1.5}$ (sample C) alloys. Zero field cooled and field cooled measurements of the sample C show a transition at 154 K. The room temperature magnetizations of samples at 5 T are respectively 56 Am²/kg (A), 34 and 45.8 Am²/kg. Qualitative analysis of XRD diffractions patterns shows that the system probably presents a complicate system. Rietveld analysis of XR diffraction patterns are in progress. From the EDAX analysis it was found that our alloys had compositions very close to the nominal one, i.e. $RFe_{4.5}Si_{1.5}$.

Tu.H-P137 - Crystal domains and magnetic glassy state in Co-ferrite nanoparticlesC.Moya¹, G. Salas^{2,3}, M.Morales³, X.Batlle¹, A. Labarta¹

1. *Departament de Física Fonamental and Institut de Nanociència i Nanotecnologia (IN2UB), Universitat de Barcelona, Barcelona, Spain*

2. *IMDEA Nanociencia, Ciudad Universitaria de Cantoblanco, Madrid, Spain*

3. *Instituto de Ciencia de Materiales de Madrid, CSIC. Madrid, Spain*

Ferrite nanoparticles with composition MFe_2O_4 ($M=Fe,Co$) are currently attracting much interest due to their potential applications in biomedicine, such as the detection of biomolecules by magnetic separation, contrast improvement in nuclear magnetic resonance imaging and the cancer treatment by magnetic hyperthermia. However, strongly sample-dependent magnetic properties have been previously reported for Co-ferrite nanoparticles, suggesting that the synthesis is affected by a number of factors limiting the reproducibility and crystal quality of the final samples, thus largely hindering their applicability [1], [2]. In our work, we present the study of three samples of 8 nm Co-ferrite particles prepared by standard methods based on the thermal decomposition of metalorganic precursors. Despite the facts that all samples have very similar stoichiometry and distribution of particle sizes, and they are all even nominally single-phase $CoFe_2O_4$ according to the conventional methods of chemical and structural characterization performed, they show strongly sample-dependent magnetic properties, ranging from bulk-like ferrimagnetism to glassy magnetic behavior. We show that the presence of crystallite domains associated with crystallographic defects throughout the particles leads to highly-frustrated ferrimagnetic cores that are responsible for the glassy phenomenology - largely spoiling the magnetic performance of the NPs-, while only samples almost free of structural imperfections show bulk-like magnetic properties.

Finally, the structural defects in monodisperse, stoichiometric Co-ferrite NPs can be understood as an additional nano-structuring procedure that tunes their final magnetic properties from bulk-like ferrimagnetism to glassy magnetism. In particular, Co-ferrite NPs with highly defective structures show outstanding magnetic properties associated with an internal enhancement of the magnetic frustration that strongly reduces both the saturation magnetization and coercive field.

[1] Peddis, D.; Cannas, C.; Piccaluga, G.; Agostinelli, E.; Fiorani, D. *Nanotechnology*. 2010, 21, 125705

[2] Cabrera, L. I.; Somoza, A.; Marco, J. F.; Serna, C. J.; Morales, M. P. J. *Nanoparticle Res.* 2012, 14, 873

TU.I-P01 - Influence of applied field direction on linearity of transition and demagnetized domain structure in stacked media

H.Saito¹, N. Tomiyama¹, R. Sugita¹

1. Department of Media And Telecommunications Engineering Ibaraki University, Japan

In order to reduce transition noise of hard disks, clarifying demagnetized domain structure is useful, because fluctuation of transition relates to the structure. The recording layers of hard disks have stacked structure, and the domain structure depends on demagnetization field direction. In this study, we clarify the influence of applied field direction on the linearity of the transition and demagnetized domain structure in the stacked media. Used stacked media in this study were a capped medium and an exchange coupled composite medium. A signal was recorded using a magnetic printing method, where the angle θ of the printing field at the time of recording was set to 30 or 90 deg. from the perpendicular direction. In-plane component of the recording field for θ of 90 deg. was larger than that for 30 deg.. From MFM observations, it was found that the linearity of the transition for both media recorded at θ of 90 deg. was higher than that of 30 deg., although these media have very different layer structure. This result relates to demagnetized domain structure. The amplitude of the leakage field from the in-plane demagnetized both media was much lower than that from the perpendicularly demagnetized ones. In the case of the perpendicular demagnetization, the domain structure of the upper-layer-etched media was almost the same as that of the non-etched media, which shows the magnetization of both upper and lower layers was integrated, while in the case of the in-plane demagnetization, the domain structure of the upper-layer-etched media much differed from that of the non-etched media, which shows the magnetization of both layer was not integrated. It is concluded that the magnetization distribution in the transition area reflects the demagnetized domain structure, and the linearity of the transition increases with increasing the in-plane component of the recording field.

TU.I-P02 - Anomalous Hall effect studies on crystalline Tb-Fe thin films

R. Pothala¹, Markandeyulu G¹

1. Indian Institute of Technology Madras, India

Rare earth - transition metallic thin films (Tb-Fe) in amorphous nature are suitable materials for magneto-optic high density data storage applications buoyed by the existence of uniaxial perpendicular magnetic anisotropy (PMA) at room temperature. In the present work, Tb_xFe_{100-x} (with $x = 11.42, 24.82, 31.08$ and 44.61) films were prepared with the substrate kept at 300 °C and PMA in crystalline films was investigated through Hall Effect measurements. Hall resistivity (HR) was measured in the temperature range 25 K - 300 K at a field of 5 kOe. The existence of PMA was observed in the films with $x = 24.82\%$, 31.08% with positive sign of the Hall loops and for the film with $x = 44.61\%$ with negative sign of the Hall loop, both at 25 K and 300 K. The compensation composition was observed to lie between $x = 32\%$ and 42% of Tb which is more compared to the compensation composition reported in the case of amorphous Tb-Fe films. All the films are seen to exhibit metallic nature in the temperature range 25 K - 300 K whereas, amorphous Tb-Fe films have been reported to exhibit semimetallic nature. The higher compensation composition of Tb, metallic nature of the films and larger HR for higher Tb containing films (larger magnetic anisotropy) and more importantly, the stability of the crystalline phase indicate that the crystalline Tb-Fe films are more suitable candidates for magneto optic data storage applications than their amorphous counterparts.

TU.I-P03 - Extraordinary hall effect based magnetic logic applications

T. Liu¹, D. Lacour¹, F. Montaigne¹, S. Le Gall², M. Hehn¹, T. Huet¹

1. Institut Jean Lamour, UMR CNRS 7198, Université de Lorraine, Vandoeuvre, France

2. LPEP

Magnetic logic devices have many potential advantages compared to traditional semiconductor logic devices, such as nonvolatility, rapid speed and low-power consumption, so that they are considered for next generation spintronics applications. Nevertheless recent proposed magnetic logic devices based on Spin valves (SVs) or magnetic tunnel junctions (MTJs) are rather complex from the material and the micro- and nano-electronic process point of view which may affect cost and reproducibility. We propose two original architectures of magnetic logic devices based on the extraordinary Hall effect (EHE) which have strong potential for logic applications because of their simplicity and scalability. The first one is a reconfigurable logic gate composed of two connected Hall crosses, and the other one is a multi-bit logic comparator which is physically composed of a chain of crosses and can compare a user input with a reference encoded by the magnetization orientations of the cross cells [1]. The latest is required in many security application fields including secure microcontrollers, SIM cards, banking cards, biometric authentication chips, and near field communication, where a logic operation of comparing the user inputs with a reference code needs to be carried out. In the context of the conventional flash technology, the reference codes are usually stored in a recording device, and is extracted and injected into the logic circuit during the comparison process. This extraction process not only causes time and energy wasting but also results in the security risk of possible exposure of reference codes to malicious user.

EHE-based devices possess simple architecture, low cost fabrication process and are obtained in single magnetic layer. Its feasibility is proved in our manuscript on two prototypes made of 4 μm and 300nm width TbCo ferrimagnetic crosses chain. Although TbCo alloy may be very interesting because it provides reliable writing procedure and very high security level (if tuned to have TCO at room temperature), other materials and writing process may also be used to improve EHE signal-to-noise ratio of the reading process as well as writing process energy consumption [1].

[1] T. Liu et al., Appl. Phys. Lett. 106, 052406 (2015)

TU.I-P04 - Energy dissipation during Landauer erasure in sub-micrometric permalloy switches: magneto-optical measurements vs micromagnetic simulations

L. Martini¹, M. Pancaldi², M. Madami¹, P. Vavassori², G. Carlotti¹, G. Gubbiotti³, S. Tacchi³, F. Hartmann⁴, M. Emmerling⁴, M. Kamp⁴, L. Worschech⁴

1. *University of Perugia - Dipartimento Di Fisica E Geologia, Perugia, Italy*

2. *CIC-NanoGune, San Sebastian, Spain*

3. *Istituto officina dei Materiali del CNR (CNR-IOM), Dipartimento di Fisica e Geologia, Perugia, Italy*

4. *Center for Complex Material Systems, Würzburg, Germany*

It is well known that bistable nanomagnetic switches can be used to store information, associating each logic state to a different equilibrium orientation of the magnetization. Here we address the question of the minimum energy required to change the information content of nanomagnetic switches consisting of elongated dots of permalloy, a crucial topic to face fundamental challenges of current technology, such as power dissipation and limits of scaling. The energy dissipated during a “reset to 1” operation, also known as Landauer erasure, was accurately measured at room temperature by vectorial magneto-optical measurements in arrays of 10 nm thick Permalloy dots prepared by e-beam lithography and lift-off. Several samples were investigated, where the longer axis D of the elliptical dots was scaled down from about 900 to 90 nm. The experimental results show that the dissipated energy increases with the dot volume and is from one to three order of magnitude above the theoretical Landauer limit of $k_B T \cdot \ln(2)$. These experimental findings are corroborated by micromagnetic simulations where the Landauer erasure is performed on a single dot and the calculated energy dissipation averaged over many cycles. The simulations confirm that when D exceeds about 200 nm one observes significant deviations from the ideal macrospin behavior, because of inhomogeneous magnetization distribution and edge effects. These phenomena lead to an average dissipated energy that is appreciably larger than the Landauer limit, in agreement with the experimental findings.

This work was supported by the European Community (FP7/2007-2013) under Grant No. 318287 “LANDAUER” and by the MIUR under PRIN Project No. 2010ECA8P3 ‘DyNanoMag’.

TU.I-P05 - Novel oxygen showering post treatment (OSP) for the robust sub-20nm magnetic tunnel junctions (MTJs) patterning process

J. Jeong^{1,2} T. Endoh^{1,3}

1. Graduate School of Engineering, Tohoku University, Japan

2. Semiconductor R&D Center, Samsung Electronics Co., Ltd., Republic of Korea

3. Center for Innovative Integrated Electronic Systems (CIES), Tohoku University, Japan

For the successful commercialization of spintronic applications, the optimal patterning technology as well as sufficient electric and magnetic properties of the magnetic tunnel junctions (MTJs) should be developed. We proposed the oxygen showering post treatment (OSP) process using non-reactive oxygen ions at the previous study to recover patterning damages of the damaged layer. However, for the sub-20nm STT-MRAM, more effective oxygen treatment should be necessary to oxidize damaged layer more selectively and to suppress over oxidations of damage-less area extremely. In this study, we studied about the best OSP conditions to maximize the electric and magnetic enhancements of the patterned MTJs around 20nm sizes by the effective damage recovery. We prepared the simple interface perpendicular anisotropy (i-PMA) MTJs and etched it as a 25nm size by hydrogen based reactive ion etching (RIE) process. With this patterned sample, we applied the non-reactive oxygen ions with various conditions of flowing time, rate and temperature to obtain the extremely controllable oxidizing condition. As a result of the OSP process to 25nm p-MTJs cell array, at the best OSP condition, the MR was increased from 99% to 116% and the I_{sw} was decreased from 41.1 μ A to 28.7 μ A compared to those of reference samples patterned with the RIE process and treated with the ion beam etching (IBE) process. In addition to electric and magnetic enhancements of MTJs array, the OSP process also reduce electric short fails from 1.4% to 0% and improve sigma distribution (\tilde{N}_{σ}) from 5.3 to 13 due to its selective oxidation of re-deposited metallic by-products generated by the physical etching process. With these results, it is verified that the optimized OSP process can recover patterning damages and improve MTJs properties at sub-20nm sizes. By the OSP treatment, we could develop the robust patterning process for sub-20nm STT-MRAM.

TU.I-P06 - Non-symmetry for faster switching in p-MTJ structure

C. Engel¹, S. Goolaup¹, W. Lew¹

1. School of Physical And Mathematical Sciences, Nanyang Technological University, Singapore

Spin-transfer torque random access memory (STT-RAM) is one of the most promising candidates for non-volatile computation in the near future due to its low power, ultrahigh endurance, non-volatility, fast speed processing and scalability. In particular, STT-RAM is attractive for replacing SRAM in L2 cache due to its ability for reducing the standby power to nearly zero by exhibiting similar power consumption and processing speed with same size. Different approaches have been introduced in order to minimize the writing power of a magnetic tunnel junction (MTJ) such as thermally assisted switching, the use of pure spin currents, STT-driven domain wall motion switching and electric field assisted switching whereas few works have looked at reducing the switching time.

In this work, we show that the introduction of geometrical asymmetry in nanostructured perpendicular MTJ (p-MTJ) greatly influences the switching speed of the device. Our model shows that this asymmetry introduces a varying in-plane demagnetizing field along the plane of the structure. This locally reduces the stability of the out-of-plane. Our micromagnetic simulations reveal that the reversal process of the free layer in the p-MTJ structure starts from the region of non-uniform demagnetization field and propagates through the structure. This in effect reduces the current needed to switch the free layer. By comparing egg-shaped and circular p-MTJ structures, our results show that reduction of switching time of up to 47% can be easily achieved. This is a remarkable reduction for a relative simple adjustment of the shape and can speed up further computational power. This in effect shows that lithographical defects inherent in the fabrication of p-MTJ structures can lower the current density and switching time of devices.

TU.I-P07 - Micromagnetic study of exchange-coupled composite bit-patterned mediaK. Son¹, D. Goll², G. Schütz¹, E. Goering¹*1. Max Planck Institute for Intelligent Systems, Heisenbergstr.3, 70569 Stuttgart, Germany**2. Institute for Materials Research, University of Aalen, Beethovenstr.1, 73430 Aalen, Germany*

Bit-patterned media (BPM) of exchange coupled composites (ECC) with perpendicular magnetization are possible candidates for ultrahigh recording densities. The hard magnetic L1₀ chemically ordered phase of FePt guarantee thermal stability with huge coercive fields. Using a soft magnetic Co layer the coercivity (H_c) could be systematically tailored for optimal data recording processes. L1₀-FePt and exchange coupled L1₀-FePt/Co composite films with different Co layers thicknesses have been prepared on MgO(100) single crystalline substrates by co-sputtering. Nanopatterns have been fabricated with thermal and ultraviolet nanoimprint lithography (TUV-NIL) and subsequent inductive coupled plasma reactive Ar-ion etching (ICP-RIE). Large arrays of regular single-domain nanodots are investigated, with 60 nm dot size / 150 nm periods. These dots have been studied by superconducting quantum interference device (SQUID) magnetometry and magnetic force microscopy (MFM). It has been ascertained for dots on patterns to have no interaction each other. The micromagnetic parameters have been determined temperature depended coercive fields distributions, which nearly follow the theoretical ideal coercive field of the micromagnetic universal relation ($\mu_0 H_c = \alpha \mu_0 2K_1/J_s - N_{eff}J_s$, microstructural parameter $\alpha \sim 1$, and $N_{eff} \sim 0$). Compared to the single layer hard magnetic L1₀-FePt pattern, the coercivity and switching field distribution (SFD) of the L1₀-FePt/Co patterns have been significantly reduced and narrowed by a factor of ~ 0.4 to ~ 0.7 , and this increases the Co thickness based on the exchange-coupling to L1₀-FePt. In addition, exchange-coupled composite bit-patterned media are used to continuously tune the effective magnetocrystalline anisotropy and the intrinsic magnetic parameters.

TU.I-P08 - A dual stacked perpendicular magnetic tunnel junction for logic application

H.K. Teoh¹, S. Goolaup¹, C. Engel¹, W.S. Lew¹

1. School of Physical And Mathematical Sciences, Nanyang Technological University, Nanyang Link, Singapore

In recent years, magnetic tunnel junctions (MTJs) have attracted great interests in the development of next generation high density non-volatile memory and logic chips. In this work, we present a novel structure for logic operation that works by exploiting the magnetization dynamics of a spatial dependent distribution of current density of a magnetic tunnel junction free layer. The logic design is a stacked p-MTJ with two small input MTJ situated on top of a larger output MTJ. The process is simple for fabrication as the deposition will be one process and the patterning is just a two-step process. We define logic "1" for parallel free and polarizer layer directions whereas a logic "0" is defined for antiparallel free and polarizer layer directions. If one input MTJ is set to "0" ("1"), a current is injected in -z-direction (+z-direction). Due to our logic architecture, the output logic state is computed at the same time when input states are set into the logic structure. Our logic scheme requires a preset stage. The output junction logic state can be changed when the current density overcome the critical current density from macro spin model. This happens only when currents passed through both input junctions. Our design prevents current lines flowing in different directions from switching the output free layer due to insufficient spin torque provided. The magnetization will only reach an unstable partial switching state which, upon removal of spin current, will relax back to its initial state. It should be noted that the non-uniform spatial distribution of the current density has been exploited for the free layer of the output junction to achieve such selective switching behavior. Our micromagnetic simulations show that various logical operations [NAND(AND),NOR(OR)] can be carried out by fixing the magnetic configuration of the polarizer layer.

TU.I-P09 - Stochastic behavior of spin transfer switching in magnetic tunnel junctions for physically unclonable function systems

T. Marukame^{1,2}, T. Tanamoto², Y. Mitani², A. Schmid¹

1. EPFL, Laussane, Switzerland

2. Toshiba corporation, Japan

Hardware security devices using physically unclonable function (PUF) offer significant advantages over software-based secure identification. We have proposed a PUF using magnetic tunnel junctions (MTJs) and a method for extracting PUF from spin transfer switching [1]. The randomness of MTJ switching is a promising property to realize secure hardware key generators. In this paper, we discuss the stochastic behavior observed in MTJs for compatibility with CMOS-based PUFs.

We measured a large number of CoFeB/MgO/CoFeB-based MTJs with a perpendicular magnetic layer for free and reference layers under magnetic field. Pulse voltages with duration ranging from 10 nano-sec to 1 micro-sec were used to measure the MTJ switching threshold. Each MTJ exhibited different voltage distributions for parallel to antiparallel (P-to-AP) and AP-to-P state transitions [1]. To evaluate thermal effects, the switching depending on the magnetic field vs. current (i.e., H-I curve) was investigated. The results show typical signatures of perpendicular MTJs. The $\gamma=dH/dI$ reduces with increasing current magnitude, suggesting thermal effects induced by the applied pulse. A region where $\gamma<0$ is clearly observed under the specific magnetic field and current. The extracted γ remains unchanged under the magnitude of the pulse, which forms a characteristic behavior in contrast to the region where $\gamma>0$. Furthermore, we observed the two curves of AP-to-P and P-to-AP overlapping in the same region where $\gamma=0$. Hence, stochastic switching occurs under the specific and unidirectional pulse, resulting in time-series data. The unpredictable data can be extracted from each MTJ in a setup consisting of the MTJs combined with certain CMOS delay detection circuits [2]. The stochastic properties demonstrate the eligibility of MTJs as a key component for CMOS-compatible PUFs.

[1] T. Marukame et al., IEEE trans. on magn. 50, #3402004, 2014

[2] M. Stanisavljevic, A. Schmid and Y. Leblebici 'Reliability of Nanoscale Circuits and Systems' Springer, 2011

TU.I-P10 - Self-initializing dual MTJ MRAM cell design

A. Khvalkovskiy¹, D. Apalkov², A. Mikhailov¹, V. Nikitin

1. *Moscow Institute of Physics And Technology, State University, Moscow, Russian Federation*

2. *Samsung Electronic Corp., Semiconductor R&D Center, Republic of Korea*

In a conventional perpendicular MRAM cell design, the reference layer (RL) should have a high thermal and magnetic stability and high spin polarization [1]. To meet these requirements, RLs are often made of two magnetic components, a high-Ku component based on high-Z (e.g. Pt/Pd) alloys, and CoFeB-based component at the MgO interface for high polarization. Since these two components often grow with different crystalline orientation, optimization of the RL design may become challenging [2]. This challenge becomes particularly strong for MTJ cells with two active MgO barriers called Dual MTJ (DMTJ), made of two oppositely directed RLs on both sides of the cell free layer (FL).

As we discuss in our paper, many of these challenges may be circumvented in a new MRAM cell design which we call Self-Initializing Dual MTJ (SID MTJ). SID MTJ has a “strong” RL (SRL) and a “weak” RL (WRL). SRL is a conventional RL like in a single-barrier MTJ cell, e.g. a SAF-coupled RL like in [3]. In contrast to it, WRL should have very low thermal stability; specifically, its switching current J_{c_WRL} should be much smaller than that of FL J_{c_FL} : $J_{c_WRL} \ll J_{c_FL}$. Once the write current pulse is applied, the spin transfer torque from FL initializes WRL antiparallel to SRL prior to the FL motion. As a result, the torque on FL doubles, for both switching directions, like for a conventional DMTJ cell design. WRL should be made of a low $M_s \cdot t$ product layer to reduce its stray field on FL. We show that SID MTJ cell with such WRL may have a matching performance to a conventional DMTJ cell, while having considerably improved growth requirements.

[1] A. V Khvalkovskiy et al., “Basic principles of STT-MRAM cell operation in memory arrays,” J. Phys. D. Appl. Phys., vol. 46, no. 7, p. 074001, Feb. 2013

[2] S. Ikeda, et al., Spin, vol. 02, no. 03, p. 1240003, Sep. 2012

[3] D. C. Worledge, et al., Appl. Phys. Lett., vol. 98, no. 2, p. 022501, 2011

TU.I-P11 - Hybrid fan-out element with magnetic quantum dot cellular automata and domain wall logic

H.Nomura¹, N.Tanigaki¹, F. Nakamura¹, S. Miura¹, R. Nakatani¹

1. Osaka University, Osaka, Japan

Magnetic quantum dot cellular automata (MQCA) [1-3] and magnetic domain wall logic (DW-logic) [4] are information processing architecture composed of magnetic materials. MQCA and DW-logic have possibilities to replace the CMOS architecture. In MQCA and DW-logic, binary state of "0" and "1" are stored with a direction of a magnetization of the nanostructure, and, logic operations are executed by applying a uniform external magnetic field (clock-field). Both architectures have advantages of information non-volatility, low-dissipation energy and operate at room temperature. However, MQCA and DW-logic have disadvantages of limitation of gate arrangements and low integration density of logic gates, respectively. Combination of the MQCA and DW-logic would compensate each disadvantage. Here we experimentally demonstrate a hybrid fan-out element with MQCA and DW-logic. Hybrid MQCA-DW-logic fan-out elements with MQCA nano-dot and v-shaped DW-logic fan-out were fabricated on Si substrate with electron-beam lithography, ion beam sputtering, and lift-off technique. The MQCA-DW-logic fan-out elements are composed of 20 nm thickness Ni₂₀at%Fe. Magnetization manipulation method based on magnetic force microscopy (MFM) was used to write initial binary states of the elements. Magnetization switching field of the v-shaped DW-logic fan-out was changed with the change of the binary state of the MQCA nano-dot. Thus, with appropriate strength of the clock-field, this hybrid MQCA-DW-logic element behaves as a fan-out element. Combination of MQCAs and DW-logic would comprise the advantages of both architectures and be exempt from their defects. Hybrid MQCA-DW-logic architecture would open a new way for developing a high functional devices.

[1] R. P. Cowburn and M. E. Welland 2000 Science 287 1466

[2] A. Imre, G. Csaba, L. Ji, A. Orlov, G. H. Bernstein and W. Porod 2006 Science 311 205

[3] H. Nomura and R. Nakatani 2011 Appl. Phys. Express 4 013004

[4] D. A. Allwood, G. Xiong and R. P. Cowburn, 2005 Science, 309, 1688

TU.I-P12 - Two Dimensional Equalisation of Shingled Write Disk

M.Abdulrazag^{1,2}, M.Ahmed¹, P.Davey¹

1. *University of Plymouth, United Kingdom*

2. *Ahmadu Bello University, Zaria, Nigeria*

Shingled magnetic media presents the potential of extending the capacity of magnetic media beyond the current limit. However it faces the problem of high complex detectors for handling the high interference that occur both from symbols in the same track and from neighbouring tracks. This paper presents a Two Dimensional process for cancelling Inter-Track Interference and Inter-Symbol Interference by combining linear and maximum likelihood (ML) equalisers. The results found show that much less complexity, less delay and better BER performance can be achieved by compressing the data more across the track rather than along the track; if ML equalisation is used across the track while linear equalisation is used along track.

TU.I-P13 - Potential of field-coupled magnetic logic circuits with perpendicular anisotropy in terms of scaling and material improvementsS.Breitkreutz-V. Gamm¹, I. Eichwald¹, G. Ziemys¹, D. Schmitt-Landsiedel¹, M. Becherer¹*1. Technische Universität München, Munich, Germany*

Perpendicular Nanomagnetic Logic (pNML) is an emerging information processing technology employing the 3-dimensional interaction of field-coupled nanomagnets with perpendicular magnetic anisotropy (PMA) to perform logic operations [1,2]. The PMA is locally tuned by focused ion beam irradiation to control the domain wall (DW) nucleation spot [3]. This allows to sensitize magnets to only specific neighbors (inputs) to provide logic operation in both 2D- and 3D-arrays of field-coupled magnets [4,5]. Physical-based compact modeling of pNML [6] is applied to investigate the behavior of a 1-bit full adder circuit in terms of progressive scaling and material improvements. The utilized models base on a well-known switching probability model [7,8] for DW nucleation, which is combined with numerical coupling field calculations [6]. Therefore, the applied model enables to simulate the magnetic behavior with respect to the magnet geometry, magnetic material, fabrication variations, clocking speed and temperature. In our simulations, the error rate e of a 1-bit full adder circuit of [4] is simulated depending on the technology node n (90nm to 7nm), clocking frequency f_{clock} (50kHz to 1GHz), effective anisotropy K_{eff} (0,5 to $2,5 \cdot 10^5 \text{ J/m}^3$), and total magnetic layer thickness t_{Co} (0,5 to 5nm) within $N = 10^5$ runs for each parameter configuration. The results show that scaling increases the coupling between the magnets and therefore improves the operational reliability (error rate decreases below $e < 10^{-4}$). Furthermore, shorter (scaled) magnets allow to increase the clocking speed f_{clock} to the +100MHz-range. Optimizations of the magnetic material enable to reduce the power consumption (lower switching fields) and also to significantly decrease the error rate.

[1] R. Stamps et al., "The 2014 Magnetism Roadmap" J. Phys. D.: Appl. Phys. 47, 333001 (2014)

[2] The 2013 Edition of the ITRS: Emerging Research Devices, <http://www.itrs.net>

[3] S. Breitkreutz et al., J. Appl. Phys. 111, 07A715 (2012)

[4] S. Breitkreutz et al., EPJ Web. Conf. 75, 05001 (2014)

[5] I. Eichwald et al., J. Appl. Phys. 113, 17B902 (2013)

[6] S. Breitkreutz et al., J. Appl. Phys. 115, 17D104 (2014)

[7] J. Engelen et al., Nanotechnology 21, 035703 (2010)

[8] M. Becherer et al., Solid-State Electronics 102, 46-51 (2014)

TU.I-P14 - Control of magnetic inactivation layer thickness in MnGa film by Kr^+ ion irradiationD. Oshima¹, T. Kato¹, S. Takahashi², Y. Sonobe², S. Iwata¹, S. Tsunashima³

1. Nagoya University, Nagoya, Japan

2. Samsung R&D Institute Japan, Republic of Korea

3. Nagoya Industrial Science Research Institute, Nagoya, Japan

It has been reported that Kr^+ ion irradiation modifies the magnetism of MnGa films from ferromagnetic to nonmagnetic due to the structural change from L1_0 ordered to A1 disordered phase and also reported that the local ion irradiation allows to fabricate lateral magnetic nanopatterning without changing the film topography [1]. In this study, we report the depth control of magnetic phase change from ferromagnetic and nonmagnetic (we refer it to as magnetic inactivation) of MnGa by ion irradiation. Kr^+ ions were irradiated to Cr (2 nm) / MnGa (15 nm) / Cr (20 nm) / MgO(001) substrates which was prepared by rf magnetron sputtering. The acceleration energy and incident angle of the Kr^+ ions were varied to control the depth of magnetic inactivation. For normal incidence of 30 keV Kr^+ ions, magnetization of MnGa completely suppressed at a dose of 1×10^{14} ions/cm². With decreasing the energy, ferromagnetism of the MnGa survived after the dose of more than 2×10^{14} ions/cm² because of the reduction of the penetration depth of Kr^+ ions. From the survived magnetization, the depth of inactivation was estimated to be 12 and 7 nm for 10 and 5 keV irradiations, respectively. Surprisingly, we found that the shape of hysteresis loops of the survived MnGa did not change from that before irradiation. This means the sharp transition between magnetically inactivated surface MnGa and survived bottom MnGa layer. Reduction of the ion incident angle was found to be effective to reduce the depth of magnetic inactivation. When the 5 keV ions were irradiated along 70° from the film normal, the depth of magnetic inactivation was reduced to 1 nm, suggesting the magnetic inactivation was controlled with a thickness resolution of 1 nm. This work was supported by the Samsung Global MRAM Innovation Program.

[1] D. Oshima et. al., IEEE Trans. Magn., vol. 49, p. 3608 (2013)

TU.I-P15 - Ultra-fast three-terminal perpendicular spin-orbit torque mram

M.Cubukcu¹, O. Boulle², N. Mikuszeit², C. Hamelin², N. Lamard⁵, L. Prejbeanu², K. Garello³, I. Miron², J. Langer⁴, B.Ocker⁴, P. Gambardella³, G. Gaudin²

1. *Unité Mixte De Physique CNRS/Thales, France*
2. *Univ. Grenoble Alpes, CNRS, CEA, INAC-SPINTEC, Grenoble, France*
3. *Department of Materials, ETH Zurich, Zürich, Switzerland*
4. *Singulus Technologies, Kahl am Main, Germany*
5. *CEA, LETI MINATEC, Grenoble, France*

The Spin-orbit torque (SOT)-MRAM is based on the discovery that a current flowing in the plane of a magnetic multilayer with structural inversion asymmetry, such as Pt/Co(0.6nm)/AlOx, exerts a torque on the magnetization, due to the spin-orbit coupling [1]. This torque can lead to the magnetization reversal, with a switching time smaller than 200 ps [2]. The key advantage of the SOT-MRAM is that write and read are decoupled due to independent current paths [3]. The SOT-MRAM thus naturally solves the reliability issues in current STT-MRAM with a potentially infinite endurance. The possibility to independently optimize the material parameters, for writing and reading, allows maximizing the magnetoresistance ratio and adjust the impedance while keeping a low writing current. Faster writing can thus be achieved for a lower energy and the read disturb issue is naturally solved, even at small sizes. In this presentation, we will present ultra-fast (down to 300 ps) bipolar and reliable writing of perpendicular three-terminal SOT-MRAM single cells. These results show that critical current of around 200 μA and a sub-100 fJ write energy at 1 ns can be achieved for 50 nm technologies. To understand experimental results, we have carried out macrospin simulations of the magnetization dynamics induced by the SOT. Our results show that SOT-MRAM is fast, reliable and low power, which is promising for non-volatile cache memory application [4].

- [1] I. M. Miron et al., Nature 476, 189 (2011)
[2] K. Garello et al., Appl. Phys. Lett. 105, 212402 (2014)
[3] M. Cubukcu et al., Appl. Phys. Lett., 104, 042406 (2014)
[4] M. Cubukcu et al., to be published (2015)

TU.I-P16 - (001) Oriented MnGa film grown on Si substrate for ion beam patterned mediaD. Oshima¹, N. Tsubasa¹, T. Kato¹, S. Iwata¹, S. Tsunashima²

1. Nagoya University, Japan

2. Nagoya Industrial Science Research Institute, Japan

We have studied magnetic patterning of MnGa films without changing the film topography by local ion beam irradiation. The MnGa film changes its magnetism from ferromagnetic to paramagnetic because of the phase change from L1₀ to A1 phase by the ion irradiation [1]. This technique is quite effective to produce low cost and high density planer bit patterned media. However, in the previous report [1], the MnGa films were grown on MgO (001) single crystal substrates to obtain (001) oriented MnGa. This is not practical as magnetic recording media, thus we studied the fabrication of (001) oriented MnGa on thermally oxidized Si substrate. The sample configuration was Cr (2nm) / Mn₅₀Ga₅₀ (15nm) / Cr (20nm) / MgO (20nm) / Ni₆₀Ta₄₀ (25nm) / substrate. The MgO layer was deposited by e-beam evaporation and the other layers were deposited by rf magnetron sputtering. The films were stacked without breaking the vacuum. From the hysteresis loop measurements, the fabricated MnGa film had a perpendicular easy axis even though the film were grown on the Si substrate although the saturation magnetization was about 150 emu/cc which was about one-third of that of the previously reported MnGa film on MgO(001) substrate. The magnetically patterned structure was fabricated using the MnGa on Si substrate by e-beam lithography followed by the 30 keV Kr irradiation with a dose of 1×10^{14} ions/cm². From the magnetic force microscope image, the magnetically patterned structure with topologically flat surface was confirmed even for the bit patterning with a pitch size of 100 nm × 100 nm (bit size of 60 nm × 60 nm). Further improvement of the (001) orientation and surface flatness of the MnGa films will be necessary to obtain bit patterned structure with pitch size as small as that for MnGa on MgO(001) substrate.

(1) D. Oshima et al., IEEE Trans. Magn., vol. 49, p. 3608 (2013)

TU.I-P18 - Investigation of p-MTJ stability for application purposes

C. Engel¹, [S. Goolaup](#)¹, H. Kheng Teoh¹, W. Siang Lew

1. School of Physical And Mathematical Sciences, Nanyang Technological University, Singapore

In this work, we studied the stability of perpendicular-magnetic tunnel junction (p-MTJ) with a synthetic antiferromagnet (SAF) as a function of the geometry and perpendicular anisotropy constant of the free layer, K_{free} . Above a threshold eccentricity, the stability of the free layer is broken for distinct K values. For elliptical p-MTJ structures, the out of plane stability is broken when the ratio between the minor and major axes is 0.8. This phenomenon happens for both the parallel and antiparallel configuration of the p-MTJ. Our results show that this behavior is due to a combination of the demagnetizing and perpendicular magnetic anisotropy field. We suspect that at distinct frequencies the symmetry of uniform magnetization precessions is broken due to a coupling between the spins aligned along the major in-plane axis and spins along the out-of-plane, leading to spin waves. These spin waves are oscillating at frequencies between the out-of-plane and in-plane magnetization oscillations with gigantically increasing amplitude. In conclusion we show that for p-MTJs the interplay between shape and uniaxial anisotropy can play a crucial role in designing stable and predictable p-MTJs state. We show that for elliptical p-MTJs the frequencies of the demagnetization and perpendicular uniaxial energy are responsible for the gigantically out of plane magnetization change while the stray field from the SAF plays a minor role.

TU.I-P19 - Data input and output method for 3D-MQCA with MFM

K. Iwaki¹, R.Wakasa¹, H.Nomura¹, R.Nakatani¹

1. Osaka University, Osaka, Japan

Magnetic quantum cellular automata (MQCA) [1], also called as nanomagnetic logic (NML), is one of a field coupled computing device, which can execute a logic operation via magneto static interaction. Recently, the focus of MQCA research has been changed from two dimensional devices to three dimensional (3D) devices [2]. For these researches, a simple and easy data input and output method, i.e., magnetization manipulation and measuring method is required. However, such method has not been developed yet. Here we propose and demonstrate 3-D magnetization manipulation and measuring method for 3D-MQCA with MFM. As a sample, Au (3 nm)/Ni-20at.%Fe (20 nm)/SiO₂ (40 nm)/Ni-20at.%Fe (20 nm) cylindroid nanodots with major/minor radius of 70 nm/40 nm were fabricated on Si substrates with electron-beam lithography, ion beam sputtering, and lift-off technique. All experiments were performed in vacuum condition at room temperature with originally developed MFM controlled by LabVIEW and commercially available cantilevers (SI-MF40). External magnetic field was used to assist the magnetization manipulation with MFM tip. Before magnetization manipulations, magnetizations of the nanodots were initialized with external magnetic field. MFM images were measured with constant height mode, to avoid a disturbance of the magnetization of nanodots with MFM tip. During a magnetization manipulation process, a jump of a phase shift of the cantilever, which corresponds to a magnetization reversal, was observed. By changing a three dimensional position of the cantilever, it is possible to select a magnetic layer for magnetization manipulation. This three dimensional magnetization manipulation method will become a powerful tool in developing a computer architecture based on 3D-MQCA. Part of this work is supported by Advanced Nano Photonics Research and Education Center in Asia and Photonics Center in Osaka University.

[1] R. P. Cowburn and M. E. Welland, Science, 287 (2000) 1466

[2] R. Lavrijsen, et. al, Nature 2013, 493, 647

TU.I-P20 - High saturation magnetization and perpendicular anisotropy of atomic layer stacking Co/Pt films sputter deposited at room temperature

N. Honda¹, T. Tsuchiya¹, H. Uchida¹, S. Saito², S. Hinata²

1. *Tohoku Institute of Technology, Japan*

2. *Tohoku University, Japan*

L11-ordered CoPt film exhibits high saturation magnetization and perpendicular magnetic anisotropy required for high density recording media(1). But, high preparation temperatures higher than 300C are needed, which would cause large agglomeration of grains. We reported a high perpendicular anisotropy field greater than 15 kOe for layer stacking Co/Pt films sputter deposited at room temperature(2). High saturation magnetization, however, was only obtained with deposition at low Ar pressures and with reduced anisotropy. We have investigated preparation conditions of layer stacking Co/Pt films for high saturation magnetization and anisotropy.

A sputtering apparatus with three magnetron cathodes was used. The atomic-layer stacking-deposition was done on a Ta(10)/Pt(10 nm) underlayer with a collimator by co-sputtering of Co and Pt while rotating the substrate holder at room temperature. Films with two or three monolayer-stacking of Co and Pt were also prepared to investigate the origin of the anisotropy. Films with a high perpendicular anisotropy field of around 15 kOe along with a high saturation magnetization of around 1000 emu/cm³, which indicates a high anisotropy of beyond 1x10⁷ erg/cm³, were obtained at an intermediate Ar pressure with controlled layer thickness. Films with more than two monolayer-stacking of Co and Pt also exhibited high anisotropy fields but with reduced saturation magnetization of around that of simple dilution of Co. The origin of high perpendicular anisotropy in these films could be attributed to the surface anisotropy. High saturation magnetization of around 1000 emu/cm³ was only obtained by monolayer stacking although the films showed only a faint ordering in XRD measurement. It was concluded that high saturation magnetization and perpendicular anisotropy of atomic layer stacking Co/Pt films was caused by micro L11-ordering.

1) H. Sato et. al., J. Appl. Phys., vol. 103, pp. 07E114-07E114-3, 2008

2) N. Honda et. al., IEEE Trans. Magn., vol. 50, no. 11, 3203104, 2014

TU.I-P21 - Dynamic magnetization reversal in NiFe wires with assistance of microwave impulse combined with 100-picosecond pulsed field

G. Okano¹, Y. Nozaki^{1,2}

1. Keio University, Tokyo, Japan

2. JST-CREST, Japan

Magnetic field required for switching can be efficiently reduced at ferromagnetic resonance (FMR) frequency. The phenomenon is called microwave-assisted magnetization reversal (MAMR). There were few experimental studies on the switching dynamics because it is difficult to reduce the duration of microwave impulse as short as sub-nanoseconds. We studied the switching dynamics by using 100-picosecond-wide pulsed field in addition to 5 GHz microwave impulse.

We measured the switching field (H_{sw}) of NiFe wire ($w = 200$ nm, $l = 4$ μ m, $t = 50$ nm) in four cases; (a) without assistance and assisted with (b) 100-picosecond pulse field alone, (c) 5 GHz microwave impulse alone, and (d) simultaneous applications of both signals in the transverse direction of NiFe wire. The pulse length is consistent with the half period of microwave field. In our previous study, we confirmed that the maximum reduction of H_{sw} appeared at 7 GHz. In the case (d), the averaged H_{sw} was lower than those of other cases. The result suggests the appearance of cooperative magnetization switching with the pulse field and microwave impulse. Thus, the cooperative switching occurs within the duration time of the pulsed field. From the multiple measurement of H_{sw} , we also found that the cooperative H_{sw} were discontinuously distributed in two field regions. Namely, there are two distinguishable processes in the cooperative magnetization reversal and it seems to be stochastic which process occurs. These results are attributable to a nonlinear dynamics of magnetization excited by a strong microwave field, i.e., an appearance of quasi-periodic or stochastic magnetization mode and a loss of uniformity in the magnetization precession due to a spin wave excitation.

TU.I-P22 - Atomic composition dependence of microwave-assisted magnetization reversal in CoCrPt-based perpendicular media

Y. Nozaki¹, T. Tanaka²

1. Dept. of Physics, Keio University, Japan

2. ISEE, Kyushu University, Japan

Microwave-assisted magnetization reversal (MAMR) is one of the promising candidates to improve the writability in strongly anisotropic perpendicular media. Recent studies on the MAMR in granular CoCrPt-based medium mainly focused on the dependence of switching field reduction on the frequency, amplitude, and duration time of microwave impulse. On the contrary, there are few studies on the medium dependence of the MAMR. In this study, we investigated an atomic composition dependence of MAMR in CoCrPt-based perpendicular medium. A 100-mm-long and 1.5- μm -wide coplanar waveguide was fabricated on a rectangular-shaped granular film consisting of 16-nm-thick CoCrPt film with a lateral size of $100 \times 1.5 \mu\text{m}^2$. The atomic composition of CoCrPt layer was set so as to realize a thermal stability coefficient Δ of 70 or 90 at room temperature. Ferromagnetic resonance (FMR) spectra of the media were measured from the frequency dependence of microwave reflection coefficient of the coplanar waveguide by vector network analyzer. The amount of magnetization reversal was evaluated from the change in the FMR frequency after applying a microwave impulse to the coplanar waveguide. The amplitude of microwave field impulse was fixed at 635 Oe which is approximately one-tenth of the static coercive field of the medium. The duration of impulse was 500 ns. The Gilbert damping constant was almost independent of the atomic composition and the value evaluated from the linewidth of FMR spectrum was 0.04. The frequency-dependent reduction in coercive field was clearly observed in both media although the reduction ratio of coercive field from the static value depended on the atomic composition. Interestingly, we found that the larger reduction ratio was realized in the medium with larger thermal stability coefficient. This is attributable to the difference in the influence of Joule heating on the switching field reduction.

TU.I-P23 - Damping constants of $\text{Ni}_x\text{Fe}_{100-x}$ ($60 < x < 80$) single crystal thin films investigated by Q-band ferromagnetic resonance analysis

T. Nishimura ¹, S. Yamanaka ¹, Y. Takahashi ¹, N. Inaba ¹, M. Ohtake ², M. Futamoto ², F. Kirino ³

1. Yamagata University, Japan

2. Chuo University, Japan

3. National University of Fine Arts and Music, Japan

Gilbert's damping constant α is an important factor to develop high frequency magnetic recording system and MRAM. The α of Ni-Fe alloy polycrystalline thin films were reported to be correlated to the magnetostriction[1]. The α values of polycrystalline specimens are overestimated, because of the distribution of the crystal orientation in the specimens. We investigated the α of Ni-Fe single crystal thin films by employing a ferromagnetic resonance (FMR) analyses at a frequency of 35 GHz.

20nm-thick $\text{Ni}_x\text{Fe}_{100-x}$ (001) single crystal thin films($60 < x < 90$) were epitaxially grown on MgO(001) single crystal substrates by a rf magnetron sputtering system. The FMR line widths ΔH of the $\text{Ni}_{88}\text{Fe}_{12}$ specimen had constant values of 195 Oe, when the spectra were measured with changing external field directions in the film plane. The α value was calculated to be 0.015 from the ΔH of 195 Oe by using the relationship of $\Delta H = 4\pi\alpha f_r/\gamma$, where g is gyromagnetic ratio, and f_r is resonance frequency. The α for the Ni-Fe specimens did not vary with the crystal directions. With decreasing Ni concentration from 88% to 80%, the α decreased from 0.015($\text{Ni}_{88}\text{Fe}_{12}$) to 0.0099($\text{Ni}_{80}\text{Fe}_{20}$). While the α gradually increased to 0.014($\text{Ni}_{63}\text{Fe}_{37}$) with the Ni concentration range from 80% to 63%. The α had the minimum value at the 80% Ni, where the magnetostriction was zero. This result probably suggests that the magnetostriction is one of the factors to bring the increase of the damping constant.

[1] R.Bonin, M.L.Schneider, T.J.Silva, and J.P.Nibarger, J. Appl. Phys., 98, 123904 (2005)

TU.I-P24 - Sputter growth on amorphous Si/SiO₂ substrates of perpendicularly-magnetized ferrimagnetic Mn₃Ge heusler thin films with giant coercivity

Y. Ferrante¹, J. Jeong², M. Samant³, C. Felser⁴, S. Parkin⁵

1. IBM Almaden Research, San José, United States

2. The Graduate School of Excellence, Mainz, Germany

3. University of Kaiserslautern, Physics Department, Kaiserslautern, Germany

4. Max Planck Institute of Microstructure Physics, Germany

5. Max Planck Institute for Chemical Physics of Solids, Germany

Over the last decade, large number of studies have been performed to find novel magnetic materials suitable for next-generation Magnetoresistive Random Access Memory (MRAM). The basic memory element of MRAM is a nanoscale device called magnetic tunnel junction (MTJ), which is nowadays switched between its two states using spin-transfer torque (STT). MTJs need to be developed using ultra-thin films of magnetic materials displaying low magnetization, high spin polarization (SP) and high perpendicular magnetic anisotropy (PMA) in order to be non-volatile, scalable to very small sizes and programmable by means of small current densities. Moreover, the growth of atomic layers of such materials onto amorphous substrates is crucial for industrial MRAM applications. Some materials among the family of Heusler alloys have been designated as possible candidates to achieve this goal. In fact, it has been previously shown that Mn-based tetragonally-distorted Heusler compounds display very high PMA, low magnetization and have been theoretically predicted to have high SP.

This work illustrates the successful growth of ultra-thin Mn₃Ge Heusler films with tetragonal D0₂₂ structure, deposited by magnetron sputtering on Si/SiO₂ substrates. These films show atomically-flat surfaces (RMS roughness of ~ 4Å) as well as low magnetization (~ 130emu/cc), with direction perpendicular to the film plane. A thickness dependence study of the Mn₃Ge films is carried out, displaying giant coercive fields of ~ 5Tesla for film thicknesses down to only 5nm. Structural, topographical and magnetic properties of films grown on amorphous substrates are also compared to Mn₃Ge films deposited on Cr-buffered MgO(001) single crystal substrates: it is shown that the properties of Mn₃Ge thin films on amorphous Si/SiO₂ substrate are superior to those on MgO(001) substrate.

These preliminary results make tetragonally-distorted Mn₃Ge alloy a promising material candidate as ferrimagnetic electrode for MTJs devices.

TH.A-P01 - Quantum degradation of the second order phase transitions

S. Stishov¹, A. Petrova¹, S. Gavrilkin², L. Klinkova³

1. Institute For High Pressure Physics of RAS, Moscow, Russian Federation

3. P. N. Lebedev Physical Institute of RAS, Moscow, Russian Federation

4. Institute of Solid State Physics of the RAS, Moscow, Russian Federation

The specific heat, magnetization and thermal expansion of single crystals of antiferromagnetic insulator EuTe were measured at temperatures down to 2 K and in magnetic fields up to 90 kOe. The Neel temperature, being 9 K at H=0, decreases with magnetic field and tends to zero at ~76 kOe, therefore forming a quantum critical point. The heat capacity and thermal expansion coefficient reveal lambda-type anomalies at the second order magnetic phase transition at low magnetic fields, evolving to simple jumps at high magnetic fields and low temperatures, well described in a fluctuation free mean - field theory. The experimental data and the corresponding analysis favor the quantum concept of effective increasing space dimensionality at low temperatures that suppresses a fluctuation divergence at the second order phase transition

TH.A-P02 - Ground state and magnetization process of a linear chain composed of coupled localized spins and mobile electrons

J.Lisárová¹, J.Strečka¹

1. Department of Physics. P. J. Safárik University, Kosice, Slovakia

Exact solution of a coupled spin-electron chain composed of localized Ising spins and mobile electrons in a magnetic field is found with the use of a transfer-matrix method. The ground-state phase diagram in the chemical potential vs. magnetic field plane consists of seven phases with different number of mobile electrons per unit cell. Except of two paramagnetic phases with either zero or four electrons per elementary unit cell, the ground-state phase diagram also contains two quantum ferromagnetic phases with one or three electrons per unit cell. The most interesting ground states are found for the system with two electrons per unit cell, in which the system resides in a quantum antiferromagnetic state at low enough fields, then it shows a quantum ferromagnetic phase at moderate fields and finally the system reaches a saturated paramagnetic phase for sufficiently strong fields. The main focus of our work was the study of magnetization process of the correlated spin-electron linear chain as a function of electron density. It is evidenced that one can generate magnetization curves with intermediate plateaus at arbitrary real value of the magnetization ranging from zero up to a saturation magnetization by a suitable choice of electron density.

TH.A-P03 - Novel quantum phase transitions of the frustrated spin nanotube

T. Sakai¹, H. Nakano², K. Hijii³, K. Okunishi⁴

1. JAEA, SPring-8, Japan

2. University of Hyogo, Japan

3. Kobe University, Japan

4. Niigata University, Japan

Recently some quantum spin systems on tube lattices, to called spin nanotubes, have been synthesized. They are expected to be interesting low-dimensional systems like the carbon nanotubes. As the first step of theoretical study on the spin nanotube, we investigate the $S=1/2$ three-leg spin tube, which is the simplest one, using the density matrix renormalization group (DMRG) and the numerical exact diagonalization (ED), combined with a precise finite-size scaling analysis named level spectroscopy[1]. The spin gap, which is one of the most interesting macroscopic quantum effects, was revealed to be open due to frustration for sufficiently strong rung exchange couplings, in contrast to the three-leg spin ladder system which is gapless. The critical point of a quantum phase transition between the gapped and gapless phases was estimated. It is consistent with the previous effective Hamiltonian approach[1-3]. We also found a new quantum phase transition to another spin-gap phase caused by the ring exchange interaction. In addition we theoretically predicted some new field-induced quantum phase transitions. A chirality-mediated novel superconductivity mechanism is also proposed.

[1]T. Sakai et al., Phys. Rev. B 78 (2008) 184415

[2]T. Sakai et al., J. Phys.: Condens. Matter 22 (2010) 403201

[3]K. Okunishi et al., Phys. Rev. B 85 (2012) 054416

TH.A-P04 - Evidencies for a non magnetic anomaly at 1K emerging from ferromagnetic $\text{Ce}_{2.1}(\text{Pd}_{1-x}\text{Ag}_x)_{1.95}\text{In}_{0.95}$ alloysJ.G. Sereni¹, M. Giovannini², M. Gómez Berisso¹, F. Gastaldo².

1. Low Temperature Division., CAB-CNEA and Conicet, San Carlos de Bariloche, Argentina
2. Dipartimento di Chimica e Chimica Industriale, Università di Genova, Genova, Italy

Magnetic and thermal properties of the Ferromagnetic (FM) $\text{Ce}_{2.1}\text{Pd}_{1.95}\text{In}_{0.95}$ solid solution were investigated to determine the $T_C \rightarrow 0$ Quantum Critical Point driven by Ag doping the Pd lattice. The increase of band electrons produced by substituting *hole-like* Pd atoms with *electron-like* Ag depresses $T_C(x)$ from $T_{C0}=4.1\text{K}$ at $x=0$ down to $T_C(x=0.5)=1.1\text{K}$ at the limit of Ag dilution. $T_C(x) \rightarrow 0$ extrapolates to a Critical Point at $x_{CP} \approx 0.62$. High temperature inverse susceptibility $1/\chi_{dc}(T)$ indicates that the effective magnetic moment $\mu_{eff} \approx 2.5\mu_B$ is close to that of the Ce^{3+} ion all along the concentration range. This feature, together with the paramagnetic temperature $\theta_p \approx -10\text{K}$, exclude significant Kondo screening effect. The $T_C(x)$ reduction is associated to a weakening of the FM magnetization and to the emergence of a specific heat C_m anomaly centered at $T_A \approx 1\text{K}$. Unexpectedly, no magnetic signal was detected by $\chi_{ac}(T)$ susceptibility measurements at $T \approx 1\text{K}$ in $x=0.2$ and 0.3 samples with respective T_C at 3.2K and 2.6K . The magnetic entropy collected at $T=4.1\text{K}(=T_{C0})$ is nearly independent of Ag concentration: $S_m(4\text{K}) \approx 0.8 R \ln 2$, suggesting a progressive transfer of FM degrees of freedom to a growing *non-magnetic* component. This shift is reversed applying magnetic field. No antecedent was found in the literature concerning a *non-magnetic* anomaly in the range of "1K" emerging from a FM system. The formation of such anomaly is attributed to an *entropy bottleneck* originated in the divergent $C_m/T = B/T^Q$ dependence for $T > T_A$ (with $Q \approx 2$) which would exceed the available $S_m = R \ln 2$ degrees of freedom at $T \approx 0.55\text{K}$.

TH.A-P05 - Tomonaga-luttinger spin liquid properties of a strong-leg heisenberg spin ladder

D. Schmidiger¹, K. Povarov¹, N. Reynolds¹, R. Bewley², T. Guidi², S. Mühlbauer³, P. Bouillot^{4,5}, C. Kollath⁶, T. Giamarchi⁷, A. Zheludev¹

1. *Neutron Scattering and Magnetism, Laboratory for Solid State Physics, ETH Zürich, Zürich, Switzerland*
2. *ISIS Facility, Rutherford Appleton Laboratory, Chilton, Didcot, United Kingdom*
3. *Forschungsneutronenquelle Heinz Maier Leibnitz (FRM II), Technische Universität München, Garching, Germany*
4. *Interventional Neuroradiology Unit, University Hospitals of Geneva, Geneva, Switzerland*
5. *Laboratory for Hydraulic Machines, Ecole Polytechnique Fédérale de Lausanne, Lausanne, Switzerland*
6. *HISKP, Universität Bonn, Bonn, Germany*
7. *DPMC-MaNEP, University of Geneva, Geneva, Switzerland*

We report a comprehensive study of the static and dynamic properties of a strong-leg Heisenberg spin ladder in its field-induced quantum critical Tomonaga Luttinger spin liquid (TLSL) phase. For this purpose, combined bulk and inelastic neutron scattering experiments were performed on the organometallic material (C₇H₁₀N)₂CuBr₄ (DIMPY), realizing the strong-leg Heisenberg spin ladder Hamiltonian with particularly weak interladder interactions [1-3].

With magneto-thermodynamic measurements, we mapped out the entire (H,T)-phase diagram. The combination of the asymptotic low-temperature behaviour of specific heat and magnetization enabled to determine the field-dependence of the TLSL parameters u and K , in quantitative agreement with numerical DMRG calculations [1].

Using inelastic neutron scattering, we observed the profound spectral changes that are accompanied by the quantum phase transition at H_{c1} [2], such as the transformation of sharp magnon modes into gapped and gapless continua. By focussing on the gapless contribution at lowest energies, we were able to observe striking scaling properties of the TLSL phase [3]. With high-resolution neutron time-of-flight spectroscopy, the T- and energy-dependent q-integrated local dynamical structure factor was determined and found to collapse onto a single curve, if shown in scaled variables [3]. In addition, the scaling curve itself was shown to be in excellent agreement with analytic QFT predictions. Due to the attractive rather than repulsive spinon-spinon interactions in strong-leg spin ladders, the observed thermodynamic and scaling properties are strikingly different from the ones previously observed in strong-rung spin ladders [4] or Heisenberg spin chains in zero field [5].

[1] D. Schmidiger et al., Phys. Rev. Lett. 108, 167201 (2012)

[2] D. Schmidiger et al., Phys. Rev. Lett. 111, 107202 (2013)

[3] K. Povarov et al., Phys. Rev. B 91, 020406R (2015)

[4] B. Thielemann et al. Phys. Rev. Lett. 102, 107204 (2009)

[5] B. Lake et al., Nat. mat. 4, 328 (2005)

TH.A-P06 - Entanglement in the one-dimensional $SU(2)\times XXZ$ spin-orbital models

A. M. Oles^{1,2}, W. You^{1,3}, P. Horsch³

1. *Max Planck Institute for Solid State Research, Stuttgart, Germany*

2. *Marian Smoluchowski Institute of Physics, Jagiellonian University, Kraków, Poland*

3. *College of Physics, Soochow University, Suzhou, People's Republic of China*

We present phase diagrams of the one-dimensional (1D) $SU(2)\times XXZ$ models with negative exchange parameter and analyze spin-orbital entanglement [1] in various ground and excited states. In the 1D $SU(2)\times Z_2$ model with Ising orbital interactions we identify a novel phase with spin-singlet dimer correlations and large spin-orbital entanglement entropy determined for an exactly solved ground state [2], while all the other phases are disentangled. Orbital quantum fluctuations away from the Ising limit do not remove this phase but are responsible for a continuous transition to the phase with coexisting antiferromagnetic and alternating orbital order. The crossover regime between the two above phases is described by two coexisting order parameters [2]. The quantum phases with spin-singlet (orbital-singlet) dimer correlations survive in the isotropic 1D $SU(2)\times SU(2)$ model. Considering the disentangled ferro-ferro phase we find one or two spin-orbital exciton bound states characterized by logarithmic scaling of the von Neumann entropy with increasing system size, unlike the other elementary excitations from the spin-orbital continuum [3]. We suggest that spin-orbital bound states can be experimentally explored using resonant inelastic x-ray scattering.

Work supported by the Polish National Science Center (NCN) Project No. 2012/04/A/ST3/00331.

[1] Andrzej M. Oles, *Journal of Physics: Condensed Matter* 24, 313201 (2012)

[2] Wen-Long You, Andrzej M. Oles, and Peter Horsch, arXiv:1501.04022 (2015)

[3] Wen-Long You, Andrzej M. Oles, and Peter Horsch, *Phys. Rev. B* 86, 094412 (2012)

TH.A-P07 - Dynamical properties of hole-doped quantum haldane chain Nd_{2-x}CaxBaNiO₅

T.Yokoo^{1,2}, S. Itoh^{1,2}, Y. Ikeda³, H.Yoshizawa³, J. Akimitsu⁴

1. High Energy Accelerator Research Organization, Japan

2. J-PARC Center, Japan

3. The University of Tokyo, Japan

4. Aoyama-Gakuin University, Japan

Quantum spins in one-dimensional (1D) chains show unusual properties such as Haldane gap and spin-Peierls state, by strong quantum nature. Particularly in the system where several physical degrees of freedom are entangled in, it opens the new paradigm of the material science. In the quantum spin systems, spin singlet is the basic starting point describing a ground state of the quantum spin chain. Another interest in quantum spin systems is the cooperation between charges and spins. The high-T_c superconductivity is one of the most fascinating examples realized in 2D CuO₂ sheet. Practically it is hard to realize the carrier doping in 1D material because the carrier localization occurs at low temperature. Here we present spin and hole dynamical properties in hole-doped 1D Haldane chain Nd_{2-x}CaxBaNiO₅, which is successfully hole doped 1D Haldane system [1,2]. The hole doped x=0.035 and x=0.1 carrier content were measured by means of pulsed neutron inelastic scattering. It is clearly observed the entire one-magnon band with 10 meV spin gap (Haldane gap) at magnetic zone center (MZC) [3]. The energy at zone boundary reaches 60 meV that is less comparing to undoped Haldane chain. On the other hand, the gap slightly increases in its energy. Nobel dynamical structures within the gap were observed upon carrier doping, showing incommensurating structures centered at MZC. This is originated by the doped-holes. The observed dynamical structures are composed of the contribution of quantum spin chains with spin gap and holes, quite similar to that observed in high-T_c superconductor. Also, at low temperature, the new excitation at E=4 meV and showing almost no momentum dependence has been observed. It is possibly originated from the crystal electric field of Nd³⁺ ions.

TH.A-P08 - Spin-orbital order in systems with orbital dilution

W. Brzezicki^{1,2}, A. M. Oles^{1,3}, M. Cuoco²

1. Marian Smoluchowski Institute of Physics, Jagiellonian University, Kraków, Poland

2. CNR-SPIN & Dipartimento di Fisica "E. R. Caianiello", Università di Salerno, Italy

3. Max Planck Institute for Solid State Research, 70569 Stuttgart, Germany

Correlated insulators with partly filled degenerate orbitals are unique systems with intrinsically frustrated superexchange which includes orbital directional interactions. This frustration is frequently removed by spin-orbital order which changes depending on the balance between ferromagnetic and antiferromagnetic exchange, as for instance in the paradigmatic Kugel-Khomski model [1]. Here we show that magnetic exchange and spin-orbital order in systems with t_{2g} orbital degrees of freedom are radically changed by orbital dilution when transition metal $3d^3$ ($S=3/2$) ions replace $4d^4$ ($S=1$) ions in ruthenium oxides, for instance in Sr_2RuO_4 . Such impurities generate new local spin-orbital order [2], either with frustrated spin defects accompanied by an immobile orbital vacancy, or doubly occupied active orbitals along $3d-4d$ bonds (orbital polarons). At finite ($x=1/8, 1/5, 1/9$) doping such defects stabilize striped patterns either with alternating magnetic domains or with islands of saturated ferromagnetic order. We find that spin-orbital entanglement [3] also plays a role and magnetic frustration can be lifted by strong quantum fluctuations in the host. The spin-orbit coupling can cause more radical modifications of the spin-orbital order [2]. We suggest how such local or global changes of the spin-orbital order induced by impurities could be detected experimentally.

Work supported by the Polish National Science Center (NCN) Project No. 2012/04/A/ST3/00331.

[1] W. Brzezicki, J. Dziarmaga, and A.M. Oles Phys. Rev. Lett. 109, 237201 (2012)

[2] W. Brzezicki, A.M. Oles, M. Cuoco, arXiv:1408.1838; Phys. Rev. X 5, in press (2015)

[3] Andrzej M. Oles, Journal of Physics: Condensed Matter 24, 313201 (2012)

TH.A-P10 - Incomplete devil's staircase in the magnetization curve of SrCu₂(BO₃)₂

M. Takigawa¹, M Horvatic², T. Waki³, S. Kraemer², C. Berthier², F. Levy-Bertrand², I. Sheikin², H. Kageyama⁴, Y. Ueda¹, F. Mila⁵

1. Institute for Solid State Physics, University of Tokyo, Kashiwanoha, Kashiwa, Chiba, Japan
2. Laboratoire National des Champs Magnetique Intenses , LNCMI-CNRS (UPR3228), UJF, UPS and INSA, Grenoble, France
3. Department of Materials Science and Engineering, Kyoto University, Kyoto, Japan
4. Department of Energy and Hydrocarbon Chemistry, Kyoto University, Kyoto, Japan
5. Institute of Theoretical Physics, Ecole Polytechnique Federale de Lausanne, Lausanne, Switzerland

We report on NMR and torque measurements in magnetic fields (H) up to 34 T on the frustrated quasi-two-dimensional spin-dimer system SrCu₂(BO₃)₂, known as the first physical representation of the Shastry-Sutherland Hamiltonian and the archetype of the S=1/2 dimer systems exhibiting quantum magnetization plateaus in its magnetization curve [1,2]. In zero magnetic field, the ground state is a singlet separated by an energy gap from the first degenerated triplet excited state. Above a critical field which closes the gap, the dimers lattice starts to fill with triplets states which are usually described as hardcore (hc) bosons hopping from site to site. In SrCu₂(BO₃)₂, the frustration strongly hinders the kinetic energy of these hc-bosons, and, at some commensurate filling of the lattice, the balance between the kinetic and the repulsive energy favors the occurrence of quantum magnetization plateaus breaking translational invariance. Our measurements reveal a sequence of magnetization plateaus at 1/8, 2/15, 1/6, and 1/4 of the saturation and two incommensurate phases below and above the 1/6 plateau. The magnetic structures inferred from NMR have been successfully described as a stripe order of triplets in all plateaus, suggesting that the incommensurate phases originate from proliferation of domain walls. We propose that the magnetization process of SrCu₂(BO₃)₂ is best described as an incomplete devil's staircase [3]. However, new theoretical calculations based on the iPEPS technique have shown that pairs of bound triplets were leading to more stable structures [4], different than those previously described in terms of dressed triplets, which are still to be confronted to the present NMR results.

[1] K. Onizuka et al., J. Phys. Soc. Jpn. 69, 1016 (2000)

[2] K. Kodama et al., Science 298, 395 (2002)

[3] M. Takigawa et al., PRL 110, 067210 (2013)

[4] P. Corboz and F. Mila, PRL 112, 147203 (2014)

TH.A-P11 - Measurements of transport and magnetic properties of layered antiferromagnet FePS₃ under pressure.

Matthew Coak¹, Y, Sebastian Haines^{1,2}, Siddarth Saxena¹

- 1. University of Cambridge, United Kingdom*
- 2. CamCool Ltd UK, United Kingdom*

FePS₃ is structurally and magnetically quasi two-dimensional, with a magnetic ground state in which spins are ordered as ferromagnetic chains coupled antiferromagnetically., with a Neel Temperature of 120K, which the application of pressure increases. At ambient pressure, it is an insulator with a direct gap of approximately 0.5 eV and a room temperature resistivity of approximately 104 Ωcm. We present the results of exploratory resistivity, magnetisation and dielectric measurements under pressure for this material. The insulating phase is suppressed at a pressure in the range 40-70 kbar giving way to a new metallic phase. As yet unexplained intermediate behaviour is seen at pressures around the transition. At high pressure, the resistivity develops linear temperature dependence similar to that observed in Cuprates. At lower temperature, there is an observed upturn in resistivity. Pressures up to 100kBar have been measured in Bridgman Anvil cells, supported by piston cylinder clamp cell data.

TH.A-P12 - Magnetic properties and structure diversity in RE₂Ni₂X hydrides

S. Maskova¹, R. V. Denys², I. Halevy³, V. Yartys², M. Giovannini⁴, L. Havela¹

1. Department of Condensed Matter Physics, Charles University, Prague, Czech Republic

2. Institute for Energy Technology, Kjeller, Norway

3. Physics Department, Nuclear Research Center Negev, Beer-Sheva, Israel

4. Department of Chemistry, University of Genova, Genova, Italy

We have been studying several RE₂Ni₂Mg compounds crystallizing in tetragonal Mo₂FeB₂ structure (P4/mbm). In this structure, RE atoms form a triangular motif bringing magnetic frustration into the system. As a consequence the magnetization typically shows several metamagnetic transitions. Magnetic properties are highly dependent on the exchange interactions between nearest (N) and next-nearest (NN) neighbors. Considering the role of the balance between the N- and NN-exchange we have decided to use the hydrogenation as the tool for weakening their absolute and relative strengths. It was found that these compounds tend to absorb up to 8 H/f.u. The crystal structure is changed to monoclinic structure (space group P21/c). The magnetic ordering temperatures of all RE-compounds studied are dramatically reduced by the hydrogenation. Such general dramatic weakening of the RKKY exchange interaction should have a strong reason - most likely the impact of hydrogenation on the system of conduction electrons. The compounds with magnesium will be compared with isostructural indides and stannides which yield different types of hydrides.

TH.A-P13 - Quantum critical point of UCoAl determined by AC magnetic susceptibility

N. Kimura¹, N. Kabeya¹, K. Ohyama¹, M. Maeda¹, H. Fujii¹, M. Kogure¹, T. Asai¹, H. Aoki¹, T. Komatsubara², T. Yamamura², I. Satoh²

1. Department of Physics, Tohoku University, Japan

2. Institute for Materials Research, Tohoku University, Japan

UCoAl is known as an itinerant-electron metamagnet. The first-order metamagnetic transition occurs at $H_m=0.6\text{T}$ and its critical temperature T_{cr} is about 11K. The non-Fermi liquid (NFL) behavior is found in the paramagnetic state. Relatively low H_m T_{cr} with the NFL behavior indicate that UCoAl is situated in a proximity to ferromagnetic order and is expected to be reachable to the so-called quantum critical point (QCP) of itinerant-electron ferromagnet by applications of pressure and magnetic field. In order to verify the existence of the QCP in UCoAl we performed the AC magnetic susceptibility measurements under pressure and determined T-P-H phase diagram. The AC magnetic susceptibility can determine the critical point (CP) precisely since its real part diverges toward the CP and its imaginary part detects a hysteresis vanishing at the CP. The obtained T-P-H phase diagram and its QCP are different from the previous report by Aoki, et al. [1]. The present study indicates that QCP is located at $P\sim 2.8\text{ GPa}$ and $H\sim 13\text{ T}$. The critical line of the metamagnetic transition changes in slope at 1.5 GPa. From the comparison between our result and the previous one, we discuss an unusual nature of the magnetic phase diagram realized in UCoAl.

[1] D. Aoki, et al.: J. Phys. Soc. Jpn. 80 (2011) 094711

TH.A-P14 - Quantum crystallization of magnetic quasiparticles in a dimer magnet $\text{Ba}_2\text{NiSi}_2\text{O}_6\text{Cl}_2$ M. Koike¹, M. Okada¹, N. Kurita¹, H. Tanaka¹, H. Uekusa¹, K. Johmoto¹, A. Matsuo², K. Kindo²

1. *Tokyo Institute of Technology, Japan*
2. *The University of Tokyo, Japan*

A spin dimer system, in which two spins are coupled by antiferromagnetic exchange interaction, has generally a gapped singlet ground state. The triplet excitations can hop to neighboring dimers and interact one another by the transverse and longitudinal components of interdimer interactions, respectively. If the frustration between interdimer interactions is imperfect, triplets are delocalized, so that magnetization slope appears in the magnetization process. On the other hand, if the frustration is perfect, triplets are localized and crystallized, which leads to a stepwise magnetization process with a plateau occurs. In this work, we synthesized single crystals of spin-one dimer magnet $\text{Ba}_2\text{NiSi}_2\text{O}_6\text{Cl}_2$ and determined its crystal structure. The crystal structure is monoclinic and is closely related to the structure of $\text{Ba}_2\text{NiSi}_2\text{O}_6\text{Cl}_2$ [1]. With decreasing temperature, the magnetic susceptibilities for H//c and H//ab exhibit rounded maxima at T=55 K and T=71 K, respectively, and decrease towards zero. These susceptibility properties indicate the presence of large single-ion anisotropy and the singlet ground state with excitation gap. It is also found that $\text{Ba}_2\text{NiSi}_2\text{O}_6\text{Cl}_2$ exhibits a stepwise magnetization process with two plateaus at one-fourth and one-half of the saturation magnetization. The 1/2 plateau manifested by the gapped triplet ground state is almost exactly given by the simple product of triplet dimers. On the other hand, the 1/4 plateau states, where the spin triplet are localized owing to the almost perfect frustration of interdimer exchange interactions, are almost exactly given by alternate product of singlet and triplet dimers. This result suggests that the frustration between interdimer interactions of this crystal is nearly perfect. We will discuss magnetic properties of $\text{Ba}_2\text{NiSi}_2\text{O}_6\text{Cl}_2$ by comparing those of $\text{Ba}_2\text{NiSi}_2\text{O}_6\text{Cl}_2$.

[1] H. Tanaka et al., J. Phys. Soc. Jpn. 83, 103701 (2014)

TH.A-P15 - Ferromagnetism in two band metals: the very strong coupling limit

C. M. Chaves¹, E. J. Calegari², S. G. Magalhaes³, A. Troper¹

1. *Centro Brasileiro de Pesquisas Fisicas, Rio de Janeiro, Brazil*

2. *Laboratorio de Teoria da Materia Condensada, Departamento de Fisica - UFSM, Santa Maria, RS, Brazil*

3. *Instituto de Fisica, Universidade Federal Fluminense, Niteroi, Rio de Janeiro, Brazil*

The main purpose of this paper is to examine the occurrence of ferromagnetism in metals at the very strong coupling regime (U tending to infinity) in the single-site approximation (SSA). The metal is described by a realistic two hybridized bands, one including Hubbard correlation and the other an uncorrelated one. We parametrize the ratio of the band widths and their centers as well.

In this method (SSA) the Hamiltonian is approximated by an effective and simpler one in which only one site retains the full correlation (U) while in the others acts an internal field, the self-energy. This field does not depend on the wave vector and is self-consistently determined by imposing the translational invariance of the problem, a coherent potential approximation (CPA) procedure. We also introduce the Roth's wave vector and spin dependent band shift W . For several total electronic occupation numbers (n_{tot}) we compare the spin dependent free energy with the corresponding paramagnetic one at $T=0$. We conclude making a critical analysis of the Roth's method for this problem arguing that the existence of a stable ferromagnetic state in this regime depends on a strong competition among W , the limit U tending to infinity, V , and on the relation between the two bare bands.

TH.A-P16 - Anomalous weak ferromagnetism of non-magnetic Sc, La, Eu, Y, Lu ion substituted RB₄ (R = Sm, Gd, Tb, Dy, Ho, Er)

B. Kang¹, S. Lee¹, M. Song¹, D. Kim², J. Kim³, B. Cho¹

1. School of Materials Science And Engineering, Gwangju Institute of Science And Technology, Republic of Korea

2. Department of Physics, POSTECH, Republic of Korea

3. Pohang Accelerator Laboratory, Republic of Korea

Recently, the weak ferromagnetism of Tb_{1-x}Y_xB₄ and Dy_{1-x}Y_xB₄ was reported. Rare earth tetraborides (RB₄) compounds belong to a geometrically frustrated magnetic system. The network of rare-earth ions, which have the same z position (z = 0), forms the Shastry-Sutherland lattice (SSL). SSL have various ground states depending on the ratio of J_{nn} (exchange interaction of nearest neighbor) and J_{nnn} (exchange interaction of next nearest neighbor). Because the non-magnetic ion substitution induced a fluctuation to the delicate equilibrium of RB₄, the result of substitution revealed the exotic weak ferromagnetism. In this study, non-magnetic Sc, Y, La, Eu, Lu ion replaced the rare-earth ion in the other RB₄ (R = Sm, Gd, Tb, Dy, Ho, Er) to find universality of weak ferromagnetism and increase the magnitude of weak ferromagnetism. As a result, we could find the weak ferromagnetism in R_{1-x}R'_xB₄ (R = Sm, Gd, Tb, Dy, Ho, Er), (R' = Sc, Y, La, Eu, Lu). The universality was confirmed. Moreover, the magnitude of weak ferromagnetism reached four times larger than Y substitution case. In order to find the origin of the weak ferromagnetism, single crystal neutron scattering and a soft x-ray magnetic circular dichroism were performed. As a result, it is confirmed that rare-earth ion manifest the weak ferromagnetism.

TH.A-P17 - Anomalous spin dynamics of coupled spin-tetramer system CuSeO₃

W.Lee¹, S. Lee¹, K.Choi¹, J. van Tol², A. Ozarowski², P. L Kuhns², Arneil P Reyes², Helmuth Berger³

1. Department of Physics, Chung-Ang University, Seoul 156-756, Republic of Korea

2. National High Magnetic Field Laboratory, Florida State University, Tallahassee, United States

3. Institute of Condensed Matter Physics, EPFL, Lausanne, Switzerland

We report high-field magnetization, ⁷⁷Se nuclear magnetic resonance (NMR), and electron spin resonance (ESR) measurements of the coupled spin-tetramer system CuSeO₃ (P21/n), which consists of strongly coupled (dimer-like) Cu(1) spins and weakly coupled Cu(2) spins. At zero field this compound undergoes long-range antiferromagnetic order at TN = 9 K. Thus, CuSeO₃ constitutes a promising candidate to investigate the interplay of inter-tetramer interactions with built-in tetrahedral frustration. We observe the half-step magnetization plateau at $\mu_0H = 42\text{-}50$ T, depending on a crystallographic orientation. This is expected for a chainlike array of tetrahedral spin clusters. With decreasing temperature both the ESR linewidth and g-factor decrease monotonically down to 50 K and then show the respective critical-like broadening and shift at TN = 9 K. The nuclear spin-lattice relaxation rates, $1/T_1$, measured at $\mu_0H = 9.9$ and 10.1 T exhibit a critical divergence at TN = 10.0 K. Noticeably, the critical temperature at finite external field is higher than the zero-field one, suggesting the significance of singlet fluctuations. In a magnetically ordered phase, both the linewidth of antiferromagnetic resonance mode and $1/T_1$ show an anomaly at $T^* = 6.0(5)$ K as evident from a change of their exponent. This result is attributed to a spin reorientation and is discussed in terms of a large difference of an energy scale between the Cu(1) and Cu(2) spins.

TH.A-P18 - Bose-einstein condensation vs. crystallization of magnons in dimer magnets $\text{Ba}_2\text{MSi}_2\text{O}_6\text{Cl}_2$ (M=Co, Cu)

M. Okada¹, N. Kurita¹, H. Tanaka¹, K. Johmoto², K. Fujii², H. Uekusa², A. Matuo³, K. Kindo³, M. Tokunaga³, H. Nojiri⁴, M. Nakamura⁵, S. Nishimoto⁶

1. Department of Physics, Tokyo Institute of Technology, Tokyo, Japan
2. Department of Chemistry, Tokyo Institute of Technology, Tokyo, Japan
3. Institute for Solid State Physics, the University of Tokyo, Tokyo, Japan
4. Institute for Materials Research, Tohoku University, Japan
5. Institute of Industrial Science, the University of Tokyo, Tokyo, Japan
6. Institute for Theoretical Solid State Physics, IFW Dresden, Germany

A quantum magnet composed of spin dimers generally has an energy gap between a singlet ground state and an excited triplet state. It is known that the magnetic-field-induced magnetic ordering in the dimer magnet can be described as Bose-Einstein condensation (BEC) of $S_z=1$ triplets (magnons). The BEC of magnons is observed in many dimer magnets. When the hopping of magnons is strongly suppressed, magnons undergo crystallization in magnetic fields owing to the repulsive interaction. The experimental realization of the magnon crystallization is little. Recently, we synthesized new dimer magnets $\text{Ba}_2\text{MSi}_2\text{O}_6\text{Cl}_2$ (M=Co and Cu) and investigated their magnetic properties via magnetization measurements using single crystals. The crystal structures of the present systems are closely related to the structure of $\text{Ba}_2\text{CuSi}_2\text{O}_6$. In analogy with the case of $\text{Ba}_2\text{CuSi}_2\text{O}_6$, the exchange network in $\text{Ba}_2\text{MSi}_2\text{O}_6\text{Cl}_2$ is expected to be a two-dimensional. With decreasing temperature, the magnetic susceptibilities of $\text{Ba}_2\text{MSi}_2\text{O}_6\text{Cl}_2$ exhibit rounded maxima and decrease rapidly, indicating the gapped ground states. We found that $\text{Ba}_2\text{CoSi}_2\text{O}_6\text{Cl}_2$ shows a sharp stepwise magnetization process with 1/2 magnetization-plateau, irrespective of the field direction. Because all the dimers are crystallographically equivalent, the possibility that there are two kinds of isolated dimer of the same number is ruled out. Thus, the stepwise magnetization process is attributed to the crystallization of magnons. The absence of magnetization slope indicates that the frustration in interdimer interactions is almost perfect. In contrast to $\text{Ba}_2\text{CoSi}_2\text{O}_6\text{Cl}_2$, $\text{Ba}_2\text{CuSi}_2\text{O}_6\text{Cl}_2$ exhibits no plateau in the magnetization process, which is indicative of weak frustration in the interdimer interactions. The non-linear slope of magnetization curve between two critical fields, where BEC of magnons occurs, is well reproduced by the exact diagonalization for the two-dimensional (2d) dimer array. $\text{Ba}_2\text{CoSi}_2\text{O}_6\text{Cl}_2$ and $\text{Ba}_2\text{CuSi}_2\text{O}_6\text{Cl}_2$ are magnetically described as strongly and weakly frustrated quasi-2d dimer magnets, respectively.

TH.A-P19 - Magneto-electric effects in the interacting dimer system TICuCl₃K. Kakihata¹, Y. Sawada¹, S. Kimura¹, K. Watanabe¹, M. Hagiwara², H. Tanaka³

1. Institute For Materials Research, Tohoku University, Japan

2. Center for Advanced High Magnetic Field Science, Osaka University, Japan

3. Tokyo Institute of Technology, Japan

TiCuCl₃ is known as the three-dimensionally coupled $S = 1/2$ antiferromagnetic dimer system, composed of Cu^{2+} spins. This material has a finite energy gap $D/k_B \sim 7.5$ K between the singlet state and the first excited triplet states. The magnetic excitation is described as Bosonic quasiparticle "triplon", which is the triplet excited on a dimer propagating through a crystal. When the energy gap is collapsed by applying a magnetic field of $H_g = D/gm_B \sim 6$ T, the quasiparticles are induced in the ground state, and then the Bose-Einstein condensation occurs, resulting in antiferromagnetic order^[1, 2]. The wave function of the field-induced phase on a dimer is described by a superposition of the singlet and triplet states, and such a superposition gives a finite expectation value of the vector spin chirality. Therefore, we expect that the spontaneous electric polarization is induced by the spin current mechanism^[3] in the magnetically ordered phase of TiCuCl₃. To confirm this expectation, we have performed pyroelectric current measurements to observe the polarization using 15 and 18 T superconducting magnets at Institute for Materials Research in Tohoku University. As a result, we succeeded in observing the appearance of the spontaneous electric polarization the field-induced antiferromagnetic ordered phase when the sample is cooled down in magnetic and electric fields applied perpendicular to (010) and (10-2) planes, respectively. The evaluated value of the electric polarization is approximately 7 mF/m² at 2 K and at 14 T. Therefore, we conclude that the spontaneous electric polarization is induced in the magnetically ordered phase of TiCuCl₃.

[1] A. Oosawa *et al.*, J. Phys. Condens. Matter. 11 (1999) 265[2] T. Nikuni *et al.*, Phys. Rev. Lett. 84 (2000) 5868[3] H. Katsura *et al.*, Phys. Rev. Lett. 95 (2005) 057205

TH.A-P20 - NMR investigations of spin dynamics and order in the BEC-type quantum antiferromagnets

M. Horvatic¹, M. Klanjsek^{1,2}, R. Blinder¹, M. Jeong^{1,3}, S. Mukhopadhyay^{1,4}, S. Krämer¹, M. S. Grbic^{1,5}, H. Mayaffre¹, C. Berthier¹

1. *Laboratoire National Des Champs Magnétiques Intenses, LNCMI-CNRS, Grenoble, France*
2. *Jozef Stefan Institute and EN-FIST Centre of Excellence, Ljubljana, Slovenia*
3. *Laboratory for Quantum Magnetism, École Polytechnique Fédérale de Lausanne, Lausanne, Switzerland*
4. *DCMP & MS, Tata Institute of Fundamental Research, Mumbai, India*
5. *Department of Physics, Faculty of Science, University of Zagreb, Zagreb, Croatia*

We report NMR investigation of three archetypal, quasi-1D, antiferromagnetic quantum spin systems in which the magnetic-field-induced phase transition can be described as Bose-Einstein condensation (BEC). The two spin-1/2 ladders compounds, $(\text{C}_5\text{H}_{12}\text{N})_2\text{CuBr}_4$ called 'BPCB' [M. Klanjsek et al., PRL 101, 137207 (2008)] and $(\text{C}_7\text{H}_{10}\text{N})_2\text{CuBr}_4$ called 'DIMPY', are respectively representative of the repulsive and attractive interaction in a description in terms of the hard-core bosons. They are perfect model systems for quantitative studies of the Tomonaga-Luttinger Liquid description, enabling us to relate the temperature dependence of the low-energy spin fluctuations, measured through $1/T_1$ NMR relaxation rate, to the type of interaction. NMR data have thus provided the first direct evidence for the attractive interaction [M. Jeong et al., PRL 111, 106404 (2013)]. Our subsequent high-field measurements demonstrated that the field dependence of $1/T_1$ provides a simple experimental criterion to distinguish between the two regimes. The third compound, $\text{NiCl}_2\text{-}4\text{SC}(\text{NH}_2)_2$ called 'DTN', contains chains of $S=1$ spins subject to single-ion anisotropy, making its low-energy Hamiltonian equivalent to the one of BPCB. While DTN is less one-dimensional, it allows better experimental access to the low-temperature 3D regime. In DTN and BPCB the $1/T_1$ data have provided the first detailed insight on quantum-critical spin dynamics, establishing the scaling behaviour and its universality for the quasi-1D regime [S. Mukhopadhyay et al., PRL 109, 177206 (2012)]. Further analysis and new data showed that the 1D regime of scaling observed in BPCB perfectly agrees with the state-of-the-art numerical predictions for hard-core bosons in 1D, while the 3D regime observed in DTN can be favourably compared with the mean-field-based theoretical prediction for hard-core bosons in 3D. The NMR data on the BEC phase in DTN provided the first insight into its low-energy dynamics. Finally, in the Br-doped DTN we established the first NMR signature of the disorder-induced Bose-glass phase.

TH.A-P21 - Magnetic polarization of the americium $J = 0$ ground state in AmFe_2

N. Magnani¹, R. Caciuffo¹, F. Wilhelm², E. Colineau¹, R. Eloirdi¹, J. Griveau¹, J. Ruzs³, P. Oppeneer³, A. Rogalev², G.H. Lander¹

1. *European Commission, Joint Research Centre, Institute For Transuranium Elements, Karlsruhe, Germany*
2. *European Synchrotron Radiation Facility, Grenoble, France*
3. *Department of Physics and Astronomy, Uppsala University, Sweden*

Ordered magnetism is a result of spin polarization of the electrons, but there are two elements in the periodic table in which the intrinsic magnetic moment is zero despite the electrons being spin-polarized: europium and americium. For the free Eu(III) and Am(III) ions the f-electron count is six, the spin and orbital moments have the same magnitude and opposite direction, and the resulting $J = 0$ ground state is non-magnetic. Nevertheless, since a large spin polarization is present, the application of a magnetic field can induce a moment by mixing with excited states. Europium, however, has a tendency towards the magnetic divalent configuration and loses its magnetism only under high pressure. Americium, in contrast, exhibits a stable trivalent oxidation state and, like most of its compounds, shows temperature independent susceptibility and no ordered magnetism.

One can expect that long-range order of the moments induced in the virtually nonmagnetic sublattice will be evident when these ions are embedded in a strong ferromagnetic matrix, because of the large molecular field created by the exchange interaction. Using the technique of x-ray magnetic circular dichroism, we show that this is the case in AmFe_2 . Our result not only confirms the previous indication on the total Am moment from neutron diffraction experiments, but by probing the orbital and the effective spin moment separately, it allows us to attribute the resultant induced moment (antiparallel to the Fe one) to significantly localized 5f electrons, a situation very different to the isostructural UFe_2 .

TH.A-P22 - Magnetic properties of single crystals of the S=2 quasi-1d heisenberg antiferromagnet MnCl₃(bpy)

M. Hagiwara¹, S.Shinozaki¹, A. Okutani¹, D.Yoshizawa¹, T. Kida¹, T.Takeuchi², O. Risset³, D.Talham³, M. Meisel⁴

1. Center For Advanced High Magnetic Field Science, Graduate School of Science, Osaka University, Toyonaka, Osaka, Japan

2. Low Temperature Center, Osaka University, Toyonaka, Osaka, Japan

3. Department of Chemistry, University of Florida, Gainesville, United States

4. Department of Physics and National High Magnetic Field Laboratory, University of Florida, Gainesville, United States

Recent theories have unveiled topological differences between one-dimensional (1D) Heisenberg antiferromagnets (HAFs) with odd and even integer spins [1, 2]. With this renewed interest, we report the experimental results of single crystal samples of MnCl₃(bpy) (bpy=2, 2'-bipyridine) (monoclinic Cc), which is regarded as a S = 2 quasi-1D HAF. The magnetic susceptibilities ($H = 0.1$ T, 2 K $\leq T \leq 300$ K) along the a^* , b , and c axes show broad maxima around 100 K. However, the magnetic signal along the c -axis (chain direction) decreases steeply with $T < 100$ K, while the responses along the other directions decrease gradually to $T \approx 25$ K, where they increase rapidly at lower temperatures. A sharp peak is observed at 11 K for the b -axis, which may correspond to the anomaly observed in a powder sample [3]. The specific heat shows a tiny peak around 11 K, suggesting long-range order. For $H \parallel c$ -axis, a spin-flop transition is seen at 22 T, while the magnetizations along the other directions show monotonic increases. Hysteresis along the b -axis below 4 T is interpreted in terms of the crystal structure.

Work supported by Kakenhi (Nos. A242440590 and A25246006) from the MEXT, Japan, by the NSF via DMR-1202033 (MWM), DMR-1405439 (DRT), and DMR-1157490 (NHMFL), and by the State of Florida.

[1] F. Pollmann *et al.*, Phys. Rev. B 85, 075125 (2012)

[2] J.A. Kjall *et al.*, Phys. Rev. B 87, 235106 (2013)

[3] M. Hagiwara *et al.*, J. Phys.: Conf. Ser. 400, 032014 (2012)

TH.A-P23 - AC susceptibility evidence for a tricritical point in the ferromagnet NdOs₄As₁₂A. Rudenko¹, Z. Henkie¹, T. Cichorek¹*1. Institute of Low Temperature And Structure Research, Polish Academy of Sciences, Poland*

Revised theories of the quantum phase transition in metallic ferromagnets point at similar results irrespective of the microscopic origin of the magnetization, i.e., the quantum phase transition from a metallic paramagnet to a ferromagnet in the absence of quenched disorder is generically discontinuous or of first order, in contrast to the second-order transition with mean-field critical behavior predicted by the Hertz theory. In particular it holds also for ferromagnets with localized magnetic moments [1].

Recent specific-heat experiments on ferromagnetic NdOs₄As₁₂, with a Curie temperature $T_C = 1.0$ K and a $\Gamma_6^{(2)}$ quartet ground state of the Nd³⁺ multiplet, revealed its anomalous low-temperature properties in finite magnetic fields [2]. While a smooth increase of T_C was observed with magnetic field applied along the easy magnetic [100] axis, for $B \parallel [111]$ we have found a qualitatively different behavior: the ferromagnetic peak is not resolved at around 1 K and, most remarkably, a clear anomaly is observed at ~ 0.7 K in $B = 0.25$ T. In a sharp contrast to NdOs₄As₁₂, the antimony-based counterpart NdOs₄Sb₁₂ ($T_C = 0.9$ K and a Γ_5 doublet ground state) exhibits an isotropic behavior in externally applied fields. Here, we present AC susceptibility evidence for a field-driven tricritical point in ferromagnetic NdOs₄As₁₂: With gradually increasing DC field up to 300 Oe applied along the hard magnetic [111] axis, both the real and imaginary components of AC susceptibility are shifted towards lower temperatures. Such a response of AC magnetometry has not been observed for $B \parallel [100]$ and in NdOs₄Sb₁₂ as well.

[1] T. R. Kirkpatrick and D. Belitz *Phys. Rev. B* 85 (2012) 134451

[2] T. Cichorek et al., *Phys. Rev. B* 90 (2014) 195123

TH.A-P24 - Ferromagnetic state of SU(3) hubbard model on the Lieb lattice

W. Nie¹, W. Zhang², H. Zhai¹

1. *Institute For Advanced Study, Tsinghua University, China*

2. *Department of Physics, Renmin University, China*

The investigation of itinerant electrons' ferromagnetism is one of the central and challenging topics in condensed matter physics. Due to the subtle sign problem of fermions, rigorous proofs for ferromagnetism of fermionic Hubbard model are very limited [1-3], which are benchmarks for the magnetic properties of the ground state. One noted example is that Lieb has proved the unsaturated ferromagnetism for the Hubbard model with SU(2) symmetry on the Lieb lattice at half filling, when the repulsive interaction is finite[3].

The systematic study of SU(N) Hubbard model at large-N limit was initiated in the context of high-T superconductivity as a theoretical tool [4]. The realization of SU(N) Hubbard has not only been theoretically proposed [5], but also has been experimentally realized by loading ultracold Yb atoms in optical lattice [6]. It calls for the theoretical prediction for the magnetic property of the ground state of SU(N) Hubbard model, for the experimental observation.

In this work, we investigate the magnetic property of the ground state of the Hubbard model with SU(3) symmetry on the Lieb lattice, with finite repulsive interaction. Our mean-field calculation shows, the ground state shows ferromagnetic order from 1/3 to 2/3 filling.

References:

[1] Y. Nagaoka, Phys. Rev. B, 147, 392 (1966)

[2] H. Tasaki, Phys. Rev. Lett. 69, 1608 (1992), A. Mielke and H. Tasaki, Commun.Math.Phys. 158, 341, (1993)

[3] E. H. Lieb, Phys. Rev. Lett. 62, 1201 (1989)

[4] I. Affleck and J. B. Marston, Phys. Rev. B 37, 3774 (1988); 39, 11538 (1989)

[5] C. Honerkamp and W. Hofstetter, Phys. Rev. Lett. 92, 170403 (2004)

[6] S. Taie, R. Yamazaki, S. Sugawa, and Y. Takahashi, Nat. Phys. 8, 825 (2012), S. Taie, Y. Takasu, S. Sugawa, R. Yamazaki, T. Tsujimoto, R. Murakami, and Y. Takahashi, Phys. Rev. Lett. 105, 190401 (2010)

TH.A-P25 - Glassy phases in dimerized quantum antiferromagnets

S. Thomson^{1,2}, C. Pedder³, F. Kruger^{2,4}

1. *University of St Andrews, United Kingdom*
2. *ISIS Neutron and Muon Facility, United Kingdom*
3. *University of Luxembourg, Luxembourg*
4. *London Centre for Nanotechnology, UCL, United Kingdom*

Quantum antiferromagnets are ideal candidates for the thorough study of the effects of disorder on strongly-interacting quantum systems. It is known that a dimerized $S=1/2$ spin system can be exactly mapped to a lattice gas of bosons with hard-core repulsion and that these bosons can condense, leading to exotic magnetically ordered states. This mapping enables us to analyse disordered quantum antiferromagnets using the existing framework developed to characterise the disordered Bose-Hubbard model. Using this, we can connect the magnetic glass phases seen in experiments with the much-studied Bose glass and Mott glass phases of disordered bosons on a lattice.

Here we present an analytic calculation of the phase diagram of a 3D dimerized quantum antiferromagnet with intra-dimer bond disorder. First we develop the formalism in the clean system, mapping it to a lattice gas of bosons and using a strong-coupling expansion around the atomic limit, followed by a momentum-shell renormalization group analysis to obtain the phase diagram. We then extend the formalism to look at the effects of disorder, establishing the phase diagram and examining the magnetic glass phases obtained as a result. We discuss their connection to recent experiments on disordered quantum antiferromagnets, as well as their analogues in optical lattice systems.

TH.A-P26 - Neutron diffraction study of proton disorder in D2O - ice

K. Siemensmeyer¹, J.-U. Hofmann¹, S. Isakov², B. Klemke¹, R. Moessner³, D.J.P. Morris⁴, D.A. Tennant⁵

1. *Helmholtz Zentrum Berlin, Germany*

2. *ETH Zürich, Zürich, Switzerland*

3. *Max-Planck Institut für Physik Komplexer Systeme, Dresden, Germany*

4. *Xavier University, Cincinnati, Ohio, United States*

5. *Oak Ridge National Laboratory, Knoxville, Tennessee, United States*

Water ice (H₂O) at low pressure can be understood as a hexagonal structure where each Oxygen atom covalently bonds to two Hydrogen atoms. Further, each bond between Oxygen atoms is occupied by only one Hydrogen atom. These are the famous ice - rules that give rise to a highly disordered ground state with a residual entropy of $R \ln(3/2)$. We have measured the diffuse scattering of a large D₂O ice crystal using neutron diffraction. Here we present an analytical model of the hydrogen configuration in water ice in contrast to previous Monte-Carlo studies.

TH.A-P27 - BaAg₂Cu[VO₄]₂ quantum magnet: local probe studies (ESR and NMR)

E.Vavilova¹, Y. Krupskaya², M. Schäpers³, A. Wolter-Giraud³, H. Grafe³, V.Kataev³, A. Müller⁴, B. Büchner³

1. *Zavoisky Physical-Technical Institute, Kazan, Russian Federation*
2. *University of Geneva, Switzerland*
3. *IFW-Dresden, Germany*
4. *University of Houston, United States*

BaAg₂TM[VO₄]₂ is a new material class with the flexible spin exchange topology. The unit cell of BaAg₂Cu[VO₄]₂ exhibits two crystallographic non-equivalent V sites located in a VO₄ tetrahedra. These VO₄ tetrahedra are connected to alternating non-equivalent Cu chains with slightly different bond angles. It creates two types of Cu chains with ferro- and anti-ferromagnetic intra-chain coupling. High-field ESR and NMR are the sensitively probes of local magnetism in BaAg₂Cu[VO₄]₂ that allows to investigate the internal field distribution in the different chains and FM and AFM correlations at low temperatures. The compound demonstrate the structure-driven tunability of magnetic couplings and can be a flexible toy model for studies of Heisenberg quantum magnets

TH.A-P28 - Slow thermodynamics in the phase separated state of the bilayered manganite $(\text{La}_{0.4}\text{Pr}_{0.6})_{1.2}\text{Sr}_{1.8}\text{Mn}_2\text{O}_7$ H. Taniguchi¹, Y. Nakamura¹, H. Takahashi¹, T. Konno¹, M. Matsukawa¹, R. Suryanarayanan²

1. Iwate University, Japan

2. Univ. Paris-Sud, Paris, France

Perovskite-type manganites fascinate many researchers with their various exotic phenomena. For example, double-layered $\text{La}_{1.2}\text{Sr}_{1.8}\text{Mn}_2\text{O}_7$ exhibits ferromagnetic-metal (FMM) to paramagnetic-insulator (PMI) transition and colossal magneto-resistance (CMR) effect. The transition temperature is suppressed by substituting Pr at La sites, and $(\text{La}_{0.4}\text{Pr}_{0.6})_{1.2}\text{Sr}_{1.8}\text{Mn}_2\text{O}_7$ exhibits metamagnetism.

To better understand thermodynamic properties of phase separated manganites, we investigated the time dependence of the remanent specific heat in $(\text{La}_{0.4}\text{Pr}_{0.6})_{1.2}\text{Sr}_{1.8}\text{Mn}_2\text{O}_7$. First, the field dependence of the specific heat was measured at several fixed temperatures. In increasing field, the specific heat was notably suppressed at a certain field, indicating the transition from PMI to FMM, which is accompanied by entropy reduction. Interestingly, the suppressed specific heat did not recover enough in decreasing field down to 0 T.

This result implies that the paramagnetic-insulating and ferromagnetic-metallic phases coexist with spatially separated. The thermodynamic phase diagram obtained from the specific heat data coincide well with that from the magnetization.

Next, we focused on the remanent specific heat and observed its relaxation at several temperatures. The relaxation curves were found to be fitted well by stretched exponential functions. This result is similar to the cases of other physical quantities like magnetization, and indicates a complicated relaxation process in $(\text{La}_{0.4}\text{Pr}_{0.6})_{1.2}\text{Sr}_{1.8}\text{Mn}_2\text{O}_7$. The relaxation time estimated from the fitting is remarkably long: it exceeds one day below 25 K.

To summarize, we examined the thermodynamic phase diagram and thermal relaxation process in the phase separated state of the bilayered manganite $(\text{La}_{0.4}\text{Pr}_{0.6})_{1.2}\text{Sr}_{1.8}\text{Mn}_2\text{O}_7$ single crystal, utilizing the specific heat measurements under magnetic field. Our findings indicate the existence of slow thermodynamics associated with magnetic frustration between double exchange and superexchange interactions.

TH.A-P29 - Pinning effect in chiral soliton lattice CrNb₃S₆

T. Honda¹, T. Ogura², Y. Kousaka^{3,4}, J. Akimitsu², Y. Yamasaki^{5,6}, H. Nakao¹, Y. Murakami¹

1. Condensed Matter Research Center and Photon Factory, Institute of Materials Structure Science, High Energy Accelerator Research Organization, Tsukuba, Japan

2. Department of Physics and Mathematics, Aoyama-Gakuin University, Sagamihara, Kanagawa, Japan

3. Graduate School of Science, Hiroshima University, Higashi-Hiroshima, Hiroshima, Japan

4. Center for Chiral Science, Hiroshima University, Higashi-Hiroshima, Hiroshima, Japan

5. Department of Applied Physics and Quantum-Phase Electronics Center (QPEC), University of Tokyo, Hongo, Tokyo, Japan

6. RIKEN Center for Emergent Matter Science (CEMS), Wako, Japan

CrNb₃S₆ is one of the chiral magnets, and forms chiral soliton lattice (CSL) by applying small magnetic fields perpendicular magnetic modulation vector q . It has been investigated by magnetic, electric transport properties measurements on single crystals and by first-principles calculations [1-2]. Quantized spatial periods of the CSL, which corresponds to topological charges, can be controlled continuously by applying magnetic fields. In order to study the magnetic-field dependence of the magnetic structure for the CSL in more detail, we performed a small-angle resonant soft x-ray scattering in a single crystal CrNb₃S₆ by using Cr L_3 -edge at BL-16A in KEK-PF, Japan.

We observed gradual decrease in the spatial period as increasing magnetic fields and higher harmonic magnetic reflections ($2q$ and $3q$) at 0.23 T, indicating the transformation of magnetic structure from the helix to the CSL. On the other hand, the spatial period was found to increase in a stepwise manner in the field-decreasing process, suggesting that the CSL is strongly pinned at some metastable states during transforming from the CSL to the helical magnetic structure [3].

References:

[1] J. Kishine, *et al.*, Prog. Theor. Phys. Suppl. 159, 82 (2005)

[2] Y. Togawa, *et al.* Phys. Rev. Lett. 108, 107202 (2012)

[3] T. Honda, *et al.* (in progress) (2015)

TH.A-P30 - Angle-resolved photoemission study of a quasi-one dimensional thermoelectric material $\text{Ba}_3\text{Co}_2\text{O}_6(\text{CO}_3)_{0.7}$

T. Ito^{1,2}, S. Kouchi¹, T. Hajiri^{1,3}, M. Matsunami^{3,4}, S. Kimura^{3,5}, Y. Shimizu⁶, Y. Kobayashi⁶, M. Itoh⁶

1. Graduate School of Engineering, Nagoya University, Nagoya, Japan
2. Nagoya University Synchrotron Radiation Research Center, Nagoya University, Nagoya, Japan
3. UVSOR Facility, Institute for Molecular Science, Okazaki, Japan
4. School of Physical Sciences, The Graduate University for Advanced Studies (SOKENDAI), Okazaki, Japan
5. Graduate School of Frontier Biosciences and Physics Department, Osaka University, Osaka, Japan
6. Graduate School of Science, Nagoya University, Nagoya, Japan

Cobalt oxides have attracted attention due to their anomalous electric/magnetic properties such as a large thermoelectric power [1]. Among the cobalt oxides, a quasi-one-dimensional cobaltate $\text{Ba}_3\text{Co}_2\text{O}_6(\text{CO}_3)_{0.7}$ has fairly large thermoelectric power, comparable to that of Na_xCoO_2 and electrical resistivity with metallic behavior above 300 K [2] and the magnetic susceptibility increases below ~ 100 K along the face-sharing CoO_6 chains [3, 4]. In order to clarify the relationship of its thermoelectric properties to the electronic states, we have investigated the electronic structure of $\text{Ba}_3\text{Co}_2\text{O}_6(\text{CO}_3)_{0.7}$ by using three-dimensional angle-resolved photoemission spectroscopy.

Here, we found at least three dispersive features with Co 3d character near the Fermi level (E_F). We also observed two dispersive bands along the CoO_6 chain at the binding energy of 1 δ 3 eV that show quasi-one dimensional electronic structure, while there is one band around 0.5 eV that has two-dimensional anomaly. From the temperature dependence, we found the spectral weight near the valence band maximum ($E_F \sim 0.5$ eV) increases at temperatures above 150 K, while one around 1 eV decreases. The results suggest that the thermodynamic properties of $\text{Ba}_3\text{Co}_2\text{O}_6(\text{CO}_3)_{0.7}$ originates from strong CoO_6 inter-chain interaction.

- [1] T. Takeuchi et al., Phys. Rev. B 69 (2004) 125410
[2] K. Iwasaki et al., J. Appl. Phys. 106 (2009) 034905
[3] H. Igarashi et al., Phys. Rev. B 89 (2014) 054431
[4] K. Igarashi et al., J. Phys. Conf. Ser. 400 (2012) 032024

TH.A-P32 - Substitution effects in an itinerant electron metamagnetic compound SrCo₂P₂I. Masaki¹, C. Michioka¹, H. Ueda¹, A. Matsuo², K. Kindo², K. Yoshimura^{1,3}

1. Graduate School of Science, Kyoto University, Japan

2. Institute for Solid State Physics, The University of Tokyo, Japan

3. Research Center for Low Temperature and Materials Sciences, Kyoto University, Japan

Layered compounds ACo₂P₂ (A = alkaline earth metals, rare earth metals) with ThCr₂Si₂-type structure (I4/mmm) generally have ferromagnetic interactions in CoP layers. For example, LaCo₂P₂ shows ferromagnetic ordering [1]. SrCo₂P₂ is a nearly ferromagnetic metal without magnetic ordering at zero magnetic field [2]. With applying high magnetic field, SrCo₂P₂ shows an itinerant metamagnetic transition from an enhanced Pauli paramagnetic state to a ferromagnetic state [3]. Such the metamagnetic transition can be observed in the vicinity of an itinerant ferromagnetic quantum critical point. Actually, SrCo₂P₂ is in the vicinity of ferromagnetic quantum point, as Jia et al. reported ferromagnetic quantum critical behavior and the quantum critical point in SrCo₂(P_{1-x}Ge_{1-x})₂ system [2].

In this work, we focused on the itinerant electron metamagnetic transition of substituted SrCo₂P₂ systems. We synthesized (Sr_{1-x}La_x)Co₂P₂ and SrCo₂(P_{1-x}Ge_{1-x})₂ substituted systems and studied their magnetic properties. (Sr_{1-x}La_x)Co₂P₂ shows ferromagnetic ordering in x > 0.5. On the other hand, SrCo₂(P_{1-x}Ge_{1-x})₂ have a ferromagnetic ground state with an intermediate substituted region of 0.3 < x < 0.675, which is consistent with previous report [2]. The metamagnetic transition cannot be observed up to 60 T in more than only 5% La and 10% Ge substitutions. The ferromagnetic phase with La and Ge substituted compounds and the field-induced ferromagnetic phase are separated in the magnetic phase diagram. These results suggest that the carrier doping effects drastically in this metamagnetic transition and that both ferromagnetic and field-induced ferromagnetic phases should originate in different bands.

[1] M. Reehuis et al., J. Magn. Magn. Mater. 138,85 (1994)

[2] S. Jia et al., nature physics 7, 207 (2011). [3] M. Imai et al., Phys. Rev. B. 90, 014407 (2014)

TH.A-P33 - Electron spin resonance in the strong-rung spin-1/2 heisenberg ladder system $\text{Cu}(\text{C}_8\text{H}_6\text{N}_2)\text{Cl}_2$

A. Ponomaryov¹, M. Ozerov¹, L. Zviagina¹, M. Uhlarz¹, J. Wosnitza^{1,2}, K. Povarov³, F. Xiao³, A. Zheludev³, C. Landee⁴, E. Čížmár⁵, A. Zvyagin^{6,7}, S. Zvyagin¹

1. *Dresden High Magnetic Field Laboratory (HLD-EMFL), Helmholtz-Zentrum Dresden-Rossendorf, Dresden, Germany*

2. *Institut für Festkörperphysik, TU Dresden, Dresden, Germany*

3. *Neutron Scattering and Magnetism, Laboratory for Solid State Physics, ETH Zürich, Switzerland*

4. *Clark University, Worcester, United States*

5. *Institute of Physics, P.J. Šafárik University, Košice, Slovakia*

6. *Max Planck Institute for the Physics of Complex Systems, Dresden, Germany*

7. *B. I. Verkin Institute for Low Temperature Physics and Engineering of the National Academy of Science of Ukraine, Kharkov 61103, Ukraine*

We report on a comprehensive angular- and temperature-dependent electron spin resonance (ESR) study of $\text{Cu}(\text{C}_8\text{H}_6\text{N}_2)\text{Cl}_2$, a spin-1/2 strong-rung two-leg ladder compound. At temperatures above $T^* = 8$ K, only a single ESR line is observed. Below T^* , the ESR line splits into two components, reflecting the presence of a finite anisotropy. The splitting is explained by taking into account a magnetic dipole-dipole interaction. The temperature dependence of the ESR linewidth above T^* is analyzed in the frame of a bosonization approach suggesting the exchange anisotropy as the main source for the ESR line broadening.

TH.A-P34 - Unusual magnetic ordering of the frustrated triangulated-kagome antiferromagnet, $\text{Cu}_9(\text{cpa})_6\text{Cl}_2 \cdot n\text{H}_2\text{O}$

A. Matsuo¹, H. Kikuchi², T. Asano², H. Nakata², N. Kasamatsu², K. Kunieda², Y. Fujii³, Y. Inagaki⁴, K. Kindo¹

1. *Institute For Solid State Physics, University of Tokyo, Japan*

2. *Department of Applied Physics, Faculty of Engineering, University of Fukui, Japan*

3. *Research Center for Development of Far-Infrared Region, University of Fukui, Japan*

4. *Department of Applied Quantum Physics, Kyushu University, Japan*

Geometrically frustrated systems, in particular kagome lattice, are interesting subjects due to the novel physics that can appear in the magnetic fields. Among many investigated actual materials, $\text{Cu}_9(\text{cpa})_6\text{Cl}_2 \cdot n\text{H}_2\text{O}$ (cpa=2-C-carboxypentionate) is noteworthy because of its unique structure, that is, Cu^{2+} ions form triangulated-kagome lattice in which a triangular lattice in kagome lattice is occupied by four small triangular lattices. This unique structure is theoretically expected to show new magnetic properties such as a 4/9-plateau in its magnetization curve [1]. We determined the concentration of water molecules “n” is 20 by the chemical analysis and investigated its magnetic properties using magnetic susceptibility, specific heat and high field magnetization measurements. Although Weiss temperature of this magnet is large, no magnetic long-range ordering (LRO) is observed above 2 K. The specific heat measurement of this magnet was performed down to about 0.3 K and no sharp peak accompanied by the occurrence of LRO is observed. On the other hand, very broad and small peak is observed at around 3 K. As increasing magnetic field this broad peak diminishes and disappears. The high field magnetization at 4.2 K measured up to 60 T in the pulsed magnetic field shows the relatively steep slope until 10 T and the monotonically increase to 60 T and reaches less than 1/3 of the saturation moment. All the results, especially magnetic susceptibility and specific heat indicate this magnet is a good frustrated system.

[1] M. Isoda et al., J. Phys. Soc. Jpn 81 (2012) 053703

TH.A-P35 - Selection rule of the direct transition in the spin gap system studied by high field ESR measurements

S. Kimura¹, K. Watanabe¹, M. Hagiwara², H. Tanaka³

1. *Institute For Materials Research, Tohoku University, Japan*

2. *Center for Advanced High Magnetic Field Science, Osaka University, Japan*

3. *Tokyo Institute of Technology, Japan*

The direct transition between the singlet and triplet states in spin gap systems, observed by electron spin resonance (ESR) measurement, is a useful phenomenon to investigate such systems, because the field dependence of the spin gap can be revealed in high accuracy. The direct transition is forbidden in principle for usual magnetic dipole transition, because the total spin quantum number should be conserved for the magnetic dipole transition. The Dzyaloshinskii-Moriya interaction or the staggered magnetic field, which is antisymmetric with exchanging the neighboring spins, was proposed as the origin of the finite probability of the direct transition [1]. However, to clarify the mechanism of the direct transition experimentally, the selection rule of the direct transition should be investigated in detail by the ESR measurements illuminating polarized electromagnetic wave to the sample. In this study, we have carried out the high field ESR measurements of the interacting dimer system KCuCl_3 in illuminating both linearly and circularly polarized electromagnetic waves at 162 GHz. KCuCl_3 is known to show the direct transition to the first excited states at wave vectors $q = [000]$ and $[001]$ [2]. Our measurements have observed curious polarization dependence of the ESR signal for the direct transition at $q = [001]$. Different from a usual magnetic dipole active ESR signal, the signal from the direct transition, observed in the static field parallel to the b-axis, is revealed to show absence of circular dichroism.

[1] T. Sakai, J. Phys. Soc. Jpn., 72 (2003) Suppl. B 53

[2] H. Tanaka, T. Takatsu, W. Shiramura, T. Kambe, H. Nojiri, T. Yamada, S. Okubo, H. Ohta, M. Motokawa, Physica B, 246-247 (1998) 545

TH.A-P36 - On the anomalous magnetism of FeGa_{3-y}Gey: combined thermodynamic, Mössbauer spectroscopy and first principles simulation studies

M. A. Avila¹, M. Cabrera-Baez¹, R. A. Ribeiro¹, J. Munevar^{1,2}, H. Micklitz², E. M. Bittar², E. Baggio-Saitovitch², J. Alvarez-Quiceno¹, J. M. Osorio-Guillen^{1,3}, G. M. Dalpian¹

1. CCNH, Universidade Federal do ABC (UFABC), Santo Andre, Brazil

2. Centro Brasileiro de Pesquisas Fisicas (CBPF), Rio de Janeiro, Brazil

3. Instituto de Fisica, Universidad de Antioquia (UdeA), Medellin, Colombia

FeGa₃ stands out among Fe-based intermetallic compounds for its diamagnetic semiconducting behavior with energy gap of 0.5 eV, and more so due to striking effects caused by chemical substitutions. Ge-doping (FeGa_{3-y}Gey) rapidly leads to a paramagnetic metallic state, followed by a magnetically ordered state for $y > 0.13$, with TM reaching 75 K for $y = 0.41$. This evolution of the electronic ground state is accompanied by anomalous magnetic behaviors that are under intense debate in the literature, including the nature of the magnetic interactions (localized vs. itinerant, ferro- vs. antiferromagnetic), non-Fermi liquid behavior, effective mass renormalization and the presence of a Quantum Critical Point. Here we present a combined study involving growth and thermodynamic characterization of FeGa_{3-y}Gey single crystals, Mössbauer spectroscopy and density functional theory (DFT) simulations, towards a better understanding of these magnetic anomalies. Low-field, temperature-dependent magnetization curves show predominantly ferromagnetic transitions for samples with $y > 0.13$, but also a smaller antiferromagnetic component which is suppressed under higher fields. Mössbauer spectra of a sample with $y = 0.27$ show two types of Fe ions with different magnetic hyperfine parameters and magnetic moments, despite the single crystallographic Fe site in the structure. DFT simulations were able to capture all these features: the distribution of Fe moments and the FM response depends on the Ge concentration but also on the Ge distribution on the Ga sites. At small Ge concentrations a localized distribution of moments in the neighboring Fe ions is favored, and in some cases an AFM component is found. We discuss the combined results in terms of a scenario wherein increasing Ge-doping leads to an evolution from mostly localized moments at small concentrations to a combination of both localized and itinerant moments in the magnetically ordered state, with respectively high and low magnetic moment distributions.

TH.A-P37 - Novel memory effects observed after temporary heating/cooling in Heisenberg spin glasses and spontaneous restoration of the spin configuration existing before

H. Mamiya¹

1. National Institute for Materials Science, Tsukuba, Japan

Spin-glass has been one of the most-studied glassy systems; however, little is known regarding their nature. In this study, we carefully reexamine the features of the slow relaxations in order to clarify the nature by a detailed comparison with the energy landscapes predicted by the theories. Samples are materials regarded as a kind of Heisenberg spin glass: a dilute magnetic alloy Cu₉₇Mn₃, a dilute magnetic semiconductor Cd₅₅Mn₄₅Te, and a geometrically frustrated magnet ZnFe₂O₄. In our typical experiments, each sample was initially subjected to a magnetic field for a significant duration (aging.) Then the field was cut off and decay of thermoremanent magnetization was recorded on various thermal histories. Consequently, we found that the decay was extremely accelerated when the sample was temporarily heated/cooled midway through the isothermal relaxation. In contrast, in the cases that the sample was sufficiently aged in the magnetic field, the thermoremanent magnetization surprisingly increased despite absence of magnetic field when the temperature returned to the original after the temporary heating/cooling. In other words, the memory in the aging period returned despite once being rejuvenated. These phenomena were commonly observed in the three samples. Because the magnetization mirrors evolution of the spin configuration, these acceleration and reversion of the decay indicate that the configuration is destabilized when the temperature changes and it is spontaneously restored when the temperature is returned to the original. Whereas such destabilization and restoration do not occur if the spin glass is simply frozen, it is possible in an energy landscape with a temperature-sensitive funnel-like structure in the explored region. This finding has thus provided fresh insight into the stereotype of glassy systems: a disordered configuration frozen in numerous meta-stable states.

TH.A-P38 - Spin liquid ground state in a vanadium based S=1/2 trimerized kagome compound

J. Orain¹, F. Bert¹, P. Mendels¹, L. Clark², F. Himeur Aidoudi², P. Lightfoot², R. Edward Morris²

1. Laboratoire de Physique des Solides, UMR 8502 CNRS, Université Paris-Sud, Orsay, France

2. School of Chemistry and EaSTChem, University of St. Andrews, St. Andrews, United Kingdom

The search for quantum spin liquid states such as the resonant valence bond state (RVB) formed by the macroscopic resonance between the various spin singlet coverings of the lattice, is a major challenge in both experimental and theoretical condensed matter research [1]. The prime candidate to host this state of matter is the S=1/2 Kagome antiferromagnet (KAFM) in two dimensions. Among the rare experimental realizations of the KAFM model the recently synthesized compound, [NH₄]₂[C₇H₁₄N][V₇O₆F₁₈] (DQVOF) [2], is the first one to host magnetically active V⁴⁺ (d1) ions rather than more usual Cu²⁺ (d9) thus allowing to investigate the effects of different perturbations to the ideal Heisenberg Hamiltonian. Further, this compound seems to be the first experimental realization of the trimerized Kagome model, formed by two different equilateral triangles, initially theoretically studied by M. Mambrini and F. Mila [3]. Our low temperature magnetization and specific heat results suggest that DQVOF is a good candidate for the S=1/2 KAFM physics despite a complex structure [4]. Besides, the low temperature specific heat and μ SR studies evidence a gapless spin liquid behaviour down to 40mK. Recent NMR studies unveil the intrinsic susceptibility of the Kagome layers which is hidden in the macroscopic measurements by the Curie like interlayer V³⁺ contribution. Under strong magnetic fields, those studies revealed a spin gap of about 15 K (J/4). As a consequence, this material exhibits an exotic excitation spectrum, with a continuum of non magnetic excitations, quite reminiscent of the short range RVB physics which could be remarkably favoured by the trimerization of the Kagome model.

[1]L. Balents, Nature 464, 199 (2010)

[2]F. H. Aidoudi and al, Nat. Chem. 3, 801 (2011)

[3]M. Mambrini and F. Mila, Eur. Phys. J. B. 17, 651-659 (2000)

[4]L. Clark and al, Phys. Rev. Lett. 110, 207208 (2013)

TH.A-P39 - Sign reversal and non-monotonic magnetocaloric effect in $\text{EuRhAl}_4\text{Si}_2$

A. Maurya¹, P. Bonville², T. Arumugam¹, S. Dhar¹

1. *Tata Institute of Fundamental Research, India*

2. *CEA, CE Saclay, DSM/IRAMIS/SPEC/LNO 91191 GIF-SUR-YVETTE, France*

The structure and magnetic properties of tetragonal quaternary $\text{EuRhAl}_4\text{Si}_2$ have been reported recently. It orders antiferromagnetically at $\sim 12\text{K}$. The isothermal magnetization along the two principle directions is highly anisotropic despite Eu^{2+} being an S-state ion which lacks crystal electric field anisotropy to the first order. The variation of entropy change, which is a measure of magnetocaloric effect, with field and temperature, calculated from the isothermal magnetization data taken at various temperatures along the principal crystallographic directions present equally unusual behavior in this compound. In the ordered state the entropy change is highly nonlinear below spin flip fields; however in the paramagnetic region, it is negative irrespective of the strength of applied magnetic field. From iso-field data, for $H//[100]$, entropy change is initially positive before a crossover temperature of 7-10 K for fields 2T-7T, reaching a maximum of -16 J/Kg K at 12 K. For $H//[001]$ the observed entropy change at 7T and at 12 K is -21 J/Kg K , which is large and comparable to the largest known values in this temperature range. The variation of the entropy vs. field plots strongly depends upon the direction of the applied magnetic field.

TH.A-P40 - Spin, charge and lattice dynamics in the frustrated Shastry-Sutherland system TmB₄

S. Gabáni¹, I. Takáčová¹, K. Siemensmeyer², A. Bogach³, N. Sluchanko³, N. Shitsevalova⁴, J. Prokleška⁵, V. Sechovsk^{2,5}, K. Falchbart¹, A. Ievdokimova⁴

1. Institute of Experimental Physics SAS, Watsonova 47, 04001 Kosice, Slovakia

2. Helmholtz-Zentrum Berlin für Materialien und Energie, Hahn-Meitner Platz 1, 14109 Berlin, Germany

3. General Physics Institute RAS, Moscow, Russian Federation

4. Institute for Problems of Materials Science NASU, Kiev, Ukraine

5. Faculty of and Mathematics and Physics, Charles University, Prague, Czech Republic

The metallic frustrated system TmB₄ with a so called Shastry-Sutherland lattice (SSL) exhibits a strong Ising-like anisotropy which orients the Tm³⁺ magnetic moments along the c-axis, and a rather complex phase diagram below $T_N \approx 11.7$ K can be observed. In the ordered antiferromagnetic state the magnetization M for magnetic field $H // c$ reaches saturation M_S at about 40 kOe accompanied by various small hysteresis loop and fractional plateaus at e.g. $M/M_S \approx 1/9, 1/7, 1/6 \dots$ (at different temperatures) followed by the main magnetization plateau at $M/M_S = 1/2$ (for all temperatures less than T_N). Those fascinating and theoretically explained [1-4] plateaus reflect various magnetic stripe structures and non-equilibrium magnetization dynamics.

In this contribution we have investigated the dynamic magnetization process of TmB₄ by measurements of M vs H at different field sweep rate of 200, 20 and 2 Oe/s at the lowest temperature 1.8 K. It is clearly demonstrated that the value of nonzero small plateau ($M/M_S < 1/2$) is elevated with the increase of stable temperature and with the decrease of magnetic field sweep rate. The received results are inconsistent with theoretical predictions by Glauber dynamics [2].

Moreover, experimental studies of the field dependence of charge mobility and of magnetostriction at 1.8 K and up to 80 kOe were carried out to specify the important role of conduction electrons in the indirect exchange interaction between Tm³⁺ magnetic ions and role of magnetoelastic interaction in the SSL of TmB₄, respectively.

[1] P. Farkašovský, H. Čenčáriková, S. Maťaš, Physical Review B 82 (2010) 054409

[2] W.C. Huang et al., Europhysics Letters 102 (2013) 37005

[3] T. Vekholyak, J. Strečka, F. Mila, K.P. Schmidt, Physical Review B 90 (2014) 134413

[4] E. Jurčišinová, M. Jurčišin, Physical Review B 90 (2014) 032108

TH.A-P41 - Zero-field spinon confinement and field-induced quantum phase transitions in the 1D XXZ antiferromagnet SrCo₂V₂O₈

A. K. Bera ¹, B. Lake ¹, A. Schneidewind ², D. Quintero-Castro ¹, B. Klemke ¹, J. Law ³, A. Mccollam ⁴, F. Essler ⁵

1. Helmholtz-Zentrum Berlin, Berlin, Germany

2. Julich Centre for Neutron Science, Garching, Germany

3. Helmholtz-Zentrum Dresden-Rossendorf, Dresden, Germany

4. High Field Magnetic Lab, Radboud University, Nijmegen, The Netherlands

5. The Rudolf Peierls Centre for Theoretical Physics, Oxford University, Oxford, United Kingdom

The study of emergent phenomena in interacting quantum systems is one of the main research topics of condensed-matter physics. Here we report experimental results of the quasi-1D Ising-like antiferromagnet SrCo₂V₂O₈.

The spin chains in SrCo₂V₂O₈ are formed by edge-shared CoO₆ (Co²⁺; 3d⁷, effective $S = 1/2$) octahedra along the *c* axis and are separated by nonmagnetic VO₄ (V⁵⁺; 3d⁰, $S = 0$) tetrahedra. In zero field, it orders antiferromagnetically below 5 K. The magnetic structure [characterized by $k = (0\ 0\ 1)$] consists of AFM chains along the *c* axis, that are arranged ferro-/antiferromagnetically along the *a/b* axes. In the pure 1D state ($T > T_N$), inelastic neutron scattering reveals a gapped continuum of spinons (spin-1/2 excitations) that are modeled nicely by the $S=1/2$ XXZ antiferromagnetic (AFM) chain with intrachain interaction constant $J = 7.0 \pm 0.1$ meV and anisotropy parameter $\varepsilon = 0.50 \pm 0.02$. Below T_N , the continuum transforms into a hierarchy of discrete excited states indicating the confinement of the spinon-pairs due to the linear interacting potential imposed by the weak interchain couplings. Interestingly, such discrete excitations are found for both the transverse and longitudinal polarizations. The unusual sharp longitudinal modes are stabilized by the anisotropy and interchain interactions. The sequence of excited states matches the zeros of the Airy function.

In an applied magnetic field the AFM ground state of SrCo₂V₂O₈ is suppressed and emerges in to a quantum-critical state known as the Tomonaga-Luttinger liquid (TLL). At low temperatures, weak interchain couplings stabilize novel ordered states at finite temperatures in the TLL regime which inherit the properties of the dominant fluctuation modes. This results into a sequence of four order-order quantum phase transitions as a function of magnetic field up to the saturation field of $H_s = 32$ T.

TH.A-P42 - Magnetic properties of the new rare earth pyrochlore Nd₂Zr₂O₇

J. Xu¹, A. T. M. Nazmul Islam¹, A. Bera¹, B. Klemke¹, J. Niedziela², M. Frontzek³, Y. Su⁴, E. Feng⁴, B. Lake¹

1. Helmholtz-Zentrum Berlin für Materialien und Energie, Berlin, Germany

2. Oak Ridge National Laboratory, Oak Ridge, United States

3. Paul Scherrer Institute, Villigen - PSI, Switzerland

4. Juelich Centre for Neutron Science JCNS, Forschungszentrum Juelich, Outstation at MLZ, Garching, Germany

Geometrically frustrated magnetic materials are ideal candidates for exhibiting large quantum mechanical spin fluctuations and the emergence of novel magnetic ground states. Over the past 20 years, many interesting and often exotic magnetic and thermodynamic phenomena have been observed in the Pyrochlore oxides which consist of highly frustrated corner-sharing tetrahedra, such as dipolar spin ice, quantum spin ice, spin liquid and spin glass. [1] Most of the studies were concentrated on the heavy Rare Earth titanate Pyrochlores which have large moments, like Dy₂Ti₂O₇, Ho₂Ti₂O₇ and Tb₂Ti₂O₇. [2-4] Here we investigate the light Rare Earth Zirconate Pyrochlore, Nd₂Zr₂O₇, using bulk properties measurements and neutron scattering. Nd₂Zr₂O₇ orders antiferromagnetically below 0.4K and has a negative Curie-Weiss temperature of ~-27K and effective moment of $\mu_{\text{eff}} \sim 3.4\mu_{\text{B}}/\text{Nd}$. It orders in the 'all-in-all-out' magnetic structure but with a much reduced Nd moment of $1.2\mu_{\text{B}}$ at 0.1K (compared to $3.3\mu_{\text{B}}$ expected for full ordering). Inelastic neutron scattering indicates that there is a large gap (~23meV) between the ground state and the first crystal field excitation state and thus strong Ising anisotropy is expected. The pinch point which is characteristic for spin ice, is also present in our neutron diffuse scattering data both below (~0.3K) and above (~0.45K) T_N . This may be because above T_N , it is a cooperative paramagnet with powder-law spin correlations due to dipolar interactions and even below the ordered state, more than 2/3 of the full moment is still fluctuating.

References:

- [1] J. S. Gardner, et al, Reviews of Modern Physics 82, 53 (2010)
- [2] T. Fennell, et al., Physical review letters, 2012. 109(1): p. 017201
- [3] Morris, et al., Science, 2009. 326(5951): p. 411-414
- [4] T. Fennell, et al., Science, 2009. 326(5951): p. 415-417

TH.A-P43 - Effective spin-1/2 model for $Tb_2Ti_2O_7$

S. Curnoe¹, S. Mukherjee²

1. *Memorial University of Newfoundland, St. John's, Canada*

2. *Brock University, Saint Catharines, Canada*

The methods of finite group theory (symmetry) are a powerful means of reducing the complexity of highly symmetric crystals such as the rare-earth pyrochlores.

A symmetry-preserving map between non-Kramers Tb_{3+} states and spin-1/2 states on a tetrahedron is used to derive an effective spin-1/2 exchange model for non-Kramers Tb_{3+} states in the pyrochlore $Tb_2Ti_2O_7$. Estimates of the exchange constants reveal that $Tb_2Ti_2O_7$ is described by a quantum spin ice Hamiltonian.

TH.A-P44 - Interplay of charge and spin fluctuations of strongly interacting electrons on the frustrated kagome lattice

K. Roychowdhury¹

1. Mpiiks, Dresden, Germany

We study electrons hopping on a kagome lattice at third filling described by an extended Hubbard Hamiltonian with on-site and nearest-neighbor repulsions in the strongly correlated limit. As a consequence of the commensurate filling and the large interactions, each triangle has precisely two electrons in the effective low-energy description, and these electrons form chains of different lengths. The effective Hamiltonian includes the ring exchange around the hexagons as well as the nearest-neighbor Heisenberg interaction. Using large-scale exact diagonalization, we find that the effective model exhibits two phases: If the charge fluctuations are small, the magnetic fluctuations confine the charges to short loops around hexagons, yielding a gapped charge-ordered phase. When the charge fluctuations dominate, the system undergoes a quantum phase transition to a resonating plaquette phase with ordered spins and gapless spin excitations. We find that a peculiar conservation law is fulfilled: the electron in the chains can be divided into two sublattices, and this division is conserved by the ring exchange term. We also discuss the possible directions of realizing a topological liquid in the similar bosonic models where importantly some of the long-range interactions are included.

Ref: PRB, 90, 035118 (2014)

TH.A-P45 - Thermodynamics of frustrated magnets: High-temperature expansion revisited

J. Richter¹, A. Lohmann¹, H.J. Schmidt²

1. *Institute for Theoretical Physics, University Magdeburg, Magdeburg, Germany*

2. *University Osnabrueck, Department of Physics, Osnabrück, Germany*

We present the high-temperature expansion (HTE) up to 10th order of the specific heat C and the uniform susceptibility χ for Heisenberg models with arbitrary exchange patterns and arbitrary spin quantum number s . We encode the algorithm in a C++ program provided at <http://www.unimagdeburg.de/jschulen/HTE10/> which allows to get explicitly the HTE series for concrete Heisenberg models [1,2]. We use our HTE scheme to study the specific heat and the susceptibility of frustrated quantum magnets. In particular, we consider magnetic systems with highly degenerate classical ground states, such as the kagome, the checkerboard, the square-kagome, the J1-J2, as well as the pyrochlore antiferromagnets. We investigate to what extent strong frustration is evident at moderate and high temperatures. Moreover, we discuss the influence of the spin quantum number s on the thermodynamic properties and compare this way quantum and classical systems.

[1] H.-J. Schmidt, A. Lohmann, and J. Richter, Phys. Rev. B 84, 104443 (2011)

[2] A. Lohmann, H.-J. Schmidt, and J. Richter, Phys. Rev. B 89, 014415 (2014)

TH.A-P47 - Chirality domain wall generated by the spin Z_2 vortex in 2d frustrated Heisenberg spin system

Pawel Rusek¹

1. Department of Theoretical Physics, Wroclaw University of Technology, Wroclaw, Poland

In frustrated spin system the rotational symmetry is completely broken. The order parameter, a rotation matrix, allows for existence of the Z_2 spin vortex (a singular point in 2d) in a system. The topology of the Z_2 spin vortex requires the change of chirality (spins on a plaquette rotate clockwise or counter-clockwise) of underlying spins to the opposite chirality on a closed path surrounding vortex. We show that in presence of a dipole spin anisotropy the region where the twist and, in the end, chirality of underlying spins change (rapidly) is shrunk to the thin band (in 2d), of a dipole length width, terminating on the Z_2 spin vortex. This band is the topologically stable soliton \hat{u} the chirality domain wall. The structure of chirality domain and chirality domain wall in the spiral phase of underdoped $La\hat{u}$ based cuprates is discussed.

TH.B-P01 - Energy gap and mixed valence state in $\text{Sm}_{1-x}\text{B}_6$ and $\text{Sm}_{1-x}\text{La}_x\text{B}_6$ kondo insulators

S.Gabáni¹, G. Pristáš¹, J. Bednarčík², E. Welter², V. Filipov³, N.Shitsevalova³, K.Flachbart¹

1. Institute of Experimental Physics SAS, Košice, Slovakia

2. Deutsches Elektronen Synchrotron DESY, Hamburg, Germany

3. Institute for Problems of Materials Science, NASU, Kiev, Ukraine

SmB_6 is a heavy fermion semiconductor with a narrow energy gap E_g at the Fermi level, also denoted as Kondo insulator, which has recently been considered to be a topological Kondo insulator, the first strongly correlated electron system to exhibit topological surface conduction states.

In this contribution we have investigated the energy gap in Sm deficient $\text{Sm}_{1-x}\text{B}_6$ (with $x = 0.03, 0.05, 0.08, 0.1$ and 0.2) sintered samples and in single crystalline solid solutions $\text{Sm}_{1-x}\text{La}_x\text{B}_6$ (with $x = 0.16, 0.28, 0.4, 0.6$) using sensitive ac-resistivity $\rho_{ac}(T)$ measurements between 2 and 300 K, as well as the mixed valence state ν_{Sm} of samarium ions in these solid solutions by X-ray absorption near edge structure (XANES) studies between 4.2 and 300 K.

From local activation energy calculated as $W(T) = d(\ln\rho_{ac}(T))/d(1/k_B T)$ we were able to determine the values of E_g . It was shown that E_g maintains up to a concentration $x = 0.2$ of vacancies and up to a concentration $x = 0.4$ of La-ions in doped samples, and that in both cases E_g decreases with the increasing x . XANES investigations, on the other hand, revealed that the mixed valence state ν_{Sm} of Sm-ions ($\nu_{Sm} \approx 2.53$ for SmB_6 at 4.2 K) increases with increasing vacancy level whereas it decreases with increasing concentration of La^{3+} ions.

The received dependences are in agreement with numerical calculations based on the spinless Falicov-Kimball model.

TH.B-P03 - Magnetic polarons in EuB₆S. Roessler¹, J. Mueller², Z. Fisk³, S. Wirth¹*1. Max Planck Institute for Chemical Physics of Solids, Dresden, Germany**2. Institute of Physics, Goethe-University Frankfurt, Frankfurt, Germany**3. Department of Physics, University of California, Irvine, United States*

Rare-earth hexaborides are an extremely interesting class of materials with a variety of exotic properties ranging from heavy fermion metallic behavior in CeB₆ to Kondo insulators with possible topological surface states in SmB₆ and YbB₆. Properties of these systems stem from the relative positions of the f-bands and the conduction bands with respect to the Fermi level, as well as their interactions. Here, the former result from the localized 4f moments, while the latter originate from either the 5d bands of the rare earth or sp bands of the B₆ molecular orbitals. EuB₆ is a ferromagnetic semimetal with unusual properties. It orders ferromagnetically with two consecutive phase transitions at T_{c1} = 15.3 K and T_{c2} = 12.6 K reaching the full ordered moments of 6.9(2) μB of the 8S_{7/2} ground state of the Eu²⁺ at 1.5 K [1]. The paramagnetic to ferromagnetic transition is accompanied by an insulator-to-metal transition as well as a colossal magnetoresistance (CMR). A model of coalescing magnetic polarons has been invoked to explain these unusual magneto-transport properties [2,3].

Here we present ac-susceptibility (also conducted in applied magnetic fields) dc-magnetization isotherms, and atomically resolved scanning tunneling microscopy/spectroscopy (STM/S) on EuB₆ single crystals. The ac-susceptibility shows a clear onset of a ferromagnetic transition at T_{c1} and a strong shift of T_{c1} to the higher temperatures in applied magnetic fields. Modified Arrott plots with conventional critical exponents display non-linear isotherms, which is in accordance with the shift of T_{c1} in magnetic fields. The conductance maps measured in zero field at T > T_{c1} display electronic phase separation with enhanced conductance regions on a length scale of 2-3 nm. These results strongly support the scenario of magnetic polarons.

[1] W. Henggeler et al., Solid State Commun. 108, 929 (1998)

[2] J. Chatterjee et al., Phys. Rev. B 69, 134423 (2004)

[3] P. Das et al., Phys. Rev. B 86, 184425 (2012)

TH.B-P04 - Anisotropic thermopower of the antiferromagnetic kondo semiconductor CeOs₂Al₁₀ doped with 5d electrons and holesT. Takabatake^{1,2}, Y. Yamada¹, J. Kawabata¹, T. Onimaru¹, Y. Muro³

1. Graduate School of Advanced Sciences of Matter, Hiroshima University, Japan
2. Institute for Advanced Materials Research, Hiroshima University, Japan
3. Faculty of Engineering, Toyama Prefectural University, Japan

Hybridization of 4f electrons with conduction band opens a gap in the renormalized band of Kondo semiconductors (KSs) such as CeNiSn, Ce₃Bi₄Pt₃, and CeOs₄P₁₂. These KSs remain paramagnetic at low temperatures. However, a KS CeOs₂Al₁₀ has been found to order antiferromagnetically at TN = 28.5 K [1], which temperature is even higher than that of the Gd counterpart. In order to understand the mechanism of the unusual AF order in the presence of hybridization gap, we have studied the effects of 5d electron and hole doping on the electrical resistivity and thermopower S. In electron-doped Ce(Os_{1-x}Ir_x)₂Al₁₀, TN gradually decreases with increasing x to 0.15, while TN in hole-doped Ce(Os_{1-y}Re_y)₂Al₁₀ disappears at a small level of doping y = 0.05 [2]. On cooling below TN in CeOs₂Al₁₀, Sa and Sc jump slightly while Sb drops from 30 to -7 microV/K, suggesting loss of a part of the Fermi surface. With increasing x, the hybridization gap feature in the resistivity disappears at x = 0.1 and development of AF correlations of localized 4f electrons manifests in the negative peak in Sa and Sc. With increasing y, by contrast, the gap feature disappears at y = 0.05 and the valence fluctuation feature manifests in the large and broad maximum in S along the three axes. These results indicate that CeOs₂Al₁₀ is located at the border between the Kondo regime of localized 4f electrons and valence fluctuation regime of itinerant 4f electrons, and the Fermi surface changes significantly by the AF ordering. In the doped systems, the parallel decreases in TN and the magnitude of the hybridization gap reveal that the gap is necessary for the unusual AF order at high TN.

[1] Y. Muro et al., PRB 81, 214401 (2010)

[2] J. Kawabata et al., PRB 89, 094404 (2014)

TH.B-P05 - Novel kondo lattices CePd₃Al₃ and CePd₄Al₄

D. Kaczorowski¹, D. Gnida¹, A. Tursina², E. Khamitcaeva², A. Griбанov²

1. *Institute of Low Temperature and Structure Research, Polish Academy of Sciences, Poland*

2. *Department of Chemistry, Lomonosov Moscow State University, Russian Federation*

The novel cerium ternaries CePd₃Al₃ and CePd₄Al₄ crystallize with the tetragonal structures being closely related to one another. Together with CePd₂Al₂, they form a new homologous series built of structural units of the CaBe₂Ge₂- and CsCl-type units. They order antiferromagnetically below 3.5 K and 2.6 K, respectively, and exhibit Kondo lattice behaviors with the characteristic energy scale of a few Kelvins. The low-temperature thermodynamic and electrical transport properties of both materials are similar to those recently reported for CePd₂Al₂.

TH.B-P06 - Friedel oscillations in strongly correlated fermionic systems- RDMFT-CTQMC approach

B. Chatterjee¹, K. Makuch¹, K. Byczuk¹

1. Institute of Theoretical Physics, Faculty of Physics, University of Warsaw, Poland

Friedel Oscillations (FO) in the presence of a single impurity is studied in the one- and two-dimensional Hubbard model. The model is solved within the real space dynamical mean-field theory using the Continuous Time Quantum Monte Carlo solver. Effects of temperature and electronic correlations on the behavior of FO are studied. We observe that the amplitudes of FO are damped and the period changes with increasing the interaction. FO becomes sharper with decreasing the temperature and also change with the dimensionality. A comparative study of the results with that from our previous studies using different approaches is presented.

TH.B-P07 - Structural and high-field ^{57}Fe Mössbauer investigations on FeSb_2

M. Reissner¹, K. Hradil², W. Steiner¹

1. *Institute of Solid State Physics, TU Wien, Wien, Austria*

2. *X-Ray Center, TU Wien, 1060 Wien, Austria*

Although intensively investigated since several decades, FeSb_2 shows still some contradicting results which have to be cleared. FeSb_2 crystallizes in the marcasite structure, where Fe has only one crystallographic site, surrounded by distorted Sb-octahedra, which are corner shared in the ab-plane and edge shared along the c-axis. These octahedra are squeezed along the apical axis. In agreement the Mössbauer spectra, can be fitted by only one quadrupole split sub-spectrum. Problems appear, however, for Mössbauer spectra taken in external magnetic fields (up to 13.5 T and at temperatures between 4.2 K and 250 K), where spectra become extremely complex [1]. An interpretation in terms of only one sub-spectrum is no longer possible and superposition of several sub-spectra was necessary to obtain reasonable fits. Neutron diffraction experiments at different temperatures on a single crystal together with X-ray powder diffraction investigation confirm that no secondary phases exist which could be responsible for the extra sub-spectra. The fact that in all published structure analyses rather high thermal coefficients were obtained, indicates that the refinement was not fully finished revealing possible presence of disorder. Further hints for such disorder result from analysis of the radial-density function obtained from high energy X-ray investigations, pointing out that approximately 30% of the Fe atoms are shifted in the basal plane out of the centre of the octahedra. Details of the results of the crystallographic investigations and their relation to the results of the high field Mössbauer analysis will be presented. The fact that the results of the magnetic and transport measurements on our sample fits well to those reported in literature indicates that the found disorder seems to be typical for this material and has to be taken into account in any future theoretical consideration.

[1] A.Farhan et al., J.Phys.:Conf. Ser. 217, 012142 (2010)

TH.B-P09 - Field dependence of the magnetic propagation vector of the heavy-fermion compound CeCu_2Ge_2 studied by neutron diffraction

M. Loewenhaupt¹, P. Geselbracht², E. Faulhaber², M. Doerr¹, O. Stockert⁵, K. Schmalzl³, K. Nemkovski⁴, M. Deppe⁵, A. Schneidewind⁴

1. IFP-TU Dresden, Germany

2. MLZ-TUM

3. JCNS at ILL

4. JCNS at MLZ

5. MPI-CPfS

CeCu_2Ge_2 , the counterpart of the heavy-fermion superconductor CeCu_2Si_2 , exhibits an incommensurate antiferromagnetically long-range ordered ground state with $\tau = (0.28 \ 0.28 \ 0.54)$ below $T(N) = 4.1$ K. The magnetism is strongly affected by a Kondo screening of the Ce 4f-moments by conduction electrons. The similar energy scale of both, Kondo and exchange interactions, results in a complex magnetic phase diagram and gives rise to potential quantum critical phenomena at very low temperatures. We present elastic neutron diffraction data using polarized as well as unpolarized neutrons obtained on a CeCu_2Ge_2 single crystal employing the cold triple axis spectrometer PANDA at FRM II as well as the instruments D23 at ILL and DNS at FRM II. At the lowest temperature for zero external magnetic field the magnetic structure can be described by an amplitude modulated spin density wave with the Ce moments lying in the basal plane with no c-component.

The field dependence of the magnetic propagation vector was measured at $T = 300$ mK in the (HHL) plane with vertical magnetic fields applied along [1-10]. We observe no change of the magnetic ordering vector for fields up to 7.5 T. In a small field range between 7.7 T and 7.9 T two magnetic Bragg peaks coexist, the first related to the original propagation vector and the second related to a slightly shifted propagation vector. Between 7.9 T and 12 T the intensity of the Bragg peak related to the second propagation vector diminishes for further increasing fields and disappears at 12.6 T.

Above 13 T, yet still well below the value of 25 T of the saturation for magnetic fields in (110) direction, the zero-field like magnetic order is lost and magnetic intensities are not to be found at incommensurate positions in the (HHL) plane anymore.

TH.B-P10 - Kondo physics in a Ni impurity embedded in O-doped Au chains

S. Di Napoli¹, M. Barral¹, P. Roura-Bas¹, A. Llois¹, A. Aligia²

1. Departamento de Física de la Materia Condensada, GlyA-CAC-CNEA, Avenida General Paz 1499, (1650) San Martín, Pcia. de Buenos Aires, Argentina and Consejo Nacional de Investigaciones Científicas y Técnicas, CONICET, Argentina

2. Centro Atómico Bariloche and Instituto Balseiro, Comisión Nacional de Energía Atómica, Bariloche, Argentina

In modern nanoscience, understanding and tailoring the electronic transport through atomic-size conductors is a duty, as it represents a powerful tool for detecting nanomagnetism. Atomic-size contacts can be experimentally obtained by different techniques, particularly in a mechanically controllable break junction (MCBJ) experiment, where the formation of one dimensional atomic chains of several kinds of elements is possible. It has been recently demonstrated that impurity-assisted chain growth leads to a strongly enhanced tendency towards chain formation, specially if the dopants are light *p-like* elements.

In this work we study the effects of the presence of oxygen atoms on the symmetry of the Au conduction bands close to the Fermi level as well as on the spin state of a Ni impurity. This symmetry determines the nature of the screening of the spin of the impurity, giving rise to the possibility of the system to exhibit an ordinary or exotic Kondo effect. In particular, we analyze the low energy physics of the system, which corresponds to a Kondo model of a spin $S=1$ screened by two conduction channels, parametrized from *ab initio* calculations. The poor man's scaling technique is applied to obtain the Kondo temperature of the system.

TH.B-P11 - Anisotropic chemical pressure effect on the antiferromagnetic kondo semiconductor $\text{Ce}(\text{Ru}_{1-x}\text{Fe}_x)_2\text{Al}_{10}$ K. Hayashi¹, Y. Muro¹, T. Fukuhara¹, T. Kuwai², J. Kawabata³, T. Takabatake⁴, M. Hagiwara⁵, K. Motoya⁵

1. Faculty of Engineering, Toyama Prefectural University, Japan

2. Graduate School of Science and Engineering, University of Toyama, Japan

3. Department of Quantum Matter, AdSM, Hiroshima University, Japan

4. IAMR, Hiroshima University, Japan

5. Department of Physics, Faculty of Science and Technology, Tokyo University of Science, Japan

An antiferromagnetic (AFM) Kondo semiconductor $\text{CeRu}_2\text{Al}_{10}$ has been studied intensively because of the peculiar AFM order at the unusually high transition temperature $T_N = 27$ K. This AFM order disappears suddenly either under pressure at $P_c = 4$ GPa or by Fe substitution at $x \sim 0.8$ in single crystalline $\text{Ce}(\text{Ru}_{1-x}\text{Fe}_x)_2\text{Al}_{10}$ grown by an Al self-flux method [1,2]. However, the decrease of T_N is gradual with x for the polycrystalline samples [3,4]. We have studied the origin of this discrepancy using both single- and poly-crystalline samples. Electron-probe microanalyses on our single-crystalline $\text{Ce}(\text{Ru}_{1-x}\text{Fe}_x)_2\text{Al}_{10}$ with $0.5 \leq x \leq 0.8$ revealed phase separation into Ru-rich region at the center of a crystal and Fe-rich one near the surface. On the other hand, no phase separation was found in polycrystalline samples. The magnetic susceptibility, electrical resistivity and specific heat measurements on the polycrystals confirmed that the AFM order disappears gradually at $x = 0.7$, in agreement with $T_N(x)$ reported previously for polycrystals [3,4]. We should remind that application of hydrostatic pressure and Fe substitution result in different lattice contractions. The rate of contraction by the hydrostatic pressure is almost isotropic up to P_c [5], while that by Fe substitution is strongly anisotropic; $\Delta a/a \approx 0.776\%$; $\Delta c/c \approx 0.776\%$; $\Delta b/b \approx 2.0\%$ [3]. Therefore, the contrasting changes in $T_N(x)$ suggest that the anomalous AFM order in $\text{CeRu}_2\text{Al}_{10}$ is more sensitive to the c-f hybridization in the ac plane than that along the b-axis.

[1] T. Nishioka et al., J. Phys. Soc. Jpn. 78 (1009) 123705

[2] T. Nishioka et al., J. Phys. Conf. Ser. 273 (2011) 012046

[3] D. T. Adroja et al., Phys. Rev. B 87 (2013) 224415

[4] K. Hayashi et al., JPS Conf. Proc. 3 (2014) 012019

[5] Y. Kawamura et al., JPS. Conf. Proc. 3 (2014) 011029

TH.B-P13 - Modification in magnetic properties of epitaxial FeSb₂ thin film on MgO

A. Duong¹, Y. Shin¹, S. Rhim¹, V. Nguyen¹, S. Cho¹

1. Department of Physics and Energy Harvest-Storage Research Center, University of Ulsan, Ulsan, Republic of Korea

FeSb₂ is Kondo insulator with a narrow band gap. In addition, it has high Seebeck coefficient and thermoelectric power factor (PF) at low temperature. [1-3] More specifically, the PF is larger than that of Bi₂Se₃ by a factor of 65. Since it is Kondo insulator with highly correlated electrons, highly peaked density of states is from eg orbitals. It possesses interesting magnetic property: It is diamagnetic at low temperature, where a crossover to paramagnetism occurs at 100 K. [4-6] In here, we report on the modified magnetic properties in epitaxial FeSb₂ thin film on MgO (100) substrate using molecular beam epitaxy (MBE). XRD pattern showed orthorhombic structure with the lattice constants of a=5.815, b=6.517, and c=3.190 Å, exhibiting the 1.74% compressive strain owing to large lattice mismatch between FeSb₂ and MgO. Magnetic phase has been changed from diamagnetism in bulk to canted antiferromagnetism in the epitaxial thin film. Temperature dependence of magnetization shown a Neel temperature (T_N) at around 50 K. Negative Magnetoresistance at below 50 K indicates a magnetic ordering in FeSb₂ thin film.

- [1] Qing Jie *et. al.*, Phys. Rev. B 86, 115121 (2012)
- [2] Kefeng Wang *et. al.*, J. Appl. Phys. 112, 013703 (2012)
- [3] Jan M. Tomczak *et. al.*, Phys. Rev. B 82, 085104 (2010)
- [4] Mani Pokhare *et. al.*, IEEE Trans. Magnetics 50, 2400304 (2014)
- [5] C. Petrovic *et. al.*, Phys. Rev. B 67, 155205 (2003)
- [6] M. S. Diakhate, *et. al.*, Phys. Rev. B 84, 125210 (2011)

TH.B-P14 - Physical properties of single-crystalline LaBe₁₃, NdBe₁₃, and SmBe₁₃

H. Hidaka¹, K. Mizuuchi¹, S. Yamazaki¹, N. Miura¹, C. Tabata¹, Y. Shimizu², T. Yanagisawa¹, H. Amitsuka¹

1. Graduate School of Science, Hokkaido University, Japan

2. The Institute for Solid State Physics, The University of Tokyo, Japan

For more than three decades, the heavy-fermion (HF) compound UBe₁₃ has attracted much attention because of emergence of unconventional superconductivity and non-Fermi liquid behavior. However, experimental studies on other MBe₁₃ compounds (M = rare earth and actinide) are small in number, especially on light rare earth systems, although they are important to understand a background feature of UBe₁₃. The MBe₁₃ compound crystallizes in the NaZn₁₃-type cubic structure, where the M ions are surrounded quasi-spherically by 24 Be atoms, namely cage-like structure. Therefore, there is a possibility that the MBe₁₃ systems exhibit novel physical phenomena attributed to the cage-like structure, such as higher multipole ordering, magnetic-field insensitive HF state, and anharmonic oscillation of the guest ion called as rattling. In the present study, we have succeeded to grow single crystals of LaBe₁₃, SmBe₁₃, and NdBe₁₃ by Al-flux method, and investigated their thermal, magnetic, and electrical transport properties of single crystalline samples, for the first time. Specific heat of non 4f-electron system LaBe₁₃ has a low-energy Einstein-phonon contribution (Einstein temperature ~ 170 K), which may be originated in the cage-like structure. In both NdBe₁₃ and SmBe₁₃, the temperature dependence of electrical resistivity shows a metallic behavior without a Kondo-like increase, suggesting a weak c-f hybridization. The localized 4f-electronic states in both compounds have been confirmed by the specific heat and magnetic-susceptibility measurements. In addition, a magnetic ordering has been observed at a transition temperature T_M = 2.6 and 8.8 K respectively in NdBe₁₃ and SmBe₁₃, which are consistent with the previous reports. By analogy with other MBe₁₃ compounds showing a helical-magnetic ordering, we discussed a possibility that these compound also undergo the helical ordering at T_M.

TH.B-P17 - Anomalous hall effect in ferromagnetic $L1_0$ -MnAl with orbital two-channel kondo effectL. J. Zhu^{1,2}, S. H. Nie¹, P. Xiong³, and J. H. Zhao¹

1. State Key Laboratory of Superlattices and Microstructures, Institute of Semiconductors, Chinese Academy of Sciences, Beijing, China

2. Institut für Physik, Martin-Luther-Universität Halle-Wittenberg, Halle, Germany

3. Department of Physics, Florida State University, Tallahassee, United States

The understanding of the anomalous Hall effect (AHE) has remained far from complete despite its long history over 130 years. The experimental studies of its scaling between longitudinal resistivity (ρ_{xx}) and anomalous Hall resistivity (ρ_{AH}) allows for clarifying the microscopic mechanisms and underlying physics. Most recent experiments firmly established a scaling of $\rho_{AH} = a_0\rho_{xx0} + b\rho_{xx}^2$ (ρ_{xx0} is the residual resistivity) in a variety of single-crystalline films (Fe, Co, Ni, $L1_0$ -Mn_{1.5}Ga, etc.) where phonon scattering dominates the temperature-dependence of resistivity [1,2]. However, the AHE in presence of chemical disorder and localization has been buried in persistent confusion. The *intrinsic* anomalous Hall conductivity b which is widely believed to originate from the band-structure effects of a perfect crystal was observed to be significantly influenced by chemical disorder in $L1_0$ -Mn_{1.5}Ga [2]. Hopping conduction was reported to give an AHE scaling of $\rho_{AH} \sim \rho_{xx}^{0.5 \sim 0.3}$ in $Ti_{1-x}Co_xO_{2-\delta}$, $Fe_{3-x}Zn_xO_4$ and (Ga,Mn)As and $\rho_{AH} \sim \rho_{xx}^0$ in polycrystalline FePt, respectively. It has also been an open questions whether weak localization and electron-electron interaction have contribution to ρ_{AH} . So far, a unified understanding of the AHE in localized systems has remains a shortage.

Here, we report the AHE in perpendicularly magnetized $L1_0$ -MnAl epitaxial films with variable chemical ordering and orbital two-channel Kondo (2CK) effect [3]. The AHE is observed to scale with $\rho_{AH} = a_0\rho_{xx0} + b\rho_{xx}^2$ at high temperatures where phonon scattering prevails, while shows significant deviation at low temperatures where orbital 2CK effect are important. This is the first evidence of contribution of orbital 2CK effect to the AHE. A remarkable tuning of the intrinsic anomalous Hall conductivity is also revealed by varying the degree of chemical ordering, indicating a topological modification of the Fermi surface [4], which is consistent with the observation in $L1_0$ -Mn_{1.5}Ga.

[1] L. J. Zhu et al., *Phys. Rev. B* 89, 220406 (R) (2014)

[2] Y. Tian et al., *Phys. Rev. Lett.* 103, 087206 (2010)

[3] L. J. Zhu, S. H. Nie, P. Xiong, P. Schlottmann, J. H. Zhao, submitted

[4] L. J. Zhu, S.H, Nie, P. Xiong, J. H. Zhao, submitted

TH.B-P18 - Point-contact spectroscopy of heavy fermion compounds CeCu₆ and CeAl₃ in magnetic field

G. Motoyama¹, S. Ogawa¹, K. Matsubayashi², K. Fujiwara¹, S. Nishigori¹, T. Mutou¹, K. Miyoshi¹, A. Yamaguchi³, A. Sumiyama³, Y. Uwatoko²

1. *Department of Material Science, Shimane University, Japan*

2. *ISSP, Tokyo University, Japan*

3. *Graduate School of Material Science, University of Hyogo, Japan*

We investigated temperature and magnetic field dependences of the point-contact spectra of heavy fermion compounds CeCu₆ and CeAl₃. We prepared fixed point-contact devices on the surface of the poly-crystalline samples. Spectrum was obtained in the form of differential resistivity (dV/dI) as a function of bias voltage. The spectra of CeCu₆ and CeAl₃ changed below T_{max} , at which there are maximum on the temperature dependence of electrical resistivity, and T_K . At the lowest temperature at 0.4 K, both spectra showed a large conductance peak. It was newly observed that both increasing rates of the magnitude of dV/dI at zero bias changed from negative curvature to positive one at each critical magnetic field of metamagnetization, although both conductance peaks on these spectra enlarged with increasing magnetic field regardless of lower or higher than the critical magnetic field.

TH.B-P19 - Anisotropy of the Kondo effect revealed by Raman scattering spectroscopy

J. Buhot^{1,2}, Y. Gallais², M. Cazayous², A. Sacuto², G. Lapertot³, D. Aoki^{3,4}, X. Montiel⁵, S. Burdin⁶, C. Pépin⁵, M. Méasson²

1. High Field Magnet Laboratory, Radboud University Nijmegen, The Netherlands
2. Laboratoire Matériaux et Phénomènes Quantiques, UMR 7162 CNRS, Université Paris Diderot - Paris 7, France
3. SPSMS, UMR-E CEA, UJF-Grenoble 1, INAC, 38054 Grenoble, France
4. IMR, Tohoku University, Oarai, Ibaraki 311-1313, Japan
5. Institut de Physique Théorique, CEA-Saclay, 91191 Gif-sur-Yvette, France
6. Condensed Matter Theory Group, CPMOH, UMR 5798, Université de Bordeaux I, 33405 Talence, France

Microscopic description of Kondo lattice systems, such as heavy-fermion materials, often assume a local, i.e., momentum-independent, hybridization between the conduction band and the local-moments on a regular lattice. In this picture, the anisotropy of the Kondo effect is not taken into account whereas such unconventional hybridization may influence the entire phase diagram of heavy fermion compounds [1]. Moreover, only very few studies report experimental signature of such effect, either in Kondo insulators or metals, and these remain indirect. We report here clear experimental evidence of anisotropic Kondo effect in metallic heavy-fermion compound URu₂Si₂, thanks to the ability of Raman spectroscopy to unveil the symmetry of the electronic excitations. We have performed polarized electronic Raman scattering on single crystals of URu₂Si₂ in all the allowed symmetries. We observe a gap opening only in two symmetries: in E_g symmetry below 100 K and in A_{1g} symmetry from 300 K. The former one, certainly related to the Kondo coherence, is consistent with optical conductivity measurements [2]. Thanks to the calculation of Raman vertices in URu₂Si₂, we discuss the k-dependence of the Kondo physics. Our results reveal a strong anisotropy of the Kondo physics in k-space.

[1] Weber et al. Phys. Rev. B, 77, 125118 (2008)

[2] D. A. Bonn, et al., Physical Review Letters, 61, 1306 (1988)

TH.B-P20 - To the origin of the singlet ground state of the Fe impurity in the archetype kondo system: CuFe

R. Radwanski^{1,2}, D. Nalecz¹, Z. Ropka²

1. Institute of Physics, Pedagogical University, 30-084 Krakow, Poland

2. Center of Solid State Physics, Snt Filip 5, 31-150 Krakow, Poland

Studies of the origin of an unexpected increase of the resistivity with decreasing temperature below about 25 K of copper containing small amounts of Fe, denoted as CuFe, has opened large experimental and theoretical field known at present as the Kondo effect. In meantime, the Kondo effect theoretical problem has been extended to different theories (Kondo lattice, multichannel Kondo effect, ...) becoming the foundation of thousand of papers devoted to heavy-fermion phenomena and strongly correlated electron systems. In the original explanation Kondo in 1964 pointed out the importance of the magnetic resistivity related with the spin degree of freedom of the magnetic impurity. The antiferromagnetic interaction of the localized spin with conduction electrons, according to the common understandings, leads to the singlet ground state of the localized spin and a cloud of conduction electrons with opposite spins fully screening the localized spin by conduction electrons. This disappearance of the local moment below temperature denoted as Kondo temperature, is seen, for instance, in the magnetic susceptibility which deviates at low temperatures from the Curie law becoming saturated for T approaching 0 K. We have re-analyzed low-temperature properties of copper with small amounts of Fe impurities, which have led years ago to the Kondo-effect theory, pointing out the formation of a singlet ground state. We claim that in CuFe (here we discussed only CuFe) there is a singlet ground state formed at the atomic scale on the Fe impurity. This singlet atomic ground state comes out if one takes into account simple crystal-field interactions and the spin-orbit coupling. Slightly above, in energy of 10-15 K, there is a magnetic doublet with a moment close to 3.0 μ_B containing, which assures large dynamics of the Fe impurity. The found singlet ground state is favored by the Jahn-Teller effect.

TH.B-P21 - CePd₂Zn₃ - a new kondo lattice antiferromagnetM. Valiska¹, J. Prokleska¹, P. Proschek¹, V. Sechovsky¹*1. Department of Condensed Matter Physics, Charles University, Prague, Czech Republic*

Single crystals of CePd₂Zn₃ have been successfully grown by Bridgman method using a sealed Mo capsule with a BN crucible. Single-crystal X-ray diffraction confirmed the hexagonal PrNi₂Al₃-type structure with the space group P6/mmm [1] with unit cell parameters $a = 539.14$ pm and $c = 430.12$ pm at RT. The crystals were subjected to measurements of magnetization (M), specific heat (Cp) and electrical resistivity (ρ) as functions of temperature ($T = 0.3 - 300$ K) and magnetic fields ($B = 0 - 14$ T) applied along the principal crystallographic directions. The low temperature anomalies of specific heat, magnetization and resistivity point to a transition to antiferromagnetic (AF) state ($T_N = 1.95$ K). Strong magnetocrystalline anisotropy with easy magnetization basal plane similar to other known isostructural CeT₂X₃ (T = transition metal, X = p-electron metal) counterparts has been revealed both in paramagnetic and AF state. The negative derivative of resistivity in the temperature interval 6 - 16K which is suppressed by a magnetic field of 8 T applied along the a-axis suggests that CePd₂Zn₃ is a Kondo lattice compound. Evolution of the Cp vs. T anomaly and large negative magnetoresistance with increasing the magnetic field applied along the a-axis reflect a metamagnetic transition at Bc around 1 T at which the AF coupling is overcome by the magnetic field. Measurements of evolution of resistivity and specific heat of crystals exerted hydrostatic pressure towards the QCP are in progress. Results will be discussed in context of magnetism in the isostructural CeT₂X₃ compounds adopting the hexagonal PrNi₂Al₃-type structure.

[1] W. Hermes, S., R. Mishra, R. Pöttgen, Chemical Monthly 139 (2008) 1143

TH.C-P01 - Doping dependent magnetism and exchange bias in $\text{CaMn}_{1-x}\text{Nb}_x\text{O}_3$

V. Markovich¹, I. Fita², A. Wisniewski², R. Puzniak², C. Martin³, D. Mogilyansky⁴, G. Jung¹, G. Gorodetsky¹

1. Department of Physics, Ben-Gurion University of the Negev, 84105 Beer-Sheva, Israel
2. Institute of Physics, Polish Academy of Sciences, Warsaw, Poland
3. Laboratoire CRISMAT, UMR 6508, ISMRA, Caen, France
4. The Ilse Katz Institute for Nanoscale Science and Technology, Ben-Gurion University of the Negev, Beer-Sheva, Israel

Magnetic and structural properties of $\text{CaMn}_{1-x}\text{Nb}_x\text{O}_3$ have been investigated. The substitution of Nb for Mn results in one-electron doping accompanied by monotonous increase of lattice parameters and unit-cell volume with increasing x . Low temperature magnetic ground state evolves from antiferromagnetic (AFM) one with weak ferromagnetic (FM) component for $x = 0.02 - 0.08$ to charge ordered C-type AFM with minority G-type AFM at $x = 0.1$. Spontaneous magnetization increases sharply with increasing x , reaches a maximum of 4.1 emu/g at $T = 10$ K for $x = 0.08$, and then decreases rapidly to 0.2 emu/g at $x = 0.1$. For $x = 0.04$ an anomalous diamagnetic behavior is observed in field cooled magnetization and remanent magnetization below Néel temperature T_N . Exchange bias (EB) effect, manifested by vertical and horizontal shifts in field cooled hysteresis loops appears in $\text{CaMn}_{0.9}\text{Nb}_{0.1}\text{O}_3$. The intrinsic EB phenomenon is caused by interface exchange coupling between nano-sized FM clusters and surrounding G-type AFM phase. The growth of FM phase volume under applied pressure is linked to progressive suppression of negative magnetization for $x = 0.04$ and to reduction of the EB effect for $x = 0.1$. EB shifts decrease monotonously with increasing temperature and vanish above 70 K, while coercive field disappears above 90 K, around T_N . Our results indicate that EB effect in $x = 0.1$ is due to Dzyaloshinsky-Moriya interactions. Hysteresis loops recorded at high maximal fields show a nonlinear increase of magnetization indicative of metamagnetic-like transition. Growth of the FM phase volume and transformation from C-type to G-type AFM in high magnetic field induced metamagnetic transition appears to be linked to complete suppression of EB effect in $\text{CaMn}_{0.9}\text{Nb}_{0.1}\text{O}_3$.

TH.C-P02 - Molecular spin dynamics analysis of complex magnetic structure on the FCC lattice in itinerant electron system

Y. Kakehashi¹, S. Nohara, S. Chandra, T. Uchida²

1. *University of the Ryukyus, Japan*

2. *Hokkaido University of Science, Japan*

Magnetic alloys on the fcc lattice such as gamma Fe-base and Mn-base alloys exhibit complex magnetic structures because of the strong frustration between the long-range ferro- and antiferro-magnetic interactions on the fcc lattice. Their formation mechanism has not yet been clarified theoretically and it is one of the current issues in magnetism. In order to understand the complex magnetic structure from the theoretical point of view, we have investigated the magnetic structure of the Hubbard model on the fcc lattice by means of the Molecular Spin Dynamics (MSD) method [1,2]. We present here the numerical results of magnetic structure. The MSD is based on the functional integral technique combined with the isothermal MD and allows us to determine automatically the complex magnetic structure for a given electron number n and temperature T . With use of $8 \times 8 \times 8$ fcc unit cells surrounded by 53248 atoms and $T/|t|=0.001$, we performed the MSD calculations. For the Coulomb interaction strength $U/|t|=8$, for example, we find that the strong ferromagnetism is stabilized from $n=2.0$ to 1.3. From $n=1.3$ to 1.2 we find a simple ferromagnetism with a small amount of holes in the up-spin band. Below $n=1.2$, the ferromagnetism collapses and the system shows the complex ferrimagnetism with small magnetization. Between $n=0.9$ and 0.6, we find complex anti-ferromagnetic structures and spin-density waves: 3Q multiple spin density waves in the vicinity of $n=0.90$, the 2Q multiple spin density waves around $n=0.75$, and the complex antiferromagnetic structure with amplitude modulation for $n=0.70$. Finally the paramagnetic state is realized below $n=0.60$. We elucidate these changes by means of the Fourier analysis.

[1] Y. Kakehashi, S. Akbar, and N. Kimura, PRB 57, 8354 (1998)

[2] T. Uchida, N. Kimura, and Y. Kakehashi, JKPS 62, 1748 (2013)

TH.C-P04 - Low-temperature spin-glass behaviour in a diluted dipolar Ising system

J. J. Alonso¹

1. Universidad de Málaga, Spain

Using Monte Carlo simulations, we study the character of the spin-glass (SG) state of a site-diluted dipolar Ising model. For concentration $x < 0.65$ these systems are known to exhibit an equilibrium spin-glass phase at low temperatures. At high dilution, well deep in the SG phase, we find spiky distributions of the overlap parameter q that are strongly sample-dependent. For the system sizes studied, the average width of spikes, and the fraction of samples with spikes higher than a certain threshold does not vary appreciably with system size. This is compared with the behaviour found for the Sherrington-Kirkpatrick and the Edwards-Anderson model.

TH.C-P07 - Magnetic control of thermopower in selected manganitesR. Mahendiran¹*1. National University of Singapore, Singapore*

Thermoelectric materials are of great interest because they can directly convert heat into electricity by generating potential difference in response to a temperature gradient. For more than half a century, the field of thermoelectrics has been dominated by semiconductors based p block elements in periodic tables such as Bi, Pb, Te etc. Transition metal oxides were not considered as promising thermoelectric materials until few years ago because majority of them have low mobility. However, the discovery of a large themopower (=100 microvolt/K) and power factor comparable to that of semiconducting Bi₂Te₃ in quasi metallic oxides based on cobalt (example Na_xCoO₂ and Ca₃Co₄O₉ etc.) has inspired focused research on thermoelectricity in TMO[1,2]. Oxides thermoelectrics is still an emerging field and much need to be understood. In this talk, I will focus on thermoelectricity in some selected magnetic transition metal oxides. Recently, we have found that thermopower in some of these oxides can be either enhanced or suppressed by external magnetic fields[3,4] In this talk, I will give overview of how electrical resistivity, thermopower and magnetic entropy change in these oxides are intertwined and what we can do to enhance the power factor and figure of merit. Special attention is given to Pr_{1-x}Sr_xMnO₃ and Nd_{1-x}Na_xMnO₃ system which encompass ferromagnetic metallic/insulating and layered antiferromagnetic quasi metallic/semiconducting phases.

[1] I. Terasaki et al., Large thermoelectric power in NaCo₂O₄ single crystals, Phys. Rev. B 56 R12685 (1997)

[2] A. Maignan et al. Perovskite manganites and layered cobaltites: potential materials for thermoelectric applications, Crystal Engineering, 5, 365, (2002)

[3] D.V.M. Repaka and R. Mahendiran, Giant magnetothermopower in charge ordered Nd_{0.75}Na_{0.25}MnO₃, Appl. Phys. Lett.103, 162408 (2013)

[4] D. V. M. Repaka, T. S. Tripathi, M. Aparnadevi, and R. Mahendiran, Magnetocaloric effect and magnetothermopower in the room temperature ferromagnet Pr_{0.6}Sr_{0.4}MnO₃, J. Appl. Phys.112, 23915 (2012)

TH.C-P08 - Physical properties of the FeRh alloys: the antiferromagnetic to ferromagnetic transition

J. Kudrnovsky¹, V. Drchal¹, I. Turek²

1. Institute of Physics AS CR, Praha, Czech Republic

2. Faculty of Mathematics and Physics, Department of Condensed Matter Physics, Charles University, Praha, Czech Republic

The electronic, magnetic, thermodynamical, and transport properties of FeRh alloys are studied from first principles. We present a unified approach to the phase stability, an estimate of exchange interactions in various magnetic phases, and transport properties including the effect of temperature which are all based on the same electronic structure model.

Emphasis is put on the transition between the ferromagnetic (FM) and antiferromagnetic (AFM) phases. Such a study is motivated by a recent suggestion of FeRh as a room-temperature antiferromagnetic memory resistor [1].

The theory predicts the order-disorder transformation from the hypothetical disordered bcc-phase into ordered B2-phase. Comparison of exchange interactions in the magnetically ordered FM and AFM phases with corresponding spin-disordered counterparts allows to identify relevant interactions which are precursors of magnetically ordered phases.

The most important result is the explanation of a dramatic decrease of the resistivity accompanying the AFM to FM phase transition [2] which is due to the spin-disorder present in the system. The study of the anisotropic magnetoresistance in the AFM phase found recently experimentally [1] is extended also to finite temperatures.

[1] X. Marti et al., Nature Materials 13, 367 (2014)

[2] M.A. de Vries, M. Loving, A.P. Mihai, L.H. Lewis, D. Heiman, and C.H. Marrows, New Journal of Physics 15, 013008 (2013)

TH.C-P09 - Magnetic properties of the RAuBi₂ (R = Ce, Pr, Nd, Gd, Sm) series of intermetallic compounds

C. B. R. Jesus¹, M. M. Piva¹, P. F. S. Rosa^{1,2}, C. Adriano¹, Z. Fisk², P. G. Pagliuso¹

1. Instituto de Física 'Gleb Wataghin', UNICAMP, Campinas-SP, Brazil

2. University of California, Irvine, United States

In this work we report the physical properties of series of intermetallic compounds RAuBi₂ (R = Ce, Pr, Nd, Gd, Sm) studied by means of x-ray powder diffraction, magnetic susceptibility, heat capacity and electrical resistivity measurements. These compounds were grown using the metallic Bi self-flux technique and they crystallize in a tetragonal ZrCuSi₂ (P4mmm) structure. Our RAuBi₂ single crystals show an antiferromagnetic ordering $T_N \geq 2.3$ K for all measured compounds. The values of T_N show a dramatic breakdown of the De Gennes factor along this series. Using a mean field model including isotropic Ruderman-Kittel-Kasuya-Yoshida (RKKY) magnetic interactions and the tetragonal crystalline electrical field (CEF), we demonstrated that one can qualitatively describe the magnetic properties and the evolution of the ordering temperature along these series. Furthermore, we compare the results present here with the properties of the isostructural series RAuBi₂ [1] and discuss the main effects associated with the chemical substitution at the transition metal (Cu or Au) site.

[1] C. B. R. Jesus, et al., *Journal of Applied Physics* 115, 17E115 (2014)

TH.C-P10 - Magnetic phase diagram of MnSi inferred from ultrasound studies

A. Petrova¹, S. Stishov¹

1. Institute For High Pressure Physics of RAS, Moscow, Russian Federation

The sound speed and attenuation were measured in the MnSi single crystal in the temperature range of 2-40 K and magnetic fields to 7 Tesla.

The magnetic phase transition in MnSi in zero magnetic field is signified by a quazi discontinuity in the c_{11} elastic constant, which suggests first order character of the transformation. The quasi discontinuities of c_{11} initially strongly decreases with magnetic field, practically disappears in the range of $\sim 0.1-0.2/0.3$ T, then recovers at $\sim 0.2/0.3-0.45/0.5$ T and again vanished at higher magnetic field. Remarkably that the region with almost zero values of in the interval $\sim 0.12-0.2/0.26$ T closely corresponds to the extent of skyrmion phase along the magnetic to paramagnetic transition. This implies that the c_{11} elastic constant is almost continuous through the transition from the skyrmion to paramagnetic phases. The recovery of discontinuities of c_{11} and the enhanced sound absorption occur at the crossing the phase transition line and the line of minima in c_{11} . The latter is a region of strong spin fluctuations, reflected in maxima of the heat capacity. Despite the fact that this region does not carry features of a real phase transition the existing powerful fluctuations at the minima of c_{11} make the mentioned crossing point similar to a critical end point, when a second order phase transition meets a first order one.

TH.C-P11 - Anomalous structural, magnetic, optical and electronic properties of GdCoO_{3-y}

S. Ovchinnikov¹, Y. Orlov¹, V. Dudnikov¹, N. Kazak¹, K. Shaikhutdinov¹

1. Kirensky Institute of Physics. Siberian Branch of Russian Academy of Sciences, Russian Federation

The interrelation of temperature induced spin crossover in the perovskite-like rare-earth cobaltates RCoO_3 is found by a variety of experimental and theoretical study of structural, magnetic, optical and electronic properties in a wide temperature range 2-1000K. It is found that spin crossover in Co^{+3} induced by lattice expansion at heating self-consistently increases the lattice expansion itself and results in the giant lattice expansion (order of magnitude large than standard anharmonic contribution) at the temperature region of maximal increase of the high spin population. The heat capacity has also the maximum in the same region. The optical transmission spectra have revealed the narrow transmission peak in the infrared region without the usual for semiconductor transparency window. The temperature dependent LDA+GTB electronic structure calculations have revealed the appearance the in-gap states due to high spin population induced by heating and off-stoichiometry. Even the small deviation from stoichiometry $y < 0.01$ is enough for the in gap state strongly decrease the semiconductor gap 0.5eV up to 0.1 eV. In solid solutions $\text{La}_{1-x}\text{Gd}_x\text{CoO}_3$ the spin gap variation results from the chemical pressure that is estimated from the Burch-Murnaghan equation of states and verified by high temperature magnetic susceptibility measurements. The spin gap variation allows to control the temperature of maximal lattice dilatation and magnetic susceptibility.

TH.C-P12 - Non-random substitutions and magnetic ordering in $\text{Fe}_{7-y}\text{M}_y\text{X}_8$ (M = Ti, Co; X = S, Se)N. Baranov^{1,2}, P. Ibrahim², N. Selezneva², A. Gubkin^{1,2}, A. Volegov², D. Shishkin^{1,2}*1. Institute of Metal Physics, RAS, Ekaterinburg, Russian Federation**2. Institute of Natural Sciences, Ural Federal University, Ekaterinburg, Russian Federation*

A comparative study of four series of pyrrhotite-type chalcogenide compounds $\text{Fe}_{7-y}\text{M}_y\text{X}_8$ (X = S, Se) with substitution of Ti or Co for iron has been performed by means of X-ray and neutron powder diffraction and magnetization measurements. The polycrystalline samples were synthesized by solid state reactions in evacuated quartz tubes. Despite the formation of different superstructures all the synthesized compounds $\text{Fe}_{7-y}\text{Ti}_y\text{X}_8$ and $\text{Fe}_{7-y}\text{Co}_y\text{X}_8$ exhibit a layered crystal structure of the NiAs-type. In $\text{Fe}_{7-y}\text{M}_y\text{X}_8$ compounds having a ferrimagnetic order at $y = 0$, the substitution of either Ti or Co for iron up to $y = 4$ is observed to result in a monotonous decrease of the magnetic ordering temperatures, while the resultant magnetization shows a non-monotonous behaviour with a minimum around $y = 1.0 - 1.5$ except $\text{Fe}_{7-y}\text{Co}_y\text{Se}_8$. The suppression of a magnetically ordered state in $\text{Fe}_{7-y}\text{M}_y\text{X}_8$ with substitutions is ascribed to nearly zero values of magnetic moments on Ti and Co ions, while the non-monotonous changes in the resultant magnetization are explained by the non-random substitution of Ti or Co for Fe in alternating metallic layers. The layer-preferential substitution is confirmed by neutron diffraction measurements. At high Ti concentrations ($y > 2$) the $\text{Fe}_{7-y}\text{Ti}_y\text{X}_8$ compounds are observed to exhibit unusually high values of the coercive field at low temperatures ($H_c = 20 - 24$ kOe), which is associated with non-zero orbital moment of Fe ions and crystal field effects.

This work was supported by RFBR (projects No 13-02-00364 and No 13-02-96038) and by the program of the Ural Branch of RAS (project No 15-17-2-22).

TH.C-P13 - Critical exponents of inhomogeneous ferromagnetic $\text{La}_{0.8}\text{Sr}_{0.2}\text{CoO}_3$ single crystalM. Nandi¹, N. Khan¹, B. Samantaray¹, P. Mandal¹, D. Prabhakaran²

1. Saha Institute of Nuclear Physics, 1/AF Bidhannagar, Calcutta, India

2. Department of Physics, Clarendon Laboratory, University of Oxford, Oxford, United Kingdom

The hole-doped cobaltite, $\text{La}_{1-x}\text{Sr}_x\text{CoO}_3$ (LSCO), is a model system to study the magneto-electronic phase separation phenomenon as the system phase separates in nano-sized metallic ferromagnetic (FM) clusters in the back ground of insulating non-FM matrix.¹ With increasing hole doping (x) the FM clusters grow in size and number and percolate at $x = 0.18$ giving rise long-ranged FM ordering. However, the phase separation extends beyond $x = 0.18$ and exists up to $x = 0.22$.¹ The system becomes homogeneous FM¹ above $x = 0.22$. Here we have determined the critical exponents of the highly inhomogeneous FM $x = 0.20$ single crystal to find how the presence of phase separation affects the nature of the transition and thereby the universality class of the pure FM LSCO system.

The compound undergoes a second order FM to paramagnetic phase transition at 176 K. The critical exponents (β , γ and δ) characterizing the transition have been estimated by different methods and are listed in Table-I together with the values predicted by theoretical models. The exponents for the present compound are found to be mean-field-like unlike 3D Heisenberg exponents observed for the $x = 0.33$ compound.² Such a large deviation of the exponents from 3D Heisenberg values is attributed to the presence of magneto-electronic inhomogeneity in this compound.³ The average exchange field originating from the percolating FM clusters in the background of non-FM matrix is responsible for the mean-field-like values of the critical exponents for the $\text{La}_{0.8}\text{Sr}_{0.2}\text{CoO}_3$ single crystal.³

Table-I

Material	Methods	β	γ	δ
$\text{La}_{0.8}\text{Sr}_{0.2}\text{CoO}_3$	Modified Arrott plot	0.497(1)	1.25(2)	3.52(5)
$\text{La}_{0.8}\text{Sr}_{0.2}\text{CoO}_3$	Kouvel-Fisher plot	0.488(5)	1.28(2)	3.62(2)
$\text{La}_{0.8}\text{Sr}_{0.2}\text{CoO}_3$	Critical isotherm plot	--	--	3.55(1)
3D Heisenberg	Theory	0.365	1.386	4.8
Mean-field	Theory	0.5	1.0	3.0
3D Ising	Theory	0.325	1.241	4.82

References:

- [1] C. He *et al.*, Phys. Rev. B 80, 214411 (2009)
 [2] N. Khan *et al.*, Phys. Rev. B 82, 064422 (2010)
 [3] N. Khan *et al.*, Phys. Rev. B 85, 214419 (2012)

TH.C-P14 - Tuning magnetostructural transformation temperature in antiperovskite compounds

E. T. Dias¹, K. R. Priolkar¹, A. K. Nigam²

1. Department of Physics, Goa University, Taleigao Plateau, Goa, India

2. Tata Institute of Fundamental Research, Dr. Homi Bhabha Road, Colaba-Mumbai, India

Magnetic refrigeration based on magnetocaloric effect (MCE) or adiabatic temperature change (ΔT_{ad}) is rapidly becoming an environmentally sound alternative to conventional vapour-cycle refrigerators due to its energy savings potential. Many new materials with large MCE have been discovered as a result of extensive research and a better understanding of this magneto-thermal property.

Mn-based antiperovskite compounds are a group of magnetic materials possessing a wide variety of magnetic structures and magnetic transitions depending on the chemical composition. They also exhibit potentially useful properties such as giant magnetoresistance, large MCE, negative thermal expansion (NTE), magnetostriction, and near zero temperature coefficient of the resistivity.

Mn_3GaC shows a first-order ferromagnetic (FM) to antiferromagnetic (AFM) transition at $T \sim 178K$ accompanied by a large change in entropy ($|\Delta S| \sim 15J/Kg-K$ at 2T equivalent to an adiabatic temperature difference of 4K) drawing interest from the point of view of application as a magnetic refrigeration material. When Tin replaces Gallium, the first-order transition temperature is increased to $T_C \sim 279K$ where the compound Mn_3SnC transforms from a paramagnetic (PM) to a non-collinear ferrimagnetic (FI) state with $|\Delta S| \sim 2.6J/Kg-K$ at 2T.

Mn_3InC is another antiperovskite compound that exhibits two first-order magnetic transformations at $T = 127K$ from AFM ground state to a FM state and a FM to PM transformation at $T \sim 430K$. Partially replacing In with Sn critically affects the two transformation temperatures. In this paper, we present a possibility of tuning these magnetic transformation temperatures to around room temperature by adjusting the ratios of Sn and In at the B-site.

TH.C-P15 - Ground-State and magnetocaloric properties of a spin-electron double-tetrahedral chain

L. Galisova¹, J. Strecka²

1. Technical University, Kosice, Slovakia

2. Pavol Jozef Šafárik University, Kosice, Slovakia

Ground state and adiabatic demagnetization process of an exactly solvable spin-electron tetrahedral chain composed of localized Ising spins regularly alternating with mobile electrons delocalized over triangular plaquettes are investigated by considering the one-third filling case and the ferromagnetic exchange interaction between mobile electrons and the localized Ising spins. Two types of ground-state degeneracy are discussed: the one arising from chiral degrees of freedom of mobile electrons and the another one appearing owing to a kinetically-driven frustration of the localized Ising spins. It is demonstrated that the investigated system may exhibit an enhanced magnetocaloric effect during the adiabatic demagnetization process manifested through magnified adiabatic cooling rate, which suggests a potential use of the investigated spin-electron system for low-temperature magnetic refrigeration.

TH.C-P16 - Investigation of magnetic and magnetoelastic properties of the unconventional heavy-fermion compound CeCu₂Ge₂ (CCG)

M. Doerr¹, S. Granovsky^{1,2}, M. Rotter^{1,3}, Z. Wang⁴, A. Schneidewind⁵, M. Loewenhaupt¹

1. Technische Universität Dresden, Institut Für Festkörperphysik, Dresden, Germany

2. Faculty of Physics, M.V. Lomonossov Moscow State University, Leninskie Gory, Moscow, Russian Federation

3. McPhase project www.mcphase.de, Dresden, Germany

4. Hochfeld-Magnetlabor Dresden, Helmholtz-Zentrum Dresden-Rossendorf, Dresden, Germany

5. Jülich Centre for Neutron Science (JCNS) at Heinz Maier-Leibnitz Zentrum (MLZ), Forschungszentrum Jülich GmbH, Garching, Germany

In general, several macroscopic measurements, including spin and lattice degrees of freedom, are necessary to map out the phase diagram of a magnetic compound. This procedure was realized at CeCu₂Ge₂ with a ground state strongly influenced by Kondo behaviour. Moreover, the challenging behaviour allows the check, whether a mean field theory succeeds in describing the physics correctly.

CeCu₂Ge₂, the counterpart of the heavy-fermion superconductor CeCu₂Si₂, exhibits an incommensurate antiferromagnetic ground state with $\tau_1 = (0.28 \ 0.28 \ 0.54)$ below the antiferromagnetic ordering temperature $T_N = 4.1$ K. The magnetism is strongly affected by a screening of the Ce 4f-moments by conduction electrons. The similar energy scales of this Kondo behaviour and magnetic exchange results in a complex magnetic phase diagram with amazing quantum critical phenomena at very-low temperatures. The magnetic properties of CeCu₂Ge₂ were studied by magnetization measurements and, using the strong magnetoelastic coupling, by magnetostrictive investigations over a wide temperature range and in fields up to 50 T. Results suggest a refinement of the proposed H-T phase diagram for [100] and [001] direction. Especially, the magnetostriction curves reveal the details clearly, e.g. the temperature dependence of the phase transition at 8 T in fields along [100], which is characterized by second-order type change of the spin-density wave vector to $\tau_2 = (0.31 \ 0.31 \ 0.54)$. Going up in field, a new phase emerges at around 12 Tesla, possibly characterized by a disordered transversal residual moment, which disappears at about 26 T.

In order to interpret the bulk measurements and the existing neutron scattering data a mean-field simulation by the McPhase program is in progress. The principal shape of magnetization and susceptibility curves as well as the proposed cycloidal magnetic-structure model is reproduced. The theoretical results demonstrate the great importance of the Kondo effect to CeCu₂Ge₂ magnetism.

TH.C-P17 - A new phase in antiferromagnets below the saturation fieldY. Kubo¹, S. Kurihara¹*1. Department of Physics, Waseda University, Tokyo, Japan*

It is known that classical square-lattice Heisenberg antiferromagnets have the Néel structure in zero magnetic field, and have a canted structure in fields H and finally saturate at H_{ms} . In the case of quantum antiferromagnets, however, there are quite strong three-magnon interactions at around $0.75 H_{\text{ms}}$ [1,2] which lead to a complete softening of a nonlinear spin-wave spectrum at a certain wave vector K_{c} at H_{c} [3]. Moreover, we get an unphysical negative spin-wave spectrum around K_{c} for $H > H_{\text{c}}$ [2,4]. We believe that the complete softening at H_{c} strongly indicates the simple canted states become unstable and a new ground state should appear in higher fields [3,4]. The main goal of this study is to clarify what is the new ground state for $H > H_{\text{c}}$. We infer from Refs. [3,4] that an incommensurate noncoplanar state, which is characterized by K_{c} , appears for $H > H_{\text{c}}$. We calculate the free energy in noncoplanar states and canted states, and find that the free energy of the noncoplanar state becomes lower than that of the canted state. Therefore, we see that the incommensurate noncoplanar states appear for $H > H_{\text{c}}$.

[1] M. E. Zhitomirsky and T. Nikuni, Phys. Rev. B 57, 5013 (1998); M. E. Zhitomirsky and A. L. Chernyshev, Phys. Rev. Lett. 82, 4536 (1999)

[2] M. Mourigal et al., Phys. Rev. B 82, 144402 (2010)

[3] Yurika Kubo and Susumu Kurihara, Phys. Rev. B 90, 014421 (2014)

[4] Yurika Kubo and Susumu Kurihara, SCES Proceedings (to be published)

TH.C-P18 - Magnetic field induced phase transition in PdCrO₂

P. Kushwaha¹, N. Nandi¹, C. Geibel¹, A.P. Mackenzie^{1,2}

1. *Max-Planck Institute, Chemical Physics of Solids, Dresden, Germany*

2. *Scottish Universities Physics Alliance, School of Physics and Astronomy, University of St. Andrews, St. Andrews, United Kingdom*

The delafossite metal PdCrO₂, which has a layered structure based on a triangular lattice, is of current interest due to its unconventional transport properties. Previous studies showed highly anisotropic metallic behavior with antiferromagnetic ordering near 38 K. Recent neutron experiments suggested that the ordered state is based on a commensurate co-planar 120° spin structure. Here we report in-plane resistivity (ρ_{ab}) measurements on single crystalline PdCrO₂. Zero field resistivity shows an excellent residual resistivity ratio (R_{300K}/R_{2K}) which is in the range of 100 - 200 for all measured crystals. The room temperature resistivity appears to be 6 $\mu\Omega$ cm which is the lowest ever measured in this system. The antiferromagnetic ordering temperature (T_N) is measured to be 38 (± 0.1) K. When a moderate magnetic field (≈ 7 Tesla) is applied perpendicular to the ab-plane, ρ_{ab} (T) smoothly increases on decreasing the temperature below 20 K. Further increase in magnetic field enhance this upturn and results in a sharp upward jump at 5 K. Iso-thermal resistivity measurements at 2 K indicate two magnetic transitions at ~ 2.8 Tesla and ~ 9.2 Tesla, but no saturation is observed up to the maximum applied field of 14 Tesla, by which field the magnetoresistance has reached 1400%. These results offer insight into the delicate interplay between Cr-derived magnetism and Pd-derived conduction in this fascinating material.

TH.C-P19 - Pressure-induced novel electronic state of Fe₇₀Ni₃₀ Invar alloy

G. Oomi¹, R. Saito², M. Ohashi³, T. Nakano⁴

1. Kurume Institute of Technology, Japan

2. Department of Physics, Kyushu University, Japan

3. Faculty of Engineering, Kanazawa University, Japan

4. Faculty of Engineering, Niigata University, Japan

It is well known that the ferromagnetic properties of Invar alloys are strongly affected by an application of pressure. Since the pressure coefficient of TC of Fe₇₀Ni₃₀ (=390K at ambient pressure) is about -60K/GPa, the ferromagnetism may disappear around 6GPa. In the present work, we made an attempt to measure the electrical resistance under high pressure and magnetic fields in order to investigate the electronic state of Fe₇₀Ni₃₀ above &GPa. The magnetoresistance (MR) at high pressure was measured below 9T and 4.2K. It is found that clear T₂ terms of the resistance appear at high pressure and the coefficients of this term were enhanced with increasing pressure, indicating an instability of electronic state or a quantum critical point. On the other hand, the MR below 10GPa is negative same as usual ferromagnets but its sign changes from negative to positive around 12 GPa suggesting a crossover from a localized moment regime to paramagnetic or a new magnetic state.

TH.C-P20 - Single crystal growth and characterization of $RNiSi_3$ ($R = Gd - Er$)D. Aristizábal¹, F. R. Arantes¹, F. N. Costa¹, F. F. Ferreira¹, R. A. Ribeiro¹, M. A. Avila¹

1. CCNH, Universidade Federal Do ABC (UFABC), Santo André, SP, 09210-580 Brazil

We have investigated the structural, magnetic, thermodynamic and transport properties of the new intermetallic series $RNiSi_3$ ($R = Gd - Er$), grown by the Sn-flux method which yields high quality plate-like single crystals. The results of the Rietveld refinement, based on X-ray powder diffraction data, show that these compounds crystallize in a layered orthorhombic structure in the $Cmmm$ space group ($SmNiGe_3$ type) with the main plate surfaces orthogonal to the crystallographic b direction, consistent with the only member previous characterized in this series, $YbNiSi_3$ [1]. Temperature dependent magnetization ($2K < T < 300K$) is anisotropic and reveals that the ground states are antiferromagnetic, with rough de Gennes scaling of T_N for the heavy rare-earths. There are also further transitions in the ordered state, indicating changes in the magnetic structure. For $R = Tb, Dy$ and Ho low-temperature magnetic isotherms up to $H=90kOe$ exhibit multiple metamagnetic transitions and alternating reversible/irreversible regions in the ordered state, which are dependent on temperature, magnetic field and crystal orientation. From this complex magnetic behavior we have built tentative magnetic phase diagrams. $HoNiSi_3$ presents at least six regions of distinct magnetic structures and is a promising candidate for the realization of the “devil's staircase” [2], involving magnetic frustration and/or long-range exchange interaction. We thank the financial support of FAPESP, CAPES and CNPq.

[1] M. A. Avila, M. Sera and T. Takabatake, *Phys. Rev. B* 70 (2004) 100409(R)[2] S. L. Bud'ko, Z. Islam, T. A. Wiener, I. R. Fisher, A. H. Lacerda, P. C. Canfield, *J. Magn. Magn. Mater.* 205 (1999) 53

TH.C-P21 - Structural and magnetic changes in $\text{Co}_x\text{Fe}_{3-x}\text{O}_4$ spinels at high pressure

G. Subías¹, V. Cuartero², J. Blasco¹, J. García¹, S. Lafuerza², S. Pascarelli², O. Mathon², C. Strohm², K. Nagai³, M. Mito³, G. Garbarino² and C. Popescu⁴

1. Instituto De Ciencia De Materiales De Aragón.CSIC-Universidad De Zaragoza, Spain

2. ESRF-The European Synchrotron, Grenoble, France

3. Faculty of Engineering, Kyushu Institute of Technology, Kitakyushu, Fukuoka, Japan

4. ALBA Synchrotron/CELLS, Cerdanyola del Vallès, 08290, Spain

We report magnetization studies to pressures of 30 GPa combined with synchrotron x-ray powder diffraction (SXRD) studies up to 40 GPa to explore the pressure-induced phase transformations of $\text{Co}_x\text{Fe}_{3-x}\text{O}_4$ ($0 < x < 2$) ferrites. All samples are ferrimagnetic and crystallize with a cubic spinel structure at ambient pressure. Room temperature Fe and Co K-edge x-ray magnetic circular dichroism (XMCD) and magnetization measurements were carried out to investigate the stability of the ferrimagnetic ground state using diamond anvil cells. By increasing pressure, the XMCD signal decrease continuously up to the highest reached pressure by ~50% in Fe_3O_4 (at 25 GPa) and by ~70% in $\text{Co}_{1.5}\text{Fe}_{1.5}\text{O}_4$ (at 16 GPa) and Co_2FeO_4 (at 21 GPa). In CoFe_2O_4 , the suppression by ~80% of the XMCD signal occurs simultaneously at both Fe and Co K-edges between 24 and 27 GPa. A continuous decrease of the dichroic signal with increasing pressure is observed at the Co K-edge, whereas the Fe K-edge dichroic intensity drops drastically. In CoFe_2O_4 , bulk magnetization measurements up to 26 GPa confirm the disappearance of ferrimagnetism and indicate an almost linear dependence of the magnetization with the magnetic field in the high pressure phase. All the samples show, coupled to the magnetic changes, structural phase transitions from the cubic spinel structure to an analogous post-spinel phase at around 20 GPa. Spinel and post-spinel phases coexist in a wide pressure range (~20–25 GPa) and the transformation is irreversible. Measurements releasing pressure revealed that the post-spinel phase is stable down to 4 GPa when it decomposes yielding a new phase with poor crystallinity. Later compression does not recover either the spinel or the post-spinel phases. This phase transformation induced by pressure explains the irreversible loss of ferrimagnetic behavior reported in these spinels.

TH.C-P23 - Spin order in FeCr₂O₄ observed by Mössbauer spectroscopyS. Nakamura^{1,2}, A. Fuwa³

1. Department of Science and Engineering, Teikyo University, 1-1 Toyosatodai, Utsunomiya, Japan

2. Advanced Research Institute of Science and Engineering, Waseda University, Tokyo, Japan

3. Faculty of Science and Engineering, Waseda University, Tokyo, Japan

A spinel oxide FeCr₂O₄ contains of Fe²⁺ ions on the A-site (tetrahedral site). The Jahn-Teller active Fe²⁺ ion causes a successive phase transition from cubic to tetragonal (135 K) and finally to orthorhombic phases (70 K). Neutron powder diffraction revealed a ferrimagnetic order below around 70 K, followed by a spiral magnetic order below 35 K. In this research, we have applied ⁵⁷Fe Mössbauer spectroscopy to investigate the magnetic structure in detail. A single crystal specimen of (100) platelet was used as an absorber. In order to obtain a single domain state in the low temperature phases, a slight compression along [001] axis was added by attaching epoxy resin on its both edges. Mössbauer spectroscopy was conducted in conventional transmission geometry by using ⁵⁷Co-in-Rh (25mCi) as γ ray source. The paramagnetic spectrum at room temperature consists of a singlet reflecting the cubic symmetry. The isomer shift is 0.937 mm/s, indicative of high spin Fe²⁺ state. With decreasing temperature, the spectrum splits into a doublet even in the cubic region due to the local and dynamical Jahn-Teller effect. The spectrum at 130 K consists of an asymmetric doublet ($I_1:I_2 \sim 3:5$) well corresponding to the single domain tetragonal phase. Below 60 K, the magnetically ordered spectrum is observed. The spectrum consists of only one component down to 40 K, which corresponds to the collinear ferrimagnetic order. Since the local structure around the Fe ion is considered to be close to that of the tetragonal phase, the Fe²⁺ spins align presumably along [110] direction. Below 35 K, however, the spectrum consists of distinct two subspectra indicating that the spins align in two different directions. One is still in [110] direction, while the other is approximately in [100] or [010] directions. This spin configuration is not consistent with a simple spiral magnetic structure.

TH.C-P25 - Single crystal growth and characteristics of $\text{Sm}_{0.7}\text{Tb}_{0.3}\text{FeO}_3$ orthoferrite single crystal with spin-reorientation in room temperature

A. Wu¹, B. Wang¹, X. Zhao¹, L. Su¹, S. Cao²

1. Shanghai Institute of Ceramics, Chinese Academy of Sciences, China

2. Department of Physics, Shanghai University, China

High quality $\text{Sm}_{0.7}\text{Tb}_{0.3}\text{FeO}_3$ single crystal has been grown by the four-mirror floating zone technique. The magnetic properties of $\text{Sm}_{0.7}\text{Tb}_{0.3}\text{FeO}_3$ single crystal were studied in the temperature range from 3 to 400 K. A clear spin reorientation behavior with the gradual transition of the Fe^{3+} magnetic moment ordering from $\{G_z, F_x\}$ -type ordering at low temperatures to $\{G_x, F_z\}$ -type ordering at high temperatures is observed in a range of 330 – 360 K, which is significantly lower than that of SmFeO_3 , while significantly higher than that of TbFeO_3 . Interestingly, below this transition, with decreasing temperature, the value of M_x increases till 3 K, which is in contrast to a pure SmFeO_3 . We ascribe this change of behavior to substitution of Sm ions for Tb ones. At temperatures 30 – 100 K hysteresis curves possess a double-loop shape with two triangular loops emerging, which is explained by the single domain-wall state of the sample. The shape of hysteresis loop depends on the values of domain wall expulsion field H_{exp} and the domain wall nucleation field H_n .

TH.C-P26 - Pressure-induced magnetic order in a gapped quantum magnet

A. Mannig¹

1. ETH Zurich, Laboratory For Solid State Physics, Neutron Scattering And Magnetism Group, Zurich, Switzerland

We present recent muon-spin relaxation and magnetic susceptibility data under applied hydrostatic pressure on the organometallic S=1 quantum magnet $\text{NiCl}_2 \cdot 4(\text{SC}(\text{NH}_2)_2)$.

The material consists of weakly coupled antiferromagnetic chains and has a spin gap resulting from large single-ion anisotropy.

Our muon spin rotation experiments provide local field dependencies on temperature as well as pressure and allow for the mapping of a detailed phase diagram up to 22 kbar. We demonstrate that the compound may be driven through two subsequent pressure-induced transitions into apparently distinct magnetically ordered phases.

Susceptibility-measurements support those results and show the potential of low-pressure transitions to be investigated by various techniques.

With $\text{NiCl}_2 \cdot 4(\text{SC}(\text{NH}_2)_2)$ we add to the very few reported pressure-induced phase transitions in quantum magnets, the recent example being the frustrated quantum spin liquid PHCC [1].

[1] M. Thede, A. Mannig, M. Månsson, D. Hübner, R. Khasanov, E. Morenzoni, and A. Zheludev, "Pressure-Induced Quantum Critical and Multicritical Points in a Frustrated Spin Liquid", Phys. Rev. Lett. 112, 087204 (2014)

TH.C-P27 - First-order magnetization process as a tool for magnetic-anisotropy description of $U_3Cu_4Ge_4$

D. Gorbunov¹, M.a Henriques^{2,3}, A. Andreev², Y. Skourski¹, M. Richter⁴, J. Wosnitza¹

1. Dresden High Magnetic Field Laboratory, Helmholtz-Zentrum Dresden-Rossendorf, Germany

2. Institute of Physics, Academy of Sciences of the Czech Republic, Prague, Czech Republic

3. CCTN, IST/CFMCUL, University of Lisbon, Nuclear and Technological Campus, Bobadela, Portugal

4. IFW Dresden, Dresden, Germany

Here, we report on high-magnetic-field investigations of a $U_3Cu_4Ge_4$ single crystal. $U_3Cu_4Ge_4$ (orthorhombic crystal structure) is a ferromagnet below 73 K and is characterized by highly localized 5f states as manifested by the spontaneous magnetic moment of 5 μ_B /f.u. at 2 K. Density-functional calculations point to a ferrimagnetic ground state. As a typical uranium-based intermetallic compound, $U_3Cu_4Ge_4$ displays very strong uniaxial magnetic anisotropy, the anisotropy field between either of two principal crystallographic directions significantly exceeds 100 T. The a axis is the easy magnetization direction. Strong anisotropy is also observed within the (bc) plane. $U_3Cu_4Ge_4$ exhibits strong magnetic hysteresis, the coercive field reaches 0.4 T. The strong magnetic anisotropy is also reflected in the specific heat and electrical resistivity both revealing gapped behavior.

In pulsed magnetic fields at 2 K, $U_3Cu_4Ge_4$ displays a type-II first-order magnetization process (FOMP) along the b axis at 25 T, while the magnetization curve along the c axis is S shaped suggesting a step-wise rotation of the magnetic moments. The critical fields of both field-induced transitions decrease with temperature. The presence of the FOMP is remarkable since it provides a tool for describing the magnetic anisotropy despite its very large value making its direct measurement impossible for $U_3Cu_4Ge_4$. Taking into account anisotropy constants up to the sixth order, we succeeded in describing the magnetization curves measured along the b axis between 2 and 60 K. At 2 K, we obtained the constants: $K_1 = 17.6$, $K_2 = -33$, $K_3 = 26$ MJ/m³. With increasing temperature the constants decrease monotonously and the higher the order of the anisotropy constant, the faster it diminishes with temperature. While the very large magnetic anisotropy of uranium intermetallics is in general hardly accessible to experiment, the present case presents an interesting counter-example.

TH.C-P28 - Substitution in LiMF₄: a playground of fundamental interactions

P. Babkevich¹, A. Finco¹, M. Jeong¹, B. Dalla Piazza¹, I. Kovacevic¹, G. Klughertz¹, K. W. Kr², D. T. Adroja³, E. Goremychkin³, T. Unruh⁴, J. Jensen⁵, H.M. Ronnow¹

1. *Laboratory for Quantum Magnetism, École Polytechnique Fédérale de Lausanne (EPFL), Lausanne, Switzerland*
2. *Department of Chemistry and Biochemistry, University of Bern, Bern, Switzerland*
3. *ISIS Facility, Rutherford Appleton Laboratory, Chilton, Didcot, United Kingdom*
4. *Forschungsneutronenquelle Heinz Maier-Leibnitz (FRM-II), Garching, Germany*
5. *Niels Bohr Institute, Copenhagen, Denmark*

Despite its fundamental nature, there exist very few studies on purely dipolar-coupled magnetic systems. Well known examples include LiHoF₄ which is an excellent realisation of an Ising system while LiErF₄ and LiYbF₄ have been found to be XY. The family of compounds, LiMF₄, where M = Ho, Er, Yb, Tm, Gd, etc are intriguing to study fundamental interactions. The crystal field environment that the M ions experience plays a crucial role in stabilising magnetism. Through careful analysis of inelastic neutron and susceptibility measurements we are able to explain and predict, in the mean-field approximation, the low-temperature phase diagrams of LiMF₄ compounds.

TH.C-P34 - dependence of morin temperature on the size of hematite nanoparticles

J. Kohout¹, T. Kmječ¹, D. Kubaniová¹, L. Kubičková¹, K. Zavřítá¹, P. Brazda², E. Santava², D. Nizoanský³, M. Klementová³, A. Lanèk³

1. Charles University In Prague, Faculty of Mathematics and Physics, Praha, Czech Republic

2. Institute of Physics ASCR, v.v.i., Praha, Czech Republic

3. Institute of Inorganic Chemistry of the ASCR, v.v.i., Husinec, Czech Republic

Bulk hematite ($\alpha\text{-Fe}_2\text{O}_3$) exhibits a spin reorientation transition from antiferromagnetic to weakly ferromagnetic state above $T_M \sim 264$ K, known as Morin transition. T_M is decreasing with particle size and for nanoparticles smaller than ~ 20 nm the Morin transition may even disappear. Nanoparticles of $\alpha\text{-Fe}_2\text{O}_3$ enriched with ^{57}Fe isotope ($\sim 95\%$) were prepared by sol-gel and nanoparticles with natural Fe by hydrothermal methods. The X-ray powder diffraction confirmed $\alpha\text{-Fe}_2\text{O}_3$ as the main phase. Various particle shapes - spheres, spindles, rhombohedra and small spheres were discerned from TEM pictures with characteristic particle sizes: 126, 42, 26 and 5.6 nm, respectively. The temperature dependence of magnetization after cooling in zero and non-zero magnetic fields was measured in a SQUID magnetometer and $T_M = 255, 215, 187$ K respectively, were derived from the rapid increase of magnetization. These data agree with theoretical dependence of T_M on the particle size [1]. The small spheres were superparamagnetic, with their magnetization curves fitted by Langevin function taking a lognormal distribution of particle sizes into account, and displayed no Morin transition. The transition was also proved by temperature dependence of Mössbauer spectra of enriched nanoparticles between 4.2 and 300 K. The ratio of the areas of two sextets ascribed to the antiferromagnetic and weakly ferromagnetic phases, gave then their relative concentrations.

[1] X. Batlle and A. Labarta J. Phys. D: Appl. Phys. 35 (2002), R15-R42

TH.C-P35 - Specific heat and ESR in borate $TbAl_3(BO_3)_4$

M. Pashchenko¹, V. Bedarev¹, M. Kobets¹, K. Dergachev¹, E. Khatsko¹, S. Gnatchenko¹, A. Zvyagin¹, T. Zajarniuk², A. Szewczyk², M. Gutowska², L. Bezmaternykh³, V. Temerov³

1. *B. Verkin Institute For Low Temperature Physics And Engineering of The National Academy of Sciences of Ukraine, Kharkiv, Ukraine*

2. *Institute of Physics, Polish Academy of Sciences, Warsaw, Poland*

3. *L.V. Kirensky Institute of Physics, Siberian Department of the Academy of Sciences, Krasnoyarsk, Russian Federation*

The rare earth aluminum borates $RAI_3(BO_3)_4$ have only one magnetic subsystem - a subsystem of rare earth ions. That is why some of these crystals can be a simple model systems for the study of spontaneous and magnetic field induced phase transitions. In this work, the specific heat and ESR were studied in order to determine parameters of interactions between the magnetic ions in the $TbAl_3(BO_3)_4$ crystal.

Investigation of temperature dependence of the specific heat allowed us to determine the magnetic ordering temperature of the rare-earth subsystem of $TbAl_3(BO_3)_4$, $T_c = 0.68$ K. The initial splitting, $\Delta \approx 1.3$ K, and the effective g-factor, $g = 16$, of the lowest quasidoublet of Tb^{3+} ion were determined from the ESR experiments. In the case of antiferromagnetic ordering, in frame of the molecular field theory, the difference between the constants of effective fields of intrasublattice interaction, λ_{11} , and intersublattice interaction λ_{12} can be calculated by using the expression: $(\lambda_{11} - \lambda_{12}) = \Delta/2 (g_{eff} \mu_B) 2 \tanh(\Delta/2T_c)$. In the case of ferromagnetic ordering, $\lambda_{12} = 0$ and λ_{11} is equal to the molecular field constant λ_0 . By fitting this expression to the experimental data we obtained $(\lambda_{11} - \lambda_{12})$ or λ_0 equal to $0.03 T^2/K$.

Low temperature magnetic ordering and small value of the effective interaction between the magnetic moments of the terbium ions allows us to make the assumption about the dipole-dipole nature of the magnetic ordering in this material.

TH.C-P36 - Towards a simple description of magnetism in heavy rare earth elements: application to magnetic refrigeration.

E. Mendive Tapia¹, J. Staunton¹

1. The University of Warwick, United Kingdom

Magnetic refrigerants are much more efficient than conventional fridges based on compression/expansion technology and are promising candidates for environmentally friendly refrigerants. Therefore, the development of simple theoretical models for their study has an important value in order to provide qualitative insights into otherwise an incredibly complex research field. Here we employ an ab-initio Disordered Local Moment Theory (DLM) to investigate the magnetic phase diagram of heavy rare earths. We focus on the study of magnetic phase transitions that are characteristic of the common valence electronic structure among them. Gd is used in order to mimic other heavy rare earths due to their chemical similitude. As a preliminary main result, we observe that FAN, distorted AFM, and CONE magnetic phases can be obtained by changing the temperature and/or the strength of an applied magnetic field without including crystal field contributions nor relativistic effects. Investigation of Helifan and other possible new magnetic structures is in process. In the long term, we seek to model the magnetism of the heavy rare earths and nanostructure potential materials exhibiting large caloric responses by scaling the exchange interaction with the Gennes factor and by including anisotropy effects as additional phenomenological terms.

TH.C-P37 - Influence of grain size in the magnetic and magnetocaloric transitions in $\text{La}_{0.5}\text{Ca}_{0.5}\text{MnO}_3$ probed by direct and indirect methods

M. Quintero^{1,2}, S. Passanante^{1,3}, I. Irurzun^{1,3}, D. Goijman¹, G. Polla¹

1. *Deperatamento De Materia Condensada, Comisión Nacional De Energía Atómica, Argentina*

2. *Escuela de Ciencia y Tecnología, Universidad Nacional de General San Martín, Argentina*

3. *Departamento de Física, Facultad de Ciencias Exactas y Naturales, UBA, Argentina*

The magnetocaloric effect has been revealed as one of the most promising topics in the study of magnetic properties, mainly motivated in the plausible use for magnetic refrigeration applications. During the last years, the increase in the complexity of the systems under study forced a careful revision to the validity of the thermodynamic models used to estimate the effect. A non adequate use can lead to inconsistencies between results obtained by different methods. In this work we used the prototypical manganite $\text{La}_{0.5}\text{Ca}_{0.5}\text{MnO}_3$ as an example of this issue. The influence of grain size in the magnetic properties of this system has been studied more than a decade ago. The presence of long range ordering is suppressed as the grain size decreases, giving place to a metastable state instead of the ground state. The differences obtained using direct and indirect methods are discussed in the framework of domain walls in the ferromagnetic phase of the system.

TH.C-P38 - High temperature magnetic properties and spin-lattice coupling of magnetoelectric epsilon-Fe₂O₃

M. Gich¹, J. Padilla¹, J. Nogués^{2,3}, J. Kreisel^{4,5}, A. Roig¹, J. Garcia-Muñoz¹

1. Institut De Ciència De Materials De Barcelona (ICMAB-CSIC), Barcelona, Spain

2. Institució Catalana de la Recerca i Estudis Avançats (ICREA), Barcelona, Spain

3. Institut Català de Nanociència i Nanotecnologia (ICN2), Barcelona, Spain

4. Luxembourg Institute of Science and Technology, Luxembourg

5. University of Luxembourg, Luxembourg

Epsilon-Fe₂O₃ is one of the less studied ferrimagnetic iron oxides and it is attracting great interest after the discovery of a huge coercivity (20 kOe)[1] and multiferroicity[2] at room temperature. Its complex structure (with four Fe³⁺ sublattices) favours magnetic frustration and successive magnetic and structural transitions. The collinear ferrimagnetic phase (T_c=500K) is substituted by two different incommensurate magnetic phases on cooling below 150K and 110K respectively [3].

We present magnetic, Raman and neutron measurements questioning the current belief that the magnetic ordering temperature of epsilon-Fe₂O₃ is ~500 K, well below that of other iron oxides such as hematite, magnetite or maghemite. Magnetometry measurements up to 925 K show non-linear behaviour under field and signs of ferrimagnetic order up to temperatures as high as 870 K. The transition to superhard ferrimagnetism upon cooling below 500 K brings about an anomalous evolution of the thermal expansion and selected bands of the Raman spectra. A temperature-dependent neutron diffraction study of these nanoparticles has revealed the presence of magnetic order well above 500 K, in agreement with magnetic measurements. Analysis of neutron data confirmed that the new high temperature ordered phase is also ferrimagnetic, although the net ferromagnetic component is significantly lowered, and it vanishes above 870 K. This temperature is similar to the Curie point in other iron oxides, indicating comparable magnetic coupling strengths.

[1] B. Jin et al. Adv.Mater. 16 (2004) 48

[2] M. Gich et al. Adv. Mater. 26 (2014) 4645

[3] M. Gich et al. Chem. Mater. 18(2006) 3889

TH.C-P39 - Charge order in magnetite below the verwey transition studied by combination of ^{57}Fe NMR and mössbauer spectroscopy

J. Kohout, K. Závěta, T. Kmječ, D. Kubániová, B. Sedlák

1. Charles University In Prague, Faculty of Mathematics and Physics, Prague, Czech Republic

Magnetite Fe_3O_4 is a multiferroic mixed-valence transition metal oxide with inverse spinel structure. At high temperatures it is cubic ($Fd\bar{3}m$) and both NMR and Mössbauer spectroscopy (MS) point to the delocalization of Fe^{2+} and Fe^{3+} ions in the octahedral B -sites. At the Verwey temperature ($T_V \approx 120\text{-}125\text{ K}$) magnetite undergoes a first order phase transition: the symmetry is lowered to monoclinic and the electric conductivity drops by more than two orders of magnitude suggesting the electron localization.

According to simple Verwey model, ferric and ferrous ions order in the B -sites which was found roughly correct in ab-initio calculation [1]. Senn [2] recently proposed the charge ordering and low-temperature superstructure of Fe_3O_4 from high-energy X-ray diffraction.

Here we present results on the charge order of a high-purity single-crystalline Fe_3O_4 determined by combination of ^{57}Fe NMR and MS. Previous NMR measurements [3-4] [found](#) 24 nonequivalent sites for iron cations - 16 octahedral and 8 tetrahedral ones agreeing with the monoclinic Cc space group.

The values of hyperfine fields from NMR spectra were used for restricting the number of free parameters when fitting the MS spectra at 4.2 K. After cooling the sample below T_V without and with an external field, the magnetic moments are normal to, and make an angle of $\sim 45^\circ$ with the plane of the thin platelet, respectively.

The isomer and quadrupole shifts of B -sites are split into two groups supporting the idea of charge localization in the MS time window of $\sim 10^{-7}\text{ s}$.

The financial support under the grant GAUK 8313 is gratefully acknowledged.

[1] K. Yamauchi et al.: Phys. Rev. B 79 (2009) 212404

[2] M.S. Senn et al.: Nature 481 (2012) 173

[3] P. Novák et al.: Phys. Rev. B 61 (2000) 1256

[4] P. Novák et al. in Ferrites: Proceedings of ICF8, Kyoto 2000, p. 131

TH.C-P40 - Magnetocaloric effect in quaternary heusler alloys

V. Prudnikov¹, I. Rodionov¹, I. Titov¹, M. Blinov¹, A. Novikov¹, E. GanÅeshina¹, A. Sokolov², I. Zakharchuk³, E. Lähderanta³, A. Granovsky¹

1. Faculty of Physics, Lomonosov Moscow State University, Mosco, Russian Federation

2. Department of Physics and Astronomy, University of Nebraska-Lincoln, Linclon, Nebraska, United States

3. Lappeenranta University of Technology, Finland

It was found that off-stoichiometric $\text{Ni}_{50}\text{Mn}_{50-x}\text{In}_x$ Heusler alloys are characterized by inhomogeneous structural and magnetic phases and in addition to the field and temperature induced magnetostructural transitions and shape memory effects, they demonstrate exchange bias, giant deformations, kinetic arrest, giant normal (direct) and inverse magnetocaloric effects, large magnetoresistance, giant anomalous Hall effect and other important properties suitable for potential practical applications ([1, 2] and references therein). Since disorder in these alloys plays a key role, even a small addition of fourth element, Z, to Ni-Mn-In alloys can drastically change their properties. We present our last experimental results on structural and magnetic phase transitions, magnetic, magnetocaloric and magneto-optical properties in quaternary Ni-Mn-In-Z (Z =Co, Cu, Al, B, Cr, Si) Heusler alloys with concentration of Ni, In and Z around 50%, 15%, and up to 5%, respectively. Bulk polycrystalline samples were obtained by the arc-melting technique, the monocrystal $\text{Ni}_{45}\text{Mn}_{36.7}\text{In}_{13.3}\text{Co}_5$ was grown by the Czochralski method, the thin films were fabricated by pulse laser deposition. The obtained results do not support the correlation between magnetic properties and the number of valence electrons per atom. Magnetic properties depend non-linearly on the fraction of Z element. The adiabatic changes of temperature in magnetic fields up to 1.8 T in the vicinity of martensitic transition reaches -2.0 K at heating the sample but does not exceed -1.0 K and can be even positive in some samples at cooling. Magneto-optical spectra were measured in the geometry of the transverse Kerr effect in the energy range 0.5-4.0 eV and did not reveal the noticeable difference in spectra profiles in martensitic and austenitic states.

[1] I. Dubenko et al., J. Magn.Magn.Mat. 324, 3530-3534 (2012)

[2] J. Liu et al., Nature Materials 11, 620-626 (2012)

The work was supported by Russian Foundation for Basic Research (Grant No 15-02-02077 and 15-52-78080)

TH.C-P41 - Enhanced NMR in entangled nuclear-electronic quantum magnet LiHoF₄

I. Kovacevic¹, P. Babkevich¹, M. Jeong¹, G. Boero¹, H. Ronnow¹

1. Ecole Polytechnique Federale De Lausanne (EPFL), Lausanne, Switzerland

Transverse-field Ising magnet LiHoF₄ is known for its electronic quantum criticality which is altered by hyperfine coupling to the nuclear spins. We focus on probing nuclear transitions (NMR) in entangled nuclear-electronic states in LiHoF₄ using a vector network analyzer (VNA) in wide frequency range up to 6 GHz and at low temperatures down to 0.15 K. Evolution of the hyperfine levels as a function of field and temperature through quantum and thermal transitions was not only measured experimentally but also simulated within the mean-field approximation. Through this approach we are able to track the evolution of the hyperfine levels as a function of field and temperature through quantum and thermal phase transitions. Our mean-field simulations show that nuclear transition amplitude is enhanced by more than two orders of magnitude due to nuclear-electronic hybridization. We find a quantitative agreement between our experiments and calculations for the resonance positions and relative transition intensities. This allows us to probe the transition energies as well as the wavefunctions of LiHoF₄. These results bring us a step closer to quantum control of hybrid nuclear-electronic states near quantum phase transition where hybridization is the largest due to avoided level crossing, and at low temperatures where hyperfine interaction is large compared to thermal fluctuations.

TH.C-P42 - Ferromagnetism in partially oxidized CuCl

T. Saerbeck¹, J. Pereiro², J. Wampler³, J. Stanley³, J. Wingert³, O. G. Shpyrko³, I. K. Schuller³

1. Institut Laue-Langevin, Grenoble, France

2. School of Physics and Astronomy, Cardiff University, Cardiff, United Kingdom

3. Department of Physics and Center for Advanced Nanoscience, University of California San Diego, La Jolla, United States

We report on the observation of ferromagnetism in bulk CuCl powders partially oxidized in air or humid environments. The phase diagram of copper-halides shows a rich diversity not only in crystalline structure, but also in magnetic and electronic properties. CuCl is reported to be a diamagnetic insulator which is highly susceptible to oxidation. Corrosion products without exception show antiferromagnetic ordering with varying transition temperature and spin structure depending on composition.

In contrast, we observe a distinct ferromagnetic transition and hysteresis with a T_c of 18 K for CuCl partially oxidized in air [1]. The amount of this new ferromagnetic phase is shown to be related to the degree of humidity and exposure time ranging from minutes to several weeks. Magnetic field modulated microwave spectroscopy (MFMMS) and SQUID magnetometry are used to identify magnetic phase transitions and compare them to the antiferromagnetic transitions in other Copper-chloride structures. Through detailed structural investigations and Rietveld analysis, the evolution of the crystallographic structure after different degree of oxidation is determined. No corrosion product of cuprous chloride can account for the observed magnetic properties. In addition, the ferromagnetic state is irreversible with respect to subsequent drying processes, but decays upon prolonged exposure to humidity. This indicates that the magnetic signal originates from an intermediate stable phase in the oxidation process of CuCl.

This work is supported by AFOSR Grant no. FA9550-14-1-0202.

[1] T. Saerbeck, J. Pereiro, J. Wampler, J. Stanley, J. Wingert, O. G. Shpyrko, and Ivan K. Schuller, *J. Magn. Magn. Mater.* 346, 161 (2013)

TH.C-P43 - Irreversibility induced by thermal cycles in phase separated manganites

J. Sacanell¹, M. Quintero¹, B. Sievers¹, L. Granja¹, G. Polla¹, P. Levy¹, F. Parisi¹

1. Departamento de Física de la Materia Condensada, Gerencia de Investigación y Aplicaciones, Comisión Nacional De Energía Atómica, San Martín, Argentina

We have studied the effect of irreversibility induced by repeated thermal cycles on the magnetization of polycrystalline samples of $\text{La}_{0.5}\text{Ca}_{0.5}\text{MnO}_3$ and $\text{La}_{0.325}\text{Pr}_{0.3}\text{Ca}_{0.375}\text{MnO}_3$. A decrease of the magnetization at different temperature ranges after cycling is obtained in the temperature range between 300 and 30 K. Both compounds are known to exhibit intrinsic submicrometric coexistence of phases and undergo a sequence of phase transitions related to structural changes. We observed that the changes induced by thermal cycling can be partially inhibited by applying magnetic field and hydrostatic pressure.

Our results suggest that the growth and coexistence of phases with different structures gives rise to microstructural tracks and strain accommodation and produces the observed irreversibility. Irrespective of the actual ground state of each compound, the effect of thermal cycling is towards an increase of the amount of the non ferromagnetic phase in both compounds.

We developed a phenomenological model to describe the observed effect in terms of a growth of one phase against the other through the contact surface between them.

TH.C-P44 - Key role of rutile structure for layered magnetism in chromium compoundsY. Kondo¹, T. Hotta¹*1. Department of Physics, Tokyo Metropolitan University, Japan*

CrCl₂ and CrF₂ with the distorted rutile-type crystal structure exhibit paramagnetism in a room temperature, but at low temperatures, they are known to show different antiferromagnetic (AF) structure. CrF₂ has the simple Néel structure in common with other fluorides, while CrCl₂ exhibits peculiar layered AF structure. Our purpose is to unveil the stabilization mechanism of such layered AF structure different from the simple Néel structure.

Since Cr ion is divalent in the halogenation chrome, we find the electron configuration 3d⁴ with one electron in e_g and three electrons in t_{2g} orbitals. We notice that this is just the same electron configuration as Mn³⁺ in manganese oxides. Here we recall that the complicated magnetism in manganese oxide is explained by the competition between the itinerant and localized natures of electrons. Namely, e_g electrons smoothly move in the ferromagnetic t_{2g} spin arrangements with the penalty of magnetic energy, while they are localized for AF t_{2g} spins with the gain of magnetic energy. The situation is well described by the so-called double-exchange model.

In this research, we try to understand the magnetic structure in chromic compounds on the basis of the double-exchange model with orbital degree of freedom. Here we consider a body centered cubic (bcc) lattice without any distortions and the TiO₂ structure (rutile structure) lattice which is obtained from the bcc lattice by pressing it along the c-axis. We find that the layered magnetic structure of CrCl₂ never appears as the ground state in the bcc lattice. When we include the distortion along the c-axis, leading to the rutile-type structure, we eventually obtain the layered magnetic structure as the ground state in a wide range of parameters space. In the poster presentation, we report the details of the ground-state phase diagram to explain the appearance of the layered magnetic phase.

TH.C-P45 - Low-temperature specific heat and magnetic ordering in R_2Pd_2In

P. Svoboda¹, S. Maskova¹, L. Havela¹, A. Kolomiets²

1. Charles University, Faculty of Math. And Physics, DCMP, Prague, Czech Republic

2. Lviv Polytechnic National Univ., Lviv, Ukraine

The series of isostructural intermetallic compounds R_2Pd_2In (R= La, Pr, Nd, Sm, Gd, Tb, Dy, Ho and Er) crystallizes in the tetragonal Mo_2FeB_2 structure type and orders antiferromagnetically at low temperatures. High quality single crystals of selected R_2Pd_2In have been grown. The zero-field low-temperature specific heat was studied in the temperature region 1.5 - 300 K using relaxation method (PPMS) for all above indicated compounds. Sharp anomalies corresponding to the Néel temperatures were observed in all magnetic compounds together with other anomalies corresponding to the order-to-order changes of magnetic phases. The detailed analysis of the specific heat yielded the magnetic part of the specific heat and magnetic entropy of all studied magnetic compounds.

TH.C-P46 - Magnetic systems at elevated temperatures by relativistic disordered local moments theory

D. Thonig¹, J. Henk², O. Eriksson¹

1. Institute of Physics and Astronomy, Uppsala University, Sweden

2. Martin Luther University Halle-Wittenberg, Germany

The mismatch of experimentally and theoretically observed temperature-dependent magnetic properties, in particular the magnetic moment, the magnon stiffness, and the Curie temperature, requires improvements in first-principles theory. The non-collinear magnetic state at elevated temperatures is described here within a relativistic disordered local moments theory. The coupling between local magnetic moments for a given magnetic configuration is obtained from first-principles calculations, allowing to map the non-collinearity to the spin temperature. Taking into account spin-orbit coupling and a spherical harmonics expansion of the atomistic exchange parameters enables us to account also for higher-order interactions, like Dzyaloshinskii-Moriya or biquadratic exchange.

We introduce to the approach and apply it to bulk ferromagnets as well as to 1-3 ML Fe on Cu(001). In combination with Monte Carlo simulations, our first principles theory is in agreement of the magnetization versus temperature dependence in the entire temperature range of $0 < T < T_c$. The temperature-dependent Heisenberg exchange exhibits a crucial dependence due to the rotation of two magnetic moments, which influences the magnetic ground state obtained from Monte Carlo simulations. Our method makes a significant contribution to a deeper understanding of the complex temperature-dependent exchange mechanisms in magnets.

TH.C-P47 - Possible decoupling of the magnetic field instabilities in the antiferromagnet CeRh₂Si₂ close to its critical pressure in pulsed magnetic fields.

D. Braithwaite¹, W. Knafo², R. Settai³, D. Aoki^{1,4}, S. Kurahashi⁵, J. Flouquet¹

1. Univ. Grenoble Alpes and CEA, INAC-SPSMS, Grenoble, France

2. Laboratoire National des Champs Magnétiques Intenses, CNRS-UJF-UPS-INSA, Toulouse, France

3. Department of Physics, Niigata University, Niigata, Japan

4. IMR, Tohoku University, Oarai, Ibaraki, Japan

5. Graduate School of Science and Technology, Niigata University, Niigata, Japan

In an Ising antiferromagnet like CeRh₂Si₂, an external magnetic field will destroy the antiferromagnetic order, and induce a polarized paramagnetic state. These two phenomena can occur concomitantly with a 1st order metamagnetic transition. Alternatively antiferromagnetic order can be destroyed at a lower field than the transition to a polarized state, with 2 characteristic fields, HC and HM. In CeRh₂Si₂ these two phenomena coincide, implying that HC>HM. However in the paramagnetic compound CeRu₂Si₂, doping with Rh induces antiferromagnetic order and a decoupling of HC and HM is found. Pressure is a clean way to tune an antiferromagnetic cerium compound to its critical point. Pressure will increase HM and decrease HC, and perhaps induce this decoupling of the characteristic fields. The experimental verification of this is challenging, requiring measurements under pressure (For CeRh₂Si₂ PC is about 1 GPa) with rather high magnetic fields (H>35T). We present a pressure cell optimized for the use in pulsed magnetic fields up to 60T, and pressures up to 4.5 GPa, at temperatures down to 1.5K. Heating effects due to the field pulse are reduced by the use of electrically insulating materials for the elements close to the sample. We report magnetoresistance measurements on a single crystal of CeRh₂Si₂. We find a continuous increase of HM with pressure, exceeding 60T at 1.5 GPa. For P<<PC only one anomaly is seen. Close to the critical pressure a broad shoulder develops on the low field side of HM. Normally a rather strong and sharp anomaly would be expected at HC, however the signature could become rather weak and broad due to the reduced value of the sublattice magnetization, and especially the steep slope of HC with pressure. We suggest that this shoulder is likely a sign of the decoupling of the 2 fields, and present the obtained phase diagram.

TH.C-P49 - Necessary conditions for the long-time variation of magnetic structure in frustrated magnetsK. Motoya¹, M. Hagihala¹, M. Matsuda²1. *Tokyo University of Science, Japan*2. *Oak Ridge National Laboratory, United States*

In uniform three-dimensional magnets, we have not expected to observe time variations in magnetic properties within an attainable time scale. Contrary to all expectations, we observed a long-time variation in the magnetic structure of the nondiluted uniform magnet CeIr_3Si_2 by means of time-resolved neutron scattering measurements.^{1,2} Subsequently, similar long-time variations in the magnetic structure were observed in some materials having competing magnetic interactions.^{3,4} All these compounds exhibit successive magnetic and multistep metamagnetic transitions. However, all materials having these two factors do not necessarily show long-time variation. In order to find necessary conditions we have studied the magnetic property of $\text{Ce}(\text{Ir-Rh})_3\text{Si}_2$ system. CeRh_3Si_2 shows magnetic transitions at $T_N=4.72\text{K}$ and $T_t=4.48\text{K}$. In the low temperature phase it shows multi-step metamagnetic transitions. [5] These properties are quite similar to those of CeIr_3Si_2 . However, our previous neutron scattering and magnetization measurements of CeRh_3Si_2 showed no time variation, which is quite different from that of CeIr_3Si_2 .

In this work, we determined the magnetic phase diagram of the $\text{Ce}(\text{Ir-Rh})_3\text{Si}_2$ system and made time-resolved neutron scattering measurements of some representative compounds. On the bases of time variation behavior of the macroscopic and neutron diffraction measurements, we have found that the presence of spontaneous magnetization in one-side structure is the necessary condition for the presence of long-time variation of magnetic structure in these compounds.

References:

1. K. Motoya et al. : J. Phys. Conference Series 200 032048 (2010)
2. T. Moyoshi et al.: J. Phys. Soc. Jpn. 81 014704 (2012)
3. K. Motoya et al. : J. Phys. Conference Series 273 012124 (2011)
4. T. Moyoshi and K. Motoya: J. Phys. Soc. Jpn. 80 034701 (2011)
5. D. Kaczowski and T. Komatsubara: Physica B 403 1362 (2008)

TH.C-P50 - Instability of ferromagnetic Fe nanoclusters produced in amorphous SiO₂ by ion implantation

K. Bharuth-Ram¹, H. Hofsaess², K. Zhang², H. Masenda³,

1. *Physics Department, Durban University of Technology, South Africa*

2. *Zweites Physikalisches Institut, University of Goettingen, Germany*

3. *Physics Department, University of the Witwatersrand, South Africa*

A 460 nm thick amorphous SiO₂ layer, formed on a Si (100) surface heated to 1000oC in oxygen atmosphere, was implanted with 57Fe to a fluence of 1 x 10¹⁶/cm² at room temperature and annealed at temperatures up to 1000oC. The implanted and annealed samples were studied by conversion electron Mössbauer spectroscopy (CEMS). The CEM spectra up to an annealing temperature of 800oC showed the presence of a singlet due to dispersed Fe ions and paramagnetic doublets with hyperfine parameters characteristic of Fe²⁺ and Fe³⁺.

The spectrum after the 1000oC anneal was dominated by a broad ferromagnetic sextet with a hyperfine field of 32 T, showing the formation Fe nanoclusters, in agreement with the observations of Zhang et al. [1] but contrary to those of Nomura et al [2].

A surprising result was that CEMS measurements performed on the annealed sample after a period of 6 months showed the complete disappearance of the ferromagnetic sextet and only the presence of a paramagnetic doublet due to Fe²⁺.

[1] G. L. Zhang et al., Appl. Phys .Lett. 61: 2527 (1992)

[2] K. Nomura and H. Reuther, J. Radioanal Nucl Chem 287: 341 -346 (2011)

TH.C-P51 - Pressure effect on the magnetic phase diagram of Nd₂RhIn₈

P. Javorský¹, M. Míšek², M. Prachařová¹, J. Kaštil², J. Prchal¹, M. Klicpera¹, M. Kratochvílová¹

1. Charles University in Prague, Faculty of Mathematics and Physics, Department of Condensed Matter Physics, Prague, Czech Republic

2. Institute of Physics ASCR, v.v.i., Praha, Czech Republic

Nd₂RhIn₈ belongs to a large group of structurally related tetragonal compounds which involve several heavy-fermion superconductors based on Ce or Pu. The occurrence of unconventional superconductivity in these compounds is closely connected to magnetic spin fluctuations, and both, the magnetism and superconductivity are believed to arise from the 4f electrons. The studies of isostructural magnetic counterparts are thus essential to investigate the evolution of the f-electron properties in these materials. We focus on Nd₂RhIn₈ which orders antiferromagnetically below $T_N = 10.7$ K. The Nd magnetic moments are oriented along the tetragonal c axis and the antiferromagnetic order is characterized by the propagation vector $(1/2 \ 1/2 \ 1/2)$. The magnetic phase diagram consists of this ground-state antiferromagnetic phase (AF1) and an additional magnetic phase (AF2) which is formed when applying magnetic field along the c axis prior to transition to the ferromagnetic state.

In this work, we present the pressure effect on the magnetic phase diagram of Nd₂RhIn₈. The magnetization under uniaxial pressure up to 5.3 kbar applied along the tetragonal c axis and the heat capacity under hydrostatic pressure were measured in magnetic fields up to 7 and 14 T, respectively. Both types of measurements reveal an increase of T_N with increasing pressure, the effect is considerably stronger for the uniaxial pressure. We conclude that T_N increases with decreasing c/a. The phase boundary between the ground-state AF1 phase and the AF2 phase shifts to higher magnetic fields with increasing pressure. The ground state phase is thus stabilized by applying pressure. The magnetic phase diagrams in hydrostatic pressures up to 30 kbar are constructed.

TH.C-P52 - Strong anisotropy and multiple phase transitions in the noncollinear incommensurate antiferromagnets EuRhGe_3 and EuIrGe_3 O. Bednarchuk¹, D. Kaczorowski¹*1. Institute of Low Temperature and Structure Research, Polish Academy of Sciences, Wroclaw, Poland*

EuRhGe_3 and EuIrGe_3 are representatives of the EuTGe_3 ($T = \text{Co, Ni, Rh, Pd, Ir, Pt}$) family that has recently been reported to exhibit nontrivial physical properties in the ordered state with a wide variety of antiferromagnetic (AFM) structures [1-3]. In this contribution, we present the low temperature physical behaviors of two representatives, namely EuRhGe_3 and EuIrGe_3 , which seem to have the most complicated antiferromagnetic arrangements within the series. Single crystals of both phases were grown using In-flux growth technique and studied along the main crystallographic directions by means of electrical transport, heat capacity, thermal expansion, magnetization and magnetic susceptibility measurements. EuRhGe_3 and EuIrGe_3 were established to order below $T_N = 11.3$ and 12.3 K, respectively, to a noncollinear AFM structure, incommensurate with the crystal lattice. Some specific features in the temperature variations of the magnetic susceptibility and the specific heat hint at the presence of amplitude modulations of the europium magnetic moments. The AFM order in the Ir-bearing compound was found to undergo an additional spin-reorientation transition at 7.5 K. The magnetic structure of EuRhGe_3 is probably of planar AFM type with an “out of ab -plane” harmonic component in the propagation wave vector. EuIrGe_3 likely orders with more complicated AFM structures which consist of several magnetic domains oriented in a canted noncollinear manner. The application of magnetic field brings about the appearance of a few other magnetic phases along both directions in EuIrGe_3 , and along the easy ab -plane in EuRhGe_3 . The two materials exhibit metallic conductivity and huge magnetoresistance effect in the AFM states.

[1] N. Kumar, P. Kumar Das, R. Kulkarni, A. Thamizhavel, S.K. Dhar, and P. Bonville, J. Phys.: Condens. Matter 24 (2012) 036005

[2] A. Maurya, P. Bonville, A. Thamizhavel, and S.K. Dhar, J. Phys.: Condens. Matter 26, 216001 (2014)

[3] O. Bednarchuk, A. Gagor, D. Kaczorowski, J. Alloys Compd. 622, 432 (2014)

TH.C-P53 - Field-induced magnetic phase transitions in Ho₇Rh₃ single crystal

T. Tsutaoka¹, K. Obata¹, A. Sherstobitov^{2,3}, E. Gerasimov³, P. Terentev³, A. Gubkin^{2,3}, N. Baranov^{2,3}

1. *Hiroshima University, Hiroshima, Japan*

The rare earth compound Ho₇Rh₃ crystallizes in the Th₇Fe₃ type hexagonal structure with the space group P6₃mc in which Ho occupies three non-equivalent sites. Ho₇Rh₃ enters an antiferromagnetic (AF) state with decreasing temperature below T_N = 34 K and shows further magnetic transformation to another magnetic state below 22 K [1, 2]. Unusual negative temperature coefficient of the electrical resistivity E in a wide temperature range above T_N was observed in Ho₇Rh₃ as well as in other R₇Rh₃ compounds such as Gd₇Rh₃ or Tb₇Rh₃.

In this study, we have performed the high-field magnetization (up to 350 kOe) and magnetoresistance (up to 120 kOe) measurements on Ho₇Rh₃ single crystals grown by the Czochralski method using a tri-arc furnace. At 4.2 K, two field-induced phase transitions were observed up to 100 kOe from the initial AF to the forced ferromagnetic (FF) state; however, the magnetization does not reach saturation even at magnetic fields up to 350 kOe. The metamagnetic transitions along the a-axis are accompanied by the large magnetoresistance effect (~40 %) in the field interval 50 -100 kOe. Meanwhile, along the c-axis, the magnetization gradually increases without saturation with increasing field up to 350 kOe. From analysis of the neutron diffraction data, the magnetic structure of Ho₇Rh₃ can be described by two propagation vectors with magnetic moments lying parallel to the c-plane. A large suppression of the electrical resistivity by the external magnetic field was observed in the paramagnetic region up to more than 100 K indicating the large magnetic contribution to total resistivity.

This work was supported by the program of the Ural Branch of RAS (Project No 15-17-2-22).

[1] T. Tsutaoka et al., J. Phys. Soc. Jpn., 70 (2001) 199

[2] T. Tsutaoka et al., Physica B, 327 (2003) 352

TH.C-P54 - High-field quantum phase transitions induced by weak three dimensionality in triangular-lattice antiferromagnets

D. Yamamoto¹, G. Marmorini², I. Danshita³

1. *Waseda Institute For Advanced Study, Japan*

2. *RIKEN, Japan*

3. *Yukawa Institute for Theoretical Physics, Japan*

We study the magnetization process of layered triangular-lattice antiferromagnets (TLAFs) by means of a numerical cluster mean-field method with a scaling scheme, motivated by the recent experiments on the spin-1/2 compound $\text{Ba}_3\text{CoSb}_2\text{O}_9$. It has been known that in TLAFs, magnetic field H and quantum or thermal fluctuations stabilize a collinear configuration with two-up and one-down spins on the three sublattices, which forms a one-third magnetization plateau in the magnetization curve. We find that taking into consideration antiferromagnetic interlayer couplings gives rise to several types of extra phase transitions among different coplanar spin configurations. In particular, a first-order transition found at ~ 0.7 of the saturation field H_s for very small interlayer coupling (less than 10 percent of intralayer coupling) explains the magnetization anomaly observed in the magnetization process of $\text{Ba}_3\text{CoSb}_2\text{O}_9$. This extra quantum phase transition at $H \sim 0.7 H_s$ is expected to occur with even infinitesimally small interlayer coupling and thus can be regarded as another common quantum effect in ideal TLAF compounds, given the unavoidable three dimensionality, in addition to the well-established one-third plateau.

TH.C-P55 - Magnetic properties of quasicrystalline (i-phase) $\text{Ti}_{45}\text{Zr}_{38}\text{Ni}_{17}$ alloy

D. Rusinek¹, J. Przewoznik¹, L. Gondek¹, A. Takasaki², A. Hoser³

1. AGH University of Science and Technology, Faculty of Physics and Applied Computer Science, Krakow, Poland

2. Department of Engineering Science and Mechanics, Shibaura Institute of Technology, Toyosu, Kotoku, Tokyo, Japan

3. Helmholtz-Zentrum Berlin, Berlin, Germany

Titanium-based amorphous and quasicrystalline alloys have very interesting properties like high strength, high corrosion resistance or hydrogen absorption properties. On the other hand, the magnetic properties of quasicrystalline alloys in Ti-Zr-Ni system were not extensively investigated. The issue of possible magnetic ordering in 3D quasicrystals is one of the very important problems in current magnetism.

Our work is focused on icosahedral $\text{Ti}_{45}\text{Zr}_{38}\text{Ni}_{17}$ alloy. This material was produced at ambient temperature by mechanical alloying using high energy planetary ball mill. The obtained amorphous alloy was heated in order to obtain the icosahedral phase. Crystal structure was examined by in-situ X-ray and neutron diffraction in ambient and non-ambient temperatures. Magnetic susceptibility was by VSM method in temperature range from 2 up to 700 K. Magnetic susceptibility shows behavior typical of Pauli-paramagnet with magnetic susceptibility hardly changing with temperature. Some anomalous behavior at low temperature as well at high temperatures were attributed to a very small amount of ferromagnetic Ni, which remain after mechanical alloying. The above finding was supported by neutron diffraction, that was made at low temperature and under external magnetic field up to 5 T. No signs of magnetic ordering at temperature of 1.7 K were noticed, hinting at absence of localized, ordered magnetic moments. The latter is in concert with isothermal magnetization curve at 2 K, where extremely small value of magnetic moment, less than $0.02 \mu_B$ per Ni atom at magnetic field of 9 T, was evidenced.

Concluding, the quasicrystalline $\text{Ti}_{45}\text{Zr}_{38}\text{Ni}_{17}$ alloy shows no long-range order down to 1.7 K, as expected for materials, in which periodicity is absent.

TH.C-P56 - Dipolar-coupled heisenberg spins system LiGdF₄

M. Jeong¹, I. Kovacevic¹, P. Babkevich¹, A. Di Lieto², H. Ronnow¹

1. *Laboratory for Quantum Magnetism, ICMP, Ecole Polytechnique, EPFL, Lausanne, Switzerland*

2. *Dipartimento di Fisica, Università di Pisa, Pisa, Italy*

The LiRF₄ family is rare systems of purely dipolar-coupled magnets. In particular, LiGdF₄ does not possess orbital angular momentum so that the crystal field interaction vanishes. This situation is completely different from other family members such as LiHoF₄ and LiErF₄ where the crystal field determines the spin symmetry and interaction sign at low temperatures: Ising ferromagnetic and XY antiferromagnetic, respectively. The competition between ferromagnetic and antiferromagnetic characters of dipolar interactions in LiGdF₄ may lead new and unconventional low-temperature phases. We investigate this unique dipolar-coupled Heisenberg system with ac susceptibility and muSR measurements. A rich set of phases both as a function of temperature below 0.2 K and a field below 1 T is evidenced by the ac susceptibility. Local probe muSR measurements further show that these low temperature phases are magnetically long-range ordered. This complex phase diagram makes strong contrast to the simple ones of LiHoF₄ [1] and LiErF₄ [2].

[1] H. M. Ronnow et al., Science 308, 389 (2005)

[2] C. Kraemer et al., Science 336, 1416 (2012)

TH.C-P57 - Ferromagnetic resonance of magnetic sublattices in Sc-substituted barium hexaferrite

R. Díaz-Pardo ¹, S. Bierlich ², G. Vazquez-Victorio ¹, J. Töpfer ², R. Valenzuela ¹

1. *National University of Mexico, Mexico*

2. *Ernst-Abbe-Hochschule Jena, Jena, Germany*

Sc-substituted hexaferrites have recently raised interest because scandium substitution allows an effective tailoring of anisotropy for many applications. On the other hand, many basic studies [1,2] have revealed that the substitution of Fe³⁺ by diamagnetic Sc³⁺ leads to unusual interactions among the magnetic sublattices in the ferrite. In this work, ferrites with the formula BaSc_xFe_{12-x}O₁₉ (x between 0 and 2.0) were prepared by reaction in the solid state at 1300°C for 6 hours. X-ray diffraction patterns confirmed the presence of a single hexagonal phase. Ferromagnetic resonance (FMR) investigation of x = 2 samples at 9.4 GHz in the 100 K - 500 K temperature range exhibited a single, broad resonance at low T (103 K); a progressive splitting into two resonance lines was observed in the 190-430 K, to finally coalesce into a single, narrow resonance line at 473 K, characteristic of a paramagnetic phase (Curie transition is ~ 460 K, as determined by magnetization measurements). These results are interpreted in terms of a substitution of Fe³⁺ by Sc³⁺ in the f sublattices; the presence of a diamagnetic cation produces a splitting of the k sublattice (with which the f sublattices sustain a strong, superexchange interaction) into two distinct sublattices, with different canting angles, and different dependence on temperature. This behavior is shown for all the compositions, exhibiting different temperature ranges and degrees of amplitude, but it is more evident for x = 2. FMR confirms therefore that it is an extremely sensitive investigation tool for complex magnetic materials.

[1] G. Albanese et al. J. Mat. Sci. 35, 4415 (2000)

[2] A. Yang et al. J. Appl. Phys. 103, 07E511 (2008)

TH.C-P58 - Extremely wide 1/3-magnetization plateau extended to megagauss magnetic fields in a distorted kagome volborthite $\text{Cu}_3\text{V}_2\text{O}_7(\text{OH})_2 \cdot 2\text{H}_2\text{O}$

T. Yamashita¹, A. Miyata¹, D. Nakamura¹, H. Ishikawa¹, Y. Okamoto², Z. Hiroi¹, S. Takeyama¹

1. *Institute For Solid State Physics, UTokyo, Japan*

2. *Graduate School of Engineering, Nagoya University, Japan*

Volborthite [$\text{Cu}_3\text{V}_2\text{O}_7(\text{OH})_2 \cdot 2\text{H}_2\text{O}$] is known as a distorted spin 1/2 kagome frustrated antiferro-magnet. Unique magnetic phase transition called orbital switching is reported for the first time in single crystals of this material [1]. High magnetic field magnetization curve of single crystal volborthite has been already reported in magnetic fields of up to 75 T. A wide 1/3-plateau was observed, starting from 30 T and it still continues up to 75 T, which is close to a limit of maximum magnetic field available by the conventional non-destructive pulse magnet. Magnetic interactions of volborthite in low-temperatures has not been clarified yet. The most promising candidate was the J1-J2-Jic model [2] based on density functional theory, which assumes two kinds of nearest-neighbor interaction, ferromagnetic J1 and antiferromagnetic inter-chain Jic and with the next-nearest-neighbor J2. The model described well the magnetization curve up to 75 T with the values of interactions J calculated based on the polycrystal structure, and depicted an end of 1/3-plateau occurred around 115 T. Thus, experimental observation above 100 T has been awaited for the verification of the model. Low-temperature magnetization measurements were conducted in ultra-high pulse magnetic fields of up to 164 T below 20 K. Megagauss magnetic field is generated by the single-turn coil method. Magnetization was obtained both by the magnetic induction method and Faraday rotation technique in megagauss magnetic fields with its pulse width of 6 fEs. It was revealed that 1/3-plateau still remained in fields up to 164 T with the giant 1/3 plateau width more than 134 T. This fact shows inadequacy of the J1-J2-Jic model mentioned above, and requests more elaboration of a theoretical model.

[1] H. Yoshida, et al., *Nature Commun.* 3, 860 (2012)

[2] O. Janson et al., *Phys. Rev. B* 82, 104434 (2010)

TH.C-P59 - First principles study on solid oxygen using van der waals density functional

M. Obata¹, I. Hamada², T. Oda^{1,3}

1. Graduate School of Natural Science And Technology, Kanazawa University, Kanazawa, Japan

2. International Center for Materials Nanoarchitectonics (WPI-MANA), National Institute for Materials Science (NIMS), Tsukuba, Japan

3. Institute of Science and Engineering, Kanazawa University, Kanazawa, Japan

Oxygen, which is one of abundant elements, has several unique characteristics. It is well known that the oxygen molecule has a spin-triplet ground state. Competition between magnetic and molecular interactions gave rich varieties of structural, electronic, and magnetic phases under the wide ranges of temperature and pressure [1,2]. The magnetism of solid oxygen is particularly interesting, as the magnetic configuration is sensitive to the relative distance between molecules owing to a short-range feature of the magnetic interaction. In order to analyze such system, the method which can describe accurately both molecular and magnetic interactions has been required. The van der Waals density functional (vdW-DF) method, which is one of promising methods to overcome the problem, has been proposed by Dion et al [3]. The extension of vdW-DF to spin-polarized (magnetic) systems, vdW-DF-GC (GC means spin-polarization-dependent gradient correction), has practically been proposed [4,5]. We used this method to investigate oxygen systems (alpha and delta phases, and molecular systems), and obtained accurate optimized structural parameters in the structures, compared with those obtained using local density and generalized gradient approximations. We found that the structural properties were determined by a delicate balance of magnetic and vdW interactions. Such balance was important not only for the molecular pairs of antiferro- or ferro-magnetic coupling within the a-b plane, but also for the out-of-plane pairs which have a much weak magnetic interaction. In the presentation, we explain the method of vdW-DF-GC and discuss the results of crystal structure and magnetic energy, compared with experimental results.

[1] I. N. Goncharenko, Phys. Rev. Lett. 94, 205701 (2005)

[2] S. Klotz et al., Phys. Rev. Lett. 104, 115501 (2010)

[3] M. Dion et al., Phys. Rev. Lett. 92, 246401 (2004)

[4] M. Obata et al., J. Phys. Soc. Jpn. 82, 093701 (2013); 84, 024715 (2015)

[5] M. Obata et al., JPS Conf. Proc., 2015, in press

TH.C-P60 - Magnetic properties of two-dimensional heisenberg antiferromagnet alpha-RbCrF₄

Y. Miura¹, H. Manaka²

1. *Suzuka National College of Technology, Japan*

2. *Kagoshima University, Japan*

Triangular spin tubes alpha-KCrF₄ and CsCrF₄, which consist of one-dimensional Heisenberg antiferromagnets along the tubes coexisting with geometrically frustrated spin systems in the triangular plane, have been studied extensively[1]. In this study, we further synthesized the series of chromium fluoride alpha-RbCrF₄[2] using return to synthetic precursor method. From X-ray powder diffraction measurements at room temperature, TIAIF₄-type crystal structure[3], i.e., the CrF₆ octahedra form a square lattice, was found. Because each plane is separated by Rb ions, two-dimensionality is expected to be good. As a result, alpha-RbCrF₄ forms an ideal two-dimensional Heisenberg antiferromagnet with $S = 3/2$. From magnetic susceptibility measurements above 2 K, antiferromagnetic long-range order appears at 29.3(1) K and the Curie-Weiss temperature is -67(3) K. Below 15 K, using return to synthetic precursor method, we found the intrinsic magnetic ground state.

[1] H. Manaka et al., J. Phys. Soc. Jpn. 78, 093701 (2009), *ibid.* 80, 084714 (2011)

[2] De Kozak, Rev. Chim. Miner, L8, 301 (1971)

[3] D. Babel, Structure and Bonding Vol.3 (Springer Berlin Heidelberg) (1967)

TH.C-P61 - Magnetic resonance in the chiral helimagnet CrNb₃S₆

D. Yoshizawa¹, J. Kishine², Y. Kousaka^{3,4}, Y. Togawa⁵, M. Mito⁶, J. Akimitsu⁷, K. Inoue^{3,4}, M. Hagiwara¹

1. *Center for Advanced High Magnetic Field Science, Graduate School of Science, Osaka University, Japan*
2. *Division of Natural and Environmental Science, The Open University of Japan, Japan*
3. *Graduate School of Science, Hiroshima University, Japan*
4. *Center for Chiral Science, Hiroshima University, Japan*
5. *Department of Physics and Electronics, Osaka Prefecture University, Japan*
6. *Faculty of Engineering, Kyusyu Institute of Technology, Japan*
7. *Department of Physics and Mathematics, Aoyama-Gakuin University, Japan*

Chirality plays an important role in the symmetrical properties of nature. In a magnetic substance with a chiral space group, a helimagnetic structure is created by the nearest neighbor (NN) exchange interaction and the Dzyaloshinsky-Moriya (DM) interaction. In particular, the DM interaction is important, because it gives chirality to the magnet. CrNb₃S₆ is one of the chiral magnetic substances. On applying the magnetic field perpendicular to the helical axis of CrNb₃S₆, the spiral structure winds down periodically, and the magnetic structure with alternate ferromagnetic and spiral domains, the so-called chiral soliton lattice (CSL), emerges [1]. This CSL state is the most characteristic feature of CrNb₃S₆. In the present study, we performed electron spin resonance (ESR) measurements in magnetic fields parallel to the helical axis to evaluate the NN exchange constant (J) and the DM constant (D) in CrNb₃S₆. We observed some ESR signals below 30 GHz. A nice fitting curve of the ESR mode is obtained by using the equation derived by J. Kishine et al. [2]. From the result, we evaluate the above constants as J/kB=-14.1 K (ferromagnetic) and D/kB=2.24 K. In addition, we observed a linear ESR mode above the saturation field (H_s) with zero energy gap at H_s in CrNb₃S₆, while such a mode appears with a finite energy gap at H_s in another chiral magnet MnSi [3].

[1] Y. Togawa, T. Koyama, K. Takayanagi, S. Mori, K. Kousaka, J. Akimitsu, S. Nishihara, K. Inoue, A. S. Ovchinnikov and J. Kishine, Phys. Rev. Lett. 108, 107202 (2012)

[2] J. Kishine and A. S. Ovchinnikov, Phys. Rev. B 79, 220405(R) (2009)

[3] M. Date, K. Okuda and K. Kadowaki, J. Phys. Soc. Jpn 42, 1555 (1977)

TH.C-P63 - I-II-III phase transitions in CeB₆ observed by high-resolution x-ray diffractionT. Inami¹, S. Michimur², T. Matsumura³, M. Sera³, Y. Haga⁴, Z. Fisk^{4,5}1. *Condensed Matter Science Division, Japan Atomic Energy Agency, Japan*2. *Research and Development Bureau, Saitama University, Japan*3. *AdSM, Hiroshima University, Japan*4. *Advanced Science Research Center, Japan Atomic Energy Agency, Japan*5. *University of California, United States*

The cubic CeB₆ is a typical compound in which orbital degrees of freedom play an important role. The G₈ ground state of the Ce 4f₁ state possesses dipole, quadrupole and octupole degrees of freedom. A phase transition from the paramagnetic phase (phase I) to the Oxy-type antiferroquadrupolar ordered phase (phase II) takes place at T_Q = 3.3K, which is followed by another phase transition to the antiferromagnetic phase (phase III) at T_N = 2.4K. Accordingly, it is expected that the crystal lattice deforms from cubic to tetragonal below T_Q. Actually, dilatometric measurements observed tetragonal deformation more than 3X10⁻⁵ below T_N, whereas the tetragonal deformation in phase II was found to be very small.[1] X-ray diffraction (XRD) is a powerful technique that measures the planar spacing d_{hkl} of the (hkl) plane in a crystal. XRD is particularly advantageous for this type of experiments, because macroscopic measurements observe a value averaged over (tetragonal) domains, while XRD discriminates domains with different planar spacings. A disadvantage of XRD is, however, its rather poor resolution Dd/d (about 10⁻⁵). High-resolution x-ray diffraction (HRXRD) is a sophisticated method that improves Dd/d. By combining a backscattering geometry and a high-resolution monochromator (HRM), one can achieve Dd/d=10⁻⁸. We hence recently utilize HRXRD for detecting tiny lattice deformation.[2] A HRXRD experiment was carried out at BL22XU in SPring-8. The sample was a CeB₆ single crystal grown by a flux method. We observed the (700) reflection. 2theta=179.53 degrees, the photon energy was about 10.5 keV, and HRM was two Si (660) channel-cut crystals. The obtained Dd/d was 4X10⁻⁶ (FWHM). A large tetragonal deformation 7X10⁻⁵ was observed at 1.7 K in phase III, while the tetragonal deformation in phase II was below the detection limit.

[1] M. Sera et al., JPSJ 57, 1412 (1988)

[2] T. Inami et al., PRB 90, 041108(R) (2014)

TH.C-P65 - Paramagnetic-diamagnetic transition in $\text{Cd}_{0.9985}\text{Dy}_{0.0010}\square_{0.0005}\text{MoO}_4$ T. Groń¹, E. Tomaszewicz², M. Piątkowska², B. Sawicki¹, M. Oboz¹, P. Urbanowicz¹1. *Institute of Physics, University of Silesia, Katowice, Poland*2. *Department of Inorganic and Analytical Chemistry, West Pomeranian University of Technology, Szczecin, Poland*

Divalent metal molybdates and tungstates with the scheelite type structure constitute a large and important class of materials. The compounds doped with rare earth ions are used as solid state lasers, scintillators and components of optoelectronic devices [1]. Our previous studies have shown the existence of new scheelite type solid solutions described as $\text{Cd}_{1-3x}\text{RE}_{2x}\square_x\text{MoO}_4$ for RE = Pr, Nd, Sm-Dy, and $0 < x \leq 0.25$, where \square are cationic vacancies [2].

The main purpose of this study was to investigate the magnetic properties of strongly diluted magnetic molybdate containing 0.001 dysprosium ions. The temperature dependence of magnetic susceptibility recorded both in zero-field-cooled (ZFC) and field-cooled (FC) mode as well as the magnetization isotherm show paramagnetic behaviour with the Curie-Weiss temperature $\theta = -6$ K, the effective magnetic moment $\mu_{\text{eff}} = 0.394 \mu_{\text{B}}/\text{f.u.}$, and the Landé factor $g = 0.049$ estimated from the Curie constant $C = 0.0194 \text{ emu}\cdot\text{K}/\text{mol}$.

The most spectacular observation here is finding of the transition from paramagnetic to diamagnetic state at the temperature $T_{\text{pd}} = 137$ K and in the magnetic field of 70 kOe. This means that at T_{pd} paramagnetic and diamagnetic components compensated.

This work was supported by Ministry of Scientific Research and Information Technology (Poland) and funded from science resources: No. 1S-0300-500-1-05-06 and No. DS-518-10-020-3101.

[1] M. Daturi, G. Busca, M.M. Borel, A. Leclaire, P. Piaggio, *J. Phys. Chem. B* 101 (1997) 4358

[2] E. Tomaszewicz, S.M. Kaczmarek, H. Fuks, *Mat. Chem. Phys.* 122 (2010) 595

TH.C-P66 - Phase transition of mobile potts model for liquid crystals

H. T. Diep¹, A. Bailly-Reyre¹

1. LPTM, UMR 8089 University of Cergy-Pontoise, CNRS, France

In this paper, we are interested in the phase transition of a mobile Potts model on a lattice with a concentration c : a Potts particle with q states interacting with its neighbors can move from a lattice site to another under the effect of temperature T . This model is interesting for several reasons among which it can describe the melting of a molecular crystal. The model of moving Potts model introduced in this paper is the first in the random category. We consider a simple cubic lattice. The lattice sites are partially filled with q -state Potts spins and each spin can move from a site to an empty nearest site. In this paper, the main results are shown for $q=6$: the Potts spin at a lattice site can take one of the 6 directions. The model is ferromagnetic $J(i,j)=J>0$ in this paper. The present model can be called the mobile Potts model to distinguish from the localized Potts model. The mobile Potts model allows to study the order-disorder phase transition associated with the Potts variable while a continuous evaporation of spins at the surface of the system takes place with increasing temperature.

We have performed the simulation by using a Monte-Carlo (MC) Metropolis algorithm. We find a first-order phase transition for high concentration, and second-order phase transition for low concentration down to a certain limit below which there is no more phase transition at a finite temperature. Results for other q at different concentrations will be shown. The mechanism leading to a transition or no transition will be presented.

TH.C-P68 - Spin frustration in the spin-1/2 Ising-Heisenberg model on triangulated Husimi lattices: exact results

C. Ekiz¹, J. Strečka

1. Department of Physics, Faculty of Science, Adnan Menderes University, Aydın, Turkey
2. Institute of Physics, Faculty of Science, P. J. Šafárik University, Košice, Slovakia

The spin-1/2 Ising-Heisenberg model on triangulated Husimi lattices is rigorously solved by combining the generalized star-triangle transformation with the method of exact recursion relations. The model defines a hybrid classical-quantum system consisting of the Ising and Heisenberg spins on recursively built lattices, which interact among themselves either through the Ising or XXZ Heisenberg nearest-neighbour interaction. Exact results for critical frontiers, total and sublattice magnetizations are obtained from a precise mapping relationship with the corresponding spin-1/2 Ising model on a pure Husimi lattice.

The effect of interaction parameters on magnetic properties of the considered model is investigated in particular. The finite-temperature phase diagram in the form of critical temperature versus the interaction ratio dependence was calculated for several values of the coordination number of the underlying Husimi lattice and the exchange anisotropy. It is demonstrated that the phase boundary between the spontaneously ordered and disordered phases essentially depend on the coordination number of the triangulated Husimi lattice. In the limiting Ising case, the critical temperature shows a monotonous decline with increasing a relative strength of the antiferromagnetic Heisenberg interaction. On the contrary, the more general Ising-Heisenberg model exhibits in a highly frustrated region a peculiar spontaneous order for the triangulated Husimi lattices with high enough coordination numbers $q > 3$ as well as reentrant phase transitions for particular value of the coordination number $q = 3$.

TH.C-P70 - Magnetism of alpha-Sr₂MO₄ (M = V, Cr) with K₂NiF₄-type structuresH. Sakurai¹*1. National Institute For Materials Science, Tsukuba, Japan*

alpha-Sr₂VO₄ is expected to have nontrivial spin- and orbital-orderings, or magnetic octapole ordering because the VO₆ octahedra are tetragonally distorted with the apical oxygen ions pulled out; the distortion leaves the d_{yz} and d_{xz} orbitals degenerated at the lowest energy level. The compound exhibits successive phase transitions at 101 K and 127 K. Magnetic susceptibility shows a small kink at 127 K and drops at 100 K without magnetic ordering. Below 101 K, a sizable Curie-Weiss term remains, and the Curie constant there is ~1/3 as large as that at the high temperatures. A magnetic ordering appears below 11 K, where only ~13% of theoretical magnetic entropy is released despite no clear sign of short-range ordering in magnetic susceptibility. On the other hand, alpha-Sr₂CrO₄ has the same distortion of the CrO₆ octahedra with 3d² electronic configuration for the Cr ions. Recent electronic band structure calculation has revealed that the d_{xy} orbital is energetically lower than the doubly degenerated d_{yz} and d_{xz} orbitals. Thus, also in the Cr compound, orbital degree of freedom remains, although the d_{xy} orbital is occupied by an electron in this case. Magnetic susceptibility and specific heat show successive phase transitions at 112 K and 140 K, which are close to the transition temperatures of the V compound. This suggests that the orbital degeneracy plays an important role in either or both of these transitions. Indeed, at the 140 K transition just a small kink appears in the susceptibility as in the case of the V compound. However, magnetic ordering occurs at 112 K, differently from the 101 K transition of the V compound. The electrons in the d_{xy} orbital may cause the difference in the magnetism between these two compounds. The magnetic susceptibility and specific heat, as well as structural data, will be presented.

TH.C-P71 - Pressure effect on transport properties of $\text{EuNi}(\text{Si}_{1-x}\text{Ge}_x)_3$ compounds

K. Uchima¹, Y. Takaesu¹, H. Akamine², M. Kakihana², K. Tomori², A. Teruya², M. Hedo³, T. Nakama³, K. Yagasaki³, K. Matsubayashi⁴, I. Uwatoko⁴

1. Okinawa Christian Junior College, Japan

2. Graduate School of Science and Engineering, University of the Ryukyus, Japan

3. Faculty of Science, University of the Ryukyus, Japan

4. Institute for Solid State Physics, University of Tokyo, Japan

The compounds of $\text{EuNi}(\text{Si}_{1-x}\text{Ge}_x)_3$ order antiferromagnetically. The Neel temperature T_N decreases monotonously with increasing the Ge concentration x . At the temperature T_C below T_N , EuNiSi_3 ($x=0$) shows an additional magnetic transition into ferromagnetic state. T_C decreases rapidly with increasing x and vanishes at the critical concentration $x \approx 0.3$. For the compound $\text{EuNi}(\text{Si}_{0.8}\text{Ge}_{0.2})_3$ which is a compound near to the boundary between the ferromagnetic and antiferromagnetic ground states in the phase diagram for $\text{EuNi}(\text{Si}_{1-x}\text{Ge}_x)_3$ system, the measurements of the electrical resistivity ρ and thermopower S have been carried out in the temperature range from 2 to 300 K under pressures up to $P=1.8$ GPa. The anomalies in $\rho(T)$ and $S(T)$ curves are observed at $T_C = 16$ K and $T_N = 34$ K. Both of T_C and T_N increase linearly with increasing pressure. The temperature variations of ρ and S of $\text{EuNi}(\text{Si}_{0.8}\text{Ge}_{0.2})_3$ at $P=1.8$ GPa are almost the same as those of $\text{EuNi}(\text{Si}_{0.9}\text{Ge}_{0.1})_3$ ($x=0.1$) at ambient pressure. The effect of pressure on T_N and T_C is opposite to that of substitution of Si by Ge, i.e., the application of pressure stabilize the ferromagnetic phase. These results indicate that the change of T_N and T_C can be attributed to the change of atomic volume induced by application of high pressure or atomic substitution.

TH.C-P74 - Application of the oguchi method for studies of the hubbard model

T. Balcerzak¹, K. Szalowski¹, M. Jascur²

1. Department of Solid State Physics, Faculty of Physics and Applied Informatics, University of Lodz, Lodz, Poland

2. Department of Theoretical Physics and Astrophysics, Faculty of Science, P. J. Safarik University, Kosice, Slovak Republic

Oguchi method in pair approximation has been extended for the investigations of the Hubbard model. The system based on a simple cubic lattice, with half-filling of the band, has been studied. In the frame of the method the grand potential has been derived, from which all thermodynamic properties can be obtained. In particular, for a prototype model of the local electric field, the ground-state and temperature phase diagram have been studied in the whole range of the Hubbard parameter U . The existence of antiferromagnetic phase has been confirmed with the critical temperature maximum value and its location vs. U being in qualitative accordance with Quantum Monte Carlo (QMC) simulations. Moreover, the quantum critical point (QCP) has been found at $T=0$, separating the antiferromagnetic and paramagnetic phases, and its position has been discussed in the context of existing literature. It can be noted that within our method the accuracy of the Néel temperature calculation improves as U increases. The extensive numerical calculations of the magnetic properties, including spin-spin and charge-charge correlation functions, have been performed and the results are illustrated in figures. It can be concluded, that the extended Oguchi method, going beyond the usual molecular field approximation, can be a potentially useful tool for the studies of magnetic properties of the Hubbard model.

TH.C-P75 - Magnetic phase diagram determination of Ce pnictides by resonant X-ray magnetic scattering

L. Paolasini¹, J. Herrero-Martin², H. Walker³, M. Kohgi⁴, K. Kuwahara⁴, K Iwasa⁵, G. Lapertot⁶

1. ESRF - The European Synchrotron, Grenoble, France

2. ALBA synchrotron light source, BP 1413, Barcelona, Spain

3. ISIS Neutron Facility, Rutherford Appleton Laboratory, Didcot, United Kingdom

4. Tokyo Metropolitan University, Tokyo, Japan

5. University of Tohoku, Sendai, Japan

6. CEA Grenoble, France

High magnetic field Resonant X-ray scattering experiments were performed to investigate the magnetic phase diagram of CeP and CeSb up to 10 Tesla. Using the Ce L₃ edge resonance, the magnetic interlayer ordering of the Ce can be studied in a great detail, and the results compared to previous neutron [1-2] and x-ray scattering results [3-4]. The energy dependence of resonances are compared in the antiferromagnetic phase at zero field with the huge enhancement found in the field-induced phases, suggesting a strong (f-p) hybridization associated to the main contribution of the Γ_8 ground state. The ferro-paramagnetic phase displays a systematic and continuous reduction of the interlayer paramagnetic modulation as a function of the applied magnetic field, showing similarities with the results of neutrons magnetic scattering experiment under applied pressure and explains the multi-step modulation of magnetic phase diagram determined by resistivity at higher temperatures.

References:

1. Rossat-Mignot, J. et al., *J. Magn. Magn. Mater.* 52, 111 (1985)
2. Kohgi, M. et al., *Physica B* 281-282, 417 (2000)
3. Hannan, A. et al., *J. of Phys. Soc. Japan* 74, 2301 (2005)
4. McMorro, D.F. et al., *J. Phys. Condens. Matter* 9, 1133 (1997)

TH.C-P76 - Extreme sensitivity of magneto-structural transitions in Ni₂MnGa-based heusler alloys to pulsed high magnetic field

J. Kastil¹, J. Kamarad¹, Z. Arnold¹, Y. Skourski², F. Albertini³

1. Institute of Physics ASCR, Prague, Czech Republic

2. Hochfeld-Magnetlabor Dresden (HLD), HZDR, Dresden, Germany

3. IMEM CNR, Parma, Italy

The study of Ni₂MnGa-based Heusler alloys is getting a significant attention due to a large variety of their interesting and usable physical properties. Their large magneto-striction that can be induced by relatively small magnetic field is widely used for many years. The diffusion-less magneto-structural transition from martensite (lower symmetry crystal phase M) to austenite (cubic L2₁ crystal structure A) is detected in most of the alloys with increasing temperature. The underlying mechanism of a shear deformation of the cubic cell is still not yet completely understood. The band Jahn-Teller mechanism was suggested to be the driving force of the transition [1].

The effect of pulsed magnetic field up to 60 T on the transition temperatures T_{M-A} , T_{A-M} and magnetization of the several different samples of Co- and In-substituted Ni₂MnGa-based alloys was studied in wide temperature range. The huge field induced non-linear decrease of T_{M-A} of about 200 K and the accompanied increase of magnetization, up to $M_A = 6.3 \mu_B/f.u$ in Ni_{1.72}Co_{0.28}Mn_{1.25}Ga_{0.75} at 2 K, verify an existence of the field induced ferromagnetic state of austenite phase in low temperatures. The observed magnetization of the ground state of both, the martensite and the austenite phases, denotes a different effect of the substitution and the off-stoichiometry on magnetic properties of the phases. The enormous nonlinear shift of transition temperature points to pronounced effect of spin polarization on the Jahn-Teller effect in these samples. The external field of 60 T seems to be high enough to suppress the Jahn-Teller distortion of crystal lattice of some of the studied alloys even at low temperatures.

[1] P J Brown, A Y Bargawi, J Crangle, K-U Neumann, K R A Ziebeck J. Phys.: Condens. Matter 11 (1999) 4715–4722

TH.C-P77 - Magnetic anisotropy in antiferromagnet GdB₆

M. Anisimov¹, V. Glushkov¹, S. Demishev¹, Shitsevalova², A. Levchenko², V. Filippov², A. Bogach¹, V. Krassnorussky¹, S. Gabani³, K. Flachbart³, N. Sluchanko¹

1. A.M. Prokhorov General Physics Institute of RAS, Moscow, Russian Federation
2. Institute for Problems of Materials Science NASU, Kyev, Ukraine
3. Institute of Experimental Physics, Slovak Academy of Science, Slovakia

In our previous reports [1-2] we have shown that unusual antiferromagnet (AF) GdB₆ ($T_{N1} \sim 15.5\text{K}$, $T_{N2} \sim 4.6\text{K}$) is characterized by the magnetic anisotropy in both AF phases. In order to investigate in details the magnetic anisotropy of GdB₆ we decided to perform the comprehensive study of Hall effect and magnetoresistance (MR) in magnetic fields $B < 8\text{T}$ oriented along the main crystallographic directions $B \parallel \langle 100 \rangle$, $\langle 110 \rangle$, $\langle 111 \rangle$ in the temperature range 2-300K. The data obtained allow to detect the several fundamental results. (i) The emergence of the anomalous Hall effect $R^{\{AHE\}}_{-H}$ in AF II phase in magnetic fields 0.7-1.5T. (ii) The appearance of considerable anisotropy of MR at $T < T_{N2}$. The 3D-diagram of the angular distribution of the charge carrier scattering reconstructed from our MR data in AF II state has the form of cross with maximal scattering along the direction $B \parallel \langle 110 \rangle$ and four caverns-satellites (along $B \parallel \langle 111 \rangle$), which disappear above 5T. (iii) The magnetic H-T phase diagram reconstructed from our data for the main crystallographic directions $B \parallel \langle 100 \rangle$, $\langle 110 \rangle$ and $\langle 111 \rangle$ contains the several additional transitions (1) at 0.7-1.7T only for the direction $B \parallel \langle 111 \rangle$ and (2) at 1.7-5T for $B \parallel \langle 111 \rangle$, $\langle 100 \rangle$. The results are discussed in terms of the complex scenario including the spin polarons formation in paramagnetic and AF I phases of GdB₆. It was proposed here that the spin polarons along with additional coherent displacement of Gd³⁺ ions from their centrosymmetric positions inside the boron cages (see [3]) are responsible for the anisotropy detected in both AF I and II states of GdB₆.

- [1] M.Anisimov et al., Sol. St. Phenom. 190, 77 (2012)
[2] M.Anisimov et al., Acta Phys. Pol. A 126, 348 (2014)
[3] M.Amara et al., Phys. Rev. B, 72 064447 (2005)

TH.C-P78 - Spin polarons and magnetic ground state in PrB₆

M.Anisimov¹, V.Glushkov¹, S.Demishev¹, N.Shitsevalova², A.Levchenko², V.Filippov², A.Bogach¹, V. Krassnorussky¹, S.Gabani³, K.Flachbart³, N.Sluchanko¹

1. Prokhorov General Physics Institute, Russian Academy of Sciences, Moscow, Russian Federation
2. Institute for Problems of Materials Science NASU, Kiev, Ukraine
3. Institute of Experimental Physics, Slovak Academy of Science, Košice, Slovakia

In current work we present investigation of magnetic, transport and thermal properties of antiferromagnet PrB₆ ($T_{N1} \sim 6.7\text{K}$, $T_{N2} \sim 4.6\text{K}$). The measurements have been performed on high quality single crystals of Pr^NB₆ with various isotope content (N=11, nat.) of boron, and before and after high temperature annealing. In order to investigate the magnetic anisotropy of PrB₆, specific heat, magnetoresistance (MR) have been measured in external magnetic field oriented along main axis B || <100>, <110>, <111>. Based on our measurements, several fundamental results have been obtained. (i) Above Neel temperature in the range T_{N1} -21K an unusual low temperature maximum of resistivity was observed in combination with spontaneous magnetization $M_{sp} \sim 1.6\text{emu/mol}$ on the initial state (before annealing) of PrB₆ samples. The anomalies detected may be explained in terms of ferromagnetic (FM) fluctuations and itinerant ferromagnetism developed in the presence of $n_{vac} \sim 1\text{-}2\%$ boron vacancies in the PrB₆ matrix. Moreover, it was found that this FM state is totally destroyed by annealing at $T_{an} \sim 1700^\circ\text{C}$. (ii) The performed study of $\Delta\rho/\rho(H)$ allowed us to estimate the magnetic parameters including the local susceptibility $\chi_{loc}(T)$ and the effective magnetic moment μ_{eff} . The calculated effective magnetic moment depends on the orientation of magnetic field and reaches the maximal values $\mu_{eff} = 2.5\mu_B$ for B || <110>, <111> and $\mu_{eff} = 4\mu_B$ for B || <100>, whereas the value of inherent moment of Pr³⁺ ions is expected to be $\mu(\Gamma_5) = 2\mu_B$. The results obtained may be attributed to the formation of magnetic clusters which are constructed from magnetic moments of Pr³⁺ ions and spin polarized domains in the conduction band of PrB₆ (5d-component of magnetism). These spin polarons of small radius $a_{sp} \sim 5\text{\AA}$ appear below 21K and are responsible for the itinerant ferromagnetism in PrB₆. Moreover, the anisotropy of PrB₆ may be explained in terms of coexistence of 4f- (local) and 5d- (itinerant) components of the magnetic structure of this unusual antiferromagnet.

TH.C-P79 - Thermodynamic properties of the S=1 heisenberg square-lattice antiferromagnet Ni(pz)₂Br₂

E. Cizmár¹, K. Ráčová¹, S. A. Zvyagin², A. Feher¹

1. Institute of Physics, Faculty of Science, P.J. Safárik University, Kosice, Slovakia

2. High Magnetic Field Laboratory (HLD-EMFL), Helmholtz-Zentrum Dresden-Rossendorf, Dresden, Germany

We report thermodynamic, magnetic and electron spin resonance (ESR) studies of the compound Ni(pz)₂Br₂ (pz is pyrazine), an S=1 Heisenberg antiferromagnet (AFM) on square lattice. Magnetic susceptibility measured in the temperature range 1.8 - 300 K reveals the presence of a strong single-ion easy-plane anisotropy ($D/k_B = 7.8$ K) and a weak AFM exchange coupling ($J/k_B = -0.9$ K), suggesting that Ni(pz)₂Br₂ is in the gapped quantum paramagnetic phase with (anti)excitons as elementary excitations [1]. The preliminary high-frequency ESR experiments on powdered samples indicate the presence of a small zero-field energy gap (~20 GHz). Such observation may suggest that Ni(pz)₂Br₂ is in the close vicinity to the quantum critical point ($D/J = 5.6$), separating the gapped quantum paramagnetic phase and a gapless planar AFM phase. Specific heat studies of Ni(pz)₂Br₂ reveal the transition into the AFM long range-ordered state at $T_N = 1.55$ K. Above 6 T the system is in the fully spin-polarized magnetically saturated phase. The analysis of magnetic entropy (calculated from specific heat measured in applied magnetic fields) yields the evidence for inverse magnetocaloric effect in fields up to 5 T (accompanied by decrease of the sample temperature during adiabatic magnetization) followed by the rapid decrease of entropy in the spin-polarized state. The enhanced release of the magnetic entropy in magnetic fields close to the saturation field suggests that this material can be potentially used as a magnetic coolant, with the efficiency comparable (or even better) with that of paramagnetic salts at temperatures below 3 K.

This work was supported by projects APVV-0132-11, VEGA 1/0145/13. S.A.Z. appreciates the support of Deutsche Forschungsgemeinschaft.

We thank M. Kajoaková for early contribution to this work - synthesis and structure determination of Ni(pz)₂Br₂.

[1] J. Oitmaa and C. J. Hamer, Phys. Rev. B 77 (2008) 224435

TH.C-P80 - Successive magnetic ordering in quasi-2D T'-La₂CuO₄

G. Pascua¹, M. Günther², P. Bonfa³, R. Hord⁴, Y.G. Pashkevich⁵, A. Suter¹, R. De Renzi³, B. Albert⁴, H. Klaus², L. Alff⁶, H. Luetkens¹

1. *Laboratory for Muon Spin Spectroscopy, Paul Scherrer Institut, Switzerland*
2. *Institut für Festkörperphysik, TU Dresden, Dresden, Germany*
3. *Dipartimento di Fisica and Unit a CNISM di Parma, Università di Parma, Italy*
4. *Eduard-Zintl-Institute of Inorganic and Physical Chemistry, TU Darmstadt, Germany*
5. *A.A. Galkin Donetsk Phystek NASU, Donetsk, Ukraine*
6. *Institute of Materials Science, TU Darmstadt, Darmstadt, Germany*

The insulating rare earth (RE) cuprates RE₂CuO₄ crystallizing in the T'-structure turn superconducting upon electron-doping. The undoped parent compounds are characterized by a very strong antiferromagnetic coupling J between the Cu moments within the CuO₂ planes and a very weak coupling J' between adjacent planes that results from the body-centered tetragonal (BCT) structure which cancels out the isotropic Heisenberg interaction of neighboring planes. Therefore this system can be considered as a very good approximation of the $S=1/2$ two-dimensional (2D) square lattice Heisenberg model which does not possess a magnetic phase transition at finite temperature. The actual process how these quasi-2D systems approach the observed 3D magnetic order has been debated to this day mainly due to the complications caused by the presence of magnetic RE elements. Recently we were able for the first time to synthesize powders of metastable T'-La₂CuO₄ and to investigate it with muon spin rotation (muSR), La-NMR, synchrotron X-ray and neutron scattering. We find that T'-La₂CuO₄ shows a series of magnetic transitions at $T = 220, 115, \text{ and } 40\text{K}$. NMR proves that below 220K the Cu moments are aligned within the CuO₂ plane due to a strong easy-plane anisotropy while muSR senses only quasi-static order with magnetic fluctuations in the MHz regime. Therefore, the system effectively undergoes a crossover from a 2D-Heisenberg to a 2D-XY behavior below $T_{\text{CO}} = 220\text{K}$. Below 115K the combined muSR and NMR data indicate the onset of static order with a symmetry allowed distribution of relative AFM spin orientations within the CuO₂ planes with respect to the neighboring layers. This physical scenario might be realized due to essentially decoupled layers and an XY anisotropy that is so small compared to the thermal energy that it does not impose a preferred spin direction. A speculative interpretation of the data would be to associate the transition at $T_{\text{KT}} = 115\text{K}$ with a Kosterlitz-Thouless transition occurring in the 2D-XY model. Only below $T_{\text{LRO}} = 40\text{K}$, the system locks-in to a special 3D long range ordered non-collinear structure.

TH.C-P81 - Study of the effective magnetic anisotropy in the MnCr_2O_4 cubic spinel

D. Tobia^{1,2,3}, J. Milano^{1,2}, M.T. Causa¹, E. L. Winkler^{1,2}

1. *Laboratorio de Resonancias Magnéticas, Centro Atómico Bariloche - CNEA, 8400 S.C. de Bariloche, Argentina*
2. *Consejo Nacional de Investigaciones Científicas y Técnicas (CONICET), Argentina*
3. *Instituto De Física "Gleb Wataghin", UNICAMP, Campinas (SP), Brazil*

The cubic spinel systems with general formula AB_2O_4 , where A, B or both sites are occupied by transition metal ions, have rich phase diagrams due to the correlations between their magnetic, electrical, and structural properties. In the particular case of the chromium spinel MnCr_2O_4 , the Cr^{3+} ions occupy the octahedral sites in a pyrochlore-like arrangement. As a consequence of this spatial array, this system exhibits magnetic frustration and unusual low temperature magnetic states. At $T_C=42\text{K}$ the MnCr_2O_4 spinel presents long-range ferrimagnetic order; as the temperature decreases below $T_H=18\text{K}$, this magnetic phase coexists with a short-range helical order, where the spin rotation axis does not coincide with the helicoidal propagation vector. In this complex scenario, the ferromagnetic resonance (FMR) spectroscopy emerges as a suitable technique because it provides microscopic information related to the exchange and magnetic anisotropy and allows extending the knowledge of the nature of the long-range ferrimagnetic order and the spiral short-range state.[1] Here we present a study of MnCr_2O_4 polycrystalline magnetic phases through dc magnetization and FMR. We describe the temperature evolution of the system by a phenomenological model that considers the different terms that contribute to the free energy density. Below T_C , the FMR spectra were modeled by a cubic magnetocrystalline anisotropy to the second order, with K_1 and K_2 anisotropy constants that define the easy magnetization axis along the $\langle 110 \rangle$ direction. At lower temperatures, the formation of a helicoidal phase was considered by including a uniaxial anisotropy axis along the $[1-10]$ propagation direction, with a K_u anisotropy constant. The values obtained from the fittings at 5K are $K_1=-2.3 \times 10^4 \text{ erg cm}^{-3}$, $K_2=6.4 \times 10^4 \text{ erg cm}^{-3}$ and $K_u=7.5 \times 10^4 \text{ erg cm}^{-3}$. [2]

[1] E. Winkler et al, Phys. Rev. B 80 (2009) 104418

[2] D. Tobia et al, J. Phys.: Condens. Matter 27 (2015) 016003

TH.C-P82 - Investigation of the relation between hysteresis and ferromagnetism in Mn_3GaC

O. Cakir¹, M. Acet², M. Farle², A. Senyshyn³, A. Wildes⁴

1. *Physics Department, Yildiz Technical University, Istanbul, Turkey*

2. *Faculty of Physics, Duisburg-Essen University, Duisburg, Germany*

3. *Forschungszentrum Neutronenquelle Heinz Maier-Leibnitz FRM-II, Technische Universität München, Germany*

4. *Institut Laue-Langevin, Grenoble, France*

Mn_3GaC among the Mn-based Antiperovskite compounds shows a first order magnetostructural transition from the antiferromagnetic state (AF) to ferromagnetic state (FM) with increasing temperature at $T_t = 165$ K accompanied with volume change. A thermal hysteresis of 3 K/T occurs at the transition. To decrease the thermal hysteresis, we have substituted 15 % of nitrogen in place of carbon. As a result, long range ferromagnetism disappeared along with the thermal hysteresis. To understand the source of the thermal hysteresis and its relation with ferromagnetism, we have undertaken neutron diffraction and neutron depolarization experiments on the Mn_3GaC and $Mn_3Ga(C_{0.85}N_{0.15})$. According to the results of neutron diffraction experiments for Mn_3GaC , the (332) nuclear reflection shows that at the transition lattice constants associated with both the AF and the FM phase coexist indicating that the system is in a heavily strained state, which can be a cause for the hysteresis. In the neutron depolarization experiments on $Mn_3Ga(C_{0.85}N_{0.15})$, the flipping ratio does not change when crossing the transition showing the absence of ferromagnetic domains around the first order transition. One factor which leads to narrow hysteresis at magnetostructural transitions is the absence of long-range ferromagnetism in the parent phase of the material.

TH.C-P83 - Magnetization study of cobalt ferrite by mean field approximationS. Ouai1, A. Benyoussef2, G. Abo3, M. Ouai4, M. Hafid5

1. *Laboratoire de Génie Physique et Environnement, Faculté des Sciences, Université Ibn Tofail, Kénitra, Morocco*
2. *Laboratory of Magnetism and Physics of High Energy, Faculty of Science, Mohammed V University, Rabat, Morocco*
3. *Department of Electrical and Computer Engineering and MINT Center, The University of Alabama, Tuscaloosa, United States*
4. *Laboratoire de Génie Physique et Environnement, Faculté des Sciences, Université Ibn Tofail, Kénitra, Morocco*
5. *Laboratoire de Génie Physique et Environnement, Faculté des Sciences, Université Ibn Tofail, Kénitra, Morocco*

Cobalt ferrite (CoFe_2O_4) is of interest for magnetoelectric transducer applications [1]. It is ferrimagnetic with an inverse spinel structure, where trivalent Fe^{3+} ions are equally distributed between A and B sites and divalent Co^{2+} ions occupy the B sites [2] and is a hard ferrite [3]. Important factors that may affect the behavior of magnetization are exchange interactions, crystal field (CF), and temperature. So in this work, we study the magnetization of cobalt ferrite with different exchange interactions and crystal fields using the mean field approximation. A variational method based on the Bogoliubov inequality for the Gibbs free energy was used within the mean field theory [4]. The effect of temperature on the magnetization of cobalt ferrite was investigated in the absence and presence of crystal fields. The effect of exchange interactions revealed different behaviors of the magnetization versus the temperature; a pure ferrimagnetic state and a frustrated magnetic behavior were observed for the cobalt ferrite. In addition, the study of the exchange interactions effect on the total magnetization shows that for strong coupling interactions, the total magnetization of the system exhibits a jump at a given temperature. A first order phase transition from ferrimagnetic to ferromagnetic phase was found at low temperature, and a second order transition from ferromagnetic to paramagnetic phase was observed at high temperature. The investigations also revealed that the phase transition temperatures depend on the crystal fields of the octahedral and tetrahedral sites. On the other hand, the magnetization curves shifted to higher temperatures when the exchange interactions values decreased.

References:

- [1] V. L. O. Brito, S. A. Cunha, L. V. Lemos, C. B. Nunes, "Magnetic properties of liquid-phase sintered CoFe_2O_4 for application in magnetoelastic and magnetoelectric transducers" *Sensors* 12, 10086-10096 (2012)
- [2] C. M. Srivastava, G. Srinivasan, N. G. Nanadikar, "Exchange constants in spinel ferrites" *Phys. Rev. B* 19, 499- 508 (1979)
- [3] B. Liu, J. Ding, J. Yi, J. Yin, Z. Dong, "Magnetic anisotropies in cobalt-nickel ferrites ($\text{Ni}_x\text{Co}_{1-x}\text{Fe}_2\text{O}_4$)" *J. Kor. Phys. Soc.* 52, 1483-1486 (2008)
- [4] H. Falk, "Inequalities of J. W. Gibbs" *Am. J. Phys.* 38, 858-869 (1970)

TH.C-P84 - Inverse and conventional magnetocaloric effects in Fe₇Se₈ single crystal

I. Radelytskyi¹, R.Szymczak¹, D. Gawryluk¹, R. Puzniak¹, M. Berkowski¹, M.Pekala², R. Diduszko³, J. Fink-Finowicki¹, H.Szymczak¹

1. *Institute of Physics PAS, Warsaw, Poland*

2. *Department of Chemistry, University of Warsaw, Poland*

3. *Tele and Radio Research Institute, Warsaw, Poland*

Iron selenide Fe₇Se₈ (3c type) has been extensively studied because of its interesting crystallographic, optical and magnetic properties. This compound is ferrimagnetic metal with high Neel temperature. Its crystal structure is hexagonal and may be derived from the NiAs-type one by introducing ordered Fe vacancies. The main purpose of this paper is to study magnetocaloric effect in this compound. The high quality single crystals of Fe₇Se₈ have been grown applying Bridgman's method. Magnetization and magnetocaloric measurements have been carried out in magnetic fields up to 50 kOe over the temperature range 4.2 to 490 K, together with analysis of the resistivity and the thermoelectric power data. The reorientation spin transition from easy c-axis to easy c-plane has been observed near the temperature T_r = 125 K. It proceeds in an abrupt fashion, as a first-order phase transition. The magnetization curves in the vicinity of this transition were shown to exhibit an S-shape behavior with a clear hysteresis. These first order metamagnetic field induced transitions have been identified above and below T_r. Conventional magnetocaloric effect related to the metamagnetic transitions has been found above T_r while below T_r inverse magnetocaloric effect is clearly seen. The critical fields of the metamagnetic transitions as a function of temperature have been measured and discussed in relation to the mechanism responsible for metamagnetic behavior of the system. The existence of both kinds of magnetocaloric effects is important from the point of view of large rotating field entropy change in Fe₇Se₈ single crystal. A second order phase transition to paramagnetic state has been studied at a Curie temperature T_c = 450 K. The magnetocaloric effect associated with this transition is weaker than those studied near T_r. The giant anisotropy of the magnetocaloric effect is discussed in relation to the magnetic anisotropy of Fe₇Se₈ crystals.

TH.C-P85 - Magnetic properties of Sm₂Fe₁₇ single crystalL. V. B. Diop¹, K. P. Skokov¹, M. D. Kuzæmin^{1,2}, D. Karpenkov¹, O. Gutfleisch¹*1. Institut für Materialwissenschaft, Technische Universität Darmstadt, Darmstadt, Germany**2. Aix-Marseille Université, IM2NP, Faculté St. Jérôme, Marseille, France*

The study of the magnetic properties of the R₂Fe₁₇ compounds (where R is a rare-earth element or yttrium) has been of interest for many years. These Fe-rich intermetallic compounds present many interesting magnetic properties. One of them is abnormalities in their ordering temperatures. Their hexagonal or rhombohedral crystallographic structures can be considered as natural multilayer systems: the Fe layers are perpendicular to the c-axis and are accompanied by dumbbell Fe pairs between them. The Fe atoms are located in four inequivalent crystal sites within the unit cell. Despite the extensive investigations devoted to the R₂Fe₁₇ compounds, there appear to have been no systematic study of the magnetic anisotropy and magnetic phase transitions in Sm₂Fe₁₇. This may be due to the difficulties associated with growing single crystals. Yet, unambiguous determination of the anisotropy constants requires single crystals. Therefore, we grew a rhombohedral single crystal of Sm₂Fe₁₇ and investigated its magnetic properties. The magnetization of the single crystal was measured in various crystallographic directions in static magnetic fields up to 14 T on a commercial Physical Property Measurement System (PPMS14 of Quantum Design). Sm₂Fe₁₇ is ferromagnetic below TC = 385 K and presents an easy-plane order. The magnetization curves recorded along the magnetic hard c-axis [001] exhibit a first-order phase transition (FOMP) at low temperatures. We have found, moreover, that the c-axis curves show a finite spontaneous magnetization. Both the magnetic anisotropy field and the critical field of the FOMP transition decrease monotonically with temperature. The obtained results show that there exist both positive and negative exchange interactions for Sm₂Fe₁₇.

TH.C-P86 - Correlating structural and magnetic properties in phase separated manganites

G. Gomez Eslava¹, L. Ghivelder¹, G. Leyva², M. Quintero², F. Parisi²

1. *Universidade Federal Do Rio De Janeiro, Brazil*

2. *Escuela de Ciencia y Tecnologia, Universidad Nacional de General San Martin, Argentina*

This work focuses on establishing the influence of structural properties on the magnetic phase separation in manganites. For this purpose, we present results in the family of compounds with general formula $\text{La}_{0.225} \text{Pr}_{0.4} (\text{Ca}_{1-x}\text{Sr}_x)_{0.375} \text{MnO}_3$, with emphasis on samples with low Sr content ($x=0.00$ e 0.05). The samples were characterized by magnetization, specific heat and resistivity measurements. High resolution X-ray diffraction (XPD) measurements allow us to establish a clear correlation between structural parameters and the observed behavior change at approximately $x=0.15$. Low temperature XPD results show the presence of lattice distortions below 230 K, related with the charge ordering. The growth of the long-range ferromagnetic (FM) phase below 100 K is explained by a decrease in the lattice distortion. It was confirmed, from neutron diffraction measurements, that in the absence of magnetic field a pseudo-CE antiferromagnetic phase is established below 170K. In addition, a decrease in the AFM phase was observed, simultaneously accompanied by a growth in the FM phase, when a magnetic field is applied. Thermal expansion and magnetostriction measurements were made using a capacitive cell. The results confirm the strong correlation between physical and structural properties in the samples. The destruction of monoclinical distortions below 100 K is reflected as the fast contraction of the sample when cooled from 100 K to 50 K. Magnetostriction measurements are in agreement with the meta-magnetic transitions observed by magnetization and NPD techniques, showing that the destruction of the CO state drives the material through a field-induced contraction process.

TH.C-P87 - Ab initio construction of magnetic phase diagrams in alloys: The case of $\text{Fe}_{1-x}\text{Mn}_x\text{Pt}$

B. Pujari¹, P. Larson¹, V. Antropov², K. Belashchenko¹

1. *University of Nebraska-Lincoln, United States*

2. *Ames Laboratory, United States*

We develop a first-principles approach to the construction of concentration-temperature magnetic phase diagrams of metallic alloys [1]. The method employs self-consistent total energy calculations based on the coherent potential approximation for partially ordered and noncollinear magnetic states and is able to account for competing interactions and multiple magnetic phases. Application to the $\text{Fe}_{1-x}\text{Mn}_x\text{Pt}$ "magnetic chameleon" system yields the sequence of five magnetic phases at $T=0$ and the c-T magnetic phase diagram in good agreement with experiment. In addition, a new low-temperature phase is predicted at the Mn-rich end. The correct first-order transitions and the Mn-rich phase are only captured if non-Heisenberg terms are included in the magnetic energy, showing the limitations of the conventional approach based on the Heisenberg model Hamiltonian. The wide applicability and predictive power of this approach makes it useful for the design of magnetic materials with desired properties.

[1] B. S. Pujari, P. Larson, V. P. Antropov, and K. D. Belashchenko, arXiv:1501.02794

TH.C-P88 - Strategies for increasing the Néel temperature of magnetoelectric antiferromagnetsS. Mu ¹, A. Wysocki ¹, K. Belashchenko ¹*1. University of Nebraska-Lincoln, United States*

Magnetoelectric antiferromagnets enable electric control of magnetism, which makes them potentially suitable for nonvolatile memory and other magnetoelectronic device applications. However, progress in device implementation is hampered by the lack of magnetoelectrics that would retain magnetic order at typical computer-core temperatures. Based on first-principles calculations, we developed strategies for increasing the Néel temperature T_N in magnetoelectric Cr_2O_3 and Fe_2TeO_6 antiferromagnets [1,2]. For Cr_2O_3 we find that, although transition-metal substitutions for Cr and N substitution for O are likely to reduce T_N , substitution of O by B is expected to increase it by 5-10% per 1% B substitution for O. Both N and B impurities introduce impurity states mediating strong hybridization and magnetic interaction between the neighboring Cr ions. While for N impurities this leads to magnetic frustration, B substitution enhances the stability of the ground antiferromagnetic state. In Fe_2TeO_6 , substitution of larger ions like Zr or Hf for tellurium increases the Fe-O-Fe superexchange angles. The compensating O vacancies tend to form bound complexes with Zr dopants, which do not degrade the electronic band gap. T_N is estimated to increase by 15% at 12.5% substitution of Zr by Te with such compensation. Substitution of N for O is favorable due to the decreased charge-transfer gap. The overall effect for N substitution in the 3- charge state compensated by O vacancies is estimated at 3-4% T_N enhancement per 1% of O substitution by N.

[1] Sai Mu, A. L. Wysocki, and K. D. Belashchenko, Phys. Rev. B 87, 054435 (2013)

[2] S. Mu and K. D. Belashchenko, J. Phys.: Condens. Matter 27, 022203 (2015)

TH.C-P89 - Effect of third element on spin state of europium in its 1-2-2 pnictides: ESR dataY. Goryunov¹, A. Nateprov²1. *E.K.Zavoisky Kazan Physical-Technical Institute, Russian Federation*2. *Institute of Applied Physics of Moldovan Academy of Sciences, Moldova*

We performed the X band ESR measurements of powder samples EuCd_2As_2 with structural type CaAl_2Si_2 at temperatures 10-300 K. This structural type, also as structural type ThCr_2Si_2 , is characterized by alternating single layers of Eu^{2+} , in which ions are located at the nodes of a plane square lattice. As in the past for other 1-2-2 europium compounds with structure type CaAl_2Si_2 was observed almost symmetric Lorentzian resonance line. The temperature dependences of the resonance field and linewidth were of the type $\sim (T-T_c)^{-1/2}$, which is indicative of spin fluctuations associated with the phase transition temperature T_c . Also at high temperatures was observed Curie – like temperature dependence of the inverse the ESR intensity with positive temperature Curie Weiss $\theta_{cw} = 16$ K, which does not coincide with $T_c = T_N \sim 7$ K. A comparative analysis of the Eu^{2+} ion g factors deviations for different 1-2-2 pnictides Eu from its value for the free electron, which corresponds to a pure spin state of the ion Eu, was made. It was found that the anion pnictides substitution effect on the g-factor Eu^{2+} is negligible (smaller 0.5%). Lattice constant is proportional to the radius of the anion Pn^{3-} pnictides with accuracy better than 1%. However, the substitution of the transition metal M^{2+} ion leads to a strong increase of the ion Eu^{2+} g - factor despite sameness of configuration of external electronic shells. Obviously, this is related to the size and distribution of the electron density remaining after filling p - orbitals of pnictides due to electrons of the Eu and the transition metal. It should be emphasized that the substitution of Zn^{2+} to Fe^{2+} in EuM_2As_2 changes the behavior of the Eu^{2+} ions layers: of adjacent europium layers are compressed and shifted by half a period along their surfaces and thus doubles the period of the structure of the ions along c -axis. The consequence of this is the metallization of the Eu layers, which is manifested in significant reduction of the g factor to smaller 2.0 and the temperature behavior of the linewidth.

TH.C-P90 - Successive component-separated magnetic transitions on pseudoternary compounds $\text{Ho}_{1-x}\text{Gd}_x\text{Rh}_2\text{Si}_2$

T. Shigeoka¹, T. Morita¹, T. Fujiwara¹, K. Matsubayashi², Y. Uwatoko²

1. *Yamaguchi University, Japan*

2. *University of Tokyo, Japan*

The ternary compound HoRh_2Si_2 shows successive component-separated magnetic transitions; the magnetic moments of c- and ab-components independently order at different temperatures, $T_{N1} = 29.1$ K and $T_{N2} = 12.1$ K, respectively [1]. This behavior may come from some frustration. Complex magnetization processes were observed at low temperatures [2]. This behavior is very interesting. In order to obtain information on the origin of this behavior, magnetic behavior of $\text{Ho}_{1-x}\text{Gd}_x\text{Rh}_2\text{Si}_2$ has been investigated by measurements of magnetization and magnetic susceptibility. Both transitions T_{N1} and T_{N2} increase with increasing x. The partial ordered phase, may be a frustration state, in $T_{N1} < T < T_{N2}$ is persisted to high concentration x. In GdRh_2Si_2 , the transition T_{N1} suddenly disappears; the frustration state goes out. Ho moments play an important role for an appearance of this partial ordered phase. Crystal field effects may be also important for this behavior.

References:

[1] T. Shigeoka, et al., J, Phys. Conf. Ser. 273, 012127 (2011)

[2] T. Shigeoka, T. Fujiwara, K. Matsubayashi, Y. Uwatoko, J, Phys. Conf. Ser. 391 012063 (2012)

TH.C-P91 - Magnetic susceptibility and anisotropy probed by terahertz spectroscopy of spin waves in rare earth orthoferrites

E. Constable^{1,2}, R. Lewis², J. Horvat², Z. Cheng², S. Cao³, S. Yuan³, G. Ma³

1. *Institut Néel, Grenoble, France*

2. *University of Wollongong, Wollongong, New South Wales, Australia*

3. *Shanghai University, Shanghai, China*

Terahertz radiation has emerged as an effective method for the study of spin dynamics in magnetic materials. The frequency range falls within the 0.1-10 meV regime making it comparable to the low-energy terms of the magnetic Hamiltonian and complementary to established methods that probe these interactions such as inelastic neutron scattering. In our recent study [PRB 90:054413 (2014)] we demonstrate how the temperature dependence of an effective anisotropy can be extracted by terahertz spectroscopy of the spin waves in a rare earth orthoferrite NdFeO₃. The results suggested a crossing of magnetic anisotropy terms as responsible for the temperature dependent spin reorientation. Here we advance that study, probing the magnetic susceptibility by the spin wave dynamics in the xy plane and along the z axis. Further refinements to the temperature dependent spin wave analysis give insights into the microscopic contributions to the magnetic anisotropy terms. The measurements are also extended to the ErFeO₃ compound which experiences different temperature dynamics for the spin reorientation. The results suggest that an interplay between magnetic dipolar and single ion anisotropies is important in the spin reorientation phenomenon.

TH.C-P92 - Picosecond emergence and control of the photo-induced magnetization across the morin transition in DyFeO₃

D. Afanasiev¹, R. Pisarev², B. Ivanov³, T. Rasing¹, A. Kimel¹

1. *Radboud University Nijmegen, Institute for Molecules and Materials, AJ Nijmegen, The Netherlands*

2. *Ioffe Physical-Technical Institute, Russian Academy of Sciences, St. Petersburg, Russia*

3. *Institute of Magnetism, National Academy of Sciences, Kiev, Ukraine*

The photo-induced phase transitions and dynamics triggered by fs laser pulses is a subject of intense and multidisciplinary research in contemporary science. In magnetism this is an especially intriguing problem since understanding the kinetics of the phase transitions is crucial for achieving the fastest possible magnetic recording and information processing.

Here we show that excitation of antiferromagnetic DyFeO₃ in the vicinity of the Morin transition with help of a single 60 fs laser pulse pushes the antiferromagnet from collinear to non-collinear spin state with the net magnetization. Imaging the photo-induced area confirms that emergence of the magnetization proceeds via a depletion of the collinear antiferromagnetic phase and reveals that the initial orientation of its antiferromagnetic vector plays a decisive role in defining the direction of the photo-induced magnetization. The measurements performed for different pump polarizations and applied magnetic fields reveal that the direction of the photo-induced magnetization depends on the polarization of the pump, so that for field below 0.4 kOe a finite fraction of the photo-induced magnetization can be aligned against the external magnetic field.

TH.C-P93 - μ SR study on the phase transition from antiferromagnetic Mott-insulator to non-magnetic metal in K-Rb alloy and Rb clusters in sodalite

T. Nakano¹, K. Tanibe¹, L. Manh Kien¹, S. Yoon^{2,3}, M. Abdel-Jawad², F. L. Pratt⁴, I. Watanabe², Y. Nozue¹

1. *Department of Physics, Osaka University, Japan*

2. *RIKEN Nishina Center, Japan*

3. *Department of Physics, The Catholic University of Korea, Republic of Korea*

4. *ISIS, Rutherford Appleton Laboratory, United Kingdom*

Sodalite is a kind of aluminosilicate zeolites where the cages with an inner diameter of 0.7 nm are arrayed in a bcc structure. Na_4^{3+} clusters arrayed in sodalite show antiferromagnetism below the Néel temperature T_N of 48 K. In the cluster, one unpaired s-electron is shared by four Na^+ ions and is confined in the cage. The antiferromagnetic ordering is realized by the exchange interaction between the s-electrons in adjacent clusters. The material is assigned to a Mott insulator. When heavier alkali elements are substituted for Na, T_N systematically increases: 72, 80, and 90-100 K for the clusters with averaged chemical compositions of K_4^{3+} , $(\text{K}_3\text{Rb})^{3+}$, and $(\text{K}_{1.5}\text{Rb}_{2.5})^{3+}$, respectively. However, a recent work has revealed that Rb_4^{3+} does not show antiferromagnetism and shows a metallic behavior. In this work, we investigate the magnetic properties of this system near the insulator-to-metal (I-M) transition in detail by utilizing μ SR. The experiments were preformed at the RIKEN-RAL Muon Facility. Zero-field μ SR spectra of the K-Rb alloy clusters ($(\text{K}_{1.7}\text{Rb}_{2.3})^{3+}$) clearly show a muon-spin precession signal with a large amplitude. This evidences that the antiferromagnetic ordering is robust in the major volume of the sample even just before the I-M transition. The internal field at the muon site is estimated to be 166 Oe at 5 K. This value is larger than that in Na_4^{3+} (92 Oe), K_4^{3+} (142 Oe), and $(\text{K}_3\text{Rb})^{3+}$ (155 Oe). The systematic increase in the size of s-electron wave function in heavier alkali metals, which has been assigned to the origin of the increase in T_N , may provide stronger Fermi contact interaction between the s-electron and μ^+ stopping near the zeolite framework. On the other hand, Rb_4^{3+} clusters show a very slow relaxation even at 2 K, which confirms the sudden disappearance of antiferromagnetic ordering after the I-M transition.

TH.C-P94 - Crystal structure and physical properties of the novel EuPdSn₂ compound

I. Čurlík^{1,2}, F. Gastaldo³, M. Giovannini³, M. Reiffers^{1,2}

1. Institute of experimental physics, Slovak academy of science, Košice, Slovakia
2. Faculty of Humanities and Natural Sciences, University of Prešov, Prešov, Slovakia
3. Department of Chemistry, University of Genova, Genova, Italy

A new intermetallic compound EuPdSn₂ has been synthesized. The pure elements have been weighed in the stoichiometric ratio inside a glove box, in order to avoid Eu oxidation, and closed in a Ta crucible. Afterwards, the compound have been synthesized by induction melting. Its crystal structure was established by X-ray powder diffraction as orthorhombic, space group *Cmcm* (No. 63) with $a = 0.4451(4)$ nm, $b = 1.1587(2)$ nm and $c = 0.7455(2)$ nm. The structure of EuPdSn₂ belongs to the MgCuAl₂ prototype, a ternary ordered variant of the Re₃B type.

In this work we present the first results of the magnetic properties, electrical resistivity and heat capacity measurements for this compound. The susceptibility dependence $\chi(T)$ follows the Curie-Weiss law above 20 K with an effective magnetic moment of $\mu_{\text{eff}} = 7.67\mu_{\text{B}}$, which is very close to the theoretical value for Eu²⁺.

Concerning the magnetic properties, an antiferromagnetic transition is observed at $T_{\text{N}} = 13$ K. All the other measurements fit well with this scenario. The magnetization dependencies $M(B)$ measured at various constant temperatures show a magnetic saturation below T_{N} . The values of electrical resistivity $\rho(T)$ at low temperatures below T_{N} increase in absolute values with the applied magnetic field due to the Lorentz force. The residual resistivity ratio $\text{RRR} = 28$ demonstrates the very good quality of this polycrystalline sample.

TH.C-P96 - Magnetic properties and negative magnetocaloric effect in Mn(Ru-Rh)AsD. Szymański¹, J. Tobola², W. Chajec¹, R. Zach¹, S. Haj-Khlifa³, D. Fruchart³, E. K. Hlil³1. *Institute of Physics, CUT, Cracow, Poland*2. *AGH University of Science and Technology, Faculty of Physics and Applied Computer Science, Cracow, Poland*3. *Institut Néel, CNRS, Grenoble, France*

We report on magnetic properties and magnetocaloric effect (MCE) of MnRu_{1-x}Rh_xAs system (SG: Fe₂P-type), which exhibits complex magnetic behaviours [1,2,3]. While the Rh content is less than 0.2, the compounds order ferromagnetically (F) with a Curie temperature (T_C), which decreases vs. x. For x>0.8, magnetic ordering is more complex and the system evidences magnetoelastic phase transitions between the antiferromagnetic (AF) and (F+AF) ordered state and the (F+AF) and paramagnetic (P) one. Based on previously analyzed XRD measurements in 80–550K temperature range [4], in this work we mainly focus on the MCE properties. The negative MCE was not yet reported for the samples with 0.8<x<1 composition range to our best knowledge. The experimental investigations of magnetic entropy changes (x=0.9, x=0.95) is analyzed by using Maxwell relation and Clausius-Clapeyron equation. Both approaches are compared and critically discussed, as previously presented for parent MnRhAs compound [2]. Moreover, magnetic properties of MnRu_{1-x}Rh_xAs are analyzed in view of electronic structure calculations using KKR and KKR-CPA methods for ordered compounds (x=0 and x=1) and disordered alloys (0<x<1), respectively.

References:

1. P. Chaudouet, Thesis INP. Grenoble (1983)
2. M. Balli, D. Fruchart, R. Zach, J. Appl Phys 115 (2014) p.203909
3. D. Szymanski, R. Zach, W. Chajec, J. Tobola, D. Fruchart and E.K. Hlil (2012) *Proceed. 18th SCTE*, Lisbon, Portugal
4. D. Szymanski, R. Zach, W. Chajec, J. Tobola, D. Fruchart and E.K. Hlil (2014) *Proceed. 19th SCTE*, Genova, Italy

TH.C-P97 - Neutron depolarisation imaging of the ferromagnetic quantum phase transition in ZrZn₂

P. Schmakat^{1,2}, M. Halder², G. Brandl^{1,2}, M. Schulz¹, S. Hayden³, R. Georgii¹, P. Böni², C. Pfleiderer²

1. *Technische Universität München, FRM II, Germany*

2. *Technische Universität München, E21, Germany*

3. *University of Bristol, Bristol, United Kingdom*

When a polarised neutron beam traverses a ferromagnetic material, the orientation and strength of the polarisation changes sensitively as a function of the ferromagnetic moment and the size of the ferromagnetic domains. We have developed an experimental set up that allows to perform neutron depolarisation imaging as a function of magnetic field. In a study of the ferromagnetic quantum phase transition in the weak itinerant ferromagnet ZrZn₂ under pressure we find, that a peculiar field dependence of the neutron depolarisation survives on the paramagnetic side of the temperature versus pressure phase diagram. This provides putative evidence for the emergence of complex magnetic textures.

TH.C-P98 - Correlation between electrical properties and antiferromagnetic ordering in brownmillerite-type $\text{Ca}_2\text{Fe}_2\text{O}_5$

I. Kagomiya¹, Y. Hirota¹, K. Kakimoto¹, A. Fuwa², S. Nakamura^{3,4}

1. *Department of Materials Science and Engineering, Nagoya Institute of Technology, Nagoya, Japan*

2. *Faculty of Science and Engineering, Waseda University, Japan*

3. *Department of Science and Engineering, Utsunomiya, Japan*

4. *Advanced Research Institute of Science and Engineering, Waseda University, Japan*

The brownmillerite $\text{Ca}_2\text{Fe}_2\text{O}_5$ possesses antiferromagnetic transition at $T_N = \sim 700$ K, which is relatively higher among magnetic iron oxides. Some studies have been reported that the $\text{Ca}_2\text{Fe}_2\text{O}_5$ shows iron charge disproportionation ($\text{Fe}^{3+} \leftrightarrow \text{Fe}^{4+} + \text{Fe}^{2+}$) in the particular temperatures.[1] We suppose that the charge disproportionation simultaneously contributes to electrical- and magnetic-properties. As a result, the correlation between electrical properties and antiferromagnetic ordering is expected in the $\text{Ca}_2\text{Fe}_2\text{O}_5$. Although there are many reported studies about electrical- or magnetic-properties of the $\text{Ca}_2\text{Fe}_2\text{O}_5$, studies and discussion about the correlation between them have been still rare. With the point of view, we try to investigate whether the correlation is present or not in the $\text{Ca}_2\text{Fe}_2\text{O}_5$. The polycrystalline $\text{Ca}_2\text{Fe}_2\text{O}_5$ was prepared by a conventional solid state reaction method. Magnetization of the $\text{Ca}_2\text{Fe}_2\text{O}_5$ was investigated by a SQUID magnetometer with oven in the temperature range of 300 - 800 K. In addition, Mössbauer spectroscopy was investigated to confirm magnetic structure and iron valence of the prepared $\text{Ca}_2\text{Fe}_2\text{O}_5$. The electrical conductivity was investigated in the temperature range of 300 - 800 K by a four-point measurement technique. It was found that activation energies estimated from Arrhenius plot of the electrical conductivity changed around T_N . The activation energy was 0.26 (0.48) eV at higher (lower) temperatures than T_N . The fact means that the electrical transport mechanism modified at the magnetic transition. From the activation energy value and the reported study[1], we suppose that the transport mechanism modified from charge transfer based on the iron charge disproportionation to polaron hole hopping at higher temperatures than T_N . It suggests that the magnetic ordering of the $\text{Ca}_2\text{Fe}_2\text{O}_5$ is closely related to presence of the charge disproportionation, because the charge transfer makes the super-exchange interaction.

[1] E. A. Smith et al., J. Sol. Stat. Chem., 2010, 183, 1670-1677

TH.C-P99 - The uniaxial pressure effect on the magnetic phase transitions in spin-lattice coupled system CuFeO_2

H. Tamatsukuri¹, S. Mitsuda¹, T. Nakajima², S. Aoki¹, S. Hosaka¹, K. Prokes³, K. Kiefer³

1. *Tokyo University of Science*

2. *RIKEN Center for Emergent Matter Science (CEMS)*

3. *Helmholtz-Centre Berlin for Materials and Energy*

The triangular lattice antiferromagnet CuFeO_2 is a strong spin-lattice coupled system, whose magnetic phase transitions are accompanied by crystal lattice distortions to relieve the geometrical spin frustration. In previous study, by the magnetic susceptibility and neutron diffraction measurements under uniaxial pressure (p) up to 100 MPa along a direction of supporting the spontaneous lattice distortions, we investigated how applied p modify the magnetic phase transition [1]. Although they observed a rise of the magnetic phase transition temperature, applied p up to 100 MPa is too small to investigate the p variation of q_0 , which is a magnetic modulation wave number at the magnetic phase transition temperature and should reflect ratios of coupling constants. In this study, we have achieved the application of p up to 600 MPa, and have performed the similar experiments. As a result, we have revealed that the value of q_0 is not changed even by applied p of 600 MPa, suggesting that coupling constants are almost invariable for applied p . In contrast, the phase transition temperature drastically increases with increasing p . This result indicates that, despite the invariable q_0 for applied p , the value of $J_{\max}(q_0)$, which is a Fourier transformed maximum value of coupling constant determining the magnetic phase transition temperature within the mean field approximation, is changed. Unlike the case in geometrically frustrated but non spin-lattice coupled system CoNb_2O_6 , in which coupling constants are easily modified by applied p [2], our results suggest that applied p does not directly affect the coupling constants, and thus spin-lattice coupled term in Hamiltonian may be essential for determining the magnetic phase transition temperature in CuFeO_2 .

[1] T. Nakajima et al., J. Phys. Soc. Japan 81, 094710 (2012)

[2] S. Kobayashi et al., Phys. Rev. B 90, 0640412 (2014)

TH.C-P100 - Quantum phase transitions and staggered dimer order in the $J_1 - J_1' - J_2$ frustrated anisotropic exchange antiferromagnetic Heisenberg model

S. Rufo¹, J.R. de Sousa^{2,3}, J.A. Plascak^{1,4,5}

1. *Universidade Federal De Minas Gerais, Brazil*

2. *Universidade Federal Do Amazonas, Brazil*

3. *National Institute of Science and Technology for Complex Systems, Brazil*

4. *Center for Simulational Physics, University of Georgia, United states*

5. *Universidade Federal da Paraíba, Brazil*

The magnetic properties of the spin-1/2 $J_1 - J_1' - J_2$ Heisenberg antiferromagnetic model with anisotropic exchange interactions is studied on a square lattice. This model is an extension of the prototypical $J_1 - J_1' - J_2$ model (when $J_1 = J_1'$) and also presents the same kind of frustration at low temperatures. The directions of the exchange interactions are: J_1 along of the x axis, J_1' along of the y axis and J_2 along the diagonal direction on a square lattice. The results have been obtained by using a variational method based on a trial vector for the ground state. The zero temperature phase diagram depends on the values of the interactions J_1, J_1', J_2 as well as on the exchange anisotropies, where the latter ones allow the Hamiltonian to vary between the classical Ising and the quantum isotropic Heisenberg models. The system presents a Néel ordered phase, a collinear antiferromagnetic phase and a disordered quantum phase between them. An interesting result points out that these exchange anisotropies play an important role regarding not only the order of the transitions between the Néel and the quantum disordered phases, but also the area of existence of the quantum disordered phase as well. We have also computed the dimerization parameter and the staggered dimer order has founded and analyzed, disagreeing with the spin-liquid picture for the intermediate phase. In addition, we can present also our results analyses about for a particular quase-one dimensional case, i.e. with no frustration parameter. We found for this case that an infinitesimal interchain coupling parameter J_1' is sufficient to stabilize a long-range order, different from some works that forecast a finite value for this coupling. That last result was published in *Phys.Rev. E 88, 34101 (2013)*.

TH.C-P103 - Low Temperature Magnetic Properties of a New Quasi-one-dimensional Organic Magnet α -2-Cl-4-F-V

Y. Kono¹, S. Kittaka¹, T. Sakakibara¹, H. Yamaguchi², Y. Hosokoshi²

1. *The Institute For Solid State Physics, The University of Tokyo, Japan*

2. *Department of Physical Science, Osaka Prefecture University, Japan*

Recently, several verdazyl radical crystals have been synthesized and found to consist of unconventional quasi-one-dimensional magnetic lattices [1,2]. They are molecular-based crystals, and each of molecules possesses the verdazyl radical, which has an $S = 1/2$ quantum spin. Chemical modification of the verdazyl radical molecule easily enables tuning of the intermolecular interactions, and it is thus useful for realizing quasi-one-dimensional quantum spin systems which have unique magnetic properties. In this study, we present low-temperature magnetic properties of a new verdazyl radical crystal α -2-Cl-4-F-V. The molecular orbital calculations of the material predicted the strongest one-dimensional antiferromagnetic interaction and three main interchain interactions between the $S = 1/2$ quantum spins. DC magnetization and heat capacity measurements have been performed at temperatures between 0.1 K and 2 K in several magnetic fields up to 7 T. The magnetization curve at 0.1 K shows gapless behavior like conventional one-dimensional quantum spin systems and saturates at about 5 T. A peak is observed in the temperature dependence of the heat capacity at 0 T, indicating that a three-dimensional ordering occurs at about 0.2 K. On the other hand, the temperature dependence of the magnetization in several magnetic fields shows a similar anomaly appearing in many of gapped spin systems, such as quantum spin ladders, differing from ordinary three-dimensional orderings. This behavior is attributed to the highly frustrated character of the interchain interactions predicted by the molecular orbital calculations.

References:

[1] H. Yamaguchi et al., Phys.Rev. Lett. 110, 157205 (2013)

[2] H. Yamaguchi et al., J. Phys. Soc. Jpn. 83, 033707 (2014)

TH.C-P104 - Effect of pressure on magnetic and transport properties in the lightly electron-doped manganite compound Sr-substituted $\text{CaMn}_{0.95}\text{Sb}_{0.05}\text{O}_3$

T. Aoyagi ¹, M. Matsukawa ¹, H. Takahashi ¹, H. Taniguchi ¹, S. Kobayashi ¹, S. Nimori ², R. Suryanarayanan ³

1. *Iwate University, Japan*

2. *National Institute for Materials Science, Tsukuba, Japan*

3. *University Paris-Sud, Paris, France*

We report on the effect of pressure of magnetic and transport properties in the lightly electron-doped manganite compound $(\text{Ca}_{1-x}\text{Sr}_x)\text{Mn}_{0.95}\text{Sb}_{0.05}\text{O}_3$ with a fixed carrier content, to better understand magnetization reversal of this system. In a weak magnetic-field-cooled measurement, diamagnetic magnetization is observed for $x < 0.15$, which changes to positive values for $x \geq 0.15$. However, with the application of pressure to the $x=0.16$ and $x=0.17$ samples, the magnetization reverses sign and diamagnetism is restored. We present a magnetic phase diagram as a function of Sr content, under ambient and hydrostatic pressures. The ac magnetic susceptibility measurement indicates the existence of magnetic frustration for the Sr-substituted samples. The low temperature negative magnetization of this system has been discussed on the basis of the local lattice distortion of MnO_6 octahedra associated with the orbital-spin coupling.

1) Y. Murano et al., Phys. Rev. B83 (2011) 054437

2) T. Fujiwara et al., J. Magn. Magn. Mater. 378 (2015) 451

TH.C-P105 - Metamagnetic transitions in $\text{La}_{0.5}\text{Pr}_{0.5}\text{Mn}_2\text{Si}_2$

E. Duman¹, M. Acet², T. Krenke³, B. Ouladdiaf⁴, E. Suard⁴

1. Ankara University, Faculty of Engineering, Department of Physics, Ankara, Turkey

2. Experimentalphysik, Duisburg-Essen University, Duisburg, Germany

3. ThyssenKrupp Electrical Steel, Gelsenkirchen, Germany

4. Institut Laue-Langevin, Grenoble, France

$\text{La}_{0.5}\text{Pr}_{0.5}\text{Mn}_2\text{Si}_2$ undergoes an antiferromagnetic-ferromagnetic transition at about 250 K. This transition can also be induced by an external magnetic field leading to a metamagnetic transition. This leads to a large change in the configurational entropy, which is useful for magnetic cooling and studying the magneto-caloric effect. We investigated the details of the spin configuration as the magnetic ordering progresses from AF to FM by neutron-diffraction techniques under magnetic fields up to 5 T and by using spectral refining methods.

TH.C-P107 - Exotic spin structures and phase transitions in a complex magnetoelectric CuB2O4 as evidenced by optical linear dichroism studies

K. Boldyrev¹, M. Popova¹, R. Pisarev², L. Bezmaternykh³

1. *Institute of Spectroscopy, Russian Academy of Sciences, Troitsk, Moscow, Russian Federation*
2. *Ioffe Physical-Technical Institute, Russian Academy of Sciences, St. Petersburg, Russian Federation*
3. *Kirensky Institute of Physics, Siberian Branch of the Russian Academy of Sciences, Krasnoyarsk, Russian Federation*

Copper metaborate CuB2O4 has a complex crystal structure (SG I42d, Z=12), in which magnetic Cu²⁺ ions (S=1/2) in the unit cell occupy two different crystallographic positions. This compound exhibits a unique combination of magnetic, magnetoelectric, linear and nonlinear optical properties. To mention some of them, Cu(4b) and Cu(8d) magnetic subsystems order magnetically at different temperatures, 21 K and ~ 8 K, respectively. Multiple frustrated and nonfrustrated antisymmetric exchange interactions within and between the 4b and 8d magnetic subsystems result in a rich complex magnetic phase diagram. Recent studies of electronic absorption spectra of CuB2O4 revealed narrow zero-phonon (ZP) exciton lines for all transitions between the crystal-field-split 3d-states of Cu²⁺ ions [1].

In this work we report on a large sublattice-sensitive optical linear dichroism (LD) on ZP exciton lines which arises below the temperature of the antiferromagnetic ordering in the crystallographically isotropic (xy)-plane of CuB2O4 [2]. We elucidate the nature of the LD attributing it to the magnetic Davydov splitting. Using this dichroism we have discovered a splitting of the phase transition at ~ 8 K into two transitions with external magnetic field dependent temperatures. Our LD data are against a simple spin helix magnetic structure reported earlier and suggest elliptical helicoidal spin structure with a temperature-dependent direction of the long axis of the spin ellipse.

To summarize, on the example of CuB2O4 we show that the discovered LD can be used as a new efficient method for revealing hidden features of magnetic structures and phase transitions in complex multi-sublattice multiferroics and magnetics. This work was supported by the RFBR Grant No 15-02-04222a and the President of the Russian Federation (Grant No MK-3521-2015.2).

[1] R. V. Pisarev, A. M. Kalashnikova, et al., Phys. Rev. B 84, 075160 (2011)

[2] K. N. Boldyrev, R. V. Pisarev, et al., arXiv:1410.8727 [cond-mat.mtrl-sci]

TH.C-P108 - Stabilizing the ferromagnetic ordering of Co nano-assemblies on graphene by dipolar interaction

C. Kuo¹, Y. Chang¹, Y. Chan¹, S. Wu¹, T. Wu¹, C. Huang¹, D. Wei²

1. *Department of Physics, National Sun Yat-Sen University, China*

2. *National Synchrotron Radiation Research Center, Taiwan*

Magnetic nano-structures may demonstrate novel electronic and magnetic properties over their material counterparts of thin films and bulk system. This is meaningful concerning the fact that micro-fabrication technology nowadays steps to nano-scale. Their integration with carbon-based materials further indicates the application in biomedics and spintronics, where the stabilization of magnetization is one of the major issues. In nano-particles, dipolar interaction is thought to dominate exchange interaction and withstand elevating temperature, so as to serve magnetic coupling. However, the capacity of magnetic anisotropy against thermal fluctuation, that is, the stability of magnetic ordering needs to be investigated.

In this work, the evolution of magnetic ordering in graphene-under-layered cobalt assemblies is reported. The quality preparation of graphene and the 3D-growth of cobalt assemblies are determined by scanning tunneling microscopy (STM). Moreover, by using x-ray magnetic circular dichroism (XMCD), the magnetic properties of cobalt assemblies are characterized. It is pointed out that for the magnetic ordering in cobalt assemblies, the coupling of cobalt particles is crucial in competing with thermal fluctuation while the magnetic anisotropy of single particle will not beat it. To confirm the mechanism for magnetic coupling, an evaluation in the framework of magnetic dipolar interaction through nano-particles is given. Accordingly, up to cobalt of 15 ML, where 'ML' stands for the equivalent monolayer of cobalt in Co/Pt(111) thin films, a phase change from superparamagnetic to ferromagnetic ordering is expected at room temperature (RT). The idea is consistent with the subsequent deposition up to 25 ML cobalt in experiments. This reveals the capability of engineering the stability of magnetization, for instance, to the onset of ferromagnetic ordering. As the magneto-static effect, dipolar interaction is insensitive to interface roughness such as some angstroms. This is about to support the advantages of magnetic nano-particles related devices.

TH.C-P109 - Thermodynamic properties of NdCu₄AuA. Bashir¹, M. Tchokonté¹, D. Britz², A. Strydom²

1. University of The Western Cape, South Africa

2. University of Johannesburg, South Africa

The studies of magnetic susceptibility, $\chi(T)$, magnetization, $\sigma(\mu_0H)$, and specific heat, $C_p(T)$, of the new antiferromagnetic (AFM) NdCu₄Au compound are reported. The room temperature X-ray diffraction analysis indicates a cubic MgCu₄Sn – type crystal structure with space group *Fm-3m* (No. 216) for the NdCu₄Au. The field cooled (FC) and Zero-field cooled (ZFC) dc $\chi(T)$ data show a coincide which suggest no evidence of an inhomogeneous magnetic ground state in this compound as a result of spin – glass – like state. The low temperature $\chi(T)$ data shows an AFM - like anomaly associated with a Néel temperature $T_N = 3.9$ K. In the paramagnetic, $\chi(T)$ data follows the Curies – Weiss law with an effective magnetic moment $\mu_{\text{eff}} = 3.42(2) \mu_B$ and a paramagnetic Weiss temperature $\theta_p = -6.96(6)$ K. The value obtained for μ_{eff} is close to the value of $3.62 \mu_B$ expected for the free Nd³⁺ - ion. $\sigma(\mu_0H)$ data shows a linear behaviour up to 7 T in the paramagnetic region at $T = 10$ K and deviation from linearity above 2.5 T in the ordering region at $T = 2$ K characteristic of metamagnetic behaviour. $C_p(T)$ data confirm AFM phase transition at $T_N = 3.5$ K close to 3.9 K observed in $\chi(T)$ result. The 4f – electron specific heat shows a Schottky – type anomaly around 25 K with energy splitting $\Delta_1 = 14.5(4)$ K and $\Delta_2 = 63(1)$ K of the Nd³⁺ ($J = 9/2$) multiplet, that are associated with the first and second excited state of the Nd³⁺ - ion. The 4f – electron entropy reaches the value of $R \ln 2$ close to the T_N at 4.2 K and saturates at the value of $R \ln(2J+1)$ at $T = 70$ K.

Keywords: NdCu₄Au, Antiferromagnetic, Crystal electric field.

TH.C-P110 - Magnetic characterization of YbMn_2Sb_2 single crystals

J. Munevar¹, F. P. Vieira¹, M. A. Avila¹, R. A. Ribeiro¹

1. CCNH, Universidade Federal do ABC (UFABC), Santo Andre, Brazil

We report the growth of high quality single crystals of the ternary intermetallic compound YbMn_2Sb_2 by the Sn-flux method, and the subsequent structural and magnetic characterization. X-ray diffraction measurements in powdered samples confirmed the trigonal structure; lattice parameters, atomic positions and atom distances as previously reported [1], where atoms of Yb separate layers of MnSb. The magnetic properties were studied via heat capacity between 2 and 300 K and magnetization measurements from 2 to 700 K. Susceptibility measurements as a function of temperature with external field perpendicular to the c axis show that the YbMn_2Sb_2 orders ferromagnetically around 580 K. Furthermore, it can be seen that the compound exhibits reduced susceptibility below 120 K, possibly caused by a spin flop process resultant of an antiferromagnetic reordering [1,2]. To observe the nature of the antiferromagnetic transition we measured the heat capacity, in which a peak is observed around 120 K. A Sommerfeld coefficient $\gamma = 2.2 \text{ mJ/mol.K}^2$ is estimated, which indicates no heavy fermion behavior. Possible contributions to the magnetic state coming from Yb are also discussed. We thank the financial support of FAPESP, CAPES and CNPq.

[1] A. V. Morozkin, O. Isnard, P. Henry, S. Granovsky, R. Nirmala, P. Manfrinetti, J. Alloys Compnd. 420 (2006) 34

[2] R. Nirmala, A. V. Morozkin, K. G. Suresh, H. D. Kim, J. Y. Kim, B. G. Park, S. J. Oh, S. K. Malik, Journal of Applied Physics 97 (2005) 10M511

TH.C-P111 - Electromagnetic waves emitted from spiral magnetic at phase transition

D. Kuzmin¹, I. Bychkov¹, A. Kamantsev², V. Koledov², V. Shavrov²

1. *Chelyabinsk State University, Russian Federation*

2. *Kotelnikov Institute of Radio-engineering and Electronics of RAS, Russian Federation*

In present work we have investigated electromagnetic waves radiation from magnetics with spin spiral ordering at phase transition to ferromagnetic state. The study cover some typical situations: fast change of the state, slow change with the linear time dependence of the spiral angle, and periodical process. It has been shown the possibility of two types emission. The first one is non-stationary terahertz radiation picosecond pulse, the second one is stationary radiation with the frequency of external field. The results of the work may be useful for both terahertz and microwave devices.

The work was supported by grants of RFBR ## 13-07-00462, 15-07-99654, and particularly by RScF # 14-22-00279

TH.C-P112 - Modeling of first order phase transitions kinetics in systems with coupled order parameters

I. Bychkov¹, D. Kuzmin¹, A. Kamantsev², V. Koledov², V. Shavrov²

1. Chelyabinsk State University, Russian Federation

2. Kotelnikov Institute of Radio-engineering and Electronics of RAS, Russian Federation

We present common 1D model of first order phase transition based on coupled solution of order parameters evolution and heat transfer equations. Such a model may be used for simulation of phase transitions in multiferroics or magnetostructural phase transitions, for example. First order phase transition process have been described by Landau-Khalatnikov-like equation with the thermodynamic potential of 2-3-4 type. Time and space distributions of the order parameters and temperature have been obtained for different heat regimes. Position and speed evolution of the interphase boundary have been calculated.

TH.C-P114 - Effect of Cu-substitution on Magnetic State of Mn₂NiGa Heusler alloy

M. Vagadia¹, A.K. Nigam¹

1. Tata Institute of Fundamental Research, Mumbai, India

Effect of Cu substitution at Ni site in Mn₂NiGa shape memory alloy, prepared by arc-melting, has been studied. Temperature dependent magnetization measurement suggests existence of martensitic phase transition near room temperature in Mn₂NiGa alloy. Magnetization isotherms measured at different temperatures near transition temperature show the occurrence of magnetocaloric effect associated with magneto-structural transformation. The maximum value of magnetic entropy change is ~ 12 J/Kg-K at 5T applied magnetic field. On the other hand, substitution of 10% Cu at Ni - site results in complete suppression of martensitic phase where the magnetization shows ferromagnetic behavior in the temperature range of 5 - 350K. Magnetoresistance (MR) measurement as a function of applied magnetic field shows slight asymmetry in MR about the direction of magnetic field in both the samples under study.

TH.C-P115 - Low-temperature properties of transition-metal and rare-earth diborides

G. Benka¹, A. Bauer¹, A. Regnat¹, C. Pfleiderer¹

1. Technische Universität München - Lehrstuhl Für Topologie Korrelierter Systeme, Germany

The class of hexagonal C32 diborides MB₂ (space group P6/mmm), where M is a transition-metal or rare-earth element, crystallize in a rather simple layered yet closest-packed hexagonal crystal structure. Still, these compounds display a wide range of magnetic and electronic properties.

Examples include ferromagnetism[1], antiferromagnetism[2] and superconductivity[3]. Taken together, tuning the C32 diborides via compositional tuning and/or by applying pressure, allows for an investigation of quantum phase transitions or changes of the Fermi surfaces topology in a simple, crystallographically unchanged environment. Additionally, the hexagonal structure may give rise to geometrical frustration.

However, presumably due to the very high melting temperatures of the C32 diborides and the resulting lack of high-quality samples, the electronic and magnetic properties of most of these compounds have not been explored in detail so far. We report a comprehensive study of high-purity polycrystals and single crystals of MB₂ (M = Cr, Mn, Nb, V, Zr, Dy, Er, Gd, Ho, Pr, Tb, Tm, Y, Yb).

All samples were prepared from 99% boron-11 enriched boron. A thorough metallurgical characterization is followed by first investigations of the low-temperature properties by means of magnetization, ac susceptibility, specific heat, and electrical transport.

As a result, our study establishes a sound basis for future experiments in this fascinating class of materials.

[1] T. Mori et al., Phys. Rev. B, 79, 104418 (2009)

[2] R. G. Barnes et al., Phys. Lett. A 29, 203 (1969) [3] J. Nagamatsu et al., Nature, 410, 63, (2001)

TH.C-P116 - CuMnSb: between local and itinerant antiferromagnetism

P. Jorba Cabré¹, A. Bauer¹, A. Regnat¹, G. Brandl¹, B. Roessli², A. Senyshyn³, M. Meven³, S. Gottlieb-Schönmeyer¹, K. Hradil⁴, Peter Böni¹, C. Pfleiderer¹

1. *Technical University of Munich - Physik Department, Munich, Germany*

2. *Laboratory of neutron scattering, PSI, Switzerland*

3. *Heinz Maier-Leibnitz Zentrum (MLZ), Munich, Germany*

4. *Universität Wien, X-ray center, Wien, Austria*

At room temperature, CuMnSb crystalizes in the cubic $C1_b$ half-Heusler structure. Other than most isostructural siblings, which order ferromagnetically at temperatures of a few hundred Kelvin, CuMnSb exhibits antiferromagnetism with a relatively low Neel temperature (≈ 55 K). We have successfully grown the first single crystals from optically float-zoned polycrystalline feed rods. After a detailed metallurgical characterization, we have collected magnetization, specific heat, electrical resistivity, Hall effect, thermal conductivity, as well as both elastic and inelastic neutron scattering data. Curiously, CuMnSb combines typical properties of local-moment and itinerant magnets in a rather unique manner. While the commensurate magnetic structure with ordered moments that correspond to the fluctuating moments is typical for local-moment magnetism, the high stability of the order in magnetic fields, and the metallic behavior of the sample, are a strong arguments in favor of itinerant magnetism. A comparably high Curie-Weiss temperature alludes to the presence of disorder-induced geometric frustration. At a lower temperature ($T^* \approx 35$ K) a second transition has been observed, corresponding to a slight reorientation of the spins of about 10° from the [111] direction. The inelastic neutron experiment revealed an interesting spin wave dispersion with a 3 meV gap closing at T_N , and an unusual broadening that could be explained by magnetic fluctuations or by anti-site disorder. Furthermore, inelastic neutron scattering under pressure, has reveal an unexpected change in the magnetic order.

TH.C-P118 - High pressure phase diagram of the singlet-ground-state magnet CsFeCl₃

N. Kurita¹, H. Tanaka¹

1. Tokyo Institute of Technology, Tokyo, Japan

CsFeCl₃ is a hexagonal ABX₃-type compound where Fe²⁺ ions with an effective S=1 form ferromagnetic spin chains along the c-axis and antiferromagnetic (AF) triangular lattices in the c-plane. Owing to the single-ion anisotropy D, the ground state becomes a spin singlet with a finite gap for the first excited state. In CsFeCl₃, the D-term overcomes the exchange interactions and hence no magnetic ordering is observed in zero field. Application of magnetic field along the c-axis suppresses the excitation gap and, above the critical field H_c~4T, an antiferromagnetically ordered state appears [1]. With applying pressure, the antiferromagnetic (AF) phase is extended toward both higher temperature and lower field regimes [2]. For further understanding of the AF phase in CsFeCl₃, we have performed magnetization measurements in the low temperature range down to 0.5 K at ambient pressure, and down to 1.8 K at several pressures up to 1.5 GPa. In the magnetization process at 0.5 K, an anomaly at 3.8 T associated with the AF transition is clearly observed, as compared to the previous result measured at 1.8 K. Together with temperature dependence of magnetic susceptibility under several fields, a more detailed field-temperature phase diagram of CsFeCl₃ is obtained at ambient pressure. With increasing pressure, H_c monotonically decreases. At high pressures exceeding the critical pressure of P_c~0.9 GPa, an anomaly associated with the AF transition is observable in a nearly zero field.

[1] T. Haseda et al., Physica B & C 108B, 841 (1981)

[2] Y. Sasaki et al., Prog. Theor. Phys. Suppl. 159, 402 (2005)

TH.C-P119 - Spin relaxation process in Cr_{1-x}Fe_{x}

S. Säubert^{1,2}, G. Benka², P. Schmakat^{1,2}, J. Kindervater³, A. Bauer², J. N. Wagner⁴, W. Häussler¹, O. Holderer¹, S. M. Shapiro⁵, P. Böni³, C. Pfleiderer²

1. *Heinz Maier-Leibnitz Zentrum (MLZ), Technische Universität München, Garching, Germany*
2. *Lehrstuhl für Topologie korrelierter Systeme, Technische Universität München, Garching, Germany*
3. *Lehrstuhl für Neutronenstreuung, Technische Universität München, Garching, Germany*
4. *Karlsruher Institute for Technology, IAM-WK, Eggenstein-Leopoldshafen, Germany*
5. *Brookhaven National Laboratory, Department of Physics, Upton, United States*

Cr_{1-x}Fe_{x} shows reentrant spin glass behaviour below a doping dependent freezing temperature $T_{\{f\}}$. In contrast to a classical spin glass, the transition at $T_{\{f\}}$ separates the spin glass state from a magnetically ordered rather than a disordered state. For low concentrations x the ordered state is antiferromagnetic and changes first to paramagnetic and subsequently to ferromagnetic state with increasing x [1, 2].

We report a study of the spin relaxation process in Cr_{1-x}Fe_{x} by means of high resolution neutron spin echo, magnetisation measurements and neutron depolarisation imaging for a wide range of concentrations x . This allows us to compare the relaxation process depending on the particular state at high temperatures. Our measurements provide an unprecedented combination of microscopic information on the spin dynamics and spin freezing on multiple length and time scales.

[1] S. K. Burke et al., J. Phys. F: Met. Phys. 13 (1983) 45 1-470 [2] S. M. Shapiro et al., Phys. Rev. B 24 (1981), 6661

TH.C-P120 - Magnetic structure of the ordered kondo compound YbNi₃Al₉ single crystal

Y. Uwatoko³, K. Munakata¹, Y. Nambu², T. Tanaka³, K. Matsubayashi³, T. Hirayama³, T. Yamashita⁴, S. Ohara⁴

1. *Comprehensive Research Organization for Science and Society, Tokai, 319-1106, Japan*

2. *Institute of Multidisciplinary Research for Advanced Materials, Tohoku University, Sendai, Japan*

3. *Institute for Solid State Physics, The University of Tokyo, Kashiwanoha, Kashiwa, Japan*

4. *Department of Engineering Physics, Electronics and Mechanics, Graduate School of Engineering, Nagoya Institute of Technology, Nagoya, Japan*

As well known, the Yb-based intermetallic compounds can induce a magnetically ordered state from a nonmagnetic state due to the hole-electron analogy of Yb magnetic 4f¹³ electrons by applying pressure. YbNi₃Al₉ displays typical characteristics of a heavy-fermion antiferromagnet with a Neel temperature of $T_N = 3.4$ K and an enhanced electronic specific heat coefficient of 100 mJ/(mol K²), reflecting a competition between the Kondo effect and the crystalline electric field (CEF) effect [1]. The crystal structure is identified as the trigonal ErNi₃Al₉-type with chiral space group R32. Recent reports on the physical properties of YbNi₃X₉ (X = Al, Ga) single crystals revealed different ground states under pressure at low temperatures [2]. In this paper, we report neutron diffraction studies of YbNi₃Al₉ that show $q = (0, 0, 0.8)$ spiral antiferromagnetic ordering below T_N , with a magnetic moment 1.2(2) μ_B per Yb that is orientated within the ab plane. We also present magnetic properties at ambient pressure.

References:

[1] S. Ohara et al., J. Phys.: Conf. Ser. 273, 012048 (2011). T. Yamashita et al., J. Phys. Soc. Jpn. 81, 034705 (2012)

[2] T. Hirayama et al., J. Phys.: Conf. Ser. 391, 012020 (2012), K. Matsubayashi et al, Phys. Rev Lett. 114, 086401 (2014)

TH.C-P122 - in MnSi

I. I. Lobanova^{1,2}, V. Glushkov^{1,2}, N. Sluchanko², S. Demishev^{1,2}

1. *Moscow Institute of Physics And Technology (State University), Moscow, Russian Federation*

2. *Prokhorov General Physics Institute of RAS, Moscow, Russian Federation*

Non-centrosymmetric B20 helical magnet MnSi attracts attention of scientific community due to pressure-induced quantum criticality [1], skyrmion lattice formed below $T_c \sim 30$ K [2] and topological Hall effect observed in this non-trivial spin texture [3]. However, the features of the spin-polarized (SP) state, into which the helical one collapses at $B > 0.6$ T, are not well understood up to now. It was recently shown that the vertical phase boundary between the SP and paramagnetic (P) states as well as the universal scaling of magnetoresistance as squared magnetization in P phase of MnSi can be explained in terms of Heisenberg type localized moments rather than within itinerant magnetism model generally applied to this system [4]. To shed more light on the charge carriers scattering the anisotropy of transverse magnetoresistance (TMR) has been studied at 2-60 K by measuring bar-shaped single crystal in magnetic field $B < 6$ T applied perpendicular to $\langle 110 \rangle$ axis. The explicit difference between temperature and field dependences of TMR for $B \parallel \langle 001 \rangle$ and $B \parallel \langle 110 \rangle$ has been detected in both SP and P phases. In moderate magnetic field $B < 2$ T the TMR anisotropy was found to change the sign at T_C , while at higher fields the transition region broadens falling into the range from 23 K to 40 K at $B = 6$ T. No distinct anomaly was observed for $B \parallel \langle 111 \rangle$, which corresponds to the pitch vector of magnetic helix formed in the ground state of MnSi. The results are discussed in terms of phase separated state formed in MnSi in vicinity of the SP-P phase transition.

[1] D. Belitz et al., Phys. Rev. Lett. 94, 247205 (2005)

[2] A. Tonomura et al., Nano Lett. 12, 1673 (2012)

[3] A. Neubauer et al., Phys. Rev. Lett. 102, 186602 (2009)

[4] S.V. Demishev et al., Phys. Rev. B 85, 045131 (2012)

TH.C-P124 - Competing interactions in $\text{Er}_x\text{Pr}_{(1-x)}\text{Co}_2$

F. Bartolomé¹, J. Bartolomé¹, L. García¹, C. Marcela Bonilla², Y. Skourski³

1. ICMA, Departamento de Física de la Materia Condensada, CSIC-Universidad de Zaragoza, Zaragoza, Spain

2. Ames Laboratory, Iowa State University, Ames, United States

3. Hochfeld-Magnetlabor Dresden, Helmholtz-Zentrum Dresden-Rossendorf, Dresden, Germany

Among the rare-earth R, transition metal T, intermetallics, the Co Laves phases are particularly interesting because of the magnetism of the 3d band in these systems is strongly influenced by the R sublattice magnetization. If the R bears a magnetic moment, the f-d exchange results in a ferro- (light R) or ferrimagnetic (heavy R) coupling between the Co and the R magnetization sublattices. High magnetic fields force ferrimagnetic RCo_2 to gradually change the antiparallel alignment between the R and the Co moments towards a ferromagnetic phase. In particular, for ErCo_2 a transition at 52 T has been reported, which was identified as Itinerant Electron Metamagnetism (IEM) [1]. On the other hand, in ferromagnetic systems (as PrCo_2) no field induced transition has been detected. The local interactions can be modified by substituting Er by Pr, changing the internal exchange fields to give rise to spin flipping transitions. In this work we have systematically measured the low-temperature high-field magnetization of $\text{Er}_x\text{Pr}_{(1-x)}\text{Co}_2$ at 4, 10, and 40 K at the Dresden High Magnetic Field Laboratory. Er substitution $\text{Er}_x\text{Pr}_{(1-x)}\text{Co}_2$ by Pr sets the condition for the system to undergo a field induced phase transition, ranging between 22 T ($x=0.1$) and 50 T ($x=0.9$). A clear jump in magnetization is observed in every diluted system. The modification on the internal exchange fields with increasing x plays the major role in modifying the critical field.

[1] J. J. M. Franse et al. Handbook of magnetic materials, Elsevier 7, 307 (1993)

TH.C-P126 - Thermal expansion and magnetostriction of Pr₃Pd₂₀Ge₆

O. Iwakami¹, Y. Yao¹, S. Abe¹, K. Matsumoto¹, G. Ano², M. Akatsu³, K. Mitsumoto¹, Y. Nemoto¹, T. Goto¹, N. Takeda⁴, H. Kitazawa⁵

1. Department of Physics, Kanazawa University, Japan
2. Graduate School of Science and Technology, Niigata University, Japan
3. Department of Physics, Niigata University, Japan
4. Faculty of Engineering, Niigata University, Japan
5. National Institute for Materials Science, Tsukuba, Japan

The clathrate compound Pr₃Pd₂₀Ge₆ is an interesting compound showing rattling motions of praseodymium (Pr) atoms, quadrupole order of 4f electrons, and hyperfine-enhanced nuclear magnetism. This compound has a Cr₂₃C₆-type cubic structure, where the Pr ions are located at two different crystallographic sites. The ground states at the 4a and 8c sites are a Γ_5 triplet and a non-Kramers Γ_3 doublet, respectively. Magnetic ordering and quadrupole ordering in Pr₃Pd₂₀Ge₆ have been studied by ultrasound and ac-susceptibility measurements [1, 2]. In the present study, we have performed thermal-expansion and magnetostriction measurements on single-crystalline sample of Pr₃Pd₂₀Ge₆ along [001] and [110] axes. The thermal expansion and magnetostriction were measured by a capacitance method in the temperature range of 2 and 30 K under the magnetic fields up to 8 T. We observed a difference of the magnetostriction between [001] and [110] axes. This lattice distortion was discussed in terms of CEF effects and symmetry strains.

[1] G. Ano et al., J. Phys. Soc. Jpn. 81, 034710 (2012)

[2] O. Iwakami et al., Phys. Rev. B 90(10), 100402 (2014)

TH.C-P127 - Synthesis and characterization of compositionally graded Fe-Rh films

N. B. Doan¹, Y. Dusch¹, G. Diguët¹, N. Dempsey¹, L. Ranno¹

1. CNRS - Institut NEEL, Grenoble, France

The chemically ordered near-equiatomic FeRh phase that exhibits an abrupt antiferromagnetic to ferromagnetic transition close to 350 K is of interest from both the viewpoint of fundamental physics and for potential applications. The latter interest is based on the fact that the magneto-structural phase transition gives rise to magneto-caloric, magneto-resistive and magneto-strictive effects. It was already shown that phase change characteristics, and thus the material's functional properties, depend on the chemical composition and degree of chemical order. Very recent studies have revealed that the transition characteristics can also be tuned through strain, controlled through epitaxial growth on single crystalline substrates with a particular lattice parameter or through the use of piezoelectric substrates. Here, we report on a study compositionally graded FeRh films deposited onto both Si and PNM-PT substrates by magnetron sputtering of composite targets. The interest of such compositionally graded films lies in the fact that both magnetic and structural properties can be studied as a function of film composition, all other deposition and annealing parameters being constant, and that the interface between ferromagnetic and antiferromagnetic zones can be studied. The film composition, as measured by EDX, was shown to vary linearly across the substrate at a rate of 5.4 at%Rh/cm. We will report on temperature and field dependent magnetization and resistivity measurements made on samples of different composition, using a VSM-SQUID and transport rig, respectively. We will then report on how the application of voltage to the piezoelectric substrate influences the phase change characteristics.

This work was funded by the EC FP 7/2007-2013 programme under grant agreement n° 310748 (DRREAM).

TH.C-P128 - Critical exponents and hall effect in iron- and cobalt-based metallic glasses

A. Rosales-Rivera¹, J. Hernandez-Parra¹, J. Lopez-Tabares¹, J. Hincapie-Bedoya¹, A. Velasquez-Salazar¹, D. Gomez-Montoya¹, J. Chavarria-Rubio¹, F. Daniel Saccone²

1. *Laboratorio De Magnetismo Y Materiales Avanzados, Universidad Nacional De Colombia, Sede Manizales, Colombia*

2. *Laboratorio de Sólidos Amorfos, INTECIN, FIUBA-CONICET, Buenos Aires, Argentina*

In this work, we investigate the universality class and the Hall effect of three different metallic glasses, namely Fe₇₀Nb₁₀B₂₀, (Fe₅₀Co₅₀)₇₅Si₅B₂₀, and Co₇₀Nb₁₀B₂₀. In so doing, we determined the critical exponents for the zero-field magnetization (β) and critical isotherm (δ) and critical temperatures from magnetization measurements. These metallic glasses were prepared as amorphous alloy ribbons by means of the melt spinning technique. The magnetization as a function of temperature of each sample was measured in the range 300-950 K using a vibrating sample magnetometer (VSM-VersaLab by Quantum Design) at fixed external magnetic fields (H). The Hall effect measurements were carried out at room temperature for applied dc magnetic field and dc electrical current varied in the range $-10 < H < 10$ kOe and $10 < I_{dc} < 50$ mA, respectively.

The present study shows that the magnetic features of Fe₇₀Nb₁₀B₂₀ and (Fe₅₀Co₅₀)₇₅Si₅B₂₀ are distinct in some aspects from the corresponding ones found in the soft magnetic metallic glass but less localized Co₇₀Nb₁₀B₂₀. In fact, the universality class of the first two metallic glasses seems to correspond to the Ising model ($\hat{O} = 0.332$), while that in the latter seems to be more near with the Heisenberg model ($\beta = 0.371$). The possible mechanisms leading to such universality classes including the spin-orbit interaction, shape anisotropies, direct exchange and itinerant exchange are analyzed. The Hall effect experiments indicate that the extraordinary Hall contribution decreases more rapidly on Co₇₀Nb₁₀B₂₀ as compared to (Fe₅₀Co₅₀)₇₅Si₅B₂₀ and Fe₇₀Nb₁₀B₂₀.

TH.D-P01 - Full potential calculation of magnetic properties of TbFe₂

M. Imaizumi¹, C. Soufen¹

1. Universidade Paulista Julio De Mesquita Filho –Unesp, Sao Paulo, Brazil

Rare-earth metals named group of lanthanides combine with Fe 3d transition metals to form a series of RFe₂ cubic phase Laves intermetallic compounds and it was thoroughly investigated during last years. These materials crystallize in the MgCu₂ (Fd m) Laves phase and exhibit a number of interesting magnetic applications. In this structure the equivalent atom to Mg atom, the Rare- Earth atom, occupies equivalent sites with cubic point symmetry. Most of these intermetallic compounds are ferromagnetic. Then ab initio calculation has been performed on magnetic properties of intermetallic compound. The Kohn - Sham equations were solved by applying the full potential linearized augmented plane wave (FPLAPW) method with spin orbit coupling(LS). In this approach the local density approximation (LDA) was substituted for (LDA+U) as exchange - correlation potential due to the strong electron - electron interaction. These calculations provide the total energy as function of volume, the total and partial densities of states and spin magnetic moment. From total energy the equilibrium lattice parameter and total energy in equilibrium volume were calculated. The spin magnetic moment was calculated from the difference between the majority and the minority total density of states below the Fermi energy. The spin magnetic moment calculated was 6.70 μ_B while the experimental value was 6.30 μ_B . Our results are in according to the values reported in the literature.

TH.D-P02 - High-field magnetoelasticity of Tm_2Co_{17}

A. V. Andreev¹, Y. Skourski², A. A. Zvyagin³, S. Yasin², S. Zherlitsyn²

1. *Institute of Physics, Academy of Sciences, Prague, Czech Republic*

2. *Dresden High Magnetic Field Laboratory, Helmholtz-Zentrum Dresden-Rossendorf Dresden, Germany*

3. *B.I. Verkin Institute for Low Temperature Physics and Engineering of the National Academy of Sciences of Ukraine, Kharkov, Ukraine*

Er_2Co_{17} and Tm_2Co_{17} (hexagonal structure) are ferrimagnets which exhibit a field-induced transition at 40 T field applied along the c axis. In spite of the similar magnetic properties, the transition in Er_2Co_{17} and Tm_2Co_{17} looks different. In Er_2Co_{17} it is clearly of the first order and corresponds to sharp rotation of the Er sublattice. In the case of Tm_2Co_{17} , the transition is attributed to a direct ferri-to-ferromagnetic transformation in a way of paramagnetic remagnetization of the Tm sublattice which is very unusual. The explanation looks reasonable but it would be useful to confirm this by different behavior of other properties at the transition. The transition in Er_2Co_{17} is accompanied by sharp anomalies in the sound velocity and magnetostriction. If the transition in Tm_2Co_{17} has indeed a different origin, it should be seen in the magnetoelastic effects accompanying the transition.

We measured sound velocity and magnetostriction in pulsed fields up to 65 T applied along the c axis of Tm_2Co_{17} single crystal grown in triarc furnace by Czochraski method. Similar to Er_2Co_{17} , the transition in Tm_2Co_{17} is accompanied by clear anomalies in the sound velocity. The observed 0.3% jump of the sound velocity at the transition is negative in Tm_2Co_{17} , whereas it is positive in Er_2Co_{17} . The magnetostriction at the transition also differs very much from that in Er_2Co_{17} . In Tm_2Co_{17} , the transition is accompanied by a smooth minimum of $0.15 \cdot 10^{-4}$ in longitudinal magnetostriction whereas in Er_2Co_{17} by a very sharp expansion of much larger magnitude ($1.2 \cdot 10^{-4}$). In the transverse mode, the effect in Tm_2Co_{17} looks as very broad minimum of low amplitude ($< 0.1 \cdot 10^{-4}$) whereas in Er_2Co_{17} as very sharp and large shrinkage ($2.6 \cdot 10^{-4}$). Thus, both the magnetoacoustics and magnetostriction are rather different in Tm_2Co_{17} and Er_2Co_{17} . This supports our idea about different nature of the field-induced transitions in these compounds.

TH.D-P03 - Ferromagnetism in UCoAl induced by Os dopingA. V. Andreev¹, K. Shirasaki², J. Sebek¹, D. I. Gorbunov^{1,3}, S. Danis⁴, T. Yamamura²*1. Institute of Physics, Academy of Sciences, Prague, Czech Republic**2. Institute for Materials Research, Tohoku University, Katahira 2-1-1, Sendai, Japan**3. Dresden High Magnetic Field Laboratory (HLD), Helmholtz-Zentrum Dresden-Rossendorf, Dresden, Germany**4. Department of Condensed Matter Physics, Charles University, Prague, Czech Republic*

UCoAl (hexagonal crystal structure) exhibits a metamagnetic transition from the paramagnetic ground state to the forced ferromagnetic state in a uniquely low transition field of 0.7 T applied along the c axis. A magnetic moment at the transition is induced on U but the state of the 5f electrons depends very drastically on the interaction with ligands. When Co is substituted by Fe, Ru, Rh, Ir, the critical field of the transition rapidly decreases and already few % doping stabilizes ferromagnetism. Opposite, Ni, Pd, Pt stabilize paramagnetism.

In the present work we studied influence of Os on the magnetism of UCoAl. The homogeneity range in the UCo_{1-x}Os_xAl system is limited to x = 0.2 with a small lattice expansion in the basal plane. Magnetization measurements performed on single crystals show that compounds with x = 0.02, 0.05, 0.10 are ferromagnets with easy c axis. The spontaneous magnetic moment M_s increases from 0.40 mB per formula unit at x = 0.02 to 0.53 mB at x = 0.10, which is almost twice larger than the magnetic moment induced at the metamagnetic transition in UCoAl. All the compounds exhibit huge magnetic anisotropy characteristic for UCoAl. Extrapolation of the a-axis magnetization curves to crossing with M = M_s gives anisotropy field H_a as 120-130 T. But this method does not take into account that the easy-axis magnetization is not saturated in the maximum applied field and grows even faster than the hard-axis one. So, the real H_a as a field of crossing of the easy- and hard-axis curves is considerably larger than these already huge values. Similarly to M_s, the Curie temperature increases with x and reaches 48 K for x = 0.10. Thus, Os stabilizes ferromagnetism in UCoAl considerably stronger than Rh and Ir and slightly stronger than Fe and Ru.

TH.D-P04 - Single crystal study of layered U_nRhIn_{3n+2} materials: case of the novel U_2RhIn_8 compoundA. Bartha¹, M. Kratochvílová¹, M. Dušek², M. Diviš¹, J. Custers¹, V. Sechovský¹

1. Department of Condensed Matter Physics, Charles University, Praha, Czech Republic

2. Department of Structure Analysis, Institute of Physics ASCR, Praha, Czech Republic

We report on the single crystal properties of the novel U_2RhIn_8 compound studied in the context of parent $URhIn_5$ [1] and UIn_3 [2] systems. The compounds were prepared by In self-flux method. U_2RhIn_8 adopts the Ho_2CoGa_8 -type structure with lattice parameters $a = 4.6056(6)$ Å and $c = 11.9911(15)$ Å. The behavior of U_2RhIn_8 strongly resembles that of related $URhIn_5$ with respect to magnetization, specific heat and resistivity showing strong magnetocrystalline anisotropy. U_2RhIn_8 orders antiferromagnetically below $T_N = 117$ K and exhibits slightly enhanced Sommerfeld coefficient $\gamma = 47$ mJ.mol⁻¹.K⁻². T_N increases with increasing c/a ratio within the $UIn_3 - URhIn_5 - U_2RhIn_8$ series contrasting with the behavior of the cerium counterparts. Magnetic field leaves the value of Néel temperature for both $URhIn_5$ and U_2RhIn_8 unaffected up to 9 T. On the other hand, T_N increases with applying hydrostatic pressure up to $T_N = 126$ K at 3.2 GPa. The character of uranium 5f electron states of U_2RhIn_8 was studied by first principles calculations based on the density functional theory combined with Hubbard model.

[1] Y. Matsumoto *et al.*, *Phys. Rev. B* 88 (2013) 045120[2] Y. Tokiwa *et al.*, *J. Phys. Soc. Jpn.* 70 (2001) 3326

TH.D-P06 - Effect of pressure on magnetothermal properties and glassy dynamics in magnetization in Nd₇Pd₃

P. Kumar¹, R. Kumar², C. Shekhar³, A. Coelho⁴, S. Gama⁴, K.G. Suresh⁵

1. *Indian Institute of Information Technology Allahabad, Allahabad, India*

2. *National Physical Laboratories, New Delhi, India*

3. *Max Planck Institute for Chemical Physics of Solids, Dresden, Germany*

4. *Instituto de Física "Gleb Wataghin", Universidade Estadual de Campinas-UNICAMP, Campinas, Brazil*

5. *Indian Institute of Technology Bombay, Mumbai, India*

We have study the effect of external pressure on the magneto thermal properties and magnetization relaxation measurements across the ferromagnetic to antiferromagnetic transition of polycrystalline compounds Nd₇Pd₃. We observed three transition temperatures T_t, T_c and T_N at 15 K, 34K and 39K respectively. The ordering temperature T_c and T_N of the Nd₇Pd₃ are found to strong dependent on pressure ($dT_c/dP=-1.9K/bar$ and $dT_N/dP=-0.31K/bar$) whereas insensitive with T_t. Large magnetic entropy change has been also observed near T_c and its sensitive with pressure also. The transition is incomplete at low temperatures with the stretched exponential relaxation behavior dominating over the power law, which is indicative of glassy dynamics or the arrest of the kinetics of the phase transition. In the intermediate temperature regime, the magnetic relaxation can be explained as a combination of both the power law and stretched exponential. We will discuss in details in full paper.

TH.D-P07 - Control of magnetic properties in alpha-Dy₂S₃ single crystal by using magnetic field

S. Ebisu¹, K. Fuji¹, Guoqing¹, Y. Shibayama¹

1. Muroran Institute of Technology, Japan

Control of magnetic properties has been attempted in alpha-Dy₂S₃ single crystal by using magnetic field. alpha-Dy₂S₃ possesses orthorhombic crystal structure having two crystallographically inequivalent Dy sites and shows successive antiferromagnetic transitions at TN1 = 11.4 K and TN2 = 6.4 K associated with various steep responses in physical properties. Such features are considered to originate from existence of metastable magnetic phases. A metastable phase induced by cooling in strong magnetic field of 18 T had been found in our previous work. In the present study, we have attempted to induce new magnetic phases by using the magnetic field of 7 T. Rotating magnetic field direction in the ac-plane of alpha-Dy₂S₃ single crystal, which is actually performed by rotation of the sample in rigid magnetic field, brings about an anomalous increase of the magnetization up to 8.4 muB/Dy-atom at 6.0 K in the magnetic field of 7 T along the a-axis. The a-direction magnetization at the same condition in the stable phase is 5.4 muB/Dy-atom. This metastable phase induced by the rotation of the magnetic field persists until 1.3 T in the process of decreasing the magnetic field. The values of the magnetization below 1.3 T are consistent with those in the stable phase. The magnetization of this metastable phase has the same magnitude as the one of the metastable phase induced by strong-field cooling at 18 T; therefore, these metastable phases are inferred to be the same. Moreover, a certain process that combines the rotating of the magnetic field with cooling the sample in the magnetic field gives rise to exchange of the features of the magnetization curves for the a- and c-direction. Consequently, the easy magnetization axis in the ac-plane switches to the c-axis after this process from the a-axis in normal situation.

TH.D-P08 - Magnetic properties of double doped UH₃-based hydrides

M. Paukov¹, I. Tkach¹, D. Drozdenko¹, P. Minárik¹, D. Kriegner¹, Z. Matej¹, S. Masková¹, L. Havela¹

1. Charles University, Prague, Czech Republic

Interaction with hydrogen is an important issue related to application of uranium and its alloys. Any contact of α -U with H leads to formation of the stable allotropic form β -UH₃, a dark pyrophoric powder, formed via the metastable α -UH₃. Bcc U-Mo and U-Zr alloys form different types of hydrides, although both are based on UH₃. While the U-Mo alloys lead to amorphous structure based on β -UH₃ (grain size 1 nm), the U-Zr alloys lead to crystalline hydrides of the α -UH₃ type, which could be therefore synthesized first time without the β -UH₃ admixture. Surprisingly their magnetic properties are very similar and both groups exhibit first an increase of Curie temperature with the concentration of dopants. Thus T_C can exceed $T = 200$ K in the Mo case. Provided the amorphous structure guaranteed by Mo, it can accept other types of dopants in addition. We tested for Ti, Fe, and Zr and investigated variations of magnetic properties. We assumed that the amorphous structure must be more accepting diverse sizes of dopant atoms. Our investigation of magnetic properties of such double doped hydrides shows ferromagnetic ordering with parameters only weakly depending on the dopants. The addition of Zr enhances T_C more than addition of Ti, addition of Fe broadens the transition and enhances magnetization per U atom.

TH.D-P09 - Hexanuclear lanthanide clusters exhibiting magnetic chilling and relaxation properties

J. Tong¹, X. Xu¹, G. Luo¹

1. Xiangyang Noncommissioned officers School, China

Polynuclear lanthanide complexes are intensively studied because of the fascinating magnetic properties, including magnetocaloric effect (MCE) and single-molecule magnetism (SMM).[1-4] And studying clusters with similar structures has considerable significance to improve our knowledge of the structure-magnetic property correlation of the LnIII complexes. In our effort to synthesize polynuclear lanthanide complexes, we have employed the homologous ligands H₂ppo and H₂Meppo, which potentially show various coordination modes that can form new polynuclear complexes. And gives rise to four analogous hexanuclear lanthanide complexes with the same skeleton, include two GdIII₆ complexes and two DyIII₆ complexes. Magnetic studies have revealed large magnetocaloric effect in the two weak antiferromagnetic GdIII₆ complexes and SMM behaviors in the two ferromagnetic DyIII₆ complexes. The differences in the nature of magnetic couplings between two GdIII₆ complexes and two DyIII₆ complexes are likely affected by the easy axes through the ligand fields and the slightly differences in structures through employed homologous ligands.

References:

1. M. Affronte, A. Ghirri, S. Carretta, G. Amoretti, S. Piligkos, G. A. Timco and R. E. P. Winpenny, *Appl. Phys. Lett.*, 2004, 84, 3468
2. M. Manoli, A. Collins, S. Parsons, A. Candini, M. Evangelisti and E. K. Brechin, *J. Am. Chem. Soc.*, 2008, 130, 11129
3. L. Bogani and W. Wernsdorfer, *Nat. Mater.*, 2008, 7, 179. 4. R. Sessoli, *Angew. Chem., Int. Ed.*, 2012, 51, 45

TH.D-P11 - Metamagnetic transition in TmCo₄Al

A.V. Andreev¹, O. Isnard^{2,3}, Y. Skourski², D.I. Gorbunov^{1,4}

1. *Institute of Physics, Academy of Sciences, Prague, Czech Republic*

2. *Université Grenoble Alpes, Institut NÉEL, Grenoble, France*

3. *CNRS, Institut NÉEL, Grenoble, France*

4. *Dresden High Magnetic Field Laboratory, Helmholtz-Zentrum Dresden-Rossendorf Dresden, Germany*

The high-field (up to 60 T) magnetization was studied on single crystal intermetallic compound TmCo₄Al having hexagonal crystal structure of CaCu₅ type. Single crystal was grown by a modified Czochralski method in triarc furnace.

TmCo₄Al is a ferrimagnet with Curie temperature $T_C=490$ K and spontaneous magnetic moment $M_s = 2.1 m_B$ per formula unit (at 4.2 K) directed along the *c* axis. The Tm sublattice dominates at low temperatures but weakens with increasing temperature faster than the Co sublattice, so above the compensation point $T_{comp} = 87$ K the total moment is along the Co sublattice.

It was found that the compound exhibits sharp metamagnetic transition with critical field of 29 T (at 4.2 K) applied along the *c* axis which corresponds to rotation of the Co sublattice. Magnetic moment of the Co sublattice (in assumption of collinear antiparallel arrangement of the Tm and Co sublattices in the ground state) can be determined from the difference between $7 m_B$ (moment of Tm³⁺ ion) and total M_s as $5 m_B$. Therefore, the observed magnetic moment $12 m_B$ after the metamagnetic transition corresponds to the forced ferromagnetic arrangement of the sublattices ($M = M_{Tm} + M_{Co}$) and no more transitions should be expected in higher fields. The critical field of the transition decreases with increasing temperature and becomes zero at T_{comp} . Above T_{comp} where the Tm sublattice is antiparallel to the field direction, no transition is observed. However, the *c*-axis susceptibility dM/dH is much larger than below T_{comp} . It points to a continuous rotation of the Tm sublattice toward the magnetic field, in contrast to the first-order process when the Co sublattice rotates.

The high-field behavior of TmCo₄Al is discussed in comparison with results on other intermetallics of Tm with 3d-metal recently studied on the single crystals (Tm₂Co₁₇, Tm₂Fe₁₇, TmFe₅Al₇).

TH.D-P12 - *I-V* characteristics in CdMoO₄:Nd³⁺ single crystal

B. Sawicki¹, E. Tomaszewicz², M. Berkowski³, H. Duda¹, T. Groń¹

1. Institute of Physics, University of Silesia, Katowice, Poland

2. Department of Inorganic and Analytical Chemistry, West Pomeranian University of Technology, Szczecin, Poland

3. Institute of Physics, Polish Academy of Sciences, Warszawa, Poland

Scheelite-type ABO₄ molybdates and tungstates form important group of materials widely used in several technical applications. They have been used as solid state scintillators and laser host materials. Doped with rare earth ions they have been applied as diode pumped solid-state lasers with very high stability of emission of nano- or femtosecond pulses.

Single crystal of new cadmium and neodymium molybdate CdMoO₄:Nd³⁺

(Cd_{0.958}Nd_{0.028}□_{0.014}MoO₄) has been successfully grown by the Czochralski method. The X-ray diffraction analysis confirmed that this solid solution crystallizes in the scheelite type structure with the space group *I*4₁/*a* [1]. Our previous studies showed paramagnetic behaviour of CdMoO₄:Nd³⁺ single crystal [2].

The main purpose of this study was to investigate the *I-V* characteristics using a KEITHLEY 6517B Electrometer/High Resistance Meter. The *I-V* characteristics, measured at 300 and 400 K showed a non-symmetric and non-linear behavior (back to back diode-like). Larger values of current in the forward direction was observed at 300 K and crystallographic plane *a* than at 400 K and crystallographic plane *c*.

This work was supported by Ministry of Scientific Research and Information Technology (Poland) and funded from science resources: No. 1S-0300-500-1-05-06 and No. DS-518-10-020-3101.

[1] E. Tomaszewicz, S.M. Kaczmarek, H. Fuks, *Mat. Chem. Phys.* 122 (2010) 595

[2] T. Groń, E. Tomaszewicz, M. Berkowski, J. Kusz, M. Oboz, *SCTE 2014 - 19th International Conference on Solid Compounds of Transition Elements*, 21-26 June 2014, Genova, Italy, Book of Abstracts, p.142

TH.D-P13 - Magnetic properties of NdPd₅Al₂

J. Zubáč¹, K. Vlaskova¹, P. Javorsky¹

1. Charles University, Faculty of Mathematics And Physics, Prague, Czech Republic

Antiferromagnetic NdPd₅Al₂ belongs to a large family of structurally related ternary tetragonal intermetallics which includes RT₅X₂, RTX₅ and R₂TX₈ compounds (R represents rare earth element or actinide, T is a transition metal and X is a p-metal). Several of these compounds are considered as archetypal unconventional heavy-fermion superconductors. We report on magnetic and physical properties of NdPd₅Al₂ as their non-superconducting magnetic analogue.

NdPd₅Al₂ crystallizes in the ZrNi₂Al₅-type structure with lattice parameters $a = 4.147 \text{ \AA}$ and $c = 14.875 \text{ \AA}$. The magnetic phase transition occurs at $T_N = 1.3 \text{ K}$. The antiferromagnetic ordering survives in magnetic fields applied perpendicular to c-axis up to 3 T; in higher fields the compound is already in the field-induced ferromagnetic state. The compound exhibits a distinct magnetocrystalline anisotropy due to the crystal field effects with c-axis as easy magnetization direction. Specific heat analysis indicates the first excited crystal field level around 40 K. The presented study is focused particularly on explanation of magnetic properties in terms of crystal field interactions and comparison to other relevant materials with similar structure.

TH.D-P15 - Searching for superconductivity in NpAl₂: a study of low temperature ground state propertiesJ. Griveau¹, E. Colineau¹, L. Martel¹, R. Eloirdi¹, R. Caciuffo¹*1. European Commission, Joint Research Centre (JRC), Institute for Transuranium Elements (ITU), Karlsruhe, Germany*

We report the results of an extensive study of the ground state properties of NpAl₂, a compound in which 5f electrons are considered to be well localized and that represents a reference system for ferromagnetism in actinides. Considerations on its bulk properties (ordering temperature T_C , 5f effective paramagnetic moment and T_C decrease with pressure) point to a strong analogy with the non-conventional superconductor UGe₂, raising questions about the possible occurrence of superconductivity at low temperature and/or under compression. Low temperature magnetic, electrical transport, and thermodynamic measurements under an external magnetic field (up to 14 T) will be reported for the first time, together with results of ²⁷Al NMR spectroscopy measurements in the paramagnetic state.

Precise dc magnetisation data confirm ferromagnetic ordering ($T_C \sim 56$ K) but also indicate that thermal treatments change the ferromagnetic characteristics of the material (from weak to moderate magnet), whilst ac magnetic susceptibility shows the presence of an anomaly at ~ 21 K not reported before. Thermal treatments also modify the anomaly of the heat capacity curve associated with magnetic order. An enhanced electronic contribution $g_e \sim 80$ mJ mol⁻¹ K⁻² clearly indicates the presence of electronic carriers. The electrical resistivity curves ($RRR > 15$), very similar to those measured for UGe₂, exhibit a slight maximum above T_C . Finally, the variable offset cumulative spectra (VOCS), acquired in the paramagnetic state by NMR spectroscopy, show a high sensitivity of the ²⁷Al nuclei spectral parameters (Knight shift and line broadening) to ferromagnetic fluctuations, even at room temperature.

This work reveals a partial delocalised nature of the 5f carriers in NpAl₂, whose bulk properties appear to be similar to those of UGe₂.

TH.D-P17 - 5d-3d antiferromagnetic spin coupling of Tm and Lu adatoms with Fe monoatomic islands on W(110) probed by spin-polarized tunneling microscopyD. Coffey^{1,2}, J. L. Diez-Ferrer¹, D. Serrate^{1,2}, M. Ciria^{2,3}, C. de la Fuente^{2,3}, J. I. Arnaudas^{1,2}

1. *Lab. de Microscopías Avanzadas - Inst. de Nanociencia de Aragón, Univ. de Zaragoza, Zaragoza, Spain*

2. *Depto. de Física de la Materia Condensada - Univ. de Zaragoza, Zaragoza, Spain*

3. *Instituto de Ciencia de Materiales de Aragón, CSIC-Univ. de Zaragoza, Zaragoza, Spain*

In Rare Earth-Transition Metal (RE-TM) compounds the RE-TM magnetic interaction proceeds via an indirect mechanism in which the 5d electrons act as the intermediary.[1] Intra-atomic exchange ferromagnetically couples the 4f and 5d spins of the RE and the interatomic direct 5d-3d exchange, associated with the hybridization of the pure TM-3d and RE-5d bands,[2] produces the final coupling between the RE and the TM spin moments. When the 5d band is less than half full and the 3d band is more than half full, the case of RE-(ferromagnetic TM) compounds, the 5d-3d exchange is antiferromagnetic and the RE and TM spins couple antiparallel. Here, we report on an extreme situation, where only adatoms of RE are adsorbed on a TM ferromagnetic monolayer. We have investigated with scanning tunneling microscopy and spectroscopy Thulium and Lutetium adatoms, deposited on iron monolayer islands, with in-plane magnetization,[3] pseudomorphically grown on a clean W(110) substrate under ultra-high vacuum conditions, at low temperature. The spin polarized differential conductance images obtained with an Fe covered tungsten tip and taken both at constant height and at constant current, show that Tm and Lu present a contrast opposite to the one shown by the respective Fe islands beneath. A possible dependence on the spin polarization shown by the adatom on the energy and vertical distance to the tip [4] has been discarded by performing the measurements at different bias and heights without appreciable modification of the reversed contrast observed between the adatom and the island. These results, combined with first-principles calculations indicate that the Lu and Tm 5d moments lie in plane and couple antiferromagnetically with their underlying iron islands, in agreement with the Campbell model even at the single atom limit.

[1] I. A. Campbell, J. Phys. F Met. Phys. 2, L47 (1972)

[2] M. S. S. Brooks and B. Johansson, in Handbook of Magnetic Materials, Buschow K. H. J. (ed.), Elsevier, Vol. 7, Chap. 3, Amsterdam (1993)

[3] N. Weber et al., Phys. Rev. B 55, 14121 (1997)

[4] N. Néel et al., Phys. Rev. B 85, 155406 (2012)

TH.D-P18 - Optical and magneto-optical interactions in Co doped CeO₂ thin films prepared by pulsed laser deposition

M. Zahradnik¹, M. Kucera¹, R. Antos¹, M. Veis¹, J. Mistrik², L. Bi³, H. Kim³, G. F. Dionne³, C. A. Ross³

1. Charles University of Prague, Faculty of Mathematics and Physics, Prague, Czech Republic

2. University of Pardubice, Department of Physics, Pardubice, Czech Republic

3. Department of Materials Science and Engineering, Massachusetts Institute of Technology, Cambridge, United States

Magnetically doped CeO₂ is a dilute magnetic semiconductor with high Curie temperature and excellent silicon compatibility [1, 2]. These properties make it a promising material for applications in integrated non-reciprocal photonic devices. Knowledge of complete permittivity tensor is necessary to enhance the non-reciprocal effect and to optimize the device functionality. Here we investigate magnetically doped thin films of Ce_{1-x}Co_xO_{2-δ} prepared by pulsed laser deposition on MgO (x = 0.05 and 0.10) and oxidized Si (x = 0.20) substrates. The samples grew as polycrystalline films with thickness ranges from 262 to 753 nm and out-of-plane easy axis. A systematic study was performed by combination of spectroscopic ellipsometry and magneto-optical (MO) Faraday and Kerr spectroscopy. Both diagonal and off-diagonal permittivity tensor components were obtained and verified by theoretical calculations confronted with experimental data. Diagonal spectra obtained from spectroscopic ellipsometry revealed two optical transitions between oxygen and cerium states. off-diagonal spectra fitted from MO Faraday spectra revealed two paramagnetic transitions involving cobalt ions. Proper spectral dependence of the permittivity tensor was confirmed by MO Kerr spectroscopy. Calculated MO Kerr effect showed excellent agreement with the experimental data. Measurements performed at temperature of liquid nitrogen excluded temperature dependence of MO Faraday effect and therefore confirmed proposed theoretical model. An essential influence of cobalt doping on the resulting ferromagnetic properties of CeO₂ was observed.

[1] A.Tiwary et al., Appl. Phys. Lett. 88 (2006) 142511

[2] L. Bi et al., J. Appl. Phys. 103 (2008) 07D138

TH.D-P19 - Deviations from Matthiessen rule and resistivity saturation effects in rare-earth metals revealed in first principles calculations

J. Glasbrenner¹, B. Pujari¹, K. Belashchenko¹

1. University of Nebraska-Lincoln, United States

According to earlier first-principles calculations [1], the spin-disorder contribution to the resistivity of rare-earth metals in the paramagnetic state is strongly underestimated if Matthiessen's rule is assumed to hold. To understand this discrepancy, the resistivity of paramagnetic Gd (and Fe for comparison) is here [2] evaluated by taking into account both spin and phonon disorder. Calculations are performed using the supercell approach within the linear muffin-tin orbital method. Phonon disorder is modeled by introducing random displacements of the atomic nuclei, and the results are compared with the case of fictitious Anderson disorder. In both cases the resistivity shows a nonlinear dependence on the square of the disorder potential, which is interpreted as a resistivity saturation effect. This effect is much stronger in Gd than in Fe. The non-linearity makes the phonon and spin-disorder contributions to the resistivity non-additive, and the standard procedure of extracting the spin-disorder resistivity by extrapolation from high temperatures becomes ambiguous. An "apparent" spin-disorder resistivity obtained through such extrapolation is in much better agreement with experiment compared to the results obtained by considering only spin disorder. By analyzing the spectral function of the paramagnetic Gd in the presence of Anderson disorder, the resistivity saturation is explained by the collapse of a large area of the Fermi surface due to the disorder-induced mixing between the electronic and hole sheets.

[1] J. K. Glasbrenner et al., Phys. Rev. B 85, 214405 (2012)

[2] J. K. Glasbrenner, B. S. Pujari, and K. D. Belashchenko, Phys. Rev. B 89, 174408 (2014)

TH.D-P20 - Crystal field effects in polymorphic compound Tblr₂Si₂T. Shigeoka¹, Y. Kurata¹, T. Nakata¹, T. Fujiwara¹, K. Matubayashi², Y. Uwatoko²

1. Yamaguchi University, Japan

2. University of Tokyo, Japan

The tetragonal ternary compound Tblr₂Si₂ exhibits polymorphism; it has two different crystallographic structures: the ThCr₂Si₂-type structure (I4/mmm, centrosymmetry: I phase) and the CaBe₂Ge₂-type one (P4/nmm, non-centrosymmetry: P phase) without changing chemical composition [1]. So this compound is suitable to study how physical properties are influenced by crystallographic symmetry. We succeeded to grow both Tblr₂Si₂ (P and I phase) single crystals and performed magnetic measurements. The compounds of both phases exhibit antiferromagnetic orderings while the magnetic behavior changes drastically depending on the symmetry. The Tblr₂Si₂ (I) has the high magnetic ordering temperature of TN=80 K and a strong magnetic anisotropy with the easy direction of the c-axis. It has two magnetic transitions at 9.5 K and 2.5 K besides TN. On the other hand, the Tblr₂Si₂ (P) has comparatively low ordering temperature of TN2=12 K and another transition temperature of TN1=5 K, and exhibits relatively weak magnetic anisotropy with the easy direction in the ab-plane. In the both compounds, anomalies, which suggest the existence of component-separated magnetic transitions, are observed on the temperature dependence of magnetic susceptibility, indicating a frustration. It is noticeable that the ab-component of magnetic moment orders at higher temperature for the P-phase compound, which is contrast to usual behavior; the c-component orders at higher temperature usually as the behavior of the I-phase compound. We think this novel behavior has been never known so far, and expect that the P-phase compound has a novel magnetic order. Crystal field effects was estimated from magnetization processes and magnetic susceptibility. Difference of magnetic anisotropy between both compounds is explain by crystal field effects.

[1] Wang-Xian Zhang, B. Lloret, Wee Lam Ng, B. Chevalier, J. Etourneau and P. Hagenmuller, Rev. Chem. Minerale, 22, 711 (1985)

TH.D-P21 - Non-equilibrium behavior of the magnetization in the helimagnetic phases of the rare earth alloys $R_{1-x}Y_x$ ($R = \text{Gd, Tb, Dy}$)T. Yamazaki¹, J. Ishiyama¹, Y. Noya¹, M. Kurihara¹, H. Yaguchi¹*1. Department of Physics, Faculty of Science And Technology, Tokyo University of Science, Japan*

The magnetic alloy system $\text{Gd}_{1-x}\text{Y}_x$ shows a para-helimagnetic phase transition at a Néel temperature, T_{N} and a heli-ferromagnetic phase transition at a Curie temperature, T_{C} in the Y-concentration range of $0.3 < x < 0.4$. In our previous study, we measured AC- and DC-magnetization of $\text{Gd}_{0.62}\text{Y}_{0.38}$ in low magnetic field, and observed non-equilibrium behavior of the magnetization along the a^* -axis in the helimagnetic phase. Features associated with the observed behavior are itemized as follows: (i) difference between the zero-field-cooled (ZFC) magnetization and the field-cooled (FC) magnetization, (ii) enhancement of the imaginary part of the AC-susceptibility, (iii) strong nonlinearity of the magnetization around T_{N} . The features (i)~(iii) are similar to those observed commonly in spin-glass systems. This similarity suggests that a novel non-equilibrium state such as a helical-glass state, which is theoretically proposed near ferromagnetic quantum critical points, is realized in the helimagnetic phase of $\text{Gd}_{0.62}\text{Y}_{0.38}$.

In order to search such glass-like behavior in analogous materials, we have investigated the magnetic properties of polycrystalline samples of Tb, Dy, their magnetically diluted alloy systems $\text{Tb}_{1-x}\text{Y}_x$ ($x = 0.14, 0.28$) and $\text{Dy}_{1-x}\text{Y}_x$ ($x = 0.03, 0.50$). Clear differences between the ZFC and FC magnetizations were observed in all of these materials, although the difference observed in Dy and $\text{Dy}_{1-x}\text{Y}_x$ was rather small. The non-linearity of the magnetization is observed only in Tb and $\text{Tb}_{0.86}\text{Y}_{0.14}$. This suggests that the non-equilibrium behavior observed in these materials relates to the strength of the ferromagnetic interaction.

TH.D-P22 - Charge density wave stabilization in $\text{LaSb}_{2-x}\text{Ce}_x$ by Ce ion substitution

R. F. Luccas^{1,2,3}, J. Hanco², A. Fente^{2,3}, N. A. Correa-Orellana^{1,2,3}, E. Climent-Pascual¹, J. Azpeitia^{1,2,3}, T. Perez-Castañeda², M. R. Osorio², N. M. Nemes^{1,3}, F. J. Mompean^{1,3}, E. Salas⁴, E. Herrera-Vasco^{2,3}, I. Guillamón^{2,3}, M. García-Hernández^{1,3}, J.G. Rodrigo^{2,3}, M.A. Ramos^{2,3}, H. Suderow^{2,3}

1. Instituto de Ciencia de Materiales de Madrid, Consejo Superior de Investigaciones Científicas (ICMM-CSIC), Madrid, Spain

2. Laboratorio de Bajas Temperaturas, Departamento de Física de la Materia Condensada, Instituto de Ciencia de Materiales Nicolás Cabrera, Condensed Matter Physics Center (IFIMAC), Universidad Autónoma de Madrid, Madrid, Spain

3. Unidad Asociada de Bajas Temperaturas y Altos Campos Magnéticos, UAM, CSIC, Cantoblanco, Madrid, Spain

4. Spiline Spanish CRG Beamline at the European Synchrotron Radiation Facilities, ESRF, Grenoble, France

CeSb_2 is a well-known layered compound having several magnetic transitions at low temperatures. On the other hand, LaSb_2 is known as a two dimensional metal that shares the same layered structure. However, a linear magnetoresistance is observed on this last system, which has been associated to some sort of charge ordering.

In this work the observation of a Charge Density Wave (CDW) order in the $\text{La}_{1-x}\text{Ce}_x\text{Sb}_2$ family compound is reported. Crystals of several compositions x ($0 < x < 1$) have been grown using flux method. Variation of the lattice parameters with x has been found. A previously unnoticed kink in the resistivity of LaSb_2 at temperatures higher than room temperature has been also found. A charge modulations superposed to the atomic lattice has been observed by Scanning Tunneling Microscopy experiments. Our results show that a CDW is present in the superconductor LaSb_2 , which is stabilized in presence of substitutional disorder at a finite x . The CDW onset temperature is observed decreasing with increasing x and competing with magnetism from Ce. The magnetic phase diagram is made from the specific heat anomalies and shows magnetic transitions for $x > 0.4$.

TH.D-P23 - Magnetic phase diagram of non-kramers Γ_3 doublet system PrPb_3 by specific heat measurementsY. Sato¹, Y. Inagaki¹, T. Kawae¹, T. Onimaru², H. Suzuki³1. *Department of Applied Quantum Physics, Kyushu University, Japan*2. *Department of Quantum Matter, Hiroshima University, Japan*3. *National Institute for Material Science, Ibaraki, Japan*

Multipolar ordering in the magnetic fields has been intensively studied during the last two decades. Especially, many studies on CeB_6 , which is the typical example to show anomalous multipolar ordered phases, have been devoted experimentally and theoretically and clarified that the field-induced multipoles have a key role on the multipolar ordered phase in the magnetic fields[1]. To reveal the concrete role, we focus on a non-Kramers Γ_3 doublet system in Pr-compounds because the Γ_3 doublet, which carries O_2^0 -type and O_2^2 -type quadrupoles, is the one of the simplest multipolar-degenerate system.

A PrPb_3 has a Γ_3 doublet as a ground state and is well known to show the antiferro quadrupolar ordering at $T_Q = 0.4$ K[2]. We measured the specific heat of the single crystal of PrPb_3 in the magnetic fields up to $H = 8$ T along [100], [110], and [111] crystalline directions. The obtained magnetic phase diagram in $H \parallel [100]$ shows the appearance of a new high-field phase above $H = 5$ T[3]. In addition, the high-field phase are also observed in $H \parallel [110]$ above $H = 6$ T, which is consistent with the previous report by magnetization measurements[4]. In the case of $H \parallel [100]$ and [110], the type and symmetry of the field-inducible multipoles is different between O_2^0 -type and O_2^2 -type quadrupole[1]. Therefore, these results indicate that the phase transition from O_2^0 -type quadrupolar ordered phase to O_2^2 -type one is induced due to the difference of the field-inducible multipole between each ordered phase.

On the other hand, the specific heats in $H \parallel [111]$ show no evidence that ordered phase exists at least above $H = 6$ T. The result can be understood by reflecting the feature that the field-inducible multipoles have the same symmetry between each quadrupoles in $H \parallel [111]$ [1].

[1] R. Shiina, et al., J. Phys. Soc. Jpn. 66 (1997) 1741

[2] E. Bucher, et al., J. Low. Temp. 2 (1972) 322

[3] Y. Sato, et al., J. Phys. Soc. Jpn. 79 (2010) 093708

[4] T. Onimaru, et al., J. Phys. Chem. Solids. 68 (2007) 2091

TH.D-P24 - Magnetic properties of CePtIn₄K. Uhlířová¹, P. Proschek¹, J. Prokleska¹*1. Charles University In Prague, Faculty of Mathematics And Physics, Department of Condensed Matter Physics, Praha , Czech Republic*

We report on single crystals growth and magnetic properties of CePtIn₄, a new indium rich Ce-Pt-In compound. Single crystals of CePtIn₄ were grown by indium flux method. The compound was characterized by microprobe analysis and x-ray diffraction. It adopts YNiAl₄ –type crystal structure similar to other recently published compounds CeNiIn₄ and EuNiIn₄ [1-3]. Specific heat, magnetization and electrical resistivity measurement have shown an antiferromagnetic transition at $T_{N1} = 2.3$ K and another transition at 0.9 K is visible in specific heat data. This behavior resembles the properties of iso-structural CeNiIn₄ and EuNiIn₄ with antiferromagnetic order below $T_{N1} = 1.4$ K and 13 K, respectively, and second order-to order magnetic transitions at lower temperatures [1-3]. However, compare to these compounds, CePtIn₄ has very low Sommerfeld coefficient $\gamma = 3$ mJ mol⁻¹K⁻². The magnetic part of entropy calculated from the specific heat data reaches value of $R \ln 2$ showing localized character of the Ce³⁺ moments. Magnetization isotherms at 1.8 K show on metamagnetic transition at field of 1T applied along the *b*-axis while magnetization measured along *a*- and *c*-axis show linear dependence up to field of 7 T. This behavior is consistent with specific heat measurements in magnetic field applied along the principal crystallographic directions; the Néel temperature quickly decreases when magnetic field is applied along the *b*-axis while in the other directions it is almost intact.

1. Kushwaha, P., et al., Crystal Growth & Design, 2014. 14(6): p. 2747-2752
2. Shishido, H., et al., Journal of the Physical Society of Japan, 2004. 73(3): p. 664-668
3. Rosa, P.F.S., et al., Journal of Magnetism and Magnetic Materials, 2014. 371: p. 5-9

TH.D-P25 - Site-selective magnetic order of neptunium in $\text{Np}_2\text{Ni}_{17}$

A. Hen¹, E. Colineau¹, R. Eloird¹, J.-C. Griveau¹, N. Magnani¹, J.-P. Sanchez², I. Halevy^{3,4}, I. Orion³, A. B. Shick⁵, R. Caciuffo¹

1. *European Commission, Joint Research Centre (JRC), Institute For Transuranium Elements (ITU), Karlsruhe, Germany*
2. *SPSMS, UMR-E CEA/UJF-Grenoble 1, INAC, Grenoble, France*
3. *Nuclear Engineering Department, Ben Gurion University, Beer-Sheva, Israel*
4. *Physics Department, Nuclear Research Center Negev, Beer-Sheva, Israel*
5. *Institute of Physics, Academy of Sciences of The Czech Republic, Prague, Czech Republic*

We report the results of a study carried out on a neptunium-transition-metal binary compound $\text{Np}_2\text{Ni}_{17}$, which has been synthesized and characterized by means of: Powder X-Ray Diffraction, SQUID magnetometry, ^{237}Np Mössbauer spectroscopy and specific heat. $\text{Np}_2\text{Ni}_{17}$ is a derived crystallographic structure of NpNi_5 [1] and is the Nickel analogue of $\text{Np}_2\text{Co}_{17}$ [2]. $\text{Np}_2\text{Ni}_{17}$ crystallized in the $\text{Th}_2\text{Ni}_{17}$ hexagonal structure (P6₃/mmc no. 194) with a room temperature lattice parameters $a = 8.28215(7)$ and $c = 8.04029(8)$ Å, containing two non-equivalent Np sites. $\text{Np}_2\text{Ni}_{17}$ exhibits an antiferromagnetic order below $T_N \sim 17.5$ K. Mössbauer spectra in the ordered state show two ordered Np sites, one with a huge ordered moment ($\mu_{\text{Np}} \sim 2.25 \mu_B$) and the other carry hardly any ordered moment at all ($\mu_{\text{Np}} \sim 0.2 \mu_B$). C_p measurements confirm the onset of an antiferromagnetic order while revealing a complex low temperature behaviour, with both electronic and magnetic Shottky anomalies that are present.

TH.E-P01 - Ab initio theory of the gilbert damping in random alloys: the torque-correlation formulation

I. Turek¹, J. Kudrnovsky², V. Drchal²

1. Institute of Physics of Materials, Acad. Sci. Czech Rep., Brno, Czech Republic

2. Institute of Physics, Acad. Sci. Czech Rep., Praha, Czech Republic

We present a formulation of the Gilbert damping tensor within the fully relativistic linear muffin-tin orbital (LMTO) method for substitutionally disordered ferromagnetic alloys. We show that the true, but random spin-torque operators in the original torque-correlation formula [1] can be replaced by non-random effective spin-torque operators, which simplifies the configurational averaging in the coherent-potential approximation (CPA) considerably.

The resulting Kubo-Greenwood formula for the Gilbert damping tensor represents thus an obvious analogy of the LMTO formula for the conductivity tensor containing non-random effective velocity operators [2]. Particular attention is paid to the related vertex corrections indispensable for an internal consistency of the theory. We prove a special Ward identity which yields several important properties of the Gilbert damping tensor: (i) its vanishing in the non-relativistic limit, (ii) its vanishing in the non-magnetic limit, and (iii) its transverse nature, i.e., the only non-zero components of the tensor are appropriate for the dynamics of small deviations of the magnetization direction from the equilibrium orientation.

The developed theory, implemented in the atomic-sphere approximation, is applied to fcc Ni-Fe and bcc Fe-V alloys. The calculated results show that the coherent part of the Gilbert damping constant is always positive, in contrast to recent results for Fe-rich Fe-V alloys based on the random spin-torque operators [1].

[1] S. Mankovsky, D. Koedderitzsch, G. Woltersdorf, H. Ebert: Phys. Rev. B 87, 014430 (2013)

[2] I. Turek, J. Kudrnovsky, V. Drchal: Phys. Rev. B 89, 064405 (2014)

TH.E-P02 - Relativistic effects on electron transport in magnetic alloys

V. Drchal¹, J. Kudrnovsky¹, I. Turek²

1. *Institute of Physics, AS CR, Prague, Czech Republic*

2. *Institute of Physics of Materials, AS CR, Prague, Czech Republic*

We study relativistic effects on electron transport in spin-polarized metals and random alloys on ab initio level using the fully relativistic tight-binding linear muffin-tin-orbital method. We employ Kubo linear-response approach adapted to disordered multisublattice systems in which the chemical disorder is described in terms of the coherent potential approximation (CPA). The CPA vertex corrections are included. We calculate both the Fermi surface and Fermi sea terms of the full conductivity tensor. We find that in cubic ferromagnetic 3d transition metals (Fe, Co, Ni) and their random binary alloys (Ni-Fe, Fe-Si) the Fermi sea term is small in comparison with the Fermi surface term, however, in more complicated structures, such as hexagonal cobalt and selected Co-based Heusler alloys, it becomes important. High values of the anisotropic magnetoresistance (AMR), found for Ni-rich alloys, are explained by a negligible disorder in the majority spin channel while a change of the sign of the anomalous Hall effect on alloying is a band-filling effect without a direct relation to the high AMR. We also study the effect of the structural long-range order and thermal spin disorder on the transport properties of partially ordered Fe-Pt alloys [2]. The main result is that all components of the resistivity tensor increase with disorder, but anomalous Hall resistivity increases much faster than the longitudinal resistivity. We find an overall good agreement between the theory and experimental data.

[1] I. Turek, J. Kudrnovsky and V. Drchal: Phys. Rev. B 89, 064405 (2014)

[2] J. Kudrnovsky, V. Drchal and I. Turek: Phys. Rev. B 89, 224422 (2014)

TH.E-P03 - Modulation of the amplitude of spin transfer torque in double barrier magnetic tunnel junctions

C. Baraduc¹, P. Clément¹, P. Coelho¹, C. Ducruet², L. Vila³, M. Chshiev¹, B. Dieny¹

1. *Spintec, Grenoble, France*

2. *Crocus Technology, Santa Clara, United States*

3. *SP2M/NM - CEA Grenoble, France*

Double barrier magnetic tunnel junctions are of particular interest concerning spin transfer torque issues. In such structures, it has been shown that spin transfer torque (STT) exerted on the magnetization of the central free layer can be enhanced [1], correlatively yielding a decrease of the critical current for STT magnetization switching [2,3], which may lead to low consumption devices. Here we show that spin transfer torque may be either enhanced or reduced depending of the magnetic configuration of the top and bottom electrodes. When their magnetizations are antiparallel, STT amplitude will be maximum, yielding an easy switching. On the contrary, if they are parallel, STT amplitude will decrease so much that the probability of switching, even at high voltages, is almost zero. Thus reading a MRAM could be performed at higher voltage with no risk of writing and consequently at higher speed. This effect could pave the way towards more reliable and faster magnetic memories. Results obtained on double junctions with reference layers composed of two pinned synthetic antiferromagnet will be presented. Both in-plane (Slonczewski's) and out-of-plane (field-like) torques are studied. Since these two torques add and subtract differently, specific effects can be observed in these dual junctions. In particular, we demonstrated magnetization switching by pure field-like torque.

[1] B. Diény et al., US patent 20050002228A1 (2005)

[2] G. Fuchs et al., Appl. Phys. Lett. 86, 152509 (2005)

[3] Z. Diao et al., Appl. Phys. Lett. 90, 132508 (2007)

TH.E-P04 - The study of the spin proximity effect from a solution of the modified boltzmann transport equations

V. Zayets¹

1. Spintronics Research Center, AIST, Japan

The spin proximity effect describes the fact that at a contact between two conductors, the spin accumulation diffuses from the conductor with a higher spin polarization to the conductor with a smaller spin polarization. For example, in the vicinity of a contact between a ferromagnetic and non-magnetic metals, in the ferromagnetic metal the equilibrium spin accumulation becomes smaller than in the bulk and the electron gas in the non-magnetic metal becomes spin-polarized. The spin proximity effect and the spin injection were studied using a solution of the modified Boltzmann transport equations [1,2]. It was found that the origin of the spin proximity effect is the spin diffusion. In contrast, the origin of the spin injection is the spin drift. It was shown that the spin injection only modifies the distribution of the spin accumulation across the contact, which was initially established due to the spin proximity effect. It was demonstrated that the electrons with energies below and above the Fermi energy contributes differently into the these effects. In the case of the spin injection, the contributions are of the opposite signs. In the case of the spin proximity effect, the contributions are of the same sign. The reason of this difference is that the electrons and the holes are drifted in the opposite directions, but they diffuses in the same direction. As result, the spin injection in a metal is not efficient, but the spin proximity effect is substantial. In a metal significant drift current is required in order to modify the distribution of the spin accumulation across a contact enough so that the spin injection can be detected.

The physical mechanism of an enlargement of spin accumulation due to the ordinary Hall effect was described.

TH.E-P05 - Resonant magnetoresistance in asymmetrical double-barrier magnetic tunnel junction

 N. Useinov¹, L. Tagirov¹

1. Kazan Federal University, Russian Federation

High tunneling magnetoresistance (TMR) is now well known in single magnetic tunnel junctions (SMTJs). Besides single-barrier, the double-barrier MTJs (DMTJs) have also been extensively studied for the novel physical phenomena and potential applications in spintronic devices [1]. In our work the resonant tunneling is studied theoretically for the asymmetrical DMTJ with a bias voltage. In this nanostructure the magnetization of the middle ferromagnetic metal layer can be aligned parallel (P) or antiparallel (AP) with respect to the fixed magnetizations of the external ferromagnetic electrodes. Analytical expression for the transmission coefficient of the DMTJ is received

$$T_{2b,s}^{P(AP)} = 1 / \left[T_{1,s}^{-1} T_{2,s}^{-1} + (T_{1,s}^{-1} - 1)(T_{2,s}^{-1} - 1) + 2 \sqrt{T_{1,s}^{-1} (T_{1,s}^{-1} - 1)} \sqrt{T_{2,s}^{-1} (T_{2,s}^{-1} - 1)} \cos \Phi_{V,s} \right],$$

which is expressed through the single-barrier transmission coefficients $T_{1,s}$ and $T_{2,s}$ taking into account the voltage drop on each barrier and spin degrees of freedom of the electron. Here, $\Phi_{V,s}$ is the characteristic phase under the applied bias. The theoretical model of the spin-polarized conduction and TMR in planar nanocontacts with different ferromagnetic metals is developed [2]. The dependences of the transmission coefficient and TMR on the applied voltage under resonant conditions, $\cos \Phi_{V,s} = -1$, are shown in Fig. 1 and Fig. 2. The parameters used in the calculations of the curves correspond to article [2].

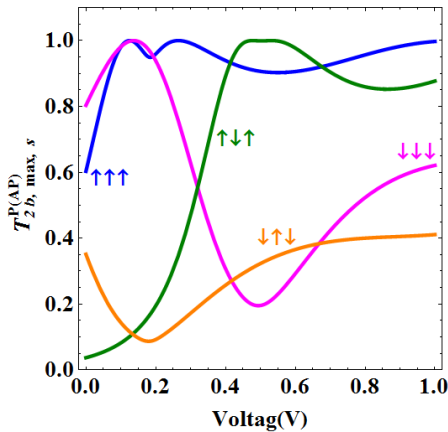


Fig. 1 Transmission coefficient vs bias in the asymmetrical DMTJ for four spin conduction channel is denoted by arrows.

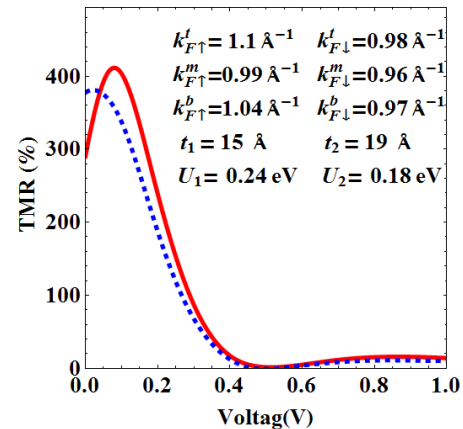


Fig. 2 TMR in the case of resonant (solid line) and non-resonant (dot line) tunnelling of electrons through the DMTJ.

Acknowledgement: The reported study was partially supported by RFBR, research project No. 14-02-00348 a.

[1] Edited by E. Tsymbal and I. Žutić. Handbook of Spin Transport and Magnetism. CRC Press Taylor & Francis Group © 2012

[2] N.Kh. Useinov, D.A. Petukhov, L.R. Tagirov, JMMM 373 27 (2015)

TH.E-P06 - Spin-pumping using the Ni₈₀Fe₂₀ thin film annealed in a magnetic field

H. Shimogiku¹, N. Hanayama², Y. Teki³, H. Tsujimoto¹, E. Shikoh¹

1. Graduate School of Engineering, Osaka City University, Japan

2. Faculty of Engineering, Osaka City University, Japan

3. Graduate School of Science, Osaka City University, Japan

The spin current by the spin-pumping with the ferromagnetic resonance (FMR) is enhanced by improving the ferromagnetic material as the spin injector. In this study, a Ni₈₀Fe₂₀ thin film, which is easily formed, was focused and the magnetic property of the Ni₈₀Fe₂₀ was controlled by annealing in a magnetic field.

A Ni₈₀Fe₂₀ (25)/Pd (10 nm in thick) bilayer sample was prepared on a SiO₂/Si substrate by using an electron-beam deposition under the vacuum of 10⁻⁶ Pa. After the depositions, the sample was annealed in the external magnetic field of 30 mT under the vacuum of 10⁻³ Pa. The maximum temperature in the annealing was set to be 673 K, and the temperature was gradually lowered. When the FMR of the A Ni₈₀Fe₂₀ of the sample was excited, a spin current was generated in the Pd layer by the spin-pumping. Then, the spin current was converted to a charge current by the inverse spin-Hall effect (ISHE) in the Pd layer, and detected as the electromotive force.

The output voltage due to the ISHE of the annealed sample was 2.60 μV when the static magnetic field direction in the annealing was parallel to that under the FMR, while that of the non-annealed sample was 1.94 μV. That is, the output voltage became 1.3 times larger by using the annealing than that without the annealing. The output voltage due to the ISHE in the Pd and the static and dynamic magnetic properties of the A Ni₈₀Fe₂₀ film were dependent on the applied magnetic field direction in the annealing. The results indicated that the spin current generation efficiency by the spin-pumping was increased by using the A Ni₈₀Fe₂₀ annealed after the film making, without using the other special techniques like an epitaxial growth in the film making process [1].

[1] H. Shimogiku, et al., cond-mat:arXiv.1407.7028 (2014)

TH.E-P08 - Enhanced giant magnetoresistance signals in lateral spin valves

G. Zahnd^{1,2}, Y. T. Van Pham^{1, 2}, W. Savero Torres^{1,2}, P. Laczkowski^{1,2}, L. Vila^{1,2}, V. Dai Nguyen^{1,2}, J.C. Rojas Sanchez^{1,2}, Alain Marty^{1,2}, C. Vergnaud^{1,2}, C. Beigné^{1, 2}, L. Notin^{1,2}, M. Jamet^{1,2}, J. Attané^{1,2}

1. *Institut Nanosciences Et Cryogenie, CEA, Grenoble, France*

2. *Université Grenoble Alpes, Grenoble, France*

The development of metallic lateral spin valves is being hampered by their low output signal. Indeed, the obtained giant magneto-resistance (GMR) is smaller than 1% and non-local measurement are used to detect such low spin signals. Nonetheless those devices are already very useful for the investigations of several basic sciences, such as spin caloritronics, spinorbitronics and all spin logics. There are several strategies to increase the output signal, such as confinement effect [1], the reduction of the spin back flow by the insertion of tunnel barriers [2] as well as innovative designs [3]. In combination of a material study and a careful design of the structures we achieved GMR signals at room temperature of 6% and we target 50 % at the 25 nm node. Indeed, the decrease of the device size is automatically associated to an increase of the output signal, due to an increase of the spin resistances as well as the decrease of the spin relaxation within the non-magnetic spin channel (bridging the spin injector and spin detector). We could thus envisioning signals comparable to that of multilayered pillars. Notably, the use of CoFe as ferromagnetic material allowed the increase by a factor of height of the spin signal compared to Py, the most commonly used material. These results are, for instance, an important step toward the use of lateral devices as reading elements in hard disk drives.

[1] P. Laczkowski, et al. *Physical Review B* 85 (22), 220404 (2012)

[2] Y. Fukuma, et al, *Nature Materials*, 10, 527~531 (2011)

[3] W. Savero Torres, et al. *Nano letters* 14 (7), 4016-4022 (2014)

TH.E-P09 - Modulation of pure spin currents with a ferromagnetic insulator

E.Villamor¹, M. Isasa¹, S. Vélez¹, A. Bedoya-Pinto¹, P. Vavassori^{1,2}, L. E. Hueso^{1,2}, F. S. Bergeret^{3,4}, F.Casanova^{1,2}

1. CIC NanoGUNE, Donostia-San Sebastian, Spain

2. IKERBASQUE, Basque Foundation for Science, Bilbao, Spain

3. Centro de Física de Materiales (CFM-MPC) Centro Mixto CSIC-UPV/EHU, Donostia-San Sebastian, Spain

4. Donostia International Physics Center (DIPC), Donostia-San Sebastian, Spain

Spintronics is a rapidly growing field that aims at using and manipulating not only the charge, but also the spin of the electron. Sophisticated applications such as hard-disk read heads and MRAMs have been introduced in the last two decades. Further progress could be achieved with pure spin currents, which are an essential ingredient in an envisioned spin-only circuit that would integrate logics and memory. One of the most robust experimental approaches to create pure spin currents is by using lateral spin valves (LSV) in a non-local geometry [1]. However, electrical manipulation of pure spin currents (via spin-orbit coupling, as proposed by Datta and Das) has a fundamental limitation, because the best spin-transport materials are those showing the lowest spin-orbit.

We propose and demonstrate an alternative way of modulating pure spin currents based on magnetic, instead of electric, gating, by taking advantage of the spin-mixing conductance concept. To that end, Co/Cu LSVs have been fabricated on top of a ferromagnetic insulator (YIG). A modulation of the pure spin current is observed as a function of the relative orientation between the magnetization of YIG and the polarization of the spin current. Such modulation is explained by solving the spin-diffusion equation and considering the spin-mixing conductance (G_r) at the Cu/YIG interface. The accuracy between the measured data and the expected modulation provides an effective way of studying the interface. From our results, $G_r \sim 4 \times 10^{11} \Omega^{-1} \text{m}^{-2}$ is obtained. An increase of this value will enhance the efficiency of the magnetic gating. This can be achieved by carefully tuning the fabrication parameters. Our experiment paves the way for novel manners of spin manipulation, bringing closer pure spin currents and logic circuits [2].

[1] E. Villamor *et al.*, Phys. Rev. B 88, 184411 (2013)

[2] E. Villamor *et al.*, Phys. Rev. B 91, 020403(R) (2015)

TH.E-P10 - Spin current transport in a Nb/Cu/NiFe tri-layer structure

K. Ohnishi^{1,2}, Y. Ono¹, M. Sakamoto¹, T. Kimura^{1,2}

1. Dept. of Physics, Kyushu University, Japan

2. Research Center for Quantum Nano-Spin Sciences, Kyushu University, Japan

The ferromagnet/superconductor hybrid structure has attracted the attention because the Cooper pair in the ferromagnet is expected to show unique transports such as 0- π transition in a Josephson junction and spin triplet supercurrent. These spin-dependent superconducting phenomena can be induced also in the nonmagnetic metal under the spin injection because the spin accumulation induced in the normal metal is similarly treated as a conduction electron state in a ferromagnet. However, the experimental study in these systems has not been performed sufficiently because of the influence of the charge current such as Joule heating and Oersted field.

In this report, we investigated spin current transport in a nanopillar-based lateral spin valve structure consisting of Permalloy(Py)/Cu/Nb trilayer, which strongly suppress the aforementioned current-induced effects.

The spin transport properties have been evaluated by measuring the nonlocal spin valve signal, namely spin signal. The spin signal below 30 K is almost constant when the Nb is in the normal metal state. When the Nb becomes superconductor below 6.8 K, the spin signal increases with decreasing the temperature. This indicates that the spin-current absorption is strongly suppressed at the Cu/Nb interface because the spin current cannot enter into the superconducting energy gap.

From this result, we can estimate the temperature dependence of the superconducting gap magnitude at the Nb/Cu interface. Moreover, around 2.3 K, we observe the superconducting proximity effect in the Cu layer. This indicates that the spin-polarized electrons and Cooper pairs coexist in the Cu layer around 2.3 K.

This is an important step for the observation of the spin dependent superconducting phenomena.

TH.E-P11 - Study of the ferromagnetic resonance properties in epitaxial FePt samples

A. Conca¹, S. Keller¹, L. Mihalceanu¹, J. Greser¹, E. Papaioannou¹, B. Hillebrands¹

1. *Fachbereich Physik And Landesforschungszentrum OPTIMAS, Technische Universität Kaiserslautern, Germany*

Metallic FM/Pt bilayers show a large increase in magnetic damping due to the presence of spin pumping, and large inverse spin Hall voltages (ISHE) are observed. In the past, most of the research has focused on polycrystalline films [1-4]. However, the study of such effects in epitaxial films can provide further insight into their nature. Here, we present studies on epitaxial Fe/Pt bilayers grown by molecular beam epitaxy. Several samples with a Fe layer with a fixed thickness of 12 nm and varying Pt thickness were studied. Additional reference samples with no Pt, capped with MgO or Al have been also measured to estimate the properties in absence of spin pumping.

A ferromagnetic resonance setup is used to measure the dependence of the Gilbert damping parameter, the effective magnetization and other parameters on the Pt thickness. The anisotropic properties are studied by the study of the coercive field H_c with a rotational MOKE setup and by the angular dependence of the resonant field. Measurements of the generated ISHE voltages are also presented and discussed in relation to the FMR data.

An increase of the damping with Pt thickness is already observed for the thinnest studied Pt thickness in comparison to the reference samples. The angular dependence of H_c shows typical sharp features originated in domain nucleation and formation of metastable domain configurations. These are not present in the angular dependence of HFMR which shows a much smoother dependence. Both show the cubic anisotropy expected for Fe although a superposed uniaxial anisotropy is observed.

- [1] E. Saitoh, et al. Appl. Phys. Lett. 88, 182509 (2006)
- [2] A. Ruiz-Calaforra, et al, submitted
- [3] O. Mosendz, et al, Phys. Rev. B 82, 214403 (2010)
- [4] A. Azevedo, et al, Phys. Rev. B 83, 144402 (2011)

TH.E-P12 - Large extrinsic spin hall effect in gold based alloys

P. Laczkowski¹, J. Rojas-Sánchez¹, W. Savero-Torres², N. Reyren¹, C. Deranlot¹, J. George¹, H. Jaffrès¹, A. Fert¹, L. Notin², C. Beigné², A. Marty², J. Attané², L. Vila²

1. UMR/CNRS-Thales and Université Paris-Sud, Palaiseau, France
2. INAC/SP2M, CEA-Université Joseph Fourier, Grenoble, France

The spin Hall effect (SHE) [1] allows for a reciprocal conversion between charge and spin currents using the spin orbit coupling which can be at the core of several promising spintronics devices. The spin orbit interaction is used to produce a transverse flow of spin or charge in response to a longitudinal excitation, these are the direct or inverse SHE. The spin Hall angle (SHA), the ratio of longitudinal and transverse electronic conductivities, is the characterizing parameter of this conversion. So far, large SHA have been reported in transition metals like Pt, Pd, W, Beta-Ta and in a few alloys with large spin orbit coupling impurities: CuIr, CuBi or CuPb [2].

In this presentation we will report on our study of the SHE induced in Au using resonant scattering on W impurities [3] by using the Non-local probe configuration in Lateral Spin Valves (LSVs). These nano-devices consist of two ferromagnetic electrodes (F) connected by a non magnetic wire (N) allowing for the injection and for the detection of pure spin currents in order to study the direct and inverse SHE by insertion of an additional spin absorbent Au_{1-x}W_x nano-wire. We will demonstrate that a correct analysis requires going further on the 1D model in order to extract the correct spin diffusion length and consequently the spin Hall angle. We will discuss the critical limit where the correction are important in the frame work of resistor model and supported by our experimental data as a function of the absorbent Au_{1-x}W_x nano-wire width.

- [1] J.E. Hirsch, PRL 83, 1834 (1999)
[2] Y. Niimi et al., PRL 106, 126601 (2011), PRL 109, 156602 (2012), PRB 89, 054401 (2014)
[3] P. Laczkowski et al., APL 104, 142403 (2014)
[4] E. Saitoh, et al., APL 88, 182509 (2006)

TH.E-P15 - Spin-orbit torque measurement by magneto-optical Kerr effect with circularly polarized lightS. Yun¹, J. Moon¹, H. Whang¹, S. Choe¹*1. Department of Physics, Seoul National University, Seoul, Republic of Korea*

Spin-orbit torque (SOT) from the interface between ferromagnet and heavy metal layers has drawn much interest due to the high efficiency in magnetization switching and domain wall motion [1, 2]. To investigate the SOT, a technique [3, 4] based on the electrical harmonic measurement of the anomalous Hall effect was proposed and extensively utilized to quantify the effective fields caused by the SOT. However, it was recently found that in the electrical measurement, a number of large artifacts exist such as the planar Hall effect, the Nernst effect and so on [5, 6] and therefore, the analysis becomes difficult and complicated. To avoid such artifacts, an optical harmonic method [7] based on the polar magneto-optical Kerr effect (p-MOKE) was recently proposed, but the p-MOKE effect also has a similar planar effect that is proportional to $\sin^2\theta$, where θ is the angle between the directions of the magnetization and the light polarization. Here, we propose that such planar effect can be systematically removed by use of a circularly polarized light, since θ rotates in the optical frequency and thus the planar effect becomes averaged out. Therefore, it is possible to quantify the pure out-of-plane component of the magnetization. The present method is applied to 5-nm Ta/1.8-nm Pd/0.3-nm Co/2.5-nm Pt samples to measure the longitudinal and transverse components of the SOT-induced effective field. The validity of the present results is confirmed in comparison to the results obtained by the electrical method with correction of the electric artifacts.

References:

1. I. M. Miron, et al., Nature 476 189 (2011)
2. I. M. Miron, et al., Nature Mater. 10 419 (2011)
3. U. H. Pi, et al., Appl. Phys. Lett. 97, 162507 (2010)
4. J. Kim, et al., Nature Mater. 12 240 (2013)
5. K. Garello, et al., Nature Nanotech. 8 587 (2013)
6. S. Woo, et al., Appl. Phys. Lett. 105 212404 (2014)
7. S. Emori, et al., Appl. Phys. Lett. 105 222401 (2014)

TH.E-P16 - Lateral spin transport in a Cu narrow strip fabricated on a magnetic insulating film

M. Kawakita¹, K. Okabe¹, T. Nomura¹, S. Yakata², T. Kimura^{1,3}

1. *Department of Physics, Kyushu University, Japan*

2. *FIT, Fukuoka, Japan*

3. *Nanospin Research Center, Kyushu University, Japan*

There has been considerable attention paid to the spin current transport in a magnetic insulator. A representative structure for this study is the magnetic/nonmagnetic hybrid structures based on YIG, where the spin current is generated by the spin pumping and the spin Seebeck effects quantitative analysis. However, the use of such spin currents makes it difficult to analyze the experimental results quantitatively.

On the other hand, nonlocal spin injection based on a lateral spin valve structure provide the reliable and quantitative information about the spin current. Since a lateral spin valve can be prepared without severe regulations, the method can be extended to the system with other magnetic insulators.

Here, we investigate the spin current transport in a magnetic insulator NiO by using a lateral spin valve structure.

The sample used for the present study consists of a CoFeAl/Cu lateral spin valve fabricated on a NiO film. Here, the interface between Cu and NiO is well cleaned by the low voltage Ar ion milling. We surely confirmed that the NiO film is real electrical insulator.

The spin transport in the NiO film has been evaluated from the nonlocal spin valve measurements. We found that the nonlocal spin valve signal with the NiO film show a strong reduction from that without NiO film although the electrical resistance of the Cu channel did not show a significant change.

This indicates that the NiO film is a strong spin absorber. We also found that the background voltage and the spin signal depends on the relative angle between the direction of the accumulated spin in the Cu channel and the magnetization direction of the NiO.

TH.E-P18 - Temperature dependence of inverse rashba-edelstein effect at metallic interfaceA. Nomura¹, T. Tashiro¹, K. Ando¹*1. Keio University, Japan*

We report temperature evolution of spin-charge conversion through the inverse Rashba-Edelstein effect (IREE) in a metallic heterostructure. Conversion between spin and charge through spin-orbit coupling is an essential function in spin-based technologies. The spin-charge conversion can be realized in solids through the spin-orbit interaction, which couples the spin of an electron to its momentum. Spin-charge conversion has been demonstrated by the inverse spin Hall effect (ISHE), arising from spin-dependent scattering of electrons by impurities in heavy metals. Most recently, the novel way of spin-charge conversion is experimentally demonstrated: the IREE [1], arising from the broken space-inversion symmetry at metallic interfaces. The IREE at a metallic interface have attracted attention recently, however, the phenomenon has not yet been understood clearly. Here, we studies that spin-charge conversion at the interface between Ag and Bi by using spin pumping. We use spin pumping to inject a spin current from a Ni₂₀Fe₈₀ layer into three different films: a Ag/Bi film, a Ag film and a Bi film and we detect the resulting charge current. Because the current of a Ni₂₀Fe₈₀/Ag/Bi film is much larger than a Ni₂₀Fe₈₀/Ag film and a Ni₂₀Fe₈₀/Bi film, spin-charge conversion in a Ni₂₀Fe₈₀/Ag/Bi film is asserted to be originated from Rashba spin-orbit coupling in a Ag/Bi heterojunction. Through measuring temperature dependence of spin-charge conversion in a Ni₂₀Fe₈₀/Ag/Bi with measured values of the temperature-dependent parameters, such as electrical resistivity, microwave absorption intensity, damping constant, and saturation magnetization, we revealed that spin-charge conversion in a Ni₂₀Fe₈₀/Ag/Bi film is almost independent of temperature. This finding provides a crucial piece of information for understanding the physics of spin currents and spin-orbit coupling in metallic heterostructures, promising substantial advances in spintronics and spin-orbitronics.

[1] J. R. Sanchez, L. Vila, G. Desfonds, S. Gambarelli, J. Attane, J. De Teresa, C. Magen, and A. Fert, *Nature Commun.* 4 (2013)

TH.E-P19 - Theoretical analysis on the anomalous hall conductivity of disordered Fe₅₀Co₅₀ alloys; effects of electron lifetime depending on the magnetic quantum number

K. Hyodo¹, A. Sakuma¹

1. Dept. of Appl. Phys., Tohoku University, Japan

The mechanism of the anomalous Hall effect in the real metals is one of the important topics in both fundamental and applied viewpoints. In the intrinsic mechanism, the effective magnetic field which drives the anomalous Hall conductivity (σ_{xy}) originates from the Berry phase of the wave function of electrons[1]. Especially, in transition metals, this Berry phase is attributed to the difference of the magnetic quantum numbers of electrons[2], which indicates that the sign of the effective field and then σ_{xy} are opposite between the hopping from the state having magnetic quantum number m to $-m$ and from $-m$ to m . In no scattering systems, finite σ_{xy} is obtained from the energy polarization between $\pm m$ states caused by the diagonal term of the spin-orbit interaction (SOI).

In this study, we focus on the finite scattering systems and σ_{xy} originated from the difference of lifetime between $+m$ and $-m$ states, which occurs from the m -dependent mixing induced by the spin-flip term in SOI. We calculated σ_{xy} of the chemically disordered Fe₅₀Co₅₀ alloys using the first-principles technique. The random alignment of atoms was considered by coherent potential approximation (CPA). The obtained result indicates that σ_{xy} from the spin-flip term of SOI is enhanced with increasing the chemical disorder. We confirmed that this effect is mainly due to the difference of spin-flip scattering rate between $+m$ and $-m$ states in the majority spin state, which is induced by the chemical disorder.

[1] N. Nagaosa *et al.*, Mod. Phys., 82, 1539-1592 (2010)

[2] H. Kontani *et al.*, Phys. Rev. B 75, 184416 (2007)

TH.E-P20 - Spin hall magnetoresistance in absence of proximity effects in Pt/CoFe₂O₄ bilayers

M. Valvidares Suarez¹, P. Gargiani¹, K. Ollefs², F. Wilhelm², E. Pellegrin¹, A. Rogalev², N. Dix³, F. Sánchez³, J. Fontcuberta³

1. ALBA Synchrotron Light Facility, Cerdanyola del Vallés, Catalonia, Spain

2. ESRF-The European Synchrotron, Grenoble, France

3. Institut de Ciència de Materials de Barcelona (ICMAB-CSIC), Bellaterra, Catalonia, Spain

Magnetoresistance has been observed in some non-magnetic metals (NM) in intimate contact with ferromagnetic insulators. Whereas magnetic proximity effects may induce the formation of magnetic moment in the metallic layer, thus allowing to account for the observed magnetoresistance, an alternative scenario, relying on the spin Hall effect and inverse spin Hall effect, has also been invoked. Indeed, experiments in NM/YIG and NM/AB₂O₄ where YIG and AB₂O₄ stand for ferromagnetic garnet and ferrites respectively can be well described within the framework of the Spin Hall effect. Still, disclosing the presence of induced moments in the NM layer is a crucial aspect to be addressed. So far this issue has been addressed in Pt/YIG bilayers with somehow contradictory findings [1, 2], that may indicate a critical role of interfaces on the observed behavior [3]. Here, we face this problem, by reporting on the magnetic properties of Pt(8 nm)/CoFe₂O₄ (30 nm) bilayers, grown in-situ, on SrTiO₃(111) substrates. We have recently shown that these bilayers display a significant magnetoresistance that we attributed to spin Hall magnetoresistance (SMR) [3]. Here, we use X-ray magnetic circular dichroism (XMCD) experiments at the Pt M₃ (2645 eV) and L_{3,2} (11564 eV) edges, performed respectively at BL29 and ID12 x-ray beamlines at the ALBA and European Synchrotron Facilities, to set an upper limit for any magnetic moment at Pt of about 0.001 μ_B /Pt atom, averaged over all Pt thickness. This observation suggests that in Pt/CoFe₂O₄, the observed SMR magnetoresistance is best described as resulting from a spin accumulation in the Pt layer, controlled by the magnetization direction of the neighboring CoFe₂O₄ layer and denies a significant magnetic proximity effect on Pt.

[1] Y. M. Lu et al, Phys. Rev. Lett. 110, 147207 (2013)

[2] S. Geprags et al, Appl. Phys. Lett. 101, 262407 (2012)

[3] M. Isasa et al, Appl. Phys. Lett. 105, 142402 (2014)

TH.E-P22 - Unidirectional spin hall magnetoresistance in ferromagnet/normal metal bilayersC. Onur Avci¹, K. Garello¹, A. Ghosh¹, M. Gabureac¹, S. F. Alvarado¹, P. Gambardella¹*1. Department of Materials, ETH Zürich, Zürich, Switzerland*

Magnetoresistance is generally invariant under magnetic field and current reversal due to the Onsager reciprocity¹. However this is not always true in noncentrosymmetric conductors where nonlinear terms can give rise to current dependence that is quadratic in the applied voltage and linear in the magnetization. We demonstrate that such conditions are realized in simple bilayer metal films where the spin-orbit interaction and spin-dependent scattering couple the current-induced spin accumulation to the electrical conductivity. We show that the longitudinal resistance of Ta/Co and Pt/Co bilayers changes when reversing the polarity of the current or the sign of the magnetization. Accordingly, we observe a decrease (increase) of the longitudinal resistance when the SHE-induced spin accumulation at the FM/NM interface is antiparallel (parallel) to the majority spin direction in the FM. This magnetoresistance effect scales linearly with current density and has opposite sign in Ta and Pt, which we associate to the modification of the interface scattering potential, induced by the spin Hall effect in these materials. The thickness and spacer layer dependence of this effect underline the substantial role of the spin Hall effect and the interfacial spin accumulation. We furthermore develop a model showing that this unidirectional spin Hall magnetoresistance² is consistent with the current-in-plane giant magnetoresistance theories^{3,4} when the second magnetic layer is removed and the spin accumulation due to the spin Hall effect is taken into account. Our results suggest a new route to altering the electric properties of metal films by control of the magnetization.

¹A. C. Smith, J. F. Janak, and R. B. Adler, *Electronic conduction in solids* (McGraw-Hill New York, 1967)

²C.O. Avci, K. Garello, A. Ghosh, M. Gabureac, S.F. Alvarado, and P. Gambardella, *ArXiv:1502.06898 [cond-mat.mes-hall]*

³P. Van Son, H. Van Kempen, and P. Wyder, *Phys. Rev. Lett.* 58, 2271 (1987)

⁴T. Valet and A. Fert, *Phys. Rev. B* 48, 7099 (1993)

TH.F.P27 - Vortex domain wall trapping via asymmetric notches

M. Voto¹, L. López Díaz¹, L. Torres Rincón¹

1. University of Salamanca, Spain

Domain walls in in-plane magnetized strips above certain cross sectional area are naturally found to have a vortex configuration (VDW) [1]. The behaviour and the potential landscape of a propagating VDW interacting with a geometrical pinning site have been studied extensively [1,2] and shown to be asymmetric with respect to the propagation direction. In particular, a VDW approaching a notch finds its equilibrium before the notch rather than at its centre. This causes a weak pinning of the wall for an anti-parallel applied field; a relevant difference compared to the potential well found for transverse domain walls [1]. It would be convenient for certain applications and experiments [3] that a VDW could be pinned at a notch by applying a low field so that it remains strongly pinned when the field is reversed. With this goal in mind, we have investigated the trapping of a VDW in a permalloy nanostrip of 300x30 nm² cross-section by means of systematic micro-magnetic simulations. Tailoring notches on both edges of the strip, we design a pinning site that enhances the asymmetric energy landscape of the VDW, determining energy barriers of different heights for a propagating VDW depending on which side the notch is approached. The potential well created this way is accessed at 12-14 mT and not escaped until up to 26 mT in both directions. This pinning site acts like a valve for VDWs and can be exploited in applications that require asymmetric propagation of Dws such as shift registers and GMR sensors in which precise propagation direction for field driven DWs is required.

[1] M. Kläui, J. Phys.: Condens. Matter 20, 313001 (2008)

[2] L. K. Bogart et al., Physical Review B 79, 054414 (2009)

[3] N. Motzko et al., Physical Review B 88, 214405 (2013)

TH.F-P01 - Field and current driven magnetic domain wall motion in disordered A₁-FePt nanowiresP. Ho¹, J. Zhang¹, J. Currivan^{1,2}, D. Bono¹, C. Ross¹1. *Massachusetts Institute of Technology, United States*2. *Harvard University, United States*

Domain wall (DW) in magnetic nanowires has technological potential in DW logic and racetrack memory devices. While an understanding of permalloy domain dynamics is well established, there are limited studies on other in-plane anisotropy ferromagnetic film. In particular, there are no reports on chemically disordered A₁-structure FePt, with a larger magnetocrystalline anisotropy K_1 of magnitude 6×10^5 erg cm⁻³. The larger anisotropy of A₁-FePt promotes thermal stability against superparamagnetism, and its spin-orbit coupling and spin polarization also differ from other transition metal alloys. An understanding of the DW dynamics in in-plane anisotropy A₁-FePt provides a useful complement to existing knowledge of DW dynamics in soft transition metal alloys and hard L₁₀-FePt. In this work, the A₁-FePt DW structure, behaviour and dynamics under the influence of a field, pulsed current and field-assisted pulsed current were studied. Arc-shaped A₁-FePt nanowires of linewidth 375 nm with 2 μm diameter injection pads were patterned. Upon an applied $H_y = 10$ kOe saturation field transverse to the nanowire, a 180° vortex DW was introduced. Translational propagation of the DW was observed at $H_x = 40$ to 80 Oe applied parallel to the wire, while complete propagation to the end of the arc occurred at $H_x = 100$ Oe. DW displacement was observed with low pulsed current densities of $2.5 - 5.0 \times 10^{11}$ A m⁻² but DW velocities were small, with values of 7×10^{-4} m s⁻¹ at 5×10^{11} A m⁻² and 1.8×10^{-2} m s⁻¹ at 2×10^{12} A m⁻². The strong spin orbit scattering and poor spin polarization limited efficient spin transfer driven DW motion. A field-assisted spin transfer torque, combination of 5.0×10^{11} A m⁻² current and a field of $H_x = 60$ Oe, drove the domain wall 1.8 μm to the end of the arc at a faster velocity.

TH.F-P03 - Simulation of the field-driven magnetic domain wall motion under the dzyaloshinskii-moriya interaction

K. Yamada¹, Y. Nakatani¹

1. *University of Electro-Communications, Tokyo, Japan*

The Dzyaloshinskii-Moriya interaction (DMI) has been a great attention in the magnetic domain wall (DW) motion[1-3]. It has been reported by the theoretical analysis that the DMI produces an effective chiral field that stabilizes Néel type walls, leading to efficient coherent motion much faster than the DW velocity of several hundred at the Walker field [1,2]. In these reports, they have studied the DW motion around the Walker field, however they have not discussed the DW motion in a high field region in which it is moved with the precessional motion. In the region, the DW velocity is affected by fluctuations of DW shape [4], and the vertical Bloch lines are nucleated and moved on the DW. In this report, we perform micromagnetic simulations and investigate the field-driven DW motion under the DMI, in particularly, in the high field region where is much higher than the Walker field.

The two-dimensional micromagnetic model is used in simulations. Nanowire structures have 1.2 nm thickness, infinite length and various widths (w) from 50 to 200 nm. The nanowire is divided by a rectangular prism with dimensions of $2.0 \times 2.0 \times 2.5$ nm³. Typical material parameters for perpendicular magnetized Co/Ni multilayer film are used. A magnetic field (H_z) is applied in the wire thickness direction, and its range is from 0 to 1.5 kOe. The DW velocity over the Walker field is not only changed by the value of DMI but also by w . The breakdowns of the DW velocity occur several times in the wires of $w = 100$ and 200 nm.

This work was supported by JSPS a Grant-in-Aid for Scientific Research (C) and for JSPS Fellows.

[1] *Europhys. Lett.* 100, 57002(2012)

[2] *Phys. Rev. Lett.* 111, 217203 (2013)

[3] *Nat. Mater.* 12, 611 (2013)

[4] *Appl. Phys. Express.* 4, 113001 (2011)

TH.F-P04 - Effect of electric current on domain wall dynamics in nanocrystalline FeCoMoB microwire

P. Klein ¹, A. Jimenez ², G. Badini-Confalonieri ², M. Vazquez ², R. Varga ¹

1. Institute of Physics, Faculty of Science, UPJS, Kosice, Slovakia

2. Instituto de Ciencia de Materiales de Madrid, CSIC, Madrid, Spain

Propagation of domain wall in thin wires is used in modern spintronics to transfer or store information. Particularly, operation speed of such devices strongly depends on the domain wall velocity. Therefore, domain wall velocity is a crucial parameter for correct work of such applications.

Glass-coated microwires with positive magnetostriction are characterized by peculiar magnetization process that runs through the single domain wall propagation. Moreover, the domain wall velocity in such wire is very fast (over 10km/s [1]). Therefore, they are ideal materials for study the single domain wall dynamics on macroscopic scale [1]. However, very few attempts have been devoted to study the effect of electric current on domain wall dynamics in bistable microwires with exception [2].

In the given contribution we have studied effect of electric current on domain wall dynamics in nanocrystalline FeCoMoB microwires. The FeCoMoB microwires were annealed by classical way in furnace above crystallization temperature at 500 oC for 1 hour in order to obtain homogeneous nanocrystalline state of metallic core. The domain wall dynamics was studied by classical Sixtus-Tonks method. Moreover, electrical current flowing through microwire was applied to produce circular magnetic field. It has been found, that electric current in one direction enhances domain wall velocity (although it decreases its mobility) while exactly opposite effect was observed in second direction of flowing electric current.

This work was supported by Project NanoCEXmat No. ITMS 26220120019, Slovak VEGA under Grant 1/0060/13, Grant APVV-0027-11.

References:

[1] P. Klein, R. Varga, and M. Vazquez, *J. Phys. D: Appl. Phys.* 47 (2014) 255001

[2] F. Beck, J. Neroti Rigue, and M. Carara, *IEEE Tran. Magn.* 49 (2013) 4699-4702

TH.F-P05 - Evidence for chiral magnetic domain-wall in ferrimagnetic GdFeCo wires

T. Tono¹, T. Taniguchi¹, K. Kim¹, T. Moriyama¹, A. Tsukamoto², T. Ono¹

1. *Institute For Chemical Research, Kyoto University, Japan*

2. *College of Science and Technology, Nihon University, Japan*

Magnetic domain-wall (DW) dynamics has been intensively investigated due to the fundamental interests as well as technological applications such as memory and logic devices. To date, ferromagnets have been mainly examined for magnetic DW motion. However, recent studies [1] have shown that ferrimagnets can be an alternative platform due to the unique properties of ferrimagnets. Ferrimagnets have two magnetic sub-lattices the magnetizations of which are aligned in the opposite direction. Their small net magnetization and a large magnetic anisotropy may respectively lead to a low critical current density for DW motion and a high thermal stability. In this presentation, we report an evidence for the chiral magnetic DW structure in ferrimagnetic GdFeCo wires. We measure a field-driven DW velocity in GdFeCo (30 nm)/ Pt (5 nm) wires by a real time DW detection technique [2]. The DW velocity increases with increasing out-of-plane magnetic field (H_z). At a threshold field, the DW velocity abruptly decreases and gradually increases again. This feature can be attributed to the change of DW dynamics from the steady motion to the precessional motion, which is known as the Walker breakdown. We next check the in-plane field dependence of the DW velocity for $H_z = 20$ mT. The DW velocity is found to exhibit a minimum at a finite in-plane field (H_m). Moreover, the sign of H_m is reversed when we change the DW structure from up-down DW to down-up DW. This result suggests that a chiral magnetic DW structure is formed in ferrimagnetic GdFeCo wires.

Acknowledgements: This work was partly supported by a Grant-in-Aid for Scientific Research (S), a Grant-in-Aid for Young Scientists (B) and a Grant-in-Aid for Scientific Research on Innovative Areas.

[1] D.-T. Ngo, et al., Appl. Phys. Express 4, 093002 (2011)

[2] M. Hayashi, et al., Phys. Rev. Lett. 96, 197207 (2006)

TH.F-P06 - Fast DW motion through the annihilation of vertical bloch lines induced by dzyaloshinskii-moriya interaction

Y. Yoshimura¹, K. Kim¹, T. Taniguchi¹, T. Tono¹, K. Ueda¹, R. Hiramatsu¹, T. Moriyama¹, Y. Nakatani², T. Ono¹

1. *Institute For Chemical Research, Kyoto University, Japan*

2. *The University of Electro-communications, Tokyo, Japan*

The vertical Bloch line (VBL), a topological defect inside a magnetic domain-wall (DW), is known to play an essential role in the two dimensional DW dynamics. A nucleation and a propagation of VBL retard the DW motion. Recently, novel type of antisymmetric exchange interaction, namely the Dzyaloshinskii-Moriya interaction (DMI), has been found to play a crucial role in the formation and the dynamics of topological objects such as magnetic soliton, vortex, and skyrmion. It thus raises an intriguing question how the DMI affects the dynamics of VBLs and DW.

We prepared two types of Co/Ni films having symmetric and asymmetric layer structures, respectively. Since the DMI is expected to exist only in asymmetric layer structure, we can elucidate the effect of DMI on the DW dynamics by comparing two different samples. An electrical time-of-flight measurement technique was employed to investigate a field-driven DW dynamics. We observed a distinct difference in the DW velocity between symmetric and asymmetric samples. The DW velocity for asymmetric Co/Ni sample was found to be 5 times larger than that for symmetric Co/Ni sample, implying that a new energy dissipation channel is opened in asymmetric Co/Ni sample. Micromagnetic simulation reveals that the DMI induces the annihilation of VBLs, resulting in the emission of spin waves. This emission of spin waves is found to be a new energy dissipation channel, which boosts up the DW velocity.

This work was partly supported by a Grant-in-Aid for Scientific Research (S), a Grant-in-Aid for Scientific Research on Innovative Areas, a Grant-in-Aid for Young Scientists (B), R&D Project for ICT Key Technology of MEXT, Research Fellowships of JSPS for young scientists and a Grant-in-Aid for Scientific Research (C).

TH.F-P07 - Magnetic origami

C. Safeer¹, E. Jué¹, A. Lopez¹, L. Buda Prejbeanu¹, S. Auffret¹, J. Vogel², S. Pizzini², O. Boulle¹, I. Miron¹, G. Gaudin¹

1. SPINTEC/INAC/CEA/Université de Grenoble Alpes, France

2. Institute Néel/CNRS/ Université de Grenoble Alpes, France

Spintronics is an emerging research field that bridges magnetism and electronics, offering multiple applications such as magnetic memories, logic devices, etc. The operation of these different devices is often based on different physical phenomenon. The device function is strongly linked to the type of excitation (electric or magnetic) as well as to the precise material parameters. We propose a new approach where the shape is used as a new parameter that defines the device behavior. Similarly to the paper origami, the objects are made of the same material, but since they have different shape they operate as different magnetic devices. This possibility is based on current induced non-collinear domain wall (DW) motion in Pt/Co/AlOx trilayers. Here, non-collinearity is defined with respect to the direction of the current flow and to that of DW motion. In all the previous experiments reported in literature, the current induced DW motion was studied in magnetic nanowires by applying current along the wire that defines the direction of the DW motion. In our experiment, the current is applied at different angles between +75 and -75 with respect to the direction of the DW motion. We observed that the DW moves in a selective way through different directions in the two dimensions. Using these observations, we could design different two dimensional shapes where the DW motion could be manipulated according to the device requirements. This led to the realization of new kinds of reversible and irreversible magnetic switches differentiated only by shape.

TH.F-P08 - Domain walls in thin film magnets/TI junctions

Y. Ferreiros¹, F. Buijnsters²

1. Instituto De Ciencias De Materiales De Madrid (ICMM), Madrid, Spain

2. Institute for Molecules and Materials, Radboud University Nijmegen, The Netherlands

The spin-transfer torque generated by the surface states of a 3D TI has recently been measured to be larger than for any other spin-transfer torque source measured so far, which encourages the applicability of thin film magnet/TI junctions for spintronic based devices. We analytically compute the effective action for the magnetization in this system with an out-of-plane domain wall (DW) configuration, at finite density and in the presence of an external electric field. We show that an electronic chiral state appears bounded to the DW carrying 1D equilibrium (finite density) and out of equilibrium (non zero electric field) dissipationless currents. We show that in addition the chiral state generates an in-plane hard axis anisotropy term in the effective action, in the direction perpendicular to the DW. We also address whether a Dzyaloshinskii-Moriya (DM) type of interaction appears, concluding that it is not the case. However we show that the 1D equilibrium current gives a term that resembles the interfacial DM interaction, but with the important difference that it is a first order term in the magnetization.

The equilibrium profile of the DW is computed as a function of the chemical potential, qualitatively reproducing the behavior of recent numerical results, and the physical explanation of the effect is shown to lie in the competition of the chiral 1D current and the induced hard axis anisotropy. We also study the motion of the DW via an external current, and show that the threshold for Walker breakdown (WB) is increased and determined by the exchange interaction. Furthermore this threshold can be further increased by both doping the TI and applying an external electric field. Having an analytic control of the Hamiltonian settles the basis for future investigations, for example addressing magnonic propagation and the appearance of a magnonic torque on the DW.

TH.F-P09 - Ultrafast dynamics of current induced motion of magnetic domain wall in permalloy sublayer in bilayer niobium-permalloy structure.

L.S. Uspenskaya¹, S.V. Egorov¹

1. Institute of Solid State Physics RAS, Moscow, Russian Federation

The electrical current switching of the magnetic state of ferromagnetic layer in hybrid ferromagnet-superconductor structures opens a new possibility to control the properties of the hybrids supposed to be used in cryoelectronics [1]. Herewith we report the results of study of the dynamic properties of magnetic domain walls in 40 nanometer thick permalloy tapes grown on niobium sublayer at their motion excited by magnetic and electric fields. The study was performed by magneto-optic visualization technique by means of yttrium iron-garnet films in temperature range 6 K - 300 K [2]. We found that on cooling from room to liquid helium temperature the coercivity of the walls shifted under the magnetic field pulses increases following thermoactivated law, and the mobility of the walls decreases according to power law like $T^{-1/4}$. Nevertheless, the mobility of the walls shifted under the current pulses increases with temperature decrease following $T^{1/3}$ dependence. The domain wall under the current excitation moves faster than under the field. The maximum velocity of the wall becomes as large as 1000 m/s at 10 K, and 4000 m/s at 6 K. The result looks absolutely surprising taking into account that the niobium transition into superconducting state takes place at $T_c = 8.5$ K, which means that main current flow occurs not in the permalloy but in the niobium layer at $T < T_c$.

[1] A.K. Feofanov, V.A. Oboznov, V.V. Bolginov et al. Implementation of superconductor/ferromagnet/superconductor pi-shifters in superconducting digital and quantum circuits. *Nature Physics* v.6, N8, 2010, pp. 593-597

[2] S. V. Egorov, A. M. Bobkov, I. V. Bobkova, L. S. Uspenskaya. Anomalously High Velocity of the Domain Walls Driven by the Electric Current in Bilayer Permalloy-Niobium Structures. *JETP Letters*, 2015, Vol. 101, No. 1, pp. 32-35

TH.F-P10 - Pure spin current injection and detection device based on magnetic domain walls

L.Vila⁵, T. Van Pham¹, W. Savero Torres², G. Zahnd³, P. Laczkowski⁴, V. Dai Nguyen⁶, J. Rojas Sanchez⁷, A. Marty⁸, C. Vergnaud⁹, C. Beigné¹⁰, L. Notin¹¹, M. Jamet¹², J. Attané¹³

1. *Institut Nanosciences Et Cryogenie, CEA, Grenoble, France*
2. *Université Grenoble Alpes, Grenoble, France*

The manipulation of pure spin currents in nanostructures generates an increasing interest, being notably the basis of two emerging research fields: The spin caloritronics [1], where the spin currents are generated by thermal gradients and the spin-orbitronics [2], where such currents are manipulated by means of the spin-orbit coupling as the spin-Hall or the Rashba effects. These spin currents can also be created by means of non-local injection in lateral spin valves (LSV), which is an attractive tool for studying spin transport properties in non-magnetic materials. Moreover, the absorption of pure spin current by a ferromagnetic element is associated to a spin transfer that can induce magnetic oscillations [4] or even lead to magnetic switching [5]. In the other hand, the manipulation of magnetic Domain Walls (Dws) in nanostructures by means of spin currents has been the subject of intense research over the last decade [6,7]. In this presentation, we report on the possibility to create switchable pure spin current sources, controlled by magnetic domain walls [8]. When the domain wall is located at a given point of the magnetic circuit, a pure spin current is injected into a nonmagnetic wire. Using the reciprocal measurement configuration, we demonstrate that the proposed device can also be used as a pure spin current detector. Thanks to its simple geometry, this device can be easily implemented in spintronics applications; in particular, a single current source can be used both to induce the domain wall motion and to generate the spin signal. Finally these DW based detector can be combined to build a AND logic function

- [1] Bauer G. E. W., et al Nature Materials 11, 391-399 (2012)
- [2] Jungwirth T., et al Nature Materials 11, 382-390 (2012)
- [4] Liu L. et al, Phys. Rev. Lett. 106, 036601 (2011)
- [5] Yang T., et al Nature Physics. 4, 851 - 854 (2008)
- [6] Parkin S.S.P., et al Science 320, 190 (2008)
- [7] Allwood D.A., et al Science 309, 1688 (2005)
- [8] W. Savero Torres, et al Nano Letter 14 (7), 4016-4022 (2014)

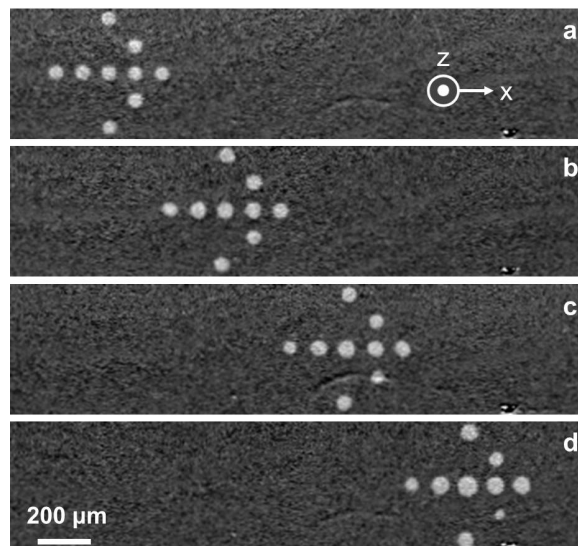
TH.F-P11 - Magnetic bubblecade memory based on chiral domain wallsK. Moon¹, D. Kim², S. Yoo^{2,3}, S. Je², B. Chun¹, W. Kim¹, B. Min³, C. Hwang¹, S. Choe²

1. Center for Nanometrology, Korea Research Institute of Standards and Science, Republic of Korea

2. Department of Physics and Astronomy, Seoul National University, Republic of Korea

3. Center for Spintronics Research, Korea Institute of Science and Technology, Republic of Korea

Up to now, there have been suggested many concepts of the unidirectional coherent magnetic domain walls (DWs) motion for next-generation promising memory and logic devices [1-3]. Such concepts based on DWs can be demonstrated by either by injecting large electric currents into nanowires [1] or by using the DW tension induced by sophisticated structural modulation [2, 3]. However these schemes require either a high threshold [1] or highly sophisticated nanofabrication processes [2, 3]. Here, we demonstrate a new scheme for unidirectional DW motion without any current injection or structural modulation. This scheme utilizes asymmetry domain expansion with respect to magnetic fields [4] induced by the Dzyaloshinskii-Moriya interaction. Due to this asymmetry, an alternating magnetic field results in a coherent motion of the DWs. Figure 1 show a proof-of-principle experiment. An arbitrary 5x5 array pattern of bubbles (Fig. 1a) is initially created on the film using the thermomagnetic writing method [5]. Under the alternating magnetic pulses, all bubbles exhibit coherent unidirectional motion, as shown by the sequential images (Figs. 1b-d and see Ref. [5]) captured during the pulses. Interestingly, the bubble-array pattern, called bubblecade, is exactly maintained even after traveling more than 1 mm (Fig. 1d). The observation of the coherent unidirectional bubbles motion can possibly replace the mechanical motion of the magnetic media, enabling a new device prototype 'magnetic bubblecade memory' with two-dimensional data-storage capability.



TH.F-P12 - Magnetization dynamics of iron garnet crystals in oscillating magnetic field

L. Pamyatnykh¹, L. Agafonov¹, D. Mekhonoshin¹, S. Pamyatnykh¹, M. Lysov¹, G. Shmatov¹

1. Ural Federal University, Russian Federation

Dynamic remagnetization mechanism was investigated based on (111) iron garnet (TbErGd)₃(FeAl)₅O₁₂ sample plate. Dependencies of stripe domains drift speed and domain walls oscillations parameters in an alternating magnetic field applied perpendicular to the sample plate were established. Parameters of the sample: saturation magnetization $M_s = 40$ Gs, constant of uniaxial magnetic anisotropy $K_u = 5500$ erg/cm³, magnetocrystalline anisotropy constant $K_1 = -3400$ erg/cm³, orthorhombic anisotropy constant $K_p = 3200$ erg/cm³. Dynamic domain structure (DDS) was revealed using magneto-optic Faraday effect and was captured using stroboscopic technique by high speed digital camera at the rates up to 1200 fps. A solid-state pulsed laser with a wavelength of 527 nm and a pulse duration of 25 ns synchronized with the alternating magnetic field was used for illumination. This allowed to obtain a series of DDS images in a successive phases of the magnetic field. The drift velocity of stripe domains, amplitude of oscillations and peak velocity of oscillations of domain walls were measured in a frequency range 25-1200 Hz for amplitudes up to 500 Oe. It was established that the character of dependencies of amplitude of oscillations and of peak velocity of oscillations of domain walls on amplitude of alternating magnetic field qualitatively changes for amplitudes that correspond to the drift of domain walls. Numerical modeling of motion of stripe domain structure with the parameters of the real sample was performed based on the model of coupled harmonic oscillators that takes dynamic attenuation into account. The results of numerical modeling are compared to the experimental results.

TH.F-P13 - Dimensional crossover in stochastic behavior of magnetic domain-wall creep motion

T. Taniguchi¹, K. Kim¹, T. Tono¹, T. Moriyama¹, T. Ono¹

1. Institute For Chemical Research, Kyoto University, Japan

It has been recently reported that the spin Hall torque (SHT) can drive a magnetic domain wall (DW) in asymmetric layer structures involving a strong Dzyaloshinskii-Moriya interaction (DMI) [1]. In order to utilize this DW driving mechanism, it is crucial to understand the microscopic DW behavior under SHT and DMI. Since a DW can be considered as an elastic string-like object, a DW generally has a roughness in two dimensional space due to the pinning sites in wires.

In this presentation, we demonstrate the crossover from two dimensional to one dimensional characteristics of the DW motion in Co/Ni nanowires with DMI. A DW can propagate with two driving forces; a magnetic field or a current invoking SHT. We compare the distributions of DW velocity in creep regime for two driving force in a different wire widths (w). While the distribution for current-driven case is about 3 times larger than that for field-driven case when $w \geq 1 \mu\text{m}$, both driving forces show similar velocity distributions when $w \lesssim 500 \text{ nm}$. The difference in the distribution for wider wires can be attributed to the difference in the DW roughness for two driving forces [2]. On the other hand, when w is reduced to w_{opt} , below which DW moves collectively [3], the difference in the DW roughness disappears and the two driving forces have the same distributions. Our findings suggest that the effective magnetic field induced by SHT is equivalent to the external field in one dimensional wires, though it is not in two dimensional wires.

[1]A.Thiaville, *et al.*, Europhys. Lett. 100, 57002 (2012)

[2]T. Taniguchi, *et al.*, Appl. Phys. Express 7, 053005 (2014)

[3]F. Cayssol, *et al.*, Phys. Rev. Lett. 92, 107202 (2004)

TH.F-P14 - Head-to-head domain wall structures in wide permalloy strips

V. Estevez¹, L. Laurson¹

1. Aalto University, Aalto, Finland

We analyze the equilibrium micromagnetic domain wall structures encountered in Permalloy strips of a wide range of thicknesses and widths, with strip widths up to several micrometers. By performing an extensive set of micromagnetic simulations, we show that the equilibrium phase diagram of the domain wall structures exhibits in addition to the previously found structures (symmetric and asymmetric transverse walls, vortex wall) also double vortex and triple vortex domain walls for large enough strip widths and thicknesses. Also several metastable domain wall structures are found for wide and/or thick strips. We discuss the details of the relaxation process from random magnetization initial states towards the stable domain wall structure and show that our results are robust with respect to changes of, e.g., the magnitude of the Gilbert damping constant and details of the initial conditions. Phys. Rev. B 91, 054407 (2015)

TH.F-P15 - Non-uniform internal degrees of freedom in field-driven extended domain walls in perpendicular media

T. Herranen¹, L. Laurson¹

1. COMP Centre of Excellence and Helsinki Institute of Physics, Department of Applied Physics, Aalto University, Aalto, Finland

Domain walls (DW) in nanostrips with perpendicular magnetic anisotropy (PMA) driven by a magnetic field along the easy axis experience a Walker breakdown (WB) [1] at the Walker field $B = B_W$. In nanostrips, the in-plane magnetization of the DW rotates uniformly around the z-axis for $B > B_W$. In this work we perform micromagnetic simulations on a wide granular CoPtCr strip with 1.2 μm width and 20 nm thickness. The disorder is generated by adding a random 10 % variation in the anisotropy magnitude in each grain. The grains are generated by Voronoi tessellation, and have an average diameter of 11.9 nm. We show that a DW in such wide strips also experiences the velocity drop related to the WB. Unlike in nanostrips, the internal magnetization of the DW in wide strips breaks into non-uniform in-plane magnetic structures for $B > B_W$. These non-uniformities are nucleated either at the sample boundaries, or due to disorder.

Analysis of the non-uniform in-plane magnetization shows that it can be described as a set of domains separated by internal domain walls. With a magnetic field pulse on a DW pinned by two notches we can generate configurations with e.g. a 180° internal DW, similar to the transverse walls in nanostrips with in-plane magnetization. These internal DW structures are stable in room temperature. The study of the field-driven dynamics of the internal DWs shows that they do not experience a WB due to the topological restrictions originating from the surrounding $\pm\hat{z}$ domains.

[1] E. Martinez. *Journal of Physics: Condensed Matter*, 24(2):024206, 2012

TH.F-P16 - Influence of asymmetric geometry on domain wall chirality detected in Y-shaped nanowires

W. Kwak¹, J. Kwon¹, B. Cho¹

1. School of Materials Science and Engineering, Gwangju Institute of Science and Technology, Republic of Korea

The control of domain wall motion in a magnetic nano-strip has received considerable attention over recent decades because many applications of spintronic devices are based on domain wall motion, including spin logic devices and race-track memory. Recently, many research groups have reported that domain wall propagation is dependent on the chirality of the domain wall in artificial structures. Domain wall chirality is generally set up by applied magnetic field, and is important for controlling the domain wall motion. However, the magnetic field used to stabilize the chirality produces an inevitable drawback for high density devices. Here, we found that the asymmetric geometry in which a nucleation pad is attached at the lower edge of a nanowire has preference for the chirality of transverse walls when the walls are injected from a nucleation pad into a magnetic nanowire. Chiralities of the injected wall were confirmed by chirality dependent propagation in a Y-shaped magnetic nanowire having a spin-valve structure. Domain wall position was detected through magnetoresistance (MR) measurement during reversal of the permalloy free layer. As a result, in this geometry, clockwise transverse walls can be stably formed in a relatively lower transverse field range than is possible with counter-clockwise walls. This is due to the tendency in which one edge defect having higher magnetostatic energy does not like to encounter a pinning site, which offers selectivity for chirality. Object oriented micromagnetic framework (OOMMF) was implemented for the investigation of domain wall nucleation in the suggested geometry and supported the experimental results. Our findings emphasize the importance of the placement of parts related to domain wall nucleation so as to control domain wall structures.

TH.F-P17 - Manipulation of domain wall motion in Ta-CoFeB-MgO ultrathin films by making use of sub-nanometer steps modulation

A. Digiacomo¹, R. Mantovan¹, N. Vernier², T. Devolder², K. Garcia², G. Tallarida¹, M. Fanciulli^{1,3}, B. Ocker⁴, L. Baldi⁵, M. Mariani⁵, D. Ravelosona²

1. *Laboratorio MDM IMM-CNR, Agrate Brianza, Italy*

2. *Institut d'Electronique Fondamentale, Université Paris-Sud, Orsay, France*

3. *Dipartimento di Scienza dei Materiali, Università di Milano Bicocca, Milano, Italy*

4. *Singulus Technology AG, Kahl am Main, Germany*

5. *Micron Semiconductor Italia S.r.l., Agrate Brianza, Italy*

Control of magnetic domain wall (DW) motion in nanowires has attracted great interest due to the possibility to develop high density non-volatile memory and logic circuits such as racetrack memory. Within the challenge of finding optimal strategies to target ultimate scaling, the use of ultrathin CoFeB layers showing perpendicular magnetic anisotropy (PMA) is particularly attracting. In this contribution we present a possible strategy for fabricating artificial pinning sites in order to manipulate DW motion in ultrathin (1 nm) CoFeB layers. Sub-nanometer steps modulation are synthesized at the surface of SiO₂-Si₃N₄ substrates, on top of which Ta/CoFeB/MgO stacks showing PMA are deposited by magnetron sputtering. The DWs dynamics in the ultrathin CoFeB layers is studied by Kerr microscopy. The propagation velocities for DWs moving “across” the steps are about two orders of magnitude lower than the velocities of DWs moving “along” the steps. Reported results demonstrate that appropriate engineering of the substrate is an efficient way to manipulate DWs in Ta/CoFeB/MgO structures. The proposed method is compatible with nanoscale dimensions and large-scale mass production, which open new opportunities for the modulation of DW motion in ultra-high density spintronics devices.

TH.F-P19 - Enhancement of spin-orbit torque and Dzyaloshinskii-Moriya interaction in Co films sandwiched by various 3d, 4d, and 5d transition metalsC. Cho¹, S. Yun¹, H. Whang¹, D. Kim¹, D. Kim¹, J. Moon¹, S. Je¹, Y. Oh², B. Park², S. Choe¹

1. Seoul National University, Republic of Korea
2. KAIST, DAEJEON, Republic of Korea

Current-induced domain-wall motion has been intensively studied over the last decades due to its promising application toward high-density and low-energy-consumption memory and logic devices. Recently, it has been found that the efficiency of the domain-wall motion can be largely enhanced by the spin-orbit torque (SOT) [1] combined with the Dzyaloshinskii-Moria interaction (DMI) [2]. In presence of the DMI caused by a broken symmetry in heavy-metal/ferromagnetic interfaces [3], the Neel-type domain-wall structure is stabilized, which then results in the domain-wall motion driven by the SOT via the spin Hall current from non-ferromagnetic heavy metals [4]. It is therefore radical to analyze the sign and magnitude of the DMI and SOT to understand their physical origin as well as to achieve memory and logic devices. In this study, we investigate the DMI and SOT of various metallic ferromagnetic films, of which the structures are Ta(5 nm)/Pt(2.5 nm)/Co(0.6 nm)/X(1.5 nm) films with various choice of X by Ti(3d), Cu(3d), Ru(4d), Pd(4d), Ta(5d), W(5d), Au(5d), and Mg. The sign and magnitude of the DMI are then measured from the asymmetric domain-wall expansion [3] as shown by Fig. 1. Figure 1 shows the asymmetric domain-wall expansion image (inset) and the domain-wall speed v with respect to the in-plane magnetic field H_x , from which the magnitude of the DMI-induced effective field H_{DMI} is determined by observing the inversion symmetry axis. The figure clearly shows that H_{DMI} is sensitive to the composition of X. The SOT is then measured by the w - $2w$ measurement method [5], as exemplified by Fig. 2 for the sample with the choice of X by Ta. The tendency of SOT and DMI will be provided a designing rule for engineering new spintronics devices.

References:

- [1] Mahdi Jamali, Phys. Rev. Lett 111, 246602 (2013)
- [2] I. M. Miron, Nature 476, 189 (2011)
- [3] S.-G. Je, Phys. Rev. B 88, 214401 (2014)
- [4] H. L. Wang, Phys. Rev. Lett. 112,197201 (2014)
- [5] A. V. Khvalkovskiy, Phys. Rev. B 87, 020402 (2013)

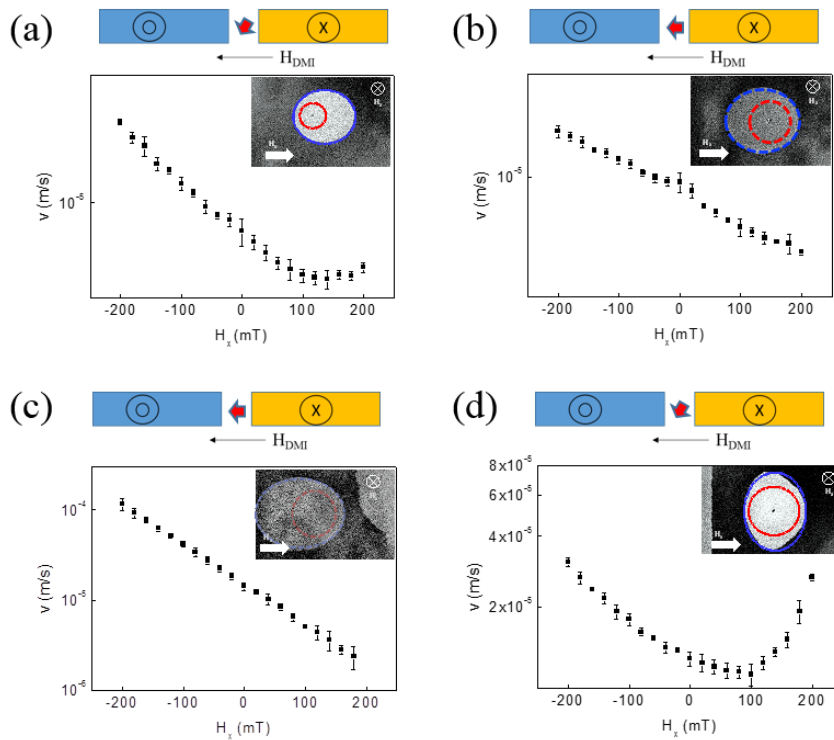


Fig 1. Asymmetric domain-wall speed v with respect to the in-plane magnetic field H_x for Ta(5 nm)/Pt(2.5 nm)/Co(0.6 nm)/X(1.5 nm) films with various choice of X by (a) Ti(3d), (b) Ru(4d), (c) W(5d), and (d) Au(5d), respectively. The inset shows the asymmetric domain-wall expansion image.

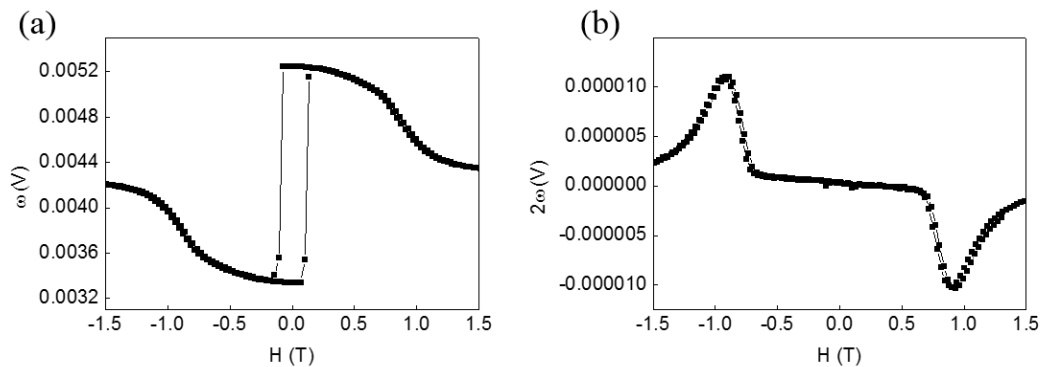


Fig 2. Results from the ω - 2ω measurement for Ta(5 nm)/Pt(2.5 nm)/Co(0.6 nm)/Ta(1.5 nm) film. (a) and (b) show the ω signal and 2ω signals, respectively.

TH.F-P20 - Quantitative scaling of magnetic avalanches in soft materials

G. Durin ^{1,2}, F. Bohn ³, M. A. Correa ³, K. Wiese ⁴, P. Le Doussal ⁴

1. *Istituto Nazionale Di Ricerca Metrologica, Torino, Italy*

2. *ISI Foundation, Torino, Italy*

3. *Universidade Federal do Rio Grande do Norte, Natal, Brazil*

4. *CNRS-Laboratoire de Physique Théorique de l'Ecole Normale Supérieure, Paris, France*

The theory of avalanches of pinned interfaces provide a series of predictions about the statistical properties of the magnetization processes in soft magnetic materials. The analysis of magnetic avalanches (Barkhausen jumps) has showed the occurrence of scaling laws with critical exponents which are well predicted by interface depinning models. For instance, polycrystalline bulk magnetic materials are well described by the so called ABBM model, which assumes to have a single domain wall moving in a random media with spatial Brownian properties. This model actually belongs to a more general class of mean-field (MF) models, which show universal properties, independent of the specific properties of a material. From this model, the average shapes of temporal avalanches is predicted to be a inverted parabola, as experimental verified in Permalloy thin films. Other materials have shown properties that go beyond the MF prediction, with different sets of critical exponents. Anyway, all these results have shown a good correspondence between models and experimental results, but failed to give a quantitative description of the magnetization dynamics. Recent advances in the theory of interfaces in random media had shed a new light in this respect, both in and beyond mean-field. In this paper, we have analyzed a large set of experimental avalanches, and compare them with new theoretical predictions. For instance, the average shape of temporal avalanches are compared with the prediction without free parameters. In addition, the average shape at fixed size is perfectly described by non-MF models, even discriminating between the small differences compared to the MF one. Good agreement is also found in presence of eddy currents in materials when MF occurs. All these results are able to offer for the first time a full quantitative comparison of the scaling properties magnetization dynamics.

TH.F-P21 - Improvement of current induced domain wall motion in TbFeCo wire on plastic substrates

A.Tsukasa¹, T. Atsushi¹, A. Hiroyuki¹

1. Toyota Technological Institute, Japan

Recently, much attention has been paid to current induced domain wall (DW) motion due to its advantage applications [1, 2]. In most reports of the current induced DW motion, Silicon substrate is often used to set magnetic wire on. To its application as a memory, the cutting cost is necessary. If it is possible to replace by an inexpensive plastic substrate it would reduce much the memory cost. It is expected that plastic substrate can be a good candidate in this case. However, there are few reports of the current driven DW motion with plastic substrate. In this study, TbFeCo/Pt wires are fabricated on plastic substrates and Si substrates by using photolithography techniques and DC sputtering.

DWs were moved along the direction of the current due to Spin Hall Effect from Pt capping layer. The threshold current densities J_{th} for DW motion are 1.34×10^{10} [A/m²] and 5.30×10^{10} [A/m²] for the wires on the plastic and Si substrate, respectively. It suggested that the current induced DW motion in TbFeCo on plastic substrates is improved effectively. The threshold current density of the plastic substrate was much smaller than that of Si substrate.

This work was supported by the Ministry of Education, Culture, Sports, Science and Technology, Japan-Supported Program for Strategic Research Foundation at Private University (2014-2019) and KAKENHI No.26630137 (2014-2016).

[1] S. S. P. Parkin, *et al*, Science.320 190 (2008)

[2] Duc-The Ngo, *et al*, Appl. Phys. Express 4 (2011) 093002

TH.F-P22 - Current induced domain wall motion along current direction in Pt/GdFeCo(110nm)/SiO₂/Si sub. magnetic nanowire

Y. Kurokawa¹, M. Kawamoto¹, H. Awano¹

1. Toyota Technological Institute, Japan

Manipulating magnetic domain wall (DW) using electric current is paid attention from the viewpoint of device application such as new type of magnetic memories. Recently, a number of experimental investigations for current induced DW motion in perpendicular magnetized magnetic wire have been reported. In our previous study, we reported that amorphous TbFeCo wire has low critical current density (J_c) because of low saturation magnetization (M_s) of that. In this study, we observe current induced DW motion of amorphous GdFeCo wire which also has low M_s .

The GdFeCo wires are fabricated by electron beam lithography and magnetron sputtering. To avoid the ambient oxidization, the wires are capped by a 2 nm thick Pt layer.

The current induced DW motion in GdFeCo wires are observed by Kerr microscope. Almost all the M_s of the GdFeCo wires are lower than 100 emu/cc. The J_c of the GdFeCo wire whose thickness is 110 nm is 7.5×10^{10} A/m². That is almost same value of the J_c of the TbFeCo and is also much lower than that of the FeNi ($\sim 10^{12}$ A/m²). Surprisingly, the direction of current induced DW motion in the GdFeCo wire is current direction. Generally, this result indicates that the DW driving force is due to spin hall effect and dzyaloshinsky-moriya interaction from the Pt interface. However, this result also indicates that these effects probably do not act only on the Pt layer interface.

This work was financially supported by the Ministry of Education, Culture, Sports, Science and Technology, Japan-Supported Program for Strategic Research Foundation at Private University (2014-2019) and KAKENHI No.26630137 (2014-2016).

TH.F-P23 - Analytical modeling of magnetic domain wall motion under applied fields and currents

S. Ali Nasser¹, B. Sarma¹, G. Durin^{1,2}, C. Serpico^{1,3}

1. *ISI Foundation, Torino, Italy*

2. *Istituto Nazionale di Ricerca Metrologica (INRIM), Torino, Italy*

3. *Dip. di Ingegneria Elettrica, University of Napoli Federico II, Italy*

Manipulating domain walls within nanostructures has many applications in the development of spintronic logic and storage devices [1]. Such applications have led to increased interest within the scientific community in developing models which can qualitatively or quantitatively describe the domain wall motion under applied fields and currents. The main analytical model for analyzing the motion of magnetic domain walls is the 1-D model for rigid transverse walls [2]. This model qualitatively describes the motion of the domain wall, while it fails to match experimental and numerical results quantitatively. Many researchers in recent years have introduced new interactions such as spin transfer torques in the 1-D model with the aim of reaching a more general model [3]. Experimentalists have also used this model to describe the motion of different domain walls, including vortex walls. It seems that in many of such attempts, formalisms are not followed accurately and the main assumptions of the model (such as the Bloch wall profile used in developing the model) are underestimated. Taking into account such flaws, the authors embarked on analytically deriving the equations of motion for a generalized domain wall under fields and currents.

In this paper, we reformulate the method to derive the equations of motion for a magnetic domain wall in nanostructures in terms of collective variable. The proposed formulation is based on the D'Alembert's principle which may be viewed as an extension of the Lagrangian formulation in presence of conservative and nonconservative forces. This formalism is then applied to analyze the motion of a rigid tilted transverse domain wall and the results are compared with micromagnetic simulations to assess the accuracy of the analytical model.

References:

- [1] R.L. Stamps, S. Breitkreutz, J. Akerman, A.V. Chumak, Y. Otani, G.E.W. Bauer, J. Thiele, M. Bowen, S.A. Majetich, M. Kläui, I.L. Prejbeanu, B. Dieny, N.M. Dempsey, B. Hillebrands: *Journal of Physics D: Applied Physics*. 47, 33 (2014)
- [2] A. Thiaville, Y. Nakatani (2006)
- [3] O. Boulle, S. Rohart, L.D. Buda-Prejbeanu, E. Ju 'e, I.M. Miron, S. Pizzini, J. Vogel, G. Gaudin, A. Thiaville: *Physical Review Letters*. 111, 21 (2013)

TH.F-P24 - Current-driven vortex domain wall motion in wire-tube nanostructures

A. Espejo^{1,2}, N. Vidal-Silva¹, J. A. López-López³, D. Goerlitz², K. Nielsch², J. Escrig^{1,4}

1. *Departamento de Física, Universidad De Santiago De Chile, Santiago, Chile*

2. *Institute of Nanostructure and Solid State Physics, University of Hamburg, Hamburg, Germany*

3. *Departamento de Física, Universidad Técnica Federico Santa María, Valparaíso, Chile*

4. *Center for the Development of Nanoscience and Nanotechnology, Santiago, Chile*

We have investigated the current-driven domain wall motion in cylindrical nanostructures comprised of a pair of nanotube and nanowire segments. Under certain values of external magnetic fields, it is possible to pin a vortex domain wall in the transition zone between the wire and tube segments. We explored the behavior of this domain wall under the action of an electron flow applied in the opposite direction to the magnetic field. Thus, for a fixed magnetic field, it is possible to release a domain wall pinned simply by increasing the intensity of the current density, or conversely, for a fixed current density, it is possible to release the domain wall simply decreasing the magnetic external field. When the domain wall remains pinned due to the competition between the current density and the magnetic external field, it exhibits a oscillation frequency close to 8 GHz. The amplitude of the oscillations increases with the current density and decreases over time. On the other hand, when the domain wall is released and propagated through the tube segment, this shows the standard separation between a steady and a precessional regime. The ability to pin and release a domain wall by varying the geometric parameters, the current density or the magnetic field, transform these wire-tube nanostructures in an interesting alternative as an on/off switch nano-transistor.

The authors acknowledge financial support from Fondecyt Grant 1150952 and the Financiamiento Basal para Centros Científicos y Tecnológicos de Excelencia, under project FB0807. CONICYT Ph.D. Program Fellowships is also acknowledged.

TH.F-P25 - Electric-current-induced dynamics of bubble domains in TbFeCo wires of various compositions with different cap layers

M. Tanaka¹, H. Kanazawa¹, S. Sumitomo¹, S. Honda², K. Mibu¹, H. Awano³

1. Nagoya Institute of Technology, Japan

2. University of Tsukuba, Japan

3. Toyota Technological Institute, Japan

Electric-current-induced dynamics of domain walls in magnetic wires is paid attention because of the potential for new spintronics devices. Some researchers have reported that the reverse or transverse forces with respect to the electron flow are induced in the current-induced dynamics of the domain walls by the spin Hall effect or Rashba effect. Bubble domains, whose domain walls do not reach the wire edges, allow us to estimate these forces from a different aspect. In this presentation, we show the current-induced forces for bubble domains in perpendicular magnetized ferrimagnetic TbFeCo wires with various saturation magnetizations with different cap layers.

TbFeCo wires with different saturation magnetizations of about 10 nm in thickness with cap Pt and Ta layers of 2 nm were fabricated on thermally oxidized Si substrates using electron-beam lithography, sputtering and a lift-off method. The width of the wires was designed to be about 10~40 μm. The magnetizations of the TbFeCo wires were set to be transition-metal-dominant and rare-earth-dominant sides. Bubble domains were induced in the wires using laser annealing under an external magnetic field. The current-induced dynamics of bubble domains was observed by polar Kerr microscopy at room temperature.

It was found that the bubble domains in the TbFeCo wires with relatively low saturation magnetizations collapsed, whereas those with relatively high saturation magnetizations grew, under a current flow. A bubble domain in the TbFeCo wire with the Pt cap layer grew to an electric current direction with a tilted angle. The tilt direction of the bubble-domain' growth in the TbFeCo wires with the transition-metal-dominant and rare-earth-dominant magnetizations are opposite each other. We discuss the composition- and the cap-layer-dependence of electric current induced dynamics of the bubble domains.

TH.F-P26 - Investigation of vortex domain wall motion in permalloy nanowire with nano-constriction

V. Parakkat¹, Anil P.S. Kumar¹

1. IISc, Bangalore, India

We have investigated the magnetic field induced reversal, in permalloy nanowire (430nm wide) attached to a nucleation pad (5micron) at one end, using localized electrical probes. The nano structure was fabricated by liftoff, of 15nm thick film grown (on SiO₂) using pulsed laser ablation. Here we utilize the anisotropic magnetoresistance of permalloy to electrically track domain wall(DW) injection from the pad, its pinning at a geometrical constriction(280nm deep) and depinning. We studied the statistics of various events in the reversal processes and observed two well defined depinning field values corresponding to vortex domain walls of different chiralities. The nucleation of DW in the nucleation pad is highly stochastic. But we could control this by applying transverse component of magnetic field which helped in tuning the probability distribution of the injection of DWs of different chiralities. Hence, we used this technique to inject DW preferentially into the NW to study its interaction with a “lambda” shaped notch.

The minor hysteresis loop measurements provided us with direct proof of the chirality dependence of the potential landscape seen by the vortex DWs at the notch and is well supported by the simulation data. We observed that there is a large difference in the values of depinning field required to move DW to left side of the notch and to the right, thus demonstrating the asymmetric nature of potential barrier at the notch, which depends on chirality of the DWs.

The pinning probability was higher for clockwise vortex DW since the potential barrier seen by it at the notch is higher compared to counter-clockwise vortex DW; this implies that a careful discretion is required for the selection of the type of DW to be used in DW based devices.

TH.F-P28 - DeltaE effect and magnetomechanical damping in the re-entrant spin glass state of ferromagnetic bulk metallic glasses

J. Torrens-Serra¹, F. Solivellas¹, S. Kustov¹

1. Universitat De Les Illes Balears, Palma de Mallorca, Spain

Ferromagnetic bulk metallic glasses are classical materials, exhibiting the re-entrant spin glass transition. The latter implies a strong decline of domain wall (DW) mobility. In the present work, the acoustic technique has been employed to follow the effect of polarizing field on the dynamics of DWs below and above the re-entrant spin glass (RSG) transition temperatures in several ferromagnetic Fe-based bulk metallic glasses (BMG). Experimentally, the dependences of deltaE effect, linear (micro- and macroeddy) and non-linear (hysteretic) magnetomechanical internal friction components at a frequency close to 90 kHz versus polarizing field have been studied between 15 and 300 K for a series of Fe-Cr-Mo-C-B BMGs with the Curie temperature from 73 to 310 K.

Above the RSG freezing temperatures, all three magnetomechanical damping components show a classical pattern: a monotonous decrease of the microeddy and hysteretic terms and a maximum in the macroeddy damping component versus magnetic field. DeltaE effect clearly shows the contributions of micro- and macroeddy relaxations.

In the RSG state, the non-linear, hysteretic damping component demonstrates an intense maximum versus field close to the position of the macroeddy current damping maximum. The formation of the maximum of non-linear damping with increasing field is concomitant with the strong variation of the functional form of the strain amplitude dependence of damping, which shows a classical Rayleigh behaviour above this "critical" field. These observations indicate that the polarizing field provokes RSG "melting", which is clearly detected by means of the acoustic technique.

TH.F-P29 - Walker breakdown of domain wall motion driven by spin waves in perpendicular magnetic anisotropy nanostrip

L. Chang¹, S. Lee¹

1. *Institute of Physics, Academia Sinica, Taiwan*

In this report, we numerically and analytically investigate the SW induced DW motion in a nanostrip with perpendicular magnetic anisotropy by means of micromagnetic simulation (OOMMF). We find the Walker breakdown in all cases of spin wave driven DW motion, as in the field driven and charge current driven DW motions. The nanostrip dimension is $4000 \times w \times t \text{ nm}^3$. The strip width w and thickness t varies from 20 to 80 nm and 2 to 10 nm, respectively. A DW at the center is subjected to a SW source 500 nm apart on the left with amplitude H_0 in the transverse direction and frequency f . When a SW approaches the DW, fluctuation of magnetization appears on the DW region, which gives rise to an effective field H_{eff} acting on the DW. The effective field exerts a torque to rotate the DW magnetization, resulting in the DW motion. The directions of the SW induce DW motion and the transmission coefficient for the propagating SW across the DW are depending on the in-plane tilt angle of the wall magnetization. The DW velocities versus amplitude of the SW for different types of DW will be presented. The oscillatory amplitude and frequency of the DW motion is analyzed. This study provided new perspectives for the control and manipulation of DW in a nanostrip.

Th.G-P01 - Reversible control of ferromagnetism in Fe₃O₄ via lithium insertion/extractionG. Wei¹, Y. Chen¹, S. Xiao¹*1. School of Physics, Shandong University, China*

Transition metal oxides have been extensively studied as anode materials for high-performance lithium ion batteries. It is notable that the redox states of these materials can be controlled by the electrochemical potential of the electrode. A reversible control of magnetism can be achieved if the charge/discharge voltage range is carefully set, because the variation of valence states of transition metal may change the exchange coupling between the d orbital electrons. With the rapid development of battery manufacturing technology, this brilliant feature makes it a new approach to achieve room-temperature magnetic control using electrochemistry method. We fabricated a miniature lithium-battery sealed in a glass tube using Fe₃O₄ as the anode. XRD and CV curves were combined to determine the suitable discharge potential limit that would allow maximum lithium insertion but avoid structural damage to the magnetic electrode. Ex situ XRD indicates when the cell is discharged to 0.8V, the patterns of the cathode are the same as those of Fe₃O₄, indicating that the cathode maintains inverse spinel structure. However, at 0.7V, some characteristic peaks of the spinel disappear and the new pattern can be assigned to Li_xFe₃O₄. An in situ magnetic measurement of Fe₃O₄ during the inserting/ extracting of Li ions was conducted in the reversible range from 3.0 to 0.8 V. A highly reversible variation in magnetic response was observed with respect to the lithium insertion/extraction process. The cycle time is only 10 min and can be further improved with a higher current. The obvious magnetic variation, fast magnetic response speed as well as uncomplicated fabrication process make this LIB styled device a promising candidate for future practical applications.

Th.G-P02 - Computer simulation of domain wall motion induced by a slope electric field

S. Murayama¹, K. Yamada¹, Y. Nakatani¹

1. *University of Electro-Communications, Tokyo, Japan*

Recently, the domain wall (DW) motion device has attracted a great deal of attention, because it will be a candidate for a nonvolatile information storage, which has a potential for reducing consumption power. In recent years, as a new method for reducing the power, the electric field-driven DW motion method has been proposed [1-3]. In this study, we perform the micromagnetic simulations, and investigate the DW motion by using a slope electric field (SEF). Since the anisotropy field in the magnetic nanowire can be changed at each position in this approach [4,5], it lead to change the DW energy at each position, and accordingly, the DW moves only by this electric field.

The size of the magnetic nanowire is 60 nm of width, 3.9 nm of height, and infinite length. The nanowire is divided by a rectangular prism with dimensions of $3.0 \times 2.0 \times 3.9 \text{ nm}^3$. Typical material parameters for Co/Ni multilayer film [6]. The effect of the SEF is realized by decreasing the K_u linearly with respect to the magnetic nanowire, and the reduction rate of the K_u is defined as ΔK_u .

The maximum velocity is 1100 cm/s at $\Delta K_u = 170 \text{ erg/cm}^3/\text{nm}$, and the DW moves to right which is the direction to decrease K_u ($x > 100 \text{ nm}$). The DW moves with the steady motion up to $\Delta K_u = 170 \text{ erg/cm}^3/\text{nm}$, and the v is proportional to ΔK_u . Above $\Delta K_u = 170 \text{ erg/cm}^3/\text{nm}$, the DW moves with the precessional motion, and the v is decreased. These phenomena are the similar with the Walker breakdown.

[1] Nat. Commun. 3, 848 (2011)

[2] Nat. Commun. 3, 888 (2012)

[3] Appl. Phys. Lett. 100, 192408 (2012)

[4] Science 315, 349 (2007)

[5] Appl. Phys. Lett. 96, 192506 (2010)

[6] Appl. Phys. Express. 1, 101303 (2008)

Th.G-P03 - Electric field control of current-induced domain wall motion

H. Kakizakai¹, K. Yamad¹, M. Kawaguchi¹, T. Koyama², D. Chiba², T. Ono¹

1. *Institute For Chemical Research, Kyoto University, Japan*

2. *The University of Tokyo, Japan*

In magnetic recording medium, information can be written by switching a magnetization direction of a magnetic material. Up to now, the switching has been realized by applying a magnetic field and/or an electric current. Domain wall (DW) displacement induced by an electric current is one of the most promising techniques. For practical applications, precise control of the DW position and its speed are desired. We have been investigating an electric field effect on magnetism using electric field-effect devices consisting of a gate electrode, an insulator layer and a ferromagnetic material. Recently, we reported that the velocity of domain wall motion induced by magnetic field can be widely modulated just by applying an electric field. In this work, we have investigated the current induced DW motion under an electric field in the absence of external magnetic field in a perpendicularly magnetized MgO/Co/Pt system. We observed the domain wall motion by means of a magneto-optical Kerr effect (MOKE) microscope through a transparent gate electrode. In this system, there is a strong Dzyaloshinsky-Moriya interaction at the interface between the Co and Pt layers due to spin orbit interaction and structural asymmetry, and the DW moves in the same direction as electric current via spin-Hall torque. The observed DW motion in this experiment was in thermally activated creep regime. The DW creep velocity decreased with increasing the gate voltage, i.e., increasing the electron density at the surface of the Co layer.

Th.G-P04 - First-principles density functional study on magnetic-anisotropy-energy non-linear variation by electric field in double Fe/MgO interfaces

D. Yoshikawa¹, M. Obata¹, S. Haraguchi¹, Y. Taguchi¹, T. Oda^{1,2}

1. Graduate School of Natural Science and Technology, Kanazawa University, Japan

2. Institute of Science and Engineering, Kanazawa University, Japan

Controlling of the magnetic anisotropy energy (MAE) by electric field (EF) is one of the most interesting techniques for exploitation in magnetic random access memory (MRAM). The magnetization direction reversal, required for writing information, has been accomplished with the technique of spin-transfer torque (STT) effect, however there has been still the fatal problem, heating problem. The control of MAE by EF can solve this problem, because the reduction of energy barrier for magnetization reversal suppresses the heat. One of the most important problems in the technology is to find the magnetic material which shows an EF-sensitive MAE. To this aim, the mechanism for a large MAE variation by EF should be understood. In this context, we have investigated electronic structures and MAEs of double Fe/MgO interfaces [2,3]. We have carried out the first-principles density functional computation for the slab models MgO/Fe/MgO and Fe/MgO/Fe, using fully relativistic ultrasoft pseudopotentials, planewave basis, and generalized gradient approximation (GGA). We estimated the MAEs in the MgO/Fe/MgO with respect to the EF. The variation ratios of MAEs with respect to the EF were obtained to be in good agreement with the experimental data [4]. We found that there was a remarkable correlation between the MAE variation and number of electrons on the interface Fe atom [3]. We calculated the orbital-angular-dependent partial density of states (PDOS) of the interface Fe atom, and found that there were very interesting features around the Fermi energy. In the presentation, we discuss dependence on the number of layers and a possible origin of MAE non-linear variations.

[1] H. Ohno, Nat. Mater. 9, 952 (2010)

[2] D. Yoshikawa et al., JPS Conf. Proc., 2015, in press

[3] D. Yoshikawa et al., Appl. Phys. Express 7, 113005 (2014)

[4] T. Nozaki et al., Appl. Phys. Express 6, 073005 (2013)

Th.G-P05 - Electric-field effect on magnetism of L10-FePt investigated by the x-ray magnetic circular dichroism spectroscopy

S. Miwa^{1,4}, K. Matsuda¹, K. Tanaka¹, T. Nozaki^{2,4}, F. Bonell¹, S. Yuasa^{2,4}, M. Suzuki³, Y. Suzuki^{1,2,4}

1. Graduate School of Engineering Science, Osaka University, Japan

2. National Institute of Advance Industrial Science and Technology (AIST), Spintronics Research center, Japan

3. Japan Synchrotron Radiation Research Institute/SPring-8, Japan

4. CREST, Japan Science Technology, Japan

Voltage control of magnetism in ferromagnetic thin-films has attracted much attention as the ultimate technology for low-power operation of spintronic devices. In particular, the voltage induced magnetic anisotropy change in ferromagnetic metals [1,2] is promising since the control is applicable for magnetic tunnel junction devices. As a mechanism of the anisotropy change, changes in the electronic occupation state of *d*-orbital and in the band structure by the electric-field-induced accumulated charge at the ferromagnet/insulator interface are plausible, which may lead to a change in the interfacial perpendicular magnetic anisotropy through the spin-orbit interaction. However, no experimental evidence to prove this mechanism has been reported. In the present study, the electric-field effect on the magnetic properties of L1₀-FePt ultrathin layer was investigated by x-ray magnetic circular dichroism (XMCD) spectroscopy at the Pt L edges.

An MgO(100)substrate/MgO(3 nm)/Cr(20 nm)/Pd(50 nm)/[Fe(1.4Å)/Pt(2.0Å)]₂/MgO(5 nm) multilayer was fabricated by molecular beam epitaxy. The FePt layer was prepared by alternate deposition of pure Fe and Pt. The film was coated with a polyimide (1500 nm) layer in the air immediately taken out of vacuum. Magnetization hysteresis loops demonstrated perpendicular magnetic anisotropy of the L1₀-FePt layer increased at a negative bias voltage, which induces charge depletion at the FePt/MgO interface. The XMCD measurement under voltage application was performed at BL39XU of SPring-8 synchrotron radiation facility. Our sum rule analysis showed that the effective spin magnetic moment ($m_{\text{spin}} - 7m_{\text{T}}$) in Pt increases about 10% under negative bias voltage, which would be correlated to the voltage induced magnetic anisotropy change in FePt.

This work was partially supported by ImpACT Program of Council for Science, Technology and Innovation. (Cabinet office, Government of Japan)

[1] M. Weisheit et al., Science 315, 349 (2007)

[2] T. Maruyama et al., Nat. Nanotechnol. 4, 158 (2009)

Th.G-P06 - Electric-field-controlled magnetization rotation and tunneling magnetoresistance of magnetic tunnel junctions at room temperature

Y. Zhao^{1,3}, P. Li¹, A. Chen¹, D. Li², S. Zhang^{1,3}, L. Yang¹, Y. Liu¹, M. Zhu¹, H. Zhang¹, X. Han²

1. *Tsinghua University, Beijing, China*

2. *Beijing National Laboratory for Condensed Matter Physics, Chinese Academy of Sciences, China*

3. *College of Science, National University of Defense Technology, China*

Magnetic tunnel junctions (MTJs) are very important for applications in field sensors, magnetic random access memories and spin logics. Recently there are a lot of efforts aiming at electric-field control of magnetism in MTJs to manipulate their electronic transport property, which could lead to ultralow-energy-consumption devices. So far two methods have been demonstrated for the electric-field control of electronic transport property in MTJs. One is the MTJ with a ferroelectric or multiferroic barrier, which works at low temperatures. Another one employs an electric field to switch the magnetic moment of ultrathin ferromagnetic layer of MTJ with voltages close to the breakdown voltage of the junctions and the assistance of a magnetic field. Therefore, electric-field modulation of tunneling magnetoresistance (TMR) at room temperature without a magnetic field is highly desired. One promising way is to employ the strain-mediated coupling in ferromagnetic/piezoelectric structure, in which remarkable electric-field controls of magnetism have been widely achieved at room temperature. Though MTJs/piezoelectric has been predicted by theory, experiment work is still lacking. We fabricated the key structure of MTJs CoFeB/AlO_x/CoFeB on Pb(Mg_{1/3}Nb_{2/3})_{0.7}Ti_{0.3}O₃ (PMN-PT) ferroelectric single crystal. Electric fields can result in a piezostain in PMN-PT, which transfers to the ferromagnetic film leading to change in magnetic anisotropy. We demonstrate a reversible, continuous magnetization rotation and manipulation of TMR at room temperature by electric fields without the assistance of a magnetic field. This work provides a new approach to manipulate the spin state and TMR of MTJs via electric fields, and should be significant for electric-field controlled spintronics.

Th.G-P07 - Underlayer material dependence of perpendicular magnetic anisotropy in CoFeB/MgO tuned by electric fields

W. Skowronski^{1,2}, T. Nozaki², Y. Shiota², S. Tamaru², K. Yakushiji², H. Kubota², A. Fukushima², S. Yuasa², Y. Suzuki²

1. AGH University of Science And Technology, Kraków, Poland

2. National Institute of Advanced Industrial Science and Technology, Ibaraki, Japan

Magnetic multilayer systems with perpendicular magnetic anisotropy (PMA) are suitable for the next generation magnetic random access memories (MRAM) due to their increased thermal stability and better scalability than in-plane magnetized systems [1]. In addition, magnetization of ultra-thin ferromagnets can be switched by ultra-fast electric-field pulses [2], or controlled in magnetic tunnel junctions (MTJs) used as magnetic field sensors [3] or radio frequency detectors [4].

We present studies on the PMA energy of thin CoFeB films deposited on metallic underlayers: Pd, Pt, Ta, Ir, W, CuN, Zr and Nb. In selected multilayer systems, we have measured CoFeB magnetic moment and the saturation field thickness dependence in order to calculate the magnetic dead layer and the PMA energy. We have repeated this investigation after annealing multilayers at various temperature up to 450°C.

The multilayer system with Ir underlayer exhibit very high interface PMA energy of 1.9 mJ/m² stable up to 300°C. By using W buffer smaller PMA of 1.2 mJ/m² is measured, however, the thermal stability is confirmed up to 450°C. In addition, we fabricated MTJ structure of CoFeB (0.88 nm)/MgO(2.5 nm)/CoFeB(5 nm) in order to investigate an influence of the electric field on PMA. We measured change of the anisotropy energy per applied electric field of up to 100 fJ/Vm. In order to prove the repeatability and high operation speed we have measured voltage induced ferromagnetic resonance up to 30 GHz in patterned MTJ driven by radio frequency stimuli, tuned by the static electric fields.

This work was partly supported by ImPACT Program of Council for Science, Technology and Innovation (Cabinet Office, Government of Japan) and by the Polish National Science Center Grant No. DEC-2012/04/M/ST7/00799.

[1] - H. Yoda et al. *Curr. Appl. Phys.* 10, e87 (2010), S. Ikeda et al. *Nature Mater.* 9, 721 (2010)

[2] - Y. Shiota et al. *Nature Mater.* 11, 39 (2012)

[3] - W. Skowronski et al. *Appl. Phys. Lett.* 101, 192401 (2012)

[4] - W. Skowronski et al. *Appl. Phys. Lett.* 105, 072409 (2014), Y. Shiota et al. *Appl. Phys. Lett.*

Th.G-P08 - Electric-Field modulation of magnetic anisotropy in the system under magnetic proximity effect

Y. Hibino¹, T. Koyama¹, A. Obinata¹, K. Miwa², S. Ono², D. Chiba¹

1. *The University of Tokyo, Tokyo, Japan*

2. *Central Research Institute of Electric Power Industry, Japan*

Electric field control of magnetism in ferromagnetic materials (FMs) using a capacitor structure has attracted a great deal of attention in the research field of spintronics [1]. Recently, the electric field manipulation of magnetism has been focused not only to the FMs but also the non-magnetic material Pt [2] and Pd. Pt and Pd is known to be an exchange-enhanced paramagnetic material, which the Stoner criterion for ferromagnetism satisfies due to the large peak in the density of states near the Fermi surface. In addition, It has been reported that the magnetic moment of Pd and Pt is induced at the interface adjacent to the FMs (magnetic proximity effect) [3]. We focused on this induced magnetic moment in Pd and manipulated its magnetism especially the perpendicular magnetic anisotropy (PMA).

We have studied the electric field effect on the PMA of perpendicular magnetized Pd/Co/Pt system. By applying electric field to the Pd layer using ionic liquid, the PMA of the whole system significantly changed up to 0.12 mJ/m² even though the Pd is non-magnetic material in ordinary. One of the possible origin of the effect is the relative change in electron occupation state of 4d orbit in the spin polarized Pd due to the proximity effect. This result indicates that the electric field effect is valid even in the ferromagnetic system created by the proximity effect.

This work was partly supported by Grant-in-Aid for Scientific Research (S) from JSPS and research grant from the Foundation for the Promotion Ion Engineering. Part of this work was performed using facilities of the Cryogenic Research Center, the University of Tokyo.

[1] H. Ohno et.al., Nature 408, 944 (2000)

[2] S. Shimizu et.al., Phys. Rev. Lett. 111, 216803 (2013) [3] M. Suzuki et.al., Phys. Rev. B 72, 054430 (2005)

Th.G-P09 - Strain mediated voltage control of metal-insulator transition in VO₂ / PMN-PT heterostructures

A. Petraru¹, R. Soni¹, H. Kohlstedt¹

1. Nanoelektronik, Technische Fakultät Der Christian-Albrechts-Universität, Zu Kiel, Germany

Vanadium oxide (VO₂) is a correlated electron material that exhibits a first-order metal-insulator phase transition (MIT) accompanied by a drastically change in electrical resistivity of up to five orders of magnitude as well a large change in infrared transmission. These properties make VO₂ potentially useful for electrical, optical and electro-optical switches and sensing applications. The transition temperature can be controlled in a relatively wide range by doping or by strain. In this work we focus on controlling the transition temperature of VO₂ in form of epitaxial thin films via strain. Thus, we choose 0.72Pb(Mg_{1/3}Nb_{2/3})-0.28PbTiO₃ (PMN-PT) piezoelectric crystalline substrates for this propose. Due to their huge piezoelectric coefficients in the order of 2500 pm/V, the PMN-PT substrates are used to impose additional amount of biaxial strain to the VO₂ films, by applying an external bias to the substrates. The films were deposited using pulsed laser deposition method, starting from a V₂O₅ ceramic target. By employing X-Ray diffraction measurements, the lattice parameters of the PMN-PT substrates and VO₂ films were measured as a function of applied bias to the substrate. We show that a reversible biaxial in-plane strain of $0.1 \pm 0.01\%$ at an electric field of $E = 10$ kV/cm is achieved by applying the E field perpendicular to the substrate plane. The strain is partly transferred to the epitaxial VO₂ film on top and acts in the (110) plane of the rutile phase of the VO₂ films. We investigate the influence of the biaxial strain on the transition temperature and on the conductive properties of the VO₂ films. Additionally, the influence of the surface charge modifications at the interface VO₂ / PMN-PT (ferroelectric) on the conductive properties of the vanadium dioxide films is investigated.

Th.G-P10 - Electric field effect on induced magnetic moment in Pd

A. Obinata¹, D. Hayakawa¹, Y. Hibino¹, T. Koyama¹, K. Miwa², S. Ono², D. Chiba¹

1. *The University of Tokyo, Japan*

2. *Central Research Institute of Electric Power Industry, Japan*

Recently, electric field control of magnetism in ultra-thin ferromagnetic metals has attracted attention in the research field of spintronics*1,*2. Electrical modulation of electron density at the surface of them plays a main role for achieving it. On the other hand, it is known that the magnetic moment is induced in Pd layer by contacting it with that of a ferromagnetic transition metal element such as Co *3 (the ferromagnetic proximity effect). We aimed to control this proximity-induced magnetic moment in Pd by applying gate electric field. For the observation of the change in the magnetic moment under gating, we deposited MgO/Pd(1.7 nm)/Co(tCo)/Pt(4.1)/Ta from the surface side on an intrinsic Si substrate by rf sputtering. The magnetic moment was confirmed to be induced in whole Pd layer at 10 K for the present Pd thickness. We fabricated an electric double layer capacitor structure with an ionic liquid as a gate insulator*2. A gate voltage V_G was applied between the bottom Pd and the top nonmagnetic Au electrode through the ionic liquid. By applying an electric field to the ferromagnetic surface of this Pd layer, a clear change in the magnetic moment below Curie temperature, which was directly measured using SQUID magnetometer, was observed. This indicates that the induced magnetic moment in non-magnetic metals by the proximity effect are electrically tunable.

This work was partly supported by Grant-in-Aid for Scientific Research (S) from JSPS and research grant from the Foundation for the Promotion Ion Engineering. Part of this work was performed using facilities of the Cryogenic Research Center, the University of Tokyo.

1. D. Chiba et al., *Nature Mater.* 10, 853 (2011)
2. K. Shimamura et al., *Appl. Phys. Lett.* 100, 122402 (2012)
3. F. J. A. den Broeder et al., *J. Appl. Phys.* 61, 4317 (1987)

Th.G-P11 - Correlation between resistive switching behavior and ferromagnetism in pure ZnO thin films

Y. Hu¹, S. Li²

1. Department of Applied Physics, National University of Kaohsiung, China

2. Institute of Electro-Optical Science and Engineering, National Cheng Kung University, China

In the past decade, zinc oxide (ZnO) doped with minute amounts of transition metal elements has been intensively investigated as a promising diluted magnetic semiconductor for possible spintronic applications. However, room temperature ferromagnetism (RT-FM) in pure or nonmagnetic-element-doped ZnO films has been frequently reported, implying that the magnetic moments arise solely from native defects. Meanwhile, the resistive switching properties that are very common in a variety of oxide thin films have also been ascribed to native defects. In this work, we prepared Ti/ZnO/Ti multilayer films by using a magnetron sputtering method with different O₂/Ar gas ratios. All of the samples were deposited on c-plane sapphire substrates at RT. Bipolar resistive switching (RS) behavior were observed in the sample grown without O₂ gas. An introduction of O₂ gas during film growth increases the set voltage and finally destroys the RS behavior. Photoluminescence results show that the intensity of the emission due to oxygen vacancies decreases with an increase in O₂/Ar gas ratio during film growth. In particular, we measured the M-H curves of the sample grown without O₂ gas in initial, high resistance (HR), and low resistance (LR) states. The pure ZnO sample with the best bipolar RS behavior is ferromagnetic in all of the states, and the saturation magnetization of the sample in LR and initial states is the largest (~1.8 emu/cm³) and smallest (~0.4 emu/cm³), respectively.

These results clearly demonstrate that the bipolar RS behavior in pure ZnO film is due to the existence of oxygen vacancies, and a voltage-controlled ferromagnetism in oxide thin film may be achieved for potential magneto-electrical device applications in the near future.

Th.G-P12 - Magnetoresistance in amorphous alloys and thin ferromagnetic films

J. Zapata Farfan¹, H. Montiel Sánchez¹, G. Alvarez Lucio²

1. Universidad Nacional Autónoma De México, Centro De Ciencias Aplicadas Y Desarrollo Tecnológico, Circuito Exterior S/N, Ciudad Universitaria, Delegación Coyoacán, México

2. Instituto Politécnico Nacional, Escuela Superior de Física y Matemáticas, México D.F. México

The phenomenon of Anisotropic Magnetoresistance (AMR) was measured in amorphous alloys and thin ferromagnetic films with the same composition. Measurements were carried out with the four probe technique, by means of a sample holder specially designed for the experimental setup, according to the electromagnet that is used, since there are no commercial devices. Ferromagnetic samples were introduced into a magnetic field with a mechanical system capable of rotating 180 degrees with the aim of detecting the angle for the highest variation of electrical resistance and make a characterization obtaining the percentage of AMR change and the easy or hard axis, according to AMR theory. All samples were swept in magnetic field between -1 to 1 T and in current in a range from 1 fA to 0.1 A in order to determine AMR, This phenomenon was first observed in Gold and Nickel to validate the system, finally it was observed a maximum electrical resistance change when the magnetic field orientation is perpendicular to the easy axis of the ferromagnetic materials and it is associated with intrinsic magnetic properties of the material. It is necessary to mention that we carried out all the instrumentation for the AMR technique.

Jennyfer Zapata want to thank the National Council for Science and Technology of Mexico (CONACYT) for the financial support.

Th.G-P13 - Voltage controlled optical and magnetic properties in ferromagnetic nanostructures studied by optical spectroscopies

L. Ohnoutek¹, L. Beran¹, R. Antos¹, M. Veis¹, A. Jun Tan², U. Bauer², G. S. D. Beach²

1. Charles University in Prague, Faculty of Mathematics and Physics, Prague, Czech Republic

2. Department of Materials Science and Engineering, Massachusetts Institute of Technology, Cambridge, Massachusetts, United States

Control of magnetization in ferromagnetic nanostructures via electric field is essential for development of novel spintronic devices. Recently, Bauer et al [1,2] reported switching of magnetic properties by electrically modulated interfacial chemistry at Co/metal-oxide interface. Detailed studies of this interface are necessary to fully understand the mechanisms responsible for magnetization changes. Magneto-optical (MO) spectroscopy and spectroscopic ellipsometry are highly sensible and non-destructive methods, which can probe magnetic and optical properties of nanostructures with depth sensitivity and provide the opportunity to study the voltage induced interface effects responsible for the changes in magnetic anisotropy as well as in optical properties of ferromagnetic nanostructures. The investigated Ta(4 nm)/Pt(3 nm)/Co(0.9 nm)/GdOx(4 nm) films were prepared by dc magnetron sputtering at room temperature under 3 mTorr Ar with a background pressure of $\sim 1 \times 10^{-7}$ Torr, on thermally-oxidized Si(100) substrates. The gadolinium oxide (GdOx) layer was sputtered from a metal Gd target at an oxygen partial pressure $\sim 5 \times 10^{-5}$ Torr. Gate electrodes of Au(5 nm) were deposited through a shadow mask. Measurements of MO Kerr rotation and ellipticity were carried out on magnetically saturated samples in polar and longitudinal configuration. The spectral range of the experiments was from 1.2 to 5.5 eV. Spectroscopic ellipsometry experiments employed Muller matrix ellipsometer Woolam RC2. The spectra were acquired for as deposited sample and for samples modified by applied voltage up to 8 V. Both spectroscopic ellipsometry as well as MO spectroscopy clearly showed changes in optical and MO properties of studied nanostructures with applied voltage. Comparison of the experimental results with theoretical models revealed the voltage induced changes at Gd/GdOx interface.

[1] Bauer, U. et al. Nature Nanotechnology 8, 411 (2014)

[2] Bauer, U. et al. Nature Materials 14, 174 (2015)

Th.G-P14 - Electric field control of superparamagnetism in Ni/Cu system using electric double layer

K. Yamada¹, H. Kakizakai¹, T. Koyama², S. Ono³, K. Miwa³, M. Kawaguchi¹, D. Chiba², T. Ono¹

1. *Institute For Chemical Research, Kyoto University, Japan*

2. *Department of Applied Physics, The University of Tokyo, Japan*

3. *Central Research Institute of Electric Power Industry, Japan*

Electric field-induced modulation of magnetic properties such as coercivity[1], magnetic anisotropy[2, 3], and Curie temperature TC[4, 5] in metallic magnets opens up a new paradigm of spintronic devices for achieving ultra-low power consumption. Recently, it has been found that an electric double layer capacitor (EDLC) provides much larger charge accumulation than a solid capacitor due to the extremely large capacitance [1, 5]. In this presentation, we demonstrate electrical modulation of blocking temperature TB in superparamagnetic Ni/Cu system by using EDLC. A Ni(1.5 nm)/Cu(1.0 nm) layer with a Ta(2.6 nm) buffer layer was deposited on a GaAs (001) substrate by rf sputtering. The Ni layer was covered with a 2-nm-thick MgO layer to protect it against oxidization. We made a capacitor structure which is composed of the Ni layer as a bottom electrode, an Au thin film as a gate electrode, and an polymer film containing ionic liquid (TMPA⁺-TFSI⁻) sandwiched between them. When a gate voltage VG is applied, the electric double layer is formed across the MgO layer, and the electric field is applied to the surface of the Ni layer. To determine the TB under the application of VG, we measured the zero-field-cooling magnetization using a superconducting quantum interference device [5]. TB was observed to increase with VG, and the amount of the change was about 8.6 K for VG = ±2 V. We ascribe the change in TB to the electric-field-induced change in magnetic anisotropy.

[1] M. Weisheit et al., *Science* 315, 349 (2007)

[2] T. Maruyama et al., *Nature Nanotechnol.* 4, 158 (2009)

[3] M. Endo et al., *Appl. Phys. Lett.* 96, 22515 (2010)

[4] D. Chiba et al., *Nature Mater.* 10, 853 (2011)

[5] K. Shimamura et al., *Appl. Phys. Lett.* 100, 122402 (2012)

Th.G-P15 - Direct imaging of reversible electric control of magnetic domains in $\text{La}_2/3\text{Sr}_1/3\text{MnO}_3$

M. Foerster¹, D. Pesquera², B. Casals², F. Sanchez², G. Herranz², L. Aballe¹, J. Fontcuberta²

1. ALBA Synchrotron Light Facility, Spain

2. Institut de Ciència de Materials de Barcelona (ICMAB-CSIC), Barcelona, Spain

Electric control of magnetic devices is a current research activity of major interest. In this direction, electric control of magnetic anisotropy via magnetoelastic coupling in magnetic films grown on piezoactuators, appears as a simple and potentially convenient strategy. However, a critical issue is the deterministic selection of the magnetization direction through strain-induced flop of the magnetization to orthogonal directions. Here we address this problem by observing the magnetic domain evolution of $\text{La}_2/3\text{Sr}_1/3\text{MnO}_3$ (LSMO) thin films grown on piezoelectric PMN-PT (001) substrates. We have used photoemission electron microscopy with X-ray magnetic circular dichroism contrast (XMCD-PEEM) to monitor in-situ the domain reconfiguration upon applying a voltage bias to the piezo substrate. Out of plane electrical fields were applied to the substrate using the LSMO as top electrode and a silver paint bottom electrode. Starting from a pre-poled state, the magnetic domain pattern in the XMCD image reflects an effective uniaxial anisotropy (twofold) of the film. Upon reversing the poling voltage applied at the piezo substrate, we observe changes in the domain pattern that indicate a biaxial (fourfold) anisotropy upon passing the substrate coercive field. Interestingly, when returning to the original poling, not only the uniaxial anisotropy is restored, but also the new domain configuration is almost identical to the previous one, i.e. the same distribution of north and south domains, which is not expected from the axial (i.e. not directional) nature of an electrically induced magnetic anisotropy mediated by strain.

Th.G-P17 - Distinguishing spin-torque from electrical modification of anisotropy in voltage-induced ferromagnetic resonance

C. Gonzalez ¹, C. Garcia ¹

1. Departamento de Fisica, Universidad Tecnica Federico Santa Maria, Valparaiso, Chile

During the last years, there has been an increasingly interest in the possibility control of magnetic dynamics by electric fields. Some recent experiments [1,2] in magnetic tunnel junction (MTJ) nanopillars have been demonstrated that the electric field can modify the magnetic perpendicular anisotropy on such devices, leading to voltage-induced ferromagnetic resonance. However, it has also been showed that there should be an important contribution of spin torque in such MTJ's response [1]. In this work, we present an analytic model to predict the magnitude and the lineshape of the voltage-induced ferromagnetic resonance, which permits distinguish the electric field and spin torque contributions to the magnetization dynamics. Our results are in good agreement with a recently published work in CoFeB/MgO/CoFeB MTJs [2]

[1] Jian Zhu et al., Phys. Rev. Lett. 108, 197203 (2012)

[2] Takayuki Nozaki et al., Nature Phys. 8, 491 (2012)

Th.G-P19 - Electrical writing of magnetic and resistive multistates in CoFe films deposited onto Pb[ZrxTi_{1-x}]O₃

V. Iurchuk¹, B. Doudin¹, J. Bran¹, Bohdan Kundys¹

1. Institut de Physique et Chimie des Matériaux de Strasbourg, France

Ever increasing miniaturization requirements stimulate large research efforts to find alternative to magnetic field methods to control magnetization in magnetoresistive memories. Use of electric field induced deformation energy of piezoelectric elements is a promising way of magnetization control. The reversible electromagnetic coupling with electric fields applied to a whole substrate was demonstrated to result in 'two states' operation [1]. However the technologically important surface electric field control, multistate operation and ability to erase the written states with electric fields have not been proven till recently [2,3]. In this work we describe the subcoercive and surface operation to write and erase remnant magnetic and resistive states in CoFe overlayer deposited on ferroelectric Pb[ZrxTi_{1-x}]O₃. Magneto- and electroresistance responses are further explored as the functions of CoFe thickness. The simplest resistance strain gage-like structure is realized as a multistate memory cell demonstrating both resistive memory (RRAM) and magnetoresistive memory (MRAM) functionalities in a single device.

References:

1. A. Brandlmaier, S. Geprägs, G. Woltersdorf, R. Gross and S. Goennenwein, J. Appl. Phys. 110 043913 (2011)
2. B. Kundys, V. Iurchuk, C. Meny, H. Majjad, B. Doudin Appl. Phys. Lett. 104, 232905 (2014)
3. V. Iurchuk, B. Doudin, B. Kundys J. Phys.: Condens. Matter 26 292202 (2014)

Th.H-P01 - Anomalous and planar righi-leduc effect in NiFe and YIG ferromagnets

B. Madon¹, D. Pham¹, D. Lacour², A. Anane³, B. Rozenn³, V. Cros³, M. Hehn², J. Wegrowe¹

1. *Ecole Polytechnique, LSI, France*

2. *Institut Jean Lamour, France*

3. *UMR CNRS Thales, France*

Nowadays electronic devices are dissipating more and more power. Hence, the use of the heat currents generated in adjacent electronic circuits for running devices (without other source of energy) is a promising strategy in terms of energy efficiency. Since 2008, a large number of publications have reported a surprising magneto-voltaic signal measured on a ferromagnetic electrode in response to a thermal excitation. In our presentation we will show that the observed magneto-voltaic signal can be accounted by anomalous (also called magnon hall) and planar Righi-Leduc effects. The Righi-Leduc effect refers to the thermal analogue of the Hall effect, for which the electric current is replaced by the heat current and the generated electric field by the temperature gradient. In both cases, the magnetic field generates a transverse force that deviates the carriers (electron, phonon, magnon) in the direction perpendicular to the current. In a ferromagnet, the magnetization plays the role of the magnetic field, and the corresponding effects are respectively called anomalous Hall and anomalous Righi-Leduc (ARL). Furthermore, a second transverse contribution due to the anisotropy, the planar Hall effect, is superimposed to the anomalous Hall effect has also a thermal counterpart named planar Righi-Leduc effect (PRL) [1]. We will report experimental evidences of those thermal counterparts in ferromagnets that are either electrical conductor (NiFe) or insulator (YIG). Varying the measurement geometry we demonstrate that the recorded magneto-voltaic signals follow the symmetry associated to ARL and PRL. Moreover their signs and amplitudes are strongly dependent on the capping layer nature. This fact is well explained by considering the presence of thermocouples in the used multilayer.

[1] J.-E. Wegrowe, H.-J. Drouhin and D. Lacour, Anisotropic magnetothermal transport and spin Seebeck effect, Phys. Rev. B 89, 094409 (2014)

Th.H-P02 - Spin-dependent Peltier effect in a lateral spin-valve device with epitaxial Heusler-compound electrodes

K. Yamasaki¹, S. Oki¹, S. Yamada¹, T. Kanashima¹, K. Hamaya^{1,2}

1. *Osaka University, Japan*

2. *Osaka University and JST-CREST, Japan*

In the field of spin caloritronics, the spin-dependent Peltier effect was experimentally detected in nanopilar spin-valve structures [1]. If giant pure spin currents are injected from a ferromagnetic material into a nonmagnetic one, one can detect the spin-dependent Peltier effect even in a lateral spin-valve (LSV) structure [2]. So far, we have developed a technique for generating giant pure spin currents at room temperature by using epitaxial Co-based Heusler-compound Co₂FeSi (CFS) films [3]. Here, we demonstrate the spin-dependent Peltier effect in a LSV with the epitaxial CFS electrodes.

We first confirmed the generation of giant pure spin currents in LSVs [3]. By using the same LSV and a second-harmonic ac lock-in technique, we observed thermally induced spin injection, so called spin-dependent Seebeck effect [4], at room temperature and obtained the spin-dependent Seebeck coefficient of $\sim -15.8 \mu\text{V/K}$. By changing terminal configuration and a thermocouple electrode in the same LSV, we detected clear spin Peltier signals under spin-injection conditions and the spin-dependent Peltier coefficient of $\sim -4.74 \text{ mV}$ was obtained. This study is the first observation of the spin-dependent Peltier effect in the LSV structure.

This work was partly supported by CREST from JST and by Grant-in-Aid for Scientific Research on Innovative Areas "Nano Spin Conversion Science" (Grant No. 26103003).

[1] J. Flipse *et al.*, *Nat. Nanotech.* 7, 166 (2012)

[2] A. Slachter *et al.*, *Phys. Rev. B.* 84, 174408 (2011)

[3] K. Hamaya *et al.*, *Phys. Rev. B.* 85, 100404(R) (2012)

[4] A. Slachter *et al.*, *Nat. Phys.* 6, 879 (2010)

Th.H-P03 - Observation of spin-dependent peltier effect using anomalous nernst effect

T. Nomura¹, G. Uematsu¹, S. Hu², T. Kimura^{1,2}

1. *Department of Physics, Kyushu University, Japan*

2. *Research Center for Quantum Nano-Spin Science, Kyushu University, Japan*

Recent development in understanding the interplay between heat and spin produces unique heat-utilizing application based on spins. A representative and fascinating phenomenon is thermal spin injection, in which excess heat can be used to produce spin current through the spin-dependent Seebeck coefficient. Recently, we have found that CoFeAl show the excellent property for the thermal spin injection because of the large spin-dependent Seebeck coefficient. According to the reciprocal relationship, a large spin-dependent Peltier coefficient will be expected at the CoFeAl/nonmagnetic-metal interface. However, because of the difficulty of the heat manipulation, it was difficult to detect the signal related to the Peltier effect. Here, we demonstrate that the spin-dependent Peltier effect can be observed by using the anomalous Nernst effect.

The sample used for the present study is a conventional lateral spin valve structure consisting of two CoFeAl wires bridged by a Cu wire. Here, the heat current induced by the spin-dependent Peltier effect at one CoFeAl/Cu interface was detected as the Anomalous Nernst voltage at the other CoFeAl/Cu interface. It should be noted that, under the electrical spin injection, the voltage due to the spin-dependent Peltier effect shows the field dependence similar to the spin valve signal under the electrical spin injection. Therefore, the spin current was created by the thermal spin injection. The field dependence of the voltage under the thermal spin injection shows a clear asymmetric behavior supporting the existence of the spin-dependent Peltier effect.

Th.H-P04 - Spin-thermoelectric voltage in the ste element using LPE YIG films grown on GGG substrates

Y. Li¹, Y. Kono², K. Mizunuma², Y. Saiga², M. Imamura¹

1. *Fukuoka Institute of Technology, Japan*

2. *DENSO CORPORATION Research Laboratories, Japan*

The voltage generated when a temperature gradient dT is applied to the element fabricated with an ultrathin platinum layer coated on an yttrium iron garnet magnetic plate is called a spin-thermoelectric (STE) voltage, and the voltage has been considered to be due to the spin Seebeck effect based on spin currents driven by a temperature gradient. We present the results of measurements on the STE voltage of a device composed of 4-10micro-m-thick YIG films grown on a 10x10x0.5mm³ gadolinium gallium garnet substrate by using liquid phase epitaxy and the Pt-coating layer applied to the YIG film surface by sputtering. Crystallinity was evaluated by an x-ray diffraction, and it was confirmed that the films were grown with high crystallinity on the GGG substrate showing the very sharp (111) diffraction spectra of 20,000 counts at $2\theta=51.56^\circ$. Magnetic characteristics of the films were measured by using VSM. The in-plane saturation field to the film surface was a small value of 25 Oe and the H_c value was ~ 1 Oe. The STE measurements were made at the probe distance of 5mm for the temperature difference dT of 30 °C. The thickness of Pt-coating was 1.4 nm. The STE voltage values of 9.3-12.2 micro-V/K observed in the elements using the 4-10micro-m-thick LPE YIG films are almost equal to the values measured for 0.5mm-thick YIG bulk plate crystals. These good results in the STE voltage measurements are considered to show that the LPE YIG films used in this SSE experiment have good crystallinity. We have studied the Pt-coating thickness dependence of the spin-Seebeck voltage in the Pt-YIG configuration for 0.5mm-thick bulk YIG plates in detail. The electric current density in the Pt-coating is discussed as well as the dependence of STE voltage on the Pt-coating thickness.

Th.H-P05 - Thermal spin current generation in Fe₃O₄/Pt thin films

R. Ramos¹, T. Kikkawa^{2, 3}, A. Anadón^{1,4}, I. Lucas^{1,5}, M. H. Aguirre^{1,4,6}, K. Uchida^{2,3,7}, H. Adachi^{3,8,9}, P. A. Algarabel^{4,10}, L. Morellón^{1,4}, S. Maekawa^{3,8,9}, E. Saitoh^{2,3,8}, M.R. Ibarra^{1,4,6}

1. Instituto De Nanociencia De Aragón, Universidad De Zaragoza, Zaragoza, Spain
2. Institute for Materials Research, Tohoku University, Sendai, Japan
3. ERATO, Japan Science and Technology Agency, Tokyo, Japan
4. Departamento de Física de la Materia Condensada, Universidad de Zaragoza, Zaragoza, Spain
5. Fundación ARAID, Zaragoza, Spain
6. Laboratorio de Microscopías Avanzadas, Universidad de Zaragoza, Zaragoza, Spain
7. PRESTO, Japan Science and Technology Agency, Kawaguchi, Saitama, Japan
8. Advanced Science Research Center, Japan Atomic Energy Agency, Tokai, Japan
9. CREST, Japan Science and Technology Agency, Sanbancho, Tokyo, Japan
10. Instituto de Ciencia de Materiales de Aragón, Universidad de Zaragoza and Consejo Superior de Investigaciones Científicas, Zaragoza, Spain

Since the discovery of the spin Seebeck effect (SSE) [1] much attention has been devoted to the study of the interaction between heat, spin and charge in magnetic systems. The SSE refers to the generation of a spin voltage upon the application of a thermal gradient, which is detected by means of the inverse spin Hall effect (ISHE). Unlike the conventional Seebeck effect which requires the presence of electronic carriers, the SSE has also been observed in insulating magnetic materials, opening the possibility to explore magnetic oxides as potential candidates for thermoelectric applications. Therefore the study of the thermomagnetic transport properties in this type of materials is of interest in order to gain insight in the spin-heat interaction. Here, we report optimization of the SSE in Fe₃O₄/Pt thin film heterostructures at room temperature by variation of several degrees of freedom of the structures. It has been previously shown that in this system the measured voltage is highly dominated by the SSE [2] and that the anomalous Nernst effect of magnetite [3] accounts for less than 1%. Our results further show that the SSE is characterized by a diffusive spin transport behavior and that the spin pumping across the Fe₃O₄/Pt is strongly affected by the interface parameters.

1. K. Uchida, S. Takahashi, K. Harii, J. Ieda, W. Koshibae, K. Ando, S. Maekawa and E. Saitoh. Nature 455, 778 (2008)
2. R. Ramos, T. Kikkawa, K. Uchida, H. Adachi, I. Lucas, M. H. Aguirre, P. Algarabel, L. Morellón, S. Maekawa, E. Saitoh and M. R. Ibarra. Appl. Phys. Lett. 102, 072413 (2013)
3. R. Ramos, M. H. Aguirre, A. Anadón, J. Blasco, I. Lucas, K. Uchida, P. A. Algarabel, L. Morellón, E. Saitoh and M. R. Ibarra. Phys. Rev. B 90, 054422 (2014)

Th.H-P06 - Magnetic field induced spin wave energy focusing

N. Perez¹, L. Lopez-Diaz¹

1. University of Salamanca, Salamanca, Spain

The capacity of spin waves to transport both energy and angular momentum as they propagate is at the heart of the emerging fields of spin caloritronics [1] and magnon spintronics [2]. To successfully translate fundamental research in these fields to technology it is crucial to be able to manipulate the flow and delivery of energy carried by spin waves in a controllable and flexible way over different length scales. An et al [3] took a first step in this direction, showing that magnetostatic surface spin waves (MSSW) allow for non-reciprocal unidirectional propagation and for remote heating at the sample edge towards which they propagate. In our work, we study these local temperature variations induced by spin wave propagation by means of a model that couples non-uniform magnetization dynamics and heat flow. We show that the remote heating reported by An et al [3] is due to geometry-induced gradual reduction of the effective field (the sample is cut at the edges, and the reduced width produces an increase of the demagnetizing field). We demonstrate that the same effect can be achieved by a reduction in the external field instead of a constriction at the edge and, furthermore, that both the location and the amount of energy to be delivered to the lattice can be controlled accurately this way. With our proposed system, up to 40\% of the magnetic energy pumped by an antenna could be delivered to a small area several millimeters away, opening the door to promising spintronic and spin caloritronic devices.

[1] G. E. W. Bauer et al, Nat. Mater 11, 391 (2012)

[2] Y. Kajiwara et al, Nature 464, 262 (2010)

[3] T. An et al, Nature Mater. 12, 549 (2013)

Th.H-P07 - Longitudinal spin seebeck effect in Bi-substituted neodymium iron garnet on GGG substrate prepared by MOD method

H. Asada¹, A. Kuwahara¹, K. Sueyasu¹, T. Ishibashi², Q. Liu², G. Lou², K. Kishimoto¹, T. Koyanagi¹

1. Yamaguchi University, Japan

2. Nagaoka University of Technology, Japan

Spin-thermoelectric coating based on a longitudinal spin-Seebeck effect (LSSE) has been demonstrated using $\text{Y}_2\text{BiFe}_5\text{O}_{12}$ formed by a metal-organic decomposition (MOD) method which is one of the most attractive techniques for preparation of large-area films at low cost[1]. In order to find out the material with large thermo-spin conversion efficiency, the systematic study for various materials is quite important. In this paper, we investigate the LSSE in Bi-substituted Neodymium Iron Garnet (Bi:NIG) prepared by MOD method and examine the dependence of thermoelectric voltage on Bi composition. Nd^{3+} has similar ionic radius (99 pm) with Bi^{3+} (102 pm) which is effective to maintain the good crystallinity when Nd is substituted by Bi. $\text{Nd}_{3-x}\text{Bi}_x\text{Fe}_5\text{O}_{12}$ films ($x=0-1$) with a thickness of approximately 200 nm were prepared on (001)-oriented GGG substrates by MOD method. After annealing (700 °C for 13 h in air), a Pt layer with a thickness of 10 nm and a size of 7x1 mm² was deposited by sputtering. The 008 diffraction peaks of Bi:NIG are observed and other phase does not be observed in the XRD patterns in all films, indicating the highly oriented Bi:NIG films are obtained. The electric voltage caused by LSSE in the Bi:NIG/Pt samples are measured by applying a temperature different of 10 K perpendicular to the film plane. By reversing the applied magnetic field, the LSSE signals of the samples indicate the clear hysteresis reflecting the M-H loop. It is clarified that the LSSE voltage increases with increasing Bi in this composition range. The amplitude of the LSSE voltage for $x=1$ is approximately two times larger than that for $x=0$. Magnetic properties of Bi:NIG films are also discussed.

[1] A. Kiriwara et al., Nature mater., 11, 686 (2012)

Th.H-P08 - Study of the magnon diffusion length in Fe₃O₄ thin films

A. Anadón^{1,2}, R. Ramos¹, I. Lucas^{1,3}, P. Algarabel^{2,5}, L. Morellón^{1,2}, M. Ibarra⁰, M. Aguirre⁰

1. Instituto De Nanociencia De Aragón, Zaragoza, Spain

2. Departamento de Física de la Materia Condensada, Zaragoza, Spain

3. Fundación ARAID, Zaragoza, Spain

4. Laboratorio de Microscopías avanzadas, Zaragoza, Spain

5. Instituto de Ciencia de Materiales de Aragón, Zaragoza, Spain

The interaction between heat and spin currents has been a very active field of study and highly boosted recently since the discovery of the Spin Seebeck effect (SSE). The mechanism and control of spin injection, detection and, in general, the optimization of SSE signal is still in progress. Here we present experimental results in agreement with the magnonic bulk thermal current model but in contrast to interface based models used for metals and semiconductors.

Fe₃O₄ epitaxial thin films with different thickness were deposited on a magnesium oxide substrate by means of pulsed laser deposition (PLD) in an ultrahigh-vacuum chamber. The quality and properties of the films were checked by X-ray diffraction, X-ray reflectivity, magnetization and resistivity vs temperature and transmission electron microscopy. Anomalous Nernst effect (ANE) and SSE measurements were performed to carefully study the characteristic dependence of thermomagnetic signal on the thickness of the magnetite. The experimental data is in agreement with reported models[1,2] where the bulk spin current is calculated macroscopically with the Boltzmann equation for the magnon flow. Following this model the estimation of the magnon diffusion length in magnetite thin films is 40 ± 10 nm.

References

[1] S. M. Rezende et al. Magnon spin-current theory for the longitudinal Spin Seebeck effect. *Physical Review B*, 89(1):014416, January 2014

[2] Steven S L Zhang and Shufeng Zhang. Magnon mediated electric current drag across a ferromagnetic insulator layer. *Physical Review Letters*, 109(August):1–5, 2012

Th.H-P09 - Optically-reconfigurable magnetic materials for the control of spin waves

M. Vogel¹, A.V. Chumak¹, E. H. Waller¹, T. Langner¹, V. I. Vasyuchka¹, B. Hillebrands¹, G. von Freymann^{1,2}

1. Department of Physics and State Research Center OPTIMAS, University of Kaiserslautern, Kaiserslautern, Germany

2. Fraunhofer-Institute for Physical Measurement Techniques IPM, Kaiserslautern, Germany

Structuring of materials is the most general approach to control wave properties in a solid body. Spin waves – eigen excitations of the electrons' spin system – are of special importance nowadays due to the large potential for applications (e.g. processing[1], filtering[2,3] or short-time storage[4] of data). While all these applications rely on pre-defined constant structures, a dynamic variation of the structures opens access to novel physical phenomena and to novel applications.

Here, we present an approach for the realization of fully-tunable two-dimensional magnetic materials. By using laser light of 532 nm wavelength and a spatial light modulator, we reconstruct computer generated holograms[5] on a 5 micrometer thick, ferrimagnetic Yttrium Iron Garnet (YIG) spin-wave waveguide. The absorbed light creates local temperature patterns (thermal landscapes) in the magnetic medium. A black absorber (including carbon black nanoparticles) painted on top of YIG increases the absorption and, thus, the contrast of the thermal landscape due to the approximately one order of magnitude smaller thermal conductivity compared to YIG. An acousto-optical modulator controls the temporal heating. The local change in temperature results in landscapes of the saturation magnetization and in the control of spin-wave characteristics. The proposed fully-reconfigurable magnetic material is demonstrated on the example of one- and two-dimensional thermal landscapes, e.g., magnonic crystals – artificial periodic magnetic lattices.

Financial support by DFG priority program SPP 1538 "Spin Caloric Transport" (project VA 735/1-2) is gratefully acknowledged.

[1] Chumak, A. V., Serga, A. A. & Hillebrands, B. *Nat. Commun.* 5, 4700 (2014)

[2] Krawczyk, M. & Grundler, D. *J. Phys.: Condens. Matter* 26, 123202 (2014)

[3] Lenk, B., Ulrichs, H., Garbs, F. & Münzenberg, M. *Phys. Rep.* 507, 107 (2011)

[4] Chumak, A. V. *et al. Phys. Rev. Lett.* 108, 257207 (2012)

[5] Ripoll, O., Kettunen, V. & Herzig, H. P. *Opt. Eng.* 43, 2549 (2004)

Th.H-P10 - Two sign changes of spin seebeck effect in compensated ferrimagnets

Y. Ohnuma^{1,2}, H. Adachi^{2,3}, E. Saitoh^{1,2,3,4}, S. Maekawa^{2,3}

1. *IMR Tohoku University, Japan*
2. *Japan Atomic Energy Agency, Japan*
3. *JST-ERATO, Japan*
4. *WPI Tohoku University, Japan*

Spin Seebeck effect is the mechanism of thermal spin injection from a ferromagnet into an attached paramagnetic metal [Uchida et al., Nature 455, 778 (2008)]. We have theoretically investigated the spin Seebeck effect in compensated ferrimagnets [Ohnuma et al., Phys. Rev. B 87, 014423 (2013)] and predicted that the sign of the spin Seebeck signal changes at the compensation temperature, which is recently confirmed by an experiment [Geprags et al., arXiv : 1405.4971 (2014)]. Interestingly, the experiment found another sign change at a lower temperature. Here we explain its origin by taking account of sublattice dependence of the exchange coupling at the ferrimagnet/paramagnet interface.

Th.H-P11 - Comprehensive study of nickel - zinc ferrites as an opportunity for spin caloritronic applications

J. Arboleda¹, O. Arnache¹, C. Ostos²

1. Grupo de Estado Sólido, Universidad de Antioquia, A. A. 1226, Medellín, Colombia

2. Grupo de Materiales Absorbentes y Catalisis, Universidad de Antioquia, A. A. 1226, Medellín, Colombia

Current developments in spin caloritronics, especially the so mentioned Longitudinal Spin Seebeck effect (LSSE), have encouraged a particular interest in the search for insulating materials with some magnetic order (ferro/ferri). Spinel mixed oxides ferrites, such as Ni-Zn ferrite oxides (NZFO), are displayed as suitable candidates for this type of edge applications. We have prepared a series of polycrystalline NZFO whose composition is $\text{Ni}_{1-x}\text{Zn}_x\text{Fe}_2\text{O}_4$, with different concentrations of Ni and Zn ($x = 0, 0.3, 0.4, 0.5, 0.7, 1$) via solid state reaction. A pretty full study using several complementary techniques (XRD, XPS, SEM, EDS, XRF, VSM, Mössbauer spectroscopy, and DC transport measurements) show a very interesting structural, magnetic and electric behavior depending of Zn concentration. Crystal structure goes from inverse spinel (Ni-ferrite, $x=0$) to normal spinel (Zn-ferrite, $x=1$) with a fairly accurate elemental composition. Intermediate concentrations exhibit mixed spinel structure. Likewise, magnetic order change from ferromagnetic to antiferromagnetic. We suggest a Yafet-Kittel magnetic ordering in the mixed ferrites, based on magnetic measurements. Further, high electrical resistivity was observed in all samples, which is desirable for LSSE measurements free for artifacts signals such as ANE. Therefore, our results show that the NZFO have physical properties with promising characteristics for different types of applications, in particular, they could be good candidates for the active field of spin caloritronic.

Th.H-P12 - Enhancement of spin-injection-induced electrical voltage using thermally excited CoFeAl film

G. Uematsu¹, T. Nomura¹, M. Kawakita¹, K. Okabe¹, S. Hu², T. Kimura^{1,2}

1. *Department of Physics, Kyushu University, Japan*

2. *Research Center for Quantum Nano-Spin Science, Kyushu University, Japan*

Enhancing the efficiency of generation of the spin current is imperative and a primary issue for the practical application of spin-based electronics, seamless device integration with the conventional complementary metal-oxide semiconductor technology is another important milestone for developing spin-based nanoelectronics. Thermal spin injection, which is a recently discovered unique characteristic of spin current, may be an innovative method for simplifying device integration without the need for electricity. Recently, we have found that CoFeAl has an excellent property for the thermal spin injection because of its unique band structure. In this paper, we focus on increasing the electrical voltage due to the thermal spin injection in a submicron-scaled lateral spin valve structure and sub-millimeter-scaled spin Hall device.

In the lateral spin valve structure, we have developed a multi-terminal ferromagnetic voltage probes.

By properly choosing the voltage probes with the optimized magnetization configuration, we have observed a large spin valve signal around 2 micro Volt by the thermal spin injection with suppressing the spurious signal induced by the anomalous Nernst effect.

In the spin Hall device, we have prepared the CoFeAl/Pt bilayer film with 200 micron in width and 600 micron in length. By creating the temperature gradient, we have observed a giant spin Hall signal over a few hundred micro volts. We have also confirmed that the voltage can be enhanced by the series connection of several spin Hall devices. This demonstration strongly enhances the potential of the CoFeAl as the material for spin-caloritronic devices.

Th.H-P13 - Utilization of antiferromagnetic electrodes in magneto-thermoelectric device for large area application

D. Kim¹, K. Lee¹, B. Park¹

1. Department of Materials Science and Engineering, KAIST Institute for the Nanocentury, KAIST, Daejeon, Republic of Korea

Magneto-thermoelectric (MTE) effect, a voltage generation due to temperature gradient in ferromagnet(FM)/non-magnet(NM) bilayers, has attracted interests because of its potential application for energy conversion well as the spin current source. The signal of the MTE strongly depends on the NM materials in which thermally-injected spin current is converted to voltage via inverse spin Hall effect (ISHE). Thus, the NM material with a large ISHE is essentially required to achieve a substantial MTE voltage. Recently, the ISHE has been reported in antiferromagnet (AFM) materials and its magnitude is comparable to those of Ta or Pt. Moreover, the AFM can be utilized for the control of magnetization reversal of the adjacent FM via exchange coupling. In this study, we investigated the MTE in the AFM IrMn/FM CoFeB structures, where the thermal voltage is generated by laser-induced vertical thermal gradient. We observed that the MTE voltage was gradually increased with IrMn thickness (t_{IrMn}) up to 10nm and slowly decreased for larger t_{IrMn} . The exchange bias between AFM and FM was developed when t_{IrMn} is thicker than 13nm. We fabricated a pair of wires of an AFM/FM bilayer, of which one ends are connected each other. The t_{IrMn} is controlled to be 10nm for one wires and 20nm for the other. As one with thicker t_{IrMn} only shows an exchange bias, we can control the relative magnetic configuration of the wires. In the antiparallel configuration, the MTE signals from each wire are opposite sign so they are added, while they are the same sign thus subtractive in parallel alignment. Furthermore, the MTE voltage could be proportionally enhanced to the number of pairs formed in magnetic thermopile. Our results demonstrate that the employment of the AFM with a large ISHE and exchange biasing can be utilized in large area application of the MTE devices.

Th.H-P14 - Longitudinal spin-seebeck effect in cobalt-ferrite epitaxial thin films with different preferential axesT. Niizeki¹, T. Kikkawa¹, K. Uchida¹, M. Oka¹, K. Z. Suzuki¹, H. Yanagihara¹, E. Kita¹, E. Saitoh¹

1. WPI-AIMR, Tohoku Univ., ERATO, IMR, Tohoku Univ., PRESTO, Inst. of Appl. Phys., Univ. of Tsukuba, CREST, JAEA

One of the most attractive outputs from “insulator spintronics” [1] is recently-proposed thermoelectric (TE) generation using magnetic insulators (MIs) as TE power sources since it has potential advantages in versatility, costs, and ubiquitousness compared with conventional semiconductor-based TE devices [2]. This epoch-making MI-based TE generation is initiated by a heat-mediated pure-spin-current creation in MIs, called spin-Seebeck effect (SSE) [3, 4], and then followed by the electric conversion via the inverse spin-Hall effect (ISHE) [5, 6] in a paramagnetic metal such as Pt adjacent to the MI. Although the SSE has been demonstrated in soft MIs so far [3, 4, 7-9], SSE in hard MIs [10,11] is recently attracting much attention from the viewpoint of both physics and application. In this study, we focused on cobalt ferrite (CFO), an exceptionally hard magnetic spinel ferrite, as an anisotropy tunable SSE material and experimentally demonstrated the longitudinal SSE (LSSE) in a bilayer of Pt/CFO grown on different substrates. Epitaxially-strained CFO thin films were prepared on MgAl₂O₄ (MAO)(110) and MgO(001) substrates by reactive rf sputtering technique. The CFO(110)/MAO(110) exhibited an in-plane uniaxial anisotropy whereas CFO(001)/MgO(001) showed a perpendicular anisotropy. Thermally generated spin voltages in those CFO films were measured via the ISHE in the polycrystalline Pt deposited on the top. External-magnetic-field (H) dependence of the LSSE voltage (V_{LSSE}) with $H \parallel [001]$ in Pt/CFO/MAO sample exhibited a magnetic hysteresis loop with a high squareness and a large coercivity, whereas that in Pt/CFO/MgO showed a nearly closed loop, reflecting the magnetic anisotropies induced by the different epitaxial strain. The magnitude of V_{LSSE} has a linear relationship with the temperature difference (ΔT), giving the relatively large $V_{\text{LSSE}}/\Delta T$ of about 3 $\mu\text{V}/\text{K}$ for CFO(110) which was kept even at zero external field. The temperature dependence of V_{LSSE} measured for various preferential axes will also be presented.

- [1] K. Kajiwara *et al.*, Nature (London) 464, 262 (2010)
- [2] A. Kiriwara *et al.*, Nat. Mater. 11, 686 (2012)
- [3] K. Uchida *et al.*, Nature (London) 455, 778 (2008)
- [4] K. Uchida *et al.*, Nat. Mater. 9, 894 (2010)
- [5] A. Azevedo *et al.*, J. Appl. Phys. 97, 10C715 (2005)
- [6] E. Saitoh *et al.*, Appl. Phys. Lett. 88, 182509 (2006)
- [7] K. Uchida *et al.*, Appl. Phys. Lett. 97, 172505 (2010)
- [8] R. Ramos *et al.*, Appl. Phys. Lett. 102, 072413 (2013)
- [9] D. Meier *et al.*, Phys. Rev. B 87, 054421 (2013)
- [10] P. Li *et al.*, Appl. Phys. Lett. 105, 242412 (2014)
- [11] T. Niizeki *et al.*, in preparation

Th.H-P15 - Spin-thermoelectric transport in quantum spin hall systems beyond linear response

S. Hwang¹, R. Lopez¹, M. Lee², D. Sanchez¹

1. Institut De Fisica Interdisciplinaria I Sistemes Complexos IFISC (CSIC-UIB), Palma de Mallorca, Spain

2. Department of Applied Physics, College of Applied Science, Kyung Hee University, Yongin, Republic of Korea

Spin-polarized transport is studied in a quantum spin Hall antidot system with a two-terminal setup [1]. Helical nature of the conducting edge states makes the screening potential at the dot region become spin dependent even without external magnetic fields nor ferromagnetic contacts. Therefore, the electric and heat currents due to voltage or temperature biases become spin polarized, where the degree of polarization can be tuned by dot energy level or the background temperature. We show that this spin-filter effect arises in the nonlinear transport regime only and has a purely interaction origin. Furthermore, our results show that a pure spin current can be generated by thermoelectric means: with a thermal bias applied, the created thermovoltage induces a spin-polarized electric current (spin Seebeck effect) for vanishingly small charge current. Analogously, pure spin heat can flow in response to a voltage shift even if the total thermal flux vanishes.

[1] Phys. Rev. B 90, 115301 (2014)

Th.H-P16 - Thermal and thermal gradient effects on microwave power spectral density of MgO based MTJ nanopillars

T. Böhnert¹, S. Serrano-Guisan¹, M. Tarequzzaman¹, J. D. Costa¹, E. Paz¹, R. Ferreira¹, P. P. Freitas¹

1. INL - International Iberian Nanotechnology Laboratory, Braga, Portugal

Theoretical studies predict that temperature gradients can be an efficient method to generate magnetic excitations (TSTTs). A deep comprehension of such heat-driven magnetization dynamics phenomena is specially required in magnetic tunnel junction (MTJ) systems as it can provide a mean to overcome scalability limitations in magnetoresistive memory (MRAM) elements as well as to explore the contribution of heat dissipation on current-induced spin torque nano-oscillators (STNOs). Here we explore the influence of temperature and thermal gradient effects on magnetization dynamics on MgO/CoFeB based MTJ nanopillars with RA of ~ 3 uOhm \cdot m. For this, high-frequency voltage noise measurements [2] (up to 20 GHz) were carried out in a temperature variable probe station enabling to compare current-biased microwave magnetization dynamics at different temperatures (Tps up to 125C) and bias voltages below the voltage breakdown ($|V_{\text{bias}}| < 400$ mV). At low Tps (~ 25 C) the power spectral density is similar for both current polarities. But an increase in Tps leads to an increase of the spectral linewidth for $V_{\text{bias}} > 0$. Note that for opposite bias voltages ($V_{\text{bias}} < 0$) almost no modification on the linewidth has been observed, whereas the total emitted power (Pout) is increased by a factor of 4. As a general trend the ferromagnetic resonance f always decreases with Tps as a signature of the reduction of the coercivity field (and therefore the overall effective magnetic field) with temperature. In order to quantify the contribution of possible TSTTs on such effects, calibration of the effective temperature and thermal gradients developed across the MTJ nanostructure and temperature dependent resistance measurements of the bottom contact line will be addressed.

[1]. S. Petit et al., PRL 98, 077203 (2007)

[2] N. Liebing et al., PRL 107, 177201 (2011) ; M. Walter et al., Nature Mater 10, 742 (2011)

Th.H-P17 - Non-equilibrium thermodynamics of the longitudinal spin seebeck effectV. Basso¹, E. Ferraro¹, A. Sola¹, A. Magni¹, M. Kuepferling¹, M. Pasquale¹*1. Istituto Nazionale di Ricerca Metrologica, Torino, Italy*

The longitudinal spin Seebeck effect (LSSE), measured in ferrimagnetic insulators, is the consequence of the transport properties of out-of-equilibrium magnons which are at the same time responsible for heat and spin currents [1]. While the microscopic physics has been already investigated in detail, the thermodynamic aspects need further investigation [2,3]. In particular we aim to define a spin Seebeck coefficient ϵ_M , relating the magnetization current to the associated thermodynamic driving in insulators. Here we employ non-equilibrium thermodynamics to state the problem with currents and forces. As the magnetization current can be absorbed and generated inside the material, we need to state a continuity equation for the non conserved magnetization. Here we choose the simple form $dM/dt + \nabla \cdot j_M = (1/\tau) (H - H_{eq}(M))$, where M is the magnetization, j_M is the magnetization current, H is the magnetic field, $H_{eq}(M)$ the magnetic equation of state at equilibrium and τ is a relaxation time associated with the damping processes. We find that gradient of $(H - H_{eq})$ takes the role of the thermodynamic driving force. The theory permits to predict the LSSE effect for different thickness and type of sensing layer. In particular we apply this theory to the LSSE experiment of Ref.[4] in which a thermally generated spin current in a ferrimagnetic insulator (YIG) diffuses into a paramagnetic metal (Pt) where is revealed by the inverse spin Hall effect (ISHE). The part of the YIG spin current which is actually injected into Pt depends on the thicknesses of the layers and on materials dependent parameters: the damping and the correlation length. Once these values are estimated, by using literature values for YIG and Pt, the comparison with LSSE experiments, gives an estimate of the value of the intrinsic spin Seebeck coefficient.

- [1] H. Adachi, K. Uchida, E. Saitoh and S. Maekawa, Rep. Prog. Phys. 76, 036501 (2013)
- [2] G. E. W. Bauer, E. Saitoh, B. J. van Wees, Nature Materials 11, 391 (2012)
- [3] M. Johnson and R. H. Silsbee, Phys. Rev. B 35, 4959 (1987)
- [4] A. Sola, M. Kuepferling, V. Basso, M. Pasquale, T. Kikkawa, K. Uchida and E. Saitoh, J. Appl. Phys. (2015) in press

Th.H-P18 - Microwave-induced spin currents in ferromagnetic-insulator|normal-metal bilayer system

V. Vasyuchka¹, M.Agrawal¹, A.Serga¹, V. Lauer¹, E. Papaioannou¹, B. Hillebrands¹

1. Department of Physics and State Research Center OPTIMAS, University of Kaiserslautern, Kaiserslautern, Germany

The generation of a pure spin current in ferromagnet|normal metal systems recently has attracted a great attention. The spin Seebeck effect is one route to generate spin current by applying a heat current to ferromagnets. In particular, the longitudinal spin Seebeck (LSSE) effect is of much importance due to its technologically promising applications. Keeping the future application in focus, a comparative study of the spin current direction (flow) for different spin-current-generation processes like spin pumping and spin Seebeck effect is very crucial. In previous studies, the direction of the spin current in these processes has been determined by combining the FMR technique with additional dc/ac or Peltier based heating techniques.

Here, we demonstrate microwaves as a simple-and-controlled heating technique to generate a thermal gradient in ferromagnetic insulator|normal metal systems to study the static and temporal dynamics of the LSSE. Experiments were conducted using a bilayer of a magnetic insulator, Yttrium Iron Garnet (YIG) 6.7 μm -thick film, and a normal metal, 10nm-thick Platinum (Pt). The static dc measurements provide crucial information about the direction of the spin current flow. The experiment demonstrates that in the LSSE a spin current flows from the normal metal (hot) towards the ferromagnet (cold), while in the spin pumping case, the flow is opposite. The temporal dynamics of the LSSE experiment manifests the sub-microsecond timescale of the effect which is slower than the spin pumping process. The thermal magnon diffusion model can explain the outcomes of the experiment and leads to conclude that the timescale of the effect relies the evolution of the vertical thermal gradient in the vicinity of the ferromagnet|normal metal interface. From our experiment, a typical magnon diffusion length of 500 nm is estimated for the YIG|Pt system.

Financial support by Deutsche Forschungsgemeinschaft (DFG) within Priority Program 1538 "Spin Caloric Transport" is gratefully acknowledged.

Th.H-P19 - Effect of strontium deficiency on structural, magnetic and magnetocaloric properties of $\text{La}_{0.65}\text{Eu}_{0.05}\text{Sr}_{0.3-x}\text{MnO}_3$ ($0 \leq x \leq 0.15$) manganite

R. Bellouz¹, A. Dinia², M. Oumezzine¹, K. Hlil³, G. Schemerber², M. Oumezzine¹

1. *Laboratoire de Physico-chimie des Matériaux, Département de Physique, Faculté des Sciences de Monastir, Université de Monastir, Tunisia*

2. *Institut de Physique et Chimie des Matériaux de Strasbourg (IPCMS) UMR 7504 CNRS-Université de Strasbourg, Strasbourg Cedex 2, France*

3. *Institut Néel, CNRS-Université J. Fourier, Grenoble, France*

We have investigated the effect of nominal strontium deficiency on the structure, magnetic and magnetocaloric properties of $\text{La}_{0.65}\text{Eu}_{0.05}\text{Sr}_{0.3-x}\text{MnO}_3$ ($x=0.05, 0.1$ and 0.15). The samples were synthesized using the Pechini sol-gel method. X-ray diffraction analysis shows that the compounds crystallize in the rhombohedral structure with the R-3C space group. Raman spectra at room temperature reveal gradual change in phonon modes, which increased with increasing nominal strontium deficiency. Magnetization as a function of temperature shows that these compounds exhibit a paramagnetic to ferromagnetic phase transition with decreasing temperature. Arrott plot analyses and a universal curve method were applied to study the order of the magnetic transition in this system. The maximum of magnetic entropy change in a magnetic field of 5T is found to be 5.44, 5.15 and 4.96 J kg⁻¹ K⁻¹ for $x=0, 0.10$ and 0.15 respectively. The relative cooling power (RCP) of $\text{La}_{0.65}\text{Eu}_{0.05}\text{Sr}_{0.3-x}\text{MnO}_3$ series is nearly 69% of pure Gd, which will be an interesting system for application in room temperature refrigeration.

Th.H-P20 - Spin-dependent thermoelectric transport in T-shaped double-quantum-dot systems

Ionel Tifrea¹, Y, Alexander Gauf¹ N, Mircea Crisan²

1. *California State University Fullerton, United States*
2. *'Babes-Bolyai' University, Cluj-Napoca, Romania*

We investigate the thermoelectric properties of a T-shaped double quantum dot system connected to two ferromagnetic electrodes whose magnetic moments are oriented at an angle θ with respect to each other. The system is modeled using a generalized Anderson Hamiltonian that accounts for finite on-site Coulomb interaction in each of the system's component quantum dots. The system's electrical conduction (G) and the fundamental thermoelectric parameters such as the Seebeck coefficient (S) and the thermal conductivity (κ), along with the system's thermoelectric figure of merit (ZT) are numerically estimated based on a Green's function formalism that includes contributions up to the Hartree-Fock level. Our results account for finite onsite Coulomb interaction terms in both component quantum dots and discuss various ways leading to an enhanced thermoelectric figure of merit for the system. We demonstrate that the presence of Fano resonances in the Coulomb blockade regime is responsible for a strong violation of the Wiedemann-Franz law and a considerable enhancement of the system's figure of merit (ZT).

Th.I-P01 - Transient exchange Interaction in a helical antiferromagnet

K. Dumesnil¹, M.C. Langner², S. Roy³, A.F. Kemper⁴, Y.D. Chuang³, S.K. Mishra³, R.B. Versteeg³, Y. Zhu², M.P. Hertlein³, T.E. Glover³, R.W. Schoenlein²

1. Institut Jean Lamour, Université de Lorraine, France

2. Materials Science Division, Lawrence Berkeley National Laboratory, United States

3. Advanced Light Source, Lawrence Berkeley National Laboratory, United States

4. Computational Science Division, Lawrence Berkeley National Laboratory, United States

The ultrafast dynamics of the uniform ferromagnetic phase in transition metals and lanthanides currently drive a strong interest to unravel the various mechanisms responsible for the demagnetization process. However, the dynamics in non-collinear phases, as observed in many lanthanides, are yet unexplored, while transiently altering the conduction electron distribution can have a profound influence on the long-range magnetic structure. In this study, time-resolved resonant x-ray scattering experiments (Ultrafast optical pump/x-ray probe) have been performed in the Dy metal to explore the dynamic response of the helical order to injection of unpolarized spins. Those measurements reveal the coupling mechanisms between the constituent spin systems, by observing the dynamics of the core spins in response to excitation of the conducting electrons responsible for the RKKY indirect exchange interaction. A reduction in the amplitude of the helical order parameter and a shift in the helical wave vector q on disparate time-scales, strongly dependent on both the pump fluence and sample temperature, have been observed. Notably, the dynamics in the helical antiferromagnetic phase (HAF) of Dy are significantly slower than those observed in the ferromagnetic (FM) phase of other Lanthanide metals. These anomalous dynamics are attributed to the relationship between the wave vector of the electronic excitation k and the wave vector of the core magnetic ordering q . In the FM phase, the electronic excitation at $k = 0$ is closely coupled to the magnetic ordering at $q = 0$. In the HAF phase, the core spin helix is concomitant with a nesting of the Fermi surface (FS). Initial ultrafast scattering of spins from the $k = 0$ excitation does not directly change the energy-minimizing configuration of the system, and the helical dynamics are driven by changes to the shape of the FS and subsequent changes to the electron distribution through scattering events.

Th.I-P02 - Antiferromagnetic writing and reading of an optical polarization state

T. Satoh^{1,2,3}, R. Lida², T. Higuchi⁴, M. Fiebig⁵, T. Shimura²

1. *Department of Physics, Kyushu University, Japan*

2. *Institute of Industrial Science, The University of Tokyo, Japan*

3. *PRESTO, Japan Science and Technology Agency, Japan*

4. *Lehrstuhl für Laserphysik, Friedrich-Alexander-Universität Erlangen-Nürnberg, Germany*

5. *Department of Materials, ETH Zurich, Switzerland*

The interaction between light and magnetism is considered a key to fast, energy-efficient data-storage technologies. Ultrafast optical magnetization control is a step in this direction. Yet, its premise remains a binary one: Light in either of two polarization states generates (writes) or adopts (reads) a magnetic bit carrying positive or negative magnetization. The fundamental limitation to just two states is overcome by employing all three degrees of freedom of optical polarization as an information carrier and representing this, in principle, arbitrary optical polarization state magnetically. Here we demonstrate this principle by using a three-sublattice antiferromagnet, hexagonal YMnO₃, for encoding the optical polarization state. Two in-plane modes and an out-of-plane mode are triggered by linearly and circularly polarized light pulses via the inverse Cotton-Mouton effect and the inverse Faraday effect, and detected by circularly and linearly polarized ones via the Cotton-Mouton effect and the Faraday effect, respectively. The control and detection represent a bijection of quantum information from polarization of pump pulse to magnetic oscillation and toward polarization of probe pulse. Also, the two-dimensional vector control of magnetic oscillation of YMnO₃ was realized by a pair of optical pulses with different polarizations.

Th.I-P03 - Ho on Pt(111) as a single-atom memory bit: a quantum master equation analysis

C. Karlewski^{1,2}, M. Marthaler¹, T. Märkl³, T. Balashov³, W. Wulfhekel^{2,3}, G. Schön^{1,2}

1. *Karlsruher Institute of Technology, TFP, Germany*

2. *Karlsruher Institute of Technology, INT, Germany*

3. *Karlsruher Institute of Technology, PI, Germany*

Due to underlying symmetries the two degenerate angular-momentum ground states of a single holmium atom (with $J=8$) on a Pt(111) surface have exceptionally long lifetimes, as observed in recent scanning tunneling microscopy studies. This opens perspectives for the application as a single-atom memory bit. For control and read-out the atom is coupled to electronic contacts. Hence the spin dynamics of the system is governed by a quantum master equation. In general it cannot be reduced to a classical master equation in the basis of the unperturbed crystal-field Hamiltonian. Rather, depending on parameters and control fields, 'environment induced superselection' principles choose the appropriate set of basis states, which in turn determines the specific relaxation channels and lifetimes. Our results suggest that in ideal situations the lifetimes should be even longer than observed in the experiment. We, therefore, investigate the influence of various perturbations. We also study the initialization process of the state of the Ho atom by applied voltage pulses and conclude that fast, high fidelity writing into the memory, on a 100ns timescale, should be possible. [arXiv:1502.02527]

Th.I-P04 - Power dependence of the inverse spin-Hall effect in Py/Pt microstructures

L. Feiler¹, K. Sentker¹, N. Kuhlmann¹, G. Meier^{1,2,3}

1. *Institut für Nanostruktur- und Festkörperphysik, ehem. Institut für Angewandte Physik und Zentrum für Mikrostrukturforschung, Universität Hamburg, Hamburg, Germany*

2. *The Hamburg Centre for Ultrafast Imaging, Hamburg, Germany*

3. *Max-Planck Institute for the Structure and Dynamics of Matter, Hamburg, Germany*

The inverse spin-Hall effect (ISHE) has lately been of strong interest due to potential spintronic applications such as read-heads for magnetic hard disc drives. We study laterally microstructured permalloy (Ni₈₀Fe₂₀)/platinum bilayers [1] that could fulfill such technological needs. The samples consist of a 30 nm thick and 2 μm × 8 μm large permalloy microelement with a 15 nm thick platinum strip on top, positioned over the signal lead of a coplanar wave-guide. The permalloy element is driven at ferromagnetic resonance by an Oersted field, generated by the waveguide. Due to this excitation spin pumping [2] occurs at the permalloy/platinum interface and a spin current is injected into the platinum layer. This spin current is detected as a voltage via the inverse spin-Hall effect [1]. To simultaneously track the magnetization dynamics of the permalloy we also probe the broadband ferromagnetic resonance (FMR) transmission with a vector-network analyzer. We observed that the voltage peak height at resonance does depend on the excitation field strength. Below 0.5 mT this dependency is linear and the peak has a Lorentzian profile that becomes slightly asymmetric, as reported by Mosendz et al. [3]. For higher field strengths we measure an abrupt nonlinear increase of the voltage and thenceforth the peaks feature a broader shape. As dominating contributions from anisotropic magnetoresistance and foldover effects have been ruled out in Ref. [3] and [4]. We assume that the pronounced occurrence of spin wave and edge modes might explain strongly enlarged ISHE voltages.

[1] E. Saitoh, M. Ueda, H. Miyajima, and G. Tatara, APL 88, 182509 (2006)

[2] Y. Tserkovnyak, A. Brataas, and G.E.W. Bauer, PRL 88, 117601 (2002)

[3] O. Mosendz, V. Vlaminck, J. E. Pearson, F. Y. Fradin, G. E. W. Bauer, S. D. Bader, and A. Hoffmann, PRB 82, 214403 (2010)

[4] Y. S. Gui, A. Wirthmann, and C.-M. Hu, PRB 80, 184422 (2009)

Th.I-P05 - Surface acoustic wave assisted magnetization switching

L. Thevenard¹, C. Gourdon¹, P. Rovillain¹, J. Duquesne¹, M. Bernard¹, A. Lemaître², J. Prieur¹, I. Camara¹

1. *Institut Des Nanosciences De Paris (CNRS/Université Pierre Marie Curie), France*

2. *Laboratoire de Photonique et Nanostructures, CNRS, Route de Nozay, Marcoussis, France*

Inverse magnetostriction is the effect by which magnetization can be changed upon application of a strain. It is particularly relevant to magnetic data storage technologies as a possible route towards induction-free data manipulation[1]. The strain modulation may be created by applying a radio frequency (rf) voltage to interdigitated transducers (IDTs), which generate surface acoustic waves (SAW). We recently demonstrated the ferromagnetic resonance (FMR) induced by a 549 MHz SAW on a 50nm layer of (Ga,Mn)(As,P)[2]. This magnetic semiconductor is an interesting system since the magnetostrictive coefficients vary strongly with temperature (up to Curie temperature $T_c \sim 90\text{K}$), and the magnetic anisotropy can be made arbitrarily weak by epitaxial growth. It is therefore an excellent test-bench to develop and validate theoretical models, and ultimately guide material engineering for all-acoustic magnetization switching. We suggest 2 possible routes for SAW-assisted out-of-plane magnetized layer switching [3]. In the first one, the field is applied in the plane of the layer and advantage is taken of the SAW-FMR effect. Numerical simulations then evidence a wide range of fields and SAW amplitudes triggering highly non-linear precessional behavior that can eventually lead to irreversible magnetization switching. In the second configuration, the field is applied anti-parallel to the magnetization, and the SAW is expected to reduce either the domain-wall energy, or switching barriers. Experiments on a 50nm thick layer of (Ga,Mn)(As,P) in this configuration have evidenced a spectacular reduction of the coercive field of up to 68% in the presence of a SAW, and at all temperatures up to T_c . For rf voltages applied slightly out of the IDTs' resonance frequency, no reduction at all is observed confirming the specific action of the SAW.

[1] W. Li, B. Buford, A. Jander, and P. Dhagat, *IEEE Trans. Magn.*, 50 (2014)

[2] L. Thevenard, C. Gourdon, J. Y. Prieur, H. J. von Bardeleben, S. Vincent, L. Becerra, L. Largeau, and J.-Y. Duquesne, *Phys. Rev. B*, 90, 094401 (2014)

[3] L. Thevenard, J.-Y. Duquesne, E. Peronne, H. J. von Bardeleben, H. Jaffrès, S. Ruttala, J.-M. George, A. Lemaître, and C. Gourdon, *Phys. Rev. B* 87, 144402 (2013)

Th.I-P06 - Enhanced magnetocrystalline anisotropy in an epitaxial array of cobalt nanowires: a ferromagnetic resonance study

I. Camara¹, V. Pierron-Bohnes¹, Y. Henry¹, C. Achkar², N. Liakakos², T. Blon², K. Soulantica², M. Respaud², M. Bailleul¹

1. *Institut de Physique et Chimie des Matériaux de Strasbourg, UMR7504 CNRS-Université de Strasbourg, Strasbourg, France*

2. *Laboratory of Physics and Chemistry of Nano-Objects, UMR 5215, INSA-UPS-CNRS, Toulouse, France*

Arrays of ferromagnetic nanowires are of considerable interest for many applications including magnetic recording, permanent magnets and microwave devices. Traditionally, the nanowires are fabricated by electrodeposition in porous membranes, which results in arrays of polycrystalline objects with relatively large diameters (10nm or above) and moderate densities (a few %). Recently, we developed a new method of epitaxial solution growth allowing us to produce single crystalline Co nanowires with 6 nm diameter arranged in ultradense hexagonal arrays [1]. Here, we report on the determination of the room-temperature magnetocrystalline anisotropy of such nanowires.

The measurements were performed using the technique of broadband ferromagnetic resonance. The nanowire array was placed on a coplanar waveguide and its microwave absorption was measured as a function of the microwave frequency and of the external magnetic field, directed either parallel or perpendicular to the nanowires. We observe unusually large resonance frequencies (40 GHz at remanence) and resonance fields (2.3T hard-axis saturation field) which we attribute to an enhanced magnetocrystalline anisotropy. By modelling the dipolar interaction in the array, we could indeed reproduce the resonance positions assuming a uniaxial anisotropy with first and second order constants $K_1=750$ kJ/m³ and $K_2=150$ kJ/m³, two values that are about 50% larger than those of bulk cobalt. This spectacular enhancement of magnetocrystalline anisotropy, which was also confirmed through independent high field magnetic torque measurements, is attributed to a sizeable surface contribution.

1. N. Liakakos et al., Nano Lett. 14, 3481–3486 (2014)

Th.I-P08 - Laser-induced ultrafast magnetization dynamic in RE-TM garnets

S. Parchenko¹, I. Yoshimine², T. Satoh^{2,3}, A. Maziewski¹, A. Stupakiewicz¹

1. *Laboratory of Magnetism, Faculty of Physics, University of Bialystok, Bialystok, Poland*

2. *Institute of Industrial Science, The University of Tokyo, Tokyo, Japan*

3. *PRESTO, Japan Science and Technology Agency, Tokyo, Japan*

We report about our study crystals of rare-earth Gd-Bi-doped iron garnets with and without Yb ions with compensation temperatures $T=96\text{K}$ and $T=218\text{K}$ and Curie temperatures $T=594\text{K}$ and $T=538\text{K}$ respectively. Ultrafast magnetization precession, induced via the inverse Faraday effect [1], was detected by time-resolved magneto-optical spectroscopy method [2]. The amplitude and frequency of the precession were studied as a function of the external magnetic field, polarization and temperature within 80-600 K range. Two separate types of oscillations were detected: magnetic field dependent mode with a frequency about few GHz caused by backward volume spin waves excitations and magnetic field independent mode with a sub-THz frequency. Strong decrease of frequencies of these modes was observed close to the compensation and Curie temperatures. The origin of the high-frequency mode could be explained by excitation of the exchange resonance between rare-earth and transition metal sublattices in garnets. Temperature dependences of the experimental data are in good agreement with proposed theoretical model. Obtained results could be important for non-thermal control of the magnetic ordering in dielectrics by polarized laser pulses. The work was supported by SYMPHONY project operated within the Foundation for Polish Science Team Program co-financed by the EU European Regional Development Fund, OPIE2007-2013.

[1] T. Satoh, et al. et al., *Nature Photonics*, vol. 6, pp. 662-666 (2012)

[2] S. Parchenko, et al. et al., *Applied Physics Letters*, vol. 103, pp. 172402-1-4 (2013)

Th.I-P09 - Stroboscopic ferromagnetic resonance detection depending on laser power

S. Yoon^{1,2}, R. D. McMichael¹

1. Center for Nanoscale Science and Technology, National Institute of Standards and Technology, Gaithersburg, United States

2. Maryland Nanocenter, University of Maryland, College Park, United States

In this presentation, we introduce a new ferromagnetic resonance (FMR) detection method using stroboscopic magneto-optical Kerr effect (MOKE). FMR is a useful method for investigating the magnetic properties of various thin films and spintronic devices. Therefore, many FMR analysis methods have been developed and improved. In particular, the availability of fast laser pulses and the non-contact nature of optical measurements have made optical approaches attractive for fast dynamic measurements. In our method, magnetization precession in a magnetized permalloy film is driven by microwave fields on a coplanar waveguide. Linearly polarized 1550 nm light is amplitude-modulated by an electro-optical modulator with the same frequency as the microwaves (1 to 10 GHz) and focused on the sample surface. The polarization of the reflected light changes depending on the phase of the spin precession. The intensity-weighted average polarization depends on the relative phase of the microwave signal and light intensity and also on the complex magnetic susceptibility. Laser powers above 10 mW induce resonance shifts that we attribute to heating. We will discuss the details of our new stroboscopic FMR measurement and the effect of laser power on magnetic properties.

Th.I-P10 - Spin wave mode identification in magnetic semiconductors

C. Gourdon¹, S. Shihab¹, H. Riahi², L. Thevenard¹, H. von Bardeleben¹, A. Lemaître³

1. *Institut Des Nanosciences De Paris-UPMC Paris06 -CNRS, UMR7588, 4 Place Jussieu, Paris, France*

2. *Laboratoire Matériaux Molécules et Applications, IPEST, Université de Carthage, La Marsa, Tunisie*

3. *Laboratoire de Photonique et Nanostructures, CNRS, UPR 20, Marcoussis, France*

Ultrafast magnetization dynamics triggered by laser pulses and detected by pump-probe experiments gives access to fast demagnetization, carrier cooling and trapping and magnetization precession times on a fs to ns time scale. This magneto-optical technique is applied both in highly absorbing materials like metals and weakly absorbing ones like ferromagnetic semiconductors. Several perpendicular standing spin waves modes (PSSW) may be excited in thin layers by laser pulses and detected through magneto-optical effects. Ferromagnetic resonance (FMR) also provides access to the frequency of those PSSWs. However the conditions for excitation and detection of the PSSW are different for the two techniques, especially in weakly absorbing materials. This is clearly revealed in GaMnAsP ferromagnetic semiconductors where two or more spin waves modes can be optically detected [1,2] whereas only one by FMR in some layers. However the spatial profile (k-number) of the PSSWs, which is of major importance for the determination of the exchange constant from the mode frequency and k-number spacing [2], is difficult to determine. We report on this mode assignment through a systematic study of optically generated and detected PSSWs in the ferromagnetic semiconductor GaMnAsP as a function of layer thickness and phosphorus alloying, for in-plane and out-of-plane magnetized samples. The assignment of the mode k-number is obtained through a detailed comparison of the mode frequencies optically detected and those obtained from FMR, when available, as well as those inferred from the exchange constant determined by domain pattern analysis. We further develop a comprehensive semi-analytical model to justify the optical observation of particular PSSWs.

[1] P. Nemeč et al., Nat. Com. 4, 1422 (2013)

[2] S. Shihab et al, <https://hal.archives-ouvertes.fr/hal-01116911>

Th.I-P11 - Ultrafast laser-induced demagnetization in multisublattice metallic magnets

T. J. Huisman¹, R. V. Mikhaylovskiy¹, A. Tsukamoto², Th. Rasing¹, A. V. Kimel¹

1. *Radboud University Nijmegen, Institute For Molecules And Materials, The Netherlands*

2. *College of Science and Technology, Nihon University, Japan*

We employed simultaneous detection of THz emission and transient magneto-optical Kerr effect (MOKE) to study ultrafast laser-induced magnetization dynamics in multisublattice magnets NdFeCo and GdFeCo amorphous alloys with in-plane magnetic anisotropy. A pure Co film was used as a reference sample. An excellent agreement between the dynamics revealed with the help of these two techniques is obtained for Co, while for GdFeCo a satisfactory quantitative agreement was observed. In contrast, for NdFeCo the THz emission reveals faster dynamics than the magneto-optical response. Note that in the multisublattice alloys, the dynamics measured with the MOKE is associated with the dynamics of the FeCo sublattice. This means that the observed mismatch for NdFeCo reveals that the Nd-sublattice exhibits MOKE-invisible and faster magnetization dynamics compared to the FeCo sublattice. Analyzing the similarities and differences of GdFeCo and NdFeCo alloys makes it clear that the orbital magnetization of Nd plays a significant role in the ultrafast demagnetization process.

Th.I-P12 - Simulation of ultrafast spin dynamics in DyCo5

A. Donges¹, S. Khmelevskiy², D. Hinzke¹, L. Szunyogh², U. Nowak¹

1. *University of Konstanz, Germany*

2. *Budapest University of Technology and Economics, Budapest, Hungary*

In search of new magnetic recording materials, allowing faster manipulation than today's hard disks, ferrimagnetic transition-metal-rare-earth compounds are of great interest. In this class of materials the so called thermally induced magnetization switching (TIMS) was discovered [1]. Here, the magnetization can be switched solely by a fs-laser-pulse without applying an external magnetic field.

Our focus is on monocrystalline ferrimagnetic DyCo5 featuring extraordinary properties, such as high magnetocrystalline anisotropy and high Curie-temperature, making it a promising candidate for data storage materials. These properties are not found in commonly used materials for studies on TIMS such as GdFeCo. Furthermore, in DyCo5 the magnetization undergoes a reorientation-transition from the in-plane to the out-of-plane direction in a temperature range between approx. 320 K and 370 K [2].

This reorientation-transition will play a crucial role for ultrafast laser excitation.

We studied both, equilibrium and dynamic magnetic properties of DyCo5 using an atomistic Heisenberg spin model, where the Heisenberg exchange parameters were calculated via the Korringa-Kohn-Rostoker-method. We perform Langevin dynamics simulations, i. e. solving the stochastic Landau-Lifshitz-Gilbert equation numerically. In our model, the laser excitation is taken into account via the two-temperature-model.

Our simulations show that in the high temperature phase, TIMS is in principle possible. However, ferromagnetic-resonance-experiments suggest a very high Gilbert-damping for DyCo5 [3], which we find to be a limiting factor concerning TIMS. In the low temperature phase our finding is, that TIMS is generally prohibited, where in response to laser excitation a transient multi-domain-state appears on the time scale of the thermal relaxation time.

This work is supported by the EU via FP7-NMP Femtospin.

[1] I. Radu, et al., *Nature*, 472 (2011)

[2] T. Tsushima, M. Ohokoshi, *JMMM*, 31-34 (1983)

[3] G. Woltersdorf, et al., *Phys.Rev.Lett.*, 102 (2009)

Th.I-P13 - Generation of ultrashort shear acoustic pulses by femtosecond laser demagnetization of magnetostrictive material terfenol

V.S. Vlasov¹, T. Parpiiev¹, V.V. Temnov¹, K. Dumensil², S. Andrieu², A. Anane³, V. Gusev¹, T. Pezeril¹

1. *Institut Molécules et Matériaux du Mans, UMR CNRS 6283, Université du Maine, Le Mans, France*

2. *Institut Jean Lamour, UMR CNRS 7198, Université de Lorraine, Vandoeuvre, France*

3. *Unité Mixte de Physique CNRS/Thales, UMR CNRS 137, Palaiseau, France*

Even in the absence of external magnetic fields magnetostrictive materials are characterized by built-in strains in the range of 0.001-1% of lattice constant [1]. Here we further explore the ultrafast magneto-acoustics in Terfenol [2] to show that femtosecond laser demagnetization of Terfenol leads to the generation of picoseconds acoustic shear pulses. Assuming a simple model of ultrafast demagnetization in high-fluence regime, when the final lattice temperature exceeds the Curie point and the length of magnetization vector drops to zero on a sub-picosecond time scale [3], we show how the ultrafast “release” of the built-in strain generates ultrashort acoustic pulses. Depending on the initial orientation of magnetization, not only longitudinal but also shear acoustic pulses can be generated by this novel physical mechanism. We also report the first experimental observations demonstrating the generation of picosecond shear acoustic pulses from single-crystal Terfenol samples. We analyze different configurations under external magnetic fields leading to the optimum conditions for the generation of shear acoustic pulses.

References:

- [1] C. de la Fuente et al., J. Phys.: Condens. Matter 16, 2959 (2004)
- [2] O. Kovalenko et al., Phys. Rev. Lett. 110, 266602 (2013)
- [3] B. Koopmans et al., Nature Materials 9, 259 (2010)

Th.I-P14 - Temperature study of ultrafast photomagnetic effect in YIG:Co garnet films

K. Szerenos¹, A. Maziewski¹, A. Stupakiewicz¹

1. Laboratory of Magnetism, Faculty of Physics, University of Bialystok, Poland

Light-induced ultrafast magnetization dynamics in Co-doped yttrium iron garnet thin films (system similar as one in [1]) were studied. Experiments were performed by means of time-resolved magneto-optical pump-probe technique using Faraday geometry. A non-thermal effect was used to induce the magnetization precession, based on photoinduced magnetic anisotropy under linear polarization of pump beam laser pulses [2]. Ultrafast magnetization dynamics were studied as a function of the external magnetic field, pump beam polarization, pump beam wavelength and temperature within 300-500 K range. The dependencies of magnetization precession amplitude, frequency, decay time and Gilbert damping parameter were investigated. Decreases of both frequency and amplitude of precession were observed near the Curie temperature in investigated garnets. The experimental results are in well agreement with simulations of ferromagnetic resonance mode frequency considering in the effective field of both magnetocrystalline and photoinduced anisotropy terms. The possibility of non-thermal control of the magnetization in ferrimagnets using linear polarization of femtosecond laser pulses is demonstrated.

This work was supported by the National Science Centre Poland for project DEC-2013/09/B/ST3/02669.

[1] F. Atoneche, et al., Phys. Rev. B, 81, 21, 214440, (2010)

[2] A. Stupakiewicz, et al., Appl. Phys. Lett., 101, 26, 262406, (2012)

Th.I-P15 - Magnetization dynamics of a dipolar chain at finite temperature

D. Laroze^{1,2}, O. Suarez¹, R. Stamps²

1. University of Glasgow, United Kingdom

2. Universidad de Tarapaca, Chile

Avalanche dynamics is studied for chains of dipolar coupled magnetic particles. We find that transient and highly nonlinear dynamics within the initial stages of a cascading reversal can drive formation of patterned domain structures that can persist until steady state is reached. We numerically integrate set of coupled Landau-Lifshitz-Bloch equations that take temperature into account. A perturbative method allows us to perform a separation of time scales such that we can compute time evolution over very long timescales. We examine in particular pattern formation produced through competition between long range dipolar coupling, that can be controlled by particle spacing, and magnetic anisotropies that can be controlled by particle shape and size.

Th.I-P16 - Time-resolved ferromagnetic resonance in ultrathin perpendicularly magnetized films: efficient nonlinear high order harmonics generation

A. Capua¹, S. Yang¹, T. Phung¹, A. Fantini¹, N. Kaminski¹, J. Woo Joeng¹, C. Rettner¹, W. Kim², S. Park², S. Parkin¹, Y. Ferrante¹

1. IBM Almaden Research Center, San Jose, United States

2. Samsung Electronics Co., Ltd, Suwon, Republic of Korea

Using a phase locked microwave RF source with a Ti:Sapphire 70 fs pulsed laser which serves as a magneto-optical Kerr effect (MOKE) probe, we study the ferromagnetic resonance of perpendicularly magnetized ultra-thin (11Å)CoFeB and (3Å)Co/(7Å)Ni/(1.5Å)Co magnetic layers in the time domain. When the system is operated at high external magnetic field compared to the crystalline anisotropy field we extract the Gilbert damping parameter in three ways; from measurement of the phase response; the magnetization amplitude spectrum and from measurement of the absorption spectrum. We show that the damping values agree well with measured values obtained from a time resolved pump-probe MOKE measurement (TR-MOKE). At low external magnetic fields which are comparable to the anisotropy field, however, the system becomes highly non-linear and higher harmonics of the basic RF frequency are efficiently generated. Additionally, we show that while in the high field regime the phase response shifts by π at the low field regime the phase response is almost zero resulting in a pure amplitude response. This behavior is due to phase compensation of two competing effects: precession about the external field and about the anisotropy field. This operation point imposes unique properties on the magnetic susceptibility.

TH.I-P17 - High-field high-repetition-rate THz sources for studying ultra-fast magnetization dynamics

S. Kovalev ¹, B. Green ¹, T. Golz ², A. Fisher ³, I. Radu ⁴, J. Seok Lee ⁵, A. Deac ¹, T. Kampfrath ⁶, N. Stojanovic ², M. Gensch ¹

1. *Hzdr, Dresden, Germany*

2. *DESY, Hamburg, Germany*

3. *SLAC National Accelerator Laboratory, Menlo Park, California, United States*

4. *Institute for Optics and Atomic Physics, Technical University Berlin and Helmholtz-Zentrum Berlin, BESSY II, Berlin, Germany*

5. *Gwangju Institute of Science and Technology (GIST), Gwangju, Republic of Korea*

6. *Fritz Haber Institute, Berlin, Germany*

THz field-driven magnetization dynamics has been in the focus of several recent highlight experiments that prove that the transient magnetic field in ps - long high field THz pulses can couple directly to the spin system and give rise to long-lived coherent excitations. In this contribution we discuss how the recent arrival of a new class of, so called, super-radiant THz sources, will allow to probe the triggered spin dynamics with unprecedented sensitivity in a frequency range from 0.1 to 3 THz. It is furthermore discussed if these high-field high-repetition rate THz sources can be utilized to employ more specific probe techniques such as e.g. time-resolved (TR) Raman/Brillouin scattering, TR ARPES measurements or spin-current measurements.

Th.I-P18 - Nonequilibrium fluctuations in nanomagnets

G. Bertotti ¹, E. Ferraro ¹, C. Serpico ²

1. *Istituto Nazionale Di Ricerca Metrologica, Torino, Italy*

2. *Università Federico II, Napoli, Italy*

Magnetization dynamics in nanomagnets are dominated by two competing features: (i) the dynamics are stochastic in nature, due to the strong fluctuations caused by the interaction with the thermal bath; (ii) in typical operations relevant to magnetic recording and spintronics applications (fast magnetization switching, high-frequency precession), the system is driven far from thermodynamic equilibrium. Such fluctuation-dominated nonequilibrium processes are governed by characteristic relations for the work and the entropy production [1,2], relations that are broadly referred to in the literature as fluctuation theorems. In this paper, we derive a fluctuation theorem for the case of stochastic magnetization dynamics in a uniformly magnetized nanomagnet. By using the path-integral form of the solutions of the Fokker-Planck equation for the dynamics under time-varying external magnetic field, we express the statistical weights of magnetization paths in terms of a specific action integral. The values of the action associated with a path and its time-reversed conjugate path are connected with the heat exchanged by the system with the thermal bath along that path. Connections of these results with known fluctuation theorems are derived, together with implications of the found fluctuation relation on the characterization of nanoscale magnetization processes. Numerical simulations are carried out in order to test the conditions under which the exponential averaging characterizing Jarzynski's and Crook's equalities [1,2] becomes relevant and leads to deviations from usual thermodynamic work relations.

[1] C. Jarzynski, "Nonequilibrium equality for free energy differences", *Phys. Rev. Lett.* 78, 2690 (1997)

[2] G. E. Crooks, "Entropy production fluctuation theorem and the nonequilibrium work relation for free energy differences", *Phys. Rev. E* 60, 2721 (1999)

Th.I-P19 - Magnetization dynamics in low-symmetry iron garnet film induced by femtosecond laser pulses

A. Kalashnikova¹, L. Shelukhin¹, V. Pavlov¹, P. Usachev¹, R. Pisarev¹

1. Ioffe Physical-Technical Institute, St Petersburg, Russian Federation

Thin films of iron garnets with generic formulae $Y_3Fe_5O_{12}$ (YIG) are the model media for developing principles of dielectrics-based spintronics [1] owing to their exceptionally narrow FMR line, high domain walls mobility, and composition-controlled magnetic anisotropy. The possibility to tune and control the magnetic anisotropy of YIG films on a subpicosecond time scale via excitation by ultrashort laser pulses can extend their functionality and link two rapidly developing areas of femtomagnetism [2] and magnonics [1].

We report on experimental magneto-optical pump-probe study of laser-induced picosecond and nanosecond magnetization dynamics in 10 micron thick rare-earth substituted iron garnet $(YPrLuBi)_3(FeGa)_5O_{12}$ film grown on a low-symmetry $Gd_3Ga_5O_{12}$ substrate of the (210) orientation. Owing to the complex magnetic anisotropy of such films dominated by the growth-induced contributions, they provide a possibility for detecting changes of anisotropy constants induced by femtosecond laser pulses.

We demonstrate that femtosecond laser pulses induce the magnetization precession in the studied film and distinguish two distinct excitation mechanisms. The first one shows dependence on pump pulse circular polarization, and thus can be identified as the ultrafast inverse Faraday effect [3]. The second mechanism appears to be dominating at low external magnetic field and depends on its sign. Thorough analysis of field and polarization dependencies shows that the magnetization precession is excited due to laser-induced change of the anisotropy parameters occurring at the picosecond time scale. Phenomenological analysis of these processes allowed us to separate relative contributions from laser-induced changes of different anisotropy parameters.

This work is supported by the Russian Government grant 14.B25.31.0025 and by the RFBR grant 15-02-09052-a.

[1] Magnonics: From Fundamentals to Applications, Ed. by S. O. Demokritov and A. N. Slavin (Springer, 2013)

[2] A. Kirilyuk, et al., Rev. Mod. Phys. 82, 2731 (2010)

[3] A. V. Kimel, et al., Nature 435, 655-657 (2005)

TH.I-P22 - Magnetic structure and ultrafast spin dynamics in GdFeCo at high magnetic fields

J. Becker^{1,2}, A. Tsukamoto³, A. Kirilyuk², T. Rasing¹, J. Kees Maan¹, P. Christianen¹, A. Kimel¹

1. *Radboud University Nijmegen, Institute for Molecules and Materials, Nijmegen, The Netherlands*

2. *High Field Magnet Laboratory, Institute for Molecules and Materials, Radboud University Nijmegen, Nijmegen, The Netherlands*

3. *College of Science and Technology, Nihon University, Chiba, Japan*

The amorphous rare earth - transition metal (RE-TM) alloy GdFeCo has been extensively studied in the recent past. This is mainly due to the intriguing phenomenon of all optical magnetic switching (AOS) that was first demonstrated in this material. AOS is thought to be strongly linked to the ferrimagnetic order of GdFeCo. A main characteristic of ferrimagnetism is the magnetization compensation temperature at which the magnetizations of the antiferromagnetically coupled RE and TM magnetic sublattices cancel each other out and the coercive field should diverge. The exact mechanism of AOS is still under discussion and many open questions concerning the compensation temperature and sublattice behavior remain due to insufficient data at fields > 1.5 T. We recently build a time resolved magneto optical Kerr effect (TR-MOKE) setup for high magnetic fields with which we investigated amorphous Gd₂₄Fe_{66.5}Co_{9.5} below, across and above the magnetization compensation temperature in fields up to 30 T. These fields allow us to closely map the static magnetic behavior of the system crossing the compensation temperature. Furthermore, using static and time resolved MOKE we find that at applied magnetic fields beyond 2 T, a significant change in the MOKE signal occurs that indicates a field induced magnetic transition. This transition can be observed below and above the compensation temperature and seems to limit the divergence of the coercive field at the compensation temperature. Furthermore, the magnetization dynamics significantly change after this field induced transition occurs. At temperatures above the compensation temperature, the (TR-)MOKE signal even changes sign upon crossing the transition field at ~2.6 T.

TH.I-P24 - Laser-induced spin precessional dynamics in FeCo/MnGa bilayers with different interfacial exchange couplings

Q. Ma¹, S. Iihama², X. Zhang¹, T. Miyazaki¹, S. Mizukami¹

1. WPI-AIMR, Tohoku University, Japan

2. Department of Applied Physics, Tohoku University, Japan

Magnetic bilayers consisting of a soft magnetic layer and hard magnetic layer with a perpendicular magnetic anisotropy (PMA) have attracted much attention because those are well suited not only for magnetic storage media but also for various spin-transfer-torque applications. However, there are few reports on spin precessional dynamics in coupled bilayers with a large perpendicular magnetic anisotropy. Here we report the effect of ferromagnetic (F) and antiferromagnetic (AF) interfacial coupling on spin precessional dynamics in the L10-MnGa/FeCo bilayers which show the F (AF) coupling for the case of Fe-rich (Co-rich) composition [1]. The epitaxial L10-MnGa (30 nm)/FexCo1-x (1.5 nm) bilayers (x=0.9, 0.1) were grown using magnetron sputtering. Polar magneto-optical Kerr effect was measured in time domain using all-optical pump-probe method (TRMOKE) with various direction of the external magnetic field direction [2]. Both the bilayers show similar dependences of precession frequency on the field direction. However, the dependences of precession amplitude on the field directions are quite different. The F-coupled bilayer shows the large precession amplitude when the field is applied near in-plane, whereas the precession disappears at certain field angle. On the other hand, the precession amplitude in the AF-coupled bilayer is monotonically changed by varying the field angle. The data for the both samples are well explained by the macro-spin model described by the Landau-Lifshitz equation taking into account of the interfacial exchange coupling and magnetic anisotropy modulated by ultrashort pulse laser [3].

This work is partially supported by Grand-in-Aid for KAKENHI for Young Researcher (A) (No. 24686001) and for Innovative Area (Nano Spin Conversion Science) (No. 26103004).

[1] Q. L. Ma et al., Phys. Rev. Lett. 112, 157202 (2014)

[2] S. Mizukami et al., Phys. Rev. Lett., 106, 117201 (2011)

[3] Q. L. Ma et al., submitted

TH.I-P25 - Microwave assisted magnetization reversal under circularly polarized field in thin exchange-coupled multilayer media

M. LoBue¹, A. Pasko¹, C. Serpico², F. Mazaleyrat¹, R. Tayade

1. SATIE - CNRS - ENS de Cachan, France

2. Dipartimento di Ingegneria Elettrica, Università di Napoli Federico II, Napoli, Italy

Microwave assisted magnetization switching (MAS) is one of the most intensely studied techniques aimed to reduce the reversal field in ultra high-density magnetic recording [1, 2, 3]. The key idea is to induce magnetization reversal by controlling the large amplitude magnetization precession excited by the application of a microwave AC magnetic field. Many authors have shown that an important reduction of the switching field, characteristic of single phase high-anisotropy materials, can be obtained by using exchange coupled multilayer media [4]. In a recent work we showed that in a soft-hard exchange coupled bilayer, with perpendicular anisotropy, zero-field switching condition is achievable under application of an in-plane circularly polarized microwave field [5]. In the previous study we showed that for thick layers (i.e. layers with thickness greater than the domain wall width of the materials) the system behave as two coupled uniform modes (i.e. P-modes [3]) and the switching process can be described using a simplified macro-spin approach. Here, using a finite difference element code to solve Landau-Lifshitz equation, we study the response of a bilayer within the very same planar geometry changing the thickness of the layers to explore under which conditions stable P-modes are still dominating the dynamics in very thin systems. The appearance of quasi periodic modes (i.e. Q-modes [3]) is studied and its influence on the stability of the system is discussed.

TH.I-P27 - Microwave linewidth broadening of FeCuNbSiB ferromagnetic films: effect of annealing

M. J. P. Alves¹, D. E. Gonzalez-Chavez¹, F. Bohn², R. L. Sommer¹

1. *Centro Brasileiro De Pesquisas Fisicas - CBPF/MCTI, Brazil*

2. *DFTE, Universidade Federal do Rio Grande do Norte – UFRN, Brazil*

We systematically investigate the annealing effects on the microwave linewidth broadening of FeCuNbSiB ferromagnetic films with thickness of 100 nm, using broadband ferromagnetic resonance and grazing incidence x-ray diffraction. The samples were annealed for 1h at several temperatures up to 400 °C. We correlate the non-uniform residual stress obtained from x-ray measurements with the ferromagnetic resonance linewidth due to effective field inhomogeneities measured from broadband FMR. We also estimate the annealing temperature effect on the Gilbert and two-magnon scattering contributions to the total FMR linewidth. In all samples we found the Gilbert damping constant is around 0.003, which is smaller than the values reported for traditional materials as NiFe and CoFeB. We show that the effective field inhomogeneities constitute the main contribution to the microwave linewidth, while this contribution is related to the non-uniform residual stress in the films which is reduced by thermal annealing. Besides we found that the two-magnon scattering contribution for the linewidth is small but not negligible for all studied samples.

Th.I-P28 - Emergence of coherent magnetization reversal at dynamic regime: a detailed vectorial-resolved angular-dependent study.

J. Camarero^{1,2}, T. Pérez¹, J. F. Cuñado^{1,2}, A. Maldonado¹, P. Perna², F. Ajejas¹, S. L. de las Heras², M. Niño², D. Cabrera², R. Guerrero²

1. *Universidad Autonoma de Madrid, Madrid, Spain*

2. *IMDEA Nanoscience, Madrid, Spain*

Systematic measurements performed as a function of the applied magnetic field sweep rate (dH/dt) support the scenario of nucleation-dominated reversal in the high dynamic regime and wall propagation-dominated reversal in the low dynamic regime [1-3]. However, studies on the angular dependence of the magnetization reversal dynamics are still lacking.

We present a detailed study on the angular dependence of the magnetization reversal dynamics in a model system with well-defined in-plane uniaxial magnetic anisotropy. Time-resolved vectorial-Kerr magnetometry measurements have been performed at room temperature over a broad range of applied magnetic field sweep rates (dH/dt), from 10^{-4} to 10^4 T/s, and for the whole angular range of applied magnetic field orientations (a_H) relative to the anisotropy axis direction. Although the angular dependence of the magnetization reversal mechanisms is preserved, thermal activated dynamical effects are observed such as increasing transition fields and widening irreversible transitions in both magnetization components when dH/dt is increased. The angular dependence of the remanence magnetization in both magnetization components does not depend on dH/dt . In contrast, thermal activated dynamical effects are found during irreversible processes and depend on a_H . Around the easy-axis directions, magnetic domain wall displacement and domain nucleation regimes govern the magnetization reversal at low and high sweep rates, respectively. Both dynamical effects are reduced as we move away from the easy-axes, vanishing along the hard-axis direction. The crossover between the two regimes increases as a_H increases. At the hard-axis direction, rotation processes govern the magnetization reversal independently of dH/dt . Remarkable, the magnetic properties become closer to the predicted ones by the coherent rotation model in the high dynamic regime, i.e., where nucleation processes are more relevant. This results in a gradual transition from a pinned to a coherent rotation like angular dependent behavior as dH/dt increases.

[1] B. Raquet, J. Magn. Magn. Mater. 150, 5 (1995)

[2] J. Camarero et al, Phys. Rev. B 64, 172402 (2001)

[3] T. Moore, et al. J. Phys.:Condens. Matter 15, 407 (2003)

Th.I-P29 - Frequency and field linewidth conversion of FMR spectra only valid for samples with negligible extrinsic linewidth contribution

Y. Wei¹, P. Svedlindh¹

1. Uppsala University, Uppsala, Sweden

Both frequency-swept and field-swept ferromagnetic resonance measurements have been carried out for a number of different samples to analyze the correlation between the experimentally measured frequency and field linewidths. We managed to fabricate FeCo thin films with almost zero extrinsic linewidth contribution, with intermediate extrinsic linewidth contribution and with significant extrinsic linewidth contribution by varying growth temperature and substrate material.

Contrary to the belief commonly held by many researchers, our experimental results indicate that the widely used conversion relation based on the derivative of the resonance condition (Kittel formula) is only valid for samples almost without extrinsic contributions to the linewidth (zero-frequency field linewidth $\Delta H_0 \approx 0$). Furthermore, a close examination of the literature reveals that previously reported results support our findings, with successful conversions related to samples with negligible extrinsic contributions and unsuccessful conversions related to samples with significant extrinsic contributions to the linewidth. A linewidth contribution ratio k_w that is defined as the ratio between the zero-frequency intercept and the slope of the field linewidth versus frequency curve is introduced to estimate the validity of linewidth conversion. It is suggested that a value of k_w smaller than about 10 GHz would yield a reasonable conversion. The findings are of great significance in providing guidance for FMR linewidth measurements and data analysis.

TH.J-P02 - Switching of the magnetic vortex core in a pac-man disk

T. Sato¹, K. Yamada¹, Y. Nakatani¹

1. University of Electro-Communications, Tokyo, Japan

The magnetic vortex structure [1] observed in a ferromagnetic circular disk has been intensively studied recently because its binary state can be used for high-density and non-volatile storage media. To realize a vortex core memory, the controlling of the core polarity and the reducing energy of the core switching are key issues. In order to solve these issues, we focus on utilizing a Pac-man (PM)-shaped disk [2,3]. The PM disk has an open slot extending from the center to the circumference, as a result, the core can be annihilated and nucleated using that part. In this work, we report micromagnetic simulations and investigated the vortex core switching using an in-plane nanosecond field and current pulses in order to study the switching mechanisms and switching conditions in the PM disk.

A three-dimensional micromagnetic model was used in the simulation. The PM disk was divided by a rectangular prism with dimensions of $2 \times 2 \times 2.5 \text{ nm}^3$. The diameter and the thickness of the PM disk were 200 nm and 40 nm, respectively. The notch depth and notch angle of the PM disk are 80 nm and 25 degree, respectively. Typical material parameters for Permalloy were used.

The minimum core switching field (current density) is reduced by 72% (75 %) compared to that of a circular disk with the same diameter and thickness. In the case of field, the core switches irregularly with respect to both the field pulse amplitude and duration. On the other hand, in the case of current, the core polarity can be controlled by the direction of applying the current [4,5].

[1] Science 289, 930 (2000)

[2] Appl. Phys. Lett. 83, 329 (2003)

[3] Phys. Rev. B 84, 014424 (2011)

[4] Appl. Phys. Express 7, 033003 (2014)

[5] Appl. Phys. Express 7, 073003 (2014)

TH.J-P03 - Vortex core reversal in patterned magnetic hybrid systems

P. Wohlhüter^{1,2}, M. Bryan^{3,4}, P. Warnicke², S. Gliga^{1,2}, S. Stevenson², G. Heldt⁵, L. Saharan⁴, A. Suszka^{1,2}, C. Moutafis², R. Chopdekar²

1. *Laboratory For Mesoscopic Systems, Department of Materials, ETH Zurich, Switzerland*

2. *Paul Scherrer Institute, Switzerland*

3. *Department of Materials Science and Engineering, University of Sheffield, United Kingdom*

4. *College of Engineering, Mathematics and Physical Sciences, University of Exeter, United Kingdom*

5. *School of Computer Science, University of Manchester, United Kingdom*

Vortices in patterned magnetic elements exhibit interesting dynamic behaviour that can be exploited for data storage and as oscillators. An essential requirement is reliable control over the vortex core polarization. It has so far been shown that the vortex core polarization can be reversed through the interaction of the vortex with magnetic fields [1], electric currents [2], or spin waves [3] in single-material structures [4]. Using scanning transmission X-ray microscopy we demonstrate a new vortex core reversal mechanism [5] in heterogeneous multilayer structures [6]. Layering and mutual imprinting of a Co/Pd multilayer with out-of-plane magnetization and a permalloy (Py) layer with in-plane magnetization results in a magnetically asymmetric heterogeneous structure, in which the vortex core in the in-plane Py film coexists with an out-of-plane maze domain pattern in the Co/Pd multilayer. We excite the vortex with an alternating magnetic field and the core polarization is determined from the sense of gyration. Simultaneously, the vortex core is displaced across domain boundaries in the Co/Pd using a static external magnetic field. We find that the sense of gyration of the vortex changes as it crosses a domain boundary of the Co/Pd multilayer, indicating the reversal of the core polarization. Micromagnetic simulations reveal a complex switching process triggered by the interaction of the vortex core with an underlying domain wall. This interaction results in the formation of a region in which the out-of-plane magnetization in the vortex core is quenched and dissolved by the propagation of two dynamically generated magnetic singularities (Bloch points). This process demonstrates the complex magnetization dynamics that can occur in heterogeneous structures and provides a new means to control the vortex core magnetization.

[1] Van Waeyenberge et al., *Nature* 444, 461 (2006)

[2] Yamada et al., *Nat Mater* 6, 269 (2007)

[3] Kammerer et al., *Nat Commun* 2, 279 (2011)

[4] Gliga et al., *J Phys Conf Ser* 303, 012005 (2011)

[5] Wohlhüter et al., *Under Review* (2015)

[6] Heldt et al., *Appl. Phys. Lett.* 104, 182401 (2014)

TH.J-P04 - Engineering 1D potential barrier for fast guided skyrmion motion

W. Gan¹, I. Purnama¹, H. Tung Fook¹, M. Ramu¹, W. Siang Lew¹

1. Nanyang Technological University, Singapore

Magnetic skyrmion, which is a topologically stable field configuration, has recently been observed in chiral ferromagnets. This potentially draws a step closer to the creation of skyrmion-based non-volatile magnetic memory. However, a long-standing fundamental issue that will hamper the progress of the “Skyrmion memory” is that the current-driven skyrmion does not follow the direction of conduction electron due to the presence of the Magnus force. The skyrmion deviates from a straight path and annihilates at the film edges eventually. In this work, we show that it is possible to counter the Magnus force and prevent it from annihilating by introducing a spatially non-uniform potential distribution along the nanowire. A few methods to implement the potential was investigated, including geometrical construction, material parameter tuning and layer coupling. Although the size of the skyrmion is usually defined by the nanowire width and its material parameters, here we demonstrate that the skyrmion can be compressed to as small as 4 nm by altering the width of the potential barrier. This greatly enhances the packing density of skyrmions on a nanowire. The skyrmion compression causes the skyrmion to be warped into an elliptical shape which is more susceptible to spin transfer torque from an applied current. Therefore, the speed of the current-driven skyrmion motion can be increased significantly by tuning the lateral dimension of the potential barrier. Lastly, we demonstrate that our proposed solution can also be imposed on curved nanotracks with steep bends to guide the skyrmion motion.

TH.J-P05 - Skyrmion pinning dynamics in nanostructures for diode and symmetric operations

H. Tung Fook¹, W. Liang Gan¹, I. Purnama¹, M. Ramu¹, W. Siang Lew¹

1. Nanyang Technological University, Singapore

Magnetic skyrmions are stable spin configurations originating from chiral interactions. There is significant scientific interest in the creation of a skyrmion-based memory device due to the high stability of skyrmions at small sizes. However, skyrmions are highly resistant to the conventional pinning used in domain-wall memory devices as they are known to skirt around the pinning sites in the magnetic film that they reside on. This poses a significant problem as the skyrmion's position becomes less predictable. In this work, we investigate the pinning effect of several geometrical structures by micromagnetic simulations. Instead of removing material to form pinning notches, our proposed structures have a patterned top layer to act as pinning "anti-notches". It was found that a single anti-notch on one side of the track acts as a diode due to the Magnus force which causes skyrmions to drift from the direction of electron flow. The threshold current required to overcome the pinning varies with notch depth and notch angle.

Our results show that anti-notches with larger depth increases the pinning strength but pinning material smaller than 5 nm in size have almost no impact on pinning. Skyrmions driven towards the pinning site are compressed at the anti-notch and the compression is higher at wider notch angles, making the skyrmion more susceptible to spin transfer torque. The depinning current peaks at certain notch angle due to skyrmion compression and repulsion by the anti-notch. Furthermore, skyrmions pinned at the anti-notch require a higher current to depin compared to skyrmions approaching at higher speeds.

To achieve reversible 2-way operation for memory device applications, we propose a symmetric anti-notch design on both sides of the nanowire. Kerbs at both longitudinal edges of the nanowire counteracts the Magnus force and restricts the skyrmion's motion to within the centre region of the nanowire.

TH.J-P06 - Skyrmion stability on curved surfacesV. L. Carvalho-Santos¹, R. G. Elias², D. Altbir²1. *Universidad De Santiago de Chile / Instituto Federal Baiano, Chile*2. *Universidad de Santiago de Chile, Chile*

During the last decade a strong interest has focused on the properties of topological structures on curved surfaces based on the fact that the surface's shape determines the physical properties of several systems. As examples, one can cite the ordering of nematic liquid crystals on a curved substrate and the local density of states of a conical graphene sheet. In the same hand, curvature is important to describe the physical properties of magnetic nanostructures. In some recent works, it was shown that toroidal nanorings can support a vortex-like magnetization for smaller sizes than cylindrical nanorings. Skyrmions were first described in nuclear physics, when Skyrme showed that topologically stable field configurations for interacting pions can occur as particle-like solutions. However, these topological structures do not appear only in particle Physics. In last two decades, skyrmions have been studied in several condensed matter systems, e.g., nematic liquid crystals, Bose-Einstein condensates, and magnetic systems. In particular, regarding magnetic systems, skyrmions are chiral spin structures with a whirling configuration which appear like a magnetization groundstate due to the competition among Exchange, anisotropy, Zeeman and Dzialoshinsky-Moriya interactions. Here we study the stability and energetics associated to topological skyrmions appearing as excitations coming from the interplay between the Heisenberg model and external magnetic fields on rotationally symmetric curved surfaces. We show that the presence of cylindrically radial and azimuthal fields coupled to the surface curvature destabilizes skyrmions which are predicted to appear when there are no magnetic fields. Weak fields shift the minima of the Heisenberg model (HM) in such way that the mapping of the spin sphere vector field is not completely done and the skyrmion-like excitation has not topological stability. On the other hand, a strong magnetic field yields stable 2π skyrmions, which has their widths diminished by the magnetic field strength.

TH.J-P07 - Spin-current induced magnetization patterns in nanomagnets

O. Volkov¹, D. Sheka², Y. Gaididei³, V. Kravchuk⁴, F. Mertens⁵

1. *Taras Shevchenko National University of Kyiv, Ukraine*

2. *Taras Shevchenko National University of Kyiv, Ukraine*

3. *Bogolyubov Institute for Theoretical Physics of the National Academy of Sciences of Ukraine, Ukraine*

4. *Bogolyubov Institute for Theoretical Physics of the National Academy of Sciences of Ukraine, Ukraine*

5. *University of Bayreuth, Germany*

We study formation of stable periodical magnetization structures in planar ferromagnetic nanosamples under the action of a transversal spin-polarized current via Slonczewski-Berger mechanism. The influence of the spin-current, whose polarization is directed along the normal to the ferromagnetic plane, leads to formation of various periodical magnetization patterns just below the saturation current. A square vortex-antivortex lattice is formed in two-dimensional films [1,2], a one-dimensional domain structure is formed in a wire [3] and various intermediate vortex-antivortex structures are formed in a stripe [4]. We developed a linear theory of instability of the saturated state for thin films under the influence of spin-polarized current and proposed a mechanism of current-induced vortex-antivortex superlattice formation. In the case of a thin nanowire with square cross-section we found that periodical domain walls structure appears for small thicknesses, for large thicknesses the periodical structure is absent and the saturation process is characterized by a hysteresis. For the case of nanostripes we also demonstrated that the dependence of the saturation current on the stripe width is nonmonotonic one. Also we found a variety of stable regular structures which appear in the process of the nanostripe saturation and studied the influence of Oersted field on them. All theoretical results are verified by micromagnetic simulations.

[1] O.M. Volkov, V.P. Kravchuk, D.D. Sheka, Yu. Gaididei, Phys. Rev. B, 84, 052404 (2011)

[2] Y. Gaididei, O.M. Volkov, V.P. Kravchuk, and D.D. Sheka, Phys. Rev. B 86, 144401 (2012)

[3] V.P. Kravchuk, O.M. Volkov, D.D. Sheka, Y. Gaididei, Phys. Rev. B. 87, 224402 (2013)

[4] O.V. Volkov, V.P. Kravchuk, D.D. Sheka, F.G. Mertens, and Yu. Gaididei, Appl. Phys. Lett. 103, 222401 (2013)

TH.J-P08 - Relation between dynamics of magnetic bubbles and electron transport

Y. Yamane¹, S. Hemmatiyani², J. Ieda^{3,4}, S. Maekawa^{3,4}, J. Sinova^{1,2,5}

1. *Institut Für Physik, Johannes Gutenberg Universität, Mainz, Germany*

2. *Department of Physics, Texas A&M University, United States*

3. *Advanced Science Research Center, Japan Atomic Energy Agency, Jaoan*

4. *ERATO, Japan Science and Technology Agency, Japan*

5. *SPICE, Johannes Gutenberg Universität, Mainz, Germany*

In the last few years, more attention has been focusing on topologically nontrivial magnetic structures, such as magnetic vortices in soft ferromagnetic nanodiscs and skyrmion lattices in chiral magnetic thin films. Another interesting example is magnetic bubble domains. A magnetic bubble carries an integer topological number N_s , the so-called skyrmion number, whose absolute value, unlike skyrmions with N_s being either +1 or -1, varies depending on the magnetic profile on the circumference of the bubble.

We theoretically study the relation between the dynamics of magnetic bubbles with different N_s and the electron transport, by investigating the effects of spin-transfer torque and spinmotive force, via which the magnetic and electronic channels interact with each other. We find that the current-driven dynamics of a bubble significantly depends on N_s . It turns out that the transverse motion with respect to the applied current is strongly suppressed as N_s increases.

Next, we demonstrate that the motion of bubble driven by magnetic field gradient induces a spin current and an accompanying electric voltage, i.e., spinmotive force[1]. The spin current along the bubble motion has its origin in the non-adiabaticity of the electron spin dynamics. We show that the measurement of the corresponding electric voltage may allow us to determine the phenomenological parameter β that describes the dissipative dynamics of the magnetization and plays an important role in its current-driven motion.

[1] Y. Yamane, S. Hemmatiyani, J. Ieda, S. Maekawa and J. Sinova, *Sci. Rep.* 4, 6901 (2014)

TH.J-P09 - Topological spin textures as emitters for multidimensional spin wave modes

V. Sluka^{1,2}, M. Weigand³, A. Kakay¹, A. Erbe¹, V. Tyberkevych⁴, A. Slavin⁴, A. Deac¹, J. Lindner¹, J. Fassbender¹, J. Raabe⁵, S. Wintz^{1,5}

1. Helmholtz-Zentrum Dresden-Rossendorf, Dresden, Germany

2. New York University, New York, United States

3. Max-Planck Institut für Intelligente Systeme, Stuttgart, Germany

4. Oakland University, Rochester, United States

5. Technische Universität Dresden, Dresden, Germany

6. Paul Scherrer Institut, Villigen Switzerland

The investigation of propagating spin waves is a key topic of magnetism research [1]. For the excitation of spin waves with short wavelengths, it was typically necessary to either use transducers with sizes on the order of the desired wavelengths (striplines or point-contacts) or to generate those spin waves parametrically by a double-frequency spatially uniform microwave signal [2]. Only recently, a novel mechanism for the local excitation of spin waves has been discovered, which overcomes the wavelength limit given by the minimum patterning size. This method utilizes the translation of natural topological defects, namely the gyration of magnetic vortex cores [3].

In the present contribution we will show that in a stacked vortex pair system with uniaxial magnetic anisotropy, spin waves of different symmetries and dimensionalities can be excited. The response of this system was imaged by means of time-resolved scanning transmission x-ray microscopy. For excitation frequencies above ~ 500 MHz, circularly spiraling spin waves occur in the same way as previously reported [3]. At the same time, however, additional plane waves are generated along the 180° domain walls that arise from the uniaxial anisotropy. Such generated waves propagate subsequently to the edge of the sample with the wave fronts remaining parallel to the walls. Interestingly, even an interference of both distinct two-dimensional spin wave symmetries (plane vs. circular spiral) can be imaged in the vicinity of the cores. When the excitation frequency is set to below ~ 500 MHz, a transition from the two-dimensional to a one-dimensional spin wave dynamics is observed. While the uniform domains remain almost free from detectable magnetic oscillations, high amplitude propagating spin waves become evident within the sharp 180° domain walls, originating from the central vortex cores.

[1] M. Madami et al., Nat. Nanotechnol. 6, 635 (2011)

[2] A. G. Gurevich and G. A. Melkov, Magnetization Oscillations and Waves. New York: CRC, 1996

[3] S. Wintz et al., Joint MMM/Intermag Abstract AC-07 (2013)

TH.J-P10 - Nonlinear behavior and mode coupling in spin transfer nano-oscillators

R. Lebrun¹, N. Locatelli¹, F. Abreu Araujo², S. Tsunegi¹, A. Jenkins¹, J. Grollier¹, H. Kubota³, K. Yakushiji³, A. Fukushima³, S. Yuasa³

1. UMR CNRS/Thales & Université Paris Sud, Paris, France

2. Université Catholique de Louvain, Belgium

3. Spintronic Research Center, AIST, Ibaraki, Japan

Spin-transfer torque reveals the potential of spintronic devices for a new generation of electronic components showing multiple functionalities, notably for microwave applications. Within this palette of new applications, spin transfer nano-oscillators (STNOs) are anticipated as being the most promising one [1]. However their usual highly nonlinear behavior has been demonstrated to be responsible of a linewidth enhancement [2], detrimental for applications. By considering a double vortex based STNO, we highlight how the tunable behavior of coupled modes provides a mean to successfully handle the properties of spin-transfer nano-oscillators. Here we investigate the spin transfer dynamics in a hybrid Magnetic Tunnel Junction with two vortices that are coupled by dipolar interaction. Depending on the relative configurations of the two vortices (core polarities or chiralities), different coupled modes are excited by spin transfer torque. Interestingly the intrinsic microwave properties of these excited modes (frequencies, spectral coherence and localizations of the modes) strongly depends on the core polarity configuration i.e. parallel (P) or antiparallel (AP). The strong impact of coupled modes on the non-linear behavior allows to combine large output emitted power (up to a few hundred nanowatts) and high quality factors ($Q > 1000$) at zero field, because of the vanishing the non-linearities in AP configuration [3].

This confirms the potential of coupled modes in order to increase the spectral coherence and the tunability of spin transfer nano-oscillators based on coupled vortices. Such a level of control on the nonlinear behavior reinforces our choice to exploit the microwave properties of collective modes for applications in advanced spintronics devices for integrated telecommunication concerns.

References:

[1] N. Locatelli, V. Cros, and J. Grollier, *Nat Mater* 13, 11 (2014)

[2] J.-V. Kim, V. Tiberkevich, and A. N. Slavin, *Phys. Rev. Lett.* 100, 017207 (2008)

[3] R. Lebrun, N. Locatelli, S. Tsunegi, J. Grollier, V. Cros, F. Abreu Araujo, H. Kubota, K. Yakushiji, A. Fukushima, and S. Yuasa, *Physical Review Applied* 2, (2014)

TH.J-P11 - Advanced dzyaloshinskii-moriya interaction meter based on angular dependence of asymmetric magnetic domain-wall motion

D. Kim¹, S. Yoo^{1,2}, D. Kim¹, B. Min², S. Choe¹

1. Department of Physics And Astronomy, Seoul National University, Republic of Korea

2. Spin Convergence Research Center, Korea Institute of Science and Technology, Republic of Korea

Recently, much attention has focused on the Dzyaloshinskii-Moriya interaction (DMI) in ferromagnetic systems for magnetic-skyrmion-racetrack memory. In order to form a skyrmion state, it is needed to have the large DMI value D about 3.5 mJ/m^2 which can be converted into the DMI-induced magnetic field $H_{\text{DMI}}=636 \text{ mT}$, where DW width is 5 nm and saturated magnetization is $1.1 \times 10^6 \text{ A/m}$. Recently, the measuring DMI technique based on asymmetric DW motion has been proposed. In this technique, H_{DMI} can be directly quantified by observing the shift H_{shift} of the symmetric axis in the DW speed $v(H_x)$ measurement with respect to the in-plane magnetic field H_x . However, in material with skyrmion state where H_{DMI} is too large ($>600 \text{ mT}$), it cannot be applicable due to limitation of the maximum strength H_{max} of the applied in-plane magnetic field. In this study, we propose an advanced technique to overcome such field-strength limit. The core idea is to utilize the dependence of H_{shift} on the tilting angle of the DWs with respect to the direction of the in-plane magnetic field. We perform that the H_{shift} measurements for the tilted DWs with various tilting angles (0° , 30° , 60° , and 90°) for Pt/Co/Pt film and then find that H_{shift} is very sensitive to tilting angle, following a simple relation $H_{\text{shift}} = H_{\text{DMI}} \cos(\theta)$. Therefore, with a large angle, H_{shift} becomes much reduced possibly less than H_{max} . The present idea can be also demonstrated to other films (Pt/Co/AlOx and Pt/Co/MgO), where H_{DMI} is even much larger than the field-strength limit of equipment, and thus enables the development of an advanced DMI meter based on asymmetric DW motion.

TH.J-P12 - Vortex core reversal by excitation of a higher vortex gyromode (flexure mode)

G. Dieterle¹, A. Gangwar^{1,2}, M. Noske¹, J. Förster¹, M. Weigand¹, I. Bykova¹, H. Stoll¹, C. H. Back², G. Schütz¹

1. Max Planck Institute for Intelligent Systems, Stuttgart, Germany

2. University of Regensburg, Department of Physics, Regensburg, Germany

Magnetic vortex core reversal by excitation of the fundamental gyromode G0 [1] or azimuthal spin waves [2] have been published before. Here we focus on higher order gyromodes, also called flexure modes, which are characterized by a strong z-dependence of their gyration radius [3,4]: one node in z-direction for G1, two nodes for G2 etc. For thinner samples these higher order gyromodes do not exist because their formation costs too much exchange energy. However, in our samples which are thick enough, Permalloy disks, 80 nm thick, 250 nm or 500 nm in diameter, vortex core switching mediated by the first order gyromode G1 could be demonstrated experimentally. Measurements have been performed by scanning transmission X-ray microscopy at the MAXYMUS endstation at the BESSY II synchrotron as well as with a table-top MOKE microscope, where a sophisticated lock-in technique was developed in order to detect the switching of the tiny vortex core, about 20 nm in diameter. Furthermore we imaged the first order gyromode mode G1 using time-resolved X-ray microscopy by exciting this mode with rotating magnetic fields with sub-switching threshold amplitudes. The time-resolved movies taken experimentally are in good agreement with our micromagnetic simulations.

In addition, hybridization will be discussed of both higher order gyromodes, G1 and G2, with azimuthal spin waves. In particular, by studying the second order gyromode G2 by micromagnetic simulations we found that this mode does not exist as a separate mode but forms, together with the first order azimuthal spin wave [2] of the same sense of rotation, one single highly hybridized mode.

[1] B. Van Waeyenberge et al. Nature 444, 7118 (2006)

[2] M. Kammerer et al. Nature Communications 2, 279 (2011)

[3] F. Boust et al. Physical Review B 70, 172408 (2004)

[4] J. Ding et al. Scientific Reports 4, 4796 (2014)

TH.J-P13 - Spin polarised current induced vortex core expulsion in magnetic tunnel junctions

A. Jenkins¹, R. LeBrun¹, E. Grimaldi¹, P. Bortolotti¹, S. Tsunegi¹, H. Kubota², K. Yakushiji², A. Fukushima², S. Yuasa², V. Cros¹

1. *Unité Mixte de Physique CNRS/Thales and Université Paris Sud, Palaiseau, France*

2. *Institute of Advanced Industrial Science and Technology (AIST), Spintronics Research Center, Ibaraki, Japan*

Spin torque nano-oscillators (STNOs) have raised considerable recent experimental interest, with potential applications including radio frequency and low energy communication devices. Our vortex-based STNO consists of a magnetic tunnel junction, where the free layer has the magnetic vortex ground state. The vortex core can be resonantly excited by a radio frequency current, I_{rf} , if the frequency of the current matches the frequency of the gyrotropic mode of the vortex.

An exciting potential functionality for STNOs is as a high frequency detector, where an rf current is applied to the STNO, resulting in a spin-torque diode induced d.c. voltage due to the mixing of the resistance and the current oscillations. A magnetic vortex has the potential to provide a high precision zero field detector, which operates at a lower frequency range (100 MHz - 2 GHz) than the standard uniform modes previously investigated.

For relatively low I_{rf} (300 μ A), the vortex shows resonant behaviour when excited by an rf current, but when I_{rf} is increased a large jump in the generated voltage is observed. This jump is associated with the core of the vortex being expelled from the disk, which has been confirmed with micromagnetic simulations. A new type of detector is proposed, based on core expulsion, displaying promising high sensitivity, large generated voltage.

Unlike the classical rectification voltage associated to the resonant mode, the magnitude of the voltage jump associated with the expulsion of the vortex core is independent of I_{rf} . The jump in voltage is actually associated with a resistance change owing to the TMR difference between the vortex state and the uniform state relative to the uniform polariser. The voltage response associated with the expulsion of the vortex core has a maximum 'effective' sensitivity, $\Delta V/P_{rf}$, of 40,000 V/W.

TH.J-P14 - Real time measurements of vortex core expulsion in magnetic tunnel junctions

A. Jenkins¹, R. LeBrun¹, E. Grimaldi¹, P. Bortolotti¹, S. Tsunegi¹, H. Kubota², K. Yakushiji², A. Fukushima², S. Yuasa², V. Cros¹

1. *Unité Mixte de Physique CNRS/Thales and Université Paris Sud, Palaiseau, France*

2. *Institute of Advanced Industrial Science and Technology (AIST), Spintronics Research Center, Ibaraki, Japan*

Spin torque nano-oscillators are a recent field of much experimental interest, owing the impressive variety of potential applications, ranging from bio-inspired neural networks to magnetic read heads, and from high frequency current sources to frequency detectors. For the latter of these potential applications, the frequency detector, the manipulation of the resistance state via high frequency currents is of significant interest, an effect which can be achieved via the resonant expulsion of the vortex core. A magnetic tunnel junction with a free layer which has a magnetic vortex at remanence is excited by both high frequency and dc currents, I_{rf} and I_{dc} , respectively. When the excitation radius of the magnetic vortex core is greater than the radius of the disk, the vortex is expelled, where the final magnetisation state (static uniform magnetisation state either parallel or antiparallel to the polariser) is determined by a small in-plane magnetic field.

We have observed that as I_{rf} approaches the critical rf current necessary to observe the expulsion, $I_{rf,crit}$, there is a finite probability of core expulsion, where the vortex is stochastically expelled but returns after a certain time. The dwell time in the expelled state depends upon of the magnitude and frequency of I_{rf} . In the absence of the in-plane magnetic field, there is an equal probability for the final state to be in either the parallel or antiparallel state, and is found experimentally that the core, and the resultant magnetisation state stochastically switches between parallel and antiparallel as a function of time.

TH.J-P15 - Time-resolved holographic imaging of magnetic vortex dynamics

N. Bukin¹, F. Ogrin¹, C. McKeever¹, E. Burgos-Parra¹, G. Beutier², M. Dupraz², G. van der Laan³

1. *University of Exeter, United Kingdom*
2. *SIMAP, INP Grenoble, France*
3. *Diamond Light Source Ltd, United Kingdom*

X-ray Holography with extended reference by autocorrelation linear differential operation (HERALDO) holds great promise for imaging magnetic materials at the nano-scale. In particular it has been demonstrated recently that in-plane magnetised thin films can be imaged with much greater ease and stability than similar techniques such as Fourier Transform Holography (FTH). Here we report our first experiments on using the HERALDO technique to obtain time-resolved measurements. As an object of study we used magnetic vortex structures formed in $2\mu\text{m} \times 2\mu\text{m}$ permalloy magnetic elements. Experiments were performed at ESRF using 16 bunch mode x-ray filling pattern. The aim of the experiments was to excite the vortex core gyration with a magnetic pulse and image different phases of gyration in a stroboscopic regime. The RF excitation of the vortex core was achieved with a CPW antennae integrated directly on top of the magnetic elements. By using different delay times between the pump and the probe allowed us to image the dynamics of the core within the sample at different stages of time from the point of excitation. Our results coincided with our predicted simulations for gyration time and amplitude. We aim to further develop this technique to be used on other, more exotic dynamic magnetic structures.

TH.J-P18 - Effect of the dzyaloshinskii-moriya interaction on the in-plane magnetization of submicronic structures

M. Cubukcu¹, J. Sampaio¹, A. Khvalkovskiy², M. Kuteifan³, D. Apalkov², V. Lomakin³, V. Cros¹, N. Reyren¹

1. Unité Mixte De Physique CNRS/Thales, France

2. Samsung Electronics, Semiconductor R&D Center (Grandis), San Jose, United States

3. Department of Electrical and Computer Engineering, University of California at San Diego, La Jolla, United States

The Dzyaloshinskii-Moriya interaction (DMI) is known to be a direct manifestation of spin-orbit coupling (SOC) in systems with broken inversion symmetry. A large DMI can be generated at the interface, which breaks the symmetry, between a material having a large SOC (e.g. Pt or Ta) and a thin ferromagnetic layer. The DMI competes with the exchange interaction and can lead to new phenomena. We will present both micromagnetic simulations and experiments showing such competition in submicronic structures with in-plane magnetization. For example, our numerical results in elliptical structures show that for small volume and large aspect ratio, a strong DMI-associated energy is taking over the shape anisotropy, and that the magnetization is aligning along the minor axis of the ellipses: As the DMI energy increases and exceeds the energy associated to the shape anisotropy, the magnetization axis switches from the major axis to the minor one. This is due to the amount of tilted spins on the edges that is increased in this configuration, effectively reducing the DMI energy. Simulations were performed to study this phenomenon as a function of the geometry and the magnetic material parameters. We then fabricated nanostructures (e.g. ellipses) made of CoFeB/Pt ultrathin bilayers using e-beam lithography. Finally, these structures are characterized by Magnetic Force microscopic measurement to verify the numerical predictions.

This work was supported by the Samsung Global MRAM Innovation Program.

TH.J-P20 - Static and dynamic skyrmion properties in confined structures with perpendicular anisotropy

R. Novak², F. Garcia¹, E. R.P. Novais³, J. Sinnecker¹, Alberto P. Guimaraes¹

1. *Centro Brasileiro de Pesquisas Físicas - RJ - Brazil*

2. *Universidade Federal de Santa Catarina - Campus Blumenau - SC - Brazil*

3. *Instituto Federal de Alagoas - IFAL - Maceió - AL - Brazil*

Skyrmions are small size stable topological structures with very good mobility that have been considered for the use in future magnetic devices in the emergent field known as “Skyrmionics” [1]. The existence of such structures is usually associated to the presence of the Dzyaloshinskii-Moriya interaction (DMI) in magnets lacking inversion symmetry or thin films with translational symmetry breaking across the interface and spin-orbit interaction in the substrate. Skyrmions are characterized by a topological charge, the skyrmion number ($S_k = +1$ or -1). Several methods have been proposed to generate isolated skyrmions in magnetic thin films with DMI, based on micromagnetic simulation [2]. An unequivocal, general-purpose way to generate isolated skyrmions in magnetic films without stringent requirements of applied current, DMI and magnetic anisotropy is still lacking. In the present work we show that by judiciously tailoring the perpendicular magnetic anisotropy (PMA) it is possible to stabilize a skyrmion without DMI. The occurrence of skyrmion in Co/Pt multilayers has already been observed by photoelectron emission microscopy (PEEM) at room temperature [3]. Since the PMA can be tailored just by changing the Co thin film thickness, the skyrmions appear only in a particular range of Co thickness. Using an exhaustive analysis of micromagnetic simulations of Co films with the appropriate geometries and several values of PMA, we describe the magnetic configuration of disks, strips and squares. Our results show the limits of applicability of these non-DMI skyrmions in suitable ranges of perpendicular anisotropy, e.g., PMA in the range of 1.1 MJ to 1.4 MJ for a disk with a diameter of 2000 nm. The winding numbers are calculated in all structures and confirm the occurrence of these isolated, stable, axially symmetric skyrmions. Dynamic properties of these non-DMI skyrmions in strips, such as the propagation velocity as a function of spin polarized current density and applied external fields will be presented.

[1] A. Fert et al. , Nat. Nanotech. 8, 152 (2013)

[2] J. Iwasaki et al. , Nat. Nanotech. 8, 742 (2013)

[3] F. Garcia et al. , Appl. Phys. Lett. 97, 022501 (2010)

TH.J-P22 - Theoretical study on spin torque diode effect of a high-magnetoresistance tunnel junction having a vortex free-layer and an in-plane polarized reference layer

H. Tsukahara¹, H. Imamura²

1. *High Energy Accelerator Research Organization, Tsukuba, Japan*

2. *National Institute of advanced industrial science and technology, Japan*

Spin torque (ST) induced dynamics of a magnetic vortex core has attracted much attention because of its potential applications as microwave oscillators[1]. The vortex-based ST oscillator (STO) exhibits comparatively narrow line-width compared with other kinds of STOs such as single-domain nano-pillars and point-contacts. ST diode (STD) is another important application of STO and it was recently demonstrated that the radiofrequency detection sensitivity of the MgO-based magnetic tunnel junction (MTJ) exceeded that of the semiconductor diode detector at a certain condition[2]. Since the out-of-plane component of ST is necessary to induce the self-oscillation of a vortex core, most studies of vortex based STO utilize the perpendicular magnetic field or perpendicularly polarized reference layer (RL). However it was shown that the in-plane current flowing through the free layer (FL) could induce the self-oscillation of a vortex core[3].

In this study we theoretically analyze the STD effect of a high-magnetoresistance tunnel junction having a vortex FL and in-plane polarized RL. The tunnel resistance and therefore the tunneling current have strong in-plane inhomogeneity because of the curling magnetic structure of the magnetic vortex in the FL. The in-plane inhomogeneity of the tunneling current produces the in-plane current flowing in the FL. By solving the Thiele equation incorporated with the ST term due to the in-plane current we show that the in-plane ac current generated by the inhomogeneity of the tunneling ac current produces the steady oscillation of the vortex core and therefore the STD voltage. The threshold current amplitude of 10 nm thick circular CoFe FL with a diameter of 200 nm and magnetoresistance ratio of 200% is obtained as 0.055 mA

[1] A. Dussaux et al., Nat. Commun. 1, 8 (2010)

[2] S. Miwa et al., Nat. Mat. 13, 50 (2014)

[3] H. Tsukahara and H. Imamura PRB 90, 14437 (2014)

TH.J-P23 - B20 FeGe thin films elaboration for skyrmions observation

C. Bouard^{1,2}, P. Warin^{1,2}, M. Jamet^{1,2}, A. Marty^{1,2}

1. CEA, INAC-SP2M, Grenoble, France

2. Univ. Grenoble Alpes, INAC-SP2M, Grenoble, France

For a few years skyrmion has become a subject of interest. This topologically protected spin structure is a promising candidate for high density storage. Lack of inversion symmetry is a crucial condition for skyrmions formation. B20 chiral ferromagnets meet this condition and have a narrow skyrmion phase. FeGe is one of those, with the highest Néel temperature. Moreover working with thin films enables to decrease the magnetic field required to the skyrmion phase. We investigated two ways of fabrication. The first one is the solid phase epitaxy of iron on germanium. The second one is the deposition of FeGe on Si (111) substrate by sputtering. We used X-ray diffraction, AFM and SEM to characterize our samples. Firstly we deposited 10 nm of iron on Ge (111) substrate by molecular beam epitaxy, followed by an annealing at various temperatures. We observed that Fe diffuses above 400 °C. The B20 phase appears at 800 °C. Yet B20 FeGe is not predominant. We also noticed strange patterns at the surface of our samples. Secondly we deposited 50 nm of FeGe on Si (111) substrate by sputtering. Si (111) is ideal since it has a lattice parameter very close to the B20-FeGe. When the substrate is not sufficiently heated during the growth, we have a polycrystalline monoclinic phase. Above 400 °C, we obtain the B20 phase. But we observe a demixing, iron diffusing in silicon. The layers are also incredibly rough. Next step is finding a good protocol by varying deposition parameters.

TH.J-P24 - Temperature dependence of the ferromagnetic resonance at the spin reorientation transition of Mn₂RhSn thin films

C. Bennati^{1,2}, A. Caprile², O. Meshcheriakova³, C. Felser³, G. Ghigo¹, M. Coisson², M. Pasquale²

1. *Department of Applied Science and Technology, Politecnico di Torino, Turin, Italy*

2. *Istituto Nazionale di Ricerca Metrologica (INRIM), Turin, Italy*

3. *Max-Planck-Institut für Chemische Physik fester Stoffe, Dresden, Germany*

Recent experimental and theoretical studies, which demonstrate a complex non collinear magnetic behavior in Mn₂RhSn [1], indicate the realistic possibility of engineering the skyrmion states in this and in similar Heusler systems. In geometrically constrained systems, the skyrmion phase persists within a wider field-temperature regime [2].

In this work we correlate the magnetization dynamics and the static magnetic properties of a Heusler thin film of Mn₂RhSn grown on MgO(001) substrate by magnetron co-sputtering of the constituents. A low temperature vector network analyzer ferromagnetic resonance (VNA-FMR) setup is used to detect the behavior of the resonance frequency peak when the temperature is varied from 8 K to 150 K. The hysteresis loops are measured with a vibrating sample magnetometer (VSM) in the same temperature interval. In both techniques, the in plane (ip)/out of plane (oop) components of magnetization are investigated, while biasing the sample with a constant external magnetic field parallel/perpendicular to the surface. From static magnetic measurements, it is found that the oop component does not change in the whole temperature range 8 - 150 K, while a significant variation in the saturation magnetization of the ip component is observed.

The FMR measurements reveal a critical temperature region where a phase transition is inferred from the behavior of the ip and oop magnetization. A minimum in the oop FMR frequency is observed at 85 K, thus the aforementioned phenomenology is interpreted as connected to the spin reorientation transition, predicted for this alloy [1]. Being this spin reorientation process accompanied by a canted state, the inset of skyrmions state is favored in the temperature range around 85 K. Moreover, applying the Kittel equations for magnetization dynamics, it has been possible to reconstruct the evolution of the value of the anisotropy field H_k with temperature.

[1] O. Meshcheriakova et al., Phys. Rev. Lett. 113, 087203 (2014)

[2] X. Z. Yu et al., Nat. Mater., 10,106 (2011)

TH.J-P25 - Observation of spin transfer torques in the transverse magnetic susceptibility of the Skyrmion lattice phase of MnSi

F. Rucker¹, A. Bauer¹, C. Schnarr¹, A. Chacón¹, P. Köhler¹, C. Pfleiderer¹

1. *Lehrstuhl für Topologie korrelierter Systeme, Technische Universität München, Garching, Germany*

In the skyrmion lattice phase of MnSi the observation of sizeable spin transfer torques [1-3] in small angle neutron scattering and the Hall resistivity for current densities already five orders of magnitude smaller as compared to conventional magnetic materials promises easy experimental access to the precise qualitative and quantitative form of the Landau Lifshitz Gilbert equation. We report measurements of the transverse magnetic susceptibility in the skyrmion lattice phase of MnSi. As our main result we find a distinct increase of the transverse susceptibility with increasing current density around the critical current density j_c . We discuss the broader implications of our experimental findings, which provide, for the first time, a direct link between a thermodynamic property and the effects of spin transfer torques in skyrmion lattices.

[1] F. Jonietz et al., Science, 330, 1648 (2010)

[2] T. Schulz et al., Nat. Phys., 8, 301 (2012)

[3] K. Everschor et al., Phys. Rev. B, 86, 054432 (2012)

TH.J-P27 - Movement of non-collinear magnetic textures driven by temperature gradients

R. Yanes Diaz ¹, D. Hinzke ¹, U. Nowak ¹

1. Universität Konstanz, Konstanz, Germany

Recently, Dzyaloshinskii-Moriya (DM) interaction has attracted attention in magnetism due to the fact that it can lead to the formation of skyrmions as well as spin spirals [1] with promising applications in spintronics [2,3]. Furthermore, temperature gradients can cause magnonic spin currents and with that spin transfer torques leading to a movement of a domain wall [4,5]. In this work, we combine both topics to analyse the dynamics of two dimensional non-collinear magnetic textures subject to a temperature gradient.

Numerical calculations of the dynamics of a spin spiral (SS), skyrmion lattices, and isolated skyrmions are carried out within an atomistic spin model using Langevin dynamics. Our results show that the SS moves towards the hotter area driven by the temperature gradient. The SS velocity depends on the sign of the temperature gradient due to chirality of the spiral.

In the case of Skyrmions, first we calculate the magnetic phase diagram and determine the isolated skyrmions and skyrmions lattice phases using Monte Carlo simulations. Later, we study the dynamics of these two phases observing here a clear difference between the movements of isolated skyrmions and skyrmions lattice. While in the isolated skyrmion case the motion is determined by the temperature gradient and the Magnus force, in the lattice case the interaction between skyrmions plays a fundamental role.

We acknowledge financial support by the DFG through SFB 767 and SPP 1538.

[1] G. Hasselberg et al, Phys. Rev. B, 91, 064402 (2015)

[2] A. Fert et al. Nature Nanotech., 8, 152, (2013)

[3] N. Nagaosa et al., Nature Nanotech., 8, 899 (2013)

[4] D. Hinzke and U. Novak, Phys. Rev. Lett, 107, 027205 (2011)

[5] F. Schlickeiser et al., Phys. Rev. Lett, 113, 097201 (2014)

TH.J-P28 - Emergent electrodynamics in $Mn_{1-x}Fe_xSi$

C.Schnarr¹, F. Rucker¹, C. Franz¹, R. Ritz¹, A. Bauer¹, C. Pfleiderer¹

1. Technische Universität München - Lehrstuhl Für Topologie Korrelierter Systeme, Germany

The emergent electrodynamics of the skyrmion lattice phase in chiral magnets comprise of an emergent magnetic field of one flux quantum per skyrmion that gives rise to an emergent electric field, when the skyrmion lattice moves under the application of spin currents exceeding a critical current density j_c [1,2]. We report a study of the emergent electrodynamics in $Mn_{1-x}Fe_xSi$, where we exploit a well understood increase of the topological Hall resistivity by an order of magnitude with increasing Fe concentration [3]. On the one hand, this allows us to track j_c for increasing emergent magnetic field in the presence of increasing disorder. On the other hand, we observe evidence for emergent electric fields even in the magnetoresistance, reflecting, in combination with the emergent electric field in the Hall signal, the direction of motion of the skyrmion lattice.

[1] F. Jonietz et al., Science 330, 6011, 1648-1651 (2010)

[2] T. Schulz et al., Nature Physics 8, 4, 301-304 (2012)

[3] C. Franz et al., Physical review letters 112, 18, 186601 (2014)

TH.J-P29 - Resonant perpendicular magnetic field induced interlayer-coupled vortex and other metastable state excitations

C. Teng¹, L. Chang², S. Lee²

1. *Academia Sinica, Taiwan*

2. *National Chengchi University, Taipei, Taiwan*

We report experimental detection of interlayer-coupled magnetic vortex core and different stable excitation states in out-of-plane magnetic field that oscillates at the eigenfrequencies of permalloy(Py)/Cu/Py trilayer disks. The samples are Ta(10)/Py(10)/Cu(3)/Py(25) (thickness in nm) disks with 2 μ m diameter, patterned via electron-beam lithography on top or in the gap of ground-signal-ground (GSG) coplanar waveguides. In-plane or out-of-plane high-frequency magnetic field can be generated by a radio frequency signal generator. We show that by using a sequence of an in-plane resonant field (H_t) and a resonant out-of-plane field (H_r), different ferromagnetic (FM) layer resonant states can be controlled in a systematic way. The two FM layers were in resonance under specific fields H_t and H_r , where the thick FM layer was in the magnetic vortex state configuration and the thin FM layer was in other stable states. When the thin FM layer is excited, the inverse spin Hall effect (ISHE) induced in the adjacent Ta layer generated dc voltage difference across the sample. We observed several peaks between 5 GHz and 7 GHz (figure 1), which were sensitive to the field. Good agreements between the experimental results and those from micro-magnetic simulations were found. Despite the complex behaviors, the interlayer-coupled state can be clearly measured at several different frequencies, thus can be useful for designing magnetic devices base on multiple magnetic resonant states.

TH.J-P30 - Antiferromagnetic Skyrmions

O. Tretiakov¹, J. Barker¹

1. Institute For Materials Research, Tohoku University, Japan

Manipulating small spin textures, which can serve as bits of information, by electric current is one of the main challenges in the field of spintronics. Ferromagnetic skyrmions attracted recently a lot of attention because they are small in size and can avoid pinning, while moved by electric current, better than other topological objects such as domain walls. Meanwhile, ferromagnetic skyrmions still have disadvantages such as the presence of stray fields and transverse dynamics, making them harder to employ for spintronic applications. In this work, we propose a novel topological object: antiferromagnetic (AFM) skyrmion. This topological texture has no stray fields and we show that its dynamics is faster compared to its ferromagnetic analogue. We find the dependence of AFM skyrmion radius on the strength of Dzyaloshinskii-Moriya interaction coming from relativistic spin-orbit effects and temperature. More importantly, we show that due to unusual topology the AFM skyrmions do not have a transverse to the current component of velocity and thus can be perfect candidates for spintronic applications.

TH.J-P31 - Skyrmion interactions with domain walls in perpendicular magnetized materials

F. Garcia-Sanchez¹, J. Kim¹, A. Vansteenkiste², B. Van Waeyenberge²

1. *Institut d'Electronique Fondamentale, Univ. Paris-Sud, Orsay, France and UMR 8622, CNRS, Orsay, France*

2. *Department of Solid State Sciences, Ghent University, Ghent, Belgium*

Skyrmions are spin configurations that possess topological charge. Due to their robustness they have been proposed as information carriers in future magnetic memory devices [1]. Key to implementing such memories are operations like the controlled creation or destruction of skyrmions. In this work we report micromagnetic simulations of the interaction between domain walls and skyrmions. We show that several of those operations can be achieved by means of a moving domain wall. It has been reported that the Dzyaloshinskii-Moriya interaction, necessary to stabilize skyrmions, gives rise to Neel walls and increased Walker fields in perpendicularly magnetized wires [2]. We show that the Walker breakdown in these materials consists of the creation of inhomogeneities along the wall. If skyrmions are stable for the corresponding applied field, then the moving domain wall periodically nucleates skyrmions. Moreover, the speed of field-driven domain walls is affected by the presence of skyrmions, which do not move under homogeneous fields. The domain wall acts as a field gradient and produces a drift in the skyrmions, where the drift component parallel to the domain wall is larger due to the gyrotropic motion of skyrmions. When the speed of the domain wall exceeds that of the drift then the skyrmion is annihilated. This behaviour presents practical features for a skyrmion memory like the creation of a skyrmion reservoir or a memory eraser. These results show the connection between different types of topological defects in magnetic materials.

[1] J. Sampaio et al. *Nature Nanotechnol.* 8, 839 (2013)

[2] A. Thiaville et al., *Europhysics Letters* 100, 57002 (2012)

TH.J-P32 - Time-dependence of the topological unwinding of skyrmions in chiral magnets

A. Chacon¹, A. Bauer¹, M. Halder¹, J. Kindervater¹, F. Rucker¹, S. Mühlbauer², C. Pfleiderer¹

1. *Technische Universität München, Germany*

2. *Heinz Meier-Leibnitz Zentrum (MLZ), Germany*

Cubic chiral helimagnets with space group P213 share a common magnetic phase diagram comprising a helical, a conical, a field-polarized, and a paramagnetic state. In addition, these materials give rise to a regular arrangement of topologically non-trivial spin whirls, the so-called skyrmion lattice [1]. Usually, in the bulk chiral magnets the latter is stabilized only in a small phase pocket in finite fields close to the helimagnetic ordering temperature. In Fe_{1-x}CoxSi, however, the skyrmion lattice may be made to exist down to the lowest temperatures, when field cooling through the skyrmion lattice phase [2]. The resulting metastable state may then decay into different topologically trivial states, subject to the detailed temperature and field history. As each skyrmion is associated with an emergent flux of precisely one flux quantum, its unwinding is accomplished through a topological defect that acts effectively as a sink of magnetic flux, i.e., a magnetic monopole [3]. A detailed understanding of the underlying processes, besides their implications for fundamental solid state research, may pave the way for spintronic applications exploiting the creation and deleting of single skyrmions in various compounds or heterostructures [4, 5]. Here, we report a comprehensive study of single-crystal Fe_{0.5}Co_{0.5}Si by means of small-angle neutron scattering, magnetization, and ac susceptibility measurements. All data have been collected as a function of temperature, magnetic field, cooling history, and, in particular, time. Depending on the details of the field and temperature history, we observe evidence for distinctively different processes of the topological unwinding.

[1] S. Mühlbauer et al., *Science* 323, 915 (2009)

[2] W. Münzer et al., *Phys. Rev. B* 81, 041203 (2010)

[3] P. Milde et al., *Science* 340, 1076 (2013)

[4] A. Fert et al., *Nature Nano.* 8, 152 (2013)

[5] N. Romming et al., *Science* 341, 636 (2013)

TH.J-P33 - Spin-mechanical torque spectroscopy of artificial pinning sites in thin magnetic disks

F. Sani^{1,2}, J. Losby^{1,2}, D. Grandmont¹, Z. Diao^{1,2}, D. Vick², K. Mohammad³, E. Salimi³, G. Bridges³, D. Thomson³, W. Hiebert²

1. *Department of Physics, University of Alberta, Canada*

2. *National Institute for Nanotechnology (NINT), Edmonton, Canada*

3. *Electrical and Computer Engineering, University of Manitoba, Canada*

Understanding the detailed effects of local inhomogeneity, intrinsic to most thin film materials used in nanomagnetic technology, becomes increasingly important as device dimensions shrink. Spatial inhomogeneity on the nanoscale can affect both static and dynamic magnetic responses [1]. Focused ion beam patterning is an elegant way to artificially-impose magnetic inhomogeneity on a very local scale. The strength and lateral dimension of the sites are tailored by varying the beam dose.

A quantitative understanding of magnetic pinning has been gained through studies of the quasi-static (Barkhausen) response of a magnetic vortex core interacting with the local energetic landscape [2,3]. An extension of nanomechanical torque magnetometry, with the capability of measuring simultaneously the DC moment and AC susceptibility [4], enables us to characterize the modifications both of statics and dynamics, arising from the presence of engineered pinning sites.

Experimental results for a Permalloy disk will be discussed, and compared to numerical micromagnetic simulations.

References:

- 1- R. L. Compton et al., PRL 97, 137202 (2006)
- 2- F. Fani Sani , et al., J. Appl. Phys. 115, 17D131 (2014)
- 3- J.A.J. Burgess et al., Science 339, 1051 (2013)
- 4- J.E. Losby, et al., Solid State Commun. (2014)

TH.J-P34 - Dynamics of magnetic vortex in disk-on-disk nanostructures

A. Ognev¹, M. Steblyi¹, A. Kolesnikov¹, A. Samardak¹, L. Chebotkevich¹, V. Novosad²

1. *Far Eastern Federal University, Vladivostok, Russian Federation*

2. *Materials Science Division and Center for Nanoscale Materials, Argonne National Laboratory, Argonne, United States*

Control of parameters of the magnetic vortex state in the disks is interesting and actual problem. In our previous studies we have showed that in a nanostructure consisting of big and small disks of permalloy, separated by a nonmagnetic Cu layer, the motion direction of the vortex core is dependent on the orientation of the applied magnetic field [1-3]. In this paper we experimentally show the effect of single-domain state in a small disk on the precession of the vortex core in a large disk. Diameter of the small and big disks are 200 and 600 nm, respectively. The disk thickness is 35 nm and the thickness of the copper layer between the disks is 3 nm. Disk-on-disk nanostructures have been fabricated on a Cr/Au waveguide. As reference samples we have used arrays consisting of single Py nanodisks with the diameter of 600 nm. Measurements of dynamic properties of the vortex have been done in a reflection mode using the vector network analyzer (VNA). The measured resonance frequency in single Py disks with diameter of 600 nm at zero field is 452 MHz, and the linewidth is 15 MHz. In the disk-on-disk nanostructure the linewidth increases up to 65 MHz, which is caused by an interaction between the small and big disks. We have showed that the change in orientation of the static in-plane magnetic field leads to a modification of a spin-wave spectrum of the nanostructure. Using micromagnetic simulations, we have analyzed the motion dynamics of the magnetic vortex in the disk-on-disk nanostructure. A good agreement between the calculated and experimentally measured data has been found.

References:

1. Steblyi, M. E.; Ognev, A. V.; Samardak, A. S.; Diga, K. S.; Chebotkevich, L. A. *IEEE Trans. Magn.*, 48, 4406 (2012)
2. Steblyi M.E., Ognev, A.V., Samardak, A.S., Chebotkevich, L.A. *Journal of Applied Physics*; 2013, 113, 17, p. 17B527 (2013)
3. Steblyi M. E., Ognev A.V., Samardak A.S., Kolesnikov A.G., Chebotkevich L.A. , Han X.F. *Applied Physics Letters* 104, p.112405 (2014)

TH.J-P35 - A Polarized neutron approach to chiral magnetism: the case of fege

F. Qian¹, H. Wilhelm², E. Lelièvre-Berna³, F. Falus³, M. Baenitz⁴, M. Schmidt⁴, J. Plomp¹, C. Pappas¹

1. *Delft University of Technology, Delft, The Netherlands*

2. *Diamond Light Source Ltd., Chilton, United Kingdom*

3. *Institut Laue-Langevin, Grenoble, France*

4. *Max Planck Institute For Chemical Physics of Solids, Dresden, Germany*

Magnetic chirality is the key ingredient to stabilize skyrmion textures and lattices, which combine fascinating properties with the potential of becoming the spintronic devices of the future. These new states of matter are generated by the anti-symmetric zylatoshinskii-Moriya interaction resulting from the absence of a center of symmetry in the crystal structure, as this occurs in thin films, metallic compounds or insulators crystallizing in the B20 structure type (space group P213). In this topical field of research polarized neutrons provide unique insight on the structure and topology of the magnetic correlations, due to the specificities of the neutron spin. The presentation will focus on the case of a multiferroic insulator Cu₂OSeO₃ which orders at TC = 58 K into a chiral helical state with a period of ~ 650 Å along the (100) direction. Polarised neutron scattering and neutron spin echo spectroscopy were used to investigate the chiral properties and dynamics in Cu₂OSeO₃. We will discuss the chiral magnetic correlations and fluctuations in the very close vicinity of TC. And then focus on a systematic study of the scattering under a magnetic field, which leads to a complex temperature-field phase diagram with a well-defined skyrmion lattice phase. We will also report the dynamic phase transitions where the skyrmion lattice phases appear and then vanish spontaneously after switching off the magnetic field. The results will be discussed in the general context of chiral magnetism.

Th.J-P37 - Spin motive force driven by the skyrmion lattice in the presence of the Rashba spin-orbit interaction

J. Ohe¹, Y. Shimada¹

1. Toho University, Japan

In a ferromagnetic metal, the dynamics of the non-uniform magnetic structure adds the spin Berry phase on the spin wave function. This geometrical phase induces the spin-dependent electromotive force that acts on the conduction electrons, called as a spin motive force. Recently, it has been pointed out theoretically that the dynamics of the skyrmion lattice induces the large spin motive force [1]. The measurable voltage is enhanced by the cascaded effect due to the phase-locked motion of skyrmions formed in a lattice structure. This non-uniform magnetic structure is realized in a chiral magnet in the presence of the Dzyaloshinskii-Moriya (DM) interaction. The DM interaction is originated from the spin-orbit interaction that may affect to the spin-motive force. In this report, we numerically investigate the spin motive force driven by the resonant motion of the skyrmion in the presence of the Rashba spin-orbit interaction. We consider the magnetic nanodisk where the boundary of the sample affects the resonant motion of the skyrmion motion. First, we show that the phase-locked motion of the skyrmion lattice is observed only in the lowest energy mode in an isolated nanodisk. We also show that the cascaded spin motive force is obtained in this lowest mode. Secondly, we show that the spin motive force is modulated by the by the Rashba spin-orbit interaction. The direction of the spin motive force is changed and the modulation of the spin motive force can be clarified by measuring the phase shift of the AC voltage. We also discuss the feedback effect that induced by the spin transfer torque due to the current by the spin motive force.

[1] Jun-ichiro Ohe and Yuhki Shimada, Appl. Phys. Lett. 103, 242403 (2013)

TH.K-P01 - Magnetic behavior of MnAs nano-ribbons

F. Fernandez Baldis^{1,2,3}, L. B. Steren^{2,3,4}, M. Tortarolo^{3,5}, M. Sirena^{1,2,3}, M. Sacchi^{3,6}, V. H. Etgens^{3,6,7}, M. Eddrief^{3,6}, M. Marangolo^{3,6}, O. Mentès⁸, B. Santos⁸, A. Locatelli⁸

1. Centro Atómico Bariloche CNEA, 8400 S. C. de Bariloche, Argentina

2. Consejo Nacional de Investigaciones Científicas y Técnicas, C1033AAJ Buenos Aires, Argentina

3. Laboratorio Internacional Franco-Argentino en Nanociencias, LIFAN

4. Centro Atómico Constituyentes CNEA, 1650 San Martín, Argentina

5. SPINTEC - CEA, France.

6. Sorbonne Universités, UPMC Univ Paris 06, UMR 7588, INSP, 4 place Jussieu, F-75005, Paris, France

7. Fédération Lavoisier Franklin, UVSQ, 78035 Versailles Cedex, France

8. Elettra Sincrotrone Trieste, Italy.

Research on MnAs films gave place to an intense activity in early 2000, due to its potential application in spintronic hybrid metal/semiconductor devices. Bulk MnAs presents a first-order magneto-structural transition that drives the system from a hexagonal ferromagnetic phase (a) to an orthorhombic paramagnetic phase (b). Instead, in MnAs thin films the a and b phases coexist in a wide temperature range below T_c (~283-313K). In the case of MnAs//GaAs(001), the a and b phases form a characteristic stripes pattern alternating ferromagnetic ridges with non-magnetic grooves along the MnAs[0001] direction (c-axis). A large magneto-crystalline anisotropy ensures that all magnetic moments are aligned along the [1120] easy axis (a-axis). X-ray photoemission electron microscopy (XPEEM) has been used for the direct imaging of magnetic domains of MnAs lithographed ribbons. We have investigated the dependence of the domain structures with films thickness and ribbons widths. The evolution of the magnetic domains structure and magnetic contrast with temperature has been studied in the ferromagnetic/paramagnetic phase coexistence temperature range. The temperature variation of the ferromagnetic signal close to the Curie temperature is strongly affected by the ribbons thickness. Results show that larger samples present domains patterns similar to films ones, composed of head-on domains separated by wedge boundaries. The magnetic domains shape and size are stable with respect to temperature. The magnetic domains of samples confined along the c-axis do not show significant change when their size is reduced. On the other hand, samples confined along the a-axis present a transition from head-on domains to regularly-stacked rectangular domains for the aspect ratio $w/t \sim 6.5$. This behavior is ascribed to the balance between shape and magneto-crystalline anisotropies. The domain walls and size of the thinner samples are nearly independent of the ribbons width while notable but systematic changes were observed in the domains of the thicker samples.

TH.K-P02 - Ferromagnetism in Pd(100) ultrathin films enhanced by distortion

S. Sakuragi¹, H. Tajiri², T. Sato¹

1. *Department of Applied Physics and Physico-Informatics, Keio University, Japan*

2. *JASRI/SPring-8, Japan*

We recently found the appearance of ferromagnetism in the ultrathin film of Pd(100) depending on the film thickness at a period which is consistent with the predictions based on d electron quantum-well (QW) state [1]. However, the spontaneous magnetization, which is comparable to that of nickel, is much higher than the value obtained from the calculation based on QW states. The magnetic enhancement of Pd(100) film is attributed to additional effects which were not assumed in the calculation. In this study, the in-situ rigorous structure analysis of ~ 16 mono layers Pd(100) ultrathin film deposited on SrTiO₃ (STO) substrate was performed using SPring-8 beam line BL13XU in order to establish a more accurate picture of ferromagnetism in Pd(100) film. As a result, the in-plane and out-of-plane lattice in Pd showed the 0.2 and 2.3% expansions compared with the bulk value, respectively. The out-of-plane lattice expansion is unexpected because the lattice mismatch between Pd and STO is 0.4% which is consistent with the in-plane expansion. Previous theoretical calculations predicted that the bulk Pd should show ferromagnetism at the 4 - 6 % lattice expansion [2]. Thus, the out-of-plane lattice expansion in Pd(100) film is also favorable to stabilize the ferromagnetism. Based this, we propose a picture that the Pd(100) ultrathin film is spontaneously distorted to stabilize the QW state to express ferromagnetism. This explains the enhancement of spontaneous magnetization in Pd(100) ultrathin film compared with the calculation through the synergistic effect of distortion and QW states.

[1] S. Sakuragi, T. Sakai, S. Urata, S. Aihara, A. Shinto, H. Kageshima, M. Sawada, H. Namatame, M. Taniguchi, and T. Sato, *Phys. Rev. B* 90, 054411 (2014)

[2] V. L. Moruzzi and P. M. Marcus, *Phys. Rev. B* 39, 471 (1989)

TH.K-P03 - MgO based tunnel junctions

L. Avilés Félix^{1,2}, J. González^{1,2}, M. Sirena^{1,2}

1. Consejo Nacional de Investigaciones Científicas y Técnicas, C1033AAJ Buenos Aires, Argentina
2. Centro Atómico Bariloche & Instituto Balseiro, Comisión Nacional de Energía Atómica-Universidad Nacional de Cuyo, San Carlos de Bariloche, Argentina

In the last years, MgO-based magnetic tunnel junctions (MTJ) with metallic electrodes (Fe, CoFe) have been widely studied due to their potential high TMR values (around 1000%). This is due to the coherent tunnelling of electrons in epitaxial MTJ.

In this work we will present the electrical and magnetic characterization of CoFe/MgO/CoFe patterned magnetic tunnel junctions grown on Si(100) and MgO(100) substrates. The obtained junctions are pillars with different areas (1600, 625, 100 and 25 μm^2) and fabricated by optical lithography. I(V) curves obtained by Conducting Atomic Force Microscopy of patterned MTJ were performed at room temperature in order to explore the reproducibility and homogeneity of their transport properties. The results show a more insulating behavior of the junctions grew on Si(100). The magnetic order of the structures was characterized by magnetization measurements so as their magnetic anisotropy and interlayer coupling. We also explored the influence of the substrate temperature during growth on the magnetic properties and the topographical features of the bottom electrode. An increase of the coercive field was achieved increasing the substrate temperature during the growth of the bottom electrode. These results are promising for the development of magnetic tunnel junctions.

TH.K-P04 - Submicrometric 2d Magnetic Domain Wall Ratchets

C. Castán-Guerrero^{1,2}, F. Valdés-Bango³, J. Herrero-Albillos^{4,1}, J. Bartolomé^{1,2}, F. Bartolomé^{1,2}, A. Hierro-Rodríguez^{5,6}, J. Martín³, M. Vélez³, JM. Alameda³, J.Sesé^{7,2}

1. Instituto de Ciencia de Materiales de Aragón, CSIC - Universidad de Zaragoza, Zaragoza, Spain
2. Dpto. de Física de la Materia Condensada, Universidad de Zaragoza, Zaragoza, Spain
3. Departamento de Física, Universidad de Oviedo - CINN, Oviedo, Spain
4. Centro Universitario de la Defensa, Zaragoza, Spain
5. IN-IFIMUP, Departamento de Física e Astronomia, Faculdade de Ciências, Universidade do Porto, Porto, Portugal
6. INESC-TEC (Coordinated by INESC-Porto), Departamento de Física e Astronomia, Faculdade de Ciências, Universidade do Porto, Porto, Portugal
7. Instituto de Nanociencia de Aragón and Laboratorio de Microscopías Avanzadas, Universidad de Zaragoza, Zaragoza, Spain

Magnetic domain walls (DWs) propagation is a relevant subject both in basic and applied science, such as the development of new technology based on DW memory or DW logic. It has already been demonstrated that a ratchet effect can be induced in the DW propagation by fabricating nanowires with asymmetric notches. The study was further extended to a 2D thin film by fabricating an array of holes with asymmetric shape and size in the tens-of-micrometers range [1]. Considering DWs as elastic lines with zero thickness, a ϕ -4 model [2] predicted the crossed-ratchet regime, in which a DW enters the array forward, and reversing the applied field causes it to propagate backward through kinks. In the present work, the study of DW propagation through 2D arrays of asymmetric holes has been extended to the limit of hole sizes of the order of the DW width, that is, about 500 nm. This closes the gap between previous studies in 1D nanowires and 2D arrays of holes in the tens-of-micrometers range.

The DW propagation through the entire array has been characterized by means of magneto-optical Kerr effect (MOKE) microscopy. On one hand, a clear ratchet effect has been observed in all the studied geometries. On the other hand, the small size of the holes hinders the kink nucleation, and thus no crossed-ratchet effect is observed. The DW morphology and local pinning at the holes have been investigated by means of X-Ray photoemission electron microscopy (XPEEM). This has provided a detailed picture of the pinning mechanism, which justifies the difficulty of nucleating a kink in the pinned DW.

- 1) A. Pérez-Junquera, V. I. Marconi, A. B. Kolton et al., Phys. Rev. Lett. 100, 037203 (2008)
- 2) V. I. Marconi, A. B. Kolton, J. A. Capitán et al., Phys. Rev. B 83, 214403 (2011)

TH.K-P05 - Direct observation of deterministic domain wall trajectory in magnetic network structures

P. Sethi¹, C. Murapaka¹, S. Goolaup¹, W. Siang Lew¹, R. Maddu¹

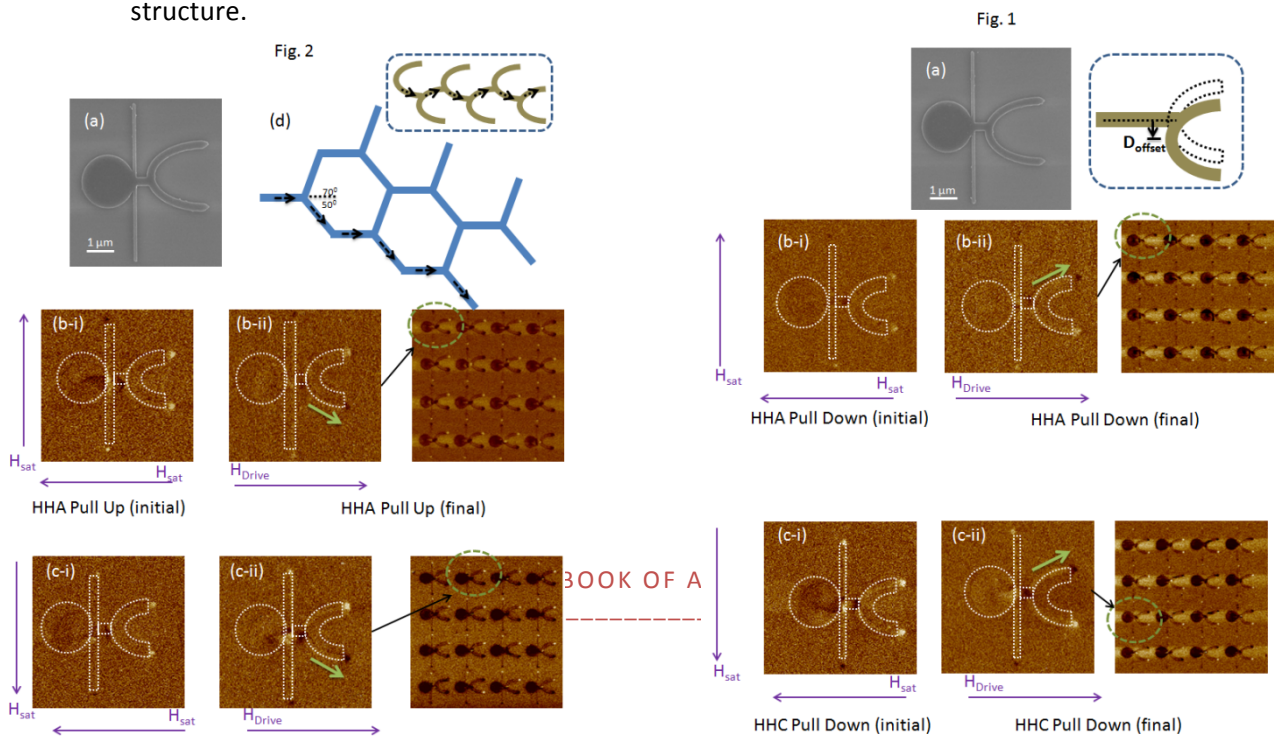
1. Nanyang Technological University, Taiwan

- [1] A. Pushp, T. Phung, C. Rettner, B. P. Hughes, S-H. Yang, L. Thomas, and S. S. P. Parkin, Nature Phys. 9, 505 (2013)
- [2] C. Murapaka, P. Sethi, S. Goolaup, R. Maddu, Y. Chen, S. H. Leong, and W. S. Lew, Appl. Phys. Exp. 7, 113003 (2014)
- [3] T. Phung, A. Pushp, C. Rettner, B. P. Hughes, S. H. Yang, and S. S. P. Parkin, Appl. Phys. Lett. 105, 222404 (2014)
- [4] K. Zeissler, S. K. Walton, S. Ladak, D. E. Read, T. Tyliczszak, L. F. Cohen, and W. R. Branford, Sci. Rep.3, 1252 (2013)
- [5] S. Ladak, D. E. Read, G. K. Perkins, L. F. Cohen, and W. R. Branford, Nature Phys. 6, 359 (2010)
- [6] N. L. Schryer, and L. R. Walker, J. Appl. Phys. 45, 5406 (1974)

Figure Captions

Fig. 1 Inset shows schematic defining asymmetry (a) SEM image of ‘pull down’ (PD) asymmetric network structure with output branch displaced in the $-y$ direction (b-i) MFM image showing initial magnetization configuration of the PD structure with transverse nanowire magnetized in the $+y$ direction (b-ii) Final magnetization configuration after head-to-head domain wall (DW) with anti-clockwise chirality (HHA) is driven to the upper branch (c-i) MFM image showing initial magnetization configuration of the PD structure with transverse nanowire magnetized in the $-y$ direction (b-ii) Final magnetization configuration after head-to-head DW with clockwise chirality (HHC) is driven to the upper branch

Fig. 2 (a) SEM image of ‘pull up’ (PU) asymmetric network structure with output branch displaced in the $+y$ direction (b-i) MFM image showing initial magnetization configuration of the PU structure with transverse nanowire magnetized in the $+y$ direction (b-ii) Final magnetization configuration after HHA is driven to the lower branch (c-i) MFM image showing initial magnetization configuration of the PU structure with transverse nanowire magnetized in the $-y$ direction (b-ii) Final magnetization configuration after HHC is driven to the lower branch (d) Asymmetric artificial Kagome type spice ice lattice depicting path followed by the DW to minimize energy. Inset showing the path followed by DW in asymmetric ‘U’ shaped network structure.



TH.K-P07 - 2D Fe-pnictide nanostructure grown on MnAs: Arsenic-bridged magnetic interactions

C. Helman^{1,2}, V. Ferrari^{2,4}, A. Llois^{2,3,4}

1. *Universidad Nacional de San Martín - Argentina*

2. *Centro Atómico Constituyentes - CNEA - Argentina*

3. *Departamento de Física - FCEN - Universidad de Buenos Aires - Argentina*

4. *Consejo Nacional de Investigaciones Científicas y Técnicas (CONICET) - Argentina*

In recent years, due to the technological importance in the realm of spintronic devices, there has been theoretical as well as experimental interest in the study of Fe films grown on metallic and on semiconducting substrates. Much effort has been devoted to the properties of nanometer thick Fe epilayers epitaxially grown on MnAs/GaAs(001)¹.

This is motivated by the future potential applications of MnAs films as active magnetic templates controlling the magnetic properties of the overlayer through temperature tuning². Within this context, the Fe monolayer (ML) coverage limit has not yet been approached.

In this presentation, we analyse the extreme case of a Fe monolayer deposited on MnAs using density functional theory.

It is found that a FeAs quasi 2D antiferromagnetic nanostructure emerges, which is magnetically almost decoupled from the substrate due to bridging effects of the arsenic atoms of the interface.

The magnetic interactions display an angular dependence characteristic of a superexchange-like behaviour, which are being modelled by a Heisenberg type Hamiltonian. The magnitude of the obtained interactions are similar to those appearing in Fe-based pnictides³. As a whole, the FeAs emerging nanostructure constitutes a 2D object which presents a nearly unsupported behaviour and that poses a challenge for heterostructure-based interface engineering.

1- C. Spezzani et al, Phys. Rev. Lett. 113, 247202 (2014)

2- M. Sacchi et al, Phys. Rev. B 81, 220401 (2010)

3- F. Ma, Z.-Y. Lu and T. Xiang, Phys. Rev. B 78, 224517 (2008)

TH.K-P08 – Resistance behavior in nanostructured $\text{La}_2/3\text{Sr}_1/3\text{MnO}_3$ thin film

I. Arango¹, M. Gomez², A. Avila³, P. Prieto^{2,4}

1. School of Materials Engineering, Universidad del Valle, Cali, Colombia

2. Thin Film Group, Department of Physics, Universidad del Valle, Cali, Colombia

3. Department of Electrical and Electronic Engineering, Universidad de Los Andes, Bogotá, Colombia

4. Center of Excellence for Novel Materials - CENM, Universidad del Valle, Cali, Colombia

$\text{La}_2/3\text{Sr}_1/3\text{MnO}_3$ (LSMO) is the most interesting compound of the manganite perovskite family due to its Curie temperature above room temperature that makes its remarkable physical properties desirable for practical applications as magnetic sensors. However, it is well known that the ferromagnetic properties of a material weaken in the presence of reduced dimensions. In this research, we have grown $\text{La}_2/3\text{Sr}_1/3\text{MnO}_3$ thin films by sputtering DC in pure oxygen atmosphere on SrTiO_3 (001) substrates at temperature of 830 °C. From x-ray diffraction (XRD) analysis, we found the Bragg peaks for LSMO thin films only (002) peaks are observed indicating a textured growth. We have characterized morphologically samples by scanning electron microscopy (SEM) and atomic force microscopy (AFM). LSMO thin film was patterned using standard UV photolithography and silver contacts bonded by copper wire were used to connect the pads to the sample holder. Dependence of resistivity with temperature shows a behavior typical of this ferromagnetic system with metal-insulator transition above 300 K. The electrical properties will be contrasted with thin film and bulk material. We carried out isothermal resistance and magnetization versus applied magnetic field loops to characterize the samples. We study the dependence of magnetic transport properties with film thickness (under 60 nm) and path size (under 1.5 micron) for potential applications like magnetic sensors.

Acknowledgements: This work was sponsored by Researchs Project No 110656933104, C.I.: 7917 COLCIENCIAS-UNIVALLE and C.I.: 7978 UNIVALLE.

TH.K-P09 - Domain Structure and magnetoresistance in Co₂MnGe zigzag structures

K. Gross¹, K. Westerholt², M. Gomez³, H. Zabel²

1. CENM, Universidad del Valle, Cali, Colombia

2. Festkörperphysik, Ruhr Universität-Bochum, Bochum, Germany

3. Grupo de Películas Delgadas, Universidad del Valle, Cali, Colombia

We report a clear manifestation of the negative contribution to the magnetoresistance due to domain walls in Co₂MnGe-Heusler submicron zigzag wires in which the domain structure, domain size and domain wall density can be well controlled. The magnetic behaviour of these systems results from the interplay between the intrinsic magneto-crystalline (K₄) anisotropy, tuneable growth induced uniaxial anisotropy ($1.2 \times 10^3 \text{ J/m}^3 < K_U < 6,1 \times 10^3 \text{ J/m}^3$) and shape anisotropy (K_S), as observed by magnetic-force microscopy (MFM) and longitudinal Kerr hysteresis loop measurements [1]. Magnetoresistance measurements were performed by the four-point method under a field applied in the plane of the wires and at different in-plane orientations at variable temperatures from 10 to 300 K. In these structures, DW-creation and annihilation occur in a coherent way. As a result, clear jumps of the resistance are detected during the transition from single-domain- to multi-domain states. At room temperature a value $RDW = -1.1\%$ was obtained; this result agrees in the order of magnitude with other experimental and theoretical findings [2,3]. The temperature dependent negative resistive contribution due to the domain wall is also discussed and compared with the existing theoretical models. Acknowledgements: This work has been partially supported by CENM-UNIVALLE and L'OREAL-UNESCO.

References:

- [1] K. Gross, P. Szary, O. Petravic, F. Brüssing, K. Westerholt and H. Zabel, Phys. Rev. B 84, 054456 (2011)
- [2] Hong, K. and Giordano, N. J. Phys.: Condens. Mater. 10 (L401)(1998)
- [3] Kent, A. D., Yu, J., Ruediger, U., and Parkin, S. S. P. J. Phys.: Condens. Mater. 13(R461) (2001)

TH.K-P10 - Surface nanostructure and magnetism of ultrathin Pd(001) films on Au(001)

T. Kawagoe¹, N. Kutsuzawa¹, K. Kondoh¹

1. *Osaka Kyoiku University, Japan*

Magnetism of Pd has been investigated for decades, e.g., ferromagnetism of ultrathin Pd films was theoretically predicted, although Pd was nonmagnetic in bulk. Increasing of a density of states (DOS) due to confinement effects is thought to be responsible for the origin of the ferromagnetism. Nevertheless, there is few direct experimental evidence of the origin of ferromagnetism. A simultaneous observation of between surface nanostructure and the spin-resolved DOS is essential for understanding the origin of the ferromagnetism of the Pd films. Here we report the surface structure and the result of differential conductivity (dI/dV) measurement of ultrathin Pd films. Experiments were performed in an UHV-MBE system equipped with an STM unit and an instrument for low-energy electron diffraction (LEED). After a cleanliness of a Au(001) reconstructed surface was confirmed by STM, Pd was then deposited on it at room temperature (RT). The LEED pattern of Pd(001) films shows a fourfold $p(1\sqrt{3}\times 1)$ structure, verifying that the Pd layers grow epitaxially on the Au(001) surface with fcc structure. The observed STM images show that the RT growth of Pd layers was dominated by an island growth mode, whereas a surface morphology of Pd layers after post-annealing (PA) at 473 K consists of atomically flat terraces. It turns out from the observed lattice constants by the LEED patterns that the Pd(001) films show lattice expansions of 4.7% for 4ML, and 3% for 12ML. We also observed strain relief patterns on the surface, when the Pd layers exceed 12 ML. The dI/dV spectra of the RT growth of Pd films are featureless. The 4ML thick of Pd(001) films after PA, however, show a distinct peak at +250 mV, which may correspond to the spin-polarized surface states of Pd(001) surface. The details of experimental results are discussed together with ex-situ magneto-optical Kerr measurements at RT.

TH.K-P11 - Controlling the size and relaxation dynamics of superferromagnetic domainsS. Bedanta¹, N. Chowdhury¹, W. Kleemann²

1. National Institute of Science Education And Research, Bhubaneswar, India

2. Physics Department, Universität Duisburg-Essen, D-47057 Duisburg, Germany

Magnetic nanoparticles below a critical radius form a single domain in which all the atomic spins are oriented along one direction. The net magnetization of such single domain magnetic nanoparticles is called as a “superspin” or “macrospin”. An ensemble of such single domain magnetic nanoparticles with dilute concentration and hence negligible inter-particle interactions will show single-particle behaviour. In this case the magnetization reversal can be explained in terms of coherent rotation of superspins as described by Stoner-Wohlfarth model. However in a dense ensemble of magnetic nanoparticles but still below physical percolation, sufficiently strong interactions can be experienced to form a “superferromagnetic (SFM)” state. [S. Bedanta et al., *Phys. Rev. Lett.* 98, 176601 (2007)].

Magnetization reversal processes using Magneto-optic Kerr microscopy in longitudinal configuration have been studied on a discontinuous metal-insulator multilayer sample $[\text{Co}_{80}\text{Fe}_{20}(1.3\text{nm})/\text{Al}_2\text{O}_3(3\text{nm})]_{10}$ showing superferromagnetic behavior. On applying the magnetic field at various angles to the in-plane easy axis we observe that both domain sizes and shapes can be changed. The reversal process by magnetizing along the easy axis (EA) is governed via domain wall motion followed by subsequent nucleation. However, as q is increased away from the easy axis, the ferromagnetic correlation strength decreases. It is found that the magnetization reversal occurs via domain wall motion and nucleation up to $q = 60^\circ$, where q is the angle between the easy axis and external magnetic field. But near to the hard axis, magnetization reversal occurs via coherent rotation of superspins. Magnetization relaxation measurements were performed at various angles between the magnetic field and the easy axis. Also relaxation time increases at increasing ϑ .

TH.K-P12 - Soft magnetic multilayered thin films for HF applications

C. Serletis¹, G. Loizos¹, G. Giannopoulos¹, T. Maity², S. Roy², N. Lupu³, G. Ababei³, H. Kijima⁴, M. Yamaguchi⁵, D. Niarchos¹

1. Institute of Nanoscience and Nanotechnology, NCSR 'Demokritos', Athens, Greece

2. Micropower-Nanomagnetics Group, Tyndall National Institute, University College Cork, Cork, Ireland

3. National Institute of R&D for Technical Physics, Iasi, Romania

4. Frontier Research Institute for Interdisciplinary Sciences (FRIS), Tohoku University, Sendai, Japan

5. Dept. of Electrical Engineering, Graduate School of Engineering, Tohoku University, Sendai, Japan

Introduction

The recent surge in demand for miniaturization of power transformers and inductors requires core materials with low energy loss, high flux density, high permeability and high operating frequency. Recent developments in magnetic materials such as CoZrO granular films and CoNiFe alloy thin films, have been evaluated for integrated devices for high frequency applications. In this work, a commercial amorphous material (Metglas® 2605HB1M) with high flux density and low loss properties at lower frequencies is used for multilayered thin films with very promising properties at higher frequencies.

Sputtering procedure

Multilayered films were prepared using a magnetron sputtering system, with a base pressure of 4×10^{-7} Torr. A composite 2-inch target from amorphous ribbon $\text{Fe}_{85-95}\text{Si}_{1-10}\text{B}_{1-10}$ (commercially known as Metglas® 2605HB1M or HB1) was used. All the depositions were performed on SiO_2 substrates at 3mTorr Ar pressure.

Experimental analysis

The structural analysis was performed by X-ray diffraction using Cu-K α radiation. In all cases, no peaks related to a crystalline phase were observed, verifying the amorphous nature of the sputtered samples.

AC hysteresis loops measurements were performed by a B-H Loop Tracer at 50Hz. It can be seen that the multilayers have the same saturation magnetization as the original material (1.62T). The coercivity varies between 80-500A/m, a very good result considering that the original material has 40A/m coercivity.

High-frequency complex permeability measurements up to 9 GHz were performed in a PMM-9G1 permeameter, The results show a constant μ' greater than 300 in all samples, with working frequency up to 900MHz, with relatively low initial μ'' . The best sample has a constant μ' , about 850.

Conclusions

The FeBSi/Al₂O₃ multilayer thin film properties in combination with their easy, fast and reproducible fabrication demonstrate that they may have applications in integrated inductive components used under high frequency in the megahertz range.

Th.K-P13 - Effect of planar magnetocrystalline anisotropy in vortex configuration of micro-scale disks

M. Martins¹, S. Parreiras^{1,2}

1. CDTN/CNEN, Belo Horizonte, Brazil

2. UFMG, Belo Horizonte, Brazil

Soft ferromagnetic dots with sub-micrometer size can exhibit in the ground state a curling spin configuration known as magnetic vortex. In the case of soft ferromagnetic materials in micron and submicron scales, small changes in shape, size and material's anisotropy can modify the energy equilibrium that defines the stable spin structure. In this work, we investigated the magnetic configuration of micron-sized $\text{Co}_{60}\text{Fe}_{40}$ and Permalloy disks by comparing the results of micromagnetic simulations and magnetic force microscopy (MFM) measurements. By comparing the results for $\text{Co}_{60}\text{Fe}_{40}$ and Permalloy it was possible to elucidate the effect of the planar magnetocrystalline anisotropy in the stability of the magnetic vortex configuration. The results for disks with diameters between 0.5 and 8 μm and nominal thickness of 20 nm showed that the anisotropy favors spins alignment and domains division, reducing vortex stability. Although the vortex is the lower energy state, the MFM results showed also different magnetic configurations. The proportion of disks in each configuration depends on the disk diameter. Additionally, a statistical analysis of the magnetic configuration distribution observed in MFM experiments was performed and compared with the simulation results.

Acknowledgements: CAPES, CNPq and FAPEMIG.

TH.K-P14 - Structural and magnetic properties of zinc ferrite thin films irradiated by slow highly charged ions

E. Gafton¹, G. Bulai¹, I. Dumitru¹, O. Caltun¹, M. Trassinelli², D. Vernhet¹

1. *Alexandru Ioan Cuza University, Faculty of Physics, Iasi, Romania*

2. *CNRS and Université Pierre et Marie Curie, INSP, UMR7588, Paris, France*

Tailoring of magnetic and structural properties of magnetic nanofilms by the slow highly charged ion irradiation is a work of interest for technological application [1]. To study the influence of such irradiation process on physical properties of zinc ferrite thin films a series of samples were fabricated in controlled condition at room temperature onto Si (111) substrates by pulsed laser deposition method (PLD) [2,3]. Structural and magnetic properties of these zinc ferrites thin films were under investigation before and after being irradiated by 90 keV neon beam. The crystallographic characterizations of the films were performed using X-ray diffraction (XRD). Information about films thicknesses were obtained with a scanning electron microscope (SEM), and profilometry measurements. The morphology of the thin films was characterized using an atomic force microscope (AFM). Vibrating sample and SQUID magnetometers were used to measure the magnetic properties of the laser ablated films. We have recorded the magnetization as a function of applied field at room temperatures (RT) and at lower temperatures (200K, 100K and 10 K) for the pristine and irradiated specimen in order to observe the change in the magnetic properties of the system under investigation. Further, thermal magnetic measurements in zero-field cooled (ZFC) and field cooled (FC) mode were carried out to understand the underlying physics responsible for the change in magnetic properties. It was observed that ion bombardment does not affect the chemical composition of the films, but changes significantly their magnetic properties. These modifications are related to local changes of the film structure during the irradiation and to the implantation of ions. More precisely, modifications of the film properties after irradiation, like coercivity, saturation magnetization, crystal lattice, etc., have been studied as a function of the ion species, the ion penetration depth and the irradiation fluence.

[1] M. Trassinelli, V.E. Gafton, M. Eddrief, V.H. Etgens, S. Hidki, E. Lacaze, E. Lamour, X. Luo, M. Marangolo, J. Mérot, C. Prigent, R. Reuschl, J.-P. Rozet, S. Steydli, D. Vernhet NIMB, Volume 317, Issue PART A, 2013, Pages 154-158

[2] Ovidiu Florin Caltun, Journal of Optoelectronics and Advanced Materials Vol. 7, No. 2, April 2005, p. 739 - 744

[3] Georgiana Dascalu, Gloria Pompilian, Bertrand Chazallon, Ovidiu Florin Caltun, Silviu Gurlui, Cristian Focsa - Applied Surface Science, Volume 278, 1 August 2013, Pages 38-42

TH.K-P15 - Effect of lattice mismatch on the morphology and magnetic properties for L1₀-ordered FePt thin filmsH. Iwama¹, M. Doi², T. Shima³

1. Tohoku Gakuin University, Japan

Recently, L1₀ FePt ordered alloy with high magnetocrystalline anisotropy ($K_u=7.0\times 10^7$ erg/cc) has attracted much attention, since they are believed to be good candidates for future magnetic devices such as next-generation ultrahigh-density magnetic storage media and biasing nanomagnets [1]. It is also thought to overcome the problem of thermal fluctuation in nano-meters scale. A lot of studies such as thin films and self-assembled nano particles have been investigated [2], [3]. However, magnetization process of FePt thin films has not been fully elucidated. In this study, in order to see the effect of lattice mismatch between FePt thin films and single crystal substrates on the magnetization process, FePt thin films have been fabricated on MgAl₂O₄ (MAO) and MgO single crystalline substrates and their structure, magnetic properties and magnetic domain structure have been investigated.

All the samples were prepared using an ultrahigh vacuum magnetron sputtering system. FePt films were prepared by co-sputtering Fe and Pt targets directly onto single crystalline MgO (100) or MAO (100) substrates. The substrates were heated to $T_s = 700$ °C during deposition. The nominal thickness of FePt film (t_{FePt}) was varied in the range between 5 and 100 nm. The magnetic properties were measured by a superconducting quantum interference device (SQUID) magnetometer. The structure analysis was performed by X-ray diffraction (XRD) with Cu $K\alpha$ radiation. The magnetic domain structure was observed by a magnetic force microscope (MFM).

From XRD patterns, in addition to a fundamental (002) peak, (001) and (003) superlattice peaks from the L1₀-FePt phase have been clearly observed for all samples. Magnetization curves for the FePt films with MgO substrate. The maximum H_c of 54.3 kOe was observed for the film with $t_{\text{FePt}} = 10$ nm. From MFM images, the single-domain structure was observed at $t_{\text{FePt}} = 10$ nm.

[1] T. Shima *et al.*, *Appl. Phys. Lett.* 99. 033516 (2006)

[2] T. Shima *et al.*, *Appl. Phys. Lett.* 81. 1050 (2002)

[3] S. Matsumoto *et al.*, *J. Phys.: Conf. Ser.* 266. 012038 (2011)

TH.K-P16 - Confinement effects in lattices of nanoskymions

J. Hagemester¹, A. Kubetzka¹, E. Vedmedenko¹, R. Wiesendanger¹

1. University of Hamburg, Germany

In this Investigation ground states of two-dimensional nanoskymions lattices in structured magnetic elements of different shape are addressed. It is demonstrated by means of Monte-Carlo simulations that the nanoskymions couple to the edges of magnetic elements and demonstrate strong confinement effects. The measure of confinement is quantified and compared with experimental Spin-polarized Scanning Tunneling Microscopy data on Fe/Ir(111).

TH.K-P17 - Splitting of spin-wave modes in periodically perturbed thin films: theory and experiment

R. A. Gallardo¹, A. Banholzer^{2,3}, K. Wagner⁴, M. Körner^{2,3}, K. Lenz², M. Farle⁴, J. Lindner², J. Fassbender^{2,3}, P. Landeros¹

1. *Departamento De Física, Universidad Técnica Federico Santa María, Valparaiso, Chile*

2. *Helmholtz-Zentrum Dresden-Rossendorf, Institute of Ion Beam Physics and Materials Research, Dresden, Germany*

3. *Technische Universität Dresden, Dresden, Germany*

4. *Fakultät für Physik and Center for Nanointegration Duisburg-Essen (CeNIDE), Universität Duisburg-Essen, Duisburg, Germany*

A joint theoretical-experimental study focusing on the description of the ferromagnetic resonance response of thin films in the presence of periodic perturbations introduced on the upper film surface is presented [1-2]. From the viewpoint of theory, these perturbations may exist in the form of any kind of one- or two-dimensional rectangular defect arrays patterned onto one surface of the magnetic film. Indeed, the defects may be pits or bumps, or ion-implanted regions with a lower saturation magnetization. The complete set of response functions, given by the components of the frequency and wave-vector dependent dynamic magnetic susceptibility tensor of the film exposed to microwave excitation, are provided and are used to explain the experimental data. This allows us to obtain the response of the system due to microwave absorption, from which the zero wave-vector spin-wave modes in the field-frequency spectra, including their intensity, are calculated. Explicit calculations for periodic defects featuring the shape of stripes, dots and rectangles are given in detail, as well as experimental results for stripe-like defects prepared either by topographical depressions or by ion implantation of thin magnetic films. The excellent agreement of the theoretical and experimental results manifests the validity of the presented model.

[1] P. Landeros and D. L. Mills, Phys. Rev. B 85, 054424 (2012)

[2] R. A. Gallardo, A. Banholzer, K. Wagner, M. Körner, K. Lenz, M. Farle, J. Lindner, J. Fassbender and P. Landeros, New J. Phys. 16, 023015 (2014)

TH.K-P18 - Electronic and spin states of SrRuO₃ thin films: an X-ray magnetic circular dichroism study

S. Agrestini¹, Z. Hu¹, C. Kuo¹, M. Haverkort¹, K. Ko¹, E. Pellegrin², M. Valvidares², J. Herrero-Martin², P. Gargiani², P. Gegenwart³

1. *Max Planck Institute For Chemical Physics of Solids, Germany*

2. *ALBA Synchrotron Light Source, Cerdanyola del Vallès, Spain*

3. *Experimental Physics VI, Center for Electronic Correlations and Magnetism, University of Augsburg, Augsburg, Germany*

4. *Physikalisches Institut, Georg-August-Universität Göttingen, Göttingen, Germany*

5. *Department of Quantum Matter, ADSM, Hiroshima University, Higashi-Hirsohima, Japan*

SrRuO₃ have received intensive research interest because it is one of the very few ferromagnetic metallic 4d transition metal oxides, with a high Curie temperature of T_c=160 K, as well as unusual negative spin polarization and magnetoresistive properties. Ru⁴⁺ has S=1 spin state, however, very recently it has been suggested that a high spin state (S=2) of Ru⁴⁺ could be stabilized on compressively in-plane strained SrRuO₃ films. We report a study of the local magnetism in thin films of SrRuO₃ grown on (111)- and (001)-oriented SrTiO₃ substrates using x-ray magnetic circular dichroism spectroscopy (XMCD) at the Ru-L_{2,3} edges. The application of the sum rules to the XMCD data gives an almost quenched orbital moment and a spin moment close to the value expected for the low spin state S = 1. Analysis of the spectral lineshape using full-multiplet cluster calculations indicates that the low spin state is quite stable and suggest that the occurrence of a transition to the high spin state S = 2 in strained thin films of SrRuO₃ is unlikely as it would be too expensive in energy.

TH.K-P19 - Characterisation of polycrystalline heusler alloys

T. Huminiuc¹, J. Sinclair¹, H. Wu¹, G. Vallejo-Fernandez¹, A. Hirohata¹

1. *University of York, United Kingdom*

Heusler alloys have significant potential for applications in spintronic devices because of their 100% spin polarisation at the Fermi level at room temperature. Some Heusler alloys exist in a ferromagnetic (F) state [1] and the others are predicted to be antiferromagnetic (AF) [2]. An antiferromagnetic Heusler alloy may be suitable to create a pinning layer via exchange bias for GMR and TMR devices. The standard alloy used for exchange bias is IrMn but Ir is a scarce element hence an alternative AF is required. Ni₂MnAl and Fe₂VAl are two Heusler alloys with potential to form an AF phase. The structural and magnetic properties of these alloys have been studied. Polycrystalline thin films of these materials were deposited using a HiTUS system. The thickness of the films was (100 - 2) nm. The samples were annealed in a vacuum furnace at a base pressure of 10⁻⁵mbar at temperatures in the range 250 to 700°C. Prior to annealing the samples exhibited a paramagnetic behaviour. It is predicted that the B2 phase of the Heusler alloys will develop an antiferromagnetic structure [3]. The degree of B2 ordering increases with both annealing time and temperature.

An increase in coercivity is observed when using Ni₂MnAl as a pinning layer for the ferromagnetic Co₂FeSi. Fe_{2.5}V_{0.5}Al is also predicted to have an antiferromagnetic phase [2]. Seed layers, heated substrate growth and doping have been investigated to promote crystallisation of the AF phase and an increase in the Neel temperature. Temperature dependent resistivity measurements are used to determine the Neel temperature of the AF Heusler alloy films.

[1] H. Endo et al, J. Phys. D: Appl. Phys. 44 (2011)

[2] D. J. Singh and I. I. Mazin, Phys. Rev. B 57, 14352 (1998)

[3] M. Acet et al, J. Appl. Phys, 92, 3867 (2002)

TH.K-P20 - Spatiotemporal Chaos induced by spin-transfer torque in Nanopillars

A. Cabanas Plana¹, A. O. Leon², D. Laroze^{1,3}, M. Clerc²

1. Instituto De Alta Investigación De La Universidad De Tarapacá, Arica, Chile

2. Depto. de Física, Facultad de Ciencias Físicas y Matemáticas, Universidad de Chile, Santiago, Chile

3. SUPA School of Physics and Astronomy, University of Glasgow, Glasgow, United Kingdom

Macroscopic system under the injection and dissipation of energy and particles can exhibit complex structures [1]. In the present work we study the pattern formation in one-dimensional nanopyllar in the presence of a spin-polarized current and an external magnetic field [2]. The combined effects of the spin-polarized current, spatial coupling, and dissipation allow for the existence of stable non-trivial uniform states as well as homogenous pattern states. These can be regular or chaotic. The temporal evolution is described by the Landau-Lifshitz-Gilbert-Sloaczewski equation [3]. We numerically characterize the dynamical behavior of the system by monitoring the Lyapunov exponents and the magnetic energy. We show that the system exhibits different types of spatiotemporal chaotic states [4] as a function of the current and intensity of the field. In addition, we find that the system presents localized chaotic patterns [5].

The authors acknowledge the research received financial support given by EPSRC under grant EP/L002922/1, FONDECYT 1120764, CEDENNA, Millennium Scientific Initiative P10-061-F, and UTA Project 8750-12.

References:

- [1] G. Nicolis et al., *Self-Organization in NonEquilibrium Systems* (Wiley, New York, 1977)
- [2] D.V. Berkov et al., *Magn. Magn. Mater.* 320, 1238-1259 (2008)
- [3] Z. Li et al., *Phys. Rev B.* 68, 024404 (2003)
- [4] D. Urzagasti et al., *Eur. Phys. J. Special Topics* 223, 141-154 (2014)
- [5] N. Verschuren et al., *Phil. Trans. R. Soc. A* 372 20140011 (2014)

TH.K-P21 - Unusual reversal process in ferromagnetic nanostructures

B. Mora¹, N. Soriano¹, C. Redondo¹, A. Arteché¹, D. Navas², R. Morales^{3,4}

1. *Dpto. de Química-Física, Universidad del País Vasco UPV/EHU, Leioa, Spain*

2. *IFIMUP-IN and Dept. Física e Astronomia, Universidade do Porto, Porto, Portugal*

3. *Dpto. de Química-Física & BCMaterials, Universidad del País Vasco UPV/EHU, Leioa, Spain*

4. *IKERBASQUE, Basque Foundation for Science, Bilbao, Spain*

Current lithography techniques have allowed the fabrication of nanostructured magnetic materials in which size, shape and order have dramatic influence on their magnetic properties [1]. In this work we show that unusual hysteresis loops with negative remanence can be achieved by patterning ferromagnetic thin films. Trench-patterned Permalloy, NiFe (Py), films were fabricated by Laser Interference lithography (LIL) and magnetically characterized by vibrating sample magnetometry (VSM). Photoresist gratings obtained by LIL were used to deposit a Ti hard mask on a 100 nm thick Py layer. The Ti mask pattern was transferred onto the Py layer by Ar+ plasma etching. Four Py-trench depths (10, 15, 25 and 50 nm) with line periodicities of 0.4 and 1.9 microns were generated by varying etching times. VSM measurements revealed the existence of hysteresis loops with negative remanence at certain directions of the applied field with respect to the line axis. A theoretical approach based on the Stoner Wohlfarth model was carried out to simulate hysteresis loops at any orientation of the external field H. We obtained an excellent agreement between both theoretical and experimental results. Moreover, this model predicts the conditions that structural and magnetic parameters of ferromagnetic patterned films should satisfy to exhibit negative remanence. Although negative remanence was observed in continuous thin films of dissimilar materials or multilayer [2], it had not been achieved in artificially patterned structures of single ferromagnetic layers. Thus, this finding illustrates a method to control the magnetization reversal of thin films by a slight surface patterning.

Work supported by Basque Country Government grant Nanoiker11, UPV/EHU UFI11/23 and MINECO FIS2013-45469.

[1] J.I. Martín, J. Nogués, K. Liu, J.L. Vicent, I.K. Schuller, J. Magn. Mater. 256 (2003) 449

[2] S. M. Valvidares, L. M. Álvarez-Prado, J. I. Martín, and J. M. Alameda, Phys. Rev. B 64 (2001) 134423

TH.K-P22 - Anisotropic magnetoresistance in nickel nanostripe fabricated by atomic force microscopy lithography

A. Pavlova¹, A. Temiryazev², M. Temiryazeva², Y. Khivintsev^{3,4}, Y. Nikulin^{3,4}, A. Dzhumaliev^{3,4}, A. Zakharov¹, Y. Filimonov^{1,3,4}

1. *Gagarin Saratov State Technical University, Saratov, Russian Federation*
2. *Fryazino Branch of Kotelnikov Institute of Radio-engineering and Electronics of Russian Academy of Sciences, Fryazino, Russian Federation*
3. *Saratov Branch of Kotelnikov Institute of Radio-engineering and Electronics of Russian Academy of Sciences, Saratov, Russian Federation*
4. *Chernyshevsky Saratov State University, Saratov, Russian Federation*

Nanostructuring can strongly affect magnetic state through the shape anisotropy effect that can be used to control anisotropic magnetoresistance (AMR) effect. In this work we applied atomic force microscopy lithography to make nanostripe out of nickel film and investigated how nanostructuring affected AMR. The studied sample was in the form of 15 nm thick and 3 micron wide nickel microstripe with contact pads on the ends for AMR measurements. In the middle of the microstripe 60 nm wide bridge-nanostripe oriented perpendicular to the microstripe was formed by scratching nickel film using atomic force microscope probe. The structure was fabricated on silicon wafer with silicon dioxide buffer layer. Resistance was measured as a function of the bias magnetic field magnitude by four-probe method at different temperatures (from 10 to 300 K) for two tangential bias field orientations: along or perpendicular to the microstripe. Measurements performed before scratching showed positive and negative change in resistance at low field relatively to resistance at saturation field for perpendicular and parallel field orientation, respectively, indicating that at zero field average magnetization is oriented at some angle to the microstripe. Temperature affected only on magnitude of AMR but not on its sign. After scratching we observed change in AMR sign at room temperature indicating that resistance in this case is mostly due to the nanostripe where current is perpendicular to the current in the microstripe. In addition, for field applied along the microstripe we observed change in AMR sign as temperature decreased. This effect might be due to thermal deformation of the structure that causes additional anisotropy field through magnetostriction.

This work was supported by Russian Foundation for Basic Research (project # 13-07-01023, 14-07-00549 and 14-07-31107).

TH.K-P23 - Magnetic domain structure and spin reorientation transition in atomically flat cobalt ferrite islands

A. Quesada¹, L. Martín-García², C. Munuera³, M. Foerster⁴, L. Aballe⁴, M. García-Hernández³, J. Fernández¹, J. de la Figuera²

1. Instituto de Cerámica y Vidrio, CSIC, Madrid, Spain

2. Instituto de Química Física Rocasolano, CSIC, Madrid, Spain

3. Instituto de Ciencia de Materiales de Madrid, CSIC, Madrid, Spain

4. Alba Synchrotron Light Facility, CELLS, Spain

Ferrimagnetic cobalt ferrite gathers a number of characteristics that make it an extremely appealing material both from fundamental and applied standpoints. Among other applications, it is frequently used in hybrid systems to exploit interfacial effects, as for instance magnetoelectric-coupling to a ferro-/piezoelectric material or exchange-coupling to ferro and antiferromagnets.[1] However, in order to rigorously study these magnetic coupling effects, an accurate control of the quality of the surfaces/interfaces and the magnetic properties is mandatory.[3,4] In this work, we employ low-energy electron microscopy (LEEM) to monitor in-situ and tailor the epitaxial growth of high quality atomically flat iron-cobalt ferrite islands on a Ru(0001) substrate. The combined LEEM/XMCD-PEEM (x-ray magnetic circular dichroism-photoemission electron microscopy) capabilities of the CIRCE beamline at ALBA allow us to characterize the electronic and structural properties of the ferrite islands, as well as the magnetic domain structure. Cobalt ferrite grows in (111) orientation, and the composition corresponds to a cobalt-rich ferrite with a nominal Fe:Co ratio of 1:1. As expected, the comparison of the magnetic domain configuration at both the Fe and Co L-edges shows a perfect match. The magnetization remains mainly in the plane, and Bloch walls separate the domains. Surprisingly, the magnetic domains are also detected at the O K-edge. In addition, MFM experiments reveal an interesting spin reorientation as a function of thickness. Thinner islands show no out-of-plane contrast. As thickness increases above 40 nm, perpendicular magnetization starts to appear. We interpret this transition as a competition between shape and magnetocrystalline anisotropy.

Acknowledgments: Research supported by EU-FP7 NANOPYME Project (No. 310516)

References:

[1] A. Quesada, F. Rubio-Marcos, J. F. Marco, F. J. Mompean, M. García-Hernández, J. F. Fernández, *Appl. Phys. Lett.* 2014, 105, 202405

[3] M. Coll, J. M. Montero Moreno, J. Gazquez, K. Nielsch, X. Obradors, T. Puig, *Adv. Funct. Mater.* 2014, 5368

[4] M. Monti, B. Santos, A. Mascaraque, O. de la Fuente, M. A. Niño, T. O. Mente, A. Locatelli, K. F. McCarty, J. F. Marco, J. de la Figuera, *Phys. Rev. B* 2012, 85, 20404

Th.K-P24 - Superexchange interaction in Fe doped manganites probed by x-ray magnetic circular dichroismA.I. Figueroa¹, G.E. Campillo², A.A. Baker^{1,3}, J.A. Osorio⁴, O.L. Arnache⁴, G. van der Laan¹*1. Magnetic Spectroscopy Group, Diamond Light Source, Didcot, United Kingdom**2. Departamento de Ciencias Básicas, Universidad de Medellín, Medellín, Colombia**3. Department of Physics, Clarendon Laboratory, University of Oxford, Oxford, United Kingdom**4. Grupo de Estado Sólido, Universidad de Antioquia, Medellín, Colombia*

Perovskite-type manganites, such as $\text{La}_{1-x}\text{Ca}_x\text{MnO}_3$ (LCMO), exhibit a variety of magneto-electronic properties depending on the concentration x . Substitution of (Ca^{2+}) ion on the La site yields the formation of Mn^{4+} in addition to the original Mn^{3+} ions. Their ferromagnetic (FM) order is caused by double-exchange (DE) via $(\text{Mn}^{3+})-(\text{O}^{2-})-(\text{Mn}^{4+})$, whereby interactions between localized spins are mediated by the hopping of itinerant electrons. In thin films, these interactions are sensitive to the preparation method and lattice mismatch, as a result competitions between orbital degrees of freedom, charge ordering and spin interaction. Doping the Mn site with Fe atoms decreases the DE and other mechanisms arise [Phys. Rev. B 77, 214430 (2008)]. In this work, the magnetic interaction between the Fe and Mn ions in $\text{La}_{2/3}\text{Ca}_{1/3}\text{Mn}_{0.97}\text{Fe}_{0.03}\text{O}_3$ (LCMFO) thin films is probed by element-selective x-ray magnetic circular dichroism (XMCD). Samples have been grown by dc magnetron sputtering on SrTiO_3 -(100) and LaAlO_3 -(100) single-crystal substrates. XMCD measurements below the FM ordering temperature under an applied field of ± 1 T at the Mn and Fe L_{2,3} absorption edges, allow determination of the contributions and relative orientations of the Mn and Fe magnetic moments. A reduction in the Mn L_{2,3} XMCD signal in the LCMFO sample compared to the parent LCMO system reveals important modifications in the magneto-electronic properties with Fe doping. The Fe L_{2,3} x-ray absorption for the LCMFO is characteristic for Fe^{3+} , and comparison with multiplet calculations [Coord. Chem. Rev. 277-278, 95-129 (2014)] suggests that the Fe dopants occupy octahedral sites in the crystal, which is consistent with Fe^{3+} substituting Mn^{3+} in LCMO. The magnetic moments of Mn and Fe are found to align antiferromagnetically, which suggests the presence of Mn-O-Fe superexchange coupling. This result is consistent with macroscopic magnetometry measurements on the LCMFO system, which show a decrease in saturation magnetization of LCMO with Fe doping.

Th.K-P25 - 360 degree magnetic domain wall injection via moving magnetic charge

J. Carter¹, D.M. Burn¹, W.R. Branford¹, L.F. Cohen¹

1. *Imperial College London*

Domain walls (DWs) in magnetic nanostructures have long been a subject of much interest¹. The majority of work so far has focused on 180 degree DWs. However, recently the field has seen promising developments in 360 degree DWs, stable topological defects consisting of two strongly-coupled 180 degree DWs of opposite chirality².

360 degree DWs have several unique properties. They are stationary under applied magnetic fields³, interact interestingly with spin-waves⁴ and have a small stray field, desirable for systems requiring high DW density⁴.

Current methods for generating 360 degree DWs rely on fabricating injection structures and applying rotating fields⁵ or current pulses⁶. These techniques are non-trivial in both device manufacture and field/current protocols.

We present a novel method for injecting 360 degree DWs into in-plane magnetised nanowires via the moving charge of an MFM tip.

Experimental evidence is presented from MFM images and supported by micromagnetic simulations. The method avoids fabricating injection structures and global field/current application. Additional benefits include localised injection via precise tip positioning and chirality selection of injected DWs.

¹ Kläui, M. – JOP: Cond. Matt. 2008

² McMichael, R.D. Donahue, M.J - IEEE Trans. Mag. 1997

³ Mascaro, M. D. Ross, C. A. – PRB 2010

⁴ Roy, P.E., Trypiniotis, T. Barnes, C. H. W. – PRB 2010

⁵ Diegel, M. Mattheis, R. Halder, E. – IEEE Trans. Mag. 2004

⁶ Oyarce, A. L., Llandro, J. Barnes, C.H.W. – APL 2013

Th.K-P26 - Crystallographical texture and coercivity in nanocrystalline thin films for magnetic recording

M. De Campos¹, J. de Castro¹, F. Sampaio da Silva¹

1. Federal Fluminense University, Niteroi, Brazil

A very important application of magnetic materials is on the thin films for magnetic recording. Miniaturization requires phases with high crystalline anisotropy as PtFe, PtCo [1] or Nd₂Fe₁₄B [2]. Perpendicular magnetic recording (PMR) [3] with textured thin films are among the possibilities for improving the areal recording density [4,5]. Relationship between magnetic properties and nanostructures as those presented by Sun et al [4] or Zhang et al [5] can be studied with the Stoner-Wohlfarth model, which predicts that a sharp (00l) texture can result in improved squareness of the hysteresis loop. Texture effects in hard nanocrystalline materials or thin films can be evaluated with the Stoner-Wohlfarth (SW) model, since the particles are single domain size and non-interacting. The texture can be introduced in the SW hysteresis by means of an experimental distribution measured by X-Ray diffraction, or theoretically by using distribution functions as Gaussian, Cauchy or Pearson VII. Any symmetrical distribution function can be used for uniaxial texture description, since it represents well the experimental texture data.

References:

- [1] J A Christodoulides, P Farber, M. Daniil, H. Okumura, G C Hadjipanayis, V. Skumryev, A. Simopoulos D. Weller. IEEE Trans. Magn.37 (2001)1292
- [2] M. Urse, M. Grigoras, N. Lupu, F. Borza, H. Chiriac. Mat. Sci. Eng. B 178 (2013) 1019
- [3] S. Iwasaki. J. Magn. Magn. Mat. 324 (2012) 244
- [4] A C Sun, F T Yuan, Jen-Hwa Hsu. Journal of Physics: Conference Series 200 (2010) 102009
- [5] L. Zhang, S.-X. Xue, Z.-G. Li, Y.-P. Liu, W.-P. Chen. Applied Physics A. 116 (2014) 1257

Th.K-P27 - Nanostructured supermalloy film on ordered metallic nanohills

J.L. Palma^{1,2}, J. Denardin^{1,2}, J. Escrig^{1,2}

1. *Departamento de Física, Universidad de Santiago de Chile, Santiago, Chile*

2. *Center for the Development of Nanoscience and Nanotechnology, CEDENNA, Santiago, Chile*

Supermalloy thin films deposited by sputtering onto nanostructured non-magnetic metals were prepared following replica-antireplica process based on porous alumina membrane. Using a high deposition rate during deposition of the non-magnetic metal on the Al pattern, we have separated the two metallic surfaces and, thus, imprinted a pattern of nanohills on a non-magnetic metallic film (such as Au, Ag or Cu). The morphology of the nanostructured Supermalloy films on ordered metallic nanohills was determined by scanning electron microscopy. Thus, we have confirmed that the ordering degree of the Al template remained after the replication and coating processes. The room temperature magnetic behavior of these thin films is also studied. Interestingly, we have found that when the external magnetic field is applied perpendicular to the substrate, the coercivity increases linearly as we increase the radius of the nanohills. These soft magnetic films can open new opportunities for magnetic field sensor applications. The authors acknowledge financial support from Fondecyt under projects 1150952, 1140195 and 3130393, and the Financiamiento Basal para Centros Científicos y Tecnológicos de Excelencia, under project FB0807.

Th.K-P28 - Interplay between of “ice-rule” and external magnetic field in inverse opal-like structures

A. Mistonov^{1,2}, I. Shishkin^{1,2}, I. Dubitskiy^{1,2}, N. Grigoryeva¹, A. Heinemann³, N. Sapoletova⁴, K. Napolskii⁴, A. Eliseev⁴, S. Grigoriev^{1,2}

1. Saint Petersburg State University, Saint Petersburg, Russia
2. Petersburg Nuclear Physics Institute, Saint Petersburg, Russia
3. Helmholtz Zentrum Geesthaht, Geesthacht, Alemania
4. Moscow State University, Moscow, Russia

We study magnetic properties of inverse opal-like structure (IOLS) based on Co. It was prepared by templating technique: the voids of face-centered-cubic (fcc) opal, which was constructed of 590 nm microspheres, were filled with Co by an electrochemical crystallization. Then, the microspheres were dissolved in toluene and free-standing ferromagnet net was obtained. The IOLS is built of unit elements, consisting of three parts: two quasitetrahedra and one quasicube with concave faces. These parts are connected by vertices along 111 directions of fcc structure. The IOLS are interesting as a 3D nanoscale analogue of spin-ice. In analogy to the “spin ice rule”, the magnetic flux conservation law for the elements of the IOLS must be fulfilled. Previously, on this basis we have developed a model for the distribution of magnetization vectors along 111 axes within the IOLS. In this work we have performed neutron small angle diffraction experiment in attempt to verify the model. During the experiment external magnetic field was directed along [111], [100] and [121] axes. Magnetic scattering intensities as a function of the field for the Bragg peaks of 202-family have been obtained. A difference between the curves for these geometries can be explained, in terms of different scenarios of the interplay between of the “ice-rule” and the field. In the first one, the field competes to the “ice-rule”, and the situation (3-in-1-out) arises, when the magnetic field breaks the ice-rule. In the second geometry the “ice-rule” and magnetic field interfere constructively, because the “ice-rule” is fulfilled, when all vectors have positive projections on the field direction, thus minimizing the Zeeman energy. In the third geometry, when one vertex is perpendicular to the field (i.e. does not depend on it), possible magnetic configurations in the IOLS are determined by the “ice-rule”.

Th.K-P29 - Effect of disorder on the magnetic and electron-transport properties of a prospective spin gapless semiconductor CoFeCrAl

P. Kharel^{1,2}, W. Zhang^{2,3}, R. Skomski^{2,3}, S. Valloppilly², Y. Huh¹, R. Fulglsby¹, S. Gilbert¹, D.J. Sellmyer^{2,3}

1. *South Dakota State University, Brookings, United States*

2. *University of Nebraska, Lincoln, United States*

3. *Department of Physics and Astronomy, University of Nebraska, Lincoln, United States*

Spin gapless semiconductors (SGS) exhibit electronic band properties similar to those of half-metallic magnets and zero-gap semiconductors. This unique combination of electronic band structures leads to several remarkable properties such as high spin polarization (100%) of both the electrons and holes and voltage-tunable spin polarization [1]. However, these properties are hindered by structural disorder in these compounds. We have investigated experimentally and by model calculations the structural, electronic, and magnetic properties of CoFeCrAl alloy in a cubic Heusler structure to understand how the magnetic and electron-transport properties are affected by the structural disorder. Our rapidly-quenched samples are polycrystalline and show a weak B2-type structural disorder. These samples are ferrimagnetic at room temperature with a Curie temperature of about 456 K, which increases to 540 K after vacuum annealing at 600 °C for 2 hours. The samples annealed at and above 650 °C show a clear signature of two-sublattice ferromagnetism. The saturation magnetization of the as-quenched sample is 1.9 μ_B /f.u., which increases to 2.1 μ_B /f.u. after annealed at 600 °C for 2 hours. The resistivity shows a nearly linear decrease with increasing temperature, from about 930 $\mu\Omega\text{cm}$ at 5 K to about 820 $\mu\Omega\text{cm}$ at 250 K, with $d\rho/dT$ of about $-5 \times 10^{-7} \Omega\text{cm/K}$. We explain this high resistivity and its temperature dependence as imperfect spin-gapless semiconducting behavior, with a negative band-gap parameter of 0.2 eV. This research is supported by Supported by US DOE-BES.

1. X. L. Wang, Phys. Rev. Lett. 100, 156404 (2008).

Th.K-P30 - Control of PEDOT orientation in conductive polymer PEDOT:PSS Film through the magnetic effects on oxygen and nitrogen gasM.A. Guziak¹, K. Hashimoto², T. Nishizaki³, Y. Honma², K. Watanabe², T. Sasaki²

1. Faculty of Science, Kagoshima University, Kagoshima, Japan

2. Institute for Materials Research, Tohoku University, Sendai, Japan

3. Faculty of Engineering, Kyushu Sangyo University, Fukuoka, Japan

Poly(3,4-ethylenedioxythiophene):poly(4-styrenesulfonate) (PEDOT:PSS), due to high electrical conductivity, visible light transparency, low cost processing and flexibility is a potential candidate for indium tin oxide (ITO) replacement. Based on the recent structural model, existence of nano-crystalline PEDOT grown in highly conductive PEDOT:PSS film, and correlation between PEDOT nano-crystallization and electrical conductivity had been reported [1]. The focus of this research is the control of PEDOT:PSS structure by means of magnetic field utilization in the course of the PEDOT:PSS film fabrication.

The solid films of PEDOT:PSS were prepared from the PEDOT:PSS aqueous dispersion (Clevios PH1000, Heraeus). For the film fabrication, a superconducting magnet was used at the maximum homogeneous field $H(0\text{mm})=10\text{T}$ and the maximum magnetic force $|H \cdot (dH/dx)|$ $H(90\text{mm})=7.5\text{T}$ in air and under N_2 and O_2 gas flow (1000 ml/min). To evaluate orientation of the PEDOT nano-crystals, polarized optical reflectivity was measured at room temperature by using a FT-IR and NIR-UV-Visible spectrometers.

Polarized infrared reflectivity spectra show Drude response with the plasma edges at the frequencies ω_p with polarization direction E being parallel to the x ($E//x$, $//H$) and y ($E//y$, $\perp H$) directions. The plasma frequency of the films fabricated under 7.5T shifts to larger ω_p of 7900 (N_2) and 9000 cm^{-1} (O_2) for $E//x$ ($//H$), but remains unchanged $\sim 7200 \text{ cm}^{-1}$ for $E//y$ ($\perp H$). On the other hand, ω_p of the films fabricated in the air, shows somewhat reverse behavior, 7200 cm^{-1} for $E//x$ ($//H$) and 8400 cm^{-1} for $E//y$ ($\perp H$). The films fabricated under 10T, shows almost no ω_p anisotropy. Independently on condition and direction, almost the same values of $\omega_p \sim 7800 \text{ cm}^{-1}$ are observed for the films fabricated at 0T. We expect that the anisotropy of ω_p arises from orientation of the PEDOT nano-crystals in these films.

[1] T.Takano et al., *Macromolecules* 45, 3859 (2012)

Th.K-P31 - Magnetic properties of Co/Pd multilayers deposited on alumina membranes.

J. Denardin¹, D. da Rosa², L. Dorneles², L. Schelp²

1. *Universidad de Santiago, Santiago, Chile*

2. *Universidade Federal de Santa Maria, Santa María, Brazil*

Magnetic films with perpendicular anisotropy (PA) are very important in the recording industry and as magnetic sensors. The research and potential applications of nano-patterned PA films is still more exciting, since the patterns can have length scales similar to the domain-wall widths and can be tailored to limit the domain-wall movements. Among the ways to produce nanostructured films, anodized alumina templates (AAO) have emerged as a low cost, simple and effective method for obtaining large areas of nano-patterns. Films deposited on top of AAO membranes with pores of different diameter and on the bottom of AAO membranes, forming bumps, shows different magnetic reversion mechanisms and can be interesting in basic and applied research in magnetism. In this work the magnetization reversal of Co/Pd multilayers deposited on different nanostructured substrates are investigated by magnetization curves, extraordinary Hall Effect and magnetic force microscopy (MFM) experiments. The magnetization curves of a Co/Pd film deposited on glass substrates shows a clear out of plane anisotropy, with $M_r = M_s$ and a two-step magnetization reversal. In the Co/Pd multilayers deposited on top of AAO membrane the coercivity and remanence are large in both in plane and out-of-plane directions, indicating a completely different mechanism of magnetization reversion than in the continuous film. From the MFM images of the continuous film it is possible to observe large stripe magnetic domains, while the MFM images for the film deposited on top of AAO membrane shows magnetic domains that are smaller and clearly pinned by the nanoporous membrane.

Th.K-P32 - Micromagnetic investigation of planar hall effect sensors for magnetic nanobeads detection

I. Firastrau¹, E. Helerea¹, M. Avram², M. Volmer¹

1. *Transilvania University of Brasov, Department of Electrical Engineering and Applied Physics, Brasov, Romania*

2. *National Institute for Research and Development in Microtechnologies, Bucharest, Romania*

Development of modern medicine led to exponential growth in demand of high sensibility magnetic field sensors, devoted to manipulation, detection and characterization of magnetic nanobeads (superparamagnetic nanoparticles) in a microfluidic system. In this context, Planar Hall Effect (PHE) sensors have gained much attention because of the high thermal stability, high field sensitivity, and low noise of the output signal. A superparamagnetic nanoparticle placed on the sensor surface generates a magnetic field that can modify the configuration of magnetic moments inside the ferromagnetic material of the sensitive layer of the sensor. In our study, the superparamagnetic nanoparticles were magnetised by an external magnetic field which can be (i) applied in the film plane or (ii) perpendicular to the film plane. Additionally, we have considered a biasing field, applied in the film plane, along the driving current, to have a better control of the linearity and sensitivity of the sensor. Using this setup, we performed full 3D micromagnetic simulations in order to investigate the magnetization dynamics of the PHE sensors in the presence of a magnetic nanoparticle. Three sensors geometries have been taken into account: cross-shaped, disk-shaped and ring-shaped structures. The sensitive layer made from Permalloy, 10-20 nm in thickness, has micrometric in-plane dimensions. The direction of the uniaxial magnetocrystalline anisotropy is parallel to the polarizing field. For each type of structure we determined a biasing field for which the maximum detection sensitivity is achieved. The micromagnetic analysis reveals, also, that the setup with the applied field perpendicular to the film plane can assure the best detection sensitivity and linearity which is confirmed by our experiments.

Acknowledgements: We wish to acknowledge the assistance and support of CNCSIS-UEFISCDI from Romania by the project PNII-PCCA, no. 2/2012

Th.K-P34 - Alternating target laser ablation deposition of Cu doped cobalt ferrite thin filmsG. Bulai¹, S. Gurlui¹, P. Rao², O. Florin Caltun¹

1. Faculty of Physics, Alexandru Ioan Cuza University, Iasi, Romania

2. Andhra University, Department of Physics, Visakhapatnam, India

Cobalt ferrite thin films are used in magnetic data storage, sensors, actuators, wave guides applications due to their interesting magnetic properties (e. g.: moderate saturation magnetization, high coercive field, large magnetostrictive coefficient and high magneto-crystalline anisotropy generated by the strong L-S coupling of the predominantly B-sited coordinated Co²⁺ ions). Copper substitutions in various typed of ferrites was reported to enhance the magnetic properties, increase the cell parameter and decrease the Curie point. The aim of this study was to compare the structural and magnetic properties of the Cu doped cobalt ferrite films obtained by pulsed laser deposition (PLD) and by alternating target laser ablation deposition (ATLAD) using CoFe₂O₄/Cu targets. For the typical PLD deposition process, various target with chemical Co_{1-x}Cu_xFe₂O₄ (x=0-0.5, 0.1 step) were synthesized using standard powder ceramic technique. The Fe₂O₃, Co₃O₄, MnO₂ and Cu₂O₃ oxide powders were mixed in the targeted proportions, ball milled for 5 h and calcined in air at 950 oC for 5 h. The final sintering step was done at 1250 oC for 2 h. For ATLAD deposition we used a stoichiometric cobalt ferrite sample obtained in the same conditions as detailed above and a pure copper target. The concentration variation was achieved by modifying the number of laser pulse incidence upon each target. The other experimental parameters such as target-substrate distance (4 cm), deposition time (60 min), pressure (~10-5 Torr) and substrate temperature (400 oC) were mentained at the same values. The structural and chemical properties of the obtained films were studied by X-ray diffraction, scanning electron microscopy/energy dispersive X-Ray spectroscopy and Raman spectroscopy while the magnetic response was investigated using a vibrating sample magnetometer. The study revealed the influence of copper doping level on thin film properties and large differences in structural characteristics induced by PLD and ATLAD techniques.

Th.K-P35 - Tailoring magnetism, magnetoresistance and interactions of nanostructured ZnO-Co films

X. Li¹, Y. Gao¹, J. Li¹, J. Jia¹, Y. Li¹, G.A. Gehring², X. Xu¹

1. Key Laboratory of Magnetic Molecules and Magnetic Information Materials of Ministry of Education and School of Chemistry and Materials Science, Shanxi Normal University, P. R. China

2. Department of Physics and Astronomy, University of Sheffield, Sheffield, United Kingdom

Extensive studies of the magnetoresistance (MR) in heterogeneous structures including ferromagnetic metal/semiconductor have been performed with a view of potential spintronic applications[1-3]. Amorphous films of ZnO containing nanoparticles of cobalt metal deposited at room temperature (RT) have small nanoparticles giving a blocking temperature (T_b) at about 20K whereas the T_b is above RT for films deposited at 400 oC, which implies that the films contain large Co nanoparticles. We study structures that combine layers with large and small nanoparticles with a ZnO spacer layer in order to utilise the coupling between the magnetic ZnO-Co layers. The bottom ZnO-Co layers were firstly deposited by magnetron sputtering at substrate temperature (T_s) of 400 oC. And when the T_s was cooled down to RT, ZnO space layers and the top ZnO-Co layers were deposited by the same method. The results show that the resistance of the ZnO-Co/ZnO/ZnO-Co trilayer sample can be considered to be a result of a parallel combination of top, bottom ZnO-Co layers, and ZnO space layer. The top ZnO-Co layer can couple with the bottom one. And the strength of the interactions can be tuned by the thickness of the ZnO space layers. Accordingly, the MR and magnetic properties are dramatically changed. Moreover, the MR of the ZnAlO-Co/ZnO/ZnO-Co sample is much larger than that of the ZnO-Co/ZnO/ZnO-Co, which implies that doping Al in ZnO of top ZnO-Co layer can dramatically enhance MR of the sandwich samples. This study is helpful to make sense the MR and interactions thus making nanostructured ZnO-based films more suitable for applications in spintronics.

The authors are grateful for the supports from NSFC (No. 51025101, 11274214, 61306109), 863 Program of China (No. 2014AA032904), and PRS of Shanxi (No. 2014-044).

[1] M. N. Baibich, J. M. Broto, et al., Phys. Rev. Lett. 61, 2472(1988)

[2] Z. Y. Quan, X. P. Zhang, et al., A.C.S Appl Mater. Interfaces 5, 3607 (2013)

[3] C. Song, X. J. Liu, et al., Appl. Phys. Lett. 91, 042106 (2007)

Th.K-P36 - Role of substrate morphology on magnetic properties of FePd thin alloy film

A. Zarzycki¹, A. Maximenko¹, M. Perzanowski¹, M. Krupinski¹, M. Marszalek¹, B. Jany², F. Krok²

1. *The Henryk Niewodniczanski Institute of Nuclear Physics Polish Academy of Sciences, Krakow, Poland*

2. *Marian Smoluchowski Institute of Physics, Jagiellonian University, Krakow, Poland*

The study concentrates on magnetic properties of L10 FePd alloy films deposited on U-shape nanopatterned substrates. The U-shape structures were formed with modified anodization process leading to the creation of nanopatterned aluminum foil with thin oxide layer on the top. Such substrates have U-shaped bowl-like structure with protruding elements at cavity edges. They show long range spatial order and have diameters varying between 60 nm and 400 nm. The L10 FePd alloys were prepared by sequential deposition of Fe and Pd multilayered system with appropriate stoichiometry and the total thickness equal to 1/8 of the U-shape diameter. The as deposited multilayers were transformed to L10 phase by annealing in vacuum at elevated temperatures (500-600 C). The magnetic characterization of obtained samples, studied with SQUID magnetometer, was supplemented with SEM and AFM/MFM measurements. The easy axis of magnetic anisotropy in all studied cases was in plane of the sample. The change of U-shape diameter from 400 nm to 60 nm resulted in the decrease of coercive field. However, the saturation field for out-of-plane geometry was smaller than for continuous films on flat substrates, indicating the role of complicated morphology of patterned samples observed in microscopy images.

Th.K-P37 - Hard/soft bilayer thin films and antidots

F. Béron¹, A. Kaidatzis², R.P. del Real³, D. Niarchos², K.R. Pirota¹, J.M. García-Martín⁴

1. *Universidade Estadual de Campinas, Campinas, Brazil*

2. *National Center for Scientific Research (NCSR) – Demokritos, Attiki, Greece*

3. *Instituto de Ciencia de Materiales (CNM-CSIC), Madrid, Spain*

4. *Instituto de Microelectrónica de Madrid (CNM-CSIC), Madrid, Spain*

Exchange coupled hard/soft bilayer thin films can be used as model systems to study the properties of exchange-spring magnets. Moreover, the inclusion of artificial defects such as nanoholes (also called antidots) helps to engineer their magnetic properties. As a result, the magnetic anisotropy, the coercivity and the remanence can be tailored by modifying the antidot diameter, the separation among them and the film thickness. In this work, bilayers of 20 nm-thick Co with 10 to 30 nm-thick Permalloy (Py) thin films and protected with 5 nm-thick Pt were fabricated by DC sputtering in a UHV system with rotating substrate to avoid any preferential direction. For comparison, the magnetic systems were prepared both in thin films and in antidots morphologies, using thermally oxidized silicon and nanoporous alumina templates as substrates, respectively. For the antidots, small (35 nm diameter, 105 nm interpore distance) and large (175 nm diameter, 275 nm interpore distance) pores geometries were compared.

In-plane magnetostatic characterization obtained by means of VSM and NanoMOKE showed that the bilayers were coupled for the Py thickness range investigated. However, careful analysis done via first-order reversal curve (FORC) technique evidenced that the coupling is worsening as the Py thickness increases, with the apparition of an additional irreversible distribution. Both local and global coercivities decrease with Py thickness, with the values for the antidots always being larger than those of the continuous films.

Th.K-P38 - Synthesis and characterization of PLD CoFe thin films as a function of composition and deposition conditions

D. Peddis¹, G. Barucca², G. Varvaro¹, A.M. Testa¹, P. Mengucci², E. Agostinelli¹, S. Laureti¹

1. ISM-CNR, Area della Ricerca RM1, Monterotondo Scalo, Roma, Italy

2. SIMAU, Università Politecnica delle Marche, Ancona, Italy

Nowadays, the emerging technologies based on spintronics devices, driven by the increasing demand for miniaturization, require a strict monitoring of the physical properties of the materials used in the spin-valve structures, which play a key role in the functioning of the GMR-TMR [1]. Among the magnetic materials used as electrodes in the spin-valve structures, the magnetically soft CoFe-based alloy, characterized by high saturation magnetization and high Curie temperature, showed the best magnetoresistive response in TMR systems with in-plane anisotropy [1]. However, the magnetic behaviour results to be strictly dependent on both composition and microstructural features of the alloy. In this work, we present a study of thin films of CoFe with 50:50 and 75:25 compositions deposited on MgO substrate by Pulsed Laser Deposition.

The effect of the deposition temperature on the crystallographic orientation is determined by means of XRD and HRTEM analysis and correlated with the anisotropic properties measured by angle dependent hysteresis loops. All the films showed a granular structure with a high degree of crystallographic order even at the lowest deposition temperature. The cubic symmetry is reflected in the angular dependence of remanent magnetization, showing a four-fold character, whose in-plane distribution is consistent with the different crystallographic orientation of the films.

This work is supported by MIUR, under project FIRB2010 - NANOREST

[1] S.S.P. Parkin et al., Nature Mater. 3 (2004) 862

Th.K-P41 - Soft X-Ray magnetic circular dichroism studies on magnetic transition metal oxide nanostructures

E. Pellegrin¹, C. Ge^{2,3}, Z. Hu⁴, S. Agrestini⁴, S.M. Valvidares¹, J. Herrero Martin¹, P. Gargiani¹, A. Barla⁵, X. Wan², W. Liang⁶

1. *Cells-Alba, Cerdanyola del Valles, Spain*
2. *Nanjing University, Nanjing, China*
3. *Jiangsu Institute of Education, Nanjing, China*
4. *Max Planck Institute for Chemical Physics of Solids, Dresden, Germany*
5. *Istituto di Struttura della Materia, ISM CNR, Trieste, Italy*
6. *National Chiao Tung University, Hsinchu, Taiwan*
7. *National Taiwan University, Taipei, Taiwan*

The inverse spinel system CoFe_2O_4 can be considered as a paradigmatic material for the study of magnetic transition metal oxides. The more recent advent of self-assembled perovskite-spinel structures has now opened new possibilities for the engineering of previously inaccessible functionalities, among others by making use of the ferromagnet-antiferromagnet interface coupling of nano-objects with an enhanced surface-to-volume ratio such as the above CoFe_2O_4 nano-pillars. The well-known “classical” core-shell particle systems may serve as another example for these interface-driven magnetic materials. We have investigated two different nanostructured transition metal oxide systems: (i) CoFe_2O_4 nano-pillars in BiFeO_3 and (ii) Co/CoO-MgO core/shell nanoparticles in MgO using soft x-ray magnetic circular dichroism (XMCD), SQUID magnetometry, and transport measurements. Single-crystalline CoFe_2O_4 has also been investigated as a bulk reference material. The results from the XMCD data indicate the importance of microscopic mechanisms such as local distortions (e.g., of CoO_6 octahedra in CoFe_2O_4 nano-pillars) as well as magnetic interactions across the ferr(i/o)magnetic/antiferromagnetic interfaces (based on the uncompensated spin model) for the bulk magnetic properties.

Th.K-P43 - Lattice effects on the magnetic and magnetoresistance properties of nanometer-Thick $\text{La}_{0.9}\text{Ba}_{0.1}\text{MnO}_3$ (LBMO) Films and LBMO/ BaTiO_3 / LBMO Heterostructures

S. Pegah Mirzadeh Vaghefi¹, M. Georg Willinger², A.A. Cardoso dos Santos Lourenço¹, V. Brás de Sequeira Amaral¹

1. *Department of Physics & CICECO, University of Aveiro, Aveiro, Portugal*

2. *Fritz Haber Institute, the Max Planck Society, Department of Inorganic Chemistry, Berlin, Germany*

We have fabricated $\text{La}_{0.9}\text{Ba}_{0.1}\text{MnO}_3$ (LBMO) thin-films and LBMO/ BaTiO_3 /LBMO (LBMBT) heterostructures, using UHV RF magnetron sputtering technique, on oriented single crystalline (100) silicon and (0001) Al_2O_3 substrates. A number of complementary methods, such as X-ray diffraction, cross section transmission electron microscopy, Piezoresponse force microscopy, magnetoresistivity and SQUID magnetometry were used to characterize local and in-depth structure features, also their physical properties.

TEM studies shows the stressed layer of LBMO on different substrates, including the BaTiO_3 thin-film in heterostructures. The different growth condition in depositions created polycrystalline structure of the films. The thicknesses of the films on Al_2O_3 , Si are 70 and 145 nm and for heterostructures are 40/30/40 nm. The mismatch between substrate and film is 0.82% for Si and 13.58% for Al_2O_3 substrate. The magnetic transition temperature (T_c) of the LBMO film on the Si and Al_2O_3 substrates are found to be 197K and 210K, respectively, slightly higher than the bulk form, 185K. The T_c of the heterostructure on silicon substrate, measured in SQUID, shows resemblance with the single layer LBMO, at 200K, while the magnetoresistance measurements shows a surprising change in transition temperature, at 250K. Local electric poling of the heterostructures was done by PFM, along with local piezoelectric hysteresis measurements to modify the nearby ferroelectric areas via the mechanical stress and field effects. Using different voltages, ranging +/-10 V to +/-30 V, one can detect electric field-induced deformation at a nanoscale and confirm the ferroelectric state of the BTO layer.

It is important to note the strain related behavior of the grown film with the substrates and the ferroelectric BaTiO_3 thin-layer, between two LBMO layers. This strain is found to influence the magnetic properties and magnetoresistive behavior of the grown film and heterostructures.

This work was developed within the project CICECO-Aveiro Institute of Materials (Ref. FCT UID/CTM/50011/2013).

Th.K-P44 - Thermal dependencies of the magnetic symmetries of low dimensionality systems, studied with novel variable temperature/full angular range vectorial MOKE technique

J.L.F. Cuñado ^{1,2}, J. Pedrosa ², F. Ajejas ¹, A. Bollero ², P. Perna ², F.J. Terán ², R. Miranda ^{1,2}, J. Camarero ^{1,2}

1. Departamento de Física de la Materia Condensada and Instituto Nicolás Cabrera, Madrid, Spain

2. Instituto Madrileño de Estudios Avanzados IMDEA nanociencia, Madrid, Spain

Magneto-optical Kerr effect (MOKE) magnetometry is one of the most widely used techniques for the characterization of magnetic nanostructures. MOKE presents high sensitivity (down to nanometer thickness), vanishing substrate effects (limited penetration depth), immunity to external fields (photon-in/photon-out approach), and relatively simple experimental implementation. We present a new versatile full angular resolved / broad temperature range / vectorial MOKE instrument, capable of probing qualitatively and quantitatively the temperature and angular dependencies of magnetization vector during the reversal processes. Quantitative studies are only possible if the apparatus can work without the need to make any manual intervention on it. The setup combines a cryostat with a vectorial v-MOKE bench. Its optical access to a motorized rotatable sample holder with azimuthal correction allows for measuring at different temperatures from 4 K up to 500 K and in the whole angular range without neither changing magnet orientation nor opening the cryostat. The measuring process is fully controlled by software. Measurements performed in a model system with competing collinear biaxial and uniaxial contributions are presented to illustrate the set-up capabilities. The temperature dependence of the effective magnetic anisotropy as well as its influence on relevant magnetic parameters are shown. The set-up provides direct views on magnetization reversal processes and magnetic transitions, unravelling magnetic symmetry effects of magnetic nanostructures.

Th.K-P46 - Sub-50 nm magnetic tunnel junctions fabrication by reactive ion etch on 150 mm wafers

A. Moskaltsova^{1,2}, S. Knudde^{1,2}, A.V. Silva^{1,2}, D.C. Leitao^{1,2}, P.P. Freitas^{1,3}, S. Cardoso^{1,2}

1. *Instituto de Engenharia de Sistemas E Computadores-Microsistemas E Nanotecnologias, Lisbon, Portugal*

2. *Department of Physics, Instituto Superior Técnico, Universidade de Lisboa, Lisbon, Portugal*

3. *INL - International Iberian Laboratory, Av. Mestre Jose Veiga, Braga, Portugal*

Today, magnetic tunnel junctions (MTJs) with tunnel magnetoresistance higher than 150% are widely used as MRAM elements and sensing devices [1]. However, efforts have been done towards reducing dimensions of the critical features towards 30nm, integrated on larger area wafers. Here we focus on MTJs nanometric pillars fabrication using Reactive Ion Etch (RIE) [2-3]. Besides material selectivity, it has shown improved wafer uniformity, being a relatively fast process, with oxide etch rates $\sim 1\text{nm/s}$. MTJs circular nanopillars were defined using electron beam lithography (EBL) and ion milling etching, with sizes from 100nm to 30nm. A thick (50 nm) metal cap layer was used to avoid damaging the free layer. A 300 nm SiO₂ layer insulated the top and bottom electrodes. With such a thick oxide becomes challenging to establish a robust electrical contact to the nanopillar. Access to nanopillars was performed by RIE with CF₄ and controlled by atomic force microscopy. Surface scans show difference in oxide thicknesses with an etch rate of $\sim 0.5\text{nm/s}$ inside $2\mu\text{m}^2$. To further extend the RIE based nanofabrication process for large area wafers, micrometric test pillars were firstly fabricated in 150 mm substrates with the following MTJ stack Si/SiO₂/Ru 40/MnIr 18/CoFe 3/ Ru 0.84/CoFe 3/Al 9+20s oxidation/CoFe 3/Ru 40 (nm). Test structures were devised and included in order to monitor RIE end point (e.g. micrometric pillars array) and map uniformity of the several steps during microfabrication over large area wafer. Transfer curves yielding 80% of working devices, square response (3.5 mT switching field) and expected resistance values (300 Ω) for RA product of $2\text{k}\Omega\mu\text{m}^2$.

[1] Ikeda et al. Appl. Phys. Lett. 93, 082508 (2008)

[2] XUE et al. IEEE TRANS. ON MAG. 50 (2014)

[3] T. Wahlbrink et al. Microelectronic Engineering 78-79 (2005) via and $\sim 0.8\text{nm}$ for larger pads.

Th.K-P47 - Enhancement of order degree and perpendicular magnetic anisotropy of L10 ordered Fe(Pt,Pd) alloy film by introducing a thin MgO cap layer

Y. Noguchi¹, M. Ohtake¹, M. Futamoto¹, F. Kirino², N. Inaba³

1. Chuo University, Japan

2. Tokyo University of the Arts, Taito, Japan

3. Yamagata University, Yamagata, Japan

FePt ordered alloy with L10 structure shows K_u greater than 10^7 erg/cm³ and the films have been investigated for HDD media and MRAM device applications. When an L10 film is formed on a (001)-oriented underlayer or substrate, the film may involve (100) crystal with the c-axis lying in the film plane in addition to (001) crystal with the c-axis perpendicular to the substrate surface. In the last Intermag conference, we reported a possibility in controlling the c-axis of FePt crystal perpendicular to the substrate surface by employing a thin MgO cap layer. In order to control the magnetic properties, replacement of Pt site in FePt structure seems useful. In the present study, 10-nm-thick Fe₅₀(Pt_xPd_{1-x})₅₀ (at.%, $x=0-1$) films with and without 2-nm-thick MgO cap layers are prepared on MgO(001) substrates by using a two-step method consisting of deposition at 200 °C followed by annealing at 600 °C. The structural and magnetic properties are investigated by RHEED, XRD, and VSM. For the investigated compositions, L10 ordered single-crystal films with the c-axis perpendicular are obtained for the samples with MgO cap layers, while crystals with the c-axis lying in-plane are included for the samples without cap layers. The values of order degree, S , estimated for the films of $x=0, 0.25, 0.5, 0.75, 1$ with and without cap layers are (0.7, 0.6), (0.7, 0.5), (0.6, 0.4), (0.7, 0.4), and (0.8, 0.6), respectively. The data show that the films with cap layers show higher order degrees and that S value becomes minimum around the Fe₅₀Pt₂₅Pd₂₅ composition. The films with cap layers show very small in-plane coercivities less than 0.8 kOe, whereas those without cap layers show coercivities around 1 kOe. An employment of MgO cap layer is effective in controlling the c-axis perpendicular, achieving higher order degree, and thus enhancing the perpendicular magnetic anisotropy.

Th.K-P48 - Magnetisation reversal in Co nanoparticle arrays on corrugated MnF₂(110) surface

S. Gastev¹, B. Krichevtsov¹, D. Baranov¹, V. Fedorov¹, S. Suturin¹, N. Sokolov¹, J.L.F. Cuñado^{2,3}, A. Bollero², J. Camarero^{2,3}

1. *Ioffe Institute, St.Petersburg, Russia*

2. *IMDEA-Nanociencia, Campus deCantoblanco, Madrid, Spain*

3. *Dpto.Física Materia Condensada & Ins. Nicolás Cabrera, UAM, Madrid, Spain*

Identifying the mechanism of magnetization reversal is the main objective of the study the properties of magnetic materials. The use of magneto-optical Kerr effect (MOKE) to accomplish this task proved to be extremely effective. In this work we applied the longitudinal Kerr effect for different orientation of in-plane magnetic field and Kerr microscopy for study of magnetization switching in Co(X nm)/ MnF₂ / CaF₂ / Si (001) epitaxial structures with X from 2 to 7 nm. Co layer represents an ensemble of nanoparticles grown on corrugated surface of MnF₂ / CaF₂ / Si (001) substrate. The magnetization vector (M) in these structures is oriented in-plane. The easy axis of magnetization (EA) is along of corrugations, i.e. [1-10] crystal direction of Si(001). Magnetic field dependencies of longitudinal Kerr effect for S-polarization of incident light ($\lambda = 633$ or 405 nm) were measured for two orientations of magnetic field: along and perpendicular to the light incidence plane. This makes it possible to carry out a vectorial analysis, i.e. get information about both the magnitude and orientation of magnetization vector during the magnetization reversal. In all structures the decrease of magnetic field from saturation to zero value is followed by rotation of magnetization M from the direction of magnetic field H to direction of EA. Then the magnetization changes its sign that is followed by appearance of zero value of $|M|$. Such behavior of magnetization evidences the magnetization reversal due to domain wall (DW) movement, that is confirmed by observation of domains by Kerr microscopy for structures with $X > 3$ nm. In structures with $X = 2$ and 3 nm the domains have been not observed but the disappearance of $|M|$ indicates the DW movement also in this case. Further increase in magnetic field results in rotation of magnetization to direction of EA.

Th.K-P49 - Morphology and magnetic properties of exchange biased natively oxidized py antidot arrays fabricated on anodized porous silicon

A. Maximenko^{1,3}, C. Cirillo², A. Zarzycki¹, M. Marszalek¹, J. Fedotova³, S. Prischepa⁴

1. *The Henryk Niewodniczanski Institute of Nuclear Physics Polish Academy of Sciences, Krakow, Poland*

2. *CNR-SPIN Salerno and Dipartimento di Fisica 'ER Caianiello', Universita degli Studi di Salerno, Fisciano, Italy*

3. *Research Institute for Nuclear Problems of Belarusian State University, Minsk, Belarus*

4. *Belarusian State University of Informatics and Radioelectronics, Minsk, Belarus*

Magnetic structures with well-defined nonmagnetic porous defects acting as pinning sites for magnetic domain walls and with exchange biased interface of ferromagnetic (FM) and antiferromagnetic (AF) layers possess larger coercivity (H_c) and exchange bias fields (HEB) in comparison to the continuous and free FM structures. This makes them attractive materials for magnetic memory devices and magnetic sensors. For the first time antidot arrays (AA) consisting of FM/AF bilayers with exchange bias (EB) were fabricated on templates of anodized porous silicon (PS) and their morphology, structure and magnetic properties with respect to different pinning mechanisms are reported. Antidot diameters (d_a) and distances between them were varied by changing PS anodization regimes. FM/AF bilayers contain permalloy and capping native thermal oxide layer constituting the superposition of NiO, FeO, Fe₂O₃ originating from natural oxidation of Py surface. To determine the influence of FM/AF interface and antidot morphology on magnetic properties of the system, oxidized and non-oxidized samples were also prepared on flat Si substrate. XRR of flat oxidized samples proved formation of 1.5 nm oxide layer made of Ni and Fe oxides. The exchange bias effect was observed only at 3 K and HEB increased from -30 Oe for AA with $d_a=15$ nm to -90 Oe for AA with $d_a=30$ nm. The H_C values of AA with $d_a=30$ nm was much larger as compared to flat samples and non-oxidized AA. This indicates that two pinning mechanisms are present in this system, one related to the interface of bilayers and the second one is associated with the substrate antidot morphology. The latter is present in the broad temperature range, whereas the other exists only at 3 K confirming that the main pinning effect is governed with the antidots.

Th.K-P55 - Selective suppression of domain wall in artificial spin ice network lattice

S. Goolaup¹, C. Sekhar Murapaka¹, W. Siang Lew¹

1. Nanyang Technological University, Singapur

Observation of magnetic monopoles and other interesting thermodynamic properties has motivated recent research interest in artificial spin ice network structures. Controlling the domain wall (DW) trajectory in magnetic network structures is crucial for the study of fundamental properties like observation of magnetic monopoles at room temperature in artificial spin ice lattice. The creation and absorption of DWs at the vertex of a network structure governs the net magnetic charge and give to rise to the formation of artificial magnetic monopole. The DW trajectory in the network structure has been shown to be dependent on the DW chirality. In this work, we show that the DW trajectory can be remotely controlled or completely suppressed by introducing an elliptical nanodot near the bifurcation in the branch of a network structure. When the DW is driven through the structure, it is observed that the magnetostatic coupling between the DW and nanodot pins the DW at the bifurcation. The magnetostatic coupling arises due to the interaction between the DW stray field and edge stray field from the nanodot. With the increase in the magnetic field, the DW annihilates at the bifurcation to generate a magnetic monopole. The annihilation of the DW and the generation of the magnetic monopole follow the conservation of topological charges in the branch network structure. By varying the distance between the bifurcation and the nanodot, different magnetization reversal processes of network structures have been observed. By selectively introducing nanodots in the array of network structures, different Dirac string configurations (i.e. arm chair and staircase) can be readily realized.

Th.L-P01 - Magnetic properties of FePt-Fe nano-composites with core/ shell structure

R. Kurosu¹, H. Iwama¹, M. Doi^{1,2}, T. Shima^{1,2}, A. Kato^{3,4}, N. Sakuma^{3,4}, H. Kishimoto^{3,4}, K. Washio^{3,4}, M. Yano^{3,4}

1. Faculty of Engineering, Tohoku Gakuin University, Miyagi, Japan
2. Technology Research Association of Magnetic Materials for High-Efficiency Motors (MagHEM), Tokyo, Japan
3. Toyota Motor Corp., Aichi, Japan
4. Higashi Fuji Branch, MagHEM, Aichi, Japan

The demand of renewable and sustainable energy drives us to develop high efficient electromagnetic conversion system. In particular, the development of high performance motors consisting of rare-earth permanent magnets are strongly needed to fulfill the automotive applications such as hybrid vehicles (HVs), plug-in hybrid vehicles (PHVs) and electric vehicles (EVs). However, due to an environmental and geometrical issues, the reduction of indispensable elements from the Nd-Fe-B sintered magnets and consequently, high performance new permanent magnets are required. In this work, in order to confirm the effect of nano-composite structure and to find the optimum configuration, ring-shaped (shell-type structure) samples embedded with another magnetic materials have been investigated. L10 ordered FePt phase and bcc-Fe phase are selected as “hard” and “soft” magnetic phase, respectively. The samples were prepared by using an ultra-high vacuum magnetron sputtering system. A Fe seed layer of 1 nm and epitaxial Au buffer layer of 40 nm were grown on a MgO (100) single crystal substrate at room temperature (R.T.). The FePt layer with the thickness of 10 nm was deposited at a substrate temperature (Ts) of 225 °C. Then, the sample was annealed at Ta = 475 °C for 1 hour. The ring-shaped FePt arrays with 2.0 mm in outer diameter were microfabricated by using an electron beam lithography followed by an Ar ion milling. Then, soft magnetic Fe was deposited and embedded into the FePt rings (shells). It is confirmed that well-defined shape of the FePt rings embedded with Fe core have been successfully prepared by a multiple microfabrication process. It was confirmed that Hc of the composite sample was improved from 4.5 kOe to 8.43 kOe after post-annealing at 500 °C for 1 hour.

Th.L-P02 - Nickel nanorod/gelatin hydrogels - tracking the genesis of a hybrid material

A. Tschöpe¹, C. Schopphoven¹, K. Birster¹, R. Birringer¹

1. Saarland University, Saarbrücken, Germany

Magnetic hybrid materials composed of ferro- or superparamagnetic particles dispersed in a soft-elastic matrix feature large changes in shape and/or elastic properties by remote magnetic stimulation. Their response depends on the applied field (homogeneous, inhomogeneous), the magnetic properties (ferro-/superparamagnetic) and spatial arrangement (textured, homogeneous) of the nanoparticles and essentially on the magneto-mechanical coupling between the particles and the non-magnetic matrix. The latter aspect is closely related to the chemical and mechanical interaction between the inorganic inclusion and the polymeric network.

The objective of the present study was to investigate the evolution of the magneto-mechanical coupling between ferromagnetic nickel nanorods and gelatin hydrogels in the course of physical or chemical gelation. For this purpose, we prepared nickel nanorods with diameters of 20 nm and average length in the range of 200-1000 nm by the AAO-template method. The nanorods were released from the template and dispersed in gelatin solutions in the semi-dilute range. We took advantage of the uniaxial ferromagnetic single domain state and the optical anisotropy of the nanorods by using them as probe particles for microrheometric characterization of their local hydrodynamic properties. Magneto-optical measurements in static and dynamic fields revealed strong chemical interaction in terms of gelatin adsorption in the sol state as well as progressive trapping of the nanorods in the polymer network during gelation.

Th.L-P03 - Domain wall pinning driven by nanoscale phase coexistence in Ni/V₂O₃ bilayers

A.F. Rodríguez¹, I. Valmianski², M. García del Muro¹, J.G. Ramírez², F. Kronast³, I.K. Schuller², A. Labarta¹, X. Batlle¹

1. *Dpt. Física Fonamental and Institut de Nanociència i Nanotecnologia (IN2UB), Universitat de Barcelona, Barcelona, Spain*

2. *Department of Physics and Center for Advanced Nanoscience, University of California San Diego, La Jolla, United States*

3. *Helmholtz-Zentrum Berlin für Materialien und Energie, Berlin, Germany*

Nanoscale manipulation of thin film magnetic properties can be achieved through proximity effects in bilayer or multilayer structures. For example, the proximity of a ferromagnetic (FM) film with a vanadium oxide results in a reversible modification of the magnetic properties due to the magnetoelastic anisotropy contribution caused by the interfacial stress [1]. Recently, large changes in coercivity and noticeable modifications of the magnetization in Ni/V₂O₃ bilayers across the structural phase transition (SPT) of V₂O₃ have been reported [1,2].

In this work, we combine photoemission electron microscopy (PEEM) with X-ray magnetic circular dichroism (XMCD) to map the temperature-driven variation of the FM domain structure of Ni (10 nm-thick) across the SPT of V₂O₃ (100 nm-thick) deposited onto a r-plane sapphire substrate. Upon crossing the SPT, the initial FM saturated state splits into a pattern of small domains with opposite orientation. The fraction of such inverted domains monotonically grows across the SPT with the predominance of one of the coexisting structural phases. The domain nucleation sites are randomly distributed across the sample for several image series, indicating that the domains are not pinned by structural defects. The analysis of the domain nucleation and growth across the SPT indicates a distribution of local transition temperatures across the sample. Furthermore, we study the lateral correlation length of the inverted domains using a radial distribution function analysis from the images.

This work was supported by MINECO (MAT2012-33037), DURSI (2009SGR856, 2014SGR220), European Union FEDER funds (Una manera de hacer Europa), and the US-DOE grant number DE-FG02-87ER-45332. A.F.R. acknowledges support from the MICIIN "Ramón y Cajal" Programme.

[1] J. de la Venta, S. Wang, J. G. Ramirez, and I. K. Schuller, *Appl. Phys. Lett.* 102, 122404 (2013)

[2] J. de la Venta et al, *Appl. Phys. Lett.* 104, 062410 (2014)

Th.L-P04 - Magnetic and microstructural investigation of $\text{Fe}_{79.7-x}\text{Ti}_x\text{B}_{20}\text{Nb}_{0.3}$ glassy alloys for hyperthermia applicationN. Lupu¹, L.C. Whitmore¹, G. Ababei¹, M. Grigoras¹, H. Chiriac¹*1. National Institute of Research and Development for Technical Physics, Iasi, Romania*

Nowadays, the use of self-regulating magnetic hyperthermia for curing cancer appears to be an extremely viable alternative. Now Fe oxides nanoparticles with superparamagnetic behavior (SPIONs) are extensively used in clinical tests involving magnetic hyperthermia. As an alternative to SPIONs, we have developed a new type of ferromagnetic material, with the nominal composition $\text{Fe}_{79.7-x}\text{Ti}_x\text{Nb}_{0.3}\text{B}_{20}$ ($x = 12, 20$ at.%) and Curie temperature in the 0-700C range depending on the Ti content, more suitable for self-regulating magnetic hyperthermia. The saturation magnetization decreases slowly by increasing the amount of Ti (from 0.7 T for 12 at.%Ti to 0.25 T for 18 at.% Ti) and the material behaves as a weak ferromagnet for 20 at.% Ti. The larger the Ti content, the more reduced the Curie temperature is. To explain this specific magnetic, especially the low TC, we investigated the microstructure using transmission electron microscopy (TEM) and energy dispersive X-ray spectroscopy (EDX). The 12 at.% Ti melt-spun ribbon is found to be amorphous, with no sign of nanocrystalline formation. EDX mapping within the amorphous matrix, shows that Fe and Ti are separated out into Fe-rich cells and Ti-rich cell-boundaries. B is also found to form a cellular distribution, but not directly related to either Fe or Ti. This phenomenon appears in electron diffraction as two overlapping sets of amorphous rings, indicating a different mean particle spacing in the two different regions. From $x = 16$ at.%, all compositions contain nanocrystals embedded within the amorphous matrix. Using EDX mapping, the nanocrystals are shown to be Ti-rich; and using electron diffraction and JEMS simulation, the nanocrystalline rings are shown to correspond to titanium diboride (TiB_2). High resolution TEM investigation, in conjunction with Crystal Maker simulation software, supports this. The size of the crystals and their phase fraction are found to increase with Ti concentration.

This work was financially supported by the CNDI-UEFISCDI Grant #148/2012 (HYPERTHERMIA). L. Whitmore acknowledges the financial support of the European Commission (FP7-REGPOT-2012-2013-1, Grant Agreement no. 316194, NANOSENS).

Th.L-P05 - Magnetic and structural characterization of hybrid CFO-YBCO nanocomposites prepared by chemical solution deposition

E. Bartolomé¹, P. Cayado², S. Ricart², E. Solano³, M. Coll², J. Ros⁴, B. Mundet², J. Gázquez², A. Medelin⁵, G. van Tedeloo⁵

1. *Escola Universitaria Salesiana de Sarriá (EUSS), Barcelona, Spain*

2. *Institut de Ciència de Materials de Barcelona (ICMAB), Bellaterra, Spain*

3. *Department of Solid State Sciences, Faculty of Sciences, Ghent University, Krijgslaan, Gent, Belgium*

4. *University Autònoma Barcelona, Dept Quim, Fac. Ciències, Barcelona, Spain*

5. *EMAT, University of Antwerp, Antwerp, Belgium*

6. *ALBA Synchrotron Light Source, Barcelona, Spain*

High T_c superconductor-ferromagnetic heterostructures constitute an appealing playground to study the interplay between flux vortices and magnetic moments. We have prepared hybrid YBCO nanocomposite epitaxial thin films on LAO substrates via a Chemical Solution Deposition technique, by introducing ex situ grown cobalt ferrite (CoFe₂O₄) nanoparticles (NPs) into the YBCO precursor solution. A one-pot, microwave radiation assisted route had to be developed to synthesize spherical, monodispersed NPs of size 5 nm that could be dispersed in the polar alcoholic solvent used for YBCO growth. The structural characterization of the nanocomposite, performed by HAADF STEM and EDS, shows that after the YBCO growth process, the NPs dissolve and the matrix contains intergrowths of a new YBaCuFeO₅/YBaFe₂O₅ phase. SQUID measurements carried out above T_c show that embedded NPs present a magnetization cycle, though the saturation value is much smaller than for synthesized CFO NPs. Besides, the critical current density J_c and T_c of the nanocomposite are decreased with respect to standard YBCO thin films due to Fe diffusion. Element-selective X-ray Absorption Spectroscopy (XAS) and X-ray magnetic dichroism (XMCD) measurements were performed at BOREAS beamline in ALBA synchrotron to gain insight into the structure and magnetic behavior of the hybrid nanocomposite. XAS&XMCD(H) measurements at the L_{2,3} edge of Fe and Cu were performed on a 16% CFO-YBCO nanocomposite at temperatures below (1.6 K) and above (60K) T_c, at fields up to 6 T. Results at the Fe-edge evidence the spinel is not present in the matrix, but a mixture of Fe³⁺/Fe²⁺ remains yielding a paramagnetic cycle. The XMCD(H) at the Cu-edge displays also paramagnetic behavior, with the magnetic moments of Cu and Fe pointing in the same direction, the Cu saturation moment being an order of magnitude smaller than in YBCO standard thin films.

Th.L-P06 - Magnetotransport properties of SrTiO_{3-δ} thin films grown by Molecular Beam Epitaxy on p-Si(001) substrates

N. Theodoropoulou¹, R. Cottier, D. Currie, B. Koehne, P. Jalili

1. *Texas State University*

SrTiO₃ (STO) films were grown on p-Si (001) and STO (001) bulk substrates using molecular beam epitaxy (MBE). Oxygen vacancies were introduced by controlling the Oxygen pressure during growth resulting in SrTiO_{3-δ} with $\delta \sim 0.02\%$ for the lowest P(O₂). The single-phase STO/Si films were of high crystalline quality as verified by x-ray diffraction, transmission electron microscopy, and atomically flat. Transport measurements were performed on the STO/Si structures in a Van der Pauw configuration. The P(O₂) during growth determines the conduction behavior which changes from strongly localized transport that fits a Variable Range Hopping (VRH) model (low P(O₂)-high disorder) to thermally activated transport (high P(O₂)-low disorder). The resistivity of the strongly disordered STO/Si films decreased from 1×10^{-2} Ohm cm to 3×10^{-2} Ohm cm as the film thickness increased (3nm-60nm) for all temperatures (T). The perpendicular magnetoresistance (MR) is positive at 300K and at T=3-20K becomes negative for low magnetic fields (H). The MR behavior combined with the Hall effect data indicates the presence of localized electrons that delocalize with H and T. To identify the origin of the resistivity thickness dependence and MR behavior, we consider different competing effects on the STO/Si heterostructure such as 1.7% compressive strain induced by lattice mismatch to Si, defects due to oxygen vacancies, the bulk STO antiferrodistortive phase transition at 105K, and structural dislocations.

Th.M-P01 - Magnetic and magnetotransport study of the crossover from antidot to dot arrays

C. Castán-Guerrero^{1,2}, J. Herrero-Albillos^{1,3}, J. Bartolomé^{1,2}, F. Bartolomé^{1,2}, P. Strichovanec¹, J. Sesé^{4,2}, L.M. García^{1,2}

1. ICMA (Universidad de Zaragoza - CSIC), Zaragoza, Spain

2. Dpto. de Física de la Materia Condensada (Universidad de Zaragoza), Zaragoza, Spain

3. Centro Universitario de la Defensa, Zaragoza, Spain

4. INA-LMA (Universidad de Zaragoza), Zaragoza, Spain

The control of magnetic properties of thin films can be achieved through the patterning of nanostructures, such as dot arrays or their negative pattern, antidot arrays. The magnetic crossover from antidot to dot regime (i.e. in series of arrays with fixed antidot diameter, d , varying the array period, p , from an array of well separated antidots when $p \gg d$ to an array of dots formed by the intersecting antidots when $p < d$) has been studied by means of MOKE magnetometry and XPEEM images of the magnetic domain structure [1]. The study revealed for the first time an intermediate regime with a dual nature, morphologically consisting on an antidot array which behaves magnetically as an array of isolated dots.

In the present study, a new series of arrays have been fabricated and characterized by magnetoresistance (MR) and MOKE magnetometry. The antidots were fabricated by means of a gallium focused ion beam, causing some damage in the edges of the antidot. This results in a broadening of the effective antidot diameter calculated from MOKE and MR measurements, d_{eff} and d_{eff}^* respectively. The morphological diameter of the holes, d , is fixed in all the fabricated arrays, and $d_{\text{eff}}^* < d_{\text{eff}} < d$. The array period p has been varied from array to array, from $p \gg d_{\text{eff}}$, belonging to the antidot regime, to $d_{\text{eff}}^* < p < d_{\text{eff}}$, which is in the magnetic dot regime, although the magnetic islands are still connected by conductive channels. Therefore, this work not only proves that the intermediate regime can be measured by MR, but opens the door to the fabrication of magnetic dot arrays which are measurable by magnetotransport techniques.

1. C. Castán-Guerrero, J. Herrero-Albillos, J. Bartolomé et al., Physical Review B 89, 144405 (2014)

Th.M-P02 - The effects of interlayer coupling on the static and dynamic behavior of $\text{Ni}_{80}\text{Fe}_{20}/\text{Ru}/\text{Ni}_{80}\text{Fe}_{20}$ Nanostripes

P. Lupo¹, Z. Haghshenasfard², L. Xiong¹, X. Ming Liu¹, M. Cottam², A. Adeyeye¹

1. *Information Storage Materials Laboratory, Department of Electrical and Computer Engineering, National University of Singapore, Singapore*

2. *Department of Physics and Astronomy, University of Western Ontario, London, Canada*

Artificial ferromagnetic nanostripe arrays have been the focus of much attention recently because of fundamental research into magnonic crystals and for their wide range of potential applications as microwave resonators, filters, non-volatile memory and spin-wave (SW) logic devices. We have studied the static and dynamic properties of systems of two $\text{Ni}_{80}\text{Fe}_{20}$ nanostripes, separated by a thin spacer stripe of Ru, using a vibrating sample magnetometer and ferromagnetic resonance (FMR) spectroscopy respectively. By varying the Ru layer thickness (in a range from 0 to about 1.6 nm) we effectively control the Ruderman-Kittel-Kasuya-Yosida (RKKY) interlayer exchange interaction, and in some cases, a biquadratic interlayer exchange. Together with the effects of varying the width of the nanostripes over the range from 90 nm to 300 nm, which changes the shape anisotropy of the samples, we can realize an overall antiferromagnetic, spin-flop, or ferromagnetic ordering of the $\text{Ni}_{80}\text{Fe}_{20}$ stripes depending on the external magnetic field applied along the length of the stripes. The switchings between states of different magnetic order are accompanied by distinctive features observed in the FMR spectra of the lowest quantized spin-wave branches. The results obtained are contrasted with those found recently for $\text{Ni}_{80}\text{Fe}_{20}/\text{Ru}/\text{Ni}_{80}\text{Fe}_{20}$ complete films [1], where there is no in-plane shape anisotropy as in the stripes. The detailed theoretical analysis of the static and dynamic behavior, which is carried out using a combination of a phenomenological magnetization-vector model, a micromagnetic simulation package, and microscopic dipole-exchange theory, provides broad confirmation of the experimental data.

[1] X M Liu, H T Nguyen, J Ding, M G Cottam, A O Adeyeye, Phys. Rev. B 90, 064428 (2014)

Th.M-P03 - Monte Carlo simulation of magnetic properties in Bit Patterned Media

O.D. Arbeláez Echeverri¹, E. Restrepo Parra¹, J.D. Agudelo Giraldo^{1,2}

1. *PCM Computational Applications, Universidad Nacional de Colombia, Manizales, Caldas, Colombia*

2. *Escuela de Materiales, Facultad de Minas, Universidad Nacional de Colombia, Medellín, Colombia*

A two dimensional geometric model of Bit Patterned Media is proposed, the model is based on the crystal structure of the materials commonly used to produce the nano islands in bit patterned materials and the possible defects that may arise from the interaction between the nano islands and the matrix material. The magnetic properties of the material are then computed using the Monte Carlo method. The Hamiltonian takes into account both the spatial and topological disorder of the sample as well as the high perpendicular anisotropy that is pursued when building bit patterned media. The main finding of the research was the double phase transition in the Magnetization observed when computing curves of Magnetization vs. Temperature, further simulations were performed in order to establish the relation of this effect with the interaction between the nano islands and the interstitial material.

Th.M-P04 - Spin-wave modes and magnetization reversal in ferromagnetic nanostructures subjected to asymmetric magnetostatic interactionsM. Pancaldi¹, J.M. Porro², S. Gliga^{3,4}, P. Landeros⁵, V. Metlushko⁶, A. Berger¹, P. Vavassori^{1,7}*1. CIC NanoGUNE, Donostia-San Sebastian, Spain**2. ISIS, Rutherford Appleton Lab, Harwell-Oxford, United Kingdom**3. Laboratory for Mesoscopic Systems, Department of Materials, ETH Zurich, Zurich, Switzerland**4. Laboratory for Micro- and Nanotechnology, Paul Scherrer Institute, Villigen PSI, Switzerland**5. Departamento de Fisica, Universidad Tecnica Federico Santa Maria, Valparaiso, Chile**6. Nanotechnology Core Facility, University of Illinois at Chicago, Chicago IL, United States**7. IKERBASQUE, Basque Science Foundation, Bilbao, Spain*

Understanding and control of the magnetization behavior in magnetic nanostructures remains a key issue in fundamental physics and for various technological applications. In this framework, the desired single-domain and Ising-like behavior is commonly achieved by exploiting the shape anisotropy in elongated nanostructures. However, the energy landscape determined by the geometry and material properties comprises various stable and metastable states, which cannot be explored under the sole action of a uniform externally applied magnetic field. We have experimentally observed that Permalloy nanobars (720 nm x 170 nm x 25 nm) arranged in a chiral square unit can form a stable vortex state of predefined chirality during system remagnetization, even if only the single-domain state is achievable in the isolated nanostructure. Measurement of 2nd order Diffracted MOKE hysteresis loops and inspection of MFM images of frozen remanent states in the chiral unit reveal the presence of a critical angle in the applied field direction, which separates the single-domain magnetization reversal path from the magnetic vortex state reversal path [1]. This mechanism has been studied by micromagnetic simulations [2] and the Dynamic Matrix Method [3] in order to trace the origin of the difference in the reversal paths in the dynamic evolution of the magnetization [4]. The symmetry breaking induced by the inhomogeneous and asymmetric interaction in the chiral unit leads to the formation of new localized dynamic end-modes: the nucleation of the vortex state is connected to the softening of the lowest frequency localized end-mode occurring at certain angles of the applied field, while a partial softening of this mode gives rise to the conventional single-domain magnetization reversal path. Our results demonstrate that localized magnetic field sources can be used to actively induce the reversal paths of nanomagnets beyond what is achievable via lateral confinement and anisotropy engineering alone.

[1] J. M. Porro et al., J. Appl. Phys. 111, 07B913 (2012)

[2] G. Carlotti et al., Physica B 435, 4 (2014)

[3] M. Grimsditch et al., Phys. Rev. B 70, 054409 (2004)

[4] F. Montoncello et al., Phys. Rev. B 77, 214402 (2008)

Th.M-P05 - Magnetic vortex states in highly anisotropic nanoislands

J.M. Porro^{1,2}, M. Pancaldi², V. Metlushko³, A. Berger², P. Vavassori^{2,4}

1. *ISIS, Rutherford Appleton Laboratory, STFC, United Kingdom*

2. *CIC nanoGUNE, San Sebastián, Spain*

3. *Nanotechnology Core Facility, University of Illinois at Chicago, Chicago, United States*

4. *IKERBASQUE, Basque Science Foundation, Bilbao, Spain*

We have fabricated arrays of elliptical ferromagnetic nanoislands, made of Permalloy, with different dimensions (smallest nanomagnets 500x120x25nm³) and aspect ratios (length/width) of 4, 5.7, and 8. They are arranged in chiral square and rectangular units formed by four nanomagnets, so that the stray fields created by each pair of parallel nanomagnets interact asymmetrically on the nanomagnets perpendicular to them. Under the action of a uniform magnetic field the only possible magnetic configuration that is induced in the nanomagnets is a single-domain state, i.e. the nanomagnets have an Ising-like bistable behavior of the magnetization. Micromagnetic simulations indicate that a vortex state, if induced, would be stable although energetically highly unfavoured with respect to the single-domain state. Here we demonstrate that indeed, under the action of asymmetric fields, it is possible to nucleate magnetic vortex states that are stable at remanence. We demonstrate experimentally [1] the existence of these vortex states by analyzing the magnetization reversal process by means of standard and diffracted MOKE magnetometry [2], and Magnetic Force Microscopy. Our micromagnetic simulations, performed using OOMMF [3], replicate the obtained experimental results.

[1] J.M.Porro et al., *J. Appl. Phys* 11, 7 07B913 (2012)

[2] P. Vavassori and M. Grimsditch, *J. Phys. Cond. Matt* 16, 9 (2004)

[3] OOMMF code developed by NIST

Th.M-P06 - Quantized energy states in spin ice due to magnetic coupling

C. Sheng Soh ¹, I. Purnama ¹, S. Krishnia ¹, W. Siang Lew ¹, R. Maddu ¹

1. School of Physical and Mathematical Sciences, Nanyang Technological University, Singapur

Spin ice structures have been used to investigate the possibility of creating magnetic monopoles when they are geometrically aligned to a vertex collectively[1]. Here, we show that the total energy of such system is quantized into several energy levels due to the coupling between the islands[2]. The energy levels are shown to be stable over a range of temperature, and it is possible to change the temperature range significantly by adjusting the strength of the coupling between the islands.

In this work, an octagonal square design with 50nm/100nm separation between the islands as shown by Figure 1(a) is being investigated. The energy values for the 8 possible magnetic configurations are calculated and shown in Figure 1(b). By running simulations on his tessellation, the density of low/medium/high energy vertices at its relaxed state is recorded and plotted against temperature (T) from 1K to 250K. The system was first randomized. Then a random island is selected to be flipped. If the energy in the vertex after flip becomes lower, the flip is accepted with a probability (P) of 1, else P is calculated using $P = e^{\frac{-\Delta E}{kT}}$. It is repeated until the system has reached equilibrium as shown in Figure 2.

The simulation results show that there is quantization in the distribution of vertices. In our design, the discrete energy levels are not observed at higher temperatures (i.e. >250K) due to minute change; however, the quantization can be observed at T<250 K. Moreover, the robustness of the quantization is shown to increase significantly as separation distance is reduced; the temperature range for the vertices fixed in the ME level is extended to ~190 K as the separation distance is reduced to 50nm. Thus, our design can potentially be used as a framework to investigate the quantization phenomenon of frustrated magnetic system at elevated temperature.

REFERENCES

- 1) C. Caste novo, R. Moessner and S. L. Sondhi, 2008, "Magnetic Monopoles in Spin Ice", *Nature*, 451, p42-45 (2008)
- 2) E. Mengotti, L.J. Heyderman, A. Fraile Rodriguez, A. Bisig, L. Le Guyader, F. Nolting, and H.B. Braun, 2008, "Building Blocks of an artificial kagome spin ice: Photoemission electron microscopy of arrays of ferromagnetic islands", *Phys. Rev. B*, 78, 144402 (2008)

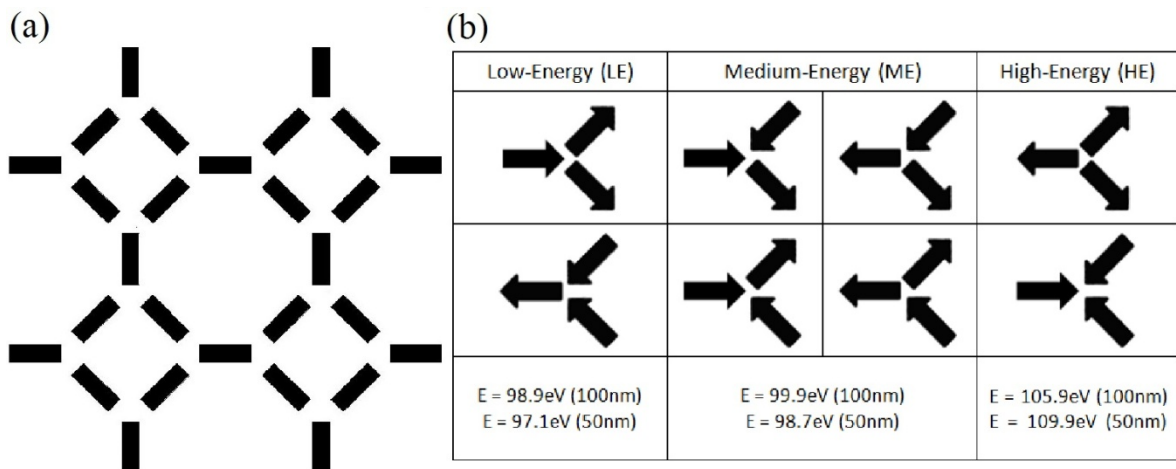


Figure 1 (a) Octagonal Square Tessellation. (b) 8 possible configurations of the Y-vertex and the energy value at 50 and 100nm separation.

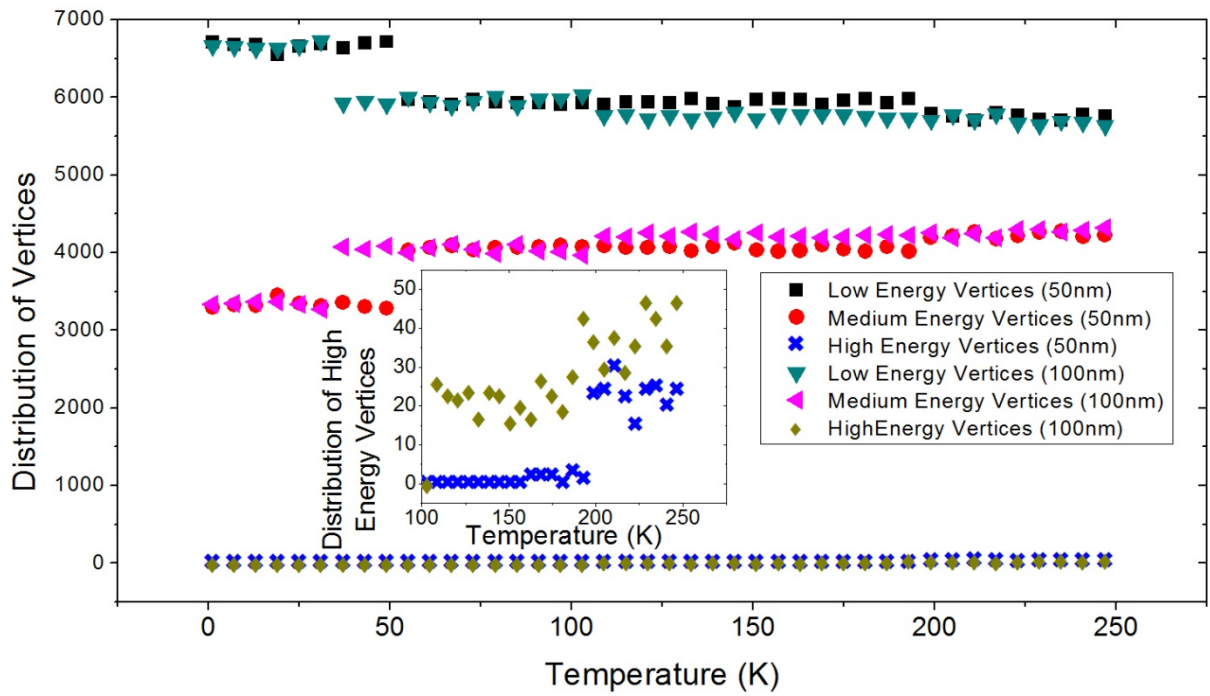


Figure 2 Number of Low/Medium/High Energy Vertices vs. Temperature at 50 and 100nm
 (inset) Number of High Energy Vertices vs. Temperature at 50 and 100nm

Th.M-P07 - Spin wave bound modes in a circular array of magnetic inclusions embedded into a ferromagnetic matrix

S. Nikitov^{1,2}, Y. Barabanenkov¹, S. Osokin^{1,2}, Dmitry Kalyabin^{1,2}

1. *Kotel'nikov Institute of Radio Engineering and Electronics of RAS, Moscow, Russia*

2. *Moscow Institute of Physics and Technology (State University), Moscow, Russia*

We have developed a theory which is capable to calculate scattering of magnetostatic spin waves propagating in a ferromagnetic film with finite array of cylindrical inclusions. We have restricted our analysis by considering magnetic inclusions having different value of magnetization in comparison with a material of the film and considering a case of a magnetic structure being saturated in a magnetic field perpendicular to the film surface.

The main result obtained in our paper is that due to spin wave multiple scattering by an ensemble of finite number of inclusions in circular array bound wave modes are excited along the path connecting inclusions. The physical origin of the bound modes propagating along circular array of inclusions is in variation of a phase a scattered magnetic potential related to a spin wave. Thus, these bound spin wave modes appear as a wave of a phase due to scattering. Scattered field spatial-phase modulation is related to spin wave reciprocity breaking due to asymmetric magnetic susceptibility tensor. Further, this fact leads to that the plane spin wave scattering by a single inclusion transforms the magnetic field potential in a form of helix lines. Such scattering can also be visible for a greater number of inclusions depending on the product of the wave number of the spin wave on distant between two nearest inclusions in circular array (collective wave parameter). If the collective wave parameter is not greater than π the helix lines appear in a scattered field. If it is greater than π the scattering spin wave potential is distributed by Bragg interference. In the case the plane wave is scattered by four inclusions specific radial nodal lines appear in a scattered field.

This work is supported by the Grant from Russian Science Foundation (Project # 14-19-00760).

Th.M-P09 - Magnetization reversal in finite size dot arrays: global configurational anisotropy

D. Bisero ^{1,5}, S. Fin ¹, A. Sarella ³, P. Vavassori ^{3,4}, B. Van de Wiele ²

1. *Dipartimento di Fisica e Scienze della Terra, Università degli Studi di Ferrara, Ferrara, Italy*
2. *Department of Electrical Energy, Systems and Automation, Ghent University, Ghent, Belgium*
3. *CIC nanoGUNE Consolider, Donostia-San Sebastian, Spain*
4. *IKERBASQUE, Basque Foundation for Science, Bilbao, Spain*
5. *CNISM, Unità di Ferrara, Ferrara, Italy*

We analyzed with MFM and MOKE finite squared (rectangular) arrays of circular (elliptical) magnetic dots and performed simulations with MuMax, a GPU-based software [1]. We showed as for limited size of the periodic arrays the transition of the magnetization during the reversal starts at the edges and corners of the array and propagates inside the pattern, so that in a restricted field range the magnetization results to be not uniformly distributed. While the shape of the dots (circular, elliptical, etc.) introduces a Configurational Anisotropy [2], we find that the finite array dimensions introduce an additional Global Configurational Anisotropy (GCA) [3]. Both effects originate at the demagnetizing interactions playing at different space scales: the dot and total array space scale, respectively. Simulations of dot arrays are often restricted to one dot assuming isolated non-interacting magnetization processes. Periodic boundary conditions are sometimes used to incorporate interdot interactions, still limiting computations to a restricted number of dots and assuming infinite lattice periodicity. Then, configurational anisotropy is accounted for, but GCA is not. We show that mutual dot interactions together with finite array dimensions have a non-negligible impact on the magnetization reversal of a dot array. We numerically and experimentally study the hysteresis properties of Permalloy (Py) arrays of 16x16 circular and elliptical dots, with thickness ranging between 10 and 25 nm and lateral size between 300 and 500 nm. In magneto-optical Kerr effect (MOKE) measurements, in-field magnetic force microscope (MFM) measurements and simulations, we find that GCA steers the magnetization reversal of the array: the dots run through different magnetization states depending on the dot location and collective magnetization processes occur, leading to transition avalanches and formation of magnetization chains. These findings are important in the development of applications that rely on a robust control of dot magnetization states in dot arrays.

[1] A. Vansteenkiste and B. Van de Wiele, *J. Magn. Magn. Mater.* 323, 2585 (2011)

[2] P. Vavassori, D. Bisero et al., *Phys. Rev. B* 72, 054405 (2005)

[3] B. Van de Wiele, S. Fin, A. Sarella, P. Vavassori and D. Bisero, *Appl. Phys. Lett.* 105, 162407 (2014)

Th.M-P10 - Magnetic properties of FeCoCu/Cu multilayer nanowire arrays

E.M. Palmero¹, C. Bran¹, C. Magen², R.P. del Real¹, F. Beron³, M. Vazquez¹

1. *ICMM-CSIC, Madrid, Spain*

2. *INA-ARAID and University of Zaragoza, Zaragoza, Spain*

3. *Instituto de Física Gleb Wataghin, Universidade Estadual de Campinas, Campinas, Brazil*

FeCo alloy nanowires have been proposed as an alternative novel family of permanent magnets with high saturation magnetization and coercivity [1]. The addition of non-magnetic materials has been proved to tailor the magnetic properties of the nanowires [2]. Series of ordered [FeCoCu(y)/Cu(x)]₁₀ multilayer nanowire arrays, with various Cu and FeCoCu layers thicknesses and constant diameter of 35nm, were fabricated by electrodeposition from a single electrolytic bath into self-assembled pores of anodic alumina membranes, in order to study the influence of magnetic and non-magnetic layer thickness on their magnetic properties. Transmission Electron Microscopy analysis confirm the segregation of layered structures, with well-defined Cu layers (fcc cubic structure) separating FeCoCu alloy layers (bcc cubic structure). Magnetic measurements indicate an overall magnetization easy axis parallel to the nanowires in all the samples. For constant FeCoCu thickness, the coercivity, remanence and susceptibility increase with Cu layer thickness, while for the series with constant Cu layer thickness, a significant decrease of susceptibility with FeCoCu thickness was observed. Complementary Henkel curves study indicates that the net inter/intra nanowires magnetostatic interactions always contribute to demagnetization of nanowires. The results show a decrease in the effective magnetostatic interactions for multilayer nanowires with thicker Cu and thinner FeCoCu layers arising from stray fields at the surface of intra-wire and adjacent inter-wires magnetic layers. FORC method was use to quantify the effect of the inter/intra nanowire magnetostatic interactions on the coercivity and interaction field distributions. For the samples with thinner FeCoCu and thicker Cu layers, sharper peak along the interaction field axis is observed, suggesting that the increase of the non-magnetic to magnetic layer thickness ratio promote the reduction in the magnetostatic interactions.

[1] L.H. Lewis and F. Jiménez-Villacorta, *Metall. Mater. Trans. A*, 44 (1), 2 (2013)

[2] Z. Liu et al., *J. Magn. Magn. Mater.*, 345, 96 (2013)

Th.M-P11 - Collective magnetic properties in nanoparticle assemblies highlighted by shape anisotropy and interparticle distances

B. Pichon¹, D. Toulemon¹, M. Pauly¹, S. Fleutot¹, S. Bégin-Colin¹

1. Institut de Physique et Chimie des Matériaux de Strasbourg, Strasbourg, Switzerland

Owing to their unique properties depending on their environment, nanoparticles are of particular interest with regard to develop the next generation of magnetic devices. Magnetic nanoparticles are featured by a single magnetic domain, and can be assimilated to elemental nanomagnets which interact together through dipolar interactions. Therefore their magnetic properties can be strongly modulated as function of the structure of their assemblies, which interparticle distances and dimensionality of the assembly are the most significant parameters to play with. Here, we report on the modulation of the collective properties of iron oxide magnetic nanoparticles assembled in films as function of the dimensionality of the assembly and of the interparticle distance by using the Langmuir-Blodgett technique [1,2] and substrate functionality by self-assembled monolayers (SAMs) of organic molecules.[3,4,5] Decreasing the dimensionality from multilayers (3D) to monolayer (2D) and finally to chains (1D) demonstrated the enhancement of the dipolar interactions thanks to shape anisotropy which forces the preferential alignment of magnetic moments in the directions of the assembly. Dipolar interactions being long range interactions, they have been also studied as function of inter particle distances.

1 Pauly, M. et al., J. Mater. Chem. 2012, 22 (13), 6343 - 6350

2 Feutot, S. et al., Nanoscale 2013, 5(4), 1507-1516

3 Pichon, B. P. et al., Langmuir, 2011, 27, 6235-6243

4 Toulemon, D. et al., Chem. Commun. 2011, 47 (43), 11954 - 11956

5 Toulemon, D. et al. Chem. Mater., 2013, 25(14), 2849-2854

Th.M-P12 - Challenges to realising topological control of domain wall transit in artificial spin ice

W. Branford¹, S. Walton¹, K. Zeissler¹, D. Burn¹, M. Chadha¹, L. Cohen¹

1. Imperial College London, London, United Kingdom

I will discuss arrays of single domain nanomagnets with frustrated interactions, known as Artificial Spin Ice. The structures studied electrically continuous permalloy honeycombs. [1-2] Here I report direct magnetic imaging studies of magnetic charge flow in artificial spin ice. [3-5]. The magnetic charge is carried by either transverse or vortex domain walls (depending on bar dimension) and the chirality of the domain wall is found to control the direction of propagation. Recently it has been shown that in isolated Y-shaped junctions that support vortex domain walls, selectivity can be robustly determined by chirality (or topology), indicating that vortex wall chirality is robust in the Walker breakdown process.[6,7] Here I will show that in Y-shaped junctions, magnetic switching in the important topologically protected regime exists only for a narrow window of field and bar geometry, which is challenging to access in field-driven Artificial Spin Ice. This work has implications for the wider field of magnetic charge manipulation for high density memory storage.

[1] S. Ladak, D. E. Read, G. K. Perkins, L. F. Cohen & W. R. Branford. Nature Physics 6, 359, (2010)

[2] W. R. Branford, S. Ladak, D. E. Read, K. Zeissler & L. F. Cohen. Science 335, 1597, (2012)

[3] S. K. Walton, K. Zeissler, et al. NJP 17, 013054, (2015)

[4] K. Zeissler, S. K. Walton, S. Ladak, D. E. Read et al. Sci. Rep. 3, 01252, (2013)

[5] S. Ladak, D. Read, T. Tyliszczak, W. R. Branford & L. F. Cohen. NJP 13, 023023, (2011)

[6] T. Phung, A. Pushp, et al. APL 105, 222404, (2014)

[7] A. Pushp, T. Phung, et al. Nature Physics 9, 505-511, (2013)

Th.M-P13 - Dipolar interactions in finite arrays of elliptical Fe(001) particles

M. Hanson¹, T. Antosiewicz^{1,2}

1. Chalmers University of Technology, Göteborg, Sweden

2. Centre of New Technologies, University of Warsaw, Warsaw, Poland

Arrays of ferromagnetic nano-sized particles are of great interest for applications. To obtain any desired functional static and dynamic magnetic properties, the individual particles as well as their interactions, determined by the design of the arrays, must be controlled. We made an extensive study of Fe ellipses prepared with their axes along the easy magnetization directions in epitaxial Fe(001) films. Here we present results from calculations of interactions in different array configurations of ellipses with axes 50 nm x 150 nm and thickness 10 nm. We show that this system is in a range where no collective effects are observed and the interactions can be tuned to either promote or delay the magnetization reversal in the individual particles.

The interaction field at different positions in a saturated array was calculated with high spatial resolution by summing the dipolar interactions from all ellipses divided into tiny cubes with 2 nm sides. As an example, for a rectangular lattice with lattice constants twice the corresponding axis of the ellipses the main component of the interaction field lies along the long axes of the ellipses and at the onset of switching it reinforces an external switching field. For a square array with 3 by 7 seven ellipses the strength is about $B_y = 11$ mT at the center. B_y decreases with the array size; being about 10 mT for 21 by 61 ellipses. The strongest interactions are felt by the ellipses at the top edge of the array; about 14 mT for the 21 by 61 array. B_y approaches 9.3 mT in the limit of large arrays.

Quasi-static micromagnetic simulations were applied to follow the array of ellipses during stepwise demagnetization. The ellipses were seen to switch individually in a range of fields, starting earlier than for corresponding single-particle switching.

Th.M-P14 - Magnetic interactions in 3d metal chains on Cu₂X/Cu(001) (X = N, O): comparison with corresponding unsupported chains

M.C. Urdaniz¹, M.A. Barral^{1,2}, A.M. Llois^{1,2}, A. Saúl^{3,4,5}

1. *Departamento de Física, Comisión Nacional de Energía Atómica, San Martín, Buenos Aires, Argentina*
2. *Departamento de Física 'Juan José Giambiagi', Facultad de Ciencias Exactas y Naturales, Universidad de Buenos Aires, Ciudad Universitaria, Buenos Aires, Argentina*
3. *CINaM, Université d'Aix Marseille-CNRS, Campus de Luminy, Marseille, France*
4. *Department of Civil and Environmental Engineering, Massachusetts Institute of Technology, Cambridge, United States*
5. *MultiScale Material Science for Energy and Environment, Cambridge, United States*

In this work we present a systematic study of the magnetic interactions within 3d transition metal chains adsorbed on Cu₂N and Cu₂O monolayers grown on Cu(001). We are interested in the particular geometric adsorption configuration which gives rise, after relaxation, to the development of diatomic TM-X (X = N, O) chains. Using Density Functional Theory we calculate the energy difference between the ferromagnetic and antiferromagnetic intrachain configurations for Ti, V, Cr, Mn, Fe, and Co. Both substrates give rise, with minor differences, to the same magnetic trends, the only chains which result being ferromagnetic after adsorption are Cr ones.

By performing similar calculations in unsupported chains and introducing a Tight-Binding model Hamiltonian based on physically reasonable assumptions we have been able to reproduce the magnetic trends obtained from the DFT calculations.

Th.M-P15 - Controlling magnetization reversal in planar nanostructures with wire-ring morphology

R. Corona ¹, A. Aranda ¹, J.L. Palma ^{1,2}, C. López ^{1,2}, J. Escrig ^{1,2}

1. Departamento de Física, Universidad de Santiago de Chile, Santiago, Chile

2. Center for the Development of Nanoscience and Nanotechnology, CEDENNA, Santiago, Chile

Magnetization reversal in planar nanowires has been controlled using structures with a larger area pad connected to a nanowire or by means of patterned variations in the planar nanowire such as notches. In this work, we have introduced a magnetic nanostructure defined as a planar nanostructure with wire-ring morphology. In particular, we have performed micromagnetic simulations to investigate how the magnetic properties (coercivity and remanence) change as a function of the geometric parameters of the nanostructure. Additionally, we observe that when the ring is very thin, the system reverses its magnetization by nucleation and propagation of domain walls along the nanowire. Conversely, when the ring has very thick walls, or directly turns into a solid cylinder, the system nucleates a vortex in the ring/cylinder, and then propagates the domain walls toward the nanowire sections. This reversal process is characterized by a step or plateau in the hysteresis curve, that is, a region in which differential magnetic susceptibility presents a local minimum or, ideally, vanishes. Finally, this nanostructure can be used in many potential applications related to the control of domain walls in planar nanowires.

The authors acknowledge financial support from Fondecyt Grant Nos. 3130393, 1150952, and 1121034, and the Financiamiento Basal para Centros Científicos y Tecnológicos de Excelencia, under Project FB0807. CONICYT Ph.D. Program Fellowships is also acknowledged. (Appl. Phys. Lett. 105, 082406.)

Th.M-P16 - Magnetostatic interactions between wire-tube nanostructures

D. Salazar-Aravena¹, J.L. Palma^{1,2}, J. Escrig^{1,2}

1. *Departamento de Física, Universidad de Santiago de Chile, Santiago, Chile*

2. *Center for the Development of Nanoscience and Nanotechnology, CEDENNA, Santiago, Chile*

We have investigated the magnetostatic interactions between wire-tube nanostructures. We have obtained that decreasing the distance between the nanostructures, decrease the coercivity of the array. Besides, when the external magnetic field is applied along the axis of the nanostructures, the two Barkhausen jumps observed for an isolated wire-tube nanostructure give rise to several minor jumps for a weakly interacting array, that eventually become a single jump for the most interacting case. Additionally, the angle at which maximum coercivity is obtained varies as a function of the center-to-center distance between the nanostructures, while that remanences obtained for arrays with different distances between the nanostructures coincide. In this way, magnetostatic interactions between wire-tube nanostructures is an interesting topic of research in connection with potential applications where it is usually desirable to avoid such interactions or at least control them. We thank K. R. Pirota and R. López-Ruiz for useful discussions. The authors acknowledge financial support from the Fondecyt Grants 3130393 and 1150952, and the Financiamiento Basal para Centros Científicos y Tecnológicos de Excelencia, under project FB0807. CONICYT Ph.D. Program Fellowships is also acknowledged.

Th.M-P17 - Spectroscopic and spatially resolved magneto-optical characterizations of 1D magnetic gratings

V. Kletecka¹, L. Beran¹, R. Antos¹, M. Veis¹

1. Charles University, Prague, Czech Republic

Magneto-optical (MO) methods are often used as high sensitive non-destructive techniques to probe physical properties of various magnetic materials down to the nanometer scale. Spatially resolved MO experiments are suited for visualization of magnetic domains larger than 0.15 μm . Samples have to be reasonably smooth, however there are many advantages such as non-destructiveness, high time resolution or easy manipulation with samples, which enables great way to analyze wide variety of nanostructured magnetic materials. In combination with spectroscopic ellipsometry (SE) as a complementary tool MO spectroscopy can provide important information about the geometrical and material properties. MO spectroscopic scatterometry combines theoretical and experimental investigation of MO spectral response of patterned periodic magnetic nanostructures.

Here we report on analyzing two types of one-dimensional gratings formed by magnetic materials, permalloy ($\text{Ni}_{81}\text{Fe}_{19}$) and nickel by specially designed MO microscopy and MO scatterometry. Periodic lamellar grooves were etched by electron-beam lithography and ion milling on a 32-nm-thick permalloy layer deposited on an Si substrate. Periodic Ni wires were fabricated by the lift-off procedure on Si substrate with a 500-nm-thick SiO_2 overlayer. For the theoretical calculations fast Fourier factorization rules with complex polarization bases were employed. Spatially resolved MO experiments provided the information about the amplitude of MO Kerr effect across the sample and allowed to estimate the thickness of magnetic material in lines and grooves separately. This demonstrated the ability our specially designed MO microscope. The half-micrometer SiO_2 layer caused significant interference in scatterometric experiments, which enabled sensitive monitoring of both the thickness and the material properties. The Ni was found partially oxidized with homogenous concentration of NiO in depth. The concentration of NiO within the Ni layer was determined equal to 52 %. The material constants of the system of Ni+NiO was modeled by the effective-medium approximation.

Th.M-P18 - Thermal ordering and correlations in an artificial two-dimensional Ising system

U. Arnalds¹, J. Chico², H. Stopfel², V. Kapaklis², O. Börenbold², M. Verschuuren³, U. Wolff⁴, V. Neu⁴, A. Bergman², B. Hjörvarsson²

1. *Science Institute, University of Iceland, Reikiavik, Iceland*

2. *Department of Physics and Astronomy, Uppsala University, Uppsala, Sweden*

3. *Philips Research Laboratories, Eindhoven, The Netherlands*

4. *IFW Dresden, Institute of Metallic Materials, Dresden, Germany*

The ability to create artificial analogues of model spin systems using lithographic techniques allows interactions and symmetries to be directly tuned through the array geometry [1]. Using magnetic microscopy tools the local ordering of individual artificial spins in relation to their neighbors can be determined and thereby the microstate of the system [2]. Here, we present a direct experimental investigation of the thermal ordering in an artificial analogue of an asymmetric two dimensional Ising system. The system is composed of a rectangular array of magnetostatically interacting elongated amorphous CoFeZr thin film islands. Below a critical thickness of the magnetic material, during the fabrication of the array, the islands are thermally fluctuating and thus the system is able to explore its phase space. Above the critical thickness the islands freeze-in resulting in an arrested state for the array corresponding to a low energy state at the fabrication temperature. Imaging the array by magnetic force microscopy the magnetization direction of individual islands can be resolved and thereby the state of an extended area of the array, composed ~10.000 islands, determined. Analyzing the pairwise correlations and ordering in the array and comparing our results to Monte-Carlo simulations we establish the array to represent a genuine artificial two-dimensional Ising system which can be analyzed in the context of nearest neighbor interactions.

[1] C. Nisoli, R. Moessneer, and P. Schiffer. *Rev. Mod. Phys.* 85, 1473 (2013)

[2] V. Kapkalis, U. B. Arnalds, A. Farhan, R. V. Chopdekar, A. Balan, A. Scholl, L. J. Heyderman, and B. Hjörvarsson. *Nature Nanotechnology* 9 (7), 514 (2014)

Th.M-P20 - Highly anisotropic dynamical magnetic properties of needle-shaped arrays of iron oxide nanocubes

E. Wetterskog¹, R. Stjernberg Bejhed¹, P. Svedlindh¹

1. Solid state physics, Department of Engineering Sciences, Uppsala University, Uppsala, Sweden

In this work we have investigated the AC-magnetic properties of needle-shaped arrays composed of monodisperse iron oxide nanocubes with average edge lengths of 9.6 and 12.6 nm. The particles are synthesized by a thermal decomposition method and assembled on a solid surface in a lateral magnetic field by an evaporative approach. This generates a hierarchical structure of needle-shaped particle arrays ($d \sim 10 \text{ \AA}$) with very long aspect ratios. The temperature dependence of the AC-susceptibility was measured both parallel and transverse to the long axes of the needle shaped arrays. The results were compared with measurements on non-interacting particles in dilute dispersions. In the needle-shaped arrays there is a significant anisotropy of the magnetic susceptibility. This effect is strongly particle size dependent and clearly differing from the behavior of the non-interacting systems meaning that the properties of the needle-shaped arrays are collective in origin. A number of other effects will also be discussed such as differing energy barrier distributions of the arrays and the dispersions, and the very large changes in magnetic susceptibility by the application of bias fields. Our results show in a dramatic fashion that collective shape and demagnetization effects can be significant and strongly influence the magnetization dynamics of nanoparticle arrays.

Th.M-P21 - Magnetostatic coupling in arrays of FeCo monolayer and bilayer long aspect ratio nanoribbons

M. Abuín¹, M.A. García², M. Maicas³, L. Pérez¹, A. Mascaraque¹

1. *Universidad Complutense de Madrid, Madrid, Spain*

2. *Consejo Superior de Investigaciones Científicas, Madrid, Spain*

3. *Universidad Politécnica de Madrid, Madrid, Spain*

Magnetic nanostructures are of great interest for the ever increasing requirements in information storage in the development of Magnetic Random Access Memories, spintronic devices, nanomagnetic logic or magnetic sensor technologies. Scientific knowledge of the magnetization behavior for the reproducible control of magnetic states is essential in these areas. This behavior depends mainly on the shape and geometry of the nanostructures as well as their relative location. Micromagnetic simulations can be used for the study of magnetization processes in large arrays of magnetic nanoelements by using Periodic Boundary Conditions (PBCs) under the assumption that all the nanostructures behave the same way. Although PBC are not absolutely convergent in 3-D they can be successfully used in large 2-D arrays.

In this work we report on the magnetostatic coupling between magnetic nanostructures in 2-D arrays of mono and bi-layer (two magnetic layers with a non-magnetic spacer) FeCo nanoribbons with dimensions 1000x100x20 (mono-layers) and 1000x100x20-10-20 (bi-layers magnetic-non magnetic-magnetic). The magnetostatic coupling between ribbons is studied as a function of the ribbon thicknesses, spacing in the array as well as other parameters. This analysis is carried out by means of micromagnetic simulations with PBCs using the LLGMicromagnetics simulator. Results are compared with magnetic measurements on FeCo arrays fabricated with sputtering and e-beam lithography. These magnetic measurements have been carried out using Diffracted Magneto-Optical Kerr Effect (D-MOKE). Results show the coupling between adjacent ribbons and how this coupling depends mainly on ribbon thicknesses and spacing. This coupling decreases rapidly when the spacing becomes larger than ribbon thickness. The zero remanent magnetization state is not found after saturation in balanced magnetic bilayers. These results agree well with magnetic measurements obtained by D-MOKE.

Th.M-P22 - Template morphology dependent control of magnetic interactions between magnetic nanostructures

K. Rumpf¹, P. Granitzer¹, P. Poelt², H. Michor³

1. *Karl-Franzens-University Graz, Institute of Physics, Graz, Austria*

2. *University of technology Graz, Institute for Electron Microscopy, Graz, Austria*

3. *Vienna University of Technology, Institute of Solid State Physics, Vienna, Austria*

This presentation discusses the fabrication of self-organized three-dimensional arrays of magnetic nanostructures with controllable magnetic properties. The magnetic structures are deposited electrochemically within a porous silicon matrix. Since the magnetic characteristics of the nanocomposite depend not only on the size, shape and mutual arrangement within the pores but also on the template morphology, the structure of the porous silicon has been modified and a correlation between these parameters has been figured out. The porous silicon templates offer a self-organized pore-arrangement with a dendritic pore-growth which cannot be suppressed completely in the investigated mesoporous regime. These porous silicon templates have been filled with diverse ferromagnetic metals and alloys by electrodeposition and the deposition process has been elucidated with respect to the roughness of the pore-walls and the resulting deposited nanostructures (wires, particles). The texture of the pore-surface plays a crucial role concerning magnetic coupling between adjacent pores. Furthermore the kind of metal is of importance, whereat for each metal the deposition parameters have to be adjusted individually. The nucleation of the metal deposition starts at surface asperities and the growth of the nanostructures can be influenced by using pulsed electrodeposition and also by the electrolyte. A study of the metal deposition dependent on the morphology and the resulting adjustability of the magnetic properties of the 3-dimensional nanostructure array will be presented.

Th.N-P01 - Superparamagnetic gold nanotriangles by microwave polyol synthesis

S. Yu¹, A. Laromaine¹, N. A. Roig¹

1. Institut de Ciència de Materials de Barcelona (ICMAB-CSIC), Campus de la UAB, Bellaterra, Spain

The combination of magnetic and optical properties in a nanomaterial offers enormous potential in bio-sensing, imaging and therapeutical applications. However, uncomplicated approaches to synthesize hybrid magneto-plasmonic nanoparticles with anisotropic plasmonic shapes avoiding cytotoxic reactants remain a huge challenge. Microwave heating is an attractive non-conventional energy source for chemical synthesis due to the high acceleration and yield of the performed chemical reactions. In comparison to conventional heating methods, microwave radiation avoids production of temperature gradients decreasing occurrences of asynchronic nucleation and heterogeneous nanocrystal growth. In addition, microwaves heats polar substances rapidly and intensely promoting selectively heat at desired sites. Thus, based on heating selectivity and the increase of the molecular motion, complex nanostructured materials can be fabricated. We will report on a facile, fast and bio-friendly microwave-assisted polyol route to synthesize gold nanotriangles decorated with a monolayer of iron oxide nanoparticles (Figure 1). The overall synthesis time is less than one hour. The obtained hybrid nanoparticles are readily dispersable in water, superparamagnetic at room temperature and display local surface plasmon resonance in the near infrared region. This is interesting since particles absorbing at the near-infrared region were reported to produce heat more efficiently compared to spherical gold nanoparticles absorbing in the UV-Vis. The effect of the reaction conditions and the magnetic and plasmonic properties of the nanoconstructs will be presented.

Th.N-P02 - Optimization of MTJ nano-contact on pn-GaAs photodetector for a high-speed non-volatile optical memory

V. Zayets¹, H. Saito², K. Ando³, S. Yuasa⁴

1. Spintronics Research Center, AIST, Ibaraki, Japan

The high-speed non-volatile optical memory has been proposed [1], which utilizes a high-speed spin injection of a spin-polarized photo current from a semiconductor-made pn-junction into a metal nanomagnet.

For the successful operation of the memory it is essential to inject photo-excited electrons from the semiconductor detector into the nanomagnet within a time interval shorter than the spin life time in the semiconductor. The spin life time in GaAs is short and it does not exceed 100 picoseconds at room temperature. In the case when the injection time is longer than the spin life time, the spin information is lost inside the semiconductor before it is injected into the nanomagnet. The injection time significantly depends on the nanocontact resistance. The lowest contact resistance is important to shorten the photocurrent injection time from the pn-photodetector to the nanomagnet.

The photocurrent was excited by 170-fs 10-pJ optical pulses at wavelength of 860 nm. The area of the MTJ nanocotact was $0.01 \mu\text{m}^2$. The tunnel magneto resistance was 100%. The injection time was measured to be 3 ns, 350 ps and 75 ps for the MTJ nanocontacts with the contact resistance of 7000, 250 and 30 Ohm μm^2 , respectively. An injection time shorter than the spin life time in GaAs was achieved. The dependence of the tunnel magneto-resistance on the light intensity was observed.

[1] V. Zayets and K. Ando, APL 94 (2009) pp. 121104

Th.N-P03 - Experimental demonstration of long-distance propagation of a surface plasmon on the surface of a ferromagnetic metal

V. Zayets¹, H. Saito², K. Ando³, S. Yuasa⁴

1. Spintronics Research Center, AIST, Ibaraki, Japan

At present, there is a significant commercial demand for an optical isolator, which can be integrated into the Photonic Integrated Circuits (PIC). An optical isolator, which utilizes unique non-reciprocal properties of surface plasmons, can be a good candidate as the integrated optical isolator [1], because of its small dimensions and its technological compatibility with the fabrication technology of the PIC. The main obstacle for a practical realization of the plasmonic isolator is the substantial propagation loss of the surface plasmons in structures containing a ferromagnetic metal [2]. Because of the high loss, a thick buffer layer of a noble metal is required between a ferromagnetic metal and a dielectric in order to observe a long-distance propagation of surface plasmons [3]. The reduction of the propagation loss of a surface plasmon is the key to make the plasmonic isolator competitive with other designs of the integrated isolator. It was demonstrated experimentally that by utilizing an optimized double-dielectric plasmonic waveguide it is possible to reduce significantly the optical loss in a plasmonic waveguide. For a Fe/SiO₂/AlGaAs double-dielectric plasmonic waveguide the low propagation loss of 0.03 dB/um was obtained. As far as we know at present it is the lowest propagation loss demonstrated for a plasmon propagating at the surface of a ferromagnetic metal. For a Co/Ti₂O₃/SiO₂ double-dielectric plasmonic waveguide integrated with a Si nanowire waveguide on a Si substrate the optical loss of 0.7 dB/um was demonstrated.

[1] V. Zayets, H. Saito, S. Yuasa, and K. Ando,, *Materials* 5, 857 (2012)

[2]. G. Armelles , A. Cebollada , A. García-Martín , and M. U. González , *Adv. Optical Mater.* 1, 10 (2013)

[3] V.V. Temnov et al. , *Nature Photon.* 4, 107 (2010)

Th.N-P04 - Using antiferromagnets as a route to tunable negative refraction

R. Macedo¹, R. Stamps¹, T. Dumelow²

1. SUPA, School of Physics and Astronomy, University of Glasgow, Glasgow, United Kingdom

2. Departamento de Física, Universidade do Estado do Rio Grande do Norte, Costa e Silva, Mossoró RN - Brazil

The phenomenon of negative refraction of a beam of electromagnetic radiation occurs when, on passing from one medium to another, the incident and refracted beams are situated at the same side of the surface normal. Here, we consider all angle negative refraction in uniaxial antiferromagnets. This phenomenon is possible when two of the principal components of the permeability tensor have opposing signs, which occurs around the magnetic resonance frequencies (typically in the terahertz range). In the absence of a magnetic field ($B_0 = 0$), the tensor component along the uniaxis is unity at all frequencies, with poles in the perpendicular components at the magnon resonance frequency (8.94 cm^{-1} in the case of MnF_2) [1]. If the uniaxis lies along the crystal surface, in the plane of incidence, the angle of refraction becomes negative immediately above this frequency. When an external magnetic field B_0 is applied perpendicular to the plane of incidence, the magnetic spins will be canted toward this field. The main effect of this is to shift the magnetic resonance frequency to higher frequencies so that, at a given frequency, the angle of refraction will change. We therefore show that antiferromagnets such as MnF_2 open the possibility of negative refraction being tuned with an external magnetic field, and also show that this can occur to such an extent that the sign of the refraction can be inverted.

[1] R. Macedo and T. Dumelow. Phys. Rev. B, 89, 035135, (2014)

Th.N-P05 - Plasmonic hollow cylindrical nanostructures fabricated by nanoimprint lithography and non-directional metallization

A. Conde-Rubio¹, M. Kovylna^{1,2}, N. Alayo³, X. Borrisé³, F. Pérez-Murano³, G.D. Hibbard², A. Labarta¹, X. Batlle¹ N

1. *Dept. Física Fonamental, Universitat de Barcelona and Institut de Nanociència i Nanotecnologia, Barcelona, Spain*

2. *Dept. Materials Science and Engineering, University of Toronto, Toronto, Canada*

3. *Instituto de Microelectrónica de Barcelona (IMB-CNM, CSIC) UAB, Barcelona, Spain*

A high-throughput, low cost process for the fabrication of hollow cylindrical nanoparticles with a precise control of their geometry and variable composition has been developed. The process is based on combining concepts from stencil and nanoimprint lithography (NIL), together with the use of non-directional metallization, allowing an accurate positioning of nanostructures in large arrays. The process starts by imprinting a trilayer structure consisting on a bottom layer of polymethyl methacrylate (PMMA) 950k MW, an intermediate thin layer of SiO₂ and a top layer of PMMA 75k MW, which are deposited on a substrate. Then, the top layer is patterned by NIL using Si dotted stamps. A dry reactive ion etching process is carried out to transfer the pattern to the bottom PMMA layer obtaining an optimal undercut for the final lift-off process. Metal deposition is performed by sputtering.

The unique properties of Au such as its chemical stability, biocompatibility and easy functionalization as well as its surface plasmon resonance which entails effects such as absorption and scattering enhancement or concentration of the electromagnetic field, make it the perfect candidate for applications in areas such as photovoltaics, sensing, and medicine. Optical absorption experiments and finite difference time domain simulations of Au hollow cylindrical nanostructures with a diameter and a height of about 400 nm and a wall and base thickness of about 30 nm demonstrate a great enhancement of the electromagnetic field, which is promising for fabricating functional devices based on surface Raman enhanced spectroscopy. This fabrication procedure also allows an easy combination of different materials making it possible to obtain multifunctional nanoparticles which could have interest for magnetoplasmonics.

This work was supported by Spanish MINECO (MAT2012-33037), Catalan DURSI (2014SGR220, 2014SGR1025), and European Union FEDER funds (Una manera de hacer Europa). A. Conde-Rubio acknowledges Spanish MINECO for a Ph.D. contract (BES-2013-065377).

Th.N-P06 - Enhancement of transverse magneto-optical intensity effect in active magneto-plasmonic structures

O. Borovkova¹, N. Khokhlov^{1,2}, A. Kalish^{1,2}, V. Belotelov^{1,2}, P. Vetoshko¹

1. *Russian Quantum Center, Moscow, Russia*

2. *Lomonosov Moscow State University, Faculty of Physics, Moscow, Russia*

Magneto-optical (MO) effects find their applications in modern data storage devices. Previously, it was shown that such effects can be significantly enhanced by the excitation of surface plasmon-polaritons (SPPs). SPPs propagating along the interface of ferromagnetic dielectric film and the nanoscaled grating of noble metal increase the MO effect in both reflected and transmitted light.

However, SPPs dissipate their energy through the interaction with metal that limits their propagation length. Moreover, the ferromagnetic material containing iron ions contributes additional losses. Thus, the problem of loss compensation and amplification of SPPs is crucial for the enhancement of the MO effect.

In our work we consider a ferromagnetic film of BiIG garnet doped by Cr ions or ions of rear-earth elements (Tb, Eu, Tm, Yb, and Nd) as a resonant amplifying medium. We address a magneto-plasmonic crystal of 1D gold grating deposited on the doped iron garnet grown on top of the non-magnetic gadolinium gallium garnet substrate. Due to the optical pump at certain frequencies of visible and IR-range dopant ions in ferromagnetic film are excited and their further emission increases the intensity and propagation length of the SPP wave. We are focused on the intensity MO effects like transverse magneto-optical Kerr effect (TMOKE) when the magnetization vector is perpendicular to the light incidence plane. We analyse the amplification of transmittance and TMOKE effect for various levels of optical gain, metal film width, and type of dopants. It is shown that by the employment of amplifying ferromagnetic film the intensity of the transmitted light can be increased by 50%. At the same time, the intensity of the TMOKE effect also increases by 50%.

The work is supported by the Russian Foundation for Basic Research (projects no. 13-02-01122, 14-02-01012)

Th.N-P07 - Faraday Rotation in (Bi, Gd, Al):YIG Films and Microcavity 1D-MPCs on their base in temperature range 300 - 20K

V.N. Berzhansky¹, A.V. Karavainikov¹, T.V. Mikhailova¹, A.R. Prokopov¹, A.N. Shaposhnikov¹, M.A. Kozhaev^{2,3}, Y. M.F. Kharchenko⁴, I.M. Lukienko⁴, O.V. Miloslavskaya⁴, Y.M. Kharchenko⁴

1. *V.I. Vernadsky Crimean Federal University, Simferopol, Russia*

2. *Russian Quantum Center, Skolkovo, Moscow, Russia*

3. *Prokhorov General Physics Institute of The RAS, Moscow, Russia*

4. *Institute for Low Temperature Physics and Engineering of the NAS of Ukraine, Kharkov, Ukraine*

1D magneto-photonic crystals (1D-MPCs) based on Bi-substituted yttrium-iron-garnet (Bi: YIG) films are very fruitful for applications in magneto-optical (MO) devices. The temperature could be one of the additional parameter allowing one to control the MO properties of 1D-MPCs, especially in the case when MO layers have a composition with a magnetic compensation temperature T_{comp} . The purpose of this research is the further study [1] of the low-temperature behavior of the optical and MO properties of single (Bi, Gd, Al)-substituted YIG films (M) prepared by reactive ion beam sputtering on GGG substrates and microcavity 1D-MPCs GGG/(TiO₂/SiO₂)₄/M/(SiO₂/TiO₂)₄ on their base. Three types of microcavity 1D-MPCs with MO films of different compositions, types of magnetic anisotropy and T_{comp} (including composition Bi_{2.8}Y_{0.2}Fe₅O₁₂ without T_{comp}) as a cavity layers were prepared and investigated.

It was found that the garnet films completely determine the MO properties of 1D-MPCs. The sign inversions of Faraday rotation angle Θ_F in the films and in MPCs are observed at the same T_{comp} and is associated with compensation of Fe- and Gd-sub-lattice magnetic moments.

In the films and in 1D-MPCs the temperature hysteresis in the $\Theta_F(T)$ dependence was observed around T_{comp} . Temperature hysteresis phenomena is caused by first-order phase transitions "collinear phase – non-collinear phase – collinear phase" and is due to the need of additional energy for the nucleation of a new magnetic phase. The observed slope of the $\Theta_F(T)$ dependence may be cause by possible inhomogeneous distribution of garnet-constituting elements along film thickness, mechanical stresses and structural inhomogeneities of the films.

The authors thank the Russian Science Foundation for support (grant # 14-32-00010).

[1]. Temperature dependence of Faraday rotation in microcavity 1D-MPC with compensation temperature / V.N. Berzhansky et al. // Intern. Conf. on Oxide Materials for Electronic Engineering (OMEE-2014), Lviv, Ukraine, May 26-30, 2014 : proceedings. – Lviv, 2014. – P. 215-216.

Th.N-P08 - One-dimensional photonic crystals with double-layered magneto-active defects

V.N. Berzhansky¹, A.V. Karavainikov¹, T.V. Mikhailova¹, A.R. Prokopov¹, A.N. Shaposhnikov¹, M.A. Kozhaev^{2,3}, M.F. Kharchenko⁴, I.M. Lukienko⁴, O.V. Miloslavskaya⁴, Y.M. Kharchenko⁴

1. *V.I. Vernadsky Crimean Federal University, Simferopol, Russia*

2. *Russian Quantum Center, Skolkovo, Moscow, Russia*

3. *Prokhorov General Physics Institute of The RAS, Moscow, Russia*

4. *Institute for Low Temperature Physics and Engineering of the NAS of Ukraine, Kharkov, Ukraine*

The basic problem in creation of one-dimensional magnetophotonic crystals (1D-MPCs) for various electronic and optical applications is the increasing of magneto-optical quality factor and finding the optimum ratio of the rotation angle of polarization plane and intensity of the light propagating through the crystal. The solution of this problem is complicated by the peculiarities of the synthesis of iron-garnet films with high Bi content (more than 1 at. / f. u.). At the first in [1] the double layer Bi-substituted iron garnet (Bi: IG) films composed of buffer layer with low Bi content and main layer with high one is proposed for synthesis of 1D-MPCs on non-garnet non-magnetic layers. As was shown the use of such films in microcavity-type structures is most effective. The aim of this research is to determine the optimal configurations and detail the magneto-optical properties of this type of structures.

Some series of microcavity 1D-MPCs of general formula $(\text{TiO}_2/\text{SiO}_2)_m/\text{M1}/\text{M2}/(\text{SiO}_2/\text{TiO}_2)_m$ with different repetition number of Bragg oxide mirrors m and double layered magneto-active defects $\text{M1}/\text{M2}$ of different compositions and thickness on the substrates of fused quartz were fabricated and investigated. Before fabrication, to determine the optimal parameters of layers the simulation of magneto-optical spectra of microcavity 1D-MPCs in transmission and reflection was performed. The obtained values of rotation angle of polarization plane of synthesized microcavity-type 1D-MPCs exceed the known experimental results by 2-3 times. The maximal values of Faraday and Kerr rotation angles are mines 20.6 deg (-66 deg/ μm) and 8.9 deg at 655 nm.

The authors thank the Russian Science Foundation for support (grant # 14-32-00010).

[1] V. N. Berzhansky, T. V. Mikhailova, A. V. Karavainikov, A. R. Prokopov, A. N. Shaposhnikov, I. N. Lukienko, Yu. N. Kharchenko, O. V. Miloslavskaya, N. F. Kharchenko, J. Magn. Soc. Jpn., 36 (1_2), 42 (2012)

Th.N-P09 - Magnetic behavior of SiO₂ opals with embedded Fe nanoparticles

C.E. Ávila Crisóstomo¹, E. Sánchez Mora¹, V. Cerdán Ramírez¹, F. Pérez Rodríguez¹

1. Instituto de Física, Benemérita Universidad Autónoma de Puebla, Heroica Puebla de Zaragoza, Mexico

Using the Stöber method, silica spheres were obtained and arranged in an fcc lattice. Fe has been introduced into void spaces of the artificial opals by means of the reduction of FeSO₄ with NaBH₄. Magnetization curves of artificial opals with Fe nanoparticles were measured by using the vibrating sample magnetometry (VSM) technique. In the measurements, the applied magnetic field was oriented along the [111] direction of the artificial crystals. In order to interpret the hysteresis cycles of magnetization, the homogenization theory developed in the work [1] has been applied. Such a theory provides explicit formulas for all the components of the permittivity and permeability tensors for a magnetodielectric photonic crystal in terms of the parameters of the inclusions and the host material in the quasistatic limit. On the basis of this homogenization theory, we have elaborated a computing program to calculate the effective permittivity and permeability of the SiO₂ opals with Fe nanoinclusions of different shape. Using the effective permeability, depending on the applied magnetic field, curves of magnetization vs magnetic field are straightforwardly calculated. The theory reproduces the general features of measured magnetization curves. In particular, the strong dependence of hysteresis loops on the Fe filling fraction, which was experimentally observed, is numerically confirmed by using an appropriate magnetic-field dependent permeability for Fe nanoparticles.

This work was partially supported by VIEP-BUAP

[1] V. Cerdán-Ramírez et al., J. Appl. Phys. 106, 103520 (2009)

Th.N-P10 - Light localization and magneto-optic enhancement in Ni and Co anti-dot arrays

E. Papaioannou¹, M. Rollinger¹, E. Melander², P. Thielen¹, E. Ístman², V. Kapaklis², M. Cinchetti¹, A. Carcia-Martin³, M. Aeschlimann¹

1. *Department of Physics and Research center OPTIMAS, Kaiserslautern, Germany*
2. *Department of Physics and Astronomy, Uppsala University, Sweden*
3. *IMM-Instituto de Microelectronica de Madrid (CNM-CSIC), Madrid, Spain*

The presence of surface plasmons in magnetic nano-structures can strongly influence the magneto-optical properties of magnetic films and multilayers [1-3]. In spite of the numerous studies on the plasmonic behaviour of magneto-plasmonic lattices and the enhanced magneto-optic signal, the physical understanding of coupling between plasmonic and magneto-optic properties is not clarified yet. Here we further elucidate the mechanisms of coupling between surface plasmons and magneto-optic properties for the case of Ni and Co antidot patterns. The antidot pattern has a hexagonal form with hole sizes ranging from 220-280 nm. With photo-emission electron microscopy (PEEM) images we show how light of different energies and polarization states is localized on the patterned magnetic surface. By using p- and s- polarized light we reveal that light takes different forms on the surfaces: either it is concentrated in bright spots that are arranged in a hexagonal lattice (use of p-light) or it forms continuous lines perpendicular to incident polarization of light (s-light). These effects are only present when the energy of the incident light is close to where excitations of surface plasmons polaritons are expected. The localization of light at the plasmonic resonances leads to a significant enhancement of the polar magneto-optic response of the patterned magnetic material. Furthermore, the type of light localization on the surface defines the size of the enhancement of the polar magneto-optic Kerr effect.

[1]E. Melander et al., Applied Physics Letters, 101, 063107, (2012)

[2] E. Th. Papaioannou et al., Phys. Rev. B 81, 054424 (2010)

[3]E. Th. Papaioannou et al., Journal of Surfaces and Interfaces of Materials 2, 40 (2015)

Th.N-P11 - Optical, magneto-optical and structural properties of Mn(2)Rh(1-x)Co(x)Sn Heusler compounds

J. Hamrle¹, K. Postava¹, J. Pistora¹, R. Silber¹, J. Enders², P. Cejpek², J. Macek², M. Veis², V. Hol², O. Meshcheriakova³

1. VSB - Technical University of Ostrava, Ostrava, Czech Republic

2. MFF, Charles University in Prague, Prague, Czech Republic

3. Max-Planck-Institut für Chemische Physik fester Stoffe, Dresden, Germany

We studied structural, optical and magneto-optical and structural properties of bulk Mn(2)Rh(1-x)Co(x)Sn Heusler compound, where Co concentration x ranges from 0 to 0.7 [1,2]. The structural properties was studied by XRD and EDAX. XRD shows that those polycrystalline samples have cubic (for x=0.7) and tetragonal (for x<0.7) lattice (space groups F-43m and I-4m2, respectively); element site occupation is within 10% of fully ordered compounds. EDAX data shows constituent element concentrations agree with the nominal ones within 5%. The optical properties was studied by ellipsometry and reflectometry. The determined permittivity reveals small optical absorption of samples in UV spectral range for all the compounds. Furthermore, at photon energy about 4.5 eV the photon absorption of Mn(2)Rh(0.7)Co(0.3)Sn compound nearly vanishes, an unusual feature for metallic systems. Furthermore, this material also provides vanishing reflectivity for s-polarized light at this photon energy range, suggesting a plasmonic behaviour of Mn(2)Rh(0.7)Co(0.3)Sn compound in this UV region. Financial support from GACR 13-30397S and EU project IT4Innovations is acknowledged.

[1] O. Meshcheriakova et al, Phys. Rev. Lett. 113, 087203 (2014)

[2] V. Alijani et al, J. Appl. Phys. 113, 063904 (2013)

Th.N-P12 - Magnetic switching of magnetoelectric plasmonic materials: from axion to toroidal electrodynamics

D. Ignatyeva ^{1,2}, A. Kalish ^{1,2}, O. Borovkova ², V. Belotelov ^{1,2}, A. Zvezdin ^{2,3,4}

1. *Lomonosov Moscow State University, Faculty of Physics, Moscow, Russia*

2. *Russian Quantum Center, Moscow, Russia*

3. *Prokhorov General Physics Institute RAS, Moscow, Russia*

4. *Moscow Institute of Physics and Technology, Dolgoprudny, Russia*

The work is devoted to the investigation of the surface plasmon polaritons (SPPs) in the metal – dielectric heterostructures containing magnetoelectric materials, chromium (III) oxide (Cr₂O₃) namely. An important feature of Cr₂O₃ is that its magnetoelectric response can be switched between axion-like and toroidal types via external magnetic field applied parallel to the crystal axis causing so-called spin-flop effect.

We analyze and classify the impact of the magnetoelectric effect on the properties of SPPs in various configurations of Cr₂O₃-metal heterostructure.

The axion-like effect causes slight rotation of the polarization ellipse of the SPP wave around the axis corresponding to the SPP propagation direction.

The impact of the toroidal effect on the SPP significantly depends on the orientation of the toroidal moment vector τ . We address three basic configurations:

1. The longitudinal configuration: τ is directed along the SPP propagation direction. The SPP propagation constant acquires non-reciprocal addition different for the SPPs propagating along τ and opposite to τ . Although the SPP polarization remains pure TM, the relations between the electromagnetic field components are slightly modified in a non-reciprocal way.

2. The transversal configuration: τ lies in the interface plane and is perpendicular to the SPP propagation direction. The plane of the SPP polarization ellipse is rotated around the axis normal to the interface.

3. The polar configuration: τ is perpendicular to the interface plane. The localization constant for the dielectric acquires small imaginary term associated with the toroidal moment and causing a slight energy leaking.

Therefore Cr₂O₃ can be considered as a unique object on which one can trace the similarities and difference between the axion-like and toroidal effects. Such magnetoelectric plasmonic heterostructure also might act as an optical tool for control of the SPP dynamics via external electric and magnetic fields.

The work is supported by RFBR (grants No.13-02-01122, 14-29-08216)

Th.N-P13 - Spin dynamics in magneto-plasmonic hybrid nanostructures

A. Capozzi ¹, T. Orlando ², M. Mariani ³, F. Pineider ⁴, M. Basini ⁵, M. Corti ², E. Umut ⁶, C. Sangregorio ⁴, A. Lascialfari ⁵, P. Ghigna ⁷

1. *Institute of Physics of Biological Systems, EPFL, Lausanne, Switzerland*

2. *Department of Physics and INSTM, University of Pavia, Pavia, Italy*

3. *Department of Physics and Astronomy, University of Bologna, Bologna, Italy*

4. *Department of Chemistry 'U. Schiff' and INSTM, University of Florence, Florence, Italy*

5. *Department of Physics and INSTM, Università degli Studi di Milano, Milano, Italy*

6. *Department of Medical Imaging Techniques, Dokuz Eylül University, Izmir, Turkey*

7. *Department of Chemistry and INSTM, University of Pavia, Pavia, Italy*

We report a broadband proton NMR study of the spin dynamics of coated maghemite and gold-maghemite hybrid nanostructures with two different geometries, namely dimers and core-shells. All the samples have a superparamagnetic behavior, displaying a blocking temperature ($T = 80$ K for maghemite, $T = 105$ K for dimer, $T = 150$ K for core-shell), and the magnetization reversal time follows the Vogel-Fulcher law. We can explain this behaviour by taking into account three different contributions to the spectral spin density, each one following the Bloembergen-Purcell-Pound (BPP) equation and characterized by a specific correlation time. Indeed, we hypothesize that: the peak at high temperatures is associated with the re-orientational motion of CH₃ and CH₂ groups of the organic coating; the peak observed at intermediate temperatures is related to the superparamagnetic blocking temperature T_B , i.e. to the Néel reversal of the magnetization; finally, the low temperature peak, whilst of still unclear origin, could be related to the surface spins dynamics of the magnetic core. The $1/T_1$ data for $T > 100$ K were successfully fitted with a BPP based heuristic model. The estimated correlation times for rotation and superparamagnetic reorientation are in good agreement with literature values for methyl group rotations and ac susceptibility data, respectively.

References:

Orlando T, Capozzi A, Umut E, Bordonali L, Mariani M, Galinetto P, Pineider F, Innocenti C, Masala P, Tabak F, Scavini M, Santini P, Corti M, Sangregorio C, Ghigna P, Lascialfari A. Spin Dynamics in Hybrid Iron Oxide-Gold Nanostructures, *The Journal of Physical Chemistry C* 119(2), 1224-1233

Th.N-P14 - Magnetoplasmonic modes in noble metal and hybrid nanoparticles

C. de Julian Fernandez^{1,2}, F. Pineider^{2,3}, V. Bonanni^{2,3}, G. Campo^{2,4}, G. Mattei⁵, A. Caneschi², C. Sangregorio^{6,2}

1. IMEM-CNR, Parma, Italy

2. Department of Chemistry, University of Florence & INSTM, Florence, Italy

3. ISTM – CNR, Milan, Italy

4. Department of Physics, University of Florence, Florence, Italy

5. Department of Physics, University of Padua, Padua, Italy

6. ICCOM – CNR, Florence, Italy

The controlled and reversible modification of the optical response of plasmonic systems, - active plasmonics- is a highly prized goal in today's research in materials science and nano-optics, due to an attractive potential for high-tech applications, from ultrasensitive refractometric sensing, to switchable plasmonic optical circuits. Magnetoplasmonics is the branch of active plasmonics that uses a magnetic field to influence surface plasmon resonance. [1] Currently, great efforts are being devoted to fully understanding the nature and effect of such interaction, with the ultimate goal of increasing its magnitude through rational design. While the magneto-optical activity of magnetic materials is a well known property, recently also important magneto-optical activity was observed in non-magnetic plasmonic materials - such as gold or silver [2,3] - in correspondence with the plasmonic resonance. In this study, using a combined approach with the aid of magnetometry and x-ray spectroscopy in addition to magneto-optics, we investigated several routes to design magnetic-plasmonic hybrid nanoparticles containing gold and iron oxides with different geometries, exhibiting different levels of conjugation, thus a variable extent of interaction of the magnetic and plasmonic functions. [4] We found that the chemical composition of the magnetic part critically affects the synergy of the two moieties; this finding paves the way to a largely rational design of material candidates for magnetoplasmonics.

This work has been financed by the Italian MIUR through FIRB projects “NanoPlasMag” (RBF100AI0), by the EC through FP7-214107-2 NANOMAGMA, and by Fondazione Cariplo through Project No. 2010-0612.

[1] G. Armelles et al. *Advanced Optical Materials* 1 (2013) 10-35

[2] B. Sepulveda et al. *Phys. Rev. Lett.* 104 (2010) 147401

[3] F. Pineider et al. *Nano Letters* 13 (2013) 4785-4789

[4] F. Pineider et al. *ACS Nano* 7 (2013) 857-866

Th.N-P15 - Nanostructural and magnetic properties in Au- Fe oxide magnetoplasmonics nanostructures

C. de Julian Fernandez ^{1,2}, F. Pineider ^{2,3}, G. Campo ², V. Bonanni ^{2,3}, P. Massala ⁴, V. Videtta ⁵, D. Pantaleone Cozzoli ⁵, M. Scavini ⁴, A. Caneschi ², P. Ghigna ⁶

1. IMEM-CNR, Milan, Italy
2. INSTM & University of Florence
3. ISTM- CNR, Milan, Italy
4. INSTM & University of Milan, Milan, Italy
5. INSTM & University of Salento, Lecce, Italy
6. INSTM & University of Pavia, Pavia, Italy
7. ICCOM – CNR, Florence, Italy

Magneto-plasmonic (MPs) is a novel concept of nanostructured materials composed by components that exhibit plasmonic and magnetic activity. However the combination of the two properties in a single nanosystems is not easy. Most of MPs are nano-heterostructures composed by ensembles noble metals and magnetic metals and oxide moieties in different morphologies like core@shell, onion-like nanoparticles, heterodimers, etc... [1-4] . Both type of properties are preserved due to the different electronic and chemical nature of the two moieties, being considered MPs nanostructures a classical example of multifunctional nanomaterials. Moreover new properties have been discovered, in particular, the enhancement of the magneto-optical response in correspondence of the plasmon excitation and the modification of the plasmon dynamics and of the magnetic properties. The chemical and physical mechanisms that will produce the such correlations are under study.

In this work we present a detailed study of the magnetic, structural and chemical properties of colloidal Au@iron oxide nano-heterostructures having both a range of core@shell morphologies, and dumbbell-like heterodimers with different dimensions. Our investigation was carried out by combining several nanostructural studies like TEM characterizations, XANES spectroscopies, Pair Distribution Function and powder X-Ray Diffractions with optical, magneto-optical and SQUID magnetometry for investigating structural, nanostructural, chemical, optical and magnetic properties. MPs nanostructures exhibit novel optical, magnetic and plasmonic features different than those of the bare nanosystems. We will show that most properties can be related to chemical and structural changes related to the synthesis process and the morphology. This work has been financed by the EC through FP7-214107-2 NANOMAGMA, and by Fondazione Cariplo through Project No. 2010-0612

- [1] L. Carbone, P. D. Cozzoli, Nano Today 5 (2010), 449
[2] G. Armelles et al. Advanced Optical Materials 1 (2013) 10
[3] F. Pineider et al. ACS Nano 7 (2013) 857
[4] S. Chandra et al Nanotechnology 25 (2014) 05570

Th.N-P16 - Novel type of highly sensitive alternating magnetic field detector based on the magnetoplasmonic crystal

V. Belyaev¹, A. Grunin², A. Fedyanin², V. Rodionova¹

1. *Immanuel Kant Baltic Federal University, Kaliningrad, Russia*

2. *Lomonosov Moscow State University, Moscow, Russia*

Continuous improvements in nanofabrication and nanocharacterization capabilities have changed predictions about the role of the metals in the development of the new optical devices and in particular of the Surface plasmon resonance (SPR) sensors. One way of increasing of the sensitivity of the SPR sensors is using of the magneto-optical (MO) effects. Using of the magnetoplasmonic crystals (MPIC) - subwavelength periodical structures made of noble and ferromagnetic metals allows one to modify MO properties by excitation of the surface plasmons at resonant conditions. Optical response of the MPICs strongly depends on the magnetization and consequently on the magnitude of the external magnetic field. This fact allows one to design and fabricate magnetic field detectors based on this effect. MPICs were fabricated by ion beam sputtering of the noble (gold or silver) and ferromagnetic (iron or nickel) metals on the substrates with different spatial profiles. After the fabrication, atomic force microscopy images of the surface were obtained in order to determine parameters of the spatial profile. Magnetic properties were measured by VSM at room temperature. MO properties were measured by a homemade setup consisting of a halogen lamp with a monochromator as the light source, Glan-Taylor prism as the polarizer and a photomultiplier tube with a lock-in amplifier as the detector. Investigation of the magnetic properties showed a non-linear dependence of the coercive force (16 - 300 Oe) and saturation magnetization (16 - 1300 Oe) on thickness and material of the ferromagnetic layer. Changing the magnetic properties it is possible to control the sensitivity and working range of the magnetic field detector based on MPIC. Dependences of MO response showed that signal-to-noise ratio is more than 200 and sensitivity is about 10^{-6} Oe. Summarizing, in this work a new type of the magnetic field detector and a way to control its parameters are represented.

Th.O-P02 - Temperature dependent magnetostrains in Mn and Ga-doped Fe-Pd ferromagnetic shape memory ribbons

M. Sofronie¹, F. Tolea¹, A. Crisan¹, M. Enculescu¹, M. Valeanu¹

1. National Institute of Materials Physics, Magurele, Romania

Ferromagnetic shape memory alloys (FSMA) have attained strong interest over the last years because of the large strains which can be obtained by the application of an external magnetic field. Fe-based FSMA are more suitable for applications, mainly due to their enhanced ductility than the well-known Ni₂MnGa alloy. The shape memory effect in disordered Fe-Pd (30 at.% Pd) is associated with an f.c.c - f.c.t. thermoelastic martensitic transformation (MT). By further cooling, an irreversible transformation occurs from f.c.t. to b.c.t. structure. The addition of a third alloying element may promote the stabilization of the fct martensite and the melt - spinning technique removes the precipitation of b.c.t. irreversible phase in Fe-Pd (30 at.% Pd) binary system. Prepared as ribbons by rapid quenched technique, these alloys are suitable for sensors designs.

The magnetic field-induced strains (MFIS) are the result of the preferential nucleation of martensitic variants with the easy magnetization direction parallel to the applied magnetic field during cooling across MT. So, high magnetocrystalline anisotropy of the martensite phase as well as large mobility of the twin boundary is required. The magnetic field assisted linear thermal expansion (LTE) measurement is an appropriate method to evaluate the influence of atomic ordering (induced by thermal treatments) on the magnetoelastic properties of highly textured ribbons.

Here we report the changes of the magnetostriction and MFIS of as prepared and thermal treated ribbons as effect of Mn and Ga substitution in Fe_{70-y}Pd₃₀X_y (X= Mn, Ga and y= 0,1,3) alloys. Results have shown a degradation of the MT characteristics and of the magnetoelastic properties for the Ga substituted alloys. In contrast, Mn substitution enhanced not only the MT temperature and the transformation enthalpy, but MFIS on the thermal treated ribbons with 3% Mn (~120x10⁻⁶) is twice that obtained on the parent alloy.

Th.O-P03 - Liquid pressure wireless stress sensor based on magnetostrictive microwires for applications in cardiovascular localized diagnostic

P. Marin¹, A. Hernando¹, A.M. Aragón¹, M. Hernando-Rydings²

1. *Instituto de Magnetismo Aplicado, Las Rozas, Spain*

2. *Hospital de Basurto, Vizcaya, Spain*

In this paper, we report a method to measure changes in a fluid pressure flowing through a flexible pipeline by means of a ring of magnetic microwire concentric to the pipeline. The detection is based on the modulated scattering of electromagnetic waves by the magnetoelastic ring. The modulation is driven by applying a bias magnetic field that tunes the magnetic permeability of the ferromagnetic microwire. The magnetostrictive character of the microwire allows pressure detection by means of magnetic permeability changes. The experimental work developed has, also, allowed the fluid pressure detection in a hydraulic circuit connected to a ventricular assist systems where a fluid with a viscosity close to blood flows.

Th.O-P05 - Electrical control of magnetostatic and magnetoelastic waves in ferrite-piezoelectric structure

Y. Khivintsev^{1,2}, Y. Filimonov^{1,2}, S. Vysotsky^{1,2}

1. SB Kotel'nikov IRE RAS, Saratov, Russia

2. Saratov State University, Saratov, Russia

Possibilities to tune wave properties through the electrical control are subject of the great interest for microwave signal processing. In this work we experimentally studied effect of electrically tuned mechanical stress on properties of the magnetostatic waves (MSW) and magnetoelastic waves (MEW) in contact structure based on yttrium iron garnet (YIG) film epitaxially grown on gadolinium gallium garnet (GGG) substrate and piezoelectric actuator. The YIG/GGG sample was placed on two separate alumina plates with microstrip antennas for MSW excitation and detection. The actuator was placed on the YIG/GGG structure in the middle and fixed mechanically using a support from above so that under voltage the actuator presses on the YIG/GGG structure and slightly bends it. External magnetic field was applied along the antennas corresponding to magnetostatic surface wave (MSSW) propagation. Scattering parameters were measured as a function of the frequency for various bias magnetic fields and voltages applied to the actuator using a vector network analyzer. At zero voltage the MSSW transmission band contained the equidistant narrow absorption peaks corresponding to the resonant interaction of the MSSW with the elastic waveguide modes of the YIG/GGG structure resulting in MEW formation. Applying voltage we observed the shift of the MSSW transmission band to higher frequencies. For the maximum voltage of 140 V extending the actuator length by 5 micron the shift was ~50 MHz. This shift can be attributed to appearance of the additional magnetic field of ~10 Oe due to the stress and magnetostriction. Also, we found effect of the voltage on the magnitude of the magnetoelastic absorption peaks that might be related with the change in distribution of the elastic oscillations across the YIG film thickness under the stress.

This work was supported by the Russian Foundation for Basic Research (13-07-12421-ofi-m, 14-07-00896-a, 13-07-00941-a)

Th.O-P06 - Preparation and characterization of porous magnetoelastic composites for magnetic field controlled flow applications

M. Krautz¹, D. Werner¹, M. Schrödner², J. Popp², A. Waske¹, J. Eckert¹

1. *Leibniz Institute for Solid State and Materials Research, Dresden, Germany*

2. *Thuringian Institute of Textile and Plastics Research e.V., Rudolstadt, Germany*

Magnetoelastic composites (MEC) based on elastic polymer matrix and a magnetic filler material, have drawn attention in various research fields, such as sensor technology, damping mechanics or biomedicine. This material class is highly responsive to an externally applied magnetic field triggering the change of intrinsic and extrinsic properties, e. g. size and shape, permeability, magnetization or mechanical behavior [1]. In our study, commercially available thermoplastics with different mechanical properties are extruded together with spherical Carbonyl-Fe particles (CIP-SQ, BASF Co.)[2]. These strands can be subsequently bundled, in order to achieve an arrangement with continuous channels for perfusion by a liquid or gaseous medium. By the application of an external magnetic field, the dipole-dipole interactions between the Fe - particles form chains, consequently the MEC strand is deformed[3,4]. In a bundle each deformed strand would lead to a change of the channel's width and therefore a change of the hydraulic pressure. In this presentation we focus on the magnetic properties of single strands as function of the polymer matrix material and the magnetic particle content. Magnetic measurements reveal that the magnetic hysteresis is crucially affected by the Young's modulus of the polymer matrix. This can be attributed to the increased particle movement in matrices with low Young's modulus. On the other hand, hysteresis is reduced with increasing filler fraction, since the modulus increases with larger particle content. This study links the evolution of the magnetization behavior as function of filler fraction and initial mechanical properties determined by the polymer matrix.

[1] J. Thévenot et al., Chem. Soc. Rev. (2013) 42

[2] G. Y. et al., Smart Mater. Struct. (2004) 13

[3] K. Zimmermann et al., Sci. J. IFToMM Problems Mech. (2014) 4

[4] A. Y. Zubarev et al., J. Magn. Magn. Mater. (2015) 377

Th.O-P07 - Oscillation of standing spin wave in nanostructured ring resonator with spin transfer torque

B. Peng¹, X. Ya², K. Imamura³, T. Tanaka⁴, K. Matsuyama⁵

1. ISEE Kyushu University Japan, Nishi, Japan

The collective magnetic excitation of spin wave (SW) is recently attracting renewed research interests from dispersive nonlinear physics and practical applications to wave-based logic or signal processing devices. Active ring resonators, made of the SW guide and an external feedback loop, have offered a stage for exploring various nonlinear SW dynamics. We report on numerical analysis on oscillation of standing spin wave (SSW) excited in a nanostructured active ring resonator, consists of a ferromagnetic nanowire (20x20 nm² cross section, 80 nm length) with perpendicular anisotropy. The following material parameter set are assumed in the simulation, $M_s = 680$ emu/cc, perpendicular anisotropy field $H_k = 5.0$ kOe, damping constant $\alpha = 0.01$. The SSW was excited with an alternative spin transfer torque assuming a spin polarized current vertically applied through a part of the wire. The magnetization direction of the overlaid fixed layer, spin polarized current source, was assumed to be in-plane, at which the most efficient SSW excitation was observed in preliminary simulations. The wave vector of the SSW is along the nanowire length. A positive feedback with proportional-integral-derivative (PID) gain control was adopted in the active ring. Stable excitation of the 1st order standing spin wave has been demonstrated with micromagnetic simulations. The stationary SSW with a pre-determined set variable of precession amplitude was attained within less than 5 ns by optimizing the PID parameters. The obtained fosc value of 7.95 GHz practically agrees with the theoretical prediction from dispersion relation of the magneto static forward volume wave. The fosc can be tuned with the value of the perpendicular anisotropy and also with the structural parameter such as the wire length.

Th.O-P08 - Enhancement of the magnetic field sensor sensitivity through tailoring of the magnetic disk profile

P. Vetoshko ^{1,4}, M. Kozhaev ^{1,3}, N. Gusev ^{1,3}, A. Zvezdin ^{1,3}, I. Syvorotka ⁵, I. Syvorotka ⁵, V. Belotelov ^{1,2}

1. Russian Quantum Center, Moscow, Russia

2. Lomonosov Moscow State University, Faculty of Physics, Moscow, Russia

3. Prokhorov General Physics Institute, Russian Academy of Sciences, Moscow, Russia

4. Kotelnikov Institute of Radio Engineering and Electronics, Russian Academy of Sciences, Moscow, Russia

5. CARAT Scientific Research Company, Lviv, Ukraine

A special place among the tools for registration of the magnetic fields is taken by magneto-modulation sensors (MMS), which are based on magnetically ordered materials. The MMS provide high energy of interaction with the measured field and the potentially high sensitivity, also they are cheap and practically feasible, and do not require cryogenic temperatures. Here we investigate MMS with a magnetic disk of epitaxial rear earth iron garnet (111) with easy plane magnetic anisotropy. Magnetization saturated (single-domain) state of the magnetic disk of the sensor is a necessary condition for achieving high sensitivity. In order to minimize noise from the electromagnetic system of the MMS, the magnetic disk must have sufficiently large magnetic susceptibility, i.e. its saturating field has to be small. At a given ratio of thickness to diameter of the sample, a magnetic disk of an oblate ellipsoid shape has the lowest saturation field. However, its practical implementation is a very complex technological problem. In this work we overcome this problem by approximation of the semi-elliptic profile of the magnetic disk by a multi-step profile fabricated by photolithography. Both theoretical and experimental studies of the capability of the multi-step profile approximation for the magnetic disk core of the MMS are conducted. Our study shows that the four-step approximation of the semi-elliptic profile of the magnetic disk significantly reduces the saturation magnetic field and, consequently, reduces the noise level of the corresponding MMS down to $10^{(-9)}$ Oe/Hz^(1/2). Further increase in the number of the approximation steps should further reduce the noise level and increase the MMS sensitivity by an order of magnitude that makes the MMS comparable to SQUID magnetometers. Main advantages of the MMS are room temperature operation and much lower cost. This work was supported by the Russian Science Foundation: grant No. 14-32-00010.

Th.O-P09 - Magnetic properties and domain structure in stress-annealed METGLAS 2714AZ

P. Sarkar¹, K. Zaveta², K. Jurek², J. Vcelak¹, P. Ripka¹,

1. *University Centre for Energy Efficient Buildings, Technical University In Prague, Czech Republic*

2. *Institute of Physics, AS CR, v. v. i., Prague, Czech Republic*

The domain structure of as-cast and stress-annealed 2.5mm wide Metglas 2714AZ was studied by means of type II magnetic contrast in SEM. The material was stress-annealed without magnetic field to obtain magnetic properties suitable for low-noise fluxgate sensor core. Various types of domain structures were observed on the shiny surface of ribbons with variations of annealing temperature (350°C and 390°C), stress (50-200 MPa) and time (5-30 minutes). The observed domain structures were compared with the processes of magnetization. During the annealing well above the Curie temperature of 250°C and below the crystallization temperature of 558°C we observed a change of the magnetic easy axis from the original longitudinal to the required transverse one, but for short annealing times the process was more complicated. The observed stripe structure with magnetization in the domain essentially transverse to ribbon direction and parallel to the easy direction leads to the demanded shape of the magnetization curve with low coercivity and remanence and linear between the saturation states. For annealing above TC the effect of ribbon cooling on the ribbon properties is decisive and we found distinct differences for annealing and cooling in the static regime or when the ribbon was moved continuously through the furnace. The latter procedure gave apparently the best properties for the intended use in fluxgate sensors. This work was supported in part by the European Union OP RDI Project under Grant CZ.1.05/2.1.00/03.0091 - University Centre for Energy Efficient Buildings and in part by the European Social Fund within the framework of realizing the project "Support of inter-sectoral mobility and quality enhancement of research teams at Czech Technical University in Prague" under Grant CZ.1.07/2.3.00/30.0034.

Th.O-P10 - GMI sensor for component integrity evaluation

P. Sarkar¹, R.K. Roy², A.K. Panda², A. Mitra², J. Vcelak¹, P. Ripka¹

1. *University Centre for Energy Efficient Buildings, Technical University, Prague, Czech Republic*

2. *CSIR-National Metallurgical Laboratory, Jamshedpur, India*

A giant magneto-impedance (GMI) based magnetic sensing device has been developed using (Co₅₀Fe₅₀)₇₄Si₈B₁₄Cr₄ microwire as the magnetic sensing core having great potential to monitor the microstructural changes that takes place in steel during in-service operation. In the present work experiment has been carried out with various test samples simulated at the laboratory condition. Experiments were conducted involving 9Cr-1Mo sample subject to various heat-treated conditions to generate various microstructure. A correlation between the GMI sensing voltages for different tempered 9Cr-1Mo steels and the corresponding hardness was found which demonstrates the usefulness of the developed sensor to monitor tempering condition of the steel. Experiment was extended for the plastically deformed 18-8 Cr-Ni (304SS) where stress induced martensite is formed. In this case GMI sensing voltage increased with percentage of deformation in steel. The formation of magnetic phase, martensite, during deformation of non-magnetic 304SS is the cause of such changes. The work was also been extended for detection of defective weld joints in 304SS oil refinery pipes collected from the petrochemical industry. The sensing device has also been used to evaluate the compressive residual behaviour in pure iron and pressure vessel steel. A field study was conducted where the developed GMI sensor was taken to the refinery unit of a petrochemical industry to find the feasibility of using the sensor for evaluation of carburization in steel which is the main cause of failure of the structure.

Th.O-P11 - Composite Fe_xO_y/TiO₂ powders - microstructure and magnetic properties

O. Zivotsky¹, J. Seidlerova², I. Safarik³, J. Lunacek¹, M. Safarikova³, K. Mamulova Kutlakova²

1. Institute of Physics, VSB-Technical University of Ostrava, Ostrava, Czech Republic

2. Nanotechnology Centre, VSB-Technical University of Ostrava, Ostrava, Czech Republic

3. Institute of Nanobiology and Structural Biology of GCRC, Academy of Sciences of the Czech Republic, Prague, Czech Republic

Titanium dioxide (occurring in three modifications: anatase, brookite and rutile), especially the anatase can be used in various technology applications such as photovoltaic solar cells, sensors and photocatalytic processes. Particles of titanium are suitable and effective as adsorbents for removal of toxic ions from aqueous solutions due to their high stability, low cost and safety toward both humans and the environment. To improve the separation of solid sorbents from liquids the composite adsorbent/magnetic particles were prepared by precipitation iron hydroxides from water solution of FeSO_{4.7}H₂O. The prepared suspension of iron hydroxides suspension was treated in a standard kitchen microwave oven (700 W, 2450 MHz) for 10 min at the maximum power. The formed magnetically responsive composite with iron oxide content was captured using an appropriate magnetic separator or NdFeB magnet. Then the magnetic TiO₂ formed was washed with water and air dried at cca 333 K.

Magnetic properties of powders were analysed by vibrating sample magnetometer (VSM) Microsense EV9. Parameters obtained from the hysteresis loop (coercive field - 1.11 kA/m, saturation magnetization - 3.38 Am²kg⁻¹) are supplemented by the thermomagnetic curve, when sample is heated up to 950 K (Curie temperature cca 878 K) and cooled back to room temperature. Dominance of negative (dipolar) magnetic interactions between particles was detected from the Henkel plot. In such a case they are produced by the magnetic moment of each particle and depend on the number of Fe atoms inside the particle. Interactions increase to their maxima at 12.72 kA/m and subsequently fall down to zero at higher fields. Marked increase of coercive field (approximately 10 times) followed by the shift of interactions maxima towards higher fields is observed after the temperature treatment (heating and cooling back to room temperature).

Th.O-P13 - Improved Microtransformer design utilizing Fe-Co magnetic core

D. Dinulovic¹, M. Haug¹, A. Gerfer¹, M. Kaiser², M. Wurz², L. Rissing²

1. *Würth Elektronik EiSos, Niedernhall, Germany*

2. *IMPT, Leibniz Universität Hannover, Hannover, Germany*

INTRODUCTION: This paper presents the design, fabrication, and characterization of on Silicon integrated micro-transformers for high frequency power applications.

Increasing trend in electronics for higher power density and mobility causes the miniaturization of power supply and therefore the miniaturization of passive components like inductors or transformers. A permanent increase of a switching frequency of an electronic power circuit sets new requirements for inductive components regarding to size and inductance and current capability. Inductors and transformers should provide smaller inductivity and smaller size. Decreasing of inductivity causes a decreasing of the inductor size and of the inductor profile height, therefore in thin-film fabricated micro microinductors and microtransformers are ideal components for fulfill this issue.

DESIGN: First fabricated microtransformer device is presented before [1]. This is a new improved design regarding to improve of a current capability and of an efficiency. The microtransformer consists of a closed CoFe magnetic core and four coils. Two coils are on the primary and two coils are on the secondary transformer side. The design was simulated using Finite Element Method (FEM). The software tool Ansys Maxwell« was applied.

The microtransformer device is fabricated using thin-film technology. As a magnetic material for the transformer core, Co-Fe alloy is chosen based on excellent magnetic properties. Co-Fe magnetic core has been deposited by Co-Fe electroplating. Coils are fabricated using Cu electroplating. Coils and magnetic core are embedded in polyimide.

The microtransformer has an inductivity of 60 nH, resistance of 300 mOhm and can be applied for current up to 1.5 A.

References:

[1] D. Dinulovic et al., JAP, 115 (17), 17A317 (2014)

Th.O-P14 - Anomalous thermal expansion in (Pr,Ca)MnO₃ due to orbital ordering

J. Tikkanen¹, H. Huhtinen¹, P. Paturi¹,

1. Wihuri Physical Laboratory, Department of Physics and Astronomy, University of Turku, Finland

The perovskite manganite family Pr(1-x)Ca(x)MnO(3) (PCMO) shows a multitude of functional properties that can be accessed by tuning the molar ratio between Pr and Ca. Species near the “half-doped” composition, Pr(0.5)Ca(0.5)MnO(3), exhibit an insulating antiferromagnetic ground state with pronounced charge and orbital ordering (CO and OO). The disruption of this state, using electromagnetic fields or mechanical stress, leads to most of the functionality of PCMO by revealing a charge-disordered, ferromagnetic metallic state.

Practical devices using PCMO will most likely employ epitaxial films of the material. The characterization of the physical properties of such films is, however, complicated by the fact that thermal expansion cannot be isolated from lattice stress due to the epitaxiality condition. To resolve the problem, we have used x-ray diffraction to measure the temperature dependence of the lattice constants of polycrystalline bulk PCMO at the Ca concentrations x=0.4 and 0.5, where CO and OO are known to be present, and also at x=0.1, where regular thermal expansion is expected. The data were obtained at temperatures from 83 K to 403 K. SQUID magnetometry was employed within the same temperature range to identify the onset of OO (or the lack thereof, for x=0.1) around 250 K.

Each of the OO species produced a distinctive structural anomaly around the onset temperature of OO, signaled by a region of negative temperature expansion just above the transition temperature. During the anomalies, unit cell volume excesses of order 0.1 % were estimated in x=0.4 and 0.5, whereas none was found in x=0.1. The magnitude of the anomalies was comparable to an expected regular thermal expansion across a temperature change of ca. 150 K. The results bear direct consequences for designing thin film devices that operate in the mentioned temperature region, since the OO anomaly will effectively modify the film-substrate lattice mismatch.

Th.O-P17 - Electromagnetic properties of Fe granular composite materials

T. Kasagi¹, T. Tsutaoka², S. Yamamoto³, K. Hatakeyama³

1. National Institute of Technology, Tokuyama College, Yamaguchi, Japan

2. Graduate School of Education, Hiroshima University, Hiroshima-shi, Japan

3. Graduate School of Engineering, University of Hyogo, Hyogo, Japan

Ferromagnetic metal granular composites (FMGC) with particle content below the electrical percolation threshold show a relatively high magnetic permeability in the GHz range. The FMGC can have the negative permeability spectra which are caused by the magnetic resonance of the ferromagnetic composite structure. This negative permeability spectrum is affected by the shape anisotropy of embedded particles [1]. The electrical conductivity of the composite structure also depends on the particle shape; the flaky particle composite shows the larger conductivity and the lower percolation threshold than the spherical particle one. Furthermore, the FMGC such as the Fe₅₀Co₅₀ flaky particle composite indicates the negative permittivity spectrum in the metallic state above the percolation threshold by the low frequency plasmonic oscillation. Hence, the high frequency permeability and permittivity spectra of FMGC can be controlled by the shape and content of dispersed particle.

In this work, the electromagnetic properties of Fe granular composite materials have been studied in the microwave frequency range. The micrometer-sized Fe spherical particles, which were heat-treated in air to suppress the eddy current effect, were used. Composite materials were prepared by mixing Fe particles with Polyphenylene sulfide resin. SEM observations revealed that both the coagulated and the isolated Fe particles were dispersed in the binder matrix. It was revealed that the low-frequency permeability of Fe composites was larger than that of the Co and Fe₅₀Co₅₀ granular composites at the same particle content. However, the Fe composites don't show the negative permeability spectrum in the microwave range. On the other hand, the Drude type negative permittivity spectrum was obtained in the metallic state at 68 vol.% particle content. This can be attributed to the low frequency plasmonic oscillation of electrons in the percolated Fe cluster chain in the Fe composite.

[1] T. Kasagi et al., J. Appl. Phys., 116 (2014) 153901

Th.O-P19 - Magneto-optical and magnetic properties of doped aluminophosphate glasses

C. Iordanescu², M. Sofronie¹, A. Catalin Galca¹, F. Tolea¹, V. Kuncser¹, M. Valeanu¹, M. Elisa², I.D. Feraru², B.A. Sava³, L. Boroica³

1. *Magnetism and Superconductivity Department, National Institute of Materials Physics, POB MG-7, Bucharest-Magurele, Romania*

2. *Optospintronics Department, National Institute for Optoelectronics INOE 2000, Bucharest-Magurele, Romania*

3. *Laser Department, National Institute for Laser, Plasma and Radiation Physics, Bucharest-Magurele, Romania*

Optical glasses with high magneto-optical effects are known to be useful for optical isolators and switches. According to the Faraday effect, a rotation of the polarization vector is observed for a light passing through specific transparent materials, if a magnetic field is applied along the wave-vector. The rotation is proportional to the passing length (l), the intensity of the magnetic field (B) and the intrinsic electric properties of the material as taken into account by the so-called Verdet constant (V). The Verdet constant itself depends on the electronic structure of the glass atoms and is it implicitly related to its magnetic properties through possible doping ions.

The effect of low-level doping with different elements (La, Y, Dy, Tb, Pb, Bi) of a new aluminophosphate glass ($\text{Li}_2\text{O}-\text{BaO}-\text{Al}_2\text{O}_3-\text{La}_2\text{O}_3-\text{P}_2\text{O}_5$) is investigated in this work, in relation to magnetic properties and specific Faraday rotations. The wavelength dependence of the Verdet constant, measured on the entire visible spectrum, was analyzed by taking into account both Westenberger's dispersion model for the diamagnetic contribution and VanVleck-Hebb theory for the paramagnetic contribution, according to the relation: $V=V_{\text{dia}}(\lambda) +V_{\text{para}}(\lambda, T)$. It was observed that the Faraday rotation is not changed as effect of doping with La or Y but it is slightly increasing for Pb and Bi doping ions (with rare-earths producing its sign change). Responsible for the Faraday rotation in Dy and Tb containing glasses was found to be the effective electric dipole transition $4f^n \rightarrow 4f^{n-1}5d^1$ corresponding to $\lambda_n=171$ nm for Dy^{3+} and $\lambda_n=216$ nm for Tb^{3+} whereas for the diamagnetic matrix, the resonance wavelength is 110 nm. The proportionality between the magnetic susceptibility and the paramagnetic Verdet constant is good for low level of rare-earth doping. A Verdet constant of 0.036 min/(cm Oe) corresponds to the glass doped with 1.2×10^{21} Tb at./cm³ and with the room temperature susceptibility of $2.18 \cdot 10^{-5}$ emu/g Oe.

Th.O-P20 - Magnetic properties of the reactive sorbents based on the CeO₂/Fe₂O₃ composite powders

J. Lunacek¹, O. Zivotsky¹, P. Janos², J. Henych^{2,3}, V. Stengl^{2,3}

1. VSB - Technical University of Ostrava, Department of Physics, Ostrava, Czech Republic

2. University of Jan Evangelista Purkyně, Faculty of the Environment, Ústí nad Labem, Czech Republic

3. AS CR v.v.i., Institute of Inorganic Chemistry, Prague, Czech Republic

Recently, new magnetically separable reactive sorbent based on γ -Fe₂O₃ (maghemite) grains and active CeO₂ surface layer which successfully decompose certain dangerous organophosphate compounds (parathion methyl, chemical warfare agents soman and VX), were discovered. The CeO₂/ α -, γ -Fe₂O₃ composite materials exhibit the different magnetic properties caused by various calcination temperature in the interval from 300 to 900°C. Vibrating sample magnetometer (VSM) EV9 was used for analysis of the powders. Magnetic properties were studied through the hysteresis loops, Henkel plots, and the switching field distribution function (SFD). All samples show the negative Henkel plots implying dominance of the dipolar interactions, according to the position of Henkel minima they can be divided into two groups. The first group consists of the powders annealed at the temperature below 600°C. Observed negative interactions start practically at zero magnetic field and reach their maxima in weak fields about 2.4 - 3.2 kA/m. Magnetic properties of the samples in the second group reflect the increasing calcination temperature from 700°C to 900°C. The nucleation magnetic fields linearly increase from 40 kA/m to 49.52 kA/m, and the minima of the Henkel plots move from 108.8 kA/m over 252.88 kA/m to 265.68 kA/m. Changes in the magnetic behavior, when the calcination temperature exceeds 600°C, are related apparently to the phase transition of the maghemite to the α -Fe₂O₃ (hematite). Rapid increase of coercive field corresponds with the growth of the crystallite sizes of the weakly ferromagnetic hematite and cerium oxide.

Th.O-P21 - Crystal structure and magnetic properties of the new R_3Pd_5 compounds (R = rare earth)

A. Provino ¹, S.K. Dhar ², N.S. Sangeetha ², P. Manfrinetti ¹, L. Petit ³, K.A. Gschneidner Jr ⁴

1. *Department of Chemistry, University of Genova, Genova, Italy*

2. *Condensed Matter Physics & Material Science, Tata Institute of Fundamental Research, Mumbai, India*

3. *Daresbury Laboratory, Daresbury Warrington, United Kingdom*

4. *Ames Laboratory, & Department of Materials Science and Engineering, Iowa State University, Ames, United States*

We report the synthesis, crystal structure and magnetic properties of the new series of compounds R_3Pd_5 (R = rare earth). The R_3Pd_5 compounds form by a peritectic reaction and adopt the orthorhombic Pu_3Pd_{5-type} structure (oS32-Cmcm); the unit cell presents two inequivalent crystallographic sites occupied by R atoms. The R_3Pd_5 compounds have been found to form for R = Sc, Y, and the heavy rare earths (Tb to Lu, including Yb).

Magnetic properties of R_3Pd_5 (R = Tb, Dy, Ho, Er, Tm and Y) have been studied by using the techniques of magnetization, heat capacity and electrical resistivity. Y_3Pd_5 is a Pauli paramagnet with a low Sommerfeld coefficient of 4.8 mJ/mol K². The other compounds are antiferromagnets, each showing two antiferromagnetic transitions, most likely associated with the separate magnetic ordering of the two distinct rare-earth sublattices. The highest Néel temperature, TN1, of 13.5 K is observed in Tb_3Pd_5 . The bulk nature of the magnetic transitions is confirmed by heat capacity which shows two peaks at temperatures corresponding closely to the peak temperatures in the magnetic susceptibility. Metamagnetic like transitions at relatively low fields are observed in Tb_3Pd_5 and Dy_3Pd_5 . Their hysteretic behavior indicates first order nature of the field induced transitions. The electrical resistivity of these compounds shows normal metallic behavior. Theoretical calculations have been performed in order to explain the antiferromagnetic behavior of these compounds.

Th.O-P22 - Controlling of demagnetizing field distribution on thin-film magnetoimpedance element for miniaturization and improvement of sensitivity

H. Kikuchi¹, S. Oe¹, H. Uetake², S. Yabukami², T. Nakai³, S. Hashi⁴, K. Ishiyama⁴

1. *Iwate University, Morioka, Japan*

2. *Tohoku Gakuin University, Miyagi, Japan*

3. *Industrial Technology Institute, Miyagi Prefectural Government, Japan*

4. *Tohoku University, Miyagi, Japan*

Magnetoimpedance (MI) element is utilized for magnetic sensor applications in various industrial fields such as biomedical field and nondestructive testing because of its higher sensitivity. Demands for a miniaturization of MI elements increase on the miniaturization of electronic devices and on the detection with high spatial resolution. MI element fabricated using a thin-film gives a solution for the demands because the configuration is compatible with integrated electronic devices. On the contrary, when a thin-film MI sensor is miniaturized, decrease in the sensitivity due to a demagnetizing field is unavoidable. To overcome the disadvantage, we controlled the distribution of demagnetizing field in the elements and evaluated the impedance characteristics of the elements. We prepared MI elements in which the sensor shapes have a typical rectangular and a quasi-ellipsoidal shape for avoiding the demagnetizing field distribution. The impedance was measured by a network analyzer and a wafer probe with an applied DC field to the elements. Impedance for both elements increase with increasing applied field and have a peak during 8 - 10 Oe, this field strength corresponds with the anisotropy field of the film. The maximum slope of the impedance (dZ/dH) for the quasi-ellipsoidal shape is larger than that for rectangular shape. On the rectangular element, the demagnetizing field near the edge increases rapidly compared with the central parts, and the change ratio of the demagnetizing field, is maxima at the end of the element, decreases toward central part and becomes constant. This distribution modifies rapid impedance changes, consequently the sensitivity is reduced. For quasi-ellipsoidal shape element, the demagnetizing field is uniform, which is attributed to keeping higher sensitivity. The evidence of the results was confirmed by the domain observations with a Kerr - effect microscope. Our results indicate a potential of a miniaturized MI element with higher sensitivity.

Th.O-P23 - Optimizing the sensing performance of fluxgate magnetometer using amorphous metallic wire cores

U. Topal¹, C. Birlikseven¹, H. Sözeri¹, H. Can¹, S. Tanrıseven¹, P. Svec Jr.², P. Svec Sr.², J. Bydzovsky³

1. *Tübytak Ume P.K: 54, Gebze-Kocaeli, Turkey*

2. *Institute of Physics, Slovak Academy of Science, Bratislava, Slovakia*

3. *Institute of Electrical Engineering, Slovak University of Technology in Bratislava, Bratislava, Slovak Republic*

In this work we present the experimental results on parallel type fluxgate magnetometer using amorphous wire cores having a diameter of 100 micrometer. Single wire with 1 cm length was put into a hollow cylindrical ceramic rod having almost same inner diameter with that of the wire and outer diameter of just 1 mm. In order to find the best core properties the wires were annealed under argon atmosphere at different temperatures and magnetic field. The driver coil and the pick up coils were wrapped over these ceramic rods. The optimal driving frequency was determined depending on the magnitude of $2f$ signal with a frequency span between 0-50 kHz at constant amplitude of ac field and constant applied DC field. After determining the optimal frequency, which is around 23-24 kHz and not reported before, the same experiment was repeated for finding optimal amplitude of ac field. Then, the sensitivity measurements and noise analysis were carried out using these optimal parameters for the driving signal. In this way we could achieve to sense DC fields as low as 1 nT (even less) with noise level of as small as several decades of $\sqrt{\text{V/Hz}}$ at 1 Hz. Besides, the V_{2f} vs H_{DC} graphs have shown perfect linearity up to 0.6 Oe with fitting parameters of 99.996. Such linearity has not been seen in such a large dynamical range till now. We also recognized that there is no hysteresis on V_{2f} -HDC graphs even after applying fields as high as 10 Oe.

Th.O-P24 - Microwave detectors based on giant and tunneling magnetoresistive devices

W. Skowroński¹, S. Ziêtek¹, P. Ogródnik^{1,2}, J. Wrona^{1,3}, P. Wiśniowski¹, A. Żywczak⁴, M. Frankowski¹, J. Chęciński¹, J. Barnaś⁵, T. Stobiecki¹

1. AGH University of Science and Technology, Department of Electronics, Krakow, Poland
2. Faculty of Physics, Warsaw University of Technology, Warsaw, Poland
3. Singulus Technologies AG, Kahl am Main, Germany
4. AGH University of Science and Technology, Academic Centre of Materials and Nanotechnology, Krakow, Poland
5. Faculty of Physics, Adam Mickiewicz University, Poznan, Poland

Ferromagnetic thin films can emit or absorb electromagnetic signals in a microwave frequency range due to spin waves excitations. By means of spin torque diode effect [1] absorption of the signal at the frequency determined by the ferromagnetic resonance can produce a DC voltage that is used in radio frequency (RF) detectors [2].

In this work we present experimental and theoretical investigations of two types of detectors based on giant magnetoresistance (GMR) and tunneling magnetoresistance (TMR) elements. The GMR stripe with multilayer structure: buffer/ PtMn(16)/ CoFe(2)/ Ru(0.85)/ CoFe(2.1)/ Cu(t)/ CoFe(1)/ NiFe(5)/ cap (thickness in nm) stripe produces a DC signal when supplied by an RF current due to the Oersted field, that drives the magnetic free layer (CoFe/NiFe) into precession via the Oersted field[3]. We will show that the detection can be realized also at the frequencies below the resonance, i.e., in a much broader range. The sensitivity dependence on the Cu spacer thickness $1.9 < t < 2.3$ nm, which influences the interlayer exchange coupling will be also discussed. The GMR stripe with the dimensions of $2.5 \times 70 \mu\text{m}^2$ and the GMR ratio of 7.4% reached the sensitivity 0.54 V/W.

On the contrary, in the TMR nanopillar device with CoFeB(2.3)/MgO(2)/CoFeB(1.6) trilayer the free layer oscillations are caused by the spin transfer torque effect. Because of greater MR ratio of up to 100 %, higher sensitivity above 10 V/W is measured. In addition, the application of the bias voltage on the top of RF signal enables us to tune the resonance frequency up to 100 MHz/V thanks to the voltage controlled magnetic anisotropy effect. Thus, we can change the peak-detection from 1.4 up to 1.6 GHz [4]. Experimental results were confirmed by the micromagnetic simulations

This work was partly supported by the Polish National Science Center Grant No. DEC-2012/04/M/ST7/00799. W.S. acknowledges the Foundation for Polish Science scholarship under START Programme.

[1] - A. A. Tulapurkar et al. Nature 438, 339 (2005)

[2] - S. Miwa et al. Nature Mater. 9, 721 (2014)

[3] - S. Ziêtek et al. Phys. Rev. B 91, 014430 (2015)

Th.O-P26 - Low temperature sintering of Sc-substituted M-type ferrite multilayers for microwave applications

J. Töpfer¹, S. Bierlich¹, F. Gellersen², A. Jacob², R. Valencuela³

1. *Univ. Appl. Sciences Jena, Jena, Germany*

2. *Techn. Univ. Hamburg, Harburg, Germany*

3. *Natl. Autonomous Univ. Mexico, Ciudad de Mexico, Mexico*

Future communication systems demand higher bandwidths and higher operating frequencies. Satellite-supported communication currently uses frequency bands up to 40 GHz. For this technology, microwave ferrites for applications in the K-band and capable of being integrated into LTCC multilayer components are required. Scandium-doped hexagonal M-type Ba-ferrites of the stoichiometric composition $\text{BaSc}_x\text{Fe}_{12-x}\text{O}_{19}$ or iron-deficient $\text{BaSc}_x\text{Fe}_{12-z-x}\text{O}_{19}$ exhibit significant potential for microwave applications such as isolators and circulators and are well suited for the required frequency range.

Sc-doped Ba ferrites with $0 \leq x \leq 2$ were prepared by the mixed oxide route. After calcination (1300 °C) as well as after sintering (1370 °C) single-phase ferrites were obtained. The sintering behavior of the ferrites was modified by the addition of BBSZ glass sintering additive and sufficient densification at 900 °C was obtained. The influence of BBSZ content and sintering temperature on microstructure formation and magnetic properties was studied. Static magnetic measurements show that both, the saturation magnetization and coercive force decrease with increasing concentration of scandium. The ferromagnetic resonance frequency of the ferrites as determined by reflectance measurements in U- and K-band (30-60 GHz) waveguide decreases with Sc content. The resonance studies in the X-band complete the investigations of the HF behavior of the ferrites. Ferrite multilayers were prepared by tape casting and stacking were co-fired at 900°C. The magnetic properties of multilayers are compared to those of sintered compacts. First results on integration of ferrite multilayer structures into LTCC multilayer architectures are reported.

Th.O-P27 - Effect of planar microantenna geometry on microwave properties of integral YIG-antenna structures

Y. Khivintsev^{1,2}, V. Sakharov¹, M. Heath³, V. Kruglyak³, Y. Filimonov^{1,2}, S. Nikitov^{2,4}

1. *Saratov Branch of Kotelnikov Institute of Radio-Engineering and Electronics of Russian Academy of Sciences, Moscow, Russia*

2. *Chernyshevsky Saratov State University, Saratov, Russia*

3. *University of Exeter, Devon, United Kingdom*

4. *Kotelnikov Institute of Radio-engineering and Electronics of Russian Academy of Sciences, Moscow, Russia*

Integral structures based on yttrium iron garnet (YIG) films and micro-sized planar microwave antennas (MAs) are promising candidates for operation of short wavelength spin waves (SWs) and miniaturisation of magnonic devices. Here, we report on the effect of the antenna geometry upon microwave properties of such YIG-MA structures. We have fabricated and tested structures with three different types of MAs. The MAs had form of either three coplanar stripes of the same width (type 1), or two coplanar stripes of the same width (type 2), or a tandem of one narrow and one wide coplanar stripes (type 3).

The structures were fabricated using a combination of photo or electron beam lithographies and magnetron sputtering followed by lift-off. The microwave characteristics of the structures were acquired using a vector network analyser along with a microwave probe station for bias magnetic field applied along the SW propagation direction.

The MAs of types 1 and 2 were found to have similar insertion loss and positions of the SW propagation bands corresponding to the different spatial harmonics of the MA structures. The MAs of type 3 were found to yield a more efficient excitation of SW within a broader frequency band. The direct electromagnetic cross-talk was minimal for type 1 MAs and maximal for type 3 MAs. The measurements of type 1 MAs with different stripe widths demonstrated a possibility to broaden the SWs excitation bands by decreasing the stripe width.

However, this was accompanied by a significant decrease in the SW excitation efficiency. In structures with type 3 MAs with 0.5 and 1 micrometre wide stripes, the excitation and propagation of sub-micrometre wavelength SWs and their resonant interaction with surface acoustic waves were observed.

This work was supported by RFBR (grants #13-07-00941, 13-07-12421, 14-07-00896) and European Community's Seventh Framework Programme (GA #247556, NoWaPhen).

Th.O-P28 - Towards integrated magnetoresistance sensors for electrical read-out in perpendicular nanomagnetic logic systems

I. Eichwald¹, S. Breitzkreutz-v. Gamm¹, G. Ziemys¹, M. Becherer¹, D. Schmitt-Landsiedel¹,

1. Technische Universität München, Munich, Germany

Perpendicular Nanomagnetic Logic (pNML) is an emerging technology providing a unique way to combine logic and memory functions [1]. Elementary computing operations are performed, exploiting purely magnetic field-interaction between nanoscale, non-volatile magnets, arranged in two- or even three-dimensions [2, 3]. Directed signal flow is achieved by one-side-irradiation of the magnets with a focused ion beam. This process sensitizes a magnet to the stray field of its nearest neighbors [4, 5]. pNML devices are low-power, radiation-hard, and can be integrated with CMOS circuits, extending their functionality.

For integration in CMOS, the magnetic signal must be translated into an electrical one. Commonly, sensors exploiting magneto-resistive effects, like GMR or MTJ are applied. Hereby, electrical resistivity changes are detected depending on the alignment of the free layer magnet (FM) to the pinned layer magnet (PM).

The challenging part for such a sensor type for pNML is, that FM must be sensitized to the stray field of its previous neighbor magnet, which performs logic operation. At the same time, the sensor reading out the magnetic information must be integrated, without interrupting the signal flow through the FM of the magneto-logic circuit. This requires a special sensor structure.

Therefore, a special two-step-patterning process is applied. FM is fabricated as a wire. The anterior half lies free and can be side-irradiated to get sensitized for the signal flow of the logic circuit. The posterior half of FM is covered by the spacer- and pinned layer, containing the sensor stack.

MOKE-measurements of the sensor confirm the sensitivity of FM in the predefined irradiated spot and the unimpeded signal flow. Resistivity changes in the sensor stack are clearly detected and show values in the 20mΩ range. These experiments prove correct functionality of the integrated sensor. However, further research will be done to further enhance resistivity change.

[1] See <http://www.itrs.net> for ITRS: Emerging Research Devices (2013)

[2] S. Breitzkreutz et al., in EPJ web of conferences 75. EDP Sciences (2014)

[3] I. Eichwald et al., Nanotechnology 25 (2014)

[4] S. Breitzkreutz et al., J. Appl. Phys. 111 (2012)

[5] I. Eichwald et al., IEEE Trans. Magn. 48 (2012)

Th.O-P29 - Optimum laser exposure for setting exchange bias in spin valve sensors

M. Almeida¹, O. Ueberschör¹, M. Müller², R. Ecke¹, H. Exner², S. Schulz¹,

1. *Fraunhofer ENAS, Chemnitz, Germany*

2. *Hochschule Mittweida, Laserinstitut, Mittweida, Germany*

The specific local alignment of the magnetization of a reference layer in spin valves has a rapidly growing significance in the implementation of monolithically integrated sensor devices. The spatial sensitivity of such sensors is defined by the exchange bias effect arising at the interface between the “pinned” ferromagnetic and the adjacent antiferromagnetic layer. The locally (re-)setting of the orientation of the exchange bias direction can be achieved through local annealing by means of a focused laser beam and subsequent cooling in the presence of a magnetic field. Particularly in the case of bottom-pinned spin valves, the parameters of such a laser exposure will also have a significant effect on the magnetic properties of the free layer, which ultimately defines the sensing characteristics. In order to analyse this effect, bottom-pinned IrMn / CoFe / Cu / NiFe-CoFe spin valves (given film order as from substrate to top) are patterned into a meander shape and further annealed using a focused pulsed laser beam. Different processing peak intensities are tested. The analysis of the electric and magnetic transport properties after this exposure shows how strongly the resistance is affected for higher intensities, as well as the effect of the laser peak intensity on the magnetic coupling between the ferromagnetic electrodes. Furthermore, this results in a decrease of the GMR. These changes are discussed as a result of the structural modifications induced by the laser exposure on the spin valve nanolayers.

Th.O-P30 - Phase stability and magnetic properties of D0₂₂-type Mn₃Ga_xGe_{1-x}H. Okada¹, T. Sasaki¹, R. Umetsu²1. *Tohoku Gakuin University, Miyagi, Japan*2. *Tohoku University, Miyagi, Japan*

Ferrimagnetic Mn₃Ga and Mn₃Ge with a tetragonal D0₂₂ structure have been expected to be candidates for spintronics materials. The compounds exhibit high uniaxial magnetic anisotropy in spite of 3d transition metal compounds, and show high Curie temperature and low magnetization. These magnetic properties are considered to be attributed to the D0₂₂ structure. It has been known that the single phase of the D0₂₂ structure is obtained in off-stoichiometric composition. In the case of Mn-Ga alloy, the D0₂₂ phase exists in the Ga-rich Mn_{75-x}Ga_{25+x} composition. On the other hand, the Mn-rich Mn_{75+x}Ge_{25-x} composition is required for obtaining the D0₂₂ single phase. In this study, we have investigated the phase stability and the magnetic properties of D0₂₂-type Mn₃Ga_xGe_{1-x} without the deficient and excess Mn.

Polycrystalline samples were prepared by arc-melting method. The ingots were annealed at 1073 K for a week, and then heated at 673 K for two weeks. The phase identification and characterization of the samples were performed by powder x-ray diffraction experiment. The phase stability was observed by differential scanning calorimetric measurement. The magnetization measurements were carried out using vibrating sample magnetometer.

The prepared samples of Mn₃Ga_xGe_{1-x} ($x = 0.3 - 0.7$) were confirmed to be single phase of the D0₂₂ structure by powder x-ray diffraction experiment at room temperature. A phase transition temperature from the ferrimagnetic D0₂₂ phase to the paramagnetic D0₁₉ phase monotonically decreases with increasing Ga content. The magnetization of the D0₂₂ phase vanishes at the transition temperature. The disappearance of the magnetization accompanied by the phase transition of the D0₂₂ phase indicates that the Curie temperature of the D0₂₂ phase is higher than the phase transition temperature. It is thought that the phase stability of the D0₂₂ phase is corresponding to the decrease of the valence electron caused by the Ga substitution.

Th.O-P31 - Excitation of a uniform rotational magnetization mode in easy-plane iron-garnet films for flux-gate sensors

P.M. Vetoshko ¹, D.V. Dodonov ^{1, 2}, M.A. Kozhaev ^{1,3}, I.I. Syvorotka ⁴, I.M. Syvorotka ⁴, A.K. Zvezdin ^{1,2,3}, V.I. Belotelov ^{1,5},

1. *Russian Quantum Center, Skolkovo, Moscow, Russia*

2. *Moscow Institute of Physics and Technology, Dolgoprudniy, Russia*

3. *Prokhorov General Physics Institute of The Russian Academy of Sciences, Moscow, Russia*

4. *Department of Crystal Physics and Technology, Scientific Research Company "Carat", Lviv, Ukraine*

5. *Lomonosov Moscow State University, Moscow, Russia*

Nowadays, iron-garnet film are of prime interest for spintronics and sensorics. In particular, ultra-sensitive flux-gate magnetometers based on the rear-earth iron-garnets were proposed and fabricated recently [1]. For getting large values of the sensitivity it must have easy-plane anisotropy and be kept in a monodomain state. For that reason, investigation of the uniform rotational magnetization mode is of importance. In this work we fabricated magnetic films suitable for the flux-gate magnetometers and investigated their magnetic properties. In the technological part of the work we fabricated 4 types of the iron-garnet samples with different degree of Fe³⁺ substitution by Sc³⁺ ions. We found experimentally a nonlinear character of the anisotropy field H_c dependence on the degree of Fe³⁺ substitution in octahedral positions. In parallel to the technological aspects, we studied theoretically magnetization dynamics in the magnetic films for the flux-gate magnetometers. A non-linear equation for the in-plane magnetization dynamics in easy-plane iron-garnets films was obtained. Conditions of the excitation of the uniform magnetization rotation in (111) plane at a constant angular speed are determined. In particular, it is found that two types of the uniform rotational modes exist. One of them is excited by a magnetic field rotating in plane. On the contrary, the second rotational mode can be excited by a rapidly varying component of the magnetic field orthogonal to the magnetic film. Using orthogonal component of the excitation magnetic field implies parametric interrelation among all three components of the magnetization. It can be used for novel types of parametric amplifiers and sensors.

This work was supported by the Russian scientific foundation (grant # 14-32-00010)

[1] Highly sensitive room temperature magnetometer based on epitaxial iron garnet film / I.I. Syvorotka et al. // V Euro-Asian Symposium 'Trends in MAGnetism': Nanomagnetism (EASTMAG-2013), Vladivostok, Russia. 15-21 September 2013, Mo-6M-I3, p.60

Th.O-P32 - Magnetoimpedance and field sensitivity in arrangement of CoFeSiB amorphous microwires

J.M. Gomez Cruz¹, H. Montiel Sánchez¹, G. Alvarez Lucio²,

1. Centro de Ciencias Aplicadas y Desarrollo Tecnológico, Universidad Nacional Autónoma de México, Delegación Coyoacán, México

2. Escuela Superior de Física y Matemáticas IPN, San Pedro Zacatenco, México D.F., México

The arrangement of amorphous wires is a new method, cheap and fast in magnetoimpedance (MI) sensor applications. For these reasons, we propose a simple design of sensor with the arrangement of two parallel CoFeSiB amorphous wires. MI and the field sensitivity in the arrangement of CoFeSiB amorphous wires were investigated at frequencies from 1 MHz to 70 MHz. Experimental results indicate that MI in CoFeSiB amorphous wires can be significantly improved. The MI maximum response occurs at frequencies between 7 MHz and 25 MHz, at higher frequencies the MI response decrease. Field sensitivity of 3.5%/Oe is obtained at 16 MHz. Sine wave colpitts oscillator at 16 MHz was designed, later this signal is pre-amplified in order to increase the current that flows through the sensing element. For the acquisition phase, we used a Freescale Microcontroller (MC9S08MM128) whose work is to attune the signal with its ADC module and subsequently, the data is sent to the PC for processing.

The authors acknowledge the financial support of PAPIME PE209915, UNAM. Juan Manuel Gómez is grateful for the scholarship provided by CONACYT Mexico.

Th.O-P33 - Paramagnetic anisotropy of amorphous silica measured by ESR and by field-induced rotational oscillation in microgravity

C. Uyeda¹, M. Yokoi¹, K. Hisayoshi¹

1. *Osaka University, Osaka, Japan*

Anisotropy of paramagnetic magnetization at the level of 10^{-7} emu/g was detected at the surface of an amorphous silica block by measuring its depth profile with spatial resolution of 50 microns [1]. The anisotropy was obtained in a synthetic block as well as in various natural samples. The magnetic unstable-axis (uni-axial) was normal to surface plane for the measured samples. Fe concentration of the samples were about 1 mol %. In the experiments, a quadrangular prism separated from the sample block (long axis was normal to surface) was cut into square plates with a length of $1.0 \text{ mm} \times 1.0 \text{ mm} \times 0.05 \text{ mm}$. Field-induced rotational oscillation of each plates with respect to applied field ($B = 0.6\text{T}$) were measured one by one in microgravity area, and its anisotropy was obtained from period of oscillation [2]. ESR measurements were performed on the same sample plates, and the anisotropy of crystal field deriving from isolated Fe ions were consistent with those obtained by the microgravity experiments [1]. The cause of anisotropy is investigated by changing the chemical composition, Fe concentration or cooling velocity of the synthesized samples. Assuming that an amorphous silica generally possesses the observed anisotropy, an amorphous particle will possess anisotropy that is uniquely determined by its 3-dimensional shape. In the case of a rod-shaped grain, a stable axis for the rod itself will be directed along the long axis of rod, since total anisotropy of particle is an integration of the uni-axial unstable anisotropy that is assigned to the local surfaces of rod [1]. Amorphous materials are believed to be isotropic at present, and application of magnetic alignment has not been considered as yet for amorphous particles.

[1] Yokoi et al, Planet., Space Sci., (2014)

[2] Uyeda et al, J. Phys. Soc. Jpn., (2010)

Th.O-P34 - Identification of weak magnetic & ferro/ferri-magnetic particles included in grain ensemble using magnetic volume force

C. Uyeda¹, K. Hisayoshi¹, K. Kuwada¹, R. Ynagihara¹,

1. Graduate School of Science, Osaka University, Osaka, Japan

Field-gradient force has been conventionally used to extract and identify of ferro (ferri)-magnetic materials because the forces that operated on the spontaneous magnetizations of these materials considerably exceeded gravity and various frictions in terrestrial condition. Solid materials are often formed as ensemble of grains composed of different materials, and it is generally desirable to extract and identify the material of individual particles of such ensemble before investigating the sample with refined devices. Such method has been well established in analyzing heterogeneous organic solutions by introducing the technique of chromatography; such procedure has not been established as yet for mixtures of heterogeneous solid grains. A principle based on magnetic volume force was previously proposed to identify various diamagnetic grains in a simple manner; here an ensemble of heterogeneous grains is released at a point located in an area of monotone decreasing field [1][2]. The material of the translating grain was identified by comparing the value of susceptibility, obtained from terminal grain velocity in the area of $B \sim 0$, with a list of compile published values. Here we extend this method on paramagnetic oxide particles with different iron concentrations. Microgravity was generated by a compact drop shaft system; duration of microgravity time was about 0.6 second. The apparatus was set inside a box which had a size of 30 x 30 x 20 cm. The compact setup was realized by introducing a magnetic-circuit that was composed of NdFeB magnets in generating the required field distribution. By proceeding the present study, the identification becomes possible for almost all the magnetic categories of solid materials.

[1] K. Hisayoshi et al: Phys., (2009)

[2] Uyeda et al, J. Phys. Soc. Jpn., (2010)

Th.O-P35 - Fast and deterministic generation of single DW in in-plane ferromagnetic nanowire using local oersted field

C. Guite¹, K. Inn Seng¹, C. Murapaka¹, R. Maddu¹, G. Sarjoosing¹, W. Siang Lew¹

1. Nanyang Technological University, Singapore

Domain walls (DWs) in magnetic nanowire have been recognised to have potentials to be used in ultra-high density storage, non-volatile logic devices and sensors. For technological applications, the creation of DW on the nanosecond timescale and perfect control of its dynamics is critical. The existing method for creating DW in the nanosecond regime using localized Oersted field always nucleates two DWs; a head-to-head (HH) and a tail-to-tail (TT) DWs. Due to the intrinsic characteristics of these DWs, they either annihilate or form a coupled DW. This results in the stochastic behaviour of DW generation in in-plane ferromagnetic nanowires. It has been previously reported that the minimum separation of two DWs for stable existence is approximately 2.5 μm . To have a reliable DW generation, an external magnetic field or long electric current pulses were used. In this work we have proposed and experimentally verified a technique for deterministic single DW generation. We exploit the stray field that emanates from the edge of the ferromagnetic nanowire conduit to overcome the mutual interaction between the DWs. Our experimental results showed that deterministic generation of DW was achieved at 10 ns pulse duration with a current density of $\sim 1.1 \times 10^{12} \text{ Am}^{-2}$ in the given device. Our simulation results showed that the injection stripe line can be placed as far as 500 nm from the edge of the nanowire, depending on the shape of the nanowire edge. Therefore in this work we show that it is possible to deterministically generate DW in in-plane ferromagnetic nanowires using localized Oersted field.

Th.O-P36 - Temperature robustness of a fluxgate current sensor with electroplated Fe-Ni-Co cores

Y. Watanabe^{1,2}, M. Otsubo², T. Yanai², M. Nakano², H. Fukunaga²

1. *Mitsubishi Electric Corp. , Amagasaki, Japan*

2. *Nagasaki Univ. , Nagasaki, Japan*

Recently, a fluxgate high-precision current sensor available for a wide temperature environment is strongly desired in the industrial market. Although the commercial sensors using Co-based amorphous or Fe-Ni-based alloys have high sensitivity, it is generally known that the sensitivity fluctuates more than 10 % as the temperature changes. We, therefore, focused on Fe-Ni-Co alloys which have higher Curie temperatures than those of Fe-Ni and Co-based amorphous alloys. In order to compare the temperature variation of the sensitivity, we fabricated two current sensors comprising each Fe-Ni and Fe-Ni-Co ring core, respectively.

An Fe₂₁Ni₇₉ or an Fe₁₅Ni₄₆Co₃₉ film with the thickness of approximately 20 micrometers was plated on the Cu ring (I.D.=36.7 mm, O.D.=44.1 mm). The turn number of excitation coil and detection coil were 100 and 300 turns, respectively. Each sensor was excited at 1 kHz by a triangular-wave current with the maximum value range from 220 to 430 mA. The temperature and dc current varied from -10 to +125 degrees and from -3 to +3 A, respectively. Moreover, a FFT signal processing was carried out for output of detection coil.

An optimization on the excitation current enabled us to obtain almost the same sensitivity of two sensors operated at 25 degrees, and the result is considered to indicate the excellent soft magnetic properties of not only the Fe-Ni ring core but also the Fe-Ni-Co ring one. Furthermore, we confirmed that the sensitivity fluctuation due to the varying temperature of the Fe-Ni-Co core was smaller than that for Fe-Ni one under the same conditions of the excitation current. The Fe-Ni-Co electroplated core, therefore, is one of effective material for a fluxgate current sensor because of the excellent temperature characteristics and equivalent sensor sensitivity in the case of using the Fe-Ni core.

Th.O-P37 - Influence of the non-magnetic material on the magnetization dynamics and spin pumping in NiFe and CoFeB multilayer systems

A. Ruiz Calaforra¹, T. Braecher¹, V. Lauer¹, P. Pirro¹, B. Heinz¹, M. Geilen¹, A.V. Chumak¹, A. Conca¹, B. Leven¹, B. Hillebrands¹

1. TU Kaiserslautern, FB Physik and Landesforschungszentrum OPTIMAS, Kaiserslautern, Germany

The inverse spin Hall effect (ISHE) has received increased interest as a new means of spin current detection. In this context, the non-magnetic (NM) material Pt has been identified as a promising material due to its large observed spin Hall angle. However, an unexpectedly large damping enhancement was observed in the ferromagnetic (FM) layer in FM/Pt bilayers. It was demonstrated that the introduction of a Cu spacer can reduce this damping enhancement. Still, the role of the spacer material on the spin current injection from the FM into the NM, as well as on the magnetization dynamics in the FM is not yet completely resolved, which calls for a more detailed study.

Here, we analyzed the influence of selected NM materials on the magnetization dynamics in the technologically relevant FM materials Ni₈₁Fe₁₉ and Co₄₀Fe₄₀B₂₀ in FM/NM/Pt and FM/Pt layer systems. By means of ferromagnetic resonance spectroscopy, we reveal that the NM materials Al and Cr have no large influence on the magnetization dynamics in an adjacent Ni₈₁Fe₁₉ layer. In contrast, an adjacent Ru, Pt as well as MgO layer increase the effective damping α_{eff} and lower the effective magnetization M_{eff} . This highlights that even in the absence of spin pumping, other interface effects affect the dynamics in the Ni₈₁Fe₁₉. In contrast, in the case of Co₄₀Fe₄₀B₂₀ only Pt has a notable influence on the dynamics in the Co₄₀Fe₄₀B₂₀ layer.

By additional measurements of the rectified DC voltage in ferromagnetic resonance in ISHE measurement, where the symmetry ratio V_s/V_a of the voltage is compared. These measurements reveal that strong spin rectification effects always leads to an output voltage. Moreover, an adjacent Pt layer in all cases results in a change of the symmetry, indicating the presence of a spin current pumped into the Pt and a consequent ISHE.

Th.O-P38 - Optimal design for performance improvement of permanent magnet assisted synchronous reluctance motor by enhancing saliency ratio

S. Seo ¹, S. Jung ¹

1. SungKyunKwan University, Seoul, South Korea

Recently, Interior Permanent Magnet Synchronous Motor(IPMSM) type motors are widely used by the high output density and efficiency. But rising cost of rare earth magnets requires substitution of IPMSM. One of the alternatives is Synchronous Reluctance Motor which has simple structure and cost-efficient. But it has low efficiency because of not using permanent magnet. Otherwise, PMA-SynRM inserts ferrite magnets into flux barriers of SynRMs to add up alignment torque. PMA-SynRM has great advantage in cost reduction compared to IPMSM by using ferrite magnets which is much cheaper than neodymium magnets. PMA-SynRM uses reluctance torque mainly and uses alignment torque adjunctively. In this paper, we increase saliency ratio to improve torque performance by various types of flux barrier and magnet. Analysis model is PMA-SynRM of internal rotational type and has 4 pole, 42 slots and rotor 5 layers. To analyze this model, we use common analyzing tool JMag to conduct 2 Dimensional Finite Element Method(2D FEM). Fractional slot distributed winding is employed because of lower cogging torque due to removal of periodicity through slots and poles. To enhance saliency ratio, we consider various shapes of flux barriers including rotating angle and magnets. Forms of flux barrier has circular barrier, sharp barrier. In the case of the magnets, design variables are thickness, length of magnet and whether it divided or not. This paper conducted 2D FEM about various models to enhance saliency ratio. In the case of flux barrier, sharp barrier type of edge of magnet and lower angle type between main and side barriers shows better performance. In the case of magnets, undivided and thick type shows better performances. Take into account overall variables, we can verify the effects on saliency ratio caused by flux barrier and magnets. When designing form of rotor for PMA-SynRM we can choose appropriate type.

Th.O-P39 - A Study on 3D design and characteristic of outer-rotor type brush-less dc motor considering upper end cover of housing

M. Seo ¹, T. Lee ¹, Y. Kim ², S. Jung ¹

1. Sungkyunkwan University, Seoul, South Korean

2. Chosun University, Gwangju, South Korea

In this study, we have dealt with a design characteristic of outer rotor type Brush-less DC (BLDC) motor applied for Engine Cooling Fan (ECF) based on a non-linear 3D Finite Element Method (FEM). The BLDC motor is used in various fields by virtue of its higher efficiency and lower cost compared with general DC motor. The driving motor for ECF is usually designed as outer rotor type since it has a decided advantage on rotation under constant speed with high inertia characteristic. The carbon steel is employed as material of a housing part and it allows the housing part roles as a rotor. When design a motor with the structure mentioned above, it is required as a requisite to consider 3D effect by implementing a non-linear FEM due to an upper end cover of housing part, which is perpendicular to the axis of rotation. We have analyzed identical models under three different conditions. One is 2D analysis model. Another is 3D analysis model without considering the upper end cover of housing. The other is 3D analysis one considering whole parts. The analysis has been performed through both a magnetic equivalent circuit method and a non-linear FEM. Finally, the results have been compared with back electro-motive force value of actual motor model. As a result, the upper end cover of housing functions as an additional flux path and the operating point on B-H curve of rotor material is shifted to non-saturation region relatively. Accordingly, magnetic flux linkage can be increased and motor size can be decreased under same input condition to satisfy ECF specification such as torque. We suggest not only analysis result but also design strategy considering both 2D and 3D FEM in this study.

Th.O-P40 - Spin lifetime in nano-particles

J. Rousseau^{1,2}, R. Morel^{1,2}, A. Brenac^{1,2}, I. Berbezier³, L. Favre³, L. Vila^{1,2}, C. Beigné^{1,2}, A. Marty^{1,2}, L. Notin^{1,2}

1. CEA Grenoble \ INAC \ SP2M \ NM, Grenoble, France
2. Univ. Grenoble Alpes, Grenoble, France
3. IM2NP, CNRS, AMU, Marseille, France

A long spin lifetime is one of the more important parameter to create high efficiency spintronic devices. This key parameter control the time during which a given spin-mediated information can be stored or manipulated.

It has been shown that, in nano-particles, the spin lifetime is strongly enhanced compare to bulk material. In very small clusters (less than 1 nm), the underlying physic is well understood and theoretical models give good agreement with experiment [1]. Longer spin lifetime has also been observed in larger cluster, even in size range where theoretical models would predict bulk value [2].

The spin lifetime in nano-clusters can be assessed by studying magneto-transport properties in the Coulomb blockade regime [3]. To do so requires to connect a unique nano-particle with two magnetic electrodes, via tunnel junctions. Such a device work as a spin-dependent single electron transistor (SD-SET). We have develop a versatile method for the fabrication of SD-SET by e-beam lithography and double angle shadow-edge evaporation technique [4]. A nano-gap is formed between the two deposited electrodes where the nano-particle is, with an underlying gate electrode. This simple and versatile device offers the possibility to study magneto-transport properties in a wide range of nano-particles. In this talk, we will present our results on germanium and cobalt clusters, and we will show how our results can be explained in regards of numerical calculations of the device.

- [1] A. Kawabata, J. Phys. Soc. Jap. 29, 902 (1970); J. Buttet et al. Phys. Rev. B, 26, 2414 (1982).
[2] P.N. Hai et al., Nat. Nanotechnol. 5, 593 (2010)
[3] A. E. Hanna et al., Phys. Rev. B 44, 5919 (1991); J. Barnás et al., Europhys. Lett. 44, 85 (1998)
[4] J. Rousseau et al., Appl. Phys. Lett. 104, 073103 (2014)

Th.O-P41 - Biosensing with magnetophotonic plasmonic heterostructures

D. Ignatyeva^{1,2}, S. Sekatskii³, M. Kozhaev^{2,4}, M. Nur-e-Alam⁵, M. Vasiliev⁵, A. Fraerman⁶, K. Alameh⁵, V. Belotelov^{1,2}

1. Lomonosov Moscow State University, Faculty of Physics, Moscow, Russia
2. Russian Quantum Center, Moscow, Russia
3. Institute of the Physics of Biological Systems, École Polytechnique Fédérale de Lausanne, Lausanne, Switzerland
4. Prokhorov General Physics Institute RAS, Moscow, Russia
5. Electron Science Research Institute, Edith Cowan University, Joondalup, Australia
6. Institute for Physics of Microstructures RAS, N.Novgorod, Russia

The operation concept of surface plasmon resonance (SPR)-sensors is based on the excitation of the surface waves under resonant conditions that experience significant variations upon the small changes of the surrounding medium.

We propose a novel type of the SPR-biosensor that is based on the combination of the plasmonic metal-dielectric structure with a magneto-optical material and photonic crystal. The several-orders of magnitude improvement of the SPR-sensor sensitivity is achieved due to the measurement of magneto-optical spectra of the transversal magneto-optical Kerr effect (that are sharper than reflection spectra) as well as the use of specially designed 1D photonic crystals as a support for ultralong-range propagating plasmons that significantly increases the quality factor of the optical resonances.

In this work, two novel types of magnetophotonic plasmonic sensor heterostructures were designed and fabricated, with the magnetic response of the first being provided by a dielectric layer (bismuth-substituted iron garnet) and the second by containing magnetic metal (cobalt). Although the structure with a magnetic metal has higher losses that decrease quality factor of the considered system its advantages are the ease of the fabrication and the low value of the saturation magnetic field. We performed experiments demonstrating the sensing process by both detecting the shift of the magneto-optical resonance position as well as its absolute value variation for the fixed wavelength and angle. The several orders of magnitude improvement of the sensitivity is caused by a very sharp magneto-optical resonance of a width of about 0.1 degrees and magnitude up to 15%. The fabricated spectral sensor sensitivity is 2300 nm/RIU (45 deg/RIU) while the magneto-optical response to the refractive index change is 10%/RIU. Estimations show that such configuration might raise the threshold sensitivity up to 10^{-8} RIU and significantly shorten the measurement time.

The work is supported by Russian Science Foundation (grant No.14-32-00010).

Th.O-P42 - Transfer torque characteristic analysis of dual-stage magnetic gear with rare-earth magnets and non rare-earth magnets

C. Kim¹, M. Kim¹, S. Jung², Y. Kim¹

1. Department of Electrical Engineering, Chosun University, Gwangju, Republic of Korea

2. School of Information and Communication Engineering, Sungkyunkwan University, Suwon, Republic of Korea

The magnetic gear that solves the physical contact problem of the mechanical gear has advantage of no mechanical friction loss, very little noise and vibration, and no need for lubricant. Due to this unique non-contact characteristic, the magnetic gear which is capable of non-contact torque transmission has replaced mechanical gear. However, the magnetic gear with a high gear ratio is disadvantageous to implement the exact gear ratio because the number of rotor poles increases. Therefore, dual-stage type magnetic gear was proposed in order to distributes the gear ratio by using two magnetic gears as to the mechanical gear is used the multi-stage in order to implement the high gear ratio. The dual-stage type magnetic gear composed of first magnetic gear for low torque, high speed and second magnetic gear for high torque, low speed. The power is input to the inner rotor of first magnetic gear when operating as a reducer. The outer rotor of first magnetic gear and inner rotor of second magnetic gear are connected in order to transmit power. As a result, the power is output through the outer rotor of second magnetic gear. However, dual-stage magnetic gear has reverse process when operating as an accelerator. The dual-stage type magnetic gear can improve the power density and efficiency compared to the conventional magnetic gear. Also, the dual-stage type magnetic gear can be designed differently permanent magnet type because the use of the two magnetic gear. Therefore, in this paper, permanent magnet material of second magnetic gear was not changed and only permanent magnet material of first magnetic gear was changed to bonded NdFeB magnet or ferrite magnet from sintered NdFeB magnet. Transfer torque and magnetic field analysis method for dual-stage magnetic gear was used numerical analysis with coupled finite element method and boundary element method.

Th.O-P43 - Design of interior permanent magnet synchronous motor for minimizing axial force by adapting novel skew method

G. Park¹, B. Son¹, Y. Kim², S. Jung¹

1. *School of Electronic and Electrical Engineering, Sungkyunkwan University, Seoul, South Korea*

2. *Department of Electrical Engineering, Chosun Universtiy, Gwangju, Republic of Korea*

Interior Permanent Magnet Synchronous Motor is applied to various fields, since it has superior power density and efficiency by utilizing reluctance torque owing to its saliency as well as alignment torque. However saliency also causes relatively higher torque ripple than the other type of motor.

One of the methods to compensate this problem is skewing. Skewing is the method of canceling the ripple of torque by skewing either rotor or stator. Skewing can reduce torque ripple and cogging torque dramatically, however it produces the unexpected axial force at the same time. This axial force can give continuous mechanical load to the part connected to the motor, and also has effect on generate noise and vibration. In this paper, V-shape skewing method is applied for designing IPMSM to reduce the axial force preventing side effect of skew, which is generation of noise, vibration and mechanical load.

Owing to the development of stacking technology, skew is applied to stator considering magnetization. It also maximizes the effect of skew with continuous configuration, unlike step-skew generally applied in rotor skewing method.

Non-skewed model, conventional-skewed model and proposed V-shape skewed model are comparatively analyzed to identify the effect of skew to axial force, and 3D numerical analysis based on Finite Element Method is conducted to consider the force in axial direction. Axial Force is calculated on both end of the rotor since most of the axial force appears at the ends. Axial force is produced due to the orientation of current flow and nonlinear magnetic flux saturation. It produces different magnitudes of axial force at each ends of the motor which resulted as the residual axial force. Proposed V-shape skewed motor also produces constant axial force, however, upper and lower parts produce axial forces in opposite direction to make net force zero.

Th.O-P44 - High sensitivity disk shaped planar Hall effect sensor for capture and detection of superparamagnetic nanoparticles

M. Volmer¹, M. Avram², A. Avram², I. Firastrau¹

1. *Transilvania University of Brasov, Brasov, Romania*

2. *National Institute for Research and Development in Microtechnologies, Bucharest, Romania*

The aim of this study is to develop high sensitivity and low cost Permalloy based planar Hall effect (PHE) sensors which can be used for various applications and, in particular, for Lab on a Chip (LOC) platforms. Using typical photolithographic technique, disk-shaped structures made from Permalloy, 1 mm diameter and 20 nm thick, were deposited on to oxidized Si substrate. No anisotropy axis has been defined. Four PHE sensors are patterned and interconnected on a chip. To control the sensor sensitivity and linearity, a biasing field has been applied along the driving current. By this, different magnetization states in the sensor layer can be generated. The strong magnetostatic interaction between the magnetic nanoparticles and the sensor magnetic layer is responsible for the actuation, capturing and sensing of magnetic particles. These aspects are explained by means of micromagnetic simulations. From aqueous solution containing maghemite nanoparticles, 10 nm mean diameter, functionalized with PEG 6000, were placed droplets with volumes between 0.2 to 1 μL over the sensor surface. Special field configuration has been used to capture the nanoparticles on the sensor surface. In addition to biasing field, a magnetic field, used to magnetize the nanoparticles, was applied perpendicular to the sensor surface in order to avoid the saturation of the PHE signal. We used different techniques to sweep the fields and the results show that high detection sensitivity, of the order of 0.1 emu/V, can be obtained for different magnetization states in the sensing layer. We observed large signal variations of the sensor output when the magnetic layer is polarized closed to the coercive state.

The authors are grateful for the financial support from the project PN2 CELLIMUNOCHIP No. 2/2012 in the frame of the National Partnership program.

Th.O-P45 - Investigation of the variation in magnetic nature of Ba - Fe magnetoplumbite with Li - Ti substitution

R.R. Deshmukh ¹, P. Bhatia ², R. Srinivasan ³

1. Institute of Chemical Technology, Prague, Czech Republic

2. Guru Nanak College of Arts, Science and Commerce, Maharashtra, India

3. University of Mumbai, Department of Physics, Mumbai, India

Pure barium ferrite and its substituted variants are synthesized;

BaFe₁₂O₁₉ - HXF Ba_{0.95}Li_{2.85}Fe_{8.55}Ti_{1.90}O₁₉- HXF1.

Ba_{1.688}Li_{0.422}Fe_{8.018}Ti_{2.532}O₁₉- HXF2.

Ba_{1.266}Li_{0.844}Fe_{7.596}Ti_{2.954}O₁₉- HXF3.

Ba_{1.688}Li_{0.844}Fe_{6.752}Ti_{3.376}O₁₉- HXF4.

Ba_{0.95}Li_{3.8}Fe_{5.7}Ti_{3.8}O₁₉- HXF5.

X-Ray diffraction studies indicate the single phase formation of hexagonal magnetoplumbite type with space group P63/mmc. The 'a' and 'c' values determined for HXF agree very well with those reported. The SEM images of the pellet surfaces show dense grain structure. An elongation of grains is also observed in substituted samples as titanium content rises. Grain size is observed to increase considerably by substitution with Li and Ti. Magnetic properties of hexaferrite are investigated. Room temperature magnetic hysteresis loops are reported. MR / Ms reduces as substitution increases with respect to pure HXF. The Hc is seen to depend on the Ti plus Li content. The normalized susceptibility vs. temperature curves are drawn. Susceptibility curve corresponding to pure HXF drops a little near room temperature, rises slowly to peak at the Curie temperature T_c = 713K which agrees well with the reported value. The curves corresponding to substituted hexaferrites are most peculiar. They could be interpreted as two Curie temperatures. With increase in Ti substitution, the separation between the two T_cs tends to increase. The Curie temperatures are observed to be higher in HXF1, HXF 3 and HXF 5 and lower in HXF2, HXF 4. The lowered T_c values demonstrate that some inter- sublattice exchange interactions are strongly diminished. The substitution of Fe³⁺ ions with Ti⁴⁺ ions in the hexaferrite reduces its intrinsically high universal magnetic anisotropy and enhances Faraday rotation in order to make it suitable for perpendicular magnetic recording.

Th.O-P46 - Multicore off-diagonal magnetoimpedance sensors utilising amorphous wires

N. Yudanov¹, A. Rudyonok¹, L. Panina^{1,2}, A. Morchenko¹, A. Zhukov³

1. *National University of Science and Technology (MISIS), Moscow, Russia*

2. *Institute for Design Problems in Microelectronics RAS, Moscow, Russia*

3. *Dept. Material Physics, Chemistry Faculty, University of San Sebastián, San Sebastian, Spain*

Magnetoimpedance (MI) sensors are attractive for realising a localised detection of weak magnetic fields owing to micro-size and high sensitivity of the MI elements. In the case of Co-rich amorphous wires of diameter 10-30 microns used as MI elements, the relative change in impedance at MHz frequencies can be over 100%/Oe. MI sensors in off-diagonal configuration [1-2] when the signal is taken from the coil mounted on the wire have a number of advantages including linearity, enhanced output voltage, and resonance detection circuitry. Utilising a pulse-driven MI and a detection coil of 600 turns the resolution of about few pT/Hz^{0.5} was achieved. However, a many-turn detection coil may be a problem considering the complexity of sensor construction, sensor-head size, and increased electronic noise. In this work, the off-diagonal impedance of a number of Co-rich glass-coated amorphous wires placed in the same coil is investigated. The wires are connected in parallel and excited by harmonic or pulsed current. The best sensitivity of about 300mV/Oe is obtained for two wires excited by a sinusoidal current and realising the resonance conditions for the detection circuit, which has only 40 turns. The full scale and linearity range are also increased more than twice in comparison with those when only one wire is used. The response drops if the distance between the wires is increased which is due to a strong effect of the magnetostatic interaction between the wires. We conclude that off-diagonal MI sensors with multiple wires can provide higher transfer function per one turn and could be advantageous for localised field detection.

[1] S.Sandacci, D. Makhnovskiy, L. Panina, K. Mohri, and Y. Honkura, *IEEE Trans. Magn.*, Vol.40, pp.3905-10, 2004

[2] T. Uchiyama, K. Mohri, Y. Honkura, and L.V. Panina, *IEEE Trans Magn*, 2012, Vol 48, pp. 3833-3839

Th.O-P47 - Magnetization and magnetic losses of powders from metallized particles at microwaves

A. Anzulevich¹, L. Butko¹, V. Buchelnikov¹, I. Bychkov¹, D. Kalganov¹

1. Chelyabinsk State University, Chelyabinsk Oblast, Russia

Powders from metallized dielectric particles have such advantages as instant microwave heating, low heat capacity of the particles and controlling the heating temperature within a narrow range. Owing to all these advantages powders from dielectric particles covered by metallic layer can be used in various fields of science and technology. For example, they would be useful as fillers in the thermal catalyst reactors in the oil refining industry or as a transfer and active agent at treatment of cancer or localized bacterial diseases.

In this work, we modeled dielectric spherical particles covered by metallic shell. To study the mechanisms of instant microwave heating of powders consisting of metallized particles, we obtained dependencies of real and imaginary parts of the effective permittivity and permeability of these powders on frequency of the incident electromagnetic wave, radius and permittivity of the particle, thickness and conductivity of the metallic shell. We used finite element method for calculation of the electromagnetic fields in the investigated model and combination of impedance lows for perfect electric conductor and perfect magnetic conductor to calculate effective electrodynamics parameters. According to obtained real part of the dynamic effective permeability the powder from such kind of particles exhibits diamagnetic properties. The imaginary part of the effective permeability is large enough compared with imaginary part of the effective permittivity and reaches its maximum values at the thickness of the metallic layer less than the skin depth. Moreover, in this case powder can be heated twice effectively than the powder consisting of entirely conductive metallic particles.

Th.O-P48 - Magnetic micro-mechanical systems for magnetic field mapping by optical effect

G. Ortiz ^{1,2,3}, M. Morcrette ^{1,2,3}, T. Dietsch ^{1,2,3}, P. Sabon ^{1,2,3}, I. Joumard ^{1,2,3}, H. Joisten ^{1,2,4}, B. Dieny ^{1,2,3}

1. Univ Grenoble Alpes, INAC-SPINTEC, Grenoble, France
2. CEA, INAC-SPINTEC, Grenoble, France
3. CNRS, SPINTEC, Grenoble, France
4. CEA, LETI, MINATEC Campus, Grenoble, France

In many areas, magnetic sensors play a very important role. Different types of sensors exist: those based on Hall effect, the magnetoresistive ones (GMR, TMR), those based on magneto-optical effects (Kerr, Faraday), etc. Optical magnetic sensors are often used to perform imaging or magnetic field mapping. A first known method to visualize magnetic fields of materials is based on magneto optical Kerr or Faraday effects. Another method for obtaining information on the intensity and direction of magnetic fields by optical visualization uses ferrofluidic materials. In this work, we propose a novel method for optical visualization of the magnetic field based on the use of magnetic flexible cantilevers. The basic idea is to create a dense assembly of cantilevers, at the micro- or nanoscale, which deform under the effect of an external magnetic disturbance. Under local magnetic perturbation, the cantilevers bend and consequently, alter the reflectivity of the system producing an image of the magnetic field to which the system is subjected. The fabricated cantilevers have micron-size dimensions and covers an area of about 1 cm * 2 cm. A magnet of 1 cm² was placed under the silicon substrate, which is perfectly opaque. Surprisingly, a magnet image appears as in transparency through the substrate due to the deflection of the cantilever caused by the magnetic field radiated by the magnet. The cantilevers were obtained by clean-room microfabrication techniques. They are made of magnetic NiFe (~ 100 nm thick) to make them deformable under the effect of a magnetic field. To allow mechanical bending, one end of the cantilevers is freed from the substrate while the other is kept attached to it. A correlation between the reflectivity modification of the surface wearing the cantilevers, and the applied magnetic field is under evaluation.

Th.O-P49 - Spin polarized transport in graphene spin valves with amorphous carbon interfacial layers

J.F. Sierra¹, B. Raes¹, I. Neumann¹, M.V. Costache¹, S.O. Valenzuela¹

1. Institut Catala de Nanociencia i Nanotecnologia (ICN2), Barcelona, Spain

We demonstrate a large enhancement of the spin accumulation in monolayer graphene following electron-beam induced deposition of an amorphous carbon layer at the ferromagnet-graphene interface. The enhancement is 10^4 -fold when graphene is deposited onto poly(methyl metacrylate) (PMMA) and exposed with sufficient electron-beam dose to cross-link the PMMA, and 10^3 -fold when graphene is deposited directly onto SiO_2 and exposed with identical dose. We attribute the difference to a more efficient carbon deposition in the former case due to an increase in the presence of compounds containing carbon, which are released by the PMMA. The amorphous carbon interface can sustain very large current densities without degrading, which leads to very large spin accumulations exceeding 20 meV at room temperature. Furthermore, Hanle measurements in large monolayer graphene flakes (20-40 μm long) deposited on SiO_2 show long spin diffusion lengths (7 μm), which corresponds to spin life times of 1.5 ns.

Surprisingly, the results are comparable to the spin life times measured in graphene on hexagonal boron nitride substrates.

Th.O-P50 - Local magnetic resonance spectroscopy with spin electronics based magnetic sensors

P.A. Guitard¹, R. Ayde¹, E. Paul¹, G. Jasmin-Lebras¹, M. Pannetier-Lecoecur¹, C. Fermon¹

1. Service de Physique de l'Etat Condensé, CEA Saclay, UMR CNRS 3680, Gif sur Yvette, France

Nuclear Magnetic Resonance Spectroscopy (NMRS) is a widely known technique for chemical and biological molecule analysis. However due to the weakness of the NMR signals, it is very difficult to work on volumes lower than a mm³. That limitation has led to the development of miniaturized sensors such as microcoils, NV centers and atomic magnetometers.

We will present our approach based on the use of Giant Magneto-Resistive sensors (GMR) as wide band magnetic sensors to detect locally the NMR signal. GMR sensors and an NMR setup have been specifically designed to have a detectivity in the range of 20pT/sqrt(Hz) and able to work with an external magnetic field up to 1 Tesla.

We will present results of NMR spectroscopy of model liquids like Ethanol on a volume of the order of 20x20x20 μm³ with two different configurations: a first one where local NMR spectroscopy can be performed in a large volume and a second one, where the liquid of interest is constrained in a small microchannel.

Th.O-P51 - Grain orientation and magnetostrictive properties of Tb-Dy-Fe alloys

X. Mu¹, C. Wang¹, X. Gao¹

1. State Key Laboratory for Advanced Metals and Materials, University of Science & Technology, Beijing, China

The microstructure and crystal orientation of Tb_{0.3}Dy_{0.7}(Fe, M)_{1.95} alloys, prepared by super high temperature directional solidification device, has been studied by XRD and electronic backscatter diffraction (EBSD) technique to find out the relationship between grain orientation and magnetostrictive properties. The results of XRD indicate that the directionally solidified alloys with different parameters (including velocity V and temperature gradient G of solid-liquid interface) have <110> crystal orientation towards sample axis. Based on the XRD data, we calculate the magnetostriction coefficients, and the calculate values disagree with the measured ones without prestress. According to EBSD maps, it is found that samples with <110> preferential orientation actually have many other grain orientations, such as <113> and <111>. Meanwhile, the highly magnetostrictive samples have more volume fraction of <110> and <111> grain orientations which orientation has larger magnetostriction than <113>. Due to the limitation of XRD in volume texture characterization, the calculated result achieved from XRD is inaccurate.

Th.O-P52 - Ultra-high frequency tunability in low-current and low-field spin torque oscillators based on perpendicular magnetic tunnel junctions

T. Le ¹, A. Eklund ², S. Chung ^{1,3}, H. Mazraati ¹, A. Nguyen ^{1,4}, M. Yamanouchi ^{5,6}, E. Enobio ⁶, S. Ikeda ^{5,6}, H. Ohno ^{5,6}, J. Akerman ^{1,3}

1. *Department of Materials and Nano Physics, School of Information and Communication Technology, KTH Royal Institute of Technology, Stockholm, Sweden*

2. *Department of Integrated Devices and Circuits, School of Information and Communication Technology, KTH Royal Institute of Technology, Stockholm, Sweden*

3. *Department of Physics, University of Gothenburg*

4. *Spintronics Research Group, Laboratory for Nanotechnology, Vietnam National University-Ho Chi Minh City, Vietnam*

5. *Laboratory for Nanoelectronics and Spintronics, RIEC, Tohoku University, Miyagi, Japan*

6. *Center for Spintronics Integrated Systems, Tohoku University, Miyagi, Japan*

All-perpendicular magnetic tunnel junctions (p-MTJs) based on CoFeB/MgO structure offer the advantages of high thermal stability, low switching current density and strong adaptability to current semiconductor technology [1] in the fabrication for spin-transfer-torque (STT) memory [2,3], Here we present a detailed study of the STT driven microwave generated signals in CoFeB/MgO/CoFeB p-MTJ nano-pillars subject to an in-plane (IP) oriented magnetic field, Owing to the different perpendicular magnetic anisotropy strengths of the two CoFeB layers, their magnetizations are tilted differently away from their equilibrium in IP fields, leading to a misalignment of their magnetizations, and consequently to substantial microwave generation. Fig. 1 show the field-dependent frequency of the STT-induced generated signal. At low fields, the frequency primarily red-shifts with field towards a minimum point, before turning to blue-shift. Clear red-shift behavior of frequency with current is also observed at low fields. The low-field red-shift dependence of frequency on the bias current implies that oscillation originates from large-angle precession around perpendicular easy axis and the precession angle increases with current, consistent with the strengthening of microwave power density with current at field <3.5 kOe (Fig. 2). In contrast, both the blue-shift behavior of frequency and weakening of microwave power at higher fields suggest a change to small-angle in-plane precession. The different behaviors are correlated to the field-dependent cosine-manner of device resistance in Fig.1-inset (a), interpreted as the misalignment between the CoFeB layer magnetizations. A broad maximum of resistance corresponds to maximum misalignment and approximately coincides with the maximum generated power. In conclusion, the microwave signals of p-MTJ nano-pillars are observed at low biases with fundamental frequencies from 5 to 10 GHz, and show ultra-high current tunability of 4.4 GHz/mA (Fig. 1-inset (b)).

[1] S. Ikeda et al., Nat. Mater. 9, 721, 2010

[2] R. Sbiaa et al., Phys. Status Solidi 5 (12), 413, 2011

[3] M. Gajek et al., Appl. Phys. Lett. 100, 132408, 2012

Th.O-P53 - Effect of Boron substitution on magnetostrictive properties of SmFe₂ and (Tb,Dy)Fe₂ intermetallic alloys

S. Dange^{1,5}, J. Pendharkar², S. Venkatraman³, M.N. Nyayate³, S.S. Vansutre^{4,5}, S. Radha⁵

1. *Physics Department, Jaihind College, Churchgate, India*
2. *Physics Department, K. J. Somaiya College, Vidyavihar, India*
3. *Physics Department, B. N. Bandodkar College, Thane, India*
4. *Physics Department, SIWS College, Wadala, India*
5. *Department of Physics, University of Mumbai, Kalina, India*

The magnetostrictive properties of Boron substituted polycrystalline samples of SmFe₂ and (Tb,Dy) Fe₂ alloys (TerFeNOL-D) for Boron substitution less than 4 at% were studied. These binary and pseudo-binary Laves phase intermetallic compounds are known to show large magnetostriction.

The ingots of the polycrystalline alloys, obtained by induction melting the constituents, were cut in slices of about 4mm x 6mm x 1mm. The magnetostrictive measurements in microstrain using the half-bridge method were done with a standard resistive strain gauge of about 3mm x 5mm in magnetic field upto 1 Tesla generated by an electromagnet.

For the (Dy_{0.27} Tb_{0.73})Fe₂B_x alloys, the parent compound (x=0) shows saturation in microstrain at fields between 0.6-0.7 Tesla, reaching a value of 1400 micron, that agrees with the earlier reported value for polycrystalline Terfenol-D alloys. The addition of Boron did not produce significant change in the structure as observed from X-ray diffraction as well as the room temperature magnetization. However, the values of microstrain decreases with increasing B concentration and the strain does not saturate up to the highest achievable field of 1.2 T.

In case of the SmFe₂B alloys, the maximum magnetostriction of about 860 microstrain was noted for the parent compound and it does not show saturation upto the highest available field of 1.2T. This value of magnetostriction goes on decreasing with addition of B up to 3 at%. An earlier study on the Boron substituted SmFe₂ alloys showed the suppression of spin reorientation observed from ac susceptibility measurements in the parent compound at a temperature of 190K. The substitution of Boron produces a reduction in the magnetostriction of these compounds without causing significant change in the structure and magnetization.

Th.O-P54 - AlOx and MgAlOx barrier based magnetic tunnel junction sensing devices for industrial application

S. Knudde^{1,2}, J. Valadeiro¹, A. Moskaltsova^{1,2}, A.V. Silva^{1,2}, D.C. Leitao^{1,2}, S. Cardoso^{1,2}

1. Inesc-Mn, Lisbon, Portugal

2. Instituto Superior Tecnico, Lisbon, Portugal

In the last decade, magnetic tunnel junctions (MTJs) research has been focused on MgO due to high tunnel magnetoresistance (TMR), ranging 200% in sensors. Still, when compared to Al₂O₃ junctions (with 50% TMR), MgO technology is expensive, while noise levels [1] place Al₂O₃ junctions as a competitive alternative for sensing devices. Another material of interest is MgAlOx: epitaxial spinel crystal MgAlOx barriers seem to provide the better of two world by both their signal and noise [2]. We explore these barriers using ion beam deposition, targeting large area and large scale production.

AlOx and MgAlOx-based MTJs were deposited from metallic targets. Deposited stacks have the structure of Glass/Ru 400A/IrMn 180A/CoFe 22A/Ru 8.5A/CoFeB 30A/Barrier/CoFeB 30A/Ru 150A. The barriers consisted of Al layers (7A,9A,11A,13A,15A) or Mg/Al multilayers (total thickness 8A to 16A), where 0.5 to 2A-thick individual layers are used to promote layer intermixing. Both were oxidized through an Ar/O remote plasma [3]. For the Mg/Al barriers, the effect of Mg seed layers to promoting the crystallinity was investigated. The MTJ stacks were microfabricated from 4 to 676µm² and aspect ratio's from 1 to 20. Linearization was achieved by shape anisotropy or external biasing. Samples were annealed at 250°C for 30minutes. Statistical data from 5000 devices was analysed and AlOx MTJs showed TMR up to 35% with 20s oxidation. Lower times of oxidation (5s,10s) resulted in TMR of 20% down to 9% for thicker barriers due to under-oxidation with RxA from 150 to 4500 Ohm.µm², consistent with previously reported values. Noise levels down to 90pV/sqrt(Hz)) were measured. MgAlOx barriers showed TMR of 20%, indicating an amorphous Al₂O₃-like behaviour. A second annealing of 2hours at 330°C was performed as in MgO for crystalization, TMR decreased, indicating the onset for a diffusion mechanism.

[1] J.Almeida,et al.J.Appl.Phys.99,08B314(2006)

[2] T.Tanaka,et al.Appl.Phys.Express 5,053003(2012)

[3] S.Cardoso,et al.IEEE Trans.magn.35,2952(1999)

Th.O-P55 - Effect of the molybdenum content on magnetic characteristics of amorphous magnetic glass coated temperature sensing microwires in biomedical applications

R. Hudak¹, R. Varga², I. Polacek¹, P. Klein², R.P. del Real³, M. Vazquez³

1. *Department of Biomedical Engineering and Measurement, Faculty of Mechanical Engineering, Technical University of Kosice, Kosice, Slovakia*

2. *Department of Condensed Matters Physics, Institute of Physics, Faculty of Science, P. J. Safarik University, Kosice, Slovakia*

3. *The Instituto de Ciencia de Materiales de Madrid, institute of the Consejo Superior de Investigaciones Cientificas, Madrid, Spain*

Validation of post-implantation processes on a tissue-implant interface requires to control several biomechanic processes including temperature changes caused by inflammation or friction, in order to prevent possible negative effects. Regarding to this, the adhesion of a amorphous magnetic glass-coated microwires (AMGCM) to surface structures of a implant can be used, to enable the wireless measurement of local human body temperature. The dimensions of the microwires (20 mm X 50 μm) simultaneously do not affect the structure, construction and biocompatibility of an implant, at significant level.

The temperature sensor suitable for such biomedical applications needs to have the sensitivity in the range of 35 - 45 °C, the Curie temperature (TC) about 300 °C and in order to achieve proper sensitivity, it is necessary to produce microwires with TC about 50°C.

To allow the amorphous magnetic glass-coated microwires measure the temperature, different contents of molybdenum were added into the metal core composition. Samples with composition of a metal core $Fe_{72}Mo_9B_{18}Cu_1$, $Fe_{71}Mo_{10}B_{18}Cu_1$, $Fe_{70}Mo_{11}B_{18}Cu_1$ were produced in order to decrease TC. During the production, samples with higher amount of molybdenum tend to crystallize, which was also confirmed by hysteresis loops measurement. $Fe_{72}Mo_9B_{18}Cu_1$ and $Fe_{71}Mo_{10}B_{18}Cu_1$ microwires remained amorphous while $Fe_{70}Mo_{11}B_{18}Cu_1$ microwire crystallized.

According to saturation magnetization measurement, the amorphous microwires in the maximum temperature of 146.85 °C, did not reach the Curie temperature.

Addition of the molybdenum exhibits possibility to decrease Curie temperature but its high melting point also increases the melting point of the master alloy, what may obstruct the production of the microwires and preservation of a nominal composition of a metal core, regarding to relatively low melting point of a Pyrex. With respect to the results achieved, the actual composition of amorphous magnetic glass-coated microwires will be the object of a further study.

Th.O-P56 - Study on the DC linear stepper motor to industrial applications

N.F. Baggio Filho¹, R. Belusso¹, F. Hoefling Santos¹, T. Francisca Baggio²

1. *Federal Institute of Rio Grande do Sul, Rio grande do Sul, Brazil*

2. *Federal University of Rio Grande do Sul, Rio grande do Sul, Brazil*

Actually, many industrial processes require a precise linear motion. Usually, this movement is achieved with the use of rotary motors combined with electrical control systems and mechanical systems such as gears, pulleys and bearings. Other types of devices are based on linear motors, where the linear motion is obtained directly. The Linear Stepper Motor (MLP), proposed by this work, is an excellent solution for industrial applications that require precise positioning and high speed. This study presents an MLP formed by a linear structure and static ferromagnetic material, and a mover structure in which three coils are mounted. Mechanical suspension systems allow a linear movement between static and mover parts, maintaining a constant air gap. The operating principle is based on the tendency of alignment of magnetic flux through the path of least reluctance. The force proportional to the intensity of the electric current and the speed proportional to the frequency of the excitation coils. The study of this device is still based on the use of a numerical and experimental analysis to verify the relationship among electric current applied and planar force developed. In addition, the magnetic field in the air gap region is also monitored.

Th.O-P57 - The development of the physical foundations of the actuator based on the magnetically bi-phase partially covered microwire

K. Chichay¹, I. Machay¹, I. Iglesias¹, J. Jimenez², M. Vazquez², N. Perov^{1,3}, V. Rodionova¹

1. *Immanuel Kant Baltic Federal University, Kaliningrad, Russia*

2. *Instituto de Ciencia de Materiales de Madrid, CSIC, Madrid, Spain*

3. *Faculty of physics, Lomonosov Moscow State University, Moscow, Russia*

There are many devices for the manipulation of the nano- and micro- objects and all of them have some disadvantages needed to overcome. In this work we propose the physical foundations of the manipulator based on the magnetically bi-phase partially covered microwires. They consist of a ferromagnetic core - amorphous glass-coated microwires, and a polycrystalline ferromagnetic shell partially covering the core along its axis.

Within our activities, we investigated the bending properties of the partially covered microwire. The bend of the partially covered microwire in the magnetic field directed parallel to the microwires axis occurs because of different signs of the magnetostriction of the core and the shell materials. So, we used following materials for preparation of the core (by Taylor-Ulitovsky technique) and of the shell (by electrodeposition and by magnetron sputtering): Fe-based(positive magnetostriction)/FeCo-based(negative magnetostriction) and FeNi(positive magnetostriction)/Co(negative magnetostriction), respectively.

Main objectives of our investigations were development of the method of the bending control of the partially covered microwires in the magnetic field, estimation of the bending value for different combinations of materials and sizes of the core and the shell and demonstration of the possibility to create a novel type of actuator.

Our measurements and theoretical estimations demonstrated that the actuators have rather good working characteristics: it is able of working at large distances - up to hundreds microns and exert strong forces to move the objects - up to tens of pN. These advantages allow to work with quite large objects. Also we demonstrated that it can have two operating regimes: control of the objects by the magnetic field or by the mechanical forces. Moreover this actuator is able to work with nontransparent objects. and the last advantage: the prototype will have a low fabrication cost and will be compact.

Th.P-P01 - The role of the coating on the degradation and hematotoxicity of magnetic nanoparticles evaluated in a rat model

L. Gutiérrez¹, A. Ruiz^{1,2}, P.R. Caceres³, D. Santos³, S.B. Chaves³, M.L. Fascineli³, M. García³, R.B. Azevedo³, M. Puerto Morales¹

1. *Instituto de Ciencia de Materiales de Madrid (ICMM/CSIC), Madrid, Spain*

2. *Centro de Estudios Avanzados de Cuba (CITMA), La Habana, Cuba*

3. *Universidade de Brasília, Brasília, Brasil*

In the last decade there has been a spectacular development of iron oxide magnetic nanoparticles (MNPs) for biomedical applications and the evaluation of their potential risk on human health has become a priority objective in nanomedicine. Our main aim in this work was to evaluate the effect of two coatings (DMSA and PEG) on two important parameters related to the risks associated to the particles: the hematotoxicity of the particles and the degradation process in different tissues. For this purpose, in vivo experiments were performed by administration of a single dose of particles to a rat model and analysis of blood and organs at different times during 30 days after administration. The hematotoxicity tests showed that, at this low dose, the particles do not affect erythropoiesis or increase the number of immature erythrocytes in the bone marrow. Interestingly, DMSA coated nanoparticles showed a significant effect on the leukocytes counts 24 h after injection that was not observed if the particles were coated with PEG. The transformations of the particles in tissues were followed by AC magnetic susceptibility measurements. Due to their iron-containing core, MNPs accumulated mainly in spleen, liver and lungs tissues, where they were quickly metabolized by the animals. In particular, the DMSA coated particles were not longer observed in the tissues 24 h after their administration. Consequently, an increased amount of ferritin, the iron storage protein, was found in liver tissues in comparison with the control ones, suggesting a rapid metabolization of maghemite into ferritin iron. The PEG coating slowed the degradation process, and particles coated with this compound were still detectable in several organs 24 h after their administration.

Knowledge on the toxicity, biodistribution, and degradation processes of these materials is fundamental for their safety evaluation before their use in biomedical applications.

Th.P-P02 - Field and frequency dependence of the SAR/ILP value in magnetic hyperthermia using magnetic multi- and single core particles

P. Southern¹, L. Bogart¹, Q. Pankhurst¹, F. Ahrentorp², A. Sarwe², J. Blomgren², C. Jonasson², F. Westphal³, C. Grüttner³, R. Costo⁴

1. *University College London, London, United Kingdom*

2. *Acreo Swedish ICT AB, Kista, Sweden*

3. *Micromod Partikeltechnologie GmbH, Rostock, Germany*

4. *Instituto de Ciencia de Materiales de Madrid, Madrid, Spain*

5. *Department of Applied Physics, Chalmers University of Technology, Göteborg, Sweden*

6. *Chalmers Industriteknik, Göteborg, Sweden*

Magnetic hyperthermia is a promising novel method in cancer therapy where an AC magnetic field induces local heating in magnetic particles. Whilst both multi-core and single core particles are used in magnetic hyperthermia applications, the heating properties and efficiency of each system are quite different. Multi-core particles comprise several single-domain nanocrystals geometrically positioned in different types of configurations, while a single-core particle only contains an individual nanocrystal. For multi-core particles, the size distribution and configuration of the nanocrystals inside the particle, together with the overall particle size distribution, gives rise to different magnetic relaxation characteristics (Brownian or Néel relaxation, or a combination of both). The value of the specific absorption rate (SAR) and/or the intrinsic loss parameter (ILP) in the particle systems depends on the applied field amplitude (H_0), excitation frequency (f) and, in some instances, the viscosity of the medium. The relationship between SAR/ILP and H_0 and f depends on the properties of the particle system as well as magnetic interactions between the nanocrystals in the multi-core particles. In this work we study the SAR/ILP values of several iron oxide multi-core and single core particles with a range of particle and nanocrystal sizes. SAR/ILP values are determined from temperature vs. time curves at different H_0 and f and are correlated with magnetic losses determined from AC susceptometry and dynamic Monte-Carlo simulations. Typical values of the SAR value of the studied particle systems are in the range of 43 W/g (corresponding to an ILP value of 1.0 nHm²kg⁻¹) at a field amplitude of 6.6 kA/m and excitation frequency 989 kHz. One of the goals is to map the relationship between SAR/ILP, dynamic magnetic loss (from AC susceptometry), and nanocrystal/particle sizes determined from TEM images, that could potentially be used to determine an optimum hyperthermia frequency for a specific nanoparticle system.

This work is supported by EC FP7 NMP NanoMag project (grant no. 604448)

Th.P-P03 - Perpendicularly magnetized particles for cancer therapies

R. Mansell¹, T. Vemulkar¹, D. Petit¹, Y. Cheng², J. Murphy³, M. Lesniak³, R. Cowburn¹

1. Cavendish Laboratory, University of Cambridge, United Kingdom

2. Tongji University School of Medicine, Shanghai, China

3. The Brain Tumor Center, University of Chicago, Chicago, United States

Mechanical disruption is an emerging form of cancer therapy where magnetic particles injected into a tumour cause physical damage to cells under an applied magnetic field. We show, both theoretically and experimentally, how magnetic particles can be optimized for this application by consideration of the symmetry and strength of their magnetic anisotropy. The torque on the magnetization of the particle from an applied magnetic field is transferred to a mechanical torque through the magnetic anisotropy. A particle with an easy axis and hard plane under a specified applied rotating magnetic field is shown to provide the maximum possible torque on the particle, independent of the relative orientation of the particle and field. Previous experiments have used easy plane, for example, magnetic vortex, particles where the existence of the easy plane allows the magnetization change without exerting a torque on the particle, reducing its effectiveness. We demonstrate this finding experimentally using an in vitro test of both easy axis and Permalloy vortex particles. The easy axis particles are made from CoFeB/Pt layers coupled by RKKY interactions through Ru spacers. The CoFeB/Pt provides perpendicular anisotropy with an easy axis and large anisotropy. The RKKY coupling leads to an antiferromagnetic ground state which prevents agglomeration. The 2 micron diameter particles are incubated with the human-derived glioma brain tumour cell line U87 for 24 hours before being subjected to a 1 T rotating field. We find that for vortex particles 12 ± 2 % of the particles are destroyed after one minute of applied field whilst for the easy axis particles 62 ± 3 % are killed. This work demonstrates how mechanical disruption of cells can be optimized by consideration of the symmetry of the particles used and provides a path for increased effectiveness of this prospective cancer therapy.

Th.P-P04 - Encapsulation of VEGF165 in magnetic PLGA nanocapsules for potential local delivery and bioactivity into human brain endothelial cells

E. Carezza¹, O. Jordan², P. Martínez-San Segundo³, R. Jirik⁴, Z. Starčuk jr⁴, G. Borchard², A. Rosell³, A. Roig¹

1. *Nanoparticles and Nanocomposites Group, Institut de Ciència de Materials de Barcelona, Consejo Superior de Investigaciones Científicas (ICMAB-CSIC), Campus de la UAB, Bellaterra, Spain.*

2. *School of Pharmaceutical Sciences, University of Geneva, University of Lausanne, Quai Ernest Ansermet 30, Geneva, Switzerland*

3. *Neurovascular Research Laboratory and Neurovascular Unit, Vall d'Hebron Institut de Recerca, Universitat Autònoma de Barcelona; Passeig Vall d'Hebron, Barcelona, Spain*

4. *Institute of Scientific Instruments, Academy of Sciences of the Czech Republic, Prague, Czech Republic*

The administration of pro-angiogenic proteins is an attractive therapeutic strategy to enhance angiogenesis after an ischemic event [1,2]. Nevertheless a labile structure and short circulation time in vivo are the main obstacles that reduce protein bioactivity and dose at the target site. Biodegradable magnetic nanomaterials, intravenously administered and accumulated at the diseased zone under an external magnetic field, may circumvent these limitations.

We report on the synthesis of poly(D,L-lactic-co-glycolic acid) (PLGA) nanocapsules (diameter less than 200 nm) loaded with the vascular endothelial growth factor-165 (VEGF165) confined into the inner core and superparamagnetic iron oxide nanoparticles (SPIONs) embedded in the polymeric shell. The system showed high encapsulation efficiencies and sustained protein release over 14 days. In vitro studies confirmed protein bioactivity after encapsulation. Moreover, through MRI measurements we demonstrated excellent T2 contrast image properties. We therefore suggest the nanoconstruct as new targeted protein delivery carrier useful in pro-angiogenic treatments, especially after an ischemic event [3].

References:

1. Rosell, A.; Morancho, A.; Navarro-Sobrino, M.; Martinez-Saez, E.; Hernandez-Guillamon, M.; Lope-Piedrafita, S.; Barcelo, V.; Borrás, F.; Penalba, A.; Garcia-Bonilla, L.; Montaner, J., Factors secreted by endothelial progenitor cells enhance neurorepair responses after cerebral ischemia in mice. *PloS one* 2013, 8 (9), e73244
2. Carezza, E.; Barceló, V.; Morancho, A.; Lisa Levander, L.; Boada, C.; Laromaine, A.; Roig A.; Montaner, J.; Rosell, A., In vitro Angiogenic Performance and in vivo Brain Targeting of Magnetized Endothelial Progenitor Cells for Neurorepair Therapies. *Nanomedicine: NBM* 2014, 10, 1 225-234
3. Carezza, E.; Jordan O.; San Segundo Martínez, P.; Jiřík, R.; Starčuk jr., Z.; Borchard, G.; Anna Rosell, A.* and Roig, A.*. Encapsulation of VEGF165 in magnetic PLGA nanocapsules for potential local delivery and bioactivity into human brain endothelial cells. *J. Mater. Chem. B*, 2015, Accepted Manuscript DOI: 10.1039/C4TB01895H

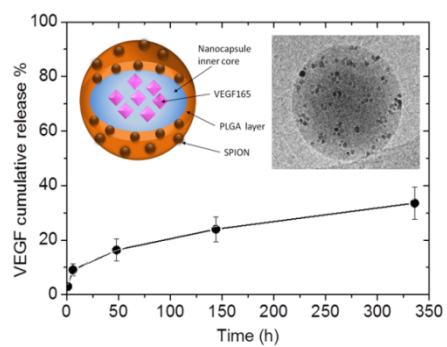


Figure caption: Protein release over a period of 2 weeks. Inset: scheme and cryo-TEM image of a PLGA nanocapsule dispersed in water

Th.P-P05 - A composite element bit design for magnetically encoded microcarriers

D. Love¹, A. Fernandez-Pacheco¹, J. Llandro¹, K. Vyas¹, J. Palfreyman¹, T. Mitrelias¹, C. Barnes¹

1. University of Cambridge, Department of Physics, Cambridge, United Kingdom

Barcoded microcarriers can be found in bioassay, point-of-care diagnostic and combinatorial chemistry applications. Encoding can be achieved using various approaches, including fluorescence, shape and magnetic based techniques [1]. Previous designs for magnetic bit encoded microcarriers [2,3] were severely limited in reliability and barcodes could only consist of up to 3-5 bits [4].

Here we present a new composite element (CE) bit design [5] that overcomes these limitations. We discuss the intricacies which govern the magnetic behaviour of the CE bit design and demonstrate how highly reliable barcodes with up to 14 bits (16,384 codes) can be fabricated. We demonstrate a multi-bit in-plane encoding and detection process, and discuss how CEs make magnetically encoded microcarriers relevant for microfluidic bioassays and modern combinatorial chemistry applications.

Furthermore, we present a new variant of the CE barcode designed to produce strong out-of-plane flux patterns, proving additional benefits to detection resolution and bit packing density. We analyse out-of-plane domains using MFM measurements and illustrate the multi-bit encoding process using MOKE imaging techniques. This talk aims to convey the significant benefits that magnetic encoding of microcarriers provides over other barcoding techniques.

[1] J. Llandro, et al., *Med. Biol. Eng. Comput.* 48, 977 (2010)

[2] R.-J. Hong, et al., *Lab on a Chip* 8, 1883 (2008)

[3] B. Hong, et al., *JAP* 105, 034701 (2009)

[4] K.N. Vyas, et al., *Biosensors* (in review)

[5] D.M. Love, et al., *RSC Advances* 5, 10211 (2015)

Th.P-P06 - Dynamically varying magnetic microstructures as NMR transducers of physiological conditions.

G. Zabow^{1,2}, S. Dodd², A. Koretsky²

1. National Institute of Standards and Technology (NIST), Boulder, United States

2. National Institutes of Health (NIH), Maryland, United States

Magnetic micro- and nanoparticles find use across many biomedical fields ranging from imaging, therapy and drug delivery, to cell separation, magnetotransfection, and even magnetic control of cell signaling pathways.

As varied as these applications are, common to all is the use of relatively simple, chemically synthesized magnetic particles.

But what additional applications might be enabled through the use of precision, microfabricated magnetic particles and / or complexes that benefit from the improved geometrical control common to top-down, lithographically defined structures?

One recent example are new multispectral magnetic resonance imaging (MRI) contrast agents that add not just contrast, but “color”, to MRI through specifically shaped magnetic microparticles with magnetic field profiles that impart unique, distinguishable NMR frequency shifts to the surrounding water[1].

Here we take this work a step further. Since different particle shapes yield different field profiles and associated NMR frequency shifts, a dynamically morphing magnetic microstructure can impart novel, geometrically dependent, dynamically varying NMR frequency shifts.

If the magnetic microstructure is designed to change shape in response to some local physiological or environmental condition, then the resulting change in microstructure field profile can transduce changes in local conditions into quantitative NMR frequency shifts in the surrounding water.

Stimuli-responsive shape-changing magnetic microparticles/structures therefore enable a new class of radio-frequency addressable sensors that can be small (and thus relatively non-invasive), that require neither electrical contact nor optical access, and that can be probed with regular NMR equipment.

In this presentation we will focus on the magnetics behind these new transducers, demonstrate, as a first example, the ability of such new shape-changing magnetic microstructures to measure local pH levels, and consider their potential for sensing other variables.

Reference:

[1] Zabow et. al., Nature 453, 1058 (2008)

Th.P-P07 - Influence of core-to-aggregate dipole interactions in the heating capacity of magnetic hyperthermia agents

C. Blanco-Andujar^{1,2}, P. Southern³, L.K. Bogart³, Q.A. Pankhurst³, C. Grüttner⁴, M. del Puerto Morales⁵, D. Ortega^{2,6,7}

1. *Institut de Physique et Chimie des Matériaux de Strasbourg (IPCMS), UMR-7504 CNRS-Université de Strasbourg, Strasbourg, France*

2. *Institute of Biomedical Engineering, University College London, London, United Kingdom*

3. *UCL Healthcare Biomagnetics Laboratory, London, United Kingdom*

4. *Micromod Partikeltechnologie GmbH, Rostock, Germany*

5. *Instituto de Ciencia de Materiales de Madrid, ICMN-CSIC, Cantoblanco, Madrid, Spain*

6. *Instituto Madrileño de Estudios Avanzados en Nanociencia (IMDEA-Nanociencia), Cantoblanco, Madrid, Spain*

7. *Unidad Asociada de Nanobiotecnología, CNB-CSIC&IMDEA Nanociencia, Ciudad Universitaria de Cantoblanco, Madrid, Spain*

Magnetic hyperthermia relies on killing cancer cells by heating biocompatible magnetic nanoparticles under alternating magnetic fields and is envisaged as one of the most promising bids of nanotechnology in cancer therapy. The role of magnetic interactions in nanoparticle systems is still regarded as a complex issue and is not fully understood, particularly in an ever-changing physical and dynamic environment such as that presented during magnetic hyperthermia. Studies of magnetic interactions rely heavily on theoretical models [1,2] and their impact on the heating performance can still not be described with ease by a single measurable characteristic.

We present an experimental study on the occurrence of interparticle interactions in a selected set of commercial and non-commercial [3] samples consisting of single-core and multi-core iron oxide nanoparticles based on the analysis of Henkel plots. The nature and intensity of the interactions are discussed and derived from DeltaM plots and the mean interaction field values estimated for each system. The role played by the core-to-aggregate ratio and the number of constituting cores on the interactions and the effect of the latter on the heating capabilities of the nanoparticles is also discussed. As a rule of thumb, samples with less intense dipole interactions between constituent nanoparticles (intra-aggregate) show better heating capabilities.

Th.P-P08 - Synergy on magneto-plasmonic nanoprobe: Combined magneto-photonic hyperthermia

J.G. Ovejero¹, E. Mazario², U. Silva³, A. Hernando¹, P. Herrasti², P. Crespo¹

1. Instituto de Magnetismo Aplicado: SalvadorVelayos (UCM), Madrid, Spain

2. Department of Physical Chemistry, Universidad Autónoma de Madrid, Cantoblanco, Madrid, Spain

3. Department of Physics of Materials, Universidad Autónoma de Madrid, Cantoblanco, Madrid, Spain

The properties of nanoparticles for biomedical applications have been largely improved in the last years [1]. Further development can be achieved by the combination of different functionalities in a single nanoprobe [2]. One very interesting approach to the multifunctionalization is the creation of hybrid nanoparticles by the conjugation of individual nanoparticles. Magneto-plasmonic hybrid nanostructure is a perfect example of a synergetic system which allows the creation of dual methods of imaging, therapy and sensing [3]. The present work studies the conjugation of silica coated nanorods (Au/SiO NR) with magnetic nanoparticles (MNP) based on different types of ferrites and their potential as dual probes for combined hyperthermia.

Both Au/SiO NR and MNP have been individually synthesized to improve their features independently. Afterwards, each part has been complementarily functionalized. On one side, APES was attached to Au/SiO NR surface to reduce their cytotoxicity and introduce reactive amine groups. While on the other side, MNP were functionalized with citric and folic acid to create carboxylic groups that allowed the nanoparticle conjugation. Electrostatic and covalent bindings have been compared as mechanism of conjugation. The later has used the EDC/NHS protocol to bond amine and carboxylic groups [4].

Au/SiO NR and MNP has been tested as efficient nanoheaters and currently magneto-photonic hyperthermia system is been used to evaluate heating power of magneto-plasmonic hybrid nanoparticles. The device developed for this purpose is able to apply high frequency AC magnetic fields and infrared radiation in a small volume at the same time. The heat dissipated by the nanoparticles is registered with an infrared camera. Dual hyperthermia presents interesting advantages against the currently used methods.

References:

[1] L. Gutierrez et al. Dalton Trans., 2015, 44: 2943–2952

[2] Michael J. Sailor and Ji-Ho Park Adv. Mater. 2012, 24: 3779–3802

[3] C. Wang, et al Angew. Chem. Int. Ed. 2009, 48: 2759 –2763

[4] Marcel J. E. Fischer Methods in Molecular Biology 2010, 627: 55-73

This work has been supported by MAT2012-37109-C02-01 and MAT2012-37109-C02-02 projects of the Spanish Ministry of Economy and Competitivity

Th.P-P09 - Stability and cellular uptake of anionic iron oxide nanoparticles for hyperthermia

D. Soukup¹, S. Moise¹, E. Cespedes², J. Dobson³, N. Telling¹

1. *Institute for Science and Technology in Medicine, Keele University, Staffordshire, United Kingdom*

2. *IMDEA NANOCIENCIA, Ciudad Universitaria de Cantoblanco*

3. *J.Crayton Pruitt Family Department of Biomedical Engineering & Department of Materials Science and Engineering, University of Florida, Gainesville, United States*

Magnetic nanoparticles (MNP) can generate heat once exposed to an alternating magnetic field which has been employed in magnetic hyperthermia. MNP are routinely tested in water based suspensions to determine the specific absorption rates (SAR). However, cell microenvironment can greatly influence the relaxation mechanism of MNP which in turn can decrease the SAR. The aim of this study is to determine the effect of cell microenvironment on magnetic response of MNP. The in situ magnetic response of anionic iron oxide nanoparticles, from water-based suspensions to cell culture media, following their cellular internalization was investigated, using a novel application of AC susceptometry. The results obtained demonstrate that cellular internalisation can disable Brownian relaxation, which has significant implications for designing suitable nanoparticles for intracellular hyperthermia applications. Further, the stability of anionic iron oxide nanoparticles in various biologically relevant solutions was also investigated. The MNP stability was tested in phosphate buffered saline (PBS) with and without foetal bovine serum (FBS) and in different dilutions of PBS to determine the effect of ionic strength, but also the protein coating from FBS, in cell culture media with and without FBS. The aim is to determine the optimal conditions with a view to minimise the clustering of MNP. We observed that the stability of MNP is micro-environment dependant and that the protein corona developed significantly increases the stability of MNP. Our results also provide evidence that the stability of MNP influences the sedimentation of nanoparticles, which in turn significantly affects cell uptake. AC susceptometry was used to monitor and quantify the uptake of MNP in live cells - a novel non-invasive method that has a potential for monitoring the uptake of MNP in vivo.

Th.P-P10 - NMR as evaluation strategy for cellular uptake of nanoparticles

T. Orlando¹, A. Paolini², F. Pineider³, E. Clementi², F. Pasi², Y. Guari⁴, J. Larionova⁴, L. Sacchi², R. Nano², M. Corti¹

1. *Department of Physics and INSTM, University of Pavia, Pavia, Italy*

2. *Department of Biology and Biotechnology, University of Pavia, Pavia, Italy*

3. *Department of Chemistry and INSTM, University of Florence, Florence, Italy*

4. *Chimie Moléculaire et Organisation du Solide, Université Montpellier II, Montpellier, France*

5. *Department of Physics, Università degli Studi di Milano, Milan, Italy*

Magnetic nanoparticles of novel synthesis can both improve the efficiency of already existing and widely used clinical techniques, like Magnetic Resonance Imaging or Magnetic Hyperthermia, and work as single multifunctional agents for theranostic purposes. However, despite the engineering background in this field is very advanced, there remain some fundamental problems involving the interaction mechanisms between nanostructures and cells. We studied the cellular uptake of rhamnose-coated magnetic nanoparticles (MNPs) in human tumor (glioblastoma) cells using a new experimental method based on ¹H Nuclear Magnetic Resonance relaxation.

After the incubation of the cells with different concentrations of MNPs, transverse nuclear magnetization relaxation process was investigated for each in vitro sample. In particular, ¹H-NMR is able to distinguish between the fast relaxing signal (T_{2,FAST}) coming from intracellular protons and the slow relaxing signal (T_{2,SLOW}) from extracellular protons. Given that the T₂ value is inversely proportional to the magnetic particle concentration, T_{2,FAST} and T_{2,SLOW} are indirect measurements of the amount of MNPs in the intracellular and in the extracellular environment, respectively. The relaxation data as a function of the MNPs concentration were fitted with a logistic curve and the uptake law for our MNPs was extracted. Furthermore, the weight of each component gives a quantitative estimation of the amount of protons in each biological environment (i.e., intra- and extracellular), allowing to follow the cellular swelling, that is directly connected to the cellular stress due to the injection of an exogenous agent in the biological system. The proposed experimental protocol, which was successfully tested also with gold nanoparticles and antitumor drug on two different cell lines, provides a new way to investigate in a quantitative way the general problem of cellular uptake for a variety of biocompatible nanostructures and drugs.

Th.P-P11 - On the double role of the magnetic anisotropy for magnetic-fluid hyperthermia

D. Serantes¹, K. Simeonidis³, M. Marciello¹, M. Angelakeris⁴, O. Chubykalo-Fesenko¹, M. del Puerto Morales¹

1. *Instituto de Ciencia de Materiales de Madrid CSIC, Madrid, Spain*

2. *UCCS Biofrontiers Center, University of Colorado, Colorado Springs, United States*

3. *Dept. of Mechanical Engineering, School of Engineering, University of Thessaly, Volos, Greece*

4. *Department of Physics, Aristotle University of Thessaloniki, Thessaloniki, Greece*

Achieving a large and well controlled heating performance according to the properties of the biological tissue are crucial milestones in the magnetic-fluid hyperthermia roadmap. Aiming to shed some light in this significant issue, here we report the double role played by the magnetic anisotropy of ellipsoidal magnetite nanoparticles to control both aspects. On the one hand, the increased effective anisotropy of the elongated particles mimics the multiplicative heating performance of chain formation in cell-like biology conditions [1], with the additional benefit of being more robust vs. thermal and/or mechanical forces. On the other hand, with the characteristics of the applied magnetic field it is possible to induce a preferential orientation of the easy magnetization axes of the particles that allows for more a better field-controlled heat release. The particles have average dimensions 250 nm/50 nm long/short axes, i.e. are comparable to the nanoparticle chains for which enhanced performance was observed [1] and, noteworthy, experiments in HeLa cells show no toxicity thus supporting their adequacy for biological use. The combined theoretical work using micromagnetic simulations explains that the unexpected frequency-dependence measured experimentally is due to a non-coherent reversal mechanism. Remarkably, from the comparison between angular-dependent experiments measured after the AC field treatment and simulations it is concluded that the induced preferential orientation of the ellipsoids point perpendicular to the AC field direction. Our results therefore demonstrate that even if Brownian rotation may be negligible regarding heat dissipation [2], it may be crucial in determining the heat dissipated by Néel reversal mechanism.

Th.P-P12 - Synthesis and characterization of magnetic nanogranular Fe₃O₄/biomimetic hydroxyapatite for potential applications in nanomedicine

L. Del Bianco¹, I. Giorgio Lesci², G. Fracasso², G. Barucca³, F. Spizzo⁴, R. Scotti⁵, L. Ciocca⁵

1. *Dipartimento di Fisica e Astronomia, Università di Bologna, Bologna, Italy*

2. *Dipartimento di Chimica 'G. Ciamician', Università di Bologna, Bologna, Italy*

3. *Dipartimento SIMAU, Università Politecnica delle Marche, Ancona, Italy*

4. *Dipartimento di Fisica e Scienze della Terra and CNISM, Università di Ferrara, Ferrara, Italy*

5. *Dipartimento di Scienze Biomediche e Neuromotorie, Università di Bologna, Bologna, Italy*

A major concern about the biomedical application of magnetic nanoparticles is their biocompatibility. A possible solution is coating them with hydroxyapatite (HA) [Ca₅(PO₄)₃OH], which is the inorganic component of biological hard tissues, e.g. bone and teeth. This approach appears especially appealing for uses in the field of bone tissue engineering.

We have synthesized a novel nanogranular system, consisting of magnetite nanoparticles embedded in biomimetic carbonate HA, through an original two-step method: i) magnetite nanoparticles are prepared by refluxing an aqueous solution of Fe(SO₄) and Fe₂(SO₄)₃ in an excess of Tetrabutylammonium hydroxide acting as surfactant; ii) the nanoparticles are coated with a Ca(OH)₂ layer, to induce the growth of HA directly on their surface, by reaction of Ca(OH)₂ with HPO₄²⁻.

Two samples have been collected with magnetite content ~ 0.8 wt. % and ~ 4 wt.%. The magnetite nanoparticles and the nanogranular material have been investigated by X-ray Diffraction, Fourier Transform Infrared Spectroscopy and Transmission Electron Microscopy. These analyses have provided structural information on the as-prepared nanoparticles (mean size ~ 6 nm) and revealed the presence of surface hydroxyl groups, which promote the growth of the HA phase featuring a nanocrystalline lamellar structure. Hysteresis loops (temperature range 5-300 K), thermal and time dependence of the magnetization under different magnetic fields and field dependence of the remanence have been measured by SQUID magnetometer. Both the as-prepared and the HA-coated magnetite nanoparticles are superparamagnetic at T=300 K. However, the magnetization relaxation process is affected by dipolar magnetic interactions of comparable strength in the three samples, also inducing the onset of a collective frozen magnetic regime below T~20 K. The results indicate that the magnetite nanoparticles form agglomerates in the as-prepared state, which are not substantially altered by the HA growth, coherently with the creation of electrostatic hydrogen bonds among the surface hydroxyl groups.

Th.P-P13 - Dynamics of CoFe₂O₄ single-core nanoparticles in viscoelastic media

H. Remmer¹, J. Dieckhoff¹, A. Tschöpe², E. Roeben³, A.M. Schmidt³, F. Ludwig¹

1. *Technische Universität Braunschweig, Institut für Elektrische Messtechnik, Linz, Austria*

2. *Universität des Saarlandes, Experimentalphysik, Graz, Austria*

3. *Universität zu Köln, Institut für Physikalische Chemie, Tübingen, Germany*

The dynamics of magnetic nanoparticles in time-varying magnetic fields in both the suspended and immobilized state have been extensively studied. In the latter case, the dynamics is determined by the Néel mechanism whereas in the former case Brownian and Néel relaxation can take place. In a Newtonian fluid and provided that the magnetic moments are magnetically blocked, the dynamics can be described by the well-known Brownian time constant with a purely real viscosity. Here we focus on the dynamics of magnetically blocked single-core nanoparticles in a viscoelastic matrix. CoFe₂O₄ nanoparticles with a mean core diameter of 15 nm, as determined from TEM and magnetization measurements, and a hydrate shell were dispersed in DI water-gelatin suspensions with gelatin contents between 2.5 and 10 wt%. After equilibrating the sample at 40°C for 60 min - thus being in the sol state - , it was rapidly cooled to 23°C and periodic measurements of the ac susceptibility and magnetorelaxation signal were performed. With increasing gelation time, a systematic shift of the maximum of the imaginary part of the ac susceptibility and a pronounced broadening were observed. In magnetorelaxometry, the characteristic time constant clearly increased. The detailed behavior depends on the given gelatin content and thus the stiffness of the gel matrix. The experimental data are analyzed applying the theoretical model by Raikher et al. [1], providing the temporal evolution of viscosity and shear module during the gelation process. Financial support by the Deutsche Forschungsgemeinschaft, DFG Priority Program 1681 is acknowledged.

[1] Yu. L. Raikher et al., Phys. Rev. E 63, 031402 (2001)

Th.P-P14 - Investigation of PEI-coated magnetic nanoparticles and their potential in nanomagnetic transfection using dynamic magnetic systems

K.K. Narayanasamy^{1,2}, M. Cruz-Acuña², L. Maldonado², C. Rinaldi², J. Dobson^{2,3,4}, N.D. Telling¹

1. *Institute of Science and Technology In Medicine, Keele University - Staffordshire, United Kingdom*

2. *2 J Crayton Pruitt Family Department of Biomedical Engineering, University of Florida - Florida, United States*

3. *3Department of Materials Science and Engineering, University of Florida - Florida, United States*

4. *Institute for Cell Engineering and Regenerative Medicine (ICERM), University of Florida - Florida, United States*

Nanomagnetic transfection is a method for delivering genes into a cell using an external magnetic force to increase the interaction between cells and magnetic nanoparticle-DNA complexes. We are developing various functionalized magnetic nanoparticles as carriers for gene delivery. Thermal decomposition, co-precipitation and flame spray methods were used to synthesise the nanoparticles allowing us to obtain different chemical compositions (magnetite, maghemite, metallic iron, and metallic cobalt), various core sizes and magnetic behaviour (magnetically blocked and superparamagnetic). MNPs used for nanomagnetic gene transfection generally consist of iron oxide cores, which respond to external magnetic fields, with cationic polyethylenimine (PEI) polyplexes for DNA adsorption. The particles were functionalized with oleic acid-PEI and citric acid-PEI to obtain different binding efficiencies. The binding and release efficiency of DNA to PEI-MNP was investigated at different pH to mimic conditions in the cell using AC susceptometry. Two oscillating dynamic magnetic systems (magnfect-nano and MICA) that enhances particle/DNA uptake through promotion of endocytosis are being used to investigate the transfection efficiency on different cell types. Future work involves a better understanding of the trafficking of the magnetic nanoparticle-DNA complex in cells when exposed to an oscillating magnetic system.

Th.P-P16 - Synthesis and characterization of surfactant coated superparamagnetic iron oxide nanoparticles for various biomedical applications

R. Srinivasan¹, N. Momin¹, A. Deshmukh²

1. *Department of Physics, University of Mumbai, Mumbai, India*

2. *Department of Biotechnology, Thakur College, Mumbai, India*

We report synthesis of superparamagnetic iron oxide nanoparticles (SPIONs) by simple chemical co-precipitation method followed by coating with surfactant (Polyethylene glycol-6000 and sodium oleate) for future biomedical applications. The synthesized particles are characterized using X-ray diffraction (XRD), Fourier transform infrared spectroscopy (FTIR), Raman, UV-visible, Dynamic light spectroscopy (DLS) and Brunauer-Emmett-Teller (BET) technique for crystal structure, average size, functional group, phase, energy band gap, hydrodynamic size and surface area determination. The surface morphology was studied by Scanning electron microscope (SEM). Magnetic properties of the synthesized particles, viz field and temperature dependent magnetization in zero field cooled and field cooled conditions between 5K-300K and up to fields of 3 Tesla have been investigated by Quantum Design physical property measurement system (QD-PPMS). Analysis of cytotoxicity of the nanoparticles was carried out by examining their effect on cell viability of human peripheral blood lymphocytes so as to assess biocompatibility for various biomedical applications. Sodium oleate coated SPIONs shows better biocompatibility as compared to the uncoated and PEG-6000 coated ones.

Th.P-P17 - Magnetic nanowires and hyperthermia: the influence of geometry and material on heat production efficiency

M.F. Contreras Gerenas¹, A. Zaher², J.E. Perez¹, A. Alfahdel¹, L.A.S. de Oliveira³, K.R. Pirota⁴, T. Ravasi¹, J. Kosel¹

1. King Abdullah University of Science and Technology, Thuwal, Saudi Arabia

2. University of British Columbia, Kelowna, Canada

3. Universidade Federal do Rio de Janeiro, Rio de Janeiro, Brazil

4. Univerdad Estadual de Campinas, Campinas, Brazil

Magnetic hyperthermia, which refers to the production of heat by magnetic nanostructures under an alternating magnetic field (AMF), is very promising using magnetic nanowires (NWs), as they have been shown to have a larger magnetic moment per unit of volume compared to nanobeads. Moreover, Fe nanowires (NWs) proved to have a higher heating efficiency compared to Fe nanobeads, when exposed to an AMF at the same concentration¹.

In this work we investigate the dependence of heating power of NWs with of different materials (Fe, Ni, and Co) and diameters (thin, 35 nm and thick, 180-300 nm). NWs with lengths of tens of microns and two different diameters were prepared using a two-step aluminum anodization process followed by electrodeposition^{2,3}. The morphology and composition of the wires are investigated using scanning and transmission electron microscopy. The magnetic properties of the NWs are studied using a vibrating sample magnetometer. After fabrication, NWs are released from the substrate and rinsed with ethanol several times.

The specific absorption rate (SAR) is commonly used to quantify the magnetic heating efficiency. SAR measurements were performed over 30 minutes for different NW concentrations using an inductive heater system that provided a field of 600 Oe at a frequency of 425 kHz. The NWs were suspended in ethanol inside of a thermally isolated tube. The ethanol's temperature was monitored with an optical temperature probe.

The results showed a strong dependence of the heating power on the magnetic properties of the NWs. The NWs with the highest SAR are those with a coercive field equal or lower to the value of the AMF applied. This effect is strongly accentuated in case of Fe and Ni, due to the magnetic single domain behavior⁴, leading to no hysteresis losses for fields less than the coercive field. Since, the coercive field is strongly controlled by the geometry⁵, the temperature increase (ΔT) of thin NWs was always lower ($< 10^\circ\text{C}$ for Fe) than the one of thick NWs ($\sim 40^\circ\text{C}$, for Fe).

1. Lin, W.-S., Lin, H.-M., Chen, H.-H., Hwu, Y.-K. & Chiou, Y.-J. Shape Effects of Iron Nanowires on Hyperthermia Treatment. *J. Nanomater.* 1–6 (2013). doi:10.1155/2013/237439

2. Masuda, H. & Fukuda, K. Ordered metal nanohole arrays made by a two-step replication of honeycomb structures of anodic alumina. *Science* (80-.). 268, 1466–8 (1995)

3. Nielsch, K., Müller, F., Li, A.-P. & Gösele, U. Uniform Nickel Deposition into Ordered Alumina Pores by Pulsed Electrodeposition. *Adv. Mater.* 12, 582–586 (2000)

4. Nielsch, K., et al. "Hexagonally ordered 100 nm period nickel nanowire arrays. *App.Phys. Let.* 79.9 (2001): 1360-1362

5. Ferre, R., et al. "Magnetization processes in nickel and cobalt electrodeposited nanowires." *Phys. Rev. B* 56.21 (1997): 14066

Th.P-P18 - The human mononuclear cells vital activity in magnetic field

N. Perov¹, L. Litvinova², V. Rodionova², I. Iglesias², V. Rodionov², V. Shupletsova², N. Sokhnevich², O. Khaziakhmatova², A. Granovsky¹

1. Faculty of Physics, Lomonosov MSU, Moscow, Russia

2. Baltic Federal University, Kaliningrad, Russia

Nowadays many industrial and medical technologies use magnetic fields with large magnetic inductions (1-5 T). However the risks arising from human exposure to these fields have not been fully determined and the possible mechanisms of the influence of relatively weak and strong dc and ac magnetic fields on human being are not understood. So it is important to get information on the magnetic field effect on the different human cells. We present our preliminary results on the vital activity of the human mononuclear cells in dc magnetic field with different strength. In the experiments there were used the mononuclear cells of healthy donors. Some experiments in the same conditions were made. The average results for all experiments were analyzed. By flow cytometry method there were evaluated the viability and total number of cells in the samples. The content of pro - and anti-inflammatory cytokines in supernatant cell cultures for all experiments was investigated with enzyme-linked immunosorbent assay. It was found the non-monotonic change of vital activity of investigated cells with magnetic field increase: till magnetic field 2000 Oe it was larger than for control series and for upper field it was less. The content of pro - and anti-inflammatory cytokines in supernatant non-monotonically depended on magnetic field strength. The maximum change with magnetic field for some parameters exceeded 50% of control value. The possible mechanism of these effects is discussed.

Th.P-P19 - A Monte Carlo study of the Susceptibility losses in heating of magnetic core/shell nanoparticles for hyperthermia

M. Vasilakaki¹, K. Trohidou¹, C. Binns²

1. *Institute of Nanoscience and Nanotechnology, NCSR "Demokritos", Aghia Paraskevi, Attiki, Greece*

2. *Department of Physics and Astronomy, University of Leicester, United Kingdom*

Optimizing the heating properties of magnetic nanoparticles is of great importance for hyperthermia applications[1].

Recent experimental results [2] show that core/shell nanoparticles could give an increased SAR compared to the magnetic oxide nanoparticles currently used.

We have developed a modified phenomenological model based on the linear Néel-Brown relaxation model to calculate the SAR due to susceptibility losses in complex nanoparticles with ferromagnetic(FM) core/ ferrimagnetic(FiM) shell [1]. We use the Monte Carlo simulations technique with the implementation of the Metropolis algorithm to study the effect of the size and shape on the magnetization behaviour of FM/FiM nanoparticles covered by a surfactant layer [3]. The simulations results for spherical, cubic, octahedral and truncated cuboctahedral nanoparticles are used as an input in our modified model for the calculation of the SAR. We find that for all the sizes and shapes the complex FM/FiM nanoparticles give higher SAR values than the pure FiM nanoparticles. For all sizes the nanoparticles with the truncated cuboctahedral shape give the highest SAR values and the cubic the lowest ones. The decrease in the surfactant thickness results in an increase of the SAR values. Our results are in good agreement with experimental findings for Fe/Fe₃O₄ nanoparticles.

[1] D. Ortega and Q. A. Pankhurst, Magnetic hyperthermia, in Nanoscience:Vol. 1: Nanostructures through Chemistry, P. O'Brien, Editor. 2013, Royal Society of Chemistry: Cambridge. p. 60-88

[2] C. Binns, P. Prieto, S. Baker, P. Howes, R. Dondi, G. Burley, L. Lari, R. Kröger, A. Pratt, S. Aktas, J. K. Mellon, J. Nanopart. Res. 2012, 14, 1136

[3] M. Vasilakaki and K.N. Trohidou, Phys. Rev. B 2009, 79, 144402

Th.P-P20 - Maghemite nanocrystal clusters for MRI diagnosis and hyperthermia medical treatment

A. Lappas¹, K. Brintakis^{1, 2}, A. Kostopoulou¹, M. Vasilakaki³, K. Trohidou³, A. Ranella¹, I. Athanassakis⁴, M. Angelakeris², A. Lascialfari⁵, A. Douvalis⁶

1. *Institute of Electronic Structure and Laser, Foundation for Research and Technology - Hellas, Vassilika Vouton, Heraklion, Greece*

2. *Department of Physics, Aristotle University of Thessaloniki, Thessaloniki, Greece*

3. *IAMPPNM, Department of Materials Science, NCSR "Demokritos", Aghia Paraskevi, Athens, Greece*

4. *Department of Biology, University of Crete, Vassilika Vouton, Heraklion, Greece*

5. *Dipartimento di Fisica, Università degli studi di Milano and INSTM, Milano, Italy*

6. *Department of Physics, University of Ioannina, Ioannina, Greece*

Cancer cure schemes are based on accurate diagnosis and treatment protocols that could have minimal side-effects for a patient. For this purpose the scientific community seeks cost-efficient advanced materials that serve the combined role of diagnosis and therapy. However, it is imperative that a so-called theranostic material is characterised in depth for its physical, chemical and biocompatibility properties.

In order to address this challenge, we have developed size-controlled (50-100 nm), water-dispersible clusters of maghemite nanoparticles (NPs), named Colloidal Nanoclusters (CNCs). Characterization techniques (including, HRTEM, X-ray scattering, Mössbauer spectroscopy, SQUID magnetometry), combined with theoretical Monte Carlo simulations have probed the microscopic mechanisms that govern the growth and magnetic behaviour of these CNCs. We have found that such controlled nanoparticle assemblies, display collective magnetic behaviour as an outcome of the intra-cluster dipolar interactions and the intra-particle exchange interactions. Our capability to engineer these interactions has a direct impact on the transverse ¹H-NMR Relaxivity (r_2), as well as on the Specific Loss Power for MRI and Hyperthermia applications, respectively. The CNCs show 4-5 times enhanced r_2 (400-500 mM⁻¹ s⁻¹) with respect to superparamagnetic contrast agents like the commercial product Endorem (100 mM⁻¹ s⁻¹). In addition, the CNCs' ferrimagnetic nature and the corresponding intra-cluster interactions provide the mechanisms for size-dependent, efficient heating response (180-420 W/g). Further on, preliminary incubation experiments of the CNCs with mice spleen cells support the low-cytotoxicity and biocompatibility of these nanosystems. We argue that all the above-mentioned characteristics pave the way for an advantageous multifunctional theranostic agent in biomedicine.

[1] A. Kostopoulou et al., *Nanoscale* 6, 3764 (2014)

[2] A. Kostopoulou et al., *Dalton Trans.* 43, 8395 (2014)

We acknowledge funding under the Action KRIPIS, project No MIS-448305 (PROENYL), of the GSRT/Ministry of Education, Greece and the European Regional Development Fund (NSRF 2007-2013)/EC

Th.P-P21 - Effect of pulsed magnetic field stimulation on circulatory diagnosis of acupuncture meridian system

H. Sook Lee¹, Y. Shin¹, D. Guwn Hwang¹

1. Dept. of Oriental Biomedical Engineering, Sangji University, Wonju-si, South Korea

Objectives: Although many previous studies related to acupuncture and magnetic field have been done, much remains unclear [1]. This study was undertaken to examine the effect of pulsed magnetic field stimulus (PMFS) on the circulatory of the acupuncture meridian system (AMS). With recent increasing attention on PMFS as non-invasive medical treatment, diverse studies are being conducted to elucidate its effects on human physiology [2]. According to traditional Chinese medicine (TCM), pericardium meridian (PC) among the twelve AMS is known as 'protector of heart' meridian and its primary function is to control the balance of heart and blood functions. In order to measure quantitatively the change of meridian circulation after PMFS, PC meridian is used due to its efficacy on diseases of the circulatory and nervous system.

Methods: After PMFS on the left side of palm, Galvanic skin response was used to measure MAX/ID score at five acupoints-PC4, PC6, PC7, PC8 and PC9 in PC meridian of the subject's right arm. Ten subjects in their 20s were participated. MAX score means initial reaction for maximum compensation of electrons in the tissue and ID means cell defense capability for maintaining the current state of the cell.

Results and Conclusions: While MAX score was out of normal range of 45-58 before PMFS, it converged to normal range after PMFS. ID score also dropped to zero after PMFS, so it tells smooth blood circulation. Our results showed that more exposure of PMFS provided MAX/ID score to be stable. For application to the circulatory diagnosis of AMS, additional experiments need with optimum conditions of exposure time and intensity of PMF as well as the subjects with heart and blood stagnation disease.

Th.P-P22 - Influence of magnetic nanoparticle surface modification on circulation time

V. Zavisova¹, M. Koneracka¹, M. Muckova², N. Tomasovicova¹, J. Kovac¹, M. Kubovcikova¹, I. Antal¹, P. Kopcansky¹

1. *Institute of Experimental Physics, Slovak Academy of Sciences, Kosice, Slovakia*

2. *Hameln, rds a.s., Modra, Slovakia*

Superparamagnetic nanoparticles have great utilization potential in drug delivery, diagnostic biosensors and as contrast agent for magnetic resonance imaging (MRI) as well. Threshold parameter for these applications is their short circulation time in bloodstream, as they are relatively quickly cleared by the reticuloendothelial system (RES). One of the ways to decrease RES clearance and prolong the circulation time is surface modification of magnetic nanoparticles.

Magnetic particles (Fe_3O_4) prepared by chemical coprecipitation method were modified by different biocompatible substances such as poly(ethylene glycol), dextran, and polyvinylpyrrolidone. Prepared samples were characterized by transmission electron microscopy (TEM), dynamic light scattering (DLS) and SQUID magnetometry. Spherical shape of magnetic core with the mean diameter of 10 nm observed by TEM was in agreement with the magnetic core diameter obtained by fitting magnetization measurements by the Langevin function. Further on, our results demonstrate that prepared samples have the hydrodynamic diameter measured by DLS ranging from 53 to 69 nm.

To evaluate the kinetics of magnetic particle uptake by RES, magnetic particles which remained in the bloodstream were detected after blood collection at preselected intervals by measuring their magnetic moment by SQUID magnetometer.

Magnetic moment of the magnetic particles in blood decreased exponentially, magnetic particles were gradually cleared by the RES. The obtained results showed that unmodified magnetic nanoparticles were trapped by RES within 1 hour. On the other hand, the magnetic nanoparticles modified by poly(ethylene glycol), dextran, and polyvinylpyrrolidone circulated in bloodstream up to 3 hours. Prolongation of the magnetic particles blood circulation time achieved by their surface modification has potential in future in vivo applications.

Acknowledgments:

This work was supported by project VEGA 0041, Ministry of Education Agency for Structural Funds of EU in frame of projects 26220220005 and 26110230097

Th.P-P23 - Resonance absorption of microwaves by tissue with ferromagnetic particles

D. Kalganov¹, L. Butko¹, A. Anzulevich¹, D. Pavlov¹

1. Chelyabinsk State University, Chelyabinsk, Russia

The wide clinical application of remote local microwave hyperthermia for treatment of superficially located malignant tumors allowed to enhance results of the treatment and, at the same time, showed limitations of this method [1]. They include: impossibility of uniform heating of tumors with sizes more than 5 cm, insufficient depth of the heating, skin burns. So, only 50% of cancer tumors of the mammary gland are managed to heat till temperature 42°C. Thus, till half part of the tumors remains insufficiently heated, which reduces effectiveness of the thermoradiotherapy of the cancer.

In order to overcome disadvantages of the local hyperthermia, it is proposed to administer into the tumors ferromagnetic microparticles. Most of these studies are still at an early stage owing to complexity of the calculation of absorption of microwave electromagnetic radiation in tissues with large values of the permittivity and containing of ferromagnetic particles. Investigation of the technical aspect allows to develop a clinically effective system of Microwave hyperthermia[2].

In this work absorption of electromagnetic radiation of range 10MHz-4GHz in system from dielectric matrix ($\epsilon = 80$) and embedded ferromagnetic particles (carbonyl iron, $r = 5\mu\text{m}$) are investigated. Dependencies of the absorption factor on the volume fraction of ferromagnetic particles in the range 0-50% are experimentally and theoretically investigated. Dependency of the absorption factor on the size of ferromagnetic particles is theoretically calculated.

The obtained dependencies indicate the presence the wide absorption maximum in the range of electromagnetic radiation 1-2,5GHz. The highest absorption is obtained for composited with 30% volume fraction of ferromagnetic particles. With decreasing particle sizes, broadening of the absorption maximum and shift it into the high frequencies are appeared.

[1] Noell, K. Thomas, et al. (1980). Microwave-induced local hyperthermia in combination with radiotherapy of human malignant tumors. *Cancer*, 45(4), 638-646

[2] Gian F. Baronzio (2006). Introduction. *Hyperthermia In Cancer Treatment. A Primer*. Medical Intelligence Unit. Berlin. Springer

Th.P-P24 - Simulation of magnetocapacitance effect in magnetic elastomers

D. Isaev¹, A. Semisalova¹, E. Kramarenko¹, Nikolai Perov¹, A. Granovsky¹

1. Lomonosov MSU, Faculty of Physics, Moscow, Russia

In this work we present the results of numerical simulation of magnetocapacitance effect in magnetorheological elastomers - the change of capacity of plane capacitor filled with magnetic elastomer and placed under the external magnetic field. The computer model of effect is based on the assumption about the displacement of magnetic particles inside the elastic matrix under the external magnetic field and the formation of chain-like structures. Such displacement of metallic particles between the planes of capacitor leads to the change of capacity, which can be considered as a change of effective dielectric permittivity of elastomer caused by magnetic field (magnetodielectric effect). In this work we simulated such effect for series of samples varying with concentration of magnetic filler, size and space distribution of particles, elastic properties of matrix. We have found the value of capacity can change up to 4%, the effect tends to saturation and has hysteretic feature due to the elastic response of matrix. The influence of orientation of magnetic field and capacitor plane was studied as well, the change of sign of the effect for parallel and perpendicular orientation was observed which is in perfect agreement with physical model we used as a base. The quantitative discrepancy between simulation and recent experiments results should be noted - the experimental value of effect was found to be up to 80%. Such big difference with simulation can be related to the simplicity of used computer model - we took into account only dipole-dipole interaction between the particles. Nevertheless, the developed model resulted in perfect qualitative agreement with all experimental data obtained earlier for Fe-based elastomers. So, the proposed model is useful to study these novel functional materials, analyze the features of magnetodielectric effect and predict the optimal composition of magnetorheological elastomers for further profound experimental study. Supported by RFBR (15-08-99554, 13-03-00914, 13-02-12443).

Th.P-P25 - Magnetic nanoparticle cryogels as hyperthermia cancer therapeutics

R. Jackson¹, P. Southern¹, J. Sullivan¹, Q. Pankhurst¹

1. UCL Healthcare Biomagnetics Laboratory, London, United Kingdom

Magnetic hyperthermia is widely thought as a promising cancer therapy in which magnetic nanoparticles are activated by an externally applied alternating magnetic field, releasing therapeutic levels of heat within cancerous tumours. The majority of magnetic nanoparticles are delivered into the body in aqueous form and rely upon the “absorbent” properties of tissue to retain the nanoparticles at the injection site, however cancerous tumours can often be highly vascular and nanoparticle retention cannot be guaranteed.

We present here a method of preparing a magnetic hyperthermia agent in the form of a flexible, facile gel system. These cryogels are biodegradable, non-toxic, gelate physically rather than chemically and can be tuned to degrade back to liquid form at a range of therapeutically useful temperatures. Further simple processes can generate a range of micron sized gel particles which can be composited with other nanoparticle systems, namely magnetic nanoparticles. The combination of these two disparate methods can generate an effective cancer therapeutic that increases adhesion to leaky vascular systems, limits unwanted diffusion to healthy tissue as well as providing a thermally self-limiting system to avoid overheating in the case of particle bioaccumulation.

Th.P-P26 - Preparation and in vitro experiments of carboxymethyl chitosan-coated Fe-Ti-Nb-B micro/nanoparticles for self-controlled magnetic hyperthermia

C. Danceanu ^{1,2}, D.D. Herea ¹, K. Palanisamy ¹, E. Radu ¹, N. Lupu ¹, H. Chiriac ¹

1. *National Institute of Research and Development for Technical Physics, Iasi, Romania*

2. *Department of Physics, "Alexandru Ioan Cuza" University, Iasi, Romania*

In this study, Fe-Ti-Nb-B magnetic nanoparticles with low Curie temperature, were embedded in chitosan matrix and used as micro-scaffolds for growing osteosarcoma cells and magnetic hyperthermia tests. The viability of the cells bound to chitosan surface was investigated against control cells before and after treatments in alternating magnetic fields (AMF). The cell viability, measured after incubation with chitosan-coated particles, in AMF-free conditions and against control cells, followed a linear increase from 220 % after 4 hours of incubation to about 450 % after 24 hours of incubation. The coated-magnetic nanoparticles are embedded into the membrane of the osteosarcoma cells, as shown by the investigation performed using an optical inverted microscope. The cells detached from the growth support in the presence of the AMF. This increase of the viability (the chitosan-coated particles offer a good support for the cells growth) is inappropriate for the cellular viability assays with high concentration of coated nanoparticles (10 mg/ml). For this reason and since the solubility of chitosan is low, the magnetic nanoparticles were coated with a chitosan derivate, caboxymethyl chitosan (CMC) and the cells were incubated with nanoparticles for 48 h, using a maximum concentration of 2 mg/ml. CMC is known to have better solubility in water, low toxicity, antimicrobial properties and apoptosis inhibitory ability. The incubation of the cells in the presence of Fe-Ti-Nb-B nanoparticles (40-200 nm in diameter) leads to a viability decrease of 5-10 % for both CMC-coated and uncoated particles. The presence of AMF leads to a temperature increase up to 46 °C and a decrease of the cell viability down to 40% was observed. Thus, the chitosan-coated magnetic nanoparticles (especially carboximetyl chitosan) could be used as thermo-seeds to kill cancerous cells through self-controlled magnetic hyperthermia and as microscaffolds to mimic a tumor environment, taking also advantage from the magnetic properties of the Fe-Ti-Nb-B particles that allows magnetic manipulation and separation.

This work was supported by a CNDI-UEFISCDI grant, Project No. 148/2012 (HYPERTHERMIA) and CNDI-UEFISCDI grant, Postdoctoral Project no. 8/2013

Th.P-P27 - Study of the optimal thermal dose in the magnetic hyperthermia with low Curie temperature particles

I. Astefanoaei¹, I. Dumitru¹, H. Chiriac², A. Stancu¹

1. *Alexandru Ioan Cuza University, Iasi, Romania*

2. *Institute of Research & Development for Technical Physics, Iasi, Romania*

Magnetic hyperthermia with low Curie temperature particles is a very promising approach in the therapy of cancer. This novel healing method offered to the scientific community convincing reasons for experimental and theoretical studies [1, 2]. The Fe-Cr-Nb-B magnetic particles (MPs) with low Curie temperature (T_c) in range of 42-44 °C have special magnetic and thermal properties for their use in magnetic hyperthermia [3, 4]. This paper analyzes the temperature field induced by the heating of the magnetic particles with low T_c in an ac magnetic field. The particles have a spatial distribution after their injection within the tumor as a result of diffusion and convection. Their spatial distribution near the injection sites (IS) was computed as a solution of the general convection-diffusion equation in a porous tissue. The ferrofluid flow within the tissue was modeled using the continuity and Darcy's equations. The ferrofluid injection rate during the injection process influences significantly the spatial distribution of the particles and temperature field within tumor. Higher values of the ferrofluid flow rate determine a strong convection of the particles to the tumor center. The FeCrNbB system determines an automatic control of tumor heating. The temperature field increases from 37°C to the Curie temperature of the particles which becomes the maximum temperature within tumor (Fig.1). The heating of tumor can be managed by controlling the Curie temperature of the MPs. Small quantities of ferrofluid 0.1 - 0.3 cm³ and implicitly a small dosage of Fe-Cr-Nb-B particles per unit gram of tumor determine a temperature rise in the therapeutic temperature range in a tumor. The ferrofluid injection rate influences significantly the spatial distribution of the particles within tumor. The FeCrNbB systems open new borders in the application of the magnetic hyperthermia with low Curie particles in the cancer therapy.

Acknowledgment:

This work was supported by a grant of the Romanian National Authority for Scientific Research, Parteneriate - HYPERTHERMIA project, no. 148/2012 and Romanian CNCS-UEFISCDI Grant Nos. Grant Nos.PN-II-RU-TE-2012-3-0449.

References:

- [1] J. Carrey, B. Mehdaoui and M. Respaud, *Journal of Applied Physics*, 109, 083921 (2011)
- [2] N. Lupu, H. Chiriac, S. Corodeanu and G. Ababei, *IEEE Trans Magn*, 47, 3791 (2011)
- [3] I. Astefanoaei, I. Dumitru, H. Chiriac and A. Stancu, *J. Appl. Phys.*, 115, 17B531 (2014)
- [4] M. Pavel and A. Stancu, *IEEE Trans. Magn.* 45, 4825 (2009)

Th.P-P28 - Bendable probes integrating ultrasensitive magnetoresistive sensors for local field detection in neurosciencesJ. Valadeiro¹, J. Amaral¹, J. Gaspar², R. Ferreira², S. Cardoso^{1,3}, P. Freitas^{1,2}*1. INESC - Microsistemas E Nanotecnologias, Lisbon, Portugal**2. International Iberian Nanotechnology Laboratory, Braga, Portugal**3. Instituto Superior Tecnico, Universidade de Lisboa, Lisbon, Portugal*

Recently a wide range of customized spintronic devices has been developed for biomedical applications [1]. In particular, the detection of neuronal activity has been pointed as a key application where the use of magnetoresistive sensors can offer unmatched advantages for local field detection [2], combined with small footprint, portability and room temperature operation [3]. The probe's design can be adapted to match the requirements of a neurological experiment, where the substrate flexibility allows a more adaptable tool able to reach further within the signal sources and thus provide in-situ detection of ultra-small local magnetic fields (pTesla range).

Giant magnetoresistive (GMR) sensors based on $\text{Ni}_{80}\text{Fe}_{20}$ 3.5/ $\text{Co}_{80}\text{Fe}_{20}$ 2.3/ Cu 2.3/ $\text{Co}_{80}\text{Fe}_{20}$ 2.3/ $\text{Mn}_{76}\text{Ir}_{24}$ 8.0 stacks and tunneling magnetoresistive (TMR) sensors $\text{Ir}_{20}\text{Mn}_{80}$ 7.5/ $\text{Co}_{70}\text{Fe}_{30}$ 2/ Ru 0.85/ $\text{Co}_{40}\text{Fe}_{40}\text{B}_{20}$ 2.6/ MgO >1/ $\text{Co}_{40}\text{Fe}_{40}\text{B}_{20}$ 3/ Ta 0.21/ $\text{Ni}_{80}\text{Fe}_{20}$ 16 (thickness in nm; alloy compositions in %) were used. These structures were incorporated in micromachined Si probes with different thicknesses (700um to 50um), allowing tunable flexibility. Si-probes were designed with two different tip configurations: (i) sharp tip (18 μm) for in-vivo experiments, to penetrate the brain and place the sensors near field sources; (ii) flat tip (104 μm) for in-vitro measurements, to place sensors on top of a brain slice without damage. The Si-probes showed a maximum bending induced stress of 300MPa, and a single TMR element with integrated flux guides ($\text{Co}_{93}\text{Zr}_{3}\text{Nb}_4$) displayed TMR=179% and sensitivity of 264%/mT. Also, a detection level of 30pT/sqrt(Hz) at 1kHz was demonstrated in partially bendable Si-probes competing with rigid technologies. The bending impact on sensor performance was evaluated, under controlled bending tests and also upon penetration into tissues/viscous media. The sensor characteristics (sensitivity, noise levels) was correlated with the Si-probe mechanical robustness. The results can provide guiding lines while selecting the optimum probe thickness for in-vivo/in-vitro experiments.

[1]P.P.Freitas et al.,LoC 12(2012) 546

[2]J.Amaral et al.,JAP 09(2011) 07B308

[3]J.Amaral et al.,IEEE Trans.Magn.49(2013) 3512

Th.P-P29 - Magnetic properties and microstructures of polymer functionalized Fe₃O₄ nanoparticles-enhanced surface plasmon resonance (SPR) biosensor

E. Suharyadi¹, S. Nuzully¹, T. Kato², S. Iwata², K. Abraha¹

1. *Department of Physics, Gadjah Mada University, Yogyakarta, Indonesia*

2. *EcoTopia Science Institute, Nagoya University, Nagoya, Japan*

Surface plasmon resonance (SPR)-based biosensor is known to be a sensitive, simple and label free optical method for detecting biomaterials that is able to do quantitative detection. For some application, biomolecules-coated magnetic nanoparticles (MNPs) are used to enhance the signal of SPR spectroscopy. Here, we report the magnetic properties of magnetite (Fe₃O₄) MNPs functionalized by polyethylene glycol (PEG-4000) polymer as SPR enhancing agents. Fe₃O₄ MNPs with various particles size of 11-20 nm have been chemically synthesized by co-precipitation method using FeSO_{4.7}H₂O and FeCl_{3.6}H₂O with ratio 1:2. The results of X-ray diffraction (XRD) and transmission electron microscopy (TEM) confirmed that Fe₃O₄ MNPs have cubic inverse spinel structure with homogeneously spherical shape. Fe₃O₄ MNPs with smaller grain size has higher response to external magnetic field and low coercivity (H_c). The saturation magnetization (M_s) Fe₃O₄ with particle size of 14 nm is 70 emu/g and then decreased by the increase of PEG-4000 concentration. M_s of PEG-coated Fe₃O₄ with 20% and 50% PEG is 60 emu/g and 37 emu/g, respectively. However, the coercivity is almost constant of about 60 Oe. The bonding analysis by Fourier transform infrared spectroscopy (FTIR) shows that surface of Fe₃O₄ MNPs can be modified with PEG-4000. The covalent bond Fe-O has been created by Fe atoms of Fe₃O₄ and O atoms of PEG-4000. It is well known that the magnetic properties of Fe₃O₄ MNPs are dependent on the particle size, morphology, crystal structure, and concentration of coating agents (PEG-4000). In addition, SPR signal has been investigated in Fe₃O₄ MNPs coated by PEG-4000 and alpha-amylase. FTIR analysis also shows that Fe₃O₄ functionalized by PEG-4000 layer can bind alpha-amylase effectively. Fe₃O₄ MNPs with smallest grain size and highest M_s have great potency to improve the performance of SPR-based biosensor.

Th.P-P30 - Protein influence on MRI contrast properties of magnetite nanoparticles

O. Strbak¹, D. Gogola¹, L. Baciak², A. Krafcik¹, M. Masarova¹, I. Antal³, M. Kubovcikova³, M. Koneracka³, V. Zavisova³, P. Kopcansky³

1. *Institute of Measurement Science SAS, Bratislava, Slovakia*

2. *Faculty of Chemical and Food Technology STU, Bratislava, Slovakia*

3. *Institute of Experimental Physics SAS, Kosice, Slovakia*

Proteins are biomarkers of many serious diseases (e.g. inflammation, cancer), and their changes in concentration levels are associated with various pathological processes. Our aim is to find out whether the presence of proteins could have an influence on the contrast properties of MRI contrast agents, affecting such desired contrast information. Secondly, it is to find the possibility for specific protein imaging in combination with contrast imaging of tissue, providing such simultaneous information about the presence of biomarker and tissue pathology, without additional invasive diagnostics.

Our model system consists of BSA as a specific protein, and magnetite nanoparticles stabilized with PEG as a carrier. MRI measurements were performed on 4.7 T (VARIAN) and 0.2 T (ESAOTE) systems. Images were acquired with standard T2 weighted protocols, and relative contrast, T2 relaxation time, and relaxivity r_2 were evaluated and compared.

The best interval for contrast imaging of our model system is in range of 4-60 $\mu\text{g/ml}$. Relative contrast of nanoparticles with and without BSA shows difference up to 20 %, affecting such signal in rate visible also to the naked eye. Differences in T2 are as follows (magnetite concentration [$\mu\text{g/ml}$] - relative T2 [%]): 0.5-19; 1-36; 2-7; 4-0.6; 7-10; 15-5; 30-1.5; 60-3; 120-2. The relaxivity values of nanoparticles are $358.73 \pm 1.4 \text{ mM}^{-1}\text{s}^{-1}$ without BSA, and $375.16 \pm 3.2 \text{ mM}^{-1}\text{s}^{-1}$ with BSA.

We showed that BSA protein influence the MRI contrast properties of magnetite nanoparticles in significant way without special optimization procedures (in the best imaging interval in rate up to 20 % for relative contrast, and up to 10 % for relative T2). On the one side, it can affect the desired contrast information from contrast agents, but on the other side, it have potential to provide the information about the presence of biomarker together with tissue pathology, without additional stressful diagnostics.

Th.P-P31 - Magneto-plasmonic nanoparticles as theranostic platforms for magnetic resonance imaging, drug delivery and NIR hyperthermia applications

I. Urriés^{1,2}, C. Muñoz^{1,2}, L. Gómez^{1,2}, C. Marquina^{3,4}, V. Sebastián^{1,2,4}, M. Arruebo^{1,2,5}, J. Santamaría^{1,2,5}

1. *Departamento de Ingeniería Química, Universidad de Zaragoza, Zaragoza, Spain*
2. *Instituto de Nanociencia de Aragón (INA), Universidad de Zaragoza, Zaragoza, Spain*
3. *Instituto de Ciencia de Materiales de Aragón (ICMA); CSIC-UZ, Zaragoza, Spain*
4. *Departamento de Física de la Materia Condensada; Universidad de Zaragoza, Zaragoza, Spain*
5. *CIBER de Bioingeniería, Biomateriales y Nanomedicina (CIBER-BBN), Spain*

PEGylated magneto-plasmonic nanoparticles consisting in a continuous but porous Au nano-shell with a hollow or semi-hollow silica interior containing magnetic cores have been successfully synthesized. Their physico-chemical characteristics have been exhaustively investigated, by means advanced electron microscopy techniques as TEM and STEM imaging, and EDS-HAADF analysis, and by UV-VIS-NIR spectroscopy, among others. The magnetic characterization has been performed by magnetization and relaxivity measurements.

The hollow interior space can be used to store drugs or other molecules of interest, whereas their magnetic characterization shows their potential as contrast agents in magnetic resonance imaging (MRI) applications. In addition, their plasmonic characteristics in the near infrared (NIR) region make them efficient in photothermal applications producing high temperature gradients after short irradiation times.

We have seen that by controlling the etching conditions the inner silica shell can be selectively dissolved to achieve a hollow or semi-hollow interior without compromising the magnetic or plasmonic characteristics of the resulting nanoparticles. Magnetic measurements (in particular relaxivity measurements) and transmission electron microscopy observations have been used to demonstrate the precise control during the etching process. At this respect, the use of these techniques has been crucial to select the optimal concentration of the etching reagent and contact time to preserve the inner superparamagnetic iron oxide nanoparticles and the plasmonic properties of the constructs.

Drug loading capabilities have been also evaluated for both semi-hollow and as-synthesized nanoparticles using Rhodamine B isothiocyanate as a model compound. The results have shown that our nanoparticles could be potentially used as “theranostic” nanoparticles, with both imaging capabilities and a dual therapeutic function (drug delivery and hyperthermia).

I. Urriés et al., *Nanoscale*, 2014, 6, 9230.

Th.P-P32 - Ferrofluids based on $Zn_xMn(1-x)Fe_2O_4@-\gamma-Fe_2O_3$ nanoparticles for heat-exchange applications

V. Pilati¹, R. Cabreira Gomes^{1,2}, G. Gomide¹, F.L. de Oliveira Paula¹, R. Aquino³, F. Augusto Tourinho⁴, G. Fabián Goya⁵, E. Dubois², R. Perzynski², J. Depeyrot¹

1. Grupo de Fluidos Complexos, Instituto de Física, Universidade de Brasília, Brasília, Brazil

2. PHENIX, Université Pierre et Marie Curie, Paris, France

3. Laboratório de Nanociência Ambiental e Aplicada LNAA, Faculdade UnB Planaltina, Brasília, Brazil

4. Grupo de Fluidos Complexos, Instituto de Química - Universidade de Brasília (UnB), Brasília, Brazil

5. Aragon Institute of Nanoscience - Universidad de Zaragoza, Zaragoza, Spain

Ferrofluids based on Zn-Mn ferrite nanoparticles constitute promising nanomaterials for heat-exchange applications such as in liquid cooling system by mean thermomagnetic effect and also as heat sources in magnetic fluid hyperthermia. Aqueous ferrofluids based on $Zn_xMn_{(1-x)}Fe_2O_4@-\gamma-Fe_2O_3$ nanoparticles were synthesized by a well proven chemical route [1] (coprecipitation followed by a surface treatment). The produced nanomaterials were characterized by chemical analysis, TEM and X-ray powder diffractogram. Magnetization measurements were performed in a VSM magnetometer for diluted fluid samples ($\Phi < 1\%$). The magneto-induced birefringence was also measured as a function of the external field. In both cases, the Langevin's formalism is applied and allows the determination of size distribution characteristics, particles magnetization and birefringence. Through DC magnetization measurements performed under ZFC procedure we obtained the temperature dependence of the magnetization in a small applied field. The curves, typical of superparamagnetic behavior, present a maximum at a temperature related to the blocking temperature. The extracted values of the anisotropy constant are approximately two orders of magnitude larger than bulk values, probably due to a surface contribution to the magnetic anisotropy. Finally, we investigated SLP in hyperthermia measurements and the pyromagnetic coefficient of nanoparticles by measuring the thermal dependence of the magnetization above 300K. Both values show that our samples are suitable for heat exchange applications. In particular the SLP values could be increased by using the exchange coupling between a hard ferrite core and a soft ferrite shell or vice versa [2].

References:

[1] J. A. Gomes, M. H. Sousa, F. A. Tourinho, R. Aquino, G. J. da Silva, J. Depeyrot, E. Dubois, R. Perzynski. J. Phys. Chem. C 112 (2008) 6220

[2] R. Cabreira Gomes, F. G. Silva, R. Aquino, P. Bonville, F. A. Tourinho, R. Perzynski, J. Depeyrot, J. Magn. Mater 368 (2014) 409

Th.P-P33 - Biodegradation of PolyChlorinated Biphenyls (PCB118) by SPION coated microbial cells of *Pseudomonas mendocina*

Radha S.¹, A. Kothare², A. Surti²

1. *Department of Physics, University of Mumbai, Mumbai, India*

2. *Department of Microbiology, Sophia College, Mumbai, India*

Polychlorinated biphenyls (PCBs) are mixtures of chlorinated hydrocarbons that have been used extensively in various industries as dielectrics, as heat exchange fluids, as paint additives and in plastics. The toxicology of PCBs is affected by the number and position of the chlorine atoms. Some of the established remedial technologies for their removal from the environment like incineration, solvent extraction, thermal desorption etc are not cost effective; hence the industries generating PCB containing wastes are tempted to discard these residues without treatment into soil or water. Bioremediation using microorganisms (free or immobilized) can be used as a biofriendly method for removal of PCBs from the environment. A novel bacterial strain degrading PCB 118 was isolated from soil identified as *Pseudomonas mendocina* strain CL-10.4. by 16S rRNA sequence analysis. PCB degrading activity was checked by GC-MS analysis and Enoic acids, Acetophenones, Acetic acids were degradation products. *Pseudomonas mendocina* cells were coated with magnetic Fe₃O₄ nanoparticles or SPIONs (Superparamagnetic Iron Oxide Nanoparticles), immobilized by external application of magnetic field. The ferrite nanoparticles synthesized by chemical co-precipitation were monodispersed in aqueous solution with an average size of 9.56 nm, magnetization of about 15emu/g and near zero coercivity indicating that the Fe₃O₄ nanoparticles had superparamagnetic properties. Degradation of PCB 118 by free and coated cells of this bacterium was studied. The rate of degradation of PCB118 coated cells was at par to the free cells with advantage of magnetic separation and possible reuse for second batch of PCB degradation.

Th.P-P34 - Interaction of superparamagnetic nanoparticles and quantum dots with pathogenic fungi: internalization and toxicity profile

N. Rispaíl¹, L. De Matteis², R. Santos³, A.S. Miguel³, L. Custardoy^{2,4}, P.S. Testillano⁵, M. del Carmen Risueño⁵, A. Pérez de Luque⁶, C. Maycock^{3,7}, P. Fevereiro^{3,7}, A. Oliva³, R. Fernández-Pacheco^{2,4}, M.R. Ibarra^{2,4,8}, J.M. de la Fuente^{9,10}, C. Marquina^{8,9}, D. Rubiales¹, E. Prats¹

1. *Instituto de Agricultura Sostenible; CSIC, Córdoba, Spain*

2. *Instituto de Nanociencia de Aragón; Universidad de Zaragoza, Zaragoza, Spain*

3. *Instituto de Tecnología Química e Biológica; Universidade Nova de Lisboa, Oeiras, Portugal*

4. *Laboratorio de Microscopías Avanzadas (LMA), Universidad de Zaragoza, Zaragoza, Spain*

5. *Centro de Investigaciones Biológicas, CSIC, Madrid, Spain*

6. *IFAPA, Centro Alameda del Obispo, Junta de Andalucía, Córdoba, Spain*

7. *Faculdade de Ciências, Universidade de Lisboa, Lisbon, Portugal*

8. *Departamento de Física de la Materia Condensada, Universidad de Zaragoza, Zaragoza, Spain*

9. *Instituto de Nanociencia de Aragón (INA), Universidad de Zaragoza, Zaragoza, Spain*

10. *Fundación ARAID, Gobierno de Aragón, Zaragoza, Spain*

For several years now, nanoscaled materials have been implemented in biotechnological applications related to animal (in particular human) cells and related pathologies. However, the use of nanomaterials in plant biology is far less widespread, although their application in this field could lead to the future development of plant biotechnology applications. For any practical use, it is crucial to elucidate the relationship between the nanomaterials and the target cells. In this work we have evaluated the behavior of two types of nanomaterials, superparamagnetic nanoparticles and quantum dots, on *Fusarium oxysporum*, a fungal species that infects an enormous range of crops causing important economic losses and is also an opportunistic human pathogen [1].

Our results indicated that both nanomaterials rapidly interacted with the fungal hypha labeling the presence of the pathogenic fungus, although they showed differential behavior with respect to internalization. Thus, whereas magnetic nanoparticles appeared to be on the cell surface, quantum dots were significantly taken up by the fungal hyphae showing their potential for the development of novel control approaches of *F. oxysporum* and related pathogenic fungi following appropriate functionalization.

In addition, the fungal germination and growth, accumulation of ROS, indicative of cell stress, and fungal viability have been evaluated at different nanomaterial concentrations showing the low toxicity of both types of nanomaterials to the fungus. This work represents the first study on the behavior of quantum dots and superparamagnetic particles on fungal cells, and constitutes the first and essential step to address the feasibility of new nanotechnology-based systems for early detection and eventual control of pathogenic fungi.

[1] Rispaíl et al., ACS Appl. Mater. Interfaces 2014, 6, 9100–9110

Th.P-P35 - Resonance frequency of alternating magnetic field stimulus on proliferation suppression of rat basophilic leukemia cancer cells

H. Park¹, J.Y. Lee¹, S. Kim¹, E. Cheong², H.S. Lee¹, D.G. Hwang¹

1. Department of Oriental Biomedical Engineering, Sangji University, Wonju, South Korea

2. Department of Biotechnology, Yonsei University, Seoul, South Korea

Frequency dependence of alternative magnetic field stimulus on proliferation of rat basophilic leukemia (RBL-2H3) cancer cells was investigated in the intermediate frequency of 500 Hz to 2 kHz. To keep constant field intensity of 5 mT as the frequency increases, we developed the switched-mode power supply with insulated gate bipolar transistor and a digitally controlled circuit which modulates a duty ratio. The alternative pulse magnetic field has a sawtooth waveform with time duration of 100 μ sec. The coil temperature of our designed stimulus system have been maintained at 37°C in incubator using a cooling system as the frequency increased. The 6-well culture plate was placed on the coil, and the cell temperature during the stimulus did not exceed 37 \pm 1.0 °C. The RBL-2H3 cells were cultured under applied magnetic field during 24 hour, and its cell morphologies and proliferation rates were analyzed. For reliability of this study, we tried to repeat the experiments 4 - 6 times during 6 months. After the cells were stimulated at 500 Hz and 2 kHz, the proliferation rates of stimulated cells were almost same as that of control cells. However, the proliferation rates in the range of 1 kHz - 1.4 kHz were suppressed up to 78 - 74% compared with control cells. And proliferation suppression of the cancer cell was found at a special frequency of 1 kHz. Further studies need to clarify physiological mechanism at this frequency. To investigate the biological change in protein after magnetic stimulus, we measured Western Blot analysis at this frequency, and found the level of ERK1/2, which is related to growth regulated protein, was much reduced than that of control cells.

Th.P-P37 - MRI tracking of the magnetite nanoparticles encapsulation in PLA spheres

M. Koneracka¹, I. Antal¹, M. Kubovcikova¹, V. Zavisova¹, O. Strbak², D. Gogola², L. Baciak³, A. Krafcik², M. Masarova², P. Kopcansky²

1. *Institute of Experimental Physics, Slovak Academy of Sciences, Kosice, Slovakia*

2. *Institute of Measurement Science, Slovak Academy of Sciences, Bratislava, Slovakia*

3. *Faculty of Chemical and Food Technology, Slovak Technical University, Bratislava, Slovakia*

Poly (D, L-lactide) (PLA) based polymers are currently widely used in biomedical applications, mainly because of their excellent biocompatible, and biodegradable properties. Although the general properties of PLA-based magnetic carriers are quite well described, there is lack of information about contrast properties of such carriers in MRI applications. We studied the relative contrast, transverse relaxation time (T₂), and transverse relaxivity (r₂) changes induced by different magnetite nanoparticles loading into PLA nanospheres. PLA-magnetite carriers were prepared by a modified nanoprecipitation method. Prepared PLA samples were divided into three groups: (i) PLA without magnetite nanoparticles, (ii) PLA with non-encapsulated magnetite nanoparticles (exterior particles), and (iii) PLA with encapsulated magnetic nanoparticles (interior particles). The last group of PLA samples was prepared with different magnetic nanoparticle input concentration (2, 5, 7, 17, 30 mg/ml), resulting in diverse loading factor of magnetic nanoparticles into PLA. MRI measurements were performed on 4.7 T system. Images were acquired with T₂-weighted Multi Echo Multi Slice (MEMS) sequence. Transverse relaxation time T₂ was obtained spectroscopically. Relative contrast (RC= [I - I₀]/I₀), relaxation time T₂, and relaxivity r₂ (R₂ = r₂C + R₂₀) values were evaluated and compared. We found that PLA itself has negligible influence on relaxation properties of medium, as well as on contrast properties of magnetic nanoparticles. The studied MRI parameters (relative contrast, T₂, r₂) of the magnetic nanoparticles encapsulated in PLA showed that we are able to distinguish between loaded and non-loaded nanoparticles, as well as to determine the rate of encapsulation.

Acknowledgments:

This work was supported within the project No. 26110230097 in frame of Structural Funds of European Union

Th.P-P39 - Magnetodes: Exploring the neuromagnetic field at the cellular level

L. Caruso¹, V. Trauchessec¹, J. Tréjo Rosillo¹, E. Paul¹, C. Fermon¹, G. Ouanounou², A. Mikroulis², F. Barbieri², T. Bal², A. Destexhe²

1. SPEC - CEA Saclay, Gif-sur-Yvette, France

2. UNIC-CNRS Gif-sur-Yvette, France

We have developed a new generation of neuroscience tools able to detect the electromagnetic signature of neurons at local scale under stimulation. We use Giant Magneto-Resistive sensors (GMR) based on spin electronics, which offer the possibility to be miniaturized and sensitive enough to probe very small magnetic fields like those emitted by the ionic currents flowing within neurons at cellular scale (in the picotesla to nanotesla range).

The probes developed called 'magnetodes', as magnetic counterpart of electrophysiological electrodes, are composed of two GMR sensors with an electrode allowing recording both magnetic and electric components at local scale. Some probes are planar, for recordings at mesoscale, and other probes with a needle shape are dedicated to microscopic scale. In this second type of probes, the sensors are located on a sharp tip allowing penetrating easily in brain's tissues.

These magnetodes reach sensitivity ranging from 3 to 12%/mT with a field level detectivity of between 50pT to 1nT/sqrt(Hz) at 100Hz, depending on the probes type. We have tested the probes in-vitro and we present the first magnetic recordings obtained.

We have also investigated the response of a neuronal array in a hippocampus slice to a magnetic stimulation and recorded responses by means of electrical recordings in the extracellular medium. Here, we will describe the first probes that have been fabricated for the in-vitro and in-vivo experiments, show results of the first magnetic recordings and responses to magnetic excitation in small assemblies of neurons.

FR.A-P01 - Topological insulators in random magnetic fields

H. Fehske¹, A. Pieper¹, I. Orue²

1. *Institute of Physics, University Greifswald, Greifswald, Germany*

2. *University of The Basque Country, Leioa, Spain*

We study the effect of random magnetic fields on the two-dimensional surface state of three-dimensional topological insulators. To this end we investigate a minimal four band model (describing weak, and strong topological insulators, as well as conventional band insulators), which is completed by terms that allow for the breaking of inversion symmetry by magnetic fields and the Zeeman effect [1]. Calculating the local density of states, the single-particle spectral function, and the conductance for a (contacted) slab geometry by exact numerical techniques based on the kernel polynomial method, we analyse how field-randomness affects the ground-state, spectral and transport properties of the resulting insulating massive Dirac fermion state. We establish a relationship to experimental angle-resolved photoemission results for magnetically doped topological insulators [2]. The effects of (nonmagnetic) surface disorder will be discussed too [3].

[1] M. Sitte, A. Rosch, E. Altman, and L. Fritz, Phys. Rev. Lett. 108, 126807 (2012)

[2] Y. L. Chen, et al. Science 329, 659 (2010)

[3] G. Schubert, H. Fehske, L. Fritz, and M. Vojta, Phys. Rev. B 85, 201105(R) (2012)

FR.A-P02 - Controlling the 2DEG states evolution at a metal/Bi₂Se₃ interface

H.J. Noh¹, J. Cheong¹, E.J. Cho¹, J. Park², J.S. Kim², I. Kim³, B.G. Park³, H.D. Kim⁴

1. Department of Physics, Chonnam National University, Gwangju, South Korea

2. Department of Physics, Pohang University of Science and Technology, Gyeongsangbuk-do, South Korea

3. Pohang Accelerator Laboratory, Pohang University of Science and Technology, Gyeongsangbuk-do, South Korea

4. Department of Physics and Astronomy, Seoul National University, Seoul, South Korea

We have demonstrated that the evolution of the two-dimensional electron gas (2DEG) system at an interface of metal and the model topological insulator (TI) Bi₂Se₃ can be controlled by choosing an appropriate kind of metal elements and by applying a low temperature evaporation procedure. In particular, we have found that only topological surface states (TSSs) can exist at a Mn/Bi₂Se₃ interface, which would be useful for implementing an electric contact with surface current channels only. Based on the ARPES and core-level x-ray photoemission spectroscopy measurements, we propose a cation intercalation model to explain our findings.

FR.A-P03 - Topological surface states in SrIrO₃ based interfaces

W. Fan¹, Y. Sun², S. Yunoki^{1,3,4}

1. *Computational Condensed Matter Physics, RIKEN, Wako, Saitama, Japan*

2. *Max Planck Institute for Chemical Physics of Solids, Dresden, Germany*

3. *Computational Quantum Matter Research Team, RIKEN Center for Emergent Matter Science (CEMS), Wako, Saitama, Japan*

4. *Computational Materials Science Research Team, RIKEN Advanced Institute for Computational Science (AICS), Kobe, Hyogo, Japan*

Recently, perovskite oxide SrIrO₃ has been proposed to be a topological semimetal hosting a Dirac point in its bulk band structure protected by crystal symmetry [1][2]. The surface states, depending on different directions, shows either a flat band ([110] surfaces) or Dirac cone ([001] surfaces) protected by either mirror symmetry or time reversal symmetry.

However, due to the metallic nature of bulk, there are mixed density of states of bulk states and topological edge states in all the Fermi surfaces. This severely impeded the observation of edge states for this material.

We propose several SrIrO₃ based interfaces by using DFT calculations together with constructing minimum Hamiltonian models. The topological surface states are explored by building slabs along different crystal directions based on maximally localized Wannier orbitals. We choose several heterostructures based on different surfaces of SrIrO₃ and show the Dirac cone edge mode can be differentiated out from bulk states. By this means, it will be much easier to discern by experimental tools such as STM or ARPES. Finally, we would like to comment on possible ways to realize other topological phases inherent in this 5d transition metal oxide.

FR.A-P04 - Metal-insulator transition in NdNiO₃ by hydrogen dopingC. Oh¹, S.Y. Heo¹, H.M. Jang¹, J. Son¹*1. Postech, Gyeongsangbuk-do, South Korea*

The rare-earth nickelate is perovskite oxide which is sensitive to the orbital occupancy of electrons. The corner sharing NiO₆ octahedra experience charge disproportionation in order to stabilize the $t_{2g}^6 e_g^1$ electrons leading Ni⁴⁺ $t_{2g}^6 e_g^0$ and Ni²⁺ $t_{2g}^6 e_g^2$ configuration. Recently, hydrogen is reversibly intercalated in SmNiO₃ leading band gap modulation and giant resistance switching. The electron configuration of hydrogen doped SmNiO₃ is modified from Ni³⁺ $t_{2g}^6 e_g^1$ to Ni²⁺ $t_{2g}^6 e_g^2$ and it suppresses charge disproportionation of NiO₆ octahedra. It opens up new directions to explore emerging electronic devices with nickelate systems. Here we report a giant resistance change in NdNiO₃ epitaxial thin films by hydrogen doping. We prepared 25 nm-thick NdNiO₃ thin film by pulsed laser deposition (PLD). Pt top electrode is utilized as hydrogen dissociating catalyst. Clear metal-to-insulator transition was observed by color change in hydrogen-treated NdNiO₃ thin films. Electrical characteristic shows the giant change of resistance. X-ray diffraction (XRD) and atomic force microscopy (AFM) datum indicate that the perovskite structure is maintained during hydrogenation accompanying unit cell expansion. We demonstrated the resistance change is related to doping concentration of hydrogen and lattice strain.

FR.A-P05 - Majorana fermions in the superconducting island

R. Akzyanov^{1,2,3}, A. Rakhmanov^{1,2,3}, A. Rozhkov^{2,3}

1. *All-Russian Research Institute of Automatics, Moscow, Russia*
2. *Moscow Institute of Physics and Technology, Moscow, Russia*
3. *Institute for Theoretical and Applied Electrodynamics, Moscow, Russia*

We investigate the properties of the edge states in the cylindrical superconducting island placed on the surface of the topological insulator in the magnetic field. We found that the Majorana fermions arise in such a system if the number of the flux quanta (vorticity) in the island is odd. The Majorana states are localized near the center of the vortex core and near the island edge. If the vorticity is even or there is no vortex in the island the Majorana states in the system are absent. We study the case of the single vortex in the island in details. We found that splitting between edge and vortex Majorana fermions is exponentially small regard to the radius of the island. We analyze the robustness of the Majorana fermion at the edge of the island. The stability of the states versus gate voltage should be performed to distinguish the edge Majorana fermion from conventional Dirac fermions. We found that the energy gap between edge Majorana fermion and the first excited state is of the order of superconducting gap induced at the surface of the topological insulator for the typical parameters value.

FR.A-P06 - Local magnetoresistance at an interface between a ferromagnetic metal and a three dimensional topological insulator due to the spin-momentum locking

Y. Ando¹, T. Hamasaki¹, F. Yang², M. Novak², S. Sasaki², K. Segawa², Y. Ando², M. Shiraishi¹

1. *Kyoto University, Kyoto, Japan*

2. *Osaka University, Osaka, Japan*

Surface state of the three-dimensional (3D) topological insulators (TIs) has been expected to represent the spin-momentum locking, i.e., spin quantization axis of the conduction electron in the TI surface state is perpendicularly locked to the carrier momentum.[1,2] Due to the spin-momentum locking, it is expected that charge current naturally induces spin polarization, whose axis and the sign can be controlled by the direction of the charge flow. Therefore, magnetoresistance at an interface between ferromagnetic metal and TI, caused by a spin polarized current in TI surface state has been expected.[3] In this presentation, we report successful detection of the local magnetoresistance at a ferromagnetic Ni₈₀Fe₂₀(Py) film / a bulk-insulating TI, Bi_{1.5}Sb_{0.5}Te_{1.7}Se_{1.3} (BSTS) interface. BSTS have been used to demonstrate the surface-dominated transport in this compound,[4] and the ARPES study has confirmed its Fermi level to be located in a bulk band gap,[5] realizing the intrinsic insulating state. In the magnetoresistance measurement, we observed a rectangular hysteresis behavior which is governed by the resistance at the interface between BSTS and the Py electrode. The interface resistance changed both with the magnetization direction of the Py electrode and with the current direction. This magnetoresistance disappeared when the BSTS device was heated to 300 K. Spin polarization of injected (extracted) spin current into (from) TI was estimated to be 0.05~0.5 %.

[1] Y. Ando, J. Phys. Soc. Jpn. 82, 102001 (2013)

[2] C. H. Li, et al., Nature Nanotech. 9, 5 (2014)

[3] A. A. Burkov and D. G. Hawthorn, PRL 105, 066802 (2010)

[4] A. A. Taskin, et al., PRL 107, 016801 (2011)

[5] T. Arakane et al., Nat. Comm. 3, 636(2012)

FR.A-P07 - Structure and induced stress of Fe on Bi₂Se₃(0001)

K. Novakoski Fischer¹, S. Ouazi¹, A. Cavallin¹, V. Sevriuk¹, D. Sander¹, J. Kirschner¹

1. Max Planck Institute of Microstructure Physics, Halle, Germany

The topological insulator Bi₂Se₃ has attracted an intense research activity since its discovery 5 years ago [1]. This is also due to the novel physics arising when doping Bi₂Se₃ with ferromagnetic impurities [1-3]. A detailed description of the stress change of Bi₂Se₃ upon Fe deposition may help to settle the debate about the distribution of magnetic atoms within the host material [4], and ultimately lead to an improved understanding of phenomena such as the topological magnetoelectric effect or the half-quantum Hall effect which are relevant to the design of new spintronic devices [2]. Here we present the first experimental study of the stress change induced by deposition of Fe on Bi₂Se₃(0001). Deposition of 0.2 ML Fe at 300 K induces a compressive stress change of -2.3 N/m. Deposition of Fe at 150 K leads to a much smaller stress change of the order of -0.1 N/m, whereas deposition at 473 K induces a stress change of -3.4 N/m. Low energy electron diffraction (LEED) reveals that the hexagonal diffraction pattern of the substrate gets blurred for Fe deposition at 150 K, whereas deposition at higher temperature of 473 K induces faint diffraction spots indicative of the formation of orthorhombic FeSe. Post-deposition annealing of films deposited at 300 K, at 600 K for 30 min triggers the formation of FeSe, as confirmed by our LEED and STM measurements. We discuss the stress results in view of a previous STM study on sub-monolayer deposition of Fe [3] and in view of epitaxial misfit between orthorhombic FeSe and hexagonal Bi₂Se₃.

[1] H. Zhang et al., Nat. Phys. 5 (2009) 438

[2] XL Qi et al., Rev. of Modern Phys. 83 (2011) 1057

[3] T. Schlenk et al., Phys. Rev. Lett. 110 (2013) 126804

[4] JM Zhang et al., Phys. Rev. B 88 (2013) 235131

FR.A-P08 - Low-energy muSR study on the tetradymite topological insulator $\text{Bi}_{1.5}\text{Sb}_{0.5}\text{TeSe}_2$

A. Shick¹, L. Havela², A. Lichtenstein³, M. Katsnelson⁴

1. *Institute of Physics, Academy of Sciences, Prague, Czech Republic*

2. *Charles University, Prague, Czech Republic*

3. *University of Hamburg, Hamburg, Germany*

4. *Radboud University, Nijmegen, The Netherlands*

The materials with strong electron correlations are important because of the fundamental properties, and the technological applications. Recently, Sm and Pu hexaborides were proposed as 3D topological insulators. The electronic structure calculations are performed combining the LDA with an exact diagonalization of the Anderson impurity model for [Sm,Pu]B₆. For the Sm atom in Sm hexaboride, intermediate valence ground state (GS) is found with the f-shell occupation of 5.6. The GS is a singlet, and the first excited triplet state 3 meV higher in the energy. The f-orbital density of states is in agreement with experimental PE spectra. It is a narrow band insulator already in LDA, with the direct band gap of 10 meV. The electron correlations increase the band gap which now becomes indirect.

For the Pu atom in Pu hexaboride, we also find intermediate valence singlet GS.

The LDA yields indirect band insulator with the band gap of 60 meV, which becomes direct when the electron correlations are included. The calculations illustrate that many-body effects are relevant to form the indirect band gap, and support the idea of "topological Kondo insulator" in SmB₆.

FR.A-P09 - Low-energy μ SR study on the tetradymite topological insulator $\text{Bi}_{1.5}\text{Sb}_{0.5}\text{TeSe}_2$

K. Matsui¹, T. Goto¹, T. Adachi¹, T. Ohtsuki¹, H. Tu², Y. Tanabe², I. Watanabe³, Z. Salman⁴, A. Suter⁴, T. Prokscha⁴

1. *Sophia University, Chiyoda, Japan*

2. *Tohoku University, Miyagi, Japan*

3. *Nishina Center, RIKEN, Saitama, Japan*

4. *Paul Scherrer Institute (PSI), Villigen, Switzerland*

The surface state of three dimensional topological insulators is characterized by a Dirac-cone dispersion which has been claimed to have a helical spin texture, where the spin vector points parallel to the surface and perpendicular to the momentum ("spin-locking"). However, the Kramers-degeneracy prevents it to be detected by magnetic resonance techniques, because of the cancellation of hyperfine field within the surface. We have addressed this problem by applying a weak field B_{par} parallel to the sample surface, which is expected to break the time-reversal symmetry and hence induce a spin cant, which must cause a finite local field perpendicular to the surface. The necessary field strength of B_{par} is roughly estimated to be 40 Oe from the criterion that the magnetic flux lines penetrate each coherent wave packet of conduction electrons, a typical size of which is determined by the inelastic scattering length to be 1 micron at 2 K.

We have applied this method on the quaternary tetradymite topological insulator $\text{Bi}_{1.5}\text{Sb}_{0.5}\text{TeSe}_2$, and investigated the effect of B_{par} by utilizing the low-energy muon spin relaxation (LE- μ SR) at PSI. The sample was 60 nm-thick film on a mica plate. The incident muon energy was set 1 keV, at which approximately 50 percent of muons stop within the surface layer of 10 nm. Under the B_{par} of 100 Oe, the muon spin relaxation at 5 K was revealed to contain the two components, the TF-oscillating part and the anomalously-fast relaxing part with $\tau \simeq 0.028 \mu\text{sec}$. The fraction of the latter showed significant dependence on the incident muon spin direction and took maximum of 50 percent when the muon spins were set perpendicular to both B_{par} and the muon momentum. This fast relaxation may be caused by a large hyperfine coupling due to the Fermi-contact interaction, and possibly reflects to the anomalous surface spin state in the topological insulator.

FR.A-P11 - Rotation effect of RuO₆ octahedron at the Sr₂RuO₄ surface on thermal transport properties

Y. Imai¹, K. Wakabayashi², M. Sigrist³

1. *Saitama University, Saitama, Japan*

2. *National Institute for Materials Science, Ibaraki, Japan*

3. *ETH Zurich, Zurich, Switzerland*

Motivated by superconductivity in Sr₂RuO₄ we investigate the thermal transport properties for a chiral p-wave superconductivity. It is well known that the low-energy properties of bulk Sr₂RuO₄ include three bands, the alpha, beta and gamma bands. The bulk Fermi level of the gamma band is close to a Lifshitz transition. The surface reconstruction doubling the unit cell occurs due to the RuO₆ octahedron rotation at c-axis oriented surfaces of Sr₂RuO₄. Since the rotation effect gives rise to the change of the Fermi surface topology, the topological property characterized by the so-called Chern number depends on the Fermi surface structure of the gamma band. While the Chern number switches at the Lifshitz transition, the chiral edge current resulting from time-reversal symmetry violation in the chiral p-wave phase is essentially unaffected around Lifshitz transition [1]. To observe the topological property directly, we consider the thermal transport property by means of the tight-binding model with electron-like Fermi surfaces corresponding to the gamma bands of Sr₂RuO₄ within a self-consistent Bogoliubov-de Gennes approach. We focus on the interplay between the topological aspect and the lattice distortion effect, and demonstrate that the thermal conductivity consists of the temperature-linear term and exponential term and thermal conductivity is directly associated with the Chern number and the gap function.

[1] Y. Imai, K. Wakabayashi and M. Sigrist: J. Phys. Soc. Jpn. 83 124712 (2014)

FR.A-P13 - Topological phase transitions in extended Hubbard-type models at half fillingS. Ejima¹, F. Lange¹, H. Fehske¹*1. Institute of Physics, University Greifswald, Greifswald, Germany*

At present symmetry-protected topological (SPT) phases attract a major attention in the physics of low dimensional systems. An example is the odd Haldane (OH) phase in the spin-1 XXZ chain [1]. Interestingly all the spin-1/2 ladder system, the extended Bose-Hubbard model with longer-range interactions at density $\rho=1$ [2], and the (Peierls-)Hubbard model with additional spin interaction at half filling [3] can be mapped onto an effective spin-1 chain system. In this work we consider extended Hubbard-type models with spin J-term at half filling. Employing the infinite density matrix renormalization group technique the degeneracy of entanglement spectra can be taken as hallmark of the formation of a SPT phase in this model. Thereby the boundary between trivial-nontrivial Haldane phases belongs to the Ising universality class with central charge $c=1/2$, similar to the OH-antiferromagnetic phase boundary in the spin-1 chain system. Likewise the neutral gap, $\Delta_n=E_1(0)-E_0(0)$, closes at the transition point (here, $E_0(M)$ and $E_1(M)$ denote the ground-state energy and first excited energy within the $M=\sum_j S_{jz}$ subspace, respectively). Decreasing the strength of the spin interaction J , the trivial-nontrivial phase boundary approaches those of the extended Hubbard-type model without spin term. This provides one means of determining the phase boundaries in the extended Hubbard model even in the weak- and intermediate-coupling regime.

[1] S. Ejima and H. Fehske, PRB 91, 045121 (2015)

[2] S. Ejima, F. Lange, H. Fehske, PRL 113, 020401 (2014)

[3] S. R. Manmana, A. M. Essin, R. M. Noack, and V. Gurarie, PRB 86, 205119 (2012)

FR.A-P14 - Tunable two-dimensional Dirac fermion gases at the surface of topological insulators

H. Aramberri¹, J.I. Cerdá¹, C. Muñoz¹

1. Instituto de Ciencia de Materiales de Madrid (ICMM) Consejo Superior de Investigaciones Científicas (CSIC), Madrid, Spain

Bi-chalcogenides, Bi₂X₃ (X=Se, Te), Topological Insulators (TIs) represent a new quantum phase defined by a bulk insulator with Z₂-invariant topology and metallic Dirac states at the surface. They exhibit a layered structure along the (0001) direction with quintuple layers (QLs) coupled through Van der Waals forces, therefore they frequently present extended structural planar defects. Via density functional theory calculations we demonstrate that in Bi₂X₃ TIs, self-doping of topological surface states can be tuned by controlling the sequence of stacking defects (SDs) inside the crystal. In particular, twin boundaries -reversal of the stacking sequence between QLs- drive large surface dopings, which achieve values of 10¹²-10¹³ e/cm² and can be adjusted by the SD distribution. Remarkably, depending on the chirality of the twin, either n- or p-type self-doping can be optionally tuned. Its origin relies on the spontaneous polarization generated by the dipole moments created at the lattice defects. Our results provide a simple explanation for the local charging of the Dirac states recently reported in epitaxial (0001) Bi₂Se₃ films [1]. This mechanism allows, by controlling the SD sequence, to fine-tune the Fermi level to the electron or hole conductive regimes and hence, to generate a preselected two-dimensional massless Dirac fermion gas with a well defined spin-helicity. Therefore, our findings open the route to the fabrication of Bi₂X₃ surfaces and nanostructures with tailored surface charge and spin densities in the absence of dopants or external electric fields. Furthermore, because of the large Rashba splitting, highly-efficient spin manipulation might be realized. In addition, in a thin film geometry two-dimensional electron and hole Dirac gases with reversed spin-helicity coexist at opposite surfaces. Consequently, thin films of Bi-chalcogenides TIs with SDs provide a playground for exotic excitations such as topological exciton condensates.

[1] Y. Liu et al. Phys. Rev. Lett, 107, 086802 (2011)

FR.A-P15 - Electrical conductivity and weak ferromagnetism at the magnetic domain walls of the all-in/all-out order in $\text{Cd}_2\text{Os}_2\text{O}_7$ T. Hirose¹, J. Yamaura², Z. Hiroi¹

1. ISSP, The University of Tokyo, Tokyo, Japan

2. MCES, Tokyo Institute of Technology, Tokyo, Japan

The pyrochlore oxide $\text{Cd}_2\text{Os}_2\text{O}_7$ show a metal-to-insulator transition at $T_{\text{MI}} = 227$ K. Below the T_{MI} , the Os^{5+} ($5d^3$) spins undergo an all-in/all-out (AIAO) magnetic order accompanied by a weak-ferromagnetism. Moreover, an unusual temperature dependence in resistivity is observed in the "insulating" state, which is strongly sample dependent [1]. Similar features have been observed in a series of Ir pyrochlore oxides $\text{R}_2\text{Ir}_2\text{O}_7$ (R: rare earth elements) and intensively discussed in terms of the Weyl semimetal [2]. In both systems, the finite electrical conductivity has been attributed to magnetic domain walls (MDWs) in the AIAO order, though there is no direct evidence for this [3, 4]. Besides, the origin of the weak ferromagnetism remains controversial. In this study, we focus on the electrical and magnetic properties of the MDWs in $\text{Cd}_2\text{Os}_2\text{O}_7$. We have observed a marked difference in the temperature dependence of resistivity below T_{MI} between field-cooling and zero-field cooling measurements on several crystals. In addition, it is found that a robust, tiny remanent magnetization emerges when a crystal is cooled in 7 T field below T_{MI} , which cannot be reversed by sweeping field between ± 7 T. These findings evidence that both the finite electrical conductivity and ferromagnetic moments are induced at MDWs, which may give a reasonable explanation to the mysteries previously observed in $\text{Cd}_2\text{Os}_2\text{O}_7$.

[1] Z. Hiroi et al., APL Mat. 3, (2015) 041501

[2] X. Wan et al., Phys. Rev. B 83 (2011) 205101

[3] K. Ueda et al., Phys. Rev. B 89 (2014) 075127

[4] Y. Yamaji et al., Phys. Rev. X 4 (2014) 021035

FR.A-P16 - The changes in surface states of La, Ce, Eu doped SmB₆

B. Kang¹, C.H. Min², M. Song¹, B. Cho¹

1. *School of Materials Science and Engineering, Gwangju Institute of Science and Technology (GIST), Gwangju, Japan*

2. *Universität Würzburg, Experimentelle Physik VII & Center for Complex Material Systems RCCM, Würzburg, Germany*

Recently, samarium hexaboride (SmB₆) has received intensive attention because its metallic surface state was found to give rise to constant resistivity at $T < 5$ K. This temperature-independent resistance has been considered a signature of topologically protected surface states. In this study, the differences of the electrical transport properties of high-quality single crystals of Sm_{1-x}RxB₆ (R = La, Ce, Eu) that were synthesized using high-temperature Al solution growth methods were investigated. When either non-magnetic La or Eu ions were lightly doped in SmB₆, the surface states were maintained. This was confirmed from the observation of the failure of Ohm's law. When the thickness of a single crystal is reduced, resistance should be inversely proportional to thickness in a normal metal. However, the resistance of non-magnetic ion doped SmB₆ was the same, due to the existence of metallic surface states. On the other hand, when magnetic Ce ion 3 % was used as the dopant, the change of resistance followed Ohm's law. As a result, the surface states were found to vanish. The metallic surface states are sensitive to magnetic ions, which break the time reversal symmetry. SmB₆ exhibits contrasting behavior depending on the presence of magnetic or non-magnetic dopants. This result indicates that SmB₆ has the required property of topological surface state protected by time reversal symmetry.

FR.A-P21 - Electronic structure and phonon modes of SmB₆

F. Kuroda¹, T. Shishido¹, T. Oguchi²

1. ADSM, Hiroshima University, Hiroshima-Shi, Japan

2. ISIR, Osaka University, Osaka, Japan

Being predicted as a Z₂ topological Kondo insulator, SmB₆ has been drawing revised attentions. Density-functional theory and related calculations show that the d-f hybridization leads to the parity-switching band inversion at X, making this material being topologically nontrivial.

Extensive efforts have been paid to observe the topologically-protected metallic surface states. Although Dirac-cone like dispersion is not seen, several experiments indicate the existence of metallic (001) surface states, which form Fermi surface around X in the surface Brillouin zone and show temperature-dependent evolution being connected with the onset of d-f hybridization in bulk.

It seems that the long-standing issue of the exotic temperature dependence of SmB₆ conductivity can be resolved by admitting the temperature evolution of surface states.

A decade ago, Ogita et al. have measured Raman scattering spectra for the RB₆ series (R= rare earth element) and found an anomaly in the T_{2g} mode of SmB₆ and divalent systems, whose origin has not been discussed well. In this talk, in order to resolve this issue and discuss its possible connection with the nontrivial electronic structure of SmB₆, we carry out first-principles calculations based on the all-electron FLAPW method with a relativistic LDA+U approximation.

The zone-center phonon modes of SmB₆, LaB₆ (trivalent representative), and CaB₆ (divalent representative) are obtained by the frozen phonon approach. The calculated frequencies of Raman-active A_{1g} and E_g modes show universal lattice-constant dependence while the T_{2g} frequency has apparent valency dependence, accounting for Ogitaüfs experiment.

We analyze the conduction states in detail. They consist of not only the Sm d states but also B 2p pi states, whose lobe extends along the B atomic displacement of T_{2g} mode, being able to screen the T_{2g} mode.

FR.A-P22 - DFT+DMFT study of composition and temperature dependent electronic structure of $\text{NiS}_{2-x}\text{Se}_x$

C.Y. Moon¹, J.H. Shim

1. Korea Research Institute of Standards and Science

2. Department of Chemistry, Pohang University of Science and Technology

The electronic correlation is known to play important roles in condensed matter systems and results in rich structures in the phase diagram of materials, often dramatically changing materials property by small adjustment of external parameters. Nickel chalcogenide alloy $\text{NiS}_{2-x}\text{Se}_x$ is a good example to exhibit such complex phase diagram where metal-insulator transition (MIT) as well as magnetic phase transition occurs by varying Se composition x , temperature, and also pressure. Although the phenomenological phase diagram itself was well established earlier, detailed nature of the each phase and the transition among them have been controversial. Here we investigate the evolution of the electronic structure of nickel chalcogenide alloy $\text{NiS}_{2-x}\text{Se}_x$ with varying composition x and temperature using the combined theoretical method of density-functional theory and dynamical mean-field theory. Using real alloy structures containing both S and Se species in the cell, we map electronic correlation strength of the alloy on the phase diagram, and observe the metal-insulator transition along both the composition and temperature axes, consistent with the experimentally established phase diagram of this alloy system. The temperature dependence of the local magnetic susceptibility is obtained and shows an evolution from typical Curie-Weiss-like behavior for insulating phases to the constant behavior for metallic phases with increasing x . Comparison of electronic structures among NiS_2 and NiSe_2 in different lattice structures suggests that the composition-driven metal-insulator transition in the alloy results from the change of the hybridization strength between Ni d and chalcogen p orbitals.

FR.A-P23 - Elastic softening in the tetrahedrite $\text{Cu}_{12}\text{Sb}_4\text{S}_{13}$

T. Suzuki^{1,2,3}, H. Goto¹, Y. Noguchi¹, S. Kamikawa¹, K. Suekuni¹, H. Tanaka¹, T. Takabatake^{1,2}, I. Ishii¹

1. Department of Quantum Matter, AdSM, Hiroshima University, Hiroshima-shi, Japan
2. Institute for Advanced Materials Research, Hiroshima University, Hiroshima-shi, Japan
3. Cryogenics and Instrumental Analysis Division, Hiroshima-shi, Japan

The tetrahedrite $\text{Cu}_{12}\text{Sb}_4\text{S}_{13}$ has a cubic structure (space group I-43m) and is expected to be a thermoelectric material. At 85 K, a metal-semiconductor phase transition accompanied by a structural change is reported by the electrical resistivity and magnetic susceptibility measurements. The origin of the phase transition has not been determined yet. To investigate the phase transition at 85 K, we measured the elastic modulus using an ultrasonic technique on polycrystalline samples. The longitudinal modulus shows elastic softening from above 300 K, suggesting that there is an instability of the structure or the electronic state, such as a band structure. The softening continues down to 85 K, and it turns into increase below 85 K accompanied by hysteresis. The phase transition is of first-order. The elastic hardening indicates disappearance of the instability by the phase transition.

FR.A-P24 - Phase diagram of graphite in the ultra-quantum limit

F. Arnold^{1,3}, A. Isidori¹, E. Kampert², B. Yager¹, M. Eschrig¹, J. Saunders¹

1. Royal Holloway, University of London, London, United Kingdom

2. Dresden High Magnetic Field Laboratory, Dresden, Germany

3. Max Planck Institute for Chemical Physics of Solids, Dresden, Germany

Semimetals like graphite are subject of renewed attention due to the unique possibility to drive these systems into their magnetic quantum limit by applying large magnetic fields. Thus graphite is an ideal model system for the study of magnetic field driven phenomena, such as charge density waves and new topological phases.

Using state of the art pulsed magnetic fields up to 60 T, we brought a single crystal of natural Tanzanian graphite in the magnetic ultra-quantum limit. By measuring its electrical transport properties, we observed a new sub-phase and phase transitions within the known resistance anomaly below 54 T. Supported by new calculations of the renormalized Landau level structure, we identified the observed phase as collinear charge-density waves in the (0,up) and (-1,down) Landau levels, where the charge-density wave associated with the (0,up) Landau level undergoes a lock-in transition at 47 T and becomes commensurate with the crystal structure. Both charge-density waves are destroyed in a first order phase transition when their respective Landau levels cross the Fermi energy at 52.3 and 54.2 T.

Extending our model to higher magnetic fields, we are able to explain the resistance anomaly above 55 T by charge-density waves in the (0,down) and (-1,up) Landau levels. In this magnetic field region graphite enters a topological state, where the bulk is isolating and the surface is characterized by chiral edge states supporting both charge and spin currents.

FR.A-P25 - Mirror-symmetric magneto optical kerr rotation of [(GeTe)₂(Sb₂Te₃)₁]_n Superlattices

B. Do⁰, H. Awano^{1,4}, Y. Saito^{2,4}, J. Tominaga^{2,4}, S. Murakami^{3,4}

1. Toyota Technological Institute, 2-12-1 Hisakata, Tempaku, Nagoya, Japan

2. Nanoelectronics Research Institute, National Institute of Advanced Industrial Science & Technology (AIST), Tsukuba, Japan

3. Department of Physics, Tokyo Institute of Technology, Tokyo, Japan

4. JST-CREST, Japan Science and Technology, 4-1-8 Honcho, Kawaguchi, Saitama, Japan

5. Institute of Materials Science, Vietnam Academy of Science and Technology, 18 Hoang Quoc Viet, Cau Giay, Ha Noi, Vietnam

Since the invention of interfacial phase change memory (iPCM), which has recently been newly named topological switching random access memory, TRAM or TSRAM, the switching energy in phase change memory (PCM) has greatly been suppressed less than 1/20. On the other hand, iPCM has recently been studied as a topological insulator (TI). Since in TI both time-reversal symmetry and spatial inversion symmetry are preserved, TI is usually non-magnetic. However, breaking the symmetries may emerge spin-related properties. Therefore, it is very interesting to confirm if iPCM changes the Kerr-rotation by the breaking of the time reversal symmetry and spatial inversion symmetry.

Superlattice structures used in the experiment were designed based on ab-initio computer simulations, and [(GeTe)₂(Sb₂Te₃)₁]_n (n = 1-20) superlattices were fabricated by r.f. magnetron sputtering using two-inch composite targets: GeTe and Sb₂Te₃.

In this study, the actual experimental results at room temperature and high temperature beyond the phase transition from RESET to SET were in good agreement with our prediction. At room temperature, the Kerr signal of the superlattice film was within noise. However, when the temperature was increased to larger than a threshold (~380 K), the Kerr signal showed several peaks at certain magnetic fields which correspond to resonant conditions induced a giant Kerr rotation. This observed Kerr signal of the SET phase is attributed to the breaking of time reversal symmetry by application of an external magnetic field as well as the degenerated electronic bands due to the replacement of a Ge atomic layer along the c-axis at high temperature. On the other hand, the threshold temperature for observing Kerr resonant peaks is in good agreement with the SET and RESET phase transition temperature observed in the electrical resistance measurements.

Acknowledgement:

This research was supported by a Grant-in-Aid for Science Research of JST-CREST, Japan

FR.A-P27 - Classification of symmetry protected topological phases by the Chern-Simons approach

T. Yoshida¹

1. *RIKEN, Saitama, Japan*

In these years, it became clear that spatial symmetries can protect topological structures; a topological crystalline insulator has been reported for SnTe [1,2]. Furthermore, nontrivial phases in correlated systems are realized not only in fermionic systems but also in bosonic and spin systems. These are referred to as symmetry protected topological (SPT) phases. Applying classification scheme based on the Chern-Simons theory [3,4], we have classified SPT phases protected by a reflection symmetry. Besides we have proposed a spin model which shows nontrivial phase protected by the reflection symmetry. This phase can be regarded as bosonic extension of topological crystalline insulator [5]. In study of fermionic systems, we have pointed out that correlation effects can reduce topological classification; topological classes in free fermion systems are reduced into those of \mathbb{Z}_N in the presence of local discrete symmetry. Here, N denotes order of the local symmetry [5].

[1] L. Fu, Phys. Rev. Lett. 106, 106802 (2011)

[2] T. H. Hsieh et al., Nat. Commun. 3, 982 (2012)

[3] Y.-M. Lu and A. Vishwanath, Phys. Rev. B 86, 125119 (2012)

[4] C.-T. Hsieh et al., arXiv:1406.0307 (2014)

[5] T. Yoshida et al. in preparation

FR.A-P28 - Shubnikov-de Haas oscillations in the antiferromagnetic superconductor HoPdBiO. Pavlosiuk¹, D. Kaczorowski¹, P. Wisniewski¹*1. Institute of Low Temperature and Structure Research Polish Academy of Sciences, Warsaw, Poland*

The compound HoPdBi, crystallizing with a cubic MgAgAs-type structure, belongs to the family of half-Heusler phases, intensively studied owing to their possible nontrivial topological properties [1]. For some materials, topologically-nontrivial state has been theoretically predicted to arise due to a specific antiferromagnetic structure [2]. HoPdBi was previously studied on polycrystalline samples only, and found to order antiferromagnetically at $T_N = 2$ K [3]. Here, we report on the physical behavior in flux-grown single crystals of HoPdBi. The magnetic susceptibility, specific heat and electrical resistivity data confirmed the antiferromagnetic ordering setting in below 2 K. Additionally, the temperature dependencies of the AC magnetic susceptibility and the electrical resistivity indicated the onset of superconductivity at $T_c = 0.7$ K. However, no clear evidence of superconducting state was revealed from the heat capacity data, alike reported for a few related non-magnetic superconductors, e.g. LuPdBi, YPtBi and LuPtBi [4-8]. Remarkably, below 50 K, the transverse magnetoresistance of HoPdBi was found to be governed by weak antilocalization effect in small magnetic fields, with phase coherence length of about 300 nm - similar as in the above mentioned non-magnetic compounds, while below 7K Shubnikov–de Haas oscillations were detected in high magnetic fields, revealing cyclotron mass of $0.3m_e$ and Berry phase close to $1/2$.

[1] H. Lin et al. Nature Mat. 9:546–549 (2010)

[2] R.S.K. Mong, A.M. Essin, and J.E. Moore, Phys. Rev. B 81:245209 (2010)

[3] K. Gofryk et al. Phys. Rev. B 84:035208 (2011)

[4] O. Pavlosiuk, D. Kaczorowski and P. Wiśniewski, Sci. Rep. in print (2015)

[5] Y. Nakajima et al. arXiv:1501.04096 (2015)

[6] P. Pagliuso et al. APS March Meeting, Baltimore, abstract: BAPS.2013.MAR.B13.13 (2013)

[7] O. Pavlosiuk, D. Kaczorowski and P. Wiśniewski, SCES'14, Grenoble, abstr.: Mo-101 (2014)

[8] E. Mun et al. Phys. Rev. B 87:075120 (2013)

FR.A-P29 - Orbital polarization, spin-spin correlations and metal-insulator transitions in the $\text{Ca}_{2-x}\text{Sr}_x\text{RuO}_4$ system

Y. Utsumi¹, D. Kasinathan¹, S. Agrestini¹, Z. Hu¹, K.T. Ko¹, M. Haverkort¹, K.D. Tsuei², Y.H. Wu², Y.F. Liao², A.C. Komarek¹

1. Max Planck Institute for Chemical Physics of Solids, Dresden, Germany

2. National Synchrotron Radiation Research Center, Hsinchu, Taiwan

The single layered perovskite system $\text{Ca}_{2-x}\text{Sr}_x\text{RuO}_4$ has been attracting a great attention because of its rich properties depending on the Ca/Sr concentration. The end material Sr_2RuO_4 is isostructural to the high-TC cuprate and is known as an unconventional spin-triplet p-wave superconductor ($T_C = 1.5$ K) [1]. With the increase in Ca substitution for Sr, the system changes from a paramagnetic metal ($2.0 > x > 0.5$) to a magnetic metal ($0.5 > x > 0.2$) accompanied by a crystal structural distortion [2]. In the Ca rich phase ($0.2 > x > 0$), the system becomes a Mott insulator. The end material Ca_2RuO_4 is an antiferromagnetic insulator below $T_N \sim 110$ K and a paramagnetic insulator between 110 and 350 K. Furthermore, Ca_2RuO_4 shows a first-order metal-insulator transition (MIT) at 350 K and becomes paramagnetic metal above 350 K accompanied by a crystal structural distortion [3]. We performed hard x-ray photoemission on $\text{Ca}_{2-x}\text{Sr}_x\text{RuO}_4$ ($x = 0, 0.09, 0.2, 2.0$) at the BL12XU beamline of SPring-8 with $h\nu \sim 6.5$ keV. High-quality single crystals of $\text{Ca}_{2-x}\text{Sr}_x\text{RuO}_4$ were cleaved insitu under the base pressure of 3×10^{-10} mbar. The valence band spectrum of Ca_2RuO_4 shows dramatic changes across the MIT. The valence band spectrum of $\text{Ca}_{1.91}\text{Sr}_{0.09}\text{RuO}_4$ displays similar temperature evolution across the MIT. Details of the changes in the spectrum as a function of temperature and composition will be critically compared to recent predictions from LDA+DMFT calculations [4].

References:

[1] Y. Maeno et al., Nature (London) 372, 532 (1994)

[2] S. Nakatsuji et al., Phys. Rev. Lett. 84, 2666 (2000)

[3] S. Nakatsuji et al., J. Phys. Soc. Jpn. 66, 1868 (1997); H. Fukazawa et al., Physica B 281-282, 613 (2000)

[4] E. Gorelov et al., Phys. Rev. Lett. 104, 22401 (2010)

FR.A-P30 - Complex magnetic ordering process at the metal insulator transition in half-frustrated $\text{Ca}_2\text{Os}_2\text{O}_7$

M. Rahn¹, R. Johnson¹, J. Vale², C. Donnerer², P. Manuel³, D. Khalyavin³, G. Nisbet⁴, Y. Guo¹, Y. Shi⁵, D. McMorrow²

1. *University of Oxford, Oxford, United Kingdom*
2. *University College London, London, United Kingdom*
3. *ISIS Facility, Rutherford Appleton Laboratory, Oxford, United Kingdom*
4. *Diamond Light Source Ltd., Oxford, United Kingdom*
5. *Institute of Physics, Beijing, China*

In 5d transition metal oxides (5d TMOs), the combination of strong spin-orbit coupling, electronic correlation and frustration produces unusual ground states. Orthorhombic calcium osmate ($\text{Ca}_2\text{Os}_2\text{O}_7$) is a "half frustrated" bad metal with an unusual phase transition at 327 K, where its resistivity increases by an order of magnitude coincident with magnetic ordering. We have investigated the magnetic ordering process by neutron powder diffraction and single crystal resonant x-ray diffraction. Our results reveal a complex reordering process, likely induced by magnetic frustration. A similar coupling of magnetic order and electronic transport characteristics has been observed in other families of 5d TMOs. Given the itinerant character of these materials, one cannot explain such behaviour in a Mott-Hubbard scenario. We hope that the interpretation of the magnetic ordering process in $\text{Ca}_2\text{Os}_2\text{O}_7$ will aid the understanding of this peculiar interplay of spin-orbit coupling, correlation and frustration.

FR.A-P31 - Doping-induced single-particle states due to magnetic excitation of a Mott insulator

M. Kohno¹

1. National Institute for Materials Science, Ibaraki, Japan

In the Mott transition, single-particle states generally emerge in the Mott gap following the doping. These states are called doping-induced states and are observed in materials such as cuprate superconductors and in various theoretical calculations. To clarify the nature of the doping-induced states, relationships with the magnetically excited states of the Mott insulator are investigated. In t-J models, using the commutator between the Hamiltonian and an electron creation operator, a weighted sum rule for the overlap between the doping-induced states in the small-doping limit and the single-spin excited states of the Mott insulator is derived. In addition, it is shown in t-J models that the spectral weight of spin-1 states for each magnetization is equal to that of spin-0 states. These results imply that in general, the magnetically excited states of the Mott insulator significantly contribute to the doping-induced states in the small-doping limit.

FR.A-P32 - Magnon waveguides from topological magnon insulators

A. Mook¹, J. Henk², I. Mertig^{1,2}

1. *Max Planck Institute for Microstructure Physics, Halle, Germany*

2. *Institute of Physics, Martin Luther University Halle-Wittenberg, Halle, Germany*

Topological magnon insulators exhibit a nontrivial topology due to the Dzyaloshinskii-Moriya interaction, which opens up band gaps in the magnon dispersion relation causing nonzero Berry curvature and nonzero Chern numbers. Obeying the bulk-boundary correspondence, topological magnon insulators host topologically nontrivial edge magnons and, consequently, energy as well as spin currents along their edges [1,2].

Bringing two topological magnon insulators into contact results in topologically protected unidirectional interface magnons. As these interface modes decay toward both bulk regions, their currents are confined to a few nanometer wide strip around the interface, which is considered a waveguide for magnons. Owing to the topological nature of the edge states, the edge currents follow any geometry.

We study theoretically interfaces of semi-infinite kagome ferromagnets in various topological phases, with a focus on the formation and the confinement of nontrivial interface magnons [3]. We analyze generic magnon dispersions with respect to the number of band gaps and the respective winding numbers. An investigation of the heat current profiles about the interface is followed by a proposal of two recipes of composing magnon waveguides with nano-scale confinement, one from topologically different phases, another from identical phases. On top of this, we identify material classes to construct these magnon waveguides.

[1] L. Zhang et al, Phys. Rev. B 87, 144101 (2013)

[2] A. Mook, J. Henk, and I. Mertig, Phys. Rev. B 89, 134409 (2014); eidem, Phys. Rev. B 90, 024412 (2014)

[3] A. Mook, J. Henk, and I. Mertig, submitted

FR.A-P33 - Magnon hall effect of topological magnon insulators

A. Mook¹, J. Henk², I. Mertig^{1,2}

1. *Max Planck Institute for Microstructure Physics, Halle, Germany*

2. *Institute of Physics, Martin Luther University Halle-Wittenberg, Halle, Germany*

The family of Hall effects has recently been extended by the magnon Hall effect (MHE). For the insulating ferromagnet $\text{Lu}_2\text{V}_2\text{O}_7$ with pyrochlore lattice Onose et al found a transverse heat current upon application of a longitudinal temperature gradient [1]. The MHE is owing to uncompensated magnon edge currents [2] that originate from the non-trivial topology of the magnon band structure of topological magnon insulators [3]. The Dzyaloshinskii-Moriya interaction opens up band gaps in the magnon dispersion relation causing nonzero Chern numbers. The transverse thermal conductivity is consequently expressed as an integral over the Berry curvature.

In our theoretical investigation [4] we deduce the rich topological phase diagram of the ferromagnetic kagome system. The bulk-boundary correspondence---the connection of the Chern numbers with the number and propagation direction of the nontrivial edge modes---holds for the topological magnon insulator. It turns out that for specific systems the transverse thermal conductivity changes sign in dependence on temperature.

Studying semi-infinite kagome systems, we explain the link between a topological phase, identified by its Chern numbers, and the flow direction of the magnon Hall heat current. Furthermore, we derive a figure of merit for the strength of the magnon Hall effect.

[1] Y. Onose et al, *Science* 329, 297 (2010)

[2] R. Matsumoto and S. Murakami, *Phys. Rev. Lett.* 106 197202 (2011); *idem*, *Phys. Rev. B* 84, 184406 (2011)

[3] L. Zhang et al, *Phys. Rev. B* 87, 144101 (2013)

[4] A. Mook, J. Henk, and I. Mertig, *Phys. Rev. B* 89, 134409 (2014); *idem*, *Phys. Rev. B* 90, 024412 (2014)

FR.A-P34 - Absence of magnetic fluctuation in the topological Kondo insulator SmB6 revealed by polarized low energy muons

P. Kumar Biswas¹, Z. Salman¹, G. Balakrishnan², M. Ciomaga Hatnean², M.R. Lees², D. McK. Paul², E. Morenzoni¹, A. Amato¹

1. Paul Scherrer Institut, Villigen, Switzerland

2. University of Warwick, Coventry, United Kingdom

We present the magnetic behavior of the 3D Kondo topological insulator SmB6 at different depth and its detailed temperature dependence using low-energy muon spin relaxation/rotation (LE-muSR) measurements. Magnetic field fluctuations which are present in the bulk of SmB6 found to decrease rapidly with decreasing depths and probably disappear completely at the surface of SmB6. This could be either due to faster fluctuation of the magnetic moments or more probably the suppression of the magnitude of the magnetic moments towards the surface. We propose that the topologically protected surface states modify the spectrum/size of magnetic field fluctuations at the surface of SmB6.

FR.A-P35 - Preparation and characterization of the topologically non-trivial half Heusler compound YPtBi

A. Kronenberg¹, H.J. Elmers¹, G. Schönhense¹, M. Jourdan¹

1. University of Mainz, Mainz, Germany

Three dimensional topological insulators present electronic surface states, which allow dissipation less spin transport. These edge channels are topologically protected by time reversal symmetry (TRS) and can therefore only be perturbed by TRS breaking i.e. magnetic impurities.

Half-Heusler materials of the family LaPtBi are predicted to show 3D-topological order [1] i.e. present topologically protected electronic surface states. Additionally, according to band structure calculations, a bulk band gap can be opened around the Fermi level by lateral strain [2]. The planned in situ spin-resolved ARUPS directly after deposition is the ideal tool to investigate the electronic structure including surface states of thin films of this material class as recently shown for highly spin polarised ferromagnetic Heusler compounds [3]. We present results on the preparation and characterization of thin films of the YPtBi compound, fabricated by magnetron sputtering from three separate elementary sputtering sources. The crystal phase forms at elevated substrate temperatures under excessive Bi flux. Investigations by x-ray diffraction reveal a preferred growth direction along the [111] or [100] axes of the crystal with in plane order depending on the choice of substrate and buffer layer. Scanning electron microscopy shows a clustered growth of the material and the formation of segregations on the film's surface, which are identified to be Bi-rich as probed by EDX.

[1] Chadov et al. Nature Materials 9, 541-545 (2010)

[2] Zhang et al. Appl. Phys. Lett. 99 071901 (2011)

[3] Jourdan et al. Nat. Commun. 5, 3974 (2014)

FR.A-P37 - Nd-ion substitution effect on f-electron multipole order of PrRu₄P₁₂K. Iwasa¹, A. Yonemoto¹, S. Takagi¹, S. Itoh², T. Yokoo², S. Ibuka², C. Sekine³, H. Sugawara⁴1. *Department of Physics, Tohoku University, Miyagi, Japan*2. *Institute of Materials Structure Science, High Energy Accelerator Research Organization, Ibaraki, Japan*3. *Graduate School of Engineering, Muroran Institute of Technology, Hokkaido, Japan*4. *Department of Physics, Kobe University, Kobe, Japan*

We studied an effect of magnetic Nd-ion substitution to the metal-nonmetal transition at $T_{MI} = 63$ K of PrRu₄P₁₂, which is accompanied by antiferro-type electric multipole ordering of Pr-ion 4f electrons in the nonmetallic phase below T_{MI} of PrRu₄P₁₂ [1]. The transition temperatures of Pr_{1-x}Nd_xRu₄P₁₂ are determined from evolution of x-ray superstructure reflection, which is caused by transformation from the simple-cubic structure above T_{MI} to the body-centered-cubic (bcc) structure below T_{MI} . The ordered multipole, characterized by the staggered alignment of inequivalent crystal-field-splitting schemes of Pr 4f² electrons in the bcc structure [2], is investigated by inelastic neutron scattering performed at the neutron spectrometer HRC installed at BL12 of MLF, J-PARC. Based on these experimental results, the ordered state in the Nd-substituted material is rather robust against the substitution concentration, x , than the La- and Ce-substituted materials [3]. We observed also low-temperature enhancement in magnetic susceptibility of Pr_{1-x}Nd_xRu₄P₁₂, which is very similar to the ferromagnetic ordering in NdRu₄P₁₂. The ferromagnetic interaction between the Pr ions and the incorporated Nd ions in Pr_{1-x}Nd_xRu₄P₁₂ assists stability of the magnetic triplet ground state of the Pr ions that appears in the antiferro-type multipole ordered phase, and reduces the site-dilution effect. Therefore, the nonmagnetic multipole ordered phase of PrRu₄P₁₂ is compatible with the magnetic perturbation.

[1] C. Sekine et al., PRL 79, 3218 (1997), Y. Kuramoto et al., Proc. Theo. Phys. Suppl. 160, 134 (2005), T. Takimoto, JPSJ 75, 034714 (2006). [2] K. Iwasa et al., PRB 72, 024414 (2005), JPSJ 74, 1930 (2005). [3] C. Sekine et al., Physica B 281&282, 300 (2000), Physica B 378-380, 211 (2006), JPSJ 80, SA024 (2011), K. Saito et al., PRB 89, 075131 (2014)

FR.A-P40 - Magnetic properties of gadolinium substituted Bi₂Te₃ single crystalsS.W. Kim¹, K. Lee¹, M.H. Jung¹*1. Sogang University, Seoul, South Korea*

Topological insulators have attracted a lot of interest in condensed matter physics because of the gapless surface state inside the bulk gap. Various quantum phenomena arising from the topological surface states could be useful for low-power electronics and error-tolerant quantum computing. Long-range magnetic ordering is a key to achieve such quantum phenomena, and it can be attained simply by magnetic impurity doping. As for a relevant system, Gd doped Bi₂Te₃ has been proposed because gadolinium is isovalently substituted for Bi and exhibits the largest magnetic moment [1]. However, no ferromagnetic order has been observed so far, and a wide variety of Gd solubility limits have been reported [2-4]. Here, we prepared single crystals of Gd_xBi_{2-x}Te₃ with various x ($= 0.04, 0.06, 0.08, 0.12, 0.15, 0.20$). All the experiments were carried out for the single crystals with shiny surface in the center part of the ingot. Although the amount of Gd substitution increased, the transport and magnetic properties did not show any big differences. For all the samples, the magnetic susceptibility data were well fitted by the Curie-Weiss law, from which the actual composition of Gd substitution was estimated in the vicinity of $x' = 0.08$. Then, a question can arise; where the excess or deficient Gd atoms are. In experimental, crumbly parts on the upper part of ingot were clearly visible. X-ray diffraction data revealed that the crumbly parts are Gd-rich or Gd-lack phases such as GdTe or BiTe for $x > 0.08$ and $x < 0.08$, respectively. These observations suggest that the most stable phase of gadolinium substituted Bi₂Te₃ is Gd_{0.08}Bi_{1.92}Te₃.

References:

- [1] Hai-Jun Zhang, Xiao Zhang, and Shou-Chen Zhang, condmat:1108.4857
- [2] Y. R. Song et al. Appl. Phys. Lett. 100, 242403 (2012)
- [3] S. Li et al. App. Phys. Lett. 102, 242412 (2013)
- [4] S. E. Harrison et al. J. Appl. Phys. 115, 023904 (2014)

FR.A-P41 - Antiferromagnetic order competing with topological state in $\text{Ce}_x\text{Bi}_{2-x}\text{Te}_3$ H.S. Lee¹, K. Lee¹, S.W. Kim¹, J. Kim¹, M.H. Jung¹, A. Jelen², S. Vrtnik², Z. Jaglicic², J. Dolinsek²

1. Department of physics, Sogang University, Seoul, South Korea

2. J. Stefan Institute and University of Ljubljana, Ljubljana, Slovenia

Topological insulator (TI) is a new material platform with time-reversal symmetry and non-trivial topology. Previous theoretical works reported that antiferromagnetic order can coexist with the topological state, even though the magnetic order breaks the time-reversal symmetry [1-3]. A candidate for antiferromagnetic topological insulator (AFTI) has been proposed to be GdBiPt [1], but only magnetic structure has been reported to be type-II antiferromagnetic [4]. The specific magnetic structure, that the magnetic moments are aligned ferromagnetically in layers which are stacked antiferromagnetically, is required for AFTI. Here, we prepared single crystals of $\text{Ce}_x\text{Bi}_{2-x}\text{Te}_3$ with various x ($= 0.04, 0.06, 0.08, 0.10, \text{ and } 0.12$). The obtained crystals were characterized by X-ray diffraction and scanning electron microscopy. The magnetic susceptibility data revealed that the Ce atoms are well substituted for Bi into Bi_2Te_3 . From the Curie-Weiss fits, we obtained that the effective magnetic moments μ_{eff} are close to $2.54 \mu_B$ for free Ce ion and the paramagnetic Curie temperatures θ_p are negatively increased from -3.04 to -59.28 K with increasing x . The magnetization data clearly showed antiferromagnetic orders around $T_N = 4$ K for $x \geq 0.08$, where θ_p suddenly increases. Only for $x = 0.06$, exotic physical properties arising from topological states were observed such as non-metallic behavior in the electrical resistivity and linear dependence of the magnetoresistance. Otherwise, for $x \geq 0.08$ the electrical resistivity is simply metallic and the magnetoresistance is parabolic. Especially, it is noteworthy that the carrier density is in an order of 10^{19} cm^{-3} for $x \geq 0.08$, while it is $\sim 10^{17} \text{ cm}^{-3}$ for $x = 0.06$. These observations propose that the antiferromagnetic order is strongly competing with the topological state in $\text{Ce}_x\text{Bi}_{2-x}\text{Te}_3$. This result seems to be contradictory to the previous works, but be reasonable by assuming type-I antiferromagnetic order.

[1] Roger S. K. Mong et al. Phys. Rev. B 81, 245206 (2010)

[2] Chen Fang et al. Phys. Rev. B 88, 085406 (2013)

[3] Chao-Xing Liu, arXiv: 1304.6455v1

[4] R. A. Muller et al. Phys. Rev. B 90, 041109(R) (2014)

FR.A-P42 - High pressure X-ray Diffraction studies on pyrochlore iridates near Metal-insulation transition

Z. Feng¹, C. Donnerer^{1,2}, J. Vale^{1,2,3}, D. Prabhakaran⁴, A. Boothroyd⁴, D. Mcmorrow^{1,2}

1. London Centre for Nanotechnology, University College London, London, United Kingdom

2. Department of Physics and Astronomy, University College London, London, United Kingdom

3. Laboratory for Quantum Magnetism, Ecole Polytechnique Federale de Lausanne (EPFL), Lausanne, Switzerland

4. Clarendon Laboratory, Department of Physics, University of Oxford, Oxford, United Kingdom

The pyrochlore $\text{Ln}_2\text{Ir}_2\text{O}_7$ (Ln=rare earth) has become a hotspot of condensed matter physics due to their tunable metal-insulator behaviour and the insight of physics. For this system, the Ln=Eu, Sm, Nd materials are of particular interests because of their setting on the proximity of Metal Insulation Transition (MIT). Previous studies have reported that the MIT can be suppressed by physical pressure [1,2]. The insight of this change is still not clear. Therefore, we carried out our investigations on the crystal structure of $\text{Ln}_2\text{Ir}_2\text{O}_7$ as a function of pressure. High pressure x-ray diffraction (XRD) was performed on Ln=Eu and Nd single crystals up to 40GPa at Diamond Light Source, United Kingdom. The pressure range is enough to suppress MIT and new long-range ordering is believed to occur at high pressure[2]. Our results reveal that there is no obvious first-order structural transition induced by the pressure, implying that lowering the cubic symmetry does not change in the electronic state and magnetic orderings of these compounds. Therefore, the magnetic order of Ir moments are likely to play a major role for the MIT.

Reference:

[1]. F. Tafti et al., Phys. Rev. B., 85, 205104 (2012) [2]. M. Sakata et al., Phys. Rev. B., 83, 041102 (2011)

FR.A-P43 - Pressure-induced semimetal-to-semiconductor transition in bismuth

P. Brown¹, K. Semeniuk¹, A. Vasiljkovic¹, F. Malte Grosche¹

1. Cavendish Laboratory, Cambridge, United Kingdom

The semimetal bismuth stands out among the elements for its extremely low carrier concentration. This arises from small electron and hole Fermi surface pockets, which result in only around one mobile electron per 100,000 atoms. Situated very close to the transition to a semiconductor, the electronic structure can be tuned further by doping with antimony or by applied hydrostatic pressure.

We investigate the electrical resistivity, Hall effect and Shubnikov de Haas oscillations of single crystal bismuth under hydrostatic pressure of up to 25 kbar in a piston cylinder pressure cell. A novel field modulation technique enables us to observe quantum oscillations down to fields below 0.2 T and temperatures above 20 K. While the temperature dependence of the resistivity is metallic at ambient pressure, it develops a pronounced kink and subsequently a maximum near 40 K with increasing pressure. The maximum shifts towards lower temperature with further increasing pressure until, above about 20 kbar, the resistivity of bismuth resembles that of a narrow-gap semiconductor.

These results suggest that the Lifshitz transition from semimetal to semiconductor can indeed be studied in bismuth at pressures less than 25 kbar; above this pressure a structural transition into a fully metallic state takes place. This makes it possible to access ultra-low carrier density states at intermediate pressures, in which the quantum limit can be reached at very low applied fields.

FR.A-P44 - Topological phases of periodically-driven system on a hexagonal lattice

M. Maksymenko¹, I. Cosma Fulga¹

1. Department of Condensed Matter Physics, Weizmann Institute of Science, , Rehovot, Israel

Characterization of topological phases in periodically driven systems can require immensely new set of topological invariants, which are defined over the full driving period. We investigate in details the phase diagram of the periodically driven two-dimensional system of fermions on the hexagonal lattice. Here the hopping integrals along the three distinct bonds are switched on and off sequentially in a stroboscopic manner implying effective chirality of the fermion hopping along the hexagon.

We find that the system exhibits a new set of topological phases for which a standard band Chern numbers fail to identify whether the phase is topologically non-trivial. Such phases can be characterized by a set of new strong and weak invariants defined over the period of time. The conductance of the finite system with different types of edges provides a clear evidence for the presence or absence of the edge-states contribution. We investigate the role of disorder as well as the possibility of breaking of rotational/translational symmetries and time periodicity.

FR.A-P46 - Weak antilocalization and magnetic field driven metal insulator transition in $\text{Bi}_2\text{Te}_{2.1}\text{Se}_{0.9}$ single crystals

B. Irfan¹, R. Chatterjee¹

1. *Indian Institute of Technology Delhi (IITD), New Delhi, India*

Topological insulators (TIs) are a new phase of matter with bulk insulating and conducting surface states. In three dimensional topological insulators such as Bi_2Se_3 , large numbers of selenium vacancies push the Fermi level inside the conduction band; due to which the charge transport is generally dominated by the bulk current in this crystal and the as grown crystals of Bi_2Te_3 are p-type because of Te-Bi exchange defects. $\text{Bi}_2\text{Te}_2\text{Se}$ is the hybrid material in which the selenium ion occupies the innermost layer in each quintuplet. This will suppress both vacancy formation and Te-Bi exchange defects. Thus, among the known topological insulators, $\text{Bi}_2\text{Te}_2\text{Se}$ with basic quintuple layer as Te-Bi-Se-Bi-Te, emerged as a promising material for studying the topological insulating properties.

In this work we present our results on $\text{Bi}_2\text{Te}_{2.1}\text{Se}_{0.9}$ single crystals grown using modified Bridgeman technique. The R-T behavior of $\text{Bi}_2\text{Te}_{2.1}\text{Se}_{0.9}$ single crystals shows a magnetic field driven metal insulator transition. The results reveal a conventional temperature dependence metallic behavior at high temperature (i.e. above 250 K) under applied magnetic field and insulating behavior at low temperatures. A sharp drop in resistance is observed in $\text{Bi}_2\text{Te}_{2.1}\text{Se}_{0.9}$ single crystals at zero magnetic field due to weak antilocalization (WAL) effect, which arises from quantum interfering nature of topological insulators. The devices were fabricated (using mechanical exfoliation technique) to investigate the effect of WAL arising from topological surface states. The WAL coefficient of conductance can be tuned by gate voltage and separated in to coherently independent channels, which in topological insulators include both the bulk conduction and topological surface conduction. We also report the experimental evidence of universal conductance fluctuation (UCF) in bulk insulating $\text{Bi}_2\text{Te}_{2.1}\text{Se}_{0.9}$ micro flakes.

FR.A-P47 - Laser-induced phase transitions of topological Kondo insulators

K. Takasan¹, M. Nakagawa¹, N. Kawakami¹

1. Department of Physics and Astronomy, Faculty of Science, Kyoto University, Kyoto, Japan

Controlling the nature of matter by laser light is an important topic in strongly correlated electron systems. We theoretically investigated how high-frequency laser field changes the nature of topological Kondo insulators. The topological Kondo insulator is a strongly correlated insulator that has a surface state protected by time-reversal symmetry (TRS) [1]. Recent theoretical and experimental studies suggest that SmB₆ is a strong candidate for the topological Kondo insulator.

By employing a prototypical model of the topological Kondo insulator [2], we treated the effect of the laser field with the effective Floquet Hamiltonian, which gives the information of the system in the high-frequency limit. It enables us to map the time-periodic systems to static systems. We treated electron correlation effects by the slave-boson method, which allows us to calculate the renormalization effect self-consistently and thus determine the Kondo temperature.

From the topological point of view, we showed how the laser light changes the topological phases of this system. We calculated the topological number at the mean field level and found how topological phase transitions occur according to laser intensity. Especially when the light is circularly polarized, we showed that the system is driven to a quantum Hall phase and a Weyl semi-metallic phase.

In terms of the heavy fermion physics, we calculated the Kondo temperature as a function of laser light intensity and discussed the intensity-temperature phase diagram. Our calculation elucidated that there are the photo-induced hopping and the photo-induced hybridization under the laser irradiation, and that these photo-induced effects change the nature of the heavy electrons in the system quantitatively.

References:

[1] M. Dzero, K. Sun, V. Galitski, and P. Coleman. Phys. Rev. Lett. 104, 106408 (2010)

[2] M. Tran, T. Takimoto, and K. Kim. Phys. Rev. B. 85, 125128 (2012)

FR.A-P49 - Spin susceptibility of mercury telluride - cadmium telluride quantum wells

M. Governale¹, T. Kernreiter¹, E. Hankiewicz², U. Zülicke¹

1. Victoria University of Wellington, Wellington, New Zealand

2. Universität Würzburg, Würzburg, Germany

(Hg,Cd)Te quantum wells exhibit a topological phase transition as a function of the well width [1]. For widths larger than the critical width, the quantum-well has an inverted band gap and becomes a two-dimensional topological insulator. In the topological phase, the system supports an odd number of chiral edge states, which give rise to the quantum spin Hall effect. The low-energy physics of these systems is well described by the 4x4 Bernevig-Hughes-Zhang model [2].

Here we calculate the static spin susceptibility of the 2D quantum-well states using a k-dot-p expansion starting from the 6x6 Kane Hamiltonian. Due to the coupling between the light-hole and conduction bands, the spin susceptibility is not proportional to the charge response function given in Ref [3]. We study the dependence of the spin-susceptibility tensor on doping both in the trivial and topological phase. We obtain analytical results in the limit of vanishing wave vector ($q=0$), while the full wave-vector dependence of the spin susceptibility is computed numerically. Interestingly, for zero doping we find a $q=0$ intrinsic contribution to the spin susceptibility that in the topological phase does not depend on the Dirac mass parameter. We discuss the physical ramifications of this unusual result, including its implications for the RKKY interaction.

Furthermore, both the in-plane and out-of-plane components of the intrinsic spin susceptibility show a maximum for a finite value of wavevector. We complete our study by calculating the edge-state contribution to the spin-susceptibility tensor.

[1] M. König, S. Wiedmann, C. Brüne, A. Roth, H. Buhmann, L. W. Molenkamp, X.-L. Qi, and S.-C. Zhang, *Science* 318, 766 (2007)

[2] B. A. Bernevig, T. L. Hughes, and S.-C. Zhang, *Science* 314, 1757 (2006)

[3] S. Juergens, P. Michetti, and B. Trauzettel, *Phys. Rev. B* 90, 115425 (2014)

FR.A-P50 - Thermopower and Nernst effect of the Kondo insulator CeRu₄Sn₆

V. Martelli¹, J. Hönel¹, J. Larrea J.^{1,2}, H. Winkler¹, A. Prokofiev¹, S. Paschen¹

1. *Institute of Solid State Physics, Vienna University of Technology, Vienna, Austria*

2. *Physics Department, University of Johannesburg, Auckland Park, South Africa*

Kondo insulators are materials in which an energy gap in the electronic density of states (DOS) opens at the Fermi level as a consequence of strong electronic correlations. The gap is thought to arise from a half-filled conduction band hybridizing with a localized f level (cf hybridization). Since correlations renormalize energy scales the gap width of Kondo insulators is of the order of 1 to 100 meV [1]. The tetragonal compound CeRu₄Sn₆ shows pronounced anisotropy between the crystallographic c axis and the directions within the tetragonal plane (a and c' directions) [2,3]: characteristics of a Kondo insulator are seen within the tetragonal plane but heavy fermion metal behaviour dominates along the c axis [3]. Thermopower is extremely sensitive to details in the electronic DOS near the Fermi level. Thus, measurements on single crystals along different crystallographic axes may shed light on the underlying electronic correlation phenomena. Here we present our investigations of the thermopower and Nernst effect of single crystalline CeRu₄Sn₆ at low temperatures and in magnetic fields, with the aim to reveal the topology of the Fermi surface and its relation to the anisotropy of the energy gap. This work was supported by the European Research Council (ERC Advanced Researcher Grant 227378), the Austrian Science Fund (projects I623-N16 and W1243), the FRC/URC of the University of Johannesburg, the European Commission (EuroMagNET II n. 22804), and the U.S. Army Research Office (grant W911NF-14-1-0496). The participation in this conference was partially supported by the Brazilian CNPq (project 401108/2014-7).

References:

- [1] G. Aeppli and Z. Fisk, *Comments Condens. Matter Phys.* 16, 155 (1992)
- [2] S. Paschen, H. Winkler, T. Nezu, M. Kriegisch, G. Hilscher, J. Custers, and A. Prokofiev *J. Phys.: Conf. Series* 200, 012156 (2010)
- [3] V. Guritanu, P. Wissgott, T. Weig, H. Winkler, J. Sichelschmidt, M. Scheffler, A. Prokofiev, S. Kimura, T. Iizuka, A. M. Strydom, M. Dressel, F. Steglich, K. Held, and S. Paschen, *Phys. Rev. B* 87, 115129 (2013)

FR.A-P51 - Spin torque diode quantitative measurements of the damping in localised magnetic modes

S. Lequeux¹, J. Sampaio¹, R. Matsumoto^{1,3}, P. Bortolotti¹, T. Devolder², A. Fukushima³, H. Kubota³, K. Yakushiji³, S. Yuasa³, V. Cros¹

1. *Unité Mixte de Physique CNRS/Thales, Palaiseau, France*

2. *Institut d'Electronique Fondamentale (IEF), Bures-sur-Yvette, France*

3. *AIST, Warrendale, United States*

Spin torque diode effect provides an efficient tool to access the resonant properties of magnetic nanostructures [1]. Indeed, injecting a microwave current through a magneto-resistive structure gives access to dynamic parameters of magnetization vibration modes like the frequency, damping or even the spin torques amplitude. While the quasi-uniform resonant mode has been largely studied, few spin torque diode experiments have concentrated on localized magnetic modes like Domain Wall (DW) resonance. Moreover, no quantitative parameters, except frequency, have ever been extracted from the rectified signals. In this study, we take advantage of the large magneto-resistance effects in MgO-based Magnetic Tunnel Junctions to perform for the first time a quantitative study of the spin torque induced resonance of a transverse DW and its adjacent domains. From the measured spectra we can clearly distinguish the signal of the DW from the signal due to domains. This allows us to extract simultaneously the dynamic parameters of the two probed vibration modes. By using a theoretical model we derive from the experimental linewidths that their damping is twice increased compared to the measured damping value of their host magnetic layer. In literature such an increase of the damping associated to localized magnetic modes has already been reported [2,3]. Several effects can be involved to explain the increase of effective damping, like transverse spin diffusion or surface roughness. In a multilayer system, the dipolar coupling between the magnetic object in one layer and its magnetic shadow projected on the bottom layer has been predicted [3] and can lead to an increase of the measured damping. We have performed micromagnetic simulations to evaluate the damping enhancement due to this dipolar coupling. Based on these results, we will discuss the contribution of the different effects to the observed damping increase in our system. This research was partly funded by the French Ministry of Defense (DGA) and the European Research Council (Stg 259068).

References:

- [1] A. A. Tulapurkar et al., Nature 438 (2005) 339
- [2] H. T. Nembach et al., Phys. Rev. Lett. 110, 117201 (2013)
- [3] J. M. B. Ndjaka et al., J Appl. Phys. 105, 023905 (2009)

FR.A-P52 - anomalous quasiparticles on the domain wall between topological insulators and spin ice compounds

I. Kanazawa¹, T. Sasaki¹

1. Department of Physics, Tokyo Gakugei University, Tokyo, Japan

Recently, one of present authors has proposed exotic quasiparticles with fractional charges in semiconductor-dot from collectively induced-charge effect on a domain wall shell[1]. In this study, we propose that there might be emergent quasiparticles with fractionalized electric charge on the domain wall between topological insulator and spin ice compounds, through the interaction between the Dirac fermions and excited magnetic monopoles.

[1] I. Kanazawa, J.of Phys.Cs 400(2012)042028

FR.A-P54 - Metal-Insulator transition in LaNiO_{3-d} thin and ultrathin films: how to disentangle disorder and doping effectsA. Senegas¹, J. Scola¹, B. Berini¹, G. Agnus², C. Vilar¹, V. Pillard², P. Lecoeur², Y. Dumont¹*1. Lab. GEMaC; Université de Versailles – CNRS, Versailles, France**2. Institut d'Electronique Fondamentale; Université Paris-Sud – CNRS, Orsay, France*

Rare-earth nickelates (RNiO_3 with R=rare earth cation) are well known to reveal a metal-insulator transition (MIT). In this series LaNiO_3 bulk shows interesting behavior for electronic devices such as paramagnetic metallic properties at all temperature and no MIT with temperature [1]. However, MIT in LaNiO_{3-d} can be triggered by several parameters (e.g. cation substitution, substrate strain and oxygen stoichiometry [2,3]) including by lowering the dimensionality [4,5]. Furthermore, even a short time exposure of the LNO films to the air atmosphere leads to the formation of a hydroxide layer on the films surface [6]. This ageing changes the films transport's properties in observed mostly in ultrathin films. Several series of epitaxial LaNiO_3 films were grown by pulsed laser deposition on STO (100) substrates, with and without protection capping. Quality of LNO films were optimized by monitoring roughness, epitaxy, thickness and homogeneity by AFM, X-ray diffraction and X-ray reflectivity. Electrical resistivity, magneto-transport and Hall Effect for thin and ultrathin LNO films were done in the range 5 - 300 K and 0 - 9 T, and after de/re-oxygenating annealing treatments. This study reveals by comparison how to disentangle effects of disorder associated to weak localisation, and of doping.

[1] X. Q. Xu, J. L. Peng, Z. Y. Li, H.L. Ju, R. L. Greene, Phys. Rev. B 48, 1112 (1993)

[2] J. Son, P. Moetakef, J. M. LeBeau, et al., Appl. Phys. Lett. 96, 062114 (2010)

[3] B. Berini, N. Keller, B. Pigeau, et al., J. Appl. Phys. 104, 103539 (2008)

[4] R. Scherwitzl, S. Gariglio, M. Gabay, et al., Phys. Rev. Lett. 106, 246403 (2011)

[5] P. A. Lee and T. V. Ramakrishnan, Rev. Mod. Phys. 57, 287 (1985)

[6] S. Mickevicius, S. Grebinskij, V. Bondarenka, et al., Acta Phys. Pol. A 112, 113 (2007)

FR.A-P56 - Fermi surface on the border of Mott transition in NiS₂

H. Chang¹, S. Friedemann², M. Gamza³, W. Coniglio⁴, D. Graf⁴, S. Tozer⁴, M. Grosche¹

1. Cavendish Laboratory, University of Cambridge, Cambridge, United Kingdom

2. HH Wills Laboratory, University of Bristol, Bristol, United Kingdom

3. Department of Physics, Royal Holloway, University of London, Egham, United Kingdom

4. National High Magnetic Field Laboratory, Tallahassee, Florida, United States

The transition from a metallic to a correlated, or Mott, insulating state is a long-standing theme of fundamental interest in condensed matter research. The nature of the Mott metal-insulator transition, the properties of the metallic and insulating state on either side of the transition, and the emergence of novel phenomena - such as high temperature superconductivity - in its vicinity have all motivated comprehensive experimental and theoretical studies.

Using quantum oscillation measurements in high magnetic fields to probe the electronic Fermi surface and effective carrier mass on the metallic side of the transition could provide much needed microscopic information. In the cuprates, such studies in samples doped into the metallic state have identified the Fermi surface structure in underdoped and overdoped regimes. Because the quantum oscillation signal is strongly suppressed in the presence of disorder, pressure rather than doping should ideally be used to reach the metallic state. We present the first observation of quantum oscillations from a pressure-metallised 3D Mott insulator. NiS₂ can be tuned through the Mott transition at a modest pressure of ~30kbar. Quantum oscillations near the Mott transition are observed with the tunnel diode oscillator technique in magnetic fields up to 31T. The main observed oscillation frequency is consistent with the Fermi surface obtained within density functional theory, whereas the effective mass is significantly enhanced over the band mass.

FR.A-P57 - Magnetic ion doping on the surface of Bi₂Se₃ topological insulatorsR. Chatterjee¹, Bushra Irfan¹*1. Indian Institute of Technology Delhi, New Delhi, India*

The effect of magnetic impurities and ferromagnetism on Dirac like conducting surface states in three dimensional topological insulators (TIs) such as Bi₂Se₃ or Bi₂Te₃ have attracted a lot of attention. The introduction of magnetic impurities breaks the time reversal symmetry and thus destroys the robust metallicity of the surface of TIs. Studies in these transition metal ion-doped TIs are usually motivated by various interesting phenomenon like quantized anomalous Hall effect, spin current, inverse spin-galvanic effect, all of which critically depend upon finding a way to break time reversal (TR) symmetry on the surface and thus use the unique TR broken spin texture for applications. In this work, we investigate the effect of Co doping (~5% to 10%) in Bi₂Se₃. We mainly focus on the result obtained on Bi_{1.8}Co_{0.2}Se₃ single crystal sample and the device prepared on mechanically exfoliated ~70 nm flake obtained from the crystal (with a technique similar to the one used for graphene). The bulk crystal resistivity measurements reveal metallic behavior, as noted by other researcher for doped Bi₂Se₃. With increasing Co-doping, the resistivities of Bi_{2-x}Co_xSe₃ (x= 0.1, 0.15, 0.2) decrease maintaining the overall metallic behavior for T > 50 K, for all samples. It is interesting to note that the crystal with high (~10%, x = 0.2) concentration of Co doping i.e. Bi_{1.8}Co_{0.2}Se₃, shows a logarithmic increase in resistivity with decreasing temperature for T <= 50 K. Although no weak antilocalization (WAL) effect is observed in this bulk Bi_{1.8}Co_{0.2}Se₃ crystal, the device prepared on nano-flake from the crystal of Bi_{1.8}Co_{0.2}Se₃, reveals a WAL feature. Above 40 K a crossover to weak localization behavior is observed in the device. Resistivity measurement on this nano-device shows a Kondo like peak at 40 K and a clear semiconducting behavior over the whole range of temperature up to 300 K is noted in the device.

FR.A-P58 - Magnetotransport and magnetic properties of single crystals of BaNiS₂: a two-dimensional semimetal with highly mobile carriers

Y. Klein¹, D. Santos-Cottin¹, M. Verseils¹, A. Gauzzi¹

1. IMPMC, University Pierre and Marie Curie, Paris, France

BaCo_{1-x}Ni_xS₂ is a two-dimensional Mott system, where electron doping drives the antiferromagnetic and insulating phase at $x = 0$ to a metallic and paramagnetic one at the critical value $x_{cr} = 0.22$ [1]. Previous studies have been mostly focused on the region near x_{cr} , whilst the metallic phase, BaNiS₂, has been relatively little studied. In particular, the available data on transport properties are limited and the carrier density and the scattering mechanism remain to be determined. For instance, the question arises whether the electron-electron or the electron-phonon scattering dominates. In order to address this point, we performed a detailed study of the magnetotransport properties, magnetic susceptibility and specific heat on high-quality single crystals. The conductivity tensor is quantitatively analyzed in terms of a three-carrier model, from which it can be stated that BaNiS₂ is a semimetal very close to the compensation. On one hand, two majority channels exhibit moderately high carrier mobilities. On the other hand, the third one is due to highly mobile holes that are attributed to strongly curved bands with a conic-like dispersion at the Fermi level. While the electronic part of the specific heat indicates weakly correlated carriers, the magnetic susceptibility is enhanced by one order of magnitude if compared to the density of state, and exhibit non-negligible temperature dependence. The supplementary paramagnetic contribution may be explained by the recently discovered and strong spin-orbit interactions in BaNiS₂ [2].

[1] J. Takeda, K. Kodama, H. Harashima, and M. Sato, J. Phys. Soc. Jpn. 63, 3564 (1994)

[2] D. Santos-Cottin et al., submitted to Phys. Rev. Lett

Fr.A-P59 - Quantum oscillations study of the Fermi surface of BaNiS₂ with enhanced spin-orbit interactions

Y. Klein¹, A. Audouard², D. Santos-Cottin¹, G. Feve³, V. Frelon³, D. Vignolles², B. Placais³, M. Verseils¹, A. Gauzzi¹

1. IMPMC - University Pierre and Marie Curie – Paris, France

2. LNCMI - INSA, UFJ, UPS – Toulouse, France

3. Laboratoire Pierre Aigrain, Ecole Normale Supérieure - University Pierre and Marie Curie – Paris, France

By a combined study of Shubnikov de Haas and de Haas van Alphen effects on high-quality single crystals of the BaNiS₂ semimetal, the Fermi surface of the latter quasi two-dimensional system is investigated. The experimental electronic properties deduced from the present paper are in accordance with recent band calculations that take into account spin-orbit coupling and Coulomb repulsion effects [1]. The analyse of quantum oscillations by the generalized Lifshitz-Kosevich formula shows the occurrence of three extremal orbits. The angular and temperature dependencies of these frequencies suggest the presence of only two pockets at the Fermi surface: a quasi two-dimensional electron-like one at the centre of the Brillouin zone compensated by a hole-like one situated at approximately mid-distance along the GM (ZA) direction. The latter pocket is made of two highly dispersed bands and contains very mobile charge carriers. The different symmetries of these two bands is an obstacle to the realisation of a Dirac symmetry.

[1] D. Santos-Cottin et al., submitted to Phys. Rev. Lett

FR.A-P60 - Magnetic and structural stability of topological-insulator/ferromagnet hybrid structures during thermal annealing procedures

M. Valiska¹, M. Vondráček², H. Steiner³, G. Springholz³, R. Tarasenko¹, V. Sechovsky¹, J. Honolka²

1. Department of Condensed Matter Physics, Charles University, Prague, Czech Republic

2. Institute of Physics, Academy of Sciences of the Czech Republic, Prague, Czech Republic

3. Institut für Halbleiter und Festkörperphysik, Johannes Kepler Universität, Linz, Austria

Topological insulators (TIs) have attracted increasing attention as a class of materials combining new fundamental physicals and potentials for applications in the field of spintronics[1]. An essential property of 3D TIs like e.g. Bi₂Se₃ is time reversal symmetry and a strong spin-orbit coupling, leading to topologically protected surface states (TSSs) and a suppression of backscattering processes in surface electronic transport. It has been predicted that magnetic atoms in the vicinity of the TSS can break time-reversal symmetry and opens efficient spin-flip channels for backscattering processes. We have shown earlier that single magnetic adatom spins situated on TI surfaces randomly fluctuate at temperatures $T \sim 4\text{K}$ [2]. In order to achieve stable exchange fields, our present work focuses on MBE-grown TI heterostructures consisting of thin surface layers of pure Bi₂Se₃ and a buried, remanently magnetized Mn-doped Bi₂Se₃ layer. The heterostructure is sealed by a protective Se capping layer. In this contribution we present an optimized Se capping and decapping procedure of Mn-doped samples under UHV conditions. Surface properties before and after decapping are controlled by EDX, PEEM and XPS measurements, and the TSS state is monitored in situ by k-PEEM. The important question of potential changes of the magnetic properties of Mn-doped layers (1 - 10%) due to diffusion effects during decapping process at elevated temperatures is addressed via extensive measurements of the bulk magnetization using SQUID. These showed no significant difference of the magnetic coupling caused by decapping process.

[1] M. Z. Hasan and C. L. Kane, Reviews of Modern Physics 82, 3045 (2010)

[2] J. Honolka, et al., Physical Review Letters 108, 256811 (2012)

FR.A-P63 - Metal-insulator transitions in elemental Yb and SrTiO₃

C. Enderlein ^{1,2}, S. Rowley ^{1,2}, J. Olivera ¹, M. Fontes ¹, S. Saxena ², G. Lonzarich ², E. Saitovitch ¹

1. CBPF, Urca, Rio de Janeiro, Brasil

2. Cavendish Laboratory, Cambridge, United Kingdom

We present results of a study in two systems Yb and SrTiO₃ which may both be readily tuned through an insulator to metal transition resulting in the formation or destruction of tiny Fermi surface pockets. In the case of Yb, ~12 kbars of pressure is enough to transform its metallic state into an insulator through a quantum critical Lifshitz transition, the point where the size of the Fermi surface is tuned continuously to zero. We study the novel transport properties around this point as a function of temperature and magnetic field and present ideas of possible new states of matter that may form at low temperatures. Pure insulating SrTiO₃ is close to a ferroelectric quantum critical point which is well understood by the quantum self-consistent phonon model and exhibits striking dielectric behaviour. By tuning with chemical substitution or gate voltages, insulating SrTiO₃ and related materials undergo a transition into the metallic state and then become superconducting. Superconductivity appears to arise in the anti-adiabatic limit where the Fermi energy is smaller than the energy scales of the pairing bosons. We discuss how the polar optical phonons present close the quantum critical point can lead to a strong binding energy for electrons over a range of carrier concentrations and present new experimental data on SrTiO₃ in its metallic and superconducting states.

Fr.A-P64 - Semi-epitaxial SmB₆ thin films prepared by the molecular beam epitaxy

H. Shishido^{1,2}, Y. Yoneda¹, T. Yoshida¹, S. Noguchi^{1,2,3}, T. Ishida^{1,2}

1. *Department of Physics and Electronics, Graduate School of Engineering, Osaka Prefecture University, Osaka, Japan*

2. *Institute of Nanofabrication Research, Osaka Prefecture University, Osaka, Japan*

3. *Nanoscience and Nanotechnology Research Center, Osaka Prefecture University, Osaka, Japan*

Rare-earth hexaboride compounds have been studied extensively for their various interesting properties. Although SmB₆ is known as a prototypical Kondo insulator [1], it has recently attracted a great deal of attention as a possible candidate of a 3D topological Kondo insulator [2]. Both theoretical and experimental works are suggestive of the appearance of topologically-protected metallic surface states at low temperatures in SmB₆ while the bulk is kept as an insulator. It is of crucial importance to realize epitaxial SmB₆ films for extending the researches. We grow thin films of SmB₆ by molecular beam epitaxy (MBE). Depositions were performed under ultra-high vacuum of below 10⁻⁶ Pa. Sm and B were evaporated by Knudsen cells with the atomic ratio of B/Sm ~ 6 on a MgO (100) substrate at temperatures from 750 to 1000 C .

Reflection high energy electron diffraction (RHEED) patterns show spotted ones indicating a relatively flat film surfaces. There are in good agreement with the surface roughness measured by the atomic force microscope (AFM). Interplane X-ray diffraction (XRD) patterns show only (00l) peaks of SmB₆, except substrate peaks. The (100) peak of SmB₆ appears as a main peak at inplane XRD patterns, while other (h k 0) peaks also observed. The phi-scan of the (100) peak shows 4 peaks in every 90 degrees, which corresponds to the four-fold symmetry of SmB₆. These results indicate that our SmB₆ thin films partly grow epitaxially. The electrical resistivity increases with decreasing temperature as a semiconductor, and becomes constant at low temperatures. These features well reproduce the tendency of the resistivity observed in bulk samples.

FR.B-P01 - The influence of Coulomb correlations on the tunneling transport through multi-electrons states in strongly coupled quantum dots

V. Mantsevich^{1,2}, N. Maslova^{1,2}, P. Arseyev^{1,2}

1. *Moscow State University, Moscow, Russia*

2. *P.N. Lebedev Physical Institute, Moscow, Russia*

We investigated tunneling processes in the system of two strongly coupled quantum dots with Coulomb correlations between localized electrons weakly interacting with the reservoirs. In the considered system the electrons number changing due to the tunneling processes leads to the modification of the energy spectrum, which is not reduced to the simple adding of Coulomb interaction value per electron. One, two, three or four electrons can be localized in the coupled QDs at the same moment, each state with fixed total charge and spin projection has it's own energy. Transitions between these states were analyzed in terms of pseudo-particle operators with constraint on the possible physical states of the system. Filling numbers of different multi-electron states, total electron occupation of quantum dots and I-V characteristics were investigated for different single electron levels positions relative to the sample Fermi level and various tunneling transfer rates.

It was shown that due to the presence of strong Coulomb correlations total electron occupation of the system can significantly decrease with increasing of applied bias when both single electron energy levels are situated below the Fermi level contrary to the situation with no correlations. Tunneling electron changes multi-particle states of QDs and pushes out electrons from the state below the Fermi level. We demonstrated that for some parameter range, the system demonstrates negative tunneling conductivity in certain ranges of the applied bias voltage due to the Coulomb correlations. We also revealed spin blockade effects in I-V characteristics of asymmetrical tunneling contact with two correlated coupled QDs. The spin blockade effect in our model manifests in the absence of a number of steps in the I-V characteristics, when asymmetrical tunneling contact is considered. We demonstrated, that correlated QDs can be used as an effective current switch key by changing the intensity of the external field.

FR.B-P02 - New state of matter

V. Shaginyan^{1,2,3}, M. Amusia^{1,2,3}, V. Stephanowich^{1,2,3}

1. *Petersburg Nuclear Physics Institute, National Research Center 'Kurchatov Institute', Moscow, Russia*
2. *Racah Institute of Physics, Hebrew University, Jerusalem, Israel*
3. *Institute of Physics, Opole University, Opole, Poland*

In many Fermi systems and compounds at zero temperature a phase transition happens that leads to a quite specific state called fermion condensation. As a signal of such a fermion condensation quantum phase transition serves unlimited increase of the effective mass of quasiparticles that determines the excitation spectrum and creates flat bands [1]. We have theoretically carried out a systematic study of the phase diagrams of strongly correlated heavy-fermion compounds, including heavy-fermion metals, high temperature superconductors, insulators with strongly correlated quantum spin liquid, quasicrystals, and two dimensional Fermi systems (like 3He), and have demonstrated that these diagrams have universal features. The obtained results are in good agreement with experimental facts. We have shown both analytically and using arguments based entirely on the experimental grounds that the data collected on these very different heavy-fermion compounds have a universal scaling behavior, and these materials with strongly correlated fermions can unexpectedly have a uniform behavior in spite of their microscopic diversity. Thus, the quantum critical physics of different heavy-fermion compounds is universal, and emerges regardless of the underlying microscopic details of compounds. This uniform behavior, induced by the universal quantum critical physics, allows us to view it as the main manifestation of the new state of matter. Our theoretical analysis of numerous experimental facts shows that the theory of fermion condensation develops completely good description of the non-Fermi liquid behavior of heavy-fermion compounds. Moreover, the fermion condensate can be considered as the universal reason for the non-Fermi liquid behavior observed in various heavy-fermion compounds [1].

[1] M. Ya. Amusia, K. G. Popov, V. R. Shaginyan, and W. A. Stephanowich, *Theory of Heavy-Fermion Compounds - Theory of Strongly Correlated Fermi-Systems*, Springer Series in Solid-State Sciences 182, (2014)

FR.B-P03 - Orbital-selective behavior and suppression of double exchange in dimerized systems

S. Streltsov^{1,2}, D. Khomskii³

1. *Institute of Metal Physics, Kiev, Ukraine*
2. *Ural Federal University, Sverdlovsk Oblast, Russia*
3. *University of Cologne, Köln, Germany*

We show that in transition metal compounds containing structural metal dimers there may exist in the presence of different orbitals a special state with partial formation of singlets by electrons on one orbital, while others are effectively decoupled and may give e.g. long-range magnetic order or stay paramagnetic. Similar situation can be realized in dimers spontaneously formed at structural phase transitions, which can be called orbital-selective Peierls transition. This can occur in case of strongly nonuniform hopping integrals for different orbitals and small intra-atomic Hund's rule coupling JH . Yet another consequence of this picture is that for odd number of electrons per dimer there exist competition between double exchange mechanism of ferromagnetism, and the formation of singlet dimer by electron on one orbital, with remaining electrons giving a net spin of a dimer. The first case is realized for strong Hund's rule coupling, typical for 3d compounds, whereas the second is more plausible for 4d-5d compounds. We discuss some implications of these phenomena, and consider examples of real systems, in which orbital-selective phase seems to be realized.

FR.B-P04 - Strong coupling theory for the Hubbard modelA. Sherman¹*1. Institute of Physics, University of Tartu, Tartu, Estonia*

In recent years, in connection with the discovery of iron-based superconductors and investigations of the influence of electron correlations on topological insulators, the interest has increased in the multi-band generalizations of the Hubbard model. For these model Hamiltonians it would be desirable to find an approach, which, being comparatively simple computationally, yields at least qualitatively correct results. As a possible candidate for such an approach the strong coupling diagram technique is considered in this work. The method is based on the expansion in powers of the kinetic energy. The elements of diagrams are on-site cumulants of creation and annihilation operators and hopping lines connecting cumulants on different sites. Despite the fact that by the construction the approach is intended for the strong coupling case, it gives the correct result for vanishing Hubbard repulsions U . The approach leads to a set of equations for the electron Green's function, which can be self-consistently solved. At half-filling, for the semi-elliptical density of states (DOS) as well as for the two-dimensional t - U and t - t' - U models these equations describe the Mott transition, which occurs at $U_c \approx 7\Delta/8$ with Δ the bandwidth. This value is close (identical for the semi-elliptical DOS) to that obtained in the Hubbard-III approximation. By the positions of maxima, shapes and their variation with momentum and electron concentration n the calculated spectral functions are close to results of Monte Carlo simulations in the range $0.7 < n < 1.3$. Also the variation of the momentum dependence of occupation numbers with U is in satisfactory agreement with Monte Carlo data at half-filling. The behavior of the Mott gap is different in the t - U and t - t' - U models [1].

[1] A. Sherman, Physica B 456, 35 (2015); arXiv:1410.8289; arXiv:1501.03587.

FR.B-P05 - First-principles theory of momentum-dependent local ansatz for correlated electrons system

S. Chandra¹, Y. Kakehashi¹

1. *University of The Ryukyus*

Variational approach is a simple and useful method to describe the ground state properties of strongly correlated electron system. We have recently developed the momentum dependent local ansatz wavefunction method (MLA) [1]. The method describes electron correlations from the weak to strong Coulomb interaction regime by making use of the two particle correlators with momentum dependent variational parameters and a hybrid starting wavefunction. The MLA describes the momentum dependence of physical quantities and therefore describes well those associated with the low energy excitations such as the effective mass, going beyond the Gutzwiller wavefunction. In order to describe the realistic system and to go beyond the first-principles Gutzwiller method [2], we have extended the MLA to the first-principles version using the tight-binding LDA+U Hamiltonian [3]. We present here the first-principles MLA and some numerical results on the correlation energy, momentum distribution function, charge fluctuations, amplitude of local moments, as well as quasiparticle weight for Fe and Fe compounds. We found the distinct momentum dependence of the momentum distribution function, and that the jump at the Fermi level is monotonically decreased with increasing Coulomb and exchange interactions, indicating mass enhancement.

[1] M. Atiqur R. Patoary and Y. Kakehashi, J. Phys. Soc. Jpn. 82 (2013) 084710

[2] T. Schickling, F. Gebhard, J. Bünemann, L. Boeri, O. K. Andersen, and W. Weber, Phys. Rev. Lett. 108 (2012) 036406

[3] Y. Kakehashi, S. Chandra, D. Rowlands, and M. Atiqur R. Patoary, Mod. Phys. Lett. B Vol. 28 (2014) 1430007

FR.B-P06 - Thermodynamic properties of solid oxide fuel cell (SOFC) cathode material- $\text{Nd}_{1-x}\text{Sr}_x\text{CoO}_{3-\delta}$ R. Thakur¹, R.K. Thakur¹, N.K. Gaur¹*1. Barkatullah University, Bhopal*

Mixed ionic-electronic conductors (MIECs) containing Co with the capability to conduct oxygen ions and electrons simultaneously have been identified as strong potential IT-SOFC cathode candidates in recent years. The fact that rare-earth perovskite-type cobaltate are most suitable as a cathode material in solid oxide fuel cells (SOFC), makes the thermal behavior of these compounds highly important. As these compounds are predominantly ionic in nature hence the lattice contributions to the specific heat at constant volume ($C_{v(\text{lattice})}$) of $\text{Nd}_{1-x}\text{Sr}_x\text{CoO}_{3-\delta}$ ($0.1 \leq x \leq 0.8$) has been studied and thereby thermal expansion is computed as function of temperature by means of Modified Rigid Ion Model (MRIM) and found to be in good agreement with experimental values. We have systematically investigated the effect of phonons on thermal properties, Debye temperature (θ_D), molecular force constant (f), Reststrahlen frequency (ν), cohesive energy (ϕ), and Gruneisen parameter (γ) for $\text{Nd}_{1-x}\text{Sr}_x\text{CoO}_{3-\delta}$ ($0.1 \leq x \leq 0.8$). Also the effect of phonons on the bulk modulus is studied using the atoms in molecules (AIM) theory for $\text{Nd}_{1-x}\text{Sr}_x\text{CoO}_{3-\delta}$ ($0.1 \leq x \leq 0.8$). We have found that the computed properties reproduce well with the available experimental data, implying that MRIM represents properly the perovskite cobaltate $\text{Nd}_{1-x}\text{Sr}_x\text{CoO}_{3-\delta}$ ($0.1 \leq x \leq 0.8$). To our knowledge some of the properties for these complicated compounds are reported for the first time.

FR.B-P07 - Metal-Insulator Transition in 1T-TaS₂:: A real-space dynamical mean-field study

Y.Y. Zhao¹, J. Sun¹, L.J. Zou², Y. Song¹

1. *Department of Physics, Beijing Normal University*

2. *Key Laboratory of materials Physics, Institute of Solid State Physics, Chinese Academy of Science, P. O. Box 1129, Hefei 230031, China*

The experimental observation of an abnormal Mott insulator to metal transition in 1T – TaS₂ was assumed to be generated by the interplay between correlation and disorder[1]. Considering the stacking disorder in this compound, we take a theoretical analysis of the interplay of interactions and off-diagonal disorder in the one-dimensional extended Anderson-Hubbard model. We employ the real-space dynamical mean-field theory[2], which can treat correlation and disorder on an equal footing, to study the competition among the hopping disorder (W'), on-site interaction U , and on-site disorder W . We find that when $U = W = 0$, the density of states has a peak at $E = 0$ with increasing hopping disorder. We use the generalized inverse participation ratio (GIPR) as a measure of the localization [2,3], and find that the system is localized at finite W' . We also find that when $W=0$ and $U \neq 0$, the density of states has a Mott gap, but also has a peak at the half of the band width at large W' . The lattice size scaling of the GIPR indicates that the localization effect of the off-diagonal disorder is much weaker than that of the on-site disorder. As a result, the Mott gap cannot be closed by the off-diagonal disorder, differing significantly from the diagonal disorder. With this method, we also discuss the dependences of the optical conductivity $\sigma(\omega = 0, T)$ with U , W and W' .

[1]E.Lahoud, O.N.Meetei, K.B.Chaska, A.Kanigel, and N.Trivedi, PRL.112,206402(2014)

[2]Yun Song, R.Wortis, and W.A.Atkinson, PRB 77,054202(2008)

[3]N.C.Murphy, R.Wortis, and W.A.Atkinson, PRB 83,184206(2011)

FR.B-P08 - NMR relaxation in the topological kondo insulator SmB₆

P. Schlottmann¹

1. Florida State University, Tallahassee, United States

SmB₆ has been predicted to be a strong topological Kondo insulator and experimentally it has been confirmed that at low temperatures the electrical conductivity only takes place at the surfaces of the crystal. We study the temperature and magnetic field dependence of the NMR Knight shift and relaxation rate arising from the topological conduction states. For the clean surface the Landau quantization of the surface states gives rise to highly degenerate discrete levels for which the Knight shift is proportional to the magnetic field B and inversely proportional to the temperature T . The relaxation rate, $1/T_1$, is not Korringa-like. For the more realistic case of a surface with a low concentration of defects (dirty limit) the scattering of the electrons leads to a broadening of the Landau levels and hence to a finite density of states. The mildly dirty surface case leads to a T -independent Knight shift proportional to B and a Korringa-like $1/T_1$ at low T [1]. The wave functions of the surface states are expected to fall off exponentially with distance from the surface giving rise to a superposition of relaxation times, i.e. a stretched exponential. It is questionable that the experimental boron 11 Knight shift and relaxation rate [2] arise from the surface states of the TKI. An alternative explanation is that the bulk susceptibility and the boron 11 NMR properties are the consequence of the in-gap bulk states originating from magnetic exciton bound states proposed by Riseborough [3].

[1] P. Schlottmann. Phys. Rev. B 90, 165127 (2014)

[2] T. Caldwell et al., Phys. Rev. B 75, 075106 (2007)

[3] P. Riseborough, Phys. Rev. B 68, 235213 (2003)

FR.B-P09 - Magnetic hyperfine field at a Cd impurity diluted in RCo₂ at finite temperatures

A.L. de Oliveira¹, C. M. Chaves², N.A. de Oliveira³, A. Troper²

1. Instituto Federal de Educacao, Ciencia e Tecnologia do Rio de Janeiro, Campus Nilopolis, Rio de Janeiro, Brazil

2. Centro Brasileiro de Pesquisas Físicas, Rio de Janeiro, Brazil

3. Instituto de Fisica, Universidade do Estado do Rio de Janeiro, Rio de Janeiro, Brazil

The local magnetic moments and the magnetic hyperfine fields at an {s-p} Cd impurity diluted in inter-metallic Laves phase compounds RCo₂ (R = Gd, Tb) at finite temperatures are calculated. For other rare earth elements (light or heavy) the pure compounds display a magnetic first order transition and are not describable by our formalism.

The host has two coupled lattices (R and Co) both having itinerant d electrons but only the rare earth lattice has localized f electrons. They all contribute to the magnetization of the host and also to the local moment and to the magnetic hyperfine field at the impurity which occupies an R site. The investigation of magnetic hyperfine field in these materials then provides valuable information on the d itinerant electrons and also on the localized 4f magnetic moments.

For the d-d electronic interaction we use the Hubbard-Stratonovich identity thus allowing the employment of functional integral; the static saddle point approximation is also used. Our model reproduces quite well the experimental data.

FR.B-P10 - Magnetism in the three-dimensional layered Lieb lattice: Higher transition temperatures via flat-band and Van Hove singularitiesK. Noda¹, K. Inaba¹, M. Yamashita¹*1. NTT Basic Research Laboratories, Kanagawa, Japan*

Realizations of two-dimensional complex optical lattices, such as the honeycomb and Kagome lattices, provide new research fields of quantum magnetism. Here, we focus on the Lieb lattice (i.e., line-centered square lattice), which was created quite recently by the Kyoto group [1]. In this lattice, the flat-band, which leads to a delta-functional divergence of the density of states (DOS), induces exotic phenomena (i.e., magnetism, superconductivity, and topological properties). However, in 2D systems, strong quantum fluctuations rule out finite temperature transitions. This fact naturally turns our attention to the three-dimensional (3D) layered Lieb lattice [1], where we addressed the ground state properties [2].

In this study, we investigate magnetism with two-component fermions in the 3D layered Lieb lattice at half-filling and finite temperatures using the dynamical mean-field theory and an analytical method. In this lattice, when the ratio of the interlayer to intra-layer hoppings changes, there appear several types of divergent DOSs, such as the delta-functional flat-band singularity (FBS) and logarithmic Van Hove singularity (VHS). First, we numerically elucidate that these two singularities change the interaction U dependence of transition temperature T_C , which drastically raise T_C . To investigate this singularity effect in detail, next we offer an analytical framework. We obtain a characteristic transition temperature specific to the FBS: $T_C/W \propto U/W$ with bandwidth W . Furthermore, using this framework, we can describe T_C in the universal form represented with the Lambert function, which includes both the characteristic and conventional dependence: $T_C/W \propto e^{-1/\rho(E_F)U}$ with the DOS at the Fermi energy $\rho(E_F)$. We also reveal that the FBS induces an anomaly of double occupancy even in the paramagnetic state above T_C , which is a precursor phenomenon to the flat-band magnetic transition.

[1] Y. Takahashi, International Conference on Atomic Physics (ICAP) 2014 abstract

[2] K. Noda, K. Inaba, and M. Yamashita, Phys. Rev. A 90, 043624 (2014)

FR.B-P11 - Steady state dynamics in a model system of strongly correlated electrons: effective temperatures near local quantum criticality

F. Zamani¹, P. Ribeiro², S. Kirchner³

1. *Max Planck Institute for Physics of Complex Systems, Dresden, Germany*
2. *Russian Quantum Center, Business-center "Ural", Skolkovo village, Odintsovo district, Moscow, Russia*
3. *Center for Correlated Matter, Zhejiang University, Zhejiang, China*

Strongly correlated systems far from equilibrium have recently generated considerable interest. This interest has mainly been spurred by experimental progress in preparing and characterizing such systems out of equilibrium. The theoretical understanding on the other hand suffers from a lack of methods that can reliably treat strongly correlated systems in and out of equilibrium at an equal footing. Here, we present our results for the thermal and non-thermal steady-state scaling functions and steady-state dynamics in a model of local quantum criticality. Our model, the pseudogap Kondo model, allows us to obtain full scaling functions in and out of equilibrium. We also study the concept of effective temperatures for correlations far from equilibrium near fully interacting as well as weak coupling fixed points. In the vicinity of each fixed point we establish the existence of an effective temperature - different at each fixed point-such that the equilibrium fluctuation-dissipation theorem is recovered. Most interestingly, steady-state scaling functions in terms of the effective temperatures coincide with the equilibrium scaling functions in terms of the equilibrium temperature. This result extends to higher correlation functions as will be explicitly demonstrated.

FR.B-P12 - Pinball liquid phase from Hund's coupling in frustrated triangular geometry

A. Ralko¹, J. Merino², S. Fratini¹

1. *Neel Institute, Grenoble, France*

2. *Universidad Autónoma de Madrid, Madrid, Spain*

Materials with competing electronic interactions on triangular lattices are a fertile ground for novel phenomena and original quantum phases, such as the spin liquid behavior observed in organic (κ -(BEDT-TTF)₂Cu₂(CN)₃, Me₃EtSb[Pd(dmit)₂]₂) and inorganic (Cs₂CuCl₄) quasi-two-dimensional materials. Geometrical frustration can play a similar role in charge ordering phenomena leading to poorly understood unconventional metallic and superconducting states. Remarkable examples are found in the quarter-filled organic salts, the layered cobaltates and the transition metal dichalcogenide 1T-TaS₂.

Motivated by AgNiO₂, a layered oxide compound with a triangular planar lattice structure, whose properties reflect a rich interplay between magnetic, orbital and charge degrees of freedom exhibiting exotic symmetry broken phases, we have analyzed a multiband microscopic model which takes explicit account of electronic correlations to demonstrate that the emergence of charge ordered phases with unconventional metallic properties is a natural outcome in frustrated triangular oxides with both strong Coulomb interactions and Hund's coupling. By using complementary technics such as DMFT, Exact Diagonalizations and Generalized Hartree-Fock, we show that the combination of on-site and off-site repulsion and Hund exchange lead to the stabilization of a robust pinball liquid phase [1,2], a quantum phase where the charges spontaneously separate into coexisting localized (pins) exhibiting Mott physics and band-like itinerant electrons (balls) moving on a honeycomb lattice. We argue that the charge ordered metallic phase of AgNiO₂ is a neat experimental realization of such pinball liquid, which explains many of the observed experimental features such as the 3-fold ordering pattern, the strong charge disproportionation, the presence of large local moments and the 'bad' metallic behavior.

[1] Jaime Merino, Arnaud Ralko and Simone Fratini, *Phys. Rev. Lett.* 111, 126403 (2013)

[2] Arnaud Ralko, Simone Fratini and Jaime Merino, arxiv:1412.4696 (2014)

FR.B-P13 - A phenomenological approach to the metamagnetism in heavy fermion compounds

K. Matsumoto¹, S. Kosaka¹, S. Murayama¹

1. Muroran Institute of Technology, Hokkaido, Japan

A phenomenological theory is developed for the metamagnetism of heavy fermion compounds by the extension of the Landau theory for phase transitions. Firstly, we write down the extended Landau free energy density for the two sub-lattice Ising antiferromagnet. In this free energy density, the higher order terms of the sub-lattice magnetizations are also included. Secondly, by minimizing this free energy density with respect to the sub-lattice magnetizations, we can determine the equilibrium quantities as the functions of the applied magnetic field.

From this analysis the crossover behavior in the high magnetic field is indicated for the extended Landau free energy density. We regard some parameters of the extended Landau free energy density as the functions of temperature. Then, we can draw the magnetic phase diagrams resemble to the observed ones for CeRu_2Si_2 and $\text{Ce}(\text{Ru}_{0.92}\text{Rh}_{0.08})_2\text{Si}_2$.^{1),2),3)} The possibility of the first order transition for the metamagnetism is discussed.

1) J. Flouquet, P. Haen, S. Raymond, D. Aoki, and G. Knebel: *Physica B*319 (2002) 251

2) C. Sekine, T. Sakakibara, H. Amitsuka, Y. Miyako, and T. Goto: *J. Phys. Soc. Jpn.* 61 (1992) 4536

3) D. Aoki, C. Paulsen, H. Kotegawa, F. Hardy, C. Meingast, P. Haen, M. Boukahil, W. Knafo, E. Ressouche, S. Raymond, and J. Flouquet: *J. Phys. Soc. Jpn.* 81 (2012) 634711

FR.B-P14 - Novel spin and orbital orderings in the layered perovskite Sr_2CrO_4

T. Ishikawa¹, T. Toriyama¹, T. Konishi¹, H. Sakurai², Y. Ohta¹

1. Chiba University, Chiba, Japan

2. National Institute for Materials Science, Ibaraki, Japan

Recently, successive phase transitions were observed in Sr_2CrO_4 with the K_2NiF_4 -type crystal structure, where the lower-temperature transition at 112 K was attributed to the Néel antiferromagnetic ordering but the higher-temperature transition at 140 K remained a mystery [1]. Since the CrO_6 octahedra in this layered perovskite are elongated along the c-axis and the Cr ions are in the Cr^{4+} ($3d^2$) oxidation state, the simple crystal-field theory predicts that there should be no orbital degrees of freedom in this system and thus this material is to be an antiferromagnetic Mott insulator with spin $S = 1$. The discovery of the successive phase transitions is therefore quite a big surprise.

We carried out the density-functional-theory-based electronic structure calculations to elucidate the origin of the observed successive phase transitions. We then obtained the electronic structure that exhibits the spin and orbital orderings in the ground state. From the analysis of the state, we found that this material consists of two subsystems: (i) a Kugel-Khomskii-type spin-orbital subsystem consisting of the dxz and d_{yz} orbitals of Cr and (ii) an antiferromagnetic Heisenberg subsystem consisting of the d_{xy} orbitals of Cr.

The two subsystems then couple via the Hund's ferromagnetic exchange interaction on the two-dimensional CrO_2 plane, and thus the novel spin-antiferro and orbital-antiferro state is realized in its ground state. We argue that the higher (lower) temperature phase transition is explained to be due to the ordering of the orbital (spin) degrees of freedom.

[1] H. Sakurai, J. Phys. Soc. Jpn. 83, 123701 (2014)

FR.B-P15 - Quantum disordered phase in the frustrated honeycomb Hubbard model

H. Nishida¹, K. Misumi¹, T. Kaneko¹, Y. Ohta¹

1. Chiba University, Chiba, Japan

The metal-insulator transition of Dirac fermions and possible occurrence of the quantum disordered (or spin-liquid) phase are studied for the frustrated honeycomb Hubbard model at half filling by means of the variational cluster approximation (VCA). The frustration in the spin degrees of freedom is introduced by the next-nearest-neighbor hopping parameters. We show that the antiferromagnetism in the Mott insulator phase is suppressed by the effects of spin frustrations in the intermediate and strong coupling regions, resulting in a possible realization of the quantum disordered (or spin-liquid) phase in the vicinity of the Dirac semimetallic phase.

This disordered phase is discussed in relation to that of the frustrated honeycomb Heisenberg model achieved in the strong-coupling region of our model.

FR.B-P16 - Charge-density wave and exciton condensation induced by Coulomb interaction and electron-phonon interaction in 1T-TiSe₂

H. Watanabe¹, K. Seki², S. Yunoki^{1,2}

1. RIKEN CEMS, Saitama, Japan

2. RIKEN, Saitama, Japan

Transition metal dichalcogenides (TMDCs) exhibit various quantum phases and have been extensively studied for more than forty years. However, the origin of these quantum phases such as charge-density wave (CDW) and superconductivity has not been fully understood because of the complicated competition among Coulomb interaction, electron-phonon interaction, and spin-orbit interaction, which are believed to be important in TMDCs. Recently, 1T-TiSe₂, one of the typical examples of TMDCs, has attracted much interests in the context of exciton condensation. The exciton condensation is a quantum phenomenon, where bound electron-hole pairs (excitons) are macroscopically condensed in a semimetal or a semiconductor. Although the exciton condensation has been proposed to be the origin of the CDW in 1T-TiSe₂, the static lattice distortion observed in CDW phase indicates a strong coupling between electron and lattice degrees of freedom and thus the band Jahn-Teller effect is also a possible origin of the CDW.

To clarify the origin of the CDW in 1T-TiSe₂, we study the two-band Hubbard model in a triangular lattice with the electron-phonon interaction. By using the variational Monte Carlo method, both the electronic and lattice degrees of freedom are treated beyond the mean-field approximation. We show that the cooperation between the Coulomb interaction and the electron-phonon interaction is essential to induce the exciton condensation and the resulting CDW phase in the model for 1T-TiSe₂. The strong-coupling BEC-type exciton condensation is proposed for 1T-TiSe₂ by investigating the nature of an electron-hole pair of the exciton. We also study the same model in a square lattice and discuss the importance of lattice structure and Fermi surface nesting on the stability of excitation condensation.

FR.B-P17 - Anomalous influence of an external magnetic field on the electron energy spectrum of ferromagnetic semiconductors with strong p,d-hybridization

A. Povzner¹, A. Volkov¹, K. Shumikhina¹

1. Ural Federal University, Sverdlovsk Oblast, Russia

Anomalous influence of an external magnetic field on the electron energy spectrum of ferromagnetic semiconductors with strong p,d-hybridization. A. A. Povzner, A. G. Volkov, K. A. Shumikhina Ural Federal University, Russia a.a.povzner@urfu.ru, agvolkov@yandex.ru.

The influence of magnetic field on properties of the hybridized pd-electrons studied for thin films of ferromagnetic semiconductors. The initial states of p-electrons were describe by model of nearly free electrons, and strongly correlated d-electrons - by Hubbard model. The total Hamiltonian includes the term electron hopping between the p- and d-states at different sites. It was show that hybridization of p- and d-electrons leads to a picture of bands, separated by hybridization gap, the states of which are splitted and shifted in energy by stochastic internal exchange and charge fields. As a result, a narrow band of heavy fermions appears in hybridization gap. The scattering of electrons by the electron density fluctuations leads to appearance strong damping of the electron states in heavy fermions band. The energy width of these states can be expressed as Γ , where μ is amplitudy of spin fluctuation, M and h are homogeny magnetization and magnetic field, T is temperature, λ is mode-mode coupling constant. The influence of magnetic field on the spectrum explains negative magnetoresistive and magnetorefractive effects. The temperature dependence of mode-mode coupling constant has a maximum in the ferromagnetic vicinity of the Curie point T_C . This fact stipulates an anomalously strong suppression of spin fluctuations by the magnetic field that leads to sharp decrease of Γ . Temperature and field dependences of Γ simultaneously describes colossal magnetoresistive and magnetorefractive effects, as well as the red shift of fundamental absorption edge. At T_C the amplitude of the spin fluctuations increases slightly. Therefore the fundamental absorption edge is almost unchanged compared to the ferromagnetic region. However, its field dependence is not anomalous.

FR.B-P18 - Quantum disordered phase in the triangular-lattice Hubbard model with next-nearest-neighbor hoppingK. Misumi¹, T. Kaneko¹, Y. Ohta¹*1. Chiba University, Chiba, Japan*

Magnetic ordering and metal-insulator transition (MIT) in the triangular-lattice Hubbard model have been one of the central issues in physics of frustrated strongly-correlated electron systems. In the isotropic triangular-lattice Hubbard model, it is known that a 120° Néel order appears in the strong-coupling region and a quantum disordered state exists near the MIT phase boundary [1,2]. Recently, the magnetic orders of the triangular-lattice J1-J2 Heisenberg model with the nearest-neighbor (J1) and next-nearest-neighbor (J2) interactions were studied by the many-variable variational Monte Carlo method, whereby the change from the 120° Néel order to the collinear order with increasing J2, as well as the quantum disordered state in-between, was predicted [3].

Motivated by such developments in the field, we here study the frustration and magnetic orders in the triangular-lattice Hubbard model at half filling with the nearest-neighbor (t_1) and next-nearest-neighbor (t_2) hopping parameters. We employ the variational cluster approach [4], which takes into account the short-range electron correlations exactly, and thus is very useful for studying the magnetic orders in the frustrated Hubbard model. We will thereby present the magnetic phase diagram of this model at zero temperature by calculating the magnetic order parameters. We will moreover show the appearance of the quantum disordered state between these two states. We will also discuss the MIT of this model by calculating the parameter dependence of the single-particle spectral function, and show that the quantum disordered state also appears in the vicinity of the MIT phase boundary.

[1] P. Sahebsara and D. Séhéal, Phys. Rev. Lett. 100, 136402 (2008)

[2] T. Yoshioka, A. Koga, and N. Kawakami, Phys. Rev. Lett. 103, 036401 (2009)

[3] R. Kaneko, S. Morita, and M. Imada, J. Phys. Soc. Jpn. 83, 093707 (2014)

[4] M. Potthoff, M. Aichhorn, and C. Dahnken, Phys. Rev. Lett. 91, 206402 (2003)

FR.B-P19 - The Hubbard model beyond the two-pole approximation: a composite operator method study

A. Avella¹

1. Università Degli Studi Di Salerno - Dipartimento Di Fisica, Milan, Italy

Within the framework of the Composite Operator Method, a three-pole solution for the two-dimensional Hubbard model is presented and analyzed in detail [1]. In addition to the two Hubbard operators, the operatorial basis comprises a third operator describing electronic transitions dressed by nearest-neighbor spin fluctuations. These latter, compared to charge and pair fluctuations, are assumed to be preeminent in the region of model-parameter space - small doping, low temperature and large on-site Coulomb repulsion - where one expects strong electronic correlations to dominate the physics of the system. This assumption and the consequent choice for the basic field, as well as the whole analytical approximation framework, have been validated through a comprehensive comparison with data for local and single-particle properties obtained by different numerical methods on varying all model parameters. The results systematically agree, both quantitatively and qualitatively, up to coincide in many cases. Many relevant features of the model, reflected by the numerical data, are exactly caught by the proposed solution and, in particular, the crossover between weak and intermediate-strong correlations as well as the shape of the occupied portion of the dispersion. A comprehensive comparison with other n-pole solutions is also reported in order to explore and possibly understand the reasons of such good performance. [Eur. Phys. J. B 87, 45 (2014)]

FR.B-P21 - The influence of the interband Coulomb interaction and the f -electron hopping on excitonic correlations in the extended Falicov Kimball model

P. Farkasovsky¹

1. Institute of Experimental Physics, Slovak Academy of Sciences, Bratislava, Slovakia

The density-matrix-renormalization-group method (DMRG) is used to examine effects of the interband Coulomb interaction between f and d electrons as well as the f -electron hopping on the stability of the excitonic phase in the one-dimensional Falicov-Kimball model (FKM) with local hybridization. It is found that the interband Coulomb interaction dramatically enhances the excitonic $P_{df} = \langle n_{d+1} n_f \rangle$ average and that this effect is especially strong in the limit of small hybridization, where the interacting $P_{df}(U)$ excitonic value is enhanced several hundred times in comparison to its non-interacting $P_{df}(U = 0)$ value. The further increase in P_{df} is observed due to the non-zero f -electron hopping, but these changes are considerable only if the d and f bands have the opposite parity. In addition, the examination of the interplay between the excitonic effects and the charge density wave (CDW) instability showed that the CDW and excitonic phase coexist up to relatively large values of local hybridization ($V \sim 0.12$). The complete phase diagram of the model in the $V - U$ plane is presented.

FR.B-P22 - Microscopic model of full magnetic phase-diagram of itinerant ferromagnet UGe₂

M. Abram¹, M. Wysokiński¹, J. Spałek^{1,2}

1. Marian Smoluchowski Institute of Physics, Jagiellonian University, ulica Łojasiewicza 11, PL-30-348 Kraków, Poland

2. Academic Centre for Materials and Nanotechnology, AGH University of Science and Technology, Aleja Mickiewicza 30, PL-30-059 Kraków, Poland

We provide [1, 2] the microscopic model which provides a fairly complete description of the electronic and magnetic properties of UGe₂. It is based on the Anderson-lattice model treated in the modified Gutzwiller approximation (SGA) [3]. We explain the appearance of the experimentally observed magnetic phases, namely strong-ferromagnetism, weak-ferromagnetism, as well as the transition to paramagnetism. We show that the sequence and evolution of those phases in the applied magnetic field can be explained in a natural manner as an effect of the competition between the Coulomb repulsion of the uranium 5f electrons and the hybridization of f-electrons with the conduction electrons [1]. We track the evolution of classical and quantum critical points in applied field, as a function of pressure, and of the total electron concentration [2]. We simulate the effect of the pressure applied to the real system. We argue, that the main effect of pressure is to change the hybridization strength. We discuss also the effect of the f-level position with the increasing pressure, as well as the possibility of crossing the Hill limit when the overlap between f-orbitals turns out to be nonzero. Our approach explains in a semiquantitative manner the recent experimental results [4].

[1] M. M. Wysokiński, M. Abram, and J. Spałek, Ferromagnetism in UGe₂: A microscopic model, Phys. Rev. B 90, 081114(R) (2014)

[2] M. M. Wysokiński, M. Abram, and J. Spałek, Criticalities in the itinerant ferromagnet UGe₂, Phys. Rev. B 91, 081108(R) (2015)

[3] M. Abram, J. Kaczmarczyk, J. Jędrak, J. Spałek, d-wave superconductivity and its coexistence with antiferromagnetism in the t-J-U model: Statistically consistent Gutzwiller approach, Phys. Rev. B 88, 094502 (2013)

[4] V. Taufour, D. Aoki, G. Knebel, and J. Flouquet, Tricritical Point and Wing Structure in the Itinerant Ferromagnet UGe₂, Phys. Rev. Lett. 105, 217201 (2010); H. Kotegawa, V. Taufour, D. Aoki, G. Knebel, and J. Flouquet, Evolution toward Quantum Critical End Point in UGe₂, J. Phys. Soc. Jpn. 80, 083703 (2011)

Support of the National Science Centre (NCN), Grant MAESTRO, No. DEC-2012/04/A/ST3/00342 and of the Foundation for Polish Science (FNP), grant TEAM is acknowledged

FR.B-P23 - Theoretical study of charge-spin-orbital fluctuations in mixed valence spinels: AlV_2O_4 and LiV_2O_4 A. Uehara¹, H. Shinaoka², Y. Motome¹1. *The University of Tokyo, Tokyo, Japan*2. *ETH Zürich, Zürich, Switzerland*

We theoretically investigate the fluctuations in charge, spin, and orbital degrees of freedom in spinel oxides AB_2O_4 . As the B cations comprise a pyrochlore lattice, the mixed valence spinels are a good playground for the interplay of multiple degrees of freedom on the geometrically frustrated lattice structure. In the present study, we focus on two spinels, AlV_2O_4 and LiV_2O_4 , which show puzzling, contrasting behavior despite the common structure: AlV_2O_4 exhibits a peculiar structural phase transition with a self-organization of seven V clusters (heptamers) at 700 K, while LiV_2O_4 does not show any transition down to the lowest temperature except for crossover to an unconventional heavy fermion state at 20-30 K. In order to clarify the origin of the contrasting behavior, we adopt the combined method between the first-principles calculation and the perturbation in terms of electron correlations. Specifically, we construct the multiband Hubbard model by the maximally-localized Wannier function analysis for the LDA band structure. We then calculate the generalized susceptibility, which includes all the information of fluctuations in charge, spin, and orbital sectors, by the random phase approximation. For AlV_2O_4 , we find that the dominant fluctuations appear in the vicinity of the center of the Brillouin zone. We unveil that peculiar charge fluctuations are sensitively enhanced by the inter-site Coulomb interaction. The enhanced fluctuations are of sigma-bonding type with strong orbital dependence. The importance of similar sigma-bonding states in the heptamer formation was suggested in the previous studies. Hence, our results provide a key for understanding of the self-organization in AlV_2O_4 . In contrast, for LiV_2O_4 , we find that the on-site interaction enhances the optical-type spin fluctuations at an incommensurate wave number. This fluctuation is enhanced at very low temperature, in the order of 10 K, which is suggestive of the peculiar heavy fermion behavior in LiV_2O_4 .

FR.B-P24 - Dynamical characteristics of the Mott transition: examination of doublon dynamics in a triangular-lattice Hubbard model

T. Sato¹, H. Tsunetsugu²

1. *RIKEN, Tokyo, Japan*

2. *The Institute for Solid State Physics, The University of Tokyo, Tokyo, Japan*

Mott transition has been understood theoretically as the singularity in the density of doublon or holon. Correlations between doublon and holon have also been studied theoretically, and it was suggested that they form a bound state in the insulating phase and the Mott transition is characterized by its binding and unbinding. Recent studies of the Mott transition include dynamical characteristics. Some theoretical groups examined dynamical spin and charge susceptibilities as optical conductivity and reported a clear difference in the spin and charge dynamics between in the metallic and in the insulating phases. However, dynamics of doublons has not been well understood. We have numerically studied dynamics of doublons near the Mott transition in the half-filled Hubbard model on a triangular lattice. By means of a cluster dynamical mean field theory with a continuous-time quantum Monte Carlo solver, we examine the change in the nearest-neighbor (NN) and on-site (OS) dynamical correlations of doublon with varying the Coulomb repulsion at a fixed temperature. Our results for the dynamical correlations show clear differences between in the metallic and in the insulating phases. We demonstrate that a NN doublon-holon pair shows a strong attractive correlation, particularly in the insulating phase, while the NN pairs of doublons or holons show a repulsive correlation. The short-time dynamics of the NN doublon and holon in the metallic phase show larger fluctuations than in the insulating phase. In the long-time region, the metallic phase has persistent fluctuations in NN configurations, while the fluctuations quickly vanish in the insulating phase. Investigating the OS dynamical correlation of doublon, we have found that the lifetime of doublon is longer in the metallic phase than in the insulating phase [Phys. Rev. B **90**, 115114 (2014)].

FR.B-P26 - Theoretical study of non-fermi liquid behavior in Pr 1-2-20 compoundsA. Tsuruta¹, K. Miyake²1. *Osaka University, Osaka, Japan*2. *Toyota Physical and Chemical Research Institute, Aichi, Japan*

Non-Fermi liquid behaviors in the resistivity have been reported in PrV₂Al₂₀ [1] and PrIr₂Zn₂₀ [2]. Namely, the electrical resistivity is proportional to $T^{0.5}$. The Specific heat increases like $C_0 - C_1 T^{0.5}$ as T decreases. The ground state of the crystalline-electrical field (CEF) of the local f -electron is considered to be the Γ_3 non-Kramers doublet in $4f^2$ configuration. Such a system with the Γ_3 CEF ground state in f^2 configuration is expected to exhibit an anomalous behavior associated with the two-channel Kondo effect. Tsuruta et al. investigated electronic states in the M -channel Anderson lattice model using the expansion from the limit of large spin-orbital degeneracy N ($1/N$ -expansion) [3]. The inclusion of the self-energy in $O((1/N)^0)$ leads to heavy electrons with degeneracy of channel and spin-orbit. In the single channel case, the imaginary part of the self-energy of conduction electrons (ISE) shows the Fermi liquid behavior: i.e. ISE is given by a form proportional to T^2 owing the inter-site correlation effects in higher order terms in power of $1/N$. In the two-channel case, however, a T -linear term in ISE at the Fermi level, in contrast to a T^2 -term in the Fermi liquid is found. However, the T -linear dependence of ISE is restricted in the asymptotic region of $T=0$, but a $T^{0.5}$ -dependence appears in a rather wide temperature region.

Because of the anomalous T -dependence of ISE, the chemical potential is given by $\mu_0 - \mu_1 T^{0.5}$, and the specific heat is given by $C_0 - C_1 T^{0.5}$. We also obtain the scaling behavior $f(T/T_K)$, T_K is the quadrupole Kondo temperature, in electrical resistivity, chemical potential, specific heat and magnetic susceptibility, explaining non-Fermi liquid properties observed in Pr 1-2-20 compounds.

[1] A. Sakai and Nakatsuji, J. Phys. Soc. Jpn. 80, 063701 (2011)

[2] T. Onimaru et. al., Phys. Rev. Lett. 106, 177001 (2011)

[3] A. Tsuruta et. al., J. Phys. Soc. Jpn. 68, 1067 (1999)

FR.B-P27 - Theory of dilution effect in orbital kondo systems

T. Mutou¹, Y. Miyamoto¹, H. Kusunose²

1. *Shimane University, Shimane, Japan*

2. *Ehime University, Ehime, Japan*

To clarify the origin of characteristic behavior in temperature dependence of transport properties observed in Pr 1-2-20 systems, the periodic Anderson model (PAM) with orbital degeneracy is investigated by the dynamical mean-field approach. In Pr 1-2-20 systems, it is considered that the characteristic behavior that is different from usual Fermi-liquid behavior arises from the orbital degrees of freedom of f electrons in Pr ions. Since there is the Coulomb repulsive interaction between these f electrons, it is also important to treat the electron correlation appropriately. In the present study, we adopt the dynamical mean-field theory (DMFT) to treat the electron correlation and use the non-crossing approximation (NCA) as an impurity solver in the DMFT scheme. The NCA is based on the perturbation theory with respect to the hybridization energy between f electrons and conduction electrons, and it is applicable to the system with orbital degeneracy. Moreover, magnetic-ion-dilution effects on the strongly correlated electron system with orbital degeneracy are also investigated. To treat dilution effects, the coherence potential approximation (CPA) is adopted. By the hybrid scheme of the DMFT and the CPA, correlation effects and dilution effects on thermodynamic properties and transport properties of the PAM with orbital degeneracy are studied.

FR.B-P28 - Excitonic phases in the two-band Hubbard model with electron-phonon couplingT. Kaneko¹, Y. Ohta¹*1. Department of Physics, Chiba University, Chiba, Japan*

The excitonic phases often referred to as the excitonic insulators were predicted half a century ago to occur in a small band-gap semiconductor or a small band-overlap semimetal and were described by the quantum condensation of excitons [1]. Recently, a number of candidate materials for the excitonic phases have been suggested [2-4]. From the theoretical standpoint, if we take into account the electron-electron interactions only, the spin-triplet excitonic phase is stabilized due to Hund's rule coupling [5]. However, the excitonic phase in the candidate materials 1T-TiSe₂ and Ta₂NiSe₅ was described in terms of the spin-singlet excitons and the importance of electron-phonon coupling was pointed out.

Motivated by the above development in the field, we investigate the stability of the spin-singlet excitonic phase in the two-band Hubbard model with electron-phonon coupling. To discuss the stability of the spin-singlet excitonic state, we use the mean field theory and variational cluster approximation. We first show that inter-band (excitonic) Coulomb interaction and electron-phonon interaction cooperatively stabilize the charge density wave (CDW) state. However, if we introduce the Hund's rule coupling, we find that the excitonic spin-density-wave (SDW) state competes with the CDW state obtained, and becomes the most stable state. The ground state phase diagram of the CDW and SDW states is drawn in the parameter space.

[1] B. I. Halperin and T. M. Rice, Rev. Mod. Phys. 40, 755 (1968)

[2] H. Cercellier et al., Phys. Rev. Lett. 99, 146403 (2007)

[3] Y. Wakisaka et al., Phys. Rev. Lett. 103, 026402 (2009)

[4] T. Kaneko et al., Phys. Rev. B 87, 035121 (2013)

[5] T. Kaneko and Y. Ohta, Phys. Rev. B 90, 245144 (2014)

FR.B-P29 - Nonequilibrium dynamics of a periodically-driven impurity spin coupled to the bath of ultracold fermions by Kondo coupling

K. Iwahori¹, N. Kawakami¹

1. Department of Physics, Kyoto University, Kyoto, Japan

The dynamics of a single impurity in a fermionic or bosonic bath is one of the fundamental problems in condensed matter physics, and plays an important role in the polaronic systems, X-ray absorption problem, Kondo effect and so on. Recently, these impurity problems are studied in the ultracold atomic systems. For example, a polaronic system is experimentally realized[1], and the realization of Kondo effect is theoretically proposed[2]. By utilizing their high controllability, dynamics of impurity driven by the time-dependent external field is also studied[3,4].

In this presentation, we study the periodically-driven impurity spin dynamics coupled to an ultracold fermionic bath by Kondo coupling. In general, it is difficult to solve the dynamics of the quantum system with periodic driving analytically. Thus we consider the case that the external field changes values discretely in time and the Hamiltonian is at the special point in the parameter space at which we can solve each time-step analytically, and thereby treat the full dynamics exactly.

We calculate the time-dependence of the impurity spin and the magnetization of bath fermions in the cases of rectangular field and sinusoidal field. As a result, we find that their characteristic behavior changes with the field-intensity, the field-frequency, and the Kondo temperature. For example, when the field-intensity is very large, the time-dependence of the impurity spin shows an oscillation whose period is inversely proportional to the field-intensity. We also find that another time scale, which is given by the inverse of the Kondo temperature, governs the response of the system to the external field.

References:

- [1] A.Schirotzek et al., Phys. Rev. Lett. 102, 230402 (2009)
- [2] J.Bauer et al., Phys. Rev. Lett. 111, 215304 (2013)
- [3] M.Knap et al., Phys. Rev. Lett. 111, 265302 (2013)
- [4] M.Knap et al., Phys. Rev. X 2, 041020(2012)

FR.B-P30 - Asymmetric thermal lineshape broadening in the dimerised antiferromagnet BaCu₂V₂O₈E. Klyushina^{1,2}, B. Lake^{1,2}, N. Islam¹, E. Wheeler³, J. Park⁴, B. Klemke¹*1. Helmholtz-Zentrum Berlin, Berlin, Germany**2. Technischen Universität Berlin, Berlin, Germany**3. Institut Laue-Langevin, Grenoble, France**4. Forschungs-Neutronenquelle Heinz Maier-Leibnitz, Munich, Germany*

Despite the conventional picture which suggests symmetric Lorentzian broadening of magnetic excitations as temperature is increased, the magnets, where the excitations strongly interact with each other, display asymmetric thermal lineshape broadening [1,2]. In present work we investigate the highly dimerised one-dimensional (1D) antiferromagnet BaCu₂V₂O₈ which is a potential candidate for the observation of asymmetric thermal line shape broadening. BaCu₂V₂O₈ has a tetragonal symmetry where the magnetic Cu²⁺ ions (spin-1/2) form alternating spiral chains along the c-axis. Our inelastic neutron scattering measurements on a single crystal of BaCu₂V₂O₈ reveal that the magnetic excitations consist of two excitation branches, which have a gap of 36meV and disperse along the L direction over the energy range 36-46 meV. Both modes are dispersionless in the H and K directions implying that the dimers are coupled together one-dimensionally along the c-direction, but with negligible coupling within the a-b plane. The large ratio of gap to bandwidth (=3.6) in BaCu₂V₂O₈ make this a candidate compound for detailed observation of asymmetric thermal lineshape broadening over a wide temperature range. The analysis of the high resolution energy scans, which were measured at the dispersion minima at different temperatures, reveals that the line shape becomes asymmetry with increasing temperature which can be attributed to strong correlations between the excitations and confirms that the excitations in highly dimerised 1D magnetic systems behave as a 1D strongly correlated gas of Bosons[2].

[1] D. L. Quintero-Castro, B. Lake, et al Phys. Rev. Lett. 109, 127206 (2012)

[2] D. Tennant, B. Lake, , et al. Phys. Rev. B 85, 014402 (2012)

FR.B-P32 - Metal-insulator transition in the two-dimensional Hubbard model studied by the dual-fermion method

A. Tanaka ¹,

1. Hiroshima University, Hiroshima, Japan

Although numbers of studies have been devoted to the metal-insulator transition in the two-dimensional Hubbard mode, it is still a subject of debate. The difficulty mainly arises from the fact that long-range antiferromagnetic order cannot be stable at finite T in two dimension because of the Mermin-Wagner theorem. Therefore, to describe the electronic state of the model, the theory must be taken into account not only the effects of the on-site Coulomb repulsion but also the long-range antiferromagnetic fluctuation properly. Unfortunately, the state-of-art dynamical mean field theory (DMFT) and its extension to the clusters are only capable for short-range correlation. However, the dual fermion approach (DFA), which is recently developed perturbative extension of DMFT, can incorporate the effects of long-range correlation.

The purpose of this study is to clarify the feature of the metal-insulator transition in the square-lattice Hubbard model at half-filling in relation to the spectral function by means of DFA. Unlike all other DFA calculations, where the continuous-time quantum Monte Carlo method is used to solve the effective Anderson impurity problem, the Lanczos exact-diagonalization technique is applied. This technique is advantageous to access low temperatures and obtain accurate spectral functions on the real axis.

The U - T phase diagram obtained in this study is completely different from that of DMFT. For large U (U/t 6.5-8.0), a drastic change in spectral shape is occurs at the metal-insulator transition and a clear pseudo-gap ~ 0.6 is appeared. On the other hand, the change is more gentle for smaller U , and the temperature at which clear gap opens is rapidly decrease with decreasing U from $T/t \sim 0.12$ and is reached $T/t < 0.01$ at $U/t=2.5$. Above this temperature non-Fermi liquid phase is present within the area where paramagnons prevail.

FR.B-P33 - Phase diagrams and phase transformations in S=1 spin- and pseudospin systemsA. Moskvina¹, Y. Panov¹, F. Rybakov², V. Konev¹, E. Vasinovich¹, V. Ulitko¹, A. Borisov²

1. Ural Federal University, Ekaterinburg, Russia

2. Institute of Metal Physics UD RAS, Ekaterinburg, Russia

At variance with quantum $s=1/2$ systems the Hamiltonian of $S=1$ spin lattices in general is characterized by several additional terms such as a single ion anisotropy, biquadratic isotropic and anisotropic exchange couplings, that results in their rich phase diagrams. Interestingly, the $S=1$ pseudospin formalism can be used to study an extended Bose-Hubbard model (EHBM) with truncation of the on-site Hilbert space to the three lowest occupation states $n = 0, 1, 2$ (semi-hard bosons). The EHBM Hamiltonian includes the on-site density-density interaction (the on-site pseudospin axial anisotropy), inter-site density-density interactions (the Ising pseudospin term), the one- and two-particle bosonic transport terms (the inter-site XY pseudospin anisotropy), and the chemical potential term (the pseudospin Zeeman coupling). Generalized non-Heisenberg effective $S=1$ pseudospin Hamiltonian does provide a physically clear description of different phases from uniform Mott insulating phases and density waves to two types of superfluids and supersolids. In the strong on-site attraction limit of the model we arrive at the Hamiltonian of the hard-core bosons which was earlier considered to explain the cuprate high- T_c superconductivity. Here we report results of the analysis of a simplified $S=1$ (pseudo)spin Hamiltonian with a two-particle transport term (inter-site biquadratic anisotropy) in frames of a generalized mean-field approximation (MFA), which takes into account the quantum description of the $S=1$ on-site states, as well as classical and quantum Monte-Carlo (QMC) technique. Using the MFA and two different QMC methods, the standard stochastic series expansion (SSE) with loop updates and a continuous time world-line QMC, we have obtained the ground-state and finite-temperature phase diagrams of the (pseudo)spin systems given different values of the coupling parameters. Making use of a special algorithm for CUDA architecture for NVIDIA graphics cards, a nonlinear conjugate-gradient method to minimize energy functional, and Monte-Carlo technique, we directly observed forming of the ground state configuration with lowering the temperature, allowing us to look upon the nucleation of the odd domain structure and vortex-like topological defects.

The work was supported by the Government of the Russian Federation Program 02.A03.21.0006 and by the Ministry of Education and Science of the Russian Federation, projects Nos. 1437 and 2725.

FR.C-P01 - Imaging of condensed quantum states in the quantum hall effect regime

J. Oswald¹, R. Römer²

1. Institute of Physics, Montanuniversity Leoben, Leoben, Austria

2. Department of Physics, University of Warwick, Coventry, United Kingdom

It has been proposed already some time ago that Wigner crystallization in the tails of the Landau levels may play an important role in the quantum Hall regime [1]. Here we use numerical simulations for modelling condensed quantum states and propose real space imaging of such highly correlated electron states by scanning gate microscopy (SGM). The ingredients for our modelling are a many particle model, that combines a self-consistent Hartree Fock calculation for the steady state with a non-equilibrium network model for the electron transport, as introduced in Ref. 2.

When there exists a condensed many particle quantum state in our electronic model system, our model shows that the response pattern of the total sample current as a function of the SGM tip position delivers detailed information about the geometry of the underlying quantum state. For the case of a ring shaped dot potential in the few electron limit it is possible to find regimes with a rigid (crystalline) charge distribution in the ring, where the SGM pattern corresponds to the probability density of the many body quantum states. The existence of the SGM image can be interpreted as the manifestation of an electron solid, since the pattern generation of the charge distribution requires a certain stability against the moving tip potential.

[1] Yang K, Haldane FDM, Rezayi EH, Physical Review B 64, 81301 (2001)

[2] C. Sohrmann, J. Oswald, R.A. Römer R.A., "Quantum percolation in the quantum Hall regime", Lecture Notes in Physics 762, pp. 163-193 (2009)

FR.C-P05 - Electronic structures and the spin-splittings in ullmannite-type structure compounds

H. Harima¹

1. Kobe University, Kobe, Japan

A variety of physical properties in crystals are produced by the interplay between electrons on the specific atomic arrangement. A mineral ullmannite NiSbS belongs to the tetrahedral class T. This is the lowest symmetry class of the isometric (cubic) system. Other ternary compound minerals called changchengite, (IrBiS) gersdosffite (NiAsS) and michenerite ((Pd, Pt)BiTe) belong to the same space group #198 (P213, T4), which is the same as for the famous MnSi. In contrast to the unique magnetic properties realized in MnSi, most of the ternary ullmannite-type compounds are known to be superconducting. This space group contains only 4 three fold and 3 two fold screw axes without space inversion symmetry, so it may be called as a non-symmorphic cubic chiral structure. Such the unique symmetry brings both the extra degeneracy and the spin-splitting in electronic band structure. The screw axes cause the supplementary degeneracy on the Brillouin zone boundary. On the contrary, the lack of the space inversion symmetry lifts the degeneracy due to the spin degree of freedom in each electronic state. Recently, very good single crystals of ullmannite-type structure, PdBiSe and NiSbS are synthesized and the Fermi surface properties are investigated by de Haas-van Alphen (dHvA) effect by Y. Onuki et al. Therefore, the electronic structure and the Fermi surfaces for both the compounds are calculated by using a full potential linearized plane wave method based on the local density approximation, including the relativistic spin-orbit interactions. The dHvA results are well reproduced by the calculated Fermi surfaces. The topology of the Fermi surfaces of both compounds is very similar, but the magnitudes of the splitting of the Fermi surfaces are very different. The large spin-splitting in PdBiSe can be understood by the strong spin-orbit interaction in Bi 6p electrons.

FR.C-P07 - Correlation-induced structural transition in one-dimensional molecular hydrogen crystal

A.P. Kądziaława¹, Andrzej Biborski², J. Spałek^{1,2}

1. Marian Smoluchowski Institute of Physics, Jagiellonian University, Kraków, Poland

2. Academic Centre for Materials and Nanotechnology, AGH University of Science and Technology, Kraków, Poland

Proper inclusion of electronic correlations plays an essential role in the hydrogen systems, especially under high pressures. It contributes to the Mott transition [1], but may also influence the crystal structure. We describe the molecular chain within the extended Hubbard model with microscopic parameters obtained via ab-initio calculations. As the framework of the computation, we use Exact Diagonalization ab Initio (EDABI) approach - a method of the wave-function renormalization, proved to be efficient for describing hydrogen systems [2], as it avoids the double-counting problem (present in LDA+U and GGA+U methods) and allows a straightforward inclusion of the long-range electronic correlations. We discuss the electronic properties of different phases by means of sampling the space of structural parameters. We observe a first-order structural transition for intermolecular distance (-- Bohr radius), between the molecular and the two separated atomic-chain configurations and discuss the impact of the electronic correlations on this transition.

The authors acknowledge the support from the National Science Centre (NCN), Grant No. DEC-2012/04/A/ST3/00342, as well as from the Foundation for Polish Science (FNP), through Grant TEAM.

[1] A. P. Kądziaława, J. Spałek, J. Kurzyk, and W. Wójcik, Eur. Phys. J. B 86, 252 (2013)

[2] A. P. Kądziaława, A. Bielas, M. Acquarone, A. Biborski, M. M. Mańska, and J. Spałek, New J. Phys. 16, 123022 (2014)

FR.C-P08 - Chemical pressure effect in SmNiC₂T. Klimczuk¹, G. Prathiba², J. Strychalska¹, T. Park²1. *Gdansk University of Technology, Gdańsk, Polonia*2. *Sungkyunkwan University(SKKU), Seoul, South Korea*

A series of Sm_{1-x}Ln_xNiC₂, where Ln=La and Lu, were synthesized by arc-melting method and annealed for 2 weeks at 850°C. Powder x-ray diffraction was used to analyze sample purity and the lattice parameters were calculated using LeBail refinement method. Physical properties were measured by means of magnetic susceptibility, electrical resistivity and heat capacity.

SmNiC₂ is a ferromagnet with relatively high Curie temperature ($T_C = 17$ K). Since Sm is located almost in the middle of the lanthanides, it gives unique opportunity of chemical doping by large La as well as small Lu metal. This way increase (La doping) or decrease (Lu doping) in the unit cell volume is expected, which might be seen as negative or positive “chemical” pressure.

The phase diagram reveals a sudden decrease of the charge density wave formation temperature (T_{CDW}) from 150K for SmNiC₂ to 55K for Sm_{0.75}La_{0.25}NiC₂. Such a decrease is not observed for Sm_{0.8}Lu_{0.2}NiC₂.

The Curie temperature decreases with both La and Lu substitution in Sm_{1-x}Ln_xNiC₂. Interestingly ferromagnetism is observed for Sm_{0.13}La_{0.87}NiC₂ and Curie temperature $T_C = 3.5$ K was estimated from the Arrot plot. Further increase of La reveals superconductivity and the highest $T_{sc} \sim 3$ K is obtained for pure LaNiC₂.

FR.D-P05 - Magnetic properties of the Ruddlesden-Popper phases $\text{Sr}_{3-x}\text{Y}_x\text{Fe}_{1.25}\text{Ni}_{0.75}\text{O}_{7-6}$ S. Kontos¹, K. Gunnarsson¹, J. Grins², D. Wardecki², G. Svensson², P. Svedlindh¹

1. Uppsala University, Uppsala, Sweden

2. Stockholm University, Stockholm, Sweden

Ruddlesden-Popper $n = 2$ member phases $\text{Sr}_{3-x}\text{Y}_x\text{Fe}_{1.25}\text{Ni}_{0.75}\text{O}_{7-6}$, $0 \leq x \leq 0.75$, have been investigated by X-ray (XRD) and neutron powder diffraction (NPD), Mössbauer spectroscopy, magnetometry and AC susceptometry. The samples were prepared at 1300 °C under nitrogen flow and subsequently air-annealed at 900 °C. The Mössbauer results show that the air-annealed samples in addition to Ni^{3+} contain both Fe^{3+} and Fe^{5+} and that the amount of Fe^{5+} increases with decreasing Y concentration. Moreover, the XRD and NPD results show that the transition metal ions exhibit octahedral (Fe^{3+} , Fe^{5+} and Ni^{3+}) and square pyramidal oxygen coordination (Fe^{3+} and Ni^{3+}), where the latter is a consequence of oxygen vacancies. The amount of octahedrally coordinated Fe/Ni cations increases with decreasing Y concentration. AC susceptibility results show that all samples exhibit properties characteristic of spin glasses. The spin glass properties are a consequence of frustrated superexchange interactions, including antiferromagnetic $\text{Fe}^{3+} - \text{Fe}^{3+}$, $\text{Fe}^{3+} - \text{Ni}^{3+}$ and $\text{Ni}^{3+} - \text{Ni}^{3+}$ interactions as well as ferromagnetic $\text{Fe}^{5+} - \text{Fe}^{3+}$ and $\text{Fe}^{5+} - \text{Ni}^{3+}$ interactions. Magnetic interactions exist in-plane of a perovskite layer, between perovskite layers in a perovskite block and between neighboring perovskite blocks. The spin glass freezing temperature shows a minimum for an yttrium concentration of $x=0.4$. The high temperature magnetization versus temperature data indicate a predominance of low-spin states for the transition metal ions at large Y concentration, while high-spin states are observed for small Y concentration. The transition between low- and high-spin states with Y concentration correlates well with the variation of the Fe/Ni-O1 bond length, where O1 corresponds to the oxygen forming bonds along the c-axis between transition metal cations in a perovskite block.

FR.D-P07 - Hidden magnetic order in P2-Na_{0.5}VO₂ found by muon-spin spectroscopy

J. Sugiyama¹, I. Umegaki¹, D. Andreica², C. Baines³, A. Amato³, M. Guignard⁴, C. Delmas⁴, M. Månsson⁵

1. *Toyota Central Research & Development Laboratories, Inc., Nagakute, Japan*

2. *Babes-Bolyai University, Cluj-Napoca, Romania*

3. *Paul Scherrer Institut, Zurich, Switzerland*

4. *ICMCB-CNRS, Pessac, France*

5. *KTH Royal Institute of Technology, Stockholm, Sweden*

The microscopic magnetic nature of a novel Na battery material, P₂-Na_{0.5}VO₂, in which V ions form a two-dimensional (2D) triangular lattice [1], has been investigated with muon-spin rotation and relaxation measurements down to 50 mK [2]. Although magnetization measurements indicated the presence of an antiferromagnetic transition at 13 K [1], the internal magnetic field due to the formation of magnetic order appears not at 13 K but at 2 K. This suggests that the magnetic anomaly at 13 K corresponds to the evolution of 2D AF correlation. Furthermore, the magnetic order observed below 2 K is found to have a wide field distribution even at 50 mK. Such wide field distribution is reasonably explained by a combination of multiple muon sites and the formation of a long-range magnetic order, as for Na_{0.75}CoO₂ [3,4,5] or Na_{0.5}CoO₂ [6], although the AF spin structure is still unknown.

[1] M. Guignard et al., *Nature Mater.* 12, 74 (2013)

[2] J. Sugiyama et al., submitted to *RSC Advances* (2015)

[3] J. Sugiyama et al., *Phys. Rev. B* 67, 214420 (2003)

[4] S. Bayrakci et al., *Phys. Rev. Lett.* 94, 157205 (2005)

[5] L. Helme et al., *Phys. Rev. Lett.* 94, 157206 (2005)

[6] G. Gasparovic et al., *Phys. Rev. Lett.* 96, 046403 (2006)

FR.D-P08 - Magnetic ground state of a two-dimensional triangular compound, CrSe₂, studied with muon-spin spectroscopy

J. Sugiyama¹, H. Nozaki¹, I. Umegaki¹, K. Miwa¹, S. Kobayashi², C. Michioka², H. Ueda², K. Yoshimura², J. Brewer^{3,4}

1. Toyota Central Research & Development Laboratories, Inc., Nagakute, Japan

2. Kyoto University, Kyoto, Japan

3. University of British Columbia, Vancouver, Canada

4. TRIUMF, Vancouver, Canada

1T-CrSe₂ belongs to a layered transition-metal dichalcogenides 1T-MX₂ family with a two dimensional triangular lattice (2DTL), where M is a transition metal and X is a chalcogen (S, Se, and Te). 1T means the phase with the layered CdI₂ structure, in which M ions form the 2DTL by the connection of edge-sharing MX₆ octahedra.

According to an early report in 1980 [1], 1T-CrSe₂ was found to undergo successive phase transitions at 180 and 160 K. That is, as temperature decreases from 300 K, magnetization increases abruptly at T_{t1}=186 K and T_{t2}=164 K, while the change in resistivity at these temperatures is less drastic [1,2]. Furthermore, very recent magnetization measurements on 1T-Cr_{1-x}V_xSe₂ and 1T-Cr_{1-x}Ti_xSe₂ indicated that the phase below 186 K is not a charge density wave state, which was proposed for TiSe₂ [3] and VSe₂ [4], but an antiferromagnetic (AF) ordered state [5], although there is no direct evidence for the presence of magnetic order.

We have therefore measured muon-spin rotation and relaxation (μ SR) spectra down to 1.8 K using powder and single crystal samples of 1T-CrSe₂. As a result, it is found that 1T-CrSe₂ enters into a static AF order phase below T_{t2}. The anisotropy of the internal magnetic field suggests that the ordered moments align in the 2DTL plane.

[1] C. F. van Bruggen et al., Physica B+C 99, 166 (1980)

[2] S. Kobayashi et al., Phys. Rev B 89, 054413 (2014)

[3] F. J. Di Salvo et al., Phys. Rev. B 14, 4321 (1976)

[4] C.F. van Bruggen and C. Haas, Solid State Commun. 20, 251 (1976)

[5] D. C. Freitas et al., Phys. Rev. B 87, 014420 (2013)

FR.D-P09 - Bipartite entanglement and quantum correlations of exact ground states of a spin-1/2 Ising-Heisenberg model on the Shastry-Sutherland lattice

J. Strečka¹, T. Verkholyak², F. Mila³, K.P. Schmidt⁴

1. Institute of Physics, Faculty of Science, P. J. Safarik University, Kosice, Slovakia

2. Institute for Condensed Matter Physics, NASU, Lviv, Ukraine

3. Institute of Theoretical Physics, Ecole Polytechnique Federale de Lausanne (EPFL), Lausanne, Switzerland

4. Lehrstuhl für Theoretische Physik I, Dortmund, Germany

The spin-1/2 Ising-Heisenberg model on the Shastry-Sutherland lattice with Heisenberg intra-dimer and Ising inter-dimer couplings exhibits five different ground states: the singlet-dimer state, the classical antiferromagnetic state, the fully polarized state, the stripe order of singlet-like states with the polarized triplet states and the checkerboard order of singlet-dimer states with the polarized triplet states. The most remarkable ground state represents a stripe order of singlet-like states and polarized triplet states, which corresponds to the one-third plateau in a zero-temperature magnetization curve. To quantify strength of the bipartite entanglement and quantum correlations between two spins coupled by the Heisenberg intra-dimer interaction, we have exactly calculated the concurrence, von Neumann entropy, Bell function and negativity. It is found that a size of entanglement measures does not depend on the magnetic field, but it basically depends on a relative ratio between the Heisenberg and Ising couplings, and respectively, whether or not a spontaneous breaking of the corresponding eigenvector is taken into account. In the former case the entanglement measures correctly reproduce a quantum nature of the stripe one-third magnetization plateau in a full range of the interaction parameters, while in the latter case the entanglement measures vanish for strong enough values of the ratio between the Ising inter-dimer and Heisenberg intra-dimer couplings.

FR.D-P11 - Unconventional spin dynamics in the spin-1/2 triangular-lattice antiferromagnet Cs_2CuBr_4

S. Zvyagin¹, M. Ozerov¹, J. Wosnitzer¹, D. Kamenskyi², M. Ikeda³, T. Fujita³, M. Hagiwara³, J. Krzystek⁴, R. Hu⁵, H. Ryu⁵

1. *Dresden High Magnetic Field Laboratory (HLD-EMFL), Helmholtz-Zentrum Dresden-Rossendorf, Dresden, Germany*

2. *Radboud University Nijmegen, High Field Magnet Laboratory, 6500 GL Nijmegen The Netherlands*

3. *Center for Advanced High Magnetic Field Science, Graduate School of Science, Osaka University, Toyonaka, Osaka, Japan*

4. *National High Magnetic Field Laboratory, Florida State University, Tallahassee, United States*

5. *Condensed Matter Physics and Materials Science Department, Brookhaven National Laboratory, Upton, NY, United States*

6. *Service de Physique Statistique, Magnétisme et Supraconductivité, UMR-E9001 CEA-INAC/UJF, 38054 Grenoble Cedex 9, France*

Magnetic excitations in Cs_2CuBr_4 , a spin-1/2 Heisenberg antiferromagnet with a distorted triangular lattice, are studied by means of high-frequency electron spin resonance (ESR) spectroscopy in magnetic fields up to 25 T. The presence of a substantial zero-field gap, $\Delta \sim 10$ K, observed above T_N , is interpreted in the frame of a triangular-lattice antiferromagnet model, indicating good agreement with results of spin-wave calculations. The excitation spectrum is found stable against the magnetic order, suggesting the presence of strong in-plane correlations in Cs_2CuBr_4 in the 3D magnetically ordered state. The peculiarities of the ESR spectrum are discussed taking into account the effect of staggered Dzyaloshinskii-Moriya interactions and two-magnon decay processes. This work was partially supported by Deutsche Forschungsgemeinschaft (DFG, Germany).

FR.D-P12 - Amorphous ferromagnetism and re-entrant magnetic glassiness in $\text{Sm}_2\text{Mo}_2\text{O}_7$

G. Prando¹, P. Carretta², A. Wolter-Giraud¹, R. Saint-Martin³, A. Revcolevschi³, B. Büchner^{1,4}

1. *Leibniz-Institut für Festkörper- und Werkstoffforschung (IFW), Dresden, Germany*

2. *Dipartimento di Fisica e Unità CNISM di Pavia, Università di Pavia, Pavia, Italy*

3. *Laboratoire de Physico- Chimie de l'Etat Solide, Université Paris-Sud, Orsay, France*

4. *Institut für Festkörperphysik, Technische Universität Dresden, Dresden, Germany*

We report on the investigation of a high-quality single crystal of $\text{Sm}_2\text{Mo}_2\text{O}_7$ by means of dc magnetometry, muon spin spectroscopy and high-harmonics ac susceptibility [1]. The magnetic phase of the Mo^{4+} sublattice develops below $T_C \sim 78$ K and is typically discussed in the literature as a conventional itinerant ferromagnetic state. However, our results clearly detect a complicated superposition of conventional and highly disordered magnetic behaviors below 78 K sharing several common features with amorphous ferromagnetic alloys and with other insulating spin-glass pyrochlore molybdates. As typical for amorphous ferromagnets, a freezing of the transverse XY spin components of Mo^{4+} below $T \sim 25$ K is evidenced, an effect otherwise known as re-entrant spin-glass phase. Our results shed new light on the overall electronic phase diagram commonly accepted for pyrochlore molybdates.

[1] G. Prando et al., Phys. Rev. B 90, 085111 (2014)

FR.D-P13 - High Frequency ESR Study of $S=1/2$ kagome lattice magnet $[\text{Cu}_3(\text{CO}_3)_2(\text{bpe})_3]_2\text{ClO}_4$

H. Ohta¹, K. Takamoto², N. Takahashi², W.M. Zhang¹, S. Okubo¹, T. Sakurai³, T. Taniguchi⁴, H. Nakata⁵, H. Kikuchi⁵, Y. Fujii⁵

1. *Molecular Photoscience Research Center, Kobe, Japan*

2. *Graduate School of Science, Kobe University, Kobe, Japan*

3. *Center for Supports to Research and Education Activities, Kobe University, Kobe, Japan*

4. *Graduate School of Science, Osaka University, Osaka, Japan*

5. *Department of Applied Physics, University of Fukui, Fukui, Japan*

$S=1/2$ Kagome antiferromagnet has attracted much attention because of its strong frustration effect. Especially the search for the ideal model substance is very important for the experimental studies. As Cu^{2+} ions ($S=1/2$) in $[\text{Cu}_3(\text{CO}_3)_2(\text{bpe})_3]_2\text{ClO}_4$ form Kagome lattice structure with 180 degrees Cu-O-Cu superexchange, $[\text{Cu}_3(\text{CO}_3)_2(\text{bpe})_3]_2\text{ClO}_4$ is a strong candidate. Kanoo et al. also suggested the small antiferromagnetic interaction from the Weiss temperature [1]. On the other hand, its ferromagnetic behaviors at low temperature are suggested from the magnetic susceptibility and NMR [2]. In order to understand these mismatches and get microscopic information of the system, we have performed high frequency ESR. Although only powder sample is available, we are able to identify the anisotropy of g-values as $g_{\text{per}}=2.150$ and $g_{\text{//}}=2.056$ by the advantages of high frequency ESR. By the detailed analyses of g-values considering the crystal fields of 3 non-equivalent Cu sites and the exchange narrowing effect, we are able to identify the mixed orbital states at each Cu site and concluded that the Goodenough-Kanamori rule cannot be applied in this case. Therefore, the Cu-O-Cu superexchange path in the system may be ferromagnetic instead of antiferromagnetic interaction. This conclusion was also supported by our high frequency ESR results below 10 K, where the abrupt rise of magnetic susceptibility is observed. There is a shift of ESR below 10 K suggesting the existence of the internal field. Our multi-frequency ESR results at 4.2 K are well explained by the ferromagnetic resonance (FMR) rather than the antiferromagnetic resonance (AFMR). In conclusion our high frequency ESR results suggest that $[\text{Cu}_3(\text{CO}_3)_2(\text{bpe})_3]_2\text{ClO}_4$ is more likely the ferromagnet rather than the antiferromagnet.

[1] P. Kanoo, et al, Dalton Trans. 26 (2009)5062

[2] H. Kikuchi, et al., JPS Conf. Proc. 3 (2014) 012019

FR.D-P14 - New spin glass material, $KV_{14}Ge_2O_{27}$

K. Harada¹

1. Department of Physics, Chuo University, Hachioji, Japan

We discovered a new SG material whose origin is attributed to a geometric frustration. After a hydrothermal reaction, black, polyhedral-shaped single crystals were obtained. It was determined that the composition of this material is $KV_{14}Ge_2O_{27}$ using single-crystal X-ray diffraction and EDS. The X-ray diffraction revealed a trigonal unit cell with space group $P\bar{3}$. Its lattice parameters are $a = 7.6309 \text{ \AA}$ and $c = 9.2195 \text{ \AA}$. In this structure, octahedra of VO_6 form two kinds of planes (plane A and B). The plane A contains also GeO_4 tetrahedral and the plane B contains also K atoms. These planes stack along the c axis in AABB sequence. A magnetic frustration is expected in this material, because V atoms form a triangle-based lattice in each plane. The field-cooled (FC) magnetic susceptibility doesn't agree with the zero-field-cooled (ZFC) susceptibility below 16 K. The ZFC susceptibility shows a cusp at 16 K. In addition, we observed a slow relaxation phenomenon of the remnant magnetization at low temperature. These behaviors indicate that a SG state appears in this material. The Weiss temperature is estimated at -370 K suggesting that this material has strong antiferromagnetic interactions. This indicates that the geometric frustration disturbs development of a long-range antiferromagnetic order.

FR.D-P15 - Single-crystal growth and magnetic properties of new frustrated magnet, $\text{Rb}_2\text{Mn}_3\text{V}_2\text{O}_{10}$ D. Otsuka¹, H. Sato¹*1. Department of Physics, Chuo University, Hachioji, Japan*

We succeeded in synthesizing a new frustrated magnet, $\text{Rb}_2\text{Mn}_3\text{V}_2\text{O}_{10}$ using a hydrothermal method. It has an interesting Mn^{2+} network, composed of hexagons connected to each other sharing their corners along the b axis and their edges along the c axis. From another viewpoint, it can be regarded as a combination of honeycomb chains and diamond chains elongated along the c axis. If the nearest neighbor exchange interaction is antiferromagnetic, we can expect interesting magnetism because of the geometric frustration. $\text{Rb}_2\text{Mn}_3\text{V}_2\text{O}_{10}$ crystallizes in a monoclinic lattice with a space group $C2/m$. The lattice parameters are $a = 15.586(2)$ Å, $b = 6.1855(5)$ Å, $c = 5.4660(4)$ Å, $\beta = 105.188(3)^\circ$ and $Z = 2$.

We measured the temperature dependence of the magnetic susceptibility of $\text{Rb}_2\text{Mn}_3\text{V}_2\text{O}_{10}$. The Weiss temperature is about -250 K, indicating strong antiferromagnetic interactions. This compound has an antiferromagnetic transition at $T_N = 40$ K. The frustration factor $f = |\theta| / T_N$ is as large as 6.25. The susceptibility has a broad maximum at about 65 K. This also suggests existence of strong frustration. Our result is in contrast with the magnetism of the isostructural compound, $\text{Na}_2\text{Ni}_3(\text{OH})_2(\text{PO}_4)_2$, which exhibits an ordinary antiferromagnetic transition.[1]

[1]O. Yakubovich et al., *Dalton Trans.* 42 (2013) 14718

FR.D-P16 - Exact solutions on the ground states of ferro- and antiferromagnetic Ising models in magnetic fields with frustration on a diamond hierarchical lattice

Y. Hirose¹, A. Oguchi¹, Y. Fukumoto¹

1. Tokyo University of Science, Tokyo, Japan

Magnetization processes of frustrated Ising models on diamond hierarchical lattices, which contain vertices with high coordination numbers, are exactly obtained at zero temperature. In antiferromagnetic systems, the magnetization cannot saturate under finite magnetic fields owing to the competition between the antiferromagnetic and Zeeman interactions and the intrinsic long-range nature of hierarchical lattices. For the zero-field classical spin-liquid phase found in [Kobayashi et al., J. Phys. Soc. Jpn. 78, 074004 (2009)], an infinitely small applied magnetic field can induce an infinitely small magnetization, despite classical Ising models that have discrete energy levels. We examine the structure of the partition function in order to obtain ground state spin-configurations and to clarify the mechanism of the “gapless spin-liquid” behavior.

FR.D-P17 - Magnetodielectric coupling behavior of single crystalline form of the geometrically frustrated spin-chain compound, $\text{Ca}_3\text{Co}_2\text{O}_6$ T. Basu¹, K.K. Iyer¹, K. Singh^{1,2}, P.L. Paulose¹, E.V. Sampathkumaran¹1. *Tata Institute of Fundamental Research, Mumbai, India*2. *UGC-DAE Consortium for Scientific Research, Indore, India*

We report some fascinating magnetodielectric (MDE) behaviors of a geometrically frustrated spin-chain compound $\text{Ca}_3\text{Co}_2\text{O}_6$, which undergoes (partially disordered) antiferromagnetic ordering (T_N) around 25 K followed additional magnetic phase transitions at lower temperatures ($T < 12\text{K}$). We find that the magnetic field (H) dependent dielectric constant at low T (<10 K) exhibits the fascinating “magnetodielectric phase coexistence” (a partial arrest of the high magnetic field dielectric phase on returning the magnetic-field to zero after the H-induced metamagnetic transition) for H//c only, irrespective of the direction of applied electric field (E); this feature is not observed for H//a. It is surprising that such a high-field-phase arrest could not be observed in isothermal magnetization data for any orientation. The T-dependence of ac susceptibility (as known in the past literature) for H//c exhibits a strong frequency (ν) dependence with a suppression under the application of H, but this ν -dependence is completely absent for the perpendicular orientation. However the strong ν -dependence in dielectric is surprisingly present for both the crystallographic directions (E//a and E//c) with a negligible influence of H, despite the existence of strong MDE coupling. The present results indicate complex relaxation behavior and/or different dynamics of electric and magnetic dipoles, although these are coupled as evidenced by MDE coupling. Another uncommon report of great interest is that, as observed in polycrystals [1], MDE coupling arising from short-range magnetic correlation within spin-chain persists even above T_N ; that is, a broad peak in dielectric constant is observed around 60-130 K when the electric-field (E) is applied along the spin (c-direction). Single crystal studies thus confirm that this geometrically frustrated compound exhibits exotic MDE coupling behavior not only below T_N , but also well above T_N due to intra-chain interactions.

[1] Tathamay Basu, *Sci. Rep.* 3, 3104 (2013)

FR.D-P18 - Magnetization process of pyrochlore-slub $\text{SrCr}_{\{9p\}}\text{Ga}_{\{12-9p\}}\text{O}_{\{19\}}$ in ultra-high magnetic fields of up to 150 T

D. Nakamura¹, S. Lee², J. Yang², H. Ueda³, K. Penc⁴, S. Takeyama¹

1. ISSP, the University of Tokyo, Tokyo, Japan

2. University of Virginia, Virginia, USA

3. Kyoto University, Kyoto, Japan

4. Hungarian Academy of Sciences, Budapest, Hungria

Pyrochlore-slub compound $\text{SrCr}_{\{9p\}}\text{Ga}_{\{12-9p\}}\text{O}_{\{19\}}$ (SCGO) possesses a spin system of Cr^{3+} ($S=3/2$), which is mainly composed by the tri-layer of Kagome lattice and triangular lattice. Therefore, SCGO is considered as a spin frustration material. The spin-glass-like behavior was observed at temperatures below 3.5 K [1]. However, the specific heat at low temperature is proportional to the square of temperature, unlike the case for other spin glass materials. A recent model calculation for SCGO shows that the quantum fluctuation induces a new glassy state called as “spin jam”, which can explain the temperature dependence of specific heat [2]. We expect that the magnetization process of SCGO also contains novel phenomena involving the quantum fluctuation.

We prepared an SCGO ($p=0.7$) crystal with 0.03 mm thickness. From the optical absorption spectra, a crystal field transition (d-d transition) was observed at 2.0 eV in the absence of magnetic field. The Faraday rotation (FR) measurement was performed in magnetic fields up to 150 T with the incident laser light setting at the edge of this absorption spectra. The obtained FR angle reflects well the magnetization curve of SCGO. The ultra-high magnetic fields are generated by the single-turn coil method. A small plateau in FR was observed at 80 T followed by the transition to the 3/7 plateau at around 120 T. The magnetization curve is well reproduced by a numerical calculation based on the classical Heisenberg model incorporating the biquadratic interaction.

[1] A. P. Ramirez, G. P. Espinosa, and A. S. Cooper, Phys. Rev. Lett. 64, 2070 (1990).

[2] I. Klich, S-H. Lee and K. Iida, Nat. Commun. 5, 3497 (2014).

FR.D-P19 - Ultrasound velocity measurements in orbital-degenerate frustrated spinel CoV_2O_4 T. Watanabe¹, S. Yamada¹, R. Koborinai², T. Katsufuji²*1. Department of Physics, College of Science and Technology (CST), Nihon University, Tokyo, Japan**2. Department of Physics, Waseda University, Tokyo, Japan*

Vanadate spinels AV_2O_4 with divalent A^{2+} ions such as Mg^{2+} , Zn^{2+} , Cd^{2+} , Mn^{2+} , Fe^{2+} , and Co^{2+} have attracted considerable interest as orbitally degenerate frustrated magnets, where the trivalent magnetic V^{3+} ions are characterized by double occupancy of the triply degenerate t_{2g} orbitals, and form a sublattice of corner-sharing tetrahedra. CoV_2O_4 is one of the vanadium spinel family which undergoes a ferrimagnetic transition at $T_{c1} = 142$ K and another phase transition at $T_{c2} = 59$ K. CoV_2O_4 is the only vanadate spinel which exhibits the absence of structural phase transition. Recent studies of structural, magnetic, and electric properties under pressure in CoV_2O_4 revealed that this compound resides closest to the itinerant electron limit in AV_2O_4 , which is due to the shortest V-V distance in AV_2O_4 . We performed ultrasound velocity measurements in CoV_2O_4 single crystal to study the spin and orbital states. The measurements were performed in all the symmetrically-independent elastic moduli of the cubic spinel, compression modulus C_{11} , tetragonal shear modulus $(C_{11}-C_{12})/2$, and trigonal shear modulus C_{44} . In temperature dependence of the elastic moduli, a discontinuous change occurs at T_{c1} in C_{11} , $(C_{11}-C_{12})/2$, and C_{44} , and at T_{c2} in C_t . Additionally, and more interestingly, the elastic moduli exhibit elastic-mode-dependent anomalous temperature variations. In the paramagnetic phase ($T > T_{c1}$), $(C_{11}-C_{12})/2$ and C_{44} exhibit softening with decreasing temperature. In the ferrimagnetic phase ($T_{c2} < T < T_{c1}$), C_{11} , $(C_{11}-C_{12})/2$, and C_{44} exhibit nonmonotonic temperature dependence. In the low-temperature phase ($T < T_{c2}$), C_{11} and $(C_{11}-C_{12})/2$ exhibit softening with a characteristic minimum with decreasing temperature. These anomalous temperature variations of the elastic moduli should originate from the coupling of lattice to the magnetic fluctuations and/or the magnetic gapped excitations. In the presentation in the conference, we would also like to report the magnetic-field effects on the elastic properties of CoV_2O_4 .

FR.D-P21 - Exploring new magnetic phases in artificial spin ices with perpendicular spin moments

I.A. Chioar^{1,2}, N. Rougemaille^{1,2}, A. Grimm^{1,2}, O. Fruchart^{1,2}, E. Wagner^{1,2}, M. Hehn³, D. Lacour³, F. Montaigne³, B. Canals^{1,2}

1. CNRS, Institut NEEL, Grenoble, France

2. Université Grenoble Alpes, Institut NEEL, Grenoble, France

3. Institut Jean Lamour, Université de Lorraine and CNRS, Vandoeuvre lès Nancy, France

Frustration is a ubiquitous concept in physics. In some cases, frustration can lead to an extensively degenerate ground state of the considered system. Pauling's description of the low-temperature proton disorder in water ice is probably the first example of frustration in condensed-matter physics and remains its paradigm [1]. At the end of the 1990s, new magnetic compounds were synthesized in which the disorder of the magnetic moments at low temperatures was analogous to the proton disorder in water ice [2]. Since then, intense work has been devoted to these frustrated spin systems. This correspondence between the physics of water ice and its magnetic counterparts has been recently extended to artificial realizations of frustrated spin systems [3].

In this contribution, magnetic frustration effects in lithographically patterned artificial kagome arrays of nanomagnets with out-of-plane magnetization are investigated using magnetic force microscopy and Monte Carlo simulations. In addition to the observation of how each individual spin locally accommodates frustration, experimental and theoretical results are compared to those found for the artificial kagome spin ice in which the nanomagnets have in-plane magnetization. In contrast with what has been recently reported [4], we demonstrate that the system with out-of-plane magnetization is characterized by a new magnetic phase [5]. However, the ground-state configuration still remains unknown.

[1] L. Pauling, J. Am. Chem. Soc. 57, 2680 (1935)

[2] M. J. Harris et al., Phys. Rev. Lett. 79, 2554 (1997)

[3] R. F. Wang et al., Nature 439, 303 (2006)

[4] S. Zhang et al., Phys. Rev. Lett. 109, 087201 (2012)

[5] I. A. Chioar et al., Phys. Rev. B 90, 064411 (2014)

FR.D-P22 - Spin glass field theory with replica Fourier transforms

I. Pimentel¹, C. De Dominicis²

1. *Departamento de Física e CFTC, Faculdade de Ciências, Universidade de Lisboa, Lisboa, Portugal*

2. *CEA Saclay Orme des Merisiers, Inst Phys Theor, Gif Sur Yvette, France*

We develop a field theory for spin glasses using replica Fourier transforms (RFT). We present the formalism for the case of replica symmetry and the case of replica symmetry breaking on an ultrametric tree, with the number of replicas n and the number of replica symmetry breaking steps R generic integers. We show how the RFT applied to the two-replica fields allows one to construct a new basis which block-diagonalizes the four-replica mass-matrix, into the replicon, anomalous and longitudinal modes. The eigenvalues are given in terms of the mass RFT and the propagators in the RFT space are obtained by inversion of the block-diagonal matrix. The formalism allows one to express any i -replica vertex in the new RFT basis and hence enables one to perform a standard perturbation expansion. We apply the formalism to calculate the contribution of the Gaussian fluctuations around the Parisi solution for the free-energy of an Ising spin glass.

[1] J. Phys. A: Math. Theor. 47, 455001 (2015)

FR.D-P23 - Nematic phases in the bilinear biquadratic Heisenberg model on the honeycomb lattice.

A. Pires¹

1. Universidade Federal de Minas Gerais, Belo Horizonte, Brazil

As it is well known, quantum spin liquids are characterized by the absence of any symmetry-breaking long-range order. In contrast to this states, spin nematic states exhibit long-range quadrupolar correlations which has no magnetic order. One interesting example where spin nematic phases could appear is the spin-1 bilinear biquadratic Heisenberg model. This model can present several interesting phases and spontaneously develop a columnar dimer order with a non-bipartite structure. In this work I will study this model in the honeycomb lattice. This lattice has the smallest coordination number in two dimensions and the effect of quantum fluctuations is the strongest.

A very convenient analytical technique to study this model (and other frustrated systems which present disordered phases and possibly new materials synthesized in the future) is the SU(3) Schwinger boson formalism (also called flavor-wave theory). I will discuss this formalism and show how it can be used to study different phases of the model and to calculate its phase diagram. I will give special attention to the ferroquadrupolar phase, which is characterized by a uniform alignment of the directors. Since quadrupolar/nematic ordering has not yet been identified unambiguously in real materials, I will present the dynamical quadrupolar structure factor, which could be, in principle, measured using resonant techniques, such as resonant inelastic x-ray scattering. This type of experiment could provide evidence for the existence of spin-nematic order.

FR.D-P24 - Magnetic field dependence of magnetoelastic interactions in $Tb_2Ti_2O_7$

M. Ruminy¹, T. Fennell¹, M. Kenzelmann²

1. Laboratory for Neutron Scattering and Imaging, Paul Scherrer Institut, Villigen, Switzerland

2. Laboratory for Developments and Methods, Paul Scherrer Institut, Villigen, Switzerland

The highly frustrated rare earth magnet $Tb_2Ti_2O_7$ enters a spin liquid regime at low temperatures which supports spin ice-like power-law correlations and a wealth of magnetoelastic effects [1-4]. These experimental observations are in stark contrast to the classically expected long-range magnetic order and/or structural phase transition - a long-standing challenge in frustrated magnetism. Recently we have discovered a microscopic coupling mechanism between the magnetic and lattice fluctuations, which forms hybrid, magnetoelastic propagating excitations via quadrupolar transition moments between the doublet groundstate and the low-lying first excited crystal field level [5,6]. Using inelastic neutron scattering, we have now studied in detail the effect of an applied magnetic field on the magnetoelastic excitation spectrum of $Tb_2Ti_2O_7$. I will show how these experiments not only boost our understanding of the coupling between spins and phonons in $Tb_2Ti_2O_7$ but also enlighten how a shift of the first crystal field excitation drives the hitherto unexplained field induced long-range antiferromagnetic ordering transition [7].

[1] Gardner et al., Rev. Mod. Phys. 82, 53 (2010)

[2] Fennell et al., PRL 109, 017201 (2012)

[3] Petit et al., PRB 86, 174403 (2012)

[4] Fritsch et al., PRB 87, 094410 (2013)

[5] Fennell et al., PRL 112, 017203 (2014)

[6] Guitteny et al., PRL 111, 087201 (2013)

[7] Rule et al., 177201 (2006)

FR.D-P25 - Unstable magnetic properties of Pd₉₉Fe₀₁ nanofilms.

L.S. Uspenskaya¹, V. Bolginov¹, I.N. Khlustikov²

1. *Institute of Solid State Physics RAS, Chernogolovka, Russia*

2. *P.L. Kapitza Institute for Physical Problems RAS, Moscow, Russia*

Bulk Pd_{1-x}Fe_x alloy is known as the material which gains the ferromagnetic properties because of high magnetic polarization of Pd already at the doping level about 0.1 - 1 %. The effective magnetic moment per Fe atom grows inversely proportional to x and reaches 12 Bohr magnetons at x ~ 0.01 [1]. Depending on x, ferromagnetic or antiferromagnetic arrangement of magnetization takes place [2]. The spontaneous magnetization of the alloys and the Curie temperature are reduced with the doping decrease and with the reduction of magnetic material volume [3,4]. The interest to the magnetic properties of weak ferromagnet nanofilms appears a few years ago with the development of cryoelectronics where such a films are suggested to be used as the layer governing electromagnetic properties of hybrid superconductor-ferromagnet-superconductor structures [5].

Herewith we report on the properties of 20 to 40 nanometers thick Pd_{1-x}Fe_x films fabricated by rf magnetron sputtering. The experiments were performed by SQUID magnetometry in temperature range 1.4 - 40 K. Temperature dependences of magnetization, coercivity and magnetic permeability were determined. Two types of magnetization loops were found depending on the range of magnetic field sweeping with the threshold value as low as 20 Oe. Large shift of Curie temperature under the applied magnetic field was observed. Huge relaxation of magnetization in all temperature range was revealed.

The results are explained taking into account the magnetic nanocluster arrangement of weak ferromagnet film which was proven by the experiments on magnetic flux penetration in Nb-PdFe bilayer films.

[1] A.M. Clogston et al. Phys. Rev. 125, 541 (1965)

[2] Y.Kondo, K.Swieca, and F.Pobell. J. Low Temp. Phys. 100, 195 (1995)

[3] T.Shinodara et al. J. Magn. Magn. Mat. 196-197, 94 (1999)

[4] L.S. Uspenskaya, A. L. Rakhmanov; L. A. Dorosinskii et al., Mater. Res. Express 1 036104 (2014)

[5] M.Yu. Kupriyanov, A.A. Golubov, and M.Sigel. Proc. of SPIE 6260, 62600S (2006)

FR.D-P26 - Low-energy dynamics of spin-1/2 square J1-J2 heisenberg antiferromagnetA. Akterskiy^{1,2}, A. Syromyatnikov^{1,3}

1. PNPI, Gatchina, St. Petersburg, Russia
2. Academic University, St. Petersburg, Russia
3. Saint Petersburg State University, St. Petersburg, Russia

Spin-1/2 J1-J2 Heisenberg antiferromagnet on the square lattice has attracted a lot of interest for a long time. One of the reasons is the relevance to cuprates, Fe-based superconductors and other materials. It has been found recently numerically [1] that this model has a singlet ground state in the range $0.41J_1 < J_2 < 0.62J_1$ that is separated from the first excited (singlet) level by a gap. It is argued in [1] that a topological quantum spin liquid phase (QSLP) is realized in the range $0.41J_1 < J_2 < 0.62J_1$. Values of the ground state energy and the gap are found numerically in [1] but the problem remains open of the low-energy sector quantitative description in QSLP. We give a physical picture of the low-energy sector in QSLP. Using a series expansion, we find an effective Hamiltonian describing an anisotropic spin-1/2 ferromagnet on the square lattice in magnetic field, which low-energy sector is fully equivalent to that of J1-J2 model in QSLP. Remarkably, this effective model possesses a long-range magnetic order. Thus, we show that QSLP in J1-J₂ antiferromagnet is equivalent to the magnet with the local order parameter. This situation is similar to that found in [2] for topological phases in Kitaev model. We discuss the effective model numerically and using the standard $1/S$ expansion and find the value of the order parameter and the elementary excitation spectrum. In particular, our results for the ground state energy and the gap values are in quantitative agreement with previous numerical findings [1].

FR.D-P27 - Novel magnetic phase transition and spin-lattice effects in the frustrated magnet CdCr₂O₄

S. Zherlitsyn¹, V. Tsurkan^{2,3}, A.A. Zvyagin^{4,5}, S. Yasin¹, S. Erfanifam¹, R. Beyer¹, M. Naumann^{1,6}, E. Green¹, J. Wosnitza^{1,6}, A. Loidl²

1. *Dresden High Magnetic Field Laboratory (HLD-EMFL), Helmholtz-Zentrum, Dresden, Germany*
2. *Experimental Physics 5, Center for Electronic Correlations and Magnetism, Institute of Physics, University of Augsburg, Augsburg, Germany*
3. *Institute for Applied Physics, Academy of Science of Moldova, Chisinau, Republic of Moldova*
4. *B.I. Verkin Institute for Low Temperature Physics and Engineering of the National Academy of Sciences of Ukraine, Kharkov, Ukraine*
5. *Max Planck Institute for the Physics of Complex Systems, Dresden, Germany*
6. *Institute for Solid State Physics, TU Dresden, Dresden, Germany*

Frustrated magnetic systems manifest a number of fascinating properties often with novel magnetic phases accompanied by magneto-structural transformations. Ultrasound studies are a powerful method to probe spin-lattice interactions and possible lattice instabilities in the frustrated magnetic systems. We present results of ultrasound investigations of the frustrated antiferromagnet CdCr₂O₄. A new magnetic phase transition has been observed below the Neel temperature, T_N = 7.8 K. This transition renormalizes the velocity and amplitude of the transverse acoustic mode c_T propagating along the crystallographic [111] direction whereas the longitudinal mode c_L propagating along the same direction is not affected. The specific heat does not show any significant change of the entropy at this transition. We argue that the magnetic transition separates two different spiral structures within the antiferromagnetic state. Furthermore, in an applied magnetic field we have observed extended metastable magneto-structural states neighboring the one-half magnetization plateau which exists in CdCr₂O₄ between 28 and 58 T. By applying an exchange-striction model we can quantitatively describe the field dependence of the sound velocity below and above the one-half magnetization plateau. Moreover, we notice a much stronger renormalization of the sound velocity in approaching T_N for the transverse mode, c_T, than for the longitudinal one, c_L, signaling that the leading contribution to the exchange-striction coupling comes from the transversal polarization of the c_T mode. The low-temperature H - T phase diagram of CdCr₂O₄ is extracted from the ultrasound experiments. Our work shows that the spin-strain coupling is crucial and determines the underlying physics of this frustrated magnetic material.

The research has been partly supported by the DFG via TRR 80 (Augsburg-Munich) and SFB 1143 (Dresden).

FR.D-P28 - Order by disorder or energetic selection of the ground state in the XY pyrochlore antiferromagnet $\text{Er}_2\text{Ti}_2\text{O}_7$, a neutron scattering study

S. Petit¹, J. Robert¹, S. Guitteny¹, I. Mirebeau¹, C. Decorse², J. Ollivier³, H. Mutka³, M. Gingras⁴

1. LLB, CEA-CNRS, Gif Sur Yvette, France

2. LPCES, Université Paris-Sud, Orsay, France

3. Institut Laue Langevin, Grenoble, France

4. Department of Physics and Astronomy, Univ of Waterloo, Waterloo, Canada.

Examples of materials where an 'order by quantum disorder' mechanism is at play to select a particular ground state are scarce [1,2]. It has been recently proposed that the antiferromagnetic XY pyrochlore $\text{Er}_2\text{Ti}_2\text{O}_7$, reveals a most convincing case of this mechanism [3,4,5]. Observation of a spin gap at zone centers was interpreted as a definitive proof of this physics [6]. We argue, however, that the magnetic anisotropy provided by the interaction-induced admixing between the crystal-field ground and excited levels gives an alternative energetic mechanism [7,8]. Random phase approximation RPA calculations based on a mean field model taking into account explicitly the crystal-electric field anisotropy reproduce quite well new high resolution inelastic neutron scattering data. These experiments point out the existence of a spin gap of 43 μeV which can be well understood within this scenario: in this energetic selection mechanism, the gap originates from the anisotropy rather than quantum fluctuations effects. The present study revives the issue of the physical origin of the experimentally broken discrete symmetry ground state in $\text{Er}_2\text{Ti}_2\text{O}_7$. It raises the question of the quantum order by disorder as the sole or even principal mechanism for the selection of the magnetic ground state in this material.

[1] C. Lacroix, Introduction to Frustrated Magnetism (Springer-Verlag, Berlin, 2011)

[2] J. Villain, R. Bidaux, J.-P. Carton, R. Conte, J. Phys 41, 1263 (1980)

[3] J. D. M. Champion et al, Phys. Rev. B, 68, 020401 (R), (2003)

[4] M. E. Zhitomirsky et al, Phys. Rev. Lett. 109, 077204 (2012)

[5] L. Savary et al, Phys. Rev. Lett. 109, 167201 (2012)

[6] K. A. Ross et al, Phys. Rev. Lett. 112 057201 (2014)

[7] S. Petit et al, Phys Rev B 90, 060410(R) (2014)

[8] P. A. McClarty et al, Journal of Physics: Conference Series 145, 012032 (2009)

FR.D-P29 - “Half-moon” excitations in the magneto-elastic spin liquid $Tb_2Ti_2O_7$

S. Petit¹, S. Guitteny¹, J. Robert¹, I. Mirebeau¹, J. Ollivier², H. Mutka², C. Decorse³

1. LLB, CEA-CNRS, Gif Sur Yvette, France

2. Institut Laue Langevin, Grenoble, France

3. LPCES, Université Paris-Sud, Orsay, France

Geometrical magnetic frustration is a central concept in condensed matter physics. In this field, rare earth pyrochlore magnets $R_2Ti_2O_7$ (R is a rare earth) play a prominent role, as they form model systems showing a rich variety of ground states, depending on the balance between dipolar, exchange interactions and crystal field [1]. The Terbium compound $Tb_2Ti_2O_7$ remains a cooperative paramagnet, or a “quantum spin ice”, with strongly correlated moments still fluctuating at 50 mK [2]. Recent time of flight neutron and triple-axis neutron scattering experiments have recently shed light in this puzzle, revealing a complex “magneto-elastic” ground state [3,4] characterized by a local constraint resulting in “pinch points” [5], analogous to the ice rule in spin ices, and supporting a low energy (bosonic) excitation [4]. Under applied field, a complex antiferromagnetic structure sets in, while the low energy excitations transform into a spin wave like mode whose dynamical structure factor is highly anisotropic, showing “half-moons” in reciprocal space [6]. This peculiar form indeed casts light on the underlying “ice rule” of $Tb_2Ti_2O_7$.

[1] J Gardner, M. Gingras and J. Greedan, Reviews of modern Physics, Vol 82 (2010)

[2] J. Gardner et al PRL 82, 1012, (1999)

[3] S. Guitteny et al PRL 111, 087201 (2013)

[4] T. Fennell et al., PRL 112, 017203 (2014)

[5] T. Fennell et al, PRL 109, 017201 (2012) and (2013)

[6] S. Petit et al, in preparation

FR.D-P30 - Spin-1/2 Heisenberg ferromagnet on the pyrochlore lattice

O. Menchyshyn¹, O. Derzhko¹, J. Richter²

1. *Institute for Condensed Matter Physics of NAS, Lviv, Ukraine*

2. *Institut für theoretische Physik, Magdeburg, Germany*

We investigate the spin-1/2 Heisenberg model on the pyrochlore lattice (three-dimensional lattice made of corner-sharing tetrahedra) with ferromagnetic nearest-neighbor interaction within 1) the linear spin-wave theory, 2) the two-time Green-function method, and 3) the quantum Monte Carlo approach. Though the pyrochlore ferromagnet has the same coordination number as the simple cubic ferromagnet (i.e., six nearest neighbors), the results for both models beyond the mean-field theory differ substantially. For example, the quantum Monte Carlo simulations yield a critical temperature of the simple cubic model of $T_c=0.839(1)$ [1], while for the pyrochlore model only $T_c=0.718(6)$ is obtained. Furthermore, we compare our findings for the pyrochlore ferromagnet with the high-temperature-expansion predictions [2] and the experimental data for $\text{Lu}_2\text{V}_2\text{O}_7$ [3].

[1] S. Wessel, Phys. Rev. B 81, 052405 (2010)

[2] A. Lohmann, H.-J. Schmidt, and J. Richter, Phys. Rev. B 89, 014415 (2014)

[3] M. Mena et al., Phys. Rev. Lett. 113, 047202 (2014)

FR.D-P32 - Magnetic field induced phase transition in Cs₂CuBr₄

D. Kamenskyi¹, J. Bruin¹, L. Peters¹, P. Gogoi¹, G. Vasylets², V. Meviediev³

1. *Radboud University, Institute for Molecules and Materials, High Field Magnet Laboratory, Nijmegen, Netherlands*

2. *V. Karazin Kharkiv National University, Faculty of Chemistry, Kharkiv, Ukraine*

3. *Division of Functional Materials Chemistry, SSI "Institute for Single Crystals" of National Academy of Science of Ukraine, Kiev, Ukraine*

The presence of qualitatively new ground states brings quantum magnets with frustrated exchange interactions into a focus of modern magnetism. A high degree of degeneracy in the ground state of frustrated magnets provides an opportunity for studying quantum phase transitions. For example, the magnetic-field-induced plateau phase at one-third of the saturation magnetization in frustrated antiferromagnets with a triangular arrangement of spins was predicted as a field-induced ground state stabilized by quantum fluctuations [1]. Cs₂CuBr₄ is an example of a frustrated magnet on a distorted triangular lattice where the plateau has been observed [2]. We report on a far infrared and magnetic torque investigation of Cs₂CuBr₄ at high magnetic fields and temperatures down to 300 mK. We observed two vibrational modes at 25.4 and 29.3 cm⁻¹ by means of far-infrared spectroscopy. High-field experiments reveal a splitting of the phonon mode between 24 and 26 T, which coincides with an anomaly observed in magnetic torque. We associate these findings with a field-induced distortion of the tetrahedral environment of Cu²⁺ ions due to the competition between Jahn-Teller and spin-orbit interactions. The external magnetic field shifts the energetic balance between those two interactions. Our findings and previous theoretical investigations [3] suggest that a wide class of quantum magnets can exhibit field-induced quantum phase transitions. Such investigations were limited in the past by the lack of sufficiently strong magnetic fields, but now the availability of continuous fields above 35 T and pulsed fields above 90T opens new possibilities.

[1] A. V. Chubukov and D. I. Golosov, *J. Phys. Condens. Matter* 3, 69 (1991)

[2] T. Ono, H. Tanaka, H. Aruga Katori, F. Ishikawa, H. Mitamura, and T. Goto, *Phys. Rev. B* 67, 104431 (2003)

[3] Kugel and D. Khomskii, *Sov. Phys. Usp.* 25, 231–256 (1982)

FR.D-P34 - Structural modulation driven spin canting in re-entrant glassy magnetic phase of $\text{Lu}_2\text{MnNiO}_6$

K. Manna¹, A.K. Bera^{3,4}, M. Jain¹, S. Elizabeth¹, S.M. Yusuf³, P.S. Anil Kumar¹

1. *Leibniz-Institute for Solid State and Materials Research, (IFW), Dresden, Germany*

2. *Department of Physics, Indian Institute of Science, Bangalore, India*

3. *Solid State Physics Division, Bhabha Atomic Research Centre, Mumbai, India*

4. *Helmholtz Zentrum Berlin für Materialien und Energie, Berlin, Germany*

Unusual spin structure of double perovskite and re-entrant spin-glass (RSG) compound $\text{Lu}_2\text{MnNiO}_6$ has been investigated using conventional magnetometry and neutron diffraction. System possesses a ferromagnetic (FM) ordering below $T_C = 40$ K and undergoes a RSG transition at, $T_g = 20$ K. Interestingly, the system retains the memory effect above T_g , till spins sustain ordering. It is found that as system cools below T_C , spins cant ferromagnetically with respect to the crystallographic 'c' axis, resulting a novel critical behavior whose exponents ($\beta = 0.241$ and $\gamma = 1.142$) doesn't match with any of the conventional model. Comprehensive study of temperature dependent neutron diffraction and first principle-based computation divulges that octahedral tilting induced structural transition and an imprinting spin-orbit interaction results this novel canted spin structure below T_C , which might be the intrinsic scenario for all RSG compounds.

FR.D-P35 - High-field raman spectroscopy measurement of the geometrically frustrated chromium spinel oxide CdCr_2O_4

Y. Sawada¹, S. Kimura¹, K. Watanabe¹, H. Ueda²

1. *Institute for Materials Research, Tohoku University, Sendai, Japan*

2. *Graduate School of Science, Kyoto University, Kyoto, Japan*

The chromium spinel oxide CdCr_2O_4 remains the paramagnetic state down to low temperature due to the strong geometrical frustration. It is known that this material undergoes the magnetic phase transition to the magnetically ordered phase at $T_N = 7.8$ K. By applying a magnetic field at low temperature, the $1/2$ magnetization plateau phase that is stable in a wide range of the magnetic field, appears at $H_c = 28$ T, accompanied by a large magnetostriction [1]. It is considered that the stability of the plateau phase originates from the lattice deformation that stems from the spin-lattice coupling. Therefore, we have performed a high field Raman spectroscopy measurement in order to clarify the lattice dynamics in the $1/2$ magnetization plateau phase.

The experiment using a single crystal of CdCr_2O_4 has been done by the high field Raman spectroscopy system utilizing the 31 T hybrid magnet in our laboratory. At zero field, three Raman peaks were observed at 131, 501, and 602 cm^{-1} below T_N . These peaks correspond to the phonon triplets of T_{2g} symmetry, for which oxygen ions displace whereas chromium is not in motion [2]. In the high field experiment, we found that the T_{2g} phonon peaks do not show clear shift at H_c . In this material, the nearest-neighbor exchange interaction between chromium ions is considered to be a sum of the antiferromagnetic direct exchange interaction and the ferromagnetic superexchange interaction through non-magnetic oxygen ions. Since our result indicates that T_{2g} modes, which involve only the vibration of oxygen and cadmium ions, is not changed by the transition to the $1/2$ magnetization plateau phase. We conclude that the direct-exchange interaction is dominant in the nearest-neighbor interaction of CdCr_2O_4 .

[1] H. Ueda et al., Phys. Rev. Lett. 94, 047202 (2005)

[2] Ch. Kant et al., Phys. Rev. B 80, 214417 (2009)

FR.D-P36 - Critical properties of a triangular lattice Ising AF/FM bilayer

M. Zukovic¹, A. Bobak¹

1. Institute of Physics, Faculty of Science, P.J. Šafárik University, Košice, Slovakia

We study by Monte Carlo simulation an Ising spin system consisting of one antiferromagnetic (AF) and one ferromagnetic (FM) triangular plane, with the respective intralayer couplings of equal strengths but opposite signs, which are coupled by a varying FM interlayer exchange. The critical behavior of the decoupled planes is notoriously well-known. The AF one shows no long-range ordered (LRO) phase down to zero temperature due to high geometrical frustration, while the FM one displays a single standard Ising universality class phase transition to the FM LRO phase. We show that introduction of a finite interlayer exchange induces drastic changes to this critical behavior. Namely, when the interlayer coupling is relatively small or comparable with the intralayer coupling we identify two separate phase transitions. The one occurring at higher temperatures is related to the transition from the paramagnetic to FM state and is of standard Ising universality class. At lower temperatures there is another phase transition that takes place only in the AF plane. At this transition spins rearrange into a ferrimagnetic state with spins on two sublattices pointing parallel and on one sublattice antiparallel to the spins on the FM plane. Finite size scaling indicates that the critical indices governing this phase transition take non-universal (not even weakly universal) values that vary with the interlayer to intralayer coupling strength ratio. Nevertheless, if the interlayer coupling becomes sufficiently strong both phase transitions disappear and the AF/FM bilayer effectively behaves as a single AF layer, showing only a noncritical anomaly in thermodynamic quantities. Thus, while a relatively weak interlayer coupling to the FM plane induces even two phase transitions in the frustrated noncritical AF plane, a sufficiently strong coupling to the AF plane impedes any LRO in the standard FM Ising model.

FR.D-P37 - Single crystal growth of tunable Cu-based quantum spin systems

P. Puphal¹, N. Van Well¹, F. Ritter¹, D.V. Sheptyakov², C. Rüegg^{2,3}, C. Krellner¹

1. *Goethe University Frankfurt, Frankfurt, Germany*

2. *Laboratory for Neutron Scattering and Imaging, Paul Scherrer Institute, Villigen, Switzerland*

3. *Department of Quantum Matter Physics, University of Geneva, Geneva, Switzerland*

We present crystal growth and analysis of the spin liquid candidate $(\text{Zn,Ga})\text{Cu}_3(\text{OH})_6\text{Cl}_2$ and the dimersystem $(\text{Ba,Sr})\text{CuSi}_2\text{O}_6$.

Herbertsmithite the spin $\frac{1}{2}$ Heisenberg antiferromagnet with a kagome lattice was proposed and proven to have a spin-liquid ground state due to the high degree of frustration. We have synthesised powder of $\text{Ga}_x\text{Cu}_{4-x}(\text{OH})_6\text{Cl}_2$, in which a doping of $x = 1$ was proposed to give a correlated Dirac metal (I. I. Mazin et. al., Nature Communications 5, 4261 (2014)). We have confirmed with EDX and magnetic measurements that Ga is built into the structure with values of. $\text{Ga}_x\text{Cu}_{4-x}(\text{OH})_6\text{Cl}_2$ shows long-range magnetic order similar to Zn-Paratacamite and with increasing x the ordering temperature decreases.

In $\text{BaCuSi}_2\text{O}_6$ triplons condense in a 2D Bose-Einstein-Condensate (BEC) at magnetic fields above 23.15 T at low temperatures accompanied by a dimensional crossover from 3D to 2D, when lowering temperature (S. E. Sebastian, et al., Phys. Rev. B 74, 180401(R) (2006)). A structural phase transition below 100 K leads to two different Cu-dimer layers, making the Hamiltonian describing the system complex (D. V. Sheptyakov et. al., Phys. Rev. B 86 014433 (2012)).

Results for strontium substitution on the barium side and investigation of the structural transition with specific heat measurements, low temperature x-ray and neutron powder diffraction surprisingly show that already small amounts of Sr ($x = 0.05$) lead to a suppression of the structural phase transition. Crystal growth in a tube furnace with a flow of oxygen was successfully employed and gave rise to Sr substituted crystals of up to $3 \times 4 \times 1 \text{ mm}^3$ and 18 mg. With increasing Sr-content the unit cell volume decreases and the intra-dimer spacing increases. The role of frustration and the dimensionality of the BEC in this system might be clarified by studying the substituted system.

FR.D-P38 - Spin -glass magnetism in RFeTi₂O₇ (R=Lu and Tb) compounds

T. Drokina¹, G. Petrakovskii¹, M. Molokeev¹, D.i Velikanov¹, A. Arauzo², J. Bartolomé²

1. *L.V. Kirensky Institute of Physics, SB RAS, Tomsk, Russia*

2. *Instituto de Ciencia de Materiales de Aragón (ICMA) and Departamento de Física Condensada, Zaragoza, Spain*

The compounds RFeTi₂O₇ (R=Lu and Tb) crystallize at room temperature in centrosymmetric orthorhombic space group Pcnb. There are five nonequivalent positions of the iron ions: the Fe ions occupy the two positions of Fe₁, Fe₂ (Fe₃) - in the octahedron consisting of the Fe₁ tetrahedron and Fe₂ (Fe₃) five-vertex, and the three positions of Fe in the mixed octahedron Fe₄ - Ti positions¹. The populations of the mixed Fe-Ti sites are different. The crystal structure features lead to the atomic disorder in the distribution of the magnetic ions in this compound. From low temperature heat capacity, magnetization and frequency dependent ac susceptibility we conclude that both compounds undergo a spin glass transition at TSG=4.5 and 6 K for Ln=Lu and Tb, respectively. Since Lu is not magnetic, in RFeTi₂O₇ the spin glass behavior is caused by the disordered distribution of the magnetic Fe³⁺ ions in the different crystallographic positions. The substitution of the magnetic and highly anisotropic Tb ion instead of Lu increases TSG because of the additional Tb-Fe exchange interaction, while the critical exponent of the frequency dependence on temperature hardly varies. The spin glass behavior in these crystalline compounds is caused by the presence of competitive interactions that lead to frustration.

[1] G.A. Petrakovskii, T.V. Drokina, D.A. Velikanov, O.A. Bayukov, M.S. Molokeev, A.V. Kartashev, A.L. Shadrina and A.A. Mitsuk, Phys. Sol. State, 54, 1813 (2012)

FR.D-P39 - Tricritical behavior in the Ising honeycomb lattice with competing interactionsA. Bobak¹, T. Lucivjansky¹, M. Zukovic¹, M. Borovsky¹, T. Balcerzak¹*1. Institute of Physics, Faculty of Science, P.J. Safarik University, Košice, Slovakia*

We study the phase diagram of the Ising antiferromagnet on the honeycomb lattice with competing interactions $J_1 < 0$ on nearest neighbor and $J_2 < 0$ on next-nearest neighbor bonds within the framework of the effective-field theory with correlations. The theory is based on different cluster sizes and allows us to treat large clusters in a simpler and more efficient computational manner. We determine the ground-state energy as a function of the frustration parameter $R = J_2 / |J_1|$. We find that the ground state is the Néel antiferromagnet for $R > -1/4$ and in the case of $R < -1/4$ the system orders in the anti-Néel states. The critical point separating these two phases lies at $R = -1/4$, where the transition temperature is suppressed to zero and the ground-state is highly degenerate. In order to determine the phase diagram of the J_1 - J_2 model and take into account effects of frustration within the present effective-field theory, it is necessary to consider at least a two-spin cluster. In particular, we have found that the critical temperature $k_B T_N / |J_1|$ versus R between the antiferromagnetic and paramagnetic phases changes from second to first order at a tricritical point. To get a more convincing evidence of the existence of a tricritical point in the phase diagram, we also consider four- and six-spin clusters. In this case, the clusters contain more information about lattice topology. On the other hand, our observations suggest that the transition line between the anti-Néel antiferromagnet and paramagnetic phases is first order for entire range of $R < -1/4$.

FR.D-P40 - Thermodynamic properties in the Kitaev spin liquids

J. Nasu¹, M. Udagawa², Y. Motome²

1. *Tokyo Institute of Technology, Tokyo, Japan*

2. *University of Tokyo, Tokyo, Japan*

Quantum spin liquid (QSL) is an exotic quantum state of matter in insulating magnets, where long-range ordering is suppressed down to the lowest temperature. Several experimental candidates of QSL have been recently nominated thus far. In their characterization, the absence of thermodynamic anomalies is experimentally regarded as a hallmark of QSL. On the other hand, the finite-temperature properties theoretically have not been well known due to the difficulty in the analysis for models with a QSL ground state such as the negative sign problem in quantum Monte Carlo (QMC) simulations. To clarify this problem, we address three kinds of Kitaev models on a honeycomb, a decorated honeycomb, and a three-dimensional hyperhoneycomb lattices. The Kitaev model is one of the solvable quantum spin models, where the ground state is given by QSLs. In addition, the Kitaev-type interaction is relevant to the recently found Ir oxides Li_2IrO_3 . Here, we investigate the finite-temperature properties in these Kitaev models by using the QMC simulation in the Majorana representation that we developed. Our method is free from any biased approximation as well as the negative sign problem. We find that these models commonly exhibit a two-stage entropy release, indicating thermal fractionalization of the quantum spins into two kinds of Majorana fermions. Moreover, there is no phase transition at nonzero temperature in the Kitaev model on the honeycomb lattice, but we find that the models on the decorated honeycomb and the hyperhoneycomb lattices exhibit the finite-temperature phase transitions. In the former case, the transition is associated with the time reversal symmetry breaking in the chiral QSL. On the other hand, in the latter case, the transition cannot be characterized within the Ginzburg-Landau-Wilson framework. We find the difference between QSL and paramagnet comes from the topological nature of the excitations.

FR.D-P41 - Dimer-dimer correlations and magnetothermodynamics of $S=1/2$ spherical kagome clusters in $W_{72}V_{30}$ and $Mo_{72}V_{30}$

Y. Fukumoto¹, N. Kunisada¹

1. Tokyo University of Science, Tokyo, Japan

Quantum-spin icosidodecahedrons are realized in $W_{72}V_{30}$ and $Mo_{72}V_{30}$. The former is expected to have the ideal symmetry I_h and exchange coupling of 115 K, and the latter is a little distorted. Icosidodecahedron can be considered as a kagome on a sphere, so the observation of resonating-valence-bond (RVB) states in $W_{72}V_{30}$ is of great interest. We present dimer-dimer correlation functions and show that the feature is similar to the kagome system. We also calculate the specific heat under magnetic fields below the spin-gap energy. It is found that there appears a low-temperature structure below 10 K, which has substantial magnetic-field dependence. The low-temperature structure comes from about 800 states, which consists of 360 non-magnetic and 440 magnetic ones. The existence of massive singlet and triplet low-energy excitations is consistent with the RVB picture. Calculated results for the distorted system $Mo_{72}V_{30}$ are also presented for comparison.

FR.D-P44 - Monte Carlo study of heisenberg antiferromagnets on breathing pyrochlore lattices

K. Aoyama¹, H. Kawamura¹

1. Department of Earth and Space Science, Graduate School of Science, Osaka University, Osaka, Japan

Geometrical frustration plays an important role in magnetism. One typical example of frustrated systems is antiferromagnets on a pyrochlore lattice which is a three dimensional network of corner-sharing tetrahedra. Due to a dominant nearest-neighbor antiferromagnetic interaction, classical Heisenberg spins on the tetrahedra cannot orient in certain fixed directions, and as a result, do not show any long range order at nonzero temperatures [1]. Recently, a new type of the pyrochlore lattice has been found in the spinel oxides, $\text{LiGaCr}_4\text{O}_8$ and $\text{LiInCr}_4\text{O}_8$ [2]. In contrast to the regular pyrochlore lattice in transition metal oxides AB_2O_4 , these materials have a 'breathing' structure consisting of an alternating array of small and large tetrahedra, because of the large size mismatch between Li^+ and $\text{Ga}^{3+}/\text{In}^{3+}$ ions at the A site. Although the geometrical frustration should still exist even in this nonuniform structure, specific heat measurements suggest a phase transition at $T= 13.8$ and 15.9 K for $\text{LiGaCr}_4\text{O}_8$ and $\text{LiInCr}_4\text{O}_8$, respectively.

Motivated by the experimental result, we theoretically investigate classical antiferromagnets on the breathing pyrochlore lattice. The results of our Monte Carlo simulations suggest that a breathing nearest-neighbor interaction does not lead to a long range order and that other intrinsic interactions are also essential in the above materials. In the presentation, we will discuss spin-lattice coupling effects on the spin ordering in this system.

[1] J. N. Reimers, Phys. Rev. B 45, 7287 (1992)

[2] Y. Okamoto, G. J. Nilsen, J. P. Attfield, and Z. Hiroi, Phys. Rev. Lett. 110, 097203 (2013)

FR.D-P45 - Ice-rule violation and magnetic monopoles hopping in artificial spin iceS. Krishnia¹, I. Purnama¹, N. C. Sheng Soh¹, W. Siang Lew¹, R. Maddu¹*1. Nanyang Technological University, Singapore, Malaysia*

Isolated elementary particles with a net magnetic charge have yet to be observed since the prediction by Dirac¹. However, recent observations of mobile quasiparticles that emerge in frustrated bulk magnetic materials when the ice rule is violated, has renewed the interest in uncovering the existence of magnetic monopoles². To direct the visualization of these monopoles and ice rule violation at macroscopic level, a set of magnetic nanostructures can be arranged in hexagonal geometry to create artificial spin ice systems³.

Fig.1(a) shows the magnetic charge configuration of ordered and monopole defects in static state of honeycomb artificial spin ice. Each vertex of the structure has a finite magnetic charge whose sign depends on the magnetization directions of the interacting single domain nanowires, as shown in Fig.1(b). The ordered ground state⁴ (no ice rule violation), which shows alternate dark and bright spots of equal intensity in magnetic force microscopy (MFM), is achieved by saturating the structure in -x direction. Our MFM results show that it is possible to break the ice rule by applying external magnetic field to flip the magnetization of one of the nanowire. As shown in dotted area of Fig2(a), after the application of +630Oe, a new magnetic particle at point A has emerged in the lattice. The MFM phase shift that corresponds to that magnetic particle is found to be three times higher than the rest of the magnetic charges (Fig.2(b)). All three spins around point A converge towards it, and thus point A can be said to behave as a magnetic sink. The emergent magnetic particle is stable at room temperature and can be termed as a "magnetic monopole defect" ($Q = \pm 3$). In conclusion, with the support of micromagnetic simulations a coherent picture of monopole creation and motion (1D Dirac strings) is studied.

References:

- [1] P. A. M. Dirac, *Proc. R. Soc. London, Ser. A* 133, 60 (1931)
- [2] M. J. Harris, S. T. Bramwell, D. F. McMorrow, T. Zeiske, and K. W. Godfrey, *Phys. Rev. Lett.* 79, 2554 (1997)
- [3] E. Mengotti, L. J. Heyderman, A. F. Rodríguez, F. Nolting, R. V. Hügli and H. B. Braun, *Nat. Phys.* 7, 68 (2011)
- [4] M. Tanaka, E. Saitoh, H. Miyajima, T. Yamaoka, and Y. Iye, *Phys. Rev. B* 73, 052411 (2006)

FR.D-P46 - Magnetic properties of the novel frustrated lattice magnet $\text{Cu}_3(\text{OH})_5(\text{NO}_3)\cdot 2\text{H}_2\text{O}$ (likasite)

H. Kikuchi¹, K. Kunieda¹, T. Asano¹, Y. Fujii², Y. Inagaki³, A. Matsuo⁴, K. Kindo⁴

1. *Department of Applied Physics, University of Fukui, Fukui, Japan*

2. *Research Center for Development of Far-Infrared Region, University of Fukui, Fukui, Japan*

3. *Department of Applied Quantum Physics, Kyushu University, Fukuoka, Japan*

4. *Institute for Solid State Physics, University of Tokyo, Tokyo, Japan*

Geometrically frustrated magnets attract much interest recently because several new magnetic phases including quantum liquid state are expected to occur in these systems. If the frustrated lattice is formed by $S=1/2$ magnetic moments, the combination of the frustration and quantum effects will lead to novel phenomena. In $\text{Cu}_3(\text{OH})_5(\text{NO}_3)\cdot 2\text{H}_2\text{O}$ (mineral name; likasite), tetrahedra composed by Cu^{2+} ($S=1/2$) ions are coupled by corner-sharing manner to make one dimensional (1D) chain along crystallographic b axis. Each 1D chains are interconnected by Cu^{2+} - Cu^{2+} bonds to form two dimensional spin lattice. This spin lattice (likasite lattice) is a novel frustrated lattice which has not been studied so far. We synthesized powder sample of likasite and studied its magnetic properties using magnetic susceptibility, specific heat and high field magnetization measurements. Weiss temperature estimated from magnetic susceptibility was -16 K, and a dominant magnetic interaction in likasite is found to be antiferromagnetic. The magnetic susceptibility had a round maximum at around 12 K, which is characteristic of low dimensional antiferromagnets. No long range magnetic order was observed down to 2 K, suggesting the good low-dimensionality of likasite. We measured the high field magnetization up to about 75 T at 1.3 K and 4.2 K. Below about 30 T, magnetization curve showed downward convex form, reflecting the low dimensional nature of this compound. The magnetization curve appeared to saturate above 40 T but the 'saturation' value was only 2/3 of the expected saturation magnetization. This result will be discussed in terms of a 2/3 magnetization plateau, which was theoretically pointed out to be stabilized in the frustrated diamond chain spin model with monomer interactions.

FR.D-P49 - Critical phenomena in two-dimensional frustrated Heisenberg models

S. Tanaka¹, R. Tamura², N. Kawashima³

1. *Waseda Institute for Advanced Study, Waseda University, Tokyo, Japan*

2. *International Center for Young Scientists, National Institute for Materials Science, Tsukuba, Japan*

3. *Institute for Solid State Physics, The University of Tokyo, Tokyo, Japan*

To quest novel phase transition behavior in frustrated systems with order parameter spaces described by direct product $SO(3) \times Z_n$, we consider the classical Heisenberg model on a distorted triangular lattice with the first nearest-neighbor and the third nearest-neighbor interactions. The order parameter space can be tuned by changing the model parameters. We focus on the case that the order parameter space is described by $SO(3) \times Z_2$. Using the Monte Carlo simulations, we found that a second-order phase transition occurs at a finite temperature, though the system we considered is two dimension. The second-order phase transition is associated with Z_2 symmetry breaking. In addition, the Z_2 vortex dissociation originated by $SO(3)$ is observed at the second-order phase transition temperature. To confirm whether the Z_2 vortex dissociation affects the critical phenomena, we perform the finite-size scaling. As a result, we confirm that the phase transition belongs to the universality class of the two-dimensional Ising model. Thus, we conclude that the Z_2 vortex dissociation does not influence the critical phenomena in the model. To our best knowledge, this is the first example that the simultaneous emergence of the Z_2 vortex dissociation at the critical point.

FR.D-P50 - Magnetic and thermal properties of an $S=1/2$ triangular lattice antiferromagnet Ba_2CoTeO_6 P. Chanlert¹, N. Kurita¹, H. Tanaka¹*1. Tokyo Institute of Technology, Tokyo, Japan*

$S=1/2$ Heisenberg Triangular Lattice Antiferromagnetic (TLAF) has been attracting considerable attention. This system exhibits quantum phase transitions such as magnetization plateau under magnetic field due to the strong frustration and the quantum fluctuation. This subject has been studied theoretically for a long time. However, experimental realization of $S=1/2$ Heisenberg TLAF is a little. Recently $Ba_3CoSb_2O_9$ was shown to be the best realization of $S=1/2$ Heisenberg TLAF [1,2].

Ba_2CoTeO_6 is considered to be other $S=1/2$ Heisenberg TLAF. Ba_2CoTeO_6 has a hexagonal structure with space group $P-3m1$ [3] in which Co^{2+} with effective spin $1/2$ is surrounded octahedrally by six O^{2-} ions. There are two Co^{2+} sites, $Co(1)$ and $Co(2)$. When considering cobalt atoms in the structure, they form a two-dimensional (2D) triangular lattice parallel to the ab -plane. In this study, we have synthesized Ba_2CoTeO_6 powder. By using X-ray powder diffraction technique, the sample was identified to be Ba_2CoTeO_6 . Magnetic properties were studied by magnetic susceptibility and specific heat measurements. The temperature dependence of magnetic susceptibility was measured at $H = 0.1$ T. With decreasing temperature, the susceptibility has a rounded maximum at about 19 K and decreases. Two susceptibility anomalies are observed at $T_{N1} = 12.0$ K and $T_{N2} = 3.2$ K. T_{N1} coincides with that reported previously. The second transition at T_{N2} was also observed in this study. Because T_{N2} is close to the ordering temperature $T_N = 3.8$ K in $Ba_3CoSb_2O_9$, and the configuration of $Co(1)O_6$ octahedra is similar to that in $Ba_3CoSb_2O_9$, we infer that spins on the $Co(2)$ sites order first at T_{N1} and then spins on the $Co(1)$ sites order next. From the specific heat measurements in magnetic fields, it was found that the low-temperature transition splits into two transitions in the field above 7 T, although the high-temperature transition is not largely affected.

References:

- [1] Y. Shirata et al., Phys. Rev. Lett. 108 (2012) 057205
- [2] T. Susuki et al., Phys. Rev. Lett. 110 (2013) 267201
- [3] S. A. Ivanov et al., Dalton Trans. 39, 5490 (2010)

FR.D-P51 - Magnetic ordering of triangular lattice antiferromagnets $\text{Ba}_3\text{NiTa}_2\text{O}_9$ and $\text{Ba}_2\text{NiTeO}_6$

S. Asai¹, M. Soda¹, K. Kasatani², T. Ono², M. Avdeev², T. Masuda¹

1. *The Institute for Solid State Physics, Tokyo University, Tokyo, Japan*

2. *Department of Physical Science, Osaka Prefecture University, Osaka, Japan*

3. *ANSTO, Lucas Heights, Australia*

Triangular-lattice antiferromagnets have attracted many experimentalists and theorists in the field of geometrically frustrated magnets. Small perturbation such as interlayer interaction, anisotropy, etc., lifts the macroscopic degeneracy of the ground, leading to an exotic magnetic state. $\text{Ba}_2\text{NiTeO}_6$ is a rare experimental realization of the bilayer equilateral triangular lattice of Ni^{2+} ions ($S = 1$). Meanwhile $\text{Ba}_3\text{NiTa}_2\text{O}_9$ is a conventional triangular antiferromagnet. Comparative study would be important for the understanding of the unique lattice in $\text{Ba}_2\text{NiTeO}_6$. Recently, bulk properties were studied in $\text{Ba}_2\text{NiTeO}_6$ and $\text{Ba}_3\text{NiTa}_2\text{O}_9$ by heat capacity and magnetic susceptibility measurements, and phase transitions were identified in both materials [1,2].

In order to investigate the magnetic states, we carried out powder neutron diffraction measurements at ECHIDNA in ANSTO. We observed magnetic Bragg peaks below the transition temperatures, and identified the magnetic propagation vectors for these oxides. The representation analyses lead to a 120 degree structure for $\text{Ba}_3\text{NiTa}_2\text{O}_9$ and collinear magnetic ordering for $\text{Ba}_2\text{NiTeO}_6$. We discuss the interlayer interactions and single-ion anisotropy of Ni^{2+} ion for $\text{Ba}_2\text{NiTeO}_6$ in terms of the crystal structure in order to clarify the origin of the difference for the magnetic structures.

[1] T. Ono et al.: 69th JPS annual meeting (2014) 27aPS-90

[2] K. Kasatani et al.: JPS 2014 autumn meeting (2014) 7aPS-133

FR.D-P52 - Spin liquid behavior in the depleted triangular antiferromagnets $Ba_3Ru_{1-x}Ir_xTi_2O_9$ S. Do¹, W. Lee¹, S. Lee¹, Y. Choi¹, K. Choi¹, S. Yoon², B. Suh², Z. Jang³, M. Lee⁴, E. Choi⁴

1. Dept. of Physics, Chung-Ang Univ.

2. Dept. of Physics, The Catholic Univ. of Korea, Bucheon, Rep. of Korea

3. Dept. of Physics, Kookmin Univ., Seoul, Rep. of Korea

4. National High Magnetic Field Laboratory, Florida State Univ., Tallahassee, Florida, United States

5. Max plank Institute for chemical physics of Solids, Dresden, Germany

We report dc and ac magnetic susceptibility, magnetic specific heat, and ZF- and LF-muon spin relaxation (μ SR) measurements of the stacked triangular antiferromagnets $Ba_3Ru_{1-x}Ir_xTi_2O_9$, which combine geometrical frustration and strong spin-orbit coupling [1,2]. The emerging issue is whether a ground state can be tuned by controlling the strength of spin-orbit coupling. The magnetic susceptibility of $Ba_3Ru_{1-x}Ir_xTi_2O_9$ show that with increasing x a Curie-Weiss temperature increases systematically from $\Theta_{CW} = -161$ K to -86 K while the effective magnetic moment decreases from $\mu_{eff} \sim 2.5 \mu_B$ for $x=0$ ($Ru^{4+}; S=1$) to $\mu_{eff} \sim 1.0 \mu_B$ for $x=1$ ($Ir^{4+}; J_{eff}=1/2$). ac magnetic susceptibility exhibits a spin freezing-like transition at $T=100$ mK for $x=0$ whereas no signature for frozen magnetic moment is observed down to 20 mK for $x=0$. The ZF- and LF- μ SR spectra reveal the development of no static magnetic moments down to 23 mK and show a persisting spin dynamics for temperatures below 1 K for all x . Taken together with ac susceptibility, we conclude that a fraction of spin freezing at $x=0$ is completely melted to a dynamically fluctuating state at $x=1$. This result suggests that strong spin-orbit coupling provides a control parameter of stabilizing spin liquid in a triangle lattice owing to extended 5d orbitals.

[1]T. Dey, et al, PRB.86.140405R(2012) [2]T. Dey, et al, Eur Phys J B.86.247(2013) [3]L. Clark et al, PRL 110, 207208 (2013)

FR.D-P53 - Substitution effect on S=1/2 frustrated magnetic cluster system $\text{Li}_2\text{AMo}_3\text{O}_8$ (A=In, Sc)Y. Haraguchi¹, C. Michioka¹, H. Ueda¹, K. Yoshimura^{1,2}*1. Department of Chemistry, Graduate School of Science, Kyoto University, Kyoto, Japan**2. Research Center for Low Temperature and Materials Sciences, Kyoto University, Kyoto, Japan*

Frustrated cluster magnets are expected to produce competition between spin frustration effects and charge fluctuation within a cluster, which possibly produces novel physics. We investigated the substitution effects on S=1/2 frustrated magnetic cluster system $\text{Li}_2\text{AMo}_3\text{O}_8$ (A=In, Sc) for the purpose of revealing details of the effect of charge fluctuations on cluster magnets. For the non-substituted compounds $\text{Li}_2\text{AMo}_3\text{O}_8$ (A=In, Sc), although their magnetic properties are attributed to the same magnetic cluster lattice, their ground states are completely different from each other; while $\text{Li}_2\text{InMo}_3\text{O}_8$ exhibits a conventional magnetic ordering with 120-degree structure, $\text{Li}_2\text{ScMo}_3\text{O}_8$ shows a spin liquid like condensation. From the ^{115}In - and ^{45}Sc -NMR studies, charge fluctuations are found to play a key role for suppression of a magnetic ordering.

For substituted compounds $\text{Li}_2\text{In}_{1-x}\text{Sc}_x\text{Mo}_3\text{O}_8$, XRD patterns of the $0 < x < 1$ samples demonstrated successful synthesis, and suggest monotonic-decrease of cell parameters from $\text{Li}_2\text{InMo}_3\text{O}_8$ to $\text{Li}_2\text{ScMo}_3\text{O}_8$.

The effective magnetic moment for $\text{Li}_2\text{In}_{1-x}\text{Sc}_x\text{Mo}_3\text{O}_8$ obtained from the high temperature Curie-Weiss fitting to magnetic susceptibility does not show the linear relation against x value and take a minimum at $x=0.5$. Moreover, it was observed that $\text{Li}_2\text{In}_{1-x}\text{Sc}_x\text{Mo}_3\text{O}_8$ with $0.3 < x < 0.9$ exhibits the disappearance of partial paramagnetic spins without magnetic orderings. Such the disappearance is also observed in the cluster magnet $\text{LiZn}_2\text{Mo}_3\text{O}_8$ with the same magnetic lattice of $\text{Li}_2\text{AMo}_3\text{O}_8$.

These facts suggest that cation-disordering suppress the low-temperature magnetic moment which comes from local dimerizations or constructions of VBS on honeycomb sublattice among cluster spins.

FR.D-P55 - Magnetic characterization of single crystalline barlowite - a structurally perfect spin-1/2 kagome system

M. Lang¹, E. Gati¹, N. Hieu Hoang¹, B. Wolf¹, H. Jeschke², F. Salvat-Pujol², R. Valenti², J.A. Schlueter³

1. *Physics Institute, Goethe University Frankfurt, Frankfurt, Germany*

2. *Institute for Theoretical Physics, Goethe-University Frankfurt, Frankfurt, Germany*

3. *Division of Materials Research, National Science Foundation, Arlington, Virginia, United States*

Quantum-spin-liquid (QSL) candidates based on spin-1/2 kagome lattices have been of high interest in recent years [1-3]. The natural mineral herbertsmithite $\text{ZnCu}_3(\text{OH})_6\text{Cl}_2$ has been considered one of the best QSL candidate systems although some ambiguities remain. Since chemical modifications of this kagome system are difficult to realize, new design strategies are necessary for synthesizing novel spin-liquid materials. The mineral barlowite $\text{Cu}_4(\text{OH})_6\text{FBr}$ reflects such a novel approach [4,5]. It contains Cu^{2+} ions in a structurally perfect kagome arrangement due to the different bonding environments adopted by the F^- and Br^- ions. Here we present a detailed magnetic characterization of small single crystals of barlowite $\text{Cu}_4(\text{OH})_6\text{FBr}$. Measurements of the magnetization and susceptibility down to 2 K and up to 5 T reveal indications for two dominant magnetic couplings of different sign and an antiferromagnetic transition at $T_N = 15$ K. The experimental findings are in good agreement with the results of density functional theory (DFT) calculations from which the Heisenberg Hamiltonian parameters are derived. By using a high temperature series expansion and the DFT-derived intra- as well as inter-kagome-plane exchange couplings, a very good fit to the susceptibility data for $T > T_N$ is obtained. The magnetic coupling between the kagome layers together with the Dzyaloshinskii-Moriya interaction, implied by the crystal's symmetry, provide a natural explanation for the canted nature of the antiferromagnetic ordering at $T_N = 15$ K giving rise to a weak ferromagnetic component.

[1] P. Mendels and F. Bert, J. Phys. Soc. Jpn. 79, 011001 (2010)

[2] P. Mendels and F. Bert, J. Phys.: Conf. Series 320, 012004 (2011)

[3] T.-H. Han et al., Nature 492, 406 (2012)

[4] T.-H. Han, J. Singleton, J. A. Schlueter, Phys. Rev. Lett. 113, 227203 (2014)

[5] H. O. Jeschke et al., arXiv:1412.4668v1

FR.D-P56 - Single-crystal high-temperature pyrochlore antiferromagnetic NaCaCo₂F₇: An NMR investigation

R. Sarkar¹, J. Krizan², F. Brückner¹, R.J. Cava², H.H. Klaus¹

1. *Technical University of Dresden, Dresden, Germany*

2. *Department of Chemistry, Princeton University, Princeton, United States*

The fluoride pyrochlore NaCaCo₂F₇ is a newly discovered frustrated pyrochlore. This possesses the large Curie Weiss theta (-140 K) albeit there is no magnetic ordering down to low temperature. The resulting frustration index of $f = \theta_{CW}/T_f \sim 56$ indicates that NaCaCo₂F₇ is highly frustrated. The small entropy loss at the freezing transition suggests magnetic entropy remains present in NaCaCo₂F₇ at 0.6 K [1]. We performed ¹⁹F and ²³Na NMR investigations on a large single crystalline sample of NaCaCo₂F₇. While ²³Na NMR -spectra reveals the presence of two inequivalent Na sites, in accordance with the local disorder of the system, below ~ 3.7 K both the ²³Na -and ¹⁹F spectra broadens considerably. Reduction of the ²³Na NMR signal intensity hints at a spin-glass state or a quasi-static field distribution in NaCaCo₂F₇. On the other hand, ¹⁹F spin-lattice relaxation rate ¹⁹(1/T₁) exhibits a peak at around ~ 3 K, at the same temperature range where ac and dc susceptibility data show a broad maximum. The overall temperature dependence of ¹⁹(1/T₁) can be modeled by the BPP theory considering a fluctuating hyperfine field with an autocorrelation function. The correlation time of the autocorrelation function exhibits an activation behavior further indicating the spin-glass state in NaCaCo₂F₇.

[1] J. W. Krizan and R. J. Cava Phys. Rev. B 89, 214401 (2014)

FR.D-P58 - Magnetic properties in a frustrated spin ladderTakanori Sugimoto¹, M. Mori², T. Tohyama¹, S. Maekawa²*1. Department of Applied Physics, Tokyo University of Science, Tokyo, Japan**2. Advanced Science Research Center, Japan Atomic Energy Agency, Ibaraki, Japan*

Recently, a new type of low-dimensional quantum spin model has attracted much attention due to successive magnetic phase transitions in a corresponding compound BiCu₂PO₆ [1]. The magnetic behaviors of the compound are well understood as a frustrated two-leg spin-ladder system, which bridges between the frustrated spin chain and the non-frustrated spin ladder with 1/2 spins [2]. A pile of studies on the frustrated spin chain and non-frustrated spin ladder has insisted that number of chains and magnitude of frustration strongly affect spin gaps in excitation spectrum. For instance, the non-frustrated spin ladder exhibits a finite spin gap, although the spin chain has no gaps without frustrations. On the other hand, a strong frustration in the spin chain causes not only a spin gap over the ground state but also another gap above 1/3 magnetized state. Therefore, the bridging model of these is worthy of study in order to clarify mechanisms of spin gaps in terms of frustration and number of chains.

We firstly investigate magnetic excitations in the frustrated two-leg spin ladder without magnetic fields by using the dynamical density-matrix renormalization-group method. We find some differences in excitation spectrum between two possible ground-state phases. The qualitative features can be understood by two different elementary excitations. Additionally, we examine magnetization processes and magnetic phase transitions. The numerical results show that magnetization plateaux emerge at $M=1/2$ and $2/3$, in addition to $1/3$ plateau and some cusps [2]. We also find out an analytical correspondence between effective models in weak and strong rung-coupling limits, which gives an explanation of the plateaux and cusps. Our study is useful to analyze experimental data of BiCu₂PO₆.

[1] Y. Kohama, et al., Phys. Rev. Lett. 109, 167204 (2012)

[2] T. Sugimoto, M. Mori, T. Tohyama, and S. Maekawa, Phys. Rev. B 87, 155143 (2013); arXiv:1409.4280

FR.D-P59 - Atomic layer deposition and characterization of triangular lattice antiferromagnetic oxide CuCrO_2

T. S. Tripathi¹, M. Karppinen¹

1. Inorganic Chemistry Department, Aalto University, Espoo, Finland

In this study, we report the atomic layer deposition (ALD) of antiferromagnetic ternary copper chromium oxide: CuCrO_2 . Copper tetramethyl heptanedionate ($\text{Cu}(\text{thd})_2$) has been used as the precursor for copper source, chromium acetyl acetonate ($\text{Cr}(\text{acac})_3$) for chromium source and ozone as the oxygen source. The growth was investigated at deposition temperatures from as low as 200 °C up to 350 °C. The effect of the process conditions and post-deposition annealing on the film structure was investigated. Atomic force microscopy revealed that the films were smooth (surface roughness ~ 0.5 nm) and uniform. The composition and stoichiometry of the films were determined by X-ray photoelectron spectroscopy and inductively coupled plasma mass spectrometry (ICP-MS).

FR.D-P60 - Specific heat of triangular spin tubes in magnetic fields

H. Manaka¹, M. Hagihala², S. Hayashida², M. Soda², T. Masuda², Y. Miura³

1. Graduate School of Science and Engineering, Kagoshima University, Kagoshima, Japan

2. Neutron Scattering Laboratory, Institute for Solid State Physics, The University of Tokyo, Tokyo, Japan

3. Suzuka National College of Technology, Suzuka, Japan

Triangular spin tubes belong to a new category of one-dimensional Heisenberg antiferromagnets along the tubes coexisting with geometrically frustrated spin systems in the triangular plane. We discovered that chromium fluoride CsCrF_4 forms ideal equilateral triangular spin tubes with $S = 3/2$ [1]. All Cr ions are at equivalent sites, and each angle of Cr-Cr-Cr in the triangular plane is 60 deg. Because superexchange interactions through the three Cr-F-Cr paths in each equilateral triangle may be kept in equilibrium at 0 K, we propose resonating spin-singlet pairs in each equilateral triangle. To clarify ground state of the spin-liquid ground state, we performed temperature dependence of specific heat $C(T)$ measurements in magnetic fields on CsCrF_4 . As a result, there is no anomaly which indicates magnetic long-range order above 0.3 K. But temperature dependence of $C(T)/T$, after exhibiting the minimum at around 1 K, exhibits

steep monotonic increase toward 0 K. The increase of $C(T)/T$ disappears, while a broad peak appears above $B = 1\text{T}$. We found that magnetic entropy is restored above $B = 1\text{T}$ because spin frustration effect is suppressed by magnetic fields.

[1] H. Manaka et al., J. Phys. Soc. Jpn. 80, 084714 (2011)

FR.D-P61 - Low temperature spin-glass behavior in nonmagnetic atom disorder compound Pr_2CuIn_3 D. X. Li¹, Y. Homma¹, F. Honda¹, T. Yamamura², D. Aoki¹

1. *Institute for Materials Research, Tohoku University, Oarai, Japan*
2. *Institute for Materials Research, Tohoku University, Senda, Japan*

Ternary intermetallic compounds with the formula R_2TX_3 (R=U or rare-earth element, T=transition element, X = Ga, In, Si, Ge) have been the subjects of intensive studies during the past years because of their intriguing physical properties. The interest in these compounds stems from the characteristic NMAD (nonmagnetic atom disorder) crystal structure, i.e., completely or partly disordered distribution of the T and X atoms on the crystallographic sites, which is expected to cause some anomalous magnetic properties. Recently, we have been paying special attention to the ternary copper indides R_2CuIn_3 . Except for the early susceptibility measurements between 4.2 and 160 K, no other magnetic properties are reported for the compounds of this family.

We present the experimental results of ac and dc susceptibility, magnetization, magnetic relaxation, specific heat, electrical resistivity and magnetic memory effect for hexagonal CaIn₂-type polycrystalline Pr_2CuIn_3 . It is found that the ac susceptibility shows an evident peak near $T_f \sim 5.4$ K, which shifts to high temperature with increasing frequency, while irreversible magnetism manifesting as the separation between FC and ZFC dc susceptibilities, long-time magnetic relaxation behavior and ZFC magnetic memory effect can be clearly observed below T_f . These features are considered as evidence for the formation of spin-glass (SG) state in Pr_2CuIn_3 . This conclusion is further confirmed by the specific heat and electrical resistivity measurements that suggest the absence of long-range magnetic ordering in this system. As important parameters characterizing the SG state, static spin freezing temperature, critical exponent and activation energy are determined from the dynamical analyses of the ac susceptibility data and compared with those obtained for other 2:1:3 compounds. We conclude that Pr_2CuIn_3 could be classified as a NMAD spin glass. The SG state in Pr_2CuIn_3 seems to originate from the continued site randomness of the non-magnetic elements, which introduce the random distribution of RKKY interactions.

FR.D-P62 - Frustrations in a mixed spin-1/2 and spin-1 Ising model with multispin exchange interactions and single-ion anisotropy on a bipartite honeycomb lattice

V. Stubna¹, M. Jascur¹

1. Department of Theoretical Physics and Astrophysics, Institute of Physics, P.J. Safarik University In Kosice, Košice, Slovakia

This work is devoted to the study of a mixed spin-1/2 and spin-1 Ising model on the honeycomb lattice. In addition to the standard pair exchange interactions and single ion-anisotropy term, we have also included into Hamiltonian unconventional three-site interactions between spin residing on the sublattice A and its nearest neighbors located on the sublattice B.

Applying the generalized form of star-triangle transformation, we have obtained an exact expression for the partition function of the system under investigation. Then, using standard relations of thermodynamics and statistical physics, we have derived exact results for the ground-state and finite temperature phase diagrams, thermal variations of the sublattice and total magnetization, correlation functions, internal energy, Helmholtz free energy, specific heat and entropy of the system. Our results clearly illustrate that due to the presence of three-site interaction term, the system exhibits very interesting physical behavior.

We have observed that the inclusion of three-site interaction causes strong competitive effects in the system, that in turn generate novel disordered phases. In particular, we have found several disordered frustrated phases exhibiting non-zero ground-state entropy. On basis of our analysis one can definitely state that the multispin interactions in magnetic systems are of extraordinary importance and deserve further investigation.

This work has been supported under grant VEGA No. 1/0331/15.

FR.D-P63 - Exact results of a mixed spin-1/2 and spin-3/2 Ising model with multispin exchange interactions and single-ion anisotropy on a decorated triangular lattice

V. Stubna¹, M. Jascur¹, K. Szaowski², T. Balcerzak²

1. *Department of Theoretical Physics and Astrophysics, Institute of Physics, P.J. Safarik University In Kosice, Kosice, Slovakia*

2. *Department of Solid State Physics, Faculty of Physics and Applied Informatics, University of Lodz, Lodz, Poland*

In this work we have obtained exact results for a mixed spin-1/2 and spin-3/2 Ising model in which, in addition to the standard pair exchange interactions, we have also considered unconventional three-site interactions between each decorating spin and its nearest neighbors. Applying the generalized decoration-iteration transformation, we have obtained an exact expression for the partition function of the decorated triangular lattice. Then, using standard relations of thermodynamics and statistical physics, we have calculated the ground-state and finite temperature phase diagrams, thermal variations of the sublattice and total magnetization, correlation functions, internal energy, Helmholtz free energy, specific heat and entropy of the system. Our results clearly indicate extraordinarily interesting influence of the three-site interaction term on physical properties of planar Ising spin systems. In particular, we have found that in the case of pure three-site interactions, the system becomes frustrated and exhibits non-zero ground-state entropy. Our results also clarify the role of coordination number and the spin value in the systems with multispin interactions. This work has been supported under grant VEGA No. 1/0234/12.

FR.D-P66 - Neutron scattering study of the quantum spin ice candidate $\text{Pr}_2\text{Zr}_2\text{O}_7$

S. Guitteny¹, J. Robert³, S. Petit¹, E. Lhotel³, A. Goukassov¹, I. Mirebeau¹, P. Bonville², C. Decorse⁴, M. Ciomaga Hatnean⁵, G. Balakrishnan⁵

1. CEA Saclay DSM/IRAMIS/Laboratoire Léon Brillouin, Gif Sur Yvette, France
2. CEA Saclay DSM/IRAMIS/SPEC, Gif Sur Yvette, France
3. Institut Néel CNRS, Grenoble, France
4. LPCES Université Paris Sud, Orsay, France
5. Department of Physics University of Warwick, Coventry, United Kingdom
6. CEA Grenoble CEA/INAC/MDN, Grenoble, France
7. Institut Laué Langevin, Grenoble, France

The pyrochlore compound $\text{Pr}_2\text{Zr}_2\text{O}_7$ is suggested to be a good candidate for displaying quantum spin ice phenomenology [1]. This is supported by recent measurements by Kimura et al showing that the elastic magnetic pattern displays a large pinch point broadening and fast fluctuations down to 50 mK. They also showed that the crystal electric field of the non-Kramers ion Pr^{3+} is consistent with an Ising anisotropy [2]. In this work, we report local susceptibility measurements carried out with polarised neutrons revealing the strong Ising-like anisotropy of the magnetic moments of the Pr^{3+} ions along the $\langle 111 \rangle$ axis. We also investigate the field induced magnetic ordering of this compound using neutron diffraction and inelastic scattering. Our neutron experiments support the existence of ferromagnetic correlations between the magnetic moments despite a negative θ_{CW} . These, together with the magnetization measurements, indicate a mixing of the two wave functions of the non-Kramers ground state which leads to fluctuations within the doublet. It is of great interest to compare these results with another quantum spin ice candidate with Ising-like non Kramers ions, namely $\text{Tb}_2\text{Ti}_2\text{O}_7$. In this compound, the coupling with the lattice written in terms of quadrupoles is likely at play involving the existence of a magneto-elastic excitation [3, 4]. However, in $\text{Pr}_2\text{Zr}_2\text{O}_7$, although we have clues for a coupling to the lattice, such features have not been observed. Moreover, one has to take into account the importance of defects which do play a role in the physics of this compound

[1] M.J.P. Gingras and P.A. McClarty, Rep. Prog. Phys. 77 056501 (2014)

[2] K. Kimura et al, Nat. Commun., 5, 1934 (2013)

[3] T. Fennell et al, Phys. Rev. Lett., 112, 017203, (2013)

[4] S. Guitteny et al, Phys. Rev. Lett., 111, 087201, (2013)

FR.D-P67 - Spin dynamics of a frustrated FCC - antiferromagnet

K. Siemensmeyer¹, D.J.P. Morris², D.A. Tennant³, A. Schneidewind⁴, K. Flachbart⁵, S. Gabani⁵, N. Shitsevalova⁶

1. Helmholtz Zentrum Berlin, Berlin, Germany

2. Xavier University, Cincinnati, Ohio, United States

3. Oak Ridge National Laboratory, Knoxville, Tennessee, United States

4. Forschungszentrum Jülich, Outstation MLZ, Garching, Germany

5. Inst. Exp.Phys., Slovak Acad. of Science, Kosice, Slovak Republic

6. Inst. for Problems of Mat Science, Ukraine Acad. of Science, Kiev, Ukraine

We investigate the dynamics of the frustrated FCC - magnet HoB12 with inelastic neutron diffraction in the paramagnetic state. Distinct regions in q - space are identified where the dynamics shows different behaviour above T_N : These are, first, so called “pinch points” of the reciprocal lattice which show static spin correlation that diverge only in the limit $T \rightarrow 0$, second, general lattice points and third nodal lines that connect reciprocal lattice points. Correlations from general lattice points show power law like temperature dependence that finally drives the antiferromagnetic (afm) ordering. The data are compared with results from classical Monte Carlo simulations as well as simulations of the dynamic behaviour in the paramagnetic and the afm ordered phase.

FR.D-P69 - Re-investigation of low-temperature magnetic phase transitions of the geometrically frustrated isosceles triangular Ising antiferromagnet CoNb₂O₆

S. Mitsuda¹, S. Hosaka¹, H. Tamatsukuri¹, H. Koorikawa¹, S. Kobayashi², T. Nakajima³, K. Prokes⁴, K. Kiefer⁴

1. *Tokyo University of Science, Tokyo, Japan*

2. *Iwate University, Morioka, Japan*

3. *RIKEN, Wako, Saitama, Japan*

4. *Helmholtz-Zentrum Berlin, Berlin, Germany*

A columbite niobate, CoNb₂O₆ is one of the model material of isosceles-triangular lattice Ising antiferromagnet, where magnetic Co²⁺ ions form quasi-one-dimensional ferromagnetic zigzag chains running along the orthorhombic c axis and form an antiferromagnetic isosceles-triangular lattice in the a-b plane. Extensive neutron diffraction measurements have demonstrated rich magnetic field (H) versus temperature (T) phase diagrams which are attributed to the competing interchain exchange interactions on the isosceles-triangular lattice.

While the H//c-T magnetic phase diagram is well studied down to 0.2K [1], neutron diffraction study of the H//a-T magnetic phase diagram is limited down to 1.8K [2]. In present study, we performed neutron diffraction and magnetization experiments down to 0.5 K on a single crystal of CoNb₂O₆ with an external magnetic field applied along the a axis, in order to investigate (i) how field-induced ferrimagnetic phase characterized by the propagation wave vectors $Q=(0,1/4,0)$ which has been suggested by H. Weitzel et al.[2] is extended to lower temperature region in the H//a-T magnetic phase diagram and (ii) how it connected with 1/2 magnetization plateau reported by T. Hanawa et al. [3] from which three up and one down spin arrangement is inferred.

As a result, we found that the field-induced ferrimagnetic phase does not exist in zero temperature limit, being consistent with that the ferrimagnetic state is degenerate at the transition magnetic field between antiferromagnetic ground state and field-induced paramagnetic state.

[1] S. Kobayashi et al., Phys. Rev. B 63, 024415 (2000)

[2] H. Weitzel et al., Phys. Rev. B 62, 12146 (2000)

[3] T. Hanawa et al., J. Phys. Soc. Jpn. 63, 2706 (1994)

FR.D-P71 - Field induced phenomena in magnetically frustrated systems $\text{Co}_{1-x}\text{M}_x\text{Al}_2\text{O}_4$ (M = Mg, Zn)

T. Naka¹, K. Sato², S. Ishii³, T. Nakane¹, N. Terada¹, M. Taguchi⁴, M. Nakayama¹, Y. Matsushita¹, A. Matsushita¹, S. Takami²

1. National Institute for Materials Science, Ibaraki, Japan

2. Institute of Multidisciplinary Research for Advanced Materials, Tohoku University, Miyagi, Japan

3. Department of Physics, Tokyo Denki University, Tokyo, Japan

4. Department of Applied Chemistry, Faculty of Science and Engineering, Chuo University, Tokyo, Japan

Magnetism of the spinel-type magnetically frustrated antiferromagnetic CoAl_2O_4 and its magnetically diluted system, $\text{Co}_{1-x}\text{M}_x\text{Al}_2\text{O}_4$; (M = Mg and Zn), are reported. These systems are partially inverted spinel oxides with magnetic cobalt ions (spin $S = 3/2$) predominately in the tetrahedral A-site. The effects of inversion and dilution were revealed when the system is field-cooled from the paramagnetic region. After the field cooling, a small ferromagnetic component was quenched at low temperatures. Magnetic anomalies associated with magnetic transitions were observed in magnetic susceptibility and specific heat. We proposed x-temperature phase diagrams in the range of $0 \leq x \leq 1$ for $\text{Co}_{1-x}\text{M}_x\text{Al}_2\text{O}_4$ (M = Mg and Zn). For the Zn-substituted system a multicritical point was indicated at $T = 3.4$ K and $x = 0.12$, where the antiferromagnetic, spin glass-like, and paramagnetic phases met. The quenched ferromagnetic moment was sharply enhanced at $x = 0.12$. While for the Mg-substituted system a phase boundary was also indicated at $x \sim 0.1$, the critical singularities observed in magnetization and specific heat were quantitatively different from those in the Zn substituted system.

FR.D-P72 - Exotic Field Induced Quantum Phase Transition of the Kagome Lattice Antiferromagnet

T. Sakai¹, H. Nakano²

1. JAEA, SPring-8, Hyogo, Japan

2. University of Hyogo, Hyogo, Japan

The kagome-lattice antiferromagnets have attracted a lot of interest in the field of the low-temperature physics. It exhibits some exotic field-induced phenomena, like a magnetization plateau, jump etc. Our previous large-scale numerical exact diagonalization study on the $S=1/2$ kagome-lattice antiferromagnet revealed that a novel field-induced phenomenon, 'the magnetization ramp', occurs at $1/3$ of the saturation magnetization[1]. It is characterized by different critical exponents between the lower-field and higher-field sides of the magnetization curve[2]. In order to clarify unconventional properties around the $1/3$ magnetization, we considered some extended lattice models; a distorted kagome lattice and distorted triangular lattice etc[3]. The ground-state magnetization curve recently obtained by the numerical exact diagonalization up to 42-spin clusters is also presented to estimate the shape in the thermodynamic limit. Our numerical exact diagonalization study also indicates that the ground state of the kagome-lattice antiferromagnet is gapless quantum spin liquid.

[1]H. Nakano and T. Sakai, J. Phys. Soc. Jpn. 79 (2010) 053707

[2]T. Sakai and H. Nakano, Phys. Rev. B 83 (2011) 100405(R)

[3]H. Nakano and T. Sakai, J. Phys. Soc. Jpn. 83 (2014) 104710

FR.D-P73 - Hidden Order in Spin-Liquid $Gd_3Ga_5O_{12}$

P. Deen^{1,2}, J. Paddison^{3,4}, H. Jacobsen^{2,1}, O. Petrenko⁵, M.T. Fernandez-Diaz⁶, A. Goodwin³

1. *European Spallation Source, Lund, Sweden*

2. *Niels Bohr Institute, University of Copenhagen, Denmark*

3. *University of Oxford, Inorganic Chemistry Laboratory, U.K.*

4. *ISIS Facility, Rutherford Appleton Laboratory, Didcot, U.K.*

5. *Department of Physics, University of Warwick, U.K.*

6. *Institut Max von Laue-Paul Langevin, Grenoble, France*

The search for new states of matter is a fundamental theme of condensed matter science. Frustrated magnetic materials are promising candidates for new states because lattice geometry suppresses conventional magnetic dipole order. Frustration thus drives novel emergent states.

$Gd_3Ga_5O_{12}$ is the canonical frustrated magnet as the compound that does not order via the pervasive “order by disorder” mechanism down to the lowest temperatures probed, 25 mK [1 and ref. therein]. Short-range correlations, determined via neutron diffraction, have long been assumed to originate from near neighbour short-range interactions.

A non-dipole (“hidden”) order has been uncovered via recent developments in Reverse Monte Carlo techniques [2] in conjunction with optimised neutron scattering instrumentation that enabled $S(Q)$ of non-isotope enriched $Gd_3Ga_5O_{12}$ to be probed. The hidden-order state of $Gd_3Ga_5O_{12}$, the only known example of a magnetic multipole crystal in a spin liquid, does not break the crystal symmetry and is built from individually fluctuating groups of spins. Indeed the multipolar order creates loops that are long-range ordered while individual spins show only short-range correlations.

[1] O. A. Petrenko, C. Ritter, M. Yethiraj, D. McK Paul, Phys. Rev. Lett. 80, 4570 (1998)

[2] J. A. M. Paddison, A. L. Goodwin, Phys. Rev. Lett. 108, 017204 (2012)

[3] J. A. M. Paddison, H. Jacobsen, O. A. Petrenko, M.T. Fernandez-Diaz, P. P. Deen, A.L. Goodwin. Under review Feb 2015

FR.D-P74 - Study of the frustrated Ising antiferromagnet on the stacked triangular lattice in the fieldM. Borovsky¹, M. Zukovic¹*1. Institute of Physics, P.J. Safarik University, Kosice, Slovakia*

Ising triangular antiferromagnet ($J_1 < 0$) on the stacked lattice is one of the simplest three-dimensional geometrically frustrated spin models. Several theoretical studies have been performed to analyse this model for the case of a ferromagnetic interlayer interaction ($J_2 > 0$) and these are in a very good agreement with the experimental results for the quasi-one-dimensional frustrated magnetic compound $\text{Ca}_3\text{Co}_2\text{O}_6$. However, the model with an antiferromagnetic interlayer interaction ($J_2 < 0$) has been studied much less. Such a model is a suitable choice for description of the material CsCoX_3 , where $X = \text{Cl}$ and Br . An applied magnetic field yields interesting new ground state phases in the system. For a weak external magnetic field ($h/|J_1| < -2J_2/|J_1|$) the nature of the exchange couplings arranges spins in the layers ferrimagnetically, while the adjacent layers are ordered antiferromagnetically. Macroscopically this phase is non-magnetic (total magnetization $m = 0$). Larger fields ($-2J_2/|J_1| < h/|J_1| < 6 - 2J_2/|J_1|$) allow ferromagnetic rearranging of the spins in one third of the chains while the ferrimagnetic ordering in the layers is preserved. This phase exhibits a plateau with $m = 1/3$ in the ground state. Above $h/|J_1| = 6 - 2J_2/|J_1|$ the system is in a paramagnetic phase ($m = 1$). This behaviour could correspond to the magnetization measurements of CsCoX_3 . The effective-field theory with correlations is applied in order to study this case. In order to verify the most interesting results we implement some progressive parallel algorithms such as population annealing, which is suitable for studying the systems with rough free-energy landscapes.

FR.D-P76 - Magnetothermal properties of the local xy-antiferromagnet Er₂Ti₂O₇

B. Wolf¹, W. Assmus¹, R. Schindler¹, S. Dörschug¹, M. Lang¹

1. Physikalisches Institut, Goethe University Frankfurt, Frankfurt, Germany

The magnetocaloric effect (MCE), i.e., temperature changes of a magnetic material in response to an adiabatic change of the magnetic field, has been successfully applied for reaching temperatures significantly below 1 K. Such a magnetic cooling is used in low-temperature laboratory experiments as a cost-efficient alternative to dilution refrigerators, and represents the cooling technique of choice in present space applications. No doubt, there is a demand on magnetic coolants exhibiting an enhanced MCE combined with a high cooling efficiency. The MCE of a material depends on the distribution of the magnetic entropy with respect to temperature and magnetic field. In a proof-of-principle-experiment we have demonstrated that the accumulation of magnetic entropy near a field-induced quantum-critical point (QCP) can be used for an efficient magnetic cooling [1]. Moreover, it has been shown that the cooling efficiency can be further increased significantly by employing materials with magnetic frustration [2]. Here we present magnetothermal data for Er₂Ti₂O₇ obtained on single crystalline as well as powder samples for 0.3 K < T < 4.5 K and magnetic fields up to 7 T. Er₂Ti₂O₇ is distinct among the family of geometrically frustrated rare-earth pyrochlores as it is the only pyrochlore antiferromagnet known so far that exhibits a strong easy-plane anisotropy. The system orders antiferromagnetically below T_N = 1.2 K into an unusual noncoplanar structure and exhibits a QCP around 1.5 T [3]. These characteristics make Er₂Ti₂O₇ particularly interesting for magnetic cooling. Especially the dT/dB-rate of Er₂Ti₂O₇ exceeds considerably that of Gadolinium Gallium Garnet, a material used for magnetic cooling in space applications.

[1] B. Wolf et al., Proc. Natl. Acad. Sci. USA 108 (17), 6862 (2011)

[2] M. Lang et al., Phys. Status Solidi B 250, 3, 457 (2013)

[3] J. P. C. Ruff et al., Phys. Rev. Lett. 101, 147205 (2008)

FR.D-P77 - Phase diagram within Kitaev - Heisenberg model

D. Gotfryd¹, J. Chaloupka², A.M. Oles^{3,4}

1. Institute of Theoretical Physics, Warsaw University, Warsaw, Poland

2. Central European Institute of Technology, Masaryk University, Brno, Czech Republic

3. Marian Smoluchowski Institute of Physics, Jagiellonian University, Kraków, Poland

4. Max Planck Institute for Solid State Research, Stuttgart, Germany

We present the phase diagram $K(J)$ for 8 – sites cluster within Kitaev – Heisenberg (KH) model. Above system is studied by means of cluster mean field method. Detailed examination of order parameters, two point correlation functions and ground state energies leads to the said phase diagram. While the diagram confirms part of recently published results for $\Gamma=0$ [1] (zigzag, stripy, spin liquid, ferromagnetic and antiferromagnetic phases) we argue that minor differences in the boundaries of the phases appear due to the shape of 8-sites cluster and specifics of cluster mean field method.

The results of [1] and [2] are compared with a recently developed analysis for $N=24$ cluster which preserves the lattice symmetry and also find the above phases, with somewhat extended range of Kitaev spin liquid phase. Furthermore the examination of $\Gamma \neq 0$ (extended KH model) region [1],[3] in phase space is presented.

Work supported by the Polish National Science Center (NCN) Project No. 2012/04/A/ST3/00331.

[1] J. G. Rau, E. Kin-Ho Lee, and H - Y Kee, Phys. Rev. Lett. 112, 077204 (2014).

[2] J. Chaloupka, G. Jackeli, and G. Khaliullin, Phys. Rev. Lett. 110, 097204 (2013).

[3] J. Chaloupka and G. Khaliullin, arXiv:1502.02587v3 (2015).

FR.D-P79 - Spiral-spin-liquid state in spinel MnSc₂S₄S. Gao¹, O. Zaharko¹, M. Ruminy¹, T. Fennell¹, T. Vladimir², Y. Su³, D. Chernyshov⁴, C. Rüegg¹*1. Laboratory for Neutron Scattering and Imaging, Paul Scherrer Institut, Villigen, Switzerland**2. Department of Experimental Physics, University of Augsburg & Institute of Applied Science, Academy of Sciences of Moldova, Chisinau, Moldavia**3. Jülich Centre for Neutron Science (FRM II), Aachen, Germany**4. Swiss-Norwegian Beam Lines, European Synchrotron Radiation Facility, France*

The spinel MnSc₂S₄ was predicted to host a special spiral-spin-liquid state above the magnetic phase transition temperature of 2.1 K. In this state, Mn²⁺ spins ($S = 5/2$) at the spinel A-sites tend to fluctuate together as spirals with propagating k-vectors distributed around the Brillouin zone boundary. Here we present the first neutron diffraction and diffuse scattering study on MnSc₂S₄ single crystals. Our diffuse scattering results strongly corroborate the proposed spiral-spin-liquid picture but the diffraction results call for some further modification of the proposed model Hamiltonian. Our crystals were grown using chemical transport reaction methods (typical size 1/1/0.5 mm). Synchrotron diffraction (BM-01A beamline at ESRF) on single crystals of the same batch didn't show any Mn/Sc anti-site disorder, confirming the high quality of our sample. Neutron diffuse scattering experiments were performed on DNS at FRM2 at selected temperatures from 1.5 to 50 K. Below 2 K, strong magnetic reflections for LRO with k vector of $[3/4 \ 3/4 \ 0]$ is observed; while above 2.9 K, these strong reflections are replaced by broad diffuse scattering intensity near the Brillouin zone boundary, just as theoretically predicted. Using Monte Carlo simulation, the main feature for the diffuse scattering can be reproduced with a model Hamiltonian with $|J_2/J_1| = 0.85$.

Neutron diffraction experiments measured on TriCS at PSI came as a surprise: the previously proposed ab-planar chiral based upon powder refinement cannot fit the single crystal data. With simulated annealing technique, we present here a new magnetic structure. It should be noted that Monte Carlo simulation with previous Hamiltonian prefers a parallel spin configuration along [1-10] direction, which is not the case for our new magnetic structure. Further modification for the Hamiltonian is needed to explain the formation of our proposed structure.

FR.D-P81 - Nonfrustrated Interlayer Order and its Relevance to the Bose-Einstein Condensation of Magnons in BaCuSi₂O₆ - an NMR, x-ray and neutron scattering, and DFT study

R. Stern¹, A. Tsirlin¹, I. Heinmaa¹, E. Joon¹, S. Krömer², M. Horvatic², C. Berthier², V. Mazurenko³, M. Valentyuk³, D. Sheptyakov⁴

1. NICPB/KBFI

2. EMFL/LNCMI / CNRS, Grenoble, France

3. Ural Federal University, Ekaterinburg, Russia

4. Laboratory of Neutron Scattering, Villigen PSI, Switzerland

5. Osaka University, Japan

Han purple (BaCuSi₂O₆) is not only an ancient pigment, but also a valuable model material for studying Bose-Einstein condensation (BEC) of magnons in high magnetic fields. In order to understand the nature of the two-dimensional BEC phase in BaCuSi₂O₆, we performed detailed ⁶³Cu and ²⁹Si NMR above the critical magnetic field, H_{c1} = 23.4 T.

We investigated the low-temperature crystal structure of BaCuSi₂O₆ with high-resolution synchrotron x-ray and neutron powder diffraction techniques and found it to be on average (ignoring the incommensurate modulation) orthorhombic, with the most probable space group *Ibam*. The Cu-Cu dimers in this material are forming two types of layers with distinctly different interatomic distances. Subtle changes also modify the partially frustrated interlayer Cu-Cu exchange paths. The two different alternating layers present in the system have very different local magnetizations close to H_{c1}; one is very weak, and its size and field dependence are highly sensitive to the nature of inter-layer coupling. Its precise value could only be determined by “on-site” ⁶³Cu NMR, and the data are fully reproduced by a model of interacting hard-core bosons in which the frustration associated to tetragonal symmetry is lifted, leading to the conclusion that the population of the less populated layers is not fully incoherent but must be partially condensed.

Using precise low-temperature structural data and extensive density-functional calculations, we elucidate magnetic couplings in this compound. The resulting magnetic model comprises two types of nonequivalent spin dimers, in excellent agreement with the ^{63,65}Cu nuclear magnetic resonance data. We further argue that leading inter-dimer couplings connect the upper site of one dimer to the bottom site of the contiguous dimer, and not the upper-to-upper and bottom- to-bottom sites, as assumed previously. This finding is verified by inelastic neutron scattering data and implies the lack of frustration between the layers of spin dimers in BaCuSi₂O₆, thus challenging existing theories of the two-dimensional-like BEC of magnons in this compound.

References:

1. “Nonfrustrated Interlayer Order and its Relevance to the Bose-Einstein Condensation of Magnons in BaCuSi₂O₆,” Vladimir V. Mazurenko, Maria V. Valentyuk, **Raivo Stern**, and, Alexander A. Tsirlin, *Physical Review Letters* 112 (10), 107202 (2014).
2. “Spatially resolved magnetization in the Bose-Einstein condensed state of BaCuSi₂O₆: Evidence for imperfect frustration,” S. Krämer, N. Laflorencie, **R. Stern**, M. Horvatic, C. Berthier, H. Nakamura, T. Kimura, and, F. Mila, *Physical Review B* 87 (18), 180405 (2013).
3. “Two types of adjacent dimer layers in the low-temperature phase of BaCuSi₂O₆,” D. V. Sheptyakov, V. Yu. Pomjakushin, **R. Stern**, I. Heinmaa, H. Nakamura, and, T. Kimura, *Physical Review B* 86 (1), 014433 (2012).
4. “Nuclear magnetic resonance evidence for a strong modulation of the Bose-Einstein condensate in BaCuSi₂O₆,” S. Kraemer, **R. Stern**, M. Horvatic, C. Berthier, T. Kimura, and, I. R. Fisher, *Physical Review B* 76 (10), 100406 (2007).

5. "Spin-triplet excitons in the $S=1/2$ gapped antiferromagnet $\text{BaCuSi}_2\text{O}_6$: Electron paramagnetic resonance studies," S. A. Zvyagin, J. Wosnitza, J. Krzystek, **R. Stern**, M. Jaime, Y. Sasago, and, K. Uchinokura, *Physical Review B* 73 (9), 094446 (2006).
6. "Magnetic-field-induced condensation of triplons in Han Purple pigment $\text{BaCuSi}_2\text{O}_6$," M. Jaime, V. F. Correa, N. Harrison, C. D. Batista, N. Kawashima, Y. Kazuma, G. A. Jorge, R. Stern, I. Heinmaa, S. A. Zvyagin, Y. Sasago, and, K. Uchinokura, *Physical Review Letters* 93 (8), 087203 (2004).

FR.D-P82 - Investigation into the magnetic properties of pyrochlore-type rare-earth hafnates

J.H. Chun¹, R.K. Kremer¹, C. Lin¹

1. MPI for Solid State Research, Stuttgart, Germany

Cubic rare-earths transition metal pyrochlores with composition $R_2TM_2O_7$ have attracted broad attention because of their unusual magnetic ground state properties related to geometrical frustration of the pyrochlores lattice. So far, the investigation focused mainly on 3d and 4d transition metal systems. The magnetic properties of rare-earths 5d TM pyrochlores are comparatively less well studied. Here we report on the single-crystal growth and the magnetic properties of some rare-earth hafnates ($R = Nd, Gd, Dy$; $TM = Hf$) of composition $R_2TM_2O_7$. $Nd_2Hf_2O_7$ and $Gd_2Hf_2O_7$ crystallize with the cubic pyrochlores structure whereas diverging reports on the structure of $Dy_2Hf_2O_7$ are available in literature. Crystals of $Gd_2Hf_2O_7$ and $Dy_2Hf_2O_7$ have been grown and their structural and magnetic properties have been investigated. Our investigations confirm $Gd_2Hf_2O_7$ and $Dy_2Hf_2O_7$ to crystallize in the cubic pyrochlores structure. Magnetic ordering below ~ 0.5 K has been observed by magnetic susceptibility and heat capacity measurements for both compounds.

FR.D-P83 - Magnetic order in pyrochlore hafnate Nd₂Hf₂O₇

V. Kumar Anand¹, A. Kumar Bera¹, J. Xu¹, T. Herrmannsdörfer², C. Ritter³, A. Nazmul Islam¹, B. Lake¹

1. Helmholtz-Zentrum Berlin für Materialien und Energie, Berlin, Germany
2. Helmholtz-Zentrum Dresden-Rossendorf, Dresden, Germany
3. Institut Laue-Langevin, Grenoble, France

The observation of spin-ice behavior and magnetic monopoles in pyrochlore titanates have created great interest in rare earth pyrochlore oxides (R³⁺)₂(T⁴⁺)₂O₇ (R = rare earth ion, T = transition metal). In the search for novel pyrochlore oxides we have investigated a pyrochlore hafnate, namely Nd₂Hf₂O₇ in which magnetic ion is Nd³⁺ in 4f³ electronic configuration having ground state 4I_{9/2} (S=3/2, L=6, J=9/2). Both polycrystalline and single crystals of Nd₂Hf₂O₇ have been synthesized and investigated by ac and dc magnetic susceptibilities, isothermal magnetization and heat capacity measurements. The heat capacity data show an upturn in Cp/T below 6 K with a value of Cp/T = 0.53 J/mol K² at 1.8 K. The ac susceptibility measurements reveal an anomaly below 0.55 K associated with a magnetic phase transition to a long range ordered state. The long range ordering is further confirmed by a neutron powder diffraction investigation. An antiferromagnetic ground state with an ordering wavevector $k = 0$ is inferred from the neutron data. The Fullprof refinement of the data reveals the magnetic structure to be all-in-all-out (where for successive tetrahedra, the four magnetic ions point alternatively all-into or all-out-of the tetrahedron) which implies antiferromagnetic interactions between the Nd³⁺ ions. The ordered state magnetic moment of 0.6 Bohr magneton at 0.1 K is much lower than the fully ordered value of 3.3 Bohr magneton for Nd³⁺ ions suggesting the persistence of dynamic correlations down to the lowest temperatures.

FR.D-P84 - Determination of critical exponents in a metallic glass: FeCrCuNbSiB

A. Rosales-Rivera¹, J. Hernandez-Parra¹, J. Lopez-Tabares¹, J. Hincapie-Bedoya¹, A. Velasquez-Salazar¹, D. Gomez-Montoya¹, F. Saccone²

1. Universidad Nacional de Colombia, Sede Manizales, Caldas, Colombia
2. Universidad de Buenos Aires, Buenos Aires, Argentina

In this work, we investigate the universality class of the $\text{Fe}_{73.5-x}\text{Cr}_x\text{Cu}_1\text{Nb}_3\text{Si}_{13.5}\text{B}_9$ metallic glasses by determining the critical exponents for the zero-field magnetization (β) and critical isotherm (δ) and critical temperatures from magnetization measurements. Furthermore, to obtain qualitative information on the possible magnetic interactions that are active in previous materials and to gain understanding of their effects on the critical exponents, we employ the Hall effect and Mössbauer spectroscopy. These metallic glasses were prepared as amorphous alloy ribbons of $\text{Fe}_{73.5-x}\text{Cr}_x\text{Cu}_1\text{Nb}_3\text{Si}_{13.5}\text{B}_9$ with $x = 0, 2, 4, 6, 8,$ and 10 by means of the melt spinning technique. The magnetization as a function of temperature of each sample was measured in the range $300\text{--}950$ K using a vibrating sample magnetometer (VSM-VersaLab by Quantum Design) at fixed external magnetic fields (H). The Hall effect measurements were carried out in the field range $-10 < H < 10$ kOe for several dc electrical currents applied to the samples at room temperature. Mössbauer spectra data were collected at room temperature and at zero-field. The radiative source was a ^{57}Co in an Rh matrix with 5 mCi. It is found that the β value shows a quasi-linear dependence on the Chromium content and, interestingly goes through values that belong to the Ising (sample with $x = 0$), XY (sample with $x = 2$) and Heisenberg (sample with $x = 4$) models, respectively, before finally deviating of any of these models in the high x region (samples with $x = 6, 8$ and 10). The δ value found varies between 3.8 and 6.1. The possible mechanisms leading to such universality classes including the spin-orbit interaction, shape anisotropies, direct exchange and itinerant exchange are analyzed.

Fr.D-P87 - Polarised neutron scattering studies of magnetic correlations in pyrochlore iridatesE. Feng¹, Y. Su¹, T. Wolf², T. Brueckel^{3,1}

1. Jülich Centre for Neutron Science JCNS, Forschungszentrum Jülich GmbH, Outstation at MLZ, Garching, Germany

2. Institut für Festkörperphysik, Karlsruhe Institute of Technology KIT, Karlsruhe, Germany

3. Jülich Centre for Neutron Science JCNS and Peter Grünberg Institut PGI, JARA-FIT, Forschungszentrum Jülich GmbH, Jülich, Germany

The metallic pyrochlore iridate compounds $A_2Ir_2O_7$, where the A sites are occupied by rare-earth local moments and the B sites by 5d transition metal Ir ions with strongly spin-orbit coupled (SOC) itinerant electrons, have attracted tremendous interests because they sit in the intersection of the two emerging research fields in condensed matter physics: quantum spin ice in frustrated magnets [1] and strongly SOC correlated phenomena [2]. For instance, due to the presence of both local ice-rule constraint and quantum fluctuation at the rare-earth A-site, a quantum spin ice ground state carrying exotic quasi-particles and fractionalized excitations could appear. On the other hand, novel topological states such as Weyl semimetals may emerge as a consequence of the strong spin-orbit coupling of the B-site 5d conduction electrons. Exotic ground states and novel magnetic phases can be resulted from complex interplay of these two phenomena. However, neutron scattering, a powerful microscopic probe to magnetism, has hardly been performed on pyrochlore iridates due to strong neutron absorption and small magnetic moment of Ir. We have recently carried out comprehensive polarized neutron scattering studies of magnetic correlations of high-quality $Nd_2Ir_2O_7$ and $Pr_2Ir_2O_7$ powder samples synthesized by solid-state reaction [3]. In $Nd_2Ir_2O_7$, a $q=0$ long-range antiferromagnetic order has been observed below $T_N \sim 20$ K, in consistence with “all-in-all-out” spin configuration as proposed in an earlier neutron diffraction investigation [4]. In $Pr_2Ir_2O_7$, magnetic diffuse scattering, a signature of short-range magnetic correlations, has been observed below 1 K. The polarized neutron scattering data has been analysed within the context of both quantum spin ice [1] and chiral spin liquid [5]. The important role of the RKKY interaction mediated by the itinerant Ir electrons will be discussed as well.

[1] M.J.P. Gingras and P.A. McClarty, Rep. Prog. Phys. 77, 056501 (2014)

[2] W. Witczak-Krempa, et al., Annu. Rev. Condens. Matter Phys. 5, 57 (2014)

[3] E. Feng, Y. Su, et al. (in preparation)

[4] K. Tomiyasu, et al., J. Phys. Soc. Jpn. 81, 034709 (2012)

[5] Y. Machida, et al., Nature 463, 210 (2010)

FR.E-P01 - Classical spin relaxation via spin-bath interaction: longitudinal vs. transverse spin-bath-coupling

S. Kun Oh¹, S.C. Yu

1. Chungbuk National University, Chungcheongbuk-do, South Korea

The system of noninteracting classical spins coupled to a heat bath consisting of one-dimensional harmonic oscillators is examined with an aim of understanding spin relaxation mechanism. Both the cases of longitudinal and transverse spin-component coupled to the modes of harmonic oscillators are studied. For the case of the longitudinal spin-component coupled to the harmonic oscillators, it is exactly solved but it does not show relaxation toward equilibrium. For the case of transverse spin-component coupled to the harmonic oscillators, it is numerically solved via geometric algorithm, and it does show some relaxation but it has nothing to do with equilibrium.

FR.E-P02 - Magnetic properties of the SPIN-1 J1-J3 heisenberg model on a triangular lattice

A. Sherman¹, P. Rubin¹, M. Schreiber²

1. *Institute of Physics, University of Tartu, Tartu, Estonia*

2. *Institute für Physik, Technische Universität, Chemnitz, Germany*

Motivated by the experimental data for NiGa₂S₄, the spin-1 Heisenberg model on a triangular lattice with the ferromagnetic nearest- and antiferromagnetic third-nearest-neighbor exchange interactions, $J_1 = -(1-p)J$ and $J_3 = pJ$, $J > 0$, is studied in the range of the parameter $0 \leq p \leq 1$. Mori's projection operator technique is used as a method which retains the rotation symmetry of spin components and does not anticipate any magnetic ordering. For zero temperature several phase transitions are observed.

At $p \approx 0.2$ the ground state is transformed from the ferromagnetic spin structure into a disordered state, which in its turn is changed to an antiferromagnetic long-range ordered state with the incommensurate ordering vector $Q \approx (1.16, 0)$ at $p \approx 0.31$. With growing p the ordering vector moves along the line $Q - Q_1$ to the commensurate point $Q_1 = (2\pi/3, 0)$ which is reached at $p = 1$. The final state with an antiferromagnetic long-range order can be conceived as four interpenetrating sublattices with the 120° spin structure on each of them. The model is able to describe the state with the incommensurate short-range order observed in NiGa₂S₄. Also our approach is able to reproduce a quadratic temperature dependence of the specific heat and dependence of the uniform spin susceptibility on T in NiGa₂S₄.

To verify the used approach the ground state energy and corresponding spin-spin correlations for small lattices are compared with exact-diagonalization results obtained with the SPINPACK code (the Lanczos exact diagonalization). The Mori's and the Lanczos results are in qualitative agreement.

FR.E-P03 - Effect of doping on magnetic properties of magnetocaloric series $(\text{Fe}_{1-x}\text{Mnx})_2\text{P}_{1-y}\text{Si}_y$

J. Goraus¹, Łukasz Hawełek², A. Kolano-Burian²

1. *University of Silesia, Institute of Physics, Uniwersytecka 4, Katowice*

2. *Institute of Non-Ferrous Metals, Gliwice, Poland*

We have calculated the magnetic quantities such as local and total magnetic moments and exchange integrals for the Fe_2P type series where iron was substituted by manganese and phosphorus was substituted by silicon. In Fe_2P type structure transition metals can occupy two Wyckoff sites - $3f$ and $3g$. We considered three structural models, where substituting the iron for the manganese lead to preference in occupation of one of the sites, as well as the model where the concentration of manganese was equal across these two sites. It is clear from our calculations, which these structural models lead to different behaviour of considered series with respect to absolute doping with the transition metal and also with respect to the silicon concentration.

FR.E-P04 - Breaking symmetry in one dimensional random chain

O. Kryvchikov¹, V. Slavin

1. ILTPE - B.Verkin Institute for Low Temperature Physics and Engineering of The National Academy of Sciences of Ukraine, Kyev, Ukraine

The ground state of interacting particles on a disordered one-dimensional host-lattice is studied by new method, using Lapunov central theorem, and verified by a direct numerical method. It is shown that if the concentration of particles is small, then randomness of the host-lattice sites positions breaks the long-range order of Generalized Wigner Crystal, replacing it by the sequence of blocks (domains) of particles with random lengths. The mean domains length as a function of the host-lattice disorder parameter is also found by both methods.

FR.E-P05 - dynamical properties of honeycomb lattice iridate Na₂IrO₃S.I. Suga¹, T. Yamada¹, T. Suzuki¹*1. University of Hyogo, Hyogo, Japan*

Honeycomb lattice iridate Na₂IrO₃ has attracted much attention, since the system can be described by a Kitaev-Heisenberg model, in which the Kitaev spin-liquid state is a possible ground state [1,2]. Several models including further neighbor interactions and/or anisotropic interactions have been proposed to explain the observed zigzag order and thermodynamic properties. However, its dynamical properties have not been fully investigated yet. In this study, we calculate dynamical spin structure factors for proposed four models [2-5] using exact numerical diagonalization. By comparing our numerical results with inelastic neutron scattering (INS) experiments [3], we find that the models in Refs. 3 and 5 well reproduce qualitative features of the experiments. However, when we focus on the scattering 'boundary' and the scattering intensity of the low energy region at the '\Gamma' symmetric point, we confirm better agreement between the numerical results for the model in Ref. 5 and the INS experiments. We thus consider that the model in Ref. 5 is most adequate to describe the INS experiments. We further perform spin-wave analyses for both models. The difference appears at the M symmetric point. The low-lying excitation is gapless there for the model in Ref. 5, while it is gapped for the model in Ref. 3. This notable difference helps us to conclude the adequate model for Na₂IrO₃, which may pave a way for realizing quantum spin liquids.

- [1] J. Chaloupka, G. Jackeli, and G. Khaliullin, Phys. Rev. Lett. 105, 027204 (2010)
- [2] J. Chaloupka, G. Jackeli, and G. Khaliullin, Phys. Rev. Lett. 110, 097204 (2013)
- [3] S. K. Choi, et al., Phys. Rev. Lett. 108, 127204 (2012)
- [4] V. M Katukiri, et al., New J. Phys. 16, 013056 (2014)
- [5] Y. Yamaji, et al., Phys. Rev. Lett. 113, 107201 (2014)

FR.E-P06 - Hybrid molecular and spin dynamics simulations of gel-based Co nanoparticle dispersions

L. Teich¹, C. Schröder¹

1. Bielefeld Institute for Applied Materials Research, University of Applied Sciences Bielefeld, Bielefeld, Germany

Dispersions of magnetic nanoparticles in conductive gel matrices exhibit promising magnetoresistive characteristics [1-3] which makes them suitable for a rational design of magnetoresistive sensor devices. This approach needs detailed knowledge of the viscous and magnetic parameters that influence the structuring processes of the nanoparticles within the dispersion and hence their magnetoresistive properties. In this regard, time-resolved simultaneous spin dynamics and molecular dynamics simulations provide crucial information which is not accessible experimentally. Here, we present a hybrid approach, which combines a modified version of HOOMD-blue [4] for molecular dynamics and a stochastic spin dynamics method that involves solving the Landau-Lifshitz equation [5]. We have applied our approach to the simulation of an ensemble of 192 monodisperse Cobalt nanoparticles. The time development of the structuring process results in the formation of vortices and chain fragments. This is in agreement with previous investigations [2].

[1] J. Meyer et al., *Smart Mater. Struct.*, 22 (2), 025032 (2013)

[2] L. Teich et al., "Efficient calculation of Low Energy Configurations of Nanoparticle Ensembles for Magnetoresistive Sensor Devices by Means of Stochastic Spin Dynamics and Monte Carlo Methods", accepted for publication in *Acta. Phys. Pol. A* (2014)

[3] T. Rempel et al., "Giant magnetoresistance effects in gel-like matrices: comparing experimental and theoretical data" accepted for publication in *Smart Mater. Struct.* (2014)

[4] J. A. Anderson et al., *J. Comp. Phys.*, 227 (10), 5342-5359 (2008)

[5] L. Engelhardt, C. Schröder, in *Molecular Cluster Magnets*, Ed. R. E. P. Winpenny, World Scientific Publishers, Singapore (2011)

FR.E-P07 - Magnetic simulation of nano-granular thin films

J.D. Agudelo Giraldo¹, J. Restrepo², E. Restrepo Parra¹

1. *Universidad Nacional de Colombia, Bogotá, Colombia*

2. *Universidad de Antioquia, Medellín, Colombia*

A new methodology for generating thin granular films was obtained according with reports of magnetic materials. The growth considered periodic boundary conditions. The Monte Carlo Method was used for a randomly grow from different seeds and subsequently for to compute magnetic properties. Metropolis algorithm was implemented for relaxation purposes. The grain boundary relaxation was obtained with Morse Potential. The Magnetic Hamiltonian was based in Heisenberg model. The sums included exchange interaction with cut radius, cubic magnetocrystalline anisotropy with temperature dependence, external magnetic field in different directions and dipolar interactions with cut radius until six times the sample length. Parallelization was necessary. The results show changes on transition temperature as function of computational thread numbers, grain size, magnetocrystalline anisotropy and cut radius. Magnetization decreases at low temperatures by cubic anisotropy effects. As a result of grain orientation, cut radius and intergranular boundaries were observed magnetic vortex formation in different points of the sample.

FR.E-P08 - Frustrated spatially anisotropic spin-1/2 Heisenberg antiferromagnet on a square lattice

V. Ilkovic¹

1. Joint Institute for Nuclear Reserch-JINR, Moscow, Russia

Frustrated spatially anisotropic spin-1/2 Heisenberg antiferromagnet on a square lattice
Vladimir Ilkovič Bogoliubov Laboratory of Theoretical Physics, JINR, 141980 Dubna, Moscow region, Russia
Permanent address: Institute of Experimental Physics, Slovak Academy of Sciences, Watsonova 47, 040 01 Kosice, Slovak Republic .
The new magnetic materials such as the layered oxide high-temperature superconductor can be well described by the Heisenberg spin model with nearest-neighbor (NN) antiferromagnetic coupling J_1 and next-nearest-neighbor (NNN) antiferromagnetic coupling J_2 . It is now well accepted that the model J_1 - J_2 exhibits two phases displaying magnetic order at small J_2 , separated by an intermediate paramagnetic phase in the interval $J_{c1} < J_2 < J_{c2}$. The ground state for $J_2 < J_{c1}$ exhibits Néel magnetic order, whereas for $J_2 > J_{c1}$ it exhibits collinear stripe order. A generalization of the frustrated J_1 - J_2 model is the J_1 - J_1' - J_2 model where J_1' is the directional anisotropy parameter. The nearest-neighbor bonds have different strength J_1 and J_1' in the x and y directions, respectively. The effect of the coupling J_1' on the Néel and stripe states is investigated. The spin-wave excitation spectrum, the magnetization and the antiferromagnetic Néel and collinear antiferromagnetic stripe order for frustrated J_1 - J_1' - J_2 Heisenberg model are calculated within the quantum many-body Green function method.

FR.E-P09 - Spontaneous magnetization and specific heat of a coupled spin-electron model on doubly decorated planar lattices

H. Cencarikova¹, J. Strecka², M. Lyra³

1. Institute of Experimental Physics, Slovak Academy of Sciences, Bratislava, Slovakia

2. Faculty of Science, P. J. Safarik University, Kosice, Slovakia

3. Instituto de Fisica, Universidade Federal de Alagoas, Maceió, Brazil

The generalized decoration-iteration transformation is adopted for an exact study of a coupled spin-electron model on 2D lattices, in which localized Ising spins reside on nodal lattice sites and mobile electrons are delocalized over pairs of decorating sites. The model takes into account a hopping term for mobile electrons, the Ising coupling between mobile electrons and localized spins, as well as, the Ising coupling between localized spins (J'). The ground state, spontaneous magnetization and specific heat are examined for both ferromagnetic ($J' > 0$) and antiferromagnetic ($J' < 0$) interaction between the localized spins. Besides reentrant transitions with only two consecutive critical points between the paramagnetic (P) and the antiferromagnetic (AF) or ferromagnetic (F) phase (P-AF/F-P) observed for $J'=0$, one may also find more peculiar reentrant transitions with three successive critical points AF/F-P-F/AF-P for a non-zero value of J' . Moreover, very interesting thermal variations of spontaneous magnetizations were found, which exhibit for the convenient electron concentration $\langle n \rangle$ a simultaneous presence of the spin/electron magnetization and staggered spin/electron magnetization, respectively. It is shown that the specific heat may also display diverse thermal dependences, which include singularities of various type for non-zero values of $\langle n \rangle$ and J' .

FR.E-P10 - Short-range order above the Curie temperature in the dynamic spin-fluctuation theory

N. Melnikov¹, B. Reser²

1. *Lomonosov Moscow State University, Moscow, Russia*

2. *Institute of Metal Physics, Russian Academy of Sciences, Ekaterinburg, Russia*

Existing theories of metallic magnetism all postulate that local magnetization remains above the Curie temperature, but there is no agreement about the extent of the short-range order in the paramagnetic phase. We study the paramagnetic spin density correlations of strong ferromagnetic metals using the dynamic spin-fluctuation theory (DSFT) [1]. Unlike the dynamic mean-field theory [2] and dynamical coherent potential approximation [3], based on the single-site approximation, the DSFT takes into account both single-site and nonlocal interactions. We obtain computational formulas for the correlation function and short-range radius in different approximations of the DSFT. Using these formulas, we calculate the short-range order above the Curie temperature in the bcc iron. Results of the calculation confirm our theoretical prediction that the inverse correlation radius increase linearly with temperature for T sufficiently large. We compare the results with other theoretical work and neutron scattering experiments.

[1] N. B. Melnikov, B. I. Reser and V. I. Grebennikov, *J. Phys.: Condens. Matter* 23 (2011) 276003

[2] A. I. Lichtenstein, M. I. Katsnelson and G. Kotliar, *Phys. Rev. Lett.* 87 (2001) 067205

[3] Y. Kakehashi and M. A. R. Patoary, *J. Phys. Soc. Jpn.* 80 (2011) 034706

FR.E-P11 - Magnetic phase transition in the spin-fluctuation theory

N. Melnikov¹, G. Paradezhenko¹

1. Lomonosov Moscow State University, Moscow, Russia

The first-order phase transition is a characteristic feature of the Gaussian approximation in the spin-fluctuation theory [1]. We present a method that takes into account the fourth-order terms in the expansion of the free energy and thus leads to a renormalization of the magnetic susceptibility [2]. To deal with the higher-order terms, we introduce partial averaging of the fluctuating fields, which is based on the Wick theorem, and is different from the decoupling of operators in mean-field theories and the Green functions in equations of motion. By example of the Ising model, we show that the renormalization of the magnetic susceptibility leads to continuous second-order phase transition, which is experimentally observed in metals. We explain the mechanism of the renormalization and show that the spin-rotational invariance is not the reason for the first-order phase transition in the spin-fluctuation theory, as it was speculated in [3].

[1] B. I. Reser and N. B. Melnikov J. Phys.: Condens. Matter 20 (2008) 285205

[2] N.B. Melnikov, G.V. Paradezhenko, Theor. Math. Phys. (2015) in press

[3] Y. Takahashi, J. Phys.: Condens. Matter 18 (2006) 521

FR.E-P12 - Generalized flavor-wave expansion for softcore bose-hubbard systems

K. Masuda¹, S. Kurihara¹, D. Yamamoto²

1. *Waseda University, Tokyo, Japan*

2. *Waseda Institute for Advanced Study, Tokyo, Japan*

We propose a systematic perturbative approach to study softcore Bose-Hubbard models by generalizing the flavor-wave theory for quantum spin systems. In previous studies, the Gutzwiller approximation has succeeded in qualitatively describing various phenomena of the Bose-Hubbard models, including the superfluid-Mott-insulator transition. On the other hand, this site-decoupled mean-field theory cannot take into account the effect of intersite correlations and quantum fluctuations, which are essential for the systems with classically degenerate ground states, e.g., strongly frustrated systems. In order to describe the fluctuation effects that are absent in the Gutzwiller approximation, we introduce auxiliary Bose fields, called the "flavor bosons," and expand the Bose-Hubbard model in powers of the flavor-boson operator. While the zeroth-order term represents the site-decoupled mean-field energy, the higher-order terms give the quantum corrections due to intersite correlations. We apply this systematic flavor-wave expansion to the Bose-Hubbard model on the square lattice and demonstrate that the quantum corrections suppress the superfluid order. The critical ratio of the hopping amplitude and the onsite interaction strength at the superfluid-Mott-insulator phase boundary asymptotically approaches the value obtained by the quantum Monte Carlo simulations as higher-order corrections are included. Building upon this result, we study several issues of current interest, including magnetic structures in spin-1 Bose gases and the ground state of frustrated Bose-Hubbard models.

FR.E-P14 - Realization of the Green's function approach for calculation of inter-atomic exchange interactions in real compounds within full-potential and pseudopotential methods based on the plane-wave basis

Z. Pchelkina^{1,2}, D. Korotin¹, S. Streltsov^{1,2}, V. Anisimov¹

1. *M N Miheev Institute of Metal Physics of Ural Branch of Russian Academy of Science, Ekaterinburg, Russia*

2. *Ural Federal University, Ekaterinburg, Russia*

The value of inter-atomic exchange interactions is one of the main characteristics of magnetic systems. In the mean-field approximation it could be extracted from the Curie-Weiss fit of experimental magnetic susceptibility data. Such estimation strongly depends on the underlying model, which is often based on structural considerations. In this regard, theoretical calculation of the exchange interactions in the real materials is hardly needed.

The exchange parameters could be calculated by mapping the Heisenberg model to the total energy difference of several magnetic configurations. To get N exchange parameters one needs to calculate the total energy for N^{+1} magnetic configurations and as a result one obtains the number without a clear physical picture (e.g. which particular orbitals are responsible for exchange processes; what is the mechanism of exchange interaction etc.).

A more general approach to derive the exchange interactions is a Green's function method, which was developed by Liechtenstein et al. in 90s. It allows to calculate the inter-atomic magnetic interactions corresponding to infinitesimal rotations of spin magnetic moments near equilibrium. Basically the calculation for one magnetic configuration will produce all exchange interactions as well as their orbital components. The Green's function approach was performed for the methods with the localised orbitals basis sets. However, nowadays in the most accurate schemes for the band structure calculations the plane-waves basis is used, e.g. full-potential (linearized) augmented plane-wave (LAPW) or pseudopotential methods.

Here we reformulate the Green's function approach to the plane-wave based electronic structure calculation methods using Wannier functions formalism. This calculation scheme is implemented in the full-potential WIEN2k and pseudopotential Quantum-ESPRESSO codes and tested on NiO compound.

The work was supported by the Russian Science Foundation through the project no. 14-22-00004.

FR.E-P15 - Spontaneous symmetry breaking in variational wave functions: When is it possible?

R. Kaneko¹, F. Becca², R. Valenti¹, C. Gros¹

1. Institut fuer Theoretische Physik, Goethe-Universitaet Frankfurt, Frankfurt, Germany

2. CNR-IOM-Democritos National Simulation Centre and International School for Advanced Studies, Trieste, Italy

The resonating valence bond (RVB) theory has been used to study and predict novel phenomena in strongly correlated electron systems. Especially, Bosonic- [Liang-Doucot-Anderson (LDA)] and Fermionic-type singlet RVB wave function are often used to investigate quantum magnetism. The LDA wave function with slowly power decaying amplitudes is shown to reproduce the magnetic long-ranged ordered state on the square Heisenberg model with accurate energy. On the other hand, the Fermionic-type singlet RVB wave function has also been extensively used to study unconventional quantum states, such as the superconducting and spin liquid states. Although there might exist a mapping between two wave functions for some special cases, it is still elusive whether the best singlet Fermionic wave functions generally allow the spontaneous symmetry breaking. To understand what kind of Fermionic RVB wave functions are possible to induce the spontaneous symmetry breaking, we investigate the magnetic properties of the Heisenberg model on the one-dimensional (1d) chain and two-dimensional (2d) square lattice. In 1d, singlet wave functions are shown to reproduce the short-range order irrespective of the power-law exponent of amplitudes. In 2d, the projected Fermi sea reproduces the long-range magnetic order, although the energy is much higher than the disordered d-wave state. To find a best wave function, which reproduces accurate energy and magnetization, we employ more flexible RVB wave functions, including general pairings and additional long-range spin Jastrow correlators. Optimized best wave function is much more improved in energy with less than 1% error from the exact result, however, the spontaneous symmetry breaking is shown to require the spin rotational SU(2) symmetry breaking.

FR.E-P16 - Functional integral calculation on the temperature dependence of the magnetic hyperfine field at a Cd impurity diluted in RZn (R = Gd, Tb, and Dy)

A.L. De Oliveira¹, C.M. Chaves², N.A. De Oliveira³, A. Troper²

1. Instituto Federal do Rio de Janeiro, Campus Nilópolis, Rio de Janeiro, Brazil

2. Centro Brasileiro de Pesquisas Físicas, Rio de Janeiro, Brazil

3. Instituto de Física Armando Dias Tavares, Universidade do Estado do Rio de Janeiro, Brazil

The study of the local magnetic moment formation and the related magnetic hyperfine fields at a s-p, noble and nd impurities diluted in GdZn and GdCd compounds at 0K have been studied both experimentally and theoretically [1]. In this work we discuss the temperature dependence of the local magnetic moment and the related magnetic hyperfine field at a non-magnetic s-p impurity, namely Cd, diluted in RZn (R = Gd, Tb, and Dy) compound. We adopt here a functional integral approach in the static approximation, which is an extension of conventional mean field calculation [2]. The temperatures ranges from 0K up to the critical temperatures T_c of these compounds, when they become paramagnetic. We calculate the perturbed densities of states and the local magnetic moments at the Cd impurity site, in each temperature. The self-consistently calculated magnetic hyperfine fields as a function of temperature are in good agreement with the available experimental data [3,4].

References:

- [1] A. L. de Oliveira, M. V. Tovar Costa, N. A. de Oliveira and A. Troper. J. Appl. Phys., 87 (2000)
- [2] A. L. de Oliveira, N. A. de Oliveira and A. Troper. J. Magn. Magn. Mater., 272-276, e631 (2004)
- [3] B. Bosh-Santos, G. A. Cabrera-Pasca and A. W. Carbonari. Hyperfine Interact., 197 (2010) 105
- [4] B. Bosh-Santos, A. W. Carbonari, G. A. Cabrera-Pasca, M. S. Costa and R. N. Saxena. J. Appl. Phys., 113 (2013) 17E136

FR.E-P17 - Hysteresis behavior of magnetic nanotubes with radial anisotropy component

V.A. Hurtado Marín¹, S. Morales Rojas¹, J.D. Agudelo Giraldo^{1,2}, E. Restrepo Parra¹

1. *PCM Computational Application, Universidad Nacional de Colombia, Manizales, Colombia*

2. *Escuela de Materiales, Facultad de Minas, Universidad Nacional de Colombia, Medellin, Colombia*

Hysteresis properties of single wall ferromagnetic nanotubes were studied on the basis of a classical Heisenberg model and Metropolis dynamics using the Monte Carlo method. The Hamiltonian involved nearest neighbor interactions for exchange energy; radial and tangential magneto-crystalline anisotropy was considered with the purpose of establish vector component correlations. The diameter of the nanotubes was selected taking into account particular observations of size effects over the critical temperature made in previous works. Our results show a typical decrease of coercive field as temperature increases at low anisotropy constant. As anisotropy increases, effects of competition with exchange interaction are observed and coercive field suddenly decreases at low temperatures. Hysteresis disappears if the applied magnetic field is not sufficient to eliminate the influence of the anisotropy over the moments configuration, even above the remanence.

FR.E-P18 - Orbital magnetism in multi-band systems

M. Ogata¹

1. Department of Physics, University of Tokyo, Tokyo, Japan

The effects of a magnetic field on electrons in solids are very complicated because of the matrix elements between different Bloch bands. This is called as the interband effects of a magnetic field. One of the typical problems for this interband effect is the orbital diamagnetism which has been discussed since Landau. We develop a general and rigorous theory of susceptibility for orbital magnetism which includes Landau-Peierls susceptibility, interband effects, and susceptibility from the core electrons. We find that a new additional contribution called Fermi-surface term exists in the susceptibility formalism. This general theory is applied to tight-binding models including triangular lattice and honeycomb lattice (or two-dimensional graphene). The results are compared with those obtained by using the Peierls phase. The effects of spin-orbit interaction are also studied.

FR.E-P20 - First principles investigation of magnetic properties of Fe-Ni-Mn-Al heusler alloys

M. Zagrebin^{1,2}, M. Klyuchnikova¹, V. Buchelnikov¹, V. Sokolovskiy¹

1. *Chelyabinsk State University, Oblast, Russia*

2. *National Research South Ural State University, Oblast, Russia*

The Fe-Ni-Mn-Al alloys system is beginning to gain a great interest due to many of its mechanical and magnetic properties and the possibility to be applied as a stainless steel and as a semisoft magnetic material. In engineering applications, they are offered as cryogenic materials, presenting high strength with low density, good toughness, good oxidation resistance and strength, and as cheap substitutes for some stainless steels. In this context, the Fe-Ni-Mn-Al alloys particularly have attracted much attention considering its promising technological applications. This has encouraged the experimental research to improve alloys performance in a large variety of applications [1,2]. The aim of this work is obtaining information of the magnetic properties (magnetic moment and magnetic exchange parameters) of the $\text{Fe}_{8-x}\text{Ni}_x\text{Mn}_4\text{Al}_4$ and $\text{Fe}_7\text{Ni}_1\text{Mn}_6\text{Al}_2$ and $\text{Fe}_7\text{Ni}_1\text{Mn}_5\text{Al}_3$ alloys. The $\text{Fe}_7\text{Ni}_1\text{Mn}_6\text{Al}_2$ and $\text{Fe}_7\text{Ni}_1\text{Mn}_5\text{Al}_3$ composition are closed to $\text{Fe}_{43.5}\text{Ni}_{7.5}\text{Mn}_{34}\text{Al}_{15}$ experimental composition with giant superelastic effect [3]. All calculations were performed using the density functional theory as part of the spin-polarized relativistic Korringa-Kohn-Rostoker (SPR-KKR) band structure code [4]. For our calculation we used the equilibrium lattice parameters. For $\text{Fe}_{8-x}\text{Ni}_x\text{Mn}_4\text{Al}_4$ alloys maximal value have Mn-Ni interactions. This interaction is FM and decreases with increasing of Ni concentration from 8.5 to 7.5 meV. The Fe-Mn interaction increases with increasing of Ni concentration approximately to 4 times. It is follow from our calculations that Fe-Ni-Mn-Al alloys are very interesting compounds and theoretical study of them allows to predict the new features of Heusler alloys.

This work was supported by Russian Science Fund No. 14-12-00570, Ministry of Education and Science RF No. 3.2021.2014/K and RFBR (grants 14-02-01085, 14-02-31189).

[1] J. Restrepo et al. *Hyperfine Interact.* 148-149 (2003) 285-293

[2] G.A.P. Alcázar, *Rev. Acad. Colomb. Cienc.* 28 (2004) 265-274

[3] T. Omori et al. *Science* 333 (2007) 68-71

[4] SPR-KKR package Version 6.3 on <http://ebert.cup.uni-muenchen.de/>

FR.E-P21 - Low temperature properties of chiral magnets with defects

O. Utesov¹, A. Syromyatnikov^{1,2}

1. Petersburg Nuclear Physics Institute NRC "Kurchatov Institute"

2. Department of Physics, Saint Petersburg State University, Saint Petersburg, Russia

We address the present study to magnets without inversion symmetry, which leads to appearance of Dzyaloshinskii-Moriya interaction (DMI). This work was motivated by the recent experimental activity in the study of noncentrosymmetric cubic magnets $Mn_{1-x}Fe_xSi$, $Fe_{1-x}Co_xGe$ etc. [1] In that research was found that magnetic chirality changes its sign at some point x_c and also helical vector x -dependence was measured.

Solid solutions at small x can be treated as system with small amount of defects. So our aim was to describe theoretically low temperature properties of chiral magnets with a small amount of defects. It consists of two parts - determine new classical ground state and calculate corrections to elementary excitations spectra and damping due to scattering on the defects. For theoretical description we used two different spin models - a cubic magnet with ferromagnetic interaction between nearest neighbors and DMI between neighbors along one of the axes and a B20 system with interactions from paper [2]. Defects were considered changing interactions constants locally.

We found that defects have a long-range impact on the spin system. All spins obey additional to pure systems rotation due to the defects, which describes by the same equations as for electrostatic dipole field. So after averaging on the disorder configurations we have a linear growth of spin rotation along one of the axes. That is equivalent to a linear in x changing of pure system helical vector. Also we study a defects impact on elementary excitations spectra and damping.

1. S.V. Grigoriev et al., Phys. Rev. Lett. 110, 207201 (2013)

2. S.V. Maleyev, Phys. Rev B 73, 174402 (2006)

FR.E-P23 - Manipulation of magnetic order in antiferromagnets by strong magnetic field

L. Smejkal¹, K. Vyborny¹

1. Institute of Physics ASCR, V. V. I., Prague, Czech Republic

Control of magnetic moment orientation in antiferromagnets (AFM) is much more involved than in ferromagnets (FM). One option to induce switching is to employ the spin-orbit torques [1], however, this remains only a theoretical proposal up to date and the approach common in experiments is to apply strong external magnetic field. Despite the fact that the consequent orientation of magnetic moments is not straightforward to infer [2], the situation is usually still more transparent than in FM/AFM multilayers where the magnetic field primarily manipulates the FM and the AFM magnetic moments follow because of the exchange spring effect [3]. In order to determine the orientation of magnetic moments as a function of the applied external field in several topical antiferromagnets including Mn₂Au, FeRh and MnTe, we generalize the Stoner-Wohlfarth model of single-domain ferromagnets. The magnetocrystalline anisotropy needed as an input to the model is determined by the first principles calculations. Experimentally, results of this analysis can be confirmed employing the anisotropic magnetoresistance in these materials.

[1] J. Zelezny et al., Phys. Rev. Lett. 113, 157201 (2014)

[2] L.D. Tung et al., J. Magn. Magn. Mat. 154, 96 (1996)

[3] B.G. Park et al., Nature Mat. 10, 347 (2011)

FR.E-P25 - Novel chiral metastable states in the discrete finite-size classical one-dimensional planar spin model with competing exchange interactions

M.G. Pini¹, A. Rettori², A.P. Popov³

1. *Istituto Dei Sistemi Complessi Del CNR (CNR-ISC), Unità Di Firenze, Florence, Italy*

2. *Dipartimento di Fisica ed Astronomia, Università degli Studi di Firenze, Sesto Fiorentino, Italy*

3. *Department of Molecular Physics, National Research Nuclear University MEPhI, Moscow, Russia*

Driven by the interest for artificially created nanoscale magnetic structures displaying a helical or spiral magnetic order (such as ultrathin films of rare-earth elements, or Fe chains deposited on a reconstructed surface [1]), we investigated the effect of finite size and open boundary conditions on the equilibrium states of a one-dimensional (1D) model of N classical planar spins with competing nearest neighbor (nn) and next nearest neighbor (nnn) intrachain exchange interactions. Using a theoretical method recently developed [2], the non-collinear magnetization profile was calculated up to $N=16$ in a systematic and accurate way [3] by finding the $(N-1)$ roots of a function in the 1D space of the first relative orientation angle. The roots were then analyzed in order to determine which of them correspond to stable, metastable or unstable states. In addition to the ground state, symmetric with respect to the center of the chain, we found metastable states of two kinds: either antisymmetric or without a definite symmetry ('ugly' states). In the ground state, the modulated configuration is non uniform along the finite chain, but the chirality of the helix does not change. In contrast, the metastable states present a change of chirality, located either in the middle of the chain (antisymmetric state) or away from it ('ugly' state). 'Ugly' states are always metastable. Antisymmetric states are metastable (unstable) for even (odd) values of N . As N grows the difference between even- N and odd- N configurations is found to decrease, and for N tending to infinity is expected to vanish.

[1] M. Menzel et al., Phys. Rev. Lett. 108, 197204 (2012)

[2] A. P. Popov et al., Phys. Rev. B 81, 054440 (2010)

[3] A. P. Popov, A. Rettori, and M. G. Pini, Phys. Rev. B 90, 134418 (2014)

FR.E-P26 - Monte Carlo investigation of magnetic properties of anisotropic transition-metal oxidesD. Ledue¹, A. Al Baalbaky¹, R. Patte¹

1. GPM UMR 6634 CNRS-Université & INSA de Rouen, Rouen, France

The delafossite CuCrO_2 is of particular interest, especially because it enters the multiferroic state in zero field with the magnetic transition [1]. In this compound, the magnetic structure below $T_N = 24 - 26$ K [2,3] is an incommensurate proper-screw magnetic structure with a propagation vector equal to $(0.3298, 0.3298, 0)$ [4] very close to the commensurate value $(1/3, 1/3, 0)$. Since several sets of exchange interactions up to the 4th neighbours have been recently proposed for CuCrO_2 [4,5] and because its magnetic properties have been widely investigated experimentally [6], we aimed here to investigate by means of Monte Carlo simulations the equilibrium magnetic properties of CuCrO_2 using the proposed exchange interaction sets. Our simulations provide the thermal variation of the internal energy $U(T)$, the specific heat $C(T)$, the order parameter $\eta(T)$, and the chiral susceptibility $\chi'(T)$ from which we can deduce the transition temperature T_N . In addition, we have calculated the linear susceptibility $\chi(T)$ at small applied field ($\chi(T) = M(T)/H$, where $M(T)$ is the magnetization) in order to estimate the Curie-Weiss temperature θ_{CW} . Finally, note that if the cooling is slow enough during the simulation, the final magnetic configuration corresponds to one of the ground states. All these results are compared to the experimental ones [6] to discuss the validity of the proposed exchange interactions sets. Our results indicate that there are differences between the final configurations obtained with the set of interactions proposed by Xue-Fan and those proposed by Frontzek et al.

[1] S. Seki, Y. Onose, Y. Tokura, Phys. Rev. Lett. 101, 067204 (2008)

[2] H. Kadowaki, H. Kikuchi, Y. Ajiro, J. Phys.: Condens. Matter 2, 4485 (1990)

[3] T. Okuda et al., Phys. Rev. B 72, 144403 (2005)

[4] M. Frontzek et al., Phys. Rev. B 84, 094448 (2011)

[5] J. Xue-Fan, Chin. Phys. B 21, 077502 (2012)

[6] T. Okuda, R. Kajimoto, M. Okawa, T. Saitoh, Int. J. Mod. Phys. B 27, 1330002-1 (2013)

FR.E-P27 - Longitudinal Spin fluctuations studies on magnetic properties of transition metal random-alloys at finite temperatures

F. Pan¹, J. Chico², A. Bergman², L. Bergqvist¹

1. Dept. of Nanomaterial Physics, Royal Institute of Technology (KTH), Stockholm, Sweden

2. Dept. of physics and astronomy, Uppsala university, Uppsala, Sweden

Using a combination of ab-initio and MC(Monte Carlo) simulations, a method that includes both transversal and longitudinal fluctuations of the magnetic moments has been developed for calculating the magnetic properties of random alloys at finite temperatures. Results demonstrate that the longitudinal fluctuations contribute to the phase transition are non-trivial, e.g. the individual moment size is reduced by about 10% up to the Curie temperature for iron. Although the standard Heisenberg model which includes the transversal fluctuation only, is sufficient for describing the critical properties of iron, the longitudinal fluctuation can play an essential role at exploring the phase transitions in Permalloy and other transition metal alloys with induced moments. We parametrized the exchange coupling for different magnetic configurations, which was calculated using the Korringa-Kohn-Rostoker (KKR) method within the coherent potential approximation (CPA) framework and fixed spin moment (FSM). Our method provides a broadening insight on the investigation of magnetic behaviour up to the Curie temperature, particularly on estimating the suppression of the atomic moments length. This extended Heisenberg model is flexible to study various magnetic systems. The method is easily extended to atomistic spin dynamics simulations.

FR.E-P28 - Magnetic moment properties of an arbitrary quantum ring contour in the presence of a magnetic field

P. Dahan¹, P. Malits¹

1. School of Engineering at Ruppin Academic Center, Emek-Hefer, Israel

The influence of an arbitrary contour of a quantum ring (QR) on the ring's magnetic moment properties is studied. The magnetic moment properties of QRs are not only of fundamental interest, but are also important due to their potential applications. The magnetic moment and oscillations are formulated in the framework of a one-dimensional model for a non-circular quantum ring [1]. In our theoretical model, the ring curvature is introduced into the orbital magnetic moment equation by means of the conformal mapping that maps the unit circle onto the QR contour.

We show that the magnetic moment, as well as other characteristics of the non-circular ring, is a periodic function of the flux, Φ/Φ_0 , and its properties are depending on the shape and order of symmetry.

We study three specific non-circular shapes of different symmetries. In the case of an elliptical QR (two axes of symmetry), our analytical results based on the conformal mapping and method of asymptotic perturbations are in good agreement with those of earlier numerical studies. To the best of our knowledge, this is the first time that explicit formulae allowing study of electronic effects are established for this contour. In particular, as the ellipse eccentricity, ϵ , and Φ/Φ_0 are satisfy the conditions $\epsilon \leq 0.6$ and $|\Phi/\Phi_0 - k| > 0.05$, k is a natural number, we have derived very simple approximate formulae for the magnetic moment, as well as for the persistent and total currents.

[1] Dahan P. and Malits P. *Physica E* 56 165–171 (2014)

FR.E-P31 - Emergence of quasi-two-dimensional ordered phase in anisotropically coupled spin ladders

S. Furuya¹, T. Giamarchi¹

1. Department of Quantum Matter Physics, University of Geneva, Geneva, France

The dimensionality plays a decisive role in the spontaneous magnetic ordering. Having severe quantum fluctuations, one-dimensional quantum antiferromagnetic systems exhibit the Tomonaga-Luttinger liquid phase that is unavailable in higher dimensional systems.

Among one-dimensional quantum antiferromagnets, the spin ladder compound is of particular interest because of controllability of the dimensionality with the temperature and the magnetic field. The spin ladder system goes through the field-induced Tomonaga-Luttinger liquid phase and reaches the three-dimensional Neel ordered phases as the temperature is decreased under the strong magnetic field. For realizing the Neel ordered phase, the interladder interaction is crucial. If the spin-spin interaction respects the rotational symmetry, the Neel ordered state breaks the U(1) symmetry around the magnetic field spontaneously. Such an ordered phase can exist only when spin ladders are coupled three-dimensionally. If spin ladders are coupled two-dimensionally, the Neel order is allowed only at zero temperature. The highly anisotropically coupled spin ladder system is placed in an intermediate situation between those two limits, whose ordered phase is yet to be understood.

In this presentation, keeping in mind a recently synthesized compound $(\text{C}_7\text{H}_{10}\text{N})_2\text{CuBr}_4$, we investigate anisotropically coupled spin ladders and discuss emergence of a quasi-two-dimensional Neel ordered phase in that system with the aid of several complementary analytical approaches: the bosonization, the variational analysis and the renormalization group analysis. We point out that the quasi-two-dimensional ordered phase has suppressed but nonzero Neel order, yielding a stepwise curve of the order parameter against the temperature.

FR.E-P34 - An extension of the Neel-Brown model of magnetization reversal

A. Roy ¹, A.P.S. Kumar ¹

1. Indian Institute of Science, Karnataka, India

The popular Neel-Brown model of magnetization reversal describes magnetization reversal of a sample by thermal excitation over an energy barrier. It uses two parameters that characterize the barrier, an energy (height) E_B , and a field H_K . The interpretation of H_K depends on the mode of reversal and it may represent an anisotropy field or a domain wall pinning field. This model predicts a decreasing coercivity and an increasing width ΔH of switching field distribution as the temperature is increased, and has been found to hold good on several occasions particularly for nano-scale systems.

Our experiment constitutes the study of switching field statistics of Permalloy ($\text{Ni}_{80}\text{Fe}_{20}$) thin films on Si(100) grown by PLD. Temperature dependence of the switching field distribution showed that the mean switching field (coercivity) increased as a function of temperature, as expected. However, ΔH increased as the temperature was lowered, contrary to the Neel-Brown model.

We have attempted to explain this anomalous behaviour by realizing that for a large system ($100\mu\text{m}$) several magnetization reversal pathways are possible, corresponding to different domain structures. Keeping the framework of the Neel-Brown model intact, we incorporated a multitude of reversal pathways in the form of a Gaussian distribution in the values of H_K (FWHM σ_{HK}). Calculations based on this model for different values of σ_{HK} show two distinct regimes. At low values of σ_{HK} , ΔH is limited by thermal broadening according to the traditional Neel-Brown expression. This regime is characterized by an increasing ΔH with temperature. For high σ_{HK} , the broadening is dominated by σ_{HK} , which masks thermal broadening. Decrease of the effective barrier $E_B/k_B T$ at increasing temperature causes the mean switching field to lie far below H_K , causing a rescaling of the distribution widths, producing temperature dependence of ΔH as observed.

FR.E-P35 - Resonating valence bond physics is not always controlled by the shortest tunneling loops

A. Ralko¹, I. Rousochatzakis²

1. *Neel Institute, Grenoble, France*

2. *School of Physics and Astronomy, University of Minnesota, Minneapolis, United States*

One of the central aspects of the nearest-neighbor valence bond (NNVB) description of magnetically disordered phases is that the dynamics is controlled by the shortest tunneling loops. Here we show that this intuitive quantum-mechanical notion can be completely wrong on account of renormalization effects that stem from virtual longer-range singlet fluctuations outside the NNVB basis.

The aim of this presentation is twofold. First, we want to unravel and establish precisely the importance of such virtual longer-range singlets in describing RVB physics, and show how the quantum dimer model (QDM) needs to become non-local in order to accurately describe the Heisenberg physics. Second, by focusing on the so-called square-kagome, a 2D spin-1/2 Heisenberg AFM with corner sharing triangles, closely related to the Kagome, we study the nature of the disordered ground state by deriving a weighted-amplitude QDM that counts for defect triangles around the loops.

As in the kagome [1], virtual singlets affect the nature of the ground state qualitatively, stabilizing an exotic valence bond crystal (VBC) that maximizes the tunneling events on the second shortest loops [2].

[1] Ioannis Rousochatzakis, Yuan Wan, Oleg Tchernyshyov, and Frederic Mila, prb 90, 100406(R) (2014)

[2] Arnaud Ralko and Ioannis Rousochatzakis, (in preparation, 2015)

FR.E-P36 - Meron crystals with spin scalar chiral stripes

R. Ozawa¹, S. Hayami¹, M. Udagawa¹, Y. Motome¹, K. Barros², G.W. Chern², C. Batista²

1. *Univ. of Tokyo, Tokyo, Japan*

2. *Los Alamos National Laboratory, New Mexico, United States*

Noncoplanar spin textures, such as skyrmion crystals, have been extensively studied not only for their intriguing transport phenomena but also their potential for applications. In most cases, the relativistic spin-orbit coupling plays an important role in the stabilization of the noncoplanar spin states. Recently, another class of noncoplanar spin textures has been found in spin-charge coupled systems in the absence of the spin-orbit coupling. These noncoplanar states are induced by the instability originating in the Fermi surface structure, which exists ubiquitously in itinerant electron systems. In this new class, a rich variety of exotic magnetism as well as peculiar transport properties is expected, depending on the band structure and electron filling.

Motivated by these new findings, we explore a further possibility for unconventional noncoplanar orders, focusing on the Fermi surface instability. Specifically, we consider the Kondo lattice model with the nearest- and third-neighbor hoppings on a square lattice. In this model, the band structure has four saddle points at the Lifshitz transition point, which give the van Hove singularity in the density of states. Such singular behavior is expected to enhance the instability of the Fermi surface. Performing an efficient numerical simulation based on the Langevin dynamics, we find that the system exhibits a new type of noncoplanar spin orders accompanied by spin scalar chiral stripes. The obtained stripes are regarded as crystals of fractionalized topological objects --- merons (half of the skyrmions). We also investigate the stabilizing mechanism by both the analytical perturbation approach with respect to the spin-charge coupling and the numerical variational calculations for the ground state.

FR.E-P39 - Volume dependence of magnetic properties in $\text{Co}_2\text{Cr}_{1-x}\text{Y}_x\text{Ga}$ (Y = Ti, V, Mn, Fe) alloys by first-principlesJ. Gonçalves¹, J. Amaral^{1,2}, N. Fortunato¹, V. Amaral¹*1. Departamento de Física and CICECO, Universidade de Aveiro, Aveiro, Portugal**2. Instituto de Física dos Materiais da Universidade do Porto, Institute of Nanoscience and Nanotechnology, Porto, Portugal*

A Curie temperature (T_C) close to room temperature, a high magnetic moment and a steep T_C dependence with volume are favorable properties for magnetocaloric applications. The latter is usually not studied in detail in Heusler alloys, and these provide a rich variety of compositions for optimization via first-principles calculations. In a previous work [1] we have examined these properties in a number of Heusler compounds of the general formula Co_2YZ . Co_2CrGa ($T_C=370$ K, $m=3 \mu_B$, and $dT_C/dV=-4.5$ K/ \AA^3) was taken as the starting point for this work. A detailed exploration of quaternary alloys is presented, with Cr site substitution by neighbor elements (Ti, V, Mn, Fe). We use the density functional KKR method and the coherent potential approximation for disorder. Heisenberg exchange constants are calculated with the magnetic force theorem, and the mean-field Curie temperature is obtained. For several concentrations, in steps of $\Delta x=0.1$ the volume change is simultaneously explored around the theoretical lattice parameters, and the change of magnetic properties is detailed, including the magnetic moments (local and total) and T_C .

Iron substitution increases the spin moment, and increases T_C away from RT, in agreement with previous studies [2]. Manganese substitution also results in increase of T_C and spin moment. The addition of vanadium decreases T_C closer to RT, although dT_C/dV becomes less negative. However, dT_C/dV can become positive and increase by application of moderate compressive strains, reaching 8 K/ \AA^3 for high concentrations of vanadium and 3% compression. This variability of dT_C/dV with dopant concentration is also found with titanium doping, where dT_C/dV similarly changes from negative to positive with increasing concentration, but is not found in iron or manganese doping, wherein dT_C/dV remains relatively constant for all concentrations and in the few percent volume changes studied, generally becoming slightly more negative with increasing volume.

1. J. N. Gonçalves et al., IEEE Trans. Magn. 50, 1301104 (2014)

2. Y. Umetsu et al., Phys. Rev. B 72, 214412 (2005); K. Kobayashi et al., J. Alloys Compd. 399, 60-63 (2005)

FR.E-P40 - Fast computational magnetic materials design via DFT calculations and a novel Monte-Carlo sampling method

N.M. Fortunato¹, C. de Oliveira Amorim¹, J.S. Amaral^{1,2}

1. Departamento de Física and CICECO, Universidade de Aveiro, Aveiro, Portugal

2. IFIMUP and IN-Institute of Nanoscience and Nanotechnology, Rua do Campo Alegre, Porto, Portugal

The end game of computational material design is to replace the high-cost and labor associated with the exhaustive experimental search for new materials, with quantum mechanical and thermodynamical modeling [1].

A common approach for predicting the magnetic properties of materials is to consider an Ising or Heisenberg-like model, solved via a Monte-Carlo method, typically by the Metropolis algorithm [2]. The required magnetic exchange parameters (J) values can be readily obtained via Density Functional Theory (DFT) methods.

While the Metropolis algorithm is the go-to method in this kind of studies, mainly due to its ease of implementation and flexibility, there are considerable drawbacks to its generalized use to determine applied magnetic field (H) and temperature (T) dependent properties. In terms of computational requirements, independent converged calculations are required for each T and H values, which can become overwhelming for detailed studies, particularly near phase transitions. Additionally, magnetovolume coupling effects, which are an important performance parameter of magnetocaloric materials, are difficult to consider, even for a simplified Domb model approach [3].

We here present an overview of the recently proposed Random Path Method (RPS) [4]. This method allows an unbiased statistical sampling of spin configurations, energy and degeneracy values of Ising and Heisenberg-like systems, leading to an approximation of the partition function coefficients. As such, the partition function obtained is generalized in terms of system parameters, such as exchange constants, external field, temperature, volume, or other homogeneous contributions to the energy.

We show a generalization of the RPS methodology to three-dimensional Ising and discretized Heisenberg-like vector models, exploring the effects of magnetic anisotropy energy (MAE), in-plane and out-of-plane exchange parameters and magnetovolume coupling. Computational performance and convergence criteria are discussed, together with finite-size effects in thermodynamic properties, obtained both via free-energy minimization and average values calculated from the partition function.

FR.E-P42 - Simulation of established linear and nonlinear hysteretic loops in coil with an iron core

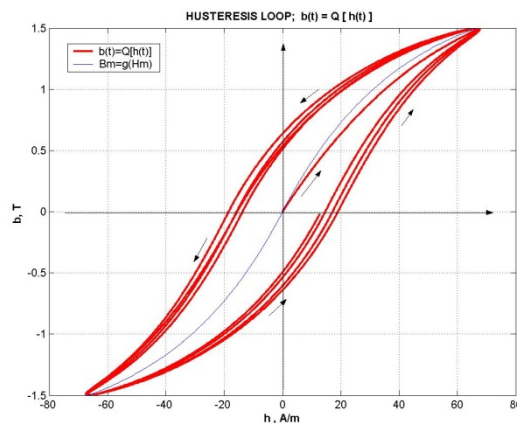
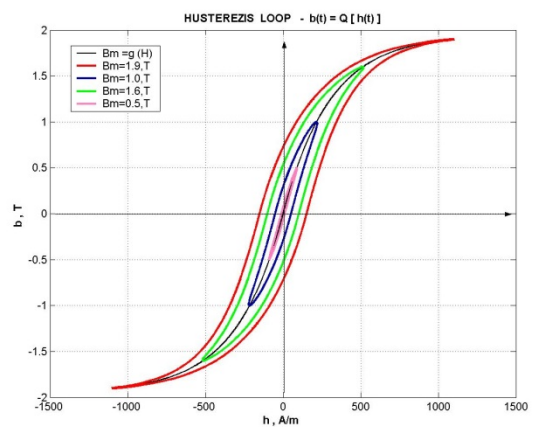
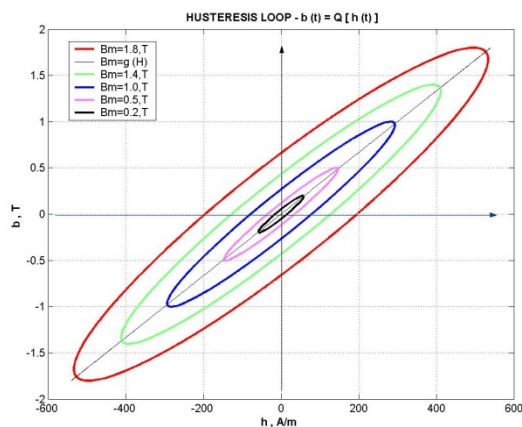
D. Danailov¹

1. Todor Kableshkov University of Transport, Sofia, Bulgaria

The paper considers a model for the simulation of an established linear and nonlinear symmetric hysteretic loop. The base magnetic material curve $B_{\mu}(H_{\mu})$, as well as magnetic chain active resistance, assigned by the $B_r(H_r)$ curve, are used in its construction. It is possible to determine remagnetization and iron losses. Hysteresis is presented by means of

pulsing functions of the type $b^{*(p)} = \vartheta[h^{*(p)}]$, where flux density $b^{*(p)} [t, b_r(t), b_{\mu}(t)]$ and magnetic field strength $h^{*(p)} [t, h_r(t), h_{\mu}(t)]$ are preliminarily expanded into two components $(b_r(t); b_{\mu}(t))$ and $(h_r(t); h_{\mu}(t))$. Parametric functions $b_r(t), b_{\mu}(t), h_r(t), h_{\mu}(t)$ are trigonometric.

A software product for the assignment of symmetric loop family has been created according to the mathematical model of hysteretic process description. Fig. 1 and fig. 2 show obtained hysteretic loop families, of linear and nonlinear hysteretic loops. The model can be also applied in dynamic hysteretic process research (fig. 3).



FR.F-P02 - Magnetism of GaSb-MnSb granular films controlled by charge carriers tunneling through the cluster-matrix Schottky barrier

A. Talantsev¹, R. Morgunov¹

1. Institute of Problems of Chemical Physics RAS, Chernogolovka, Russia

Ferromagnetic clusters incorporated in semiconductor crystal lattice attract significant attention because interplay between their electrical and magnetic properties is possible in the wide temperature range [1]. In our work, we have studied series of GaSb(59 %) - MnSb(41 %) thin films with different carrier concentrations from $N_h = 4 \cdot 10^{18}$ to $N_h = 4 \cdot 10^{20} \text{ cm}^{-3}$ at 300 K. Clear concentration dependence of saturation magnetization $M_{\text{sat}}(N_h)$ was observed. At lower carrier concentrations ($\sim 4 \cdot 10^{18}$) the $M_{\text{sat}}(N_h)$ dependence is linear corresponding to spin-dependent tunneling under the Schottky barriers on the cluster-matrix bounds. At higher carrier concentration $M_{\text{sat}}(N_h)$ dependence becomes non-linear and magnetization saturates at $N_h = 2 \cdot 10^{20} \text{ cm}^{-3}$ reaching the value $M_{\text{sat}} = 3.6$ Bohr's magnetons, which is in good agreement with the highest saturation magnetization, obtained from electronic calculations for MnSb [2]. At higher carrier concentrations the width of Schottky barrier becomes comparable with charge carrier wavelength. This fact allows over-barrier transitions of charge carriers from matrix into clusters. These transitions are responsible to non-linear $M_{\text{sat}}(N_h)$ dependence. To investigate tunneling conductivity separately from over-barrier motion, we have carried out magnetization and carrier concentration measurements at 2 K. At this temperature carrier concentrations were decreased down to $2 \cdot 10^{17} \text{ cm}^{-3}$, and only linear part of $M_{\text{sat}}(N_h)$ was observed.

[1] Masrour, R., R., Hlil, E. K., Hamedoun, M., Benyoussef, A., Mounkachi, O., & El Moussaoui, H. 'Electronic and Magnetic Properties of MnSb Compounds.' *Journal of Superconductivity and Novel Magnetism* (2015): 1-5

[2] Coehoorn, R., Hass, C., de Groot, R.A. "Electronic structure of MnSb" *Phys. Rev. B.* 31, 1980
This work is supported by RFBR (grant 13-07-12027)

FR.F-P03 - Magnetically induced transition from hopping-type to band-type conduction in Mn-doped ZnO

A. Ruotolo¹, X. Wang², S. Qi¹, R. Lortz³, J. Wang³

1. City University of Hong Kong, Tat Chee Ave, Hong Kong

2. Chinese Academy of Science, Beijing, China

3. Hong Kong University of Science and Technology, Clear Water Bay, Hong Kong

We here show that a negative magnetoresistance as large as several hundreds percent can be induced in simple zinc oxide (ZnO) doped with manganese (Mn). This anomalous effect was found to appear in oxygen-deficient films and to increase with the concentration of dopant. By combining magnetoresistive measurements with magneto-photoluminescence, we demonstrate that the effect can be explained as the result of a magnetically induced transition from hopping-type to band-type conduction where the activation energy is caused by the sp-d exchange interaction. The study was carried out on films of $Zn_{1-x}Mn_xO$ with $x = 0$ (pure ZnO), 0.02, 0.04 and 0.08 grown by pulsed laser deposition on sapphire substrates. The films showed n-type conductivity, regardless temperature. Oxygen vacancies (VO's) were introduced in the films by increasing the temperature of the substrate and decreasing the oxygen partial pressure during growth. As the temperature is reduced, the resistivity of the films increases with distinct signatures of a transition from band- to hopping-conduction. A sharp decrease of resistance of the Mn-substituted films was measured when an external magnetic field was applied. The change of resistivity was found to increase with the concentration of Mn. The magnetic activation of electrons to the band conduction was probed by resorting to magneto-photoluminescence measurements.

FR.F-P04 - The magnetic phase diagram of Mn-Doped GeTe crystals

M. Kriener¹, Y. Kaneko¹, X.Z. Yu¹, Y. Tokura^{1,2}, Y. Taguchi¹

1. RIKEN Center for Emergent Matter Science (CEMS), Wako, Saitama, Japan

2. Department of Applied Physics and Quantum-Phase Electronics Center (QPEC), University of Tokyo, Hongo, Tokyo, Japan

GeTe has attracted huge interest for decades: It is one of the first examples among the many-valley semiconductors in which superconductivity was found [1]. Later it came into the focus of research as an ingredient for thermoelectrical materials [2] and more recently due to its large Rashba-spin splitting [3]. Moreover, GeTe exhibits a ferroelectric distortion. Since Mn doping leads to the formation of a diluted magnetic semiconductor [4], the system is also discussed as a possible multiferroic material [5]. The polar distortion is suppressed with increasing Mn concentration x and eventually disappears above approximately $x \approx 0.15$ where the high-temperature cubic structure is retained down to low temperatures. Here we investigate the magnetic phase diagram of bulk $\text{Ge}_{1-x}\text{Mn}_x\text{Te}$ ($x \leq 0.25$) with respect to the polar distortion by means of high-resolution transport, thermodynamic, and microscopic measurements. The magnetic exchange interaction is found to strongly depend on the crystal-growth method. One can get control of it by carefully varying the growth recipe of stoichiometrically mixed powders. Such modifications lead to deviations from the previously reported linear dependence of the ordering temperature on x [4].

[1] R. A. Hein et al., Phys. Rev. Lett. 12, 320 (1964)

[2] D. M. Rowe, Proc. IEEE 125, 1113 (1978)

[3] D. Di Sante et al., Adv. Mater. 25, 509 (2013)

[4] R. W. Cochrane et al., Phys. Rev. B 9, 3013 (1974)

[5] H. Przybylinska et al., Phys. Rev. Lett. 112, 047202 (2014)

FR.F-P06 - Systematic study of AMR in (Ga,Mn)As

Z. Kaspar¹, K. Olejnik¹, K. Vyborny¹, V. Novak¹, T. Jungwirth¹

1. Institute of Physics ASCR, V.V.I., Prague, Czech Republic

We systematically study the anisotropic magnetoresistance (AMR) on a series of optimized (Ga,Mn)As samples [1]. The crystalline and non-crystalline contributions to the AMR were separated [2] and an apparent higher-order term (of six-fold symmetry) was identified to be an artefact resulting from the presence of magnetic anisotropy of the material and of the residual fields of external superconducting magnets. In the broad range of nominal Mn concentrations from 2 to 11%, we find the non-crystalline contribution to dominate, although the crystalline terms become relatively more important for higher doping levels. We compare these findings with the Boltzmann transport calculations based on the k.p mean-field kinetic-exchange model [3] and discuss the level of agreement of AMR components term by term. For some terms, the model turns out to be very sensitive to the input Luttinger parameters (taken from the clean GaAs host material), yet the dominant non-crystalline term is largely independent of the model details demonstrating the applicability of this model to the highly disordered dilute magnetic semiconductor.

[1] P. Nemeč et al., Nature Communications 4, 1422 (2013). [2] E. de Ranieri et al., New Journal of Physics 10, 065003 (2008)

[3] K. Vyborny et al., Physical Review B 80, 165204 (2009)

FR.F-P07 - Magnetic properties of the CeO₂-Co system

M. Paulin¹, A. Leyva¹, J. Sacanell¹

1. Departamento de Física de la Materia Condensada, Gerencia de Investigación y Aplicaciones, Centro Atómico Constituyentes, Comisión Nacional de Energía Atómica, Río Negro, Argentina

The development of spintronics has promoted the study of materials with strong coupling between their electric and magnetic properties. For that kind of applications, the materials should have a high spin polarization and also present structural compatibility with existing semiconductors. Among materials that meet these requirements are the diluted magnetic oxides such as Co doped CeO₂. The pure compound is a diamagnetic insulator, but on doping with magnetic ions like, the system can become paramagnetic or ferromagnetic. The great capability to accommodate oxygen vacancies in its structure can be the responsible for this particular behavior however, some results could also be explained in terms of small segregation of magnetic impurities. In order to determine the contribution of each of them, we performed X-ray absorption near edge structure (XANES) and Magnetization measurements in oxidizing and reducing conditions as we observed that the FM contribution is enhanced as we increase the time of the thermal treatments in vacuum. Those systematic experiments allows us to establish a relation between ferromagnetism and oxygen content of the samples.

FR.F-P08 - Spin correlations in the lightly doped semiconductor oxide Mn:ZnO

A. Wildes¹, D. Lançon^{1,2}, G. Nilsen¹, H. Rønnow², A. Magrez²

1. *Institut Laue-Langevin, Grenoble, France*

2. *École Polytechnique Fédérale de Lausanne, Lausanne, Switzerland*

ZnO is a wide-gap semiconductor that, on light doping with another transition metal for the zinc, is reported to have room temperature ferromagnetism. These reports have resulted in a flurry of interest, as such a material would have applications in spintronic materials. It is possible to manufacture some of these materials in bulk, although the processes used can result in phase segregation and clustering. We have used magnetometry and neutron scattering with polarization analysis to determine the spin correlations in ZnO lightly doped with manganese. The samples were manufactured via a solid-state synthesis method, or via a thermal decomposition of hydrozincite. Our results show clear evidence for ferromagnetism in 3% doped samples made by solid-state synthesis, however there is also clear phase segregation of the manganese into MnO and ZnMn₂O₄. The decomposed hydrozincite samples also showed clear ferromagnetism at 3% doping, however they also showed the formation of MnO nanoparticles. Lower doping of Mn in the decomposed hydrozincite samples resulted in superparamagnetic behaviour with no evidence of phase segregation and with indications of ferromagnetic short-ranged order.

FR.F-P09 - Magnetic band splitting of Ga_{1-x}Mn_xAs estimated by magnetic circular dichroism spectroscopy

K. Ando¹, H. Tanaka², V. Zayets¹, H. Saito¹

1. National Institute of Advanced Industrial Science and Technology (AIST), Japan

2. Ohio University, Athens, United States

Ga_{1-x}Mn_xAs is a canonical III-V diluted magnetic semiconductor (DMS). In spite of intensive studies reported in nearly two decades from its discovery, its band structure is still under heated debate. Because Mn-related impurity bands makes the interpretation of the optical spectroscopic data extremely difficult [1], even the most important characteristic parameter of DMS, i.e. magnetic band splitting (Zeeman splitting), had not been reported until quite recently [2]. In this study, we report the band splitting of high quality Ga_{1-x}Mn_xAs samples by using magnetic circular dichroism (MCD) spectroscopy. Ga_{1-x}Mn_xAs thin films were grown by MBE method. The InP substrates were removed by chemical etching. MCD spectra were measured between 0.62 eV and 4.0 eV. Around 3 eV, which corresponds to the L critical points (c.p.) optical transitions of GaAs, strong and characteristic MCD structures were observed. Analyses of the MCD spectral shape clearly indicated that E1-c.p. is magnetically split with at least 7 meV at 6 K in a x = 0.03 sample. The Zeeman splitting at E0-c.p., which is known to be typically 16 times larger than that at E1-c.p. in zinc-blend type DMS, was thus estimated to be larger than 110 meV. With Mn concentration, the MCD structures showed a shift to the lower energy which quickly saturated with Mn concentration far below x=0.01. This red-shift with quick saturation suggests that the s, p-d exchange interaction of Ga_{1-x}Mn_xAs has a very localized nature.

[1] K. Ando, H. Saito, K. Agarwal, M. Debnath and V. Zayets, Phys. Rev. Lett. 100, 067204 (2008)

[2] H. Tanaka, W. M. Jadwisieniczak, H. Saito, V. Zayets, S. Yuasa and K. Ando, J. Phys. D 47, 355001 (2014)

FR.F-P10 - Magnetic properties of Mn doped crystalline and amorphous Ge thin film grown on Si(111)

A.C. Önel¹, L. Çolakerol Arslan, B. Toydemir, M. Ertas

1. Gebze Technical University, Kocaeli, Turkey

We report on the structural and magnetic properties of Mn-doped Ge thin films grown by thermal diffusion. X-ray diffraction, X-ray photoelectron (XPS), and electron spin resonance (ESR) spectroscopies were applied to investigate crystallinity, the local structure and magnetism of the Mn doped Ge films grown on Si (111) by molecular beam epitaxy in monocrystalline and amorphous forms. We have found out that the distribution of Mn atoms inside the Ge layer and resulting properties are affected by the thickness, crystal quality and roughness of the Ge layer. The results show that for Mn doped crystalline Ge film, most of the Mn atoms diffused into the deep region of Ge without forming any secondary phase. Both magnetic and structural investigations indicate that only few percent of Mn atoms are in the ionic form with a valency of +2 and Mn atoms in crystalline Ge ferromagnetically interact. When a thin highly strained monocrystalline Ge film is formed on Si (111), Mn atoms travel through the Ge layer and form ferromagnetic MnSi nanodots at the interface. For amorphous film, on the other hand, both chemical shift in the Mn 2p peak position and changes in the core level line-shape reveal the formation of Ge-Mn phase in the surface region. ZFC and FC curves of amorphous film exhibits low temperature irreversibility just below $T_c=300K$, indicating the existence of ferromagnetic nanoparticles of Mn_5Ge_3 incorporated into the amorphous film. Similar to the thin Mn_5Ge_3 films, amorphous film shows uniaxial magnetic anisotropy with easy axis parallel to the film surface. Thermal diffusion doping strategy on thin crystalline Ge is a reachable path toward Si based DMS for future semiconductor spintronics devices.

FR.F-P11 - Femtosecond optical excitation of spin resonances in the easy-plane antiferromagnet semiconductor EuTe

R. Subkhangulov¹, R. Mikhaylovskiy¹, B. Ivanov², A. Henriques³, P. Rappl⁴, E. Abramof⁴, T. Rasing¹, A. Kimel¹

1. *Institute for Molecules and Materials, Radboud University Nijmegen, Nijmegen, Netherlands*

2. *Institute of Magnetism, Kiev, Ukraine*

3. *Instituto de Fisica, Universidade de Sao Paulo, Sao Paulo, Brazil*

4. *LAS-INPE, Sao Jose dos Campos, Brazil*

Understanding laser-induced spin dynamics in magnetic materials is a cornerstone for high-speed spintronics and magnetic recording. Here we investigated the ultrafast spin dynamics in the model Heisenberg antiferromagnetic semiconductor EuTe. We employed a time-resolved all-optical pump-probe technique at a temperature of 1.7 K and magnetic fields up to 70 kG applied in the plane of the sample. We demonstrate that the optically excited electrons from the 4f to 5d EuTe band trigger antiferromagnetic spin precession consisting of two modes, in accordance with the theoretical model for an easy plane antiferromagnet.

Analyzing the efficiency of the excitation of the modes as a function of the applied magnetic field we found that the antiferromagnetic spin precession is induced by the ferromagnetic 5d-4f exchange interaction, which is high in comparison with the antiferromagnetic f-f exchange. The d-f exchange in EuTe, in particular, gives rise to the isotropic magneto refractive effect.

It is manifested as a modulation of the bandgap of EuTe at the antiferromagnetic resonance frequency and can be monitored by measuring the pump induced reflectivity changes in the probe beam. We found that the antiferromagnetic spin precession is triggered at magnetic fields higher than that of the spin flop transition at ~1 kG, and lower than that of spin flip transition at ~70 kG. We found that at magnetic fields, corresponding to the crossing of the two modes, the amplitudes of both modes are strongly enhanced; meanwhile the damping is strongly suppressed. The amplitude enhancement can be explained by a weak coupling of the two antiferromagnetic modes, which can be due to a small non-collinearity of the external magnetic field to the sample plane. We show that the damping suppression can be explained by accounting possible modification of the damping by the 5d electrons.

Published partially in: Scientific Reports 4, 4368, 2014

FR.F-P12 - The effects of different precursors in the production of target for pulsed laser deposition on the magnetism of cobalt doped ZnO films

W. Dizayee¹, M. Ying², S.M. Heald³, H.J. Blythe¹, A.M. Fox¹, G.A. Gehring¹

1. *Department of Physics and Astronomy, Hicks Building, University of Sheffield, Sheffield, United Kingdom*
2. *Key Laboratory of Beam Technology and Material Modification of Ministry of Education, College of Nuclear Science and Technology, Beijing Normal University, Beijing, China*
3. *Advanced Photon Source, Argonne National Laboratory, Argonne, United States*

Zn_{0.95}Co_{0.05}O films have been prepared by pulsed laser deposition, PLD, using three different solid state targets formed from different precursors; ZnO and metallic Co, CoO and Co₂O₃ to investigate if the amount of oxygen in the precursor material is important and mimics the well-studied effects of changing the oxygen content in the PLD chamber. Films of thickness 700nm were grown at base pressure using each of the targets; we found that all the films contained a fraction of the Co ions in metallic Co and the rest as Co²⁺. The film grown with CoO was the most ordered and contained the smallest fraction of Co ions in metallic Co (9%). Its magnetic circular dichroism signal, MCD, showed no evidence of inclusions of CoO. The film grown with metallic Co in the target contained the largest fraction of Co ions in metallic Co (24%). All three films showed ferromagnetic behavior at low temperatures with small coercive fields (~100Oe). However this magnetization had vanished by room temperature. In all cases the size of the magnetization measured at low temperatures was larger than the amount that would be expected from the measured amount of metallic cobalt. Films were also deposited using the target made from metallic Co in 10mTorr and 100mTorr of O₂, of thickness 300nm and 100nm respectively, and x-ray and optical MCD measurements showed that the metallic fraction had vanished, the crystal quality dramatically improved. Furthermore the substantial ferromagnetic signal (~10emu/cm³) had become almost independent of temperature. Hence a conclusion of this work is that the choice of precursor is important and that adding oxygen in the growth chamber does not appear to be equivalent to including more oxygen in the target. Furthermore the highest quality and most useful films may be made by using metallic cobalt in the preparation of the target and including some oxygen in the growth chamber. This result disagrees strongly with what is found when the target was made using Co₂O₃. when including oxygen in the growth chamber reduces the magnetization.

FR.F-P13 - Direct observation of Dresselhaus effect in zinc blend structure InSb

W. Jung¹, J. Hong², S. Cho¹, B. Kim¹, M. Leandersson³, T. Balasubramanian³, S. Kimura⁴, J. Shim², C. Kim¹

1. *Institute of Physics and Applied Physics, Yonsei University, Seoul, Korea*
2. *Department of Chemistry, Pohang University of Science and Technology, Pohang, Korea*
3. *MAX IV Laboratory, Lund University, Lund, Sweden*
4. *UVSOR Facility, Institute for Molecular Science and The Graduate University for Advanced Studies, Okazaki, Japan*

We have performed circular dichroism angle-resolved photoemission spectroscopy (ARPES) experiments on InSb. Our results show that InSb surface has very strong circular dichroism (CD) signal, indicating probable existence of orbital angular momentum (OAM). In nonmagnetic semi-conductor samples, net OAM in the bulk should be normally zero because of the symmetric electric potential. However, non-zero OAM can appear when there is an inversion symmetry breaking (ISB) which is caused of zinc blend structure and cleaved surface. We find that the dichroism has momentum dependence which, in our view, comes from modulation in the internal electric field in InSb. Heavy hole band shows a Rashba type OAM modulation and warping effects. Light hole band has a the Dresselhaus type OAM modulation. Rashba and Dresselhaus type OAM chiralities coexist in each hole bands. From these results, we suggest new effective Hamiltonians in the form of HLD and HLRD for the Dresselhaus and rst order of RashbaDresselhaus Hamiltonian.

FR.F-P15 - Effect of Ge layer thickness on formation of Mn₅Ge₃ Thin Film on Si (111)

B. Toydemir¹, A. Can Önel¹, M. Ertap¹, L. Çolakerol Arslan¹

1. Gebze Technical University, Kocaeli, Turkey

Injection of spin polarized current via ferromagnetic materials into the Si based semiconductors is the most important requirement to develop such spin-based devices. For this purpose, a lot of attention has been devoted to the development of epitaxial ferromagnetic compounds due to their high Curie temperature, high spin polarization and compatibility with the recent technology. Among these materials, Mn₅Ge₃ is an appealing candidate with its high spin injection efficiency, high spin polarization and room temperature ferromagnetism. Numerous investigations on the fabrication of epitaxial Mn₅Ge₃ films directly grown on Ge showed that growth conditions play a significant role in the magnetic and structural properties of this material. However, a detailed investigation of the growth of thin Mn₅Ge₃ film on the Si substrate has not been carried out so far, although such information is crucial for such a system to be combined with the existing Si technology.

Epitaxial ferromagnetic Mn₅Ge₃ thin films were deposited on Ge/Si (111) substrates by molecular beam epitaxy using solid phase epitaxy. The role of Ge layer thickness and surface morphology on the formation of epitaxial Mn₅Ge₃ films and their magnetic properties were examined. Both structural and magnetic investigation results indicate that Mn₅Ge₃ thin film is formed above a critical Ge layer thickness and it shows perpendicular magnetic anisotropy with magnetic anisotropy increased with decreasing temperature. On the other hand, below critical thickness, Mn atoms directly diffuse into Si underlayer and form a ferromagnetic MnSi phase below a Curie point of about 250K. X-ray photoelectron spectroscopy (XPS) measurements also confirm the diffusion of Mn atoms from Ge towards Si. These results show that high crystallinity and defect free Mn₅Ge₃ can be epitaxially grown on Si substrate, despite an 8% lattice mismatch between Mn₅Ge₃ and Si (111).

FR.F-P16 - Defect-induced magnetism in graphite through neutron irradiation

Y. Wang¹, P. Pochet², C.A. Jenkins³, E. Arenholz³, G. Bukalis⁴, S. Gemming¹, M. Helm¹, S. Zhou¹

1. *Helmholtz-Zentrum Dresden-Rossendorf, Institute of Ion Beam Physics and Materials Research, Dresden, Germany*
2. *Univ. Grenoble Alpes, INAC-SP2M, Grenoble, France*
3. *Advanced Light Source, Lawrence Berkeley National Laboratory, Berkeley, California, United States*
4. *Helmholtz-Zentrum Berlin für Materialien und Energie, Lise-Meitner-Campus, Berlin, Germany*

We have investigated the variation in the magnetization of highly ordered pyrolytic graphite (HOPG) after neutron irradiation, which introduces defects in the bulk sample and consequently gives rise to a large magnetic signal. We observe strong paramagnetism in HOPG, increasing with the neutron fluence. The induced paramagnetism can be well correlated with structural defects by comparison with density-functional theory calculations. In addition to the in-plane vacancies, the transplanar defects also contribute to the magnetization. The lack of any magnetic order between the local moments is possibly due to the absence of hydrogen/nitrogen chemisorption, or the magnetic order cannot be established at all in the bulk form.

FR.F-P19 - Influence of manganese ions environment in octahedral sublattice on the properties of triple-substituted manganitesV. Karpasyuk¹, A. Badelin¹, D. Merkulov¹, S. Estemirova², I. Derzhavin¹

1. Astrakhan State University, Oblast, Russia

2. Institute for Metallurgy, Ural Division of RAS

The purpose of present research is to establish the regularities in dependencies of unit cell volume (v), magnetization (σ) and Curie temperature (T_c) upon concentration and electron configuration of substituent Me^{2+} in manganites $La_{1-c}Sr_cMn^{3+}_{1-c-x-2y}Mn^{4+}_{c+2y}Me^{2+}_{0.5x}Ge^{4+}_{0.5x}O_{3+y}$, where $Me^{2+}=Mg^{2+}(2p^6)$, $Zn^{2+}(3d^{10})$, $Ni^{2+}(3d^8)$, $c=0.2+x$ ($x=0.05; 0.10; 0.15$).

Polycrystalline samples were prepared by traditional ceramic processing. The final sintering step was performed in air at 1473 K. In order to provide stoichiometric oxygen content ($y=0$), obtained samples were annealed in vacuum (partial oxygen pressure 10^{-1} Pa) at 1223 K.

It was found that T_c of all samples increases as a functions of "x", but v and σ decrease. Magnetization of Mg-contained manganites decreases most sharply.

After annealing, characteristics of manganites changed in the following way: the values of v of all Ni-substituted manganites diminished, while v of Mg- and Zn-contained samples with $x=0.05$ increased; magnetization of all manganites and T_c of compositions with 3d substituents did not practically alter, while Curie point of Mg-contained compositions with $x=0.15$ greatly lowered.

Interpretation of experimental results is based on the assumption that, owing to Coulomb interaction, Me^{2+} ions shield Mn^{4+} , breaking double-exchange bonds, and Ge^{4+} dilutes sublattice of Jahn-Teller ions Mn^{3+} . These processes are associated with the formation of clusters enriched with the pairs of different valence cations. Besides that, competing exchange interactions, interionic distances and the effect of composition on the value of y are taken into account.

This research was supported by the Ministry of Education and Science of Russian Federation (State order project 334).

FR.F-P20 - Low temperature magnetization and Electron Spin Resonance studies in $\text{SrSn}_{1-x}\text{Fe}_x\text{O}_3$ ($x=0.05$ to 0.1)H. Kumar N.¹, Radhika K.¹*1. Department of Physics, IIT MADRAS, Tamil Nadu, India*

Oxide Dilute magnetic semiconductors (DMS) continue to be attractive due to the possibility of realizing room temperature ferromagnetism required for spintronic device applications [1, 2]. Perovskite oxides exhibit many interesting physical phenomenon such as superconductivity, colossal magnetoresistance etc. Perovskite based DMS can lead to the fabrication of novel devices, with hetero junction of materials with dissimilar properties [3]. Hence it is interesting to explore possibilities of inducing magnetic interaction by suitable substitutions of ferromagnetic elements. Fe substituted SrSnO_3 gives rise to room temperature (RT) ferromagnetic response for concentrations above 4% with Curie temperature around 600 K. However the low temperature magnetic measurement exhibit anomalous characteristics. In order to understand the nature of magnetic interactions in this system and the dependence of it on Fe concentration we have synthesized compounds with Fe concentration in the range 5% - 10 % and investigated their properties. The M-H isotherms recorded at 5K and 13K differs from the ones recorded at 100 K, 200 K and 300 K. The magnetization shows saturation in the isothermal field sweep measured at room temperature. Lack of saturation is observed in the low temperature regime which may arise from either magnetic anisotropy or due to the presence of mixed magnetic phases. Zero field cooled (ZFC) and field cooled (FC) measurements were carried out in the temperature range 5 K - 300 K at an applied field of 100 Oe. As the concentration of Fe increases, drastic changes are observed in the shape of the ZFC and FC curves. Electron spin resonance (ESR) spectra for all samples have shown broad asymmetric spectra at room temperature. A slight shift towards left in the spectra is observed at 77 K and a change in line shape can also be seen for samples. These observations indicate the presence of strong magnetic interactions in the material.

References:

- [1] T. Dietl, Nature materials. 9, 12 (2010)
- [2] W. Prellier, A Fouchet and B Mercey, , J. Phys: Condens Matter, 15, R1583 (2003)
- [3] G. Prathiba, S. Venkatesh and N. Harish Kumar, , Solid State Comm.,150, 1436 (2010)

FR.F-P21 - Complex magnetic response of SrSn_{1-x}Fe_xO_{3-δ} (x=0, 0.05 and 0.08) nano sticksH. Kumar N.¹, Radhika K.¹*1. Department of Physics, IIT MADRAS, Tamil Nadu, India*

In SrSnO₃ substitution of 5% Fe not only induces ferromagnetism but also reduces resistivity by a few orders of magnitude. But in the nanocrystalline form a substantial reduction in the magnetic moment was observed. In order to strengthen the magnetic interactions without altering its semiconducting and optical characteristics the Fe concentration was increased to 8% and the magnetic properties were investigated by DC magnetization and electron spin resonance measurements. Nanocrystalline SrSn_{1-x}Fe_xO_{3-δ} (x=0, 0.05 and 0.08) were prepared by co precipitation method. The X-ray Diffraction analysis showed that the samples have crystallized in nearly single phase. Scanning electron microscope images showed stick shaped grains with average width 50 nm. The 5% Fe sample exhibits paramagnetism at room temperature (RT) but shows nonlinear magnetic response below 50K with increase in magnetic moment and anisotropy while ferromagnetic response is observed at room temperature in the 8% Fe sample. The magnetization is hysteretic at 5K and the magnetization curve looks distinctly different than that of 5% Fe sample. For the 8% Fe sample Zero field cooled and Field cooled curves show a large bifurcation from low temperature to RT which confirms that the sample retains its ferromagnetic characteristics upto room temperature. Magnetic phase transition with Curie temperatures 725 K and 848 K respectively is observed for 5% and 8% Fe samples with sharper transition for the latter. The broad electron spin resonance spectra at RT indicate the presence of strong magnetic interactions among the dipoles in both the samples. The spectra of 5% Fe doped sample looks more symmetric. A small peak is observed with g= 4.3 which may originate from Fe³⁺ ions having paramagnetic behavior. At 77 K, the spectrum of 8% Fe sample is broader but for 5% Fe sample it is sharper and highly asymmetric suggesting complex magnetic interactions in the latter.

References:

- [2] G. Prathiba, S. Venkatesh and N. Harish Kumar, , *Solid State Comm.*, 150, 1436 (2010)
- [3] Jörg Bohnemanna, *Chemical Engineering Journal* 155, 905 (2009)
- [4] R. Berger et al., *J. Magn. Magn. Mater.* 234, 535 (2001)

FR.F-P22 - Large magnetoresistance in diluted magnetic semiconductors in quasi-two dimensional geometry

I. Kanazawa¹, T. Sasaki¹

1. Department of Physics, Tokyo Gakugei University, Tokyo, Japan

Large magnetoresistance effects in diluted magnetic semiconductors(DMS) have been reported [1]. In addition, interesting phenomena such as the photo-induced magnetic polaron in DMS has been discovered [2]. These works stimulated us to the study of the carrier-induced magnetic solitons, which is an interesting and challenging subject. Kanazawa [3] has discussed the localization mechanism in the metal-insulator transition, using the gauge-invariant Lagrangian density for the hole-induced magnetic solitons. In this study, we have discussed the large magnetoresistance effects in DMS in quasi-two dimensional geometry, extending the previous formula[4]

[1] S.Katsumoto et al.,Mater.Sci.Eng.B84,88(2001)

[2] S. Koshihara et al. Phys. Rev. Lett. 78,4617(1997)

[3] I. Kanazawa,Physica E21,961(2004)

[4]I. Kanazawa,Phys. Lett.A355,4111(2006)

FR.F-P24 - Mössbauer and magnetic study of $\text{Ni}_x\text{Co}_{1-x}\text{Fe}_2\text{O}_4$ nanoferrites

J. Msomi¹, B. Ndlovu¹, T. Moyo¹

1. University of Kwazulu-Natal, Durban, South Africa

Ni-Co nano crystalline ferrites having the general formula $\text{Ni}_x\text{Co}_{1-x}\text{Fe}_2\text{O}_4$ ($0 \leq x \leq 1.0$, in steps of 0.1) were synthesized by glycol-thermal route. X-ray powder diffraction (XRD) and Fourier transform infrared (FTIR) spectroscopy were carried out to investigate the structural properties of the samples. XRD patterns indicate the formation of spinel structure of the prepared compounds. FTIR data confirmed the XRD results. ^{57}Fe Mössbauer spectroscopy and SQUID measurements were used to investigate the magnetic properties. The Mössbauer spectra indicate ordered magnetic spin state in all the compounds. The 'S' shaped hysteresis curves with almost zero coercive recorded at 300 K is characteristic of the superparamagnetic nature of the fine particles. The changes in the saturation magnetization and coercive fields as a function of composition or sample measuring temperature were observed.

FR.F-P26 - Magnetic properties of V- and Ta-doped alpha-Fe₂O₃ films

S.J. Liu¹, L.W. Juang¹, Y.Z. Lin², J.H. Hsieh²

1. *Thin Film Laboratory, National Taiwan Normal University, Taipei City, Taiwan*

2. *Department of Materials Engineering, Mingchi University of Technology, Taipei City, Taiwan*

V- and Ta-doped alpha-Fe₂O₃ films were fabricated by using magnetron co-sputtering technique. The valence state of both V and Ta doped in the films is 5+, which is higher than that of Fe³⁺. Moreover, the ionic radii of V⁵⁺ and Ta⁵⁺ ions are respectively smaller and larger than that of Fe³⁺ ions. The effects of electron doping and lattice strains induced by impurity doping on the magnetic properties of the doped Fe₂O₃ films were investigated, as well as electrical and optical properties. Density functional theory calculations were performed to further clarify the mechanism causing the variation of physical properties of doped alpha-Fe₂O₃.

FR.F-P28 - Nanoscale tin oxide undoped and doped by 3-d elements: Synthesis and magnetic properties

D. Nazarov¹, P. Matveeva¹, N. Bobrysheva¹, O. Osmolowskaya¹, V. Smirnov¹, M. Osmolowsky¹

1. Saint Petersburg State University, Institute of Chemistry, Saint Petersburg, Russia

SnO₂ attracts enormous interest caused by a variety of areas of its application, such as a gas sensors, catalysts, solar cells, optoelectronics, Li-ion batteries. Presence of the room temperature ferromagnetism (RTF) in the nanosized doped and pristine SnO₂ causes concern to this oxide as the material for spintronic. In spite of extensively theoretical and experimental studying of the RTF in the diluted magnetic semiconductors the nature and cause of the ferromagnetism in the tin dioxide is still not fully elucidated.

In this work we have investigated the influence of the size, dimension, composition, nature and concentrations of dopants on the magnetic properties of undoped and chromium, iron, copper doped SnO₂ nanoparticles and nanofilms.

Undoped and doped nanoparticles were obtained by sol-gel method. SnCl₄, FeCl₃, Cr₂(SO₄)₃ and Cu(NO₃)₂ were used as tin, iron, chromium and copper sources, respectively. Doping element concentration varied from 1 to 20%. Pristine tin oxide nanofilms (4-32 nm) were deposited on silicon (100) and quartz substrate by Atomic Layer Deposition (ALD) method using tetraethyl tin (IV) and ozone or hydrogen peroxide.

The nanopowders were characterized by XRD, TEM, BET, TGA, DTA, Mossbauer, Raman and luminescence spectroscopy. Ellipsometry, AFM, SEM, XPS and XRD methods were used to characterize nanofilms. Magnetic properties for all samples were studied by Vibrating Sample Magnetometry (VSM) method.

Presence of RTF was found in both undoped and doped samples. It has been found that the formation of RTF mainly determined by the postprocessing (calcination, vacuum treatment) and concentration of dopants for the nanoparticles and for the films the thickness performs a crucial role.

The reported study was supported by RFBR, research project № 14-03-31053 mol_a. Scientific research were performed at the "Center for optical and laser materials research", "X-ray Diffraction Studies", "Physical Methods of Surface Investigation" and "Nanocomposite" Centers of St. Petersburg State University.

FR.F-P29 - Magnetic anisotropy energy studies in highly Co-doped ZnO by ab initio calculations

A. Lusakowski¹, [W. Szuszkiewicz](#)¹

1. Institute of Physics Polish Academy of Sciences, Warsaw, Poland

ZnO is well known and intensively investigated wide-gap semiconductor with the wurtzite type crystal structure. Both the transition-metal doped thin layers and bulk crystals of this compound or diluted magnetic semiconductors (DMS) grown on the basis of ZnO attract still a lot of attention due to continuous interest in materials for possible future applications in the area of spintronics. In particular, the ZnO crystals containing Co exhibit interesting magnetic properties and have been the topic of several recent papers.

The aim of the present work is the theoretical analysis of the magnetic anisotropy energy (MAE) for a Co-doped ZnO crystal. In the paper we discuss the results of extensive ab initio calculations of the MAE for 2x2x2 ZnO supercell containing 32 atoms with one Zn ion replaced by the Co ion. It is demonstrated that the effect of spin polarization of the surrounding atoms caused by the Co ion is almost limited to the four nearest oxygen neighbours only. As it could be expected, the influence of the Zn and O spin-orbit coupling on the MAE magnitude is very weak and one may claim that the magnetic anisotropy of Co is a single ion type anisotropy. On the contrary, the MAE is extremely sensitive to the lattice geometry and to the nearest neighbourhood of Co ion. The direction of magnetization easy axis is well reproduced by the calculations performed for the ZnO lattice parameter values. However, there exists a significant discrepancy between experimental and theoretical MAE value, the latter one is about one order of magnitude smaller than the former.

This work was supported in part by the Grant No UMO-2011/03/B/ST3/02664 from the National Science Centre (Poland) and by PL-Grid Infrastructure.

FR.F-P30 - Magnetic properties of the MOVPE and implanted GaN:Mn films

M. Marysko¹, Z. Sofer², D. Sedmidubsk², J. Hejtmánek¹, K. Jurek¹, V. Laguta¹, J. Stejskal², P. ěimek², A. Macková³, V. Havránek³

1. *Institute of Physics, ASCR, v.v.i. , Prague, Czech Republic*
2. *Dep. of Inorganic Chemistry, Inst. of Chemical Technology, Prague, Czech Republic*
3. *Nuclear Physics Institute of the ASCR, v.v.i., Prague, Czech Republic*
4. *Forschungszentrum Julich, Institute of BioNanosystems, Julich, Germany*
5. *Faculty of Mathematics and Physics, Charles University, Prague, Czech Republic*
6. *Peter Grunberg Institute (PG1-9), Julich, Germany*

The metal-organic vapour phase epitaxy (MOVPE) and implantation process were used to prepare GaN:Mnx (x=0.1-0.4) thin films on the sapphire substrates. The samples were characterized by the SIMS, disorder density analysis and the Mn content was determined by the electron microprobe method. The EPR measurement at the X band yielded information on the absence of Mn²⁺ ions in the films. The detailed SQUID measurements showed the zero ferromagnetic and, in the low temperature region, relatively large paramagnetic (PM) moment of the samples. The magnetization curves at T=2 K and temperature dependence of the PM susceptibility were measured for the parallel and perpendicular orientation of the magnetic field with respect to the film plane. The results were interpreted in terms of the molecular field approximation starting from the spin Hamiltonian for the Mn³⁺ ion [1],[2]. In contrast to nearly single crystal character of the MOVPE films, for which the m(H) curves exhibit a clearly pronounced anisotropy with the easy axis in the plane, the anisotropy of the implanted films is very small which suggests that the Mn³⁺ ions are in a disordered state. The PM susceptibility follows the Curie-Weiss law and a special attention was given to the Weiss temperature giving information on the possible exchange interaction between the Mn³⁺ ions. The evaluated value of the Weiss temperature was found to depend on the applied field and the value extrapolated to zero field approaches zero which would point to the ensemble of non-interacting Mn³⁺ ions. On the other hand, the dependence on the applied field could be ascribed to a part of the Mn³⁺ ions exhibiting ferromagnetic and antiferromagnetic exchange interactions.

[1] W. Stefanowicz et al. , Phys. Rev. B 81, 235210 (2010)

[2] A. Alsaad, Physica B440, 184425 (2010)

FR.F-P31 - Transport properties in the ferromagnetic semiconductor gadolinium nitride

B. Ruck¹, T. Maity¹, H. Warring¹, E.M. Anton¹, C.M. Lee¹, J. Chan¹, S. Granville¹, F. Natali¹, J. Trodahl¹

1. Victoria University of Wellington, Wellington, New Zealand

Gadolinium nitride is one of the rare examples of an intrinsic magnetic semiconductor [1], which makes it of particular interest for use in spintronics studies. As a semiconductor its conductivity is controlled by doping, with most GdN samples being heavily n-type doped by large concentrations of nitrogen vacancies. The concentration of such vacancies can be controlled by varying the growth conditions [2], and we have recently shown that Mg doping can passivate the donors to give semi-insulating GdN [3]. However, fundamental questions regarding the nature of the dopant levels and their influence on the electrical transport remain unanswered. Here we will present the transport properties, including temperature dependent resistivity, magnetoresistance, anisotropic magnetoresistance, and Hall effect, from a series of samples that span the range from insulating to degenerately doped. The data can be understood in terms of an evolution from isolated impurity levels in the insulating material to an impurity band that merges with the conduction band at heavy doping levels. The overall behaviour is reminiscent of that seen in dilute magnetic semiconductor such as (Ga,Mn)As.

[1] F. Natali, B.J. Ruck, N.O.V. Plank, H.J. Trodahl, S. Granville, C. Meyer, and W.R.L. Lambrecht, Rare-earth mononitrides, *Prog. Mats. Sci.* 58, 1316 (2013)

[3] F. Natali, B.J. Ruck, H.J. Trodahl, Do Le Binh, S. Vezian, B. Damilano, Y. Cordier, F. Semond, and C. Meyer, Role of magnetic polarons in ferromagnetic GdN, *Phys. Rev. B* 87, 035202 (2013)

[4] C.-M. Lee, H. Warring, S. Vezian, B. Damilano, S. Granville, M. Al Khalfioui, Y. Cordier, H.J. Trodahl, B.J. Ruck and F. Natali, Highly resistive Mg-doped GdN films, *Appl. Phys. Lett.* 106, 022401 (2015).

FR.H-P01 - Magnetoresistive memory with recording by the electric field

A. Morosov¹, A. Sigov², D. Vinokurov²

1. *Moscow Institute of Physics and Technology (State University), Moscow, Russia*

2. *Moscow State Technical University of Radioengineering, Electronics and Automation, Moscow, Russia*

To realize a magnetoresistive random-access memory cell with recording by the electric field one needs to turn by 90° the magnetization of one of ferromagnetic layers entering the magnetic tunnel junction that consists of two conducting ferromagnetic layers separated by the dielectric interlayer. The parallel orientation of magnetizations of these layers serves to write “zero”, while the mutually perpendicular orientation of magnetizations is used to write “unity”. To switch the magnetization of one of ferromagnetic layers, the additional electrosensitive layer neighboring with the selected ferromagnetic layer is used. One possible mechanism of interaction between these layers is the interaction due to the elastic deformations transferred from one layer to another. If the reorientation occurs between two equilibrium positions existed in the absence of the interaction with the electrosensitive layer (two easy axes in the layer plane caused by the crystalline symmetry), there is the lower limit of about 100 nm for the bit size because of the occurrence of the superparamagnetic threshold. Promising directions for the development of the magnetoresistive memory switched by the electric field are the memory based on the exchange interaction between the ferromagnetic layer and multiferroic BiFeO₃ layer [1], as well as the memory based on the elastic interaction between the ferromagnetic layer and the layer of ferroelectric-ferroelastic (the “long-leg” memory [2]), in which the magnetization direction of the ferromagnetic layer is determined by the deformation direction of the electrosensitive layer in the absence of the electric field.

[1] A. Morosov, Phys. Solid State 56 (5), 865 (2014)

[2] A. Morosov and A. Sigov, J. Appl. Phys. 115, 223909 (2014)

FR.H-P02 - Intrinsic magnetoresistance in metal films on ferromagnetic insulators

V. Grigoryan¹, W. Guo¹, J. Xiao¹, G. Bauer^{2,3}

- 1. Department of Physics and State Key Laboratory of Surface Physics, Fudan University, Shanghai, China*
- 2. Kavli Institute of NanoScience, Delft University of Technology, Delft, The Netherlands*
- 3. Institute for Materials Research and WPI-AIMR, Tohoku University, Sendai, Japan*

We predict a magnetoresistance induced by the interfacial Rashba spin orbit coupling in a normal metal-ferromagnetic insulator bilayer system. This new magnetoresistance depends on the angle between current and magnetization directions as the recent discovered 'spin Hall magnetoresistance' mechanism caused by a combined action of spin Hall and inverse spin Hall effects. Due to the identical phenomenology we question the true origin of the spin Hall magnetoresistance and propose that a normal metal film thickness dependence measurement can clarify which effect, the interfacial Rashba or the bulk spin Hall effect, is responsible for the new magnetoresistance.

FR.H-P03 - Interface influence on the properties of Co₉₀Fe₁₀ films on soft magnetic underlayers - magnetostrictive and Mössbauer spectrometry studies

T. Szumiata¹, M. Gzik-Szumiata¹, K. Brzózka¹, B. Górka¹, M. Gawroński¹, A. Caruana Finkel², N. Reeves-McLaren², N.A. Morley²

1. *Department of Physics, Faculty of Mechanical Engineering, University of Technology and Humanities in Radom, Radom, Poland*

2. *Department of Materials Science and Engineering, University of Sheffield, Sheffield, United Kingdom*

The main aim of the work was to understand the correlation between magnetostrictive properties and microstructure of 25 nm thick Co₉₀Fe₁₀ films deposited on soft magnetic underlayers. The investigated magnetic bilayers were grown on silicon substrates using a RF sputtering deposition system with 3 targets: Co₉₀Fe₁₀, Ni₈₁Fe₁₉ (permalloy), and METGLAS 2605SC of Fe₈₁B_{13.5}Si_{3.5}C₂ composition [1]. The magnetostriction constant was measured by the Villari Effect using a magneto-optic Kerr effect (MOKE) magnetometer. Crystalline and magnetic microstructure has been examined with 57Fe-based conversion electrons Mössbauer spectrometry (CEMS). In the case of Co₉₀Fe₁₀ on 25 nm and 35 nm thick METGLAS underlayers one can resolve in Mössbauer spectra two hyperfine field distributions (high-field and medium-field ones) corresponding to these two constituents of bilayers. Analogical distributions describe the spectra of Co₉₀Fe₁₀ bilayers on 25nm and 35 nm thick Ni₈₁Fe₁₉ underlayers, however an additional low-field, smeared component has been observed. It has been attributed to the interface layer (of partially disordered structure) between magnetostrictive and soft magnetic layer. Such interpretation is backed up by the obtained linear correlation between mean hyperfine field value and magnetostriction constant of the films. The investigated bilayers are good candidates for MagMEMS devices, like FeGa-based films [2].

[1] A. Caruana Finkel, N. Reeves-McLaren, N. A. Morley; J. Magn. Magn. Mat. 357 (2014) 87-92

[2] A. Javed, N. A. Morley, T. Szumiata, M. R. J. Gibbs; Appl. Surf. Sci. 257 (2011) 5977-5983

FR.H-P07 - Interfacial-scattering-induced enhancement of the anomalous Hall effect in uniform Fe nanocluster-assembled films

D. Peng¹, J. Wang¹, W. Mi², L. Wang¹

1. Department of Materials Science and Engineering, College of Materials, Xiamen University, Xiamen, China

2. Department of Applied Physics, Tianjin University, Tianjin, China

More than a century ago, the anomalous Hall effect (AHE) in ferromagnets was found. The large AHE made them become the potential candidates for the practical applications in the field of Hall sensors, magnetic logic devices, etc [1, 2]. But the AHE mechanisms are still a controversial issue. Recently, extensive studies have been devoted to understand the influence factors of AHE [3-5]. However, so far, there has been no report on the granular size effects on AHE. Although the AHE is strongly related to the granular size, it is difficult to investigate the size effect on the AHE in the granular films due to their wide size distribution. In this work, we studied the cluster size ($d=4.3-16.1$ nm) dependence of the anomalous Hall effect in uniform Fe nanocluster-assembled films prepared by the plasma-gas-condensation method. In particular, a large enhancement of AHE is observed at $d=4.3$ nm, which is almost four orders of magnitude larger than bulk Fe. The saturated anomalous Hall resistivity (RA_{xy}) shows a sharp decrease as d increases from 4.3 to 10.1 nm and a slight decrease with further increasing d to 16.1 nm. Moreover, the relations between the RA_{xy} and longitudinal resistivity (R_{xx}) were also discussed in details. Results show that in double-logarithmic scales, RA_{xy} decreases with the increase of R_{xx} , obeying a new scaling relation of $\log(RA_{xy}/R_{xx}) = a_0 + b_0 \log R_{xx}$, which originates from the interfacial scattering to the AHE and longitudinal resistivity.

[1] E. H. Hall, Ph.D. thesis, Johns Hopkins University, 1880

[2] J. Xu et al., Appl. Phys. Lett. 102 (2013) 162401

[3] Z. B. Guo et al., Phys. Rev. B 86 (2012) 104433

[4] J. Y. Zhang et al., Appl. Phys. Lett. 102 (2013) 102404

[5] L. Wu et al., Phys. Rev. B 87 (2013)155307

FR.H-P08 - Thermal stability of an interface-stabilized skyrmion lattice

S. Krause¹, A. Sonntag¹, J. Hermenau¹, R. Wiesendanger¹

1. University of Hamburg, Hamburg, Germany

Skyrmions are topologically protected field configurations with particle-like properties. They are in the focus of many ongoing investigations due to their potential application for future spintronic devices. Using spin-polarized scanning tunneling microscopy (SP-STM) at low temperature ($T = 11$ K), a lattice of nanoskyrmions has been shown to be the ground state of the one-atomic-layer thick Fe/Ir(111) surface [1]. In our recent SP-STM studies we investigated the influence of temperature onto the Fe/Ir(111) nanoskyrmionic lattice. The experiments reveal that the lattice is stable against thermal agitation up to $T = 27.4$ K. Further elevating T to 28.0 K results in a fading of the magnetic SP-STM contrast, indicating a phase transition into the paramagnetic state. By slowly varying T we elaborate a very sharp phase transition at $T = 27.8$ K. [2] At second monolayer Fe step edges the skyrmionic lattice is found to persist even to higher T , which is attributed to pinning. The experimental results will be presented and discussed in terms of magnetic corrugation amplitude of the skyrmion lattice and pinning decay length.

[1] S. Heinze et al., Nat. Phys. 7, 713 (2011)

[2] A. Sonntag et al., Phys. Rev. Lett. 113, 077202 (2014)

FR.H-P09 - Effect of the ion bombardment on the magnetic and transport properties of space-less manganite/metal pseudo spin valves

K.W. Lin ¹, Q. Shao ², W. Rong Luo ¹, H.F. Wong ³, C.W. Leung ³, A. Ruotolo ²

1. *Department of Materials Science and Engineering, National Chung Hsing University, Taichung, Taiwan*

2. *Department of Physics and Materials Science, City University of Hong Kong, Kowloon, Hong Kong SAR, China*

3. *Department of Applied Physics and Materials Research Centre, The Hong Kong Polytechnic University, Hung Hom, Kowloon, Hong Kong, China*

A magnetically dead layer exists at the surface of manganites. This dead layer can be used as a non-magnetic natural barrier at the interface of manganite/magnetic-metal bilayers for space-less pseudo spin-valves [1,2]. Ideally, magnetism should be completely suppressed at the interface of the bilayer to achieve maximum magnetoresistive effect. This can be achieved by ion bombardment. We investigated the effect of Ar⁺ ion bombardment on the magnetic and magneto-transport properties of La_{0.7}Sr_{0.3}MnO₃/Permalloy (LSMO/Py) bilayers. LSMO films were grown by pulsed laser deposition (PLD) on (100) SrTiO₃ single crystal substrates. The LSMO films showed a Curie temperature larger than room temperature, as measured by a vibrating sample magnetometer. The surface of the LSMO films was bombarded by Ar ion-beam for different periods (t_{bomb} = 1 to 10 mins.) with an End Hall ion source. Py was subsequently deposited by a Kaufmann ion source using the ion-beam sputtering deposition technique. Atomic Force Microscope (AFM) measurements show that, for the power used here, the bombardment did not significantly increase surface roughness. Magnetization versus temperature (M vs T) measurements showed that the magnetic layers could be independently reversed. Low dose bombardment was effective in increasing decoupling between the layers as compared to the case of untreated interface. This could lead to enhanced giant magnetoresistive effect in patterned devices.

[1] A. Ruotolo et al., Appl. Phys. Lett. 88, 252504 (2006)

[2] W. F. Cheng et al., J. Appl. Phys. 103, 103903 (2008)

FR.H-P10 - Ferromagnetic resonance measurements in sub-nanometer Fe films

H. Mizuno¹, T. Moriyama¹, M. Kawaguchi¹, M. Nagata¹, K. Tanaka¹, T. Koyama², D. Chiba², T. Ono¹

1. Institute for Chemical Research, Kyoto University, Kyoto, Japan
2. The University of Tokyo, Tokyo, Japan

Interfacial effects in magnetic multilayers are a key phenomenology for the recent spintronic research developments involving the spin Hall effect, the Rashba effect, voltage-induced magnetism, and the Dzyaloshinskii-Moriya interaction. Since the interfacial effects become more and more pronounced as the ferromagnetic films get thinner, it is desirable to measure the magnetic properties in the thinnest limit of magnetic films. In this study, we show that our ferromagnetic resonance (FMR) measurement technique is sensitive enough to characterize the various static and dynamic magnetic properties of the sub-nanometers (~ 0.56 nm) Fe films. We prepare Ta 3.0 nm/Pt 1.5 nm /Fe x nm/MgO 2.0 nm ($x=0.56-0.86$) films grown on a GaAs(001) substrate. The film is patterned into the 40 μm wide strip. A microwave current is applied along the strip and a rectified dc voltage across the strip is measured akin to the spin torque FMR technique [1]. With the frequency bandwidth of 40 GHz, we extract the Landé g -factor, the Gilbert damping constant α , and the effective demagnetizing field $4\pi M_{\text{eff}}$ from which the perpendicular magnetic anisotropy (PMA) is estimated.

It is found that both the g -factor and the PMA linearly decrease with increasing the reciprocal of x , implying the PMA correlates with the anisotropy of the orbital moment at the Pt/Fe interface [2]. The measurement results clearly capture the magnetic properties of sub-nanometer ferromagnetic films where the interface effects dominate. Especially, the capability of the g -factor extraction in our measurement will be very helpful for characterizing ultra-thin films with various interfacial effects perturbed by spin-orbit interactions.

[1] Sankey, et al., PRL 96, 227601 (2006)

[2] Shaw, et al., PRB 87, 054416 (2013) This work was partly supported by a Grant-in-Aid for Scientific Research (S), a Grant-in-Aid for Young Scientists (B), and a Grant-in-Aid for Scientific Research on Innovative Areas.

FR.H-P11 - Study on spin-orbit interaction in an MgO/Co/Pd trilayer with annealing

S. Kim^{1,2}, M. Kim¹, J. Ko¹, J. Hong¹

1. Department of Material Science and Engineering, Yonsei University, Seoul, South Korea

2. Institute for Chemical Research, Kyoto University, Tokyo, Japan

The spin-orbit interaction (SOI) is well known to depend on the atomic environment. Crystalline and chemical structures are critical to observe the spin-orbit coupled phenomena, such as perpendicular magnetic anisotropy (PMA), spin-orbit torque (SOT) and Dzyaloshinskii-Moriya interaction (DMI). Magnetic trilayers composed of non-magnetic metal/ferromagnet/oxide have been intensively studied during the last five years since they have shown the SOT effect due to strong SOI. Because the thickness of ferromagnets was on a nanometer scale, the interfacial structure can dominate the behavior of the ferromagnets in the trilayer. Essential to understand is a quantitative study about how the interfacial state in the structure affects the spin-orbit coupled phenomena, which has not been fully explored before. In this talk, we present that a thermal treatment changed the chemical and structural states in an MgO/Co/Pd trilayer and as a result, both volumetric and interfacial magnetic anisotropy changed accordingly. Varying the annealing temperature, two important phenomena were discovered: 1) the metallic Co/Pd interface contributes more to magnetic anisotropy than the MgO/Co one does, and 2) the stress developed in the MgO/Co layer during annealing induces magnetoelastic anisotropy of the trilayer. X-ray magnetic circular dichroism (XMCD) study proves that the spin-orbit interaction was significantly enhanced due to atomic intermixing and lattice strain in the trilayer induced during annealing, which led to strong PMA in the trilayer. Our experimental results will make it clear how spin-orbit interaction is affected by chemical and structural modification through thermal annealing.

FR.H-P12 - Anomalous hall conductivity at uncompensated antiferromagnetic interfacesK. Nakamura¹, M. Ikuta¹, T. Akiyama¹, T. Ito¹*1. Mie University, Tsu, Japan*

Interest in antiferromagnets has increased towards atomic-scale data storage/spintronic applications that may overcome a superparamagnetic issue [1] while a key challenge remains in understanding magnetocrystalline anisotropy (MCA) and sensing ways of the magnetic states since the lack of net magnetic moment in the antiferromagnets make measurements difficult. Here, we demonstrate from first principles calculations that an anomalous Hall conductivity, being proportional to the magnetization of uncompensated spins at antiferromagnetic film surfaces/interfaces, enables a characterization of the magnetic states. Calculations were carried out by using the full-potential linearized augmented plane wave method [2], in which the anomalous Hall conductivity was obtained by applying the Kubo formula of the linear response theory. We confirmed that the MCA energy in a prototype Cr₂O₃(0001) thin film shows the magnetic easy axis along perpendicular to the film plane with the MCA energy of 0.45 meV, which arises from the surface Cr 3d states appeared in the bulk band gap. By capping a nonmagnetic metallic layer (Au) on the Cr₂O₃(0001) surface, the magnetic easy axis remains along the perpendicular and the anomalous Hall conductivity results in $0.1 \times 10^{15} \text{ s}^{-1}$; the magnitude predicted is enough for experimental measurements. The uncompensated spin alignment at the Cr₂O₃(0001) interface plays an important role where the interface Cr d states highly couple to the conduction electrons in the Au layer.

[1] Loth et. al., Science 335, 196 (2012)

[2] Nakamura, et. al., PRB 67, 014420 (2003); Wimmer et. al., PRB 24, 864 (1981); Weinert et. al., PRB 26, 4571 (1982)

FR.H-P13 - Influence of roughness in ultrathin Co/Ni multilayered films with perpendicular magnetic anisotropy: reduction or enhancement?

D. Gopman¹, A. Chen¹, L. Chen², G. Rowlands³, R. Shull¹

1. *Materials Science and Engineering Division, NIST, Gaithersburg, United States*

2. *Center for Nanoscale Science and Technology, NIST, Gaithersburg, United States*

3. *Applied and Engineering Physics, Cornell University, Ithaca, New York, United States*

The perpendicular magnetic anisotropy (PMA) of thin films is sensitive to surface and interfacial roughness. Established roughness anisotropy models are limited to films much thicker than the roughness amplitude (low roughness limit), and may not be applicable to technologically-relevant magnetic films of several monolayer thickness. To better understand the evolution of PMA in the low and high roughness limit, we grew films on substrates displaying a range of roughness amplitudes. We observe distinct roughness amplitude regimes: low and high roughness characterized by decreasing PMA, and an intermediate range associated with increasing PMA. We present magnetic and morphological measurements on Co/Ni multilayered films grown on SiO₂/Si substrates with designed roughness amplitudes. By controlling the duration of a reactive ion etch, we tuned the roughness amplitude from 0.3 nm to 12 nm. Using sputtering, we grew a magnetic thin film of Ta(3)/Pt(2)/[Co(0.15)/Ni(0.6)]₈/Co(0.3)/Pt(2)/Ta(3), simultaneously on the series of substrates. (Numbers in parentheses indicate thicknesses in nm.) Using ferromagnetic resonance spectroscopy, vibrating sample magnetometry and atomic force microscopy, we present the evolution of the effective perpendicular anisotropy field (H_{eff}) and saturation magnetization (M_S) with roughness. The H_{eff} of the film series decreases slightly from 184.4 ± 0.3 mT with increasing roughness (R_q) at the lowest roughness amplitudes, but for $R_q > 3.5$ nm H_{eff} begins systematically increasing at a fast rate with roughness, reaching a maximum of 240 ± 2.4 mT near $R_q = 8$ nm. Substrates in the series exceeding 8 nm roughness exhibit lower H_{eff} , presumably a ramification of changes in the film growth process as it develops into a combination of discontinuous island growth and interstitial filling as the substrate roughness becomes comparable and larger than the film thickness. M_S decreases continuously with roughness, perhaps due to increased chemical reactivity/disorder. These results could suggest distinct roughness contributions to surface and volume anisotropies.

FR.H-P14 - Probing Co/Pd interfaces by the extraordinary hall effect.

A. Gerber¹, A. Segal¹, G. Winer¹

1. Tel Aviv University, Tel Aviv-Yafo, Israel

We used measurements of the magnitude and polarity of the extraordinary Hall effect to identify and characterize the alloyed interfaces in Co/Pd bi-layer and multi-layer structures. As far as the EHE is concerned, Co/Pd multilayers with monoatomic thickness of Co layers behave as alloys with an effective concentration corresponding to the thickness ratio between the Co and Pd layers. Intermixing leading to formation of interfacial alloys occurs during the deposition and continues either as a natural aging or due to post-deposition annealing. An effective natural alloying time at room temperature is about 100 days while thickness of the intermixed layer is of order of 1 nm. Multilayers and homogeneous Co-Pd alloys demonstrate positive or negative EHE polarity when an effective Pd content is respectively below or above the mark of about 75%. We found a direct correlation between changes in the EHE signal occurring due to a gradual alloying of the interface and coercivity of the hysteresis loops in Co/Pd bi-layers. This is a straightforward evidence that perpendicular magnetic anisotropy in heterogeneous Co/Pd systems is due to formation of strained interfacial CoPd alloys. As a general note, our results put in doubt the very existence of sharp alloy-free interfaces between Co and Pd or other miscible elements.

FR.H-P15 - Mechanism and control of antiferromagnetic coupling in Fe/Fe₃O₄ junctions

J. Inoue¹, S. Honda¹, H. Yanagihara¹, E. Kita¹, H. Itoh², K. Mibu³

1. Faculty of Pure and Applied Sciences, University of Tsukuba, Tsukuba, Japan

2. Department of Pure and Applied Physics, Kansai University, Osaka, Japan

3. Graduate School of Engineering, Nagoya Institute of Technology, Aichi, Japan

The antiferromagnetic (AF) exchange coupling between two ferromagnetic layers in trilayers is an essential feature for spintronics applications such as hard-disk drive and spin-valve sensors. Recently, a rather strong AF coupling, ~ 1 erg/cm², has been observed in Fe(001)/Fe₃O₄ junctions [1], which may have potential applicability to spintronics devices. It has been proposed theoretically that control of the magnitude of the AF coupling is possible by inserting thin Co or Mn layers between Fe and Fe₃O₄ layers [2]. The mechanism of the AF coupling, however, remains to be clarified. Purposes of present study are to confirm the theoretical prediction experimentally, and to clarify the mechanism of the AF coupling in Fe/Fe₃O₄ junctions.

Magnetization curve (M-H loop) was measured for Fe/Fe₃O₄ junctions in which a thin Co (Mn) film is inserted, and the M-H loops are analyzed by adopting several models which include bilinear, biquadratic, and magnetization twisting near the interface. The analyses indicate that the bilinear term is dominant in AF coupling and rather independent of the Mn layer thickness while it decreases with increasing Co layer thickness, in agreement with the theoretical prediction. The analyses further show that the magnetization twisting is crucial for the M-H loop fitting, and that the biquadratic term may not be neglected completely, suggesting an importance of roughness at the interface.

We performed first-principles calculations to clarify possible mechanism of the AF coupling. It was found that ideally epitaxial junctions give always ferromagnetic (F) coupling, while extra Fe atoms located on hollow sites of Fe₃O₄ mediate AF coupling between Fe and Fe₃O₄ layers. Coexistence of the F and AF couplings may produce frustration in alignment of Fe and Fe₃O₄ magnetizations resulting in the biquadratic exchange interaction.

[1] H. Yanagihara et al., Appl. Phys. Exp. 1, 111303 (2008)

[2] J. Inoue et al., Phys. Rev. B 85, 184431 (2012)

FR.H-P16 - Reversed behavior studies of angle-dependent magneto-optical Kerr rotation in magnetic/optical birefringent system

C. Su¹, C. Lin¹, G. Chern¹

1. National Chiayi University, Chiayi City, Taiwan

In a magnetic/optical spin material system, the interface problem always directly reflects its structural character from the magnetic layer or the beneath optical layer. We used a common magneto-optic Kerr effect (MOKE) magnetometry method through angle-dependent detection in the incident plane. The low-vibration homemade horizontal optical platform is suitable for studying a perpendicular spin system, ultrathin magnetic structure Ta/CoFeB/MgO film, (3)/(1.5)/(1) in nanometer thick. The experimental result for this sample is interesting that we found a reversed hysteresis loop behavior between 69 and 70 degrees. The angle of hysteresis flipping is dependent of the covering thickness of Ta. The direction of Kerr rotation is reversed from clockwise to counterclockwise only in the out-of-plane MOKE configuration. The reason of the reversed hysteresis loop originates from the optical properties of the interface structure between the magnetic film and optical underlayer. We use an equation considering anisotropic birefringence of the optical material, and compare the data by simulation of the polar magneto-optical Kerr effect. The ordering thickness of the anisotropic optical layer plays an important role in the reversed character of magneto-optic effects. This finding is very important for future spintronics application of any ultrathin device which is already fabricated and can be examined without any structural destruction.

FR.H-P17 - Reduction of the mean magnetic moment of Ni clusters embedded in Ag

A. García-Prieto ^{1,2}, A. Arteché ³, F. Aguilera-Granja ^{4,5}, M. B. Torres ⁶, I. Orue ⁷, J. Alonso ², L. Fernández Barquín ⁸, M. L. Fdez-Gubieda ^{2,3}

1. *Dpto. Física Aplicada I, Universidad Del País Vasco UPV/EHU, Bilbao, Spain*

2. *BCMaterials, Derio, Spain*

3. *Dpto. Electricidad y Electrónica, Universidad del País Vasco UPV/EHU, Leioa, Spain*

4. *Instituto de Física, Universidad Autónoma de San Luis Potosí, San Luis Potosí, Mexico*

5. *DIPC Donostia International Physics Center, San Sebastián, Spain*

6. *Dpto. de Matemáticas y Computación, Universidad de Burgos, Burgos, Spain*

7. *SGIker, Universidad del País Vasco UPV/EHU, Leioa, Spain*

8. *CITIMAC, Universidad de Cantabria, Santander, Spain*

Magnetic properties of materials change drastically from the bulk size to the nanoscale [1]. This is due to surface effects, which become increasingly important and need to be taken into account when analyzing the magnetic properties at the nanoscale.

In this work we combine experimental results with Density Functional Theory (DFT) calculations to show that Ni clusters embedded in an Ag matrix become non-magnetic below a cluster size of around 6 atoms. Experimental measurements have been performed on a DC-sputtered Ni₆Ag₉₄ nanogranular thin film. The film structure investigated by means of Extended X-ray Absorption Fine Structure (EXAFS) confirms that the film is composed of sub-nanometre sized Ni particles. The magnetic analysis highlights a strongly reduced magnetic signal that is 62% lower than the bulk value. DFT calculations performed on Ni_m clusters of selected sizes (m=1 to 6, 10 and 13) embedded in an Ag bulk matrix confirm that Ni clusters below 6 atoms become non-magnetic due to charge transfer between the Ni sp and d orbitals. This explains the loss of magnetic signal observed experimentally as being due to the coexistence of small non-magnetic Ni clusters together with slightly larger ones that do hold a full magnetic moment.

[1] Bader S. (2006). Colloquium: Opportunities in nanomagnetism. Rev. Mod. Phys., 1-15

FR.H-P18 - First-principles study on the vertical spin texture of anomalous rashba effect in Tl/Si(111) and Tl/Si(110)

H. Nakano ¹, H. Kato ¹, M. Obata ¹, D. Yoshikawa ¹, N. Kitagawa ¹, K. Sakamoto ², T. Oda ^{1,3}

1. Graduate School of Natural Science and Technology, Kanazawa University, Kanazawa, Japan

2. Department of Nanomaterials Science, Chiba University, Chiba, Japan

3. Institute of Science and Engineering, Kanazawa University, Kanazawa, Japan

The heavy-element-covered semiconductor surfaces show a giant Rashba-type spin splitting and many experiments have been reported for spintronics applications. In particular, the surface of Tl/Si(111) has been known to show out-of-plane spin textures in the surface bands [1,2]. This is novel, compared with a normal Rashba spin texture, in which the spin lies within the surface plane. However, the vertical spin configuration may be useful, because of the suppressed spin scattering. The silicon based materials are still recommended as a new material in the next generation electronics (spintronics). In these contexts, it is important to clarify electronic structures in the surface electronic structure. In this work, we studied the surface systems of Tl/Si(111) and Tl/Si(110), in which the system has a triangular lattice network of Tl atoms on the respective silicon substrate. The systems have a single Tl monolayer (ML), and 16 Si MLs, and is terminated with the hydrogen. We carried out a fully relativistic first-principles computation based on the density functional theory. The Rashba effect is taken into account through the bi-spinor wavefunctions and fully relativistic ultrasoft pseudopotentials. The artificial surface electric polarization was excluded by using an effective screened medium method.

We revealed that the surface in Tl/Si(110) has vertical spin textures at around the parts of momentum space, which corresponds to the K-bar points of Tl/Si(111). We calculated the distribution of the surface states given at a constant energy. This result agreed well with the corresponding experimental result. In the presentation, we explain the electronic structures and the spin textures, and discuss the similarity between two surface electronic structures and doping effect for realizing surface current carriers.

[1] K. Sakamoto et al., Phys. Rev. Lett. 102, 096805 (2009)

[2] K. Sakamoto et al., Nat. Commun. 4, 2073 (2013)

FR.H-P20 - Magnetoelastic coupling between NiFe thin film and ferroelastic substrateP. Graczyk^{1,2}, R. Schöfer^{3,4}, A. Trzaskowska¹, B. Mróz^{1,2}*1. Faculty of Physics, Adam Mickiewicz University, Umultowska 85, Poznań, Poland**2. NanoBioMedical Centre, Adam Mickiewicz University, Umultowska 85, Poznań, Poland**3. Leibniz Institute for Solid State and Materials Research Dresden, Institute for Metallic Materials, Dresden, Germany**4. Dresden University of Technology, Institute for Materials Science, Dresden, Germany*

Strain is the most important linker in multiferroic devices that utilize magnetoelectric coupling [1-3]. It links piezoelectricity of one material with magnetoelasticity (usually magnetostriction) of another material. Strain in ferromagnetic layer affects magnetocrystalline anisotropy and may change the axis of easy magnetization. Magnetoelectric coupling in multiferroic heterostructures has been frequently reported experimentally and theoretical model for a monodomain magnetic layer has been proposed [4]. Recently a magnetoelectric cells with resistive readout have been demonstrated [5] as a new step towards designing of magnetoelectric random access memory. The purpose of this research was a comprehensive investigation of magnetoelastic effect in multiferroic heterostructures and its quantitative description with the use of existing theory of magnetism. Magnetoelastic coupling between ferroelastic substrates (LiCsSO_4 , KH_2PO_4 and $\text{Gd}_2(\text{MoO}_4)_3$) and thin $\text{Ni}_{85}\text{Fe}_{15}$ layer has been studied by different techniques. Measurements revealed strong influence of a strain onto magnetic properties of a layer. Significant, continuous and reversible drop of longitudinal magnetization in NiFe film cooled below substrate phase transition temperature has been observed by SQUID magnetometry. As imaged by Kerr microscope, magnetic domains strictly copy the pattern of elastic domains of a substrate. This also affects the frequency of magnetostatic surface spin waves, which were investigated by Brillouin spectroscopy. Results have been quantitatively compared with micromagnetic simulations, which describe observed effects as a strain-driven reorientations of magnetic moments, taking into account peculiar multidomain pattern of a substrate. Thus, we have successfully linked theoretical predictions of spin-reorientation transitions [4] with experiment.

[1] Velev, J.P. et al., Multiferroic and magnetoelectric materials and interfaces, *Phil. Trans. R. Soc. A* 2011, 369, pp. 3069-3097

[2] Wang, Y. et al., Multiferroic magnetoelectric composite nanostructures, *NPG Asia Mater.* 2010, 2, pp. 61-68

[3] Eerenstein, W. et al., Multiferroic and magnetoelectric materials, *Nature* 2006, Vol. 442, pp. 759-765

[4] Pertsev, N.A., Giant magnetoelectric effect via strain-induced spin reorientation transitions in ferromagnetic films, *Phys. Rev. B* 2008, Vol. 78, 212102

[5] Han, X., et al., Demonstration of magnetoelectric memory cell in (110) $[\text{Pb}(\text{Mg}_{1/2}\text{Nb}_{2/3})\text{O}_3]_{0.68}\text{-}[\text{PbTiO}_3]_{0.32}/\text{Ru}/\text{FeCo}$ heterostructures, *Appl. Phys. Lett.* 2014, 105, 122402

FR.H-P21 - Magnetic and electric transport properties of $\text{LaFe}_{0.5}\text{Co}_{0.5}\text{O}_3$ perovskite system: effect of annealing temperatureC. A. López¹, J. Lohr², M. E. Saleta³, J. Curiale⁴, R. D. Sánchez⁵*1. Instituto de Investigaciones en Tecnología Química - Universidad Nacional de San Luis, Argentina**2. Centro Atómico Bariloche- Comisión Nacional Energía Atómica, Río Negro, Argentina**3. Universidade Estadual de Campinas -UNICAP, Campinas, Brazil**4. Centro Atómico Bariloche- Comisión Nacional Energía Atómica, Río Negro, Argentina**5. Centro Atómico Bariloche- Comisión Nacional Energía Atómica, Río Negro, Argentina*

The perovskite-like compound $\text{LaFe}_{0.5}\text{Co}_{0.5}\text{O}_3$ have attracted significant attention for more than a decade, mainly because of their magnetoelectric and multiferroic properties.^[1,2] In this work we present the synthesis, structure, magnetism and electric transport properties of different grain size $\text{LaFe}_{0.5}\text{Co}_{0.5}\text{O}_3$ perovskites.

Different compounds have been synthesized by citrate method and then annealed 12 hours at different temperatures (T_{anneal}) between 600 and 1200 °C. The crystallographic characterization was performed by X-ray powder diffraction, the best Rietveld refinement was obtained with a rhombohedral structure ($R\bar{3}c$) at room temperature. Also from the X-ray data, we observe the increase of the grain size increasing T_{anneal} . The temperature and field dependence of the magnetization evidences a ferrimagnetic transition (T_C) around 250 K in all cases. Differences in field cooled cooling, field cooled warming and zero-field cooled magnetization suggest the presence of different magnetic states (Ferri and Antiferro) below T_C whose ratio change with temperature. Impedance and DC resistivity were characterized as a function of temperature. The resistivity shows a semiconducting-like or thermally activated behavior. From impedance spectroscopy (IS) characterization, we calculated different complex functions as: impedance (Z^*), dielectric modulus (M^*), permittivity (ϵ^*); and loss tangent ($\tan \delta$). The conduction process is dominated by a long-range mechanism in all samples. This process is related to a single relaxations peak in $\tan \delta$ plots. However, imaginary part of Z^* and M^* functions show two different relaxations process, which are linked to the grain and grain boundary effects. From this behavior we found the increase of the grain boundary effect as the T_{anneal} decreases. On the other hand, we observed a subtle effect of T_{anneal} on the studied magnetic properties. However, differences on the contact between ceramic grains becomes much more important on the transport properties (IS and DC resistivity). As a final remark, our work shows how the synthesis protocol is a powerful tool in the search of specific properties of these kinds of oxides.

(1) Fiebig, M, et. al.. Nature (London, U.K.) 2002, 419, 818–820

(2) Kimura, T., et. al. Nature (London, U.K.) 2003, 426, 55–58

FR.H-P22 - First-principles studies on the electronic and magnetic properties of (001) surfaces of half-Heusler X(X=Li and Na)CaB

D. Kim¹, B. Bialek², J. Il Lee²

1. *Halla University, Wonju-si, South Korea*

2. *Inha University, Incheon, South Korea*

Half-metals, substances that act as conductors to electrons with one spin orientation, but as insulators or semiconductors to electrons in the other spin orientation, have been attracted much attention as candidates for application to spintronics as, for example, multilayer spin valves systems, spin injectors, and/or spin transistors. Recently, an exotic class of half-metals not containing a transition metal element in their structure emerged due to results of computational study with the use of first-principles methods. Specifically, half-Heusler compounds, XCaB, (X=Li, Na, and K) were found to be half-metallic [1]. It is crucial to have information on the surface properties of materials for the spintronics application. In this study, we investigated the electronic and the magnetic properties of (001) surfaces of two of the mentioned half-Heusler compounds, namely LiCaB and NaCaB. The full-potential linearized augmented plane wave method [2] with the generalized gradient approximation [3] was used to calculate the surface electronic properties. We considered two possible terminations of the (001) surfaces, i.e., alkali metal termination and CaB-termination. From the calculated local density of states, we found that the half-metallicity is not retained at all the surfaces. The magnetic moments of the Li or Na atom at the (001) surface decrease to nearly zero. The magnetic moments of B atom of CaB-terminated surface in LiCaB is 0.51 bohr magneton, and that of NaCaB compound is 0.05 bohr magneton. Due to a delocalization of p-electrons at the surfaces the values of magnetic moments on Ca atoms in both systems are close to zero, even though in the bulk structures Ca atoms exhibit noticeable magnetization.

[1] R. Umamaheswari, M. Yogeswari, and G. Kalpana, *J. Magn. Magn. Mater.* 350 (2014) 167

[2] E. Wimmer, H. Krakauer, M. Weinert, and A. J. Freeman, *Phys. Rev. B* 24 (1981) 864

[3] J. P. Perdew, K. Burke and M. Ernzerhof, *Phys. Rev. Lett.* 77 (1996) 3865

FR.H-P24 - Optical characterization of quantum hall effect devices with a cap layer passivated by silicon monolayers

L. Zamora-Peredo ¹, I. Cortes-Meztizo ¹, L. García-González ¹, J. Hernandez-Torres ¹, I. Martínez-Veliz ¹, M. Perez-Caro ², M. Ramirez-López ², Y. Casallas-Moreno ², Z. Rivera-Ivarez ², A. Conde-gallardo ²

1. *Centro de Investigación en Micro y Nanotecnología, Universidad Veracruzana, Xalapa Enriquez, Mexico*

2. *Departamento de Física, Centro de Investigación y de Estudios Avanzados del IPN, Ciudad de Mexico, Mexico*

In this study, the effect of the surface electric field over the optical and electrical properties of quantum Hall effect (QHE) devices were analyzed using photorefectance and QHE measurements. AlGaAs/GaAs heterostructures were grown by MBE with a GaAs cap layer passivated by one and two silicon monolayers. Photorefectance spectra show wide-period Franz-Keldysh oscillations between 1.42 and 1.70 eV originated by the surface electric field. For sample without silicon monolayer the surface electric field is near to 5×10^7 V/m whilst sample with 1 Si-ML has 2.9×10^7 V/m and 1.7×10^7 V/m for the sample with 2 ML. the electric field decreases near to 66%. By QHE measurements we have found the electron density varied between 5.3 and 9×10^{11} cm⁻², which increases as the surface electric field decreases. Furthermore, Raman measurements have been used to study the passivated surface.

Keywords:

QHE, 2DEG, photorefectance, AlGaAs/GaAs heterostructure

Acknowledgements:

We acknowledge the partial financial supports of CONACYT-SENER, Mexico, through the contract No. 151076.

FR.H-P25 - Electronic reconstructions at manganite interfaces driven by chemical and structural symmetry breaking

D. Pesquera¹, A. Barla², F. Bondino³, E. Magnano³, M. Valvidares⁴, J. Herrero⁴, P. Gargiani⁴, E. Pellegrin⁴, N. Dix¹, F. Sánchez¹

1. *Institut de Ciència de Materials de Barcelona (ICMAB-CSIC), Campus UAB, Bellaterra, Spain*

2. *Istituto di Struttura della Materia, ISM CNR, Area Science Park Basovizza, Italy*

3. *IOM-CNR, S.S. 14 km 163.5, Area Science Park Basovizza, Italy*

4. *ALBA Synchrotron Light Source, Cerdanyola del Valles, Barcelona, Spain*

The emergent physical properties displayed by transition-metal oxide (TMO) heterostructures are originated by the charge, spin and orbital reconstructions occurring at interfaces [1]. However, the mechanisms driving these reconstructions, largely discussed in the last years, are still under debate. Manganites represent a prototypical system to explore oxides interface phenomena. In manganite thin films it is now understood that, at free surfaces, the reduced coordination of Mn ions leads to an imbalance of the orbital population in the surface layers [2], which is expected to originate the commonly found electrically and magnetically inert character of ultrathin films. However, at interfaces with other oxides, the transition metal crystal field will be modified in a different manner dependent upon the component layers.

By means of X-ray absorption linear dichroism we study the influence of oxide epitaxial capping layers on the Mn-3d orbital occupancy of manganite films with composition $\text{La}_{0.7}\text{Sr}_{0.3}\text{MnO}_3$. Probing with different capping materials (SrTiO_3 , LaAlO_3 , SrZrO_3) and thicknesses we find a clear dependence of the Mn electron distribution on the structural characteristics of the capping layers. We also demonstrate the correlation of these electronic reconstructions with the magnetic properties of the films, which is crucial for the implementation of these materials in magnetic tunnel junctions.

[1] H. Y. Hwang, Y. Iwasa, M. Kawasaki, B. Keimer, N. Nagaosa, and Y. Tokura, *Nat. Mater.* 11, 103 (2012)

[2] D. Pesquera, G. Herranz, A. Barla, E. Pellegrin, F. Bondino, E. Magnano, F. Sánchez, and J. Fontcuberta, *Nat. Commun.* 3, 1189 (2012)

FR.H-P27 - Investigations on interface magnetism of Fe-containing heusler alloy films through mössbauer spectroscopic measurements

K. Mibu¹, A. Okubo¹, N. Nakatani¹, M. Tanaka¹

1. Nagoya Institute of Technology, Nagoya, Japan

The interface magnetism of Fe-containing Heusler alloy films, such as Co₂FeGe, was examined through magnetic hyperfine fields at the interfacial Fe sites derived from ⁵⁷Fe Mössbauer spectra, absorption spectra of gamma-rays by the ⁵⁷Fe nuclei in the film. The samples were prepared on MgO(001) substrates using alternate deposition of an atomic layer (or a half an atomic layer) of the constituent elements. The Fe atoms at the interfacial regions were made of the Mössbauer-sensitive ⁵⁷Fe isotope, and those at the inner part of the films were of the Mössbauer-inert ⁵⁶Fe isotope, so that interface-sensitive measurements can be performed. To examine whether the interfacial atomic species can be controlled or not, the deposition sequence of the constituent elements was tested to be changed in four ways.

For the Co₂FeGe/MgO interfaces, the magnitude of the magnetic hyperfine field was obtained to be around 34 - 35 T at room temperature, which was almost the same as the value at the inner part of the Heusler alloy layer. The values were not different among the samples prepared with different deposition sequences (therefore nominally with different interfacial atomic species). The evidence of controllability of the interfacial atomic species was not obtained.

In magnetic tunnel junctions or giant magnetoresistance multilayers using Heusler alloys as ferromagnetic layers, a strong reduction in magnetoresistance is generally observed when the temperature approaches from low temperatures to room temperature. This change may have relation with some instability of the magnetization at the interfacial region, but the above result indicates that the interfacial magnetization has no special anomaly, at least for the Co₂FeGe/MgO(001) system. The results for other material combinations will also be shown in the presentation.

FR.H-P28 - Magnetism of Ru monolayer - first principles calculations -

Y. Kitaoka¹, K. Nakamura², H. Imamura¹

1. *National Institute of Advanced Industrial Science and Technology (AIST), Spintronics Research Center, Japan*

2. *Department of Physics Engineering, Mie University, Tsu, Japan*

The study of magnetism in nano-structures composed of 4d transition metal elements is to pave the way for new materials sciences and technologies. It is well known that bulk 4d transition metals are non-magnetic. However, there are recent experimental and theoretical investigations showing ferromagnetism for some of these 4d transition metals thin films on noble metal substrate. For example, Y. Sun et al. demonstrated that application of an external electric field can induce and modulate ferromagnetism on an otherwise paramagnetic Pd metal thin-film surface[1]. Until now most researches are focused on Pd films since Pd is very close to fulfill the Stoner criterion of ferromagnetism. By contrast, little attention has been paid to the magnetism of the other 4d transition metals.

Here, we investigate the magnetism of the free-standing Ru monolayer and that on MgO(001) substrate by using first-principles FLAPW method [2]. Results predict that the free-standing Ru monolayer shows ferromagnetic properties with the magnetic anisotropy (MA) energy of 3.4 meV/atom, which means it has a perpendicular magnetic anisotropy. For the free-standing Ru monolayer with the same lattice constant as the bulk MgO the easy axis of magnetization changes to in-plane (planar magnetic anisotropy). For the Ru monolayer on MgO(001) substrate the magnetization remains and the MA energy is 1.52 meV/atom (perpendicular magnetic anisotropy). The change of easy axis between the free-standing Ru monolayer and Ru/MgO multilayer is explained by the hybridization between the Ru d_{z^2} and O p_z orbitals at the metal-substrate interface as discussed in Fe/MgO interface [3].

[1] Y. Sun, J. D. Burton, E. Y. Tsybal, PRB 81, 064413 (2010)

[2] K. Nakamura, T. Ito, A. J. Freeman, L. Zhong, J. Fernandez-de-Castro, PRB, 67, 014420 (2003)

[3] K. Nakamura, T. Akiyama, T. Ito, M. Weinert, A. J. Freeman, PRB 81, 220409R (2010)

FR.H-P29 - The influence of interfacial dzyaloshinskii-moriya interaction strength on the magnetic structure of thin films under magnetic field

C. Wu¹, C. Kuo²

1. Department of Physics, Chung Yuan Christian University, Chungli, Taiwan

2. Department of Physics, National Sun Yat-Sen University, Kaohsiung, Taiwan

The magnetic skyrmions have attracted much attention recently due to their potential applications in spintronics. They arise from the spin-orbit coupling in non-central symmetric systems, such as the MnSi bulk material, or the interface between a magnetic thin film and a strong spin-orbit coupled adjacent layer. The coupling in such cases is called Dzyaloshinskii-Moriya interaction (D). The influence of this interaction strength on the magnetic structure of thin films plays a key role to understand the behavior of magnetic skyrmions. We study the influence of D values on the magnetic structures of thin films to obtain the phase diagram of the magnetic skyrmions under magnetic fields by using the micromagnetism simulation (OOMMF code). The skyrmion state is found to exist only when the D is larger than a certain finite value and when the magnetic field is less than the saturation field, which increases linearly with the increasing D value. In the skyrmion state, the stripe domains and isolated skyrmions can co-exist. When the magnetic field is increased, the stripe domains shrink toward skyrmions, resulting in isolated skyrmions. The diameter of the isolated skyrmions decreases with the increasing field. When the saturation field is reached, all of the skyrmions are smeared out and the sample changes to a ferromagnetic single domain state. This is provided as the guideline for designing the magnetic skyrmions for further applications in spintronics.

FR.H-P31 - Magnetic properties of ordered CoO nanostructures on Co/Fe(001)

A. Brambilla¹, A. Picone¹, G. Dario¹, R. Michele¹, G. Berti¹, A. Calloni¹, F. Boschini¹, H. Hedayat¹, E. Carpena², C. Dallera¹

1. Dipartimento Di Fisica, Politecnico di Milano, Milan, Italy

2. IFN-CNR, Dipartimento di Fisica, Politecnico di Milano, piazza Leonardo da Vinci, Milano, Italy

3. Laboratorio TASC, IOM-CNR, Basovizza, Trieste, Italy

Intriguing magnetic properties can be obtained in systems containing antiferromagnetic (AF) transition metal (TM) oxides both by low-dimensionality and by proximity to ferromagnetic (F) layers. So far, we have investigated both chemical [1] and magnetic [2] properties of a rich record of Fe/AF (NiO, CoO) layered structures [3].

One of the most critical issues concerning the interfaces between TM mono-oxides and a reactive TM is the high degree of chemical mixing at the interfaces [1]. We have observed, through scanning tunneling microscopy combined with Auger, photoemission, and X-ray absorption spectroscopies, that the layer-by-layer growth of an ultrathin (1 nm) Co buffer layer prior to CoO deposition prevents, in particular growth conditions, the different elements to react and mix at the interface. When this occurs, we also observe a dislocation-driven nanostructuring of CoO, which grows in square islands, whose lateral sizes (tens of nanometers) increase with CoO coverage.

On such samples, peculiar hysteresis loops are observed, whose reversal is characterized by the nucleation of 90° in plane domains when the magnetic field is applied along one of the Fe easy axes. On the other hand, when the field is moved away from the easy axes, jumps in the loops are seen, which interestingly resemble those observed on exchange spring multilayers, thus suggesting the presence of different magnetically active components. When performing element specific hysteresis loops by XMCD, it is revealed that the transverse component observed in the loop arise only upon CoO formation and that it can be attributed to both Fe and Co magnetic moments close to the interface.

[1] A. Brambilla, et al., Thin Solid Films 516, 7519 (2008)

[2] M. Finazzi, et al., Phys. Rev. Lett. 97, 097202 (2006)

[3] M. Finazzi, L. Duò, and F. Ciccacci, Surf. Sci. Rep. 64, 139 (2009)

FR.H-P33 - Magnetic properties of tetra-phenyl-porphyrins adsorbed on metal surfaces

M. Panighel⁰, G. Di Santo¹, M. Caputo¹, A. Goldoni¹

1. Elettra-Sincrotrone Trieste S.C.p.A., Trieste, Italy

2. Università degli Studi di Trieste, Trieste, Italy

3. Institut Català de Nanociència i Nanotecnologia (ICN2), Campus UAB, Bellaterra, Spain

Within the next few years the traditional semiconductor technology will reach its essential size limit. The use of organic molecules as single functional units in metal-organic based devices could overcome this limitation. However, the success of this approach strongly depends on the understanding of the interaction of the molecules with metallic substrates which determines the electronic and magnetic properties of these interfaces.

Organic molecules such as porphyrins can be deposited in the sub-monolayer regime on single crystal surfaces in ultra high vacuum and geometrically ordered structures can be obtained from this procedure [1]. Taking advantage of the flexibility in choosing their molecular substituents, in combination with the presence of active sites of interactions with metals [2-4], this kind of molecules can be used to fabricate two-dimensional arrays of metallic centres with nanometric spacing, making them promising candidates for applications in emerging fields like spintronics and molecular electronics.

By means of XPS, NEXAFS and XMCD techniques we studied the self-assembly, metalation and magnetic properties of tetra-phenyl-porphyrins (TPP) on metal substrate. Focusing on the magnetic coupling of two layers of molecules with a ferromagnetic thin film, we will show that, in the case of a MnTPP layer on FeTPP/Fe(110), the magnetic coupling extends to the second molecular layer, and its magnetization is opposite with respect to the substrate [5].

References:

[1] G. Di Santo et al., Chem. Eur. J. 18 (2012) 12619

[2] M. Panighel et al., J. Phys. Conf. Ser. 470 (2013) 012012

[3] G. Di Santo et al., J. Phys. Chem. C 115 (2011) 4155

[4] A. Goldoni et al., ACS Nano 6 (2012) 10800

[5] M. Panighel et al., Oral. Comm., SINFO II, 25-27 June 2014, Trieste

FR.H-P34 - Magnetic coupling of MnTPP(Cl) molecules to magnetic substrates investigated by X-ray photo-emission electron microscopy

M. Baljozovic¹, J. Girovsky¹, M. Buzzi², C. Wöckerlin³, D. Siewert⁴, J. Nowakowski¹, P. M. Oppeneer⁵, F. Nolting², T. A. Jung¹, N. Ballav⁶

1. *Laboratory For Micro and Nanotechnology, Paul Scherrer Institute, Villigen, Switzerland*

2. *Swiss Light Source, Paul Scherrer Institute, Villigen, Switzerland*

3. *LNS, EPFL, Lausanne, Switzerland*

4. *University of Basel, Basel, Switzerland*

5. *Uppsala University, Uppsala, Sweden*

6. *Indian Institute of Science Education and Research (IISER), Pune, India*

Magnetism at the nanoscale and especially the magnetism of the square-planar metalloporphyrins and -phthalocyanines adsorbed on (magnetic) substrates has attracted considerable attention. Several reports showed that when adsorbed on ferromagnetic (FM) substrates such magnetic molecules possess an exchange induced magnetic moment [1, 2, 3]. Furthermore, the magnetic moment of ad-molecules can be tailored by the introduction of a non-magnetic spacer layer in between molecules and the substrate [3] or by means of a chemical stimulus (i.e. by coordination with ligands like NO, NH₃, CO) [3,4,5]. In this contribution we use X-ray Photo-Emission Electron Microscopy (X-PEEM) combined with X-ray Magnetic Circular Dichroism (XMCD) to investigate the magnetic exchange coupling between Mn-porphyrin molecules and (1) native FM Co (001) substrates; (2) oxygen-terminated Co (001) substrates and (3) FM Co (001) substrates covered with a Cr spacer layer with increasing thickness. Specifically, we investigate spatial variations in the magnetic coupling of the molecules, their chemical state as well as the spatial distribution of the respective elements at the surface of the sample by combination of PEEM and XMCD in a direct spectro-microscopy correlation [5].

[1] A. Scheybal et al., Chem. Phys. Lett., 411, 214 (2005)

[2] Wende et al., Nat. Mater. 6, 516 (2007)

[3] N. Ballav et al., J. Phys. Chem. Lett. 4, 2303 (2013)

[4] C. Wöckerlin et al., Chem. Sci. 3, 3154 (2012)

[5] J. Girovsky et al., Chem. Commun. 50, 5190 (2014)

FR.I-P02 - Implementation of broadband magnetic susceptibility meter based on broadband lock-in amplifier techniques

J. Lu¹, C. Guo¹, X. Shao¹, B. Shen¹

1. State Key Laboratory of Magnetism, Institute of Physics, Chinese Academy of Sciences, Beijing, China

Measuring magnetic susceptibility of spintronic materials in a wide frequency window is important for exploring high performance soft magnetic materials with high permeability in high frequency, researching magnetic resonance phenomena and understanding the order-disorder transition of superconducting vortex configuration. To fully investigate magnetic dynamics behaviors of various spin related materials, it is necessary to use broadband magnetic susceptibility measurement system. Conventionally, magnetic susceptibility meters have four types: 3-coil system, impedance measurement, cavity resonance and vector network analyzers. Unfortunately, none of them could continuously work from low frequency (below 1 Hz) to high frequency (above 1 GHz). The current poster introduces a new type of magnetic susceptibility meter, which can measure not only linear magnetic susceptibility but also higher-order magnetic susceptibility in broad frequency range from low frequency to above 1 GHz. We implement the broadband magnetic susceptibility measurement system based on broadband lock-in amplifier techniques. We have studied broadband lock-in amplifier (LIA) and its application to multifunctional electromagnetic measurement system for many years, with continuous improvement on bandwidth and precision. The magnetic susceptibility measurement system takes advantage of a specially designed sample holder compatible to high frequency coaxial cables and dynamical compensation. To enhance the convenience of physical research, our broadband measurement system can easily be connected and integrated to different types of environments, such as temperature and magnetic field.

FR.I-P03 - Controllable measurements of magnetic hysteresis and Barkhausen noise

A. Stupakov¹, O. Perevertov¹, V. Zablotskii¹

1. Institute of Physics ASCR, Prague, Czech Republic

We developed a novel setup for accurate measurements of the magnetic hysteresis and Barkhausen noise (BN) with two distinctive features. First, the magnetic field is measured directly by an array of Hall sensors. Second, a digital feedback loop adjusts the waveform of the magnetic induction or field to the prescribed sinusoidal/triangular shape. This method gives physically accurate and repeatable results, which are independent of a specific design of the magnetizing circuit. In particular, the measurements can be performed in a magnetically open configuration, i.e. with a several mm air-gap between the ac magnet and a tested sample [1]. This provides new possibilities for further development of the measurement standards and industrial non-destructive techniques. The enhanced performance of the setup was clearly demonstrated on the measurements at constant field/induction rates allowing the physically correct study of the magnetization dynamics in ferromagnetic steels and alloys. Interesting results were obtained for the BN signal originating from a sub-surface irreversible motion of the magnetic domain walls. The shape of the BN rms profile was found to correlate with the surface field rate dH/dt ; e.g., the measurements of magnetically soft materials at the constant field rate (triangular field waveform) reduce a typical two-peak profile to a usual single-peak one [2]. Similar to the hysteresis loss behavior, the BN signal was shown to follow a nearly square root dependence on the magnetizing frequency.

[1] O. Stupakov, "System for controllable magnetic measurement with direct field determination," *J. Magn. Magn. Mater.*, 324 (2012) 631

[2] O. Stupakov, "Stabilization of Barkhausen noise readings by controlling a surface field waveform," *Meas. Sci. Technol.*, 25 (2014) 015604

FR.I-P04 - Resonant X-ray magnetic scattering at helium-3 temperatures in high magnetic fields at beamline P09 at PETRA III at DESY

S. Francoual¹, J. Stempfer¹, J. Warren², Y. Liu³, A. Skaugen¹, S. Poli², J. Blume¹, F. Wolff-Fabris⁴, P. Canfield^{5,6}, T. Lograsso^{3,5}

1. *Deutsches Elektronen-Synchrotron, Hamburg, Germany*

2. *Cryogenic Ltd., London, United Kingdom*

3. *Division of Materials Sciences and Engineering, Ames Laboratory, Ames, Iowa, United States*

4. *Hochfeld-MagnetlaborDresden, Helmholtz-Zentrum Dresden-Rossendorf, Dresden, Germany*

5. *Department of Materials Science and Engineering, Iowa State University, Ames, Iowa, United States*

6. *Department of Physics and Astronomy, Iowa State University, Ames, Iowa, United States*

The resonant scattering and diffraction beamline P09 at PETRA III at DESY is equipped with a 14 T vertical field split-pair magnet. A Helium-3 refrigerator is available that can be fitted inside the magnet's variable temperature insert. Here we present the results of a series of experiments aimed at determining the beam conditions permitting operations with the He-3 insert. By measuring the tetragonal-to-orthorhombic phase transition occurring at 2.1 K in the Jahn-Teller compound TmVO_4 , we find that the photon flux at P09 must be attenuated by 4 orders of magnitude for the sample to remain at temperatures below 800 mK. Despite such a reduction of the incident flux and the subsequent use of a Cu(111) analyzer, the resonant X-ray magnetic scattering signal at the Tm L_{III} absorption edge associated with the spin-density-wave in $\text{TmNi}_2\text{B}_2\text{C}$ below 1.5 K is intense enough to permit for a complete study in magnetic field and at sub-Kelvin temperatures to be carried out.

FR.I-P05 - Measurement of the DC properties of permanent magnets using a Pulsed Field Magnetometer.

M. Hall¹, N. Hillier¹, S. Harmon¹, S. Turner¹

1. National Physical Laboratory, Middlesex, United Kingdom

In the design of electric motors that use NdFeB magnets the intrinsic coercivity exhibited determines the maximum operating temperature that can be used. A convenient method for measuring this quantity and the changes exhibited with temperature is Pulsed Field Magnetometry (PFM). The pulsed magnetic field applied to the magnet allows the full BH curve to be measured in milliseconds. This is important since when determining the DC properties of permanent magnets, the increase in the magnetic field necessary for reversal of polarization should be performed quasi statically to avoid introducing dynamic errors such as magnetic viscosity.

The measured intrinsic coercivity is known to increase when the polarization reversal time (PRT), the time taken to reduce polarization from 90% to zero, is below a material dependent threshold.

Since industrial measurement systems require a high throughput of measurements, the errors that dynamic measurements, such as the PFM, introduce need to be evaluated. In this paper a detailed study is reported on magnets with intrinsic coercivities ranging from 640 kA/m to 2000 kA/m, measured using a National Measurement Institute grade electromagnetic system. For each magnet a PRT between 2 to 600 seconds was used. The dependence of the measured intrinsic coercivity on the PRT was analysed using published models and a method for correcting the dynamically measured values from a PFM to obtain the required DC value is presented. This work shows that an electromagnet measurement of DC intrinsic coercivity, where the PRT is too short, cannot be used to calibrate the PFM. The effect of saturating the electromagnet's yokes on the measured demagnetization curve will also be presented, which despite producing unphysical reversal behaviour, is shown to still yield the correct intrinsic coercivity.

FR.I-P06 - A giant magneto-impedance magnetometer for magnetic nondestructive detection of corrosion activity

I.a Bardin ¹, V. Bautin ¹, S. Gudoshnikov ¹, B. Ljubimov ², N. Usov ²

1. *National University of Science and Technology MISiS, Moscow, Russia*

2. *Pushkov Institute of Terrestrial Magnetism, Ionosphere and Radio Wave Propagation RAS, Oblast, Russia*

It has recently been demonstrated [1] that the GMI magnetometer [2] with a sensitivity of approximately 10^{-6} Oe is able to measure the distribution of very weak magnetic fields, of amplitude $H \sim 10^{-4}$ Oe, of corrosion currents existing near an isolated corrosion center of diameter 0.15 cm, simulating pitting corrosion. In this paper we study the magnetic field distribution near the long zinc strip of width 0.12 cm in the copper sample placed in a weak solution of sulfuric acid, which simulates another common type of electrochemical corrosion, the so-called intergranular corrosion. In addition, we study the magnetic field distribution for two corrosion centers of small diameters, depending on the distance between them. The experimental results are compared with the corresponding numerical simulation data. The approximation of the isolated corrosion centers [1] is proved to hold for the case when the distance between the corrosion centers is more or of the order of their diameters. Consequently, the magnetic field distribution for the pitting corrosion, when the corrosion centers are typically scarce and randomly distributed, can be described with reasonable accuracy as a superposition of the magnetic fields of the individual corrosion centers.

We acknowledge funding from Russian Ministry of Education and Science (Grant RFMEF157-514X0011).

[1] I.V. Bardin, V.A. Bautin, S.A. Gudoshnikov, B.Ya. Ljubimov and N.A. Usov. *AIP Advances* 5, 017143 (2015)

[2] N.A. Usov and S.A. Gudoshnikov, *J. Appl. Phys.* 113, 243902 (2013)

FR.I-P07 - CAMEA - Continuous angle multiple-energy analysis a novel neutron spectrometer

F. Groitl^{1,2}, D. Graf³, J. Okkels Birk², M. Markó⁴, M. Bartkowiak³, U. Filges³, R. Müller³, C. Niedermayer², C. Rüegg², H. Ronnow¹

1. *Laboratory for Quantum Magnetism, École Polytechnique Fédérale de Lausanne, 1015 Lausanne, Switzerland*
2. *Laboratory for Neutron Scattering and Imaging, Paul Scherrer Institut, Villigen, Switzerland*
3. *Laboratory for Developments and Methods, Paul Scherrer Institut, Villigen, Switzerland*
4. *Neutron Spectroscopy Department, Wigner Research Centre for Physics, Budapest, Hungary*

The novel neutron spectrometer concept CAMEA (Continuous Angle Multiple Energy Analyzer), developed in collaboration between University of Copenhagen, Danish Technical University, Paul Scherrer Institute (PSI) and École Polytechnique Fédérale de Lausanne (EPFL), will be installed at SINQ at PSI, Switzerland, and will replace the cold triple-axis spectrometer RITA-II. The novelty of the CAMEA design is that it employs a series of several upwards scattering analyser arcs behind each other. This allows each analyser to collect neutrons over different energy ranges and a large solid angle that are measured simultaneously by position sensitive detectors. The result is that in a single data-acquisition an entire constant-energy line in the horizontal scattering plane is recorded for a quasi-continuous angular coverage of about 60°, where tremendous gains in data collection rates can be achieved. Combined, this will result in a state-of-the-art spectrometer, which will be particularly suited for parametric studies under extreme conditions requiring restrictive sample environments such as high magnetic field magnets or pressure cells, and for small samples of novel materials. This project is a joint venture of the Laboratory for Neutron Scattering and Imaging (LNS, PSI), Laboratory for Developments and Methods (LDM, PSI) and the Laboratory for Quantum Magnetism (LQM, EPFL) financed by the R'Equip program of the Swiss National Science Foundation (SNF) and the EPFL.

We will present the instrument concept, performance simulations, technical solutions and prototype verifications.

[1] Reports on the CAMEA projects can be found here: <http://lqm.epfl.ch/page-66994-en.html>

[2] P.G. Freeman, J.O. Birk, M. Marko, M. Bertelsen, J. Larsen, N.B. Christensen, K. Lefmann, J. Jacobsen, Ch. Niedermayer, F. Juranyi and H.M. Ronnow, EPJ Web of Conferences 83, 03005 (2015)

FR.I-P08 - Application of electroplated magnetic gratings for high-resolution position sensing

Z. Xu¹, B. Tseng², C. Hung¹, C. Chang², S. Wang³, T. Chin², C.Sung¹

1. *Department of Power Mechanical Engineering, National Tsing Hua University, Hsinchu City, Taiwan*

2. *Department of Materials Science & Engineering, Feng Chia University, Taichung City, Taiwan*

3. *Department of Mechanical Engineering, National United University, Miaoli Country, Taiwan*

Unlike optical encoders, magnetic encoders are applicable in a harsh environment involving dust, oil and splash fluids. To improve the resolution of a magnetic sensing system, the pole pitch has to be fine enough. However, conventional magnetization process requires a complicate magnetizing system and time consuming. It is difficult to achieve pole pitches finer than 1 mm. This paper proposes a new method to prepare magnetic gratings by using lithography to define grooves of photoresist then to electroplate permanent magnetic layer of CoP into grooves. The gratings are magnetized in unison by a single pulsed field in a solenoid. Magnetic gratings were designed and simulated by a commercial software Maxwell, including magnetic properties, demagnetizing factors, and magnetization directions. Then suitable shapes and thickness with respect to time were also simulated by the software Consol. CoP layers were electroplated with various power modes that included pulsed current, pulsed voltage, constant current and constant voltage. Magnetic hysteresis loops were measured by a vibrating sample magnetometer. After the magnetic grating was magnetized with a solenoid coil by a single pulse, the resultant magnetic flux density was detected by using a Hall sensor. According to experimental results, the best electroplating conditions were: pH 4.52 at 246J under constant current mode. The best magnetic properties in a parallel field are: Br 550 mT and Hc 76.9 kA/m at the current density 5 mA/cm². The shapes of the gratings are well patterned by lithography and electroplating to have a 400-um-pitch and a 200-um-width. After magnetization, the peak-to-peak amplitude of Bz is 6.2 mT at parallel magnetizing, and the half periodicity of the sinusoidal magnetic flux density from the grating is 200 um. These are crucial for decoding the signal by a thousand fold to obtain a resolution approaches 200 nm for incremental positioning.

FR.I-P09 - In-situ magnetic studies on Li_xCoO_2 battery cathodes during charging/discharging

S. Topolovec¹, H. Kren², G. Klinser¹, S. Koller², H. Krenn³, R. Würschum¹

1. *Institute of Materials Physics, Graz University of Technology, Graz, Austria*

2. *VARTA Micro Innovation GmbH, Graz, Austria*

3. *Institute of Physics, University of Graz, Graz, Austria*

In-situ magnetic measurements during electrochemical charging, with the purpose to tune magnetic properties by electrochemical processes, have recently attracted considerable attention (i.e. [1-3]). As the magnetic properties of the technologically important Li-ion battery electrode materials are sensitive to phase composition, structural disorder, defects and the oxidation state of the transition metals ions [4], such in-situ magnetic studies could also be used to provide insights into the electronic and chemical processes during charging.

Based on our recent electrochemical in-situ experiments in a SQUID [2,3] we have designed an electrochemical cell allowing in-situ measurements of the magnetic susceptibility of commercially used battery electrodes during charging/discharging. This is demonstrated by the example of Li_xCoO_2 cathodes, which show reversible variations of the magnetic susceptibility χ of up to 167% with lithium de-/intercalation. For lithium contents $1 > x \geq 0.77$ the susceptibility χ , which is mainly attributed to a Pauli-paramagnetic component, varies linear with charging. This indicates a linear rise of $D(E_F)$ with Li extraction. For $x < 0.77$ the variation of χ can be assigned to alterations of the Co oxidation state, revealing that in addition to Co also O undergoes partial oxidation during charging. An observed further increase of χ at the beginning of the discharging process may indicate the formation of Co^{2+} during reduction. The sensitive in-situ technique opens up a new pathway for studying the kinetics of the atomic processes underlying the charging-induced property variations in solids.

[1] M. Weisheit et al., *Science* 315 (2009) 349

[2] S. Topolovec et al., *J. Magn. Magn. Mater.* 329 (2013) 43

[3] E.-M. Steyskal et al., *Beilstein J. Nanotechnol.* 4 (2013) 394

[4] N. A. Chernova et al., *J. Mater. Chem.* 21 (2011) 9865

FR.I-P11 - A new bench concept for measuring magnetic fields of big closed structures

J. Campmany¹, J. Marcos¹, V. Massana¹, C. Colldelram¹, L. Ribó¹, F. Becheri¹

1. CELLS - ALBA Synchrotron, Barcelona, Spain

The measurement of big closed magnetic structures is becoming a challenge of great interest. The main reason is the tendency towards building accelerators with high magnetic fields produced by small gap magnets, as well as the development of cryogenic or superconducting narrow-gap insertion devices. Usual approach, based on side-measurements made with a Hall probe mounted on the tip of a motorized arm based on a long granite bench is no more applicable to such closed structures. So, new concepts and approaches have been developed, mainly based on complex devices that insert a Hall probe inside the magnetic structure maintaining the desired position by close-loop controls. The main problem of these devices is that they are not general-purpose oriented: they need a special vacuum chamber, require a specific geometry of the magnetic structure, or does not provide 3D field-map measurements. We present in this paper a new bench that has been built at ALBA synchrotron that is simple, multi-purpose and can be a general solution for measuring big closed structures. Motion control is done via ICEpap using the new trigger feature that has been implemented in this motor controller.

FR.I-P12 - New improvements in magnetic measurements laboratory of the ALBA synchrotron facility

J. Campmany¹, J. Marcos¹, V. Massana¹

1. CELLS - ALBA Synchrotron, Barcelona, Spain

ALBA synchrotron facility has a complete ID laboratory to characterize and produce the insertion devices and magnetic devices needed to satisfy the requirements of ALBA user's community. The laboratory is provided with a Hall-probe bench working in on-the-fly measurement mode allowing the measurement field maps of big magnetic structures with high accuracy, both in magnetic field magnitude and position. The whole control system of this bench is based on TANGO. The Hall probe calibration range extends between sub-Gauss to 2 Tesla with an accuracy of 100 ppm. Apart from the Hall probe bench, the ID laboratory has a flipping coil bench dedicated to measure field integrals and a Helmholtz Coil bench specially designed to characterize pure permanent magnetic blocks. Also, a fixed stretched wire bench is used to measure field integrals of magnet sets. This device is specifically dedicated to insertion devices construction. Finally, the laboratory is equipped with a Rotating coil bench, specially designed for measuring multipolar devices used in accelerators, as quadrupoles, sextupoles, etc. Last improvements of the magnetic measurements laboratory of ALBA synchrotron include the design and manufacturing of very thin 3D Hall probe heads, the design and manufacturing of coil sensors for the Rotating coil bench based on multilayered PCB, and the improvement of calibration methodology in order to improve the accuracy of the measurements. ALBA magnetic measurements laboratory is open for external contractors, and has been widely used by national and international institutes as CERN, ESRF or CIEMAT, as well as magnet manufacturing companies, as ANTEC, TESLA or I3M. In this paper we will present the main features of the measurement benches as well as the last improvements made so far.

FR.I-P13 - Magnetic vector potential formulation for stress intensity factor calculation by eddy current testing

S. Harzallah¹, M. Chabaat¹, S. bensaad¹

1. University of Sciences and Technology Houari Boumediene, Bab Ezzouar, Algeria

A new method for computing the Stress Intensity Factor (SIF) by measuring and testing related Eddy currents is considered. In the process, a magnetic vector is provided on the basis of formulation taken from the theoretical set up. Thus, results of relevant applications are obtained to check the theory consistency. A simulation by a numerical approach using the finite element method is employed to detect cracks and damaged zones in Magnetic materials and eventually to study their propagation. Crucial parameter such as a SIF is determined. This method has emerged as one of the most efficient technique for prospecting cracks in materials, evaluating SIFs and analyzing crack's growth in the context of linear elastic fracture mechanics (LEFM). Crack's growth is analyzed as a model by combining the maximum circumferential stress criteria with the critical plane for predicting the direction of crack's propagation in magnetic materials. On the other side, SIF for these models are calculated using the domain form of the J-integral. This latest is an important parameter in LEFM for the integrity assessment of structures containing cracks. It is proven herein that these measurements give the intensity of a stress field in the vicinity of a crack tip and also allow the possibility of analyzing crack's growth until a catastrophic failure.

FR.I-P14 - Numerical modeling of Barkhausen magnetic noise

A. Zaoui¹, L. Cherifi¹

1. Ecole Militaire Polytechnique, Bordj El Bahri, Algeria

In this work, a numerical modeling of Barkhausen magnetic noise (MBN) phenomenon is proposed. The developed model is based on the coupling between the quasi-static formulation of Maxwell's equations using the vector magnetic potential A and the microscopic model of BN. The resolution of this model is obtained by the finite difference method where the microscopic model of BN is introduced at the level of each discretization cells. The numerical model has enabled us first, to plot the hysteresis loop, and also to get the BN.

An experimental test bench is built and the simulated signal obtained from the numerical model is similar to measured one. The numerical model is developed for the study and the tuning parameters of the BN nondestructive evaluation technique.

The MBN signal obtained for different types of metals is presented and the effect of the different metallurgical treatment techniques is highlighted on the response of the signal.

FR.I-P15 - Radiation pressure excitation of low temperature atomic force & magnetic force microscope (LT-AFM/MFM) for imaging

O. Karc^{2 1}, U. Celik¹, Y. Uysalli², H. Ozgur Ozer³, A. Oral²

1. *NanoMagnetics Instruments Ltd., Ivedik, Turkey*

2. *Orta Dogu Teknik Universitesi, Ankara, Turkey*

3. *Istanbul Technical University, Istanbul, Turkey*

We describe a novel method for excitation of Atomic Force Microscope (AFM) cantilevers by means of radiation pressure for imaging in an AFM for the first time. Piezo excitation is the most common method for cantilever excitation. However, it has quite a few drawbacks like causing spurious resonance peaks and non-ideal Lorentzian curves. Radiation pressure excitation is an alternative method for cantilever excitation^{1,2,3} however it has never been used for imaging before.

A fiber optic interferometer with 1310 nm laser was used both to measure the deflection of cantilever and apply a force to the cantilever in a LT-AFM/MFM from NanoMagnetics Instruments. The laser power was modulated sinusoidally at the cantilever's resonance frequency utilizing a digital Phase Lock Loop (PLL). The force exerted by the radiation pressure on a perfectly reflecting surface by a laser beam of power P is $F = 2P/c$. For 3 mW laser power, the force exerted by radiation pressure is calculated to be 20 pN for 5 N/m cantilever, which will deflect the cantilever 4 pm. Typical Q factor in air is 200 and the final amplitude of oscillation will be 8 nm. We can obtain much larger Q values, $\sim 8,000$ and hence larger oscillation amplitudes when we evacuate the system to 2.5×10^{-4} mbar. The cantilever's stiffness can be accurately calibrated by using the radiation pressure. We shall demonstrate tapping mode AFM image of a calibration grating at 300 K and MFM images of a harddisk sample with radiation pressure excitation at 300 K and 4 K.

1D. W. Weld, A. Kapitulnik, arXiv:cond-mat/0606394v2, (2006)

2O. Marti et. Al., Ultramicroscopy 42-44, 345 (1992)

3T. Aoki, M. Hiroshima, K. Kitamura, M. Takunaga and T. Yanagida, Ultramicroscopy 70, 45 (1997)

FR.I-P16 - 1fm/VHz Noise Level Low Temperature Atomic Force & Magnetic Force Microscope (LT-AFM/MFM) in 20mK-300K Temperature Range

O. Karc^{2 1}, U. Celik¹, M. Dede¹, A. Oral²

1. *NanoMagnetics Instruments Ltd. , Ivedik, Turkey*

2. *Orta Dogu Teknik Universitesi, Ankara, Turkey*

We describe the design of a new low temperature Fabry-Perot interferometer for LT-AFM/MFM operating in 20mK-300K Temperature range. We used a multilayer dielectric mirror coated optical fiber to achieve 1fm/VHz Noise Level, while the shot noise limit was 0.16fm/VHz. The fibre can be brought very close to the cantilever using a dedicated 2mm stroke piezo nanopositioner integrated in the piezo tube scanner. The same nanopositioner is used to park the fibre to a safe parking location during cantilever exchange. The LT-AFM/MFM can be used between 6 μ W-3mW laser power. We have demonstrated performance of the LT-AFM/MFM by imaging a hard disk sample between 1.5-300K and Abrikosov vortex lattice in BSCCO single crystal at 4K.

FR.I-P17 - An ultra-low temperature scanning hall probe microscope (SHPM) for magnetic imaging below 40 mK

O. Karc^{2 1}, J. Piatek², P. Jorba², M. Dede¹, H. Ronnow², A. Oral³

1. *NanoMagnetics Instruments Ltd., Ivedik, Turkey*

2. *Laboratory for Quantum Magnetism, Ecole Polytechnique Federale de Lausanne (EPFL), Lausanne, Switzerland*

3. *Orta Dogu Teknik Universitesi, Ankara, Turkey*

We describe the design of a low temperature scanning Hall probe microscope (SHPM) for a dilution refrigerator system. A detachable SHPM head with 25.4 mm OD and 200 mm length is integrated at the end of the mixing chamber base plate of the dilution refrigerator insert (Oxford Instruments, Kelvinox MX-400) by means of a dedicated docking station. It is also possible to use this detachable SHPM head with a variable temperature insert (VTI) for 2 K–300 K operations. A microfabricated 1 μ m size Hall sensor (GaAs/AlGaAs) with integrated scanning tunneling microscopy (STM) tip was used for magnetic imaging. The field sensitivity of the Hall sensor was better than 1 mG/ \sqrt Hz at 1 kHz bandwidth at 4 K. Both the domain structure and topography of LiHoF₄, which is a transverse-field Ising model ferromagnet which orders below TC=1.53 K, was imaged simultaneously below 40 mK.

FR.I-P18 - Broadband dynamic permeability measurements of a single micronic ferromagnetic flake

A. Adenot-Engelvin¹, M. Ledieu¹, J. Neige², N. Vukadinovic³

1. CEA Le Ripault, Monts, France

2. Sherbrooke OEM, Sherbrook, Canada

3. Dassault Aviation, Saint-Claud, France

Ferromagnetic flakes made of FeSiAl or of soft magnetic alloys are widely used as ferromagnetic constituents in composites for electromagnetic shielding of RFID antennas [S. Yoshida et al, J. Appl. Phys., vol. 85, n°8, pp. 4636- 4638, 1999]. The high-frequency response of such composites is usually measured by means of coaxial line or shorted microstrip techniques. In the last case, the zero-field permeability spectra measured on NiFeMo flake composites revealed a low-frequency resonance below 100 MHz, recently interpreted as an embedded vortex translation mode, and a broad high-frequency resonance above 2 GHz corresponding to the natural ferromagnetic resonance [J. Neige et al, Appl. Phys. Lett., vol. 102, p. 242401, 2013]. An open question is how to connect the permeability spectrum of such composites with that of a single flake. To tackle this issue a setup has been developed to measure the permeability measurement of a micrometric flake, free from couplings. The RF excitation is obtained by a copper micro-loop, which acts like an electrical short circuit between the inner and the outer conductors of a small diameter coaxial line. This setup allows the application of a static magnetic field in the plane of the flake. The dynamic permeability measurements of single flakes were performed in the frequency range 1 MHz-20 GHz [J. Neige et al, Appl. Phys. Lett., vol. 104, p. 162402, 2014]. The zero-field permeability spectrum shows two main contributions: a resonance at 50 MHz and the natural spin resonance at 2.8 GHz, in accordance with the composite permeability spectrum. In addition, it is shown that the edge roughness of flake affects the permeability spectrum. Permeability measurements have been performed on square-shaped samples of similar size. By analogy with these samples, a shouldering appearing at intermediate frequency in the single flake spectrum has been identified as domain wall excitations.

FR.I-P19 - Nuclear GISAXS superstructure peaks for characterization of antiferromagnetically ordered nanostripes

L. Dzemiantsova^{1,2}, K. Schlage², L. Bocklage^{1,2}, H. Wille², D. Erb², G. Meier^{1,3}, R. Roehlsberger^{1,2}

1. *The Hamburg Centre of Ultrafast Imaging, Hamburg, Germany*

2. *Deutsches Elektronen Synchrotron, Hamburg, Germany*

3. *Max-Planck Institute for the Structure and Dynamics of Matter, Hamburg, Germany*

Magnetic superstructure reflections have been extensively used for more than twenty years to characterize the vertical spin profile in multilayer structures like antiferromagnetically coupled superlattices. To investigate the lateral spin configuration of ordered nanostructure patterns, we employ a new scattering technique based on resonant GISAXS superstructure peaks, namely grazing incidence nuclear small-angle X-ray scattering (nuclear GISAXS). This synchrotron based x-ray scattering technique is highly sensitive to the magnetic moment orientation and uniquely offers a background free nuclear signal. We perform GINSAXS at the Dynamics beamline P01 at PETRA III to study the lateral magnetic configuration in isotopically enriched permalloy nanostripes during magnetic reversal and to detect a ferro- and an antiferromagnetic state. The origin of this state is the difference in nanostripes which are with and without pads for nucleation of domain walls. We measure a conventional GISAXS pattern of the sample, exhibiting a large number of diffraction maxima, where the angular spacing is determined by the lateral distance of the stripes (250 nm). We find that the nuclear GISAXS line scan of the saturated sample is characterized by diffraction maxima at the same angular position as the electronically scattered GISAXS intensity. Additional strong nuclear superstructure peaks appear when the sample is brought into the antiferromagnetic state. The field dependent intensity of these resonant GISAXS superstructure peaks is a powerful measure of the antiferromagnetic contribution in the sample and is highly suitable to study the lateral saturation behavior. With GINSAXS, it will be possible to magnetically characterize complex ordered structures such as spin ice and skyrmions with sub-nm resolution, even under different conditions of pressure and temperature which is hardly accessible for most surface-sensitive magnetic techniques. The technique can be further developed to study spin dynamics from selected parts of a periodic sample.

FR.I-P20 - Investigation of vortex chirality via local hysteresis loops measured by magnetic force microscopy

M. Coisson ¹, G. Barrera ^{1,2}, F. Celegato ¹, A. Manzin ¹, F. Vinai ¹, P. Tiberto ¹

1. INRIM, Torino, Italy

2. University of Torino, Chemistry Department, Torino, Italy

Magnetic force microscopy (MFM) is a valuable technique to investigate the reversal mechanisms of the magnetisation in patterned films that are not accessible to magneto-optical methods. A field-dependent MFM-derived technique has been recently exploited to measure local hysteresis loops (LHL) on sub-micrometric magnetic structures, consisting in repeatedly scanning the same profile of the sample by disabling the slow scan axis while synchronously changing the magnetic field. A suitable analysis of the phase channel in pass 2 provides a means of investigating the magnetisation reversal processes. In the present work, this technique is exploited to control and measure the vortex chirality on square dots of Ni₈₀Fe₂₀ (lateral size 800 nm, thickness 30 nm) prepared by EBL. LHL are significantly affected by vortex chirality: when it is inverted between the first and second loop branch, symmetric hysteresis loops are observed, whereas when the chirality is preserved the LHL turn out to be asymmetric. Micromagnetic simulations have been performed on dots having the same shape, size and composition to calculate their domain configuration as a function of the applied field, by also taking into account the tip-sample interaction. The corresponding MFM images have been calculated from the magnetisation distribution in the dot. These simulated MFM images, that correspond to the experimental ones, allow the determination of the LHL as if they were measured by the exploited MFM-derived technique. The experimental loops shape and their different symmetries have been accurately reproduced. The tip-sample interaction turned out to have negligible effects on the magnetisation configuration of the dot, but can be exploited to induce vortex nucleation along a specific dot edge, and therefore to accurately control vortex chirality. Via LHL measurements, these effects can be observed and the results of the simulations have been experimentally confirmed.

FR.I-P21 - Transversal mapping of Gd concentration in UO₂-Gd₂O₃ nuclear fuel pellets

D. Tobia^{1,2}, E. L. Winkler¹, J. Milano¹, A. Butera¹, R. Kempf³, L. Bianchi⁴, F. Kaufmann⁴

1. *Laboratorio de Resonancias Magnéticas, Centro Atómico Bariloche - CNEA and CONICET, 8400 S.C. de Bariloche, Argentina*

2. *Instituto de Física "Gleb Wataghin", UNICAMP, Campinas (SP), Brazil*

3. *División Caracterización de Combustibles Avanzados, Gerencia Ciclo Combustible Nuclear, Centro Atómico Constituyentes - CNEA, San Martín, Pcia. de Buenos Aires, Argentina*

4. *Departamento de Combustibles Avanzados, Gerencia Ciclo Combustible Nuclear, Centro Atómico Constituyentes - CNEA, San Martín, Pcia. de Buenos Aires, Argentina*

One of the major challenges of the nuclear industry is the research and development of new materials in order to extend the fuel lifetime, increase the burn-up and optimize the power density distribution. With this aim Gd is usually incorporated into the UO₂ nuclear fuel as a burnable poison, due to its high cross section for neutron absorption. However, the fabrication process of the solid solution (U, Gd)O₂ and the amount of Gd incorporated could affect some physical and chemical properties, that can eventually alter the proper and safe performance of this fuel in reactors, as well as the stability in storage and disposal conditions. Within this frame, it is crucial the search of new and more precise analysis techniques that allow a better characterization of Gd content and distribution in the fuel pellets.[1] Due to its high sensitivity, electron paramagnetic resonance spectroscopy (EPR) emerges as an excellent candidate to carry out this goal. In this work we present a method to measure with a very high precision the transversal mapping of the Gd concentration in UO₂-Gd₂O₃ nuclear fuel pellets by EPR.[2]The quantification of Gd³⁺ ions in the UO₂ matrix was made from the direct comparison with a Gd₂O₃ reference sample. The simple protocol employed allows to determine the relative concentration of Gd in UO₂ with an error smaller than 5%. The nominal concentration in the pellets is UO₂: 7.5% Gd₂O₃. However, a concentration gradient was found, which indicates that the Gd₂O₃ amount diminishes towards the edges of the pellets. The concentration varies from (9.3 ± 0.5)% in the center to (5.8 ± 0.3)% in one of the edges.

[1] F. Zaldivar Escola et al, Journal of Nuclear Materials 435 (2013) 17-24

[2] D. Tobia et al, Journal of Nuclear Materials 451 (2014) 207-210

FR.I-P22 - Diffraction-limited optical imaging of ferroelectricity and magnetism

O. Vlasin¹, B. Casals¹, N. Dix¹, F. Sánchez¹, G. Herranz¹

1. *Icmab-Csic, Bellaterra, Spain*

The electrical polarization in ferroelectrics as well as the magnetization in ferromagnets can be exploited for digital processing and storage. In this regard, a deep understanding of the dynamics and the local response of these materials is crucial for the comprehension of the mechanisms underlying the endurance, retention and fatigue effects in ferroelectric or magnetic devices. Optics is particularly well suited to peer noninvasively into the local responses of both ferroelectric and magnetic properties. Although the spatial lateral resolution cannot beat the ultimate nanoscale resolution of scanning proximity probes, light polarization comes along with the advantage of being sensitive to magnetism and ferroelectricity simultaneously, giving optics an edge over other experimental approaches.

Here we present a comprehensive experimental methodology that exploits electro-optics and magneto-optics as probes of ferroelectricity and magnetism, respectively. For that purpose, confocal optical microscopy was adapted to measure the rotation and ellipticity of the polarization of light with diffraction-limited lateral resolution. As a showcase study, we have imaged the birefringence of ferroelectric BaTiO₃ and manganite La_{2/3}Sr_{1/3}MnO₃ thin films. In the particular case of the ferroelectric, we further disentangled the contributions arising from electro-optics -linked to ferroelectricity- as well as strain - arising from converse piezoelectricity-, so that both properties were mapped out simultaneously. Remarkably, in spite of the high quality of the films under study, the optical imaging displayed inhomogeneous spatial distributions of both ferroelectric- magnetic- and strain-related responses, so that they exhibited significant fluctuations in the scale of the micrometer. Our work underscores the relevance and impact that these variations may have when ferroelectric or magnetic materials are downscaled to small sizes.

FR.I-P24 - Magnetic classification in wet-mode: proofs of concept, and applications.

P. Augusto ¹, T. Castelo-Grande ², A. M Estevez ¹, P. M Costa ¹, D. Barbosa ², C. Torrente ¹

1. APLICAMA - Dep. Chem Engineering - Fac Chem Sciences - Univ Salamanca

2. LEPAPE, Departamento de Engenharia Química, Faculdade de Engenharia da Universidade do Porto, Rua Dr. Roberto Frias, Porto, PORTUGAL

We have developed recently an indirect proof of concept (POC) of magnetic classification in wet mode. This POC, was accompanied by another one, concerning fundamental background theory and simulations. Both POC's proved the feasibility of the process and specially have allowed to determine the influence of some of the force balances and some of the main parameters in fluid media. Based on the preliminary results we are now ready to develop, design and control a larger scale device for future applications, and to strength the proof of concept by direct determination.

Bearing in mind the systems and trajectories obtained we were able to conclude that magnetic classification was able to be achieved with the classes differences shown in Table 1.

Magnetic array touching the walls		$\frac{F_{m1}}{F_{m2}} = \frac{BVB_1}{BVB_2}$	$\frac{F_{m1}}{F_{m2}}$	$extrapolated \frac{\chi_{L1}}{\chi_{L2}} = \frac{F_{m1}}{F_{m2}}$	Magnetic array touching the walls		$\frac{F_{m1}}{F_{m2}} = \frac{BVB_1}{BVB_2}$	$\frac{F_{m1}}{F_{m2}}$	$extrapolated \frac{\chi_{L1}}{\chi_{L2}} = \frac{F_{m1}}{F_{m2}}$
B (T)	BVB (T ² /m)	1.4073	1.4073	1.4073	B (T)	BVB (T ² /m)	1.7452	1.7452	1.7452
0.0972	-2.5936				0.0972	-2.5936			
Magnetic array about 2mm of the wall					Magnetic array about 5mm of the wall				
B (T)	BVB (T ² /m)	0.0824	-1.8430	0.0676	B (T)	BVB (T ² /m)	-1.4861		
0.0824	-1.8430				0.0676	-1.4861			

Magnetic array about 2mm of the wall		$\frac{F_{m1}}{F_{m2}} = \frac{BVB_1}{BVB_2}$	$\frac{F_{m1}}{F_{m2}}$	$extrapolated \frac{\chi_{L1}}{\chi_{L2}} = \frac{F_{m1}}{F_{m2}}$
B (T)	BVB (T ² /m)	1.7112	1.7112	1.7112
0.0995	-3.1058			
Magnetic array about 5mm of the wall		0.0812	-1.8150	
B (T)	BVB (T ² /m)			
0.0812	-1.8150			

Table 1. Results obtained.

Developing this processing techniques allow us to selectively separate and purify several substances at the same step and in the same device, especially in what concerns biomedical applications (ranging from diagnostics until treatment of diseases), mineral processing, water treatment and recycling, as modern technologies are still very limited regarding this goal. The main applications and the improved given by magnetic classification will be also detailed.

FR.I-P26 - Elastic scattering of electron vortex beams through magnetic matter

A. Edström¹, A. Lubk², V. Grillo⁰, J. Ruzs¹

1. *Uppsala University, Uppsala, Sweden*

2. *Technische Universität Dresden, Dresden, Germany*

3. *CNR-Istituto Nanoscienze, Centro S3, Via G. Campi 213/a, Modena, Italy*

4. *CNR-IMEM Parco Area delle Scienze 37/A, Parma, Italy*

Recently, electron vortex beams, i.e. electron beams carrying orbital angular momentum (OAM), have gained much attention as a promising route to measure magnetic properties of materials with high spatial resolution in inelastic electron scattering experiments. One challenge to still overcome is poor signal to noise ratio. Due to recent progression in producing beams with very high OAM (in the order of 100xPlanck's constant) [1], a new route to overcome this could potentially be elastic scattering of high OAM vortex beams. In order to investigate this possibility, we derive a model to describe the magnetic interaction of vortex beams with magnetic matter and, based on this model, present simulations evaluating this potential route to atomic resolution magnetic measurements.

[1] B. McMorrnan et al, Science 331 (2011)

FR.I-P27 - A firmware-defined digital direct-sampling NMR spectrometer for condensed-matter physics

M. Pikulski¹, T. Shiroka^{1,2}, H. Rudolf Ott¹, J. Mesot^{1,2}

1. Laboratorium für Festkörperphysik, ETH Zürich, Zürich, Switzerland

2. Paul Scherrer Institut, Villigen, Switzerland

Nuclear magnetic resonance (NMR) instrumentation employed in condensed-matter physics typically relies on purpose-built hardware, which in most cases involves analog signal-processing components. This approach implies high initial costs and/or significant constructional efforts. By contrast, modern high-performance radio- processing devices are capable of directly sampling and emitting signals throughout the NMR frequency range. In addition, they often feature field-programmable gate arrays (FPGAs), which allow for real-time control and data processing. Hence, fully soft- and firmware-defined solutions are feasible, promising unprecedented levels of flexibility. We report the implementation of a novel type of NMR spectrometer applying these techniques and demonstrate its ability to meet the special demands of condensed-matter NMR. Besides regular laboratory- applications, our approach may be interesting in situations where the number of repeated acquisitions is limited, such as low-temperature and pulsed magnetic-field experiments, since it combines large bandwidth and accurate data acquisition.

FR.I-P28 - Quantitative analysis of shadow X-ray magnetic circular dichroism photo-emission electron microscopy

S. Jamet^{1,2}, S. Da-Col^{1,2}, N. Rougemaille^{1,2}, A. Wartelle^{1,2}, A. Locatelli³, T. Onur Mentès³, B. Santos Burgos³, S. Bochmann⁴, J. Bachmann⁴, R. Afid^{1,2}

1. *Univ. Grenoble Alpes, Institut NEEL, Grenoble, France*

2. *CNRS, Institut NEEL, Grenoble, France*

3. *Elettra - Sincrotrone Trieste S.C.p.A., Trieste, Italy*

4. *Univ Erlangen, Department of Chemistry, Germany*

Shadow X-ray Magnetic Circular Dichroism Photo-Emission Electron Microscopy (XMCD-PEEM) is a recent technique, in which the photon intensity in the shadow of an object lying on a surface, may be used to gather information about the inner magnetic structure of the object. It is attractive as both surface information (through usual photo-emission from the object) and volume information may in principle be extracted, whose combination may be crucial to identify complex three-dimensional magnetization textures. Recently we applied it to formally identify the Bloch-point domain wall in cylindrical nanowires 100nm in diameter [PRB89, 180405 (2014)].

Our ongoing purpose is to lay the basis of a quantitative analysis for this technique. We first discuss the principle and implementation of a method to simulate the contrast expected from an arbitrary micromagnetic state. The simulation is based on finite elements micromagnetics. The intensity of X-ray beams is computed along their path in matter, depending on the dichroic contrast and the local direction of magnetization. From this, the magnetic image is simulated quantitatively both at the surface of the magnetic object, and in its shadow. An excellent agreement is shown with both test cases and experiments.

We also discuss instrumental settings having an impact on the contrast and spatial resolution. For instance, the strength of both dichroism and the absorption length may be changed through the choice of the absorption edge, and adapted to each situation. In principle the contrast in the shadow increases for higher absorption, however in practice it is limited by the S/N ratio, and also the background level of the PEEM, which we evidenced experimentally. The microscope extraction voltage and plane of focus may also be used, to enhanced the surface or the volume contrast.

FR.I-P29 - Magnetic moment measurement utilizing single magnetometer and levenberg-marquardt algorithm

M. Nowicki¹, D. Jackiewicz², R. Szewczyk¹

1. *Institute of Metrology and Biomedical Engineering, Warsaw University of Technology, Warsaw, Poland*

2. *Industrial Research Institute for Automation and Measurements, Warsaw, Poland*

Helmholtz coils connected to the integrator are a well-known method of magnetic moment measurement, taking also into account the magnet geometry. The coils themselves must have proper dimensions for the measured object. Besides this, standardized magnets are often needed to calibrate the system. Therefore, it is a problematic procedure for a single measurement, or the small-scale production testing. In the paper, a procedure for magnetic moment measurement, utilizing single sensitive magnetometer is described. The object under test, for example a permanent magnet, is swept along the sensitive axis of the stationary magnetometer, and the magnetic field strength is recorded, as well as the sample's precise position. The results of measurement are then processed in the Matlab software, and the non-linear least squares curve fitting is done using the Levenberg-Marquardt algorithm. The fitting is performed for the magnetic dipole magnetic field strength versus distance equation. The important factor is that the distance of the first measurement point from the measured object is also treated as unknown, and thus not essential to perform the procedure. Therefore only the information of the magnetic field strength value in measurement points, and the distance between them, is needed for the magnetic moment measurement. To evaluate the proposed method, a laboratory test stand was constructed. The first part of the test stand consist of the Helmholtz coil and precise fluxmeter setup for the reference magnetic moment measurement. The second part consist of magnetoresistive magnetometer, and a linear table for sample manipulation. The measurements of the magnetic moment were done for the Alnico, NdFeB and SmCo permanent magnets. High reproducibility of the results was achieved, with better than 5% accuracy. Additionally, with proper scaling, the proposed method allows for magnetic moment measurement of larger and more complicated objects, for which the standard method would be impractical.

FR.I-P30 - In-situ observation for reaction sintering behavior of Bi-Mn alloy in high magnetic fields

D. Miyazaki¹, Y. Mitsui¹, K. Abematsu¹, K. Takahashi², S. Uda², K. Watanabe², K. Koyama¹

1. Faculty of Science, Kagoshima University, Kagoshima, Japan

2. Institute for Materials Research, Tohoku University, Miyagi, Japan

The application of high magnetic fields for synthesizing process of magnetic material have been performed for controlling phase equilibrium, microstructure, diffusion, and so on. Recently, it was found that the reaction sintering of ferromagnetic MnBi phase is also influenced by magnetic fields [1].

For understanding the magnetic field effect on synthesizing process of MnBi, in-situ observation is one of the important techniques. Recently, we have developed an in-situ observation system with differential thermal analysis (DTA) in high magnetic fields, which is utilized by combining the cryogen-free superconducting magnet with 100 mm room temperature bore [2]. In this study, in order to investigate the magnetic field effect on reaction sintering process from Bi + Mn to ferromagnetic MnBi, in-situ observation of reaction sintering were carried out.

The pellets of Bi-50at.%Mn and Bi-20at.%Mn were prepared by pressing the mixed powder Mn and Bi. The heat treatments were carried out at 520 K for 6 hours in a zero field and 10 T. Here, the annealing temperature was just below the eutectic temperature of Bi and Mn. So that, ferromagnetic MnBi phase is synthesized by solid-state reaction.

For Bi-20at.%Mn, it is found that the surface of the sample slightly changed during the reaction in 10 T. After the heat treatment, the sample shows ferromagnetism, resulting the synthesis of ferromagnetic MnBi phase from Bi and Mn. On the other hand, reaction process is not observed clearly from DTA signal because the reaction is very slow.

[1] Y. Mitsui, et al., J. Alloy. Compd. 615 (2014) 131-134

[2] D. Miyazaki, et al., Abstract of 6th International workshop on Materials Analysis and Processing in magnetic fields, pp72 (2014)

FR.I-P31 - Development of a rapid temperature scanning system for pulsed magnetic fields and its applications

K. Mochizuki¹, Y. Kohama¹, K. Kindo¹

1. International MegaGauss Science Laboratory, The Institute For Solid State Physics, The University of Tokyo, Tokyo, Japan

A pulsed magnet provides us a way to access the extremely high magnetic field range (above 50 T) and is an effective tool to explore exotic physical properties of the strongly correlated materials such as high-T_c superconductors, heavy fermions and so on. However, owing to the short time duration of a pulsed magnet at best a few seconds, it was difficult to measure a temperature dependence of a physical property under pulsed magnetic fields. To overcome this difficulty, we have developed an apparatus that has a short relaxation time of 0.01-1 ms between the sample and the platform on which a film thermometer and a film heater are deposited, and have succeeded in measuring temperature dependencies of the specific heat and resistivity on a short time-scale of pulsed magnetic fields.[1] More recently, we have found that this apparatus also enables to measure other physical quantities (dielectric polarization) as a function of temperature. In this poster presentation, we will describe the details of our measurements and discuss an advantage (and disadvantage) of using our apparatus.

[1] Kenji MOCHIDZUKI et al., in preparation

FR.I-P32 - Application of thermal expansion and magnetostriction measurements using PPMS

S. Tateno¹, N. Kishii¹, M. Ohashi¹

1. Kanazawa University, Ishikawa, Japan

We report a bridge circuit-type detector that has a simple structure and high accuracy with a low degree of error when measuring thermal expansion and magnetostriction by a strain gage method using a commercial PPMS (physical property measurement system, Quantum Design). A compact bridge circuit is connected between a cryostat and the bridge board, which is the primary hardware component on the Model 6000 PPMS controller. Thermal expansion and magnetostriction is calculated from the resistance of the bridge and the bridge voltage, which is measured by the operation of a standard PPMS resistivity option. Its performance is demonstrated by measuring the temperature and the magnetic field dependences of the expansion of some rare earth compounds.

FR.I-P34 - High-frequency ESR measurements of lightly phosphorous doped silicon at low temperatures and their extension to lower temperatures for high B/T ratio

Y. Fujii¹, S. Mitsudo¹, K. Morimoto², T. Mizusaki¹, M. Gwak³, S. Lee³, A. Fukuda⁴, A. Matsubara⁵, T. Ueno⁶, S. Lee⁷

1. *Research Center for Development of Far-Infrared Region, University of Fukui, Fukui, Japan*

2. *Department of Applied Physics, Faculty of Engineering, University of Fukui, Fukui, Japan*

3. *Division of Materials Science, Korea Basic Science Institute (KBSI), Daejeon, Korea*

4. *Department of Physics, Hyogo College of Medicine, Nishinomiya, Japan*

5. *Research Center for Low Temperature and Materials Sciences, Kyoto University, Kyoto, Japan*

6. *Graduate School of Medicine, Kyoto University, Kyoto, Kyoto, Japan*

7. *Department of Physics, Korea Advanced Institute of Science and Technology, Daejeon, Korea*

8. *Wihuri Physical Laboratory, Department of Physics and Astronomy, University of Turku, Turku, Finland*

One of the most practical quantum computer designs reported so far is the system consisting of phosphorus (P) atoms in silicon (Si) crystal as proposed by B. Kane [1]. However, experimental demonstration has not been done yet. One of the remaining unknown properties of this device essential for the realization of Kane's model is spin dynamics including dynamic nuclear polarization phenomena at very low temperatures below 0.1 K and under high magnetic fields above 2 T. These conditions are required for Kane's model. In order to investigate the feasibility of Kane's model, we have been studying phosphorous-doped silicon (Si:P) by magnetic resonance [2]. In Si:P, the donor electrons are well localized around the donor ions if the donor concentration is below the critical doping concentration, $n_c = 3.7 \times 10^{18} \text{ cm}^{-3}$, while they are delocalized above n_c . We have measured T1 and T2 relaxation times of donor electrons in Si:P with the concentration $n = 6.5 \times 10^{16} \text{ cm}^{-3}$ with a W-band (94 GHz) pulsed ESR system. The spin-lattice relaxation rate $1/T_1$ rapidly decreases with decreasing temperature below 30 K down to approximately 4 K. Below 4 K, $1/T_1 \sim T$ due to the phonon-direct relaxation mechanism. These behaviors are qualitatively the same as the data extrapolated from X-band ESR data and our previous data from cw-ESR measurements at 80 GHz [2], though the measured values from pulsed ESR are slightly smaller than them. In order to study the spin dynamics of ^{31}P in the mK regime, we have constructed a magnetic resonance system with a $^3\text{He}/^4\text{He}$ dilution refrigerator and succeeded to detect ESR of Si:P with this system. We will also report the detail of this system.

[1] B.E. Kane, Nature 393 (1998) 133

[2] M. Song et al., J. Phys.: Condens. Matter 22 (2010) 206001, and references therein

FR.I-P36 - Functional properties of newly developed Hall-effect sensors made of graphene

M. Kachniarz¹, O. Petruk¹, M. Oszwa|dowski¹, J. Salach², T. Ciuk³, W. Strupiński³, R. Szewczyk¹, W. Winiarski¹

1. *Industrial Research Institute for Automation and Measurements PIAP*

2. *Warsaw University of Technology, Institute of Metrology and Biomedical Engineering, Warsaw, Poland*

3. *Institute of Electronic Materials Technology, Warsaw, Poland*

The Hall-effect sensors are used in many industrial applications and are the most common type of sensors in the market of industrial measurements of magnetic field [1]. Paper presents newly developed Hall-effect sensors made of graphene for measurements of magnetic flux density.

Graphene is a 2-dimensional crystalline allotrope of carbon, where atoms are organized into sp²-bonded hexagonal pattern [2]. Recent studies indicates that graphene, with high electron mobility (up to 5 000 cm²/Vs) [3] and carrier concentration, allows to obtain significantly higher sensitivity than materials used for Hall-effect sensors so far.

The investigated graphene Hall-effect structure was manufactured using new and original method based on Chemical Vapor Deposition (CVD). Graphene layer was grown on the Si face of SiC substrate in hot-wall CVD Aixtron VP508 reactor.

Digitally controlled measurement system, utilizing Helmholtz coils as a source of reference magnetic field, was developed to measure basic functional properties of graphene structures.

Investigated graphene Hall-effect structure is characterized by low value of offset voltage (3,4 mV with supply current value 10 mA) and significantly high sensitivity (4,92·10⁻¹ V/T with 10 mA supply current). Both sensitivity and offset voltage are proportional to the supply current. Sensitivity of the structure has high stability over time. The relative deviation from the average value is lower than 0,2%. Value of offset voltage is decreasing over time at an average rate of 0,006 mV/h. Measured sheet resistance of the structure is 247 Ω/sq. The obtained results confirmed that graphene may be the good material for Hall-effect sensors.

[1] Magnetic Field Sensors Market by Type, Technology, Applications & Geography – Forecasts & Analysis to 2013 – 2020. MarketsandMarkets (2014)

[2] Krupka, J., Strupinski, W., Applied Phys. Letts., 96 (2010)

[3] Tokarczyk, M., Kowalski, G., Mozdzonek, M., et al., Applied Phys. Letts., 103(2013)

FR.I-P37 - M-H loop tracer for low frequency measurements: ribbons, powders and wires

J.J. Suñol⁴, J. Bonastre¹, I. Santandreu², Ll. Escoda³

1. University of Girona, Girona, Spain

Measurement of a hysteresis loop is a very simple and fast method to characterize ferromagnetic materials. In this work, a high-performance home-made M-H loop tracer has been developed to measure low frequency magnetic hysteresis loops of soft magnetic samples. Commercially available hysteresis loop tracers and magnetic devices are usually designed for hard magnetic materials. The measurement setup is based on digital signal processing (with data acquisition cards). Several requirements are needed in this device as: noise reduction, flux compensation and voltage integration. Sensitivity and accuracy is compared with those of home-made devices described in the literature. Equivalent or high performance is found. The system has been successfully tested in samples from: a) ribbons of crystalline ferromagnetic Heusler shape memory alloys, b) glass coated microwires of soft magnetic amorphous alloys and c) powders of amorphous and nanocrystalline samples produced by mechanical alloying. Results were compared with those obtained in the same samples in commercial equipments. Next evolution of this measuring system is the application of external forces to take into account the effect of stress on the magnetic response of these alloys. Acknowledgements: Financial support from project MAT2013-47231-C2-2-P.

FR.I-P38 - Hexapod Hall scanner for high-resolution magnetic imaging

G. K. Perkins¹, M. Kustov¹, L. F. Cohen¹

1. *Blackett Laboratory, Imperial College London, London, United Kingdom*

Scanning Hall probe microscopy is a powerful magnetic quantitative imaging technique that offers a unique combination of a large scan range with a submicron lateral resolution and a large measured magnetic field range [1-3].

In this work we report the design, construction and performance of a scanning Hall probe microscope (SHPM) which uses six bending piezoelectric actuators that are arranged in a hexagonal configuration and kinematically coupled. This arrangement allows both translation and rotation of a mounted Hall probe along the three Cartesian coordinates. Keeping such general advantages of the technique as the large scan range and the submicron resolution (provided that a high-resolution Hall probe is used), the constructed SHPM offers a unique opportunity of the *in situ* adjustment of the alignment of the sensor with respect to the sample surface that enhances the lateral resolution of the imaging device. The SHPM is compact measuring 25 mm across, and is designed to be fitted into the bore of a cryogenic environment such as those equipped with a superconducting magnet for temperature- and magnetic field-dependent imaging.

[1] A. Oral, S.J. Bending, M. Henini, *Appl. Phys. Lett.* 69, 9, (1996)

[2] V.V. Khotkevych, M.V. Milošević, S.J. Bending, *Rev. Sci. Instrum.* 79,123708, (2008)

[3] Chiu-Chun Tang, Hui-Ting Lin, Sing-Lin Wu, Tse-Jun Chen, M. J. Wang, D. C. Ling, C. C. Chi, and Jeng-Chung Chen, *Rev. Sci. Instrum.* 85, 083707 (2014)

Acknowledgement: The work was funded by European Community's 7th Framework Programme under Grant agreement 310748 "DRREAM" and the UK EPSRC grant EP/G060940/1.

FR.I-P39 - Discrete inverse transformation for eddy-current tomography based on whitney finite edge element method

P. Nowak¹, R. Szewczyk², M. Urbanski², J. Ruokolainen³, P. Raback³

1. *Industrial Research Institute for Automation and Measurements PIAP, Al.Jerozolimskie, Warsaw, Poland*

2. *Institute of Metrology and Biomedical Engineering, Warsaw University of Technology, Warsaw, Poland,*

3. *CSC - IT Center for Science, Espoo, Finland*

Eddy current tomography is a method for non-destructive testing of ferromagnetic and non-ferromagnetic but conductive, materials. Tested element is placed between exciting and sensing coil. Alternate current in exciting coil induces eddy currents in the tested element, which affect signal picked by the sensing coil. Variation of phase and amplitude of sensed signal is caused by variation of conductivity and permeability of the tested element, which are caused by element's defects.

Forward transformation in eddy –current tomography with utilization of Whitney finite edge element method was previously reported [1]. The expected measurement results can be calculated with finite-element method, knowing only the shape, conductivity, and permeability of the sample.

On the base of measurements of exemplary elements [2] and system for calculation of forward transformation, discrete inverse tomography transformation was applied. Values of conductivity and permeability of the model elements are discretely changed, then forward transformation is applied. Calculation results were compared with the real object measurements, and proper changes were applied in the next iteration, until the assumed compliance level was achieved. Discrete optimization was performed only on the element edges, therefore calculation time was significantly faster.

The results show acceptable element shape reconstruction, with visible indentation in place of the sample discontinuity. Further research will be conducted in order to achieve higher reconstruction accuracy and lower computation time.

[1]- Szewczyk, Roman, et al. "Forward transformation for high resolution eddy current tomography using Whitney elements."

[2]- Salach, Jacek. "Non-destructive Testing of Cylindrical Ferromagnetic and Non-magnetic Materials Using Eddy Current Tomography." *Mechatronics-Ideas for Industrial Application*. Springer International Publishing, 2015. 373-380

FR.I-P40 - Comparison of different geometries for membrane based AC calorimeters

M. Bratko¹, D. Caplin¹, L.F. Cohen¹, Y.V. Bugoslavsky²

1. *Imperial College London, United Kingdom*

2. *Cryogenic Limited, London, United Kingdom*

AC calorimetry is an alternative to differential scanning calorimetry and relaxation methods. One of its main advantages is the measurement speed. During the measurement the sample is excited by a heat wave from a local heater resulting in temperature oscillations in the sample. Due to the capacitive load of the sample the temperature oscillation lags between the power excitation. The heat capacity can be calculated from the temperature oscillations phase and amplitude based on a simple AC-circuit model of the thermodynamic setup. Here we study a SiN-membrane based AC calorimeter suitable for measurement of extremely small samples of the order of a few micrograms in magnetic field [1]. We compare two types of membranes with different spatial arrangements of the essential elements: heater, sample, temperature sensor. We study the system response as a function of frequency and observe that both geometries deviate from the simple thermodynamic model but in significantly different ways. By considering these deviations within the context of the spatial arrangements of the essential elements on the membrane we were able to identify the limiting assumptions in the simple model and optimise the operating conditions for accurate calibration and measurement.

[1] Minakov A.A. et al., Review of Scientific Instruments 76, 043906 (2005)

This work was funded by the EPSRC under an Imperial College Knowledge Transfer Secondment.

FR.I-P41 - Magnetometry based on asymmetric coupled mechanical oscillators

T. Mühl¹, J. Körner¹, C. F. Reiche¹, B. Büchner⁰

1. IFW Dresden, Dresden, Germany

2. Institut für Festkörperphysik, Dresden, Germany

In cantilever magnetometry, the field-dependent frequency shift and damping of a small mechanical oscillator is used to measure magnetic moments, anisotropy fields, switching fields, and magnetic fluctuations of tiny samples that are attached to the oscillator [1]. An increase of sensitivity of such mechanical magnetometers can be achieved by decreasing their effective spring constants. This is usually accompanied by a reduction of their spatial dimensions, which may require more sophisticated detection methods. A high-sensitivity magnetometer might be based on a one-side clamped carbon nanotube [2].

By discussing the rich behavior of a simple asymmetric coupled harmonic oscillator model, we present a co-resonant sensor concept which combines a conventional cantilever oscillator and a low-stiffness nanowire oscillator. Even though the spring constants and the effective masses of the two partial systems differ by orders of magnitude, the nanowire oscillator strongly influences the cantilever oscillation if nanowire and cantilever have similar resonance frequencies. Thus, the magnetic interaction of a nanosized sample attached to the nanowire with an external field leads to a notable frequency shift of the coupled system which can be measured at the cantilever by conventional means.

We prepared a co-resonant oscillator that is composed of an iron-filled carbon nanotube (FeCNT) and a Si cantilever forming a coupled flexural oscillation system. Frequency matching of the partial oscillators has been achieved by deposition of materials at the FeCNT free end. The measured field-dependent frequency shift of the coupled oscillator system is several orders of magnitude larger than that of a corresponding single-cantilever magnetometer, which is in agreement with our calculations.

[1] B. C. Stipe, H. J. Mamin, T. D. Stowe, T. W. Kenny, and D. Rugar, Phys. Rev. Lett. 86, 2874 (2001)

[2] S. Philippi, U. Weissker, T. Mühl, A. Leonhardt, and B. Büchner, J. Appl. Phys. 110, 084319 (2011)

FR.I-P42 - Surface flaws detection in low conductivity titanium alloys using magnetoresistive devices

F. Franco¹, F. Cardoso¹, L. Rosado⁰, R. Ferreira⁴, S. Cardoso^{1,2}, P. Freitas⁰

1. INESC - *Microsistemas E Nanotecnologias*
2. Instituto Superior Técnico, *Universidade de Lisboa*
3. INESC - *Investigação e Desenvolvimento*
4. *International Iberian Nanotechnology Laboratory*

Typically inductive sensors used for Eddy current testing (ECT) display limited sensitivity in a low frequency range and poor spatial resolution, being nowadays surpassed by magnetoresistive (MR) sensors with improved spatial resolution, high sensitivity and bandwidth [1]. Therefore, MR-ECT tools are of high impact even with surface contaminations, which is impossible with common liquid penetrate testing. In particular, ECT reliability is critical for low conductivity titanium alloys broadly integrated in aerospace industries due to their high strength/weight ratio [2].

A TA6Valpha titanium mock-up with a single defect (0.6mmx100umx50um) was characterized using MR-ECT probes. Probe A consisted of 10 magnetic tunnel junctions (MTJs) in series (each 10x4um², total area=22x96um²) for enhanced spatial resolution and Probe B is an array of 72 MTJs (each 50x50um², total area=500x500um²) for improved detectivity, both based on IrMn/CoFe/Ru/CoFeB/MgO/CoFeB stacks [1].

Probes A and B were biased with 180µApp and 1.65mApp, respectively, at 4999kHz (fb) while the excitation line was biased with 2App at 5MHz (fH), promoting a confined and intense EC density at the surface. The magnetic information was modulated at fH-fb, avoiding the electric biasing component (fb) and electromagnetic coupling (fH). Sample topography was partially removed by assembling the probes in a differential configuration.

With enhanced sensitivity (1.5x) and larger area, Probe B revealed a maximum signal amplitude increase of 7.6x (Vout(max)=6uV). However as the sample-sensor distance increases, a compromise between number of sensors and their intrinsic noise has to be met. Finite element simulations allowed us to access the influence of the total array area versus each sensor's noise. For a width of 500um, we demonstrate that probe B is close to the total area that maximizes the signal-to-noise ratio.

[1] F. Cardoso et al. IEEE Trans. Magn. 50 (2014) 6201304

[2] R. Boyer et al. Mat. Sc. Eng. A 213 (1996) 103

FR.I-P43 - Local magnetic measurements in multi-layered nanowires observed by electron holography

D. Reyes¹, C. Gatel^{1,2}, N. Biziere¹, T. Wade³, B. Warot-Fonrose¹

1. CEMES-CNRS, Toulouse, France
2. Université Paul Sabatier, Toulouse, France
3. LSI, Ecole Polytechnique, Palaiseau, France

Magnetic multilayered structures are studied for various applications like nano-oscillators, as multilayered nanowires can be used as a spin transfer torque system. In this kind of systems, a spin polarized current can transfer its angular momentum to a ferromagnet layer, inducing a torque on its magnetization. Thus, the magnetic moment can switch to another state or oscillate around its equilibrium position at microwave frequencies. The possibility in multilayers to couple multiple individual oscillators allows an increased power for RF signal generator. In this work we demonstrate how the advanced quantitative electron microscopy techniques allow for the complete description of magnetic nanowires, for both structural and magnetic properties that can not be achieved by standard method.

We have studied the magnetic configuration in multilayered Co/Cu nanowires. We will show that electron holography is mandatory to observe the magnetic configuration in such small magnetic volumes. The acquisition and treatment methods will be detailed. The interpretation of the magnetic states needs combined structural and chemical characterization to estimate the thickness and the crystallinity of the layers, two geometrical parameters required for meaningful simulations.

The 60 nm diameter wires are characterized by chemical imaging (EFTEM) in order to know the distribution of cobalt and copper along the wire, 24nm thick Co and 14nm thick Cu layers are observed. Detailed EELS analysis show that 15% of Cu is mixed in the cobalt layers.

FR.I-P44 - Highly sensitive very low temperature and high field faraday magnetometer

O. Florea¹, E. Lhotel¹, J. Mocellin¹, Y. Launay¹, S. Dufresnes¹

1. Institut Neel, Grenoble, France

We present the development of a new Faraday Magnetometer, which will allow performing absolute magnetization measurements with a high sensitivity (10^{-8} A.m² = 10^{-5} emu) in extreme conditions: at very low temperature, down to 30 mK, and high applied magnetic fields, up to 16 T.

Our objective is to be able to probe the entanglement in quantum frustrated molecules as well as exploring the field induced phases at very low temperature in exotic materials such as frustrated magnets or ferromagnetic superconductors. The principle is to use a capacitive detection to measure the Faraday force induced on a magnetized sample in presence of a field gradient.

The originality of our magnetometer compared to similar systems [1,2] is two fold : i) We have developed an electronic detection system which involves a cold amplifier stage in the 3He-4He dilution fridge to improve the sensitivity of the capacitive measurement. ii) We have designed two capacitive sensors to probe a large variety of physical systems: a 'usual' sample holder, made using a 3D printer, suitable for samples with strong magnetic signals or large samples and a MEMS (MicroElectroMechanical System) made of a suspended nanofabricated silicon membrane, able to reach a high sensitivity.

[1] T. Sakakibara et al, Jpn. J. Appl. Phys. 33,5067 (1994)

[2] D. Slobinsky et al., Rev. Sci. Instrum 83, 125104 (2012)

FR.I-P45 - Sub-nanosecond time-resolved scanning magneto-optical microscope utilizing near-field optics

J. Rudge¹, H. Xu¹, J. Kolthammer¹, Y. Hong², B. Choi¹

1. *Dept. of Physics and Astronomy, University of Victoria, Saanich, Canada*

2. *Dept. of Electrical and Computer Engineering, University of Alabama, Tuscaloosa, United States*

Magnetization dynamics in patterned magnetic elements is fertile ground for fundamental research that also leads to novel technological applications. In many studies of magnetization dynamics in micron-sized elements, the ultrafast magnetization processes have been investigated using time-resolved magneto-optical Kerr effect (TR-MOKE) techniques, with sub-micron spatial resolution and ~50 ps temporal resolution. The biggest drawback of TR-MOKE is its spatial resolution, which is diffraction-limited due to the use of conventional optics. With the continuing demand for faster, more compact technological applications, this limit to spatial resolution is becoming a significant problem. One way of bypassing the diffraction limit in magnetic imaging is with near-field scanning optical microscopy (NSOM), which utilises evanescent waves at sub-wavelength distances from the sample surface. In this study we combined a near-field scanning optical microscope and magneto-optical contrast and successfully developed a new magnetic microscope, i.e., time-resolved near-field scanning magneto-optical microscope (TR-NSMOM). By taking advantage of the high temporal resolution of time-resolved Kerr microscope and the sub-wavelength spatial resolution of a near-field microscope, we achieved a temporal resolution of ~50 ps and a spatial resolution of < 100 nm. In order to demonstrate the spatiotemporal magnetic imaging capability of this microscope, the magnetic field pulse induced gyrotropic vortex dynamics occurring in 1 μm diameter, 20 nm thick CoFeB circular disks has been investigated. The microscope provides sub-wavelength resolution magnetic images of the gyrotropic motion of the vortex core at a resonance frequency of ~240 MHz. The details of the vortex dynamics are reconstructed using micromagnetic modeling based on time integration of the Landau-Lifshitz-Gilbert (LLG) equation.

FR.I-P46 - Oxide wizard as a new tool to probe magnetic properties at the nanoscale.

P. Torruella¹, L. Yedra¹, E. Xuriguera², M. Estrader³, A. López-Ortega⁴, M. Baró⁵, J. Nogués⁶, M. Roldan⁷, M. Varela⁷, S. Estradé¹, F. Peiró¹

1. Dept. Electrònica, Universitat de Barcelona, Barcelona, Spain
2. Dept. Enginyeria Química, Universitat de Barcelona, Barcelona, Spain
3. Dept. Química Inorgànica, Universitat de Barcelona, Barcelona, Spain
4. Dipt. di Chimica, Università degli Studi di Firenze, Florence, Italy
5. Dept. Física, Universitat Autònoma de Barcelona, Barcelona, Spain
6. Institut Català de Nanociència i Nanotecnologia
7. Dept. Física Aplicada III, Universidad Complutense de Madrid, Madrid, Spain

It is well-known that the oxidation state of rare-earth and transition metals cations in different types of oxides governs its magnetic properties. Electron Energy Loss Spectroscopy (EELS), has repeatedly shown to be a technique that can access this type of information at the nanoscale [1-2], and even with atomic resolution [3]. However, as datasets become increasingly larger, the treatment of the data can be complicated. It can even be biased as it involves arbitrary choices of values such as integrating windows, peak onsets etc. In this work we developed a new software (Oxide Wizard) that evaluates the most important parameters of rare-earth and transition metals EEL spectra that can be related with their oxidation state, and we show how this information can solve material science problems related to magnetism [4].

FR.I-P47 - Probing nano- and micro- magnetism with very small angle neutron scattering instrument KWS-3

Z. Fu¹, V. Pipich¹, K. Ono², S. Siegfried³, T. Brückel⁴

1. Forschungszentrum Jülich GmbH, Jülich, Germany

2. High Energy Accelerator Research Organization (KEK), Ibaraki, Japan

3. Helmholtz Zentrum Geesthacht, Geesthacht, Japan

4. Forschungszentrum Jülich GmbH, Jülich, Germany

KWS-3 is a very small angle neutron scattering (VSANS) instrument operated at the Research Neutron Source Heinz-Maier Leibnitz (FRM-II) in Garching, Germany. The principle of this instrument is to form a one-to-one image of an entrance aperture on a 2D position sensitive detector by neutron reflection from a double-focusing toroidal mirror. The instrument has two fixed and one flexible sample position, covering a scattering vector Q range between $4 \cdot 10^{-5}$ and $2 \cdot 10^{-2} \text{ \AA}^{-1}$. Correspondingly the structural and magnetic properties of microstructures with sizes from 10 \mu m to 50 nm can be investigated on KWS-3. For example, VSANS measurements at KWS-3 have been performed on sintered (Nd, Dy)-Fe-B magnets, which have grain sizes ranging from several hundred nanometers to a few micrometers. Field-dependent VSANS patterns of sintered and Dy-free magnets were measured and revealed that the sizes of the magnetic microstructures increase with the sizes of crystal grains, giving valuable information on the high coercivity mechanism in this series of permanent magnets with wide automotive applications. Another example is the field-dependent VSANS measurement on the Fe-doped CoGe alloys at various temperatures below 200 K. This experiment identifies the k -value of the helical phase in the half-doped sample and confirms the disappearance of the helical peak at a critical Co-concentration is true even down to $Q = 4 \cdot 10^{-4} \text{ \AA}^{-1}$, which might be difficult to reach using normal SANS. Given the implementations of polarization option and more sophisticated sample environment in the near future, VSANS instrument KWS-3 is a powerful tool to investigate magnetic microstructures ranging from nanoscale to microscale.

FR.I-P48 - Software development for investigating magneto-optical and non-linear effects in nanofluids

R. Srinivasan¹, C. Pai¹, S. Mohan^{1,3}, N. Momin¹, Muthurajan H.², Nagarajan R.³

1. Department of Physics, University of Mumbai, Mumbai, India

2. Centre for Nanoscience and Nanotechnology, University of Mumbai, Mumbai, India

3. UM-DAE Centre for Excellence in Basic Sciences, University of Mumbai, Mumbai, India

In this paper, we present the instrumentation software developed for studying non-linear and magneto-optical effects in nanofluids. Laser beam (He-Ne, 632 nm, 10 mW) transmission studies through nanofluid samples are carried out. In-house software contains modules for control and data processing.

Laser beam transmitted through nanofluid shows thermal lensing along with higher order non-linear effects like self-diffraction and magneto-optical effects. In case of magnetic nanofluids, refractive index gradient arising due to thermal and concentration diffusion of particles is found to be tunable with external magnetic field. Control module in the software generates customized magnetic field varying with time. Self diffraction patterns show variation with magnetic field resulting into temporal variation of non-linear refractive index. Separate module has been developed for processing the images of self-diffraction patterns and storing optical transmission data.

This paper presents laser interaction studies carried out with dispersions of Fe₃O₄ nanoparticles (40 nm, 30 mg/ml in Hexane) where a non-linear optical response in form of self diffraction patterns is observed. On the other hand, laser transmission through smaller sized Fe₃O₄ particles (8-10 nm, 10 mg/ml in Water) show speckle like forward scattered patterns tunable with external magnetic field. The simple experimental set-up and associated software system is useful for understanding colloidal dynamics, non-linear, magneto-optical response of nanofluids and the possible applications for development of optofluidic sensors.

FR.I-P49 - Three axis vector magnet for low temperature magnetic imaging

J. Azpeitia^{1,2,3}, R. F. Luccas^{1,2,3}, M. Rocci^{3,4}, C. León^{3,4}, J. Santamaría^{3,4}, M. García-Hernández^{1,2,3}, C. Munuera^{1,2,3}, H. Suderow^{2,5}

1. Instituto de Ciencia de Materiales de Madrid, Consejo Superior de Investigaciones Científicas (ICMM-CSIC), Madrid, Spain
2. Unidad Asociada de Bajas Temperaturas y Altos Campos Magnéticos, UAM-CSIC, Cantoblanco, Madrid, Spain
3. Unidad Asociada de Laboratorio de Heteroestructuras con aplicación en Spintronica, UCM-CSIC, Cantoblanco, Madrid, Spain
4. Departamento de Física Aplicada III, Universidad Complutense, Ciudad Universitaria, Madrid, Spain
5. Laboratorio de Bajas Temperaturas, Departamento de Física de la Materia Condensada, Instituto de Ciencia de Materiales Nicolás Cabrera, Condensed Matter Physics Center (IFIMAC), Facultad de Ciencias Universidad Autónoma de Madrid, Madrid, Spain

Three axis vector magnet for low temperature magnetic imaging Scanning probe measurements, i.e. STM or MFM, in vectorial magnetic field systems is a growing research area, which can be used, in superconductors or magnets, to establish internal anisotropies and, for example, observe possible vortex lattice transitions in the mixed state of superconductors [1]. In this work we present a three axis vector magnet system for cryogenic scanning probe microscopy, which has been developed and successfully used in conjunction with a liquid helium temperature Magnetic Force Microscopy (MFM) [2]. We discuss the magnet support as well as the homogeneity of the fields achieved in the sample space. We obtain tilted fields in any direction of space, with a maximum field of 5T along the Z axis and 1.2T in the XY plane. We further present the evolution of (ferro)magnetic domains, first on a test sample (HDD) and subsequently on a nanostructured manganite thin film, with temperature, magnetic strength and direction.

[1]H. F. Hess, C. Murray, and J. V. Waszczak, Phys. Rev. B 50, 16528 (1994)

[2] J. A. Galvis et al., Rev. Sci. Instrum. 86, 013706 (2015)

FR.I-P50 - Using of ambient magnetic field information in diagnosis of electric motor

P. Szulim¹, S. Gontarz¹

1. Warsaw University of Technology, Institute of Vehicles, Warsaw, Poland

In this paper, the authors present theoretical basis of using external magnetic fields surrounding electric machines like BLDC motors or generators to diagnose their technical state. Conducted analytical calculation was verified on the test stand with the BLDC motor subjected to some mechanical faults. The problem of determining the technical condition of an electric machine has not been resolved yet. Many new publications related to this topic can bear witness to this. However, the demand for reliable diagnosis can be easily observed in case of complicated technical systems which perform important functions, which takes place for example in the energy industry. It turns out, that an unambiguous statement of specified mechanical faults occurrence may not necessarily be distinguished on sufficient level, because of the lack of diagnostic methods. An interesting alternative can be using external magnetic field that comes from rotors and windings, as a source of diagnostic information. A significant part of this field is confined in the motor armature but measuring of some residual values can have diagnostic validity. In this paper, the complete analytical 2D model of the electric BLDC motor was shown, allowing for the derivation of some analytical relationships between the specified mechanical faults like eccentricity, torque pulsation, unbalanced load, demagnetization, and distribution of instantaneous values of magnetic field vector on the outside of investigated motor. The topic of analytical modeling of electric brushless motors has been an object of intensive work for the last 40 years. Achievements from this area were used in this paper. The result of analytical modeling will be verified by test stand investigations where the investigated motor works in different load conditions. Three axial magnetometer made of magneto-resistive elements was used to wide band measurements. Using these elements allows for the precise measurement of three components of vector field with high sensitivity and linearity. In this paper, the analysis of influence of chosen mechanical faults on diagnosis signal under time-frequency analysis, will be presented. The results will be compared with the classic CSA analysis where advantages of presented method will be clearly depicted.

FR.I-P51 - Passive identification of magneto-mechanical phenomena in process of fatigue of steel and cast

S. Gontarz¹, J. Dybala¹, P. Szulim¹

1. Warsaw University of Technology, Institute of Vehicles, Warsaw, Poland

Fatigue process in steel materials leads to changes in their structure, that modify their magnetic properties also. The influence of fatigue is so large, that this material in the presence of earth magnetic field yields measurable view in the form of characteristics changes of magnetic fields near steel materials. In work one was verified abilities of identification magneto-mechanical phenomena in a fatigue process of steel and cast. To do this test stand based on MTS machine had been modified. Measurement was realized in contactless manner using FluxGate magnetometers. Analysis of signals was oriented on determination of a degree of material fatigue and quantitative characteristic of changes that had place for the analyzed materials.

A

A. Ávila, M.	Abdallah, A.	Th.P-P29
TH.C-P20	Mo.L-P50	Abrahams, I.
A. García, F.	ABDALLAH, I.	TU.D-P5
FR.D-P65	Mo.H-P18	Abram, M.
A. Justino Nunes, C.	Abdelgawad, A.	FR.B-P22
FR.D-P65	Fr.H.2_I1	WE.F2_O6
A. Lograsso, T.	Abdel-Jawad, M.	Abramof, E.
Mo.H-P107	TH.C-P93	FR.F-P11
A. Ribeiro, R.	Abdellatif, A.	Abreu Araujo, F.
TH.C-P20	Mo.A-P6	Th.I.3_O4
A. Ross, C.	Abd-Lefdil, M.	TH.J-P10
TU.A.1_O5	TU.A-P8	Abreu Ávila, M.
Aanand, K.	Abdul-Jabbar, G.	Mo.C-P5
MO.D.1_O5	Th.D.1_I4	Abrikosov, I.
Ababaei, G.	Abdulrazaq, M.B.	WE.E2_O2
TU.H-P96	TU.I-P12	Abrikosov, I.A.
Ababei, G.	Abe, N.	TU.C.3_O4
TH.K-P12	Mo.C-P19	Abuín, M.
Th.L-P4	TU.A.-59	Th.M-P21
TU.H-P92	TU.A-P60	Acet, M.
Aballe, L.	TU.A-P61	TH.C-P105
FR.I.2_O3	Abel, F.M.	TH.C-P82
MO.E.1_I1	MO.B.3_O4	TU.C.3_O3
Th.G-P15	Abematsu, K.	WE.D.1_O3
TH.K-P23	FR.I-P30	Acevedo Salas, U.
Abbate, M.	TU.H-P82	TU.A-P42
TU.E-P17	Abemtsu, K.	Achkar, C.
	Fr.A.1_O2	Th.G.2_O3
	Abernathy, D.	Th.I.3_O3
	MO.D.3_O3	Th.I-P6
	Ablett, J.	Adachi, H.
	Th.C.3_O2	Th.H-P10
	Abo, G.	Th.H-P5
	TH.C-P83	WE.I.2_O4
	Abolhassani, M.R.	Adachi, T.
	TU.E-P13	FR.A-P9
	TU.E-P27	TU.E-P16
	Aboljadayel, R.	Adachi, Y.
	Mo.H-P106	Mo.L-P71
	Abouhaswa, A.	Adams, T.
	Mo.A-P12	TU.C-P30
	Abraha, K.	Adanakova, O.
		Mo.I-P34
		Adelmann, P.
		Mo.A-P110

Adelnia, F. TU.D-P7	TU.A-P74	Mo.L-P65
Adenot-Engelvin, A. FR.I-P18	Agatsuma, T. Th.C.3_O3	Ahrentorp, F. Th.P-P2
Adeyeye, A. Mo.G-P6 TH.C.1_I1 Th.M-P2	Agbelele, A. Th.E.1_I1	TU.B.3_O2
Adeyeye, A.O. TH.G.1_O2	Agnus, G. FR.A-P54	Aichhorn, M. Fr.D.3_O1
Adler, P. Mo.B-P9 TU.E-P28	Agostinelli, E. MO.B.1_O2 Mo.I-P35 Th.K-P38	Aidoudi, F.H. TH.A-P38 TU.D.1_O4
Adriano, C. Mo.A-P48 TH.C-P9	TU.B.2_O3 TU.E.3_O3 TU.F-P53	Aimon, N. MO.F.2_I1
Adroja, D. Mo.G-P25	Agramunt, S. Mo.J-P5	Ajejas, F. Mo.H-P99 Mo.I-P37 TH.I-P28 Th.K-P44 TU.A-P91
Adroja, D.T. Mo.C-P17 TH.C-P28 WE.H.2_O5	Agramunt-Puig, S. Mo.F.2_O5	Akabane, E. TU.C-P10
Aeppli, G. TU.D-P13	Agrawal, M. Fr.G.1_O5 MO.H.2_O2 Th.H-P18	Akagi, Y. Fr.F.2_I1
Aeschlimann, M. Mo.E-P11 Th.N-P10	Agrestini, S. FR.A-P29 TH.K-P18 Th.K-P41	Akaki, M. Mo.B-P12 TU.A-P73
Æwik, J. Mo.L-P15 Mo.L-P3	Agudelo Giraldo, J.D. FR.E-P17 FR.E-P7 Th.M-P3	Akamine, H. TH.C.1_O2 TH.C-P71
Aezami, A. TU.E-P13 TU.E-P27	Aguilera-Granja, F. FR.H-P17	Akansel, S. TU.E-P42
Afanasiev, D. TH.C-P92	Aguirre, M.H. Th.B.3_O2 Th.H-P5 Th.H-P8	Akatsu, M. TH.C-P126 TU.B-P48
Affronte, M. MO.I.2_O5	Ahmad, R. Mo.H-P96	Akbari, A. Fr.B.3_O3 Mo.A-P99
Afid, R. FR.I-P28 Mo.K-P26	Ahmadi, T. FR.I-P1	Akça, G. Mo.L-P69
Afrass, M.A. Mo.A-P103	Ahmed, M.Z. TU.I-P12	Akdogan, N.G. Mo.I-P5
Agafonov, L. TH.F-P12	Ahn, F. Mo.A-P22	Akerman, J. Th.O-P52
Agarwal, V.	Ahn, J.	Åkerman, J. Mo.F-P19 Mo.F-P25 Mo.F-P4

Mo.F-P8	TU.F-P94	Alexe, M.
MO.H.2_04	Albargi, H.	Th.E.2_02
TU.J.2_11	TU.A-P57	Alfadhel, A.
Akimitsu, J.	Alberca, A.	TU.I.2_04
Th.A.2_02	Fr.B.2_01	WE.F.1_02
TH.A-P29	TU.E.1_03	Alfahdel, A.
TH.A-P7	Albert, B.	Th.P-P17
TH.C-P61	TH.C-P80	Alff, L.
TU.C.2_02	Albert, F.	Mo.H-P29
TU.C.2_04	TU.SYM_1	TH.C-P80
Akiyama, T.	Albertini, F.	TU.A-P31
FR.H-P12	MO.C.2_11	Alfonsov, A.
Akiyama-Hasegawa, K.	TH.C-P76	TH.A-P9
TU.F-P4	TU.E-P28	Th.D.3_02
Akmaldinov, K.	TU.G-P10	Algarabel, P.
Mo.H-P67	TU.G-P16	MO.C.3_03
Mo.I-P4	TU.J.2_04	Mo.H-P101
TU.G.3_02	WE.D.1_03	Mo.H-P40
Aktaş, B.	Albille, J.	Mo.H-P55
TU.H-P48	TU.A-P91	Mo.L-P47
TU.H-P49	Albino, M.	Th.B.3_02
Akterskiy, A.	TU.B.2_04	Th.H-P5
FR.D-P26	TU.E.3_02	Th.H-P8
Akyol, M.	TU.F-P60	TU.A-P24
Mo.L-P69	TU.F-P64	TU.A-P26
Th.I.2_01	Albisetti, E.	TU.A-P45
Akzyanov, R.	Th.H.1_04	TU.A-P86
FR.A-P5	Th.H.2_04	TU.C.1_04
Mo.B-P19	TU.G.3_05	Alho, B.
TU.E-P2	TU.I.1_04	Mo.L-P5
Al Baalbaky, A.	Albrecht, M.	Ali, K.
FR.E-P26	Fr.I.3_01	TH.B-P16
Alameda, J.M.	TU.J.1_05	Ali, N.
Fr.H.3_02	Aleksandrov, Y.	Mo.L-P3
Mo.H-P98	TU.H.1_11	Aliev, A.
TH.H.3_02	Alekseev, P.	Mo.L-P74
TH.K-P4	TU.B-P16	Mo.L-P89
TU.G-P11	TU.B-P20	Th.B.1_05
TU.J.1_03	Aleshkevych, P.	Aligia, A.A.
Alameh, K.	TU.D-P2	TH.B-P10
Th.O-P41	TU.D-P3	Alisultanov, Z.
Alayo, N.	Alet, F.	Mo.J-P7
Th.N-P5	FR.B-P31	Aliyeva, S.
Alba Venero, D.	Alexandrakis, V.	FR.F-P5
TU.F-P102	TU.H-P81	Allão Cassaro, R.

TU.D-P14	Altmann, P.	TU.A-P79
Allende, S.	Mo.D-P31	TU.H-P131
FR.E-P38	Alvarado, S.F.	Amaral, V.
Mo.J-P18	TH.E-P22	FR.E-P39
Th.G.2_I1	Alvarenga, T.	Mo.H-P90
Allia, P.	Mo.L-P5	Amaral, V.B.S.
TH.E3_O4	Álvarez Lucio, G.	Th.K-P43
Alling, B.	Mo.H-P48	Amato, A.
TU.C.3_O4	Th.G-P12	FR.A-P34
Allwood, D.	Th.O-P32	FR.D-P7
Fr.G.1_O4	Álvarez, G.	TU.C.2_O3
Th.G.2_O6	Mo.H-P47	Ambrozic, B.
Al-Mahdawi, M.	TU.H-P127	MO.F.2_O6
Mo.F-P13	Álvarez, J.V.	Amico, L.
Mo.F-P17	FR.E-P37	TU.D-P13
Almeida, A.	Álvarez-Hérault, J.	Amiri, P.K.
TU.A-P46	TU.G.3_O2	Th.I.2_O1
Almeida, J.	Álvarez-Prado, L.M.	Amirov, A.
TU.F-P44	Fr.H.3_O2	TU.A-P85
Almeida, M.	TU.J.1_O3	Amitsuka, H.
Th.O-P29	Álvarez-Quiceno, J.C.	MO.A.1_O4
Alnassar, M.	TH.A-P36	TH.B-P14
Mo.L-P45	Alvaro, A.	TU.A-P67
WE.F.1_O2	TU.F-P72	TU.B-P45
Alonso, J.	Alves, E.	TU.B-P48
Fr.B.1_O2	TU.A-P65	TU.B-P50
Fr.C.2_O4	Alves, M.J.P.	Ammar, S.
FR.H-P17	TH.I-P27	Mo.I-P12
MO.B.1_O3	Alves-Santos, O.	Mo.L-P50
Alonso, J.A.	Th.I.2_O6	TU.A.2_O3
Th.G.3_O3	Alzate Cardona, J.D.	TU.A-P42
Alonso, J.J.	TH.C-P22	TU.H-P36
TH.C-P4	Alzate, J.G.	Amorim, C.O.
Alonso, M.	Th.I.2_O1	FR.E-P40
Mo.H-P108	Amakai, Y.	TU.A-P65
TU.C.1_O5	Mo.A-P74	Amou, Y.
Alp, E.E.	TU.B-P46	TU.E.2_O4
TU.D.3_O4	TU.B-P56	Amusia, M.
Altbir, D.	Amaral, J.	FR.B-P2
FR.E-P38	FR.E-P39	Anadón Barcelona, A.
Th.E.3_O2	Mo.H-P90	Th.B.3_O2
Th.G.2_I1	Th.P-P28	Anadón, A.
TH.J-P6	Amaral, J.S.	Th.H-P5
Altenhof, A.	FR.E-P40	Th.H-P8
Fr.I.3_O4	TU.A-P65	Anahory, Y.

Mo.H-P81
Anand, V.K.
 FR.D-P83
Anane, A.
 MO.J.3_O3
 Th.H-P1
 Th.I-P13
 TU.I.1_O2
 WE.I.2_O3
Anders, A.G.
 Mo.L-P7
Andersen, B.M.
 TU.E.2_O3
Andersson, G.
 TU.G-P14
Andersson, M.
 WE.D.1_O4
Andersson, M.S.
 TU.F-P30
 TU.F-P52
Ando, K.
 FR.F-P9
 TH.E-P18
 Th.N-P2
 Th.N-P3
Ando, Y.
 FR.A-P6
 FR.H-P26
 Mo.D-P23
 Mo.D-P4
 MO.F.3_O1
 Mo.H-P78
 Th.F.1_O4
 Th.I.2_O3
 Th.O-P18
 TU.A-P66
 TU.F-P7
 TU.H-P106
 TU.H-P70
Andrade, A.M.H.
 Mo.H-P10
 Mo.H-P7
Andrade, B.
 TU.A-P41
 TU.A-P55

TU.A-P56
Andrade, L.
 Mo.L-P90
Andrade, V.
 Mo.K-P3
André, G.
 TU.B-P11
Andre, J.M.
 MO.E.1_O2
Andreev, A.
 Th.A.2_O1
 TH.C-P27
 TH.D-P11
 TH.D-P2
 TH.D-P3
 WE.C.2_O2
Andreev, N.
 TU.A-P57
 TU.E-P12
Andreica, D.
 FR.D-P7
 TU.C.2_O3
 TU.C-P2
Andrejka, F.
 TU.A.2_O5
 TU.H-P133
Andrieu, S.
 Th.I-P13
Angelakeris, M.
 Th.P-P11
 Th.P-P20
Angervo, I.
 Mo.H-P19
Angevaare, J.
 MO.SYM_2
Anikin, M.
 Mo.L-P72
Anil Kumar, P.S.
 FR.D-P34
Anisimov, M.
 TH.C-P77
 TH.C-P78
 TU.B-P59
Anisimov, V.
 FR.E-P14

Annaorazov, M.
 Mo.L-P92
Ano, G.
 TH.C-P126
Ansaldo, E.
 Mo.B-P6
 TU.B-P3
 TU.C-P2
Ansalone, P.
 Mo.J-P21
Ansermet, J.
 Fr.F.2_O2
Antal, I.
 Th.P-P22
 Th.P-P30
 Th.P-P37
 TU.F-P48
Antal, V.
 Mo.L-P19
Anthony, R.
 TU.H-P26
Antohe, V.A.
 Th.I.3_O4
Anton, E.M.
 FR.F-P31
 Mo.A-P91
Antonov, V.
 Fr.E.1_O2
Antos, R.
 TH.D-P18
 Th.G-P13
 TU.H-P85
Antoš, R.
 Mo.L-P20
 Th.M-P17
Antosiewicz, T.
 Th.M-P13
Antropov, V.
 Fr.D.3_O4
 TH.C-P87
Antunes De Oliveira, N.
 MO.D.2_O5
Anwar, M.S.
 Mo.A-P66
Anzulevich, A.

Th.O-P47
Th.P-P23
Aoki, D.
FR.D-P61
Mo.A-P59
Mo.A-P95
Mo.L-P64
TH.B-P19
TH.C-P47
TU.B-P35
TU.B-P39
TU.B-P43
TU.B-P48
TU.C-P25
TU.E-P20
TU.F.1_02
WE.F2_03
WE.F2_07
WE.H.2_11
Aoki, H.
TH.A-P13
TU.A-P7
TU.B-P52
TU.B-P77
Aoki, K.
TU.A-P52
Aoki, S.
TH.C-P99
Aoki, Y.
Mo.A-P89
TU.B-P58
TU.B-P8
TU.C-P19
Aoyagi, T.
TH.C-P104
Aoyama, K.
FR.D-P44
Apalkov, D.
Mo.F-P15
TH.J-P18
TU.I-P10
Aparecida da Silva, E.
TH.J-P16
Aplesnin, S.
FR.F-P1

Mo.D-P1
Mo.D-P6
TU.A-P4
Apolinário, A.
Mo.L-P90
Appel, P.
MO.E.2_03
Appino, C.
TU.H-P10
TU.H-P6
Aqeel, A.
Th.A.2_03
Aquino, R.
Mo.I-P13
Th.P-P32
TU.F-P114
Aragón Muriel, A.
TU.F-P27
Aragón, A.M.
TU.H-P98
Aragón, A.M.
Fr.A.1_04
Th.O-P3
Arai, H.
MO.H.2_05
Mo.J-P4
WE.D.2_02
Arai, M.
FR.D-P1
Arakawa, E.
TU.B-P46
Arakawa, Y.
Mo.A-P52
Araki, K.
Mo.A-P111
Mo.A-P40
TU.B-P27
TU.B-P57
Araki, S.
Mo.A-P46
TU.B-P37
WE.F2_03
Aramberri, H.
FR.A-P14
Aranda, A.

Th.M-P15
Arango, I.
TH.K-P8
Arantes, F.
TU.F-P110
Araújo, J.P.
Mo.K-P27
Mo.L-P47
Mo.L-P90
TU.A-P89
TU.E.2_05
Arauzo, A.
FR.D-P38
Aravena, D.
Mo.E-P6
Arbeláez Echeverri, O.D.
Th.M-P3
Arboleda, J.D.
Th.H-P11
Arcila Forero, J.F.
FR.A-P19
Arcon, D.
MO.I.1_05
Ardu, A.
TU.F-P67
TU.F-P68
Arenal, R.
Tu.B.2_02
TU.F-P57
Arenholz, E.
FR.F-P16
Arèon, D.
Tu.C.3_05
Ariando, .
FR.C-P9
TU.C-P34
Arima, T.H.
Mo.C-P19
TU.A.-59
TU.A-P22
TU.A-P60
TU.A-P61
TU.A-P7
Aristizábal, D.
TH.C-P20

Arita, R. Tu.A.3_05	Arumugam, T. TH.A-P39	Ashida, K. Mo.A-P86
Arnache, O. Th.H-P11	Arvan, B. WE.B.2_11	Asmat-Uceda, M. Fr.I.1_02
Arnache, O.L. Th.K-P24	Aryal, A. Mo.L-P3	Asokan, K. Mo.H-P23
Arnalds, U. Th.M-P18	Asa, M. Th.G-P9	Assmus, W. TU.A-P15
Arnau, A. MO.J.2_03	TU.G.3_05 WE.G2_05	Astefanoaei, I. Mo.J-P14
Arnaudás, J.I. Mo.H-P75 Mo.J-P9 Mo.K-P28 TH.D-P17	Asada, H. Mo.H-P92 Th.H-P7	Astretsov, A. Th.G.1_04
Arnold, F. FR.A-P24	Asadullin, F. Mo.G-P21	Astudillo Lagos, J.A. TU.A-P95
Arnold, Z. TH.C-P76	Asai, S. FR.D-P51	Aswartham, S. Mo.A-P20
Aroca, C. MO.E.1_03 TH.C.1_04	Asai, T. TH.A-P13	Athanassakis, I. Th.P-P20
Arora, S.K. FR.D-P47	Asali, A. TU.H-P107 TU.H-P108 TU.H-P110	Atitoaie, A. Mo.K-P30
Arras, R. FR.H-P5 Th.C.2_02 TU.C.1_04	Asano, H. Mo.H-P66 TU.A-P72 TU.E-P18	Atsushi, T. TH.F-P21
Arruda, L.M. MO.I.2_03	Asano, T. FR.D-P46 Mo.A-P89	Attané, J.P Fr.G.3_04 Mo.D-P27 Mo.D-P30 MO.F.1_05 MO.F.3_02 TH.E-P12 TH.E-P8 TU.G-P27
Arruebo, M. Th.P-P31	Th.A-P34 TU.C-P19	Atxitia, U. FR.F.2_05
Arsenijevic, S. TU.C-P31	Asato, M. Mo.J-P1 TU.E-P1	Audouard, A. Fr.A-P59
Arseyev, P. FR.B-P1	Aschauer, U. TU.A-P24	Auffret, S. Mo.H-P67 TH.F-P7 TU.J.1_11 TU.J.2_03
Arshad, M.S. MO.F.2_06	Aseguinolaza, I.R. Mo.L-P93	Augusto Tourinho, F. Mo.I-P13
Artacho, E. Mo.A-P56	Asenjo, A. Fr.E.2_03 Mo.I-P26 Mo.J-P8 Th.F.3_11 WE.F.1_04	Augusto, P.
Arteche, A. FR.H-P17 TH.K-P21		
Aruga Katori, H. TU.E-P16		

FR.I-P24
 TU.F-P72
 TU.F-P73
Auslender, M.
 Mo.C-P16
Avci, C.O.
 TH.E-P22
Avdeev, M.
 FR.D-P51
 Mo.A-P69
 TU.A-P23
Avelino Pasa, A.
 TU.F-P75
Avella, A.
 FR.B-P19
 Fr.E.2_O4
 Mo.A-P51
Avignon, M.
 TU.E-P23
Ávila Crisóstomo, C.E.
 Th.N-P9
Ávila Osses, J.I.
 Th.K-P42
Ávila, A.
 TH.K-P8
Ávila, M.
 Mo.A-P33
Ávila, M.A.
 TH.A-P36
 TH.C-P110
Avilés Félix, L.
 MO.C.1_O2
 TH.K-P3
Avram, A.M.
 Th.O-P44
Avram, M.
 Th.K-P32
 Th.O-P44
Avvakumov, I.
 Mo.A-P71
Avzuragova, V.
 TU.C-P25
Awad, A.
 MO.H.2_O4
Awana, V.

Mo.L-P94
 TU.E-P6
Awana, V.P.S.
 TU.G-P25
Awano, H.
 FR.A-P25
 TH.C.1_O2
 TH.F-P22
 TH.F-P25
Ayas, A.O.
 Mo.L-P69
Ayde, R.
 Th.O-P50
Azarevich, A.
 Mo.A-P85
Azevedo, A.
 Mo.H-P9
 Th.I.2_O6
 WE.G2_I1
Azevedo, G.M.
 Mo.I-P16
Azevedo, J.
 Mo.L-P90
Azevedo, R.B.
 Th.P-P1
Aziz, F.
 Mo.H-P23
 Mo.H-P24
Azpeitia, J.
 FR.I-P49
 TH.D-P22
Azuma, K.
 TU.H-P58
Azuma, M.
 Mo.A-P31

B

B. G., F.
 TU.H-P100
Baar, S.
 Mo.A-P74
Baaziz, W.
 Mo.I-P21

Babić, E.
 WE.A.2_O2
Babkevich, P.
 Mo.A-P55
 TH.C-P28
 TH.C-P41
 TH.C-P56
Babkin, R.
 Fr.C.3_O2
Baby K. B., A.
 TU.A-P58
Bachmann, J.
 FR.I-P28
Baciak, L.
 Th.P-P30
 Th.P-P37
Back, C.H.
 Fr.G.1_O3
 TH.J-P12
Backen, A.
 TU.H-P97
Backes, D.
 Th.C.2_O4
Backes, S.
 Fr.B.2_O2
Baczewski, L.T.
 Mo.H-P82
 Th.G.2_O4
Badelin, A.
 FR.F-P19
Badía-Romano, L.
 MO.I.2_O4
 Tu.F-P123
 WE.J.2_I1
Badica, P.
 TU.A-P32
Badini-Confalonieri, G.A.
 TH.F-P4
Badoi, A.
 TU.F-P108
Badoux, S.
 MO.A.2_I1
 MO.A.2_O3
Bae, J.S.
 Mo.D-P24

Mo.H-P25	Bai, W.	FR.F-P13
Bae, K.H.	MO.F.2_I1	Balbashov, A.
TU.H-P44	Baibich, M.N.	Mo.L-P87
TU.H-P47	TU.H-P135	Balbashov, A.M.
Bae, Y.J	Bailleul, M.	TU.A-P18
Mo.E-P10	Mo.G-P5	Balcells, L.
Mo.E-P12	Th.G.2_O3	MO.C.2_O2
Mo.H-P102	Th.I.3_O3	Mo.H-P108
Baek, S.H.	Th.I-P6	Mo.H-P54
Mo.A-P21	Bailly-Reyre, A.	Mo.H-P57
WE.A.1_O6	TH.C-P66	TU.A-P99
Baenitz, M.	Baines, C.	Balcerzak, T.
TH.J-P35	FR.D-P7	FR.D-P39
Bagani, K.	MO.A-P2	FR.D-P63
FR.H-P4	MO.D.3_O1	TH.C-P74
TH.C-P5	TU.C-P2	Baldi, L.
Baggio Filho, N.F.	Bajorek, A.	TH.F-P17
Th.O-P16	TU.H-P12	Baldrati, L.
Th.O-P56	Bak, Z.	Th.G-P9
Baggio Saitovitch, E.M.	Mo.A-P16	TU.G.3_O5
Mo.I-P1	Baker, A.A.	WE.G2_O5
Baggio, T.F.	MO.H.2_I1	Balédent, V.
Th.O-P16	Th.K-P24	TU.A-P6
Th.O-P56	Baker, S.	TU.B-P44
Baggio-Saitovitch, E.	Mo.I-P32	Balents, L.
Mo.I-P39	Baker, T.E.	TH.SP-1
Mo.I-P8	WE.J.2_O3	Balint, N.
TH.A-P36	Bal, T.	TU.I.3_O3
TU.F-P58	Th.P-P39	Baljozovic, M.
TU.G-P5	Balachandran, J.	FR.H-P34
Baghizadeh, A.	MO.B.1_O4	TU.D-P12
TU.A-P79	TU.F-P90	Balke, B.
Baglo, J.	WE.SYM_3	Fr.D.2_O2
MO.A.2_O2	Balakrishnan, G.	Balla, P.
Baguès, N.	FR.A-P10	TU.A-P25
Mo.H-P57	FR.A-P34	Ballav, N.
Bahadur, D.	FR.D-P54	FR.H-P34
WE.SYM_5	FR.D-P66	TU.D-P12
Bahamida, S.	TU.D.2_I1	Ballon, G.
Mo.I-P18	Balashov, T.	Mo.I-P13
Bahiana, M.	MO.J.2_O3	TU.C-P31
FR.E-P38	Th.I-P3	Ballou, G.
Th.G.2_I1	Balasubramanian, B.	Mo.C-P17
Bai, H.	TU.F-P76	Ballou, R.
Mo.A-P63	Balasubramanian, T.	TU.A-P43

TU.D.2_O3	Th.M-P7	FR.H-P25
Balogh, J.	Baraduc, C.	MO.J.2_O5
Mo.H-P83	TH.E-P3	Th.G.3_O4
Baltazar, S.	TU.H.1_O2	Th.K-P41
Fr.B.1_O5	TU.J.1_I1	Barman, R.
Baltic, R.	Baral, A.	Mo.I-P36
Fr.I.3_O3	Fr.J.2_O3	Barmin, Y.
Baltz, V.	Barandiaran, J.M.	FR.E-P22
Mo.F-P9	FR.SP-3	Barnas, J.
MO.G.2_O3	Mo.L-P41	Mo.C-P25
Mo.H-P67	Mo.L-P93	Th.O-P24
Mo.I-P4	Th.A.3_O1	Barnes, C.
TU.G.2_O4	TU.I.2_O3	MO.D.3_O2
TU.G.3_O2	Baranger, H.	Mo.H-P106
Balymov, K.	TU.C-P6	Mo.H-P95
Mo.I-P34	Baranov, N.	Mo.H-P96
Balz, C.	Mo.A-P12	Th.P-P5
Th.D.3_O1	Mo.L-P23	WE.B.2_O5
Balzer, K.	Mo.L-P83	Barnes, C.H.W.
Th.F.2_O4	TH.C-P12	Fr.B.1_O3
Banasik, M.	TH.C-P53	Barnsley, L.
Mo.H-P105	Barbara, B.	Fr.H.2_O5
Bandyopadhyay, B.	Mo.B-P13	Baró, M.
Mo.A-P88	Barbe, F.	FR.I-P46
TU.F-P47	MO.G.2_O3	MO.B.1_I1
Banerjee, K.	Barbieri, F.	Baró, M.D.
Mo.B-P23	Th.P-P39	TU.F-P87
Banerjee, S.	Barbosa, D.	Barone, P.
FR.H-P4	FR.I-P24	TU.A-P14
TH.C-P5	TU.F-P73	Baroudi, K.
Bang, D.	Barbosa, M.	TH.A-P9
TH.C.1_O2	TU.A-P89	Barral, M.A.
Banholzer, A.	Barcza, A.	TH.B-P10
TH.K-P17	Mo.L-P56	Th.M-P14
Banuazizi, S.A.H.	Bardin, I.	TU.G-P21
Mo.F-P25	FR.I-P6	Barrera, G.
Bao, J.	Bärenbold, O.	FR.I-P20
Th.C.3_O1	Th.M-P18	MO.C.2_I1
Bao, Z.	Barilo, S.	MO.F.2_O2
TU.G.2_O5	TU.A-P98	Mo.I-P18
Bapna, M.	Barišić, N.	TH.E3_O4
Fr.H.2_I1	MO.A.2_O3	Barreto, P.
Baptiste, B.	Barker, J.	Mo.I-P8
Mo.A-P31	TH.J-P30	Barrio, M.
Barabanenkov, Y.	Barla, A.	Th.B.1_O3

Barros, K.

FR.E-P36

Barrozo, P.

Mo.L-P21

Barsukov, I.

MO.H.2_O3

TU.G-P27

Barth, S.

Th.G.2_O2

Bartha, A.

TH.D-P4

Bartha, C.

TU.A-P32

Barthélémy, A.

MO.F.1_O5

Th.E.1_I1

TU.A-P100

TU.A-P91

Barthem, V.M.T.S.

MO.G.1_O5

Th.I.1_O5

Bartkowiak, M.

Fr.E.2_O5

FR.I-P7

Mo.A.1_O5

TU.A-P51

Bartnik, A.

Th.C.2_O5

TU.G-P28

Bartok, A.

Fr.F.3_O2

Mo.L-P26

Bartolomé, E.

Th.L-P5

Bartolomé, F.

MO.I.2_O4

TH.C-P124

TH.K-P4

Th.M-P1

Tu.F-P123

TU.F-P16

TU.J.1_O4

TU.J.3_O2

WE.J.2_I1

Bartolomé, J.

FR.D-P38

MO.I.2_O4

TH.C-P124

TH.K-P4

Th.M-P1

TU.F-P16

TU.J.1_O4

TU.J.3_O2

WE.J.2_I1

Barton, C.

Mo.H-P51

Barturen, M.

TU.G-P21

Barua, R.

Th.B.1_O4

Barucca, G.

Th.K-P38

Th.P-P12

TU.E.3_O3

TU.G.3_O1

Barzca, A.

Mo.L-P70

Mo.L-P79

Th.B.3_O1

Basaran, A.C.

MO.E.3_I1

Mo.I-P24

Tu.G.2_I1

TU.G.2_O2

Bascones, E.

Fr.J.1_O2

Bashir, A.

TH.C-P109

Bashir, M.

WE.J.1_O2

Basina, G.

TU.F-P100

Basini, M.

Th.N-P13

Basso, V.

Mo.L-P79

Mo.L-P85

Th.A.1_O5

Th.B.3_O1

Th.B.3_O3

Th.H-P17

TU.H-P121

Bastien, G.

WE.F2_O3

Basu, T.

FR.D-P17

TU.A-P19

Bataev, D.

Mo.L-P80

Bataille, A.M.

TU.B-P11

Bataronov, I.

FR.E-P22

Batdalov, A.

Mo.L-P74

Mo.L-P89

Th.B.1_O5

Batista, C.

Fr.A.1_O3

FR.E-P36

Batlle, X.

Fr.E.2_O3

MO.E.3_I1

Mo.H-P80

Mo.I-P24

Th.C.2_O3

Th.L-P3

Th.N-P5

TU.B.3_O3

Tu.F-P123

TU.F-P79

TU.F-P80

Tu.G.2_I1

Tu.H-P137

Batlogg, B.

MO.A.3_O4

Baudelet, F.

Th.C.3_O2

Bauer, A.

MO.H.3_O3

TH.C-P115

TH.C-P116

TH.C-P119

TH.J-P25

TH.J-P28

TH.J-P32	Becher, C.	Mo.C-P12
TU.B-P75	TU.A-P24	Th.J.2_O2
TU.C-P30	Becherer, M.	Beigné, C.
TU.H.3_O3	Th.O-P28	Fr.G.3_O4
WE.H.1_O3	TU.I-P13	Mo.D-P27
Bauer, E.	Becheri, F.	Mo.D-P30
Fr.A.1_O3	FR.I-P11	MO.F.3_O2
Fr.B.3_O1	Beck, F.	TH.E-P12
TU.B-P33	Mo.I-P20	TH.E-P8
TU.F.3_O1	Becker, C.	Th.O-P40
TU.H.2_O2	Th.B.2_O2	Bejhed, R.S.
TU.H.2_O5	Becker, J.	Th.H.1_O3
WE.H.2_O3	Fr.J.2_O4	Th.H.2_O5
Bauer, E.D.	TH.I-P22	Belaiche, M.
MO.A.1_O2	Becker, K.W.	Fr.F-P33
MO.A.2_O5	TU.B-P4	Belashchenko, K.
TU.B-P15	Bedanta, S.	Fr.D.3_O4
Bauer, G.	Mo.H-P41	TH.C-P87
FR.H-P2	TH.K-P11	TH.C-P88
Bauer, U.	Bedarev, V.	TH.D-P19
Th.G-P13	TH.C-P35	TU.E-P30
Baumbach, R.	Bednarchuk, O.	Belayachi, A.
MO.A.2_O5	TH.C-P52	TU.A-P8
TU.F.3_O1	Bednarcik, J.	Belik, A.
Bautin, V.	TH.B-P1	TU.A-P38
FR.I-P6	Bedoya-Pinto, A.	Belkacem, W.
Baykal, A.	Fr.I.3_O4	TU.F-P93
TU.H-P48	MO.J.2_I1	Bell, G.
TU.H-P49	TH.E-P9	TU.E-P48
Bazaliy, Y.B.	Beesetty, N.S.	Bellin, C.
Mo.F-P12	Mo.B-P7	TU.A-P76
Mo.F-P28	Bégin, D.	Belliveau, H.
Béa, H.	Mo.I-P21	MO.C.3_O1
Mo.F-P9	Begin-Colin, S.	Mo.H-P44
Beach, G.	Th.H.2_O3	Bellouz, R.
WE.I.1_I1	Bégin-Colin, S.	Mo.L-P4
Béard, J.	Mo.I-P21	Belmeguenai, M.
MO.A.2_O3	Th.M-P11	MO.H.1_O4
Beardsley, R.	Beginin, E.	TU.G-P17
Mo.G-P22	Mo.H-P21	Belo, J.H.
Th.G.2_O6	Beguivin, A.	Mo.L-P47
Beaud, P.	TU.J.2_O5	Belochapkine, S.
TU.E.1_O6	Behera, N.	TU.H-P74
Becca, F.	Mo.F-P14	Belotelov, V.
FR.E-P15	Behnia, K.	Th.N-P12

Th.N-P6	Benyoussef, A.	Mo.H-P88
Th.O-P31	Fr.F-P33	Th.M-P18
Th.O-P41	MO.A-P1	TU.I.3_O2
Th.O-P8	TH.C-P83	Bergmann, C.
Beltrán, J.I.	Bera, A.K.	TU.C-P9
Fr.G.2_I2	FR.D-P34	Bergqvist, L.
WE.G.1_O4	FR.D-P83	FR.E-P27
Belusso, R.	TH.A-P41	Mo.H-P88
Th.O-P16	TH.A-P42	TU.I.3_O2
Th.O-P56	Beran, L.	Bergström, L.
Belyaev, B.	Mo.H-P78	TU.F-P87
Mo.H-P93	Mo.H-P8	Berini, B.
Belyaev, V.	Mo.L-P20	FR.A-P54
Th.N-P16	Th.G-P13	Berkov, D.
Ben Dor, O.	Th.M-P17	Fr.A.2_O3
Th.I.2_O2	TU.A.1_O5	Mo.F-P1
BEN GHZAIEL, T.	Berbezier, I.	TU.H-P3
TU.H-P130	Th.O-P40	Berkowski, M.
BENASSAYAG, G.	Berganza, E.	TH.D-P12
Mo.H-P18	Th.F.3_I1	Bernal-Villamil, I.
Bencok, P.	WE.F.1_O4	TU.E-P22
Th.J.1_O3	Bergeal, N.	Bernand-Mantel, A.
Bendele, M.	Mo.A-P58	MO.G.1_O5
Mo.A-P8	MO.C.1_O2	Mo.I-P28
Bender, P.	Bergeard, N.	Bernard, M.
TU.F-P102	Th.F.2_I1	Th.I-P5
Benedict, L.	Bergenti, I.	Bernard, R.
Fr.D.3_O4	FR.H-P30	MO.C.1_O2
Benedikt, E.	Mo.H-P94	MO.J.3_O3
TH.J-P21	Berger, A.	WE.I.2_O3
Benfatto, L.	MO.C.3_O1	Bernard-Carlsson, L.
WE.A.2_O3	Th.I.3_O4	Mo.L-P86
Benka, G.	Th.M-P4	Bernhard, B.H.
TH.C-P115	Th.M-P5	TU.B-P65
TH.C-P119	Berger, H.	Bernhard, C.
WE.D.1_O2	FR.D-P42	Fr.B.2_O1
Bennati, C.	MO.G.3_O3	Bernien, M.
Mo.L-P79	MO.H.3_O3	MO.I.2_O3
Th.A.1_O5	TH.A-P17	Beron, F.
Th.B.3_O3	Tu.C.3_O5	Th.E.3_O2
TH.J-P24	Bergeret, F.S.	Th.M-P10
bensaad, S.	TH.E-P9	Béron, F.
FR.I-P13	WE.A.2_O1	Th.K-P37
Benton, O.J.	Bergman, A.	TU.D-P15
Th.D.2_O3	FR.E-P27	Bersweiler, M.

TU.G.3_03	Fr.F.3_02	Bialek, B.
TU.G-P1	Mo.L-P26	FR.H-P22
TU.I.3_01	Mo.L-P63	TU.E-P24
Bert, F.	Bessonov, V.	Bianchi, A.D.
FR.D-P78	Mo.G-P16	MO.D.3_01
TH.A-P38	Beuran, M.	Bianchi, L.
TU.C.2_03	TU.F-P5	FR.I-P21
TU.D.1_04	Beutier, G.	Bibes, M.
Bertacco, R.	TH.J-P15	MO.F.1_05
Th.G.3_04	Bewley, R.	Th.E.1_11
Th.G-P9	TH.A-P5	TU.A-P100
Th.H.1_04	Beyer, R.	TU.A-P91
Th.H.2_04	FR.D-P27	Biborski, A.
TU.G.3_05	Bezergheanu, A.	FR.C-P7
TU.I.1_04	Mo.L-P62	Biegger, F.
WE.G2_05	TU.F-P93	Th.G.2_02
Bertaina, S.	Bezmaternykh, L.	Bieñkowski, A.
Mo.B-P13	TH.C-P107	TU.H-P104
TU.A-P75	TH.C-P35	TU.H-P59
Berthier, C.	TU.A-P11	Bierdel, M.
MO.I.1_03	TU.A-P87	Mo.L-P48
TH.A-P10	TU.H-P31	Bierlich, S.
TH.A-P20	Bhardwaj, R.	TH.C-P57
Berti, G.	TU.F-P99	Th.O-P26
FR.H-P31	Bharuth-Ram, K.	Biernacka, M.
Mo.H-P85	TH.C-P50	TU.E-P41
Bertinshaw, J.	TU.G.1_05	Biffin, A.
TU.A-P23	Bhat, M.A.	MO.SYM_5
Bertoli, S.	Mo.F-P7	Bigot, J.Y.
Th.G-P9	Bhat, S.V.	Th.F.1_02
TU.G.3_05	TU.F-P89	Bihlmayer, G.
WE.G2_05	Bhatia, P.	Mo.C-P23
Bertoni, G.	Th.O-P45	Bill, A.
TU.F-P95	Bhatia, P.G.	WE.J.2_03
Bertotti, G.	TU.H-P105	Billette, J.
Mo.J-P19	Bhatnagar, D.	Th.D.3_04
Mo.J-P20	TU.H-P103	Billinge, S.
Mo.J-P21	Bhattacharyya, A.	Th.J.1_02
Th.I-P18	WE.H.2_05	Biner, D.
Bertran, F.	Bhoi, D.	Mo.B-P15
WE.G.1_05	Th.A.1_03	Bingham, N.
Berzhansky, V.N.	Bi, L.	Mo.H-P37
Th.N-P7	TH.D-P18	Binns, C.
Th.N-P8	Biagioni, P.	Mo.I-P32
Bessais, L.	Mo.D-P30	Th.P-P19

Bird, M.	Fr.B.1_O4	TU.SYM_5
Fr.E.2_O5	TU.F-P59	Blum, C.G.F.
Birèáková, Z.	WE.C.2_O4	Mo.A-P20
TU.H-P45	Blanco-Andujar, C.	Blumberg, G.
Birk, J.O.	Th.H.2_O3	TU.F.3_O1
FR.I-P7	Th.P-P7	Blume, J.
Birlikseven, C.	Blanco-Roldán, C.	FR.I-P4
Th.O-P23	Fr.H.3_O2	Blythe, H.
Biro, L.P.	Mo.H-P98	TU.A-P57
MO.I.1_I1	TH.H.3_O2	TU.G.1_O4
Birringer, R.	Blasco, J.	Blythe, H.J.
Th.L-P2	MO.C.3_O3	FR.F-P12
Birster, K.	Th.A.1_O1	Bobak, A.
Th.L-P2	TH.C-P21	FR.D-P36
Bisero, D.	TU.A-P10	FR.D-P39
Th.M-P9	TU.A-P13	Bobba, F.
Bisig, A.	TU.A-P24	Mo.A-P35
Fr.I.1_I1	TU.A-P26	BOBO, J.F.
Bisogni, V.	TU.A-P9	Mo.H-P18
Fr.B.2_O3	TU.E.1_O2	Bobrysheva, N.
Biswas, A.	Blázquez, J.	FR.F-P28
Fr.H.1_O4	MO.D.2_O3	Bochmann, S.
Th.B.1_I1	Mo.L-P14	FR.I-P28
Biswas, D.	Th.B.1_I1	Bocklage, L.
TH.B-P16	TU.A.2_O5	FR.I-P19
Biswas, P.	Bleif, H.J.	TU.C.1_O2
Mo.A-P100	Fr.E.2_O5	TU.I.1_O5
Biswas, P.K.	Blinder, R.	WE.E.1_O3
FR.A-P34	TH.A-P20	Bode, M.
TU.A-P53	Blinov, I.V.	TH.I.1_I1
Bitla, Y.	Mo.H-P35	Boehm, M.
TU.E-P8	Blinov, M.	MO.E.2_O2
Bittar, E.M.	Mo.L-P3	TU.B-P23
TH.A-P36	TH.C-P40	Boehnke, A.
Bittner, F.	Blomgren, J.	WE.I.2_O5
Mo.L-P57	Th.P-P2	Boeije, M.
Biziere, N.	TU.B.3_O2	Mo.L-P16
FR.I-P43	Blon, T.	Boeni, P.
Mo.H-P18	Fr.E.1_I1	Fr.I.1_O3
We.F.1_O3	Fr.E.3_O4	Boero, G.
Blaas-Schenner, C.	Th.G.2_O3	TH.C-P41
Fr.B.3_O1	Th.I.3_O3	Bogach, A.
Blanchard, P.	Th.I-P6	Th.A-P40
Th.O-P25	Blügel, S.	TH.C-P77
Blanco, J.A.	MO.F.3_O2	TH.C-P78

TU.B-P32	Bonanni, V.	Fr.E.3_04
TU.B-P59	Th.N-P14	Bonn, D.
Bogart, L.	Th.N-P15	MO.A.2_11
Th.P-P2	TU.B.2_04	MO.A.2_02
Bogart, L.K.	TU.E.3_02	TU.A.3_01
Th.P-P7	Bonastre, J.	Bonnilla, F.
Bohm, M.	FR.I-P37	Fr.E.1_11
Mo.B-P15	TU.H-P99	Bono, D.
Bohmer, A.E.	Bondarev, A.	TH.F-P1
Tu.A.3_05	FR.E-P22	Bonville, P.
Bohn, F.	Bondino, F.	FR.D-P66
Mo.H-P10	FR.H-P25	TH.A-P39
Mo.H-P7	Th.G.3_04	TU.C.2_03
Mo.H-P9	Bondioli, F.	Boothroyd, A.
TH.F-P20	TH.E3_04	FR.A-P30
TH.I-P27	Bonell, F.	FR.A-P42
Böhnert, T.	Th.G-P5	Th.A.2_06
Th.H-P16	WE.G2_16	Th.G.3_02
WE.I.2_11	Bonetti, M.	WE.A1_01
Bolaños, A.	Th.B.1_02	Borchard, G.
TU.F-P27	Bonfa, P.	Th.P-P4
Bolaños, G.	TH.C-P80	Borchers, J.
TU.A-P95	Bonfà, P.	TU.E.1_04
Boldyrev, K.	Mo.A-P102	Bordet, P.
TH.C-P107	Mo.A-P103	TU.A-P76
TU.A-P87	Mo.A-P37	Bordignon, S.
Boldyrev, K.N.	Bonfiglioli, E.	Mo.A-P103
Fr.C.3_02	Mo.H-P3	TU.D-P7
Bolginov, V.	Mo.I-P38	Bordonali, L.
FR.D-P25	Mo.I-P40	TU.D-P7
Bollani, M.	TU.G.3_01	Borisov, A.
Mo.D-P30	Böni, P.	FR.B-P33
Bollero, A.	Mo.H-P100	Borme, J.
Fr.A.1_04	Mo.H-P12	Mo.F-P21
MO.D.1_02	Mo.H-P56	TU.H.1_05
Mo.H-P99	Mo.H-P70	TU.I.1_03
Mo.I-P15	TH.C-P116	Born, N.O.
Mo.I-P37	TH.C-P119	WE.D.1_05
TH.I-P28	TH.C-P97	Boroica, L.
Th.K-P44	TU.C-P30	Th.O-P19
TU.G.2_04	TU.H.3_03	Borovkova, O.
TU.I.3_03	WE.H.1_03	Th.N-P12
Bombardi, A.	Bonilla, C.M.	Th.N-P6
Th.E.1_03	TH.C-P124	Borovsky, M.
TU.E.1_01	Bonilla, F.	FR.D-P39

FR.D-P74	WE.H.1_05	FR.H-P31
Borrisé, X.	WE.I.1_02	Mo.H-P85
Mo.I-P24	Boulon, M.E.	Bramwell, S.
Th.N-P5	MO.I.2_11	Fr.D.1_11
Borrmann, H.	Bourassa, A.	Bran, C.
TU.B-P36	Mo.F-P27	Mo.J-P8
Borsa, F.	Bourdarot, F.	Th.M-P10
TU.D-P7	Th.D.3_04	TU.G-P15
Bortolotti, P.	Bourges, P.	WE.B.2_11
FR.A-P51	Th.E.2_11	WE.F.1_04
MO.J.3_03	Bousseksou, A.	Bran, J.
TH.J-P13	MO.J.2_04	Th.G-P19
TH.J-P14	Bouzehouane, K.	Brandl, G.
TU.H.1_04	MO.H.3_02	TH.C-P116
TU.I.1_02	WE.I.1_03	TH.C-P97
Borys, P.	Bowe, S.	Brando, M.
Mo.H-P31	Mo.G-P22	WE.H.2_04
Borza, F.	Th.G.2_06	Branford, W.
TU.H-P117	Bowman, R.	MO.F.2_04
Boscher, J.E.	WE.J.1_02	Th.M-P12
Mo.G-P15	Bozhko, D.A.	WE.B.2_04
Boschini, F.	Mo.G-P13	Brataas, A.
FR.H-P31	MO.H.2_02	TU.SYM_4
Bosch-Santos, B.	TU.E.3_11	Bratko, M.
TH.D-P10	Bozzo, B.	FR.I-P40
Boseggia, S.	MO.C.2_02	Mo.L-P70
Th.G.3_02	Mo.H-P54	Mo.L-P79
Bossini, D.	Mo.H-P57	Braun, H.B.
MO.J.3_01	Th.A.1_01	Mo.J-P22
Bossoni, L.	TU.A-P93	Braun, J.
Mo.A-P103	Bracanovic, D.	Fr.D.2_02
Bottegoni, F.	MO.E.2_05	Brázda, P.
Mo.D-P30	Brächer, T.	TH.C-P34
Böttger, R.	MO.H.2_02	Bréard, Y.
Mo.H-P82	Braecher, T.	TU.H-P78
Bouard, C.	Th.O-P37	Brechet, S.
TH.J-P23	Brahlek, M.	Fr.F.2_02
Bouhassoune, M.	Mo.B-P23	Breitkreutz-v. Gamm, S.
Fr.I.3_02	Braithwaite, D.	Th.O-P28
Bouillot, P.	TH.C-P47	TU.I-P13
TH.A-P5	TU.B-P44	Brenac, A.
Boulle, O.	TU.B-P70	Th.O-P40
TH.F-P7	TU.C-P25	Brenig, W.
TU.I-P15	TU.F.1_02	TH.A-P37
TU.J.1_02	Brambilla, A.	Brewer, J.

FR.D-P8	Brubach, J.	Buchanan, K.
Mo.B-P6	TU.A-P43	Fr.I.1_O2
TU.B-P3	Brucas, R.	Buchelnikov, V.
TU.C-P2	Th.H.1_O3	FR.E-P20
Brey, L.	Bruck, E.	Mo.L-P75
WE.G.1_O4	TU.F-P38	Mo.L-P77
Breznay, N.	Brück, E.	Mo.L-P80
MO.SYM_5	MO.D.2_O2	Th.O-P47
Brianèin, J.	Mo.L-P16	Buchepalli, V.
TU.A-P82	Bruck, E.H.	TU.E-P32
TU.C-P12	MO.D.2_O4	Büchner, B.
Briatico, J.	TU.F-P37	Fr.B.2_O6
MO.C.1_O2	Brückel, T.	FR.D-P12
Briceño, S.	FR.I-P47	FR.I-P41
TU.F-P2	Mo.H-P41	Mo.A-P103
Bridges, G.	Brückner, F.	Mo.A-P20
TH.J-P33	Mo.A-P100	Mo.A-P22
Bridoux, G.	Brückner, F.	Mo.B-P7
WE.I.2_I2	FR.D-P56	MO.E.2_O1
Brinis, D.	Brueckel, T.	TH.A-P27
TU.F-P23	Fr.D-P87	TH.A-P9
Brinkman, A.	Bruin, J.	Th.D.3_O2
MO.SYM_2	Fr.D.2_O4	TU.E-P6
Brintakis, K.	FR.D-P32	Buchter, A.
Th.P-P20	Brukhardt, U.	MO.E.2_O1
TU.F-P21	Mo.B-P9	Buda-Prejbeanu, L.
Britz, D.	Brune, H.	Mo.F-P24
TH.C-P109	Fr.I.3_O3	TU.J.1_O2
Broholm, C.	Brunner, B.	WE.H.1_O5
Th.D.2_I1	Mo.A-P36	WE.I.1_O2
Brombacher, C.	Bruno, F.Y.	Buechner, B.
TU.J.1_O5	WE.G.1_O4	Mo.A-P21
Brookes, N.	Brunt, D.	Mo.A-P98
FR.I-P23	FR.D-P54	MO.E.1_O5
TU.B-P5	Bryan, M.	WE.A.1_O6
TU.J.1_O4	Fr.G.1_O4	Bugoslavsky, Y.V.
Brooks, C.	TH.J-P3	FR.I-P40
TU.E.1_O4	Bryson, J.F.J.	Buhot, J.
Brooks, J.	Fr.E.2_O2	TH.B-P19
Tu.A.3_O5	Brzezicki, W.	WE.F2_O7
Brooks, J.S.	TH.A-P8	Buijnsters, F.
Th.G.3_O1	Brzózka, K.	Mo.G-P19
Brown, P.	FR.H-P3	Mo.G-P27
FR.A-P43	Bucci, F.	TH.F-P8
Mo.A-P110	Mo.A-P50	Bukalis, G.

FR.F-P16
Bukin, N.
 TH.J-P15
Bulai, G.
 TH.K-P14
 Th.K-P34
 TU.F-P42
Bułka, B.
 Mo.D-P9
Bumbach, R.E.
 Fr.H.1_02
Bunau, O.
 TU.J.3_02
Bünemann, J.
 WE.E2_05
Bunyaev, S.
 Mo.H-P43
Buragohain, P.
 TU.G-P23
Burdin, D.
 TH.C.1_03
Burdin, S.
 TH.B-P19
 Th.D.2_02
Burdusel, M.
 TU.A-P32
Bureš, R.
 TU.H-P41
 TU.H-P45
Bürgler, D.E.
 WE.J.2_11
Burgos, S.
 WE.D.2_16
Burgos-Parra, E.
 TH.J-P15
Burkhanov, G.
 Mo.L-P49
Burkhardt, U.
 TU.B-P36
Burn, D.
 MO.F.2_04
 Th.M-P12
 WE.B.2_04
Burriel, R.
 Th.B.3_04

Bursik, J.
 Fr.B.3_01
 TU.F-P20
Bury, P.
 TU.F-P29
 TU.F-P91
Burzuri, E.
 Mo.E-P4
Bushinsky, M.
 TH.C-P69
Bussetti, G.
 Mo.H-P85
Bussmann-Holder, A.
 WE.C.1_02
Bustos, H.
 TU.H-P37
Butch, N.
 TU.B-P21
 TU.B-P22
 TU.D.2_02
Butera, A.
 FR.I-P21
Butko, L.
 Th.O-P47
 Th.P-P23
Butkovièová, D.
 TU.G.1_03
Büttner, F.
 Fr.I.1_11
Butzke, C.
 TU.C-P4
Buzzi, M.
 FR.H-P34
Bychkov, I.
 Mo.L-P8
 TH.C-P111
 TH.C-P112
 Th.O-P47
 TU.A-P92
Byczuk, K.
 TH.B-P6
Bydzovsky, J.
 Th.O-P23
Bykova, I.
 TH.J-P12

Byun, J.Y.
 TU.H-P88

C

C. Aragonez, A.
 Mo.E-P6
C. Jiles, D.
 Mo.H-P107
C. Lourenço, A.
 TU.H-P116
C. Onbasli, M.
 TU.A.1_05
Cabanas Plana, A.M.
 TH.K-P20
Cabanas, A.
 Mo.F-P16
Cabreira Gomes, R.
 Th.P-P32
Cabrera Baez, M.
 Mo.C-P5
Cabrera, D.
 TH.I-P28
 TU.F-P106
Cabrera-Baez, M.
 TH.A-P36
Cabrera-Pasca, G.
 TH.D-P10
 TU.F-P45
Caceres, P.R.
 Th.P-P1
Caciuffo, R.
 TH.A-P21
 TH.D-P15
 TH.D-P25
 TU.G.2_05
Cadogan, S.
 Mo.L-P31
Cagnon, L.
 FR.I-P28
 Mo.K-P26

Cai, H.	Mo.I-P37	Caneira Gomes, R.
Mo.D-P10	TH.I-P28	Th.B.1_O2
Cakir, Ö.	Th.K-P44	Caneiro, A.
TH.C-P82	TU.A-P91	Mo.B-P8
Cakmakoglu, Y.I.	TU.G.2_O4	Caneschi, A.
TU.H-P25	TU.I.3_O3	MO.I.2_I1
Çakýr, A.	Cameron, A.	Th.N-P14
WE.D.1_O3	MO.D.3_O3	Th.N-P15
Calatayud, M.P.	Caminale, M.	TU.B.2_O4
WE.SYM_1	Mo.A-P19	Canevet, E.
Calbucci, M.	Campanini, M.	MO.I.1_O3
Mo.H-P94	MO.C.2_I1	Th.D.1_O2
Caldas, A.	Campbell, S.	Canfield, P.
Mo.L-P5	Mo.L-P31	FR.I-P4
Caldas, H.	Campillo, G.E.	MO.A.2_O5
FR.B-P25	Th.K-P24	Cannas, C.
Mo.A-P14	Campion, R.	TU.F-P67
Mo.A-P49	Fr.G.3_O2	TU.F-P68
Calderón Piñar, F.	MO.C.1_O5	Cano, A.
TU.A-P42	MO.F.1_O3	TU.A-P43
Calderon, M.J.	Campmany, J.	Cantoni, M.
WE.G.1_O4	FR.I-P11	Th.G-P9
Caldonazo, T.	FR.I-P12	TU.G.3_O5
TU.F-P26	Campo, G.	WE.G2_O5
Calegari, E.	Th.N-P14	Cao, C.
Mo.A-P76	Th.N-P15	Mo.A-P75
TU.B-P41	TU.B.2_O4	Cao, G.
Calegari, E.J.	TU.E.3_O2	Mo.A-P75
TH.A-P15	Campo, J.	Th.C.3_O1
Calloni, A.	TH.C-P106	Cao, S.
FR.H-P31	TU.C.2_O4	TH.C-P25
Mo.H-P85	Campos, A.	TH.C-P91
Calmels, L.	Mo.K-P3	Caplin, A.
FR.H-P5	Campos, C.L.A.V.	Mo.L-P70
Caltun, O.F.	Mo.K-P2	Caplin, D.
TH.K-P14	Campos, E.	FR.I-P40
Th.K-P34	WE.SYM_1	Mo.L-P79
Camara, I.	Can, H.	Caporaso, M.
Th.G.2_O3	Th.O-P23	MO.F.2_O2
Th.I.3_O3	Canals, B.	Capozzi, A.
Th.I-P5	Fr.D.1_O3	Th.N-P13
Th.I-P6	FR.D-P21	Caprile, A.
Camarero, J.	MO.I.1_O3	Fr.E.2_O4
MO.D.1_O2	Canaparo, R.	TH.J-P24
Mo.H-P99	MO.F.2_O2	Capua, A.

Th.I-P16	Carretta, P.	MO.J.2_I1
Caputo, M.	FR.D-P12	TH.E-P9
Mo.F-P33	Mo.A-P102	Th.I.2_O4
Caranivi, P.	Mo.A-P103	Casiraghi, A.
Mo.F-P16	Carrey, J.	Mo.H-P76
Carara, M.	MO.J.2_O4	TU.A-P77
Mo.H-P9	Th.H.1_O2	Caslin, K.
Mo.I-P17	Carrillo Flores, D.M.	Mo.B-P25
Mo.I-P20	FR.H-P35	WE.C.1_O2
Carbonari, A.	Carter Gartside, J.	Casola, F.
TH.D-P10	Th.K-P25	Mo.G-P28
TU.F-P45	Carugo, D.	Casoli, F.
Carcia-Martin, A.	Fr.H.2_O5	MO.C.2_I1
Th.N-P10	Caruso, L.	TU.G-P10
Cardoso, F.	Th.P-P39	TU.G-P16
FR.I-P42	Carva, K.	TU.J.2_O4
Cardoso, S.	Mo.D-P12	Castán-Guerrero, C.
FR.I-P42	Carvajal Quiroz, E.	TH.K-P4
Mo.H-P43	Mo.H-P49	Th.M-P1
Th.K-P46	Carvajal, E.	Castañeda Guzman, R.
Th.O-P54	Mo.A-P25	Mo.H-P48
Th.P-P28	Carvalho, A.	Castelnovo, C.
TU.I.1_O3	Mo.L-P32	Fr.D.1_O4
Carenza, E.	Mo.L-P5	Castelo-Grande, T.
Th.P-P4	Carvalho, M.D.	FR.I-P24
Carlotti, G.	Mo.H-P101	TU.F-P72
Mo.F-P20	Carvalho-Santos, V.	TU.F-P73
Mo.G-P23	Mo.B-P31	Castillejo, M.
MO.SP-2	TH.J-P6	TU.I.3_O3
TU.I-P4	Carvalho, C.	Castillo-Sepúlveda, S.
Carminati, R.	MO.B.1_I1	FR.E-P38
Th.G.1_I1	Casa, D.	Castle, E.
Caro Patiño, J.	WE.F2_O5	Mo.L-P29
MO.D.2_O5	Casagrande Denardin, J.	Castro Merino, I.L.
Caroca-Canales, N.	Mo.K-P21	Mo.I-P1
TU.B-P13	TU.H-P68	Castro, G.R.
Caron, L.	Casallas-Moreno, Y.	WE.J.2_I1
MO.D.2_O2	FR.H-P24	Castro, M.
MO.D.2_O4	Casals, B.	TU.A-P95
Carpene, E.	FR.I-P22	Casula, M.
FR.H-P31	MO.C.3_O4	Th.C.3_O2
Carpenter, M.A.	Th.G-P15	Catalin Galca, A.
WE.D.1_O5	Casanova, F.	Mo.H-P15
Carreras, S.	Fr.I.3_O4	Cattoni, A.
Mo.H-P13	MO.F.3_O3	Th.H.1_O4

Causa, M.T. TH.C-P81	FR.I-P16	Chae, K.H. TU.A-P15
Cava, R. FR.D-P56 TH.A-P9	Cencarikova, H. FR.D-P13	Chaix, L. TU.A-P43
Cavalcanti, P. TU.F-P1	Cerda, J.I. Mo.E-P6	Chajec, W. TH.C-P96
Cavallin, A. FR.A-P7	Cerdá, J.I. FR.A-P14	Chajewski, G. Mo.A-P107 TU.B-P74
Cavill, S. Mo.G-P22 Th.G.2_O6	Cerdán Ramírez, V. Th.N-P9	Chalker, J. Fr.F.1_O4
Cayado, P. Th.L-P5	Cermak, P. Mo.A-P32 TU.B-P75 TU.C-P33	Chaloupka, J. FR.D-P77
Cazayous, M. TH.B-P19 Th.E.1_I1 WE.F2_O7	Čermák, P. TU.B-P72	Chan, J. FR.F-P31
Ceballos, G. MO.J.2_O3	Cerullo, G. MO.J.3_O1	Chan, M. MO.A.2_O3
Cebollada, F. Mo.H-P108 TU.C.1_O5	Cervera, S. Mo.L-P86	Chan, Y. TH.C-P108
Cecchini, R. FR.H-P30	Cesari, E. Mo.L-P24	Chandra, M. Mo.H-P23 Mo.H-P24
Ceci, P. Fr.H.2_O2	Cespedes, E. Th.P-P9	Chandra, S. FR.B-P5 Th.B.1_I1 TH.C-P2
Cedervall, J. TU.H-P111 WE.D.1_O4	Cezar, J.C. Fr.A.1_O3	Chandra, V.R. FR.D-P68
Cejpek, P. Mo.H-P8 Mo.L-P20 Th.N-P11	Cha, H.R. TU.H-P112	Chandrasekhar, K.D. FR.D-P42
Celebrano, M. Mo.D-P30	Cha, J. TU.A-P78	Chang, C. FR.I-P8
Celegato, F. FR.I-P20 MO.F.2_O2 Mo.I-P18 TU.G-P16	Chabaat, M. FR.I-P13	Chang, C.L. Th.I-P7
Celgato, F. MO.C.2_I1	Chaboy, J. TU.B-P34	Chang, F. TU.A-P23
Celik, U. FR.I-P15	Chacon, A. Mo.H-P70 TH.J-P32	Chang, H. FR.A-P56 Fr.C.2_O2 MO.H.2_O3
	Chacón, A. TH.J-P25	Chang, J. Mo.A-P72 Mo.D-P16 Mo.D-P18 Mo.D-P24
	Chadha, M. MO.F.2_O4 Th.M-P12 WE.B.2_O4	
	Chadov, S. Fr.D.2_O2 Th.N-P11	

Mo.D-P26 Th.G.3_O1 Chang, K.	TU.A-P6 Chaudhary, S.	Fr.C.2_O4 Fr.G.2_I1 Chen, C.
MO.H.3_O4 Chang, K.C.	Mo.F-P14 Mo.H-P91 TU.E-P42 TU.F-P11 Chaudret, B.	TU.H-P69 Chen, C.C.
WE.D.2_I1 Chang, L.J.	MO.B.3_O3 Th.I.3_O3 Chavarria-Rubio, J.	TU.F-P88 Chen, C.T.
TH.F-P29 TH.J-P29 Chang, S.	TH.C-P128 Chaves, C.M.	TU.E-P8 Chen, J.
MO.I.1_O2 Chang, Y.	FR.B-P9 FR.E-P16 Mo.A-P76 TH.A-P15 Chaves, S.B.	Mo.A-P70 Mo.L-P35 TU.B-P67 WE.F.2_I1 Chen, J.M.
Mo.A-P13 Chang, Y.M.	Th.P-P1 Che, L.	Mo.L-P35 TU.A-P21 Chen, J.W.
TH.C-P108 TU.A-P44 Chang, Y.Y.	Mo.A-P27 Chebotaev, N.	TU.F-P66 Chen, K.
Mo.A-P13 Chanlert, P.	Mo.L-P67 Chebotkevich, L.	TU.G.2_O3 Chen, L.
FR.D-P50 Chantrell, R.	TH.J-P34 Chechenin, N.	FR.H-P13 Th.E.2_O5 Chen, P.
FR.F.2_O5 Fr.J.2_I2 Mo.J-P16 TU.G-P18 Chaplier, G.	Mo.I-P27 Chêciński, J.	Mo.H-P39 Chen, P.J.
TU.H-P102 Chapon, L.	Th.O-P24 Cheglakov, G.	Mo.H-P39 Chen, Q.
Mo.C-P17 Tu.C.3_O5 TU.D.2_O3 TU.E.1_O1 Chareev, D.	Mo.H-P106 Chegonda, M.	TU.C-P29 Chen, S.
Mo.A-P101 Chashin, D.	TU.H-P75 Cheikhrouhou Koubaa, W.	Th.G-P16 Chen, S.A.C.
TH.C.1_O3 Chatterjee, B.	Mo.L-P50 Chekanova, L.	TU.A-P21 Chen, S.C.
TH.B-P6 Chatterjee, R.	Mo.H-P38 Chełkowska, G.	Mo.H-P6 TU.G-P3 TU.G-P8 Chen, S.T.
FR.A-P46 TU.A-P80 TU.H-P103 Chatterjee, S.	TU.H-P12 Chen, A.	TU.G-P3 Chen, T.Y.
Mo.L-P18 Chattopadhyay, S.	FR.H-P13 MO.C.2_I4 Th.G-P6 WE.G2_O4 Chen, B.	FR.D-P42 Chen, X.
	Fr.B.2_O4 Chen, Y.	Mo.A-P109 Mo.A-P112 Chen, Y.

Mo.A-P27	Fr.G.1_04	FR.E-P27
MO.H.2_03	Chesman, C.	Mo.H-P88
MO.SYM_4	Mo.H-P9	Th.M-P18
Th.G-P1	Cheung, S.	Chien, C.L.
TU.B-P67	Fr.B.2_04	PLENARY2
TU.F-P33	Fr.C.2_04	Chien, N.
TU.H.2_02	Fr.G.2_11	TU.E-P8
Chen, Y.C.	Fr.I.1_03	Chiesi, V.
TU.H-P29	Chiang, C.	Mo.C.2_11
TU.H-P35	TU.A-P54	Chikina, A.
Chen, Y.Q.	Chiang, C.W.	TU.B-P30
Mo.A-P4	TU.A-P54	Chikoïdze, E.
Chen, Z.	Chiang, J.C.	Mo.C.3_05
Th.E.2_05	Mo.B-P9	Chikov, A.
TU.B-P67	Chiari, M.	Mo.A-P71
Cheng, Y.	Th.H.2_04	Childress, L.
Th.P-P3	Chiba, D.	Mo.F-P27
Cheng, Z.	FR.H-P10	Chin, T.S.
TH.C-P91	Mo.H-P16	FR.I-P8
Cheong, E.	TH.C.1_02	Chin, Y.
Th.P-P35	Th.G-P10	TU.E-P8
Cheong, J.	Th.G-P14	Chinni, F.
FR.A-P2	Th.G-P3	Mo.I-P38
Cheong, S.W.	Th.G-P8	Mo.I-P40
Th.E.2_11	Chiba, T.	TU.G.3_01
TU.E.1_01	Mo.J.3_04	Chioar, I.A.
Cherifi, L.	Chichay, K.	Fr.D.1_03
FR.I-P14	Th.O-P57	FR.D-P21
Cherifi, R.O.	TU.A-P94	Chiou, J.Y.
TU.A-P100	TU.H-P125	TU.G-P3
Chern, G.	TU.H-P129	TU.G-P8
FR.E-P36	Chichkov, V.	Chiriac, H.
FR.H-P16	TU.A-P57	Mo.K-P30
TU.D.1_11	TU.E-P12	Th.L-P4
Chernenko, V.	Chicinas, H.F.	Th.P-P26
FR.SP-3	TU.H-P119	Th.P-P27
Mo.L-P41	TU.H-P120	TU.A.1_11
Mo.L-P93	TU.H-P122	TU.H-P101
Chernyshev, A.L.	Chicinas, I.	TU.H-P117
Mo.B-P7	TU.H-P119	TU.H-P92
Chernyshev, S.	TU.H-P120	TU.H-P96
TU.D.2_14	TU.H-P122	Chirkova, A.
Chernyshov, D.	TU.H-P23	Mo.L-P23
FR.D-P79	TU.H-P24	Mo.L-P83
Chertopalov, S.	Chico, J.	Chirside, C.

TU.E-P49	TU.H-P69	Chorro, M.
Christopher, N.	Choi, D.	TU.J.1_O4
MO.D.1_O5	Mo.J-P11	Chou, F.
Chistyakov, O.	Choi, E.	Th.K-P41
Mo.L-P49	FR.D-P52	Chowdhury, N.
Chizhik, A.	Choi, E.S.	Mo.H-P41
TU.A.1_O3	Tu.A.3_O5	TH.K-P11
Cho, B.	Choi, G.	Chowdhury, P.
FR.A-P16	TU.H-P72	MO.J.3_O2
Mo.D-P13	TU.H-P90	Christensen, M.
TH.A-P16	Choi, H.C.	Mo.I-P11
TH.F-P16	Th.E.2_O5	Mo.I-P15
Cho, C.G.	Choi, H.J.	Mo.L-P38
TH.F-P19	Mo.D-P16	TU.F-P41
Cho, C.W.	Choi, H.Y.	TU.F-P46
Mo.H-P25	TU.A-P28	TU.F-P55
Cho, D.Y.	TU.A-P29	TU.H-P34
FR.A-P17	Choi, K.	Christensen, N.B.
Cho, E.	FR.D-P52	Mo.A-P72
FR.A-P2	Choi, K.D.	Christian, M.
Cho, J.	TU.H-P89	Mo.H-P36
Fr.I.2_O5	Choi, K.W.	Christianen, P.
Mo.C-P7	TH.A-P17	Fr.J.2_O4
Mo.G-P24	Choi, M.	TH.I-P22
WE.G.1_O2	Mo.J-P11	Chshiev, M.
Cho, M.R.	Choi, S.	Mo.F-P9
Mo.D-P25	MO.SYM_5	TH.E-P3
Cho, S.	TU.H-P32	Th.J.3_I1
FR.F-P13	Choi, S.J.	TU.J.1_I1
Mo.H-P36	TU.H-P21	Chu, C.W.
Mo.H-P79	Choi, W.J.	TU.E.2_O2
TH.B-P13	Mo.A-P100	Chu, K.
TU.E-P4	Choi, Y.	Th.E.2_O5
Choa, Y.H.	FR.D-P52	Chu, Y.H.
TU.H-P84	Mo.H-P34	Th.K-P41
Choe, S.B.	Th.G.3_O3	TU.E-P8
TH.E-P15	Choi, Y.J.	Chua, M.
TH.F-P11	TU.A-P28	MO.B.3_O2
TH.F-P19	TU.A-P29	Chua, M.J.
TH.J-P11	Choi-Yim, H.	Th.O-P4
Choi, B.	TU.H-P5	Chuang, Y.D.
FR.I-P45	Chong, S.	Th.I-P1
Th.F.2_O2	Mo.A-P91	TU.E.1_O6
Choi, C.	Chopdekar, R.	Chubycalo-Fesenko, O.
Mo.L-P65	TH.J-P3	Mo.J-P16

Chubykalo-Fesenko, O.	Cicek, M.M.	TU.F-P101
FR.F.2_O5	Mo.L-P43	Ciubotariu, O.T.
Mo.I-P29	Cichelero, R.	Mo.H-P30
Mo.I-P30	Mo.I-P19	Ciubotaru, F.
Mo.J-P8	Mo.I-P22	Fr.G.1_O2
Th.P-P11	Cichorek, T.	Ciuk, T.
TU.G.2_O4	TH.A-P23	FR.I-P36
Chudnovsky, E.	Cid Barreno, R.	Cizek, J.
TU.C.2_I1	TU.G-P11	TU.F-P20
Chulkov, E.V.	Cieslar, M.	Čižmár, E.
TU.B-P30	WE.C.2_O2	TH.A-P33
Chumak, A.	Cifuentes, Z.	Cizmas, C.B.
Fr.G.1_O2	Th.H.1_O5	Mo.L-P62
MO.H.2_O2	Cimorra, C.	TU.F-P93
Th.H-P9	MO.D.3_O2	Clark, L.
Th.O-P37	Mo.H-P106	TH.A-P38
TU.I.1_I1	WE.B.2_O5	TU.D.1_O4
Chun, B.S.	Cinchetti, M.	Clarke, S.
TH.F-P11	Mo.E-P11	WE.A1_O1
Chun, J.H.	Th.N-P10	Claus, C.
FR.D-P82	Ciobanu, C.S.	TU.C-P26
Th.D.1_O2	TU.F-P5	Clausen, P.
Chunchu, V.	Ciocca, L.	Mo.G-P13
TU.A-P58	Th.P-P12	TU.E.3_I1
Chung, C.H.	Ciomaga Hatnean, M.	Clement, P.Y.
Mo.A-P13	FR.A-P10	TU.J.1_I1
TU.C-P3	FR.D-P66	Clément, P.Y.
TU.C-P6	TU.D.2_I1	TH.E-P3
WE.E2_O4	Ciria, M.	Clementi, E.
Chung, M.H.	Mo.H-P75	Th.P-P10
Th.A.2_O5	Mo.J-P9	Clementyev, E.
Chung, S.	Mo.K-P28	TU.B-P16
Mo.F-P25	TH.D-P17	Clerc, M.
Th.O-P52	Cirillo, C.	TH.K-P20
Chuvilin, A.	Th.K-P49	Climent-Pascual, E.
Fr.E.1_O3	Císařová, I.	TH.D-P22
Fr.I.3_O4	TU.B-P28	Coak, M.
Chzhan, V.	Cisneros, J.	TH.A-P11
Mo.L-P49	Mo.H-P54	Cobos, P.
Ciccacci, F.	Cisneros-Fernández, J.	MO.E.1_O3
FR.H-P31	MO.C.2_O2	Coelho, A.
Mo.D-P30	TU.A-P99	Mo.K-P3
Mo.H-P85	Cisternas, E.	Mo.L-P27
Ciccarelli, C.	TU.F-P15	TH.D-P6
TU.SYM_4	Čitošlu, S.	TU.F-P98

Coelho, P.

TH.E-P3
TU.I.1_03

Coey, J.M.D.

FR.C-P9
Mo.G-P30

Coffey, D.

Mo.J-P9
Mo.K-P28
TH.D-P17

Cohen, L.

Fr.F.3_02
FR.I-P38
FR.I-P40
MO.F.2_04
Mo.L-P70
Mo.L-P79
Th.B.3_01
Th.M-P12
WE.B.2_04

Coisson, M.

FR.I-P20
MO.F.2_02
Mo.I-P18
TH.J-P24

Çolakeroğlu Arslan, L.

FR.F-P10
FR.F-P15

Coldea, M.

TU.H-P24

Coldea, R.

MO.SYM_5

Coleman, P.

Fr.C.2_11

Colin, C.

Th.I.1_05
TU.D.2_11
TU.D.3_01

Colineau, E.

TH.A-P21
TH.D-P15
TH.D-P25

Colino, J.M.

TU.F-P52

Colis, S.

Mo.B-P14

MO.H.1_04

Coll, M.

Th.L-P5

Coll, R.

Mo.L-P78

Collidelram, C.

FR.I-P11

Collet, M.

MO.J.3_03
TU.I.1_02

Collin, S.

WE.I.1_03

Collins, S.

Th.G.3_02

Collins-McIntyre, L.J.

MO.H.2_11

Combier, T.

TU.C-P25
WE.H.2_11

Comfort, J.

TU.C.1_02

Comin, R.

MO.A.2_04

Conca, A.

TH.E-P11
Th.O-P37

Conca, D.

Th.H.1_04

Concas, G.

TU.B.2_03
TU.F-P67

TU.F-P68

TU.F-P81

Conde Gallardo, A.

Mo.H-P47
Mo.H-P48

Conde, A.

MO.D.2_03
Mo.L-P13
Mo.L-P14

Th.B.1_11

TU.A.2_05

Conde-gallardo, A.

FR.H-P24

Conder, K.

Mo.A-P8
TU.A-P51

Conde-Rubio, A.

Mo.H-P80
Th.N-P5

Condó, A.M.

Mo.K-P19

Cong, P.T.

TU.B-P48

Coniglio, W.

FR.A-P56
Fr.C.2_02
Th.C-P03

Constable, E.

TH.C-P91

Conta, G.

MO.F.2_02

Conte, R.L.

Fr.I.2_05

Continentino, M.

FR.B-P25
Mo.A-P14
Mo.A-P29
Mo.A-P49
Mo.A-P77

Continenza, A.

Mo.A-P50
TU.E-P6

Contreras Gerenas, M.F.

Th.P-P17

Contreras, M.

Mo.K-P7

Cooper, J.

Fr.B.1_03
Mo.A-P28
Mo.H-P95
TU.A.3_01

Copolla, P.

TU.F-P114

Corbetta, M.

FR.H.3_01
Fr.H.3_04

Córdoba, R.

Mo.K-P16

Mo.K-P31	Th.N-P13	Mo.K-P14
Cornejo, D.	Th.P-P10	Cours, R.
Mo.K-P19	TU.F-P60	WE.J.1_O2
TU.F-P110	Cortijo, A.	Cowburn, R.
Cornia, A.	WE.A.2_O3	Th.H.3_O3
Mo.E-P4	Costa, B.	Th.P-P3
Corodeanu, S.	Mo.K-P12	TU.F-P118
TU.A.1_I1	Mo.K-P13	TU.J.2_O5
TU.H-P101	Costa, H.D.	WE.J.1_I1
TU.H-P92	TU.F-P98	Cozzoli, D.P.
Corona, R.	Costa, I.	Th.N-P15
Th.M-P15	TU.F-P43	Crespo, P.
Coronado, E.	TU.F-P44	Th.P-P8
Fr.I.3_O4	Costa, J.D.	Crete, D.
MO.J.2_I1	Mo.F-P21	TU.I.1_O2
PLENARY4	Th.H-P16	Cretich, M.
Coronado, M.J.	Th.I.1_O3	Th.H.2_O4
Th.H.1_O5	TU.H.1_O5	Crisan, A.
Corrêa, M.A.	Costa, N.	Th.O-P2
Mo.H-P10	Mo.A-P104	Crisan, A.D.
Mo.H-P7	Costa, P.M.	Mo.L-P53
Mo.H-P9	FR.I-P24	Crisan, M.
TH.F-P20	Costache, M.	Th.H-P20
Correa-Orellana, A.	WE.I.2_I2	Cristian Tanase, L.
TH.D-P22	Costache, M.V.	Mo.H-P15
TU.E-P47	Fr.F.3_I1	Cros, V.
Corredor, E.	Th.O-P49	FR.A-P51
Th.H.1_O5	Costo, R.	MO.F.1_O5
Corredor, E.C.	Th.P-P2	Mo.F-P15
Mo.H-P75	TU.B.3_O2	MO.H.3_O2
Mo.K-P28	TU.F-P102	MO.J.3_O3
Correia, J.G.	Copkun, M.	Th.H-P1
TU.A-P89	TU.F-P101	TH.J-P10
Correia, M.R.	Cotta, A.	TH.J-P13
TU.A-P65	TU.G-P7	TH.J-P14
Corró Moyà, M.L.	Cottam, M.	TH.J-P18
Fr.E.1_O4	Mo.K-P6	TU.H.1_O3
TU.C.3_O2	Th.M-P2	TU.H.1_O4
Corte-León, H.	Cottier, R.	TU.I.1_O2
Fr.E.1_O2	Th.L-P6	WE.I.1_O3
Cortés-Meztizo, I.	Couet, S.	WE.I.1_O5
FR.H-P24	WE.D.2_O3	WE.I.2_O3
Cortés-Ortuño, D.	Coura, P.	Cruz Reyes, G.J.
WE.F.1_O5	Mo.K-P12	FR.A-P39
Corti, M.	Mo.K-P13	Cruz, M.

Mo.A-P25
 Mo.H-P101
Cruz-Acuña, M.
 Th.P-P14
Cruz-Irisson, M.
 Mo.H-P49
Csaba, G.
 TU.I.1_04
Csach, K.
 Mo.A-P38
 TU.F-P49
 TU.F-P50
 TU.H-P39
Cuadrado, R.
 TU.G-P18
Cuartero, V.
 TH.C-P21
 TU.A-P13
 TU.A-P9
Cubukcu, M.
 Mo.F-P15
 TH.J-P18
 TU.I-P15
Cuccoli, A.
 Fr.F.2_04
Cuchet, L.
 TU.J.1_11
 TU.J.2_03
Cucolo, A.M.
 Mo.A-P35
Cuellar, F.
 WE.A.2_01
Cuevas, J.C.
 TH.G.1_02
Cugini, F.
 MO.D.2_11
Cunha, J.
 Mo.B-P11
Cunha, R.
 Th.I.2_06
Cunha, T.
 TU.F-P43
 TU.F-P44
Cuñado, J.L.F.
 TH.I-P28

TU.A-P91
 TU.G.2_04
 TU.I.3_03
Cuoco, M.
 TH.A-P8
Cuppens, J.
 Mo.H-P81
Curcio, C.
 Mo.L-P79
 Th.B.3_03
 TU.H-P121
Curiale, J.
 FR.H-P21
Curnoe, S.
 Th.A-P43
Currie, D.
 Th.L-P6
Currivan, J.A.
 TH.F-P1
Curtis, J.
 TU.I.1_04
Custardoy, L.
 Th.H.1_05
 Th.P-P34
 TU.F-P57
Custers, J.
 TH.D-P4
 WE.A.1_03
Cuya, J.
 MO.B.1_04
 TU.F-P90
Cyr-Choinière, O.
 MO.A.2_11
Czapkiewicz, M.
 Mo.H-P105
Czerner, M.
 WE.I.2_05

D

D. Matsuda, T.

Mo.A-P89
D´Albuquerque E Castro, J.
 FR.E-P38
Da Cas Viegas, A.
 Th.K-P40
 Th.K-P42
da Rosa, D.
 Th.K-P31
da Silva Neto, E.
 MO.A.2_04
da Silva, F.G.
 TU.F-P114
Dabkowska, H.
 TU.D.2_02
D'Acapito, F.
 TU.J.1_05
Da-Col, S.
 FR.I-P28
 Mo.K-P26
Daene, M.
 Fr.D.3_04
D'Agostino, D.
 Mo.A-P35
Dahan, P.
 FR.E-P28
 Mo.D-P29
Daisenberger, D.
 Mo.A-P109
Dakovski, G.L.
 TU.E.1_06
Dal Conte, S.
 MO.J.3_01
Dalla Piazza, B.
 TH.C-P28
Dallera, C.
 FR.H-P31
d'Allivy Kelly, O.
 MO.J.3_03
 TU.I.1_02
Dalmas de Rotier, P.
 MO.A-P2
Dalpian, G.M.
 TH.A-P36
Damascelli, A.
 MO.A.2_04

Damay, F.	Fr.B.1_03	de Oliveira, N.A.
TU.B-P11	Das, B.	FR.B-P9
TU.E.1_05	TU.F-P76	de Almeida, P.T.
D'Amico, I.	Das, D.	TU.D-P15
WE.E2_03	Mo.L-P18	de Andrade, A.
Damin, F.	TU.B-P14	Mo.I-P17
Th.H.2_04	Das, I.	de Andrade, A.M.H.
Dan, N.H.	Mo.L-P17	Mo.I-P20
TU.H-P4	Das, S.	de Azevedo, W.M.
Danailov, D.	Mo.A-P47	TU.F-P1
FR.E-P42	Mo.H-P23	de Bergevin, F.
Danceanu, C.	Mo.H-P24	Th.J.2_04
Th.P-P26	Dasari, N.R.	de Campos, M.
Dange, S.	TU.B-P24	Th.K-P26
Th.O-P53	d'Astuto, M.	TU.H-P65
Dani, I.	Mo.A-P31	TU.H-P66
MO.A-P1	Th.C.3_02	de Castro, J.
Daniel, F.	Daumont, C.J.M.	Th.K-P26
Th.H.2_02	Th.E.1_02	TU.H-P65
Danilyuk, A.	Davarpanah, A.	De Dominicis, C.
TU.B.3_01	MO.D.2_04	FR.D-P22
Daniš, S.	Davey, P.	de Franca, C.A.
TH.D-P3	TU.I-P12	Mo.K-P2
TU.G.2_05	David, P.	de Groot, R.
Danshita, I.	Mo.I-P28	Mo.L-P16
TH.C-P54	Davies, C.	De Hosson, J.T.M.
TU.C.3_01	Fr.G.1_04	TU.H-P39
Dantz, M.	Mo.G-P9	de Jong, S.
Fr.B.2_03	Davies, J.	TU.E.1_06
Th.G.3_01	Mo.H-P103	De Julian Fernández, C.
Danzenbächer, S.	Dávila, Y.G.	Th.N-P14
TU.B-P30	Mo.K-P2	Th.N-P15
Daou, R.	Davydov, V.Y.	TU.B.2_04
FR.C-P2	Fr.C.3_02	TU.F-P19
WE.H.2_04	Day, J.	de Julián Fernández, C.
d'Aquino, M.	MO.A.2_02	TU.E.3_02
MO.G.2_14	TU.A.3_01	TU.F-P95
Mo.J-P19	Dayal, V.	de la Figuera, J.
Mo.J-P20	FR.F-P32	FR.I.2_03
Mo.J-P21	Dayen, J.F.	TH.K-P23
Darine, E.D.	MO.E.1_02	TU.I.3_03
Th.H.2_02	Mo.E-P5	de la Fuente Rodríguez, M.
Dario, G.	MO.J.2_02	TU.B-P33
FR.H-P31	de Oliveira, A.L.	TU.F-P59
Darr, J.A.	FR.B-P9	de la Fuente, C.

Mo.J-P9	de Sousa, M.A.	FR.D-P73
TH.D-P17	Mo.I-P16	TU.D.1_03
de la Fuente, J.M.	De Sousa, V.	Deftels, C.
Th.H.1_05	TH.C-P121	TU.C-P31
Th.P-P34	De Teresa, J.M.	Degen, C.
TU.F-P57	Mo.H-P55	MO.H.3_04
de la Presa, P.	Mo.K-P16	Deger, C.
FR.H-P35	Mo.K-P17	Mo.G-P3
De La Venta, J.	Th.B.2_11	Degiorgi, L.
TU.A.2_11	Th.I.2_04	WE.A.1_05
TU.G.2_02	TU.C.1_04	Degiovanni, I.P.
de las Heras, S.L.	De Toro, J.A.	Fr.E.2_04
TH.I-P28	TU.F-P30	Deguchi, H.
TU.A-P91	TU.F-P52	TU.F-P7
De Loubens, G.	TU.F-P94	Deguchi, K.
MO.J.3_03	De Visser, A.	Fr.B.3_04
De Matteis, L.	Fr.C.1_02	Mo.A-P80
Th.H.1_05	MO.SYM_2	Mo.A-P81
Th.P-P34	Deac, A.	TU.C-P18
TU.F-P57	Th.I-P17	TU.H.2_11
de' Medici, L.	TH.J-P9	Dejneka, A.
Mo.A-P97	TU.H.1_11	Fr.H.2_03
De Mendizabal, I.	Deac, I.G.	Fr.H.2_04
MO.E.1_03	Mo.L-P62	Dekadjevi, D.
De Milly, X.	Dean, M.M.P.	Mo.H-P53
MO.J.3_03	Mo.A-P31	Del Bianco, L.
De Oliveira, A.J.A.	Dean, P.	Mo.H-P3
TU.A-P76	Th.J.1_04	Mo.H-P94
De Oliveira, A.L.	Debord, R.	Mo.I-P35
FR.E-P16	Th.A.2_04	Mo.I-P38
de Oliveira, L.A.S.	deBrion, S.	Mo.I-P40
Th.P-P17	TU.A-P43	Th.P-P12
De Oliveira, N.A.	Decorse, C.	TU.G.3_01
FR.E-P16	FR.D-P28	del Puerto Morales, M.
de Pedro, I.	FR.D-P29	Th.P-P2
TU.D-P5	FR.D-P66	del Real, R.P.
TU.F-P59	Dede, M.	Mo.J-P8
De Renzi, R.	FR.I-P16	Th.K-P37
Mo.A-P102	FR.I-P17	Th.M-P10
Mo.A-P103	Dediu, V.A.	TU.G.2_04
Mo.A-P37	FR.H-P30	WE.F.1_04
TH.C-P80	Mo.H-P94	Del Valle, J.
TU.E-P6	Deen, L.	Mo.E-P8
de Sousa, J.R.	Mo.K-P16	WE.B.2_16
TH.C-P100	Deen, P.	Delaët, B.

Mo.F-P24	Mo.K-P20	Desfond, G.
Delczeg, E.	Th.K-P27	WE.G.1_O5
WE.D.1_O4	Th.K-P31	Desfonds, G.
Deledda, S.	Deng, G.	Mo.D-P27
Fr.A.1_O4	TU.A-P23	MO.F.1_O5
MO.D.1_O2	TU.A-P51	Deshmukh, A.
TU.H-P98	Deng, M.J.	Th.P-P16
Delin, A.	Mo.L-P35	Deshmukh, R.R.
TU.I.3_O2	Deng, Z.	Th.O-P45
Della Pace, R.D.	Fr.G.2_I1	Désilets-Benoît, A.
Mo.H-P9	Denisova, E.	MO.D.3_O1
Delmas, C.	Mo.H-P38	Destexhe, A.
FR.D-P7	TU.H-P55	Th.P-P39
Del-Valle, N.	Dennis, C.	Detlefs, B.
Mo.F.2_O5	TU.F-P63	Mo.I-P35
Mo.J-P5	Denys, R.V.	Deumal, M.
Demaille, D.	TH.A-P12	TU.J.3_O1
Th.C.2_O2	Deorani, P.	Deus, F.
Demcak, S.	Mo.B-P23	FR.B-P25
TU.H-P39	Depeyrot, J.	Mo.A-P14
Demidenko, O.	Mo.I-P13	Deutsch, M.
TU.A-P4	Th.P-P32	TU.C.2_O3
Demidov, V.	TU.F-P114	Devolder, T.
Fr.G.1_I1	Deppe, M.	FR.A-P51
Demishev, S.	TH.B-P9	TH.F-P17
Mo.A-P85	TU.B-P66	Dey, S.
TH.C-P122	Deranlot, C.	FR.H-P4
TH.C-P77	MO.H.3_O2	Dhagat, P.
TH.C-P78	TH.E-P12	MO.J.3_O2
TU.B-P32	TU.A-P91	DHAOUI, W.
TU.B-P59	TU.J.1_O4	TU.H-P130
Demmel, F.	WE.A.2_O1	Dhar, A.
Th.D.1_I4	WE.I.1_O3	MO.D.1_O5
Demokritov, S.	Dergachev, K.	Dhar, S.K.
Fr.G.1_I1	TH.C-P35	TH.A-P39
Demouchy, G.	Derory, A.	Th.O-P21
Th.B.1_O2	TU.B.3_O1	Dhara, S.
Dempsey, N.	Dery, H.	Mo.A-P88
Fr.A.2_O5	MO.F.3_O3	TU.F-P47
Fr.E.1_O2	Derzhavin, I.	Dhesi, S.
Mo.L-P91	FR.F-P19	WE.B.2_O5
TH.C-P127	Derzhko, O.	di Bona, A.
TU.H-P63	FR.D-P30	TU.G-P10
TU.H-P97	Desautels, R.	di Cesare Mannelli, L.
Denardin, J.	TU.F-P107	Fr.H.2_O2

Di Giorgio, C. Mo.A-P35	TU.C.1_03 Dieterle, G.	TU.A-P8 Dinulovic, D.
Di Lieto, A. TH.C-P56	TH.J-P12 Dietl, T.	Mo.L-P25 Th.O-P13
Di Marco, I. Tu.G.1_02	MO.SP-3 Dietsch, T.	Dionne, G.F. TH.D-P18
Di Napoli, S. TH.B-P10	Th.O-P48 Diez-Ferrer, J.L.	Diop, L.V.B. TH.C-P85
Di Santo, G. FR.H-P33	Mo.J-P9 TH.D-P17	TU.E-P29 Dirba, I.
Diao, Z. TH.J-P33	Díez-Perez, I. Mo.E-P6	Mo.H-P29 Disseler, S.
Dias, E.T. Fr.C.3_01	Digiacomio, A. TH.F-P17	TU.E.1_04 Diviš, M.
Díaz Michelena, M. TH.C.1_04	Diguët, G. Mo.L-P91	TH.D-P4 WE.C.2_02
Díaz, J. Mo.H-P98 TU.G-P11	TH.C-P127 Diko, P.	Dix, N. FR.H-P25 FR.I-P22
Díaz, M. MO.E.1_03	Mo.L-P19 Dilmieva, E.	Mo.A-P58 TH.E-P20
Díaz-Pardo, R. TH.C-P57	Mo.L-P37 Mo.L-P74	Th.K-P45 Dizayee, W.
Dib, H. Th.H.2_03	Th.B.1_05 Dimitriadis, V.	FR.F-P12 TU.G.1_04
Diduszko, R. TH.C-P84	Mo.I-P29 Mo.I-P30	Djuraev, D. TH.C-P30
Dieckhoff, J. Th.P-P13	Dincer, I. Mo.L-P42	Dkhil, B. Th.E.1_11 TU.A-P100
Diego, M. TU.F-P73	Mo.L-P43 Dinesh Kumar, S.	Dlamini, W.B. TU.F-P104 TU.F-P105
Dieny, B. MO.G.2_03 Mo.H-P67 Mo.I-P4 TH.E-P3 Th.O-P48 TU.G.2_04 TU.G.3_02 TU.J.1_11 TU.J.2_03	TU.H-P80 Ding, C. Fr.B.2_04 Fr.C.2_04 Fr.G.2_11 Ding, H. Mo.H-P28 Ding, J. Fr.E.3_02 MO.C.3_02 Ding, Z. Mo.H-P28 Dinia, A. Mo.B-P14 Mo.L-P4	Dobak, S. FR.A-P25 Do, S. FR.D-P52 Dobak, S. TU.H-P51 Dobrea, V. TU.H-P117

TU.H-P92	Donner, W.	Mo.B-P13
Dobrota, C.	TU.A-P31	TU.A-P75
FR.E-P33	Donnerer, C.	TU.B-P63
Dobrynin, A.	FR.A-P30	TU.C-P26
Th.J.1_03	FR.A-P42	TU.H.2_04
Th.J.1_04	Donolato, M.	Drobac, &
Dobson, J.	Th.H.2_05	WE.A.2_02
Th.P-P14	Döntgen, J.	Drobosyuk, M.
Th.P-P9	Mo.L-P76	Mo.L-P80
Dodd, S.	D'Orazio, F.	Droghetti, A.
Th.P-P6	Mo.I-P31	Fr.I.3_04
Dodonov, D.V.	Dorneles, L.	Drokina, T.
Th.O-P31	Th.K-P31	FR.D-P38
Doenni, A.	Dörschug, S.	Drozdenko, D.
Mo.B-P5	FR.D-P76	TH.D-P8
Doerr, M.	dos Santos Dias, M.	WE.C.2_02
TH.B-P9	Fr.I.3_02	Drulis, H.
TH.C-P16	Dos Santos, A.	Mo.L-P49
Doi, M.	TU.E.2_05	DSwain, A.
Mo.H-P26	Dosanjh, P.	WE.SYM_5
TH.K-P15	MO.A.2_02	Dubenko, I.
Th.L-P1	Doto, H.	Mo.L-P3
TU.H-P28	TU.B-P35	Dubey, S.
Doiron-Leyraud, N.	TU.B-P39	FR.F-P17
MO.A.2_I1	Dou, Y.	Dubiel, S.
Dolci, M.	Th.K-P41	Th.A.1_06
Mo.I-P21	Doudin, B.	Dubitskiy, I.
Dolezal, P.	Fr.B.1_I1	Mo.J-P12
Mo.A-P54	MO.J.2_02	Th.K-P28
TU.B-P23	Th.G-P19	Dubois, E.
Dolgov, O.V.	Douvalis, A.	Mo.I-P13
Mo.A-P26	Th.P-P20	Th.B.1_02
Dolinšek, J.	TU.F-P21	Th.P-P32
FR.A-P41	Drchal, V.	Dubowik, J.
Mo.A-P18	TH.C-P8	TU.C.3_04
Dominguez, C.	TH.E-P1	Dubs, C.
Mo.H-P4	TH.E-P2	MO.H.2_02
Donac, A.	Drechsler, S.L.	Duc, F.
TU.H-P92	Mo.A-P20	Th.D.3_04
Donati, F.	Th.D.2_04	TU.B-P44
Fr.I.3_03	Dreifus, D.	TU.C-P31
Donges, A.	TU.A-P76	Duch, M.
Th.I-P12	Dreiser, J.	Fr.H.3_02
Donnelly, C.	Fr.I.3_03	Duchamp, M.
WE.E.1_04	Dressel, M.	TU.H-P42

Ducruet, C.

Mo.D-P27
 MO.F.3_O2
 Mo.I-P4
 TH.E-P3
 TU.G.3_O2

Duda, H.

TH.D-P12
 TU.H-P50
 TU.H-P53

Dudnikov, V.

TH.C-P11

Dudrova, E.

TU.H-P52

Dufresnes, S.

FR.I-P44

Dugay, J.

MO.J.2_O4

Duine, R.

Mo.C-P8

Duman, E.

TH.C-P105

Dumas, R.

Mo.C-P22
 Mo.F-P4
 Mo.F-P8
 MO.H.2_O4

Dumelow, T.

FR.H-P19
 Th.N-P4

Dumensil, K.

Th.I-P13

Dumesnil, K.

Th.I-P1
 TU.G.3_O3
 TU.G-P1
 TU.I.3_O1
 WE.G2_O4

Dumitrache, F.

TU.F-P108

Dumitru, I.

Mo.J-P14
 TH.K-P14
 Th.P-P27
 TU.F-P42

Dumont, Y.

FR.A-P54
 MO.C.3_O5

Duncan, W.

TU.C-P23
 TU.C-P32
 TU.C-P33

Dung, N.H.

MO.D.2_O2

Dunin-Borkowski, R.

MO.D.3_O2
 TU.H-P42

Dunn, A.

Th.P-P15

Dunsiger, S.

Fr.I.1_O3

Duò, L.

FR.H-P31
 Mo.H-P85

Duong, A.T.

Mo.H-P36
 Mo.H-P79
 TH.B-P13

Duong, L.D.

WE.G2_I6

Dupraz, M.

TH.J-P15

Dupuis, V.

TU.F-P25

Duque, J.

TU.B-P61
 TU.F-P43
 TU.F-P44
 TU.F-P98
 TU.H-P79

Duquesne, J.Y.

Th.I-P5

Durak, G.

Mo.L-P42

Durin, G.

TH.F-P20
 TH.F-P23

Durisin, M.

TU.E-P5

Dürrenfeld, P.

Mo.F-P19

Mo.F-P4
 Mo.F-P8
 MO.H.2_O4

Dusch, Y.

TH.C-P127

Dusek, J.

TU.A.1_O5

Dusek, M.

WE.A.1_O3

Dušek, M.

TH.D-P4

Dushenko, S.

Mo.D-P4

Dussaux, A.

MO.H.3_O4
 TU.H.1_O4

Dutoit, C.E.

Mo.B-P13
 TU.A-P75

Dutra, R.

Mo.G-P29

Dutta, P.

Mo.L-P18

DuttaGupta, S.

MO.H.1_O3

Dutton, S.E.

Mo.A-P56

Dutz, S.

TU.F-P71
 TU.F-P78

Duy Khanh, N.

Mo.C-P19

Dvornik, M.

Mo.F-P8

Dwyer, M.

MO.A.2_O5

Dyakonov, V.

FR.F-P5

Dybala, J.

FR.I-P51

Dynowska, E.

Mo.H-P82
 TU.G-P28

Dyrdal, A.

Mo.C-P25	Mo.L-P86	Eisaki, H.
Dzemiantsova, L.	TH.K-P1	Fr.C.3_O3
FR.I-P19	TU.G-P21	Mo.B-P18
MO.C.2_O3	We.E.1_O5	TU.A-P50
Dzhumaliev, A.	Edelman, I.	TU.A-P52
TH.K-P22	TU.E-P12	TU.A-P53
Dzhun, I.	TU.F-P88	Èisárová, J.
Mo.I-P27	Edmonds, K.	TH.A-P2
Dziom, V.	MO.C.1_O5	EIXENBERGER, J.
TU.A-P11	Mo.G-P22	TU.F-P40
	Th.G.2_O6	Èižmár, E.
E	Edström, A.	TH.C-P79
	Fr.A.1_I1	TU.D-P4
	FR.I-P26	Ejima, S.
	MO.E.1_O4	FR.A-P13
E. W. Bauer, G.	Edvinsson, T.	Ekhholm, M.
Mo.J.3_O4	TU.F-P101	TU.C.3_O4
Ebels, U.	Efimov, V.	Ekicibil, A.
Mo.F-P24	TH.C-P69	Mo.L-P69
Mo.F-P26	Efremov, D.	Th.I.2_O1
Eber, N.	Mo.A-P26	Ekino, T.
Tu.F-P122	WE.A.1_O6	TU.B-P19
Éber, N.	Efthimiadis, K.G.	Ekiz, C.
TU.F-P49	Mo.J-P15	TH.C-P68
TU.F-P50	Egawa, G.	Eklund, A.
Ebert, H.	MO.E.2_O4	Th.O-P52
Fr.D.2_O2	Eggenschwiler, F.	Ekonomoov, N.
Mo.J-P2	Mo.B-P22	TH.C.1_O3
Ebisu, S.	Egorov, S.V.	El Bahraoui, t.
TH.D-P7	TH.F-P9	TU.A-P8
Ebke, D.	WE.J.2_O2	el Hichou, A.
TH.J-P21	Eguchi, G.	TU.C.3_O2
Echevarria-Bonet, C.	Mo.D-P23	El Hog, S.
TU.B-P33	Th.I.2_O3	TU.C.1_O3
TU.F-P59	Eguchi, K.	El Kenz, A.
Ecke, R.	Mo.H-P72	Fr.F-P33
Th.O-P29	Ehresmann, A.	elahi, M.
Eckert, J.	TU.G.2_O2	TU.E-P13
Mo.L-P44	Eichwald, I.	TU.E-P27
Mo.L-P48	Th.O-P28	Elender, M.
Th.O-P6	TU.I-P13	TU.A-P53
TU.D.3_O3	Eilers, F.	Elerman, Y.
Eckstein, M.	Mo.A-P30	Mo.L-P42
Th.F.2_O4	Einsle, J.	Mo.L-P43
Eddrief, M.	WE.J.1_O2	El-Gendy, A.A.

Mo.I-P25	Enderlein, C.	TU.A-P48
Elias, R.G.	FR.A-P63	Eremin, I.
TH.J-P6	Enders, J.	Mo.A-P22
Elies, P.	Th.N-P11	Mo.A-P99
Mo.H-P53	Endo, A.	Erfanifam, S.
Elin, A.	Mo.B-P17	FR.D-P27
Mo.J-P6	Endo, R.	Ericsson, T.
Elisa, M.	TU.H.2_04	WE.D.1_04
Th.O-P19	WE.F2_04	Eriksson, K.
Eliseev, A.	Endoh, T.	Th.H.1_03
Th.K-P28	TU.I-P5	Eriksson, O.
Elizabeth, S.	Ener, S.	Fr.A.1_11
FR.D-P34	Fr.A.1_11	Mo.H-P88
TH.C-P73	Th.A.3_02	TH.C-P46
Elizalde Galindo, J.T.	TU.H-P29	Ermawan, E.
FR.H-P35	TU.H-P43	TU.H-P77
Eljarrat, A.	TU.H-P95	Ernst, A.
Th.K-P45	Engel, A.	Fr.D.2_11
Tu.B.2_02	Mo.A-P91	Fr.D.3_02
Elkaim, E.	Engel, C.	Ernst, S.
TU.E.1_05	TU.I-P18	TU.C-P30
ElMassalami, M.	TU.I-P6	Erofeev, D.
Mo.A-P104	TU.I-P8	TU.A-P87
Elmers, H.J.	Enobio, E.	Erokhin, S.
FR.A-P35	Th.O-P52	Fr.A.2_03
Fr.D.2_02	Entel, P.	TU.H-P3
Eloird, R.	Mo.L-P75	Ershing, K.
TH.D-P25	Eom, C.	Th.K-P40
Eloirdi, R.	Th.E.1_03	Ertap, M.
TH.A-P21	Eom, M.	FR.F-P10
TH.D-P15	WE.A.1_04	FR.F-P15
Elovaara, T.	Era, H.	Erten, O.
Mo.H-P20	TU.H-P33	Fr.C.2_11
Mo.H-P52	Erb, D.	Escamilla, R.
Emi, N.	FR.I-P19	Mo.A-P25
FR.A-P55	Th.I.3_01	Eschrig, M.
Emmerling, M.	TU.C.1_02	FR.A-P24
TU.I-P4	TU.I.1_05	Escobar, O.
Emoto, H.	WE.E.1_03	Mo.I-P17
Th.I.2_03	Erbe, A.	Escobar, R.
Enculescu, M.	TH.J-P9	FR.E-P38
Th.O-P2	Eremenko, V.	Escoda, L.
Enderle, M.	TU.A-P18	FR.I-P37
Mo.G-P25	Eremin, E.	Mo.L-P78
Th.D.1_02	TH.D-P16	Escote, M.

Mo.K-P3	MO.B.1_I1	MO.D.2_O4
Escrig, J.	Th.K-P45	Fabbrici, S.
Mo.K-P20	Estrader, M.	MO.C.2_I1
Mo.K-P21	FR.I-P46	TU.E-P28
Mo.K-P27	MO.B.1_I1	TU.J.2_O4
TH.F-P24	Tu.B.2_O2	Fabbris, G.
Th.K-P27	TU.F-P87	Mo.A-P33
Th.M-P15	Etcheberry, A.	Fáberová, M.
Th.M-P16	MO.C.3_O5	TU.H-P41
TU.H-P68	Etgens, V.	TU.H-P45
Escudero, R.	Mo.L-P86	Fabiatti, L.M.
Mo.A-P68	Th.C.2_O2	Mo.K-P19
Eskildsen, M.R.	TH.K-P1	Fabrèges, X.
Mo.A-P105	We.E.1_O5	TU.A-P43
Espejo, Á.	Èurlík, I.	TU.B-P44
TH.F-P24	WE.C.2_O3	TU.C-P31
Espeso, J.I.	Èurlík, I.	Fähler, S.
TU.B-P33	TH.C-P94	Mo.H-P63
TU.B-P34	Evans, R.	WE.D.1_I1
Espinola, M.	Fr.J.2_I2	Fahlman, M.
MO.C.3_O4	Mo.J-P16	Fr.I.3_O4
Essafi, K.	Evgeny, .	Failamani, F.
Th.D.2_O3	Mo.H-P22	WE.H.2_O3
Esser, S.	Ewings, R.	Faini, G.
TH.K-P18	WE.A1_O1	We.E.1_O5
Essler, F.	Exner, H.	Fajardo Tolosa, F.E.
TH.A-P41	Th.O-P29	Th.O-P1
Estemirova, S.	Ez-Zahraouy, H.	Fak, B.
FR.F-P19	MO.A-P1	Th.D.1_O2
Esteve, J.		WE.C.2_O4
Fr.H.3_O2	F	WE.H.2_O5
Estevez, A.M.		Fåk, B.
FR.I-P24		MO.G.3_O2
TU.F-P72	F Cohen, L.	Falchbart, K.
TU.F-P73	Th.K-P25	Th.A-P40
Estevez, V.	F. Cuñado, J.L.	Falduti, G.
TH.F-P14	Mo.H-P99	Th.H.2_O4
Estrada, F.	Mo.I-P37	Faleev, S.
Th.I.2_O6	Th.K-P44	WE.J.1_O5
TU.E-P23	F. Ferreira, F.	Falus, F.
Estrade, S.	TH.C-P20	TH.J-P35
Tu.B.2_O2	F. Kaneko, U.	Falvo, E.
TU.F-P87	FR.D-P65	Fr.H.2_O2
Estradé, S.	F. Miao, X.	Fan, F.
FR.I-P46		TU.I-P17

Fan, R.	Th.E.1_02	Fedorov, V.
Th.J.1_03	Farrer, I.	Mo.I-P14
TU.F-P94	Mo.H-P96	Fedotova, J.
Fan, W.	Fascineli, M.L.	Th.K-P49
FR.A-P3	Th.P-P1	WE.E.1_02
Mo.C-P3	Fasolino, A.	Fedyanin, A.
Fanciulli, M.	Mo.G-P19	Th.N-P16
TH.F-P17	Mo.G-P27	Feher, A.
TU.G.1_05	Fassbender, J.	Mo.L-P7
Fanfarillo, L.	Mo.H-P82	TH.C-P79
Fr.J.1_02	TH.J-P9	TU.D-P4
WE.A.2_03	TH.K-P17	Feher, T.
Fang, H.	TU.H.1_11	TU.G-P15
Mo.L-P84	Fatale, S.	Fehske, H.
TU.H-P111	Th.G.3_01	FR.A-P1
Fang, M.	Fatuzzo, C.G.	FR.A-P13
Mo.A-P112	Th.G.3_01	Feiler, L.
Fani Sani, F.	Faulhaber, E.	Th.I-P4
TH.J-P33	TH.B-P9	TU.F-P36
Fantechi, E.	TU.B-P66	Felder, D.
Fr.H.2_02	TU.C-P33	Th.H.2_03
TU.F-P64	Faundez, J.	Felser, C.
Fantini, A.	TU.F-P15	Fr.D.2_02
Th.I-P16	Fauqué, B.	MO.SYM_4
Farberovich, O.	Mo.C-P12	Th.A.1_02
FR.G-P1	Faurie, D.	TH.J-P21
Farias Mancilla, R.	TU.G-P17	TH.J-P24
FR.H-P35	Fauth, F.	Th.N-P11
Farias, S.	TU.B-P33	TU.E-P28
TU.F-P103	Favre, L.	TU.G-P16
Farjami Shayesteh, S.	Th.O-P40	TU.I-P24
Mo.B-P1	Fayziev, S.	TU.J.2_04
Farkas, D.	TH.C-P29	WE.D.1_05
TU.A-P25	Fayzullin, R.	WE.J.1_05
Farkasovsky, P.	Mo.L-P77	Feng, C.
FR.B-P21	Mo.L-P80	Mo.A-P75
Farle, M.	Fazlali, M.	Feng, E.
Mo.H-P63	Mo.F-P8	Fr.D-P87
TH.C-P82	Fdez-Gubieda, M.L.	TH.A-P42
TH.K-P17	Fr.B.1_02	Feng, Z.
TU.C.3_03	FR.H-P17	FR.A-P42
TU.G-P27	TU.B-P33	Fr.D.2_04
WE.B.2_11	TU.F-P59	Th.G.3_02
WE.D.1_03	Fecher, G.	WE.F.2_11
Farokhipoor, S.	TU.E-P28	Fennell, A.

MO.D.3_01	TU.E.2_02	Ferrer, S.
TU.E.2_03	Fernández-Díaz, M.T.	Fr.H.3_02
Fennell, T.	FR.D-P73	MO.E.1_I1
FR.D-P24	TU.C.2_03	Ferrero, M.
FR.D-P79	Fernández-Outon, L.E.	WE.E2_02
Fente, A.	MO.G.1_05	Ferrie, A.
TH.D-P22	Fernández-Pacheco, A.	TU.F-P33
Feraru, I.D.	Mo.K-P17	Ferrón, A.
Th.O-P19	Th.P-P5	Fr.F.1_03
Ferguson, A.	TU.J.2_05	Fert, A.
TU.SYM_4	Fernández-Pacheco, R.	MO.F.1_05
Ferhat, K.	Th.H.1_05	MO.H.3_02
MO.I.3_03	Th.P-P34	TH.E-P12
Fermon, C.	Fernández-Rossier, J.	TH.I.1_04
Th.O-P50	Fr.F.1_03	Th.J.3_I1
Th.P-P39	Ferrante, Y.	WE.G.1_05
Fernandes dos Santos, L.	Th.I-P16	WE.I.1_03
TU.C-P8	TU.I-P24	Fertey, P.
Fernández Baldís, F.	WE.J.1_05	TU.A-P6
TH.K-P1	Ferrari, A.	Fetisov, L.
We.E.1_05	Mo.D-P30	TU.A-P94
Fernández Barquin, L.	Ferrari, V.	Fetisov, Y.
TU.B-P33	TH.K-P7	TH.C.1_03
TU.B-P34	Ferraro, E.	TU.A-P94
Fernández Barquín, L.	Th.H-P17	Feve, G.
Fr.B.1_02	Th.I-P18	Fr.A-P59
FR.H-P17	WE.H.1_04	Fevereiro, P.
TU.D-P5	Ferraro, F.J.	Th.P-P34
TU.F-P102	Mo.I-P28	Fidler, J.
TU.F-P59	Ferraz, A.	Fr.A.1_I1
TU.F-P82	Th.D.2_02	TU.H-P107
Fernández Scarioni, A.	Ferreira, L.P.	TU.H-P108
WE.H.1_04	Mo.H-P101	TU.H-P110
Fernández, A.B.	Ferreira, N.	TU.H-P81
TH.C.1_04	TU.F-P103	WE.B.2_I1
Fernández, E.	TU.F-P113	Fidrysiak, M.
TU.I.2_03	Ferreira, R.	Mo.A-P34
Fernández, J.F.	FR.I-P42	Fiebig, M.
Fr.A.1_04	Mo.F-P21	MO.H.3_04
MO.D.1_02	Th.H-P16	Th.I-P2
Mo.I-P15	Th.P-P28	TU.A-P24
TH.K-P23	TU.H.1_05	Figueiras, F.
Fernández, M.P.	WE.I.2_I1	TU.A-P65
Mo.L-P90	Ferreiros, Y.	Figueroa, A.I.
Fernández-Baca, J.	TH.F-P8	MO.H.2_I1

Th.K-P24	TH.C-P28	TH.B-P3
TU.F-P16	Finkel, A.C.	TH.C-P63
TU.J.1_04	FR.H-P3	TH.C-P9
TU.J.3_02	Finkel, P.	TU.B-P2
Figueroa, S.J.A.	TH.C.1_05	TU.B-P77
Mo.K-P9	TU.A-P12	TU.F.1_11
Fijałkowski, M.	TU.E.2_01	Fita, I.
TU.B-P1	Finkelstein, G.	Mo.I-P41
TU.E-P19	TU.C-P6	TH.C-P1
TU.H-P53	WE.E2_04	Fitsimmons, M.
Filar, K.	Fink-Finowicki, J.	WE.G2_04
TU.A-P40	TH.C-P84	Fitta, M.
Filges, U.	Fiolka, C.	TU.A-P46
FR.I-P7	Th.C-P03	TU.A-P82
Filho, J.	Fiorani, D.	Fittipaldi Antonio Vecchione, R.
TU.F-P77	MO.B.1_02	Th.G.3_01
Filimonov, Y.	Mo.I-P32	Flachbart, K.
Mo.G-P10	Mo.I-P35	FR.D-P67
TH.K-P22	TU.E.3_03	Mo.A-P85
Th.O-P27	TU.F-P53	TH.B-P1
Th.O-P5	TU.F-P67	TH.C-P77
TU.H-P54	TU.F-P68	TH.C-P78
Filipek, E.	Firastrau, I.	TU.B-P32
TU.H-P53	Th.K-P32	TU.B-P59
Filipov, V.	Th.O-P44	Flansberry, Z.
Mo.A-P85	Fischer, G.	Mo.F-P27
TH.B-P1	Mo.H-P33	Flatt, J.
TH.C-P78	Fischer, J.	Th.E.3_01
TU.B-P20	FR.H.3_01	Fleaca, C.
Filippov, V.	TU.E-P28	TU.F-P108
TH.C-P77	Fischer, J.A.	Fleutot, S.
TU.B-P32	Fr.H.3_04	Th.M-P11
TU.B-P59	Mo.A-P19	Flint, R.
Filomeno, C.	Fischer, P.	TU.F.3_02
Th.B.1_02	Fr.E.1_05	Florea, O.
Fin, S.	Fr.I.2_04	FR.I-P44
Th.M-P9	Mo.H.3_01	TU.D.1_03
Fina, I.	TU.C.1_11	Florentina Chirila, C.
Th.E.2_02	WE.H.1_02	Mo.H-P15
Finazzi, M.	Fischer, T.	Flores-Arias, Y.
FR.H-P31	TU.F-P12	TU.A.2_03
Mo.D-P30	Fisher, A.	Flores-Martinez, N.
Mo.H-P85	Th.I-P17	TU.H-P36
Finco, A.	Fisk, Z.	Flouquet, J.
MO.G.3_04	Fr.C.1_06	

Mo.A-P59	MO.C.3_04	Mo.A-P77
TH.C-P47	Mo.H-P84	Fracasso, G.
TU.C-P25	Th.E.2_02	Th.P-P12
TU.F.1_02	TH.E-P20	Fraerman, A.
WE.F2_03	Th.G.3_04	Th.O-P41
WE.H.2_11	Th.G-P15	Fraile Rodríguez, A.
Flovik, V.	Th.K-P45	MO.E.3_11
Th.I.1_02	TU.A-P62	Mo.I-P24
Fnidiki, A.	TU.A-P63	Th.L-P3
Mo.I-P18	Fontes, M.	TU.F-P79
Fock, J.	FR.A-P63	WE.F.1_04
TU.F-P102	Fook, H.T.	Franchesin, G.
Focsa, C.	TH.J-P4	TU.H-P36
TU.F-P42	TH.J-P5	Francis, A.
Fodor-Csorba, K.	Forgan, E.M.	Fr.G.1_04
TU.F-P49	Mo.A-P105	Franco Peñalosa, R.
TU.F-P50	Fornara, M.	FR.A-P19
Foerster, M.	Fr.H.2_02	FR.A-P20
Fr.I.1_11	Forro, L.	Franco Peñaloza, R.
FR.I.2_03	TU.C-P31	FR.A-P39
MO.E.1_11	Förster, J.	Franco, F.
Th.G-P15	TH.J-P12	FR.I-P42
TH.K-P23	Fort, D.	FRANCO, N.
Foerster, T.	TU.B-P5	TU.F-P40
Mo.A-P98	Fortes Brollo, M.E.	Franco, V.
Fohtung, E.	TU.F-P18	Fr.C.3_04
WE.G2_04	Fortunato, N.	MO.D.2_03
Folcke, E.	FR.E-P39	Mo.H-P37
TU.F-P85	Fortunato, N.M	Mo.L-P13
TU.F-P86	FR.E-P40	Mo.L-P14
TU.H-P78	TU.H-P116	Mo.L-P40
Fomicheva, L.	TU.H-P131	Th.B.1_11
TU.C.2_03	Foury-Leylekian, P.	TU.A.2_05
Fondacaro, A.	TU.A-P6	François, M.
FR.I-P23	Fowley, C.	Mo.L-P50
Fonseca, J.	TU.H.1_11	Francoval, S.
Mo.B-P30	Fox, A.M	FR.I-P4
Mo.B-P31	FR.F-P12	Frandsen, B.
Fontaíña-Troitiño, N.	Fox, A.M.	Fr.B.2_04
TU.B.2_11	TU.A-P57	Fr.C.2_04
Fontcuberta i Morral, A.	Fox, M.	Fr.G.2_11
MO.E.2_01	TU.G.1_04	Fr.I.1_03
Fontcuberta, J.	Foxon, T.	Th.J.1_02
FR.H-P25	MO.C.1_05	Frandsen, C.
Mo.A-P58	Foyevtsova, K.	TU.F-P102

Frangou, L.	Fr.A.1_I1	Fuji, K.
Mo.I-P4	Fr.C.3_O4	TH.D-P7
TU.G.3_O2	Frings, P.	Fujii, H.
Franke, K.	Th.D.3_O4	TH.A-P13
Fr.G.3_O3	Frisk, A.	Fujii, K.
Mo.H-P76	TU.G-P14	TH.A-P18
Frankowski, M.	Fritsch, V.	Fujii, T.
Th.O-P24	TU.H.2_O3	TH.C.1_O2
Franz, C.	Frollo, I.	Fujii, Y.
TH.J-P28	Th.P-P30	FR.D-P13
TU.B-P75	Th.P-P37	FR.D-P46
TU.C-P30	Frömter, R.	FR.I-P34
WE.I.2_O5	Mo.H-P75	Mo.B-P21
Fratini, S.	Mo.H-P76	Th.A-P34
FR.B-P12	Frontera, C.	Fujima, N.
Freeland, J.	MO.C.2_O2	Mo.J-P1
Fr.A.1_O5	Mo.H-P54	TU.E-P1
TU.F-P107	Mo.H-P57	Fujimori, A.
Freeman, M.	Th.B.1_O3	Fr.I.1_O3
TH.J-P33	TU.A-P99	TU.B-P55
Freeman, P.	Frontzek, M.	Fujimori, S.I.
Mo.A-P32	Mo.A.1_O5	TU.B-P55
Freitas, P.	Mo.A-P55	Fujimoto, S.
FR.I-P42	MO.D.3_O1	Fr.B.3_O2
Mo.H-P43	TH.A-P42	Fujimura, K.
Th.H-P16	Fruchart, D.	Mo.A-P46
Th.I.1_O3	TH.C-P96	Mo.A-P84
Th.K-P46	Fruchart, O.	Fujio, M.
Th.P-P28	FR.D-P21	Mo.L-P71
TU.H.1_O5	Mo.K-P26	Fujisaki, K.
TU.I.1_O3	WE.F.1_I1	Mo.L-P54
Frelon, V.	Fu, X.	Fujisawa, M.
Fr.A-P59	Th.C.2_O2	Mo.B-P21
Fresard, R.	Fu, Y.	Fujita, H.
FR.C-P2	MO.F.1_O5	Mo.A-P78
Friedemann, S.	TU.G-P27	Fujita, T.
FR.A-P56	Fu, Z.	FR.D-P11
Fr.C.2_O2	Fr.A.3_O3	Mo.A-P53
WE.H.2_O4	FR.I-P47	Fujiwara, K.
Friedland, L.	Fuchs, J.N.	Mo.A-P44
TU.F-P31	TU.I.3_O4	Mo.A-P79
Friedlein, J.	Fuertes, A.B.	Mo.A-P83
Fr.I.3_O1	Fr.B.1_O4	Mo.L-P60
WE.G2_O2	Fügenschuh, A.	TH.B-P18
Fries, M.	TU.I-P25	TU.B-P54

Fujiwara, N.

Fr.B.2_05
Mo.A-P60

Fujiwara, T.

TH.C-P113
TH.C-P90
TH.D-P20

Fukami, S.

MO.H.1_03
MO.H.1_05

Fukuda, A.

FR.I-P34

Fukuda, K.

TU.B-P38

Fukuhara, T.

TH.B-P11
TU.B-P40

Fukumoto, Y.

FR.D-P16
FR.D-P41

Fukunaga, H.

Mo.L-P54
Th.O-P36
TU.H-P38
TU.H-P58
TU.H-P86

Fukunaga, M.

Mo.H-P71
TU.F-P90

Fukushima, A.

Th.G-P7
TH.J-P10
TH.J-P13
TH.J-P14
TU.H.1_03
TU.H.1_04
WE.D.2_05
WE.G2_I6
WE.G2_03
WE.I.1_05

Fukushima-, A.

FR.A-P51

Fulga, I.C.

FR.A-P44

Fulglsby, R.

Th.K-P29

Fullerton, E.

Fr.J.2_I1
Mo.H-P53
WE.G2_04

Funk, A.

Mo.L-P44
TU.D.3_03

Furnemont, A.

WE.D.2_03

Furukawa, I.

TU.F-P90

Furukawa, N.

Th.E.2_03

Furukawa, S.

Th.E.2_I1

Furukawa, Y.

Fr.D.2_03

Furuuchi, T.

TU.H-P28

Furuya, S.

FR.E-P31
Mo.B-P15

Fuseya, Y.

Mo.C-P12
Th.I.2_03

Fushiya, K.

TU.B-P58
TU.C-P19

Fusil, S.

Th.E.1_I1

Futamoto, M.

Fr.A.3_02
Th.K-P47
TU.I-P23

Fuwa, A.

Mo.H-P71
TH.C-P23
TH.C-P98
TU.E-P16

Fuzer, J.

TU.H-P51
TU.H-P52

Füzer, J.

TU.H-P41

TU.H-P45

Fuzerova, J.

TU.H-P52

G

G. Ovejero, J.

Th.P-P8

Gaal, R.

TU.C-P31

Gabani, S.

FR.D-P67
Mo.A-P85
TH.B-P1
TH.C-P77
TH.C-P78
TU.B-P32
TU.B-P59

Gabáni, S.

Th.A-P40

Gabor, M.

MO.H.1_04
TU.G-P17

Gabureac, M.

TH.E-P22

Gafton, E.V.

TH.K-P14

Gafton, V.

Mo.L-P86

Gai, Z.

TU.E.2_05

Gaididei, Y.

Fr.E.3_01
Mo.K-P23
TH.J-P7
TU.F-P83

Galca, A.C.

Th.O-P19

Galceran, R.

MO.C.2_02
Mo.H-P54

Galcerán, R.	Gamino, M.	García Prieto, A.
TU.A-P99	Mo.H-P10	Fr.B.1_O2
Galdun, L.	Mo.H-P7	García Sanchez, F.
TU.E-P5	Gamza, M.	Mo.F-P24
TU.E-P9	FR.A-P56	Mo.H-P31
Galić, S.	Fr.C.2_O2	García, C.
WE.A.2_O2	Mo.A-P109	Mo.C-P22
Galisova, L.	TU.C-P33	Mo.H-P44
TH.C-P15	Gamzatov, A.	Th.G-P17
Gallagher, B.	Mo.L-P89	TU.E-P5
Fr.G.3_O2	Gan, W.	García, D.
MO.C.1_O5	TH.J-P4	TU.A-P76
Mo.G-P22	Gan, W.L.	TU.F-P26
Th.G.2_O6	Fr.E.3_O2	García, F.
Gallais, Y.	TH.J-P5	TH.J-P20
TH.B-P19	Gan'shina, E.	García, J.
WE.F2_O7	TH.C-P40	TH.C-P21
Gallardo, R.	Gandra, L.	TU.A-P10
WE.F.1_O5	MO.SYM_5	TU.A-P13
Gallardo, R.A.	Ganesh, K.R.	TU.A-P9
TH.K-P17	TU.G-P23	TU.E.1_O2
Gallas, J.	Ganguli, A.K.	García, J.A.
Mo.F-P16	TU.A-P80	TU.F-P54
Gallego, S.	Gangwar, A.	García, K.
TU.E-P22	Fr.G.1_O3	MO.H.3_O2
Galyas, A.	TH.J-P12	Th.E.1_I1
FR.F-P1	Ganzhorn, M.	TH.F-P17
Mo.D-P6	MO.E.2_O3	García, L.M.
Gama, S.	Gao, F.	TH.C-P124
TH.D-P6	Mo.A-P27	TH.K-P4
Gambardella, P.	TU.B-P67	Th.M-P1
Fr.I.2_I1	Gao, S.	TU.F-P16
Fr.I.3_O3	FR.D-P79	TU.J.1_O4
Mo.C-P23	Gao, X.	TU.J.3_O2
MO.J.2_O3	Th.O-P51	García, M.
TH.E-P22	Gao, Y.	Th.P-P1
TU.I-P15	Th.K-P35	García, M.A.
TU.J.3_O3	Garanin, D.	Th.M-P21
Gambarelli, S.	TU.C.2_I1	García, V.
Mo.D-P27	Garbarino, G.	Th.E.1_I1
MO.F.1_O5	TH.C-P21	García-Arribas, A.
MO.F.3_O2	García Del Muro, M.	Mo.K-P4
WE.G.1_O5	MO.E.3_I1	TU.I.2_O3
Gambashidze, G.	Th.C.2_O3	García-Barriocanal, J.
Mo.A-P100	Th.L-P3	WE.G.1_O4

García-Flores, A.F.	FR.H-P25	TU.I-P15
TU.F-P26	Mo.H-P84	TU.J.1_02
García-García, A.	Mo.H-P98	WE.H.1_05
Mo.H-P43	MO.J.2_05	WE.I.1_02
Mo.H-P55	TH.E-P20	Gaudisson, T.
García-González, L.	TH.K-P18	Mo.I-P12
FR.H-P24	Th.K-P41	Mo.L-P50
García-Hernández, M.	Gargiano, P.	TU.A.2_03
FR.I-P49	Th.L-P5	TU.H-P36
Mo.I-P15	Garitaonandia, J.	Gauf, A.
TH.D-P22	TU.A.2_02	Th.H-P20
TH.K-P23	Garlea, O.	Gaulin, B.
TU.E-P47	MO.I.1_02	TU.D.2_02
TU.G-P15	Garnero, C.	Gaur, N.K.
TU.I.3_03	MO.B.3_03	FR.B-P6
WE.G.1_04	Garst, M.	Mo.C-P2
García-Lekue, A.	MO.H.3_03	Mo.F-P7
MO.J.2_03	TU.C-P30	TH.J.3_02
García-Martín, A.	WE.H.1_03	TU.A-P70
TH.G.1_02	Garzón Posada, A.O.	TU.H-P2
García-Martín, J.M.	Th.O-P1	Gautam, S.
Th.K-P37	Gaspar, J.	TU.A-P15
TU.G-P4	Th.P-P28	TU.F-P99
García-Muñoz, J.L.	Gastaldo, F.	Gauthier, N.
Mo.C-P9	TH.A-P4	MO.D.3_01
Th.A.1_01	TH.C-P94	Gauzzi, A.
TH.C-P38	Gastev, S.	FR.A-P58
Th.J.1_03	Mo.I-P14	Fr.A-P59
TU.A-P10	Gataullin, E.	Mo.A-P31
TU.A-P83	TU.F-P82	TU.A-P76
TU.A-P93	Gatel, C.	Gaviko, V.
García-Prieto, A.	Fr.E.1_11	Mo.L-P73
FR.H-P17	Fr.E.3_04	Gavilán, H.
TU.B-P33	FR.I-P43	TU.F-P61
García-Saiz, A.	Mo.K-P17	Gavilano, J.
TU.D-P5	We.F.1_03	Mo.A.1_05
García-Sánchez, F.	WE.J.1_02	Mo.A-P105
TH.J-P31	Gati, E.	MO.A-P2
WE.G.1_03	FR.D-P55	Gavrilkin, S.
Garello, K.	Gaudenzi, R.	Mo.A-P85
TH.E-P22	Mo.E-P4	TH.A-P1
TU.I-P15	Gaudet, J.	TU.B-P59
Gargallo-Caballeroa, R.	TU.D.2_02	Gawronski, P.
FR.I.2_03	Gaudin, G.	Mo.J-P8
Gargiani, P.	TH.F-P7	Gawroński, M.

FR.H-P3 Gawryluk, D.	Geilhufe, J. Fr.I.1_I1	Geselbracht, P. TH.B-P9
TH.C-P84 Gazeau, F.	Gellersen, F. Th.O-P26	TU.B-P66 Geshev, J.
FR.SP-2 Gázquez, J.	Gemmer, J. TH.A-P37	Mo.I-P16 Mo.I-P19
Mo.A-P58 Th.L-P5 Gàzquez, J.	Gemming, S. FR.F-P16	Mo.I-P22 Mo.I-P39
Th.E.2_O2 Gdovinova, V.	FR.G.2_O3 Genç, F.	Ghafari, M. FR.H-P23
Tu.F-P122 Ge, C.	TU.H-P49 Generalov, A.	Ghelardini, C. Fr.H.2_O2
Th.K-P41 Gegenwart, P.	TU.B-P30 Genovese, M.	Ghica, C. Mo.H-P15
Mo.C-P13 Th.D.1_O3 TH.K-P18 Gehring, G.	Fr.E.2_O4 Gensch, M.	Ghigna, P. Th.N-P13 Th.N-P15 TU.E.3_O2
TU.A-P57 TU.G.1_O4 Gehring, G.A.	Th.F.2_O5 Th.I-P17 George, J.	Ghigo, G. Th.A.1_O5 TH.J-P24
FR.F-P12 Th.K-P35 Geibel, C.	TH.E-P12 George, J.M.	Ghirardini, L. Mo.D-P30
Mo.A-P83 TH.C-P18 TU.B-P12 TU.B-P13 TU.B-P14 TU.B-P26 TU.B-P30 TU.B-P63 TU.C-P26 TU.C-P9 TU.F.1_I1 TU.F.1_O3 WE.H.2_O4 Geiger, D.	MO.F.1_O5 MO.F.3_O2 MO.H.3_O2 WE.G.1_O5 WE.I.1_O3 George, S.	Ghirri, A. TU.F-P53 Ghivelder, L. Th.B.3_O1 TH.C-P86 Ghorbani-Zavareh, M. Mo.L-P39 Ghosh, A. TH.E-P22 Ghosh, H. TU.A-P39 Ghosh, S. MO.A.3_O3 Mo.H-P58 Giamarchi, T. FR.E-P31 Mo.B-P15 TH.A-P5 Giannini, E. TU.C-P31 Giannopoulos, G. Mo.H-P63
TU.C-P20 TU.C-P29 Geiger, P.	TU.G-P14 George, T.	
Mo.L-P56 Geilen, M.	TU.F-P76 Georges, J.M.	
Th.O-P37	Mo.D-P27 Georgii, R.	
	TH.C-P97 Gerardino, A.	
	TU.G.3_O1 Gerasimov, E.	
	TH.C-P101 TH.C-P53 Gerber, A.	
	FR.H-P14 Gercsi, Z.	
	Th.B.3_O1 Gerfer, A.	
	Th.O-P13	

TH.K-P12 TU.E.3_03 TU.G-P4 Giblin, S.	TH.C-P94 Giriat, G. TU.F.1_05 Giridhar, M. FR.F-P32 Girovsky, J. FR.H-P34 TU.D-P12 Gislason, H.P. TU.G.1_05 Givord, D. Fr.A.2_05 MO.G.1_05 Th.I.1_05 TU.H-P63 TU.H-P97 Gjoka, M. TU.H-P136 Gladii, O. Mo.G-P5 Glasbrenner, J. TH.D-P19 Glatzel, P. Mo.A-P97 MO.B.1_11 Glaum, R. Mo.B-P26 Gluga, S. TH.J-P3 Th.M-P4 WE.E.1_04 Glomm, W.R. TU.B.2_03 Gloskovskii, A. Fr.D.2_02 Glover, S. TU.E-P48 Glover, T.E. Th.I-P1 Glushkov, V. Mo.A-P85 TH.C-P122 TH.C-P77 TH.C-P78 TU.B-P32	TU.B-P59 Gnatchenko, S. TH.C-P35 Gnida, D. TH.B-P5 TU.C-P17 Gobbi, M. MO.F.3_03 MO.J.2_11 Godel, F. Mo.E-P5 MO.J.2_02 Godinho, M. Mo.H-P101 Goering, E. Fr.G.1_03 Mo.I-P10 TU.H-P29 TU.H-P35 TU.I-P7 Goerlitz, D. TH.F-P24 Goetze, O. TU.E-P53 Gog, T. WE.F2_05 Gogoi, P. FR.D-P32 Gogola, D. Th.P-P30 Th.P-P37 Goh, S.K. Mo.A-P112 Gohda, Y. Fr.A.2_04 TU.E-P36 Goijman, D. TH.C-P37 Goikhman, A. Mo.H-P104 Goiriena, M. Mo.K-P4 Gojzewski, H. TU.F-P71 TU.F-P78
---	--	--

Goko, T. Fr.I.1_03	TU.B-P34	MO.C.1_02
Golasinski, K. MO.D.1_02	Gómez, A. TU.A-P95	González Vivas, L. TU.J.1_04
Gölden, D. Mo.H-P29	WE.B.2_16	González, C. Mo.C-P22
Golden, M. MO.SYM_2	Gómez, L. Th.P-P31	Th.G-P17
Goldman, A.I. Fr.D.2_03	Gómez, M.E. Mo.H-P14	González, D. TU.G-P15
Goldoni, A. FR.H-P33	Mo.H-P4	González, E.M. WE.B.2_16
Goll, D. TU.I-P7	TH.K-P8	González, J. TH.K-P3
Golosov, D. Th.J.3_03	TH.K-P9	TU.A.1_03
Golosovsky, I. MO.B.1_11	TU.A-P86	González, J.M. Mo.H-P108
TU.F-P87	TU.F-P24	TU.C.1_05
Golovenchits, E. TU.A-P64	Gómez-Iriarte, G.A. Mo.H-P13	González, L.E. TU.F-P24
Goltz, T. Fr.B.2_06	Gómez-Miralles, S. MO.J.2_11	González, M. TU.F-P73
TU.C-P9	Gómez-Montoya, D. FR.D-P84	González-Calbet, J.M. TU.J.1_04
Golubov, A.A. Mo.A-P26	TH.C-P128	González-Chavez, D.E. Mo.G-P29
Golz, T. Th.I-P17	Gómez-Polo, C. TU.D.3_02	Mo.G-P31
Gomes Da Silva, F. Mo.I-P13	Gomide, G. Th.P-P32	TH.I-P27
Gomes, A. Mo.L-P32	Gomide, G.S. TU.F-P114	González-Legarreta, L. TU.H-P133
TH.C-P121	Goncalves, A. Fr.B.3_01	González-Melendi, P. Th.H.1_05
Gomes, L. Mo.H-P90	Th.A.2_01	Gooch, M. TU.E.2_02
Gomes, Y. Mo.B-P30	TU.G-P27	Good, J. MO.E.2_05
Gómez Berisso, M. TH.A-P4	Gonçalves, A.P. WE.C.2_03	Goodwin, A. FR.D-P73
Gómez Cruz, J.M. Th.O-P32	Gonçalves, J. FR.E-P39	Gook, J.H. Mo.H-P102
Gómez Eslava, G.R. TH.C-P86	Gonçalves, J.N. TU.A-P89	Goolaup, S. Mo.K-P29
Gómez sal, J.C. TU.B-P33	TU.H-P131	Th.G.2_05
	Gonda, Y. TU.E-P11	TH.K-P5
	Gondek, Ł. TH.C-P55	Th.K-P55
	Gontarz, S. FR.I-P50	TU.I-P18
	FR.I-P51	TU.I-P6
	Gonzales Sutter, J.	

TU.I-P8 WE.J.1_O4 Gopman, D.	FR.D-P77 Goto, H.	Gradhand, M.
FR.H-P13 Goraus, J.	FR.A-P23	Th.I.2_O4
FR.E-P3 TU.B-P1 TU.E-P19 Gorbunov, D.	Mo.A-P111 Mo.A-P40 Mo.A-P42 Mo.A-P53 Goto, T.	Graf, D.
Th.A.2_O1 TH.C-P27 TH.D-P11 TH.D-P3 Gordon, E.	FR.A-P9 Mo.B-P16 Mo.B-P17 Mo.B-P18 TH.C-P126 TU.E-P37 Gotou, H.	FR.A-P56 FR.I-P7 Th.C-P03 Tu.A.3_O5 TU.H.2_O2 Grafe, H.J.
Mo.B-P25 Gordon, R.	Mo.A-P23 Gottlieb-Schönmeyer, S.	TH.A-P27 TH.A-P9 Th.D.3_O2 Gräfe, J.
Th.F.2_O2 Goremychkin, E.	TH.C-P116 Gottschall, T.	Fr.G.1_O3 Mo.I-P10 Granada, M.
TH.C-P28 Th.E.2_I1 Górka, B.	Fr.C.3_O4 Mo.L-P76 Mo.L-P83 Gouder, T.	Mo.K-P9 Granado, E.
FR.H-P3 Görlitz, D.	TU.G.2_O5 Goukassov, A.	FR.D-P65 Mo.A-P48 Granados, C.
Th.G.2_I1 Gornakov, V.	FR.D-P66 Gourdon, C.	TU.H-P34 Granados-Miralles, C.
MO.C.2_I4 Gorobets, O.	Th.I-P10 Th.I-P5 Gourgout, A.	Mo.I-P15 TU.F-P55 Grande, P.L.
Mo.H-P42 Gorobets, Y.	Mo.A-P59 Governale, M.	Mo.I-P16 Grandmont, D.
Gorodetsky, G.	FR.A-P49 MO.A.3_O2 Mo.A-P91 Goya, G.	TH.J-P33 Granitzer, P.
TH.C-P1 Gorria, P.	Th.P-P32 TU.F-P111 WE.SYM_1 Goyal, N.	Th.E.3_O3 Th.M-P22 Granja, L.
Fr.B.1_O4 TU.B-P33 TU.F-P59 Gorría, P.	TU.F-P99 Gràcia-Condal, A.	TH.C-P43 Granovsky, A.
TU.A.1_O4 Goryunov, Y.	Th.B.1_O3 Graczyk, P.	Mo.L-P3 TH.C-P40 Th.P-P18 Th.P-P24 Granovsky, S.
TH.C-P89 Goswami, P.	FR.H-P20	TH.C-P16 Granville, S.
Fr.C.1_O1 Mo.A-P5 Mo.B-P3 Gotfryd, D.		FR.F-P31 Mo.A-P91 Grasso, S.

Mo.L-P29 Graziosi, P.	Th.L-P4 TU.H-P96 Grigoriev, S.	WE.D.2_I6 Grockowiak, A.
Mo.H-P94 Grazú, V.	Mo.H-P61 Mo.I-P14 Mo.J-P12 Th.K-P28 Grigoryan, V.	Th.C-P03 Groitzl, F.
TU.F-P57 Grbic, M.S.	FR.H-P2 Grigoryeva, N.	FR.I-P7 Grollier, J.
TH.A-P20 Grça, M.	Mo.H-P61 Mo.J-P12 Th.K-P28 Grillo, V.	FR.A-P51 MO.H.1_I1 TH.J-P10 TU.H.1_O3 TU.H.1_O4 TU.I.1_O2 WE.I.1_O5 Groñ, T.
TU.A-P79 Gredig, T.	FR.I-P26 MO.C.2_I1 Grimaldi, E.	TH.C-P65 TH.D-P12 TU.H-P50 TU.H-P53 Gros, C.
TU.J.3_O2 Green, A.	TH.J-P13 TH.J-P14 TU.H.1_O3 TU.H.1_O4 TU.I.1_O2 Grin, Y.	FR.E-P15 Gros, I.
Th.D.1_I4 Green, B.	TU.I.1_O2 Grimm, A.	Th.E.1_I1 Grosche, M.
Th.I-P17 Green, E.	FR.D-P21 Grin, Y.	FR.A-P43 FR.A-P56 Fr.C.2_O2 FR.E-P41 Mo.A-P110 Mo.A-P70 TU.C-P23 TU.C-P32 TU.C-P33 WE.F.2_I1 Gross, K.
Fr.D.1_O2 FR.D-P27 TU.H.2_O3 Greenblatt, M.	TU.B-P36 Grinenko, V.	Mo.H-P14 TH.K-P9 Gross, R.
TU.A-P6 Greene, L.H.	Mo.A-P20 Grins, J.	TU.C-P20 Guar, R.
MO.A.2_O5 Greene, R.	FR.D-P5 Grioni, M.	Fr.B.1_O3 Grube, K.
MO.A.2_O4 Gregori, G.	Th.G.3_O1 Grisewood, N.	Fr.H.1_O2 Fr.H.1_O3 Mo.A-P110 Mo.A-P30
TU.H-P29 Greneche, J.M.	Mo.J-P22 Grishin, S.	
Mo.J-P10 TU.E.3_O2 Grenèche, J.M.	Fr.G.1_O4 Grissonanche, G.	
TU.H-P36 Grenier, B.	MO.A.2_I1 Gritsenko, C.	
MO.I.1_O3 Th.D.1_I4 Greser, J.	Mo.I-P27 Griveau, J.C.	
TH.E-P11 Greven, M.	TH.A-P21 TH.D-P15 TH.D-P25 Grobis, M.	
MO.A.2_O3 Gribanov, A.		
TH.B-P5 TU.C-P14 Grigera, S.A.		
TU.C-P28 Grigoras, M.		

TU.B-P63
 TU.H.2_03
Grübel, S.
 TU.E.1_06
Grundler, D.
 MO.E.2_01
 MO.H.3_03
 WE.H.1_03
Gruner, D.
 Mo.A-P20
Gruner, M.
 Mo.L-P75
 TU.D.3_04
Gruner, M.E.
 WE.D.1_11
Gruner, T.
 TU.B-P12
 TU.B-P14
Grunin, A.
 Mo.H-P104
 Th.N-P16
Gruszecki, P.
 Fr.I.2_02
 Mo.G-P11
Grutter, A.
 MO.C.3_01
Grüttner, C.
 Th.P-P2
 Th.P-P7
 TU.B.3_02
Grytsiv, A.
 WE.H.2_03
Gschneidner Jr, K.
 FR.SP-1
 Mo.L-P47
 Th.O-P21
Gspan, C.
 Th.G.2_02
Gu, B.
 Fr.G.2_11
 TH.I.1_04
 Th.I.2_05
Gu, G.
 Mo.A-P21
Gu, Y.

We.A.2_04
Gualdi, A.
 TU.A-P76
Guari, Y.
 Th.P-P10
 TU.F-P2
Gubbins, M.
 WE.J.1_02
Gubbiotti, G.
 Mo.G-P23
 Mo.H-P3
 TU.G-P10
 TU.I-P4
Gubkin, A.
 TH.C-P12
 TH.C-P53
Gudim, I.
 TH.D-P16
 TU.A-P48
 TU.A-P87
Gudoshnikov, S.
 FR.I-P6
 TU.A.1_02
Guerrero, R.
 Mo.I-P37
 TH.I-P28
Guerrero, S.
 Mo.G-P25
Guerrini, A.
 Fr.H.2_02
Guesdon, A.
 TU.E.1_05
Guetari, R.
 Mo.L-P63
Guguchia, Z.
 Mo.A-P22
 Mo.A-P8
Guiblin, N.
 TU.A-P100
Guidi, T.
 TH.A-P5
 Th.D.3_01
 Th.E.2_11
Guignard, M.
 FR.D-P7

Guillamón, I.
 TH.D-P22
Guillou, F.
 Mo.L-P16
Guimarães, A.P.
 TH.J-P20
Guimarães, J.
 Mo.I-P19
Guitard, P.A.
 Th.O-P50
Guitarra, S.
 Mo.B-P8
Guite, C.
 Th.O-P35
Guitteny, S.
 FR.D-P28
 FR.D-P29
 FR.D-P66
 TU.D.2_11
Guittoum, A.
 Mo.I-P18
Guizar-Sicairos, M.
 WE.E.1_04
Gukasov, A.
 TU.B-P11
 WE.C.2_05
Gukassov, A.
 Th.A.2_01
Gumeniuk, R.
 TU.B-P36
Gunderov, D.
 TU.H-P124
Gunnarson, K.
 Mo.L-P84
Gunnarsson, K.
 FR.D-P5
 Th.H.1_03
 TU.H-P111
Gunnlaugsson, H.P.
 TU.G.1_05
Günter, C.
 Fr.I.1_11
Günther, M.
 TH.C-P80
Guo, C.

FR.I-P2
 Mo.A-P27
 TU.B-P67
Guo, W.
 FR.H-P2
Guo, Y.
 FR.A-P30
 Th.A.2_O6
Guoqing, .
 TH.D-P7
Gupta, A.
 MO.D.1_O5
Gupta, L.
 TU.A-P80
Gural'skiy, L.C.
 MO.J.2_O4
Gurlui, S.
 Th.K-P34
 TU.F-P42
Gusev, N.
 Th.O-P8
Gusev, V.
 Th.I-P13
Gusin, P.
 FR.E-P29
Gusliyenko, K.
 Fr.I.1_I4
 Mo.K-P5
Gusmão, M.
 Mo.B-P11
Gustafsson, S.
 Th.P-P2
 TU.B.3_O2
Guterding, D.
 Fr.B.2_O2
Gutfleisch, O.
 Fr.A.1_I1
 Fr.A.2_O2
 Fr.C.3_O4
 MO.D.1_O4
 Mo.H-P29
 Mo.L-P39
 Mo.L-P48
 Mo.L-P56
 Mo.L-P76

Mo.L-P83
 PLENARY 5
 Th.A.3_O2
 TH.C-P85
 TU.C.3_O3
 TU.D.3_O4
 TU.H-P118
 TU.H-P124
 TU.H-P29
 TU.H-P43
 TU.H-P95
Gutierrez, A.
 TU.C.1_O5
Gutiérrez, D.
 Mo.K-P18
 Th.G.3_O4
 TU.A-P62
Gutiérrez, L.
 Th.P-P1
 TU.F-P61
Gutowska, M.
 TH.C-P35
 TU.E-P41
Güttler, M.
 TU.B-P30
Gutzeit, N.
 Mo.H-P17
Guziak, M.A.
 Th.K-P30
Guzik, M.N.
 MO.D.1_O2
 TU.H-P98
Guzmán, J.
 Mo.I-P26
Guzman, R.
 MO.C.3_O3
 TU.A-P24
 TU.A-P45
Guzmán, R.
 TU.A-P26
Guzowska, U.
 Mo.G-P16
Gvasaliya, S.
 Mo.B-P7
Gwak, M.

FR.I-P34
Gzik-Szumiata, M.
 FR.H-P3
H
H. Belo, J.
 Mo.H-P107
Haag, N.
 Mo.E-P11
Hachisu, M.
 TU.F-P10
 TU.F-P69
 TU.F-P70
Hackamer, A.
 Mo.L-P15
Hadipour, H.
 Mo.B-P1
Hadjipanayis, C.
 TU.F-P100
Hadjipanayis, G.
 MO.B.3_O4
 Mo.I-P25
 Mo.I-P30
 Th.A.3_O1
 TU.E.3_O3
 TU.F-P100
 TU.F-P76
Haen, P.
 TU.B-P44
Haese-Seiler, M.
 Mo.H-P56
Haese-Seiller, M.
 Mo.H-P100
 Mo.H-P12
Haettel, R.
 Th.I.1_O5
Hafermann, H.
 TU.B-P60
Hafid, M.
 TH.C-P83
Hafner, D.
 TU.B-P63

Haga, Y.	TH.C-P78	Mo.H-P76
MO.A.1_O4	Hajiri, T.	Hamann, S.
TH.C-P63	Mo.H-P66	TU.H-P81
TU.B-P35	TH.A-P30	Hamasaki, T.
TU.B-P43	TU.A-P72	FR.A-P6
TU.B-P55	TU.E-P18	Mo.B-P18
TU.B-P77	Hajisalem, G.	Hamaya, K.
Hägele, D.	Th.F.2_O2	Mo.D-P17
Mo.L-P76	Haj-Khlifa, S.	Mo.D-P19
Hagemeister, J.	TH.C-P96	Th.H-P2
MO.E.3_O3	Haku, T.	Hamelin, C.
TH.K-P16	Mo.B-P2	TU.I-P15
Häggström, L.	Halbedel, B.	Hamlin, J.J.
WE.D.1_O4	Mo.H-P17	Fr.H.1_O2
Haghshenasfard, Z.	Haldar, A.	Hammerath, F.
Mo.K-P6	Fr.I.1_O2	Mo.A-P103
Th.M-P2	Halder, M.	Hammouda, T.
Hagihala, M.	Mo.L-P51	TU.E.1_O5
FR.D-P60	TH.C-P97	Hamrle, J.
TH.C-P49	TH.J-P32	Fr.D.3_O3
Hagiwara, M.	Halevy, I.	Mo.H-P78
FR.D-P11	TH.A-P12	Th.N-P11
Mo.B-P12	TH.D-P25	Han, D.S.
Mo.B-P20	Hall, M.	Fr.I.2_O5
TH.A-P19	FR.I-P5	Mo.K-P31
TH.A-P22	TU.H-P16	WE.G.1_O2
TH.A-P35	TU.H-P27	Han, H.S.
TH.B-P11	Hallas, A.	Mo.H.3_O1
TH.C-P61	Fr.B.2_O4	Han, J.H.
Tu.E-P51	Fr.C.2_O4	Mo.G-P2
Hagjipanayis, G.	Halley, D.	Han, S.H.
Mo.I-P5	Fr.B.1_I1	Mo.D-P24
Hagymasi, I.	MO.E.1_O2	Han, X.
Fr.J.1_O3	Mo.E-P5	Mo.K-P10
MO.I.1_I1	MO.J.2_O2	Th.G-P6
Hai, X.	Halpin, F.	Hanayama, N.
TU.D.3_O1	Th.E.3_O1	TH.E-P6
Haidar, M.	Hals, K.	Hancock, J.
Mo.F-P8	TU.SYM_4	WE.F2_O5
Mo.G-P5	Hamada, I.	Hänel, J.
Haim, A.	TH.C-P59	FR.A-P50
Mo.A-P13	Hamada, K.	Hanfland, M.
Haines, S.	FR.A-P53	Mo.B-P25
TH.A-P11	Hämäläinen, S.	Hankiewicz, E.
Hairullin, E.	Fr.G.3_O3	FR.A-P49

Hanko, J.	Harish Kumar, N.	Th.O-P22
TH.D-P22	FR.F-P20	TU.H-P38
HANNA, C.	FR.F-P21	Hashimoto, K.
TU.F-P40	TU.E-P32	Th.K-P30
Hanneken, C.	Harmon, S.	Hashimoto, T.
Th.C.2_I1	FR.I-P5	Mo.B-P17
Hansen, M.F.	TU.H-P16	Hashimoto, Y.
Th.H.2_O5	TU.H-P27	MO.J.3_O1
TU.F-P102	Harnagea, L.	Hashinaka, T.
Hansen, T.	Fr.B.2_O6	TU.H-P85
TU.C.2_O3	Harres, A.	TU.H-P94
TU.E.1_O5	Mo.I-P16	Haskel, D.
Hanson, M.	Mo.I-P19	Mo.A-P33
Th.M-P13	Mo.I-P22	Mo.H-P34
Hara, R.	Harrison, N.	Th.G.3_O3
Mo.H-P1	MO.A.2_O3	Haskova, V.
Harada, K.	Harrison, R.J.	TU.E-P5
FR.D-P14	Fr.E.2_O2	Haslbeck, F.
Harada, M.	Hartmann, F.	TU.C-P30
Mo.B-P6	TU.I-P4	TU.H.3_O3
TU.C-P2	Hartmann, S.	Hasnip, P.
Haraguchi, S.	TU.F.1_I1	TU.E-P48
Th.G-P4	Hartmann, T.	Hatakeyama, K.
Haraguchi, Y.	Mo.A-P22	Th.O-P17
FR.D-P53	Hartwig, S.	TU.I.2_O5
Harasawa, T.	Mo.A-P98	Hatakeyama, Y.
WE.J.1_O3	WE.C.2_O5	MO.A.1_O3
Hardoň, Š.	Haruna, D.	Hatnean, M.C.
TU.F-P29	TU.H-P7	FR.A-P34
TU.F-P91	Harzallah, S.	Hatton, P.
Hardtdegen, H.	FR.I-P13	Th.J.1_O4
FR.F-P30	Hase, M.	Hauet, T.
Hardy, F.	Mo.B-P18	Th.I.3_O4
Mo.A-P97	Mo.B-P5	TU.I-P3
Tu.A.3_O5	TU.A-P50	Haug, M.
Hardy, W.	TU.A-P52	Mo.L-P25
MO.A.2_I1	TU.A-P53	Th.O-P13
MO.A.2_O2	Hase, T.	Haule, K.
TU.A.3_O1	TU.E-P48	TU.F.3_O1
Hari Babu, V.	Hasegawa, T.	Häußler, W.
Mo.H-P84	Mo.H-P51	TU.C-P30
Harima, H.	TU.B-P53	TU.H.3_O3
FR.C-P5	TU.D-P8	WE.H.1_O3
TU.E-P20	TU.H-P132	Häussler, W.
TU.E-P44	Hashi, S.	TH.C-P119

Havela, L.	TU.H-P38	WE.I.2_O3
FR.A-P8	Hayashibara, H.	Heid, R.
Mo.L-P49	Mo.H-P64	Mo.A-P30
TH.A-P12	Hayashida, S.	Heiliger, C.
TH.C-P45	FR.D-P60	WE.I.2_O5
TH.D-P8	TU.A-P27	Heinemann, A.
TU.G.2_O5	TU.A-P90	Th.K-P28
WE.C.2_O2	Hayashita, T.	Heinz, B.
Haverkort, M.	Mo.B-P17	Th.O-P37
FR.A-P29	Hayden, S.	Heish, H.C.
TH.K-P18	TH.C-P97	Mo.K-P1
Haverkort, M.W.	Hayward, T.	Hejtmánek, J.
TU.B-P5	Th.G.2_O6	FR.F-P30
Havránek, V.	He, Q.	Held, K.
FR.F-P30	TU.E-P8	Fr.J.1_I4
Haw, S.C.	He, S.	Heldt, G.
TU.A-P21	Mo.D-P13	TH.J-P3
Hawelek, L.	Heald, S.	Helerea, E.
FR.E-P3	TU.G.1_O4	Th.K-P32
TU.E-P41	Heald, S.M.	Helm, M.
Hawng, T.Y.	FR.F-P12	FR.F-P16
TU.H-P84	Heath, M.	FR.F-P18
Hayakawa, D.	Th.O-P27	FR.G.2_O3
Th.G-P10	Hebert, S.	Mo.D-P10
Hayakawa, K.	FR.C-P2	Helman, C.
Mo.H-P1	Heczko, O.	TH.K-P7
Hayami, S.	Mo.L-P20	TU.G-P21
FR.E-P36	Hedayat, H.	Helton, J.S.
Mo.C-P15	FR.H-P31	Fr.D.2_O3
TU.A-P81	Hedo, M.	Hemeda, O.
Hayashi, J.	TH.C-P71	TU.A-P35
Mo.A-P4	TU.E-P20	Hemmatiyani, S.
Hayashi, K.	TU.E-P44	TH.J-P8
FR.A-P55	Hehn, M.	Hen, A.
TH.B-P11	Fr.D.1_O3	TH.D-P25
TU.B-P38	FR.D-P21	Henk, J.
WE.H.2_O5	Mo.D-P8	FR.A-P32
Hayashi, M.	MO.H.1_O4	FR.A-P33
TU.SYM_3	Th.F.2_I1	TH.C-P46
WE.G.1_O3	Th.H-P1	Henkie, Z.
Hayashi, N.	Th.I.3_O4	TH.A-P23
Mo.K-P10	TU.G.3_O3	Henriques, A.
Hayashi, S.	TU.G-P1	FR.F-P11
TU.E-P31	TU.I.3_O1	Henriques, M.
Hayashi, Y.	TU.I-P3	Th.A.2_O1

TH.C-P27	Fr.A.1_04	TU.A-P93
WE.C.2_03	Semi Plenary	TU.E.1_02
Henry, F.	Th.O-P3	Herrmannsdörfer, T.
Mo.D-P30	Th.P-P8	Fr.D.1_02
Henry, P.	TU.H-P98	FR.D-P83
TU.D.1_03	TU.I.2_06	Herrnberger, A.
Henry, Y.	Hernando-Rydings, M.	Mo.H-P100
Fr.B.1_11	Th.O-P3	Mo.H-P12
Mo.G-P5	Herranen, T.	Mo.H-P56
MO.J.2_02	TH.F-P15	Hertlein, M.
Th.I.3_03	Herranz, G.	Th.I-P1
Th.I-P6	FR.I-P22	Hervault, A.
Henych, J.	Mo.A-P58	Th.P-P15
Th.O-P20	MO.C.3_04	Hervieu, M.
Heo, S.Y.	Mo.H-P84	TU.E.1_05
FR.A-P4	Th.G.1_03	Hervieux, P.A.
Herbrych, J.	Th.G-P15	TU.F-P31
TH.A-P37	TU.A-P63	Herzer, G.
Herea, D.D.	Herranz, O.	Mo.L-P13
Th.P-P26	Th.G.1_03	TU.A.2_02
Hering, E.N.	Herrasti, P.	Hesjedal, T.
TU.B-P70	Th.P-P8	MO.H.2_11
Hermanns, C.F.	Herrera-Aragon, F.	Mo.H-P70
MO.I.2_03	MO.G.1_05	Hess, C.
Hermenau, J.	Herrera-Vasco, E.	Mo.A-P20
FR.H-P8	TH.D-P22	Mo.A-P98
WE.G2_02	Herrero Albillos, J.	Mo.B-P7
Hermet, P.	Fr.E.2_02	Hettiarachchi, G.P.
TU.E.1_05	Mo.L-P47	TU.E-P37
Hernandez-Parra, J.	TH.K-P4	Heyderman, L.
FR.D-P84	Th.M-P1	Mo.H-P37
Hernández Paz, J.F.	TU.A-P13	TH.J-P3
FR.H-P35	WE.B.2_05	Heyderman, L.J.
Hernández, I.	Herrero Martin, J.	WE.E.1_04
TU.D-P5	Th.K-P41	Hibbard, G.D.
Hernández, J.M.	Herrero, J.	Th.N-P5
Th.C.2_04	FR.H-P25	Hibino, Y.
TU.B.3_01	MO.J.2_05	Mo.H-P16
Hernández-Parra, J.C.	Th.L-P5	Th.G-P10
TH.C-P128	Herrero-Martin, J.	Th.G-P8
Hernández-Torres, J.	TH.C-P75	Hidaka, H.
FR.H-P24	Th.J.1_03	TH.B-P14
Hernando Grande, A.	TH.K-P18	TU.A-P67
FR.H-P35	Herrero-Martín, J.	TU.B-P45
Hernando, A.	Th.A.1_01	TU.B-P48

TU.B-P50	Hillenbrand, R.	Mo.H-P16
Hidki, S.	Fr.I.3_O4	Mo.I-P2
Mo.L-P86	Hiller, S.	TH.K-P19
Hiebert, W.	Mo.B-P8	TU.E-P48
TH.J-P33	Hillier, A.	Hiroi, M.
Hierro-Rodriguez, A.	WE.H.2_O5	Mo.L-P66
Fr.H.3_O2	Hillier, N.	Hiroi, Z.
TU.J.1_O3	FR.I-P5	FR.A-P15
Hierro-Rodríguez, A.	TU.H-P16	FR.A-P17
Mo.H-P98	TU.H-P27	TH.C-P58
TH.K-P4	Hillion, A.	Hirose, S.
Hiess, A.	TU.F-P25	TU.E-P18
WE.C.2_O4	Hills, V.A.	Hirose, T.
Higa, N.	MO.C.1_O5	FR.A-P15
TH.B-P8	Hinata, S.	Hirose, Y.
TU.E-P44	TU.I-P20	FR.D-P16
Higashinaka, R.	Hincapie Fresneda, A.F.	TU.B-P35
Mo.A-P89	FR.A-P20	TU.B-P39
TU.B-P58	Hincapie-Bedoya, J.	TU.B-P42
TU.B-P8	FR.D-P84	TU.B-P43
TU.C-P19	TH.C-P128	Hirota, Y.
Higgins, J.	Hinokihara, T.	TH.C-P98
MO.A.2_O4	TU.B-P18	Hirotaki, K.
Higuchi, K.	Hinzke, D.	TU.H-P86
TU.A-P7	Th.I-P12	Hirotsu, Y.
Higuchi, T.	TH.J-P27	TU.H-P14
Th.I-P2	Hirabayashi, H.	Hiroyuki, A.
Higuchi, Y.	TU.B-P51	TH.F-P21
Mo.B-P6	Hirai, D.	Hirsch, K.
Hihath, J.	TU.E-P11	TU.F-P56
Mo.E-P6	Hiraka, H.	Hirschberger, M.
Hijii, K.	TU.C.2_O2	TU.C-P32
TH.A-P3	Hirakawa, M.	TU.C-P33
Hildebrandt, E.	TU.B-P46	Hisayoshi, K.
Mo.H-P29	Hiramatsu, R.	Th.O-P33
Hillebrands, B.	TH.F-P6	Th.O-P34
Fr.G.1_O2	Hirata, Y.	Hitotsukabuto, H.
Fr.G.1_O5	TU.A-P50	TU.B-P56
Mo.G-P13	TU.A-P52	Hjörvarsson, B.
MO.H.2_O2	Hirayama, T.	Mo.H-P100
TH.E-P11	TH.C-P120	Th.M-P18
Th.H-P18	Hirian, R.	WE.B.2_O3
Th.H-P9	TU.H-P23	Hlil, E.K.
Th.O-P37	TU.H-P24	Mo.L-P4
TU.E.3_I1	Hirohata, A.	TH.C-P96

Hneda, M.	Mo.L-P20	Mo.B-P9
Mo.B-P11	Th.N-P11	Höppner, M.
Ho, P.	TU.E-P46	TU.B-P30
TH.F-P1	Homma, Y.	Hord, R.
Ho, P.C.	FR.D-P61	TH.C-P80
TU.B-P50	Mo.A-P95	Horibe, Y.
Ho, T.	Mo.L-P64	TU.H-P33
Mo.L-P22	Honda, F.	Horiuchi, T.
Ho, T.A.	FR.D-P61	TU.H-P33
TU.F-P17	Mo.A-P87	Horsch, P.
Hoang, N.H.	Mo.A-P95	TH.A-P6
FR.D-P55	Mo.L-P64	Horvat, A.
Hoarau, C.	TU.B-P35	Fr.D.3_O1
TU.H.1_O2	TU.B-P39	Horvat, J.
Höfer, K.	TU.B-P42	TH.C-P91
Th.B.2_O2	TU.B-P43	Horvatic, M.
Hoffman, J.	TU.E-P20	TH.A-P10
TH.I.3_O5	Honda, N.	TH.A-P20
Hoffmann, A.	TU.I-P20	Hosaka, S.
TH.I.3_O5	Honda, S.	FR.D-P69
TH.SP-2	FR.H-P15	TH.C-P99
Hoffmann, J.U.	TH.F-P25	Th.D.3_O3
Mo.B-P29	Honda, T.	Hoser, A.
Hoffmann, M.	TH.A-P29	TH.C-P55
TU.E.1_O6	Hong, J.	Hoshino, H.
Hofmann, J.U.	Fr.A.1_11	Fr.H.3_O3
TH.A-P26	FR.F-P13	Hoshino, T.
Hofsaess, H.	FR.H-P11	Mo.J-P1
TH.C-P50	TU.G-P22	TU.E-P1
Holanda, J.	Hong, J.I.	Hosokoshi, Y.
Mo.K-P2	Mo.H.3_O1	TH.C-P103
Holanda, L.M.	WE.H.1_O2	Hosono, H.
TU.B-P2	Hong, S.	Fr.B.2_O5
Holderer, O.	TU.A-P78	Mo.A-P60
TH.C-P119	Hong, Y.K.	Hosoya, Y.
Holdsworth, P.	FR.I-P45	Mo.B-P17
Fr.D.1_11	Honma, Y.	Hossain, Z.
Holladay, B.	Th.K-P30	TU.B-P14
WE.G2_O4	Honolka, J.	Hotta, T.
Holler, M.	FR.A-P60	Th.C.3_O3
WE.E.1_O4	Hoof, N.	TH.C-P44
Holm, S.	WE.G.1_O2	TU.E-P14
TU.E.2_O3	Hoovinakatte, N.	Hotta, Y.
Holý, V.	Mo.H-P81	Fr.A.3_O2
Mo.D-P12	Hopkins, E.J.	Houshang, A.

Mo.F-P4
MO.H.2_04

Hovorka, O.

Th.I.3_04

Howald, L.

MO.A-P2

Howczak, O.

WE.E2_06

Hradil, K.

Mo.A-P32

TH.B-P7

TH.C-P116

Hrkac, G.

TH.J-P3

Hsiao, Y.F.

TU.A-P44

Hsieh, J.H.

FR.F-P26

Hsu, H.S.

TU.F-P88

Hsu, P.J.

MO.G.3_04

Hu, C.K.

Tu.F-P122

Hu, M.Y.

TU.D.3_04

Hu, R.

FR.D-P11

MO.I.1_02

TU.E.1_04

Hu, S.

TH.E-P14

Th.H-P12

Th.H-P3

Hu, X.

WE.H.1_04

Hu, Y.

TU.E.1_03

Hu, Y.M.

Mo.H-P69

Th.G-P11

Hu, Z.

FR.A-P29

Mo.B-P9

TH.K-P18

Th.K-P41

TU.A-P21

TU.B-P5

TU.B-P67

Huang, B.T.

Th.B.1_02

Huang, C.H.

TH.C-P108

Huang, K.

TU.B-P21

TU.B-P48

Huang, S.

TU.E.1_06

Huang, S.S.

WE.D.2_11

Huang, S.W.

TU.E.1_03

Huang, Y.

Fr.B.2_03

Fr.C.1_02

WE.C.2_05

Huang, Y.H.

TU.F-P66

Huang, Y.K.

MO.SYM_2

Huber, L.

TU.E.1_06

Huber, M.

Mo.H-P81

Hübl, H.

TU.C-P20

Huckfeldt, H.

TU.G.2_02

Hudak, R.

Th.O-P55

Huecker, M.

Mo.A-P21

Huerta, L.

Mo.A-P25

Huesges, Z.

TU.B-P26

Hueso, L.

Fr.I.3_04

Hueso, L.E.

MO.F.3_03

MO.J.2_11

TH.E-P9

Th.I.2_04

Hug, H.J.

MO.E.2_06

Th.I.3_04

Hugonnet, B.

Th.A.3_04

Huh, S.

Mo.B-P9

Huh, Y.

Th.K-P29

Huhtinen, H.

Mo.H-P19

Mo.H-P20

Mo.H-P52

Th.O-P14

Huisman, T.

Th.F.1_03

Huisman, T.J

Th.I.1_03

Th.I-P11

Huminiuc, T.

TH.K-P19

Hung, C.Y.

FR.I-P8

Hunter, E.

Fr.D.2_04

Th.G.3_02

Huq, A.

Mo.A-P102

Huráková, M.

Mo.A-P38

TU.H-P39

Hurdequint, H.

TU.G-P22

Hurtado Marín, V.A.

FR.E-P17

Husain, S.

TU.E-P42

Hüsges, Z.

TU.H.2_03

Hussain, T.

Mo.H-P96

Hutchison, W.

Mo.L-P31
Huth, M.
 Th.G.2_O2
 WE.B.2_O2
Huthwelker, T.
 WE.E.1_O4
Huxley, A.
 Mo.A-P61
 Mo.A-P73
 Th.D.1_I4
Hwang, C.
 MO.I.1_I1
 TH.F-P11
Hwang, D.G.
 Th.P-P21
 Th.P-P35
Hwang, S.Y.
 Th.H-P15
Hyodo, K.
 TH.E-P19
 TU.F-P10
 TU.F-P69
 TU.F-P70
 TU.H-P109
Hyun, J.M.
 TU.D-P10
 TU.E-P40

I

I. Stepanov, V.
 Mo.I-P13
Iacocca, E.
 Mo.F-P4
 Mo.F-P8
 MO.H.2_O4
Iakovleva, M.
 Th.D.3_O2
Ibarra, A.
 TU.F-P111
Ibarra, M.R.
 MO.C.3_O3
 Mo.H-P55

Mo.K-P17
 Th.B.2_I1
 Th.B.2_O3
 Th.B.3_O2
 Th.H.1_O5
 Th.H-P5
 Th.H-P8
 Th.I.2_O4
 Th.P-P34
 TU.A-P26
 TU.A-P86
 TU.C.1_O4
 TU.F-P111
 TU.F-P57
 WE.H.2_O2
 WE.SYM_1
Ibrahim, P.
 TH.C-P12
Ibuka, S.
 FR.A-P37
Ichinose, T.
 TU.A-P66
Ichiyanagi, Y.
 TU.F-P10
 TU.F-P62
 TU.F-P69
 TU.F-P70
Ido, H.
 TU.E-P3
Ido, M.
 Mo.A-P74
Idrobo, J.C.
 MO.E.1_O4
Idzikowski, B.
 Mo.L-P40
 TU.H-P46
Ieda, J.
 TH.J-P8
Ienaga, K.
 Fr.D.3_O2
Ievdokimova, A.
 Th.A-P40
Iga, F.
 FR.A-P55
 Th.D.3_O4

TU.B-P38
 TU.B-P53
Iglesias, I.
 Th.O-P57
 Th.P-P18
 TU.H-P125
 TU.H-P129
Iglesias, O.
 Mo.K-P11
 TU.B.3_O3
 TU.F-P65
Iglesias-Freire, O.
 Th.F.3_I1
Iglesias-Freire, Ó.
 Fr.E.2_O3
Ignatyeva, D.
 Th.N-P12
 Th.O-P41
Iguchi, M.
 TU.E-P39
Iguchi, S.
 Mo.B-P17
Ihara, Y.
 TU.B-P45
Iida, R.
 Th.I-P2
Iihama, S.
 Th.F.1_O4
 TH.I-P24
Iimura, S.
 Fr.B.2_O5
 Mo.A-P60
Ikeda, A.
 TU.A.-59
 TU.A-P60
Ikeda, H.
 Mo.A-P30
 Tu.A.3_O5
Ikeda, M.
 FR.D-P11
Ikeda, N.
 TU.C.2_O2
Ikeda, R.
 MO.A.1_O3
Ikeda, S.

Th.O-P52	Fr.A.3_O2	TU.D-P8
Ikeda, Y.	Th.K-P47	Iñiguez, J.
TH.A-P7	TU.I-P23	Th.E.1_O2
Ikedo, Y.	Inagaki, H.	Ionescu, A.
TU.A-P47	TU.B-P50	Fr.B.1_O3
Ikuta, M.	Inagaki, Y.	Mo.H-P106
FR.H-P12	FR.D-P46	Mo.H-P95
Ilkovic, S.	FR.H-P36	Mo.H-P96
WE.C.2_O3	FR.I-P25	Iordanescu, C.R.
Ilkovic, V.	Th.A-P34	Th.O-P19
FR.E-P8	TH.D-P23	Ipatov, M.
Ilver, L.	Th.K-P33	Mo.L-P12
Tu.G.1_O2	Inami, N.	Mo.L-P78
Im, M.Y.	FR.H-P26	Ipus, J.
Mo.H.3_O1	Mo.I-P2	Th.B.1_11
WE.H.1_O2	TU.H-P132	Ipus, J.J.
Imai, M.	TU.H-P57	Mo.L-P14
TU.C-P2	Inami, T.	Irfan, B.
Imai, Y.	TH.C-P63	FR.A-P46
FR.A-P11	Inchausti, X.	Irons, H.
Imaizumi, M.	TH.G.1_O2	TU.D-P13
TH.D-P1	Infante, I.C.	Irurzun, I.
Imamura, H.	TU.A-P100	TH.C-P37
FR.H-P28	Innocenti, C.	Irvine, A.
MO.H.2_O5	Fr.H.2_O2	Fr.G.3_O2
Mo.J-P4	TU.B.2_O4	Th.G.2_O6
TH.J-P22	TU.F-P60	TU.SYM_4
WE.D.2_O2	TU.F-P64	Isaev, D.
WE.D.2_O5	Inokuchi, T.	Th.P-P24
imamura, K.	Mo.D-P17	Isakov, S.
Mo.G-P4	Inosov, D.	TH.A-P26
Th.O-P7	Mo.A-P100	Isasa, M.
Imamura, M.	MO.D.3_O3	TH.E-P9
Th.H-P4	Inoue, D.	Th.I.2_O4
Imazato, M.	TU.B-P76	Isella, G.
TU.G-P24	Inoue, I.H.	Mo.D-P30
Imura, K.	FR.A-P45	Ishibashi, T.
Fr.B.3_O4	Inoue, J.I.	Th.H-P7
Mo.A-P80	FR.H-P15	TU.H-P114
Mo.A-P81	TU.G-P13	TU.H-P85
TU.C-P18	TU.G-P9	TU.H-P87
TU.H.2_11	Inoue, K.	TU.H-P94
Inaba, K.	TH.C-P61	Ishida, K.
FR.B-P10	TU.C.2_O2	WE.F2_O4
Inaba, N.	TU.C.2_O4	Ishida, T.

Fr.A-P64	Isidori, A.	Ito, N.
Ishida, Y.	FR.A-P24	TU.A.2_02
Fr.C.2_05	Isikawa, Y.	Ito, T.
Ishiguro, R.	TU.B-P9	FR.H-P12
Mo.A-P66	Iskhakov, R.	Mo.B-P18
Ishihara, K.	Mo.H-P38	TH.A-P30
TU.B-P56	TU.H-P55	Th.E.2_04
Ishii, H.	Islam, A.T.M.N	TU.A-P50
Mo.A-P46	FR.D-P83	TU.A-P52
Ishii, I.	TH.A-P42	TU.A-P53
FR.A-P23	Islam, N.	TU.E-P3
Mo.A-P111	FR.B-P30	Itoh, H.
Mo.A-P40	Th.D.3_01	FR.H-P15
Mo.A-P53	Islam, S.	Itoh, M.
Ishii, K.	Th.K-P33	Mo.A-P90
TU.B-P38	Islam, Z.	Mo.C-P21
WE.F2_05	MO.SYM_5	TH.A-P30
Ishii, S.	Isnard, O.	TU.E-P38
FR.D-P71	Mo.B-P11	TU.E-P39
Ishikado, M.	TH.D-P11	Itoh, S.
FR.D-P1	TU.E-P29	FR.A-P37
Ishikawa, H.	TU.H-P119	FR.I-P33
TH.C-P58	TU.H-P120	TH.A-P7
TU.H-P70	TU.H-P122	TU.A-P90
Ishikawa, M.	TU.H-P23	Iunin, Y.L.
Mo.D-P17	TU.H-P24	Mo.H-P39
Ishikawa, T.	Isobe, H.	Iurchuk, V.
FR.B-P14	Mo.E-P7	Th.G-P19
Mo.A-P52	Isobe, M.	Ivanov, A.
TU.H-P57	FR.A-P12	TU.B-P20
Ishimasa, T.	Mo.A-P39	Ivanov, B.
Fr.B.3_04	TU.B-P3	FR.F-P11
TU.C-P18	TU.E-P39	TH.C-P92
TU.H.2_11	ITAKURA, M.	Ivanov, I.
Ishio, S.	TU.H-P70	Fr.E.1_03
MO.B.1_04	Ito, E.	Mo.L-P45
Mo.H-P51	Mo.E-P12	WE.F.1_02
TU.H-P132	Ito, F.	Ivanov, V.Y.
Ishiyama, J.	TU.H-P56	TU.A-P11
TH.D-P21	Ito, K.	TU.A-P30
Ishiyama, K.	Mo.H-P51	TU.A-P93
Th.O-P22	TU.A-P72	TU.A-P98
TU.H-P38	Ito, M.	Ivanovskaya, V.
Ishizaka, T.	Fr.A.2_05	TU.A-P100
Mo.A-P23	TU.H-P63	Ivanshin, V.

J

TU.B-P62
TU.F-P82

Ivantsov, R.

TU.F-P88

Iwahori, K.

FR.B-P29

Iwakami, O.

TH.C-P126

Iwaki, K.

TU.I-P19

Iwama, H.

Mo.H-P26
TH.K-P15
Th.L-P1

Iwano, K.

Mo.J-P13
TU.H-P57

Iwasa, K.

FR.A-P37
TH.C-P75

Iwasaki, J.

TU.H.3_O2

Iwata, S.

Th.P-P29
TU.H-P114
TU.I-P14
TU.I-P16

Iwazaki, Y.

TU.E-P36

Iyer, K.K.

FR.D-P17
TU.A-P19

Izawa, K.

Th.J.2_O2
TU.C-P22
TU.C-P27

Izotov, A.

Mo.H-P93

Izquierdo, J.L.

TU.A-P95

Izumi, T.

Mo.E-P7

J. Terán, F.

Th.K-P44

Jaafar, M.

Th.F.3_I1

Jaccard, D.

TU.F.1_O5

Jackiewicz, D.

FR.I-P29
TU.H-P59

Jackson, R.

Th.P-P25

Jacob, A.

Th.O-P26

Jacobsen, H.

FR.D-P73
TU.D.1_O3

Jacques, V.

Th.E.1_I1

Jacquet, E.

MO.F.1_O5
MO.J.3_O3
TU.A-P100

Jacyna, I.

TU.G-P28

Jaffrès, H.

Mo.D-P27
MO.F.1_O5
MO.F.3_O2
TH.E-P12
WE.I.1_O3

Jaglicic, Z.

FR.A-P41
Mo.A-P18

Jaglièiaè, Z.

TU.A-P46

Jahangiri, J.

Mo.B-P1

Jaime, M.

TU.H.2_O2

Jain, A.

Mo.C-P14

Jain, M.

FR.D-P34

Jain, P.

TU.A-P80

Jakhina, E.

Mo.L-P87

Jakubowski, M.

Th.C.2_O5

Jalili, P.

Th.L-P6

Jamet, M.

Fr.G.3_O4
Mo.D-P27
Mo.D-P30
MO.F.1_O5
MO.F.3_O2
TH.E-P8
TH.J-P23
WE.G.1_O5

Jamet, S.

FR.I-P28
Mo.K-P26
WE.F.1_I1

Jamon, D.

Tu.F-P122

Janda, T.

Fr.G.3_O2
TU.G.1_O3

Jander, A.

MO.J.3_O2

Jang, B.K.

Th.E.2_O5
TU.A-P36

Jang, D.

FR.D-P52

Jang, H.

TU.A-P36

Jang, H.J.

Mo.E-P2

Jang, H.M.

FR.A-P4

Jang, J.

TU.A-P6

Jang, P.

TU.H-P72

TU.H-P90	Javaheri, M.	FR.F-P16
Jang, T.	TU.C-P26	Jensen, J.
TU.H-P20	Javorsky, P.	TH.C-P28
Jang, T.S.	Mo.A-P54	WE.C.2_O4
TU.H-P44	TH.D-P13	Jenuš, P.
TU.H-P47	TU.B-P23	Mo.I-P11
Jang, Y.J.	Javorský, P.	TU.H-P34
Mo.C-P20	TH.C-P51	Jeon, B.Y.
TU.G-P20	TU.B-P72	Mo.L-P33
Jang, Z.	Jazbec, S.	Jeon, G.S.
FR.D-P52	Mo.A-P18	Th.E.2_I1
Jankovský, O.	Je, S.G.	Jeon, K.W.
FR.F-P30	TH.F-P11	TU.H-P84
Janos, P.	TH.F-P19	Jeong, H.G
Th.O-P20	Jean, M.	FR.A-P17
Janoschek, M.	TU.F-P85	Jeong, J.
Fr.A.1_O3	TU.F-P86	Fr.C.3_O3
TU.B-P21	TU.H-P61	Th.E.2_I1
TU.B-P48	TU.H-P62	TU.I-P24
WE.H.1_O3	Jedryka, E.	TU.I-P5
Jansen, M.	TU.A-P62	WE.J.1_O5
Th.A.1_O2	TU.A-P63	Jeong, M.
Jansen, R.	Jeffries, J.	TH.A-P20
Mo.D-P22	Fr.C.1_O4	TH.C-P28
Janusonis, J.	TU.B-P21	TH.C-P41
Th.I-P7	TU.B-P22	TH.C-P56
Jany, B.	TU.B-P73	Jeong, Y.H.
Th.K-P36	Jelen, A.	Fr.H.1_O4
WE.E.1_O2	FR.A-P41	TU.A-P16
Jaouen, N.	Mo.A-P18	TU.A-P17
WE.G2_O4	Jellyman, E.	TU.A-P36
Jaramillo, D.S.	Mo.A-P105	Jeschke, H.
Th.A.3_O1	Jen, S.U.	FR.D-P55
Jarrige, I.	Mo.L-P1	Jeschke, H.O.
WE.F2_O5	TU.G-P8	Fr.B.2_O2
Jascur, M.	Jenei, Z.	Jesenska, E.
FR.D-P62	Fr.C.1_O4	TU.H-P85
FR.D-P63	Jenkins, A.	Jesus, C.B.R.
TH.C-P74	TH.J-P10	TH.C-P9
Jasmin-Lebras, G.	TH.J-P13	Jhajhria, D.
Th.O-P50	TH.J-P14	Mo.H-P91
Jaubert, L.	TU.H.1_O3	Ji, H.
Fr.D.1_O4	TU.H.1_O4	TH.A-P9
Jaubert, L.D.C	TU.I.1_O2	Jia, C.
Th.D.2_O3	Jenkins, C.A.	Mo.K-P10

TU.A-P97	Jin, W.	MO.C.3_05
Jia, J.	Mo.A-P57	Jonasson, C.
Th.K-P35	Jin, Y.	Th.P-P2
Jia, M.	TU.F-P33	TU.B.3_02
Mo.H-P28	Jiraskova, Y.	Jonnard, P.
Jia, Q.	TU.F-P20	MO.E.1_02
WE.G2_04	Jiřík, R.	Jorba Cabre, P.
Jiang, W.	Th.P-P4	TU.B-P75
Mo.A-P27	Jo, M.H.	Jorba Cabré, P.
Th.C.3_01	Mo.D-P16	TH.C-P116
TU.B-P67	Jo, W.	Jorba, P.
Jiang, Y.	TU.A-P78	FR.I-P17
MO.A.2_04	Jo, Y.J.	Jordan, O.
Mo.H-P65	TU.A-P28	Th.P-P4
Jiang, Y.W	TU.A-P29	Joshi, N.
TU.A-P44	Joeng, J.W.	MO.E.2_06
Jiao, L.	Th.I-P16	Jouan, A.
Th.C.3_01	Johanns, K.E.	Mo.A-P58
TU.F.1_11	Mo.L-P56	Joulié, S.
TU.H.2_02	Johansen, T.	Th.C.2_02
Jiménez, A.	TU.F-P12	Joumard, I.
TH.F-P4	Johansson, C.	Mo.I-P4
Jiménez, E.	Th.P-P2	Th.O-P48
Mo.I-P31	TU.B.3_02	TU.G.3_02
Jiménez, J.	TU.F-P102	Jourdan, M.
Th.O-P57	Johmoto, K.	FR.A-P35
TU.H-P129	TH.A-P14	Fr.D.2_02
Jiménez-Cavero, P.	TH.A-P18	Juang, J.Y.
Mo.H-P2	Johnson, J.	TU.A-P44
Mo.H-P40	TU.E.1_06	Juang, L.W.
Jiménez-Romero, E.	Johnson, R.	FR.F-P26
FR.I-P23	FR.A-P30	Jué, E.
Jin, C.	MO.SYM_5	TH.F-P7
Fr.B.2_04	Th.E.1_03	WE.I.1_02
Fr.C.2_04	Johnson, S.L.	Juhin, A.
Fr.G.2_11	TU.E.1_06	MO.B.1_11
Fr.I.1_03	Johnston, D.C.	Th.C.3_02
Jin, C.Q.	Fr.D.2_03	Julfakyan, K.
Fr.B.2_03	Johnston, K.	Mo.K-P7
Jin, H.J.	TU.G.1_05	Julian, C.
TU.A-P78	Joisten, H.	Th.H.2_02
Jin, H.S.	Th.O-P48	Julian, S.
FR.A-P17	Joly, L.	TU.A.3_01
Jin, H.W.	Fr.B.1_11	TU.E-P33
Mo.D-P25	Jomard, F.	Julian, S.R.

TU.C-P28
Jun Tan, A.
 Th.G-P13
Jun, H.W.
 TU.H-P17
Jung, C.U.
 Mo.D-P25
Jung, G.
 TH.C-P1
Jung, H.
 Mo.E-P12
 TU.H-P22
Jung, J.
 Mo.F-P17
 Mo.I-P9
Jung, M.H.
 FR.A-P40
 Mo.G-P24
 TU.A-P36
Jung, S.
 TU.H-P5
Jung, S.Y.
 Th.O-P38
 Th.O-P39
 Th.O-P42
 Th.O-P43
Jung, T.A.
 FR.H-P34
 TU.D-P12
Jung, W.
 FR.F-P13
Jungfleisch, M.B
 MO.H.2_02
Jungwirth, T.
 FR.F-P6
 Fr.G.3_02
 MO.C.1_05
 MO.F.1_11
 MO.F.1_03
 TU.G.1_03
Junquera, C.
 WE.SYM_1
Juraszek, J.
 Th.E.1_11
 TU.H-P61

TU.H-P62
Jurchescu, O.
 Mo.E-P2
Jurek, K.
 FR.F-P30
 Th.O-P9
Jurga, S.
 Mo.I-P25
Juríková, A.
 Mo.A-P38
 TU.F-P49
 TU.F-P50
 TU.H-P39

K

Kabanov, Y.P.
 MO.C.2_14
Kabatova, M.
 TU.H-P52
Kabeya, N.
 TH.A-P13
Kachniarz, M.
 FR.I-P36
 TU.H-P104
Kaczmarczyk, J.
 WE.E2_05
Kaczorowski, D.
 FR.A-P28
 Fr.C.1_03
 Mo.A-P107
 TH.B-P5
 TH.C-P52
 TU.C-P17
Kadam, M.
 Mo.H-P53
Kadowaki, K.
 Mo.A-P52
Kądzielawa, A.P.
 FR.C-P7
Kaeswurm, B.
 Fr.C.3_04
 Mo.L-P56

Kagayama, T.
 Mo.A-P78
Kageyama, H.
 TH.A-P10
Kagomiya, I.
 TH.C-P98
Kaidatzis, A.
 Th.K-P37
 TU.G-P4
Kaido, C.
 TU.H-P33
Kaido, D.
 TU.B-P76
Kainuma, R.
 Mo.L-P71
Kaiser, M.
 Th.O-P13
Kaiser, V.
 Fr.D.1_11
Kajihara, R.
 TU.A-P73
Kakay, A.
 MO.D.3_02
 TH.J-P9
 TU.H.1_11
Kakazei, G.
 Mo.H-P43
 Mo.H-P55
Kakehashi, Y.
 FR.B-P5
 TH.C-P2
 Th.J.1_05
Kakihana, M.
 TH.C-P71
Kakihata, K.
 TH.A-P19
Kakimaru, R.
 Mo.H-P92
Kakimoto, K.I.
 TH.C-P98
Kakiuchi, K.
 TU.E-P3
Kakizakai, H.
 Th.G-P14
 Th.G-P3

Kakurai, K.	FR.D-P11	Kanazawa, N.
FR.D-P1	FR.D-P32	Fr.I.1_O3
Kalashnikova, A.	Kamikawa, S.	MO.H.3_O4
Th.I-P19	FR.A-P23	Kanchanavatee, N.
Kalganov, D.	Mo.A-P111	TU.B-P48
Th.O-P47	Mo.A-P40	Kandpal, L.M.
Th.P-P23	Mo.A-P53	TU.A-P74
Kalinin, Y.	Kamilov, I.	TU.G-P25
Mo.H-P38	TU.A-P85	Kandukuri, S.C
Kalinowski, L.	Kamimori, T.	TH.B-P16
TU.B-P1	TU.H-P7	Kaneko, H.
TU.E-P19	Kaminski, N.	Fr.D.1_O2
Kalish, A.	Th.I-P16	Kaneko, R.
Th.N-P12	Kamiya, K.	FR.E-P15
Th.N-P6	TU.C-P18	Kaneko, T.
Kalitsov, A.	Kamiyama, T.	FR.A-P53
Mo.F-P9	TU.C.2_O4	FR.B-P15
Kalyabin, D.	Kamp, M.	FR.B-P18
Th.M-P7	TU.I-P4	FR.B-P28
Kamalakar, V.	Kampert, E.	Mo.A-P41
MO.J.2_O2	FR.A-P24	Kaneko, Y.
Kamantsev, A.	Mo.A-P98	Fr.A.3_O3
Mo.L-P37	Kampfrath, T.	FR.F-P4
Mo.L-P74	Th.I-P17	Kang, B.
Mo.L-P8	Kamran, M.	FR.A-P16
Th.B.1_O5	Mo.A-P62	Mo.D-P13
TH.C-P111	Kamusella, S.	TH.A-P16
TH.C-P112	Fr.B.2_O6	Kang, B.S
Kamarad, J.	Mo.A-P100	FR.F-P14
TH.C-P76	Kamzin, A.	Kang, M.K
Kamazawa, K.	TU.F-P62	TU.H-P84
FR.D-P1	Kamzin, A.S.	Kang, S.J
Kambe, S.	Mo.H-P51	Mo.A-P66
TU.H.2_O5	Kanak, J.	Kang, S.K.
Kambe, T.	Mo.H-P105	Mo.C-P7
Mo.A-P86	Kanao, T.	Kang, W.
TU.D-P9	WE.D.2_O4	Mo.C-P12
Kamble, B.	Kanashima, T.	Th.J.2_O2
Mo.A-P99	Mo.D-P19	Kanjilal, D.
Kamenev, K.	Th.H-P2	Mo.H-P58
Mo.A-P61	Kanazawa, H.	TU.A-P15
Mo.A-P73	TH.F-P25	Kanoda, K.
Kameno, M.	Kanazawa, I.	MO.I.3_O4
MO.F.3_O1	FR.A-P52	Kanomata, T.
Kamenskyi, D.	FR.F-P22	Mo.L-P71

TU.E-P21

Kanski, J.

Tu.G.1_O2

Kanungo, S.

Th.A.1_O2

Kaňuchová, M.

Mo.L-P19

Kao, T.H.

Mo.C-P21

Kapa, S.R.

MO.E.2_O4

Kapaklis, V.

Th.M-P18

Th.N-P10

WE.B.2_O3

Kappenberger, R.

Mo.A-P103

Kar, G.S.

WE.D.2_O3

Karavainikov, A.

Th.N-P7

Th.N-P8

Karcý, O.

FR.I-P15

FR.I-P16

FR.I-P17

Karel, J.

TU.E-P28

TU.G-P16

TU.J.2_O4

Karlewski, C.

Th.I-P3

Karlsson, K.

Tu.G.1_O2

Karnad, G.

Fr.I.2_O5

Karnaushenko, D.

TU.C.1_I1

Karpasyuk, V.

FR.F-P19

Karpenkov, D.

TU.H-P124

Karpenkov, D.Y.

Fr.A.1_I1

TH.C-P85

TU.H-P43

Karpinski, J.

Mo.A-P37

Karppinen, M.

FR.D-P59

Karube, S.

WE.E.1_I1

Kasagi, T.

Th.O-P17

TU.I.2_O5

Kasahara, A.

Th.C.3_O4

Kasahara, S.

Tu.A.3_O5

Kasai, S.

Mo.G-P7

Mo.G-P8

Kasamatsu, N.

Th.A-P34

Kasatani, K.

FR.D-P51

Kashiwagi, T.

Mo.A-P52

Kasinathan, D.

FR.A-P29

Kasiviswanathan, S.

TH.C-P117

Kaspar, Z.

FR.F-P6

Kastil, J.

TH.C-P76

Kaštil, J.

TH.C-P51

Kataev, V.

TH.A-P27

TH.A-P9

Th.D.3_O2

TU.E-P6

Katano, S.

TU.B-P51

KATAO, H.

TU.H-P70

Kato, A.

Fr.A.3_O3

MO.D.1_O4

Th.L-P1

TU.H-P115

TU.H-P63

Kato, H.

FR.H-P18

TU.H-P106

Kato, T.

Th.P-P29

TU.H-P114

TU.I-P14

TU.I-P16

Kato, Y.

Mo.C-P21

Katoh, K.

Mo.A-P111

Mo.A-P40

TU.B-P27

TU.B-P57

Katori, H.

TU.C-P10

Katrych, S.

Mo.A-P37

Katsnelson, M.I.

FR.A-P8

Fr.F.1_O5

Mo.G-P19

Mo.G-P27

Katsufuji, T.

FR.D-P19

Katsunori, K.

Mo.G-P24

Katter, M.

Mo.L-P56

Mo.L-P70

Mo.L-P79

Th.A.3_O3

Th.B.3_O1

Kaufmann, F.

FR.I-P21

Kaur, D.

Mo.I-P36

Kavaldzhiev, M.

Th.M-P8

Kavas, H.

TU.H-P48

TU.H-P49	Kawamura, N.	Keller, L.
Kaveèanský, V.	Fr.D.3_O2	Mo.A-P55
Mo.L-P19	TU.B-P25	Mo.B-P5
TU.C-P12	Kawamura, Y.	Mo.B-P6
Kawabata, J.	Mo.A-P23	TU.A-P51
TH.B-P11	Mo.A-P4	Keller, N.
TH.B-P4	TU.B-P56	MO.C.3_O5
TU.B-P19	Kawana, D.	Keller, S.
Kawachi, S.	TU.A-P90	TH.E-P11
Th.E.2_O4	Kawano, M.	Keller, T.
TU.A-P50	Mo.D-P19	Mo.H-P70
Kawae, T.	Kawano-Furukawa, H.	Kemper, A.
FR.H-P36	Mo.A-P105	Th.I-P1
FR.I-P25	Kawasaki, Y.	Kempf, R.
Mo.I-P23	FR.A-P12	FR.I-P21
TH.D-P23	Kawase, T.	Kent, A.
Th.K-P33	Mo.B-P18	Mo.F-P23
Kawagoe, T.	Kawashima, N.	Mo.G-P15
TH.K-P10	FR.D-P49	Th.I.1_O2
Kawaguchi, M.	Kawata, T.	Kent, A.D.
FR.H-P10	TH.B-P8	Th.C.2_O4
Th.G-P14	Kaya, M.	Kenzelmann, M.
Th.G-P3	Mo.L-P43	FR.D-P24
Kawaguchi, N.	Kayser, P.	Mo.A.1_O5
Fr.B.2_O5	Th.G.3_O3	MO.A-P2
Mo.A-P60	Kazak, N.	MO.D.3_O1
Kawahara, H.	TH.C-P11	TU.A-P51
Mo.G-P12	TU.H-P31	Kermarrec, E.
Kawakami, N.	Kazakova, O.	TU.D.2_O2
FR.A-P47	Fr.E.1_O2	Kermorvant, J.
FR.B-P29	Mo.A-P15	TU.I.1_O2
TU.C-P21	Th.H.3_O3	Kern, P.
TU.F.1_O4	Ke, L.	Mo.I-P17
Kawakita, M.	Fr.D.3_O4	Kern, P.R.
Mo.I-P23	Keavney, D.J.	Mo.I-P20
TH.E-P16	MO.B.1_I1	Kernreiter, T.
Th.H-P12	Kechrakos, D.	FR.A-P49
Kawakita, Y.	Mo.I-P29	Kerouad, M.
FR.D-P1	Mo.I-P30	Mo.K-P32
Kawamoto, M.	Keinzle, P.	TU.F-P112
TH.F-P22	MO.C.3_O1	Keune, W.
Kawamura, H.	Keiper, T.	TU.D.3_O4
FR.D-P44	Mo.D-P21	Kézmárki, I.
Mo.H-P1	Keller, H.	TU.A-P25
TU.D.1_O2	Mo.A-P8	Khaidukov, Y.

Mo.H-P34
Khajetoorians, A.A.
 Fr.I.3_O2
Khalid, M.
 FR.F-P18
Khalid, N.
 Mo.H-P96
Khalyavin, D.
 FR.A-P30
 Mo.C-P17
 Th.A.2_O6
 TU.A-P38
 TU.D.2_O3
Khalyavin, D.D.
 TU.A.3_O2
Khamitcaeva, E.
 TH.B-P5
Khan, N.
 Th.A.1_O3
 TH.C-P13
 TU.G-P2
Khannanov, B.
 TU.A-P64
Khanov, L.
 Mo.L-P74
 Mo.L-P89
 Th.B.1_O5
Kharchenko, M.F.
 Th.N-P7
 Th.N-P8
Kharchenko, Y.
 Th.N-P7
 Th.N-P8
Kharel, P.
 Th.K-P29
Khasanov, R.
 Mo.A-P22
 Mo.A-P37
 Mo.A-P8
 TU.E-P6
Khashab, N.
 Mo.K-P7
Khatsko, E.
 TH.C-P35
Khaydukov, Y.

Mo.H-P70
Khaziakhmatova, O.
 Th.P-P18
Khim, S.
 Mo.A-P20
Khivintsev, Y.
 Mo.G-P10
 TH.K-P22
 Th.O-P27
 Th.O-P5
 TU.H-P54
Khlustikov, I.N.
 FR.D-P25
Khmelevskiy, S.
 Th.I-P12
 TU.G.3_O4
Khokhlov, N.
 Th.N-P6
Khomskii, D.
 FR.B-P3
 Mo.C-P10
 WE.C.1_I4
Khoroshilov, A.
 Mo.A-P85
 TU.B-P32
Khovaylo, V.
 TU.H-P124
Khurshid, H.
 MO.B.1_O3
 TU.F-P65
Khvalkovskiy, A.
 Mo.F-P15
 TH.J-P18
 TU.I-P10
Kida, T.
 Mo.B-P20
 TH.A-P22
 Tu.E-P51
Kiefer, K.
 FR.D-P69
 TH.C-P99
 Th.D.3_O3
Kien, L.M.
 TH.C-P93
 TU.E-P37

Kihou, K.
 Mo.A-P105
Kijima, H.
 TH.K-P12
Kikkawa, T.
 Th.H-P14
 Th.H-P5
Kikuchi, H.
 FR.D-P13
 FR.D-P46
 Mo.B-P21
 Th.A-P34
 Th.O-P22
 TU.H-P56
Kikuchi, S.
 Mo.A-P92
Kikuchi, Y.
 Mo.A-P92
Kikugawa, N.
 Th.G.3_O1
 Tu.A.3_O5
Kılıç Çetin, S.
 Mo.L-P69
Kilinc, H.
 Mo.H-P44
Kim Chong, O.
 TU.F-P8
Kim, Be.
 FR.F-P13
Kim, Bu.
 Mo.C-P20
 TU.G-P20
Kim, Bum.
 Mo.C-P14
Kim, Ch.
 FR.F-P13
 WE.A.1_O4
Kim, Ch.Ho.
 Th.O-P42
Kim, D.H.
 TU.H-P15
Kim, Da.Je.
 TU.F.1_I1
Kim, Da.Ye.
 TH.F-P19

Kim, Da.Yu.	Mo.D-P26	Kim, Jun.
TH.J-P11	Kim, I.	WE.A.1_O4
Kim, De.Hy.	FR.A-P2	Kim, Ka.Ji.
TU.F-P14	Kim, J.	TH.F-P13
Kim, Do.	WE.F2_O5	TH.F-P5
Mo.C-P20	Kim, J.N.	TH.F-P6
Mo.L-P65	MO.A.1_O2	Kim, Kw.Eu.
TU.G-P20	Kim, Ja.Yo.	TU.A-P36
TU.H-P69	Mo.C-P11	Kim, Ky
Kim, Do.Ch.	TH.A-P16	Mo.A-P45
FR.H-P22	TU.H-P13	Kim, Ky.Se.
TU.E-P24	WE.A.1_O4	FR.F-P14
Kim, Do.Hw.	Kim, Je.Hy.	Kim, Ky.Wa
Mo.C-P11	TU.G-P22	FR.A-P17
TH.A-P16	Kim, Ji.	Kim, Ky.Wh
Kim, Do.Jn.	Mo.C-P20	Fr.G.3_O1
Th.H-P13	TU.G-P20	Kim, Mi.
Kim, Du.Ho.	Kim, Ji.He.	FR.H-P11
TH.F-P11	Mo.D-P24	Kim, Mi.Se.
TH.F-P19	Kim, Jin.	Th.O-P42
TH.J-P11	FR.A-P41	Kim, Miy.
Kim, Gy.Mi.	Kim, Ji-Se	Th.A.2_O5
TU.H-P84	Mo.E-P10	TU.E-P40
Kim, Ha.	Kim, Jiw.	Kim, N.
Th.A.2_O5	Th.F.1_O2	TU.E-P10
TU.D-P10	Kim, Ji-Wo	Kim, N.H.
TU.E-P40	Mo.H-P25	Fr.I.2_O5
Kim, Ha.Su.	Kim, Jo.He.	WE.G.1_O2
Mo.D-P26	TU.F-P3	Kim, P.
Kim, Hu.Eu.	Kim, Jo.Vo	Fr.C.2_O4
TU.H-P32	Mo.H-P31	Kim, R.
Kim, Hu.Su.	TH.J-P31	TU.E-P10
TH.D-P18	WE.G.1_O3	Kim, S.Y.
Kim, Hy.Do.	Kim, Jon.	FR.A-P17
FR.A-P2	Mo.J-P11	Kim, Sa.
TU.E-P34	TU.H-P84	FR.H-P11
Kim, Hy.Ji.	Kim, Ju.Se.	Kim, Sh.Ae.
Mo.A-P56	Fr.I.2_O5	Th.E.2_I1
Kim, Hy.Ju.	WE.G.1_O2	Kim, So.
TU.H-P20	Kim, Ju.Su.	Mo.A-P45
TU.H-P44	FR.A-P2	Kim, So.W.
TU.H-P47	WE.A.1_O6	FR.A-P40
Kim, Hyu.J.	Kim, Ju.Yo.	FR.A-P41
Mo.D-P18	Mo.H-P95	Kim, Su.
Mo.D-P24	Mo.H-P96	TU.H-P22

TU.H-P5	TH.I-P22	WE.H.1_03
TU.H-P64	Kimel, A.V.	Kindo, K.
Kim, Sun.	Th.I.1_03	FR.D-P46
Th.P-P35	Th.I-P11	FR.I-P31
Kim, T.	Kim-Ngan, N.T.H.	MO.I.2_02
Th.F.2_05	WE.C.2_02	TH.A-P14
Kim, Ta.He.	Kimoto, T.	TH.A-P18
Mo.E-P10	Mo.D-P23	TH.A-P32
Mo.E-P12	Kimura, A.	Th.A-P34
Mo.H-P102	Fr.C.2_05	TU.A-P47
Kim, Ta.Ho.	Mo.L-P41	TU.B-P38
TU.H-P20	Kimura, N.	King, S.
TU.H-P44	TH.A-P13	TU.F-P94
TU.H-P47	Th.J.1_05	King, W.
Kim, Won.	TU.B-P77	TU.I.1_04
TH.F-P11	Kimura, S.	Kino, R.
Kim, Woo.	FR.D-P35	TU.A-P52
Th.I-P16	FR.F-P13	Kinoshita, Y.
Kim, Wooi.	Mo.H-P51	MO.E.2_04
WE.D.2_03	TH.A-P19	Kioussis, N.
Kim, Yeo.	TH.A-P35	TU.J.2_02
WE.A.1_04	TU.A.-59	Kipgen, L.
Kim, Yo.Ba.	TU.A-P60	MO.I.2_03
Th.E.2_05	Kimura, S.I.	Kirby, B.
Kim, Yo.Baek	TH.A-P30	MO.C.3_01
Th.E.2_11	TU.B-P52	Mo.H-P103
Kim, Yo.Ja.	Kimura, T.	WE.G2_04
Th.O-P39	Mo.A-P86	Kirchner, S.
Th.O-P42	Mo.B-P20	FR.B-P11
Th.O-P43	Mo.G-P17	Th.J.2_11
Kim, Yon.	Mo.G-P18	TU.F.1_11
Mo.B-P10	Mo.H-P59	Kirichenko, E.
Kim, You.K.	Mo.I-P23	TU.C-P1
Mo.B.3_01	TH.E-P10	Kirilyuk, A.
Kimata, M.	TH.E-P14	Fr.J.2_04
TH.I.1_04	TH.E-P16	MO.E.3_02
Kimchi, I.	Th.H-P12	Th.F.1_11
MO.SYM_5	Th.H-P3	TH.I-P22
Kimel, A.	Kinane, C.	Kirino, F.
FR.F-P11	Mo.H-P95	Fr.A.3_02
Fr.J.2_04	Kindervater, J.	Th.K-P47
MO.J.3_01	TH.C-P119	TU.I-P23
TH.C-P92	TH.J-P32	Kirk, E.
Th.F.1_03	TU.C-P30	WE.E.1_04
Th.G.1_05	TU.H.3_03	Kirman, M.

TU.D-P1	Kitahama, Y.	MO.J.3_03
Kirschner, J.	Mo.A-P84	Klein, P.
FR.A-P7	Kitamoto, Y.	TH.F-P4
FR.H.3_01	Fr.E.3_03	Th.O-P55
Fr.H.3_04	Kitanovski, A.	Klein, Y.
Mo.A-P19	Mo.L-P48	FR.A-P58
Mo.E-P11	Kitaoka, Y.	Fr.A-P59
Kiryasova, O.	FR.H-P28	TU.A-P76
Mo.G-P10	Mo.A-P87	Kleiner, R.
Kiryukhin, V.	Kitazawa, H.	MO.E.2_01
Th.E.2_11	Mo.L-P55	Klementová, M.
Kishii, N.	TH.C-P126	TH.C-P34
FR.I-P32	Kitou, A.	Klemke, B.
TU.B-P9	FR.A-P45	FR.B-P30
Kishimoto, H.	Kittaka, S.	Mo.B-P29
Th.L-P1	MO.A.1_04	TH.A-P26
TU.H-P63	Mo.A-P81	TH.A-P41
Kishimoto, K.	Th.C.3_04	TH.A-P42
Mo.H-P92	TH.C-P103	Klemmer, T.
Th.H-P7	TU.E.2_04	TU.G-P18
Kishimoto, Y.	Kittler, W.	Kletečka, V.
FR.A-P12	TU.H.2_03	Th.M-P17
Kishine, J.I.	Klanjsek, M.	Klicpera, M.
TH.C-P61	MO.I.1_05	Mo.A-P54
TU.C.2_02	TH.A-P20	TH.C-P51
Kisielewski, J.	Klar, D.	TU.B-P23
Th.C.2_05	TU.D.3_04	TU.B-P28
Kiss, L.	Klaur, M.	Kliemt, K.
Mo.H-P83	Fr.I.2_05	TU.C-P26
Kiswandhi, A.	Kläui, M.	TU.C-P4
Tu.A.3_05	Fr.D.2_02	WE.H.2_04
Kita, E.	Th.F.3_12	Klimczuk, T.
FR.H-P15	Klauss, H.H.	FR.C-P8
Mo.F-P18	Fr.B.2_06	Mo.A-P96
Th.H-P14	FR.D-P56	Klinger, D.
TU.E-P43	Mo.A-P100	TU.G-P28
TU.G-P9	TH.C-P80	Klinkova, L.
TU.H-P87	Th.D.3_02	TH.A-P1
Kitagawa, I.	TU.C-P9	Klinser, G.
TU.H-P19	Kleemann, W.	FR.I-P9
Kitagawa, N.	TH.K-P11	Klos, J.W.
FR.H-P18	Kleibert, A.	Mo.G-P26
Kitagawa, S.	FR.H-P34	Klos, J.W.
Mo.A-P46	TU.D-P12	Mo.G-P6
TU.B-P37	Klein, O.	Klughertz, G.

TH.C-P28
 TU.F-P31
Klyatskaya, S.
 TU.J.3_O3
Klyuchnikova, M.
 FR.E-P20
Klyushina, E.
 FR.B-P30
Kmjec, T.
 TU.A-P20
Kmječ, T.
 TH.C-P39
Kmjeè, T.
 TH.C-P34
Knafo, W.
 TH.C-P47
 Th.D.3_O4
 TU.B-P44
 TU.C-P31
Knebel, G.
 TU.F.1_O2
 WE.F2_O3
Knee, C.
 TU.D.1_O3
Kneidinger, F.
 TU.C-P14
Knobel, M.
 Th.E.3_O2
 TU.F-P18
 TU.F-P39
 TU.F-P6
Knudde, S.
 Th.K-P46
 Th.O-P54
Knyazev, D.
 Fr.C.1_O5
 Mo.A-P101
Knyazev, Y.
 TU.H-P31
Ko, J.
 FR.H-P11
Ko, K.T.
 FR.A-P29
 TH.K-P18
Ko, K.Y.

TU.A-P36
Kobata, M.
 TU.B-P55
Kobayashi, K.
 Mo.A-P74
Kobayashi, N.
 MO.C.1_O4
 TU.H-P109
Kobayashi, S.
 FR.D-P69
 FR.D-P8
 TH.C-P104
 Th.D.3_O3
Kobayashi, T.
 Mo.A-P46
 Mo.A-P83
Kobayashi, T.C.
 MO.I.2_O2
 TU.B-P37
Kobayashi, Y.
 Mo.A-P90
 Mo.C-P21
 TH.A-P30
 TU.E-P38
 TU.E-P39
Kobe, S.
 MO.F.2_O6
 Mo.I-P11
 Th.A.3_O3
 TU.H-P34
 TU.H-P42
Kobets, M.
 TH.C-P35
Kobljanskyj, Y.V.
 MO.H.2_O2
Koborinai, R.
 FR.D-P19
Koch, R.
 Mo.D-P14
 Mo.D-P20
 TU.J.3_O4
Kocjan, A.
 TU.H-P42
Kocsis, V.
 TU.A-P22

TU.A-P25
Koda, A.
 TU.C.2_O2
Kodam, U.
 Mo.C-P4
Koehne, B.
 Th.L-P6
Koelle, D.
 MO.E.2_O1
Koerner, J.
 MO.E.1_O5
Koga, A.
 TU.B-P60
Kogias, G.
 TU.H-P9
Kogure, M.
 TH.A-P13
Koh, Y.
 WE.A.1_O4
KOHAMA, Y.
 FR.I-P31
Kohda, M.
 Mo.D-P31
Kohei, T.
 TU.B-P57
Kohgi, M.
 TH.C-P75
Kohiki, S.
 TU.F-P4
Köhler, A.
 TH.J-P21
Köhler, J.
 WE.C.1_O2
Köhler, P.
 TH.J-P25
Kohlstedt, H.
 FR.A-P26
Kohno, A.
 TU.F-P7
Kohno, M.
 FR.A-P31
Kohout, J.
 TH.C-P34
 TH.C-P39
 TU.A-P20

Koichiro, I. Th.K-P33	Koller, S. FR.I-P9	TU.F-P49 TU.F-P50
Koike, H. MO.F.3_O1	Kollo, L. TU.H-P25	Konev, V. FR.B-P33
Koike, K. TU.H-P106 TU.H-P70	Kolomiets, A. TH.C-P45	Kong, Y.X. Mo.J-P7
Koike, M. Mo.D-P4 TH.A-P14	Kolthammer, J. FR.I-P45	KONGARA, M.R. TU.F-P40
Koirala, N. Mo.B-P23	Komanicky, V. Mo.L-P12	König, J. MO.A.3_O2 Mo.K-P15
Kokanovic, I. Mo.A-P28 TU.A.3_O1	Komarek, A.C. FR.A-P29 TH.K-P18	Konishi, T. FR.B-P14 Mo.A-P41 Mo.A-P42
Kokh, K. Fr.C.2_O5	Komatsu, T. TU.H-P87	Konno, T. Mo.H-P74 TH.A-P28
Kokubun, J. Th.J.2_O4	Komatsubara, T. TH.A-P13	Kono, Y. TH.C-P103 Th.H-P4 TU.E.2_O4
Kolano-Burian, A. FR.E-P3	Komissarov, I. TU.B.3_O1	Konoto, M. WE.D.2_O5
Kolbe, M. Fr.D.2_O2	Komissinskiy, P. Mo.H-P29 TU.A-P31	Konstantinovic, Z. Mo.H-P54 Mo.H-P57 Th.C.2_O3
Kolchugina, N. Mo.L-P15 Mo.L-P49	Komori, F. Fr.D.3_O2	Kontani, H. Fr.B.2_O5
Koledov, V. Mo.L-P37 Mo.L-P74 Mo.L-P77 Mo.L-P8 Mo.L-P89 Th.B.1_O5 TH.C-P111 TH.C-P112	Kondo, A. TU.B-P38	Kontos, S. FR.D-P5 Mo.L-P84 TU.H-P111
Kolesnikov, A. TH.J-P34	Kondo, K. Mo.D-P11	Koo, H.Cheon. Mo.D-P24
Kollar, P. TU.H-P51 TU.H-P52	Kondo, M. Mo.A-P44 Mo.A-P79	Koo, H.Chul Mo.D-P26
Kollár, P. TU.H-P41 TU.H-P45	Kondo, Y. TH.C-P44	Koo, J.W. Fr.I.2_O5
Kollath, C. TH.A-P5	Kondoh, K. TH.K-P10	Koo, T.Y. Mo.H-P60 Th.E.2_O5 TU.A-P36
	Kondou, K. WE.E.1_I1	Koopmans, B.
	Kondratiev, V. Th.O-P25	
	Koneracka, M. Th.P-P22 Th.P-P30 Th.P-P37 TU.F-P48	
	Koneracká, M.	

Fr.I.2_05	Korshunov, M.	Kousaka, Y.
Mo.K-P16	Mo.A-P26	Th.A.2_02
Mo.K-P31	Kosaka, M.	Th.A-P29
WE.G.1_02	TU.B-P51	Th.C-P61
Koorikawa, H.	Kosaka, S.	TU.C.2_02
FR.D-P69	FR.B-P13	TU.C.2_04
Kopcansky, P.	Kosel, J.	Kouyaté, M.
Th.P-P22	Fr.E.1_03	Th.B.1_02
Th.P-P30	Mo.K-P25	Kovac, J.
Th.P-P37	Mo.K-P7	Th.P-P22
Tu.F-P122	Mo.L-P45	TU.F-P48
TU.F-P32	Th.M-P8	TU.F-P71
TU.F-P48	Th.P-P17	TU.F-P78
TU.F-P71	TU.I.2_04	TU.F-P84
TU.F-P78	WE.F.1_02	TU.H-P133
Kopcanský, P.	Koshkid'ko, Y.	Kovac, P.
TU.F-P29	Mo.L-P15	Mo.A-P36
TU.F-P49	Mo.L-P3	Kovacevic, I.
TU.F-P50	Kostin, V.	Th.C-P28
Kopčanský, P.	FR.I-P10	Th.C-P41
TU.F-P91	Kostishyn, V.	Th.C-P56
Koplak, O.	TU.A-P35	Kovacs, A.
MO.F.1_02	TU.E.2_06	MO.D.3_02
Koralewski, M.	Kostopoulou, A.	Kovács, A.
TU.F-P32	Th.P-P20	TU.H-P42
Korelis, P.	TU.F-P21	Kováè, J.
Mo.H-P12	Kostylev, M.	Mo.L-P19
Mo.H-P56	Mo.G-P5	TU.H-P46
Koretsky, A.	Kostyuchenko, N.	Kovalev, S.
Th.P-P6	TU.A-P30	Th.F.2_05
Körner, J.	Kota, Y.	Th.I-P17
FR.I-P41	TU.E-P7	Kovylina, M.
Körner, M.	Kotani, A.	MO.E.3_11
Th.K-P17	WE.F2_05	Mo.H-P80
Kornowicz, A.	Kothare, A.	Mo.I-P24
TU.D-P2	Th.P-P33	Th.N-P5
TU.D-P3	Kotov, L.	Tu.F-P123
Koroleva, L.	Mo.G-P20	Koyama, K.
Mo.L-P87	Mo.G-P21	Fr.A.1_02
Koroteev, Y.M.	Kouchi, S.	FR.I-P30
TU.B-P30	Th.A-P30	Mo.L-P52
Korotin, D.	Koumouras, K.	Mo.L-P66
FR.E-P14	Mo.H-P88	TU.E-P35
Korovina, Y.	Kourtis, S.	TU.H-P82
Th.O-P25	MO.I.3_02	Koyama, T.

FR.A-P12	Krämer, K.W.	WE.H.2_O4
FR.A-P55	Mo.B-P15	Kremer, R.
FR.H-P10	Krämer, S.	Th.D.1_O2
Mo.H-P16	TH.A-P20	WE.C.1_O2
TH.C.1_O2	Krasovskii, E.E.	Kremer, R.K.
Th.G-P10	Mo.C-P23	FR.D-P82
Th.G-P14	Krassnorussky, V.	Mo.B-P25
Th.G-P3	TH.C-P77	Mo.B-P26
Th.G-P8	Kratochvilova, M.	Kren, H.
Koyanagi, T.	WE.A.1_O3	FR.I-P9
Mo.H-P92	Kratochvílová, M.	Krenke, T.
Th.H-P7	TH.C-P51	TH.C-P105
Koza, M.M.	TH.D-P4	Krenn, H.
TU.B-P23	TU.A-P82	FR.I-P9
WE.H.2_O5	Krause, S.	Kreuzpaintner, W.
Kozeki, T.	FR.H-P8	Mo.H-P100
TH.C.1_O2	Fr.I.3_O1	Mo.H-P12
Koželj, P.	WE.G2_O2	Mo.H-P56
Mo.A-P18	Krautz, M.	Kreyszig, A.
Kozhaev, M.	Th.O-P6	Fr.D.2_O3
Th.O-P41	TU.D.3_O4	Kriegner, D.
Th.O-P8	Kravchuk, V.	Th.A.2_O1
Kozhaev, M.A.	Fr.E.3_O1	TH.D-P8
Th.N-P7	Mo.K-P23	Kriener, M.
Th.N-P8	TH.J-P7	FR.F-P4
Th.O-P31	TU.F-P83	Krinitina, T.P.
Kozhevnikov, A.	Kravtsov, E.A.	Mo.H-P35
Mo.G-P10	Mo.H-P34	Krishnan, K.
Kozhitov, L.	Krawczyk, M.	WE.SYM_2
TU.E.2_O6	Fr.I.2_O2	Krishnan, R.
Kozub, A.	Mo.G-P11	TU.H-P75
Mo.A-P96	Mo.G-P16	Krishnia, S.
Kr, K.W.	Mo.G-P26	FR.D-P45
TH.C-P28	Mo.G-P6	Th.M-P6
Kraemer, S.	Kreisel, A.	Krivorotov, I.
TH.A-P10	TU.E.2_O3	MO.H.2_O3
Krafcik, A.	Kreisel, J.	TU.G-P27
Th.P-P30	Mo.C-P9	Krizan, J.
Th.P-P37	TH.C-P38	FR.D-P56
Kraken, M.	Krellner, C.	Krok, F.
TU.C-P23	FR.D-P37	Th.K-P36
Kral, D.	TU.B-P63	WE.E.1_O2
Mo.H-P78	TU.C-P26	Krompiewski, S.
Kramarenko, E.	TU.C-P4	Mo.J-P3
Th.P-P24	TU.F.1_I1	Kronast, F.

Fr.E.1_05	FR.E-P4	Mo.H-P78
Fr.E.2_02	Krzysteczko, P.	Mo.I-P6
Fr.I.2_04	Fr.E.1_02	Kubovcikova, M.
MO.E.3_I1	WE.H.1_04	Th.P-P22
Th.L-P3	Krzystek, J.	Th.P-P30
TU.A-P100	FR.D-P11	Th.P-P37
TU.C.1_I1	Krzyzewski, A.	TU.F-P48
Kronenberg, A.	TU.D-P2	TU.F-P91
FR.A-P35	TU.D-P3	Kucera, M.
Fr.D.2_02	Kubacka, T.	TH.D-P18
Kronmüller, H.	TU.E.1_06	TU.A.1_05
TU.H-P29	Kubaniova, D.	Kuch, W.
Kruchkov, A.	TU.A-P20	MO.I.2_03
Mo.B-P24	Kubániová, D.	Kuchko, A.
Krueger, B.	TH.C-P34	Mo.H-P42
Fr.I.1_I1	TH.C-P39	Kúdelčík, J.
Krug, I.	Kübel, C.	TU.F-P29
TU.A-P24	Th.A.3_02	TU.F-P91
Krüger, A.	Kubetzka, A.	Kudo, K.
MO.I.2_03	MO.G.3_04	Mo.A-P46
Krüger, D.	Th.C.2_I1	Mo.A-P84
MO.I.2_03	TH.K-P16	Mo.A-P86
Kruger, F.	Kubièková, L.	WE.D.2_04
TH.A-P25	TH.C-P34	Kudrevatykh, N.
Th.D.1_I4	Kubinová, Š.	Mo.L-P72
Kruger, P.	Fr.H.2_03	Kudrnovsky, J.
TU.J.3_02	Fr.H.2_04	Fr.D.3_03
Kruglyak, V.	Kubo, K.	TH.C-P8
Fr.G.1_04	TU.B-P10	TH.E-P1
Mo.G-P9	Kubo, Y.	TH.E-P2
Mo.H-P42	TH.C-P17	Kudrnovský, J.
Th.G.1_05	Kubota, H.	Mo.D-P12
Th.O-P27	FR.A-P51	Kuepferling, M.
Krull, C.	MO.H.2_05	Th.A.1_05
TU.J.3_03	Th.G-P7	Th.B.3_03
Krupinski, M.	TH.J-P10	Th.H-P17
Th.I.3_02	TH.J-P13	TU.H-P121
Th.K-P36	TH.J-P14	WE.H.1_04
Krupskaya, Y.	TU.H.1_03	Kuerbanjiang, B.
TH.A-P27	TU.H.1_04	Mo.H-P16
Kruthovostovs, R.	WE.D.2_05	TU.E-P48
Fr.I.3_04	WE.G2_I6	TU.E-P49
Krylov, V.	WE.G2_03	Kuga, K.
TH.D-P10	Kubota, T.	TU.B-P2
Kryvchikov, O.	Mo.F-P6	TU.C-P16

Kugel, K. Mo.C-P10	Kumar, S. FR.H-P4	Mo.L-P79
Kuhlmann, N. Th.I-P4 TU.F-P36	Kumar, V. FR.D-P47	Kura, H. TU.H-P38
Kuhn, S.J. Mo.A-P105	Kumisbek, G. Mo.J-P17	Kurahashi, S. TH.C-P47 TU.B-P43
Kuhns, P.L. TH.A-P17	Kummer, K. FR.I-P23 TU.B-P30 TU.B-P5	Kurant, Z. Th.C.2_O5 TU.G-P28
Kukula, Z. TU.H-P50	Kun, H.S. Mo.A-P62	Kurata, Y. TH.D-P20
Kulda, J. MO.E.2_O2	Kuncevich, A. Th.A.1_O4	Kurbakov, A. Th.A.1_O4
Kulesh, N. Mo.I-P34	Kuncser, A. Mo.H-P15	Kurebayashi, H. TU.SYM_4
Kulkarni, A. TU.A-P31	Kuncser, V. Mo.H-P15 Th.O-P19	Kurihara, M. TH.D-P21
Kumar, A. TU.E-P42	Kundys, B. Th.G-P19 TU.A-P3	Kurihara, S. FR.E-P12 TH.C-P17
Kumar, A.P. TU.F-P81	Kung, H.H. TU.F.3_O1	Kurihashi, Y. WE.J.1_O3
Kumar, A.P.S. FR.E-P34 Mo.H-P77 Mo.H-P86 Mo.H-P87 Mo.H-P97 TH.F-P26 TU.G-P23	Kunieda, K. FR.D-P46 Th.A-P34	Kurinjimala, R. TU.C-P14
Kumar, D. Mo.F-P7 Mo.G-P6 TU.F-P11	Kunikata, S. Mo.A-P81	Kurita, N. FR.D-P50 TH.A-P14 TH.A-P18 TH.C-P118
Kumar, N. FR.A-P45	Kunisada, N. FR.D-P41	Kurlyandskaya, G. Mo.I-P26 TU.I.2_O3
Kumar, P. Mo.H-P58 Mo.L-P46 TH.D-P6	Kunitsyna, E. TH.D-P5	Kurniawan, B. Mo.L-P67 TH.A-P31 TU.H-P77
Kumar, P.A. TU.B.2_O3	Kuo, C. TU.G-P27	Kuroda, F. FR.A-P21
Kumar, R. FR.D-P47 Mo.L-P46 TH.D-P6	Kuo, C.C. FR.H-P29 TH.C-P108	Kuroe, H. Mo.B-P18 Mo.B-P5 TU.A-P50 TU.A-P52 TU.A-P53 TU.A-P73
	Kuo, C.Y. Mo.B-P9 TH.K-P18	
	Kuo, P.C. Mo.H-P6 TU.G-P3	
	Kupferling, M.	

Kurokawa, Y. TH.F-P22	Kuwik, P. Mo.H-P46	Mo.I-P13
Kurosawa, T. Mo.A-P72 Mo.A-P74	Kuz'min, M.D. TH.C-P85	L. Schlagel, D. Mo.H-P107
Kuroshima, H. TU.E-P44	Kuzian, R. Th.D.2_04	L\`Ohneysen, H.V. Tu.A.3_05
Kurosu, R. Th.L-P1	Kuzmenko, A. TU.A-P11	Laad, M. Mo.A-P47
Kurowska, B. Th.G.2_04	Kuzmenko, A.M. TU.A-P11	Labarta, A. Fr.E.2_03 MO.E.3_11
Kushwaha, P. TH.C-P18 TU.B-P13	Kuzmin, D. Mo.L-P8 TH.C-P111 TH.C-P112	Mo.H-P80 Mo.I-P24 Th.C.2_03 Th.L-P3 Th.N-P5
Kustov, M. Fr.F.3_02 FR.I-P38	Kuz'min, M.D. Fr.A.1_11 TU.H-P43	TU.B.3_03 Tu.F-P123 TU.F-P79 TU.F-P80 Tu.H-P137
Kustov, S. Fr.E.1_04 TH.F-P28 TU.C.3_02	Kuznetsov, A. Mo.A-P85 TH.C-P78	Labaye, Y. Mo.J-P10
Kusunose, H. FR.B-P27 Mo.C-P15	Kuzovnikov, A. TU.H-P55	Labunov, V. TU.B.3_01
Kuswik, P. Mo.G-P26	Kuzovnikova, L. TU.H-P55	Lacaze, E. Mo.L-P86
Kuteifan, M. Mo.F-P15 TH.J-P18	Kwak, W. TH.F-P16	Lach, S. Fr.I.3_04
Kutsuzawa, N. TH.K-P10	Kwon, H.W. TU.H-P112 TU.H-P13	Lachman, E. Mo.H-P81
Kuwada, K. Th.O-P34	Kwon, J. TH.F-P16	Lacoste, B. Mo.F-P26
Kuwahara, A. Th.H-P7	Kwon, S. TU.H-P32	Lacour, D. Fr.D.1_03 FR.D-P21 Mo.D-P8 MO.H.1_04 Th.H-P1 Th.I.3_04 TU.G.3_03 TU.G-P1 TU.I.3_01 TU.I-P3 WE.I.2_03
Kuwahara, H. Mo.B-P12 Th.E.2_04 TU.A-P53 TU.A-P73	Kwon, Y.S. Mo.A-P100 TU.B-P52	
Kuwahara, K. TH.C-P75	L	
Kuwai, T. TH.B-P11 TU.B-P40	L. Hadimani, R. Mo.H-P107	
	L. Raikher, Y.	Lacroix, C.

Mo.G-P30 Th.D.2_O2	Fr.E.2_O5 Mo.A-P108	Mo.A-P98
Lacroix, L.M.	TH.A-P41	Lanèok, A.
Fr.E.1_I1 Fr.E.3_O4 MO.B.3_O3	TH.A-P42 Th.D.3_O1	TH.C-P34
Laczkowski, P.	Laktionova, M.	Lang, M.
Fr.G.3_O4 Mo.D-P27 MO.F.3_O2 TH.E-P12 TH.E-P8 WE.I.1_O3	Mo.A-P38	FR.D-P55 FR.D-P76
Lado, J.L.	Laliena, V.	Lange, F.
Fr.F.1_O3	TH.C-P106	FR.A-P13
Laflorencie, N.	Lalis, D.M.	Langenberg, A.
FR.B-P31	TU.B-P65	TU.F-P56
Lafuerza Bielsa, S.	Lamard, N.	Langenberg, E.
Mo.A-P97	TU.I-P15	MO.C.3_O3 TU.A-P24 TU.A-P26 TU.A-P45
Lafuerza, S.	Lamekhov, S.	Langer, J.
TH.C-P21 TU.A-P13 TU.E.1_O2	TU.A-P92	TU.I-P15
Laggoun, A.	Lamour, E.	Langford, R.M.
Mo.I-P18 TU.F-P23	Mo.L-P86	Fr.B.1_O3
Lago-Cachón, D.	Lampen-Kelley, P.	Langner, M.C.
TU.F-P54	TU.F-P65	Th.I-P1
Laguna-Marco, M.A.	Lampronti, G.	Langner, T.
Th.G.3_O3	Mo.A-P70 WE.F.2_I1	Th.H-P9
Laguta, V.	Lamrani, F.	Langouche, G.
FR.F-P30	Fr.F-P33	TU.G.1_O5
Laguta, V.V.	Lamura, G.	Langridge, S.
TU.A-P20	Mo.A-P102 Mo.A-P103 Mo.A-P37	Mo.H-P95
Lähderanta, E.	Lançon, D.	Lapertot, G.
Mo.L-P3 TH.C-P40	Fr.G.2_O4	TH.B-P19 TH.C-P75 TU.B-P44 TU.B-P70 TU.F.1_O5 WE.F2_O7 WE.H.2_I1
Lahti, P.	Landee, C.	LaPierre, R.R.
TU.D-P14	TH.A-P33	TU.C-P8
Lai, C.H.	Lander, G.H.	Lappas, A.
Mo.H-P62 WE.D.2_I1	TH.A-P21	Th.P-P20 TU.F-P21
Lake, B.	Landeros, P.	Lardé, R.
FR.B-P30 FR.D-P83	Mo.K-P18 Mo.K-P8 TH.K-P17 Th.M-P4 WE.F.1_O5	Mo.H-P67 TU.F-P86 TU.H-P61 TU.H-P62
	Landers, J.	
	TU.D.3_O4	
	Landínez Téllez, D.A.	
	Th.O-P1	
	Landsgesell, S.	

Largeron, C.	Mo.I-P35	Le Doussal, P.
Mo.D-P30	Th.K-P38	TH.F-P20
Lari, L.	TU.E.3_03	Le Fèvre, P.
TU.E-P48	TU.F-P67	WE.G.1_05
TU.E-P49	TU.F-P68	Le Gall, S.
Larionova, J.	TU.J.1_05	Mo.D-P8
Th.P-P10	Laurson, L.	TU.I-P3
TU.F-P2	TH.F-P14	Le Hur, K.
Laromaine, A.	TH.F-P15	WE.E2_04
Th.N-P1	Lausmann, A.	Le Marchand, G.
Laroze, D.	Mo.A-P76	Th.C.3_02
MO.D3_04	TU.B-P41	Le Normand, F.
Mo.F-P16	Laviano, F.	TU.B.3_01
Th.I-P15	Th.A.1_05	Le Roy, D.
TH.K-P20	Lavorato, G.	TU.H-P97
Larrea J., J.	MO.B.1_02	Le, A.T.
FR.A-P50	TU.F-P53	Mo.L-P22
TU.C-P29	Lavrijsen, R.	Le, D.
Larrea Jimenez, J.A.	WE.G.1_02	Mo.G-P25
TU.B-P7	Lavrov, A.	Le, M.D.
Larsen, J.	TH.D-P14	Fr.C.3_03
TU.E.2_03	Law, J.	Th.E.2_11
Larson, P.	Mo.A-P98	Le, T.
TH.C-P87	TH.A-P41	Th.O-P52
Lascialfari, A.	Law, J.Y.	Leandersson, M.
Th.N-P13	MO.D.2_03	FR.F-P13
Th.P-P10	Lawicki, A.	Tu.G.1_02
Th.P-P20	TU.F-P56	Lebert, B.W.
TU.D-P7	Lazarov, V.	Mo.A-P31
TU.F-P60	Mo.H-P16	Th.C.3_02
Lau, J.	TU.E-P48	Lebrun, R.
TU.E.1_04	TU.E-P49	TH.J-P10
Lau, J.W.	Lázpita, P.	TH.J-P13
Mo.H-P62	Mo.L-P24	TH.J-P14
Lau, T.	Lazukin, V.	TU.H.1_03
TU.F-P56	Mo.L-P73	TU.H.1_04
Laubschat, C.	Lazúrová, J.	TU.I.1_02
TU.B-P30	TU.A-P82	Leca, A.
Lauer, V.	Le Breton, J.M	Mo.H-P15
MO.H.2_02	Mo.H-P67	Lechevallier, L.
Th.H-P18	TU.F-P85	Mo.H-P67
Th.O-P37	TU.F-P86	Lecoeur, P.
Launay, Y.	TU.H-P61	FR.A-P54
FR.I-P44	TU.H-P62	Ledieu, M.
Laureti, S.	TU.H-P78	FR.I-P18

Ledue, D.	Th.H.3_03	Lee, Ny.Jo.
FR.E-P26	TU.J.2_05	Mo.E-P10
MO.G.2_03	Lee, Ji.Su.	Mo.E-P12
TU.F-P23	Mo.B.3_01	Mo.H-P102
Lee, Bo	Lee, Ji.You.	Lee, S.R.
TU.F-P14	Th.P-P35	Mo.A-P66
Lee, Bo.Wh.	Lee, Jin.	Lee, Sa.Ga.
TU.H-P15	TU.B-P67	FR.I-P34
Lee, C.	Lee, Jo.Seo.	Lee, Se.Rae.
Mo.E-P12	Th.F.2_05	TU.H-P20
Lee, C.H.	Th.I-P17	TU.H-P44
Mo.A-P105	Lee, Ju.Goo.	TU.H-P47
Lee, Chang.M	TU.H-P112	Lee, Seong.
FR.F-P31	Lee, Ju.Gu.	Th.E.2_11
Lee, Chih.H	TU.H-P13	Lee, Seun.
TU.A-P21	Lee, Ju.Sik	FR.D-P18
Lee, D.Y.	TU.A-P36	TU.A-P17
Mo.H-P25	Lee, Ki.Do.	Lee, Shan.Fa.
Lee, Hank.	TU.H-P17	TH.F-P29
MO.H.2_03	Lee, Ki-Su.	TH.J-P29
Lee, Ho.Sa	Mo.H.3_01	Lee, Soj.
TU.H-P20	Mo.K-P22	TU.E-P43
Lee, Hy.Seo.	WE.H.1_02	Lee, Soon.
FR.A-P41	Lee, Kuy.Ji.	FR.I-P34
Lee, Hy.Soo.	Fr.G.3_01	Lee, Su. Seok
Th.P-P21	Lee, Kye.Do.	Mo.H.3_01
Th.P-P35	Th.H-P13	Lee, Su.Seo.
TU.H-P64	Lee, Kyujo.	TU.F-P30
Lee, Hy.Woo.	FR.A-P40	TU.F-P52
Fr.G.3_01	FR.A-P41	TU.F-P94
TU.H-P17	Lee, Mi.Ta.	Lee, Su.Yu.
Lee, Hyuny.	TU.A-P21	Mo.D-P25
Mo.G-P2	Lee, Mi.Woo	Lee, Suhe.
Lee, J.I.	TU.H-P20	FR.D-P52
FR.H-P22	TU.H-P44	TH.A-P17
TU.E-P24	TU.H-P47	Lee, Sukm.
Lee, J.Mi.	Lee, Minch.	WE.G.1_02
TU.A-P21	Th.H-P15	Lee, Sungh.
Lee, Jeon.	Lee, Minh.	Mo.J-P11
Mo.D-P13	Fr.I.1_03	Lee, Sung.
Lee, Ji.Hon.	Lee, Minse.	TH.A-P16
Th.E.2_05	FR.D-P52	Lee, Sunw.
TU.A-P36	Lee, Na.	TU.H-P21
Lee, Ji.Hy.	TU.A-P28	TU.H-P32
Mo.A-P86	TU.A-P29	Lee, Tae.Yon

Th.O-P39
Lee, Taek.

Mo.I-P9
Lee, Wonj.

FR.D-P52
TH.A-P17
Lee, Wooyo.

TU.H-P22
TU.H-P64
Lee, Yongw.

TU.A-P17
Lee, Yun.Hi.

Mo.D-P18
Lee, Yuns.

TU.E-P4
Lees, M.

FR.A-P10
Lees, M.R.

FR.A-P34
TU.D.2_I1
Lefevre, F.

TU.H-P78
Lefevre, P.

TU.I.3_O1
Lefmann, K.

Mo.A-P72
TU.E.2_O3
Lefrançois, E.

Mo.C-P17
TU.D.2_O3
Lefter, C.

MO.J.2_O4
Legeza, O.

Fr.J.1_O3
Leguen, K.

MO.E.1_O2
Legut, D.

Fr.D.3_O3
Lei, Q.

TU.B-P29
Lei, Z.

TU.H-P33
Leitao, D.

TU.I.1_O3
Leitao, D.C.

Th.K-P46
Th.O-P54
Leithe-Jasper, A.

TU.B-P36
Leitner, M.

Th.A.2_O7
WE.D.1_O2
Lejay, P.

Mo.C-P17
MO.I.1_O3
TU.A-P43
TU.B-P15
TU.D.2_O3
WE.C.2_O4
Lejeune, B.

Th.B.1_O4
Lelièvre-berna, E.

Th.D.3_O4
TH.J-P35
Lemaître, A.

Th.I-P10
Th.I-P5
Lendínez, S.

Th.C.2_O4
Lenertz, M.

Mo.B-P14
Lenoble, O.

Mo.D-P8
Lenoir, B.

Mo.C-P12
Lenz, K.

TH.K-P17
Leon Vanegas, A.O.

Mo.A-P19
Leon, A.O.

TH.K-P20
Leon, C.

Mo.E-P8
WE.G.1_O4
León, C.

FR.I-P49
Leonel, S.

Mo.K-P12
Mo.K-P13
Mo.K-P14

Léotin, J.

TU.C-P31
Lepalovskij, V.

Mo.I-P26
Lepeshev, A.

TU.H-P55
Lepetit, M.B.

TU.A-P6
Lequeux, S.

FR.A-P51
Lesci, I.G.

Th.P-P12
Lesne, E.

MO.F.1_O5
Lesniak, M.

Th.P-P3
Lesseux, G.

TU.F-P26
Lesseux, G.G.

TU.B-P2
Lesueur, J.

Mo.A-P58
MO.C.1_O2
Leszczynski, B.

Mo.I-P25
Letellier, F.

Mo.H-P67
Leu, B.

TU.B-P21
Leung, C.W.

FR.H-P9
Levatic, I.

MO.G.3_O3
Levchenko, A.

TH.C-P77
TH.C-P78
TU.B-P59
Leven, B.

Fr.G.1_O2
Th.O-P37
Levy, P.

TH.C-P43
Levy-Bertrand, F.

TH.A-P10
Th.D.1_I4

Lew, W.S.	TU.B-P35	Th.I-P6
FR.D-P45	TU.B-P39	Liang, K.C.
Fr.E.3_O2	TU.B-P43	TU.E.2_O2
Mo.K-P29	Li, D.X.	Liang, R.
Th.G.2_O5	FR.D-P61	MO.A.2_I1
TH.J-P4	Mo.L-P64	MO.A.2_O2
TH.J-P5	Li, G.	TU.A.3_O1
TH.K-P5	Mo.L-P36	Liang, W.I.
Th.K-P55	Li, J.	Th.K-P41
Th.M-P6	Mo.H-P28	Liao, J.W.
Th.O-P35	Th.K-P35	Mo.H-P62
TU.I-P18	Li, L.	WE.D.2_I1
TU.I-P6	Mo.D-P21	Liao, Y.F.
TU.I-P8	TU.D-P8	FR.A-P29
WE.J.1_O4	Li, O.	TU.B-P15
Lewinska, S.	TU.F-P88	Lichtenstein, A.
TU.D-P2	Li, P.	FR.A-P8
TU.D-P3	Th.G-P6	Fr.F.1_O5
Lewinski, J.	Li, S.	Liébana Viñas, S.
TU.D-P2	TU.E-P38	WE.B.2_I1
TU.D-P3	Li, S.S.	Liebing, N.
Lewińska, S.	Th.G-P11	WE.H.1_O4
Mo.H-P82	Li, W.	WE.I.2_I1
Th.G.2_O4	TU.E.3_O3	Lightfoot, P.
Lewis, L.	Li, X.	TH.A-P38
Th.B.1_O4	Mo.L-P34	TU.D.1_O4
Lewis, R.	Th.I.2_O1	Lilienblum, M.
TH.C-P91	Th.K-P35	TU.A-P24
Leyva, A.	TU.G.1_O4	Lim, M.
FR.F-P7	Li, Y.	Th.P-P15
Leyva, G.	MO.A.2_O3	Lim, S.H.
TH.C-P86	MO.D3_O4	TU.H-P47
Lhotel, E.	Th.H-P4	Lima Jr, E.
FR.D-P66	Th.K-P35	MO.B.1_O2
FR.I-P44	Li, Z.	TU.F-P53
TU.D.1_O3	MO.B.3_O2	Lima Jr., E.
TU.D.2_I1	Th.O-P4	TU.F-P111
TU.D.2_O3	TU.I-P17	Lima Lopes, A.M.
Lhoutellier, G.	Li, Z.A.	TU.A-P89
MO.G.2_O3	WE.B.2_I1	TU.E.2_O5
Li, B.H.	Li, Z.D.	Lima, J.S.
TH.E-P13	Mo.H-P69	TU.F-P98
Li, D.	Liakakos, N.	Lima, R.
Mo.A-P95	Th.G.2_O3	TU.F-P43
Th.G-P6	Th.I.3_O3	Lin, C.

FR.D-P82	Lippert, T.	Liu, S.J.
Lin, C.L.	TU.E.1_03	FR.F-P26
FR.H-P16	Liscio, F.	Liu, T.
Lin, C.R.	Mo.H-P94	TU.I-P3
TU.F-P88	Lisiecki, F.	Liu, X.
Lin, C.Y.	Mo.G-P26	Mo.I-P21
TU.C-P6	Lithgow, C.	Liu, X.M.
Lin, G.	Mo.A-P61	Th.M-P2
TU.C.1_11	Litterst, F.J.	Liu, Y.
Lin, H.J.	TU.F-P58	FR.G.2_03
TU.E-P8	Litterst, J.	FR.I-P4
Lin, J.C.	TU.C-P23	MO.E.1_02
TU.E-P8	Litvinova, A.	Mo.I-P21
Lin, J.Y.	TU.H-P125	Th.G-P6
TU.A-P44	Litvinova, L.	TU.F-P51
Lin, K.	Th.P-P18	Ljubimov, B.
TU.A-P54	Liu, C.	FR.I-P6
TU.C-P14	Mo.J-P1	Llandro, J.
Lin, K.W.	TU.E-P1	MO.D.3_02
FR.H-P9	TU.F-P14	Th.P-P5
Mo.I-P7	TU.H-P15	WE.B.2_05
Lin, P.A.	Liu, E.	Llobet, J.
TU.A-P21	TH.C-P31	Mo.I-P24
Lin, T.	TH.C-P32	Llois, A.M.
WE.D.2_03	WE.D.2_03	TH.B-P10
Lin, X.	Liu, H.J.	TH.K-P7
Th.J.2_02	TU.E-P8	Th.M-P14
Lin, Y.C.	Liu, H.T.	TU.G-P21
Mo.L-P1	TU.B-P67	Lloveras, P.
Lin, Y.Z.	Liu, J.	Th.B.1_03
FR.F-P26	Fr.I.1_02	Lo, W.T.
Lindner, J.	TU.C.3_03	Mo.I-P7
TH.J-P9	Liu, K.	Lobanova, I.I.
TH.K-P17	Mo.H-P62	TH.C-P122
TU.H.1_11	Liu, L.	LoBue, M.
Lindner, P.	Fr.B.2_04	Fr.F.3_02
Fr.I.3_01	Fr.C.2_04	Mo.L-P26
Ling, D.	Fr.G.2_11	TH.I-P25
TU.A-P54	Fr.I.1_03	Locatelli, A.
Ling, D.C.	Liu, N.	Fr.D.1_03
TU.A-P54	Fr.E.3_02	FR.I-P28
Linh, Di.C	Liu, Q.	Mo.K-P26
TU.F-P17	Th.H-P7	TH.K-P1
Link, J.	Liu, R.R.	TU.J.1_02
TU.H-P25	TU.E-P8	WE.H.1_05

Locatelli, N.	TU.I.2_06	Lorenz, B.
TH.J-P10	López González, D.	TU.E.2_02
TU.H.1_04	Mo.H-P76	Lorenzer, K.
Lochner, E.	TU.A-P77	TU.B-P7
Mo.D-P21	Lopez Molina, E.	Lorenzo, E.
Loewenhaupt, M.	Mo.H-P47	Th.D.3_04
TH.B-P9	López Moreno, E.	Lorenzo, J.E.
TH.C-P16	Mo.H-P48	Th.D.1_11
TU.B-P66	Lopez Noda, R.	Lortz, R.
Lofink, F.	TU.A-P42	FR.F-P3
Mo.H-P75	Lopez, A.	Losby, J.
Logg, P.	TH.F-P7	TH.J-P33
WE.F.2_11	López, C.	Lostun, M.
Lograsso, T.	Th.M-P15	TU.H-P92
FR.I-P4	López, C.A.	TU.H-P96
Lograsso, T.A.	FR.H-P21	Lott, D.
Th.B.2_03	Lopez, J.A.	TU.G.2_03
Lohmann, A.	TU.F-P24	Lottini, E.
Th.A-P45	Lopez, R.	TU.F-P19
Löhneysen, H.V.	Th.H-P15	TU.F-P95
Fr.H.1_02	Lopez-conesa, L.	Lou, G.
Fr.H.1_03	Tu.B.2_02	Th.H-P7
Lohr, J.	Lopez-Díaz, L.	TU.H-P114
FR.H-P21	Th.H-P6	TU.H-P85
Loidl, A.	López-López, J.A.	TU.H-P94
FR.D-P27	TH.F-P24	Loulidi, M.
Loizos, G.	López-López, M.	Fr.F-P33
TH.K-P12	FR.H-P24	Lounis, S.
Lokamani, M.	Lopez-Mir, L.	Fr.I.3_02
TU.A.2_02	MO.C.2_02	Lourenço, A.
Lomakin, V.	TU.A-P99	Mo.H-P90
Mo.F-P15	Lopez-Ortega, A.	Lourenço, A.A.C.
TH.J-P18	Tu.B.2_02	Th.K-P43
Lonzarich, G.	TU.F-P87	Love, D.
FR.A-P63	López-Ortega, A.	MO.D.3_02
FR.E-P41	FR.I-P46	Mo.H-P106
Lopera Muñoz, W.	MO.B.1_11	Th.P-P5
Mo.H-P14	TU.F-P19	WE.B.2_05
Lopes da Silva, R.	TU.F-P95	Lovell, E.
TH.J-P16	López-Ruiz, R.	Mo.L-P70
Lopes, P.	TU.D-P15	Mo.L-P79
Mo.L-P5	TU.F-P18	Th.B.3_01
López Díaz, L.	Lopez-Tabares, J.	Lovesey, S.W.
TH.F-P27	FR.D-P84	TU.A.3_02
Lopez Dominguez, V.	TH.C-P128	Loy, D.

WE.J.1_O4	Th.P-P13	Luo, Z.
Loyau, V.	TU.B.3_O2	Mo.D-P2
TU.H-P102	Luetkens, H.	Mo.D-P5
Lu, J.	Fr.B.2_O6	Lupi, M.
FR.I-P2	Mo.A-P100	Th.H.1_O4
Mo.D-P21	TH.C-P80	Lupo, P.
Lu, K.T.	Th.D.3_O1	Th.M-P2
Mo.L-P35	Th.D.3_O2	TU.G-P10
TU.A-P21	TU.C-P23	TU.G-P16
Lü, W.	Luis Prieto, J.	TU.J.2_O4
FR.C-P9	MO.J.3_O3	Lupu, N.
Lu, X.	Luis, F.	TH.K-P12
Mo.A-P27	WE.C.2_I6	Th.L-P4
TU.B-P67	Luitz, D.	Th.P-P26
Lu, Y.	FR.B-P31	TU.A.1_I1
Mo.D-P8	Luke, G.	TU.H-P117
Luan, J.	Fr.B.2_O4	TU.H-P92
TU.H-P67	Fr.C.2_O4	TU.H-P96
Lubk, A.	Fr.G.2_I1	Lusakowski, A.
FR.I-P26	Fr.I.1_O3	FR.F-P29
Lucas, I.	Lukienko, I.M.	Lutsev, L.
Mo.H-P2	Th.N-P7	Mo.D-P15
Mo.H-P40	Th.N-P8	Th.G.1_O4
Mo.J-P8	Lum, I.K.	Luu, T.
Th.B.2_I1	Fr.H.1_O2	TU.F-P8
Th.B.3_O2	Lunacek, J.	Lužnik, J.
Th.H-P5	Th.O-P11	Mo.A-P18
Th.H-P8	Th.O-P20	Luzón, J.
TU.C.1_O4	Lunov, O.	MO.I.2_O4
Lucas, S.	Fr.H.2_O3	Lyberatos, A.
TU.H.2_O3	Fr.H.2_O4	MO.G.2_O2
Luccas, R.F.	Luo, C.W.	Lyder Andersen, H.
FR.I-P49	TU.A-P44	TU.F-P46
TH.D-P22	Luo, F.	Lynn, J.
TU.E-P47	Mo.K-P10	TU.B-P21
Lucivjansky, T.	Luo, G.	TU.B-P73
FR.D-P39	TH.D-P9	TU.E.1_O4
Łuczak,, J.	Luo, W.	Lynn, J.W.
Mo.D-P9	Mo.I-P7	Fr.D.2_O3
Ludszuweit, M.	Luo, W.R.	Lyra, M.
TU.I-P25	FR.H-P9	FR.E-P9
Ludwig, A.	Luo, X.	Lysov, M.
Mo.L-P76	TU.E.1_O4	TH.F-P12
TU.H-P81	Luo, Y.	
Ludwig, F.	Mo.A-P75	

M

M Burn, D.	Macedo, M.	FR.D-P45
Th.K-P25	TU.A-P41	Mo.K-P29
M Strydom, A.	TU.A-P55	Th.G.2_05
TH.C-P73	TU.A-P56	TH.K-P5
M. Andersen, B.	Macêdo, M.	Th.M-P6
WE.A1_02	TU.F-P103	Th.O-P35
M. L. Lopes, A.	Macedo, R.	Madon, B.
Mo.H-P107	FR.H-P19	Th.H-P1
M. Pereira, A.	Th.N-P4	WE.I.2_03
Mo.H-P107	Macedo, W.	Madugundo, R.
Mo.L-P90	TU.G-P7	Th.A.3_01
M. R, M.	Macedo, W.A.A.	Maeda, M.
FR.F-P32	MO.G.1_05	TH.A-P13
M. Ro;Nnov, H.	TU.F-P87	Maekawa, S.
TU.C-P29	Macek, J.	FR.D-P58
Ma, F.	Th.N-P11	Fr.G.2_11
MO.C.3_02	Machay, I.	MO.G.3_01
Ma, G.	Th.O-P57	Th.H-P10
TH.C-P91	TU.H-P125	Th.H-P5
Ma, Q.	Machida, K.	TH.I.1_04
Mo.H-P89	MO.A.1_04	Th.I.2_05
TH.I-P24	Th.C.3_04	TH.J-P8
TU.G-P12	Machida, Y.	TU.SP-2
Ma, Y.	Th.J.2_02	WE.I.2_04
Mo.A-P36	TU.C-P22	Maeno, Y.
Maan, J.K.	TU.C-P27	Fr.C.2_04
Fr.J.2_04	Macia, F.	MO.A.1_11
TH.I-P22	Th.C.2_04	Mo.A-P66
Maât, N.	Macià, F.	Th.C.3_04
TU.F-P85	Mo.G-P15	Maenosono, S.
TU.F-P86	Th.I.1_02	Th.P-P15
TU.H-P61	Mackenzie, A.P.	Magalhaes, S.
TU.H-P62	TH.C-P18	Mo.A-P76
TU.H-P78	TU.C-P28	Magalhães, S.
Maccaferri, N.	Mackova, A.	FR.D-P80
TH.G.1_02	TU.G.2_05	TU.B-P41
Maccariello, D.	Macková, A.	Magalhaes, S.G.
Mo.H-P99	FR.F-P30	TH.A-P15
Mo.I-P37	MacLaren, D.	Magda, G.
Maccherozzi, F.	FR.H-P30	MO.I.1_11
WE.B.2_05	Madami, M.	Magén Domínguez, C.
	Mo.G-P23	Mo.L-P47
	TU.G-P10	Magen, C.
	TU.I-P4	Fr.E.1_11
	Maddu, R.	MO.C.2_11

MO.C.3_O3	Th.M-P21	TU.D.3_O4
Th.I.2_O4	Maignan, A.	Makino, A.
Th.M-P10	FR.C-P2	TU.A.1_I1
TU.A-P24	Mailman, A.	TU.H-P14
TU.A-P45	TU.E-P33	TU.H-P67
TU.A-P86	Mairoser, T.	Maksymenko, M.
Magén, C.	Mo.H-P100	FR.A-P44
Mo.H-P2	Mo.H-P12	FR.D-P68
Mo.H-P40	Mo.H-P56	Maksymov, A.
Mo.H-P55	Maiti, K.	Fr.F.2_O3
Mo.K-P16	TH.B-P16	Makuch, K.
Mo.K-P17	Maity, T.	TH.B-P6
Th.B.2_I1	FR.F-P31	Makuta, H.
Th.E.1_O2	TH.K-P12	Mo.H-P26
TU.A-P26	Majer, J.	Malago, P.
TU.C.1_O4	TU.C-P20	Fr.I.2_O2
WE.J.2_I1	Majetich, S.	Malagò, P.
Magnani, N.	Fr.H.2_I1	Mo.I-P38
TH.A-P21	Maji, B.	Maldonado, A.
TH.D-P25	TH.C-P5	TH.I-P28
Magnano, E.	Majjæ Renjo, M.	Maldonado, L.
FR.H-P25	Mo.L-P81	Th.P-P14
Th.G.3_O4	Major, M.	Maletinsky, P.
Magnavita, E.T.	TU.A-P31	MO.E.2_O3
TU.B-P2	Majumdar, P.	Malinowski, G.
Magni, A.	FR.C-P6	Th.F.2_I1
Fr.E.2_O4	FR.D-P64	malits, p.
Th.H-P17	Majumdar, S.	FR.E-P28
Magnus, F.	Mo.E-P9	Maljuk, A.
TU.G-P14	Mo.H-P20	Th.D.3_O2
Magrez, A.	Mo.H-P52	Malkin, B.
Fr.G.2_O4	Th.B.1_O3	TU.A-P87
Mahdavifar, S.	Majumder, A.	Malles, S.
Mo.B-P1	TU.A-P58	TU.F-P97
Mahender, C.	Majumder, S.	Malta, M.
Mo.H-P50	FR.H-P4	Mo.K-P9
Mahendiran, R.	Makarov, D.	Malterre, D.
Fr.F.3_O3	Fr.E.1_O5	TU.B-P62
Mo.L-P59	Fr.E.3_O1	Malyshev, A.
TH.C-P7	Fr.I.2_O4	Th.A.1_O4
TU.A-P1	MO.E.3_O2	Mamiya, H.
Mahendru, D.	TU.C.1_I1	Th.A-P45
WE.B.2_O5	TU.F-P83	TU.F-P90
Maicas, M.	TU.J.1_O5	WE.SYM_3
TH.C.1_O4	Makarov, S.	Mamiyev, Z.

FR.F-P5
Mammeri, F.
 Mo.I-P12
Mamulova Kutlakova, K.
 Th.O-P11
Manabe, A.
 Fr.A.3_03
 TU.H-P115
 TU.H-P63
Manago, T.
 Mo.G-P7
 Mo.G-P8
Manaka, H.
 FR.D-P60
 Mo.B-P16
 TH.C-P60
Manami, K.
 Mo.L-P60
Manchanda, P.
 TU.F-P76
Mandal, P.
 Th.A.1_03
 TH.C-P13
 TU.G-P2
Manfredi, G.
 TU.F-P31
Manfrinetti, P.
 Th.O-P21
Mangin, S.
 Th.F.2_11
 Th.I.3_04
Manley, M.
 TU.B-P21
Manna, K.
 FR.D-P34
Manna, L.
 TU.F-P21
Manna, S.K
 TU.H-P100
Manna, S.K.
 TU.H-P134
Mannhart, J.
 Mo.H-P100
 Mo.H-P12
 Mo.H-P56

Manni, S.
 Mo.C-P13
Mannig, A.
 MO.I.1_04
 TH.C-P26
Mannini, M.
 MO.I.2_11
Manosa, L.
 MO.D.1_11
Mansell, R.
 Mo.H-P95
 Th.H.3_03
 Th.P-P3
 TU.F-P116
 TU.J.2_05
Månsson, M.
 FR.D-P7
 Mo.A.1_05
 Mo.B-P6
 TU.A-P27
 TU.C-P2
Mansurova, M.
 Mo.G-P14
Mantovan, R.
 TH.F-P17
 TU.G.1_05
Mantsevich, V.
 FR.B-P1
Manuel, P.
 FR.A-P30
 FR.D-P10
 Th.A.2_06
 TU.A-P38
 TU.D.2_03
Manzin, A.
 FR.I-P20
Mañosa, L.
 Th.B.1_03
 Th.B.1_04
Mao, Q.
 Mo.A-P112
Mao, X.
 Fr.C.1_02
Maple, B.
 TU.B-P21

Maple, M.B.
 Fr.H.1_02
 TU.B-P48
 TU.B-P50
Marangolo, M.
 Mo.L-P86
 TH.K-P1
 TU.G-P21
Marcano Aguado, N.
 Mo.L-P47
Marcano, L.
 Fr.B.1_02
Marcano, N.
 MO.C.3_03
 Th.B.2_11
Marchi, F.
 Fr.E.1_02
Marchisio, E.
 Th.H.2_04
Marciello, M.
 Th.P-P11
Marcilhac, B.
 TU.I.1_02
Marcin, J.
 TU.A.2_05
 TU.H-P133
 TU.H-P46
Marco, J.F.
 FR.I.2_03
 TU.I.3_03
Marcos, J.
 FR.I-P11
 FR.I-P12
Marcus, M.A.
 MO.E.3_11
 Mo.I-P24
Mardegan, J.
 Mo.A-P33
Margaris, G.
 Mo.H-P83
 Mo.I-P33
Margineanu, M.B.
 Mo.K-P7
Marhieu, R.
 Mo.G-P15

Mariani, M.	TU.C.3_01	TU.C.2_03
TH.F-P17	Maroutian, T.	TU.C-P30
Th.N-P13	WE.G2_04	WE.H.1_03
TU.D-P7	Marozau, I.	Martin, S.Y.
Mariano, Q.	Fr.B.2_01	TU.H.1_02
TH.C-P43	Marques, D.	Martina, K.
Marin, C.	TU.F-P94	MO.F.2_02
Th.D.1_I1	Marques-Ferreira, P.	Martin-Delgado, M.A.
Marin, L.	FR.D-P65	TU.D-P13
TU.C.1_04	Marquina, C.	Martinelli, A.
Marín, L.	Th.H.1_05	Mo.A-P102
TU.A-P86	Th.P-P31	Martínez de Baños, L.
Marin, P.	Th.P-P34	TU.A-P26
Th.O-P3	TU.F-P111	Martinez, B.
TU.I.2_06	TU.F-P57	MO.C.2_02
Marín, P.	Marrows, C.	Mo.H-P108
Fr.A.1_04	MO.D3_04	Mo.H-P54
TU.H-P98	Marsilius, M.	TU.A-P99
Marin, S.	Mo.L-P13	Martínez, B.
Th.D.1_I1	Marszalek, M.	Mo.H-P57
Marinca, T.F.	Th.I.3_02	Martinez, E.
TU.H-P119	Th.K-P36	WE.I.1_04
TU.H-P120	WE.E.1_02	Martinez, E.L.
TU.H-P122	Marszałek, M.	Mo.A-P68
Marinica, O.	Th.K-P49	Martínez, G.
TU.F-P108	Martel, L.	TU.H-P135
Marioni, M.A.	TH.D-P15	Martínez-Blanco, D.
Th.I.3_04	Martelli, V.	Fr.B.1_04
Markandeyulu, G.	FR.A-P50	Martínez-Casado, F.J.
Mo.C-P4	TU.B-P7	TU.E-P46
Mo.L-P2	Martens, U.	Martínez-García, J.C.
TU.A-P58	WE.I.2_05	TU.A.1_04
TU.I-P2	Marthaler, M.	TU.F-P54
Märkl, T.	Th.I-P3	Martínez-Pérez, M.J.
Th.I-P3	Martin, C.	MO.E.2_01
Markó, M.	TH.C-P1	Martínez-San Segundo3, P.
FR.I-P7	TU.E.1_05	Th.P-P4
Markou, A.	Martin, E.	Martinez-Velarte, M.C.
Mo.H-P63	TU.F-P73	Th.B.2_03
Mo.I-P5	Martín, J.I.	Martínez-Velarte, M.C.
Markovich, V.	Fr.H.3_02	Th.B.2_I1
Mo.I-P41	TH.H.3_02	Th.I.2_04
TH.C-P1	TH.K-P4	Martínez-Veliz, I.
Marmorini, G.	TU.J.1_03	FR.H-P24
TH.C-P54	Martin, N.	Martín-García, L.

FR.I.2_03	TH.A-P12	TH.C-P21
TH.K-P23	Mašková, S.	TU.B-P44
Martini, L.	TH.C-P45	Matij, Z.
TU.I-P4	TH.D-P8	TU.E-P46
Martino, L.	Maslova, N.	Matos, I.
TU.H-P121	FR.B-P1	TU.F-P45
Martins, G.	Massala, P.	Matsubara, A.
Mo.A-P77	Th.N-P15	FR.I-P34
Martins, M.	Massana, V.	Matsubayashi, K.
Th.K-P13	FR.I-P11	TH.B-P18
Marty, A.	FR.I-P12	TH.C-P113
Fr.G.3_04	Massango, H.	TH.C-P120
Mo.D-P27	TU.I.2_05	TH.C-P71
Mo.D-P30	Masseboeuf, A.	TH.C-P90
TH.E-P12	WE.J.1_02	TU.B-P17
TH.E-P8	Massetti, M.	TU.B-P43
TH.J-P23	Th.H.2_04	TU.E-P20
Th.O-P40	Masuda, K.	Matsuda, F.
WE.G.1_05	FR.E-P12	TU.C-P21
Marukame, T.	Masuda, T.	Matsuda, K.
TU.I-P9	FR.D-P51	Th.G-P5
Marynowska, A.	FR.D-P60	WE.G2_I6
Mo.H-P82	Mo.B-P2	Matsuda, M.
Maryško, M.	TU.A-P27	TH.C-P49
FR.F-P30	TU.A-P90	Matsuda, T.D.
Masaki, I.	Masuko, M.	TU.B-P58
TH.A-P32	Mo.B-P17	TU.B-P8
Masarova, M.	Masumoto, H.	TU.C-P19
Th.P-P30	MO.C.1_04	WE.H.2_I1
Th.P-P37	Matczak, M.	Matsuda, Y.
Mascaraque, A.	Mo.G-P26	Tu.A.3_05
Th.M-P21	Mo.H-P46	TU.A.-59
Maschke, K.	Matej, Z.	TU.H.2_04
Fr.F.2_02	Th.A.2_01	WE.F2_04
Maseboeuf, A.	TH.D-P8	Matsuda, Y.H.
Fr.E.1_I1	WE.C.2_02	Mo.B-P10
Masenda, H.	Materne, P.	MO.I.2_02
TH.C-P50	Fr.B.2_06	TU.A-P60
TU.G.1_05	Mathieu, R.	Matsui, K.
Mashirov, A.	Mo.I-P32	FR.A-P9
Mo.L-P37	TU.B.2_03	Mo.B-P16
Mo.L-P74	TU.F-P30	Matsuishi, S.
Mo.L-P77	TU.F-P52	Fr.B.2_05
Th.B.1_05	TU.F-P81	Mo.A-P60
Maskova, S.	Mathon, O.	Matsukawa, M.

TH.A-P28	Th.A-P34	Th.K-P49
TH.C-P104	TU.A-P47	WE.E.1_O2
Matsukawa, S.	Matsushita, A.	Mayaffre, H.
Fr.B.3_O4	FR.D-P71	TH.A-P20
TU.C-P18	Matsushita, M.	Maycock, C.
TU.H.2_I1	Mo.H-P66	Th.P-P34
Matsukura, F.	Matsushita, Y.	Mayer, C.
MO.H.1_O5	FR.D-P71	TU.D.3_O1
Matsumoto, K.	Mo.B-P5	Mayer, J.
FR.B-P13	Matsuura, K.	TU.H-P42
Mo.A-P64	Mo.C-P19	Mayergoyz, I.D.
TH.C-P126	TU.A-P61	Mo.J-P19
Th.D.1_O3	Matsuyama, K.	Mo.J-P20
TU.B-P76	Mo.G-P4	Mo.J-P21
TU.C-P27	Th.O-P7	Mayoral, A.
Matsumoto, K.T.	Mattei, G.	TU.F-P111
TU.B-P49	Th.N-P14	Mayoral, Á.
TU.C-P13	Matty, M.	TU.F-P57
Matsumoto, M.	Fr.H.2_I1	Mayr, S.
TU.A-P27	Matubayashi, K.	Mo.H-P100
TU.G-P9	TH.D-P20	Mo.H-P12
Matsumoto, R.	Matuo, A.	Mo.H-P56
FR.A-P51	TH.A-P18	Mazaleyrat, F.
MO.H.2_O5	Matveeva, P.	Fr.F.3_O2
WE.I.1_O5	FR.F-P28	Mo.L-P26
Matsumoto, T.	Matwiejczyk, A.	TH.I-P25
WE.D.2_I6	TU.E-P41	TU.H-P102
Matsumoto, Y.	Maurel, L.	TU.H-P130
Th.A.2_O2	MO.C.3_O3	TU.H-P36
TU.B-P52	Mo.H-P40	Mazalova, V.
TU.B-P55	TU.A-P24	FR.G-P1
TU.B-P77	TU.A-P26	Mazario, E.
TU.B-P78	TU.A-P45	Th.P-P8
TU.F.3_O3	Maurits W., H.	Mazet, T.
Matsumura, C.	WE.H.2_I6	TU.B-P62
Mo.A-P83	Maurya, A.	Maziewski, A.
Matsumura, T.	TH.A-P39	Mo.G-P16
TH.C-P63	Mavani, K.	Mo.G-P26
Matsunami, M.	Mo.H-P24	Th.C.2_O5
TH.A-P30	Mavani, K.R.	Th.I-P14
Matsuo, A.	Mo.H-P23	Th.I-P8
FR.D-P46	Mawass, M.	TU.A.1_O3
MO.I.2_O2	Fr.I.1_I1	TU.G-P28
TH.A-P14	Maximenko, A.	Mazin, I.
TH.A-P32	Th.K-P36	Th.A.2_O6

Mazraati, H. Th.O-P52	WE.F2_07 Méasson, M.A.	TU.E.3_I1 Mellado, P.
Mazzoli, C. Th.J.1_03	TH.B-P19 Mecena, G.	Th.D.2_05 Mello, A.
Mazzone, D. Mo.A.1_05 MO.A-P2	TU.B-P61 TU.H-P79 Meckenstock, R.	Mo.H-P13 Melnikov, N.
McCall, S. Fr.C.1_04	TU.C.3_03 Meda, A.	FR.E-P10 FR.E-P11 Melnikova, L.
McCandless, G. MO.SYM_5	Fr.E.2_04 Medarde, M.	TU.F-P32 Melo Mendonça, T.
McCann, D. Mo.A-P73	TU.A-P51 Medelin, A.	TU.A-P89 Melo, L.
McCollam, A. TH.A-P41 TU.A.3_01	Th.L-P5 Meffre, A.	TU.I.1_03 Melo, T.
McDonald, R. MO.A.2_03 MO.SYM_5	Fr.E.3_04 Meguro, A.	Mo.B-P30 Melzer, M.
McEwen, K.A. TU.B-P5	TU.H-P94 Mehdiyev, T.	TU.C.1_I1 Mena, M.
McGuinness, P. TU.H-P34 TU.H-P42	FR.F-P5 Mehmedi, Z.	Mo.G-P25 Menad, N.E.
McGuinness, P.J. Mo.I-P11	TU.H-P48 Meier, D.	TU.H-P61 Ménard, D.
McGuire, M.A. Mo.A-P102	MO.H.3_04 TU.A-P24 Meier, G.	Mo.G-P30 Menchyshyn, O.
McHenry, M.E. Mo.L-P58	FR.I-P19 MO.C.2_03 Th.I-P4 TU.F-P36 WE.H.1_02 Meingast, C.	FR.D-P30 Mendels, P.
McKeever, C. TH.J-P15	Mo.A-P97 Tu.A.3_05 Meisel, M.	FR.D-P78 TH.A-P38 TU.D.1_04 Mendes, A.M.
McMichael, R.D. Th.I-P9	TH.A-P22 Mekhonoshin, D.	Mo.L-P90 Mendes, J.
McMorrow, D. FR.A-P30 FR.A-P42 Fr.D.2_04 Mo.G-P25 Th.G.3_02	TH.F-P12 Melander, E.	Th.I.2_06 Mendive Tapia, E.
McMorrow, D.F. Mo.B-P15	Th.N-P10 Melikyan, A.	TH.C-P36 Mendonça, C.
McQueeney, R.J. Fr.D.2_03	Mo.A-P106 Melkov, G.A.	TU.H-P79 Mendoza Zelis, P.
Measson, M.A.	Mo.G-P13 MO.H.2_02	TU.F-P6 Mendoza, A.
		TU.H-P127 Meneses, C.
		TU.F-P43 TU.F-P44

TU.F-P77	TH.J-P7	Mibu, K.
Meneses, T.	Mertens, S.	Fr.H.3_03
TU.B-P61	WE.D.2_03	FR.H-P15
TU.F-P98	Mertig, I.	FR.H-P27
TU.H-P79	FR.A-P32	TH.F-P25
Mengucci, P.	FR.A-P33	Mican, S.
Th.K-P38	Mertz, D.	TU.H-P23
Menshikova, M.	Th.H.2_03	TU.H-P24
Mo.J-P6	Merz, M.	Michalik, J.M.
Mentes, O.	TU.H-P35	Th.B.2_11
TH.K-P1	Mesa Uña, J.L.	Michel, A.
WE.H.1_05	TH.C.1_04	Mo.H-P102
Mentes, T.O.	Mesa, J.L.	Michele, R.
Fr.D.1_03	MO.E.1_03	FR.H-P31
FR.I-P28	Meshcheriakova, O.	Michels, A.
Mo.K-P26	TH.J-P21	TU.A.2_02
TU.J.1_02	TH.J-P24	TU.H-P3
Mentink, J.	Th.N-P11	TU.H-P40
Th.F.2_04	Mesot, J.	Michimur, S.
Meny, C.	FR.I-P27	TH.C-P63
MO.B.3_03	MO.A.3_04	Michimura, S.
MO.E.1_02	Mo.A-P72	Th.D.3_04
Mo.E-P5	Mo.B-P22	TU.B-P51
Mo.H-P79	Messner, I.	Michioka, C.
Th.G.2_03	TU.C-P14	FR.D-P53
TU.F-P51	Messori, M.	FR.D-P8
Menzel, A.	TH.E3_04	TH.A-P32
WE.E.1_04	Metlushko, V.	TU.C-P2
Menzel, D.	Th.M-P4	Michor, H.
Mo.H-P61	Th.M-P5	Fr.B.3_01
Mercier, A.	Meven, M.	Th.M-P22
TU.H-P102	TH.C-P116	TU.C-P14
Mereacre, V.	Meviediev, V.	WE.H.2_03
MO.I.2_04	FR.D-P32	Micklitz, H.
Merentsov, A.	Meyer, F.	TH.A-P36
Mo.A-P12	Th.H.2_03	Miclea, C.F.
Mériguet, G.	Mi, J.W.	TU.B-P69
Th.B.1_02	TU.A-P44	Midya, A.
Merino, J.	Mi, W.	Th.A.1_03
FR.B-P12	FR.H-P7	Mignot, J.M.
Merkulov, D.	Miao, P.	TU.B-P11
FR.F-P19	TU.C.2_04	TU.B-P20
Merodio, P.	Miao, X.F.	TU.F.3_04
Mo.F-P9	MO.D.2_02	Migowski, P.
Mertens, F.	Mo.L-P16	TU.D-P5

Miguel, A.S. Th.P-P34	Millán, Á. TU.F-P16	Mino, M. Mo.G-P12
Miguel, J. MO.I.2_O3	Miller, C. MO.C.3_O1	Miraglia, S. TU.D.3_O1
Mihalceanu, L. TH.E-P11	Miller, C.W. Mo.H-P44	Miranda, M.G.M. TU.H-P135
Mihalik, M. TU.A-P18 TU.A-P46 TU.A-P82 TU.C-P12	Miller, M. Mo.L-P15	Miranda, R. Mo.H-P99 Mo.I-P37 MO.SP-1 TH.I-P28 Th.K-P44 TU.A-P91 TU.G.2_O4
Mikage, H. Mo.A-P4	Millington, A. Fr.B.2_O4	Mirebeau, I. FR.D-P28 FR.D-P29 FR.D-P66 TU.C.2_O3 TU.D.2_I1 TU.F-P87
Mikhailov, A. TU.I-P10	Millis, A.J. PLENARY 1	Miron, I.M. TH.F-P7 TU.I-P15
Mikhailova, A. Mo.L-P15	Miloslavskaya, O. Th.N-P7 Th.N-P8	Miron, M. WE.I.1_O2
Mikhailova, T.V. Th.N-P7 Th.N-P8	Milton, F.P. TU.A-P76	Mirzadeh Vaghefi, S.P. Th.K-P43
Mikhaylovskiy, R. FR.F-P11 Th.F.1_O3 Th.G.1_O5	Milyaev, M.A. Mo.H-P35	Míšek, M. TH.C-P51
Mikhaylovskiy, R.V. Th.I.1_O3 Th.I-P11	Mimura, K. TU.B-P38	Mishra, S.K. Th.I-P1
Mikroulis, A. Th.P-P39	Min, B.C. Mo.D-P16 Mo.D-P24 TH.F-P11 TH.J-P11	Misiuna, P. Th.G.2_O4
Mikulics, M. FR.F-P30	Min, B.I. Mo.A-P45	Miskuf, J. Mo.A-P38 TU.F-P49 TU.F-P50 TU.H-P39
Mikuszeit, N. Mo.I-P31 TU.I-P15	Min, C.H. FR.A-P16	Misoka, K. Mo.B-P18
Mila, F. FR.D-P9 TH.A-P10	Minar, J. Fr.D.2_O2 Mo.J-P2	Missell, F.P. TU.H-P74
Milano, J. FR.I-P21 TH.C-P81 TU.G-P21	Minárik, P. TH.D-P8	Missiaen, J.M. Th.A.3_O4
Milińska, E. Th.G.2_O4	Mineev, V. MO.G.3_O2	
Milita, S. Mo.H-P94	Minegishi, M. TU.B-P76	
	Minei, M. TU.E-P44	
	Minikayev, R. TU.G-P28	
	Mino, J. Mo.L-P12	

Mistonov, A.

Mo.H-P61
Mo.J-P12
Th.K-P28

Mistrik, J.

TH.D-P18
TU.A.1_05

Misumi, K.

FR.B-P15
FR.B-P18

Mitamura, H.

TU.E.2_04

Mitani, S.

Mo.G-P7
Mo.G-P8
WE.G.1_03

Mitani, Y.

TU.I-P9

Mito, M.

TH.C-P21
TH.C-P61
TU.F-P7

Mito, T.

FR.A-P12
FR.A-P55

Mitome, M.

TU.F-P4

Mitra, A.

Mo.L-P11
Mo.L-P58
Th.O-P10
TU.D.3_02

Mitrelias, T.

Th.P-P5

Mitroova, Z.

TU.F-P32

Mitroová, Z.

TU.F-P49

Mitróová, Z.

TU.F-P50

Mitsen, K.

Mo.A-P85
TU.B-P59

Mitsuda, S.

FR.D-P69

TH.C-P99

Th.D.3_03

Mitsudo, S.

FR.I-P34

Mitsui, Y.

Fr.A.1_02
FR.I-P30
Mo.L-P66
TU.E-P35
TU.H-P82

Mitsumata, C.

Mo.F-P10
Mo.J-P13
TU.H-P57

Mitsumoto, K.

TH.C-P126

Mitsuoka, D.

Mo.A-P46

Miura, D.

TU.H-P91

Miura, N.

TH.B-P14
TU.A-P67
TU.B-P45

Miura, O.

TU.C-P19

Miura, S.

TU.I-P11

Miura, Y.

FR.D-P60
Mo.B-P16
TH.C-P60

Miwa, K.

FR.D-P8
Th.G-P10
Th.G-P14
Th.G-P8
TU.C-P2

Miwa, S.

Th.G-P5
WE.G2_I6
WE.G2_03

Mix, T.

MO.D.1_03

Miyagawa, K.

MO.I.3_04

Miyagawa, M.

TU.C.2_02

Miyahara, S.

Th.E.2_03

Miyake, A.

Th.E.2_04
TU.A-P47
TU.A-P50

Miyake, K.

FR.B-P26
Fr.J.1_I1
TU.B-P18
TU.C-P15

Miyakoshi, S.

FR.A-P53

Miyamachi, T.

Fr.D.3_02

Miyamoto, Y.

FR.B-P27

Miyamura, H.

MO.B.1_04
TU.F-P90

Miyata, A.

Fr.D.1_05
TH.C-P58

Miyazaki, D.

FR.I-P30

MIYAZAKI, T.

Mo.H-P89
TH.I-P24
TU.G-P12
TU.H-P70

Miyoshi, K.

Mo.A-P44
Mo.A-P79
Mo.L-P60
TH.B-P18
TU.B-P54

Mizokawa, T.

MO.A.3_01

Mizuguchi, M.

Mo.F-P10
Mo.H-P74
TU.G-P6

Mizuguchi, Y. TU.C-P19	Mo.A-P91	TU.B-P50
Mizukami, S. Mo.E-P7 Mo.H-P89 Th.F.1_04 TH.I-P24 TU.G-P12	Mogilyansky, D. TH.C-P1	Momin, N. FR.I-P48 Th.P-P16
Mizukami, T. Mo.A-P84	Mohammad, K. TH.J-P33	Momono, N. Mo.A-P72 Mo.A-P74 TU.B-P46 TU.B-P56
Mizukami, Y. WE.F2_04	Mohammed, H. Mo.K-P25	Mompeán, F. TU.I.3_03
Mizuki, j. Mo.A-P78	Mohan, A. Mo.B-P7	Mompean, F.J. TH.D-P22 TU.E-P47
Mizumaki, M. TU.B-P25	Mohan, S. FR.I-P48	Mompeán, F.J. Mo.I-P15
Mizuno, H. FR.H-P10	Mohanan, V.P. Mo.H-P87	Momsen, N.C.R. TU.E.2_03
Mizuno, Y. TU.H-P106	Mohanty, J. Fr.I.1_11	Monceau, P. Th.D.1_11
Mizunuma, K. Th.H-P4	Mohseni, F. TU.H-P116	Monecke, M. Mo.H-P30
Mizusaki, T. FR.I-P34	Mohseni, M. Mo.F-P25	Monsen, Å. Mo.G-P15
Mizushima, K. WE.D.2_04	Moise, S. Th.P-P9	Montaigne, F. Fr.D.1_03 FR.D-P21 Mo.D-P8 Th.I.3_04 TU.G.3_03 TU.I-P3
Mizuuchi, K. TH.B-P14	Mojsic, A. TU.I-P25	Montambaux, G. TU.I.3_04
Mliki, N. Mo.L-P63 TU.F-P93	Molcan, M. TU.F-P71 TU.F-P78	Monteblanco, E. Mo.F-P24 Mo.G-P29
Mocellin, J. FR.I-P44	Molchanova, A.D. Fr.C.3_02	Monteiro, P. Mo.H-P106
Mochidzuki, K. FR.I-P31	Mole, R. Mo.A-P32	Monti, M. FR.I.2_03 TU.I.3_03
Modic, K. MO.A.2_03 MO.SYM_5	Molèanová, Z. TU.C-P12	Monticelli, M. Th.H.1_04
Moessner, R. Fr.D.1_11 Fr.D.1_04 FR.D-P68 MO.SYM_1 TH.A-P26	Mølholt, T.E. TU.G.1_05	Montiel Sánchez, H. Th.G-P12
Moghaddam, A.	Möller, J. MO.I.1_04	
	Molnar, D. Mo.A-P56	
	Molnar, G. MO.J.2_04	
	Molokeev, M. FR.D-P38 FR.F-P1	
	Mombetsu, S. TU.B-P48	

Th.O-P32
Montiel Sánchez, M.H.

Mo.H-P48
Montiel, H.

Mo.H-P47
 TU.H-P127

Montiel, X.
 TH.B-P19

Mook, A.
 FR.A-P32
 FR.A-P33

Moon, C.Y.
 FR.A-P22

Moon, H.
 TU.H-P22
 TU.H-P64

Moon, J.
 TH.E-P15
 TH.F-P19

Moon, K.
 TH.F-P11

Moon, K.W.
 TU.H-P84

Moon, S.J.
 FR.A-P17

Mora, B.
 TH.K-P21
 Tu.G.2_I1

Morales Rojas, S.
 FR.E-P17
 FR.E-P19

Morales, M.P.
 Th.H.1_I1
 Th.P-P1
 Th.P-P11
 Th.P-P7
 TU.B.3_O2
 TU.F-P61
 TU.F-P80
 Tu.H-P137

Morales, R.
 MO.E.3_I1
 Mo.H-P44
 Mo.I-P24
 TH.K-P21

Tu.G.2_I1
Morán, O.

TU.A-P95
Morchenko, A.

Th.O-P46
 TU.A-P35

Morcrette, M.
 Th.O-P48

Moreau-Luchaire, C.
 MO.H.3_O2

Moreira, A.
 TU.A-P46

Morel, R.
 Th.O-P40

Morelli, A.
 Th.E.2_O2

Morellon, L.
 MO.C.3_O3
 Th.B.2_O3

Morellón, L.
 Mo.H-P2
 Mo.H-P40
 Mo.H-P55

Th.B.2_I1
 Th.B.3_O2

Th.H-P5
 Th.H-P8
 Th.I.2_O4

TU.A-P26
 TU.A-P86
 TU.C.1_O4

Moreno Ortega, R.
 Mo.J-P16

Moreno-Ramirez, L.M.
 Mo.L-P14

Moreno-Ramírez, L.M.
 MO.D.2_O3
 Mo.L-P13

Morenzoni, E.
 FR.A-P34
 Fr.I.1_O3

Moretti Sala, M.
 Mo.C-P17

Moretti, S.
 WE.I.1_O4

Morgunov, R.
 FR.F-P2

MO.F.1_O2
 TH.D-P5

TU.D-P1

Mori, K.
 TU.F-P10
 TU.F-P62

TU.F-P69
 TU.F-P70

Mori, M.
 FR.D-P58
 MO.G.3_O1
 Th.I.2_O5

Morice, C.
 Mo.A-P56

Morimoto, K.
 FR.I-P34

Morimoto, S.
 TU.F-P10
 TU.F-P69
 TU.F-P70

Morin, M.
 TU.A-P51

Morioka, R.
 FR.A-P12

Morishima, M.
 TU.E-P44

Morishita, K.
 Mo.A-P44
 Mo.A-P79

Morita, T.
 TH.C-P90

Moriyama, T.
 FR.H-P10

TH.F-P13
 TH.F-P5
 TH.F-P6

Morjan, I.
 TU.F-P108

Morley, N.
 FR.H-P3

Morley, S.
 MO.D3_O4

Moro-Lagares, M.

Th.B.2_O3	TH.C-P49	TU.F-P22
WE.H.2_O2	Motoyama, G.	TU.F-P96
Moroni, M.	Mo.A-P44	Mravlje, J.
Mo.A-P103	Mo.A-P79	Fr.D.3_O1
Morooka, A.	Mo.L-P60	WE.E2_O2
WE.J.1_O3	TH.B-P18	Mróz, B.
Morosov, A.	TU.B-P54	FR.H-P20
FR.H-P1	Mott, D.	Mruczkiewicz, M.
Morozov, A.	Th.P-P15	Mo.G-P16
Mo.L-P87	Motte, J.F.	Mo.G-P26
Morris, D.	Fr.E.1_O2	Msomi, J.
FR.D-P67	Moudřík, J.	FR.F-P24
TH.A-P26	TU.B-P28	FR.F-P25
Morris, R.E.	Mougin, A.	TU.F-P104
TH.A-P38	WE.I.1_O3	TU.F-P105
TU.D.1_O4	Moulin, J.F.	Msomi, J.Z.
Mortensen, A.Z.	Mo.H-P100	TU.B.2_O5
Mo.L-P38	Mo.H-P12	TU.F-P96
Moskaltsova, A.	Mo.H-P56	Mu, S.
Th.K-P46	Moura-Melo, W.	TH.C-P88
Th.O-P54	Mo.B-P30	TU.E-P30
Moskvin, A.	Mo.B-P31	Mu, X.
FR.B-P33	Moutafis, C.	Th.O-P51
Mo.A-P71	Fr.I.1_I1	Muckova, M.
TU.C.2_O5	MO.H.3_O2	Th.P-P22
Mossang, E.	TH.J-P3	Mudryk, Y.
Mo.I-P28	Moutis, N.	FR.SP-1
Mostovoy, M.	Mo.I-P30	Mo.L-P47
Th.E.1_O2	Mouton, L.	Muduli, P.
Mota, A.C.	Mo.I-P12	Mo.F-P19
TU.B-P69	Movshovich, R.	Muehl, T.
Mota, D.	TU.B-P69	MO.E.1_O5
TU.A-P46	Moya, C.	Muela, A.
Motelica-Heino, M.	Fr.E.2_O3	Fr.B.1_O2
TU.F-P5	TU.B.3_O3	Mueller, E.
Motevalli, M.	TU.F-P79	WE.E.1_O4
TU.D-P5	TU.F-P80	Mueller, J.
Motome, Y.	Tu.H-P137	TH.B-P3
FR.B-P23	Moyer, J.	Mufti, N.
FR.D-P40	TU.E.1_O4	TU.C-P9
FR.E-P36	Moyo, T.	Mugarza, A.
Mo.C-P15	FR.F-P24	Mo.C-P23
TU.A-P81	FR.F-P25	MO.J.2_O3
Motoya, K.	TU.F-P104	TU.J.3_O3
TH.B-P11	TU.F-P105	Mühl, T.

FR.I-P41	TU.C-P11	Murakami, T.
MO.E.2_O1	Munakata, K.	TU.H-P56
Mühlbauer, S.	TH.C-P120	Murakami, Y.
Mo.H-P70	Mundet, B.	TH.A-P29
TH.A-P5	Th.L-P5	Mural, Z.
TH.J-P32	Mundy, J.	TU.H-P25
WE.H.1_O3	TU.E.1_O4	Muramatsu, A.
Mukai, K.	Munevar, J.	TU.F-P35
TU.E-P31	TH.A-P36	Murapaka, C.
Mukherjee, P.	TH.C-P110	Th.G.2_O5
TU.F-P76	Munoz, M.	TH.K-P5
Mukherjee, S.	MO.J.3_O3	Th.K-P55
Th.A-P43	Munoz, M.C.	Th.O-P35
TU.E.2_O3	Mo.J-P16	Murayama, S.
Mukhin, A.	Munsch, P.	FR.B-P13
TU.A-P11	Th.C.3_O2	Th.G-P2
Mukhin, A.A	Munsie, T.	TU.B-P46
Th.J.1_O3	Fr.B.2_O4	TU.B-P56
TU.A-P11	Fr.C.2_O4	TU.B-P76
TU.A-P30	Munuera, C.	Murazumi, T.
TU.A-P93	FR.I-P49	TU.B-P48
TU.A-P98	TH.K-P23	TU.B-P50
Mukhopadhyay, S.	Münzenberg, M.	Murgulescu, I.
TH.A-P20	Mo.G-P14	TU.H-P117
Mukuda, H.	WE.I.2_O5	Muro, Y.
Mo.A-P87	Muñiz, P.	TH.B-P11
Mullegger, S.	TU.F-P52	TH.B-P4
TU.J.3_O4	TU.F-P94	Th.J.1_O4
Müller, A.	Muñoz Rodríguez, D.	TU.B-P19
TH.A-P27	Fr.B.1_O2	TU.B-P40
Müller, B.	Muñoz, C.	WE.H.2_O5
MO.E.2_O1	FR.A-P14	Murphy, J.
Muller, D.	Th.P-P31	Th.P-P3
TU.E.1_O4	Muñoz, M.	Murugesan, S.
Müller, J.	Mo.H-P99	Th.P-P38
Mo.H-P17	Muñoz, M.C.	Muscas, G.
WE.B.2_O2	Fr.G.2_I2	TU.B.2_O3
Müller, K.H.	WE.G.1_O4	TU.F-P67
MO.D.1_O3	Muraca, D.	TU.F-P68
TU.H-P118	TU.F-P18	TU.F-P81
Müller, M.	TU.F-P39	Mushnikov, N.
Th.O-P29	TU.F-P6	Mo.L-P73
Müller, R.	Murakami, S.	TH.C-P101
FR.I-P7	FR.A-P25	Musial, A.
Mulligan, M.	WE.G.1_I1	TU.H-P46

Musinu, A.

TU.F-P67
TU.F-P68

Mustaqima, M.

TU.H-P15

Muthurajan, H.

FR.I-P48

Mutka, H.

FR.D-P28
FR.D-P29
FR.D-P66
Mo.A-P72

Mutou, E.

Mo.A-P44

Mutou, T.

FR.B-P27
TH.B-P18

Myasoedov, Y.

Mo.H-P81

Mydosh, J.

TU.A.3_O4
TU.F.3_O1
WE.C.2_O5

Myronov, M.

Mo.D-P4

Myrzakhmet, M.

Mo.J-P17

N

N. Costa, F.

TH.C-P20

Nachbaur, V.

TU.F-P85
TU.F-P86
TU.H-P61
TU.H-P62
TU.H-P78

Nachiappan, M.S.

Th.P-P38

Nadeem, K.

Mo.A-P7

Nadvornik, L.

Fr.G.3_O2

Nagai, K.

TH.C-P21

Naganuma, H.

FR.H-P26

Th.F.1_O4

Th.O-P18

TU.A-P66

Nagaosa, N.

Fr.I.1_O3

TU.H.3_O2

Nagarajan, R.

FR.I-P48

Nagasawa, N.

TU.B-P49

TU.C-P22

Nagasawa, T.

WE.D.2_O4

Nagata, H.

TU.B-P38

Nagata, M.

FR.H-P10

Nagel, P.

TU.H-P35

Nagel, U.

TU.A-P25

Naggert, H.

MO.I.2_O3

Nagler, S.E.

Mo.A-P102

Nahm, H.H.

Fr.C.3_O3

Naidoo, D.

TU.G.1_O5

Nail, C.

WE.A.2_O1

Naito, A.

FR.A-P38

Najjari, N.

Fr.B.1_I1

Naka, T.

FR.D-P71

Nakagawa, F.

Mo.A-P53

Nakagawa, K.

Mo.B-P21

Nakagawa, M.

FR.A-P47

Nakagawa, R.

Mo.L-P28

Nakagawa, S.

Mo.H-P64

Nakagawa, T.

Mo.H-P72

Nakai, T.

Th.O-P22

Nakajima, K.

Fr.C.3_O3

FR.D-P1

Th.E.2_I1

Nakajima, T.

FR.D-P69

TH.C-P99

Th.D.3_O3

TU.A-P22

Nakama, T.

TH.C-P71

TU.E-P20

TU.E-P44

Nakamae, S.

Th.B.1_O2

Nakamura, A.

TU.E-P20

TU.E-P44

Nakamura, D.

FR.D-P18

Mo.B-P10

TH.C-P58

Nakamura, F.

Fr.C.2_O4

TU.I-P11

Nakamura, K.

FR.A-P12

FR.H.3_O1

FR.H-P12

FR.H-P28

Nakamura, M.

TH.A-P18

Nakamura, O.

TU.B-P17

Nakamura, S.	FR.H-P27	Nandi, S.
Mo.F-P5	Nakatani, R.	Mo.A-P57
Mo.H-P71	TU.I-P11	Nandy, A.K.
TH.C-P23	TU.I-P19	MO.F.3_O2
TH.C-P98	Nakatani, Y.	Nano, R.
TU.B-P27	Mo.F-P5	Th.P-P10
TU.B-P57	TH.F-P3	Nanto, D.
TU.E-P16	TH.F-P6	Mo.L-P67
Nakamura, T.	Th.G-P2	TU.H-P77
WE.G2_I6	TH.J-P2	Napolskii, K.
Nakamura, Y.	Nakatsuji, S.	Th.K-P28
TH.A-P28	TU.B-P2	Naranjo-Uribe, A.
TU.F-P4	TU.B-P47	Mo.C-P5
Nakane, T.	TU.C-P16	Narasiwodeyar, S.
FR.D-P71	TU.F.3_O3	MO.A.2_O5
Nakano, H.	Nakaya, M.	Narayanamy, K.K.
FR.D-P72	TU.F-P35	Th.P-P14
FR.H-P18	Nakayama, M.	Nardone, M.
TH.A-P3	Fr.B.3_O4	Mo.E-P8
Nakano, M.	FR.D-P71	Narsinga Rao, G.
Mo.L-P54	Mo.G-P7	TU.F-P66
Th.O-P36	TU.C-P18	Nascimento, V.
TU.H-P38	Nalbandyan, V.	Mo.I-P39
TU.H-P58	Th.A.1_O4	Nasi, L.
TU.H-P86	Nalecz, D.	MO.C.2_I1
Nakano, T.	Fr.D.2_O5	TU.G-P16
TH.C-P19	TH.B-P20	TU.J.2_O4
TH.C-P93	TU.B-P64	Nasseri, S.A.
TU.E-P31	Namatame, H.	TH.F-P23
TU.E-P37	TU.B-P38	Nasu, J.
Nakao, A.	Namazu, T.	FR.D-P40
TU.A-P61	TH.C.1_O2	Natali, F.
Nakao, H.	Nambu, Y.	FR.F-P31
TH.A-P29	TH.C-P120	Mo.A-P91
Nakao, M.	Namiki, T.	Mo.D-P3
TU.E-P26	TU.B-P29	Nateprov, A.
Nakashima, T.	TU.B-P31	TH.C-P89
Mo.A-P89	Nan, W.Z.	Natoli, C.R.
TU.C-P19	Mo.L-P33	TU.J.3_O2
Nakata, H.	Nandi, M.	Naumann, M.
FR.D-P13	Th.A.1_O3	FR.D-P27
Th.A-P34	TH.C-P13	Navarro Chávez, O.
Nakata, T.	TU.G-P2	Mo.H-P49
TH.D-P20	Nandi, N.	Navarro, E.
Nakatani, N.	TH.C-P18	Mo.H-P108

TU.C.1_05

Navarro, O.

TU.E-P23

Navas, D.

Mo.H-P44

TH.K-P21

Tu.G.2_11

Navau, C.

Mo.F.2_05

Mo.J-P5

TU.I.2_02

Nayak, A.K.

WE.D.1_05

Nayak, C.

TU.C-P11

Nazarov, D.

FR.F-P28

Ncube, M.

TU.G.1_05

Ndlovu, B.

FR.F-P24

Neamtu, B.V.

TU.H-P119

TU.H-P120

TU.H-P122

Nedelko, N.

TU.D-P2

TU.D-P3

Nedelkoski, Z.

TU.E-P48

Nehme, Z.

Mo.J-P10

Neibecker, P.

Th.A.2_07

WE.D.1_02

Neige, J.

FR.I-P18

Nekrasov, I.

Mo.A-P22

Nemati, Z.

MO.B.1_03

Nemec, P.

Fr.G.3_02

Nemes, N.M.

TH.D-P22

TU.G-P15

TU.I.3_03

WE.G.1_04

Nemkovski, K.

TH.B-P9

TU.B-P20

Nemoto, Y.

TH.C-P126

Nemtsev, I.

TU.H-P55

Nenkov, K.

Mo.L-P15

Mo.L-P23

Nesterenko, S.

TU.C-P27

Netsu, N.

TU.A-P61

Neu, E.

MO.E.2_03

Neu, V.

MO.E.1_05

MO.E.2_06

Th.M-P18

TU.G.2_04

WE.J.2_05

Neubauer, A.

TU.C-P23

TU.C-P32

TU.C-P33

Neumann, I.

Fr.F.3_11

Th.O-P49

WE.I.2_12

Neumann, R.

Th.G.2_11

Nevidomskyy, A.

Fr.C.1_01

Ngema, N.

FR.F-P25

TU.F-P96

NGuyen Ba, D.

Mo.L-P91

Nguyen Thi, M.H.

Mo.H-P36

Nguyen Van, Q.

Mo.H-P36

Nguyen, A.

Th.O-P52

Nguyen, B.D.

TH.C-P127

Nguyen, D.H.

TU.C-P20

Nguyen, K.

TU.A-P61

Nguyen, T.

TU.F-P37

TU.F-P38

Nguyen, T.T.K.

Th.P-P15

Nguyen, V.D.

Fr.G.3_04

TH.E-P8

Nguyen, V.Q.

TH.B-P13

Nhalil, H.

TH.C-P73

Niarchos, D.

Mo.H-P63

TH.K-P12

Th.K-P37

TU.E.3_03

TU.G-P4

TU.H-P136

niayfar, M.

TU.E-P13

Nica, M.

FR.E-P33

Nichols, C.I.O'B

Fr.E.2_02

Nickel, F.

MO.I.2_03

Nicklas, M.

WE.D.1_05

Niclas, M.

TU.B-P69

Nicolaou, A.

Mo.A-P31

Nicolas, H.

Th.H.2_02

Nicolas, J.

MO.E.1_I1	Mo.H-P39	Nishida, R.
Nicolodi, S.	Nikitin, A.	TU.F-P35
Th.K-P40	Fr.C.1_O2	Nishigori, S.
Nicotina, A.	Nikitin, S.	Mo.L-P60
Th.B.3_O1	TH.D-P14	TH.B-P18
Niculescu, A.M.	Nikitin, V.	TU.B-P54
TU.F-P108	TU.I-P10	Nishihara, S.
Nie, S.	Nikitov, S.	TU.C.2_O2
TH.B-P17	Fr.G.1_O4	Nishikawa, S.
Niebieskikwiat, D.	Mo.H-P21	TU.A-P50
Mo.B-P8	Th.M-P7	TU.A-P52
TH.I.3_O5	Th.O-P27	Nishimoto, K.
Niedermayer, C.	Niklowitz, P.	Mo.A-P87
FR.I-P7	Mo.A-P109	Nishimoto, N.
Mo.A-P72	TU.C-P32	Mo.A-P86
MO.D.3_O1	TU.C-P33	Nishimoto, S.
Niedziela, J.	Nikulin, Y.	TH.A-P18
TH.A-P42	TH.K-P22	Th.D.2_O4
Niehaus, O.	Nilsen, G.	Nishimura, A.
WE.C.2_O5	Fr.G.2_O4	FR.I-P25
Niensch, K.	MO.D.3_O1	Nishimura, K.
Mo.K-P20	Nimec, P.	TU.B-P29
TH.F-P24	TU.G.1_O3	TU.B-P31
Th.G.2_I1	Nimori, S.	Nishimura, T.
Niemann, R.	TH.C-P104	TU.I-P23
WE.D.1_I1	Ning, F.	Nishine, K.
Nigam, A.	Fr.B.2_O4	Mo.A-P23
TH.C-P114	Fr.C.2_O4	Nishiuchi, T.
Nigam, A.K.	Fr.G.2_I1	TU.H-P19
Fr.C.3_O1	MO.F.1_O4	Nishiwaki, M.
TH.C-P117	Ninomiya, H.	Mo.H-P66
Nii, Y.	Th.A.2_O2	TU.E-P18
Mo.C-P19	Ninomiya, M.	Nishiyama, K.
Niimi, Y.	TU.H-P87	FR.A-P12
TH.I.1_O4	TU.H-P94	FR.A-P55
WE.E.1_I1	Niño, M.A.	Nishizaki, T.
Niizeki, T.	Mo.H-P99	Th.K-P30
Mo.F-P18	Mo.I-P37	Nisoli, C.
Th.H-P14	TH.I-P28	TU.D.1_I1
Niki, H.	Nisbet, G.	Nistor, C.
TH.B-P8	FR.A-P30	TU.J.3_O3
TU.E-P44	Nishida, H.	Niyaifar, M.
Nikitenko, V.	FR.B-P15	TU.E-P27
MO.C.2_I4	Nishida, K.	Niyazov, L.
Nikitenko, V.I.	TU.A-P73	TH.C-P29

TH.C-P30	Nojima, T.	Noske, M.
Nizhankovskii, V.	TU.B-P27	Fr.G.1_O3
Mo.L-P37	TU.B-P57	TH.J-P12
TU.A-P40	Nojiri, H.	Notargiacomo, A.
Nižďanský, D.	TH.A-P18	TU.G.3_O1
TH.C-P34	Tu.C.3_O5	Notin, L.
Nobe, K.	Nolas, G.	Fr.G.3_O4
TU.C-P18	Th.B.1_I1	TH.E-P12
TU.H.2_I1	Nolting, F.	TH.E-P8
Nobrega, E.	FR.H-P34	Th.O-P40
Mo.L-P5	Nomura, A.	Novais, E.R.P.
Noda, K.	TH.E-P18	TH.J-P20
FR.B-P10	Nomura, H.	Novak, M.
Noguchi, S.	TU.I-P11	FR.A-P6
Fr.A-P64	TU.I-P19	TU.D-P14
Noguchi, Y.	Nomura, K.	Novak, M.A.
FR.A-P23	Th.B.2_O4	TU.D-P15
Mo.A-P111	Nomura, T.	Novak, P.
Mo.A-P40	MO.I.2_O2	TU.H-P128
Th.K-P47	TH.E-P14	TU.H-P89
Nogues, J.	TH.E-P16	Novak, R.
Tu.B.2_O2	Th.H-P12	TH.J-P20
TU.F-P87	Th.H-P3	Novak, V.
Nogués, J.	TU.A.-59	FR.F-P6
FR.I-P46	TU.A-P60	MO.C.1_O5
MO.B.1_I1	Nonaka, Y.	TU.SYM_4
MO.B.1_O5	Fr.B.2_O4	Novák, V.
Mo.C-P9	Nordblad, P.	MO.F.1_O3
Mo.F.2_O5	Mo.G-P15	TU.G.1_O3
Mo.I-P33	Mo.I-P32	Novakoski Fischer, K.
TH.C-P38	TU.F-P30	FR.A-P7
TU.F-P64	TU.F-P52	Novello, N.
Noh, H.J.	WE.D.1_O4	Fr.A.3_O1
FR.A-P2	Nori, F.	Novikov, A.
Noh, T.W.	Mo.B-P19	TH.C-P40
FR.A-P17	TU.E-P2	Novitskii, N.
Mo.A-P66	Norman, M.	Th.G.1_O4
Nohara, M.	Mo.A-P106	Novoa, J.J.
Mo.A-P46	Normile, P.	TU.J.3_O1
Mo.A-P84	TU.F-P94	Novosad, V.
Mo.A-P86	Normile, P.S.	TH.J-P34
Nohara, S.	TU.F-P30	Novosel, N.
TH.C-P2	TU.F-P52	WE.A.2_O2
Noheda, B.	Nose, M.	Nowak, P.
Th.E.1_O2	MO.C.1_O4	FR.I-P39

Nowak, S.

Mo.I-P12
Mo.L-P50

Nowak, U.

Th.I-P12
Th.J-P27
TU.G.3_O4

Nowakowski, J.

FR.H-P34
TU.D-P12

Nowicki, M.

FR.I-P29
TU.H-P59

Noya, Y.

Th.D-P21

Nozaki, H.

FR.D-P8
Mo.B-P6
TU.B-P3
TU.C-P2

Nozaki, T.

Fr.H.3_O3
MO.G.1_O4
Th.G-P5
Th.G-P7
WE.G2_I6
WE.G2_O3

Nozaki, Y.

Mo.F-P22
TU.I-P21
TU.I-P22

Nozue, T.

Mo.H-P71

Nozue, Y.

Th.C-P93
TU.E-P31
TU.E-P37

Ntallis, N.

Mo.J-P15

Nunez-Regueiro, M.

Mo.A-P94

Nur-e-Alam, M.

Th.O-P41

Nuzully, S.

Th.P-P29

Nuzzi, D.

Fr.F.2_O4

Nyayate, M.N.

Th.O-P53

Nyman, M.

Mo.H-P52



Ó Mathúna, C.

TU.H-P26

O'Neill, C.

Th.D.1_I4

Oakley, R.

TU.E-P33

Obaida, M.

TU.E-P5

Obata, K.

Th.C-P53

Obata, M.

FR.H-P18
Th.C-P59
Th.G-P4

Oberdick, S.

Fr.H.2_I1

Obinata, A.

Mo.H-P16
Th.G-P10
Th.G-P8

Oboz, M.

Th.C-P65

Obradors, X.

Th.SP-3

Ocelík, V.

TU.H-P39

Ochiai, A.

TU.B-P27
TU.B-P57

Ocker, B.

Th.F-P17
TU.I-P15

Oda, M.

Mo.A-P72

Mo.A-P74

Oda, R.

TU.A-P73

Oda, T.

FR.H-P18
Th.C-P59
Th.G-P4

Oe, S.

Th.O-P22

Oehler, F.

Mo.H-P95
Mo.H-P96

Elebarski, A.

TU.E-P19

Oepen, H.P.

Mo.H-P75
Mo.H-P76

Ogasawara, A.

TU.G-P24

Ogata, M.

Mo.J-P23

OGAWA, D.

TU.H-P106
TU.H-P70

Ogawa, S.

Th.B-P18

Ogawa, T.

TU.H-P33
TU.H-P38

Ogita, N.

TU.B-P53
TU.D-P8

Ognev, A.

Th.J-P34

O'Grady, K.

Th.E.3_O1

Ogrin, F.

Th.J-P15

Ogrodnik, P.

Th.O-P24

Oguchi, A.

FR.D-P16

Oguchi, T.

FR.A-P21

TU.A-P14
 TU.E-P25
Ogura, T.
 TH.A-P29
 TU.C.2_O2
 TU.C.2_O4
Oguz, K.
 Mo.G-P30
Oh, C.
 FR.A-P4
Oh, J.
 Fr.C.3_O3
Oh, S.
 Mo.B-P23
Oh, S.H.
 TU.A-P78
Oh, S.K.
 FR.E-P1
 TU.F-P17
Oh, Y.
 Mo.G-P2
 TH.F-P19
Oh, Y.S.
 TU.E.1_O4
Ohara, S.
 Th.A.2_O2
 TH.C-P120
 TU.B-P77
 TU.B-P78
Ohashi, M.
 FR.I-P32
 TH.C-P19
 TU.B-P9
Ohe, J.I.
 Th.J-P37
Ohgushi, K.
 Fr.D.1_O5
 TU.A-P90
Ohira-Kawamura, S.
 Fr.C.3_O3
 FR.D-P1
Ohishi, K.
 Th.A.2_O2
 TU.C.2_O2
Ohja, S.

MO.F.2_I1
Ohldag, H.
 TU.A-P36
Ohnishi, K.
 Mo.H-P59
 TH.E-P10
Ohno, H.
 MO.H.1_O3
 MO.H.1_O5
 Th.O-P52
 WE.B.2_O2
Ohno, T.
 Mo.L-P55
Ohno, Y.
 WE.B.2_O2
Ohnoutek, L.
 Th.G-P13
 TU.H-P85
Ohnuma, S.
 MO.C.1_O4
Ohnuma, Y.
 Th.H-P10
 WE.I.2_O4
Ohta, H.
 FR.D-P13
 TU.C-P10
 TU.E-P16
Ohta, T.
 TU.B-P31
Ohta, Y.
 FR.A-P53
 FR.B-P14
 FR.B-P15
 FR.B-P18
 FR.B-P28
 Mo.A-P41
 Mo.A-P42
Ohtake, K.
 Mo.L-P52
Ohtake, M.
 Fr.A.3_O2
 Th.K-P47
 TU.I-P23
Ohtani, T.
 TU.A-P88

Ohtsubo, Y.
 WE.G.1_O5
Ohtsuki, T.
 FR.A-P9
Ohyama, K.
 TH.A-P13
Oikawa, T.
 MO.F.3_O1
Ok, J.M.
 WE.A.1_O6
Oka, H.
 Fr.H.3_O4
 Mo.A-P19
Oka, K.
 Mo.B-P18
 TU.A-P50
 TU.A-P52
 TU.A-P53
Oka, M.
 Th.H-P14
Okabe, K.
 Mo.I-P23
 TH.E-P16
 Th.H-P12
Okada, H.
 Th.O-P30
Okada, M.
 TH.A-P14
 TH.A-P18
Okamoto, Y.
 FR.D-P78
 TH.C-P58
Okane, T.
 TU.B-P55
Okano, G.
 TU.I-P21
Okayasu, S.
 MO.E.2_O4
Oki, S.
 Mo.D-P19
 Th.H-P2
Okubo, A.
 FR.H-P27
Okubo, S.
 FR.D-P13

Okunishi, K.	TU.E-P12	Th.G-P8
TH.A-P3	Ollivier, J.	Ono, T.
Okutani, A.	FR.D-P28	FR.D-P51
Mo.B-P12	FR.D-P29	FR.H-P10
Mo.B-P20	FR.D-P66	TH.F-P13
TH.A-P22	Mo.A-P72	TH.F-P5
Tu.E-P51	MO.D.3_O1	TH.F-P6
Ólafsson, S.	TU.A-P43	Th.G-P14
TU.G.1_O5	Olsson, E.	Th.G-P3
Olalde Velasco, P.	Th.P-P2	Ono, Y.
Fr.B.2_O3	TU.B.3_O2	Mo.H-P59
Olalde-Velasco, P.	Omori, Y.	TH.E-P10
Th.G.3_O1	TH.I.1_O4	Onoda, S.
Olejník, K.	Önel, A.C.	Mo.B-P27
FR.F-P6	FR.F-P10	TU.D.1_O5
Fr.G.3_O2	FR.F-P15	Onozaki, N.
Olejník, K.	Ong, C.K.	TU.E.2_O4
MO.F.1_O3	TU.A-P5	Onuki, Y.
TU.G.1_O3	Onimaru, T.	Mo.A-P87
Olekšáková, D.	Mo.A-P64	TU.E-P20
TU.H-P41	TH.B-P4	TU.E-P44
Oles, A.M.	Th.D.1_O3	Oogane, M.
FR.D-P77	TH.D-P23	FR.H-P26
TH.A-P6	TU.B-P49	Th.F.1_O4
TH.A-P8	TU.C-P13	Th.O-P18
Oleszak, D.	TU.C-P22	TU.A-P66
TU.E-P41	TU.C-P27	Oomaru, K.
Oliva, A.	Onji, T.	Mo.F-P5
Th.P-P34	TU.B-P37	Oomi, G.
Oliveira, G.	Ono, A.	TH.C-P19
Mo.L-P90	Th.O-P18	Opazo-Damiani, M.
TU.E.2_O5	Ono, K.	WE.F.1_O5
Oliveira, N.	Fr.A.3_O3	Opherden, L.
Mo.L-P5	FR.H-P26	Fr.D.1_O2
Olivera, J.	FR.I-P47	Opletal, P.
FR.A-P63	Mo.I-P2	TU.C-P7
Olivetti, E.	Mo.J-P13	Oppemeer, P.M.
Th.A.1_O5	TU.H-P115	TU.D-P12
Olivetti, E.S	TU.H-P132	Oppeneer, P.M.
TU.H-P121	TU.H-P57	FR.H-P34
Olle, M.	Ono, M.	TH.A-P21
MO.J.2_O3	Mo.A-P105	Orain, J.C.
Ollefs, K.	Ono, S.	FR.D-P78
TH.E-P20	Th.G-P10	TH.A-P38
TU.C.3_O3	Th.G-P14	TU.D.1_O4

Oral, A.	TU.B-P2	Mo.K-P8
FR.I-P15	O'Shea, K.	Otani, Y.
FR.I-P16	FR.H-P30	TH.I.1_04
FR.I-P17	Oshima, D.	WE.E.1_11
Ordoñez, J.E.	TU.I-P14	Otsubo, M.
Mo.H-P4	TU.I-P16	Mo.L-P54
TU.A-P86	Oshima, K.	Th.O-P36
Oreg, Y.	TU.D-P9	Otsuka, D.
Mo.A-P13	Oshima, S.	FR.D-P15
Orendáè, M.	TU.H-P86	Otsuka, H.
Mo.L-P7	Osiak, K.	FR.E-P32
Orendáèová, A.	TU.I.2_06	Otsuki, J.
Mo.L-P7	Osman, N.	Mo.A-P17
Orio, M.	TU.F-P22	Ott, F.
TU.A-P75	Osmolowskaya, O.	TU.G-P28
Orion, I.	FR.F-P28	Ott, H.R.
TH.D-P25	Osmolowsky, M.	FR.I-P27
Orlando, T.	FR.F-P28	MO.A.3_04
Th.N-P13	Osokin, S.	Mo.B-P22
Th.P-P10	Th.M-P7	Ottaviano, L.
TU.D-P7	Osorio, J.A..	Mo.E-P8
TU.F-P60	Th.K-P24	Otxoa, R.
Orlov, Y.	Osorio, M.R.	Fr.G.3_02
TH.C-P11	TH.D-P22	Ou, X.
Orozco, J.M.	Osorio-Guillen, J.M.	TU.I-P17
TU.F-P39	TH.A-P36	Ouaissa, M.
Orrù, F.	Osorio-Guillén, J.M.	TH.C-P83
TU.F-P67	Mo.C-P5	Ouaissa, S.
TU.F-P68	Ostler, T.	TH.C-P83
Ortega, D.	FR.F.2_05	Ouanounou, G.
Th.P-P7	Fr.J.2_12	Th.P-P39
TU.F-P106	Östman, E.	Ouazi, S.
Ortix, C.	Th.N-P10	FR.A-P7
TU.E-P6	WE.B.2_03	FR.H.3_01
Ortiz, G.	Ostos, C.	Ouchri, M.
Th.O-P48	Th.H-P11	Fr.F-P33
Orue, I.	Oswald, J.	Oujja, M.
FR.A-P1	FR.C-P1	TU.I.3_03
FR.H-P17	Oszwa³dowski, M.	Ouladdiaf, B.
Osanai, Y.	FR.I-P36	Fr.B.1_03
FR.A-P55	Ota, M.	FR.D-P54
TU.B-P38	Mo.G-P8	TH.C-P105
Oscarsson, S.	Ota, S.	TU.B-P28
Th.H.1_03	TH.C.1_02	Oumezzine, M.
Oseroff, S.B.	Otálora, J.	Mo.H-P15

Mo.L-P4
Ourry, L.
Mo.I-P12
Ovari, T.A.
Mo.K-P30
TU.H-P101
TU.H-P92
Ovchinnikov, S.
TH.C-P11
TU.F-P88
TU.H-P31
WE.J.2_I1
Ovchinnikova, E.N.
Th.J.2_O4
Owada, A.
FR.H-P26
Owen, J.
Fr.H.2_O5
Oyanagi, M.
WE.J.1_O3
Oyarzun, S.
Mo.D-P27
MO.F.1_O5
MO.F.3_O2
WE.G.1_O5
Oyola, D.
TU.H-P37
Ozaki, T.
Fr.A.2_O4
Ozarowski, A.
TH.A-P17
Ozawa, R.
FR.E-P36
Özçelik, B.
Mo.L-P69
Ozdemir, M.
Mo.G-P3
Ozer, H.O.
FR.I-P15
Özer, S.
MO.E.2_O6
Ozerov, M.
FR.D-P11
TH.A-P33
Ozherelyev, V.

FR.E-P22
Ozono, K.
Mo.L-P66
P
P. Amaral, R.
FR.D-P65
P. Araújo, J.
Mo.H-P107
P. D., B.
TU.E-P32
P. del Real, R.
Th.O-P55
P. Freitas, P.
Mo.F-P21
P. Ivanov, I.
Mo.K-P25
P. Skokov, K.
Mo.L-P39
P.V., M.
TU.E-P32
Pablo-Navarro, J.
Mo.K-P17
Paczeńska, A.
TU.H-P53
Paddison, J.
FR.D-P73
Padilla, J.
Mo.C-P9
TH.C-P38
Padilla-Pantoja, J.
Th.A.1_O1
TU.A-P93
Padrón-Hernández, E.
Mo.K-P2
Paglione, J.
TU.B-P73
Pagliuso, P.
TU.B-P2
Pagliuso, P.G.
Mo.A-P48
TH.C-P9

Pai, C.
FR.I-P48
Pailhes, S.
Th.A.2_O4
Paiva, T.
Mo.A-P104
Pajić, D.
WE.A.2_O2
Pajskr, K.
TU.B-P72
Pal, A.
TU.E-P6
Pal, S.K.
TU.H-P118
TU.H-P95
Palacio Morales, A.
WE.H.2_I1
Palacio, F.
TU.F-P16
Palacio-Morales, A.
TU.F.1_O2
Palacios, E.
Th.B.3_O4
Palanisamy, K.
Th.P-P26
Palermo, V.
Mo.E-P8
Palfreyman, J.
Th.P-P5
Palma, J.L.
Mo.K-P20
Mo.K-P21
Th.K-P27
Th.M-P15
Th.M-P16
TU.H-P68
Palmero, E.M.
Th.M-P10
WE.B.2_I1
WE.F.1_O4
Palomares, F.
Mo.H-P108
TU.C.1_O5
Palstra, T.T.M.
Th.A.2_O3

Paltiel, Y.	TU.E.2_06	Mo.H-P40
Th.I.2_02	Panke, J.	Mo.H-P55
Pamyatnykh, L.	Mo.G-P14	TU.A-P24
TH.F-P12	Pankhurst, Q.	TU.A-P26
Pamyatnykh, S.	Th.P-P2	TU.A-P45
TH.F-P12	Th.P-P25	TU.A-P86
Pan, D.	Th.P-P7	Parisi, F.
Mo.D-P21	Pannetier-Lecoeur, M.	TH.C-P43
Pan, F.	Th.O-P50	TH.C-P86
FR.E-P27	Th.P-P39	Park, B.H.
TU.I.3_02	Pannunzio Miner, E.	Mo.D-P25
Pan, Y.	TU.A-P99	Park, Bye.Gy
Fr.C.1_02	Panov, Y.	FR.A-P2
MO.SYM_2	FR.B-P33	WE.A.1_04
Panagiotopoulos, I.	Mo.A-P71	Park, Byo.Gu.
Mo.H-P63	Paolasini, L.	MO.H.1_02
Mo.I-P30	TH.C-P75	Mo.K-P22
Mo.I-P5	Paolini, A.	TH.F-P19
Panasevich, A.	Th.P-P10	Th.H-P13
TU.A-P4	Papaioannou, E.	Park, E.
Pancaldi, M.	TH.E-P11	MO.A.1_02
Th.M-P4	Th.H-P18	Park, G.J.
Th.M-P5	Th.N-P10	Th.O-P43
TU.I.1_04	Papp, A.	Park, Hye.
TU.I-P4	TU.I.1_04	Th.P-P35
Panda, A.K.	Pappas, C.	Park, Hyu.
Mo.L-P11	TH.J-P35	FR.A-P17
Mo.L-P58	Pappas, S.	Park, J.G.
Th.O-P10	WE.B.2_03	Fr.C.3_03
Pandey, A.	Paradezhenko, G.	Th.E.2_11
Fr.D.2_03	FR.E-P11	Park, Ji.Yo.
Pandey, S.	Parakkat, V.M.	Mo.D-P25
Mo.L-P3	Mo.H-P77	Park, Jit.
Pandya, D.K.	TH.F-P26	FR.B-P30
Mo.F-P14	TU.G-P23	Mo.A-P100
Mo.H-P91	Paramanik, T.	MO.D.3_03
TU.F-P11	Mo.L-P17	Park, Joon.
Pang, G.	Parazzoli, D.	FR.A-P2
Mo.A-P27	Th.H.1_04	Park, Kb.
Th.C.3_01	Parchenko, S.	TU.F-P3
Panighel, M.	Th.I-P8	Park, Ky.
FR.H-P33	Parcollet, O.	Mo.E-P4
Panina, L.	WE.E2_02	Park, S.
Th.O-P46	Pardo, J.A.	Th.I-P16
TU.A-P35	MO.C.3_03	Park, Se.Yo.

TU.A-P28	TU.C-P29	FR.E-P26
TU.A-P29	Pascua, G.	MO.G.2_O3
Park, Sun.	TH.C-P80	TU.F-P23
Mo.H-P25	Pascual, J.I.	Patthey, L.
Park, Tae.Eo.	TU.J.3_O2	TU.E.1_O6
Mo.D-P16	WE.H.2_O2	Paturi, P.
Park, Tus.	Pashchenko, M.	Mo.H-P19
FR.C-P8	TH.C-P35	Mo.H-P20
MO.A.1_O2	Pashkevich, Y.	Mo.H-P52
Park, W.K.	Fr.C.3_O2	Th.O-P14
MO.A.2_O5	TH.C-P80	Paudyal, D.
Park, Youn.	Pasi, F.	FR.SP-1
Mo.D-P16	Th.P-P10	Paukov, M.
Parker, G.	Pasko, A.	Mo.L-P49
MO.G.2_O2	Fr.F.3_O2	TH.D-P8
WE.D.2_I6	Mo.L-P26	WE.C.2_O2
Parkes, D.	TH.I-P25	Paul, A.
Mo.G-P22	TU.H-P102	Mo.H-P100
Th.G.2_O6	Pasquale, M.	Mo.H-P12
Parkin, S.	Fr.E.2_O4	Mo.H-P56
Th.I-P16	Th.H-P17	Paul, D.M.
TH.J-P21	TH.J-P24	FR.A-P34
TU.I-P24	Passamani Caetano, E.	Paul, E.
WE.J.1_O5	Mo.I-P1	Th.O-P50
Parkkinen, K.	TU.F-P58	Th.P-P39
TU.B-P63	Passanante, S.	Paula, F.L.O.
Parpiiev, T.	TH.C-P37	Th.P-P32
Th.I-P13	Passos, D.	TU.F-P114
Parreiras, S.	TU.A-P46	Paulin, M.
Th.K-P13	Pasuk, I.	FR.F-P7
Pasa, A.A.	Mo.H-P15	Paulose, P.
Th.K-P40	Pasztorova, J.	FR.D-P17
Th.K-P42	Mo.A-P54	TH.C-P95
Pascal, C.	Patel, V.	Paulsen, C.
Th.H.2_O2	Th.E.3_O1	Th.D.1_I1
Pascarelli, S.	Pati, S.P.	Pauly, M.
TH.C-P21	Fr.H.3_O3	Th.M-P11
TU.B-P44	MO.G.1_O4	Pauselli, M.
TU.J.1_O4	Patil, S.	Mo.F-P20
Paschen, S.	TH.C-P95	Pautrat, A.
FR.A-P50	Patnaik, S.	TU.H-P78
Fr.H.1_I1	MO.C.1_O3	Pavlosiuk, O.
TH.B-P12	TU.A-P39	FR.A-P28
TU.B-P7	TU.A-P80	Fr.C.1_O3
TU.C-P20	Patte, R.	Pavlov, D.

Th.P-P23	MO.D.1_O2	Fr.B.2_O3
Pavlov, V.	Mo.I-P15	Mo.A-P31
Th.G.1_O4	TU.G.2_O4	Penc, K.
Th.I-P19	TU.I.3_O3	FR.D-P18
Pavlova, A.	Pedrosa, J.	TU.A-P25
TH.K-P22	Mo.H-P99	Pendharkar, J.
Paz, E.	Mo.I-P37	Th.O-P53
Mo.F-P21	Th.K-P44	Peng, B.
Th.H-P16	Pedruzzi Nascimento, V.	Th.O-P7
Th.I.1_O3	Mo.I-P1	Peng, D.
TU.H.1_O5	Peiró, F.	FR.H-P7
WE.I.2_I1	FR.I-P46	Peng, X.
Pchelkina, Z.	MO.B.1_I1	TH.B-P17
FR.E-P14	Th.K-P45	Pentcheva, R.
PECASSOU, B.	Tu.B.2_O2	WE.B.2_I1
Mo.H-P18	TU.F-P87	Penton-Madriral, A.
Pechan, M.J.	Peixoto, B.	Mo.H-P13
MO.B.1_I1	TU.H-P79	Peña, G.
Pecharsky, V.	Pekala, M.	Th.O-P1
FR.SP-1	TH.C-P84	Pépin, C.
Pecharsky, V.K.	Pelegrini, F.	TH.B-P19
Mo.L-P47	Mo.I-P16	Th.D.2_O2
Pedder, C.	Mo.I-P39	TU.A.3_O3
TH.A-P25	Mo.I-P8	Pereira, A.
Peddis, D.	Peleiderer, C.	Mo.B-P30
MO.B.1_O2	TU.C-P32	Mo.B-P31
Mo.I-P35	Peřka, J.	Mo.K-P20
Th.K-P38	Th.C.2_O5	Mo.K-P21
TU.B.2_O3	Pellegrin, E.	Mo.L-P47
TU.E.3_O2	FR.H-P25	TU.H-P68
TU.E.3_O3	MO.E.1_I1	Pereira, A.M.
TU.E-P31	Mo.H-P84	TU.E.2_O5
TU.F-P53	MO.J.2_O5	Pereira, J.
TU.F-P67	TH.E-P20	TU.G.3_O2
TU.F-P68	TH.K-P18	Pereira, L.G.
TU.J.1_O5	Th.K-P41	Mo.I-P16
Pedds, D.	Pellegrini, E.	Mo.I-P22
Mo.I-P32	Th.L-P5	Pereira, L.M.C.
Pedra, P.	Pellegrino, T.	TU.G.1_O5
TU.F-P77	TH.H.2_I1	Pereira, M.
Pedro, S.	Pellicciari, J.	Mo.H-P90
Mo.K-P3	Th.G.3_O1	Pereira, M.J.
Pedrolo, B.	Pellicer, E.	TU.H-P116
TU.B-P41	Mo.F.2_O5	Pereiro, E.
Pedrosa, F.J.	Pelliciari, J.	Fr.H.3_O2

Pereiro, J.	Th.N-P5	Perzynski, R.
TH.C-P42	Périgo, E.A.	Mo.I-P13
Perevertov, O.	TU.H-P40	Th.B.1_O2
FR.I-P3	Perkins, G.K.	Th.P-P32
TU.H-P30	FR.I-P38	Pesquera, D.
Pérez Alcázar, G.A.	Perna, P.	FR.H-P25
TU.F-P27	Mo.H-P99	Th.G.3_O4
TU.F-P28	Mo.I-P37	Th.G-P15
TU.H-P11	TH.I-P28	TU.A-P63
TU.H-P37	Th.K-P44	Peters, L.
Pérez de Luque, A.	TU.A-P91	FR.D-P32
Th.H.1_O5	Perna, S.	Peters, R.
Th.P-P34	MO.G.2_I4	TU.F.1_O4
Pérez del Real, R.	Mo.J-P19	Petit, D.
TU.H-P129	Mo.J-P20	Th.P-P3
Perez Pelaez, R.	Mo.J-P21	TU.F-P117
FR.E-P37	Perov, N.	TU.J.2_O5
Pérez Rodríguez, F.	Th.O-P57	Petit, L.
Th.N-P9	Th.P-P18	Th.O-P21
Pérez, E.	Th.P-P24	Petit, S.
Th.M-P8	TU.H-P125	FR.D-P28
Pérez, E.J.	Perren, G.	FR.D-P29
Mo.K-P7	MO.I.1_O4	FR.D-P66
Pérez, J.E.	Perret, E.	MO.I.1_O3
Th.P-P17	Fr.B.2_O1	Th.E.2_I1
Pérez, L.	Perring, T.	TU.A-P43
Th.M-P21	Mo.G-P25	TU.D.2_I1
Pérez, M.	TU.D-P13	Petrakovskii, G.
MO.E.1_O3	Perring, T.G.	FR.D-P38
TH.C.1_O4	Fr.C.3_O3	Petraru, A.
Pérez, N.	Perrozzi, F.	FR.A-P26
Fr.E.2_O3	Mo.E-P8	Petrashov, V.
Th.H-P6	Perry, R.	Mo.A-P15
TU.F-P79	Fr.D.2_O4	Petrenko, O.
Pérez, T.	Mo.G-P25	FR.D-P54
TH.I-P28	Th.G.3_O2	FR.D-P73
Perez-Caro, M.	TU.C-P28	Petříček, V.
FR.H-P24	Pershin, Y.V.	Th.A.2_O1
Perez-Castañeda, T.	MO.F.3_O4	Petrisor jr., T.
TH.D-P22	Perumal, A.	TU.G-P17
Pérez-Mato, J.M.	TU.G-P2	Petroff, F.
TU.A-P83	Perzanowski, M.	TU.J.1_O4
Perez-Muñoz, A.	Th.K-P36	Petroutchik, A.
Mo.E-P8	Perzynska, K.	Mo.H-P82
Pérez-Murano, F.	TU.E-P41	Petrov, M.

TH.D-P14
Petrova, A.
 TH.A-P1
 TH.C-P10
Petrova, O.
 Th.D.2_05
Petrovic, C.
 FR.D-P11
 MO.I.1_02
Petrovic, T.
 Mo.L-P25
Petruk, O.
 FR.I-P36
Petry, W.
 Th.A.2_07
 WE.D.1_02
Petti, D.
 Th.H.1_04
 Th.H.2_04
 TU.G.3_05
 TU.I.1_04
Peyre, V.
 Th.B.1_02
Pezeril, T.
 Th.I-P13
Pfau, B.
 Fr.I.1_11
Pfau, H.
 WE.H.2_04
Pfleiderer, C.
 MO.H.3_03
 Mo.H-P70
 TH.C-P115
 TH.C-P116
 TH.C-P119
 TH.C-P97
 TH.J-P25
 TH.J-P28
 TH.J-P32
 TU.B-P75
 TU.C-P23
 TU.C-P30
 TU.C-P33
 TU.H.3_03
 TU.SYM_2

WE.H.1_03
Pham, D.C.
 Th.H-P1
 WE.I.2_03
Pham, S.T.
 Mo.E-P7
Pham, T.V.
 Fr.G.3_04
 TH.E-P8
PhamHuu, C.
 MO.E.1_02
 TU.F-P51
Phan, M.H.
 MO.B.1_03
 Th.B.1_11
 TU.F-P65
Phan, T.L.
 Mo.L-P22
 Mo.L-P33
 TU.F-P17
 TU.H-P4
Phark, S.H.
 FR.H.3_01
 Fr.H.3_04
Phillips, L.C.
 TU.A-P100
Phung, T.
 Th.I-P16
Phuoc, N.N.
 TU.A-P5
Pi, T.W.
 Mo.B-P9
 TU.A-P21
Piamba Jimenez, J.F.
 TU.F-P28
Piamonteze, C.
 TU.F-P79
Piantek, M.
 TU.J.3_02
 WE.H.2_02
Piatek, J.
 FR.I-P17
Piątkowska, M.
 TH.C-P65
 TU.H-P50

Piazzì, M.
 Mo.L-P85
 Th.B.3_03
Piccaluga, G.
 TU.F-P67
 TU.F-P68
Pichon, B.
 Mo.I-P21
 Th.M-P11
Picone, A.
 FR.H-P31
 Mo.H-P85
Picozzi, S.
 Mo.C-P17
 TU.A-P14
 WE.C.1_1.1
Piéchon, F.
 TU.I.3_04
Pieper, A.
 FR.A-P1
Pierron-Bohnes, V.
 Th.I.3_03
 Th.I-P6
Pierunek, N.
 Mo.L-P40
Pikul, A.
 Mo.A-P107
 TU.B-P74
Pikulski, M.
 FR.I-P27
 MO.A.3_04
 Mo.A-P72
 Mo.B-P22
Pilati, V.
 Th.P-P32
Pillard, V.
 FR.A-P54
Pilo Gonzalez, J.
 Mo.H-P49
Pimenov, A.
 TU.A-P11
Pimentel, I.
 FR.D-P22
Pimentel, J.
 Mo.A-P104

Pineider, F.

Th.N-P13
Th.N-P14
Th.N-P15
Th.P-P10
TU.B.2_O4
TU.E.3_O2

Pingstone, D.

TU.E-P49

Pinho Oliveira, G.N.

TU.A-P89

Pini, M.G.

FR.E-P25
TU.G-P10

Pinna, D.

Mo.F-P23

Pinteala, M.

TU.F-P42

Pinto, R.

Mo.G-P31

Piotrowski, S.

Fr.H.2_I1

Piovano, A.

Th.A.2_O6

Piovarèi, S.

Mo.L-P19

Pipich, V.

FR.I-P47

Piquerel, R.

Mo.C-P23

Piroux, L.

Th.I.3_O4

Pires, A.

FR.D-P23
Mo.H-P107

Pirogov, A.

Mo.L-P72
TH.C-P101

Pirota, K.

Th.E.3_O2
TU.F-P18

Pirota, K.R.

Th.K-P37
Th.P-P17
TU.D-P15

Pirro, P.

MO.H.2_O2
Th.O-P37

Pisarev, R.

Fr.C.3_O2
MO.J.3_O1
TH.C-P107
TH.C-P92
Th.F.1_O3
Th.G.1_O4
Th.I-P19

Pistora, J.

Mo.H-P78
Th.N-P11

Piva, M.M.

TH.C-P9

Pizani, P.S.

TU.A-P76

Pizzini, S.

TH.F-P7
TU.J.1_O2
WE.H.1_O5
WE.I.1_O2

Plá Cid, C.C.

TU.F-P75

Placais, B.

Fr.A-P59

Plamadeala, E.

TU.C-P11

Planes, A.

MO.D.1_I1
Th.B.1_O3
Th.B.1_O4

Plank, H.

Th.G.2_O2

Plascak, J.A.

TH.C-P100

Platunov, M.

TU.H-P31

Platunov, M.S.

WE.J.2_I1

Pleshev, D.

Mo.G-P21

Plomp, J.

TH.J-P35

Plugaru, N.

TU.A-P32

Pochet, P.

FR.F-P16

Pochylski, M.

TU.F-P32

Podlesnyak, A.

TH.D-P14

Podlucky, R.

Fr.B.3_O1

Podolskiy, A.

Mo.A-P38

Poelt, P.

Th.E.3_O3
Th.M-P22

Poetardji, S.

TU.H-P77

Poettgen, R.

WE.C.2_O5

Poggini, L.

MO.I.2_I1

Poggio, M.

MO.E.2_O1

Pogorelov, Y.

Mo.H-P55

Pohlit, M.

WE.B.2_O2

Poiendar, M.

TU.E.1_O5

Polacek, I.

Th.O-P55

Poleshikov, S.

Mo.G-P21

Poli, S.

FR.I-P4

Polian, A.

Th.C.3_O2
TU.A-P76

Politova, G.

Mo.L-P49

Polla, G.

TH.C-P37
TH.C-P43

Pomar, A.

Mo.H-P54

Mo.H-P57 Pomjakushin, V.	MO.D.2_I1 MO.D.2_O2 Porcher, F.	Povzner, A. FR.B-P17
Mo.B-P5 Mo.B-P6 TU.A-P93 Pomjakushina, E.	TU.B-P11 Porod, W. TU.I.1_O4 Porras-Montenegro, N.	Powroznik, W. Mo.H-P105 Poyurovskiy, L. WE.E2_O2
Mo.A-P8 TU.A-P51 Pomm, M.	TU.F-P24 Porrati, F. Th.G.2_O2 WE.B.2_O2	Pozo-López, G. Mo.K-P19 Prabhakaran, D. FR.A-P42 Mo.A-P32 TH.C-P13 Th.G.3_O2
Mo.H-P100 Mo.H-P12 Mo.H-P56 Ponce, A.	Th.M-P4 Th.M-P5 Portemont, C. TU.G.3_O2	Prabhu, R. Mo.H-P50 Prachařová, M. TH.C-P51 TU.B-P72
TU.G-P7 Pong, W.F. Mo.K-P1 TU.A-P54 Ponomaryov, A.	Mo.A-P100 MO.D.3_O3 Pospíšil, J. TU.B-P28	Pracht, U.S. TU.H.2_O4 Pradhan, L. WE.SYM_5 Pradhan, N. FR.F-P17
TH.A-P33 Pop, V. TU.H-P23 TU.H-P24 Popescu, C.	Th.N-P11 Pothala, R. Mo.L-P2 TU.I-P2	Pradipto, A.M. Mo.C-P17 Prado, Y. Fr.I.3_O4 Prajapat, M. Mo.H-P23 Mo.H-P24
TH.C-P21 Popkov, S. TH.D-P14 Popov, A.	Poudel, N. TU.E.2_O2 Poulsen, J. Mo.A-P109	Pramanick, S. Th.B.1_O3 Prando, G. FR.D-P12 Mo.A-P103 Mo.A-P22 TH.A-P9 TU.E-P6
Th.F.1_O3 Popov, A.I. TU.A-P30 Popov, A.P.	TU.C-P32 TU.C-P33 Pourovskij, L. Fr.D.3_O1	Prasad, S. Mo.H-P50 TU.H-P75 Prat-Camps, J. TU.I.2_O2 Prathiba, G.
FR.E-P25 Popov, V.V. Mo.H-P35 Popov, Y.F.	TU.C-P33 Pourret, A. Mo.A-P59 TU.F.1_O2 WE.H.2_I1	
TU.A-P30 Popova, M. Fr.C.3_O2 TH.C-P107 TU.A-P87 Popova, O.	Poux, A. TU.B-P44 Povarov, K. Mo.B-P4 TH.A-P33	
MO.C.3_O5 Popp, J. Th.O-P6 Porcari, G.	Povarov, K.Y. TH.A-P5	

FR.C-P8 Prats, E.	TU.B.3_01 Pristas, G.	Prokscha, T. FR.A-P9
Th.P-P34 Pratt, A.	TH.B-P1 TU.C-P29	MO.C.3_03 Proschek, P.
Mo.E-P10 Pratt, F.L.	Prochaska, L. TU.C-P20	TH.B-P21 TH.D-P24
TH.C-P93 Prchal, J.	Proctor, T. TU.C.2_I1	Proshin, Y. Mo.A-P69
Mo.A-P54 TH.C-P51	Prodan, A.M. TU.F-P5	Proskurina, E. TU.C.2_02
Predoi, D. TU.F-P5	Prodius, D. MO.I.2_04	Prosnikov, M.A. Fr.C.3_02
Pregelj, M. Tu.C.3_05	Proença, M.P. Mo.K-P27	Protasov, A. Mo.L-P73
Prejbeanu, I.L. TU.J.1_I1	Profeta, G. Mo.A-P50	Prots, Y. Mo.B-P9
Prejbeanu, L. Mo.F-P26	TU.E-P6 Proglyado, V.V.	Proust, C. MO.A.2_I1
TH.F-P7 TU.I-P15	Mo.H-P35 Prokes, K.	Provenzano, V. Mo.H-P62
Prévost, B. MO.D.3_01	FR.D-P69 Fr.E.2_05	Provino, A. Th.O-P21
Prida, V. TU.E-P9	Mo.A-P98 Mo.B-P29	Prudnikov, P. Mo.J-P6
Prieto, J.L. Mo.H-P99	TH.C-P99 Th.D.3_03	TH.C-P48 Prudnikov, V.
Prieto, P. TH.K-P8	WE.C.2_05 Prokhnenko, O.	Mo.J-P6 Mo.L-P3
TU.A-P86 Prieto, P.A.	Fr.E.2_05 Th.D.3_01	TH.C-P40 TH.C-P48
Mo.H-P14 Prieur, J.Y.	Prokleška, J. Th.A.2_01	Prusik, K. TU.H-P12
Th.I-P5 Prigent, C.	Th.A-P40 TH.B-P21	Przewoznik, J. Th.A.1_06
Mo.L-P86 Prima-Garcia, H.	TH.D-P24 TU.B-P28	TH.C-P55 Psaruk, I.
MO.J.2_I1 Princep, A.	TU.C-P7 WE.A.1_03	Mo.A-P38 Psycharis, V.
Th.A.2_06 Prinsloo, A.	Prokofiev, A. FR.A-P50	Mo.H-P63 TU.G-P4
Mo.H-P53 Priolkar, K.R.	TH.B-P12 TU.B-P7	TU.H-P136 Puente-Orench, I.
Fr.C.3_01 Prischepa, S.	Prokopov, A.R. Th.N-P7	Fr.B.1_04 Pujari, B.
Th.K-P49	Th.N-P8	TH.C-P87

TH.D-P19
TU.E-P30
Pulko, B.
Mo.L-P48
Punith Kumar, V.
FR.F-P32
Punnoose, A.
TU.F-P40
Puphal, P.
FR.D-P37
Purnama, I.
FR.D-P45
TH.J-P4
TH.J-P5
Th.M-P6
Pusep, Y.
TU.C-P8
Putti, M.
Mo.A-P102
Mo.A-P37
Putz, S.
TU.C-P20
Puzniak, R.
Mo.I-P41
TH.C-P1
TH.C-P84
Pylypovskiy, O.
Fr.E.3_01
TU.F-P83

Q

Qaiumzadeh, A.
Mo.C-P8
Qi, H.
MO.E.2_04
Qi, S.
FR.F-P3
Qi, Y.
Th.E.2_05
Qian, F.
TH.J-P35
Qing, L.

MO.F.3_03
Qiu, X.G.
Mo.A-P7
Qiu, Z.Q.
MO.G.1_11
Qu, F.
TU.H-P29
Quang, T.
TU.E-P40
Quercia, A.
MO.G.2_14
Mo.J-P19
Mo.J-P20
Mo.J-P21
Quesada, A.
Fr.A.1_04
MO.D.1_02
Mo.I-P15
TH.K-P23
Quetz, A.
Mo.L-P3
Quintanilla, J.
TU.D-P13
Quintero Castro, D.
TU.B-P66
Quintero, M.
TH.C-P86
Quintero, M.H.
TH.C-P37
Quintero-Castro, D.
TH.A-P41
Quirós, C.
Fr.H.3_02
Mo.H-P98
TH.H.3_02
Quispe-Marcatoma, J.
TU.G-P5
Qureshi, N.
FR.D-P54
TU.A-P98

R

R Branford, W.
Th.K-P25
R. Arantes, F.
TH.C-P20
R. Aseguinolaza, I.
FR.SP-3
R. Cavicchia, D.
Mo.I-P31
R. Sani, S.
Mo.F-P25
Raab, B.
TU.C-P14
Raabe, J.
MO.H.3_02
TH.J-P3
TH.J-P9
WE.E.1_04
Raback, P.
FR.I-P39
Rack, A.
TU.D.3_03
Rackham, J.
Mo.H-P106
Rączová, K.
TH.C-P79
Radaelli, G.
Th.G.3_04
TU.A-P62
Radaelli, P.
Th.E.1_03
TU.E.1_01
Radelytskyi, I.
TH.C-P84
Radetinac, A.
TU.A-P31
Radha, S.
Th.O-P53
Th.P-P33
Radhika, K.
FR.F-P20
FR.F-P21

Radjai Sani, S. Mo.F-P4	TU.A.2_I1	TU.G-P10
Rado, C. Th.A.3_O4	Ramirez-López, M. FR.H-P24	Rao, P. Th.K-P34
Radu, E. Th.P-P26	Ramos, A.Y. MO.G.1_O5	Raoux, A. TU.I.3_O4
Radu, I. Th.I-P17	Ramos, C.A. TU.F-P110	Raposo, V. WE.I.1_O4
Radulov, I.A. Fr.A.1_I1	Ramos, M.A. TH.D-P22	Rappl, P. FR.F-P11
Radwanski, R. Fr.D.2_O5 TH.B-P20 TU.B-P64	Ramos, R. Th.B.3_O2 Th.H-P5 Th.H-P8	Rascón, A. TU.F-P54
Raes, B. Th.O-P49	Ramos, S.M. TU.B-P70	Raselli, A.R. TU.A-P53
Raevsky, I.P. TU.A-P20	Ramsay, A. Fr.G.3_O2	Rasing, T. FR.F-P11 Fr.J.2_O4 MO.E.3_O2 MO.J.3_O1 TH.C-P92 Th.F.1_O3 Th.G.1_O5 Th.I.1_O3 Th.I-P11 TH.I-P22
Raghavendra Reddy, V. Mo.C-P4	Ramshaw, B. MO.A.2_O3	Rata, D. Th.B.2_O2
Raghuvanshi, N. Mo.A-P82	Ramu, M. Fr.E.3_O2 TH.J-P4 TH.J-P5	Ratcliff, W. TU.E.1_O4
Rahn, M. FR.A-P30 WE.A1_O1	Rana, K.G. TH.J-P21	Rathore, S.S. TU.A-P33 TU.A-P34
Rakhmanov, A. FR.A-P5 Mo.B-P19 TU.E-P2	Ranchal, R. MO.E.1_O3	Rauch, D. TU.C-P23
Ralko, A. FR.B-P12 FR.E-P35 MO.I.3_O3	Rando, E. Mo.J-P18	Ravasi, T. Mo.K-P7 Th.P-P17
Ramakrishnan, M. Fr.B.2_O1 TU.E.1_O3	Ranella, A. Th.P-P20	Ravelosona, D. TH.F-P17
Ramasse, Q.M. MO.D.1_O4	Ranganathan, R. TU.G-P2	Ravichandran, J. Fr.C.2_O4
Ramesh, G. TU.H-P80	Ranjbar, M. Mo.F-P8 MO.H.2_O4	Ravot, D. Th.A.2_O4
Ramesh, R. Fr.C.2_O4	Ranjbar, R. TU.G-P12	Ray, M.K. TH.C-P5
Ramírez, J.G. MO.E.3_I1 Th.L-P3	Ranno, L. MO.G.1_O5 Mo.I-P28 Mo.L-P91 TH.C-P127	Rayaprol, S.
	Ranzieri, P. MO.C.2_I1	

Mo.C-P17	Mo.B-P4	TU.A-P43
Raymond, S.	Reichl, C.	TU.A-P83
MO.A-P2	Mo.D-P31	TU.A-P93
MO.I.1_O3	Reichlova, H.	TU.A-P98
Razdolski, I.	Fr.G.3_O2	Restrepo Parra, E.
MO.E.3_O2	Reiffers, M.	FR.E-P17
Razumovskaya, O.	TH.C-P94	FR.E-P7
TU.A-P85	WE.C.2_O3	TH.C-P22
Real, J.A.	Reis, M.	Th.M-P3
Mo.E-P6	Mo.K-P3	Restrepo, J.
Reardon, C.	Mo.L-P9	FR.E-P7
Mo.G-P22	Reiss, G.	Mo.K-P11
Th.G.2_O6	MO.G.1_O3	Rettig, L.
Rebled Corsellas, J.M.	WE.H.1_O4	Fr.B.2_O1
Th.K-P45	WE.I.2_I1	TU.E.1_O3
Rebollar, E.	WE.I.2_O5	Rettner, C.
TU.I.3_O3	Reiss, P.	Th.I-P16
Redondo, C.	FR.E-P41	Rettori, A.
TH.K-P21	Mo.A-P110	FR.E-P25
Tu.G.2_I1	Mo.A-P112	TU.G-P10
Reece, M.	WE.F.2_I1	Rettori, C.
Mo.L-P29	Reissner, M.	Mo.C-P5
Reehuis, M.	Mo.A-P36	TU.B-P2
Th.D.3_O1	TH.B-P7	TU.F-P26
Reeves-McLaren, N.	Th.E.3_O3	Reuse, F.
FR.H-P3	Reith, D.	Fr.F.2_O2
Regnat, A.	Fr.B.3_O1	Reuther, J.
TH.C-P115	Remenyi, G.	Th.D.3_O1
TH.C-P116	Th.D.1_I1	Reuvekamp, P.G.
TU.B-P75	Remmer, H.	Mo.B-P26
Regnault, L.P.	Th.P-P13	WE.C.1_O2
MO.D.3_O1	Ren, Z.	Revcolevschi, A.
MO.I.1_O3	TU.F.1_O5	FR.D-P12
Th.D.1_I1	Repaka, D.V.M.	Mo.B-P7
Th.D.3_O4	Mo.L-P59	Th.D.1_I1
TU.A-P43	Reser, B.	Reyes, A.P.
Reibel, C.	FR.E-P10	TH.A-P17
Th.A.2_O4	Respaud, M.	Reyes, D.
Reiche, C.F.	Th.G.2_O3	FR.I-P43
FR.I-P41	Th.H.1_O2	Mo.A-P29
MO.E.1_O5	Th.I.3_O3	We.F.1_O3
MO.E.2_O1	Th.I-P6	Reynolds, N.
Reichel, L.	Ressouche, E.	TH.A-P5
Mo.H-P63	FR.D-P66	Reyren, N.
Reichert, A.	MO.A-P2	Mo.D-P27

MO.F.1_05	FR.I-P11	TU.F-P68
MO.F.3_02	Ricart, S.	Rinaldi-Montes, N.
Mo.F-P15	Th.L-P5	Fr.B.1_04
MO.H.3_02	Riccardi, E.	Rincón Domínguez, T.
TH.E-P12	TU.I.2_06	Mo.H-P76
TH.J-P18	Richardson, D.	Ripka, P.
WE.G.1_05	Mo.K-P24	Th.O-P10
WE.I.1_03	Richie-Halford, A.	Th.O-P9
Rezhikova, I.	WE.J.2_03	Riseborough, P.
TH.D-P5	Richter, C.	Th.J.2_05
Rezende, S.	Mo.E-P2	TU.B-P41
Th.I.2_06	Richter, J.	Rispail, N.
WE.G2_I1	FR.D-P30	Th.P-P34
Rezende, S.M.	Th.A-P45	Risset, O.
Mo.H-P9	Th.D.2_04	TH.A-P22
Reznichenko, L.	TU.E-P53	Rissing, L.
TU.A-P85	Richter, M.	Th.O-P13
Reznik, D.	TH.C-P27	Risueño, M.C.
Fr.I.1_03	Richter, P.	Th.H.1_05
Rhein, F.	Mo.H-P30	Th.P-P34
MO.E.2_06	Richy, J.	Ritman-Meer, T.
Rheingans, B.	Mo.H-P53	MO.E.2_05
TU.H-P29	Riedemann, T.M.	Ritter, C.
Rhen, F.M.F.	Th.B.2_03	FR.D-P37
Mo.K-P24	Riedo, E.	FR.D-P83
TU.H-P74	TU.I.1_04	Mo.C-P14
Rhie, K.	Riego, P.	Th.A.1_01
Mo.C-P20	MO.C.3_01	TH.C-P69
TU.G-P20	Righi, L.	WE.H.2_05
Rhim, S.H.	TU.J.2_04	Ritter, F.
TH.B-P13	WE.D.1_03	TU.A-P10
Riahi, H.	Rigue, J.	Ritz, R.
Th.I-P10	Mo.I-P17	TH.J-P28
Rial, J.	Rigue, J.N.	Riva, M.
MO.D.1_02	Mo.I-P20	Mo.H-P85
Ribas-Arino, J.	Riley, G.	Rivadulla, F.
TU.J.3_01	Fr.I.1_02	Mo.H-P2
Ribeiro, P.	Rinaldi, C.	TH.H.3_I1
FR.B-P11	Th.G-P9	Rivas, M.
Mo.L-P5	Th.P-P14	TU.A.1_04
Ribeiro, R.A.	TU.G.3_05	TU.F-P54
TH.A-P36	WE.G2_05	Rivas-Murías, B.
TH.C-P110	Rinaldi, D.	Mo.H-P2
TU.B-P2	TU.F-P53	TU.B.2_I1
Ribó, L.	TU.F-P67	Rivera-Álvarez, Z.

FR.H-P24

Riyat, R.

Mo.A-P105

Roa Rojas, J.

Th.O-P1

Robert, J.

FR.D-P28

FR.D-P29

FR.D-P66

TU.B-P11

TU.D.2_I1

Robert, S.

Mo.D-P8

TU.G-P1

Robinet, E.

Th.H.2_O3

Robisc, N.

TU.C-P14

Roca, A.G.

TU.F-P64

TU.F-P87

Rocci, M.

FR.I-P49

Mo.E-P8

Rocco, D.

Mo.K-P3

Rocha dos Santos, R.

Mo.A-P104

Rocha, J.

TU.A-P65

Rodionov, I.

Mo.L-P3

TH.C-P40

Rodionov, V.

Mo.L-P92

Th.P-P18

Rodionova, V.

Mo.H-P104

Mo.I-P27

Mo.L-P61

Mo.L-P92

Th.N-P16

Th.O-P57

Th.P-P18

TU.A-P94

TU.H-P125

Rodmacq, B.

TU.J.1_I1

TU.J.2_O3

Rodrigo, C.

TU.A-P91

Rodrigo, J.G.

TH.D-P22

Rodrigues Pereira, A.

TH.J-P16

Rodrigues, A.R.

TU.F-P1

Rodríguez Fernández, J.

Mo.L-P47

TU.B-P34

TU.D-P5

TU.F-P59

Rodríguez González, L.A.

TU.C.1_O4

Rodriguez, B.

TU.F-P73

Rodriguez, I.

Mo.L-P41

Rodriguez, J.

Th.D.3_O1

Rodriguez, J.M.

TU.F-P72

Rodriguez, L.A.

Fr.E.1_I1

TU.A-P86

Rodríguez, L.A.

Mo.K-P16

Mo.K-P17

Rodriguez-Carvajal, J.

Th.J.1_I1

TU.A-P51

Rodríguez-González, B.

TU.B.2_I1

Rodriguez-Rodriguez, G.

TH.H.3_O2

Rodríguez-Suárez, R.

Th.I.2_O6

Rodríguez-Velamazán, J.A.

TU.A-P10

TU.A-P9

Roeben, E.

Th.P-P13

Roehlsberger, R.

FR.I-P19

TU.I.1_O5

Roessler, S.

TH.B-P3

Roessler, U.

TU.C.2_O3

Roessli, B.

TH.C-P116

TU.A-P27

Rogalev, A.

MO.I.2_I1

MO.I.2_O4

TH.A-P21

TH.E-P20

Th.J.2_O4

TU.B-P70

TU.C.3_O3

TU.E-P12

TU.H-P31

TU.J.1_O4

TU.J.3_O2

Roger, M.

Th.B.1_O2

Rogers, S.

TU.F-P102

Rogl, P.

Fr.B.3_O1

TU.C-P14

WE.H.2_O3

Rohan, J.

TU.H-P26

Rohart, S.

Th.J.3_I1

WE.I.1_O2

Röhlsberger, R.

MO.C.2_O3

Th.I.3_O1

TU.C.1_O2

WE.E.1_O3

Roig, A.

Mo.C-P9

TH.C-P38

Th.E.2_O2	FR.C-P1	Rosado, L.
Th.N-P1	Romera, M.	FR.I-P42
Th.P-P4	Mo.F-P24	Rosales-Rivera, A.
WE.SYM_4	Mo.F-P26	FR.D-P84
Rojas, D.P.	Romero, S.	TH.C-P128
TU.B-P33	TU.H-P66	Rosas Huerta, J.L.
TU.B-P34	Romming, N.	Mo.H-P49
TU.F-P59	MO.E.3_O3	Rosell, A.
TU.F-P82	Th.C.2_I1	Th.P-P4
Rojas, Y.A.	Ronning, F.	Rosenberg, R.
TU.H-P37	Fr.A.1_O3	Fr.A.1_O3
Rojas-Ayala, C.	Fr.C.1_O6	Rosner, H.
TU.F-P58	MO.A.1_O2	Th.D.2_O4
Rojas-Sanchez, J.C.	MO.A.2_O5	TU.C-P9
Mo.D-P27	TU.H.2_O5	Ross, C.A.
MO.F.3_O2	Rønnow, H.M.	MO.F.2_I1
Rojas-Sánchez, J.C.	Fr.G.2_O4	TH.D-P18
Fr.G.3_O4	FR.I-P17	TH.F-P1
MO.F.1_O5	FR.I-P7	Ross, K.
TH.E-P12	Mo.A-P55	TU.D.2_O2
TH.E-P8	Mo.A-P72	Rossi, L.
WE.G.1_O5	Mo.B-P24	Mo.I-P31
WE.I.1_O3	TH.C-P28	Rossier, J.
Roldán Cuenya, B.	TH.C-P41	Fr.F.1_I1
TU.D.3_O4	TH.C-P56	Rossigny, A.
Roldan, M.	Th.G.3_O1	TU.F-P86
FR.I-P46	Th.G.3_O2	Rößler, S.
Rollinger, M.	TU.B-P7	Mo.H-P75
Th.N-P10	Rööm, T.	Mo.H-P76
Rols, S.	TU.A-P25	TU.F.1_I1
TU.B-P20	Ropka, Z.	Rößler, U.K.
TU.B-P23	Fr.D.2_O5	Fr.I.2_O4
Romachevsky, K.E.	TH.B-P20	TU.C.1_I1
TU.F-P62	TU.B-P64	Rotarescu, C.
Roman, M.	Roqueta, J.	Mo.K-P30
Mo.A-P96	MO.C.2_O2	Rotaru, A.
Romanova, O.	Mo.H-P57	MO.J.2_O4
Mo.D-P1	Rortais, F.	Rott, K.
Mo.D-P6	Mo.D-P27	WE.H.1_O4
Romanova, T.	Mo.D-P30	WE.I.2_I1
Fr.C.1_O5	MO.F.3_O2	WE.I.2_O5
Mo.A-P101	Ros, J.	Rotter, M.
Romanus, H.	Th.L-P5	TH.C-P16
Mo.H-P17	Rosa, P.F.S.	TU.B-P66
Römer, R.	TH.C-P9	WE.C.2_O4

Roudebush, J.	Roy, S.	Mo.A-P91
TH.A-P9	Th.I-P1	Mo.D-P3
Rougemaille, N.	TH.K-P12	Rucker, F.
Fr.D.1_O3	Royanian, E.	TH.J-P25
FR.D-P21	Fr.B.3_O1	TH.J-P28
FR.I-P28	Roychowdhury, K.	TH.J-P32
Mo.K-P26	TH.A-P44	WE.H.1_O3
WE.F.1_I1	Royer, F.	Rudenko, A.
Rouquette, J.	Tu.F-P122	TH.A-P23
TU.E.1_O5	Rozenberg, E.	Rudge, J.
Roura-Bas, P.	Mo.C-P16	FR.I-P45
TH.B-P10	Rozenn, B.	Rudolph, J.
Rousochatzakis, I.	Th.H-P1	Mo.L-P76
FR.E-P35	Rozet, J.P.	Rudyonok, A.
Rousseau, J.	Mo.L-P86	Th.O-P46
Th.O-P40	Rozhkov, A.	Rueff, J.P.
Roux, S.	FR.A-P5	Th.C.3_O2
MO.E.2_O2	Mo.B-P19	TU.B-P44
Rovillain, P.	TU.E-P2	Rüegg, C.
Th.I-P5	Rozman, K.Z.	FR.D-P37
Rowe, M.	MO.F.2_O6	FR.D-P79
Fr.A.1_O5	Ruben, M.	FR.I-P7
TU.B.3_O4	TU.J.3_O3	Mo.A-P55
TU.F-P107	Rubí, D.	Mo.B-P15
Rowlands, G.	Th.E.1_O2	Mo.G-P25
FR.H-P13	Rubi, K.	Th.C-P03
Rowley, S.	Fr.F.3_O3	Th.G.3_O1
FR.A-P63	Rubiales, D.	Rüffer, R.
Roy Chowdhury, R.	Th.H.1_O5	Th.E.1_I1
Mo.A-P88	Th.P-P34	WE.E.1_O3
TU.F-P47	Rubín, J.	Rufo, S.
Roy, A.	MO.I.2_O4	TH.C-P100
FR.E-P34	TU.J.1_O4	Ruiz Bustos, R.
Mo.H-P77	WE.J.2_I1	FR.D-P10
Mo.H-P86	Rubin, P.	Ruiz Calaforra, A.
Mo.H-P87	FR.E-P2	Th.O-P37
Mo.H-P97	Rubio, H.	Ruiz, A.
Roy, P.	TU.G-P11	Mo.H-P108
Fr.G.3_O2	Rubio-Marcos, F.	Th.P-P1
Mo.L-P16	MO.D.1_O2	Ruiz, E.
TU.A-P43	Mo.I-P15	Mo.E-P6
Roy, R.K.	Rubio-Zuazo, J.	Ruiz, L.
Mo.L-P11	WE.J.2_I1	TU.J.1_O4
Mo.L-P58	Ruck, B.	Ruminy, M.
Th.O-P10	FR.F-P31	FR.D-P24

FR.D-P79

Rumpf, K.

Th.E.3_O3

Th.M-P22

Ruo Berchera, I.

Fr.E.2_O4

Ruokolainen, J.

FR.I-P39

Ruotolo, A.

FR.F-P3

FR.H-P9

Mo.H-P5

Mo.I-P7

Rusek, P.

Th.A-P47

Rushforth, A.

Mo.G-P22

Th.G.2_O6

Rusinek, D.

TH.C-P55

Rusponi, S.

Fr.I.3_O3

Russier, V.

Mo.L-P26

Rusz, J.

Fr.A.1_I1

FR.I-P26

MO.E.1_O4

TH.A-P21

WE.C.2_O3

Ryabukhina, M.V.

Mo.H-P34

Ryazanov, V.

WE.J.2_I6

Ryba, T.

TU.E-P5

TU.E-P9

Rybakov, F.

FR.B-P33

Rychly, J.

Mo.G-P26

Mo.G-P6

Ryll, H.

Th.D.3_O1

Ryu, H.

FR.D-P11

S**S Nair, H.**

TH.C-P73

S. Amaral, J.

MO.D.2_O4

TU.H-P116

S. Amaral, V.

MO.D.2_O4

S. D. Beach, G.

Th.G-P13

S. Duque, J.G.

FR.D-P65

S. H., R.

Mo.H-P36

Sabogal Suárez, D.A.

TH.C-P22

Sabon, P.

Th.O-P48

Saboungie, M.L.

TU.F-P65

Sacanell, J.

FR.F-P7

TH.C-P43

Sacchi, L.

Th.P-P10

Sacchi, M.

TH.K-P1

Saccone, F.

FR.D-P84

Saccone, F.D.

TH.C-P128

Sacuto, A.

TH.B-P19

WE.F2_O7

Sadakov, A.

Fr.C.1_O5

Mo.A-P101

Sadovnikov, A.

Fr.G.1_O4

Mo.H-P21

Mo.H-P22

Sadowski, J.

Tu.G.1_O2

Saenrang, W.

Th.E.1_O3

Saerbeck, T.

TH.C-P42

TU.A.2_I1

TU.E-P48

TU.G.2_O2

Safarik, I.

Th.O-P11

Safarikova, M.

Th.O-P11

Safeer, C.

TH.F-P7

Safranski, C.

MO.H.2_O3

Sagayama, H.

Mo.C-P19

TU.A-P61

TU.A-P7

Saghir, M.

FR.A-P10

Saha, J.

MO.C.1_O3

TU.A-P80

Saha, R.

TH.C-P117

Saha, S.

FR.C-P9

TU.B-P73

Saharan, L.

TH.J-P3

Sahashi, M.

Fr.H.3_O3

Mo.F-P13

Mo.F-P17

MO.G.1_O4

Sahlberg, M.

Mo.L-P84

TU.H-P111

WE.D.1_O4

Sahling, S.

Th.D.1_I1

Sahu, B.

Mo.H-P50
TU.H-P75

Said, A.

TU.B-P21

Saidani, M.

TU.F-P93

Saiful, I.

FR.H-P36

Saiga, Y.

Th.H-P4

Sailaubekuly, R.

Mo.J-P17

Sainctavit, P.

MO.B.1_I1

Saini, N.L.

MO.A.3_O1

Saint-Martin, R.

FR.D-P12

Saint-Paul, M.

Mo.A-P6

Saito, H.

FR.F-P9
Mo.D-P22
MO.E.2_O4
Th.N-P2
Th.N-P3
TU.A-P67
TU.B-P45
TU.I-P1

Saito, K.

Fr.A.3_O3
TU.B-P11
TU.H-P115

Saito, R.

TH.C-P19
TU.H-P106

Saito, S.

TU.I-P20

Saito, Y.

FR.A-P25
Mo.D-P17

Saitoh, E.

PLENARY3
Th.H-P10

Th.H-P14

Th.H-P5
WE.I.2_O4

Saitoh, Y.

Mo.L-P41

TU.B-P55

Sakaguchi, R.

TU.H-P106

Sakai, A.

Th.D.1_O3
TU.B-P47
TU.F.3_O3
TU.H.2_O3

Sakai, H.

TU.H.2_O5

Sakai, M.

TU.B-P17

Sakai, O.

TU.B-P52

Sakai, T.

FR.D-P72
TH.A-P3

Sakai, Y.

TU.B-P19

Sakakibara, T.

MO.A.1_O4
Mo.A-P81
Th.C.3_O4
TH.C-P103
TU.E.2_O4

Sakami, T.

TU.A-P88

Sakamoto, K.

FR.H-P18
Mo.F-P17

Sakamoto, M.

Mo.H-P59
TH.E-P10

Sakat, E.

Mo.D-P30

Sakawaki, S.

Mo.H-P92

Sakharov, V.

Mo.G-P10
Th.O-P27

TU.H-P54

Saksl, K.

TU.E-P5

Sakuma, A.

TH.E-P19
TU.E-P7
TU.H-P109
TU.H-P91

Sakuma, N.

Th.L-P1
TU.H-P115
TU.H-P63

Sakuragi, S.

TH.K-P2

Sakurai, H.

FR.B-P14
Mo.A-P39
Mo.B-P6
Mo.C-P21
TH.C-P70
TU.B-P3
TU.E-P39

Sakurai, T.

FR.D-P13

Sala, A.

TU.J.1_O2
WE.H.1_O5

Sala, G.

Mo.D-P8

Salach, J.

FR.I-P36
TU.H-P104
TU.H-P93

Salamon, M.

Mo.B-P8

Salas, E.

TH.D-P22

Salas, G.

TU.F-P106
Tu.H-P137

Salazar Mejía, C.

Mo.L-P32
WE.D.1_O5

Salazar-Alvarez, G.

MO.B.1_I1

Tu.B.2_O2	WE.J.1_O5	TH.E-P20
TU.F-P87	Samantaray, B.	Th.G.3_O4
Salazar-Aravena, D.	TH.C-P13	Th.G-P15
Th.M-P16	TU.G-P2	Th.K-P45
Salce, B.	Samardak, A.	TU.A-P62
TU.C-P25	TH.J-P34	TU.A-P63
Salem, M.	Samoshkina, Y.	Sánchez, J.P.
TU.A-P35	TU.E-P12	TH.D-P25
Saleta, M.E.	Sampaio da Silva, F.	Sánchez, R.D.
FR.H-P21	Th.K-P26	FR.H-P21
Mo.A-P48	Sampaio, J.	Mo.K-P9
Mo.K-P9	FR.A-P51	Sanchez-Portal, D.
Salez, T.	Mo.F-P15	MO.J.2_O3
Th.B.1_O2	MO.H.3_O2	Sandeman, K.
Salgado, M.	TH.J-P18	Mo.L-P85
Fr.B.1_O5	WE.I.1_O3	Sander, D.
Salgueiriño, V.	WE.I.1_O5	FR.A-P7
TU.B.2_I1	Sampathkumaran, E.V.	FR.H.3_O1
WE.B.2_I1	FR.D-P17	Fr.H.3_O4
Salikhov, R.	Mo.C-P17	Mo.A-P19
Mo.H-P63	TU.A-P19	Sandilands, L.J.
WE.B.2_I1	Samsel-Czeka, M.	FR.A-P17
Salimi, E.	Mo.A-P107	Sandiumenge, F.
TH.J-P33	Samuely, P.	Mo.H-P57
Salinas, H.	Mo.A-P85	Sando, D.
Mo.K-P11	Sanathkumar, R.	Th.E.1_I1
Salis, G.	TH.C-P73	Sangeetha, N.S.
Mo.D-P31	Sánchez Mora, E.	Th.O-P21
Salman, Z.	Th.N-P9	Sangiao, S.
FR.A-P34	Sanchez, A.	Th.B.2_I1
FR.A-P9	FR.A-P10	Sangregorio, C.
Salmon, L.	Mo.F.2_O5	Fr.H.2_O2
MO.J.2_O4	Mo.J-P5	Th.N-P13
Saloaro, M.	TU.F-P73	Th.N-P14
Mo.H-P19	TU.I.2_O2	Th.N-P15
Salomon, S.	Sánchez, C.W.	TU.B.2_O4
Mo.L-P76	Mo.H-P14	TU.E.3_O2
Salvan, G.	Sanchez, D.	TU.F-P19
Mo.H-P30	Th.H-P15	TU.F-P60
Salvat-Pujol, F.	Sánchez, F.	TU.F-P64
FR.D-P55	FR.H-P25	TU.F-P95
Samaniego, J.	FR.I-P22	Sanina, V.
TU.D.3_O2	Mo.A-P58	TU.A-P64
Samant, M.	Mo.H-P84	Sankar, R.
TU.I-P24	Th.E.2_O2	Th.K-P41

Sankey, J.	Sanvito, S.	TU.H-P85
Mo.F-P27	Fr.I.3_O4	TU.H-P87
Sanna, S.	MO.G.2_I1	TU.H-P94
Mo.A-P102	Sanz, M.	Sasaki, R.
Mo.A-P103	TU.I.3_O3	TU.H-P91
Mo.A-P22	Saouma, F.	Sasaki, S.
Mo.A-P37	TU.A-P6	FR.A-P6
TU.E-P6	Sapkota, A.	Sasaki, T.
Santamaria, J.	Fr.D.2_O3	FR.A-P52
Mo.E-P8	Sapoletova, N.	FR.F-P22
Th.E.1_I4	Th.K-P28	Mo.B-P17
WE.G.1_O4	Sarella, A.	Mo.B-P18
Santamaría, J.	Th.M-P9	MO.F.3_O1
FR.I-P49	Sarjoosing, G.	Th.K-P30
Th.P-P31	Th.O-P35	Th.O-P30
Santana, P.J.S.	Sarkar, A.	TU.A-P7
Mo.L-P21	Mo.D-P14	TU.H-P56
Santandreu, I.	Mo.D-P20	Saslow, W.
FR.I-P37	Sarkar, P.	WE.I.2_O6
Šantavá, E.	Th.O-P10	Satake, Y.
TH.C-P34	Th.O-P9	TH.C-P102
Santiso, J.	Sarkar, R.	Sato, C.
Mo.H-P57	Fr.B.2_O6	TU.F-P18
Santo, K.	FR.D-P56	Sato, F.
Mo.D-P19	Mo.A-P100	Mo.K-P12
Santos Burgos, B.	Sarkar, T.	Mo.K-P13
Fr.D.1_O3	WE.D.1_O4	Mo.K-P14
FR.I-P28	Sarma, B.	Sato, H.
Santos, D.	TH.F-P23	FR.D-P15
Th.P-P1	Saroun, J.	MO.H.1_O5
Santos, F.H.	MO.E.2_O2	TU.A-P47
Th.O-P16	Sarrao, J.L.	TU.B-P38
Th.O-P56	MO.A.2_O5	TU.B-P8
Santos, R.	TU.B-P15	Sato, K.
Th.P-P34	Sarsenov, A.	FR.D-P71
Santos, Y.	Mo.J-P17	Mo.H-P74
TU.A-P41	Sarwe, A.	TU.H-P14
TU.A-P56	Th.P-P2	Sato, M.
Santos-Cottin, D.	TU.B.3_O2	FR.D-P1
FR.A-P58	Sasai, R.	Mo.A-P90
Fr.A-P59	Mo.L-P60	Th.F.1_O5
Santosh Babu, G.	Sasaki, I.	Sato, N.K.
Mo.H-P41	TU.H-P33	Fr.B.3_O4
Santucci, S.	Sasaki, M.	Mo.A-P80
Mo.E-P8	TU.H-P114	Mo.A-P81

TU.C-P18
 TU.H.2_I1
Sato, R.

WE.D.2_O4
Sato, S.

Mo.E-P7
Sato, T.

FR.B-P24
 Mo.F-P5
 TH.J-P2
 TH.K-P2
Sato, Y.

TH.D-P23
Satoh, I.

TH.A-P13
Satoh, S.

TU.B-P43
Satoh, T.

Th.I-P2
 Th.I-P8
Saturin, S.

Mo.I-P14
Satyarathi, P.S.

Mo.H-P58
Säubert, S.

TH.C-P119
Saúl, A.

Th.M-P14
Saunders, J.

FR.A-P24
Saunin, V.

TU.H-P55
Saura-Múzquiz, M.

TU.F-P55
Saurina, J.

TU.H-P99
Sava, B.A.

Th.O-P19
Savary, L.

MO.I.3_O1
Savero-Torres, W.

Fr.G.3_O4
 TH.E-P12
 TH.E-P8
Savici, A.

MO.I.1_O2
Savin, P.

Mo.I-P26
Sawada, Y.

FR.D-P35
 TH.A-P19
Sawatzki, S.

Th.A.3_O2
 TU.H-P29
Sawicki, B.

TH.C-P65
 TH.D-P12
 TU.H-P50
Sawicki, M.

TU.G.1_I1
Saxena, R.

TU.F-P45
Saxena, S.

FR.A-P63
 TH.A-P11
Saxena, S.S.

Mo.A-P56
Sayed Hassan, R.

Mo.J-P10
Sboychakov, A.

Mo.B-P19
 Mo.C-P10
 TU.E-P2
Scagnoli, V.

TU.E.1_O3
 WE.E.1_O4
Scaramucci, A.

TU.A-P51
Scavini, M.

Th.N-P15
Schaefer, R.

TU.A.2_O2
Schafer, D.

Mo.I-P16
 Mo.I-P39
Schäfer, R.

FR.H-P20
 Mo.H-P46
Schäfer, S.

Th.A.2_O3

Schäffer, T.

TU.E.2_O3
Schaffert, S.

Fr.I.1_I1
Schaller, V.

Th.P-P2
 TU.B.3_O2
Schäpers, M.

TH.A-P27
Scheerer, G.W.

TU.F.1_O5
Schefer, J.

Mo.A.1_O5
Scheffler, M.

TU.B-P63
 TU.C-P26
 TU.H.2_O4
Scheidt, E.W.

Fr.B.3_O1
Schell, J.

TU.A-P89
Schelp, L.

Th.K-P31
Schemerber, G.

Mo.L-P4
Scheneider, M.

Fr.I.1_I1
Scherer, M.

MO.D.3_O2
Schickling, T.

WE.E2_O5
Schiebl, M.

TU.A-P11
Schiemer, J.

WE.D.1_O5
Schierle, E.

Mo.A-P108
 MO.I.2_O3
 TU.A-P13
 TU.H-P31
Schiffer, P.

TU.D.1_I1
 TU.E.1_O4
Schindler, R.

FR.D-P76

Schirone, S.	Mo.I-P22	TU.C-P33
Mo.C-P23	Schmidt, L.	Schnelle, W.
Schlage, K.	MO.G.3_O4	TU.B-P36
FR.I-P19	Schmidt, M.	Schoenemann, R.
Th.I.3_O1	FR.D-P80	Th.D.3_O1
TU.C.1_O2	MO.D.3_O3	Schoenlein, R.W.
TU.I.1_O5	Mo.I-P10	Th.I-P1
WE.E.1_O3	TH.J-P35	Scholl, A.
Schlenhoff, A.	TU.F-P41	MO.E.3_I1
Fr.I.3_O1	Schmidt, O.	Mo.I-P24
WE.G2_O2	Fr.E.3_O1	Schön, G.
Schlom, D.	MO.E.3_O2	Th.I-P3
TU.E.1_O4	TU.F-P83	Schönemann, R.
Schlottmann, P.	Schmidt, O.G.	Fr.D.1_O2
FR.B-P8	Fr.E.1_O5	Schönhense, G.
TU.C-P5	Fr.I.2_O4	FR.A-P35
Schlueter, J.A.	TU.C.1_I1	Fr.D.2_O2
FR.D-P55	Schmitt, D.	Schönherr, P.
Schmakat, P.	WE.C.2_O4	MO.H.3_O4
TH.C-P119	Schmitt, T.	Schönmann, R.
TH.C-P97	Fr.B.2_O3	TU.B-P75
Schmalzl, K.	Mo.A-P31	Schopphoven, C.
TH.B-P9	Th.G.3_O1	Th.L-P2
TU.B-P26	Schmitt-Landsiedel, D.	TU.F-P63
TU.B-P66	Th.O-P28	Schöppner, C.
Schmehl, A.	TU.I-P13	TU.C.3_O3
Mo.H-P100	Schnarr, C.	Schorr, S.
Mo.H-P12	TH.J-P25	TH.C-P69
Mo.H-P56	TH.J-P28	Schottenhamel, W.
Schmerber, G.	Schneider, C.	Mo.A-P22
TU.A-P8	TU.E.1_O3	Schreck, M.
Schmid, A.	Schneider, H.C.	Fr.I.3_O1
TU.I-P9	Fr.J.2_O3	Schrefl, T.
Schmidiger, D.	Schneider, HC	Fr.A.2_I1
TH.A-P5	Fr.J.2_O3	Schreiber, M.
Schmidt, A.M.	Schneider, M.	FR.E-P2
Th.P-P13	TH.K-P18	Schreier, M.
Schmidt, B.	Schneidewind, A.	Mo.J.3_O4
FR.D-P48	FR.D-P67	Schröder, C.
Schmidt, H.	MO.D.3_O3	FR.E-P6
Mo.H-P58	TH.A-P41	MO.G.1_O3
Th.A-P45	TH.B-P9	Schrödner, M.
Schmidt, J.E.	TH.C-P16	Th.O-P6
FR.D-P9	TU.B-P66	Schuller, I.K.
Mo.I-P19	TU.B-P75	MO.E.3_I1

Mo.I-P24	MO.H.3_O3	Mo.A-P55
TH.C-P42	Schweiss, P.	Sefrioui, Z.
Th.L-P3	Fr.H.1_O2	Mo.E-P8
TU.A.2_I1	Mo.A-P30	WE.G.1_O4
Tu.G.2_I1	Schwenk, J.	Segal, A.
TU.G.2_O2	Th.I.3_O4	FR.H-P14
TU.J.3_O2	Sciancalepore, C.	Segawa, K.
Schultz, L.	TH.E3_O4	FR.A-P6
MO.D.1_O3	Scigaj, M.	Seguí, C.
MO.E.1_O5	Mo.A-P58	Mo.L-P24
MO.E.2_O6	Scola, J.	Seidel, J.
Mo.L-P57	FR.A-P54	Mo.E-P11
Mo.L-P83	Scopel, W.	Seidlerova, J.
TU.G.2_O4	FR.H-P32	Th.O-P11
TU.H-P118	Scotti, R.	Seifert, M.
WE.D.1_I1	Th.P-P12	TU.G.2_O4
WE.J.2_O5	Sculze, M.	Seine, G.
Schulz, M.	Mo.A-P98	Th.C.2_O2
TH.C-P97	Sebastian, S.	Seiner, H.
Schulz, S.	Mo.A-P47	WE.D.1_I1
Th.O-P29	Šebek, J.	Seiro, S.
Schulz, T.	TH.D-P3	Mo.A-P83
Fr.I.1_I1	Secchi, A.	TU.B-P30
Fr.I.2_O5	Fr.F.1_O5	TU.F.1_I1
Schumacher, D.	MO.J.3_O1	Sekatskii, S.
TU.C.1_O2	Sechovsky, V.	Th.O-P41
Schumacher, H.W.	MO.E.2_O2	Seki, K.
Fr.E.1_O2	WE.A.1_O3	FR.B-P16
WE.H.1_O4	Sechovský, V.	Mo.A-P41
WE.I.2_I1	FR.A-P60	Seki, S.
Schuppler, S.	Th.A-P40	Fr.I.1_O3
TU.H-P35	TH.B-P21	Seki, T.
Schütte, C.	TH.D-P4	Mo.F-P6
TU.H.3_O2	TU.B-P28	WE.D.2_O2
Schütte, G.	TU.C-P7	Sekine, A.
TU.H-P29	Sedlák, B.	Th.B.2_O4
Schütz, G.	TH.C-P39	Sekine, C.
Fr.G.1_O3	Sedlmaier, S.	FR.A-P37
Mo.I-P10	WE.A1_O1	Mo.A-P23
TH.J-P12	Sedmidubský, D.	Mo.A-P4
TU.H-P35	FR.F-P30	TH.B-P8
TU.I-P7	Seemann, K.	Sekine, T.
Schwarz, T.	TU.C-P32	Mo.B-P18
MO.E.2_O1	TU.C-P33	Mo.B-P5
Schwarze, T.	Sefat, A.S.	TU.A-P50

TU.A-P52	Seo, S.	Mo.F-P21
TU.A-P53	MO.A.1_O2	Th.H-P16
Selezneva, N.	Th.O-P38	TU.H.1_O5
Mo.A-P12	Seo, S.H.	WE.I.2_I1
TH.C-P12	Mo.A-P100	Serrano-Ramón, L.
Sellmyer, D.J.	Seo, Y.	Mo.K-P17
MO.B.3_O4	TU.H-P69	Serrao, C.
Th.K-P29	Sera, M.	Fr.C.2_O4
TU.F-P76	Mo.A-P53	Serrate, D.
Semeniuk, K.	TH.C-P63	Mo.J-P9
FR.A-P43	TU.B-P11	Th.B.2_O3
Mo.A-P110	Serantes, D.	TH.D-P17
Mo.A-P70	Th.P-P11	WE.H.2_O2
WE.F.2_I1	TU.G.2_O4	Servent, F.
Semenova, E.	Serebryakova, O.	Th.A.3_O4
Mo.F-P1	TU.F-P34	Sesé, J.
Semisalova, A.	Serebryannikov, A.E.	MO.E.2_O1
Th.P-P24	Mo.G-P11	TH.K-P4
Sen, K.	Sereni, J	Th.M-P1
Fr.B.2_O1	TU.C-P14	Sessoli, R.
Senba, S.	Sereni, J.	MO.I.2_I1
Mo.H-P92	TH.A-P4	Sethi, P.
Senegas, A.	Serga, A.A.	TH.K-P5
FR.A-P54	Fr.G.1_O2	Settai, R.
Seng, K.I.	Fr.G.1_O5	Mo.A-P87
Th.O-P35	Mo.G-P13	TH.C-P47
Sengupta, P.	MO.H.2_O2	TU.B-P35
Fr.F.1_O2	Th.H-P18	TU.B-P39
Senthil, T.	TU.E.3_I1	TU.B-P42
MO.I.3_O1	Serin, V.	TU.B-P43
Sentker, K.	Th.C.2_O2	Severing, A.
Th.I-P4	Serletis, C.	TU.B-P15
Senyshyn, A.	TH.K-P12	TU.B-P5
TH.C-P116	Serpe, L.	WE.H.2_I6
TH.C-P82	MO.F.2_O2	Sevriuk, V.
TU.B-P75	Serpico, C.	FR.A-P7
Seo, H.Y.	MO.G.2_I4	Seyfarth, G.
Mo.H-P73	Mo.J-P19	TU.F.1_O2
Seo, J.	Mo.J-P20	Shabadi, V.
WE.A.1_O4	Mo.J-P21	TU.A-P31
Seo, M.	TH.F-P23	Shadrov, V.
Th.O-P39	Th.I-P18	TU.H-P54
Seo, M.S.	TH.I-P25	Shaginyan, V.
TU.A-P28	WE.H.1_O4	FR.B-P2
TU.A-P29	Serrano-Guisan, S.	TU.C-P1

Shah, W.	Th.E.3_O2	Mo.A-P75
Mo.C-P1	TU.F-P39	Shengelaya, A.
Shahee, A.	TU.F-P6	Mo.A-P8
Mo.F-P7	Sharmin, S.	Sheppard, C.
Shaik Bastien Dalla Piazza, N.E.	Mo.F-P18	Mo.H-P53
Th.G.3_O1	TU.G-P9	Sheptyakov, D.V.
Shaikhutdinov, K.	Sharp, P.	FR.D-P37
TH.C-P11	WE.E2_O3	TU.A-P51
Shames, A.	Shavrov, V.	Sheridan, R.
Mo.C-P16	Mo.G-P20	Mo.L-P29
Shamonin, M.	Mo.G-P21	Sherman, A.
TU.A-P94	Mo.L-P37	FR.B-P4
Shannon, N.	Mo.L-P74	FR.E-P2
Fr.F.2_I1	Mo.L-P77	Sherstobitov, A.
Shao, Q.	Mo.L-P8	TH.C-P53
FR.H-P9	Mo.L-P89	Sheshukova, S.
Mo.H-P5	Th.B.1_O5	Mo.H-P21
Shao, X.	TH.C-P111	Shevyrtaov, S.
FR.I-P2	TH.C-P112	Mo.L-P61
Shao, Y.	TU.A-P92	Mo.L-P92
TU.A-P54	Shayestehaminzadeh, S.	Shi Ping, Z.
Shapiro, S.M.	TU.G.1_O5	Mo.A-P62
TH.C-P119	Shaykhutdinov, K.	Shi, S.
Shaposhnikov, A.	TH.D-P14	Fr.I.3_O4
Th.N-P7	Shcheglov, V.	Shi, Y.
Th.N-P8	Mo.G-P20	FR.A-P30
Sharaevski, Y.	Mo.G-P21	Th.A.2_O6
Mo.H-P21	Sheikin, I.	Shibata, D.
Sharaevskii, Y.	TH.A-P10	Th.C.3_O4
Fr.G.1_O4	WE.F2_O3	Shibata, K.
Sharma, G.	Sheka, D.	TU.B-P51
MO.C.1_O3	Fr.E.3_O1	Shibauchi, T.
TU.A-P39	Mo.K-P23	Tu.A.3_O5
Sharma, J.	TH.J-P7	TU.H.2_O4
Mo.L-P27	TU.F-P83	WE.F2_O4
Mo.L-P30	Shekhar, C.	Shibayama, Y.
Sharma, P.	Mo.L-P46	TH.D-P7
Th.H.2_O4	MO.SYM_4	Shick, A.
TU.A.1_I1	TH.D-P6	FR.A-P8
TU.H-P67	Shelukhin, L.	Shick, A.B.
Sharma, R.	Th.I-P19	TH.D-P25
Mo.F-P19	Shen, B.G.	Shields, B.
Sharma, S.	FR.I-P2	MO.E.2_O3
Mo.L-P56	Shen, C.	Shiga, M.
	Mo.A-P63	TU.J.3_O1

Shigematsu, E.	Mo.C-P21	MO.F.3_O1
Mo.D-P23	TH.A-P30	Th.I.2_O3
Shigeoka, T.	TH.B-P14	Shinozaki, K.
TH.C-P113	TU.C-P25	TU.H-P87
TH.C-P90	Shimmura, S.	Shinozaki, S.
TH.D-P20	TU.B-P45	TH.A-P22
Shihab, S.	Shimogiku, H.	Shintani, K.
Th.I-P10	TH.E-P6	TH.B.2_O5
Shiina, R.	Shimokawa, T.	Shiokawa, Y.
TU.A-P27	TU.D.1_O2	Mo.F-P13
Shiino, T.	Shimomura, N.	Mo.F-P17
Mo.K-P22	Fr.H.3_O3	Shiota, Y.
Shikoh, E.	MO.G.1_O4	Th.G-P7
TH.E-P6	Shimoya, N.	WE.G2_I6
Th.I.2_O3	Mo.L-P54	WE.G2_O3
Shim, H.J.	Shimozawa, M.	Shiozawa, S.
Mo.H-P73	TU.H.2_O4	TU.A-P61
Shim, I.B.	WE.F2_O4	Shirahata, Y.
Mo.H-P73	Shimura, T.	Fr.G.3_O3
Shim, J.H.	Th.I-P2	Shirai, K.
FR.A-P22	Shimura, Y.	Mo.L-P41
FR.F-P13	TU.E.2_O4	Shirai, T.
MO.A.1_O2	Shin, E.	Mo.A-P83
Mo.D-P18	Th.A.2_O5	Shiraishi, K.
Th.E.2_O5	Shin, J.	TU.H-P58
Shima, T.	Mo.D-P26	Shiraishi, M.
Mo.H-P26	Shin, S.	FR.A-P6
Mo.L-P28	Fr.C.2_O5	Mo.D-P23
TH.K-P15	Shin, Y.	Mo.D-P4
Th.L-P1	MO.B.3_O3	MO.F.3_O1
TU.H-P28	Mo.E-P5	Th.I.2_O3
Shimada, K.	Mo.H-P36	Shirakawa, T.
TU.B-P38	Mo.H-P79	Mo.C-P3
Shimada, Y.	TH.B-P13	Shirane, T.
Th.J-P37	Th.G.2_O3	FR.I-P35
TU.C-P22	Th.P-P21	Shirasaki, K.
Shimamoto, K.	TU.F-P51	TH.D-P3
TU.E.1_O3	Shin, Y.J.	Shiroka, T.
Shimizu, K.	Mo.A-P66	FR.I-P27
Mo.A-P78	Mo.B-P10	MO.A.3_O4
TU.E-P3	Shinaoka, H.	Mo.A-P103
Shimizu, O.	FR.B-P23	Mo.A-P37
WE.J.1_O3	Shinjo, T.	Mo.B-P22
Shimizu, Y.	Mo.D-P23	Shiryayev, S.
MO.A.1_O4	Mo.D-P4	TU.A-P98

Shishido, H.

Fr.A-P64
WE.F2_04

Shishido, T.

FR.A-P21

Shishidou, T.

TU.A-P14
TU.E-P15

Shishkin, D.

Mo.L-P23
TH.C-P12

Shishkin, I.

Mo.H-P61
Mo.J-P12
Th.K-P28

Shitsevalova, N.

FR.D-P67
Mo.A-P85
Th.A-P40
TH.B-P1
TH.C-P77
TH.C-P78
TU.B-P20
TU.B-P32
TU.B-P59

Shmatov, G.

TH.F-P12

Shockley, A.

FR.D-P78

Shoji, T.

Fr.A.3_03
MO.D.1_04
TU.H-P115
TU.H-P63

Shombert, H.H.

Mo.K-P2

Shpyrko, O.G.

TH.C-P42
WE.G2_04

Shu, L.

TU.H-P112

Shull, R.

FR.H-P13
MO.C.2_I4
Mo.H-P39

TU.F-P63

Shumikhina, K.

FR.B-P17

Shupletsova, V.

Th.P-P18

Shuvaev, A.

TU.A-P11

Shvets, I.

FR.D-P47

Si, B.

Mo.A-P63

Mo.A-P75

Si, Q.

Fr.H.1_03
TU.F.1_I1
WE.E2_07

Sibille, R.

Mo.A.1_05

Mo.L-P50

Sichelschmidt, J.

FR.D-P65

TU.C-P26

Sideris, E.

Mo.I-P30

Sidorenko, A.

TH.B-P12

TU.C-P20

Siegfried, S.

FR.I-P47

Siemensmeyer, K.

FR.D-P67
Mo.A-P108
TH.A-P26
Th.A-P40

Sierra, J.F.

Fr.F.3_I1

Th.O-P49

Sievers, S.

WE.H.1_04

Siewert, D.

FR.H-P34

TU.D-P12

Sigov, A.

FR.H-P1

Sigrist, M.

FR.A-P11

Mo.A-P92

Sikolenko, V.

TH.C-P69

Sikora, M.

MO.B.1_I1

Silber, R.

Mo.H-P78

Th.N-P11

Silotri, S.

TU.C-P3

Silva Valencia, J.

FR.A-P19

FR.A-P20

FR.A-P39

Silva, A.

TU.I.1_03

Silva, A.V.

Th.K-P46

Th.O-P54

Silva, C.

Mo.H-P101

Silva, E.F.D.

Mo.H-P10

Mo.H-P7

Mo.H-P9

TH.C-P121

Silva, N.

Mo.H-P90

Silva, P.

TU.F-P2

Silva, R.B.D

Mo.H-P10

Mo.H-P7

Silva, R.C.D.

Mo.H-P101

Silva, S.

TU.B-P61

TU.H-P79

Silva, U.

Th.P-P8

Silvani, R.

Mo.G-P23

Silwal, P.

Mo.H-P62

Sim, H.	TU.A-P37	Mo.D-P1
Fr.C.3_O3	Singh, N.	TU.A-P4
Šimek, P.	MO.D.1_O5	Siwach, P.K.
FR.F-P30	Singh, S.B.	TU.A-P74
Simeoni, G.	Mo.K-P1	TU.G-P25
Th.D.3_O1	TU.A-P54	Sizaret, S.
Simeonidis, K.	Singh, Y.	TU.F-P5
Th.P-P11	Th.D.3_O1	Skaugen, A.
Simon, E.	Singha, A.	FR.I-P4
TU.G.3_O4	Fr.I.3_O3	Skidanov, V.
Simonelli, L.	Singleton, J.	Mo.H-P45
MO.A.3_O1	TU.H.2_O2	Skokov, K.
Simonet, V.	Sinha, A.K.	Fr.C.3_O4
MO.I.1_O3	TU.A-P37	Mo.L-P83
TU.A-P43	TU.A-P39	TU.H-P124
TU.D.2_O3	Sinha, J.	Skokov, K.P.
Sims, Z.C.	WE.G.1_O3	Fr.A.1_I1
Mo.A-P55	Sinha, S.	Mo.L-P48
Simutis, G.	WE.G2_O4	TH.C-P85
Mo.B-P7	Sinitsyn, N.A.	TU.H-P43
Sinclair, J.	MO.F.3_O4	Skokov, M.
TH.K-P19	Sinnecker, J.P.	TU.H-P95
Singh, A.	Mo.H-P13	Skomski, R.
MO.A.3_O3	TH.J-P20	Th.K-P29
Singh, G.	Sinova, J.	TU.F-P76
Mo.A-P58	TH.J-P8	Skornia, P.
TU.B.2_O3	Sipr, O.	TU.H-P12
TU.F-P30	Mo.J-P2	Skoropata, E.
TU.F-P52	Siqueira, J.	Fr.A.1_O5
TU.F-P89	Mo.I-P17	TU.B.3_O4
TU.F-P94	Siqueira, J.V.	Skorupa, W.
Singh, H.	Mo.I-P20	FR.F-P18
TU.A-P37	Sirena, M.	Skorvanek, I.
TU.A-P39	MO.C.1_O2	TU.A.2_O5
Singh, H.K.	TH.K-P1	TU.H-P133
Mo.L-P94	TH.K-P3	TU.H-P46
TU.A-P74	We.E.1_O5	Skoulatos, M.
TU.G-P25	Sirenko, V.	Th.C-P03
Singh, J.P.	TU.A-P18	Skourski, Y.
TU.A-P15	Sirhan, K.	Mo.L-P39
Singh, K.	TU.C-P14	TH.C-P124
FR.D-P17	Sitnikov, A.	TH.C-P27
FR.D-P47	Mo.H-P38	TH.C-P76
TU.A-P19	Sitnikov, M.	TH.D-P11
Singh, M.N.	FR.F-P1	TH.D-P2

Skowroński, W.	FR.E-P23	FR.D-P60
Th.G-P7	Smidman, M.	TU.A-P27
Th.O-P24	Th.C.3_01	TU.A-P90
WE.G2_I6	TU.B-P67	Soderžnik, M.
Skrotzki, R.	Smidt, T.	Th.A.3_03
Fr.D.1_02	MO.SYM_5	Sofer, Z.
Skumiel, A.	Smigaj, W.	FR.F-P30
Mo.I-P25	Mo.G-P11	Sofronie, M.
TU.F-P71	Smirnov, A.N.	Mo.L-P53
TU.F-P78	Fr.C.3_02	Th.O-P19
Skumryev, V.	Smirnov, V.	Th.O-P2
Th.J.1_03	FR.F-P28	Softwedel, O.
TU.A-P93	Smith, A.	Mo.H-P70
TU.A-P98	MO.H.2_03	Soh, C.S.
Slavin, A.	Snelder, M.	FR.D-P45
TH.J-P9	MO.SYM_2	Th.M-P6
Slavin, V.	Sniadecki, Z.	Sohn, C.H
FR.E-P4	TU.E-P45	FR.A-P17
Slawska-Waniewska, A.	Śniadecki, Z.	Sokhonevich, N.
Mo.H-P82	Mo.L-P40	Th.P-P18
Th.G.2_04	TU.H-P46	Sokol, J.
TU.D-P2	Snoeck, E.	TU.I-P25
TU.D-P3	Fr.E.1_I1	Sokolov, A.
Ślebarski, A.	Fr.E.3_04	TH.C-P40
TU.B-P1	Mo.H-P18	TU.E-P12
TU.H-P53	Mo.K-P16	Sokolov, D.
Slimani Tlemčani, T.	Mo.K-P17	Th.D.1_I4
TU.A-P8	Th.E.1_02	Sokolov, N.
Slipko, V.A.	TU.C.1_04	Mo.I-P14
MO.F.3_04	WE.J.1_02	Sokolov, V.
Sluchanko, N.	So, J.	Mo.D-P6
Mo.A-P85	TU.A-P72	Sokolovskiy, V.
Th.A-P40	Soares, M.	FR.E-P20
TH.C-P122	FR.I-P23	Mo.L-P75
TH.C-P77	TU.J.3_03	Sola, A.
TH.C-P78	Šobán, Z.	Th.H-P17
TU.B-P32	Fr.G.3_02	WE.H.1_04
TU.B-P59	MO.F.1_03	Solano, E.
Sluka, V.	Sobierajski, R.	Th.L-P5
TH.J-P9	Th.C.2_05	Soldusova, A.
Sluka, V.A.	TU.G-P28	Mo.J-P6
TU.H.1_I1	Soda, J.	Soler, E.
Smeibidl, P.	Mo.A-P74	WE.SYM_1
Fr.E.2_05	Soda, M.	Solignac, A.
Šmejkal, L.	FR.D-P51	WE.G.1_02

Solivelles, F.	Sonobe, Y.	Mo.H-P13
TH.F-P28	TU.I-P14	Souza, E.
Sologub, O.	Soriano Gomez, N.S.	FR.H-P32
Fr.B.3_O1	Mo.H-P44	Souza, J.A.
Solovev, P.	TH.K-P21	TU.F-P45
Mo.H-P93	Soriano, L.	Sözeri, H.
Šoltésová, D.	TU.C.1_O5	Th.O-P23
TU.D-P4	Soriano, N.	TU.H-P48
Solyom, J.	Tu.G.2_I1	TU.H-P49
Fr.J.1_O3	Sorrentino, A.	Spaldin, N.A.
Solzi, M.	Fr.H.3_O2	TU.A-P24
MO.D.2_I1	Sort, J.	TU.A-P51
MO.D.2_O2	Mo.F.2_O5	Spalek, J.
Sommer, C.	Sothmann, B.	FR.B-P22
Mo.K-P7	MO.A.3_O2	FR.C-P7
Sommer, R.	Mo.K-P15	WE.E2_O5
Mo.G-P31	Soufen, C.	WE.E2_O6
Sommer, R.L.	TH.D-P1	WE.F2_O6
Mo.G-P29	Soukup, D.	Spallek, J.
TH.I-P27	Th.P-P9	TU.B-P75
Son, B.	Soulantica, K.	Spasova, M.
Th.O-P43	MO.B.3_O3	TU.G-P27
Son, J.	Th.G.2_O3	WE.B.2_I1
FR.A-P4	Th.I.3_O3	Speliotis, T.
Son, K.	Th.I-P6	TU.E.3_O3
TU.I-P7	Sousa de Oliveira, L.A.	Spencer-Smith, A.
Song, C.	Mo.H-P13	MO.G.3_O1
Mo.L-P35	Sousa, C.T.	Spiegelberg, J.
Song, J.	Mo.K-P27	MO.E.1_O4
Mo.H-P60	Sousa, G.	Spiesser, A.
Song, J.D.Ç	Mo.A-P77	Mo.D-P22
Mo.B-P10	Sousa, M.	Spinu, L.
Song, M.	Mo.I-P8	Fr.F.2_O3
FR.A-P16	TU.F-P58	Spizzo, F.
TH.A-P16	TU.G-P5	Mo.H-P3
TU.H-P22	Sousa, R.C.	Mo.I-P38
TU.H-P64	TU.J.1_I1	Mo.I-P40
Song, Y.	TU.J.2_O3	Th.P-P12
FR.B-P7	Sousa, V.	TU.G.3_O1
MO.F.3_O3	Mo.L-P5	Springell, R.
Soni, R.	Southern, P.	Th.G.3_O2
FR.A-P26	Th.P-P2	Springholz, G.
Sonntag, A.	Th.P-P25	FR.A-P60
FR.H-P8	Th.P-P7	Srikanth, H.
WE.G2_O2	Souza, D.M.	MO.B.1_O3

Mo.I-P30	TU.A-P10	Stegmann, P.
Th.B.1_I1	Stanley, D.C.	Mo.K-P15
TU.F-P65	MO.B.1_I1	Stein, D.
Srinivas, V.	Stanley, J.	Mo.F-P23
TH.C-P117	TH.C-P42	Stein, W.D.
TU.F-P97	Starčuk, Z.	Fr.E.2_O5
Srinivasan, R.	Th.P-P4	Steinbrecher, M.
FR.I-P48	Starodub, V.	Fr.I.3_O2
Th.O-P45	TU.D-P4	Steiner, H.
Th.P-P16	Staruch, M.	FR.A-P60
Srivastava, A.	TH.C.1_O5	Steiner, U.
Mo.L-P94	TU.A-P12	MO.D.3_O2
Srivastava, O.	TU.E.2_O1	Steiner, W.
Mo.L-P94	Stashkov, A.	TH.B-P7
Srivastava, P.	FR.I-P10	Steinigeweg, R.
Mo.H-P58	Stasinopoulus, I.	TH.A-P37
Srivastava, S.K.	WE.H.1_O3	Steinke, N.J.
Th.I.3_O4	Stasinopoulos, I.	Mo.H-P95
Srivastva, R.C.	MO.H.3_O3	Stejskal, J.
TU.A-P15	Staub, U.	FR.F-P30
Stadler, S.	Fr.B.2_O1	Stengl, V.
Mo.L-P3	TU.A.3_O2	Th.O-P20
Stadtmüller, B.	TU.E.1_O3	Stepanov, A.
Mo.E-P11	TU.E.1_O6	Mo.B-P13
Stahn, J.	Stanton, J.	TU.A-P75
Fr.B.2_O1	TH.C-P36	Stepanow, S.
Mo.H-P100	Steadman, P.	Fr.I.3_O3
Mo.H-P12	Th.J.1_O3	TU.J.3_O3
Mo.H-P56	Stebliy, M.	Stephanovich, V.
Stamm, C.	TH.J-P34	TU.C-P1
TU.J.3_O3	Steckel, F.	Stephanowich, V.
Stamps, R.	Mo.A-P20	FR.B-P2
FR.H-P19	Steeves, G.	Stepniak, A.
MO.D3_O4	Th.F.2_O2	Mo.A-P19
Mo.H-P31	Stefanoski, S.	Steppke, A.
Th.I-P15	Th.B.1_I1	WE.H.2_O4
Th.N-P4	Steffens, P.	Steren, L.B.
TU.H.3_I1	MO.E.2_O2	MO.C.1_O2
Stancu, A.	Steglich, F.	Mo.H-P13
FR.E-P33	Mo.A-P83	TH.K-P1
Mo.J-P14	TU.B-P26	We.E.1_O5
Th.P-P27	TU.B-P63	Stergiou, B.
Stanislavchuk, T.	TU.F.1_I1	Mo.L-P88
TU.A-P87	TU.H.2_O2	TU.H-P126
Stankiewicz, J.	WE.H.2_O4	Stern-Taulats, E.

Th.B.1_O3	Stojanovic, N.	Mo.H-P62
Th.B.1_O4	Th.I-P17	Strohm, C.
Stevenson, S.	Stoleriu, L.	TU.B-P44
TH.J-P3	FR.E-P33	Strömberg, M.
Steydli, S.	Stoll, H.	Th.H.1_O3
Mo.L-P86	Fr.G.1_O3	Th.H.2_O5
Stiles, M.	TH.J-P12	Strupiński, W.
Fr.G.3_O1	Stopfel, H.	FR.I-P36
Stillwell, R.	MO.E.2_O6	Strychalska, J.
Fr.C.1_O4	Th.M-P18	FR.C-P8
TU.B-P22	WE.B.2_O3	Mo.A-P96
Stingaciu, M.	Storni, M.	Strydom, A.
Mo.I-P11	Mo.G-P25	TH.C-P109
Mo.I-P15	Strbak, O.	TU.B-P7
Mo.L-P38	Th.P-P30	TU.C-P24
Stipe, B.	Th.P-P37	Strydom, A.M.
WE.D.2_I6	Streda, P.	WE.H.2_O5
Stishov, S.	Mo.D-P7	Stubna, V.
TH.A-P1	Strečka, J.	FR.D-P62
TH.C-P10	FR.D-P9	FR.D-P63
Stjernberg Bejhed, R.	FR.E-P9	Studer, A.
Th.M-P20	TH.A-P2	Mo.L-P31
TU.B.3_O2	TH.C-P15	Stuesser, N.
Stobiecki, F.	TH.C-P68	Fr.E.2_O5
Mo.H-P46	Streltsov, S.	Stuhr, U.
Stobiecki, T.	FR.B-P3	Mo.G-P25
Mo.H-P105	FR.E-P14	TU.E.2_O3
Th.O-P24	Mo.C-P10	Stupakiewicz, A.
Stock, C.	Strepfer, J.	Th.I-P14
Th.D.1_I4	FR.I-P4	Th.I-P8
Stockem, I.	Streubel, R.	TU.A.1_O3
MO.G.1_O3	Fr.E.1_O5	Stupakov, A.
Stockert, O.	Fr.I.2_O4	FR.I-P3
Fr.H.1_O3	TU.C.1_I1	Sturm, T.
TH.B-P9	Štrichovanec, P.	WE.J.2_O5
TU.B-P26	Mo.H-P101	Su, C.W.
TU.B-P63	Mo.H-P55	FR.H-P16
TU.B-P66	Th.M-P1	Su, L.
TU.H.2_O3	Stride, E.	TH.C-P25
Stognij, A.	Fr.H.2_O5	Su, Y.
Mo.G-P16	Strigari, F.	FR.D-P79
Th.G.1_O4	TU.B-P15	Fr.D-P87
TU.H-P54	TU.B-P5	Mo.A-P57
Stojak Repa, K.	WE.H.2_I6	TH.A-P42
MO.B.1_O3	Stritch, K.B.	Suard, E.

TH.C-P105 Suarez, O.	TU.A-P81 Sugiyama, H.	Mo.H-P6 Sun, T.H.
Th.I-P15 Suárez, R.	Mo.D-P17 Sugiyama, J.	TU.G-P8 Sun, X.
WE.G2_I1 Subías, G.	FR.D-P7 Sugiyama, T.	MO.J.2_I1 Sun, Y.
TH.C-P21 TU.A-P10 TU.A-P13 TU.A-P9 TU.E.1_O2 Subiyanto, I.	FR.D-P8 Mo.B-P6 TU.B-P3 TU.C-P2 Suh, B.	FR.A-P3 Sun, Y.Y. TU.E.2_O2 Sun, Z.
TH.A-P31 Subkhangulov, R.	Mo.I-P6 Suharyadi, E.	Mo.F-P2 Sundermann, M.
FR.F-P11 Th.G.1_O5 Subramanian, V.	FR.D-P52 Th.P-P29 Sukhostavets, O.	TU.B-P15 TU.B-P5 WE.H.2_I6 Sung, C.
TU.H-P80 Suderow, H.	Fr.I.1_I4 Sullivan, J.	FR.I-P8 Sung, K.
FR.I-P49 TH.D-P22 TU.E-P47 Suekuni, K.	Th.P-P25 Süllow, S.	Mo.I-P9 Sung, N.
FR.A-P23 Sueyasu, K.	TU.C-P23 Sulpice, A.	Mo.C-P14 Suñol, J.
Th.H-P7 Suga, S.I.	Mo.I-P13 Sumida, K.	FR.I-P37 Mo.L-P78 TU.H-P99 Suresh, K.G.
FR.E-P5 Sugawara, A.	Fr.C.2_O5 Mo.L-P41 Sumitomo, S.	Mo.L-P27 Mo.L-P30 Mo.L-P46 Mo.L-P51 TH.D-P6 Suresh, P.
TU.H-P19 Sugawara, H.	TH.F-P25 Sumiyama, A.	Mo.L-P51 Sürgers, C.
FR.A-P37 Sugihara, A.	TH.B-P18 Fr.B.3_O2 Sun, C.	Mo.H-P33 Surija, V.
Mo.E-P7 TU.G-P12 Sugimoto, A.	TU.F-P65 Sun, D.	MO.G.3_O3 Suriñach, S.
TU.B-P19 Sugimoto, T.	TU.C-P28 WE.H.2_O4 Sun, J.	Mo.B.1_I1 Surmach, M.
FR.D-P58 Sugimoto, Y.	FR.B-P7 Sun, I.	Mo.A-P100 Surti, A.
Mo.A-P66 Sugita, R.	Mo.H-P28 Mo.K-P10 Sun, S.J.	Th.P-P33 Suryanarayanan, R.
Mo.H-P1 TU.I-P1 Sugita, Y.	Mo.A-P13 Sun, T.	TH.A-P28

TH.C-P104
Sushkov, O.
 MO.G.3_O1
Susner, M.A.
 Mo.A-P55
Suszka, A.
 Mo.H-P37
 TH.J-P3
Suter, A.
 FR.A-P9
 TH.C-P80
Sutherland, M.
 Mo.A-P112
Suto, H.
 WE.D.2_O4
Suwada, Y.
 Mo.A-P83
Suzuki, A.
 Fr.A.3_O2
Suzuki, H.
 Fr.D.1_O2
 TH.D-P23
 TU.C-P27
Suzuki, J.
 Mo.A-P74
Suzuki, J.I.
 TU.C.2_O2
Suzuki, K.
 Mo.E-P7
 TU.A.2_O2
 TU.E.2_O4
 TU.G-P12
Suzuki, K.Z.
 Th.H-P14
Suzuki, M.
 Th.G-P5
 Tu.A.3_O5
 TU.F.1_O2
 WE.G2_I6
Suzuki, T.
 FR.A-P23
 FR.E-P5
 Mo.A-P111
 Mo.A-P40
 Mo.A-P53

MO.F.3_O1
 TU.A-P88
Suzuki, Y.
 Mo.G-P24
 Th.G-P5
 Th.G-P7
 WE.G2_I6
 WE.G2_O3
Svalov, A.V.
 Mo.I-P26
 Mo.I-P34
 Mo.K-P4
 Mo.L-P93
 TU.I.2_O3
Svec Jr., P.
 Th.O-P23
Svec Sr., P.
 Th.O-P23
Svec, P.
 TU.H-P133
Svedlindh, P.
 FR.D-P5
 Mo.L-P84
 Th.H.1_O3
 Th.H.2_O5
 Th.I-P29
 Th.M-P20
 TU.B.3_O2
 TU.E-P42
 TU.F-P101
 TU.F-P102
 TU.H-P111
Sveklo, I.
 Th.C.2_O5
Svensson, G.
 FR.D-P5
Svoboda, P.
 MO.E.2_O2
 TH.C-P45
Swagten, H.
 Fr.I.2_O5
 WE.G.1_O2
Swain, N.
 FR.C-P6
 FR.D-P64

Swanson, J.
 Th.B.2_O2
Swerts, J.
 WE.D.2_O3
Syassen, K.
 Mo.B-P25
Sydney Dutra Folly, W.
 TU.F-P75
Sykora, S.
 TU.B-P4
Syková, E.
 Fr.H.2_O3
 Fr.H.2_O4
Syromyatnikov, A.
 FR.D-P26
 FR.E-P21
 Mo.J-P12
Syvorotka, I.
 Th.O-P31
 Th.O-P8
Szabo, P.
 Mo.A-P85
 TU.E-P5
Szaller, D.
 TU.A-P25
Szałowski, K.
 FR.D-P63
 TH.C-P74
Szerenos, K.
 Th.I-P14
Szewczyk, A.
 TH.C-P35
 TU.E-P41
Szewczyk, R.
 FR.I-P29
 FR.I-P36
 FR.I-P39
 TU.H-P104
 TU.H-P18
 TU.H-P59
Szkudlarek, A.
 Th.I.3_O2
Szlawska, M.
 TU.C-P17
Szulim, P.

FR.I-P50	MO.A.2_03	TU.C-P27
FR.I-P51	Tacchi, S.	WE.H.2_05
Szumiata, T.	Mo.G-P23	Takada, S.
FR.H-P3	Mo.H-P3	Mo.B-P21
Szunyogh, L.	TU.G-P10	Takáèová, I.
Mo.J-P16	TU.I-P4	Th.A-P40
Th.I-P12	Tagirov, L.	Takaesu, Y.
TU.G.3_04	TH.E-P5	TH.C-P71
Szuskiewicz, W.	Taguchi, K.	Takagi, H.
FR.F-P29	TH.B.2_05	Mo.A-P39
TU.G-P28	Taguchi, M.	TU.B-P3
Szymanski, D.	FR.D-P71	TU.E-P39
TH.C-P96	Taguchi, Y.	Takagi, S.
Szymanski, K.	FR.F-P4	FR.A-P37
TU.E-P41	Th.G-P4	Takagi, Y.
Szymański, B.	TU.A-P22	Mo.H-P72
Mo.H-P46	TU.A-P25	Takahashi, H.
Szymczak, H.	Tahiri, N.	TH.A-P28
TH.C-P84	MO.A-P1	TH.C-P104
Szymczak, R.	Taibi, M.	Takahashi, K.
TH.C-P84	TU.A-P8	Fr.A.1_02
	Taillefer, L.	FR.I-P30
	MO.A.2_11	Mo.L-P52
	Tainosho, T.	Mo.L-P66
	Mo.F-P18	TU.H-P82
	Taira, A.	Takahashi, M.
	TU.H-P82	Mo.F-P22
	Tajiri, H.	Takahashi, Mi.
	TH.K-P2	Mo.A-P80
T. A., L.	Tajiri, T.	Takahashi, N.
TU.H-P100	TU.F-P7	FR.D-P13
T. Gomes, I.	Taka, H.	Takahashi, S.
Mo.H-P107	Mo.E-P7	Mo.J.3_04
T. Sousa, C.	Takabatake, T.	Takahashi, Sh.
Mo.L-P90	FR.A-P23	TU.I-P14
Tabachnikova, E.	Mo.A-P64	Takahashi, Yu.
Mo.A-P38	TH.B-P11	Fr.D.3_02
Tabares, J.A.	TH.B-P4	Takahashi, Yut.
TU.F-P27	Th.D.1_03	TU.I-P23
TU.H-P11	Th.J.1_04	Takahei, Yuu.
Tabata, C.	TU.B-P19	Mo.A-P86
TH.B-P14	TU.B-P38	Takaira, Y.
TU.A-P67	TU.B-P49	TH.E-P14
TU.B-P45	TU.C-P13	Takakura, H.
Tabis, W.	TU.C-P22	TU.C-P18

Takami, S.	TU.H-P14	Tamaru, S.
FR.D-P71	Takenobu, T.	Th.G-P7
Takamiya, K.	TH.C.1_O2	WE.G2_O3
TU.B-P54	Takeuchi, A.	Tamatsukuri, H.
Takamoto, K.	TH.E-P17	FR.D-P69
FR.D-P13	TU.A.1_I1	TH.C-P99
Takamura, Y.	Takeuchi, J.	Th.D.3_O3
Mo.H-P64	Mo.A-P44	Tamion, A.
Takanashi, K.	Mo.A-P79	TU.F-P25
Mo.F-P6	Mo.L-P60	Tamisari, M.
Mo.H-P74	Takeuchi, T.	Mo.H-P3
Mo.I-P6	TH.A-P22	Mo.I-P38
TU.G-P6	TU.B-P35	Mo.I-P40
WE.D.2_O2	TU.B-P42	TU.G.3_O1
Takano, H.	TU.B-P43	Tamura, R.
Mo.A-P74	TU.E-P20	FR.D-P49
TU.B-P46	Takeyama, S.	Mo.B-P5
TU.B-P56	Fr.D.1_O5	Mo.L-P55
Takano, M.	FR.D-P18	Tan, C.B.
Mo.K-P10	Mo.B-P10	Fr.E.3_O2
Takano, Y.	MO.I.2_O2	Tan, H.
Mo.A-P78	TH.C-P58	Mo.A-P112
Takasaki, A.	TU.A.-59	Tan, R.
TH.C-P55	TU.A-P60	MO.J.2_O4
Takasan, K.	Takezawa, M.	Th.H.1_O2
FR.A-P47	TU.H-P33	Tanabe, Y.
Takase, K.	Takigawa, M.	FR.A-P9
FR.A-P38	TH.A-P10	Tanahashi, M.
Takata, H.	TU.B-P47	TU.B-P51
FR.H-P36	Takita, Y.	Tanaka, A.
Th.K-P33	TU.B-P38	FR.B-P32
Takayanagi, H.	Talantcev, A.	Mo.B-P9
Mo.A-P66	MO.F.1_O2	TH.K-P18
Takeda, A.	Talantsev, A.	TU.B-P15
Mo.A-P81	FR.F-P2	TU.B-P5
Takeda, H.	TH.D-P5	Tanaka, H.
TU.B-P47	TU.D-P1	FR.A-P23
Takeda, N.	Taleb-Ibrahimi, A.	Tanaka, Hi.
TH.C-P126	WE.G.1_O5	FR.F-P9
Takeda, Y.	Talham, D.	TU.B-P57
Mo.L-P41	TH.A-P22	Tanaka, Hid.
TU.B-P55	Tallarida, G.	FR.D-P50
Takemori, N.	TH.F-P17	Mo.H-P66
TU.B-P60	Tamarit, J.L.	TH.A-P14
Takenaka, K.	Th.B.1_O3	TH.A-P18

TH.A-P19	TU.I-P11	WE.J.2_I1
TH.A-P35	Taniguchi, H.	Tarequzzaman, M.
TH.C-P118	TH.A-P28	Mo.F-P21
Tanaka, K.	TH.C-P104	Th.H-P16
Fr.B.3_O4	Taniguchi, M.	Tarequzzman, M.
Tanaka, Kaz.	Fr.C.2_O5	TU.H.1_O5
Th.G-P5	Mo.L-P41	Tashima, M.
WE.G2_I6	TU.B-P38	Mo.G-P7
Tanaka, Ken.	Taniguchi, Tai.	Tashiro, Takah.
FR.H-P10	FR.A-P55	TH.E-P18
Tanaka, M.	Taniguchi, Tak.	Tashiro, Takay.
FR.H-P27	TU.B-P47	Mo.H-P74
TH.F-P25	Taniguchi, Taku.	TU.G-P6
Tanaka, Mas.	TH.F-P13	Taskaev, S.
Mo.A-P78	TH.F-P5	Mo.L-P77
Tanaka, R.	TH.F-P6	Mo.L-P80
FR.I-P35	Taniguchi, Tom.	TU.H-P124
Tanaka, S.	WE.G.1_O3	Tateiwa, N.
FR.D-P49	WE.I.2_O6	TU.B-P77
Mo.L-P55	Taniguchi, Tos.	Tateno, S.
Tanaka, T.	FR.D-P13	FR.I-P32
Mo.G-P4	TANIIKE, T.	TU.B-P9
Th.O-P7	Th.P-P15	Tatetsu, Y.
TU.I-P22	Taniyama, T.	Fr.A.2_O4
Tanaka, To.	Fr.G.3_O3	Taubenheim, C.
TH.C-P120	TU.H-P94	TU.H.2_O3
Tanaka, Y.	Tano, Y.	Tavares, B.
FR.B-P20	Mo.A-P66	TU.C-P8
Tanaka, Yu.	Tanrýseven, S.	Tavares, P.
TH.B.2_O5	Th.O-P23	TU.A-P46
Tanamoto, T.	Tao, J.	TU.A-P65
TU.I-P9	Mo.L-P82	Tawfik, A.E.
Tang, Y.	TU.D-P11	TU.A-P35
MO.A.2_O3	Tao, Q.	Tayade, R.
Tange, H.	Mo.A-P63	TH.I-P25
TU.E-P43	Tapasztó, L.	Tchernyshyov, O.
TU.H-P7	MO.I.1_I1	Th.D.2_O5
Tani, K.	Tarafder, K.	Tchoula Tchokonté, M.
Mo.A-P87	TU.D-P12	TH.C-P109
Tanibe, K.	Tarassenko, R.	Te Velthuis, S.G.E.
TH.C-P93	FR.A-P60	MO.C.1_I1
Tanida, H.	TU.E-P46	Tear, S.
Mo.A-P53	Tarasov, E.	TU.E-P49
TU.B-P11	Mo.L-P72	Tebi, S.
Tanigaki, N.	Tarasov, I.	TU.J.3_O4

Teich, L.	Teoh, H.K.	Th.P-P34
FR.E-P6	TU.I-P18	Tetean, R.
Teixeira, J.M.	TU.I-P8	Mo.L-P62
Mo.H-P43	Terada, N.	Tetienne, J.
Mo.H-P98	FR.D-P71	Th.E.1_I1
TU.J.1_O3	Mo.B-P5	Tezuka, M.
Teixeira, R.	TU.A-P38	TU.C-P21
TU.A-P89	TU.A-P47	Tezuka, N.
Tejada, J.	Terán, F.	Mo.D-P17
TU.B.3_O1	TH.I-P28	Thakur, R.
TU.SP-3	Teran, F.J.	FR.B-P6
Teki, Y.	TU.F-P106	Mo.C-P2
TH.E-P6	Terasaki, A.	TH.J.3_O2
Teleanu, G.	TU.F-P56	TU.A-P70
TU.F-P5	Terashima, T.	TU.H-P2
Telegin, A.	Tu.A.3_O5	Thakur, R.K.
Mo.L-P67	TU.H.2_O4	FR.B-P6
Telegin, S.	WE.F2_O4	Mo.C-P2
TU.H-P55	Terent'ev, K.	TU.A-P70
Telling, N.	TH.D-P14	TU.H-P2
Th.P-P14	Terentev, P.	Thalmeier, P.
Th.P-P9	TH.C-P53	Fr.B.3_O3
Temerov, V.	Tereshchenko, O.	FR.D-P48
TH.C-P35	Fr.C.2_O5	Th.B.2_O2
TH.D-P16	Tereshina, E.	Thanh, N.T.K.
TU.A-P48	Mo.L-P49	Fr.B.1_O3
Temiryazev, A.	TU.G.2_O5	Thanh, T.D.
TH.K-P22	Tereshina, I.	Mo.L-P22
Temiryazeva, M.	Mo.L-P37	Mo.L-P33
TH.K-P22	Mo.L-P49	TU.F-P17
Temnov, V.	Mo.L-P8	TU.H-P4
MO.E.3_O2	Ternes, M.	Thede, M.
Th.I-P13	Fr.I.3_O2	Mo.B-P22
Tence, M.	Terris, B.	Theodoropoulou, N.
TU.F-P57	WE.D.2_I6	Th.L-P6
Teng, C.	Teruya, A.	Thevenard, L.
TH.J-P29	TH.C-P71	Th.I-P10
Tennant, D.	TU.E-P20	Th.I-P5
FR.D-P67	Testa, A.M.	Thiaville, A.
TH.A-P26	Mo.H-P94	Th.J.3_I1
TENNE, D.	Mo.I-P35	WE.I.1_O2
TU.E.1_O4	Th.K-P38	Thiel, L.
TU.F-P40	TU.E.3_O3	MO.E.2_O3
Tenya, K.	Testillano, A.M.	Thielen, P.
Th.C.3_O4	Th.H.1_O5	Th.N-P10

Thiem, S.	MO.F.2_O2	Tiwari, R.
Fr.F.1_O4	Mo.I-P18	FR.C-P6
Thiemann, M.	TH.E3_O4	Tiwari, S.
TU.B-P63	TU.G-P16	TU.A-P49
Thirion, C.	Tierno, P.	Tizianel, S.
TU.H.1_O2	TU.F-P12	Fr.A.3_O1
WE.F.1_I1	TU.F-P13	Tjeng, L.H.
Thoma, P.	Tietze, T.	FR.A-P29
Mo.H-P30	TU.H-P35	Mo.B-P9
Thomas, A.	Tifrea, I.	Th.B.2_O2
WE.H.2_I6	Th.H-P20	TH.K-P18
Thomas, B.	Tighe, C.	TU.B-P15
Mo.A-P57	Fr.B.1_O3	TU.B-P5
Thomas, C.	Tikkanen, J.	TU.F.1_I1
Th.D.2_O2	Mo.H-P52	WE.H.2_I6
Thomas, W.	Th.O-P14	Tkach, I.
WE.I.2_O5	Tikuiðis, K.K.	TH.D-P8
Thompson, J.	Mo.H-P8	WE.C.2_O2
Fr.A.1_O3	Timco, G.	Tkàè, V.
Fr.C.1_O6	TU.D-P7	Mo.L-P7
TU.H.2_O2	Timko, M.	Tobash, P.H.
TU.SP-1	Tu.F-P122	MO.A.2_O5
Thompson, J.D.	TU.F-P29	Tobey, R.I.
MO.A.1_O2	TU.F-P71	Th.I-P7
MO.A.2_O5	TU.F-P78	Tobia, D.
TU.B-P15	TU.F-P91	FR.I-P21
TU.H.2_O5	Timm, C.	Mo.A-P48
Thomson, D.	Fr.B.2_O6	MO.B.1_O2
TH.J-P33	Timmis, J.	TH.C-P81
Thomson, J.D.	Th.E.3_O1	TU.F-P87
TU.B-P69	Timofeev, A.	Tobita, Y.
Thomson, S.	TU.E.2_O6	TU.B-P38
TH.A-P25	Timopheev, A.	Tobola, J.
Thomson, T.	TU.J.1_I1	TH.C-P96
Mo.H-P51	Tito, M.A.	Toda, Y.
TH.J-P3	TU.C-P8	Mo.F-P13
Thonig, D.	Titov, I.	Togawa, Y.
TH.C-P46	Mo.L-P3	TH.C-P61
Tian, B.	TH.C-P40	Togushova, Y.
Th.H.1_O3	TU.C.3_O3	Mo.A-P26
Tian, D.	Titov, M.	Tohyama, T.
TU.E-P33	Mo.C-P8	FR.D-P58
Tiberto, P.	Tiusan, C.	Toji, T.
FR.I-P20	MO.H.1_O4	TU.E-P44
MO.C.2_I1	TU.G-P17	Tokiwa, Y.

Mo.C-P13	Tomiyama, N.	Mo.A-P42
Tokunaga, M.	TU.I-P1	Torras, N.
TH.A-P18	Tomori, K.	Fr.H.3_O2
Th.E.2_O4	TH.C-P71	Torrejon, J.
TU.A-P47	Tonai, H.	WE.G.1_O3
TU.A-P50	TU.B-P25	Torrens-Serra, J.
Tokunaga, Y.	Tong, J.P.	TH.F-P28
Th.F.2_O5	Mo.L-P82	Torrente, C.
TU.A-P22	TH.D-P9	FR.I-P24
TU.A-P25	TU.D-P11	TU.F-P72
TU.A-P61	Tonnerre, J.M.	TU.F-P73
TU.H.2_O5	WE.G2_O4	Torres Molina, T.
Tokura, Y.	Tono, T.	TU.F-P111
FR.F-P4	TH.F-P13	Torres Rincón, L.
Fr.I.1_O3	TH.F-P5	TH.F.P27
MO.H.3_O4	TH.F-P6	Torres, M.B.
Th.F.2_O5	Tonon, X.	FR.H-P17
TU.A-P22	Th.D.3_O4	Torres, T.
TU.A-P25	Topal, U.	WE.SYM_1
Tola, P.	Th.O-P23	Torresi, R.M.
TU.F-P14	TU.H-P48	Mo.K-P9
Tolea, F.	TU.H-P49	Torruella, P.
Mo.L-P53	Töpfer, J.	FR.I-P46
Th.O-P19	TH.C-P57	Tu.B.2_O2
Th.O-P2	Th.O-P26	Tortarolo, M.
Tolentino, H.C.N.	Topic, M.	TH.K-P1
MO.G.1_O5	Mo.L-P74	Toscano, D.
Tomaru, S.	Th.B.1_O5	Mo.K-P12
TU.B-P43	Topole, M.	Mo.K-P13
Tomasovicová, N.	Mo.I-P11	Mo.K-P14
Th.P-P22	TU.H-P34	Toson, P.
Tu.F-P122	Topolovec, S.	Fr.A.1_I1
TU.F-P49	FR.I-P9	TU.H-P107
TU.F-P50	Toreh, K.R.N.	TU.H-P108
Tomaszewicz, E.	Mo.D-P25	TU.H-P110
TH.C-P65	Torelli, P.	WE.B.2_I1
TH.D-P12	FR.H-P31	Tosoni, O.
TU.H-P50	TU.G.1_O5	Th.A.3_O4
Tomczak, Y.	Torii, S.	Toth- Katona, T.
WE.D.2_O3	TU.C.2_O4	Tu.F-P122
Tominaga, J.	Torija, M.	Toth, S.
FR.A-P25	Mo.H-P103	Th.D.3_O1
Tomita, T.	Toriyama, T.	Th.G.3_O1
TU.C-P16	FR.B-P14	Toulemon, D.
TU.F.3_O3	Mo.A-P41	Mo.I-P12

Th.M-P11 Toulouse, C.	Mo.A-P47 Tripathy, D.	FR.H-P20 Tsai, T.
Th.E.1_I1 Tourinho, F.A.	TH.G.1_O2 Trisnanto, S.B.	TU.A-P44 Tsai, W.F.
Th.P-P32 TU.F-P114 Tournus, F.	Fr.E.3_O3 Trodahl, J.	Mo.A-P13 Tsakaloudi, V.
TU.F-P25 Toussaint, J.C.	FR.F-P31 Mo.A-P91 Mo.D-P3 Trohidou, K.	TU.A.2_O4 Tschöpe, A.
FR.I-P28 Mo.K-P26 WE.F.1_I1 Toydemir, B.	MO.B.1_I1 MO.B.1_O5 Mo.H-P83 Mo.I-P32 Mo.I-P33 Mo.J-P15 Th.P-P19 Th.P-P20 TU.F-P21 TU.F-P87 Troiani, H.	Th.L-P2 Th.P-P13 TU.F-P63 Tseng, B.H.
FR.F-P10 FR.F-P15 Toyoda, M.	Mo.L-P35 Mo.L-P35 Tserkovnyak, Y.	FR.I-P8 Tseng, Y.C.
Mo.A-P90 TU.E-P25 TOYODA, S.	Mo.L-P35 Tsiantos, V.	Mo.L-P35 Tsiantos, V.
TU.A.-59 TU.A-P60 Tozer, S.	Th.P-P19 Th.P-P20 TU.F-P21 TU.F-P87 Troiani, H.	TU.SYM_4 Tsiantos, V.
FR.A-P56 Fr.C.2_O2 Th.C-P03 Trassin, M.	TU.F-P53 Troiani, H.E.	Mo.I-P29 Tsubasa, N.
TU.A-P24 Trassinelli, M.	MO.B.1_O2 Mo.K-P9 Trojának, F.	TU.I-P16 Tsuchimoto, S.
Mo.L-P86 TH.K-P14 Trauchessec, V.	Fr.G.3_O2 TU.G.1_O3 Troncoso, R.	TU.B-P29 Tsuchiura, H.
Th.P-P39 Tréjo Rosillo, J.	WE.F.1_O5 Troper, A.	Mo.A-P92 TU.G-P13 TU.H-P128 TU.H-P89 Tsuchiya, T.
Th.P-P39 Treossi, E.	FR.B-P9 FR.E-P16 Mo.A-P76 TH.A-P15 Troyanchuk, I.	Mo.I-P6 TU.I-P20 Tsuei, K.D.
Mo.E-P8 Tretiakov, O.	TH.C-P69 Trujillo Hernandez, J.S.	FR.A-P29 TU.B-P15 Tsujii, H.
TH.J-P30 Tricard, S.	TU.F-P27 TU.H-P11 Trujillo, J.S.	FR.H-P36 Th.K-P33 Tsujii, N.
MO.J.2_O4 Tripathi, S.	TU.H-P37 Trung, J.S.	WE.F2_O5 Tsujimoto, H.
TU.H-P35 Tripathi, T.S.	MO.D.2_O2 Trzaskowska, A.	TH.E-P6 Tsujimoto, M.
FR.D-P59 Tripathi, V.		TU.B-P47 TU.F.3_O3 Tsujimoto, Y.

Mo.B-P2
 TU.A-P38
Tsukahara, H.
 TH.J-P22
 TU.H-P57
Tsukamoto, A.
 Fr.J.2_O4
 Th.F.2_O3
 TH.F-P5
 Th.I-P11
 TH.I-P22
 TU.G-P24
Tsukasa, A.
 TH.F-P21
Tsunashima, S.
 TU.I-P14
 TU.I-P16
Tsunegi, S.
 TH.J-P10
 TH.J-P13
 TH.J-P14
 TU.H.1_O3
 TU.H.1_O4
Tsunetsugu, H.
 FR.B-P24
Tsuneyuki, S.
 Fr.A.2_O4
 TU.E-P11
 TU.E-P36
Tsunoda, R.
 TU.B-P42
Tsurkan, V.
 FR.D-P27
Tsurui, T.
 TU.H-P87
Tsuruta, A.
 FR.B-P26
 TU.B-P18
Tsutaoka, T.
 TH.C-P53
 Th.O-P17
 TU.I.2_O5
Tsutsumi, Y.
 MO.A.1_O4
Tsuya, D.

TU.F-P4
Tsvyashchenko, A.
 TU.C.2_O3
Tu, H.
 FR.A-P9
Tu, K.
 MO.F.2_I1
Tuczek, F.
 MO.I.2_O3
Tukmachev, D.
 Fr.H.2_O3
Tumelero, M.A.
 Th.K-P42
Turcaud, J.
 Mo.L-P79
Turculet, C.
 TU.F-P5
Turek, I.
 TH.C-P8
 TH.E-P1
 TH.E-P2
 TU.F-P20
 WE.C.2_O2
Turmanian, T.
 Mo.H-P103
Turner, J.J.
 TU.E.1_O6
Turner, S.
 FR.I-P5
 TU.F-P95
 TU.H-P16
 TU.H-P27
Tursina, A.
 TH.B-P5
 TU.C-P26
Turta, C.
 MO.I.2_O4
Tusche, C.
 Mo.E-P11
Txoperena, O.
 MO.F.3_O3
Tybell, T.
 Mo.G-P15
Tyberkevych, V.
 TH.J-P9

Tyliszczak, T.
 Fr.E.2_I1
Tzavellas, A.
 Mo.I-P30
Tzitzios, V.
 MO.B.3_O4
 Mo.I-P25
 Mo.I-P30
 TU.F-P100


U

Uchida, H.
 TU.I-P20
Uchida, K.
 Th.H-P14
Uchida, K.I.
 Th.H-P5
Uchida, T.
 TH.C-P2
 Th.J.1_O5
Uchikoshi, T.
 Mo.B-P2
Uchima, K.
 TH.C-P71
 TU.E-P20
Uda, S.
 FR.I-P30
Udagawa, M.
 Fr.D.1_O4
 FR.D-P40
 FR.E-P36
 TU.B-P53
 TU.D-P8
Udby, L.
 Mo.A-P72
Udod, L.
 FR.F-P1
Ueberschär, O.
 Th.O-P29
Ueda, H.
 FR.D-P18
 FR.D-P35

FR.D-P53	FR.H-P26	TU.C-P13
FR.D-P8	FR.I-P34	Umetsu, R.
Fr.F.2_I1	TU.H-P115	Mo.L-P66
Mo.B-P27	TU.H-P132	Th.O-P30
TH.A-P32	Ueno, Y.	TU.E-P21
Ueda, K.	FR.H-P36	TU.E-P35
FR.A-P55	Th.K-P33	TU.H-P82
Mo.H-P66	Üestüener, K.	Umetsu, R.Y.
TH.F-P6	Th.A.3_O3	Fr.A.1_O2
TU.A-P72	Uetake, H.	Mo.L-P71
TU.E-P18	Th.O-P22	Umezawa, T.
Ueda, S.	Ugendar, K.	TU.B-P54
Mo.L-P41	TU.A-P58	Umut, E.
TU.B-P38	Uhlarz, M.	Th.N-P13
TU.G-P6	TH.A-P33	Ünal, A.A.
Ueda, T.	Uhlířová, K.	TU.A-P100
TU.B-P78	Mo.H-P8	Unruh, T.
Ueda, Y.	TH.D-P24	TH.C-P28
FR.A-P12	TU.A-P82	Uozumi, T.
Fr.C.2_O3	TU.E-P46	TU.B-P25
Mo.H-P92	WE.A.1_O3	Upadhyaya, P.
TH.A-P10	Uji, S.	Th.I.2_O1
Uehara, A.	Tu.A.3_O5	Upton, M.
FR.B-P23	Ukleev, V.	WE.F2_O5
Uekusa, H.	Mo.I-P14	Urazhdin, S.
TH.A-P14	Ulfat, I.	Fr.G.1_I1
TH.A-P18	Tu.G.1_O2	Urbánek, M.
Ueland, B.G.	Ulitko, V.	Mo.H-P8
Fr.D.2_O3	FR.B-P33	Urbaniak, M.
Uematsu, G.	Ulrich, C.	Mo.H-P46
Th.H-P12	TU.A-P23	Urbaniak-Kucharczyk, A.
Th.H-P3	Ulyanov, M.	Mo.H-P68
Uemura, Y.	Mo.L-P80	Urbano, R.R.
Fr.B.2_O4	Ulysse, C.	Mo.A-P48
Fr.C.2_O4	We.E.1_O5	TU.B-P2
Fr.G.2_I1	Umeda, K.	TU.F-P26
Fr.I.1_O3	MO.I.3_O4	Urbanowicz, P.
Uen, T.M.	Umegaki, I.	TH.C-P65
TU.A-P44	FR.D-P7	TU.H-P50
Uenishi, K.	FR.D-P8	Urbanski, M.
TU.A-P67	TU.B-P3	FR.I-P39
Uenisi, K.	TU.C-P2	Urcelay-Olabarria, I.
TU.C-P13	Umeo, K.	TU.A-P83
Ueno, T.	Mo.A-P64	TU.A-P93
Fr.A.3_O3	TU.B-P49	Urdaniz, M.C.

Th.M-P14
Urdíroz-Urricelqui, U.
 Tu.F-P123
Uribe-Laverde, M.A.
 Fr.B.2_O1
Urreta, S.E.
 Mo.K-P19
Urriés, I.
 Th.P-P31
Usachev, P.
 Th.G.1_O4
 Th.I-P19
Useinov, N.
 TH.E-P5
Ushio, J.
 TU.H-P19
Usov, N.
 FR.I-P6
 TU.A.1_O2
 TU.F-P34
Uspenskaya, L.S.
 FR.D-P25
 TH.F-P9
 WE.J.2_O2
Ustinov, V.V.
 Mo.H-P34
 Mo.H-P35
Usui, T.
 Mo.B-P20
Utesov, O.
 FR.E-P21
Utsumi, Y.
 FR.A-P29
Uwatoko, Y.
 TH.B-P18
 TH.C-P113
 TH.C-P120
 TH.C-P71
 TH.C-P90
 TH.D-P20
 TU.B-P17
 TU.B-P43
 TU.C-P16
 TU.E-P20
Uyeda, C.

Th.O-P33
 Th.O-P34
Uysalli, Y.
 FR.I-P15


V. Korff Schmising, C.
 Fr.I.1_I1
v. Löhneysen, H.
 Mo.H-P33
 TU.B-P63
 TU.H.2_O3
V. Naletov, V.
 MO.J.3_O3
V. Rodionova, V.
 TU.H-P129
Vackar, J.
 Mo.J-P2
Václavu, M.
 FR.F-P30
Vagadia, M.
 TH.C-P114
Vaia, R.
 Fr.F.2_O4
Vajda, A.
 TU.F-P49
 TU.F-P50
Valadeiro, J.
 Th.O-P54
 Th.P-P28
 TU.I.1_O3
Valcarcel, R.
 Fr.H.3_O2
Valdés-Bango, F.
 Mo.H-P98
 TH.K-P4
Vale, J.
 FR.A-P30
 FR.A-P42
 Th.G.3_O2

Valeanu, M.
 Mo.L-P53
 Th.O-P19
 Th.O-P2
Valencia, S.
 TU.A-P100
Valencuela, R.
 Th.O-P26
Valenti, R.
 Fr.B.2_O2
 FR.D-P55
 FR.E-P15
 WE.E2_I1
Valenzuela, B.
 WE.A.2_O3
Valenzuela, R.
 TH.C-P57
 TU.A.2_O3
 TU.A-P42
 TU.H-P36
Valenzuela, S.O.
 Fr.F.3_I1
 Th.O-P49
 WE.I.2_I2
Valeri, S.
 TU.G-P10
Vališka, M.
 FR.A-P60
 Mo.D-P12
 Th.A.2_O1
 TH.B-P21
Valiullin, A.A.
 Mo.H-P51
Valldor, M.
 Mo.B-P9
Vallejo-Fernandez, G.
 Th.E.3_O1
 TH.K-P19
Valloppilly, S.
 Th.K-P29
Valmianski, I.
 MO.E.3_I1
 Th.L-P3
 TU.A.2_I1
Valvidares Suarez, M.

TH.E-P20	van Lierop, J.	Varier, S.R.
Valvidares, M.	Fr.A.1_05	TH.B-P16
FR.H-P25	Mo.I-P7	Varnakov, S.N.
Mo.H-P84	TU.B.3_04	WE.J.2_11
MO.J.2_05	TU.F-P107	Vartiainen, I.
TH.K-P18	Van Loosdrecht, P.H.M.	WE.E.1_04
Th.L-P5	Th.A.2_03	Varvaro, G.
Valvidares, S.M.	van Tedeloo, G.	Mo.H-P94
Mo.H-P98	Th.L-P5	Mo.I-P35
Th.K-P41	Van Tilburg, L.	Th.K-P38
TU.G-P11	Mo.G-P19	TU.E.3_03
Van de Wiele, B.	Van Tol, J.	TU.F-P81
Fr.G.3_03	Mo.B-P13	TU.H-P81
Th.M-P9	TH.A-P17	TU.J.1_05
van den Brink, J.	Van Waeyenberge, B.	Vas'kovskiy, V.
Th.D.2_04	TH.J-P31	Mo.I-P26
WE.A.1_06	Van Well, N.	Vasilakaki, M.
van der Laan, G.	FR.D-P37	MO.B.1_11
MO.H.2_11	Vaňatka, M.	MO.B.1_05
TH.J-P15	Mo.H-P8	Mo.H-P83
Th.K-P24	Vancso, P.	Th.P-P19
WE.C.2_11	MO.I.1_11	Th.P-P20
van der Linden, P.	Vansteenkiste, A.	TU.F-P21
FR.I-P23	TH.J-P31	TU.F-P87
TU.B-P44	Vansutre, S.S.	Vasile, E.
van der Marel, D.	Th.O-P53	TU.F-P108
TU.C-P31	Varela, M.	Vasilenko, O.
Van Der Sar, T.	FR.I-P46	FR.I-P10
Mo.G-P28	MO.B.1_11	Vasili, H.B.
van der Zant, H.S.J.	Varga, M.	MO.J.2_05
Mo.E-P4	TU.H-P133	Vasiliev, M.
van Dijk, N.	Varga, R.	Th.O-P41
Mo.L-P16	Mo.L-P12	Vasiliev, S.
TU.F-P37	TH.F-P4	FR.I-P34
TU.F-P38	Th.O-P55	Vasilikaki, M.
Van Dijken, S.	TU.E-P5	Mo.I-P32
Fr.G.3_03	TU.E-P9	Vasiljkovic, A.
Mo.H-P76	Vargas, D.	FR.A-P43
TU.A-P77	TU.F-P73	Vasinovich, E.
Van Duijn, J.	Vargas, J.M.	FR.B-P33
FR.D-P10	Th.E.3_02	Vas'kovskiy, V.
Van Elshocht, S.	Vargova, Z.	Mo.I-P34
WE.D.2_03	Mo.L-P12	Vásquez-Mansilla, M.
Van Horne, N.	TU.E-P5	TU.G-P21
MO.H.3_02	TU.E-P9	VASUNDHARA, M.

TU.F-P97

Vasylets, G.

FR.D-P32

TU.D-P4

Vasyuchka, V.I.

Fr.G.1_02

Fr.G.1_05

Mo.G-P13

MO.H.2_02

Th.H-P18

Th.H-P9

TU.E.3_11

Vautrin, C.

Mo.D-P8

Vavassori, P.

TH.E-P9

TH.G.1_02

Th.M-P4

Th.M-P5

Th.M-P9

TU.I.1_04

TU.I-P4

Vavilova, E.

TH.A-P27

TH.A-P9

Th.D.3_02

Vavra, M.

TU.A-P46

Vaz de Araujo, A.C.

TU.F-P1

Vaz, C.

MO.H.3_02

Vaz, C.A.F.

Fr.I.1_11

Mo.H-P37

Vaz, M.

TU.D-P14

Vaz, M.G.F.

TU.D-P15

Vazquez Zubiate, L.

FR.H-P35

Vázquez, M.

Mo.I-P26

Mo.J-P8

Mo.K-P12

Mo.K-P20

Mo.K-P27

Mo.L-P45

TH.F-P4

Th.M-P10

Th.O-P55

Th.O-P57

TU.G.2_04

TU.G-P15

TU.H-P129

TU.H-P68

WE.F.1_02

WE.F.1_04

Vazquez-Victorio, G.

TH.C-P57

Vcelak, J.

Th.O-P10

Th.O-P9

Vecchini, C.

TU.E.1_01

Vedeneev, S.I.

Fr.C.1_05

Vedmedenko, E.

MO.E.3_03

MO.G.1_02

TH.K-P16

Veeturi, S.

TU.H-P134

Veinthal, R.

TU.H-P25

Veis, M.

Mo.H-P78

Mo.H-P8

Mo.L-P20

TH.D-P18

Th.G-P13

Th.M-P17

Th.N-P11

TU.A.1_05

TU.H-P85

Veitemillas- Verdaguier, S.

TU.F-P61

Vekas, L.

TU.F-P108

Vela, S.

TU.J.3_01

Velasquez-Salazar, A.

FR.D-P84

TH.C-P128

Vélez, M.

Fr.H.3_02

TH.H.3_02

TH.K-P4

TU.J.1_03

Vélez, S.

TH.E-P9

Velez-Fort, E.

FR.I-P23

Velikanov, D.

FR.D-P38

TU.F-P88

Vemulkar, T.

Th.P-P3

TU.F-P115

Venkataramani, N.

Mo.H-P50

TU.H-P100

TU.H-P75

Venkatesan, S.

Th.E.1_02

Venkatesan, T.

FR.C-P9

TU.C-P34

Venkatraman, S.

Th.O-P53

Ventura, J.

Mo.H-P43

Mo.K-P27

Mo.L-P90

Th.I.1_03

TU.H.1_05

Verbenko, I.

TU.A-P85

Verdín, E.

Mo.A-P25

Vergnaud, C.

Fr.G.3_04

Mo.D-P27

Mo.D-P30

MO.F.3_02

TH.E-P8 Vergnaux, C.	Vidal-Silva, N. TH.F-P24	TU.A-P46 Vilela-Leão, L.
WE.G.1_O5 Verkholyak, T.	Videtta, V. Th.N-P15	Th.I.2_O6 Villa, L.
FR.D-P9 Vernhet, D.	Vidhyadhiraja, N. TU.B-P24	Mo.D-P27 Villamor, E.
Mo.L-P86 TH.K-P14 Vernier, N.	Vieira Silva, A. Mo.H-P43	TH.E-P9 Th.I.2_O4 Villanova Vidal, E.
TH.F-P17 Véronique, G.	Vieira, F.P. TH.C-P110	Th.M-P8 Villegas, J.
Th.H.2_O2 Verrucchi, P.	Vieira, J. TU.A-P79	MO.C.1_O2 Villegas, J.E.
Fr.F.2_O4 Verschuuren, M.	Vieira, J.M. TU.H-P116	Tu.G.2_I1 WE.A.2_O1 Vinai, F.
Th.M-P18 Verseils, M.	Viennois, R. Th.A.2_O4	FR.I-P20 MO.F.2_O2 Vinai, G.
FR.A-P58 Fr.A-P59 TU.A-P76 Verso, A.	TU.C-P31 Vigneron, J. MO.C.3_O5	FR.H-P31 Vincent, C. Th.H.2_O2 Vinokurov, D.
WE.A.2_O1 Versteeg, R.	Vignolle, B. MO.A.2_I1 MO.A.2_O3	FR.H-P1 Viqueira, M.S. Mo.K-P19 Viret, M.
Th.I-P1 Versteeg, R.B.	Vignolles, D. Fr.A-P59	Th.B.2_I1 Virginie, S. Mo.C-P17 Visani, C.
Th.A.2_O3 Veselov, A.	Viirok, J. TU.A-P25	WE.A.2_O1 Vishwanath, A. MO.SYM_5 Vitos, L.
Mo.G-P10 Vetoshko, P.	Vijayabaskaran, T. WE.J.2_O4	Mo.L-P36 Vitta, S. TU.A-P33 TU.A-P34 TU.A-P49 WE.J.2_O4 Vladimir, T.
Th.N-P6 Th.O-P31 Th.O-P8 Viana, D.	Viktor, V. TU.A-P82	FR.D-P79 Vlaminck, V. TH.I.3_O5
Mo.B-P30 Vianden, R.	Vila, L. Fr.G.3_O4 Mo.D-P30 MO.F.1_O5 MO.F.3_O2 TH.E-P12 TH.E-P3 TH.E-P8 Th.O-P40 TU.G-P27 Vilanova Vidal, E.	
TU.F-P45 Vicario, C.	TH.E-P12 TH.E-P3 TH.E-P8 Th.O-P40 TU.G-P27 Vilar, C. FR.A-P54 Vilarinho, R.	
TU.E.1_O6 Vicent, J.L.		
Mo.E-P8 WE.B.2_I6 Vick, A.		
Mo.I-P2 Vick, D.		
TH.J-P33		

Vlasin, O.	Volkov, O.	TH.F.P27
FR.I-P22	TH.J-P7	Vovk, A.
Vlaskova, K.	Volkov, O.M.	Mo.H-P101
TH.D-P13	Mo.K-P23	Mo.H-P55
Vlasov, V.	Volmer, M.	Vrtnik, S.
Mo.G-P20	Th.K-P32	FR.A-P41
Mo.G-P21	Th.O-P44	Mo.A-P18
Vlasov, V.S.	Vomir, M.	Vu, P.
Th.I-P13	Th.F.1_02	TU.J.2_02
Vock, S.	von Bardeleben, H.J.	Vukadinovic, N.
MO.E.1_05	Th.I-P10	FR.I-P18
MO.E.2_06	von Bergmann, K.	Vyalikh, D.
WE.J.2_05	MO.E.3_03	TU.B-P30
Voesch, W.	MO.G.3_04	TU.F.1_03
TU.C-P26	Th.C.2_11	Vyalikh, D.V.
Vogel, A.	WE.H.1_11	TU.B-P13
WE.H.1_02	von der Ehe, M.	Vyas, K.
Vogel, E.	WE.I.2_05	Th.P-P5
TU.F-P15	von Freymann, G.	Vyborny, K.
Vogel, J.	Th.H-P9	FR.F-P6
TH.F-P7	von Issendorff, B.	Výborný, K.
TU.J.1_02	TU.F-P56	FR.E-P23
WE.H.1_05	von Löhneysen, H.	Vysotsky, S.
WE.I.1_02	Mo.A-P110	Mo.G-P10
Vogel, M.	Mo.A-P30	Th.O-P5
Th.H-P9	von Molnair, S.	TU.H-P54
Vögler, M.	Mo.D-P21	W
Mo.L-P56	von Ranke, P.	
Vohra, Y.	MO.D.2_05	
Fr.C.1_04	Mo.L-P5	Wäckerlin, A.
Vojta, M.	TH.C-P121	TU.D-P12
WE.E2_04	Vondrackova, B.	Wäckerlin, C.
Vojtek, V.	WE.A.1_03	FR.H-P34
TU.H-P41	WE.C.2_02	Fr.I.3_03
Vojtková, L.	Vondráèek, M.	TU.D-P12
Mo.L-P19	FR.A-P60	Wade, J.
Volegov, A.	Vondráèková, B.	Mo.E-P10
Mo.L-P23	TU.E-P46	Wade, T.
TH.C-P101	Vorob'ev, G.P.	FR.I-P43
TH.C-P12	TU.A-P30	We.F.1_03
Volkov, A.	Vorobiev, A.	Wadley, P.
FR.B-P17	Mo.I-P14	MO.C.1_05
Volkov, N.	Voronov, V.	Waerenborgh, J.C.
TH.D-P16	TU.B-P59	WE.C.2_03
TU.A-P48	Voto, M.	

Wagner, E.	Wampler, J.	Wang, R.
FR.D-P21	TH.C-P42	TU.B-P73
Wagner, J.N.	Wan, X.	Wang, S.
TH.C-P119	Th.K-P41	FR.I-P8
Wagner, K.	Wang, B.	Wang, Shi.
TH.K-P17	TH.C-P25	Mo.D-P14
Wahl, U.	Wang, C.	Mo.D-P20
TU.G.1_05	Th.O-P51	Wang, Sim.
Wahlström, E.	Wang, C.C.	TU.A.2_11
Mo.G-P15	Mo.L-P35	Wang, T.
Th.I.1_02	Wang, C.H.	Mo.F-P2
Waizner, J.	Mo.H-P6	Wang, W.
MO.H.3_03	Wang, C.M.	TH.C-P31
Wakabayashi, K.	Mo.H-P6	TH.C-P32
FR.A-P11	Wang, D.	Wang, X.
Wakaoji, H.	Fr.B.2_04	FR.F-P3
FR.I-P25	Wang, H.	Mo.D-P21
Wakasa, R.	Mo.D-P21	Wang, Xia.
TU.I-P19	Mo.H-P65	TU.A-P23
Wakeham, N.	Wang, Han.	Wang, Y.
Fr.C.1_06	Mo.A-P112	Mo.B-P23
TU.H.2_05	Wang, Hon.	Wang, Y.F.
Waki, T.	TU.I-P17	Mo.K-P1
TH.A-P10	Wang, J	TU.A-P54
Wakiya, K.	Mo.L-P31	Wang, Y.Q.
Mo.A-P64	Wang, J.	TU.E.2_02
TU.B-P49	Mo.L-P31	Wang, Yong.
TU.C-P13	Wang, Jian.	Fr.C.1_06
Waliszewski, J.	FR.F-P3	Wang, Yun.
TU.E-P41	Wang, Jie	Mo.A-P27
Walker, H.	TU.F-P33	Th.C.3_01
TH.C-P75	Wang, Jin.	TU.B-P67
Th.G.3_02	TU.E.2_02	Wang, Yut.
Waller, E.H.	Wang, Jun.	FR.F-P16
Th.H-P9	FR.H-P7	FR.G.2_03
Wallisch, W.	Wang, K.L.	Wang, Z.
TU.H-P81	Th.I.2_01	Fr.D.1_02
Walser, M.P.	Wang, L.	TH.C-P16
Mo.D-P31	FR.H-P7	Wang, Zhi.
Walsworth, R.	Wang, Ling.	Mo.F-P2
Mo.G-P28	TU.F-P33	Wani, R.
Walton, A.	Wang, M.	TU.B-P24
Mo.L-P29	Mo.G-P22	Wanklyn, B.M.
Walton, S.	Wang, Q.	TU.A-P6
Th.M-P12	WE.G2_04	Warczewski, J.

FR.E-P29	Watanabe, S.	Th.I-P29
Ward, S.	Fr.J.1_I1	Weichselbaumer, S.
Mo.B-P15	TU.B-P25	MO.H.3_O3
Wardecki, D.	TU.C-P15	Weigand, M.
FR.D-P5	Watanabe, T.	Fr.I.1_I1
Warin, P.	FR.D-P19	MO.H.3_O2
TH.J-P23	Watanabe, Y.	TH.J-P12
Warnicke, P.	Mo.L-P54	TH.J-P9
Fr.I.1_I1	Th.O-P36	Weinen, J.
MO.H.3_O2	TU.H-P58	TU.B-P15
TH.J-P3	Watanuki, R.	Weinl, M.
Warot, B.	TU.E.2_O4	Fr.I.3_O1
Th.C.2_O2	Watashige, T.	Weir, S.
Warot-Fonrose, B.	Tu.A.3_O5	Fr.C.1_O4
Fr.E.3_O4	Waterfield Price, N.	TU.B-P22
FR.I-P43	Th.E.1_O3	Weis, C.
We.F.1_O3	Watier, Y.	TU.D.3_O4
Warren, J.	Mo.B-P9	Weise, B.
FR.I-P4	Watkins-Curry, P.	Mo.L-P48
Warring, H.	MO.SYM_5	Weiss, S.
FR.F-P31	Wawro, A.	MO.A.3_O2
Mo.D-P3	Mo.H-P82	Wells, J.
Wartelle, A.	Th.C.2_O5	Th.H.3_O3
FR.I-P28	Th.G.2_O4	Welter, E.
Washio, K.	TU.G-P28	TH.B-P1
Th.L-P1	Weber, A.	Wen, C.
Waske, A.	Mo.H-P41	Mo.H-P6
Mo.L-P44	Weber, K.	TU.G-P3
Mo.L-P48	TU.C-P9	Wen, C.K.
Th.O-P6	Weerasinghe, J.	TU.G-P8
TU.D.3_O3	TU.E-P30	Wen, H.
Watanabe, H.	Wegrowe, J.	Mo.A-P97
FR.B-P16	Th.H-P1	Wen, W.
Watanabe, I.	WE.I.2_O3	WE.D.2_I1
FR.A-P9	Wegscheider, W.	Wende, H.
TH.C-P93	Mo.D-P31	TU.C.3_O3
TU.A-P53	Wehinger, B.	TU.D.3_O4
Watanabe, K.	Th.C-P03	Weng, Z.
FR.D-P35	Wei, D.	Mo.A-P27
Mo.L-P52	TH.C-P108	Th.C.3_O1
TH.A-P19	Wei, G.	TU.H.2_O2
TH.A-P35	Th.G-P1	Wermeille, D.
TU.D.1_O2	Wei, T.Y.	Th.D.1_I4
Watanabe, Kaz.	FR.D-P42	Werner, D.
FR.I-P30	Wei, Y.	Th.O-P6

Werwinski, M.Fr.A.1_11
TU.E-P45**Weschke, E.**FR.F-P18
Mo.A-P108
MO.I.2_03
TU.H-P31**Westerholt, K.**

TH.K-P9

Westphal, F.Th.P-P2
TU.B.3_02**Wetterskog, E.**Th.M-P20
TU.B.3_02
TU.F-P101
TU.F-P102**Weyer, G.**

TU.G.1_05

Whang, H.TH.E-P15
TH.F-P19**Whangbo, M.H.**

Mo.B-P25

Wheeler, E.FR.B-P30
Th.D.3_01**Wheelwright, J.**

Th.G.2_06

White, J.

TU.A-P27

White, J.S.

Mo.A-P55

Whitmore, L.C.

Th.L-P4

Wiater, M.

Th.G.2_04

Widiez, J.Mo.D-P27
MO.F.3_02**Wiebe, J.**

Fr.I.3_02

Wiedemann, B.

Mo.H-P12

Mo.H-P56

Mo.H-P70

Wiedmann, S.

MO.SYM_2

Wiedwald, U.

WE.B.2_11

Wiendlocha, B.

Mo.A-P96

Wierschem, K.

Fr.F.1_11

Wiese, K.

TH.F-P20

Wiesendanger, R.

FR.H-P8

Fr.I.3_01

Fr.I.3_02

MO.E.3_03

MO.G.3_04

Th.C.2_11

TH.K-P16

WE.G2_02

Wildes, A.

Fr.G.2_04

TH.C-P82

TU.D.1_03

Wilhelm, F.

MO.I.2_11

MO.I.2_04

TH.A-P21

TH.E-P20

Th.J.2_04

TU.B-P70

TU.C.3_03

TU.H-P31

TU.J.3_02

Wilhelm, H.

Mo.A-P109

TH.J-P35

Wilhem, F.

TU.J.1_04

Wille, H.

FR.I-P19

TU.C.1_02

TU.I.1_05

WE.E.1_03

Willers, T.

TU.B-P15

Willinger, M.G.

Th.K-P43

Wilson, M.

Fr.B.2_04

Fr.C.2_04

Wilson, N.

Mo.L-P56

Windsor, W.

TU.E.1_03

Windsor, W.Y.

Fr.B.2_01

Winer, G.

FR.H-P14

Wingert, J.

TH.C-P42

Winiarski, W.

FR.I-P36

Winkler, E.L.

FR.I-P21

MO.B.1_02

TH.C-P81

TU.F-P53

TU.F-P87

Winkler, H.

FR.A-P50

TH.B-P12

Winpenny, R.

TU.D-P7

Winter, S.

TU.E-P33

Wintz, S.

TH.J-P9

Wirth, S.

TH.B-P3

TU.F.1_11

Wisniewski, A.

Mo.I-P41

TH.C-P1

Wiśniewski, P.

FR.A-P28

Fr.C.1_03

Mo.A-P107

Th.O-P24

Witas, P.	FR.D-P12	TH.K-P19
TU.B-P1	Mo.A-P22	Wu, Hua
TU.E-P19	TH.A-P27	TU.I-P17
Woelfle, P.	Wong, D.W.	Wu, J.W.
WE.E2_O4	Fr.E.3_O2	MO.B.3_O3
Wohlhüter, P.	Wong, H.F.	Mo.E-P5
MO.H.3_O2	FR.H-P9	Wu, K.H.
TH.J-P3	Wong, K.L.	TU.A-P44
Woike, T.	Th.I.2_O1	Wu, M.
TU.C-P9	Woo, C.S.	MO.H.2_O3
Wojciechowski, T.	Th.E.2_O5	Wu, M.W.
Th.G.2_O4	Woodcock, T.G.	Mo.D-P8
Wojcieszuk, D.	MO.D.1_O3	Wu, S.Y.
FR.E-P29	MO.D.1_O4	TH.C-P108
Wojcik, M.	Mo.L-P57	Wu, T.H.
TU.A-P62	Mo.L-P83	TH.C-P108
TU.A-P63	Worschech, L.	Wu, Y.
Wojtowicz, T.	TU.I-P4	FR.A-P29
Th.G.2_O4	Wosnitza, J.	MO.B.3_O2
Wojtyniak, M.	Fr.D.1_O2	MO.C.3_O2
TU.H-P12	FR.D-P11	Mo.H-P28
Wölbing, R.	FR.D-P27	Mo.H-P65
MO.E.2_O1	Mo.L-P39	Wulf, E.
Wolf, B.	TH.A-P33	Mo.B-P4
FR.D-P55	TH.C-P27	Wulfhekel, W.
FR.D-P76	Wosnitza, Joch.	Th.I-P3
Wolf, T.	TU.B-P48	Wunderlich, J.
Fr.D-P87	Wren, T.	Fr.G.3_O2
Mo.A-P110	Mo.A-P15	Wurmehl, S.
Mo.A-P30	Wroczynskij, Y.	Fr.B.2_O6
Mo.A-P97	Mo.I-P7	Mo.A-P103
Tu.A.3_O5	TU.B.3_O4	Mo.A-P20
Wolf, W.	Wrona, J.	Mo.A-P22
Fr.B.3_O1	Mo.H-P105	Mo.A-P98
Wolff, U.	Th.O-P24	Th.D.3_O2
MO.E.2_O6	Wu, A.	Würschum, R.
Th.M-P18	TH.C-P25	FR.I-P9
Wolff-Fabris, F.	Wu, C.B.	Wurz, M.
FR.I-P4	FR.H-P29	Th.O-P13
Wollmann, L.	wu, G.	Wysocki, A.
TU.E-P28	TH.C-P31	TH.C-P88
Wolter, A.U.B.	TH.C-P32	Wysokiński, M.
Mo.A-P103	Wu, H.C.	FR.B-P22
Mo.A-P20	FR.D-P42	WE.F2_O6
Wolter-Giraud, A.	Wu, H.J.	Wyss, M.

MO.E.2_O1

X

Xi, X.

Mo.A-P111
Mo.A-P40
TU.A-P88

Xianggang, Q.

Mo.A-P62

Xiao, F.

TH.A-P33

Xiao, J.

FR.H-P2

Xiao, S.

Th.G-P1

Xiao, Y.

Mo.A-P57

Xing, L.

Fr.B.2_O4

Xiong, L.

Th.M-P2

Xiong, P.

Mo.D-P21

Xu, B.

Fr.A.2_O2

Xu, D.

TH.E-P13

Xu, F.

TU.A-P72

Xu, H.

FR.I-P45
Th.F.2_O2

Xu, J.

FR.D-P83
TH.A-P42

Xu, Jia

Mo.H-P27
Mo.L-P34

Xu, X.

Mo.L-P71

Xu, Xiaoh.

Th.K-P35

Xu, Xue.

Mo.L-P82

TH.D-P9

TU.D-P11

Xu, Z.H.

FR.I-P8

Xu, Zh.

Mo.A-P63
Mo.A-P75
TU.C-P29

Xu, Zhuo

Th.I.2_O5

Xuriguera, E.

FR.I-P46

Y

Ya, X.

Mo.G-P4
Th.O-P7

Yaacob, N.

TU.E.3_O2

Yaacoub, N.

Mo.J-P10
TU.H-P36

Yabukami, S.

Th.O-P22

Yacoby, A.

Mo.G-P28

Yagasaki, K.

TH.C-P71

Yager, B.

FR.A-P24

Yaguchi, H.

TH.D-P21

Yakata, S.

Mo.G-P17
Mo.G-P18

Mo.H-P59

Mo.I-P23

TH.E-P16

Yakhou-Harris, F.

FR.I-P23

Yako, H.

Mo.F-P6

Yakovlev, I.

WE.J.2_I1

Yakushiji, K.

FR.A-P51

Th.G-P7

TH.J-P10

TH.J-P13

TH.J-P14

TU.H.1_O3

TU.H.1_O4

WE.D.2_O5

WE.I.1_O5

Yakushiji, Kei

WE.G2_I6

Yamad, K.

Th.G-P3

Yamada, A.

TU.B-P8

Yamada, Kaz.

FR.D-P1

Yamada, Kei.

Mo.F-P5

TH.F-P3

Th.G-P2

TH.J-P2

Yamada, Khi.

Th.G-P14

Yamada, M.

Fr.A.3_O2

Yamada, S.

FR.D-P19

Yamada, Shig.

TU.A-P7

Yamada, Shin.

Mo.D-P19

Th.H-P2

TU.E-P48

Yamada, T.

FR.E-P5

Yamada, Y.

TH.B-P4

TU.B-P19

Yamagami, H.

TU.B-P55

TU.B-P77

Yamaguchi, A.	Mo.G-P18	Yanagihara, H.
TH.B-P18	Mo.G-P8	FR.H-P15
Yamaguchi, H.	Yamanouchi, M.	Mo.F-P18
TH.C-P103	Th.O-P52	Th.H-P14
Yamaguchi, M.	Yamaoka, H.	TU.G-P9
TH.K-P12	Mo.A-P78	TU.H-P87
Yamaji, T.	WE.F2_05	Yanagisawa, T.
MO.H.2_05	Yamasaki, K.	TH.B-P14
Yamakawa, Y.	Th.H-P2	TU.A-P67
Fr.B.2_05	Yamasaki, Y.	TU.B-P48
Yamamoto, D.	TH.A-P29	TU.B-P50
FR.E-P12	Yamashita, M.	Yanai, T.
TH.C-P54	FR.B-P10	Mo.L-P54
TU.C.3_01	Yamashita, T.	Th.O-P36
Yamamoto, E.	TH.C-P120	TU.H-P38
MO.A.1_04	TH.C-P58	TU.H-P58
TU.B-P55	Yamashiya, T.	TU.H-P86
TU.B-P77	TU.C-P18	Yanes Diaz, R.
Yamamoto, I.	Yamauchi, K.	TH.J-P27
TU.E.2_04	TU.A-P14	Yanes-Diaz, R.
Yamamoto, S.	TU.E-P25	TU.G.3_04
Th.O-P17	Yamauchi, T.	Yanez, W.
TU.I.2_05	FR.A-P12	TH.I.3_05
Yamamoto, T.	Fr.C.2_03	Yang, B.Y.
Mo.F-P6	Yamaura, J.	WE.D.2_11
Yamamoto, Y.	FR.A-P15	Yang, C.H.
Mo.A-P78	FR.A-P17	Th.E.2_05
Yamamura, R.	Yamaura, K.	TU.A-P36
TU.E-P14	Mo.B-P2	Yang, D.J.
Yamamura, T.	Yamazaki, S.	Mo.L-P82
FR.D-P61	TH.B-P14	TU.D-P11
Mo.L-P64	Yamazaki, Tak.	Yang, F.
TH.A-P13	TU.F-P10	FR.A-P6
TH.D-P3	TU.F-P69	Yang, H.D.
Yamanaka, S.	TU.F-P70	FR.D-P42
TU.I-P23	Yamazaki, Te.	Yang, Hong.
Yamanaka, T.	TH.D-P21	Th.J.3_11
WE.F2_04	Yan, B.	Yang, Hung.
Yamane, Y.	Fr.C.1_02	Mo.C-P21
Mo.A-P64	MO.SYM_4	Yang, Hyun.
TH.J-P8	Th.A.1_02	Mo.B-P23
Yamani, Z.	Yan, C.	Yang, I.
TU.E.2_03	Mo.K-P10	TU.A-P16
Yamanoi, K.	Yan, S.	Yang, J.
Mo.G-P17	Mo.F-P12	FR.D-P18

Mo.A-P112	Yaresko, A.	FR.F-P12
Yang, L.	Mo.C-P6	Yiu, Y.
Th.G-P6	Yartys, V.	Mo.A-P102
TU.B-P67	TH.A-P12	Ynagihara, R.
Yang, L.T.	Yashima, M.	Th.O-P34
TU.A-P54	Mo.A-P87	Yodoshi, N.
Yang, P.	Yasin, S.	TU.H-P67
Th.E.2_05	FR.D-P27	Yogi, M.
Yang, S.	TH.D-P2	TH.B-P8
Th.I-P16	TU.B-P48	TU.E-P44
Yang, X.	Yasin, S.M.	Yokoi, M.
Mo.A-P63	TH.C-P117	Th.O-P33
Mo.A-P75	Yasuoka, H.	Yokoo, T.
Yang, Y.	TU.H.2_05	FR.A-P37
Fr.E.3_02	Ye, F.	TH.A-P7
MO.B.3_02	TU.E.2_02	TU.A-P90
MO.C.3_02	Ye, J.	Yokota, H.
Yang, Z.	Mo.H-P100	Mo.H-P71
Th.O-P4	Mo.H-P12	Yokotani, Y.
Yang, Zhi.	Mo.H-P56	Mo.G-P17
MO.B.3_02	Ye, M.	Mo.G-P18
MO.C.3_02	Fr.C.2_05	Yokoyama, T.
Yano, K.	Mo.L-P41	Mo.H-P72
TU.B-P31	Yedra, L.	Yoneda, Y.
TU.E-P43	FR.I-P46	Fr.A-P64
Yano, M.	Th.K-P45	Yonemoto, A.
Fr.A.2_05	Tu.B.2_02	FR.A-P37
Fr.A.3_03	Yeninas, S.	Yonezawa, S.
MO.D.1_04	Fr.D.2_03	Mo.A-P66
Th.L-P1	Yershov, K.	Th.C.3_04
TU.H-P115	Mo.K-P23	Yoo, S.C.
TU.H-P63	Yi, M.	TH.F-P11
Yanushkevich, K.	Fr.A.2_02	TH.J-P11
FR.F-P1	Yibolie	Yoo, S.I.
TU.A-P4	Mo.L-P16	TU.H-P21
Yanuskevich, K.	Yim, C.	TU.H-P32
Mo.D-P6	TH.A-P9	Yoon, J.
Yao, C.	Yim, H.	Mo.G-P24
Mo.A-P36	TU.H-P113	Yoon, Seun.
Yao, Y.	Yin, Yul.	Th.I-P9
TH.C-P126	Mo.C-P22	Yoon, Sung.
Yaochen, S.Q.	Yin, Yux.	FR.D-P52
Mo.H-P5	Fr.I.2_05	TH.C-P93
Yaouanc, A.	WE.G.1_02	York, S.
MO.A-P2	Ying, M.	FR.A-P10

Yoshida, H. Tu.E-P51	TH.A-P7	TU.H-P77
Yoshida, M. TU.B-P47	Yoshizawa, K. TU.E-P36	Yu, Sim. Th.N-P1
Yoshida, O. Fr.C.3_03	You, C. Fr.I.2_05	Yu, X.Z. FR.F-P4
Yoshida, T. TU.C-P22	Mo.C-P7	Yu, Xue. Mo.D-P21
TU.C-P27	Mo.G-P24	Yuan, H. Mo.A-P27
Yoshida, Tak. Fr.A-P64	WE.G.1_02	Th.C.3_01
Yoshida, Tsu. FR.A-P27	You, J. TU.H-P21	TU.B-P67
Yoshii, T. TU.C.2_02	TU.H-P32	TU.H.2_02
Yoshikawa, D. FR.H-P18	You, T.S. Mo.L-P33	Yuan, S. TH.C-P91
Th.G-P4	You, W. TH.A-P6	Yuan, Y. Mo.D-P10
Yoshikawa, H. Th.F.2_03	Young Yong, N. TU.F-P8	Yuasa, S. TH.J-P13
Yoshikawa, Y. TU.B-P76	Young, A. Mo.H-P81	TH.J-P14
Yoshimine, I. Th.I-P8	Yousupov, D. TU.A-P85	Yuasa, Shin. FR.A-P51
Yoshimura, K. FR.D-P53	Yu, G. Th.I.2_01	Mo.D-P22
FR.D-P8	Yu, H. Mo.H-P65	MO.H.2_05
TH.A-P32	Yu, J. TU.E-P10	Th.G-P5
TU.C-P2	TU.H-P112	Th.G-P7
Yoshimura, S. MO.E.2_04	TU.H-P13	TH.J-P10
Yoshimura, Y. TH.F-P6	Yu, J.F. TU.A.3_01	Th.N-P2
Yoshinaga, S. TU.E-P35	Yu, N.T.C. Mo.I-P2	Th.N-P3
Yoshioka, T. Mo.A-P92	Yu, R. Mo.A-P31	TU.H.1_03
TU.G-P13	Yu, S. Mo.L-P22	TU.H.1_04
TU.H-P128	Yu, S.C. Mo.L-P33	WE.D.2_05
TU.H-P89	Yu, Se.Ch. FR.E-P1	WE.G2_I6
Yoshizawa, D. Mo.B-P12	FR.F-P14	WE.G2_03
TH.A-P22	Mo.L-P67	WE.I.1_05
TH.C-P61	TU.F-P17	Yudanov, N. Th.O-P46
Yoshizawa, H. TU.H-P4	TU.H-P4	Yue, M. TH.C-P31
		TH.C-P32
		Yun, S.J. TH.E-P15
		TH.F-P19
		Yun, Seok. TU.H-P47
		Yunoki, S.

FR.A-P3
FR.B-P16
Mo.C-P3
Yusuf, S.M.

FR.D-P34
Yuya, F.
Mo.G-P24
Yüzüak, E.
Mo.L-P42

Z

Zabel, H.
TH.K-P9

Zabila, Y.
WE.E.1_02

Zablotskii, V.
Fr.H.2_03
Fr.H.2_04
FR.I-P3

Zabow, G.
Th.P-P6

Zach, R.
TH.C-P96

Zadro, K.
WE.A.2_02

Zagar, K.
TU.H-P42

Zagrebin, M.
FR.E-P20

Zaharko, O.
FR.D-P79
Mo.A.1_05
Tu.C.3_05

Zaher, A.
Th.P-P17

Zahn, D.R.T.
Mo.H-P30

Zahnd, G.
Fr.G.3_04
TH.E-P8

Zahradnik, M.
TH.D-P18
TU.A.1_05

TU.H-P85
Zaim, A.

Mo.K-P32
TU.F-P112

Zaim, N.
Mo.K-P32
TU.F-P112

Zajarniuk, T.
TH.C-P35
TU.E-P41

Zakharchuk, I.
Mo.L-P3
TH.C-P40

Zakharov, A.
TH.K-P22

Zaleski, K.
Mo.I-P25
TU.C.3_04

Zaleski, P.
TU.E-P41

Zaliznyak, I.
Mo.B-P7
MO.I.1_02

Zamani, F.
FR.B-P11

Zambrano, G.
TU.F-P24

Zamorano, R.
Mo.H-P47

TU.H-P127
Zamora-Peredo, L.

FR.H-P24
Zamudio-Bayer, V.

TU.F-P56
Zanardelli, M.
Fr.H.2_02

Zaoui, A.
FR.I-P14

Zapata Farfan, J.
Th.G-P12

Zapien, J.A.
Mo.H-P5

Zardán Gómez de la Torre, T.
Th.H.2_05

Zarzycki, A.

Th.I.3_02
Th.K-P36
Th.K-P49
WE.E.1_02

Zaspalis, V.
Mo.L-P88
TU.A.2_04
TU.H-P126
TU.H-P9

Zaum, S.
Fr.H.1_02
Fr.H.1_03

Závěta, K.
TH.C-P39
Th.O-P9
TU.A-P20

Zavisova, V.
Th.P-P22

Th.P-P30
Th.P-P37
Tu.F-P122
TU.F-P48

Zavisová, V.
TU.F-P49

Závisová, V.
TU.F-P50

Závita, K.
TH.C-P34

Zayets, V.
FR.F-P9
TH.E-P4

Th.N-P2
Th.N-P3

Zehani, K.
Fr.F.3_02
Mo.L-P26
Mo.L-P63

Zehner, J.
Th.E.3_01

Zeissler, K.
Th.M-P12
WE.B.2_04

Zeitler, U.
MO.SYM_2

Zeldov, E.

Mo.H-P81	Mo.J-P7	MO.I.1_04
Zelenak, V.	Mo.L-P34	TH.A-P33
TU.F-P84	Zhang, W.M.	TH.A-P5
Zelenakova, A.	FR.D-P13	Zheng, F.
TU.F-P84	Zhang, X.	MO.E.2_04
Zemen, J.	Th.A.2_06	Zheng, K.
Mo.L-P85	Zhang, Xian.	Mo.K-P10
Zenatti, A.	Mo.E-P7	Zheng, Y.
Mo.K-P3	Mo.H-P89	Mo.L-P86
Zeng, L.	TH.I-P24	Zherlitsyn, S.
TU.B.3_02	Zhang, Xiao.	FR.D-P27
Zeng, S.W.	Mo.D-P2	TH.D-P2
TU.C-P34	Mo.D-P5	TU.B-P48
Zentková, M.	Zhang, Y.	Zhigadlo, N.
TU.A-P18	TU.H-P67	MO.A.3_04
TU.A-P46	Zhang, Yian.	Mo.A-P37
TU.A-P82	Mo.A-P36	Zhitomirsky, M.
TU.C-P12	Zhang, Yiw.	FR.D-P11
Zhan, Q.	MO.C.1_04	Mo.B-P24
TU.E-P8	Zhang, Z.	TU.D.2_14
Zhang, C.	Th.C.3_02	Zhou, S.
MO.H.1_03	Zhang, Ze	FR.F-P16
MO.H.1_05	Mo.K-P10	FR.F-P18
Zhang, F.C.	Zhao, J.	FR.G.2_03
Mo.A-P13	Mo.D-P21	Mo.D-P10
Zhang, H.	Mo.H-P65	Mo.H-P58
TH.C-P31	TH.B-P17	Zhou, W.
TH.C-P32	Zhao, K.	WE.D.2_02
Th.G-P6	Fr.G.2_11	Zhu, C.
Zhang, J.	Zhao, X.	Fr.J.2_12
Mo.F.2_05	MO.A.2_03	Zhu, J.X.
Th.C.3_01	Zhao, Xian.	Fr.A.1_03
TH.F-P1	TH.C-P25	TU.H.2_05
TU.C.2_04	Zhao, Y.	Zhu, L.
Zhang, K.	Fr.D.2_03	TH.B-P17
Mo.L-P82	Zhao, Yang.	Zhu, M.
TH.C-P50	FR.B-P7	Th.G-P6
Zhang, S.	Zhao, Yong.	Zhu, S.
Mo.H-P70	Th.G-P6	Fr.C.2_05
Th.G-P6	Zharkov, S.	Mo.L-P41
TU.D.1_11	TU.F-P88	Zhu, Y.
Zhang, W.	Zheludev, A.	Th.I-P1
Mo.A-P7	Mo.B-P22	Zhu, Y.M.
Th.K-P29	Mo.B-P4	TU.E-P8
Zhang, W.D.	Mo.B-P7	Zhu, Yao.

TH.E-P13 Zhu, Z.	MO.C.1_O2 Zinin, A.	Mo.A-P91 Zukovic, M.
Mo.C-P12	Mo.L-P72	FR.D-P36
Mo.H-P27	Zivieri, R.	FR.D-P39
Mo.L-P34	Mo.H-P3	FR.D-P74
Zhukov, A.	Zivkovic, I.	Zülicke, U.
Mo.L-P12	MO.G.3_O3	FR.A-P49
Mo.L-P61	Zivotsky, O.	Župan, J.
Th.O-P46	Th.O-P11	Mo.L-P81
TU.A.1_O3	Th.O-P20	Žužek Rožman, K.
TU.E-P9	TU.F-P20	Mo.I-P11
Zhukova, V.	Zmorayová, K.	TU.H-P34
Mo.L-P12	Mo.L-P19	Zvereva, E.
Mo.L-P61	Zobelli, A.	Th.A.1_O4
TU.E-P9	TU.A-P100	Zvezdin, A.
Zhumageldin, U.	Zocco, D.A	Th.F.1_O3
Mo.J-P17	Fr.H.1_O2	Th.N-P12
Zhuravlev, I.	Mo.A-P30	Th.O-P31
Fr.D.3_O4	Zong, B.	Th.O-P8
Zickler, G.A.	MO.C.3_O2	TU.A-P30
TU.H-P107	Zoppellaro, G.	Zviagina, L.
TU.H-P108	Th.E.3_O2	TH.A-P33
TU.H-P110	Zorin, A.	Zvyagin, A.
Ziebeck, G.A.	MO.E.2_O1	TH.A-P33
Fr.B.1_O3	Zorko, A.	TH.C-P35
Ziegler, C.	Tu.C.3_O5	Zvyagin, A.A.
Fr.I.3_O4	Zotos, X.	FR.D-P27
Ziemys, G.	TH.A-P37	TH.D-P2
Th.O-P28	Zou, L.	Zvyagin, S.
TU.I-P13	FR.B-P7	TH.A-P33
Zierold, R.	Zou, W.	Zvyagin, S.A.
Mo.K-P20	Th.K-P41	TH.C-P79
Ziêtek, S.	Zou, Y.	Zwicknagl, G.
Th.O-P24	Th.K-P41	WE.F2_O2
Zighem, F.	Zou, Yang.	Zysler, R.
MO.H.1_O4	Mo.A-P70	MO.B.1_O2
TU.G-P17	WE.F.2_I1	TU.F-P53
Ziman, T.	Zubáč, J.	TU.F-P87
TH.I.1_O4	TH.D-P13	Zyuzin, A.
Th.I.2_O5	TU.B-P72	TU.E.2_O6
Zimmer, F.	Zubavichus, Y.	Zywczak, A.
FR.D-P80	TU.H-P31	Mo.H-P105
Zimmermann, S.	Zucolotto, B.	Żywczak, A.
Th.D.3_O2	TU.F-P75	Th.O-P24
Zimmers, A.	Zuelicke, U.	

